FUNDAMENTALS OF

BIOCHEMISTRY

THIRD EDITION

Life at the Molecular Level

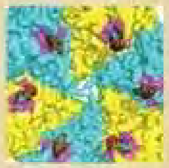

Donald Voet Judith G. Voet Charlotte W. Pratt

VISIT…

LANZAROTE
Caliente.com

Success in Biochemistry is just a click away...

Every one of your students has the potential to make a difference. And realizing that potential starts right here, in your course.

When students succeed in your course—when they stay on-task and make the breakthrough that turns confusion into confidence—they are empowered to realize the possibilities for greatness that lie within each of them. We know your goal is to create an environment where students reach their full potential and experience the exhilaration of academic success that will last them a lifetime. *WileyPLUS* can help you reach that goal.

Wiley**PLUS** is an online suite of resources—including the complete text—that will help your students:

- come to class better prepared for your lectures
- get immediate feedback and context-sensitive help on assignments and quizzes
- track their progress throughout the course

> "I just wanted to say how much this program helped me in studying… I was able to actually see my mistakes and correct them. … I really think that other students should have the chance to use *WileyPLUS*."
>
> Ashlee Krisko, *Oakland University*

---

www.wileyplus.com

88% of students surveyed said it improved their understanding of the material.*

FOR INSTRUCTORS

WileyPLUS is built around the activities you perform in your class each day. With WileyPLUS you can:

Prepare & Present

Create outstanding class presentations using a wealth of resources such as enhanced art, PowerPoint slides containing text art optimized for presentation, animated figures, Guided Explorations, Interactive Exercises (featuring Jmol rendered 3D molecules), and kinemages. You can even add materials you have created yourself.

Create Assignments

Automate the assigning and grading of homework or quizzes by using the provided question banks, featuring over 700 conceptual questions, with detailed answer feedback.

Track Student Progress

Keep track of your students' progress and analyze individual and overall class results.

Now Available with
WebCT, eCollege, and ANGEL Learning!

> "It has been a great help, and I believe it has helped me to achieve a better grade."
>
> Michael Morris,
> *Columbia Basin College*

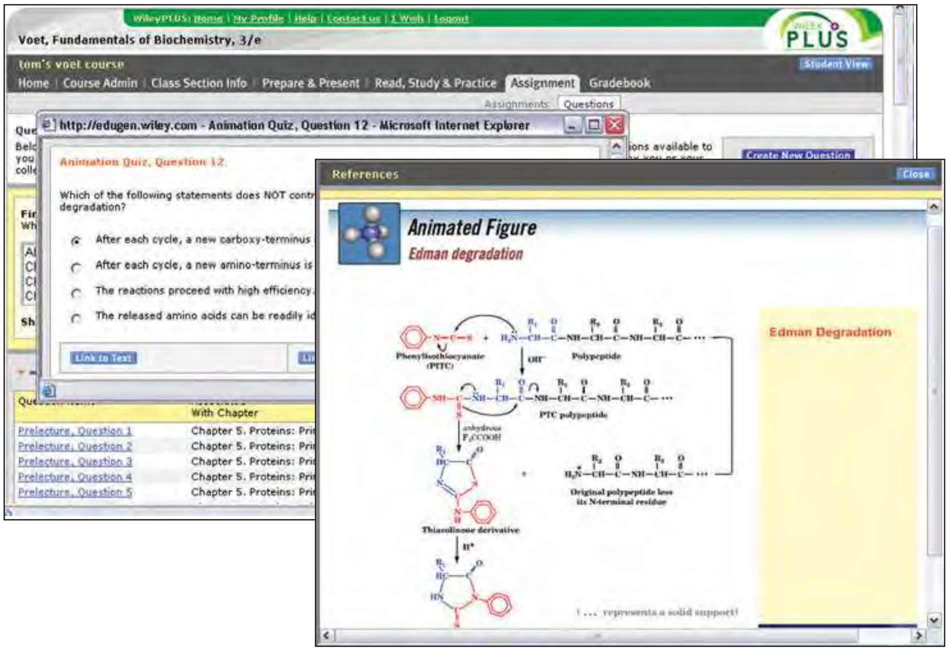
WileyPLUS: Home | My Profile | Help | Contact us | I Wish | Logout
Voet, Fundamentals of Biochemistry, 3/e
tom's voet course
Home | Course Admin | Class Section Info | Prepare & Present | Read, Study & Practice | Assignment | Gradebook
Student View
Assignments | Questions
Create New Question
http://edugen.wiley.com - Animation Quiz, Question 12 - Microsoft Internet Explorer
Animation Quiz, Question 12
Link to Text
With Chapter
References
Close
Animated Figure
Edman degradation
Edman Degradation
Phenylisothiocyanate (PTIC)
Polypeptide
OH^-
PTC polypeptide
anhydrous F_3CCOOH
Thiazolinone derivative
Original polypeptide less its N-terminal residue
H^+
(. . . represents a solid support)

Which of the following statements does NOT contr
degradation?

- ● After each cycle, a new carboxy-terminus
- ○ After each cycle, a new amino-terminus is
- ○ The reactions proceed with high efficiency.
- ○ The released amino acids can be readily id

ions available to

	With Chapter
Prelecture, Question 1	Chapter 5. Proteins: Pri
Prelecture, Question 2	Chapter 5. Proteins: Pri
Prelecture, Question 3	Chapter 5. Proteins: Pri
Prelecture, Question 4	Chapter 5. Proteins: Pri
Prelecture, Question 5	Chapter 5. Proteins: Pri

FOR STUDENTS

You have the potential to make a difference!

WileyPLUS is a powerful online system packed with features to help you make the most of your potential and get the best grade you can!

With WileyPLUS you get:

- A complete online version of your text and other study resources.
- Problem-solving help, instant grading, and feedback on your homework and quizzes.
- The ability to track your progress and grades throughout the term.

For more information on what *WileyPLUS* can do to help you and your students reach their potential, please visit www.wileyplus.com/experience.

82% of students surveyed said it made them better prepared for tests. *

*Based upon 7,000 responses to student surveys in academic year 2006-2007.

WILEY PLUS

THIRD EDITION

FUNDAMENTALS OF
Biochemistry
LIFE AT THE MOLECULAR LEVEL

Donald Voet
University of Pennsylvania

Judith G. Voet
Swarthmore College, Emeritus

Charlotte W. Pratt
Seattle Pacific University

WILEY

John Wiley & Sons, Inc.

IN MEMORY OF WILLIAM P. JENCKS

scholar, teacher, friend

Vice-President & Executive Publisher	Kaye Pace
Associate Publisher	Petra Recter
Marketing Manager	Amanda Wainer
Assistant Editor	Alyson Rentrop
Senior Production Editor	Sandra Dumas
Production Manager	Dorothy Sinclair
Director of Creative Services	Harry Nolan
Cover Design	Madelyn Lesure
Text Design	Laura C. Ierardi
Photo Department Manager	Hilary Newman
Photo Editors	Hilary Newman, Sheena Goldstein
Illustration Editor	Sigmund Malinowski
Pathways of Discovery Portraits	Wendy Wray
Senior Media Editor	Thomas Kulesa
Production Management Services	Suzanne Ingrao/Ingrao Associates

Background Photo Cover Credit: Lester Lefkowitz/Getty Images

Inset Photo Credits: Based on X-ray structures by (left to right) Thomas Steitz, Yale University; Daniel Koshland, Jr., University of California at Berkeley; Emmanual Skordalakis and James Berger, University of California at Berkeley; Nikolaus Grigorieff and Richard Henderson, MRC Laboratory of Molecular Biology, U.K.; Thomas Steitz, Yale University.

This book was set in 10/12 Times Ten by Aptara and printed and bound by Courier/Kendallville. The cover was printed by Phoenix Color Corporation.

This book is printed on acid free paper. ∞

Copyright © 2008 by Donald Voet, Judith G. Voet, and Charlotte W. Pratt. All rights reserved.

No part of this publication may be reproduced, stored in a retrieval system or transmitted in any form or by any means, electronic, mechanical, photocopying, recording, scanning or otherwise, except as permitted under Sections 107 or 108 of the 1976 United States Copyright Act, without either the prior written permission of the Publisher, or authorization through payment of the appropriate per-copy fee to the Copyright Clearance Center, Inc., 222 Rosewood Drive, Danvers, MA 01923, website www.copyright.com. Requests to the Publisher for permission should be addressed to the Permissions Department, John Wiley & Sons, Inc., 111 River Street, Hoboken, NJ 07030-5774, (201)748-6011, fax (201)748-6008, website http://www.wiley.com/go/permissions.

To order books or for customer service, please call 1-800-CALL WILEY (225-5945).

ISBN-13 978-0470-12930-2

Printed in the United States of America

10 9 8 7 6 5 4 3 2 1

About the Authors

Donald Voet received a B.S. in Chemistry from the California Institute of Technology, a Ph.D. in Chemistry from Harvard University with William Lipscomb, and did postdoctoral research in the Biology Department at MIT with Alexander Rich. Upon completion of his postdoctoral research, Don took up a faculty position in the Chemistry Department at the University of Pennsylvania where, for the past 38 years, he has taught a variety of biochemistry courses as well as general chemistry. His major area of research is the X-ray crystallography of molecules of biological interest. He has been a visiting scholar at Oxford University, the University of California at San Diego, and the Weizmann Institute of Science in Israel. Together with Judith G. Voet, he is Co-Editor-in-Chief of the journal *Biochemistry and Molecular Biology Education*. He is a member of the Education Committee of the International Union of Biochemistry and Molecular Biology. His hobbies include backpacking, scuba diving, skiing, travel, photography, and writing biochemistry textbooks.

Judith ("Judy") Voet received her B.S. in Chemistry from Antioch College and her Ph.D. in Biochemistry from Brandeis University with Robert H. Abeles. She has done postdoctoral research at the University of Pennsylvania, Haverford College, and the Fox Chase Cancer Center. Her main area of research involves enzyme reaction mechanisms and inhibition. She taught Biochemistry at the University of Delaware before moving to Swarthmore College. She taught there for 26 years, reaching the position of James H. Hammons Professor of Chemistry and Biochemistry before going on "permanent sabbatical leave." She has been a visiting scholar at Oxford University, University of California, San Diego, University of Pennsylvania, and the Weizmann Institute of Science, Israel. She is Co-Editor-in-Chief of the journal *Biochemistry and Molecular Biology Education*. She has been a member of the Education and Professional Development Committee of the American Society for Biochemistry and Molecular Biology as well as the Education Committee of the International Union of Biochemistry and Molecular Biology. Her hobbies include hiking, backpacking, scuba diving, and tap dancing.

Charlotte Pratt received her B.S. in Biology from the University of Notre Dame and her Ph.D. in Biochemistry from Duke University under the direction of Salvatore Pizzo. Although she originally intended to be a marine biologist, she discovered that Biochemistry offered the most compelling answers to many questions about biological structure–function relationships and the molecular basis for human health and disease. She conducted postdoctoral research in the Center for Thrombosis and Hemostasis at the University of North Carolina at Chapel Hill. She has taught at the University of Washington and currently teaches at Seattle Pacific University. In addition to working as an editor of several biochemistry textbooks, she has co-authored *Essential Biochemistry* and previous editions of *Fundamentals of Biochemistry*.

Brief Contents

PART I **INTRODUCTION**

1 | Introduction to the Chemistry of Life 1
2 | Water 22

PART II **BIOMOLECULES**

3 | Nucleotides, Nucleic Acids, and Genetic Information 39
4 | Amino Acids 74
5 | Proteins: Primary Structure 91
6 | Proteins: Three-Dimensional Structure 125
7 | Protein Function: Myoglobin and Hemoglobin, Muscle Contraction, and Antibodies 176
8 | Carbohydrates 219
9 | Lipids and Biological Membranes 245
10 | Membrane Transport 295

PART III **ENZYMES**

11 | Enzymatic Catalysis 322
12 | Enzyme Kinetics, Inhibition, and Control 363
13 | Biochemical Signaling 405

PART IV **METABOLISM**

14 | Introduction to Metabolism 448
15 | Glucose Catabolism 485
16 | Glycogen Metabolism and Gluconeogenesis 530
17 | Citric Acid Cycle 566
18 | Electron Transport and Oxidative Phosphorylation 596
19 | Photosynthesis 640
20 | Lipid Metabolism 677
21 | Amino Acid Metabolism 732
22 | Mammalian Fuel Metabolism: Integration and Regulation 791

PART V **GENE EXPRESSION AND REPLICATION**

23 | Nucleotide Metabolism 817
24 | Nucleic Acid Structure 848
25 | DNA Replication, Repair, and Recombination 893
26 | Transcription and RNA Processing 942
27 | Protein Synthesis 985
28 | Regulation of Gene Expression 1037

Solutions to Problems SP-1
Glossary G-1
Index I-1

Contents

Preface xviii

Acknowledgments xxi

Instructor and Student Resources xxiii

Guide to Media Resources xxv

PART I INTRODUCTION

1 Introduction to the Chemistry of Life 1

1 The Origin of Life 2
- **A.** Biological Molecules Arose from Inorganic Materials 2
- **B.** Complex Self-replicating Systems Evolved from Simple Molecules 3

2 Cellular Architecture 5
- **A.** Cells Carry Out Metabolic Reactions 5
- **B.** There Are Two Types of Cells: Prokaryotes and Eukaryotes 7
- **C.** Molecular Data Reveal Three Evolutionary Domains of Organisms 9
- **D.** Organisms Continue to Evolve 11

3 Thermodynamics 11
- **A.** The First Law of Thermodynamics States That Energy Is Conserved 12
- **B.** The Second Law of Thermodynamics States That Entropy Tends to Increase 13
- **C.** The Free Energy Change Determines the Spontaneity of a Process 14
- **D.** Free Energy Changes Can Be Calculated from Equilibrium Concentrations 15
- **E.** Life Obeys the Laws of Thermodynamics 17

BOX 1-1 **PATHWAYS OF DISCOVERY**
Lynn Margulis and the Theory of Endosymbiosis 10

BOX 1-2 **PERSPECTIVES IN BIOCHEMISTRY**
Biochemical Conventions 13

2 Water 22

1 Physical Properties of Water 23
- **A.** Water Is a Polar Molecule 23
- **B.** Hydrophilic Substances Dissolve in Water 25
- **C.** The Hydrophobic Effect Causes Nonpolar Substances to Aggregate in Water 26
- **D.** Water Moves by Osmosis and Solutes Move by Diffusion 29

2 Chemical Properties of Water 30
- **A.** Water Ionizes to Form H$^+$ and OH$^-$ 30
- **B.** Acids and Bases Alter the pH 32
- **C.** Buffers Resist Changes in pH 34

BOX 2-1 **BIOCHEMISTRY IN HEALTH AND DISEASE**
The Blood Buffering System 36

PART II BIOMOLECULES

3 Nucleotides, Nucleic Acids, and Genetic Information 39

1 Nucleotides 40

2 Introduction to Nucleic Acid Structure 43
- **A.** Nucleic Acids Are Polymers of Nucleotides 43
- **B.** The DNA Forms a Double Helix 44
- **C.** RNA Is a Single-Stranded Nucleic Acid 47

3 Overview of Nucleic Acid Function 47
- **A.** DNA Carries Genetic Information 48
- **B.** Genes Direct Protein Synthesis 49

4 Nucleic Acid Sequencing 50
- **A.** Restriction Endonucleases Cleave DNA at Specific Sequences 51
- **B.** Electrophoresis Separates Nucleic Acid According to Size 52
- **C.** DNA Is Sequenced by the Chain-Terminator Method 53
- **D.** Entire Genomes Have Been Sequenced 57
- **E.** Evolution Results from Sequence Mutations 58

5 Manipulating DNA 59
- **A.** Cloned DNA Is an Amplified Copy 60
- **B.** DNA Libraries Are Collections of Cloned DNA 62
- **C.** DNA Is Amplified by the Polymerase Chain Reaction 65
- **D.** Recombinant DNA Technology Has Numerous Practical Applications 67

BOX 3-1 **PATHWAYS OF DISCOVERY**
Francis Collins and the Gene for Cystic Fibrosis 56

BOX 3-2 **PERSPECTIVES IN BIOCHEMISTRY**
DNA Fingerprinting 66

BOX 3-3 **PERSPECTIVES IN BIOCHEMISTRY**
Ethical Aspects of Recombinant DNA Technology 70

4 Amino Acids 74

1 Amino Acid Structure 74
- **A.** Amino Acids Are Dipolar Ions 75

B. Peptide Bonds Link Amino Acids 78
C. Amino Acid Side Chains Are Nonpolar, Polar, or Charged 78
D. The p*K* Values of Ionizable Groups Depend on Nearby Groups 81
E. Amino Acid Names Are Abbreviated 81

2 Stereochemistry 82

3 Amino Acid Derivatives 86
A. Protein Side Chains May Be Modified 86
B. Some Amino Acids Are Biologically Active 86

BOX 4-1 **PATHWAYS OF DISCOVERY**
William C. Rose and the Discovery of Threonine 75

BOX 4-2 **PERSPECTIVES IN BIOCHEMISTRY**
The *RS* System 85

BOX 4-3 **PERSPECTIVES IN BIOCHEMISTRY**
Green Fluorescent Protein 87

5 Proteins: Primary Structure 91

1 Polypeptide Diversity 91

2 Protein Purification and Analysis 94
A. Purifying a Protein Requires a Strategy 94
B. Salting Out Separates Proteins by Their Solubility 97
C. Chromatography Involves Interaction with Mobile and Stationary Phases 98
D. Electrophoresis Separates Molecules According to Charge and Size 101

3 Protein Sequencing 104
A. The First Step Is to Separate Subunits 104
B. The Polypeptide Chains Are Cleaved 107
C. Edman Degradation Removes a Peptide's First Amino Acid Residue 109
D. Mass Spectrometry Determines the Molecular Masses of Peptides 110
E. Reconstructed Protein Sequences Are Stored in Databases 112

4 Protein Evolution 114
A. Protein Sequences Reveal Evolutionary Relationships 114
B. Proteins Evolve by the Duplication of Genes or Gene Segments 117

BOX 5-1 **PATHWAYS OF DISCOVERY**
Frederick Sanger and Protein Sequencing 105

6 Proteins: Three-Dimensional Structure 125

1 Secondary Structure 127
A. The Planar Peptide Group Limits Polypeptide Conformations 127
B. The Most Common Regular Secondary Structures Are the α Helix and the β Sheet 129
C. Fibrous Proteins Have Repeating Secondary Structures 134
D. Most Proteins Include Nonrepetitive Structure 139

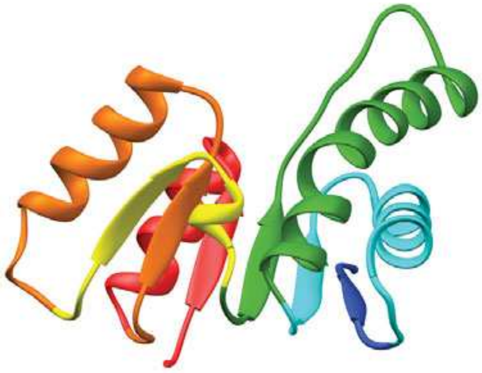

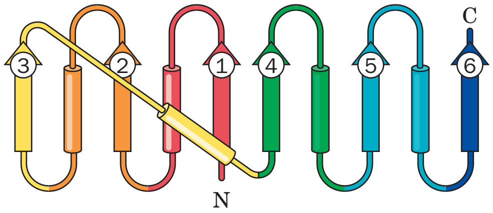

2 Tertiary Structure 140
A. Most Protein Structures Have Been Determined by X-Ray Crystallography or Nuclear Magnetic Resonance 141
B. Side Chain Location Varies with Polarity 145
C. Tertiary Structures Contain Combinations of Secondary Structure 146
D. Structure Is Conserved More than Sequence 150
E. Structural Bioinformatics Provides Tools for Storing, Visualizing, and Comparing Protein Structural Information 151

3 Quaternary Structure and Symmetry 154

4 Protein Stability 156
A. Proteins Are Stabilized by Several Forces 156
B. Proteins Can Undergo Denaturation and Renaturation 158

5 Protein Folding 161
A. Proteins Follow Folding Pathways 161
B. Molecular Chaperones Assist Protein Folding 165
C. Some Diseases Are Caused by Protein Misfolding 168

BOX 6-1 **PATHWAYS OF DISCOVERY**
Linus Pauling and Structural Biochemistry 130

BOX 6-2 **BIOCHEMISTRY IN HEALTH AND DISEASE**
Collagen Diseases 137

BOX 6-3 **PERSPECTIVES IN BIOCHEMISTRY**
Thermostable Proteins 159

BOX 6-4 **PERSPECTIVES IN BIOCHEMISTRY**
Protein Structure Prediction and Protein Design 163

7 Protein Function: Myoglobin and Hemoglobin, Muscle Contraction, and Antibodies 176

1 Oxygen Binding to Myoglobin and Hemoglobin 177
- **A.** Myoglobin Is a Monomeric Oxygen-Binding Protein 177
- **B.** Hemoglobin Is a Tetramer with Two Conformations 181
- **C.** Oxygen Binds Cooperatively to Hemoglobin 184
- **D.** Hemoglobin's Two Conformations Exhibit Different Affinities for Oxygen 186
- **E.** Mutations May Alter Hemoglobin's Structure and Function 194

2 Muscle Contraction 197
- **A.** Muscle Consists of Interdigitated Thick and Thin Filaments 198
- **B.** Muscle Contraction Occurs When Myosin Heads Walk Up Thin Filaments 205
- **C.** Actin Forms Microfilaments in Nonmuscle Cells 207

3 Antibodies 209
- **A.** Antibodies Have Constant and Variable Regions 210
- **B.** Antibodies Recognize a Huge Variety of Antigens 212

BOX 7-1 **PERSPECTIVES IN BIOCHEMISTRY** Other Oxygen-Transport Proteins 181

BOX 7-2 **PATHWAYS OF DISCOVERY** Max Perutz and the Structure and Function of Hemoglobin 182

BOX 7-3 **BIOCHEMISTRY IN HEALTH AND DISEASE** High-Altitude Adaptation 192

BOX 7-4 **PATHWAYS OF DISCOVERY** Hugh Huxley and the Sliding Filament Model 200

BOX 7-5 **PERSPECTIVES IN BIOCHEMISTRY** Monoclonal Antibodies 213

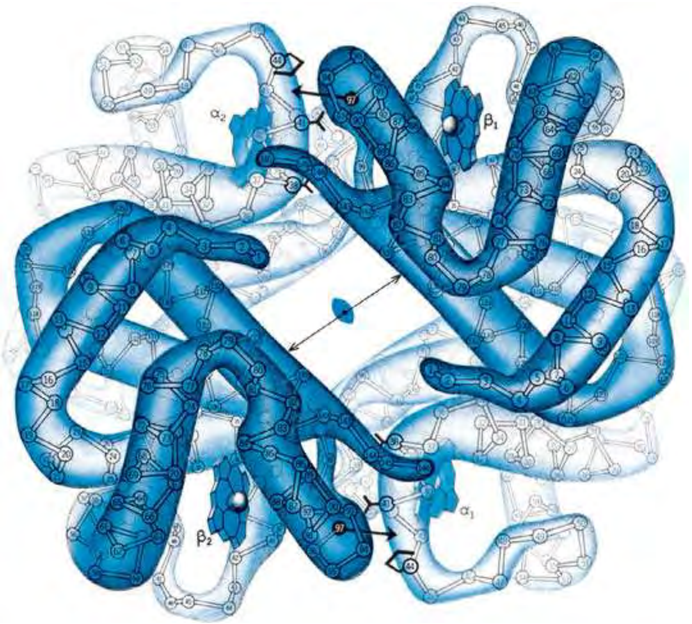

© Irving Geis/HHMI

8 Carbohydrates 219

1 Monosaccharides 220
- **A.** Monosaccharides Are Aldoses or Ketoses 220
- **B.** Monosaccharides Vary in Configuration and Conformation 221
- **C.** Sugars Can Be Modified and Covalently Linked 224

2 Polysaccharides 226
- **A.** Lactose and Sucrose Are Disaccharides 227
- **B.** Cellulose and Chitin Are Structural Polysaccharides 228
- **C.** Starch and Glycogen Are Storage Polysaccharides 230
- **D.** Glycosaminoglycans Form Highly Hydrated Gels 232

3 Glycoproteins 234
- **A.** Proteoglycans Contain Glycosaminoglycans 234
- **B.** Bacterial Cell Walls Are Made of Peptidoglycan 235
- **C.** Many Eukaryotic Proteins Are Glycosylated 238
- **D.** Oligosaccharides May Determine Glycoprotein Structure, Function, and Recognition 240

BOX 8-1 **BIOCHEMISTRY IN HEALTH AND DISEASE** Lactose Intolerance 227

BOX 8-2 **PERSPECTIVES IN BIOCHEMISTRY** Artificial Sweeteners 228

BOX 8-3 **BIOCHEMISTRY IN HEALTH AND DISEASE** Peptidoglycan-Specific Antibiotics 238

9 Lipids and Biological Membranes 245

1 Lipid Classification 246
- **A.** The Properties of Fatty Acids Depend on Their Hydrocarbon Chains 246
- **B.** Triacylglycerols Contain Three Esterified Fatty Acids 248
- **C.** Glycerophospholipids Are Amphiphilic 249
- **D.** Sphingolipids Are Amino Alcohol Derivatives 252
- **E.** Steroids Contain Four Fused Rings 254
- **F.** Other Lipids Perform a Variety of Metabolic Roles 257

2 Lipid Bilayers 260
- **A.** Bilayer Formation Is Driven by the Hydrophobic Effect 260
- **B.** Lipid Bilayers Have Fluidlike Properties 261

3 Membrane Proteins 263
- **A.** Integral Membrane Proteins Interact with Hydrophobic Lipids 263
- **B.** Lipid-Linked Proteins Are Anchored to the Bilayer 267
- **C.** Peripheral Proteins Associate Loosely with Membranes 269

4 Membrane Structure and Assembly 269
- **A.** The Fluid Mosaic Model Accounts for Lateral Diffusion 270
- **B.** The Membrane Skeleton Helps Define Cell Shape 272
- **C.** Membrane Lipids Are Distributed Asymmetrically 274
- **D.** The Secretory Pathway Generates Secreted and Transmembrane Proteins 278

E. Intracellular Vesicles Transport Proteins 282
F. Proteins Mediate Vesicle Fusion 287

BOX 9-1 **BIOCHEMISTRY IN HEALTH AND DISEASE** Lung Surfactant 250

BOX 9-2 **PATHWAYS OF DISCOVERY** Richard Henderson and the Structure of Bacteriorhodopsin 266

BOX 9-3 **BIOCHEMISTRY IN HEALTH AND DISEASE** Tetanus and Botulinum Toxins Specifically Cleave SNAREs 288

10 Membrane Transport 295

1 Thermodynamics of Transport 296

2 Passive-Mediated Transport 297
A. Ionophores Carry Ions across Membranes 297
B. Porins Contain β Barrels 298
C. Ion Channels Are Highly Selective 299
D. Aquaporins Mediate the Transmembrane Movement of Water 306
E. Transport Proteins Alternate between Two Conformations 307

3 Active Transport 311
A. The (Na^+–K^+)–ATPase Transports Ions in Opposite Directions 311
B. The Ca^{2+}–ATPase Pumps Ca^{2+} Out of the Cytosol 313
C. ABC Transporters Are Responsible for Drug Resistance 314
D. Active Transport May Be Driven by Ion Gradients 316

BOX 10-1 **PERSPECTIVES IN BIOCHEMISTRY** Gap Junctions 308

BOX 10-2 **PERSPECTIVES IN BIOCHEMISTRY** Differentiating Mediated and Nonmediated Transport 309

BOX 10-3 **BIOCHEMISTRY IN HEALTH AND DISEASE** The Action of Cardiac Glycosides 313

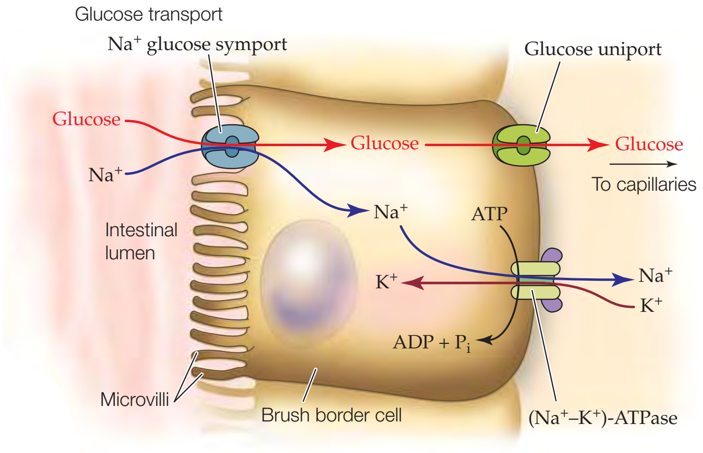

PART III ENZYMES

11 Enzymatic Catalysis 322

1 General Properties of Enzymes 323
A. Enzymes Are Classified by the Type of Reaction They Catalyze 324
B. Enzymes Act on Specific Substrates 325
C. Some Enzymes Require Cofactors 326

2 Activation Energy and the Reaction Coordinate 328

3 Catalytic Mechanisms 330
A. Acid–Base Catalysis Occurs by Proton Transfer 331
B. Covalent Catalysis Usually Requires a Nucleophile 333
C. Metal Ion Cofactors Act as Catalysts 335
D. Catalysis Can Occur through Proximity and Orientation Effects 336
E. Enzymes Catalyze Reactions by Preferentially Binding the Transition State 338

4 Lysozyme 339
A. Lysozyme's Catalytic Site Was Identified through Model Building 340
B. The Lysozyme Reaction Proceeds via a Covalent Intermediate 343

5 Serine Proteases 347
A. Active Site Residues Were Identified by Chemical Labeling 348
B. X-Ray Structures Provided Information about Catalysis, Substrate Specificity, and Evolution 348
C. Serine Proteases Use Several Catalytic Mechanisms 352
D. Zymogens Are Inactive Enzyme Precursors 357

BOX 11-1 **PERSPECTIVES IN BIOCHEMISTRY** Effects of pH on Enzyme Activity 332

BOX 11-2 **PERSPECTIVES IN BIOCHEMISTRY** Observing Enzyme Action by X-Ray Crystallography 342

BOX 11-3 **BIOCHEMISTRY IN HEALTH AND DISEASE** Nerve Poisons 349

BOX 11-4 **BIOCHEMISTRY IN HEALTH AND DISEASE** The Blood Coagulation Cascade 358

12 Enzyme Kinetics, Inhibition, and Control 363

1 Reaction Kinetics 364
A. Chemical Kinetics Is Described by Rate Equations 364
B. Enzyme Kinetics Often Follows the Michaelis–Menten Equation 366
C. Kinetic Data Can Provide Values of V_{max} and K_M 372
D. Bisubstrate Reactions Follow One of Several Rate Equations 375

2 Enzyme Inhibition 377
A. Competitive Inhibition Involves Inhibitor Binding at an Enzyme's Substrate Binding Site 377

B. Uncompetitive Inhibition Involves Inhibitor Binding to the Enzyme–Substrate Complex 381
C. Mixed Inhibition Involves Inhibitor Binding to Both the Free Enzyme and the Enzyme–Substrate Complex 382

3 Control of Enzyme Activity 386
A. Allosteric Control Involves Binding at a Site Other Than the Active Site 386
B. Control by Covalent Modification Often Involves Protein Phosphorylation 390

4 Drug Design 394
A. Drug Discovery Employs a Variety of Techniques 394
B. A Drug's Bioavailability Depends on How It Is Absorbed and Transported in the Body 396
C. Clinical Trials Test for Efficacy and Safety 396
D. Cytochromes P450 Are Often Implicated in Adverse Drug Reactions 398

BOX 12-1 **PERSPECTIVES IN BIOCHEMISTRY** Isotopic Labeling 367
BOX 12-2 **PATHWAYS OF DISCOVERY** J.B.S. Haldane and Enzyme Action 369
BOX 12-3 **PERSPECTIVES IN BIOCHEMISTRY** Kinetics and Transition State Theory 372
BOX 12-4 **BIOCHEMISTRY IN HEALTH AND DISEASE** HIV Enzyme Inhibitors 384

13 Biochemical Signaling 405

1 Hormones 406
A. Pancreatic Islet Hormones Control Fuel Metabolism 407
B. Epinephrine and Norepinephrine Prepare the Body for Action 409
C. Steroid Hormones Regulate a Wide Variety of Metabolic and Sexual Processes 410
D. Growth Hormone Binds to Receptors in Muscle, Bone, and Cartilage 411

2 Receptor Tyrosine Kinases 412
A. Receptor Tyrosine Kinases Transmit Signals across the Cell Membrane 413
B. Kinase Cascades Relay Signals to the Nucleus 416
C. Some Receptors Are Associated with Nonreceptor Tyrosine Kinases 422
D. Protein Phosphatases Are Signaling Proteins in Their Own Right 425

3 Heterotrimeric G Proteins 428
A. G Protein–Coupled Receptors Contain Seven Transmembrane Helices 429
B. Heterotrimeric G Proteins Dissociate on Activation 430
C. Adenylate Cyclase Synthesizes cAMP to Activate Protein Kinase A 432
D. Phosphodiesterases Limit Second Messenger Activity 435

4 The Phosphoinositide Pathway 436
A. Ligand Binding Results in the Cytoplasmic Release of the Second Messengers IP_3 and Ca^{2+} 437
B. Calmodulin Is a Ca^{2+}-Activated Switch 438
C. DAG Is a Lipid-Soluble Second Messenger That Activates Protein Kinase C 440
D. Epilog: Complex Systems Have Emergent Properties 442

BOX 13-1 **PATHWAYS OF DISCOVERY** Rosalyn Yalow and the Radioimmunoassay (RIA) 408
BOX 13-2 **PERSPECTIVES IN BIOCHEMISTRY** Receptor–Ligand Binding Can Be Quantitated 414
BOX 13-3 **BIOCHEMISTRY IN HEALTH AND DISEASE** Oncogenes and Cancer 421
BOX 13-4 **BIOCHEMISTRY IN HEALTH AND DISEASE** Drugs and Toxins That Affect Cell Signaling 435
BOX 13-5 **BIOCHEMISTRY IN HEALTH AND DISEASE** Anthrax 444

PART IV METABOLISM

14 Introduction to Metabolism 448

1 Overview of Metabolism 449
A. Nutrition Involves Food Intake and Use 449
B. Vitamins and Minerals Assist Metabolic Reactions 450
C. Metabolic Pathways Consist of Series of Enzymatic Reactions 451
D. Thermodynamics Dictates the Direction and Regulatory Capacity of Metabolic Pathways 455
E. Metabolic Flux Must Be Controlled 457

2 "High-Energy" Compounds 459
A. ATP Has a High Phosphoryl Group-Transfer Potential 460
B. Coupled Reactions Drive Endergonic Processes 462
C. Some Other Phosphorylated Compounds Have High Phosphoryl Group-Transfer Potentials 464
D. Thioesters Are Energy-Rich Compounds 468

3 Oxidation–Reduction Reactions 469
A. NAD^+ and FAD Are Electron Carriers 469
B. The Nernst Equation Describes Oxidation–Reduction Reactions 470
C. Spontaneity Can Be Determined by Measuring Reduction Potential Differences 472

4 Experimental Approaches to the Study of Metabolism 475
A. Labeled Metabolites Can Be Traced 475
B. Studying Metabolic Pathways Often Involves Perturbing the System 477
C. Systems Biology Has Entered the Study of Metabolism 477

BOX 14-1 **PERSPECTIVES IN BIOCHEMISTRY** Oxidation States of Carbon 453
BOX 14-2 **PERSPECTIVES IN BIOCHEMISTRY** Mapping Metabolic Pathways 454
BOX 14-3 **PATHWAYS OF DISCOVERY** Fritz Lipmann and "High-Energy" Compounds 460
BOX 14-4 **PERSPECTIVES IN BIOCHEMISTRY** ATP and ΔG 462

15 Glucose Catabolism 485

1 Overview of Glycolysis 486

2 The Reactions of Glycolysis 489

- **A.** Hexokinase Uses the First ATP 489
- **B.** Phosphoglucose Isomerase Converts Glucose-6-Phosphate to Fructose-6-Phosphate 490
- **C.** Phosphofructokinase Uses the Second ATP 491
- **D.** Aldolase Converts a 6-Carbon Compound to Two 3-Carbon Compounds 492
- **E.** Triose Phosphate Isomerase Interconverts Dihydroxyacetone Phosphate and Glyceraldehyde-3-Phosphate 494
- **F.** Glyceraldehyde-3-Phosphate Dehydrogenase Forms the First "High-Energy" Intermediate 497
- **G.** Phosphoglycerate Kinase Generates the First ATP 499
- **H.** Phosphoglycerate Mutase Interconverts 3-Phosphoglycerate and 2-Phosphoglycerate 499
- **I.** Enolase Forms the Second "High-Energy" Intermediate 500
- **J.** Pyruvate Kinase Generates the Second ATP 501

3 Fermentation: The Anaerobic Fate of Pyruvate 504

- **A.** Homolactic Fermentation Converts Pyruvate to Lactate 505
- **B.** Alcoholic Fermentation Converts Pyruvate to Ethanol and CO_2 506
- **C.** Fermentation Is Energetically Favorable 509

4 Regulation of Glycolysis 510

- **A.** Phosphofructokinase Is the Major Flux-Controlling Enzyme of Glycolysis in Muscle 511
- **B.** Substrate Cycling Fine-Tunes Flux Control 514

5 Metabolism of Hexoses Other than Glucose 516

- **A.** Fructose Is Converted to Fructose-6-Phosphate or Glyceraldehyde-3-Phosphate 516
- **B.** Galactose Is Converted to Glucose-6-Phosphate 518
- **C.** Mannose Is Converted to Fructose-6-Phosphate 520

6 The Pentose Phosphate Pathway 520

- **A.** Oxidative Reactions Produce NADPH in Stage 1 522
- **B.** Isomerization and Epimerization of Ribulose-5-Phosphate Occur in Stage 2 523
- **C.** Stage 3 Involves Carbon–Carbon Bond Cleavage and Formation 523
- **D.** The Pentose Phosphate Pathway Must Be Regulated 524

BOX 15-1 **PATHWAYS OF DISCOVERY** Otto Warburg and Studies of Metabolism 488

BOX 15-2 **PERSPECTIVES IN BIOCHEMISTRY** Synthesis of 2,3-Bisphosphoglycerate in Erythrocytes and Its Effect on the Oxygen Carrying Capacity of the Blood 502

BOX 15-3 **PERSPECTIVES IN BIOCHEMISTRY** Glycolytic ATP Production in Muscle 510

BOX 15-4 **BIOCHEMISTRY IN HEALTH AND DISEASE** Glucose-6-Phosphate Dehydrogenase Deficiency 526

16 Glycogen Metabolism and Gluconeogenesis 530

1 Glycogen Breakdown 532

- **A.** Glycogen Phosphorylase Degrades Glycogen to Glucose-1-Phosphate 534
- **B.** Glycogen Debranching Enzyme Acts as a Glucosyltransferase 536
- **C.** Phosphoglucomutase Interconverts Glucose-1-Phosphate and Glucose-6-Phosphate 537

2 Glycogen Synthesis 540

- **A.** UDP–Glucose Pyrophosphorylase Activates Glucosyl Units 540
- **B.** Glycogen Synthase Extends Glycogen Chains 541
- **C.** Glycogen Branching Enzyme Transfers Seven-Residue Glycogen Segments 543

3 Control of Glycogen Metabolism 545

- **A.** Glycogen Phosphorylase and Glycogen Synthase Are Under Allosteric Control 545
- **B.** Glycogen Phosphorylase and Glycogen Synthase Undergo Control by Covalent Modification 545
- **C.** Glycogen Metabolism Is Subject to Hormonal Control 550

4 Gluconeogenesis 552

- **A.** Pyruvate Is Converted to Phosphoenolpyruvate in Two Steps 554
- **B.** Hydrolytic Reactions Bypass Irreversible Glycolytic Reactions 557
- **C.** Gluconeogenesis and Glycolysis Are Independently Regulated 558

5 Other Carbohydrate Biosynthetic Pathways 560

BOX 16-1 **PATHWAYS OF DISCOVERY** Carl and Gerty Cori and Glucose Metabolism 533

BOX 16-2 **BIOCHEMISTRY IN HEALTH AND DISEASE** Glycogen Storage Diseases 538

BOX 16-3 **PERSPECTIVES IN BIOCHEMISTRY** Optimizing Glycogen Structure 544

BOX 16-4 **PERSPECTIVES IN BIOCHEMISTRY** Lactose Synthesis 560

17 Citric Acid Cycle 566

1 Overview of the Citric Acid Cycle 567

2 Synthesis of Acetyl-Coenzyme A 570

- **A.** Pyruvate Dehydrogenase Is a Multienzyme Complex 570
- **B.** The Pyruvate Dehydrogenase Complex Catalyzes Five Reactions 572

3 Enzymes of the Citric Acid Cycle 576

- **A.** Citrate Synthase Joins an Acetyl Group to Oxaloacetate 577
- **B.** Aconitase Interconverts Citrate and Isocitrate 578
- **C.** NAD^+-Dependent Isocitrate Dehydrogenase Releases CO_2 579

- **D.** α-Ketoglutarate Dehydrogenase Resembles Pyruvate Dehydrogenase 580
- **E.** Succinyl-CoA Synthetase Produces GTP 580
- **F.** Succinate Dehydrogenase Generates FADH$_2$ 582
- **G.** Fumarase Produces Malate 583
- **H.** Malate Dehydrogenase Regenerates Oxaloacetate 583

4 Regulation of the Citric Acid Cycle 583
- **A.** Pyruvate Dehydrogenase Is Regulated by Product Inhibition and Covalent Modification 585
- **B.** Three Enzymes Control the Rate of the Citric Acid Cycle 585

5 Reactions Related to the Citric Acid Cycle 588
- **A.** Other Pathways Use Citric Acid Cycle Intermediates 588
- **B.** Some Reactions Replenish Citric Acid Cycle Intermediates 589
- **C.** The Glyoxylate Cycle Shares Some Steps with the Citric Acid Cycle 590

BOX 17-1 **PATHWAYS OF DISCOVERY** Hans Krebs and the Citric Acid Cycle 569

BOX 17-2 **BIOCHEMISTRY IN HEALTH AND DISEASE** Arsenic Poisoning 576

BOX 17-3 **PERSPECTIVES IN BIOCHEMISTRY** Evolution of the Citric Acid Cycle 592

18 Electron Transport and Oxidative Phosphorylation 596

1 The Mitochondrion 597
- **A.** Mitochondria Contain a Highly Folded Inner Membrane 597
- **B.** Ions and Metabolites Enter Mitochondria via Transporters 599

2 Electron Transport 600
- **A.** Electron Transport Is an Exergonic Process 601
- **B.** Electron Carriers Operate in Sequence 602
- **C.** Complex I Accepts Electrons from NADH 604
- **D.** Complex II Contributes Electrons to Coenzyme Q 609
- **E.** Complex III Translocates Protons via the Q Cycle 611
- **F.** Complex IV Reduces Oxygen to Water 615

3 Oxidative Phosphorylation 618
- **A.** The Chemiosmotic Theory Links Electron Transport to ATP Synthesis 618
- **B.** ATP Synthase Is Driven by the Flow of Protons 622
- **C.** The P/O Ratio Relates the Amount of ATP Synthesized to the Amount of Oxygen Reduced 629
- **D.** Oxidative Phosphorylation Can Be Uncoupled from Electron Transport 630

4 Control of Oxidative Metabolism 631
- **A.** The Rate of Oxidative Phosphorylation Depends on the ATP and NADH Concentrations 631
- **B.** Aerobic Metabolism Has Some Disadvantages 634

BOX 18-1 **PERSPECTIVES IN BIOCHEMISTRY** Cytochromes Are Electron-Transport Heme Proteins 610

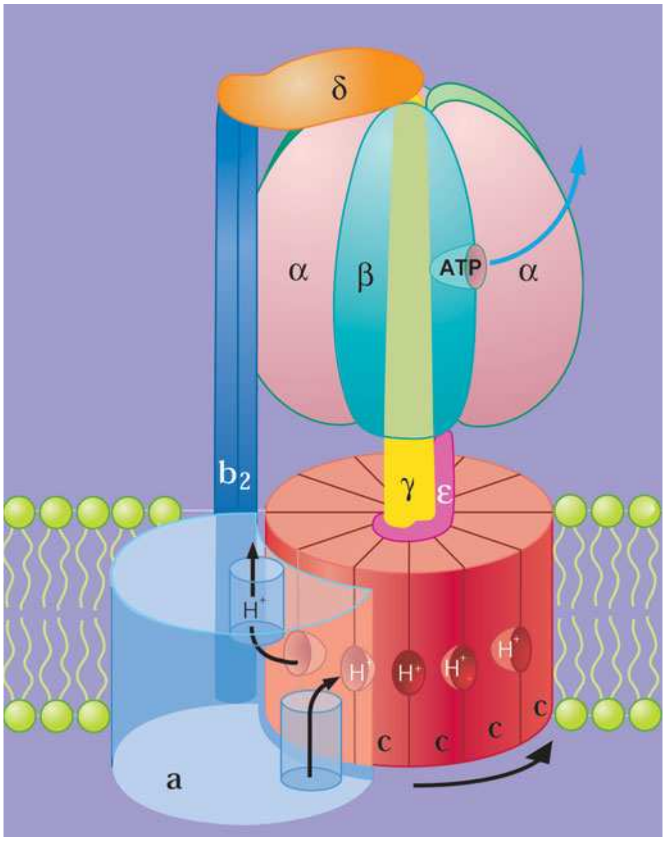

BOX 18-2 **PATHWAYS OF DISCOVERY** Peter Mitchell and the Chemiosmotic Theory 619

BOX 18-3 **PERSPECTIVES IN BIOCHEMISTRY** Bacterial Electron Transport and Oxidative Phosphorylation 621

BOX 18-4 **PERSPECTIVES IN BIOCHEMISTRY** Uncoupling in Brown Adipose Tissue Generates Heat 632

BOX 18-5 **BIOCHEMISTRY IN HEALTH AND DISEASE** Oxygen Deprivation in Heart Attack and Stroke 635

19 Photosynthesis 640

1 Chloroplasts 641
- **A.** The Light Reactions Take Place in the Thylakoid Membrane 641
- **B.** Pigment Molecules Absorb Light 643

2 The Light Reactions 645
- **A.** Light Energy Is Transformed to Chemical Energy 645
- **B.** Electron Transport in Photosynthetic Bacteria Follows a Circular Path 647
- **C.** Two-Center Electron Transport Is a Linear Pathway That Produces O$_2$ and NADPH 650
- **D.** The Proton Gradient Drives ATP Synthesis by Photophosphorylation 661

3 The Dark Reactions 663
- **A.** The Calvin Cycle Fixes CO$_2$ 663
- **B.** Calvin Cycle Products Are Converted to Starch, Sucrose, and Cellulose 668
- **C.** The Calvin Cycle Is Controlled Indirectly by Light 670
- **D.** Photorespiration Competes with Photosynthesis 671

BOX 19-1 **PERSPECTIVES IN BIOCHEMISTRY** Segregation of PSI and PSII 662

20 Lipid Metabolism 677

1 Lipid Digestion, Absorption, and Transport 678
- **A.** Triacylglycerols Are Digested before They Are Absorbed 678
- **B.** Lipids Are Transported as Lipoproteins 680

2 Fatty Acid Oxidation 685
- **A.** Fatty Acids Are Activated by Their Attachment to Coenzyme A 686
- **B.** Carnitine Carries Acyl Groups across the Mitochondrial Membrane 686
- **C.** β Oxidation Degrades Fatty Acids to Acetyl-CoA 688
- **D.** Oxidation of Unsaturated Fatty Acids Requires Additional Enzymes 690
- **E.** Oxidation of Odd-Chain Fatty Acids Yields Propionyl-CoA 692
- **F.** Peroxisomal β Oxidation Differs from Mitochondrial β Oxidation 698

3 Ketone Bodies 698

4 Fatty Acid Biosynthesis 701
- **A.** Mitochondrial Acetyl-CoA Must Be Transported into the Cytosol 701
- **B.** Acetyl-CoA Carboxylase Produces Malonyl-CoA 702
- **C.** Fatty Acid Synthase Catalyzes Seven Reactions 703
- **D.** Fatty Acids May Be Elongated and Desaturated 707
- **E.** Fatty Acids Are Esterified to Form Triacylglycerols 711

5 Regulation of Fatty Acid Metabolism 711

6 Synthesis of Other Lipids 714
- **A.** Glycerophospholipids Are Built from Intermediates of Triacylglycerol Synthesis 714
- **B.** Sphingolipids Are Built from Palmitoyl-CoA and Serine 717
- **C.** C$_{20}$ Fatty Acids Are the Precursors of Prostaglandins 718

7 Cholesterol Metabolism 721
- **A.** Cholesterol Is Synthesized from Acetyl-CoA 721
- **B.** HMG-CoA Reductase Controls the Rate of Cholesterol Synthesis 725
- **C.** Abnormal Cholesterol Transport Leads to Atherosclerosis 727

BOX 20-1 **BIOCHEMISTRY IN HEALTH AND DISEASE** Vitamin B$_{12}$ Deficiency 696

BOX 20-2 **PATHWAYS OF DISCOVERY** Dorothy Crowfoot Hodgkin and the Structure of Vitamin B$_{12}$ 697

BOX 20-3 **PERSPECTIVES IN BIOCHEMISTRY** Triclosan: An Inhibitor of Fatty Acid Synthesis 708

BOX 20-4 **BIOCHEMISTRY IN HEALTH AND DISEASE** Sphingolipid Degradation and Lipid Storage Diseases 720

21 Amino Acid Metabolism 732

1 Protein Degradation 732
- **A.** Lysosomes Degrade Many Proteins 732
- **B.** Ubiquitin Marks Proteins for Degradation 733
- **C.** The Proteasome Unfolds and Hydrolyzes Ubiquitinated Polypeptides 734

2 Amino Acid Deamination 738
- **A.** Transaminases Use PLP to Transfer Amino Groups 738
- **B.** Glutamate Can Be Oxidatively Deaminated 742

3 The Urea Cycle 743
- **A.** Five Enzymes Carry out the Urea Cycle 743
- **B.** The Urea Cycle Is Regulated by Substrate Availability 747

4 Breakdown of Amino Acids 747
- **A.** Alanine, Cysteine, Glycine, Serine, and Threonine Are Degraded to Pyruvate 748
- **B.** Asparagine and Aspartate Are Degraded to Oxaloacetate 751
- **C.** Arginine, Glutamate, Glutamine, Histidine, and Proline Are Degraded to α-Ketoglutarate 751
- **D.** Isoleucine, Methionine, and Valine Are Degraded to Succinyl-CoA 753
- **E.** Leucine and Lysine Are Degraded Only to Acetyl-CoA and/or Acetoacetate 758
- **F.** Tryptophan Is Degraded to Alanine and Acetoacetate 758
- **G.** Phenylalanine and Tyrosine Are Degraded to Fumarate and Acetoacetate 760

5 Amino Acid Biosynthesis 763
- **A.** Nonessential Amino Acids Are Synthesized from Common Metabolites 764
- **B.** Plants and Microorganisms Synthesize the Essential Amino Acids 769

6 Other Products of Amino Acid Metabolism 774
- **A.** Heme Is Synthesized from Glycine and Succinyl-CoA 775
- **B.** Amino Acids Are Precursors of Physiologically Active Amines 780
- **C.** Nitric Oxide Is Derived from Arginine 781

7 Nitrogen Fixation 782
- **A.** Nitrogenase Reduces N$_2$ to NH$_3$ 783
- **B.** Fixed Nitrogen Is Assimilated into Biological Molecules 786

BOX 21-1 **BIOCHEMISTRY IN HEALTH AND DISEASE** Homocysteine, a Marker of Disease 755

BOX 21-2 **BIOCHEMISTRY IN HEALTH AND DISEASE** Phenylketonuria and Alcaptonuria Result from Defects in Phenylalanine Degradation 762

BOX 21-3 **BIOCHEMISTRY IN HEALTH AND DISEASE** The Porphyrias 778

22 Mammalian Fuel Metabolism: Integration and Regulation 791

1 Organ Specialization 792
- **A.** The Brain Requires a Steady Supply of Glucose 793
- **B.** Muscle Utilizes Glucose, Fatty Acids, and Ketone Bodies 794
- **C.** Adipose Tissue Stores and Releases Fatty Acids and Hormones 795
- **D.** Liver Is the Body's Central Metabolic Clearinghouse 796
- **E.** Kidney Filters Wastes and Maintains Blood pH 798
- **F.** Blood Transports Metabolites in Interorgan Metabolic Pathways 798

2 Hormonal Control of Fuel Metabolism 799

3 Metabolic Homeostasis: The Regulation of Energy Metabolism, Appetite, and Body Weight 804
- **A.** AMP-Dependent Protein Kinase Is the Cell's Fuel Gauge 804
- **B.** Adiponectin Regulates AMPK Activity 806
- **C.** Leptin Is a Satiety Hormone 806
- **D.** Ghrelin and PYY$_{3-36}$ Act as Short-Term Regulators of Appetite 807
- **E.** Energy Expenditure Can Be Controlled by Adaptive Thermogenesis 808

4 Disturbances in Fuel Metabolism 809
- **A.** Starvation Leads to Metabolic Adjustments 809
- **B.** Diabetes Mellitus Is Characterized by High Blood Glucose Levels 811
- **C.** Obesity Is Usually Caused by Excessive Food Intake 814

BOX 22-1 **PATHWAYS OF DISCOVERY** Frederick Banting and Charles Best and the Discovery of Insulin 812

PART V GENE EXPRESSION AND REPLICATION

23 Nucleotide Metabolism 817

1 Synthesis of Purine Ribonucleotides 818
- **A.** Purine Synthesis Yields Inosine Monophosphate 818
- **B.** IMP Is Converted to Adenine and Guanine Ribonucleotides 821
- **C.** Purine Nucleotide Biosynthesis Is Regulated at Several Steps 822
- **D.** Purines Can Be Salvaged 823

2 Synthesis of Pyrimidine Ribonucleotides 824
- **A.** UMP Is Synthesized in Six Steps 824
- **B.** UMP Is Converted to UTP and CTP 826
- **C.** Pyrimidine Nucleotide Biosynthesis Is Regulated at ATCase or Carbamoyl Phosphate Synthetase II 827

3 Formation of Deoxyribonucleotides 828
- **A.** Ribonucleotide Reductase Converts Ribonucleotides to Deoxyribonucleotides 828
- **B.** dUMP Is Methylated to Form Thymine 834

4 Nucleotide Degradation 839
- **A.** Purine Catabolism Yields Uric Acid 839
- **B.** Some Animals Degrade Uric Acid 842
- **C.** Pyrimidines Are Broken Down to Malonyl-CoA and Methylmalonyl-CoA 845

BOX 23-1 **BIOCHEMISTRY IN HEALTH AND DISEASE** Inhibition of Thymidylate Synthesis in Cancer Therapy 838

BOX 23-2 **PATHWAYS OF DISCOVERY** Gertrude Elion and Purine Derivatives 844

24 Nucleic Acid Structure 848

1 The DNA Helix 849
- **A.** DNA Can Adopt Different Conformations 849
- **B.** DNA Has Limited Flexibility 855
- **C.** DNA Can Be Supercoiled 857
- **D.** Topoisomerases Alter DNA Supercoiling 859

2 Forces Stabilizing Nucleic Acid Structures 864
- **A.** DNA Can Undergo Denaturation and Renaturation 864
- **B.** Nucleic Acids Are Stabilized by Base Pairing, Stacking, and Ionic Interactions 866
- **C.** RNA Structures Are Highly Variable 868

3 Fractionation of Nucleic Acids 872
- **A.** Nucleic Acids Can Be Purified by Chromatography 872
- **B.** Electrophoresis Separates Nucleic Acids by Size 872

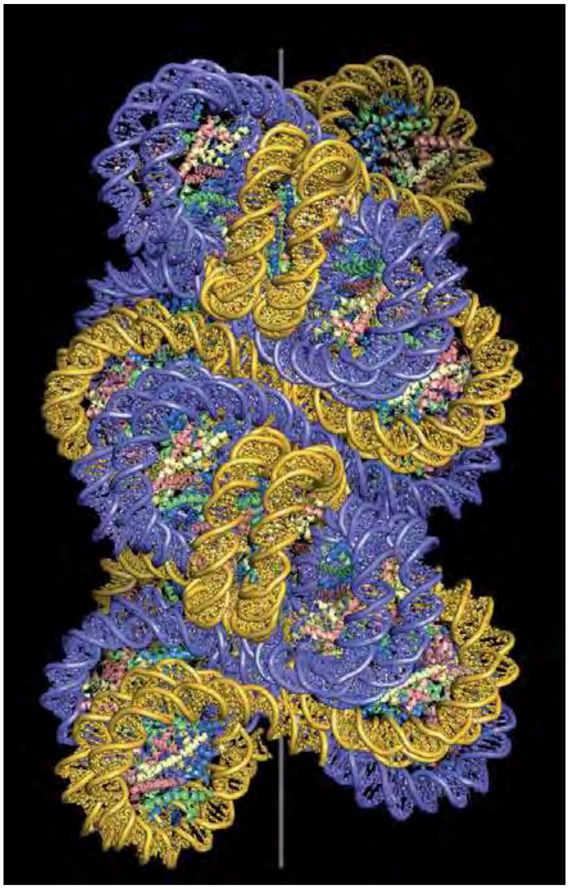

4 DNA–Protein Interactions 874
- **A.** Restriction Endonucleases Distort DNA on Binding 875
- **B.** Prokaryotic Repressors Often Include a DNA-Binding Helix 876
- **C.** Eukaryotic Transcription Factors May Include Zinc Fingers or Leucine Zippers 879

5 Eukaryotic Chromosome Structure 883
- **A.** Histones Are Positively Charged 884
- **B.** DNA Coils around Histones to Form Nucleosomes 884
- **C.** Chromatin Forms Higher-Order Structures 887

BOX 24-1 **PATHWAYS OF DISCOVERY** Rosalind Franklin and the Structure of DNA 850

BOX 24-2 **BIOCHEMISTRY IN HEALTH AND DISEASE** Inhibitors of Topoisomerases as Antibiotics and Anticancer Chemotherapeutic Agents 865

BOX 24-3 **PERSPECTIVES IN BIOCHEMISTRY** The RNA World 871

25 DNA Replication, Repair, and Recombination 893

1 Overview of DNA Replication 894

2 Prokaryotic DNA Replication 896
- **A.** DNA Polymerases Add the Correctly Paired Nucleotide 896
- **B.** Replication Initiation Requires Helicase and Primase 903
- **C.** The Leading and Lagging Strands Are Synthesized Simultaneously 904
- **D.** Replication Terminates at Specific Sites 908
- **E.** DNA Is Replicated with High Fidelity 909

3 Eukaryotic DNA Replication 910
- **A.** Eukaryotes Use Several DNA Polymerases 910
- **B.** Eukaryotic DNA Is Replicated from Multiple Origins 911
- **C.** Telomerase Extends Chromosome Ends 914

4 DNA Damage 916
- **A.** Environmental and Chemical Agents Generate Mutations 916
- **B.** Many Mutagens Are Carcinogens 919

5 DNA Repair 920
- **A.** Some Damage Can Be Directly Reversed 920
- **B.** Base Excision Repair Requires a Glycosylase 921
- **C.** Nucleotide Excision Repair Removes a Segment of a DNA Strand 923
- **D.** Mismatch Repair Corrects Replication Errors 924
- **E.** Some DNA Repair Mechanisms Introduce Errors 925

6 Recombination 926
- **A.** Homologous Recombination Involves Several Protein Complexes 926
- **B.** DNA Can Be Repaired by Recombination 932
- **C.** Transposition Rearranges Segments of DNA 934

BOX 25-1 **PATHWAYS OF DISCOVERY** Arthur Kornberg and DNA Polymerase I 898

BOX 25-2 **PERSPECTIVES IN BIOCHEMISTRY** Reverse Transcriptase 912

BOX 25-3 **BIOCHEMISTRY IN HEALTH AND DISEASE** Telomerase, Aging, and Cancer 915

BOX 25-4 **PERSPECTIVES IN BIOCHEMISTRY** DNA Methylation 918

BOX 25-5 **PERSPECTIVES IN BIOCHEMISTRY** Why Doesn't DNA Contain Uracil? 921

26 Transcription and RNA Processing 942

1 Prokaryotic RNA Transcription 943
- **A.** RNA Polymerase Resembles Other Polymerases 943
- **B.** Transcription Is Initiated at a Promoter 943
- **C.** The RNA Chain Grows from the 5′ to 3′ End 947
- **D.** Transcription Terminates at Specific Sites 950

2 Transcription in Eukaryotes 952
- **A.** Eukaryotes Have Several RNA Polymerases 953
- **B.** Each Polymerase Recognizes a Different Type of Promoter 958
- **C.** Transcription Factors Are Required to Initiate Transcription 960

3 Posttranscriptional Processing 965
- **A.** Messenger RNAs Undergo 5′ Capping, Addition of a 3′ Tail, and Splicing 965
- **B.** Ribosomal RNA Precursors May Be Cleaved, Modified, and Spliced 976
- **C.** Transfer RNAs Are Processed by Nucleotide Removal, Addition, and Modification 980

BOX 26-1 **PERSPECTIVES IN BIOCHEMISTRY** Collisions between DNA Polymerase and RNA Polymerase 949

BOX 26-2 **BIOCHEMISTRY IN HEALTH AND DISEASE** Inhibitors of Transcription 954

BOX 26-3 **PATHWAYS OF DISCOVERY** Richard Roberts and Phillip Sharp and the Discovery of Introns 968

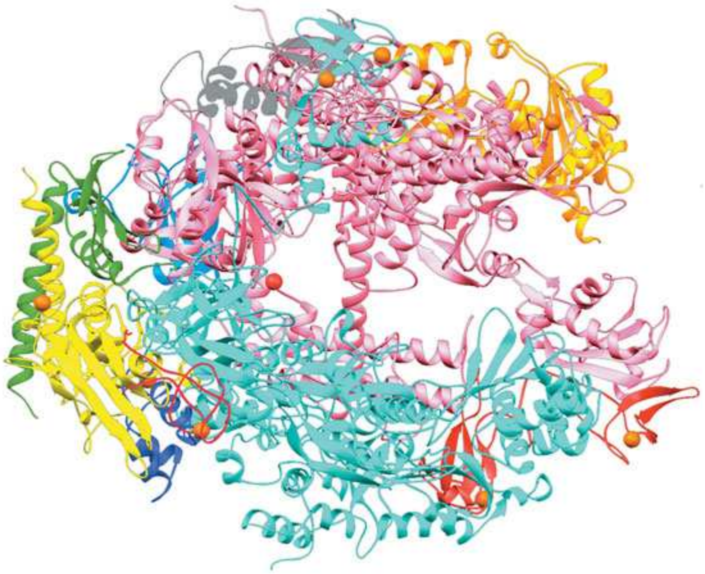

27 Protein Synthesis 985

1 The Genetic Code 986
- **A.** Codons Are Triplets That Are Read Sequentially 986
- **B.** The Genetic Code Was Systematically Deciphered 987
- **C.** The Genetic Code Is Degenerate and Nonrandom 988

2 Transfer RNA and Its Aminoacylation 991
- **A.** All tRNAs Have a Similar Structure 991
- **B.** Aminoacyl–tRNA Synthetases Attach Amino Acids to tRNAs 994
- **C.** A tRNA May Recognize More than One Codon 998

3 Ribosomes 1000
- **A.** The Prokaryotic Ribosome Consists of Two Subunits 1001
- **B.** The Eukaryotic Ribosome Is Larger and More Complex 1007

4 Translation 1008
- **A.** Chain Initiation Requires an Initiator tRNA and Initiation Factors 1010
- **B.** The Ribosome Decodes the mRNA, Catalyzes Peptide Bond Formation, Then Moves to the Next Codon 1014
- **C.** Release Factors Terminate Translation 1026

5 Posttranslational Processing 1028
- **A.** Ribosome-Associated Chaperones Help Proteins Fold 1028
- **B.** Newly Synthesized Proteins May Be Covalently Modified 1029

BOX 27-1 **PERSPECTIVES IN BIOCHEMISTRY** Evolution of the Genetic Code 990

BOX 27-2 **PERSPECTIVES IN BIOCHEMISTRY** Expanding the Genetic Code 1000

BOX 27-3 **BIOCHEMISTRY IN HEALTH AND DISEASE** The Effects of Antibiotics on Protein Synthesis 1024

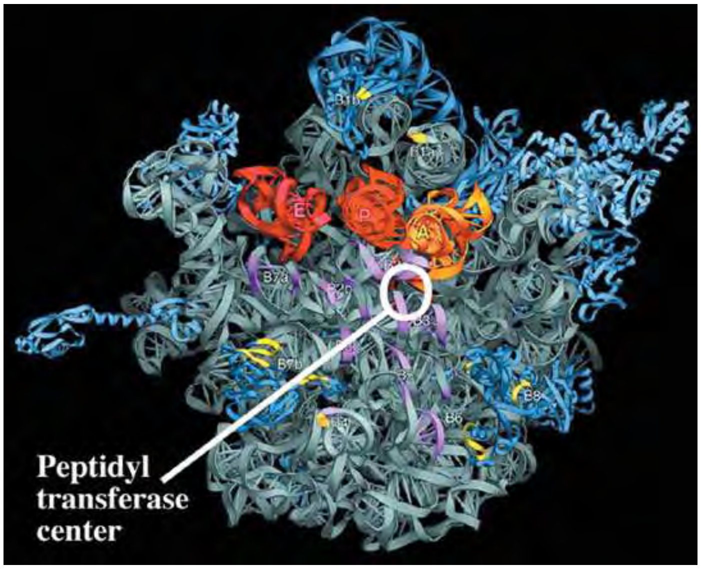

28 Regulation of Gene Expression 1037

1 Genome Organization 1038
- **A.** Gene Number Varies among Organisms 1038
- **B.** Some Genes Occur in Clusters 1042
- **C.** Eukaryotic Genomes Contain Repetitive DNA Sequences 1043

2 Regulation of Prokaryotic Gene Expression 1046
- **A.** The *lac* Operon Is Controlled by a Repressor 1046
- **B.** Catabolite-Repressed Operons Can Be Activated 1050
- **C.** Attenuation Regulates Transcription Termination 1051
- **D.** Riboswitches Are Metabolite-Sensing RNAs 1054

3 Regulation of Eukaryotic Gene Expression 1055
- **A.** Chromatin Structure Influences Gene Expression 1055
- **B.** Eukaryotes Contain Multiple Transcriptional Activators 1067
- **C.** Posttranscriptional Control Mechanisms Include RNA Degradation 1073
- **D.** Antibody Diversity Results from Somatic Recombination and Hypermutation 1077

4 The Cell Cycle, Cancer, and Apoptosis 1081
- **A.** Progress through the Cell Cycle Is Tightly Regulated 1081
- **B.** Tumor Suppressors Prevent Cancer 1084
- **C.** Apoptosis Is an Orderly Process 1086
- **D.** Development Has a Molecular Basis 1090

BOX 28-1 **BIOCHEMISTRY IN HEALTH AND DISEASE** Trinucleotide Repeat Diseases 1044

BOX 28-2 **PERSPECTIVES IN BIOCHEMISTRY** X Chromosome Inactivation 1057

BOX 28-3 **PERSPECTIVES IN BIOCHEMISTRY** Nonsense-Mediated Decay 1074

APPENDICES

Solutions to Problems SP-1

Glossary G-1

Index I-1

Preface

The last several years have seen enormous advances in biochemistry, particularly in the areas of structural biology and bioinformatics. Against this backdrop, we asked *What do students of modern biochemistry really need to know and how can we, as authors, help them in their pursuit of this knowledge?* We concluded that it is more important than ever to provide a solid biochemical foundation, rooted in chemistry, to prepare students for the scientific challenges of the future. With that in mind, we re-examined the contents of *Fundamentals of Biochemistry,* focusing on basic principles and striving to polish the text and improve the pedagogy throughout the book so that it is even more accessible to students. At the same time, we added new material in a way that links it to the existing content, mindful that students assimilate new information only in the proper context. We believe that students are best served by a textbook that is complete, clearly written, and relevant to human health and disease.

New For The Third Edition

The newest edition of *Fundamentals of Biochemistry* includes significant changes and updates to the contents. These changes include:

- A new chapter, Chapter 13, on Biochemical Signaling covers the role of hormones, receptors, G proteins, second messengers, and other aspects of inter- and intracellular communication. Placing these topics in a single chapter allows more comprehensive coverage of this rapidly changing field, which is critical for understanding such processes as fuel metabolism and cancer growth.
- Chapter 14 (Introduction to Metabolism) includes a new discussion of vitamins, minerals, and macronutrients, as part of a more wholistic approach to human metabolism. Expanded coverage of DNA chip technology and applications reflects growth in this area. In addition, a section on Systems Biology describes the cutting-edge fields of genomics, transcriptomics, proteomics, and metabolomics, along with some relevant laboratory techniques.
- P/O ratios have been updated throughout the metabolism chapters (so that each electron pair from NADH corresponds to 2.5 rather than 3 ATP) to match the most recent research findings.
- Chapter 22 (Mammalian Fuel Metabolism: Integration and Regulation) has been extensively revised to incorporate recent advances in human metabolic studies, with a new section on metabolic homeostasis that includes a discussion of appetite and body weight regulation. New material on AMP-dependent protein kinase and the hormone adiponectin describes some of the newly discovered biochemistry behind metabolic regulation.
- Other additions to the third edition were prompted by advances in many different fields, for example, new information on the analysis of short tandem repeats for DNA fingerprinting, bacterial biofilms, viral membrane fusion events, structures and functions of ABC transporters such as P-glycoprotein responsible for drug resistance, chromatin structure, elements involved in initiating RNA transcription, and posttranscriptional protein processing.

We have given significant thought to the pedagogy within the text and have concentrated on fine-tuning and adding

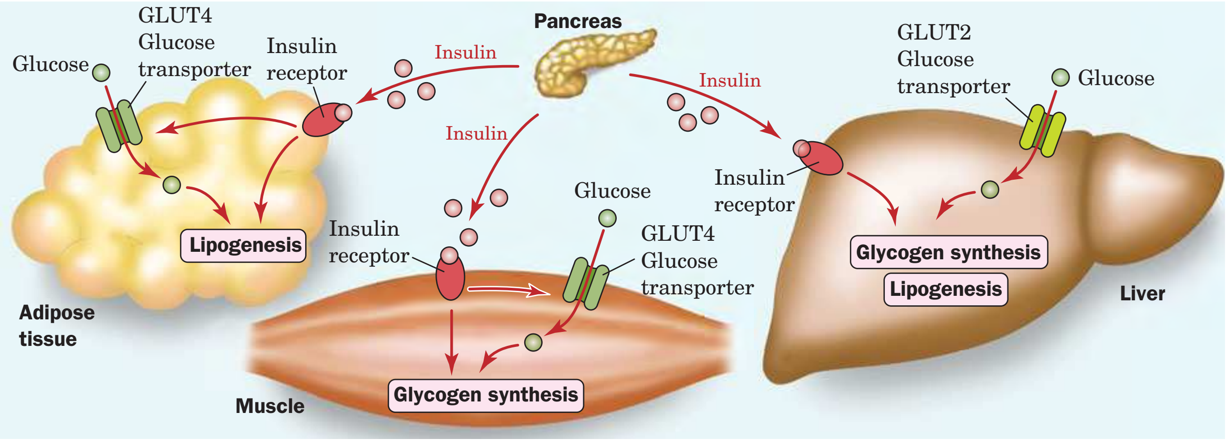

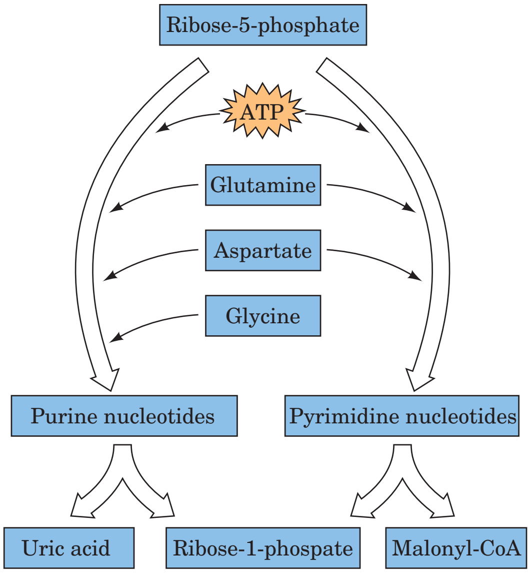

some new elements to promote student learning. These enhancements include the following:

- Numerous macromolecular structures are displayed with newly revealed details, and well over 100 figures have been replaced with state-of-the-art molecular graphics.
- Seven metabolic overview figures have been reworked to better emphasize their physiological relevance.
- Three new Pathways of Discovery Boxes have been added to focus on the scientific contributions of Lynn Margulis (Chapter 1), Rosalyn Yalow (Chapter 13), and Gertrude Elion (Chapter 23). These provide a better sense of history and emphasize that the study of biochemistry is a human endeavor.
- **Learning Objectives** placed at the beginning of each section of a chapter guide students as they read.
- Each section concludes with a set of study questions, entitled **Check Your Understanding,** to provide a quick review of the preceding material.
- Thirty new end-of-chapter problems with complete solutions have been added to provide students with more opportunities to apply their knowledge.
- New **overview figures** summarize multistep metabolic pathways and the interrelationships among them.

Organization

As in the second edition, the text begins with two introductory chapters that discuss the origin of life, evolution, thermodynamics, the properties of water, and acid–base chemistry. Nucleotides and nucleic acids are covered in Chapter 3, since an understanding of the structures and functions of these molecules supports the subsequent study of protein evolution and metabolism.

Four chapters (4 through 7) explore amino acid chemistry, methods for analyzing protein structure and sequence, secondary through quaternary protein structure, protein folding and stability, and structure–function relationships in hemoglobin, muscle proteins, and antibodies. Chapter 8 (Carbohydrates), Chapter 9 (Lipids and Biological Membranes), and Chapter 10 (Membrane Transport) round out the coverage of the basic molecules of life.

The next three chapters examine proteins in action, introducing students first to enzyme mechanisms (Chapter 11), then shepherding them through discussions of enzyme kinetics, the effects of inhibitors, and enzyme regulation (Chapter 12). These themes are continued in Chapter 13, which describes the components of signal transduction pathways.

Metabolism is covered in a set of chapters, beginning with an introductory chapter (Chapter 14) that provides an overview of metabolic pathways, the thermodynamics of "high-energy" compounds, and redox chemistry. Central metabolic pathways are presented in detail (e.g., glycolysis, glycogen metabolism, and the citric acid cycle in Chapters 15–17) so that students can appreciate how individual enzymes catalyze reactions and work in concert to perform complicated biochemical tasks. Chapters 18 (Electron Transport and Oxidative Phosphorylation) and 19 (Photosynthesis) complete a sequence that emphasizes energy-producing pathways. Not all pathways are covered in full detail, particularly those related to lipids (Chapter 20), amino acids (Chapter 21), and nucleotides (Chapter 23). Instead, key enzymatic reactions are highlighted for their interesting chemistry or regulatory importance. Chapter 22, on the integration of metabolism, discusses organ specialization and metabolic regulation in mammals.

Five chapters describe the biochemistry of nucleic acids, beginning with Chapter 24, which discusses the structure of

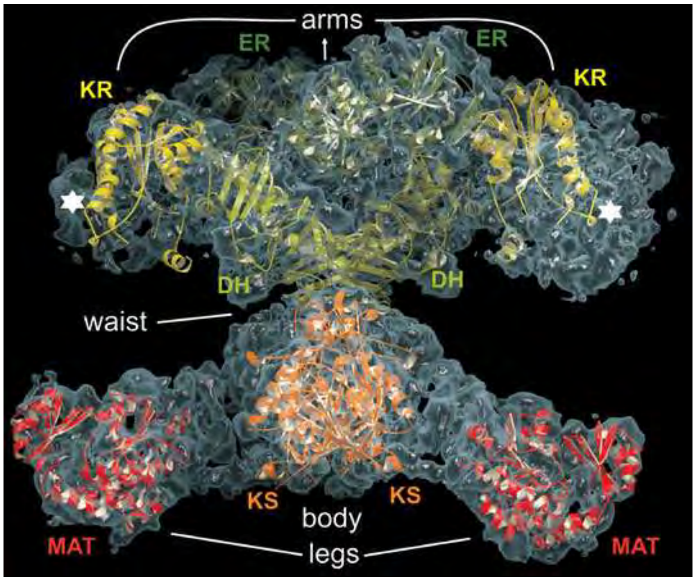

DNA and its interactions with proteins. Chapters 25–27 cover the processes of replication, transcription, and translation, highlighting the functions of the RNA and protein molecules that carry out these processes. Chapter 28 deals with a variety of mechanisms for regulating gene expression, including the histone code and the roles of transcription factors and their relevance to cancer and development.

Traditional Pedagogical Strengths

Successful pedagogical elements from the first and second editions of *Fundamentals of Biochemistry* have been retained. Among these are:

- the division of chapters into **numbered sections** for easy navigation
- **key sentences** printed in italic to assist with quick visual identification
- boldfaced **key terms**
- a **list of terms** at the end of each chapter, with the **page numbers** where the terms are first defined
- a comprehensive **glossary containing over 1200 terms** in an appendix
- **overview figures** for many metabolic processes
- figures illustrating **detailed enzyme mechanisms** throughout the text
- **sample calculations**
- **PDB identification codes** in the figure legend for each molecular structure so that students can download and explore structures on their own.
- Enrichment material, including clinical correlations, technical descriptions, and historical perspectives placed in **text boxes**.
- a **numbered summary** at the end of each chapter
- an expanded set of **problems** (with **complete solutions** in an appendix)
- a list of references for each chapter, selected for their relevance and user-friendliness.

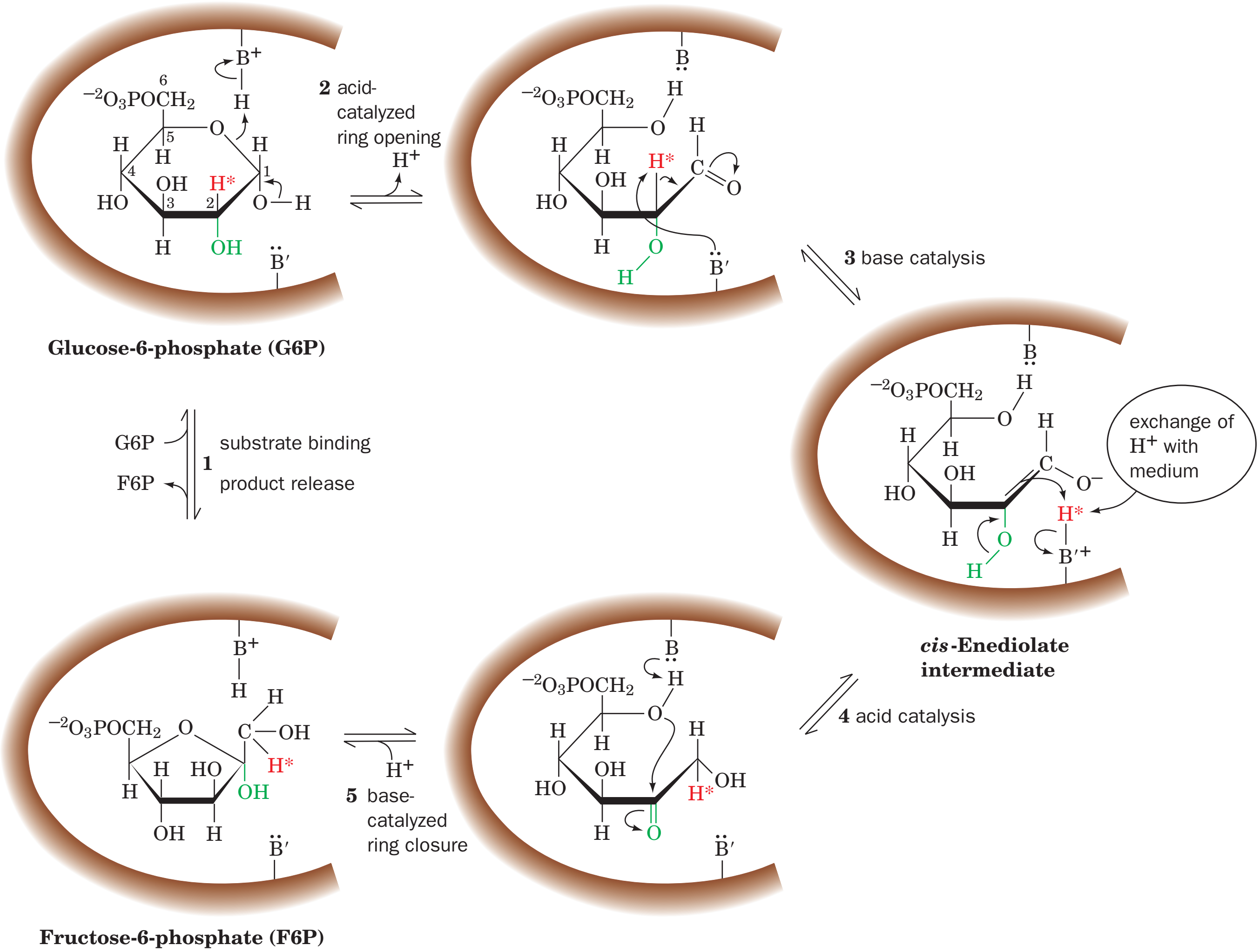
Glucose-6-phosphate (G6P)
2 acid-catalyzed ring opening
H^+
3 base catalysis
exchange of H^+ with medium
cis-**Enediolate intermediate**
G6P
F6P
1
substrate binding
product release
4 acid catalysis
5 base-catalyzed ring closure
H^+
Fructose-6-phosphate (F6P)
$^{-2}O_3POCH_2$
B^+
B'
B'^+
H^*

Acknowledgments

This textbook is the result of the dedicated effort of many individuals, several of whom deserve special mention: Laura Ierardi cleverly combined text figures and tables in designing each of the textbook's pages. Suzanne Ingrao, our Production Coordinator, skillfully managed the production of the textbook. Madelyn Lesure designed the book's typography and cover. Kevin Molloy, our Acquisitions Editor, skillfully organized and managed the project until his departure, and Petra Recter, Associate Publisher, saw us through to publication. Hilary Newman and Elyse Rieder acquired many of the photographs in the textbook and kept track of all of them. Connie Parks, our copy editor, put the final polish on the manuscript and eliminated large numbers of grammatical and typographical errors. Sandra Dumas was our in-house Production Editor at Wiley. Sigmund Malinowski coordinated the illustration program, with contributions from Joan Kalkut and artist Elizabeth Morales. Amanda Wainer spearheaded the marketing campaign. Special thanks to Geraldine Osnato and Aly Rentrop, Project Editors, who coordinated and managed an exceptional supplements package, and to Tom Kulesa, Media Editor, who substantially improved and developed the media resources, website, and WileyPLUS program. Thanks go also to Ann Shinnar for her careful review of the Test Bank.

The atomic coordinates of many of the proteins and nucleic acids that we have drawn for use in this textbook were obtained from the Research Collaboratory for Structural Bioinformatics Protein Data Bank. We created these drawings using the molecular graphics programs RIBBONS by Mike Carson; GRASP by Anthony Nicholls, Kim Sharp, and Barry Honig; and PyMOL by Warren DeLano.

The interactive computer graphics diagrams that are presented on the website that accompanies this textbook are either Jmol images or Kinemages. Jmol is a free, open source, interactive, web browser applet for manipulating molecules in three dimensions. It is based on the program RasMol by Roger Sayle, which was generously made publicly available. The Jmol images in the Interactive Exercises were generated by Stephen Rouse. Kinemages are displayed by the program KiNG, which was written and generously provided by David C. Richardson who also wrote and provided the program PREKIN, which DV and JGV used to help generate the Kinemages. KiNG (Kinemage, Next Generation) is an interactive system for three-dimensional vector graphics that runs on Windows, Mac OS X, and Linux/Unix systems.

The Internet Resources and Student Printed Resources were prepared by the following individuals. Bioinformatics Exercises: Paul Craig, Rochester Institute of Technology, Rochester, New York; Online Homework Exercises and Classroom Response Questions: Rachel Milner and Adrienne Wright, University of Alberta, Edmonton, Alberta, Canada; Online Self-Study Quizzes: Steven Vik, Southern Methodist University, Dallas, Texas; Case Studies: Kathleen Cornely, Providence College, Providence, Rhode Island; Student Companion: Akif Uzman, University of Houston-Downtown, Houston, Texas; Test Bank: Marilee Benore-Parsons, University of Michigan-Dearborn, Dearborn, Michigan and Robert Kane, Baylor University, Waco, Texas.

We wish to thank those colleagues who have graciously devoted their time to offer us valuable comments and feedback as it relates to our textbook. Our reviewers include:

ALABAMA
Michael E. Friedman, *Auburn University*
CALIFORNIA
Marjorie A. Bates, *University of California Los Angeles*
Lukas Buehler, *University of California San Diego*
Charles E. Bowen, *California Polytechnic University*
Richard Calendar, *University of California Berkeley*
Gopal Iyer, *University of California Los Angeles*
Carla Koehler, *University of California Los Angeles*
Michael A. Marletta, *University of California Berkeley*
Douglas McAbee, *California State University Long Beach*
Angelika Niema, *Keck Graduate Institute*
Tim Osborne, *University of California Irvine*
Stanley M. Parsons, *University of California Santa Barbara*
Leigh Plesniak, *University of San Diego*
Christian K. Roberts, *University of California Los Angeles*
Pam Stacks, *San Jose State University*
Koni Stone, *California State University Stanislaus*
Leon Yengoyan, *San Jose State University*
FLORIDA
Fazal Ahmad, *University of Miami School of Medicine*
Peggy R. Borum, *University of Florida Gainesville*
Glenn Cunningham, *University of Central Florida*
Frans Huijing, *University of Miami School of Medicine*
Robley J. Light, *Florida State University*
David J. Merkler, *University of South Florida Tampa*
Thomas L. Selby, *University of Central Florida*
GEORGIA
Giovanni Gadda, *Georgia State University*
Stephan Quirk, *Georgia Institute of Technology*
ILLINOIS
Jeffrey A. Frick, *Illinois Wesleyan University*
Lowell P. Hager, *University of Illinois Urbana-Champaign*
Robert MacDonald, *Northwestern University*
Stephen Meredith, *University of Chicago*
Ken Olsen, *Loyola University*
Phoebe A. Rice, *University of Chicago*
Gary Spedding, *Butler University*
INDIANA
Thomas Goyne, *Valparaiso University*
Ann L. Kirchlmaier, *Purdue University West Lafayette*

IOWA

Donald Beitz, *Iowa State University*
LaRhee Henderson, *Drake University*

KANSAS

Lawrence C. Davis, *Kansas State University*
Michael Keck, *Emporia State University*

KENTUCKY

Steven R. Ellis, *University of Louisville*
Stefan Paula, *Northern Kentucky University*

LOUISIANA

Marion L. Carroll, *Xavier University of Louisiana*
Jim D. Karam, *Tulane University Health Sciences Center*
Eric R. Taylor, *University of Louisiana at Lafayette*
Candace Timpte, *University of New Orleans*
William C. Wimley, *Tulane University Health Sciences Center*

MAINE

Gale Rhodes, *University of Southern Maine*

MARYLAND

Bonnie Diehl, *Johns Hopkins University*
J. Norman Hansen, *University of Maryland*
Jason D. Kahn, *University of Maryland College Park*
Tom Stanton, *University of Maryland Shady Grove*

MASSACHUSETTS

Robert D. Lynch, *University of Massachusetts Lowell*
Lynmarie K. Thompson, *University of Massachusetts*
Adele Wolfson, *Wellesley College*
Michael B. Yaffe, *Massachusetts Institute of Technology*

MICHIGAN

Kenneth Balazovich, *University of Michigan Ann Arbor*
Deborah Heyl-Clegg, *Eastern Michigan University*
Michael LaFontaine, *Ferris State University*
Kathleen V. Nolta, *University of Michigan*
Robert Stach, *University of Michigan Flint*
Marty Thompson, *Michigan Technical University*

MISSISSIPPI

Jeffrey Evans, *University of Southern Mississippi*
Kenneth O. Willeford, *Mississippi State University*
Robert P. Wilson, *Mississippi State University*

MISSOURI

Mark E. Martin, *University of Missouri Columbia*
William T. Morgan, *University of Missouri Kansas City*
Michael R. Nichols, *University of Missouri St Louis*
Peter Tipton, *University of Missouri Columbia*

MONTANA

Larry L. Jackson, *Montana State University*
Martin Teintze, *Montana State University*

NEBRASKA

Ruma Banerjee, *University of Nebraska*
Frank A. Kovack, *University of Nebraska*

NEVADA

Bryan Spangelo, *University of Nevada Las Vegas*

NEW HAMPSHIRE

Anita S. Kline, *University of New Hampshire*

NEW JERSEY

Cathy Yang, *Rowan University*

NEW MEXICO

James Hageman, *New Mexico State University*

NEW YORK

Jacquelyn Fetrow, *University of Albany*
Burt Goldberg, *New York University*
Martin Horowitz, *New York Medical College*
Terry Platt, *University of Rochester*
Raghu Sarma, *State University of New York at Stony Brook*
Scott Severance, *Canisius College*
Ann E. Shinnar, *Touro College*
Burton Tropp, *Queens College CUNY*
Joseph T. Warden, *Rensselaer Polytechnic Institute*

NORTH CAROLINA

Arno L. Greenleaf, *Duke University*

OHIO

Caroline Breitenberger, *The Ohio State University*
Susan C. Evans, *Ohio University*
Dave Mascotti, *John Carroll University*
Gary E. Means, *Ohio State University*
Daniel Smith, *University of Akron*
John Turchi, *Wright State University*

OKLAHOMA

Paul F. Cook, *University of Oklahoma*
Kenneth Weed, *Oral Roberts University*

PENNSYLVANIA

Michael Borenstein, *Temple University*
David J. Edwards, *University of Pittsburgh*
Jan Feng, *Temple University*
Diane W. Husic, *East Stroudsburg University*
Teh-hui Kao, *Pennsylvania State University*
Laura Mitchell, *St. Joseph's University*
Allen T. Phillips, *Pennsylvania State University*
Philip A. Rea, *University of Pennsylvania*
Michael Sypes, *Pennsylvania State University*
George Tuszynski, *Temple University*
Joan Wasilewski, *The University of Scranton*
Michelle W. Wien, *Saint Joseph's University*
Bruce Wightman, *Muhlenberg College*
Michael Wilson, *Temple University*

RHODE ISLAND

Kathleen Cornely, *Providence College*
Mary Louise Greeley, *Salve Regina University*
Kimberly Mowry, *Brown University*

SOUTH CAROLINA

Jessup M. Shivley, *Clemson University*
Kerry Smith, *Clemson University*
Takita Felder Sumter, *Winthrop University*

SOUTH DAKOTA

Joel E. Houglum, *South Dakota State University*
Daniel Cervantes Laurean, *South Dakota State University*

TENNESSEE

Scott Champney, *East Tennessee State University*
Paul C. Kline, *Middle Tennessee State University*
Gerald Stuffs, *Vanderbilt University*
Jubran M. Wakim, *Middle Tennessee State University*

TEXAS

Helen Cronenberger, *University of Texas San Antonio*
Joseph Eichberg, *University of Houston*
George E. Fox, *University of Houston*
Edward D. Harris, *Texas A&M University*
David W. Hoffman, *University of Texas at Austin*
Bob Kane, *Baylor University*
Barrie Kitto, *University of Texas at Austin*
W. E. Kurtin, *Trinity University*
Glen B. Legge, *University of Houston*
Robert Renthal, *University of Texas San Antonio*
Linda J. Roman, *University of Texas San Antonio*
Rick Russell, *University of Texas Austin*
Jane Torrie, *Tarrant County College Northwest*
Akif Uzman, *University of Houston-Downtown*
Steven B. Vik, *Southern Methodist University*
Linette M. Watkins, *Southwest Texas State University*
William Widger, *University of Houston*
Ryland E. Young, *Texas A&M University*

UTAH

Scott A. Ensign, *Utah State University*
Steven W. Graves, *Brigham Young University*

VIRGINIA

Robert F. Diegelmann, *Virginia Commonwealth University*
William M. Grogan, *Virginia Commonwealth University*
Jeff Kushner, *James Madison University*

WASHINGTON

Ronald Brosemer, *Washington State University*
Michael D. Griswold, *Washington State University*
Christine M. Smith, *University of Puget Sound*
Steve Sylvester, *Washington State University Vancouver*
David C. Teller, *University of Washington*

WEST VIRGINIA

Giri R. Sura, *West Virginia State University*

WISCONSIN

Lisa C. Kroutil, *University of Wisconsin River Falls*

AUSTRALIA

Graham Parslow, *University of Melbourne*

Instructor and Student Resources

INTERNET RESOURCES

WileyPLUS

Provided at **no charge** when packaged with a new textbook or available for purchase stand alone.

Text and *WileyPLUS* bundle: 978-0-470-28104-8

***WileyPLUS* stand alone: 978-0-470-10207-7**

WileyPLUS combines the complete, dynamic online text with all the teaching and learning resources you need, in an easy-to-use system. ***WileyPLUS*** allows you to deliver all or a portion of your course online. With ***WileyPLUS*** you can:

- Create and assign online homework that is automatically graded and closely correlated to the text. Over 750 conceptually-based questions, organized by chapter and topic, offer students practice with instant feedback that explains why an answer choice is right or wrong.
- Manage your students' results in the online gradebook.
- Build media-rich class presentations.
- Customize your course to meet your course objectives.
- Additional valuable resources in electronic format. These include:
  - New! ***Bioinformatics Exercises:*** A set of newly updated exercises covering the contents and uses of databases related to nucleic acids, protein sequences, protein structures, enzyme inhibition, and other topics. These exercises use real data sets, pose specific questions, and prompt students to obtain information from online databases and to access the software tools for analyzing such data.
  - ***Guided Explorations:*** 30 self-contained presentations, many with narration, employ extensive animated computer graphics to enhance student understanding of key topics.
  - ***Interactive Exercises:*** 59 molecular structures from the text have been rendered in Jmol, a browser-independent interface for manipulating structures in three dimensions, and paired with questions designed to facilitate comprehension of concepts. A tutorial for using Jmol is also provided.
  - ***Kinemages:*** A set of 22 exercises comprising 55 three-dimensional images of selected proteins and nucleic acids that can be manipulated by users as suggested by accompanying text.
  - ***Animated Figures:*** 67 figures from the text, illustrating various concepts, techniques, and processes, are presented as brief animations to facilitate learning.
  - New! ***Online Homework Exercises:*** Over 750 conceptually-based questions, which you can sort by chapter and/or topic, may be assigned as graded homework or additional practice. Each question features immediate, descriptive feedback for students that explains why an answer is right or wrong.
  - New! ***Online Self-Study Quizzes:*** Quizzes to accompany each chapter consisting of multiple choice, true/false and fill in the blank questions, with instant feedback to help students master concepts.
  - New! ***Online Prelecture Questions:*** Each chapter includes multiple choice questions that address common student misconceptions.
  - ***Case Studies:*** A set of 33 case studies use problem-based learning to promote understanding of biochemical concepts. Each case presents data from the literature and asks questions that require students to apply principles to novel situations, often involving topics from multiple chapters in the textbook.
  - New! ***"Take Note!" Workbook:*** Available for download in PDF format, this contains the most important figures, diagrams, and art from the text that illustrate key concepts. Each page contains ample space for note taking and writing.
  - New! ***Wiley Encyclopedia of Chemical Biology:*** Most chapters include a link to a carefully selected article from the ***Wiley Encyclopedia of Chemical Biology.*** This is the first reference work in the widely expanding field of chemical biology. Links to relevant articles will facilitate deeper research and encourage additional reading.

INTERNET RESOURCES

Most of the ***"additional resources"*** listed above (i.e., Bioinformatics Exercises, etc.) can also be accessed at the following URL: http://www.wiley.com/college/voet.

PRINTED STUDENT RESOURCE

Student Companion to *Fundamentals of Biochemistry 3E*

Offered at no **additional charge** when purchased with a new textbook or can be purchased separately:

Text and *Student Companion* bundle: 978-0-470-28439-1
***Student Companion* separately: 978-0-470-22842-5**

This newly updated study resource is designed to help students master basic concepts and to enhance their analytic skills. Each chapter contains a summary, a review of essential concepts, and additional problems.

INSTRUCTOR RESOURCES

These can be accessed through ***WileyPLUS.***

- **PowerPoint Slides** of all the figures and tables in the text. The figures are optimized for classroom projection, with bold leader lines and large labels, and are also available for importing individually as jpeg files from the *Wiley Image Gallery*.
- **Test Bank** with almost 1,200 questions, containing a variety of question types (multiple choice, matching, fill in the blank, and short answer). Each question is keyed to the relevant section in the text as well as to the key topic and is rated by difficulty level. (Tests can be created and administered online or with test-generator software.)
- New! **Classroom Response Questions ("clicker questions") for each chapter.** These interactive questions, for classroom response systems, facilitate classroom participation and discussion. These questions can also be used by instructors as prelecture questions that help gauge students' knowledge of overall concepts, while addressing common misconceptions.
- New! Access to the **Molecular and Life Sciences Visual Library** which provides a large collection of figures from a variety of Wiley Life Science texts, including *Cell and Molecular Biology 5E* by Gerald Karp and *Principles of Genetics 4E* by D. Peter Snustad and Michael J. Simmons. These can be used in lecture presentations.

If you wish to gain access to ***Instructor Resources*** (PowerPoint, Test Bank, etc.) but do not wish to access them through *WileyPLUS,* please contact your local Wiley sales representative. You can locate your Wiley sales representative by clicking *"Who's My Rep?"* after typing in your school affiliation at the following URL: www.wiley.com/college.

Guide to Media Resources

The book website (www.wiley.com/college/voet) offers the following resources to enhance student understanding of biochemistry. These are all keyed to figures or sections in the text. They are called out in the text with a red mouse icon or margin note.

Chapter		Media Type	Title	Text Reference
2	Water	Animated Figure	Titration curves for acetic acid, phosphate, and ammonia	Fig. 2-17
		Animated Figure	Titration of polyprotic acid	Fig. 2-18
		Case Study	1. Acute Aspirin Overdose: Relationship to the Blood Buffering	Pg. 38
3	Nucleotides, Nucleic Acids, and Genetic Information	Guided Exploration	1. Overview of transcription and translation	Section 3-3B
		Guided Exploration	2. DNA sequence determination by the chain-terminator method	Section 3-4C
		Guided Exploration	3. PCR and site-directed mutagenesis	Section 3-5C
		Interactive Exercise	1. Three-dimensional structure of DNA	Fig. 3-6
		Animated Figure	Construction of a recombinant DNA molecule	Fig. 3-26
		Animated Figure	Cloning with bacteriophage λ	Fig. 3-27
		Animated Figure	Site-directed mutagenesis	Fig. 3-30
		Kinemage	2-1. Structure of DNA	Fig. 3-6
		Kinemage	2-2. Watson-Crick base pairs	Fig. 3-8
		Bioinformatics Exercise	Chapter 3. Databases for the Storage and "Mining" of Genome Sequences	Pg. 72
5	Proteins: Primary Structure	Guided Exploration	4. Protein sequence determination	Section 5-3
		Guided Exploration	5. Protein evolution	Section 5-4A
		Animated Figure	Enzyme-linked immunosorbent assay	Fig. 5-3
		Animated Figure	Ion exchange chromatography	Fig. 5-6
		Animated Figure	Gel filtration chromatography	Fig. 5-7
		Animated Figure	Edman degradation	Fig. 5-15
		Animated Figure	Generating overlapping fragments to determine the amino acid sequence of a polypeptide	Fig. 5-18
		Case Study	2. Histidine-Proline-rich Glycoprotein as a Plasma pH Sensor	Pg. 123
		Bioinformatics Exercise	Chapter 5. Using Databases to Compare and Identify Related Protein Sequences	Pg. 124
6	Proteins: Three-Dimensional Structure	Guided Exploration	6. Stable helices in proteins: the α helix	Section 6-1B
		Guided Exploration	7. Hydrogen bonding in β sheets	Section 6-1B
		Guided Exploration	8. Secondary structures in proteins	Section 6-2C
		Interactive Exercise	2. Glyceraldehyde-3-phosphate dehydrogenase	Fig. 6-31
		Animated Figure	The α helix	Fig. 6-7
		Animated Figure	β sheets	Fig. 6-9
		Animated Figure	Symmetry in oligomeric proteins	Fig. 6-34
		Animated Figure	Mechanism of protein disulfide isomerase	Fig. 6-42
		Kinemage	3-1. The peptide group	Fig. 6-2, 6-4, 6-5
		Kinemage	3-2. The α helix	Fig. 6-7
		Kinemage	3-3. β sheets	Fig. 6-9, 6-10, 6-11
		Kinemage	3-4. Reverse turns	Fig. 6-14
		Kinemage	4-1, 4-2. Coiled coils	Fig. 6-15
		Kinemage	4-3, 4-4. Collagen	Fig. 6-18
		Kinemage	5. Cytochrome *c*	Fig. 6-27, 6-32
		Case Study	4. The Structure of Insulin	Pg. 174
		Case Study	5. Characterization of Subtilisin from the Antarctic Psychrophile *Bacillus* TA41	Pg. 174
		Case Study	6. A Collection of Collagen Cases	Pg. 174
		Bioinformatics Exercise	Chapter 6. Visualizing Three-Dimensional Protein Structures	Pg. 174

Chapter	Media Type	Title	Text Reference
7 Protein Function: Myoglobin and Hemoglobin, Muscle Contraction, and Antibodies	Interactive Exercise	3. Structure of a mouse antibody	Fig. 7-38
	Animated Figure	Oxygen-binding curve of hemoglobin	Fig. 7-6
	Animated Figure	Movements of heme and F helix in hemoglobin	Fig. 7-8
	Animated Figure	The Bohr effect	Fig. 7-11
	Animated Figure	Effect of BPG and CO_2 on hemoglobin	Fig. 7-13
	Animated Figure	Mechanism of force generation in muscle	Fig. 7-32
	Kinemage	6-1. Myoglobin structure	Fig. 7-1, 7-3
	Kinemage	6-2, 6-3. Hemoglobin structure	Fig. 7-5
	Kinemage	6-3. BPG binding to hemoglobin	Fig. 7-14
	Kinemage	6-4. Conformational changes in hemoglobin	Fig. 7-8
	Kinemage	6-5. Changes at α_1–β_2/α_2–β_1 interfaces in hemoglobin	Fig. 7-9
	Case Study	8. Hemoglobin, the Oxygen Carrier	Pg. 217
	Case Study	9. Allosteric Interactions in Crocodile Hemoglobin	Pg. 217
	Case Study	10. The Biological Roles of Nitric Oxide	Pg. 217
8 Carbohydrates	Kinemage	7-1. D-Glucopyranose, α and β anomers	Fig. 8-4, 8-5
	Kinemage	7-2. Sucrose	Section 8-2A
	Kinemage	7-3. Hyaluronate	Fig. 8-12
	Kinemage	7-4. Structure of a complex carbohydrate	Fig. 8-19
9 Lipids and Biological Membranes	Guided Exploration	9. Membrane structure and the fluid mosaic model	Section 9-4A
	Interactive Exercise	4. Model of phospholipase A_2 and glycerophospholipid	Fig. 9-6
	Animated Figure	Secretory pathway	Fig. 9-35
	Kinemage	8-1. Bacteriorhodopsin	Fig. 9-22
	Kinemage	8-3. OmpF porin	Fig. 9-23
10 Membrane Transport	Interactive Exercise	5. The K^+ channel selectivity filter	Fig. 10-5
	Animated Figure	Model for glucose transport	Fig. 10-13
	Case Study	3. Carbonic Anhydrase II Deficiency	Pg. 320
	Case Study	14. Shavings from the Carpenter's Bench: The Biological Role of the Insulin C-peptide	Pg. 320
	Case Study	17. A Possible Mechanism for Blindness Associated with Diabetes: Na^+-Dependent Glucose Uptake by Retinal Cells	Pg. 320
11 Enzymatic Catalysis	Guided Exploration	10. The catalytic mechanism of serine proteases	Section 11-5C
	Interactive Exercise	6. Pancreatic RNase S	Fig. 11-9
	Interactive Exercise	7. Carbonic anhydrase	Fig. 11-13
	Interactive Exercise	8. Hen egg white lysozyme	Fig. 11-17
	Animated Figure	Effect of preferential transition state binding	Fig. 11-15
	Animated Figure	Chair and half-chair conformations	Fig. 11-18
	Kinemage	9. Hen egg white lysozyme-catalytic mechanism	Fig. 11-17, 11-19, 11-21
	Kinemage	10-1. Structural overview of a trypsin/inhibitor complex	Fig. 11-25, 11-31
	Kinemage	10-2. Evolutionary comparisons of proteases	Fig. 11-28
	Kinemage	10-3. A transition state analog bound to chymotrypsin	Fig. 11-30
	Case Study	11. Nonenzymatic Deamidization of Asparagine and Glutamine Residues in Proteins	Pg. 362
12 Enzyme Kinetics, Inhibition, and Control	Guided Exploration	11. Michaelis-Menten kinetics, Lineweaver-Burk plots, and enzyme inhibition	Section 12-1
	Interactive Exercise	9. HIV protease	Box 12-4
	Animated Figure	Progress curve for an enzyme-catalyzed reaction	Fig. 12-2
	Animated Figure	Plot of initial velocity versus substrate concentration	Fig. 12-3
	Animated Figure	Double-reciprocal (Lineweaver-Burk) plot	Fig. 12-4
	Animated Figure	Lineweaver-Burk plot of competitive inhibition	Fig. 12-7
	Animated Figure	Lineweaver-Burk plot of uncompetitive inhibition	Fig. 12-8
	Animated Figure	Lineweaver-Burk plot of mixed inhibition	Fig. 12-9
	Animated Figure	Plot of v_o versus [aspartate] for ATCase	Fig. 12-10
	Kinemage	11-1. Structure of ATCase	Fig. 12-12, 12-13
	Kinemage	11-2. Conformational changes in ATCase	Fig. 12-13
	Kinemage	14-1. Glycogen phosphorylase	Fig. 12-14

Chapter	Media Type	Title	Text Reference
	Kinemage	14-2 and 14-3. Conformational changes in glycogen phosphorylase	Fig. 12-15
	Case Study	7. A Storage Protein from Seeds of *Brassica nigra* Is a Serine Protease Inhibitor	Pg. 403
	Case Study	12. Production of Methanol in Ripening Fruit	Pg. 403
	Case Study	13. Inhibition of Alcohol Dehydrogenase	Pg. 403
	Case Study	15. Site-Directed Mutagenesis of Creatine Kinease	Pg. 403
	Case Study	19. Purification of Rat Kidney Sphingosine Kinease	Pg. 403
	Bioinformatics Exercise	Chapter 12. Enzyme Inhibitors and Rational Drug Design	Pg. 404
13 Biochemical Signaling	Guided Exploration	12. Hormone signaling by the receptor tyrosine kinase system	Section 13-2A
	Guided Exploration	13. Hormone signaling by the adenylate cyclase system	Section 13-3C
	Interactive Exercise	10. X-ray structure of human growth hormone (hGH)	Fig. 13-3
	Interactive Exercise	11. Tyrosine kinase domain of insulin receptor	Fig. 13-5
	Interactive Exercise	12. A heterotrimeric G protein	Fig. 13-19
	Interactive Exercise	13. C subunit of protein kinase A	Fig. 13-21
	Animated Figure	The Ras signaling cascade	Fig. 13-7
	Animated Figure	The phosphoinositide signaling system	Fig. 13-24
	Kinemage	15. cAMP-dependent protein kinase (PKA)	Fig. 13-21
	Kinemage	16-1 The structure of calmodulin	Fig. 13-27
	Kinemage	16-2 Calmodulin complex with target polypeptide	Fig. 13-28
14 Introduction to Metabolism	Interactive Exercise	14. Conformational changes in *E. coli* adenylate kinase	Fig. 14-9
	Case Study	16. Allosteric Regulation of ATCase	Pg. 484
	Bioinformatics Exercises	Chapter 14. Metabolic Enzymes, Microarrays, and Proteomics	Pg. 484
15 Glucose Catabolism	Guided Exploration	14. Glycolysis overview	Section 15-1
	Interactive Exercise	15. Conformational changes in yeast hexokinase	Fig. 15-2
	Interactive Exercise	16. Yeast TIM in complex with 2-phosphoglycolate	Fig. 15-6
	Interactive Exercise	17. TPP binding to pyruvate decarboxylase	Fig. 15-19
	Animated Figure	Overview of glycolysis	Fig. 15-1
	Animated Figure	Mechanism of aldolase	Fig. 15-5
	Animated Figure	Mechanism of GAPDH	Fig. 15-9
	Animated Figure	PFK activity versus F6P concentration	Fig. 15-23
	Kinemage	12-1, 12-2 Triose phosphate isomerase	Fig. 15-6
	Kinemage	13-1 Phosphofructokinase	Fig. 15-22
	Kinemage	13-2 Allosteric changes in phosphofructokinase	Fig. 15-24
	Case Study	18. Purification of Phosphofructokinase 1-C	Pg. 529
	Case Study	20. NAD$^+$-dependent Glyceraldehyde-3-Phosphate Dehydrogenase from *Thermoproteus tenax*	Pg. 529
16 Glycogen Metabolism and Gluconeogenesis	Guided Exploration	15. Control of glycogen metabolism	Section 16-3B
	Animated Figure	Overview of glucose metabolism	Fig. 16-1
	Animated Figure	Major phosphorylation and dephosphorylation systems in glycogen metabolism	Fig. 16-13
	Animated Figure	Comparison of gluconeogenesis and glycolysis	Fig. 16-15
	Animated Figure	Transport of PEP and oxaloacetate from mitochondrion to cytosol	Fig. 16-20
	Animated Figure	Pathway for dolichol-PP-oligosaccharide synthesis	Fig. 16-27
	Case Study	22. Carrier-Mediated Uptake of Lactate in Rat Hepatocytes	Pg. 564
	Case Study	26. The Role of Specific Amino Acids in the Peptide Hormone Glucagon in Receptor Binding and Signal Transduction	Pg. 564
17 Citric Acid Cycle	Guided Exploration	16. Citric acid cycle overview	Section 17-1
	Interactive Exercise	18. Conformational changes in citrate synthase	Fig. 17-9
	Animated Figure	Overview of oxidative fuel metabolism	Fig. 17-1
	Animated Figure	Reactions of the citric acid cycle	Fig. 17-2
	Animated Figure	Regulation of the citric acid cycle	Fig. 17-16
	Animated Figure	Amphibolic functions of the citric acid cycle	Fig. 17-17
	Case Study	21. Characterization of Pyruvate Carboxylase from *Methanobacterium thermoautotrophicum*	Pg. 595

Chapter	Media Type	Title	Text Reference
18 Electron Transport and Oxidative Phosphorylation	Guided Exploration	17. Electron transport and oxidative phosphorylation overview	Section 18-2B
	Guided Exploration	18. The Q cycle	Section 18-2E
	Guided Exploration	19. F_1F_0-ATP synthase and the binding change mechanism	Section 18-3B
	Interactive Exercise	19. Complex III	Fig. 18-14
	Interactive Exercise	20. Cytochrome *c* residues involved in intermolecular complex formation	Fig. 18-16
	Interactive Exercise	21. Bovine heart cyctochrome *c* oxidase	Fig. 18-17
	Interactive Exercise	22. F_1-ATP synthase	Fig. 18-22
	Animated Figure	The mitochondrial electron transport chain	Fig. 18-8
	Animated Figure	Coupling of electron transport and ATP synthesis	Fig. 18-20
	Animated Figure	The binding change mechanism of ATP synthesis	Fig. 18-24
	Animated Figure	Coordinated control of glycolysis and the citric acid cycle	Fig. 18-29
	Kinemage	5. Cytochrome *c*	Fig. 18-16
	Case Study	24. Uncoupling Proteins in Plants	Pg. 639
	Case Study	27. Regulation of Sugar and Alcohol Metabolism in *Saccharomyces cerevisiae*	Pg. 639
	Case Study	33. Modification of Subunit *c* from Bovine Mitochondrial ATPase	Pg. 639
19 Photosynthesis	Guided Exploration	20. Two-center photosynthesis (Z-scheme) overview	Section 19-2C
	Interactive Exercise	23. Light-harvesting complex LH-2	Fig. 19-5
	Interactive Exercise	24. *Rb. sphaeroides* reaction center	Fig. 19-8
	Interactive Exercise	25. Ferredoxin	Fig. 19-22
	Interactive Exercise	26. Ferredoxin–NADP$^+$ reductase	Fig. 19-23
	Animated Figure	Electronic states of chlorophyll	Fig. 19-6
	Animated Figure	The Calvin cycle	Fig. 19-26
	Animated Figure	Mechanism of RuBP carboxylase	Fig. 19-28
	Kinemage	8-2 Photosynthetic reaction center	Fig. 19-8, 19-9
20 Lipid Metabolism	Interactive Exercise	27. Active site of medium-chain acyl-CoA dehydrogenase	Fig. 20-13
	Interactive Exercise	28. X-Ray structure of methylmalonyl-CoA mutase	Fig. 20-18
	Animated Figure	Receptor-mediated endocytosis	Fig. 20-8
	Animated Figure	β-oxidation pathway of fatty acyl-CoA	Fig. 20-12
	Animated Figure	Comparison of fatty acid β oxidation and fatty acid biosynthesis	Fig. 20-23
	Animated Figure	Reaction sequence for biosynthesis of fatty acids	Fig. 20-26
	Case Study	23. The Role of Uncoupling Proteins in Obesity	Pg. 731
21 Amino Acid Metabolism	Interactive Exercise	29. Ubiquitin	Fig. 21-1
	Interactive Exercise	30. The bifunctional enzyme tryptophan synthase	Fig. 21-35
	Interactive Exercise	31. *A vinelandii* nitrogenase	Fig. 21-41
	Animated Figure	Mechanism of PLP-dependent transamination	Fig. 21-8
	Animated Figure	The urea cycle	Fig. 21-9
22 Mammalian Fuel Metabolism: Integration and Regulation	Interactive Exercise	32. Human leptin	Fig. 22-13
	Animated Figure	The Cori cycle	Fig. 22-6
	Animated Figure	The glucose-alanine cycle	Fig. 22-7
	Animated Figure	GLUT4 activity	Fig. 22-8
	Case Study	25. Glycogen Storage Diseases	Pg. 816
	Case Study	28. The Bacterium *Helicobacter pylori* and Peptic Ulcers	Pg. 816
	Case Study	30. Phenylketonuria	Pg. 816
23 Nucleotide Metabolism	Interactive Exercise	33. *E coli* ribonucleotide reductase	Fig. 23-9
	Interactive Exercise	34. Human dihydrofolate reductase	Fig. 23-17
	Interactive Exercise	35. Murine adenosine deaminase	Fig. 23-20
	Animated Figure	Metabolic pathway for *de novo* biosynthesis of IMP	Fig. 23-1
	Animated Figure	Control of purine biosynthesis pathway	Fig. 23-4
	Animated Figure	The *de novo* synthesis of UMP	Fig. 23-5
	Animated Figure	Regulation of pyrimidine biosynthesis	Fig. 23-8
24 Nucleic Acid Structure	Guided Exploration	21. DNA structures	Section 24-1A
	Guided Exploration	22. DNA supercoiling	Section 24-1C

Chapter	Media Type	Title	Text Reference
	Guided Exploration	23. Transcription factor–DNA interactions	Section 24-4B
	Guided Exploration	24. Nucleosome structure	Section 24-5B
	Interactive Exercise	36. An RNA-DNA helix	Fig. 24-4
	Interactive Exercise	37. Yeast topoisomerase II	Fig. 24-16
	Interactive Exercise	38. A hammerhead ribozyme	Fig. 24-26
	Interactive Exercise	39. A portion of phage 434 repressor in complex with target DNA	Fig. 24-32
	Interactive Exercise	40. *E. coli trp* repressor–operator complex	Fig. 24-33
	Interactive Exercise	41. *E. coli met* repressor–operator complex	Fig. 24-34
	Interactive Exercise	42. A three-zinc finger segment of Zif268 in complex with DNA	Fig. 24-35
	Interactive Exercise	43. GAL4 DNA-binding domain in complex with DNA	Fig. 24-36
	Interactive Exercise	44. GCN4 bZIP region in complex with DNA	Fig. 24-38
	Interactive Exercise	45. Max binding to DNA	Fig. 24-39
	Animated Figure	UV absorbance spectra of native and heat-denatured DNA	Fig. 24-19
	Animated Figure	Example of DNA melting curve	Fig. 24-20
	Kinemage	17-1, 17-4, 17-5, 17-6. Structures of A, B, and Z DNAs	Fig. 24-2
	Kinemage	17-2. Watson-Crick base pairs	Fig. 24-1
	Kinemage	17-3. Nucleotide sugar conformations	Fig. 24-7
	Kinemage	18-1. *Eco*RI endonuclease in complex with DNA	Fig. 24-30
	Kinemage	18-2. *Eco*RV endonuclease in complex with DNA	Fig. 24-31
	Kinemage	19. 434 phage repressor in complex with DNA	Fig. 24-32
	Kinemage	20. GCN4 leucine zipper motif	Fig. 24-37
	Case Study	31. Hyperactive Dnase I Variants: A Treatment for Cystic Fibrosis	Pg. 892
25 DNA Replication, Repair, and Recombination	Guided Exploration	25. The replication of DNA in *E. coli*	Section 25-2B
	Interactive Exercise	46. *E. coli* DNA Pol I Klenow fragment with double-helical DNA	Fig. 25-10
	Interactive Exercise	47. *E. coli* Tus in complex with Ter-containing DNA	Fig. 25-19
	Interactive Exercise	48. Structure of PCNA	Fig. 25-20
	Interactive Exercise	49. HIV reverse transcriptase	Box 25-2
	Animated Figure	Meselson and Stahl experiment	Fig. 25-1
	Animated Figure	Holliday model of general recombination	Fig. 25-36
	Case Study	32. Glucose-6-Phosphate Dehydrogenase Activity and Cell Growth	Pg. 941
26 Transcription and RNA Processing	Interactive Exercise	50. RNA polymerase II	Fig. 26-12
	Interactive Exercise	51. TATA-binding protein in complex with TATA box	Fig. 26-16
	Interactive Exercise	52. Self-splicing group I intron from *Tetrahymena*	Fig. 26-30
27 Protein Synthesis	Guided Exploration	26. The structure of tRNA	Section 27-2
	Guided Exploration	27. The structures of aminoacyl–tRNA synthetases and their interactions with tRNAs	Section 27-2B
	Guided Exploration	28. Translational initiation	Section 27-4A
	Guided Exploration	29. Translational elongation	Section 27-4B
	Interactive Exercise	53. Ribosomal subunits in complex with three tRNAs and an mRNA	Fig. 27-17
	Interactive Exercise	54. Elongation factor EF-Tu in its complexes with GDP and GMPPNP	Fig. 27-29
	Kinemage	21-1. Structure of yeast tRNA^{Phe}	Fig. 27-5
	Kinemage	21-2. Modified bases in tRNAs	Fig. 27-4
	Kinemage	22. Structure of GlnRS–tRNA^{Gln}–ATP	Fig. 27-8
	Case Study	29. Pseudovitamin D Deficiency	Pg. 1035
28 Regulation of Gene Expression	Guided Exploration	30. The regulation of gene expression by the *lac* repressor system	Section 28-2A
	Interactive Exercise	55. CAP–cAMP dimer in complex with DNA	Fig. 28-13
	Interactive Exercise	56. Glucocorticoid receptor DNA-binding domain in complex with DNA	Fig. 28-33
	Interactive Exercise	57. Cdk2 phosphorylated at Thr 160	Fig. 28-41
	Interactive Exercise	58. DNA-binding domain of human p53 in complex with its target DNA	Fig. 28-42
	Interactive Exercise	59. Engrailed protein homeodomain in complex with its target DNA	Fig. 28-53

Clinical Applications

Acidosis and alkalosis (p. 36)
Gene therapy (p. 69)
Scurvy and collagen diseases (p. 137)
Amyloidoses and Alzheimer's disease (p. 168)
Transmissible spongiform encephalopathies (TSEs) (p. 170)
High-altitude adaptation (p. 192)
Hemolytic anemia and polycythemia (p. 194)
Sickle-cell anemia and malaria (p. 195)
Muscular dystrophy (p. 205)
Autoimmune diseases (p. 214)
Lactose intolerance (p. 227)
Penicillin and vancomycin (p. 238)
ABO blood groups (p. 242)
Lung surfactant (p. 250)
Sphingolipid storage diseases (p. 253)
Steroid hormones (p. 255)
Addison's and Cushing's diseases (p. 255)
I-cell disease (p. 286)
Tetanus and botulinum toxins (p. 288)
Cardiac glycosides and heart failure (p. 313)
Drug resistance (p. 314)
Cystic fibrosis (p. 315)
Nerve poisons (p. 349)
Acute pancreatitis (p. 357)
Blood coagulation (p. 358)
Methanol poisoning (p. 379)
HIV enzyme inhibitors (p. 384)
Drug design (p. 394)
Clinical trials (p. 397)
Drug–drug interactions (p. 398)
Insulin and glucagon (p. 407)
Epinephrine and norepinephrine (p. 409)
Growth disorders (p. 411)
Klinefelter's and Turner's syndromes (p. 411)
Oncogenes and cancer (p. 421)
Leukemia (p. 424)
Bubonic plague (p. 426)
Cholera and pertussis (p. 435)
Viagra action (p. 436)
Anthrax (p. 444)
Vitamin deficiency diseases (p. 450)
Erythrocyte enzyme deficiencies (p. 502)
Beriberi (p. 508)
Fructose intolerance and galactosemia (p. 518)
Glucose-6-phosphate dehydrogenase deficiency (p. 526)
Glycogen storage diseases (p. 538)
Bacitracin (p. 563)
Arsenic poisoning (p. 576)
Myocardial infarction and stroke (p. 635)
Low- and high-density lipoproteins (LDL & HDL) (p. 681)
Sudden infant death syndrome (SIDS) (p. 688)
Pernicious anemia (p. 696)
Aspirin and nonsteroidal anti-inflammatory drugs (NSAIDs) (p. 719)
COX-2 inhibitors (p. 719)
Statins and atherosclerosis (p. 727)
Hypercholesterolemia (p. 728)
Hyperammonemia (p. 742)
Folic acid and spina bifida and anencephaly (p. 755)
Phenylketonuria and alcaptonuria (p. 762)
Porphyria (p. 778)
Diabetes (p. 811)
Obesity (p. 814)
Starvation (p. 809)
Metabolic syndrome (p. 815)
Lesch-Nyhan syndrome (p. 824)
Toxoplasmosis (p. 826)
Antifolates (p. 838)
Severe combined immunodeficiency disease (SCID) (p. 840)
Gout (p. 843)
Topoisomerase inhibitors (p. 865)
Telomerase, aging, and cancer (p. 915)
Mutagenesis and carcinogenesis (p. 919)
Xeroderma pigmentosum and Cockayne's syndrome (p. 924)
Antibiotics that inhibit transcription (p. 954)
Antibiotics that inhibit translation (p. 1024)
Trinucleotide repeat diseases (p. 1094)
Genomic imprinting and Prader-Willi and Angelman syndromes (p. 1067)
Generation of antibody diversity (p. 1077)
Tumor suppressors: p53 and pRb (p. 1084)

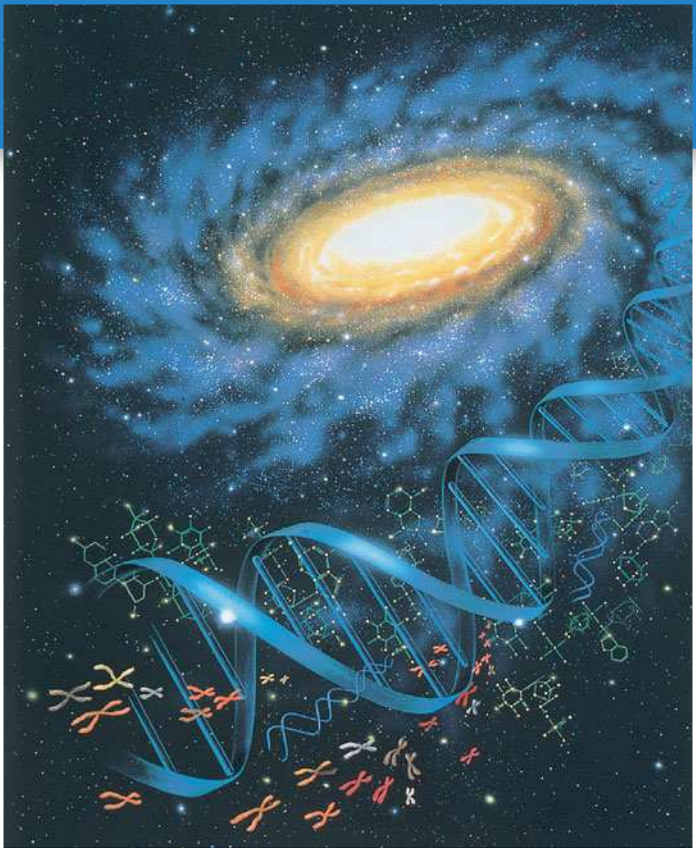

1

Introduction to the Chemistry of Life

Early earth, a tiny speck in the galaxy, contained simple inorganic molecules that gave rise to the first biological macromolecules. These, in turn, gained the ability to self-organize and self-replicate, eventually forming cellular life-forms. [Lynette Cook/Photo Researchers.]

Biochemistry is, literally, the study of the chemistry of life. Although it overlaps other disciplines, including cell biology, genetics, immunology, microbiology, pharmacology, and physiology, biochemistry is largely concerned with a limited number of issues:

1. What are the chemical and three-dimensional structures of biological molecules?
2. How do biological molecules interact with each other?
3. How does the cell synthesize and degrade biological molecules?
4. How is energy conserved and used by the cell?
5. What are the mechanisms for organizing biological molecules and coordinating their activities?
6. How is genetic information stored, transmitted, and expressed?

Biochemistry, like other modern sciences, relies on sophisticated instruments to dissect the architecture and operation of systems that are inaccessible to the human senses. In addition to the chemist's tools for separating, quantifying, and otherwise analyzing biological materials, biochemists take advantage of the uniquely biological aspects of their subject by examining the evolutionary histories of organisms, metabolic systems, and individual molecules. In addition to its obvious implications for human health, biochemistry reveals the workings of the natural world, allowing us to understand and appreciate the unique and mysterious condition that we call life. In this introductory chapter, we will review some aspects of chemistry and biology—including chemical evolution, the different types of cells, and basic principles of thermodynamics—in order to help put biochemistry in context and to introduce some of the themes that recur throughout this book.

■ CHAPTER CONTENTS

1 The Origin of Life
  A. Biological Molecules Arose from Inorganic Materials
  B. Complex Self-replicating Systems Evolved from Simple Molecules
2 Cellular Architecture
  A. Cells Carry Out Metabolic Reactions
  B. There Are Two Types of Cells: Prokaryotes and Eukaryotes
  C. Molecular Data Reveal Three Evolutionary Domains of Organisms
  D. Organisms Continue to Evolve
3 Thermodynamics
  A. The First Law of Thermodynamics States That Energy Is Conserved
  B. The Second Law of Thermodynamics States That Entropy Tends to Increase
  C. The Free Energy Change Determines the Spontaneity of a Process
  D. Free Energy Changes Can Be Calculated from Equilibrium Concentrations
  E. Life Obeys the Laws of Thermodynamics

1 The Origin of Life

LEARNING OBJECTIVES

- Understand that simple inorganic compounds combined to form more complex molecules through a process of chemical evolution.
- Become familiar with the common functional groups and linkages in biological molecules.

Certain biochemical features are common to all organisms: the way hereditary information is encoded and expressed, for example, and the way biological molecules are built and broken down for energy. The underlying genetic and biochemical unity of modern organisms suggests they are descended from a single ancestor. Although it is impossible to describe exactly how life first arose, paleontological and laboratory studies have provided some insights about the origin of life.

A | Biological Molecules Arose from Inorganic Materials

Living matter consists of a relatively small number of elements (Table 1-1). For example, C, H, O, N, P, Ca, and S account for ~97% of the dry weight of the human body (humans and most other organisms are ~70% water). Living organisms may also contain trace amounts of many other elements, including B, F, Al, Si, V, Cr, Mn, Fe, Co, Ni, Cu, Zn, As, Se, Br, Mo, Cd, I, and W, although not every organism makes use of each of these substances.

Table 1-1 Most Abundant Elements in the Human Body[a]

Element	Dry Weight (%)
C	61.7
N	11.0
O	9.3
H	5.7
Ca	5.0
P	3.3
K	1.3
S	1.0
Cl	0.7
Na	0.7
Mg	0.3

[a] Calculated from Frieden, E., *Sci. Am.* **227**(1), 54–55 (1972).

The earliest known fossil evidence of life is ~3.5 billion years old (Fig. 1-1). The preceding **prebiotic era,** which began with the formation of the earth ~4.6 billion years ago, left no direct record, but scientists can experimentally duplicate the sorts of chemical reactions that might have given rise to living organisms during that billion-year period.

The atmosphere of the early earth probably consisted of small, simple compounds such as H_2O, N_2, CO_2, and smaller amounts of CH_4 and NH_3. In the 1930s, Alexander Oparin and J. B. S. Haldane independently suggested that ultraviolet radiation from the sun or lightning discharges caused the molecules of the primordial atmosphere to react to form simple **organic** (carbon-containing) **compounds.** This process was replicated in 1953 by Stanley Miller and Harold Urey, who subjected a mixture of H_2O, CH_4, NH_3, and H_2 to an electric discharge for about a week. The resulting solution contained water-soluble organic compounds, including several amino acids (which are components of proteins) and other biochemically significant compounds.

The assumptions behind the Miller–Urey experiment, principally the composition of the gas used as a starting material, have been challenged by some scientists who have suggested that the first biological molecules were generated in a quite different way: in the dark and under water. Hydrothermal vents in the ocean floor, which emit solutions of metal

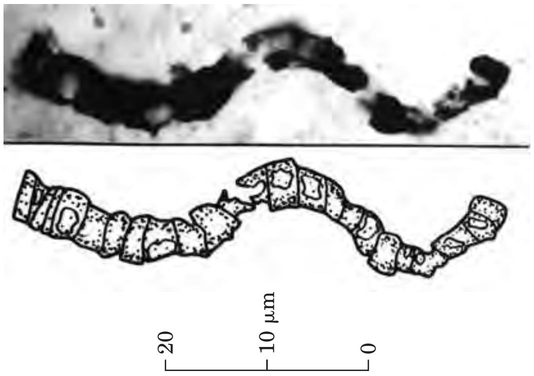

Figure 1-1 | Microfossil of filamentous bacterial cells. This fossil (shown with an interpretive drawing) is from ~3.4-billion-year-old rock from Western Australia. [Courtesy of J. William Schopf, UCLA.]

sulfides at temperatures as high as 400°C (Fig. 1-2), may have provided conditions suitable for the formation of amino acids and other small organic molecules from simple compounds present in seawater.

Whatever their actual origin, the early organic molecules became the precursors of an enormous variety of biological molecules. These can be classified in various ways, depending on their composition and chemical reactivity. A familiarity with organic chemistry is useful for recognizing the **functional groups** (reactive portions) of molecules as well as the **linkages** (bonding arrangements) among them, since these features ultimately determine the biological activity of the molecules. Some of the common functional groups and linkages in biological molecules are shown in Table 1-2.

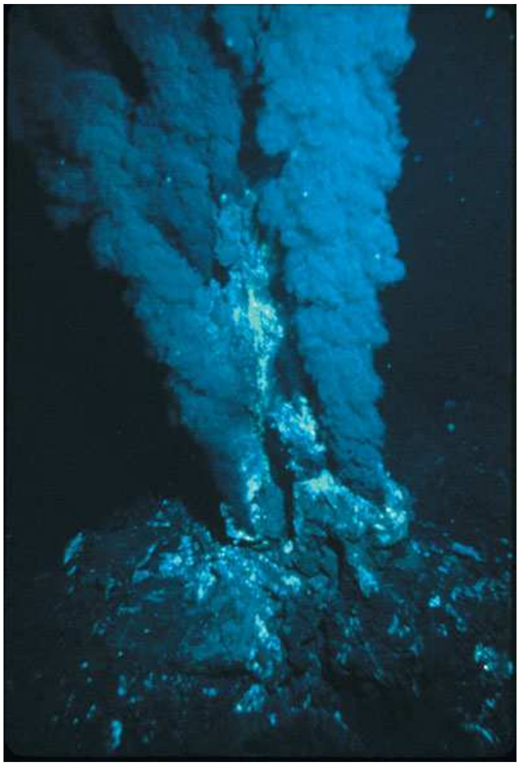

Figure 1-2 | A hydrothermal vent. Such ocean-floor formations are known as "black smokers" because the metal sulfides dissolved in the superheated water they emit precipitate on encountering the much cooler ocean water. [© J. Edmond. Courtesy of Woods Hole Oceanographic Institution.]

B | Complex Self-replicating Systems Evolved from Simple Molecules

During a period of chemical evolution, simple organic molecules condensed to form more complex molecules or combined end-to-end as **polymers** of repeating units. In a **condensation reaction,** the elements of water are lost. The rate of condensation of simple compounds to form a stable polymer must therefore be greater than the rate of **hydrolysis** (splitting by adding the elements of water; Fig. 1-3). In the prebiotic environment, minerals such as clays may have catalyzed polymerization reactions and sequestered the reaction products from water. The size and composition of prebiotic macromolecules would have been limited by the availability of small molecular starting materials, the efficiency with which they could be joined, and their resistance to degradation.

Obviously, *combining different functional groups into a single large molecule increases the chemical versatility of that molecule,* allowing it to perform chemical feats beyond the reach of simpler molecules. (This principle of emergent properties can be expressed as "the whole is greater than the sum of its parts.") Separate macromolecules with complementary arrangements of functional groups can associate with each other (Fig. 1-4), giving rise to more complex molecular assemblies with an even greater range of functional possibilities.

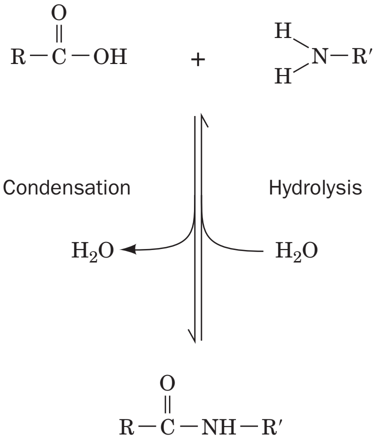

Figure 1-3 | Reaction of a carboxylic acid with an amine. The elements of water are released during condensation. In the reverse process—hydrolysis—water is added to cleave the amide bond. In living systems, condensation reactions are not freely reversible.

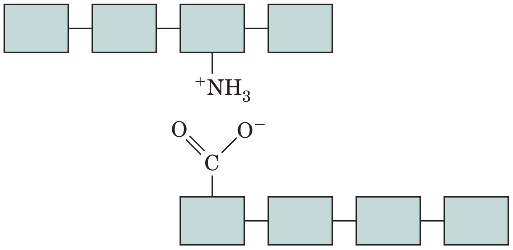

Figure 1-4 | Association of complementary molecules. The positively charged amino group interacts electrostatically with the negatively charged carboxylate group.

Table 1-2 Common Functional Groups and Linkages in Biochemistry

Compound Name	**Structure**[a]	**Functional Group or Linkage**
Amine[b]	$\mathrm{RNH_2}$ or $\mathrm{R\overset{+}{N}H_3}$ $\mathrm{R_2NH}$ or $\mathrm{R_2\overset{+}{N}H_2}$ $\mathrm{R_3N}$ or $\mathrm{R_3\overset{+}{N}H}$	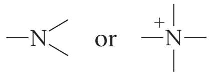 $\mathrm{-N\langle}$ or $\mathrm{-\underset{|}{\overset{|}{\overset{+}{N}}}-}$ (amino group)
Alcohol	ROH	—OH (hydroxyl group)
Thiol	RSH	—SH (sulfhydryl group)
Ether	ROR	—O— (ether linkage)
Aldehyde	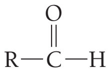 $\mathrm{R-\overset{O}{\overset{\|}{C}}-H}$	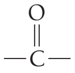 $\mathrm{-\overset{O}{\overset{\|}{C}}-}$ (carbonyl group)
Ketone	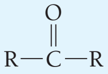 $\mathrm{R-\overset{O}{\overset{\|}{C}}-R}$	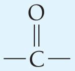 $\mathrm{-\overset{O}{\overset{\|}{C}}-}$ (carbonyl group)
Carboxylic acid[b]	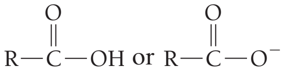 $\mathrm{R-\overset{O}{\overset{\|}{C}}-OH}$ or $\mathrm{R-\overset{O}{\overset{\|}{C}}-O^-}$	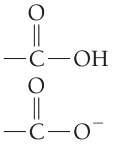 $\mathrm{-\overset{O}{\overset{\|}{C}}-OH}$ (carboxyl group) or $\mathrm{-\overset{O}{\overset{\|}{C}}-O^-}$ (carboxylate group)
Ester	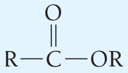 $\mathrm{R-\overset{O}{\overset{\|}{C}}-OR}$	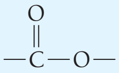 $\mathrm{-\overset{O}{\overset{\|}{C}}-O-}$ (ester linkage) 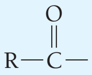 $\mathrm{R-\overset{O}{\overset{\|}{C}}-}$ (acyl group)[c]
Thioester	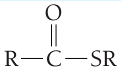 $\mathrm{R-\overset{O}{\overset{\|}{C}}-SR}$	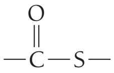 $\mathrm{-\overset{O}{\overset{\|}{C}}-S-}$ (thioester linkage) 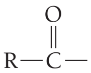 $\mathrm{R-\overset{O}{\overset{\|}{C}}-}$ (acyl group)[c]
Amide	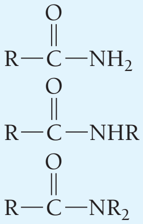 $\mathrm{R-\overset{O}{\overset{\|}{C}}-NH_2}$ $\mathrm{R-\overset{O}{\overset{\|}{C}}-NHR}$ $\mathrm{R-\overset{O}{\overset{\|}{C}}-NR_2}$	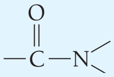 $\mathrm{-\overset{O}{\overset{\|}{C}}-N\langle}$ (amido group) 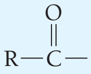 $\mathrm{R-\overset{O}{\overset{\|}{C}}-}$ (acyl group)[c]
Imine (Schiff base)[b]	$\mathrm{R{=}NH}$ or $\mathrm{R{=}\overset{+}{N}H_2}$ $\mathrm{R{=}NR}$ or $\mathrm{R{=}\overset{+}{N}HR}$	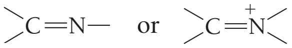 $\mathrm{\rangle C{=}N-}$ or $\mathrm{\rangle C{=}\overset{+}{N}\langle}$ (imino group)
Disulfide	R—S—S—R	—S—S— (disulfide linkage)
Phosphate ester[b]	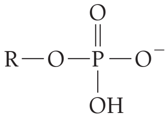 $\mathrm{R-O-\underset{OH}{\underset{|}{\overset{O}{\overset{\|}{P}}}}-O^-}$	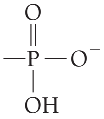 $\mathrm{-\underset{OH}{\underset{|}{\overset{O}{\overset{\|}{P}}}}-O^-}$ (phosphoryl group)
Diphosphate ester[b]	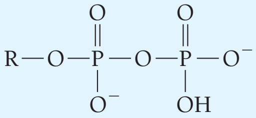 $\mathrm{R-O-\underset{O^-}{\underset{|}{\overset{O}{\overset{\|}{P}}}}-O-\underset{OH}{\underset{|}{\overset{O}{\overset{\|}{P}}}}-O^-}$	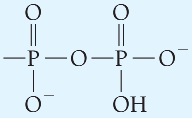 $\mathrm{-\underset{O^-}{\underset{|}{\overset{O}{\overset{\|}{P}}}}-O-\underset{OH}{\underset{|}{\overset{O}{\overset{\|}{P}}}}-O^-}$ (phosphoanhydride group)
Phosphate diester[b]	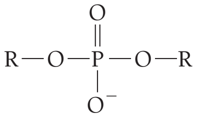 $\mathrm{R-O-\underset{O^-}{\underset{|}{\overset{O}{\overset{\|}{P}}}}-O-R}$	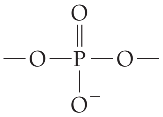 $\mathrm{-O-\underset{O^-}{\underset{|}{\overset{O}{\overset{\|}{P}}}}-O-}$ (phosphodiester linkage)

---

[a] R represents any carbon-containing group. In a molecule with more than one R group, the groups may be the same or different.

[b] Under physiological conditions, these groups are ionized and hence bear a positive or negative charge.

[c] If attached to an atom other than carbon.

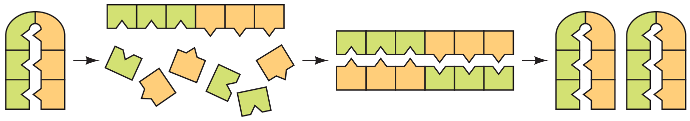

Figure 1-5 | Replication through complementarity. In this simple case, a polymer serves as a template for the assembly of a complementary molecule, which, because of intramolecular complementarity, is an exact copy of the original.

Specific pairing between complementary functional groups permits one member of a pair to determine the identity and orientation of the other member. *Such complementarity makes it possible for a macromolecule to* ***replicate,*** *or copy itself, by directing the assembly of a new molecule from smaller complementary units.* Replication of a simple polymer with intramolecular complementarity is illustrated in Fig. 1-5. A similar phenomenon is central to the function of DNA, where the sequence of bases on one strand (e.g., A-C-G-T) absolutely specifies the sequence of bases on the strand to which it is paired (T-G-C-A). When DNA replicates, the two strands separate and direct the synthesis of complementary daughter strands. Complementarity is also the basis for transcribing DNA into RNA and for translating RNA into protein.

A critical moment in chemical evolution was the transition from systems of randomly generated molecules to systems in which molecules were organized and specifically replicated. Once macromolecules gained the ability to self-perpetuate, the primordial environment would have become enriched in molecules that were best able to survive and multiply. The first replicating systems were no doubt somewhat sloppy, with progeny molecules imperfectly complementary to their parents. Over time, **natural selection** would have favored molecules that made more accurate copies of themselves.

CHECK YOUR UNDERSTANDING

Summarize the major stages of chemical evolution.
Be able to identify the functional groups and linkages in Table 1-2.
Describe what occurs during a condensation reaction and a hydrolysis reaction.

2 Cellular Architecture

The types of systems described so far would have had to compete with all the other components of the primordial earth for the available resources. A selective advantage would have accrued to a system that was sequestered and protected by boundaries of some sort. How these boundaries first arose, or even what they were made from, is obscure. One theory is that membranous **vesicles** (fluid-filled sacs) first attached to and then enclosed self-replicating systems. These vesicles would have become the first cells.

LEARNING OBJECTIVES

- Understand the advantages of compartmentation and enzymes in cellular chemistry.
- Know the differences between prokaryotes and eukaryotes.
- Become familiar with the major eukaryotic organelles.
- Understand the relationship between archaebacteria, eubacteria, and eukaryotes.
- Understand the central principles of evolution by natural selection.

A | Cells Carry Out Metabolic Reactions

The advantages of **compartmentation** are several. In addition to receiving some protection from adverse environmental forces, an enclosed system can maintain high local concentrations of components that would otherwise diffuse away. More concentrated substances can react more readily, leading to increased efficiency in polymerization and other types of chemical reactions.

A membrane-bounded compartment that protected its contents would gradually become quite different in composition from its surroundings. Modern cells contain high concentrations of ions, small molecules, and large molecular aggregates that are found in only traces—if at all—outside the

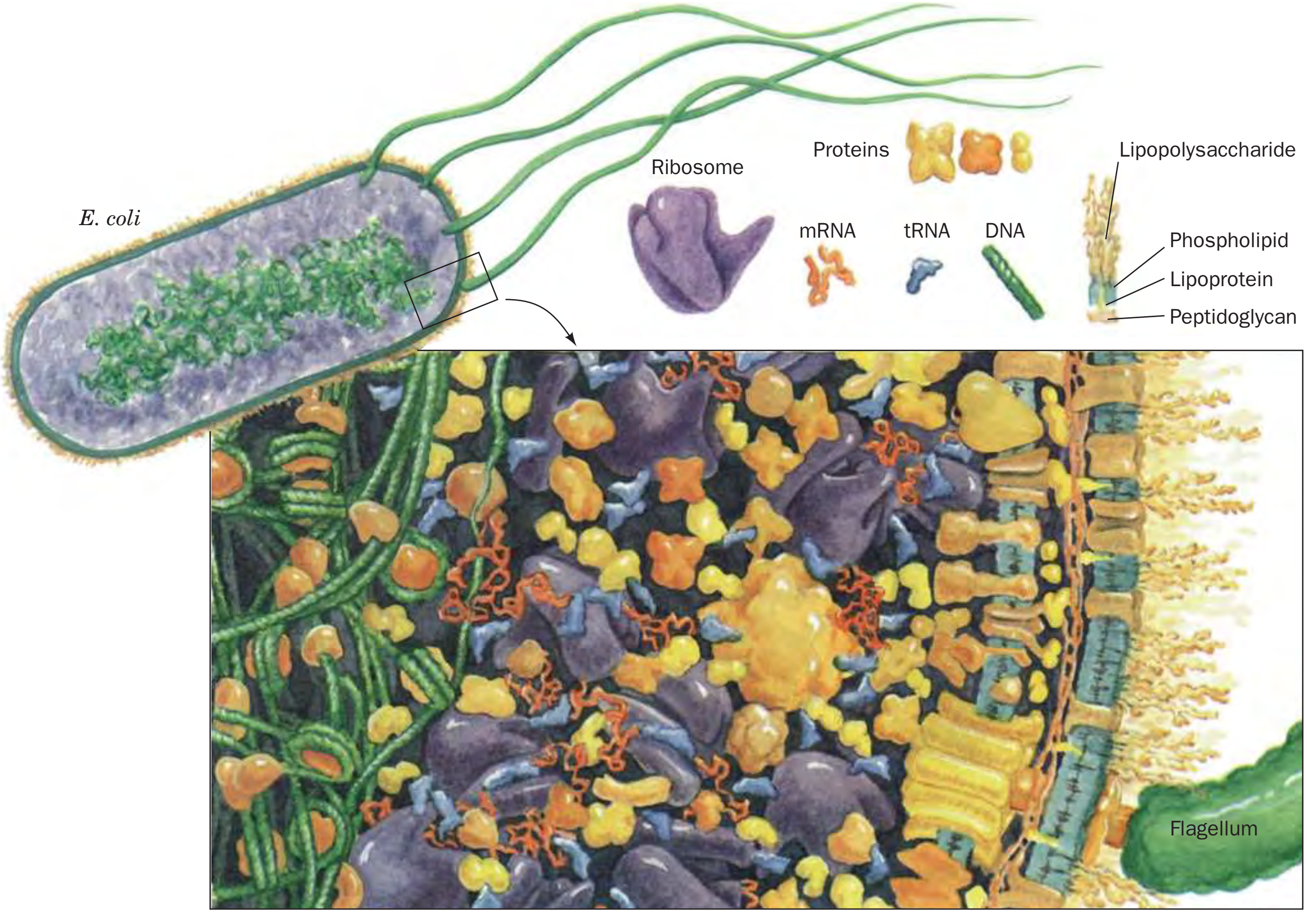

Figure 1-6 | Cross section of an *E. coli* cell. The right side of the drawing shows the multilayered cell wall and membrane. The cytoplasm in the middle region of the drawing is filled with ribosomes engaged in protein synthesis. The left side of the drawing contains a dense tangle of DNA. This drawing corresponds to a millionfold magnification. Only the largest macromolecules and molecular assemblies are shown. In a living cell, the remaining space in the cytoplasm would be crowded with smaller molecules and water (the water molecules would be about the size of the period at the end of this sentence). [After a drawing by David Goodsell, UCLA.]

cell. For example, the ***Escherichia coli* (*E. coli*)** cell contains millions of molecules representing some 3000 to 6000 different compounds (Fig. 1-6). A typical animal cell may contain 100,000 different types of molecules.

Early cells depended on the environment to supply building materials. As some of the essential components in the prebiotic soup became scarce, natural selection favored organisms that developed mechanisms for synthesizing the required compounds from simpler but more abundant **precursors.** The first metabolic reactions may have used metal or clay **catalysts** (a catalyst is a substance that promotes a chemical reaction without itself being changed). In fact, metal ions are still at the heart of many chemical reactions in modern cells. Some catalysts may also have arisen from polymeric molecules that had the appropriate functional groups.

In general, biosynthetic reactions require energy; hence the first cellular reactions also needed an energy source. The eventual depletion of preexisting energy-rich substances in the prebiotic environment would have stimulated the development of energy-producing metabolic pathways. For example, photosynthesis evolved relatively early to take advantage of a practically inexhaustible energy supply, the sun. However, the accumulation of O_2 generated from H_2O by photosynthesis (the modern atmosphere is 21% O_2) presented an additional challenge to organisms adapted to life in an oxygen-poor atmosphere. Metabolic refinements eventually permitted organisms not only to avoid oxidative damage but to use O_2 for oxidative metabolism, a much more efficient form of energy metabolism than anaerobic metabolism. Vestiges of ancient life can be seen in the anaerobic metabolism of certain modern organisms.

Early organisms that developed metabolic strategies to synthesize biological molecules, conserve and utilize energy in a controlled fashion, and replicate within a protective compartment were able to propagate in an ever-widening range of habitats. Adaptation of cells to different external conditions ultimately led to the present diversity of species. Specialization of individual cells also made it possible for groups of differentiated cells to work together in multicellular organisms.

B | There Are Two Types of Cells: Prokaryotes and Eukaryotes

All modern organisms are based on the same morphological unit, the cell. There are two major classifications of cells: the **eukaryotes** (Greek: *eu,* good or true + *karyon,* kernel or nut), which have a membrane-enclosed **nucleus** encapsulating their DNA; and the **prokaryotes** (Greek: *pro,* before), which lack a nucleus. *Prokaryotes, comprising the various types of bacteria, have relatively simple structures and are almost all unicellular* (although they may form filaments or colonies of independent cells). *Eukaryotes, which are multicellular as well as unicellular, are vastly more complex than prokaryotes.* (**Viruses** are much simpler entities than cells and are not classified as living because they lack the metabolic apparatus to reproduce outside their host cells.)

Prokaryotes are the most numerous and widespread organisms on the earth. This is because their varied and often highly adaptable metabolisms suit them to an enormous variety of habitats. Prokaryotes range in size from 1 to 10 μm and have one of three basic shapes (Fig. 1-7): spheroidal (cocci), rodlike (bacilli), and helically coiled (spirilla). Except for an outer

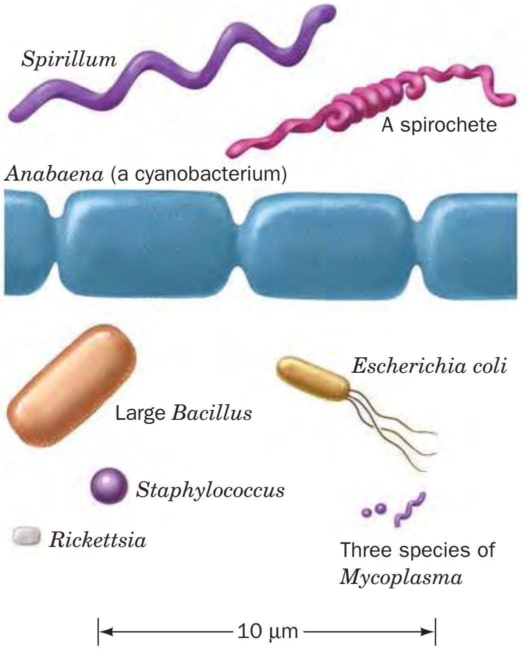

Figure 1-7 | Scale drawings of some prokaryotic cells.

cell membrane, which in most cases is surrounded by a protective cell wall, nearly all prokaryotes lack cellular membranes. However, the prokaryotic **cytoplasm** (cell contents) is by no means a homogeneous soup. Different metabolic functions are believed to be carried out in different regions of the cytoplasm (Fig. 1-6). The best characterized prokaryote is *Escherichia coli,* a 2 μm by 1 μm rodlike bacterium that inhabits the mammalian colon.

Eukaryotic cells are generally 10 to 100 μm in diameter and thus have a thousand to a million times the volume of typical prokaryotes. It is not size, however, but a profusion of membrane-enclosed **organelles** that best characterizes eukaryotic cells (Fig. 1-8). In addition to a nucleus, eukaryotes have an **endoplasmic reticulum,** the site of synthesis of many cellular components, some of which are subsequently modified in the **Golgi apparatus.** The bulk of aerobic metabolism takes place in **mitochondria** in almost all eukaryotes, and photosynthetic cells contain **chloroplasts.** Other organelles, such as **lysosomes** and **peroxisomes,** perform specialized functions. **Vacuoles,** which are more prominent in plant cells, usually function as storage depots. The **cytosol** (the cytoplasm minus its membrane-bounded organelles) is organized by the **cytoskeleton,** an extensive array of filaments that also gives the cell its shape and the ability to move.

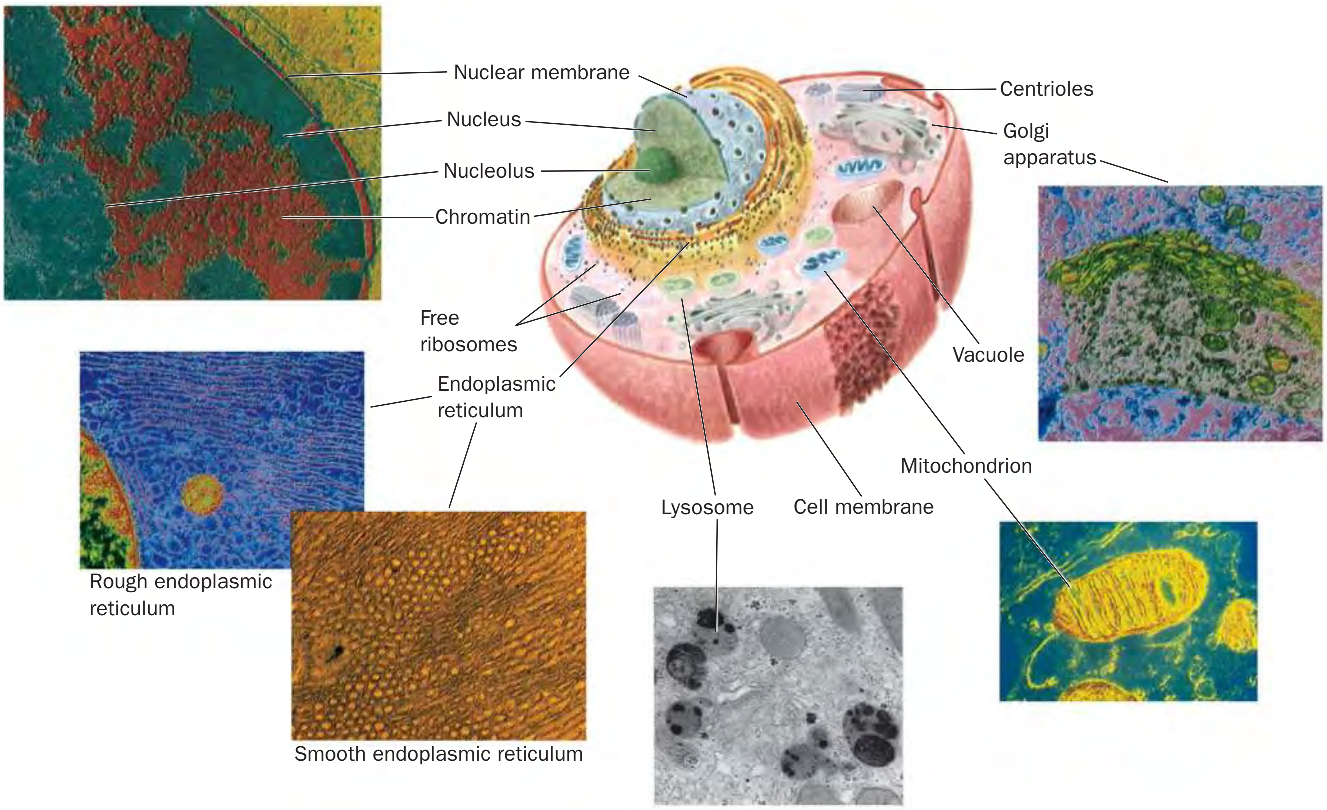

■ **Figure 1-8 | Diagram of a typical animal cell accompanied by electron micrographs of its organelles.** Membrane-bounded organelles include the nucleus, endoplasmic reticulum, lysosome, peroxisome (not pictured), mitochondrion, vacuole, and Golgi apparatus. The nucleus contains chromatin (a complex of DNA and protein) and the nucleolus (the site of ribosome synthesis). The rough endoplasmic reticulum is studded with ribosomes; the smooth endoplasmic reticulum is not. A pair of centrioles help organize cytoskeletal elements. A typical plant cell differs mainly by the presence of an outer cell wall and chloroplasts in the cytosol. [Nucleus: Tektoff-RM, CNRI/Photo Researchers; rough endoplasmic reticulum and Golgi apparatus: Secchi-Lecaque/Roussel-UCLAF/CNRI/Photo Researchers; smooth endoplasmic reticulum: David M. Phillips/Visuals Unlimited; mitochondrion: CNRI/Photo Researchers; lysosome: Biophoto Associates/Photo Researchers.]

The various organelles that compartmentalize eukaryotic cells represent a level of complexity that is largely lacking in prokaryotic cells. Nevertheless, prokaryotes are more efficient than eukaryotes in many respects. Prokaryotes have exploited the advantages of simplicity and miniaturization. Their rapid growth rates permit them to occupy ecological niches in which there may be drastic fluctuations of the available nutrients. In contrast, the complexity of eukaryotes, which renders them larger and more slowly growing than prokaryotes, gives them the competitive advantage in stable environments with limited resources. It is therefore erroneous to consider prokaryotes as evolutionarily primitive compared to eukaryotes. Both types of organisms are well adapted to their respective lifestyles.

C | Molecular Data Reveal Three Evolutionary Domains of Organisms

The practice of lumping all prokaryotes in a single category based on what they lack—a nucleus—obscures their metabolic diversity and evolutionary history. Conversely, the remarkable morphological diversity of eukaryotic organisms (consider the anatomical differences among, say, an amoeba, an oak tree, and a human being) masks their fundamental similarity at the cellular level. Traditional taxonomic schemes (**taxonomy** is the science of biological classification), which are based on gross morphology, have proved inadequate to describe the actual relationships between organisms as revealed by their evolutionary history (**phylogeny**).

Biological classification schemes based on reproductive or developmental strategies more accurately reflect evolutionary history than those based solely on adult morphology. But *phylogenetic relationships are best deduced by comparing polymeric molecules—RNA, DNA, or protein—from different organisms.* For example, analysis of RNA led Carl Woese to group all organisms into three domains (Fig. 1-9). The **archaea** (also known as **archaebacteria**) are a group of prokaryotes that are as distantly related to other prokaryotes (the **bacteria,** sometimes called **eubacteria**) as both groups are to eukaryotes **(eukarya).** The archaea include some unusual organisms: the **methanogens** (which produce CH_4), the **halobacteria** (which thrive in concentrated brine solutions), and certain **thermophiles** (which inhabit hot springs).The pattern of branches in Woese's diagram indicates the divergence of different types of organisms (each branch point represents a common ancestor). The three-domain scheme also shows that animals, plants, and fungi constitute only a small portion of all life-forms. Such phylogenetic trees supplement the fossil record, which provides a patchy record of life prior to about 600 million years before the present (multicellular organisms arose about 700–900 million years ago).

It is unlikely that eukaryotes are descended from a single prokaryote, because the differ-

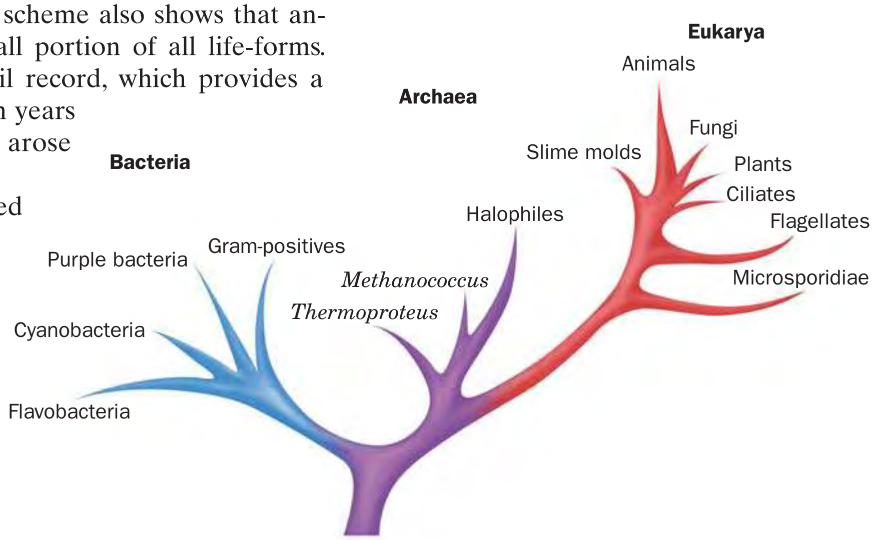

■ **Figure 1-9 | Phylogenetic tree showing three domains of organisms.** The branches indicate the pattern of divergence from a common ancestor. The archaea are prokaryotes, like bacteria, but share some features with eukaryotes. [After Wheelis, M.L., Kandler, O., and Woese, C.R., *Proc. Natl. Acad. Sci.* **89,** 2931 (1992).]

BOX 1-1 **PATHWAYS OF DISCOVERY**

Lynn Margulis and the Theory of Endosymbiosis

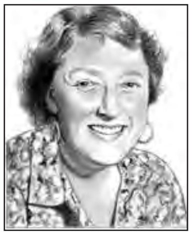

Lynn Margulis (1938–)

After growing up in Chicago and enrolling in the University of Chicago at age 16, Lynn Margulis intended to be a writer. Her interest in biology was sparked by a required science course for which she read Gregor Mendel's accounts of his experiments with the genetics of pea plants. Margulis continued her studies at the University of Wisconsin Madison and at the University of California Berkeley, earning a doctorate in 1963. Her careful consideration of cellular structures led her to hypothesize that eukaryotic cells originated from a series of endosymbiotic events involving multiple prokaryotes. The term *endo* (Greek: within) refers to an arrangement in which one cell comes to reside inside another. This idea was considered outrageous at the time (1967), but many of Margulis's ideas have since become widely accepted.

Endosymbiosis as an explanation for the origin of mitochondria had been proposed by Ivan Wallin in 1927, who noted the similarity between mitochondria and bacteria in size, shape, and cytological staining. Wallin's hypothesis was rejected as being too fantastic and was ignored until it was taken up again by Margulis. By the 1960s, much more was known about mitochondria (and chloroplasts), including the fact that they contained DNA and reproduced by division. Margulis did not focus all her attention on the origin of individual organelles but instead sought to explain the origin of the entire eukaryotic cell, which also includes centrioles, another possible bacterial relic. Her paper, "On the Origin of Mitosing cells," was initially rejected by several journals before being accepted by the *Journal of Theoretical Biology.* The notion that a complex eukaryotic cell could arise from a consortium of mutually dependent prokaryotic cells was incompatible with the prevailing view that evolution occurred as a series of small steps. Evolutionary theory of the time had no room for the dramatic amalgamation of cells—and their genetic material—that Margulis had proposed. Nevertheless, the outspoken Margulis persisted, and by the time she published *Symbiosis in Cell Evolution* in 1981, much of the biological community had come on board.

Two main tenets of Margulis's theory, that mitochondria are the descendants of oxygen-respiring bacteria and chloroplasts were originally photosynthetic bacteria, are almost universally accepted. The idea that the eukaryotic cytoplasm is the remnant of an archaebacterial cell is still questioned by some biologists. Margulis is in the process of collecting evidence to support a fourth idea, that cilia and flagella and some sensory structures such as the light-sensing cells of the eye are descendants of free-living spirochete bacteria. Margulis's original prediction that organelles such as mitochondria could be isolated and cultured has not been fulfilled. However, there is ample evidence for the transfer of genetic material between organelles and the nucleus, consistent with Margulis's theory of endosymbiosis. In fact, current theories of evolution include the movement of genetic material among organisms, as predicted by Margulis, in addition to small random mutations as agents of change.

Perhaps as an extension of her work on bacterial endosymbiosis, Margulis came to recognize that the interactions among many different types of organisms as well as their interactions with their physical environment constitute a single self-regulating system. This notion is part of the Gaia hypothesis proposed by James Lovelock, which views the entire earth as one living entity (Gaia was a Greek earth goddess). However, Margulis has no patience with those who seek to build a modern mythology based on Gaia. She is adamant about the importance of using scientific tools and reasoning to discover the truth and is irritated by the popular belief that humans are the center of life on earth. Margulis understands that human survival depends on our relationships with waste-recycling, water-purifying, and oxygen-producing bacteria, with whom we have been evolving, sometimes endosymbiotically, for billions of years.

Sagan, L., On the origin of mitosing cells, *J. Theor. Biol.* **14,** 255–274 (1967).

ences between bacteria and eukaryotes are so profound. Instead, eukaryotes probably evolved from the association of archaebacterial and eubacterial cells. The eukaryotic genetic material includes features that suggest an archaebacterial origin. In addition, the mitochondria and chloroplasts of modern eukaryotic cells resemble bacteria in size and shape, and both types of organelles contain their own genetic material and protein synthetic machinery. Evidently, as Lynn Margulis proposed, mitochondria and chloroplasts evolved from free-living bacteria that formed **symbiotic** (mutually beneficial) relationships with a primordial eukaryotic cell (Box 1-1). In fact, certain eukaryotes that lack mitochondria or chloroplasts permanently harbor symbiotic bacteria.

D | Organisms Continue to Evolve

The natural selection that guided prebiotic evolution continues to direct the evolution of organisms. Richard Dawkins has likened evolution to a blind watchmaker capable of producing intricacy by accident, although such an image fails to convey the vast expanse of time and the incremental, trial-and-error manner in which complex organisms emerge. Small **mutations** (changes in an individual's genetic material) arise at random as the result of chemical damage or inherent errors in the replication process. *A mutation that increases the chances of survival of the individual increases the likelihood that the mutation will be passed on to the next generation.* Beneficial mutations tend to spread rapidly through a population; deleterious changes tend to die along with the organisms that harbor them.

The theory of evolution by natural selection, which was first articulated by Charles Darwin in the 1860s, has been confirmed through observation and experimentation. It is therefore useful to highlight several important—and often misunderstood—principles of evolution:

1. ***Evolution is not directed toward a particular goal.*** It proceeds by random changes that may affect the ability of an organism to reproduce under the prevailing conditions. An organism that is well adapted to its environment may fare better or worse when conditions change.
2. ***Variation among individuals*** allows organisms to adapt to unexpected changes. This is one reason why genetically homogeneous populations (e.g., a corn crop) are so susceptible to a single challenge (e.g., a fungal blight). A more heterogeneous population is more likely to include individuals that can resist the adversity and recover.
3. ***The past determines the future.*** New structures and metabolic functions emerge from preexisting elements. For example, insect wings did not erupt spontaneously but appear to have developed gradually from small heat-exchange structures.
4. ***Evolution is ongoing,*** although it does not proceed exclusively toward complexity. An anthropocentric view places human beings at the pinnacle of an evolutionary scheme, but a quick survey of life's diversity reveals that simpler species have not died out or stopped evolving.

CHECK YOUR UNDERSTANDING

What is the role of compartmentation in cellular chemistry?

List the differences between prokaryotes and eukaryotes.

How are the three evolutionary domains of organisms related to each other?

Summarize the process of evolution by natural selection.

3 Thermodynamics

LEARNING OBJECTIVES

- Understand the first and second laws of thermodynamics and how they apply to living systems.
- Understand the relationship between free energy, enthalpy, and entropy.
- Understand the meaning of spontaneity for a biological process.
- Understand the relationship between equilibrium constants and free energy changes.

The normal activities of living organisms—moving, growing, reproducing—demand an almost constant input of energy. Even at rest, organisms devote a considerable portion of their biochemical apparatus to the acquisition and utilization of energy. The study of energy and its effects on matter falls under the purview of **thermodynamics** (Greek: *therme,* heat + *dynamis,* power). Although living systems present some practical challenges to thermodynamic analysis, *life obeys the laws of thermodynamics.* Understanding thermodynamics is important not only for describing a particular process—such as a biochemical reaction—in terms that can be quantified, but also for predicting whether that process *can* actually occur, that is, whether the process is spontaneous. To begin, we will review the fundamental laws of thermodynamics. We will then turn our attention to free energy and how it relates to chemical reactions. Finally, we will look at how biological systems deal with the laws of thermodynamics.

A | The First Law of Thermodynamics States That Energy Is Conserved

In thermodynamics, a **system** is defined as the part of the universe that is of interest, such as a reaction vessel or an organism; the rest of the universe is known as the **surroundings.** The system has a certain amount of **energy, *U*.** *The first law of thermodynamics states that energy is conserved;* it can be neither created nor destroyed. However, when the system undergoes a change, some of its energy can be used to perform work. The energy change of the system is defined as the difference between the **heat (*q*)** absorbed by the system from the surroundings and **work (*w*)** done by the system on the surroundings. The Greek letter Δ (Delta) indicates change.

$$\Delta U = U_{\text{final}} - U_{\text{initial}} = q - w \qquad [1\text{-}1]$$

Heat is a reflection of random molecular motion, whereas work, which is defined as force times the distance moved under its influence, is associated with organized motion. Force may assume many different forms, including the gravitational force exerted by one mass on another, the expansional force exerted by a gas, the tensional force exerted by a spring or muscle fiber, the electrical force of one charge on another, and the dissipative forces of friction and viscosity. Because energy can be used to perform different kinds of work, it is sometimes useful to speak of energy taking different forms, such as mechanical energy, electrical energy, or chemical energy—all of which are relevant to biological systems.

Most biological processes take place at constant pressure. Under such conditions, the work done by the expansion of a gas (pressure–volume work) is $P\Delta V$. Consequently, it is useful to define a new thermodynamic quantity, the **enthalpy** (Greek: *enthalpein,* to warm in), abbreviated ***H*:**

$$H = U + PV \qquad [1\text{-}2]$$

Then, when the system undergoes a change at constant pressure,

$$\Delta H = \Delta U + P\Delta V = q_P - w + P\Delta V \qquad [1\text{-}3]$$

where $\boldsymbol{q_P}$ is defined as the heat at constant pressure. Since we already know that in this system $w = P\Delta V$,

$$\Delta H = q_P - P\Delta V + P\Delta V = q_P \qquad [1\text{-}4]$$

In other words, the change in enthalpy is equivalent to heat. Moreover, the volume changes in most biochemical reactions are insignificant ($P\Delta V \approx 0$), so the differences between their ΔU and ΔH values are negligible, and hence the energy change for the reacting system is equivalent to its enthalpy change. Enthalpy, like energy, heat, and work, is given units of joules. (Some commonly used units and biochemical constants and other conventions are given in Box 1-2.)

Thermodynamics is useful for indicating the spontaneity of a process. A **spontaneous process** occurs without the input of additional energy from outside the system. (Thermodynamic spontaneity has nothing to do with how quickly a process occurs.) The first law of thermodynamics, however, cannot by itself determine whether a process is spontaneous. Consider two objects of different temperatures that are brought together. Heat spontaneously flows from the warmer object to the cooler one, never vice versa. Yet either process would be consistent with the first law of thermodynamics since the aggregate energy of the two objects does not change. Therefore, an additional criterion of spontaneity is needed.

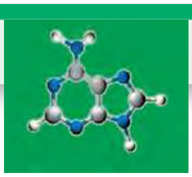

BOX 1-2 PERSPECTIVES IN BIOCHEMISTRY

Biochemical Conventions

Modern biochemistry generally uses Système International (SI) units, including meters (m), kilograms (kg), and seconds (s) and their derived units, for various thermodynamic and other measurements. The following table lists the commonly used biochemical units, some useful biochemical constants, and a few conversion factors.

Units

Energy, heat, work	joule (J)	$kg \cdot m^2 \cdot s^{-2}$ or $C \cdot V$
Electric potential	volt (V)	$J \cdot C^{-1}$

Prefixes for units

mega (M)	10^6	nano (n)	10^{-9}
kilo (k)	10^3	pico (p)	10^{-12}
milli (m)	10^{-3}	femto (f)	10^{-15}
micro (μ)	10^{-6}	atto (a)	10^{-18}

Conversions

angstrom (Å)	10^{-10} m
calorie (cal)	4.184 J
kelvin (K)	degrees Celsius (°C) + 273.15

Constants

Avogadro's number (*N*)	6.0221×10^{23} molecules $\cdot$ mol^{-1}
Coulomb (C)	6.241×10^{18} electron charges
Faraday ($\mathcal{F}$)	96,485 $C \cdot mol^{-1}$ or 96,485 $J \cdot V^{-1} \cdot mol^{-1}$
Gas constant (*R*)	8.3145 $J \cdot K^{-1} \cdot mol^{-1}$
Boltzmann constant (k_B)	1.3807×10^{-23} $J \cdot K^{-1}$ (*R/N*)
Planck's constant (*h*)	6.6261×10^{-34} $J \cdot s$

Throughout this text, molecular masses of particles are expressed in units of **daltons (D),** which are defined as l/12th the mass of a ^{12}C atom (1000 D = 1 **kilodalton, kD**). Biochemists also use **molecular weight,** a dimensionless quantity defined as the ratio of the particle mass to l/12th the mass of a ^{12}C atom, which is symbolized $\boldsymbol{M_r}$ (for relative molecular mass).

B | The Second Law of Thermodynamics States That Entropy Tends to Increase

According to the second law of thermodynamics, spontaneous processes are characterized by the conversion of order to disorder. In this context, disorder is defined as the number of energetically equivalent ways, ***W,*** of arranging the components of a system. To make this concept concrete, consider a system consisting of two bulbs of equal volume, one of which contains molecules of an ideal gas (Fig. 1-10). When the stopcock connecting the bulbs is open, the molecules become randomly but equally distributed between the two bulbs. The equal number of gas molecules in each bulb is not the result of any law of motion; it is because the probabilities of all other distributions of the molecules are so overwhelmingly small. Thus, the probability of all the molecules in the system spontaneously rushing into the left bulb (the initial condition) is nil, even though the energy and enthalpy of this arrangement are exactly the same as those of the evenly distributed molecules.

The degree of randomness of a system is indicated by its **entropy** (Greek: *en,* in + *trope,* turning), abbreviated ***S*:**

$$S = k_B \ln W \qquad [1\text{-}5]$$

where $\boldsymbol{k_B}$ is the **Boltzmann constant.** The units of S are $J \cdot K^{-1}$ (absolute temperature, in units of kelvins, is a factor because entropy varies with temperature; e.g., a system becomes more disordered as its temperature rises). The most probable arrangement of a system is the one that maximizes W and hence S. Thus, if a spontaneous process, such as the one shown in Fig. 1-10, has overall energy and enthalpy changes (ΔU and ΔH) of zero, its entropy change (ΔS) must be greater than zero; that is,

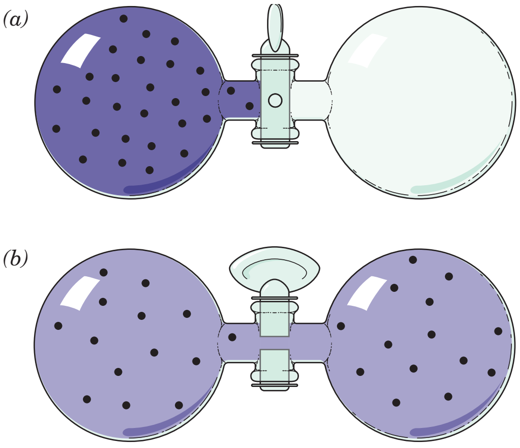

■ **Figure 1-10 | Illustration of entropy.** In (*a*), a gas occupies the leftmost of two equal-sized bulbs and hence the entropy is low. When the stopcock is opened (*b*), the entropy increases as the gas molecules diffuse back and forth between the bulbs and eventually become distributed evenly, half in each bulb.

the number of equivalent ways of arranging the final state must be greater than the number of ways of arranging the initial state. Furthermore, because

$$\Delta S_{\text{system}} + \Delta S_{\text{surroundings}} = \Delta S_{\text{universe}} > 0 \qquad [1\text{-}6]$$

all processes increase the entropy—that is, the disorder—of the universe.

In chemical and biological systems, it is impractical, if not impossible, to determine the entropy of a system by counting all the equivalent arrangements of its components (W). However, there is an entirely equivalent expression for entropy that applies to the constant-temperature conditions typical of biological systems: for a spontaneous process,

$$\Delta S \geq \frac{q}{T} \qquad [1\text{-}7]$$

Thus, the entropy change in a process can be experimentally determined from measurements of heat.

C | The Free Energy Change Determines the Spontaneity of a Process

The spontaneity of a process cannot be predicted from a knowledge of the system's entropy change alone. For example, 2 mol of H_2 and 1 mol of O_2, when sparked, react to form 2 mol of H_2O. Yet two water molecules, each of whose three atoms are constrained to stay together, are more ordered than are the three diatomic molecules from which they formed. Thus, the reaction occurs with a decrease in the system's entropy.

What, then, is the thermodynamic criterion for a spontaneous process? Equations 1-4 and 1-7 indicate that at constant temperature and pressure

$$\Delta S \geq \frac{q_P}{T} = \frac{\Delta H}{T} \qquad [1\text{-}8]$$

Thus,

$$\Delta H - T\Delta S \leq 0 \qquad [1\text{-}9]$$

This is the true criterion for spontaneity as formulated, in 1878, by J. Willard Gibbs. He defined the **Gibbs free energy** (***G***, usually called just **free energy**) as

$$G = H - TS \qquad [1\text{-}10]$$

The change in free energy for a process is ΔG. Consequently, spontaneous processes at constant temperature and pressure have

$$\boxed{\Delta G = \Delta H - T\Delta S < 0} \qquad [1\text{-}11]$$

Such processes are said to be **exergonic** (Greek: *ergon,* work). Processes that are not spontaneous have positive ΔG values ($\Delta G > 0$) and are said to be **endergonic;** they must be driven by the input of free energy. If a process is exergonic, the reverse of that process is endergonic and vice versa. Thus, the ΔG value for a process indicates whether the process can occur spontaneously in the direction written. Processes at **equilibrium,** those in which the forward and reverse reactions are exactly balanced, are characterized by $\Delta G = 0$. For the most part, only changes in free energy, enthalpy, and entropy (ΔG, ΔH, and ΔS) can be measured, not their absolute values (G, H, and S).

A process that is accompanied by an increase in enthalpy ($\Delta H > 0$), which opposes the process, can nevertheless proceed spontaneously if the

Table 1-3 Variation of Reaction Spontaneity (Sign of ΔG) with the Signs of ΔH and ΔS

ΔH	ΔS	$\Delta G = \Delta H - T\Delta S$
−	+	The reaction is both enthalpically favored (exothermic) and entropically favored. It is spontaneous (exergonic) at all temperatures.
−	−	The reaction is enthalpically favored but entropically opposed. It is spontaneous only at temperatures *below* $T = \Delta H/\Delta S$.
+	+	The reaction is enthalpically opposed (endothermic) but entropically favored. It is spontaneous only at temperatures *above* $T = \Delta H/\Delta S$.
+	−	The reaction is both enthalpically and entropically opposed. It is nonspontaneous (endergonic) at all temperatures.

entropy change is sufficiently positive ($\Delta S > 0$; Table 1-3). Conversely, a process that is accompanied by a decrease in entropy ($\Delta S < 0$) can proceed if its enthalpy change is sufficiently negative ($\Delta H < 0$). It is important to emphasize that *a large negative value of ΔG does not ensure that a process such as a chemical reaction will proceed at a measurable rate. The rate depends on the detailed mechanism of the reaction, which is independent of ΔG.*

Free energy as well as energy, enthalpy, and entropy are **state functions.** In other words, their values depend only on the current state or properties of the system, not on how the system reached that state. Therefore, *thermodynamic measurements can be made by considering only the initial and final states of the system and ignoring all the stepwise changes in enthalpy and entropy that occur in between*. For example, it is impossible to directly measure the energy change for the reaction of glucose with O_2 in a living organism because of the numerous other simultaneously occurring chemical reactions. But since ΔG depends on only the initial and final states, the combustion of glucose can be analyzed in any convenient apparatus, using the same starting materials (glucose and O_2) and end products (CO_2 and H_2O) that would be obtained *in vivo*.

D | Free Energy Changes Can Be Calculated from Equilibrium Concentrations

The entropy (disorder) of a substance increases with its volume. For example, a collection of gas molecules, in occupying all of the volume available to it, maximizes its entropy. Similarly, dissolved molecules become uniformly distributed throughout their solution volume. Entropy is therefore a function of concentration.

If entropy varies with concentration, so must free energy. Thus, *the free energy change of a chemical reaction depends on the concentrations of both its reacting substances (reactants) and its reaction products.* This phenomenon has great significance because many biochemical reactions operate spontaneously in either direction depending on the relative concentrations of their reactants and products.

Equilibrium Constants Are Related to ΔG. The relationship between the concentration and the free energy of a substance A is approximately

$$\overline{G}_A = \overline{G}_A^\circ + RT \ln [A] \qquad [1\text{-}12]$$

where $\overline{\boldsymbol{G}}_{\mathbf{A}}$ is known as the **partial molar free energy** or the **chemical potential** of A (the bar indicates the quantity per mole), $\overline{\boldsymbol{G}}^{\circ}_{\mathbf{A}}$ is the partial molar free energy of A in its **standard state,** R is the gas constant, and [A] is the molar concentration of A. Thus, for the general reaction

$$aA + bB \rightleftharpoons cC + dD$$

the free energy change is

$$\Delta G = c\overline{G}_C + d\overline{G}_D - a\overline{G}_A - b\overline{G}_B \qquad [1\text{-}13]$$

and

$$\Delta G^{\circ} = c\overline{G}^{\circ}_C + d\overline{G}^{\circ}_D - a\overline{G}^{\circ}_A - b\overline{G}^{\circ}_B \qquad [1\text{-}14]$$

because free energies are additive and the free energy change of a reaction is the sum of the free energies of the products less those of the reactants. Substituting these relationships into Eq. 1-12 yields

$$\Delta G = \Delta G^{\circ} + RT \ln\left(\frac{[C]^c[D]^d}{[A]^a[B]^b}\right) \qquad [1\text{-}15]$$

where ΔG° is the free energy change of the reaction when all of its reactants and products are in their standard states (see below). Thus, the expression for the free energy change of a reaction consists of two parts: (1) a constant term whose value depends only on the reaction taking place and (2) a variable term that depends on the concentrations of the reactants and the products, the stoichiometry of the reaction, and the temperature.

For a reaction at equilibrium, there is no *net* change because the free energy change of the forward reaction exactly balances that of the reverse reaction. Consequently, $\Delta G = 0$, so Eq. 1-15 becomes

$$\boxed{\Delta G^{\circ} = -RT \ln K_{eq}} \qquad [1\text{-}16]$$

where K_{eq} is the familiar **equilibrium constant** of the reaction:

$$K_{eq} = \frac{[C]^c_{eq}[D]^d_{eq}}{[A]^a_{eq}[B]^b_{eq}} = e^{-\Delta G^{\circ}/RT} \qquad [1\text{-}17]$$

The subscript "eq" denotes reactant and product concentrations at equilibrium. (The equilibrium condition is usually clear from the context of the situation, so equilibrium concentrations are usually expressed without this subscript.) *The equilibrium constant of a reaction can therefore be calculated from standard free energy data and vice versa* (see Sample Calculation 1-1).

SAMPLE CALCULATION 1-1

The standard free energy change for a reaction is $-15\ \text{kJ} \cdot \text{mol}^{-1}$. What is the equilibrium constant for the reaction?

Since ΔG° is known, Eq. 1-17 can be used to calculate K_{eq}. Assume the temperature is 25°C (298 K):

$$K_{eq} = e^{-\Delta G^{\circ}/RT}$$

$$K_{eq} = e^{-(-15{,}000\ \text{J}\cdot\text{mol}^{-1})/(8.314\ \text{J}\cdot\text{K}^{-1}\cdot\text{mol}^{-1})(298\ \text{K})}$$

$$K_{eq} = e^{6.05}$$

$$K_{eq} = 426$$

***K* Depends on Temperature.** The manner in which the equilibrium constant varies with temperature can be seen by substituting Eq. 1-11 into Eq. 1-16 and rearranging:

$$\ln K_{eq} = \frac{-\Delta H^{\circ}}{R}\left(\frac{1}{T}\right) + \frac{\Delta S^{\circ}}{R} \qquad [1\text{-}18]$$

where H° and S° represent enthalpy and entropy in the standard state. Equation 1-18 has the form $y = mx + b$, the equation for a straight line. A plot of $\ln K_{eq}$ versus $1/T$, known as a **van't Hoff plot,** permits the values of ΔH° and ΔS° (and hence ΔG°) to be determined from measurements of K_{eq} at two (or more) different temperatures. This method is often more practical than directly measuring ΔH and ΔS by calorimetry (which measures the heat, q_P, of a process).

Biochemists Have Defined Standard-State Conventions. In order to compare free energy changes for different reactions, it is necessary to express ΔG values relative to some standard state (likewise, we refer the elevations of geographic locations to sea level, which is arbitrarily assigned the height of zero). According to the convention used in physical chemistry, a solute is in its standard state when the temperature is 25°C, the pressure is 1 atm, and the solute has an **activity** of 1 (activity of a substance is its concentration corrected for its nonideal behavior at concentrations higher than infinite dilution).

The concentrations of reactants and products in most biochemical reactions are usually so low (on the order of millimolar or less) that their activities are closely approximated by their molar concentrations. Furthermore, because biochemical reactions occur near neutral pH, biochemists have adopted a somewhat different standard-state convention:

1. The activity of pure water is assigned a value of 1, even though its concentration is 55.5 M. This practice simplifies the free energy expressions for reactions in dilute solutions involving water as a reactant, because the $[H_2O]$ term can then be ignored.
2. The hydrogen ion (H^+) activity is assigned a value of 1 at the physiologically relevant pH of 7. Thus, the biochemical standard state is pH 7.0 (neutral pH, where $[H^+] = 10^{-7}$ M) rather than pH 0 ($[H^+] =$ 1 M), the physical chemical standard state, where many biological substances are unstable.
3. The standard state of a substance that can undergo an acid–base reaction is defined in terms of the total concentration of its naturally occurring ion mixture at pH 7. In contrast, the physical chemistry convention refers to a pure species whether or not it actually exists at pH 0. The advantage of the biochemistry convention is that the total concentration of a substance with multiple ionization states, such as most biological molecules, is usually easier to measure than the concentration of one of its ionic species. Since the ionic composition of an acid or base varies with pH, however, the standard free energies calculated according to the biochemical convention are valid only at pH 7.

Under the biochemistry convention, the standard free energy changes of reactions are customarily symbolized by $\Delta G^{\circ\prime}$ to distinguish them from physical chemistry standard free energy changes, ΔG°. If a reaction includes neither H_2O, H^+, nor an ionizable species, then $\Delta G^{\circ\prime} = \Delta G^\circ$.

E | Life Obeys the Laws of Thermodynamics

At one time, many scientists believed that life, with its inherent complexity and order, somehow evaded the laws of thermodynamics. However, elaborate measurements on living animals are consistent with the conservation of energy predicted by the first law. Unfortunately, experimental verification of the second law is not practicable, since it requires dismantling an organism to its component molecules, which would result in its irreversible death. Consequently, it is possible to assert only that the entropy of living matter is less than that of the products to which it decays. *Life persists, however, because a system (a living organism) can be ordered* *at the expense of disordering its surroundings to an even greater extent.* In other words, the total entropy of the system plus its surroundings increases, as required by the second law. Living organisms achieve order by disordering (breaking down) the nutrients they consume. Thus, the entropy content of food is as important as its energy content.

Living Organisms Are Open Systems. Classical thermodynamics applies primarily to reversible processes in **isolated systems** (which cannot exchange matter or energy with their surroundings) or in **closed systems** (which can only exchange energy). An isolated system inevitably reaches equilibrium. For example, if its reactants are in excess, the forward reaction will proceed faster than the reverse reaction until equilibrium is attained ($\Delta G = 0$), at which point the forward and reverse reactions exactly balance each other. In contrast, **open systems,** which exchange both matter and energy with their surroundings, can reach equilibrium only after the flow of matter and energy has stopped.

Living organisms, which take up nutrients, release waste products, and generate work and heat, are open systems and therefore can never be at equilibrium. They continuously ingest high-enthalpy, low-entropy nutrients, which they convert to low-enthalpy, high-entropy waste products. The free energy released in this process powers the cellular activities that produce the high degree of organization characteristic of life. If this process is interrupted, the system ultimately reaches equilibrium, which for living things is synonymous with death. An example of energy flow in an open system is illustrated in Fig. 1-11. Through photosynthesis, plants convert radiant energy from the sun, the primary energy source for life on the earth, to the chemical energy of carbohydrates and other organic substances. The plants, or the animals that eat them then metabolize these substances to power such functions as the synthesis of biomolecules, the maintenance of intracellular ion concentrations, and cellular movements.

Living Things Maintain a Steady State. Even in a system that is not at equilibrium, matter and energy flow according to the laws of thermodynamics. For example, materials tend to move from areas of high concentration to areas of low concentration. This is why blood takes up O_2 in the lungs, where O_2 is abundant, and releases it to the tissues, where O_2 is scarce.

Living systems are characterized by being in a **steady state.** This means that all flows in the system are constant so that the system does not change

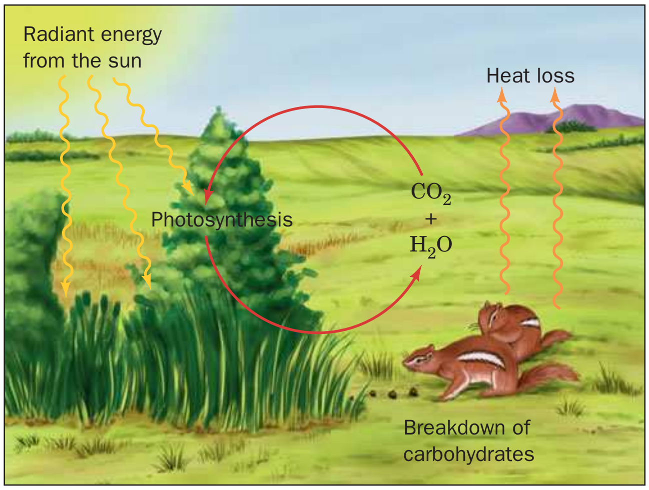

Figure 1-11 | **Energy flow in the biosphere.** Plants use the sun's radiant energy to synthesize carbohydrates from CO_2 and H_2O. Plants or the animals that eat them eventually metabolize the carbohydrates to release their stored free energy and thereby return CO_2 and H_2O to the environment.

with time. Energy flow in the biosphere (Fig. 1-11) is an example of a system in a steady state. Slight perturbations from the steady state give rise to changes in flows that restore the system to the steady state. In all living systems, energy flow is exclusively “downhill” ($\Delta G < 0$). In addition, nature is inherently dissipative, so the recovery of free energy from a biochemical process is never total and some energy is always lost to the surroundings.

Enzymes Catalyze Biochemical Reactions. Nearly all the molecular components of an organism can potentially react with each other, and many of these reactions are thermodynamically favored (spontaneous). Yet only a subset of all possible reactions actually occur to a significant extent in a living organism. The rate of a particular reaction depends not on the free energy difference between the initial and final states but on the actual path through which the reactants are transformed to products. Living organisms take advantage of catalysts, substances that increase the rate at which the reaction approaches equilibrium without affecting the reaction’s ΔG. Biological catalysts are referred to as **enzymes,** most of which are proteins.

Enzymes accelerate biochemical reactions by physically interacting with the reactants and products to provide a more favorable pathway for the transformation of one to the other. Enzymes increase the rates of reactions by increasing the likelihood that the reactants can interact productively. Enzymes cannot, however, promote reactions whose ΔG values are positive.

A multitude of enzymes mediate the flow of energy in every cell. As free energy is harvested, stored, or used to perform cellular work, it may be transferred to other molecules. And although it is tempting to think of free energy as something that is stored in chemical bonds, chemical energy can be transformed into heat, electrical work, or mechanical work, according to the needs of the organism and the biochemical machinery with which it has been equipped through evolution.

CHECK YOUR UNDERSTANDING

Explain the first and second laws of thermodynamics.
How does the free energy change for a process depend on its enthalpy and entropy changes? What makes a process spontaneous?
How is the free energy change for a chemical reaction related to the equilibrium constant?
How does life persist despite the laws of thermodynamics?

SUMMARY

1. A model for the origin of life proposes that organisms ultimately arose from simple organic molecules that polymerized to form more complex molecules capable of replicating themselves.
2. Compartmentation gave rise to cells that developed metabolic reactions for synthesizing biological molecules and generating energy.
3. All cells are either prokaryotic or eukaryotic. Eukaryotic cells contain a variety of membrane-bounded organelles.
4. Phylogenetic evidence groups organisms into three domains: archaea, bacteria, and eukarya.
5. Natural selection determines the evolution of species.
6. The first law of thermodynamics (energy is conserved) and the second law (spontaneous processes increase the disorder of the universe) apply to biochemical processes. The spontaneity of a process is determined by its free energy change ($\Delta G = \Delta H - T\Delta S$): spontaneous reactions have $\Delta G < 0$ and nonspontaneous reactions have $\Delta G > 0$.
7. The equilibrium constant for a process is related to the standard free energy change for that process.
8. Living organisms are open systems that maintain a steady state.

KEY TERMS

prebiotic era	**2**
organic compound	**2**
functional group	**3**
linkage	**3**
polymer	**3**
condensation reaction	**3**
hydrolysis	**3**
replication	**5**
natural selection	**5**
vesicle	**5**
compartmentation	**5**
precursor	**6**
catalyst	**6**
eukaryote	**7**
nucleus	**7**
prokaryote	**7**
virus	**7**
cytoplasm	**8**
organelle	**8**
endoplasmic reticulum	**8**
Golgi apparatus	**8**
mitochondrion	**8**
chloroplast	**8**
lysosome	**8**

peroxisome	**8**
vacuole	**8**
cytosol	**8**
cytoskeleton	**8**
taxonomy	**9**
phylogeny	**9**
archaea	**9**
bacteria	**9**
eukarya	**9**
methanogens	**9**
halobacteria	**9**
thermophiles	**9**
symbiosis	**10**
mutation	**11**
thermodynamics	**11**
system	**12**
surroundings	**12**
U	**12**
q	**12**
w	**12**
H	**12**
q_P	**12**
spontaneous process	**12**
D	**13**
kD	**13**
W	**13**
S	**13**
k_B	**13**
G	**14**
exergonic	**14**
endergonic	**14**
equilibrium	**14**
state function	**15**
$\overline{G}_A$	**16**
$\overline{G}_A^\circ$	**16**
standard state	**16**
equilibrium constant	**16**
van't Hoff plot	**16**
activity	**17**
isolated system	**18**
closed system	**18**
open system	**18**
steady state	**18**
enzyme	**19**

PROBLEMS

1. Identify the circled functional groups and linkages in the compound below.

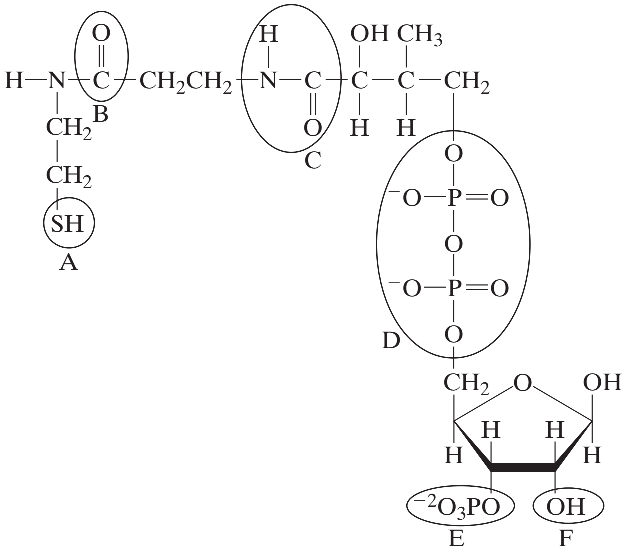

2. Why is the cell membrane not an absolute barrier between the cytoplasm and the external environment?

3. A spheroidal bacterium with a diameter of 1 μm contains two molecules of a particular protein. What is the molar concentration of the protein?

4. How many glucose molecules does the cell in Problem 3 contain when its internal glucose concentration is 1.0 mM?

5. (a) Which has greater entropy, liquid water at 0°C or ice at 0°C? (b) How does the entropy of ice at −5°C differ, if at all, from its entropy at −50°C?

6. Does entropy increase or decrease in the following processes?

   (a) $N_2 + 3\ H_2 \longrightarrow 2\ NH_3$

   (b)

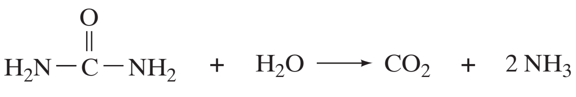

$$H_2N-\overset{\overset{\displaystyle O}{\|}}{C}-NH_2 + H_2O \longrightarrow CO_2 + 2\ NH_3$$

Urea

   (c)

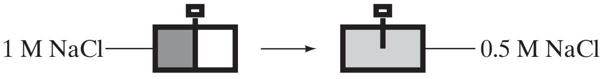

   (d)

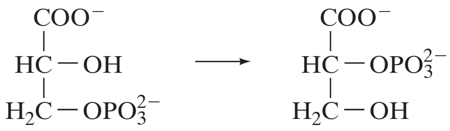

3-Phosphoglycerate **2-Phosphoglycerate**

7. Consider a reaction with $\Delta H = 15$ kJ and $\Delta S = 50\ \text{J} \cdot \text{K}^{-1}$. Is the reaction spontaneous (a) at 10°C, (b) at 80°C?

8. Calculate the equilibrium constant for the reaction

$$\text{glucose-1-phosphate} + H_2O \longrightarrow \text{glucose} + H_2PO_4^-$$

at pH 7.0 and 25°C ($\Delta G^{\circ\prime} = -20.9\ \text{kJ} \cdot \text{mol}^{-1}$).

9. Calculate $\Delta G^{\circ\prime}$ for the reaction $A + B \rightleftharpoons C + D$ at 25°C when the equilibrium concentrations are [A] = 10 μM, [B] = 15 μM, [C] = 3 μM, and [D] = 5 μM. Is the reaction exergonic or endergonic under standard conditions?

10. $\Delta G^{\circ\prime}$ for the isomerization reaction

$$\text{glucose-1-phosphate (G1P)} \rightleftharpoons \text{glucose-6-phosphate (G6P)}$$

is $-7.1\ \text{kJ} \cdot \text{mol}^{-1}$. Calculate the equilibrium ratio of [G1P] to [G6P] at 25°C.

11. For the reaction $A \longrightarrow B$ at 298 K, the change in enthalpy is $-7\ \text{kJ} \cdot \text{mol}^{-1}$ and the change in entropy is $-25\ \text{J} \cdot \text{K}^{-1} \cdot \text{mol}^{-1}$. Is the reaction spontaneous? If not, should the temperature be increased or decreased to make the reaction spontaneous?

12. For the conversion of reactant A to product B, the change in enthalpy is $7\ \text{kJ} \cdot \text{mol}^{-1}$ and the change in entropy is $20\ \text{J} \cdot \text{K}^{-1} \cdot \text{mol}^{-1}$. Above what temperature does the reaction become spontaneous?

13. Label the following statements true or false:

    (a) A reaction is said to be spontaneous when it can proceed in either the forward or reverse direction.

    (b) A spontaneous process always happens very quickly.

    (c) A nonspontaneous reaction will proceed spontaneously in the reverse direction.

    (d) A spontaneous process can occur with a large decrease in entropy.

14. Two biochemical reactions have the same $K_{eq} = 5 \times 10^8$ at temperature $T_1 = 298$ K. However, Reaction 1 has $\Delta H^\circ =$

$-28\ \text{kJ} \cdot \text{mol}^{-1}$ and Reaction 2 has $\Delta H° = +28\ \text{kJ} \cdot \text{mol}^{-1}$. The two reactions utilize the same reactants. Your lab partner has proposed that you can get more of the reactants to proceed via Reaction 2 rather than Reaction 1 by lowering the temperature of the reaction. Will this strategy work? Why or why not? How much would the temperature have to be raised or lowered in order to change the value of K_2/K_1 from 1 to 10?

REFERENCES

Origin and Evolution of Life

Anet, F.A.L., The place of metabolism in the origin of life, *Curr. Opin. Chem. Biol.* **8,** 654–659 (2004). [Discusses various hypotheses proposing that life originated as a self-replicating system or as a set of catalytic polymers.]

Bada, J.L. and Lazcano, A., Prebiotic soup—revisiting the Miller experiment, *Science* **300,** 745–756 (2003).

Nisbet, E.G. and Sleep, N.H., The habitat and nature of early life, *Nature* **409,** 1083–1091 (2001). [Explains some of the hypotheses regarding the early earth and the origin of life, including the possibility that life originated at hydrothermal vents.]

Cells

Baldauf, S.L., The deep roots of eukaryotes, *Science* **300,** 1703–1706 (2003). [Describes some recent discoveries that raise questions about the taxonomy of eukaryotes.]

Campbell, N.A. and Reece, J.B., *Biology* (7th ed.), Benjamin/Cummings (2005). [This and other comprehensive general biology texts provide details about the structures of prokaryotes and eukaryotes.]

DeLong, E.F. and Pace, N.R., Environmental diversity of bacteria and archaea, *Syst. Biol.* **593,** 470–478 (2001). [Describes some of the challenges of classifying microbial organisms among the three domains.]

Goodsell, D.S., A look inside the living cell, *Am. Scientist* **80,** 457–465 (1992); *and* Inside a living cell, *Trends Biochem. Sci.* **16,** 203–206 (1991).

Lodish, H., Berk, A., Matsudaria, P., Kaiser, C. A., Krieger, M., Scott, M.P., Zipursky, S.L., and Darnell, J., *Molecular Cell Biology* (5th ed.), Chapter 5, W.H. Freeman (2004). [This and other cell biology textbooks offer thorough reviews of cellular structure.]

Thermodynamics

Tinoco, I., Jr., Sauer, K., Wang, J.C., and Puglisi, J.C., *Physical Chemistry. Principles and Applications in Biological Sciences* (4th ed.), Chapters 2–5, Prentice-Hall (2002). [Most physical chemistry texts treat thermodynamics in some detail.]

van Holde, K.E., Johnson, W.C., and Ho, P.S., *Principles of Physical Biochemistry* (2nd ed.), Chapters 2 and 3, Prentice-Hall (2006).

2

Water

Coral reefs support a variety of vertebrates and invertebrates. The water that surrounds them is critical for their existence, acting as a solvent for biochemical reactions and determining the structures of the macromolecules. [Georgette Douwma/Taxi/Getty Images.]

CHAPTER CONTENTS

1 Physical Properties of Water
  A. Water Is a Polar Molecule
  B. Hydrophilic Substances Dissolve in Water
  C. The Hydrophobic Effect Causes Nonpolar Substances to Aggregate in Water
  D. Water Moves by Osmosis and Solutes Move by Diffusion
2 Chemical Properties of Water
  A. Water Ionizes to Form H^+ and OH^-
  B. Acids and Bases Alter the pH
  C. Buffers Resist Changes in pH

MEDIA RESOURCES

(Available at www.wiley.com/college/voet)
Animated Figure 2-17. Titration curves for acetic acid, phosphate, and ammonia
Animated Figure 2-18. Titration of a polyprotic acid
Case Study 1. Acute Aspirin Overdose: Relationship to the Blood Buffering System

Any study of the chemistry of life must include a study of water. Biological molecules and the reactions they undergo can be best understood in the context of their aqueous environment. Not only are organisms made mostly of water (about 70% of the mass of the human body is water), they are surrounded by water on this, the "blue planet." Aside from its sheer abundance, water is central to biochemistry for the following reasons:

1. Nearly all biological molecules assume their shapes (and therefore their functions) in response to the physical and chemical properties of the surrounding water.
2. The medium for the majority of biochemical reactions is water. Reactants and products of metabolic reactions, nutrients as well as waste products, depend on water for transport within and between cells.
3. Water itself actively participates in many chemical reactions that support life. Frequently, the ionic components of water, the H^+ and OH^- ions, are the true reactants. In fact, the reactivity of many functional groups on biological molecules depends on the relative concentrations of H^+ and OH^- in the surrounding medium.

All organisms require water, from the marine creatures who spend their entire lives in an aqueous environment to terrestrial organisms who must guard their watery interiors with protective skins. Not surprisingly, living organisms can be found wherever there is liquid water—in hydrothermal vents as hot as 121°C and in the cracks and crevices between rocks hundreds of meters beneath the surface of the earth. Organisms that survive desiccation do so only by becoming dormant, as seeds or spores.

An examination of water from a biochemical point of view requires a look at the physical properties of water, its powers as a solvent, and its chemical behavior—that is, the nature of aqueous acids and bases.

1 Physical Properties of Water

The colorless, odorless, and tasteless nature of water belies its fundamental importance to living organisms. Despite its bland appearance to our senses, water is anything but inert. Its physical properties—unique among molecules of similar size—give it unparalleled strength as a solvent. And yet its limitations as a solvent also have important implications for the structures and functions of biological molecules.

LEARNING OBJECTIVES

- Understand that water molecules are polar and form irregular hydrogen-bonded networks in the liquid state.
- Know the noncovalent forces that act on biomolecules.
- Understand why polar and ionic substances dissolve in water.
- Understand that the hydrophobic effect is the tendency for water to exclude nonpolar groups in order to maximize the entropy of water molecules.
- Understand the processes of osmosis and diffusion.

A | Water Is a Polar Molecule

A water molecule consists of two hydrogen atoms bonded to an oxygen atom. The O—H bond distance is 0.958 Å (1 Å = 10^{-10} m), and the angle formed by the three atoms is 104.5° (Fig. 2-1). The hydrogen atoms are not arranged linearly, because the oxygen atom's four sp^3 hybrid orbitals extend roughly toward the corners of a tetrahedron. Hydrogen atoms occupy two corners of the tetrahedron, and the nonbonding electron pairs of the oxygen atom occupy the other two corners (in a perfectly tetrahedral molecule, such as methane, CH_4, the bond angles are 109.5°).

Water Molecules Form Hydrogen Bonds. The angular geometry of the water molecule has enormous implications for living systems. Water is a **polar** molecule: the oxygen atom with its unshared electrons carries a partial negative charge ($\delta-$) of $-0.66e$, and the hydrogen atoms each carry a partial positive charge ($\delta+$) of $+0.33e$, where e is the charge of the electron. Electrostatic attractions between the dipoles of water molecules are crucial to the properties of water itself and to its role as a biochemical solvent. Neighboring water molecules tend to orient themselves so that the O—H bond of one water molecule (the positive end) points toward one of the electron pairs of the other water molecule (the negative end). The resulting directional intermolecular association is known as a **hydrogen bond** (Fig. 2-2).

In general, a hydrogen bond can be represented as D—H···A, where D—H is a weakly acidic "donor" group such as O—H, N—H, or sometimes S—H, and A is a weakly basic "acceptor" atom such as O, N, or occasionally S. Hydrogen bonds are structurally characterized by an H···A distance that is at least 0.5 Å shorter than the calculated **van der Waals distance** (the distance of closest approach between two nonbonded atoms). In water, for example, the O···H hydrogen bond distance is ~1.8 Å versus 2.6 Å for the corresponding van der Waals distance.

A single water molecule contains two hydrogen atoms that can be "donated" and two unshared electron pairs that can act as "acceptors," so

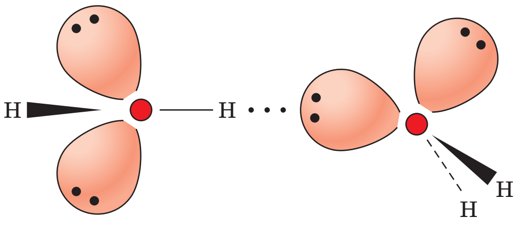

Figure 2-2 | A hydrogen bond in water. The strength of the interaction is maximal when the O—H covalent bond of one molecule points directly toward the lone-pair electron cloud of the other.

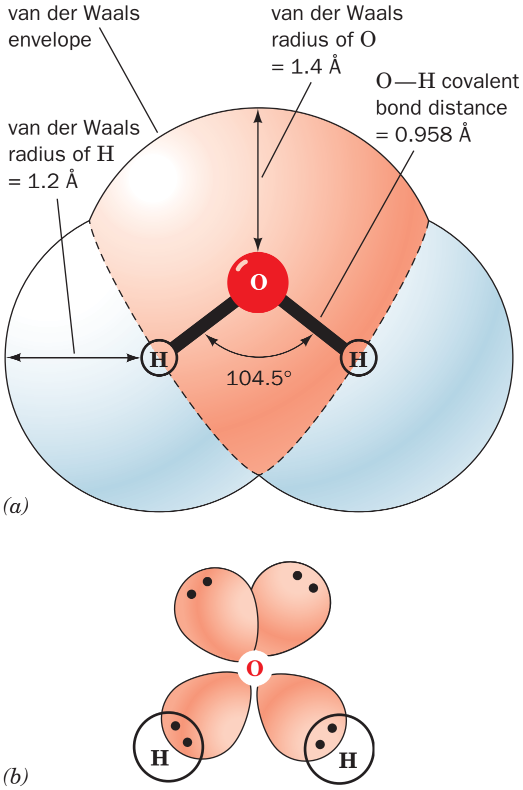
van der Waals envelope
van der Waals radius of O = 1.4 Å
O—H covalent bond distance = 0.958 Å
van der Waals radius of H = 1.2 Å
O
H
H
104.5°
(a)
O
H
H
(b)

Figure 2-1 | Structure of the water molecule. (*a*) The shaded outline represents the van der Waals envelope, the effective "surface" of the molecule. (*b*) The oxygen atom's sp^3 orbitals are arranged tetrahedrally. Two orbitals contain nonbonding electron pairs (lone pairs).

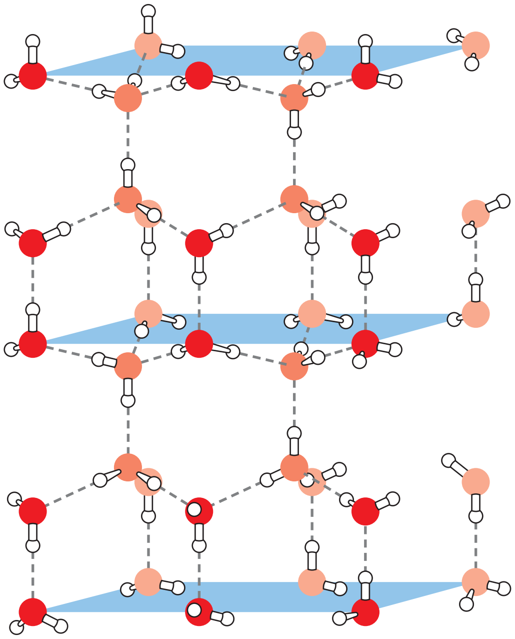

Figure 2-3 | **The structure of ice.** Each water molecule interacts tetrahedrally with four other water molecules. Oxygen atoms are red and hydrogen atoms are white. Hydrogen bonds are represented by dashed lines. [After Pauling, L., *The Nature of the Chemical Bond* (3rd ed.), p. 465, Cornell University Press (1960).]

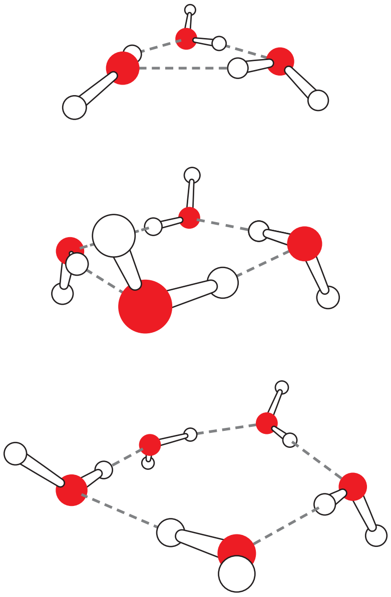

Figure 2-4 | **Rings of water molecules.** These models, containing three, four, or five molecules, are based on theoretical predictions and spectroscopic data. [After Liu, K., Cruzan, J.D., and Saykally, R.J., *Science* **271,** 929 (1996).]

each molecule can participate in a maximum of four hydrogen bonds with other water molecules. Although the energy of an individual hydrogen bond ($\sim$20 $\text{kJ}\cdot\text{mol}^{-1}$) is relatively small (e.g., the energy of an O—H covalent bond is 460 $\text{kJ}\cdot\text{mol}^{-1}$), the sheer number of hydrogen bonds in a sample of water is the key to its remarkable properties.

Ice Is a Crystal of Hydrogen-Bonded Water Molecules. The structure of ice provides a striking example of the cumulative strength of many hydrogen bonds. X-Ray and neutron diffraction studies have established that water molecules in ice are arranged in an unusually open structure. Each water molecule is tetrahedrally surrounded by four nearest neighbors to which it is hydrogen bonded (Fig. 2-3). As a consequence of its open structure, water is one of the very few substances that expands on freezing (at 0°C, liquid water has a density of 1.00 $\text{g}\cdot\text{mL}^{-1}$, whereas ice has a density of 0.92 $\text{g}\cdot\text{mL}^{-1}$).

The expansion of water on freezing has overwhelming consequences for life on the earth. Suppose that water contracted on freezing, that is, became more dense rather than less dense. Ice would then sink to the bottoms of lakes and oceans rather than float. This ice would be insulated from the sun so that oceans, with the exception of a thin surface layer of liquid in warm weather, would be permanently frozen solid (the water at great depths, even in tropical oceans, is close to 4°C, its temperature of maximum density). Thus, the earth would be locked in a permanent ice age and life might never have arisen.

The melting of ice represents the collapse of the strictly tetrahedral orientation of hydrogen-bonded water molecules, although hydrogen bonds between water molecules persist in the liquid state. In fact, liquid water is only $\sim$15% less hydrogen bonded than ice at 0°C. Indeed, the boiling point of water is 264°C higher than that of methane, a substance with nearly the same molecular mass as H_2O but which is incapable of hydrogen bonding (substances with similar intermolecular associations and equal molecular masses should have similar boiling points). This difference reflects the extraordinary internal cohesiveness of liquid water resulting from its intermolecular hydrogen bonding.

The Structure of Liquid Water Is Irregular. Because each molecule of liquid water reorients about once every 10^{-12} s, very few experimental techniques can explore the instantaneous arrangement of these water molecules. Theoretical considerations and spectroscopic evidence suggest that molecules in liquid water are each hydrogen bonded to four nearest neighbors, as they are in ice. These hydrogen bonds are distorted, however, so the networks of linked molecules are irregular and varied. For example, three- to seven-membered rings of hydrogen-bonded molecules commonly occur in liquid water (Fig. 2-4), in contrast to the six-membered rings characteristic of ice (Fig. 2-3). Moreover, these networks continually break up and re-form every 2×10^{-11} s or so. *Liquid water therefore consists of a rapidly fluctuating, three-dimensional network of hydrogen-bonded H_2O molecules.*

Hydrogen Bonds and Other Weak Interactions Influence Biological Molecules. Biochemists are concerned not just with the strong covalent bonds that define chemical structure but with the weak forces that act under relatively mild physical conditions. The structures of most biological molecules are determined by the collective influence of many individually weak interactions. The weak electrostatic forces that interest biochemists include ionic interactions, hydrogen bonds, and van der Waals forces.

Table 2-1 Bond Energies in Biomolecules

Type of Bond	**Example**	**Bond Strength ($\mathbf{kJ \cdot mol^{-1}}$)**
Covalent	O—H	460
	C—H	414
	C—C	348
Noncovalent		
Ionic interaction	$—COO^{-}\cdots{}^{+}H_3N—$	86
van der Waals forces		
Hydrogen bond	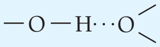	20
Dipole–dipole interaction	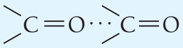	9.3
London dispersion forces	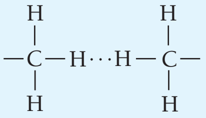	0.3

The strength of association of ionic groups of opposite charge depends on the chemical nature of the ions, the distance between them, and the polarity of the medium. In general, the strength of the interaction between two charged groups (i.e., the energy required to completely separate them in the medium of interest) is less than the energy of a covalent bond but greater than the energy of a hydrogen bond (Table 2-1).

The noncovalent associations between neutral molecules, collectively known as **van der Waals forces,** arise from electrostatic interactions among permanent or induced dipoles (the hydrogen bond is a special kind of dipolar interaction). Interactions among permanent dipoles such as carbonyl groups (Fig. 2-5*a*) are much weaker than ionic interactions. A permanent dipole also induces a dipole moment in a neighboring group by electrostatically distorting its electron distribution (Fig. 2-5*b*). Such dipole–induced dipole interactions are generally much weaker than dipole–dipole interactions.

At any instant, nonpolar molecules have a small, randomly oriented dipole moment resulting from the rapid fluctuating motion of their electrons. This transient dipole moment can polarize the electrons in a neighboring group (Fig. 2-5*c*), so that the groups are attracted to each other. These so-called **London dispersion forces** are extremely weak and fall off so rapidly with distance that they are significant only for groups in close contact. They are, nevertheless, extremely important in determining the structures of biological molecules, whose interiors contain many closely packed groups.

(*a*) Interactions between permanent dipoles

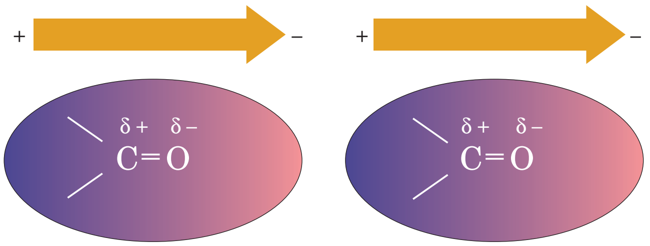

(*b*) Dipole–induced dipole interactions

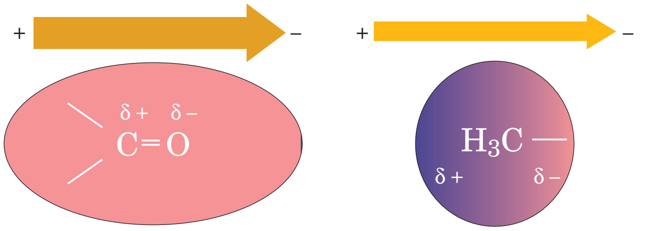

(*c*) London dispersion forces

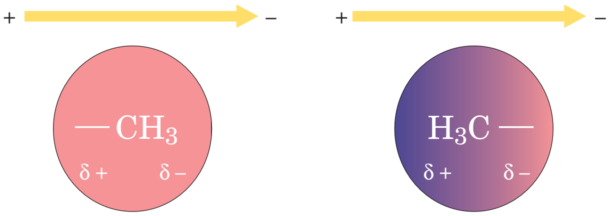

Figure 2-5 | **Dipole–dipole interactions.** The strength of each dipole is indicated by the thickness of the accompanying arrow. (*a*) Interaction between permanent dipoles. (*b*) Dipole–induced dipole interaction. (*c*) London dispersion forces.

B | Hydrophilic Substances Dissolve in Water

Solubility depends on the ability of a solvent to interact with a solute more strongly than solute particles interact with each other. Water is said to be the "universal solvent." Although this statement cannot literally be true, water certainly dissolves more types of substances and in greater amounts than any other solvent. In particular, the polar character of water makes

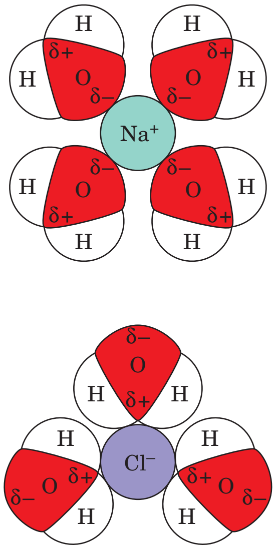

Figure 2-6 | Solvation of ions. The dipoles of the surrounding water molecules are oriented according to the charge of the ion. Only one layer of solvent molecules is shown.

it an excellent solvent for polar and ionic materials, which are said to be **hydrophilic** (Greek: *hydro,* water + *philos,* loving). On the other hand, nonpolar substances are virtually insoluble in water ("oil and water don't mix") and are consequently described as **hydrophobic** (Greek: *phobos,* fear). Nonpolar substances, however, are soluble in nonpolar solvents such as CCl_4 and hexane. This information is summarized by another maxim, "like dissolves like."

Why do salts such as NaCl dissolve in water? Polar solvents, such as water, weaken the attractive forces between oppositely charged ions (such as Na^+ and Cl^-) and can therefore hold the ions apart. (In nonpolar solvents, ions of opposite charge attract each other so strongly that they coalesce to form a solid salt.) An ion immersed in a polar solvent such as water attracts the oppositely charged ends of the solvent dipoles (Fig. 2-6). The ion is thereby surrounded by one or more concentric shells of oriented solvent molecules. Such ions are said to be **solvated** or, when water is the solvent, to be **hydrated.**

The water molecules in the hydration shell around an ion move more slowly than water molecules that are not involved in solvating the ion. In bulk water, the energetic cost of breaking a hydrogen bond is low because another hydrogen bond is likely to be forming at the same time. The cost is higher for the relatively ordered water molecules of the hydration shell. The energetics of solvation also play a role in chemical reactions, since a reacting group must shed its **waters of hydration** (the molecules in its hydration shell) in order to closely approach another group.

The bond dipoles of uncharged polar molecules make them soluble in aqueous solutions for the same reasons that ionic substances are water soluble. The solubilities of polar and ionic substances are enhanced when they carry functional groups, such as hydroxyl (OH), carbonyl (C═O), carboxylate (COO^-), or ammonium (NH_3^+) groups, that can form hydrogen bonds with water as illustrated in Fig. 2-7. Indeed, water-soluble biomolecules such as proteins, nucleic acids, and carbohydrates bristle with just such groups. Nonpolar substances, in contrast, lack hydrogen-bonding donor and acceptor groups.

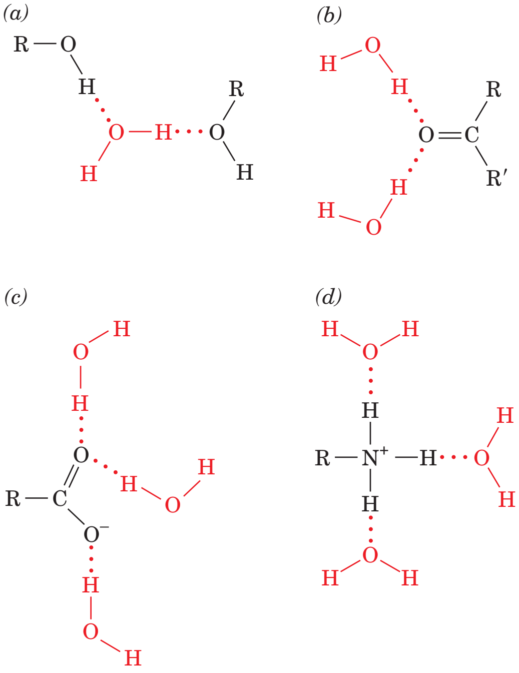

Figure 2-7 | Hydrogen bonding by functional groups. Water forms hydrogen bonds with (*a*) hydroxyl groups, (*b*) keto groups, (*c*) carboxylate ions, and (*d*) ammonium ions.

C | The Hydrophobic Effect Causes Nonpolar Substances to Aggregate in Water

When a nonpolar substance is added to an aqueous solution, it does not dissolve but instead is excluded by the water. *The tendency of water to minimize its contacts with hydrophobic molecules is termed the* ***hydrophobic effect.*** Many large molecules and molecular aggregates, such as proteins, nucleic acids, and cellular membranes, assume their shapes at least partially in response to the hydrophobic effect.

Consider the thermodynamics of transferring a nonpolar molecule from an aqueous solution to a nonpolar solvent. In all cases, the free energy change is negative, which indicates that such transfers are spontaneous processes (Table 2-2). Interestingly, these transfer processes are either endothermic (positive ΔH) or isothermic ($\Delta H = 0$); that is, it is enthalpically more or less equally favorable for nonpolar molecules to dissolve in water as in nonpolar media. In contrast, the entropy change (expressed as $-T\Delta S$) is large and negative in all cases. Clearly, the transfer of a hydrocarbon from an aqueous medium to a nonpolar medium is entropically driven (i.e., the free energy change is mostly due to an entropy change).

Entropy, or "randomness," is a measure of the order of a system (Section 1-3B). If entropy increases when a nonpolar molecule leaves an aqueous solution, entropy must decrease when the molecule enters water.

Table 2-2 Thermodynamic Changes for Transferring Hydrocarbons from Water to Nonpolar Solvents at 25°C

Process	ΔH ($kJ \cdot mol^{-1}$)	$-T\Delta S$ ($kJ \cdot mol^{-1}$)	ΔG ($kJ \cdot mol^{-1}$)
CH_4 in $H_2O \rightleftharpoons CH_4$ in C_6H_6	11.7	−22.6	−10.9
CH_4 in $H_2O \rightleftharpoons CH_4$ in CCl_4	10.5	−22.6	−12.1
C_2H_6 in $H_2O \rightleftharpoons C_2H_6$ in benzene	9.2	−25.1	−15.9
C_2H_4 in $H_2O \rightleftharpoons C_2H_4$ in benzene	6.7	−18.8	−12.1
C_2H_2 in $H_2O \rightleftharpoons C_2H_2$ in benzene	0.8	−8.8	−8.0
Benzene in $H_2O \rightleftharpoons$ liquid benzene[a]	0.0	−17.2	−17.2
Toluene in $H_2O \rightleftharpoons$ liquid toluene[a]	0.0	−20.0	−20.0

[a] Data measured at 18°C.

Source: Kauzmann, W., *Adv. Protein Chem.* **14,** 39 (1959).

This decrease in entropy when a nonpolar molecule is solvated by water is an experimental observation, not a theoretical conclusion. Yet the entropy changes are too large to reflect only the changes in the conformations of the hydrocarbons. Thus the entropy changes must arise mainly from some sort of ordering of the water itself. What is the nature of this ordering?

The extensive hydrogen-bonding network of liquid water molecules is disrupted when a nonpolar group intrudes. A nonpolar group can neither accept nor donate hydrogen bonds, so the water molecules at the surface of the cavity occupied by the nonpolar group cannot hydrogen bond to other molecules in their usual fashion. In order to maximize their hydrogen-bonding ability, these surface water molecules orient themselves to form a hydrogen-bonded network enclosing the cavity (Fig. 2-8). This orientation constitutes an ordering of the water structure since the number of ways that water molecules can form hydrogen bonds around the surface of a nonpolar group is fewer than the number of ways they can form hydrogen bonds in bulk water.

Unfortunately, the ever-fluctuating nature of liquid water's basic structure has not yet allowed a detailed description of this ordering process. One model proposes that water forms icelike hydrogen-bonded "cages" around the nonpolar groups. The water molecules of the cages are tetrahedrally hydrogen bonded to other water molecules, and the ordering of water molecules extends several layers beyond the first hydration shell of the nonpolar solute.

The unfavorable free energy of hydration of a nonpolar substance caused by its ordering of the surrounding water molecules has the net result that the nonpolar substance tends to be excluded from the aqueous phase. This is because the surface area of a cavity containing an aggregate of nonpolar molecules is less than the sum of the surface areas of the cavities that each of these molecules would individually occupy (Fig. 2-9). *The*

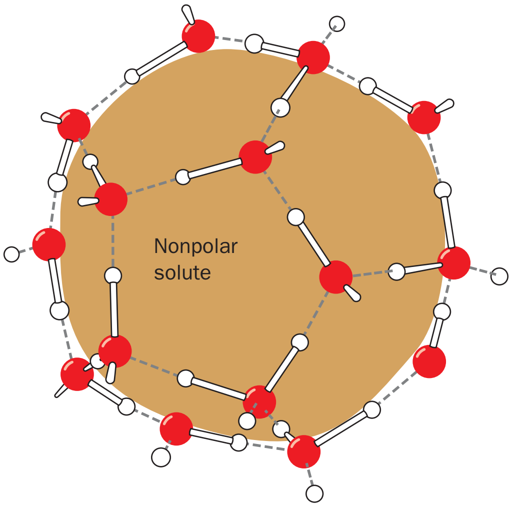

■ **Figure 2-8 | Orientation of water molecules around a nonpolar solute.** In order to maximize their number of hydrogen bonds, water molecules form a "cage" around the solute. Dashed lines represent hydrogen bonds.

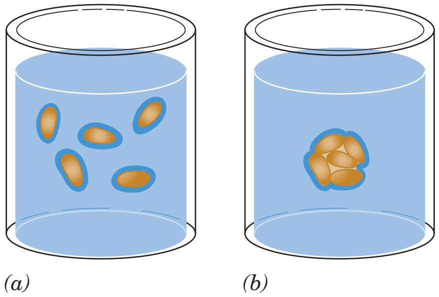

■ **Figure 2-9 | Aggregation of nonpolar molecules in water.** (*a*) The individual hydration of dispersed nonpolar molecules (*brown*) decreases the entropy of the system because their hydrating water molecules (*dark blue*) are not as free to form hydrogen bonds. (*b*) Aggregation of the nonpolar molecules increases the entropy of the system, since the number of water molecules required to hydrate the aggregated solutes is less than the number of water molecules required to hydrate the dispersed solute molecules. This increase in entropy accounts for the spontaneous aggregation of nonpolar substances in water.

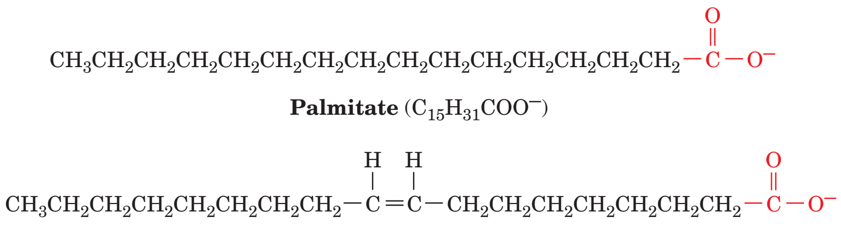

$$\mathrm{CH_3CH_2CH_2CH_2CH_2CH_2CH_2CH_2CH_2CH_2CH_2CH_2CH_2CH_2CH_2}-\overset{\overset{\displaystyle \mathrm{O}}{\|}}{\mathrm{C}}-\mathrm{O^-}$$

Palmitate ($C_{15}H_{31}COO^-$)

$$\mathrm{CH_3CH_2CH_2CH_2CH_2CH_2CH_2CH_2}-\overset{\overset{\displaystyle \mathrm{H}}{|}}{\mathrm{C}}=\overset{\overset{\displaystyle \mathrm{H}}{|}}{\mathrm{C}}-\mathrm{CH_2CH_2CH_2CH_2CH_2CH_2CH_2}-\overset{\overset{\displaystyle \mathrm{O}}{\|}}{\mathrm{C}}-\mathrm{O^-}$$

Oleate ($C_{17}H_{33}COO^-$)

■ **Figure 2-10 | Fatty acid anions (soaps).** Palmitate and oleate are amphiphilic compounds; each has a polar carboxylate group and a long nonpolar hydrocarbon chain.

aggregation of the nonpolar groups thereby minimizes the surface area of the cavity and therefore maximizes the entropy of the entire system. In a sense, the nonpolar groups are squeezed out of the aqueous phase.

Amphiphiles Form Micelles and Bilayers. *Most biological molecules have both polar (or charged) and nonpolar segments and are therefore simultaneously hydrophilic and hydrophobic.* Such molecules, for example, fatty acid ions (soaps; Fig. 2-10), are said to be **amphiphilic** or **amphipathic** (Greek: *amphi,* both; *pathos,* suffering). How do amphiphiles interact with an aqueous solvent? Water tends to hydrate the hydrophilic portion of an amphiphile, but it also tends to exclude the hydrophobic portion. Amphiphiles consequently tend to form structurally ordered aggregates. For example, **micelles** are globules of up to several thousand amphiphilic molecules arranged so that the hydrophilic groups at the globule surface can interact with the aqueous solvent while the hydrophobic groups associate at the center, away from the solvent (Fig. 2-11*a*). Of course, the model presented in Fig. 2-11*a* is an oversimplification, since it is geometrically impossible for all the hydrophobic groups to occupy the center of the micelle. Instead, the amphipathic molecules pack in a more disorganized fashion that buries most of the hydrophobic groups and leaves the polar groups exposed (Fig. 2-12).

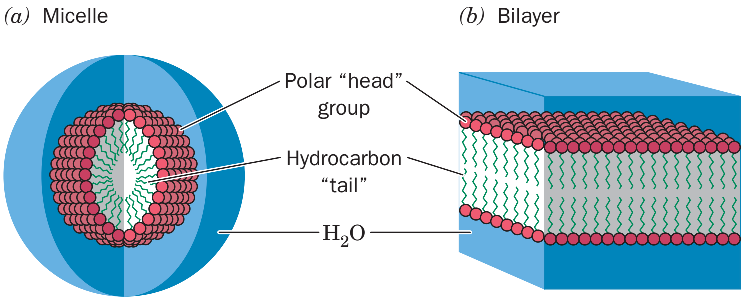

■ **Figure 2-11 | Structures of micelles and bilayers.** In aqueous solution, the polar head groups of amphipathic molecules are hydrated while the nonpolar tails aggregate by exclusion from water. (*a*) A micelle is a spheroidal aggregate. (*b*) A bilayer is an extended planar aggregate.

Alternatively, amphiphilic molecules may arrange themselves to form **bilayered** sheets or vesicles in which the polar groups face the aqueous phase (Fig. 2-11*b*). In both micelles and bilayers, the aggregate is stabilized by the hydrophobic effect, the tendency of water to exclude hydrophobic groups.

The consequences of the hydrophobic effect are often called hydrophobic forces or hydrophobic "bonds." However, the term *bond* implies a dis-

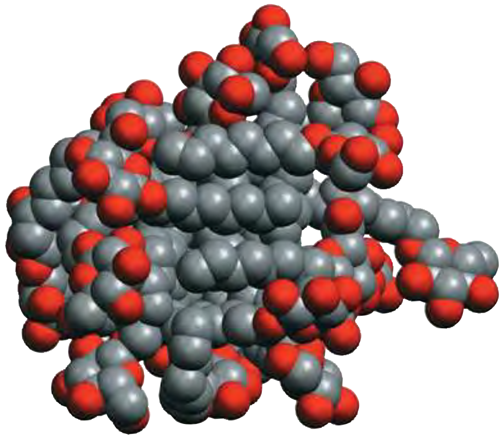

■ **Figure 2-12 | Model of a micelle.** Twenty molecules of octyl glucoside (an eight-carbon chain with a sugar head group) are shown in space-filling form in this computer-generated model. The polar O atoms of the glucoside groups are red and C atoms are gray. H atoms have been omitted for clarity. Computer simulations indicate that such micelles have an irregular, rapidly fluctuating structure (unlike the symmetric aggregate pictured in Fig. 2-11*a*) such that portions of the hydrophobic tails are exposed on the micelle surface at any given instant. [Courtesy of Michael Garavito and Shelagh Ferguson-Miller, Michigan State University.]

crete directional relationship between two entities. The hydrophobic effect acts indirectly on nonpolar groups and lacks directionality. Despite the temptation to attribute some mutual attraction to a collection of nonpolar groups excluded from water, their exclusion is largely a function of the entropy of the surrounding water molecules, not some "hydrophobic force" among them (the London dispersion forces between the nonpolar groups are relatively weak).

D | Water Moves by Osmosis and Solutes Move by Diffusion

The fluid inside cells and surrounding cells in multicellular organisms is full of dissolved substances ranging from small inorganic ions to huge molecular aggregates. The concentrations of these solutes affect water's **colligative properties,** the physical properties that depend on the concentration of dissolved substances rather than on their chemical features. For example, solutes depress the freezing point and elevate the boiling point of water by making it more difficult for water molecules to crystallize as ice or to escape from solution into the gas phase.

Osmotic pressure also depends on the solute concentration. When a solution is separated from pure water by a semipermeable membrane that permits the passage of water molecules but not solutes, water tends to move into the solution in order to equalize its concentration on both sides of the membrane. **Osmosis** is the movement of solvent from a region of high concentration (here, pure water) to a region of relatively low concentration (water containing dissolved solute). The **osmotic pressure** of a solution is the pressure that must be applied to the solution to prevent the inward flow of water; it is proportional to the concentration of the solute (Fig. 2-13). For a 1 M solution, the osmotic pressure is 22.4 atm. Consider the implications of osmotic pressure for living cells, which are essentially semipermeable sacs of aqueous solution. In order to minimize osmotic influx of water, which would burst the relatively weak cell membrane, many animal cells are surrounded by a solution of similar osmotic pressure (so there is no net flow of water). Another strategy, used by most plants and bacteria, is to enclose the cell with a rigid cell wall that can withstand the osmotic pressure generated within.

When an aqueous solution is separated from pure water by a membrane that is permeable to both water and solutes, solutes move out of the solution even as water moves in. The molecules move randomly, or **diffuse,** until the concentration of the solute is the same on both sides of the membrane. At this point, equilibrium is established; that is, there is no further *net* flow of water or solute (although molecules continue to move in and

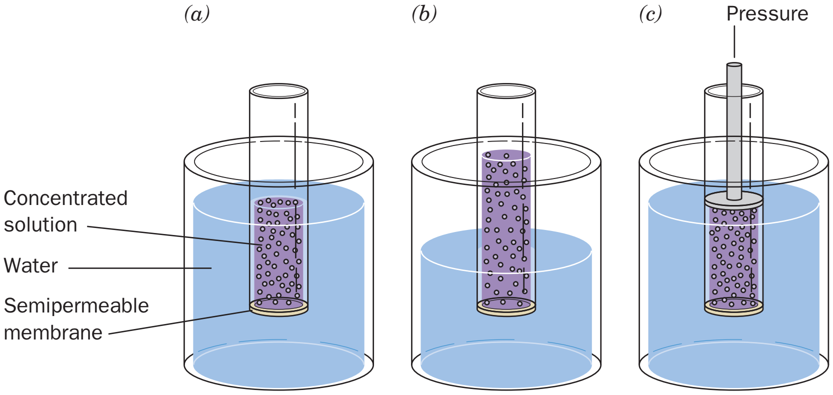

Figure 2-13 | Osmotic pressure. (*a*) A water-permeable membrane separates a tube of concentrated solution from pure water. (*b*) As water moves into the solution by osmosis, the height of the solution in the tube increases. (*c*) The pressure that prevents the influx of water is the osmotic pressure (22.4 atm for a 1 M solution).

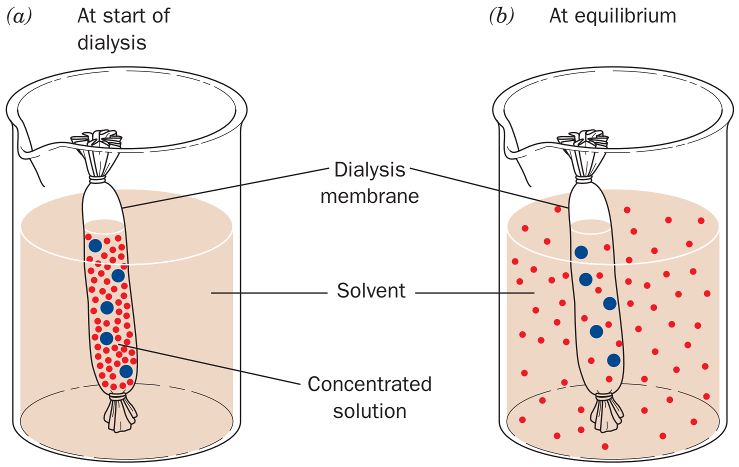

■ **Figure 2-14 | Dialysis.** (*a*) A concentrated solution is separated from a large volume of solvent by a dialysis membrane (shown here as a tube knotted at both ends). Only small molecules can diffuse through the pores in the membrane. (*b*) At equilibrium, the concentrations of small molecules are nearly the same on either side of the membrane, whereas the macromolecules remain inside the dialysis bag.

out through the membrane). Note that the tendency for solutes to diffuse from an area of high concentration to an area of low concentration (i.e., down a concentration gradient) is thermodynamically favored because it is accompanied by an increase in entropy.

Diffusion of solutes is the basis for the laboratory technique of **dialysis.** In this process, solutes smaller than the pore size of the dialysis membrane freely exchange between the sample and the bulk solution until equilibrium is reached (Fig. 2-14). Larger substances cannot cross the membrane and remain where they are. Dialysis is particularly useful for separating large molecules, such as proteins or nucleic acids, from smaller molecules. Because small solutes (and water) move freely between the sample and the surrounding medium, dialysis can be repeated several times to replace the sample medium with another solution.

■ **CHECK YOUR UNDERSTANDING**

Compare hydrogen bonding in ice and in liquid water.
Describe the nature and relative strength of covalent bonds, ionic interactions, and van der Waals interactions (hydrogen bonds, dipole–dipole interactions, and London dispersion forces).
Explain why polar substances dissolve in water while nonpolar substances do not.
What is the role of entropy in the hydrophobic effect?
Explain why amphiphiles form micelles in water.
How does osmosis differ from diffusion? Which process occurs during dialysis?

2 Chemical Properties of Water

LEARNING OBJECTIVES

- Understand that water ionizes to form hydronium ions and hydroxide ions.
- Understand that an acid can donate a proton and a base can accept a proton.
- Understand how acids and bases affect the pH of a solution.
- Understand the relationship between pH and p*K* for a solution of weak acid.
- Understand how a buffer works.

Water is not just a passive component of the cell or extracellular environment. By virtue of its physical properties, water defines the solubilities of other substances. Similarly, water's chemical properties determine the behavior of other molecules in solution.

A | Water Ionizes to Form H^+ and OH^-

Water is a neutral molecule with a very slight tendency to ionize. We express this ionization as

$$H_2O \rightleftharpoons H^+ + OH^-$$

There is actually no such thing as a free proton (H^+) in solution. Rather, the proton is associated with a water molecule as a **hydronium ion,** H_3O^+. The association of a proton with a cluster of water molecules also gives rise to structures with the formulas $H_5O_2^+$, $H_7O_3^+$, and so on. For simplicity, however, we often represent these ions by H^+. The other product of water's ionization is the **hydroxide ion,** OH^-.

The proton of a hydronium ion can jump rapidly to another water molecule and then to another (Fig. 2-15). For this reason, the mobilities of H^+ and OH^- ions in solution are much higher than for other ions, which must move through the bulk water carrying their waters of hydration. ***Proton***

***jumping** is also responsible for the observation that acid–base reactions are among the fastest reactions that take place in aqueous solution.*

The ionization (dissociation) of water is described by an equilibrium expression in which the concentration of the parent substance is in the denominator and the concentrations of the dissociated products are in the numerator:

$$K = \frac{[H^+][OH^-]}{[H_2O]} \tag{2-1}$$

K is the **dissociation constant** (here and throughout the text, quantities in square brackets symbolize the molar concentrations of the indicated substances, which in many cases are only negligibly different from their activities; Section 1-3D). Because the concentration of the undissociated H_2O ($[H_2O]$) is so much larger than the concentrations of its component ions, it can be considered constant and incorporated into K to yield an expression for the ionization of water,

$$K_w = [H^+][OH^-] \tag{2-2}$$

The value of $\boldsymbol{K_w}$**,** the ionization constant of water, is 10^{-14} at 25°C.

Pure water must contain equimolar amounts of H^+ and OH^-, so $[H^+] = [OH^-] = (K_w)^{1/2} = 10^{-7}$ M. Since $[H^+]$ and $[OH^-]$ are reciprocally related by Eq. 2-2, when $[H^+]$ is greater than 10^{-7} M, $[OH^-]$ must be correspondingly less and vice versa. Solutions with $[H^+] = 10^{-7}$ M are said to be **neutral,** those with $[H^+] > 10^{-7}$ M are said to be **acidic,** and those with $[H^+] < 10^{-7}$ M are said to be **basic.** Most physiological solutions have hydrogen ion concentrations near neutrality. For example, human blood is normally slightly basic with $[H^+] = 4.0 \times 10^{-8}$ M.

The values of $[H^+]$ for most solutions are inconveniently small and thus impractical to compare. A more practical quantity, which was devised in 1909 by Søren Sørenson, is known as the **pH:**

$$\text{pH} = -\log[H^+] = \log\frac{1}{[H^+]} \tag{2-3}$$

The higher the pH, the lower is the H^+ concentration; the lower the pH, the higher is the H^+ concentration (Fig. 2-16). The pH of pure water is

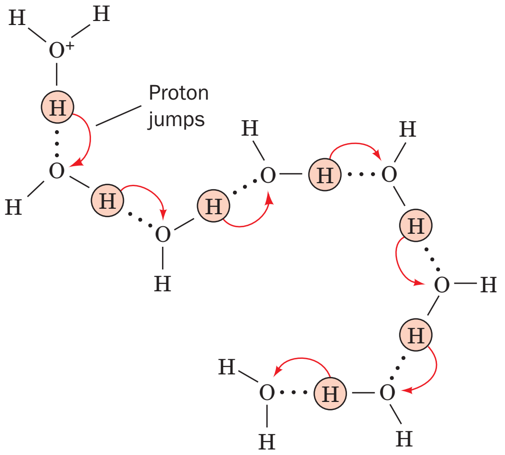

Figure 2-15 | Proton jumping. Proton jumps occur more rapidly than direct molecular migration, accounting for the observed high ionic mobilities of hydronium ions (and hydroxide ions) in aqueous solutions.

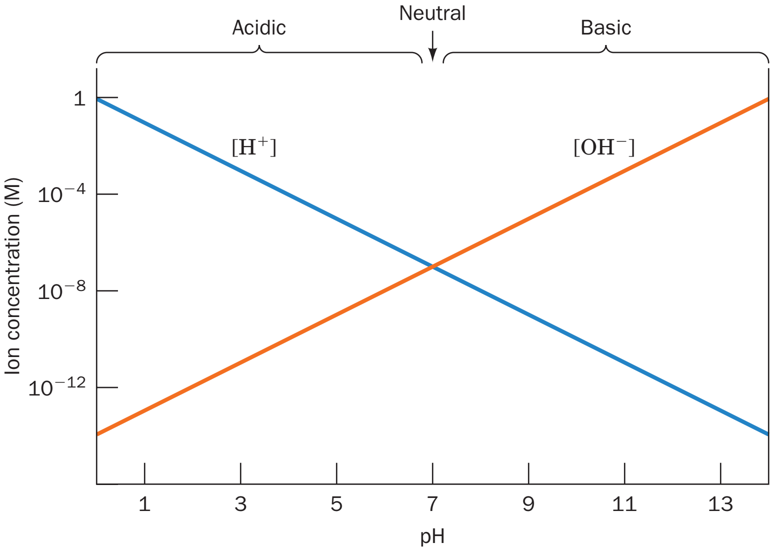

Figure 2-16 | Relationship of pH and the concentrations of H^+ and OH^- in water. Because the product of $[H^+]$ and $[OH^-]$ is a constant (10^{-14}), $[H^+]$ and $[OH^-]$ are reciprocally related. Solutions with relatively more H^+ are acidic (pH < 7), solutions with relatively more OH^- are basic (pH > 7), and solutions in which $[H^+] = [OH^-] = 10^{-7}$ M are neutral (pH = 7). Note the logarithmic scale for ion concentration.

SAMPLE CALCULATION 2-1

If 1.0×10^{-4} mole of H^+ (as HCl) is added to 1 liter of pure water, what is the final pH of the solution?

Pure water has a pH of 7, so its $[H^+] = 10^{-7}$ M. The added H^+ has a concentration of 10^{-4} M, which overwhelms the $[H^+]$ already present.

The total $[H^+]$ is therefore 1.0×10^{-4} M, so that the pH is equal to $-\log[H^+] = -\log(1.0 \times 10^{-4}) = 4$.

Table 2-3 pH Values of Some Common Substances

Substance	pH
1 M NaOH	14
Household ammonia	12
Seawater	8
Blood	7.4
Milk	7
Saliva	6.6
Tomato juice	4.4
Vinegar	3
Gastric juice	1.5
1 M HCl	0

7.0, whereas acidic solutions have pH < 7.0 and basic solutions have pH > 7.0 (see Sample Calculation 2-1). Note that solutions that differ by one pH unit differ in $[H^+]$ by a factor of 10. The pH values of some common substances are given in Table 2-3.

B | Acids and Bases Alter the pH

H^+ and OH^- ions derived from water are fundamental to the biochemical reactions we shall encounter later in this book. Biological molecules, such as proteins and nucleic acids, have numerous functional groups that act as acids or bases, for example, carboxyl and amino groups. These molecules influence the pH of the surrounding aqueous medium, and their structures and reactivities are in turn influenced by the ambient pH. An appreciation of acid–base chemistry is therefore essential for understanding the biological roles of many molecules.

An Acid Can Donate a Proton. According to a definition formulated in 1923 by Johannes Brønsted and Thomas Lowry, *an **acid** is a substance that can donate a proton, and a **base** is a substance that can accept a proton.* Under the Brønsted–Lowry definition, an acid–base reaction can be written as

$$HA + H_2O \rightleftharpoons H_3O^+ + A^-$$

An acid (HA) reacts with a base (H_2O) to form the **conjugate base** of the acid (A^-) and the **conjugate acid** of the base (H_3O^+). Accordingly, the acetate ion (CH_3COO^-) is the conjugate base of acetic acid (CH_3COOH), and the ammonium ion (NH_4^+) is the conjugate acid of ammonia (NH_3). The acid–base reaction is frequently abbreviated

$$HA \rightleftharpoons H^+ + A^-$$

with the participation of H_2O implied. An alternative expression for a basic substance B is

$$HB^+ \rightleftharpoons H^+ + B$$

The Strength of an Acid Is Specified by Its Dissociation Constant. The equilibrium constant for an acid–base reaction is expressed as a dissociation constant with the concentrations of the "reactants" in the denominator and the concentrations of the "products" in the numerator:

$$K = \frac{[H_3O^+][A^-]}{[HA][H_2O]} \qquad [2\text{-}4]$$

In dilute solutions, the water concentration is essentially constant, 55.5 M ($1000 \text{ g}\cdot\text{L}^{-1}/18.015 \text{ g}\cdot\text{mol}^{-1} = 55.5$ M). Therefore, the term $[H_2O]$ is customarily combined with the dissociation constant, which then takes the form

$$K_a = K[H_2O] = \frac{[H^+][A^-]}{[HA]} \qquad [2\text{-}5]$$

For brevity, however, we shall henceforth omit the subscript "*a*."

The dissociation constants of some common acids are listed in Table 2-4. Because acid dissociation constants, like $[H^+]$ values, are sometimes cumbersome to work with, they are transformed to **p*K*** values by the formula

$$pK = -\log K \qquad [2\text{-}6]$$

which is analogous to Eq. 2-3.

Table 2-4 Dissociation Constants and p*K* Values at 25°C of Some Acids

Acid	K	pK
Oxalic acid	5.37×10^{-2}	1.27 (pK_1)
H_3PO_4	7.08×10^{-3}	2.15 (pK_1)
Formic acid	1.78×10^{-4}	3.75
Succinic acid	6.17×10^{-5}	4.21 (pK_1)
Oxalate$^-$	5.37×10^{-5}	4.27 (pK_2)
Acetic acid	1.74×10^{-5}	4.76
Succinate$^-$	2.29×10^{-6}	5.64 (pK_2)
2-(*N*-Morpholino)ethanesulfonic acid (MES)	8.13×10^{-7}	6.09
H_2CO_3	4.47×10^{-7}	6.35 (pK_1)[a]
Piperazine-*N*,*N*′-bis(2-ethanesulfonic acid) (PIPES)	1.74×10^{-7}	6.76
$H_2PO_4^-$	1.51×10^{-7}	6.82 (pK_2)
3-(*N*-Morpholino)propanesulfonic acid (MOPS)	7.08×10^{-8}	7.15
N-2-Hydroxyethylpiperazine-*N*′-2-ethanesulfonic acid (HEPES)	3.39×10^{-8}	7.47
Tris(hydroxymethyl)aminomethane (Tris)	8.32×10^{-9}	8.08
NH_4^+	5.62×10^{-10}	9.25
Glycine (amino group)	1.66×10^{-10}	9.78
HCO_3^-	4.68×10^{-11}	10.33 (pK_2)
Piperidine	7.58×10^{-12}	11.12
HPO_4^{2-}	4.17×10^{-13}	12.38 (pK_3)

[a] The pK for the overall reaction $CO_2 + H_2O \rightleftharpoons H_2CO_3 \rightleftharpoons H^+ + HCO_3^-$; see Box 2-1.

Source: Dawson, R.M.C., Elliott, D.C., Elliott, W.H., and Jones, K.M., *Data for Biochemical Research* (3rd ed.), pp. 424–425, Oxford Science Publications (1986); *and* Good, N.E., Winget, G.D., Winter, W., Connolly, T.N., Izawa, S., and Singh, R.M.M., *Biochemistry* **5,** 467 (1966).

Acids can be classified according to their relative strengths, that is, their abilities to transfer a proton to water. The acids listed in Table 2-4 are known as **weak acids** because they are only partially ionized in aqueous solution ($K < 1$). Many of the so-called mineral acids, such as $HClO_4$, HNO_3, and HCl, are **strong acids** ($K \gg 1$). Since strong acids rapidly transfer all their protons to H_2O, *the strongest acid that can stably exist in aqueous solutions is* H_3O^+. Likewise, *there can be no stronger base in aqueous solutions than* OH^-. Virtually all the acid–base reactions that occur in biological systems involve H_3O^+ (and OH^-) and weak acids (and their conjugate bases).

The pH of a Solution Is Determined by the Relative Concentrations of Acids and Bases. The relationship between the pH of a solution and the concentrations of an acid and its conjugate base is easily derived. Equation 2-5 can be rearranged to

$$[H^+] = K\frac{[HA]}{[A^-]} \qquad [2\text{-}7]$$

Taking the negative log of each term (and letting pH = $-\log[H^+]$; Eq. 2-3) gives

$$\text{pH} = -\log K + \log\frac{[A^-]}{[HA]} \qquad [2\text{-}8]$$

SAMPLE CALCULATION 2-2

Calculate the pH of a 2 L solution containing 10 mL of 5 M acetic acid and 10 mL of 1 M sodium acetate.

First, calculate the concentrations of the acid and conjugate base, expressing all concentrations in units of moles per liter.

Acetic acid: (0.010 L)(5 M)/(2 L)
= 0.025 M

Sodium acetate: (0.010 L)(1 M)/(2 L)
= 0.005 M

Substitute the concentrations of the acid and conjugate base into the Henderson–Hasselbalch equation. Find the p*K* for acetic acid in Table 2-4.

$$\text{pH} = \text{p}K + \log([\text{acetate}]/[\text{acetic acid}])$$

$$\text{pH} = 4.76 + \log(0.005/0.025)$$

$$\text{pH} = 4.76 - 0.70$$

$$\text{pH} = 4.06$$

Substituting p*K* for $-\log K$ (Eq. 2-6) yields

$$\boxed{\text{pH} = \text{p}K + \log\frac{[\text{A}^-]}{[\text{HA}]}} \qquad [2\text{-}9]$$

This relationship is known as the **Henderson–Hasselbalch equation.** *When the molar concentrations of an acid (HA) and its conjugate base (A^-) are equal, $\log([A^-]/[HA]) = \log 1 = 0$, and the pH of the solution is numerically equivalent to the pK of the acid.* The Henderson–Hasselbalch equation is invaluable for calculating, for example, the pH of a solution containing a known quantity of a weak acid and its conjugate base (see Sample Calculation 2-2). However, since the Henderson–Hasselbalch equation does not account for the ionization of water itself, it is not useful for calculating the pH of solutions of strong acids or bases. For example, in a 1 M solution of a strong acid, $[\text{H}^+] = 1$ M and the pH is 0. In a 1 M solution of a strong base, $[\text{OH}^-] = 1$ M, so $[\text{H}^+] = K_w/[\text{OH}^-] = 1 \times 10^{-14}$ M and the pH is 14.

C | Buffers Resist Changes in pH

Adding a 0.01-mL droplet of 1 M HCl to 1 L of pure water changes the pH of the water from 7 to 5, which represents a 100-fold increase in $[\text{H}^+]$. Such a huge change in pH would be intolerable to most biological systems, since even small changes in pH can dramatically affect the structures and functions of biological molecules. Maintaining a relatively constant pH is therefore of paramount importance for living systems. To understand how this is possible, consider the titration of a weak acid with a strong base.

Figure 2-17 shows how the pH values of solutions of acetic acid, H_2PO_4^-, and ammonium ion (NH_4^+) vary as OH^- is added. **Titration curves** such as these can be constructed from experimental observation or by using the Henderson–Hasselbalch equation to calculate points along the curve (see Sample Calculation 2-3). When OH^- reacts with HA, the products are A^- and water:

$$\text{HA} + \text{OH}^- \rightleftharpoons \text{A}^- + \text{H}_2\text{O}$$

Several details about the titration curves in Fig. 2-17 should be noted:

1. The curves have similar shapes but are shifted vertically along the pH axis.
2. The pH at the midpoint of each titration is numerically equivalent to the p*K* of its corresponding acid; at this point, $[\text{HA}] = [\text{A}^-]$.

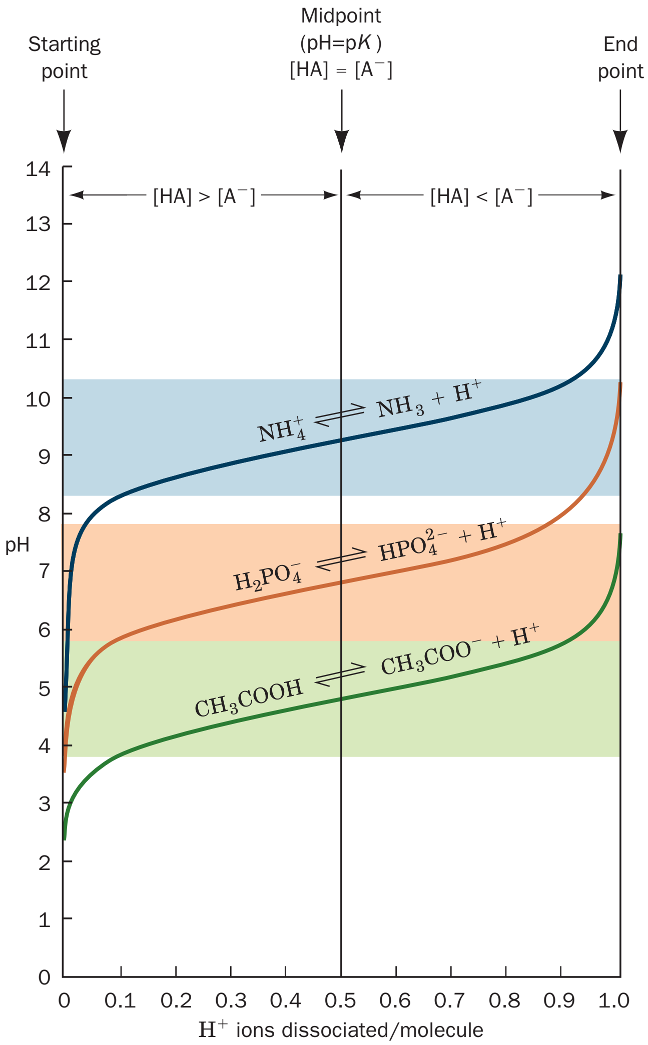

■ **Figure 2-17 | Titration curves for acetic acid, phosphate, and ammonia.** At the starting point, the acid form predominates. As strong base (e.g., NaOH) is added, the acid is converted to its conjugate base. At the midpoint of the titration, where pH = p*K*, the concentrations of the acid and the conjugate base are equal. At the end point (equivalence point), the conjugate base predominates, and the total amount of OH^- that has been added is equivalent to the amount of acid that was present at the starting point. The shaded bands indicate the pH ranges over which the corresponding solution can function as a buffer. **See the Animated Figures.**

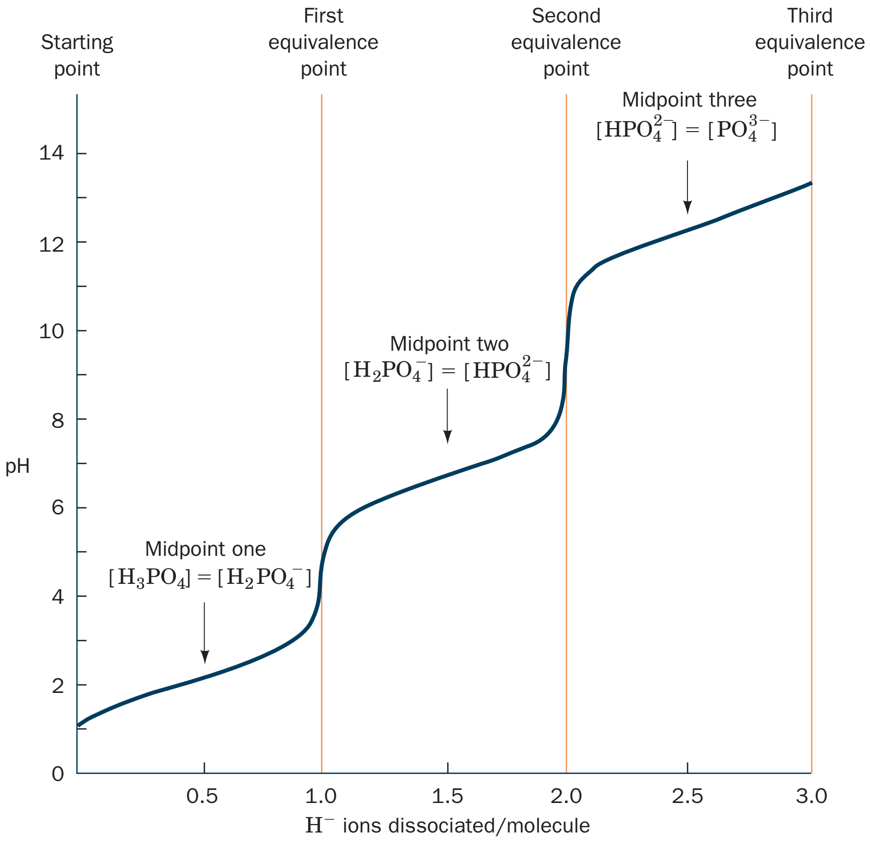

Figure 2-18 | Titration of a polyprotic acid. The first and second equivalence points for titration of H_3PO_4 occur at the steepest parts of the curve. The pH at the midpoint of each stage provides the pK value of the corresponding ionization. **See the Animated Figures.**

3. The slope of each titration curve is much lower near its midpoint than near its wings. This indicates that *when [HA] ≈ [A⁻], the pH of the solution is relatively insensitive to the addition of strong base or strong acid.* Such a solution, which is known as an acid–base **buffer,** resists pH changes because small amounts of added H^+ or OH^- react with A^- or HA, respectively, without greatly changing the value of $\log([A^-]/[HA])$.

Substances that can lose more than one proton, or undergo more than one ionization, such as H_3PO_4 or H_2CO_3, are known as **polyprotic acids.** The titration curves of such molecules, as illustrated in Fig. 2-18 for H_3PO_4, are more complicated than the titration curves of monoprotic acids such as acetic acid. A polyprotic acid has multiple pK values, one for each ionization step. H_3PO_4, for example, has three dissociation constants because the ionic charge resulting from one proton dissociation electrostatically inhibits further proton dissociation, thereby increasing the values of the corresponding pK values. Similarly, a molecule with more than one ionizable group has a discrete pK value for each group. In a biomolecule that contains numerous ionizable groups with different pK values, the many dissociation events may yield a titration curve without any clear "plateaus."

Biological fluids, both intracellular and extracellular, are heavily buffered. For example, the pH of the blood in healthy individuals is closely

SAMPLE CALCULATION 2-3

Calculate the pH of a 1 L solution containing 0.1 M formic acid and 0.1 M sodium formate before and after the addition of 1 mL of 5 M NaOH. How much would the pH change if the NaOH were added to 1 L of pure water?

According to Table 2-4, the pK for formic acid is 3.75. Since [formate] = [formic acid], the $\log([A^-]/[HA])$ term of the Henderson–Hasselbalch equation is 0 and pH = pK = 3.75. The addition of 1 mL of NaOH does not significantly change the volume of the solution, so the [NaOH] is (0.001 L)(5 M)/(1 L) = 0.005 M.

Since NaOH is a strong base, it completely dissociates, and $[OH^-] = [NaOH] = 0.005$ M. This OH^- reacts with formic acid to produce formate and H_2O. Consequently, the concentration of formic acid decreases and the concentration of formate increases by 0.005 M.

The new formic acid concentration is 0.1 M − 0.005 M = 0.095 M, and the new formate concentration is 0.1 M + 0.005 M = 0.105 M. Substituting these values into the Henderson–Hasselbalch equation gives

$$\text{pH} = \text{p}K + \log([\text{formate}]/[\text{formic acid}])$$

$$\text{pH} = 3.75 + \log(0.105/0.095)$$

$$\text{pH} = 3.75 + 0.04$$

$$\text{pH} = 3.79$$

In the absence of the formic acid buffering system, the $[H^+]$ and therefore the pH can be calculated directly from K_w. Since $K_w = [H^+][OH^-] = 10^{-14}$,

$$[H^+] = \frac{10^{-14}}{[OH^-]} = \frac{10^{-14}}{(0.005)} = 2 \times 10^{-12}\ \text{M}$$

$$\text{pH} = -\log[H^+] = -\log(2 \times 10^{-12}) = 11.7$$

BOX 2-1 **BIOCHEMISTRY IN HEALTH AND DISEASE**

The Blood Buffering System

Bicarbonate is the most significant buffer compound in human blood; other buffering agents, including proteins and organic acids, are present at much lower concentrations. The buffering capacity of blood depends primarily on two equilibria: (1) between gaseous CO_2 dissolved in the blood and carbonic acid formed by the reaction

$$CO_2 + H_2O \rightleftharpoons H_2CO_3$$

and (2) between carbonic acid and bicarbonate formed by the dissociation of H^+:

$$H_2CO_3 \rightleftharpoons H^+ + HCO_3^-$$

The overall p*K* for these two sequential reactions is 6.35. (The further dissociation of HCO_3^- to CO_3^{2-}, $pK = 10.33$, is not significant at physiological pH.)

When the pH of the blood falls due to metabolic production of H^+, the bicarbonate–carbonic acid equilibrium shifts toward more carbonic acid. At the same time, carbonic acid loses water to become CO_2, which is then expired in the lungs as gaseous CO_2. Conversely, when the blood pH rises, relatively more HCO_3^- forms. Breathing is adjusted so that increased amounts of CO_2 in the lungs can be reintroduced into the blood for conversion to carbonic acid. In this manner, a near-constant hydrogen ion concentration can be maintained. The kidneys also play a role in acid–base balance by excreting HCO_3^- and NH_4^+.

Disturbances in the blood buffer system can lead to conditions known as **acidosis,** with a pH as low as 7.1, or **alkalosis,** with a pH as high as 7.6. (Deviations of less than 0.05 pH unit from the "normal" value of 7.4 are not significant.) For example, obstructive lung diseases that prevent efficient expiration of CO_2 can cause respiratory acidosis. Hyperventilatin accelerates the loss of CO_2 and causes respiratory alkalosis. Overproduction of organic acids from dietary precursors or sudden surges in lactic acid levels during exercise can lead to metabolic acidosis.

Acid–base imbalances are best alleviated by correcting the underlying physiological problem. In the short term, acidosis is commonly treated by administering $NaHCO_3$ intravenously. Alkalosis is more difficult to treat. Metabolic alkalosis sometimes responds to KCl or NaCl (the additional Cl^- helps minimize the secretion of H^+ by the kidneys), and respiratory alkalosis can be ameliorated by breathing an atmosphere enriched in CO_2.

controlled at pH 7.4 (see Box 2-1). The phosphate and bicarbonate ions in most biological fluids are important buffering agents because they have p*K*s in this range (Table 2-4). Moreover, many biological molecules, such as proteins and some lipids, as well as numerous small organic molecules, bear multiple acid–base groups that are effective buffer components in the physiological pH range.

The concept that the properties of biological molecules vary with the acidity of the solution in which they are dissolved was not fully appreciated before the twentieth century. Many early biochemical experiments were undertaken without controlling the acidity of the sample, so the results were often poorly reproducible. Nowadays, biochemical preparations are routinely buffered to simulate the properties of naturally occurring biological fluids. A number of synthetic compounds have been developed for use as buffers; some of these are included in Table 2-4. The **buffering capacity** of these weak acids (their ability to resist pH changes on addition of acid or base) is maximal when $pH = pK$. It is helpful to remember that a weak acid is in its useful buffer range within one pH unit of its p*K* (e.g., the shaded regions of Fig. 2-17). Above this range, where the ratio $[A^-]/[HA] > 10$, the pH of the solution changes rapidly with added strong base. A buffer is similarly impotent with the addition of strong acid when its p*K* exceeds the pH by more than one unit.

In the laboratory, the desired pH of the buffered solution determines which buffering compound is selected. Typically, the acid form of the compound and one of its soluble salts are dissolved in the (nearly equal) molar ratio necessary to provide the desired pH and, with the aid of a pH meter, the resulting solution is fine-tuned by titration with strong acid or base.

■ CHECK YOUR UNDERSTANDING

What are the products of water's ionization? How are these related by K_w?

Describe how to calculate pH from the concentration of H^+ or OH^-.

Define *acid* and *base.* What is the relationship between the strength of an acid and its p*K* value?

List some uses for the Henderson–Hasselbalch equation.

Be able to sketch a titration curve, and label its parts, for a monoprotic and a polyprotic acid.

What are the properties of useful buffer?

SUMMARY

1. Water is essential for all living organisms.
2. Water molecules can form hydrogen bonds with other molecules because they have two H atoms that can be donated and two unshared electron pairs that can act as acceptors.
3. Liquid water is an irregular network of water molecules that each form up to four hydrogen bonds with neighboring water molecules.
4. Hydrophilic substances such as ions and polar molecules dissolve readily in water.
5. The hydrophobic effect is the tendency of water to minimize its contacts with nonpolar substances.
6. Water molecules move from regions of high concentration to regions of low concentration by osmosis; solutes move from regions of high concentration to regions of low concentration by diffusion.
7. Water ionizes to H^+ (which represents the hydronium ion, H_3O^+) and OH^-.
8. The concentration of H^+ in solutions is expressed as a pH value; in acidic solutions $pH < 7$, in basic solutions $pH > 7$, and in neutral solutions $pH = 7$.
9. Acids can donate protons and bases can accept protons. The strength of an acid is expressed as its p*K*.
10. The Henderson–Hasselbalch equation relates the pH of a solution to the p*K* and concentrations of an acid and its conjugate base.
11. Buffered solutions resist changes in pH within about one pH unit of the p*K* of the buffering species.

KEY TERMS

polar	**23**
hydrogen bond	**23**
van der Waals distance	**23**
van der Waals forces	**25**
London dispersion forces	**25**
hydrophilic	**26**
hydrophobic	**26**
solvation	**26**
hydration	**26**
waters of hydration	**26**
hydrophobic effect	**26**
amphiphilic	**28**
amphipathic	**28**
micelle	**28**
bilayer	**28**
colligative properties	**29**
osmosis	**29**
osmotic pressure	**29**
diffusion	**29**
dialysis	**30**
hydronium ion	**30**
hydroxide ion	**30**
proton jumping	**30**
dissociation constant	**31**
K_w	**31**
neutral solution	**31**
acidic solution	**31**
basic solution	**31**
pH	**31**
acid	**32**
base	**32**
conjugate base	**32**
conjugate acid	**32**
p*K*	**32**
weak acid	**33**
strong acid	**33**
Henderson–Hasselbalch equation	**34**
titration curve	**34**
buffer	**35**
polyprotic acid	**35**
acidosis	**36**
alkalosis	**36**
buffering capacity	**36**

PROBLEMS

1. Identify the potential hydrogen bond donors and acceptors in the following molecules:

(a)

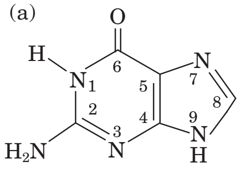

(b)

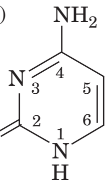

(c)

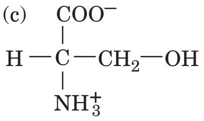

$\mathrm{H{-}C(COO^-)(NH_3^+){-}CH_2{-}OH}$

2. Occasionally, a C—H group can form a hydrogen bond. Why would such a group be more likely to be a hydrogen bond donor group when the C is next to N?

3. Rank the water solubility of the following compounds:

(a) $H_3C{-}CH_2{-}O{-}CH_3$

(b)

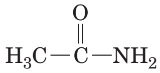

$H_3C{-}C({=}O){-}NH_2$

(c)

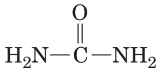

$H_2N{-}C({=}O){-}NH_2$

(d) $H_3C{-}CH_2{-}CH_3$

(e)

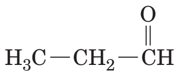

$H_3C{-}CH_2{-}CH({=}O)$

4. Where would the following substances partition in water containing palmitic acid micelles? (a) $^+H_3N{-}CH_2{-}COO^-$, (b) $^+H_3N{-}(CH_2)_{11}{-}COO^-$, (c) $H_3C{-}(CH_2)_{11}{-}COO^-$

5. Explain why water forms nearly spherical droplets on the surface of a freshly waxed car. Why doesn't water bead on a clean windshield?

6. Describe what happens when a dialysis bag containing pure water is suspended in a beaker of seawater. What would happen if the dialysis membrane were permeable to water but not solutes?

7. Draw the structures of the conjugate bases of the following acids:

(a)

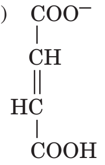

$\mathrm{COO^-{-}CH{=}HC{-}COOH}$

(b)

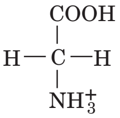

$\mathrm{H{-}C(COOH)(NH_3^+){-}H}$

(c)

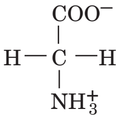

$\mathrm{H{-}C(COO^-)(NH_3^+){-}H}$

(d)

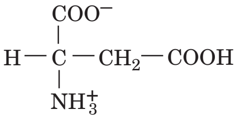

$\mathrm{H{-}C(COO^-)(NH_3^+){-}CH_2{-}COOH}$

8. Indicate the ionic species that predominates at pH 4, 8, and 11 for (a) ammonia and (b) phosphoric acid.
9. Calculate the pH of a 200 mL solution of pure water to which has been added 50 mL of 1 mM HCl.
10. Calculate the pH of a 1 L solution containing (a) 10 mL of 5 M NaOH, (b) 10 mL of 100 mM glycine and 20 mL of 5 M HCl, and (c) 10 mL of 2 M acetic acid and 5 g of sodium acetate (formula weight 82 $\mathrm{g \cdot mol^{-1}}$).
11. Calculate the standard free energy change for the dissociation of HEPES.
12. A solution is made by mixing 50 mL of 2.0 M K_2HPO_4 and 25 mL of 2.0 M KH_2PO_4. The solution is diluted to a final volume of 200 mL. What is the pH of the final solution?
13. What is the pK of the weak acid HA if a solution containing 0.1 M HA and 0.2 M A^- has a pH of 6.5?
14. How many grams of sodium succinate (formula weight 140 $\mathrm{g \cdot mol^{-1}}$) and disodium succinate (formula weight 162 $\mathrm{g \cdot mol^{-1}}$) must be added to 1 L of water to produce a solution with pH 6.0 and a total solute concentration of 50 mM?
15. Estimate the volume of a solution of 5 M NaOH that must be added to adjust the pH from 4 to 9 in 100 mL of a 100 mM solution of phosphoric acid.
16. (a) Would phosphoric acid or succinic acid be a better buffer at pH 5? (b) Would ammonia or piperidine be a better buffer at pH 9? (c) Would HEPES or Tris be a better buffer at pH 7.5?
17. You need a buffer at pH 7.5 for use in purifying a protein at 4°C. You have chosen Tris, pK 8.08, $\Delta H° = 50\ \mathrm{kJ \cdot mol^{-1}}$. You carefully make up 0.01 M Tris buffer, pH 7.5 at 25°C, and store it in the cold box to equilibrate it to the temperature of the purification. When you measure the pH of the temperature-equilibrated buffer it has increased to 8.1. What is the explanation for this increase? How can you avoid this problem?
18. Glycine hydrochloride ($\mathrm{Cl^-H_3N^+CH_2COOH}$) is a diprotic acid that contains a carboxylic acid group and an ammonium group and is therefore called an amino acid. It is often used in biochemical buffers.
    (a) Which proton would you expect to dissociate at a lower pH, the proton of the carboxylic acid group or the ammonium group?
    (b) Write the chemical equations describing the dissociation of the first and second protons of $\mathrm{Cl^-H_3N^+CH_2COOH}$.
    (c) A solution containing 0.01 M $\mathrm{Cl^-H_3N^+CH_2COOH}$ and 0.02 M of the monodissociated species has pH = 2.65. What is the pK of this dissociation?
    (d) In analogy with Figure 2-18, sketch the titration curve of this diprotic acid.

CASE STUDY

Case 1 (available at www.wiley.com/college/voet)

Acute Aspirin Overdose: Relationship to the Blood Buffering System

Focus concept: The carbonic acid–bicarbonate buffering system responds to an overdose of aspirin.

Prerequisite: Chapter 2

- Principles of acids and bases, including pK and the Henderson–Hasselbalch equation
- The carbonic acid–bicarbonate blood buffering system

REFERENCES

Finney, J.L., Water? What's so special about it? *Phil. Trans. R. Soc. Lond. B Biol. Sci.* **29,** 1145–1163 (2004). [Includes discussions of the structure of water molecules, hydrogen bonding, structures of ice and liquid water, and how these relate to biological function.]

Gerstein, M. and Levitt, M., Simulating water and the molecules of life, *Sci Am.* **279**(11), 101–105 (1998). [Describes the structure of water and how water interacts with other molecules.]

Good, N.E., Winget, G.D., Winter, W., Connolly, T.N., Izawa, S., and Singh, R.M.M., Hydrogen ion buffers for biological research, *Biochemistry* **5,** 467–477 (1966). [A classic paper on laboratory buffers.]

Halperin, M.L. and Goldstein, M.B., *Fluid, Electrolyte, and Acid–Base Physiology: A Problem-Based Approach* (3rd ed.), W.B. Saunders (1999). [Includes extensive problem sets with explanations of basic science as well as clinical effects of acid–base disorders.]

Jeffrey, G.A. and Saenger, W., *Hydrogen Bonding in Biological Structures,* Chapters 1, 2, and 21, Springer (1994). [Reviews hydrogen bond chemistry and its importance in small molecules and macromolecules.]

Segel, I.H., *Biochemical Calculations* (2nd ed.), Chapter 1, Wiley (1976). [An intermediate level discussion of acid–base equilibria with worked-out problems.]

Tanford, C., *The Hydrophobic Effect: Formation of Micelles and Biological Membranes* (2nd ed.), Chapters 5 and 6, Wiley–Interscience (1980). [Discusses the structures of water and micelles.]

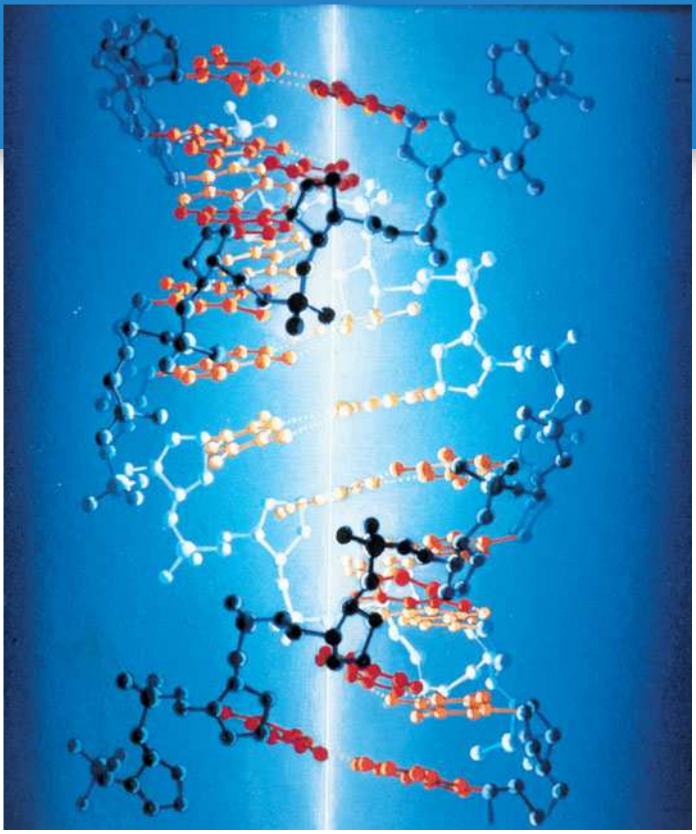

3

Nucleotides, Nucleic Acids, and Genetic Information

A DNA molecule consists of two strands that wind around a central axis, shown here as a glowing wire. [Illustration, Irving Geis. Image from the Irving Geis Collection/Howard Hughes Medical Institute. Rights owned by HHMI. Reproduction by permission only.]

■ CHAPTER CONTENTS

1 Nucleotides

2 Introduction to Nucleic Acid Structure
- **A.** Nucleic Acids Are Polymers of Nucleotides
- **B.** DNA Forms a Double Helix
- **C.** RNA Is a Single-Stranded Nucleic Acid

3 Overview of Nucleic Acid Function
- **A.** DNA Carries Genetic Information
- **B.** Genes Direct Protein Synthesis

4 Nucleic Acid Sequencing
- **A.** Restriction Endonucleases Cleave DNA at Specific Sequences
- **B.** Electrophoresis Separates Nucleic Acids According to Size
- **C.** DNA Is Sequenced by the Chain-Terminator Method
- **D.** Entire Genomes Have Been Sequenced
- **E.** Evolution Results from Sequence Mutations

5 Manipulating DNA
- **A.** Cloned DNA Is an Amplified Copy
- **B.** DNA Libraries Are Collections of Cloned DNA
- **C.** DNA Is Amplified by the Polymerase Chain Reaction
- **D.** Recombinant DNA Technology Has Numerous Practical Applications

■ MEDIA RESOURCES

(Available at www.wiley.com/college/voet)

Guided Exploration 1. Overview of transcription and translation
Guided Exploration 2. DNA sequence determination by the chain-terminator method
Guided Exploration 3. PCR and site-directed mutagenesis
Interactive Exercise 1. Three-dimensional structure of DNA
Animated Figure 3-26. Construction of a recombinant DNA molecule
Animated Figure 3-27. Cloning with bacteriophage λ
Animated Figure 3-30. Site-directed mutagenesis
Kinemage Exercise 2-1. Structure of DNA
Kinemage Exercise 2-2. Watson–Crick base pairs
Bioinformatics Exercises Chapter 3. Databases for the Storage and "Mining" of Genome Sequences

Despite obvious differences in lifestyle and macroscopic appearance, organisms exhibit striking similarity at the molecular level. The structures and metabolic activities of all cells rely on a common set of molecules that includes amino acids, carbohydrates, lipids, and nucleotides, as well as their polymeric forms. Each type of compound can be described in terms of its chemical makeup, its interactions with other molecules, and its physiological function. We begin our survey of biomolecules with a discussion of the **nucleotides** and their polymers, the **nucleic acids.**

Nucleotides are involved in nearly every facet of cellular life. Specifically, they participate in oxidation–reduction reactions, energy transfer, intracellular signaling, and biosynthetic reactions. Their polymers, the nucleic acids DNA and RNA, are the primary players in the storage and decoding of genetic information. Nucleotides and nucleic acids also perform structural and catalytic roles in cells. No other class of molecules participates in such varied functions or in so many functions that are essential for life.

Evolutionists postulate that the appearance of nucleotides permitted the evolution of organisms that could harvest and store energy from their surroundings and, most importantly, could make copies of themselves. Although the chemical and biological details of early life-forms are the subject of speculation, it is incontrovertible that life as we know it is inextricably linked to the chemistry of nucleotides and nucleic acids.

In this chapter, we briefly examine the structures of nucleotides and the nucleic acids DNA and RNA. We also consider how the chemistry of these molecules allows them to carry biological information in the form of a sequence of nucleotides. This information is expressed by the transcription of a segment of DNA to yield RNA, which is then translated to form protein. Because a cell's structure and function ultimately depend on its genetic makeup, we discuss how genomic sequences provide information about evolution, metabolism, and disease. Finally, we consider some of the techniques used in manipulating DNA in the laboratory. In later chapters, we will examine in greater detail the participation of nucleotides and nucleic acids in metabolic processes. Chapter 24 includes additional information about nucleic acid structures, DNA's interactions with proteins, and DNA packaging in cells, as a prelude to several chapters discussing the roles of nucleic acids in the storage and expression of genetic information.

1 Nucleotides

LEARNING OBJECTIVE

- Become familiar with the structures and nomenclature of the eight common nucleotides.

Nucleotides are ubiquitous molecules with considerable structural diversity. *There are eight common varieties of nucleotides, each composed of a nitrogenous base linked to a sugar to which at least one phosphate group is also attached.* The bases of nucleotides are planar, aromatic, heterocyclic molecules that are structural derivatives of either **purine** or **pyrimidine** (although they are not synthesized *in vivo* from either of these organic compounds).

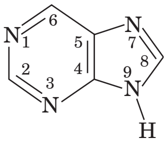
Purine

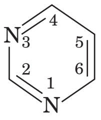
Pyrimidine

The most common purines are **adenine (A)** and **guanine (G),** and the major pyrimidines are **cytosine (C), uracil (U),** and **thymine (T).** The purines form bonds to a five-carbon sugar (a pentose) via their N9 atoms, whereas pyrimidines do so through their N1 atoms (Table 3-1).

In **ribonucleotides,** the pentose is **ribose,** while in **deoxyribonucleotides** (or just **deoxynucleotides**), the sugar is **2′-deoxyribose** (i.e., the carbon at position 2′ lacks a hydroxyl group).

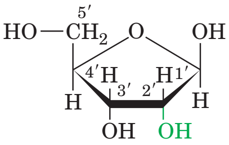
Ribose

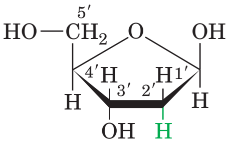
Deoxyribose

Table 3-1 Names and Abbreviations of Nucleic Acid Bases, Nucleosides, and Nucleotides

Base Formula	Base (X = H)	Nucleoside (X = ribose[a])	Nucleotide[b] (X = ribose phosphate[a])
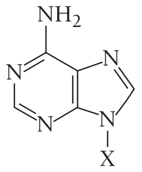	Adenine Ade A	Adenosine Ado A	Adenylic acid Adenosine monophosphate AMP
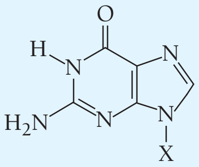	Guanine Gua G	Guanosine Guo G	Guanylic acid Guanosine monophosphate GMP
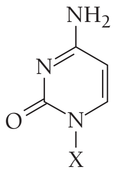	Cytosine Cyt C	Cytidine Cyd C	Cytidylic acid Cytidine monophosphate CMP
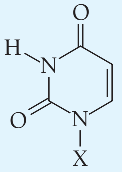	Uracil Ura U	Uridine Urd U	Uridylic acid Uridine monophosphate UMP
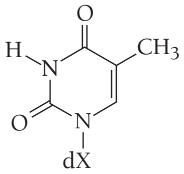	Thymine Thy T	Deoxythymidine dThd dT	Deoxythymidylic acid Deoxythymidine monophosphate dTMP

[a] The presence of a 2′-deoxyribose unit in place of ribose, as occurs in DNA, is implied by the prefixes “deoxy” or “d.” For example, the deoxynucleoside of adenine is deoxyadenosine or dA. However, for thymine-containing residues, which rarely occur in RNA, the prefix is redundant and may be dropped. The presence of a ribose unit may be explicitly implied by the prefix “ribo.”

[b] The position of the phosphate group in a nucleotide may be explicitly specified as in, for example, 3′-AMP and 5′-GMP.

Note that the “primed” numbers refer to the atoms of the pentose; “unprimed” numbers refer to the atoms of the nitrogenous base.

In a ribonucleotide or a deoxyribonucleotide, one or more phosphate groups are bonded to atom C3′ or atom C5′ of the pentose to form a 3′-nucleotide or a 5′-nucleotide, respectively (Fig. 3-1). When the phosphate group is absent, the compound is known as a **nucleoside.** A 5′-nucleotide can therefore be called a nucleoside-5′-phosphate. Nucleotides most commonly contain one to three phosphate groups at the C5′ position and are called nucleoside monophosphates, diphosphates, and triphosphates.

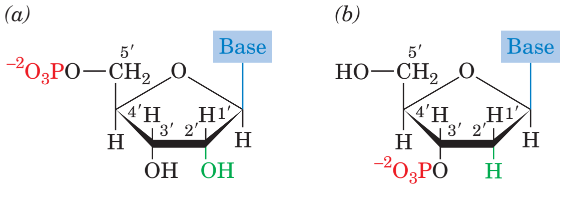

5′-Ribonucleotide **3′-Deoxynucleotide**

Figure 3-1 | Chemical structures of nucleotides. (*a*) A 5′-ribonucleotide and (*b*) a 3′-deoxynucleotide. The purine or pyrimidine base is linked to C1′ of the pentose and at least one phosphate (*red*) is also attached. A nucleoside consists only of a base and a pentose.

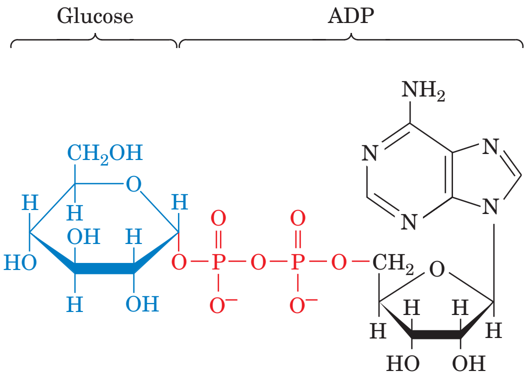

Figure 3-2 | ADP–glucose. In this nucleotide derivative, glucose (*blue*) is attached to adenosine (*black*) by a diphosphate group (*red*).

The structures, names, and abbreviations of the common bases, nucleosides, and nucleotides are given in Table 3-1. Ribonucleotides are components of **RNA (ribonucleic acid),** whereas deoxynucleotides are components of **DNA (deoxyribonucleic acid).** Adenine, guanine, and cytosine occur in both ribonucleotides and deoxynucleotides (accounting for six of the eight common nucleotides), but uracil primarily occurs in ribonucleotides and thymine occurs in deoxynucleotides. Free nucleotides, which are anionic, are almost always associated with the counterion Mg^{2+} in cells.

Nucleotides Participate in Metabolic Reactions. The bulk of the nucleotides in any cell are found in polymeric forms, as either DNA or RNA, whose primary functions are information storage and transfer. However, free nucleotides and nucleotide derivatives perform an enormous variety of metabolic functions not related to the management of genetic information.

Perhaps the best known nucleotide is **adenosine triphosphate (ATP),** a nucleotide containing adenine, ribose, and a triphosphate group. ATP is often mistakenly referred to as an energy-storage molecule, but it is more accurately termed an energy carrier or energy transfer agent. The process of photosynthesis or the breakdown of metabolic fuels such as carbohydrates and fatty acids leads to the formation of ATP from **adenosine diphosphate (ADP):**

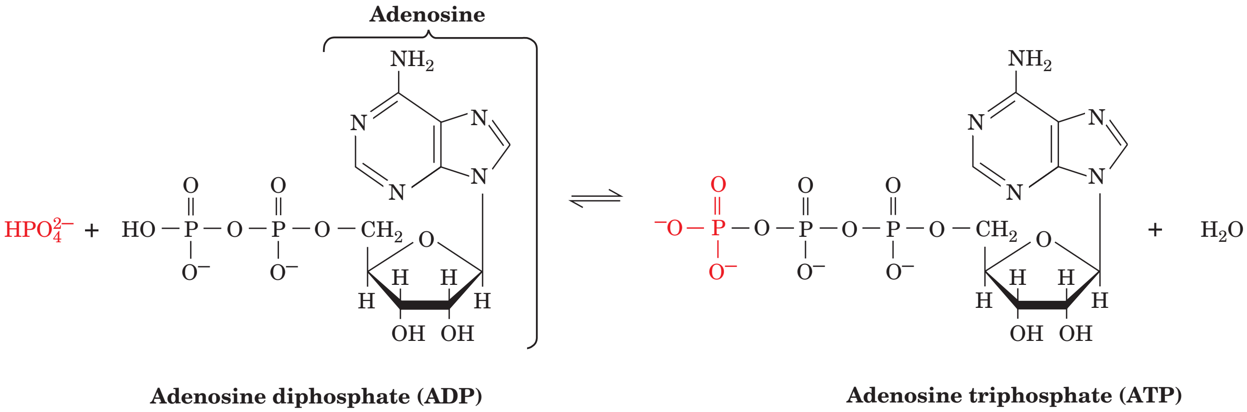

ATP diffuses throughout the cell to provide energy for other cellular work, such as biosynthetic reactions, ion transport, and cell movement. The chemical potential energy of ATP is made available when it transfers one (or two) of its phosphate groups to another molecule. This process can be represented by the reverse of the preceding reaction, namely, the hydrolysis of ATP to ADP. (As we shall see in later chapters, the interconversion of ATP and ADP in the cell is not freely reversible, and free phosphate groups are seldom released directly from ATP.) The degree to which ATP participates in routine cellular activities is illustrated by calculations indicating that while the concentration of cellular ATP is relatively moderate (~5 mM), humans typically recycle their own weight of ATP each day.

Nucleotide derivatives participate in a wide variety of metabolic processes. For example, starch synthesis in plants proceeds by repeated additions of glucose units donated by ADP–glucose (Fig. 3-2). Other nucleotide derivatives, as we shall see in later chapters, carry groups that undergo oxidation–reduction reactions. The attached group, which may be a small molecule such as glucose (Fig. 3-2) or even another nucleotide, is typically linked to the nucleotide through a mono- or diphosphate group.

CHECK YOUR UNDERSTANDING

Describe the general structure of a nucleoside and a nucleotide.

Describe the difference between a ribonucleotide and a deoxyribonucleotide.

2 Introduction to Nucleic Acid Structure

LEARNING OBJECTIVES

- Understand how nucleotides are linked together to form nucleic acids.
- Become familiar with the structural features of the DNA double helix.

Nucleotides can be joined to each other to form the polymers that are familiar to us as RNA and DNA. In this section, we describe the general features of these nucleic acids. Nucleic acid structure is considered further in Chapter 24.

A | Nucleic Acids Are Polymers of Nucleotides

The nucleic acids are chains of nucleotides whose phosphates bridge the 3′ and 5′ positions of neighboring ribose units (Fig. 3-3). The phosphates of these **polynucleotides** are acidic, so at physiological pH, nucleic acids are polyanions. The linkage between individual nucleotides is known as a **phosphodiester bond,** so named because the phosphate is esterified to two ribose units. Each nucleotide that has been incorporated into the polynucleotide is known as a **nucleotide residue.** The terminal residue whose C5′

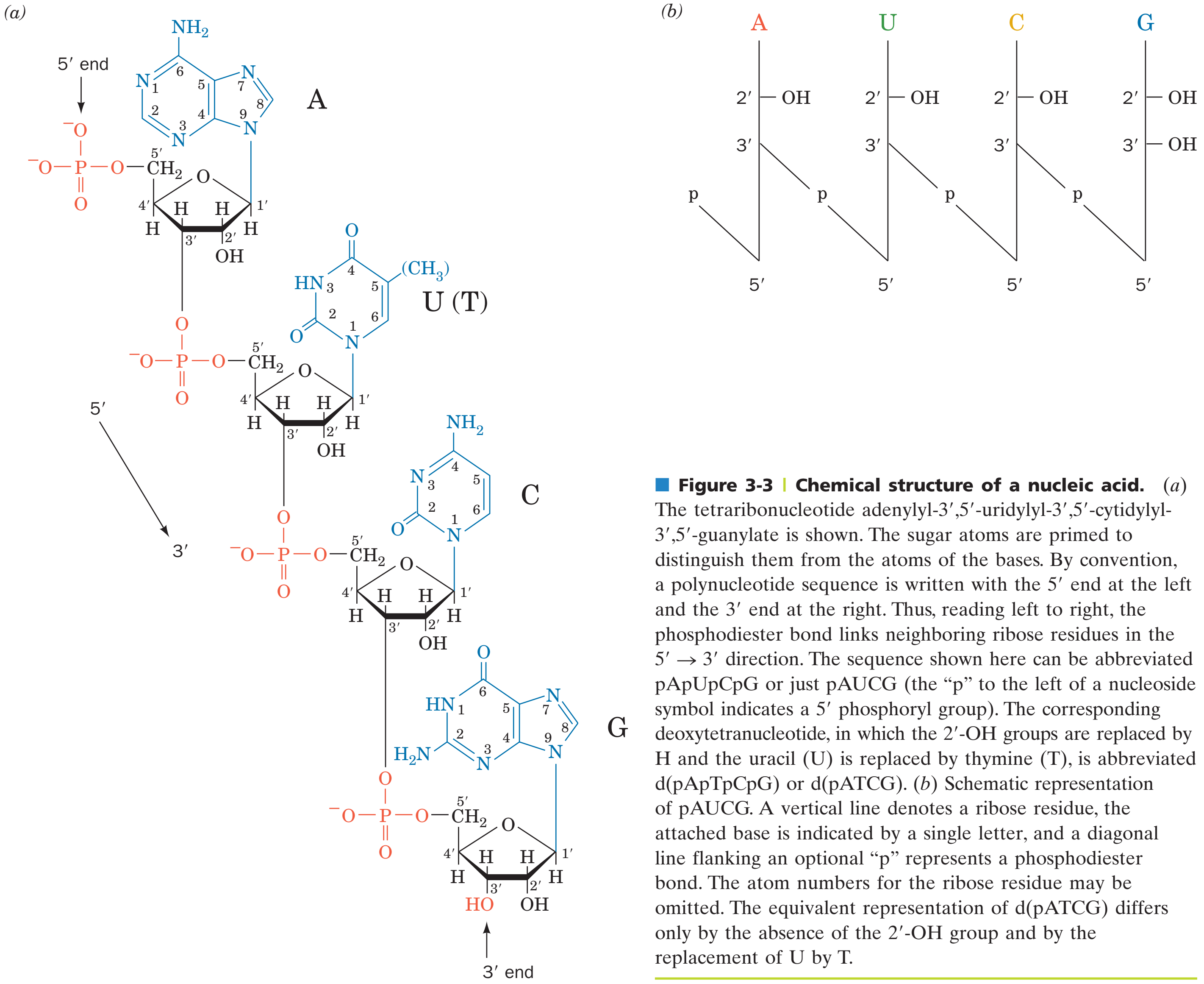

Figure 3-3 | Chemical structure of a nucleic acid. (*a*) The tetraribonucleotide adenylyl-3′,5′-uridylyl-3′,5′-cytidylyl-3′,5′-guanylate is shown. The sugar atoms are primed to distinguish them from the atoms of the bases. By convention, a polynucleotide sequence is written with the 5′ end at the left and the 3′ end at the right. Thus, reading left to right, the phosphodiester bond links neighboring ribose residues in the 5′ → 3′ direction. The sequence shown here can be abbreviated pApUpCpG or just pAUCG (the "p" to the left of a nucleoside symbol indicates a 5′ phosphoryl group). The corresponding deoxytetranucleotide, in which the 2′-OH groups are replaced by H and the uracil (U) is replaced by thymine (T), is abbreviated d(pApTpCpG) or d(pATCG). (*b*) Schematic representation of pAUCG. A vertical line denotes a ribose residue, the attached base is indicated by a single letter, and a diagonal line flanking an optional "p" represents a phosphodiester bond. The atom numbers for the ribose residue may be omitted. The equivalent representation of d(pATCG) differs only by the absence of the 2′-OH group and by the replacement of U by T.

is not linked to another nucleotide is called the **5′ end,** and the terminal residue whose C3′ is not linked to another nucleotide is called the **3′ end.** By convention, the sequence of nucleotide residues in a nucleic acid is written, left to right, from the 5′ end to the 3′ end.

The properties of a polymer such as a nucleic acid may be very different from the properties of the individual units, or **monomers,** before polymerization. As the size of the polymer increases from **dimer, trimer, tetramer,** and so on through **oligomer** (Greek: *oligo,* few), physical properties such as charge and solubility may change. In addition, *a polymer of nonidentical residues has a property that its component monomers lack—namely, it contains information in the form of its sequence of residues.*

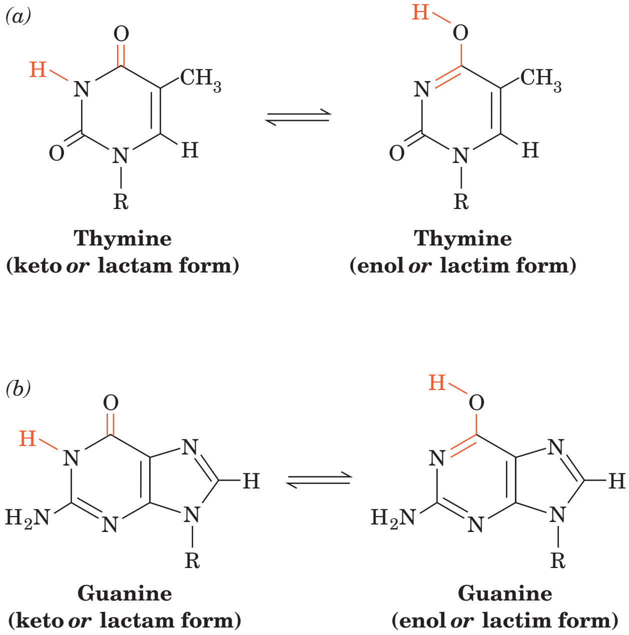
(a)
Thymine (keto or lactam form)
Thymine (enol or lactim form)
(b)
Guanine (keto or lactam form)
Guanine (enol or lactim form)

Figure 3-4 | Tautomeric forms of bases. Some of the possible tautomeric forms of (*a*) thymine and (*b*) guanine are shown. Cytosine and adenine can undergo similar proton shifts.

Chargaff's Rules Describe the Base Composition of DNA. Although there appear to be no rules governing the nucleotide composition of typical RNA molecules, DNA has equal numbers of adenine and thymine residues (A = T) and equal numbers of guanine and cytosine residues (G = C). These relationships, known as **Chargaff's rules,** were discovered in the late 1940s by Erwin Chargaff, who devised the first reliable quantitative methods for the compositional analysis of DNA.

DNA's base composition varies widely among different organisms. It ranges from ~25 to 75 mol % G + C in different species of bacteria. However, it is more or less constant among related species; for example, in mammals G + C ranges from 39 to 46%. The significance of Chargaff's rules was not immediately appreciated, but we now know that the structural basis for the rules derives from DNA's double-stranded nature.

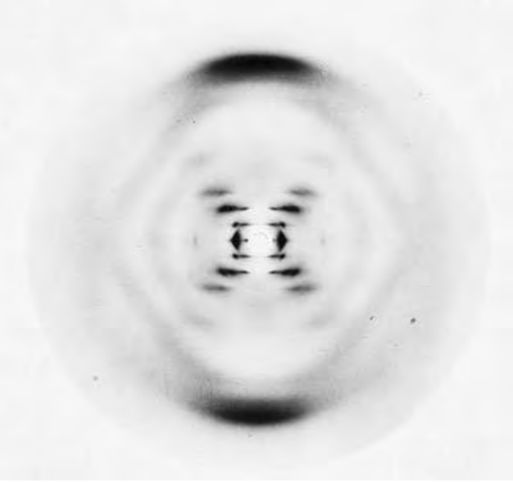

Figure 3-5 | An X-ray diffraction photograph of a vertically oriented DNA fiber. This photograph, taken by Rosalind Franklin, provided key evidence for the elucidation of the Watson–Crick structure. The central X-shaped pattern indicates a helix, whereas the heavy black arcs at the top and bottom of the diffraction pattern reveal the spacing of the stacked bases (3.4 Å). [Courtesy of Maurice Wilkins, King's College, London.]

B | DNA Forms a Double Helix

The determination of the structure of DNA by James Watson and Francis Crick in 1953 is often said to mark the birth of modern molecular biology. The **Watson–Crick structure** of DNA not only provided a model of what is arguably the central molecule of life, it also suggested the molecular mechanism of heredity. Watson and Crick's accomplishment, which is ranked as one of science's major intellectual achievements, was based in part on two pieces of evidence in addition to Chargaff's rules: the correct tautomeric forms of the bases and indications that DNA is a helical molecule.

The purine and pyrimidine bases of nucleic acids can assume different tautomeric forms (**tautomers** are easily converted isomers that differ only in hydrogen positions; Fig. 3-4). X-Ray, nuclear magnetic resonance (NMR), and spectroscopic investigations have firmly established that the nucleic acid bases are overwhelmingly in the keto tautomeric forms shown in Fig. 3-3. In 1953, however, this was not generally appreciated. Information about the dominant tautomeric forms was provided by Jerry Donohue, an office mate of Watson and Crick and an expert on the X-ray structures of small organic molecules.

Evidence that DNA is a helical molecule was provided by an X-ray diffraction photograph of a DNA fiber taken by Rosalind Franklin (Fig. 3-5). The appearance of the photograph enabled Crick, an X-ray crystallographer by training, to deduce (a) that DNA is a helical molecule and (b) that its planar aromatic bases form a stack that is parallel to the fiber axis.

The limited structural information, along with Chargaff's rules, provided few clues to the structure of DNA; Watson and Crick's model sprang mostly from their imaginations and model-building studies. Once the Watson–Crick model had been published, however, its basic simplicity combined with its obvious biological relevance led to its rapid acceptance. Later investigations have confirmed the general accuracy of the Watson–Crick model, although its details have been modified.

The Watson–Crick model of DNA has the following major features:

1. Two polynucleotide chains wind around a common axis to form a **double helix** (Fig. 3-6).
2. The two strands of DNA are **antiparallel** (run in opposite directions), but each forms a right-handed helix. (The difference between a right-handed and a left-handed helix is shown in Fig. 3-7.)

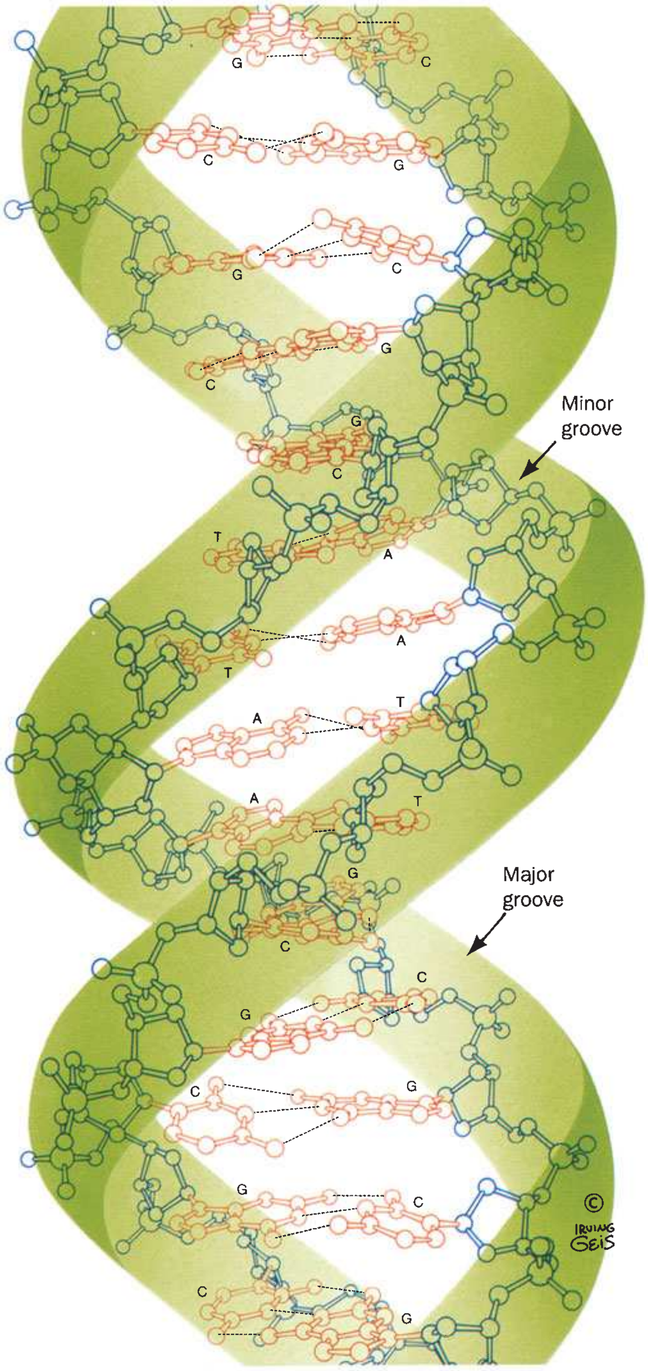

■ **Figure 3-6 | Three-dimensional structure of DNA.** The repeating helix is based on the structure of the self-complementary dodecamer d(CGCGAATTCGCG) determined by Richard Dickerson and Horace Drew. The view in this ball-and-stick model is perpendicular to the helix axis. The sugar–phosphate backbones (*blue, with green ribbon outlines*) wind around the periphery of the molecule. The bases (*red*) form hydrogen-bonded pairs that occupy the core. H atoms have been omitted for clarity. The two strands run in opposite directions. [Illustration, Irving Geis. Image from the Irving Geis Collection/Howard Hughes Medical Institute. Rights owned by HHMI. Reproduction by permission only.] **See Interactive Exercise 1 and Kinemage Exercise 2-1.**

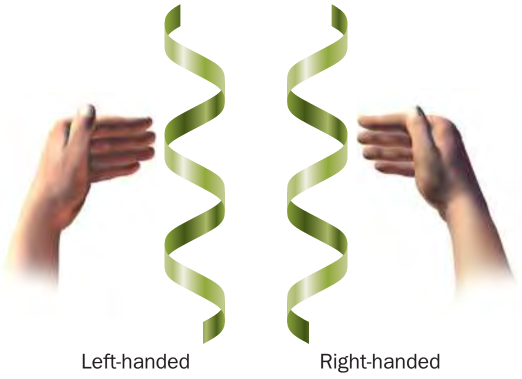

■ **Figure 3-7 | Diagrams of left- and right-handed helices.** In each case, the fingers curl in the direction the helix turns when the thumb points in the direction the helix rises. Note that the handedness is retained when the helices are turned upside down.

3. The bases occupy the core of the helix and sugar–phosphate chains run along the periphery, thereby minimizing the repulsions between charged phosphate groups. The surface of the double helix contains two grooves of unequal width: the **major** and **minor grooves.**
4. Each base is hydrogen bonded to a base in the opposite strand to form a planar **base pair.** The Watson–Crick structure can accommodate only two types of base pairs. Each adenine residue must pair with a thymine residue and vice versa, and each guanine residue must pair with a cytosine residue and vice versa (Fig. 3-8). These hydrogen-bonding interactions, a phenomenon known as **complementary base pairing,** result in the specific association of the two chains of the double helix.

The Watson–Crick structure can accommodate any sequence of bases on one polynucleotide strand if the opposite strand has the complementary

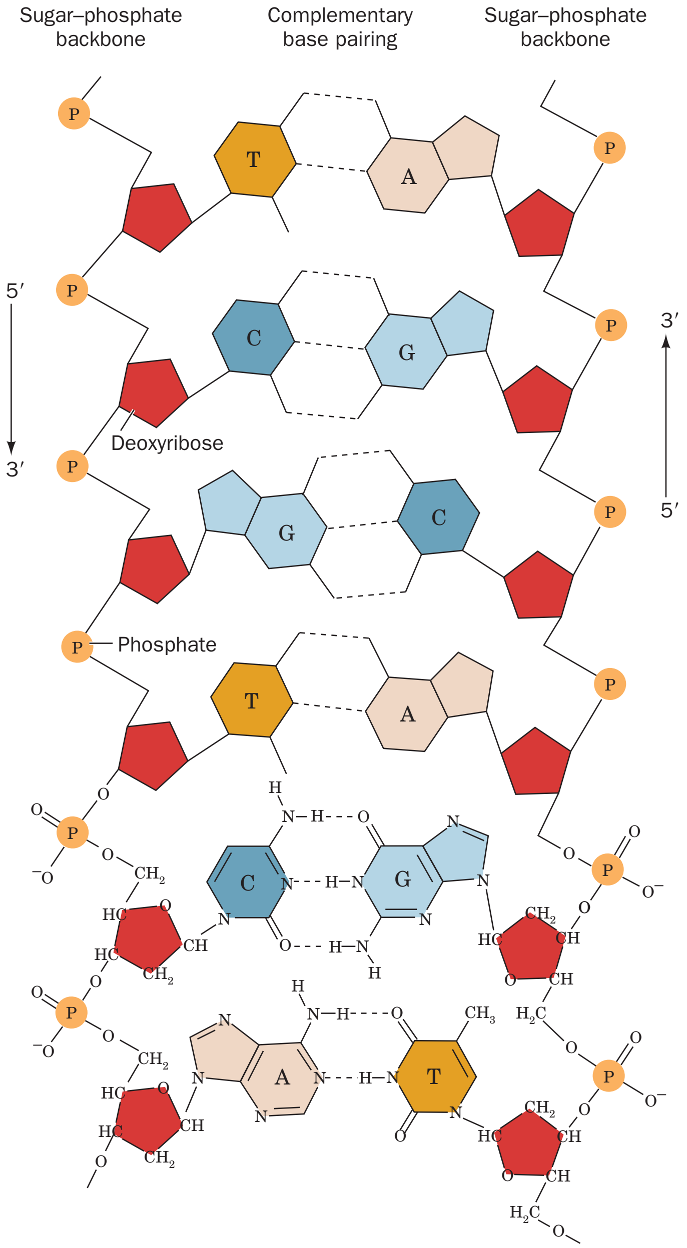
Sugar–phosphate backbone
Complementary base pairing
Sugar–phosphate backbone
5′
3′
3′
5′
P
T
A
C
G
G
C
T
A
Deoxyribose
Phosphate
H
N—H- - -O
N
C
N- - -H—N
G
N
N
O- - -H—N
H
CH
CH_2
HC
O
HC
O
P
O
^-O
CH_2
CH
H
N—H- - -O
CH_3
N
A
N- - -H—N
T
N
N
O
H_2C
O
P
O
O^-
HC
CH
CH

■ **Figure 3-8** | **Complementary strands of DNA.** Two polynucleotide chains associate by base pairing to form double-stranded DNA. A pairs with T, and G pairs with C by forming specific hydrogen bonds. **See Kinemage Exercise 2-2.**

base sequence. This immediately accounts for Chargaff's rules. More importantly, it suggests that *each DNA strand can act as a* ***template*** *for the synthesis of its complementary strand and hence that hereditary information is encoded in the sequence of bases on either strand.*

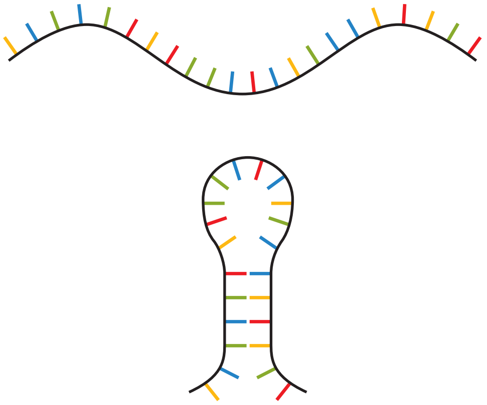

Figure 3-9 | Formation of a stem–loop structure. Base pairing between complementary sequences within an RNA strand allows the polynucleotide to fold back on itself.

Most DNA Molecules Are Large. The extremely large size of DNA molecules is in keeping with their role as the repository of a cell's genetic information. Of course, an organism's **genome,** its unique DNA content, may be allocated among several **chromosomes** (Greek: *chromos,* color + *soma,* body), each of which contains a separate DNA molecule. Note that many organisms are **diploid;** that is, they contain two equivalent sets of chromosomes, one from each parent. Their content of unique **(haploid)** DNA is half their total DNA. For example, humans are diploid organisms that carry 46 chromosomes per cell; their haploid number is therefore 23.

Because of their great lengths, DNA molecules are described in terms of the number of base pairs **(bp)** or thousands of base pairs **(kilobase pairs,** or **kb).** Naturally occurring DNAs vary in length from ~5 kb in small DNA-containing viruses to well over 250,000 kb in the largest mammalian chromosomes. Although DNA molecules are long and relatively stiff, they are not completely rigid. We shall see in Chapter 24 that the DNA double helix forms coils and loops when it is packaged inside the cell. Furthermore, depending on the nucleotide sequence, DNA may adopt slightly different helical conformations. Finally, in the presence of other cellular components, the DNA may bend sharply or the two strands may partially unwind.

C | RNA Is a Single-Stranded Nucleic Acid

Single-stranded DNA is rare, occurring mainly as the hereditary material of certain viruses. In contrast, RNA occurs primarily as single strands, which usually form compact structures rather than loose extended chains (double-stranded RNA is the hereditary material of certain viruses). An RNA strand—which is identical to a DNA strand except for the presence of 2′-OH groups and the substitution of uracil for thymine—can base-pair with a complementary strand of RNA or DNA. As expected, A pairs with U (or T in DNA), and G with C. Base pairing often occurs intramolecularly, giving rise to **stem–loop** structures (Fig. 3-9) or, when loops interact with each other, to more complex structures.

The intricate structures that can potentially be adopted by single-stranded RNA molecules provide additional evidence that RNA can do more than just store and transmit genetic information. Numerous investigations have found that certain RNA molecules can specifically bind small organic molecules and can catalyze reactions involving those molecules. These findings provide substantial support for theories that *many of the processes essential for life began through the chemical versatility of small polynucleotides* (a situation known as the **RNA world**). We will further explore RNA structure and function in Section 24-2C.

CHECK YOUR UNDERSTANDING

Describe the double-helical structure of DNA.
List the structural differences between DNA and RNA.

3 Overview of Nucleic Acid Function

LEARNING OBJECTIVE

- Understand that genetic information is contained in the sequence of nucleotides in DNA and can be expressed through its transcription into RNA, which is then translated into protein.

DNA is the carrier of genetic information in all cells and in many viruses. Yet a period of over 75 years passed from the time the laws of inheritance were discovered by Gregor Mendel until the biological role of DNA was elucidated. Even now, many details of how genetic information is expressed and transmitted to future generations are still unclear.

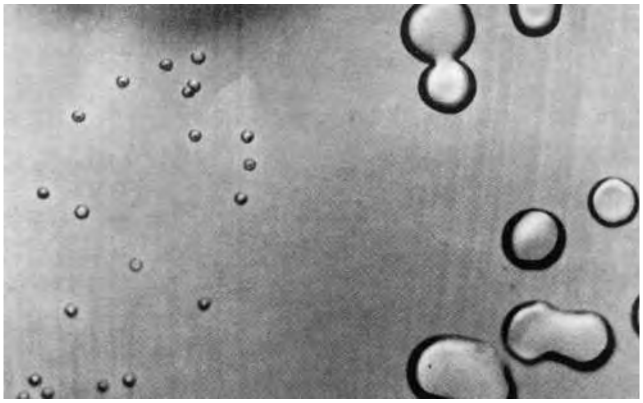

■ **Figure 3-10 | Transformed pneumococci.** The large colonies are virulent pneumococci that resulted from the transformation of nonpathogenic pneumococci (smaller colonies) by DNA extracted from the virulent strain. We now know that this DNA contained a gene that was defective in the nonpathogenic strain. [From Avery, O.T., MacLeod, C.M., and McCarty, M., *J. Exp. Med.* **79,** 153 (1944). Copyright © 1944 by Rockefeller University Press.]

Mendel's work with garden peas led him to postulate that an individual plant contains a pair of factors (which we now call **genes**), one inherited from each parent. But Mendel's theory of inheritance, reported in 1866, was almost universally ignored by his contemporaries, whose knowledge of anatomy and physiology provided no basis for its understanding. Eventually, genes were hypothesized to be part of chromosomes, and the pace of genetic research greatly accelerated.

A | DNA Carries Genetic Information

Until the 1940s, it was generally assumed that genes were made of protein, since proteins were the only biochemical entities that, at the time, seemed complex enough to serve as agents of inheritance. Nucleic acids, which had first been isolated in 1869 by Friedrich Miescher, were believed to have monotonously repeating nucleotide sequences and were therefore unlikely candidates for transmitting genetic information.

It took the efforts of Oswald Avery, Colin MacLeod, and Maclyn McCarty to demonstrate that DNA carries genetic information. Their experiments, completed in 1944, showed that DNA—not protein—extracted from a virulent (pathogenic) strain of the bacterium *Diplococcus pneumoniae* was the substance that **transformed** (permanently changed) a nonpathogenic strain of the organism to the virulent strain (Fig. 3-10). Avery's discovery was initially greeted with skepticism, but it influenced Erwin Chargaff, whose rules (Section 3-2A) led to subsequent models of the structure and function of DNA.

The double-stranded, or duplex, nature of DNA facilitates its **replication.** When a cell divides, each DNA strand acts as a template for the assembly of its complementary strand (Fig. 3-11). Consequently, every progeny cell contains a complete DNA molecule (or a complete set of DNA molecules in organisms whose genomes contain more than one chromosome). Each DNA molecule consists of one parental strand and one daughter strand. Daughter strands are synthesized by the stepwise polymerization of nucleotides that specifically pair with bases on the parental strands. The mechanism of replication, while straightforward in principle, is exceedingly complex in the cell, requiring a multitude of cellular factors to proceed with fidelity and efficiency, as we shall see in Chapter 25.

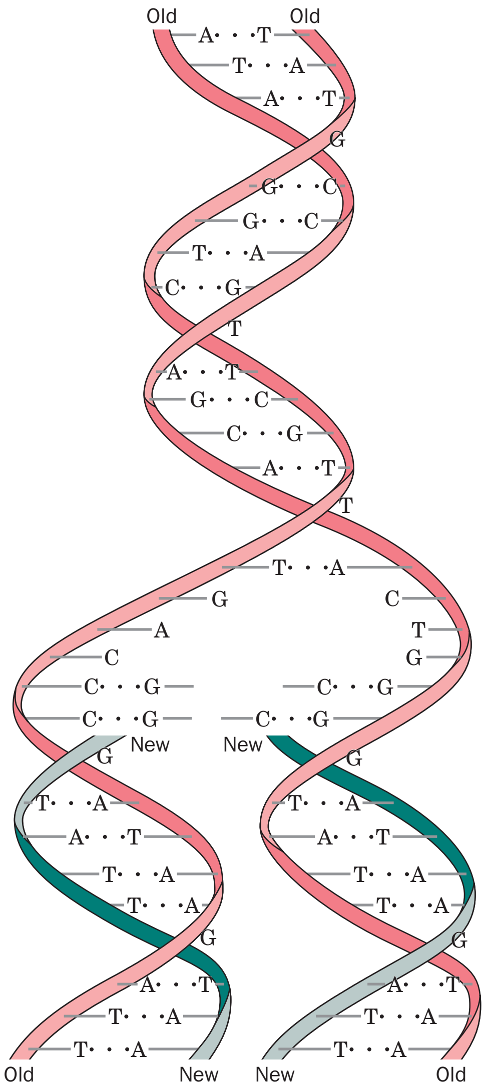

■ **Figure 3-11 | DNA replication.** Each strand of parental DNA (*red*) acts as a template for the synthesis of a complementary daughter strand (*green*). Thus, the resulting double-stranded molecules are identical.

B | Genes Direct Protein Synthesis

The question of how sequences of nucleotides control the characteristics of organisms took some time to be answered. In experiments with the mold *Neurospora crassa* in the 1940s, George Beadle and Edward Tatum found that *there is a specific connection between genes and enzymes, the one gene–one enzyme theory.* Beadle and Tatum showed that mutant varieties of *Neurospora* that were generated by irradiation with X-rays required additional nutrients in order to grow. Presumably, the offspring of the radiation-damaged cells lacked the specific enzymes necessary to synthesize those nutrients.

The link between DNA and enzymes (nearly all of which are proteins) is RNA. *The DNA of a gene is* ***transcribed*** *to produce an RNA molecule that is complementary to the DNA. The RNA sequence is then* ***translated*** *into the corresponding sequence of amino acids to form a protein* (Fig. 3-12). These transfers of biological information are summarized in the so-called **central dogma of molecular biology** formulated by Crick in 1958 (Fig. 3-13).

Just as the daughter strands of DNA are synthesized from free deoxynucleoside triphosphates that pair with bases in the parent DNA strand, RNA strands are synthesized from free ribonucleoside triphosphates that pair with the complementary bases in one DNA strand of a gene (transcription is described in greater detail in Chapter 26). The RNA that corresponds to a protein-coding gene (called **messenger RNA,** or **mRNA**) makes its way to a **ribosome,** an organelle that is itself composed largely of RNA **(ribosomal RNA,** or **rRNA).** At the ribosome, each set of three nucleotides in the mRNA pairs with three complementary nucleotides in a small RNA molecule called a **transfer RNA,** or **tRNA** (Fig. 3-14). Attached to each tRNA molecule is its corresponding amino acid. The ribosome catalyzes the joining of amino acids, which are the monomeric units of proteins (protein synthesis is described in detail in Chapter 27). Amino acids are added to the growing protein chain according to the order in which the tRNA molecules bind to the mRNA. Since the nucleotide sequence of the mRNA in turn reflects the sequences of nucleotides in the gene, DNA directs the synthesis of proteins. It follows that alterations to the genetic material of an organism **(mutations)** may manifest themselves as proteins with altered structures and functions.

Using techniques that are described in the following sections and in other parts of this book, researchers can compile a catalog of all the

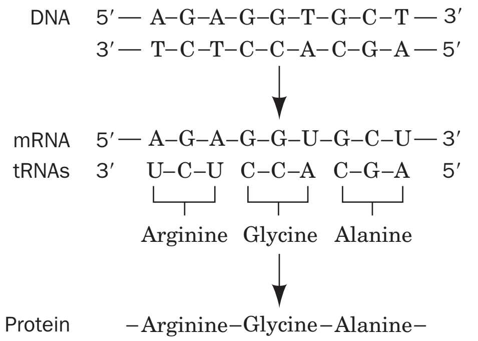

DNA
5′— A–G–A–G–G–T–G–C–T — 3′
3′— T–C–T–C–C–A–C–G–A — 5′
mRNA
5′— A–G–A–G–G–U–G–C–U — 3′
tRNAs
3′
U–C–U
C–C–A
C–G–A
5′
Arginine
Glycine
Alanine
Protein
–Arginine–Glycine–Alanine–

Figure 3-12 | Transcription and translation. One strand of DNA directs the synthesis of messenger RNA (mRNA). The base sequence of the transcribed RNA is complementary to that of the DNA strand. The message is translated when transfer RNA (tRNA) molecules align with the mRNA by complementary base pairing between three-nucleotide segments known as **codons.** Each tRNA carries a specific amino acid. These amino acids are covalently joined to form a protein. Thus, the sequence of bases in DNA specifies the sequence of amino acids in a protein.

See Guided Exploration 1
Overview of transcription and translation.

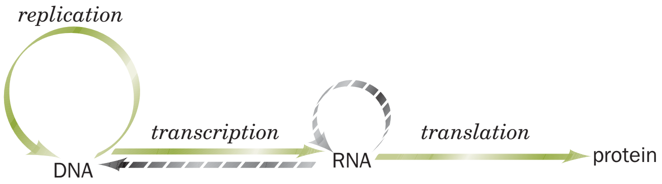

Figure 3-13 | The central dogma of molecular biology. Solid arrows indicate the types of information transfers that occur in all cells: DNA directs its own replication to produce new DNA molecules; DNA is transcribed into RNA; RNA is translated into protein. Dashed lines represent information transfers that occur only in certain organisms.

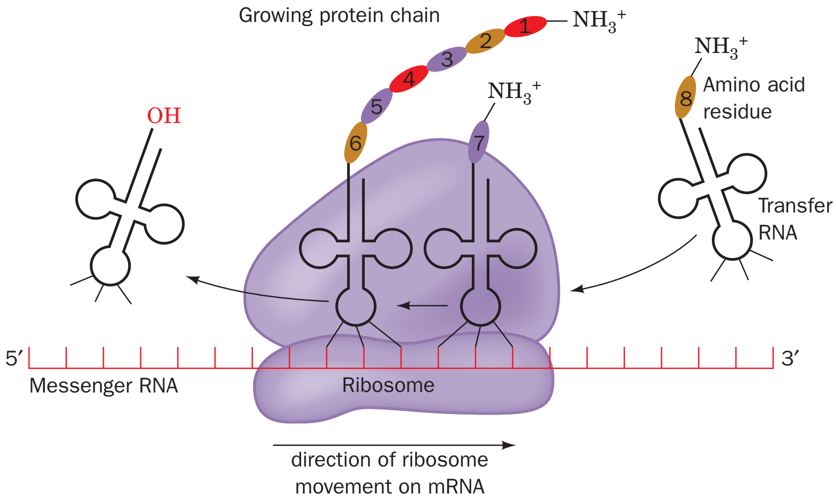

Figure 3-14 | Translation. tRNA molecules with their attached amino acids bind to complementary three-nucleotide sequences (codons) on mRNA. The ribosome facilitates the alignment of the tRNA and the mRNA, and it catalyzes the joining of amino acids to produce a protein chain. When a new amino acid is added, the preceding tRNA is ejected, and the ribosome proceeds along the mRNA.

information encoded in an organism's DNA. The study of the genome's size, organization, and gene content is known as **genomics.** By analogy, **transcriptomics** refers to the study of gene expression, which focuses on the set of mRNA molecules, or **transcriptome**, that is transcribed from DNA under any particular set of circumstances. Finally, **proteomics** is the study of the proteins (the **proteome**) produced as a result of transcription and translation. Although an organism's genome remains essentially unchanged throughout its lifetime, its transcriptome and proteome may vary significantly among different types of tissues, developmental stages, and environmental conditions.

CHECK YOUR UNDERSTANDING

Summarize the central dogma of molecular biology.

4 Nucleic Acid Sequencing

LEARNING OBJECTIVES

- Understand why restriction endonucleases are useful for generating DNA fragments.
- Understand the steps required to sequence DNA by the chain-terminator method.
- Understand what kinds of information have been provided by sequencing the human genome.
- Understand that changes in DNA allow evolution to occur.

Much of our current understanding of protein structure and function rests squarely on information gleaned not from the proteins themselves, but indirectly from their genes. *The ability to determine the sequence of nucleotides in nucleic acids has made it possible to deduce the amino acid sequences of their encoded proteins and, to some extent, the structures and functions of those proteins. Nucleic acid sequencing has also revealed information about the regulation of genes.* Certain portions of genes that are not actually transcribed into RNA nevertheless influence how often a gene is transcribed and translated, that is, **expressed.** Moreover, efforts to elucidate the sequences in hitherto unmapped regions of DNA have led to the discovery of new genes and new regulatory elements. *Once in hand, a nucleic acid sequence can be duplicated, modified, and expressed, making it possible to study proteins that could not otherwise be obtained in useful quantities.* In this section, we describe how nucleic acids are sequenced and what information the sequences may reveal. In the following section, we discuss the manipulation of purified nucleic acid sequences for various purposes.

The overall strategy for sequencing any polymer of nonidentical units is

1. Cleave the polymer into specific fragments that are small enough to be fully sequenced.
2. Determine the sequence of residues in each fragment.
3. Determine the order of the fragments in the original polymer by repeating the preceding steps using a degradation procedure that yields a set of fragments that overlap the cleavage points in the first step.

The first efforts to sequence RNA used nonspecific enzymes to generate relatively small fragments whose nucleotide composition was then determined by partial digestion with an enzyme that selectively removed nucleotides from one end or the other (Fig. 3-15). Sequencing RNA in this manner was tedious and time-consuming. Using such methods, it took Robert Holley seven years to determine the sequence of a 76-residue tRNA molecule.

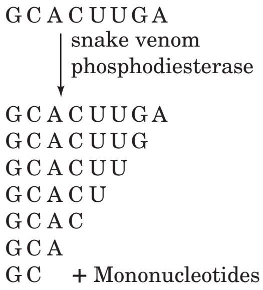

Figure 3-15 | Determining the sequence of an oligonucleotide using nonspecific enzymes. The oligonucleotide is partially digested with snake venom phosphodiesterase, which breaks the phosphodiester bonds between nucleotide residues, starting at the 3′ end of the oligonucleotide. The result is a mixture of fragments of all lengths, which are then separated. Comparing the base composition of a pair of fragments that differ in length by one nucleotide establishes the identity of the 3′-terminal nucleotide in the larger fragment. Analysis of each pair of fragments reveals the sequence of the original oligonucleotide.

After 1975, dramatic progress was made in nucleic acid sequencing technology. The advances were made possible by the discovery of enzymes that could cleave DNA at specific sites and by the development of rapid sequencing techniques for DNA. The advent of modern molecular cloning techniques (Section 3-5) also made it possible to produce sufficient quantities of specific DNA to be sequenced. These cloning techniques are necessary because most specific DNA sequences are normally present in a genome in only a single copy.

A | Restriction Endonucleases Cleave DNA at Specific Sequences

Many bacteria are able to resist infection by **bacteriophages** (viruses that are specific for bacteria) by virtue of a **restriction–modification system.** The bacterium modifies certain nucleotides in specific sequences of its own DNA by adding a methyl (—CH_3) group in a reaction catalyzed by a **modification methylase.** A **restriction endonuclease,** which recognizes the same nucleotide sequence as does the methylase, cleaves any DNA that has not been modified on at least one of its two strands. (An **endonuclease** cleaves a nucleic acid within the polynucleotide strand; an **exonuclease** cleaves a nucleic acid by removing one of its terminal residues.) This system destroys foreign (phage) DNA containing a recognition site that has not been modified by methylation. The host DNA is always at least half methylated, because although the daughter strand is not methylated until shortly after it is synthesized, the parental strand to which it is paired is already modified (and thus protects both strands of the DNA from cleavage by the restriction enzyme).

Type II restriction endonucleases are particularly useful in the laboratory. These enzymes cleave DNA within the four- to eight-base sequence that is recognized by their corresponding modification methylase. (Type I and Type III restriction endonucleases cleave DNA at sites other than their recognition sequences.) Over 3000 Type II restriction enzymes with over 200 different recognition sequences have been characterized. Some of the more widely used restriction enzymes are listed in Table 3-2. A

Table 3-2 Recognition and Cleavage Sites of Some Restriction Enzymes

Enzyme	Recognition Sequence[a]	Microorganism
*Alu*I	AG↓CT	*Arthrobacter luteus*
*Bam*HI	G↓GATCC	*Bacillus amyloliquefaciens* H
*Bgl*I	GCCNNNNN↓NGGC	*Bacillus globigii*
*Bgl*II	A↓GATCT	*Bacillus globigii*
*Eco*RI	G↓AATTC	*Escherichia coli* RY13
*Eco*RII	↓CC$\left(\begin{smallmatrix}A\\T\end{smallmatrix}\right)$GG	*Escherichia coli* R245
*Eco*RV	GAT↓ATC	*Escherichia coli* J62 pLG74
*Hae*II	RGCGC↓Y	*Haemophilus aegyptius*
*Hae*III	GG↓CC	*Haemophilus aegyptius*
*Hind*III	A↓AGCTT	*Haemophilus influenzae* R_d
*Hpa*II	C↓CGG	*Haemophilus parainfluenzae*
*Msp*I	C↓CGG	*Moraxella* species
*Pst*I	CTGCA↓G	*Providencia stuartii* 164
*Pvu*II	CAG↓CTG	*Proteus vulgaris*
*Sal*I	G↓TCGAC	*Streptomyces albus* G
*Taq*I	T↓CGA	*Thermus aquaticus*
*Xho*I	C↓TCGAG	*Xanthomonas holcicola*

[a] The recognition sequence is abbreviated so that only one strand, reading 5′ to 3′, is given. The cleavage site is represented by an arrow (↓). R, Y, and N represent a purine nucleotide, a pyrimidine nucleotide, and any nucleotide, respectively.

Source: Roberts, R.J. and Macelis, D., REBASE—the restriction enzyme database, http://rebase.neb.com.

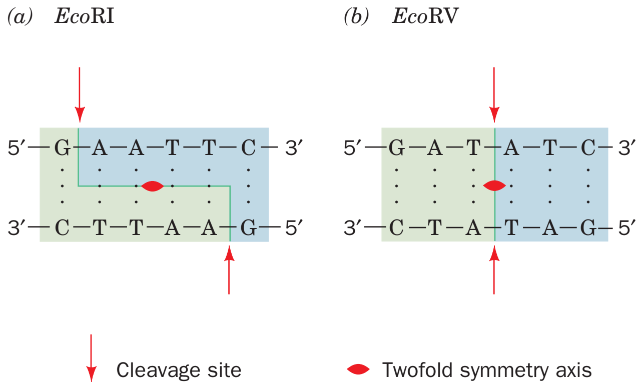

Figure 3-16 | Restriction sites. The recognition sequences for Type II restriction endonucleases are palindromes, sequences with a twofold axis of symmetry. (*a*) Recognition site for *Eco*RI, which generates DNA fragments with sticky ends. (*b*) Recognition site for *Eco*RV, which generates blunt-ended fragments.

restriction enzyme is named by the first letter of the genus and the first two letters of the species of the bacterium that produced it, followed by its serotype or strain designation, if any, and a roman numeral if the bacterium contains more than one type of restriction enzyme. For example, *Eco*RI is produced by *E. coli* strain RY13.

Interestingly, most Type II restriction endonucleases recognize and cleave palindromic DNA sequences. A **palindrome** is a word or phrase that reads the same forward or backward. Two examples are "refer" and "Madam, I'm Adam." In a palindromic DNA segment, the sequence of nucleotides is the same in each strand, and the segment is said to have twofold symmetry (Fig. 3-16). Most restriction enzymes cleave the two strands of DNA at positions that are staggered, producing DNA fragments with complementary single-strand extensions. Restriction fragments with such **sticky ends** can associate by base pairing with other restriction fragments generated by the same restriction enzyme. Some restriction endonucleases cleave the two strands of DNA at the symmetry axis to yield restriction fragments with fully base-paired **blunt ends.**

B | Electrophoresis Separates Nucleic Acids According to Size

Treating a DNA molecule with a restriction endonuclease produces a series of precisely defined fragments that can be separated according to size. **Gel electrophoresis** is commonly used for the separation. In principle, a charged molecule moves in an electric field with a velocity proportional to its overall charge density, size, and shape. For molecules with a relatively homogeneous composition (such as nucleic acids), shape and charge density are constant, so the velocity depends primarily on size. Electrophoresis is carried out in a gel-like matrix, usually made from **agarose** (carbohydrate polymers that form a loose mesh) or **polyacrylamide** (a more rigid cross-linked synthetic polymer). The gel is typically held between two glass plates (Fig. 3-17). The molecules to be separated are applied to one end of the gel, and the molecules move through the pores in the matrix under the influence of an electric field. Smaller molecules move more rapidly through the gel and therefore migrate farther in a given time.

Following electrophoresis, the separated molecules may be visualized in the gel by an appropriate technique, such as addition of a stain that binds tightly to the DNA or by radioactive labeling. Depending on the dimensions of the gel and the visualization technique used, samples containing less than a nanogram of material can be separated and detected by gel electrophoresis. Several samples can be electrophoresed simultaneously. For example, the fragments obtained by digesting a DNA sample with

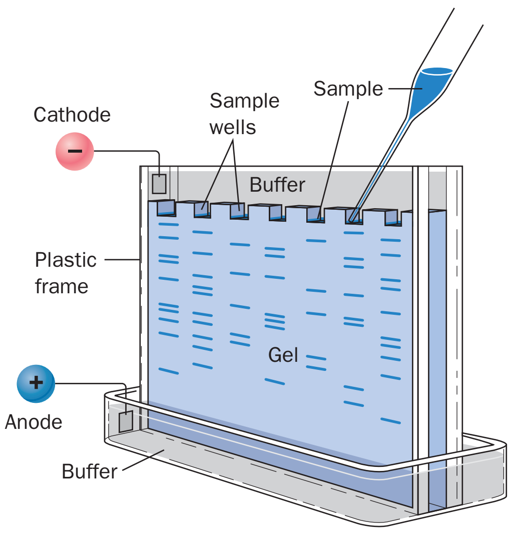

Figure 3-17 | Apparatus for gel electrophoresis. Samples are applied in slots at the top of the gel and electrophoresed in parallel lanes. Negatively charged molecules such as DNA migrate through the gel matrix toward the anode in response to an applied electric field. Because smaller molecules move faster, the molecules in each lane are separated according to size. Following electrophoresis, the separated molecules may be visualized by staining, fluorescence, or a radiographic technique.

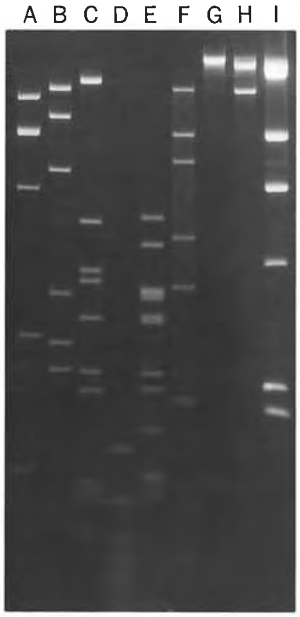

Figure 3-18 | Electrophoretogram of restriction digests. The plasmid pAgK84 has been digested with (A) *Bam*HI, (B) *Pst*I, (C) *Bgl*II, (D) *Hae*III, (E) *Hinc*II, (F) *Sac*I, (G) *Xba*I, and (H) *Hpa*I. Lane I contains bacteriophage λ digested with *Hind*III as a standard since these fragments have known sizes. The restriction fragments in each lane are made visible by fluorescence against a black background. [From Slota, J.E. and Farrand, S.F., *Plasmid* **8,** 180 (1982). Copyright © 1982 by Academic Press.]

different restriction endonucleases can be visualized side by side (Fig. 3-18). The sizes of the various fragments can be determined by comparing their electrophoretic mobilities to the mobilities of fragments of known size.

C | DNA Is Sequenced by the Chain-Terminator Method

Here we discuss the most commonly used procedure for sequencing DNA, the **chain-terminator method,** which was devised by Frederick Sanger. The first step in this procedure is to obtain single polynucleotide strands. Complementary DNA strands can be separated by heating, which breaks the hydrogen bonds between bases. Next, polynucleotide fragments that terminate at positions corresponding to each of the four nucleotides are generated. Finally, the fragments are separated and detected.

The Chain-Terminator Method Uses DNA Polymerase. The chain-terminator method (also called the **dideoxy method**) uses an *E. coli* enzyme to make complementary copies of the single-stranded DNA being sequenced. The enzyme is a fragment of **DNA polymerase I,** one of the enzymes that participates in replication of bacterial DNA (Section 25-2A). Using the single DNA strand as a template, DNA polymerase I assembles the four deoxynucleoside triphosphates **(dNTPs),** dATP, dCTP, dGTP, and dTTP, into a complementary polynucleotide chain that it elongates in the 5′→3′ direction (Fig. 3-19).

See Guided Exploration 2
DNA sequence determination by the chain-terminator method.

DNA polymerase I can sequentially add deoxynucleotides only to the 3′ end of a polynucleotide. Hence, replication is initiated in the presence of a

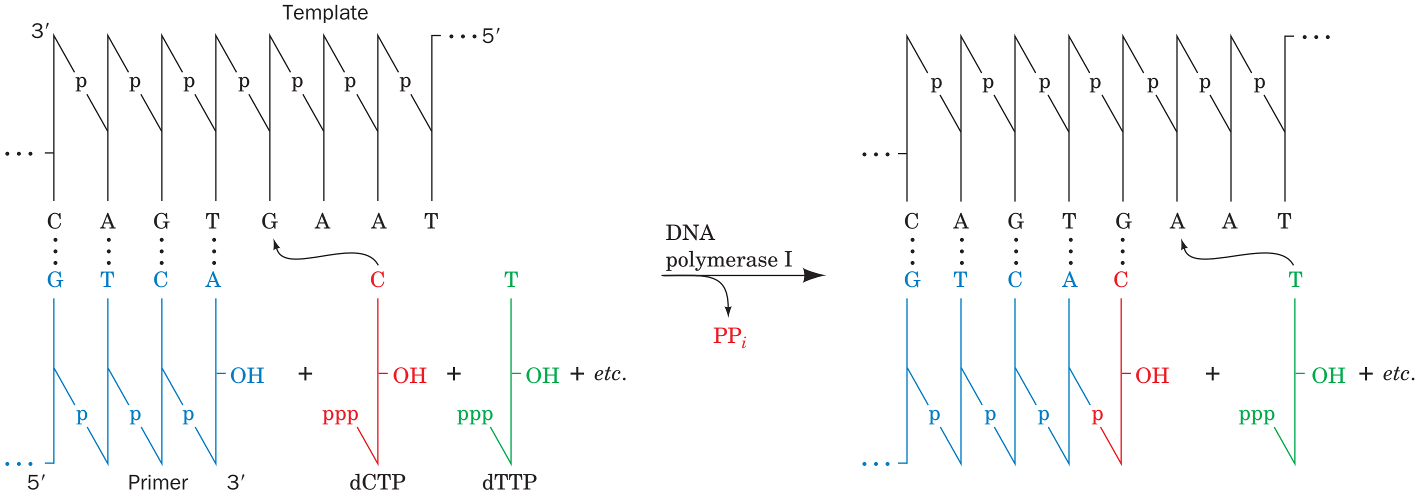

Figure 3-19 | Action of DNA polymerase I. Using a single DNA strand as a template, the enzyme elongates the primer by stepwise addition of complementary nucleotides. Incoming nucleotides pair with bases on the template strand and are joined to the growing polynucleotide strand in the 5′ → 3′ direction. The polymerase-catalyzed reaction requires a free 3′-OH group on the growing strand. **Pyrophosphate** ($P_2O_7^{4-}$; PP_i) is released with each nucleotide addition.

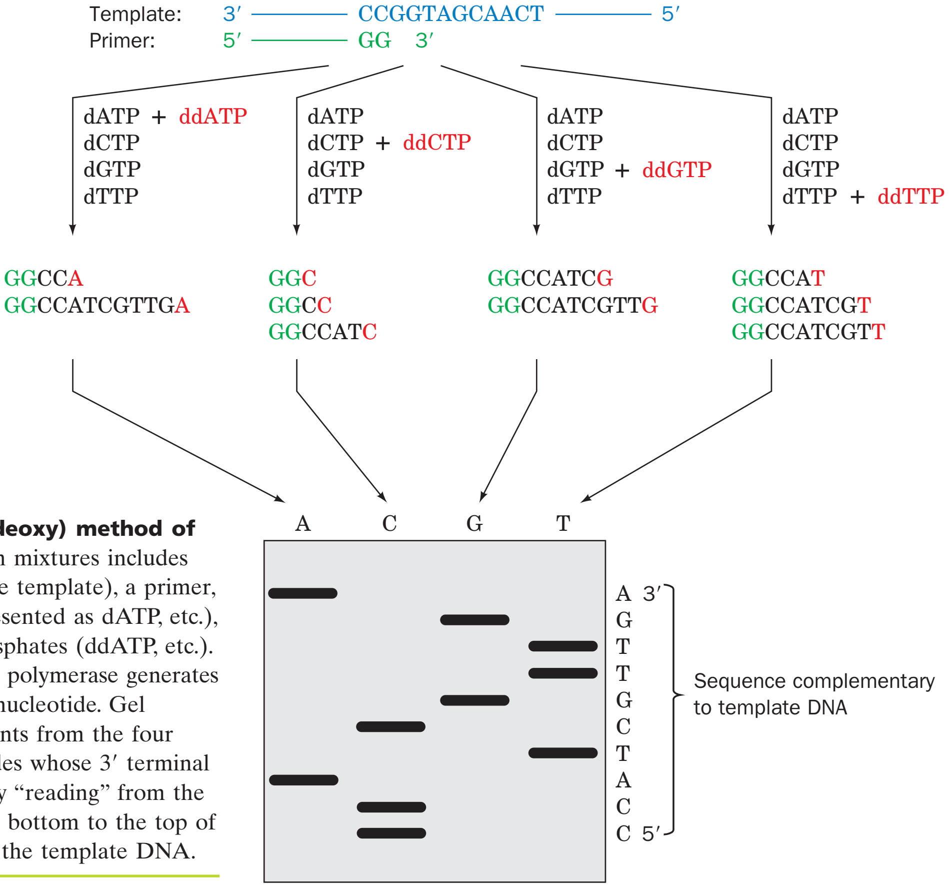
Template: 3′ CCGGTAGCAACT 5′
Primer: 5′ GG 3′
dATP + ddATP
dCTP
dGTP
dTTP
dATP
dCTP + ddCTP
dGTP
dTTP
dATP
dCTP
dGTP + ddGTP
dTTP
dATP
dCTP
dGTP
dTTP + ddTTP
GGCCA
GGCCATCGTTGA
GGC
GGCC
GGCCATC
GGCCATCG
GGCCATCGTTG
GGCCAT
GGCCATCGT
GGCCATCGTT
A
C
G
T
A 3′
G
T
T
G
C
T
A
C
C 5′
Sequence complementary to template DNA

Figure 3-20 | The chain-terminator (dideoxy) method of DNA sequencing. Each of the four reaction mixtures includes the single-stranded DNA to be sequenced (the template), a primer, the four deoxynucleoside triphosphates (represented as dATP, etc.), and one of the four dideoxynucleoside triphosphates (ddATP, etc.). Extension of the primer by the action of DNA polymerase generates stretches of DNA terminating with a dideoxynucleotide. Gel electrophoresis in parallel lanes of the fragments from the four reaction mixtures yields a set of polynucleotides whose 3′ terminal residues are known. The sequence obtained by "reading" from the smallest fragment to the largest (i.e., from the bottom to the top of the gel) is complementary to the sequence of the template DNA.

short polynucleotide (a **primer**) that is complementary to the 3′ end of the template DNA and thus becomes the 5′ end of the new strand. The primer base-pairs with the template strand, and nucleotides are sequentially added to the 3′ end of the primer. If the DNA being sequenced is a restriction fragment, as it usually is, it begins and ends with a restriction site. The primer can therefore be a short DNA segment with the sequence of this restriction site.

DNA Synthesis Terminates after Specific Bases. In the chain-terminator technique (Fig. 3-20), the DNA to be sequenced is incubated with DNA polymerase I, a suitable primer, and the four dNTP **substrates** (reactants in enzymatic reactions) for the polymerization reaction. The reaction mixture also includes a "tagged" compound, either one of the dNTPs or the primer. The tag, which may be a radioactive isotope (e.g., ^{32}P) or a fluorescent label, permits the products of the polymerase reaction to be easily detected.

The key component of the reaction mixture is a small amount of a **2′,3′-dideoxynucleoside triphosphate (ddNTP),**

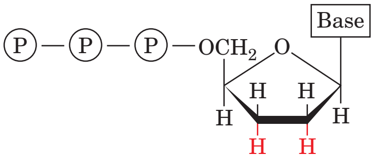
P
P
P
OCH2
O
Base
H
H
H
H
H
H

2′,3′-Dideoxynucleoside triphosphate

which lacks the 3′-OH group of deoxynucleotides. *When the dideoxy analog is incorporated into the growing polynucleotide in place of the corresponding normal nucleotide, chain growth is terminated because addition of the next nucleotide requires a free 3′-OH.* By using only a small amount of the ddNTP, a series of truncated chains is generated, each of which ends with the dideoxy analog at one of the positions occupied by the corresponding base.

Relatively modest sequencing tasks use four reaction mixtures, each with a different ddNTP, and the reaction products are electrophoresed in parallel lanes. The lengths of the truncated chains indicate the positions where the dideoxynucleotide was incorporated. Thus, the sequence of the replicated strand can be directly read from the gel (Fig. 3-21). The gel must have sufficient resolving power to separate fragments that differ in length by only one nucleotide. Two sets of gels, one run for a longer time than the other, can be used to obtain the sequence of up to 800 bases of DNA. Note that the sequence obtained by the chain-terminator method is complementary to the DNA strand being sequenced.

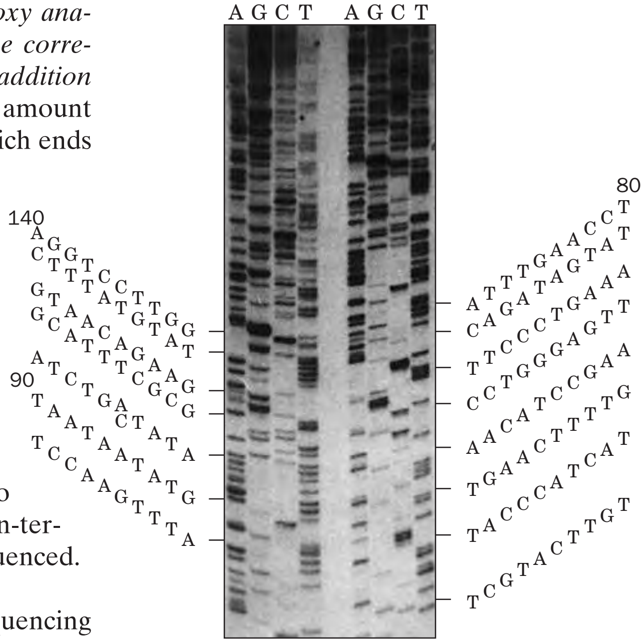

■ **Figure 3-21 | An autoradiogram of a sequencing gel.** The positions of radioactive DNA fragments produced by the chain-terminator method were visualized by laying X-ray film over the gel after electrophoresis. A second loading of the gel (the four lanes at right) was made 90 min after the initial loading in order to obtain the sequences of the smaller fragments. The deduced sequence of 140 nucleotides is written along the side. [From Hindley, J., DNA sequencing, *in* Work, T.S. and Burdon, R.H. (Eds.), *Laboratory Techniques in Biochemistry and Molecular Biology,* Vol. 10, p. 82, Elsevier (1983). Used by permission.]

Large Sequencing Projects Are Automated. Large-scale sequencing operations are accelerated by automation. In a variation of the chain-terminator method, the primers used in the four chain-extension reactions are each linked to a different fluorescent dye. The separately reacted mixtures are combined and subjected to gel electrophoresis in a single lane. As each fragment exits the bottom of the gel, its terminal base is identified by its characteristic fluorescence (Fig. 3-22) with an error rate of ~1%.

In the most advanced systems, the sequencing gel is contained in an array of up to 96 capillary tubes (rather than in a slab-shaped apparatus), sample preparation and sample loading are performed by robotic systems, and electrophoresis and data analysis are fully automated. These systems can simultaneously sequence 96 DNA samples averaging ~600 bases each with a turnaround time of ~2.5 hr and hence can identify up to 550,000 bases per day—all with only ~15 min of human attention (a skilled

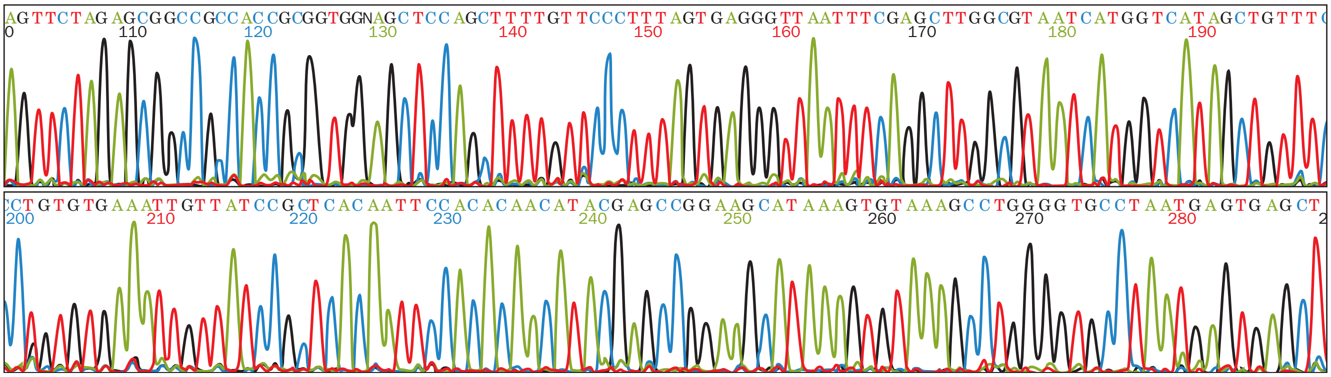

■ **Figure 3-22 | Automated DNA sequencing.** In this variant of the technique, a different fluorescent dye is attached to the primer in each of the four reaction mixtures in the chain-terminator procedure. The four reaction mixtures are combined for electrophoresis. Each of the four colored curves therefore represents the electrophoretic pattern of fragments containing one of the dideoxynucleotides: Green, red, black, and blue peaks correspond to fragments ending in ddATP, ddTTP, ddGTP, and ddCTP, respectively. The 3′-terminal base of each oligonucleotide, identified by the fluorescence of its gel band, is indicated by a single letter (A, T, G, or C). This portion of the readout corresponds to nucleotides 100–290 of the DNA segment being sequenced. [Courtesy of Mark Adams, The Institute for Genomic Research, Rockville, Maryland.]

BOX 3-1 **PATHWAYS OF DISCOVERY**

Francis Collins and the Gene for Cystic Fibrosis

Francis S. Collins (1950–)

By the mid-twentieth century, the molecular basis of several human diseases was appreciated. For example, sickle-cell anemia (Section 7-1E) was known to be caused by an abnormal hemoglobin protein. Studies of sickle-cell hemoglobin eventually revealed the underlying genetic defect, a mutation in a hemoglobin gene. It therefore seemed possible to trace other diseases to defective genes. But for many genetic diseases, even those with well-characterized symptoms, no defective protein had yet been identified. One such disease was cystic fibrosis, which is characterized mainly by the secretion of thick mucus that obstructs the airways and creates an ideal environment for bacterial growth. Cystic fibrosis is the most common inherited disease in individuals of northern European descent, striking about 1 in 2500 newborns and leading to death by early adulthood due to irreversible lung damage. It was believed that identifying the molecular defect in cystic fibrosis would lead to better understanding of the disease and to the ability to design more effective treatments.

Enter Francis Collins, who began his career by earning a doctorate in physical chemistry but then enrolled in medical school to take part in the molecular biology revolution. As a physician-scientist, Collins developed methods for analyzing large stretches of DNA in order to home in on specific genes, including the one that, when mutated, causes cystic fibrosis. By analyzing the DNA of individuals with the disease (who had two copies of the defective gene) and of family members who were asymptomatic carriers (with one normal and one defective copy of the gene), Collins and his team localized the cystic fibrosis gene to the long arm of chromosome 7. They gradually closed in on a DNA segment that appears to be present in a number of mammalian species, which suggests that the segment contains an essential gene. The cystic fibrosis gene was finally identified in 1989. Collins had demonstrated the feasibility of identifying a genetic defect in the absence of other molecular information.

Once the cystic fibrosis gene was in hand, it was a relatively straightforward process to deduce the probable structure and function of the encoded protein, which turned out to be a membrane channel for chloride ions. When functioning normally, the protein helps regulate the ionic composition and viscosity of extracellular secretions. Discovery of the cystic fibrosis gene also made it possible to design tests to identify carriers so that they could take advantage of genetic counseling.

Throughout Collins' work on the cystic fibrosis gene and during subsequent hunts for the genes that cause neurofibromatosis and Huntington's disease, he was mindful of the ethical implications of the new science of molecular genetics. Collins has been a strong advocate for protecting the privacy of genetic information. At the same time, he recognizes the potential therapeutic use of such information. In his tenure as director of the human genome project, he was committed to making the results freely and immediately accessible, as a service to researchers and the individuals who might benefit from new therapies based on molecular genetics.

Riordan, J.R., Rommens, J.M., Kerem, B.-S., Alon, N., Rozmahel, R., Grzelczak, Z., Zielensky, J., Lok, S., Plavsic, N., Chou, J.-L., Drumm, M.L., Iannuzzi, M.C., Collins, F.S., and Tsui, L.-C., Identification of the cystic fibrosis gene: Cloning and characterization of complementary DNA, *Science* **245,** 1066–1073 (1989).

operator can identify only ~25,000 bases per year using the above-described manual methods). Sequencing the 3.2-billion-bp human genome required hundreds of such advanced sequencing systems.

Databases Store Nucleotide Sequences. The results of sequencing projects large and small are customarily deposited in online databases such as GenBank (see the Bioinformatics Exercises). Over 150 billion nucleotides in 80 million sequences have been recorded as of late 2006.

Nucleic acid sequencing has become so routine that directly determining a protein's amino acid sequence (Section 5-3) is generally far more time-consuming than determining the base sequence of its corresponding gene. In fact, nucleic acid sequencing is invaluable for studying genes whose products have not yet been identified. If the gene can be sequenced, the probable function of its protein product may be deduced by comparing the base sequence to those of genes whose products are already characterized (see Box 3-1).

D Entire Genomes Have Been Sequenced

The advent of large-scale sequencing techniques brought to fruition the dream of sequencing entire genomes. However, the major technical hurdle in sequencing all the DNA in an organism's genome is not the DNA sequencing itself but, rather, assembling the tens of thousands to tens of millions of sequenced segments (depending on the size of the genome) into contiguous blocks and assigning them to their correct chromosomal positions. To do so required the development of automated sequencing protocols and mathematically sophisticated computer algorithms.

The first complete genome sequence to be determined, that of the bacterium *Haemophilus influenzae,* was reported in 1995 by Craig Venter. By mid-2007, the complete genome sequences of over 500 prokaryotes had been reported (with many more being determined) as well as those of dozens of eukaryotes, including humans, human pathogens, plants, and laboratory organisms (Table 3-3).

The determination of the ~3.2-billion-nucleotide human genome sequence was a gargantuan undertaking involving hundreds of scientists working in two groups, one led by Venter and the other by Francis Collins (Box 3-1), Eric Lander, and John Sulston. After over a decade of intense

Table 3-3 Some Sequenced Genomes

Organism	Genome Size (kb)	Number of Chromosomes
Mycoplasma genitalium (human parasite)	580	1
Rickettsia prowazekii (putative relative of mitochondria)	1,112	1
Haemophilus influenzae (human pathogen)	1,830	1
Escherichia coli (human symbiont)	4,639	1
Saccharomyces cerevisiae (baker's yeast)	11,700	16
Plasmodium falciparum (protozoan that causes malaria)	30,000	14
Caenorhabditis elegans (nematode)	97,000	6
Arabidopsis thaliana (dicotyledonous plant)	117,000	5
Drosophila melanogaster (fruit fly)	137,000	4
Oryza sativa (rice)	390,000	12
Danio rerio (zebra fish)	1,700,000	25
Gallus gallus (chicken)	1,200,000	40
Mus musculus (mouse)	2,500,000	20
Homo sapiens	3,200,000	23

effort, the “rough draft” of the human genome sequence was reported in early 2001 and the “finished” sequence was reported in mid-2003. This stunning achievement promises to revolutionize the way both biochemistry and medicine are viewed and practiced, although it is likely to require many years of further effort before its full significance is understood. Nevertheless, numerous important conclusions can already be drawn, including these:

1. About half the human genome consists of repeating sequences of various types.
2. Up to 60% of the genome is transcribed to RNA.
3. Only 1.1% to 1.4% of the genome (~2% of the transcribed RNA) encodes protein.
4. The human genome appears to contain only ~23,000 protein-encoding genes [also known as **open reading frames (ORFs)**] rather than the 50,000 to 140,000 ORFs that had previously been predicted. This compares with the ~6000 ORFs in yeast, ~13,000 in *Drosophila,* ~18,000 in *C. elegans,* and ~26,000 in *Arabidopsis* (although these numbers will almost certainly change as our ability to recognize ORFs improves).
5. Only a small fraction of human proteins are unique to vertebrates; most occur in other if not all life-forms.
6. Two randomly selected human genomes differ, on average, by only 1 nucleotide per 1250; that is, any two people are likely to be >99.9% genetically identical.

The obviously greater complexity of humans (vertebrates) relative to invertebrate forms of life is unlikely to be due to the not-much-larger numbers of ORFs that vertebrates encode. Rather, it appears that vertebrate proteins themselves are more complex than those of invertebrates; that is, vertebrate proteins tend to have more domains (modules) than invertebrate proteins, and these modules are more often selectively expressed through **alternative gene splicing** (a phenomenon in which a given gene transcript can be processed in multiple ways so as to yield different proteins when translated; Section 26-3A). Thus, many vertebrate genes encode several different although similar proteins.

E | Evolution Results from Sequence Mutations

One of the richest rewards of nucleic acid sequencing technology is the information it provides about the mechanisms of evolution. The chemical and physical properties of DNA, such as its regular three-dimensional shape and the elegant process of replication, may leave the impression that genetic information is relatively static. In fact, *DNA is a dynamic molecule, subject to changes that alter genetic information.* For example, the mispairing of bases during DNA replication can introduce errors known as **point mutations** in the daughter strand. Mutations also result from DNA damage by chemicals or radiation. More extensive alterations in genetic information are caused by faulty **recombination** (exchange of DNA between chromosomes) and the **transposition** of genes within or between chromosomes and, in some cases, from one organism to another. All these alterations to DNA provide the raw material for natural selection. When a mutated gene is transcribed and the messenger RNA is subsequently translated, the resulting protein may have properties that confer some advantage to the individual. As a beneficial change is passed from generation to

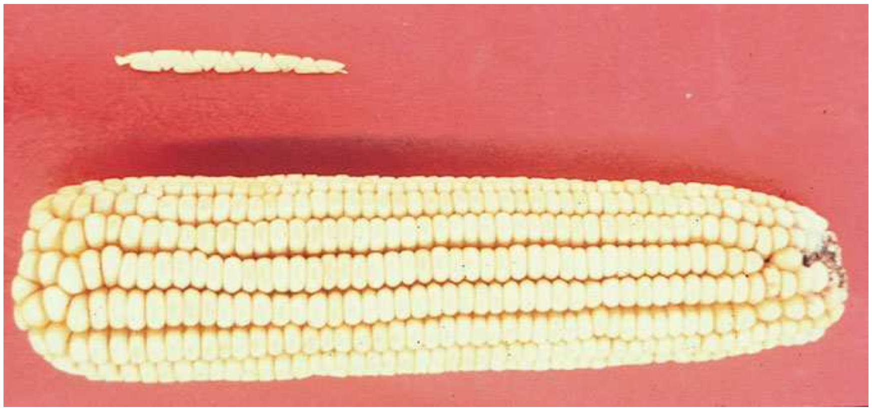

Figure 3-23 | Maize and teosinte. Despite the large differences in phenotype—maize (*bottom*) has hundreds of easily chewed kernels whereas teosinte (*top*) has only a few hard, inedible kernels—the plants differ in only a few genes. The ancestor of maize is believed to be a mutant form of teosinte in which the kernels were more exposed. [John Doebley/Visuals Unlimited.]

generation, it may become part of the standard genetic makeup of the species. Of course, many changes occur as a species evolves, not all of them simple and not all of them gradual.

Phylogenetic relationships can be revealed by comparing the sequences of similar genes in different organisms. The number of nucleotide differences between the corresponding genes in two species roughly indicates the degree to which the species have diverged through evolution. The regrouping of prokaryotes into archaea and bacteria (Section 1-2C) according to rRNA sequences present in all organisms illustrates the impact of sequence analysis.

Nucleic acid sequencing also reveals that species differing in **phenotype** (physical characteristics) are nonetheless remarkably similar at the molecular level. For example, humans and chimpanzees share 98–99% of their DNA. Studies of corn (maize) and its putative ancestor, teosinte, suggest that the plants differ in only a handful of genes governing kernel development (teosinte kernels are encased by an inedible shell; Fig. 3-23).

Small mutations in DNA are apparently responsible for relatively large evolutionary leaps. This is perhaps not so surprising when the nature of genetic information is considered. A mutation in a gene segment that does not encode protein might interfere with the binding of cellular factors that influence the timing of transcription. A mutation in a gene encoding an RNA might interfere with the binding of factors that affect the efficiency of translation. Even a minor rearrangement of genes could disrupt an entire developmental process, resulting in the appearance of a novel species. Notwithstanding the high probability that most sudden changes would lead to diminished individual fitness or the inability to reproduce, the capacity for sudden changes in genetic information is consistent with the fossil record. Ironically, the discontinuities in the fossil record that are probably caused in part by sudden genetic changes once fueled the adversaries of Charles Darwin's theory of evolution by natural selection.

CHECK YOUR UNDERSTANDING

Explain how the restriction–modification system operates.
Summarize the steps in the chain-terminator procedure for sequencing DNA.
What proportion of the human genome is transcribed? Translated?
Explain how evolution can result from a mutation in DNA.

5 Manipulating DNA

LEARNING OBJECTIVES

- Understand how recombinant DNA molecules are constructed and propagated.
- Understand that a DNA library is a collection of cloned DNA segments that can be screened to find a particular gene.
- Understand that the polymerase chain reaction copies and thereby amplifies a defined segment of DNA.
- Understand that recombinant DNA technology can be used to manipulate genes for protein expression or for the production of transgenic organisms.

Along with nucleic acid sequencing, techniques for manipulating DNA *in vitro* and *in vivo* (in the test tube and in living systems) have produced dramatic advances in biochemistry, cell biology, and genetics. In many cases, this **recombinant DNA technology** has made it possible to purify specific DNA sequences and to prepare them in quantities sufficient for study. Consider the problem of isolating a unique 1000-bp length of chromosomal DNA from *E. coli*. A 10-L culture of cells grown at a density of

$\sim 10^{10}$ cells · mL^{-1} contains only $\sim$0.1 mg of the desired DNA, which would be all but impossible to separate from the rest of the DNA using classical separation techniques (Sections 5-2 and 24-3). *Recombinant DNA technology, also called* ***molecular cloning*** *or* ***genetic engineering,*** *makes it possible to isolate, amplify, and modify specific DNA sequences.*

A | Cloned DNA Is an Amplified Copy

The following approach is used to obtain and amplify a segment of DNA:

1. A fragment of DNA of the appropriate size is generated by a restriction enzyme, by PCR (Section 3-5C), or by chemical synthesis.
2. The fragment is incorporated into another DNA molecule known as a **vector,** which contains the sequences necessary to direct DNA replication.
3. The vector—with the DNA of interest—is introduced into cells, where it is replicated.
4. Cells containing the desired DNA are identified, or selected.

Cloning refers to the production of multiple identical organisms derived from a single ancestor. The term **clone** refers to the collection of cells that contain the vector carrying the DNA of interest or to the DNA itself. In a suitable host organism, such as *E. coli* or yeast, large amounts of the inserted DNA can be produced.

Cloned DNA can be purified and sequenced (Section 3-4). Alternatively, if a cloned gene is flanked by the properly positioned regulatory sequences for RNA and protein synthesis, the host may also produce large quantities of the RNA and protein specified by that gene. Thus, cloning provides materials (nucleic acids and proteins) for other studies and also provides a means for studying gene expression under controlled conditions.

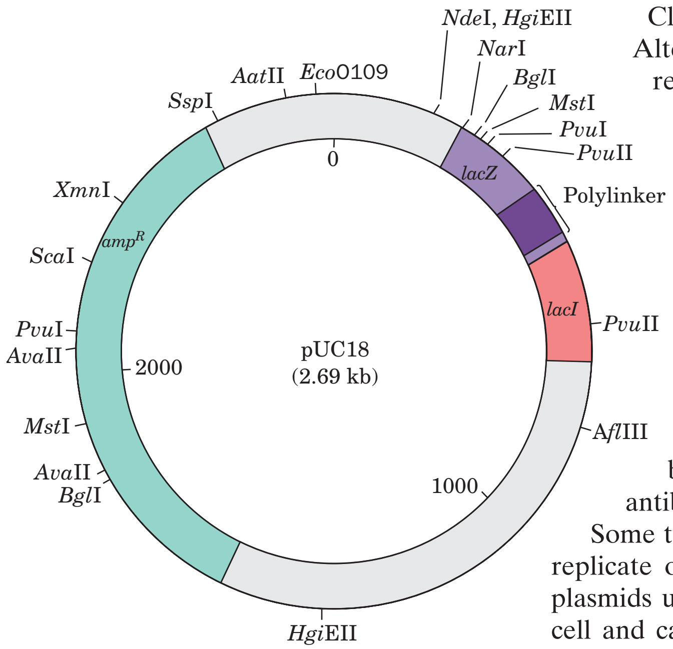

Figure 3-24 | The plasmid pUC18. As shown in this diagram, the circular plasmid contains multiple restriction sites, including a **polylinker** sequence that contains 13 restriction sites that are not present elsewhere on the plasmid. The three genes expressed by the plasmid are *amp*^{R}, which confers resistance to the antibiotic **ampicillin;** *lacZ,* which encodes the enzyme **β-galactosidase;** and *lacI,* which encodes a factor that controls transcription of *lacZ* (as described in Section 28-2A).

Cloning Vectors Carry Foreign DNA. A variety of small, autonomously replicating DNA molecules are used as cloning vectors. **Plasmids** are circular DNA molecules of 1 to 200 kb found in bacteria or yeast cells. Plasmids can be considered molecular parasites, but in many instances they benefit their host by providing functions, such as resistance to antibiotics, that the host lacks.

Some types of plasmids are present in one or a few copies per cell and replicate only when the bacterial chromosome replicates. However, the plasmids used for cloning are typically present in hundreds of copies per cell and can be induced to replicate until the cell contains two or three thousand copies (representing about half of the cell's total DNA). The plasmids that have been constructed for laboratory use are relatively small, replicate easily, carry genes specifying resistance to one or more antibiotics, and contain a number of conveniently located restriction endonuclease sites into which foreign DNA can be inserted. Plasmid vectors can be used to clone DNA segments of no more than $\sim$10 kb. The *E. coli* plasmid designated **pUC18** (Fig. 3-24) is a representative cloning vector ("pUC" stands for plasmid-Universal Cloning).

Bacteriophage λ (Fig. 3-25) is an alternative cloning vector that can accommodate DNA inserts up to 16 kb. The central third of the 48.5-kb phage genome is not required for infection and can therefore be replaced by foreign DNAs of similar size. The resulting **recombinant,** or **chimera** (named after the mythological monster with a lion's head, goat's body, and serpent's tail), is packaged into phage particles that can then be introduced into the host cells. One advantage of using phage vectors is that the recombinant DNA is produced in large amounts in easily purified form. **Baculoviruses,** which infect insect cells, are similarly used for cloning in cultures of insect cells.

Much larger DNA segments—up to several hundred kilobase pairs—can be cloned in large vectors known as **bacterial artificial chromosomes (BACs)** or **yeast artificial chromosomes (YACs).** YACs are linear DNA molecules that contain all the chromosomal structures required for normal replication and segregation during yeast cell division. BACs, which replicate in *E. coli,* are derived from circular plasmids that normally replicate long regions of DNA and are maintained at the level of approximately one copy per cell (properties similar to those of actual chromosomes).

Ligase Joins Two DNA Segments. A DNA segment to be cloned is often obtained through the action of restriction endonucleases. Most restriction enzymes cleave DNA to yield sticky ends (Section 3-4A). Therefore, as Janet Mertz and Ron Davis first demonstrated in 1972, *a restriction fragment can be inserted into a cut made in a cloning vector by the same restriction enzyme* (Fig. 3-26). The complementary ends of the two DNAs form base pairs **(anneal)** and the sugar–phosphate backbones are covalently **ligated,** or spliced together, through the action of an enzyme named **DNA ligase.** (A ligase produced by a bacteriophage can also join blunt-ended restriction fragments.) A great advantage of using a restriction enzyme to construct a recombinant DNA molecule is that the DNA insert can later be precisely excised from the cloned vector by cleaving it with the same restriction enzyme.

Selection Detects the Presence of a Cloned DNA. The expression of a chimeric plasmid in a bacterial host was first demonstrated in 1973 by Herbert Boyer and Stanley Cohen. A host bacterium can take up a plasmid when the two are mixed together, but the vector becomes permanently established in its bacterial host (transformation) with an efficiency of only ~0.1%. However, a single transformed cell can multiply without limit, producing large quantities of recombinant DNA. Bacterial cells are typically plated on a semisolid growth medium at a low enough density that discrete colonies, each arising from a single cell, are visible.

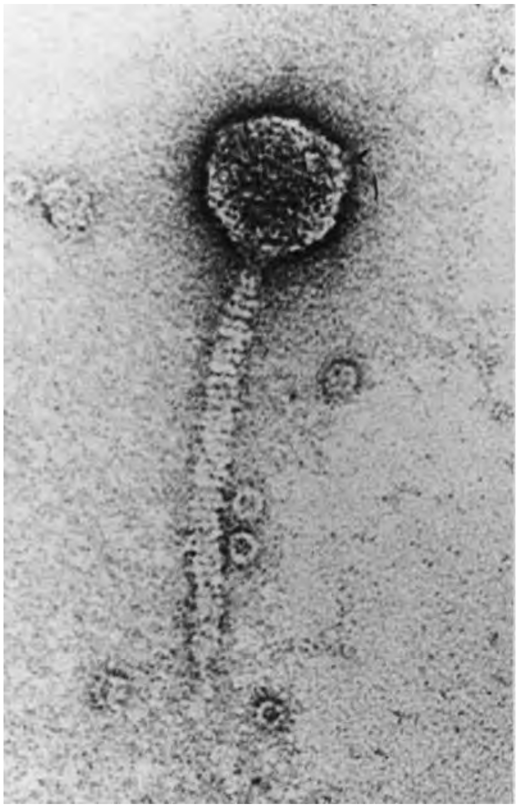

Figure 3-25 | **Bacteriophage λ.** During phage infection, DNA contained in the "head" of the phage particle enters the bacterial cell, where it is replicated ~100 times and packaged to form progeny phage. [Electron micrograph courtesy of A.F. Howatson. From Lewin, B., *Gene Expression,* Vol. 3, Fig. 5.23, Wiley (1977).]

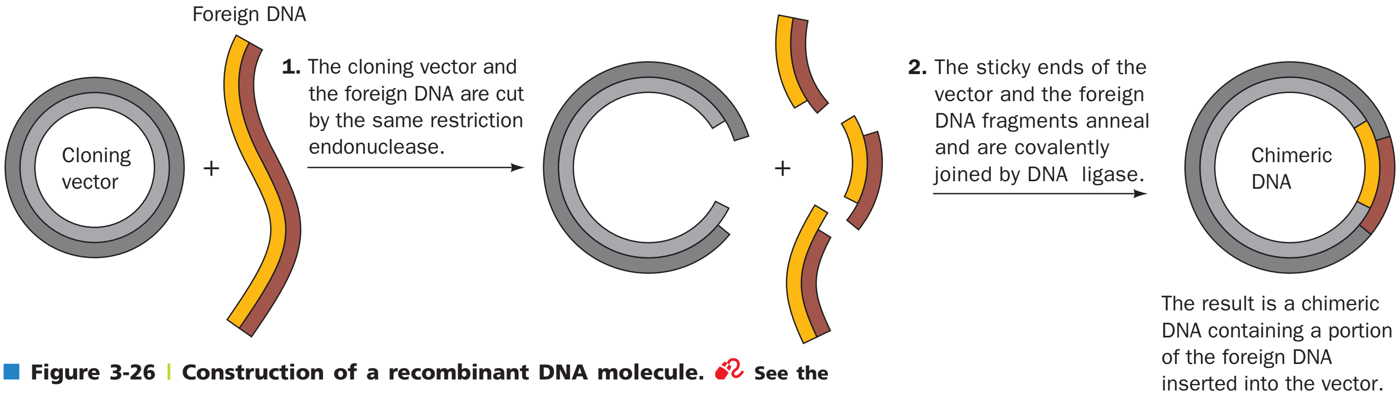

Foreign DNA
Cloning vector
+
1. The cloning vector and the foreign DNA are cut by the same restriction endonuclease.
+
2. The sticky ends of the vector and the foreign DNA fragments anneal and are covalently joined by DNA ligase.
Chimeric DNA
The result is a chimeric DNA containing a portion of the foreign DNA inserted into the vector.

Figure 3-26 | **Construction of a recombinant DNA molecule.** **See the Animated Figures.**

It is essential to select only those host organisms that have been transformed and that contain a properly constructed vector. In the case of plasmid transformation, selection can be accomplished through the use of antibiotics and/or chromogenic (color-producing) substances. For example, the *lacZ* gene in the pUC18 plasmid (see Fig. 3-24) encodes the enzyme β-galactosidase, which cleaves the colorless compound **X-gal** to a blue product:

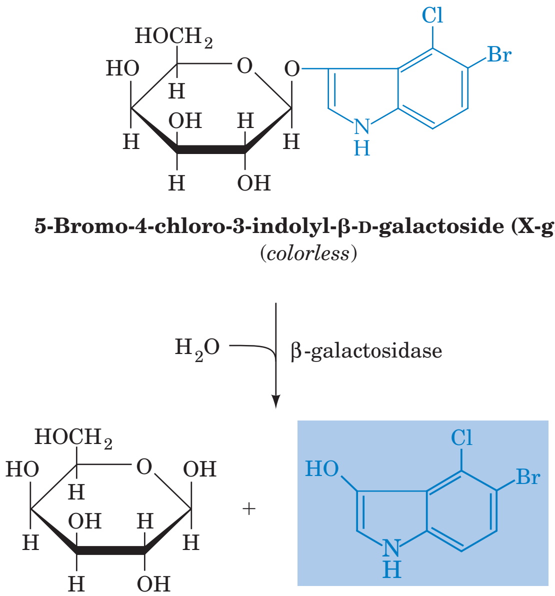

5-Bromo-4-chloro-3-indolyl-β-D-galactoside (X-gal)
(*colorless*)

β-D-Galactose **5-Bromo-4-chloro-3-hydroxyindole**
(*blue*)

Cells of *E. coli* that have been transformed by an unmodified pUC18 plasmid form blue colonies. However, if the plasmid contains a foreign DNA insert in its polylinker region, the colonies are colorless because the insert interrupts the protein-coding sequence of the *lacZ* gene and no functional β-galactosidase is produced. Bacteria that have failed to take up any plasmid are also colorless due to the absence of β-galactosidase, but these cells can be excluded by adding the antibiotic ampicillin to the growth medium (the plasmid includes the gene *amp*^{R}, which confers ampicillin resistance). Thus, successfully transformed cells form colorless colonies in the presence of ampicillin. Genes such as amp^R are known as **selectable markers.**

Genetically engineered bacteriophage λ vectors contain restriction sites that flank the dispensable central third of the phage genome. This segment can be replaced by foreign DNA, but the chimeric DNA is packaged in phage particles only if its length is from 75 to 105% of the 48.5-kb wild-type λ genome (Fig. 3-27). Consequently, λ phage vectors that have failed to acquire a foreign DNA insert are unable to propagate because they are too short to form infectious phage particles. Of course, the production of infectious phage particles results not in a growing bacterial colony but in a **plaque,** a region of lysed bacterial cells, on a culture plate containing a "lawn" of the host bacteria. The recombinant DNA—now much amplified—can be recovered from the phage particles in the plaque.

B | DNA Libraries Are Collections of Cloned DNA

In order to clone a particular DNA fragment, it must first be obtained in relatively pure form. The magnitude of this task can be appreciated by considering that, for example, a 1-kb fragment of human DNA represents

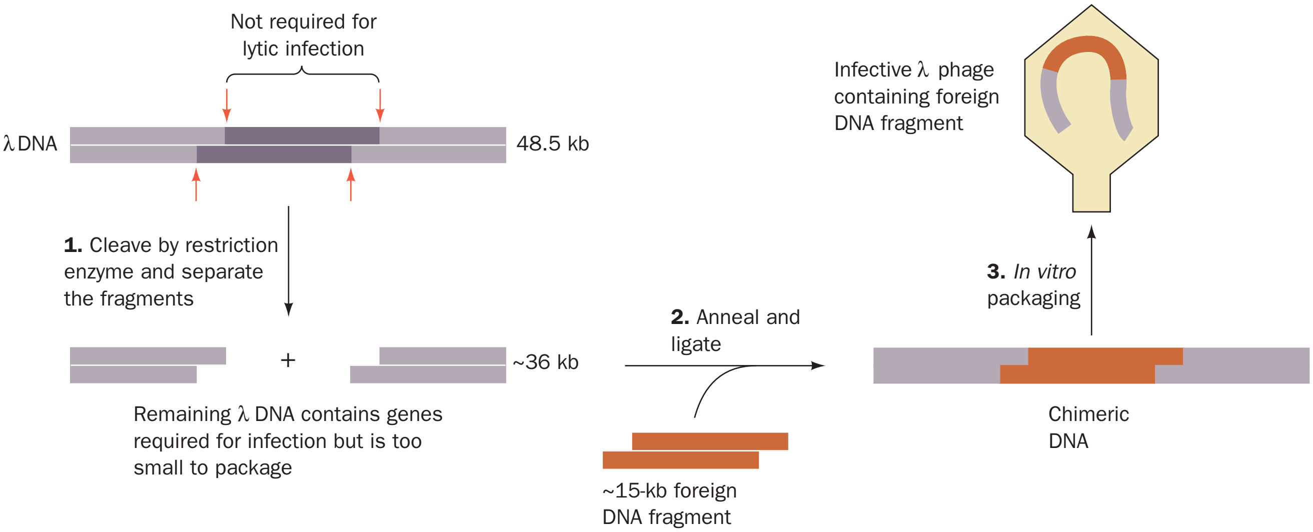
Not required for lytic infection
λ DNA
48.5 kb
1. Cleave by restriction enzyme and separate the fragments
+
~36 kb
Remaining λ DNA contains genes required for infection but is too small to package
2. Anneal and ligate
~15-kb foreign DNA fragment
Chimeric DNA
3. *In vitro* packaging
Infective λ phage containing foreign DNA fragment

■ **Figure 3-27 | Cloning with bacteriophage λ.** Removal of a nonessential portion of the phage genome allows a segment of foreign DNA to be inserted. The DNA insert can be packaged into an infectious phage particle only if the insert DNA has the appropriate size. **See the Animated Figures.**

only 0.000031% of the 3.2 billion-bp human genome. Of course, identifying a particular DNA fragment requires knowing something about its nucleotide sequence or its protein product. In practice, it is usually more difficult to identify a particular DNA fragment from an organism and then clone it than it is to clone all the organism's DNA that might contain the DNA of interest and then identify the clones containing the desired sequence.

A Genomic Library Includes All of an Organism's DNA. The cloned set of all DNA fragments from a particular organism is known as its **genomic library.** Genomic libraries are generated by a procedure known as **shotgun cloning.** The chromosomal DNA of the organism is isolated, cleaved to fragments of clonable size, and inserted into a cloning vector. The DNA is usually fragmented by partial rather than exhaustive restriction digestion so that the genomic library contains intact representatives of all the organism's genes, including those that contain restriction sites. DNA in solution can also be mechanically fragmented **(sheared)** by rapid stirring.

Given the large size of the genome relative to a gene, the shotgun cloning method is subject to the laws of probability. The number of randomly generated fragments that must be cloned to ensure a high probability that a desired sequence is represented at least once in the genomic library is calculated as follows: The probability P that a set of N clones contains a fragment that constitutes a fraction f, in bp, of the organism's genome is

$$P = 1 - (1 - f)^N \qquad [3\text{-}1]$$

Consequently,

$$N = \log(1 - P)/\log(1 - f) \qquad [3\text{-}2]$$

Thus, in order for P to equal 0.99 for fragments averaging 10 kb in length, $N = 2162$ for the 4600-kb *E. coli* chromosome and 63,000 for the 137,000-kb *Drosophila* genome. The use of BAC- or YAC-based genomic libraries with their large fragment lengths therefore greatly reduces the effort necessary to obtain a given gene segment from a large genome. After a BAC- or YAC-based clone containing the desired DNA has been identified (see below), its large DNA insert can be further fragmented and cloned again **(subcloned)** to isolate the target DNA.

A cDNA Library Represents Expressed Genes. A different type of DNA library contains only the expressed sequences from a particular cell type. Such a **cDNA library** is constructed by isolating all the cell's mRNAs and then copying them to DNA using a specialized type of DNA polymerase known as **reverse transcriptase** because it synthesizes DNA using RNA templates (Box 25-2). The **complementary DNA (cDNA)** molecules are then inserted into cloning vectors to form a cDNA library.

A Library Is Screened for the Gene of Interest. Once the requisite number of clones is obtained, the genomic library must be **screened** for the presence of the desired gene. This can be done by a process known as **colony** or ***in situ* hybridization** (Latin: *in situ,* in position; Fig. 3-28). The cloned yeast colonies, bacterial colonies, or phage plaques to be tested are transferred, by **replica plating,** from a master plate to a nitrocellulose filter (replica plating is also used to transfer colonies to plates containing different growth media). Next, the filter is treated with NaOH, which lyses the cells or phages and separates the DNA into single strands, which preferentially bind to the nitrocellulose. The filter is then dried to fix the DNA in place and incubated with a labeled **probe.** The probe is a short segment of DNA or RNA whose sequence is complementary to a portion of the DNA of interest. After washing away unbound probe, the presence of the probe on the nitrocellulose is detected by a technique appropriate for the label used (e.g., exposure to X-ray film for a radioactive probe, a process known as **autoradiography,** or illumination with an appropriate wavelength for a fluorescent probe). Only those colonies or plaques containing the desired gene bind the probe and are thereby detected. The corresponding clones can then be retrieved from the master plate. Using this technique, a

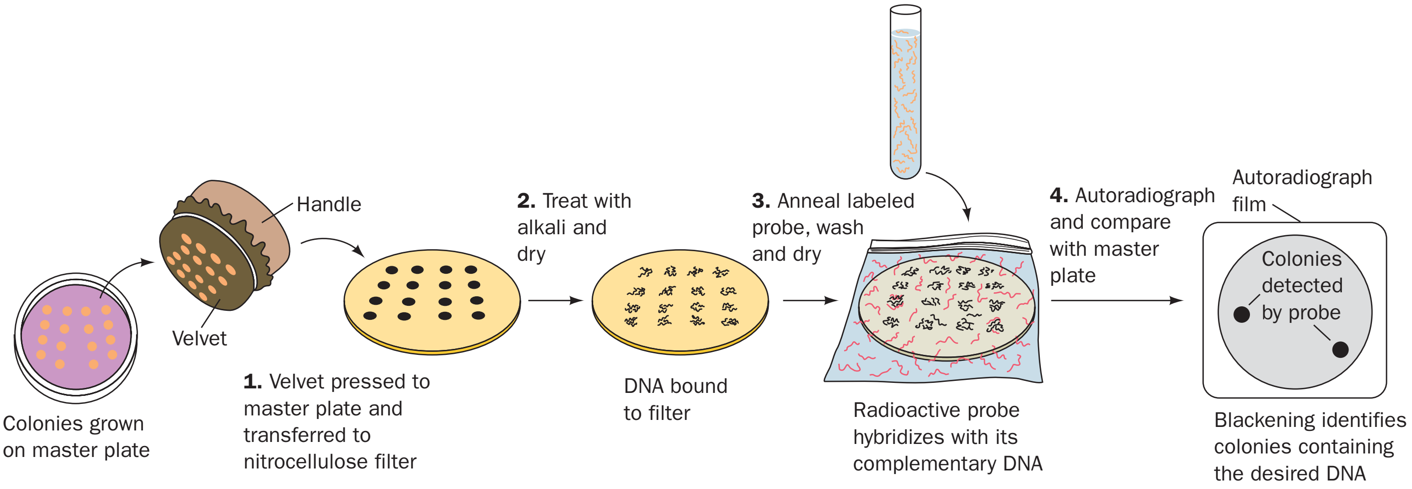
Handle
Velvet
Colonies grown on master plate
1. Velvet pressed to master plate and transferred to nitrocellulose filter
2. Treat with alkali and dry
DNA bound to filter
3. Anneal labeled probe, wash and dry
Radioactive probe hybridizes with its complementary DNA
4. Autoradiograph and compare with master plate
Autoradiograph film
Colonies detected by probe
Blackening identifies colonies containing the desired DNA

■ **Figure 3-28 | Colony (*in situ*) hybridization.** Colonies are transferred from a "master" culture plate by replica plating. Clones containing the DNA of interest are identified by the ability to bind a specific probe. Here, binding is detected by laying X-ray film over the dried filter. Since the colonies on the master plate and on the filter have the same spatial distribution, positive colonies are easily retrieved.

human genomic library of ~1 million clones can be readily screened for the presence of one particular DNA segment.

Choosing a probe for a gene whose sequence is not known requires some artistry. The corresponding mRNA can be used as a probe if it is available in sufficient quantities to be isolated. Alternatively, if the amino acid sequence of the protein encoded by the gene is known, the probe may be a mixture of the various synthetic oligonucleotides that are complementary to a segment of the gene's inferred base sequence. Several disease-related genes have been isolated using probes specific for nearby markers, such as repeated DNA sequences, that were already known to be genetically linked to the disease genes.

C | DNA Is Amplified by the Polymerase Chain Reaction

Although molecular cloning techniques are indispensable to modern biochemical research, the **polymerase chain reaction (PCR)** is often a faster and more convenient method for amplifying a specific DNA. Segments of up to 6 kb can be amplified by this technique, which was devised by Kary Mullis in 1985. *In PCR, a DNA sample is separated into single strands and incubated with DNA polymerase, dNTPs, and two oligonucleotide primers whose sequences flank the DNA segment of interest. The primers direct the DNA polymerase to synthesize complementary strands of the target DNA* (Fig. 3-29). Multiple cycles of this process, each doubling the amount of the target DNA, geometrically amplify the DNA starting from as little as a single gene copy. In each cycle, the two strands of the duplex DNA are separated by heating, the primers are annealed to their complementary segments on the DNA, and the DNA polymerase directs the synthesis of the complementary strands. The use of a heat-stable DNA polymerase, such as ***Taq* polymerase** isolated from *Thermus aquaticus,* a bacterium that thrives at 75°C, eliminates the need to add fresh enzyme after each round of heating (heat inactivates most enzymes). Hence, in the presence of sufficient quantities of primers and dNTPs, PCR is carried out simply by cyclically varying the temperature.

Twenty cycles of PCR increase the amount of the target sequence around a millionfold (~2^{20}) with high specificity. Indeed, PCR can amplify a target DNA present only once in a sample of 10^5 cells, so this method can be used without prior DNA purification. The amplified DNA can then be sequenced or cloned.

PCR amplification has become an indispensable tool. Clinically, it is used to diagnose infectious diseases and to detect rare pathological events such as mutations leading to cancer. Forensically, the DNA from a single hair or sperm can be am-

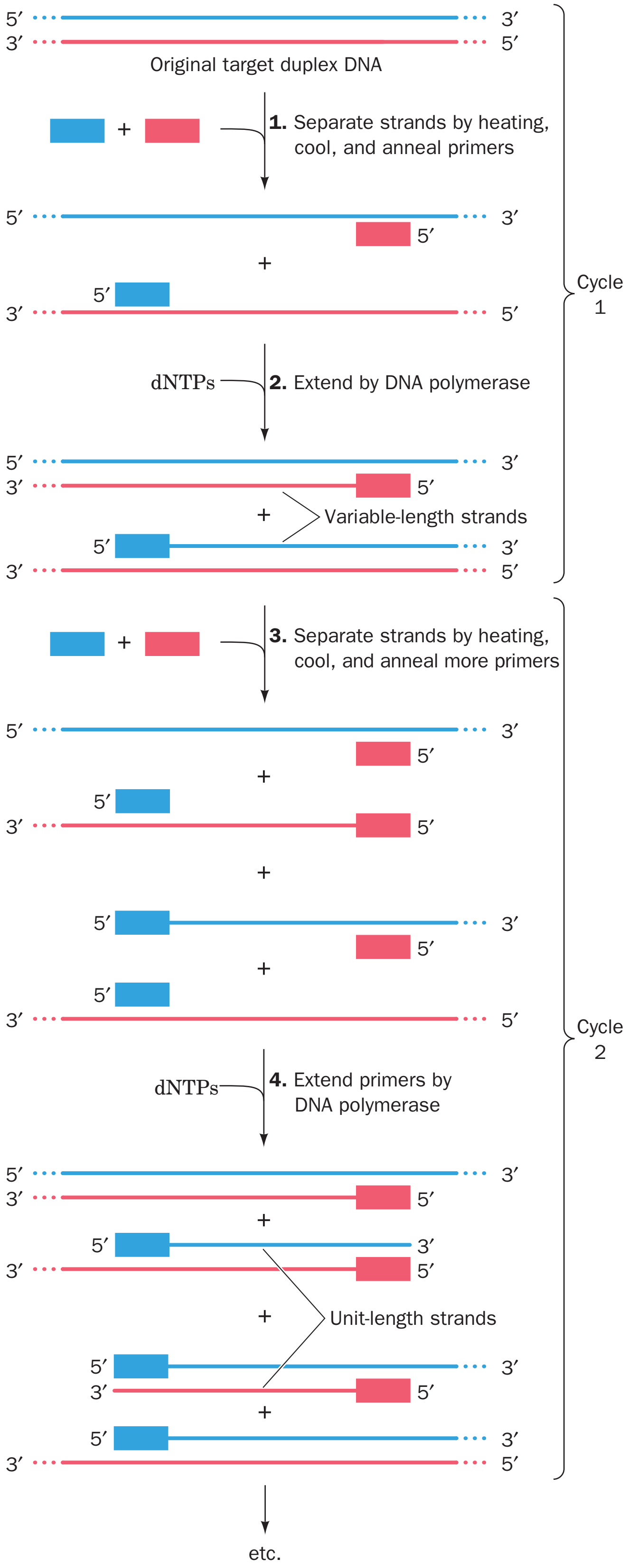
5′
3′
Original target duplex DNA
+
1. Separate strands by heating, cool, and anneal primers
Cycle 1
dNTPs
2. Extend by DNA polymerase
Variable-length strands
3. Separate strands by heating, cool, and anneal more primers
Cycle 2
dNTPs
4. Extend primers by DNA polymerase
Unit-length strands
etc.

■ **Figure 3-29 | The polymerase chain reaction (PCR).** In each cycle of the reaction, the strands of the duplex DNA are separated by heating, the reaction mixture is cooled to allow primers to anneal to complementary sequences on each strand, and DNA polymerase extends the primers. The number of "unit-length" strands doubles with every cycle after the second cycle. By choosing primers specific for each end of a gene, the gene can be amplified over a millionfold.

BOX 3-2 **PERSPECTIVES IN BIOCHEMISTRY**

DNA Fingerprinting

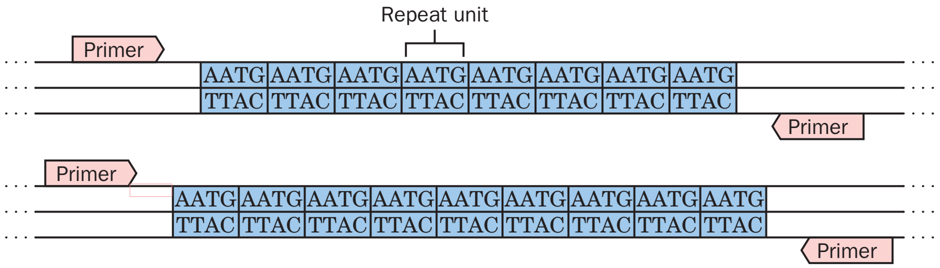
Repeat unit
Primer
AATG AATG AATG AATG AATG AATG AATG AATG
TTAC TTAC TTAC TTAC TTAC TTAC TTAC TTAC
Primer
Primer
AATG AATG AATG AATG AATG AATG AATG AATG AATG
TTAC TTAC TTAC TTAC TTAC TTAC TTAC TTAC TTAC
Primer

Forensic DNA testing takes advantage of DNA sequence variations or **polymorphisms** that occur among individuals. Many genetic polymorphisms have no functional consequences because they occur in regions of the DNA that contain many repetitions but do not encode genes (although if they are located near a "disease" gene, they can be used to track and identify the gene). Modern **DNA fingerprinting** methods examine these noncoding repetitive DNA sequences in samples that have been amplified by PCR.

Tandemly repeated DNA sequences occur throughout the human genome and include **short tandem repeats (STRs),** which contain variable numbers of repeating segments of two to seven base pairs. The most popular STR sites for forensic use contain tetranucleotide repeats. The number of repeats at any one site on the DNA varies between individuals, even within a family. Each different number of repeats at a site is called an **allele,** and each individual can have two alleles, one from each parent. Since PCR is the first step of the fingerprinting process, only a tiny amount (~1 ng) of DNA is needed. The region of DNA containing the STR is amplified by PCR using primers that are complementary to the unique (nonrepeating) sequences flanking the repeats.

The amplified products are separated by electrophoresis and detected by the fluorescent tag on their primers. An STR allele is small enough (<500 bp) that DNA fragments differing by a four-base repeat can be readily differentiated. The allele designation for each STR site is generally the number of times a repeated unit is present. STR sites that have been selected for forensic use generally have 7 to 30 different alleles.

In the example shown here, the upper trace shows the fluorescence of the electrophoretogram of reference standards (the set of all possible alleles, each identified by the number of repeat units, from 13 to 23). The lower trace corresponds to the sample being tested, which contains two alleles, one with 16 repeats and one with 18 repeats. Several STR sites can be analyzed simultaneously by using the appropriate primers and tagging them with different fluorescence dyes.

The probability of two individuals having matching DNA fingerprints depends on the number of STR sites examined and the number of alleles at each site. For example, if a pair of alleles at one site occurs in the population with a frequency of 10% (1/10), and a pair of alleles at a second site occurs with a frequency of 5% (1/20), then the probability that the DNA fingerprints from two individuals would match at both sites is 1 in 200 (1/10 × 1/20; the probabilities of independent events are multiplied). By examining multiple STR sites, the probability of obtaining matching fingerprints by chance becomes exceedingly small.

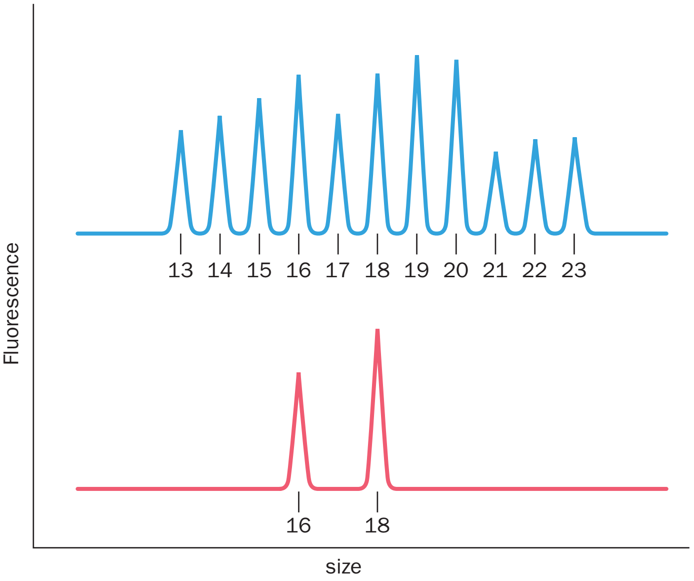

See Guided Exploration 3
PCR and site-directed mutagenesis.

plified by PCR so that it can be used to identify the donor (Box 3-2). Traditional ABO blood-type analysis requires a coin-sized drop of blood; PCR is effective on pinhead-sized samples of biological fluids. Courts now consider DNA sequences as unambiguous identifiers of individuals, as are fingerprints, because the chance of two individuals sharing extended sequences of DNA is typically one in a million or more. In a few cases, PCR has dramatically restored justice to convicts who were released from prison on the basis of PCR results that proved their innocence—even many years after the crime-scene evidence had been collected.

D | Recombinant DNA Technology Has Numerous Practical Applications

The ability to manipulate DNA sequences allows genes to be altered and expressed in order to obtain proteins with improved functional properties or to correct genetic defects.

Cloned Genes Can Be Expressed. The production of large quantities of scarce or novel proteins is relatively straightforward only for bacterial proteins: A cloned gene must be inserted into an **expression vector,** a plasmid that contains properly positioned transcriptional and translational control sequences. The production of a protein of interest may reach 30% of the host's total cellular protein. Such genetically engineered organisms are called **overproducers.** Bacterial cells often sequester large amounts of useless and possibly toxic (to the bacterium) protein as insoluble inclusions, which sometimes simplifies the task of purifying the protein.

Bacteria can produce eukaryotic proteins only if the recombinant DNA that carries the protein-coding sequence also includes bacterial transcriptional and translational control sequences. Synthesis of eukaryotic proteins in bacteria also presents other problems. For example, many eukaryotic genes are large and contain stretches of nucleotides **(introns)** that are transcribed and excised before translation (Section 26-3A); bacteria lack the machinery to excise the introns. In addition, many eukaryotic proteins are posttranslationally modified by the addition of carbohydrates or by other reactions. These problems can be overcome by using expression vectors that propagate in eukaryotic hosts, such as yeast or cultured insect or animal cells.

Table 3-4 lists some recombinant proteins produced for medical and agricultural use. In many cases, purification of these proteins directly from human or animal tissues is unfeasible on ethical or practical grounds.

Table 3-4 Some Proteins Produced by Genetic Engineering

Protein	Use
Human insulin	Treatment of diabetes
Human growth hormone	Treatment of some endocrine disorders
Erythropoietin	Stimulation of red blood cell production
Colony-stimulating factors	Production and activation of white blood cells
Coagulation factors IX and X	Treatment of blood clotting disorders (hemophilia)
Tissue-type plasminogen activator	Lysis of blood clots after heart attack and stroke
Bovine growth hormone	Production of milk in cows
Hepatitis B surface antigen	Vaccination against hepatitis B

Expression systems permit large-scale, efficient preparation of the proteins while minimizing the risk of contamination by viruses or other pathogens from tissue samples.

Site-Directed Mutagenesis Alters a Gene's Nucleotide Sequence. After isolating a gene, it is possible to modify the nucleotide sequence to alter the amino acid sequence of the encoded protein. **Site-directed mutagenesis,** a technique pioneered by Michael Smith, *mimics the natural process of evolution and allows predictions about the structural and functional roles of particular amino acids in a protein to be rigorously tested in the laboratory*.

Synthetic oligonucleotides are required to specifically alter genes through site-directed mutagenesis. An oligonucleotide whose sequence is identical to a portion of the gene of interest except for the desired base changes is used to direct replication of the gene. The oligonucleotide hybridizes to the corresponding **wild-type** (naturally occurring) sequence if there are no more than a few mismatched base pairs. Extension of the oligonucleotide, called a primer, by DNA polymerase yields the desired altered gene (Fig. 3-30). The altered gene can then be inserted into an appropriate vector. A mutagenized primer can also be used to generate altered genes by PCR.

Transgenic Organisms Contain Foreign Genes. For many purposes it is preferable to tailor an intact organism rather than just a protein—true genetic engineering. Multicellular organisms expressing a gene from another organism are said to be **transgenic,** and the transplanted foreign gene is called a **transgene.**

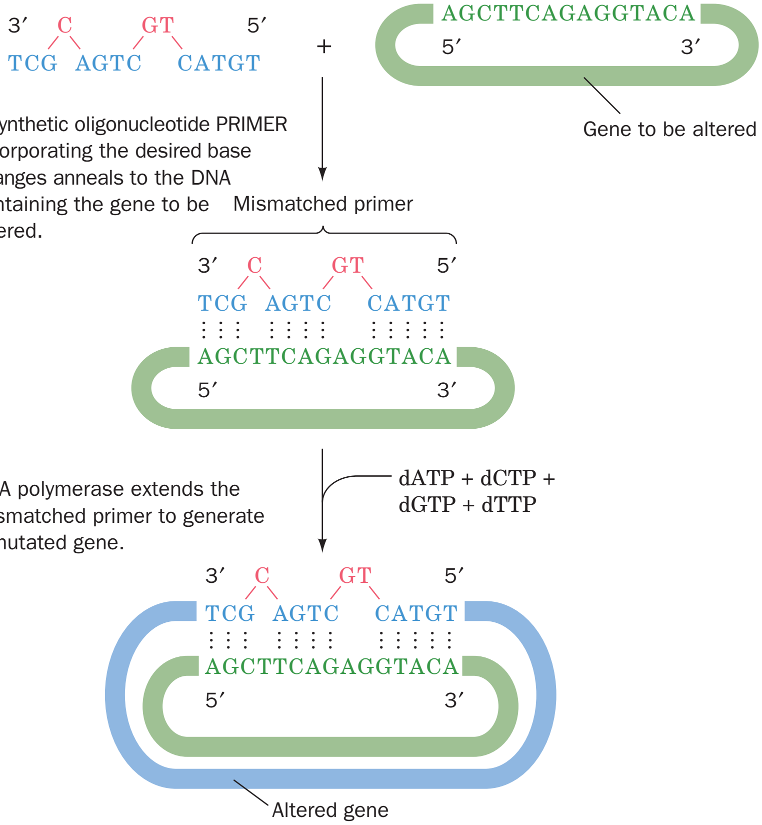

1. A synthetic oligonucleotide PRIMER incorporating the desired base changes anneals to the DNA containing the gene to be altered.

2. DNA polymerase extends the mismatched primer to generate a mutated gene.

Figure 3-30 | Site-directed mutagenesis. The altered gene can be inserted into a suitable cloning vector to be amplified, expressed, or used to generate a mutant organism. **See the Animated Figures.**

For the change to be permanent, that is, heritable, a transgene must be stably integrated into the organism's germ cells. For mice, this is accomplished by microinjecting cloned DNA encoding the desired altered characteristics into a fertilized egg and implanting it into the uterus of a foster mother. A well-known example of a transgenic mouse contains extra copies of a growth hormone gene (Fig. 3-31).

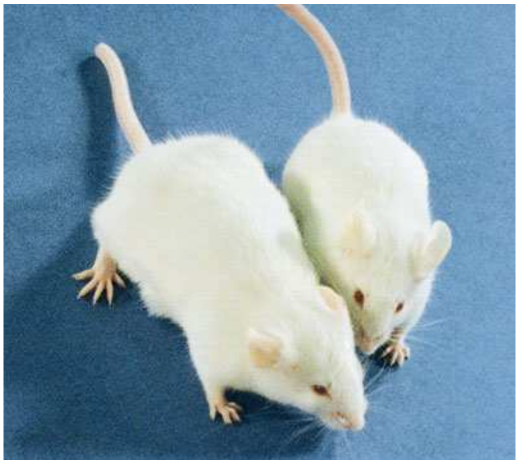

Figure 3-31 | Transgenic mouse. The gigantic mouse on the left was grown from a fertilized ovum that had been microinjected with DNA containing the rat growth hormone gene. He is nearly twice the weight of his normal littermate on the right. [Courtesy of Ralph Brinster, University of Pennsylvania.]

Transgenic farm animals have also been developed. Ideally, the genes of such animals could be tailored to allow the animals to grow faster on less food or to be resistant to particular diseases. Some transgenic farm animals have been engineered to secrete medically useful proteins into their milk. Harvesting such a substance from milk is much more cost-effective than producing the same substance in bacterial cultures.

One of the most successful transgenic organisms is corn (maize) that has been genetically modified to produce a protein that is toxic to plant-eating insects (but harmless to vertebrates). The toxin is synthesized by the soil microbe *Bacillus thuringiensis.* The toxin gene has been cloned into corn in order to confer protection against the European corn borer, a commercially significant pest that spends much of its life cycle inside the corn plant, where it is largely inaccessible to chemical insecticides. The use of "Bt corn," which is now widely planted in the United States, has greatly reduced the need for such toxic substances.

Transgenic plants have also been engineered for better nutrition. For example, researchers have developed a strain of rice with foreign genes that encode enzymes necessary to synthesize **β-carotene** (an orange pigment that is the precursor of **vitamin A**) and a gene for the iron-storage protein **ferritin.** The genetically modified rice, which is named "golden rice" (Fig. 3-32), should help alleviate vitamin A deficiencies (which afflict some 400 million people) and iron deficiencies (an estimated 30% of the world's population suffers from iron deficiency). Other transgenic plants include freeze-tolerant strawberries and slow-ripening tomatoes.

There is presently a widely held popular suspicion, particularly in Europe, that genetically modified or "GM" foods will somehow be harmful. However, extensive research, as well as considerable consumer experience, has failed to reveal any deleterious effects caused by GM foods (see Box 3-3).

Transgenic organisms have greatly enhanced our understanding of gene expression. Animals that have been engineered to contain a defective gene or that lack a gene entirely (a so-called **gene knockout**) also serve as experimental models for human diseases.

Genetic Defects Can Be Corrected. **Gene therapy** is the transfer of new genetic material to the cells of an individual in order to produce a therapeutic effect. Although the potential benefits of this as yet rudimentary technology are enormous, there are numerous practical obstacles to overcome. For example, the retroviral vectors (RNA-containing viruses) commonly used to directly introduce genes into humans can provoke a fatal immune response.

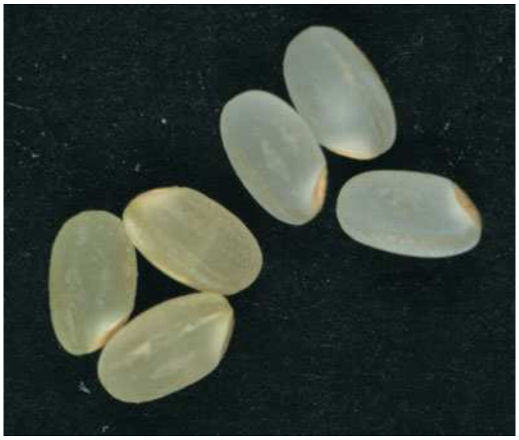

Figure 3-32 | Golden rice. The white grains on the right are the wild type. The grains on the left have been engineered to store up to three times more iron and to synthesize β-carotene, which gives them their yellow color. [Courtesy of Ingo Potrykus.]

BOX 3-3 PERSPECTIVES IN BIOCHEMISTRY

Ethical Aspects of Recombinant DNA Technology

In the early 1970s, when genetic engineering was first discussed, little was known about the safety of the proposed experiments. After considerable debate, during which there was a moratorium on such experiments, regulations for recombinant DNA research were drawn up. The rules prohibit obviously dangerous experiments (e.g., introducing the gene for diphtheria toxin into *E. coli,* which would convert this human symbiont into a deadly pathogen). Other precautions limit the risk of accidentally releasing potentially harmful organisms into the environment. For example, many vectors must be cloned in host organisms with special nutrient requirements. These organisms are unlikely to survive outside the laboratory.

The proven value of recombinant DNA technology has silenced nearly all its early opponents. Certainly, it would not have been possible to study some pathogens, such as the virus that causes AIDS, without cloning. The lack of recombinant-induced genetic catastrophes so far does not guarantee that recombinant organisms won't ever adversely affect the environment. Nevertheless, the techniques used by genetic engineers mimic those used in nature—that is, mutation and selection—so natural and man-made organisms are fundamentally similar. In any case, people have been breeding plants and animals for several millennia already, and for many of the same purposes that guide experiments with recombinant DNA.

There are other ethical considerations to be faced as new genetic engineering techniques become available. Bacterially produced human growth hormone is now routinely prescribed to increase the stature of abnormally short children. However, should athletes be permitted to use this protein, as some reportedly have, to increase their size and strength? Few would dispute the use of gene therapy, if it can be developed, to cure such genetic defects as sickle-cell anemia (Section 7-1E) and Lesch–Nyhan syndrome (Section 23-1D). If, however, it becomes possible to alter complex (i.e., multigene) traits such as athletic ability and intelligence, which changes would be considered desirable and who would decide whether to make them? Should gene therapy be used only to correct an individual's defects, or should it also be used to alter genes in the individual's germ cells so that succeeding generations would not inherit the defect? If it becomes easy to determine an individual's genetic makeup, should this information be used in evaluating applicants for educational and employment opportunities or for health insurance? These conundrums have led to the creation of a branch of philosophy, named **bioethics,** designed to deal with them.

The only documented success of gene therapy in humans has occurred in children with a form of **severe combined immunodeficiency disease (SCID)** known as **SCID-X1,** which without treatment would have required their isolation in a sterile environment to prevent fatal infection. SCID-X1 is caused by a defect in the gene encoding **γc cytokine receptor,** whose action is essential for proper immune system function. Bone marrow cells (the precursors of white blood cells) were removed from the bodies of SCID-X1 victims, incubated with a vector containing a normal γc cytokine receptor gene, and returned to their bodies. The transgenic bone marrow cells restored immune system function. However, because the viral vector integrates into the genome at random, the location of the transgene may affect the expression of other genes, triggering cancer. At least two children have developed leukemia (a white blood cell cancer) as a result of gene therapy for SCID-X1.

CHECK YOUR UNDERSTANDING

What are the roles of the vector and DNA ligase in cloning DNA?

Explain how cells containing recombinant DNA are selected.

What is a DNA library and how can it be screened for a particular gene?

Describe the steps required to amplify a DNA segment by PCR.

Explain how site-directed mutagenesis can be used to produce an altered protein in bacterial cells.

What is the difference between manipulating a gene for gene therapy and for producing a transgenic organism?

SUMMARY

1. Nucleotides consist of a purine or pyrimidine base linked to ribose to which at least one phosphate group is attached. RNA is made of ribonucleotides; DNA is made of deoxynucleotides (which contain 2′-deoxyribose).
2. In DNA, two antiparallel chains of nucleotides linked by phosphodiester bonds form a double helix. Bases in opposite strands pair: A with T, and G with C.

3. Single-stranded nucleic acids, such as RNA, can adopt stem–loop structures.
4. DNA carries genetic information in its sequence of nucleotides. When DNA is replicated, each strand acts as a template for the synthesis of a complementary strand.
5. According to the central dogma of molecular biology, one strand of the DNA of a gene is transcribed into mRNA. The RNA is then translated into protein by the ordered addition of amino acids that are bound to tRNA molecules that base-pair with the mRNA at the ribosome.
6. Restriction endonucleases that recognize certain sequences of DNA are used to specifically cleave DNA molecules.
7. Gel electrophoresis is used to separate and measure the sizes of DNA fragments.
8. In the chain-terminator method of DNA sequencing, the sequence of nucleotides in a DNA strand is determined by enzymatically synthesizing complementary polynucleotides that terminate with a dideoxy analog of each of the four nucleotides. Polynucleotide fragments of increasing size are separated by electrophoresis to reconstruct the original sequence.
9. Mutations and other changes to DNA are the basis for the evolution of organisms.
10. In molecular cloning, a fragment of foreign DNA is inserted into a vector for amplification in a host cell. Transformed cells can be identified by selectable markers.
11. Genomic libraries contain all the DNA of an organism. Clones harboring particular DNA sequences are identified by screening procedures.
12. The polymerase chain reaction amplifies selected sequences of DNA.
13. Recombinant DNA methods are used to produce wild-type or selectively mutagenized proteins in cells or entire organisms.

KEY TERMS

nucleotide **39**
nucleic acid **39**
nucleoside **41**
RNA **42**
DNA **42**
polynucleotide **43**
phosphodiester bond **43**
nucleotide residue **43**
5′ end **44**
3′ end **44**
monomer **44**
dimer **44**
trimer **44**
tetramer **44**
oligomer **44**
Chargaff’s rules **44**
tautomer **44**
double helix **45**
antiparallel **45**
major groove **46**
minor groove **46**
complementary base pairing **46**
genome **47**
chromosome **47**
diploid **47**
haploid **47**
bp **47**
kb **47**
stem–loop **47**
gene **48**
transformation **48**
replication **48**
transcription **49**
translation **49**
central dogma of molecular biology **49**
mRNA **49**
ribosome **49**
rRNA **49**
tRNA **49**
genomics **50**
transcriptomics **50**
proteomics **50**
gene expression **50**
bacteriophage **51**
restriction–modification system **51**
modification methylase **51**
restriction endonuclease **51**
endonuclease **51**
exonuclease **51**
palindrome **52**
sticky ends **52**
blunt ends **52**
gel electrophoresis **52**
chain-terminator procedure **53**
dNTP **53**
primer **54**
ddNTP **54**
ORF **58**
alternative gene splicing **58**
point mutation **58**
recombination **58**
transposition **58**
phenotype **59**
recombinant DNA technology **59**
vector **60**
cloning **60**
clone **60**
plasmid **60**
recombinant DNA **61**
BAC **61**
YAC **61**
anneal **61**
ligation **61**
selectable marker **62**
plaque **62**
DNA library **62**
genomic library **63**
shotgun cloning **63**
reverse transcriptase **64**
cDNA **64**
screening **64**
colony (*in situ*) hybridization **64**
replica plating **64**
probe **64**
autoradiography **64**
PCR **65**
polymorphism **66**
DNA fingerprinting **66**
STR **66**
allele **66**
expression vector **67**
overproducer **67**
intron **67**
site-directed mutagenesis **68**
wild type **68**
transgenic organism **68**
transgene **68**
gene knockout **69**
gene therapy **69**

PROBLEMS

1. Kinases are enzymes that transfer a phosphoryl group from a nucleoside triphosphate. Which of the following are valid kinase-catalyzed reactions?
   (a) ATP + GDP → ADP + GTP
   (b) ATP + GMP → AMP + GTP
   (c) ADP + CMP → AMP + CDP
   (d) AMP + ATP → 2 ADP
2. A diploid organism with a 45,000-kb haploid genome contains 21% G residues. Calculate the number of A, C, G, and T residues in the DNA of each cell in this organism.

3. A segment of DNA containing 20 base pairs includes 7 guanine residues. How many adenine residues are in the segment? How many uracil residues are in the segment?

4. Draw the tautomeric forms of (a) adenine and (b) cytosine.

5. The adenine derivative hypoxanthine can base-pair with both cytosine and adenine. Show the structures of these base pairs.

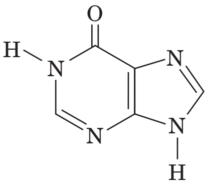

Hypoxanthine

6. Explain why the strands of a DNA molecule can be separated more easily at $\text{pH} > 11$.

7. How many different amino acids could theoretically be encoded by nucleic acids containing four different nucleotides if (a) each nucleotide coded for one amino acid; (b) consecutive sequences of two nucleotides coded for one amino acid; (c) consecutive sequences of three nucleotides coded for one amino acid; (d) consecutive sequences of four nucleotides coded for one amino acid?

8. The recognition sequence for the restriction enzyme *Taq*I is T↓CGA. Indicate the products of the reaction of *Taq*I with the DNA sequence shown.

5′–ACGTCGAATC–3′
3′–TGCAGCTTAG–5′

9. Using the data in Table 3-2, identify restriction enzymes that (a) produce blunt ends; (b) recognize and cleave the same sequence (called **isoschizomers**); (c) produce identical sticky ends.

10. Describe the outcome of a chain-terminator sequencing procedure in which (a) too little ddNTP is added; (b) too much ddNTP is added; (c) too few primers are present; (d) too many primers are present.

11. Calculate the number of clones required to obtain with a probability of 0.99 a specific 5-kb fragment from *C. elegans* (Table 3-3).

12. Describe how to select recombinant clones if a foreign DNA is inserted into the polylinker site of pUC18 and then introduced into *E. coli* cells.

13. Describe the possible outcome of a PCR experiment in which (a) one of the primers is inadvertently omitted from the reaction mixture; (b) one of the primers is complementary to several sites in the starting DNA sample; (c) there is a single-stranded break in the target DNA sequence, which is present in only one copy in the starting sample; (d) there is a double-stranded break in the target DNA sequence, which is present in only one copy in the starting sample.

14. Write the sequences of the two 12-residue primers that could be used to amplify the following DNA segment by PCR.

ATAGGCATAGGCCCATATGGCATAAGG-
CTTTATAATATGCGATAGGCGCTGGTCAG

15. (a) Why is a genomic library larger than a cDNA library for a given organism?

    (b) Why do cDNA libraries derived from different cell types within the same organism differ from each other?

16. A blood stain from a crime scene and blood samples from four suspects were analyzed by PCR using fluorescent primers associated with three STR loci: D3S1358, vWA, and FGA. The resulting electrophoretograms are shown below. The numbers beneath each peak identify the allele (upper box) and the height of the peak in relative fluorescence units (lower box).

    (a) Since everyone has two copies of each chromosome and therefore two alleles of each gene, what accounts for the appearance of only one allele at some loci?

    (b) Which suspect is a possible source of the blood?

    (c) Could the suspect be identified using just one of the three STR loci?

    (d) What can you conclude about the amount of DNA obtained from Suspect 1 compared to Suspect 4?

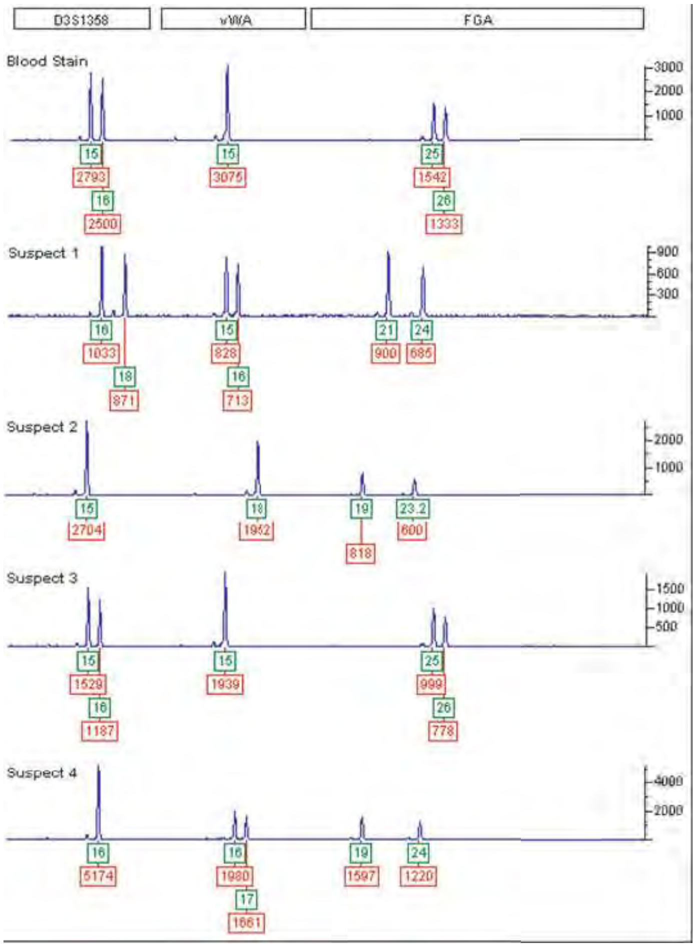

[From Thompson, W.C., Ford, S., Doom, T., Raymer, M., and Krane, D.E., Evaluating forensic DNA evidence: Essential elements of a competent defense review, *The Champion* **27,** 16–25 (2003).]

BIOINFORMATICS EXERCISES

Bioinformatics Exercises are available at www.wiley.com/college/voet.

Chapter 3

Databases for the Storage and "Mining" of Genome Sequences

1. **Finding Databases.** Locate databases for genome sequences and explore the meaning of terms related to them.
2. **The Institute for Genomic Research.** Explore a prokaryotic genome and find listings for eukaryotic genomes.
3. **Analyzing a DNA Sequence.** Given a DNA sequence, identify its open reading frame and translate it into a protein sequence.
4. **Sequence Homology.** Perform a BLAST search for homologs of a protein sequence.
5. **Plasmids and Cloning.** Predict the sizes of the fragments produced by the action of various restriction enzymes on plasmids.

REFERENCES

DNA Structure and Function

Bloomfield, V.A., Crothers, D.M., and Tinoco, I., Jr., *Nucleic Acids. Structures, Properties, and Functions,* University Science Books (2000).

Dickerson, R.E., DNA structure from A to Z, *Methods Enzymol.* **211,** 67–111 (1992). [Describes the various crystallographic forms of DNA.]

Thieffry, D., Forty years under the central dogma, *Trends Biochem. Sci.* **23,** 312–316 (1998). [Traces the origins, acceptance, and shortcomings of the idea that nucleic acids contain biological information.]

Watson, J.D. and Crick, F.H.C., Molecular structure of nucleic acids, *Nature* **171,** 737–738 (1953); *and* Genetical implications of the structure of deoxyribonucleic acid, *Nature* **171,** 964–967 (1953). [The seminal papers that are widely held to mark the origin of modern molecular biology.]

DNA Sequencing

Galperin, M.Y., The molecular biology database collection: 2007 update, *Nucleic Acids Res.* **35,** Database issue D3–D4 (2007). [This article cites 968 databases covering various aspects of molecular biology, biochemistry, and genetics. Additional articles in the same issue provide more information on individual databases. Freely available at http://nar.oxfordjournals.org.]

Graham, C.A. and Hill, A.J.M. (Eds.), *DNA Sequencing Protocols* (2nd ed.), Humana Press (2001).

Higgins, D. and Taylor, W. (Eds.), *Bioinformatics. Sequence, Structure and Databanks,* Oxford University Press (2000).

International Human Genome Sequencing Consortium, initial sequencing and analysis of the human genome, *Nature* **409,** 860–921 (2001); *and* Venter, J.C., *et al.,* the sequence of the human genome, *Science* **291,** 1304–1351 (2001). [These and other papers in the same issues of *Nature* and *Science* describe the data that constitute the draft sequence of the human genome and discuss how this information can be used in understanding biological function, evolution, and human health.]

International Human Genome Sequencing Consortium, finishing the euchromatic sequence of the human genome, *Nature* **431,** 931–945 (2004). [Describes the most up-to-date version of the human genome sequence.]

Recombinant DNA Technology

Ausubel, F.M., Brent, R., Kingston, R.E., Moore, D.D., Seidman, J.G., Smith, J.A., and Struhl, K., *Short Protocols in Molecular Biology* (5th ed.), Wiley (2002).

Nicholl, D.S.T., *An Introduction to Genetic Engineering* (2nd ed.), Cambridge University Press (2002).

Pingoud, A., Fuxreiter, M., Pingoud, V., and Wende, W., Type II restriction endonucleases: structure and mechanism, *Cell. Mol. Life Sci.* **62,** 685–707 (2005). [Includes an overview of different types of restriction enzymes.]

Sambrook, J., and Russell, D. *Molecular Cloning* (3rd ed.), Cold Spring Harbor Laboratory (2001). [A three-volume "bible" of laboratory protocols with accompanying background explanations.]

4

Amino Acids

In addition to the well-known taste sensations of sweet, sour, salty, and bitter is umami, the taste sensation elicited by monosodium glutamate (MSG), an amino acid commonly used as a flavor enhancer. [Jackson Vereen/Foodpix/PictureArts Corp.]

CHAPTER CONTENTS

1 Amino Acid Structure
- **A.** Amino Acids Are Dipolar Ions
- **B.** Peptide Bonds Link Amino Acids
- **C.** Amino Acid Side Chains Are Nonpolar, Polar, or Charged
- **D.** The p*K* Values of Ionizable Groups Depend on Nearby Groups
- **E.** Amino Acid Names Are Abbreviated

2 Stereochemistry

3 Amino Acid Derivatives
- **A.** Protein Side Chains May Be Modified
- **B.** Some Amino Acids Are Biologically Active

LEARNING OBJECTIVES

- Know the overall structure of an amino acid and the structures of the 20 different R groups.
- Understand how peptide bonds link amino acid residues in a polypeptide.
- Understand that amino acids include ionizable groups whose p*K* values vary when the amino acid is part of a polypeptide.

When scientists first turned their attention to nutrition, early in the nineteenth century, they quickly discovered that natural products containing nitrogen were essential for the survival of animals. In 1839, the Dutch chemist G. J. Mulder coined the term **protein** (Greek: *proteios,* primary) for this class of compounds. The physiological chemists of that time did not realize that proteins were actually composed of smaller components, amino acids, although the first amino acids had been isolated in 1830. In fact, for many years, it was believed that substances from plants—including proteins—were incorporated whole into animal tissues. This misconception was laid to rest when the process of digestion came to light. After it became clear that ingested proteins were broken down to smaller compounds containing amino acids, scientists began to consider the nutritive qualities of those compounds (Box 4-1).

Modern studies of proteins and amino acids owe a great deal to nineteenth and early twentieth century experiments. We now understand that nitrogen-containing amino acids are essential for life and that they are the building blocks of proteins. The central role of amino acids in biochemistry is perhaps not surprising: Several amino acids are among the organic compounds believed to have appeared early in the earth's history (Section 1-1A). Amino acids, as ancient and ubiquitous molecules, have been co-opted by evolution for a variety of purposes in living systems. We begin this chapter by discussing the structures and chemical properties of the common amino acids, including their stereochemistry, and end with a brief summary of the structures and functions of some related compounds.

1 Amino Acid Structure

The analyses of a vast number of proteins from almost every conceivable source have shown that *all proteins are composed of 20 "standard" amino acids.* Not every protein contains all 20 types of amino acids, but most proteins contain most if not all of the 20 types.

The common amino acids are known as **α-amino acids** because they have a primary amino group ($-NH_2$) as a substituent of the **α carbon** atom, the carbon next to the carboxylic acid group ($-COOH$; Fig. 4-1).

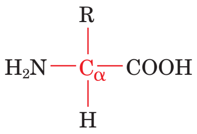

$$H_2N-\overset{\displaystyle R}{\underset{\displaystyle H}{C_\alpha}}-COOH$$

Figure 4-1 | General structure of an α-amino acid. The R groups differentiate the 20 standard amino acids.

BOX 4-1 **PATHWAYS OF DISCOVERY**

William C. Rose and the Discovery of Threonine

William C. Rose (1887–1985)

Identifying the amino acid constituents of proteins was a scientific challenge that grew out of studies of animal nutrition. At the start of the twentieth century, physiological chemists (the term *biochemist* was not yet used) recognized that not all foods provided adequate nutrition. For example, rats fed the corn protein zein as their only source of nitrogen failed to grow unless the amino acids tryptophan and lysine were added to their diet. Knowledge of metabolism at that time was mostly limited to information gleaned from studies in which intake of particular foods in experimental subjects (including humans) was linked to the urinary excretion of various compounds. Results of such studies were consistent with the idea that compounds could be transformed into other compounds, but clearly, nutrients were not wholly interchangeable.

At the University of Illinois, William C. Rose focused his research on nutritional studies to decipher the metabolic relationships of nitrogenous compounds. Among other things, his studies of rat growth and nutrition helped show that purines and pyrimidines were derived from amino acids but that those compounds could not replace dietary amino acids.

In order to examine the nutritional requirements for individual amino acids, Rose hydrolyzed proteins to obtain their component amino acids and then selectively removed certain amino acids. In one of his first experiments, he removed arginine and histidine from a hydrolysate of the milk protein casein. Rats fed on this preparation lost weight unless the amino acid histidine was added back to the food. However, adding back arginine did not compensate for the apparent requirement for histidine. These results prompted Rose to investigate the requirements for all the amino acids. Using similar experimental approaches, Rose demonstrated that cysteine, histidine, and tryptophan could not be replaced by other amino acids.

From preparations based on hydrolyzed proteins, Rose moved to mixtures of pure amino acids. Thirteen of the 19 known amino acids could be purified, and the other six synthesized. However, rats fed these 19 amino acids as their sole source of dietary nitrogen lost weight. Although one possible explanation was that the proportions of the pure amino acids were not optimal, Rose concluded that there must be an additional essential amino acid, present in naturally occurring proteins and their hydrolysates but not in his amino acid mixtures.

After several years of effort, Rose obtained and identified the missing amino acid. In work published in 1935, Rose showed that adding this amino acid to the other 19 could support rat growth. Thus, the twentieth and last amino acid, threonine, was discovered.

Experiments extending over the next 20 years revealed that 10 of the 20 amino acids found in proteins are nutritionally essential, so that removal of one of these causes growth failure and eventually death in experimental animals. The other 10 amino acids were considered "dispensable" since animals could synthesize adequate amounts of them.

Rose's subsequent work included verifying the amino acid requirements of humans, using graduate students as subjects. Knowing which amino acids were required for normal health—and in what amounts—made it possible to evaluate the potential nutritive value of different types of food proteins. Eventually, these findings helped guide the formulations used for intravenous feeding.

McCoy, R.H., Meyer, C.E., and Rose, W.C., Feeding experiments with mixtures of highly purified amino acids. VIII. Isolation and identification of a new essential amino acid, *J. Biol. Chem.* **112,** 283–302 (1935). [Freely available at http://www.jbc.org.]

The sole exception is proline, which has a secondary amino group (—NH—), although for uniformity we shall refer to proline as an α-amino acid. The 20 standard amino acids differ in the structures of their side chains **(R groups).** Table 4-1 displays the names and complete chemical structures of the 20 standard amino acids.

A | Amino Acids Are Dipolar Ions

The amino and carboxylic acid groups of amino acids readily ionize. The pK values of the carboxylic acid groups (represented by pK_1 in Table 4-1) lie in a small range around 2.2, while the pK values of the α-amino groups (pK_2) are near 9.4. *At physiological pH (~7.4), the amino groups are protonated and the carboxylic acid groups are in their conjugate base (carboxylate) form* (Fig. 4-2). An amino acid can therefore act as both an acid and a base.

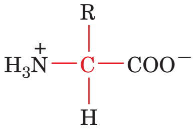

$$H_3\overset{+}{N}-\underset{H}{\overset{R}{C}}-COO^-$$

Figure 4-2 | A dipolar amino acid. At physiological pH, the amino group is protonated and the carboxylic acid group is unprotonated.

Table 4-1 Covalent Structures and Abbreviations of the "Standard" Amino Acids of Proteins, Their Occurrence, and the p*K* Values of Their Ionizable Groups

Name, Three-letter Symbol, and One-letter Symbol	Structural Formula[a]	Residue Mass (D)[b]	Average Occurrence in Proteins (%)[c]	pK_1 α-COOH[d]	pK_2 $\alpha\text{-}NH_3^+$[d]	pK_R Side Chain[d]
Amino acids with nonpolar side chains						
Glycine Gly G	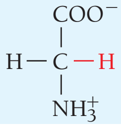 $H-\overset{COO^-}{\underset{NH_3^+}{C}}-H$	57.0	7.2	2.35	9.78	
Alanine Ala A	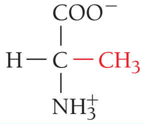 $H-\overset{COO^-}{\underset{NH_3^+}{C}}-CH_3$	71.1	7.8	2.35	9.87	
Valine Val V	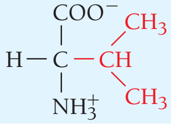	99.1	6.6	2.29	9.74	
Leucine Leu L	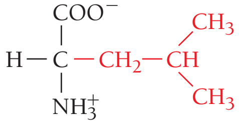	113.2	9.1	2.33	9.74	
Isoleucine Ile I	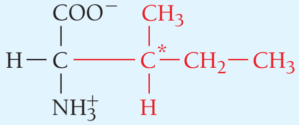	113.2	5.3	2.32	9.76	
Methionine Met M	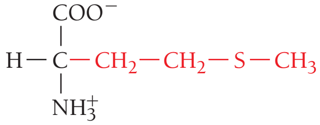 $H-\overset{COO^-}{\underset{NH_3^+}{C}}-CH_2-CH_2-S-CH_3$	131.2	2.2	2.13	9.28	
Proline Pro P	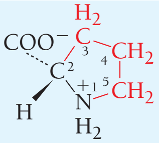	97.1	5.2	1.95	10.64	
Phenylalanine Phe F	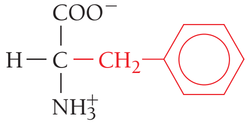	147.2	3.9	2.20	9.31	
Tryptophan Trp W	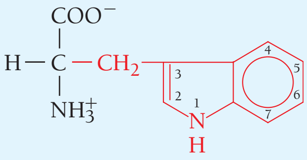	186.2	1.4	2.46	9.41	

---

[a] The ionic forms shown are those predominating at pH 7.0 (except for that of histidine[f]) although residue mass is given for the neutral compound. The C_α atoms, as well as those atoms marked with an asterisk, are chiral centers with configurations as indicated according to Fischer projection formulas (Section 4-2). The standard organic numbering system is provided for heterocycles.

[b] The residue masses are given for the neutral residues. For the molecular masses of the parent amino acids, add 18.0 D, the molecular mass of H_2O, to the residue masses. For side chain masses, subtract 56.0 D, the formula mass of a peptide group, from the residue masses.

[c] Calculated from a database of nonredundant proteins containing 300,688 residues as compiled by Doolittle, R.F., *in* Fasman, G.D. (Ed.), *Predictions of Protein Structure and the Principles of Protein Conformation,* Plenum Press (1989).

[d] Data from Dawson, R.M.C., Elliott, D.C., Elliott, W.H., and Jones, K.M., *Data for Biochemical Research* (3rd ed.), pp. 1–31, Oxford Science Publications (1986).

Table 4-1 (continued)

Name, Three-letter Symbol, and One-letter Symbol	Structural Formula[a]	Residue Mass (D)[b]	Average Occurrence in Proteins (%)[c]	pK_1 α-COOH[d]	pK_2 α-NH_3^+[d]	pK_R Side Chain[d]
Amino acids with uncharged polar side chains						
Serine Ser S	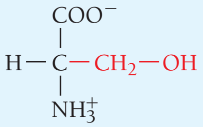	87.1	6.8	2.19	9.21	
Threonine Thr T	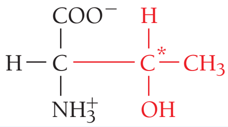	101.1	5.9	2.09	9.10	
Asparagine[e] Asn N	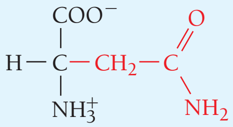	114.1	4.3	2.14	8.72	
Glutamine[e] Gln Q	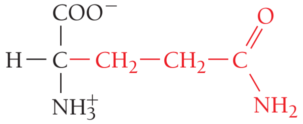	128.1	4.3	2.17	9.13	
Tyrosine Tyr Y	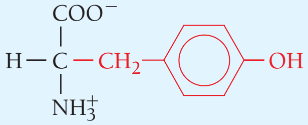	163.2	3.2	2.20	9.21	10.46 (phenol)
Cysteine Cys C	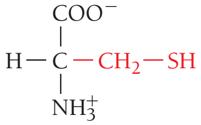	103.1	1.9	1.92	10.70	8.37 (sulfhydryl)
Amino acids with charged polar side chains						
Lysine Lys K	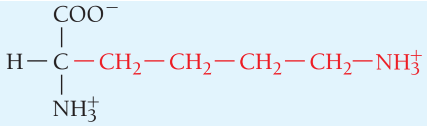	128.2	5.9	2.16	9.06	10.54 (ε-NH_3^+)
Arginine Arg R	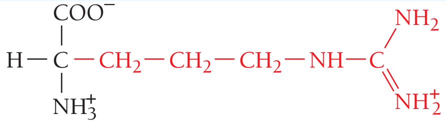	156.2	5.1	1.82	8.99	12.48 (guanidino)
Histidine[f] His H	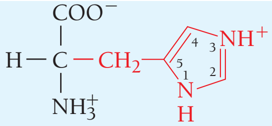	137.1	2.3	1.80	9.33	6.04 (imidazole)
Aspartic acid[e] Asp D	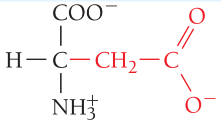	115.1	5.3	1.99	9.90	3.90 (β-COOH)
Glutamic acid[e] Glu E	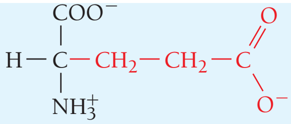	129.1	6.3	2.10	9.47	4.07 (γ-COOH)

---

[e] The three- and one-letter symbols for asparagine *or* aspartic acid are Asx and B, whereas for glutamine *or* glutamic acid they are Glx and Z. The one-letter symbol for an undetermined or "nonstandard" amino acid is X.

[f] Both neutral and protonated forms of histidine are present at pH 7.0, since its pK_R is close to 7.0.

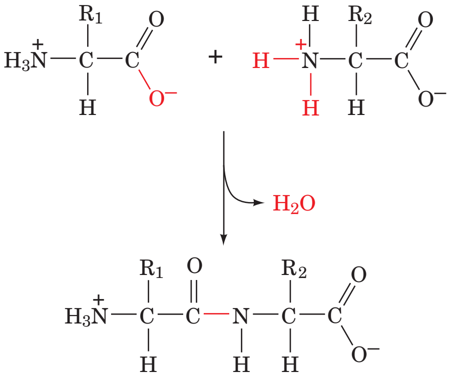

Figure 4-3 | Condensation of two amino acids. Formation of a CO—NH bond with the elimination of a water molecule produces a dipeptide. The peptide bond is shown in red. The residue with a free amino group is the N-terminus of the peptide, and the residue with a free carboxylate group is the C-terminus.

Table 4-1 also lists the pK values for the seven side chains that contain ionizable groups (pK_R).

Molecules such as amino acids, which bear charged groups of opposite polarity, are known as **dipolar ions** or **zwitterions.** Amino acids, like other ionic compounds, are more soluble in polar solvents than in nonpolar solvents. As we shall see, the ionic properties of the side chains influence the physical and chemical properties of free amino acids and amino acids in proteins.

B | Peptide Bonds Link Amino Acids

Amino acids can be polymerized to form chains. This process can be represented as a **condensation reaction** (bond formation with the elimination of a water molecule), as shown in Fig. 4-3. The resulting CO—NH linkage, an amide linkage, is known as a **peptide bond.**

Polymers composed of two, three, a few (3–10), and many amino acid units are known, respectively, as **dipeptides**, **tripeptides**, **oligopeptides**, and **polypeptides.** These substances, however, are often referred to simply as "peptides." After they are incorporated into a peptide, the individual amino acids (the monomeric units) are referred to as amino acid **residues.**

Polypeptides are linear polymers rather than branched chains; that is, each amino acid residue participates in two peptide bonds and is linked to its neighbors in a head-to-tail fashion. The residues at the two ends of the polypeptide each participate in just one peptide bond. The residue with a free amino group (by convention, the leftmost residue, as shown in Fig. 4-3) is called the **amino terminus** or **N-terminus.** The residue with a free carboxylate group (at the right) is called the **carboxyl terminus** or **C-terminus.**

Proteins are molecules that contain one or more polypeptide chains. *Variations in the length and the amino acid sequence of polypeptides are major contributors to the diversity in the shapes and biological functions of proteins,* as we shall see in succeeding chapters.

C | Amino Acid Side Chains Are Nonpolar, Polar, or Charged

The most useful way to classify the 20 standard amino acids is by the polarities of their side chains. According to the most common classification scheme, there are three major types of amino acids: (1) those with

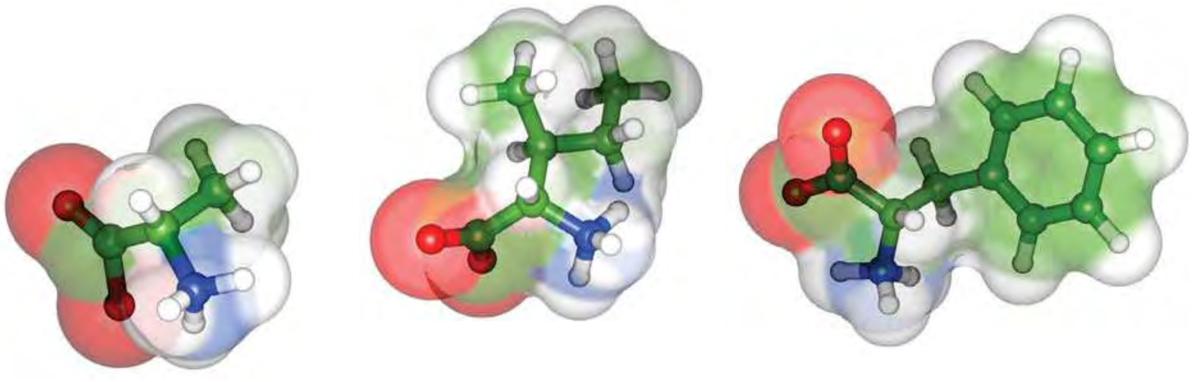

Alanine Isoleucine Phenylalanine

■ **Figure 4-4** | **Some amino acids with nonpolar side chains.** The amino acids are shown as ball-and-stick models embedded in transparent space-filling models. The atoms are colored according to type with C green, H white, N blue, and O red.

nonpolar R groups, (2) those with uncharged polar R groups, and (3) those with charged polar R groups.

The Nonpolar Amino Acid Side Chains Have a Variety of Shapes and Sizes. Nine amino acids are classified as having nonpolar side chains. The three-dimensional shapes of some of these amino acids are shown in Fig. 4-4. **Glycine** has the smallest possible side chain, an H atom. **Alanine, valine, leucine,** and **isoleucine** have aliphatic hydrocarbon side chains ranging in size from a methyl group for alanine to isomeric butyl groups for leucine and isoleucine. **Methionine** has a thioether side chain that resembles an *n*-butyl group in many of its physical properties (C and S have nearly equal electronegativities, and S is about the size of a methylene group). **Proline** has a cyclic pyrrolidine side group. **Phenylalanine** (with its phenyl moiety) and **tryptophan** (with its indole group) contain aromatic side groups, which are characterized by bulk as well as nonpolarity.

Uncharged Polar Side Chains Have Hydroxyl, Amide, or Thiol Groups. Six amino acids are commonly classified as having uncharged polar side chains (Table 4-1 and Fig. 4-5). **Serine** and **threonine** bear hydroxylic R groups of different sizes. **Asparagine** and **glutamine** have amide-bearing side chains of different sizes. **Tyrosine** has a phenolic group (and, like phenylalanine and tryptophan, is aromatic). **Cysteine** is unique among the

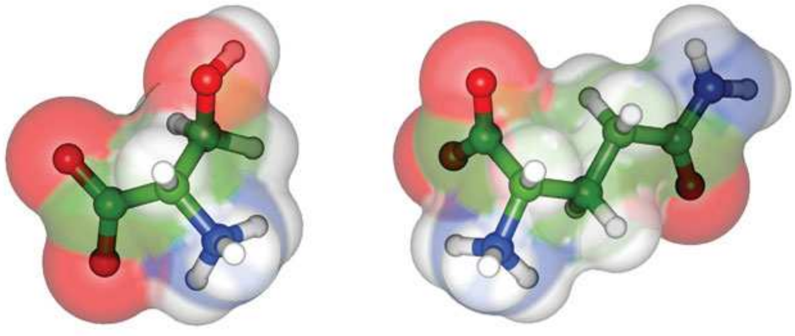

Serine Glutamine

■ **Figure 4-5** | **Some amino acids with uncharged polar side chains.** Atoms are represented and colored as in Fig. 4-4. Note the presence of electronegative atoms on the side chains.

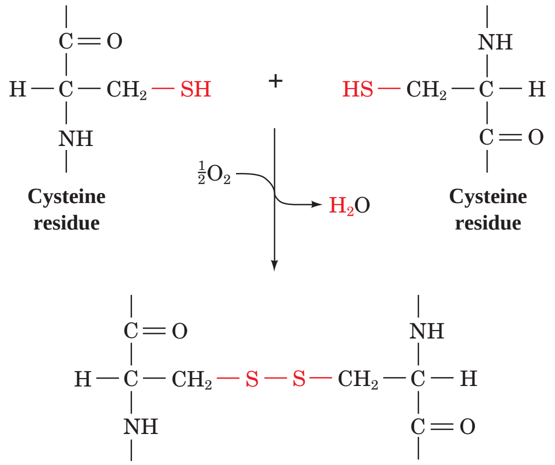

Figure 4-6 | Disulfide-bonded cysteine residues. The disulfide bond forms when the two thiol groups are oxidized.

20 amino acids in that it has a thiol group that can form a disulfide bond with another cysteine through the oxidation of the two thiol groups (Fig. 4-6).

Charged Polar Side Chains Are Positively or Negatively Charged. Five amino acids have charged side chains (Table 4-1 and Fig. 4-7). The side chains of the basic amino acids are positively charged at physiological pH values. **Lysine** has a butylammonium side chain, and **arginine** bears a guanidino group. As shown in Table 4-1, **histidine** carries an imidazolium moiety. Note that only histidine, with a pK_R of 6.04, readily ionizes within the physiological pH range. Consequently, both the neutral and cationic forms occur in proteins. In fact, the protonation–deprotonation of histidine side chains is a feature of numerous enzymatic reaction mechanisms.

The side chains of the acidic amino acids, **aspartic acid** and **glutamic acid,** are negatively charged above pH 3; in their ionized state, they are often referred to as **aspartate** and **glutamate.** Asparagine and glutamine are, respectively, the amides of aspartic acid and glutamic acid.

The allocation of the 20 amino acids among the three different groups is somewhat arbitrary. For example, glycine and alanine, the smallest of the amino acids, and tryptophan, with its heterocyclic ring, might just as well be classified as uncharged polar amino acids. Similarly, tyrosine and cysteine, with their ionizable side chains, might also be thought of as charged polar amino acids, particularly at higher pH values. In fact, the deprotonated side chain of cysteine (which contains the thiolate anion, S^-) occurs in a variety of enzymes, where it actively participates in chemical reactions.

Inclusion of a particular amino acid in one group or another reflects not just the properties of the isolated amino acid, but its behavior when it is part of a polypeptide. The structures of most polypeptides depend on a tendency for polar and ionic side chains to be hydrated and for nonpolar side chains to associate with each other rather than with water. This property of polypeptides is the hydrophobic effect (Section 2-1C) in action. As we shall see, the chemical and physical properties of amino acid side chains also govern the chemical reactivity of the polypeptide. It is worthwhile studying the structures of the 20 standard amino acids in order to

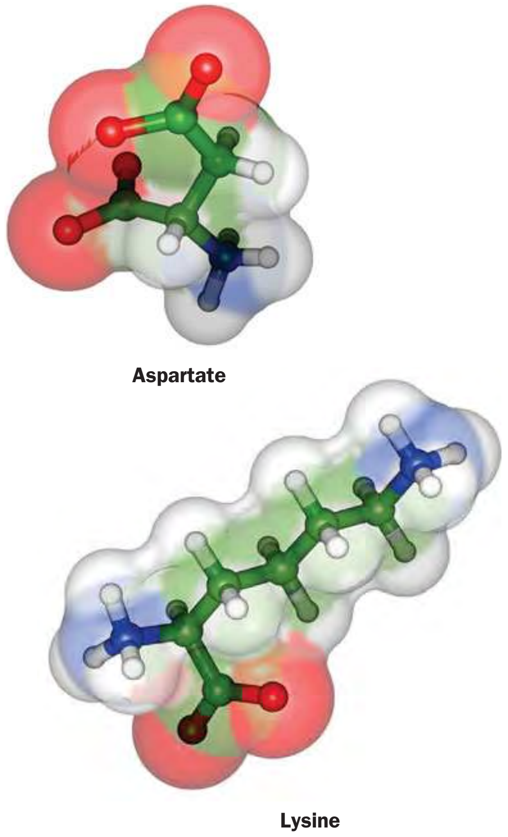

Figure 4-7 | Some amino acids with charged polar side chains. Atoms are represented and colored as in Fig. 4-4.

appreciate how they vary in polarity, acidity, aromaticity, bulk, conformational flexibility, ability to cross-link, ability to hydrogen bond, and reactivity toward other groups.

D | The p*K* Values of Ionizable Groups Depend on Nearby Groups

The α-amino acids have two or, for those with ionizable side chains, three acid–base groups. At very low pH values, these groups are fully protonated, and at very high pH values, these groups are unprotonated. At intermediate pH values, the acidic groups tend to be unprotonated, and the basic groups tend to be protonated. Thus, for the amino acid glycine, below pH 2.35 (the p*K* value of its carboxylic acid group), the $^+H_3NCH_2COOH$ form predominates. Above pH 2.35, the carboxylic acid is mostly ionized but the amino group is still mostly protonated ($^+H_3NCH_2COO^-$). Above pH 9.78 (the p*K* value of the amino group), the $H_2NCH_2COO^-$ form predominates. Note that *in aqueous solution, the un-ionized form (H_2NCH_2COOH) is present only in vanishingly small quantities*.

The pH at which a molecule carries no net electric charge is known as its **isoelectric point, p*I*.** For the α-amino acids,

$$pI = \tfrac{1}{2}(pK_i + pK_j) \qquad [4\text{-}1]$$

where K_i and K_j are the dissociation constants of the two ionizations involving the neutral species. For monoamino, monocarboxylic acids such as glycine, K_i and K_j represent K_1 and K_2. However, for aspartic and glutamic acids, K_i and K_j are K_1 and K_R, whereas for arginine, histidine, and lysine, these quantities are K_R and K_2.

Of course, amino acid residues in the interior of a polypeptide chain do not have free α-amino and α-carboxyl groups that can ionize (these groups are joined in peptide bonds; Fig. 4-3). Furthermore, the p*K* values of all ionizable groups, including the N- and C-termini, usually differ from the p*K* values listed in Table 4-1 for free amino acids. For example, the p*K* values of α-carboxyl groups in unfolded proteins range from 3.5 to 4.0. In the free amino acids, the p*K* values are much lower, because the positively charged ammonium group electrostatically stabilizes the COO^- group, in effect making it easier for the carboxylic acid group to ionize. Similarly, the p*K* values for α-amino groups in proteins range from 7.5 to 8.5. In the free amino acids, the p*K* values are higher, due to the electron-withdrawing character of the nearby carboxylate group, which makes it more difficult for the ammonium group to become deprotonated. In addition, the three-dimensional structure of a folded polypeptide chain may bring polar side chains and the N- and C-termini close together. The resulting electrostatic interactions between these groups may shift their p*K* values up to several pH units from the values for the corresponding free amino acids. For this reason, the p*I* of a polypeptide, which is a function of the p*K* values of its many ionizable groups, is not easily predicted and is usually determined experimentally.

E | Amino Acid Names Are Abbreviated

The three-letter abbreviations for the 20 standard amino acids given in Table 4-1 are widely used in the biochemical literature. Most of these abbreviations are taken from the first three letters of the name of the corresponding amino acid and are pronounced as written. The symbol **Glx**

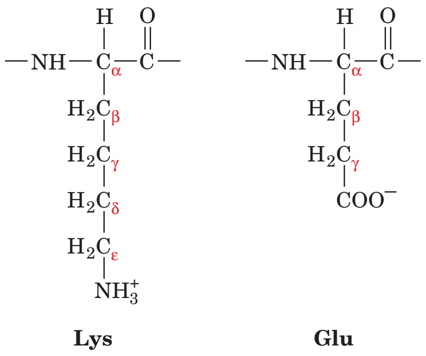

Figure 4-8 | Greek nomenclature for amino acids. The carbon atoms are assigned sequential letters in the Greek alphabet, beginning with the carbon next to the carbonyl group.

indicates Glu or Gln, and similarly, **Asx** means Asp or Asn. This ambiguous notation stems from laboratory experience: Asn and Gln are easily hydrolyzed to Asp and Glu, respectively, under the acidic or basic conditions often used to recover them from proteins. Without special precautions, it is impossible to tell whether a detected Glu was originally Glu or Gln, and likewise for Asp and Asn.

The one-letter symbols for the amino acids are also given in Table 4-1. This more compact code is often used when comparing the amino acid sequences of several similar proteins. Note that the one-letter symbol is usually the first letter of the amino acid's name. However, for sets of residues that have the same first letter, this is true only of the most abundant residue of the set.

Amino acid residues in polypeptides are named by dropping the suffix, usually **-ine,** in the name of the amino acid and replacing it by **-yl.** Polypeptide chains are described by starting at the N-terminus and proceeding to the C-terminus. The amino acid at the C-terminus is given the name of its parent amino acid. Thus, the compound

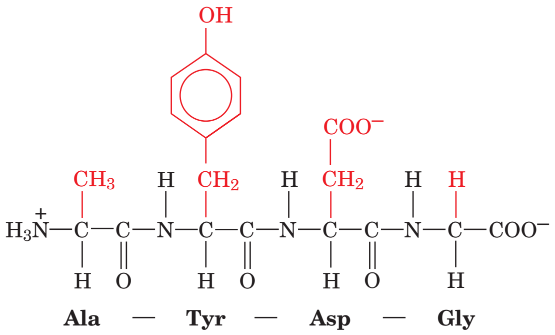

is called alanyltyrosylaspartylglycine. Obviously, such names for polypeptide chains of more than a few residues are extremely cumbersome. The tetrapeptide above can also be written as Ala-Tyr-Asp-Gly using the three-letter abbreviations, or AYDG using the one-letter symbols.

The various atoms of the amino acid side chains are often named in sequence with the Greek alphabet, starting at the carbon atom adjacent to the peptide carbonyl group. Therefore, as Fig. 4-8 indicates, the Lys residue is said to have an ε-amino group and Glu has a γ-carboxyl group. Unfortunately, this labeling system is ambiguous for several amino acids. Consequently, standard numbering schemes for organic molecules are also employed (and are indicated in Table 4-1 for the heterocyclic side chains).

CHECK YOUR UNDERSTANDING

Describe the overall structure of an amino acid.

Be able to identify the peptide bonds, amino acid residues, and the N- and C-termini of a polypeptide.

Draw the structures of the 20 standard amino acids and give their one- and three-letter abbreviations.

Classify the 20 standard amino acids by polarity, structure, type of functional group, and acid–base properties.

Why do the p*K* values of ionizable groups differ between free amino acids and amino acid residues in polypeptides?

LEARNING OBJECTIVES

- Understand that amino acids and other biological compounds are chiral molecules whose configurations can be depicted by Fischer projections.
- Understand that amino acids in proteins all have the L stereochemical configuration.

2 Stereochemistry

With the exception of glycine, all the amino acids recovered from polypeptides are **optically active;** that is, they rotate the plane of polarized light. The direction and angle of rotation can be measured using an instrument known as a **polarimeter** (Fig. 4-9).

Optically active molecules are asymmetric; that is, they are not superimposable on their mirror image in the same way that a left hand is not

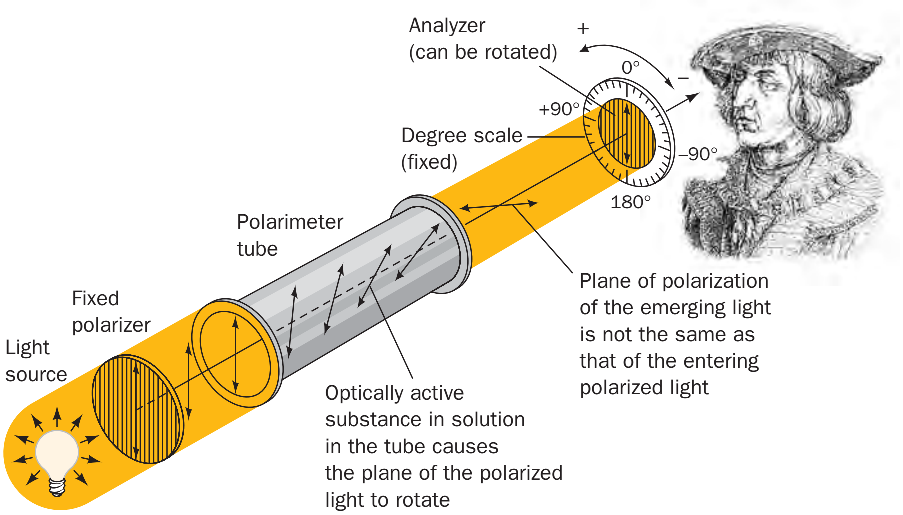
Analyzer
(can be rotated)
+
0°
–
+90°
Degree scale
(fixed)
–90°
180°
Polarimeter
tube
Fixed
polarizer
Light
source
Optically active
substance in solution
in the tube causes
the plane of the polarized
light to rotate
Plane of polarization
of the emerging light
is not the same as
that of the entering
polarized light

■ **Figure 4-9 | Diagram of a polarimeter.** This device is used to measure optical rotation.

superimposable on its mirror image, a right hand. This situation is characteristic of substances containing tetrahedral carbon atoms that have four different substituents. For example, the two molecules depicted in Fig. 4-10 are not superimposable; they are mirror images. The central atoms in such molecules are known as **asymmetric centers** or **chiral centers** and are said to have the property of **chirality** (Greek: *cheir,* hand). The C_α atoms of the amino acids (except glycine) are asymmetric centers. Glycine, which has two H atoms attached to its C_α atom, is superimposable on its mirror image and is therefore not optically active. Many biological molecules in addition to amino acids contain one or more chiral centers.

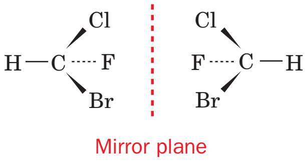
Cl
H
C
F
Br
Cl
F
C
H
Br
Mirror plane

■ **Figure 4-10 | The two enantiomers of fluorochlorobromomethane.** The four substituents are tetrahedrally arranged around the central carbon atom. A dotted line indicates that a substituent lies behind the plane of the paper, a wedged line indicates that it lies above the plane of the paper, and a thin line indicates that it lies in the plane of the paper. The mirror plane relating the enantiomers is represented by a vertical dashed line.

Chiral Centers Give Rise to Enantiomers. Molecules that are nonsuperimposable mirror images are known as **enantiomers** of one another. Enantiomeric molecules are physically and chemically indistinguishable by most techniques. *Only when probed asymmetrically, for example, by plane-polarized light or by reactants that also contain chiral centers, can they be distinguished or differentially manipulated.*

Unfortunately, there is no clear relationship between the structure of a molecule and the degree or direction to which it rotates the plane of polarized light. For example, leucine isolated from proteins rotates polarized light 10.4° to the left, whereas arginine rotates polarized light 12.5° to the right. (The enantiomers of these compounds rotate polarized light to the same degree but in the opposite direction.) It is not yet possible to predict optical rotation from the structure of a molecule or to derive the **absolute configuration** (spatial arrangement) of chemical groups around a chiral center from optical rotation measurements.

The Fischer Convention Describes the Configuration of Asymmetric Centers. Biochemists commonly use the **Fischer convention** to describe different forms of chiral molecules. In this system, the configuration of the groups around an asymmetric center is compared to that of **glyceraldehyde,** a molecule with one asymmetric center. In 1891, Emil Fischer proposed that the spatial isomers, or **stereoisomers,** of glyceraldehyde

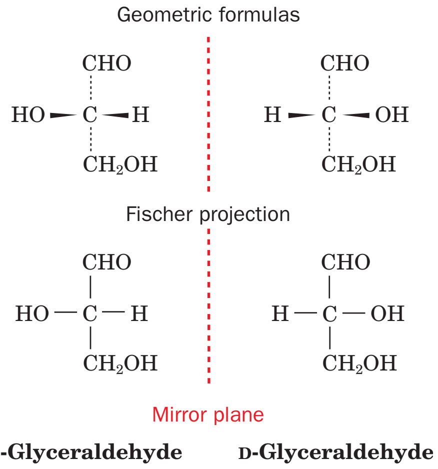

Figure 4-11 | The Fischer convention. The enantiomers of glyceraldehyde are shown as geometric formulas (*top*) and as Fischer projections (*bottom*). In a Fischer projection, horizontal lines represent bonds that extend above the page and vertical lines represent bonds that extend below the page (in some Fischer projections, the central chiral carbon atom is not shown explicitly).

be designated D-glyceraldehyde and L-glyceraldehyde (Fig. 4-11). The prefix L (note the use of a small uppercase letter) signified rotation of polarized light to the left (Greek: *levo,* left), and the prefix D indicated rotation to the right (Greek: *dextro,* right) by the two forms of glyceraldehyde. Fischer assigned the prefixes to the structures shown in Fig. 4-11 without knowing whether the structure on the left and the structure on the right were actually **levorotatory** and **dextrorotatory,** respectively. Only in 1949 did experiments confirm that Fischer's guess was indeed correct.

Fischer also proposed a shorthand notation for molecular configurations, known as **Fischer projections,** which are also given in Fig. 4-11. In the Fischer convention, horizontal bonds extend above the plane of the paper and vertical bonds extend below the plane of the paper.

The configuration of groups around any chiral center can be related to that of glyceraldehyde by chemically converting the groups to those of glyceraldehyde. For α-amino acids, the amino, carboxyl, R, and H groups around the C_α atom correspond to the hydroxyl, aldehyde, CH_2OH, and H groups, respectively, of glyceraldehyde.

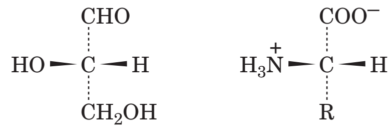

L-Glyceraldehyde **L-α-Amino acid**

Therefore, L-glyceraldehyde and L-α-amino acids are said to have the same **relative configuration.** *All amino acids derived from proteins have the L stereochemical configuration;* that is, they all have the same relative configuration around their C_α atoms. Of course, the L or D designation of an amino acid does not indicate its ability to rotate the plane of polarized light. Many L-amino acids are dextrorotatory.

The Fischer system has some shortcomings, particularly for molecules with multiple asymmetric centers. Each asymmetric center can have two possible configurations, so a molecule with n chiral centers has 2^n different possible stereoisomers. Threonine and isoleucine, for example, each have two chiral carbon atoms, and therefore each has four stereoisomers, or two pairs of enantiomers. [The enantiomers (mirror images) of the L forms are the D forms.] For most purposes, the Fischer system provides an adequate description of biological molecules. A more precise nomenclature system is also occasionally used by biochemists (see Box 4-2).

Life Is Based on Chiral Molecules. Consider the ordinary chemical synthesis of a chiral molecule, which produces a **racemic mixture** (containing equal amounts of each enantiomer). In order to obtain a product with net asymmetry, a chiral process must be employed. One of the most striking characteristics of life is its production of optically active molecules. *Biosynthetic processes almost invariably produce pure stereoisomers.* The fact that the amino acid residues of proteins all have the L configuration is just one example of this phenomenon. Furthermore, because most biological molecules are chiral, a given molecule—present in a single enantiomeric form—will bind to or react with only a single enantiomer of another compound. For example, a protein made of L-amino acid residues that reacts with a particular L-amino acid does not readily react with the D form of that amino acid. An otherwise identical synthetic protein made of D-amino acid residues, however, readily reacts only with the corresponding D-amino acid.

D-Amino acid residues are components of some relatively short (<20 residues) bacterial polypeptides. These polypeptides are perhaps most

BOX 4-2 **PERSPECTIVES IN BIOCHEMISTRY**

The *RS* System

A system to unambiguously describe the configurations of molecules with more than one asymmetric center was devised in 1956 by Robert Cahn, Christopher Ingold, and Vladimir Prelog. In the **Cahn–Ingold–Prelog** or ***RS* system,** the four groups surrounding a chiral center are ranked according to a specific although arbitrary priority scheme: Atoms of higher atomic number rank above those of lower atomic number (e.g., —OH ranks above —CH_3). If the first substituent atoms are identical, the priority is established by the next atom outward from the chiral center (e.g., —CH_2OH takes precedence over —CH_3). The order of priority of some common functional groups is

$$SH > OH > NH_2 > COOH > CHO > CH_2OH > C_6H_5 > CH_3 > H$$

The prioritized groups are assigned the letters W, X, Y, Z such that their order of priority ranking is W > X > Y > Z. To establish the configuration of the chiral center, it is viewed from the asymmetric center toward the Z group (lowest priority). If the order of the groups W → X → Y is clockwise, the configuration is designated *R* (Latin: *rectus,* right). If the order of W → X → Y is counterclockwise, the configuration is designated *S* (Latin: *sinistrus,* left).

L-Glyceraldehyde is (*S*)-glyceraldehyde because the three highest priority groups are arranged counterclockwise when the H atom (*dashed lines*) is positioned behind the chiral C atom (*large circle*).

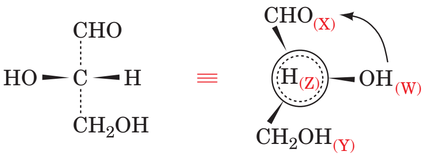

L-Glyceraldehyde **(*S*)-Glyceraldehyde**

All the L-amino acids in proteins are (*S*)-amino acids except cysteine, which is (*R*)-cysteine because the S in its side chain increases its priority. Other closely related compounds with the same designation under the Fischer DL convention may have different representations under the *RS* system. The *RS* system is particularly useful for describing the chiralities of compounds with multiple asymmetric centers. Thus, L-threonine can also be called (2*S*,3*R*)-threonine.

widely distributed as constituents of bacterial cell walls (Section 8-3B). The presence of the D-amino acids renders bacterial cell walls less susceptible to attack by the **peptidases** (enzymes that hydrolyze peptide bonds) that are produced by other organisms to digest bacteria. Likewise, D-amino acids are components of many bacterially produced peptide antibiotics. Most peptides containing D-amino acids are not synthesized by the standard protein synthetic machinery, in which messenger RNA is translated at the ribosome by transfer RNA molecules with attached L-amino acids (Chapter 27). Instead, the D-amino acids are directly joined together by the action of specific bacterial enzymes.

The importance of stereochemistry in living systems is also a concern of the pharmaceutical industry. *Many drugs are chemically synthesized as racemic mixtures, although only one enantiomer has biological activity.* In most cases, the opposite enantiomer is biologically inert and is therefore packaged along with its active counterpart. This is true, for example, of the anti-inflammatory agent **ibuprofen,** only one enantiomer of which is physiologically active (Fig. 4-12). Occasionally, the inactive enantiomer of a useful drug produces harmful effects and must therefore be eliminated from the racemic mixture. The most striking example of this is the drug **thalidomide** (Fig. 4-13), a mild sedative whose inactive enantiomer causes

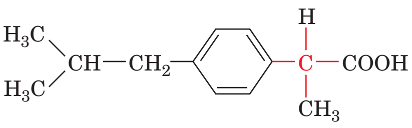

Ibuprofen

■ **Figure 4-12** | **Ibuprofen.** Only the enantiomer shown has anti-inflammatory action. The chiral carbon is red.

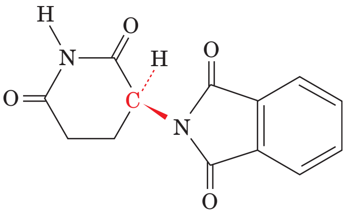

Thalidomide

■ **Figure 4-13** | **Thalidomide.** This drug was widely used in Europe as a mild sedative in the early 1960s. Its inactive enantiomer (not shown), which was present in equal amounts in the formulations used, causes severe birth defects in humans when taken during the first trimester of pregnancy. Thalidomide was often prescribed to alleviate the nausea (morning sickness) that is common during this period.

severe birth defects. Partly because of the unanticipated problems caused by inactive drug enantiomers, **chiral organic synthesis** has become an active area of medicinal chemistry.

CHECK YOUR UNDERSTANDING

Be able to identify the chiral carbons in the amino acids shown in Table 4-1.
Explain how the Fischer convention describes the absolute configuration of a chiral molecule.

3 Amino Acid Derivatives

LEARNING OBJECTIVES

- Understand that the side chains of amino acid residues in proteins may be covalently modified.
- Understand that some amino acids and amino acid derivatives function as hormones and regulatory molecules.

The 20 common amino acids are by no means the only amino acids that occur in biological systems. “Nonstandard” amino acid residues are often important constituents of proteins and biologically active peptides. In addition, many amino acids are not constituents of polypeptides at all but independently play a variety of biological roles.

A | Protein Side Chains May Be Modified

The “universal” genetic code, which is nearly identical in all known lifeforms (Section 27-1), specifies only the 20 standard amino acids of Table 4-1. Nevertheless, many other amino acids, some of which are shown in Fig. 4-14, are components of certain proteins. *In almost all cases, these unusual amino acids result from the specific modification of an amino acid residue after the polypeptide chain has been synthesized*.

Amino acid modifications include the simple addition of small chemical groups to certain amino acid side chains: hydroxylation, methylation, acetylation, carboxylation, and phosphorylation. Larger groups, including lipids and carbohydrate polymers, are attached to particular amino acid residues of certain proteins. The free amino and carboxyl groups at the N- and C-termini of a polypeptide can also be chemically modified. These modifications are often important, if not essential, for the function of the protein. In some cases, several amino acid side chains together form a novel structure (Box 4-3).

B | Some Amino Acids Are Biologically Active

The 20 standard amino acids undergo a bewildering number of chemical transformations to other amino acids and related compounds as part of their normal cellular synthesis and degradation. In a few cases, the intermediates of amino acid metabolism have functions beyond their immediate

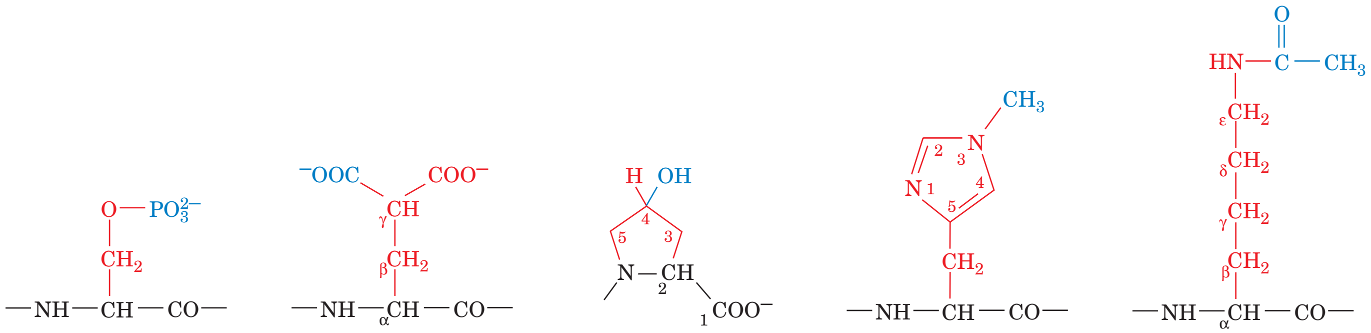

***O*-Phosphoserine** **γ-Carboxyglutamate** **4-Hydroxyproline** **3-Methylhistidine** **ε-*N*-Acetyllysine**

Figure 4-14 | Some modified amino acid residues in proteins. The side chains of these residues are derived from one of the 20 standard amino acids after the polypeptide has been synthesized. The standard R groups are red, and the modifying groups are blue.

BOX 4-3 **PERSPECTIVES IN BIOCHEMISTRY**

Green Fluorescent Protein

Genetic engineers often link a protein-coding gene to a "reporter gene," for example, the gene for an enzyme that yields a colored reaction product. The intensity of the colored compound can be used to estimate the level of expression of the engineered gene. One of the most useful reporter genes is the one that codes for **green fluorescent protein (GFP).** This protein, from the bioluminescent jellyfish *Aequorea victoria,* fluoresces with a peak wavelength of 508 nm (green light) when irradiated by ultraviolet or blue light (optimally 400 nm).

Green fluorescent protein is nontoxic and intrinsically fluorescent; it requires no substrate or small molecule cofactor to fluoresce as do other highly fluorescent proteins. Consequently, when the gene for green fluorescent protein is linked to another gene, the level of expression of the fused genes can be measured noninvasively by fluorescence microscopy.

[© 1999 Steven Haddock and Trevor Rivers/Monterey Bay Aquarium Research Institute, Monterey, California.]

Green fluorescent protein consists of a chain of 238 amino acid residues. The light-emitting group is a derivative of three consecutive amino acids: Ser, Tyr, and Gly. After the protein has been synthesized, the three amino acids undergo spontaneous cyclization and oxidation. The carbonyl C atom of Ser forms a covalent bond to the amino N atom contributed by Gly, followed by the elimination of water and the oxidation of the C_α—C_β bond of Tyr to a double bond. The resulting structure contains a system of conjugated double bonds that gives the protein its fluorescent properties.

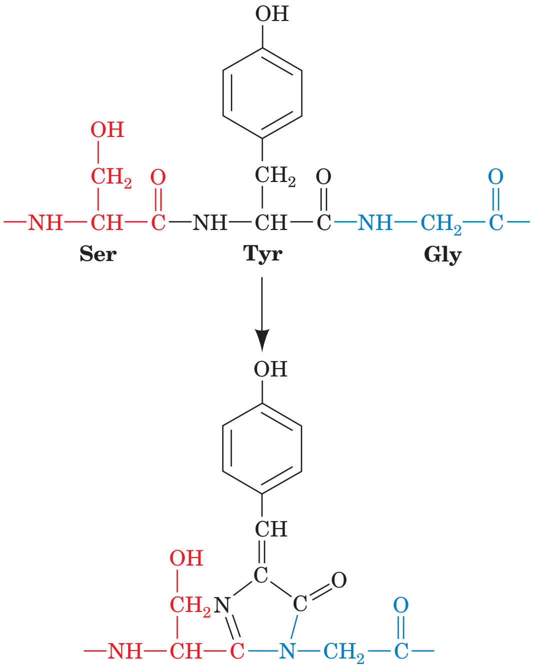

Fluorophore of green fluorescent protein

Cyclization between Ser and Gly is probably rapid, and the oxidation of the Tyr side chain (by O_2) is probably the rate-limiting step of fluorophore generation. Genetic engineering has introduced site-specific mutations that enhance fluorescence intensity and shift the wavelength of the emitted light to different colors, thereby making it possible to simultaneously monitor the expression of two or more different genes.

use as precursors or degradation products of the 20 standard amino acids. Moreover, many amino acids are synthesized not to be residues of polypeptides but to function independently. We shall see that many organisms use certain amino acids to transport nitrogen in the form of amino

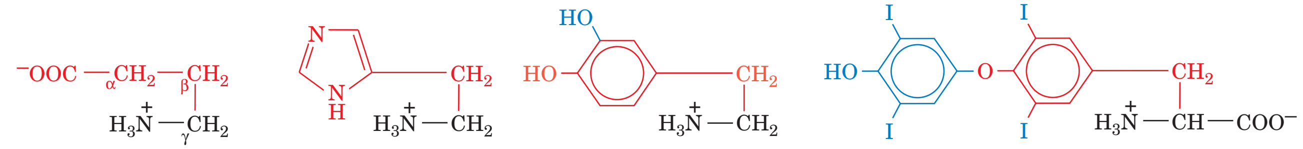

γ-Aminobutyric acid (GABA) **Histamine** **Dopamine** **Thyroxine**

Figure 4-15 | Some biologically active amino acid derivatives. The remaining portions of the parent amino acids are black and red, and additional groups are blue.

groups (Section 21-2A). Amino acids may also be oxidized as metabolic fuels to provide energy (Section 21-4). In addition, amino acids and their derivatives often function as chemical messengers for communication between cells (Fig. 4-15). For example, glycine, **γ-aminobutyric acid (GABA;** a glutamine decarboxylation product), and **dopamine** (a tyrosine derivative) are **neurotransmitters,** substances released by nerve cells to alter the behavior of their neighbors. **Histamine** (the decarboxylation product of histidine) is a potent local mediator of allergic reactions. **Thyroxine** (another tyrosine derivative) is an iodine-containing thyroid hormone that generally stimulates vertebrate metabolism.

Many peptides containing only a few amino acid residues have important physiological functions as hormones or other regulatory molecules. One nearly ubiquitous tripeptide called **glutathione** plays a role in cellular metabolism. Glutathione is a Glu–Cys–Gly peptide in which the γ-carboxylate group of the glutamate side chain forms an **isopeptide bond** with the amino group of the Cys residue (so called because a peptide bond is taken to be the amide bond formed between an α-carboxylate and an α-amino group of two amino acids). Two of these tripeptides (abbreviated **GSH**) undergo oxidation of their SH groups to form a dimeric disulfide-linked structure called **glutathione disulfide (GSSG):**

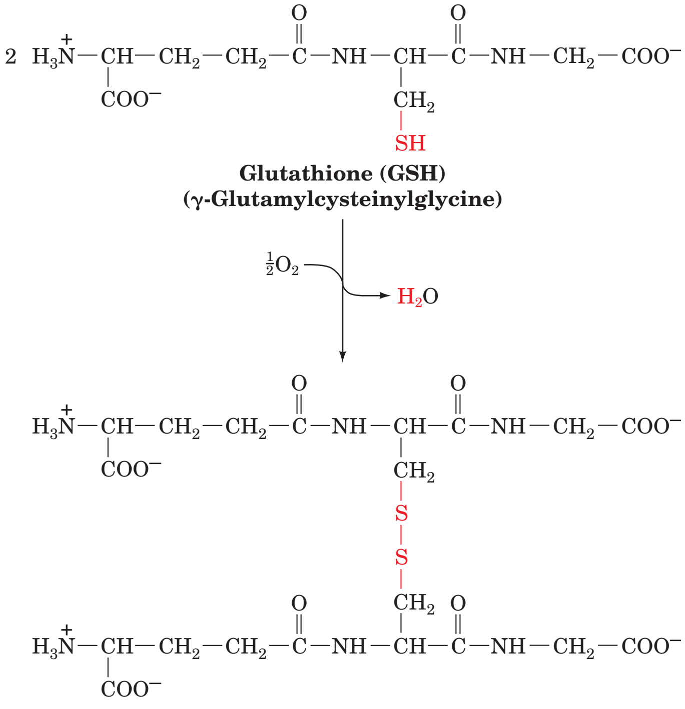

Glutathione (GSH)
(γ-Glutamylcysteinylglycine)

Glutathione disulfide (GSSG)

Glutathione helps inactivate oxidative compounds that could potentially damage cellular structures, since the oxidation of GSH to GSSG is accompanied by the reduction of another compound (shown as O_2 above):

$$2\ \mathrm{GSH} + \mathrm{X}_{oxidized} \rightarrow \mathrm{GSSG} + \mathrm{X}_{reduced}$$

GSH must then be regenerated in a separate reduction reaction.

CHECK YOUR UNDERSTANDING

List some covalent modifications of amino acids in proteins.

List some functions of amino acid derivatives.

SUMMARY

1. At neutral pH, the amino group of an amino acid is protonated and its carboxylic acid group is ionized.
2. Proteins are polymers of amino acids joined by peptide bonds.
3. The 20 standard amino acids can be classified as nonpolar (Gly, Ala, Val, Leu, Ile, Met, Pro, Phe, Trp), uncharged polar (Ser, Thr, Asn, Gln, Tyr, Cys), and charged (Lys, Arg, His, Asp, Glu).
4. The p*K* values of the ionizable groups of amino acids may be altered when the amino acid is part of a polypeptide.
5. Amino acids are chiral molecules. Only L-amino acids are found in proteins (some bacterial peptides contain D-amino acids).
6. Amino acids may be covalently modified after they have been incorporated into a polypeptide.
7. Individual amino acids and their derivatives have diverse physiological functions.

KEY TERMS

protein	**74**
α-amino acid	**74**
α carbon	**74**
R group	**75**
zwitterion	**78**
condensation reaction	**78**
peptide bond	**78**
dipeptide	**78**
tripeptide	**78**
oligopeptide	**78**
polypeptide	**78**
residue	**78**
N-terminus	**78**
C-terminus	**78**
p*I*	**81**
optical activity	**82**
polarimeter	**82**
chiral center	**83**
chirality	**83**
enantiomers	**83**
absolute configuration	**83**
Fischer convention	**83**
stereoisomers	**83**
levorotatory	**84**
dextrorotatory	**84**
Fischer projection	**84**
racemic mixture	**84**
Cahn–Ingold–Prelog (*RS*) system	**85**
peptidase	**85**
neurotransmitter	**88**
isopeptide bond	**88**

PROBLEMS

1. Identify the amino acids that differ from each other by a single methyl or methylene group.
2. The 20 standard amino acids are called α-amino acids. Certain β-amino acids are found in nature. Draw the structure of β-alanine (3-amino-*n*-propionate).
3. Identify the hydrogen bond donor and acceptor groups in asparagine.
4. Draw the dipeptide Asp-His at pH 7.0.
5. Calculate the number of possible pentapeptides that contain one residue each of Ala, Gly, His, Lys, and Val.
6. Determine the net charge of the predominant form of Asp at (a) pH 1.0, (b) pH 3.0, (c) pH 6.0, and (d) pH 11.0.
7. Calculate the p*I* of (a) Ala, (b) His, and (c) Glu.
8. A sample of the amino acid tyrosine is barely soluble in water. Would a polypeptide containing only Tyr residues, poly(Tyr), be more or less soluble, assuming the total number of Tyr groups remains constant?
9. Circle the chiral carbons in the following compounds:

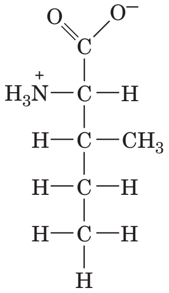

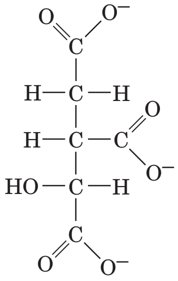

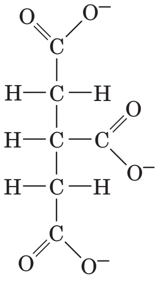

10. Draw the four stereoisomers of threonine.
11. The two $C_\alpha H$ atoms of Gly are said to be prochiral, because when one of them is replaced by another group, C_α becomes chiral. Draw a Fischer projection of Gly and indicate which H must be replaced with CH_3 to yield D-Ala.
12. The bacterially produced antibiotic gramicidin A forms channels in cell membranes that allow the free diffusion of Na^+

and K^+ ions, thereby killing the cell. This peptide consists of a sequence of D- and L-amino acids. The sequence of a segment of five amino acids in gramicidin A is R–Gly–L-Ala–D-Leu–L-Ala–D-Val–R′. Complete the Fischer projection below by adding the correct group to each vertical bond.

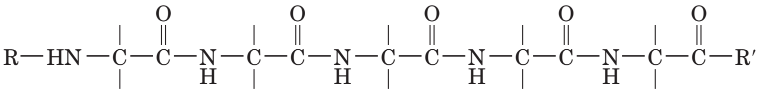

13. Describe isoleucine (as shown in Table 4-1) using the *RS* system.
14. Some amino acids are synthesized by replacing the keto group (C═O) of an organic acid known as an α-keto acid with an amino group ($C{-}NH_3^+$). Identify the amino acids that can be produced this way from the following α-keto acids:

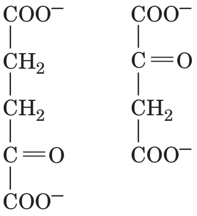

15. Identify the amino acid residue from which the following groups are synthesized:

(a)

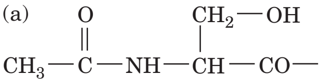

$$CH_3-\overset{\overset{\displaystyle O}{\|}}{C}-NH-\overset{\overset{\displaystyle CH_2-OH}{|}}{CH}-CO-$$

(b)

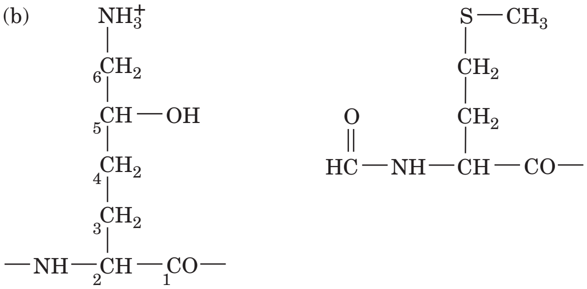

16. Draw the peptide ATLDAK. (a) Calculate its approximate p*I*. (b) What is its net charge at pH 7.0?
17. The protein insulin consists of two polypeptides termed the A and B chains. Insulins from different organisms have been isolated and sequenced. Human and duck insulins have the same amino acid sequence with the exception of six amino acid residues, as shown below. Is the p*I* of human insulin lower than or higher than that of duck insulin?

Amino acid residue	A8	A9	A10	B1	B2	B27
Human	Thr	Ser	Ile	Phe	Val	Thr
Duck	Glu	Asn	Pro	Ala	Ala	Ser

REFERENCES

Barrett, G.C. and Elmore, D.T., *Amino Acids and Peptides,* Cambridge University Press (2001). [Includes structures of the common amino acids along with a discussion of their chemical reactivities and information on analytical properties.]

Lamzin, V.S., Dauter, Z., and Wilson, K.S., How nature deals with stereoisomers, *Curr. Opin. Struct. Biol.* **5,** 830–836 (1995). [Discusses proteins synthesized from D-amino acids.]

Solomons, G. and Fryhle, C., *Organic Chemistry* (9th ed.), Chapter 5, Wiley (2008). [A discussion of chirality. Most other organic chemistry textbooks contain similar material.]

5

Proteins: Primary Structure

The great variation in structure and function among proteins reflects the astronomical variation in the sequences of their component amino acids: There are far more possible amino acid sequences than there are stars in the universe. [PhotoDisc, Inc./Getty Images.]

MEDIA RESOURCES

(Available at www.wiley.com/college/voet)
Guided Exploration 4. Protein sequence determination
Guided Exploration 5. Protein evolution
Animated Figure 5-3. Enzyme-linked immunosorbent assay
Animated Figure 5-6. Ion exchange chromatography
Animated Figure 5-7. Gel filtration chromatography
Animated Figure 5-15. Edman degradation
Animated Figure 5-18. Generating overlapping fragments to determine the amino acid sequence of a polypeptide
Case Study 2. Histidine–Proline-Rich Glycoprotein as a Plasma pH Sensor
Bioinformatics Exercises Chapter 5. Using Databases to Compare and Identify Related Protein Sequences

CHAPTER CONTENTS

1 Polypeptide Diversity

2 Protein Purification and Analysis
- **A.** Purifying a Protein Requires a Strategy
- **B.** Salting Out Separates Proteins by Their Solubility
- **C.** Chromatography Involves Interaction with Mobile and Stationary Phases
- **D.** Electrophoresis Separates Molecules According to Charge and Size

3 Protein Sequencing
- **A.** The First Step Is to Separate Subunits
- **B.** The Polypeptide Chains Are Cleaved
- **C.** Edman Degradation Removes a Peptide's First Amino Acid Residue
- **D.** Mass Spectrometry Determines the Molecular Masses of Peptides
- **E.** Reconstructed Protein Sequences Are Stored in Databases

4 Protein Evolution
- **A.** Protein Sequences Reveal Evolutionary Relationships
- **B.** Proteins Evolve by the Duplication of Genes or Gene Segments

Proteins are at the center of action in biological processes. Nearly all the molecular transformations that define cellular metabolism are mediated by protein catalysts. Proteins also perform regulatory roles, monitoring extracellular and intracellular conditions and relaying information to other cellular components. In addition, proteins are essential structural components of cells. A complete list of known protein functions would contain many thousands of entries, including proteins that transport other molecules and proteins that generate mechanical and electrochemical forces. And such a list would not account for the thousands of proteins whose functions are not yet fully characterized or, in many cases, are completely unknown.

One of the keys to deciphering the function of a given protein is to understand its structure. Like the other major biological macromolecules, the nucleic acids (Section 3-2) and the polysaccharides (Section 8-2), proteins are polymers of smaller units. But unlike many nucleic acids, proteins do not have uniform, regular structures. This is, in part, because the 20 kinds of amino acid residues from which proteins are made have widely differing chemical and physical properties (Section 4-1C). The sequence in which these amino acids are strung together can be analyzed directly, as we describe in this chapter, or indirectly, via DNA sequencing (Section 3-4). In either case, amino acid sequence information provides insights into the chemical and physical properties of proteins, their relationships to other proteins, and ultimately, their mechanisms of action in living organisms. After a brief introduction to the variety in protein structure we will examine some methods for purifying and analyzing proteins, procedures for determining the sequence of amino residues, and finally, some approaches to understanding protein evolution.

1 Polypeptide Diversity

LEARNING OBJECTIVE

- Understand that the size and composition of polypeptides exhibit tremendous but not unlimited variety.

Like all polymeric molecules, proteins can be described in terms of levels of organization, in this case, their primary, secondary, tertiary, and quaternary structures. *A protein's* ***primary structure*** *is the amino acid sequence of its polypeptide chain,* or chains if the protein consists of more than one polypeptide. An example of an amino acid sequence is given in Fig. 5-1. Each residue is linked to the next via a peptide bond (Fig. 4-3). Higher levels of protein structure—secondary, tertiary, and quaternary—refer to the three-dimensional shapes of folded polypeptide chains and will be described in the next chapter.

Proteins are synthesized *in vivo* by the stepwise polymerization of amino acids in the order specified by the sequence of nucleotides in a gene. The direct correspondence between one linear polymer (DNA) and another (a polypeptide) illustrates the elegant simplicity of living systems and allows us to extract information from one polymer and apply it to the other.

The Theoretical Possibilities for Polypeptides Are Unlimited. With 20 different choices available for each amino acid residue in a polypeptide chain, it is easy to see that a huge number of different protein molecules are possible. For a protein of n residues, there are 20^n possible sequences. A relatively small protein molecule may consist of a single polypeptide chain of 100 residues. There are $20^{100} \approx 1.27 \times 10^{130}$ possible unique polypeptide chains of this length, a quantity vastly greater than the estimated number of atoms in the universe (9×10^{78}). Clearly, evolution has produced only a tiny fraction of the theoretical possibilities—a fraction that nevertheless represents an astronomical number of different polypeptides.

Actual Polypeptides Are Somewhat Limited in Size and Composition. In general, proteins contain at least 40 residues or so; polypeptides smaller than that are simply called **peptides.** The largest known polypeptide chain belongs to the 34,350-residue **titin,** a giant (3816 kD) protein that helps arrange the repeating structures of muscle fibers (Section 7-2A). However, *the vast majority of polypeptides contain between 100 and 1000 residues* (Table 5-1). **Multisubunit proteins** contain several identical and/or nonidentical chains called **subunits.** Some proteins are synthesized as single polypeptides that are later cleaved into two or more chains that remain associated; **insulin** is such a protein (Fig. 5-1).

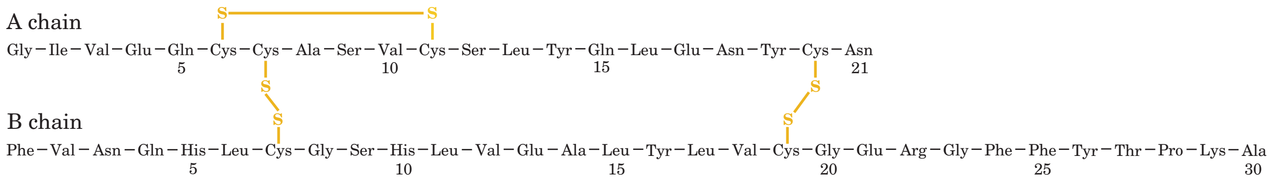
A chain
S
S
Gly – Ile – Val – Glu – Gln – Cys – Cys – Ala – Ser – Val – Cys – Ser – Leu – Tyr – Gln – Leu – Glu – Asn – Tyr – Cys – Asn
5
10
15
21
S
S
S
S
B chain
Phe – Val – Asn – Gln – His – Leu – Cys – Gly – Ser – His – Leu – Val – Glu – Ala – Leu – Tyr – Leu – Val – Cys – Gly – Glu – Arg – Gly – Phe – Phe – Tyr – Thr – Pro – Lys – Ala
5
10
15
20
25
30

Figure 5-1 | The primary structure of bovine insulin. Note the intrachain and interchain disulfide bond linkages.

Table 5-1 Compositions of Some Proteins

Protein	Amino Acid Residues	Subunits	Protein Molecular Mass (D)
Proteinase inhibitor III (bitter gourd)	30	1	3,427
Cytochrome *c* (human)	104	1	11,617
Myoglobin (horse)	153	1	16,951
Interferon-γ (rabbit)	288	2	33,842
Chorismate mutase (*Bacillus subtilis*)	381	3	43,551
Triose phosphate isomerase (*E. coli*)	510	2	53,944
Hemoglobin (human)	574	4	61,986
RNA polymerase (bacteriophage T7)	883	1	98,885
Nucleoside diphosphate kinase (*Dictyostelium discoideum*)	930	6	100,764
Pyruvate decarboxylase (yeast)	2,252	4	245,456
Glutamine synthetase (*E. coli*)	5,616	12	621,264
Titin (human)	34,350	1	3,816,188

The size range in which most polypeptides fall probably reflects the optimization of several biochemical processes:

1. Forty residues appears to be near the minimum for a polypeptide chain to fold into a discrete and stable shape that allows it to carry out a particular function.
2. Polypeptides with many hundreds of residues may approach the limits of efficiency of the protein synthetic machinery. The longer the polypeptide (and the longer its corresponding mRNA), the greater the likelihood of introducing errors during transcription and translation.

In addition to these mild constraints on size, polypeptides are subject to more severe limitations on amino acid composition. The 20 standard amino acids do not appear with equal frequencies in proteins. (Table 4-1 lists the average occurrence of each amino acid residue.) For example, the most abundant amino acids in proteins are Leu, Ala, Gly, Ser, Val, and Glu; the rarest are Trp, Cys, Met, and His.

Because each amino acid residue has characteristic chemical and physical properties, its presence at a particular position in a protein influences the properties of that protein. In particular, as we shall see, the three-dimensional shape of a folded polypeptide chain is a consequence of the intramolecular forces among its various residues. In general, a protein's hydrophobic residues cluster in its interior, out of contact with water, whereas its hydrophilic side chains tend to occupy the protein's surface.

The characteristics of an individual protein depend more on its amino acid sequence than on its amino acid composition per se, for the same reason that "kitchen" and its anagram "thicken" are quite different words. In addition, many proteins consist of more than just amino acid residues. They may form complexes with metal ions such as Zn^{2+} and Ca^{2+}, they may covalently or noncovalently bind certain small organic molecules, and they may be covalently modified by the posttranslational attachment of groups such as phosphates and carbohydrates.

■ **CHECK YOUR UNDERSTANDING**

Explain why polypeptides have such variable sequences.

What factors limit the size and composition of polypeptides?

2 Protein Purification and Analysis

LEARNING OBJECTIVES

- Understand that environmental conditions affect a protein's stability during purification.
- Understand that an assay is used to quantify a protein during purification.
- Understand that increasing the salt concentration causes selective "salting out" (precipitation) of proteins with different solubilities.
- Understand how a protein's ionic charge, polarity, size, and ligand-binding ability influence its chromatographic behavior.
- Understand that gel electrophoresis and its variations can separate proteins according to charge, size, and isoelectric point.

Purification is an all but mandatory step in studying macromolecules, but it is not necessarily easy. Typically, a substance that makes up <0.1% of a tissue's dry weight must be brought to ~98% purity. Purification problems of this magnitude would be considered unreasonably difficult by most synthetic chemists! The following sections outline some of the most common techniques for purifying and, to some extent, characterizing proteins and other macromolecules. Most of these techniques can be used, sometimes in modified form, for nucleic acids and other types of biological molecules.

A | Purifying a Protein Requires a Strategy

The task of purifying a protein present in only trace amounts was once so arduous that many of the earliest proteins to be characterized were studied in part because they are abundant and easily isolated. For example, hemoglobin, which accounts for about one-third the weight of red blood cells, has historically been among the most extensively studied proteins. Most of the enzymes that mediate basic metabolic processes or that are involved in the expression and transmission of genetic information are common to all species. For this reason, a given protein is frequently obtained from a source chosen primarily for convenience, for example, tissues from domesticated animals or easily obtained microorganisms such as *E. coli* and *Saccharomyces cerevisiae* (Baker's yeast).

The development of molecular cloning techniques (Section 3-5) allows almost any protein-encoding gene to be isolated from its parent organism, specifically altered (genetically engineered) if desired, and expressed at high levels in a microorganism. Indeed, the cloned protein may constitute up to 40% of the microorganism's total cell protein (Fig. 5-2). This high level of protein production generally renders the cloned protein far easier to isolate than it would be from its parent organism (in which it may occur in vanishingly small amounts).

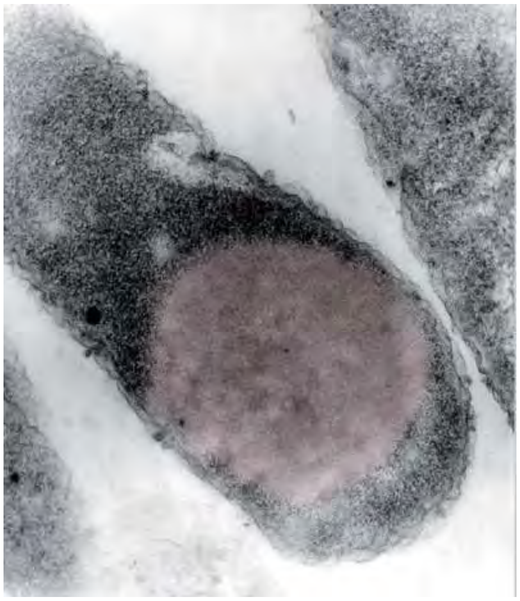

Figure 5-2 | Inclusion body. A genetically engineered organism that produces large amounts of a foreign protein often sequesters it in **inclusion bodies.** This electron micrograph shows an inclusion body of the protein prochymosin in an *E. coli* cell. [Courtesy of Teruhiko Beppu, Nikon University, Japan.]

The first step in the isolation of a protein or other biological molecule is to get it out of the cell and into solution. Many cells require some sort of mechanical disruption to release their contents. Most of the procedures for lysing cells use some variation of crushing or grinding followed by filtration or centrifugation to remove large insoluble particles. If the target protein is tightly associated with a lipid membrane, a detergent or organic solvent may be used to solubilize the lipids and recover the protein.

pH, Temperature, and Other Conditions Must Be Controlled to Keep Proteins Stable. Once a protein has been removed from its natural environment, it becomes exposed to many agents that can irreversibly damage it. These influences must be carefully controlled at all stages of a purification process. The following factors should be considered:

1. ***pH.*** Biological materials are routinely dissolved in buffer solutions effective in the pH range over which the materials are stable (buffers are described in Section 2-2C). Failure to do so could cause their **denaturation** (structural disruption), if not their chemical degradation.
2. ***Temperature.*** The thermal stability of proteins varies. Although some proteins denature at low temperatures, most proteins denature at high temperatures, sometimes only a few degrees higher than their native environment. Protein purification is normally carried out at temperatures near 0°C.

3. ***Presence of degradative enzymes.*** Destroying tissues to liberate the molecule of interest also releases degradative enzymes, including **proteases** and **nucleases.** Degradative enzymes can be inhibited by adjusting the pH or temperature to values that inactivate them (provided this does not adversely affect the protein of interest) or by adding compounds that specifically block their action.
4. ***Adsorption to surfaces.*** Many proteins are denatured by contact with the air–water interface or with glass or plastic surfaces. Hence, protein solutions are handled so as to minimize foaming and are kept relatively concentrated.
5. ***Long-term storage.*** All the factors listed above must be considered when a purified protein sample is to be kept stable. In addition, processes such as slow oxidation and microbial contamination must be prevented. Protein solutions are sometimes stored under nitrogen or argon gas (rather than under air, which contains ~21% O_2) and/or are frozen at −80°C or −196°C (the temperature of liquid nitrogen).

Proteins Are Quantified by Assays. Purifying a substance requires some means for quantitatively detecting it. Accordingly, an **assay** must be devised that is specific for the target protein, highly sensitive, and convenient to use (especially if it must be repeated at every stage of the purification process).

Among the most straightforward protein assays are those for enzymes that catalyze reactions with readily detected products, because *the rate of product formation is proportional to the amount of enzyme present.* Substances with colored or fluorescent products have been developed for just this purpose. If no such substance is available for the enzyme being assayed, the product of the enzymatic reaction may be converted, by the action of another enzyme, to an easily quantified substance. This is known as a **coupled enzymatic reaction.** Proteins that are not enzymes can be detected by their ability to specifically bind certain substances or to produce observable biological effects.

Immunochemical procedures are among the most sensitive of assay techniques. **Immunoassays** use **antibodies,** proteins produced by an animal's immune system in response to the introduction of a foreign substance (an **antigen**). Antibodies recovered from the blood serum of an immunized animal or from cultures of immortalized antibody-producing cells bind specifically to the original protein antigen.

A protein in a complex mixture can be detected by its binding to its corresponding antibodies. In one technique, known as a **radioimmunoassay (RIA),** the protein is indirectly detected by determining the degree to which it competes with a radioactively labeled standard for binding to the antibody. Another technique, the **enzyme-linked immunosorbent assay (ELISA),** has many variations, one of which is diagrammed in Fig. 5-3.

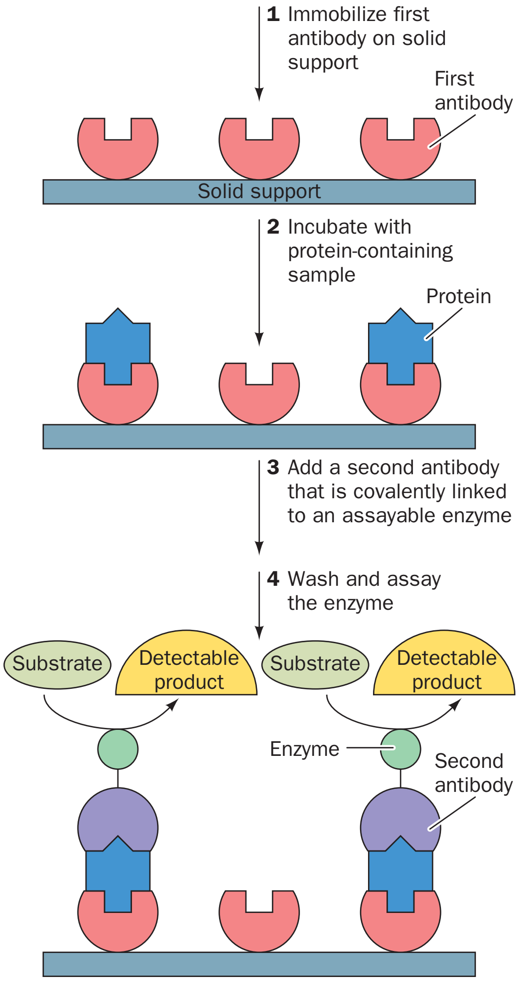
1 Immobilize first antibody on solid support
First antibody
Solid support
2 Incubate with protein-containing sample
Protein
3 Add a second antibody that is covalently linked to an assayable enzyme
4 Wash and assay the enzyme
Substrate
Detectable product
Substrate
Detectable product
Enzyme
Second antibody

Figure 5-3 | **Enzyme-linked immunosorbent assay.** (**1**) An antibody against the protein of interest is immobilized on an inert solid such as polystyrene. (**2**) The solution to be assayed is applied to the antibody-coated surface. The antibody binds the protein of interest, and other proteins are washed away. (**3**) The protein–antibody complex is reacted with a second protein-specific antibody to which an enzyme is attached. (**4**) Binding of the second antibody–enzyme complex is measured by assaying the activity of the enzyme. The amount of substrate converted to product indicates the amount of protein present. **See the Animated Figures.**

Protein Concentrations Can Be Determined by Spectroscopy. The concentration of a substance in solution can be measured by **absorbance spectroscopy.** A solution containing a solute that absorbs light does so according to the **Beer–Lambert law,**

$$A = \log\frac{I_0}{I} = \varepsilon c l \qquad [5\text{-}1]$$

where $\boldsymbol{A}$ is the solute's **absorbance** (alternatively, its **optical density**), I_0 is the intensity of the incident light at a given wavelength λ, I is its transmitted intensity at λ, $\boldsymbol{\varepsilon}$ is the **absorptivity** (alternatively, the **extinction**

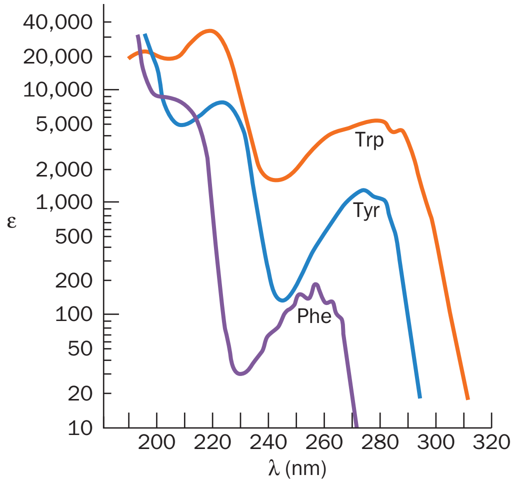

Figure 5-4 | UV absorbance spectra of phenylalanine, tryptophan, and tyrosine. Here the **molar absorptivity** (ε when *c* is expressed in $\text{mol} \cdot \text{L}^{-1}$) for each aromatic amino acid is displayed on a log scale. [After Wetlaufer, D.B., *Adv. Prot. Chem.* **7,** 310 (1962).]

coefficient) of the solute at λ, *c* is its concentration, and *l* is the length of the light path in centimeters. The value of ε varies with λ; a plot of *A* or ε versus λ for the solute is called its **absorption spectrum.** If the value of ε for a substance is known, then its concentration can be spectroscopically determined.

Polypeptides absorb strongly in the ultraviolet (UV) region of the spectrum (λ = 200 to 400 nm) largely because their aromatic side chains (those of Phe, Trp, and Tyr) have particularly large extinction coefficients in this spectral region (ranging into the tens of thousands when *c* is expressed in $\text{mol} \cdot \text{L}^{-1}$; Fig. 5-4). However, polypeptides do not absorb visible light (λ = 400 to 800 nm) so that they are colorless. Nevertheless, if a protein has a **chromophore** that absorbs in the visible region of the spectrum, this absorbance can be used to assay for the presence of the protein in a mixture of other proteins.

In order to follow the purification of a protein, it is important to measure the total amount of protein at every stage of the purification. Absorbance spectroscopy at 280 nm is a convenient way of doing so. However, since many substances that are likely to be present during a protein purification procedure (e.g., nucleic acids) also absorb UV light, and since proteins vary in their proportion of light-absorbing aromatic residues, spectroscopic measurements in the UV region can only provide estimates of the amount of protein present (although they can accurately determine the amount of a pure protein of known molar absorptivity). Moreover, spectroscopic methods are only moderately sensitive to proteins; they can minimally detect 50 to 100 μg of protein per milliliter.

Several techniques have been developed to circumvent these difficulties. For example, in the **Bradford assay,** the binding of the dye **Coomassie brilliant blue**

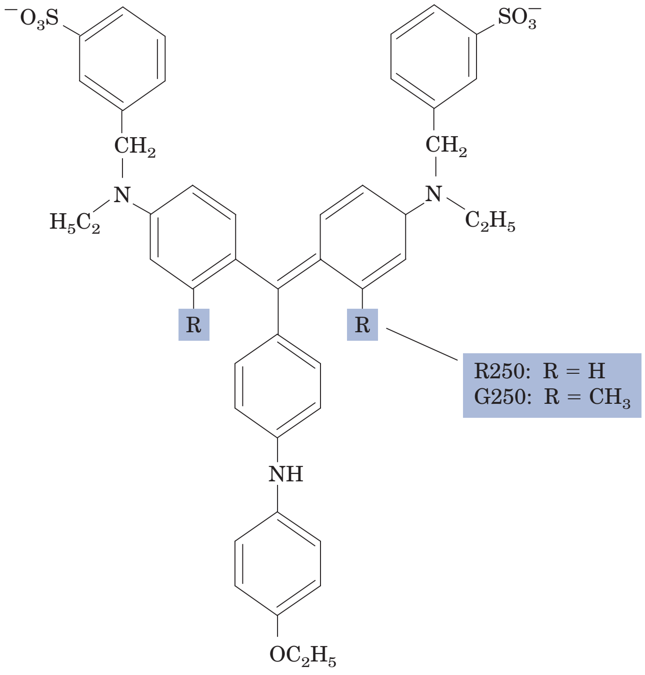

Coomassie brilliant blue

to protein in acidic solution causes the dye's absorption maximum to shift from 465 nm to 595 nm. Hence the absorbance at 595 nm in a Bradford assay provides a direct measure of the amount of protein present. In addition, the Bradford assay is highly sensitive; it can detect as little as 1 μg of protein per milliliter.

Purification Is a Stepwise Process. Proteins are purified by **fractionation procedures.** In a series of independent steps, the various physicochemical properties of the protein of interest are used to separate it progressively from other substances. The idea is not necessarily to minimize the loss of the desired protein, but to *eliminate selectively the other components of the mixture so that only the required substance remains.*

Protein purification is considered as much an art as a science, with many options available at each step. While a trial-and-error approach can work, knowing something about the target protein (or the proteins it is to be separated from) simplifies the selection of fractionation procedures. Some of the procedures we discuss and the protein characteristics they depend on are as follows:

Protein Characteristic	Purification Procedure
Solubility	Salting out
Ionic Charge	Ion exchange chromatography Electrophoresis Isoelectric focusing
Polarity	Hydrophobic interaction chromatography
Size	Gel filtration chromatography SDS-PAGE
Binding Specificity	Affinity chromatography

B | Salting Out Separates Proteins by Their Solubility

Because a protein contains multiple charged groups, its solubility depends on the concentrations of dissolved salts, the polarity of the solvent, the pH, and the temperature. Some or all of these variables can be manipulated to selectively precipitate certain proteins while others remain soluble.

The solubility of a protein at low ion concentrations increases as salt is added, a phenomenon called **salting in.** The additional ions shield the protein's multiple ionic charges, thereby weakening the attractive forces between individual protein molecules (such forces can lead to aggregation and precipitation). However, as more salt is added, particularly with sulfate salts, the solubility of the protein again decreases. This **salting out** effect is primarily a result of the competition between the added salt ions and the other dissolved solutes for molecules of solvent. At very high salt concentrations, so many of the added ions are solvated that there is significantly less bulk solvent available to dissolve other substances, including proteins.

Since different proteins have different ionic and hydrophobic compositions and therefore precipitate at different salt concentrations, salting out is the basis of one of the most commonly used protein purification procedures. Adjusting the salt concentration in a solution containing a mixture of proteins to just below the precipitation point of the protein to be purified eliminates many unwanted proteins from the solution (Fig. 5-5). Then, after removing the precipitated proteins by filtration or centrifugation, the salt concentration of the remaining solution is increased to precipitate the desired protein. This procedure results in a significant purification and concentration of large quantities of protein. Ammonium

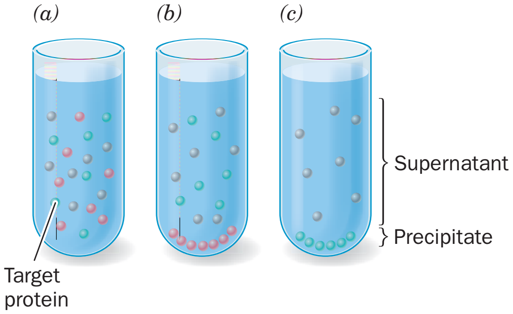

Figure 5-5 | Fractionation by salting out. (*a*) The salt of choice, usually ammonium sulfate, is added to a solution of macromolecules to a concentration just below the precipitation point of the protein of interest. (*b*) After centrifugation, the unwanted precipitated proteins (*red spheres*) are discarded and more salt is added to the supernatant to a concentration sufficient to salt out the desired protein (*green spheres*). (*c*) After a second centrifugation, the protein is recovered as a precipitate, and the supernatant is discarded.

Table 5-2 Isoelectric Points of Several Common Proteins

Protein	p*I*
Pepsin	<1.0
Ovalbumin (hen)	4.6
Serum albumin (human)	4.9
Tropomyosin	5.1
Insulin (bovine)	5.4
Fibrinogen (human)	5.8
γ-Globulin (human)	6.6
Collagen	6.6
Myoglobin (horse)	7.0
Hemoglobin (human)	7.1
Ribonuclease A (bovine)	9.4
Cytochrome *c* (horse)	10.6
Histone (bovine)	10.8
Lysozyme (hen)	11.0
Salmine (salmon)	12.1

sulfate, $(NH_4)_2SO_4$, is the most commonly used reagent for salting out proteins because its high solubility (3.9 M in water at 0°C) allows the preparation of solutions with high ionic strength. The pH may be adjusted to approximate the isoelectric point (p*I*) of the desired protein because a protein is least soluble when its net charge is zero. The p*I*'s of some proteins are listed in Table 5-2.

C | Chromatography Involves Interaction with Mobile and Stationary Phases

The process of **chromatography** (Greek: *chroma,* color + *graphein,* to write) was discovered in 1903 by Mikhail Tswett, who separated solubilized plant pigments using solid adsorbents. In most modern chromatographic procedures, a mixture of substances to be fractionated is dissolved in a liquid (the "mobile" phase) and percolated through a column containing a porous solid matrix (the "stationary" phase). As solutes flow through the column, they interact with the stationary phase and are retarded. The retarding force depends on the properties of each solute. If the column is long enough, substances with different rates of migration will be separated. The chromatographic procedures that are most useful for purifying proteins are classified according to the nature of the interaction between the protein and the stationary phase.

Early chromatographic techniques used strips of filter paper as the stationary phase, whereas modern column chromatography uses granular derivatives of cellulose, agarose, or dextran (all carbohydrate polymers) or synthetic substances such as cross-linked polyacrylamide or silica. **High-performance liquid chromatography (HPLC)** employs automated systems with precisely applied samples, controlled flow rates at high pressures (up to 5000 psi), a chromatographic matrix of specially fabricated 3- to 300-μm-diameter glass or plastic beads coated with a uniform layer of chromatographic material, and on-line sample detection. This greatly improves the speed, resolution, and reproducibility of the separation—features that are particularly desirable when chromatographic separations are repeated many times or when they are used for analytical rather than preparative purposes.

Ion Exchange Chromatography Separates Anions and Cations. In **ion exchange chromatography,** charged molecules bind to oppositely charged groups that are chemically linked to a matrix such as cellulose or agarose. Anions bind to cationic groups on **anion exchangers,** and cations bind to anionic groups on **cation exchangers.** Perhaps the most frequently used anion exchanger is a matrix with attached **diethylaminoethyl (DEAE)** groups, and the most frequently used cation exchanger is a matrix bearing **carboxymethyl (CM)** groups.

$$\begin{array}{ll}\text{DEAE:} & \text{Matrix}-CH_2-CH_2-NH(CH_2CH_3)_2^+ \\ \text{CM:} & \text{Matrix}-CH_2-COO^-\end{array}$$

Proteins and other **polyelectrolytes** (polyionic polymers) that bear both positive and negative charges can bind to both cation and anion exchangers. *The binding affinity of a particular protein depends on the presence of other ions that compete with the protein for binding to the ion exchanger and on the pH of the solution, which influences the net charge of the protein.*

The proteins to be separated are dissolved in a buffer of an appropriate pH and salt concentration and are applied to a column containing the ion exchanger. The column is then washed with the buffer (Fig. 5-6). As

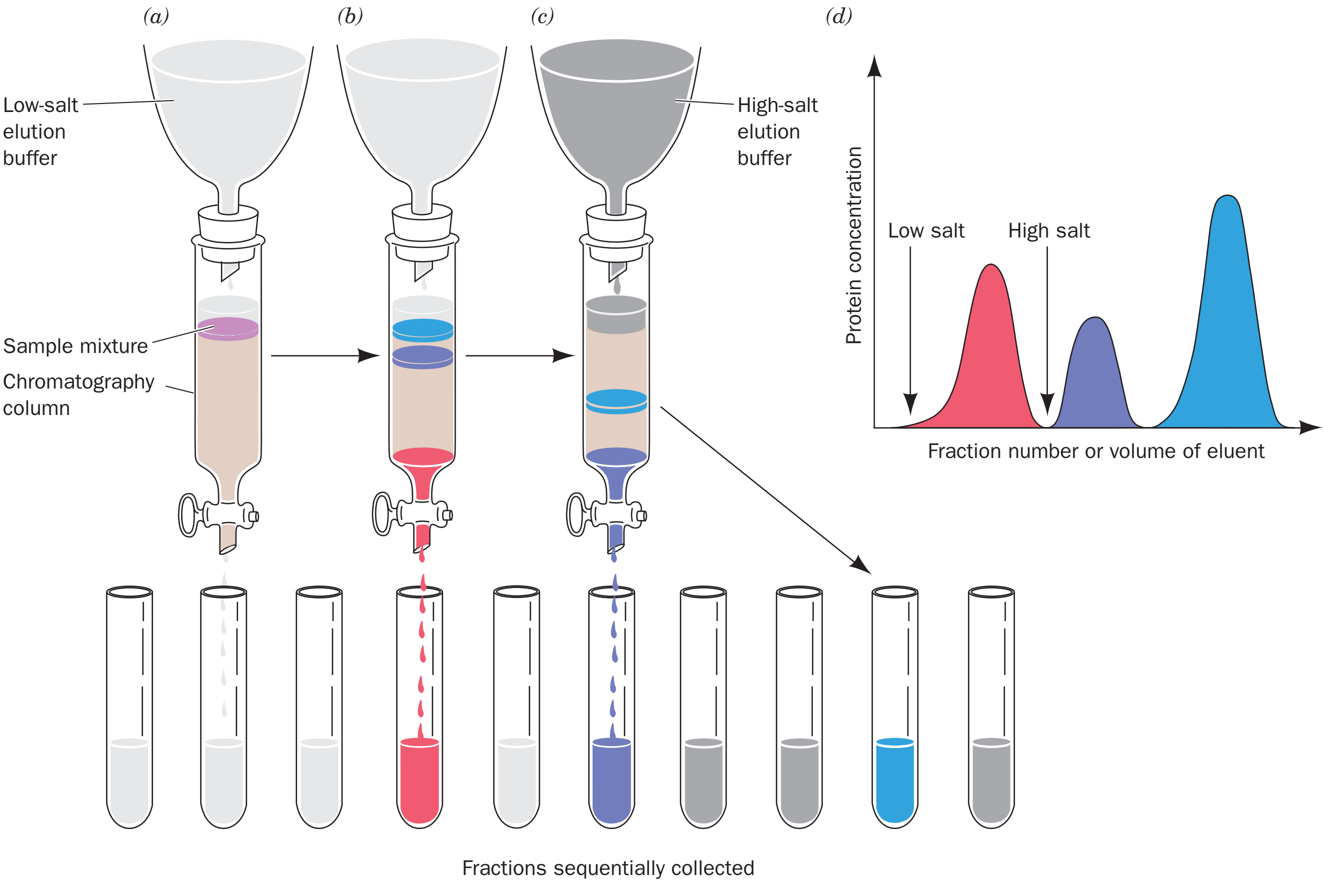

Figure 5-6 | Ion exchange chromatography. The tan region of the column represents the ion exchanger and the colored bands represent proteins. (*a*) A mixture of proteins dissolved in a small volume of buffer is applied to the top of the matrix in the column. (*b*) As elution progresses, the proteins separate into discrete bands as a result of their different affinities for the exchanger. In this diagram, the first protein (*red*) has passed through the column and has been isolated as a separate fraction. The other proteins remain near the top of the column. (*c*) The salt concentration in the eluant is increased to elute the remaining proteins. (*d*) The elution diagram of the protein mixture from the column. **See the Animated Figures.**

the column is washed, proteins with relatively low affinities for the ion exchanger move through the column faster than proteins that bind with higher affinities. The column effluent is collected in a series of fractions. Proteins that bind tightly to the ion exchanger can be **eluted** (washed through the column) by applying a buffer, called the **eluant,** that has a higher salt concentration or a pH that reduces the affinity with which the matrix binds the protein. The column effluent can be monitored for the presence of protein by measuring its absorbance at 280 nm. The eluted fractions can also be tested for the protein of interest using a more specific assay.

Hydrophobic Interaction Chromatography Purifies Nonpolar Molecules. Hydrophobic interactions between proteins and the chromatographic matrix can be exploited to purify the proteins. In **hydrophobic interaction chromatography,** the matrix material is lightly substituted with octyl or phenyl groups. At high salt concentrations, nonpolar groups on the surface of proteins "interact" with the hydrophobic groups; that is, both types of groups are excluded by the polar solvent (hydrophobic effects are augmented by increased ionic strength). The eluant is typically an aqueous buffer with decreasing salt concentrations, increasing concentrations of detergent (which disrupts hydrophobic interactions), or changes in pH.

Gel Filtration Chromatography Separates Molecules According to Size. In **gel filtration chromatography** (also called **size exclusion** or **molecular sieve chromatography**), molecules are separated according to their size and shape. The stationary phase consists of gel beads containing pores that span a relatively narrow size range. The pore size is typically determined by the extent of cross-linking between the polymers of the gel material. If an aqueous solution of molecules of various sizes is passed through a column containing such "molecular sieves," the molecules that are too large to pass through the pores are excluded from the solvent volume inside the gel beads. *These large molecules therefore traverse the column more rapidly than small molecules that pass through the pores* (Fig. 5-7). Because the pore size in any gel varies to some degree, gel filtration can be used to separate a range of molecules; larger molecules with access to fewer pores elute sooner (i.e., in a smaller volume of eluant) than smaller molecules that have access to more of the gel's interior volume.

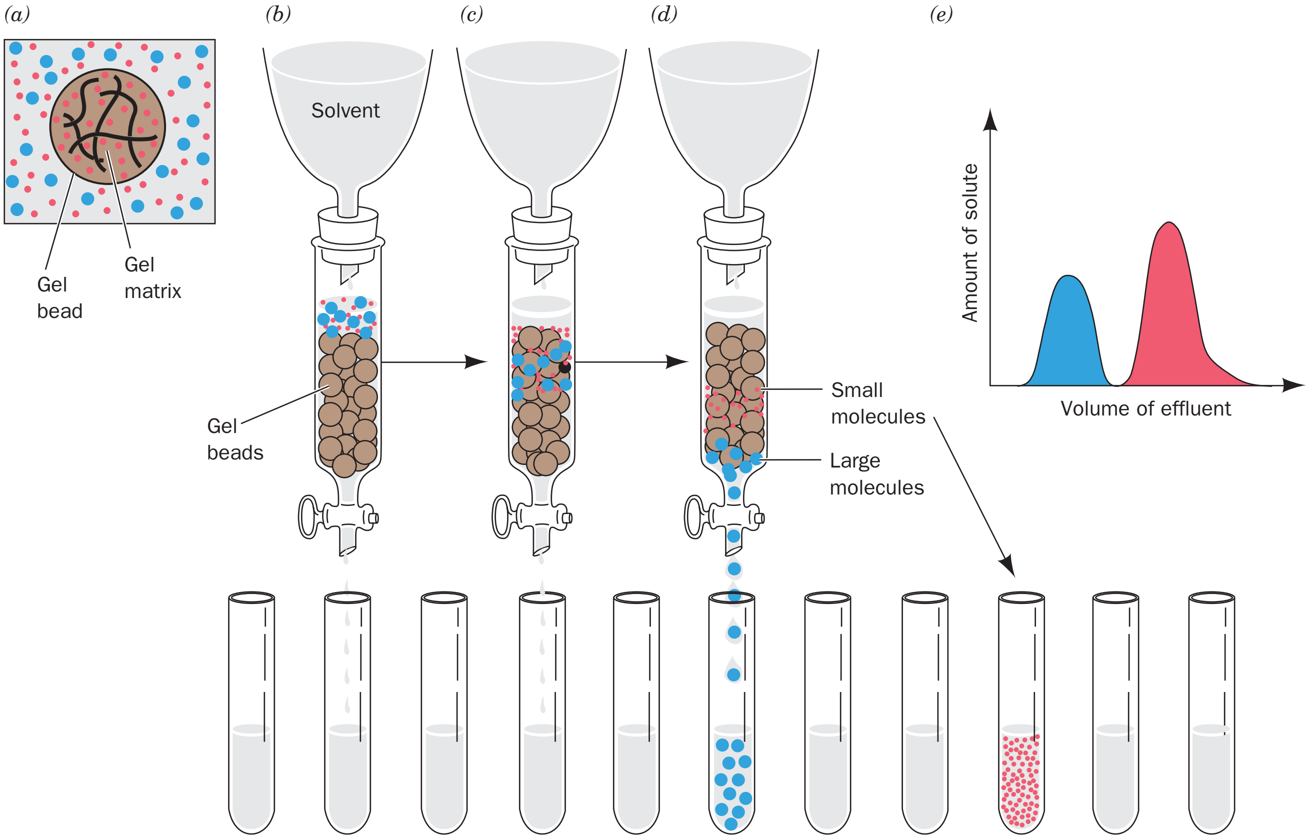

■ **Figure 5-7 | Gel filtration chromatography.** (*a*) A gel bead consists of a gel matrix (*wavy solid lines*) that encloses an internal solvent space. Small molecules (*red dots*) can freely enter the internal space of the gel bead. Large molecules (*blue dots*) cannot penetrate the gel pores. (*b*) The sample solution is applied to the top of the column (the gel beads are represented as brown spheres). (*c*) The small molecules can penetrate the gel and consequently migrate through the column more slowly than the large molecules that are excluded from the gel. (*d*) The large molecules elute first and are collected as fractions. Small molecules require a larger volume of solvent to elute. (*e*) The elution diagram, or chromatogram, indicating the complete separation of the two components. **See the Animated Figures.**

Within the size range of molecules separated by a particular pore size, there is a linear relationship between the relative elution volume of a substance and the logarithm of its molecular mass (assuming the molecules have similar shapes). If a given gel filtration column is calibrated with several proteins of known molecular mass, the mass of an unknown protein can be conveniently estimated by its elution position.

Affinity Chromatography Exploits Specific Binding Behavior. A striking characteristic of many proteins is their ability to bind specific molecules tightly but noncovalently. This property can be used to purify such proteins by **affinity chromatography** (Fig. 5-8). In this technique, a molecule (a **ligand**) that specifically binds to the protein of interest (e.g., a nonreactive analog of an enzyme's substrate) is covalently attached to an inert matrix. *When an impure protein solution is passed through this chromatographic material, the desired protein binds to the immobilized ligand, whereas other substances are washed through the column with the buffer.* The desired protein can then be recovered in highly purified form by changing the elution conditions to release the protein from the matrix. The great advantage of affinity chromatography is its ability to exploit the desired protein's unique biochemical properties rather than the small differences in physicochemical properties between proteins exploited by other chromatographic methods. Accordingly, the separation power of affinity chromatography for a specific protein is often greater than that of other chromatographic techniques.

Affinity chromatography columns can be constructed by chemically attaching small molecules or proteins to a chromatographic matrix. In **immunoaffinity chromatography,** an antibody is attached to the matrix in order to purify the protein against which the antibody was raised. In all cases, the ligand must have an affinity high enough to capture the protein of interest but not so high as to prevent the protein's subsequent release without denaturing it. The bound protein can be eluted by washing the column with a solution containing a high concentration of free ligand or a solution of different pH or ionic strength.

In **metal chelate affinity chromatography,** a divalent metal ion such as Zn^{2+} or Ni^{2+} is attached to the chromatographic matrix so that proteins bearing metal-chelating groups (e.g., multiple His side chains) can be retained. Recombinant DNA techniques (Section 3-5) can be used to append a segment of six consecutive His residues, known as a **His-Tag,** to the N- or C-terminus of the polypeptide to be isolated. This creates a metal ion-binding site that allows the recombinant protein to be purified by metal chelate chromatography. After the protein has been eluted, usually by altering the pH, the His-Tag can be removed by the action of a specific protease whose recognition sequence separates the $(His)_6$ sequence from the rest of the protein.

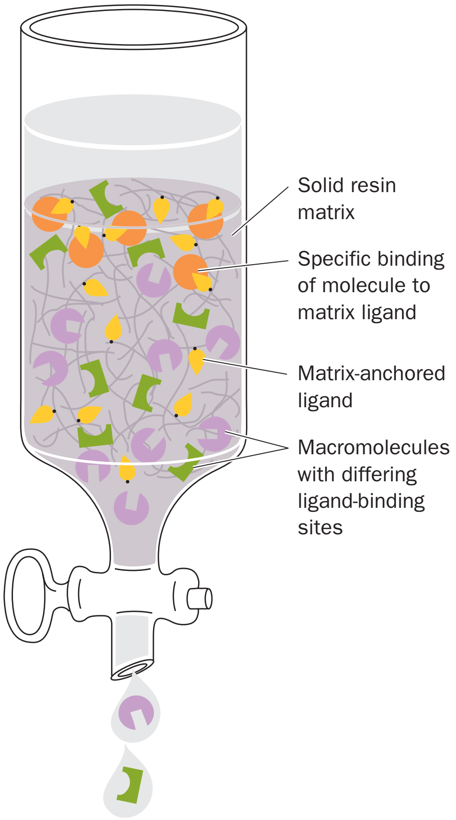
Solid resin matrix
Specific binding of molecule to matrix ligand
Matrix-anchored ligand
Macromolecules with differing ligand-binding sites

Figure 5-8 | **Affinity chromatography.** A ligand (shown here in *yellow*) is immobilized by covalently binding it to the chromatographic matrix. The cutout squares, semicircles, and triangles represent ligand-binding sites on macromolecules. Only certain molecules (represented by *orange circles*) specifically bind to the ligand. The other components are washed through the column.

D | Electrophoresis Separates Molecules According to Charge and Size

Electrophoresis, the migration of ions in an electric field, is described in Section 3-4B. **Polyacrylamide gel electrophoresis (PAGE)** of proteins is typically carried out in agarose or polyacrylamide gels with a characteristic pore size, so *the molecular separations are based on gel filtration (size and shape) as well as electrophoretic mobility (electric charge).* However, electrophoresis differs from gel filtration in that the electrophoretic mobility of smaller molecules is greater than the mobility of larger molecules

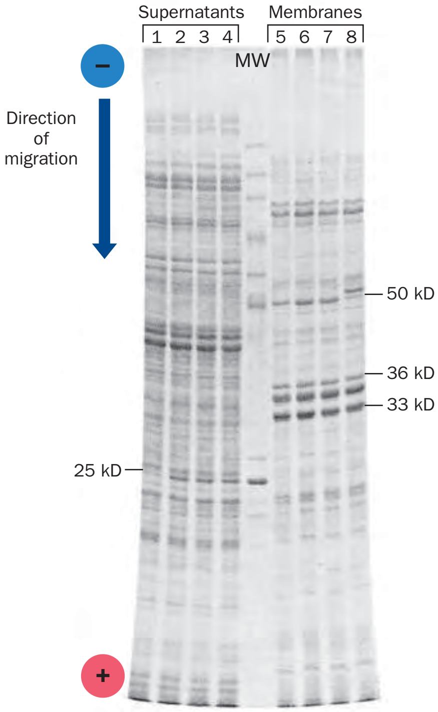

Figure 5-9 | SDS-PAGE. Samples of supernatants (*left*) and membrane fractions (*right*) from a preparation of the bacterium *Salmonella typhimurium* were electrophoresed in parallel lanes on a 35-cm-long by 0.8-mm-thick polyacrylamide slab. The lane marked MW contains molecular weight standards. [Courtesy of Giovanna F. Ames, University of California at Berkeley.]

with the same charge density. The pH of the gel is high enough (usually about pH 9) so that nearly all proteins have net negative charges and move toward the positive electrode when the current is switched on. Molecules of similar size and charge move as a band through the gel.

Following electrophoresis, the separated bands may be visualized in the gel by an appropriate technique, such as soaking the gel in a solution of a stain that binds tightly to proteins (e.g., Coomassie brilliant blue). If the proteins in a sample are radioactive, the gel can be dried and then clamped over a sheet of X-ray film. After a time, the film is developed and the resulting **autoradiograph** shows the positions of the radioactive components by a blackening of the film. If an antibody to a protein of interest is available, it can be used to specifically detect the protein on a gel in the presence of many other proteins, a process called **immunoblotting** or **Western blotting** that is similar to ELISA (Fig. 5-3). Depending on the dimensions of the gel and the visualization technique used, samples containing less than a nanogram of protein can be separated and detected by gel electrophoresis.

SDS-PAGE Separates Proteins by Mass. In one form of polyacrylamide gel electrophoresis, the detergent sodium dodecyl sulfate (SDS)

$$[CH_3{-}(CH_2)_{10}{-}CH_2{-}O{-}SO_3^-]Na^+$$

is used to denature proteins. Amphiphilic molecules (Section 2-1C) such as SDS interfere with the hydrophobic interactions that normally stabilize proteins. Proteins assume a rodlike shape in the presence of SDS. Furthermore, most proteins bind SDS in a ratio of about 1.4 g SDS per gram protein (about one SDS molecule for every two amino acid residues). The large negative charge that the SDS imparts masks the proteins' intrinsic charge. The net result is that SDS-treated proteins have similar shapes and charge-to-mass ratios. ***SDS-PAGE** therefore separates proteins purely by gel filtration effects,* that is, according to molecular mass. Figure 5-9 is an example of the resolving power and the reproducibility of SDS-PAGE.

In SDS-PAGE, the relative mobilities of proteins vary approximately linearly with the logarithm of their molecular masses (Fig. 5-10). Consequently, the molecular mass of a protein can be determined with about 5 to 10% accuracy by electrophoresing it together with several "marker" proteins of known molecular masses that bracket that of the protein of interest. Because SDS disrupts noncovalent interactions between polypeptides, SDS-PAGE yields the molecular masses of the subunits of multisubunit proteins. The possibility that subunits are linked

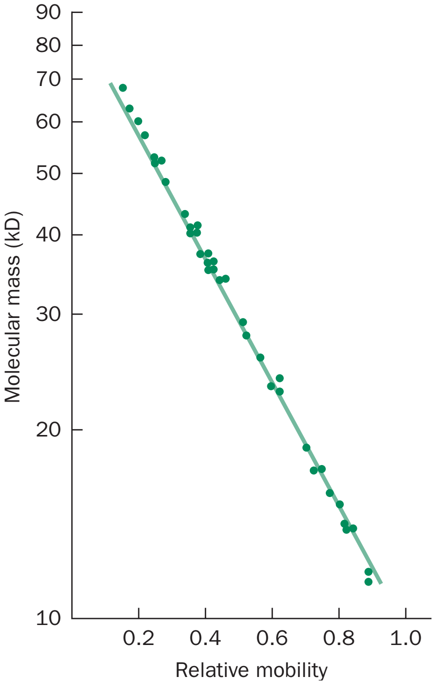

Figure 5-10 | Logarithmic relationship between the molecular mass of a protein and its electrophoretic mobility in SDS-PAGE. The masses of 37 proteins ranging from 11 to 70 kD are plotted. [After Weber, K. and Osborn, M., *J. Biol. Chem.* **244,** 4406 (1969).]

by disulfide bonds can be tested by preparing samples for SDS-PAGE in the presence and absence of a reducing agent, such as **2-mercaptoethanol** ($HSCH_2CH_2OH$), that breaks these bonds (Section 5-3A).

Capillary Electrophoresis Rapidly Separates Charged Molecules. Although gel electrophoresis in its various forms is highly effective at separating charged molecules, it can require up to several hours and is difficult to quantitate and automate. These disadvantages are largely overcome through the use of **capillary electrophoresis (CE),** a technique in which electrophoresis is carried out in very thin capillary tubes (20- to 100-μm inner diameter). Such narrow capillaries rapidly dissipate heat and hence permit the use of very high electric fields, which reduces separation times to a few minutes. The CE techniques have extremely high resolution and can be automated in much the same way as is HPLC, that is, with automatic sample loading and on-line sample detection. Since CE can separate only small amounts of material, it is largely limited to use as an analytical tool.

Two-Dimensional Electrophoresis Resolves Complex Mixtures of Proteins. A protein has charged groups of both polarities and therefore has an isoelectric point, p*I*, at which it is immobile in an electric field. *If a mixture of proteins is electrophoresed through a solution or gel that has a stable pH gradient in which the pH smoothly increases from anode to cathode, each protein will migrate to the position in the pH gradient corresponding to its pI.* If a protein molecule diffuses away from this position, its net charge will change as it moves into a region of different pH and the resulting electrophoretic forces will move it back to its isoelectric position. Each species of protein is thereby "focused" into a narrow band about its p*I*. This type of electrophoresis is called **isoelectric focusing (IEF).**

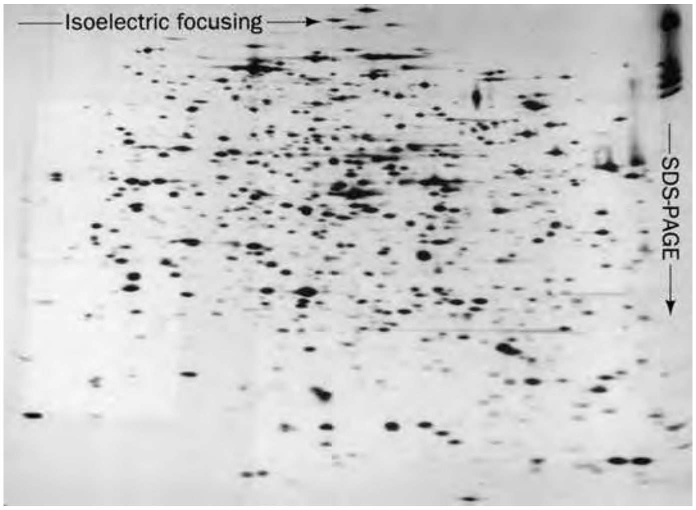

Figure 5-11 | **Two-dimensional gel electrophoresis.** In this example, *E. coli* proteins that had been labeled with ^{14}C-amino acids were subjected to isoelectric focusing (horizontally) followed by SDS-PAGE (vertically). Over 1000 spots can be resolved in the autoradiogram shown here. [Courtesy of Patrick O'Farrell, University of California at San Francisco.]

IEF can be combined with SDS-PAGE in an extremely powerful separation technique named **two-dimensional (2D) gel electrophoresis.** First, a sample of proteins is subjected to IEF in one direction, and then the separated proteins are subjected to SDS-PAGE in the perpendicular direction. This procedure generates an array of spots, each representing a protein (Fig. 5-11). Up to 5000 proteins have been observed on a single two-dimensional electrophoretogram.

Two-dimensional gel electrophoresis is a valuable tool for **proteomics,** a field of study that involves cataloguing all of a cell's expressed proteins with emphasis on their quantitation, localization, modifications, interactions, and activities. Individual protein spots in a stained 2D gel can be excised with a scalpel, destained, and the protein eluted from the gel fragment for identification and/or characterization, often by mass spectrometry (Section 5-3D). 2D electrophoretograms can be analyzed by computer after they have been scanned and digitized. This facilitates the detection of variations in the positions and intensities of protein spots in samples obtained from different tissues or under different growth conditions. Numerous reference 2D gels are publicly available for this purpose in the Web-accessible databases listed at http://us.expasy.org/ch2d/. These databases contain images of 2D gels of a variety of organisms and tissues and identify many of their component proteins. Their use is illustrated in Bioinformatics Exercise 5-4 (www.wiley.com/college/voet).

CHECK YOUR UNDERSTANDING

What are some environmental conditions that must be controlled while purifying a protein?
Describe how a protein may be quantified by an assay or by absorbance spectroscopy.
Explain how salting out is used in protein fractionation.
Describe the basis for separating proteins by ion exchange, hydrophobic interaction, gel filtration, and affinity chromatography.
Describe the processes of gel electrophoresis, SDS-PAGE, and 2D gel electrophoresis.

LEARNING OBJECTIVES

- Understand the steps required to sequence a protein, including N-terminal analysis, disulfide bond cleavage, chain fragmentation, Edman degradation (or mass spectrometry), and sequence reconstruction.
- Understand the importance of protein sequence databases.

See Guided Exploration 4
Protein sequence determination.

3 Protein Sequencing

Once a pure sample of protein has been obtained, it may be used for a variety of purposes. But if the protein has not previously been characterized, the next step is often determining its sequence of amino acids. Frederick Sanger determined the first known protein sequence, that of bovine insulin, in 1953, thereby definitively establishing that proteins have unique covalent structures (Box 5-1). Since then, many additional proteins have been sequenced, and the sequences of many more proteins have been inferred from their DNA sequences. All told, the amino acid sequences of hundreds of thousands of polypeptides are now known. Such information is valuable for the following reasons:

1. Knowledge of a protein's amino acid sequence is prerequisite for determining its three-dimensional structure and is essential for understanding its molecular mechanism of action.
2. Sequence comparisons among analogous proteins from different species yield insights into protein function and reveal evolutionary relationships among the proteins and the organisms that produce them.
3. Many inherited diseases are caused by mutations that result in an amino acid change in a protein. Amino acid sequence analysis can assist in the development of diagnostic tests and effective therapies.

Sanger's determination of the sequence of insulin's 51 residues (Fig. 5-1) took about 10 years and required ~100 g of protein. Procedures for primary structure determination have since been so refined and automated that most proteins can be sequenced within a few hours or days using only a few micrograms of material. Regardless of the technique used, the basic approach for sequencing proteins is similar to the procedure developed by Sanger. *The protein must be broken down into fragments small enough to be individually sequenced, and the primary structure of the intact protein is then reconstructed from the sequences of overlapping fragments* (Fig. 5-12). Such a procedure, as we have seen (Section 3-4C), is also used to sequence DNA.

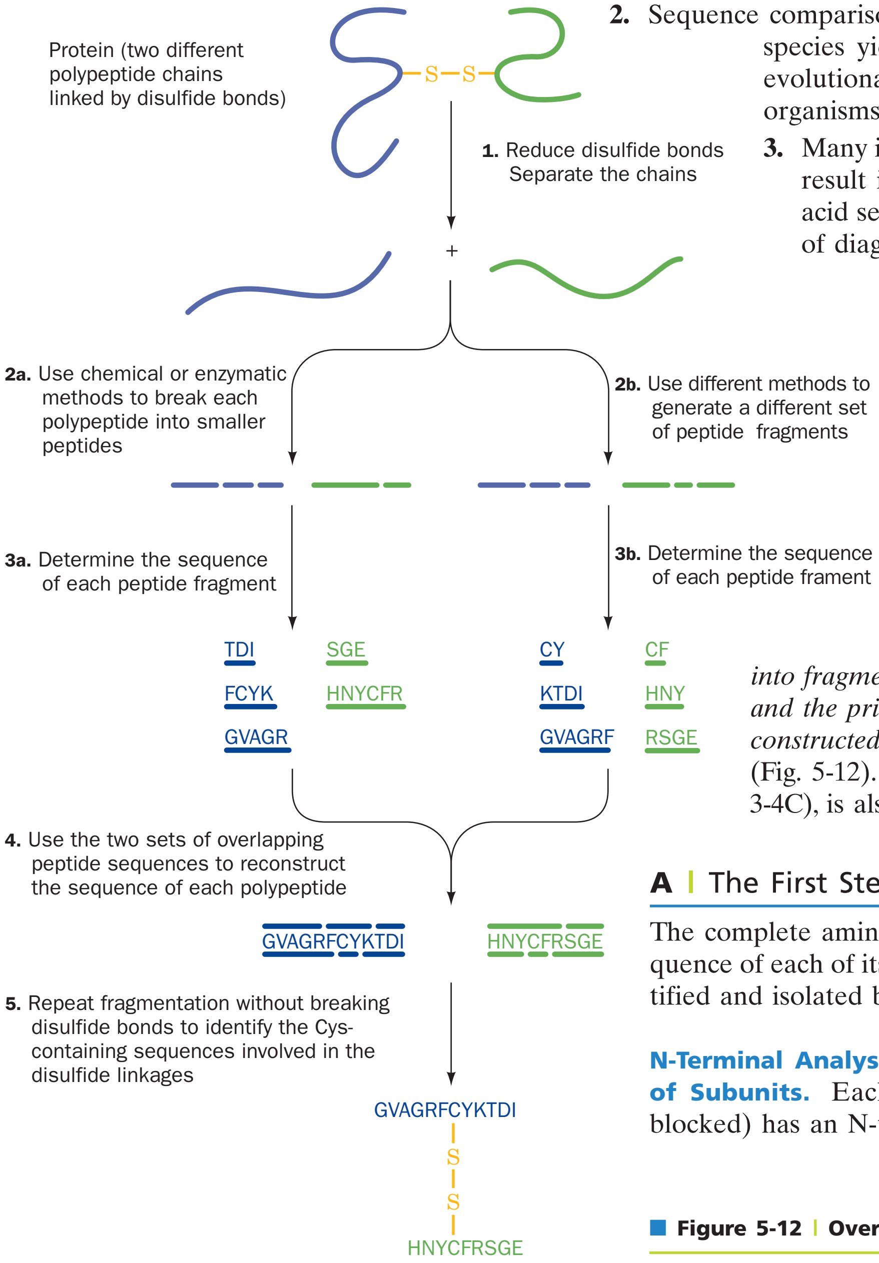
Protein (two different polypeptide chains linked by disulfide bonds)
S—S
1. Reduce disulfide bonds Separate the chains
+
2a. Use chemical or enzymatic methods to break each polypeptide into smaller peptides
2b. Use different methods to generate a different set of peptide fragments
3a. Determine the sequence of each peptide fragment
3b. Determine the sequence of each peptide frament
TDI
SGE
FCYK
HNYCFR
GVAGR
CY
CF
KTDI
HNY
GVAGRF
RSGE
4. Use the two sets of overlapping peptide sequences to reconstruct the sequence of each polypeptide
GVAGRFCYKTDI
HNYCFRSGE
5. Repeat fragmentation without breaking disulfide bonds to identify the Cys-containing sequences involved in the disulfide linkages
GVAGRFCYKTDI
S
S
HNYCFRSGE

Figure 5-12 | Overview of protein sequencing.

A | The First Step Is to Separate Subunits

The complete amino acid sequence of a protein includes the sequence of each of its subunits, if any, so the subunits must be identified and isolated before sequencing begins.

N-Terminal Analysis Reveals the Number of Different Types of Subunits. Each polypeptide chain (if it is not chemically blocked) has an N-terminal residue. *Identifying this "end group"*

BOX 5-1 **PATHWAYS OF DISCOVERY**

Frederick Sanger and Protein Sequencing

Frederick Sanger (1918–)

At one time, many biochemists believed that proteins were amorphous "colloids" of variable size, shape, and composition. This view was largely abandoned by the 1940s, when it became possible to determine the amino acid composition of a protein, that is, the number of each kind of constituent amino acid. However, such information revealed nothing about the order in which the amino acids were combined. In fact, skeptics still questioned whether proteins even had unique sequences. One plausible theory was that proteins were populations of related molecules that were probably assembled from shorter pieces. Some studies went so far as to describe the rules governing the relative stoichiometries and spacing of the various amino acids in proteins.

During the 1940s, the accuracy of amino acid analysis began to improve as a result of the development of chromatographic techniques for separating amino acids and the use of the reagent **ninhydrin,** which forms colored adducts with amino acids, to chemically quantify them (previous methods used cumbersome biological assays). Frederick Sanger, who began his work on protein sequencing in 1943, used these new techniques as well as classic organic chemistry. Sanger did not actually set out to sequence a protein; his first experiments were directed toward devising a better method for quantifying free amino groups such as the amino groups corresponding to the N-terminus of a polypeptide.

Sanger used the reagent 2,4-dinitrofluorobenzene, which forms a yellow dinitrophenyl (DNP) derivative at terminal amino groups without breaking any peptide bonds.

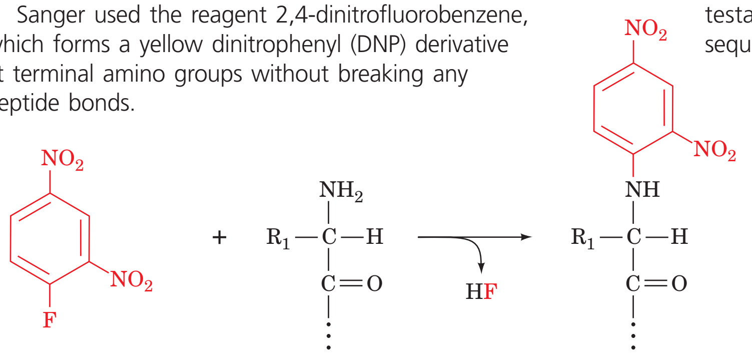

2,4-Dinitrofluorobenzene (DNFB) **Polypeptide** **DNP-Polypeptide**

When the protein is subsequently hydrolyzed to break its peptide bonds, the N-terminal amino acid retains its DNP label and can be identified when the hydrolysis products are separated by chromatography. Sanger found that some DNP-amino acid derivatives were unstable during hydrolysis, so this step had to be shortened. In comparing the results of long and short hydrolysis times, Sanger observed extra yellow spots corresponding to dipeptides or other small peptides with intact peptide bonds. He could then isolate the dipeptides and identify the second residue. Sanger's genius was to recognize that by determining the sequences of overlapping small peptides from an incompletely hydrolyzed protein, the sequence of the intact protein could be determined.

An enormous amount of work was required to turn the basic principle into a sound laboratory technique for sequencing a protein. Sanger chose insulin as his subject, because it was one of the smallest known proteins. Insulin contains 51 amino acids in two polypeptide chains (called A and B). The sequence of the 30 residues in the B chain was completed in 1951, and the sequence of the A chain (21 residues) in 1953. Because the two chains are linked through disulfide bonds, Sanger also endeavored to find the optimal procedure for cleaving those bonds and then identifying their positions in the intact protein, a task he completed in 1955.

Sanger's work of over a decade, combining his expertise in organic chemistry (the cleavage and derivatization reactions) with the development of analytical tools for separating and identifying the reaction products, led to his winning a Nobel prize in 1958 [he won a second Nobel prize in 1980, for his invention of the chain-terminator method of nucleic acid sequencing (Section 3-4C)]. A testament to Sanger's brilliance is that his basic approaches to sequencing polypeptides and nucleic acids are still widely used.

Publication of the sequence of insulin in 1955 convinced skeptics that a protein has a unique amino acid sequence. Sanger's work also helped catalyze thinking about the existence of a genetic code that would link the amino acid sequence of a protein to the nucleotide sequence of DNA, a molecule whose structure had just been elucidated in 1953.

Sanger, F., Sequences, sequences, sequences, *Annu. Rev. Biochem.* **57,** 1–28 (1988). [A scientific autobiography that provides a glimpse of the early difficulties in sequencing proteins.]

Sanger, F., Thompson, E.O.P., and Kitai, R., The amide groups of insulin, *Biochem. J.* **59,** 509–518 (1955).

can establish the number of chemically distinct polypeptides in a protein. For example, insulin has equal amounts of the N-terminal residues Gly and Phe, which indicates that it has equal numbers of two nonidentical polypeptide chains.

The N-terminus of a polypeptide can be determined by several methods. The fluorescent compound **5-dimethylamino-1-naphthalenesulfonyl chloride (dansyl chloride)** reacts with primary amines to yield dansylated polypeptides

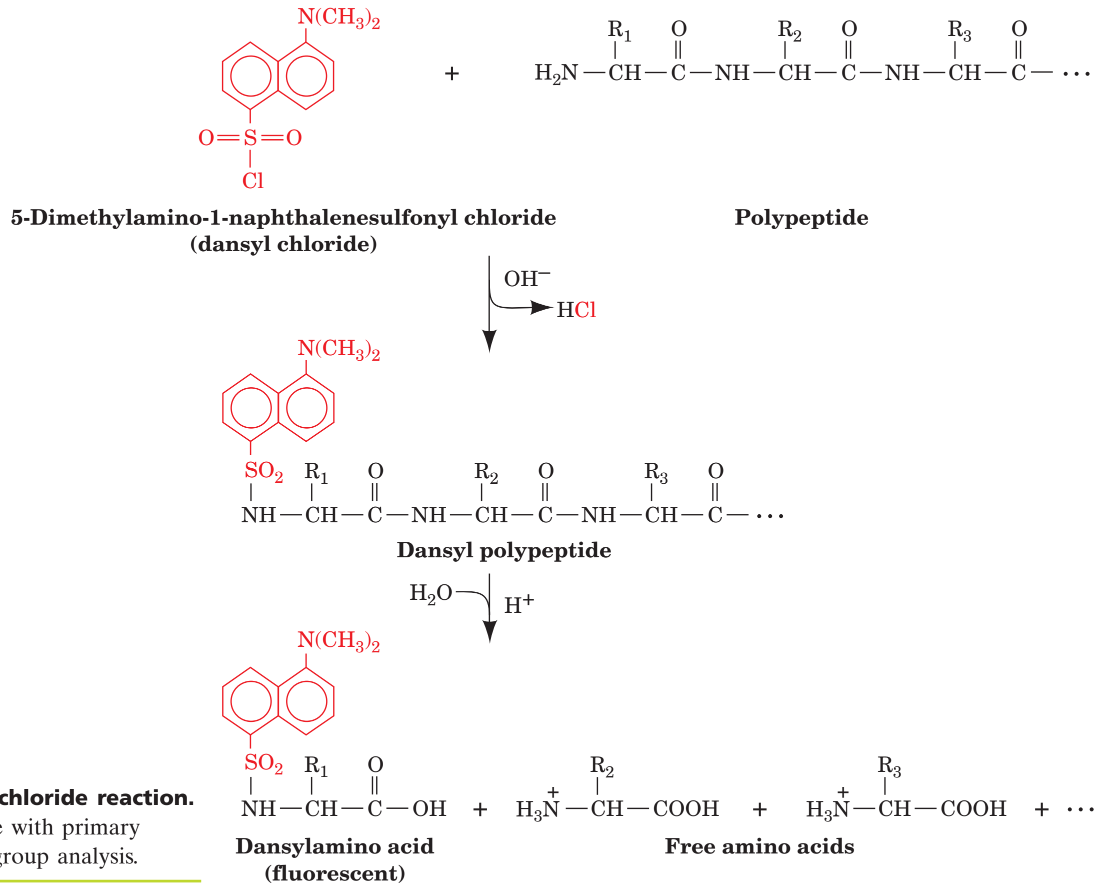
5-Dimethylamino-1-naphthalenesulfonyl chloride
(dansyl chloride)
Polypeptide
OH⁻
HCl
Dansyl polypeptide
H₂O
H⁺
Dansylamino acid
(fluorescent)
Free amino acids

Figure 5-13 | The dansyl chloride reaction. The reaction of dansyl chloride with primary amino groups is used for end group analysis.

(Fig. 5-13). The treatment of a dansylated polypeptide with aqueous acid at high temperature hydrolyzes its peptide bonds. This liberates the dansylated N-terminal residue, which can then be separated chromatographically from the other amino acids and identified by its intense yellow fluorescence. The N-terminal residue can also be identified by performing the first step of Edman degradation (Section 5-3C), a procedure that liberates amino acids one at a time from the N-terminus of a polypeptide.

Disulfide Bonds between and within Polypeptides Are Cleaved.

Disulfide bonds between Cys residues must be cleaved to separate polypeptide chains—if they are disulfide-linked—and to ensure that polypeptide chains are fully linear (residues in polypeptides that are "knotted" with disulfide bonds may not be accessible to all the enzymes and reagents for sequencing). Disulfide bonds can be reductively cleaved by treating them with 2-mercaptoethanol or another **mercaptan** (compounds that contain an —SH group):

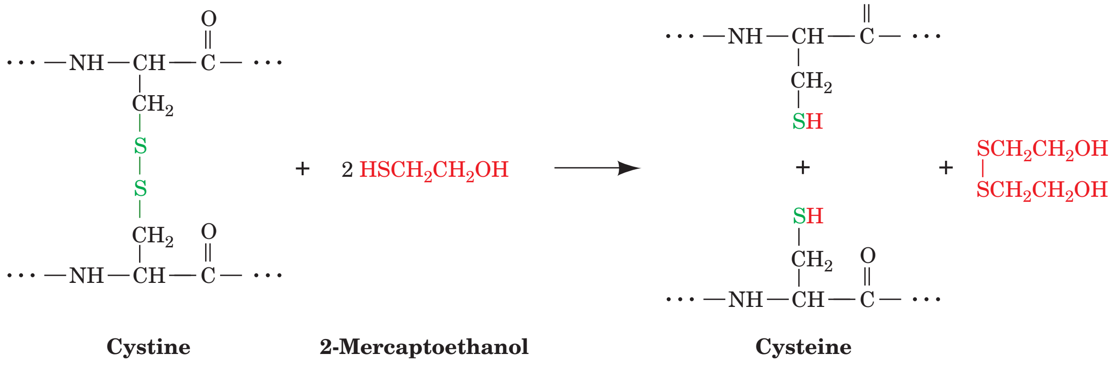
Cystine
2-Mercaptoethanol
Cysteine

The resulting free sulfhydryl groups are then alkylated, usually by treatment with **iodoacetate,** to prevent the re-formation of disulfide bonds through oxidation by O_2:

$$\text{Cys}-\text{CH}_2-\text{SH} + \text{ICH}_2\text{COO}^- \longrightarrow \text{Cys}-\text{CH}_2-\text{S}-\text{CH}_2\text{COO}^- + \text{HI}$$

Cysteine **Iodoacetate** ***S*-Carboxymethylcysteine (CM-Cys)**

B | The Polypeptide Chains Are Cleaved

Polypeptides that are longer than 40 to 100 residues cannot be directly sequenced and must therefore be cleaved, either enzymatically or chemically, to specific fragments that are small enough to be sequenced. Various **endopeptidases** (enzymes that catalyze the hydrolysis of internal peptide bonds, as opposed to **exopeptidases,** which catalyze the hydrolysis of N- or C-terminal residues) can be used to fragment polypeptides. Both endopeptidases and exopeptidases (which collectively are called **proteases**) have side chain requirements for the residues flanking the scissile peptide bond (i.e., the bond that is to be cleaved; Table 5-3). The digestive enzyme **trypsin** has the greatest specificity and is therefore the most valuable member of the arsenal of endopeptidases used to fragment polypeptides. It cleaves peptide bonds on the C side (toward the carboxyl terminus) of the positively charged residues Arg and Lys if the next residue is not Pro.

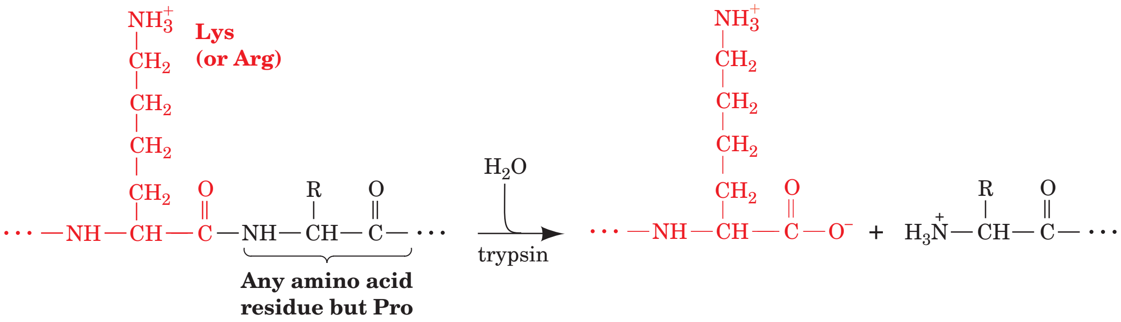

$$\cdots-\text{NH}-\underset{\text{(CH}_2)_4\text{NH}_3^+}{\text{CH}}-\overset{\text{O}}{\overset{\|}{\text{C}}}-\text{NH}-\overset{\text{R}}{\text{CH}}-\overset{\text{O}}{\overset{\|}{\text{C}}}-\cdots \xrightarrow[\text{trypsin}]{\text{H}_2\text{O}} \cdots-\text{NH}-\underset{\text{(CH}_2)_4\text{NH}_3^+}{\text{CH}}-\overset{\text{O}}{\overset{\|}{\text{C}}}-\text{O}^- + \text{H}_3\overset{+}{\text{N}}-\overset{\text{R}}{\text{CH}}-\overset{\text{O}}{\overset{\|}{\text{C}}}-\cdots$$

Table 5-3 Specificities of Various Endopeptidases

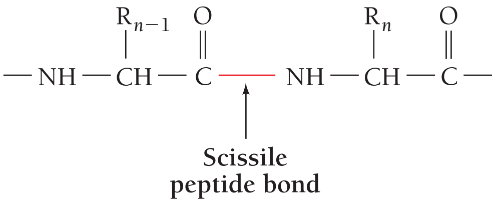

$$-\text{NH}-\overset{\text{R}_{n-1}}{\text{CH}}-\overset{\text{O}}{\overset{\|}{\text{C}}}-\text{NH}-\overset{\text{R}_n}{\text{CH}}-\overset{\text{O}}{\overset{\|}{\text{C}}}-$$

Enzyme	**Source**	**Specificity**	**Comments**
Trypsin	Bovine pancreas	R_{n-1} = positively charged residues: Arg, Lys; $R_n \neq$ Pro	Highly specific
Chymotrypsin	Bovine pancreas	R_{n-1} = bulky hydrophobic residues: Phe, Trp, Tyr; $R_n \neq$ Pro	Cleaves more slowly for R_{n-1} = Asn, His, Met, Leu
Elastase	Bovine pancreas	R_{n-1} = small neutral residues: Ala, Gly, Ser, Val; $R_n \neq$ Pro	
Thermolysin	*Bacillus thermoproteolyticus*	R_n = Ile, Met, Phe, Trp, Tyr, Val; $R_{n-1} \neq$ Pro	Occasionally cleaves at R_n = Ala, Asp, His, Thr; heat stable
Pepsin	Bovine gastric mucosa	R_n = Leu, Phe, Trp, Tyr; $R_{n-1} \neq$ Pro	Also others; quite nonspecific; pH optimum = 2
Endopeptidase V8	*Staphylococcus aureus*	R_{n-1} = Glu	

The other endopeptidases listed in Table 5-3 exhibit broader side chain specificities than trypsin and often yield a series of peptide fragments with overlapping sequences. However, through **limited proteolysis,** that is, by adjusting reaction conditions and limiting reaction times, these less specific endopeptidases can yield a set of discrete, nonoverlapping fragments.

Several chemical reagents promote peptide bond cleavage at specific residues. The most useful of these, **cyanogen bromide** (CNBr), cleaves on the C side of Met residues (Fig. 5-14).

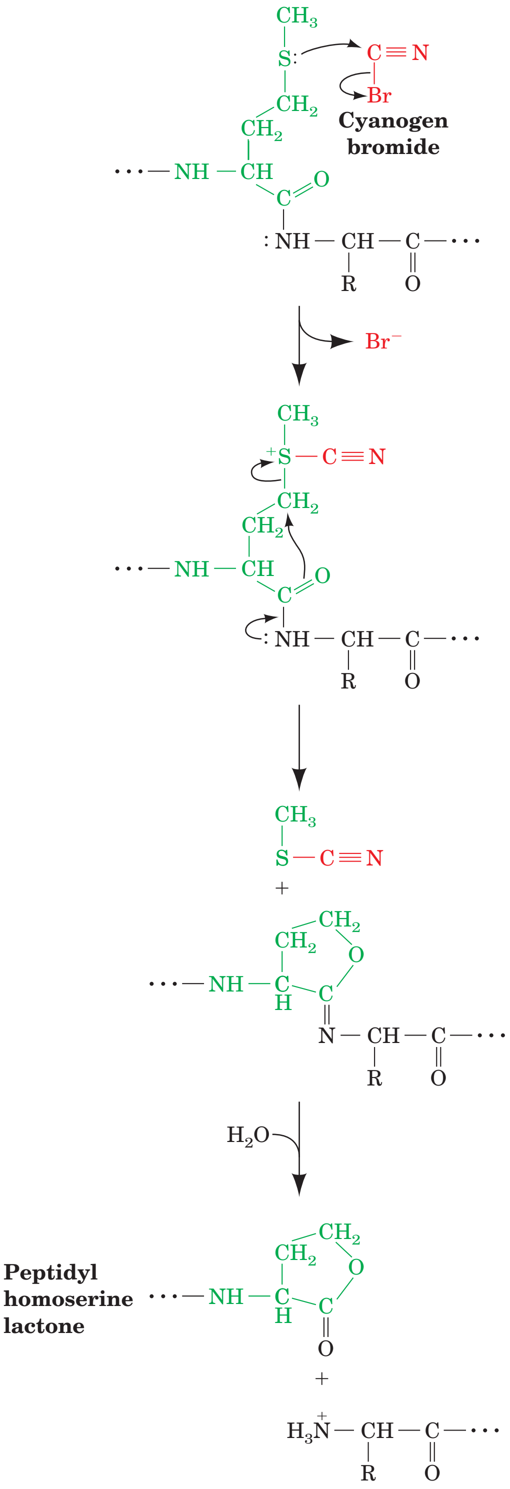

Figure 5-14 | Cyanogen bromide cleavage of a polypeptide. CNBr reacts specifically with Met residues, resulting in cleavage of the peptide bond on their C-terminal side. The newly formed C-terminal residue forms a cyclic structure known as a **peptidyl homoserine lactone.**

C | Edman Degradation Removes a Peptide's First Amino Acid Residue

Once the peptide fragments formed through specific cleavage reactions have been isolated, their amino acid sequences can be determined. This can be accomplished through repeated cycles of **Edman degradation.** In this process (named after its inventor, Pehr Edman), **phenylisothiocyanate** (**PITC;** also known as **Edman's reagent**) reacts with the N-terminal amino group of a polypeptide under mildly alkaline conditions to form a **phenylthiocarbamyl (PTC)** adduct (Fig. 5-15). This product is treated with anhydrous **trifluoroacetic acid,** which cleaves the N-terminal residue as a thiazolinone derivative but does not hydrolyze other peptide bonds. Edman degradation therefore releases the N-terminal amino acid residue but leaves intact the rest of the polypeptide chain. The thiazolinone-amino acid is selectively extracted into an organic solvent and is converted to the more stable **phenylthiohydantoin (PTH)** derivative by treatment with aqueous acid. This PTH-amino acid can later be identified by chromatography. Thus, *it is possible to determine the amino acid sequence of a polypeptide chain from the N-terminus inward by subjecting the polypeptide to repeated cycles of Edman degradation and, after every cycle, identifying the newly liberated PTH-amino acid.*

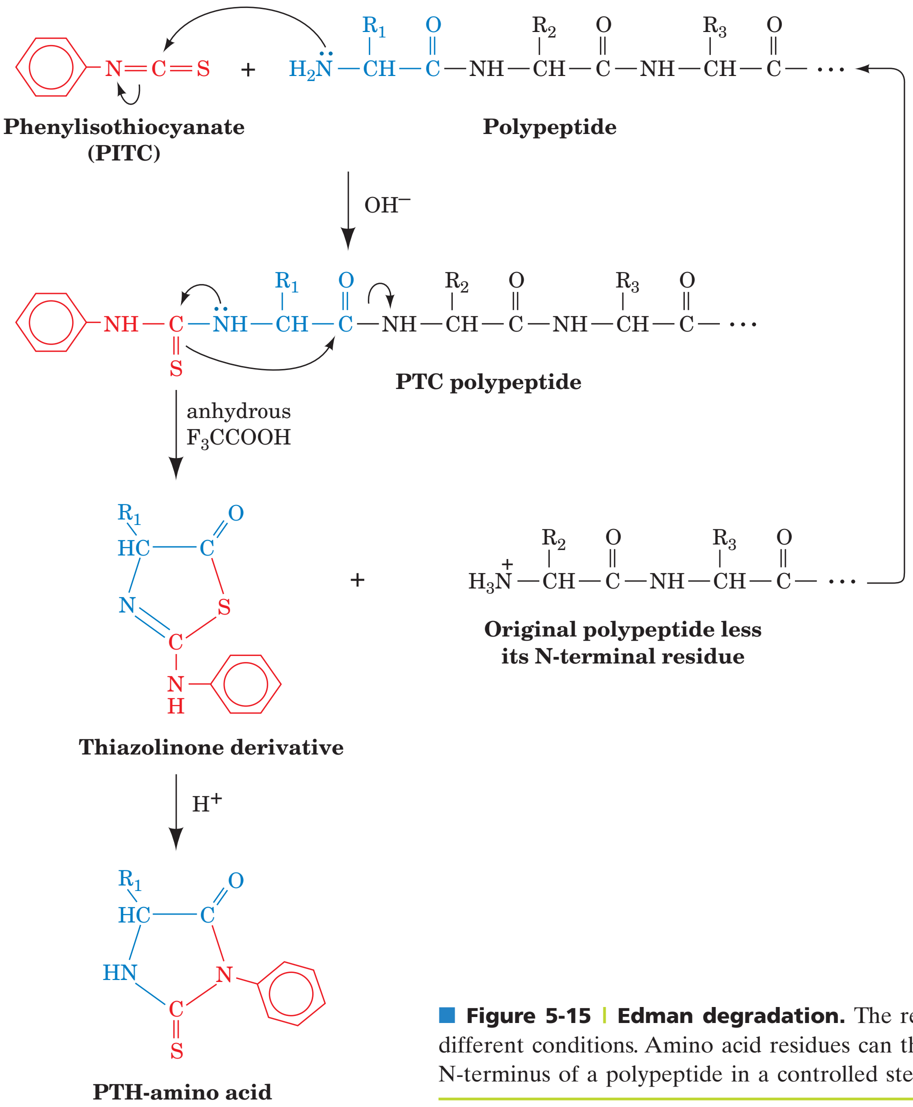

Phenylisothiocyanate (PITC)
Polypeptide
OH^-
PTC polypeptide
anhydrous F_3CCOOH
Thiazolinone derivative
Original polypeptide less its N-terminal residue
H^+
PTH-amino acid

Figure 5-15 | Edman degradation. The reaction occurs in three stages, each requiring different conditions. Amino acid residues can therefore be sequentially removed from the N-terminus of a polypeptide in a controlled stepwise fashion. **See the Animated Figures.**

The Edman degradation technique has been automated and refined, resulting in great savings of time and material. In modern instruments, the peptide sample is dried onto a disk of glass fiber paper, and accurately measured quantities of reagents are delivered and products removed as vapors in a stream of argon at programmed intervals. Up to 100 residues can be identified before the cumulative effects of incomplete reactions, side reactions, and peptide loss make further amino acid identification unreliable. Since less than a picomole of a PTH-amino acid can be detected and identified, sequence analysis can be carried out on as little as 5 to 10 pmol of a peptide (<0.1 μg—an invisibly small amount).

D | Mass Spectrometry Determines the Molecular Masses of Peptides

Mass spectrometry has emerged as an important technique for characterizing and sequencing polypeptides. Mass spectrometry accurately measures the mass-to-charge (m/z) ratio for ions in the gas phase (where m is the ion's mass and z is its charge). Until about 1985, macromolecules such as proteins and nucleic acids could not be analyzed by mass spectrometry. This was because macromolecules were destroyed during the production of gas-phase ions, which required vaporization by heating followed by ionization via bombardment with electrons.

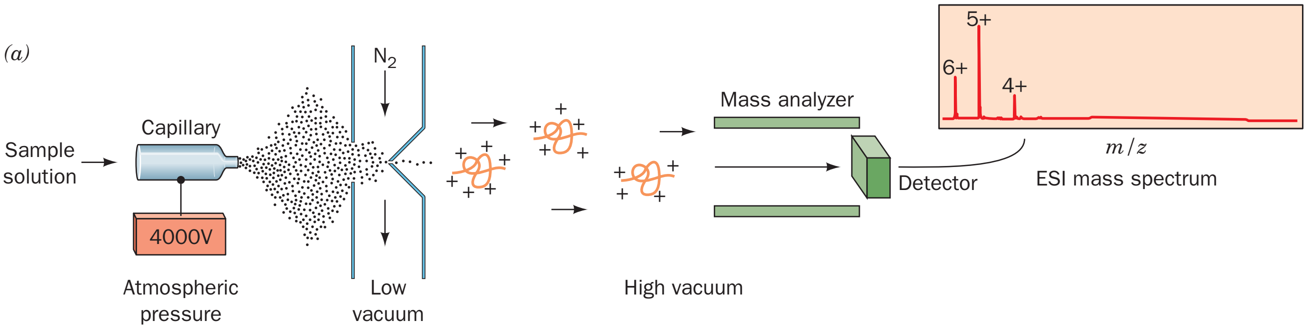

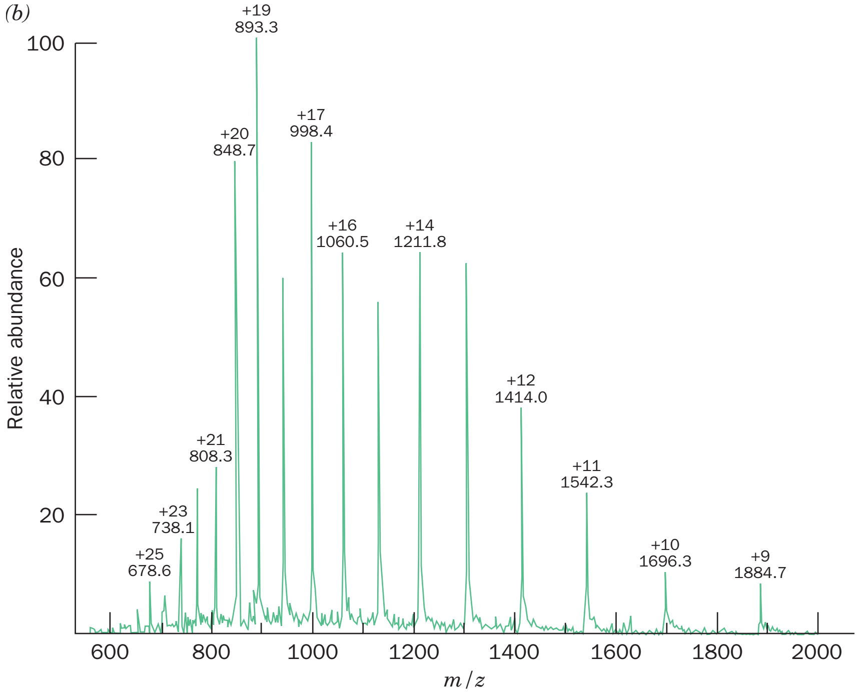

Figure 5-16 | Electrospray ionization mass spectrometry (ESI). (*a*) Dry N_2 gas promotes the evaporation of solvent from charged droplets containing the protein of interest, leaving gas-phase ions, whose charge is due to the protonation of Arg and Lys residues. The mass spectrometer then determines the mass-to-charge ratio of these ions. The resulting mass spectrum consists of a series of peaks corresponding to ions that differ by a single ionic charge and the mass of one proton). [After Fitzgerald, M.C. and Siuzdak, G., *Chem. Biol.* **3,** 708 (1996).] (*b*) The ESI mass spectrum of horse heart **apomyoglobin** (myoglobin that lacks its Fe ion). The measured m/z ratios and the inferred charges for most of the peaks are indicated. The data provided by this spectrum permit the mass of the original molecule to be calculated (see Sample Calculation 5-1). [After Yates, J.R., *Methods Enzymol.* **271,** 353 (1996).]

Newer techniques have addressed this shortcoming. For example, in the **electrospray ionization (ESI)** technique, a solution of a macromolecule such as a peptide is sprayed from a narrow capillary tube maintained at high voltage (~4000 V), forming fine highly charged droplets from which the solvent rapidly evaporates (Fig. 5-16*a*). This yields a series of gas-phase macromolecular ions that typically have ionic charges in the range +0.5 to +2 per kilodalton. The charges result from the protonation of basic side chains such as Arg and Lys. The ions are directed into the mass spectrometer, which measures their m/z values with an accuracy of >0.01% (Fig. 5-16*b*). Consequently, determining an ion's z permits its molecular mass to be determined with far greater accuracy than by any other method.

Short polypeptides (<25 residues) can be directly sequenced though the use of a tandem mass spectrometer (Fig. 5-17; two mass spectrometers coupled in series). The first mass spectrometer functions to select and separate the peptide ion of interest from peptide ions of different masses as well as any contaminants that may be present. The selected peptide ion is then passed into a collision cell, where it collides with chemically inert atoms such as helium. The energy thereby imparted to the peptide ion causes it to fragment predominantly at only one of its several peptide bonds, thereby yielding one or two charged fragments per original ion. The molecular masses of the numerous charged fragments so produced are then determined by the second mass spectrometer.

By comparing the molecular masses of successively larger members of a family of fragments, the molecular masses and therefore the identities of the corresponding amino acid residues can be determined. The sequence of an entire polypeptide can thus be elucidated (although mass spectrometry cannot distinguish the isomeric residues Ile and Leu because they have exactly the same mass, and it cannot always reliably distinguish Gln and Lys residues because their molecular masses differ by only 0.036 D).

Computerization of the mass-comparison process has reduced the time required to sequence a short polypeptide to only a few minutes (one cycle of Edman degradation may take an hour). The reliability of this process has been increased through the computerized matching of a measured mass spectrum with those of peptides of known sequence as maintained in databases. Mass spectrometry can also be used to sequence peptides with chemically blocked N-termini (which prevents Edman degradation) and to characterize other posttranslational modifications such as the addition of phosphate or carbohydrate groups.

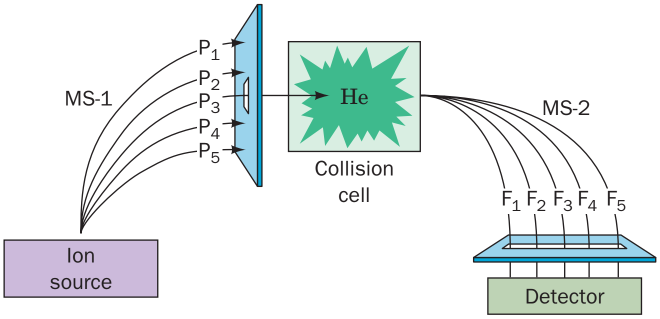

■ **Figure 5-17 | Tandem mass spectrometry in peptide sequencing.** Electrospray ionization (ESI), the ion source, generates gas-phase peptide ions, labeled P_1, P_2, etc., from a digest of the protein to be sequenced. These peptides are separated by the first mass spectrometer (MS-1) according to their m/z values, and one of them (here, P_3) is directed into the collision cell, where it collides with helium atoms. This treatment breaks the peptide into fragments (F_1, F_2, etc.), which are directed into the second mass spectrometer (MS-2) for determination of their m/z values. [After Biemann, K. and Scoble, H.A., *Science* **237,** 992 (1987).]

SAMPLE CALCULATION 5-1

An ESI mass spectrum such as that of apomyoglobin (Fig. 5-16*b*) contains a series of peaks, each corresponding to the m/z ratio of an $(M + nH)^{n+}$ ion. Two successive peaks in this mass spectrum have measured m/z ratios of 1414.0 and 1542.3. What is the molecular mass of the original apomyoglobin molecule, how does it compare with the value given for it in Table 5-1, and what are the charges of the ions causing these peaks?

The first peak (p_1 = 1414.0) arises from an ion with charge z and mass M + z, where M is the molecular mass of the original protein. Then the adjacent (p_2 = 1542.3) peak, which is due to an ion with one less proton, has charge $z - 1$ and mass $M + z - 1$. The m/z ratios for these ions, p_1 and p_2, are therefore given by the following expressions.

$$p_1 = (M + z)/z$$

$$p_2 = (M + z - 1)/(z - 1)$$

These two linear equations can readily be solved for their unknowns, M and z. Solve the first equation for M.

$$M = z(p_1 - 1)$$

Then plug this result into the second equation.

$$p_2 = \frac{z(p_1 - 1) + z - 1}{z - 1} = \frac{zp_1 - 1}{z - 1}$$

$$zp_2 - p_2 = zp_1 - 1$$

$$z = (p_2 - 1)/(p_2 - p_1)$$

$$M = (p_2 - 1)/(p_1 - 1)/(p_2 - p_1)$$

Plugging in the values for p_1 and p_2,

$$M = (1542.3 - 1)(1414.0 - 1)/(1542.3 - 1414.0)$$

$$= 16{,}975 \text{ D}$$

which is only 0.14% larger than the 16,951 D for horse apomyoglobin given in Table 5-1. For the charge on ion 1,

$$z = (1542.3 - 1)/(1542.3 - 1414.0) = 12$$

The ionic charge on ion 2 is 12 − 1 = 11.

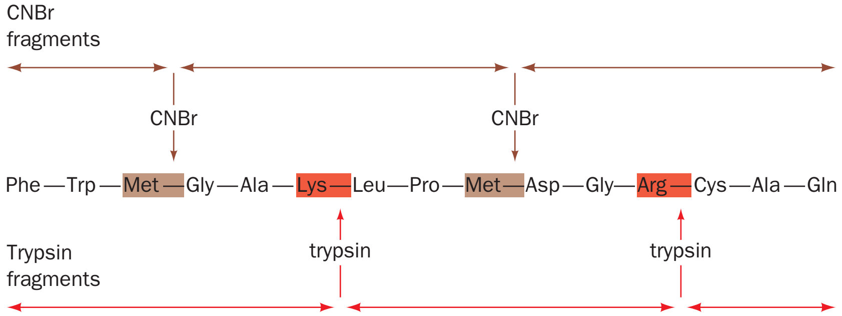

Figure 5-18 | Generating overlapping fragments to determine the amino acid sequence of a polypeptide. In this example, two sets of overlapping peptide fragments are made by using trypsin to cleave the polypeptide after all its Arg and Lys residues and, in a separate reaction, using CNBr to cleave it after all its Met residues. **See the Animated Figures.**

E | Reconstructed Protein Sequences Are Stored in Databases

After individual peptide fragments have been sequenced, their order in the original polypeptide must be elucidated. This is accomplished by conducting a second round of protein cleavage with a reagent of different specificity and then comparing the amino acid sequences of the overlapping sets of peptide fragments (Fig. 5-18).

The final step in an amino acid sequence analysis is to determine the positions (if any) of the disulfide bonds. This can be done by cleaving a sample of the protein, with its disulfide bonds intact, to yield pairs of peptide fragments, each containing a single Cys, that are linked by a disulfide bond. After isolating a disulfide-linked polypeptide fragment, the disulfide bond is cleaved and alkylated (Section 5-3A), and the sequences of the two peptides are determined (Fig. 5-19). The various pairs of such polypeptide fragments are identified by comparing their sequences with that of the protein, thereby establishing the locations of the disulfide bonds.

Sequences Are Recorded in Databases. After a protein's amino acid sequence has been determined, the information is customarily deposited in a public database. Databases for proteins as well as DNA sequences are accessible via the Internet (Table 5-4). Electronic links between databases allow rapid updates and cross-checking of sequence information.

Most sequence databases use similar conventions. For example, consider the annotated protein sequence database named UniProt. A sequence record in UniProt begins with the protein's ID code in the form X_Y, where X is a short mnemonic indicating the protein's name (for example, CYC for cytochrome *c* and HBA for hemoglobin α chain) and Y is a five-character identification code indicating the protein's biological source, which usually consists of the first three letters of the genus and the first two letters of the species [e.g., CANFA for *Canis familiaris* (dog)], although for most commonly encountered organisms, Y is self-explanatory (e.g., BOVIN or ECOLI). This is followed by an accession number, which is assigned by the database as a way of identifying an entry even if its ID code must be changed (for example, see Fig. 5-20). The entry continues with the date the sequence was entered into the database and when it was last modified and annotated, a list of pertinent references (which are linked to PubMed), a description of the protein, and its links to other databases. A Feature Table describes regions or sites of interest in the protein such as disulfide bonds, posttranslational modifications, binding sites, and conflicts between different references. The entry ends with the length of the peptide in residues, its molecular weight, and finally, its sequence using the one-letter amino acid code.

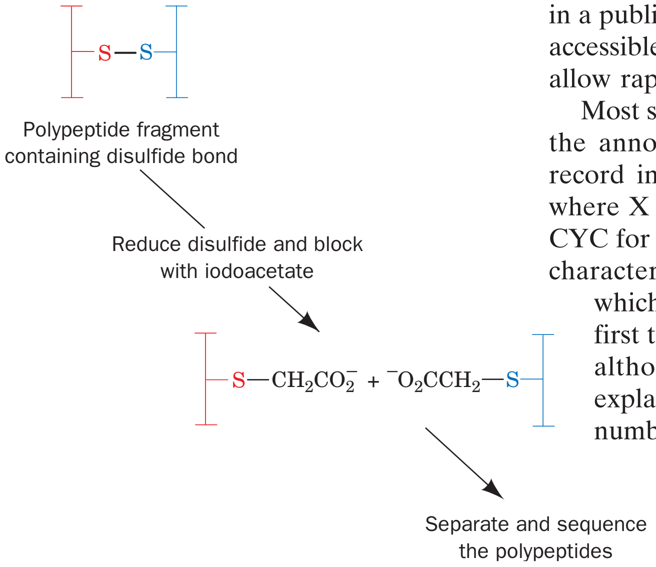
S—S
Polypeptide fragment containing disulfide bond
Reduce disulfide and block with iodoacetate
S—CH₂CO₂⁻ + ⁻O₂CCH₂—S
Separate and sequence the polypeptides

Figure 5-19 | Determining the positions of disulfide bonds. In this method, disulfide-linked peptide fragments from a protein are reductively cleaved and separately sequenced to identify the positions of the disulfide bonds in the intact protein.

Table 5-4 Internet Addresses for the Major Protein and DNA Sequence Data Banks

Data Banks Containing Protein Sequences

ExPASy Proteomics Server: http://expasy.org/

Protein Information Resource (PIR): http://pir.georgetown.edu/

Protein Research Foundation (PRF): http://www4.prf.or.jp/

UniProt: http://www.ebi.uniprot.org/

Data Banks Containing Gene Sequences

GenBank: http://www.ncbi.nlm.nih.gov/Genbank/

European Bioinformatics Institute (EBI): http://www.ebi.ac.uk

DBGET/Integrated Database Retrieval System: GenomeNet@http://www.genome.jb/

Armed with the appropriate software (which is often publicly available at the database sites), a researcher can search a database to find proteins with similar sequences in various organisms. The sequence of even a short peptide fragment may be sufficient to "fish out" the parent protein or its counterpart from another species.

Amino acid sequence information is no less valuable when the nucleotide sequence of the corresponding gene is also known, because the protein sequence provides information about protein structure that is not revealed by nucleic acid sequencing (see Section 3-4). For example, only direct protein sequencing can reveal the locations of disulfide bonds in proteins. In addition, many proteins are modified after they are synthesized. For example, certain residues may be excised to produce the "mature" protein (insulin, shown in Fig. 5-1, is actually synthesized as an 84-residue polypeptide that is proteolytically processed to its smaller two-chain form). Amino acid side chains may also be modified by the addition of carbohydrates, phosphate groups, or acetyl groups, to name only a few. Although some of these modifications occur at characteristic amino acid sequences and are therefore identifiable in nucleotide sequences, only the actual protein sequence can confirm whether and where they occur.

CHECK YOUR UNDERSTANDING

Summarize the steps involved in sequencing a protein.

Why is it important to identify the N-terminal residue(s) of a protein?

What are some advantages of sequencing peptides by mass spectrometry rather than by Edman degradation?

What types of information can be retrieved from a protein sequence database?

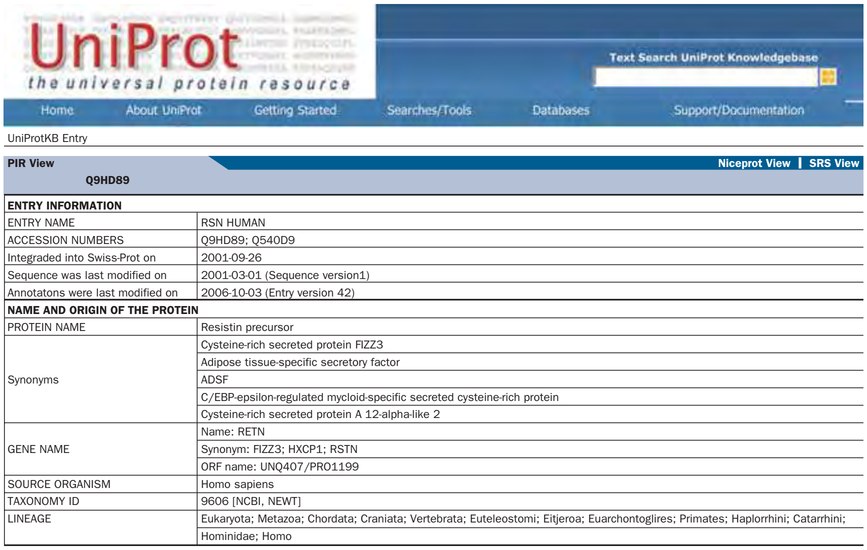

UniProtKB Entry

PIR View

Q9HD89

ENTRY INFORMATION	
ENTRY NAME	RSN HUMAN
ACCESSION NUMBERS	Q9HD89; Q540D9
Integraded into Swiss-Prot on	2001-09-26
Sequence was last modified on	2001-03-01 (Sequence version1)
Annotatons were last modified on	2006-10-03 (Entry version 42)
NAME AND ORIGIN OF THE PROTEIN	
PROTEIN NAME	Resistin precursor
Synonyms	Cysteine-rich secreted protein FIZZ3 Adipose tissue-specific secretory factor ADSF C/EBP-epsilon-regulated mycloid-specific secreted cysteine-rich protein Cysteine-rich secreted protein A 12-alpha-like 2
GENE NAME	Name: RETN Synonym: FIZZ3; HXCP1; RSTN ORF name: UNQ407/PRO1199
SOURCE ORGANISM	Homo sapiens
TAXONOMY ID	9606 [NCBI, NEWT]
LINEAGE	Eukaryota; Metazoa; Chordata; Craniata; Vertebrata; Euteleostomi; Eitjeroa; Euarchontoglires; Primates; Haplorrhini; Catarrhini; Hominidae; Homo

Figure 5-20 | The initial portion of a UniProt entry. This information pertains to the protein **resistin,** which is produced by adipose (fat) tissue and may play a role in diabetes (Section 22-4B). The complete entry includes additional information and references as well as the protein's sequence. [From http://www.pir.uniprot.org/.]

Table 5-5 Amino Acid Sequences of Cytochromes *c* from 38 Species[a]

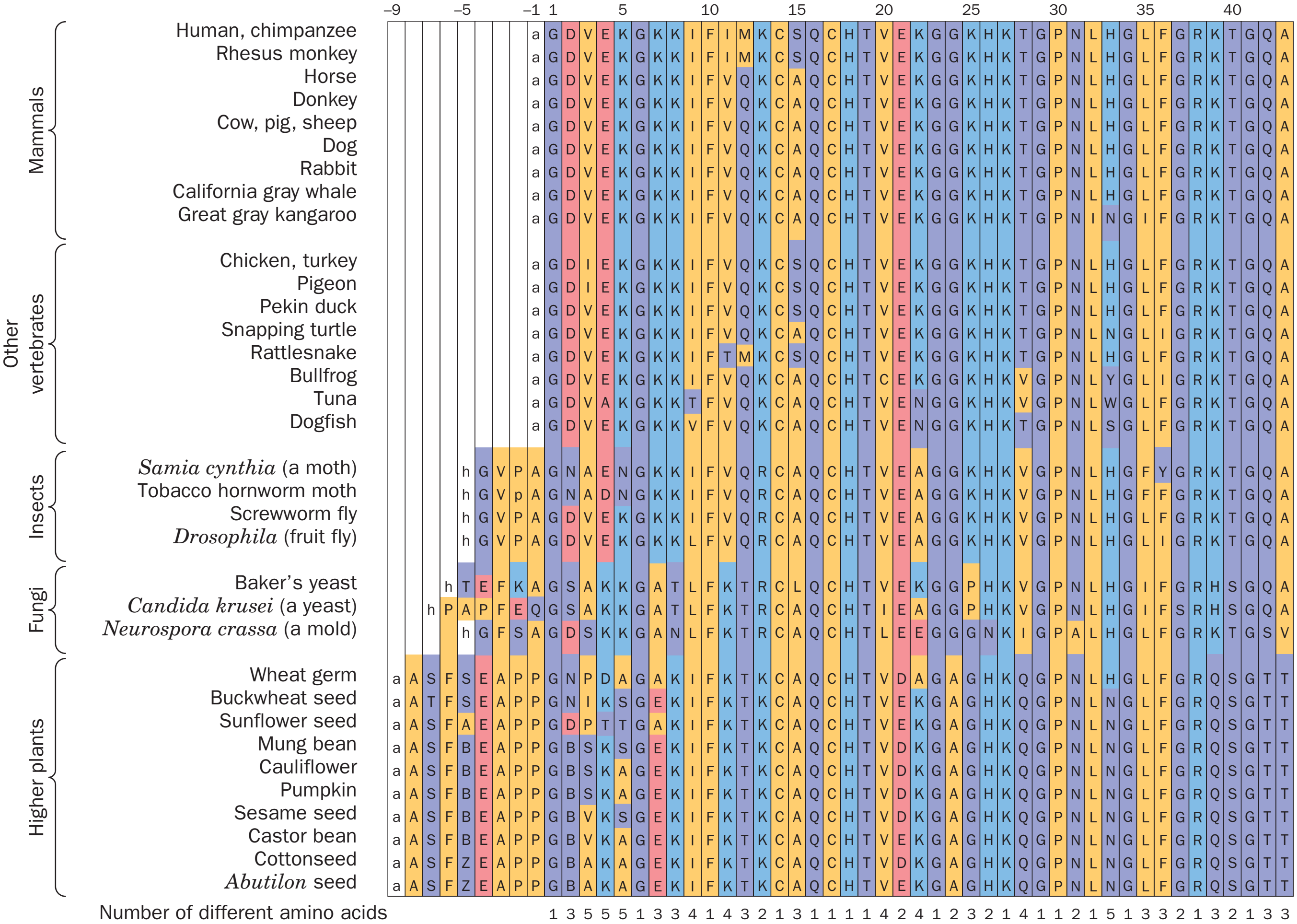

		–9				–5				–1	1				5					10					15					20					25					30					35					40			
Mammals	Human, chimpanzee									a	G	D	V	E	K	G	K	K	I	F	I	M	K	C	S	Q	C	H	T	V	E	K	G	G	K	H	K	T	G	P	N	L	H	G	L	F	G	R	K	T	G	Q	A
	Rhesus monkey									a	G	D	V	E	K	G	K	K	I	F	I	M	K	C	S	Q	C	H	T	V	E	K	G	G	K	H	K	T	G	P	N	L	H	G	L	F	G	R	K	T	G	Q	A
	Horse									a	G	D	V	E	K	G	K	K	I	F	V	Q	K	C	A	Q	C	H	T	V	E	K	G	G	K	H	K	T	G	P	N	L	H	G	L	F	G	R	K	T	G	Q	A
	Donkey									a	G	D	V	E	K	G	K	K	I	F	V	Q	K	C	A	Q	C	H	T	V	E	K	G	G	K	H	K	T	G	P	N	L	H	G	L	F	G	R	K	T	G	Q	A
	Cow, pig, sheep									a	G	D	V	E	K	G	K	K	I	F	V	Q	K	C	A	Q	C	H	T	V	E	K	G	G	K	H	K	T	G	P	N	L	H	G	L	F	G	R	K	T	G	Q	A
	Dog									a	G	D	V	E	K	G	K	K	I	F	V	Q	K	C	A	Q	C	H	T	V	E	K	G	G	K	H	K	T	G	P	N	L	H	G	L	F	G	R	K	T	G	Q	A
	Rabbit									a	G	D	V	E	K	G	K	K	I	F	V	Q	K	C	A	Q	C	H	T	V	E	K	G	G	K	H	K	T	G	P	N	L	H	G	L	F	G	R	K	T	G	Q	A
	California gray whale									a	G	D	V	E	K	G	K	K	I	F	V	Q	K	C	A	Q	C	H	T	V	E	K	G	G	K	H	K	T	G	P	N	L	H	G	L	F	G	R	K	T	G	Q	A
	Great gray kangaroo									a	G	D	V	E	K	G	K	K	I	F	V	Q	K	C	A	Q	C	H	T	V	E	K	G	G	K	H	K	T	G	P	N	I	N	G	I	F	G	R	K	T	G	Q	A
Other vertebrates	Chicken, turkey									a	G	D	I	E	K	G	K	K	I	F	V	Q	K	C	S	Q	C	H	T	V	E	K	G	G	K	H	K	T	G	P	N	L	H	G	L	F	G	R	K	T	G	Q	A
	Pigeon									a	G	D	I	E	K	G	K	K	I	F	V	Q	K	C	S	Q	C	H	T	V	E	K	G	G	K	H	K	T	G	P	N	L	H	G	L	F	G	R	K	T	G	Q	A
	Pekin duck									a	G	D	V	E	K	G	K	K	I	F	V	Q	K	C	S	Q	C	H	T	V	E	K	G	G	K	H	K	T	G	P	N	L	H	G	L	F	G	R	K	T	G	Q	A
	Snapping turtle									a	G	D	V	E	K	G	K	K	I	F	V	Q	K	C	A	Q	C	H	T	V	E	K	G	G	K	H	K	T	G	P	N	L	N	G	L	I	G	R	K	T	G	Q	A
	Rattlesnake									a	G	D	V	E	K	G	K	K	I	F	T	M	K	C	S	Q	C	H	T	V	E	K	G	G	K	H	K	T	G	P	N	L	H	G	L	F	G	R	K	T	G	Q	A
	Bullfrog									a	G	D	V	E	K	G	K	K	I	F	V	Q	K	C	A	Q	C	H	T	C	E	K	G	G	K	H	K	V	G	P	N	L	Y	G	L	I	G	R	K	T	G	Q	A
	Tuna									a	G	D	V	A	K	G	K	K	T	F	V	Q	K	C	A	Q	C	H	T	V	E	N	G	G	K	H	K	V	G	P	N	L	W	G	L	F	G	R	K	T	G	Q	A
	Dogfish									a	G	D	V	E	K	G	K	K	V	F	V	Q	K	C	A	Q	C	H	T	V	E	N	G	G	K	H	K	T	G	P	N	L	S	G	L	F	G	R	K	T	G	Q	A
Insects	*Samia cynthia* (a moth)					h	G	V	P	A	G	N	A	E	N	G	K	K	I	F	V	Q	R	C	A	Q	C	H	T	V	E	A	G	G	K	H	K	V	G	P	N	L	H	G	F	Y	G	R	K	T	G	Q	A
	Tobacco hornworm moth					h	G	V	p	A	G	N	A	D	N	G	K	K	I	F	V	Q	R	C	A	Q	C	H	T	V	E	A	G	G	K	H	K	V	G	P	N	L	H	G	F	F	G	R	K	T	G	Q	A
	Screwworm fly					h	G	V	P	A	G	D	V	E	K	G	K	K	I	F	V	Q	R	C	A	Q	C	H	T	V	E	A	G	G	K	H	K	V	G	P	N	L	H	G	L	F	G	R	K	T	G	Q	A
	Drosophila (fruit fly)					h	G	V	P	A	G	D	V	E	K	G	K	K	L	F	V	Q	R	C	A	Q	C	H	T	V	E	A	G	G	K	H	K	V	G	P	N	L	H	G	L	I	G	R	K	T	G	Q	A
Fungi	Baker's yeast				h	T	E	F	K	A	G	S	A	K	K	G	A	T	L	F	K	T	R	C	L	Q	C	H	T	V	E	K	G	G	P	H	K	V	G	P	N	L	H	G	I	F	G	R	H	S	G	Q	A
	Candida krusei (a yeast)			h	P	A	P	F	E	Q	G	S	A	K	K	G	A	T	L	F	K	T	R	C	A	Q	C	H	T	I	E	A	G	G	P	H	K	V	G	P	N	L	H	G	I	F	S	R	H	S	G	Q	A
	Neurospora crassa (a mold)					h	G	F	S	A	G	D	S	K	K	G	A	N	L	F	K	T	R	C	A	Q	C	H	T	L	E	E	G	G	G	N	K	I	G	P	A	L	H	G	L	F	G	R	K	T	G	S	V
Higher plants	Wheat germ	a	A	S	F	S	E	A	P	P	G	N	P	D	A	G	A	K	I	F	K	T	K	C	A	Q	C	H	T	V	D	A	G	A	G	H	K	Q	G	P	N	L	H	G	L	F	G	R	Q	S	G	T	T
	Buckwheat seed	a	A	T	F	S	E	A	P	P	G	N	I	K	S	G	E	K	I	F	K	T	K	C	A	Q	C	H	T	V	E	K	G	A	G	H	K	Q	G	P	N	L	N	G	L	F	G	R	Q	S	G	T	T
	Sunflower seed	a	A	S	F	A	E	A	P	P	G	D	P	T	T	G	A	K	I	F	K	T	K	C	A	Q	C	H	T	V	E	K	G	A	G	H	K	Q	G	P	N	L	N	G	L	F	G	R	Q	S	G	T	T
	Mung bean	a	A	S	F	B	E	A	P	P	G	B	S	K	S	G	E	K	I	F	K	T	K	C	A	Q	C	H	T	V	D	K	G	A	G	H	K	Q	G	P	N	L	N	G	L	F	G	R	Q	S	G	T	T
	Cauliflower	a	A	S	F	B	E	A	P	P	G	B	S	K	A	G	E	K	I	F	K	T	K	C	A	Q	C	H	T	V	D	K	G	A	G	H	K	Q	G	P	N	L	N	G	L	F	G	R	Q	S	G	T	T
	Pumpkin	a	A	S	F	B	E	A	P	P	G	B	S	K	A	G	E	K	I	F	K	T	K	C	A	Q	C	H	T	V	D	K	G	A	G	H	K	Q	G	P	N	L	N	G	L	F	G	R	Q	S	G	T	T
	Sesame seed	a	A	S	F	B	E	A	P	P	G	B	V	K	S	G	E	K	I	F	K	T	K	C	A	Q	C	H	T	V	D	K	G	A	G	H	K	Q	G	P	N	L	N	G	L	F	G	R	Q	S	G	T	T
	Castor bean	a	A	S	F	B	E	A	P	P	G	B	V	K	A	G	E	K	I	F	K	T	K	C	A	Q	C	H	T	V	E	K	G	A	G	H	K	Q	G	P	N	L	N	G	L	F	G	R	Q	S	G	T	T
	Cottonseed	a	A	S	F	Z	E	A	P	P	G	B	A	K	A	G	E	K	I	F	K	T	K	C	A	Q	C	H	T	V	D	K	G	A	G	H	K	Q	G	P	N	L	N	G	L	F	G	R	Q	S	G	T	T
	Abutilon seed	a	A	S	F	Z	E	A	P	P	G	B	A	K	A	G	E	K	I	F	K	T	K	C	A	Q	C	H	T	V	E	K	G	A	G	H	K	Q	G	P	N	L	N	G	L	F	G	R	Q	S	G	T	T
	Number of different amino acids										1	3	5	5	5	1	3	3	4	1	4	3	2	1	3	1	1	1	1	4	2	4	1	2	3	2	1	4	1	1	2	1	5	1	3	3	2	1	3	2	1	3	3

[a] The amino acid side chains have been shaded according to their polarity characteristics so that an invariant or conservatively substituted residue is identified by a vertical band of a single color. The letter a at the beginning of the chain indicates that the N-terminal amino group is acetylated; an h indi-cates that the acetyl group is absent.

Source: After Dickerson, R.E., *Sci. Am.* 226(4); 58–72 (1972), with corrections from Dickerson, R.E., and Timkovich, R., *in* Boyer, P.D. (Ed.), *The Enzymes* (3rd ed.), Vol. 11, pp. 421–422, Academic Press (1975). Table, Irving Geis/Geis Archives Trust, Copyright Howard Hughes Medical Institute. Reproduced with permission.

4 Protein Evolution

LEARNING OBJECTIVES

- Understand that sequence comparisons reveal the evolutionary relationships between proteins.
- Understand how protein families evolve by the duplication and divergence of genes encoding protein domains.
- Understand that the rate of evolution varies from protein to protein.

Because an organism's genetic material specifies the amino acid sequences of all its proteins, changes in genes due to random mutation can alter a protein's primary structure. A mutation in a protein is propagated only if it somehow increases, or at least does not decrease, the probability that its owner will survive to reproduce. Many mutations are deleterious or produce lethal effects and therefore rapidly die out. On rare occasions, however, a mutation arises that improves the fitness of its host. This is the essence of **evolution** by **natural selection.**

See Guided Exploration 5
Protein evolution.

A | Protein Sequences Reveal Evolutionary Relationships

The primary structures of a given protein from related species closely resemble one another. Consider **cytochrome *c*,** a protein found in nearly all eukaryotes. Cytochrome *c* is a component of the mitochondrial electron-

Table 5-5 (continued)

	45					50					55					60					65					70					75					80					85					90					95					100				104
P	G	Y	S	Y	T	A	A	N	K	N	K	G	I	I	W	G	E	D	T	L	M	E	Y	L	E	N	P	K	K	Y	I	P	G	T	K	M	I	F	V	G	I	K	K	K	E	E	R	A	D	L	I	A	Y	L	K	K	A	T	N	E
P	G	Y	S	Y	T	A	A	N	K	N	K	G	I	I	W	G	E	D	T	L	M	E	Y	L	E	N	P	K	K	Y	I	P	G	T	K	M	I	F	V	G	I	K	K	K	E	E	R	A	D	L	I	A	Y	L	K	K	A	A	N	E
P	G	F	T	Y	T	D	A	N	K	N	K	G	I	T	W	K	E	E	T	L	M	E	Y	L	E	N	P	K	K	Y	I	P	G	T	K	M	I	F	A	G	I	K	K	K	T	E	R	E	D	L	I	A	Y	L	K	K	A	T	N	E
P	G	F	S	Y	T	D	A	N	K	N	K	G	I	T	W	K	E	E	T	L	M	E	Y	L	E	N	P	K	K	Y	I	P	G	T	K	M	I	F	A	G	I	K	K	K	T	E	R	E	D	L	I	A	Y	L	K	K	A	T	N	E
P	G	F	S	Y	T	D	A	N	K	N	K	G	I	T	W	G	E	E	T	L	M	E	Y	L	E	N	P	K	K	Y	I	P	G	T	K	M	I	F	A	G	I	K	K	K	G	E	R	E	D	L	I	A	Y	L	K	K	A	T	N	E
P	G	F	S	Y	T	D	A	N	K	N	K	G	I	T	W	G	E	E	T	L	M	E	Y	L	E	N	P	K	K	Y	I	P	G	T	K	M	I	F	A	G	I	K	K	T	G	E	R	A	D	L	I	A	Y	L	K	K	A	T	K	E
V	G	F	S	Y	T	D	A	N	K	N	K	G	I	T	W	G	E	D	T	L	M	E	Y	L	E	N	P	K	K	Y	I	P	G	T	K	M	I	F	A	G	I	K	K	K	D	E	R	A	D	L	I	A	Y	L	K	K	A	T	N	E
V	G	F	S	Y	T	D	A	N	K	N	K	G	I	T	W	G	E	E	T	L	M	E	Y	L	E	N	P	K	K	Y	I	P	G	T	K	M	I	F	A	G	I	K	K	K	G	E	R	A	D	L	I	A	Y	L	K	K	A	T	N	E
P	G	F	T	Y	T	D	A	N	K	N	K	G	I	I	W	G	E	D	T	L	M	E	Y	L	E	N	P	K	K	Y	I	P	G	T	K	M	I	F	A	G	I	K	K	K	G	E	R	A	D	L	I	A	Y	L	K	K	A	T	N	E
E	G	F	S	Y	T	D	A	N	K	N	K	G	I	T	W	G	E	D	T	L	M	E	Y	L	E	N	P	K	K	Y	I	P	G	T	K	M	I	F	A	G	I	K	K	K	S	E	R	V	D	L	I	A	Y	L	K	D	A	T	S	K
E	G	F	S	Y	T	D	A	N	K	N	K	G	I	T	W	G	E	D	T	L	M	E	Y	L	E	N	P	K	K	Y	I	P	G	T	K	M	I	F	A	G	I	K	K	K	A	E	R	A	D	L	I	A	Y	L	K	Q	A	T	A	K
E	G	F	S	Y	T	D	A	N	K	N	K	G	I	T	W	G	E	D	T	L	M	E	Y	L	E	N	P	K	K	Y	I	P	G	T	K	M	I	F	A	G	I	K	K	K	S	E	R	A	D	L	I	A	Y	L	K	D	A	T	A	K
E	G	F	S	Y	T	E	A	N	K	N	K	G	I	T	W	G	E	E	T	L	M	E	Y	L	E	N	P	K	K	Y	I	P	G	T	K	M	I	F	A	G	I	K	K	K	A	E	R	A	D	L	I	A	Y	L	K	D	A	T	S	K
V	G	Y	S	Y	T	A	A	N	K	N	K	G	I	I	W	G	D	D	T	L	M	E	Y	L	E	N	P	K	K	Y	I	P	G	T	K	M	V	F	T	G	L	S	K	K	K	E	R	T	N	L	I	A	Y	L	K	E	K	T	A	A
A	G	F	S	Y	T	D	A	N	K	N	K	G	I	T	W	G	E	D	T	L	M	E	Y	L	E	N	P	K	K	Y	I	P	G	T	K	M	I	F	A	G	I	K	K	K	G	E	R	Q	D	L	I	A	Y	L	K	S	A	C	S	K
E	G	Y	S	Y	T	D	A	N	K	S	K	G	I	V	W	N	N	D	T	L	M	E	Y	L	E	N	P	K	K	Y	I	P	G	T	K	M	I	F	A	G	I	K	K	K	G	E	R	Q	D	L	V	A	Y	L	K	S	A	T	S	-
Q	G	F	S	Y	T	D	A	N	K	S	K	G	I	T	W	Q	Q	E	T	L	R	I	Y	L	E	N	P	K	K	Y	I	P	G	T	K	M	I	F	A	G	L	K	K	K	S	E	R	Q	D	L	I	A	Y	L	K	K	T	A	A	S
P	G	F	S	Y	S	N	A	N	K	A	K	G	I	T	W	G	D	D	T	L	F	E	Y	L	E	N	P	K	K	Y	I	P	G	T	K	M	V	F	A	G	L	K	K	A	N	E	R	A	D	L	I	A	Y	L	K	E	S	T	K	-
P	G	F	S	Y	S	N	A	N	K	A	K	G	I	T	W	Q	D	D	T	L	F	E	Y	L	E	N	P	K	K	Y	I	P	G	T	K	M	V	F	A	G	L	K	K	A	N	E	R	A	D	L	I	A	Y	L	K	Q	A	T	K	-
A	G	F	A	Y	T	N	A	N	K	A	K	G	I	T	W	Q	D	D	T	L	F	E	Y	L	E	N	P	K	K	Y	I	P	G	T	K	M	I	F	A	G	L	K	K	P	N	E	R	G	D	L	I	A	Y	L	K	S	A	T	K	-
A	G	F	A	Y	T	N	A	N	K	A	K	G	I	T	W	Q	D	D	T	L	F	E	Y	L	E	N	P	K	K	Y	I	P	G	T	K	M	I	F	A	G	L	K	K	P	N	E	R	G	D	L	I	A	Y	L	K	S	A	T	K	-
Q	G	Y	S	Y	T	D	A	N	I	K	K	N	V	L	W	D	E	N	N	M	S	E	Y	L	T	N	P	X	K	Y	I	P	G	T	K	M	A	F	G	G	L	K	K	E	K	D	R	N	D	L	I	T	Y	L	K	K	A	C	E	-
Q	G	Y	S	Y	T	D	A	N	K	R	A	G	V	E	W	A	E	P	T	M	S	D	Y	L	E	N	P	X	K	Y	I	P	G	T	K	M	A	F	G	G	L	K	K	A	K	D	R	N	D	L	V	T	Y	M	L	E	A	S	K	-
D	G	Y	A	Y	T	D	A	N	K	Q	K	G	I	T	W	D	E	N	T	L	F	E	Y	L	E	N	P	X	K	Y	I	P	G	T	K	M	A	F	G	G	L	K	K	D	K	D	R	N	D	I	I	T	F	M	K	E	A	T	A	-
A	G	Y	S	Y	S	A	A	N	K	N	K	A	V	E	W	E	E	N	T	L	Y	D	Y	L	L	N	P	X	K	Y	I	P	G	T	K	M	V	F	P	G	L	X	K	P	Q	D	R	A	D	L	I	A	Y	L	K	K	A	T	S	S
A	G	Y	S	Y	S	A	A	N	K	N	K	A	V	T	W	G	E	D	T	L	Y	E	Y	L	L	N	P	X	K	Y	I	P	G	T	K	M	V	F	P	G	L	X	K	P	Q	E	R	A	D	L	I	A	Y	L	K	D	S	T	E	-
A	G	Y	S	Y	S	A	A	N	K	N	M	A	V	I	W	E	E	N	T	L	Y	D	Y	L	E	N	P	X	K	Y	I	P	G	T	K	M	V	F	P	G	L	X	K	P	Q	E	R	A	D	L	I	A	Y	L	K	T	S	T	A	-
A	G	Y	S	Y	S	T	A	N	K	N	M	A	V	I	W	E	E	K	T	L	Y	D	Y	L	E	N	P	X	K	Y	I	P	G	T	K	M	V	F	P	G	L	X	K	P	Q	D	R	A	D	L	I	A	Y	L	K	E	S	T	A	-
A	G	Y	S	Y	S	A	A	N	K	N	K	A	V	E	W	E	E	K	T	L	Y	D	Y	L	E	N	P	X	K	Y	I	P	G	T	K	M	V	F	P	G	L	X	K	P	Q	D	R	A	D	L	I	A	Y	L	K	E	A	T	A	-
P	G	Y	S	Y	S	A	A	N	K	N	R	A	V	I	W	E	E	K	T	L	Y	D	Y	L	E	N	P	X	K	Y	I	P	G	T	K	M	V	F	P	G	L	X	K	P	Q	D	R	A	D	L	I	A	Y	L	K	E	A	T	A	-
P	G	Y	S	Y	S	A	A	N	K	N	M	A	V	I	W	G	E	N	T	L	Y	D	Y	L	E	N	P	X	K	Y	I	P	G	T	K	M	V	F	P	G	L	X	K	P	Q	E	R	A	D	L	I	A	Y	L	K	E	A	T	A	-
A	G	Y	S	Y	S	A	A	N	K	N	M	A	V	Q	W	G	E	N	T	L	Y	A	Y	L	E	N	P	X	K	Y	I	P	G	T	K	M	V	F	P	G	L	X	K	P	Q	D	R	A	D	L	I	A	Y	L	K	E	A	T	A	-
A	G	Y	S	Y	S	A	A	N	K	N	M	A	V	Q	W	G	E	N	T	L	Y	D	Y	L	E	N	P	X	K	Y	I	P	G	T	K	M	V	F	P	G	L	X	K	P	Q	D	R	A	D	L	I	A	Y	L	K	E	S	T	A	-
P	G	Y	S	Y	S	A	A	N	K	N	M	A	V	N	W	G	E	N	T	L	Y	D	Y	L	E	N	P	X	K	Y	I	P	G	T	K	M	V	F	P	G	L	X	K	P	Q	D	R	A	D	L	I	A	Y	L	K	E	S	T	A	-
6	1	2	3	1	2	5	1	1	2	6	4	3	2	7	1	7	4	5	2	2	5	4	1	1	3	1	1	1	1	1	1	1	1	1	1	1	3	1	5	1	2	2	1	6	9	2	1	7	2	2	2	2	2	2	2	6	4	4	5	4

Hydrophilic, acidic: D Asp E Glu

Hydrophilic, basic: H His K Lys R Arg X TrimethylLys

Polar, uncharged: B Asn or Asp G Gly N Asn Q Gln
S Ser T Thr W Trp Y Tyr Z Gln or Glu

Hydrophobic: A Ala C Cys F Phe I Ile L Leu
M Met P Pro V Val

transport system (Section 18-2), which is believed to have taken its present form between 1.5 and 2 billion years ago, when organisms developed mechanisms for aerobic respiration. Emanuel Margoliash, Emil Smith, and others have elucidated the amino acid sequences of the cytochromes *c* from over 100 eukaryotic species ranging in complexity from yeast to humans. The cytochromes *c* from different species are single polypeptides of 104 to 112 residues. The sequences of 38 of these proteins are arranged in Table 5-5 to show the similarities between vertically aligned residues (the residues have been color-coded according to their physical properties). A survey of the aligned sequences (bottom line of Table 5-5) shows that at 38 positions (23 positions in the complete set of >100 sequences), the same amino acid appears in all species. Most of the remaining positions are occupied by chemically similar residues in different organisms. In only eight positions does the sequence accommodate six or more different residues.

According to evolutionary theory, *related species have evolved from a common ancestor, so it follows that the genes specifying each of their proteins must likewise have evolved from the corresponding gene in that ancestor.* The sequence of the ancestral cytochrome *c* is accessible only indirectly, by examining the sequences of extant proteins.

Sequence Comparisons Provide Information on Protein Structure and Function. *In general, comparisons of the primary structures of* ***homologous proteins*** *(evolutionarily related proteins) indicate which of the protein's residues are essential to its function, which are less significant, and which have little specific function.* Finding the same residue at a particular position in the amino acid sequence of a series of related proteins suggests that the chemical or structural properties of that so-called **invariant residue** uniquely suit it to some essential function of the protein. For example, its side chain may be necessary for binding another molecule or for participating in a catalytic reaction. Other amino acid positions may have less stringent side chain requirements and can therefore accommodate residues with similar characteristics (e.g., Asp or Glu, Ser or Thr, etc.); such positions are said to be **conservatively substituted.** On the other hand, a particular amino acid position may tolerate many different amino acid residues, indicating that the functional requirements of that position are rather nonspecific. Such a position is said to be **hypervariable.**

Why is cytochrome *c*—an ancient and essential protein—not identical in all species? Even a protein that is well adapted to its function, that is, one that is not subject to physiological improvement, nevertheless continues evolving. The random nature of mutational processes will, in time, change such a protein in ways that do not significantly affect its function, a process called ***neutral drift*** (deleterious mutations are, of course, rapidly rejected through natural selection). Hypervariable residues are apparently particularly subject to neutral drift.

Phylogenetic Trees Depict Evolutionary History. Far-reaching conclusions about evolutionary relationships can be drawn by comparing the amino acid sequences of homologous proteins. The simplest way to assess evolutionary differences is to count the amino acid differences between proteins. For example, the data in Table 5-5 show that primate cytochromes *c* more nearly resemble those of other mammals than they do those of insects (8–12 differences among mammals versus 26–31 differences between mammals and insects). Similarly, the cytochromes *c* of fungi differ as much from those of mammals (45–51 differences) as they do from those of insects (41–47) or higher plants (47–54). The order of these differences largely parallels that expected from classical taxonomy, which is based primarily on morphological rather than molecular characteristics.

The sequences of homologous proteins can be analyzed by computer to construct a **phylogenetic tree,** a diagram that indicates the ancestral relationships among organisms that produce the protein. The phylogenetic tree for cytochrome *c* is sketched in Fig. 5-21. Similar trees have been derived for other proteins. Each branch point of the tree represents a putative common ancestor for all the organisms above it. The distances between branch points are expressed as the number of amino acid differences per 100 residues of the protein. Such trees present a more quantitative measure of the degree of relatedness of the various species than macroscopic taxonomy can provide.

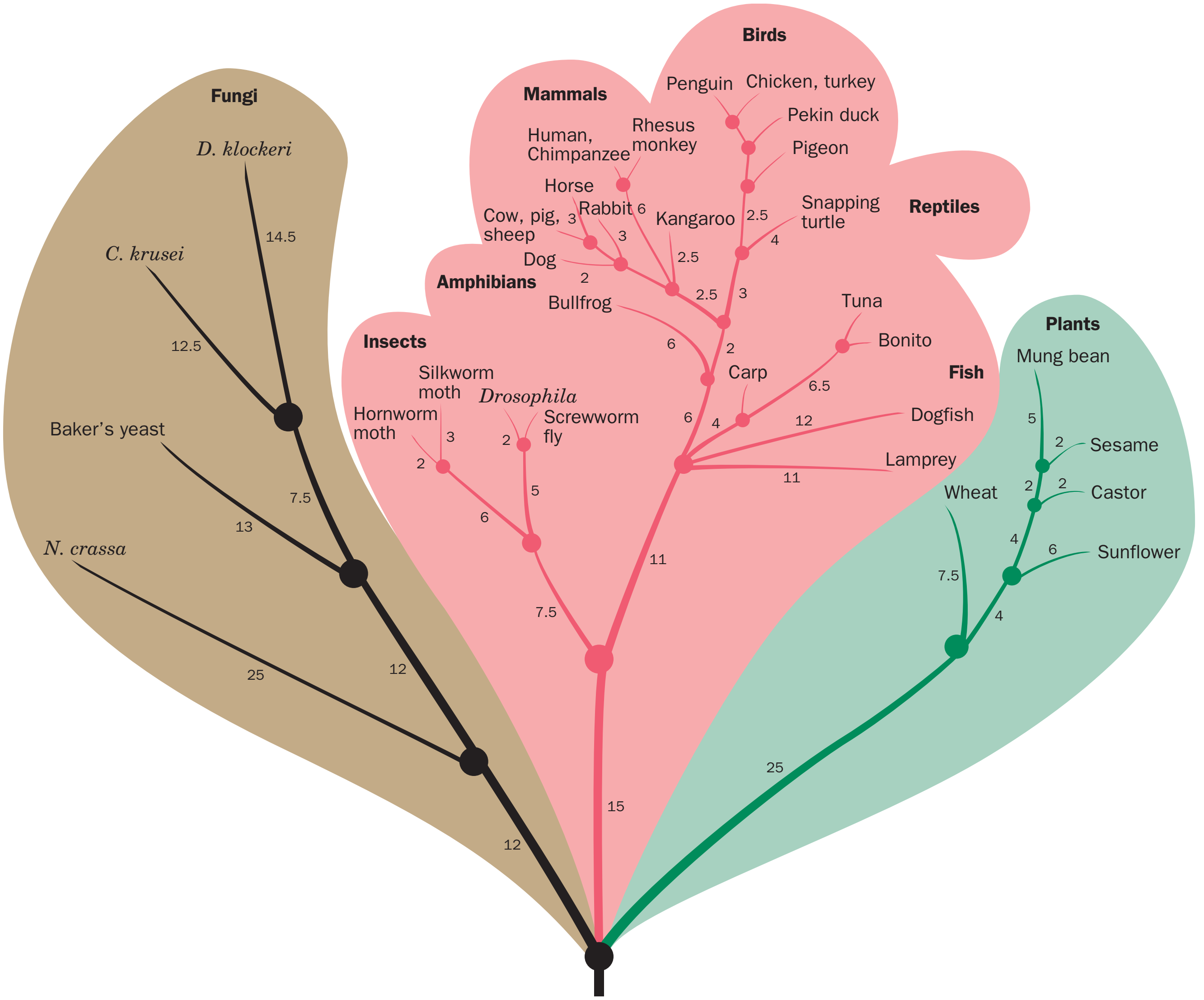
Fungi
D. klockeri
14.5
C. krusei
12.5
Baker's yeast
7.5
13
N. crassa
25
12
12
Mammals
Human, Chimpanzee
Rhesus monkey
Horse
Cow, pig, sheep
3
Rabbit
6
3
3
Kangaroo
Dog
2
2.5
2.5
Amphibians
Bullfrog
Birds
Penguin
Chicken, turkey
Pekin duck
Pigeon
Snapping turtle
2.5
4
3
Reptiles
Tuna
Bonito
Fish
Carp
6
2
6.5
6
4
12
Dogfish
Lamprey
11
Insects
Silkworm moth
Drosophila
Hornworm moth
Screwworm fly
3
2
2
5
6
7.5
11
15
Plants
Mung bean
5
2
Sesame
2
2
Castor
Wheat
4
6
Sunflower
7.5
4
25

Figure 5-21 | Phylogenetic tree of cytochrome *c*. Each branch point represents an organism ancestral to the species connected above it. The number beside each branch indicates the number of inferred differences per 100 residues between the cytochromes *c* of the flanking branch points or species. [After Dayhoff, M.O., Park, C.M., and McLaughlin, P.J., *in* Dayhoff, M.O. (Ed.), *Atlas of Protein Sequence and Structure, p.* 8, National Biomedical Research Foundation (1972).]

Note that the evolutionary distances from all modern cytochromes *c* to the lowest point, the earliest common ancestor producing this protein, are approximately the same. Thus, "lower" organisms do not represent life-forms that appeared early in history and ceased to evolve further. The cytochromes *c* of all the species included in Fig. 5-21—whether called "primitive" or "advanced"—have evolved to about the same extent.

B | Proteins Evolve by the Duplication of Genes or Gene Segments

The effort to characterize protein evolution and create databases of related proteins was pioneered by Margaret Dayhoff beginning in the 1960s. Since then, around one million protein sequences have been catalogued as the result of direct protein sequencing or DNA sequencing projects.

This has led to the development of mathematically sophisticated computer algorithms to identify similarities between sequences. These search protocols can detect similarities between proteins that have evolved to the extent that their amino acid sequences are <20% identical and have acquired several sequence insertions and/or deletions of various lengths. The use of such sequence alignment programs, which are publicly available, is demonstrated in Bioinformatics Exercises 5-1 and 5-2 (www.wiley.com/college/voet).

Analysis of a large number of proteins indicates that evolutionarily conserved sequences are often segments of about 40 to 200 residues, called **domains.** Originally, this term referred to a portion of discrete protein structure, but the usage has expanded to include the corresponding amino acid sequence. As we shall see in Section 6-20, structural similarities between two domains may be apparent even when the sequences have few residues in common.

Protein domains can be grouped into an estimated 1000–1400 different families, but about half of all known domains fall into just 200 families. Most protein families have only a few members, and 10–20% of proteins appear to be unique, although it is also possible that they represent family members whose sequences have simply diverged beyond recognition. Domains whose sequences are more than about 40% identical usually have the same function; domains with less than about 25% sequence identity usually perform different roles.

Protein Families Can Arise through Gene Duplication. It is not surprising that proteins with similar functions have similar sequences; such proteins presumably evolved from a common ancestor. Homologous proteins with the same function in different species (e.g., the cytochromes *c* shown in Table 5-5) are said to be **orthologous.**

Within a species, similar proteins arise through **gene duplication,** an aberrant genetic recombination event in which one member of a chromosome pair acquires both copies of the primordial gene (genetic recombination is discussed in Section 25-6). Following duplication, the sequences may diverge as mutations occur over time. *Gene duplication is a particularly efficient mode of evolution because one copy of the gene evolves a new function through natural selection while its counterpart continues to direct the synthesis of the original protein.* Two independently evolving genes that are derived from a duplication event are said to be **paralogous.** In prokaryotes, approximately 60% of protein domains have been duplicated; in many eukaryotes the figure is ~90%, and in humans, ~98%.

The **globin family** of proteins provides an excellent example of evolution through gene duplication and divergence. **Hemoglobin,** which transports O_2 from the lungs (or gills or skin) to the tissues, is a tetramer with the subunit composition $\alpha_2\beta_2$ (i.e., two α polypeptides and two β polypeptides). The sequences of the α and β subunits are similar to each other and to the sequence of the protein **myoglobin,** which facilitates oxygen diffusion through muscle tissue (hemoglobin and myoglobin are discussed in more detail in Chapter 7). The primordial globin probably functioned simply as an oxygen-storage protein. Gene duplication allowed one globin to evolve into a monomeric hemoglobin α chain. Duplication of the α chain gene gave rise to the paralogous gene for the β chain. Other members of the globin family include the β-like γ chain that is present in fetal hemoglobin, an $\alpha_2\gamma_2$ tetramer, and the β-like ε and α-like ζ chains that appear together early in embryogenesis as $\zeta_2\varepsilon_2$ hemoglobin. Primates contain a relatively recently duplicated globin, the β-like δ chain, which appears as a minor component (~1%) of adult hemoglobin. Although the $\alpha_2\delta_2$ hemoglobin has no known unique function, perhaps it may eventually evolve one. The genealogy of the members of the globin family is diagrammed in Fig. 5-22. The human genome also contains the relics of globin genes that are not expressed. These **pseudogenes** can be considered the dead ends of protein evolution. Note that a duplicated and therefore initially superfluous gene has only a limited time to evolve a new functionality that provides a selective advantage to its host before it is inactivated through mutation, that is, becomes a pseudogene.

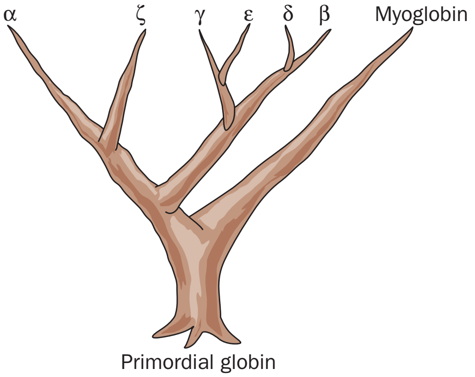

Figure 5-22 | Genealogy of the globin family. Each branch point represents a gene duplication event. Myoglobin is a single-chain protein. The globins identified by Greek letters are subunits of hemoglobins.

The Rate of Sequence Divergence Varies. The sequence differences between orthologous proteins can be plotted against the time when, according to the fossil record, the species producing the proteins diverged. The plot for a given protein is essentially linear, indicating that its mutations accumulate at a constant rate over a geological time scale. However, rates of evolution vary among proteins (Fig. 5-23). This does not imply that the rates of mutation of the DNAs specifying those proteins differ, but rather that *the rate at which mutations are accepted into a protein varies.*

A major contributor to the rate at which a protein evolves is the effect of amino acid changes on the protein's function. For example, Fig. 5-23 shows that **histone H4,** a protein that binds to DNA in eukaryotes (Section 24-5A), is among the most highly conserved proteins (the histones H4 from peas and cows, species that diverged 1.2 billion years ago, differ by only two conservative changes in their 102 residues). Evidently, histone H4 is so finely tuned to its function of packaging DNA in cells that it is extremely intolerant of any mutations. Cytochrome *c* is only slightly more tolerant. It is a relatively small protein that binds to several other proteins. Hence, any changes in its amino acid sequence must be compatible with all its binding partners (or they would have to simultaneously mutate to accommodate the altered cytochrome *c*, an unlikely event). Hemoglobin, which functions as a free-floating molecule, is subject to less selective pressure than histone H4 or cytochrome *c,* so its surface residues are more easily substituted by other amino acids. The **fibrinopeptides** are ~20-residue fragments that are cleaved from the vertebrate protein **fibrinogen** to induce blood clotting. Once they have been removed, the fibrinopeptides are discarded, so that they are subject to little selective pressure to maintain their amino acid sequences.

The rate of protein evolution also depends on the protein's structural stability. For example, a mutation that slowed the rate at which a newly synthesized polypeptide chain folds into its functional three-dimensional shape could affect the cell's survival, even if the protein ultimately functioned normally. Such mutations would be especially critical for proteins that are produced at high levels, since the not-yet-folded proteins could swamp the cell's protein-folding mechanisms. In fact, the genes for highly expressed proteins appear to evolve more slowly than the genes for rarely expressed proteins.

Mutational changes in proteins do not account for all evolutionary changes among organisms. The DNA sequences that control the expression of proteins (Chapters 26, 27, and 28) are also subject to mutation. These sequences control where, when, and how much of the corresponding protein is made. Thus, although the proteins of humans and chimpanzees are >99% identical on average (e.g., their cytochromes *c* are

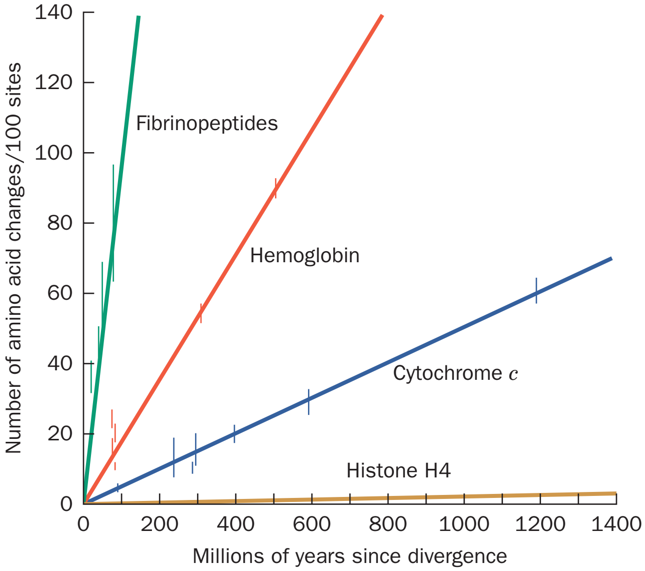

Figure 5-23 | Rates of evolution of four proteins. The graph was constructed by plotting the number of different amino acid residues in the proteins on two sides of a branch point of a phylogenetic tree versus the time, according to the fossil record, since the corresponding species diverged from their common ancestor. [Illustration, Irving Geis/Geis Archives Trust. Copyright Howard Hughes Medical Institute. Reproduced with permission.]

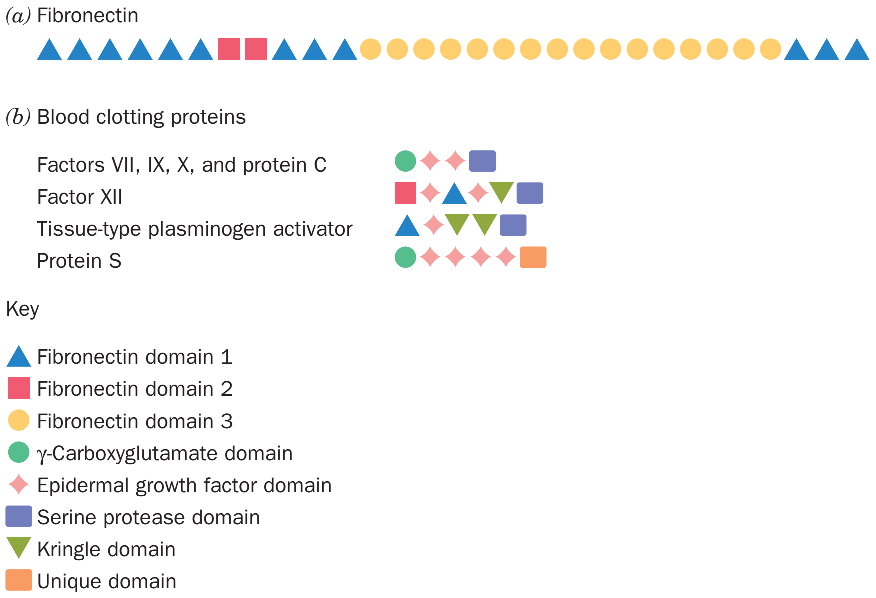
(a) Fibronectin
(b) Blood clotting proteins
Factors VII, IX, X, and protein C
Factor XII
Tissue-type plasminogen activator
Protein S
Key
Fibronectin domain 1
Fibronectin domain 2
Fibronectin domain 3
γ-Carboxyglutamate domain
Epidermal growth factor domain
Serine protease domain
Kringle domain
Unique domain

■ **Figure 5-24 | Construction of some multidomain proteins.** Each shape represents a segment of ~40–100 residues that appears, with some sequence variation, several times in the same protein or in a number of related proteins. (*a*) **Fibronectin,** an ~500-kD protein of the extracellular matrix, is composed mostly of repeated domains of three types. (*b*) Some of the proteins that participate in blood clotting are built from a small set of domains. (The epidermal growth factor domain is so named because it was first observed as a component of **epidermal growth factor.**) [After Baron, M., Norman, D.G., and Campbell, I.D., *Trends Biochem. Sci.* **16,** 14 (1991).]

identical), their anatomical and behavioral differences are so great that they are classified as belonging to different families.

Many Proteins Contain Domains That Occur in Other Proteins. Gene duplication is not the only mechanism that generates new proteins. Analysis of protein sequences has revealed that many proteins, particularly those made by eukaryotes, are mosaics of sequence motifs or domains of about 40–100 amino acid residues. These domains occur in several other proteins in the same organism and may be repeated numerous times within a given protein (Fig. 5-24*a*). For example, most of the proteins involved in blood clotting are composed of sets of smaller domains (Fig. 5-24*b*). The sequence identity between homologous domains is imperfect since each domain evolves independently. The functions of individual domains are not always known: Some appear to have discrete activities, such as catalyzing a certain chemical reaction or binding a particular molecule, but others may merely be spacers or scaffolding for other domains.

We shall see in Section 25-6C how gene segments encoding protein domains are copied and inserted into other positions in a genome to generate new genes that encode proteins with novel sequences. Such domain shuffling is a much faster process than the duplication of an entire gene followed by its evolution of a new functionality. Nevertheless, both mechanisms have played important roles in the evolution of proteins.

■ CHECK YOUR UNDERSTANDING

How can sequence comparisons reveal which amino acid residues are essential for a protein's function?

Explain how the number of amino acid differences between homologous proteins can be used to construct a phylogenetic tree.

Explain the origin of orthologous proteins, paralogous proteins, and multidomain proteins.

Why do different proteins appear to evolve at different rates?

SUMMARY

1. The properties of proteins depend largely on the sizes and sequences of their component polypeptides.
2. Protein purification requires controlled conditions such as pH and temperature, and a means to quantify the protein (an assay).
3. Fractionation procedures are used to purify proteins on the basis of solubility, charge, polarity, size, and binding specificity.
4. Differences in solubility permit proteins to be concentrated and purified by salting out.
5. Chromatography, the separation of soluble substances by their rate of movement through an insoluble matrix, is a technique for purifying molecules by charge (ion exchange chromatography), hydrophobicity (hydrophobic interaction chromatography), size (gel filtration chromatography), and binding specificity (affinity chromatography). Binding and elution often depend on the salt concentration and pH.
6. Electrophoresis separates molecules by charge and size; SDS-PAGE separates them primarily by size. 2D electrophoresis can resolve thousands of proteins.
7. Analysis of a protein's sequence begins with end group analysis, to determine the number of different subunits, and the cleavage of disulfide bonds.
8. Polypeptides are cleaved into fragments suitable for sequencing by Edman degradation, in which residues are removed, one at a time, from the N-terminus. Peptides can also be sequenced by mass spectrometry.
9. A protein's sequence is reconstructed from the sequences of overlapping peptide fragments and from information about the locations of disulfide bonds. The sequences of numerous proteins are archived in publicly available databases.
10. Proteins evolve through changes in primary structure. Protein sequences can be compared to construct phylogenetic trees and to identify essential amino acid residues.
11. New proteins arise as a result of the duplication of genes or gene segments specifying protein domains, followed by their divergence.

KEY TERMS

primary structure **92**
peptide **92**
multisubunit protein **92**
subunit **92**
denaturation **94**
protease **95**
nuclease **95**
assay **95**
coupled enzymatic reaction **95**
immunoassay **95**
antibody **95**
antigen **95**
RIA **95**
ELISA **95**
Beer–Lambert law **95**
absorbance (A) **95**
absorptivity (ε) **95**
chromophore **96**
Bradford assay **96**
fractionation procedure **97**
salting in **97**
salting out **97**
chromatography **98**
HPLC **98**
ion exchange chromatography **98**
anion exchanger **98**
cation exchanger **98**
polyelectrolyte **98**
elution **99**
eluant **99**
hydrophobic interaction chromatography **99**
gel filtration chromatography **100**
affinity chromatography **101**
ligand **101**
immunoaffinity chromatography **101**
metal chelate affinity chromatography **101**
PAGE **101**
autoradiography **102**
immunoblot (Western blot) **102**
SDS-PAGE **102**
capillary electrophoresis **103**
IEF **103**
two-dimensional (2D) gel electrophoresis **103**
proteomics **103**
mercaptan **106**
endopeptidase **107**
exopeptidase **107**
limited proteolysis **108**
Edman degradation **109**
mass spectrometry **110**
ESI **111**
homologous proteins **116**
invariant residue **116**
conservative substitution **116**
hypervariable residue **116**
neutral drift **116**
phylogenetic tree **116**
domain **118**
orthologous proteins **118**
gene duplication **118**
paralogous proteins **118**
pseudogenes **119**

PROBLEMS

1. Which peptide has greater absorbance at 280 nm?
   A. Gln–Leu–Glu–Phe–Thr–Leu–Asp–Gly–Tyr
   B. Ser–Val–Trp–Asp–Phe–Gly–Tyr–Trp–Ala
2. Protein X has an absorptivity of 0.4 $\text{mL}\cdot\text{mg}^{-1}\cdot\text{cm}^{-1}$ at 280 nm. What is the absorbance at 280 nm of a 2.0 $\text{mg}\cdot\text{mL}^{-1}$ solution of protein X? (Assume the light path is 1 cm.)
3. You are using ammonium sulfate to purify protein Q (pI = 5.0) by salting out from a solution at pH 7.0. How should you adjust the pH of the mixture to maximize the amount of protein Q that precipitates?
4. (a) In what order would the amino acids Arg, His, and Leu be eluted from a carboxymethyl column at pH 6? (b) In what

order would Glu, Lys, and Val be eluted from a diethylaminoethyl column at pH 8?

5. Consult Table 5-1 to complete the following: (a) On a plot of absorbance at 280 nm versus elution volume, sketch the results of gel filtration of a mixture containing human cytochrome *c* and bacteriophage T7 RNA polymerase and identify each peak. (b) Sketch the results of SDS-PAGE of the same protein mixture showing the direction of migration and identifying each band.

6. Explain why a certain protein has an apparent molecular mass of 90 kD when determined by gel filtration and 60 kD when determined by SDS-PAGE in the presence or absence of 2-mercaptoethanol. Which molecular mass determination is more accurate?

7. Determine the subunit composition of a protein from the following information:

   Molecular mass by gel filtration: 200 kD

   Molecular mass by SDS-PAGE: 100 kD

   Molecular mass by SDS-PAGE with 2-mercaptoethanol:
   40 kD and 60 kD

8. What fractionation procedure could be used to purify protein 1 from a mixture of three proteins whose amino acid compositions are as follows?

   1. 25% Ala, 20% Gly, 20% Ser, 10% Ile, 10% Val, 5% Asn, 5% Gln, 5% Pro
   2. 30% Gln, 25% Glu, 20% Lys, 15% Ser, 10% Cys
   3. 25% Asn, 20% Gly, 20% Asp, 20% Ser, 10% Lys, 5% Tyr

   All three proteins are similar in size and p*I*, and there is no antibody available for protein 1.

9. Purification of Myoglobin (Mb). Purification tables are often used to keep track of the yield and purification of a protein. The specific activity is a ratio of the amount of the protein of interest, in this case Mb, obtained at a given step (μmol or enzyme units) divided by the amount (mg) of total protein. The yield is the ratio of the amount of the protein of interest obtained at a given step (μmol or enzyme units) divided by the original amount present in the crude extract, often converted to percent yield by multiplying by 100. The fold purification is the ratio of the specific activity of the purified protein to that of the crude preparation.

   (a) For the purification table below, calculate the specific activity, % yield, and fold purification for the empty cells.

   (b) Which step—DEAE or affinity chromatography—causes the greatest loss of Mb?

   (c) Which step causes the greater purification of Mb?

   (d) If you wanted to use only one purification step, which technique would you choose?

10. Explain why the dansyl chloride treatment of a single polypeptide chain followed by its complete acid hydrolysis yields several dansylated amino acids.

11. Identify the first residue obtained by Edman degradation of cytochrome *c* from (a) *Drosophila,* (b) baker's yeast, and (c) wheat germ (see Table 5-5).

12. You must cleave the following peptide into smaller fragments. Which of the proteases listed in Table 5-3 would be likely to yield the most fragments? The fewest?

    NMTQGRCKPVNTFVHEPLVDVQNVCFKE

13. Electrospray ionization mass spectrometry (ESI-MS) of proteins involves creating positively charged ions of the protein and separating them according to their mass-to-charge ratio (m/z).

    (a) What causes the different positive charges on different particles of the protein?

    (b) The amino acid composition (in numbers of residues per chain) of hen egg-white lysozyme (HEWL) is as follows:

P	2	Y	3	N	14	H	1
D	7	M	2	L	8	E	2
C	8	R	11	G	12	F	3
A	12	I	6	K	6	V	6
S	10	W	6	T	7	Q	3

    What is the maximum positive charge that can be present on a HEWL ion?

    (c) The ESI-MS spectrum below was obtained for HEWL.

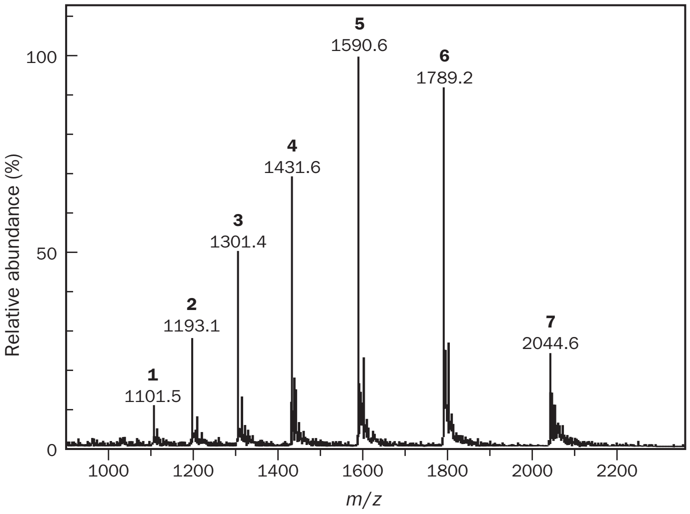

Using peaks 5 and 6, calculate the molecular mass of HEWL (see Sample Calculation 5-1). [Spectrum obtained from http://www.astbury.leeds.ac.uk/facil/MStut/mstutorial.htm]

    (d) What is the charge on the ion that makes peak 5?

Purification Table for Problem 9

Purification step	mg total protein	μmol Mb	Specific activity (μmol Mb/mg total protein)	% yield	fold purification
1. Crude extract	1550	0.75	100	1	
2. DEAE-cellulose chromatography	550	0.35			
3. Affinity chromatography	5.0	0.28			

14. You wish to determine the sequence of a short peptide. Cleavage with trypsin yields three smaller peptides with the sequences Leu–Glu, Gly–Tyr–Asn–Arg, and Gln–Ala–Phe–Val–Lys. Cleavage with chymotrypsin yields three peptides with the sequences Gln–Ala–Phe, Asn–Arg–Leu–Glu, and Val–Lys–Gly–Tyr. What is the sequence of the intact peptide?

15. Separate cleavage reactions of a polypeptide by CNBr and chymotrypsin yield fragments with the following amino acid sequences. What is the sequence of the intact polypeptide?

    CNBr treatment

    1. Arg–Ala–Tyr–Gly–Asn
    2. Leu–Phe–Met
    3. Asp–Met

    Chymotrypsin

    4. Met–Arg–Ala–Tyr
    5. Asp–Met–Leu–Phe
    6. Gly–Asn

16. You wish to determine the sequence of a polypeptide that has the following amino acid composition.

    1 Ala 4 Arg 2 Asn 3 Asp 4 Cys 3 Gly 1 Gln 4 Glu
    1 His 1 Lys 1 Met 1 Phe 2 Pro 4 Ser 2 Tyr 1 Trp

    (a) What is the maximum number of peptides you can expect if you cleave the polypeptide with cyanogen bromide?

    (b) What is the maximum number of peptides you can expect if you cleave the polypeptide with chymotrypsin?

    (c) Analysis of the intact polypeptide reveals that there are no free sulfhydryl groups. How many disulfide bonds are likely to be present?

    (d) How many different arrangements of disulfide bonds are possible?

17. Treatment of a polypeptide with 2-mercaptoethanol yields two polypeptides:

    1. Ala–Val–Cys–Arg–Thr–Gly–Cys–Lys–Asn–-Phe–Leu
    2. Tyr–Lys–Cys–Phe–Arg–His–Thr–Lys–Cys–Ser

    Treatment of the intact polypeptide with trypsin yields fragments with the following amino acid compositions:

    3. (Ala, Arg, Cys$_2$, Ser, Val)
    4. (Arg, Cys$_2$, Gly, Lys, Thr, Phe)
    5. (Asn, Leu, Phe)
    6. (His, Lys, Thr)
    7. (Lys, Tyr)

    Indicate the positions of the disulfide bonds in the intact polypeptide.

18. You wish to sequence the light chain of a protease inhibitor from the *Brassica nigra* plant. Cleavage of the light chain by trypsin and chymotrypsin yields the following fragments. What is the sequence of the light chain?

    Chymotrypsin

    1. Leu–His–Lys–Gln–Ala–Asn–Gln–Ser–Gly–Gly–Gly–Pro–Ser
    2. Gln–Gln–Ala–Gln–His–Leu–Arg–Ala–Cys–Gln–Gln–Trp
    3. Arg–Ile–Pro–Lys–Cys–Arg–Lys–Phe

    Trypsin

    4. Arg
    5. Ala–Cys–Gln–Gln–Trp–Leu–His–Lys
    6. Cys–Arg
    7. Gln–Ala–Asn–Gln–Ser–Gly–Gly–Gly–Pro–Ser
    8. Phe–Gln–Gln–Ala–Gln–His–Leu–Arg
    9. Ile–Pro–Lys
    10. Lys

19. In site-directed mutagenesis experiments, Gly is often successfully substituted for Val, but Val can rarely substitute for Gly. Explain.

20. Below is a list of the first 10 residues of the B helix in myoglobin from different organisms.

Position	1	2	3	4	5	6	7	8	9	10
Human	D	I	P	G	H	G	Q	E	V	L
Chicken	D	I	A	G	H	G	H	E	V	L
Alligator	K	L	P	E	H	G	H	E	V	I
Turtle	D	L	S	A	H	G	Q	E	V	I
Tuna	D	Y	T	T	M	G	G	L	V	L
Carp	D	F	E	G	T	G	G	E	V	L

Based on this information, which positions (a) appear unable to tolerate substitutions, (b) can tolerate conservative substitution, and (c) are highly variable?

CASE STUDY

Case 2 (available at www.wiley.com/college/voet)
Histidine–Proline-Rich Glycoprotein as a Plasma pH Sensor

Focus concept: A histidine–proline-rich glycoprotein may serve as a plasma sensor and regulate local pH in extracellular fluid during ischemia or metabolic acidosis.

Prerequisites: Chapters 4 and 5

- Acidic/basic properties of amino acids
- Amino acid structure and protein structure

BIOINFORMATICS EXERCISES

Bioinformatics Exercises are available at www.wiley.com/college/voet.

Chapter 5

Using Databases to Compare and Identify Related Protein Sequences

1. **Obtaining Sequences from BLAST.** Using a known protein sequence, find and retrieve the sequences of related proteins from other organisms.
2. **Multiple Sequence Alignment.** Examine the various sequences for similarities.
3. **Phylogenetic Trees.** Set up and interpret phylogenetic trees to explore the evolutionary relationships between related protein sequences.
4. **Interpreting Mass Spectral Data.** Learn about different types of mass spectrometry and how to correctly interpret the data they generate.
5. **One-Dimensional Electrophoresis.** Perform an SDS-PAGE electrophoresis simulation with known and unknown proteins.
6. **Two-Dimensional Electrophoresis.** Explore the predicted and observed electrophoretic parameters (p*I*, molecular mass, and fragmentation pattern) for a known protein.

REFERENCES

Protein Purification

Boyer, R.F., *Biochemistry Laboratory: Modern Theory and Techniques*, Benjamin Cummings (2006).

Janson, J.-C. (Ed.), *Protein Purification: Principles, High Resolution Methods, and Applications* (3rd ed.), Wiley (2007). [Contains detailed discussions of a variety of chromatographic and electrophoretic separation techniques.]

Tanford, C. and Reynolds, J., *Nature's Robots: A History of Proteins,* Oxford University Press (2001). [Descriptions of some early discoveries related to the nature of proteins and their purification and analysis.]

Wilson, K. and Walker, J.M. (Eds.), *Principles and Techniques of Biochemistry and Molecular Biology* (6th ed.), Cambridge University Press (2005). [Includes reviews of spectroscopy, electrophoresis, and chromatography.]

Protein Sequencing

Aebersold, R. and Mann, M., Mass spectrometry-based proteomics, *Nature* **422,** 198–207 (2003). [Describes some of the methods of mass spectrometric analysis of proteins as well as current and potential applications.]

Findlay, J.B.C. and Geisow, M.J. (Eds.), *Protein Sequencing. A Practical Approach,* IRL Press (1989).

Galperin, M.Y., The molecular biology database collection: 2007 update, *Nucleic Acids Res.* **35,** Database issue D3–D4 (2007). [This and other articles in this Database Issue describe the features and potential uses of various protein and DNA sequence databases. Freely available at http://nar.oxfordjournals.org.]

Protein Evolution

Baxevanis, A.D. and Ouellette, B.F.F. (Eds.), *Bioinformatics, A Practical Guide to the Analysis of Genes and Proteins* (3rd ed.), Wiley-Interscience (2005).

Doolittle, R.F., Feng, D.-F., Tsang, S., Cho, G., and Little, E., Determining divergence times of the major kingdoms of living organisms with a protein clock, *Science* **271,** 470–477 (1996). [Demonstrates how protein sequences can be used to draw phylogenetic trees.]

Mount, D.W., *Bioinformatics: Sequence and Genome Analysis* (2nd ed.), Cold Spring Harbor Laboratory Press (2004).

Pál, C., Papp, B., and Lercher, M.J., An integrated view of protein evolution, *Nature Reviews Genetics* **7,** 337–348 (2006). [Discusses some of the factors that contribute to the variable rate of evolution among proteins, including protein dispensability and expression level.]

6

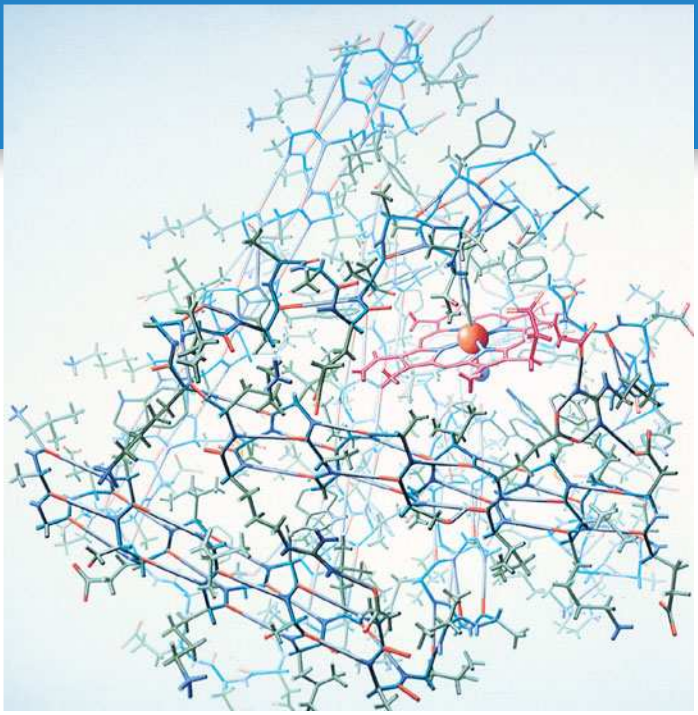

Proteins: Three-Dimensional Structure

The atomic structure of myoglobin, is drawn here as a stick model. Noncovalent forces stabilize its three-dimensional structure. [Illustration, Irving Geis. Image from the Irving Geis Collection/Howard Hughes Medical Institute. Rights owned by HHMI. Reproduction by permission only.]

■ MEDIA RESOURCES

(Available at www.wiley.com/college/voet)

Guided Exploration 6. Stable helices in proteins: the α helix
Guided Exploration 7. Hydrogen bonding in β sheets
Guided Exploration 8. Secondary structures in proteins
Interactive Exercise 2. Glyceraldehyde-3-phosphate dehydrogenase
Animated Figure 6-7. The α helix
Animated Figure 6-9. β sheets
Animated Figure 6-34. Symmetry in oligomeric proteins
Animated Figure 6-42. Mechanism of protein disulfide isomerase
Kinemage 3-1. The peptide group
Kinemage 3-2. The α helix
Kinemage 3-3. β sheets
Kinemage 3-4. Reverse turns
Kinemage 4-1, 4-2. Coiled coils
Kinemage 4-3, 4-4. Collagen
Kinemage 5. Cytochrome *c*
Case Study 4. The Structure of Insulin
Case Study 5. Characterization of Subtilisin from the Antarctic Psychrophile *Bacillus* TA41
Case Study 6. A Collection of Collagen Cases
Bioinformatics Exercises. Chapter 6. Visualizing Three-Dimensional Protein Structures

■ CHAPTER CONTENTS

1 Secondary Structure
- **A.** The Planar Peptide Group Limits Polypeptide Conformations
- **B.** The Most Common Regular Secondary Structures Are the α Helix and the β Sheet
- **C.** Fibrous Proteins Have Repeating Secondary Structures
- **D.** Most Proteins Include Nonrepetitive Structure

2 Tertiary Structure
- **A.** Most Protein Structures Are Determined by X-Ray Crystallography or Nuclear Magnetic Resonance
- **B.** Side Chain Location Varies with Polarity
- **C.** Tertiary Structures Contain Combinations of Secondary Structure
- **D.** Structure Is Conserved More than Sequence
- **E.** Structural Bioinformatics Provides Tools for Storing, Visualizing, and Comparing Protein Structural Information

3 Quaternary Structure and Symmetry

4 Protein Stability
- **A.** Proteins Are Stabilized by Several Forces
- **B.** Proteins Can Undergo Denaturation and Renaturation

5 Protein Folding
- **A.** Proteins Follow Folding Pathways
- **B.** Molecular Chaperones Assist Protein Folding
- **C.** Some Diseases Are Caused by Protein Misfolding

For many years, it was thought that proteins were colloids of random structure and that the enzymatic activities of certain crystallized proteins were due to unknown entities associated with an inert protein carrier. In 1934, J.D. Bernal and Dorothy Crowfoot Hodgkin showed that a crystal of the protein **pepsin** yielded a discrete diffraction pattern when placed in an X-ray beam. This result provided convincing evidence that pepsin was not a random colloid but an ordered array of atoms organized into a large yet uniquely structured molecule.

Even relatively small proteins contain thousands of atoms, almost all of which occupy definite positions in space. The first X-ray structure of a protein, that of sperm whale myoglobin, was reported in 1958 by John Kendrew and co-workers. At the time—only 5 years after James Watson and Francis Crick had elucidated the simple and elegant structure of DNA (Section 3-2B)—protein chemists were chagrined by the complexity and apparent lack of regularity in the structure of myoglobin. In retrospect, such irregularity seems essential for proteins to fulfill their diverse biological roles. However, comparisons of the nearly 50,000 protein structures now known have revealed that proteins actually exhibit a remarkable degree of structural regularity.

As we saw in Section 5-1, the primary structure of a protein is its linear sequence of amino acids. In discussing protein structure, three further levels of structural complexity are customarily invoked:

- **Secondary structure** is the local spatial arrangement of a polypeptide's backbone atoms without regard to the conformations of its side chains.
- **Tertiary structure** refers to the three-dimensional structure of an entire polypeptide, including its side chains.
- Many proteins are composed of two or more polypeptide chains, loosely referred to as subunits. A protein's **quaternary structure** refers to the spatial arrangement of its subunits.

The four levels of protein structure are summarized in Fig. 6-1.

In this chapter, we explore secondary through quaternary structure, including examples of proteins that illustrate each of these levels. We also discuss the process of protein folding and the forces that stabilize folded proteins.

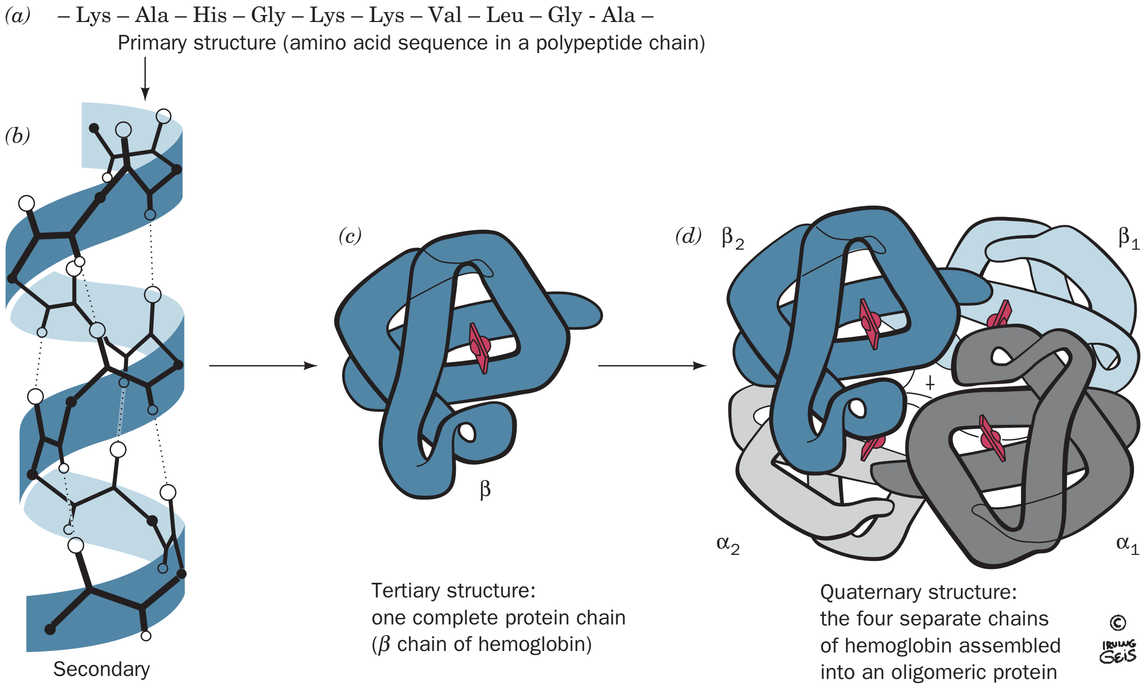
(a)
– Lys – Ala – His – Gly – Lys – Lys – Val – Leu – Gly - Ala –
Primary structure (amino acid sequence in a polypeptide chain)
(b)
(c)
β
(d)
β2
β1
α2
α1
© Irving Geis

Secondary structure (helix)

Tertiary structure: one complete protein chain (β chain of hemoglobin)

Quaternary structure: the four separate chains of hemoglobin assembled into an oligomeric protein

Figure 6-1 | Levels of protein structure. (*a*) Primary structure, (*b*) secondary structure, (*c*) tertiary structure, and (*d*) quaternary structure. [Illustration, Irving Geis. Image from the Irving Geis Collection/Howard Hughes Medical Institute. Rights owned by HHMI. Reproduction by permission only.]

1 Secondary Structure

Protein secondary structure includes the regular polypeptide folding patterns such as helices, sheets, and turns. However, before we discuss these basic structural elements, we must consider the geometric properties of peptide groups, which underlie all higher order structures.

LEARNING OBJECTIVES

- Understand that the planar character of the peptide group limits the conformational flexibility of the polypeptide chain.
- Become familiar with the α helix and the β sheet.
- Understand the structures of the fibrous proteins α keratin and collagen.

A | The Planar Peptide Group Limits Polypeptide Conformations

Recall from Section 4-1B that a polypeptide is a polymer of amino acid residues linked by amide (peptide) bonds. In the 1930s and 1940s, Linus Pauling and Robert Corey determined the X-ray structures of several amino acids and dipeptides in an effort to elucidate the conformational constraints on a polypeptide chain. These studies indicated that *the* ***peptide group*** *has a rigid, planar structure as a consequence of resonance interactions that give the peptide bond ~40% double-bond character:*

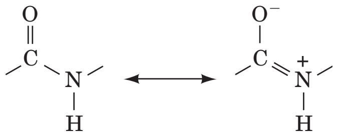

This explanation is supported by the observations that a peptide group's C—N bond is 0.13 Å shorter than its N—C_α single bond and that its C═O bond is 0.02 Å longer than that of aldehydes and ketones. The planar conformation maximizes π-bonding overlap, which accounts for the peptide group's rigidity.

Peptide groups, with few exceptions, assume the **trans conformation,** in which successive C_α atoms are on opposite sides of the peptide bond joining them (Fig. 6-2). The **cis conformation,** in which successive C_α atoms are on the same side of the peptide bond, is ~8 kJ · mol^{-1} less stable than the trans conformation because of steric interference between neighboring side chains. However, this steric interference is reduced in peptide bonds to Pro residues, so *~10% of the Pro residues in proteins follow a cis peptide bond.*

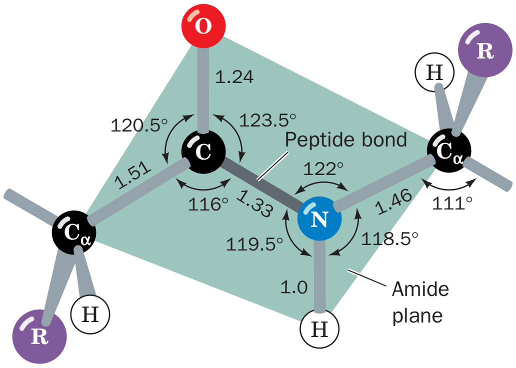

Figure 6-2 | The trans peptide group. The bond lengths (in angstroms) and angles (in degrees) are derived from X-ray crystal structures. [After Marsh, R.E. and Donohue, J., *Adv. Protein Chem.* **22,** 249 (1967).]

See Kinemage Exercise 3-1.

Torsion Angles between Peptide Groups Describe Polypeptide Chain Conformations. The **backbone** or **main chain** of a protein refers to the atoms that participate in peptide bonds, ignoring the side chains of the amino acid residues. The backbone can be drawn as a linked sequence of rigid planar peptide groups (Fig. 6-3). *The conformation of the backbone*

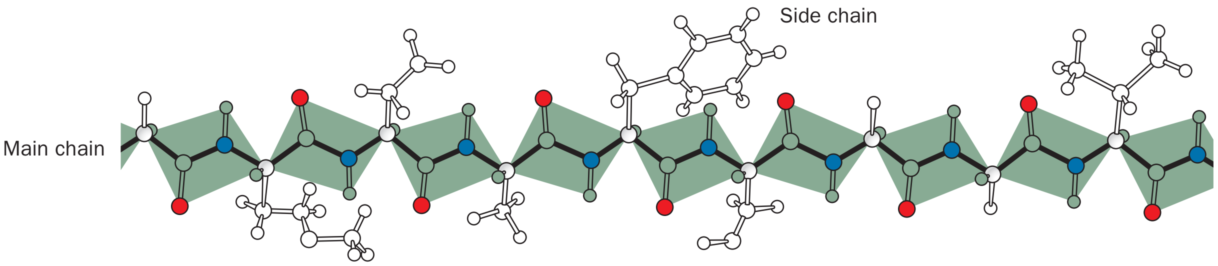

Figure 6-3 | Extended conformation of a polypeptide. The backbone is shown as a series of planar peptide groups. [Illustration, Irving Geis. Image from the Irving Geis Collection/Howard Hughes Medical Institute. Rights owned by HHMI. Reproduction by permission only.]

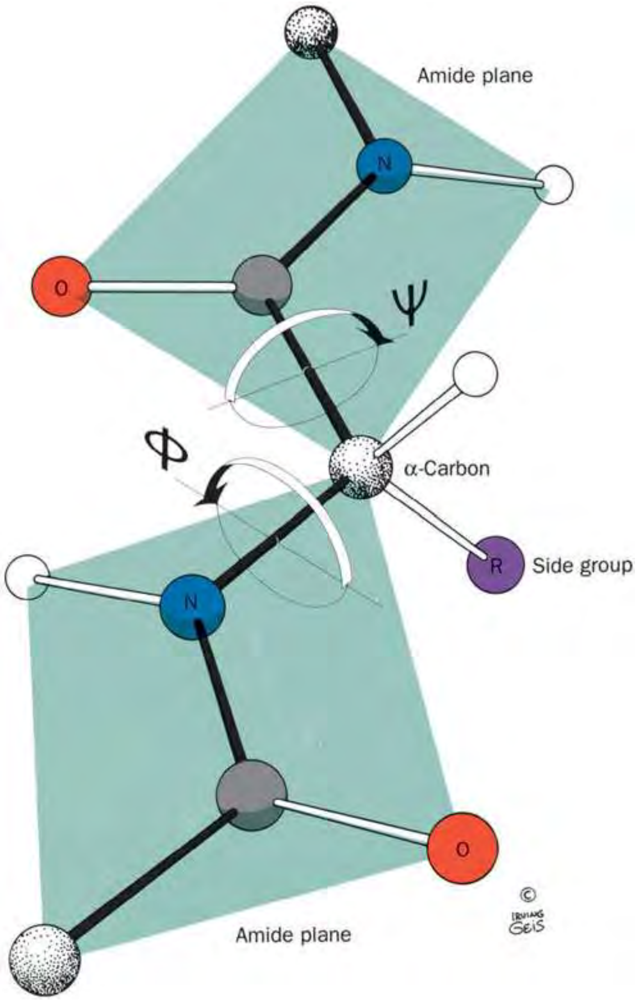

Figure 6-4 | Torsion angles of the polypeptide backbone. Two planar peptide groups are shown. The only reasonably free movements are rotations around the C_α—N (measured as ϕ) and the C_α—C bond (measured as ψ). By convention, both ϕ and ψ are 180° in the conformation shown and increase, as indicated, when the peptide plane is rotated in the clockwise direction as viewed from C_α. [Illustration, Irving Geis. Image from the Irving Geis Collection/Howard Hughes Medical Institute. Rights owned by HHMI. Reproduction by permission only.] **See Kinemage Exercise 3-1.**

can therefore be described by the ***torsion angles*** (also called **dihedral angles** or rotation angles) *around the* C_α*—N bond (ϕ) and the* C_α*—C bond (ψ) of each residue* (Fig. 6-4). These angles, **ϕ** and **ψ**, are both defined as 180° when the polypeptide chain is in its fully extended conformation and increase clockwise when viewed from C_α.

The conformational freedom and therefore the torsion angles of a polypeptide backbone are sterically constrained. Rotation around the C_α—N and C_α—C bonds to form certain combinations of ϕ and ψ angles will cause the amide hydrogen, the carbonyl oxygen, or the substituents of C_α of adjacent residues to collide (e.g., Fig. 6-5). Certain conformations of longer polypeptides can similarly produce collisions between residues that are far apart in sequence.

The Ramachandran Diagram Indicates Allowed Conformations of Polypeptides. The sterically allowed values of ϕ and ψ can be calculated.

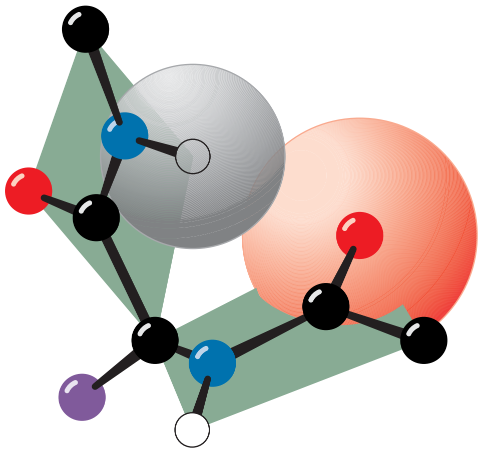

Figure 6-5 | Steric interference between adjacent peptide groups. Rotation can result in a conformation in which the amide hydrogen of one residue and the carbonyl oxygen of the next are closer than their van der Waals distance. [Illustration, Irving Geis. Image from the Irving Geis Collection/Howard Hughes Medical Institute. Rights owned by HHMI. Reproduction by permission only.] 7 **See Kinemage Exercise 3-1.**

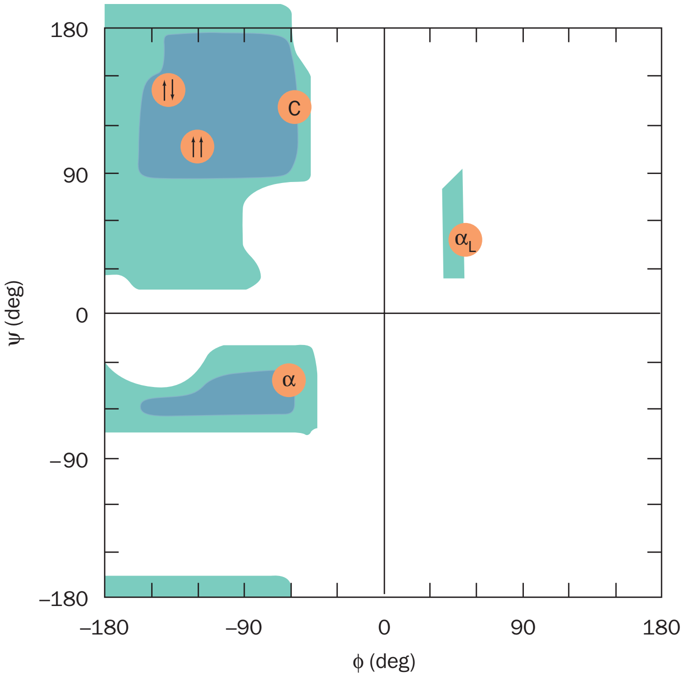

■ **Figure 6-6 | The Ramachandran diagram.** The blue-shaded regions indicate the sterically allowed ϕ and ψ angles for all residues except Gly and Pro. The green-shaded regions indicate the more crowded (outer limit) ϕ and ψ angles. The orange circles represent conformational angles of several secondary structures: α, right-handed α helix; ↑↑, parallel β sheet; ↑↓, antiparallel β sheet; C, collagen helix; α_L, left-handed α helix.

Sterically forbidden conformations, such as the one shown in Fig. 6-5, have ϕ and ψ values that would bring atoms closer than the corresponding van der Waals distance (the distance of closest contact between nonbonded atoms). Such information is summarized in a **Ramachandran diagram** (Fig. 6-6), which is named after its inventor, G. N. Ramachandran.

Most areas of the Ramachandran diagram (most combinations of ϕ and ψ) represent forbidden conformations of a polypeptide chain. Only three small regions of the diagram are physically accessible to most residues. The observed ϕ and ψ values of accurately determined structures nearly always fall within these allowed regions of the Ramachandran plot. There are, however, some notable exceptions:

1. The cyclic side chain of Pro limits its range of ϕ values to angles of around −60°, making it, not surprisingly, the most conformationally restricted amino acid residue.
2. Gly, the only residue without a C_β atom, is much less sterically hindered than the other amino acid residues. Hence, its permissible range of ϕ and ψ covers a larger area of the Ramachandran diagram. At Gly residues, polypeptide chains often assume conformations that are forbidden to other residues.

B | The Most Common Regular Secondary Structures Are the α Helix and the β Sheet

A few elements of protein secondary structure are so widespread that they are immediately recognizable in proteins with widely differing amino acid sequences. Both the **α helix** and the **β sheet** are such elements; they are called **regular secondary structures** because they are composed of sequences of residues with repeating ϕ and ψ values.

See Guided Exploration 6
Stable helices in proteins: the α helix.

The α Helix Is a Coil. Only one polypeptide helix has both a favorable hydrogen bonding pattern and ϕ and ψ values that fall within the fully allowed regions of the Ramachandran diagram: the α helix. Its discovery by

BOX 6-1 **PATHWAYS OF DISCOVERY**

Linus Pauling and Structural Biochemistry

(Linus Pauling, 1901–1994)

Linus Pauling, the only person to have been awarded two unshared Nobel prizes, is clearly the dominant figure in twentieth-century chemistry and one of the greatest scientific figures of all time. He received his B.Sc. in chemical engineering from Oregon Agricultural College (now Oregon State University) in 1922 and his Ph.D. in chemistry from the California Institute of Technology in 1925, where he spent most of his career.

The major theme throughout Pauling's long scientific life was the study of molecular structures and the nature of the chemical bond. He began this career by using the then recently invented technique of X-ray crystallography to determine the structures of simple minerals and inorganic salts. At that time, methods for solving the phase problem (Box 7-2) were unknown, so X-ray structures could only be determined using trial-and-error techniques. This limited the possible molecules that could be effectively studied to those with few atoms and high symmetry such that their atomic coordinates could be fully described by only a few parameters (rather than the three-dimensional coordinates of each of its atoms). Pauling realized that the positions of atoms in molecules were governed by fixed atomic radii, bond distances, and bond angles and used this information to make educated guesses about molecular structures. This greatly extended the complexity of the molecules whose structures could be determined.

In his next major contribution, occurring in 1931, Pauling revolutionized the way that chemists viewed molecules by applying the then infant field of quantum mechanics to chemistry. Pauling formulated the theories of orbital hybridization, electron-pair bonding, and resonance and thereby explained the nature of covalent bonds. This work was summarized in his highly influential monograph, *The Nature of the Chemical Bond,* which was first published in 1938.

In the mid-1930s, Pauling turned his attention to biological chemistry. He began these studies in collaboration with his colleague, Robert Corey, by determining the X-ray structures of several amino acids and dipeptides. At that time, the X-ray structural determination of even such small molecules required around a year of intense effort, largely because the numerous calculations required to solve a structure had to be made by hand (electronic computers had yet to be invented). Nevertheless, these studies led Pauling and Corey to the conclusions that the peptide bond is planar, which Pauling explained from resonance considerations (Section 6-1A), and that hydrogen bonding plays a central role in maintaining macromolecular structures.

In the 1940s, Pauling made several unsuccessful attempts to determine whether polypeptides have any preferred conformations. Then, in 1948, while visiting Oxford University, he was confined to bed by a cold. He eventually tired of reading detective stories and science fiction and again turned his attention to proteins. By folding drawings of polypeptides in various ways, he discovered the α helix, whose existence was rapidly confirmed by X-ray studies of α keratin (Section 6-1C). This work was reported in 1951, and later that year Pauling and Corey also proposed both the parallel and antiparallel β pleated sheets. For these ground-breaking insights, Pauling received the Nobel Prize in Chemistry in 1954, although α helices and β sheets were not actually visualized until the first X-ray structures of proteins were determined, five to ten years later.

Pauling made numerous additional pioneering contributions to biological chemistry, most notably that the heme group in hemoglobin changes its electronic state on binding oxygen (Section 7-1A), that vertebrate hemoglobins are $\alpha_2\beta_2$ heterotetramers (Section 7-1B), that the denaturation of proteins is caused by the unfolding of their polypeptide chains, that sickle-cell anemia is caused by a mutation in the β chain of normal adult hemoglobin (the first so-called molecular disease to be characterized; Section 7-1E), that molecular complementarity plays an important role in antibody–antigen interactions (Section 7-3B) and by extension all macromolecular interactions, that enzymes catalyze reactions by preferentially binding their transition states (Section 11-3E), and that the comparison of the sequences of the corresponding proteins in different organisms yields evolutionary insights (Section 5-4).

Pauling was also a lively and stimulating lecturer who for many years taught a general chemistry course [which one of the authors of this textbook (DV) had the privilege of taking]. His textbook, *General Chemistry,* revolutionized the way that introductory chemistry was taught by presenting it as a subject that could be understood in terms of atomic physics and molecular structure. For a book of such generality, an astounding portion of its subject matter had been elucidated by its author. Pauling's amazing grasp of chemistry was demonstrated by the fact that he dictated each chapter of the textbook in a single sitting.

By the late 1940s, Pauling became convinced that the possibility of nuclear war posed an enormous danger to humanity and calculated that the radioactive fallout from each aboveground test of a nuclear bomb would ultimately cause cancer in thousands of people. He therefore began a campaign to educate the public about the hazards of bomb testing and nuclear war. The political climate in the United States at the time was such that the government considered Pauling to be subversive and his passport was revoked (and only returned two weeks before he was to leave for Sweden to receive his first Nobel prize). Nevertheless, Pauling persisted in this campaign, which culminated, in 1962, with the signing of the first Nuclear Test Ban Treaty. For his efforts, Pauling was awarded the 1962 Nobel Peace Prize.

Pauling saw science as the search for the truth, which included politics and social causes. In his later years, he became a vociferous promoter of what he called orthomolecular medicine, the notion that large doses of vitamins could ward off and cure many human diseases, including cancer. In the best known manifestation of this concept, Pauling advocated taking large doses of vitamin C to prevent the common cold and lessen its symptoms, advice still followed by millions of people, although the medical evidence supporting this notion is scant. It should be noted, however, that Pauling, who followed his own advice, remained active until he died in 1994 at the age of 93.

Linus Pauling in 1951, through model building, ranks as one of the landmarks of structural biochemistry (Box 6-1).

The α helix (Fig. 6-7) is right-handed; that is, it turns in the direction that the fingers of a right hand curl when its thumb points in the direction that the helix rises (Fig. 3-7). The α helix has 3.6 residues per turn and a **pitch** (the distance the helix rises along its axis per turn) of 5.4 Å. The α helices of proteins have an average length of ~12 residues, which corresponds to over three helical turns, and a length of ~18 Å.

In the α helix, the backbone hydrogen bonds are arranged such that the peptide C═O bond of the nth residue points along the helix axis toward the peptide N—H group of the (n + 4)th residue. This results in a strong

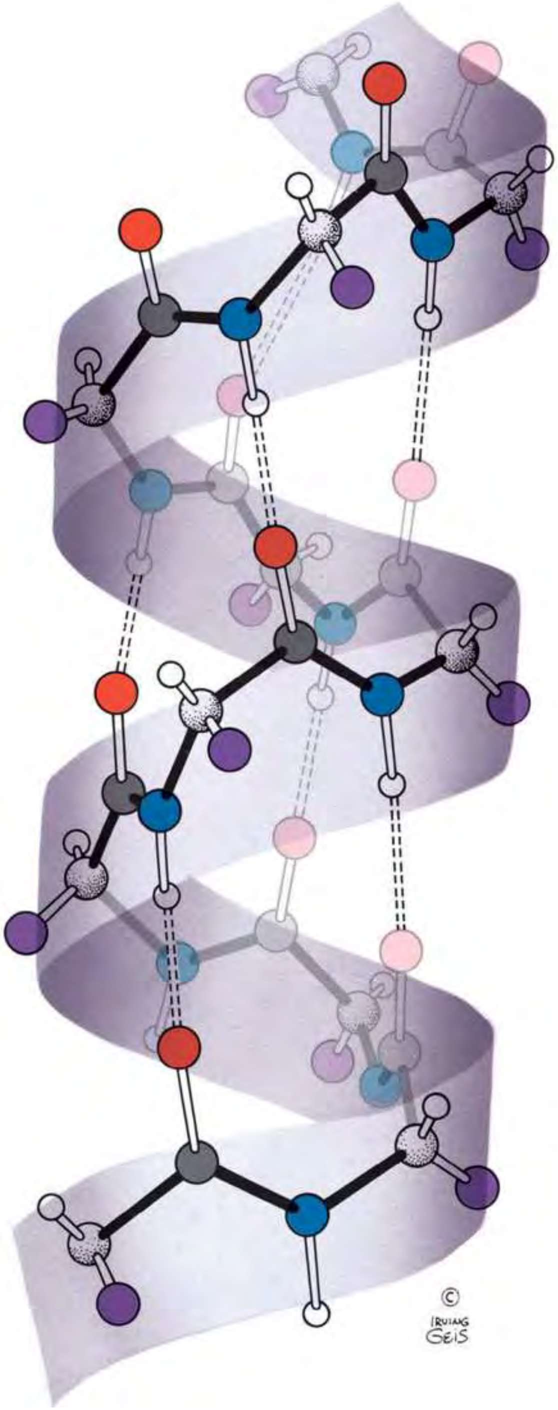

Figure 6-7 | **The α helix.** This right-handed helical conformation has 3.6 residues per turn. Dashed lines indicate hydrogen bonds between C═O groups and N—H groups that are four residues farther along the polypeptide chain. [Illustration, Irving Geis. Image from the Irving Geis Collection/Howard Hughes Medical Institute. Rights owned by HHMI. Reproduction by permission only.] **See Kinemage Exercise 3-2 and the Animated Figures.**

hydrogen bond that has the nearly optimum N···O distance of 2.8 Å. Amino acid side chains project outward and downward from the helix (Fig. 6-8), thereby avoiding steric interference with the polypeptide backbone and with each other. The core of the helix is tightly packed; that is, its atoms are in van der Waals contact.

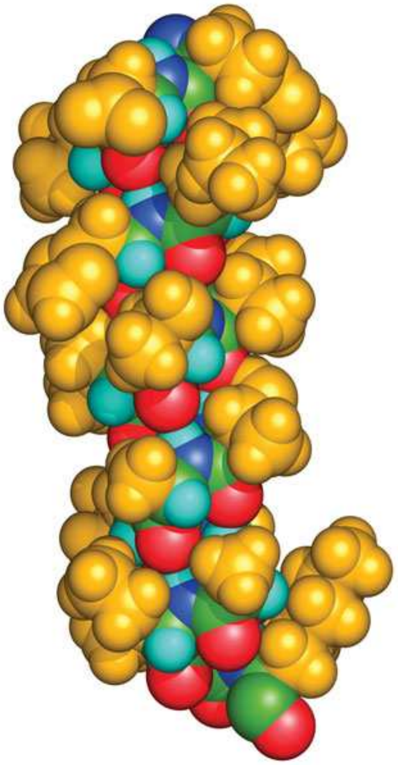

Figure 6-8 | Space-filling model of an α helix. The backbone atoms are colored according to type with C green, N blue, O red, and H cyan. The side chains (*gold*) project away from the helix. This α helix is a segment of sperm whale myoglobin. [Based on an X-ray structure by Ilme Schlichting, Max Planck Institut für Molekulare Physiologie, Dortmund, Germany. PDBid 1A6M (for the definition of "PDBid" see Section 6-2E).]

β Sheets Are Formed from Extended Chains. In 1951, the same year Pauling proposed the α helix, Pauling and Corey postulated the existence of a different polypeptide secondary structure, the β sheet. Like the α helix, the β sheet uses the full hydrogen-bonding capacity of the polypeptide backbone. *In β sheets, however, hydrogen bonding occurs between neighboring polypeptide chains rather than within one* as in an α helix.

Sheets come in two varieties:

1. The **antiparallel β sheet,** in which neighboring hydrogen-bonded polypeptide chains run in opposite directions (Fig. 6-9*a*).
2. The **parallel β sheet,** in which the hydrogen-bonded chains extend in the same direction (Fig. 6-9*b*).

The conformations in which these β structures are optimally hydrogen bonded vary somewhat from that of the fully extended polypeptide shown in Fig. 6-3. They therefore have a rippled or pleated edge-on appearance (Fig. 6-10) and for that reason are sometimes called "pleated sheets." Successive side chains of a polypeptide chain in a β sheet extend to opposite sides of the sheet with a two-residue repeat distance of 7.0 Å.

See Guided Exploration 7
Hydrogen bonding in β sheets.

(*a*) **Antiparallel**

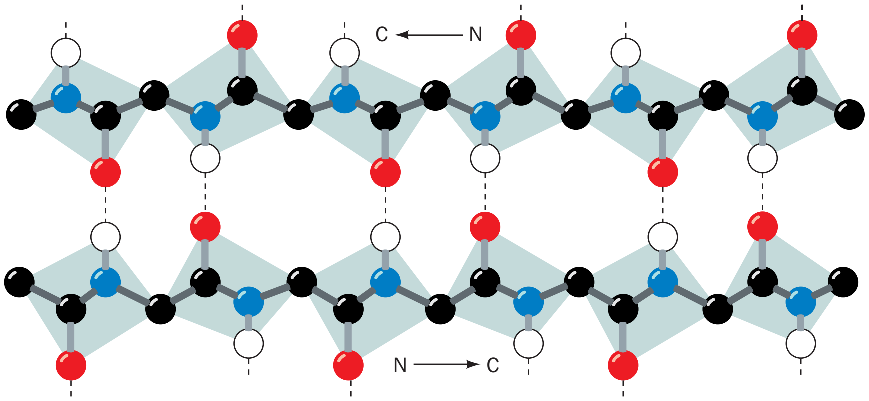

(*b*) **Parallel**

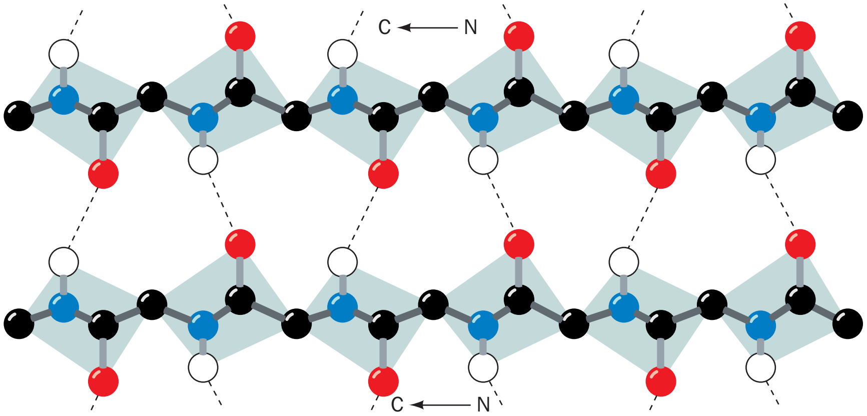

Figure 6-9 | β Sheets. Dashed lines indicate hydrogen bonds between polypeptide strands. Side chains are omitted for clarity. (*a*) An antiparallel β sheet. (*b*) A parallel β sheet. [Illustration, Irving Geis. Image from the Irving Geis Collection/Howard Hughes Medical Institute. Rights owned by HHMI. Reproduction by permission only.] **See Kinemage Exercise 3-3 and the Animated Figures.**

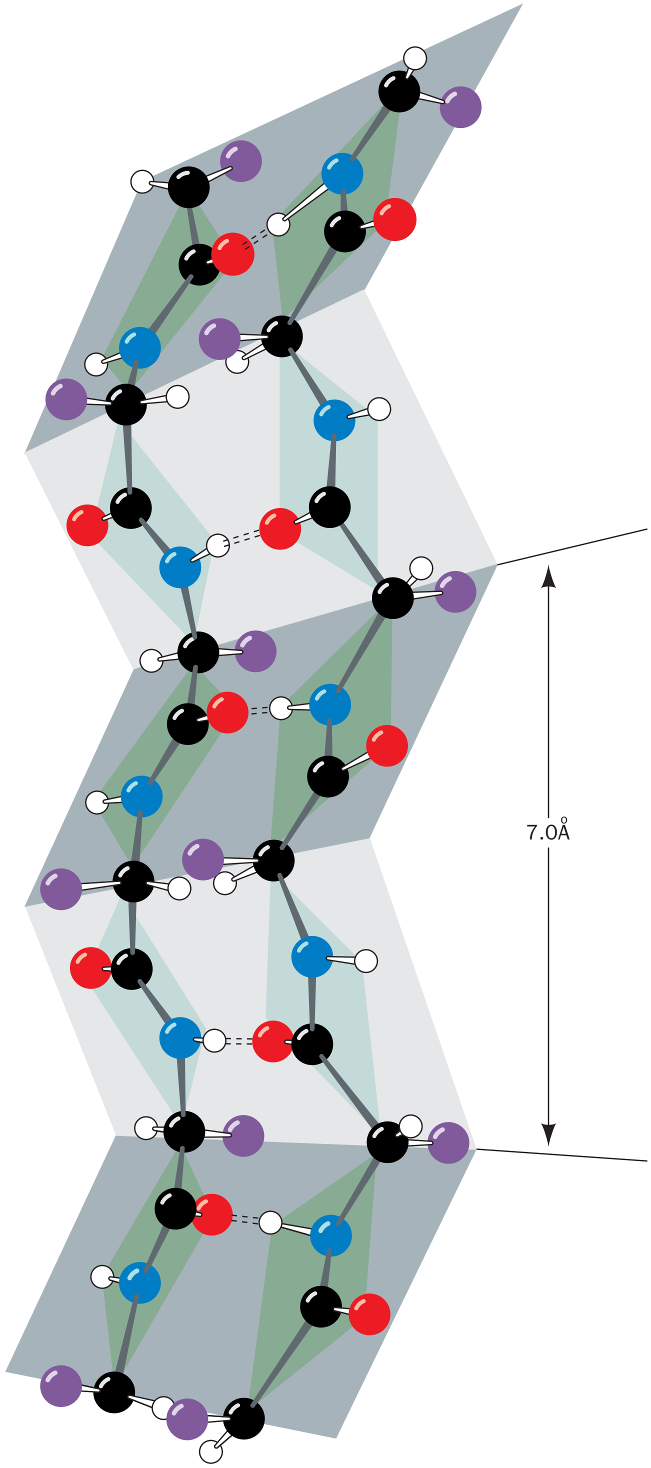

Figure 6-10 | **Pleated appearance of a β sheet.** Dashed lines indicate hydrogen bonds. The R groups (*purple*) on each polypeptide chain alternately extend to opposite sides of the sheet and are in register on adjacent chains. [Illustration, Irving Geis. Image from the Irving Geis Collection/Howard Hughes Medical Institute. Rights owned by HHMI. Reproduction by permission only.] **See Kinemage Exercise 3-3.**

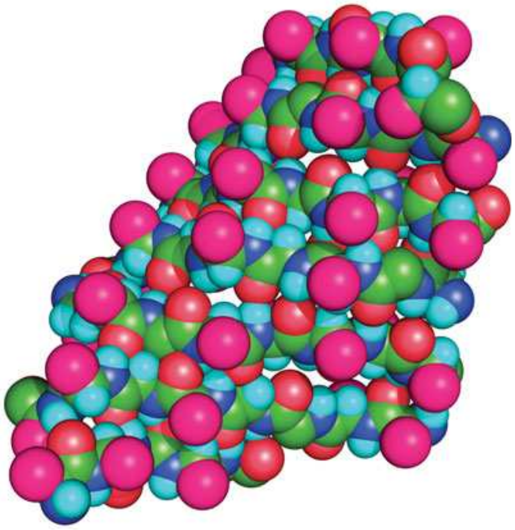

Figure 6-11 | **Space-filling model of a β sheet.** The backbone atoms are colored according to type with C green, N blue, O red, and H cyan. The R groups are represented by large magenta spheres. This seven-stranded antiparallel β sheet, which is shown with its polypeptide strands approximately horizontal, is from the jack bean protein **concanavalin A.** [Based on an X-ray structure by Gerald Edelman, The Rockefeller University. PDBid 2CNA.] **See Kinemage Exercise 3-3.**

β Sheets in proteins contain 2 to as many as 22 polypeptide strands, with an average of 6 strands. Each strand may contain up to 15 residues, the average being 6 residues. A seven-stranded antiparallel β sheet is shown in Fig. 6-11.

Parallel β sheets containing fewer than five strands are rare. This observation suggests that parallel β sheets are less stable than antiparallel β sheets, possibly because the hydrogen bonds of parallel sheets are distorted compared to those of the antiparallel sheets (Fig. 6-9). β Sheets containing mixtures of parallel and antiparallel strands frequently occur.

β Sheets almost invariably exhibit a pronounced right-handed twist when viewed along their polypeptide strands (Fig. 6-12). Conformational energy calculations indicate that the twist is a consequence of interactions between chiral L-amino acid residues in the extended polypeptide chains. The twist distorts and weakens the β sheet's interchain hydrogen bonds. The geometry of a particular β sheet is thus a compromise between optimizing the conformational energies of its polypeptide chains and preserving its hydrogen bonding.

The **topology** (connectivity) of the polypeptide strands in a β sheet can be quite complex. The connection between two antiparallel strands may be just a small loop (Fig. 6-13*a*), but the link between tandem parallel strands must be a crossover connection that is out of the plane of the β sheet (Fig. 6-13*b*). The connecting link in either case can be extensive, often containing helices (e.g., Fig. 6-12).

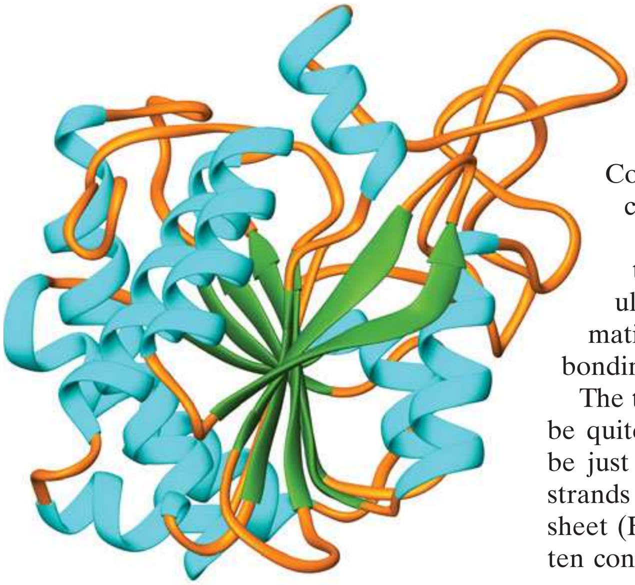

■ **Figure 6-12** | **X-Ray structure of bovine carboxypeptidase A.** The polypeptide backbone is drawn in ribbon form with α helices depicted as cyan coils, the strands of the β sheet represented by green arrows pointing toward the C-terminus, and its remaining portions portrayed by orange worms. Side chains are not shown. The eight-stranded β sheet forms a saddle-shaped curved surface with a right-handed twist. [Based on an X-ray structure by William Lipscomb, Harvard University. PDBid 3CPA.]

Turns Connect Some Units of Secondary Structure. Polypeptide segments with regular secondary structure such as α helices or the strands of β sheets are often joined by stretches of polypeptide that abruptly change direction. Such **reverse turns** or **β bends** (so named because they often connect successive strands of antiparallel β sheets; Fig. 6-13*a*) almost always occur at protein surfaces. They usually involve four successive amino acid residues arranged in one of two ways, Type I and Type II, that differ by a 180° flip of the peptide unit linking residues 2 and 3 (Fig. 6-14). Both types of turns are stabilized by a hydrogen bond, although deviations from these ideal conformations often disrupt this hydrogen bond. In Type II turns, the oxygen atom of residue 2 crowds the C_β atom of residue 3, which is therefore usually Gly. Residue 2 of either type of turn is often Pro since it can assume the required conformation.

C | Fibrous Proteins Have Repeating Secondary Structures

Proteins have historically been classified as either **fibrous** or **globular,** depending on their overall morphology. This dichotomy predates methods for determining protein structure on an atomic scale and does not do justice to proteins that contain both stiff, elongated, fibrous regions as well as more compact, highly folded, globular regions. Nevertheless, the division helps emphasize the properties of fibrous proteins, which often have a protective, connective, or supportive role in living organisms. The two well-characterized fibrous proteins we discuss here—keratin and collagen—are highly elongated molecules whose shapes are dominated by a single type of secondary structure. They are therefore useful examples of these structural elements.

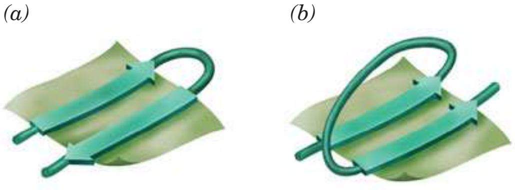

■ **Figure 6-13** | **Connections between adjacent strands in β sheets.** (*a*) Antiparallel strands may be connected by a small loop. (*b*) Parallel strands require a more extensive crossover connection. [After Richardson, J.S., *Adv. Protein Chem.* **34,** 196 (1981).]

α Keratin Is a Coiled Coil. **Keratin** is a mechanically durable and relatively unreactive protein that occurs in all higher vertebrates. It is the principal component of their horny outer epidermal layer and its related appendages such as hair, horn, nails, and feathers. Keratins have been classified as either α keratins, which occur in mammals, or β keratins, which occur in birds and reptiles. Humans have over 50 keratin genes that are expressed in a tissue-specific manner.

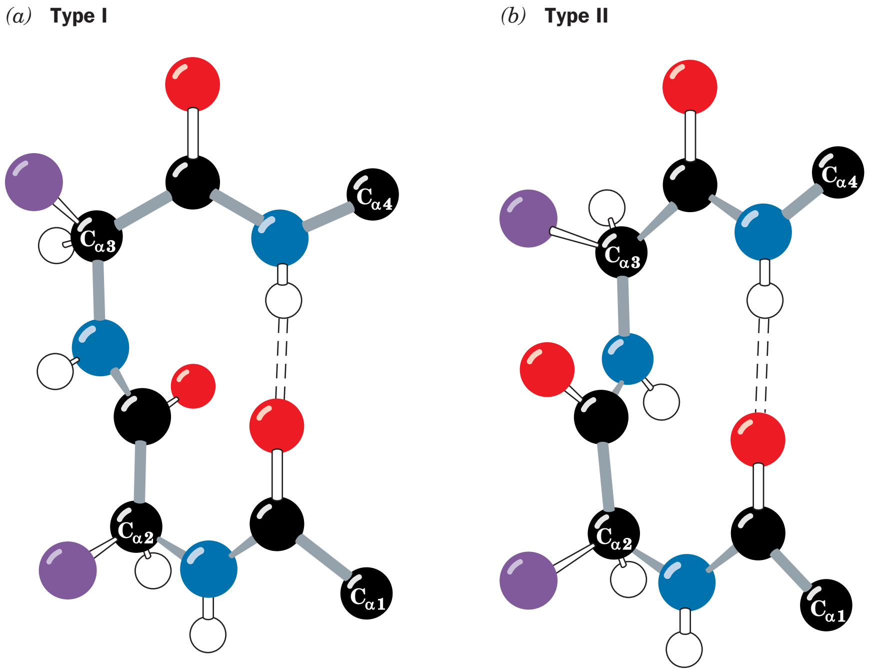
(a) **Type I**
(b) **Type II**

Figure 6-14 | **Reverse turns in polypeptide chains.** Dashed lines represent hydrogen bonds. (*a*) Type I. (*b*) Type II. [Illustration, Irving Geis. Image from the Irving Geis Collection/Howard Hughes Medical Institute. Rights owned by HHMI. Reproduction by permission only.] **See Kinemage Exercise 3-4.**

The X-ray diffraction pattern of α keratin resembles that expected for an α helix (hence the name α keratin). However, α keratin exhibits a 5.1-Å spacing rather than the 5.4-Å distance corresponding to the pitch of the α helix. This discrepancy is the result of *two α keratin polypeptides, each of which forms an α helix, twisting around each other to form a left-handed coil*. The normal 5.4-Å repeat distance of each α helix in the pair is thereby tilted relative to the axis of this assembly, yielding the observed 5.1-Å spacing. The assembly is said to have a **coiled coil** structure because each α helix itself follows a helical path.

The conformation of α keratin's coiled coil is a consequence of its primary structure: The central ∼310-residue segment of each polypeptide chain has a 7-residue pseudorepeat, *a-b-c-d-e-f-g,* with nonpolar residues predominating at positions *a* and *d*. Since an α helix has 3.6 residues per turn, α keratin's *a* and *d* residues line up along one side of each α helix (Fig. 6-15*a*). The hydrophobic strip along one helix associates with the hydrophobic strip on another helix. Because the 3.5-residue repeat in α keratin is slightly smaller than the 3.6 residues per turn of a standard α helix, the two keratin helices are inclined about 18° relative to one another, resulting in the coiled coil arrangement (Fig. 6-15*b*). Coiled coils also occur in numerous other proteins, some of which are globular rather than fibrous.

The higher order structure of α keratin is not well understood. The N- and C-terminal domains of each polypeptide facilitate the assembly of

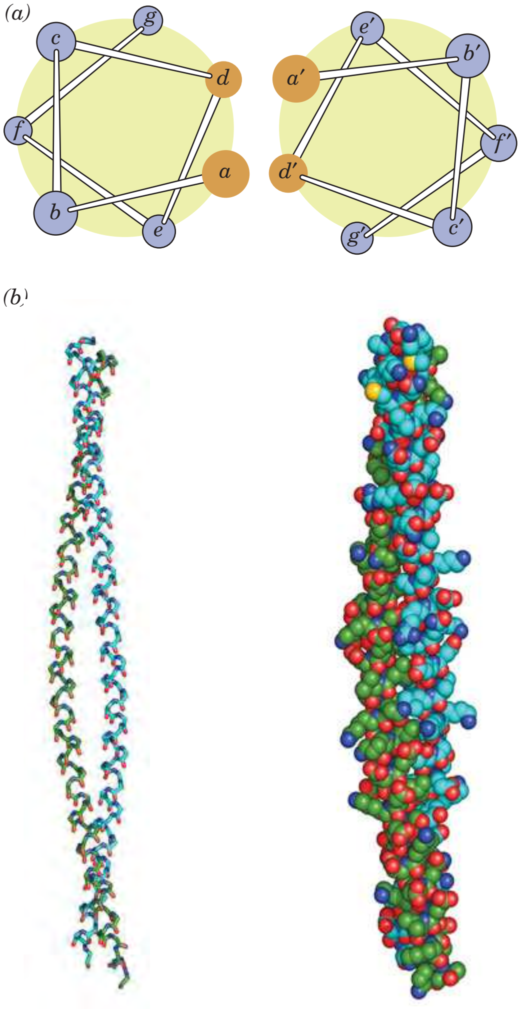

Figure 6-15 | **A coiled coil.** (*a*) View down the coil axis showing the alignment of nonpolar residues along one side of each α helix. The helices have the pseudorepeating sequence *a-b-c-d-e-f-g* in which residues *a* and *d* are predominately nonpolar. [After McLachlan, A.D. and Stewart, M., *J. Mol. Biol.* **98,** 295 (1975).] (*b*) Side view of the polypeptide backbones in stick form (*left*) and of the entire polypeptides in space-filling form (*right*). The atoms are colored according to type with C green in one chain and cyan in the other, N blue, O red, and S yellow. The 81-residue chains are parallel with their N-terminal ends above. Note that in the space-filling model the side chains of the two polypeptides contact each other. This coiled coil is a portion of the muscle protein tropomyosin (Section 7-2A). [Based on an X-ray structure by Carolyn Cohen, Brandeis University. PDBid 1IC2.] **See Kinemage Exercises 4-1 and 4-2.**

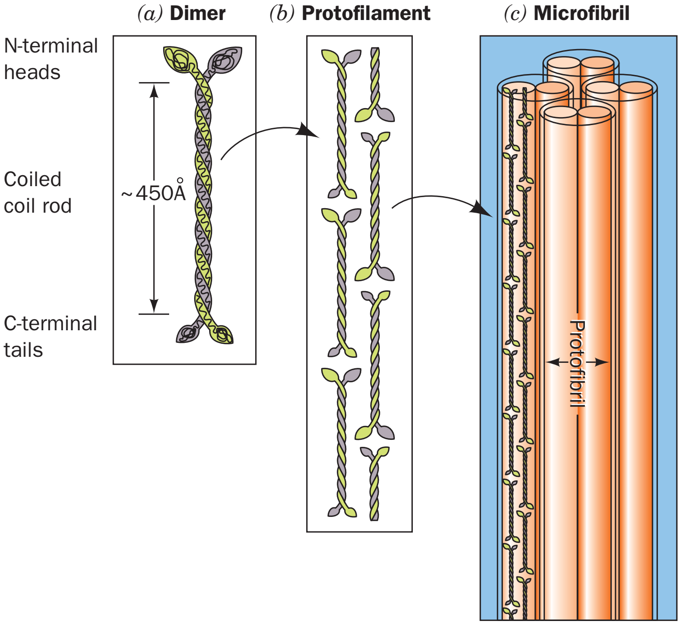

Figure 6-16 | Higher order α keratin structure. (*a*) Two keratin polypeptides form a dimeric coiled coil. (*b*) Protofilaments are formed from two staggered rows of head-to-tail associated coiled coils. (*c*) Protofilaments dimerize to form a protofibril, four of which form a microfibril. The structures of the latter assemblies are poorly characterized.

coiled coils (dimers) into protofilaments, two of which constitute a protofibril (Fig. 6-16). Four protofibrils constitute a microfibril, which associates with other microfibrils to form a macrofibril. A single mammalian hair consists of layers of dead cells, each of which is packed with parallel macrofibrils.

α Keratin is rich in Cys residues, which form disulfide bonds that cross-link adjacent polypeptide chains. The α keratins are classified as "hard" or "soft" according to whether they have a high or low sulfur content. Hard keratins, such as those of hair, horn, and nail, are less pliable than soft keratins, such as those of skin and callus, because the disulfide bonds resist deformation. The disulfide bonds can be reductively cleaved by disulfide interchange with mercaptans (Section 5-3A). Hair so treated can be curled and set in a "permanent wave" by applying an oxidizing agent that reestablishes the disulfide bonds in the new "curled" conformation. Conversely, curly hair can be straightened by the same process.

The springiness of hair and wool fibers is a consequence of the coiled coil's tendency to recover its original conformation after being untwisted by stretching. If some of its disulfide bonds have been cleaved, however, an α keratin fiber can be stretched to over twice its original length. At this point, the polypeptide chains assume a β sheet conformation. β Keratin, such as that in feathers, exhibits a β-like pattern in its native state.

Collagen Is a Triple Helix. **Collagen,** which occurs in all multicellular animals, is the most abundant vertebrate protein. Its strong, insoluble fibers are the major stress-bearing components of connective tissues such as bone, teeth, cartilage, tendon, and the fibrous matrices of skin and blood vessels. A single collagen molecule consists of three polypeptide chains. Mammals have at least 33 genetically distinct chains that are assembled into at least 20 collagen varieties found in different tissues in the same individual. One of the most common collagens, called Type I, consists of two α_1(I) chains and one α_2(I) chain. It has a molecular mass of ~285 kD, a width of ~14 Å, and a length of ~3000 Å.

Collagen has a distinctive amino acid composition: Nearly one-third of its residues are Gly; another 15 to 30% of its residues are Pro and

4-hydroxyprolyl (Hyp). 3-Hydroxyprolyl and **5-hydroxylysyl (Hyl)** residues also occur in collagen, but in smaller amounts.

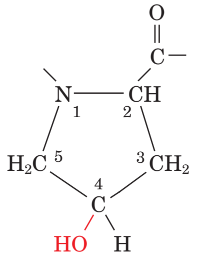

4-Hydroxyprolyl residue (Hyp)

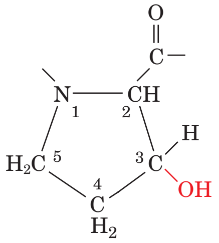

3-Hydroxyprolyl residue

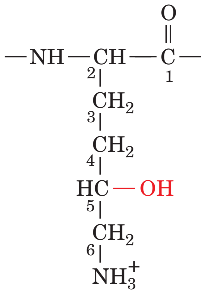

5-Hydroxylysyl residue (Hyl)

These nonstandard residues are formed after the collagen polypeptides are synthesized. For example, Pro residues are converted to Hyp in a reaction catalyzed by **prolyl hydroxylase.** This enzyme requires **ascorbic acid (vitamin C)** to maintain its activity.

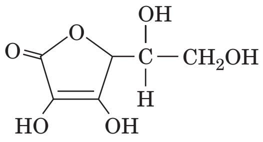

Ascorbic acid (vitamin C)

The disease **scurvy** results from the dietary deficiency of vitamin C (Box 6-2).

The amino acid sequence of a typical collagen polypeptide consists of monotonously repeating triplets of sequence Gly-X-Y over a segment of

BOX 6-2 BIOCHEMISTRY IN HEALTH AND DISEASE

Collagen Diseases

Some collagen diseases have dietary causes. In scurvy (caused by vitamin C deficiency), Hyp production decreases because prolyl hydroxylase requires vitamin C. Thus, in the absence of vitamin C, newly synthesized collagen cannot form fibers properly, resulting in skin lesions, fragile blood vessels, poor wound healing, and, ultimately, death. Scurvy was common in sailors whose diets were devoid of fresh foods on long voyages. The introduction of limes to the diet of the British navy by the renowned explorer Captain James Cook alleviated scurvy and led to the nickname "limey" for the British sailor.

The disease **lathyrism** is caused by regular ingestion of the seeds from the sweet pea *Lathyrus odoratus,* which contain a compound that specifically inactivates lysyl oxidase (see below). The resulting reduced cross-linking of collagen fibers produces serious abnormalities of the bones, joints, and large blood vessels.

Several rare heritable disorders of collagen are known. Mutations of Type I collagen, which constitutes the major structural protein in most human tissues, usually result in **osteogenesis imperfecta** (brittle bone disease). The severity of this disease varies with the nature and position of the mutation: Even a single amino acid change can have lethal consequences. For example, the central Gly → Ala substitution in the model polypeptide shown in Fig. 6-18 locally distorts the already internally crowded collagen helix. This ruptures the hydrogen bond from the backbone N—H of each Ala (normally Gly) to the carbonyl group of the adjacent Pro in a neighboring chain, thereby reducing the stability of the collagen structure. Mutations may affect the structure of the collagen molecule or how it forms fibrils. These mutations tend to be dominant because they affect either the folding of the triple helix or fibril formation even when normal chains are also involved.

Many collagen disorders are characterized by deficiencies in the amount of a particular collagen type synthesized, or by abnormal activities of collagen-processing enzymes such as lysyl hydroxylase and lysyl oxidase. One group of at least 10 different collagen-deficiency diseases, the **Ehlers–Danlos syndromes,** are all characterized by the hyperextensibility of the joints and skin. The "India-rubber man" of circus fame had an Ehlers–Danlos syndrome.

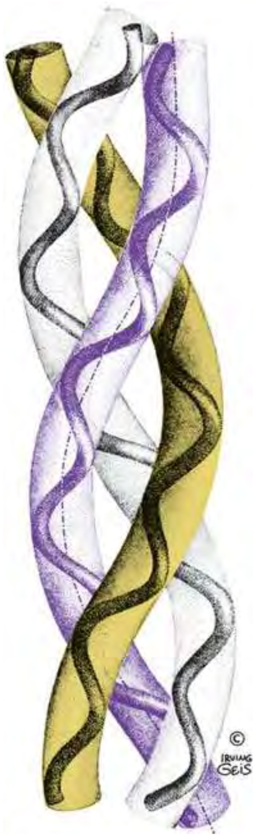

Figure 6-17 | The collagen triple helix. Left-handed polypeptide helices are twisted together to form a right-handed superhelical structure. [Illustration, Irving Geis. Image from the Irving Geis Collection/Howard Hughes Medical Institute. Rights owned by HHMI. Reproduction by permission only.]

$\sim$1000 residues, where X is often Pro and Y is often Hyp. Hyl sometimes appears at the Y position. Collagen's Pro residues prevent it from forming an α helix (Pro residues cannot assume the α-helical backbone conformation and lack the backbone N—H groups that form the intrahelical hydrogen bonds shown in Fig. 6-7). Instead, *the collagen polypeptide assumes a left-handed helical conformation with about three residues per turn. Three parallel chains wind around each other with a gentle, right-handed, ropelike twist to form the triple-helical structure of a collagen molecule* (Fig. 6-17).

This model of the collagen structure has been confirmed by Barbara Brodsky and Helen Berman, who determined the X-ray crystal structure of a collagen-like model polypeptide. Every third residue of each polypeptide chain passes through the center of the triple helix, which is so crowded that only a Gly side chain can fit there. This crowding explains the absolute requirement for a Gly at every third position of a collagen polypeptide chain. The three polypeptide chains are staggered so that a Gly, X, and Y residue occurs at each level along the triple helix axis (Fig. 6-18*a*). The peptide groups are oriented such that the N—H of each Gly makes a strong hydrogen bond with the carbonyl oxygen of an X (Pro) residue on a neighboring chain (Fig. 6-18*b*). The bulky and relatively inflexible Pro and Hyp residues confer rigidity on the entire assembly.

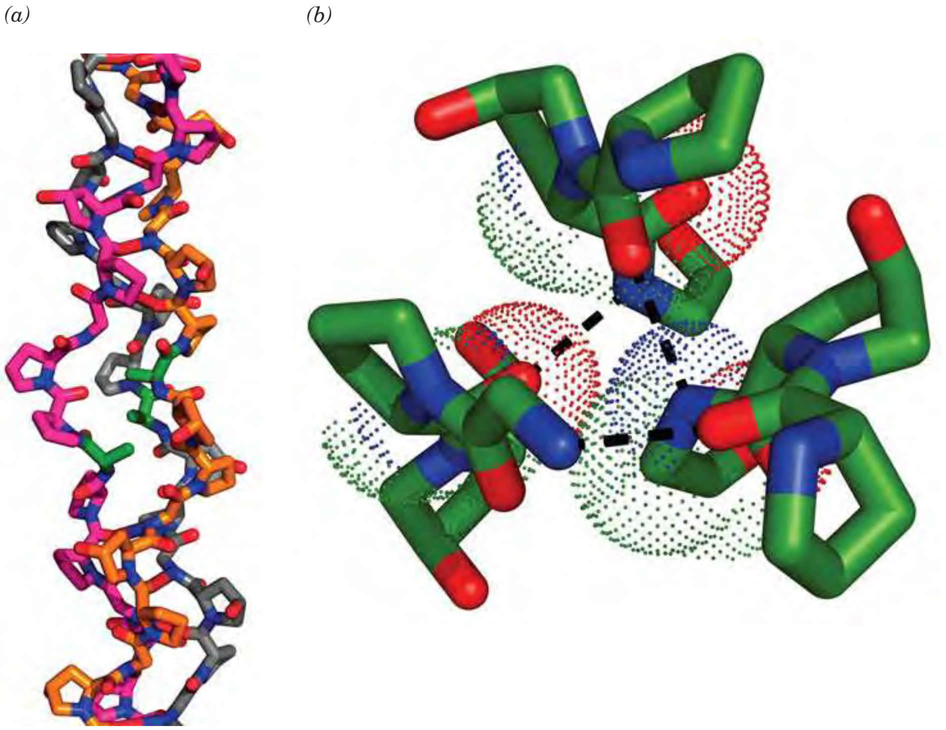

Figure 6-18 | Structure of a collagen model peptide. In this X-ray structure of (Pro-Hyp-Gly)$_{10}$, the fifth Gly of each peptide has been replaced by Ala. (*a*) A stick model of the middle portion of the triple helix oriented with its N-termini at the bottom. The C atoms of the three chains are colored orange, magenta, and gray. The N and O atoms on all chains are blue and red. Note how the replacement of Gly with the bulkier Ala (C atoms green) distorts the triple helix. (*b*) This view from the N-terminus down the helix axis shows the interchain hydrogen-bonding associations. Three consecutive residues from each chain are shown in stick form (C atoms green). Hydrogen bonds are represented by dashed lines from Gly N atoms to Pro O atoms in adjacent chains. Dots represent the van der Waals surfaces of the backbone atoms of the central residue in each chain. Note the close packing of the atoms along the triple helix axis. [Based on an X-ray structure by Helen Berman, Rutgers University, and Barbara Brodsky, UMDNJ–Robert Wood Johnson Medical School. PDBid 1CAG.]
See Kinemage Exercises 4-3 and 4-4.

■ **Figure 6-19 | A reaction pathway for cross-linking side chains in collagen.** The first step is the lysyl oxidase–catalyzed oxidative deamination of Lys to form the aldehyde allysine. Two allysines then undergo an aldol condensation to form allysine aldol. This product can react with His to form aldol histidine, which can in turn react with 5-hydroxylysine to form a Schiff base (an imine bond), thereby cross-linking four side chains.

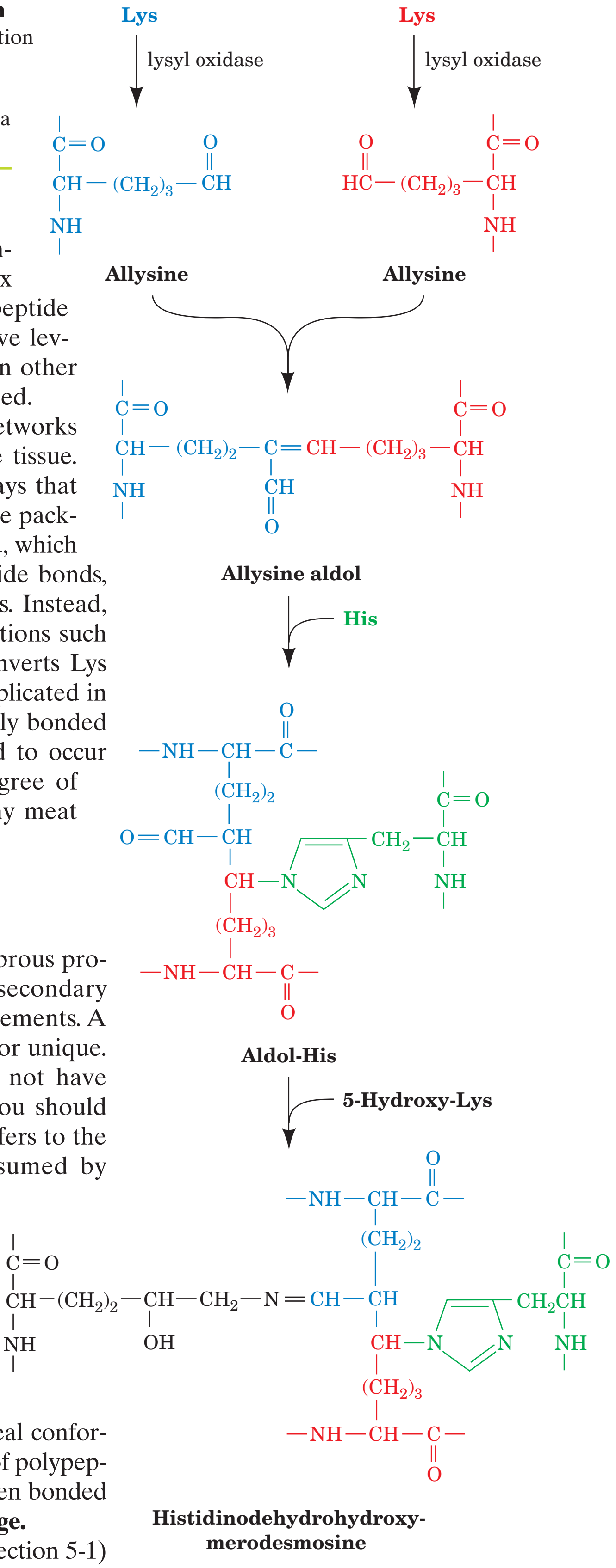

Collagen's well-packed, rigid, triple-helical structure is responsible for its characteristic tensile strength. The twist in the helix cannot be pulled out under tension because its component polypeptide chains are twisted in the opposite direction (Fig. 6-17). Successive levels of fiber bundles in high-quality ropes and cables, as well as in other proteins such as keratin (Fig. 6-16), are likewise oppositely twisted.

Several types of collagen molecules assemble to form loose networks or thick fibrils arranged in bundles or sheets, depending on the tissue. The collagen molecules in fibrils are organized in staggered arrays that are stabilized by hydrophobic interactions resulting from the close packing of triple-helical units. Collagen is also covalently cross-linked, which accounts for its poor solubility. The cross-links cannot be disulfide bonds, as in keratin, because collagen is almost devoid of Cys residues. Instead, the cross-links are derived from Lys and His side chains in reactions such as those shown in Fig. 6-19. **Lysyl oxidase,** the enzyme that converts Lys residues to those of the aldehyde **allysine,** is the only enzyme implicated in this cross-linking process. Up to four side chains can be covalently bonded to each other. The cross-links do not form at random but tend to occur near the N- and C-termini of the collagen molecules. The degree of cross-linking in a particular tissue increases with age. This is why meat from older animals is tougher than meat from younger animals.

D | Most Proteins Include Nonrepetitive Structure

The majority of proteins are globular proteins that, unlike the fibrous proteins discussed above, may contain several types of regular secondary structure, including α helices, β sheets, and other recognizable elements. A significant portion of a protein's structure may also be irregular or unique. Segments of polypeptide chains whose successive residues do not have similar ϕ and ψ values are sometimes called coils. However, you should not confuse this term with the appellation **random coil,** which refers to the totally disordered and rapidly fluctuating conformations assumed by **denatured** (fully unfolded) proteins in solution. In **native** (folded) proteins, *nonrepetitive structures are no less ordered than are helices or β sheets; they are simply irregular and hence more difficult to describe.*

Sequence Affects Secondary Structure. *Variations in amino acid sequence as well as the overall structure of the folded protein can distort the regular conformations of secondary structural elements.* For example, the α helix frequently deviates from its ideal conformation in the initial and final turns of the helix. Similarly, a strand of polypeptide in a β sheet may contain an "extra" residue that is not hydrogen bonded to a neighboring strand, producing a distortion known as a **β bulge.**

Many of the limits on amino acid composition and sequence (Section 5-1) may be due in part to conformational constraints in the three-dimensional structure of proteins. For example, a Pro residue produces a

Table 6-1 Propensities of Amino Acid Residues for α Helical and β Sheet Conformations

Residue	P_α	P_β
Ala	1.42	0.83
Arg	0.98	0.93
Asn	0.67	0.89
Asp	1.01	0.54
Cys	0.70	1.19
Gln	1.11	1.10
Glu	1.51	0.37
Gly	0.57	0.75
His	1.00	0.87
Ile	1.08	1.60
Leu	1.21	1.30
Lys	1.16	0.74
Met	1.45	1.05
Phe	1.13	1.38
Pro	0.57	0.55
Ser	0.77	0.75
Thr	0.83	1.19
Trp	1.08	1.37
Tyr	0.69	1.47
Val	1.06	1.70

Source: Chou, P.Y. and Fasman, G.D., *Annu. Rev. Biochem*. **47,** 258 (1978).

kink in an α helix or β sheet. Similarly, steric clashes between several sequential amino acid residues with large branched side chains (e.g., Ile and Tyr) can destabilize α helices.

Analysis of known protein structures by Peter Chou and Gerald Fasman revealed the propensity *P* of a residue to occur in an α helix or a β sheet (Table 6-1). Chou and Fasman also discovered that certain residues not only have a high propensity for a particular secondary structure but they tend to disrupt or break other secondary structures. Such data are useful for predicting the secondary structures of proteins with known amino acid sequences.

The presence of certain residues outside of α helices or β sheets may also be nonrandom. For example, α helices are often flanked by residues such as Asn and Gln, whose side chains can fold back to form hydrogen bonds with one of the four terminal residues of the helix, a phenomenon termed **helix capping.** Recall that the four residues at each end of an α helix are not fully hydrogen bonded to neighboring backbone segments (Fig. 6-7).

CHECK YOUR UNDERSTANDING

Explain why the conformational freedom of peptide bonds is limited.
Summarize the features of an α helix and a parallel and antiparallel β sheet.
What distinguishes regular and irregular secondary structure?
What properties do fibrous proteins confer on substances such as hair and bones?

2 Tertiary Structure

LEARNING OBJECTIVES

- Understand how the techniques of X-ray crystallography and NMR spectroscopy are used to determine protein structure.
- Understand why nonpolar residues occur in the protein interior and polar residues on the exterior.
- Understand that a protein's tertiary structure consists of secondary structural elements that combine to form motifs and domains.
- Understand that, over time, a protein's structure is more highly conserved than its sequence.
- Become familiar with the type of information that is available from bioinformatics databases and programs.

The tertiary structure of a protein describes the folding of its secondary structural elements and specifies the positions of each atom in the protein, including its side chains. This information is deposited in a database and is readily available via the Internet, which allows the tertiary structures of a variety of proteins to be analyzed and compared. The common

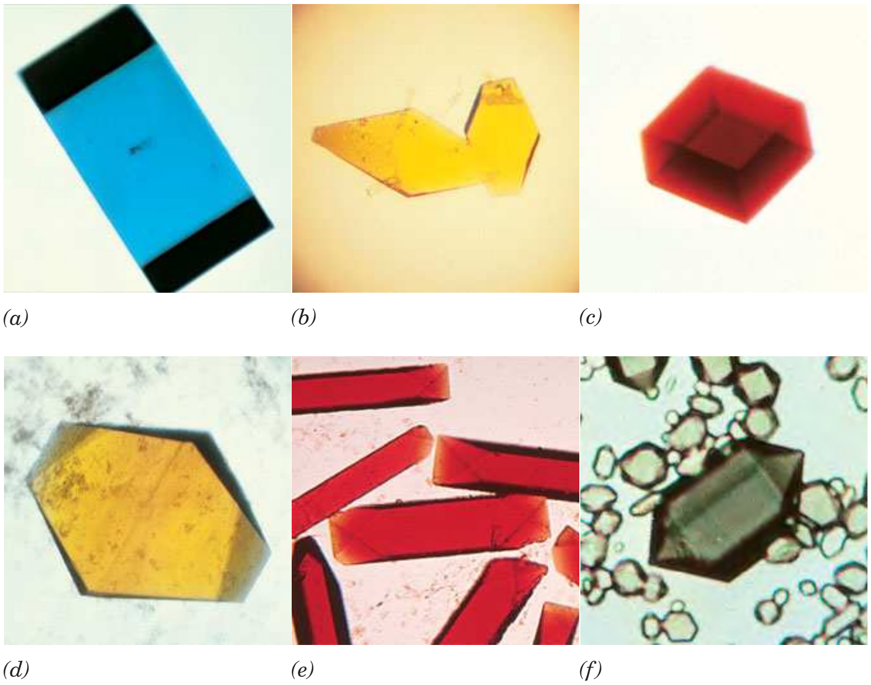

Figure 6-20 | **Protein crystals.** (*a*) Azurin from *Pseudomonas aeruginosa,* (*b*) flavodoxin from *Desulfovibrio vulgaris,* (*c*) rubredoxin from *Clostridium pasteurianum,* (*d*) azidomet myohemerythrin from the marine worm *Siphonosoma funafuti,* (*e*) lamprey hemoglobin, and (*f*) bacteriochlorophyll *a* protein from *Prosthecochloris aestuarii.* These crystals are colored because the proteins contain light-absorbing groups; proteins are colorless in the absence of such groups. [Parts *a–c* courtesy of Larry Siecker, University of Washington; Parts *d* and *e* courtesy of Wayne Hendrikson, Columbia University; and Part *f* courtesy of John Olsen, Brookhaven National Laboratories, and Brian Matthews, University of Oregon.]

features of protein tertiary structures reveal much about the biological functions of proteins and their evolutionary origins.

A | Most Protein Structures Are Determined by X-Ray Crystallography or Nuclear Magnetic Resonance

***X-Ray crystallography** is a technique that directly images molecules.* X-Rays must be used to do so because, according to optical principles, the uncertainty in locating an object is approximately equal to the wavelength of the radiation used to observe it (covalent bond distances and the wavelengths of the X-rays used in structural studies are both ~1.5 Å; individual molecules cannot be seen in a light microscope because visible light has a minimum wavelength of 4000 Å). There is, however, no such thing as an X-ray microscope because there are no X-ray lenses. Rather, a crystal of the molecule to be imaged (e.g., Fig. 6-20) is exposed to a collimated beam of X-rays and the resulting **diffraction pattern,** which arises from the regularly repeating positions of atoms in the crystal, is recorded by a radiation detector or, now infrequently, on photographic film (Fig. 6-21). The X-rays used in structural studies are produced by laboratory X-ray generators or, now commonly, by **synchrotrons,** particle accelerators that produce X-rays of far greater intensity. The intensities of the diffraction maxima (darkness of the spots on a film) are then used to construct mathematically the three-dimensional image of the crystal structure through methods that are beyond the scope of this text. In what follows, we discuss some of the special problems associated with interpreting the X-ray crystal structures of proteins.

X-Rays interact almost exclusively with the electrons in matter, not the nuclei. An X-ray structure is therefore an image of the **electron density** of the object under study. Such **electron density maps** are usually presented with the aid of computer graphics as one or more sets of **contours,** in

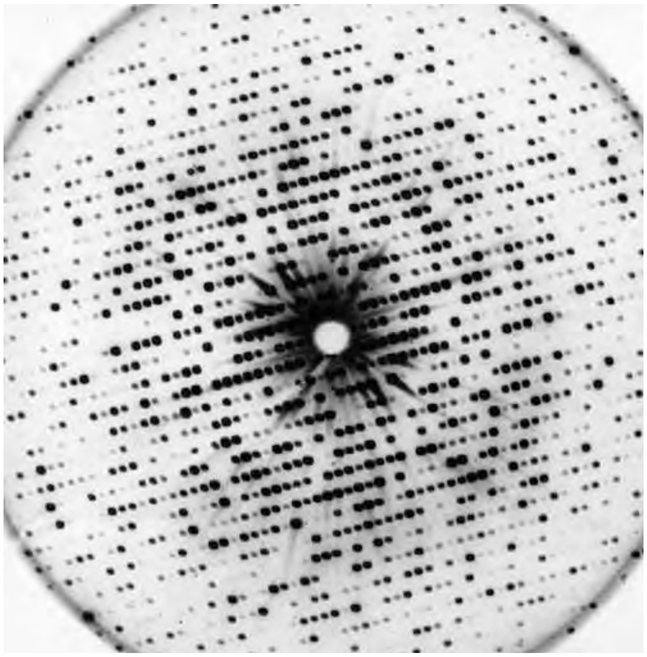

Figure 6-21 | **An X-ray diffraction photograph of a crystal of sperm whale myoglobin.** The intensity of each diffraction maximum (the darkness of each spot) is a function of the crystal's electron density. [Courtesy of John Kendrew, Cambridge University, U.K.]

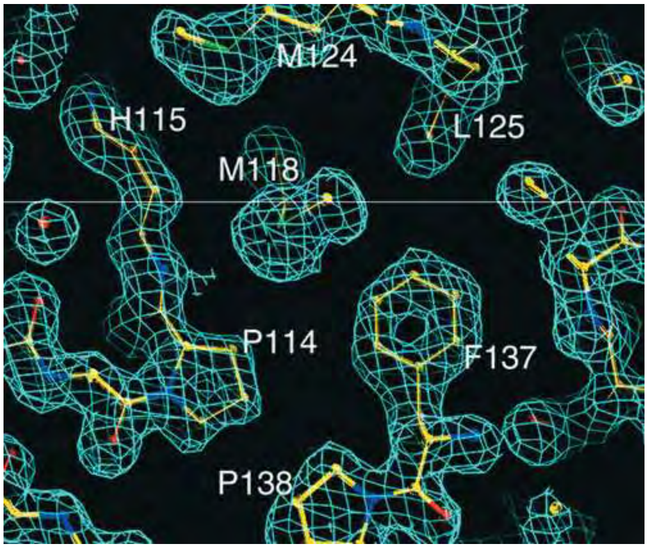

■ **Figure 6-22 | A thin section through a 1.5-Å-resolution electron density map of a protein that is contoured in three dimensions.** Only a single contour level (*cyan*) is shown, together with a ball-and-stick model of the corresponding polypeptide segments colored according to atom type with C yellow, N blue, and O red. A water molecule is represented by a red sphere. [Courtesy of Xinhua Ji, NCI–Frederick Cancer Research and Development Center, Frederick, Maryland.]

which a contour represents a specific level of electron density in the same way that a contour on a topographic map indicates locations that have a particular altitude. A portion of an electron density map of a protein is shown in Fig. 6-22.

Most Protein Crystal Structures Exhibit Less Than Atomic Resolution.

The molecules in protein crystals, as in other crystalline substances, are arranged in regularly repeating three-dimensional lattices. Protein crystals, however, differ from those of most small organic and inorganic molecules in being highly hydrated; they are typically 40 to 60% water by volume. The aqueous solvent of crystallization is necessary for the structural integrity of the protein crystals, because water is required for the structural integrity of native proteins themselves (Section 6-4).

The large solvent content of protein crystals gives them a soft, jellylike consistency so that their molecules usually lack the rigid order characteristic of crystals of small molecules such as NaCl or glycine. The molecules in a protein crystal are typically disordered by more than an angstrom, so the corresponding electron density map lacks information concerning structural details of smaller size. The crystal is therefore said to have a resolution limit of that size. Protein crystals typically have resolution limits in the range 1.5 to 3.0 Å, although some are better ordered (have higher resolution, that is, a lesser resolution limit) and many are less ordered (have lower resolution).

Since an electron density map of a protein must be interpreted in terms of its atomic positions, the accuracy and even the feasibility of a crystal structure analysis depends on the crystal's resolution limit. Indeed, the inability to obtain crystals of sufficiently high resolution is a major limiting factor in determining the X-ray crystal structure of a protein or other macromolecule. Figure 6-23 indicates how the quality (degree of focus) of an electron density map varies with its resolution limit. At 6-Å resolution, the presence of a molecule the size of diketopiperazine is difficult to discern. At 2.0-Å resolution, its individual atoms cannot yet be distinguished, although its molecular shape has become reasonably evident. At 1.5-Å resolution, which roughly corresponds to a bond distance, individual atoms become partially resolved. At 1.1-Å resolution, atoms are clearly visible.

Most protein crystal structures are too poorly resolved for their electron density maps to reveal clearly the positions of individual atoms (e.g.,

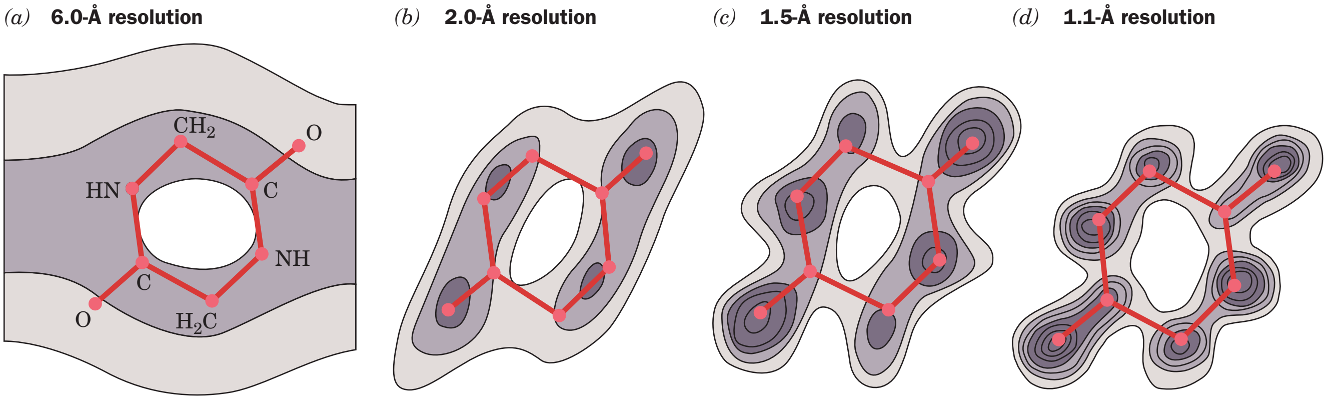

■ **Figure 6-23 | Electron density maps of diketopiperazine at different resolution levels.** Hydrogen atoms are not visible in these maps because of their low electron density. [After Hodgkin, D.C., *Nature* **188,** 445 (1960).]

Fig. 6-23). Nevertheless, the distinctive shape of the polypeptide backbone usually permits it to be traced, which, in turn, allows the positions and orientations of its side chains to be deduced (e.g., Fig. 6-22). Yet side chains of comparable size and shape, such as those of Leu, Ile, Thr, and Val, cannot always be differentiated (hydrogen atoms, having just one electron, are visible only if the resolution limit is less than ~1.2 Å). Consequently, a protein structure cannot be elucidated from its electron density map alone, but knowing the primary structure of the protein permits the sequence of amino acid residues to be fitted to the electron density map. Mathematical refinement can then reduce the uncertainty in the crystal structure's atomic positions to as little as 0.1 Å.

Most Crystalline Proteins Maintain Their Native Conformations. Does the structure of a protein in a crystal accurately reflect the structure of the protein in solution, where globular proteins normally function? Several lines of evidence indicate that *crystalline proteins assume very nearly the same structures that they have in solution:*

1. A protein molecule in a crystal is essentially in solution because it is bathed by solvent of crystallization over all of its surface except for the few, generally small patches that contact neighboring protein molecules.
2. In cases where different crystal forms of a protein have been analyzed, or when a crystal structure has been compared to a solution structure (determined by NMR; see below), the molecules have virtually identical conformations. Evidently, crystal packing forces do not greatly perturb the structures of protein molecules.
3. Many enzymes are catalytically active in the crystalline state. Since the activity of an enzyme is very sensitive to the positions of the groups involved in binding and catalysis (Chapter 11), the crystalline enzymes must have conformations that closely resemble their solution conformations.

Protein Structures Can Be Determined by NMR. The basis of **nuclear magnetic resonance (NMR)** is the observation that an atomic nucleus, such as a proton (a hydrogen nucleus), resonates in an applied magnetic field in a way that is sensitive to its electronic environment and its interactions with nearby nuclei. The development of NMR techniques, since the mid-1980s,

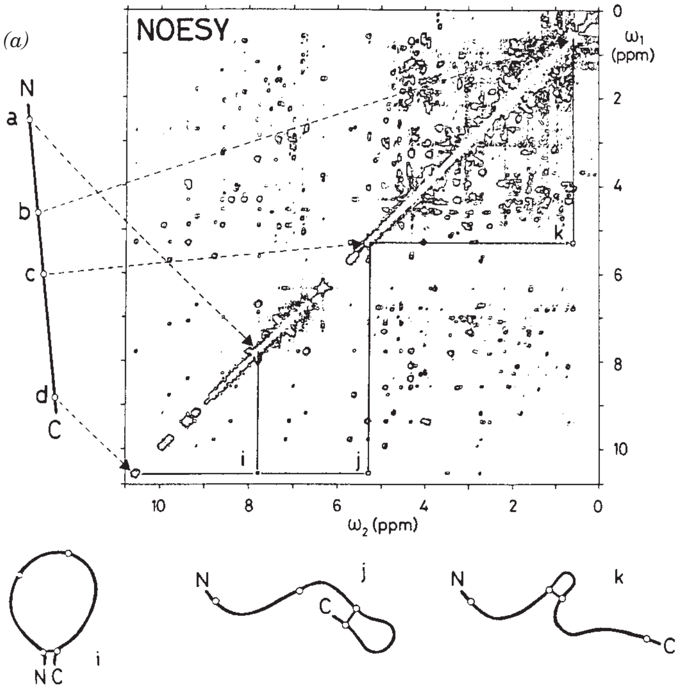

Figure 6-24 | NOESY spectrum of a protein. The diagonal represents the conventional one-dimensional NMR spectrum presented as a contour plot. Note that it is too crowded with peaks to be directly interpretable (even a small protein has hundreds of protons). The cross (off-diagonal) peaks each arise from the interaction of two protons that are <5 Å apart in space (their one-dimensional NMR peaks are located where horizontal and vertical lines intersect the diagonal). The line to the left of the spectrum represents the extended polypeptide chain with its N- and C-termini labeled N and C and the positions of four protons labeled a to d. The dashed arrows indicate the diagonal NMR peaks to which these protons give rise. Cross peaks, such as i, j, and k, each located at the intersection of the corresponding horizontal and vertical lines, show that two protons are <5 Å apart. These distance relationships are schematically drawn as three looped structures of the polypeptide chain below the spectrum. The assignment of a distance relationship between two protons in a polypeptide requires that the NMR peaks to which they give rise and their positions in the polypeptide be known, which requires that the polypeptide's amino acid sequence has been previously determined. [After Wüthrich, K., *Science* **243,** 45 (1989).]

in large part by Kurt Wüthrich, has made it possible to determine the three-dimensional structures of small globular proteins in aqueous solution.

A protein's conventional (one-dimensional) NMR spectrum is crowded with overlapping peaks, since even a small protein has hundreds of protons. This problem is addressed by **two-dimensional (2D) NMR spectroscopy,** which yields additional peaks arising from the interactions of protons that are less than 5 Å apart. Correlation spectroscopy (COSY) provides interatomic distances between protons that are covalently connected through one or two other atoms, such as the H atoms attached to the N and C_α of the same amino acid (corresponding to the ϕ torsion angle). Nuclear Overhauser spectroscopy (NOESY) provides interatomic distances for protons that are close in space although they may be far apart in the protein sequence. An example of a NOESY spectrum is shown in Fig. 6-24.

Interatomic distance measurements, along with knowledge of the protein's sequence and known geometric constraints such as covalent bond distances and angles, group planarity, chirality, and van der Waals radii, are used to compute the protein's three-dimensional structure. However, since interproton distance measurements are imprecise, they cannot imply a unique structure but rather are consistent with an ensemble of closely related structures. Consequently, an NMR structure of a protein (or another macromolecule) is often presented as a sample of structures that are consistent with the data (e.g., Figure 6-25). The "tightness" of a bundle of such structures is indicative both of the accuracy with which the structure is known, which in the most favorable cases is roughly comparable to that of an X-ray crystal structure with a resolution of 2 to 2.5 Å, and of the conformational fluctuations that the protein undergoes (Section 6-4A). Although present NMR methods are limited to determining the structures of macromolecules with molecular masses no greater than ~40 kD, recent advances in NMR technology suggest that this limit may soon increase to ~100 kD or more.

NMR methods, besides validating the structures of proteins analyzed by X-ray crystallography (or in some cases identifying protein residues that

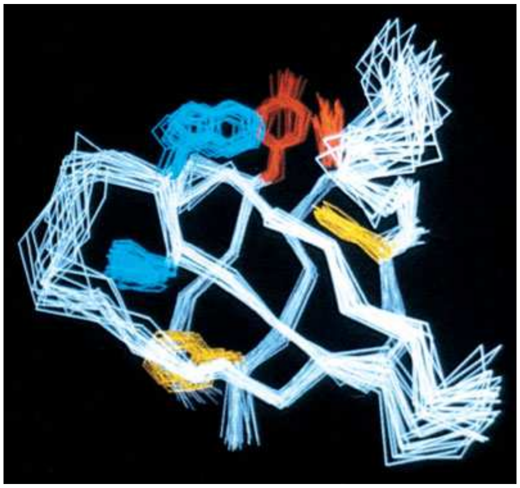

Figure 6-25 | The NMR structure of a protein. The drawing represents 20 superimposed structures of a 64-residue polypeptide comprising the **Src protein SH3 domain** (Section 13-1B). The polypeptide backbone (its connected C_α atoms) is white, and its Phe, Tyr, and Trp side chains are yellow, red, and blue, respectively. The polypeptide backbone folds into two 3-stranded antiparallel β sheets that form a sandwich. [Courtesy of Stuart Schreiber, Harvard University.]

are perturbed by crystallization), can determine the structures of proteins and other macromolecules that fail to crystallize. Moreover, since NMR can probe motions over time scales spanning 10 orders of magnitude, it can also be used to study protein folding and dynamics (Section 6-5).

Proteins Can Be Depicted in Different Ways. The huge number of atoms in proteins makes it difficult to visualize them using the same sorts of models employed for small organic molecules. Ball-and-stick representations showing all or most atoms in a protein (as in Figs. 6-7 and 6-10) are exceedingly cluttered, and space-filling models (as in Figs. 6-8 and 6-11) obscure the internal details of the protein. Accordingly, computer-generated or artistic renditions (e.g., Fig. 6-12) are often more useful for representing protein structures. The course of the polypeptide chain can be followed by tracing the positions of its C_α atoms or by representing helices as helical ribbons or cylinders and β sheets as sets of flat arrows pointing from the N- to the C-termini.

B | Side Chain Location Varies with Polarity

In the years since Kendrew solved the structure of myoglobin, nearly 50,000 protein structures have been reported. No two are exactly alike, but they exhibit remarkable consistencies. The primary structures of globular proteins generally lack the repeating sequences that support the regular conformations seen in fibrous proteins. However, *the amino acid side chains in globular proteins are spatially distributed according to their polarities:*

1. The nonpolar residues Val, Leu, Ile, Met, and Phe occur mostly in the interior of a protein, out of contact with the aqueous solvent. The hydrophobic effects that promote this distribution are largely responsible for the three-dimensional structure of native proteins.
2. The charged polar residues Arg, His, Lys, Asp, and Glu are usually located on the surface of a protein in contact with the aqueous solvent. This is because immersing an ion in the virtually anhydrous interior of a protein is energetically unfavorable.
3. The uncharged polar groups Ser, Thr, Asn, Gln, and Tyr are usually on the protein surface but also occur in the interior of the molecule. When buried in the protein, these residues are almost always hydrogen bonded to other groups; in a sense, the formation of a hydrogen

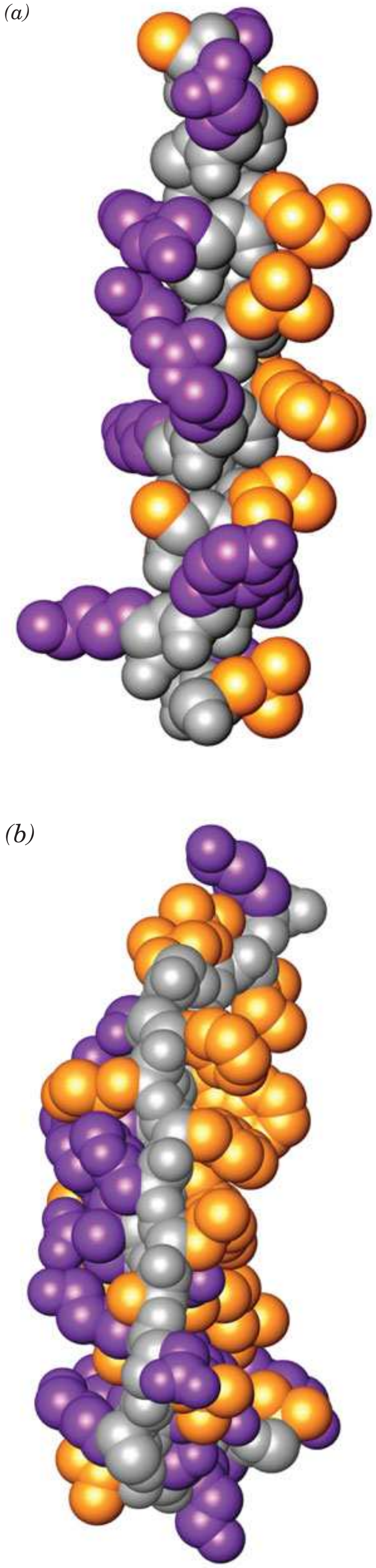

Figure 6-26 | Side chain locations in an α helix and a β sheet. In these space-filling models, the main chain is gray, nonpolar side chains are gold, and polar side chains are magenta. (*a*) An α helix from sperm whale myoglobin. Note that the nonpolar residues are primarily on one side of the helix. (*b*) An antiparallel β sheet from concanavalin A (*side view*). The protein interior is to the right and the exterior is to the left. [Based on X-ray structures by Ilme Schlichting, Max Planck Institut für Molekulare Physiologie, Dortmund, Germany, and Gerald Edelman, The Rockefeller University. PDBids 1A6M and 2CNA.]

bond "neutralizes" their polarity. This is also the case with the polypeptide backbone.

These general principles of side chain distribution are evident in individual elements of secondary structure (Fig. 6-26) as well as in whole proteins (Fig. 6-27). Polar side chains tend to extend toward—and thereby help form—the protein's surface, whereas nonpolar side chains largely extend toward—and thereby occupy—its interior. Turns and loops joining secondary structural elements usually occur at the protein surface.

Most proteins are quite compact, with their interior atoms packed together even more efficiently than the atoms in a crystal of small organic molecules. Nevertheless, the atoms of protein side chains almost invariably have low-energy arrangements. Evidently, interior side chains adopt relaxed conformations despite the profusion of intramolecular interactions. Closely packed protein interiors generally exclude water. When water molecules are present, they often occupy specific positions where they can form hydrogen bonds, sometimes acting as a bridge between two hydrogen-bonding protein groups.

C | Tertiary Structures Contain Combinations of Secondary Structure

Globular proteins—each with a unique tertiary structure—are built from combinations of secondary structural elements. The proportions of α helices and β sheets and the order in which they are connected provide an informative way of classifying and analyzing protein structure.

Certain Combinations of Secondary Structure Form Motifs. Groupings of secondary structural elements, called **supersecondary structures** or **motifs,** occur in many unrelated globular proteins:

1. The most common form of supersecondary structure is the **βαβ motif,** in which an α helix connects two parallel strands of a β sheet (Fig. 6-28*a*).
2. Another common supersecondary structure, the **β hairpin** motif, consists of antiparallel strands connected by relatively tight reverse turns (Fig. 6-28*b*).
3. In an **αα motif,** two successive antiparallel α helices pack against each other with their axes inclined. This permits energetically favorable intermeshing of their contacting side chains (Fig. 6-28*c*). Similar associations stabilize the coiled coil conformation of α keratin and tropomyosin (Fig. 6-15*b*), although their helices are parallel rather than antiparallel.
4. In the **Greek key motif** (Fig. 6-28*d;* named after an ornamental design commonly used in ancient Greece; see inset), a β hairpin is folded over to form a 4-stranded antiparallel β sheet.

See Guided Exploration 8
Secondary structures in proteins.

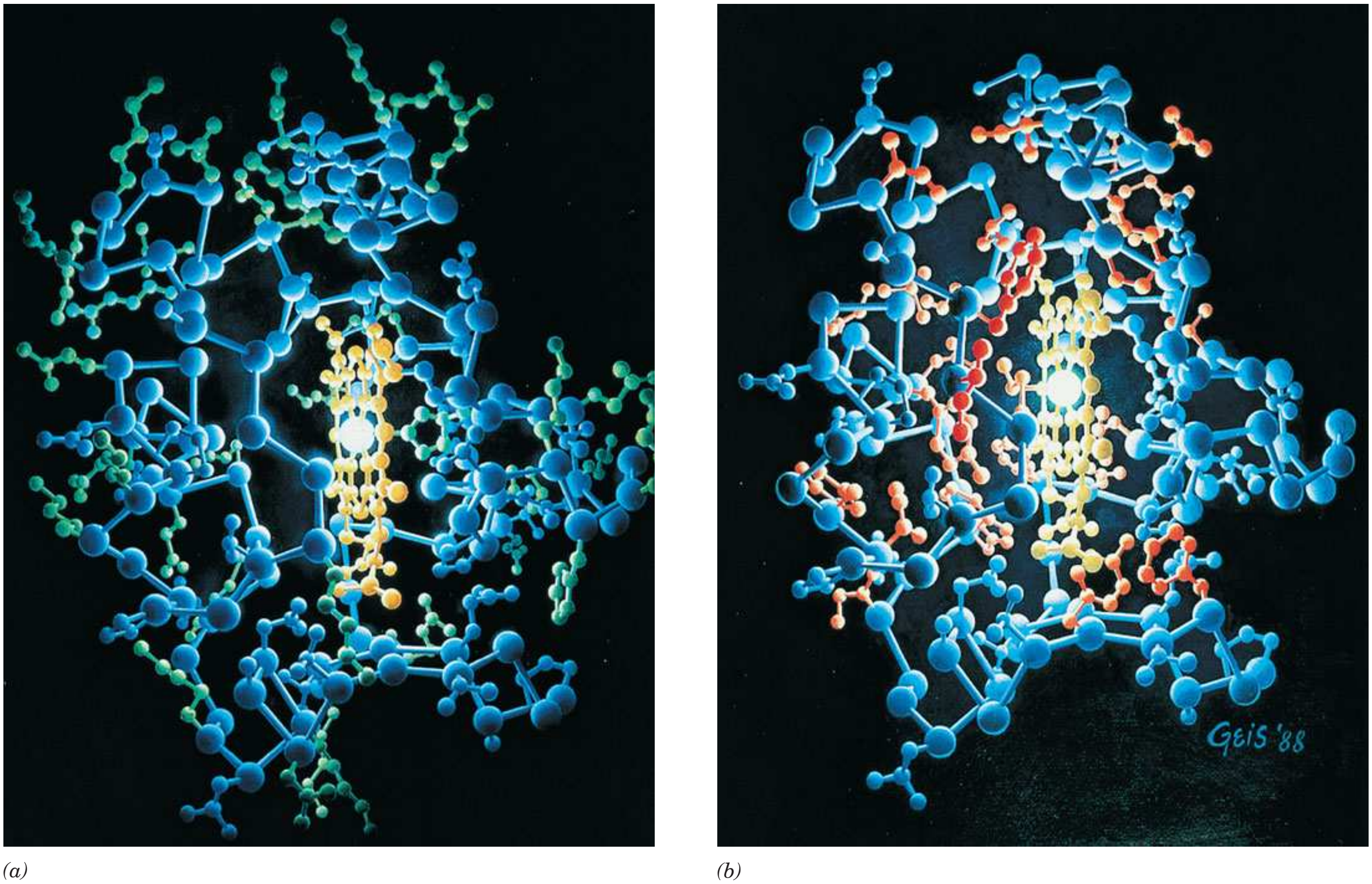

■ **Figure 6-27** | **Side chain distribution in horse heart cytochrome c.** In these paintings, based on an X-ray structure determined by Richard Dickerson, the protein is illuminated by its single iron atom centered in a heme group. Hydrogen atoms are not shown. In (*a*) the hydrophilic side chains are green, and in (*b*) the hydrophobic side chains are orange. [Illustration, Irving Geis. Image from the Irving Geis Collection/Howard Hughes Medical Institute. Rights owned by HHMI. Reproduction by permission only.] **See Kinemage Exercise 5.**

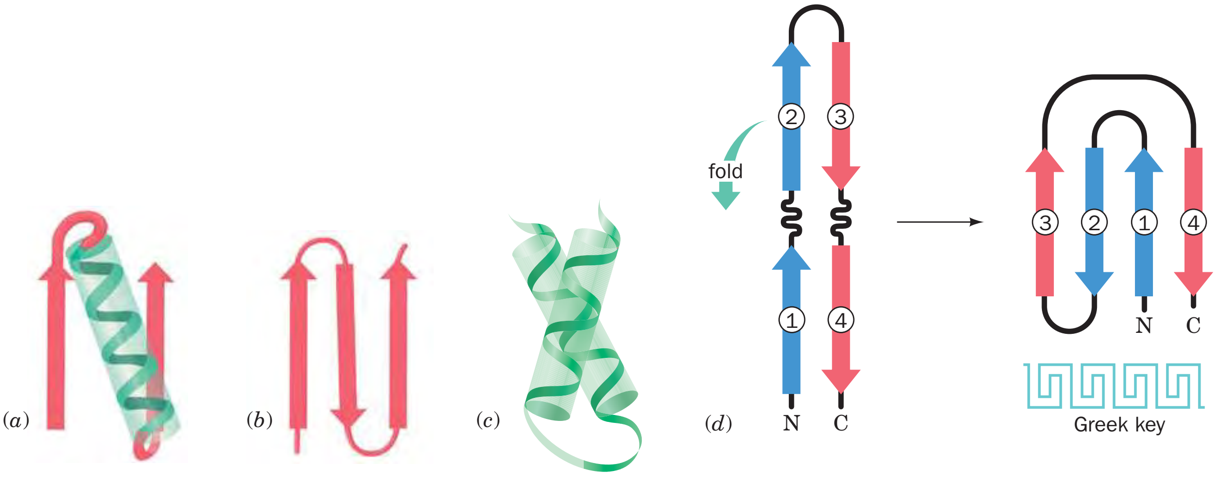

■ **Figure 6-28** | **Schematic diagrams of supersecondary structures.** (*a*) A βαβ motif, (*b*) a β hairpin motif, (*c*) an αα motif, and (*d*) a Greek key motif, showing how it is constructed from a folded-over β hairpin. The polypeptide backbones are drawn as ribbons, with β strands shown as flat arrows pointing from N- to C-terminus, and α helices represented by cylinders.

Most Proteins Can Be Classified as α, β, or α/β. The major types of secondary structural elements occur in globular proteins in varying proportions and combinations. Some proteins, such as *E. coli* **cytochrome b_{562}** (Fig. 6-29*a*), consist only of α helices spanned by short connecting links and are therefore classified as **α proteins.** Others, such as immunoglobulins, contain the **immunoglobulin fold** (Fig. 6-29*b*), and are called **β proteins** because they have a large proportion of β sheets and are devoid of α helices. Most proteins, however, including **lactate dehydrogenase** (Fig. 6-29*c*) and carboxypeptidase A (Fig. 6-12), are known as **α/β proteins** because they largely consist of mixtures of both types of secondary structure (proteins, on average contain ~31% α helix and ~28% β sheet).

The α, β, and α/β classes of proteins can be further subdivided by their **topology,** that is, according to how their secondary structural elements are connected. For example, extended β sheets often roll up to form **β barrels.** Three different types of 8-stranded β barrels, each with a different topology, are shown in Fig. 6-30. Two of these (Fig. 6-30*a* and *b*) are all-β structures containing multiple β hairpin motifs. The third, known as an **α/β barrel** (Fig. 6-30*c*), can be considered as a set of overlapping βαβ motifs (and is a member of the α/β class of proteins).

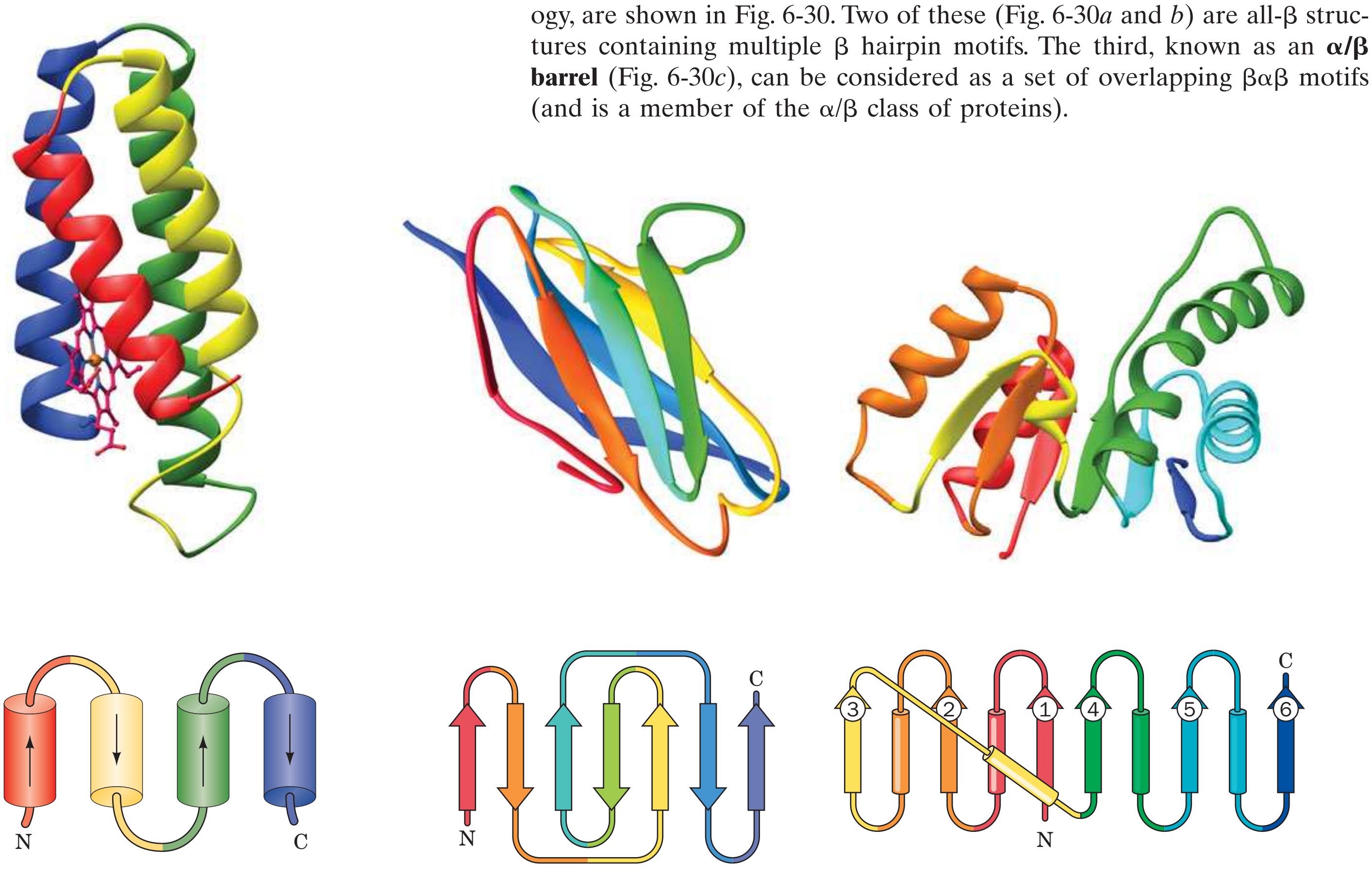

(a) *(b)* *(c)*

Figure 6-29 | A selection of protein structures. The proteins are represented by their peptide backbones, drawn in ribbon form, with β strands shown as flat arrows pointing from N- to C-terminus and α-helices depicted as coils. The polypeptide chain is colored, from N- to C-terminus, in rainbow order from red to blue. Below each drawing is the corresponding topological diagram indicating the connectivity of its helices (cylinders) and β strands (flat arrows). (*a*) *E. coli* **cytochrome b_{562}** (106 residues), which forms an up–down–up–down 4-helix bundle. Its bound heme group is shown in ball-and-stick form with C magenta, N blue, O red, and Fe orange. (*b*) The N-terminal domain of the human immunoglobulin fragment **Fab New** (103 residues) showing its immunoglobulin fold. The polypeptide chain is folded into a sandwich of 3- and 4-stranded antiparallel β sheets. (*c*) The N-terminal domain of dogfish lactate dehydrogenase (163 residues). It contains a 6-stranded parallel β sheet in which the crossovers between β strands all contain an α helix that forms a right-handed helical turn with its flanking β strands. [Based on X-ray structures by (*a*) F. Scott Matthews, Washington University School of Medicine; (*b*) Roberto Poljak, The Johns Hopkins School of Medicine; and (*c*) Michael Rossmann, Purdue University. PDBids (*a*) 256B, (*b*) 7FAB, and (*c*) 6LDH.]

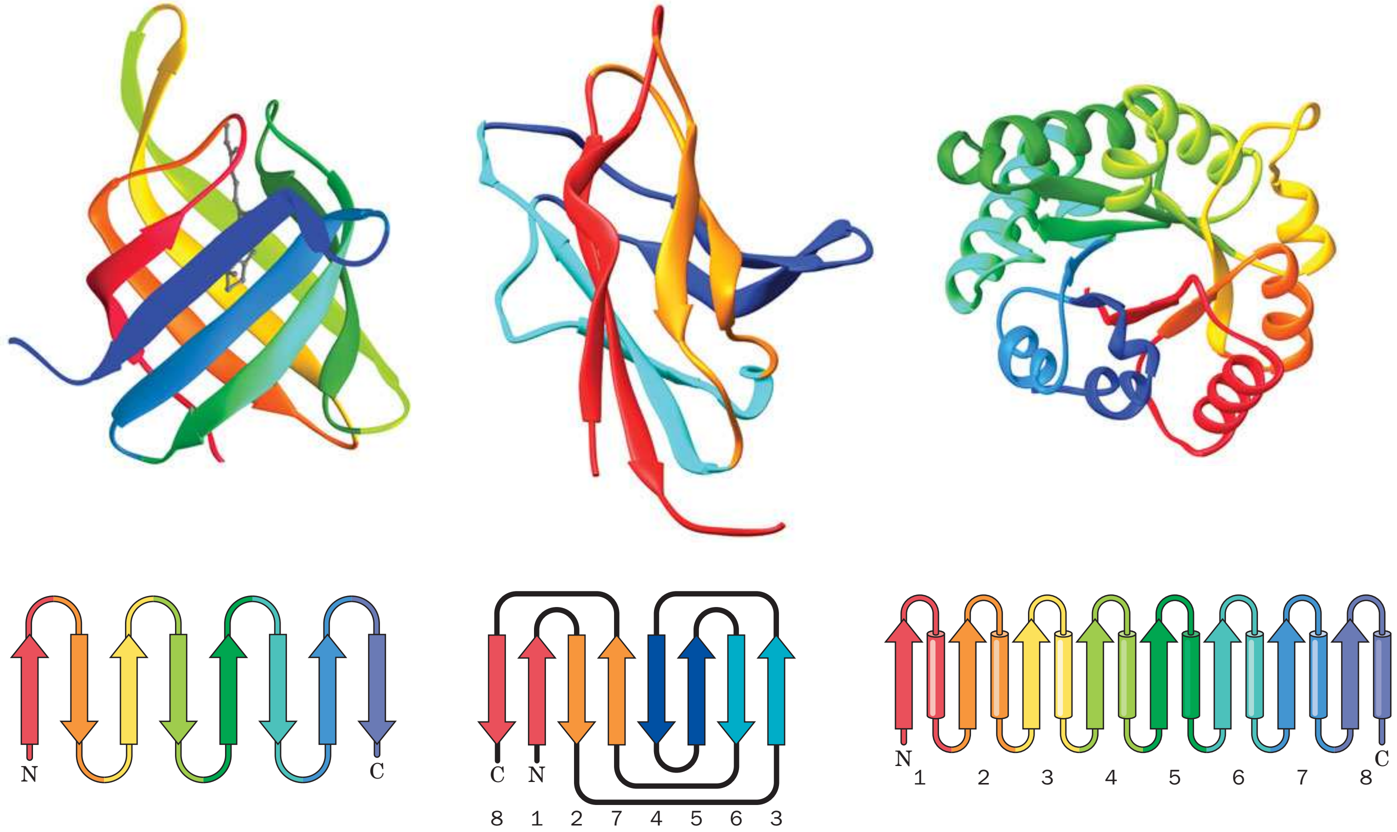

(*a*) (*b*) (*c*)

Figure 6-30 | X-Ray structures of β barrels. Each polypeptide is drawn and colored and accompanied by its corresponding topological diagram as is described in the legend to Fig. 6-29. (*a*) Human **retinol binding protein** showing its 8-stranded up-and-down β barrel (residues 1–142 of the 182-residue protein). Note that each β strand is linked via a short loop to its clockwise-adjacent strand as seen from the top. The protein's bound retinol molecule is represented by a gray ball-and-stick model. (*b*) **Peptide-*N*^{4}-(*N*-acetyl-β-D-glucosaminyl)asparagine amidase F** from *Flavobacterium meningosepticum* (residues 1–140 of the 340-residue enzyme). Note how its 8-stranded β barrel is formed by rolling up a 4-segment β hairpin. Here the two β strands in each segment of the β hairpin are colored alike with strands 1 and 8 (the N- and C-terminal strands) red, strands 2 and 7 orange, strands 3 and 6 cyan, and strands 4 and 5 blue. This motif, which is known as a **jelly roll** or **Swiss roll barrel,** is so named because of its topological resemblance to the rolled-up pastries. (*c*) Chicken muscle **triose phosphate isomerase** (**TIM;** 247 residues) forms a so-called **α/β barrel** in which 8 pairs of alternating β strands and α helices roll up to form an inner barrel of 8 parallel β strands surrounded by an outer barrel of 8 parallel α helices. The protein is viewed approximately along the axis of the α/β barrel. Note that the α/β barrel is essentially a series of linked βαβ motifs. [Based on X-ray structures by (a) T. Alwyn Jones, Biomedical Center, Uppsala, Sweden; (b) Patrick Van Roey, New York State Department of Health, Albany, New York; and (c) David Phillips, Oxford University, Oxford, U.K. PDBids (a) 1RBP, (b) 1PNG, and (c) 1TIM.]

Large Polypeptides Form Domains. Polypeptide chains containing more than ~200 residues usually fold into two or more globular clusters known as **domains,** which give these proteins a bi- or multilobal appearance. Each subunit of the enzyme **glyceraldehyde-3-phosphate dehydrogenase,**

for example, has two distinct domains (Fig. 6-31). Most domains consist of 40 to 200 amino acid residues and have an average diameter of ~25 Å. An inspection of the various protein structures diagrammed in this chapter reveals that domains consist of two or more layers of secondary structural elements. The reason for this is clear: At least two such layers are required to seal off a domain's hydrophobic core from its aqueous environment.

A polypeptide chain wanders back and forth within a domain, but neighboring domains are usually connected by only one or two polypeptide segments. *Consequently, many domains are structurally independent units that have the characteristics of small globular proteins.* Nevertheless, the domain structure of a protein is not necessarily obvious since its domains may make such extensive contacts with each other that the protein appears to be a single globular entity.

Domains often have a specific function such as the binding of a small molecule. In Fig. 6-31, for example, the dinucleotide NAD^+ (nicotinamide adenine dinucleotide; Fig. 11-4) binds to the N-terminal domain of glyceraldehyde-3-phosphate dehydrogenase. Michael Rossmann has shown that a βαβαβ unit, in which the β strands form a parallel sheet with α helical connections, often acts as a nucleotide-binding site. Two of these βαβαβ units combine to form a domain known as a **dinucleotide-binding fold,** or **Rossmann fold.** Glyceraldehyde-3-phosphate dehydrogenase's N-terminal domain contains such a fold, as does lactate dehydrogenase (Fig. 6-29*c*). In some multidomain proteins, binding sites occupy the clefts between domains; that is, small molecules are bound by groups from two domains. In such cases, the relatively pliant covalent connection between the domains allows flexible interactions between the protein and the small molecule.

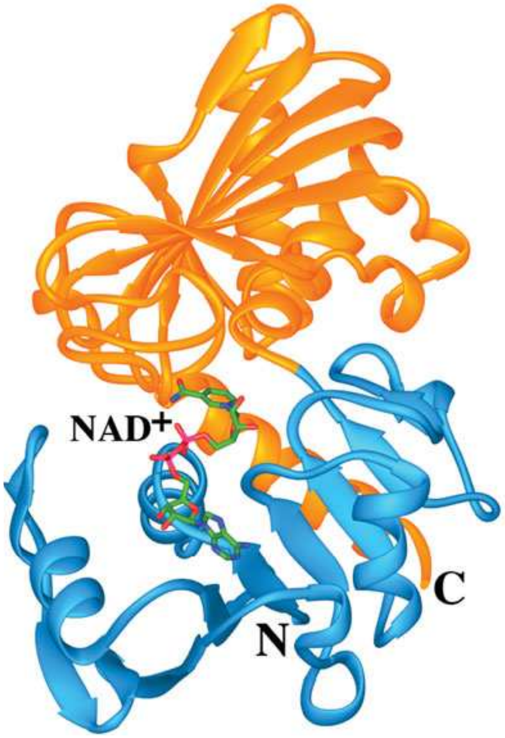

■ **Figure 6-31 | The two-domain protein glyceraldehyde-3-phosphate dehydrogenase.** The N-terminal domain (*light blue*) binds NAD^+ (drawn in stick form and colored according to atom type with C green, N blue, O red, and P magenta), and the C-terminal domain (*orange*) binds glyceraldehyde-3-phosphate (not shown). [Based on an X-ray structure by Alan Wonacott, Imperial College, London, U.K. PDBid 1GD1.] **See Interactive Exercise 2.**

D | Structure Is Conserved More than Sequence

The many thousands of known protein structures, comprising an even greater number of separate domains, can be grouped into families by examining the overall paths followed by their polypeptide chains. Although it is estimated that there are as many as 1400 different protein domain families, approximately 200 different folding patterns account for about half of all known protein structures. As described in Section 5-4B, the domain is the fundamental unit of protein evolution. Apparently, the most common protein domains are evolutionary sinks—domains that arose and persisted because of their ability (1) to form stable folding patterns; (2) to tolerate amino acid deletions, substitutions, and insertions, thereby making them more likely to survive evolutionary changes; and/or (3) to support essential biological functions.

Polypeptides with similar sequences tend to adopt similar backbone conformations. This is certainly true for evolutionarily related proteins that carry out similar functions. For example, the cytochromes *c* of different species are highly conserved proteins with closely similar sequences (Table 5-5) and three-dimensional structures.

Cytochrome *c* occurs only in eukaryotes, but prokaryotes contain proteins, known as ***c*-type cytochromes,** which perform the same general function (that of an electron carrier). The *c*-type cytochromes from different species exhibit only low degrees of sequence similarity to each other and to eukaryotic cytochromes *c*. Yet their X-ray structures are clearly similar, particularly in polypeptide chain folding and side chain packing in the protein interior (Fig. 6-32). The major structural differences among *c*-type cytochromes lie in the various polypeptide loops on their surfaces. The

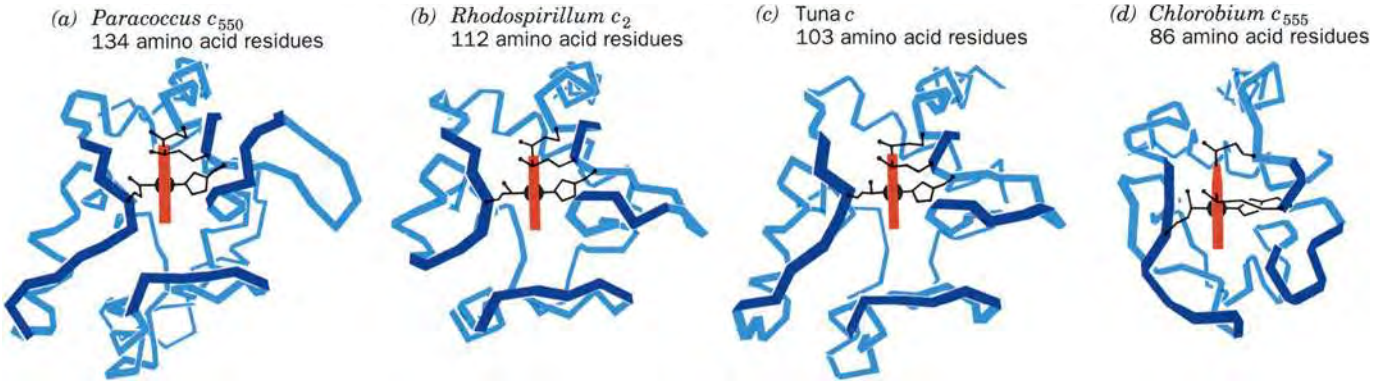

Figure 6-32 | Three-dimensional structures of *c*-type cytochromes. The polypeptide backbones (*blue*) are shown in analogous orientations such that their heme groups (*red*) are viewed edge-on. The Cys, Met, and His side chains that covalently link the heme to the protein are also shown. (*a*) Cytochrome c_{550} from *Paracoccus denitrificans*, (*b*) cytochrome c_2 from *Rhodospirillum rubrum*, (*c*) cytochrome *c* from tuna, and (*d*) cytochrome c_{555} from *Chlorobium limicola*. [Illustration, Irving Geis. Image from the Irving Geis Collection/Howard Hughes Medical Institute. Rights owned by HHMI. Reproduction by permission only.] **See Kinemage Exercise 5.**

sequences of the *c*-type cytochromes have diverged so far from one another that, in the absence of their X-ray structures, they can be properly aligned only through the use of mathematically sophisticated computer programs. Thus, *it appears that the essential structural and functional elements of proteins, rather than their amino acid residues, are conserved during evolution*.

E | Structural Bioinformatics Provides Tools for Storing, Visualizing, and Comparing Protein Structural Information

The data obtained by X-ray crystallography, NMR spectroscopy, and certain other techniques take the form of three-dimensional coordinates describing the spatial positions of atoms in molecules. This kind of information can be easily stored, displayed, and compared, much like sequence information obtained by nucleotide or protein sequencing methods (see Sections 3-4 and 5-3). **Bioinformatics** is the rapidly growing discipline that deals with the burgeoning amount of information related to molecular sequences and structures. **Structural bioinformatics** is a branch of bioinformatics that is concerned with how macromolecular structures are displayed and compared. Some of the databases and analytical tools that are used in structural bioinformatics are listed in Table 6-2.

The Protein Data Bank Is the Repository for Structural Information. The atomic coordinates of nearly 50,000 macromolecular structures, including proteins, nucleic acids, and carbohydrates, are archived in the **Protein Data Bank (PDB).** Indeed, most scientific journals that publish macromolecular structures require that authors deposit their structure's coordinates in the PDB.

Each independently determined structure in the PDB is assigned a unique four-character identifier (its PDBid). For example, the PDBid for the structure of sperm whale myoglobin is 1MBO. A coordinate file begins with information that identifies the macromolecule, its source (the organism from which it was obtained), the author(s) who determined the structure, and key journal references. The file continues with a synopsis of how the structure was determined together with indicators of its accuracy.

Table 6-2 Structural Bioinformatics Internet Addresses

Structural Databases
Protein Data Bank (PDB): http://www.rcsb.org/pdb/
Nucleic Acid Database: http://ndbserver.rutgers.edu/
Molecular Modeling Database (MMDB): http://www.ncbi.nlm.nih.gov/Structure/index.shtml
Most Representative NMR Structure in an Ensemble: http://pqs.ebi.ac.uk/pqs-nmr.html
PQS Protein Quaternary Structure Query Form at the EBI: http://pqs.ebi.ac.uk/
Molecular Graphics Programs
Cn3D: http://www.ncbi.nlm.nih.gov/Structure/CN3D/cn3d.shtml
Jmol: http://jmol.sourceforge.net/
KiNG: http://kinemage.biochem.duke.edu/
FirstGlance: http:// molvis.sdsc.edu/fgij/index.htm
Swiss-PDB Viewer (Deep View): http://us.expasy.org/spdbv/
Structural Classification Algorithms
CATH (*C*lass, *A*rchitecture, *T*opology, and *H*omologous superfamily): http://www.cathdb.info/latest/index.html
CE (*C*ombinatorial *E*xtension of optimal pathway): http://cl.sdsc.edu/
FSSP (*F*amily of *S*tructurally *S*imilar *P*roteins): http://www.ebi.ac.uk/dali/
SCOP (*S*tructural *C*lassification *O*f *P*roteins): http://scop.mrc-lmb.cam.ac.uk/scop/
VAST (*V*ector *A*lignment *S*earch *T*ool): http://www.ncbi.nlm.nih.gov/Structure/VAST/vast.shtml

The sequences of the structure's various chains are then listed together with the descriptions and formulas of its so-called HET (for heterogen) groups, which are molecular entities that are not among the "standard" amino acid or nucleotide residues (for example, organic molecules, nonstandard residues such as Hyp, metal ions, and bound water molecules). The positions of the structure's secondary structural elements and its disulfide bonds are then provided.

The bulk of a PDB file consists of a series of records (lines), each of which provides the three-dimensional (x, y, z) coordinates in angstroms of one atom in the structure. All atoms are labeled either ATOM (for a "standard" amino acid or nucleotide residue) or HETATM (for any other atom). Each atom is identified by a serial number, an atom name (for example, C and O for an amino acid residue's carbonyl C and O atoms, CA and CB for C_α and C_β atoms), the name of the residue, and a letter to identify the chain to which it belongs (for structures that have more than one chain). For NMR-based structures, the PDB file contains a full set of records for each member of the ensemble of structures (the most representative member of such a coordinate set can be obtained from another database; see Table 6-2).

A particular PDB file may be located according to its PDBid or, if this is unknown, by searching with a variety of criteria including a protein's name, its source, the author(s), key words, and/or the experimental technique used to determine the structure. Selecting a particular macromolecule in the PDB initially displays a summary page with options for viewing the structure (either statically or interactively), for viewing or downloading the coordinate file, and for classifying or analyzing the structure in terms of its geometric properties and sequence. The **Nucleic Acid Database (NDB)** archives the atomic coordinates of structures that contain nucleic acids, using roughly the same format as PDB files.

Molecular Graphics Programs Interactively Show Macromolecules in Three Dimensions. The most informative way to examine a macromolecular structure is through the use of molecular graphics programs that permit the user to interactively rotate a macromolecule and thereby perceive its three-dimensional structure. This impression may be further enhanced by simultaneously viewing the macromolecule in stereo. Most molecular graphics programs use PDB files as input. The programs described here can be downloaded from the Internet addresses listed in Table 6-2, some of which also provide instructions for the program's use.

Jmol, which functions as both a Web browser–based applet or as a standalone program, allows the user to display user-selected macromolecules in a variety of colors and formats (e.g., wire frame, ball-and-stick, backbone, space-filling, and cartoons). The Interactive Exercises on the website that accompanies this textbook (http://wiley.com/college/voet/) all use Jmol. **FirstGlance** uses Jmol to display macromolecules via a user-friendly interface. **KiNG,** which also has Web browser–based and standalone versions, displays the so-called **Kinemages** on this textbook's accompanying website. KiNG provides a generally more author-directed user environment than does Jmol. Macromolecules can be displayed directly from their corresponding PDB page using either Jmol or KiNG. The **Swiss-PDB Viewer** (also called **Deep View**), in addition to displaying molecular structures, provides tools for basic model building, homology modeling, energy minimization, and multiple sequence alignment. One advantage of the Swiss-PDB Viewer is that it allows users to easily superimpose two or more models.

Structure Comparisons Reveal Evolutionary Relationships. Most proteins are structurally related to other proteins, since *evolution tends to conserve the structures of proteins rather than their sequences*. The computational tools described below facilitate the classification and comparison of protein structures. These programs can be accessed directly via their Internet addresses and in some cases through the PDB. Studies using these programs yield functional insights, reveal distant evolutionary relationships that are not apparent from sequence comparisons, generate libraries of unique folds for structure prediction, and provide indications as to why certain types of structures are preferred over others.

1. ***CATH*** (for *C*lass, *A*rchitecture, *T*opology, and *H*omologous superfamily), as its name suggests, categorizes proteins in a four-level structural hierarchy: (1) Class, the highest level, places the selected protein in one of four levels of gross secondary structure (e.g., Mainly α, Mainly β, α/β, and Few Secondary Structures); (2) Architecture, the gross arrangement of secondary structure; (3) Topology, which depends on both the overall shape of the protein domain and the connectivity of its secondary structural elements; and (4) Homologous Superfamily, which identifies the protein as a member of a group that shares a common ancestor.
2. ***CE*** (for *C*ombinatorial *E*xtension of the optimal path) finds all proteins in the PDB that can be structurally aligned with the query structure to within user-specified geometric criteria. CE can optimally align and display two user-selected structures.
3. ***FSSP*** (*F*amily of *S*tructurally *S*imilar *P*roteins) lists the protein structures that, at least in part, structurally resemble the query protein. It is based on continuously updated all-against-all comparisons of the protein structures in the PDB, using a program called **Dali.**

4. ***SCOP*** (*S*tructural *C*lassification *O*f *P*roteins) classifies protein structures based mainly on manually generated topological considerations according to a six-level hierarchy: Class (e.g., all-α, all-β, α/β), Fold (based on the arrangement of secondary structural elements), Superfamily (indicative of distant evolutionary relationships based on structural criteria and functional features), Family (indicative of near evolutionary relationships based on sequence as well as on structure), Protein, and Species. SCOP permits the user to navigate through its treelike hierarchical organization and lists the known members of any particular branch.
5. ***VAST*** (*V*ector *A*lignment *S*earch *T*ool), a component of the National Center for Biotechnology Information (NCBI) Entrez system, reports a precomputed list of proteins of known structure that structurally resemble the query protein ("structure neighbors"). The VAST system uses the **Molecular Modeling Database (MMDB),** an NCBI-generated database that is derived from PDB coordinates but in which molecules are represented by connectivity graphs rather than sets of atomic coordinates. VAST displays the superposition of the query protein in its structural alignment with up to five other proteins using the molecular graphics program **Cn3D.** VAST also reports a precomputed list of proteins that are similar to the query protein in sequence ("sequence neighbors").

■ CHECK YOUR UNDERSTANDING

List some of the relative advantages and disadvantages of using X-ray crystallography and NMR spectroscopy to determine the structure of a protein.

Why do turns and loops most often occur on the protein surface? Which side chains usually occur on a protein's surface? in its interior?

Describe some of the common protein structural motifs.

Explain why a protein's sequence evolves faster than its structure.

Summarize the types of information provided in a PDB file.

Why is it useful to compare protein structures in addition to protein sequences?

3 Quaternary Structure and Symmetry

LEARNING OBJECTIVES

- Understand that some proteins contain multiple subunits, usually arranged symmetrically.

Most proteins, particularly those with molecular masses >100 kD, consist of more than one polypeptide chain. These polypeptide subunits associate with a specific geometry. The spatial arrangement of these subunits is known as a protein's quaternary structure.

There are several reasons why multisubunit proteins are so common. In large assemblies of proteins, such as collagen fibrils, the advantages of subunit construction over the synthesis of one huge polypeptide chain are analogous to those of using prefabricated components in constructing a building: Defects can be repaired by simply replacing the flawed subunit; the site of subunit manufacture can be different from the site of assembly into the final product; and the only genetic information necessary to specify the entire edifice is the information specifying its few different self-assembling subunits. In the case of enzymes, increasing a protein's size tends to better fix the three-dimensional positions of its reacting groups. *Increasing the size of an enzyme through the association of identical subunits is more efficient than increasing the length of its polypeptide chain since each subunit has an active site. More importantly, the subunit construction of many enzymes provides the structural basis for the regulation of their activities* (Sections 7-3B and 12-3).

Subunits Usually Associate Noncovalently. A multisubunit protein may consist of identical or nonidentical polypeptide chains. Hemoglobin, for example, has the subunit composition $\alpha_2\beta_2$ (Fig. 6-33). Proteins with more than one subunit are called **oligomers,** and their identical units are called **protomers.** A protomer may therefore consist of one polypeptide chain or several unlike polypeptide chains. In this sense, hemoglobin is a dimer of αβ protomers.

The contact regions between subunits resemble the interior of a single-subunit protein: They contain closely packed nonpolar side chains, hydrogen bonds involving the polypeptide backbones and their side chains, and, in some cases, interchain disulfide bonds. However, the subunit interfaces of proteins that dissociate *in vivo* have lesser hydrophobicities than do permanent interfaces.

Subunits Are Symmetrically Arranged. In the vast majority of oligomeric proteins, the protomers are symmetrically arranged; that is, each protomer occupies a geometrically equivalent position in the oligomer. Proteins cannot have inversion or mirror symmetry, however, because bringing the protomers into coincidence would require converting chiral L residues to D residues. Thus, *proteins can have only* ***rotational symmetry.***

In the simplest type of rotational symmetry, **cyclic symmetry,** protomers are related by a single axis of rotation (Fig. 6-34*a*). Objects with two-, three-, or *n*-fold rotational axes are said to have C_2, C_3, or C_n symmetry, respectively. C_2 symmetry is the most common; higher cyclic symmetries are relatively rare.

Dihedral symmetry (D_n), a more complicated type of rotational symmetry, is generated when an *n*-fold rotation axis intersects a twofold rotation axis at right angles (Fig. 6-34*b*). An oligomer with D_n symmetry consists of 2*n* protomers. D_2 symmetry is the most common type of dihedral symmetry in proteins.

Other possible types of rotational symmetry are those of a tetrahedron, cube, and icosahedron (Fig. 6-34*c*). Some multienzyme complexes and spherical viruses are built on these geometric plans.

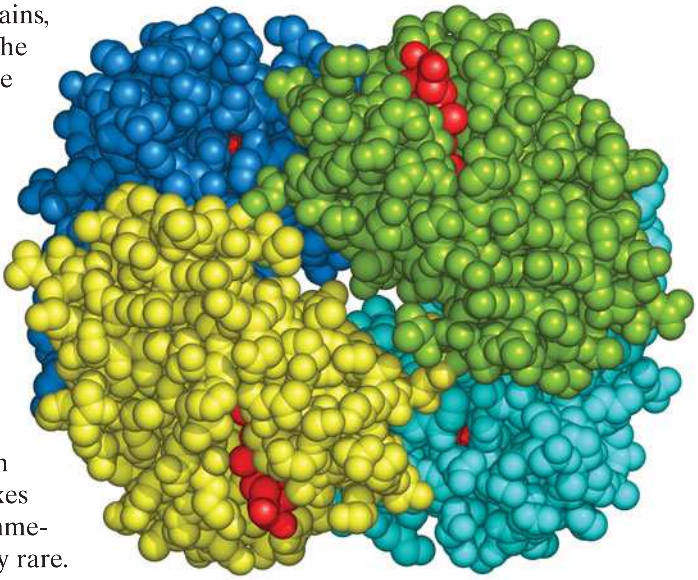

Figure 6-33 | Quaternary structure of hemoglobin. In this space-filling model, the α_1, α_2, β_1, and β_2 subunits are colored yellow, green, cyan, and blue, respectively. Heme groups are red. [Based on an X-ray structure by Max Perutz, MRC Laboratory of Molecular Biology, Cambridge, U.K. PDBid 2DHB.]

CHECK YOUR UNDERSTANDING

List the advantages of multiple subunits in proteins.

Why can't proteins have mirror symmetry?

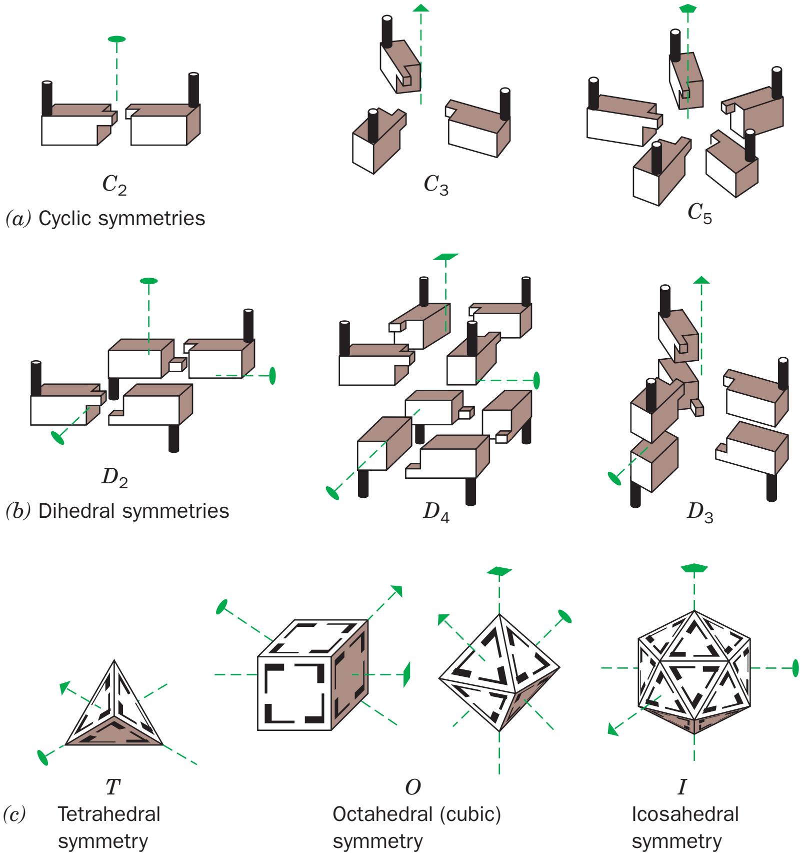

Figure 6-34 | Symmetries of oligomeric proteins. The oval, the triangle, the square, and the pentagon at the ends of the dashed green lines indicate, respectively, the unique twofold, threefold, fourfold, and fivefold rotational axes of the objects shown. (*a*) Assemblies with cyclic symmetry. (*b*) Assemblies with dihedral symmetry. In these objects, a twofold axis is perpendicular to another rotational axis. (*c*) Assemblies with the rotational symmetries of a tetrahedron, a cube or octahedron, and an icosahedron. [Illustration, Irving Geis. Image from the Irving Geis Collection/Howard Hughes Medical Institute. Rights owned by HHMI. Reproduction by permission only.]

See the Animated Figures.

4 Protein Stability

LEARNING OBJECTIVES

- Understand that protein stability depends primarily on hydrophobic effects and secondarily on electrostatic interactions.
- Understand that a protein that has been denatured may undergo renaturation.

Incredible as it may seem, thermodynamic measurements indicate that *native proteins are only marginally stable under physiological conditions*. The free energy required to denature them is ~0.4 $\text{kJ} \cdot \text{mol}^{-1}$ per amino acid residue, so a fully folded 100-residue protein is only about 40 $\text{kJ} \cdot \text{mol}^{-1}$ more stable than its unfolded form (for comparison, the energy required to break a typical hydrogen bond is ~20 $\text{kJ} \cdot \text{mol}^{-1}$). The various noncovalent influences on proteins—hydrophobic effects, electrostatic interactions, and hydrogen bonding—each have energies that may total thousands of kilojoules per mole over an entire protein molecule. Consequently, a protein structure is the result of a delicate balance among powerful countervailing forces.

A | Proteins Are Stabilized by Several Forces

Protein structures are governed primarily by hydrophobic effects and, to a lesser extent, by interactions between polar residues, and by other types of bonds.

The Hydrophobic Effect Has the Greatest Influence on Protein Stability. *The hydrophobic effect, which causes nonpolar substances to minimize their contacts with water* (Section 2-1C), *is the major determinant of native protein structure.* The aggregation of nonpolar side chains in the interior of a protein is favored by the increase in entropy of the water molecules that would otherwise form ordered "cages" around the hydrophobic groups. The combined hydrophobic and hydrophilic tendencies of individual amino acid residues in proteins can be expressed as **hydropathies** (Table 6-3). The greater a side chain's hydropathy, the more likely it is to occupy the interior of a protein and vice versa. Hydropathies are good predictors of which portions of a polypeptide chain are inside a protein, out of contact with the aqueous solvent, and which portions are outside (Fig. 6-35).

Table 6-3 Hydropathy Scale for Amino Acid Side Chains

Side Chain	Hydropathy
Ile	4.5
Val	4.2
Leu	3.8
Phe	2.8
Cys	2.5
Met	1.9
Ala	1.8
Gly	−0.4
Thr	−0.7
Ser	−0.8
Trp	−0.9
Tyr	−1.3
Pro	−1.6
His	−3.2
Glu	−3.5
Gln	−3.5
Asp	−3.5
Asn	−3.5
Lys	−3.9
Arg	−4.5

Source: Kyte, J. and Doolittle, R.F., *J. Mol. Biol.* **157,** 110 (1982).

Site-directed mutagenesis experiments in which individual interior residues have been replaced by a number of others suggest that the factors that affect stability are, in order, the hydrophobicity of the substituted residue, its steric compatibility, and, last, the volume of its side chain.

Electrostatic Interactions Contribute to Protein Stability. In the closely packed interiors of native proteins, van der Waals forces, which are relatively weak (Section 2-1A), are nevertheless an important stabilizing influence. This is because these forces only act over short distances and hence are lost when the protein is unfolded.

Perhaps surprisingly, *hydrogen bonds, which are central features of protein structures, make only minor contributions to protein stability*. This is because hydrogen-bonding groups in an unfolded protein form hydrogen bonds with water molecules. Thus the contribution of a hydrogen bond to the stability of a native protein is the small difference in hydrogen bonding free energies between the native and unfolded states (−2 to 8 $\text{kJ} \cdot \text{mol}^{-1}$ as determined by site-directed mutagenesis studies). Nevertheless, hydrogen bonds are important determinants of native protein structures, because if a protein folded in a way that prevented a hydrogen bond from forming, the stabilizing energy of that hydrogen bond would be lost. Hydrogen bonding therefore fine-tunes tertiary structure by "selecting"

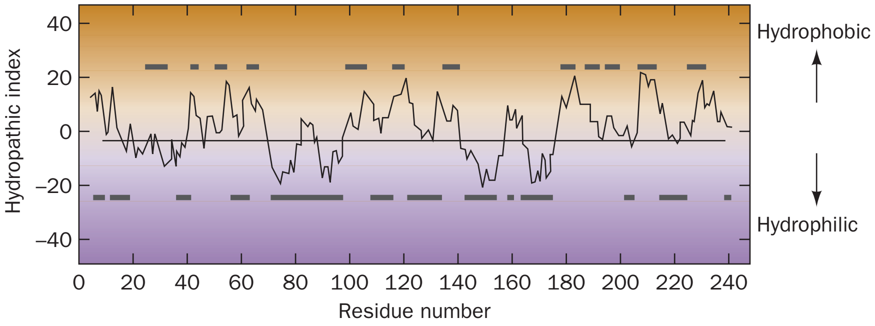

Figure 6-35 | **A hydropathic index plot for bovine chymotrypsinogen.** The sum of the hydropathies of nine consecutive residues is plotted versus residue sequence number. A large positive hydropathic index indicates a hydrophobic region of the polypeptide, whereas a large negative value indicates a hydrophilic region. The upper bars denote the protein's interior regions, as determined by X-ray crystallography, and the lower bars denote the protein's exterior regions. [After Kyte, J. and Doolittle, R.F., *J. Mol. Biol.* **157,** 111 (1982).]

the unique native structure of a protein from among a relatively small number of hydrophobically stabilized conformations.

The association of two ionic protein groups of opposite charge (e.g., Lys and Asp) is known as an **ion pair** or **salt bridge.** About 75% of the charged residues in proteins are members of ion pairs that are located mostly on the protein surface (Fig. 6-36). Despite the strong electrostatic attraction between the oppositely charged members of an ion pair, these interactions contribute little to the stability of a native protein. This is because the free energy of an ion pair's charge–charge interactions usually fails to compensate for the loss of entropy of the side chains and the loss of solvation free energy when the charged groups form an ion pair. This accounts for the observation that ion pairs are poorly conserved among homologous proteins.

Disulfide Bonds Cross-Link Extracellular Proteins. Disulfide bonds (Fig. 4-6) within and between polypeptide chains form as a protein folds to its native conformation. Some polypeptides whose Cys residues have been derivatized or mutagenically replaced to prevent disulfide bond formation can still assume their fully active conformations, suggesting that disulfide bonds are not essential stabilizing forces. They may, however, be

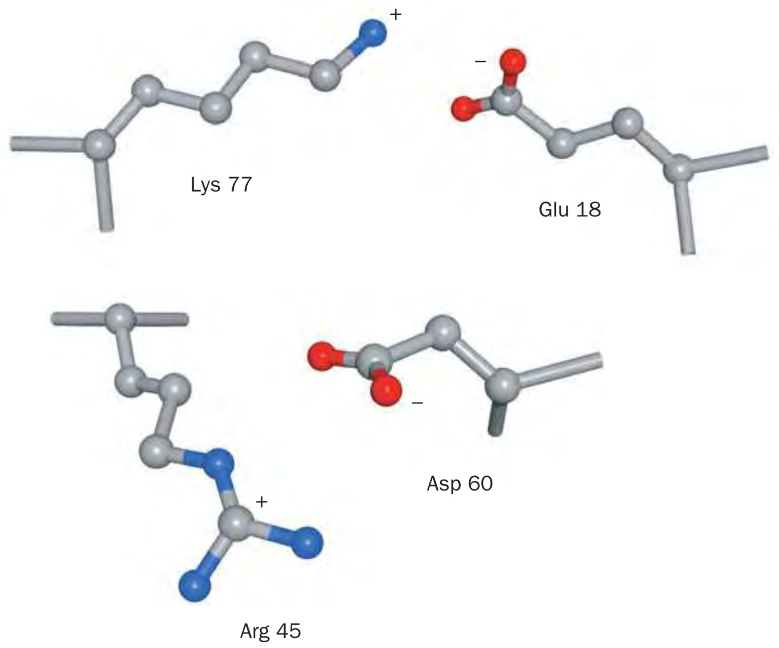

Figure 6-36 | **Examples of ion pairs in myoglobin.** In each case, oppositely charged side chain groups from residues far apart in sequence closely approach each other through the formation of ion pairs.

important for "locking in" a particular backbone folding pattern as the protein proceeds from its fully extended state to its mature form.

Disulfide bonds are rare in intracellular proteins because the cytoplasm is a reducing environment. Most disulfide bonds occur in proteins that are secreted from the cell into the more oxidizing extracellular environment. The relatively hostile extracellular world (e.g., uncontrolled temperature and pH) apparently requires the additional structural constraints conferred by disulfide bonds.

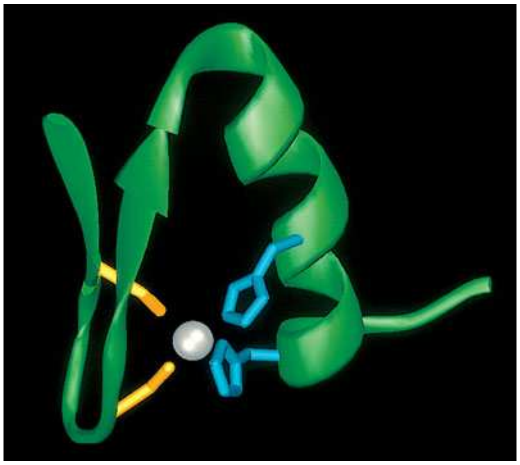

Figure 6-37 | A zinc finger motif. This structure, from the DNA-binding protein **Zif268,** is known as a Cys_2–His_2 zinc finger because the zinc atom (*silver sphere*) is coordinated by two Cys residues (*yellow*) and two His residues (*cyan*). [Based on an X-ray structure by Carl Pabo, MIT. PDBid 1ZAA.]

Metal Ions Stabilize Some Small Domains. Metal ions may also function to internally cross-link proteins. For example, at least ten motifs collectively known as **zinc fingers** have been described in nucleic acid–binding proteins. These structures contain about 25–60 residues arranged around one or two Zn^{2+} ions that are tetrahedrally coordinated by the side chains of Cys, His, and occasionally Asp or Glu (Fig. 6-37). The Zn^{2+} ion allows relatively short stretches of polypeptide chain to fold into stable units that can interact with nucleic acids. Zinc fingers are too small to be stable in the absence of Zn^{2+}. Zinc is ideally suited to its structural role in intracellular proteins: Its filled *d* electron shell permits it to interact strongly with a variety of ligands (e.g., sulfur, nitrogen, or oxygen) from different amino acid residues. In addition, zinc has only one stable oxidation state (unlike, for example, copper and iron), so it does not undergo oxidation–reduction reactions in the cell.

Proteins Are Dynamic Structures. The plethora of forces acting to stabilize proteins as well as the static way that their structures are usually portrayed may leave the false impression that proteins have fixed and rigid structures. In fact, proteins are flexible and rapidly fluctuating molecules whose structural mobilities are functionally significant. Groups ranging in size from individual side chains to entire domains or subunits may be displaced by up to several angstroms through random intramolecular movements or in response to a trigger such as the binding of a small molecule. Extended side chains, such as Lys, and the N- and C-termini of polypeptide chains are especially prone to wave around in solution because there are few forces holding them in place.

Theoretical calculations by Martin Karplus indicate that a protein's native structure probably consists of a large collection of rapidly interconverting conformations that have essentially equal stabilities (Fig. 6-38). Conformational flexibility, or **breathing,** with structural displacement of up to ~2 Å, allows small molecules to diffuse in and out of the interior of certain proteins.

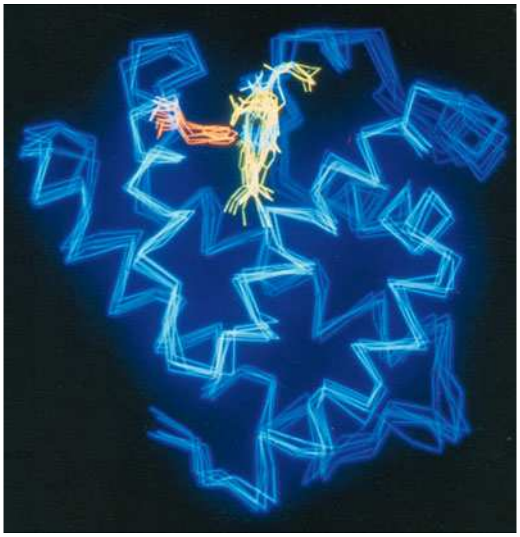

Figure 6-38 | Molecular dynamics of myoglobin. Several "snapshots" of the protein calculated at intervals of 5×10^{-12} s are superimposed. The backbone is blue, the heme group is yellow, and the His side chain linking the heme to the protein is orange. [Courtesy of Martin Karplus, Harvard University.]

B | Proteins Can Undergo Denaturation and Renaturation

The low conformational stabilities of native proteins make them easily susceptible to denaturation by altering the balance of the weak nonbonding forces that maintain the native conformation. Proteins can be denatured by a variety of conditions and substances:

1. Heating causes a protein's conformationally sensitive properties, such as optical rotation (Section 4-2), viscosity, and UV absorption, to change abruptly over a narrow temperature range. Such a sharp transition indicates that the entire polypeptide unfolds or "melts" **cooperatively,** that is, nearly simultaneously. Most proteins have melting temperatures that are well below 100°C. Among the exceptions are the proteins of thermophilic bacteria (Box 6-3).

BOX 6-3 PERSPECTIVES IN BIOCHEMISTRY

Thermostable Proteins

Certain species of bacteria known as **hyperthermophiles** grow at temperatures near 100°C. They live in such places as hot springs and submarine hydrothermal vents, with the most extreme, the archaebacterium *Pyrolobus fumarii,* able to grow at temperatures as high as 113°C. These organisms have many of the same metabolic pathways as do **mesophiles** (organisms that grow at "normal" temperatures). Yet most mesophilic proteins denature at temperatures where hyperthermophiles thrive. What is the structural basis for the thermostability of hyperthermophilic proteins?

The difference in the thermal stabilities of the corresponding (hyper)thermophilic and mesophilic proteins does not exceed $\sim$100 kJ·mol^{-1}, the equivalent of a few noncovalent interactions. This is probably why comparisons of the X-ray structures of hyperthermophilic enzymes with their mesophilic counterparts have failed to reveal any striking differences between them. These proteins exhibit some variations in secondary structure but no more than would be expected for homologous proteins from distantly related mesophiles. However, several of these thermostable enzymes have a superabundance of salt bridges on their surfaces, many of which are arranged in extensive networks containing up to 18 side chains.

The idea that salt bridges can stabilize a protein structure appears to contradict the conclusion of Section 6-4A that ion pairs are, at best, marginally stable. The key to this apparent paradox is that *the salt bridges in thermostable proteins form networks.* Thus, the gain in charge–charge free energy on associating a third charged group with an ion pair is comparable to that between the members of this ion pair, whereas the free energy lost on desolvating and immobilizing the third side chain is only about half that lost in bringing together the first two side chains. The same, of course, is true for the addition of a fourth, fifth, etc., side chain to a salt bridge network.

Not all thermostable proteins have such a high incidence of salt bridges. Structural comparisons suggest that these proteins are stabilized by a combination of small effects, the most important of which are an increased size of the protein's hydrophobic core, an increased size in the interface between its domains and/or subunits, and a more tightly packed core as evidenced by a reduced surface-to-volume ratio.

The fact that the proteins of hyperthermophiles and mesophiles are homologous and carry out much the same functions indicates that mesophilic proteins are by no means maximally stable. This, in turn, strongly suggests *that the marginal stability of most proteins under physiological conditions (averaging* $\sim$*0.4 kJ·mol*$^{-1}$ *of amino acid residues) is an essential property that has arisen through natural selection.* Perhaps this marginal stability helps confer the structural flexibility that many proteins require to carry out their physiological functions.

2. pH variations alter the ionization states of amino acid side chains, thereby changing protein charge distributions and hydrogen-bonding requirements.
3. Detergents associate with the nonpolar residues of a protein, thereby interfering with the hydrophobic interactions responsible for the protein's native structure.
4. The **chaotropic agents** guanidinium ion and urea,

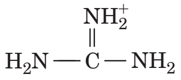

$$H_2N{-}\overset{\overset{\displaystyle NH_2^+}{\|}}{C}{-}NH_2$$

Guanidinium ion

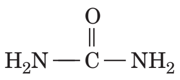

$$H_2N{-}\overset{\overset{\displaystyle O}{\|}}{C}{-}NH_2$$

Urea

in concentrations in the range 5 to 10 M, are the most commonly used protein denaturants. Chaotropic agents are ions or small organic molecules that increase the solubility of nonpolar substances in water. Their effectiveness as denaturants stems from their ability to disrupt hydrophobic interactions, although their mechanism of action is not well understood.

Many Denatured Proteins Can Be Renatured. In 1957, the elegant experiments of Christian Anfinsen on **ribonuclease A (RNase A)** showed that proteins can be denatured reversibly. RNase A, a 124-residue single-chain protein, is completely unfolded and its four disulfide bonds reductively

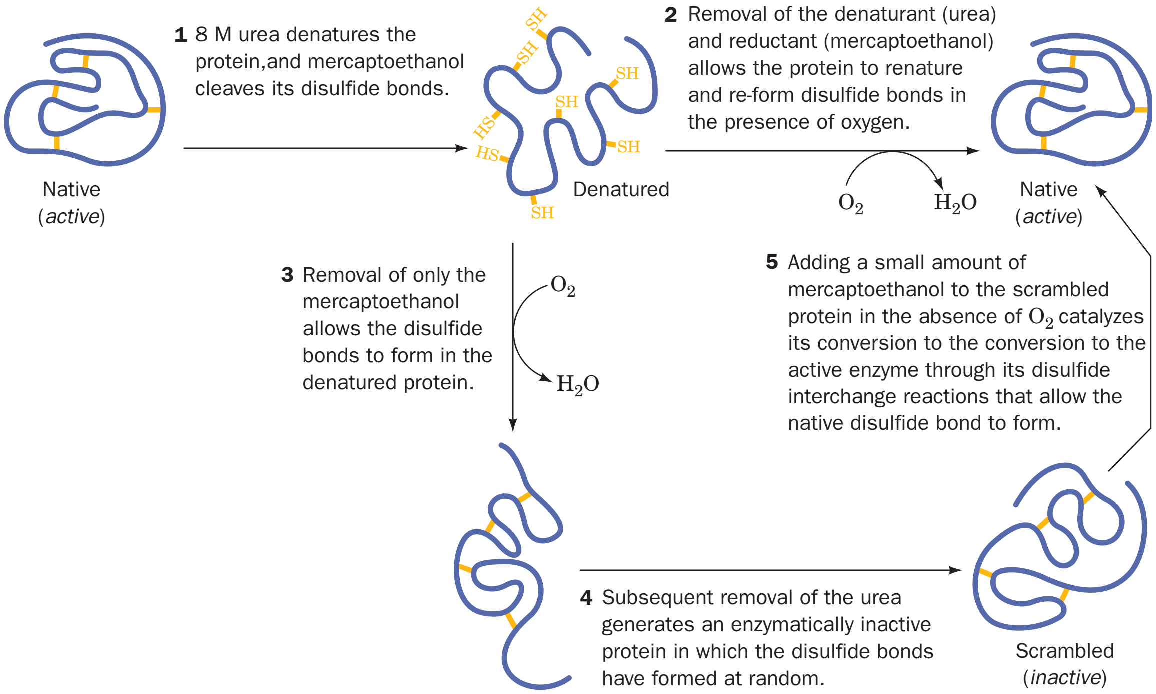

1 8 M urea denatures the protein,and mercaptoethanol cleaves its disulfide bonds.

2 Removal of the denaturant (urea) and reductant (mercaptoethanol) allows the protein to renature and re-form disulfide bonds in the presence of oxygen.

3 Removal of only the mercaptoethanol allows the disulfide bonds to form in the denatured protein.

4 Subsequent removal of the urea generates an enzymatically inactive protein in which the disulfide bonds have formed at random.

5 Adding a small amount of mercaptoethanol to the scrambled protein in the absence of O_2 catalyzes its conversion to the conversion to the active enzyme through its disulfide interchange reactions that allow the native disulfide bond to form.

Figure 6-39 | Denaturation and renaturation of RNase A. The polypeptide is represented by a purple line, with its disulfide bonds in yellow.

cleaved in an 8 M urea solution containing 2-mercaptoethanol. Dialyzing away the urea and reductant and exposing the resulting solution to O_2 at pH 8 (which oxidizes the SH groups to form disulfides) yields a protein that is virtually 100% enzymatically active and physically indistinguishable from native RNase A (Fig. 6-39). The protein must therefore **renature** spontaneously.

The renaturation of RNase A demands that its four disulfide bonds re-form. The probability of one of the eight Cys residues randomly forming a disulfide bond with its proper mate among the other seven Cys residues is 1/7; that of one of the remaining six Cys residues then randomly forming its proper disulfide bond is 1/5; etc. Thus the overall probability of RNase A re-forming its four native disulfide links at random is

$$\frac{1}{7} \times \frac{1}{5} \times \frac{1}{3} \times \frac{1}{1} = \frac{1}{105}$$

Clearly, the disulfide bonds do not randomly re-form under renaturing conditions, since, if they did, only 1% of the refolded protein would be catalytically active. Indeed, if the RNase A is reoxidized in 8 M urea so that its disulfide bonds re-form while the polypeptide chain is a random coil, then after removal of the urea, the RNase A is, as expected, only ~1% active (Fig. 6-39, Steps 3–4). This "scrambled" protein can be made fully active by exposing it to a trace of 2-mercaptoethanol, which breaks the improper disulfide bonds and allows the proper bonds to form. *Anfinsen's work demonstrated that proteins can fold spontaneously into their native conformations under physiological conditions. This implies that a protein's primary structure dictates its three-dimensional structure.*

CHECK YOUR UNDERSTANDING

Describe the forces that stabilize proteins, and rank their relative importance.

Summarize the results of Anfinsen's experiment with RNase A.

5 Protein Folding

LEARNING OBJECTIVES

- Understand that a folding protein follows a pathway from high energy and high entropy to low energy and low entropy.
- Understand that molecular chaperones assist protein folding via an ATP-dependent bind-and-release mechanism.
- Understand how amyloid diseases result from protein misfolding.

Studies of protein stability and renaturation suggest that protein folding is directed largely by the residues that occupy the interior of the folded protein. But *how* does a protein fold to its native conformation? One might guess that this process occurs through the protein's random exploration of all the conformations available to it until it eventually stumbles onto the correct one. A simple calculation first made by Cyrus Levinthal, however, convincingly demonstrates that this cannot possibly be the case: Assume that an n-residue protein's 2^n torsion angles, ϕ and ψ, each have three stable conformations. This yields $3^{2n} \approx 10^n$ possible conformations for the protein (a gross underestimate because we have completely neglected its side chains). Then, if the protein could explore a new conformation every 10^{-13} s (the rate at which single bonds reorient), the time t, in seconds, required for the protein to explore all the conformations available to it is

$$t = \frac{10^n}{10^{13}}$$

For a small protein of 100 residues, $t = 10^{87}$ s, which is immensely greater than the apparent age of the universe (20 billion years, or 6×10^{17} s). Clearly, proteins must fold more rapidly than this.

A | Proteins Follow Folding Pathways

Experiments have shown that many proteins fold to their native conformations in less than a few seconds. This is because *proteins fold to their native conformations via directed pathways rather than stumbling on them through random conformational searches.* Thus, as a protein folds, its conformational stability increases sharply (i.e., its free energy decreases sharply), which makes folding a one-way process. A hypothetical folding pathway is diagrammed in Fig. 6-40.

Experimental observations indicate that protein folding begins with the formation of local segments of secondary structure (α helices and β sheets). This early stage of protein folding is extremely rapid, with much of the native secondary structure in small proteins appearing within 5 ms of the initiation of folding. Since native proteins contain compact hydrophobic cores, it is likely that the driving force in protein folding is what has been termed a **hydrophobic collapse.** The collapsed state is known as a **molten globule,** a species that has much of the secondary structure of the native protein but little of its tertiary structure. Theoretical studies suggest that helices and sheets form in part because they are particularly compact ways of folding a polypeptide chain.

Over the next 5 to 1000 ms, the secondary structure becomes stabilized and tertiary structure begins to form. During this intermediate stage, the nativelike elements are thought to take the form of subdomains that are not yet properly docked to form domains. In the final stage of folding, which for small single-domain proteins occurs over the next few seconds, the protein undergoes a series of complex motions in which it attains its

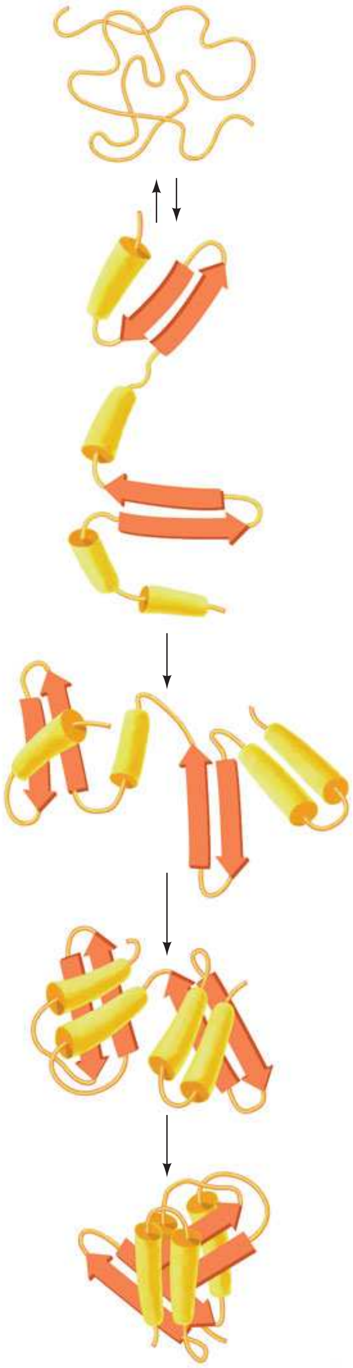

Figure 6-40 | Hypothetical protein folding pathway. This example shows a linear pathway for folding a two-domain protein. [After Goldberg, M.E., *Trends Biochem. Sci.* **10,** 389 (1985).]

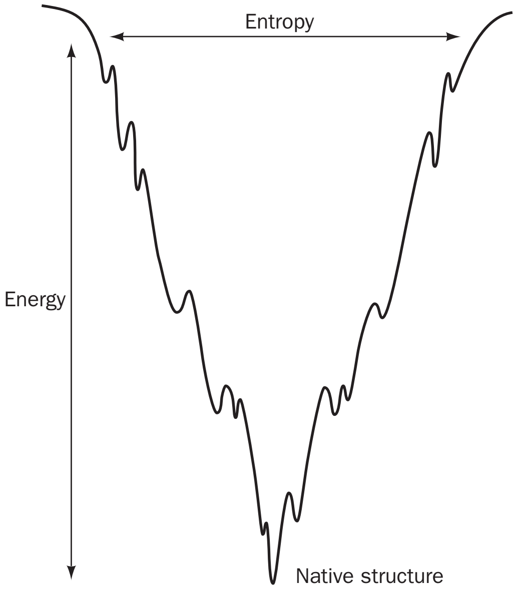

Figure 6-41 | Energy–entropy diagram for protein folding. The width of the diagram represents entropy, and the depth, the energy. The unfolded polypeptide proceeds from a high-entropy, disordered state (*wide*) to a single low-entropy (*narrow*), low-energy native conformation. [After Onuchic, J.N., Wolynes, P.G., Luthey-Schulten, Z., and Socci, N.D., *Proc. Natl. Acad. Sci.* **92,** 3626 (1995).]

relatively stable internal side chain packing and hydrogen bonding while it expels the remaining water molecules from its hydrophobic core.

In multidomain and multisubunit proteins, the respective units then assemble in a similar manner, with a few slight conformational adjustments required to produce the protein's native tertiary or quaternary structure. Thus, *proteins appear to fold in a hierarchical manner, with small local elements of structure forming and then coalescing to yield larger elements, which coalesce with other such elements to form yet larger elements, etc*.

Folding, like denaturation, appears to be a cooperative process, with small elements of structure accelerating the formation of additional structures. A folding protein must proceed from a high-energy, high-entropy state to a low-energy, low-entropy state. This energy–entropy relationship, which is diagrammed in Fig. 6-41, is known as a **folding funnel.** An unfolded polypeptide has many possible conformations (high entropy). As it folds into an ever-decreasing number of possible conformations, its entropy and free energy decrease. The energy–entropy diagram is not a smooth valley but a jagged landscape. Minor clefts and gullies represent conformations that are temporarily trapped until, through random thermal activation, they overcome a slight "uphill" free energy barrier and can then proceed to a lower energy conformation. Evidently, *proteins have evolved to have efficient folding pathways as well as stable native conformations*.

Understanding the process of protein folding as well as the forces that stabilize folded proteins is essential for elucidating the rules that govern the relationship between a protein's amino acid sequence and its three-dimensional structure. Such information will prove useful in predicting the structures of the hundreds of thousands of proteins that are known only from their sequences (Box 6-4).

BOX 6-4 **PERSPECTIVES IN BIOCHEMISTRY**

Protein Structure Prediction and Protein Design

Around one million protein sequences are known, yet the structures of only $\sim$50,000 of these proteins have been determined. Consequently, there is a need to develop robust techniques for predicting a protein's structure from its amino acid sequence. This represents a formidable challenge but promises great rewards in terms of understanding protein function, identifying diseases related to abnormal protein sequences, and designing drugs to alter protein structure or function.

There are several major approaches to protein structure prediction. The simplest and most reliable approach, **homology modeling,** aligns the sequence of interest with the sequence of a homologous protein or domain of known structure—compensating for amino acid substitutions, insertions, and deletions—through modeling and energy minimization calculations. This method yields reliable models for proteins that have as little as 25% sequence identity with a protein of known structure, although, of course, the accuracy of the model increases with the degree of sequence identity. The emerging field of **structural genomics,** which seeks to determine the X-ray structures of all representative domains, is aimed at expanding this predictive technique. The identification of structural homology is likely to provide clues as to a protein's function even with imperfect structure prediction.

Distantly related proteins may be structurally similar even though they have diverged to such an extent that their sequences show no obvious resemblance. **Threading** is a computational technique that attempts to determine the unknown structure of a protein by ascertaining whether it is consistent with a known protein structure. It does so by placing (threading) the unknown protein's residues along the backbone of a known protein structure and then determining whether the amino acid side chains of the unknown protein are stable in that arrangement. This method is not yet reliable, although it has yielded encouraging results.

Empirical methods based on experimentally determined statistical information such as the α helix and β sheet propensities deduced by Chou and Fasman (Table 6-1) have been moderately successful in predicting the secondary structures of proteins. Their main drawback is that neighboring residues in a polypeptide sometimes exert strong influence on a given residue's tendency to form a particular secondary structure.

Since the native structure of a protein ultimately depends on its amino acid sequence, it should be possible, in principle, to predict the structure of a protein based only on its chemical and physical properties (e.g., the hydrophobicity, size, hydrogen-bonding propensity, and charge of each of its amino acid residues). Such ***ab initio*** (from the beginning) methods are still only moderately successful in predicting the structures of small polypeptides.

Protein design, the experimental inverse of protein structure prediction, has provided insights into protein folding and stability. Protein design attempts to construct an amino acid sequence that will form a structure such as a sandwich of β sheets or a bundle of α helices. The designed polypeptide is then chemically or biologically synthesized, and its structure is determined. Experimental results suggest that the greatest challenge of protein design may lie not in getting the polypeptide to fold to the desired conformation but in preventing it from folding into other unwanted conformations. In this respect, science lags far behind nature.

The first wholly successful *de novo* (beginning anew) protein design, accomplished by Stephen Mayo, was for a 28-residue ββα motif that has a backbone conformation designed to resemble a zinc finger (Fig. 6-37) but that contains no stabilizing metal ions. A computational design process considered the interactions among side chain and backbone atoms, screened all possible amino acid sequences, and, in order to take into account side chain flexibility, tested all sets of energetically allowed torsion angles for each side chain. The number of amino acid sequences to be tested was limited to 1.9×10^{27}, representing 1.1×10^{62} possible conformations! The design process yielded an optimal sequence of 28 residues, which was chemically synthesized and its structure determined by NMR spectroscopy. The designed protein, called FSD-1, closely resembled its predicted structure, and its backbone conformation (blue) was nearly superimposable on that of a known zinc finger motif (red). Although FSD is relatively small, it folds into a unique stable structure, thereby demonstrating the power of protein design techniques.

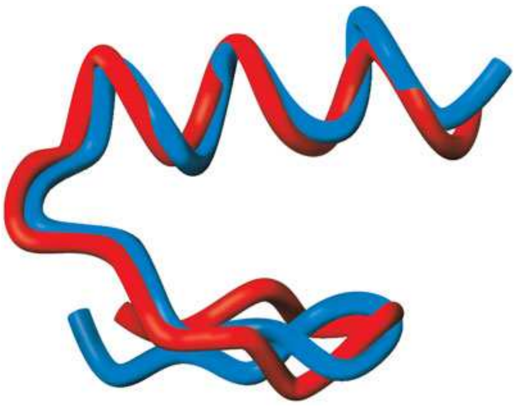

[Photo courtesy of Stephen Mayo, California Institute of Technology.]

Protein Disulfide Isomerase Acts During Protein Folding. Even under optimal experimental conditions, proteins often fold more slowly *in vitro* than they fold *in vivo*. One reason is that folding proteins often

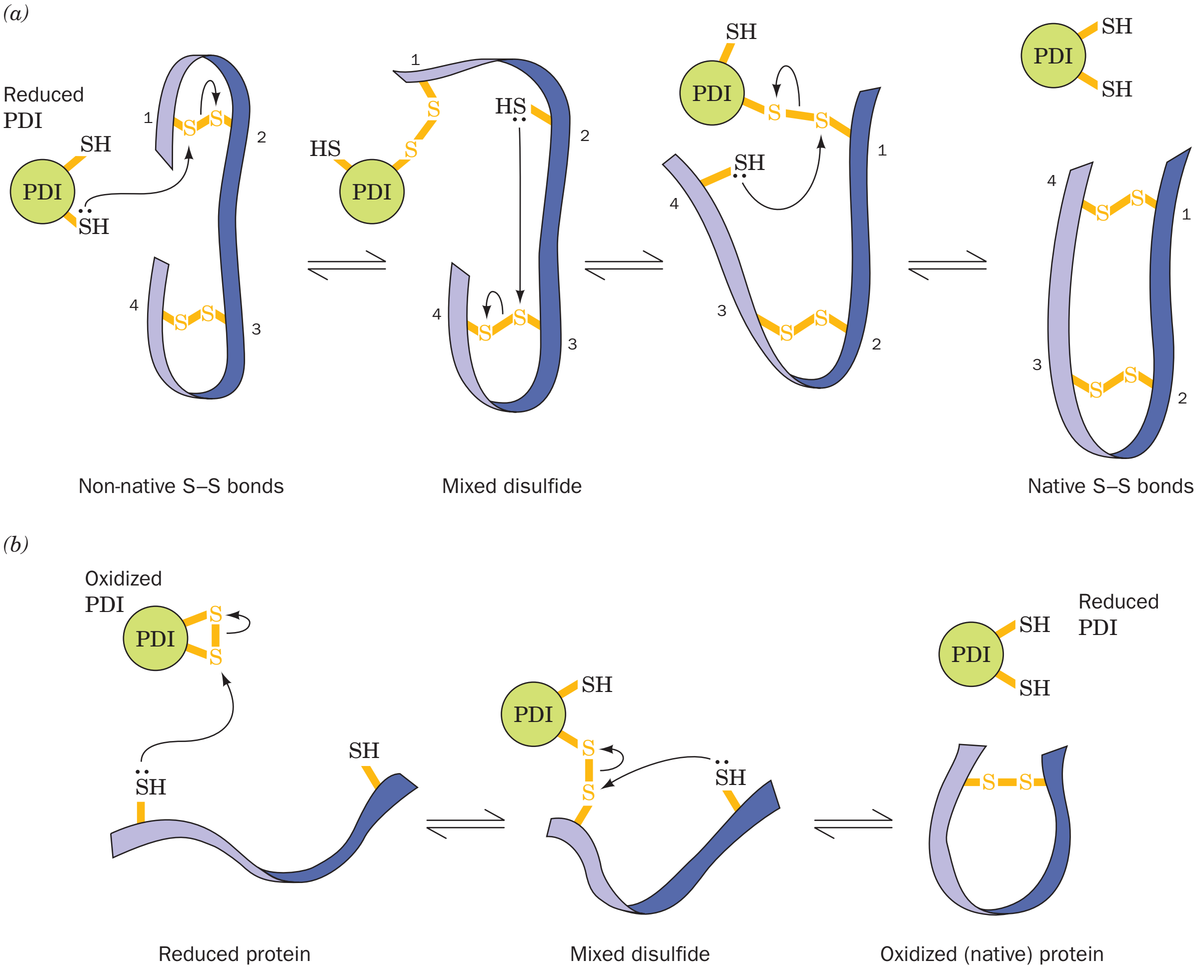
(a)
Reduced PDI
PDI
SH
SH
1
2
3
4
S
S
S
S
Non-native S–S bonds
HS
PDI
S
S
HS
1
2
3
4
S
S
Mixed disulfide
SH
PDI
S
S
SH
1
2
3
4
S
S
PDI
SH
SH
4
1
3
2
S
S
S
S
Native S–S bonds
(b)
Oxidized PDI
PDI
S
S
SH
SH
Reduced protein
PDI
SH
S
S
SH
Mixed disulfide
Reduced PDI
PDI
SH
SH
S
S
Oxidized (native) protein

Figure 6-42 | Mechanism of protein disulfide isomerase. (*a*) Reduced (SH-containing) PDI catalyzes the rearrangement of a polypeptide's non-native disulfide bonds via disulfide interchange reactions to yield native disulfide bonds. (*b*) Oxidized (disulfide-containing) PDI catalyzes the initial formation of a polypeptide's disulfide bonds through the formation of a mixed disulfide. Reduced PDI can then react with a cellular oxidizing agent to regenerate oxidized PDI. **See the Animated Figures.**

form disulfide bonds not present in the native proteins, and then slowly form native disulfide bonds through the process of disulfide interchange. **Protein disulfide isomerase (PDI)** catalyzes this process. Indeed, the observation that RNase A folds so much faster *in vivo* than *in vitro* led Anfinsen to discover this enzyme.

PDI binds to a wide variety of unfolded polypeptides via a hydrophobic patch on its surface. A Cys—SH group on reduced (SH-containing) PDI reacts with a disulfide group on the polypeptide to form a mixed disulfide and a Cys—SH group on the polypeptide (Fig. 6-42*a*). Another disulfide group on the polypeptide, brought into proximity by the spontaneous folding of the polypeptide, is attacked by this Cys—SH group. The newly liberated Cys—SH group then repeats this process with another disulfide bond, and so on, ultimately yielding the polypeptide containing only native disulfide bonds, along with regenerated PDI.

Oxidized (disulfide-containing) PDI also catalyzes the initial formation of a polypeptide's disulfide bonds by a similar mechanism (Fig. 6-42*b*). In this case, the reduced PDI reaction product must be reoxidized by cellular oxidizing agents in order to repeat the process.

B | Molecular Chaperones Assist Protein Folding

Proteins begin to fold as they are being synthesized, so the renaturation of a denatured protein *in vitro* may not entirely mimic the folding of a protein *in vivo*. In addition, proteins fold *in vivo* in the presence of extremely high concentrations of other proteins with which they can potentially interact. ***Molecular chaperones** are essential proteins that bind to unfolded and partially folded polypeptide chains to prevent the improper association of exposed hydrophobic segments that might lead to non-native folding as well as polypeptide aggregation and precipitation.* This is especially important for multidomain and multisubunit proteins, whose components must fold fully before they can properly associate with each other. Molecular chaperones also induce misfolded proteins to refold to their native conformations.

Many molecular chaperones were first described as **heat shock proteins (Hsp)** because their rate of synthesis is increased at elevated temperatures. Presumably, the additional chaperones are required to recover heat-denatured proteins or to prevent misfolding under conditions of environmental stress.

Chaperone Activity Requires ATP. There are several classes of molecular chaperones in both prokaryotes and eukaryotes, including (1) the **Hsp70** family of proteins, which function as monomers; (2) the **chaperonins,** which are large multisubunit proteins; (3) the **Hsp90** proteins, which are mainly involved with the folding of proteins involved with signal transduction such as **steroid receptors** (Section 28-3B); and (4) **trigger factor,** which associates with the ribosome to prevent the improper folding of polypeptides as they are being synthesized (Section 27-5A). All of these molecular chaperones operate by binding to an unfolded or aggregated polypeptide's solvent-exposed hydrophobic surface and subsequently releasing it, often repeatedly, in a manner that facilitates its proper folding. Molecular chaperones are **ATPases,** that is, enzymes that catalyze the hydrolysis of ATP (adenosine triphosphate) to ADP (adenosine diphosphate) and P_i (inorganic phosphate):

$$\text{ATP} + \text{H}_2\text{O} \rightarrow \text{ADP} + \text{P}_i$$

The favorable free energy change of ATP hydrolysis drives the chaperone's bind-and-release reaction cycle.

Hsp70 proteins are highly conserved 70-kD proteins in both prokaryotes and eukaryotes. An Hsp70 chaperone, which functions in association with the **cochaperone** protein **Hsp40,** appears to bind to a newly synthesized polypeptide as it emerges from the ribosome. The chaperone changes its shape so that it binds the polypeptide loosely or tightly depending on whether ATP is bound (before the hydrolysis reaction) or ADP is bound (after hydrolysis). The repeated binding and release of small hydrophobic regions on the new polypeptide may prevent its premature folding. Other chaperones apparently complete the job begun by the Hsp70 proteins. The Hsp70 proteins also function to unfold proteins in preparation for their transport through membranes (Section 9-4D) and to subsequently refold them.

The GroEL/ES Chaperonin Forms Closed Chambers in Which Proteins Fold. The chaperonins in *E. coli* consist of two types of subunits named **GroEL** and **GroES.** The X-ray structure of a GroEL–GroES–$(\text{ADP})_7$

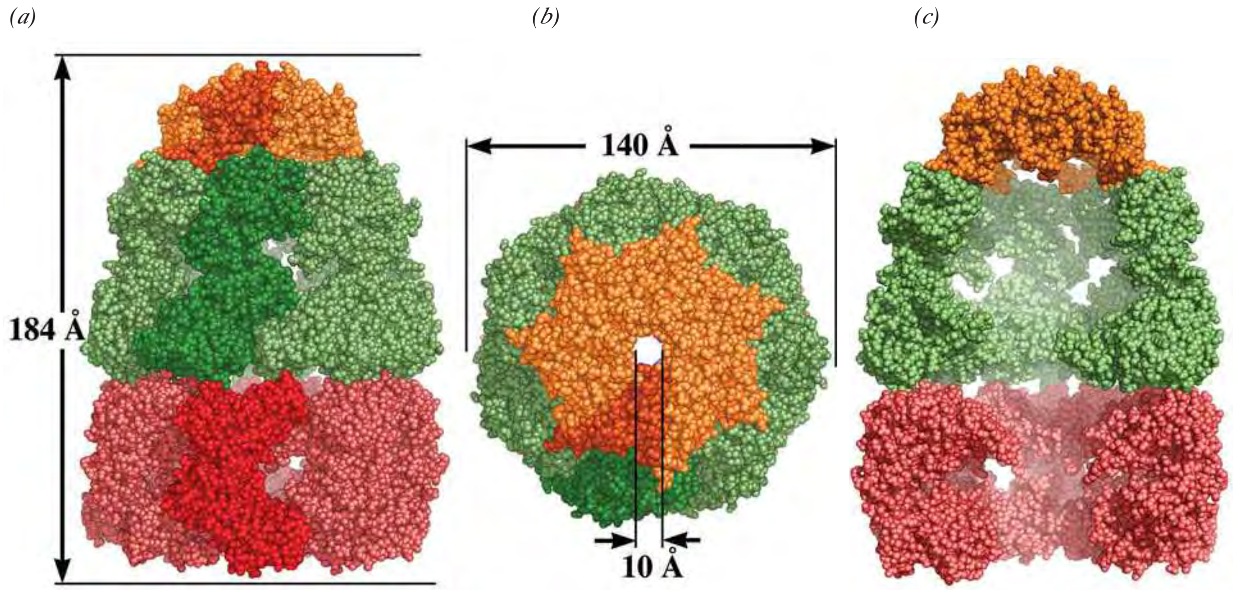

■ **Figure 6-43** | **X-Ray structure of the GroEL–GroES–(ADP)$_7$ complex.** (*a*) A space-filling drawing as viewed perpendicularly to the complex's sevenfold axis with the GroES ring orange, the cis ring of GroEL green, and the trans ring of GroEL red with one subunit of each ring shaded more brightly. The dimensions of the complex are indicated. Note the different conformations of the two GroEL rings. The ADPs, whose binding sites are in the base of each cis ring GroEL subunit, are not seen because they are surrounded by protein. (*b*) As in Part *a* but viewed along the sevenfold axis. (*c*) As in Part *a* but with the two GroEL subunits closest to the viewer in both the cis and trans rings removed to expose the interior of the complex. The level of fog increases with the distance from the viewer. Note the much larger size of the cavity formed by the cis ring and GroES in comparison to that of the trans ring. [Based on an X-ray structure by Paul Sigler, Yale University. PDBid 1AON.]

complex (Fig. 6-43), determined by Arthur Horwich and Paul Sigler, reveals fourteen identical 549-residue GroEL subunits arranged in two stacked rings of seven subunits each. This complex is capped at one end by a domelike heptameric ring of 97-residue GroES subunits to form a bullet-shaped complex with C_7 symmetry. The two GroEL rings each enclose a central chamber with a diameter of ~45 Å in which partially folded proteins fold to their native conformations. A barrier in the center of the complex (Fig. 6-43*c*) prevents a folding protein from passing between the two GroEL chambers. The GroEL ring that contacts the GroES heptamer is called the cis ring; the opposing GroEL ring is known as the trans ring.

ATP Binding and Hydrolysis Drive the Conformational Changes in GroEL/ES. Each GroEL subunit has a binding pocket for ATP that catalyzes the hydrolysis of its bound ATP to ADP + P_i. When the cis ring subunits hydrolyze their bound ATP molecules and release the product P_i, the protein undergoes a conformational change that widens and elongates the cis inner cavity so as to more than double its volume from 85,000 Å^3 to 175,000 Å^3. (In the structure shown in Fig. 6-43, the cis ring has already hydrolyzed its seven molecules of ATP to ADP.) The expanded cavity can enclose a partially folded substrate protein of at least 70 kD. *All seven subunits of the GroEL ring act in concert; that is, they are mechanically linked such that they change their conformations simultaneously*.

The cis and trans GroEL rings undergo conformational changes in a reciprocating fashion, with events in one ring influencing events in the other ring. The entire GroEL/ES chaperonin complex functions as follows (Fig. 6-44):

1. One GroEL ring that has bound 7 ATP also binds an improperly folded substrate protein, which associates with hydrophobic patches

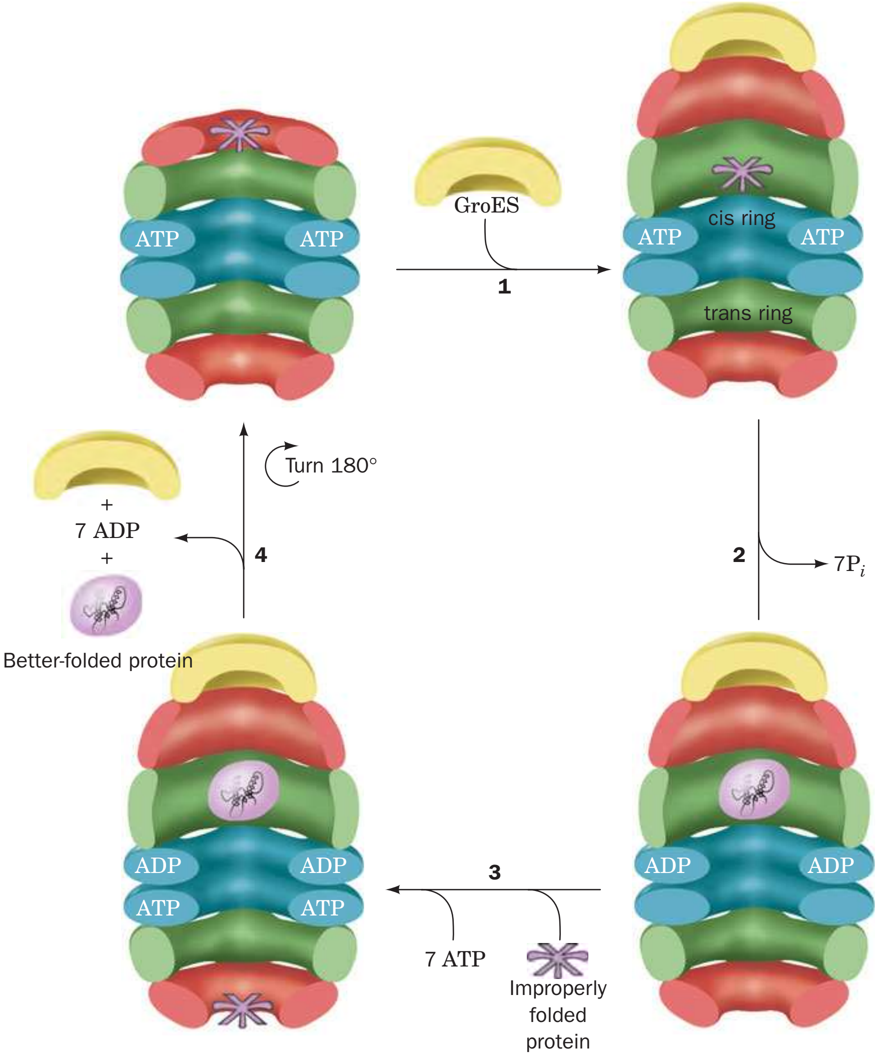

Figure 6-44 | Reaction cycle of the GroEL/ES chaperonin. The protein complex is drawn in cutaway form with the rings formed by each subunit's equatorial, intermediate, and apical domains colored blue, green, and red, respectively. See the text for an explanation.

that line the inner wall of the GroEL chamber. The GroES cap then binds to the GroEL ring like a lid on a pot, thereby inducing a conformational change in the resulting cis ring that buries the hydrophobic patches, thereby depriving the substrate protein of its binding sites. This releases the substrate protein into the now enlarged and closed cavity, where it commences folding. The cavity, which is now lined only with hydrophilic groups, provides the substrate protein with an isolated microenvironment that prevents it from nonspecifically aggregating with other misfolded proteins. Moreover, the conformational change that buries GroEL's hydrophobic patches stretches and thereby partially unfolds the improperly folded substrate protein before it is released. This rescues the substrate protein from a local energy minimum in which it had become trapped (Fig. 6-41) thereby permitting it to continue its conformational journey down the folding funnel toward its native state (the state of lowest free energy.

2. Within ~13 s (the time the substrate protein has to fold), the cis ring catalyzes the hydrolysis of its 7 bound ATPs to ADP + P_i and the P_i is released. The absence of ATP's γ phosphate group weakens the interactions that bind GroES to GroEL.
3. A second molecule of improperly folded substrate protein binds to the trans ring followed by 7 ATP. Conformational linkages between

the cis and trans rings prevent the binding of both substrate protein and ATP to the trans ring until the ATP in the cis ring has been hydrolyzed.

4. The binding of substrate protein and ATP to the trans ring conformationally induces the cis ring to release its bound GroES, 7 ADP, and the presumably now better-folded substrate protein. This leaves ATP and substrate protein bound only to the trans ring of GroEL, which now becomes the cis ring as it binds GroES.

Steps 1 through 4 are then repeated. The GroEL/ES system expends 7 ATPs per folding cycle. If the released substrate protein has not achieved its native state, it may subsequently rebind to GroEL (a substrate protein that has achieved its native fold lacks exposed hydrophobic groups and hence cannot rebind to GroEL). It requires an average of 24 folding cycles for a protein to attain its native state, which necessitates the hydrolysis of 168 ATPs (which appears to be a profligate use of ATP but constitutes only a small fraction of the thousands of ATPs that must be hydrolyzed to synthesize a typical polypeptide and its component amino acids). Because protein folding occurs alternately in the two GroEL rings, the proper functioning of the chaperonin requires both GroEL rings, even though their two cavities are unconnected.

Eukaryotic cells contain the chaperonin **TRiC,** with double rings of eight nonidentical subunits, each of which resembles a GroEL subunit. However, the TRiC proteins contain an additional segment that acts as a built-in lid, so the complex encloses a polypeptide chain and mediates protein folding without the assistance of a GroES-like cap. Like its bacterial counterpart, TRiC operates in an ATP-dependent fashion.

Experiments indicate that the GroEL/ES system interacts with only a subset of *E. coli* proteins, most with molecular masses in the range 20 to 60 kD. These proteins tend to contain two or more α/β domains that mainly consist of open β sheets. Such proteins are expected to fold only slowly to their native state because the formation of hydrophobic β sheets requires a large number of specific long-range interactions. Proteins dissociate from GroEL/ES after folding, but some frequently revisit the chaperonin, apparently because they are structurally labile or prone to aggregate and must return to GroEL for periodic maintenance.

C | Some Diseases Are Caused by Protein Misfolding

Most proteins in the body maintain their native conformations or, if they become partially denatured, are either renatured through the auspices of molecular chaperones or are proteolytically degraded (Section 21-1). However, at least 20 different—and usually fatal—human diseases are associated with the extracellular deposition of normally soluble proteins in certain tissues in the form of insoluble fibrous aggregates (Table 6-4). The aggregates are known as **amyloids,** a term that means starchlike because it was originally thought that the material resembled starch.

The diseases known as **amyloidoses** are a set of relatively rare inherited diseases in which mutant forms of normally occurring proteins [e.g., **lysozyme,** an enzyme that hydrolyzes bacterial cell walls (Section 11-4), and **fibrinogen,** a blood plasma protein that is the precursor of **fibrin,** which forms blood clots (Box 11-4)] accumulate in a variety of tissues as amyloids. The symptoms of amyloidoses usually do not become apparent until the third to seventh decade of life and typically progress over 5 to 15 years, ending in death.

Table 6-4 Some Protein Misfolding Diseases

Disease	Defective Protein
Alzheimer's disease	Amyloid-β protein
Amyotrophic lateral sclerosis	Superoxide dismutase
Huntington's disease	Huntingtin with polyglutamate expansion
Lysozyme amyloidosis	Lysozyme
Hereditary renal amyloidosis	Fibrinogen
Parkinson's disease	α-Synuclein
Transmissible spongiform encephalopathies (TSEs)	Prion protein

Amyloid-β Protein Accumulates in Alzheimer's Disease. **Alzheimer's disease,** a neurodegenerative condition that strikes mainly the elderly, causes devastating mental deterioration and eventual death (it affects ~10% of those over 65 and ~50% of those over 85). It is characterized by brain tissue containing abundant amyloid **plaques** (deposits) surrounded by dead and dying neurons (Fig. 6-45). The amyloid plaques consist mainly of fibrils of a 40- to 42-residue protein named **amyloid-β protein (Aβ).** Aβ is a fragment of a 770-residue membrane protein called the **Aβ precursor protein (βPP),** whose normal function is unknown. Aβ is excised from βPP in a multistep process through the actions of two proteolytic enzymes dubbed **β-** and **γ-secretases.** The neurotoxic effects of Aβ begin even before significant amyloid deposits appear (see below).

The age dependence of Alzheimer's disease suggests that Aβ deposition is an ongoing process. Indeed, several rare mutations in the βPP gene that increase the rate of Aβ production result in the onset of Alzheimer's disease as early as the fourth decade of life. A similar phenomenon occurs in individuals with **Down's syndrome,** a condition characterized by mental retardation and a distinctive physical appearance caused by the trisomy (3 copies per cell) of chromosome 21 rather than the normal two copies. These individuals invariably develop Alzheimer's disease by their 40th year because the gene encoding βPP is located on chromosome 21 and hence individuals with Down's syndrome produce βPP and presumably Aβ at an accelerated rate. Consequently, a promising strategy for halting the progression of Alzheimer's disease is to develop drugs that inhibit the action of the β- and/or γ-secretases so as to decrease the rate of Aβ production.

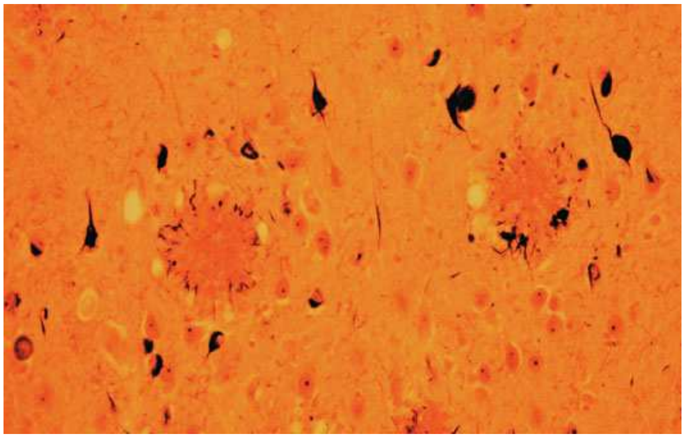

Figure 6-45 | Brain tissue from an individual with Alzheimer's disease. The two circular objects in this photomicrograph are plaques that consist of amyloid deposits of Aβ protein surrounded by a halo of neurites (axons and dendrites) from dead and dying neurons. [Courtesy of Dennis Selkoe and Marcia Podlisny, Harvard University Medical School.]

Prion Diseases Are Infectious. Certain diseases that affect the mammalian central nervous system were originally thought to be caused by "slow viruses" because they take months, years, or even decades to develop. Among them are **scrapie** (a neurological disorder of sheep and goats), **bovine spongiform encephalopathy (BSE** or **mad cow disease),** and **kuru** (a degenerative brain disease in humans that was transmitted by ritual cannibalism among the Fore people of Papua New Guinea; *kuru* means "trembling"). There is also a sporadic (spontaneously arising) human disease with similar symptoms, **Creutzfeldt–Jakob disease (CJD),** which strikes one person per million per year and which may be identical to kuru. In all of these invariably fatal diseases, neurons develop large vacuoles that give brain tissue a spongelike microscopic appearance. Hence the diseases are collectively known as **transmissible spongiform encephalopathies (TSEs).**

Unlike other infectious diseases, *the TSEs are not caused by a virus or microorganism.* Indeed, extensive investigations have failed to show that they are associated with any nucleic acid. Instead, as Stanley Pruisner demonstrated for scrapie, the infectious agent is a protein called a **prion** (for *pro*teinaceous *in*fectious particle that lacks nucleic acid) and hence TSEs are alternatively called **prion diseases.** The scrapie prion, which is named **PrP** (for *Pr*ion *P*rotein), consists of 208 mostly hydrophobic residues. This hydrophobicity causes partially proteolyzed PrP to aggregate as clusters of rodlike particles that closely resemble the amyloid fibrils seen on electron microscopic examination of prion-infected brain tissue (Fig. 6-46). These fibrils presumably form the amyloid plaques that accompany the neuronal degeneration in TSEs.

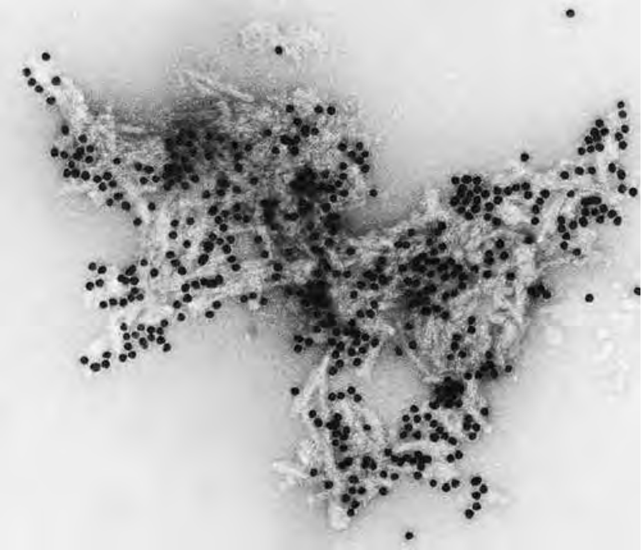

■ **Figure 6-46 | Electron micrograph of a cluster of partially proteolyzed prion rods.** The black dots are colloidal gold beads that are coupled to anti-PrP antibodies adhering to the PrP. [Courtesy of Stanley Pruisner, University of California at San Francisco Medical Center.]

How are prion diseases transmitted? PrP is the product of a normal cellular gene that has no known function (genetically engineered mice that fail to express PrP appear to be normal). Infection of cells by prions somehow alters the PrP protein. Various methods have demonstrated that the scrapie form of PrP (PrP^{Sc}) is identical to normal cellular PrP (PrP^{C}) in sequence but differs in secondary and/or tertiary structure. This suggests that *PrP^{Sc} induces PrP^{C} to adopt the conformation of PrP^{Sc}*, that is, a small amount of PrP^{Sc} triggers the formation of additional PrP^{Sc} from PrP^{C}, which triggers more PrP^{Sc} to form, and so on. This accounts for the observation that mice that do not express the gene encoding PrP cannot be infected with scrapie.

Human PrP^{C} consists of a disordered (and hence unseen) 99-residue N-terminal "tail" and a 110-residue C-terminal globular domain containing three α helices and a short two-stranded antiparallel β sheet (Fig. 6-47*a*). Unfortunately, the insolubility of PrP^{Sc} has precluded its structural

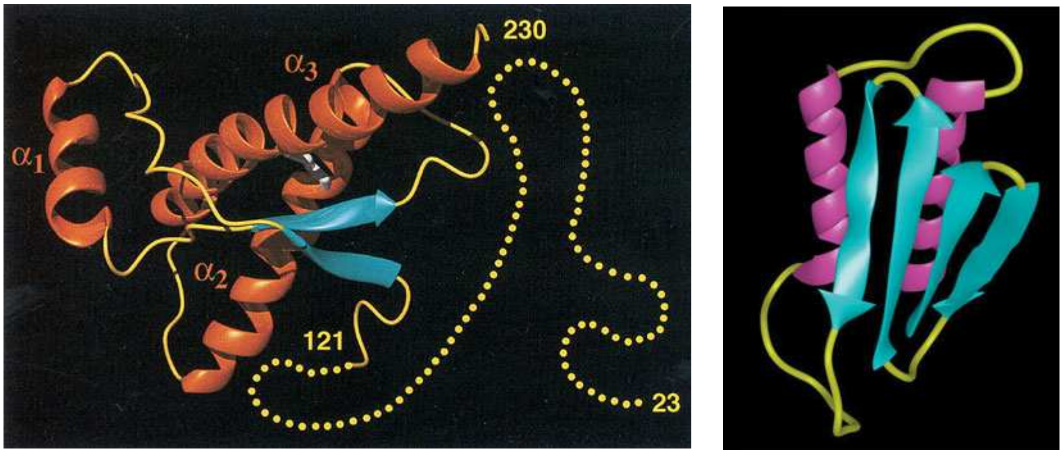

(*a*) (*b*)

■ **Figure 6-47 | Prion protein conformations.** (*a*) The NMR structure of human prion protein (PrP^{C}). Its flexibly disordered N-terminal "tail" (residues 23–121) is represented by yellow dots (the protein's N-terminal 22 residues have been posttranslationally excised). (*b*) A plausible model for the structure of PrP^{Sc}. [Part *a* courtesy of Kurt Wüthrich, Eidgenössische Technische Hochschule, Zurich, Switzerland. Part *b* courtesy of Fred Cohen University of California at San Francisco.]

determination, but spectroscopic methods indicate that it has a lower α helix content and a higher β sheet content than PrP^C. This suggests that the protein has refolded (Fig. 6-47*b*). The high β sheet content of PrP^{Sc} presumably facilitates the aggregation of PrP^{Sc} as amyloid fibrils (see below).

Prion diseases can be transmitted by the consumption of nerve tissue from infected individuals, as illustrated by the incidence of BSE. This disease was unknown before 1985 but reached epidemic proportions among cattle in the U.K. in 1993. The rise in BSE reflects the practice, beginning in the 1970s, of feeding cattle preparations of meat-and-bone meal that were derived from other animals by a method that failed to inactivate prions. The BSE epidemic abated due to the banning of such feeding in 1988, together with the slaughter of a large number of animals at risk for having BSE. However, it is now clear that BSE was transmitted to humans who ate meat from BSE-infected cattle: Some 160 cases of so-called **new variant CJD** have been reported to date, almost entirely in the U.K., many of which occurred in teenagers and young adults. Yet before 1994, CJD under the age of 40 was extremely rare. It should be noted that the transmission of BSE from cattle to humans was unexpected: Scrapie-infected sheep have long been consumed worldwide and yet the incidence of CJD in mainly meat-eating countries such as the U.K. (in which sheep are particularly abundant) was no greater than that in largely vegetarian countries such as India.

Amyloid Fibrils Are β Sheet Structures. The amyloid fibers that characterize the amyloidoses, Alzheimer's disease, and the TSEs are built from proteins that exhibit no structural or functional similarities in their native states. In contrast, the appearance of their fibrillar forms is strikingly similar. Spectroscopic analysis of amyloid fibrils indicates that they are rich in β structure, with individual β strands oriented perpendicular to the fiber axis (Fig. 6-48). Furthermore, the ability to form amyloid fibrils is not unique to the small set of proteins associated with specific diseases. Under the appropriate conditions, almost any protein can be induced to aggregate. Thus, *the ability to form amyloid may be an intrinsic property of all polypeptide chains*.

A variety of experiments indicate that amyloidogenic mutant proteins are significantly less stable than their wild-type counterparts (e.g., they have significantly lower melting temperatures). This suggests that the partially unfolded, aggregation-prone forms are in equilibrium with the native conformation even under conditions in which the native state is thermodynamically stable [keep in mind that the equilibrium ratio of unfolded (U) to native (N) protein molecules in the reaction $N \rightleftharpoons U$ is governed by Eq. 1-17: $K_{eq} = [U]/[N] = e^{-\Delta G^{\circ\prime}/RT}$, where $\Delta G^{\circ\prime}$ is the standard free energy of unfolding,

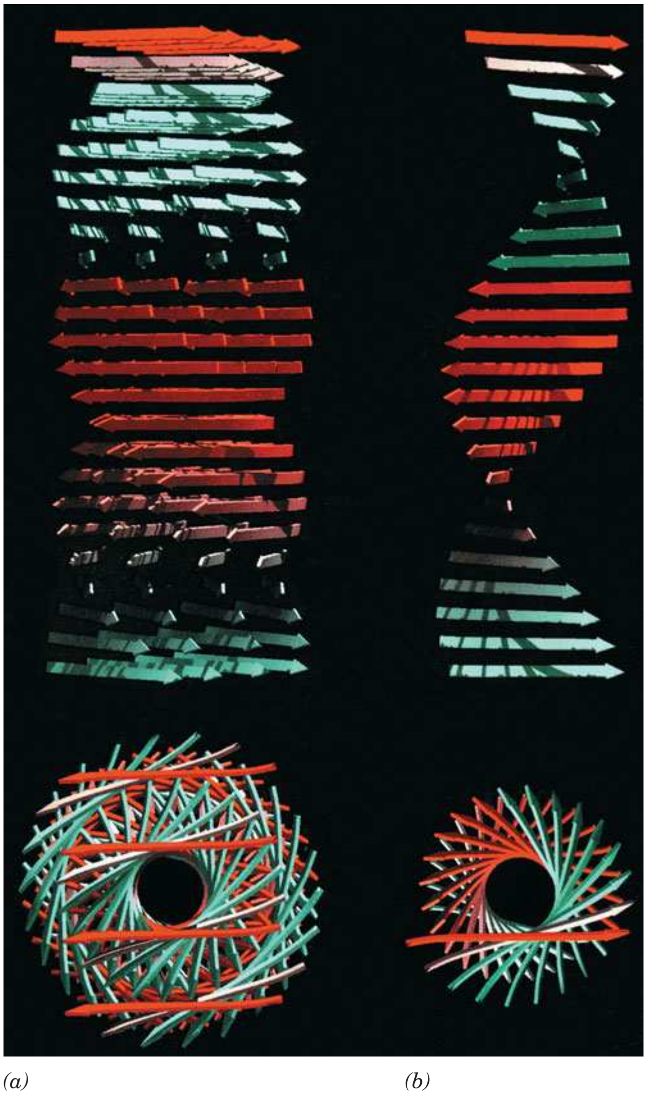
(a) *(b)*

■ **Figure 6-48 | Model of an amyloid fibril.** (*a*) The model, based on X-ray fiber diffraction measurements, is viewed normal to the fibril axis (*above*) and along the fibril axis (*below*). The arrowheads indicate the path but not necessarily the direction of the β strands. (*b*) A single β sheet, which is shown for clarity. The loop regions connecting the β strands have unknown structure. [Courtesy of Colin Blake, Oxford University, Oxford, U.K., and Louise Serpell, University of Cambridge, U.K.]

so that as $\Delta G^{\circ\prime}$ decreases, the equilibrium proportion of U increases]. It is therefore likely that fibril formation is initiated by the association of the β domains of two or more partially unfolded amyloidogenic proteins to form a more extensive β sheet. This would provide a template or nucleus for the recruitment of additional polypeptide chains to form the growing fibril. Since most amyloid diseases require several decades to become symptomatic, the development of an amyloid nucleus must be a rare event. Once an amyloid fiber begins to grow, however, its development is more rapid.

The factors that trigger amyloid formation remain obscure, even when mutations (in the case of hereditary amyloidoses) or infection (in the case of TSEs) appear to be the cause. After it has formed, an amyloid fibril is virtually indestructible under physiological conditions, possibly due to the large number of main-chain hydrogen bonds that must be broken in order to separate the individual polypeptide strands (side chain interactions are less important in stabilizing β sheets). It seems likely that protein folding pathways have evolved not only to allow polypeptides to assume stable native structures but also to avoid forming interchain hydrogen bonds that would lead to fibril formation.

Are fibrillar deposits directly responsible for the neurodegeneration seen in many amyloid diseases? A growing body of evidence suggests that cellular damage begins when the misfolded proteins first aggregate but are still soluble. For example, in mouse models of Alzheimer's disease, cognitive impairment is evident before amyloid plaques develop. Other experiments show that the most infectious prion preparations contain just 14–28 PrP^{Sc} molecules, that is, a nucleus for a fibril, not the fibril itself. Even a modest number of misfolded protein molecules could be toxic if they prevented the cell's chaperones from assisting other more critical proteins to fold. The appearance of extracellular—and sometimes intracellular—amyloid fibrils may simply represent the accumulation of protein that has overwhelmed the cellular mechanisms that govern protein folding or the disposal of misfolded proteins.

CHECK YOUR UNDERSTANDING

Describe the energy and entropy changes that occur during protein folding.

How does protein renaturation *in vitro* differ from protein folding *in vivo*?

Explain the role of ATP in the action of Hsp70 and GroEL/ES.

What are amyloid fibrils, what is their origin, and why are they harmful?

SUMMARY

1. Four levels of structural complexity are used to describe the three-dimensional shapes of proteins.
2. The conformational flexibility of the peptide group is described by its ϕ and ψ torsion angles.
3. The α helix is a regular secondary structure in which hydrogen bonds form between backbone groups four residues apart. In the β sheet, hydrogen bonds form between the backbones of separate polypeptide segments.
4. Fibrous proteins are characterized by a single type of secondary structure: α keratin is a left-handed coil of two α helices, and collagen is a left-handed triple helix with three residues per turn.
5. The structures of proteins have been determined mainly by X-ray crystallography and NMR spectroscopy.
6. The nonpolar side chains of a globular protein tend to occupy the protein's interior, whereas the polar side chains tend to define its surface.
7. Protein structures can be classified on the basis of motifs, secondary structure content, topology, or domain architecture. Structural elements are more likely to be evolutionarily conserved than are amino acid sequences.
8. The field of structural bioinformatics is concerned with the storage, visualization, analysis, and comparison of macromolecular structures.
9. The individual subunits of multisubunit proteins are usually symmetrically arranged.
10. Native protein structures are only slightly more stable than their denatured forms. The hydrophobic effect is the primary determinant of protein stability. Hydrogen bonding and ion pairing contribute relatively little to a protein's stability.
11. Studies of protein denaturation and renaturation indicate that the primary structure of a protein determines its three-dimensional structure.
12. Proteins fold to their native conformations via directed

pathways in which small elements of structure coalesce into larger structures.

13. Molecular chaperones facilitate protein folding *in vivo* by repeatedly binding and releasing a polypeptide in an ATP-dependent manner and providing it with an isolated microenvironment in which to fold.

14. Diseases caused by protein misfolding include the amyloidoses, Alzheimer's disease, and the transmissible spongiform encephalopathies (TSEs).

KEY TERMS

secondary structure	**126**
tertiary structure	**126**
quaternary structure	**126**
peptide group	**127**
trans conformation	**127**
cis conformation	**127**
backbone	**127**
torsion (dihedral) angle	**128**
ϕ	**128**
ψ	**128**
Ramachandran diagram	**129**
α helix	**129**
regular secondary structure	**129**
pitch	**131**
antiparallel β sheet	**132**
parallel β sheet	**132**
topology	**134**
reverse turn (β bend)	**134**
fibrous protein	**134**
globular protein	**134**
coiled coil	**135**
random coil	**139**
denaturation	**139**
native structure	**139**
β bulge	**139**
helix cap	**140**
X-ray crystallography	**141**
diffraction pattern	**141**
electron density	**141**
contour map	**141**
NMR	**143**
supersecondary structure (motif)	**146**
βαβ motif	**146**
β hairpin	**146**
αα motif	**146**
β barrel	**148**
α/β barrel	**148**
domain	**149**
dinucleotide-binding (Rossmann) fold	**150**
structural bioinformatics	**151**
oligomer	**154**
protomer	**154**
rotational symmetry	**155**
cyclic symmetry	**155**
dihedral symmetry	**155**
hydropathy	**156**
ion pair (salt bridge)	**157**
zinc finger	**158**
breathing	**158**
cooperativity	**158**
chaotropic agent	**159**
renaturation	**160**
hydrophobic collapse	**161**
molten globule	**161**
homology modeling	**163**
threading	**163**
ab initio	**163**
molecular chaperone	**165**
heat shock protein	**165**
chaperonin	**165**
ATPase	**165**
amyloid	**168**
Alzheimer's disease	**169**
transmissible spongiform encephalopathies (TSEs)	**169**
Creutzfeldt–Jakob disease	**169**
prion	**170**

PROBLEMS

1. Draw a cis peptide bond and identify the groups that experience steric interference.

2. Helices can be described by the notation n_m, where n is the number of residues per helical turn and m is the number of atoms, including H, in the ring that is closed by the hydrogen bond. (a) What is this notation for the α helix? (b) Is the 3_{10} helix steeper or shallower than the α helix?

3. Calculate the length in angstroms of a 100-residue segment of the α keratin coiled coil.

4. Hydrophobic residues usually appear at the first and fourth positions in the seven-residue repeats of polypeptides that form coiled coils. (a) Why do polar or charged residues usually appear in the remaining five positions? (b) Why is the sequence Ile–Gln–Glu–Val–Glu–Arg–Asp more likely than the sequence Trp–Gln–Glu–Tyr–Glu–Arg–Asp to appear in a coiled coil?

5. Globular proteins are typically constructed from several layers of secondary structure, with a hydrophobic core and a hydrophilic surface. Is this true for a fibrous protein such as α keratin?

6. The digestive tract of the larvae of clothes moths is a strongly reducing environment. Why is this beneficial to the larvae?

7. Describe the primary, secondary, tertiary, and quaternary structures of collagen.

8. Explain why gelatin, which is mostly collagen, is nutritionally inferior to other types of protein.

9. Is it possible for a native protein to be entirely irregular, that is, without α helices, β sheets, or other repetitive secondary structure?

10. (a) Is Trp or Gln more likely to be on a protein's surface? (b) Is Ser or Val less likely to be in the protein's interior? (c) Is Leu or Ile less likely to be found in the middle of an α helix? (d) Is Cys or Ser more likely to be in a β sheet?

11. What types of rotational symmetry are possible for a protein with (a) four or (b) six identical subunits?

12. You are performing site-directed mutagenesis to test predictions about which residues are essential for a protein's function. Which of each pair of amino acid substitutions listed below would you expect to disrupt protein structure the most? Explain.
    (a) Val replaced by Ala or Phe.
    (b) Lys replaced by Asp or Arg.
    (c) Gln replaced by Glu or Asn.
    (d) Pro replaced by His or Gly.

13. Laboratory techniques for randomly linking together amino acids typically generate an insoluble polypeptide, yet a naturally occurring polypeptide of the same length is usually soluble. Explain.
14. Given enough time, can all denatured proteins spontaneously renature?
15. Describe the intra- and intermolecular bonds or interactions that are broken or retained when collagen is heated to produce gelatin.
16. Under physiological conditions, polylysine assumes a random coil conformation. Under what conditions might it form an α helix?
17. It is often stated that proteins are quite large compared to the molecules they bind. However, what constitutes a large number depends on your point of view. Calculate the ratio of the volume of a hemoglobin molecule (65 kD) to that of the four O_2 molecules that it binds and the ratio of the volume of a typical office (4 × 4 × 3 m) to that of the typical (70-kg) office worker that occupies it. Assume that the molecular volumes of hemoglobin and O_2 are in equal proportions to their molecular masses and that the office worker has a density of 1.0 g/cm^3. Compare these ratios. Is this the result you expected?
18. Which of the following polypeptides is most likely to form an α helix? Which is least likely to form a β strand?
    (a) CRAGNRKIVLETY
    (b) SEDNFGAPKSILW
    (c) QKASVEMAVRNSG
19. The X-ray crystallographic analysis of a protein often fails to reveal the positions of the first few and/or the last few residues of a polypeptide chain. Explain.

CASE STUDIES

Case 4 (available at www.wiley.com/college/voet)
The Structure of Insulin

Focus concept: The primary structure of insulin is examined, and the sequences of various animal insulins are compared.

Prerequisites: Chapters 4, 5, and 6

- Amino acid structure
- Protein architecture
- Basic immunology

Case 5
Characterization of Subtilisin from the Antarctic Psychrophile* Bacillus *TA41

Focus concept: The structural features involved in protein adaptation to cold temperatures are explored.

Prerequisite: Chapter 6

- Protein architecture
- Principles of protein folding

Case 6
A Collection of Collagen Cases

Focus concept: Factors important in the stability of collagen are examined.

Prerequisites: Chapters 4, 5, and 6

- Amino acid structures and properties
- Primary and secondary structure
- Basic collagen structure

BIOINFORMATICS EXERCISES

Bioinformatics Exercises are available at www.wiley.com/college/voet.

Chapter 6
Visualizing Three-Dimensional Protein Structures

1. **Obtaining Structural Information.** Compare different secondary structure predictions for a given protein sequence, then inspect its X-ray crystallographic structure.
2. **Exploring the Protein Data Bank.** Learn how to locate and download specific protein structure files, sequences, and images. Explore additional educational resources such as Molecule of the Month and links to additional structural biology resources.
3. **Using RasMmol and PyMol.** Examine a protein structure file and use basic molecular modeling programs to visualize the protein and highlight selected features.
4. **Protein Families.** Identify homologous proteins in other structural databases.

REFERENCES

General

Bourne, P.E. and Weissig, H. (Eds.), *Structural Bioinformatics,* Wiley-Liss (2003).

Branden, C. and Tooze, J., *Introduction to Protein Structure* (2nd ed.), Garland Publishing (1999). [A well-illustrated book with chapters introducing amino acids and protein structure, plus chapters on specific proteins categorized by their structure and function.]

Goodsell, D.S., Visual methods from atoms to cells, *Structure* **13,** 347–454 (2005). [Discusses several ways of depicting different features of molecular structures.]

Goodsell, D.S. and Olson, J., Structural symmetry and protein function, *Annu. Rev. Biophys. Biomol. Struct.* **29,** 105–153 (2000).

Lesk, A.M., *Introduction to Protein Science,* Oxford University Press (2004).

Petsko, G.A. and Ringe, D., *Protein Structure and Function,* New Science Press (2004).

Fibrous Proteins

Brodsky, B. and Persikov, A.V., Molecular structure of the collagen triple helix, *Adv. Protein Chem.* **70,** 301–339 (2005).

Macromolecular Structure Determination

McPherson, A., *Macromolecular Crystallography,* Wiley (2002).

Rhodes, G., *Crystallography Made Crystal Clear: A Guide for Users of Macromolecular Models* (3rd ed.), Academic Press (2006). [Includes overviews, methods, and discussions of model quality.]

Wider, G. and Wüthrich, K., NMR spectroscopy of large molecules and multimolecular assemblies in solution, *Curr. Opin. Struct. Biol*. **9,** 594–601 (1999).

Protein Stability

Fersht, A., *Structure and Mechanism in Protein Science,* Chapter 11, Freeman (1999).

Karplus, M. and McCammon, J.A., Molecular dynamics simulations of biomolecules, *Nature Struct. Biol.* **9,** 646–652 (2002).

Protein Folding

Fitzkee, N.C., Fleming, P.J., Gong, H., Panasik, N., Jr., Street, T.O., and Rose, G.D., Are proteins made from a limited parts list? *Trends Biochem. Sci.* **30,** 73–80 (2005).

Onuchic, J.N. and Wolynes, P.G., Theory of protein folding, *Curr. Opin. Struct. Biol.* **14,** 70–75 (2004).

Schueler-Furman, O., Wang, C., Bradley, P., Misura, K., and Baker, D., Progress in modeling of protein structures and interactions, *Science* **310,** 638–642 (2005).

Young, J.C., Agashe, V.R., Siegers, K., and Hartl, F.U., Pathways of chaperone-mediated protein folding in the cytosol, *Nature Reviews Mol. Cell Biol.* **5,** 781–791 (2004). [Summarizes the types and activities of chaperones that function in prokaryotes and eukaryotes.]

Protein Misfolding Diseases

Dobson, C.M., Protein folding and misfolding, *Nature* **426,** 884–890 (2003).

Selkoe, D.J., Cell biology of protein misfolding: the examples of Alzheimer's and Parkinson's diseases, *Nature Cell Biol.* **6,** 1054–1061 (2004). [Describes the relationship between protein misfolding and cellular pathology.]

Weissmann, C., The state of the prion, *Nature Reviews Microbiol.* **2,** 861–862 (2004).

7

Protein Function: Myoglobin and Hemoglobin, Muscle Contraction, and Antibodies

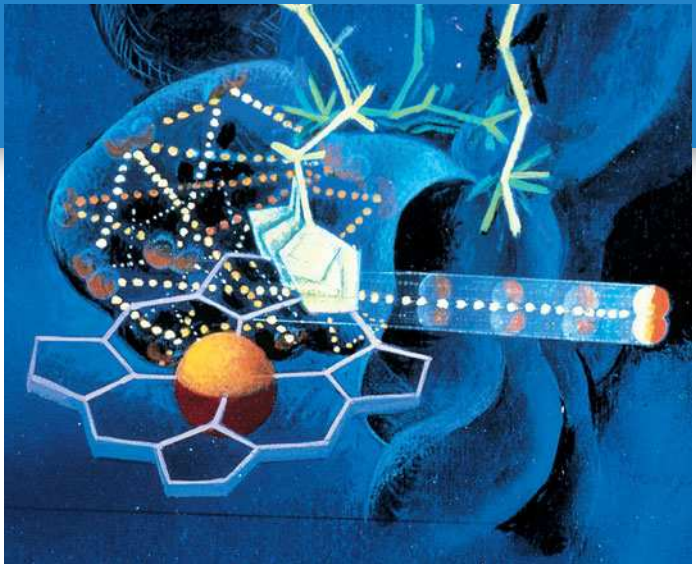

The structure of a protein determines its biological role. The oxygen-binding site of myoglobin is structured so that O_2 can bind or, as pictured here, escape from the protein. [Illustration, Irving Geis. Image from the Irving Geis Collection/Howard Hughes Medical Institute. Rights owned by HHMI. Reproduction by permission only.]

■ CHAPTER CONTENTS

1 Oxygen Binding to Myoglobin and Hemoglobin
  - **A.** Myoglobin Is a Monomeric Oxygen-Binding Protein
  - **B.** Hemoglobin Is a Tetramer with Two Conformations
  - **C.** Oxygen Binds Cooperatively to Hemoglobin
  - **D.** Hemoglobin's Two Conformations Exhibit Different Affinities for Oxygen
  - **E.** Mutations May Alter Hemoglobin's Structure and Function

2 Muscle Contraction
  - **A.** Muscle Consists of Interdigitated Thick and Thin Filaments
  - **B.** Muscle Contraction Occurs When Myosin Heads Walk Up Thin Filaments
  - **C.** Actin Forms Microfilaments in Nonmuscle Cells

3 Antibodies
  - **A.** Antibodies Have Constant and Variable Regions
  - **B.** Antibodies Recognize a Huge Variety of Antigens

■ MEDIA RESOURCES

(available at www.wiley.com/college/voet)
Interactive Exercise 3. Structure of a mouse antibody
Animated Figure 7-6. Oxygen-binding curve of hemoglobin
Animated Figure 7-8. Movements of heme and F helix in hemoglobin
Animated Figure 7-11. The Bohr effect
Animated Figure 7-13. Effect of BPG and CO_2 on hemoglobin
Animated Figure 7-32. Mechanism of force generation in muscle
Kinemage 6-1. Myoglobin structure
Kinemage 6-2, 6-3. Hemoglobin structure
Kinemage 6-3. BPG binding to hemoglobin
Kinemage 6-4. Conformational changes in hemoglobin
Kinemage 6-5. Changes at α_1–β_2/α_2–β_1 interfaces in hemoglobin
Case Study 8. Hemoglobin, the Oxygen Carrier
Case Study 9. Allosteric Interactions in Crocodile Hemoglobin
Case Study 10. The Biological Roles of Nitric Oxide

The preceding two chapters have painted a broad picture of the chemical and physical properties of proteins but have not delved deeply into their physiological functions. Nevertheless, it should come as no surprise that the structural complexity and variety of proteins allow them to carry out an enormous array of specialized biological tasks. For example, the enzyme catalysts of virtually all metabolic reactions are proteins (we consider enzymes in detail in Chapters 11 and 12). Genetic information would remain locked in DNA were it not for the proteins that participate in decoding and transmitting that information. Remarkably, the thousands of proteins that participate in building, supporting, recognizing, transporting, and transforming cellular components act with incredible speed and accuracy and in many cases are subject to multiple regulatory mechanisms.

The specialized functions of proteins, from the fibrous proteins we examined in Section 6-1C to the precisely regulated metabolic enzymes we discuss in later chapters, can all be understood in terms of how proteins bind to and interact with other components of living systems. In this chapter, we focus on three sets of proteins: the oxygen-binding proteins myoglobin and hemoglobin, the actin and myosin proteins responsible for muscle contraction, and antibody molecules. The molecular structures and physiological roles of these proteins are known in detail, and their proper functioning is vital for human health. In addition, these proteins serve as models for many of the proteins we will examine later when we discuss metabolism and the management of genetic information.

1 Oxygen Binding to Myoglobin and Hemoglobin

We begin our study of protein function with two proteins that reversibly bind molecular oxygen (O_2). **Myoglobin,** the first protein whose structure was determined by X-ray crystallography, is a small protein with relatively simple oxygen-binding behavior. **Hemoglobin,** a tetramer of myoglobin-like polypeptides, is a more complicated protein that functions as a sophisticated system for delivering oxygen to tissues throughout the body. The efficiency with which hemoglobin binds and releases O_2 is reminiscent of the specificity and efficiency of metabolic enzymes. It is worthwhile to study hemoglobin's structure and function because many of the theories formulated to explain O_2 binding to hemoglobin also explain the control of enzyme activity.

A | Myoglobin Is a Monomeric Oxygen-Binding Protein

Myoglobin is a small intracellular protein in vertebrate muscle. Its X-ray structure, determined by John Kendrew in 1959, revealed that most of myoglobin's 153 residues are members of eight α helices (traditionally labeled A through H) that are arranged to form a globular protein with approximate dimensions 44 × 44 × 25 Å (Fig. 7-1).

LEARNING OBJECTIVES

- Understand that myoglobin, with its single heme prosthetic group, exhibits a hyperbolic O_2-binding curve.
- Understand that hemoglobin can adopt the deoxy (T) or oxy (R) conformation, which differ in their O_2-binding affinity.
- Understand that oxygen binding triggers conformational changes in hemoglobin so that oxygen binds to the protein cooperatively, yielding a sigmoidal binding curve.
- Understand how the Bohr effect and BPG alter oxygen binding and transport by hemoglobin *in vivo*.
- Understand that amino acid mutations in hemoglobin can alter oxygen binding and cause disease.

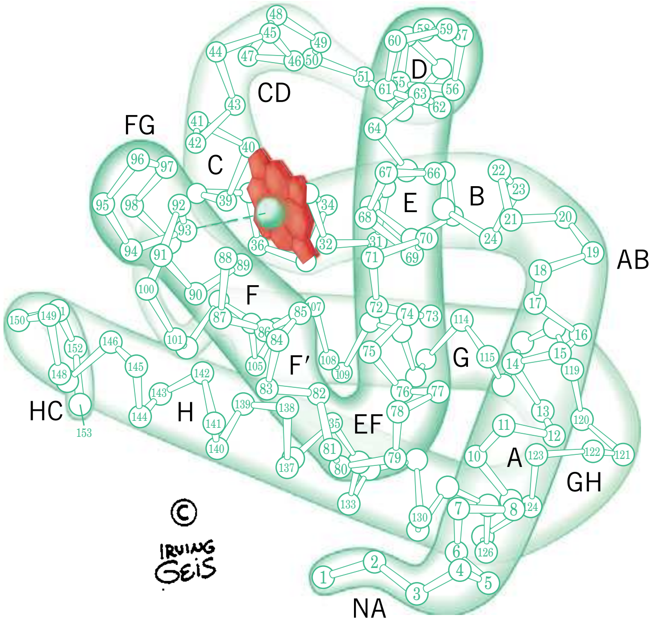

Figure 7-1 | Structure of sperm whale myoglobin. This 153-residue monomeric protein consists of eight α helices, labeled A through H, that are connected by short polypeptide links (the last half of what was originally thought to be the EF corner has been shown to form a short helix that is designated the F′ helix). The heme group is shown in red. [Illustration, Irving Geis. Image from the Irving Geis Collection/Howard Hughes Medical Institute. Rights owned by HHMI. Reproduction by permission only.] **See Kinemage Exercise 6-1.**

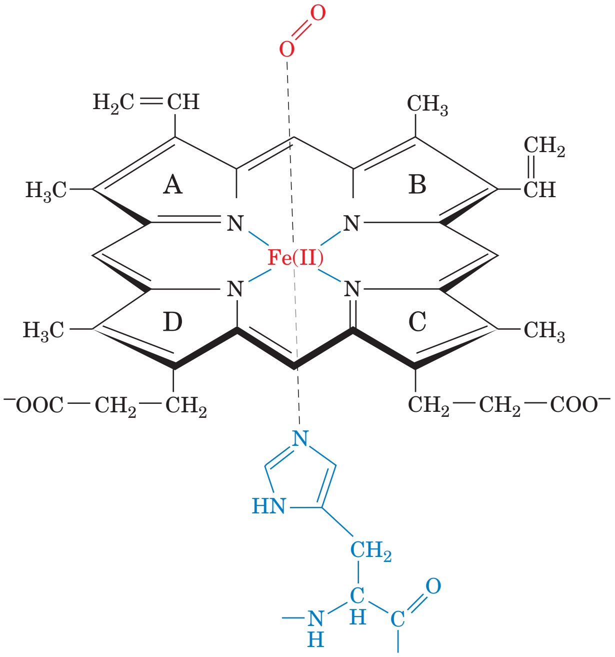

Figure 7-2 | The heme group. The central Fe(II) atom is shown liganded to four N atoms of the porphyrin ring, whose pyrrole groups are labeled A–D. The heme is a conjugated system, so all the Fe—N bonds are equivalent. The Fe(II) is also liganded to a His side chain and, when it is present, to O_2. The six ligands are arranged at the corners of an octahedron centered on the Fe ion (octahedral geometry).

Myoglobin Contains a Heme Prosthetic Group. Myoglobin, other members of the globin family of proteins (Section 5-4B), and a variety of other proteins such as cytochrome *c* (Sections 5-4A and 6-2D) all contain a single **heme** group (Fig. 7-2). The heme is tightly wedged in a hydrophobic pocket between the E and F helices in myoglobin. The heterocyclic ring system of heme is a **porphyrin** derivative containing four **pyrrole** groups (labeled A–D) linked by methene bridges (other porphyrins vary in the substituents attached to rings A–D). The Fe(II) atom at the center of heme is coordinated by the four porphyrin N atoms and one N from a His side chain (called, in a nomenclature peculiar to myoglobin and hemoglobin, His F8 because it is the eighth residue of the F helix). A molecule of oxygen (O_2) can act as a sixth ligand to the iron atom. His E7 (the seventh residue of helix E) hydrogen bonds to the O_2 with the geometry shown in Fig. 7-3. Two hydrophobic side chains on the O_2-binding side of the heme, Val E11 and Phe CD1 (the first residue in the segment between helices C and D), help hold the heme in place. These side chains presumably swing aside as the protein "breathes" (Section 6-4A), allowing O_2 to enter and exit.

When exposed to oxygen, the Fe(II) atom of isolated heme is irreversibly oxidized to Fe(III), a form that cannot bind O_2. The protein portion of myoglobin (and of hemoglobin, which contains four heme groups in four globin chains) prevents this oxidation and makes it possible for O_2 to bind reversibly to the heme group. **Oxygenation** alters the electronic

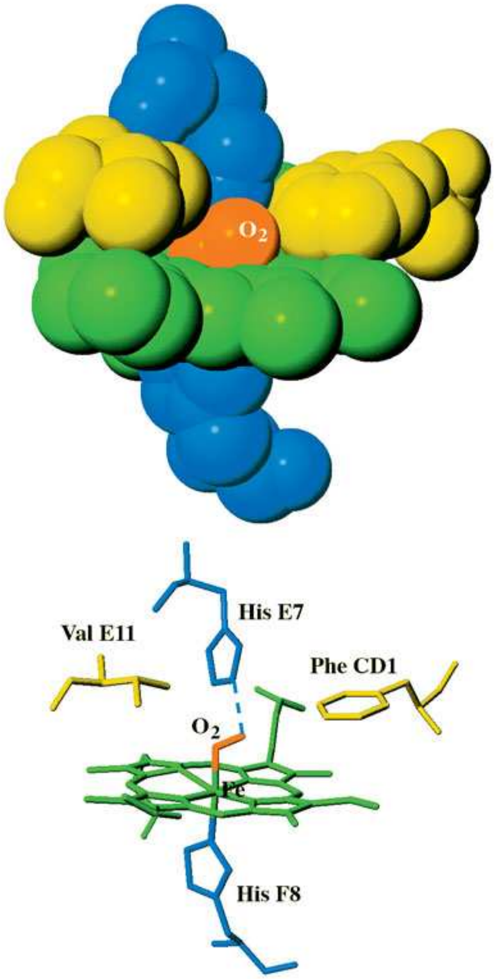

Figure 7-3 | The heme complex in myoglobin. In the upper drawing, atoms are represented in space-filling form (H atoms are not shown). The lower drawing shows the corresponding skeletal model with a dashed line representing the hydrogen bond between His E7 and the bound O_2. [Based on an X-ray structure by Simon Phillips, MRC Laboratory of Molecular Biology, Cambridge, U.K. PDBid 1MBO.]
See Kinemage Exercise 6-1.

state of the Fe(II)–heme complex, as indicated by its color change from dark purple (the color of hemoglobin in venous blood) to brilliant scarlet (the color of hemoglobin in arterial blood). Under some conditions, the Fe(II) of myoglobin or hemoglobin becomes oxidized to Fe(III) to form **metmyoglobin** or **methemoglobin,** respectively; these proteins are responsible for the brown color of old meat and dried blood.

In addition to O_2, certain other small molecules such as CO, NO, and H_2S can bind to heme groups in proteins. These other compounds bind with much higher affinity than O_2, which accounts for their toxicity. CO, for example, has 200-fold greater affinity for hemoglobin than does O_2.

Myoglobin Binds O_2 to Facilitate Its Diffusion. Although myoglobin was originally thought to be only an oxygen-storage protein, it is now apparent that *its major physiological role is to facilitate oxygen diffusion in muscle* (the most rapidly respiring tissue under conditions of high exertion). The rate at which O_2 can diffuse from the capillaries to the tissues is limited by its low solubility in aqueous solution ($\sim 10^{-4}$ M in blood). Myoglobin increases the effective solubility of O_2 in muscle cells, acting as a kind of molecular bucket brigade to boost the O_2 diffusion rate. The oxygen-storage function of myoglobin is probably significant only in aquatic mammals such as seals and whales, whose muscle myoglobin concentrations are around 10-fold greater than those in terrestrial mammals (which is one reason why Kendrew chose the sperm whale as a source of myoglobin for his X-ray crystallographic studies). Nevertheless, mice in which the gene for myoglobin has been "knocked out" are apparently normal, although their muscles are lighter in color than those of wild-type mice. This experiment suggests that myoglobin is not required by muscles under normal metabolic conditions. In contrast, a recently discovered myoglobin-like protein in the brain, dubbed **neuroglobin,** may be essential for boosting O_2 concentrations in neural tissues, which are metabolically highly active. For example, the brain constitutes only about 2% of the mass of a human body, but it consumes about 20% of the available oxygen.

Myoglobin's Oxygen-Binding Curve Is Hyperbolic. The reversible binding of O_2 to myoglobin **(Mb)** is described by a simple equilibrium reaction:

$$\text{Mb} + \text{O}_2 \rightleftharpoons \text{MbO}_2$$

The dissociation constant, K, for the reaction is

$$K = \frac{[\text{Mb}][\text{O}_2]}{[\text{MbO}_2]} \qquad [7\text{-}1]$$

Note that biochemists usually express equilibria in terms of dissociation constants, the reciprocal of the association constants favored by chemists. The O_2 dissociation of myoglobin can be characterized by its **fractional saturation, Y_{O_2},** which is defined as the fraction of O_2-binding sites occupied by O_2:

$$Y_{O_2} = \frac{[\text{MbO}_2]}{[\text{Mb}] + [\text{MbO}_2]} \qquad [7\text{-}2]$$

Y_{O_2} ranges from zero (when no O_2 is bound to the myoglobin molecules) to one (when the binding sites of all the myoglobin molecules are occupied). Equation 7-1 can be rearranged to

$$[\text{MbO}_2] = \frac{[\text{Mb}][\text{O}_2]}{K} \qquad [7\text{-}3]$$

When this expression for $[\mathrm{MbO_2}]$ is substituted into Eq. 7-2, the fractional saturation becomes

$$Y_{\mathrm{O_2}} = \frac{\dfrac{[\mathrm{Mb}][\mathrm{O_2}]}{K}}{[\mathrm{Mb}] + \dfrac{[\mathrm{Mb}][\mathrm{O_2}]}{K}} \qquad [7\text{-}4]$$

Factoring out the $[\mathrm{Mb}]/K$ term in the numerator and denominator gives

$$Y_{\mathrm{O_2}} = \frac{[\mathrm{O_2}]}{K + [\mathrm{O_2}]} \qquad [7\text{-}5]$$

Since O_2 is a gas, its concentration is conveniently expressed by its **partial pressure, $p\mathrm{O_2}$** (also called the oxygen tension). Equation 7-5 can therefore be expressed as

$$Y_{\mathrm{O_2}} = \frac{p\mathrm{O_2}}{K + p\mathrm{O_2}} \qquad [7\text{-}6]$$

This equation describes a rectangular ***hyperbola*** *and is identical in form to the equations that describe a hormone binding to its cell-surface receptor or a small molecular substrate binding to the active site of an enzyme.* This hyperbolic function can be represented graphically as shown in Fig. 7-4. At low $p\mathrm{O_2}$, very little O_2 binds to myoglobin ($Y_{\mathrm{O_2}}$ is very small). As the $p\mathrm{O_2}$ increases, more O_2 binds to myoglobin. At very high $p\mathrm{O_2}$, virtually all the O_2-binding sites are occupied and myoglobin is said to be **saturated** with O_2.

The steepness of the hyperbola for a simple binding event, such as O_2 binding to myoglobin, increases as the value of K decreases. This means that *the lower the value of K, the tighter is the binding.* K is equivalent to the concentration of ligand at which half of the binding sites are occupied. In other words, when $p\mathrm{O_2} = K$, myoglobin is half-saturated with oxygen. This can be shown algebraically by substituting $p\mathrm{O_2}$ for K in Eq. 7-6:

$$Y_{\mathrm{O_2}} = \frac{p\mathrm{O_2}}{K + p\mathrm{O_2}} = \frac{p\mathrm{O_2}}{2p\mathrm{O_2}} = 0.5 \qquad [7\text{-}7]$$

Thus, K can be operationally defined as the value of $p\mathrm{O_2}$ at which $Y = 0.5$ (Fig. 7-4).

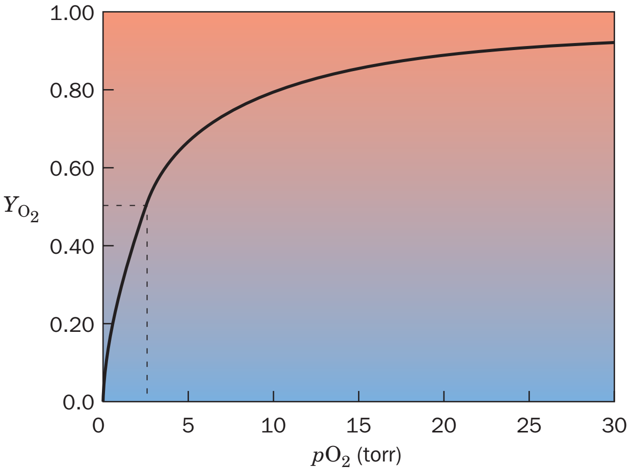

Figure 7-4 | Oxygen-binding curve of myoglobin. Myoglobin is half-saturated with O_2 ($Y_{\mathrm{O_2}} = 0.5$) at an oxygen partial pressure ($p\mathrm{O_2}$) of 2.8 torr (*dashed lines*). The hyperbolic shape of myoglobin's binding curve is typical of the simple binding of a small molecule to a protein. The background is shaded to indicate the color change that myoglobin undergoes as it binds O_2.

It is convenient to define K as $\boldsymbol{p_{50}}$, that is, the oxygen pressure at which myoglobin is 50% saturated. The p_{50} for myoglobin is 2.8 torr (760 torr = 1 atm). Over the physiological range of $p\mathrm{O_2}$ in the blood (100 torr in arterial blood and 30 torr in venous blood), myoglobin is almost fully saturated with oxygen; for example, $Y_{\mathrm{O_2}} = 0.97$ at $p\mathrm{O_2} = 100$ torr and 0.91 at 30 torr. Consequently, *myoglobin efficiently relays oxygen from the capillaries to muscle cells.*

Myoglobin, a single polypeptide chain with one heme group and hence one oxygen-binding site, is a useful model for other binding proteins. Even proteins with multiple binding sites for the same small molecule, or **ligand,** may generate hyperbolic binding curves like myoglobin's. *A hyperbolic binding curve occurs when ligands interact independently with their binding sites.* In practice, the affinity of a ligand for its binding protein may not be known. Constructing a binding curve such as the one shown in Fig. 7-4 may provide this information.

B | Hemoglobin Is a Tetramer with Two Conformations

Hemoglobin, the intracellular protein that gives red blood cells their color, is one of the best-characterized proteins and was one of the first proteins to be associated with a specific physiological function (oxygen transport). Animals that are too large (>1 mm thick) for simple diffusion to deliver sufficient oxygen to their tissues have circulatory systems containing hemoglobin or a protein of similar function that does so (Box 7-1).

Mammalian hemoglobin, as we saw in Fig. 6-33, is an $\alpha_2\beta_2$ tetramer (a dimer of $\alpha\beta$ protomers). The α and β subunits are structurally and evolutionarily related to each other and to myoglobin. The structure of hemoglobin was determined by Max Perutz (Box 7-2). Only about 18% of the residues are identical in myoglobin and in the α and β subunits of hemoglobin, but the three polypeptides have remarkably similar tertiary structures (hemoglobin subunits follow the myoglobin helix-labeling system, although

BOX 7-1 **PERSPECTIVES IN BIOCHEMISTRY**

Other Oxygen-Transport Proteins

The presence of O_2 in the earth's atmosphere and its utility in the oxidation of metabolic fuels have driven the evolution of various mechanisms for storing and transporting oxygen. Small organisms rely on diffusion to supply their respiratory oxygen needs. However, since the rate at which a substance diffuses varies inversely with the square of the distance it must diffuse, organisms of >1-mm thickness overcome the constraints of diffusion with circulatory systems and boost the limited solubility of O_2 in water with specific O_2-transport proteins.

Many invertebrates, and even some plants and bacteria, contain heme-based O_2-binding proteins. Single-subunit and multimeric hemoglobins are found both as intracellular proteins and as extracellular components of blood and other body fluids. The existence of hemoglobin-like proteins in some species of bacteria is evidence of gene transfer from animals to bacteria at one or more points during evolution. In bacteria, these proteins may function as sensors of environmental conditions such as local O_2 concentration. In some leguminous plants, the so-called **leghemoglobins** bind O_2 that would otherwise interfere with nitrogen fixation carried out by bacteria that colonize plant root nodules (Section 21-7). The **chlorocruorins,** which occur in some annelids (e.g., earthworms), contain a somewhat differently derivatized porphyrin than that in hemoglobin, which accounts for the green color of chlorocruorins.

The two other types of O_2-binding proteins, **hemerythrin** and **hemocyanin** (neither of which contains heme groups), occur only in invertebrate animals. Hemerythrin, which occurs in only a few species of marine worms, is an intracellular protein with a subunit mass of ~13 kD. It contains two Fe atoms liganded by His and acidic residues. It is violet-pink when oxygenated and colorless when deoxygenated.

Hemocyanins, which are exclusively extracellular, transport O_2 in mollusks and arthropods. The molluscan and arthropod hemocyanins are large multimeric proteins that differ in their primary through quaternary structures. However, their oxygen-binding sites are highly similar, consisting of a pair of copper atoms, each liganded by three His residues.

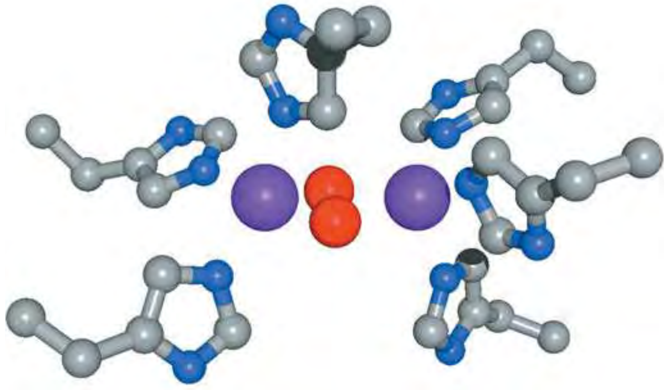

[Figure based on an X-ray structure by Wim Hol, University of Washington School of Medicine. PDBid 1OXY.]

In this model of the O_2-binding site of hemocyanin from the horseshoe crab *Limulus polyphemus,* atoms are colored according to type with C gray, N blue, O red, and Cu purple. The otherwise colorless complex turns blue when it binds O_2.

Hemocyanins must be present at high concentrations in order to function efficiently as oxygen carriers. For example, octopus **hemolymph** (its equivalent of blood) contains about 100 mg/mL hemocyanin. In order to minimize the osmotic pressure of so much protein, hemocyanins form multimeric structures with masses as great as 9×10^6 D in some species. Hemocyanins are often the predominant extracellular protein and may therefore have additional functions as buffers against pH changes and osmotic fluctuations. In some invertebrates, hemocyanins may serve as a nutritional reserve, for example, during metamorphosis or molting.

BOX 7-2 **PATHWAYS OF DISCOVERY**

Max Perutz and the Structure and Function of Hemoglobin

Max Perutz (1914–2002)

The determination of the three-dimensional structures of proteins has become so commonplace that it is difficult to appreciate the challenges that faced the first protein crystallographers. Max Perutz was a pioneer in this area, spending many years determining the structure of hemoglobin at atomic resolution and then using this information to explain the physiological function of the protein.

In 1934, two years before Perutz began his doctoral studies in Cambridge, J.D. Bernal and Dorothy Crowfoot Hodgkin had placed a crystal of the protein pepsin in an X-ray beam and obtained a diffraction pattern. Perutz tried the same experiment with hemoglobin, chosen because of its abundance, ease of crystallization, and obvious physiological importance. Hemoglobin crystals yielded diffraction patterns with thousands of diffraction maxima (called reflections), the result of X-ray scattering by the thousands of atoms in each protein molecule. At the time, X-ray crystallography had been used to determine the structures of molecules containing no more than around 40 atoms, so the prospect of using the technique to determine the atomic structure of hemoglobin seemed impossible. Nevertheless, Perutz took on the challenge and spent the rest of his long career working with hemoglobin.

In X-ray crystallography, the intensities and the positions of the reflections can be readily determined but the values of their phases (the relative positions of the wave peaks, the knowledge of which is as important as wave amplitude for image reconstruction) cannot be directly measured. Although computational techniques for determining the values of the phases had been developed for small molecules, methods for solving this so-called phase problem for such complex entities as proteins seemed hopelessly out of reach. In 1952, Perutz realized that the method of isomorphous replacement might suffice to solve the phase problem for hemoglobin. In this method, a heavy atom such as an Hg^{2+} ion, which is rich in electrons (the particles that scatter X-rays), must bind to specific sites on the protein without significantly disturbing its structure (which would change the positions of the reflections). If this causes measurable changes in the intensities of the reflections, these differences would provide the information to determine their phases. With trepidation followed by jubilation, Perutz observed that Hg-doped hemoglobin crystals indeed yielded reflections with measurable changes in intensity but no changes in position. Still, it took another 5 years to obtain the three-dimensional structure of hemoglobin at low (5.5-Å) resolution and it was not until 1968, some 30 years after he began the project, that he determined the structure of hemoglobin at near atomic (2.8-Å) resolution. In the meantime, Perutz's colleague John Kendrew used the method of isomorphous replacement to solve the structure of myoglobin, a smaller and simpler relative of hemoglobin. For their groundbreaking work, Perutz and Kendrew were awarded the 1962 Nobel Prize in Chemistry.

For Perutz, obtaining the structure of hemoglobin was only part of his goal of understanding hemoglobin. For example, functional studies indicated that the four oxygen-binding sites of hemoglobin interacted, as if they were in close contact, but Perutz's structure showed that the binding sites lay in deep and widely separated pockets. Perutz was also intrigued by the fact that crystals of hemoglobin prepared in the absence of oxygen would crack when they were exposed to air (the result, it turns out, of a dramatic conformational change). Although many other researchers also turned their attention to hemoglobin, Perutz was foremost among them in ascribing oxygen-binding behavior to protein structural features. He also devoted considerable effort to relating functional abnormalities in mutant hemoglobins to structural changes.

Perutz's groundbreaking work on the X-ray crystallography of proteins paved the way for other studies. For example, the first X-ray structure of an enzyme, lysozyme, was determined in 1965. The nearly 50,000 macromolecular structures that have been obtained since then owe a debt to Perutz and his decision to pursue an "impossible" task and to follow through on his structural work to the point where he could use his results to explain biological phenomena.

Perutz, M.F., Rossmann, M.G., Cullis, A.F., Muirhead, H., Will, G., and North, A.C.T., Structure of haemoglobin: A three-dimensional Fourier synthesis at 5.5 Å resolution, obtained by X-ray analysis. *Nature* **185,** 416–422 (1960).

the α chain has no D helix). The αβ protomers of hemoglobin are symmetrically related by a twofold rotation (i.e., a rotation of 180° brings the protomers into coincidence). In addition, hemoglobin's structurally similar α and β subunits are related by an approximate twofold rotation (pseudosymmetry) whose axis is perpendicular to that of the exact twofold rotation. Thus, hemoglobin has exact C_2 symmetry and pseudo-D_2 symmetry (Section 6-3; objects with D_2 symmetry have the rotational symmetry of a tetrahedron). The hemoglobin molecule has overall dimensions of about $64 \times 55 \times 50$ Å.

Oxygen binding alters the structure of the entire hemoglobin tetramer, so the structures of **deoxyhemoglobin** (Fig. 7-5*a*) and **oxyhemoglobin** (Fig. 7-5*b*) are noticeably different. In both forms of hemoglobin, the α and β subunits form extensive contacts: Those at the α_1–β_1 interface (and its α_2–β_2 symmetry equivalent) involve 35 residues, and those at the α_1–β_2 (and α_2–β_1) interface involve 19 residues. These associations are predominantly hydrophobic, although numerous hydrogen bonds and several ion pairs are also involved. Note, however, that the α_1–α_2 and β_1–β_2 interactions are tenuous at best because these subunit pairs are separated by an

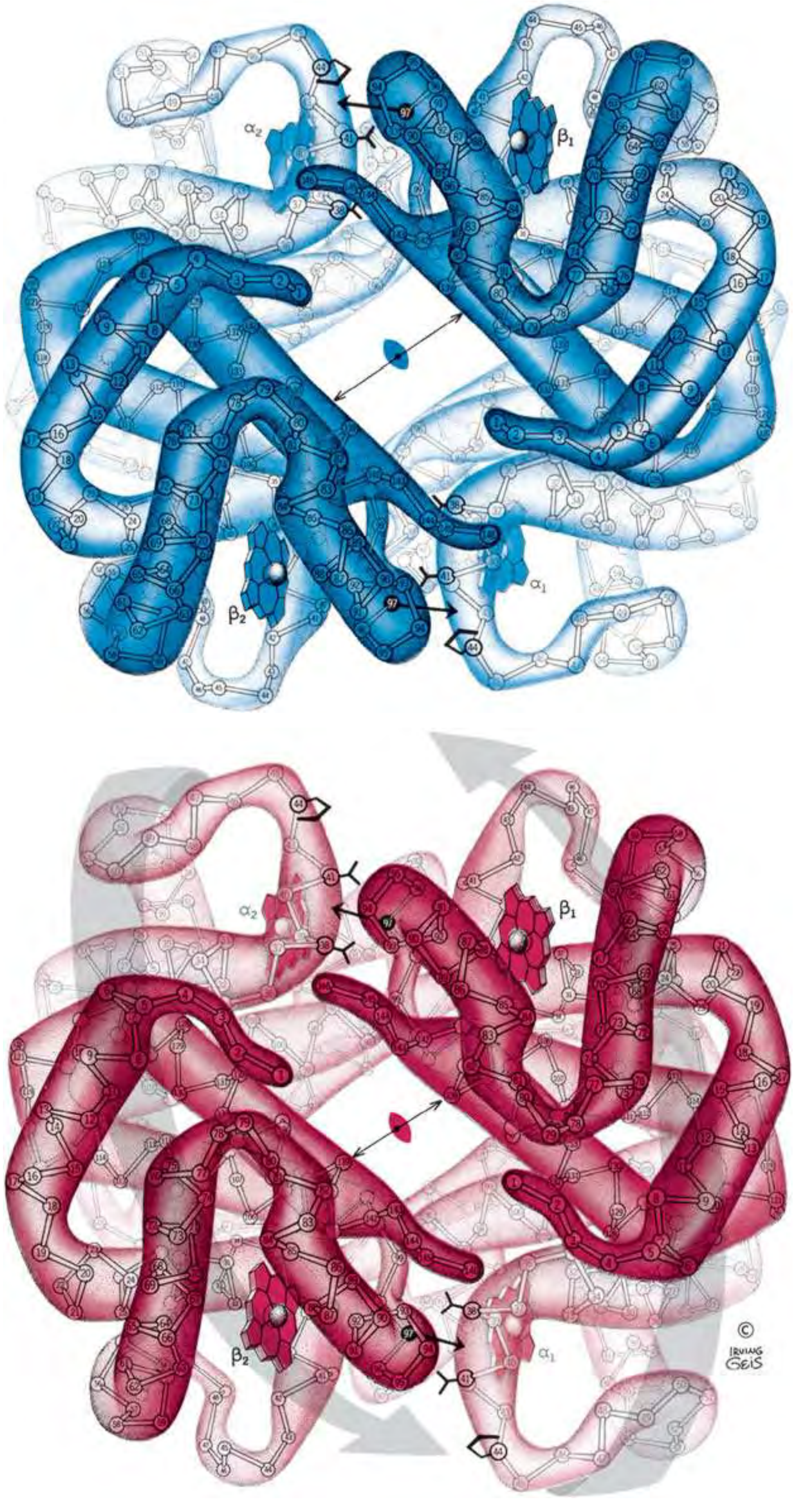

Figure 7-5 | Hemoglobin structure. (*a*) Deoxyhemoglobin and (*b*) oxyhemoglobin. The $\alpha_1\beta_1$ protomer is related to the $\alpha_2\beta_2$ protomer by a twofold axis of symmetry (*lenticular symbol*), which is perpendicular to the page. Oxygenation causes one protomer to rotate ~15° relative to the other, bringing the β chains closer together (compare the lengths of the double-headed arrows) and shifting the contacts between subunits at the α_1–β_2 and α_2–β_1 interfaces (some of the relevant side chains are drawn in black). The large gray arrows in *b* indicate the molecular movements that accompany oxygenation. [Illustration, Irving Geis. Image from the Irving Geis Collection/Howard Hughes Medical Institute. Rights owned by HHMI. Reproduction by permission only.] **See Kinemage Exercises 6-2 and 6-3.**

~20-Å-diameter solvent-filled channel that parallels the 50-Å length of hemoglobin's exact twofold axis (Fig. 7-5).

When oxygen binds to hemoglobin, the α_1–β_2 (and α_2–β_1) contacts shift, producing a change in quaternary structure. Oxygenation rotates one αβ dimer ~15° with respect to the other αβ dimer (gray arrows in Fig. 7-5*b*), which brings the β subunits closer together and narrows the solvent-filled central channel (Fig. 7-5). Some atoms in the α_1–β_2 and α_2–β_1 interfaces shift by as much as 6 Å (oxygenation causes such extensive quaternary structural changes that crystals of deoxyhemoglobin shatter on exposure to O_2). This structural rearrangement is a crucial element of hemoglobin's oxygen-binding behavior.

C | Oxygen Binds Cooperatively to Hemoglobin

Hemoglobin has a p_{50} of 26 torr (i.e., hemoglobin is half-saturated with O_2 at an oxygen partial pressure of 26 torr), which is nearly 10 times greater than the p_{50} of myoglobin. Moreover, hemoglobin does not exhibit a myoglobin-like hyperbolic oxygen-binding curve. Instead, O_2 binding to hemoglobin is described by a **sigmoidal** (S-shaped) **curve** (Fig. 7-6). *This permits the blood to deliver much more O_2 to the tissues than if hemoglobin had a hyperbolic curve with the same p_{50}* (dashed line in Fig. 7-6). For example, hemoglobin is nearly fully saturated with O_2 at arterial oxygen pressures ($Y_{O_2} = 0.95$ at 100 torr) but only about half-saturated at venous oxygen pressures ($Y_{O_2} = 0.55$ at 30 torr). This 0.40 difference in oxygen saturation, a measure of hemoglobin's ability to deliver O_2 from the lungs to the tissues, would be only 0.25 if hemoglobin exhibited hyperbolic binding behavior.

In any binding system, a sigmoidal curve is diagnostic of a ***cooperative*** *interaction between binding sites.* This means that the binding of a ligand to one site affects the binding of additional ligands to the other sites. In the case of hemoglobin, O_2 binding to one subunit increases the O_2 affinity of the remaining subunits. The initial slope of the oxygen-binding curve (Fig. 7-6) is low, as hemoglobin subunits independently compete for the first O_2. However, an O_2 molecule bound to one of hemoglobin's subunits increases the O_2-binding affinity of its other subunits, thereby accounting for the increasing slope of the middle portion of the sigmoidal curve.

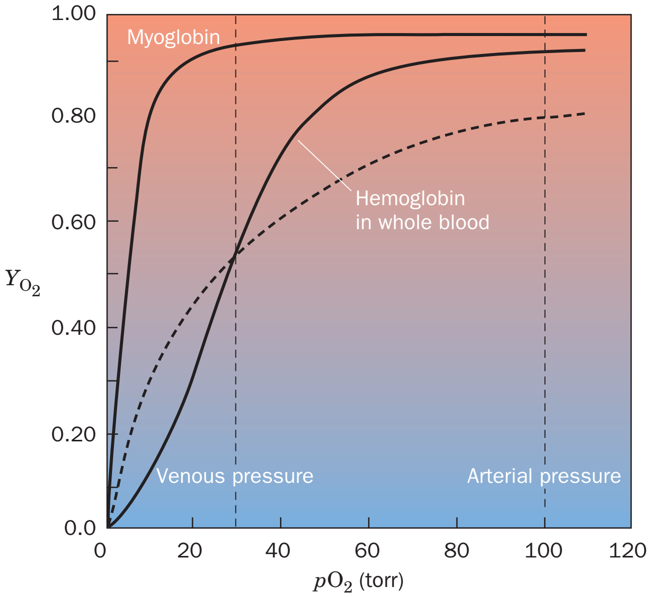

Figure 7-6 | Oxygen-binding curve of hemoglobin. In whole blood, hemoglobin is half-saturated at an oxygen pressure of 26 torr. The normal sea level values of human arterial and venous pO_2 are indicated (atmospheric pO_2 is 160 torr at sea level). The O_2-binding curve for myoglobin is included for comparison. The dashed line is a hyperbolic O_2-binding curve with the same p_{50} as hemoglobin. The background is shaded to indicate the color change that hemoglobin undergoes as it binds O_2. **See the Animated Figures.**

The Hill Equation Describes Hemoglobin's O_2-Binding Curve. The earliest attempt to analyze hemoglobin's sigmoidal O_2 dissociation curve was formulated by Archibald Hill in 1910. Hill assumed that hemoglobin **(Hb)** bound *n* molecules of O_2 in a single step,

$$\text{Hb} + n\text{O}_2 \rightarrow \text{Hb(O}_2)_n$$

that is, with infinite cooperativity. Thus, in analogy with the derivation of Eq. 7-6,

$$Y_{O_2} = \frac{(pO_2)^n}{(p_{50})^n + (pO_2)^n} \qquad [7\text{-}8]$$

which is known as the **Hill equation.** Like Eq. 7-6, it describes the degree of saturation of hemoglobin as a function of pO_2.

Infinite O_2 binding cooperativity, as Hill assumed, is a physical impossibility. Nevertheless, *n* may be taken to be a nonintegral parameter related to the degree of cooperativity among interacting hemoglobin subunits rather than the number of subunits that bind O_2 in one step. The Hill equation can then be taken as a useful empirical curve-fitting relationship rather than as an indicator of a particular model of ligand binding.

The quantity n, the ***Hill constant,*** *increases with the degree of cooperativity of a reaction and therefore provides a convenient although simplistic characterization of a ligand-binding reaction.* If $n = 1$, Eq. 7-8 describes a hyperbola as does Eq. 7-6 for myoglobin, and the O_2-binding reaction is said to be **noncooperative.** If $n > 1$, the reaction is described as being **positively cooperative,** because O_2 binding increases the affinity of hemoglobin for further O_2 binding (cooperativity is infinite in the limit that $n = 4$, the number of O_2 binding sites in hemoglobin). Conversely, if $n < 1$, the reaction is said to be **negatively cooperative,** because O_2 binding would then reduce the affinity of hemoglobin for subsequent O_2 binding.

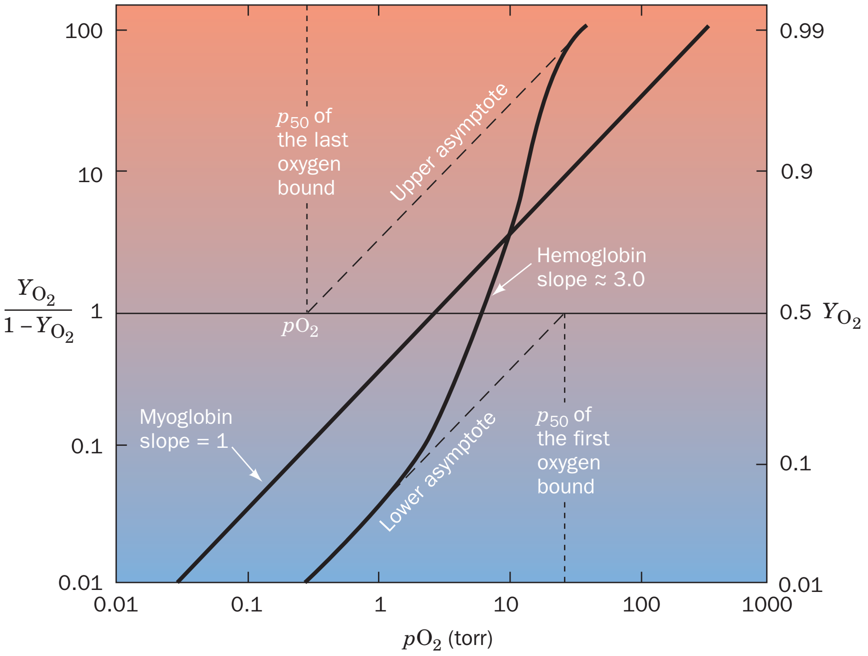

Figure 7-7 | Hill plots for myoglobin and purified hemoglobin. Note that this is a log–log plot. At $pO_2 = p_{50}$, $Y_{O_2}/(1 - Y_{O_2}) = 1$. [The p_{50} for hemoglobin *in vivo* is higher than the p_{50} of purified hemoglobin due to its binding of certain substances present in the red cell (see below).]

The Hill coefficient, n, and the value of p_{50} that best describe hemoglobin's saturation curve can be graphically determined by rearranging Eq. 7-8. First, divide both sides by $1 - Y_{O_2}$:

$$\frac{Y_{O_2}}{1 - Y_{O_2}} = \frac{\dfrac{(pO_2)^n}{(p_{50})^n + (pO_2)^n}}{1 - Y_{O_2}} = \frac{\dfrac{(pO_2)^n}{(p_{50})^n + (pO_2)^n}}{1 - \dfrac{(pO_2)^n}{(p_{50})^n + (pO_2)^n}} \quad [7\text{-}9]$$

Factoring out the $[(p_{50})^n + (pO_2)^n]$ term gives

$$\frac{Y_{O_2}}{1 - Y_{O_2}} = \frac{(pO_2)^n}{[(p_{50})^n + (pO_2)^n] - (pO_2)^n} = \frac{(pO_2)^n}{(p_{50})^n} \quad [7\text{-}10]$$

Taking the log of both sides yields a linear equation:

$$\log\left(\frac{Y_{O_2}}{1 - Y_{O_2}}\right) = n\log pO_2 - n\log p_{50} \quad [7\text{-}11]$$

The linear plot of $\log[Y_{O_2}/(1 - Y_{O_2})]$ versus $\log pO_2$, the **Hill plot,** has a slope of n and an intercept on the $\log pO_2$ axis of $\log p_{50}$ (recall that the linear equation $y = mx + b$ describes a line with a slope of m and an x intercept of $-b/m$).

Figure 7-7 shows the Hill plots for myoglobin and purified hemoglobin. For myoglobin, the plot is linear with a slope of 1, as expected. Although all subunits of hemoglobin do not bind O_2 in a single step as was assumed in deriving the Hill equation, its Hill plot is essentially linear for values of Y_{O_2} between 0.1 and 0.9. When $pO_2 = p_{50}$, $Y_{O_2} = 0.5$, and

$$\frac{Y_{O_2}}{1 - Y_{O_2}} = \frac{0.5}{1 - 0.5} = 1.0 \quad [7\text{-}12]$$

As can be seen in Fig. 7-7, this is the region of maximum slope, whose value is customarily taken to be the Hill coefficient, n. For normal human hemoglobin, the Hill coefficient is between 2.8 and 3.0; that is, hemoglobin's oxygen binding is highly, but not infinitely, cooperative. Many abnormal hemoglobins exhibit smaller Hill coefficients (Section 7-1E), indicating that they have a less than normal degree of cooperativity.

At Y_{O_2} values near zero, when few hemoglobin molecules have bound even one O_2 molecule, the Hill plot for hemoglobin assumes a slope of 1 (Fig. 7-7, lower asymptote) because the hemoglobin subunits independently compete for O_2 as do molecules of myoglobin. At Y_{O_2} values near 1, when at least three of hemoglobin's four O_2-binding sites are occupied, the Hill plot also assumes a slope of 1 (Fig. 7-7, upper asymptote) because the few remaining unoccupied sites are on different molecules and therefore bind O_2 independently.

Extrapolating the lower asymptote in Fig. 7-7 to the horizontal axis indicates, according to Eq. 7-11, that $p_{50} = 30$ torr for binding the first O_2 to purified hemoglobin. Likewise, extrapolating the upper asymptote yields $p_{50} = 0.3$ torr for binding hemoglobin's fourth O_2. Thus, *the fourth O_2 binds to hemoglobin with 100-fold greater affinity than the first*. This difference, as we shall see below, is entirely due to the influence of the globin chain on the O_2 affinity of heme.

D | Hemoglobin's Two Conformations Exhibit Different Affinities for Oxygen

The cooperativity of oxygen binding to hemoglobin arises from the effect of the ligand-binding state of one heme group on the ligand-binding affinity of another. Yet the hemes are 25 to 37 Å apart—too far to interact electronically. Instead, information about the O_2-binding status of a heme group is mechanically transmitted to the other heme groups by motions of the protein. These movements are responsible for the different quaternary structures of oxy- and deoxyhemoglobin depicted in Fig. 7-5.

Oxygen Binding to Hemoglobin Triggers a Conformational Change from T to R. On the basis of the X-ray structures of oxy- and deoxyhemoglobin, Perutz formulated a mechanism for hemoglobin oxygenation. *In the* ***Perutz mechanism,*** *hemoglobin has two stable conformational states, the* ***T state*** *(the conformation of deoxyhemoglobin) and the* ***R state*** *(the conformation of oxyhemoglobin).* The conformations of all four subunits in T-state hemoglobin differ from those in the R state. Oxygen binding initiates a series of coordinated movements that result in a shift from the T state to the R state within a few microseconds:

1. In the T state, the Fe(II) in each of the four hemes is situated ~0.6 Å out of the heme plane because of a pyramidal doming of the porphyrin group toward His F8 (Fig. 7-8). O_2 binding changes the heme's electronic state, which shortens the Fe—$N_{porphyrin}$ bonds by ~0.1 Å and causes the porphyrin doming to subside. Consequently, during the T → R transition, the Fe(II) moves into the center of the heme plane.
2. The Fe(II) drags the covalently linked His F8 along with it. However, the direct movement of His F8 by 0.6 Å toward the heme plane would cause it to collide with the heme. To avoid this steric clash, the attached F helix tilts and translates by ~1 Å across the heme plane.
3. The changes in tertiary structure are coupled to a shift in the arrangement of hemoglobin's four subunits. The largest change produced by the T → R transition is the result of movements of residues at the α_1–β_2 and α_2–β_1 interfaces; in other words, at the interface between the two protomeric units of hemoglobin. In the T state, His

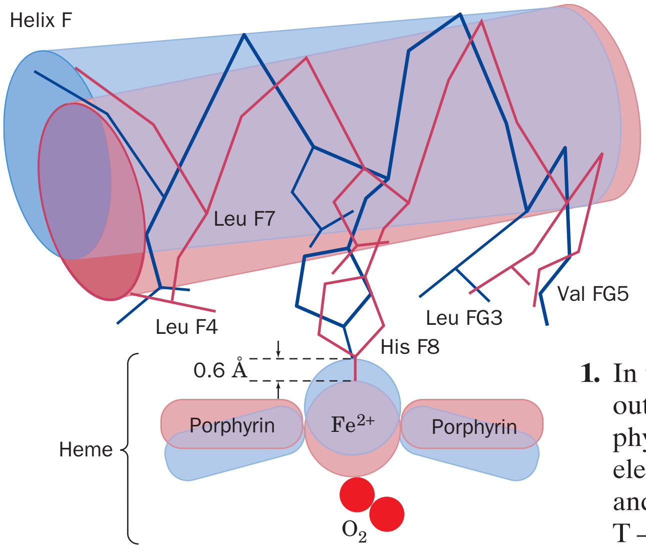

■ **Figure 7-8 | Movements of the heme and the F helix during the T → R transition in hemoglobin.** In the T form (*blue*), the Fe is 0.6 Å above the center of the domed porphyrin ring. On assuming the R form (*red*), the Fe moves into the plane of the now undomed porphyrin, where it can more tightly bind O_2, and, in doing so, pulls His F8 and its attached F helix with it. **See Kinemage Exercise 6-4 and the Animated Figures.**

97 in the β chain contacts Thr 41 in the α chain (Fig. 7-9*a*). In the R state, His 97 contacts Thr 38, which is positioned one turn back along the C helix (Fig. 7-9*b*). In both conformations, the "knobs" on one

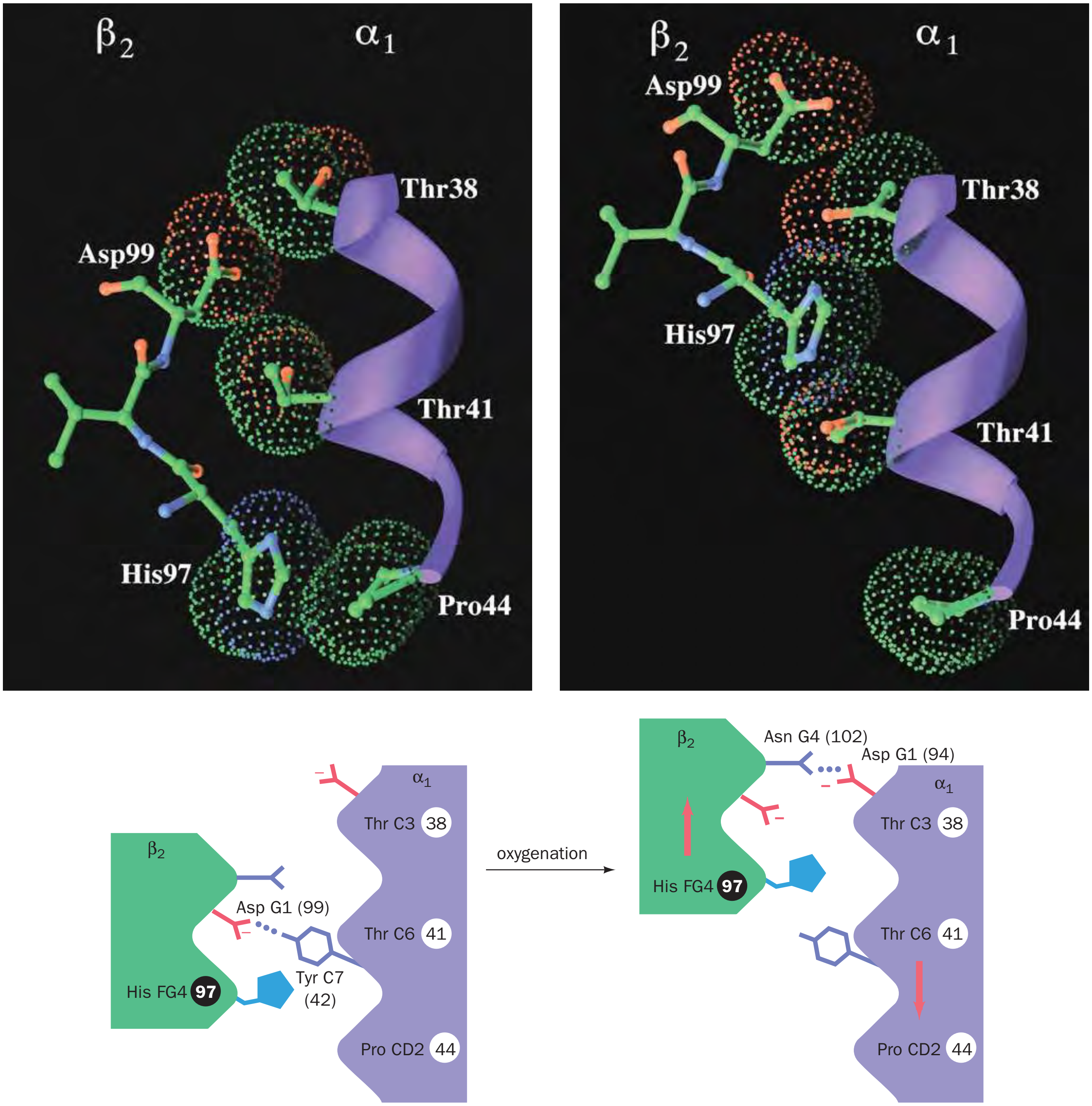
β_2
α_1
Thr38
Asp99
Thr41
His97
Pro44
β_2
α_1
Asp99
Thr38
His97
Thr41
Pro44
α_1
Thr C3 38
β_2
Asp G1 (99)
Thr C6 41
His FG4 97
Tyr C7 (42)
Pro CD2 44
oxygenation
β_2
Asn G4 (102)
Asp G1 (94)
α_1
Thr C3 38
His FG4 97
Thr C6 41
Pro CD2 44

(*a*) **T State (deoxy)**

(*b*) **R State (oxy)**

■ **Figure 7-9 | Changes at the α_1–β_2 interface during the T → R transition in hemoglobin.** (*a*) The T state and (*b*) the R state. In the upper drawings, the C helix is represented by a purple ribbon, the contacting residues forming the α_1C–β_2FG contact are shown in ball-and-stick form colored by atom type (C green, N blue, and O red), and their van der Waals surfaces are outlined by like-colored dots. The lower drawings are the corresponding schematic diagrams of the α_1C–β_2FG contact. Upon a T → R transformation, the β_2FG region shifts by one turn along the α_1C helix with no stable intermediate (note how in both conformations, the knobs formed by the side chains of His 97β and Asp 99β fit between the grooves on the C helix formed by the side chains of Thr 38α, Thr 41α, and Pro 44α). The subunits are joined by different hydrogen bonds in the two quaternary states. Figure 7-5 provides another view of these interactions. [Based on X-ray structures by Giulio Fermi, Max Perutz, and Boaz Shaanan, MRC Laboratory of Molecular Biology, Cambridge, U.K. PDBids (*a*) 2HHB and (*b*) 1HHO.] **See Kinemage Exercise 6-5.**

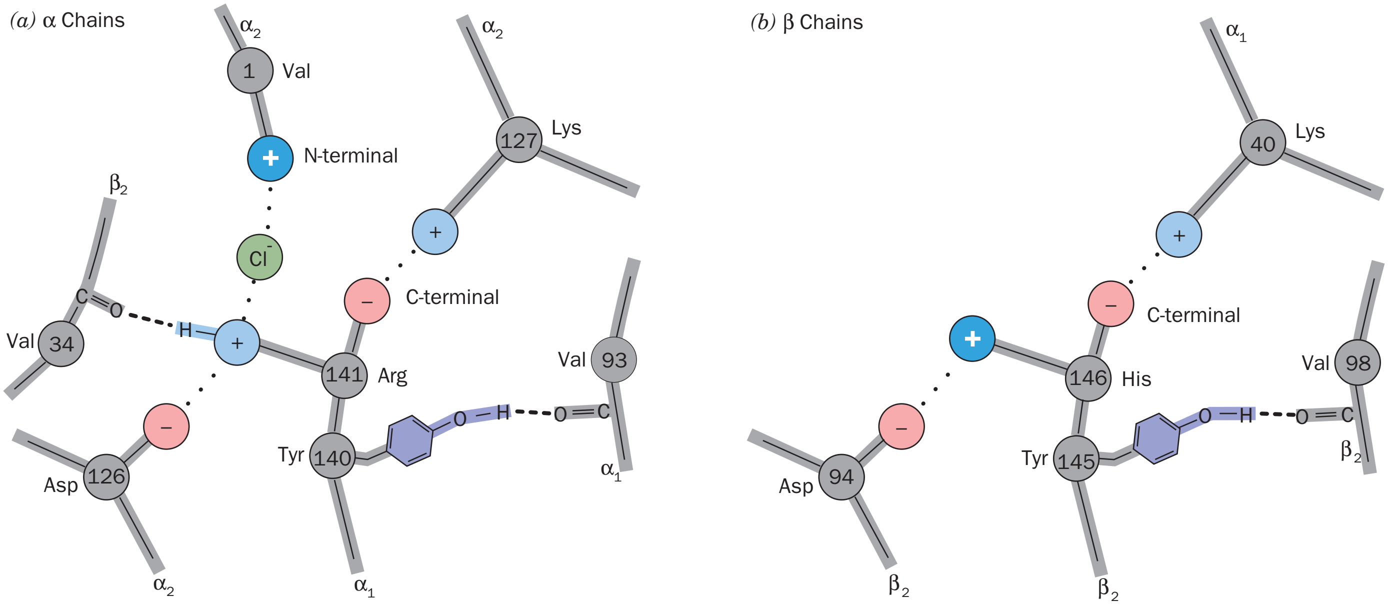

■ **Figure 7-10 | Networks of ion pairs and hydrogen bonds in deoxyhemoglobin.** These bonds, which involve the last two residues of (*a*) the α chains and (*b*) the β chains, are ruptured in the T → R transition. Two groups that become partially deprotonated in the R state (part of the Bohr effect) are indicated by white plus signs. [Illustration, Irving Geis. Image from the Irving Geis Collection/Howard Hughes Medical Institute. Rights owned by HHMI. Reproduction by permission only.]

subunit mesh nicely with the "grooves" on the other. An intermediate position would be severely strained because it would bring His 97 and Thr 41 too close together (i.e., knobs on knobs).

4. The C-terminal residues of each subunit (Arg 141α and His 146β) in T-state hemoglobin each participate in a network of intra- and intersubunit ion pairs (Fig. 7-10) that stabilize the T state. However, the conformational shift in the T → R transition tears away these ion pairs in a process that is driven by the energy of formation of the Fe—O_2 bonds.

The essential feature of hemoglobin's T → R transition is that *its subunits are so tightly coupled that large tertiary structural changes within one subunit cannot occur without quaternary structural changes in the entire tetrameric protein.* Hemoglobin is limited to only two quaternary forms, T and R, because the intersubunit contacts shown in Fig. 7-9 act as a binary switch that permits only two stable positions of the subunits relative to each other. The inflexibility of the α_1–β_1 and α_2–β_2 interfaces requires that the T → R shift occur simultaneously at both the α_1–β_2 and α_2–β_1 interfaces. No one subunit or dimer can greatly change its conformation independently of the others.

We are now in a position to structurally rationalize the cooperativity of oxygen binding to hemoglobin. The T state of hemoglobin has low O_2 affinity, mostly because of the 0.1 Å greater length of its Fe—O_2 bond relative to that of the R state (e.g., the blue structure shown in Fig. 7-8). Experimental evidence indicates that when at least one O_2 has bound to each αβ dimer, the strain in the T-state hemoglobin molecule is sufficient to tear away the C-terminal ion pairs, thereby snapping the protein into the R state. All the subunits are thereby simultaneously converted to the R-state conformation whether or not they have bound O_2. Unliganded subunits in the R-state conformation have increased oxygen affinity because they are already in the O_2-binding conformation. This accounts for the high O_2 affinity of nearly saturated hemoglobin.

The Bohr Effect Enhances Oxygen Transport. The conformational changes in hemoglobin that occur on oxygen binding decrease the p*K*'s of several groups. Recall that the tendency for a group to ionize depends on its microenvironment, which may include other ionizable groups. For example, in T-state hemoglobin, the N-terminal amino groups of the α subunits and the C-terminal His of the β subunits are positively charged and participate in ion pairs (see Fig. 7-10). The formation of ion pairs increases the p*K* values of these groups (makes them less acidic and therefore less likely to give up their protons). In R-state hemoglobin, these ion pairings are absent, and the p*K*'s of the groups decrease (making them more acidic and more likely to give up protons). Consequently, under physiological conditions, hemoglobin releases ~0.6 protons for each O_2 it binds. Conversely, increasing the pH, that is, removing protons, stimulates hemoglobin to bind more O_2 at lower oxygen pressures (Fig. 7-11). This phenomenon is known as the **Bohr effect** after Christian Bohr (father of the physicist Niels Bohr), who first reported it in 1904.

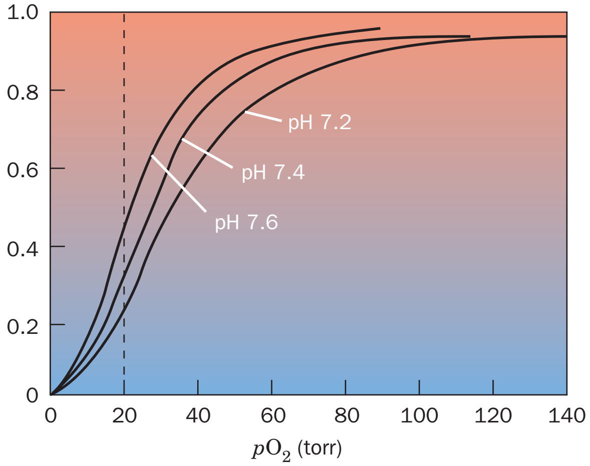

Figure 7-11 | **The Bohr effect.** The O_2 affinity of hemoglobin increases with increasing pH. The dashed line indicates the pO_2 in actively respiring muscle. [After Benesch, R.E. and Benesch, R., *Adv. Protein Chem.* **28,** 212 (1974).] **See the Animated Figures.**

The Bohr effect has important physiological functions in transporting O_2 from the lungs to respiring tissue and in transporting the CO_2 produced by respiration back to the lungs (Fig. 7-12). The CO_2 produced by respiring tissues diffuses from the tissues to the capillaries. This dissolved CO_2 forms bicarbonate (HCO_3^-) only very slowly, by the reaction

$$CO_2 + H_2O \rightleftharpoons H^+ + HCO_3^-$$

However, in the **erythrocyte** (red blood cell; from the Greek: *erythrose,* red + *kytos,* a hollow vessel), the enzyme **carbonic anhydrase** greatly accelerates this reaction. Accordingly, most of the CO_2 in the blood is carried in the form of bicarbonate (in the absence of carbonic anhydrase, bubbles of CO_2 would form in the blood).

In the capillaries, where pO_2 is low, the H^+ generated by bicarbonate formation is taken up by hemoglobin in forming the ion pairs of the T

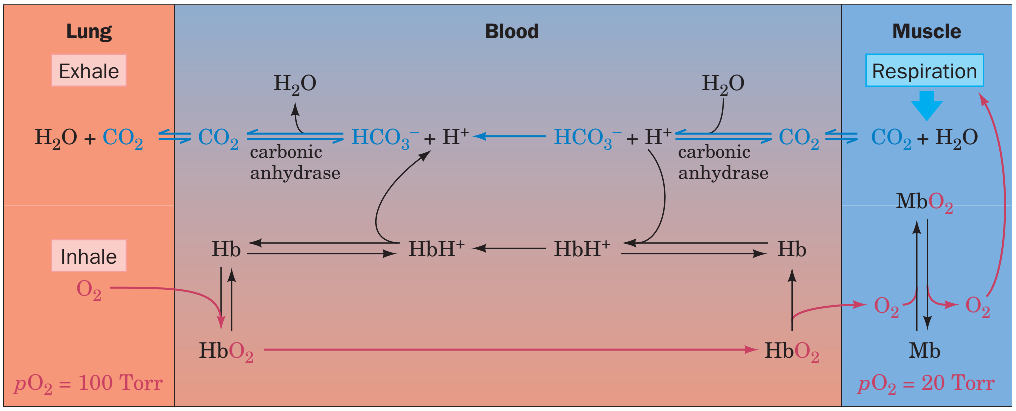

Figure 7-12 | **The roles of hemoglobin and myoglobin in O_2 and CO_2 transport.** Oxygen is inhaled into the lungs at high pO_2, where it binds to hemoglobin in the blood. The O_2 is then transported to respiring tissue, where the pO_2 is low. The O_2 therefore dissociates from the Hb and diffuses into the tissues, where it is used to oxidize metabolic fuels to CO_2 and H_2O. In rapidly respiring muscle tissue, the O_2 first binds to myoglobin (whose oxygen affinity is higher than that of hemoglobin). This increases the rate at which O_2 can diffuse from the capillaries to the tissues by, in effect, increasing its solubility. The Hb and CO_2 (mostly as HCO_3^-) are then returned to the lungs, where the CO_2 is exhaled.

state, thereby inducing hemoglobin to unload its bound O_2. This H^+ uptake, moreover, facilitates CO_2 transport by stimulating bicarbonate formation. Conversely, in the lungs, where pO_2 is high, O_2 binding by hemoglobin disrupts the T-state ion pairs to form the R state, thereby releasing the Bohr protons, which recombine with bicarbonate to drive off CO_2. These reactions are closely matched, so they cause very little change in blood pH (see Box 2-1).

The Bohr effect provides a mechanism whereby additional oxygen can be supplied to highly active muscles, where the pO_2 may be <20 torr. Such muscles generate lactic acid (Section 15-3A) so fast that they lower the pH of the blood passing through them from 7.4 to 7.2. At a pO_2 of 20 torr, hemoglobin releases ~10% more O_2 at pH 7.2 than it does at pH 7.4 (Fig. 7-11).

CO_2 also modulates O_2 binding to hemoglobin by combining reversibly with the N-terminal amino groups of blood proteins to form **carbamates:**

$$\text{R—NH}_2 + \text{CO}_2 \rightleftharpoons \text{R—NH—COO}^- + \text{H}^+$$

The T (deoxy) form of hemoglobin binds more CO_2 as carbamate than does the R (oxy) form. When the CO_2 concentration is high, as it is in the capillaries, the T state is favored, stimulating hemoglobin to release its bound O_2. The protons released by carbamate formation further promote O_2 release through the Bohr effect. Although the difference in CO_2 binding between the oxy and deoxy states of hemoglobin accounts for only ~5% of the total blood CO_2, it is nevertheless responsible for around half the CO_2 transported by the blood. This is because only ~10% of the total blood CO_2 is lost through the lungs in each circulatory cycle.

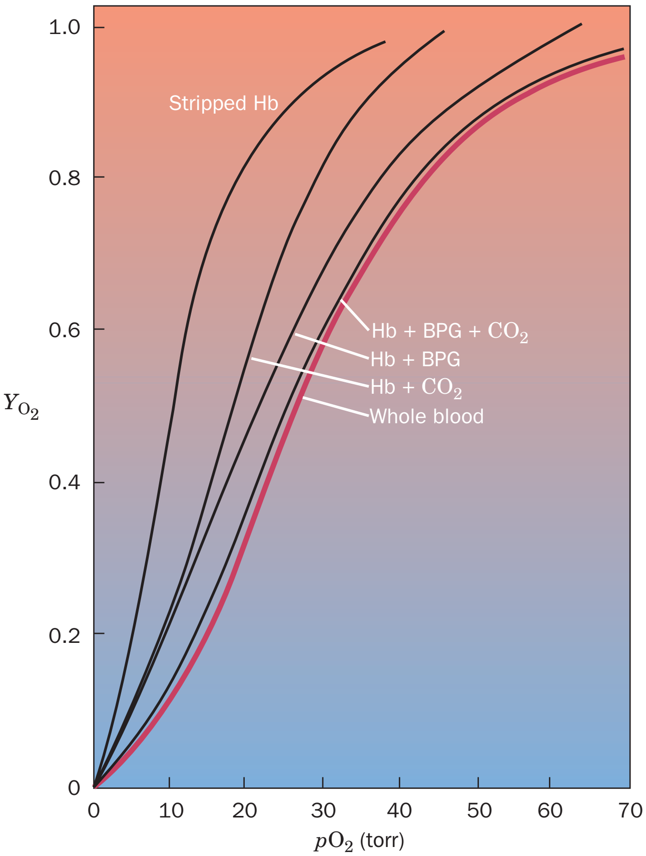

Figure 7-13 | The effects of BPG and CO_2 on hemoglobin's O_2 dissociation curve. Stripped hemoglobin (*left*) has higher O_2 affinity than whole blood (*red curve*). Adding BPG or CO_2 or both to hemoglobin shifts the dissociation curve back to the right (lowers hemoglobin's O_2 affinity). [After Kilmartin, J.V. and Rossi-Bernardi, L., *Physiol. Rev.* **53,** 884 (1973).] **See the Animated Figures.**

Bisphosphoglycerate Binds to Deoxyhemoglobin. Highly purified ("stripped") hemoglobin has a much greater oxygen affinity than hemoglobin in whole blood (Fig. 7-13). This observation led Joseph Barcroft, in 1921, to speculate that blood contains some other substance besides CO_2 that affects oxygen binding to hemoglobin. This compound is **D-2,3-bisphosphoglycerate (BPG).**

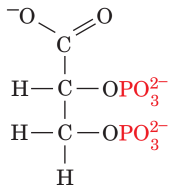

D-2,3-Bisphosphoglycerate (BPG)

BPG binds tightly to deoxyhemoglobin but only weakly to oxyhemoglobin. *The presence of BPG in mammalian erythrocytes therefore decreases hemoglobin's oxygen affinity by keeping it in the deoxy conformation.* In other vertebrates, different phosphorylated compounds elicit the same effect.

BPG has an indispensable physiological function: In arterial blood, where pO_2 is ~100 torr, hemoglobin is ~95% saturated with O_2, but in venous blood, where pO_2 is ~30 torr, it is only 55% saturated (Fig. 7-6). Consequently, in passing through the capillaries, hemoglobin unloads ~40% of its bound O_2. In the absence of BPG, little of this bound O_2 would be released since hemoglobin's O_2 affinity is increased, thus shifting its O_2 dissociation curve significantly toward lower pO_2 (Fig. 7-13, *left*). BPG also plays an important role in adaptation to high altitudes (Box 7-3).

The X-ray structure of a BPG–deoxyhemoglobin complex shows that BPG binds in the central cavity of deoxyhemoglobin (Fig. 7-14). The anionic groups of BPG are within hydrogen-bonding and ion-pairing distances of the N-terminal amino groups of both β subunits. The T → R transformation brings the two βH helices together, which narrows the central cavity (compare Figs. 7-5*a* and 7-5*b*) and expels the BPG. It also widens the distance between the β N-terminal amino groups from 16 to 20 Å, which prevents their simultaneous hydrogen bonding with BPG's phosphate groups. BPG therefore binds to and stabilizes only the T conformation of hemoglobin by cross-linking its β subunits. This shifts the T $\rightleftharpoons$ R equilibrium toward the T state, which lowers hemoglobin's O_2 affinity.

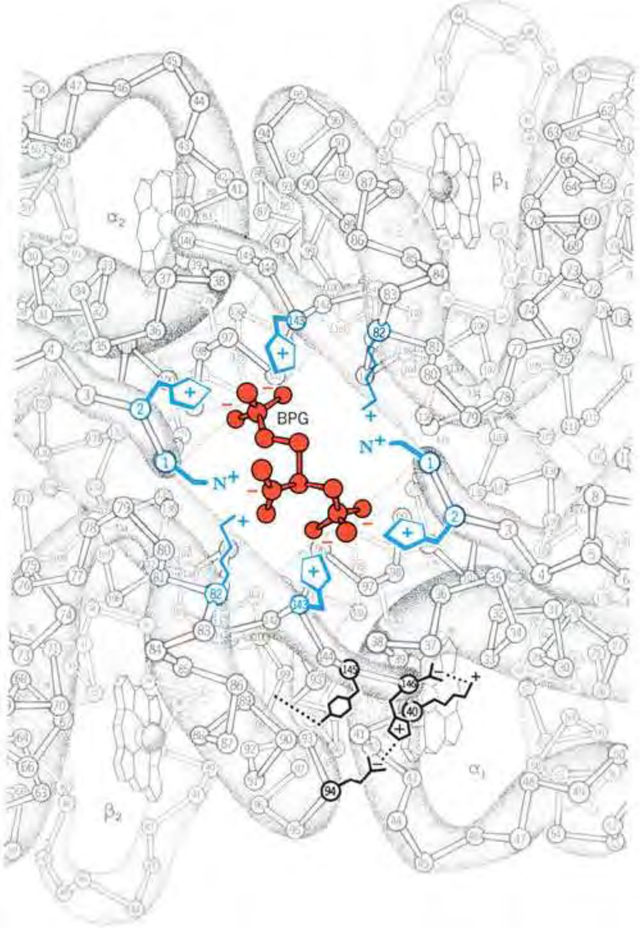

Figure 7-14 | Binding of BPG to deoxyhemoglobin. BPG (*red*) binds in hemoglobin's central cavity. The BPG, which has a charge of −5 under physiological conditions, is surrounded by eight cationic groups (*blue*) extending from the two β subunits. In the R state, the central cavity is too narrow to contain BPG. Some of the ion pairs and hydrogen bonds that help stabilize the T state (Fig. 7-10*b*) are indicated at the lower right. [Illustration, Irving Geis. Image from the Irving Geis Collection/Howard Hughes Medical Institute. Rights owned by HHMI. Reproduction by permission only.] **See Kinemage Exercise 6-3.**

Fetal Hemoglobin Has Low BPG Affinity. The effects of BPG also help supply the fetus with oxygen. A fetus obtains its O_2 from the maternal circulation via the placenta. The concentration of BPG is the same in adult and fetal erythrocytes, but BPG binds more tightly to adult hemoglobin than to fetal hemoglobin. The higher oxygen affinity of fetal hemoglobin facilitates the transfer of O_2 to the fetus.

Fetal hemoglobin has the subunit composition $\alpha_2\gamma_2$ in which the γ subunit is a variant of the β chain (Section 5-4B). Residue 143 of the β chain of adult hemoglobin has a cationic His residue, whereas the γ chain has an uncharged Ser residue. The absence of this His eliminates a pair of interactions that stabilize the BPG–deoxyhemoglobin complex (Fig. 7-14).

BOX 7-3 BIOCHEMISTRY IN HEALTH AND DISEASE

High-Altitude Adaptation

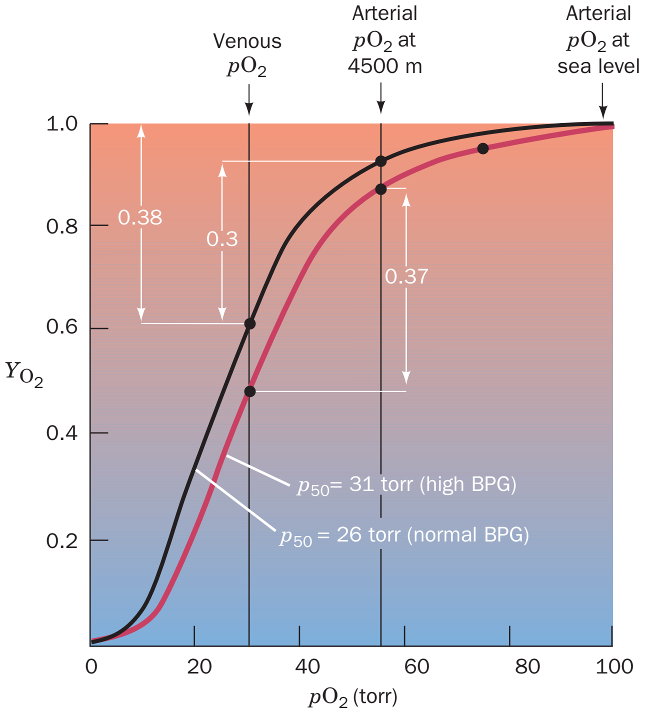

Atmospheric pressure decreases with altitude, so that the oxygen pressure at 3000 m (10,000 feet) is only ~110 torr, 70% of its sea-level pressure. A variety of physiological responses are required to maintain normal oxygen delivery (without adaptation, $p\mathrm{O}_2$ levels of 85 torr or less result in mental impairment).

High-altitude adaptation is a complex process that involves increases in the number of erythrocytes and the amount of hemoglobin per erythrocyte. It normally requires several weeks to complete. Yet, as is clear to anyone who has climbed to high altitude, even a 1-day stay there results in a noticeable degree of adaptation. This effect results from a rapid increase in the amount of BPG synthesized in erythrocytes (from ~4 mM to ~8 mM; BPG cannot cross the erythrocyte membrane). As illustrated by plots of Y_{O_2} versus $p\mathrm{O}_2$, the high altitude–induced increase in BPG causes the O_2-binding curve of hemoglobin to shift from its sea-level position (*black line*) to a lower affinity position (*red line*). At sea level, the difference between arterial and venous $p\mathrm{O}_2$ is 70 torr (100 torr − 30 torr), and hemoglobin unloads 38% of its bound O_2. However, when the arterial $p\mathrm{O}_2$ drops to 55 torr, as it does at an altitude of 4500 m, hemoglobin would be able to unload only 30% of its O_2. High-altitude adaptation (which decreases the amount of O_2 that hemoglobin can bind in the lungs but, to a greater extent, increases the amount of O_2 it releases at the tissues) allows hemoglobin to deliver a near-normal 37% of its bound O_2. BPG concentrations also increase in individuals suffering from disorders that limit the oxygenation of the blood **(hypoxia),** such as various anemias and cardiopulmonary insufficiency.

The BPG concentration in erythrocytes can be adjusted more rapidly than hemoglobin can be synthesized (Box 15-2; erythrocytes lack nuclei and therefore cannot synthesize proteins). An altered BPG level is also a more sensitive regulator of oxygen delivery than an altered respiratory rate. Hyperventilation, another early response to high altitude, may lead to respiratory alkalosis (Box 2-1). Interestingly, individuals in long-established Andean and Himalayan populations exhibit high lung capacity, along with high hemoglobin levels and, often, enlarged right ventricles (reflecting increased cardiac output), compared to individuals from low-altitude populations.

In contrast to the mechanism of human adaptation to high altitude, most mammals that normally live at high altitudes (e.g., the llama) have genetically altered hemoglobins that have higher O_2-binding affinities than do their sea-level cousins. Thus, both raising and lowering hemoglobin's p_{50} can provide high-altitude adaptation.

Hemoglobin Is a Model Allosteric Protein. The cooperativity of oxygen binding to hemoglobin is a classic model for the behavior of many other multisubunit proteins (including many enzymes) that bind small molecules. In some cases, binding of a ligand to one site increases the affinity of other binding sites on the same protein (as in O_2 binding to hemoglobin). In other cases, a ligand decreases the affinity of other binding sites (as when BPG binding decreases the O_2 affinity of hemoglobin). All these effects are the result of **allosteric interactions** (Greek: *allos,* other + *stereos,* solid or space). *Allosteric effects, in which the binding of a ligand at one site affects the binding of another ligand at another site, generally require interactions among subunits of oligomeric proteins.* The $\mathrm{T} \rightarrow \mathrm{R}$ transition in hemoglobin subunits explains the difference in the oxygen affinities of oxy- and deoxyhemoglobin. Other proteins exhibit similar

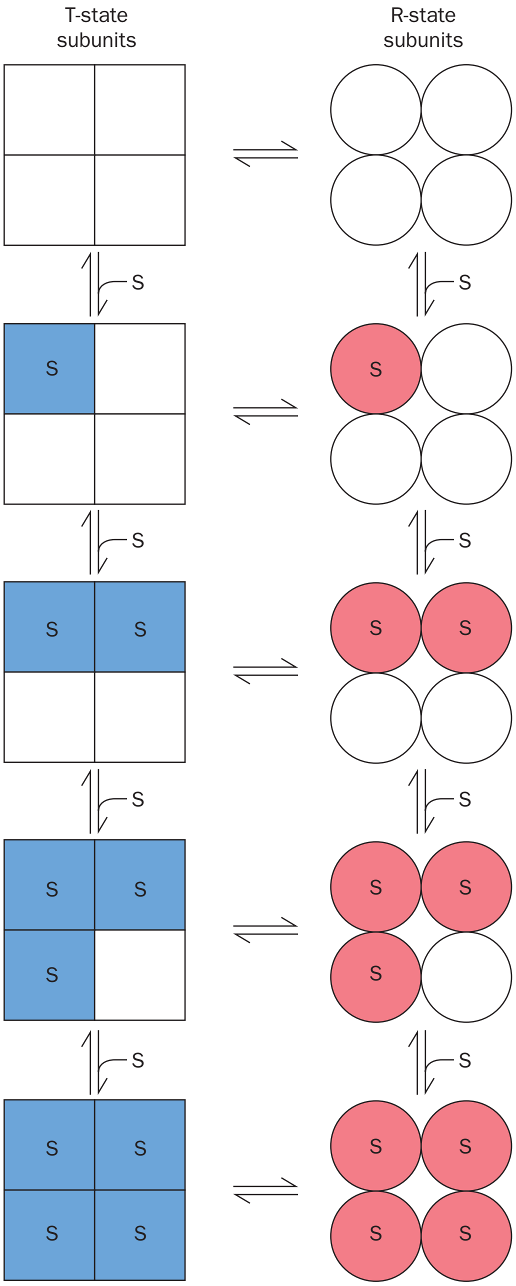

■ **Figure 7-15 | The symmetry model of allosterism.** Squares and circles represent T- and R-state subunits, respectively, of a tetrameric protein. The T and R states are in equilibrium regardless of the number of ligands (represented by S) that have bound to the protein. All the subunits must be in either the T or the R form; the model does not allow combinations of T- and R-state subunits in the same protein.

conformational shifts, although the molecular mechanisms that underlie these phenomena are not completely understood.

Two models that account for cooperative ligand binding have received the most attention. One of them, the **symmetry model** of allosterism, formulated in 1965 by Jacques Monod, Jeffries Wyman, and Jean-Pierre Changeux, is defined by the following rules:

1. An allosteric protein is an oligomer of symmetrically related subunits (although the α and β subunits of hemoglobin are only pseudosymmetrically related).
2. Each oligomer can exist in two conformational states, designated R and T; these states are in equilibrium.
3. The ligand can bind to a subunit in either conformation. *Only the conformational change alters the affinity for the ligand*.
4. *The molecular symmetry of the protein is conserved during the conformational change*. The subunits must therefore change conformation in a concerted manner; in other words, there are no oligomers that simultaneously contain R- and T-state subunits.

The symmetry model is diagrammed for a tetrameric binding protein in Fig. 7-15. If a ligand binds more tightly to the R state than to the T state, ligand binding will promote the T → R shift, thereby increasing the affinity of the unliganded subunits for the ligand.

One major objection to the symmetry model is that it is difficult to believe that oligomeric symmetry is perfectly preserved in all proteins, that is, that the T → R shift occurs simultaneously in all subunits regardless of the number of ligands bound. In addition, the symmetry model can account only for positive cooperativity, although some proteins exhibit negative cooperativity.

An alternative to the symmetry model is the **sequential model** of allosterism, proposed by Daniel Koshland. According to this model, ligand binding induces a conformational change in the subunit to which it binds, and cooperative interactions arise through the influence of those conformational changes on neighboring subunits. The conformational changes occur sequentially as more ligand-binding sites are occupied (Fig. 7-16). The ligand-binding affinity of a subunit varies with its conformation and may be higher or lower than that of the subunits in the ligand-free protein.

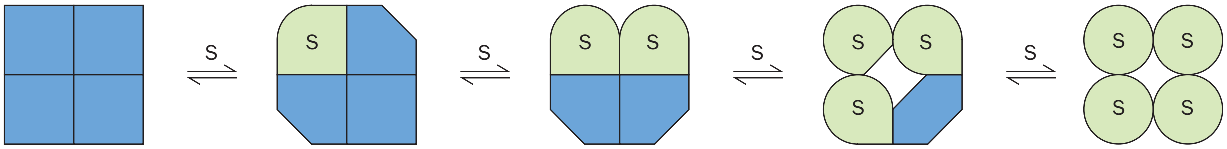

■ **Figure 7-16 | The sequential model of allosterism.** Ligand binding progressively induces conformational changes in the subunits, with the greatest changes occurring in those subunits that have bound ligand. The symmetry of the oligomeric protein is not preserved in this process as it is in the symmetry model.

Thus, proteins that follow the sequential model of allosterism may be positively or negatively cooperative.

If the mechanical coupling between subunits in the sequential model is particularly strong, the conformational changes occur simultaneously and the oligomer retains its symmetry, as in the symmetry model. Thus, the symmetry model of allosterism may be considered to be an extreme case of the more general sequential model.

Oxygen binding to hemoglobin exhibits features of both models. The quaternary T → R conformational change is concerted, as the symmetry model requires. Yet ligand binding to the T state does cause small tertiary structural changes, as the sequential model predicts. These minor conformational shifts are undoubtedly responsible for the buildup of strain that eventually triggers the T → R transition. It therefore appears that the complexity of ligand–protein interactions in hemoglobin and other proteins allows binding processes to be fine-tuned to the needs of the organism under changing internal and external conditions. We shall revisit allosteric effects when we discuss enzymes in Chapter 12.

E | Mutations May Alter Hemoglobin's Structure and Function

Before the advent of recombinant DNA techniques, mutant hemoglobins provided what was an almost unique opportunity to study structure–function relationships in proteins. This is because, for many years, hemoglobin was the only protein of known structure that had a large number of well-characterized naturally occurring **variants.** The examination of individuals with physiological disabilities, together with the routine electrophoretic screening of human blood samples, has led to the discovery of nearly 950 variant hemoglobins, >90% of which result from single amino acid substitutions in a globin polypeptide chain. Indeed, about 5% of the world's human population are carriers of an inherited variant hemoglobin.

Not all hemoglobin variants produce clinical symptoms, but some abnormal hemoglobin molecules do cause debilitating diseases (~300,000 individuals with serious hemoglobin disorders are born every year; naturally occurring hemoglobin variants that are lethal are, of course, never observed). Table 7-1 lists several of these hemoglobin variants. Mutations that destabilize hemoglobin's tertiary or quaternary structure alter hemoglobin's oxygen-binding affinity (p_{50}) and reduce its cooperativity (Hill coefficient). Moreover, the unstable hemoglobins are degraded by the erythrocytes, and their degradation products often cause the erythrocytes to **lyse** (break open). The resulting **hemolytic anemia** (anemia is a deficiency of red blood cells) compromises O_2 delivery to tissues.

Certain mutations at the O_2-binding site of either the α or β chain favor the oxidation of Fe(II) to Fe(III). Individuals carrying the resulting methemoglobin subunit exhibit **cyanosis,** a bluish skin color, due to the presence of methemoglobin in their arterial blood. These hemoglobins have reduced cooperativity (Hill coefficient ~1.2 compared to a maximum value of 2, since only two subunits in each of these methemoglobins can bind oxygen).

Mutations that increase hemoglobin's oxygen affinity lead to increased numbers of erythrocytes in order to compensate for the less than normal amount of oxygen released in the tissues. Individuals with this condition, which is named **polycythemia,** often have a ruddy complexion.

A Single Amino Acid Change Causes Sickle-Cell Anemia. Most harmful hemoglobin variants occur in only a few individuals, in many of whom the mutation apparently originated. However, ~10% of African-

Table 7-1 Some Hemoglobin Variants

Name[a]	Mutation	Effect
Hammersmith	Phe CD1(42)$\beta \rightarrow$ Ser	Weakens heme binding
Bristol	Val E11(67)$\beta \rightarrow$ Asp	Weakens heme binding
Bibba	Leu H19(136)$\alpha \rightarrow$ Pro	Disrupts the H helix
Savannah	Gly B6(24)$\beta \rightarrow$ Val	Disrupts the B–E helix interface
Philly	Tyr C1(35)$\beta \rightarrow$ Phe	Disrupts hydrogen bonding at the α_1–β_1 interface
Boston	His E7(58)$\alpha \rightarrow$ Tyr	Promotes methemoglobin formation
Milwaukee	Val E11(67)$\beta \rightarrow$ Glu	Promotes methemoglobin formation
Iwate	His F8(87)$\alpha \rightarrow$ Tyr	Promotes methemoglobin formation
Yakima	Asp G1(99)$\beta \rightarrow$ His	Disrupts a hydrogen bond that stabilizes the T conformation
Kansas	Asn G4(102)$\beta \rightarrow$ Thr	Disrupts a hydrogen bond that stabilizes the R conformation

[a] Hemoglobin variants are usually named after the place where they were discovered (e.g., hemoglobin Boston).

Americans and as many as 25% of black Africans carry a single copy of (are **heterozygous** for) the gene for **sickle-cell hemoglobin (hemoglobin S).** Individuals who carry two copies of (are **homozygous** for) the gene for hemoglobin S suffer from **sickle-cell anemia,** in which deoxyhemoglobin S forms insoluble filaments that deform erythrocytes (Fig. 7-17). In this painful, debilitating, and often fatal disease, the rigid, sickle-shaped cells cannot easily pass through the capillaries. Consequently, in a sickle-cell "crisis," the blood flow to some tissues may be completely blocked, resulting in tissue death. In addition, the mechanical fragility of the misshapen cells results in hemolytic anemia. Heterozygotes, whose hemoglobin is ~40% hemoglobin S, usually lead a normal life, although their erythrocytes have a shorter than normal lifetime.

In 1945, Linus Pauling hypothesized that sickle-cell anemia was the result of a mutant hemoglobin, and in 1949 he showed that the mutant hemoglobin had a less negative ionic charge than normal adult hemoglobin. This was the first evidence that a disease could result from an alteration in the molecular structure of a protein. Furthermore, since sickle-cell anemia is an inherited disease, a defective gene must be responsible for the abnormal protein. Nevertheless, the molecular defect in sickle-cell hemoglobin was not identified until 1956, when Vernon Ingram showed that hemoglobin S contains Val rather than Glu at the sixth position of each β chain. This was the first time an inherited disease was shown to arise from a specific amino acid change in a protein.

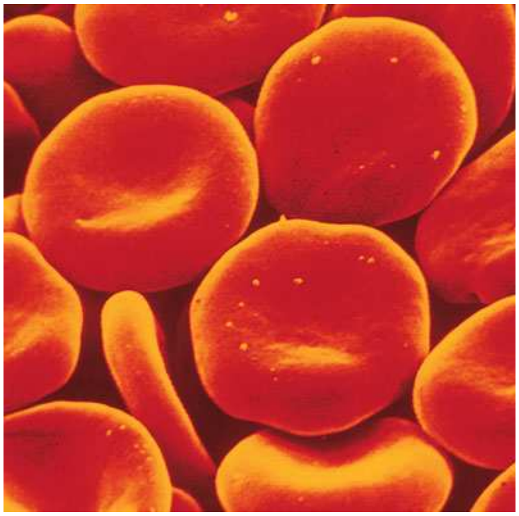

(a)

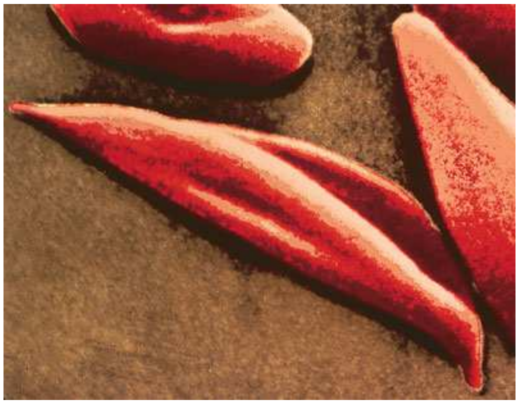

(b)

■ **Figure 7-17 | Scanning electron micrographs of human erythrocytes.** (*a*) Normal erythrocytes are flexible biconcave disks that can tolerate slight distortions as they pass through the capillaries (many of which have smaller diameters than erythrocytes). (*b*) Sickled erythrocytes from an individual with sickle-cell anemia are elongated and rigid and cannot easily pass through capillaries. [(a) David M. Phillips/Visuals Unlimited; (b) Bill Longcore/Photo Researchers, Inc.]

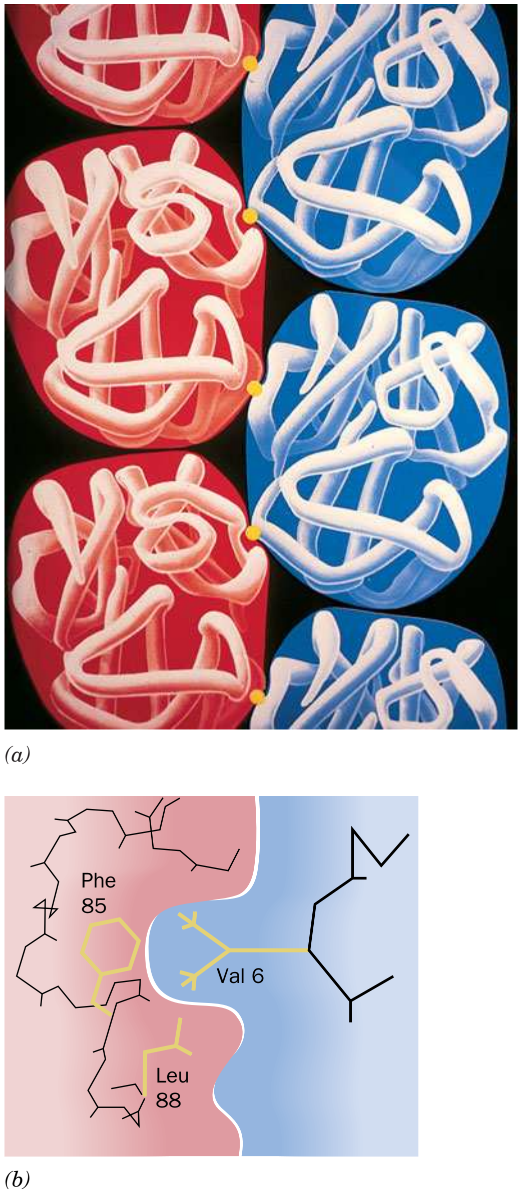

Figure 7-18 | Structure of a deoxyhemoglobin S fiber. (*a*) The arrangement of deoxyhemoglobin S molecules in the fiber. Only three subunits of each deoxyhemoglobin S molecule are shown. (*b*) The side chain of the mutant Val 6 in the β_2 chain of one hemoglobin S molecule (yellow knob in Part *a*) binds to a hydrophobic pocket on the β_1 subunit of a neighboring deoxyhemoglobin S molecule. [Illustration, Irving Geis. Image from the Irving Geis Collection/Howard Hughes Medical Institute. Rights owned by HHMI. Reproduction by permission only.]

The X-ray structure of deoxyhemoglobin S has revealed that one mutant Val side chain in each hemoglobin S tetramer nestles into a hydrophobic pocket on the surface of a β subunit in another hemoglobin tetramer (Fig. 7-18). This intermolecular contact allows hemoglobin S tetramers to form linear polymers. Aggregates of 14 strands that wind around each other form fibers extending throughout the length of the erythrocyte (Fig. 7-19). The hydrophobic pocket on the β subunit cannot accommodate the normally occurring Glu side chain, and the pocket is absent in oxyhemoglobin. Consequently, neither normal hemoglobin nor oxyhemoglobin S can polymerize. In fact, hemoglobin S fibers dissolve essentially instantaneously on oxygenation, so none are present in arterial blood. The danger of sickling is greatest when erythrocytes pass through the capillaries, where deoxygenation occurs. The polymerization of hemoglobin S molecules is time and concentration dependent, which explains why blood flow blockage occurs only sporadically (in a sickle-cell “crisis”).

Interestingly, many hemoglobin S homozygotes have only a mild form of sickle-cell anemia because they express relatively high levels of fetal hemoglobin, which contains γ chains rather than the defective β chains. The fetal hemoglobin dilutes the hemoglobin S, making it more difficult for hemoglobin S to aggregate during the 10–20 s it takes for an erythrocyte to travel from the tissues to the lungs for reoxygenation. The administration of **hydroxyurea,** the first and as yet the only effective treatment for sickle-cell anemia, ameliorates the symptoms of sickle-cell anemia by increasing the fraction of cells containing fetal hemoglobin (although the mechanism whereby hydroxyurea acts is unknown).

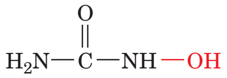

$$H_2N-\overset{\overset{\displaystyle O}{\|}}{C}-NH-OH$$

Hydroxyurea

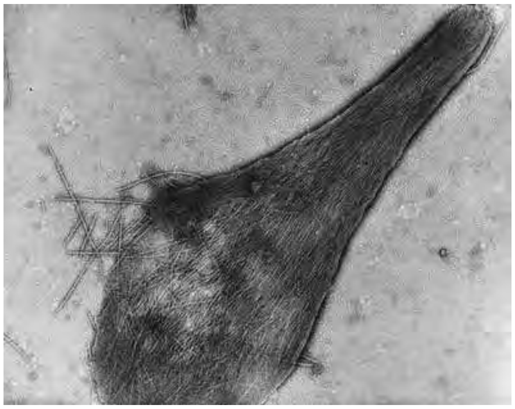

Figure 7-19 | Electron micrograph of deoxyhemoglobin S fibers spilling out of a ruptured erythrocyte. [Courtesy of Robert Josephs, University of Chicago.]

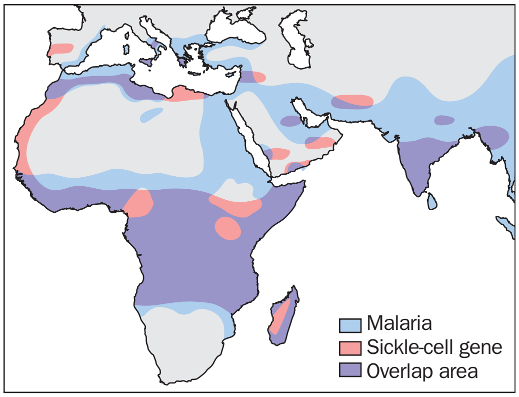

Figure 7-20 | Correspondence between malaria and the sickle-cell gene. The blue areas of the map indicate regions where malaria is or was prevalent. The pink areas represent the distribution of the gene for hemoglobin S. Note the overlap (*purple*) of the distributions.

Hemoglobin S Protects Against Malaria. Before the advent of modern palliative therapies, individuals with sickle-cell anemia rarely survived to maturity. Natural selection has not minimized the prevalence of the hemoglobin S variant, however, because heterozygotes are more resistant to **malaria,** an often lethal infectious disease. Of the 2.5 billion people living within malaria-endemic areas, 100 million are clinically ill with the disease at any given time and around 1 million, mostly very young children, die from it each year. Malaria is caused by the mosquito-borne protozoan *Plasmodium falciparum,* which resides within an erythrocyte during much of its 48-h life cycle. Infected erythrocytes adhere to capillary walls, causing death when cells impede blood flow to a vital organ.

The regions of equatorial Africa where malaria is a major cause of death coincide closely with those areas where the sickle-cell gene is prevalent (Fig. 7-20), thereby suggesting that the sickle-cell gene confers resistance to malaria. How does it do so? Plasmodia increase the acidity of infected erythrocytes by ~0.4 pH units. The lower pH favors the formation of deoxyhemoglobin via the Bohr effect, thereby increasing the likelihood of sickling in erythrocytes that contain hemoglobin S. Erythrocytes damaged by sickling are normally removed from the circulation by the spleen. During the early stages of a malarial infection, parasite-enhanced sickling probably allows the spleen to preferentially remove infected erythrocytes. In the later stages of infection, when the parasitized erythrocytes attach to the capillary walls (presumably to prevent the spleen from removing them from the circulation), sickling may mechanically disrupt the parasite. Consequently, heterozygous carriers of hemoglobin S in a malarial region have an adaptive advantage: They are more likely to survive to maturity than individuals who are homozygous for normal hemoglobin. Thus, in malarial regions, the fraction of the population who are heterozygotes for the sickle-cell gene increases until their reproductive advantage is balanced by the correspondingly increased proportion of homozygotes (who, without modern medical treatment, die in childhood).

2 Muscle Contraction

One of the most striking characteristics of living things is their capacity for organized movement. Such phenomena occur at all structural levels and include such diverse vectorial processes as the separation of replicated chromosomes during cell division, the beating of flagella and cilia, and, most obviously, muscle contraction. In this section, we consider the structural

CHECK YOUR UNDERSTANDING

Describe the O_2-binding behavior of myoglobin in terms of pO_2 and K. How is K defined?
Explain the structural basis for cooperative oxygen binding to hemoglobin.
Describe how myoglobin and hemoglobin function in delivering O_2 from the lungs to respiring tissues.
What is the physiological relevance of the Bohr effect and BPG?
Explain why mutations can increase or decrease the oxygen affinity and cooperativity of hemoglobin. How can the body compensate for these changes?

LEARNING OBJECTIVES

- Understand that myosin is a motor protein that undergoes conformational changes as it hydrolyzes ATP.
- Understand how the sliding filament model of muscle contraction describes the movement of thick filaments relative to thin filaments.
- Understand how the globular protein actin can form structures such as microfilaments and the thin filaments of muscle.

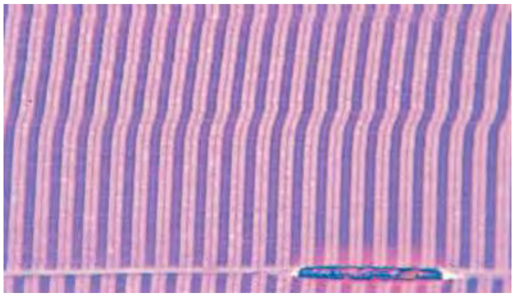

Figure 7-21 | Photomicrograph of a muscle fiber. The longitudinal axis of the fiber is horizontal (perpendicular to the striations). The alternating pattern of dark A bands and light I bands from multiple in-register myofibrils is clearly visible. [J.C. Revy, CNRI/Photo Researchers.]

and chemical basis of movement in **striated muscle,** one of the best understood mobility systems.

A | Muscle Consists of Interdigitated Thick and Thin Filaments

The voluntary muscles, which include the skeletal muscles, have a striated (striped) appearance when viewed by light microscopy (Fig. 7-21). Such muscles consist of long multinucleated cells (the muscle fibers) that contain parallel bundles of **myofibrils** (Greek: *myos,* muscle; Fig. 7-22). Electron micrographs show that muscle striations arise from the banded structure of multiple in-register myofibrils. The bands are formed by alternating regions of greater and lesser electron density called **A bands** and **I bands,** respectively (Fig. 7-23). The myofibril's repeating unit, the **sarcomere** (Greek: *sarkos,* flesh), is bounded by **Z disks** at the center of each I band. The A band is centered on the **H zone,** which in turn is centered on the **M disk.** The A band contains 150-Å-diameter **thick filaments,** and the I band contains 70-Å-diameter **thin filaments.** The two sets of filaments are linked by cross-bridges where they overlap.

A contracted muscle can be as much as one-third shorter than its fully extended length. The contraction results from a decrease in the length of the sarcomere, caused by reductions in the lengths of the I band and the H zone (Fig. 7-24*a*). These observations, made by Hugh Huxley in 1954

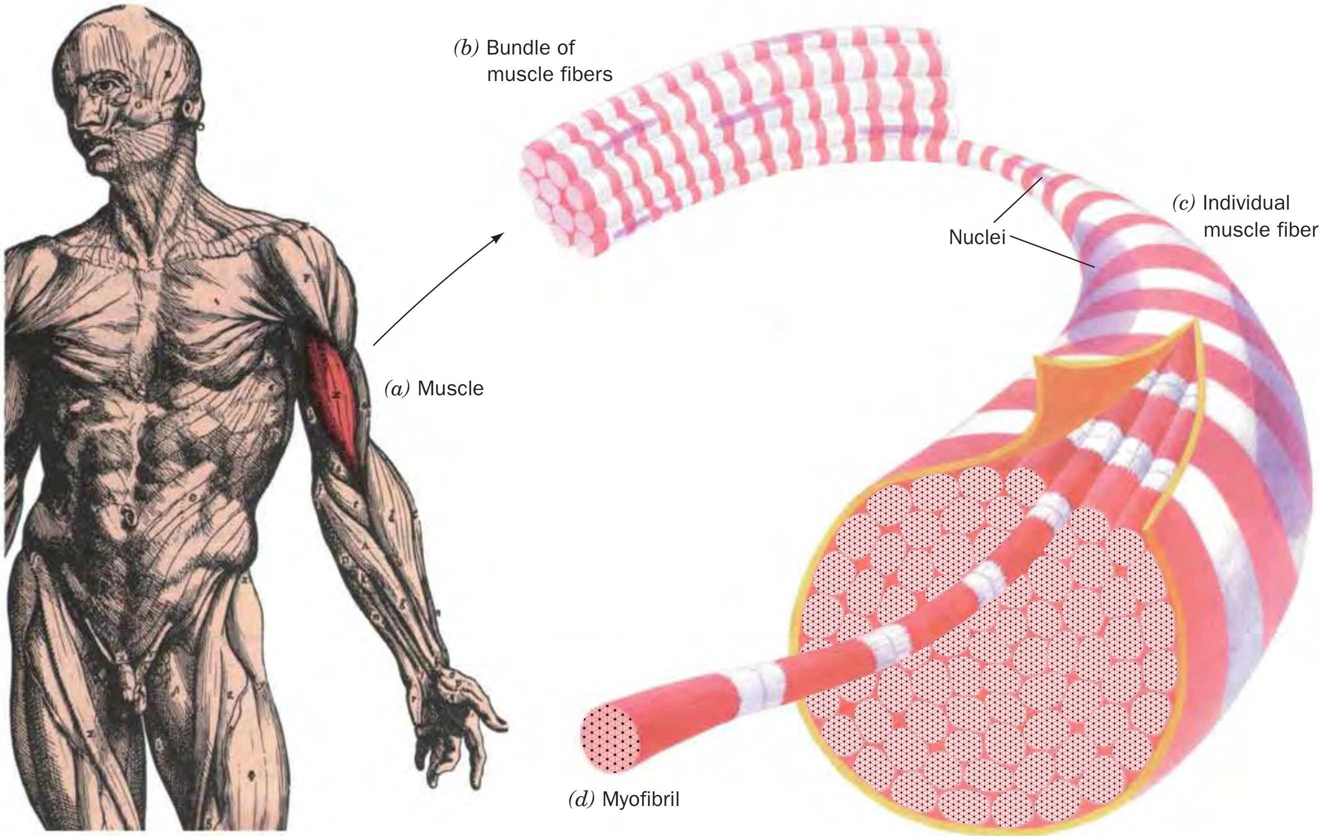

Figure 7-22 | Skeletal muscle organization. A muscle (*a*) consists of bundles of muscle fibers (*b*), each of which is a long, thin, multinucleated cell (*c*) that may run the length of the muscle. Muscle fibers contain bundles of laterally aligned myofibrils (*d*), which in turn consist of bundles of alternating thick and thin filaments.

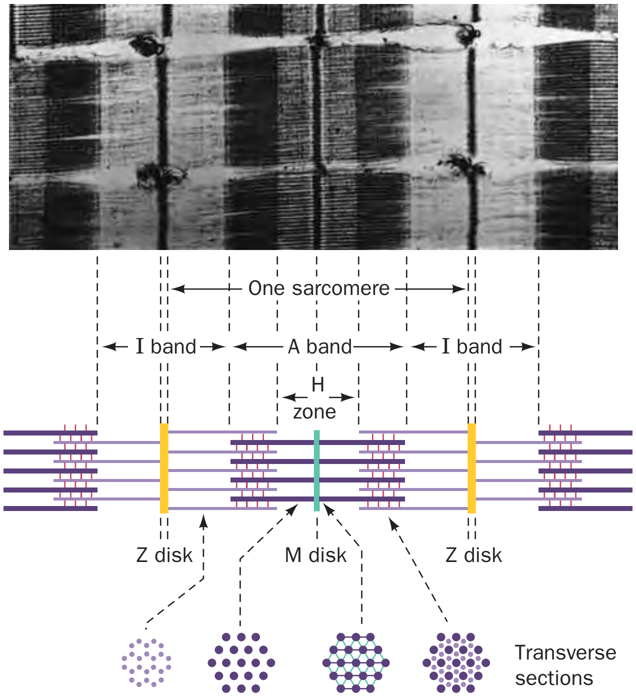

Figure 7-23 | **Anatomy of the myofibril.** The electron micrograph shows parts of three myofibrils, which are separated by horizontal gaps. The accompanying interpretive drawing shows the major features of the myofibril: the light I band, which contains only thin filaments; the A band, whose dark H zone contains only thick filaments and whose darker outer segments contain overlapping thick and thin filaments; the Z disk, to which the thin filaments are anchored; and the M disk, which arises from a bulge at the center of each thick filament. The myofibril's functional unit, the sarcomere, is the region between two successive Z disks. [Courtesy of Hugh Huxley, Brandeis University.]

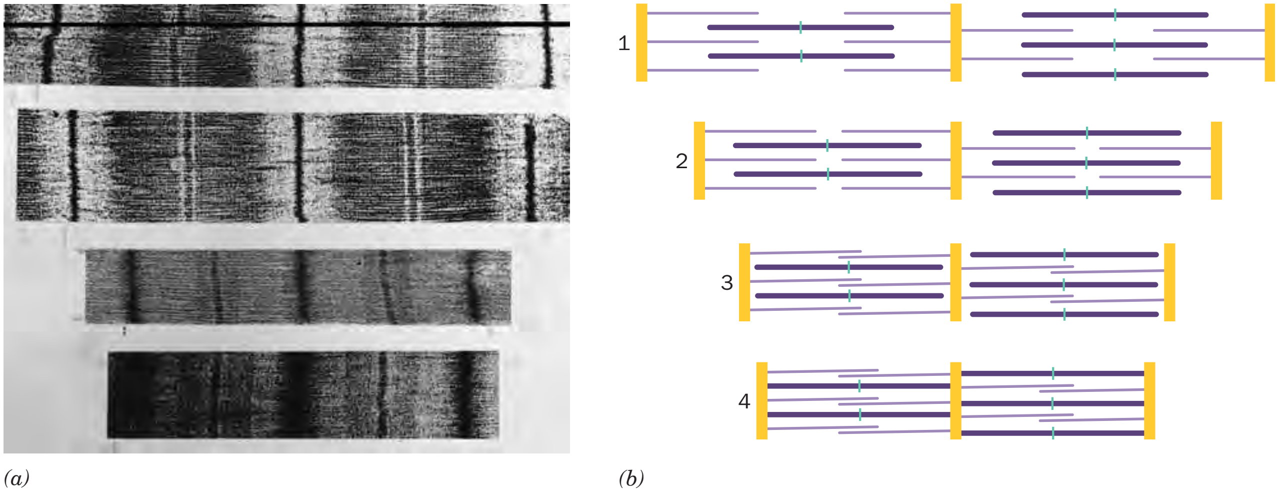

Figure 7-24 | **Myofibril contraction.** (*a*) Electron micrographs showing myofibrils in progressively more contracted states. The lengths of the I band and H zone decrease on contraction, whereas the lengths of the thick and thin filaments remain constant. (*b*) Interpretive drawings showing interpenetrating sets of thick and thin filaments sliding past each other. [Courtesy of Hugh Huxley, Brandeis University.]

BOX 7-4 **PATHWAYS OF DISCOVERY**

Hugh Huxley and the Sliding Filament Model

Hugh Huxley (1924–)

The mechanism of muscle action has fascinated scientists for hundreds if not thousands of years. The first close look at muscle fibers came in 1682, when Antoni van Leeuwenhoek's early microscope revealed a pattern of thin longitudinal fibers. In the modern era, research on muscle has followed one of two approaches. First, it is possible to study muscle as an energy-transducing system, in which metabolic energy is generated and consumed. This line of research received a tremendous boost in the 1930s with the discovery that ATP is the energy source for muscle contraction. The second approach involves treating muscle as a mechanical system, that is, sorting out its rods and levers. Ultimately, a molecular approach united the mechanical and energetic aspects of muscle research. The insights of Hugh Huxley made this possible.

The molecular characterization of muscle did not occur overnight. In 1859, Willi Kühne isolated a proteinaceous substance from muscle tissue that he named "myosin" (almost certainly a mixture of many proteins), but it tended to aggregate and was therefore not as popular a study subject as the more soluble proteins such as hemoglobin. A major breakthrough in muscle protein chemistry came in 1941, when the Hungarian biochemist Albert Szent-Györgyi showed that two types of protein could be extracted from ground muscle by a solution with high salt concentration (Szent-Györgyi also contributed to the elucidation of the citric acid cycle; Box 17-1). Extraction for 20 minutes yielded a protein he named myosin A but which is now called myosin. However, extraction overnight yielded a second protein which he named myosin B but is now called actomyosin. It soon became apparent that myosin B was a mixture of two proteins, myosin and a new protein which was named actin. Further work showed that threads of actomyosin contracted to ~10% of their original length in the presence of ATP. Since actin and myosin alone do not contract in the presence of ATP, the contraction must have resulted from their interaction. However, it took another decade to develop a realistic model of how myosin and actin interact.

A number of theories had been advanced to explain muscle contraction. According to one theory, the cytoplasm of muscle cells moved like that of an amoeba. Other theories proposed that muscle fibers took up and gave off water or repelled and attracted other fibers electrostatically. Linus Pauling, who had recently discovered the structures of the α helix and β sheet (Box 6-1), ventured that myosin could change its length by shifting between the two protein conformations. Huxley formulated an elegant—and correct—explanation in his sliding filament model for muscle contraction.

In 1948, Huxley began his doctoral research at Cambridge University in the United Kingdom, in the laboratory of John Kendrew (who 10 years later determined the first X-ray structure of a protein, that of myoglobin; Section 7-1A). There, through X-ray studies on frog muscle fibers, Huxley established that the X-ray diffraction pattern changes with the muscle's physiological state. Furthermore, he showed that muscle contained two sets of parallel fibers, rather than one, and that these fibers were linked together by multiple cross-links. These observations became the germ for further research, which he carried out at MIT in 1953 and 1954. He teamed up with Jean Hanson, a Briton who was also working at MIT. Hanson made good use of her knowledge of muscle physiology and her expertise in phase-contrast microscopy, a technique that could visualize the banded patterns of muscle fibers. Huxley and Hanson observed rabbit muscle fibers under different experimental conditions, making precise measurements of the width of the A and I bands in sarcomeres (Fig. 7-23). In one experiment, they extracted myosin from the muscle fiber, noted the loss of the dark A band, and concluded that the A band consists of myosin. When they extracted both actin and myosin, all identifiable structure was lost, and they concluded that actin is present throughout the sarcomere.

When ATP was added, the muscle slowly contracted, and Huxley and Hanson were able to measure the shortening of the I band. The A band maintained a constant length but became darker. A muscle fiber under the microscope could also be stretched by pulling on the coverslip. As the muscle "relaxed," the I band increased in width and the A band became less dense. Measurements were made for muscle fibers contracted to 60% of their original length and stretched to 120% of their original length.

The key to the sliding filament model that Huxley described and subsequently refined is that the individual molecules (that is, their observable fibrous forms) do not shrink or extend but instead slide past each other. During contraction, actin filaments (thin filaments) in the I band are drawn into the A band, which consists of stationary myosin-containing filaments (thick filaments). During stretching, the actin filaments withdraw from the A band. Similar conclusions were reached by the team of Andrew Huxley (no relation to Hugh) and Rolf Niedergerke, who were examining the contraction of living frog muscle fibers. Both groups published their work in back-to-back papers in *Nature* in 1954.

Hugh Huxley went on to supply additional details to his sliding filament model. For example, he showed that myosin forms cross-bridges with actin fibers. However, these bridges are asymmetric, pointing in opposite directions in the two halves of the sarcomere. This arrangement allows myosin to pull thin filaments in opposite directions toward the center of the sarcomere (Fig. 7-24).

While Huxley was describing the mechanism of muscle contraction, Watson and Crick discovered the structure of DNA, and Max Perutz made a decisive breakthrough in the use of heavy metal atoms to solve the phase problem in his X-ray studies of hemoglobin (Box 7-2). Collectively, these discoveries indicated the tremendous potential for describing biological phenomena in molecular terms. Subsequent studies of muscle contraction have used electron microscopy, X-ray crystallography, and enzymology to probe the fine details of the sliding filament model, including the structure of myosin's lever arm, the composition of the thin filament, and the exact role of ATP in triggering conformational changes that generate mechanical force.

Huxley, H.E. and Hanson, J., Changes in the cross-striations of muscle during contraction and stretch and their structural interpretation, *Nature* **173,** 973–976 (1954).

(Box 7-4), are explained by the **sliding filament model** in which interdigitated thick and thin filaments slide past each other (Fig. 7-24*b*). Thus, during a contraction, a muscle becomes shorter, and because its total volume does not change, it also becomes thicker.

Thick Filaments Consist Mainly of Myosin. Vertebrate thick filaments are composed almost entirely of a single type of protein, **myosin,** which consists of six polypeptide chains: two 220-kD **heavy chains** and two pairs of different **light chains,** the so-called **essential** and **regulatory light chains (ELC** and **RLC)** that vary in size between 15 and 22 kD, depending on their source. X-Ray structure determinations by Ivan Rayment and Hazel Holden of the N-terminal half of the myosin heavy chain, the so-called **myosin head,** reveals that it forms an elongated (55 × 165 Å) globular head to which one subunit each of ELC and RLC bind (Fig. 7-25*a*). The C-terminal half of the heavy chain forms a long fibrous α-helical tail, two of which associate to form a left-handed coiled coil. Thus, *myosin consists of a 1600-Å-long rodlike segment with two globular heads* (Fig. 7-25*b*). The

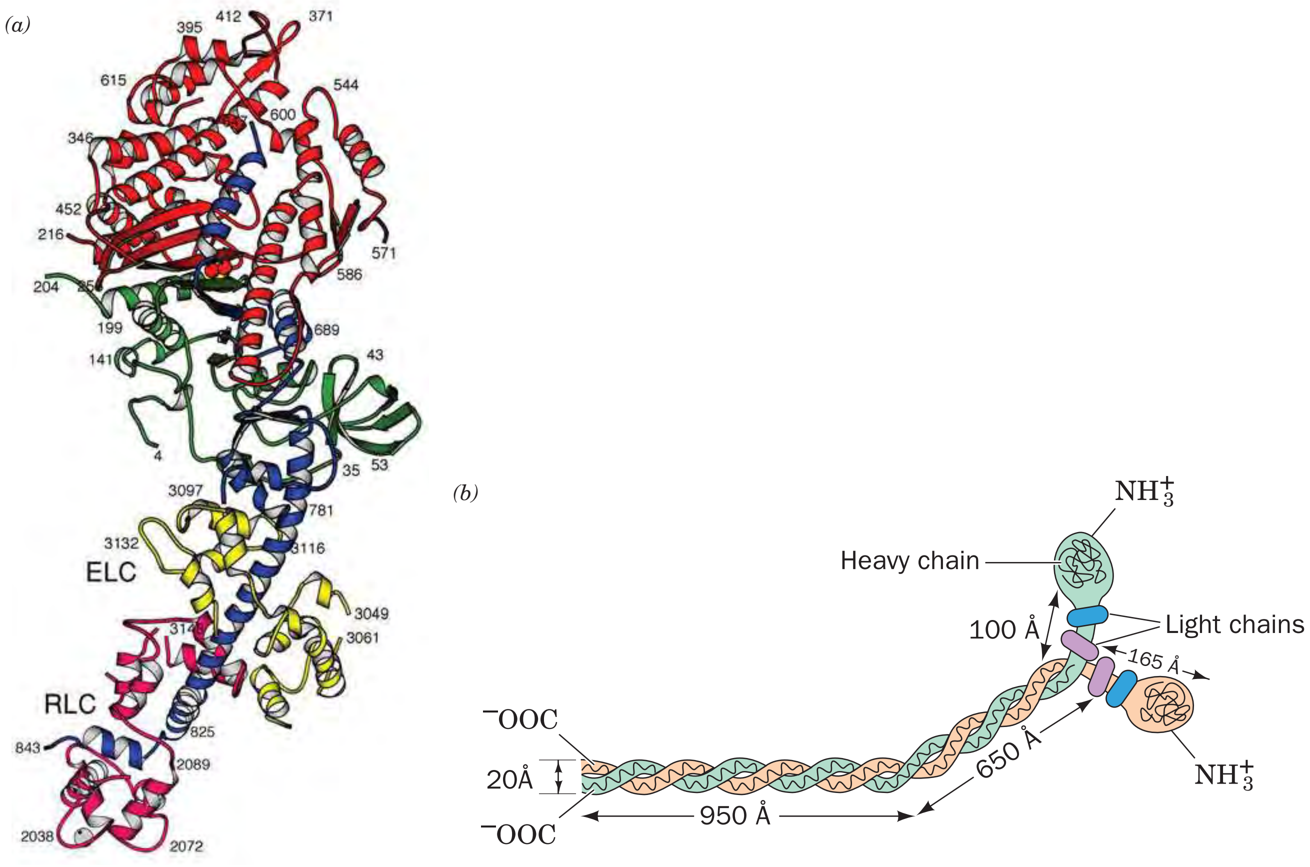

Figure 7-25 | Structure of myosin. (*a*) A ribbon diagram of the myosin head from chicken muscle. The heavy chain's 25-, 50-, and 20-kD segments are green, red, and blue, respectively, and its essential and regulatory light chains, RLC and ELC, are magenta and yellow. Residue numbers are indicated at various positions, with 2000 and 3000 being added to those of the RLC and ELC to distinguish them from the heavy chain. A sulfate ion, shown in space-filling form (*red*), is bound near the confluence of the three heavy chain segments, where it occupies the binding site of ATP's β-phosphate group. An RLC-bound Ca^{2+} ion (*lower left*) is represented by a gray ball. [Courtesy of Ivan Rayment and Hazel Holden, University of Wisconsin. PDBid 2MYS.] (*b*) Diagram of the myosin molecule. Its two identical heavy chains (*green and orange*) each have an N-terminal globular head and an α-helical tail. Between the head and tail is an α helix, the lever arm, that associates with the two kinds of light chains (*light blue and lavender*). The tails wind around each other to form a 1600-Å-long parallel coiled coil.

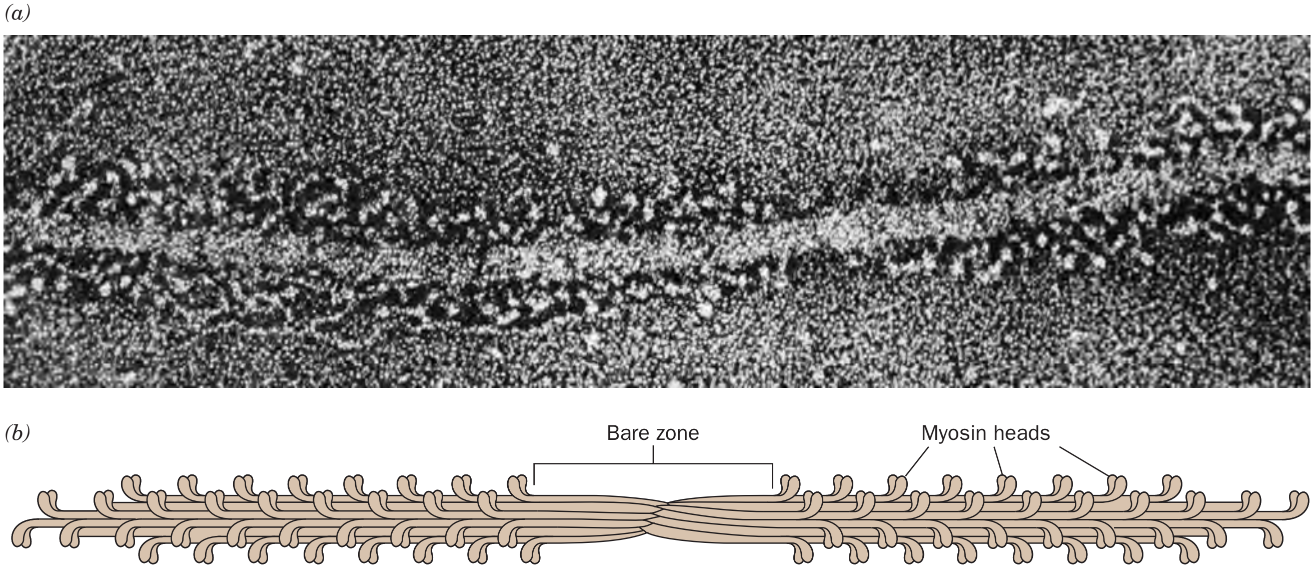

■ **Figure 7-26 | Structure of the thick filament.** (*a*) Electron micrograph showing the myosin heads projecting from the thick filament. [From Trinick, J. and Elliott, A., *J. Mol. Biol.* **131,** 135 (1977).] (*b*) Drawing of a thick filament, in which several hundred myosin molecules form a staggered array with their globular heads pointing away from the filament.

amino acid sequence of myosin's α-helical tail is characteristic of coils such as those in keratin (Section 6-1C): It has a seven-residue pseudorepeat, *a-b-c-d-e-f-g,* with nonpolar residues predominating at positions *a* and *d.*

Under physiological conditions, several hundred myosin molecules aggregate to form a thick filament. The rodlike tails pack end to end in a regular staggered array, leaving the globular heads projecting to the sides on both ends (Fig. 7-26). These myosin heads form the cross-bridges to thin filaments in intact myofibrils. The myosin head, which is an **ATPase** (ATP-hydrolyzing enzyme), has its ATP-binding site located in a 13-Å-deep V-shaped pocket.

Thin Filaments Consist Mainly of Actin. Thin filaments consist mainly of polymers of **actin,** the most abundant cytosolic protein in eukaryotes (comprising ~20% of the protein in muscle cells and up to 15% of the protein in nonmuscle cells). In its monomeric form, this ~375-residue protein is known as **G-actin** (G for globular); when polymerized, it is called **F-actin** (F for fibrous). Each actin subunit has binding sites for ATP and a Ca^{2+} or Mg^{2+} ion that are located in a deep cleft (Fig. 7-27). ATP hydrolysis to ADP + P_i is not required for actin polymerization but occurs afterward (Section 7-2C).

The fibrous nature of F-actin and its variable fiber lengths has thwarted its crystallization in a manner suitable for X-ray crystallographic analysis. Consequently, our current understanding of the atomic structure of F-actin is based on electron micrographs (Fig. 7-28*a*) together with low resolution models based on X-ray studies of oriented gels of F-actin into which high resolution atomic models of G-actin have been fitted (Fig. 7-28*b*). These models indicate that the actin polymer is a double-stranded helix of subunits in which each subunit contacts four others. Each actin subunit has

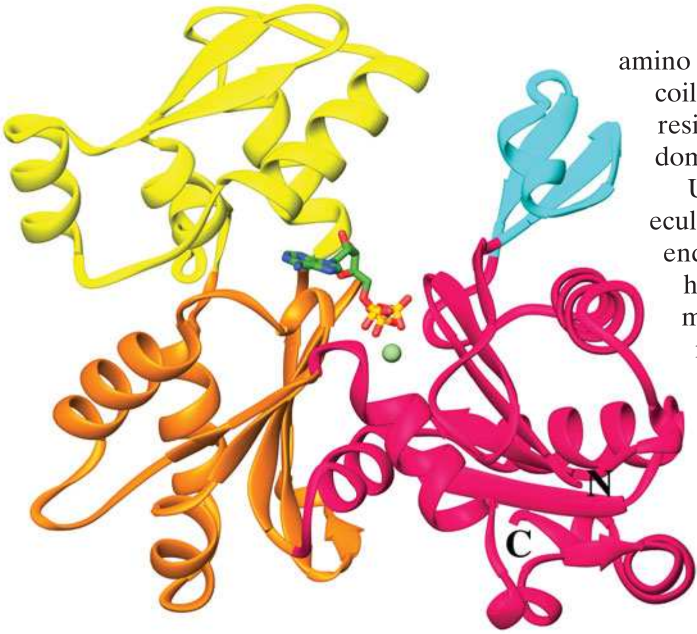

■ **Figure 7-27 | X-Ray structure of rabbit muscle actin.** The four domains of the protein are colored cyan, magenta, orange, and yellow, and the N- and C-termini are labeled. A nonhydrolyzable ATP analog, adenosine-5′-(β,γ-imido)triphosphate, drawn in stick form and colored according to atom type (C green, N blue, O red, and P gold), binds at the bottom of a deep cleft between the domains. The Ca^{2+} ion is represented by a light green sphere. [Based on an X-ray structure by Roberto Dominguez, Boston Biomedical Research Institute, Watertown, Massachusetts. PDBid 1NWK.]

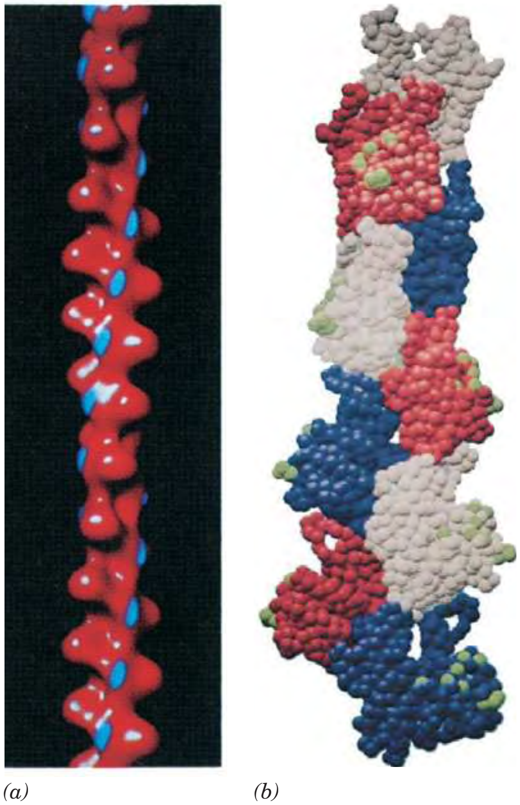

Figure 7-28 | Structure of the actin filament. (*a*) Cryoelectron microscopy–based image. The tropomyosin binding sites (see below) are blue. [Courtesy of Daniel Safer, University of Pennsylvania, and Ronald Milligan, The Scripps Research Institute, La Jolla, California.] (*b*) Model based on fitting the known X-ray structure of the actin monomer to the X-ray fiber diffraction pattern of F-actin. Actin monomers are shown in space-filling representation, in alternating blue, red, and white, with each amino acid residue represented by a sphere. The lowest monomer shown is oriented identically to that in Fig. 7-27. The residues that cross-linking studies indicate form the myosin-binding site (see below) are green. [Courtesy of Wolfgang Kabsch and Kenneth Holmes, Max-Planck-Institute für medizinische Forschung, Heidleberg, Germany.]

the same head-to-tail orientation (e.g., all the nucleotide-binding clefts open upward in Fig. 7-28*b*), so the assembled fiber has a distinct polarity. The end of the fiber toward which the nucleotide-binding sites open is known as the **(−) end,** and its opposite end is the **(+) end.** The (+) ends of the thin filaments bind to the Z disk (Fig. 7-23).

Each of muscle F-actin's monomeric units can bind a single myosin head (Fig. 7-29), probably by ion pairing and by the association of hydrophobic patches on each protein. Electron micrographs indicate that the myosin heads bound to an F-actin filament all have the same orientation

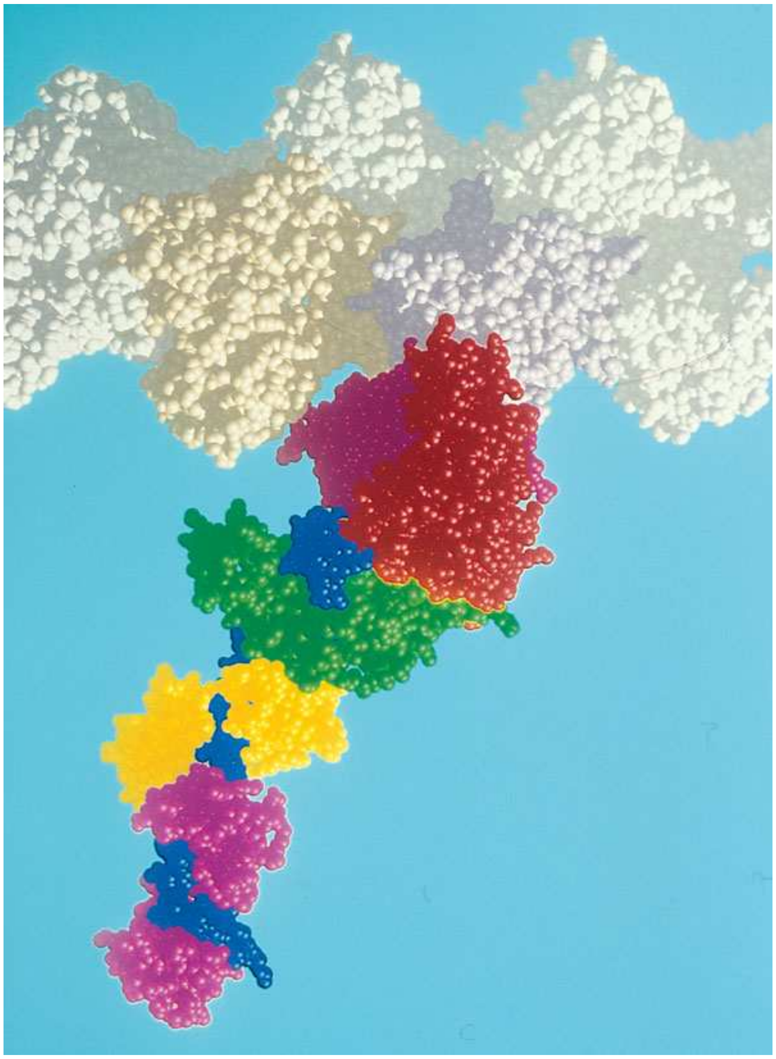

Figure 7-29 | Model of the myosin–actin interaction. This space-filling model was constructed from the X-ray structures of actin and the myosin head and electron micrographs of their complex. The actin filament is at the top. The myosin head globular regions are red and green, its α-helical lever arm is blue, and the light chains are yellow and purple. The coiled-coil tail is not shown. An ATP-binding site is located in a cleft in the red domain of the myosin head. In a myofibril, every actin monomer has the potential to bind a myosin head, and the thick filament has many myosin heads projecting from it. [Courtesy of Ivan Rayment and Hazel Holden, University of Wisconsin.]

(Fig. 7-30) and that in thin filaments that are still attached to the Z disk, the myosin heads all point away from the Z disk.

Tropomyosin and Troponin Are Thin Filament Components. Myosin and actin, the major components of muscle, account for 60 to 70% and 20 to 25% of total muscle protein, respectively. Of the remainder, two proteins that are associated with the thin filaments are particularly prominent:

1. **Tropomyosin,** a homodimer whose two 284-residue α-helical subunits wrap around each other to form a parallel coiled coil that extends nearly the entire 400-Å length of the molecule (a portion of which is shown in Fig. 6-15*b*). Multiple copies of these rod-shaped proteins are joined head-to-tail to form cables wound in the grooves of the F-actin helix such that each tropomyosin molecule contacts seven consecutive actin subunits in a quasi-equivalent manner (Fig. 7-30).
2. **Troponin,** which consists of three subunits: **TnC,** a Ca^{2+}-binding protein; **TnI,** which binds to actin; and **TnT,** an elongated molecule, which binds to tropomyosin at its head-to-tail junctions. The X-ray structure of troponin in complex with four Ca^{2+} ions (Fig. 7-31), determined by Robert Fletterick, reveals that TnI closely resembles the myosin light chains and that the inhibitory segment of TnI binds to TnC's rigid central helix in this Ca^{2+}-activated state.

The tropomyosin–troponin complex, as we shall see below, regulates muscle contraction by controlling the access of the myosin heads to their binding site on actin.

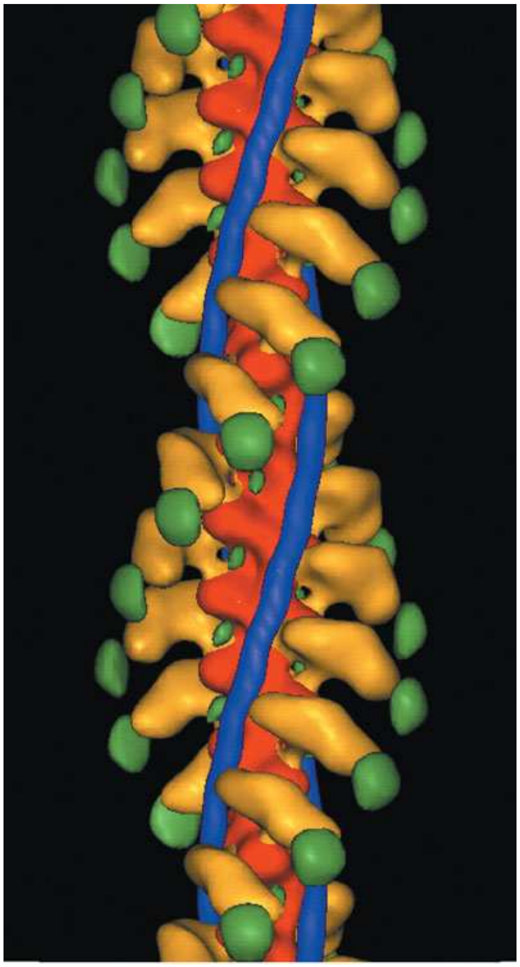

Figure 7-30 | Cryoelectron microscopy–based image at <25-Å resolution of a thin filament decorated with myosin heads. F-actin is red, tropomyosin is blue, the myosin motor domain is yellow, yellow, and the essential light chain is green. The helical filament has a pitch (rise per turn) of 370 Å. [Courtesy of Ronald Milligan, The Scripps Research Institute, La Jolla, California.]

Muscle Contains Numerous Minor Proteins That Organize Its Structure. Other proteins serve to form the Z disk and the M disk and to organize the arrays of thick and thin filaments. For instance, **α-actinin,** a rodlike homodimeric protein that cross-links F-actin filaments, is localized in the Z disk's interior and is therefore thought to attach oppositely oriented thin filaments to the Z disk.

One of the more unusual muscle proteins, **titin,** the longest known polypeptide chain (34,350 residues), is composed of ~300 repeating

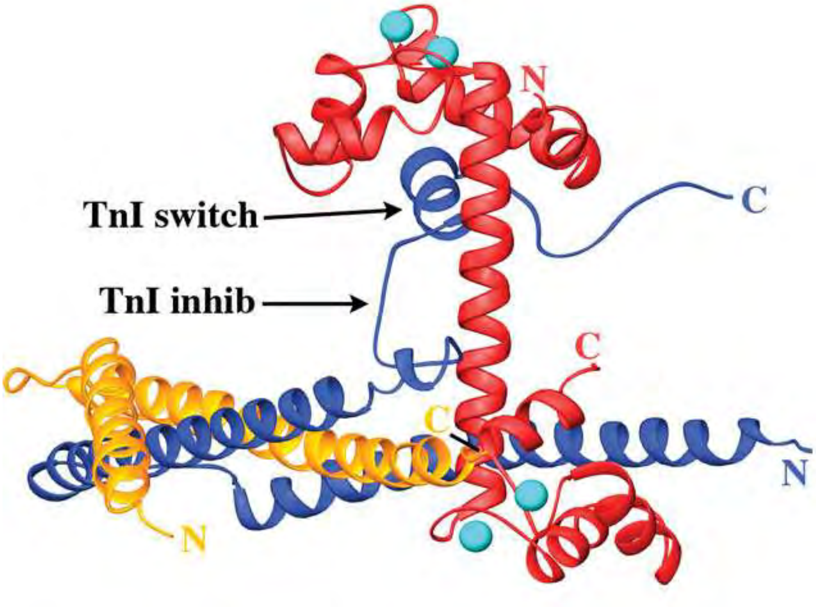

Figure 7-31 | X-Ray structure of chicken skeletal muscle troponin. TnC is red, TnI is blue, and TnT is gold. The four Ca^{2+} ions bound by TnC are represented by cyan spheres. [Based on an X-ray structure by Robert Fletterick, University of California at San Francisco. PDBid 1YTZ.]

globular domains. Three to six titin molecules associate with each thick filament, spanning the 1-μm distance between the M and Z disks. Titin is believed to function as a molecular bungee cord to keep the thick filament centered on the sarcomere: During muscle contraction, it compresses as the sarcomere shortens, but when the muscle relaxes, titin resists sarcomere extension past the starting point.

Nebulin, which is also extremely large (6669 residues), is a mainly α-helical protein that is associated with the thin filament. It is thought to set the length of the thin filament by acting as a template for actin polymerization. This length is held constant by **tropomodulin,** which caps the (−) end of the thin filament (the end not attached to the Z disk), thereby preventing further actin polymerization and depolymerization. **CapZ** (also called **β-actinin**) is an α-actinin-associated heterodimer that similarly caps the (+) end of F-actin.

The M disk (Fig. 7-23) arises from the local enlargement of in-register thick filaments. Two proteins that are associated with this structure, **myomensin** and **M-protein,** bind to titin and are therefore likely to participate in thick filament assembly, as does the thick filament–associated **myosin-binding protein C.**

Duchenne muscular dystrophy (DMD) and the less severe **Becker muscular dystrophy (BMD)** are both sex-linked muscle-wasting diseases. In DMD, which has an onset age of 2 to 5 years, muscle degeneration exceeds muscle regeneration, causing progressive muscle weakness and ultimately death, typically due to respiratory disorders or heart failure, usually by age 25. In BMD, the onset age is 5 to 10 years and there is an overall less progressive course of muscle degeneration and a longer (sometimes normal) life span than in individuals with DMD.

The gene responsible for DMD/BMD encodes a 3685-residue protein named **dystrophin,** which has a normal abundance in muscle tissue of 0.002%. Individuals with DMD usually have no detectable dystrophin in their muscles, whereas those with BMD mostly have dystrophins of altered sizes. Evidently, the dystrophins of individuals with DMD are rapidly degraded, whereas those of individuals with BMD are semifunctional.

Dystrophin is a member of a family of flexible rod-shaped proteins that includes other actin-binding cytoskeletal components. Dystrophin associates on the inner surface of the muscle plasma membrane with a transmembrane glycoprotein complex, where it helps anchor F-actin to the extracellular matrix and thereby protects the plasma membrane from being torn by the mechanical stress of muscle contraction. Although such small tears are common in muscle cells, they occur much more frequently in dystrophic cells, leading to a greatly increased rate of cell death.

B | Muscle Contraction Occurs When Myosin Heads Walk Up Thin Filaments

In order to complete our description of muscle contraction we must determine how ATP hydrolysis is coupled to the sliding filament model. If the sliding filament model is correct then it would be impossible for a myosin cross-bridge to remain attached to the same point on a thin filament during muscle contraction. Rather, it must repeatedly detach and then reattach itself at a new site further along the thin filament toward the Z disk. This, in turn, suggests that *muscular tension is generated through the interaction of myosin cross-bridges with thin filaments.* The actual contractile force is provided by ATP hydrolysis. Thus, myosin is a **motor protein** that converts the chemical energy of ATP hydrolysis to the mechanical energy of movement. Edwin Taylor formulated a model for myosin-mediated ATP hydrolysis, which has been refined by the structural studies of Rayment, Holden, and Ronald Milligan as follows (Fig. 7-32):

1. ATP binds to a myosin head in a manner that causes myosin's actin-binding site to open up and release its bound actin.

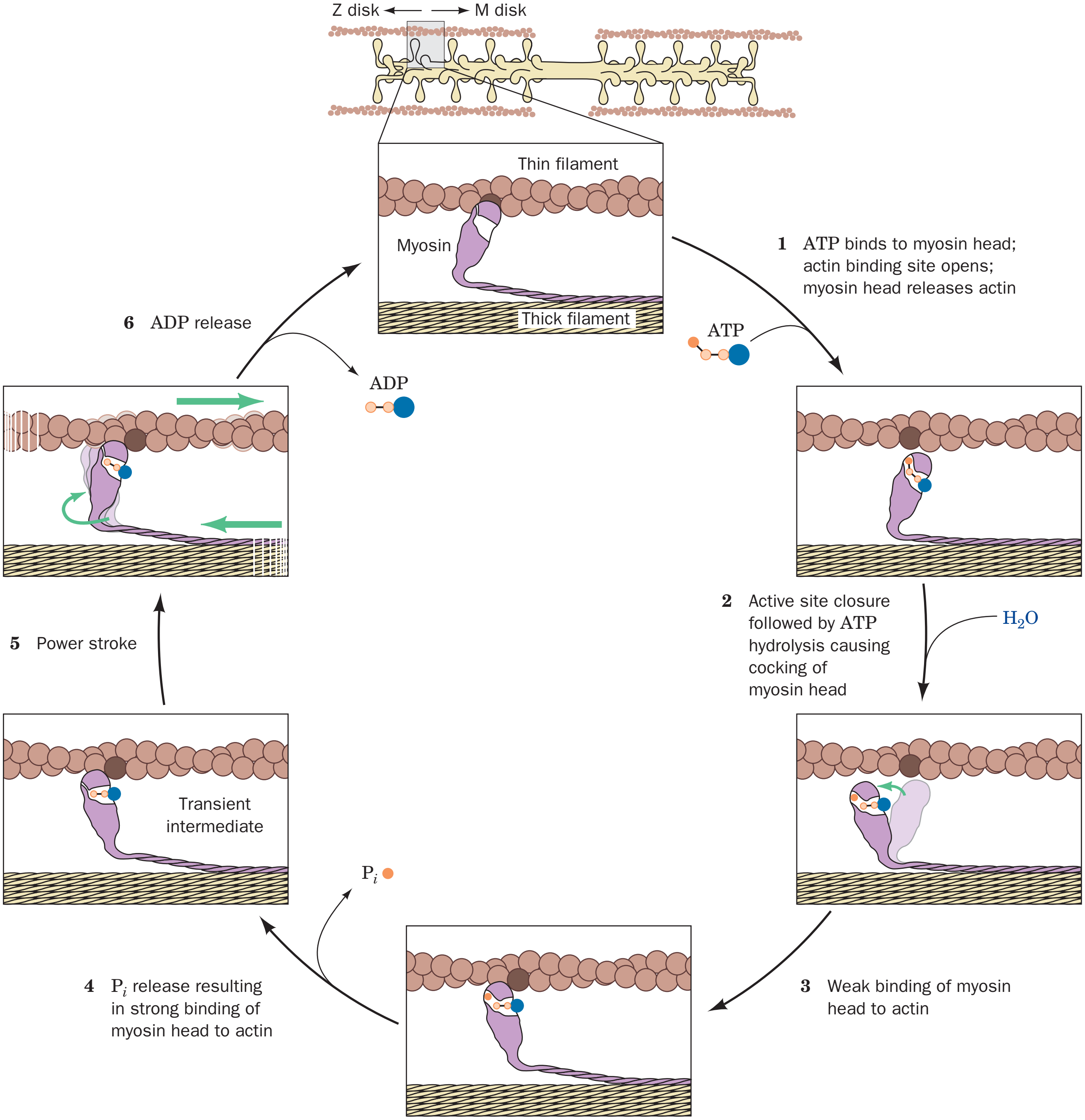
Z disk
M disk
Thin filament
Myosin
Thick filament
1 ATP binds to myosin head; actin binding site opens; myosin head releases actin
ATP
2 Active site closure followed by ATP hydrolysis causing cocking of myosin head
H_2O
3 Weak binding of myosin head to actin
4 P_i release resulting in strong binding of myosin head to actin
P_i
Transient intermediate
5 Power stroke
6 ADP release
ADP

■ **Figure 7-32 | Mechanism of force generation in muscle.** The myosin head "walks" up the actin thin filament through a unidirectional cyclic process that is driven by ATP hydrolysis to ADP and P_i. Only one myosin head is shown. The actin monomer to which the myosin head is bound at the beginning of the cycle is more darkly colored for reference. [After Rayment, I. and Holden, H., *Curr. Opin. Struct. Biol.* **3,** 949 (1993).] **See the Animated Figures.**

2. Myosin's active site (distinct from its actin-binding site) closes around the ATP. The resulting hydrolysis of the ATP to ADP + P_i "cocks" the myosin head, that is, puts it into its "high energy" conformation in which it is approximately perpendicular to the thick filament.
3. The myosin head binds weakly to an actin monomer that is closer to the Z disk than the one to which it had been bound previously.
4. Myosin releases P_i, which causes its actin-binding site to close, thereby increasing its affinity for actin.
5. The resulting transient state is immediately followed by the power stroke, a conformational shift that sweeps the myosin head's C-terminal tail by an estimated ~100 Å toward the Z disk relative to the actin-binding site on its head, thus translating the attached thin filament by this distance toward the M disk.
6. ADP is released, thereby completing the cycle.

Because the reaction cycle involves several steps, some of which are irreversible (e.g., ATP hydrolysis and P_i release), the entire cycle is unidirectional. The ~500 myosin heads on every thick filament asynchronously cycle through this reaction sequence about five times each per second during a strong muscular contraction. *The myosin heads thereby "walk" or "row" up adjacent thin filaments toward the Z disk with the concomitant contraction of the muscle.* Although myosin is dimeric, its two heads function independently.

Calcium Triggers Muscle Contraction. Highly purified actin and myosin can contract regardless of the Ca^{2+} concentration, but preparations containing intact thin filaments contract only in the presence of Ca^{2+}, due to the regulatory action of troponin C (Fig. 7-31). Stimulation of a myofibril by a nerve impulse results in the release of Ca^{2+} from the **sarcoplasmic reticulum** (a system of flattened vesicles derived from the endoplasmic reticulum). As a result, the intracellular [Ca^{2+}] increases from ~10^{-7} to ~10^{-5} M. The higher calcium concentration triggers the conformational change in the troponin–tropomyosin complex that exposes the site on actin where the myosin head binds (Fig. 7-33). When the myofibril [Ca^{2+}] is low (Ca^{2+} is rapidly pumped back into the sarcoplasmic reticulum by ATP-requiring Ca^{2+} pumps; Section 10-3B), the troponin–tropomyosin complex assumes its resting conformation, blocking myosin binding to actin and causing the muscle to relax.

C | Actin Forms Microfilaments in Nonmuscle Cells

Although actin and myosin are most prominent in muscle, they also occur in other tissues. In fact, actin is ubiquitous and is usually the most abundant cytoplasmic protein in eukaryotic cells, typically accounting for 5 to 10% of their total protein. Nonmuscle actin forms ~70-Å-diameter fibers known as **microfilaments** that can be visualized by **immunofluorescence microscopy** (in which a fluorescent-tagged antibody is used to "stain" the

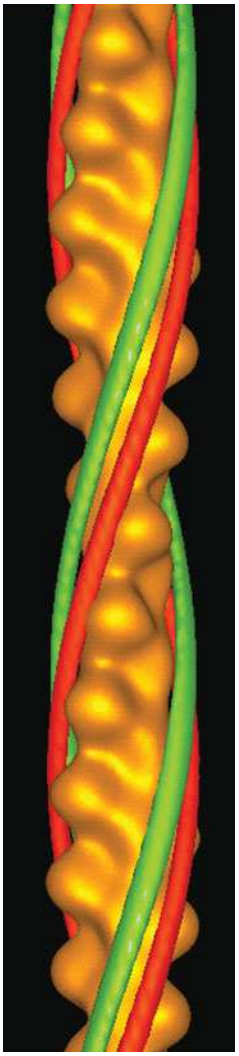

■ **Figure 7-33 | Comparison of the positions of tropomyosin on the thin filament in the absence and presence of Ca^{2+}.** In this superposition of cryoelectron microscopy–based images, the F-actin filament is gold, the tropomyosin in the absence of Ca^{2+} is red, and that in the presence of Ca^{2+} is green. [Courtesy of William Lehman, Boston University School of Medicine.]

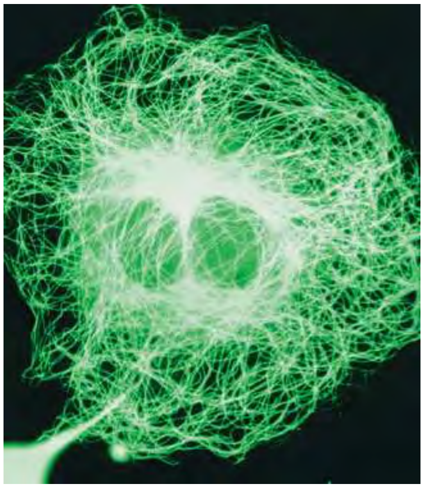

Figure 7-34 | Actin microfilaments. The microfilaments in a fibroblast resting on the surface of a culture dish are revealed by immunofluorescence microscopy using a fluorescently labeled antibody to actin. When the cell begins to move, the filaments disassemble. [Courtesy of John Victor Small, Austrian Academy of Sciences, Salzburg.]

actin to which it binds; Fig. 7-34). In nonmuscle cells, actin plays an essential role in many processes, including changes in cell shape, cell division, endocytosis, and organelle transport.

Microfilament Treadmilling Can Mediate Locomotion. ATP–G-actin binds to both ends of an F-actin filament but with a greater affinity for its (+) end (hence its name). This polymerization activates F-actin subunits to hydrolyze their bound ATP to ADP + P_i with the subsequent dissociation of P_i. The resulting conformation change reduces the affinity of an ADP–F-actin subunit for its neighboring subunits relative to that of ATP–F-actin. Since F-actin–catalyzed ATP hydrolysis occurs more slowly than actin polymerization and F-actin's bound nucleotide does not exchange with those in solution (its nucleotide-binding site is blocked by its associated subunits), F-actin's more recently polymerized and hence predominantly ATP-containing subunits occur largely at its (+) end, whereas its (−) end consists mainly of less recently polymerized and hence predominantly ADP-containing subunits. The lesser affinity of ADP-containing actin subunits for F-actin results in their net dissociation from the (−) end of the polymer.

The steady state (when the microfilament maintains a constant length) occurs when the net rate of addition of subunits at the (+) end matches the net rate of dissociation of subunits at the (−) end. Then, *subunits that have added to the (+) end move toward the (−) end where they dissociate, a process called* ***treadmilling*** (Fig. 7-35). Thus, a fluorescently labeled actin monomer is seen to move from the (+) end of the microfilament toward its (−) end. Treadmilling is driven by the free energy of ATP hydrolysis and hence is not at equilibrium.

The directional growth of actin filaments exerts force against the plasma membrane, allowing a cell to extend its cytoplasm in one direction. If the cytoplasmic protrusion anchors itself to the underlying surface, then the cell can use the adhesion point for traction in order to advance further.

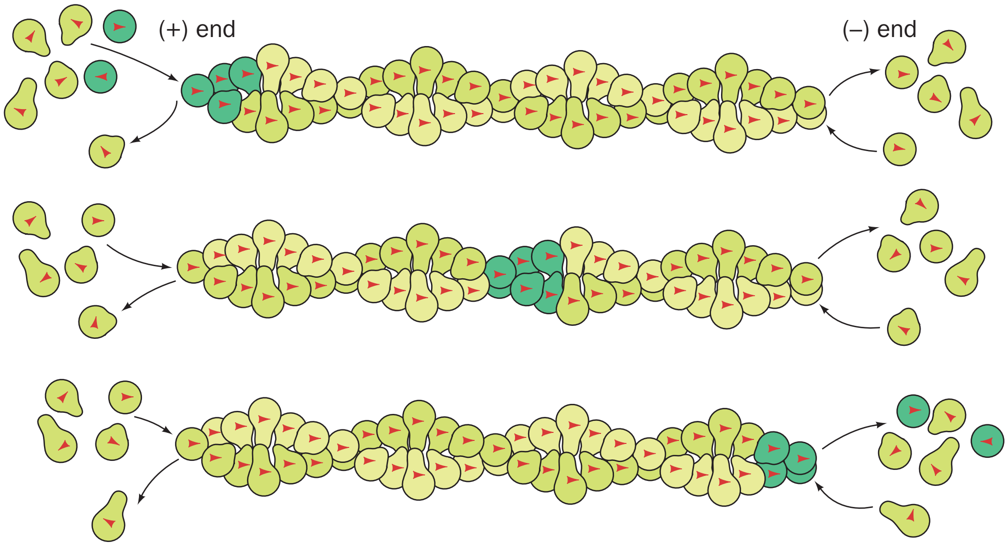

Figure 7-35 | Microfilament treadmilling. In the steady state, actin monomers continually add to the (+) end of the filament (*left*) but dissociate at the same rate from the (−) end (*right*). The filament thereby maintains a constant length while its component monomers translocate from left to right.

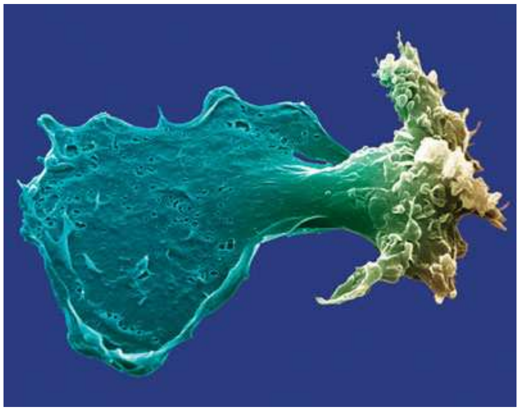

Figure 7-36 | Scanning electron micrograph of a crawling cell. The leading edge of the cell (*left*) is ruffled where it has become detached from the surface and is in the process of extending. The cell's trailing edge or tail (*right*), which is still attached to the surface, is gradually pulled toward the leading edge. The rate of actin polymerization is greatest at the leading edge. [© David Phillips/Visuals Unlimited.]

In order for the cell to crawl, however, the trailing edge of the cell must release its contacts with the surface while newer contacts are being made at the leading edge (Fig. 7-36). In addition, as microfilament polymerization proceeds at the leading edge, depolymerization must occur elsewhere in the cell, since the pool of G-actin is limited. A variety of actin-binding proteins modulate the rate of actin depolymerization and repolymerization *in vivo*.

Actin-mediated cell locomotion, that is, amoeboid motion, is the most primitive mechanism of cell movement. Nevertheless, virtually all eukaryotic cells undertake some version of it, even if it involves just a small patch of actin near the cell surface. More extensive microfilament rearrangements are essential for cells such as neutrophils (a type of white blood cell) that travel relatively long distances to sites of infection or inflammation.

CHECK YOUR UNDERSTANDING

Explain how myosin structure relates to its function as a motor protein.

Draw a diagram of the components of a sarcomere.

Explain the molecular basis of the sliding filament model of muscle contraction.

Describe the process of treadmilling in a microfilament.

How does a microfilament differ from the thin filament in a myofibril?

3 Antibodies

LEARNING OBJECTIVES

- Understand the overall structure of immunoglobulins,
- Understand how the immune system generates a diversity of antibodies to bind a variety of different antigens.

All organisms are continually subject to attack by other organisms, including disease-causing microorganisms and viruses. In higher animals, these **pathogens** may penetrate the physical barrier presented by the skin and mucous membranes (a first line of defense) only to be identified as foreign invaders and destroyed by the **immune system.** Two types of immunity have been distinguished:

1. **Cellular immunity,** which guards against virally infected cells, fungi, parasites, and foreign tissue, is mediated by **T lymphocytes** or **T cells,** so called because they develop in the thymus.
2. **Humoral immunity** (*humor* is an archaic term for fluid), which is most effective against bacterial infections and the extracellular phases of viral infections, is mediated by an enormously diverse collection of related proteins known as **antibodies** or **immunoglobulins.** Antibodies are produced by **B lymphocytes** or **B cells,** which in mammals mature in the bone marrow.

In this section we focus on the structure, function, and generation of antibodies.

The immune response is triggered by the presence of a foreign macromolecule, often a protein or carbohydrate, known as an ***antigen.*** B cells display immunoglobulins on their surfaces. If a B cell encounters an antigen that binds to its particular immunoglobulin, it engulfs the antigen–antibody complex, degrades it, and displays the antigen fragments on the cell surface.

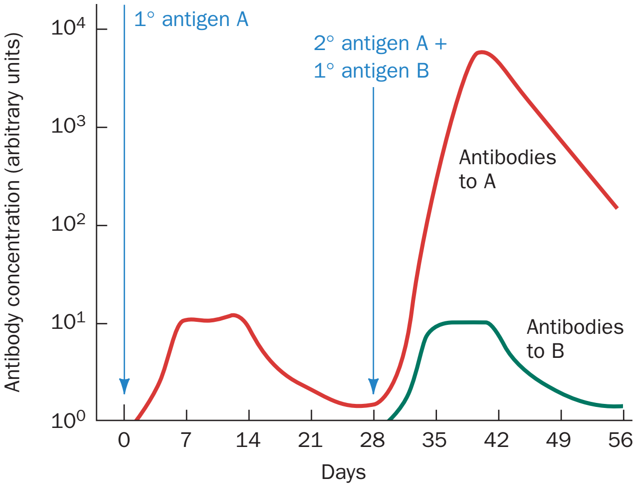

■ **Figure 7-37 | Primary and secondary immune responses.** Antibodies to antigen A appear in the blood following primary immunization on day 0 and secondary immunization on day 28. Antigen B is included in the secondary immunization to demonstrate the specificity of immunological memory for antigen A. The secondary response to antigen A is both faster and greater than the primary response.

T cells then stimulate the B cell to proliferate. Most of the B cell progeny are circulating cells that secrete large amounts of the antigen-specific antibody. These antibodies can bind to additional antigen molecules, thereby marking them for destruction by other components of the immune system. Although most B cells live only a few days unless stimulated by their corresponding antigen, a few long-lived **memory B cells** can recognize antigen several weeks or even many years later and can mount a more rapid and massive immune response (called a secondary response) than B cells that have not yet encountered their antigen (Fig. 7-37).

A | Antibodies Have Constant and Variable Regions

The immunoglobulins form a related but enormously diverse group of proteins. All immunoglobulins contain at least four subunits: two identical ~23-kD **light chains (L)** and two identical 53- to 75-kD **heavy chains (H).** These subunits associate by disulfide bonds and by noncovalent interactions to form a roughly Y-shaped symmetric molecule with the formula $(LH)_2$ (Fig. 7-38).

The five classes of immunoglobulin **(Ig)** differ in the type of heavy chain they contain and, in some cases, in their subunit structure (Table 7-2). For example, **IgM** consists of five Y-shaped molecules arranged around a central **J subunit; IgA** occurs as monomers, dimers, and trimers. The various immunoglobulin classes also have different physiological functions. IgM is most effective against microorganisms and is the first immunoglobulin to

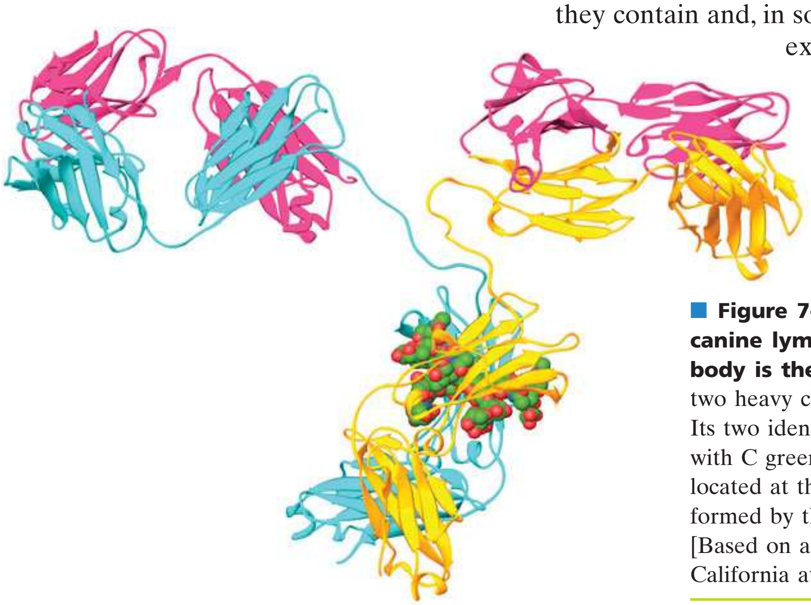

■ **Figure 7-38 | X-Ray structure of a murine antibody against canine lymphoma (a type of cancer against which this antibody is therapeutically useful).** It is shown in ribbon form with its two heavy chains gold and cyan and its two light chains both magenta. Its two identical carbohydrate chains are drawn in space-filling form with C green, N blue, and O red. The antigen-combining sites are located at the ends of the two approximately horizontal Fab arms formed by the association of the light chains with the heavy chains. [Based on an X-ray structure by Alexander McPherson, University of California at Irvine. PDBid 1IGT.] **See Interactive Exercise 3.**

Table 7-2 Classes of Human Immunoglobulins

Class	Heavy Chain	Light Chain	Subunit Structure	Molecular Mass (kD)
IgA	α	κ or λ	$(\alpha_2\kappa_2)_n\mathrm{J}^a$ or $(\alpha_2\lambda_2)_n\mathrm{J}^a$	360–720
IgD	δ	κ or λ	$\delta_2\kappa_2$ or $\delta_2\lambda_2$	160
IgE	ε	κ or λ	$\varepsilon_2\kappa_2$ or $\varepsilon_2\lambda_2$	190
IgG[b]	γ	κ or λ	$\gamma_2\kappa_2$ or $\gamma_2\lambda_2$	150
IgM	μ	κ or λ	$(\mu_2\kappa_2)_5\mathrm{J}$ or $(\mu_2\lambda_2)_5\mathrm{J}$	950

[a] n = 1, 2, or 3.

[b] IgG has four subclasses, IgG1, IgG2, IgG3, and IgG4, which differ in their γ chains.

be secreted in response to an antigen. **IgG,** the most common immunoglobulin, is equally distributed between the blood and the extravascular fluid. IgA occurs predominantly in the intestinal tract and defends against pathogens by adhering to their antigenic sites so as to block their attachment to epithelial (outer) surfaces. **IgE,** which is normally present in the blood in minute concentrations, protects against parasites and has been implicated in allergic reactions. **IgD,** which is also present in small amounts, has no clearly known function. Our discussion of antibody structure will focus on IgG.

IgG can be cleaved through limited proteolysis with the enzyme **papain** into three ~50-kD fragments: two identical **Fab fragments** and one **Fc fragment.** The Fab fragments are the "arms" of the Y-shaped antibody and contain an entire L chain and the N-terminal half of an H chain (Fig. 7-39). These fragments contain IgG's antigen-binding sites (the "ab" in Fab

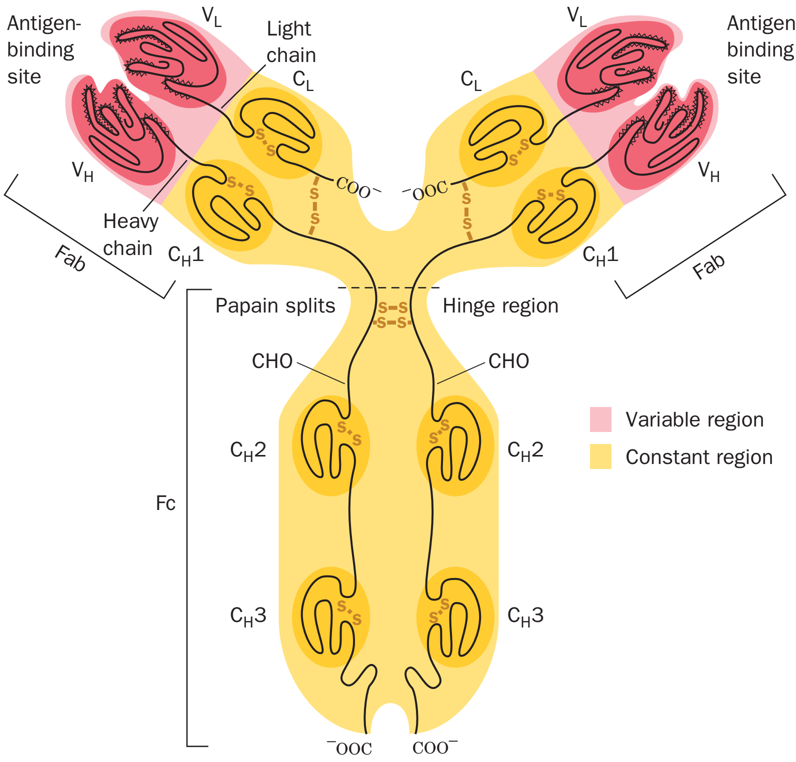

Figure 7-39 | Diagram of human immunoglobulin G (IgG). Each light chain contains a variable (V_L) and a constant (C_L) region, and each heavy chain contains one variable (V_H) and three constant (C_H1, C_H2, and C_H3) regions. Each of the variable and constant domains contains a disulfide bond, and the four polypeptide chains are linked by disulfide bonds. The proteolytic enzyme papain cleaves IgG at the hinge region to yield two Fab fragments and one Fc fragment. CHO represents carbohydrate chains. [Illustration, Irving Geis. Image from Irving Geis Collection/Howard Hughes Medical Institute. Rights owned by HHMI. Reproduction by permission only.]

stands for *a*ntigen *b*inding). The Fc portion ("c" because it *c*rystallizes easily) derives from the "stem" of the antibody and consists of the C-terminal halves of two H chains. The arms of the Y are connected to the stem by a flexible hinge region. The hinge angles may vary, so an antibody molecule may not be perfectly symmetrical (e.g., Fig. 7-38).

Although all IgG molecules have the same overall structure, IgGs that recognize different antigens have different amino acid sequences. The light chains of different antibodies differ mostly in their N-terminal halves. These polypeptides are therefore said to have a **variable region, V_L** (residues 1 to 108), and a **constant region, C_L** (residues 109 to 214). Comparisons of H chains, which have 446 residues, reveal that H chains also have a variable region, **V_H,** and a constant region, **C_H.** As indicated in Fig. 7-39, the C_H region consists of three ~110-residue segments, **C_H1, C_H2,** and **C_H3,** which are homologous to each other and to C_L. In fact, all the constant and variable regions resemble each other in sequence and in disulfide-bonding pattern. These similarities suggest that the six different homology units of an IgG evolved through the duplication of a primordial gene encoding an ~110-residue protein.

B | Antibodies Recognize a Huge Variety of Antigens

The immunoglobulin homology units all have the same characteristic **immunoglobulin fold:** a sandwich composed of three- and four-stranded antiparallel β sheets that are linked by a disulfide bond (Fig. 6-29*b*). Nevertheless, the basic immunoglobulin structure must accommodate an enormous variety of antigens. The ability to recognize antigens resides in three loops in the variable domain (Fig. 7-40). Most of the amino acid variation among antibodies is concentrated in these three short segments, called **hypervariable** sequences. As hypothesized by Elvin Kabat, the hypervariable sequences line an immunoglobulin's antigen-binding site, so that their amino acids determine its binding specificity.

Scientists have determined the X-ray structures of Fab fragments from **monoclonal antibodies** (Box 7-5) and monospecific antibodies isolated from patients with **multiple myeloma** (a disease in which a cancerous B cell proliferates and produces massive amounts of a single immunoglobulin; immunoglobulins purified from ordinary blood are heterogeneous and hence cannot be used for detailed structural studies). As predicted by the positions of the hypervariable sequences, the antigen-binding site is located at the tip of each Fab fragment in a crevice between its V_L and V_H domains.

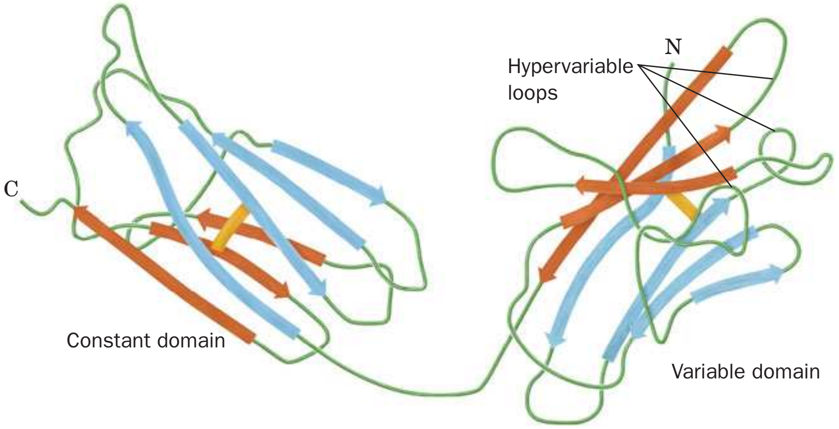

■ **Figure 7-40 | Immunoglobulin folds in a light chain.** Both the constant and variable domains consist of a sandwich of a four-stranded antiparallel β sheet (*blue*) and a three-stranded antiparallel β sheet (*orange*) that are linked by a disulfide bond (*yellow*). The positions of the three hypervariable sequences in the variable domain are indicated. [After Schiffer, M., Girling, R.L., Ely, K.R., and Edmundson, A.B., *Biochemistry* **12,** 4628 (1973).]

BOX 7-5 PERSPECTIVES IN BIOCHEMISTRY

Monoclonal Antibodies

Introducing a foreign molecule into an animal induces the synthesis of large amounts of antigen-specific but heterogeneous antibodies. One might expect that a single lymphocyte from such an animal could be cloned (allowed to reproduce) to yield a harvest of homogeneous immunoglobulin molecules. Unfortunately, lymphocytes do not grow continuously in culture. In the late 1970s, however, César Milstein and Georges Köhler developed a technique for immortalizing such cells so that they can grow continuously and secrete virtually unlimited quantities of a specific antibody. Typically, lymphocytes from a mouse that has been immunized with a particular antigen are harvested and fused with mouse myeloma cells (a type of blood system cancer), which can multiply indefinitely (see figure). The cells are then incubated in a selective medium that inhibits the synthesis of purines, which are essential for myeloma growth [the myeloma cells lack the enzyme **hypoxanthine phosphoribosyl transferase (HPRT),** which could otherwise participate in a purine nucleotide salvage pathway; Section 23-1D]. The only cells that can grow in the selective medium are fused cells, known as **hybridoma cells,** that combine the missing HPRT (it is supplied by the lymphocyte) with the immortal attributes of the myeloma cells. Clones derived from single fused cells are then screened for the presence of antibodies to the original antigen. Antibody-producing cells can be grown in large quantities in tissue culture or as semisolid tumors in mouse hosts.

Monoclonal antibodies are used to purify macromolecules (Section 5-2), to identify infectious diseases, and to test for the presence of drugs and other substances in body tissues. Because of their purity and specificity and, to some extent, their biocompatibility, monoclonal antibodies also hold considerable promise as therapeutic agents against cancer and other diseases. In fact, the monoclonal antibody known as **Herceptin** binds specifically to the growth factor receptor **HER2** that is overexpressed in about one-quarter of breast cancers. Herceptin binding to HER2 blocks its growth-signaling activity, thereby causing the tumor to stop growing or even regress.

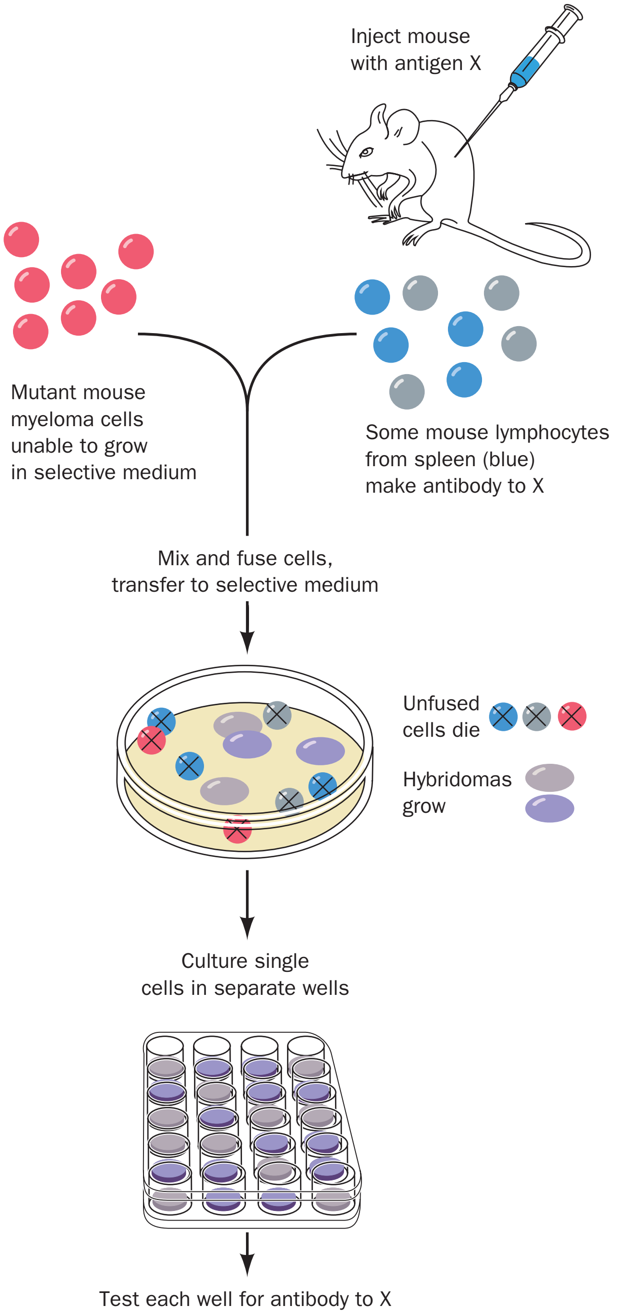
Inject mouse with antigen X
Mutant mouse myeloma cells unable to grow in selective medium
Some mouse lymphocytes from spleen (blue) make antibody to X
Mix and fuse cells, transfer to selective medium
Unfused cells die
Hybridomas grow
Culture single cells in separate wells
Test each well for antibody to X

The association between antibodies and their antigens involves van der Waals, hydrophobic, hydrogen bonding, and ionic interactions. Their dissociation constants range from 10^{-4} to 10^{-10} M, comparable (or even greater) in strength to the associations between enzymes and their substrates. The specificity and strength of an antigen–antibody complex are a function of the exquisite structural complementarity between the antigen and the

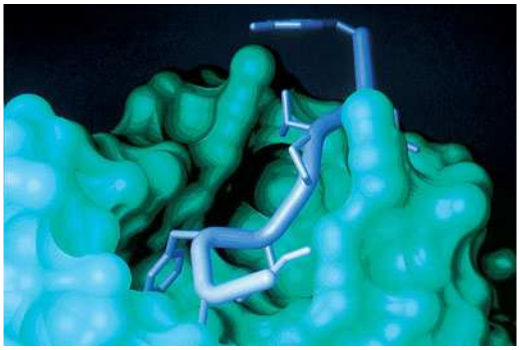

■ **Figure 7-41 | Interaction between an antigen and an antibody.** This X-ray structure shows a portion of the solvent-accessible surface of a monoclonal antibody Fab fragment (*green*) with a stick model of a bound nine-residue fragment of its peptide antigen (*lavender*). [Courtesy of Ian Wilson, The Scripps Research Institute, La Jolla, California. PDBid 1HMM.]

antibody (e.g., Fig. 7-41). These are also the features that make antibodies such useful laboratory reagents (Fig. 5-3, for example).

Most immunoglobulins are divalent molecules; that is, they can bind two identical antigens simultaneously (IgM and IgA are multivalent). A foreign substance or organism usually has multiple antigenic regions, and a typical immune response generates a mixture of antibodies with different specificities. Divalent binding allows antibodies to cross-link antigens to form an extended lattice (Fig. 7-42), which hastens the removal of the antigen and triggers B cell proliferation.

Antibody Diversity Results from Gene Rearrangement and Mutation. A novel antigen does not direct a B cell to begin manufacturing a new immunoglobulin to which it can bind. Rather, *an antigen stimulates the proliferation of a preexisting B cell whose antibodies happen to recognize the antigen.* The immune system has the potential to produce an enormous number of different antibodies, probably $>10^{18}$. Even though this number is so large that an individual can synthesize only a small fraction of its potential immunoglobulin repertoire during its lifetime, this fraction is still sufficient to react with almost any antigen the individual might encounter. Yet the number of immunoglobulin genes is far too small to account for the observed level of antibody diversity. The diversity in antibody sequences arises instead from genetic changes during B lymphocyte development.

Each chain of an immunoglobulin molecule is encoded by multiple DNA segments: V, J, and C segments for the light chains, and V, D, J, and C segments for heavy chains. These segments are joined together by **somatic recombination** during B cell development before being transcribed and translated into protein. The process is called somatic (Greek: *soma,* body) to distinguish it from the recombination that occurs in reproductive cells. Because there are multiple versions of the V, D, J, and C segments in the genome, the combinatorial possibilities are enormous. In addition, the recombination process sometimes adds or deletes nucleotides at the junctions between gene segments, further contributing to the diversity of the encoded protein. The generation of antibody diversity is further discussed in Section 28-3D.

Additional changes can occur after a B cell has encountered its antigen and begun secreting antibody molecules. As the antibody-producing B cells divide, their rate of immunoglobulin gene mutation increases dramatically, favoring the substitution of one nucleotide for another and leading to an average of one amino acid change for every cell generation. This process, which is called **somatic hypermutation,** permits the antigen specificity of the antibody to be fine-tuned over many cell generations, because the rate of B cell proliferation increases with the antigen-binding affinity of the antibody it produces.

The Immune System Loses Its Tolerance in Autoimmune Diseases. Another remarkable property of the immune system is that its power is unleashed only against foreign substances and not against any of the tens of thousands of endogenous (self) molecules of various sorts. Virtually all macromolecules are potentially antigenic, as can be demonstrated by transplanting tissues from one individual to another, even within a species. This incompatibility presents obvious challenges for therapies ranging from routine blood transfusions to multiple organ transplants.

The mechanism whereby an individual's immune system distinguishes self from non-self is poorly understood. It begins to operate around the time of birth and must be ongoing, since new lymphocytes arise throughout

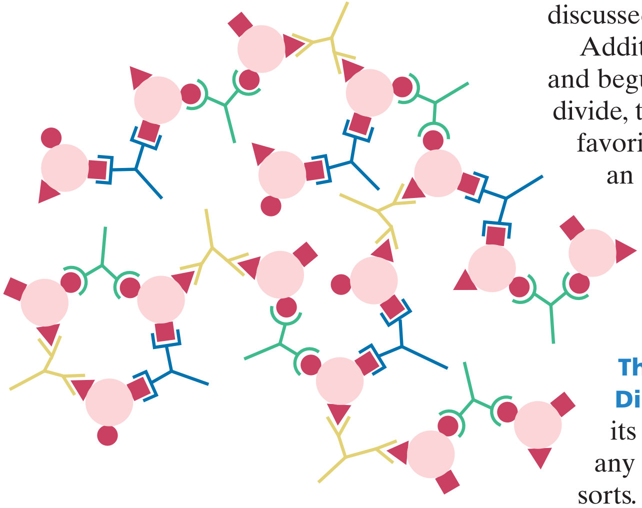

■ **Figure 7-42 | Antigen cross-linking by antibodies.** A mixture of divalent antibodies that recognizes the several different antigenic regions of an intruding particle such as a toxin molecule or a bacterium can form an extensive lattice of antigen and antibody molecules.

Table 7-3 Some Autoimmune Diseases

Disease	Target Tissue	Major Symptoms
Addison's disease	Adrenal cortex	Low blood glucose, muscle weakness, Na^+ loss, K^+ retention, increased susceptibility to stress
Crohn's disease	Intestinal lining	Intestinal inflammation, chronic diarrhea
Graves' disease	Thyroid gland	Oversecretion of thyroid hormone resulting in increased appetite accompanied by weight loss
Insulin-dependent diabetes mellitus	Pancreatic β cells	Loss of ability to make insulin
Multiple sclerosis	Myelin sheath of nerve fibers in brain and spinal cord	Progressive loss of motor control
Myasthenia gravis	Acetylcholine receptors at nerve–muscle synapses	Progressive muscle weakness
Psoriasis	Epidermis	Hyperproliferation of the skin
Rheumatoid arthritis	Connective tissue	Inflammation and degeneration of the joints
Systemic lupus erythematosus	DNA, phospholipids, other tissue components	Rash, joint and muscle pain, anemia, kidney damage, mental dysfunction

an individual's lifetime. Occasionally, the immune system loses tolerance to some of its self-antigens, resulting in an **autoimmune disease.**

All the body's organ systems are theoretically susceptible to attack by an immune system that has lost its self-tolerance, but some tissues are attacked more often than others. Some of the most common autoimmune diseases are listed in Table 7-3. The symptoms of a particular disease reflect the type of tissue with which the autoantibodies react. In general, autoimmune diseases are chronic, often with periods of remission, and their clinical severity may differ among individuals.

The loss of tolerance to one's own antigens may result from an innate malfunctioning of the mechanism by which the immune system distinguishes self from non-self, possibly precipitated by an event, such as trauma or infection, in which tissues that are normally sequestered from the immune system are exposed to lymphocytes. For example, breaching the blood–brain barrier may allow lymphocytes access to the brain or spinal cord, and injury may allow access to the spaces at joints, which are not normally served by blood vessels. There is also evidence that some autoimmune diseases are caused by antibodies to certain viral or bacterial antigens that cross-react with endogenous substances because of chance antigenic similarities. Some diseases, such as systemic lupus erythematosus, represent a more generalized breakdown of the immune system, so that antibodies to many endogenous substances (e.g., DNA and phospholipids) may be generated.

CHECK YOUR UNDERSTANDING

Identify the domains of an immunoglobulin molecule.
What is the source of antibody diversity?
How do autoimmune diseases arise?

SUMMARY

1. Myoglobin, a monomeric heme-containing muscle protein, reversibly binds a single O_2 molecule.
2. Hemoglobin, a tetramer with pseudo-D_2 symmetry, has distinctly different conformations in its oxy and deoxy states.
3. Oxygen binds to hemoglobin in a sigmoidal fashion, indicating cooperative binding.
4. O_2 binding to a heme group induces a conformational change in the entire hemoglobin molecule that includes movements

at the subunit interfaces and the disruption of ion pairs. The result is a shift from the T to the R state.

5. CO_2 promotes O_2 dissociation from hemoglobin through the Bohr effect. BPG decreases hemoglobin's O_2 affinity by binding to deoxyhemoglobin.
6. The symmetry and sequential models of allosterism explain how binding of a ligand at one site affects binding of another ligand at a different site.
7. Hemoglobin variants have revealed structure–function relationships. Hemoglobin S produces the symptoms of sickle-cell anemia by forming rigid fibers in its deoxy form.
8. The thick filaments of a sarcomere are composed of the motor protein myosin and the thin filaments are composed mainly of actin.
9. The heads of myosin molecules in thick filaments form bridges to actin in thin filaments such that the detachment and reattachment of the myosin heads cause the thick and thin filaments to slide past each other during muscle contraction. The contractile force derives from conformational changes in myosin that are triggered by ATP hydrolysis.
10. In nonmuscle cells, actin forms microfilaments, which are components of the cytoskeleton. Microfilaments are dynamic structures whose growth and regression are responsible for certain types of cell movement.
11. The immune system responds to foreign macromolecules through the production of antibodies (immunoglobulins).
12. The Y-shaped IgG molecule consists of two heavy and two light chains. The two antigen-binding sites are formed by the hypervariable sequences in the variable domains at the ends of a heavy and a light chain.
13. Antibody diversity results from somatic recombination during B cell development and from somatic hypermutation.

KEY TERMS

heme	**178**
oxygenation	**178**
Y_{O_2}	**179**
pO_2	**180**
hyperbolic curve	**180**
saturation	**180**
p_{50}	**180**
ligand	**180**
sigmoidal curve	**184**
cooperative binding	**184**
Hill equation	**184**
Hill coefficient	**185**
noncooperative binding	**185**
positive cooperativity	**185**
negative cooperativity	**185**
Perutz mechanism	**186**
T state	**186**
R state	**186**
Bohr effect	**189**
erythrocyte	**189**
allosteric interaction	**192**
symmetry model	**193**
sequential model	**193**
variant	**194**
lyse	**194**
anemia	**194**
cyanosis	**194**
polycythemia	**194**
heterozygote	**195**
homozygote	**195**
sickle-cell anemia	**195**
striated muscle	**198**
myofibril	**198**
sarcomere	**198**
thick filament	**198**
thin filament	**198**
sliding filament model	**201**
(−) end	**203**
(+) end	**203**
motor protein	**205**
microfilament	**207**
treadmilling	**208**
pathogen	**209**
immune system	**209**
cellular immunity	**209**
lymphocyte	**209**
humoral immunity	**209**
immunoglobulin (Ig)	**209**
antigen	**209**
memory B cell	**210**
Fab fragment	**211**
Fc fragment	**211**
variable region	**212**
constant region	**212**
immunoglobulin fold	**212**
hypervariability	**212**
monoclonal antibody	**212**
multiple myeloma	**212**
somatic recombination	**214**
somatic hypermutation	**214**
autoimmune disease	**215**

PROBLEMS

1. Estimate K from the following data describing ligand binding to a protein.

[Ligand] (mM)	Y
0.25	0.30
0.50	0.45
0.80	0.56
1.4	0.66
2.2	0.80
3.0	0.83
4.5	0.86
6.0	0.93

2. Which set of binding data is likely to represent cooperative ligand binding to an oligomeric protein?

(a)

[Ligand] (mM)	Y
0.1	0.3
0.2	0.5
0.4	0.7
0.7	0.9

(b)

[Ligand] (mM)	Y
0.2	0.1
0.3	0.3
0.4	0.6
0.6	0.8

3. In active muscles, the pO_2 may be 10 torr at the cell surface and 1 torr at the mitochondria (the organelles where oxidative metabolism occurs). Use Eq. 7-6 to show how myoglobin ($p_{50} = 2.8$ torr) facilitates the diffusion of O_2 through these cells.

4. In humans, the urge to breathe results from high concentrations of CO_2 in the blood; there are no direct physiological sensors of blood pO_2. Skindivers often hyperventilate (breathe rapidly and deeply for several minutes) just before making a dive in the belief that this will increase the O_2 content of their blood. (a) Does it do so? (b) Use your knowledge of hemoglobin function to evaluate whether this practice is useful.
5. Drinking a few drops of a commercial preparation called "vitamin O," which consists of oxygen and sodium chloride dissolved in water, is claimed to increase the concentration of oxygen in the body. (a) Use your knowledge of oxygen transport to evaluate this claim. (b) Would vitamin O be more or less effective if it were infused directly into the bloodstream?
6. Is the p_{50} higher or lower than normal in (a) hemoglobin Yakima and (b) hemoglobin Kansas? Explain.
7. Hemoglobin S homozygotes who are severely anemic often have elevated levels of BPG in their erythrocytes. Is this a beneficial effect?
8. In hemoglobin Rainier, Tyr 145β is replaced by Cys, which forms a disulfide bond with another Cys residue in the same subunit. This prevents the formation of ion pairs that normally stabilize the T state. How does hemoglobin Rainier differ from normal hemoglobin with respect to (a) oxygen affinity, (b) the Bohr effect, and (c) the Hill coefficient?
9. The crocodile, which can remain under water without breathing for up to 1 h, drowns its air-breathing prey and then dines at its leisure. An adaptation that aids the crocodile in doing so is that it can utilize virtually 100% of the O_2 in its blood whereas humans, for example, can extract only ~65% of the O_2 in their blood. Crocodile Hb does not bind BPG. However, crocodile deoxyHb preferentially binds HCO_3^-. How does this help the crocodile obtain its dinner?
10. Some primitive animals have a hemoglobin that consists of two identical subunits.
    (a) Sketch an oxygen-binding curve for this protein.
    (b) What is the likely range of the Hill coefficient for this hemoglobin?
11. Is myosin a fibrous protein or a globular protein? Explain.
12. A myosin head can undergo five ATP hydrolysis cycles per second, each of which moves an actin monomer by ~100 Å. How is it possible for an entire sarcomere to shorten by 1000 Å in this same period?
13. **Rigor mortis,** the stiffening of muscles after death, is caused by depletion of cellular ATP. Describe the molecular basis of rigor.
14. Explain why a microfilament is polar whereas a filament of keratin is not.
15. Give the approximate molecular masses of an immunoglobulin G molecule analyzed by (a) gel filtration chromatography, (b) SDS-PAGE, and (c) SDS-PAGE in the presence of 2-mercaptoethanol.
16. Explain why the variation in V_L and V_H domains of immunoglobulins is largely confined to the hypervariable loops.
17. Why do antibodies raised against a native protein sometimes fail to bind to the corresponding denatured protein?
18. Antibodies raised against a macromolecular antigen usually produce an antigen–antibody precipitate when mixed with that antigen. Explain why no precipitate forms when (a) Fab fragments from those antibodies are mixed with the antigen; (b) antibodies raised against a small antigen are mixed with that small antigen; and (c) the antibody is in great excess over the antigen and vice versa.

CASE STUDIES

Case 8 (available at www.wiley.com/college/voet)
Hemoglobin, the Oxygen Carrier

Focus concept: A mutation in the gene for hemoglobin results in an altered protein responsible for the disease sickle-cell anemia. An understanding of the biochemistry of the disease may suggest possible treatments.

Prerequisite: Chapter 7

- Hemoglobin structure and function

Case 9
Allosteric Interactions in Crocodile Hemoglobin

Focus concept: The effect of allosteric modulators on oxygen affinity for crocodile hemoglobin differs from that of other species.

Prerequisite: Chapter 7

- Hemoglobin structure and function

Case 10
The Biological Roles of Nitric Oxide

Focus concept: Nitric oxide, a small lipophilic molecule, acts as a second messenger in blood vessels.

Prerequisite: Chapter 7

- Hemoglobin structure and function

REFERENCES

Myoglobin and Hemoglobin

Ackers, G.K. and Holt, J.M., Asymmetric cooperativity in a symmetric tetramer: human hemoglobin, *J. Biol. Chem.* **281,** 11441–11443 (2006). [A brief review of hemoglobin's allosteric behavior.]

Allison, A.C., The discovery of resistance to malaria of sickle-cell heterozygotes, *Biochem. Mol. Biol. Educ.* **30,** 279–287 (2002).

Dickerson, R.E. and Geis, I., *Hemoglobin,* Benjamin/Cummings (1983). [A beautifully written and lavishly illustrated treatise on the structure, function, and evolution of hemoglobin.]

Hsia, C.C.W., Respiratory function of hemoglobin, *New Engl. J. Med.* **338,** 239–247 (1998). [A short review of hemoglobin's physiological role.]

Judson, H.F., *The Eighth Day of Creation* (Expanded edition), Chapters 9 and 10, Cold Spring Harbor Laboratory Press (1996). [Includes a fascinating historical account of how our present perception of hemoglobin structure and function came about.]

Nagel, R.L., Haemoglobinopathies due to structural mutations, *in* Provan, D. and Gribben, J. (Eds.), *Molecular Haematology,* pp. 121–133, Blackwell Science (2000).

Perutz, M.F., Wilkinson, A.J., Paoli, M., and Dodson, G.G., The stereochemical mechanism of the cooperative effects in hemoglobin revisited, *Annu. Rev. Biophys. Biomol. Struct*. **27,** 1–34 (1998).

Strasser, B.J., Sickle-cell anemia, a molecular disease, *Science* **286,** 1488–1490 (1999). [A short history of Pauling's characterization of sickle-cell anemia.]

Actin and Myosin

Cooper, J.A. and Schafer, D.A., Control of actin assembly and disassembly at filament ends, *Curr. Opin. Cell Biol.* **12,** 97–103 (2000). [Provides an overview of the principles of microfilament dynamics and some of the key protein players.]

Craig, R. and Woodhead, J.L., Structure and function of myosin filaments, *Curr. Opin. Struct. Biol.* **16,** 204–212 (2006). [Includes details of myosin and thick filament structure, including its arrangement in the sarcomere.]

Schliwa, M. and Woehlke, G., Molecular motors, *Nature* **422,** 759–765 (2003). [Includes reviews of myosin and other motor proteins.]

Spudich, J.A., The myosin swinging cross-bridge model, *Nature Rev. Mol. Cell Biol.* **2,** 387–391 (2001). [Summarizes the history and current state of models for myosin action.]

Antibodies

Davies, D.R. and Cohen, G.H., Interactions of protein antigens with antibodies, *Proc. Natl. Acad. Sci.* **93,** 7–12 (1996).

Harris, L.J., Larson, S.B., Hasel, K.W., Day, J., Greenwood, A., and McPherson, A., The three-dimensional structure of an intact monoclonal antibody for canine lymphoma, *Nature* **360,** 369–372 (1992). [The first high-resolution X-ray structure of an intact IgG.]

Janeway, C.A., Jr., Travers, P., Walport, M., and Shlomchik, M.J., *Immunobiology 6: The Immune System in Health and Disease*, Garland Science (2004).

Marrack, P., Kappler, J., and Kotzin, B.L., Autoimmune disease: why and where it occurs, *Nature Medicine* **7,** 899–905 (2001).

8

Carbohydrates

Sugars are relatively simple molecules that can be linked together in various ways to form larger molecules, for example, starch. This storage form of carbohydrate is the primary source of energy in many foods, including bread, rice, and pasta. [Charles D. Winters/Photo Researchers.]

CHAPTER CONTENTS

1 Monosaccharides
  - **A.** Monosaccharides Are Aldoses or Ketoses
  - **B.** Monosaccharides Vary in Configuration and Conformation
  - **C.** Sugars Can Be Modified and Covalently Linked

2 Polysaccharides
  - **A.** Lactose and Sucrose Are Disaccharides
  - **B.** Cellulose and Chitin Are Structural Polysaccharides
  - **C.** Starch and Glycogen Are Storage Polysaccharides
  - **D.** Glycosaminoglycans Form Highly Hydrated Gels

3 Glycoproteins
  - **A.** Proteoglycans Contain Glycosaminoglycans
  - **B.** Bacterial Cell Walls Are Made of Peptidoglycan
  - **C.** Many Eukaryotic Proteins Are Glycosylated
  - **D.** Oligosaccharides May Determine Glycoprotein Structure, Function, and Recognition

MEDIA RESOURCES

(available at www.wiley.com/college/voet)

Kinemage 7-1. D-Glucopyranose, α and β anomers

Kinemage 7-2. Sucrose

Kinemage 7-3. Hyaluronate

Kinemage 7-4. Structure of a complex carbohydrate

Carbohydrates or **saccharides** (Greek: *sakcharon,* sugar) are the most abundant biological molecules. They are chemically simpler than nucleotides or amino acids, containing just three elements—carbon, hydrogen, and oxygen—combined according to the formula $(C \cdot H_2O)_n$, where $n \geq 3$. The basic carbohydrate units are called **monosaccharides.** There are numerous different types of monosaccharides, which, as we discuss below, differ in their number of carbon atoms and in the arrangement of the H and O atoms attached to the carbons. Furthermore, monosaccharides can be strung together in almost limitless ways to form **polysaccharides.**

Until the 1960s, carbohydrates were thought to have only passive roles as energy sources (e.g., glucose and starch) and as structural materials (e.g., cellulose). Carbohydrates, as we shall see, do not catalyze complex chemical reactions as do proteins, nor do carbohydrates replicate themselves as do nucleic acids. And because polysaccharides are not built according to a genetic "blueprint," as are nucleic acids and proteins, they tend to be much more heterogeneous—both in size and in composition—than other biological molecules.

However, it has become clear that the innate structural variation in carbohydrates is fundamental to their biological activity. The apparently haphazard arrangements of carbohydrates on proteins and on the surfaces of cells are the key to many recognition events between proteins and between cells. An understanding of carbohydrate structure, from the simplest monosaccharides to the most complex branched polysaccharides, is essential for appreciating the varied functions of carbohydrates in biological systems.

1 Monosaccharides

LEARNING OBJECTIVES

- Be able to recognize monosaccharides and their derivatives.
- Understand how monosaccharides cyclize to form two different anomers.
- Understand that a glycosidic bond links two monosaccharides.

Monosaccharides, or simple sugars, are synthesized from smaller precursors that are ultimately derived from CO_2 and H_2O by photosynthesis.

A | Monosaccharides Are Aldoses or Ketoses

Monosaccharides are aldehyde or ketone derivatives of straight-chain polyhydroxy alcohols containing at least three carbon atoms. They are classified according to the chemical nature of their carbonyl group and the number of their C atoms. If the carbonyl group is an aldehyde, the sugar is an **aldose.** If the carbonyl group is a ketone, the sugar is a **ketose.** The smallest monosaccharides, those with three carbon atoms, are **trioses.**

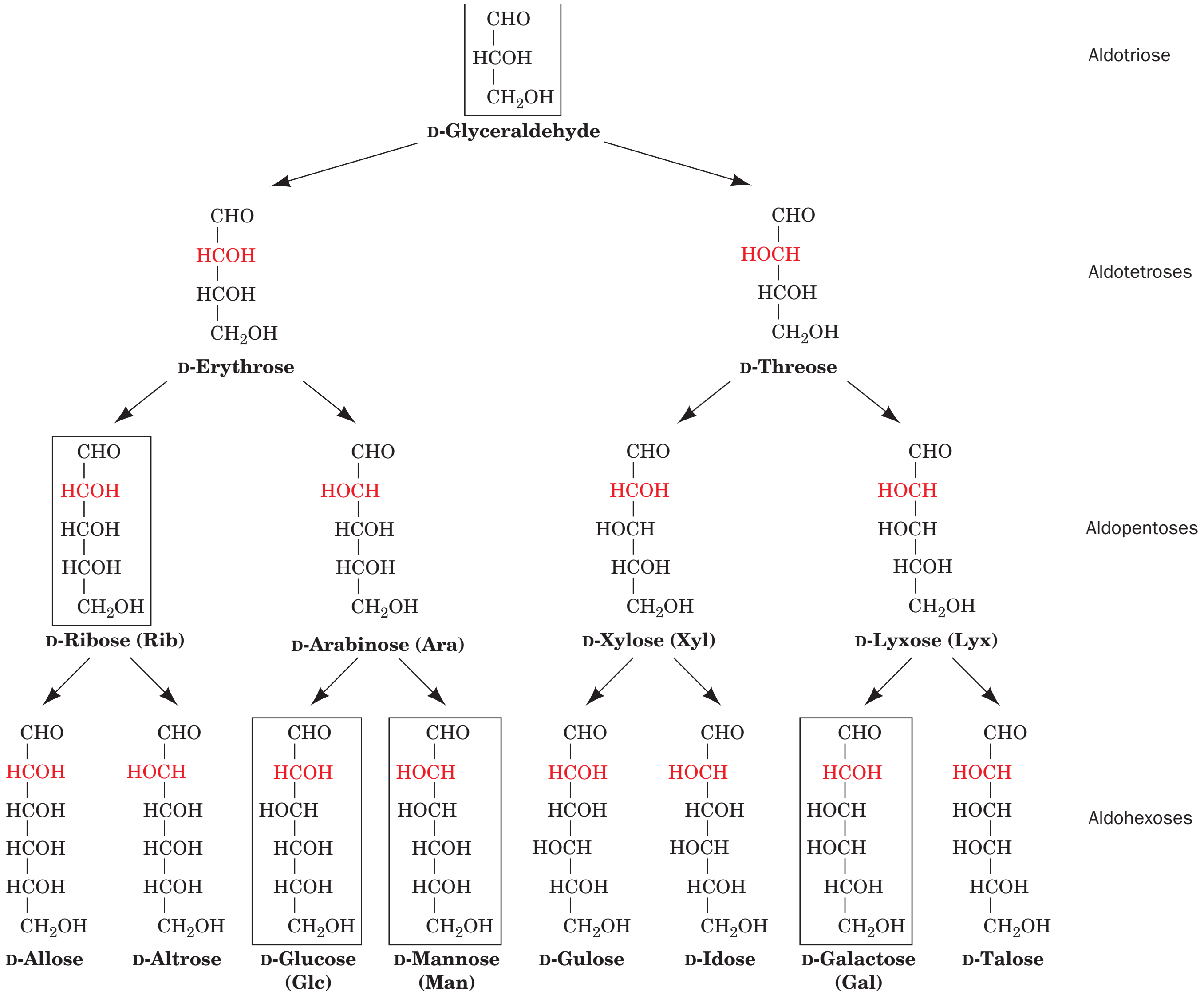
D-Glyceraldehyde
Aldotriose
D-Erythrose
D-Threose
Aldotetroses
D-Ribose (Rib)
D-Arabinose (Ara)
D-Xylose (Xyl)
D-Lyxose (Lyx)
Aldopentoses
D-Allose
D-Altrose
D-Glucose (Glc)
D-Mannose (Man)
D-Gulose
D-Idose
D-Galactose (Gal)
D-Talose
Aldohexoses

Figure 8-1 | The D-aldoses with three to six carbon atoms. The arrows indicate stereochemical relationships (not biosynthetic pathways). The configuration around C2 (*red*) distinguishes the members of each pair of monosaccharides. The L counterparts of these 15 sugars are their mirror images. The biologically most common aldoses are boxed.

Those with four, five, six, seven, etc. C atoms are, respectively, **tetroses, pentoses, hexoses, heptoses,** etc.

The aldohexose **D-glucose** has the formula $(C \cdot H_2O)_6$:

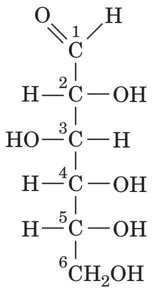

D-Glucose

All but two of its six C atoms, C1 and C6, are chiral centers, so D-glucose is one of $2^4 = 16$ possible stereoisomers. The stereochemistry and nomenclature of the D-aldoses are presented in Fig. 8-1. The assignment of D or L is made according to the Fischer convention (Section 4-2): *D sugars have the same absolute configuration at the asymmetric center farthest from their carbonyl group as does D-glyceraldehyde* (i.e., the —OH at C5 of D-glucose is on the right in a Fischer projection). The L sugars are the mirror images of their D counterparts. Because L sugars are biologically much less abundant than D sugars, the D prefix is often omitted.

Sugars that differ only by the configuration around one C atom are known as **epimers** of one another. Thus, D-glucose and **D-mannose** are epimers with respect to C2. The most common aldoses include the six-carbon sugars glucose, mannose, and **galactose.** The pentose **ribose** is a component of the ribonucleotide residues of RNA. The triose **glyceraldehyde** occurs in several metabolic pathways.

The most common ketoses are those with their ketone function at C2 (Fig. 8-2). The position of their carbonyl group gives ketoses one less asymmetric center than their isomeric aldoses, so a ketohexose has only $2^3 = 8$ possible stereoisomers (4 D sugars and 4 L sugars). The most common ketoses are **dihydroxyacetone, ribulose,** and **fructose,** which we shall encounter in our studies of metabolism.

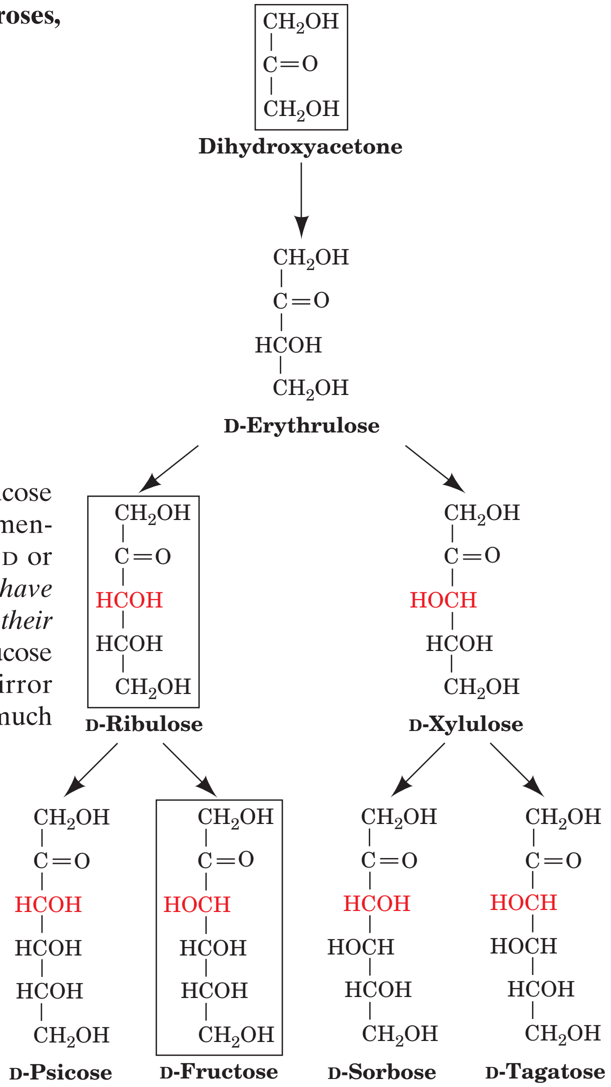

Figure 8-2 | The D-ketoses with three to six carbon atoms. The configuration around C3 (*red*) distinguishes the members of each pair. The biologically most common ketoses are boxed.

B | Monosaccharides Vary in Configuration and Conformation

Alcohols react with the carbonyl groups of aldehydes and ketones to form **hemiacetals** and **hemiketals,** respectively:

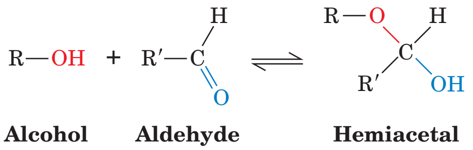

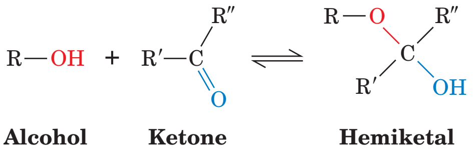

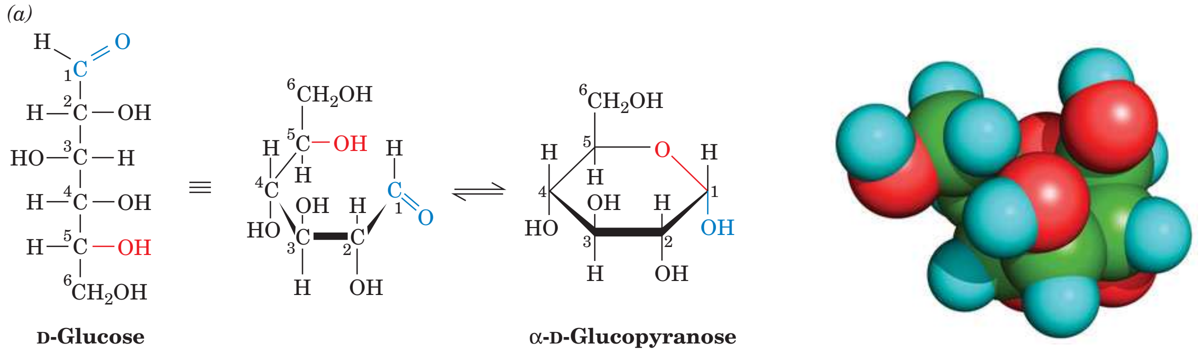
(a)
H
O
C
H—C—OH
HO—C—H
H—C—OH
H—C—OH
CH₂OH
≡
CH₂OH
C—OH
H
H
C
OH
H
C
O
HO
C
C
H
OH
⇌
CH₂OH
O
H
H
H
OH
H
HO
OH
H
OH
1
2
3
4
5
6

D-Glucose (linear form)

α-D-Glucopyranose (Haworth projection)

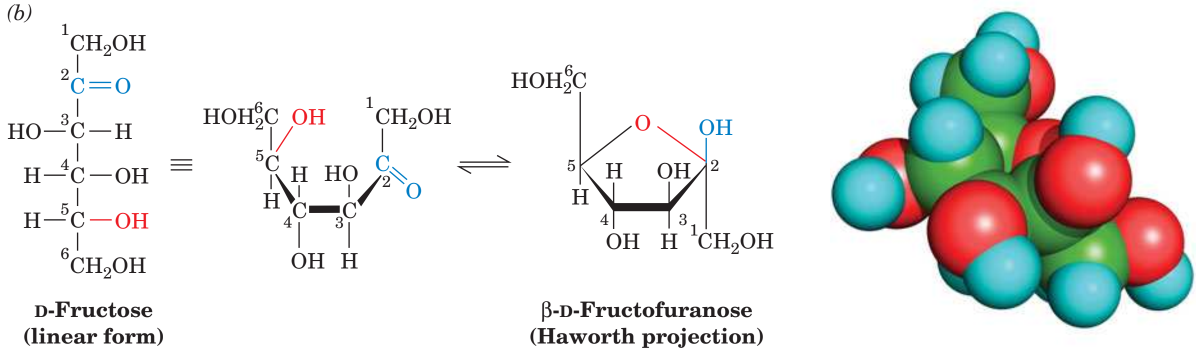
(b)
CH₂OH
C=O
HO—C—H
H—C—OH
H—C—OH
CH₂OH
≡
HOH₂C
OH
CH₂OH
C
H
HO
C
O
H
C
C
OH
H
⇌
HOH₂C
O
OH
H
OH
H
OH
H
CH₂OH
1
2
3
4
5
6

D-Fructose (linear form)

β-D-Fructofuranose (Haworth projection)

Figure 8-3 | Cyclization of glucose and fructose. (*a*) The linear form of D-glucose yielding the cyclic hemiacetal α-D-glucopyranose. (*b*) The linear form of D-fructose yielding the hemiketal β-D-fructofuranose. The cyclic sugars are shown as both Haworth projections and space-filling models with C green, H cyan, and O red.

The hydroxyl and either the aldehyde or the ketone functions of monosaccharides can likewise react intramolecularly to form cyclic hemiacetals and hemiketals (Fig. 8-3). The configurations of the substituents of each carbon atom in these sugar rings are conveniently represented by their **Haworth projections,** in which the heavier ring bonds project in front of the plane of the paper and the lighter ring bonds project behind it.

A sugar with a six-membered ring is known as a **pyranose** in analogy with **pyran,** the simplest compound containing such a ring. Similarly, sugars with five-membered rings are designated **furanoses** in analogy with **furan:**

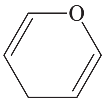

Pyran

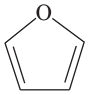

Furan

The cyclic forms of glucose and fructose with six- and five-membered rings are therefore known as **glucopyranose** and **fructofuranose,** respectively.

Cyclic Sugars Have Two Anomeric Forms. When a monosaccharide cyclizes, the carbonyl carbon, called the **anomeric carbon,** becomes a chiral center with two possible configurations. The pair of stereoisomers that differ in configuration at the anomeric carbon are called **anomers.** In

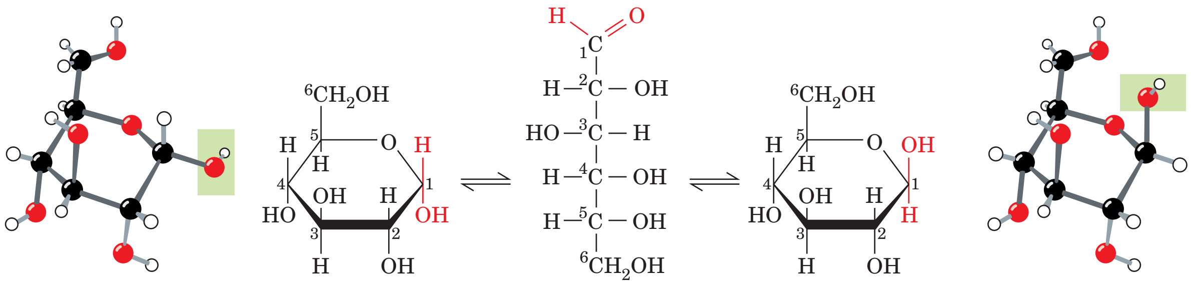

α-D-Glucopyranose **D-Glucose (linear form)** **β-D-Glucopyranose**

Figure 8-4 | **α and β anomers.** The monosaccharides α-D-glucopyranose and β-D-glucopyranose, drawn as Haworth projections and ball-and-stick models, interconvert through the linear form. They differ only by their configuration about the anomeric carbon, C1. **See Kinemage Exercise 7-1.**

the **α anomer,** the OH substituent of the anomeric carbon is on the opposite side of the sugar ring from the CH_2OH group at the chiral center that designates the D or L configuration (C5 in hexoses). The other form is known as the **β anomer** (Fig. 8-4).

The two anomers of D-glucose have slightly different physical and chemical properties, including different optical rotations (Section 4-2). *The anomers freely interconvert in aqueous solution,* so at equilibrium, D-glucose is a mixture of the β anomer (63.6%) and the α anomer (36.4%). The linear form is normally present in only minute amounts.

Sugars Can Adopt Different Conformations. A given hexose or pentose can assume pyranose or furanose forms. In principle, hexoses and larger sugars can form rings of seven or more atoms, but such rings are rarely observed because of the greater stabilities of the five- and six-membered rings. The internal strain of three- and four-membered rings makes them less stable than the linear forms.

The use of Haworth formulas may lead to the erroneous impression that furanose and pyranose rings are planar. This cannot be the case, however, because all the atomic orbitals in the ring atoms are tetrahedrally (sp^3) hybridized. The pyranose ring, like the cyclohexane ring, can assume a chair conformation, in which the substituents of each atom are arranged tetrahedrally. Of the two possible chair conformations, the one that predominates is the one in which the bulkiest ring substituents occupy **equatorial** positions rather than the more crowded **axial** positions (Fig. 8-5).

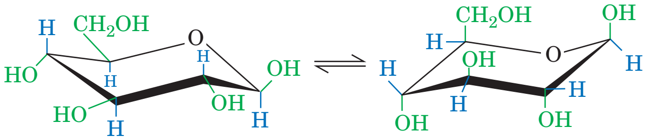

Figure 8-5 | **The two chair conformations of β-D-glucopyranose.** In the conformation on the left, which predominates, the relatively bulky OH and CH_2OH substituents all occupy equatorial positions, where they extend alternately above and below the ring. In the conformation on the right (drawn in ball-and-stick form in Fig. 8-4, *right*), the bulky groups occupy the more crowded axial (vertical) positions. **See Kinemage Exercise 7-1.**

Only β-D-glucose can simultaneously have all five of its non-H substituents in equatorial positions. Perhaps this is why glucose is the most abundant monosaccharide in nature.

Furanose rings can also adopt different conformations, whose stabilities depend on the arrangements of bulky substituents. Note that a monosaccharide can readily shift its *conformation,* because no bonds are broken in the process. The shift in *configuration* between the α and β anomeric forms or between the pyranose and furanose forms, which requires breaking and re-forming bonds, occurs slowly in aqueous solution. Other changes in configuration, such as **epimerization,** do not occur under physiological conditions without the appropriate enzyme.

C | Sugars Can Be Modified and Covalently Linked

Because the cyclic and linear forms of aldoses and ketoses do interconvert, these sugars undergo reactions typical of aldehydes and ketones.

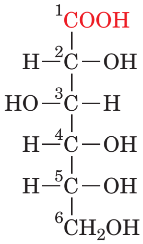

D-Gluconic acid

1. Oxidation of an aldose converts its aldehyde group to a carboxylic acid group, thereby yielding an **aldonic acid** such as **gluconic acid** *(at left)*. Aldonic acids are named by appending the suffix *-onic acid* to the root name of the parent aldose.

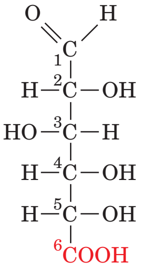

D-Glucuronic acid

2. Oxidation of the primary alcohol group of aldoses yields **uronic acids,** which are named by appending *-uronic acid* to the root name of the parent aldose, for example, **D-glucuronic acid** *(at left)*. Uronic acids can assume the pyranose, furanose, and linear forms.
3. Aldoses and ketoses can be reduced under mild conditions, for example, by treatment with $NaBH_4$, to yield polyhydroxy alcohols known as **alditols,** which are named by appending the suffix *-itol* to the root name of the parent aldose. **Ribitol** is a component of flavin coenzymes (Fig. 14-12), and **glycerol** and the cyclic polyhydroxy alcohol ***myo*-inositol** are important lipid components (Section 9-1). **Xylitol** is a sweetener that is used in "sugarless" gum and candies:

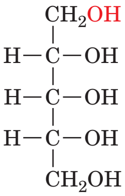

Ribitol

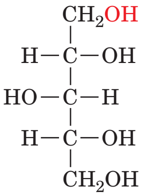

Xylitol

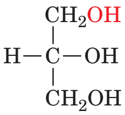

Glycerol

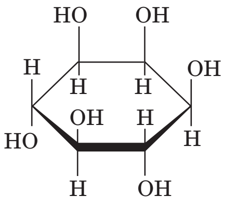

***myo*-Inositol**

4. Monosaccharide units in which an OH group is replaced by H are known as **deoxy sugars.** The biologically most important of these is **β-D-2-deoxyribose,** the sugar component of DNA's sugar–phosphate backbone (Section 3-2B). **L-Fucose** is one of the few L sugar components of polysaccharides.

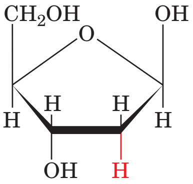

β-D-2-Deoxyribose

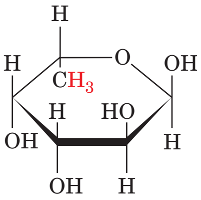

α-L-Fucose

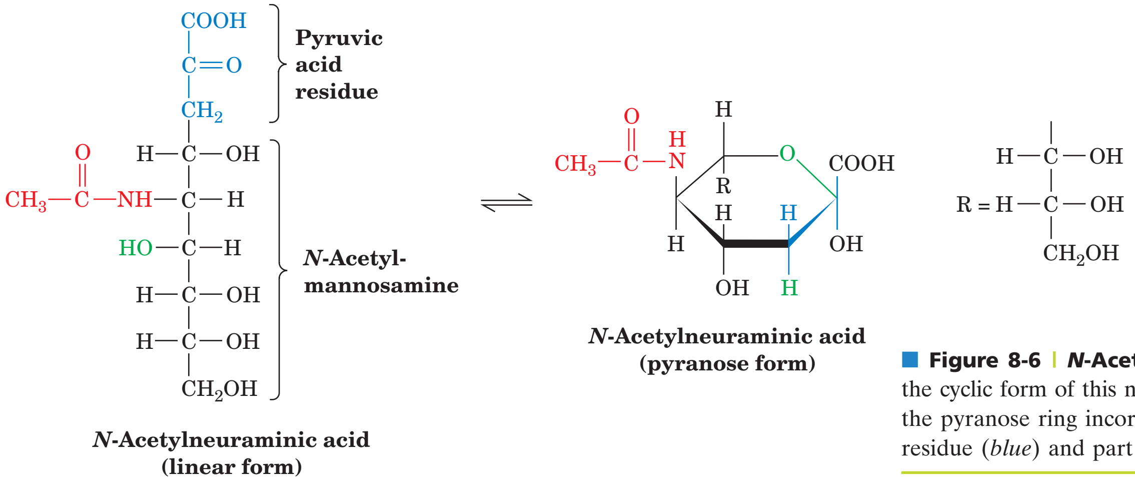
COOH
C=O
CH$_2$
Pyruvic acid residue
H—C—OH
CH$_3$—C—NH—C—H
HO—C—H
H—C—OH
H—C—OH
CH$_2$OH
N-Acetyl-mannosamine
N-Acetylneuraminic acid (linear form)
CH$_3$—C—N
H
O
R
COOH
OH
N-Acetylneuraminic acid (pyranose form)
R = H—C—OH
H—C—OH
CH$_2$OH

Figure 8-6 | ***N*-Acetylneuraminic acid.** In the cyclic form of this nine-carbon monosaccharide, the pyranose ring incorporates the pyruvic acid residue (*blue*) and part of the mannose moiety.

5. In **amino sugars,** one or more OH groups have been replaced by an amino group, which is often acetylated. **D-Glucosamine** and **D-galactosamine** are the most common:

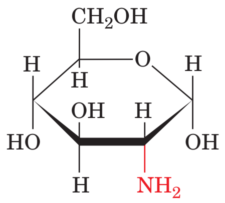
CH$_2$OH
O
HO
OH
NH$_2$

α-D-Glucosamine
(2-amino-2-deoxy-
α-D-glucopyranose)

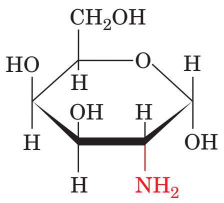
CH$_2$OH
O
HO
OH
NH$_2$

α-D-Galactosamine
(2-amino-2-deoxy-
α-D-galactopyranose)

***N*-Acetylneuraminic acid,** which is derived from ***N*-acetylmannosamine** and **pyruvic acid** (Fig. 8-6), is an important constituent of **glycoproteins** and **glycolipids** (proteins and lipids with covalently attached carbohydrate). *N*-Acetylneuraminic acid and its derivatives are often referred to as **sialic acids.**

Glycosidic Bonds Link the Anomeric Carbon to Other Compounds. The anomeric group of a sugar can condense with an alcohol to form **α-** and **β-glycosides** (Greek: *glykys*, sweet; Fig. 8-7). The bond connecting the anomeric carbon to the alcohol oxygen is termed a **glycosidic bond.**

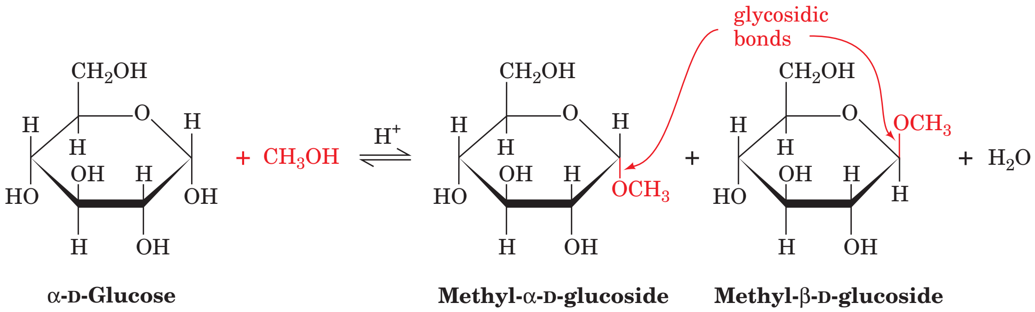
glycosidic bonds
CH$_2$OH
+ CH$_3$OH
H$^+$
OCH$_3$
+
+ H$_2$O
α-D-Glucose
Methyl-α-D-glucoside
Methyl-β-D-glucoside

Figure 8-7 | **Formation of glycosides.** The acid-catalyzed condensation of α-D-glucose with methanol yields an anomeric pair of **methyl-D-glucosides.**

N-Glycosidic bonds, which form between the anomeric carbon and an amine, are the bonds that link D-ribose to purines and pyrimidines in nucleic acids:

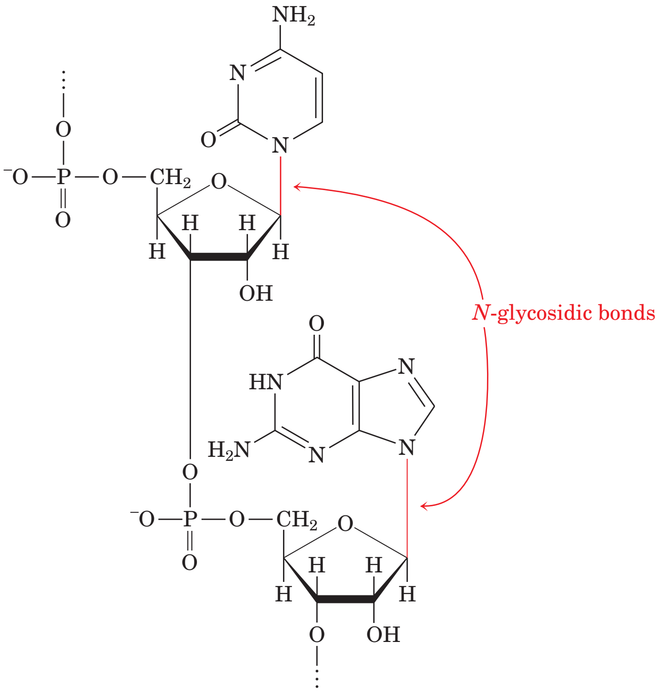

Like peptide bonds, glycosidic bonds hydrolyze extremely slowly under physiological conditions in the absence of appropriate hydrolytic enzymes. Consequently, an anomeric carbon that is involved in a glycosidic bond cannot freely convert between its α and β anomeric forms. Saccharides bearing anomeric carbons that have not formed glycosides are termed **reducing sugars,** because the free aldehyde group that is in equilibrium with the cyclic form of the sugar reduces mild oxidizing agents. Identification of a sugar as **nonreducing** is evidence that it is a glycoside.

CHECK YOUR UNDERSTANDING

How does an aldose differ from a ketose?
Show how aldoses and ketoses can form five- and six-membered rings.
Explain why anomers of a monosaccharide can interconvert whereas epimers cannot.
Describe aldonic acids, uronic acids, alditols, deoxy sugars, and amino sugars.
Explain why a sugar can form at least two different glycosides.

2 Polysaccharides

LEARNING OBJECTIVES

- Be able to describe the monosaccharide units and their linkages in the common polysaccharides.
- Understand how the physical properties of polysaccharides relate to their biological functions.

Polysaccharides, which are also known as ***glycans,*** *consist of monosaccharides linked together by glycosidic bonds.* They are classified as **homopolysaccharides** or **heteropolysaccharides** if they consist of one type or more than one type of monosaccharide. Although the monosaccharide sequences of heteropolysaccharides can, in principle, be even more varied than those of proteins, many are composed of only a few types of monosaccharides that alternate in a repetitive sequence.

Polysaccharides, in contrast to proteins and nucleic acids, form branched as well as linear polymers. This is because glycosidic linkages can be made to any of the hydroxyl groups of a monosaccharide. Fortunately for structural biochemists, most polysaccharides are linear and those that branch do so in only a few well-defined ways.

A complete description of an **oligosaccharide** or polysaccharide includes the identities, anomeric forms, and linkages of all its component monosaccharide units. Some of this information can be gathered through the use of specific **exoglycosidases** and **endoglycosidases,** enzymes that hydrolyze monosaccharide units in much the same way that exopeptidases and endopeptidases cleave amino acid residues from polypeptides (Section 5-3B). NMR measurements are also invaluable in determining both sequences and conformations of polysaccharides.

A | Lactose and Sucrose Are Disaccharides

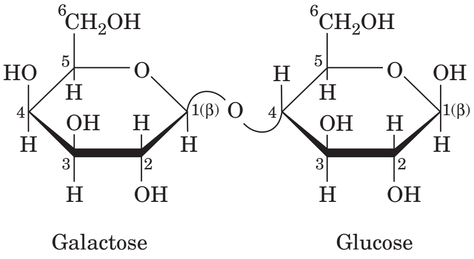

Lactose

Oligosaccharides containing three or more residues are relatively rare, occurring almost entirely in plants. **Disaccharides,** the simplest polysaccharides, are more common. Many occur as the hydrolysis products of larger molecules. However, two disaccharides are notable in their own right. **Lactose** *(at right)*, for example, occurs naturally only in milk, where its concentration ranges from 0 to 7% depending on the species (Box 8-1). The systematic name for lactose, *O*-β-D-galactopyranosyl-(1→4)-D-glucopyranose, specifies its monosaccharides, their ring types, and how they are linked together. The symbol (1→4) combined with the β in the prefix indicates that the glycosidic bond links C1 of the β anomer of galactose to O4 of glucose. Note that lactose has a free anomeric carbon on its glucose residue and is therefore a reducing sugar.

The most abundant disaccharide is **sucrose,**

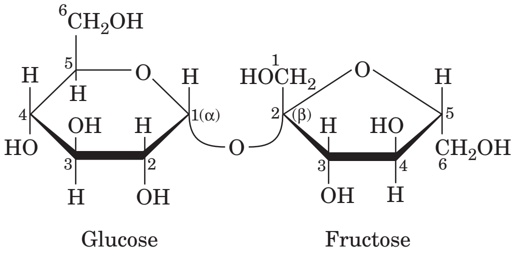

Sucrose

the major form in which carbohydrates are transported in plants. Sucrose is familiar to us as common table sugar (**see Kinemage Exercise 7-2).** The systematic name for sucrose, *O*-α-D-glucopyranosyl-(1→2)-β-D-fructofuranoside, indicates that the anomeric carbon of each sugar (C1 in glucose and C2 in fructose) participates in the glycosidic bond and hence sucrose is not a reducing sugar. Noncarbohydrate molecules that mimic the taste of sucrose are used as sweetening agents in foods and beverages (Box 8-2).

BOX 8-1 BIOCHEMISTRY IN HEALTH AND DISEASE

Lactose Intolerance

In infants, lactose (also known as milk sugar) is hydrolyzed by the intestinal enzyme **β-D-galactosidase** (or **lactase**) to its component monosaccharides for absorption into the bloodstream. The galactose is enzymatically converted (epimerized) to glucose, which is the primary metabolic fuel of many tissues.

Since mammals are unlikely to encounter lactose after they have been weaned, most adult mammals have low levels of β-galactosidase. Consequently, much of the lactose they might ingest moves through their digestive tract to the colon, where bacterial fermentation generates large quantities of CO_2, H_2, and irritating organic acids. These products cause the embarrassing and often painful digestive upset known as **lactose intolerance.**

Lactose intolerance, which was once considered a metabolic disturbance, is actually the norm in adult humans, particularly those of African and Asian descent. Interestingly, however, β-galactosidase levels decrease only mildly with age in descendants of populations that have historically relied on dairy products for nutrition throughout life. Modern food technology has come to the aid of milk lovers who develop lactose intolerance: Milk in which the lactose has been hydrolyzed enzymatically is widely available.

BOX 8-2 PERSPECTIVES IN BIOCHEMISTRY

Artificial Sweeteners

Artificial sweeteners are added to processed foods and beverages to impart a sweet taste without adding calories. This is possible because the compounds mimic sucrose in its interactions with taste receptors but either are not metabolized or contribute very little to energy metabolism because they are used at such low concentrations.

Naturally occurring saccharides, such as fructose, are slightly sweeter than sucrose. Honey, which contains primarily fructose, glucose, and maltose (a glucose disaccharide), is about 1.5 times as sweet as sucrose. How is sweetness measured? There is no substitute for the human sense of taste, so a panel of individuals sample solutions of a compound and compare them to a reference solution containing sucrose. The very sweet compounds listed below must be diluted significantly before testing in this manner.

Compound	Sweetness Relative to Sucrose
Acesulfame	200
Alitame	2000
Aspartame	180
Saccharin	350
Sucralose	600

One of the oldest artificial sweeteners is saccharin, discovered in 1879 and commonly consumed as Sweet'N Low®. In the 1970s, extremely high doses of saccharin were found to cause cancer in laboratory rats. Such doses are now considered to be so far outside of the range used for sweetening as to be of insignificant concern to users.

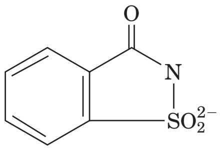

Saccharin

Aspartame, the active ingredient in NutraSweet® and Equal®, was approved for human use in 1981 and is currently the market leader:

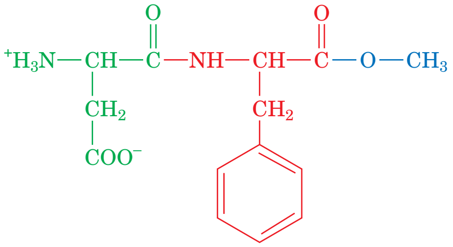

Aspartylphenylalanine methyl ester (aspartame)

Unlike saccharin, which is not metabolized by the human body, aspartame is broken down into its components: aspartate (*green*), phenylalanine (*red*), and methanol (*blue*). The Asp and Phe, like all amino acids, can be metabolized, so aspartame is not calorie-free. Methanol in large amounts is toxic; however, the amount derived from an aspartame-sweetened drink is comparable to the amount naturally present in the same volume of fruit juice. Individuals with the genetic disease **phenylketonuria,** who are unable to metabolize phenylalanine, are advised to avoid ingesting excess Phe in the form of aspartame (or any other polypeptide). The greatest drawback of aspartame may be its instability to heat, which makes it unsuitable for baking. In addition, aspartame in soft drinks hydrolyzes over a period of months and hence loses its flavor.

Acesulfame is sometimes used in combination with aspartame, since the two compounds act synergistically (i.e., their sweetness when combined is greater than the sum of their individual sweetnesses).

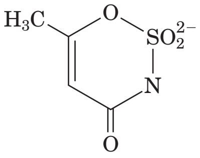

Acesulfame

Other artificial sweeteners are derivatives of sugars, such as sucralose (Splenda®; see Problem 8-9), or of aspartame (e.g., alitame). Some plant extracts (e.g., *Stevia*) are also used as artificial sweeteners.

The market for artificial sweeteners is worth several billion dollars annually. But surprisingly, the most successful sweetening agents have not been the result of dedicated research efforts. Instead, they were discovered by chance or mishap. For example, aspartame was discovered in 1965 by a synthetic chemist who unknowingly got a small amount of the compound on his fingers and happened to lick them. Sucralose came to light in 1975 when a student was asked to "test" a compound and misunderstood the directions as "taste" the compound.

B | Cellulose and Chitin Are Structural Polysaccharides

Plants have rigid cell walls that can withstand osmotic pressure differences between the extracellular and intracellular spaces of up to 20 atm. In large plants, such as trees, the cell walls also have a load-bearing function.

Cellulose, the primary structural component of plant cell walls (Fig. 8-8), accounts for over half of the carbon in the biosphere: Approximately 10^{15} kg of cellulose is estimated to be synthesized and degraded annually.

Cellulose is a linear polymer of up to 15,000 D-glucose residues linked by β(1→4) glycosidic bonds:

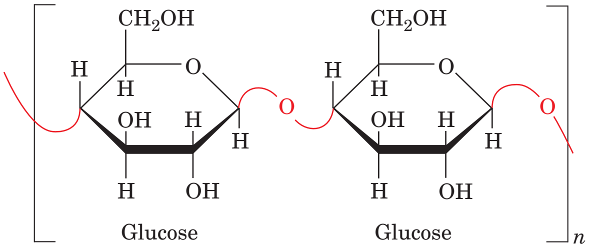

Cellulose

X-Ray and other studies of cellulose fibers reveal that cellulose chains are flat ribbons in which successive glucose rings are turned over 180° with respect to each other. This permits the C3—OH group of each glucose residue to form a hydrogen bond with the ring oxygen (O5) of the next residue. Parallel cellulose chains form sheets with interchain hydrogen bonds, including O2—H···O6 and O6—H···O3 bonds (Fig. 8-9). Stacks of these sheets are held together by hydrogen bonds and van der Waals interactions. This highly cohesive structure gives cellulose fibers exceptional strength and makes them water insoluble despite their hydrophilicity. In plant cell walls, the cellulose fibers are embedded in and cross-linked by a matrix containing other polysaccharides and **lignin,** a plasticlike phenolic

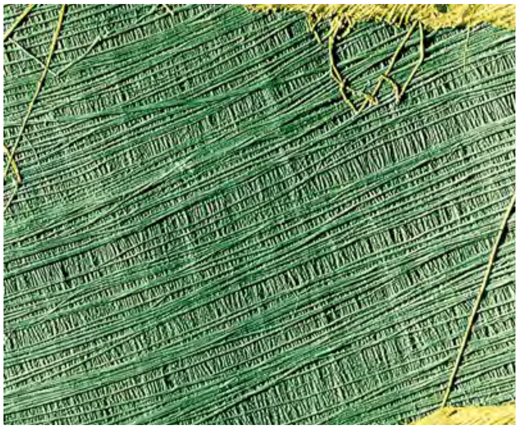

Figure 8-8 | Electron micrograph of cellulose fibers. The cellulose fibers in this sample of cell wall from the alga *Chaetomorpha* are arranged in layers. [Biophoto Associates/ Photo Researchers.]

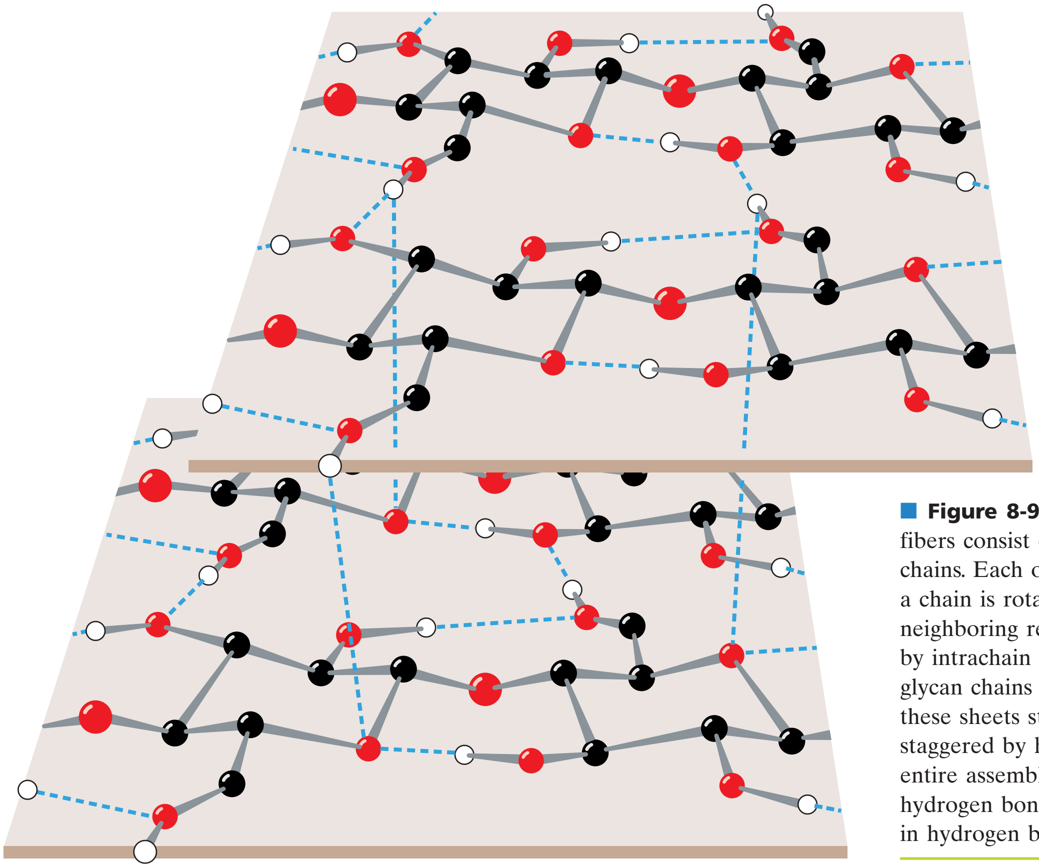

Figure 8-9 | Model of cellulose. Cellulose fibers consist of ~40 parallel, extended glycan chains. Each of the β(1→4)-linked glucose units in a chain is rotated 180° with respect to its neighboring residues and is held in this position by intrachain hydrogen bonds (*dashed lines*). The glycan chains line up laterally to form sheets, and these sheets stack vertically so that they are staggered by half the length of a glucose unit. The entire assembly is stabilized by intermolecular hydrogen bonds. Hydrogen atoms not participating in hydrogen bonds have been omitted for clarity.

polymer. The resulting composite material can withstand large stresses because the matrix evenly distributes the stresses among the cellulose reinforcing elements.

Although vertebrates themselves do not possess an enzyme capable of hydrolyzing the β(1→4) linkages of cellulose, the digestive tracts of herbivores contain symbiotic microorganisms that secrete a series of enzymes, collectively known as **cellulases,** that do so. The same is true of termites. Nevertheless, the degradation of cellulose is a slow process because its tightly packed and hydrogen-bonded glycan chains are not easily accessible to cellulase and do not separate readily even after many of their glycosidic bonds have been hydrolyzed. Thus, cows must chew their cud, and the decay of dead trees by fungi and other organisms generally takes many years.

Chitin is the principal structural component of the exoskeletons of invertebrates such as crustaceans, insects, and spiders and is also present in the cell walls of most fungi and many algae. It is therefore almost as abundant as cellulose. Chitin is a homopolymer of β(1→4)-linked *N*-acetyl-D-glucosamine residues:

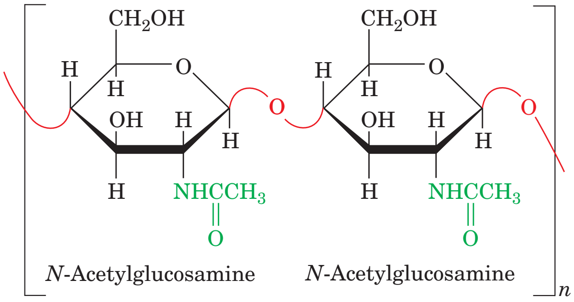

Chitin

It differs chemically from cellulose only in that each C2—OH group is replaced by an acetamido function. X-Ray analysis indicates that chitin and cellulose have similar structures.

C | Starch and Glycogen Are Storage Polysaccharides

Starch is a mixture of glycans that plants synthesize as their principal energy reserve. It is deposited in the chloroplasts of plant cells as insoluble granules composed of **α-amylose** and **amylopectin.** α-Amylose is a linear polymer of several thousand glucose residues linked by α(1→4) bonds:

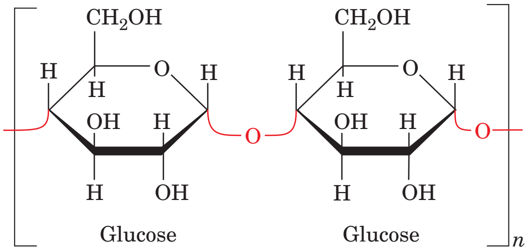

α-Amylose

Note that although α-amylose is an isomer of cellulose, it has very different structural properties. While cellulose's β-glycosidic linkages cause it to assume a tightly packed, fully extended conformation (Fig. 8-9), α-amylose's α-glycosidic bonds cause it to adopt an irregularly aggregating helically coiled conformation (Fig. 8-10).

Figure 8-10 | **α-Amylose.** This regularly repeating polymer forms a left-handed helix. Note the great differences in structure and properties that result from changing α-amylose's α(1→4) linkages to the β(1→4) linkages of cellulose (Fig. 8-9). [Illustration, Irving Geis/Geis Archives Trust. Copyright Howard Hughes Medical Institute. Reproduced with permission.]

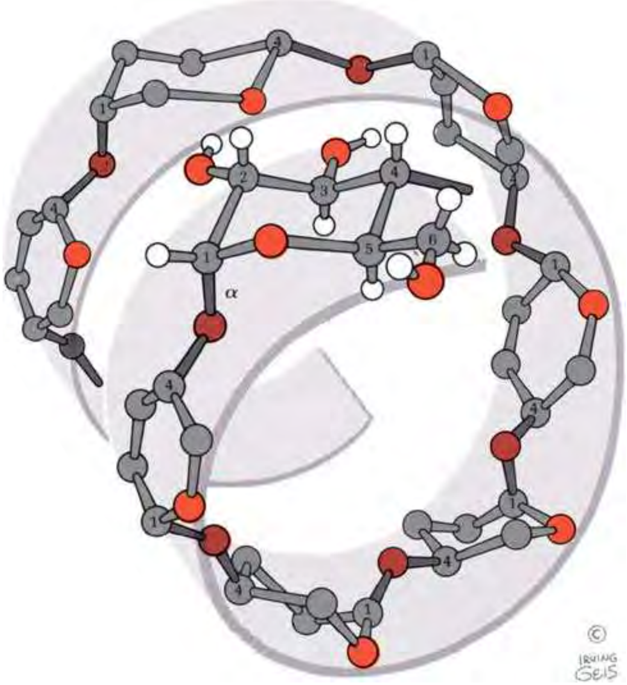

Amylopectin consists mainly of α(1→4)-linked glucose residues but is a branched molecule with α(1→6) branch points every 24 to 30 glucose residues on average:

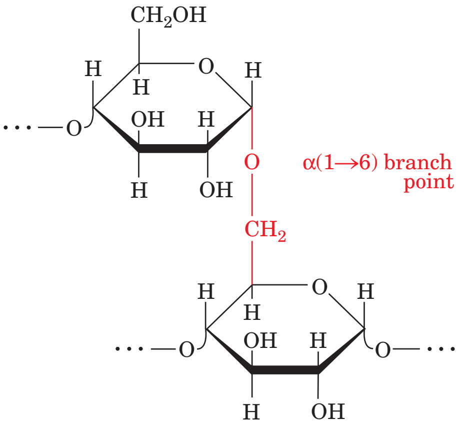

Amylopectin

Amylopectin molecules contain up to 10^6 glucose residues, making them some of the largest molecules in nature. The storage of glucose as starch greatly reduces the large intracellular osmotic pressure that would result from its storage in monomeric form, because osmotic pressure is proportional to the number of solute molecules in a given volume (Section 2-1D). Starch is a reducing sugar, although it has only one residue, called the **reducing end,** that lacks a glycosidic bond.

The digestion of starch, the main carbohydrate source in the human diet, begins in the mouth. Saliva contains an **amylase,** which randomly hydrolyzes the α(1→4) glycosidic bonds of starch. Starch digestion continues in the small intestine under the influence of pancreatic amylase, which degrades starch to a mixture of small oligosaccharides. Further hydrolysis by an **α-glucosidase,** which removes one glucose residue at a time, and by a **debranching enzyme,** which hydrolyzes α(1→6) as well as α(1→4) bonds, produces monosaccharides that are absorbed by the intestine and transported to the bloodstream.

Glycogen, the storage polysaccharide of animals, is present in all cells but is most prevalent in skeletal muscle and in liver, where it occurs as cytoplasmic granules (Fig. 8-11). The primary structure of glycogen resembles that of amylopectin, but glycogen is more highly branched, with branch points occurring every 8 to 14 glucose residues. In the cell, glycogen is degraded for metabolic use by **glycogen phosphorylase,** which phosphorolytically cleaves glycogen's α(1→4) bonds sequentially inward from its nonreducing ends. *Glycogen's highly branched structure, which has many nonreducing ends, permits the rapid mobilization of glucose in times of metabolic need*. The α(1→6) branches of glycogen are cleaved by **glycogen debranching enzyme** (glycogen breakdown is discussed further in Section 16-1).

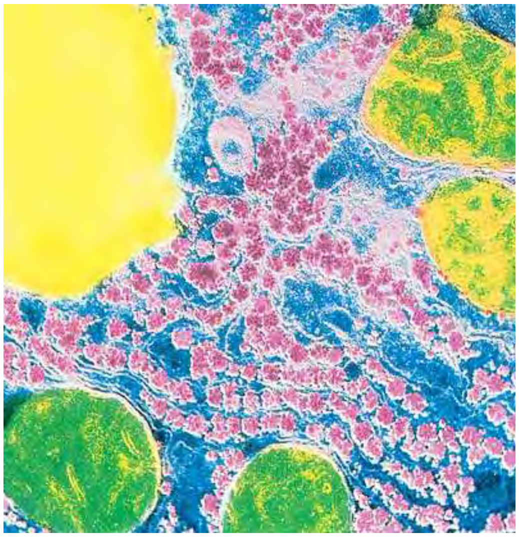

Figure 8-11 | **Glycogen granules in a liver cell.** In this photomicrograph, glycogen granules are pink, the greenish objects are mitochondria, and the yellow object is a fat globule. The glycogen content of liver may reach 10% of its net weight. [CNRI/Science Photo Library/Photo Researchers.]

D | Glycosaminoglycans Form Highly Hydrated Gels

The extracellular spaces, particularly those of connective tissues such as cartilage, tendon, skin, and blood vessel walls, contain collagen (Section 6-1C) and other proteins embedded in a gel-like matrix that is composed largely of **glycosaminoglycans.** These unbranched polysaccharides consist of alternating uronic acid and hexosamine residues. Solutions of glycosaminoglycans have a slimy, mucuslike consistency that results from their high viscosity and elasticity.

Hyaluronate Acts as a Shock Absorber and Lubricant. **Hyaluronic acid (hyaluronate)** is an important glycosaminoglycan component of connective tissue, synovial fluid (the fluid that lubricates joints), and the vitreous humor of the eye. Hyaluronate molecules are composed of 250 to 25,000 β(1→4)-linked disaccharide units that consist of D-glucuronic acid and ***N*-acetyl-D-glucosamine (GlcNAc)** linked by a β(1→3) bond (Fig. 8-12). Hyaluronate is an extended, rigid molecule whose numerous repelling anionic groups bind cations and water molecules. In solution, hyaluronate occupies a volume ~1000 times that in its dry state.

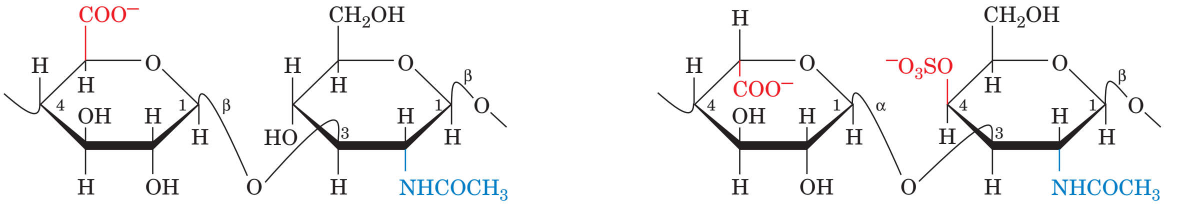

D-Glucuronate N-Acetyl-D-glucosamine

Hyaluronate

L-Iduronate N-Acetyl-D-galactosamine-4-sulfate

Dermatan sulfate

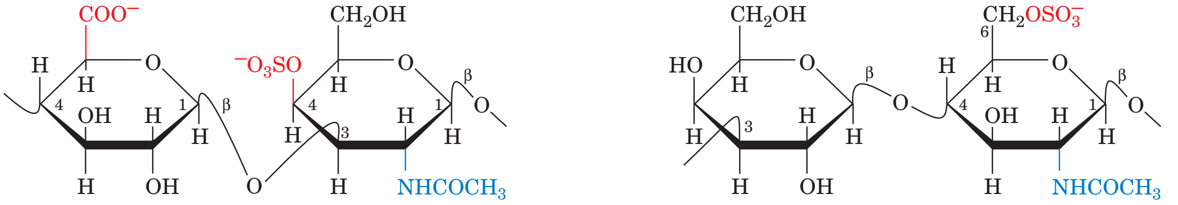

D-Glucuronate N-Acetyl-D-galactosamine-4-sulfate

Chondroitin-4-sulfate

D-Galactose N-Acetyl-D-glucosamine-6-sulfate

Keratan sulfate

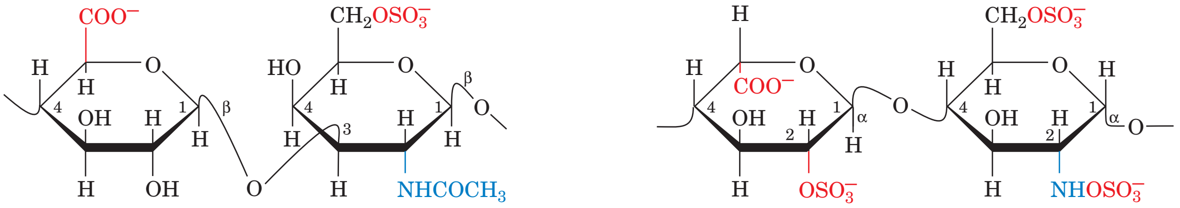

D-Glucuronate N-Acetyl-D-galactosamine-6-sulfate

Chondroitin-6-sulfate

L-Iduronate-2-sulfate N-Sulfo-D-glucosamine-6-sulfate

Heparin

Figure 8-12 | Repeating disaccharide units of some glycosaminoglycans. The anionic groups are shown in red and the *N*-acetylamido groups are shown in blue. **See Kinemage Exercise 7-3.**

Hyaluronate solutions have a viscosity that is shear dependent (an object under shear stress has equal and opposite forces applied across its opposite faces). At low shear rates, hyaluronate molecules form tangled masses that greatly impede flow; that is, the solution is quite viscous. As the shear stress increases, the stiff hyaluronate molecules tend to line up with the flow and thus offer less resistance to it. This viscoelastic behavior makes hyaluronate solutions excellent biological shock absorbers and lubricants.

Some Glycosaminoglycans Are Sulfated. The other common glycosaminoglycans shown in Fig. 8-12 consist of 50 to 1000 sulfated disaccharide units. **Chondroitin-4-sulfate** and **chondroitin-6-sulfate** differ only in the sulfation of their ***N*-acetylgalactosamine (GalNAc)** residues. **Dermatan sulfate** is derived from chondroitin by enzymatic epimerization of the C5 of glucuronate residues to form **iduronate** residues. **Keratan sulfate** (not to be confused with the fibrous protein keratin; Section 6-1C) is the most heterogeneous of the major glycosaminoglycans in that its sulfate content is variable and it contains small amounts of fucose, mannose, GlcNAc, and sialic acid. **Heparin** is also variably sulfated, with an average of 2.5 sulfate residues per disaccharide unit, which makes it the most highly charged polymer in mammalian tissues (Fig. 8-13).

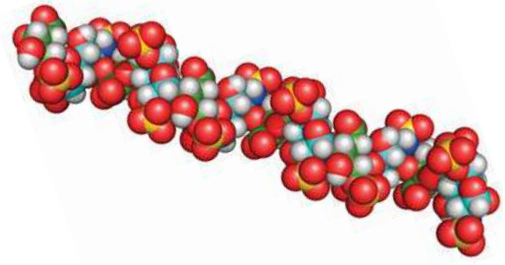

Figure 8-13 | NMR structure of heparin. The polymer shown here in space-filling form contains six pairs of iduronate and glucosamine residues. Atoms are colored according to type with iduronate C green, glucosamine C cyan, H white, N blue, O red, and S yellow. Note the high density of anionic sulfate groups. [Based on an NMR structure by Barbara Mulloy and Mark Forster, National Institute for Biological Standards and Control, Herts, U.K. PDBid 1HPN.]

In contrast to the other glycosaminoglycans, heparin is not a constituent of connective tissue but occurs almost exclusively in the intracellular granules of the mast cells that occur in arterial walls. It inhibits the clotting of blood, and its release, through injury, is thought to prevent runaway clot formation. Heparin is therefore in wide clinical use to inhibit blood clotting, for example, in postsurgical patients.

Heparan sulfate, a ubiquitous cell-surface component as well as an extracellular substance in blood vessel walls and brain, resembles heparin but has a far more variable composition with fewer *N*- and *O*-sulfate groups and more *N*-acetyl groups. Heparan sulfate plays a critical role in development and in wound healing. Various **growth factors** bind to heparan sulfate, and the formation of complexes of the glycosaminoglycan, the growth factor, and the growth factor receptor is required to initiate cell differentiation and proliferation. Specific sulfation patterns on heparan sulfate are required for the formation of these ternary complexes.

Plants Produce Pectin. Plants do not synthesize glycosaminoglycans, but the **pectins,** which are major components of cell walls, may function similarly as shock absorbers. Pectins are heterogeneous polysaccharides with a core of α(1→4)-linked galacturonate residues interspersed with the hexose **rhamnose:**

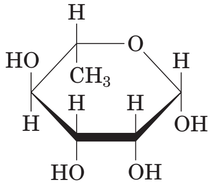

Rhamnose

The galacturonate residues may be modified by the addition of methyl and acetyl groups. Other polysaccharide chains, some containing the pentoses arabinose and xylose and other sugars, are attached to the galacturonate. The aggregation of pectin molecules to form bundles requires divalent cations (usually Ca^{2+}), which form cross-links between the anionic carboxylate groups of neighboring galacturonate residues. The tendency for

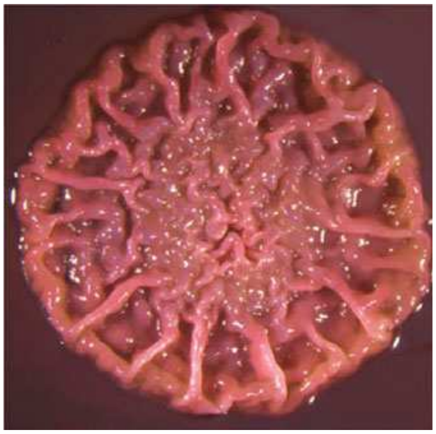

Figure 8-14 | A *Pseudomonas aeruginosa* biofilm. Bacterial colonies growing on the surface of an agar plate form a biofilm with complex architecture. [Courtesy of Roberto Kolter, Harvard Medical School,]

pectin to form highly hydrated gels is exploited in the manufacture of jams and jellies, to which pectin is often added to augment the endogenous pectin content of the fruit.

Bacterial Biofilms Are a Type of Extracellular Matrix. Outside the laboratory, bacteria are most often found growing on surfaces as a **biofilm,** an association of cells in a semisolid matrix (Fig. 8-14). The extracellular material of the biofilm consists mostly of highly hydrated polysaccharides such as anionic poly-D-glucuronate, poly-*N*-acetylglucosamine, cellulose-like molecules, and acetylated glycans. A biofilm is difficult to characterize, as it typically houses a mixture of species, and the proportions of its component polysaccharides can vary over time and space.

The gel-like consistency of a biofilm, for example, the plaque that forms on teeth, prevents bacterial cells from being washed away and protects them from desiccation. Biofilms that develop on medical apparatus, such as catheters, are problematic because they offer a foothold for pathogenic organisms and create a barrier to soluble antimicrobial agents.

CHECK YOUR UNDERSTANDING

Compare and contrast the structures and functions of cellulose, chitin, starch, and glycogen.

How do the physical properties of glycosaminoglycans and similar molecules relate to their biological roles?

3 Glycoproteins

LEARNING OBJECTIVES

- Understand that proteoglycans are large, glycosaminoglycan-containing proteins.
- Understand that bacterial cell walls consist of glycan chains cross-linked by peptides.
- Understand that the oligosaccharide chains covalently attached to eukaryotic glycoproteins may play a role in protein structure and recognition.

Many proteins are actually glycoproteins, with carbohydrate contents varying from <1% to >90% by weight. Glycoproteins occur in all forms of life and have functions that span the entire spectrum of protein activities, including those of enzymes, transport proteins, receptors, hormones, and structural proteins. The polypeptide chains of glycoproteins, like those of all proteins, are synthesized under genetic control. Their carbohydrate chains, in contrast, are enzymatically generated and covalently linked to the polypeptide without the rigid guidance of nucleic acid templates. For this reason, glycoproteins tend to have variable carbohydrate composition, a phenomenon known as **microheterogeneity.** Characterizing the structures of carbohydrates—and their variations—is one goal of the field of **glycomics,** which complements the studies of genomics (for DNA) and proteomics (for proteins).

A | Proteoglycans Contain Glycosaminoglycans

Proteins and glycosaminoglycans in the extracellular matrix aggregate covalently and noncovalently to form a diverse group of macromolecules known as **proteoglycans.** Electron micrographs (Fig. 8-15*a*) and other evidence indicate that proteoglycans have a bottlebrush-like molecular architecture, with "bristles" noncovalently attached to a filamentous hyaluronate "backbone." The bristles consist of a **core protein** to which glycosaminoglycans, most often keratan sulfate and chondroitin sulfate, are covalently linked (Fig. 8-15*b*). The interaction between the core protein and the hyaluronate is stabilized by a **link protein.** Smaller oligosaccharides are usually attached to the core protein near its site of attachment to hyaluronate. These oligosaccharides are glycosidically linked to the protein via the amide N of specific Asn residues (and are therefore known as ***N*-linked oligosaccharides;** Section 8-3C). The keratan

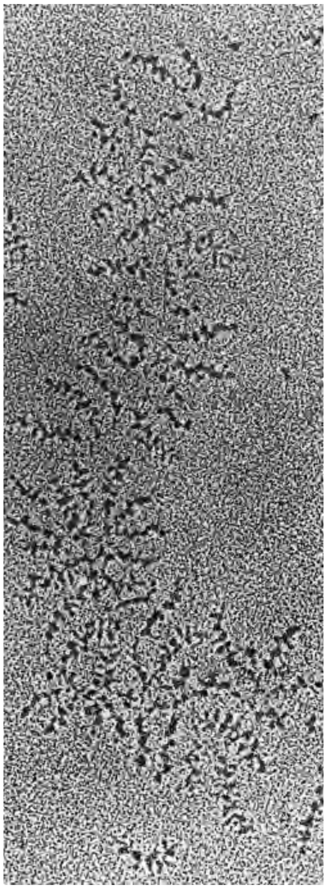

■ **Figure 8-15 | A proteoglycan.** *(a)* Electron micrograph showing a central strand of hyaluronate, which supports numerous projections. [From Caplan, A.I., *Sci. Am.* **251**(4), 87 (1984). Copyright © Scientific American, Inc. Used by permission.] *(b)* Bottlebrush model of the proteoglycan shown in Part *a*. Numerous core proteins are noncovalently linked to the central hyaluronate strand. Each core protein has three saccharide-binding regions.

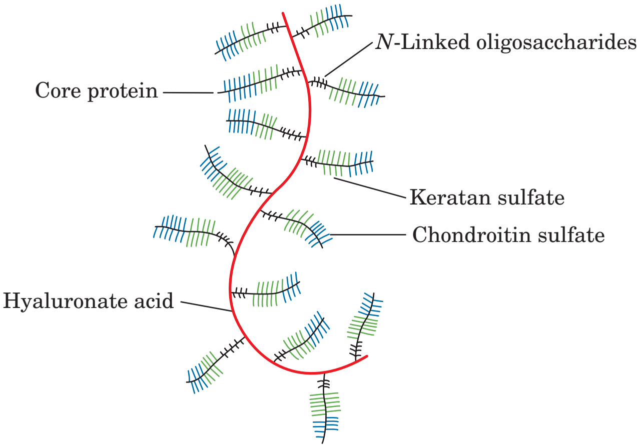

sulfate and chondroitin sulfate chains are glycosidically linked to the core protein via oligosaccharides that are covalently bonded to side chain O atoms of specific Ser or Thr residues (i.e., ***O*-linked oligosaccharides**).

Altogether, a central strand of hyaluronate, which varies in length from 4000 to 40,000 Å, can have up to 100 associated core proteins, each of which binds ~50 keratan sulfate chains of up to 250 disaccharide units and ~100 chondroitin sulfate chains of up to 1000 disaccharide units each. This accounts for the enormous molecular masses of many proteoglycans, which range up to tens of millions of daltons.

The extended brushlike structure of proteoglycans, together with the polyanionic character of their keratan sulfate and chondroitin sulfate components, cause these complexes to be highly hydrated. Cartilage, which consists of a meshwork of collagen fibrils that is filled in by proteoglycans, is characterized by its high resilience: The application of pressure on cartilage squeezes water away from the charged regions of its proteoglycans until charge–charge repulsions prevent further compression. When the pressure is released, the water returns. Indeed, the cartilage in the joints, which lacks blood vessels, is nourished by this flow of liquid brought about by body movements. This explains why long periods of inactivity cause cartilage to become thin and fragile.

B | Bacterial Cell Walls Are Made of Peptidoglycan

Bacteria are surrounded by rigid cell walls (Fig. 1-6) that give them their characteristic shapes (Fig. 1-7) and permit them to live in **hypotonic** (less than intracellular salt concentration) environments that would otherwise

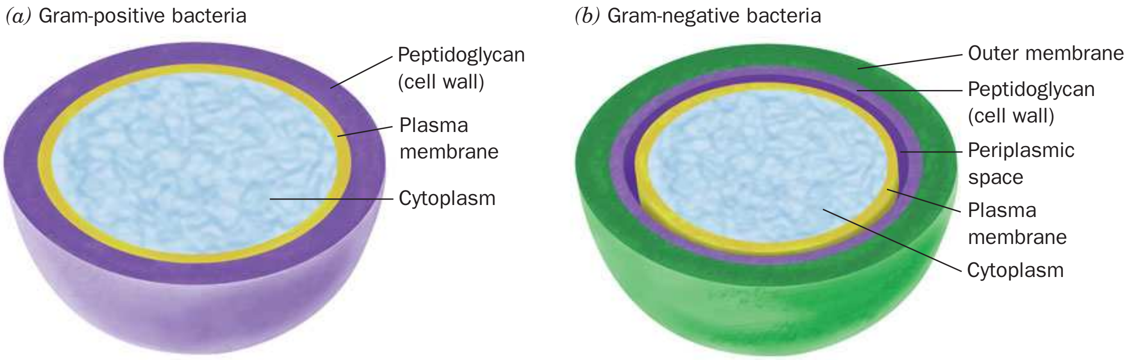
(a) Gram-positive bacteria
Peptidoglycan (cell wall)
Plasma membrane
Cytoplasm
(b) Gram-negative bacteria
Outer membrane
Peptidoglycan (cell wall)
Periplasmic space
Plasma membrane
Cytoplasm

■ **Figure 8-16** | **Bacterial cell walls.** This diagram compares the cell envelopes of (*a*) gram-positive bacteria and (*b*) gram-negative bacteria.

cause them to swell osmotically until their plasma (cell) membranes lysed (burst). Bacterial cell walls are of considerable medical significance because they are, in part, responsible for bacterial **virulence** (disease-evoking power). In fact, the symptoms of many bacterial diseases can be elicited in animals merely by injecting bacterial cell walls. Furthermore, bacterial cell wall components are antigenic (Section 7-3B), so such injections often invoke immunity against these bacteria.

Bacteria are classified as **gram-positive** or **gram-negative** according to whether or not they take up Gram stain (a procedure developed in 1884 by Christian Gram in which heat-fixed cells are successively treated with the dye crystal violet and iodine and then destained by ethanol or acetone). Gram-positive bacteria (Fig. 8-16*a*) have a thick cell wall (~250 Å) surrounding their plasma membrane, whereas gram-negative bacteria (Fig. 8-16*b*) have a thin cell wall (~30 Å) covered by a complex outer membrane. This outer membrane functions, in part, to exclude substances toxic to the bacterium, including Gram stain. This accounts for the observation that gram-negative bacteria are more resistant to antibiotics than are gram-positive bacteria.

The cell walls of bacteria consist of covalently linked polysaccharide and polypeptide chains, which form a baglike macromolecule that completely encases the cell. This framework, whose structure was elucidated in large part by Jack Strominger, is known as a **peptidoglycan.** Its polysaccharide component consists of linear chains of alternating β(1→4)-linked GlcNAc and ***N*-acetylmuramic acid** (Latin: *murus,* wall). The lactic acid group of *N*-acetylmuramic acid forms an amide bond with a D-amino acid–containing tetrapeptide to form the peptidoglycan repeating unit (Fig. 8-17). Neighboring parallel peptidoglycan chains are covalently cross-linked through their tetrapeptide side chains, although only ~40% of possible cross-links are made.

In the bacterium *Staphylococcus aureus,* whose tetrapeptide has the sequence L-Ala-D-isoglutamyl-L-Lys-D-Ala, the cross-link consists of a pentaglycine chain that extends from the terminal carboxyl group of one tetrapeptide to the ε-amino group of the Lys in a neighboring tetrapeptide. A model based on the NMR structure of a synthetic segment of peptidoglycan suggests that in the bacterial cell, the glycan chains are perpendicular to the plasma membrane and, with their peptide cross-links, form a honeycomb-like structure with spaces that could accommodate proteins that are known to penetrate the cell wall (Fig. 8-18).

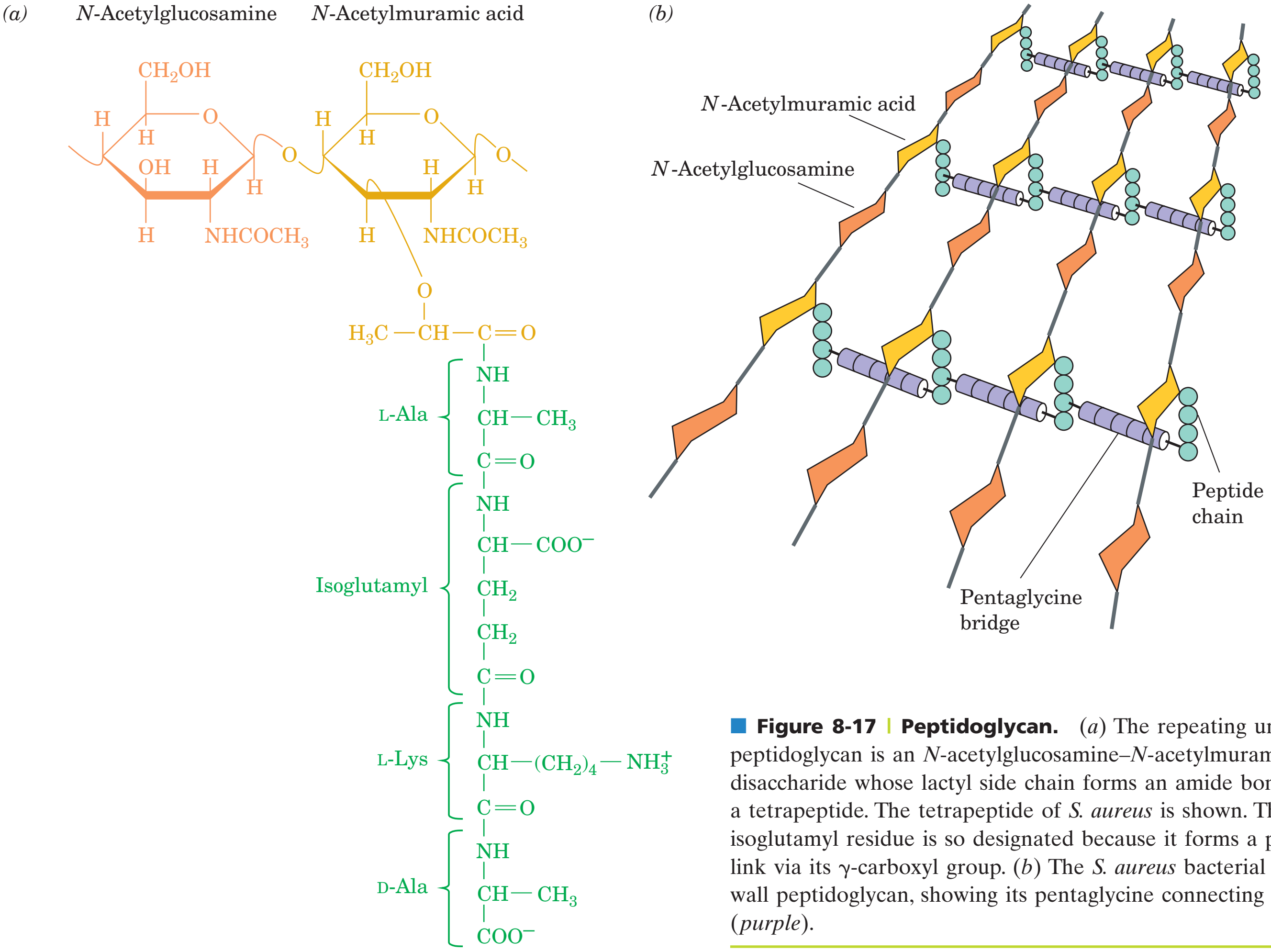
(a)
N-Acetylglucosamine
N-Acetylmuramic acid
CH₂OH
O
H
OH
NHCOCH₃
H₃C—CH—C=O
L-Ala
NH
CH—CH₃
C=O
Isoglutamyl
CH—COO⁻
CH₂
L-Lys
CH—(CH₂)₄—NH₃⁺
D-Ala
COO⁻
(b)
N-Acetylmuramic acid
N-Acetylglucosamine
Peptide chain
Pentaglycine bridge

Figure 8-17 | Peptidoglycan. (*a*) The repeating unit of peptidoglycan is an *N*-acetylglucosamine–*N*-acetylmuramic acid disaccharide whose lactyl side chain forms an amide bond with a tetrapeptide. The tetrapeptide of *S. aureus* is shown. The isoglutamyl residue is so designated because it forms a peptide link via its γ-carboxyl group. (*b*) The *S. aureus* bacterial cell wall peptidoglycan, showing its pentaglycine connecting bridges (*purple*).

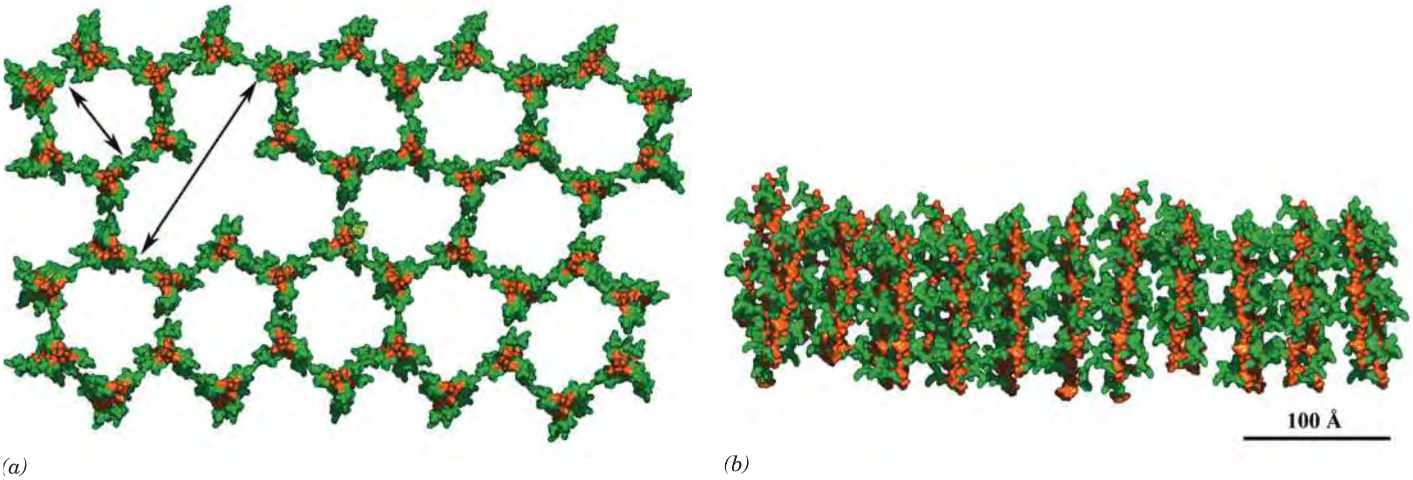

(*a*)

(*b*)

Figure 8-18 | Model of a bacterial cell wall. The glycan chains, each consisting of eight disaccharide repeats, are orange, and their peptide extensions are green (the pentaglycine cross-links are not included in this model). (*a*) Top view, showing pores (indicated by arrows) that could accommodate peptidoglycan-synthesizing enzymes or other proteins. (*b*) Side view, parallel to the plane of the plasma membrane. [Courtesy of Shahriar Mobashery, University of Notre Dame.]

BOX 8-3 BIOCHEMISTRY IN HEALTH AND DISEASE

Peptidoglycan-Specific Antibiotics

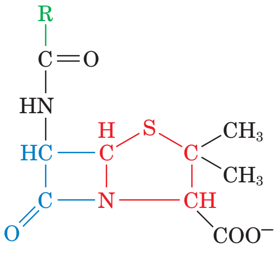

Penicillin

In 1928, Alexander Fleming noticed that the chance contamination of a bacterial culture plate with the mold *Penicillium notatum* resulted in the lysis of the bacteria in the vicinity of the mold. This was caused by the presence of **penicillin,** an antibiotic secreted by the mold. Penicillin contains a thiazolidine ring (*red*) fused to a β-lactam ring (*blue*). A variable R group is bonded to the β-lactam ring via a peptide link.

Penicillin specifically binds to and inactivates enzymes that cross-link the peptidoglycan strands of bacterial cell walls. Since cell wall expansion in growing cells requires that their rigid cell walls be opened up for the insertion of new cell wall material, exposure of growing bacteria to penicillin results in cell lysis. However, since no human enzyme binds penicillin specifically, it is not toxic to humans and is therefore therapeutically useful.

Most bacteria that are resistant to penicillin secrete the enzyme **penicillinase** (also called **β-lactamase**), which inactivates penicillin by cleaving the amide bond of its β-lactam ring. Attempts to overcome this resistance have led to the development of β-lactamase inhibitors such as **sulbactam** that are often prescribed as mixtures with penicillin derivatives.

Multiple drug resistant bacteria are a growing problem. For many years, **vancomycin,** the so-called antibiotic of last resort, has been used to treat bacterial infections that do not succumb to other antibiotics. Vancomycin inhibits the transpeptidation (cross-linking) reaction of bacterial cell wall synthesis by binding to the peptidoglycan precursor. However, bacteria can become resistant to vancomycin by acquiring a gene that allows cell wall synthesis from a slightly different precursor sequence, to which vancomycin binds much less effectively.

One limitation of drugs such as vancomycin and penicillin, particularly for slow-growing bacteria, is that the drug may halt bacterial growth without actually killing the cells. For this reason, effective antibacterial treatments may require combinations of antibiotics over a course of several weeks.

The D-amino acids of peptidoglycans render them resistant to proteases, which are mostly specific for L-amino acids. However, **lysozyme,** an enzyme that is present in tears, mucus, and other vertebrate body secretions, as well as in egg whites, catalyzes the hydrolysis of the β(1→4) glycosidic linkage between *N*-acetylmuramic acid and *N*-acetylglucosamine (the structure and mechanism of lysozyme are examined in detail in Section 11-4). The cell wall is also compromised by antibiotics that inhibit its biosynthesis (Box 8-3).

C | Many Eukaryotic Proteins Are Glycosylated

Almost all the secreted and membrane-associated proteins of eukaryotic cells are **glycosylated.** Oligosaccharides are covalently attached to proteins by either *N*-glycosidic or *O*-glycosidic bonds.

N-Linked Oligosaccharides Are Attached to Asparagine. *In N-linked oligosaccharides, GlcNAc is invariably β-linked to the amide nitrogen of an Asn residue in the sequence Asn-X-Ser or Asn-X-Thr, where X is any amino acid except possibly Pro or Asp:*

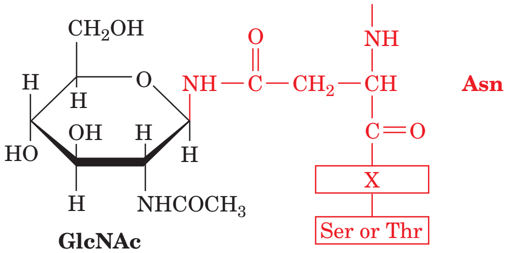

GlcNAc

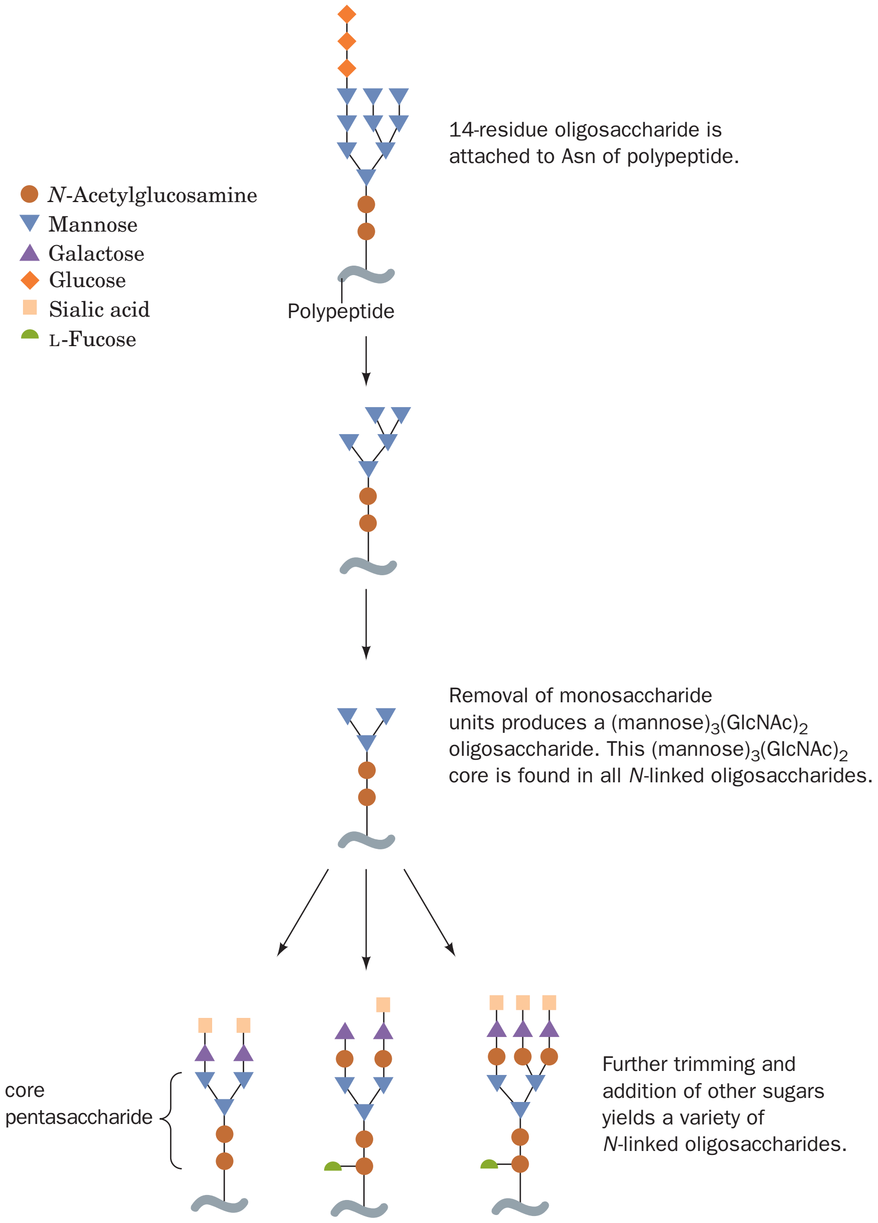

● *N*-Acetylglucosamine
▼ Mannose
▲ Galactose
◆ Glucose
■ Sialic acid
◓ L-Fucose
14-residue oligosaccharide is attached to Asn of polypeptide.
Polypeptide
Removal of monosaccharide units produces a (mannose)$_3$(GlcNAc)$_2$ oligosaccharide. This (mannose)$_3$(GlcNAc)$_2$ core is found in all *N*-linked oligosaccharides.
core pentasaccharide
Further trimming and addition of other sugars yields a variety of *N*-linked oligosaccharides.

■ **Figure 8-19** | **Synthesis of *N*-linked oligosaccharides.** The addition of a (mannose)$_9$(glucose)$_3$(GlcNAc)$_2$ oligosaccharide is followed by removal of monosaccharides as catalyzed by glycosidases, and the addition of other monosaccharides as catalyzed by glycosyltransferases. The core pentasaccharide occurs in all *N*-linked oligosaccharides. [Adapted from Kornfeld, R. and Kornfeld, S., *Annu. Rev. Biochem*. **54**, 640 (1985).] **See Kinemage Exercise 7-4.**

N-Glycosylation occurs **cotranslationally,** that is, while the polypeptide is being synthesized. Proteins containing *N*-linked oligosaccharides typically are glycosylated and then processed as elucidated, in large part, by Stuart Kornfeld (Fig. 8-19):

1. An oligosaccharide containing 9 mannose residues, 3 glucose residues, and 2 GlcNAc residues is attached to the Asn of a growing polypeptide chain that is being synthesized by a ribosome associated with the endoplasmic reticulum (Section 16-5).
2. Some of the sugars are removed during processing, which begins in the lumen (internal space) of the endoplasmic reticulum and continues in the Golgi apparatus (Fig. 1-8). Enzymatic trimming is accomplished by glucosidases and mannosidases.
3. Additional monosaccharide residues, including GlcNAc, galactose, fucose, and sialic acid, are added by the action of specific **glycosyltransferases** in the Golgi apparatus.

The exact steps of *N*-linked oligosaccharide processing vary with the identity of the glycoprotein and the battery of endoglycosidases in the cell, but all *N*-linked oligosaccharides have a common core pentasaccharide with the following structure:

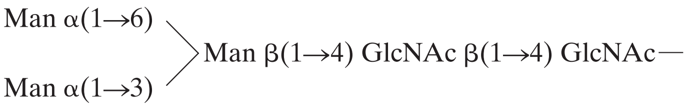

$$\left.\begin{array}{l}\text{Man }\alpha(1\rightarrow6)\\ \\ \text{Man }\alpha(1\rightarrow3)\end{array}\right\rangle \text{Man }\beta(1\rightarrow4)\text{ GlcNAc }\beta(1\rightarrow4)\text{ GlcNAc}—$$

In some glycoproteins, processing is limited, leaving "high-mannose" oligosaccharides; in other glycoproteins, extensive processing generates large oligosaccharides containing several kinds of sugar residues. *There is enormous diversity among the oligosaccharides of N-linked glycoproteins*. Indeed, even glycoproteins with a given polypeptide chain exhibit considerable microheterogeneity, presumably as a consequence of incomplete glycosylation and lack of absolute specificity on the part of glycosidases and glycosyltransferases.

O-Linked Oligosaccharides Are Attached to Serine or Threonine. The most common *O*-glycosidic attachment involves the disaccharide core *β-galactosyl-(1→3)-α-N-acetylgalactosamine linked to the OH group of either Ser or Thr:*

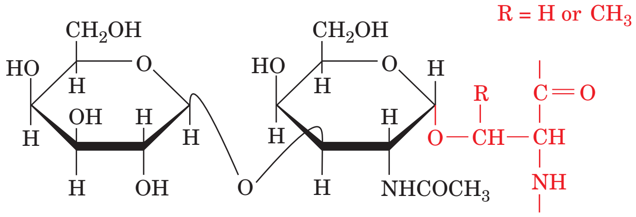

β-Galactosyl-(1→3)-α-*N*-acetylgalactosaminyl-Ser/Thr

Less commonly, galactose, mannose, and xylose form *O*-glycosides with Ser or Thr. Galactose also forms *O*-glycosidic bonds to the 5-hydroxylysyl residues of collagen (Section 6-1C). *O*-Linked oligosaccharides vary in size from a single galactose residue in collagen to the chains of up to 1000 disaccharide units in proteoglycans.

O-Linked oligosaccharides are synthesized in the Golgi apparatus by the serial addition of monosaccharide units to a completed polypeptide chain. Synthesis starts with the transfer of GalNAc to a Ser or Thr residue on the polypeptide. *N*-Linked oligosaccharides are transferred to an Asn in a specific amino acid sequence, but *O*-glycosylated Ser and Thr residues are not members of any common sequence. Instead, the locations of glycosylation sites are specified only by the secondary or tertiary structure of the polypeptide. *O*-Glycosylation continues with stepwise addition of sugars by the corresponding glycosyltransferases. The energetics and enzymology of oligosaccharide synthesis are discussed further in Section 16-5.

D | Oligosaccharides May Determine Glycoprotein Structure, Function, and Recognition

A single protein may contain several *N*- and *O*-linked oligosaccharide chains, although different molecules of the same glycoprotein may differ in the sequences, locations, and numbers of covalently attached carbohydrates (the variant species of a glycoprotein are known as its **glycoforms**). This heterogeneity makes it difficult to assign discrete biological functions to oligosaccharide chains. In fact, certain glycoproteins synthesized by cells that lack particular oligosaccharide-processing enzymes appear to function normally despite abnormal or absent glycosylation. In other cases, however, glycosylation may affect a protein's structure, stability, or activity.

Oligosaccharides Help Define Protein Structure. Oligosaccharides are usually attached to proteins at sequences that form surface loops or turns. Since sugars are hydrophilic, the oligosaccharides tend to project away from the protein surface. Because carbohydrate chains are often conformationally mobile, oligosaccharides attached to proteins can occupy time-averaged volumes of considerable size (Fig. 8-20). In this way, an oligosaccharide can shield a protein's surface, possibly modifying its activity or protecting it from proteolysis.

In addition, some oligosaccharides may play structural roles by limiting the conformational freedom of their attached polypeptide chains. Since *N*-linked oligosaccharides are added as the protein is being synthesized, the attachment of an oligosaccharide may help determine how the protein folds. In addition, the oligosaccharide may help stabilize the folded conformation of a polypeptide by reducing backbone flexibility. In particular, *O*-linked oligosaccharides, which are usually clustered in heavily glycosylated segments of a protein, may help stiffen and extend the polypeptide chain.

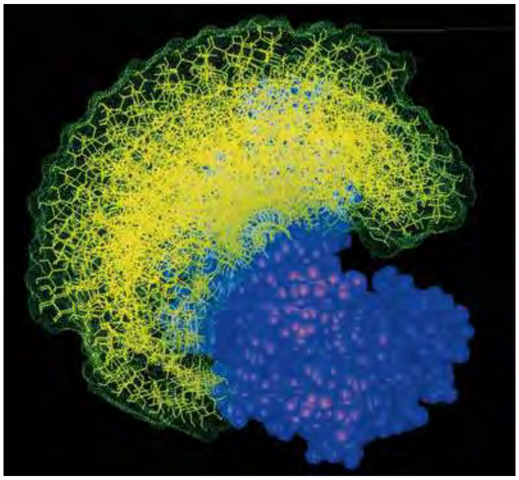

■ **Figure 8-20 | Model of oligosaccharide dynamics.** The allowed conformations of a $(GlcNAc)_2(mannose)_{5-9}$ oligosaccharide (*yellow*) attached to the bovine pancreatic enzyme **ribonuclease B** (*purple*) are shown in superimposed "snapshots." [Courtesy of Raymond Dwek, Oxford University, U.K.]

Oligosaccharides Mediate Recognition Events. The many possible ways that carbohydrates can be linked together to form branched structures gives them the potential to carry more biological information than either nucleic acids or proteins of similar size. For example, two different nucleotides can make only two distinct dinucleotides, but two different hexoses can combine in 36 different ways (although not all possibilities are necessarily realized in nature).

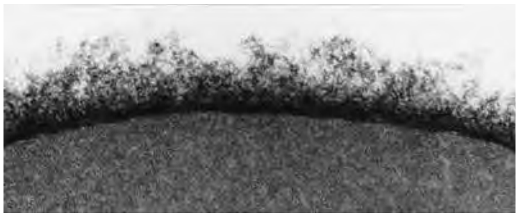

■ **Figure 8-21 | Electron micrograph of the erythrocyte surface.** Its thick (up to 1400 Å) carbohydrate coat, which is called the **glycocalyx,** consists of closely packed oligosaccharides attached to cell-surface proteins and lipids. [Courtesy of Harrison Latta, UCLA.]

The first evidence that unique combinations of carbohydrates might be involved in intercellular communication came with the discovery that all cells are coated with sugars in the form of **glycoconjugates** such as glycoproteins and glycolipids. The oligosaccharides of glycoconjugates form a fuzzy layer up to 1400 Å thick in some cells (Fig. 8-21).

Additional evidence that cell-surface carbohydrates have recognition functions comes from **lectins** (proteins that bind carbohydrates), which are ubiquitous in nature and frequently appear on the surfaces of cells. Lectins are exquisitely specific: They can recognize individual monosaccharides in particular linkages to other sugars in an oligosaccharide (this property also makes lectins useful laboratory tools for isolating glycoproteins and oligosaccharides). Protein–carbohydrate interactions are typically characterized by extensive hydrogen bonding (often including bridging water molecules) and the van der Waals packing of hydrophobic sugar faces against aromatic side chains (Fig. 8-22).

Proteins known as **selectins** mediate the attachment between **leukocytes** (circulating white blood cells) and the surfaces of endothelial cells (the

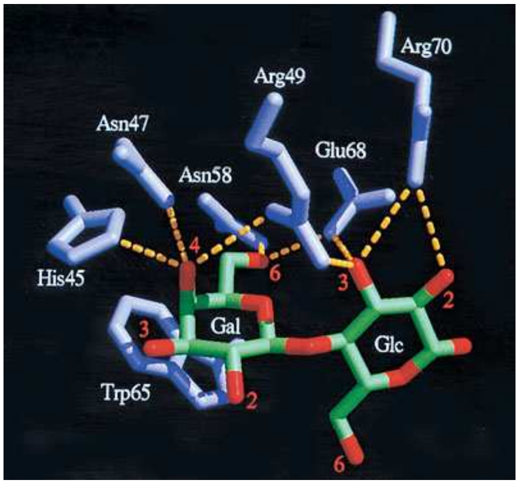

■ **Figure 8-22 | Carbohydrate binding by a lectin.** Human **galectin-2** binds β-galactosides, such as lactose, primarily through their galactose residue. The galactose and glucose residues are shown in green (with red O atoms), and the lectin amino acid side chains are shown in violet. Hydrogen bonds between the side chains and the sugar residues are shown as dashed yellow lines. [Courtesy of Hakon Leffler, University of California at San Francisco. PDBid 1HLC.]

Table 8-1 Structures of the A, B, and H Antigenic Determinants in Erythrocytes

Type	Antigen[a]
H	Galβ(1→4)GlcNAc··· ↑1,2 L-Fucα
A	GalNAcα(1→3)Galβ(1→4)GlcNAc··· ↑1,2 L-Fucα
B	Galα(1→3)Galβ(1→4)GlcNAc··· ↑1,2 L-Fucα

[a] Gal, Galactose; GalNAc, *N*-acetylgalactosamine; GlcNAc, *N*-acetylglucosamine; L-Fuc, L-fucose.

■ CHECK YOUR UNDERSTANDING

Describe the general structures of proteoglycans, peptidoglycans, and glycosylated proteins.

List the major biological functions of proteoglycans and peptidoglycans.

Explain the difference between *N*- and *O*-linked oligosaccharides.

How do oligosaccharides participate in biological recognition?

cells that line blood vessels). Leukocytes constitutively (continually) express selectins on their surface; endothelial cells transiently display their own selectins in response to tissue damage from infection or mechanical injury. The selectins recognize and bind specific oligosaccharides on cell-surface glycoproteins. Reciprocal selectin–oligosaccharide interactions between the two cell types allow the endothelial cells to “capture” circulating leukocytes, which then crawl past the endothelial cells on their way to eliminate the infection or help repair damaged tissues.

Other cell–cell recognition phenomena depend on oligosaccharides. For example, proteins on the surface of mammalian spermatozoa recognize GlcNAc or galactose residues on the glycoproteins of the ovum as part of the binding and activation events during fertilization. Many viruses, bacteria, and eukaryotic parasites invade their target tissues by first binding to cell-surface carbohydrates.

Oligosaccharides Are Antigenic Determinants. The carbohydrates on cell surfaces are some of the best known immunochemical markers. For example, the **ABO blood group antigens** are oligosaccharide components of glycoproteins and glycolipids on the surfaces of an individual’s cells (not just red blood cells). Individuals with type A cells have A antigens on their cell surfaces and carry anti-B antibodies in their blood; those with type B cells, which bear B antigens, carry anti-A antibodies; those with type AB cells, which have both A and B antigens, carry neither anti-A nor anti-B antibodies; and type O individuals, whose cells bear neither antigen, carry both anti-A and anti-B antibodies. Consequently, the transfusion of type A blood into a type B individual, for example, results in an anti-A antibody–A antigen reaction, which agglutinates (clumps together) the transfused erythrocytes, resulting in an often fatal blockage of blood vessels.

Table 8-1 lists the oligosaccharides found in the **A, B,** and **H antigens** (type O individuals have the H antigen). These occur at the nonreducing ends of the oligosaccharides. The H antigen is the precursor oligosaccharide of A and B antigens. Type A individuals have a 303-residue glycosyltransferase that specifically adds a GalNAc residue to the terminal position of the H antigen. In type B individuals, this enzyme, which differs by four amino acid residues from that of type A individuals, instead adds a galactose residue. In type O individuals, the enzyme is inactive because its synthesis terminates after its 115th residue.

SUMMARY

1. Monosaccharides, the simplest carbohydrates, are classified as aldoses or ketoses.
2. The cyclic hemiacetal and hemiketal forms of monosaccharides have either the α or β configuration at their anomeric carbon but are conformationally variable.
3. Monosaccharide derivatives include aldonic acids, uronic acids, alditols, deoxy sugars, amino sugars, and α- and β-glycosides.
4. Polysaccharides consist of monosaccharides linked by glycosidic bonds.
5. Cellulose and chitin are polysaccharides whose β(1 → 4) linkages cause them to adopt rigid and extended structures.
6. The storage polysaccharides starch and glycogen consist of α-glycosidically linked glucose residues.
7. Glycosaminoglycans are unbranched polysaccharides containing uronic acid and amino sugars that are often sulfated.
8. Proteoglycans are enormous molecules consisting of hyaluronate with attached core proteins that bear numerous glycosaminoglycans and oligosaccharides.

9. Bacterial cell walls are made of peptidoglycan, a network of polysaccharide and polypeptide chains.
10. Glycosylated proteins may contain *N*-linked oligosaccharides (attached to Asn) or *O*-linked oligosaccharides (attached to Ser or Thr) or both. Different molecules of a glycoprotein may contain different sequences and locations of oligosaccharides.
11. Oligosaccharides play important roles in determining protein structure and in cell-surface recognition phenomena.

KEY TERMS

carbohydrate	**219**
monosaccharide	**219**
polysaccharide	**219**
aldose	**220**
ketose	**220**
epimer	**221**
hemiacetal	**221**
hemiketal	**221**
Haworth projection	**222**
pyranose	**222**
furanose	**222**
anomeric carbon	**222**
α anomer	**223**
β anomer	**223**
aldonic acid	**224**
uronic acid	**224**
alditol	**224**
deoxy sugar	**224**
amino sugar	**225**
glycoprotein	**225**
glycolipid	**225**
α-glycoside	**225**
β-glycoside	**225**
glycosidic bond	**225**
reducing sugar	**226**
glycan	**226**
homopolysaccharide	**226**
heteropolysaccharide	**226**
oligosaccharide	**226**
exoglycosidase	**226**
endoglycosidase	**226**
disaccharide	**227**
starch	**230**
glycogen	**231**
growth factor	**233**
glycosaminoglycan	**233**
biofilm	**234**
microheterogeneity	**234**
glycomics	**234**
proteoglycan	**234**
N-linked oligosaccharide	**234**
O-linked oligosaccharide	**235**
gram-positive	**236**
gram-negative	**236**
peptidoglycan	**236**
glycosylation	**238**
oligosaccharide processing	**240**
glycoforms	**240**
glycoconjugate	**241**
lectin	**241**
leukocyte	**241**
ABO blood group antigens	**242**

PROBLEMS

1. How many stereoisomers are possible for (a) a ketopentose, (b) a ketohexose, and (c) a ketoheptose?
2. Which of the following pairs of sugars are epimers of each other?
   (a) D-sorbose and D-psicose
   (b) D-sorbose and D-fructose
   (c) D-fructose and L-fructose
   (d) D-arabinose and D-ribose
   (e) D-ribose and D-ribulose
3. The sucrose substitute tagatose (Fig. 8-2) is produced by hydrolyzing lactose and then chemically converting one of the two resulting aldoses to a ketose. Which residue of lactose gives rise to tagatose?
4. Draw the furanose and pyranose forms of D-ribose.
5. Are (a) D-glucitol, (b) D-galactitol, and (c) D-glycerol optically active?
6. Draw a Fischer projection of L-fucose. L-Fucose is the 6-deoxy form of which L-hexose?
7. (a) Deduce the structure of the disaccharide trehalose from the following information: Complete hydrolysis yields only D-glucose; it is hydrolyzed by α-glucosidase but not β-glucosidase; and it does not reduce Cu^{2+} to Cu^{+}. (b) When exposed to dehydrating conditions, many plants and invertebrates synthesize large amounts of trehalose, which enables them to survive prolonged desiccation. What properties of the trehalose molecule might allow it to act as a water substitute?
8. How many different disaccharides of D-glucopyranose are possible?
9. The artificial sweetener sucralose is a derivative of sucrose with the formal name 1,6-dichloro-1,6-dideoxy-β-D-fructofuranosyl-4-chloro-4-deoxy-α-D-galactopyranoside. Draw its structure.
10. How many reducing ends are in a molecule of glycogen that contains 10,000 residues with a branch every 10 residues?
11. Is amylose or amylopectin more likely to be a long-term storage polysaccharide in plants?
12. “Nutraceuticals” are products that are believed to have some beneficial effect but are not strictly defined as either food or drug. Why might an individual suffering from osteoarthritis be tempted to consume the nutraceutical glucosamine?
13. Calculate the net charge of a chondroitin-4-sulfate molecule containing 100 disaccharide units.
14. The core of pectin molecules is a polymer of α(1→4)-linked D-galacturonate. Draw one of its residues.
15. Draw the structure of the O-type oligosaccharide (the H antigen, described in Table 8-1).
16. Glycogen is treated with dimethyl sulfate, which adds a methyl group to every free OH group. Next, the molecule is hydrolyzed to break all the glycosidic bonds between glucose residues. The reaction products are then chemically analyzed.
   (a) How many different types of methylated glucose molecules are obtained?
   (b) Draw the structure of the one that is most abundant.

REFERENCES

Branda, S.S., Vik, A., Friedman, L., and Kolter, R., Biofilms: the matrix revisited, *Trends Microbiol.* **13,** 20–26 (2005). [Summarizes the general features of biofilms and ways of studying them.]

Esko, J.D. and Lindahl, U., Molecular diversity of heparan sulfate, *J. Clin. Invest.* **108,** 169–173 (2001). [Reviews the structure, function, and biosynthesis of heparan sulfate–containing proteoglycans.]

Meroueh, S.O., Bencze, K.Z., Hesek, D., Lee, M., Fisher, J.F., Stemmler, T.L., and Mobashery, S., Three-dimensional structure of the bacterial cell wall peptidoglycan, *Proc. Natl. Acad. Sci.* **103,** 4404–4409 (2006).

Mitra, N., Sinha, S., Ramya, T.N.C., and Surolia, A., *N*-Linked oligosaccharides as outfitters for glycoprotein folding, form and function, *Trends Biochem. Sci.* **31,** 156–163 and 251 (2006). [Summarizes the ways in which oligosaccharides can influence glycoprotein structure.]

Sharon, N. and Lis, H., History of lectins: from hemagglutinins to biological recognition molecules, *Glycobiology* **14,** 53R–62R (2004). [A historical account of lectin research and applications.]

Spiro, R.G., Protein glycosylation: nature, distribution, enzymatic formation, and disease implications of glycopeptide bonds, *Glycobiology* **12,** 43R–56R (2002). [Catalogs the various ways in which saccharides are linked to proteins, and describes the enzymes involved in glycoprotein synthesis.]

Varki, A., Cummings, R., Esko, J., Freeze, H., Hart, G., and Marth, J. (Eds.), *Essentials of Glycobiology,* Cold Spring Harbor Laboratory Press (1999).

9

Lipids and Biological Membranes

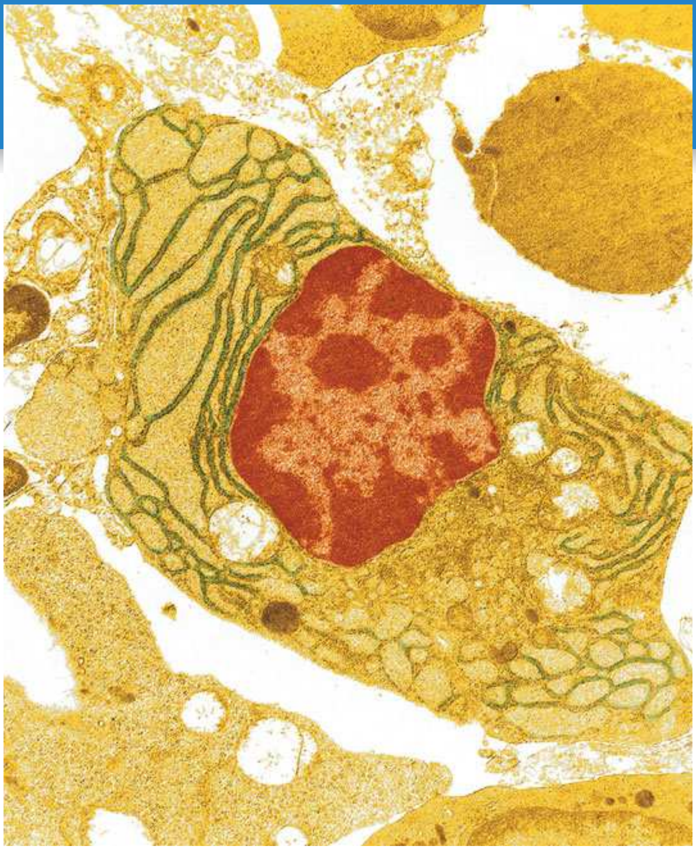

Due to their hydrophobicity, lipids do not mix freely with the aqueous phase but instead can form bilayers. Membranes, which consist of a lipid bilayer and the proteins embedded in it, surround the cytoplasm of all cells and delineate discrete metabolic compartments within cells. [©ISM/Phototake.]

CHAPTER CONTENTS

1 Lipid Classification
  A. The Properties of Fatty Acids Depend on Their Hydrocarbon Chains
  B. Triacylglycerols Contain Three Esterified Fatty Acids
  C. Glycerophospholipids Are Amphiphilic
  D. Sphingolipids Are Amino Alcohol Derivatives
  E. Steroids Contain Four Fused Rings
  F. Other Lipids Perform a Variety of Metabolic Roles
2 Lipid Bilayers
  A. Bilayer Formation Is Driven by the Hydrophobic Effect
  B. Lipid Bilayers Have Fluidlike Properties
3 Membrane Proteins
  A. Integral Membrane Proteins Interact with Hydrophobic Lipids
  B. Lipid-Linked Proteins Are Anchored to the Bilayer
  C. Peripheral Proteins Associate Loosely with Membranes
4 Membrane Structure and Assembly
  A. The Fluid Mosaic Model Accounts for Lateral Diffusion
  B. The Membrane Skeleton Helps Define Cell Shape
  C. Membrane Lipids Are Distributed Asymmetrically
  D. The Secretory Pathway Generates Secreted and Transmembrane Proteins
  E. Intracellular Vesicles Transport Proteins
  F. Proteins Mediate Vesicle Fusion

MEDIA RESOURCES

(available at www.wiley.com/college/voet)
Guided Exploration 9. Membrane structure and the fluid mosaic model
Interactive Exercise 4. Model of phospholipase A_2 and glycerophospholipid
Animated Figure 9-35. Secretory pathway
Kinemage 8-1. Bacteriorhodopsin
Kinemage 8-3. OmpF porin

Lipids (Greek: *lipos,* fat) are the fourth major group of molecules found in all cells. Unlike nucleic acids, proteins, and polysaccharides, lipids are not polymeric. However, they do aggregate, and it is in this state that they perform their most obvious function as the structural matrix of biological membranes.

Lipids exhibit greater structural variety than the other classes of biological molecules. To a certain extent, lipids constitute a catchall category of substances that are similar only in that they are largely hydrophobic and only sparingly soluble in water. In general, lipids perform three biological functions (although certain lipids apparently serve more than one purpose in some cells):

1. Lipid molecules in the form of lipid bilayers are essential components of biological membranes.
2. Lipids containing hydrocarbon chains serve as energy stores.
3. Many intra- and intercellular signaling events involve lipid molecules.

In this chapter we examine the structures and physical properties of the most common types of lipids. Next, we look at the properties of the lipid bilayer and the proteins that are situated within it. Finally, we explore current models of membrane structure. The following chapter examines membrane transport phenomena. The participation of lipids in intracellular signaling is discussed in Section 13-4.

1 Lipid Classification

LEARNING OBJECTIVES

- Become familiar with the structures and nomenclature of the major classes of lipids, including fatty acids, triacylglycerols, glycerophospholipids, sphingolipids, and steroids.
- Understand how hydrocarbon chain length affects a lipid's physical properties.
- Understand the physiological roles of lipids as membrane components, energy-storage molecules, and signaling molecules.

Lipids are substances of biological origin that are soluble in organic solvents such as chloroform and methanol. Hence, they are easily separated from other biological materials by extraction into organic solvents. Fats, oils, certain vitamins and hormones, and most nonprotein membrane components are lipids. In this section, we discuss the structures and physical properties of the major classes of lipids.

A | The Properties of Fatty Acids Depend on Their Hydrocarbon Chains

***Fatty acids** are carboxylic acids with long-chain hydrocarbon side groups* (Fig. 9-1). They usually occur in esterified form as major components of the various lipids described in this chapter. The more common biological fatty acids are listed in Table 9-l. In higher plants and animals, the predominant fatty acid residues are those of the C_{16} and C_{18} species: **palmitic, oleic, linoleic,** and **stearic acids.** Fatty acids with <14 or >20 carbon atoms are uncommon. Most fatty acids have an even number of carbon

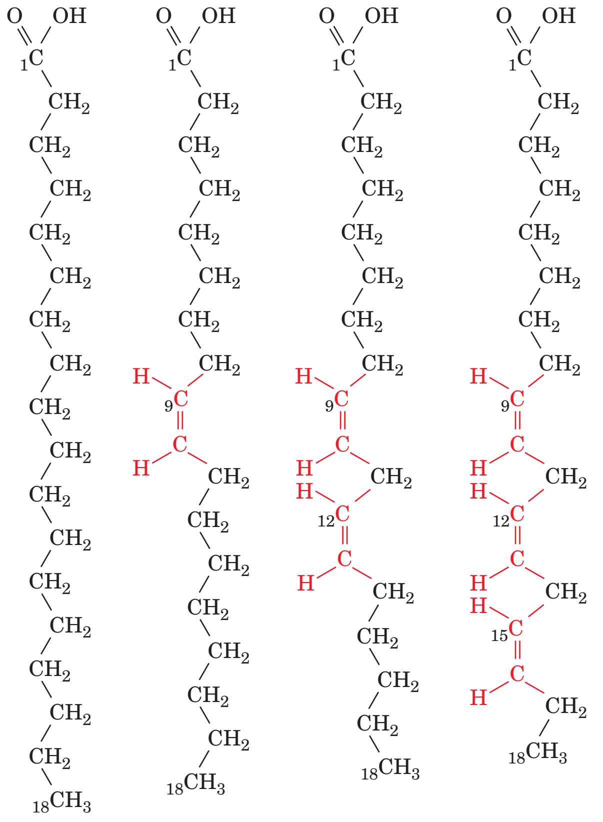

Figure 9-1 | The structural formulas of some C_{18} fatty acids. The double bonds all have the cis configuration.

Table 9-1 The Common Biological Fatty Acids

Symbol[a]	Common Name	Systematic Name	Structure	mp (°C)
Saturated fatty acids				
12:0	Lauric acid	Dodecanoic acid	$CH_3(CH_2)_{10}COOH$	44.2
14:0	Myristic acid	Tetradecanoic acid	$CH_3(CH_2)_{12}COOH$	53.9
16:0	Palmitic acid	Hexadecanoic acid	$CH_3(CH_2)_{14}COOH$	63.1
18:0	Stearic acid	Octadecanoic acid	$CH_3(CH_2)_{16}COOH$	69.6
20:0	Arachidic acid	Eicosanoic acid	$CH_3(CH_2)_{18}COOH$	77
22:0	Behenic acid	Docosanoic acid	$CH_3(CH_2)_{20}COOH$	81.5
24:0	Lignoceric acid	Tetracosanoic acid	$CH_3(CH_2)_{22}COOH$	88
Unsaturated fatty acids (all double bonds are cis)				
16:1*n*–7	Palmitoleic acid	9-Hexadecanoic acid	$CH_3(CH_2)_5CH{=}CH(CH_2)_7COOH$	−0.5
18:1*n*–9	Oleic acid	9-Octadecanoic acid	$CH_3(CH_2)_7CH{=}CH(CH_2)_7COOH$	12
18:2*n*–6	Linoleic acid	9,12-Octadecadienoic acid	$CH_3(CH_2)_4(CH{=}CHCH_2)_2(CH_2)_6COOH$	−5
18:3*n*–3	α-Linolenic acid	9,12,15-Octadecatrienoic acid	$CH_3CH_2(CH{=}CHCH_2)_3(CH_2)_6COOH$	−11
18:3*n*–6	γ-Linolenic acid	6,9,12-Octadecatrienoic acid	$CH_3(CH_2)_4(CH{=}CHCH_2)_3(CH_2)_3COOH$	−11
20:4*n*–6	Arachidonic acid	5,8,11,14-Eicosatetraenoic acid	$CH_3(CH_2)_4(CH{=}CHCH_2)_4(CH_2)_2COOH$	−49.5
20:5*n*–3	EPA	5,8,11,14,17-Eicosapentaenoic acid	$CH_3CH_2(CH{=}CHCH_2)_5(CH_2)_2COOH$	−54
22:6*n*–3	DHA	4,7,10,13,16,19-Docosohexenoic acid	$CH_3CH_2(CH{=}CHCH_2)_6CH_2COOH$	−44
24:1*n*–9	Nervonic acid	15-Tetracosenoic acid	$CH_3(CH_2)_7CH{=}CH(CH_2)_{13}COOH$	39

[a] Number of carbon atoms:Number of double bonds. For unsaturated fatty acids, the quantity "*n*–*x*" indicates the position of the last double bond in the fatty acid, where *n* is its number of C atoms, and *x* is the position of the last double-bonded C atom counting from the methyl-terminal (ω) end.

Source: LipidBank (http://www.lipidbank.jp)

atoms because they are biosynthesized by the concatenation of C_2 units (Section 20-4).

Over half of the fatty acid residues of plant and animal lipids are **unsaturated** (contain double bonds) and are often **polyunsaturated** (contain two or more double bonds). Bacterial fatty acids are rarely polyunsaturated but are commonly branched, hydroxylated, or contain cyclopropane rings.

Table 9-1 indicates that the first double bond of an unsaturated fatty acid commonly occurs between its C9 and C10 atoms counting from the carboxyl C atom. This bond is called a Δ^9- or 9-double bond. In polyunsaturated fatty acids, the double bonds tend to occur at every third carbon atom (e.g., $—CH{=}CH—CH_2—CH{=}CH—$) and so are not conjugated (as in $—CH{=}CH—CH{=}CH—$). Two important classes of polyunsaturated fatty acids are designated as ω-3 or ω-6 fatty acids, a nomenclature that identifies the last double-bonded carbon atom as counted from the methyl terminal (ω) end of the chain. **α-Linolenic acid** and linoleic acid (Fig. 9-1) are examples of such fatty acids.

Saturated fatty acids (which are fully reduced or "saturated" with hydrogen) are highly flexible molecules that can assume a wide range of conformations because there is relatively free rotation around each of their C—C bonds. Nevertheless, their lowest energy conformation is the fully extended conformation, which has the least amount of steric interference between neighboring methylene groups. The melting points (mp) of saturated fatty acids, like those of most substances, increase with their molecular mass (Table 9-1).

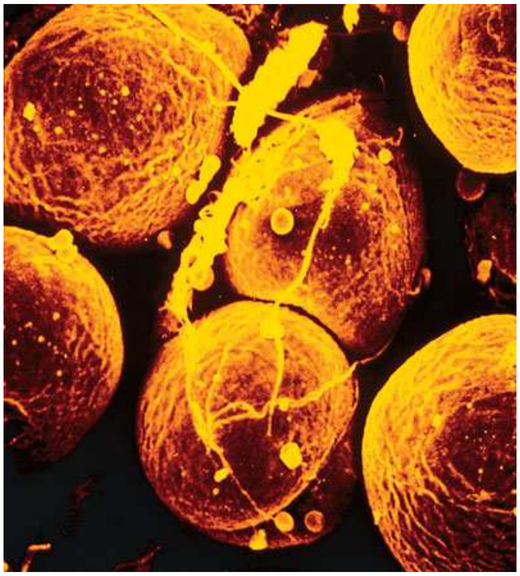

Figure 9-2 | Scanning electron micrograph of adipocytes. Each adipocyte contains a fat globule that occupies nearly the entire cell. [Fred E. Hossler/Visuals Unlimited.]

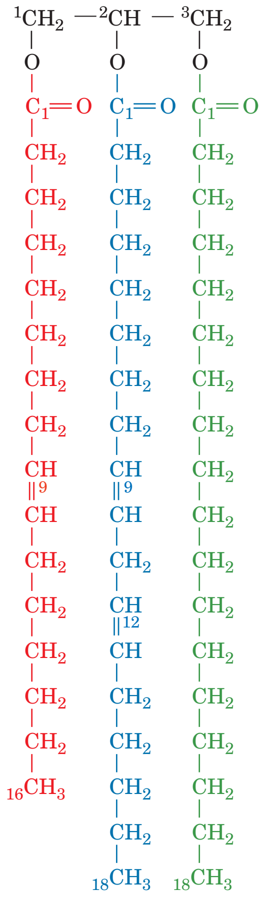

1-Palmitoleoyl-2-linoleoyl-3-stearoylglycerol

Fatty acid double bonds almost always have the cis configuration (Fig. 9-1). This puts a rigid 30° bend in the hydrocarbon chain. Consequently, unsaturated fatty acids pack together less efficiently than saturated fatty acids. The reduced van der Waals interactions of unsaturated fatty acids cause their melting points to decrease with the degree of unsaturation. The fluidity of lipids containing fatty acid residues likewise increases with the degree of unsaturation of the fatty acids. This phenomenon, as we shall see, has important consequences for biological membranes.

B | Triacylglycerols Contain Three Esterified Fatty Acids

The fats and oils that occur in plants and animals consist largely of mixtures of **triacylglycerols** (also called **triglycerides**). These nonpolar, water-insoluble substances are fatty acid triesters of **glycerol:**

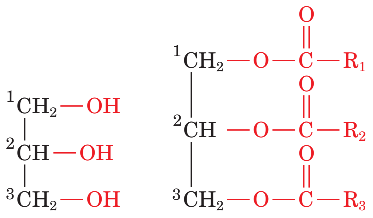

Glycerol **Triacylglycerol**

Triacylglycerols function as energy reservoirs in animals and are therefore their most abundant class of lipids even though they are not components of cellular membranes.

Triacylglycerols differ according to the identity and placement of their three fatty acid residues. Most triacylglycerols contain two or three different types of fatty acid residues and are named according to their placement on the glycerol moiety, for example, **1-palmitoleoyl-2-linoleoyl-3-stearoylglycerol** *(at left)*. Note that the *-ate* ending of the name of the fatty acid becomes *-oyl* in the fatty acid ester. **Fats** and **oils** (which differ only in that fats are solid and oils are liquid at room temperature) are complex mixtures of triacylglycerols whose fatty acid compositions vary with the organism that produced them. Plant oils are usually richer in unsaturated fatty acid residues than animal fats, as the lower melting points of oils imply.

Triacylglycerols Function as Energy Reserves. Fats are a highly efficient form in which to store metabolic energy. This is because triacylglycerols are less oxidized than carbohydrates or proteins and hence yield significantly more energy per unit mass on complete oxidation. Furthermore, triacylglycerols, which are nonpolar, are stored in anhydrous form, whereas glycogen (Section 8-2C), for example, binds about twice its weight of water under physiological conditions. *Fats therefore provide about six times the metabolic energy of an equal weight of hydrated glycogen.*

In animals, **adipocytes** (fat cells; Fig. 9-2) are specialized for the synthesis and storage of triacylglycerols. Whereas other types of cells have only a few small droplets of fat dispersed in their cytosol, adipocytes may be almost entirely filled with fat globules. **Adipose tissue** is most abundant in a subcutaneous layer and in the abdominal cavity. The fat content of normal humans (21% for men, 26% for women) allows them to survive starvation for 2 or 3 months. In contrast, the body's glycogen supply, which functions as a short-term energy store, can provide for the body's energy needs for less than a day. The subcutaneous fat layer also provides thermal insulation, which is particularly important for warm-blooded aquatic

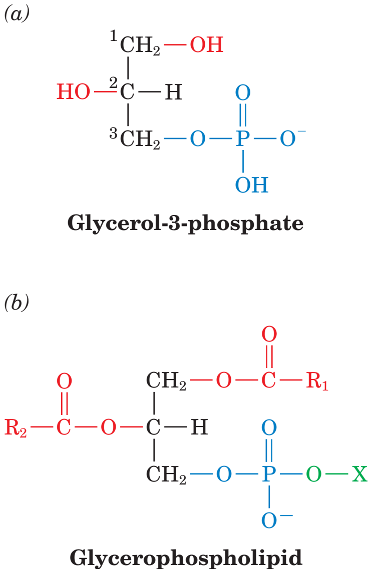
(a) Glycerol-3-phosphate

(b) Glycerophospholipid

■ **Figure 9-3 | Structure of glycerophospholipids.** (*a*) The backbone, L-glycerol-3-phosphate. (*b*) The general formula of the glycerophospholipids. R_1 and R_2 are the long-chain hydrocarbon tails of fatty acids, and X is derived from a polar alcohol (Table 9-2). Note that glycerol-3-phosphate and glycerophospholipid are chiral compounds.

animals, such as whales, seals, geese, and penguins, which are routinely exposed to low temperatures.

C | Glycerophospholipids Are Amphiphilic

Glycerophospholipids (or **phosphoglycerides**) are the major lipid components of biological membranes. They consist of **glycerol-3-phosphate** whose C1 and C2 positions are esterified with fatty acids. In addition, the phosphoryl group is linked to another usually polar group, X (Fig. 9-3). *Glycerophospholipids are therefore amphiphilic molecules with nonpolar aliphatic (hydrocarbon) "tails" and polar phosphoryl-X "heads."*

The simplest glycerophospholipids, in which X = H, are **phosphatidic acids;** they are present in only small amounts in biological membranes. In the glycerophospholipids that commonly occur in biological membranes, the head groups are derived from polar alcohols (Table 9-2). Saturated C_{16} or C_{18} fatty acids usually occur at the C1 position of the glycerophospholipids,

Table 9-2 The Common Classes of Glycerophospholipids

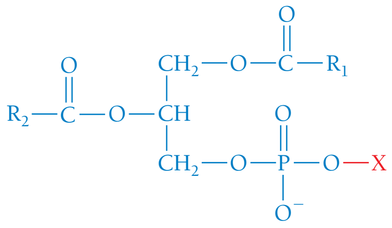

Name of X—OH	Formula of —X	Name of Phospholipid
Water	—H	Phosphatidic acid
Ethanolamine	$—CH_2CH_2NH_3^+$	Phosphatidylethanolamine
Choline	$—CH_2CH_2N(CH_3)_3^+$	Phosphatidylcholine (lecithin)
Serine	$—CH_2CH(NH_3^+)COO^-$	Phosphatidylserine
myo-Inositol	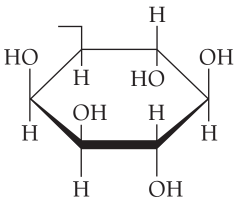	Phosphatidylinositol
Glycerol	$—CH_2CH(OH)CH_2OH$	Phosphatidylglycerol
Phosphatidylglycerol	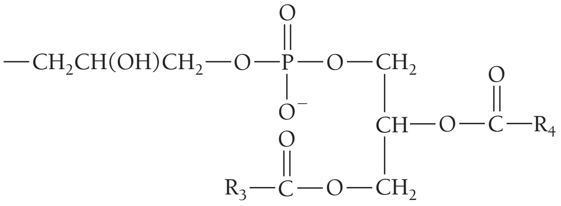	Diphosphatidylglycerol (cardiolipin)

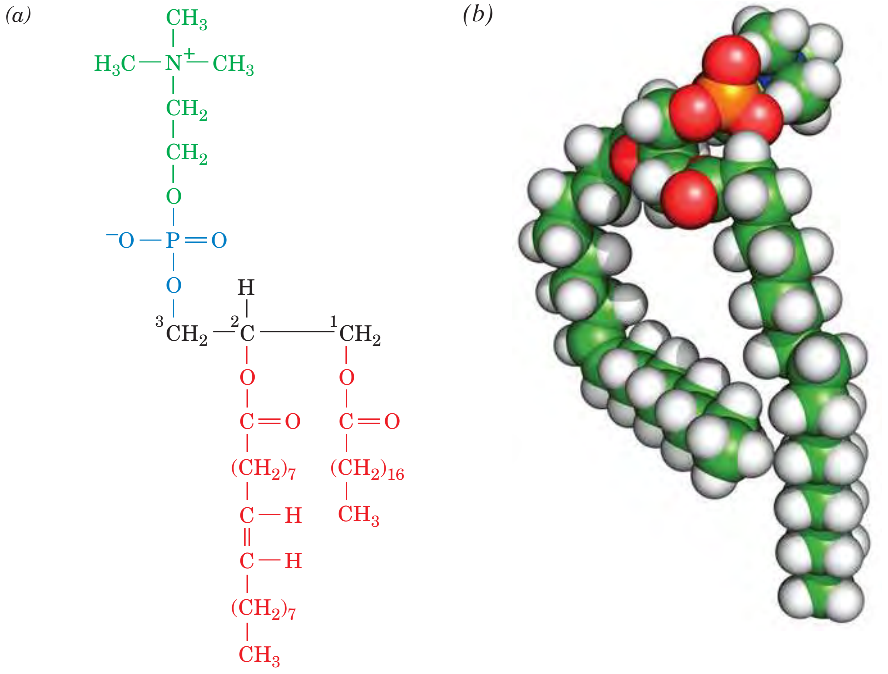

1-Stearoyl-2-oleoyl-3-phosphatidylcholine

■ **Figure 9-4 | The glycerophospholipid 1-stearoyl-2-oleoyl-3-phosphatidylcholine.** (*a*) Molecular formula in Fischer projection. (*b*) Energy-minimized space-filling model with C green, H white, N blue, O red, and P orange. Note how the unsaturated oleoyl chain (*left*) is bent compared to the saturated stearoyl chain. [Based on coordinates provided by Richard Venable and Richard Pastor, NIH, Bethesda, Maryland.]

and the C2 position is often occupied by an unsaturated C_{16} to C_{20} fatty acid. Individual glycerophospholipids are named according to the identities of these fatty acid residues (e.g., Fig. 9-4). A glycerophospholipid containing two palmitoyl chains is an important component of **lung surfactant** (Box 9-1).

Phospholipases Hydrolyze Glycerophospholipids. The chemical structures—including fatty acyl chains and head groups—of glycerophos-

BOX 9-1 BIOCHEMISTRY IN HEALTH AND DISEASE

Lung Surfactant

Dipalmitoyl phosphatidylcholine (DPPC) is the major lipid of lung surfactant, the protein–lipid mixture that is essential for normal pulmonary function. The surfaces of the cells that form the alveoli (small air spaces of the lung) are coated with surfactant, which decreases the alveolar surface tension. Lung surfactant contains 80 to 90% phospholipid by weight, and 70 to 80% of the phospholipid is phosphatidylcholine, mostly the dipalmitoyl species.

Because the palmitoyl chains of DPPC are saturated, they tend to extend straight out without bending. This allows close packing of DPPC molecules, which are oriented in a single layer with their nonpolar tails toward the air and their polar heads toward the alveolar cells. When air is expired from the lungs, the volume and surface area of the alveoli decrease. The collapse of the alveolar space is prevented by the surfactant, because the closely packed DPPC molecules resist compression. Reopening a collapsed air space requires a much greater force than expanding an already open air space.

Lung surfactant is continuously synthesized, secreted, and recycled by alveolar cells. Because surfactant production is low until just before birth, premature infants are at risk of developing **respiratory distress syndrome,** which is characterized by difficulty in breathing due to alveolar collapse. The syndrome can be treated by introducing exogenous surfactant into the lungs. A related condition in adults **(adult respiratory distress syndrome)** is characterized by insufficient surfactant, usually secondary to other lung injury. This condition, too, can be treated with exogenous surfactant.

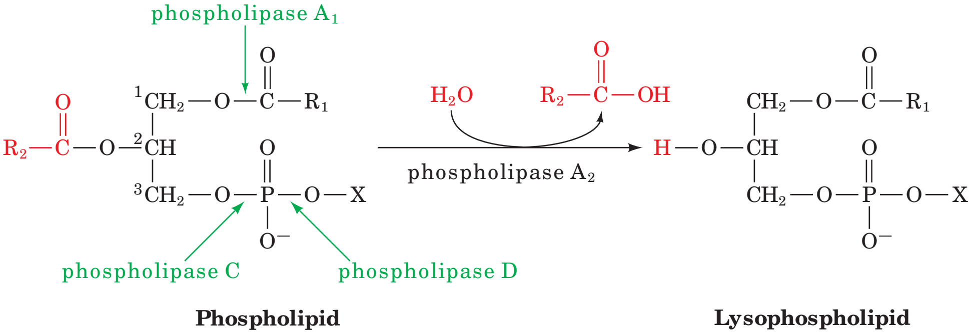

Figure 9-5 | **Action of phospholipases.** Phospholipase A_2 hydrolytically excises the C2 fatty acid residue from a triacylglycerol to yield the corresponding lysophospholipid. The bonds hydrolyzed by other types of phospholipases, which are named according to their specificities, are also indicated.

pholipids can be determined from the products of the hydrolytic reactions catalyzed by enzymes known as **phospholipases.** For example, **phospholipase A_2** hydrolytically excises the fatty acid residue at C2, leaving a **lysophospholipid** (Fig. 9-5). Lysophospholipids, as their name implies, are powerful detergents that disrupt cell membranes, thereby lysing cells. Bee and snake venoms are rich sources of phospholipase A_2. Other types of phospholipases act at different sites in glycerophospholipids, as shown in Fig. 9-5.

Enzymes that act on lipids have fascinated biochemists because the enzymes must gain access to portions of the lipids that are buried in a nonaqueous environment. Phospholipases A_2, which constitute some of the best understood lipid-specific enzymes, are relatively small proteins (~14 kD, ~125 amino acid residues). The X-ray structure of phospholipase A_2 from cobra venom suggests that the enzyme binds a glycerophospholipid molecule such that its polar head group fits into the enzyme's active site, whereas the hydrophobic tails, which extend beyond the active site, interact with several aromatic side chains (Fig. 9-6).

Lipases specific for triacylglycerols and membrane lipids catalyze their degradation *in vivo*. Occasionally, the hydrolysis products are not destined for further degradation but instead serve as intra- and extracellular signal molecules. For example, **lysophosphatidic acid (1-acyl-glycerol-3-phosphate),** which is not actually lytic since it has a small head group (an unsubstituted phosphate group), is produced by hydrolysis of membrane lipids in blood platelets and injured cells and stimulates cell growth as part of the wound-repair process. **1,2-Diacylglycerol,** derived from membrane lipids by the action of **phospholipase C,** is an intracellular signal molecule that activates a **protein kinase** (Section 13-4C; kinases catalyze ATP-dependent phosphoryl-transfer reactions).

Plasmalogens Contain an Ether Linkage. **Plasmalogens** are glycerophospholipids in which the C1 substituent of the glycerol moiety is

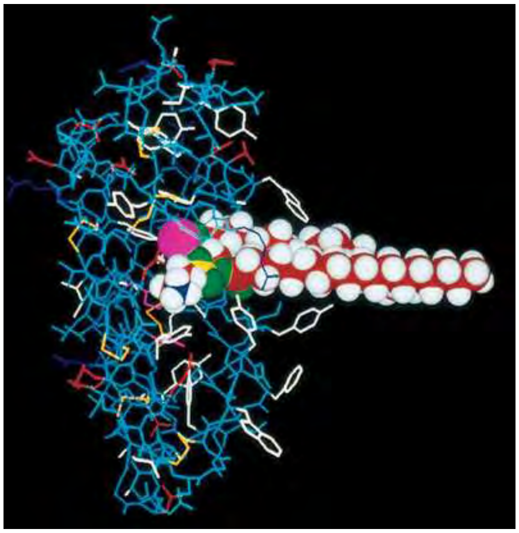

Figure 9-6 | **Model of phospholipase A_2 and a glycerophospholipid.** The X-ray structure of the enzyme from cobra venom is shown with a space-filling model of dimyristoyl phosphatidylethanolamine in its active site as located by NMR methods. A Ca^{2+} ion in the active site is shown in magenta. [Courtesy of Edward A. Dennis, University of California at San Diego.] **See Interactive Exercise 4.**

linked via an α,β-unsaturated ether linkage in the cis configuration rather than through an ester linkage:

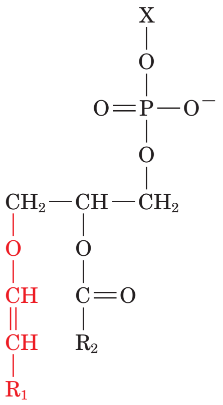
X
O
O=P—O⁻
O
CH₂—CH—CH₂
O
O
CH
C=O
CH
R₂
R₁

A plasmalogen

Ethanolamine, choline, and serine (Table 9-2) form the most common plasmalogen head groups. The functions of most plasmalogens are not well understood. Because the vinyl ether group is easily oxidized, plasmalogens may react with oxygen free radicals, by-products of normal metabolism, thereby preventing free-radical damage to other cell constituents.

D | Sphingolipids Are Amino Alcohol Derivatives

Sphingolipids are also major membrane components. Their function in cells was at first mysterious, so they were named after the Sphinx. Most sphingolipids are derivatives of the C_{18} amino alcohol **sphingosine,** whose double bond has the trans configuration. The *N*-acyl fatty acid derivatives of sphingosine are known as **ceramides:**

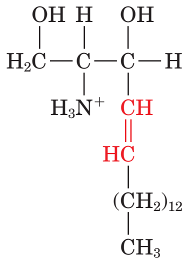
OH H OH
H₂C—C—C—H
H₃N⁺ CH
HC
(CH₂)₁₂
CH₃

Sphingosine

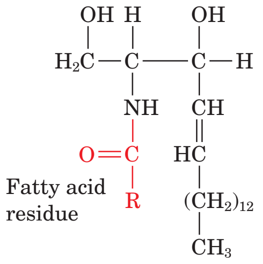
OH H OH
H₂C—C——C—H
NH CH
O=C HC
Fatty acid residue
R
(CH₂)₁₂
CH₃

A ceramide

Ceramides are the parent compounds of the more abundant sphingolipids:

1. ***Sphingomyelins,*** the most common sphingolipids, are ceramides bearing either a phosphocholine (Fig. 9-7) or a phosphoethanolamine head group, so they can also be classified as **sphingophospholipids.** They typically make up 10 to 20 mol % of plasma membrane lipids. *Although sphingomyelins differ chemically from phosphatidylcholine and phosphatidylethanolamine, their conformations and charge distributions are quite similar* (compare Figs. 9-4 and 9-7). The membranous myelin sheath that surrounds and electrically insulates many nerve cell axons is particularly rich in sphingomyelins (Fig. 9-8).
2. ***Cerebrosides*** are ceramides with head groups that consist of a single sugar residue. These lipids are therefore **glycosphingolipids. Galactocerebrosides** and **glucocerebrosides** are the most prevalent.

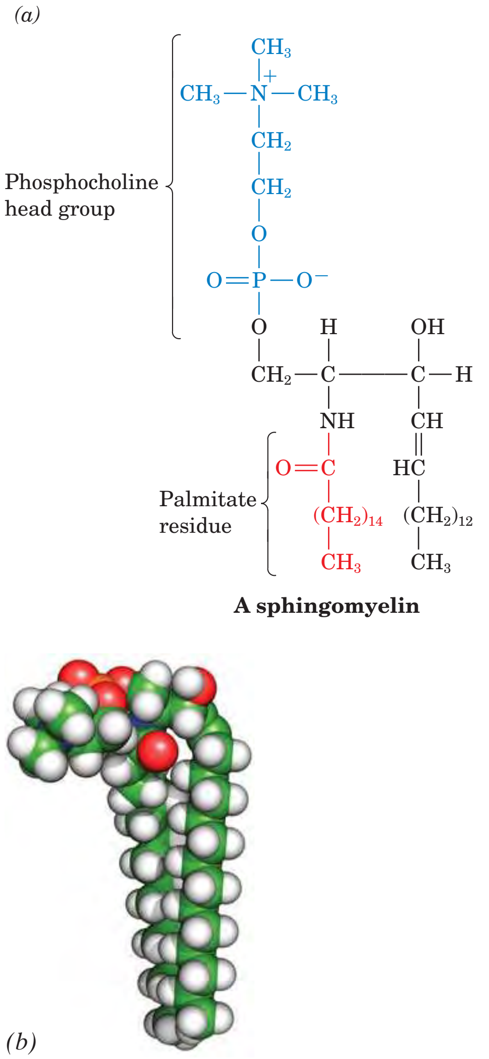
(a)
CH₃
CH₃—N⁺—CH₃
CH₂
CH₂
O
O=P—O⁻
O H OH
CH₂—C——C—H
NH CH
O=C HC
(CH₂)₁₄ (CH₂)₁₂
CH₃ CH₃
Phosphocholine head group
Palmitate residue
A sphingomyelin
(b)

Figure 9-7 | A sphingomyelin. (*a*) Molecular formula. (*b*) Energy-minimized space-filling model with C green, H white, N blue, O red, and P orange. [Based on coordinates provided by Richard Venable and Richard Pastor, NIH, Bethesda, Maryland.]

Cerebrosides, in contrast to phospholipids, lack phosphate groups and hence are nonionic.

3. ***Gangliosides*** are the most complex glycosphingolipids. They are ceramides with attached oligosaccharides that include at least one sialic acid residue. The structures of **gangliosides G_{M1}, G_{M2},** and **G_{M3},** three of the over 60 that are known, are shown in Fig. 9-9. Gangliosides are primarily components of cell-surface membranes and constitute a significant fraction (6%) of brain lipids.

Gangliosides have considerable physiological and medical significance. Their complex carbohydrate head groups, which extend beyond the surfaces of cell membranes, act as specific receptors for certain pituitary glycoprotein hormones that regulate a number of important physiological functions. Gangliosides are also receptors for certain bacterial protein toxins such as **cholera toxin.** There is considerable evidence that gangliosides are specific determinants of cell–cell recognition, so they probably have an important role in the growth and differentiation of tissues as well as in carcinogenesis. Disorders of ganglioside breakdown are responsible for several hereditary **sphingolipid storage diseases,** such as **Tay-Sachs disease,** which are characterized by an invariably fatal neurological deterioration in early childhood.

Sphingolipids, like glycerophospholipids, are a source of smaller lipids that have discrete signaling activity. Sphingomyelin itself, as well as the ceramide portions of more complex sphingolipids, appear to specifically modulate the activities of protein kinases and **protein phosphatases** (enzymes that remove phosphoryl groups from proteins) that are involved in regulating cell growth and differentiation.

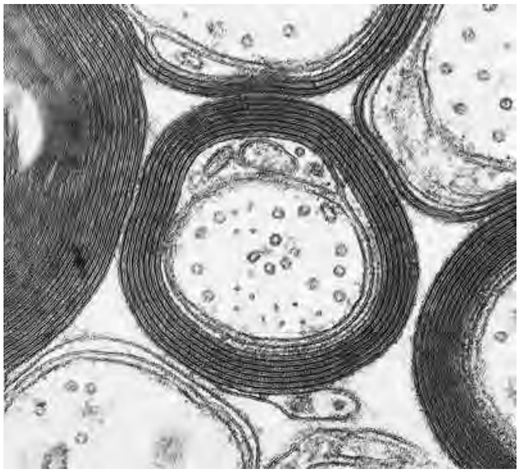

■ **Figure 9-8 | Electron micrograph of myelinated nerve fibers.** This cross-sectional view shows the spirally wrapped membranes around each nerve axon. The myelin sheath may be 10–15 layers thick. Its high lipid content makes it an electrical insulator. [Courtesy of Cedric S. Raine, Albert Einstein College of Medicine.]

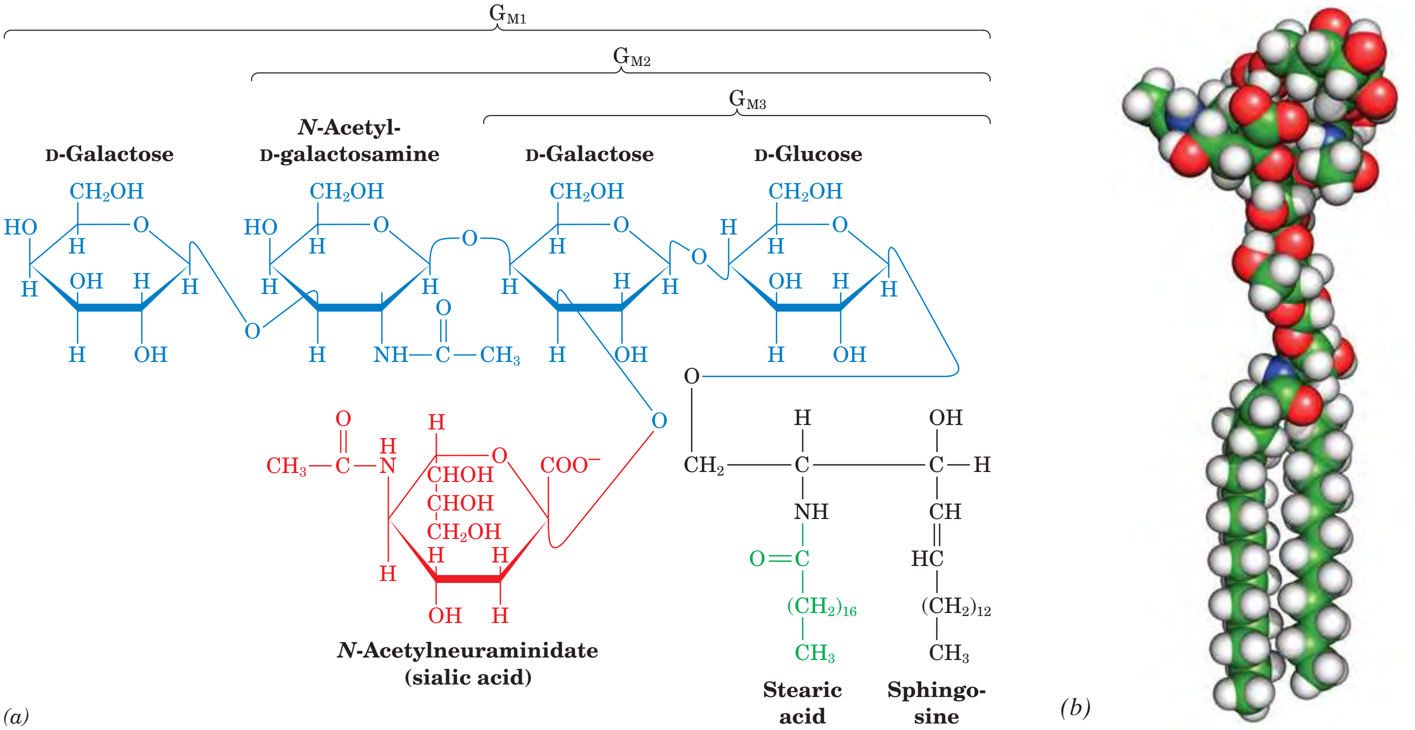

■ **Figure 9-9 | Gangliosides.** (*a*) Structural formula of gangliosides G_{M1}, G_{M2}, and G_{M3}. Gangliosides G_{M2} and G_{M3} differ from G_{M1} only by the sequential absences of the terminal D-galactose and *N*-acetyl-D-galactosamine residues. Other gangliosides have different oligosaccharide head groups. (*b*) Energy-minimized space-filling model of G_{M1} with C green, H white, N blue, and O red. [Based on coordinates provided by Richard Venable and Richard Pastor, NIH, Bethesda, Maryland.]

E | Steroids Contain Four Fused Rings

Steroids, which are mostly of eukaryotic origin, are derivatives of **cyclopentanoperhydrophenanthrene,**

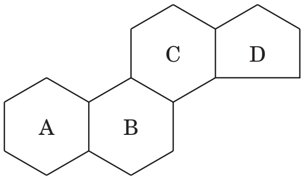

Cyclopentanoperhydrophenanthrene

a compound that consists of four fused, nonplanar rings (labeled A–D). The much maligned **cholesterol,** which is the most abundant steroid in animals, is further classified as a **sterol** because of its C3-OH group (Fig. 9-10). Cholesterol is a major component of animal plasma membranes, typically constituting 30 to 40 mol % of plasma membrane lipids. Its polar OH group gives it a weak amphiphilic character, whereas its fused ring system provides it with greater rigidity than other membrane lipids. Cholesterol can also be esterified to long-chain fatty acids to form **cholesteryl esters,** for example:

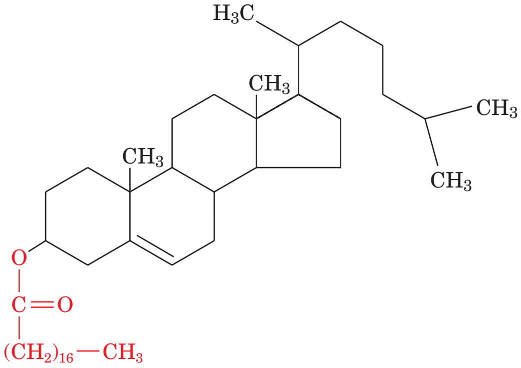

Cholesteryl stearate

Plants contain little cholesterol but synthesize other sterols. Yeast and fungi also synthesize sterols, which differ from cholesterol in their aliphatic side chains and number of double bonds. Prokaryotes contain little, if any, sterol.

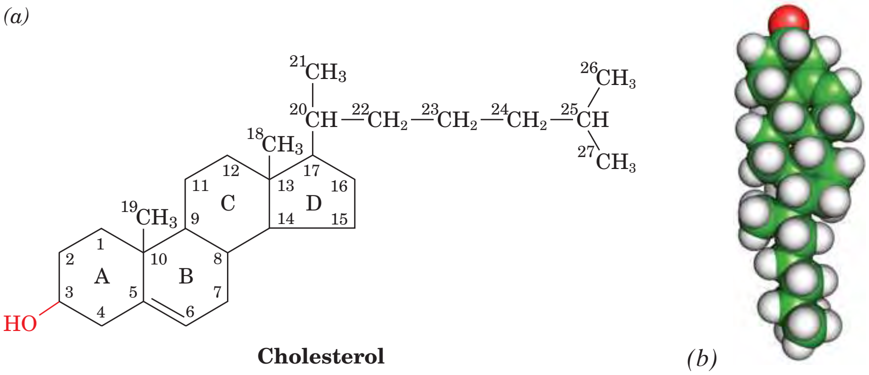

Cholesterol

Figure 9-10 | Cholesterol. (*a*) Structural formula with the standard numbering system. (*b*) Energy-minimized space-filling model with C green, H white, and O red. [Based on coordinates provided by Richard Venable and Richard Pastor, NIH, Bethesda, Maryland.]

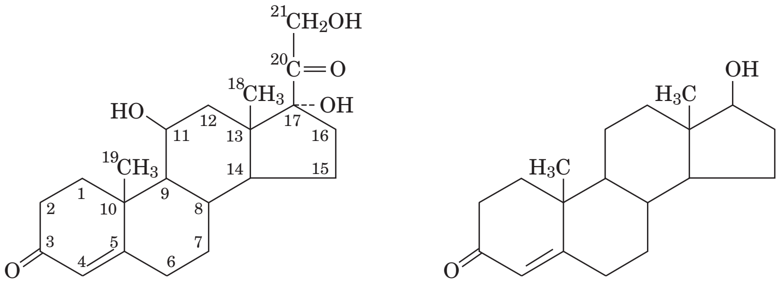

Cortisol (hydrocortisone)
(a glucocorticoid)

Testosterone
(an androgen)

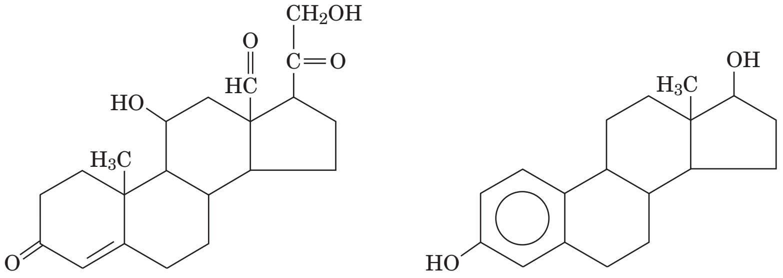

Aldosterone
(a mineralocorticoid)

β-Estradiol
(an estrogen)

Figure 9-11 | Some representative steroid hormones.

In mammals, cholesterol is the metabolic precursor of **steroid hormones,** substances that regulate a great variety of physiological functions. The structures of some steroid hormones are shown in Fig. 9-11. Steroid hormones are classified according to the physiological responses they evoke:

1. The **glucocorticoids,** such as **cortisol** (a C_{21} compound), affect carbohydrate, protein, and lipid metabolism and influence a wide variety of other vital functions, including inflammatory reactions and the capacity to cope with stress.
2. **Aldosterone** and other **mineralocorticoids** regulate the excretion of salt and water by the kidneys.
3. The **androgens** and **estrogens** affect sexual development and function. **Testosterone,** a C_{19} compound, is the prototypic androgen (male sex hormone), whereas **β-estradiol,** a C_{18} compound, is an estrogen (female sex hormone).

Glucocorticoids and mineralocorticoids are synthesized by the cortex (outer layer) of the adrenal gland. Both androgens and estrogens are synthesized by testes and ovaries (although androgens predominate in testes and estrogens predominate in ovaries) and, to a lesser extent, by the adrenal cortex. Because steroid hormones are water insoluble, they bind to proteins for transport through the blood to their target tissues.

Impaired adrenocortical function, either through disease or trauma, results in **Addison's disease,** which is characterized by **hypoglycemia** (decreased amounts of glucose in the blood), muscle weakness, Na^+ loss, K^+ retention, impaired cardiac function, and greatly increased susceptibility to stress. The victim, unless treated by the administration of glucocorticoids and mineralocorticoids, slowly languishes and dies without any particular pain or distress. Conversely, adrenocortical hyperfunction, which is often caused by a tumor of the adrenal cortex, results in **Cushing's syndrome,** which is characterized by fatigue, **hyperglycemia** (increased amount of glucose in the blood), **edema** (water retention), and a redistribution of body fat to yield a characteristic "moon face."

Vitamin D Regulates Ca^{2+} Metabolism. The various forms of **vitamin D,** which are really hormones, are sterol derivatives in which the steroid B ring is disrupted between C9 and C10:

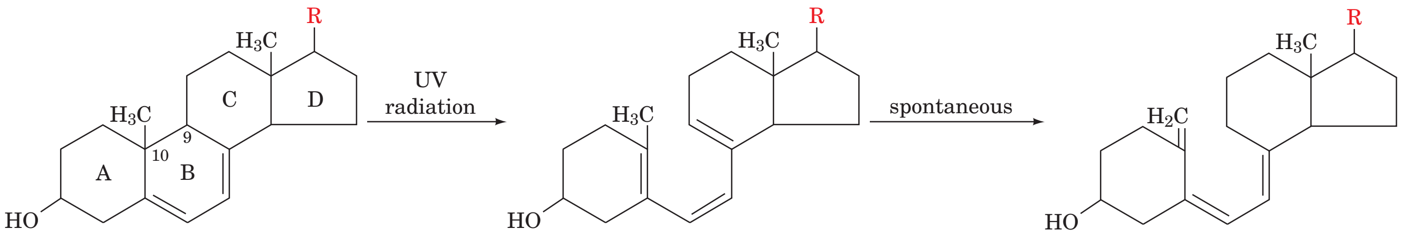

R = X 7-Dehydrocholesterol
R = Y Ergosterol

R = X Vitamin D_3 (cholecalciferol)
R = Y Vitamin D_2 (ergocalciferol)

X =

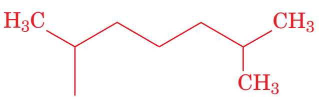

Y =

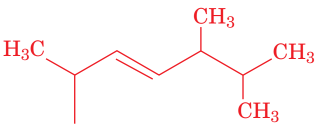

Vitamin D_2 (ergocalciferol) is nonenzymatically formed in the skin of animals through the photolytic action of UV light on the plant sterol **ergosterol,** a common milk additive, whereas the closely related **vitamin D_3 (cholecalciferol)** is similarly derived from **7-dehydrocholesterol** (hence the saying that sunlight provides vitamin D).

Vitamins D_2 and D_3 are inactive; the active forms are produced through their enzymatic hydroxylation (addition of an OH group) carried out by the liver (at C25) and by the kidney (at C1) to yield **1α,25-dihydroxycholecalciferol:**

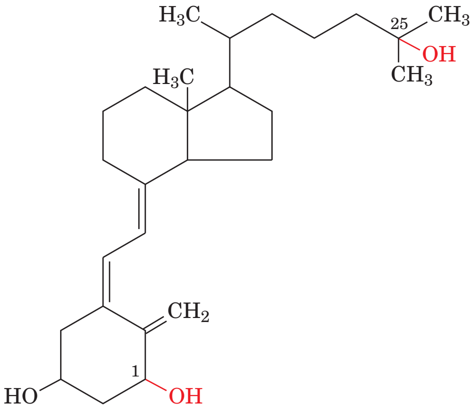

1α,25-Dihydroxycholecalciferol

Active vitamin D increases serum $[Ca^{2+}]$ by promoting the intestinal absorption of dietary Ca^{2+}. This increases the deposition of Ca^{2+} in bones and teeth. Vitamin D deficiency produces **rickets** in children, a disease characterized by stunted growth and deformed bones caused by insufficient bone mineralization. Although rickets was first described in 1645, it was not until the early twentieth century that eating animal fats, particularly fish liver oils, was shown to prevent this deficiency disease. Rickets can also be prevented by exposing children to sunlight or just UV light in the wavelength range 230 to 313 nm, regardless of their diets.

Since vitamin D is water insoluble, it can accumulate in fatty tissues. Excessive intake of vitamin D over long periods results in **vitamin D intoxication.** The consequent high serum [Ca^{2+}] results in aberrant calcification of soft tissues and in the development of kidney stones, which can cause kidney failure. The observation that the level of skin pigmentation in indigenous human populations tends to increase with their proximity to the equator is explained by the hypothesis that skin pigmentation functions to prevent vitamin D intoxication by filtering out excessive solar radiation.

F | Other Lipids Perform a Variety of Metabolic Roles

In addition to the well-characterized lipids that are found in large amounts in cellular membranes, many organisms synthesize compounds that are not membrane components but are classified as lipids on the basis of their physical properties. For example, lipids occur in the waxy coatings of plants, where they protect cells from desiccation by creating a water-impermeable barrier.

Isoprenoids Are Built from Five-Carbon Units. Among the compounds that are not structural components of membranes—although they are soluble in the lipid bilayer—are the **isoprenoids,** which are built from five-carbon units with the same carbon skeleton as **isoprene.**

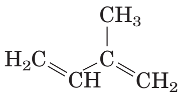

Isoprene

For example, the isoprenoid **ubiquinone** (also known as **coenzyme Q**) is reversibly reduced and oxidized in the mitochondrial membrane (its activity is described in more detail in Section 18-2C). Mammalian ubiquinone consists of 10 isoprenoid units.

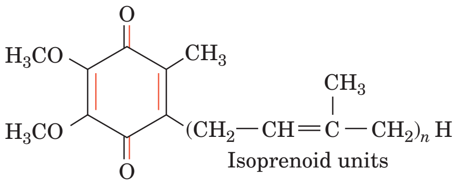

Coenzyme Q (CoQ) or ubiquinone

The plant kingdom is rich in isoprenoid compounds, which serve as pigments, molecular signals (hormones and pheromones), and defensive agents. Indeed, over 25,000 isoprenoids (also known as **terpenoids**), which are mostly of plant, fungal, and bacterial origin, have been characterized. During the course of evolution, vertebrate metabolism has co-opted several of these compounds for other purposes. Some of these compounds (e.g., vitamin D) are known as **fat-soluble vitamins** (**vitamins** are organic substances that an animal requires in small amounts but cannot synthesize and hence must acquire in its diet).

Vitamin A, or **retinol** *(at right)*, is derived mainly from plant products such as **β-carotene** [a red pigment that is present in green vegetables as well as carrots (after which it is named) and tomatoes; Section 19-1B]. Retinol is oxidized to its corresponding aldehyde, **retinal,** which functions

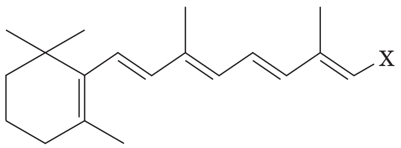

X = CH_2OH **Retinol (vitamin A)**
X = CHO **Retinal**

as the eye's photoreceptor at low light intensities. Light causes the retinal to isomerize, triggering, via a complex signaling pathway, an impulse through the optic nerve. A severe deficiency of vitamin A can lead to blindness. Retinoic acid also has hormonelike properties in that it stimulates tissue repair. It is used to treat severe acne and skin ulcers and is also used cosmetically to eliminate wrinkles.

Vitamin K is a lipid synthesized by plants (as **phylloquinone**) and bacteria (as **menaquinone):**

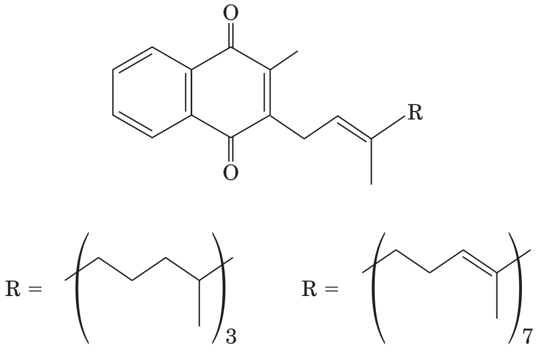

Phylloquinone
(vitamin K_1)

Menaquinone
(vitamin K_2)

About half of the daily requirement for humans is supplied by intestinal bacteria. Vitamin K participates in the carboxylation of Glu residues in some of the proteins involved in blood clotting (vitamin K is named for the Danish word *Koagulation*). Vitamin K deficiency prevents this carboxylation, and the resulting inactive clotting proteins lead to excessive bleeding. Compounds that interfere with vitamin K function are the active ingredients in some rodent poisons.

Vitamin E is actually a group of compounds whose most abundant member is **α-tocopherol:**

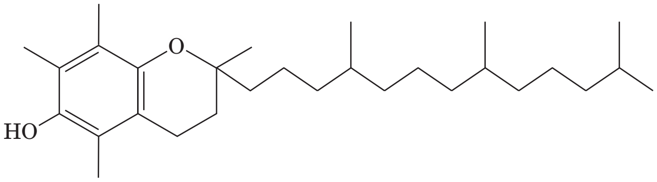

α-Tocopherol
(vitamin E)

This highly hydrophobic molecule is incorporated into cell membranes, where it functions as an antioxidant that prevents oxidative damage to membrane proteins and lipids. A deficiency of vitamin E elicits a variety of nonspecific symptoms, which makes the deficiency difficult to detect. The popularity of vitamin E supplements rests on the hypothesis that vitamin E protects against oxidative damage to cells and hence reduces the effects of aging.

Eicosanoids Are Derived from Arachidonic Acid. Other less common lipids are derived from relatively abundant membrane lipids. **Prostaglandins** (e.g., Fig. 9-12) were discovered in the 1930s by Ulf von Euler, who thought they were produced by the prostate gland. Prostaglandins and related compounds—**prostacyclins, thromboxanes, leukotrienes,** and **lipoxins**—are known collectively as **eicosanoids** because they are all C_{20} compounds (Greek: *eikosi,* twenty). *The eicosanoids act at very low concentrations and*

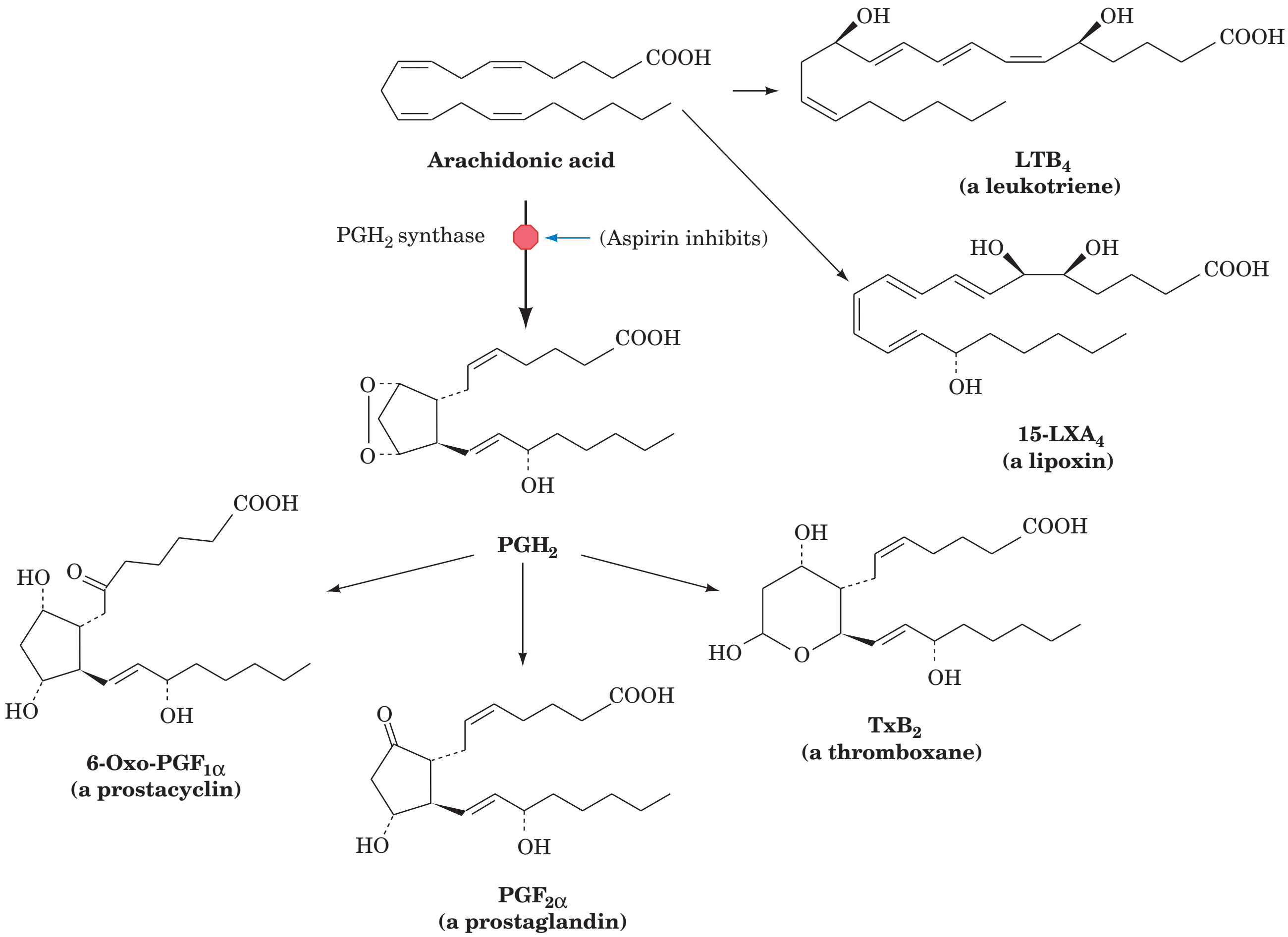
COOH
Arachidonic acid
OH
OH
COOH
LTB$_4$
(a leukotriene)
PGH$_2$ synthase
(Aspirin inhibits)
HO
OH
COOH
OH
15-LXA$_4$
(a lipoxin)
COOH
O
O
OH
PGH$_2$
COOH
HO
O
HO
OH
6-Oxo-PGF$_{1\alpha}$
(a prostacyclin)
O
COOH
HO
OH
PGF$_{2\alpha}$
(a prostaglandin)
OH
COOH
HO
O
OH
TxB$_2$
(a thromboxane)

■ **Figure 9-12** | **Eicosanoids.** Arachidonate is the precursor of prostaglandins (PG), prostacyclins, thromboxanes (Tx), and lipoxins (LX). Arachidonate also leads to leukotrienes. Although only a single example of each type of eicosanoid is shown, each has numerous physiologically significant derivatives, which are designated by letters and subscripts (e.g., **PGH$_2$** for **prostaglandin H$_2$**).

are involved in the production of pain and fever, and in the regulation of blood pressure, blood coagulation, and reproduction. Unlike most other types of hormones, eicosanoids are not transported by the bloodstream to their sites of action but tend to act locally, close to the cells that produced them. In fact, most eicosanoids decompose within seconds or minutes, which limits their effects on nearby tissues. The synthesis of the eicosanoids is discussed in Section 20-6C.

In humans, the most important eicosanoid precursor is **arachidonic acid,** a polyunsaturated fatty acid with four double bonds (Table 9-1). Arachidonate is stored in cell membranes as the C2 ester of **phosphatidylinositol** (Table 9-2) and other phospholipids. The fatty acid residue is released by the action of phospholipase A$_2$ (Fig. 9-5).

The specific products of arachidonate metabolism are tissue-dependent. For example, platelets produce thromboxanes almost exclusively, but endothelial cells (which line the walls of blood vessels) predominantly synthesize prostacyclins. Interestingly, thromboxanes stimulate vasoconstriction and platelet aggregation (which helps initiate blood clotting), while prostacyclins elicit the opposite effects. Thus, the two substances act in opposition to maintain a balance in the cardiovascular system.

■ CHECK YOUR UNDERSTANDING

How do lipids differ from the three other major classes of biological molecules?

How does unsaturation affect the physical properties of fatty acids or the membrane lipids to which they are esterified?

Compare the structures and physical properties of triacylglycerols, glycerophospholipids, and sphingolipids.

Summarize the functions of steroids and eicosanoids.

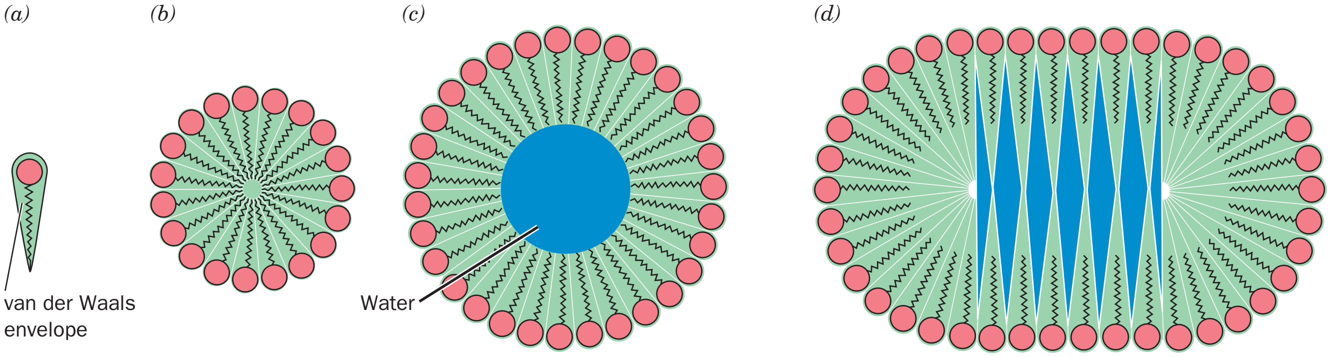

Figure 9-13 | Aggregates of single-tailed lipids. The tapered van der Waals envelope of these lipids (*a*) permits them to pack efficiently to form a spheroidal micelle (*b*). The diameter of the micelles depends on the length of the tails. Spheroidal micelles composed of many more lipid molecules than the optimal number (*c*) would have an unfavorable water-filled center (*blue*). Such micelles could flatten out to collapse the hollow center, but as these ellipsoidal micelles become elongated (*d*), they also develop water-filled spaces.

2 Lipid Bilayers

LEARNING OBJECTIVES

- Understand why certain amphiphilic molecules form bilayers.
- Understand that the bilayer is a fluid structure in which lipids rapidly diffuse laterally.

In living systems, lipids are seldom found as free molecules but instead associate with other molecules, usually other lipids. In this section, we discuss how lipids aggregate to form micelles and bilayers. We are concerned with the physical properties of lipid bilayers because these aggregates form the structural basis for biological membranes.

A | Bilayer Formation Is Driven by the Hydrophobic Effect

In aqueous solutions, amphiphilic molecules such as soaps and detergents form micelles (globular aggregates whose hydrocarbon groups are out of contact with water; Section 2-1C). This molecular arrangement eliminates unfavorable contacts between water and the hydrophobic tails of the amphiphiles and yet permits the solvation of the polar head groups.

The approximate size and shape of a micelle can be predicted from geometrical considerations. Single-tailed amphiphiles, such as soap anions, form spheroidal or ellipsoidal micelles because of their tapered shapes (their hydrated head groups are wider than their tails; Fig. 9-13*a,b*). The number of molecules in such a micelle depends on the amphiphile, but for many substances it is on the order of several hundred. Too few lipid molecules would expose the hydrophobic core of the micelle to water, whereas too many would give the micelle an energetically unfavorable hollow center (Fig. 9-13*c*). Of course, a large micelle could flatten out to eliminate this hollow center, but the resulting decrease of curvature at the flattened surfaces would also generate empty spaces (Fig. 9-13*d*).

The two hydrocarbon tails of glycerophospholipids and sphingolipids give these amphiphiles a somewhat rectangular cross section (Fig. 9-14*a*). The steric requirements of packing such molecules together yields large disklike micelles (Fig. 9-14*b*) that are really extended bimolecular leaflets. These **lipid bilayers** are ~60 Å thick, as measured by electron microscopy and X-ray diffraction techniques, the value expected for more or less fully extended hydrocarbon tails.

A suspension of phospholipids (glycerophospholipids or sphingomyelins) can form **liposomes**—closed, self-sealing solvent-filled

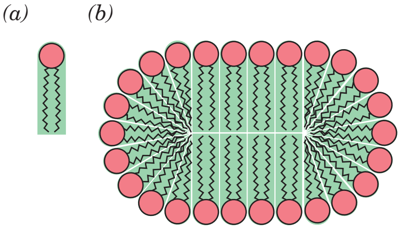

Figure 9-14 | Bilayer formation by phospholipids. The cylindrical van der Waals envelope of these lipids (*a*) causes them to form extended disklike micelles (*b*) that are better described as lipid bilayers.

Figure 9-15 | Electron micrograph of a liposome. Its wall, as the accompanying diagram indicates, consists of a lipid bilayer. [Courtesy of Walther Stoeckenius, University of California at San Francisco.]

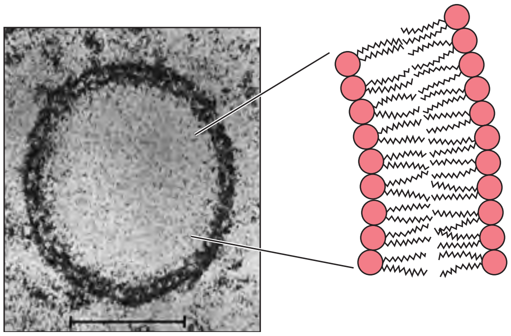

vesicles that are bounded by only a single bilayer (Fig. 9-15). They typically have diameters of several hundred angstroms and, in a given preparation, are rather uniform in size. Once formed, liposomes are quite stable and can be purified by dialysis, gel filtration chromatography, or centrifugation. Liposomes whose internal environment differs from the surrounding solution can therefore be readily prepared. Liposomes serve as models of biological membranes and also hold promise as vehicles for drug delivery since they are absorbed by many cells through fusion with the plasma membrane.

B | Lipid Bilayers Have Fluidlike Properties

*The transfer of a lipid molecule across a bilayer (Fig. 9-16a), a process termed **transverse diffusion** or a **flip-flop,** is an extremely rare event.* This is because a flip-flop requires the hydrated, polar head group of the lipid to pass through the anhydrous hydrocarbon core of the bilayer. The flip-flop rates of phospholipids have half-times of several days or more. In contrast to their low flip-flop rates, *lipids are highly mobile in the plane of the bilayer* (**lateral diffusion;** Fig. 9-16*b*). It has been estimated that lipids in a membrane can diffuse the 1-μm length of a bacterial cell in ~1 s. Because of the mobilities of the lipids, the lipid bilayer can be considered to be a two-dimensional fluid.

The interior of the lipid bilayer is in constant motion due to rotations around the C—C bonds of the lipid tails. Various physical measurements suggest that the interior of the bilayer has the viscosity of light machine oil. This feature of the bilayer core is evident in **molecular dynamics simulations,** in which the time-dependent positions of atoms are predicted from calculations of the forces acting on them (Fig. 9-17). The viscosity of the bilayer increases dramatically closer to the lipid head groups, whose rotation is limited and whose lateral mobility is more constrained by interactions between other polar or charged head groups.

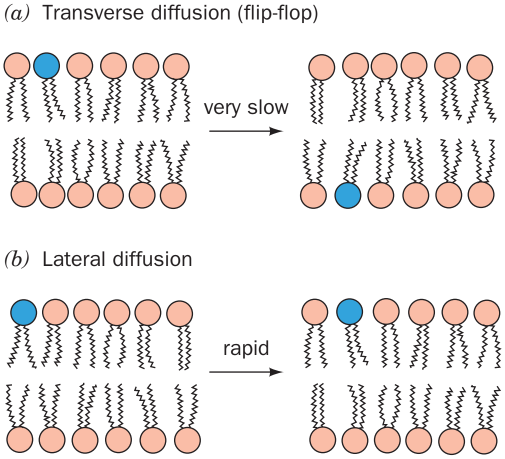

Figure 9-16 | Phospholipid diffusion in a lipid bilayer. (*a*) Transverse diffusion (a flip-flop) is defined as the transfer of a phospholipid molecule from one bilayer leaflet to the other. (*b*) Lateral diffusion is defined as the pairwise exchange of neighboring phospholipid molecules in the same bilayer leaflet.

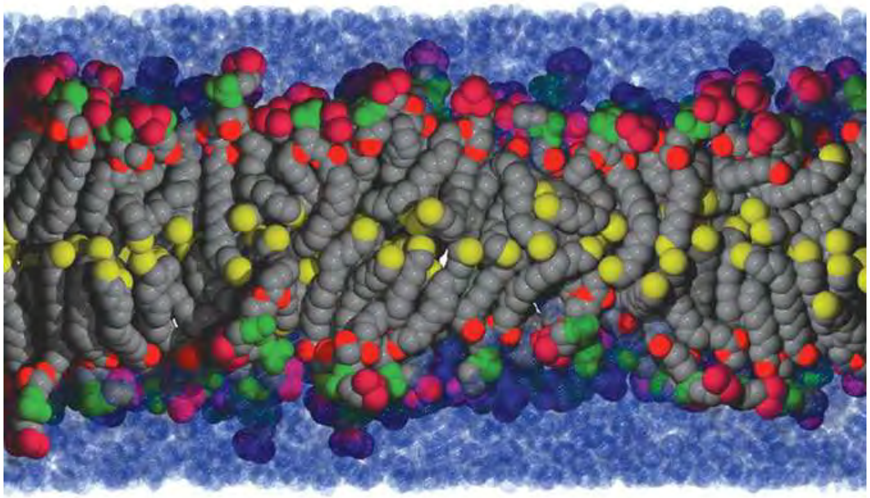

Figure 9-17 | Model (snapshot) of a lipid bilayer at an instant in time. The conformations of dipalmitoyl phosphatidylcholine molecules in a bilayer surrounded by water were modeled by computer. Atom colors are chain and glycerol C gray except terminal methyl C yellow, ester O red, phosphate P and O green, and choline C and N magenta. Water molecules are represented by translucent blue spheres (those near the bilayer appear dark because they overlap head group atoms). [Courtesy of Richard Pastor and Richard Venable, NIH, Bethesda, Maryland.]

Note that the hydrophobic tails of the lipids shown in Fig. 9-17 are not stiffly regimented as Fig. 9-16 might suggest, but instead bend and interdigitate. A typical biological membrane includes many different lipid molecules, some of whose tails are of different lengths or are kinked due to the presence of double bonds. Under physiological conditions, highly mobile chains fill any gaps that might form between lipids in the bilayer interior.

The model bilayer shown in Fig. 9-17 indicates that the phospholipids bob up and down to some degree. This is also the case in naturally occurring membranes, which contain a variety of different lipid head groups that must nestle among each other. The polar nature of the outer surface of the bilayer extends from the head groups to the carbonyl groups of the ester and amide bonds that link the fatty acyl chains. Consequently, water molecules penetrate a lipid bilayer to a depth of up to 15 Å, avoiding only the central ~30 Å hydrocarbon core.

The Fluidity of a Lipid Bilayer Is Temperature-Dependent. *As a lipid bilayer cools below a characteristic* **transition temperature,** *it undergoes a sort of phase change in which it becomes a gel-like solid; that is, it loses its fluidity* (Fig. 9-18). Above the transition temperature, the highly mobile lipids are in a state known as a **liquid crystal** because they are ordered in some directions but not in others. The bilayer is thicker in the gel state than in the liquid crystal state due to the stiffening of the hydrocarbon tails at lower temperatures.

The transition temperature of a bilayer increases with the chain length and the degree of saturation of its component fatty acid residues for the same reasons that the melting points of fatty acids increase with these quantities. The transition temperatures of most biological membranes are in the range 10 to 40°C. Bacteria and cold-blooded animals such as fish modify (through lipid synthesis and degradation) the fatty acid compositions of their membrane lipids with ambient temperature so as to maintain a constant level of fluidity. Thus, the fluidity of biological membranes is one of their important physiological attributes.

Cholesterol, which by itself does not form a bilayer, decreases membrane fluidity because its rigid steroid ring system interferes with the motions of

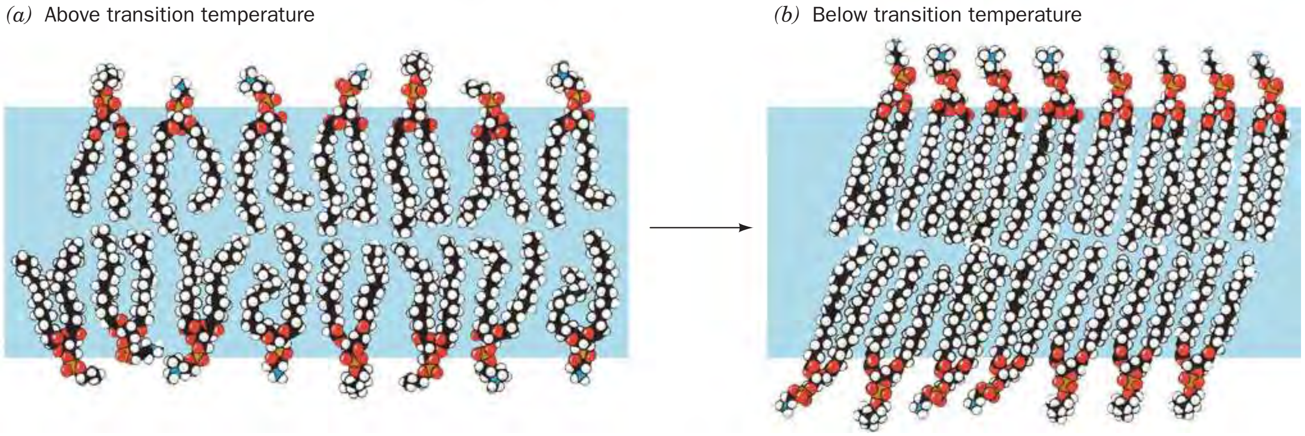
(*a*) Above transition temperature
(*b*) Below transition temperature

Figure 9-18 | Phase transition in a lipid bilayer. (*a*) Above the transition temperature, both the lipid molecules as a whole and their nonpolar tails are highly mobile in the plane of the bilayer. (*b*) Below the transition temperature, the lipid molecules form a much more orderly array to yield a gel-like solid. [After Robertson, R.N., *The Lively Membranes,* pp. 69–70, Cambridge University Press (1983).]

the fatty acid side chains in other membrane lipids. It also broadens the temperature range of the phase transition. This is because cholesterol inhibits the ordering of fatty acid side chains by fitting in between them. Thus, cholesterol functions as a kind of membrane plasticizer.

CHECK YOUR UNDERSTANDING

Why do glycerophospholipids—but not fatty acids—form bilayers?

Explain why lateral diffusion of membrane lipids is faster than transverse diffusion.

What factors influence the fluidity of a bilayer?

3 Membrane Proteins

LEARNING OBJECTIVES

- Understand that integral membrane proteins contain a transmembrane structure consisting of α helices or a β barrel with a hydrophobic surface.
- Understand that lipid-linked proteins have a covalently attached prenyl group, fatty acyl group, or glycosylphosphatidylinositol group.
- Understand that peripheral membrane proteins interact with proteins or lipids at the membrane surface.

Biological membranes contain proteins as well as lipids. The exact lipid and protein components and the ratio of protein to lipid varies with the identity of the membrane. For example, the lipid-rich myelinated membranes that surround and insulate certain nerve axons (Fig. 9-8) have a protein-to-lipid ratio of 0.23, whereas the protein-rich inner membrane of mitochondria, which mediates numerous chemical reactions, has a protein-to-lipid ratio of 3.2. Eukaryotic plasma membranes are typically ~50% protein.

Membrane proteins catalyze chemical reactions, mediate the flow of nutrients and wastes across the membrane, and participate in relaying information about the extracellular environment to various intracellular components. Such proteins carry out their functions in association with the lipid bilayer. They must therefore interact to some degree with the hydrophobic core and/or the polar surface of the bilayer. In this section, we examine the structures of some membrane proteins, which are classified by their mode of interaction with the membrane.

A | Integral Membrane Proteins Interact with Hydrophobic Lipids

Integral or **intrinsic proteins** (Fig. 9-19) associate tightly with membranes through hydrophobic effects and can be separated from membranes only by treatment with agents that disrupt membranes. For example, detergents such as sodium dodecyl sulfate (Section 5-2D) solubilize membrane proteins by replacing the membrane lipids that normally surround the protein. The hydrophobic portions of the detergent molecules coat the hydrophobic regions of the protein, and the polar head groups render the detergent–protein complex soluble in water. Chaotropic agents such as guanidinium ion and urea (Section 6-4B) disrupt water structure, thereby reducing the hydrophobic effect, the primary force stabilizing the association of the protein with the membrane. Some integral proteins bind lipids so tenaciously that they can be freed from them only under denaturing conditions.

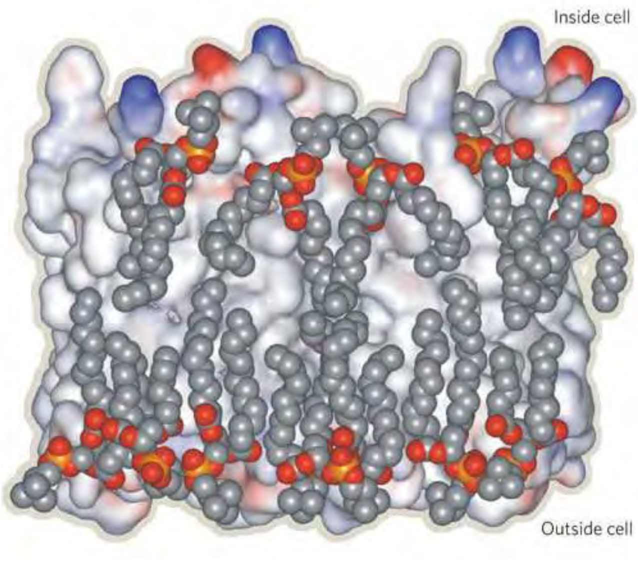

Figure 9-19 | Structure of the integral membrane protein aquaporin-0 (AQP0) in association with lipids. The protein is represented by its surface diagram, which is colored according to charge (red negative, blue positive, and white uncharged). Tightly bound molecules of dimyristoylphosphatidylcholine are drawn in space-filling form with O red, P orange, and C gray. Note how the lipid tails closely conform to the nonpolar surface of the protein, thereby solvating it. The arrangement of the two rows of lipid molecules, with phosphate–phosphate distances of ~35 Å, matches the dimensions of a lipid bilayer. [Courtesy of Anthony Lee, University of Southampton, Southampton, U.K. Based on an electron crystallography structure by Stephen Harrison and Thomas Walz, Harvard Medical School.]

Once they have been solubilized, integral proteins can be purified by many of the protein fractionation methods described in Section 5-2. Since these proteins tend to aggregate and precipitate in aqueous solution, their solubility frequently requires the presence of detergents or water-miscible organic solvents such as butanol or glycerol.

Integral Proteins Are Asymmetrically Oriented Amphiphiles. *Integral proteins are amphiphiles; the protein segments immersed in a membrane's nonpolar interior have predominantly hydrophobic surface residues, whereas those portions that extend into the aqueous environment are by and large sheathed with polar residues.* This was first demonstrated through **surface labeling,** a technique employing agents that react with proteins but cannot penetrate membranes. For example, the extracellular domain of an integral protein binds antibodies elicited against it, but its cytoplasmic domain will do so only if the membrane has been ruptured. Membrane-impermeable protein-specific reagents that are fluorescent or radioactively labeled can be similarly employed. Alternatively, proteases, which digest only the solvent-exposed portions of an integral protein, may be used to identify the membrane-immersed portions of the protein. These techniques revealed, for example, that the erythrocyte membrane protein **glycophorin A** has three domains (Fig. 9-20): (1) a 72-residue externally

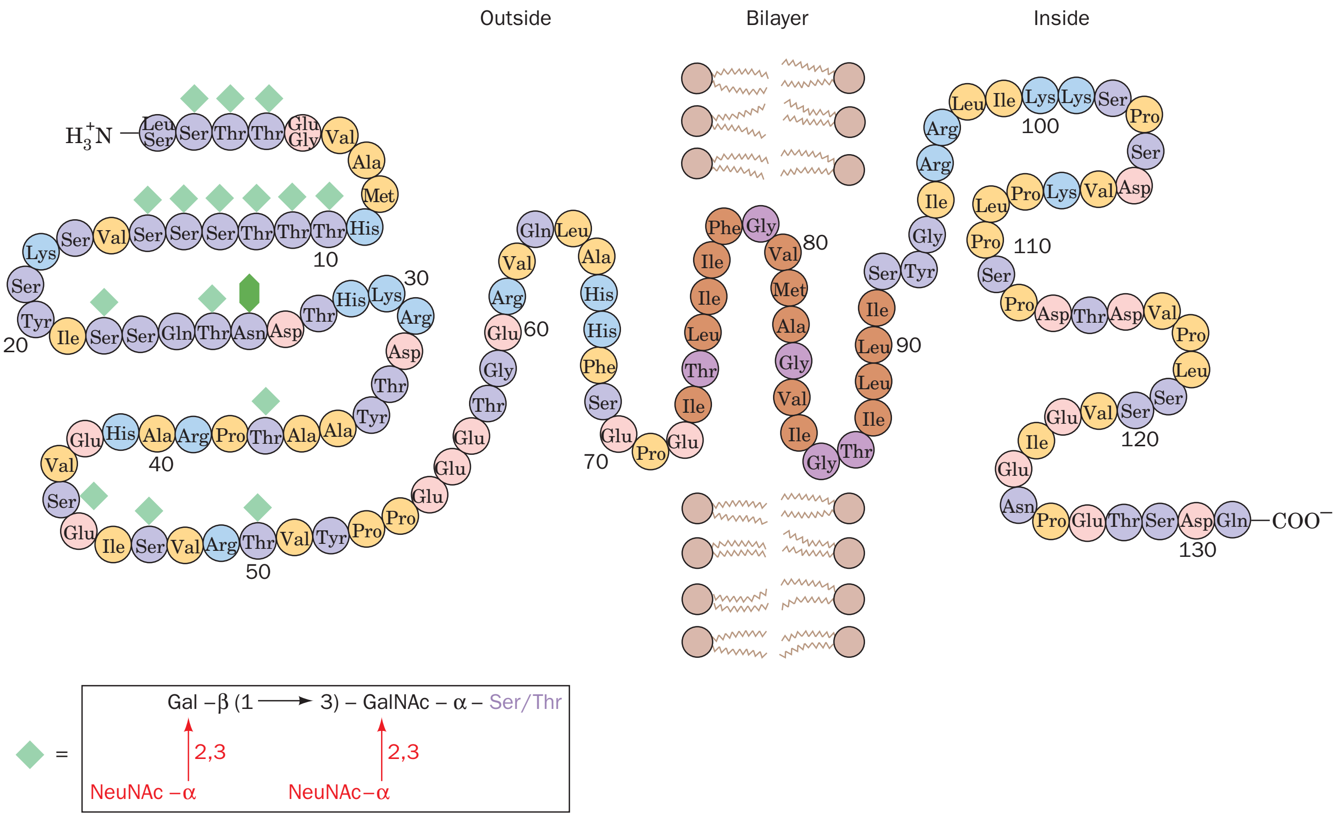
Outside
Bilayer
Inside
$H_3\overset{+}{N}$ —
Leu Ser Ser Thr Thr Glu Gly Val Ala Met His Thr Thr Thr Ser Ser Ser Val Ser Lys Ser Tyr Ile Ser Ser Gln Thr Asn Asp Thr His Lys Arg Asp Thr Tyr Ala Ala Thr Pro Arg Ala His Glu Val Ser Glu Ile Ser Val Arg Thr Val Tyr Pro Pro Glu Glu Glu Thr Gly Glu Arg Val Gln Leu Ala His His Phe Ser Glu Pro Glu Ile Thr Leu Ile Ile Phe Gly Val Met Ala Gly Val Ile Gly Thr Ile Leu Leu Ile Ser Tyr Gly Ile Arg Arg Leu Ile Lys Lys Ser Pro Ser Asp Val Lys Pro Leu Pro Ser Pro Asp Thr Asp Val Pro Leu Ser Ser Val Glu Ile Glu Asn Pro Glu Thr Ser Asp Gln
—COO⁻
10
20
30
40
50
60
70
80
90
100
110
120
130
=
Gal –β (1 ⟶ 3) – GalNAc – α – Ser/Thr
2,3
2,3
NeuNAc –α
NeuNAc –α

Figure 9-20 | Human erythrocyte glycophorin A. The protein bears 15 *O*-linked oligosaccharides (*green diamonds*) and one that is *N*-linked (*dark green hexagon*) on its extracellular domain. The predominant sequence of the *O*-linked oligosaccharides is also shown (NeuNAc = *N*-acetylneuraminic acid). The protein's transmembrane portion (*brown and purple*) consists of 19 sequential predominantly hydrophobic residues. Its C-terminal portion, which is located on the membrane's cytoplasmic face, is rich in anionic (*pink*) and cationic (*blue*) residues. There are two common genetic variants of glycophorin A: Glycophorin A^M has Ser and Gly at positions 1 and 5, whereas glycophorin A^N has Leu and Glu at these positions. [After Marchesi, V.T., *Semin. Hematol.* **16,** 8 (1979).]

located N-terminal domain that bears 16 carbohydrate chains; (2) a 19-residue sequence, consisting almost entirely of hydrophobic residues, that spans the erythrocyte cell membrane; and (3) a 40-residue cytoplasmic C-terminal domain that has a high proportion of charged and polar residues. Thus, glycophorin A is a **transmembrane (TM) protein;** that is, it completely spans the membrane.

Studies of a variety of biological membranes have established that *biological membranes are asymmetric in that a particular membrane protein is invariably located on only one particular face of a membrane, or in the case of a transmembrane protein, oriented in only one direction with respect to the membrane.* However, no protein is known to be completely buried in a membrane; that is, all membrane-associated proteins are at least partially exposed to the aqueous environment.

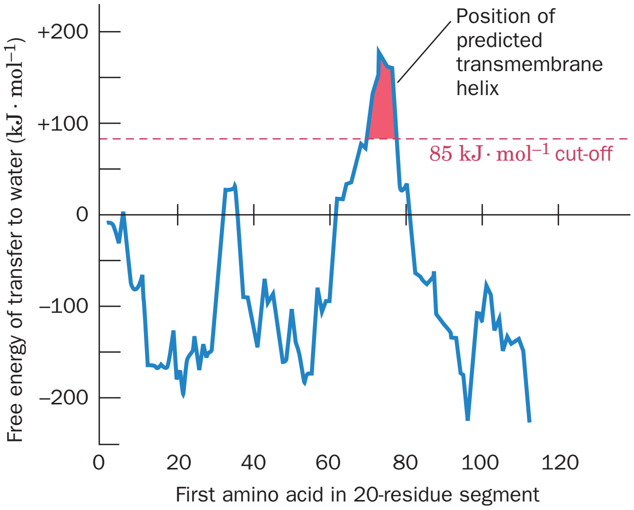

Figure 9-21 | Identification of glycophorin A's transmembrane domain. The calculated free energy change in transferring 20-residue-long α-helical segments from the interior of a membrane to water is plotted against the position of the segment's first residue. Peaks higher than +85 kJ · mol^{-1} indicate a transmembrane helix. [After Engelman, D.M., Steitz, T.A., and Goldman, A., *Annu. Rev. Biophys. Biophys. Chem.* **15,** 343 (1986).]

Transmembrane Proteins May Contain α Helices. In order for a polypeptide chain to penetrate or span the lipid bilayer, it must have hydrophobic side chains that contact the lipid tails and it must shield its polar backbone groups. This second requirement is met by the formation of secondary structure that satisfies the hydrogen-bonding capabilities of the polypeptide backbone. Consequently, all known TM segments of integral membrane proteins consist of either α helices or β sheets. For example, glycophorin A's 19-residue TM sequence almost certainly forms an α helix. The existence of such a TM helix can be predicted by comparing the free energy change in transferring α-helical polypeptide segments from the nonpolar interior of a membrane to water (Fig. 9-21). Alternatively, a potential TM sequence can be identified by reference to hydropathy indices such as those in Table 6-3. Methods for predicting the position of a TM α helix are useful because the difficulty in crystallizing integral membrane proteins has permitted relatively few of their X-ray structures to be determined.

Nigel Unwin and Richard Henderson used **electron crystallography** (Box 9-2) to determine the structure of the integral membrane protein **bacteriorhodopsin.** This 247-residue homotrimeric protein, which is produced by the halophilic (salt-loving) archaebacterium *Halobacterium salinarum* (it grows best in 4.3 M NaCl), is a light-driven proton pump: It generates a proton concentration gradient across the cell membrane that powers ATP synthesis by a mechanism discussed in Section 18-3B. A covalently bound retinal (Section 9-1F) is the protein's light-absorbing group. Bacteriorhodopsin consists largely of a bundle of seven ~25-residue α-helical rods that span the lipid bilayer in directions almost perpendicular to the bilayer plane (Fig. 9-22). As expected, the amino acid side chains that contact the lipid tails are highly hydrophobic. Successive membrane-spanning helices are connected in head-to-tail fashion by hydrophilic loops of varying size. This arrangement places the protein's charged residues near the surfaces of the membrane in contact with the aqueous environment.

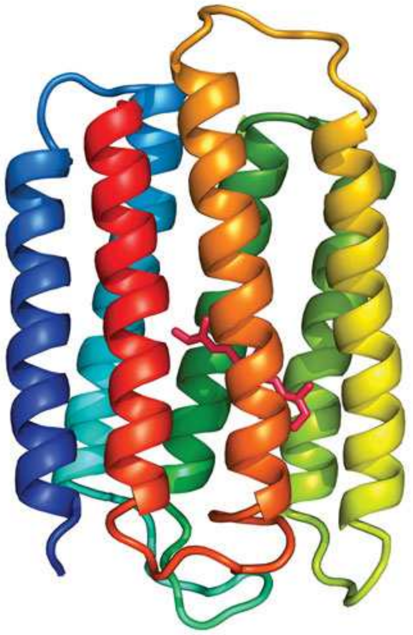

Figure 9-22 | The structure of bacteriorhodopsin. The protein is shown in ribbon form as viewed from within the membrane plane and colored in rainbow order from its N-terminus (*blue*) to its C-terminus (*red*). Its covalently bound retinal is drawn in stick form (*magenta*). [Based on an X-ray structure by Nikolaus Grigorieff and Richard Henderson, MRC Laboratory of Molecular Biology, Cambridge, U.K. PDBid 2BRD.] **See Kinemage Exercise 8-1.**

BOX 9-2 **PATHWAYS OF DISCOVERY**

Richard Henderson and the Structure of Bacteriorhodopsin

Richard Henderson (1945–)

Richard Henderson, like a number of other pioneering structural biologists, began his career as a physicist. He turned his attention to membrane proteins because of their importance in cellular metabolic, transport, and signaling phenomena. Unlike globular proteins, which are soluble in aqueous solution from which they can often be crystallized, integral membrane proteins aggregate in aqueous solution and hence can only be kept in solution by the presence of a suitable detergent. In spite of this, such solubilized proteins rarely crystallize in a manner suitable for X-ray analysis (and none had been made to do so at the time that Henderson began his studies). To circumvent this obstacle, Henderson adapted the technique of electron crystallography to macromolecules, using the membrane protein bacteriorhodopsin as his subject.

Bacteriorhodopsin was discovered in 1967, and its function as a proton pump was described shortly thereafter. The protein is synthesized by halophilic archaebacteria such as *H. salinarum* (formerly known as *H. halobium*). In addition to bacteriorhodopsin, the archaeal rhodopsin family includes chloride-pumping and sensory proteins. Similar proteins have also been identified in eubacteria and in unicellular eukaryotes. What made bacteriorhodopsin attractive as a research subject is its relatively small size (248 residues), its stability, and—most importantly—its unusual proclivity to form ordered two-dimensional arrays in the bacterial cell membrane. In *H. salinarum,* such arrays, which occur as 0.5-μm-wide patches, are known as purple membranes due to the color of the protein's bound retinal molecule. Each purple membrane patch, which is essentially a two-dimensional crystal, consists of 75% bacteriorhodopsin and 25% lipid.

At the time that Henderson began his structural studies of bacteriorhodopsin, the X-ray structures of only around a dozen different globular proteins had been reported. Henderson, working with Nigel Unwin, adapted the principles of X-ray crystallography to the two-dimensional bacteriorhodopsin crystals by measuring the diffraction intensities generated by the electron beam from an electron microscope impinging on a purple membrane patch (as explained by the wave–particle duality, electrons, like all particles, have wavelike properties with a wavelength, $\lambda = h/mv$, where h is Planck's constant, m is the particle mass, and v is its velocity). It was necessary to use an electron beam rather than X-rays because the electron microscope can focus its electron beam on the microscopically small purple membrane patches. Nevertheless, only very low electron beam intensities could be used because otherwise the resulting radiation damage would destroy the purple membrane. Consequently, to obtain diffraction data of sufficiently high signal-to-noise ratio, the diffraction patterns of around one hundred or more purple membrane samples had to be averaged.

Working at the limits of the available technology, Henderson and Unwin, in 1975, published a low-resolution model for the structure of bacteriorhodopsin. This was the first glimpse of an integral membrane protein. Its seven transmembrane helices were clearly visible as columns of electron density that were approximately perpendicular to the plane of the membrane. However, to obtain three-dimensional diffraction data, a two-dimensional crystal must be systematically tilted relative to the electron beam. Mechanical limitations that prevented the sample from being tilted to the degree necessary to obtain a full three-dimensional data set as well as other technical difficulties therefore yielded a model that had a resolution of 7 Å in the plane of the membrane, but only 14 Å in a perpendicular direction. Consequently, the polypeptide loops connecting the seven helices could not be discerned, nor were the protein's associated retinal molecule or any of its side chains visible. However, over the next 15 years, developments in electron microscopy, such as the use of better electron sources and liquid-helium temperatures to minimize radiation damage to the sample, permitted Henderson to extend the resolution of the bacteriorhodopsin structure to 3.5 Å in the plane of the membrane and 10 Å in the perpendicular direction. The resulting electron density map clearly revealed the positions of several bulky aromatic residues and the bound retinal and permitted the loops connecting the transmembrane helices to be visualized. Thus, electron crystallography has become a useful tool for determining the structures of a variety of proteins that can be induced to form two-dimensional arrays as well as those that form very thin three-dimensional crystals.

Henderson's groundbreaking work on bacteriorhodopsin made a seminal contribution to the growing body of biochemical, genetic, spectroscopic, and structural studies of bacteriorhodopsin. This information, together with more recent high-resolution X-ray structures derived from three-dimensional crystals of bacteriorhodopsin, obtained by crystallizing the protein in a lipid matrix, have led to a detailed understanding of the mechanism of the light-induced structural changes through which bacteriorhodopsin pumps protons out of the bacterial cell.

Henderson, R. and Unwin, P.N., Three-dimensional model of purple membrane obtained by electron microscopy, *Nature* **257,** 28–32 (1975).

Henderson, R., Baldwin, J.M., Ceska, T.A., Zemlin, F., Beckmann, E., and Downing, K.H., Model for the structure of bacteriorhodopsin based on high-resolution electron cryo-microscopy, *J. Mol. Biol*. **213,** 899–929 (1990).

Hydrophobic effects, as we saw in Section 6-4A, are the dominant forces stabilizing the three-dimensional structures of water-soluble globular proteins. However, since the TM regions of integral membrane proteins are immersed in nonpolar environments, what stabilizes their structures? Analysis of integral protein structures indicates that their interior residues have hydrophobicities comparable to those of water-soluble proteins. However, the membrane-exposed residues of these proteins, on average, are even more hydrophobic than their interior residues. Thus, *the difference between integral proteins and water-soluble proteins is only skin-deep: Their interiors are similar, but their surface polarities are consistent with the polarities of their environments*.

Some Transmembrane Proteins Contain β Barrels. A protein segment immersed in the nonpolar interior of a membrane must fold so that it satisfies the hydrogen-bonding potential of its polypeptide backbone. An α helix can do so as can an antiparallel β sheet that rolls up to form a barrel (a β barrel; Section 6-2C). Transmembrane β barrels of known structure consist of 8 to 22 strands. The number of strands must be even to permit the β sheet to close up on itself with all strands antiparallel.

β Barrels occur in **porins,** which are channel-forming proteins in the outer membrane of gram-negative bacteria (Section 8-3B). The outer membrane protects the bacteria from hostile environments while the porins permit the entry of small polar solutes such as nutrients. Porins also occur in eukaryotes in the outer membranes of mitochondria and chloroplasts (consistent with the descent of these organelles from free-living gram-negative bacteria; Section 1-2C).

Bacterial porins are monomers or trimers of identical 30- to 50-kD subunits. X-Ray structural studies show that most porin subunits consist largely of at least a 16-stranded antiparallel β barrel that forms a solvent-accessible central channel with a length of ~55 Å and a minimum diameter of ~7 Å (Fig. 9-23). As expected, the side chains of the protein's membrane-exposed surface are nonpolar, thereby forming a ~27-Å-high hydrophobic band encircling the trimer (Fig. 9-23*c*). This band is flanked by more polar aromatic side chains (Table 6-3) that form interfaces with the head groups of the lipid bilayer (Fig. 9-23*c*). In contrast, the side chains at the solvent-exposed surface of the protein, including those lining the walls of the aqueous channel, are polar. Possible mechanisms for the solute selectivity of porins are discussed in Section 10-2B.

B | Lipid-Linked Proteins Are Anchored to the Bilayer

Some membrane-associated proteins contain covalently attached lipids that anchor the protein to the membrane. The lipid group, like any modifying group, may also mediate protein–protein interactions or modify the structure and activity of the protein to which it is attached. **Lipid-linked**

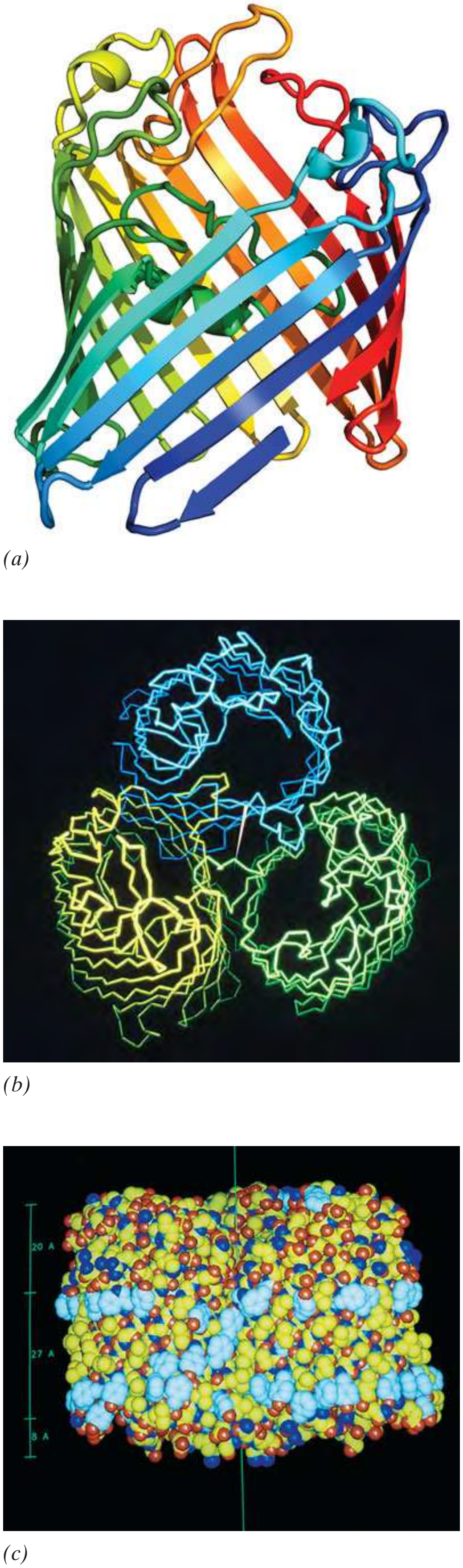

■ **Figure 9-23 | X-Ray structure of the *E. coli* OmpF porin.** (*a*) A ribbon diagram of the 16-stranded monomer colored in rainbow order from its N-terminus (*blue*) to its C-terminus (*red*). (*b*) The C_α backbone of the trimer viewed ~30° from its threefold axis of symmetry, showing the pore through each subunit. (*c*) A space-filling model of the trimer viewed perpendicular to its threefold axis (*vertical green line*). N atoms are blue, O atoms are red, and C atoms are yellow, except those in the side chains of aromatic residues, which are white. The aromatic groups appear to delimit an ~27-Å-high hydrophobic band (*scale at left*) that is immersed in the nonpolar portion of the bacterial outer membrane (with the cell's exterior at the tops of Parts *a* and *c*). [Part *a* based on an X-ray structure by and Parts *b* and *c* courtesy of Tilman Schirmer and Johan Jansonius, University of Basel, Switzerland. PDBid 1OPF.] **See Kinemage Exercise 8-3.**

proteins come in three varieties: prenylated proteins, fatty acylated proteins, and glycosylphosphatidylinositol-linked proteins. A single protein may contain more than one covalently linked lipid group.

Prenylated proteins have covalently attached lipids that are built from isoprene units (Section 9-1F). The most common isoprenoid groups are the C_{15} **farnesyl** and C_{20} **geranylgeranyl** residues:

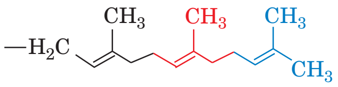

Farnesyl residue

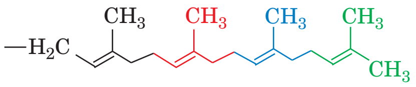

Geranylgeranyl residue

The most common prenylation site in proteins is the C-terminal tetrapeptide C-X-X-Y, where C is Cys and X is often an aliphatic amino acid residue. Residue Y influences the type of prenylation: Proteins are farnesylated when Y is Ala, Met, or Ser and geranylgeranylated when Y is Leu. In both cases, the prenyl group is enzymatically linked to the Cys sulfur atom via a thioether linkage. The X-X-Y tripeptide is then proteolytically excised, and the newly exposed terminal carboxyl group is esterified with a methyl group, producing a C-terminus with the structure

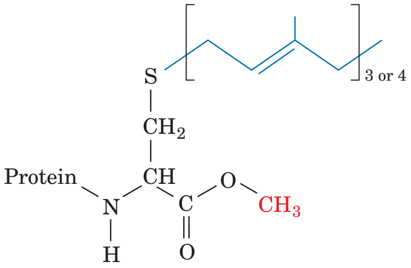

Two kinds of fatty acids, myristic acid and palmitic acid, are linked to membrane proteins. Myristic acid, a biologically rare saturated C_{14} fatty acid, is appended to a protein via an amide linkage to the α-amino group of an N-terminal Gly residue. **Myristoylation** is stable: The fatty acyl group remains attached to the protein throughout its lifetime. Myristoylated proteins are located in a number of subcellular compartments, including the cytosol, endoplasmic reticulum, plasma membrane, and the nucleus.

In **palmitoylation,** the saturated C_{16} fatty acid palmitic acid is joined in thioester linkage to a specific Cys residue. Palmitoylated proteins occur almost exclusively on the cytoplasmic face of the plasma membrane, where many participate in transmembrane signaling. The palmitoyl group can be removed by the action of **palmitoyl thioesterases,** suggesting that reversible palmitoylation may regulate the association of the protein with the membrane and thereby modulate the signaling processes.

Glycosylphosphatidylinositol-linked proteins (GPI-linked proteins) occur in all eukaryotes but are particularly abundant in some parasitic protozoa, which contain relatively few membrane proteins anchored by transmembrane polypeptide segments. Like glycoproteins and glycolipids, GPI-linked proteins are located only on the exterior surface of the plasma membrane.

The core structure of the GPI group consists of phosphatidylinositol (Table 9-2) glycosidically linked to a linear tetrasaccharide composed of

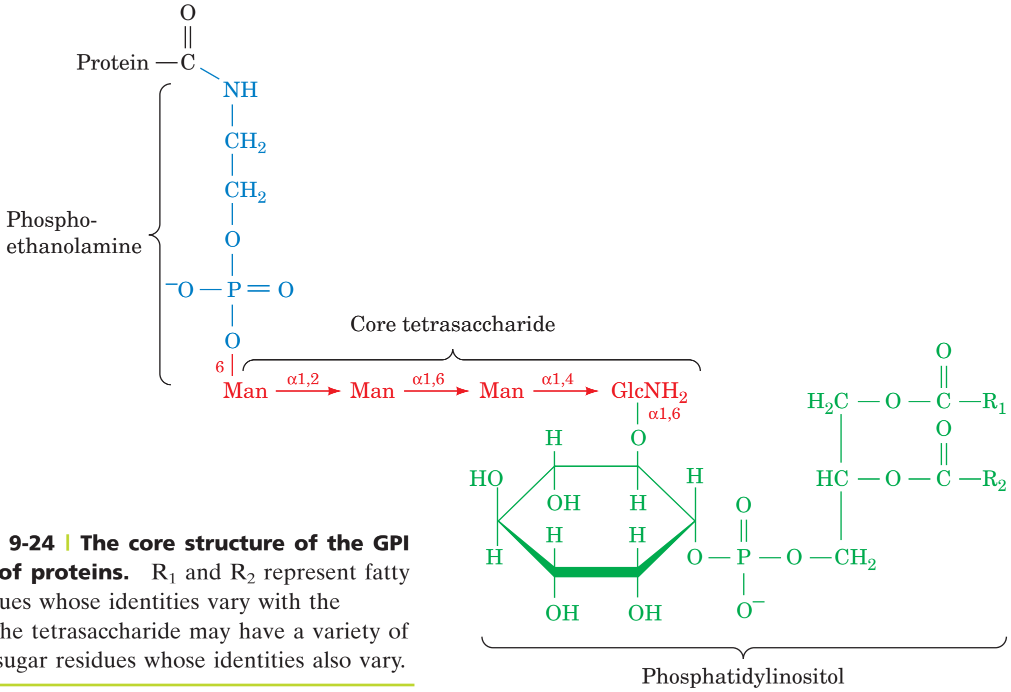

Figure 9-24 | The core structure of the GPI anchors of proteins. R_1 and R_2 represent fatty acid residues whose identities vary with the protein. The tetrasaccharide may have a variety of attached sugar residues whose identities also vary.

three mannose residues and one glucosaminyl residue (Fig. 9-24). The mannose at the nonreducing end of this assembly forms a phosphodiester bond with a phosphoethanolamine residue that is amide-linked to the protein's C-terminal carboxyl group. The core tetrasaccharide is generally substituted with a variety of sugar residues that vary with the identity of the protein. There is likewise considerable diversity in the fatty acid residues of the phosphatidylinositol group.

C | Peripheral Proteins Associate Loosely with Membranes

Peripheral or **extrinsic proteins,** unlike integral membrane proteins or lipid-linked proteins, can be dissociated from membranes by relatively mild procedures that leave the membrane intact, such as exposure to high ionic strength salt solutions or pH changes. Peripheral proteins do not bind lipid and, once purified, behave like water-soluble proteins. They associate with membranes by binding at their surfaces, most likely to certain lipids or integral proteins, through electrostatic and hydrogen-bonding interactions. Cytochrome *c* (Sections 5-4A, 6-2D, and 18-2E) is a peripheral membrane protein that is associated with the outer surface of the inner mitochondrial membrane. At physiological pH, cytochrome *c* is cationic and can interact with negatively charged phospholipids such as phosphatidylserine and phosphatidylglycerol.

CHECK YOUR UNDERSTANDING

Explain the differences between integral and peripheral membrane proteins.
What are the two types of secondary structures that occur in transmembrane proteins?
Describe the covalent modifications of lipid-linked proteins.

4 Membrane Structure and Assembly

LEARNING OBJECTIVES

- Understand how the arrangement and interactions of membrane lipids and proteins are described by the fluid mosaic model.
- Understand that the membrane skeleton gives the cell shape yet is flexible.
- Understand that lipids are not distributed uniformly throughout a membrane.
- Understand how the secretory pathway describes the transmembrane passage of membrane and secreted proteins.
- Understand that different types of coated vesicles transport proteins between cellular compartments.
- Understand the role of SNAREs in vesicle fusion.

Membranes were once thought to consist of a phospholipid bilayer sandwiched between two layers of unfolded polypeptide. This sandwich model, which is improbable on thermodynamic grounds, was further discredited by electron microscopic visualization of membranes and other experimental approaches. More recent studies have revealed insights into the fine structure of membranes, including a surprising degree of heterogeneity. In this section, we consider the arrangement of membrane proteins and lipids and examine some of the mechanisms by which these components move throughout the cell.

A | The Fluid Mosaic Model Accounts for Lateral Diffusion

See Guided Exploration 9
Membrane structure
and the fluid mosaic model.

The demonstrated fluidity of artificial lipid bilayers (Section 9-2B) suggests that biological membranes have similar properties. This idea was proposed in 1972 by S. Jonathan Singer and Garth Nicolson in their unifying theory of membrane structure known as the **fluid mosaic model.** In this model, integral proteins are visualized as "icebergs" floating in a two-dimensional lipid "sea" in a random or mosaic distribution (Fig. 9-25). A key element of the model is that integral proteins can diffuse laterally in the lipid matrix unless their movements are restricted by association with other cell components. This model of membrane fluidity explained the earlier experimental results of Michael Edidin, who fused cultured cells and observed the intermingling of their differently labeled cell-surface proteins (Fig. 9-26).

The rates of diffusion of proteins in membranes can be determined from measurements of **fluorescence recovery after photobleaching (FRAP).** In this technique, a **fluorophore** (fluorescent group) is specifically attached to a membrane component in an immobilized cell or in an artificial membrane system. An intense laser pulse focused on a very small area (~3 μm^2) destroys (bleaches) the fluorophore there (Fig. 9-27). The rate at which the bleached area recovers its fluorescence, as monitored by fluorescence microscopy, indicates the rate at which unbleached and bleached fluorophore-labeled molecules laterally diffuse into and out of the bleached area.

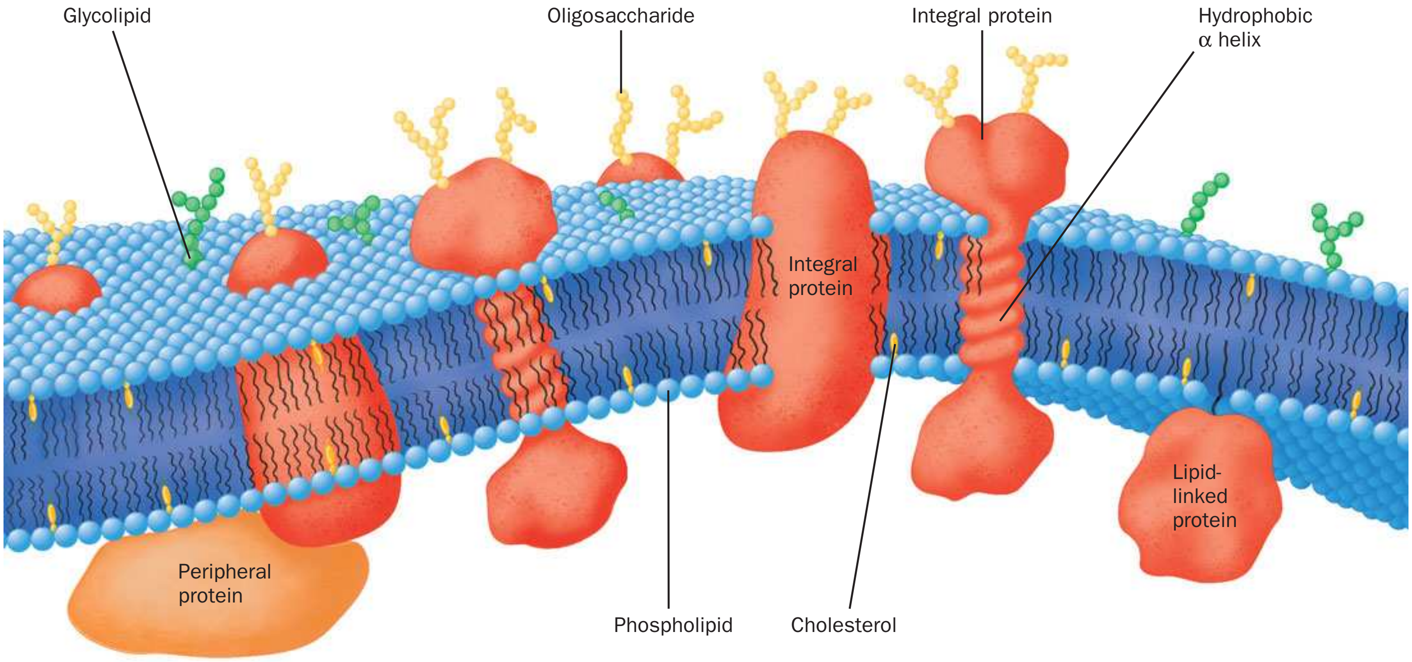

■ **Figure 9-25 | Diagram of a plasma membrane.** Integral proteins (*orange*) are embedded in a bilayer composed of phospholipids (*blue head groups attached to wiggly tails*) and cholesterol (*yellow*). The carbohydrate components (*green and yellow beads*) of glycoproteins and glycolipids occur on only the external face of the membrane. Most membranes contain a higher proportion of protein than is depicted here.

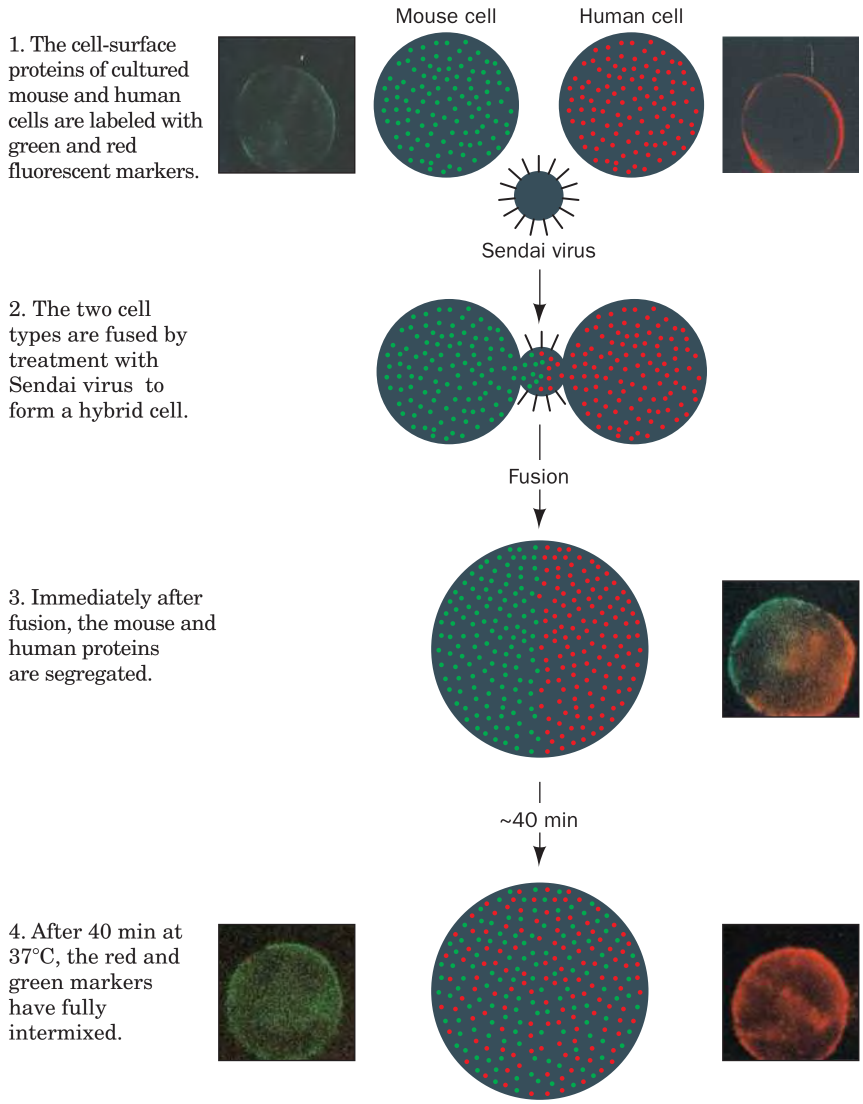
Mouse cell
Human cell
1. The cell-surface proteins of cultured mouse and human cells are labeled with green and red fluorescent markers.
Sendai virus
2. The two cell types are fused by treatment with Sendai virus to form a hybrid cell.
Fusion
3. Immediately after fusion, the mouse and human proteins are segregated.
~40 min
4. After 40 min at 37°C, the red and green markers have fully intermixed.

■ **Figure 9-26 | Fusion of mouse and human cells.** The accompanying photomicrographs (in square boxes) were taken through filters that allowed only red or green light to reach the camera. [Immunofluorescence photomicrographs courtesy of Michael Edidin, The Johns Hopkins University.]

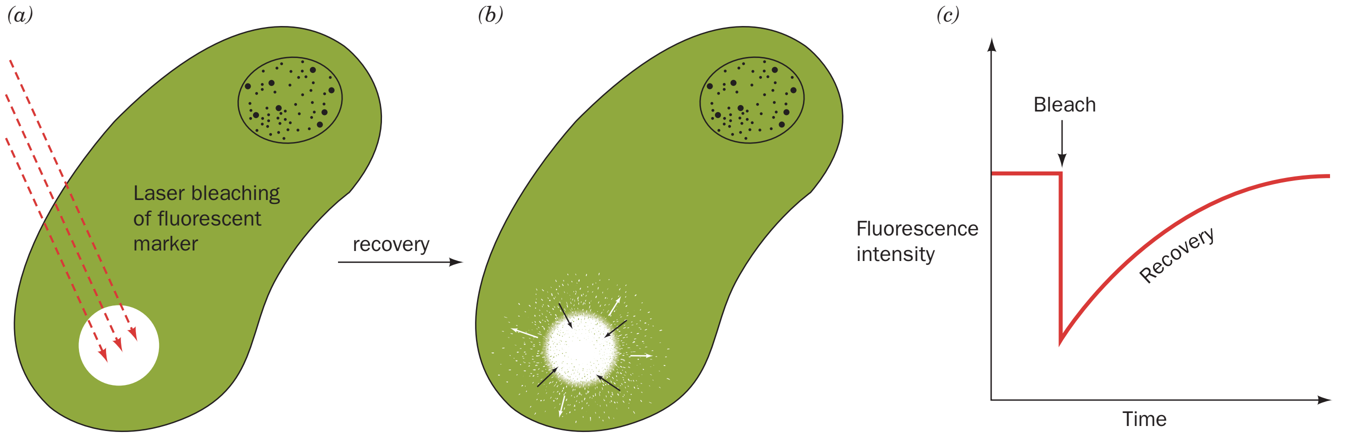
(a)
Laser bleaching of fluorescent marker
recovery
(b)
(c)
Bleach
Fluorescence intensity
Recovery
Time

■ **Figure 9-27 | The fluorescence recovery after photobleaching (FRAP) technique.** (*a*) An intense laser light pulse bleaches the fluorescent markers (*green*) from a small region of an immobilized cell that has a fluorophore-labeled membrane component. (*b*) The fluorescence of the bleached area recovers as the bleached molecules laterally diffuse out of it and intact fluorescent molecules diffuse into it. (*c*) The fluorescence recovery rate depends on the diffusion rate of the labeled molecule.

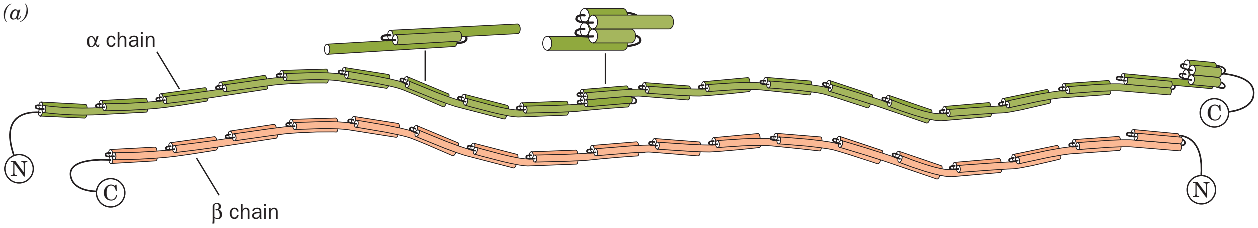

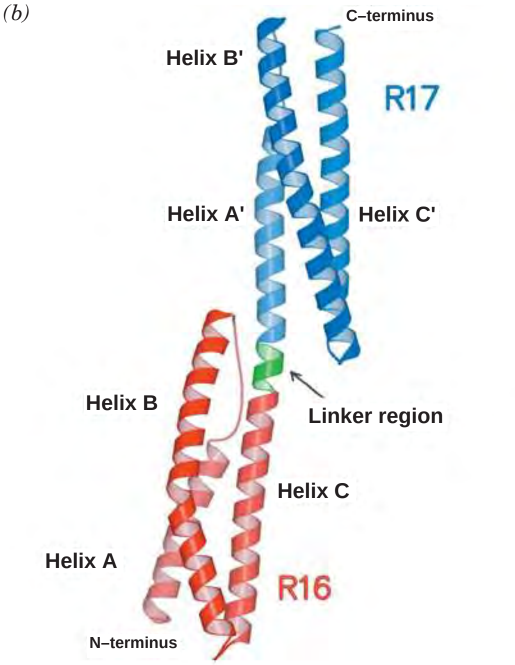

Figure 9-28 | Structure of spectrin. (*a*) Structure of an αβ dimer. Both of these antiparallel polypeptides contain multiple 106-residue repeats, which are thought to form flexibly connected triple-helical bundles. Two of these heterodimers join, head to head, to form an $(\alpha\beta)_2$ heterotetramer. [After Speicher, D.W. and Marchesi, V. *Nature* **311,** 177 (1984).] (*b*) The X-ray structure of two consecutive repeats of chicken brain α-spectrin. Each of these 106-residue repeats consists of an up–down–up triple-helical bundle in which the C-terminal helix of the first repeat (*red*) is continuous, via a 5-residue helical linker (*green*), with the N-terminal helix of the second repeat (*blue*). The helices within each triple-helical bundle wrap around each other in a gentle left-handed supercoil. [Courtesy of Alfonso Mondragón, Northwestern University. PDBid 1CUN.]

FRAP measurements demonstrate that membrane proteins vary in their lateral diffusion rates. Some 30 to 90% of these proteins are freely mobile; they diffuse at rates only an order of magnitude or so slower than those of the much smaller lipids, so they can diffuse the 20-μm length of a eukaryotic cell within an hour. Other proteins diffuse more slowly, and some are essentially immobile due to submembrane attachments.

B | The Membrane Skeleton Helps Define Cell Shape

Studies of membrane structure and composition often make use of erythrocyte membranes, since these are relatively simple and easily isolated. A mature mammalian erythrocyte lacks organelles and carries out few metabolic processes; it is essentially a membranous bag of hemoglobin. Erythrocyte membranes can be obtained by osmotic lysis, which causes the cell contents to leak out. The resulting membranous particles are known as erythrocyte **ghosts** because, on return to physiological conditions, they reseal to form colorless particles that retain their original shape but are devoid of cytoplasm.

A normal erythrocyte's biconcave disklike shape (Fig. 7-17*a*) ensures the rapid diffusion of O_2 to its hemoglobin molecules by placing them no further than 1 μm from the cell surface. However, the rim and the dimple regions of an erythrocyte do not occupy fixed positions on the cell membrane. This can be demonstrated by anchoring an erythrocyte to a microscope slide by a small portion of its surface and inducing the cell to move laterally with a gentle flow of buffer. A point originally on the rim of the erythrocyte will move across the dimple to the rim on the opposite side of the cell. Evidently, the membrane rolls across the cell while maintaining its shape, much like the tread of a tractor. This remarkable mechanical property of the erythrocyte membrane results from the presence of a submembranous network of proteins that function as a membrane "skeleton."

The fluidity and flexibility imparted to an erythrocyte by its membrane skeleton have important physiological consequences. A slurry of solid particles of a size and concentration equal to that of red cells in blood has flow characteristics approximating those of sand. Consequently, in order for blood to flow at all, much less for its erythrocytes to squeeze through capillary blood vessels smaller in diameter than they are, erythrocyte membranes, with their membrane skeletons, must be fluidlike and easily deformable.

The protein **spectrin,** so called because it was discovered in erythrocyte ghosts, accounts for ~75% of the erythrocyte membrane skeleton. It is composed of two similar polypeptide chains, a 280-kD α subunit and a 246-kD β subunit, which each consist of repeating 106-residue segments that fold into triple-stranded α-helical coiled coils (Fig. 9-28). These large polypeptides are loosely intertwined to form a flexible wormlike αβ dimer that is ~1000 Å long. Two such heterodimers further associate in a head-

■ **Figure 9-29 | The human erythrocyte membrane skeleton.** *(a)* An electron micrograph of an erythrocyte membrane skeleton that has been stretched to an area 9 to 10 times greater than that of the native membrane. Stretching makes it possible to obtain clear images of the membrane skeleton, which in its native state is densely packed and irregularly flexed. Note the predominantly hexagonal network composed of spectrin tetramers. [Courtesy of Daniel Branton, Harvard University.] *(b)* A model of the erythrocyte membrane skeleton with an inset showing its relationship to the intact erythrocyte. The junctions between spectrin tetramers include actin and tropomyosin (Section 7-2) and **band 4.1 protein** (named after its position in an SDS-PAGE electrophoretogram). [After Goodman, S.R., Krebs, K.E., Whitfield, C.F., Riederer, B.M., and Zagen, I.S., *CRC Crit. Rev. Biochem*. **23,** 196 (1988).]

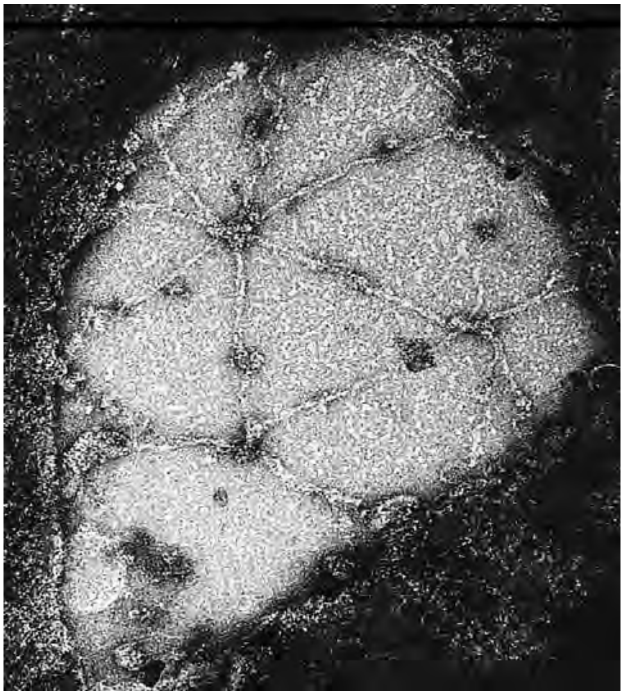

(a)

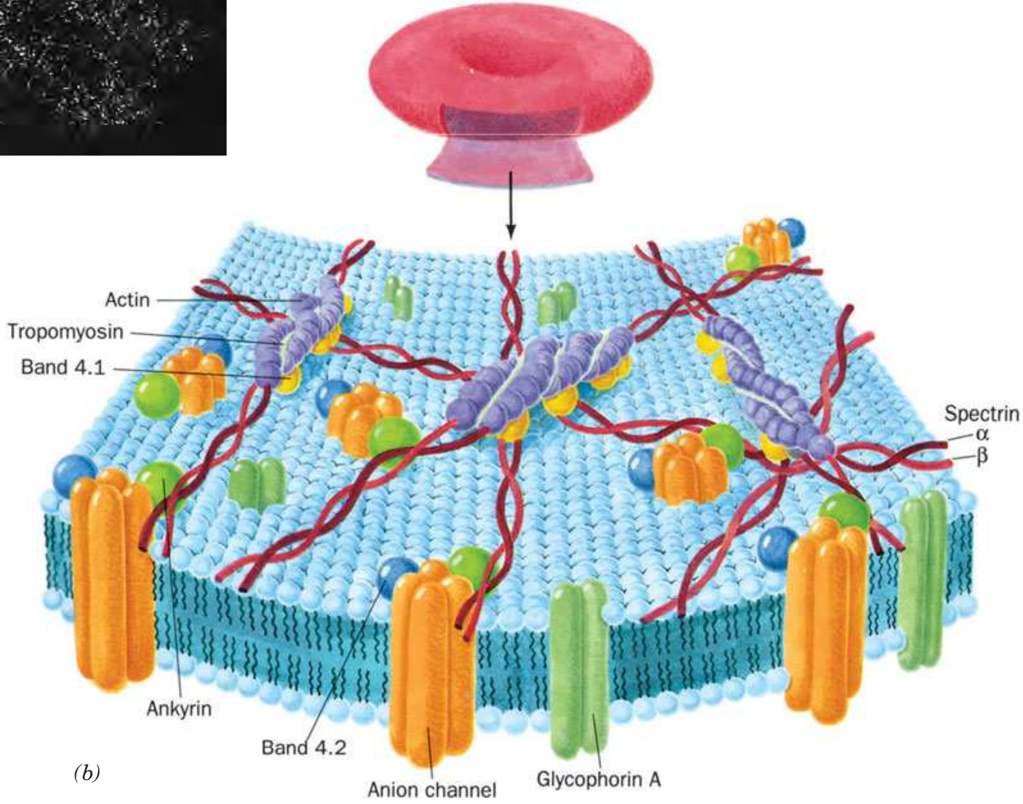

(b)

to-head manner to form an $(\alpha\beta)_2$ tetramer. Spectrin is a homolog of dystrophin, the muscle protein that is defective in muscular dystrophy (Section 7-2A).

There are ~100,000 spectrin tetramers per cell, and they are cross-linked at both ends by attachments to other cytoskeletal proteins. Together, these proteins form a dense and irregular protein meshwork that underlies the erythrocyte plasma membrane (Fig. 9-29). A defect or deficiency in spectrin synthesis causes **hereditary spherocytosis,** in which erythrocytes are spheroidal and relatively fragile and inflexible. Individuals with the disease suffer from anemia due to erythrocyte lysis and the removal of spherocytic cells by the spleen (which normally functions to

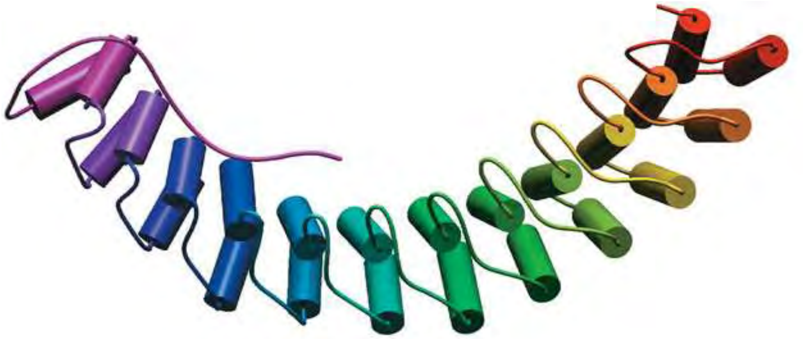

■ **Figure 9-30 | The X-ray structure of human ankyrin repeats 13 to 24.** The individual repeats are colored in rainbow order with repeat 13 red and repeat 24 violet. [Courtesy of Peter Michaely, University of Texas Southwestern Medical Center, Dallas, Texas. PDBid 1N11.]

filter out aged and hence inflexible erythrocytes from the blood at the end of their ~120-day lifetimes).

Spectrin also associates with an 1880-residue protein known as **ankyrin,** which binds to an integral membrane ion channel protein. This attachment anchors the membrane skeleton to the membrane. Immunochemical studies have revealed spectrin-like and ankyrin-like proteins in a variety of tissues, in addition to erythrocytes. Ankyrin's N-terminal 798-residue segment consists almost entirely of 24 tandem ~33-residue repeats known as **ankyrin repeats** (Fig. 9-30), which also occur in a variety of other proteins. Each ankyrin repeat consists of two short (8- or 9-residue) antiparallel α helices followed by a long loop. These structures are arranged in a right-handed helical stack. The entire assembly forms an elongated concave surface that is postulated to bind various integral proteins as well as spectrin.

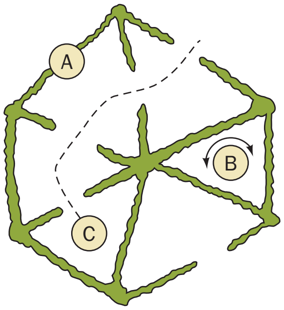

■ **Figure 9-31 | Model rationalizing the various mobilities of membrane proteins.** Protein A, which interacts tightly with the underlying cytoskeleton, is immobile. Protein B is free to rotate within the confines of the cytoskeletal "fences." Protein C diffuses by traveling through "gates" in the cytoskeleton. The diffusion of some membrane proteins is not affected by the cytoskeleton. [After Edidin, M., *Trends Cell Biol*. **2,** 378 (1992).]

The interaction of membrane components with the underlying skeleton helps explain why integral membrane proteins exhibit different degrees of mobility within the membrane: Some integral proteins are firmly attached to elements of the cytoskeleton or are trapped within the spaces defined by those "fences." Other membrane proteins may be able to squeeze through gaps or "gates" between cytoskeletal components, whereas still other proteins can diffuse freely without interacting with the cytoskeleton at all (Fig. 9-31). Support for this **gates and fences model** comes from the finding that partial destruction of the cytoskeleton results in freer protein diffusion.

C | Membrane Lipids Are Distributed Asymmetrically

The lipid and protein components of membranes do not occur in equal proportions on the two sides of biological membranes. For example, *membrane glycoproteins and glycolipids are invariably oriented with their carbohydrate moieties facing the cell's exterior*. The asymmetric distribution of certain membrane lipids between the inner and outer leaflets of a membrane was first established through the use of phospholipases (Section 9-1C). Phospholipases cannot pass through membranes, so phospholipids on only the external surface of intact cells are susceptible to hydrolysis by these enzymes. Such studies reveal that lipids in biological membranes are asymmetrically distributed (e.g., Fig. 9-32). How does this asymmetry arise?

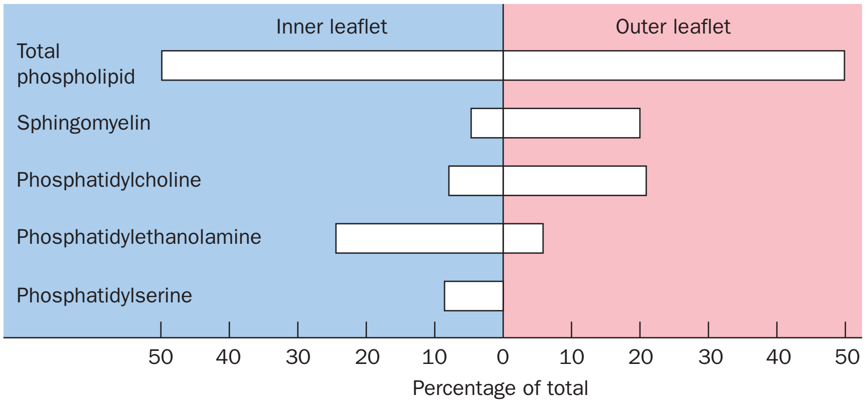

Figure 9-32 | Asymmetric distribution of membrane phospholipids in the human erythrocyte membrane. The phospholipid content is expressed as mol %. [After Rothman, J.E. and Lenard, J., *Science* **194,** 1744 (1977).]

In eukaryotes, the enzymes that synthesize membrane lipids are mostly integral membrane proteins of the **endoplasmic reticulum** (**ER;** the interconnected membranous vesicles that occupy much of the cytosol; Fig. 1-8), whereas in prokaryotes, lipids are synthesized by integral membrane proteins in the plasma membrane. Hence, membrane lipids are fabricated on site. Eugene Kennedy and James Rothman demonstrated this to be the case in bacteria through the use of selective labeling. They gave growing bacteria a 1-minute pulse of $^{32}PO_4^{3-}$ in order to radioactively label the phosphoryl groups of only the newly synthesized phospholipids. Immediately afterward, they added **trinitrobenzenesulfonic acid (TNBS),** a membrane-impermeable reagent that combines with phosphatidylethanolamine (**PE;** Fig. 9-33). Analysis of the resulting doubly labeled membranes showed that none of the TNBS-labeled PE was

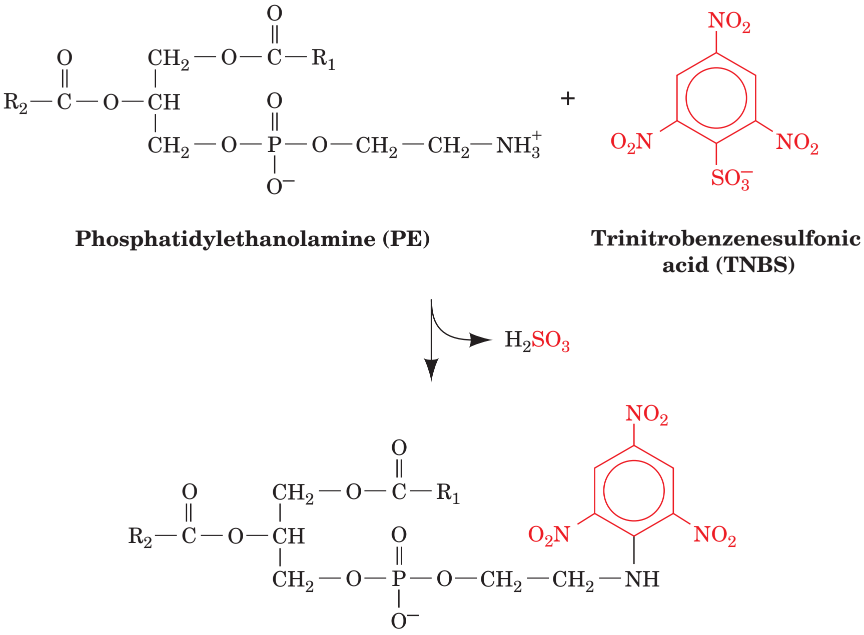
Phosphatidylethanolamine (PE)
Trinitrobenzenesulfonic acid (TNBS)
H_2SO_3

Figure 9-33 | The reaction of TNBS with phosphatidylethanolamine.

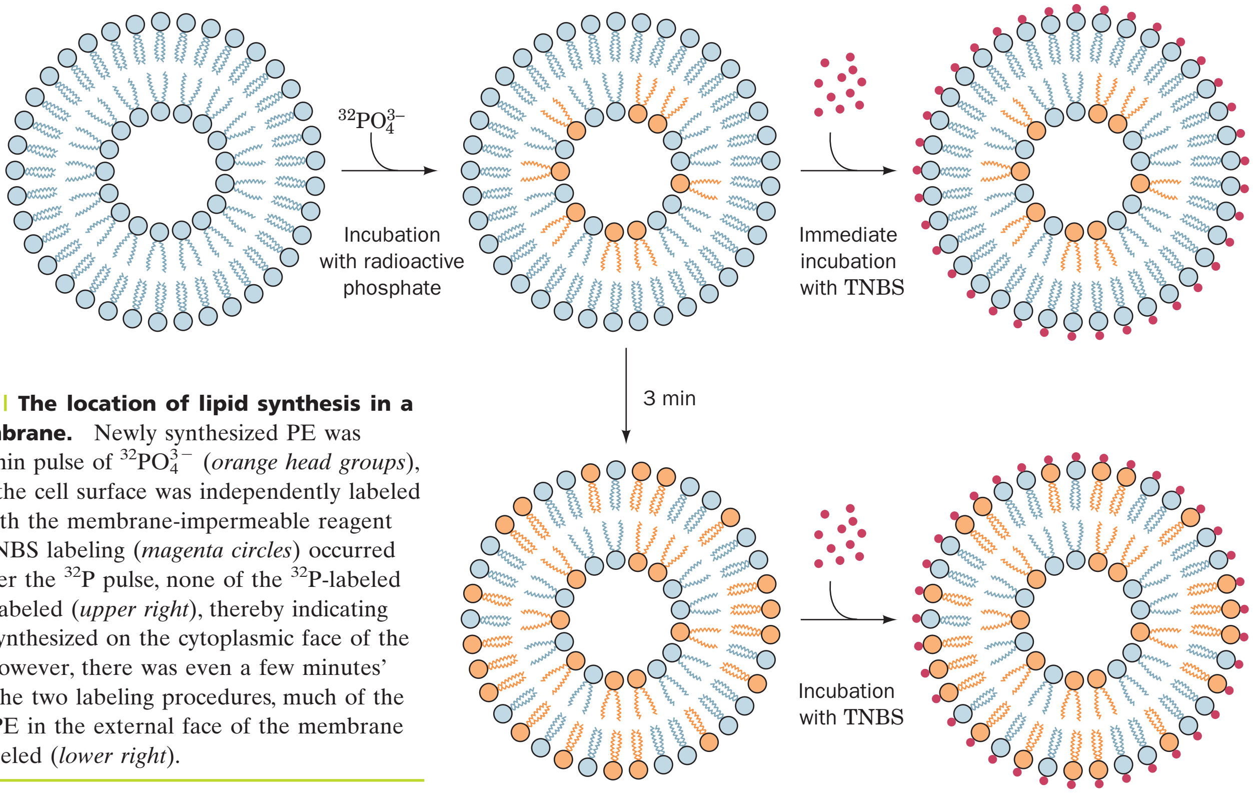
$^{32}PO_4^{3-}$
Incubation with radioactive phosphate
Immediate incubation with TNBS
3 min
Incubation with TNBS

Figure 9-34 | The location of lipid synthesis in a bacterial membrane. Newly synthesized PE was labeled by a 1-min pulse of $^{32}PO_4^{3-}$ (*orange head groups*), and the PE on the cell surface was independently labeled by treatment with the membrane-impermeable reagent TNBS. When TNBS labeling (*magenta circles*) occurred immediately after the ^{32}P pulse, none of the ^{32}P-labeled PE was TNBS labeled (*upper right*), thereby indicating that the PE is synthesized on the cytoplasmic face of the membrane. If, however, there was even a few minutes' delay between the two labeling procedures, much of the TNBS-labeled PE in the external face of the membrane was also ^{32}P labeled (*lower right*).

radioactively labeled. This observation indicates that *newly made PE is synthesized on the cytoplasmic face of the membrane* (Fig. 9-34, *upper right*).

However, if an interval of only 3 minutes was allowed to elapse between the $^{32}PO_4^{3-}$ pulse and the TNBS addition, about half of the ^{32}P-labeled PE was also TNBS labeled (Fig. 9-34, *lower right*). This observation indicates that the flip-flop rate of PE in the bacterial membrane is ~100,000-fold greater than it is in bilayers consisting of only phospholipids (where the flip-flop rates have half-times of many days).

How do phospholipids synthesized on one side of the membrane reach its other side so quickly? Phospholipid flip-flops in bacteria as well as eukaryotes appear to be facilitated in two ways:

1. Membrane proteins known as **flipases** catalyze the flip-flops of specific phospholipids. These proteins tend to equilibrate the distribution of their corresponding phospholipids across a bilayer; that is, the net transport of a phospholipid is from the side of the bilayer with the higher concentration of the phospholipid to the opposite side. Such a process, as we shall see in Section 10-1, is a form of **facilitated diffusion.**
2. Membrane proteins known as **phospholipid translocases** transport specific phospholipids across a bilayer in a process that is driven by ATP hydrolysis. These proteins can transport certain phospholipids from the side of a bilayer that has the lower concentration of the phospholipid to the opposite side, thereby establishing a nonequilibrium distribution of the phospholipid. Such a process, as we shall see in Section 10-3, is a form of **active transport.**

The observed distribution of phospholipids across membranes (e.g., Fig. 9-32) therefore appears to arise from the membrane orientations of the enzymes that synthesize phospholipids combined with the countervailing tendencies of ATP-dependent phospholipid translocases that generate asymmetric phospholipid distributions and flipases that equilibrate these distributions. The importance of these lipid transport systems is demonstrated by the observation that the presence of phosphatidylserine on the exteriors of many cells induces blood clotting (i.e., it is an indication of tissue damage) and, in erythrocytes, marks the cell for removal from the circulation.

In all cells, *new membranes are generated by the expansion of existing membranes*. In eukaryotic cells, lipids synthesized on the cytoplasmic face of the ER are transported to other parts of the cell by membranous vesicles that bud off from the ER and fuse with other cellular membranes. These vesicles also carry membrane proteins.

Lipid Rafts Are Membrane Subdomains. *Lipids and proteins in membranes can also be laterally organized*. Thus the plasma membranes of many eukaryotic cells have two or more distinct domains that have different functions. For example, the plasma membranes of epithelial cells (the cells lining body cavities and free surfaces) have an **apical domain,** which faces the lumen (interior) of the cavity and often has a specialized function (such as the absorption of nutrients in intestinal brush border cells), and a **basolateral domain,** which covers the remainder of the cell. These two domains, which do not intermix, have different compositions of both lipids and proteins.

In addition, the hundreds of different lipids and proteins within a given plasma membrane domain may not be uniformly mixed but instead often segregate to form **microdomains** that are enriched in certain lipids and proteins. This may result from specific interactions between integral membrane proteins and particular types of membrane lipids. Divalent metal ions, notably Ca^{2+}, which bind to negatively charged lipid head groups such as those of phosphatidylserine, may also cause clustering of these lipids.

One type of microdomain, termed a **lipid raft,** appears to consist of closely packed glycosphingolipids (which occur only in the outer leaflet of the plasma membrane) and cholesterol. By themselves, glycosphingolipids cannot form bilayers because their large head groups prevent the requisite close packing of their predominantly saturated hydrophobic tails. Conversely, cholesterol by itself does not form a bilayer due to its small head group. It is therefore likely that *the glycosphingolipids in lipid rafts associate laterally via weak interactions between their carbohydrate head groups, and the voids between their tails are filled in by cholesterol*.

Owing to the close packing of their component lipids and the long, saturated sphingolipid tails, sphingolipid–cholesterol rafts have a more ordered or crystalline arrangement than other regions of the membrane and are more resistant to solubilization by detergents. The rafts may diffuse laterally within the membrane. Certain proteins preferentially associate with the rafts, including many GPI-linked proteins and some of the proteins that participate in transmembrane signaling processes (Chapter 13). This suggests that lipid rafts, which are probably present in all cell types, function as platforms for the assembly of complex intercellular signaling systems. Several viruses, including influenza virus, measles virus, Ebola virus, and HIV, localize to lipid rafts, which therefore appear to be the sites from which these viruses enter uninfected cells and bud from infected cells. It should be noted that lipid rafts are highly dynamic structures that rapidly exchange both proteins and lipids with their surrounding membrane as a consequence of the weak and transient interactions between membrane components.

Caveolae (Latin for small caves), which are ~75-nm-diameter flask-shaped invaginations (infoldings) on the plasma membrane, are specialized forms of lipid rafts that are associated with ~21-kD integral proteins named **caveolins.** Caveolae, which occur mainly on muscle and epithelial cells, participate in **endocytosis** (the internalization of receptor-bound ligands; Section 20-1B) as well as intercellular signaling.

D | The Secretory Pathway Generates Secreted and Transmembrane Proteins

In contrast to membrane lipids, membrane proteins do not change their orientation in the membrane after they are synthesized. Membrane proteins, like all proteins, are ribosomally synthesized under the direction of messenger RNA templates (translation is discussed in Chapter 27). The polypeptide grows from its N-terminus to its C-terminus by the stepwise addition of amino acid residues. Ribosomes may be free in the cytosol or bound to the ER to form the **rough endoplasmic reticulum** (**RER,** so called because of the knobby appearance its bound ribosomes give it; Fig. 1-8). *Free ribosomes synthesize mostly soluble and mitochondrial proteins, whereas membrane-bound ribosomes manufacture transmembrane proteins and proteins destined for secretion, operation within the ER, and incorporation into* ***lysosomes*** (Fig. 1-8; membranous vesicles containing a battery of hydrolytic enzymes that degrade and recycle cell components). The latter proteins initially appear in the ER.

Secreted and Transmembrane Proteins Pass through the ER Membrane. How are RER-destined proteins differentiated from other proteins? And how do these large, relatively polar molecules pass through the RER membrane? These processes occur via the **secretory pathway,** which was first described by Günter Blobel, Cesar Milstein, and David Sabatini around 1975. Since ~25% of the various proteins synthesized by all types of cells are integral proteins and many others are secreted, *~40% of the various types of proteins that a cell synthesizes must be processed via the secretory pathway or some other protein targeting pathway*. Here we outline the secretory pathway, which is diagrammed in Fig. 9-35:

1. *All secreted, ER-resident, and lysosomal proteins, as well as many TM proteins, are synthesized with leading (N-terminal) 13- to 36-residue* ***signal peptides.*** These signal peptides consist of a 6- to 15-residue hydrophobic core flanked by several relatively hydrophilic residues that usually include one or more basic residues near the N-terminus (Fig. 9-36). Signal peptides otherwise have little sequence similarity. However, a variety of evidence indicates they form α helices in nonpolar environments.
2. When the signal peptide first protrudes beyond the ribosomal surface (when the polypeptide is at least ~40 residues long), the **signal recognition particle (SRP),** a 325-kD complex of six different polypeptides and a 300-nucleotide RNA molecule, binds to both the signal peptide and the ribosome (Section 27-5B). At the same time, the SRP's bound **guanosine diphosphate** (**GDP;** the guanine analog of ADP) is replaced by **guanosine triphosphate** (**GTP;** the guanine analog of ATP). The resulting conformational change in the SRP causes the ribosome to arrest further polypeptide growth, thereby preventing the RER-destined protein from being released into the cytosol.

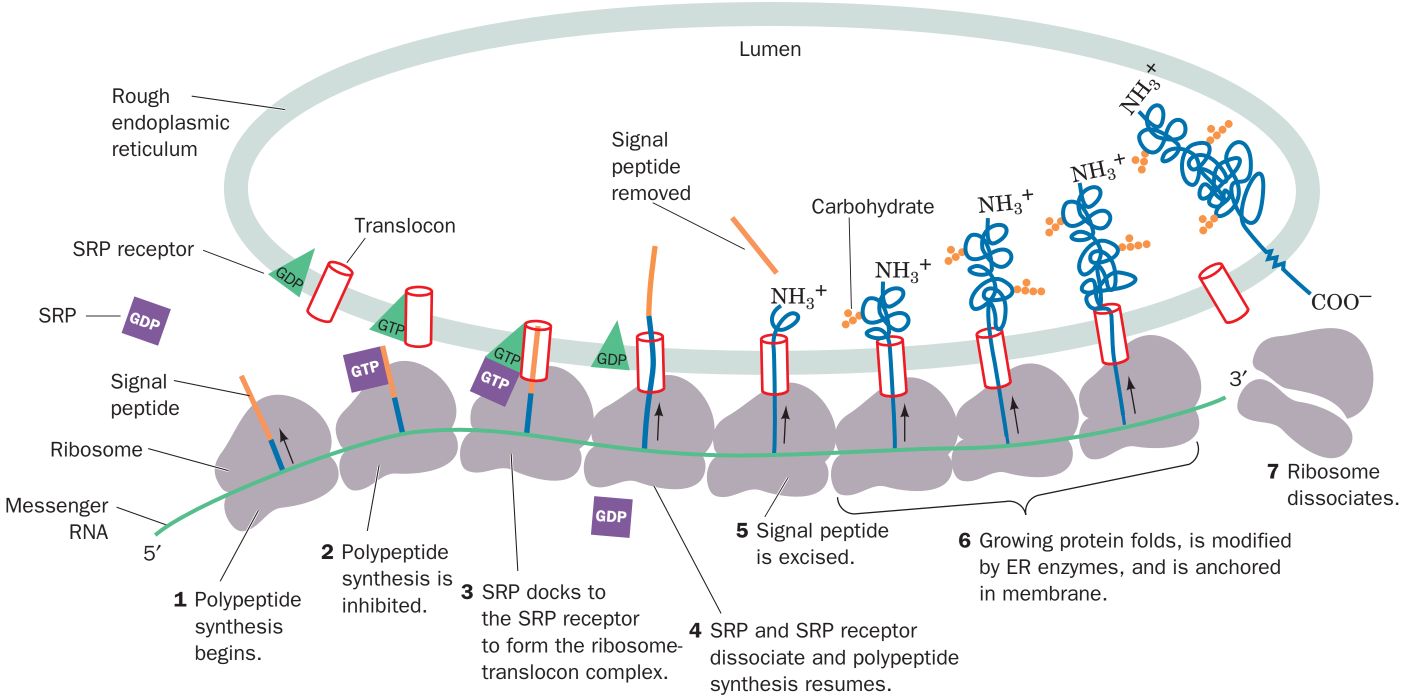
Lumen
Rough endoplasmic reticulum
Signal peptide removed
Carbohydrate
Translocon
SRP receptor
GDP
SRP
GDP
GTP
GTP
GTP
GTP
GDP
GDP
Signal peptide
Ribosome
Messenger RNA
5′
3′
NH_3^+
NH_3^+
NH_3^+
NH_3^+
NH_3^+
COO^-
1 Polypeptide synthesis begins.
2 Polypeptide synthesis is inhibited.
3 SRP docks to the SRP receptor to form the ribosome-translocon complex.
4 SRP and SRP receptor dissociate and polypeptide synthesis resumes.
5 Signal peptide is excised.
6 Growing protein folds, is modified by ER enzymes, and is anchored in membrane.
7 Ribosome dissociates.

■ **Figure 9-35** | **The ribosomal synthesis, membrane insertion, and initial glycosylation of an integral protein via the secretory pathway.** Details are given in the text. **See the Animated Figures.**

3. The SRP–ribosome complex diffuses to the RER surface, where it binds to the **SRP receptor (SR;** also called **docking protein)** in complex with the **translocon,** a protein pore in the ER membrane through which the growing polypeptide will be extruded. In forming the SR–translocon complex, the SR's bound GDP is replaced by GTP.

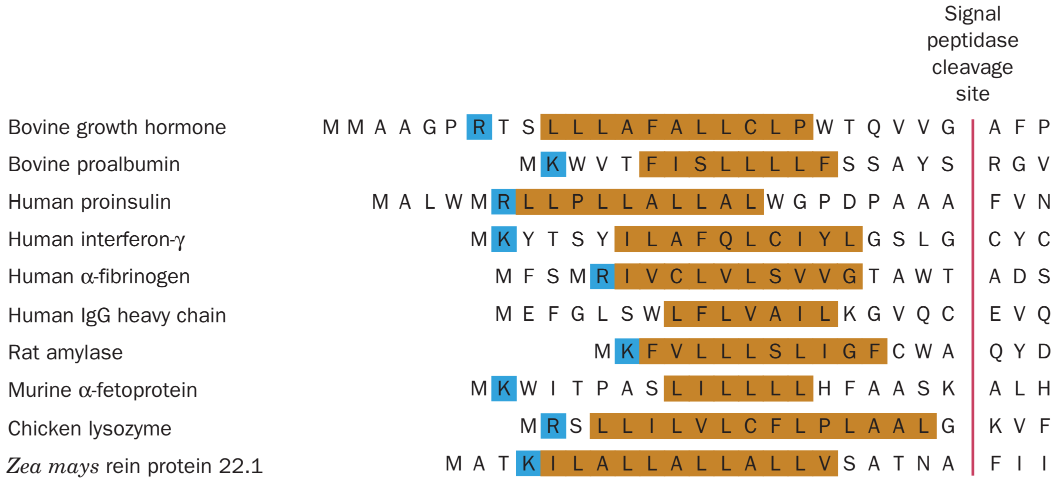

		Signal peptidase cleavage site
Bovine growth hormone	M M A A G P R T S L L L A F A L L C L P W T Q V V G	A F P
Bovine proalbumin	M K W V T F I S L L L L F S S A Y S	R G V
Human proinsulin	M A L W M R L L P L L A L L A L W G P D P A A A	F V N
Human interferon-γ	M K Y T S Y I L A F Q L C I Y L G S L G	C Y C
Human α-fibrinogen	M F S M R I V C L V L S V V G T A W T	A D S
Human IgG heavy chain	M E F G L S W L F L V A I L K G V Q C	E V Q
Rat amylase	M K F V L L L S L I G F C W A	Q Y D
Murine α-fetoprotein	M K W I T P A S L I L L L L H F A A S K	A L H
Chicken lysozyme	M R S L L I L V L C F L P L A A L G	K V F
Zea mays rein protein 22.1	M A T K I L A L L A L L A L L V S A T N A	F I I

■ **Figure 9-36** | **The N-terminal sequences of some eukaryotic preproteins.** The hydrophobic cores (*brown*) of most signal peptides are preceded by basic residues (*blue*). [After Watson, M.E.E., *Nucleic Acids Res.* **12,** 5147–5156 (1984).]

4. The SRP and SR stimulate each other to hydrolyze their bound GTP to GDP (which is energetically equivalent to ATP hydrolysis), resulting in conformational changes that causes them to dissociate from each other and from the ribosome–translocon complex. This permits the bound ribosome to resume polypeptide synthesis such that the growing polypeptide's N-terminus passes through the translocon into the lumen of the ER. Most ribosomal processes, as we shall see in Section 27-4, are driven by GTP hydrolysis.
5. Shortly after the signal peptide enters the ER lumen, it is specifically cleaved from the growing polypeptide by a membrane-bound **signal peptidase** (polypeptide chains with their signal peptide still attached are known as **preproteins;** signal peptides are alternatively called **presequences**).
6. The nascent (growing) polypeptide starts to fold to its native conformation, a process that is facilitated by its interaction with the ER-resident chaperone protein Hsp70 (Section 6-5B). Enzymes in the ER lumen then initiate **posttranslational modification** of the polypeptide, such as the specific attachments of "core" carbohydrates to form glycoproteins (Section 8-3C) and the formation of disulfide bonds as facilitated by protein disulfide isomerase (Section 6-5A). Once the protein has folded, it cannot be pulled back through the membrane. Secretory, ER-resident, and lysosomal proteins pass completely through the RER membrane into the lumen. TM proteins, in contrast, contain one or more hydrophobic ~20-residue **membrane anchor** sequences that remain embedded in the membrane.
7. When the synthesis of the polypeptide is completed, it is released from both the ribosome and the translocon. The ribosome detaches from the RER, and its two subunits dissociate.

The secretory pathway also functions in prokaryotes for the insertion of certain proteins into the cell membrane (whose exterior is equivalent to the ER lumen). Indeed, all forms of life yet tested have homologous SRPs, SRs, and translocons. Nevertheless, it should be noted that cells have several mechanisms for installing proteins in or transporting them through membranes. For example, cytoplasmically synthesized proteins that reside in the mitochondrion reach their destinations via mechanisms that are substantially different from that of the secretory pathway.

The Translocon Is a Multifunctional Transmembrane Pore. In 1975, Blobel postulated that protein transport through the RER membrane is mediated by an aqueous TM channel. However, it was not until 1991 that he was able to experimentally demonstrate its existence. These channels, now called translocons, enclose aqueous pores that completely span the ER membrane, as shown by linking nascent polypeptide chains to fluorescent dyes whose fluorescence is sensitive to the polarity of their environment. The channel-forming component of the translocon is a heterotrimeric protein named **Sec61** in mammals and **SecY** in prokaryotes. This protein is conserved throughout all kingdoms of life and hence is likely to have a similar structure and function in all organisms.

The X-ray structure of the SecY complex from the archaeon *Methanococcus jannaschii* reveals that the α, β, and γ subunits, respectively, have 10, 1, and 1 TM α helices (Fig. 9-37). The α subunit's TM helices are wrapped around an hourglass-shaped channel whose minimum diameter is ~3 Å. The channel is blocked at its extracellular end by a short

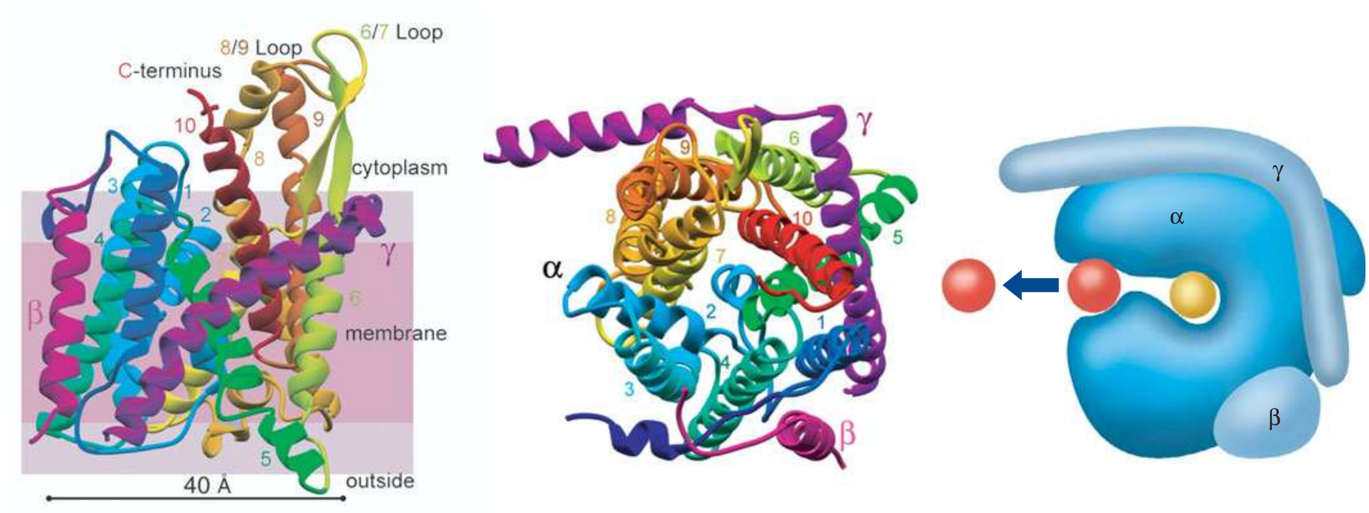

(a) *(b)* *(c)*

Figure 9-37 | Structure and function of the *M. jannaschii* SecY complex. (*a*) X-Ray structure of the complex, with shading indicating the positions of membrane phospholipid head groups (*gray*) and hydrocarbon tails (*violet*). The α subunit of SecY is colored in rainbow order from its N-terminus (*dark blue*) to its C-terminus (*red-orange*), the β subunit is red, and the γ subunit is magenta. (*b*) View of SecY from the cytosol. The translocon's putative lateral gate is on the left between helices 2 and 7. (*c*) Model for the insertion of a TM helix into a membrane. The translocon (*blue*) is viewed as in Part *b*. A polypeptide chain (*yellow*) is shown bound in the translocon's pore during its translocation through the membrane, and a signal-anchor sequence (*red*) is shown passing through the translocon's lateral gate and being released into the membrane (*arrow*). [Parts *a* and *b* courtesy of Stephen Harrison and Tom Rapoport, Harvard Medical School. PDBid 1RH5. Part *c* after a drawing by Dobberstein, B. and Sinning, I., *Science* **303,** 320 (2004).]

relatively hydrophilic helix (blue unnumbered helix in Figs. 9-37*a* and *b*). It is proposed that an incoming signal peptide pushes this helix aside and hence that the helix functions as a plug to prevent small molecules from leaking across the membrane in the absence of a translocating polypeptide. The maximum diameter of an extended polypeptide is ~12 Å and that of an α helix is ~14 Å. In order for SecY to function as a channel for translocating polypeptides, the central pore must expand, a structural change that would require relatively simple hingelike motions involving conserved Gly residues.

In addition to forming a conduit for soluble proteins to pass through the membrane, *the translocon must mediate the insertion of an integral protein's TM segments into the membrane*. The X-ray structure of SecY suggests that this occurs by the opening of the C-shaped α subunit, as is diagramed in Fig. 9-37*c*, to permit the lateral installation of the TM segment into the membrane.

The signal peptides of many TM proteins are not cleaved by signal peptidase but, instead, are inserted into the membrane. Such so-called ***signal-anchor sequences*** *may be oriented with either their N- or C-termini in the cytosol.* If the N-terminus is installed in the cytosol, then the polypeptide must have looped around before being inserted into the membrane. Moreover, for **polytopic** (multispanning) TM proteins such as the SecY α subunit itself, this must occur for each successive TM helix. Since it seems unlikely that the SecY channel could expand to simultaneously accommodate numerous TM helices, these helices are probably installed in the membrane one or two at a time. The mechanisms by which the translocon recognizes TM segments are not well understood. For example, the experimental deletion or insertion of a TM helix in a polytopic protein does not necessarily change the membrane orientations of the succeeding TM helices; when two successive TM helices have the same preferred orientation, one of them may be forced out of the membrane.

E | Intracellular Vesicles Transport Proteins

Shortly after their polypeptide synthesis is completed, partially processed transmembrane, secretory, and lysosomal proteins appear in the Golgi apparatus (Fig. 1-8). This 0.5- to 1.0-μm-diameter organelle consists of a stack of three to six or more (depending on the species) flattened and functionally distinct membranous sacs known as **cisternae,** where further posttranslational processing, mainly glycosylation, occurs (Section 8-3C). The Golgi stack (Fig. 9-38) has two distinct faces, each composed of a network of interconnected membranous tubules: the **cis Golgi network (CGN),** which is opposite the ER and is the port through which proteins enter the Golgi apparatus; and the **trans Golgi network (TGN),** through which processed proteins exit to their final destinations. The intervening Golgi stack contains at least three different types of sacs, the **cis, medial,** and **trans cisternae,** each of which contains different sets of glycoprotein-processing enzymes.

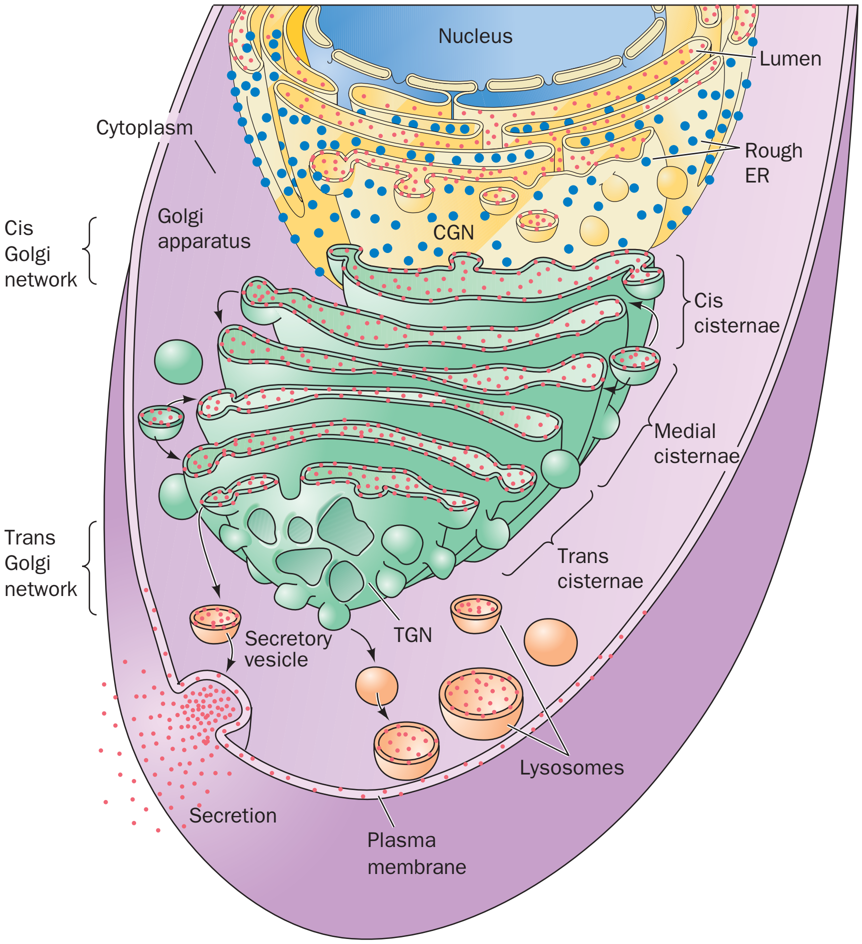

Figure 9-38 | The posttranslational processing of proteins. Membrane, secretory, and lysosomal proteins are synthesized by RER-associated ribosomes (*blue dots*; *top*). As they are synthesized, the proteins (*red dots*) are either injected into the lumen of the ER or inserted into its membrane. After initial processing in the ER, the proteins are encapsulated in vesicles that bud off from the ER membrane and subsequently fuse with the cis Golgi network (CGN). The proteins are progressively processed in the cis, medial, and trans cisternae of the Golgi. Finally, in the trans Golgi network (TGN; *bottom*), the completed glycoproteins are sorted for delivery to their final destinations: the plasma membrane, **secretory vesicles,** or lysosomes, to which they are transported by yet other vesicles.

Proteins transit from one end of the Golgi stack to the other while being modified in a stepwise manner. The proteins are transported via two mechanisms:

1. They are conveyed between successive Golgi compartments in the cis to trans direction as cargo within membranous vesicles that bud off of one compartment and fuse with a successive compartment, a process known as forward or **anterograde transport.**
2. They are carried as passengers in Golgi compartments that transit the Golgi stack; that is, the cis cisternae eventually become trans cisternae, a process called **cisternal progression** or **maturation.** (Golgi-resident proteins may migrate backward by **retrograde transport** from one compartment to the preceding one via membranous vesicles.)

Upon reaching the trans Golgi network, the now mature proteins are sorted and sent to their final cellular destinations.

Membrane, Secretory, and Lysosomal Proteins Are Transported in Coated Vesicles. The vehicles in which proteins are transported between the RER, the different compartments of the Golgi apparatus, and their final destinations are known as **coated vesicles** (Fig. 9-39). This is because these 60- to 150-nm-diameter membranous sacs are initially encased on their outer (cytosolic) faces by specific proteins that act as flexible scaffolding in promoting vesicle formation. A vesicle buds off from its membrane

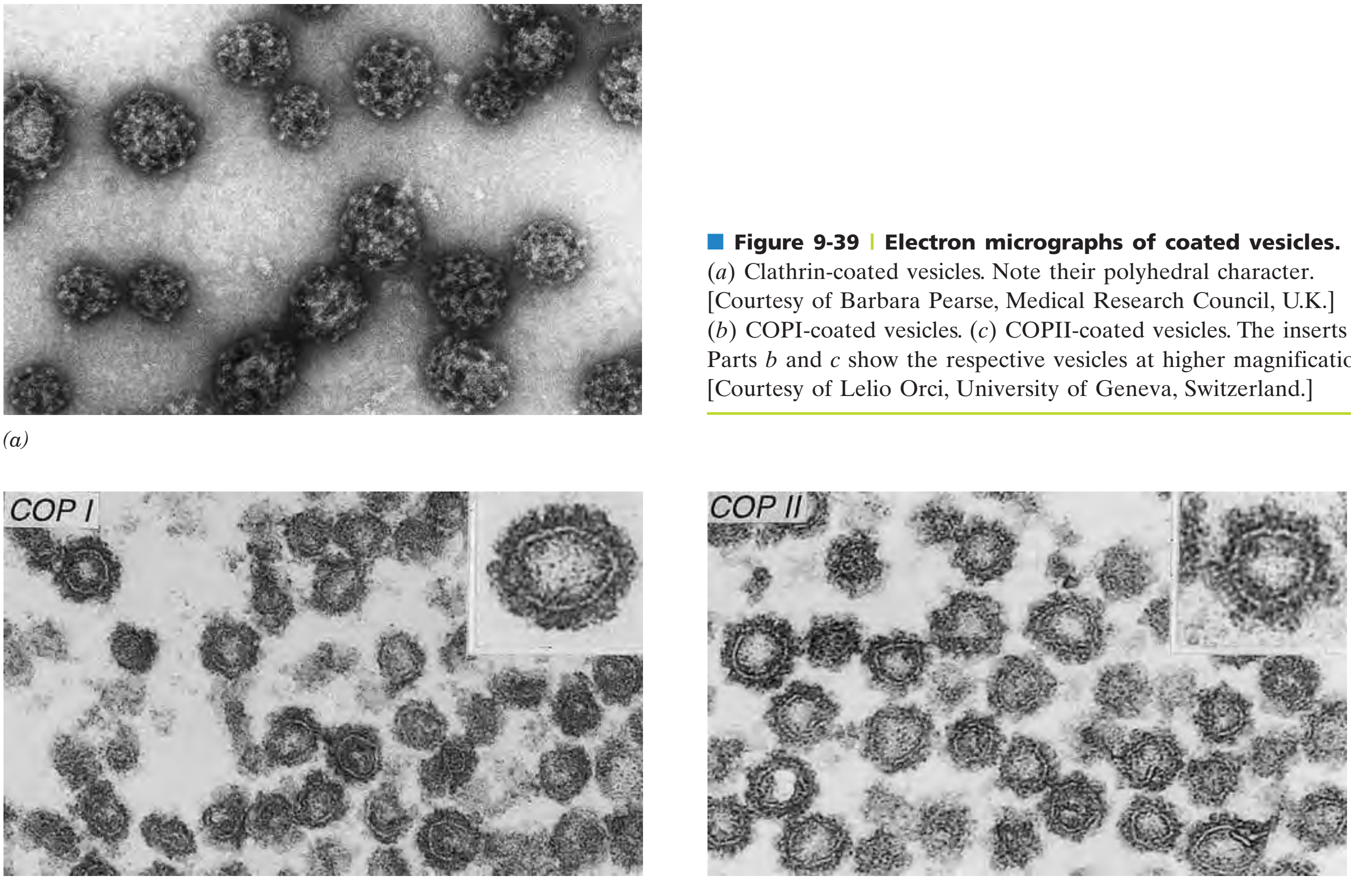

(*a*)

(*b*)

(*c*)

Figure 9-39 | Electron micrographs of coated vesicles. (*a*) Clathrin-coated vesicles. Note their polyhedral character. [Courtesy of Barbara Pearse, Medical Research Council, U.K.] (*b*) COPI-coated vesicles. (*c*) COPII-coated vesicles. The inserts in Parts *b* and *c* show the respective vesicles at higher magnification. [Courtesy of Lelio Orci, University of Geneva, Switzerland.]

of origin and later fuses to its target membrane. *This process preserves the orientation of the transmembrane protein (Fig. 9-40), because the lumens of the ER and the Golgi cisternae are topologically equivalent to the outside of the cell.* This explains why the carbohydrate moieties of integral glycoproteins and the GPI anchors of GPI-linked proteins occur only on the external surfaces of plasma membranes.

The three known types of coated vesicles are characterized by their protein coats:

1. **Clathrin** (Fig. 9-39*a*), a protein that forms a polyhedral framework around vesicles that transport TM, GPI-linked, and secreted proteins from the Golgi to the plasma membrane (see below).
2. **COPI** protein (Fig. 9-39*b;* COP for *co*at *p*rotein), which forms a fuzzy rather than a polyhedral coating about vesicles that carry out both the anterograde and retrograde transport of proteins between successive Golgi compartments. In addition, COPI-coated vesicles

Figure 9-40 | Fusion of a vesicle with the plasma membrane. The inside of the vesicle and the exterior of the cell are topologically equivalent. Fusion of the vesicle with the plasma membrane preserves the orientation of the integral proteins embedded in the vesicle bilayer because the same side of the protein is always immersed in the cytosol. Note that soluble proteins packaged inside a secretory vesicle that fuses with the plasma membrane would be released outside the cell.

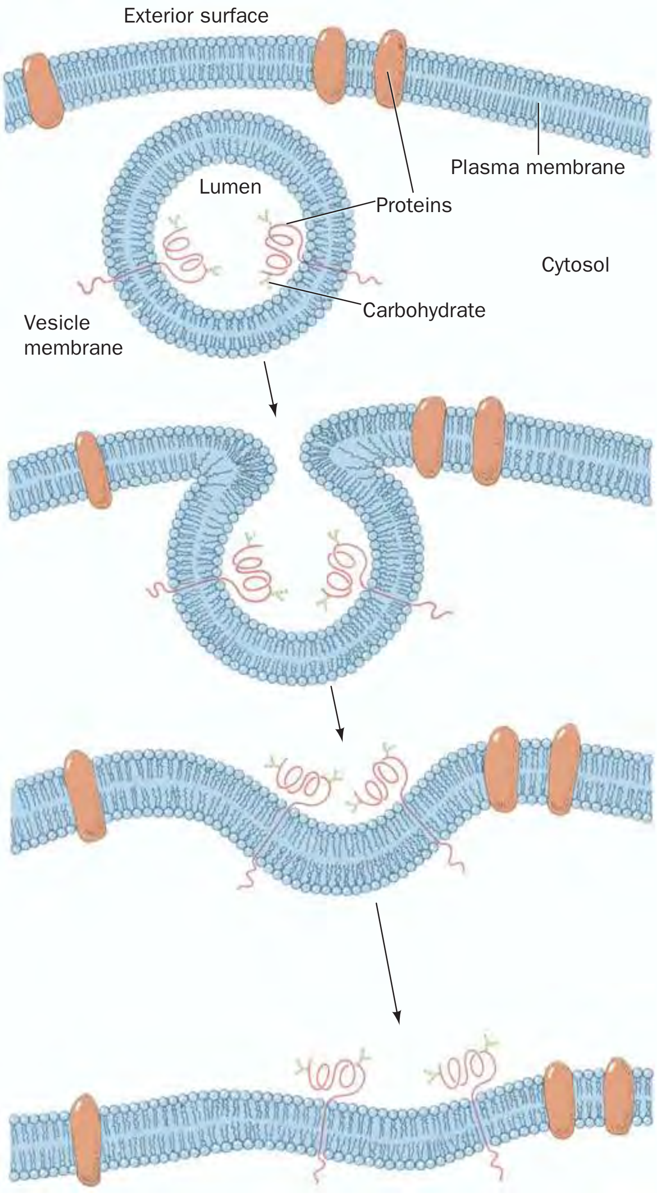

return escaped ER-resident proteins from the Golgi back to the ER (see below). The COPI protomer, which contains seven different subunits, is named **coatomer.**

3. **COPII** protein (Fig. 9-39*c*), which transports proteins from the ER to the Golgi. The COPII vesicle components are then returned to the ER by COPI-coated vesicles (the COPI vesicle components entering the ER are presumably recycled by COPII-coated vesicles). The COPII coat consists of two conserved protein heterodimers.

All of the above coated vesicles also bear receptors that bind the proteins being transported, as well as proteins that mediate the fusion of these vesicles with their target membranes (Section 9-4F).

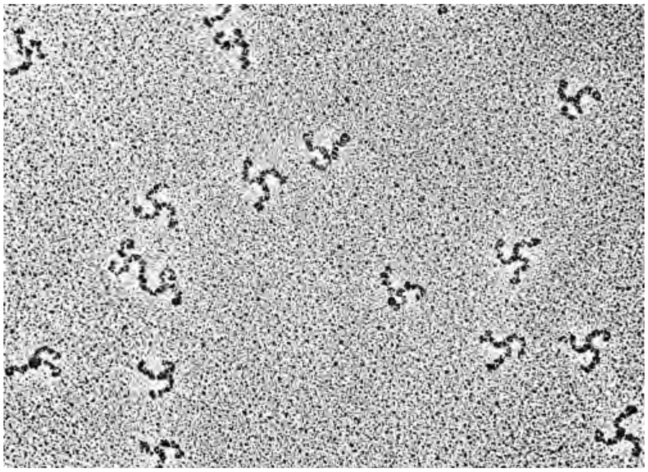

Figure 9-41 | **An electron micrograph of triskelions.** The variable orientations of their legs is indicative of their flexibility. [Courtesy of Daniel Branton, Harvard University.]

Clathrin Forms Flexible Cages. Clathrin-coated vesicles are structurally better characterized than those coated with COPI or COPII. The clathrin network is built from proteins known as **triskelions** (Fig. 9-41), which consist of three heavy chains (190 kD) that each bind one of two homologous light chains (24–27 kD). The triskelions assemble to form a polyhedral cage in which each vertex is the center (hub) of a triskelion and the ~150-Å-long edges are formed by the overlapping legs of four triskelions (Fig. 9-42). The clathrin light chains are not required for clathrin cage assembly. In fact, they inhibit heavy chain polymerization *in vitro,* suggesting that they play a regulatory role in clathrin cage formation in the cytosol.

A clathrin polyhedron, which has 12 pentagonal faces and a variable number of hexagonal faces, is the most parsimonious way of enclosing a spheroidal object in a polyhedral cage. The volume enclosed by a clathrin polyhedron increases with the number of hexagonal faces. The structure shown in Fig. 9-42*a* is ~600 Å in diameter. *In vivo,* clathrin-coated vesicles are typically at least ~1200 Å in diameter.

The triskelion legs, which have a total length of ~450 Å, exhibit considerable flexibility (Fig. 9-41). This is a functional necessity for the

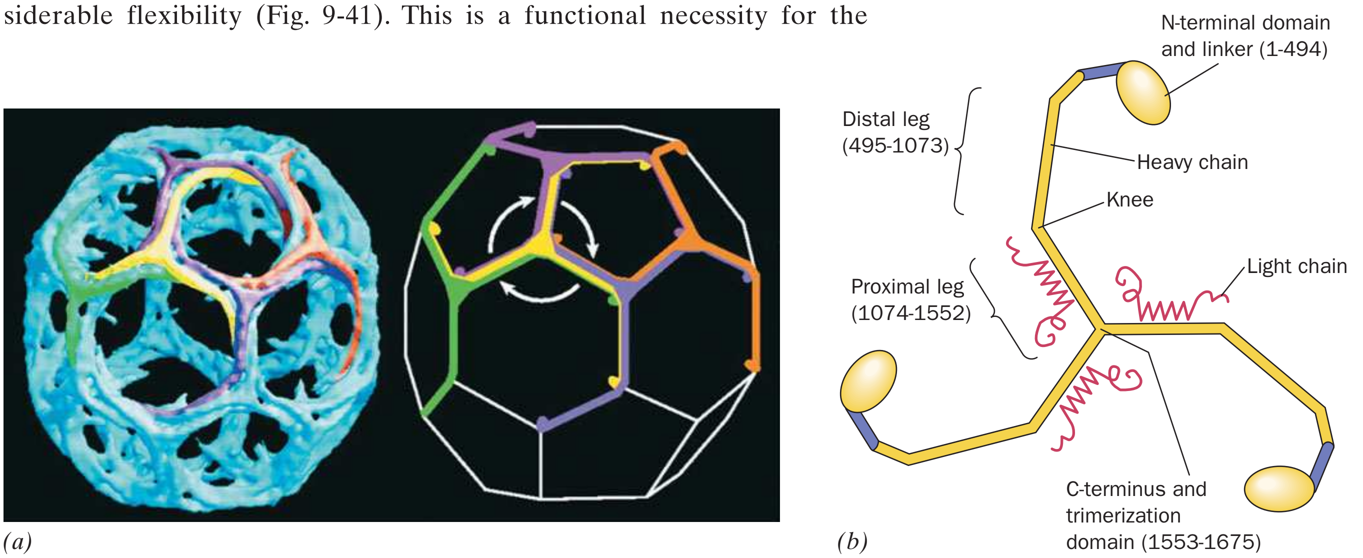
(a)
(b)
N-terminal domain and linker (1-494)
Distal leg (495-1073)
Heavy chain
Knee
Light chain
Proximal leg (1074-1552)
C-terminus and trimerization domain (1553-1675)

Figure 9-42 | **The anatomy of a clathrin-coated vesicle.** (*a*) A cryoelectron microscopy–based image of a clathrin cage at 21 Å resolution with its triskelions differently colored. As the accompanying diagram (*right*) indicates, a triskelion is centered on each of this polyhedral cage's 36 vertices, its edges are formed by the legs of adjacent triskelions, and the linker and N-terminal domains of each clathrin heavy chain project inward. [Electron micrograph by Barbara Pearse and courtesy of H.T. McMahon, MRC Laboratory for Molecular Biology, Cambridge, U.K.] (*b*) Schematic diagram of a triskelion indicating its structural subdivisions.

formation of different-sized vesicles as well as for the budding of a vesicle from a membrane surface, which requires a large change in its curvature. The clathrin heavy chains appear to flex mainly along a segment of the knee (Fig. 9-42*b*) between the proximal and distal legs that is free of contacts with other molecules in clathrin cages.

In addition to transporting membrane and secretory proteins between the Golgi apparatus and the plasma membrane, clathrin-coated vesicles participate in **endocytosis.** In this process (discussed in Section 20-1B), a portion of the plasma membrane invaginates to form a clathrin-coated vesicle that engulfs specific proteins from the extracellular medium and then transports them to intracellular destinations.

Proteins Are Directed to the Lysosome by Carbohydrate Recognition Markers. The signals that direct particular proteins to the various types of coated vesicles for transport between cellular compartments are not entirely understood. However, the trafficking of lysosomal proteins is known to depend on their oligosaccharides. A clue to the nature of this process was provided by the human hereditary defect known as **I-cell disease** (alternatively, **mucolipidosis II**) which, in homozygotes, is characterized by severe progressive psychomotor retardation, skeletal deformities, and death by age 10. The lysosomes in the connective tissue of I-cell disease victims contain large inclusions (after which the disease is named) of glycosaminoglycans and glycolipids as a result of the absence of several lysosomal hydrolases. These enzymes are synthesized on the RER with their correct amino acid sequences, but rather than being dispatched to the lysosomes, are secreted into the extracellular medium. This misdirection results from the absence of a mannose-6-phosphate recognition marker on the carbohydrate moieties of these hydrolases because of a deficiency of an enzyme required for mannose phosphorylation of the lysosomal proteins. The mannose-6-phosphate residues are normally bound by a receptor in the coated vesicles that transports lysosomal hydrolases from the Golgi apparatus to the lysosomes. No doubt, other glycoproteins are directed to their intracellular destinations by similar carbohydrate markers.

ER-Resident Proteins Have the C-Terminal Sequence KDEL. Most soluble ER-resident proteins in mammals have the C-terminal sequence KDEL (HDEL in yeast), KKXX, or KXKXXX (where X represents any amino acid residue), whose alteration results in the secretion of the resulting protein. By what means are these proteins selectively retained in the ER? Since many ER-resident proteins freely diffuse within the ER, it seems unlikely that they are immobilized by membrane-bound receptors within the ER. Rather, ER-resident proteins, like secretory and lysosomal proteins, readily leave the ER via COPII-coated vesicles, but ER-resident proteins are promptly retrieved from the Golgi and returned to the ER in COPI-coated vesicles. Indeed, coatomer binds the Lys residues in the C-terminal KKXX motif of transmembrane proteins, which presumably permits it to gather these proteins into COPI-coated vesicles. Furthermore, genetically appending KDEL to the lysosomal protease **cathepsin D** causes it to accumulate in the ER, but it nevertheless acquires an *N*-acetylglucosaminyl-1-phosphate group, a modification that is made in an early Golgi compartment. Presumably, a membrane-bound receptor in a post-ER compartment binds the KDEL signal and the resulting complex is returned to the ER in a COPI-coated vesicle. **KDEL receptors** have, in fact, been identified in yeast and humans. However, the observation that former KDEL proteins whose KDEL sequences have been deleted are, nevertheless, secreted relatively slowly suggests that there are mechanisms for retaining these proteins in the

ER by actively withholding them from the bulk flow of proteins through the secretory pathway.

F | Proteins Mediate Vesicle Fusion

In all cells, *new membranes are generated by the expansion of existing membranes*. In eukaryotes, this process occurs mainly via vesicle trafficking in which a vesicle buds off from one membrane (e.g., that of the Golgi apparatus) and fuses to a different membrane (e.g., the plasma membrane or that of the lysosome), thereby transferring both lipids and proteins from the parent to the target membrane.

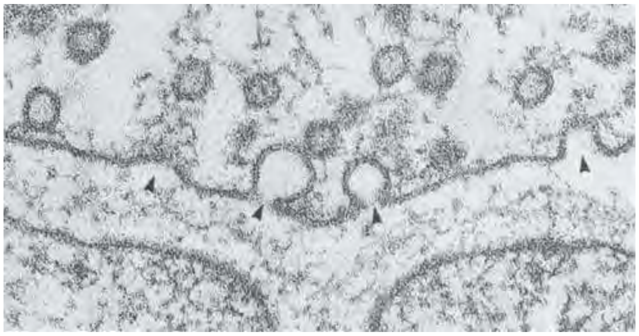
(*a*)

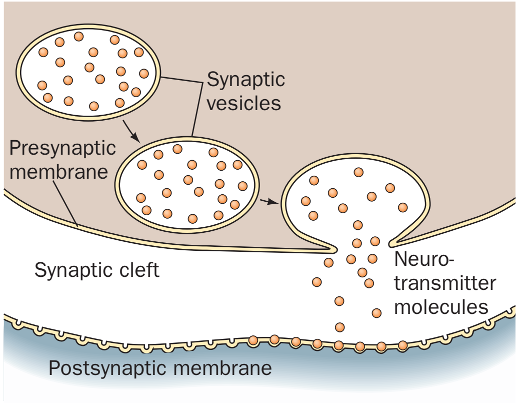
(*b*)

Figure 9-43 | Vesicle fusion at a synapse. (*a*) An electron micrograph of a frog neuromuscular synapse. Synaptic vesicles are undergoing fusion (*arrows*) with the presynaptic plasma membrane (*top*). [Courtesy of John Heuser, Washington University School of Medicine, St. Louis, Missouri.] (*b*) This process discharges the neurotransmitter contents of the synaptic vesicles into the synaptic cleft, the space between the neuron and the muscle cell (the postsynaptic cell).

On arriving at its target membrane, a vesicle fuses with it, thereby releasing its contents on the opposite side of the target membrane (Fig. 9-40). We have already seen how proteins are transported from the ER through the Golgi apparatus and secreted by this mechanism. Other substances are also secreted in this way. For example (Fig. 9-43), when a nerve impulse in a presynaptic cell reaches a **synapse** [the junction between neurons (nerve cells) or between neurons and muscles], it triggers the fusion of **neurotransmitter**-containing **synaptic vesicles** with the **presynaptic membrane** (a specialized section of the neuron's plasma membrane). This releases the neurotransmitter (a small molecule) into the ~200-Å-wide **synaptic cleft** (the process whereby membranous vesicles fuse with the plasma membrane to release their contents outside the cell is called **exocytosis**). In less than 0.1 ms, the neurotransmitter diffuses across the synaptic cleft to the **postsynaptic membrane,** where it binds to specific receptors that then trigger the continuation of the nerve impulse or muscle contraction in the postsynaptic cell.

Biological membranes do not spontaneously fuse. Indeed, being negatively charged, they strongly repel each other at short distances. This repulsive force must be overcome if biological membranes are to fuse. How do vesicles fuse and why do they fuse only with their target membranes?

Extensive investigations, in large part by James Rothman, have identified numerous proteins that mediate vesicle fusion with their target membranes. Among these are integral or lipid-linked proteins known as **SNAREs. R-SNAREs** (which contain conserved Arg residues) usually associate with vesicle membranes, and **Q-SNAREs** (which contain conserved Gln residues) usually associate with target membranes. Interactions among these proteins, as we shall see, firmly anchor the vesicle to the target membrane, a process called docking.

The X-ray structure of a core SNARE complex is shown in Fig. 9-44. Four parallel ~65-residue α helices wrap around each other with a gentle left-handed twist. For the most part,

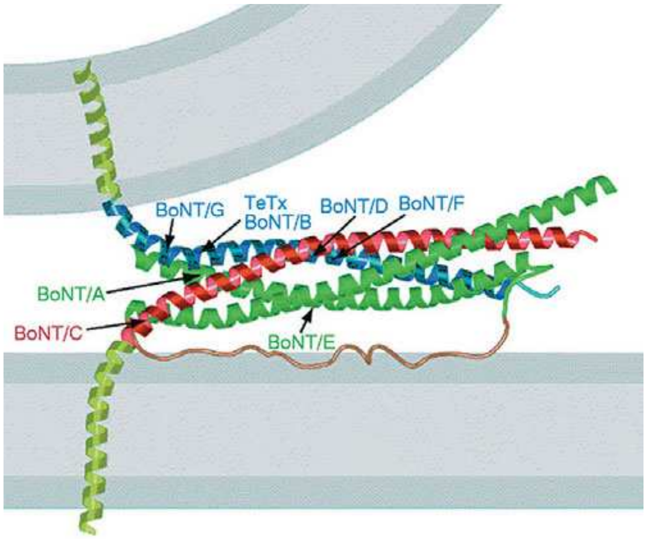

Figure 9-44 | X-Ray structure of a SNARE complex modeled between two membranes. The complex includes an R-SNARE (**syntaxin,** *red*) and two Q-SNARES (**synaptobrevin,** *blue,* and **SNAP-25,** *green,* a two-Q-domain–containing Q-SNARE) for a total of four helices, which are shown here as ribbons. The transmembrane C-terminal extensions of syntaxin and synaptobrevin are modeled as helices (*yellow-green*). The peptide segment connecting the two Q-domain helices of SNAP-25 is speculatively represented as an unstructured loop (*brown*). The loop is anchored to the membrane via Cys-linked palmitoyl groups (*not shown*). The cleavage sites for various clostridial neurotoxins (causing tetanus and botulism; Box 9-3) are indicated by the arrows. [Courtesy of Axel Brünger, Yale University. PDBid 1SFC.]

BOX 9-3 BIOCHEMISTRY IN HEALTH AND DISEASE

Tetanus and Botulinum Toxins Specifically Cleave SNAREs

The frequently fatal infectious diseases **tetanus** (which arises from wound contamination) and **botulism** (a type of food poisoning) are caused by certain anaerobic bacteria of the genus *Clostridium*. These bacteria produce extremely potent protein neurotoxins that inhibit the release of neurotransmitters into synapses. In fact, botulinum toxins are the most powerful known toxins; they are ∼10 million times more toxic than cyanide.

There are seven serologically distinct types of botulinum neurotoxins, designated **BoNT/A** through **BoNT/G,** and one type of tetanus neurotoxin, **TeTx.** Each of these homologous proteins is synthesized as a single ∼150-kD polypeptide chain that is cleaved by host proteases to yield an ∼50-kD light chain and an ∼100-kD heavy chain. The heavy chains bind to specific types of neurons and facilitate the uptake of the light chain by endocytosis. *Each light chain is a protease that cleaves its target SNARE at a specific site* (see Fig. 9-44). SNARE cleavage prevents the formation of the core complex and thereby halts the exocytosis of synaptic vesicles. The heavy chain of TeTx specifically binds to inhibitory neurons (which function to moderate excitatory nerve impulses) and is thereby responsible for the spastic paralysis characteristic of tetanus. The heavy chains of the BoNTs instead bind to motor neurons (which innervate muscles) and thus cause the flaccid paralysis characteristic of botulism.

The administration of carefully controlled quantities of botulinum toxin ("Botox") is medically useful in relieving the symptoms of certain types of chronic muscle spasms. Moreover, this toxin is being used cosmetically: Its injection into the skin relaxes the small muscles causing wrinkles and hence these wrinkles disappear for ∼3 months.

the sequence of each helix has the expected seven-residue repeat, $(a\text{-}b\text{-}c\text{-}d\text{-}e\text{-}f\text{-}g)_n$, with residues a and d hydrophobic (Section 6-1C). However, the central layer of side chains along the length of the four-helix bundle includes an Arg residue from the R-SNARE that is hydrogen bonded to three Gln side chains, one from each of the Q-SNARE helices. These highly conserved polar residues are sealed off from the aqueous environment so that their interactions serve to bring the four helices into proper register. Since cells contain numerous different R-SNAREs and Q-SNAREs, it seems likely that their interactions are at least partially responsible for the specificity that vesicles exhibit in fusing with their target membranes. Bacterial proteases that cleave SNAREs interfere with vesicle fusion, with serious consequences (Box 9-3).

SNAREs Facilitate the Fusion of Membranes by Bringing Them Together. The association of an R-SNARE on a vesicle with Q-SNAREs on its target membrane brings the two bilayers into close proximity. But what induces the fusion of the juxtaposed lipid bilayers? According to one model, mechanical stresses arising from the formation of SNARE complexes expel lipid molecules from their bilayer. This, it is hypothesized, results in the formation of a transient structure with lipids from the opposing bilayer, a process that culminates in bilayer fusion (Fig. 9-45). However, *in vitro,* this process takes 30 to 40 minutes, whereas the fusion of a synaptic vesicle with the presynaptic membrane requires ∼0.3 ms. This argues that other proteins also participate in inducing bilayer fusion and, indeed, several other proteins have been implicated.

Membrane-Enveloped Viruses Infect Their Target Cells Using Viral Fusion Proteins. Many viruses, including those causing influenza and AIDS, arise by budding from the plasma membrane of a virus-infected cell, much like the budding of a vesicle from a membrane. In order to

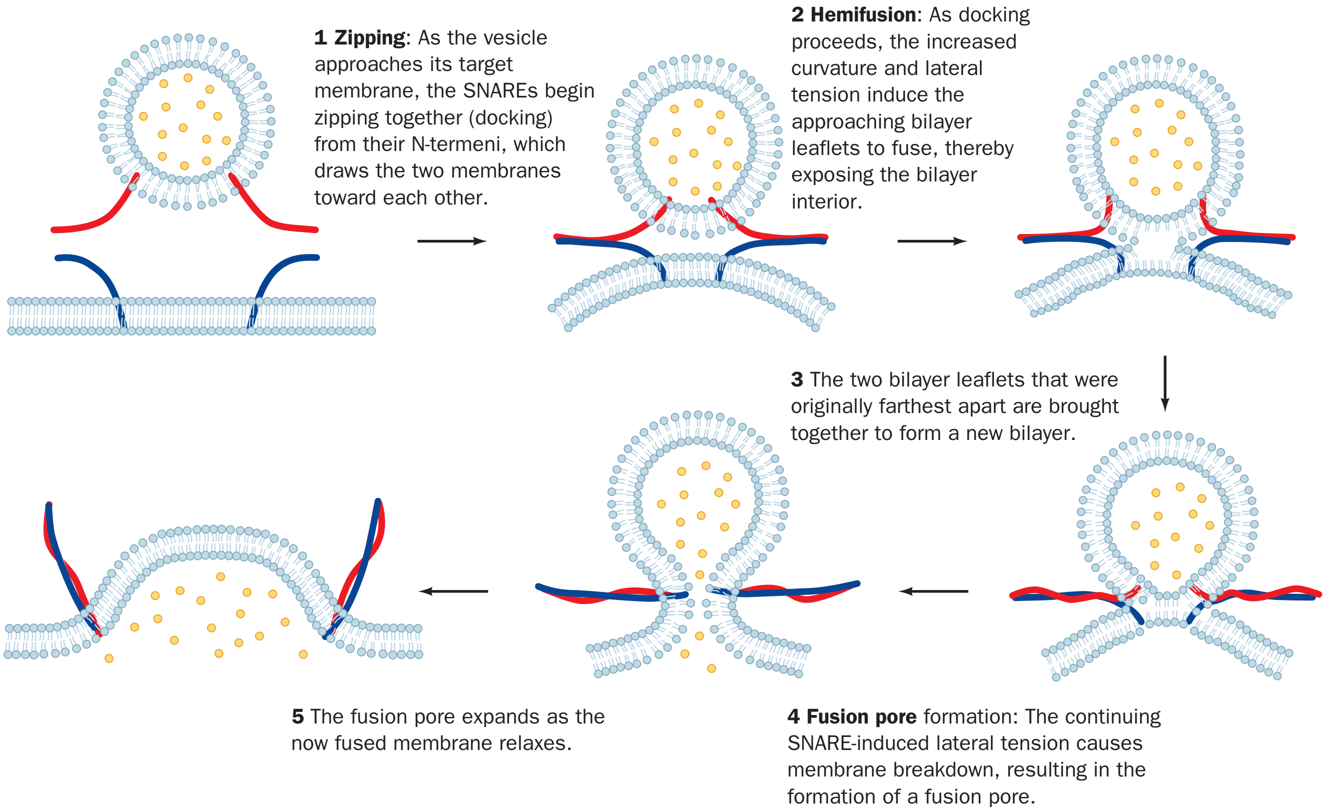

1 Zipping: As the vesicle approaches its target membrane, the SNAREs begin zipping together (docking) from their N-termeni, which draws the two membranes toward each other.

2 Hemifusion: As docking proceeds, the increased curvature and lateral tension induce the approaching bilayer leaflets to fuse, thereby exposing the bilayer interior.

3 The two bilayer leaflets that were originally farthest apart are brought together to form a new bilayer.

4 Fusion pore formation: The continuing SNARE-induced lateral tension causes membrane breakdown, resulting in the formation of a fusion pore.

5 The fusion pore expands as the now fused membrane relaxes.

Figure 9-45 | **A model for SNARE-mediated vesicle fusion.** Here R-SNAREs and Q-SNAREs are schematically represented by red and blue worms. [After a drawing by Chen, Y.A. and Scheller, R.H., *Nature Rev. Mol. Cell Biol*. **2,** 98 (2001).]

infect a new cell, the membrane of the resulting **membrane-enveloped virus** must fuse with a membrane in its target cell so as to deposit the virus' cargo of nucleic acid in the cell's cytoplasm. Such membrane fusion events are mediated by protein systems that differ from those responsible for the vesicle fusion events we discussed above. As an example, let us discuss how **influenza virus** mediates membrane fusion (other membrane-enveloped viruses use similar systems). Virus-mediated membrane fusion occurs in three stages:

1. Host cell recognition by the virus.
2. Activation of the viral membrane fusion machinery.
3. Fusion of the viral membrane with a host cell membrane so as to release the viral genome into the host cell cytoplasm.

The major integral protein component of the membrane that envelops influenza virus is named **hemagglutinin (HA)** because it causes erythrocytes to agglutinate (clump together). HA, a so-called **viral fusion protein,** mediates influenza host cell recognition by binding to specific glycoproteins that act as cell-surface receptors. These glycoproteins (glycophorin A in erythrocytes; Section 9-3A) bear terminal *N*-acetylneuraminic acid (sialic acid; Fig. 8-6) residues on their carbohydrate groups. HA is synthesized as a homotrimer of 550-residue subunits that are each anchored to

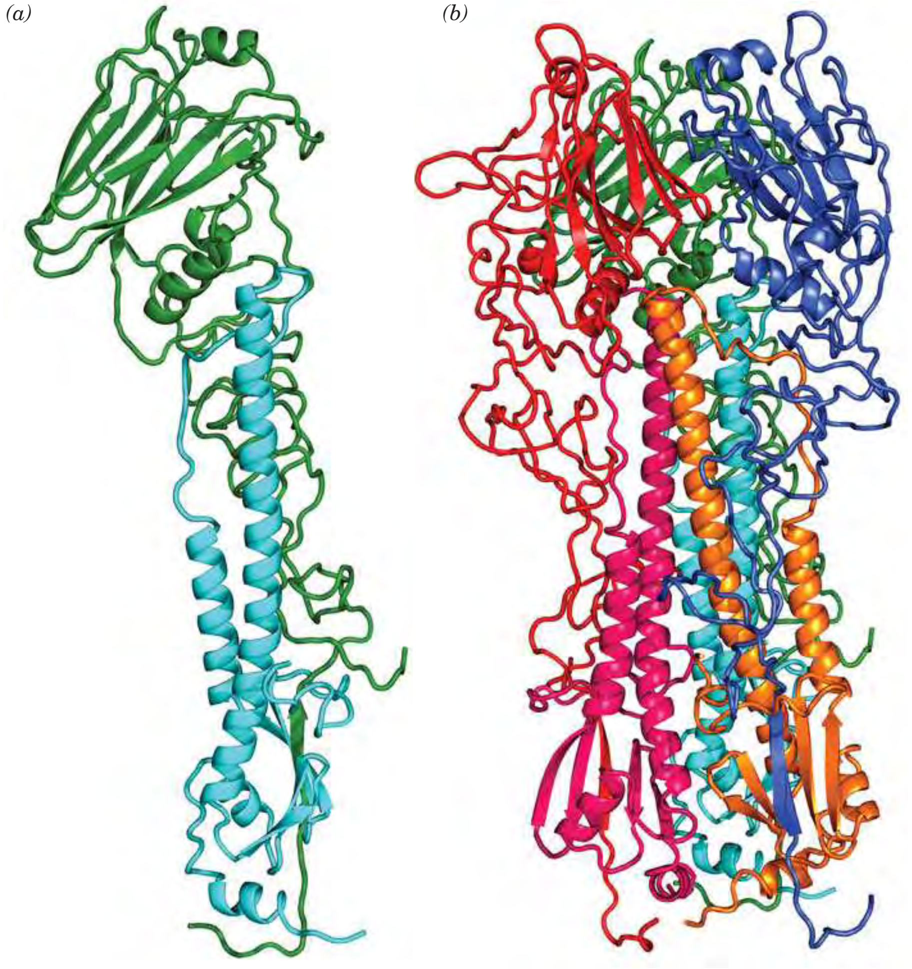

Figure 9-46 | X-Ray structure of influenza hemagglutinin. (*a*) Ribbon diagram of the BHA monomer. HA1 is green and HA2 is cyan. (*b*) Ribbon diagram of the BHA trimer. Each HA1 and HA2 chain is drawn in a different color. The orientations of the green HA1 and the cyan HA2 are the same as in Part *a*. [Based on an X-ray structure by John Skehel, National Institute for Medical Research, London, U.K., and Don Wiley, Harvard University. PDBid 4HMG.]

the membrane by a single transmembrane helix (residues 524–540). However, HA's Arg 329 is posttranslationally excised by host cell proteases to yield two peptides, designated HA1 and HA2, that remain linked by a disulfide bond.

After binding to the plasma membrane of its host cell, an influenza virus particle is taken into the cell by the invagination of the membrane via a process known as **receptor-mediated endocytosis** (Section 20-1B) that superficially resembles the reverse of the fusion of a vesicle with a membrane (Fig. 9-40). The resulting intracellular vesicle with the virus bound to its inner surface then fuses with a vesicle known as an **endosome** that has an internal pH of ~5. The consequent drop in pH triggers a conformational change in which the N-terminal end of HA2, a conserved, hydrophobic, ~24-residue segment known as a **fusion peptide,** inserts into the host cell's endosomal membrane, thereby tightly linking it to the viral membrane preparatory to their fusion.

Our understanding of how HA mediates the fusion of viral and host cell membranes is based largely on X-ray structural studies by Don Wiley and John Skehel. HA's hydrophobic membrane anchor interferes with its crystallization. However, the proteolytic removal of HA's transmembrane helix yields a crystallizable protein named BHA, whose X-ray structure reveals that it consists of a globular region that is perched on a long fibrous stalk projecting from the viral membrane surface (Fig. 9-46*a*). The globular region contains the sialic acid–binding pocket, whereas the

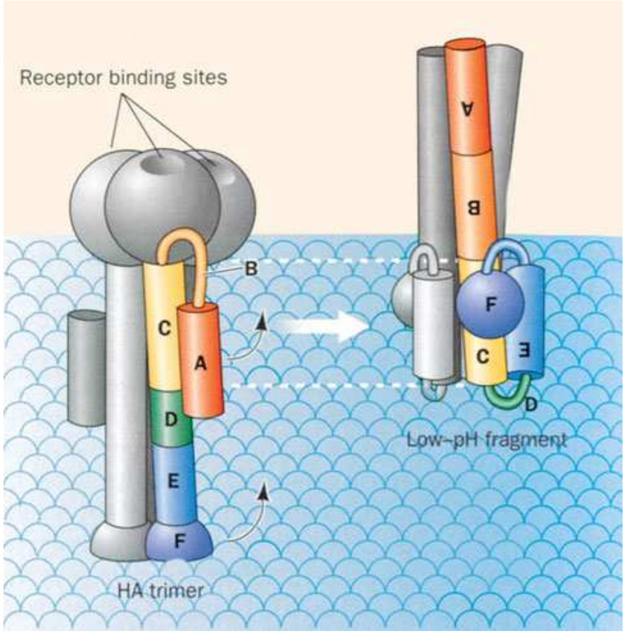

Figure 9-47 | Schematic drawing comparing the structures of BHA and TBHA2. This drawing indicates the positions and heights above the viral membrane surface of TBHA2's various structural elements in the HA trimer (*left*) and in its low-pH form (*right*). In the low-pH form, the fusion peptide would protrude well above the receptor-binding heads where it would presumably insert itself into the endosomal membrane.

fibrous stalk includes a remarkable 76-Å-long (53 residues in 14 turns) α helix. The dominant interaction stabilizing BHA's trimeric structure is a triple-stranded coiled coil consisting of the long α helices from each of its protomers (Fig. 9-46*b*). Curiously, BHA's fusion peptides are buried in its hydrophobic interior, ~100 Å from the sialic acid–binding sites at the "top" of the protein.

In the endosome, HA undergoes a dramatic conformational change (Fig. 9-47), the nature of which was elucidated by the X-ray structure of a portion of BHA named TBHA2 that consists of BHA's long helix and some of its flanking regions. In this conformational change, segments A and B at the N-terminus of TBHA2 (the red and orange segments in Fig. 9-47) undergo a jackknife-like movement of ~100 Å in a way that extends the top of the long helix by ~10 helical turns toward the endosomal membrane. This translocates the fusion peptide (which is absent in TBHA2 but would extend beyond its N-terminus at the top of segment A) by at least 100 Å above its position in BHA, thereby allowing it to insert into the host membrane. At the same time, the long helix is shortened from the bottom by similar shifts of segments D and E (green and blue in Fig. 9-47). These conformational changes, which simultaneously occur in several closely spaced HA molecules in the viral membrane, draw together the viral and host membranes so as to facilitate their fusion in a manner similar to that postulated for SNARE complexes.

CHECK YOUR UNDERSTANDING

Describe the fluid mosaic model.

Explain how the membrane skeleton influences membrane protein distribution.

What are the functions of flipases and phospholipid translocases?

Describe the structure of a lipid raft.

Summarize the steps of the secretory pathway, including the function of the translocon.

Describe how a membrane protein, a secreted protein, and a lysosomal protein are transported from the RER to their final destination.

Describe how SNAREs and viral fusion proteins such as hemagglutinin act to bring specific membranes close together and trigger their fusion.

SUMMARY

1. Lipids are a diverse group of molecules that are soluble in organic solvents and, in contrast to other major types of biomolecules, do not form polymers.
2. Fatty acids are carboxylic acids whose chain lengths and degrees of unsaturation vary.
3. Adipocytes and other cells contain stores of triacylglycerols, which consist of three fatty acids esterified to glycerol.
4. Glycerophospholipids are amphiphilic molecules that contain two fatty acid chains and a polar head group.

5. The sphingolipids include sphingomyelins, cerebrosides, and gangliosides.
6. Cholesterol, steroid hormones, and vitamin D are all based on a four-ring structure.
7. The arachidonic acid derivatives prostaglandins, prostacyclins, thromboxanes, leukotrienes, and lipoxins are signaling molecules that have diverse physiological roles.
8. Glycerophospholipids and sphingolipids form bilayers in which their nonpolar tails associate with each other and their polar head groups are exposed to the aqueous solvent.
9. Although the transverse diffusion of a lipid across a bilayer is extremely slow, lipids rapidly diffuse in the plane of the bilayer. Bilayer fluidity varies with temperature and with the chain lengths and degree of saturation of its component fatty acid residues.
10. The proteins of biological membranes include integral (intrinsic) proteins that contain one or more transmembrane α helices or a β barrel. In all cases, the membrane-exposed surface of the protein is hydrophobic.
11. Other membrane-associated proteins may be anchored to the membrane via isoprenoid, fatty acid, or glycosylphosphatidylinositol (GPI) groups. Peripheral (extrinsic) proteins are loosely associated with the membrane surface.
12. The fluid mosaic model of membrane structure accounts for the lateral diffusion of membrane proteins and lipids.
13. The arrangement of membrane proteins may depend on their interactions with an underlying protein skeleton, as in the erythrocyte.
14. Membrane proteins and lipids are distributed asymmetrically in the two leaflets and may form domains such as lipid rafts.
15. Transmembrane (TM), secretory, and lysosomal proteins are synthesized by means of the secretory pathway. A signal peptide directs a growing polypeptide chain through the RER membrane via a protein pore called the translocon, which also functions to laterally install TM proteins into the RER membrane.
16. Coated vesicles transport membrane-embedded and luminal proteins from the ER to the Golgi apparatus for further processing, and from there to other membranes. The proteins coating these vesicles may consist largely of clathrin, which forms polyhedral cages, or COPI or COPII, which form coats with an amorphous appearance.
17. The fusion of vesicles with membranes occurs via a complex process that involves SNAREs. These form four-helix bundles that bring two membranes into proximity, which in turn induces membrane fusion.
18. Viral fusion proteins mediate the fusion of membrane-enveloped viruses such as influenza virus with their host cell membranes so as to release the viral nucleic acids into the host cell cytoplasm.

KEY TERMS

lipid	**245**
fatty acid	**246**
saturation	**247**
triacylglycerol	**248**
fats	**248**
oils	**248**
adipocyte	**248**
glycerophospholipid	**249**
phosphatidic acid	**249**
phospholipase	**251**
lysophospholipid	**251**
plasmalogen	**251**
sphingolipid	**252**
ceramide	**252**
sphingomyelin	**252**
cerebroside	**252**
ganglioside	**253**
steroid	**254**
sterol	**254**
glucocorticoid	**255**
mineralocorticoid	**255**
androgen	**255**
estrogen	**255**
isoprenoid	**257**
vitamin	**257**
prostaglandin	**258**
eicosanoid	**258**
lipid bilayer	**260**
liposome	**260**
transverse diffusion	**261**
lateral diffusion	**261**
transition temperature	**262**
integral (intrinsic) protein	**263**
transmembrane (TM) protein	**265**
electron crystallography	**265**
prenylation	**268**
myristoylation	**268**
palmitoylation	**268**
GPI-linked protein	**268**
peripheral (extrinsic) protein	**269**
fluid mosaic model	**270**
fluorescence recovery after photobleaching (FRAP)	**270**
gates and fences model	**274**
flipase	**276**
lipid raft	**277**
endocytosis	**278**
secretory pathway	**278**
signal peptide	**278**
signal recognition particle (SRP)	**278**
SRP receptor (SR)	**279**
translocon	**279**
coated vesicles	**283**
clathrin	**284**
exocytosis	**287**
SNARE	**287**
membrane-enveloped virus	**289**
hemagglutinin	**289**
viral fusion protein	**289**

PROBLEMS

1. Does *trans*-oleic acid have a higher or lower melting point than *cis*-oleic acid? Explain.
2. How many different types of triacylglycerols could incorporate the fatty acids shown in Fig. 9-1?
3. Which triacylglycerol yields more energy on oxidation: one containing three residues of linolenic acid or three residues of stearic acid?
4. Draw the structure of a glycerophospholipid that has a saturated C_{16} fatty acyl group at position 1, a monounsaturated C_{18} fatty acyl group at position 2, and an ethanolamine head group.
5. What products are obtained when 1-palmitoyl-2-oleoyl-3-phosphatidylserine is hydrolyzed by (a) phospholipase A_1; (b) phospholipase A_2; (c) phospholipase C; (d) phospholipase D?

6. Which of the glycerophospholipid head groups listed in Table 9-2 can form hydrogen bonds?
7. Does the phosphatidylglycerol "head group" of cardiolipin (Table 9-2) project out of a lipid bilayer like other glycerophospholipid head groups?
8. In some autoimmune diseases, an individual develops antibodies that recognize cell constituents such as DNA and phospholipids. Some of the antibodies react with both DNA and phospholipids. What is the structural basis for this cross-reactivity?
9. Most hormones, such as peptide hormones, exert their effects by binding to cell-surface receptors. However, steroid hormones do so by binding to cytosolic receptors. How is this possible?
10. Animals cannot synthesize linoleic acid (a precursor of arachidonic acid) and therefore must obtain this **essential fatty acid** from their diet. Explain why cultured animal cells can survive in the absence of linoleic acid.
11. Why can't triacylglycerols be significant components of lipid bilayers?
12. Why would a bilayer containing only gangliosides be unstable?
13. When bacteria growing at 20°C are warmed to 30°C, are they more likely to synthesize membrane lipids with (a) saturated or unsaturated fatty acids, and (b) short-chain or long-chain fatty acids? Explain.
14. (a) How many turns of an α helix are required to span a lipid bilayer (~30 Å across)? (b) What is the minimum number of residues required? (c) Why do most transmembrane helices contain more than the minimum number of residues?
15. The distance between the C_α atoms in a β sheet is ~3.5 Å. Can a single 9-residue segment with a β conformation serve as the transmembrane portion of an integral membrane protein?
16. Are the following lipid samples likely to correspond to the inner or outer leaflet of a eukaryotic plasma membrane? (a) 20% phosphatidylcholine, 15% phosphatidylserine, 65% other lipids. (b) 35% phosphatidylcholine, 15% gangliosides, 5% cholesterol, 45% other lipids.
17. Describe the labeling pattern of glycophorin A when a membrane-impermeable protein-labeling reagent is added to (a) a preparation of solubilized erythrocyte proteins; (b) intact erythrocyte ghosts; and (c) erythrocyte ghosts that are initially leaky and then immediately sealed and transferred to a solution that does not contain the labeling reagent.
18. Predict the effect of a mutation in signal peptidase that narrows its specificity so that it cleaves only between two Leu residues.
19. Explain why a drug that interferes with the disassembly of a SNARE complex would block neurotransmission.

REFERENCES

Lipids and Membrane Structure

Edidin, M., Lipids on the frontier: a century of cell-membrane bilayers, *Nature Rev. Mol. Cell Biol.* **4,** 414–418 (2003). [A short account of the history of the study of membranes.]

Engelman, D.M., Membranes are more mosaic than fluid, *Nature* **438,** 578–580 (2005). [A brief review updating the classic model with more proteins and variable bilayer thickness.]

Gurr, M.I., Harwood, J.L., and Frayn, K.N., *Lipid Biochemistry: An Introduction* (5th ed.), Blackwell Science (2002).

Nagle, J.F. and Tristram-Nagle, S., Lipid bilayer structure, *Curr. Opin. Struct. Biol*. **10,** 474–480 (2000). [Explains why it is difficult to quantitatively describe the structure of the lipid bilayer.]

Vance, D.E. and Vance, J. (Eds.), *Biochemistry of Lipids, Lipoproteins, and Membranes* (4th ed.), Elsevier (2002).

Membrane Proteins

Fleishman, S.J., Unger, V.M., and Ben-Tal, N., Transmembrane protein structures without X-rays, *Trends Biochem. Sci.* **31,** 106–113 (2006). [Discusses how information about TM proteins can be obtained from a limited number of known protein structures.]

Grum, V.L., Li, D., MacDonald, R.I., and Mondragón, A., Structures of two repeats of spectrin suggest models of flexibility, *Cell* **98,** 523–535 (1999).

Popot, J.-L. and Engelman, D.M., Helical membrane protein folding, stability, and evolution, *Annu. Rev. Biochem*. **69,** 881–922 (2000). [Shows a number of protein structures and discusses many features of transmembrane proteins.]

Sharom, F.J., and Lehto, M.T., Glycosylphosphatidylinositol-anchored proteins: structure, function, and cleavage by phosphatidylinositol-specific phospholipase C, *Biochem. Cell Biol.* **80,** 535–549 (2002). [Includes a discussion of the GPI anchor and its importance for protein localization and function.]

Subramaniam, S., The structure of bacteriorhodopsin: an emerging consensus, *Curr. Opin. Struct. Biol*. **9,** 462–468 (1999). [Compares the six structures of bacteriorhodopsin that have been independently determined by electron or X-ray crystallography and finds them to be remarkably similar.]

Wimley, W.C., The versatile β-barrel membrane protein, *Curr. Opin. Struct. Biol.* **13,** 404–411 (2003). [Reviews the basic principles of construction for transmembrane β barrels.]

Zhang, F.L. and Casey, P.J., Protein prenylation: molecular mechanisms and functional consequences, *Annu. Rev. Biochem*. **65,** 241–269 (1996).

The Secretory Pathway

Alder, N.N. and Johnson, A.E., Cotranslational membrane protein biogenesis at the endoplasmic reticulum, *J. Biol. Chem.* **279,** 22787–22790 (2004).

Keenan, R.J., Fraymann, D.M., Stroud, R.M., and Walter, P., The signal recognition particle, *Annu. Rev. Biochem*. **70,** 755–775 (2001).

van den Berg, B., Clemons, W.M., Jr., Collinson, I., Modis, Y., Hartmann, E., Harrison, S.C., and Rapaport, T.A., X-Ray structure of a protein-conducting channel, *Nature* **427,** 36–44 (2004). [The X-ray structure of SecY.]

Vesicle Trafficking

Brodsky, F.M., Chen, C.-Y., Knuehl, C., Towler, M.C., and Wakeham, D.E., Biological basket weaving: formation and function of clathrin-coated vesicles, *Annu. Rev. Cell Dev. Biol*. **17,** 515–568 (2001).

Kirchhausen, T., Clathrin, *Annu. Rev. Biochem*. **69,** 677–706 (2000).

Membrane Fusion

Skehel, J.J and Wiley, D.C., Receptor binding and membrane fusion in virus entry: The influenza hemagglutinin, *Annu. Rev. Biochem.* **69,** 531–569 (2000).

Ungar, D. and Hughson, F.M., SNARE protein structure and function, *Annu. Rev. Cell Dev. Biol.* **19,** 493–517 (2003).

Ungermann, C. and Langosch, D., Functions of SNAREs in intracellular membrane fusion and lipid bilayer mixing. *J. Cell Sci.* **118,** 3819–3828 (2005).

10

Membrane Transport

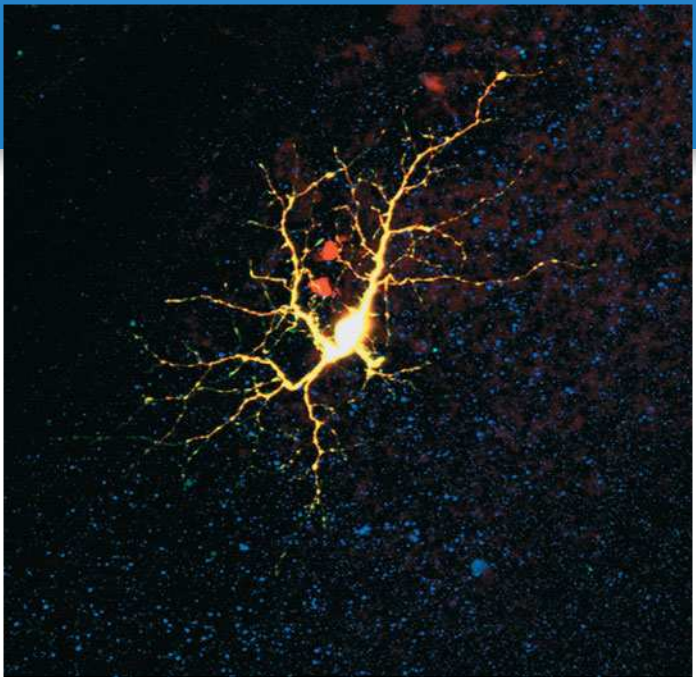

The impermeable membranes of cells, including those of neurons such as that pictured here, permit the establishment of a membrane potential, which changes when certain membrane proteins allow ions to flow into or out of the cell. [David Becker/Photo Researchers.]

CHAPTER CONTENTS

1 Thermodynamics of Transport

2 Passive-Mediated Transport

- **A.** Ionophores Carry Ions across Membranes
- **B.** Porins Contain β Barrels
- **C.** Ion Channels Are Highly Selective
- **D.** Aquaporins Mediate the Transmembrane Movement of Water
- **E.** Transport Proteins Alternate between Two Conformations

3 Active Transport

- **A.** The (Na^+–K^+)–ATPase Transports Ions in Opposite Directions
- **B.** The Ca^{2+}–ATPase Pumps Ca^{2+} Out of the Cytosol
- **C.** ABC Transporters Are Responsible for Drug Resistance
- **D.** Active Transport May Be Driven by Ion Gradients

MEDIA RESOURCES

(available at www.wiley.com/college/voet)

Interactive Exercise 5. The K^+ channel selectivity filter

Animated Figure 10-13. Model for glucose transport

Case Study 3. Carbonic Anhydrase II Deficiency

Case Study 14. Shavings from the Carpenter's Bench: The Biological Role of the Insulin C-peptide

Case Study 17. A Possible Mechanism for Blindness Associated with Diabetes: Na^+-Dependent Glucose Uptake by Retinal Cells

Cells are separated from their environments by plasma membranes. Eukaryotic cells, in addition, are compartmentalized by intracellular membranes that form the boundaries and internal structures of their various organelles. Biological membranes present formidable barriers to the passage of ionic and polar substances, so *these substances can traverse membranes only through the action of specific* ***transport proteins.*** Such proteins are therefore required to mediate the transmembrane movements of ions, such as Na^+, K^+, Ca^{2+}, and Cl^-, as well as metabolites such as pyruvate, amino acids, sugars, and nucleotides, and even water. Transport proteins are also responsible for all biological electrochemical phenomena such as neurotransmission. More complicated processes (e.g., endocytosis) are required to move larger substances such as proteins and macromolecular aggregates across membranes.

We begin our discussion of membrane transport by considering the thermodynamics of this process. We will then examine the structures and mechanisms of several different types of transport systems.

1 Thermodynamics of Transport

LEARNING OBJECTIVE

- Understand the thermodynamics of mediated and nonmediated membrane transport.

The diffusion of a substance between two sides of a membrane

$$\mathrm{A}(out) \rightleftharpoons \mathrm{A}(in)$$

thermodynamically resembles a chemical equilibration. We saw in Section 1-3D that the free energy of a solute, A, varies with its concentration:

$$\overline{G}_{\mathrm{A}} = \overline{G}_{\mathrm{A}}^{\circ\prime} = RT\ln[\mathrm{A}] \qquad [10\text{-}1]$$

where $\overline{G}_{\mathrm{A}}$ is the **chemical potential** (partial molar free energy) of A (the bar indicates quantity per mole) and $\overline{G}_{\mathrm{A}}^{\circ\prime}$ is the chemical potential of its standard state. Thus, a difference in the concentrations of the substance on two sides of a membrane generates a **chemical potential difference:**

$$\Delta\overline{G}_{\mathrm{A}} = \overline{G}_{\mathrm{A}}(in) - \overline{G}_{\mathrm{A}}(out) = RT\ln\left(\frac{[\mathrm{A}]_{in}}{[\mathrm{A}]_{out}}\right) \qquad [10\text{-}2]$$

SAMPLE CALCULATION 10-1

Show that $\Delta G < 0$ when Ca^{2+} ions move from the endoplasmic reticulum (where $[\mathrm{Ca}^{2+}] = 1$ mM) to the cytosol (where $[\mathrm{Ca}^{2+}] = 0.1$ μM). Assume $\Delta\Psi = 0$.
The cytosol is *in* and the endoplasmic reticulum is *out*.

$$\Delta G = RT\ln\frac{[\mathrm{Ca}^{2+}]_{in}}{[\mathrm{Ca}^{2+}]_{out}} = RT\ln\frac{10^{-7}}{10^{-3}}$$

$$= RT(-9.2)$$

Hence, ΔG is negative.

Consequently, if the concentration of A outside the membrane is greater than that inside, $\Delta\overline{G}_{\mathrm{A}}$ for the transfer of A from outside to inside will be negative and the spontaneous net flow of A will be inward. If, however, [A] is greater inside than outside, $\Delta\overline{G}_{\mathrm{A}}$ is positive and an inward net flow of A can occur only if an exergonic process, such as ATP hydrolysis, is coupled to it to make the overall free energy change negative (see Sample Calculation 10-1).

The transmembrane movement of ions also results in charge differences across the membrane, thereby generating an electrical potential difference, $\Delta\Psi = \Psi(in) - \Psi(out)$, where **ΔΨ** is termed the **membrane potential.** Consequently, if A is ionic, Eq. 10-2 must be amended to include the electrical work required to transfer a mole of A across the membrane from outside to inside:

$$\Delta\overline{G}_{\mathrm{A}} = RT\ln\left(\frac{[\mathrm{A}]_{in}}{[\mathrm{A}]_{out}}\right) + Z_{\mathrm{A}}\mathcal{F}\Delta\Psi \qquad [10\text{-}3]$$

where Z_{A} is the ionic charge of A; $\mathcal{F}$, the Faraday constant, is the charge of a mole of electrons (96,485 $\mathrm{C\cdot mol^{-1}}$; C is the symbol for coulomb); and $\overline{G}_{\mathrm{A}}$ is now termed the **electrochemical potential** of A. The membrane potentials of living cells are commonly as large as −100 mV (inside negative; note that $1\ \mathrm{V} = 1\ \mathrm{J\cdot C^{-1}}$), which for a 50-Å-thick membrane corresponds to a voltage gradient of 200,000 $\mathrm{V\cdot cm^{-1}}$. Hence, the last term in Eq. 10-3 is often significant for ionic substances, particularly in mitochondria (Chapter 18) and in neurotransmission (Section 10-2C).

Transport May Be Mediated or Nonmediated. There are two types of transport processes: **nonmediated transport** and **mediated transport.** Nonmediated transport occurs through simple diffusion. In contrast, mediated transport occurs through the action of specific carrier proteins. The driving force for the nonmediated flow of a substance through a medium is its chemical potential gradient. Thus, *the substance diffuses in the direction that eliminates its concentration gradient, at a rate proportional to the magnitude of the gradient. The rate of diffusion of a substance also depends on its solubility in the membrane's nonpolar core*. Consequently, nonpolar molecules such as steroids and O_2 readily diffuse through biological membranes by nonmediated transport, according to their concentration gradients across the membranes.

Mediated transport is classified into two categories depending on the thermodynamics of the system:

1. **Passive-mediated transport,** or **facilitated diffusion,** in which a specific molecule flows from high concentration to low concentration.
2. **Active transport,** in which a specific molecule is transported from low concentration to high concentration, that is, against its concentration gradient. Such an endergonic process must be coupled to a sufficiently exergonic process to make it favorable (i.e., $\Delta G < 0$).

CHECK YOUR UNDERSTANDING

Explain why the free energy change of membrane transport depends on both the concentration and charge of the transported substance.

Explain the differences between mediated and nonmediated transport across membranes.

2 Passive-Mediated Transport

LEARNING OBJECTIVES

- Understand the overall structure and mechanism of ionophores, porins, ion channels, aquaporins, and transport proteins.
- Understand the protein features that make passive-mediated transport systems specific for a solute.
- Understand the importance of gating in ion channels.
- Understand that membrane proteins may mediate uniport, symport, and antiport transport.

Substances that are too large or too polar to diffuse across lipid bilayers on their own may be conveyed across membranes via proteins or other molecules that are variously called **carriers, permeases, channels,** and **transporters.** These transporters operate under the same thermodynamic principles but vary widely in structure and mechanism, particularly as it relates to their selectivity.

A | Ionophores Carry Ions across Membranes

Ionophores are organic molecules of diverse types, often of bacterial origin, that increase the permeability of membranes to ions. These molecules often exert an antibiotic effect by discharging the vital ion concentration gradients that cells actively maintain.

There are two types of ionophores:

1. ***Carrier ionophores,*** *which increase the permeabilities of membranes to their selected ion by binding it, diffusing through the membrane, and releasing the ion on the other side* (Fig. 10-1*a*). For net transport to occur, the uncomplexed ionophore must then return to the original side of the membrane ready to repeat the process. Carriers therefore share the common property that *their ionic complexes are soluble in nonpolar solvents.*
2. ***Channel-forming ionophores,*** *which form transmembrane channels or pores through which their selected ions can diffuse* (Fig. 10-1*b*).

Both types of ionophores transport ions at a remarkable rate. For example, a single molecule of the carrier ionophore **valinomycin** transports up to 10^4 K^+ ions per second across a membrane. However, *since ionophores*

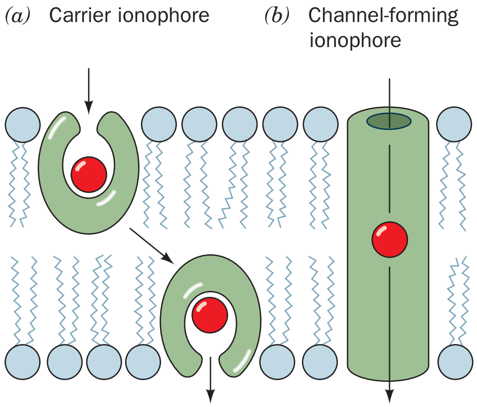

Figure 10-1 | Ionophore action. (*a*) Carrier ionophores transport ions by diffusing through the lipid bilayer. (*b*) Channel-forming ionophores span the membrane with a channel through which ions can diffuse.

(a)

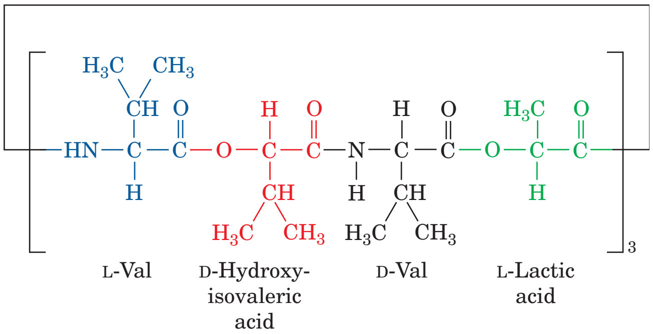

Valinomycin

(b)

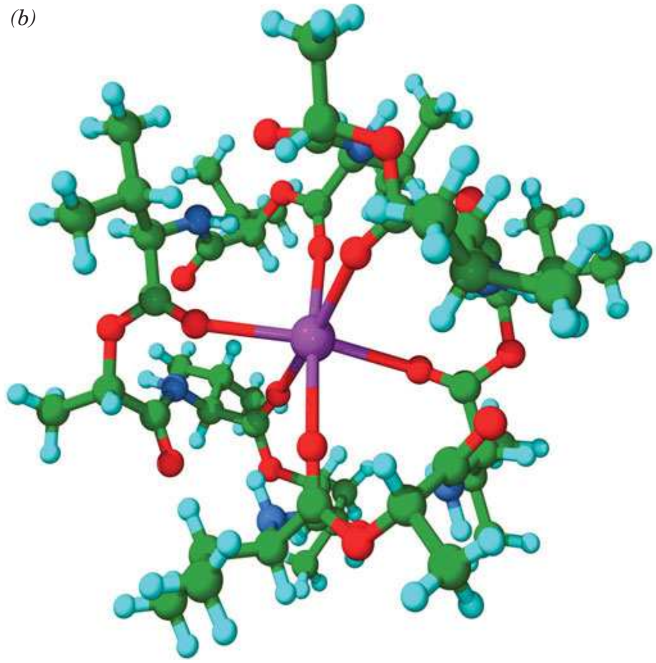

■ **Figure 10-2** | **Valinomycin.** (*a*) This cyclic ionophore contains ester and amide bonds and D- as well as L-amino acids. (*b*) X-Ray structure of valinomycin in complex with a K^+ ion colored according to atom type (C green, H cyan, N blue, O red, and K^+ purple). Note that the K^+ ion is octahedrally coordinated by the carbonyl oxygen atoms of its six Val residues. [Based on an X-ray structure by Max Dobler, ETH, Zürich, Switzerland.]

passively permit ions to diffuse across a membrane in either direction, their effect can only be to equilibrate the concentrations of their selected ions across the membrane.

Valinomycin, which is one of the best characterized ionophores, specifically binds K^+. It is a cyclic molecule containing D- and L-amino acid residues that participate in ester linkages as well as peptide bonds (Fig. 10-2*a*). The X-ray structure of valinomycin's K^+ complex (Fig. 10-2*b*) indicates that the K^+ ion is octahedrally coordinated by the carbonyl groups of its six Val residues, and the cyclic valinomycin backbone surrounds the K^+ coordination shell. The methyl and isopropyl side chains project outward to provide the complex with a nonpolar exterior that makes it soluble in the hydrophobic cores of lipid bilayers.

The K^+ ion (ionic radius, $r = 1.33$ Å) fits snugly into valinomycin's coordination site, but the site is too large for Na^+ ($r = 0.95$ Å) or Li^+ ($r = 0.60$ Å) to coordinate with all six carbonyl oxygens. Valinomycin therefore has 10,000-fold greater binding affinity for K^+ than for Na^+. No other known substance discriminates better between Na^+ and K^+.

B | Porins Contain β Barrels

The porins, introduced in Section 9-3A, are β barrel structures with a central aqueous channel. In the *E. coli* OmpF porin (Fig. 9-23), the channel is constricted to form an elliptical pore with a minimum cross section of 7×11 Å. Consequently, solutes of more than ~600 D are too large to pass through the channel. OmpF is weakly cation selective; other porins are more selective for anions. In general, the size of the channel and the residues that form its walls determine what types of substances can pass through.

Solute selectivity is elegantly illustrated by **maltoporin.** This bacterial outer membrane protein facilitates the diffusion of **maltodextrins,** which are the α(1→4)-linked glucose oligosaccharide degradation products of starch (Section 8-2C). The X-ray structure of *E. coli* maltoporin reveals that the protein is structurally similar to OmpF porin but is a homotrimer of 18-stranded rather than 16-stranded antiparallel β barrels. Three long loops from the extracellular face of each maltoporin subunit fold inward into the barrel, thereby constricting the channel near the center of the membrane to a diameter of ~5 Å and giving the channel an hourglass-like cross section. The channel is lined on one side with a series of six contiguous aromatic side chains arranged in a left-handed helical path that matches the left-hand helical curvature of α-amylose (Fig. 8-10). This so-called greasy slide extends from one end of the channel, through its constriction, to the other end (Fig. 10-3).

How does the greasy slide work? The hydrophobic faces of the maltodextrin glucose residues stack on aromatic side chains, as is often observed in complexes of sugars with proteins. The glucose hydroxyl groups, which are arranged in two strips along opposite edges of the maltodextrins, form numerous hydrogen bonds with polar and charged side chains that line the channel. Tyr 118, which protrudes into the channel opposite the greasy slide, apparently functions as a steric barrier that only permits the passage of near-planar groups such as glucosyl residues. Thus, the hook-shaped sucrose (a glucose–fructose disaccharide) passes only very slowly through the maltoporin channel.

At the start of the translocation process, the entering glucosyl residue interacts with the readily accessible end of the greasy slide in the extracellular vestibule of the channel. Further translocation along the helical channel requires the maltodextrin to follow a screwlike path that maintains the helical structure of the oligosaccharide, much like the movement of a bolt through a nut, thereby excluding molecules of comparable size that have different shapes. *The translocation process is unlikely to encounter any large energy barrier due to the smooth surface of the greasy slide and the multiple polar groups at the channel constriction that would permit the essentially continuous exchange of hydrogen bonds as a maltodextrin moves through the constriction.*

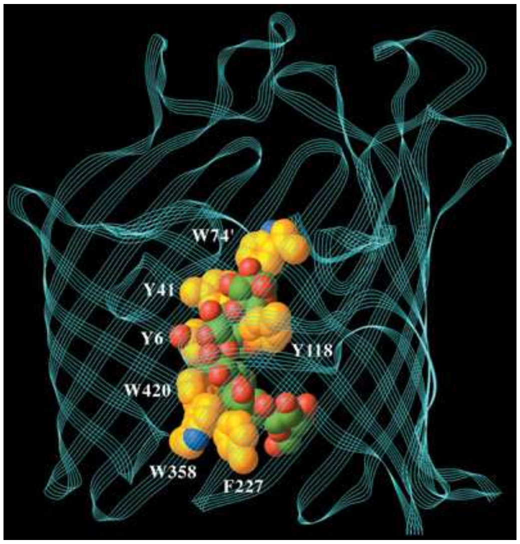

Figure 10-3 | Structure of a maltoporin subunit in complex with a malto-dextrin of six glycosyl units. The polypeptide backbone of this *E. coli* protein is represented by a cyan ribbon. Five glucose residues of maltodextrin and the aromatic side chains lining the transport channel are shown in space-filling form with N blue, O red, protein C gold, and glucosyl C green. The "greasy slide" consists of the aromatic side chains of six residues. Tyr 118, which projects into the channel, helps restrict passage to glucosyl residues. [Based on an X-ray structure by Tilman Schirmer, University of Basel, Basel, Switzerland. PDBid 1MPO.]

C | Ion Channels Are Highly Selective

All cells contain ion-specific channels that allow the rapid passage of ions such as Na^+, K^+, and Cl^-. The movement of these ions through such channels, along with their movement through active transporters (discussed in Section 10-3), is essential for maintaining osmotic balance, for signal transduction (Section 13-4A), and for effecting changes in membrane potential that are responsible for neurotransmission. Mammalian cells, for example, maintain a nonequilibrium distribution of ions on either side of the plasma membrane: ~150 mM Na^+ and ~4 mM K^+ in the extracellular fluid, and ~12 mM Na^+ and ~140 mM K^+ inside the cell.

The Structure of the KcsA K^+ Channel Explains Its Selectivity and Speed. Potassium ions passively diffuse from the cytoplasm to the extracellular space through transmembrane proteins known as **K^+ channels.** Although there is a large diversity of K^+ channels, even within a single organism, all of them have similar sequences, exhibit comparable permeability characteristics, and most importantly, are at least 10,000-fold more permeable to K^+ than Na^+. Since this high selectivity (around the same as that of valinomycin; Section 10-2A) implies energetically strong interactions between K^+ and the protein, how can the K^+ channel maintain its observed nearly diffusion-limited throughput rate of up to 10^8 ions per second (a 10^4-fold greater rate than that of valinomycin)?

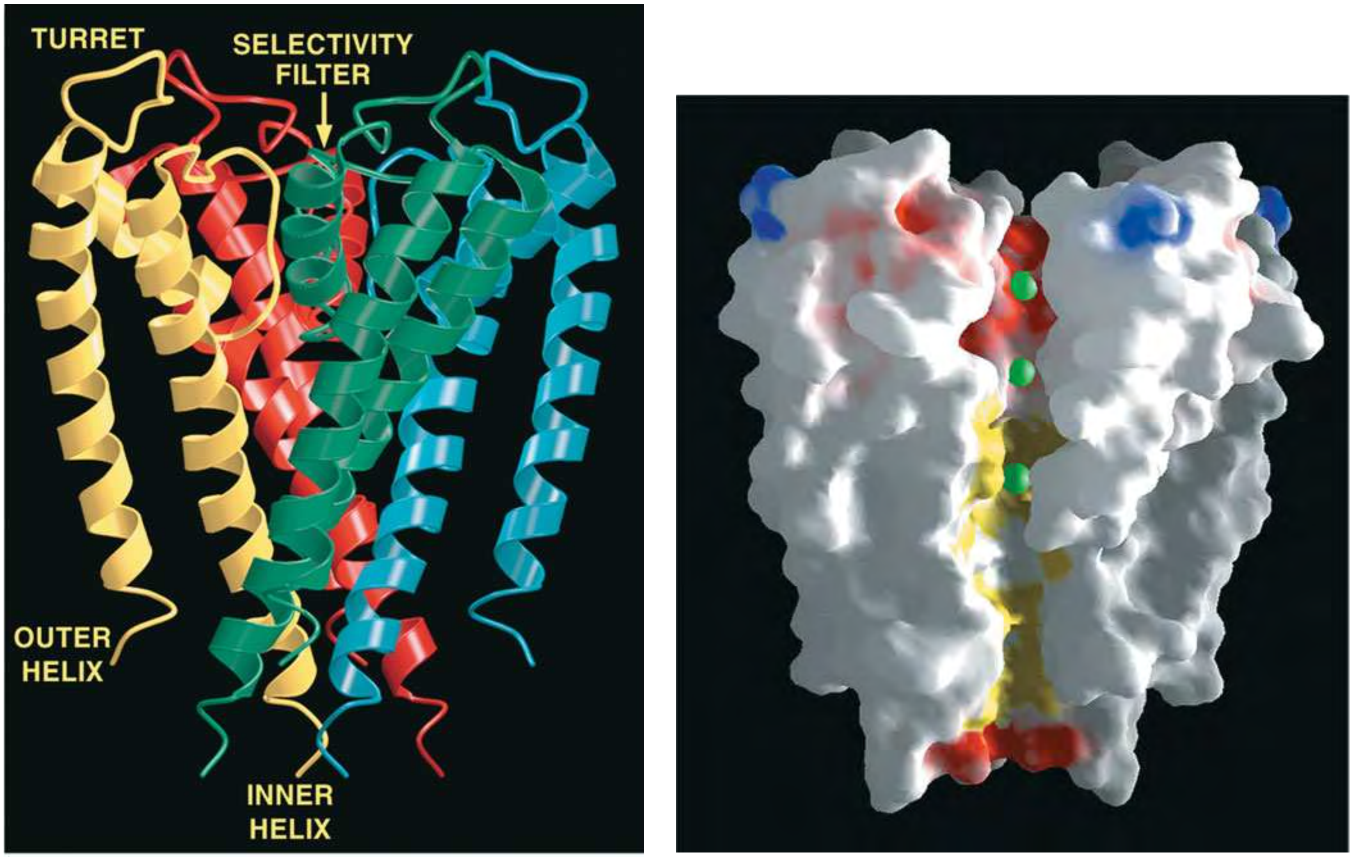

(a)

(b)

Figure 10-4 | X-Ray structure of the KcsA K^+ channel. (*a*) Ribbon diagram of the tetramer as viewed from within the plane of the membrane, with the cytoplasm below and the extracellular region above. The protein's fourfold axis of rotation is vertical and each of its identical subunits is differently colored. Each subunit has an inner helix that forms part of the central pore, an outer helix that contacts the membrane interior, and a turret that projects out into the extracellular space. The selectivity filter at the extracellular end of the protein allows the passage of K^+ ions but not Na^+ ions. (*b*) Cutaway diagram viewed similarly to Part *a* in which the K^+ channel is represented by its solvent-accessible surface. The surface is colored according to its physical properties with negatively charged areas red, uncharged areas white, positively charged areas blue, and hydrophobic areas of the central pore yellow. K^+ ions are represented by green spheres. [Courtesy of Roderick MacKinnon, Rockefeller University. PDBid 1BL8.]

One of the best characterized ion channels is a K^+ channel from *Streptomyces lividans* named **KcsA.** This 158-residue integral membrane protein, like all known K^+ channels, functions as a homotetramer. The X-ray structure of KcsA's N-terminal 125-residue segment, determined by Roderick MacKinnon, reveals that each of its subunits contains two nearly parallel transmembrane helices plus a shorter helix (Fig. 10-4*a*). Four such subunits associate to form a fourfold symmetric assembly surrounding a central pore. The four inner helices, which largely form the pore, pack against each other near the cytoplasmic side of the membrane much like the poles of an inverted teepee. The four outer helices, which face the lipid bilayer, buttress the inner helices. The central pore can accommodate several K^+ ions (Fig. 10-4*b*).

The 45-Å-long central pore has variable width: It starts at its cytoplasmic side as an ~6-Å-diameter tunnel whose entrance is lined with four anionic side chains (red area at the bottom of Fig. 10-4*b*) that presumably attract cations and repel anions. The pore then widens to form an ~10-Å-diameter cavity. These regions of the central pore are wide enough so that a K^+ ion could move through them in its hydrated state. However, the upper part of the pore, called the selectivity filter, narrows to 3 Å, thereby forcing a transiting K^+ ion to shed its waters of hydration. The walls of the pore and the cavity are lined with hydrophobic groups that interact minimally with diffusing ions (yellow area of the pore in Fig. 10-4*b*). However, the selectivity filter (red area of the pore at the top of Fig. 10-4*b*) is lined with closely spaced main chain carbonyl oxygens of residues from a TVGYG "signature sequence" that is highly conserved in all K^+ channels.

How does the K^+ channel discriminate so acutely between K^+ and Na^+ ions? The main chain O atoms lining the selectivity filter form a stack of rings (Fig. 10-5, *top*) that provide a series of closely spaced sites of appropriate dimensions for coordinating dehydrated K^+ ions but not the smaller Na^+ ions. The structure of the protein surrounding the selectivity filter suggests that the diameter of the pore is rigidly maintained, thus making the energy of a dehydrated Na^+ in the selectivity filter considerably higher than that of hydrated Na^+ and thereby accounting for the K^+ channel's high selectivity for K^+ ions.

What is the function of the cavity? Energy calculations indicate that an ion moving through a narrow transmembrane pore must surmount an energy barrier that is maximal at the center of the membrane. The existence of the cavity reduces this electrostatic destabilization by surrounding the ion with polarizable water molecules (Fig. 10-5, *bottom*). The cavity holds ~40 additional water molecules, which are disordered and therefore not seen in the X-ray structure. Remarkably, the K^+ ion occupying the cavity is liganded by 8 ordered water molecules located at the corners of a square antiprism (a cube with one face twisted by 45° with respect to the opposite face). K^+ in aqueous solution is known to have such an inner hydration shell but it had never before been visualized.

How does KcsA support such a high throughput of K^+ ions (up to 10^8 ions per second)? Figure 10-5 shows a string of regularly spaced K^+ ions: four in the selectivity filter and two more just outside it on its extracellular (top) side. Such closely spaced positive ions would strongly repel one another and hence represent a high energy situation. However, the X-ray structure is an average of many KcsA molecules, and a variety of evidence indicates that within a single channel, the K^+ ions in the pore actually alternate with water molecules. This arrangement means that each K^+ ion is surrounded by O atoms (from H_2O or protein carbonyl groups) at each position along the selectivity filter. As a K^+ ion moves into the selectivity filter from the cavity, it exchanges some of its hydrating water molecules for protein ligands, then does the reverse to restore its hydration shell when it exits the selectivity filter to enter the extracellular solution. Within the selectivity filter, the ligands are spaced and oriented such that there is little free energy change ($<12\ kJ \cdot mol^{-1}$) as a K^+ ion moves to successive positions. This level free energy landscape allows the rapid movement of K^+ ions through the ion channel. In

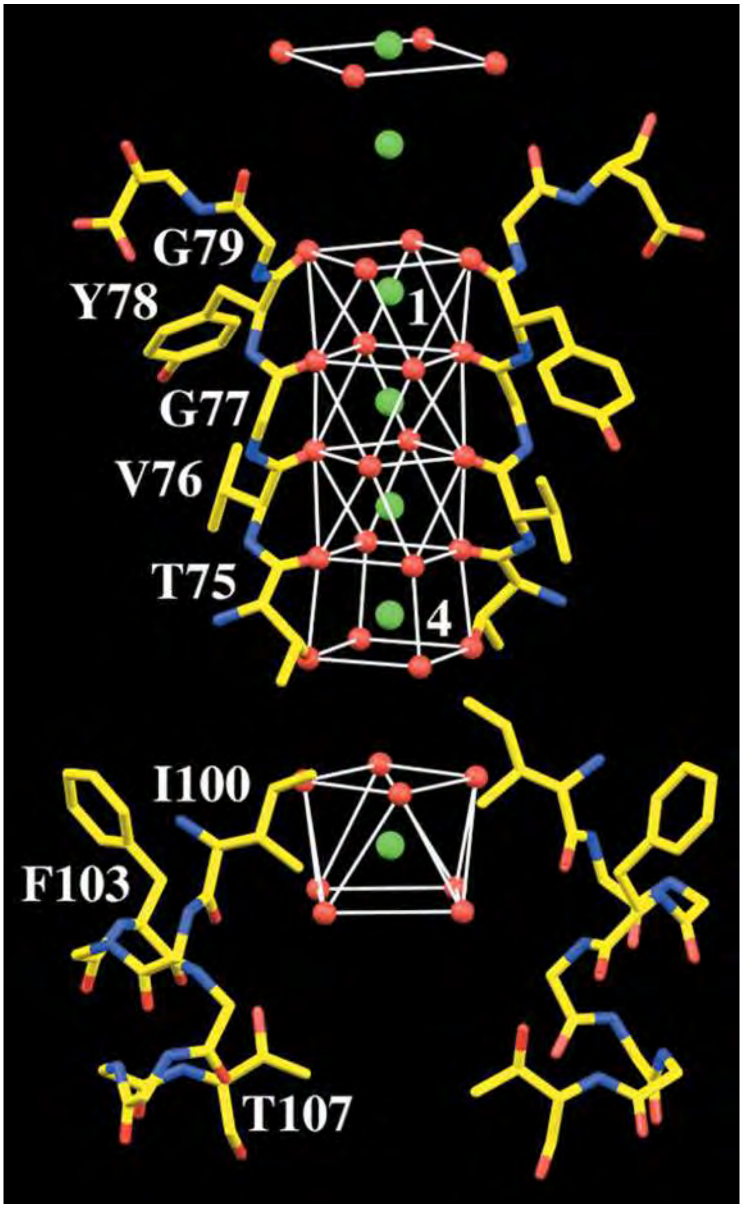

Figure 10-5 | Portions of the KcsA K^+ channel responsible for its ion selectivity. The protein is viewed similarly to Fig. 10-4 but with the front and back subunits omitted for clarity. The residues forming the cavity (*bottom*) and selectivity filter (*top*) are shown with atoms colored according to type (C yellow, N blue, O red, and K^+ ions represented by green spheres). The water and protein O atoms that ligand the K^+ ions, including those contributed by the front and back subunits, are represented by red spheres. The coordination polyhedra formed by these O atoms are outlined by thin white lines. [Based on an X-ray structure by Roderick MacKinnon, Rockefeller University. PDBid 1K4C.] **See Interactive Exercise 5.**

addition, mutual electrostatic repulsions between successive K^+ ions balance the attractive interactions holding these ions in the selectivity filter and hence further facilitate their rapid transit.

Ion Channels Are Gated. The physiological functions of ion channels depend not only on their exquisite ion specificity and speed of transport but also on their ability to be selectively opened or closed. For example, the ion gradients across cell membranes, which are generated by specific energy-driven pumps (Section 10-3), are discharged through Na^+ and K^+ channels. However, the pumps could not keep up with the massive fluxes of ions passing through the open channels, so *ion channels are normally shut and only open transiently to perform some specific task for the cell.* The opening and closing of ion channels, a process known as **gating,** can occur in response to a variety of stimuli:

1. **Mechanosensitive channels** open in response to local deformations in the lipid bilayer. Consequently, they respond to direct physical stimuli such as touch, sound, and changes in osmotic pressure.
2. **Ligand-gated channels** open in response to an extracellular chemical stimulus such as a neurotransmitter.
3. **Signal-gated channels** open on intracellularly binding a Ca^{2+} ion or some other signaling molecule (Section 13-4A).
4. **Voltage-gated channels** open in response to a change in membrane potential. Multicellular organisms contain numerous varieties of voltage-gated channels, including those responsible for generating nerve impulses.

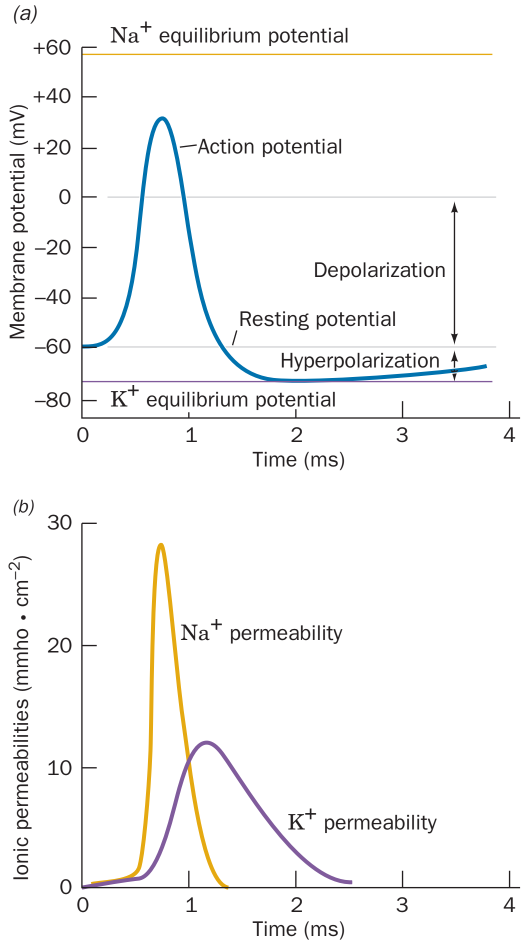

Figure 10-6 | Time course of an action potential. (*a*) The neuron membrane undergoes rapid depolarization, followed by a nearly as rapid hyperpolarization and then a slow recovery to its resting potential. (*b*) The depolarization is caused by a transient increase in Na^+ permeability (conductance), whereas the hyperpolarization results from a more prolonged increase in K^+ permeability that begins a fraction of a millisecond later. [After Hodgkin, A.L. and Huxley, A.F., *J. Physiol.* **117,** 530 (1952).]

Nerve Impulses Are Propagated by Action Potentials. As an example of the functions of voltage-gated channels, let us consider electrical signaling events in neurons (nerve cells). The stimulation of a neuron, a cell specialized for electrical signaling, causes Na^+ channels to open so that Na^+ ions spontaneously flow into the cell. The consequent local increase in membrane potential induces neighboring voltage-gated Na^+ channels to open. The resulting local **depolarization** of the membrane induces nearby voltage-gated K^+ channels to open. This allows K^+ ions to spontaneously flow out of the cell in a process called **repolarization** (Fig. 10-6). However, well before the distribution of Na^+ and K^+ ions across the membrane equilibrates, the Na^+ and K^+ channels spontaneously close. Yet, because depolarization of a membrane segment induces the voltage-gated Na^+ channels in a neighboring membrane segment to open, which induces their neighboring voltage-gated Na^+ channels to open, etc., a wave of transient change in the membrane potential, called an **action potential,** travels along the length of the nerve cell (which may be over 1 m long). The action potential, which travels at ~10 m/s, propagates in one direction only because, after the ion channels have spontaneously closed, they resist reopening until the membrane potential has regained its resting value, which takes a few milliseconds (Fig. 10-6).

As an action potential is propagated along the length of a nerve cell, it is continuously renewed so that its signal strength remains constant (in contrast, an electrical impulse traveling down a wire dissipates as a consequence of resistive and capacitive effects). Nevertheless, the relative ion imbalance responsible for the resting membrane potential is small; only a tiny fraction of a nerve cell's Na^+–K^+ gradient (which is generated by ion pumps; Section 10-3A) is discharged by a single nerve impulse (only one K^+ ion per 3000–300,000 in the cytosol is exchanged for extracellular Na^+ as indicated by measurements with radioactive Na^+). A nerve cell can therefore transmit a nerve impulse every few milliseconds without letup. This capacity to fire rapidly is an essential feature of neuronal communications: Since action potentials all have the same amplitude, the magnitude of a stimulus is conveyed by the rate at which a nerve fires.

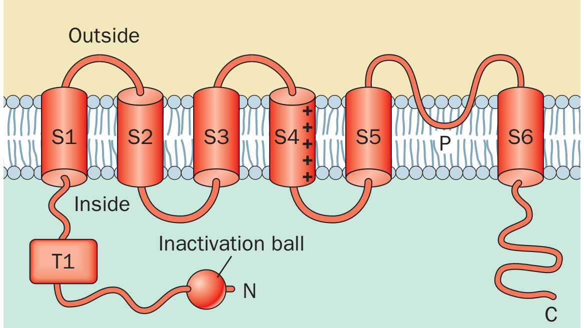

Figure 10-7 | Topology of voltage-gated K^+ channel subunits.

Voltage Gating in Kv Channels Is Triggered by the Motion of a Positively Charged Protein Helix. The subunits of all voltage-gated K^+ channels contain an ~220-residue N-terminal cytoplasmic domain, an ~250-residue transmembrane domain consisting of six helices, S1 to S6, and an ~150-residue C-terminal cytoplasmic domain (Fig. 10-7). S5 and S6 are respectively homologous to the outer and inner transmembrane helices of the KcsA channel (Fig. 10-4), and their intervening P-loop, which forms the selectivity filter, includes the same TVGYG signature sequence that occurs in KcsA. In the voltage-gated K^+ channels known as **Kv channels,** a conserved, cytoplasmic, ~100-residue so-called T1 domain precedes the transmembrane domain.

Kv channels closely resemble the KcsA channel in their tetrameric pore structure, but what is the nature of the gating machinery in the voltage-gated ion channels? The ~19-residue S4 helix, which contains around five positively charged side chains spaced about every three residues on an otherwise hydrophobic polypeptide, appears to act as a voltage sensor. Various experimental approaches indicate that when the membrane potential increases (the inside becomes less negative), the S4 helix is pulled toward the extracellular side of the membrane.

The X-ray structure of a Kv channel from rat brain named **Kv1.2** (Fig. 10-8) shows how gating might occur. As the membrane begins to depolarize, the four conserved Arg residues on the S4 helix are drawn

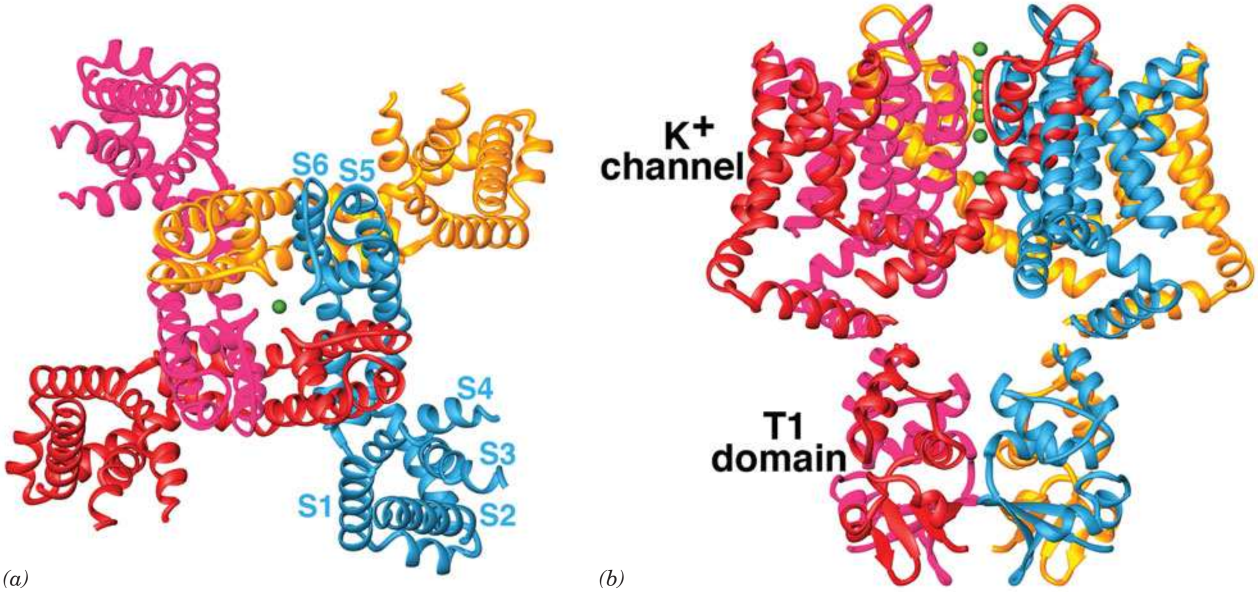

Figure 10-8 | X-Ray structure of the Kv1.2 voltage-gated K^+ channel. (*a*) View along the tetrameric protein's fourfold axis from the extracellular side of the membrane in which it is embedded. Each of its four identical subunits is colored differently, and the T1 domain has been omitted for clarity. The fragmented appearance of the polypeptide chains is due to the high mobilities of the missing segments. The S5 and S6 helices with their intervening P loops form the pore for K^+ ions (delineated by green spheres). Helices S1 to S4 form a separate intramembrane voltage-sensing domain that associates with the S5 and S6 helices of the clockwise adjacent subunit. (*b*) View perpendicular to that in Part *a* with the extracellular side of the membrane above. The pore and voltage sensing domains span a distance of 30 Å, the thickness of the membrane's hydrophobic core. The T1 domain, which occupies the cytoplasm, forms the vestibule of the transmembrane K^+ channel. The four large openings between the T1 domain and the K^+ channel are the portals through which K^+ ions enter the K^+ channel. [Based on an X-ray structure by Roderick MacKinnon, Rockefeller University. PDBid 2A79.]

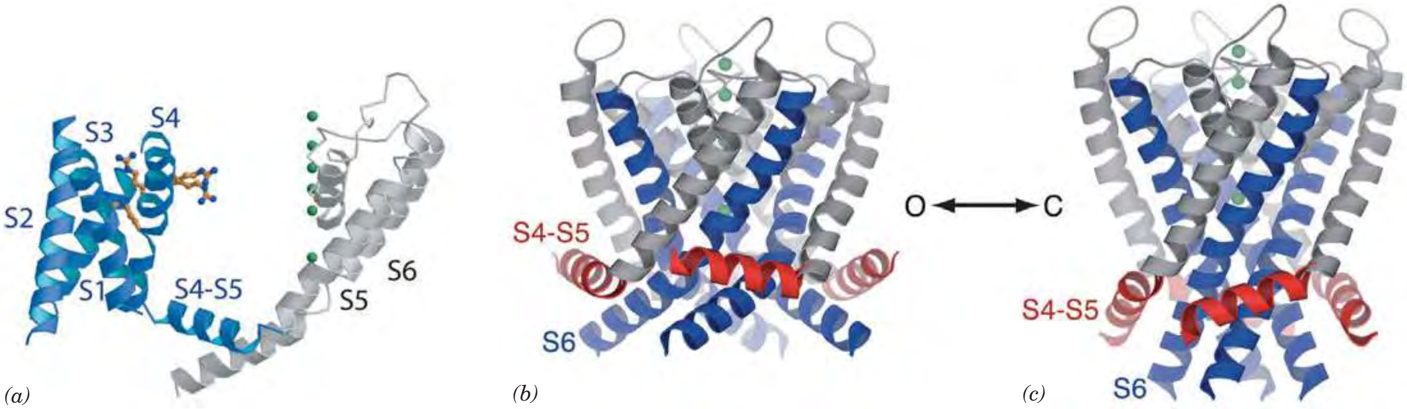

Figure 10-9 | Operation of the transmembrane domain of the Kv1.2 voltage-gated K$^+$ channel. (*a*) Side view of a single subunit with its extracellular side at the top. The pore-forming helices (S5 and S6) are gray, and the voltage-sensor domain (helices S1–S4) is blue. The S4–S5 linker helix (not drawn in Fig. 10-7), which is parallel to the membrane surface, connects the voltage-sensing domain to the domain forming the K$^+$ pore (delineated by green spheres). Four Arg residues on S4 are shown in ball-and-stick form with C atoms gold and N atoms blue. Two of these residues interact with the protein, and two project into the lipid bilayer. (*b*) Side view of the channel tetramer in its open conformation. The S5 helices are gray, the S6 helices are blue, and the S4–S5 linker helix is red. (*c*) Hypothetical model of the channel in its closed conformation, colored as in Part *b*. The downward movement of the Arg-bearing S4 helix (not shown in this drawing) pushes down on the S4–S5 linker helix to pinch off the pore at its cytoplasmic end (*bottom*). [Courtesy of Roderick MacKinnon, Rockefeller University. PDBid 2A79.]

toward the extracellular surface (up in Fig. 10-9), pulling on the S4-S5 linker helix (not drawn in Fig. 10-7) and with it the S5 helix. This splays the ends of the S6 helices so as to enlarge the intracellular entrance to the K$^+$ channel (Fig. 10-9*b*). During repolarization, as the cell interior becomes more negative, the positively charged S4 helix drops back toward the cytoplasmic side of the membrane, pressing down on the S4-S5 lever to close off the channel (Fig. 10-9*c*).

Ion Channels Have a Second Gate. Electrophysiological measurements indicate that Kv channels spontaneously close a few milliseconds after opening and do not reopen until after the membrane has regained its resting membrane potential. Evidently, *the Kv channel contains two voltage-sensitive gates, one to open the channel on an increase in membrane potential and one to inactivate it a short time later*. This inactivation of the Kv channel is abolished by proteolytically excising its N-terminal 20-residue segment, whose NMR structure is a ball-like assembly. In the intact Kv channel, this "inactivation ball" is tethered to the end of a flexible 65-residue peptide segment (Fig. 10-7), suggesting that channel inactivation normally occurs when the ball swings around to bind in the mouth of the open K$^+$ pore, thereby blocking the passage of K$^+$ ions. The mobility of this "ball and chain" is presumably why it is not visible in the X-ray structure of Kv1.2 (Fig. 10-8).

The T1 tetramer does not have an axial channel, so the inactivation ball must find its way to block the central pore through the side portals between the T1 tetramer and the central pore (Fig. 10-8*b*). These portals, which are 15 to 20 Å across, are lined with negatively charged groups that presumably attract K$^+$ ions.

The cytoplasmic entrance to the K$^+$ channel pore is only 6 Å in diameter, too narrow to admit the inactivation ball. Therefore, it appears that the ball peptide must unfold in order to enter the pore. The first 10 residues of the unfolded ball peptide are predominantly hydrophobic and presumably make contact with the hydrophobic residues lining the Kv channel pore. The next 10 residues, which are largely hydrophilic and contain several cationic groups, bind to anionic groups lining the entrance to the side portals in T1. Thus, the inactivation peptide acts more like a snake than a ball and chain. A Kv channel engineered so that only one subunit has an inactivation peptide still becomes inactivated but at one-fourth the rate of normal Kv channels. Apparently, any of the normal Kv channel's four inactivation peptides can block the channel and it is simply a matter of chance as to which one does so.

Other Voltage-Gated Cation Channels Contain a Central Pore. Voltage-gated Na^+ and Ca^{2+} channels appear to resemble K^+ channels, although rather than forming homotetramers, they are monomers of four consecutive domains, each of which is homologous to the K^+ channel, separated by often large cytoplasmic loops. These domains presumably assume a pseudotetrameric arrangement about a central pore resembling that of voltage-gated K^+ channels. This structural homology suggests that voltage-gated ion channels share a common architecture in which differences in ion selectivity arise from precise stereochemical variations within the central pore. However, outside of their conserved transmembrane core, voltage-gated ion channels with different ion selectivities are highly divergent. For example, the T1 domain of Kv channels is absent in other types of voltage-gated ion channels.

Cl^- Channels Differ from Cation Channels. **Cl^- channels,** which occur in all cell types, permit the transmembrane movement of chloride ions along their concentration gradient. In mammals, the extracellular Cl^- concentration is ~120 mM and the intracellular concentration is ~4 mM.

ClC Cl^- channels form a large family of anion channels that occur widely in both prokaryotes and eukaryotes. The X-ray structures of ClC Cl^- channels from two species of bacteria, determined by MacKinnon, reveal, as biophysical measurements had previously suggested, that ClC Cl^- channels are homodimers with each subunit forming an anion-selective pore (Fig. 10-10). Each subunit consists mainly of 18 mostly transmembrane α helices that are remarkably tilted with respect to the membrane plane and have variable lengths compared to the transmembrane helices in other integral proteins of known structures.

The specificity of the Cl^- channel results from an electrostatic field established by basic amino acids on the protein surface, which helps funnel anions toward the pore, and by a selectivity filter formed by the N-terminal ends of several α helices. Because the polar groups of an α helix are all aligned (Fig. 6-7), it forms a strong electrical dipole with its N-terminal end positively charged. This feature of the selectivity filter helps attract Cl^- ions, which are specifically coordinated by main chain amide nitrogens and side chain hydroxyls from Ser and Tyr residues. A positively charged residue such as Lys or Arg, if it were present in

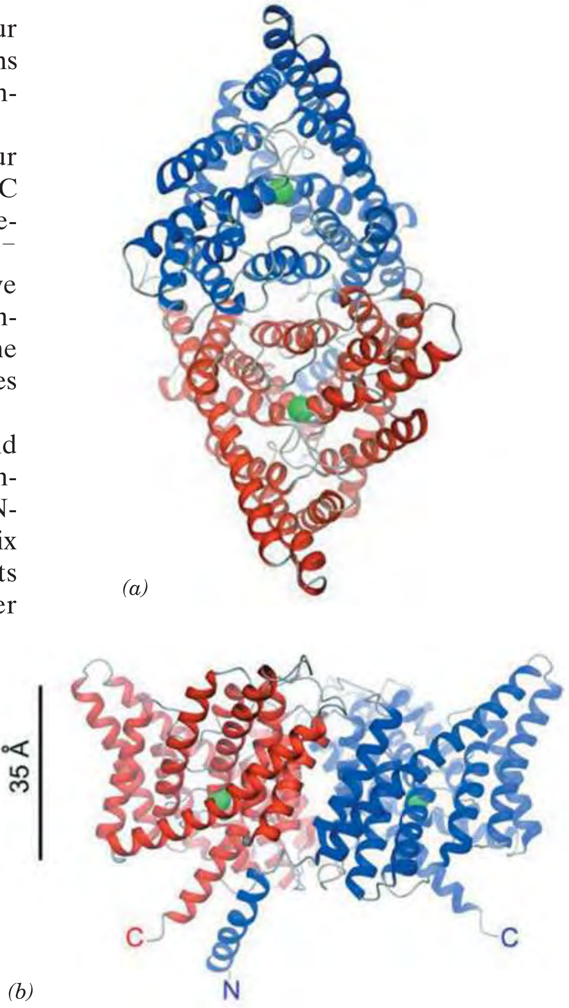

Figure 10-10 | **X-Ray structure of the ClC Cl^- channel from *Salmonella typhimurium*.** Each subunit of the homodimer contains 18 α helices of variable lengths. (*a*) View from the extracellular side of the membrane. The two subunits are colored blue and red. The green spheres represent Cl^- ions in the selectivity filter. (*b*) View from within the membrane with the extracellular surface above. The scale bar indicates the thickness of the membrane. [Courtesy of Roderick MacKinnon, Rockefeller University. PDBid 1KPL.]

the selectivity filter, would probably bind a Cl^- ion too tightly to facilitate its rapid transit through the channel.

Unlike the K^+ channel, which has a central aqueous cavity (Fig. 10-4*b*), the Cl^- channel is hourglass-shaped, with its narrowest part in the center of the membrane and flanked by wider aqueous "vestibules." A conserved Glu side chain projects into the pore. This group would repel other anions, suggesting that rapid Cl^- flux requires a protein conformational change in which the Glu side chain moves aside. Another anion could push the Glu away, which explains why some Cl^- channels appear to be activated by Cl^- ions; that is, they open in response to a certain concentration of Cl^- in the extracellular fluid.

D | Aquaporins Mediate the Transmembrane Movement of Water

The observed rapid passage of water molecules across biological membranes had long been assumed to occur via simple diffusion that was made possible by the small size of water molecules and their high concentrations in biological systems. However, certain cells, such as those in the kidney, can sustain particularly rapid rates of water transport, which can be reversibly inhibited by mercuric ions. This suggested the existence of previously unrecognized protein pores that conduct water through biological membranes. The first of these elusive proteins was discovered in 1992 by Peter Agre, who named them **aquaporins.**

Aquaporins are widely distributed in nature; plants may have as many as 50 different aquaporins. The 11 mammalian aquaporins that have been identified are expressed at high levels in tissues that rapidly transport water, including kidneys, salivary glands, and lacrimal glands (which produce tears). Aquaporins permit the passage of water molecules at an extremely high rate ($\sim 3 \times 10^9$ per second) but do not permit the transport of solutes (e.g., glycerol or urea) or ions, including, most surprisingly, protons (really hydronium ions; H_3O^+), whose free passage would discharge the cell's membrane potential.

The most extensively characterized member of the aquaporin family, **AQP1,** is a homotetrameric glycoprotein. Its X-ray and electron crystallographic structures reveal that each of its subunits consists mainly of six transmembrane α helices plus two shorter helices that lie within the bilayer (Fig. 10-11). These helices are arranged so as to form an elongated hourglass-shaped central pore that, at its narrowest point, the so-called constriction region, is ~2.8 Å wide, which is the van der Waals diameter of a water molecule (Fig. 10-12). Much of the pore is lined with hydrophobic groups whose lack of strong interactions with water molecules hastens their passage through the pore. However, for a water molecule to transit the constriction region, it must shed its associated waters of hydration. This is facilitated by the side chains of highly conserved Arg and His residues as well as several backbone carbonyl groups that form hydrogen bonds to a transiting water molecule and hence readily displace its associated water molecules, much as occurs with K^+ in the selectivity filter of the KcsA channel (Section 10-2C).

If water were to pass through aquaporin as an uninterrupted chain of hydrogen-bonded molecules, then protons would pass even more rapidly through the channel via proton jumping (Fig. 2-15; in order for more than one such series of proton jumps to occur, each water molecule in the chain must reorient such that one of its protons forms a hydrogen bond to the next water molecule in the chain). However, aquaporin interrupts this

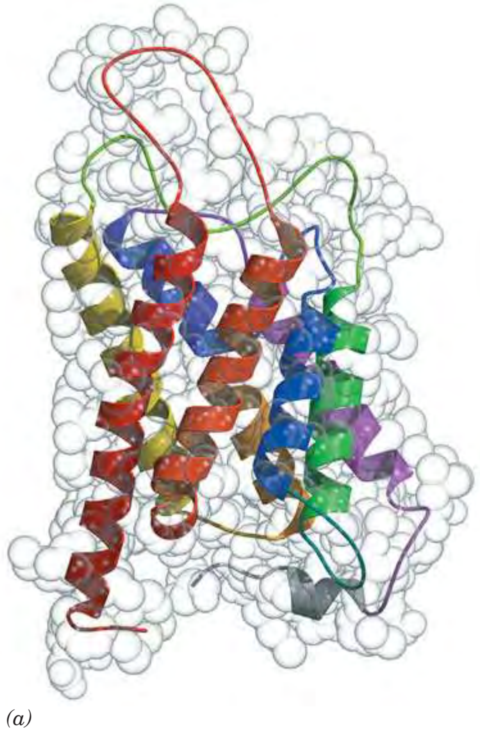

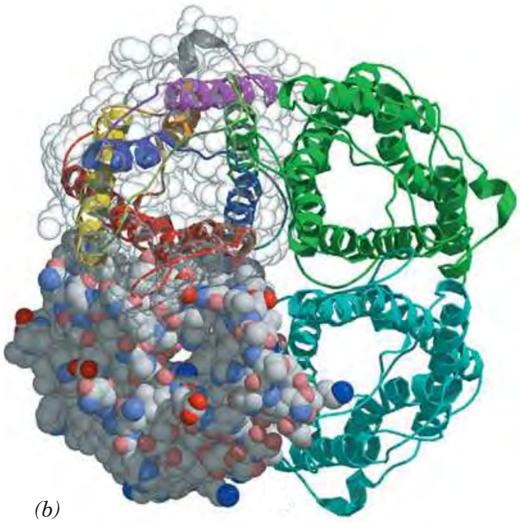

Figure 10-11 | X-Ray structure of the aquaporin AQP1 from bovine erythrocytes. (*a*) Superimposed ribbon and space-filling models of an aquaporin subunit as viewed from within the membrane with its extracellular surface above. The eight helical segments are drawn with different colors. (*b*) View of the aquaporin tetramer from the extracellular surface. Each subunit forms a water-transport channel, which is visible in the space-filling subunit model at the lower left. [Courtesy of Bing Jap, University of California at Berkeley. PDBid 1J4N.]

process by forming hydrogen bonds from the side chain NH_2 groups of two highly conserved Asn residues to a water molecule that is centrally located in the pore (Fig. 10-12). Consequently, although this central water molecule can readily donate hydrogen bonds to its neighboring water molecules in the hydrogen-bonded chain, it cannot accept one from them nor reorient, thereby severing the “proton-conducting wire.”

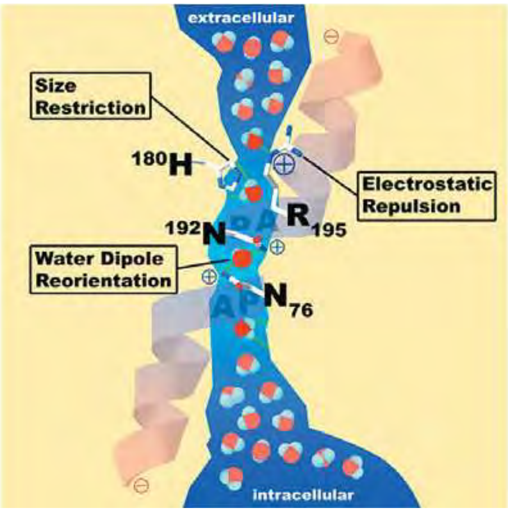

Figure 10-12 | Schematic drawing of the water-conducting pore of aquaporin AQP1. The pore is viewed from within the membrane with the extracellular surface above. The positions of residues critical for preventing the passage of protons, other ions, and small molecule solutes are indicated. [Courtesy of Peter Agre, The Johns Hopkins School of Medicine.]

E | Transport Proteins Alternate between Two Conformations

Up to this point, we have examined the structures and functions of membrane proteins that form a physical passageway for small molecules, ions, or water. Membrane proteins known as **connexins** also form such channels, in the form of **gap junctions** between cells (see Box 10-1). However, not all membrane transport proteins offer a discrete bilayer-spanning pore. Instead, some proteins undergo conformational changes to move substances from one side of the membrane to the other. The **erythrocyte glucose transporter** (also known as **GLUT1**) is such a protein.

Biochemical evidence indicates that GLUT1 has glucose-binding sites on both sides of the membrane. John Barnett showed that adding a propyl group to glucose C1 prevents glucose binding to the outer surface of the membrane, whereas adding a propyl group to C6 prevents binding to the inner surface. He therefore proposed that this transmembrane protein has two alternate conformations: one with the glucose site facing the external cell surface, requiring O1 contact and leaving O6 free, and the other with the glucose site facing the internal cell surface, requiring O6 contact and leaving O1 free. Transport apparently occurs as follows (Fig. 10-13):

1. Glucose binds to the protein on one face of the membrane.
2. A conformational change closes the first binding site and exposes the binding site on the other side of the membrane (transport).
3. Glucose dissociates from the protein.
4. The transport cycle is completed by the reversion of GLUT1 to its initial conformation in the absence of bound glucose (recovery).

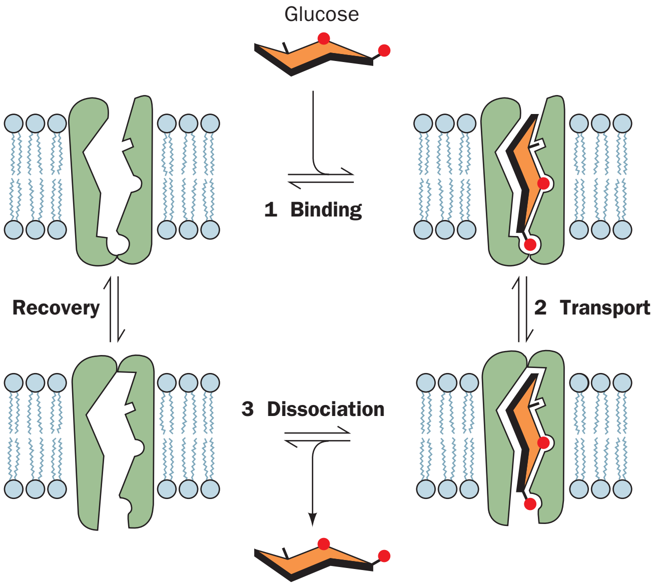

Figure 10-13 | Model for glucose transport. The transport protein alternates between two mutually exclusive conformations. The glucose molecule (*red*) is not drawn to scale. [After Baldwin, S.A. and Lienhard, G.E., *Trends Biochem. Sci.* **6,** 210 (1981).] **See the Animated Figures.**

BOX 10-1 PERSPECTIVES IN BIOCHEMISTRY

Gap Junctions

Most eukaryotic cells are in metabolic as well as physical contact with neighboring cells. This contact is brought about by tubular particles, named **gap junctions,** that join discrete regions of neighboring plasma membranes much like hollow rivets. The gap junction consists of two apposed plasma membrane–embedded complexes. Small molecules and ions, but not macromolecules, can pass between cells via the gap junction's central channel.

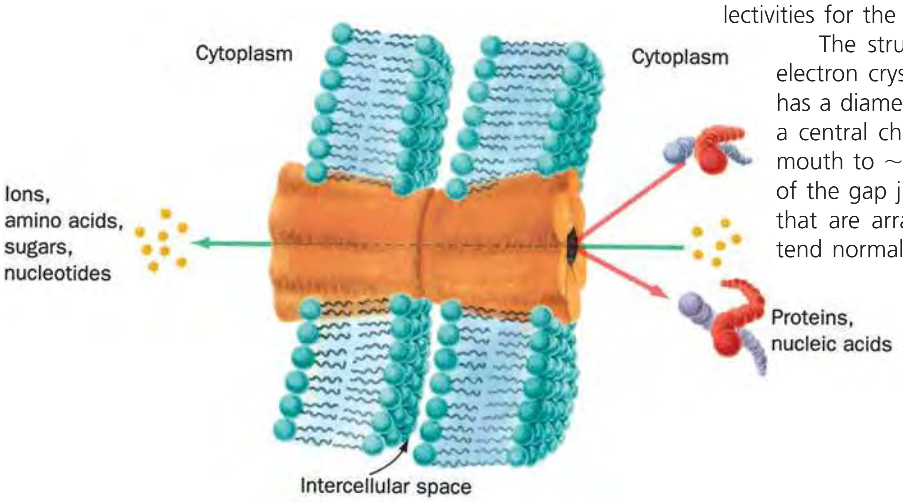

These intercellular channels are so widespread that many whole organs are continuous from within. Thus, *gap junctions are important intercellular communication channels*. For example, the synchronized contraction of heart muscle is brought about by flows of ions through gap junctions, and gap junctions serve as conduits for some of the substances that mediate embryonic development.

Mammalian gap junction channels are 16 to 20 Å in diameter, which Werner Loewenstein established by microinjecting single cells with fluorescent molecules of various sizes and observing with a fluorescence microscope whether the fluorescent probe passed into neighboring cells. The molecules and ions that can pass freely between neighboring cells are limited in molecular mass to a maximum of ~1000 D; macromolecules such as proteins and nucleic acids cannot leave a cell via this route.

The diameter of a gap junction channel varies with Ca^{2+} concentration: The channels are fully open when the Ca^{2+} level is $<10^{-7}$ M and become narrower as the Ca^{2+} concentration increases until, above 5×10^{-5} M, they close. This shutter system is thought to protect communities of interconnected cells from the otherwise catastrophic damage that would result from the death of even one of their members. Cells generally maintain very low cytosolic Ca^{2+} concentrations ($<10^{-7}$ M) by actively pumping Ca^{2+} out of the cell as well as into their mitochondria and endoplasmic reticulum (Section 10-3B). Ca^{2+} floods back into leaky or metabolically depressed cells, thereby inducing closure of their gap junctions and sealing them off from their neighbors.

Gap junctions are constructed from a single sort of protein subunit known as a **connexin.** A single gap junction consists of two hexagonal rings of connexins, called **connexons,** one from each of the adjoining plasma membranes. A given animal expresses numerous genetically distinct connexins, with molecular masses ranging from 25 to 50 kD. At least some connexons may be formed from two or more species of connexins, and the gap junctions joining two cells may consist of two different types of connexons. These various types of gap junctions presumably differ in their selectivities for the substances they transmit.

The structure of a cardiac gap junction, determined by electron crystallography, reveals a symmetrical assembly that has a diameter of ~70 Å, a length of ~150 Å, and encloses a central channel whose diameter varies from ~40 Å at its mouth to ~15 Å in its interior. The transmembrane portions of the gap junction each contain 24 rods of electron density that are arranged with hexagonal symmetry and which extend normal to the membrane plane.

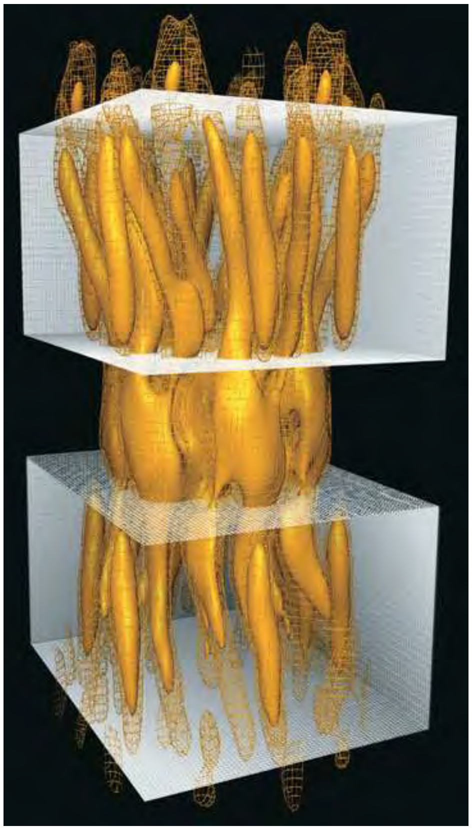

Here, the electron density at two different levels is represented by the solid and mesh contours (*gold*), whereas the white boxes indicate the positions of the cell membranes.

[Electron crystal structure courtesy of Mark Yeager, The Scripps Research Institute, La Jolla, California.]

BOX 10-2 **PERSPECTIVES IN BIOCHEMISTRY**

Differentiating Mediated and Nonmediated Transport

Glucose and many other compounds can enter cells by a nonmediated pathway; that is, they slowly diffuse into cells at a rate proportional to their membrane solubility and their concentrations on either side of the membrane. This is a linear process: The **flux** (rate of transport per unit area) of a substance across the membrane increases with the magnitude of its concentration gradient (the difference between its internal and external concentrations). If the same substance, say glucose, moves across a membrane by means of a transport protein, its flux is no longer linear. This is one of four characteristics that distinguish mediated from nonmediated transport:

1. ***Speed and specificity.*** The solubilities of the chemically similar sugars D-glucose and D-mannitol in a synthetic lipid bilayer are similar. However, the rate at which glucose moves through the erythrocyte membrane is four orders of magnitude faster than that of D-mannitol. The erythrocyte membrane must therefore contain a system that transports glucose and that can distinguish D-glucose from D-mannitol.
2. ***Saturation.*** The rate of glucose transport into an erythrocyte does not increase infinitely as the external glucose concentration increases: The rate gradually approaches a maximum. Such an observation is evidence that a specific number of sites on the membrane are involved in the transport of glucose. At high [glucose], the transporters become saturated, much like myoglobin becomes saturated with O_2 at high pO_2 (Fig. 7-4). As expected, the plot of glucose flux versus [glucose] (*above right*) is hyperbolic. The nonmediated glucose flux increases linearly with [glucose] but would not visibly depart from the baseline on the scale of the graph.

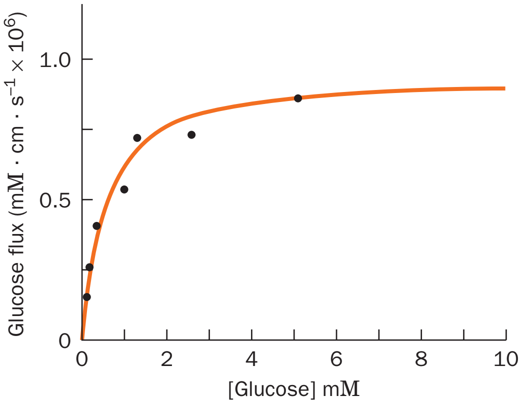

3. ***Competition.*** The above curve is shifted to the right in the presence of a substance that competes with glucose for binding to the transporter; for example, 6-*O*-benzyl-D-galactose has this effect. Competition is not a feature of nonmediated transport, since no transport protein is involved.
4. ***Inactivation.*** Reagents that chemically modify proteins and hence may affect their functions may eliminate the rapid, saturatable flux of glucose into the erythrocyte. The susceptibility of the erythrocyte glucose transport system to protein-modifying reagents is additional proof that it is a protein.

[Graph based on data from Stein, W.D., *Movement of Molecules across Membranes,* p. 134, Academic Press (1967).]

This transport cycle can occur in either direction, according to the relative concentrations of intracellular and extracellular glucose. GLUT1 provides a means of equilibrating the glucose concentration across the erythrocyte membrane without any accompanying leakage of small molecules or ions (as might occur through an always-open channel such as a porin).

All known transport proteins appear to be asymmetrically situated transmembrane proteins that alternate between two conformational states in which the ligand-binding sites are exposed, in turn, to opposite sides of the membrane. Such a mechanism is analogous to the T → R allosteric transition of proteins such as hemoglobin (Section 7-1B). In fact, many of the features of ligand-binding proteins such as myoglobin and hemoglobin also apply to transport proteins (Box 10-2).

Biochemical analyses indicate that GLUT1 has 12 membrane-spanning α helices and probably forms a tetramer in the membrane. This protein belongs to a large family of transporters whose structures have not been as well characterized as those of channel-type proteins. The 6.5-Å-resolution electron crystal structure of a bacterial **oxalate transporter** named **OxlT** reveals that its 12 transmembrane helices are arranged around a central

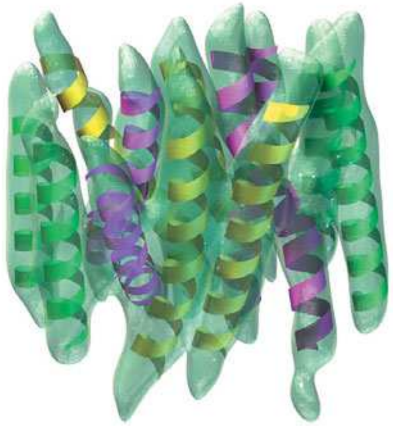

Figure 10-14 | Electron crystal structure of oxalate transporter OxlT from *Oxalobacter formigenes*. Twelve α helices have been fitted to the electron density map, which has a resolution of 6.5 Å. The green helices are nearly perpendicular to the plane of the membrane; yellow helices include a bend; and magenta helices are both bent and curved to match the electron density. Segments linking the helices are not resolved. [Courtesy of Sriram Subramaniam, NIH, Bethesda, Maryland.]

cavity, which presumably represents a substrate-binding site (Fig. 10-14). The protein exhibits a high degree of symmetry between its cytoplasmic and external halves, which is consistent with its ability to transport substances both into and out of the cell. The structure shown in Fig. 10-14 probably corresponds to a conformational intermediate that is not fully accessible to either the cytoplasmic or extracellular face of the membrane.

Some transporters can transport more than one substance. For example, the bacterial oxalate transporter transports **oxalate** into the cell and transports **formate** out.

$$^{-}\text{OOC}{-}\text{COO}^{-} \qquad \text{H}{-}\text{COO}^{-}$$

Oxalate **Formate**

Some transport proteins move more than one substance at a time. Hence, it is useful to categorize mediated transport according to the stoichiometry of the transport process (Fig. 10-15):

1. A **uniport** involves the movement of a single molecule at a time. GLUT1 is a uniport system.
2. A **symport** simultaneously transports two different molecules in the same direction.
3. An **antiport** simultaneously transports two different molecules in opposite directions.

CHECK YOUR UNDERSTANDING

What are the similarities and differences among ionophores, porins, ion channels, and passive-mediated transport proteins?

Explain how and why ion channels are gated.

Use the terminology of allosteric proteins to discuss the operation of proteins that carry out uniport, symport, and antiport transport processes.

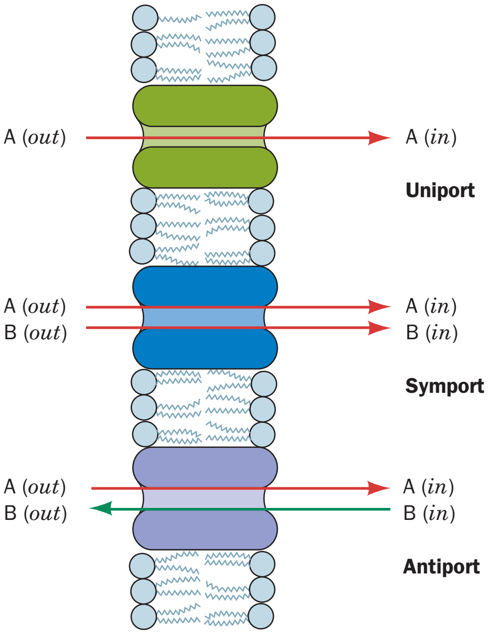

Figure 10-15 | Uniport, symport, and antiport translocation systems.

3 Active Transport

LEARNING OBJECTIVES

- Understand how pumps use the free energy of ATP to transport ions against their gradient.
- Understand that ABC transporters move amphipathic substances from one side of the membrane to the other.
- Understand the difference between primary and secondary active transport.

Passive-mediated transporters, including porins, ion channels, and proteins such as GLUT1, facilitate the transmembrane movement of substances according to the relative concentrations of the substance on either side of the membrane. For example, the glucose concentration in the blood plasma (~5 mM) is generally higher than in cells, so GLUT1 allows glucose to enter the erythrocyte to be metabolized. Many substances, however, are available on one side of a membrane in lower concentrations than are required on the other side of the membrane. Such substances must be actively and selectively transported across the membrane against their concentration gradients.

Active transport is an endergonic process that, in most cases, is coupled to the hydrolysis of ATP. Several families of ATP-dependent transporters have been identified:

1. **P-type ATPases** undergo phosphorylation as they transport cations such as Na^+, K^+, and Ca^{2+} across the membrane.
2. **F-type ATPases** are proton-transporting complexes located in mitochondria and bacterial membranes. Instead of using the free energy of ATP to pump protons against their gradient, these proteins operate in reverse in order to synthesize ATP, as we shall see in Section 18-3.
3. **V-type ATPases** resemble the F-type ATPases and occur in plant vacuoles and acidic vesicles such as animal lysosomes.
4. **A-type ATPases** transport anions across membranes.
5. **ABC transporters** are named for their *A*TP-*b*inding *c*assette and transport a wide variety of substances, including ions, small metabolites, and drug molecules.

In this section, we examine two P-type ATPases and an ABC transporter; these proteins carry out **primary active transport.** In **secondary active transport,** the free energy of the electrochemical gradient generated by another mechanism, such as an ion-pumping ATPase, is used to transport a neutral molecule against its concentration gradient.

A | The $(Na^+–K^+)$–ATPase Transports Ions in Opposite Directions

One of the most thoroughly studied active transport systems is the **$(Na^+–K^+)$–ATPase** in the plasma membranes of higher eukaryotes, which was first characterized by Jens Skou. This transmembrane protein consists of two types of subunits: a 110-kD nonglycosylated α subunit that contains the enzyme's catalytic activity and ion-binding sites, and a 55-kD glycoprotein β subunit of unknown function. Sequence analysis suggests that the α subunit has eight transmembrane α-helical segments and two large cytoplasmic domains. The β subunit has a single transmembrane helix and a large extracellular domain. The protein may function as an $(\alpha\beta)_2$ tetramer *in vivo* (Fig. 10-16).

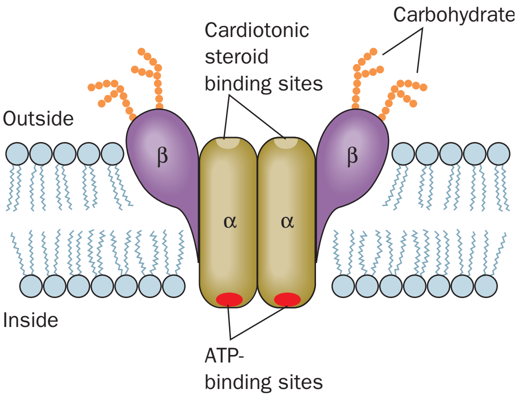

Figure 10-16 | $(Na^+–K^+)$–ATPase. This diagram shows the transporter's putative dimeric structure and its orientation in the plasma membrane. Cardiotonic steroids (Box 10-3) bind to the external surface of the transporter so as to inhibit transport.

The $(Na^+–K^+)$–ATPase is often called the **$(Na^+–K^+)$ pump** because it pumps Na^+ out of and K^+ into the cell with the concomitant hydrolysis of intracellular ATP. The overall stoichiometry of the reaction is

$$3\,Na^+(in) + 2\,K^+(out) + ATP + H_2O \rightleftharpoons 3\,Na^+(out) + 2\,K^+(in) + ADP + P_i$$

The $(Na^+–K^+)$–ATPase is an antiport that generates a charge separation across the membrane, since three positive charges exit the cell for every two that enter. This extrusion of Na^+ enables animal cells to control their water content osmotically; *without functioning (Na^+–K^+)–ATPases to maintain a low internal [Na^+], water would osmotically rush in to such an extent that animal cells, which lack cell walls, would swell and burst.* The electrochemical gradient generated by the (Na^+–K^+)–ATPase is also responsible for the electrical excitability of nerve cells (Section 10-2C). In fact, all cells expend a large fraction of the ATP they produce (up to 70% in nerve cells) to maintain their required cytosolic Na^+ and K^+ concentrations.

The key to the (Na^+–K^+)–ATPase is the phosphorylation of a specific Asp residue of the transport protein. ATP phosphorylates the transporter only in the presence of Na^+, whereas the resulting aspartyl phosphate residue is subject to hydrolysis only in the presence of K^+. This suggests that the (Na^+–K^+)–ATPase has two conformational states (called E_1 and E_2) with different structures, different catalytic activities, and different ligand specificities. The protein appears to operate in the following manner (Fig. 10-17):

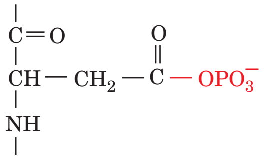

$$\begin{array}{l} | \\ C{=}O \\ | \\ CH-CH_2-\overset{\overset{O}{\|}}{C}-OPO_3^- \\ | \\ NH \\ | \end{array}$$

Aspartyl phosphate residue

1. The transporter in the E_1 state binds three Na^+ ions inside the cell and then binds ATP to yield an $E_1 \cdot ATP \cdot 3\ Na^+$ complex.
2. ATP hydrolysis produces ADP and a "high-energy" aspartyl phosphate intermediate $E_1{\sim}P \cdot 3\ Na^+$ (here "~" indicates a "high-energy" bond).
3. This "high-energy" intermediate relaxes to its "low-energy" conformation, E_2—$P \cdot 3\ Na^+$, and releases its bound Na^+ outside the cell.
4. E_2—P binds two K^+ ions from outside the cell to form an E_2—$P \cdot 2\ K^+$ complex.
5. The phosphate group is hydrolyzed, yielding $E_2 \cdot 2\ K^+$.

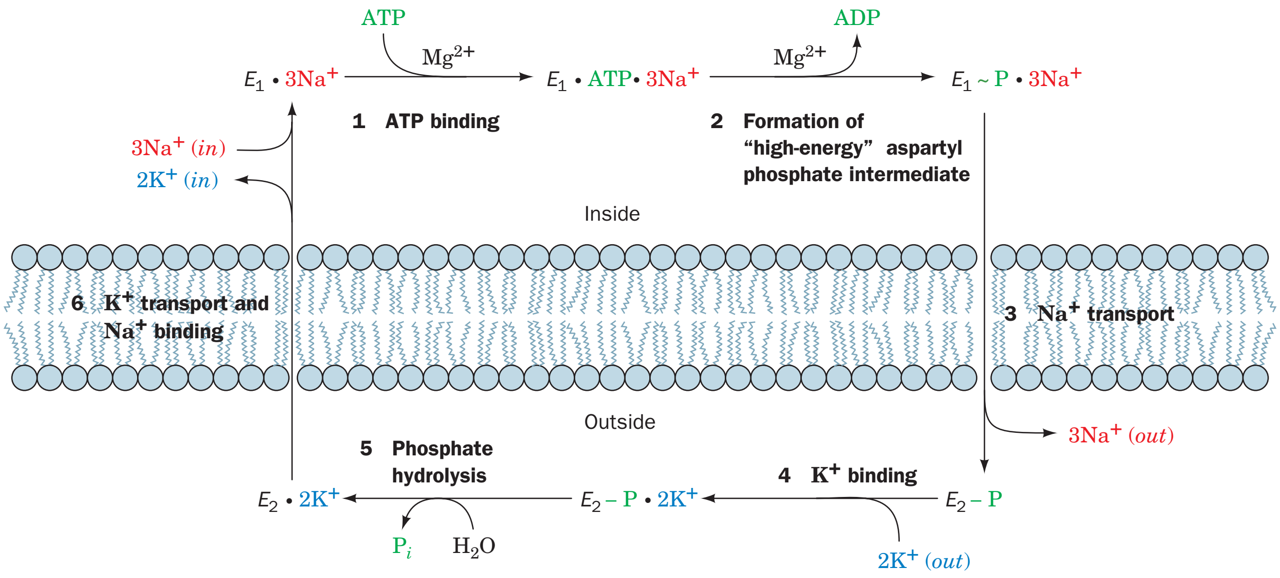
ATP
Mg2+
ADP
Mg2+
E1 • 3Na+
E1 • ATP• 3Na+
E1 ~ P • 3Na+
1 ATP binding
2 Formation of "high-energy" aspartyl phosphate intermediate
3Na+ (in)
2K+ (in)
Inside
6 K+ transport and Na+ binding
3 Na+ transport
Outside
3Na+ (out)
5 Phosphate hydrolysis
4 K+ binding
E2 • 2K+
E2 – P • 2K+
E2 – P
Pi
H2O
2K+ (out)

Figure 10-17 | **Scheme for the active transport of Na^+ and K^+ by the (Na^+–K^+)–ATPase.**

BOX 10-3 **BIOCHEMISTRY IN HEALTH AND DISEASE**

The Action of Cardiac Glycosides

The cardiac glycosides are natural products that increase the intensity of heart muscle contraction. Indeed, **digitalis,** an extract of purple foxglove leaves, which contains a mixture of cardiac glycosides including **digitalin** (see figure below), has been used to treat congestive heart failure for centuries. The cardiac glycoside **ouabain** (pronounced wabane), a product of the East African ouabio tree, has been long used as an arrow poison.

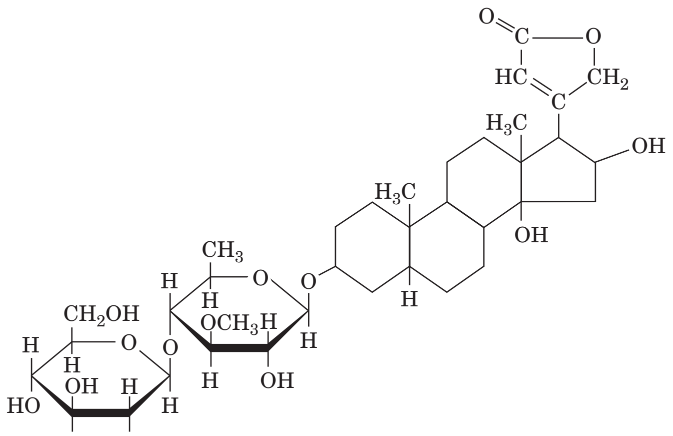

Digitalin

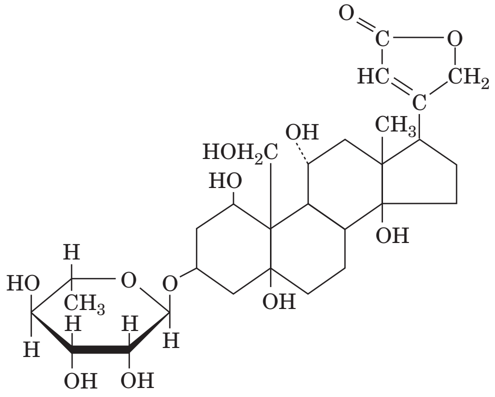

Ouabain

These two steroids, which are still among the most commonly prescribed cardiac drugs, inhibit the $(Na^+–K^+)$–ATPase by binding strongly to an externally exposed portion of the protein (Fig. 10-16) so as to block Step 5 in Fig. 10-17. The resultant increase in intracellular $[Na^+]$ stimulates the cardiac $(Na^+–Ca^{2+})$ antiport system, which pumps Na^+ out of and Ca^{2+} into the cell, ultimately boosting the $[Ca^{2+}]$ in the sarcoplasmic reticulum. Thus, the release of Ca^{2+} to trigger muscle contraction (Section 7-2B) produces a larger than normal increase in cytosolic $[Ca^{2+}]$, thereby intensifying the force of cardiac muscle contraction. Ouabain, which was once thought to be produced only by plants, has recently been discovered to be an animal hormone that is secreted by the adrenal cortex and functions to regulate cellular $[Na^+]$ and overall body salt and water balance.

6. $E_2 \cdot 2\ K^+$ changes conformation, releases its two K^+ ions inside the cell, and replaces them with three Na^+ ions, thereby completing the transport cycle.

Although each of the above reaction steps is individually reversible, the cycle, as diagramed in Fig. 10-17, circulates only in the clockwise direction under normal physiological conditions. This is because ATP hydrolysis and ion transport are coupled vectorial (unidirectional) processes. The vectorial nature of the reaction cycle results from the alternation of some of the steps of the exergonic ATP hydrolysis reaction (Steps 1 + 2 and Step 5) with some of the steps of the endergonic ion transport process (Steps 3 + 4 and Step 6). Thus, *neither reaction can go to completion unless the other one also does*. Study of the $(Na^+–K^+)$–ATPase has been greatly facilitated by the use of glycosides that inhibit the transporter (Box 10-3).

B | The Ca^{2+}–ATPase Pumps Ca^{2+} Out of the Cytosol

Transient increases in cytosolic $[Ca^{2+}]$ trigger numerous cellular responses including muscle contraction (Section 7-2B), the release of neurotransmitters,

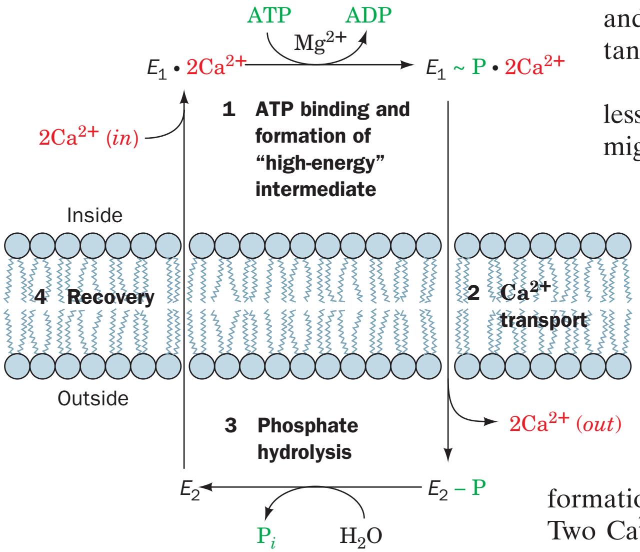

Figure 10-18 | Scheme for the active transport of Ca^{2+} by the Ca^{2+}–ATPase. Here (*in*) refers to the cytosol and (*out*) refers to the outside of the cell for plasma membrane Ca^{2+}–ATPase or the lumen of the endoplasmic reticulum (or sarcoplasmic reticulum) for the Ca^{2+}–ATPase of that membrane.

and glycogen breakdown (Section 16-3). Moreover, Ca^{2+} is an important activator of oxidative metabolism (Section 18-4).

The [Ca^{2+}] in the cytosol (~0.1 μM) is four orders of magnitude less than it is in the extracellular spaces [~1500 μM; intracellular Ca^{2+} might otherwise combine with phosphate to form $Ca_3(PO_4)_2$, which has a maximum solubility of only 65 μM]. This large concentration gradient is maintained by the active transport of Ca^{2+} across the plasma membrane and the endoplasmic reticulum (the sarcoplasmic reticulum in muscle) by a **Ca^{2+}–ATPase.** This **Ca^{2+} pump** actively pumps two Ca^{2+} ions out of the cytosol at the expense of ATP hydrolysis, while countertransporting two or three protons. The mechanism of the Ca^{2+}–ATPase (Fig. 10-18) resembles that of the $(Na^+–K^+)$–ATPase (Fig. 10-17).

The superimposed X-ray structures of the Ca^{2+}–ATPase from rabbit muscle sarcoplasmic reticulum in its E_1 and E_2 conformations, determined by Chikashi Toyoshima, are shown in Fig. 10-19. Two Ca^{2+} ions bind within a bundle of 10 transmembrane helices. Three additional domains form a large structure on the cytoplasmic side of the membrane. The differences between the Ca^{2+}-bound (E_1) and the Ca^{2+}-free (E_2) structures indicate that the transporter undergoes extensive rearrangements, particularly in the positions of the cytoplasmic domains but also in the Ca^{2+}-transporting membrane domain, during the reaction cycle. These changes apparently mediate communication between the Ca^{2+}-binding sites and the ~80-Å-distant site where bound ATP is hydrolyzed.

C | ABC Transporters Are Responsible for Drug Resistance

The inability of anticancer drugs to kill cancer cells is frequently traced to the overexpression of a membrane protein known as **P-glycoprotein.** This member of the ABC class of transporters pumps a variety of amphiphilic substances—including many drugs—out of the cell, so that it is also called a **multidrug resistance (MDR) transporter.** Similar proteins in bacteria contribute to their antibiotic resistance.

The **ABC transporters,** which pump ions, sugars, amino acids, and other polar and nonpolar substances, are built from four modules: two highly conserved cytoplasmic nucleotide-binding domains, and two transmembrane domains that typically contain six transmembrane helices each. In bacteria, the four domains are contained on two or four separate polypeptides, and in eukaryotes, a single polypeptide includes all four domains. Bacterial ABC transporters mediate the uptake as well as the efflux of a variety of compounds, whereas their eukaryotic counterparts apparently

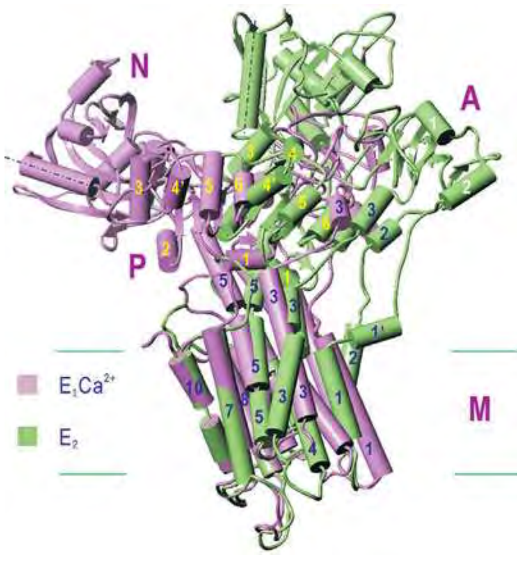

Figure 10-19 | X-Ray structures of the Ca^{2+}-free and Ca^{2+}-bound Ca^{2+}–ATPase. The Ca^{2+}-free form, E_2, is green with black helix numbers, and the Ca^{2+}-bound form, E_1Ca^{2+}, is violet with yellow helix numbers. These proteins, which are superimposed on their transmembrane domains, are viewed from within the membrane with the cytosolic side up. Ten transmembrane helices form the M (for membrane) domain, ATP binds to the N (for nucleotide-binding) domain, the Asp residue that is phosphorylated during the reaction cycle is located on the P (for phosphorylation) domain, and the A (for actuator) domain is so named because it participates in the transmission of major conformational changes. Dashed lines highlight the orientations of a helix in the N domain in the two conformations and the horizontal lines delineate the membrane. [Courtesy of Chikashi Toyoshima, University of Tokyo, Japan. PDBids 1EUL and 1WIO.]

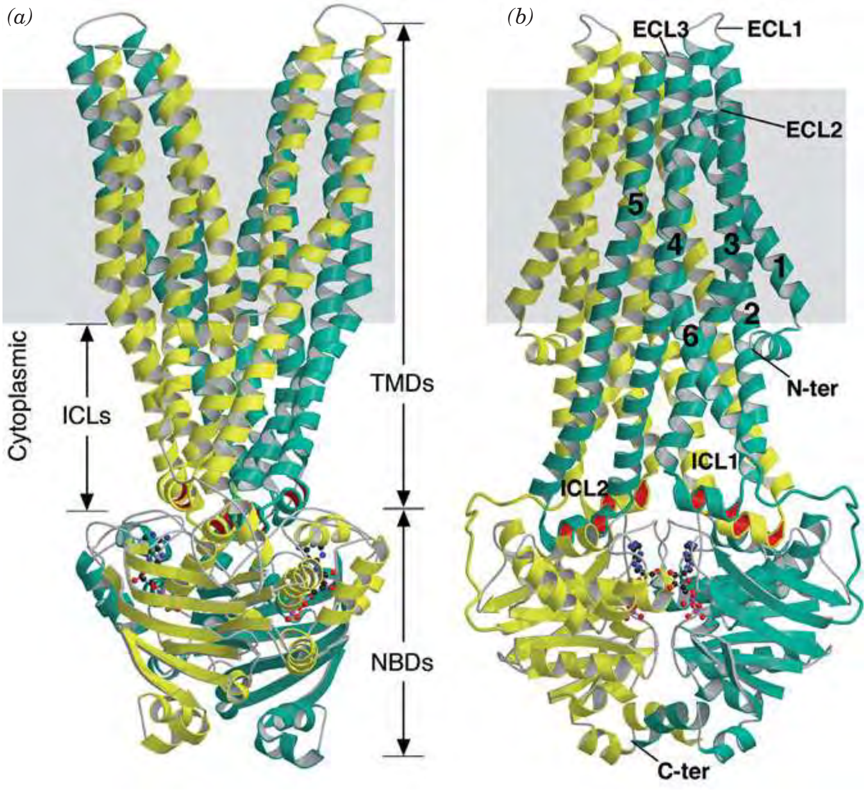

Figure 10-20 | **X-Ray structure of the ABC transporter Sav1866 from *Staphylococcus aureus.*** (*a*) Ribbon diagram of the homodimeric protein in which its subunits are colored yellow-green and turquoise. The protein is viewed parallel to the membrane with its extracellular surface at the top. The transmembrane domains (TMDs), nucleotide-binding domains (NBDs), and intracellular loops (ICLs) are indicated, and the gray box marks the approximate location of the lipid bilayer. (*b*) Same model, rotated 90° around its vertical molecular twofold axis. Its bound ADP molecules are drawn in ball-and-stick form. The transmembrane helices of the turquoise subunit are numbered, and several extracellular loops (ECL) and intracellular loops (ICL) are indicated. [Courtesy of Kaspar Locher, ETH, Zurich, Switzerland. PDBid 2HYD.]

operate only as exporters that transport material out of the cell or into intracellular compartments such as the endoplasmic reticulum.

The X-ray structure of a bacterial ABC transporter called **Sav1866,** which shows significant homology to human P-glycoprotein, provides some clues about how the ABC transporters function. The two identical subunits of Sav1866 are extensively intertwined, with three helices from each subunit forming each of the two arms of the V-shaped transmembrane domain (Fig. 10-20*a*). Two ATP-binding sites are located at the interface between the subunits in the nucleotide-binding domains. Conformational changes resulting from ATP binding and hydrolysis in this part of the protein appear to be transmitted to the transmembrane domains via small movements in two short intracellular helices (ICL; Fig. 10-20*b*) that are oriented parallel to the membrane. These so-called coupling helices interact with the nucleotide-binding domain of the opposite subunit, permitting the two subunits of the transporter to move in concert.

In the nucleotide-bound state drawn in Fig. 10-20, the transmembrane domains define a cavity that is accessible to the outer leaflet of the bilayer and the extracellular space. ATP hydrolysis presumably triggers a conformational change that exposes the cavity to the cytosol and the inner leaflet. Thus, ATP-driven conformational changes would allow the transporter to bind a molecule from inside the cell or from the inner leaflet and release it outside the cell or into the outer leaflet (hence the transporter would operate as a flipase for lipid-soluble substances). In its outward-facing conformation, the cavity is lined primarily with polar and charged residues, which would favor the release of hydrophobic substances such as drug molecules.

CFTR Is an ABC Transporter. Only one of the thousands of known ABC transporters functions as an ion channel rather than a pump: the **cystic fibrosis transmembrane conductance regulator (CFTR).** This 1480-residue protein, which is defective in individuals with the inherited disease cystic fibrosis (Box 3-1), allows Cl^- ions to flow out of the cell, following their concentration gradient. ATP binding to CFTR's two nucleotide-binding domains appears to open the Cl^- channel, and the hydrolysis of one ATP closes it (the other ATP remains intact). However, the CFTR channel can open only if its regulatory domain (which is unique among ABC transporters) has been phosphorylated, thus regulating the flow of ions across the membrane. CFTR does not exhibit high specificity for Cl^- ions, suggesting that the channel lacks a selectivity filter analogous to that in the KcsA K^+ channel (Section 10-2C).

The maintenance of electrical neutrality requires that the Cl^- ions transported by the CFTR be accompanied by positively charged ions, mainly Na^+. The transported ions are osmotically accompanied by water, thus maintaining the proper level of fluidity in secretions of the airways, intestinal tract, and the ducts of the pancreas, testes, and sweat glands. Although over 1000 mutations of the CFTR have been described, in about 70% of cystic fibrosis cases, Phe 508 of the CFTR has been deleted. Even though this mutant CFTR is functional, it is improperly folded and hence is degraded before it can be installed in the plasma membrane.

Homozygotes for defective or absent CFTRs have problems in many of their above organs but especially in their lungs (heterozygotes are asymptomatic). This is because the reduced Cl^- export results in thickened mucus that the lungs cannot easily clear. Since the flow of mucus is the major way in which the lungs eliminate foreign particles such as bacteria, individuals with cystic fibrosis suffer from chronic lung infections leading to progressive lung damage and early death.

D | Active Transport May Be Driven by Ion Gradients

Systems such as the (Na^+–K^+)–ATPase generate electrochemical gradients across membranes. The free energy stored in an electrochemical gradient (Eq. 10-3) can be harnessed to power various endergonic physiological processes. For example, cells of the intestinal epithelium take up dietary glucose by Na^+-dependent symport (Fig. 10-21). The immediate energy source for this "uphill" transport process is the Na^+ gradient. This process is an example of secondary active transport because *the Na^+ gradient in these cells is maintained by the (Na^+–K^+)–ATPase.* The Na^+–glucose transport system concentrates glucose inside the cell. Glucose is then transported into the capillaries through a passive-mediated glucose uniport (which resembles GLUT1; Fig. 10-13). Thus, since glucose enhances Na^+ resorption, which in turn enhances water resorption, glucose, in addition to salt and water, should be fed to individuals suffering from salt and water losses due to diarrhea.

Lactose Permease Requires a Proton Gradient. Gram-negative bacteria such as *E. coli* contain several active transport systems for concentrating sugars. One extensively studied system, **lactose permease** (also known as **galactoside permease**), *utilizes the proton gradient across the bacterial cell membrane to cotransport H^+ and lactose.* The proton gradient is metabolically generated through oxidative metabolism in a manner similar to that in mitochondria (Section 18-2). The electrochemical potential gradient created by both these systems is used mainly to drive the synthesis of ATP.

Lactose permease is a 417-residue monomer that, like GLUT1 and the oxalate transporter (Section 10-2E), to which it is distantly related,

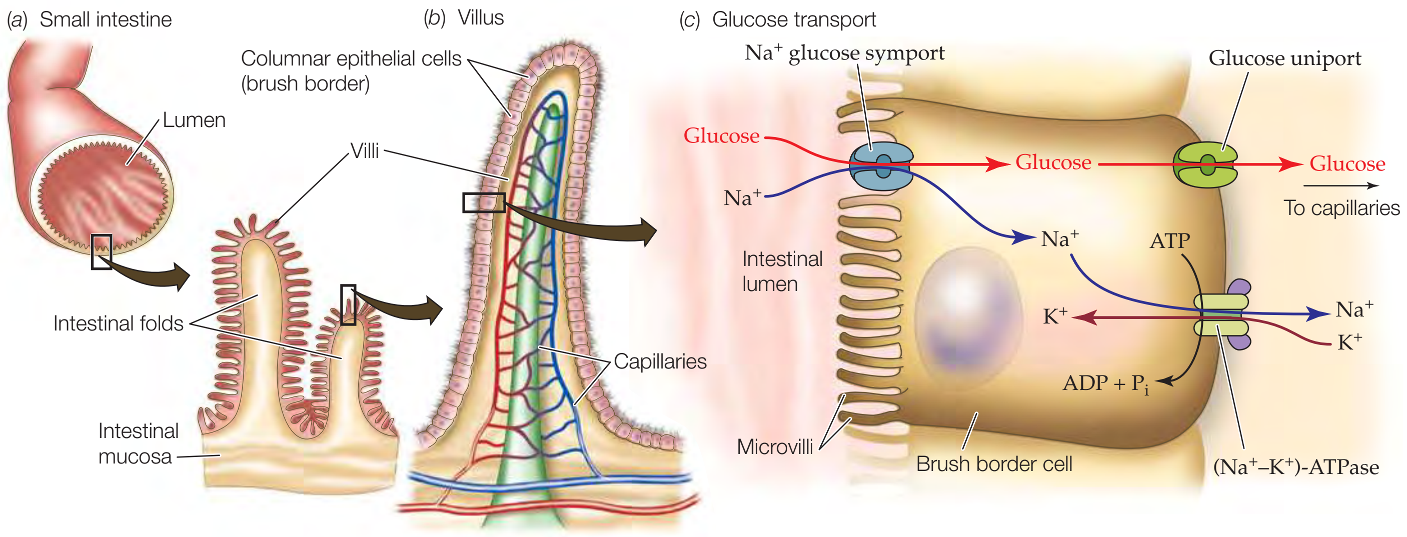
(a) Small intestine
Lumen
Intestinal folds
Intestinal mucosa
(b) Villus
Columnar epithelial cells (brush border)
Villi
Capillaries
(c) Glucose transport
Na+ glucose symport
Glucose uniport
Glucose
Na+
Glucose
Glucose
To capillaries
Intestinal lumen
Na+
ATP
K+
Na+
K+
ADP + Pi
Microvilli
Brush border cell
(Na+–K+)-ATPase

Figure 10-21 | Glucose transport in the intestinal epithelium. The brushlike villi lining the small intestine greatly increase its surface area (*a*), thereby facilitating the absorption of nutrients. The brush border cells from which the villi are formed (*b*) concentrate glucose from the intestinal lumen in symport with Na^+ (*c*), a process that is driven by the $(Na^+–K^+)$–ATPase, which is located on the capillary side of the cell and functions to maintain a low internal $[Na^+]$. The glucose is exported to the bloodstream via a separate passive-mediated uniport system similar to GLUT1.

consists largely of 12 transmembrane helices with its N- and C-termini in the cytoplasm. Like $(Na^+–K^+)$–ATPase, it has two major conformational states (Fig. 10-22):

1. E-1, which has a low-affinity lactose-binding site facing the interior of the cell.
2. E-2, which has a high-affinity lactose-binding site facing the exterior of the cell.

Ronald Kaback established that E-1 and E-2 can interconvert only when their H^+- and lactose-binding sites are either both filled or both empty. This prevents dissipation of the H^+ gradient without cotransport of lactose into the cell. It also prevents transport of lactose out of the cell since this would require cotransport of H^+ against its concentration gradient.

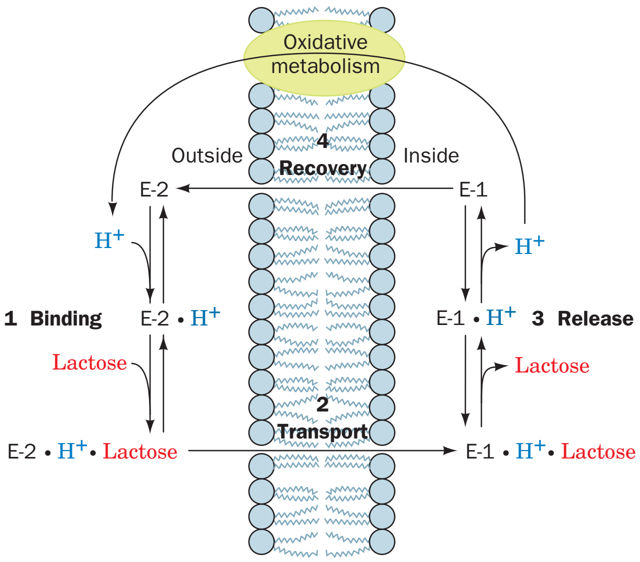
Oxidative metabolism
Outside
Inside
4 Recovery
E-2
E-1
H+
H+
1 Binding
E-2 • H+
E-1 • H+
3 Release
Lactose
Lactose
2 Transport
E-2 • H+• Lactose
E-1 • H+• Lactose

Figure 10-22 | Scheme for the cotransport of H^+ and lactose by lactose permease in *E. coli*. H^+ binds first to E-2 outside the cell, followed by lactose. They are sequentially released from E-1 inside the cell. E-2 must bind to lactose and H^+ in order to change conformation to E-1, thereby cotransporting these substances into the cell. E-1 changes conformation to E-2 when neither lactose nor H^+ is bound, thus completing the transport cycle.

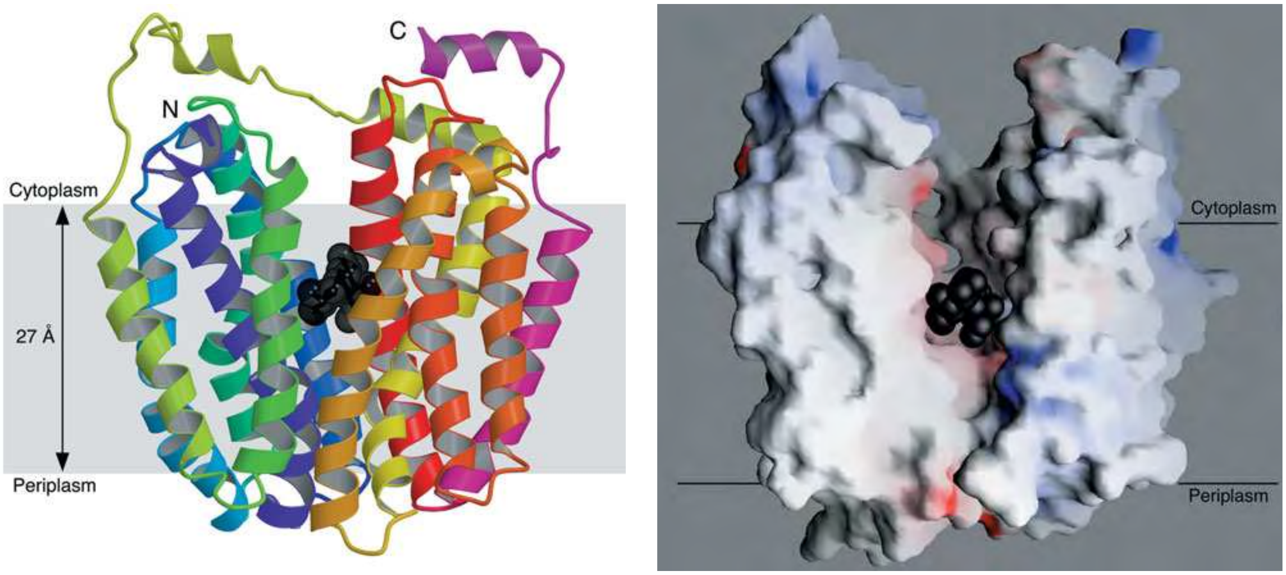

(a) *(b)*

■ **Figure 10-23 | X-Ray structure of lactose permease from *E. coli.*** (*a*) Ribbon diagram as viewed from the membrane with the cytoplasmic side up. The protein's 12 transmembrane helices are colored in rainbow order from the N-terminus (*purple*) to the C-terminus (*pink*). The bound lactose analog is represented by black spheres. (*b*) Surface model viewed as in Part *a* but with the two helices closest to the viewer in Part *a* removed to reveal the lactose-binding cavity. The surface is colored according to its electrostatic potential with positively charged areas blue, negatively charged areas red, and neutral areas white. [Courtesy of H. Ronald Kaback, UCLA. PDBid 1PV7.]

The X-ray structure of lactose permease in complex with a tight-binding lactose analog, determined by Kaback and So Iwata, reveals that this protein consists of two structurally similar and twofold symmetrically positioned domains containing six transmembrane helices each (Fig. 10-23*a*). A large internal hydrophilic cavity is open to the cytoplasmic side of the membrane (Fig. 10-23*b*) so that the structure represents the E-1 state of the protein. The lactose analog is bound in the cavity at a position that is approximately equidistant from both sides of the membrane, consistent with the model that the lactose-binding site is alternately accessible from each side of the membrane (e.g., Fig. 10-13). Arg, His, and Glu residues that mutational studies have implicated in proton translocation are located in the vicinity of the lactose-binding site.

■ CHECK YOUR UNDERSTANDING

Distinguish passive-mediated transport, active transport, and secondary active transport.

Explain why the (Na^+–K^+)–ATPase and the Ca^{2+}–ATPase carry out transport in one direction only.

Explain why a multidrug resistance ABC transporter would operate as a flipase.

SUMMARY

1. The mediated and nonmediated transport of a substance across a membrane is driven by its chemical potential difference.
2. Ionophores facilitate ion diffusion by binding an ion, diffusing through the membrane, and then releasing the ion; or by forming a channel.
3. Porins form β barrel structures about a central channel that is selective for anions, cations, or certain small molecules.
4. Ion channels mediate changes in membrane potential by allowing the rapid and spontaneous transport of ions. Ion channels are highly solute-selective and open and close (gate) in response to various stimuli. Nerve impulses involve ion channels.
5. Aquaporins contain channels that allow the rapid transmembrane diffusion of water but not protons.
6. Transport proteins such as GLUT1 alternate between two conformational states that expose the ligand-binding site to opposite sides of the membrane.
7. Active transport, in most cases, is driven by ATP hydrolysis. In the (Na^+–K^+)–ATPase and Ca^{2+}–ATPase, ATP hydrolysis and ion transport are coupled and vectorial.
8. ABC transporters use ATP hydrolysis to trigger conformational changes that move substances, including amphiphilic molecules, from one side of the membrane to the other.

9. In secondary active transport, an ion gradient maintained by an ATPase drives the transport of another substance. For example, the transport of lactose into a cell by lactose permease is driven by the cotransport of H^+.

KEY TERMS

chemical potential	**296**
$\Delta\Psi$	**296**
electrochemical potentia	**296**
nonmediated transport	**296**
mediated transport	**296**
passive-mediated transport	**297**
active transport	**297**
ionophore	**297**
gating	**302**
mechanosensitive channel	**302**
ligand-gated channel	**302**
signal-gated channel	**302**
voltage-gated channel	**302**
depolarization	**302**
repolarization	**302**
action potential	**302**
aquaporin	**306**
gap junction	**307**
uniport	**310**
symport	**310**
antiport	**310**
primary active transport	**313**
secondary active transport	**313**
ABC transporter	**314**

PROBLEMS

1. Indicate whether the following compounds are likely to cross a membrane by nonmediated or mediated transport: (a) ethanol, (b) glycine, (c) cholesterol, (d) ATP.

2. Rank the rate of transmembrane diffusion of the following compounds:

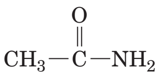
$CH_3-\overset{\overset{O}{\|}}{C}-NH_2$

A. Acetamide

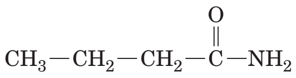
$CH_3-CH_2-CH_2-\overset{\overset{O}{\|}}{C}-NH_2$

B. Butyramide

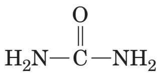
$H_2N-\overset{\overset{O}{\|}}{C}-NH_2$

C. Urea

3. Calculate the free energy change for glucose entry into cells when the extracellular concentration is 5 mM and the intracellular concentration is 3 mM.

4. (a) Calculate the chemical potential difference when intracellular $[Na^+] = 10$ mM and extracellular $[Na^+] = 150$ mM at 37°C. (b) What would the electrochemical potential be if the membrane potential were -60 mV (inside negative)?

5. For the problem in Sample Calculation 10-1, calculate ΔG at 37°C when the membrane potential is (a) -50 mV (cytosol negative) and (b) $+150$ mV. In which case is Ca^{2+} movement in the indicated direction thermodynamically favorable?

6. What happens to K^+ transport by valinomycin when the membrane is cooled below its transition temperature?

7. How long would it take 100 molecules of valinomycin to transport enough K^+ to change the concentration inside an erythrocyte of volume 100 μm^3 by 10 mM? (Assume that the valinomycin does not also transport any K^+ out of the cell, which it really does, and that the valinomycin molecules inside the cell are always saturated with K^+.)

8. The rate of movement (flux) of a substance X into cells was measured at different concentrations of X to construct the following graph.
   (a) Does this information suggest that the movement of X into the cells is mediated by a protein transporter? Explain.
   (b) What additional experiment could you perform to verify that a transport protein is or is not involved?

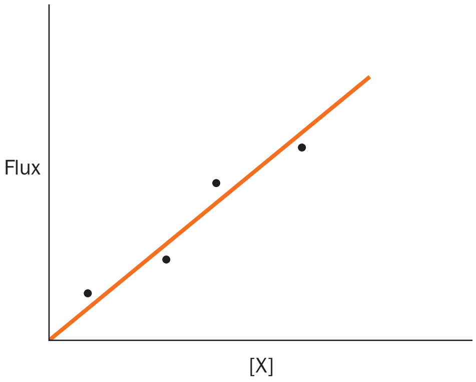

9. If the ATP supply in the cell shown in Fig. 10-21*c* suddenly vanished, would the intracellular glucose concentration increase, decrease, or remain the same?

10. Endothelial cells and pericytes in the retina of the eye have different mechanisms for glucose uptake. The figure shows the rate of glucose uptake for each type of cell in the presence of increasing amounts of sodium. What do these results reveal about the glucose transporter in each cell type?

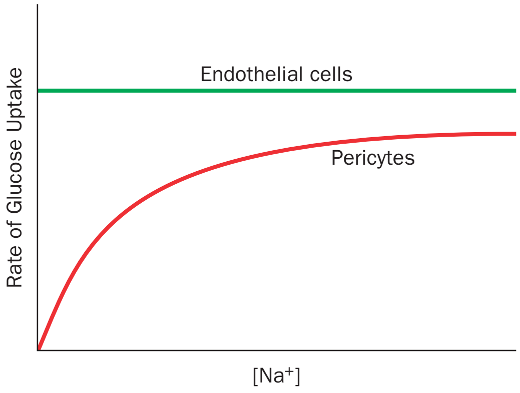

11. The compound shown below is the antiparasitic drug miltefosine.

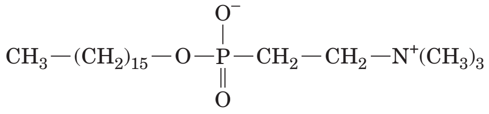

$$\mathrm{CH_3{-}(CH_2)_{15}{-}O{-}\overset{\overset{O^-}{|}}{\underset{\underset{O}{\|}}{P}}{-}CH_2{-}CH_2{-}N^+(CH_3)_3}$$

Miltefosine

(a) Is this compound a glycerophospholipid?

(b) How does miltefosine likely cross the parasite cell membrane?

(c) In what part of the cell would the drug tend to accumulate? Explain.

(d) Miltefosine binds to a protein that also binds some sphingolipids and some glycerophospholipids. What feature common to all these compounds is recognized by the protein? The protein does not bind triacylglycerols.

12. In eukaryotes, ribosomes (approximate mass 4×10^6 D) are assembled inside the nucleus, which is enclosed by a double membrane. Protein synthesis occurs in the cytosol. (a) Could a protein similar to a porin or the glucose transporter be responsible for transporting ribosomes into the cytoplasm? Explain. (b) Would free energy be required to move a ribosome from the nucleus to the cytoplasm? Why or why not?

13. In addition to neurons, muscle cells undergo depolarization, although smaller and slower than in the neuron, as a result of the activity of the acetylcholine receptor.

(a) The acetylcholine receptor is also a gated ion channel. What triggers the gate to open?

(b) The acetylcholine receptor/ion channel is specific for Na^+ ions. Would Na^+ ions flow in or out? Why?

(c) How would the Na^+ flow through the ion channel change the membrane potential?

14. Cells in the wall of the mammalian stomach secrete HCl at a concentration of 0.15 M. The secreted protons, which are derived from the intracellular hydration of CO_2 by carbonic anhydrase, are pumped out by an (H^+–K^+)–ATPase antiport. A K^+–Cl^- cotransporter is also required to complete the overall transport process. (a) Calculate the pH of the secreted HCl. How does this compare to the cytosolic pH (7.4)? (b) Write the reaction catalyzed by carbonic anhydrase. (c) Draw a diagram to show how the action of both transport proteins results in the secretion of HCl.

15. Why would overexpression of an MDR transporter in a cancer cell make the cancer more difficult to treat?

CASE STUDIES

Case Study 3 (available at www.wiley.com/college/voet)
Carbonic Anhydrase II Deficiency

Focus concept: Carbonic anhydrase plays a role in normal bone tissue formation.

Prerequisites: Chapters 2, 3, 4, and 10

- Amino acid structure
- The carbonic acid/bicarbonate blood buffering system
- Membrane transport proteins
- Basic genetics

Case Study 14

Shavings from the Carpenter's Bench: The Biological Role of the Insulin C-peptide

Focus concept: Recent experiments indicate that the insulin C-peptide, which is removed on conversion of proinsulin to insulin, may have biological activity in its own right.

Prerequisites: Chapters 4, 6, and 10

- Amino acid structure
- Principles of protein folding
- Membrane transport proteins

Case Study 17

A Possible Mechanism for Blindness Associated with Diabetes: Na^+-Dependent Glucose Uptake by Retinal Cells

Focus concept: Glucose transport into cells can influence collagen synthesis, which causes the basement membrane thickening associated with diabetic retinopathy.

Prerequisite: Chapter 10

- Transport proteins
- (Na^+–K^+)–ATPase and active transport

REFERENCES

Busch, W. and Saier, M.H., Jr., The transporter classification (TC) system, 2002, *Crit. Rev. Biochem. Mol. Biol.* **37,** 287–337 (2002). [Summarizes the classification of the nearly 400 families of transport systems and their distribution among the three domains of life.]

Dutzler, R., Schirmer, T., Karplus, M., and Fischer, S., Translocation mechanism of long sugar chains across the maltoporin membrane channel, *Structure* **10,** 1273–1284 (2002).

Gouaux, E. and MacKinnon, R., Principles of selective ion transport in channels and pumps, *Science* **310,** 1461–1465 (2005). [Compares several transport proteins of known structure and discusses the selectivity of Na^+, K^+, Ca^{2+}, and Cl^- transport.]

Unger, V.M., Kumar, N.M., Gilula, N.B., and Yeager, M., Three-dimensional structure of a recombinant gap junction membrane channel, *Science* **283,** 1176–1180 (1999).

Walmsley, A.R., Barrett, M.P., Bringaud, F., and Gould, G.W., Sugar transporters from bacteria, parasites, and mammals: structure–activity relationships, *Trends Biochem. Sci.* **22,** 476–481 (1998). [Provides structure–function analysis of sugar transporters with 12 transmembrane helices.]

Ion Channels

Dutzler, R., The ClC family of chloride channels and transporters, *Curr. Opin. Struct. Biol.* **16,** 439–446 (2006).

Dutzler, R., Campbell, E.B., Cadene, M., Chait, B.T., and MacKinnon, R., X-Ray structure of a ClC chloride channel at 3.0 Å reveals the molecular basis of anion selectivity, *Nature* **415,** 287–294 (2002).

Jiang, Y., Lee, A., Chen, J., Ruta, V., Cadene, M., Chait, B.T., and MacKinnon, R., X-Ray structure of a voltage-dependent K^+ channel, *Nature* **423,** 33–41 (2003).

Long, S.B., Campbell, E.B., and MacKinnon, R., Voltage sensor of Kv1.2: Structural basis of electromechanical coupling, *Science* **30,** 903–908 (2005).

Aquaporins

King, L.S., Kozono, D., and Agre, P., From structure to disease: The evolving tale of aquaporin biology, *Nat. Rev. Mol. Cell Biol.* **5,** 687–698 (2004).

Sui, H., Han, B.-G., Lee, J.K., and Jap, B.K., Structural basis of water-specific transport through the AQP1 water channel, *Nature* **414,** 872–878 (2001).

Active Transporters

Abramson, J., Smirnova, I., Kasho, V., Verner, G., Kaback, H.R., and Iwata, S., Structure and mechanism of the lactose permease of *Escherichia coli, Science* **301,** 610–615 (2003).

Dawson, R.J.P. and Locher, K.P., Structure of a bacterial multidrug ABC transporter, *Nature* **443,** 180–185 (2006). [The structure of Sav1866.]

Hille, B., *Ionic Channels of Excitable Membranes* (3rd ed.), Sinauer Associates (2001).

Kaplan, J.H., Biochemistry of Na,K-ATPase, *Annu. Rev. Biochem.* **71,** 511–535 (2002).

Toyoshima, C. and Nomura, H., Structural changes in the calcium pump accompanying the dissociation of calcium, *Nature* **418,** 605–611 (2002); *and* Toyoshima, C., Nomura, H., and Sugita, Y., Structural basis of ion pumping by Ca^{2+}-ATPase of sarcoplasmic reticulum, *FEBS Lett.* **555,** 106–110 (2003).

11

Enzymatic Catalysis

Like these acrobats, enzymes typically act with great speed and precision, interacting with a substrate to facilitate chemical transformation. [David Madison/Stone/Getty Images.]

CHAPTER CONTENTS

1 General Properties of Enzymes
- **A.** Enzymes Are Classified by the Type of Reaction They Catalyze
- **B.** Enzymes Act on Specific Substrates
- **C.** Some Enzymes Require Cofactors

2 Activation Energy and the Reaction Coordinate

3 Catalytic Mechanisms
- **A.** Acid–Base Catalysis Occurs by Proton Transfer
- **B.** Covalent Catalysis Usually Requires a Nucleophile
- **C.** Metal Ion Cofactors Act as Catalysts
- **D.** Catalysis Can Occur through Proximity and Orientation Effects
- **E.** Enzymes Catalyze Reactions by Preferentially Binding the Transition State

4 Lysozyme
- **A.** Lysozyme's Catalytic Site Was Identified through Model Building
- **B.** The Lysozyme Reaction Proceeds via a Covalent Intermediate

5 Serine Proteases
- **A.** Active Site Residues Were Identified by Chemical Labeling
- **B.** X-Ray Structures Provide Information about Catalysis, Substrate Specificity, and Evolution
- **C.** Serine Proteases Use Several Catalytic Mechanisms
- **D.** Zymogens Are Inactive Enzyme Precursors

MEDIA RESOURCES

(available at www.wiley.com/college/voet)

Guided Exploration 10. The catalytic mechanism of serine proteases
Interactive Exercise 6. Pancreatic RNase S
Interactive Exercise 7. Carbonic anhydrase
Interactive Exercise 8. Hen egg white lysozyme
Animated Figure 11-15. Effect of preferential transition state binding
Animated Figure 11-18. Chair and half-chair conformations
Kinemage 9. Hen egg white lysozyme—catalytic mechanism
Kinemage 10-1. Structural overview of a trypsin/inhibitor complex
Kinemage 10-2. Evolutionary comparisons of proteases
Kinemage 10-3. A transition state analog bound to chymotrypsin
Case Study 11. Nonenzymatic Deamidization of Asparagine and Glutamine Residues in Proteins

Living systems are shaped by an enormous variety of biochemical reactions, nearly all of which are mediated by a series of remarkable biological catalysts known as enzymes. **Enzymology,** the study of enzymes, has its roots in the early days of biochemistry; both disciplines evolved together from nineteenth century investigations of fermentation and digestion. Initially, the inability to reproduce most biochemical reactions in the laboratory led Louis Pasteur and others to assume that living systems were endowed with a "vital force" that permitted them to evade the laws of nature governing inanimate matter. Some investigators, however, notably Justus von Liebig, argued that biological processes were caused by the action of chemical substances that were then known as "ferments." Indeed, the name "enzyme" (Greek: *en,* in + *zyme,* yeast) was coined in 1878 in an effort to emphasize that there is something *in* yeast, as opposed to the yeast itself, that catalyzes the reactions of fermentation. Eventually, Eduard Buchner showed that a cell-free yeast extract could in fact carry out the synthesis of ethanol from glucose (**alcoholic fermentation;** Section 15-3B):

$$C_6H_{12}O_6 \rightarrow 2\ CH_3CH_2OH + 2\ CO_2$$

This chemical transformation actually proceeds in 12 enzyme-catalyzed steps.

The chemical composition of enzymes was not firmly established until 1926, when James Sumner crystallized jack bean **urease,** which catalyzes the hydrolysis of urea to NH_3 and CO_2, and demonstrated that these crystals consist of protein. Enzymological experience since then has amply demonstrated that most enzymes are proteins.

Certain species of RNA molecules known as **ribozymes** also have enzymatic activity. These include ribosomal RNA, which catalyzes the formation of peptide bonds between amino acids. In fact, laboratory experiments have produced ribozymes that can catalyze reactions similar to those required for replicating DNA, transcribing it to RNA, and attaching amino acids to transfer RNA. These findings are consistent with a precellular world in which RNA molecules enjoyed a more exalted position as the catalytic workhorses of biochemistry. The present-day RNA catalysts are presumably vestiges of this earlier "RNA world." Proteins have largely eclipsed RNA as cellular catalysts, probably because of the greater chemical versatility of proteins. Whereas nucleic acids are polymers of four types of chemically similar monomeric units, proteins have at their disposal 20 types of amino acids with a greater variety of functional groups.

This chapter is concerned with one of the central questions of biochemistry: How do enzymes work? We shall see that enzymes increase the rates of chemical reactions by lowering the free energy barrier that separates the reactants and products. Enzymes accomplish this feat through various mechanisms that depend on the arrangement of functional groups in the enzyme's **active site,** the region of the enzyme where catalysis occurs. In this chapter, we describe these mechanisms, along with examples that illustrate how enzymes combine several mechanisms to catalyze biological reactions. The following chapter includes a discussion of enzyme kinetics, the study of the rates at which such reactions occur.

1 General Properties of Enzymes

LEARNING OBJECTIVES

- Understand that enzymes differ from ordinary chemical catalysts in reaction rate, reaction conditions, reaction specificity, and control.
- Understand the molecular basis for the stereospecificity and geometric specificity of enzymes.
- Understand the functions and types of enzyme cofactors.

Biochemical research since Pasteur's era has shown that, although enzymes are subject to the same laws of nature that govern the behavior of other substances, enzymes differ from ordinary chemical catalysts in several important respects:

1. ***Higher reaction rates.*** The rates of enzymatically catalyzed reactions are typically 10^6 to 10^{12} times greater than those of the corresponding uncatalyzed reactions (Table 11-1) and are at least several orders of magnitude greater than those of the corresponding chemically catalyzed reactions.
2. ***Milder reaction conditions.*** Enzymatically catalyzed reactions occur under relatively mild conditions: temperatures below 100°C, atmospheric pressure, and nearly neutral pH. In contrast, efficient chemical

Table 11-1 Catalytic Power of Some Enzymes

Enzyme	Nonenzymatic Reaction Rate (s^{-1})	Enzymatic Reaction Rate (s^{-1})	Rate Enhancement
Carbonic anhydrase	1.3×10^{-1}	1×10^{6}	7.7×10^{6}
Chorismate mutase	2.6×10^{-5}	50	1.9×10^{6}
Triose phosphate isomerase	4.3×10^{-6}	4300	1.0×10^{9}
Carboxypeptidase A	3.0×10^{-9}	578	1.9×10^{11}
AMP nucleosidase	1.0×10^{-11}	60	6.0×10^{12}
Staphylococcal nuclease	1.7×10^{-13}	95	5.6×10^{14}

Source: Radzicka, A. and Wolfenden, R., *Science* **267,** 91 (1995).

catalysis often requires elevated temperatures and pressures as well as extremes of pH.

3. ***Greater reaction specificity.*** Enzymes have a vastly greater degree of specificity with respect to the identities of both their **substrates** (reactants) and their products than do chemical catalysts; that is, enzymatic reactions rarely have side products.
4. ***Capacity for regulation.*** The catalytic activities of many enzymes vary in response to the concentrations of substances other than their substrates. The mechanisms of these regulatory processes include allosteric control, covalent modification of enzymes, and variation of the amounts of enzymes synthesized.

A | Enzymes Are Classified by the Type of Reaction They Catalyze

Before delving further into the specific properties of enzymes, a word on nomenclature is in order. Enzymes are commonly named by appending the suffix *-ase* to the name of the enzyme's substrate or to a phrase describing the enzyme's catalytic action. Thus, urease catalyzes the hydrolysis of urea, and **alcohol dehydrogenase** catalyzes the oxidation of primary and secondary alcohols to their corresponding aldehydes and ketones by removing hydrogen. Since there were at first no systematic rules for naming enzymes, this practice occasionally resulted in two different names being used for the same enzyme or, conversely, in the same name being used for two different enzymes. Moreover, many enzymes, such as **catalase** (which mediates the dismutation of H_2O_2 to H_2O and O_2), were given names that provide no clue to their function. In an effort to eliminate this confusion and to provide rules for rationally naming the rapidly growing number of newly discovered enzymes, a scheme for the systematic functional classification and nomenclature of enzymes was adopted by the International Union of Biochemistry and Molecular Biology (IUBMB).

Enzymes are classified and named according to the nature of the chemical reactions they catalyze. There are six major classes of enzymatic reactions (Table 11-2), as well as subclasses and sub-subclasses. Each enzyme is assigned two names and a four-part classification number. Its **alternative name** is convenient for everyday use and is often an enzyme's previously used trivial name. Its **systematic** or **official name** is used when ambiguity must be minimized; it is the name of its substrate(s) followed by a word ending in *-ase* specifying the type of reaction the enzyme catalyzes according to its major group classification. For example, the enzyme whose alternative name is aconitase (Section 17-3B) has the systematic name aconitate hydratase and the Classification number EC 4.2.1.3 ("EC"

Table 11-2 Enzyme Classification According to Reaction Type

Classification	Type of Reaction Catalyzed
1. Oxidoreductases	Oxidation–reduction reactions
2. Transferases	Transfer of functional groups
3. Hydrolases	Hydrolysis reactions
4. Lyases	Group elimination to form double bonds
5. Isomerases	Isomerization
6. Ligases	Bond formation coupled with ATP hydrolysis

stands for Enzyme Commission, and the numbers represent the class, subclass, sub-subclass, and its arbitrarily assigned serial number in its sub-subclass). For our purposes, the recommended name of an enzyme is usually adequate. However, EC classification numbers are increasingly used in various Internet-accessible databases (Box 14-2). Systematic names and EC classification numbers can be obtained via the Internet (http://expasy.org/enzyme/).

B | Enzymes Act on Specific Substrates

The noncovalent forces through which substrates and other molecules bind to enzymes are similar in character to the forces that dictate the conformations of the proteins themselves (Section 6-4A). Both involve van der Waals, electrostatic, hydrogen bonding, and hydrophobic interactions. In general, a substrate-binding site consists of an indentation or cleft on the surface of an enzyme molecule that is complementary in shape to the substrate **(geometric complementarity).** Moreover, the amino acid residues that form the binding site are arranged to specifically attract the substrate (**electronic complementarity,** Fig. 11-1). Molecules that differ in shape or functional group distribution from the substrate cannot productively bind to the enzyme. X-Ray studies indicate that the substrate-binding sites of most enzymes are largely preformed but undergo some conformational change on substrate binding (a phenomenon called **induced fit**). The complementarity between enzymes and their substrates is the basis of the "lock-and-key" model of enzyme function first proposed by Emil Fischer in 1894. As we shall see, such specific binding is necessary but not sufficient for efficient catalysis.

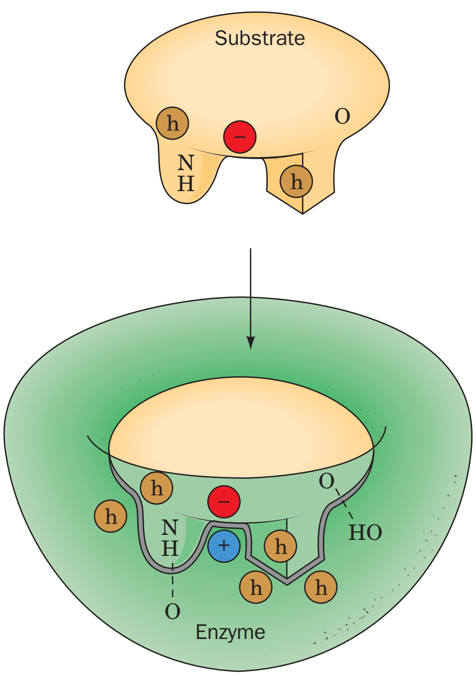

Figure 11-1 | An enzyme–substrate complex. The geometric and the electronic complementarity between the enzyme and substrate depend on noncovalent forces. Hydrophobic groups are represented by an h in a brown circle, and dashed lines represent hydrogen bonds.

Enzymes Are Stereospecific. Enzymes are highly specific both in binding chiral substrates and in catalyzing their reactions. This **stereospecificity** arises because enzymes, by virtue of their inherent chirality (proteins consist of only L-amino acids), form asymmetric active sites. For example, the enzyme **aconitase** catalyzes the interconversion of citrate and isocitrate in the citric acid cycle (Section 17-3B):

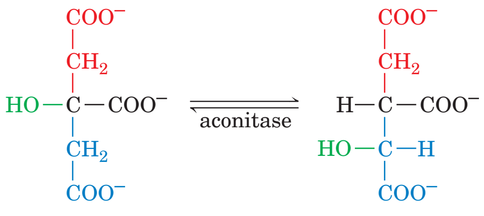

$$\begin{array}{c} \text{COO}^- \\ | \\ \text{CH}_2 \\ | \\ \text{HO}-\text{C}-\text{COO}^- \\ | \\ \text{CH}_2 \\ | \\ \text{COO}^- \end{array} \underset{\text{aconitase}}{\rightleftharpoons} \begin{array}{c} \text{COO}^- \\ | \\ \text{CH}_2 \\ | \\ \text{H}-\text{C}-\text{COO}^- \\ | \\ \text{HO}-\text{C}-\text{H} \\ | \\ \text{COO}^- \end{array}$$

Citrate **Isocitrate**

Citrate is a **prochiral** molecule; that is, it can become chiral through the substitution of one of its two carboxymethyl ($-\text{CH}_2\text{COO}^-$) groups (chirality is discussed in Section 4-2). These groups are chemically equivalent but occupy different positions relative to the OH and COO^- groups (likewise, your body is bilaterally symmetric but has distinguishable right and left sides). Aconitase can therefore distinguish between them because citrate interacts asymmetrically with the surface of the enzyme by making a three-point attachment (Fig. 11-2). Because there is only one productive way for citrate to bind to the enzyme, only one of its $-\text{CH}_2\text{COO}^-$ groups reacts to form isocitrate. The stereospecificity of aconitase is by no means unusual. As we consider biochemical reactions, we shall find that *nearly all enzymes that participate in chiral reactions are absolutely stereospecific.*

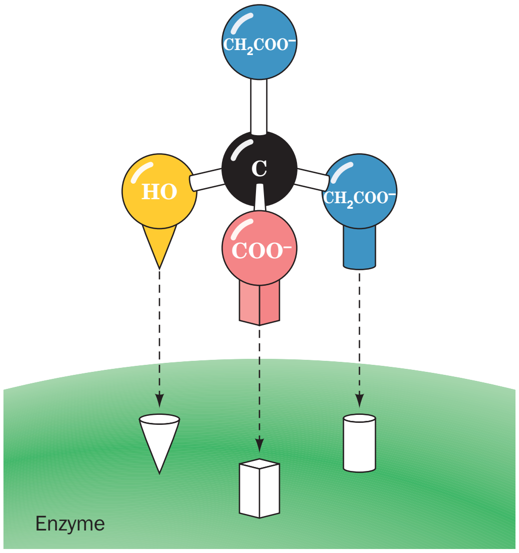

Figure 11-2 | Stereospecificity in substrate binding. The specific binding of a prochiral molecule, such as citrate, in an enzyme active site allows the enzyme to differentiate between prochiral groups.

Enzymes Vary in Geometric Specificity. The stereospecificity of enzymes is not particularly surprising in light of the complementarity of an enzyme's binding site for its substrate. A substance of the wrong chirality will not fit productively into an enzymatic binding site for much the same reason that you cannot fit your right hand into your left glove. In addition to their stereospecificity, however, most enzymes are quite selective about the identities of the chemical groups on their substrates. Indeed, such **geometric specificity** is a more stringent requirement than is stereospecificity.

Enzymes vary considerably in their degree of geometric specificity. A few enzymes are absolutely specific for only one compound. Most enzymes, however, catalyze the reactions of a small range of related compounds although with different efficiencies. For example, alcohol dehydrogenase catalyzes the oxidation of **ethanol** (CH_3CH_2OH) to **acetaldehyde** (CH_3CHO) faster than it oxidizes **methanol** (CH_3OH) to **formaldehyde** (H_2CO) or **isopropanol** [$(CH_3)_2CHOH$] to **acetone** [$(CH_3)_2CO$], even though methanol and isopropanol differ from ethanol by only the deletion or addition of a CH_2 group.

Some enzymes, particularly digestive enzymes, are so permissive in their ranges of acceptable substrates that their geometric specificities are more accurately described as preferences. Some enzymes are not even very specific in the type of reaction they catalyze. For example, chymotrypsin, in addition to its ability to mediate peptide bond hydrolysis, also catalyzes ester bond hydrolysis.

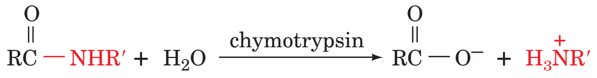

$$R\overset{\overset{\displaystyle O}{\|}}{C}-NHR' + H_2O \xrightarrow{\text{chymotrypsin}} R\overset{\overset{\displaystyle O}{\|}}{C}-O^- + H_3\overset{+}{N}R'$$

Peptide

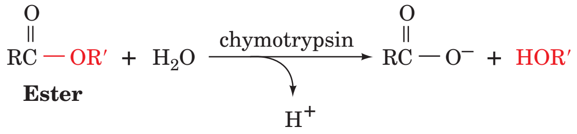

$$R\overset{\overset{\displaystyle O}{\|}}{C}-OR' + H_2O \xrightarrow{\text{chymotrypsin}} R\overset{\overset{\displaystyle O}{\|}}{C}-O^- + HOR' + H^+$$

Ester

This property makes it convenient to measure chymotrypsin activity using small synthetic esters as substrates. Such permissiveness is much more the exception than the rule. Indeed, most intracellular enzymes function *in vivo* to catalyze a particular reaction on a particular substrate.

C | Some Enzymes Require Cofactors

The functional groups of proteins, as we shall see, can facilely participate in acid–base reactions, form certain types of transient covalent bonds, and take part in charge–charge interactions. They are, however, less suitable for catalyzing oxidation–reduction reactions and many types of group-transfer processes. Although enzymes catalyze such reactions, they can do so only in association with small **cofactors,** which essentially act as the enzymes' "chemical teeth" (Fig. 11-3).

Cofactors may be metal ions, such as Cu^{2+}, Fe^{3+}, or Zn^{2+}. The essential nature of these cofactors explains why organisms require trace amounts of certain elements in their diets. It also explains, in part, the toxic effects of certain heavy metals. For example, Cd^{2+} and Hg^{2+} can replace Zn^{2+} (all are in the same group of the periodic table) in the active sites of certain enzymes, including RNA polymerase, and thereby render these enzymes inactive.

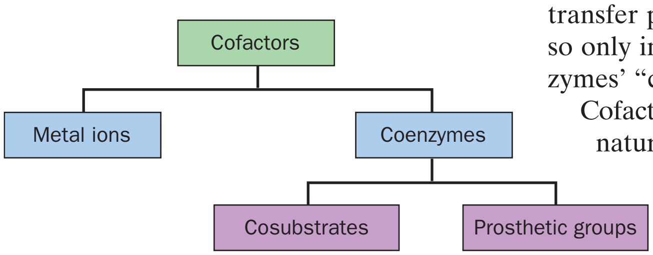

Figure 11-3 | Types of cofactors.

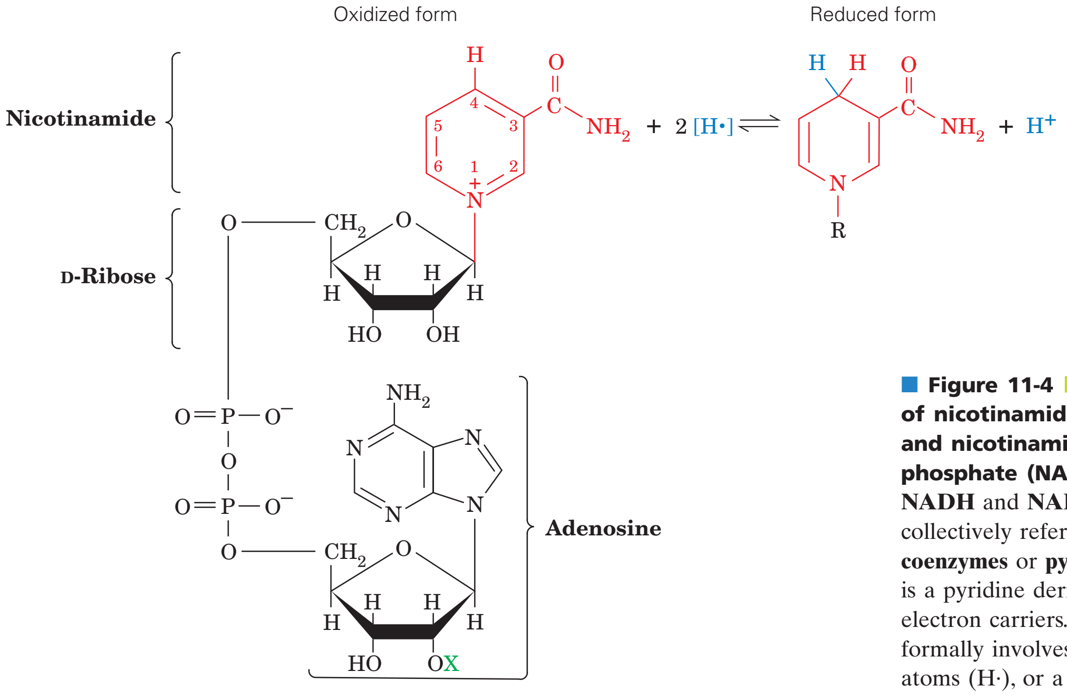

X = H **Nicotinamide adenine dinucleotide (NAD^+)**
X = PO_3^{2-} **Nicotinamide adenine dinucleotide phosphate ($NADP^+$)**

Figure 11-4 | The structures and reaction of nicotinamide adenine dinucleotide (NAD^+) and nicotinamide adenine dinucleotide phosphate ($NADP^+$). Their reduced forms are **NADH** and **NADPH.** These substances, which are collectively referred to as the **nicotinamide coenzymes** or **pyridine nucleotides** (nicotinamide is a pyridine derivative), function as intracellular electron carriers. Reduction (addition of electrons) formally involves the transfer of two hydrogen atoms (H·), or a hydride ion and a proton ($H{:}^- + H^+$). Note that only the nicotinamide ring is changed in the reaction.

Cofactors may also be organic molecules known as **coenzymes.** Some cofactors are only transiently associated with a given enzyme molecule, so that they function as **cosubstrates**. **Nicotinamide adenine dinucleotide (NAD^+)** and **nicotinamide adenine dinucleotide phosphate ($NADP^+$)** are examples of cosubstrates (Fig. 11-4). For instance, NAD^+ is an obligatory oxidizing agent in the alcohol dehydrogenase **(ADH)** reaction:

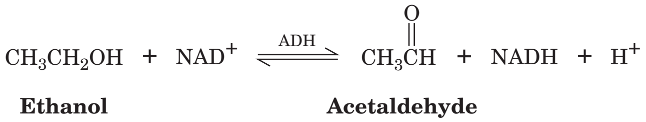

$$CH_3CH_2OH + NAD^+ \xrightleftharpoons{\text{ADH}} CH_3\overset{\overset{\displaystyle O}{\|}}{C}H + NADH + H^+$$

Ethanol **Acetaldehyde**

The product NADH dissociates from the enzyme for eventual reoxidation to NAD^+ in an independent enzymatic reaction.

Other cofactors, known as **prosthetic groups,** are permanently associated with their protein, often by covalent bonds. For example, a heme prosthetic group (Fig. 7-2) is tightly bound to proteins known as **cytochromes** (Fig. 6-32 and Box 18-1) through extensive hydrophobic and hydrogen-bonding interactions together with covalent bonds between the heme and specific protein side chains.

A catalytically active enzyme–cofactor complex is called a **holoenzyme.** The enzymatically inactive protein resulting from the removal of a holoenzyme's cofactor is referred to as an **apoenzyme;** that is,

$$\text{apoenzyme } (\textit{inactive}) + \text{cofactor} \rightleftharpoons \text{holoenzyme } (\textit{active})$$

Coenzymes Must Be Regenerated. Coenzymes are chemically changed by the enzymatic reactions in which they participate. *In order to complete the catalytic cycle, the coenzyme must return to its original state.* For a transiently bound coenzyme (cosubstrate), the regeneration reaction may be catalyzed by a different enzyme as we have seen to be the case for NAD^+. However, for a prosthetic group, regeneration occurs as part of the enzyme reaction sequence.

CHECK YOUR UNDERSTANDING

What properties distinguish enzymes from other catalysts?
What factors influence an enzyme's substrate specificity?
Why are cofactors required for some enzymatic reactions?
What is the relationship between cofactors, coenzymes, cosubstrates, and prosthetic groups?

LEARNING OBJECTIVE

- Understand that an enzyme affects the free energy along the path of a chemical reaction but not the overall free energy change.

2 Activation Energy and the Reaction Coordinate

Much of our understanding of how enzymes catalyze chemical reactions comes from **transition state theory,** which was developed in the 1930s, principally by Henry Eyring. Consider a bimolecular reaction involving three atoms, such as the reaction of a hydrogen atom with diatomic hydrogen (H_2) to yield a new H_2 molecule and a different hydrogen atom:

$$H_A{-}H_B + H_C \longrightarrow H_A + H_B{-}H_C$$

In this reaction, H_C must approach the diatomic molecule $H_A{-}H_B$ so that, at some point in the reaction, there exists a high-energy (unstable) complex represented as $H_A{---}H_B{---}H_C$. In this complex, the $H_A{-}H_B$ covalent bond is in the process of breaking while the $H_B{-}H_C$ bond is in the process of forming. The point of highest free energy is called the **transition state** of the system.

Reactants generally approach one another along the path of minimum free energy, their so-called **reaction coordinate.** A plot of free energy versus the reaction coordinate is called a **transition state diagram** or **reaction coordinate diagram** (Fig. 11-5). The reactants and products are states of minimum free energy, and the transition state corresponds to the highest point of the diagram. For the H + H_2 reaction, the reactants and products have the same free energy (Fig. 11-5*a*). If the atoms in the reacting system are of different types, such as in the reaction

$$A + B \longrightarrow X^{\ddagger} \longrightarrow P + Q$$

where A and B are the reactants, P and Q are the products, and $X^{\ddagger}$ represents the transition state, the transition state diagram is no longer symmetrical because there is a free energy difference between the reactants and products (Fig. 11-5*b*). In either case, $\boldsymbol{\Delta G^{\ddagger}}$**,** the free energy

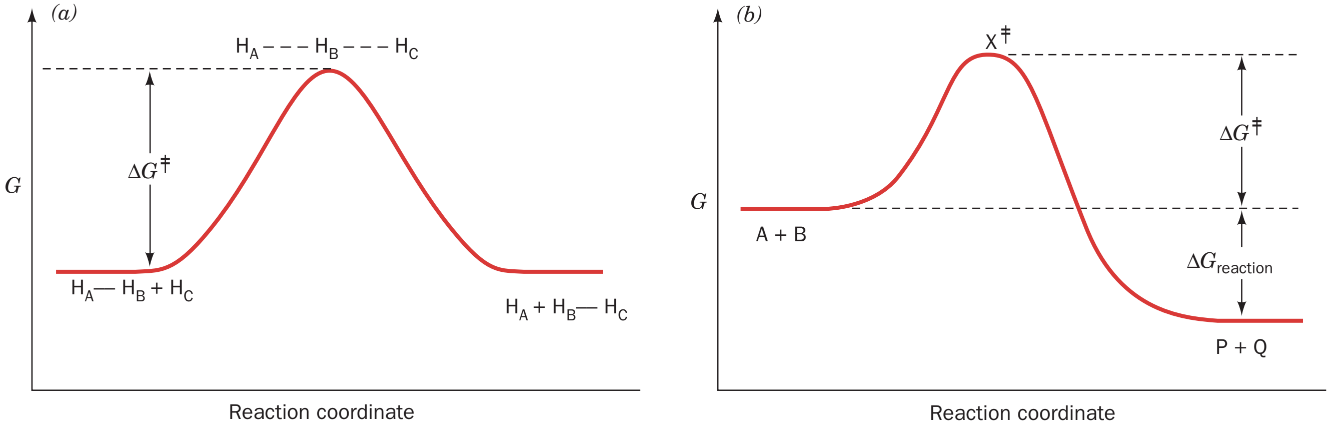

Figure 11-5 | Transition state diagrams. (*a*) The H + H_2 reaction. The reactants and products correspond to low free energy structures. The point of highest free energy is the transition state, in which the reactants are partially converted to products. $\Delta G^{\ddagger}$ is the free energy of activation, the difference in free energy between the reactants and the transition state, $X^{\ddagger}$. (*b*) Transition state diagram for the reaction A + B → P + Q. This is a spontaneous reaction; that is, $\Delta G_{\text{reaction}} < 0$ (the free energy of P + Q is less than the free energy of A + B).

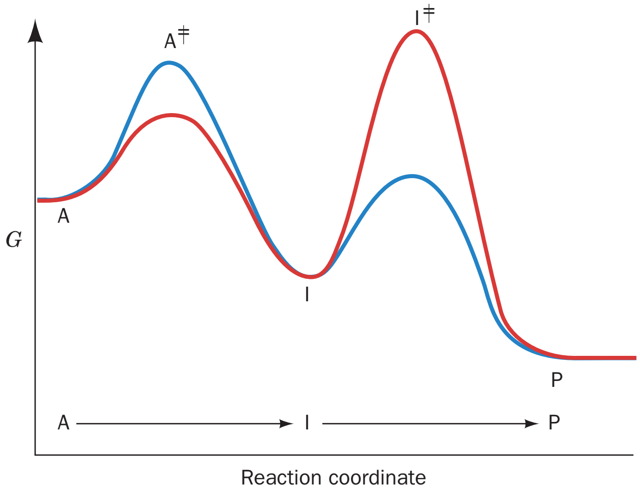

Figure 11-6 | **Transition state diagram for a two-step reaction.** The blue curve represents a reaction (A → I → P) whose first step is rate determining, and the red curve represents a reaction whose second step is rate determining.

of the transition state less that of the reactants, is known as the **free energy of activation.**

Passage through the transition state requires only 10^{-13} to 10^{-14} s, so the concentration of the transition state in a reacting system is small. Hence, the decomposition of the transition state to products (or back to reactants) is postulated to be the rate-determining process of the overall reaction. Thermodynamic arguments lead to the conclusion that the reaction rate is proportional to $e^{-\Delta G^{\ddagger}/RT}$, where R is the gas constant and T is the absolute temperature. Thus, *the greater the value of* $\Delta G^{\ddagger}$, *the slower the reaction rate*. This is because the larger the $\Delta G^{\ddagger}$, the smaller the number of reactant molecules that have sufficient thermal energy to achieve the transition state free energy.

Chemical reactions commonly consist of several steps. For a two-step reaction such as

$$\mathrm{A} \longrightarrow \mathrm{I} \longrightarrow \mathrm{P}$$

where I is an intermediate of the reaction, there are two transition states and two activation energy barriers. The shape of the transition state diagram for such a reaction reflects the relative rates of the two steps (Fig. 11-6). If the activation energy of the first step is greater than that of the second step, then the first step is slower than the second step, and conversely, if the activation energy of the second step is greater. In a multistep reaction, the step with the highest transition state free energy acts as a "bottleneck" and is therefore said to be the **rate-determining step** of the reaction.

Catalysts Reduce $\Delta G^{\ddagger}$. *Catalysts act by providing a reaction pathway with a transition state whose free energy is lower than that in the uncatalyzed reaction* (Fig. 11-7). The difference between the values of $\Delta G^{\ddagger}$ for the uncatalyzed and catalyzed reactions, $\Delta\Delta G^{\ddagger}_{\text{cat}}$, indicates the efficiency of the catalyst. The **rate enhancement** (ratio of the rates of the catalyzed and uncatalyzed reactions) is given by $e^{\Delta\Delta G^{\ddagger}_{\text{cat}}/RT}$. Hence, at 25°C (298 K), a 10-fold rate enhancement requires a $\Delta\Delta G^{\ddagger}_{\text{cat}}$ of only 5.71 $\text{kJ} \cdot \text{mol}^{-1}$, which is less than half the free energy of a typical hydrogen bond. Similarly, a

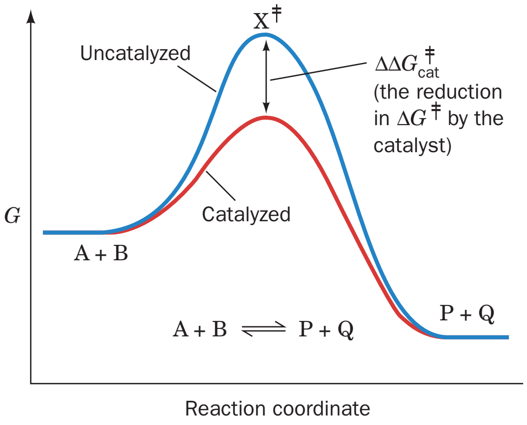

Figure 11-7 | **Effect of a catalyst on the transition state diagram of a reaction.** Here $\Delta\Delta G^{\ddagger}_{\text{cat}} = \Delta G^{\ddagger}(\text{uncat}) - \Delta G^{\ddagger}(\text{cat})$.

millionfold rate acceleration occurs when $\Delta\Delta G^{\ddagger}_{\text{cat}} \approx 34\ \text{kJ}\cdot\text{mol}^{-1}$, a small fraction of the free energy of most covalent bonds. Thus, from a theoretical standpoint, tremendous catalytic efficiency seems within reach of the reactive groups that occur in the active sites of enzymes. How these groups actually function at the atomic level is the subject of much of this and other chapters.

Note that a catalyst lowers the free energy barrier by the same amount for both the forward and reverse reactions (Fig. 11-7). Consequently, a catalyst equally accelerates the forward and reverse reactions. Keep in mind also that while a catalyst can accelerate the conversion of reactants to products (or products back to reactants), the likelihood of the net reaction occurring in one direction or the other depends only on the free energy difference between the reactants and the products. If $\Delta G_{\text{reaction}} < 0$, the reaction proceeds spontaneously from reactants toward products; if $\Delta G_{\text{reaction}} > 0$, the reverse reaction proceeds spontaneously. *An enzyme cannot alter $\Delta G_{\text{reaction}}$; it can only decrease $\Delta G^{\ddagger}$ to allow the reaction to approach equilibrium (where the rates of the forward and reverse reactions are equal) more quickly than it would in the absence of a catalyst.* The actual velocity with which reactants are converted to products is the subject of kinetics (Section 12-1).

■ CHECK YOUR UNDERSTANDING

Sketch and label the various parts of transition state diagrams for a reaction with and without a catalyst.

What is the relationship between ΔG and $\Delta G^{\ddagger}$?

3 Catalytic Mechanisms

LEARNING OBJECTIVES

- Understand the chemical basis for acid–base catalysis, covalent catalysis, and metal ion catalysis.
- Understand how enzymes accelerate reactions through proximity and orientation effects and by preferential binding of the transition state.

Enzymes achieve their enormous rate accelerations via the same catalytic mechanisms used by chemical catalysts. Enzymes have simply been better designed through evolution. Enzymes, like other catalysts, reduce the free energy of the transition state ($\Delta G^{\ddagger}$); that is, *they stabilize the transition state of the catalyzed reaction.* What makes enzymes such effective catalysts is their specificity of substrate binding combined with their arrangement of catalytic groups. As we shall see, however, the distinction between substrate-binding groups and catalytic groups is somewhat arbitrary.

Much can be learned about enzymatic reaction mechanisms by examining the corresponding nonenzymatic reactions of model compounds. Both types of reactions can be described using the **curved arrow convention** to trace the electron pair rearrangements that occur in going from reactants to products. The movement of an electron pair (which may be either a lone pair or a pair forming a covalent bond) is symbolized by a curved arrow emanating from the electron pair and pointing to the electron-deficient center attracting the electron pair. For example, imine **(Schiff base)** formation, a biochemically important reaction between an amine and an aldehyde or ketone, is represented as follows:

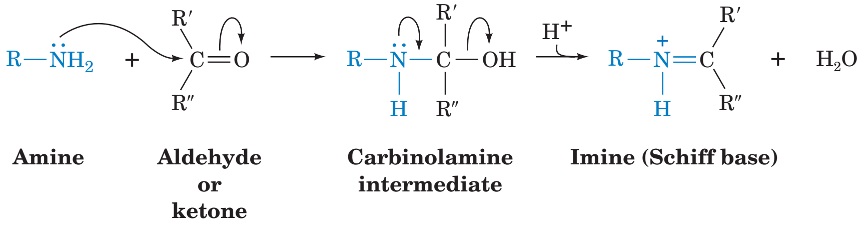

In the first reaction step, the amine's unshared electron pair adds to the electron-deficient carbonyl carbon while one electron pair from its C=O double bond transfers to the oxygen atom. In the second step, the unshared electron pair on the nitrogen atom adds to the electron-deficient carbon atom with the elimination of water. *At all times, the rules of chemical* *reason apply to the system:* For example, there are never five bonds to a carbon atom or two bonds to a hydrogen atom.

The types of catalytic mechanisms that enzymes employ have been classified as

1. Acid–base catalysis
2. Covalent catalysis
3. Metal ion catalysis
4. Proximity and orientation effects
5. Preferential binding of the transition state complex

In this section, we consider each of these types of mechanisms in turn.

A | Acid–Base Catalysis Occurs by Proton Transfer

***General acid catalysis** is a process in which proton transfer from an acid lowers the free energy of a reaction's transition state.* For example, an uncatalyzed keto–enol tautomerization reaction occurs quite slowly as a result of the high free energy of its carbanion-like transition state (Fig. 11-8*a;* the transition state is drawn in square brackets to indicate its instability). Proton donation to the oxygen atom (Fig. 11-8*b*), however, reduces the carbanion character of the transition state, thereby accelerating the reaction.

*A reaction may also be stimulated by **general base catalysis** if its rate is increased by proton abstraction by a base* (e.g., Fig. 11-8*c*). Some reactions may be simultaneously subject to both processes; these are **concerted acid–base catalyzed reactions.**

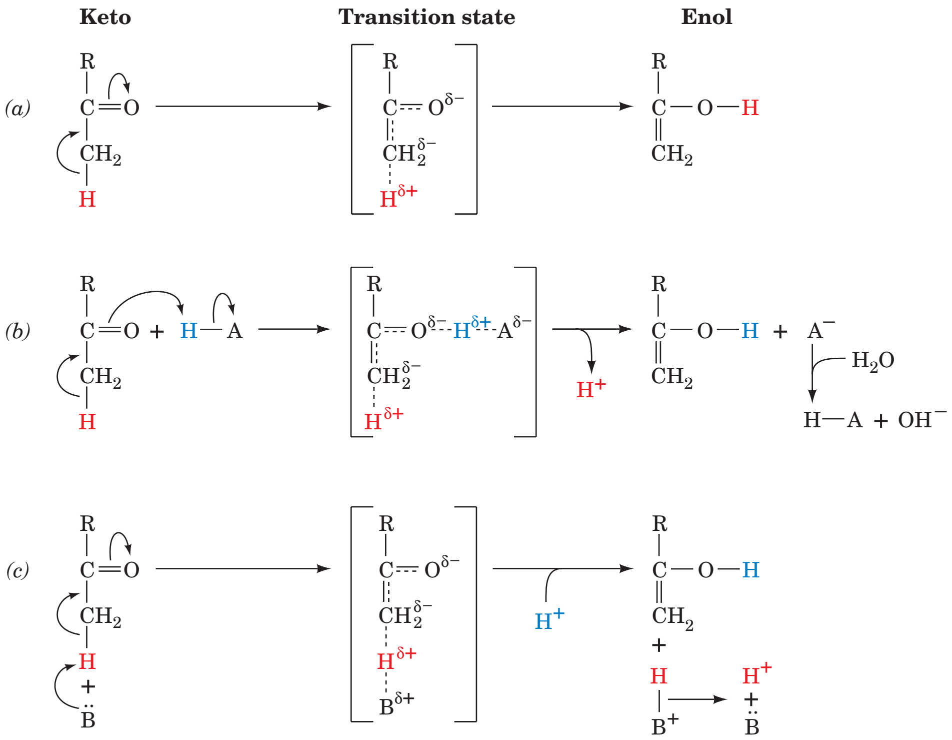

■ **Figure 11-8 | Mechanisms of keto–enol tautomerization.** (*a*) Uncatalyzed. (*b*) General acid catalyzed. (*c*) General base catalyzed. The acid is represented as H—A and the base as $\ddot{B}$.

BOX 11-1 **PERSPECTIVES IN BIOCHEMISTRY**

Effects of pH on Enzyme Activity

Most enzymes are active within only a narrow pH range, typically 5 to 9. This is a result of the effects of pH on a combination of factors: (1) the binding of substrate to enzyme, (2) the ionization states of the amino acid residues involved in the catalytic activity of the enzyme, (3) the ionization of the substrate, and (4) the variation of protein structure (usually significant only at extremes of pH).

The rates of many enzymatic reactions exhibit bell-shaped curves as a function of pH. For example, the pH dependence of the rate of the reaction catalyzed by **fumarase** (Section 17-3G) produces the following curve:

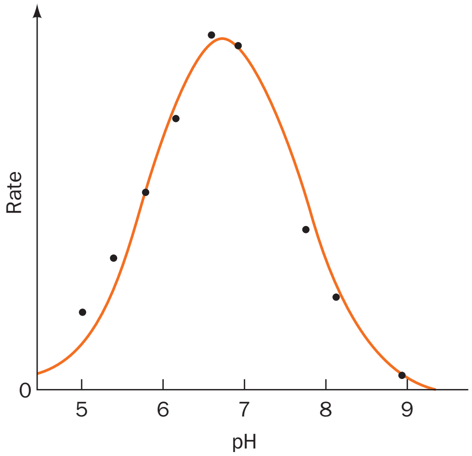

Such curves reflect the ionization of certain amino acid residues that must be in a specific ionization state for enzymatic activity. The observed p*K*'s (the inflection points of the curve) often provide valuable clues to the identities of the amino acid residues essential for enzymatic activity. For example, an observed p*K* of ~4 suggests that an Asp or Glu residue is essential to the enzyme. Similarly, p*K*'s of ~6 or ~10 suggest the participation of a His or a Lys residue, respectively. However, the p*K* of a given acid–base group may vary by as much as several pH units from its expected value, depending on its microenvironment (e.g., an Asp residue in a nonpolar environment or in close proximity to another Asp residue would attract protons more strongly than otherwise and hence have a higher p*K*). Furthermore, pH effects on an enzymatic rate may reflect denaturation of the enzyme rather than protonation or deprotonation of specific catalytic residues. The replacement of a particular residue by site-directed mutagenesis or comparisons of enzyme variants generated by evolution is a more reliable approach to identifying residues that are required for substrate binding or catalysis.

[Figure adapted from Tanford, C., *Physical Chemistry of Macromolecules,* p. 647, Wiley (1961).]

Many types of biochemical reactions are susceptible to acid and/or base catalysis. The side chains of the amino acid residues Asp, Glu, His, Cys, Tyr, and Lys have p*K*'s in or near the physiological pH range (Table 4-1), which permits them to act as acid and/or base catalysts. Indeed, *the ability of enzymes to arrange several catalytic groups around their substrates makes concerted acid–base catalysis a common enzymatic mechanism.* The catalytic activity of these enzymes is sensitive to pH, since the pH influences the state of protonation of side chains at the active site (Box 11-1).

RNase A Is an Acid–Base Catalyst. **Bovine pancreatic RNase A** provides an example of enzymatically mediated acid–base catalysis. This digestive enzyme (Fig. 11-9) is secreted by the pancreas into the small

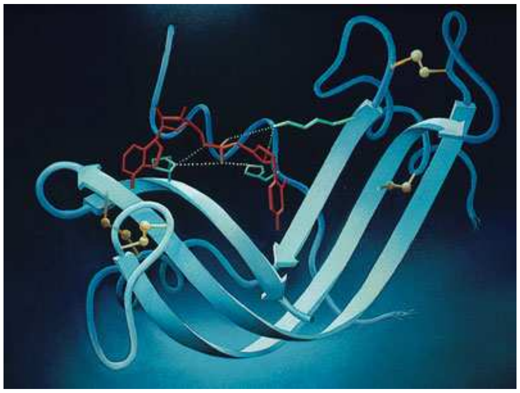

Figure 11-9 | X-Ray structure of bovine pancreatic RNase S. A nonhydrolyzable substrate analog, the dinucleotide phosphonate UpcA (*red*), is bound in the active site. RNase S is a catalytically active form of RNase A in which the peptide bond between residues 20 and 21 has been hydrolyzed. [Illustration, Irving Geis/Geis Archives Trust. Copyright Howard Hughes Medical Institute. Reproduced by permission.] **See Interactive Exercise 6.**

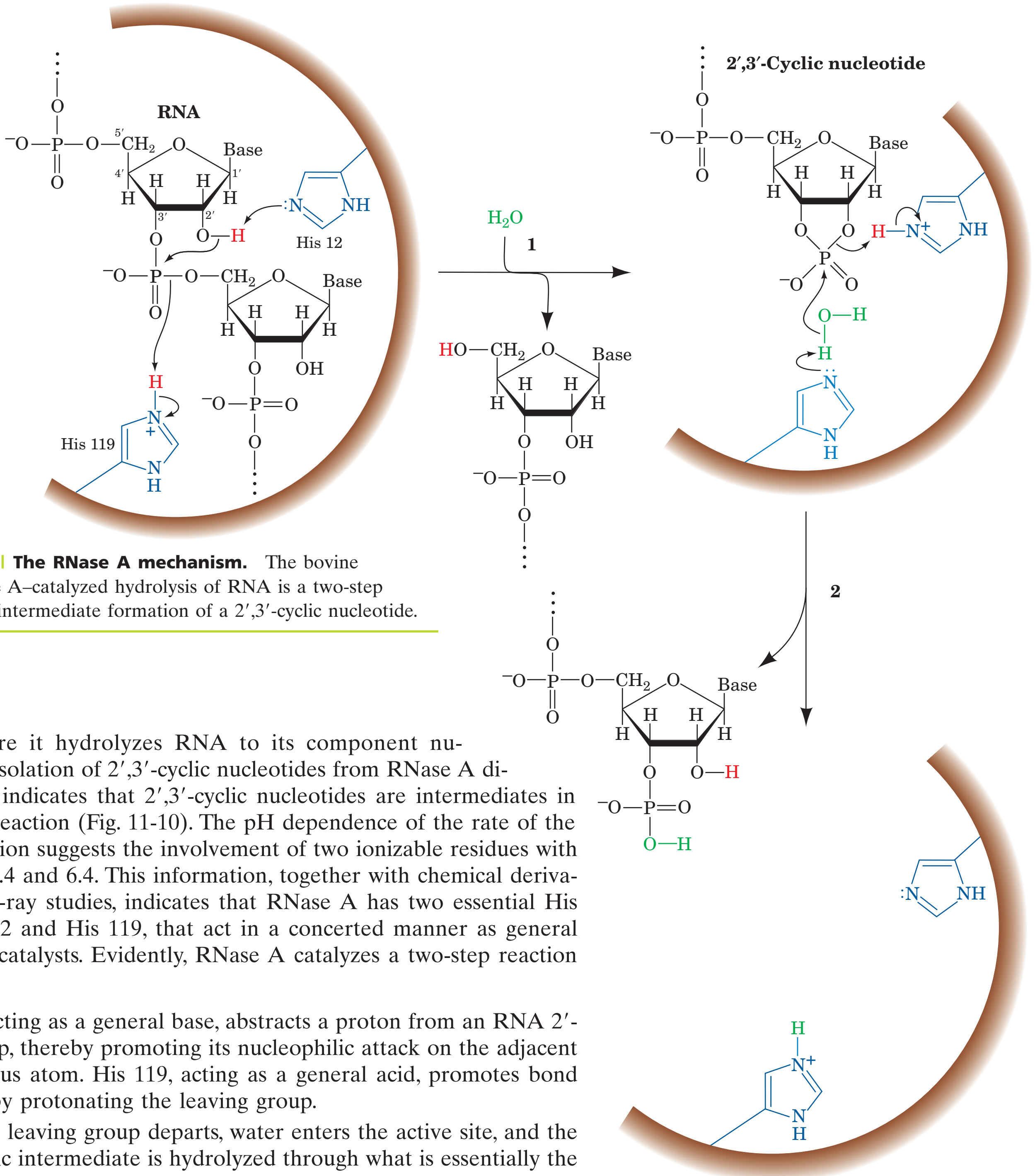

Figure 11-10 | The RNase A mechanism. The bovine pancreatic RNase A–catalyzed hydrolysis of RNA is a two-step process with the intermediate formation of a 2′,3′-cyclic nucleotide.

intestine, where it hydrolyzes RNA to its component nucleotides. The isolation of 2′,3′-cyclic nucleotides from RNase A digests of RNA indicates that 2′,3′-cyclic nucleotides are intermediates in the RNase A reaction (Fig. 11-10). The pH dependence of the rate of the RNase A reaction suggests the involvement of two ionizable residues with pK values of 5.4 and 6.4. This information, together with chemical derivatization and X-ray studies, indicates that RNase A has two essential His residues, His 12 and His 119, that act in a concerted manner as general acid and base catalysts. Evidently, RNase A catalyzes a two-step reaction (Fig. 11-10):

1. His 12, acting as a general base, abstracts a proton from an RNA 2′-OH group, thereby promoting its nucleophilic attack on the adjacent phosphorus atom. His 119, acting as a general acid, promotes bond scission by protonating the leaving group.
2. After the leaving group departs, water enters the active site, and the 2′,3′-cyclic intermediate is hydrolyzed through what is essentially the reverse of the first step. Thus, His 12 now acts as a general acid and His 119 as a general base to yield the hydrolyzed RNA and the enzyme in its original state.

B | Covalent Catalysis Usually Requires a Nucleophile

***Covalent catalysis** accelerates reaction rates through the transient formation of a catalyst–substrate covalent bond.* Usually, this covalent bond is formed by the reaction of a nucleophilic group on the catalyst with an electrophilic group on the substrate, and hence this form of catalysis is often also called

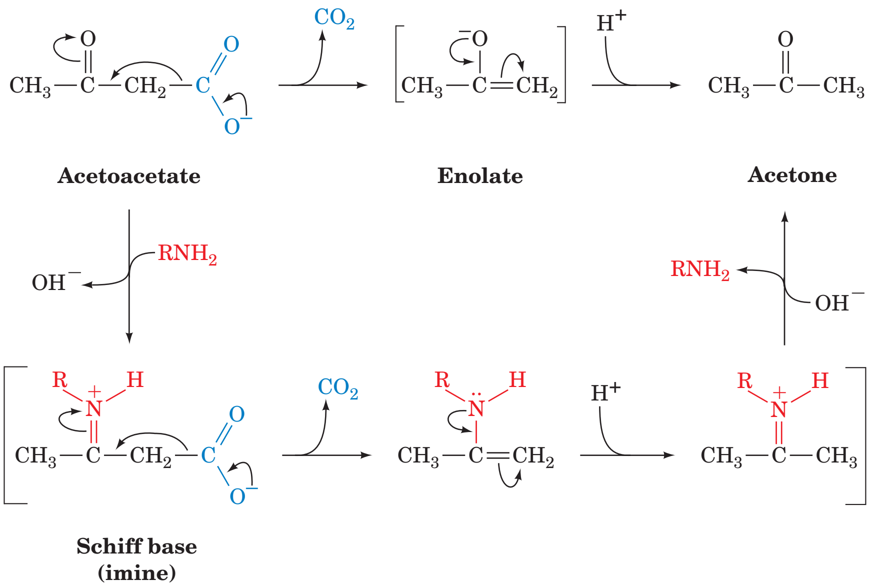

■ **Figure 11-11 | The decarboxylation of acetoacetate.** The uncatalyzed reaction mechanism is at the top, and the mechanism as catalyzed by primary amines is at the bottom.

nucleophilic catalysis. The decarboxylation of acetoacetate, as chemically catalyzed by primary amines, is an example of such a process (Fig. 11-11). In the first stage of this reaction, the amine, a nucleophile, attacks the carbonyl group of acetoacetate to form a Schiff base (imine bond):

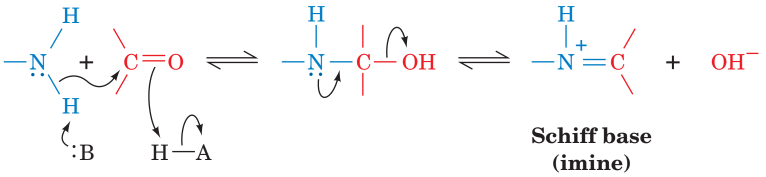

The protonated nitrogen atom of the covalent intermediate then acts as an electron sink (Fig. 11-11, *bottom*) to reduce the high-energy enolate character of the transition state. The formation and decomposition of the Schiff base occurs quite rapidly so that it is not the rate-determining step of this reaction.

Covalent catalysis can be conceptually decomposed into three stages:

1. The nucleophilic reaction between the catalyst and the substrate to form a covalent bond.
2. The withdrawal of electrons from the reaction center by the now electrophilic catalyst.
3. The elimination of the catalyst, a reaction that is essentially the reverse of stage 1.

The nucleophilicity of a substance is closely related to its basicity. Indeed, the mechanism of nucleophilic catalysis resembles that of base catalysis except that, instead of abstracting a proton from the substrate, the catalyst nucleophilically attacks the substrate to form a covalent bond. Biologically important nucleophiles are negatively charged or contain unshared electron pairs that easily form covalent bonds with electron-deficient centers (Fig. 11-12*a*). Electrophiles, in contrast, include groups that are positively

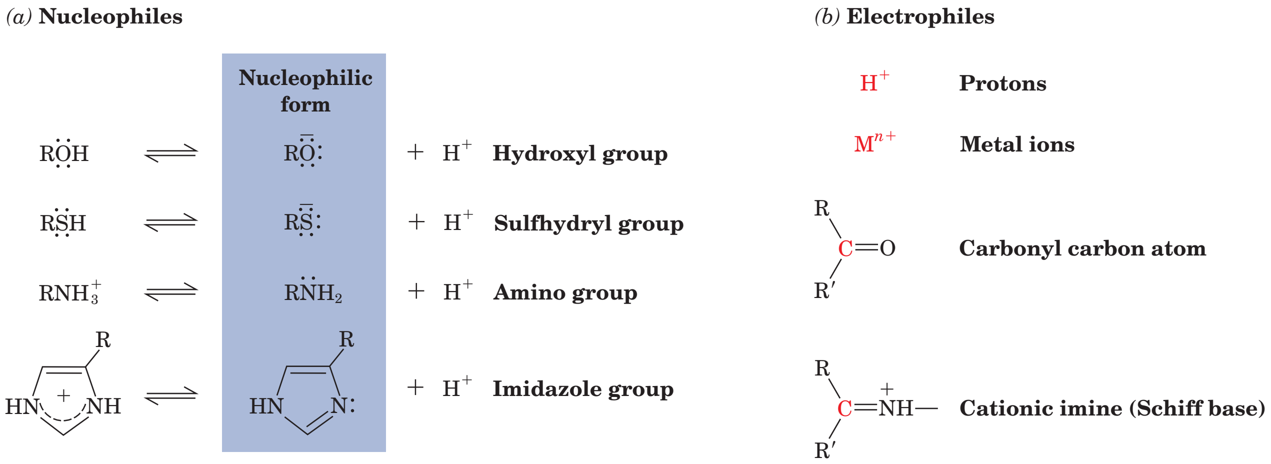

Figure 11-12 | Biologically important nucleophilic and electrophilic groups. (*a*) Nucleophilic groups such as hydroxyl, sulfhydryl, amino, and imidazole groups are nucleophiles in their basic forms. (*b*) Electrophilic groups contain an electron-deficient atom (*red*).

charged, contain an unfilled valence electron shell, or contain an electronegative atom (Fig. 11-12*b*).

An important aspect of covalent catalysis is that *the more stable the covalent bond formed, the less easily it can decompose in the final steps of a reaction.* A good covalent catalyst must therefore combine the seemingly contradictory properties of high nucleophilicity and the ability to form a good leaving group, that is, to easily reverse the bond formation step. Groups with high polarizability (highly mobile electrons), such as imidazole and thiol groups, have these properties and hence make good covalent catalysts. Functional groups in proteins that act in this way include the unprotonated amino group of Lys, the imidazole group of His, the thiol group of Cys, the carboxyl group of Asp, and the hydroxyl group of Ser. In addition, several coenzymes, notably **thiamine pyrophosphate** (Section 15-3B) and **pyridoxal phosphate** (Section 21-2A), function in association with their apoenzymes as covalent catalysts. The large variety of covalently linked enzyme–substrate reaction intermediates that have been isolated demonstrates that enzymes commonly employ covalent catalytic mechanisms.

C | Metal Ion Cofactors Act as Catalysts

Nearly one-third of all known enzymes require metal ions for catalytic activity. This group of enzymes includes the **metalloenzymes,** which contain tightly bound metal ion cofactors, most commonly transition metal ions such as Fe^{2+}, Fe^{3+}, Cu^{2+}, Mn^{2+}, or Co^{2+}. These catalytically essential metal ions are distinct from ions such as Na^+, K^+, or Ca^{2+}, which often play a structural rather than a catalytic role in enzymes. Ions such as Mg^{2+} and Zn^{2+} may be either structural or catalytic.

Metal ions participate in the catalytic process in three major ways:

1. By binding to substrates to orient them properly for reaction.
2. By mediating oxidation–reduction reactions through reversible changes in the metal ion's oxidation state.
3. By electrostatically stabilizing or shielding negative charges.

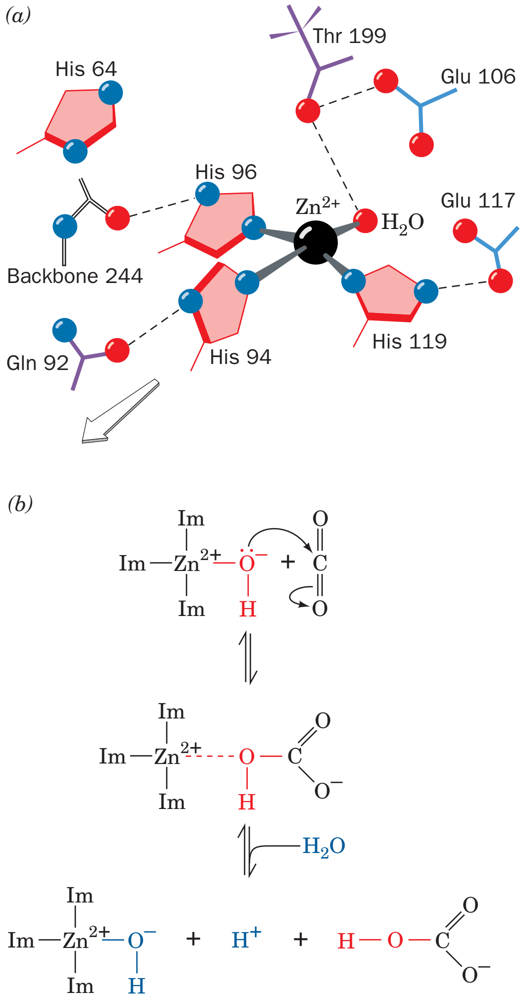

■ **Figure 11-13 | The role of Zn^{2+} in carbonic anhydrase.** (*a*) The active site of the human enzyme. In the X-ray structure, the Zn^{2+} ion is coordinated by three imidazole groups and a water molecule. The arrow points toward the opening of the active site cavity. [After Sheridan, R.P. and Allen, L.C., *J. Am. Chem. Soc.* **103,** 1545 (1981).] **See Interactive Exercise 7.** (*b*) The reaction catalyzed by carbonic anhydrase. Im represents the His imidazole group.

In many metal ion–catalyzed reactions, the metal ion acts in much the same way as a proton to neutralize negative charge. Yet metal ions are often much more effective catalysts than protons because metal ions can be present in high concentrations at neutral pH (where $[H^+] = 10^{-7}$ M) and may have charges greater than +1.

A metal ion's charge also makes its bound water molecules more acidic than free H_2O and therefore a source of nucleophilic OH^- ions even below neutral pH. An excellent example of this phenomenon occurs in the catalytic mechanism of carbonic anhydrase (Box 2-1), a widely occurring enzyme that catalyzes the reaction

$$CO_2 + H_2O \rightleftharpoons HCO_3^- + H^+$$

Carbonic anhydrase contains an essential Zn^{2+} ion that the enzyme's X-ray structure indicates lies at the bottom of a 15-Å-deep active site cleft, where it is tetrahedrally coordinated by three evolutionarily invariant His side chains and an H_2O molecule (Fig. 11-13*a*). The Zn^{2+}-polarized H_2O ionizes to form OH^-, which nucleophilically attacks the enzyme-bound CO_2 to yield HCO_3^- (Fig. 11-13*b*). The proton produced in the reaction is shuttled to the enzyme's surface through base catalysis that is facilitated by a fourth His residue (His 64). The enzyme's catalytic site is then regenerated by the binding of another H_2O to the Zn^{2+} ion.

D | Catalysis Can Occur through Proximity and Orientation Effects

Although enzymes employ catalytic mechanisms that resemble those of organic model reactions, they are far more catalytically efficient than the models. Such efficiency must arise from the specific physical conditions at enzyme catalytic sites that promote the corresponding chemical reactions. The most obvious effects are **proximity** and **orientation:** Reactants must come together with the proper spatial relationship for a reaction to occur. Consider the bimolecular reaction of imidazole with ***p*-nitrophenylacetate.**

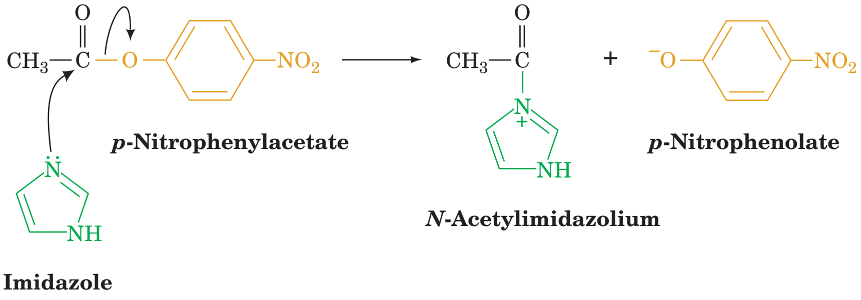

The progress of the reaction is conveniently monitored by the appearance of the intensely yellow ***p*-nitrophenolate** ion. The related intramolecular reaction

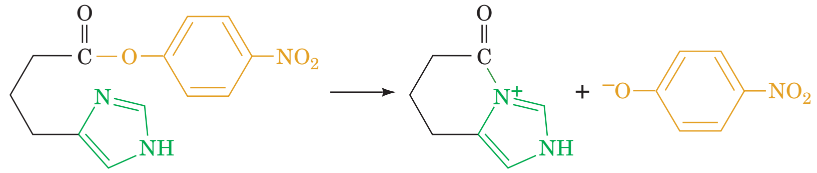

occurs about 24 times faster. Thus, when the imidazole is covalently attached to the reactant, it is 24 times more effective than when it is free in solution. This rate enhancement results from both proximity and orientation effects.

By simply binding their substrates, enzymes facilitate their catalyzed reactions in four ways:

1. Enzymes bring substrates into contact with their catalytic groups and, in reactions with more than one substrate, with each other. However, calculations based on simple model systems suggest that such proximity effects alone can enhance reaction rates by no more than a factor of ~5.
2. Enzymes bind their substrates in the proper orientations for reaction. Molecules are not equally reactive in all directions. Rather, *they react most readily if they have the proper relative orientation*. For example, in an S_N2 (bimolecular nucleophilic substitution) reaction, the incoming nucleophile optimally attacks its target along the direction opposite to that of the bond to the leaving group (Fig. 11-14). Reacting atoms whose approaches deviate by as little as 10° from this optimum direction are significantly less reactive. It is estimated that properly orienting substrates can increase reaction rates by a factor of up to ~100. Enzymes, as we shall see, align their substrates and catalytic groups so as to optimize reactivity.
3. Charged groups may help stabilize the transition state of the reaction, a phenomenon termed **electrostatic catalysis.** The charge distribution around the active sites of enzymes may also guide polar substrates toward their binding site.
4. Enzymes freeze out the relative translational and rotational motions of their substrates and catalytic groups. This is an important aspect of catalysis because, in the transition state, the reacting groups have

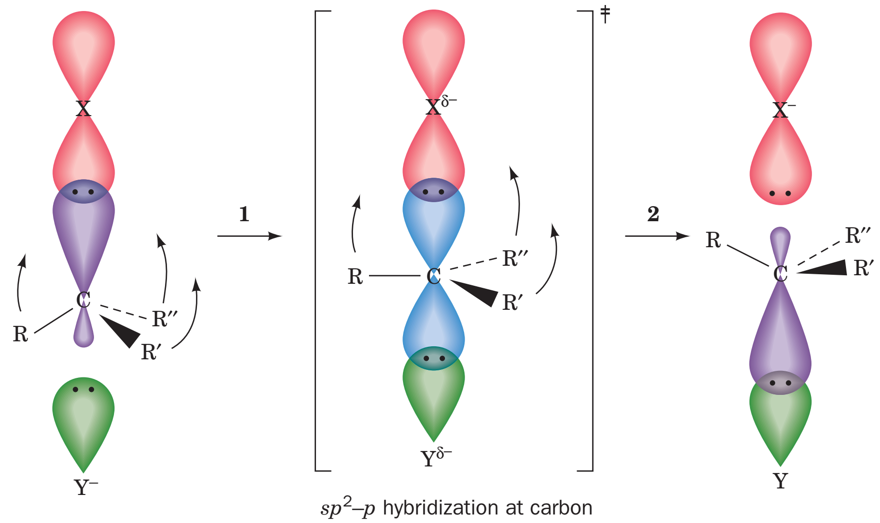

Figure 11-14 | The geometry of an S_N2 reaction. **(1)** The attacking nucleophile, Y^-, must approach the tetrahedrally coordinated and hence sp^3-hybridized C atom along the direction opposite that of its bond to the leaving group, X. In the transition state of the reaction, the C atom becomes trigonal bipyramidally coordinated and hence sp^2–p hybridized, with the p orbital (*blue*) forming partial bonds to X and Y. The three sp^2 orbitals form bonds to the C atom's three other substituents (R, R′, and R″), which have shifted their positions into the plane perpendicular to the X—C—Y axis (*curved arrows*). Any deviation from this optimal geometry would increase the free energy of the transition state, $\Delta G^\ddagger$, and hence reduce the rate of the reaction. **(2)** The transition state then decomposes to products in which R, R′, and R″ have inverted their positions about the C atom, which has rehybridized to sp^3, and X^- has been released.

little relative motion. Indeed, experiments with model compounds suggest that *this effect can promote rate enhancements of up to* $\sim 10^7$!

Bringing substrates and catalytic groups together in a reactive orientation orders them and therefore has a substantial entropic penalty. The free energy required to overcome this entropy loss is supplied by the binding energy of the substrate(s) to the enzyme and contributes to the decreased $\Delta\Delta G^{\ddagger}$.

E | Enzymes Catalyze Reactions by Preferentially Binding the Transition State

The rate enhancements effected by enzymes are often greater than can be reasonably accounted for by the catalytic mechanisms discussed so far. However, we have not yet considered one of the most important mechanisms of enzymatic catalysis: *An enzyme may bind the transition state of the reaction it catalyzes with greater affinity than its substrates or products.* When taken together with the previously described catalytic mechanisms, preferential transition state binding explains the observed rates of enzyme-catalyzed reactions.

The original concept of transition state binding proposed that enzymes mechanically strained their substrates toward the transition state geometry through binding sites into which undistorted substrates did not properly fit. Such strain promotes many organic reactions. For example, the rate of the reaction

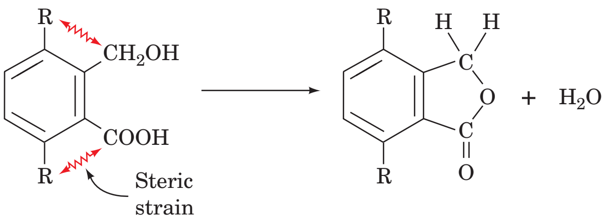

Steric strain

is 315 times faster when R is CH_3 rather than H because of the greater steric repulsion between the CH_3 groups and the reacting groups. The strained reactant more closely resembles the transition state of the reaction than does the corresponding unstrained reactant. Thus, as was first suggested by Linus Pauling and further amplified by Richard Wolfenden and Gustav Lienhard, *enzymes that preferentially bind the transition state structure increase its concentration and therefore proportionally increase the reaction rate*.

The more tightly an enzyme binds its reaction's transition state relative to the substrate, the greater is the rate of the catalyzed reaction relative to that of the uncatalyzed reaction; that is, catalysis results from the preferential binding and therefore the stabilization of the transition state relative to the substrate (Fig. 11-15). In other words, the free energy difference between an enzyme–substrate complex (ES) and an enzyme–transition state complex ($ES^{\ddagger}$) is less than the free energy difference between S and $S^{\ddagger}$ in an uncatalyzed reaction.

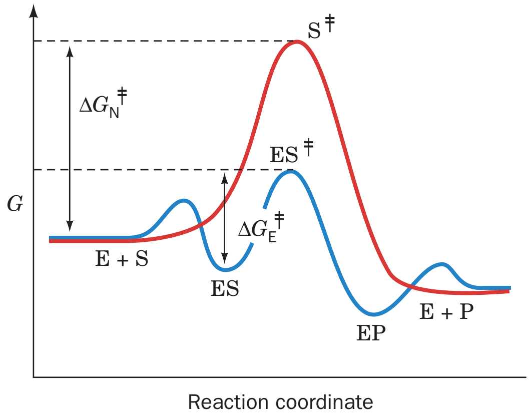

■ **Figure 11-15 | Effect of preferential transition state binding.** The reaction coordinate diagram for a hypothetical enzyme-catalyzed reaction involving a single substrate is blue, and the diagram for the corresponding uncatalyzed reaction is red. $\Delta G_{\mathrm{N}}^{\ddagger}$ is the free energy of activation for the nonenzymatic reaction and $\Delta G_{\mathrm{E}}^{\ddagger}$ is the free energy of activation for the enzyme-catalyzed reaction. The small dips in the reaction coordinate diagram for the enzyme-catalyzed reaction arise from the binding of substrate and product to the enzyme. **See the Animated Figures.**

As we saw in Section 11-2, the rate enhancement of a catalyzed reaction is given by $e^{\Delta\Delta G^{\ddagger}_{\text{cat}}/RT}$, where $\Delta\Delta G^{\ddagger}_{\text{cat}}$ is the difference in the values of $\Delta G^{\ddagger}$ for the uncatalyzed (ΔG_{N}) and the catalyzed (ΔG_{E}) reactions. Thus, a rate enhancement of 10^6, which requires that an enzyme bind its transition state complex with 10^6-fold higher affinity than its substrate, corresponds to a 34.2 $\text{kJ} \cdot \text{mol}^{-1}$ stabilization at 25°C, roughly the free energy of two hydrogen bonds. Consequently, the enzymatic binding of a transition state by two hydrogen bonds that cannot form when the substrate first binds to the enzyme should result in a rate enhancement of $\sim 10^6$ based on this effect alone.

It is commonly observed that an enzyme binds poor substrates, which have low reaction rates, as well as or even better than good ones, which have high reaction rates. Thus, a good substrate does not necessarily bind to its enzyme with high affinity, but it does so on activation to the transition state.

Transition State Analogs Are Enzyme Inhibitors. *If an enzyme preferentially binds its transition state, then it can be expected that* ***transition state analogs,*** *stable molecules that geometrically and electronically resemble the transition state, are potent inhibitors of the enzyme.* For example, the reaction catalyzed by **proline racemase** from *Clostridium sticklandii* is thought to occur via a planar transition state:

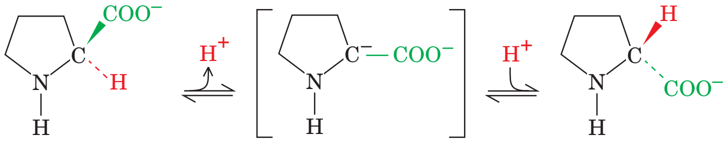

L-Proline **Planar transition state** **D-Proline**

Proline racemase is inhibited by the planar analogs of proline, **pyrrole-2-carboxylate** and **Δ-1-pyrroline-2-carboxylate,**

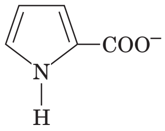

Pyrrole-2-carboxylate

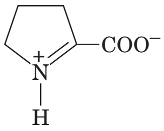

Δ-1-Pyrroline-2-carboxylate

both of which bind to the enzyme with 160-fold greater affinity than does proline. These compounds are therefore thought to be analogs of the transition state in the proline racemase reaction.

Hundreds of transition state analogs for various enzymes have been reported. Some are naturally occurring antibiotics. Others were designed to investigate the mechanism of particular enzymes or to act as specific enzyme inhibitors for therapeutic or agricultural use. Indeed, *the theory that enzymes bind transition states with higher affinity than substrates has led to a rational basis for drug design based on the understanding of specific enzyme reaction mechanisms* (Section 12-4).

4 Lysozyme

In the remainder of this chapter, we investigate the catalytic mechanisms of some well-characterized enzymes. In doing so, we shall see how enzymes apply the catalytic principles described in the preceding section.

CHECK YOUR UNDERSTANDING

Describe how protein functional groups can act as acid and base catalysts.
Explain how nucleophiles function as covalent catalysts.
List the ways in which metal ions participate in catalysis.
What roles do proximity and orientation play in enzymatic catalysis?
Why is it unlikely that nonenzymatic catalysts operate by preferentially binding the transition state?

LEARNING OBJECTIVES

- Understand the general features of substrate binding to lysozyme.
- Understand lysozyme's catalytic mechanisms and how these have been experimentally verified.

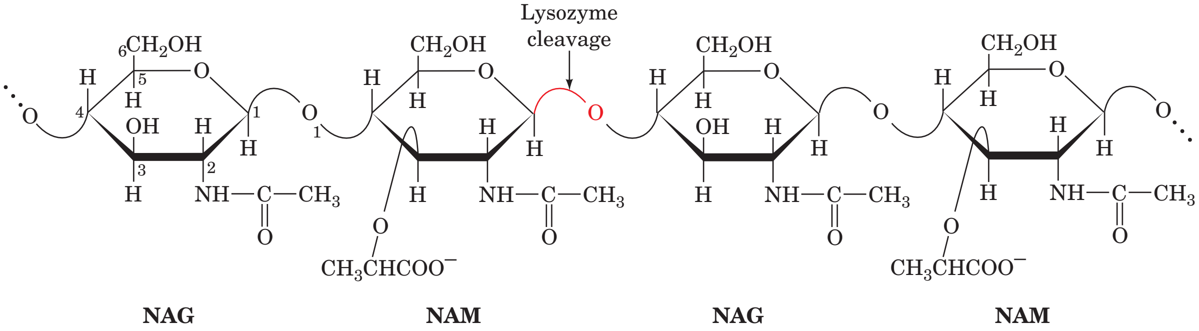

Figure 11-16 | The lysozyme cleavage site. The enzyme cleaves after a β(1→4) linkage in the alternating NAG—NAM polysaccharide component of bacterial cell walls.

Lysozyme is an enzyme that destroys bacterial cell walls. It does so by hydrolyzing the β(1→4) glycosidic linkages from ***N*-acetylmuramic acid (NAM** or **MurNAc)** to ***N*-acetylglucosamine (NAG** or **GlcNAc)** in cell wall peptidoglycans (Fig. 11-16 and Section 8-3B). It likewise hydrolyzes β(1→4)-linked poly(NAG) (chitin; Section 8-2B), a cell wall constituent of most fungi as well as the major component of the exoskeletons of insects and crustaceans. Lysozyme occurs widely in the cells and secretions of vertebrates, where it probably functions as a bactericidal agent or helps dispose of bacteria after they have been killed by other means.

Hen egg white (HEW) lysozyme is the most widely studied species of lysozyme and is one of the mechanistically best understood enzymes. It is a rather small protein (14.3 kD) whose single polypeptide chain consists of 129 amino acid residues and is internally cross-linked by four disulfide bonds. Lysozyme catalyzes the hydrolysis of its substrate at a rate that is $\sim 10^8$-fold greater than that of the uncatalyzed reaction.

A | Lysozyme's Catalytic Site Was Identified through Model Building

The X-ray structure of HEW lysozyme, which was elucidated by David Phillips in 1965 (and hence was the first enzyme to have its structure determined), shows that the protein molecule is roughly ellipsoidal in shape with dimensions 30 × 30 × 45 Å (Fig. 11-17). *Its most striking feature is a prominent cleft, the substrate-binding site, that traverses one face of the molecule.*

The elucidation of an enzyme's mechanism of action requires a knowledge of the structure of its enzyme–substrate complex. This is because, even if the active site residues have been identified through chemical and physical means, their three-dimensional arrangement relative to the substrate as well as to each other must be known in order to understand how the enzyme works. However, an enzyme binds its good substrates only transiently before it catalyzes a reaction and releases products. Consequently, much of our structural knowledge of enzyme–substrate complexes comes from X-ray studies of enzymes in their complexes with substrate analogs that bind but do not react or react very slowly (but see Box 11-2).

Phillips' X-ray structure of lysozyme includes the trisaccharide $(NAG)_3$, which is only slowly hydrolyzed by lysozyme. However, the enzyme efficiently catalyzes the hydrolysis of substrates containing at least six saccharide units,

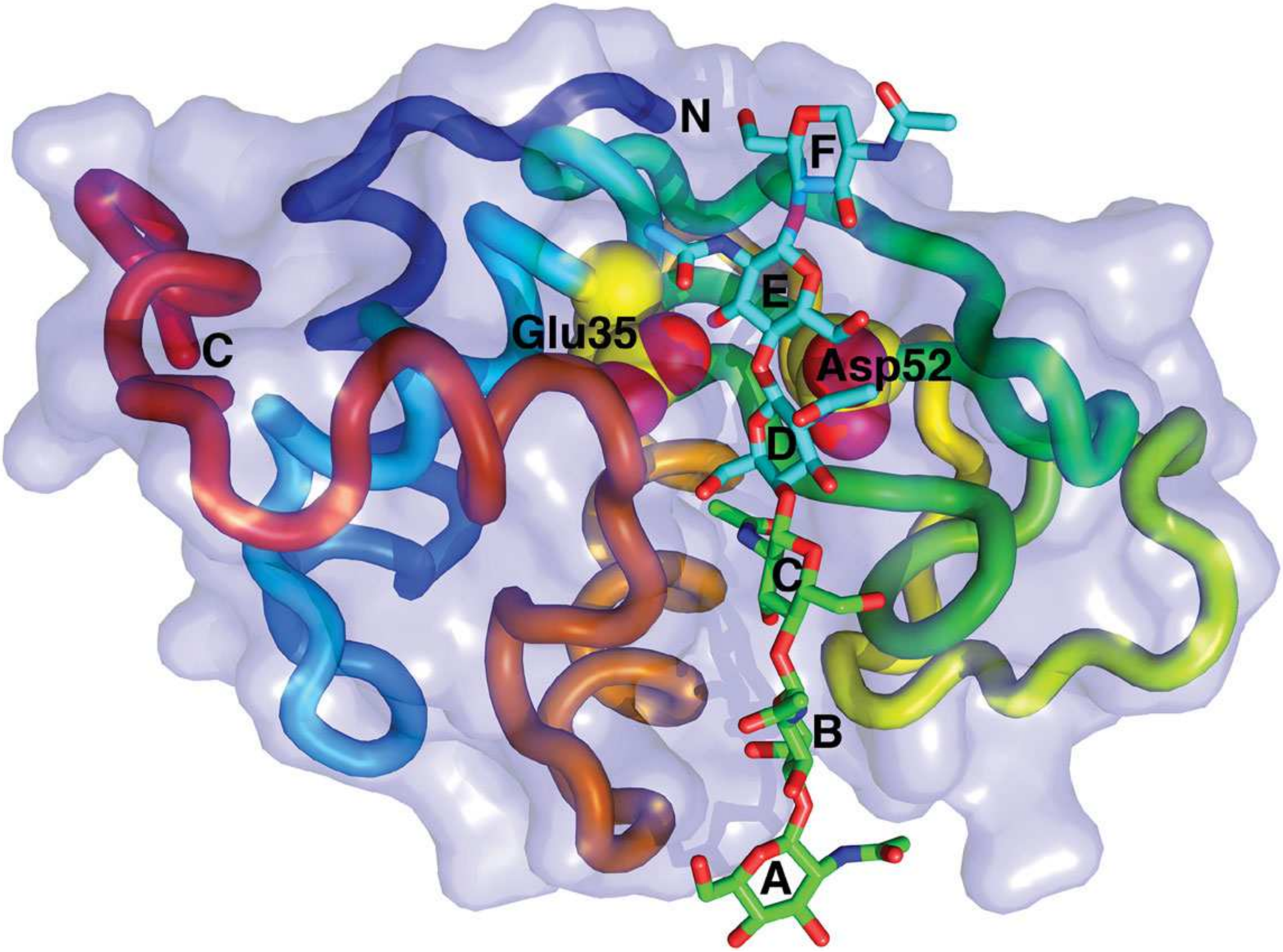

■ **Figure 11-17 | X-Ray structure of HEW lysozyme in complex with (NAG)$_6$.** The protein is represented by its transparent molecular surface with its polypeptide chain in worm form colored in rainbow order from blue at its N-terminus to red at its C-terminus. The (NAG)$_6$, which is drawn in stick form with its sugar rings designated A, at its nonreducing end, through F, at its reducing end, binds in a deep cleft in the enzyme surface. Rings A, B, and C (colored according to atom type with C green, N blue, and O red) are observed in the X-ray structure of the complex of (NAG)$_3$ with lysozyme; the positions of rings D, E, and F (C atoms cyan) were inferred by model building. The side chains of lysozyme's active site residues, Glu 35 and Asp 52, which are drawn in space-filling form (C atoms yellow), catalyze the hydrolysis of the glycosidic bond between rings D and E. [Based on an X-ray structure by David Phillips, Oxford University. PDBid 1HEW.] **See Interactive Exercise 8 and Kinemage Exercise 9.**

so Phillips used model building to investigate how a larger substrate could bind to the enzyme. Lysozyme's active site cleft is long enough to accommodate an oligosaccharide of six residues (designated A to F in Fig. 11-17). However, the fourth residue (D) appeared unable to bind to the enzyme because its C6 and O6 atoms too closely contacted protein

BOX 11-2 PERSPECTIVES IN BIOCHEMISTRY

Observing Enzyme Action by X-Ray Crystallography

The atomic rearrangements that occur during catalysis are to some extent observable during X-ray crystallographic analysis. Because protein crystals are mostly solvent, not only are the native structures of proteins preserved in the crystalline state, but often their catalytic functions are also intact. Substrates can diffuse through solvent channels in the crystal into the enzyme's active site. However, an enzyme rapidly converts its substrates to products. For this reason, the chemical transformations during an enzymatic reaction would be accessible only from "before and after" snapshots, that is, from the structure of the enzyme in the absence of substrate and, in some cases, the structure of the enzyme with its loosely bound products. Several approaches have been used to get around this limitation.

The X-ray structures of enzymes in complexes with slow-reacting substrates may be determined. In this approach, the substrate must remain stably bound to the enzyme for the several hours that are usually required to measure the crystal's X-ray diffraction intensities. Alternatively, an unreactive substrate analog can be used. In this case, the molecule binds much as a substrate would but is not subject to the catalytic reaction. This approach yields somewhat incomplete information, however, since some of the molecular interactions that allow catalysis to occur are missing or distorted. Nevertheless, such data, along with knowledge of nonenzymatic reaction mechanisms, often allow the enzymatic reaction mechanism to be deduced with a fair degree of certainty. Indeed, most of our present structural knowledge of enzyme–substrate interactions is based on this technique.

Enzymatic reactions, like all chemical reactions, are temperature sensitive. Therefore, cooling a crystallized enzyme can significantly slow the rate at which it reacts with a substrate that diffuses to it. For example, cooling a crystal to less than 50 K can slow reaction times from less than a microsecond to hours or days, long enough to measure a set of X-ray diffraction intensities.

Another approach, which has been successfully used to investigate the atomic events at the heme group of myoglobin, solves two problems inherent in analyzing rapid biochemical events. First, taking a "snapshot" of an enzyme in action requires a short exposure time, in analogy to conventional photography. Accordingly, very intense radiation must be used, in this case an X-ray beam generated by a synchrotron (a type of "atom smasher" in which electrons are accelerated around a circular track to near light speed, thereby emitting X-radiation many orders of magnitude more intense than that available from conventional X-ray generators). Second, all the molecules in the crystal must act simultaneously; otherwise, the data will be "blurry." In a study of CO dissociation from myoglobin (the CO binds to myoglobin in much the same way as does O_2 but much more tightly), the molecules were made to dissociate from the heme on cue by a flash of laser light with a duration of a few nanoseconds. Subsequent molecular motions, ultimately leading to the recombination of the CO with myoglobin, were monitored at intervals of microseconds to milliseconds. With refinements, this experimentally complicated technique may eventually prove useful for documenting the operations of enzymes, whose catalytic cycles are complete within nanoseconds.

---

side chains and residue C. This steric interference could be relieved by distorting the glucose ring from its normal chair conformation to that of a half-chair (Fig. 11-18). This distortion moves the C6 group from its normal

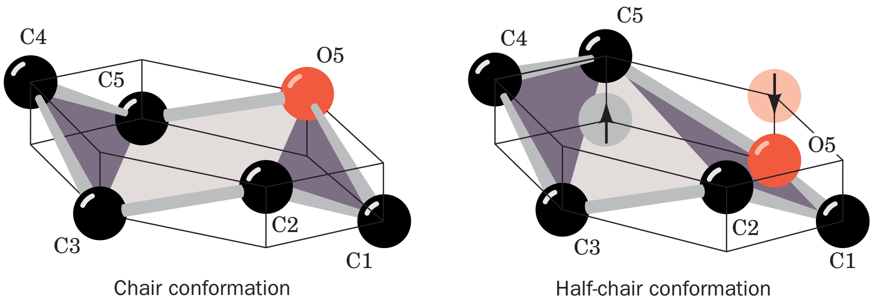

Figure 11-18 | Chair and half-chair conformations. Hexose rings normally assume the chair conformation. However, binding to lysozyme distorts the D ring into the half-chair conformation in which atoms C1, C2, C5, and O5 are coplanar. **See the Animated Figures.**

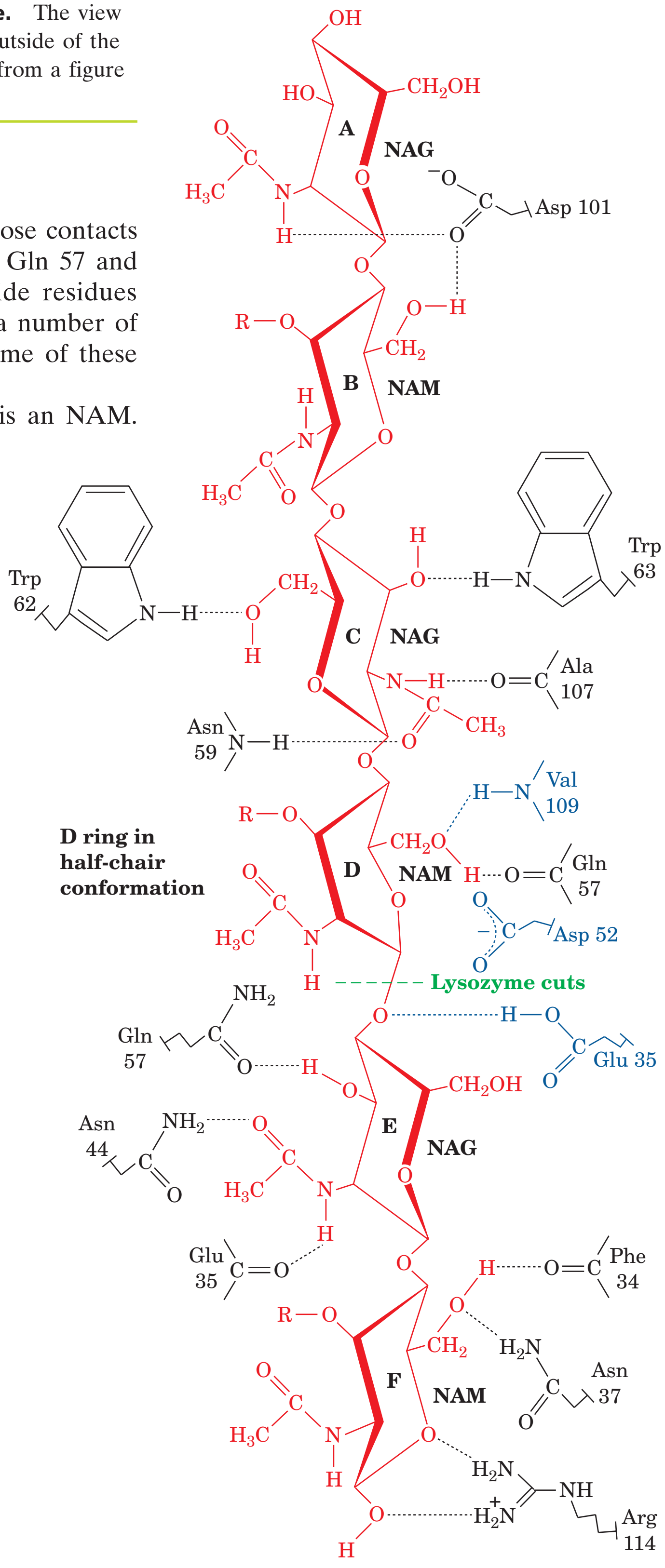
OH
HO
CH$_2$OH
A
NAG
$^-$O
Asp 101
O—H
R—O
CH$_2$
B
NAM
H$_3$C
Trp 62
Trp 63
N—H
H—N
C
NAG
Ala 107
CH$_3$
Asn 59
Val 109
CH$_2$O
D ring in half-chair conformation
D
NAM
Gln 57
Asp 52
Lysozyme cuts
NH$_2$
Gln 57
H—O
Glu 35
CH$_2$OH
E
NAG
Asn 44
Glu 35
Phe 34
H$_2$N
Asn 37
F
NAM
NH
H$_2$N$^+$
Arg 114

■ **Figure 11-19 | The interactions of lysozyme with its substrate.** The view is into the binding cleft with the heavier edges of the rings facing the outside of the enzyme and the lighter ones against the bottom of the cleft. [Modified from a figure by Irving Geis.] **See Kinemage Exercise 9.**

equatorial position to an axial position, where it makes no close contacts and can hydrogen bond to the backbone carbonyl group of Gln 57 and the backbone amido group of Val 109. The other saccharide residues apparently bind to the enzyme without distortion and with a number of favorable hydrogen-bonding and van der Waals contacts. Some of these hydrogen bonds are diagrammed in Fig. 11-19.

In the enzyme's natural substrate, every second residue is an NAM. Model building, however, indicated that the enzyme could not accommodate a lactyl side chain in subsites C or E. Hence, the NAM residues must bind at positions B, D, and F, as drawn in Fig. 11-19. Moreover, since lysozyme hydrolyzes (NAG)$_6$ between residues D and E, it must cleave the glycosidic bond in its natural substrate between the NAM residue in subsite D and the NAG residue in subsite E.

The bond that lysozyme cleaves was identified by allowing lysozyme to catalyze the hydrolysis of (NAG)$_3$ in $H_2{}^{18}O$. The bond cleaved could either be between C1 and the bridge oxygen O1 or between O1 and C4 of the next sugar ring. The product of the hydrolysis reaction had ^{18}O bonded to the C1 atom of its newly liberated reducing terminus, thereby demonstrating that bond cleavage occurs between C1 and O1:

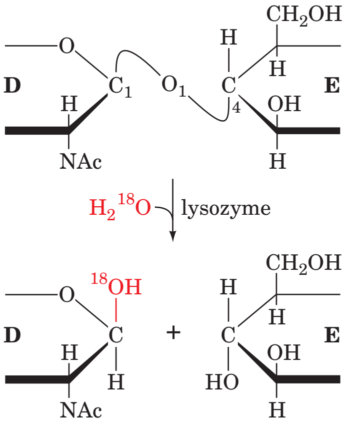
CH$_2$OH
D
C$_1$
O$_1$
C
4
E
H
OH
NAc
$H_2{}^{18}O$
lysozyme
^{18}OH
+
HO

In addition, this reaction occurs with retention of configuration so that the D-ring product remains the β anomer.

B | The Lysozyme Reaction Proceeds via a Covalent Intermediate

The reaction catalyzed by lysozyme, the hydrolysis of a glycoside, is the conversion of an acetal to a hemiacetal. Nonenzymatic acetal hydrolysis is an acid-catalyzed reaction that involves the protonation of a reactant

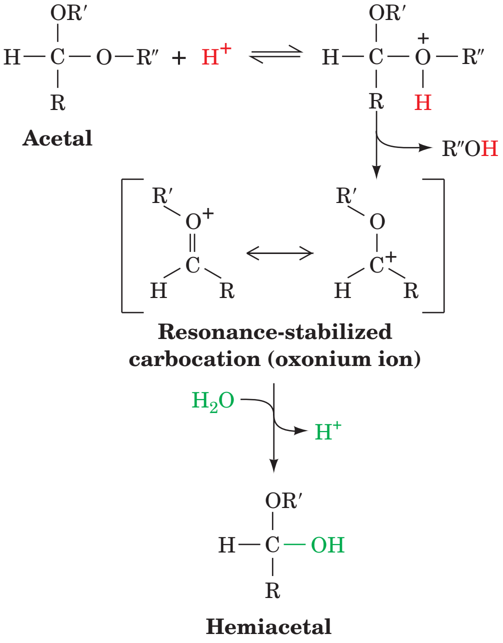

Figure 11-20 | The mechanism of the nonenzymatic acid-catalyzed hydrolysis of an acetal to a hemiacetal. The reaction involves the protonation of one of the acetal's oxygen atoms followed by cleavage of its C—O bond to form an alcohol (R″OH) and a resonance-stabilized carbocation (oxonium ion). The addition of water to the oxonium ion forms the hemiacetal and regenerates the H^+ catalyst. Note that the oxonium ion's C, O, H, R, and R′ atoms all lie in the same plane.

oxygen atom followed by cleavage of its C—O bond (Fig. 11-20). This results in the transient formation of a resonance-stabilized carbocation that is called an **oxonium ion.** To attain resonance stabilization, the oxonium ion's R and R′groups must be coplanar with its C, O, and H atoms. The oxonium ion then adds water to yield the hemiacetal and regenerate the acid catalyst. An enzyme that mediates acetal hydrolysis should therefore include an acid catalyst and possibly a group that can stabilize an oxonium ion transition state.

Glu 35 and Asp 52 Are Lysozyme's Catalytic Residues. The only functional groups in the immediate vicinity of lysozyme's reactive center that have the required catalytic properties are the side chains of Glu 35 and Asp 52. These side chains, which are disposed to either side of the glycosidic linkage to be cleaved (Fig. 11-17), have markedly different environments. Asp 52 is surrounded by several conserved polar residues with which it forms a complex hydrogen-bonded network. Asp 52 is therefore predicted to have a normal p*K*; that is, it should be unprotonated and hence negatively charged throughout the 3 to 8 pH range over which lysozyme is catalytically active. Thus, Asp 52 can function to electrostatically stabilize an oxonium ion. In contrast, the carboxyl group of Glu 35 is nestled in a predominantly nonpolar pocket where it is likely to remain protonated at unusually high pH values for carboxyl groups. This residue can therefore act as an acid catalyst. Studies using protein-modifying reagents and site-directed mutagenesis (e.g., changing Asp 52 to Asn and Glu 35 to Gln) have verified that these residues are catalytically important.

Lysozyme's catalytic mechanism occurs as follows (Fig. 11-21):

1. The enzyme attaches to a bacterial cell wall by binding to a hexasaccharide unit. This distorts the D residue toward the half-chair conformation.
2. Glu 35 transfers its proton to the O1 atom bridging the D and E rings, thereby facilitating cleavage of the C1—O1 bond (general acid catalysis). This step converts the D ring to a resonance-stabilized oxonium ion transition state whose formation is facilitated by the strain distorting it to the half-chair conformation (catalysis by the preferential binding of the transition state). The positively charged oxonium ion is stabilized by the presence of the nearby negatively charged Asp 52 carboxylate group (electrostatic catalysis). The E-ring product is released.
3. The Asp 52 carboxylate group nucleophilically attacks the now electron-poor C1 of the D ring to form a covalent glycosyl–enzyme intermediate (covalent catalysis).
4. Water replaces the E-ring product in the active site.
5. Hydrolysis of the covalent bond with the assistance of Glu 35 (general base catalysis), which involves another oxonium ion transition state, regenerates the active site groups. The enzyme then releases the D-ring product, completing the catalytic cycle.

The double-displacement mechanism diagrammed in Fig. 11-21 allows the incoming water molecule to attach to the same face of the D residue as the E residue it replaces. Consequently, the configuration of the D residue is retained. A single-displacement reaction, in which water directly displaces the leaving group, would invert the configuration at C1 of the D ring between the substrate and product, a result that is not observed.

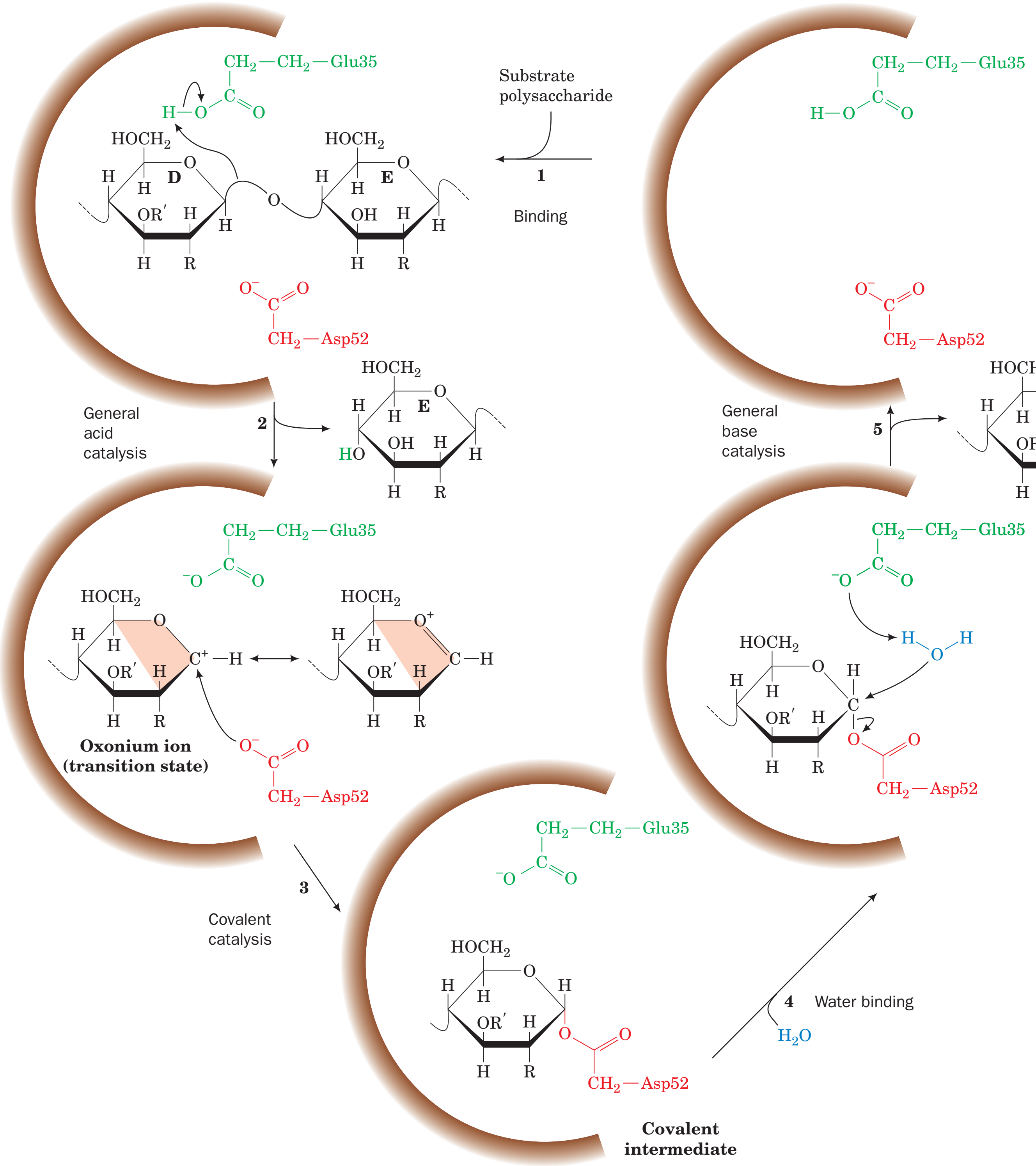
CH2—CH2—Glu35
H—O
C=O
HOCH2
D
E
O
H
OH
OR′
R
Substrate polysaccharide
1
Binding
O⁻
C=O
CH2—Asp52
General acid catalysis
2
HO
General base catalysis
5
OH
C⁺—H
O⁺
C—H
Oxonium ion (transition state)
H
O
H
3
Covalent catalysis
4
Water binding
H2O
Covalent intermediate

■ **Figure 11-21 | The lysozyme reaction mechanism.** Glu 35 acts as an acid catalyst, and Asp 52 acts as a covalent catalyst. Only the substrate D and E rings are shown. R represents the *N*-acetyl group at C2, and R′ represents the CH_3CHCOO^- group at C3. The resonance-stabilized oxonium ion transition state requires that C1, C2, C5, and O5 be coplanar (*shading*), creating a half-chair conformation. Step 5 includes the participation of an oxonium ion transition state that is not shown.

See Kinemage Exercise 9.

Experimental Evidence Supports the Role of Strain in the Lysozyme Mechanism. Many of the structural and mechanistic investigations of lysozyme have focused on the catalytic role of strain. For example, the X-ray structure of lysozyme in complex with NAM—NAG—NAM shows that the trisaccharide binds, as predicted, to the B, C, and D subsites of lysozyme, *with the NAM in the D subsite distorted to the half-chair conformation.* This strained conformation is stabilized by a strong hydrogen bond between the D ring O6 and the backbone NH of Val 109 (as predicted by model building; Fig. 11-19). Indeed, the mutation of Val 109 to Pro, which lacks the NH group to make such a hydrogen bond, inactivates the enzyme.

As we have discussed in Section 11-3E, an enzyme that catalyzes a reaction by the preferential binding of its transition state has a greater binding affinity for an inhibitor that has the transition state geometry (a transition state analog) than it does for its substrate. The δ-lactone analog of $(NAG)_4$ (Fig. 11-22), which binds tightly to lysozyme, is a transition state analog of lysozyme since *this compound's lactone ring has the half-chair conformation that geometrically resembles the proposed oxonium ion transition state of the substrate's D ring*. X-Ray studies confirm that this inhibitor binds to lysozyme such that the lactone ring occupies the D subsite in a half-chair-like conformation.

Despite the foregoing, *the role of substrate distortion in lysozyme catalysis has been questioned.* Nathan Sharon and David Chipman determined that the NAG lactone inhibitor (Fig. 11-22) binds to the D subsite with only 9.2 $kJ \cdot mol^{-1}$ greater affinity than does NAG. This quantity, as is explained in Section 11-3E, corresponds to no more than an ~40-fold rate enhancement for the lysozyme reaction, suggesting that strain in the D ring is not a major contributor to lysozyme's ~10^8-fold rate enhancement. However, this unexpectedly small free energy difference is explained by the observation that an undistorted NAG ring can be modeled into lysozyme's D subsite as it occurs in the X-ray structure of its complex with NAM—NAG—NAM. In contrast, NAM's bulky lactyl side chain prevents it from binding to the D subsite in this manner.

Mass Spectrometry and X-Ray Crystallography Provide Support for Covalent Catalysis. The existence of a covalent reaction intermediate has also been difficult to verify. The lifetime of a glucosyl oxonium ion in water is ~10^{-12} s. In order for such a short-lived intermediate to be experimentally observed, its rate of formation must be made significantly greater than its rate of breakdown. To do this, Stephen Withers capitalized on three phenomena. First, if the reaction goes through an oxonium ion transition state, its formation should be slowed by the electron-withdrawing effects of substituting F (the most electronegative element) at C2 of the D ring.

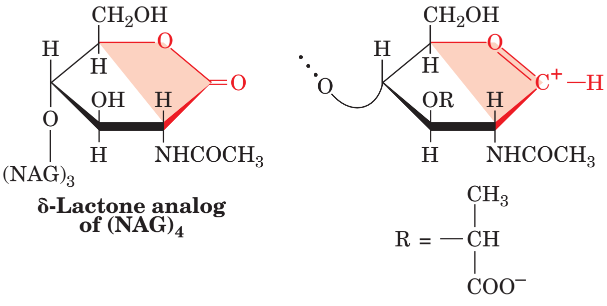

δ-Lactone analog of $(NAG)_4$

Lysozyme transition state

Figure 11-22 | Transition state analog inhibition of lysozyme. The δ-lactone analog of $(NAG)_4$ (*left*) resembles the transition state of the lysozyme reaction (*right*). Note that atoms C1, C2, C5, and O5 in each structure are coplanar (as indicated by shading), consistent with the half-chair conformation of the hexose ring.

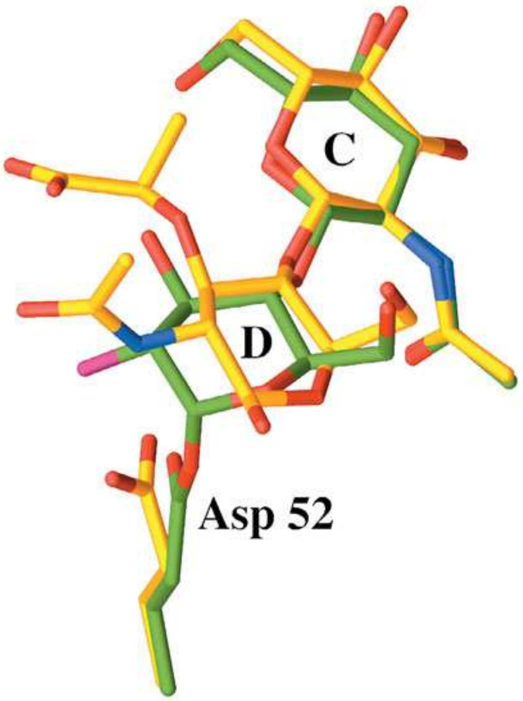

Figure 11-23 | Position of the D ring during catalysis by lysozyme. The position of the substrate's C and D rings and the catalytic Asp 52 are shown in superimposed X-ray structures of the covalent complex between E35Q lysozyme and NAG2FGlcF (C green, N blue, O red, and F magenta) and the noncovalent complex between lysozyme and a NAM—NAG—NAM substrate (C yellow, N blue, and O red). Note that the covalent bond between Asp 52 and C1 of the D ring forms when the D ring in the noncovalent complex relaxes from its distorted half-chair conformation to an undistorted chair conformation and the side chain of Asp 52 undergoes a 45° rotation about its C_α—C_β bond. [Based on X-ray structures by David Vocadlo and Stephen Withers, University of British Columbia, Vancouver, Canada; *and* Michael James, University of Alberta, Edmonton, Canada. PDBid 1H6M.]

Second, mutating Glu 35 to Gln (E35Q) removes the general acid–base catalyst, further slowing all steps involving the oxonium ion transition state. Third, substituting an additional F atom at C1 of the D ring accelerates the formation of the intermediate because this F is a good leaving group without the need of general acid catalysis. Making all three of these changes should increase the rate of formation of the proposed covalent intermediate relative to its breakdown and hence should result in its accumulation. Withers therefore incubated E35Q HEW lysozyme with NAG-β(1→4)-2-deoxy-2-fluoro-β-D-glucopyranosyl fluoride **(NAG2FGlcF):**

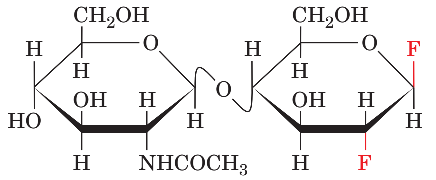

NAG2FGlcF

Electrospray ionization mass spectrometry (ESI-MS; Section 5-3D) of this reaction mixture revealed a sharp peak at 14,683 D, consistent with the formation of the proposed covalent intermediate [lysozyme has a molecular mass of 14,314 D and that of the NAG-β(1→4)-2-deoxy-2-fluoro-β-D-glucopyranosyl group is 369 D].

The X-ray structure of this covalent complex reveals an ~1.4-Å-long covalent bond between C1 of the D ring and a side chain carboxyl O of Asp 52 (Fig. 11-23). This D ring adopts an undistorted chair conformation, thus indicating that it is a reaction intermediate rather than an approximation of the transition state. The superposition of this covalent complex with that of the above-described complex of NAM—NAG—NAM with wild-type HEW lysozyme reveals how this covalent bond forms (Fig. 11-23). The shortening of the 3.2-Å distance between the D ring C1 and the Asp 52 O in the NAM—NAG—NAM complex to ~1.4 Å in the covalent complex occurs as the D ring relaxes from the half-chair to the chair conformation and the Asp 52 side chain rotates ~45° about its C_α—C_β bond.

CHECK YOUR UNDERSTANDING

Explain the importance of conformation in the D ring of a lysozyme substrate.

Describe the catalytic mechanisms employed by lysozyme.

5 Serine Proteases

LEARNING OBJECTIVES

- Understand how chemical labeling and structural analysis can identify an enzyme's catalytic residues and substrate-binding determinants.
- Understand how serine proteases mediate peptide bond hydrolysis and stabilize the reaction's transition state.
- Understand that zymogens are the inactive precursors of enzymes.

Our next example of enzymatic mechanisms is a diverse and widespread group of proteolytic enzymes known as the **serine proteases,** so named because they have a common catalytic mechanism involving a peculiarly reactive Ser residue. The serine proteases include digestive enzymes from prokaryotes and eukaryotes, as well as more specialized proteins that participate in development, blood coagulation (clotting), inflammation, and numerous other processes. In this section, we focus on some of the best studied serine proteases: chymotrypsin, trypsin, and elastase.

A | Active Site Residues Were Identified by Chemical Labeling

Chymotrypsin, trypsin, and elastase are digestive enzymes that are synthesized by the pancreas and secreted into the duodenum (the small intestine's upper loop). All these enzymes catalyze the hydrolysis of peptide (amide) bonds but with different specificities for the side chains flanking the scissile (to be cleaved) peptide bond. Chymotrypsin is specific for a bulky hydrophobic residue preceding the scissile bond, trypsin is specific for a positively charged residue, and elastase is specific for a small neutral residue (Table 5-3). Together, they form a potent digestive team.

Chymotrypsin's catalytically important groups were identified by chemical labeling studies. A diagnostic test for the presence of the active site Ser of serine proteases is its reaction with **diisopropylphosphofluoridate (DIPF),** which irreversibly inactivates the enzyme *(at left)*. Other Ser residues, including those on the same protein, do not react with DIPF. *DIPF reacts only with Ser 195 of chymotrypsin, thereby demonstrating that this residue is the enzyme's active site Ser.* This specificity makes DIPF and related compounds extremely toxic (Box 11-3).

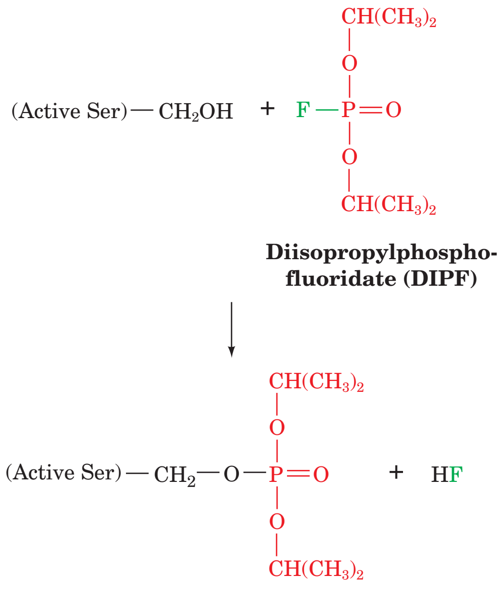
Diisopropylphosphofluoridate (DIPF)

DIP–Enzyme

A second catalytically important residue, His 57, was discovered through **affinity labeling.** In this technique, a substrate analog bearing a reactive group specifically binds at the enzyme's active site, where it reacts to form a stable covalent bond with a nearby susceptible group (these reactive substrate analogs have been dubbed the "Trojan horses" of biochemistry). The affinity labeled group(s) can subsequently be isolated and identified.

Chymotrypsin specifically binds **tosyl-L-phenylalanine chloromethylketone (TPCK)** because of its resemblance to a Phe residue (one of chymotrypsin's preferred substrate residues). Active site–bound TPCK's chloromethylketone group is a strong alkylating agent; it reacts only with His 57 (Fig. 11-24), thereby inactivating the enzyme. Trypsin, which prefers basic residues, is similarly inactivated by **tosyl-L-lysine chloromethylketone:**

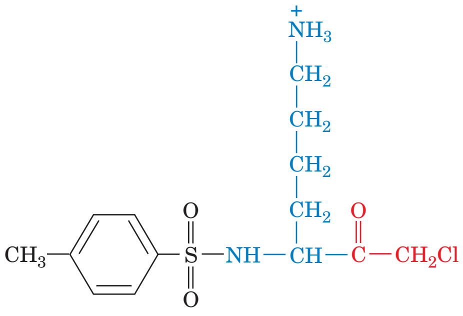
Tosyl-L-lysine chloromethylketone

B | X-Ray Structures Provide Information about Catalysis, Substrate Specificity, and Evolution

Chymotrypsin, trypsin, and elastase are strikingly similar: The primary structures of these ~240-residue enzymes are ~40% identical (for comparison, the α and β chains of human hemoglobin have 44% sequence

BOX 11-3 **BIOCHEMISTRY IN HEALTH AND DISEASE**

Nerve Poisons

The use of DIPF as an enzyme-inactivating agent came about through the discovery that organophosphorus compounds such as DIPF are potent nerve poisons. The neurotoxicity of DIPF arises from its ability to inactivate **acetylcholinesterase,** an enzyme that catalyzes the hydrolysis of **acetylcholine:**

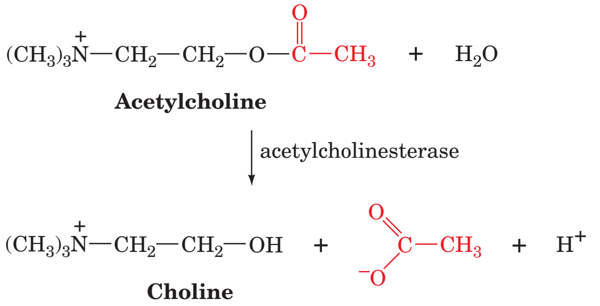

The esterase activity of acetylcholinesterase, like that of chymotrypsin (Section 11-1B), requires a reactive Ser residue.

Acetylcholine is a **neurotransmitter:** It transmits nerve impulses across certain types of **synapses** (junctions between nerve cells). Acetylcholinesterase in the synapse normally degrades acetylcholine so that the nerve impulse has a duration of only a millisecond or so. The inactivation of acetylcholinesterase prevents hydrolysis of the neurotransmitter. As a result, the acetylcholine receptor, which is a Na^+–K^+ channel, remains open for longer than normal, thereby interfering with the regular sequence of nerve impulses. DIPF is so toxic to humans (death occurs through the inability to breathe) that it has been used militarily as a nerve gas. Related compounds, such as **parathion** and **malathion,** are useful insecticides because they are far more toxic to insects than to mammals.

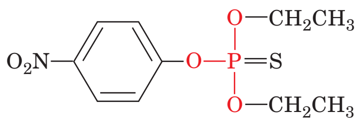

Parathion

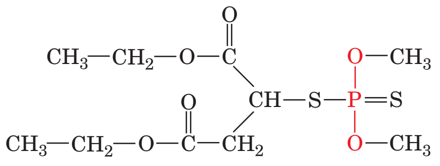

Malathion

Neurotoxins such as DIPF and **sarin** (which gained notoriety after its release by terrorists in a Tokyo subway in 1995) are inactivated by the enzyme **paraoxonase.**

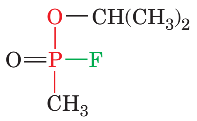

Sarin

This enzyme occurs as two isoforms (one has Arg at position 192 and the other has Gln) with different activities, and individuals express widely differing levels of the enzyme. These factors may account for the large observed differences in individuals' sensitivity to nerve poisons.

identity). Furthermore, all these enzymes have a reactive Ser and a catalytically essential His. It therefore came as no surprise when their X-ray structures all proved to be closely related.

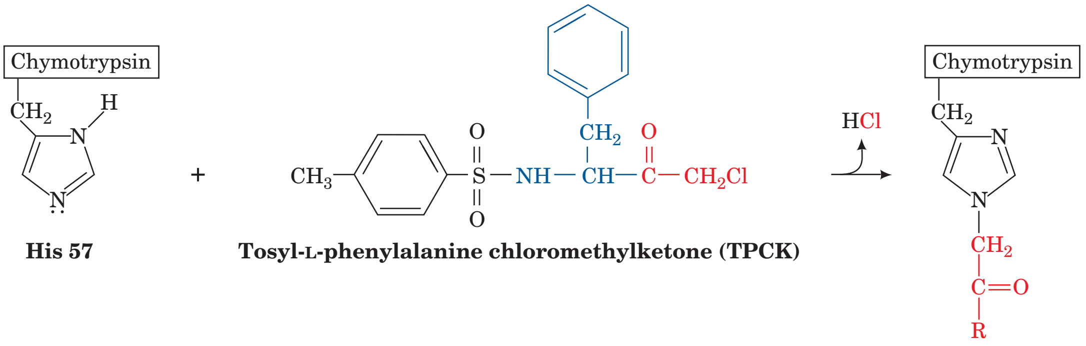

■ **Figure 11-24 | Reaction of TPCK with His 57 of chymotrypsin.**

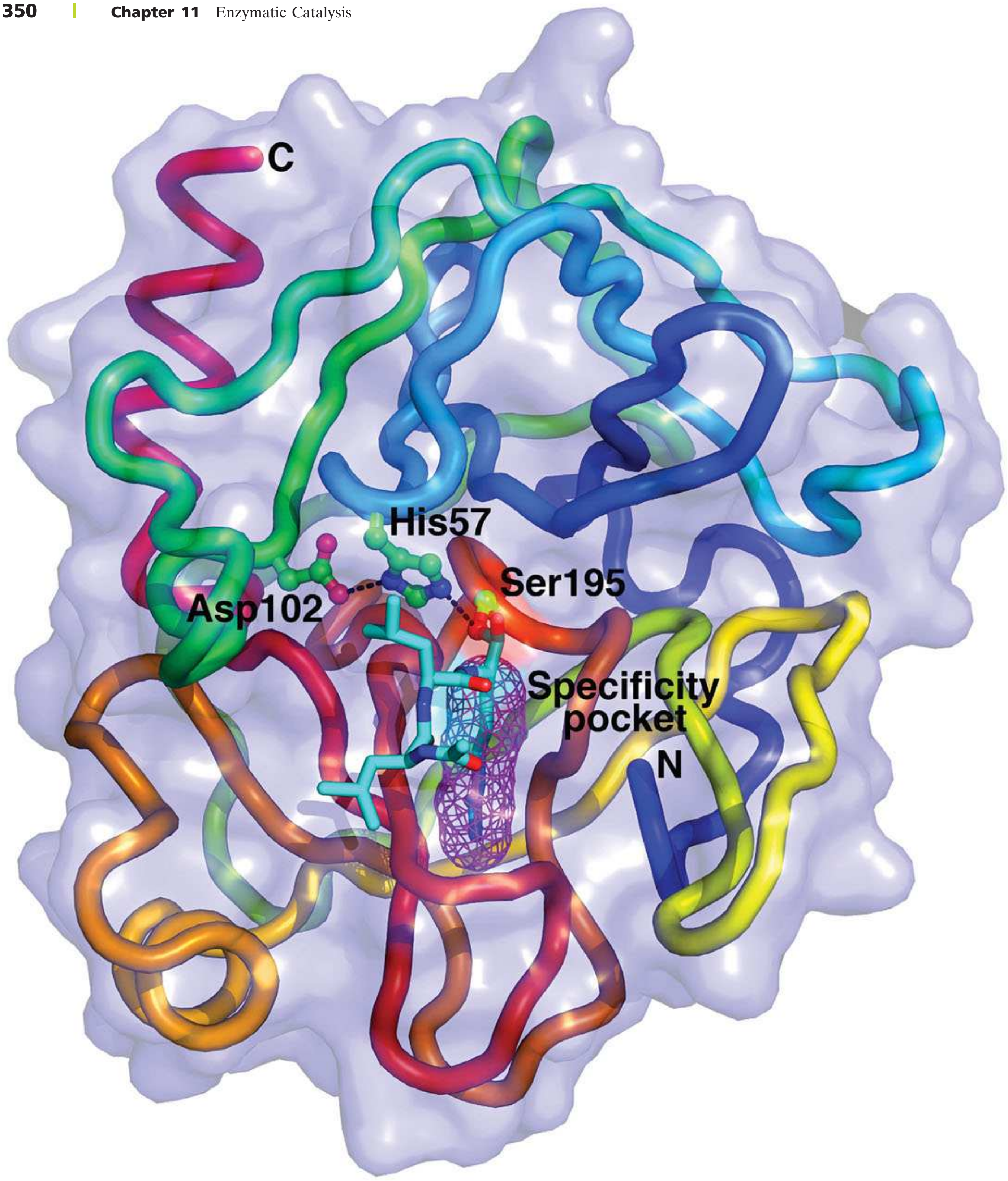

■ **Figure 11-25** | **X-Ray structure of bovine trypsin in covalent complex with its inhibitor leupeptin.** The protein is represented by its transparent molecular surface with its polypeptide chain in worm form colored in rainbow order from blue at its N-terminus to red at its C-terminus. The side chains of the catalytic triad, Ser 195, His 57, and Asp 102, are drawn in ball-and-stick form colored according to atom type (C green, N blue, O red) with hydrogen bonds represented by dashed black lines. **Leupeptin** (acetyl-Leu-Leu-Arg in which the terminal carboxyl group is replaced by —CHO) is drawn in stick form (C cyan, N blue, O red) with its Arg side chain occupying the enzyme's specificity pocket (*magenta mesh*). [Based on an X-ray structure by Daniel Koshland, Jr., University of California at Berkeley. PDBid 2AGI.] **See Kinemage Exercise 10-1.**

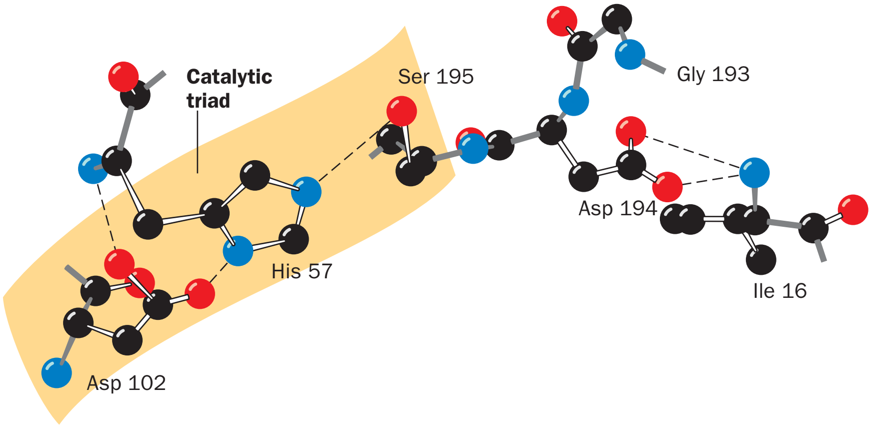

■ **Figure 11-26** | **The active site residues of chymotrypsin.** The view is in approximately the same direction as in Fig. 11-25. The catalytic triad consists of Ser 195, His 57, and Asp 102. [After Blow, D.M. and Steitz, T.A., *Annu. Rev. Biochem.* **39,** 86 (1970).]

The structure of bovine chymotrypsin was elucidated in 1967 by David Blow. This was followed by the determination of the structures of bovine trypsin (Fig. 11-25) by Robert Stroud and Richard Dickerson, and porcine elastase by David Shotton and Herman Watson. Each of these proteins is folded into two domains, both of which have extensive regions of antiparallel β sheets in a barrel-like arrangement but contain little helix. For convenience in comparing the structures of these three enzymes, we shall assign them the same residue numbering system—that of bovine **chymotrypsinogen,** the 245-residue precursor of chymotrypsin (Section 11-5D).

In all three structures, the catalytically essential His 57 and Ser 195 residues are located in the enzyme's substrate-binding site (center of Fig. 11-25). The X-ray structures also show that Asp 102, which is present in all serine proteases, is buried in a nearby solvent-inaccessible pocket. *These three invariant residues form a hydrogen-bonded constellation referred to as the **catalytic triad*** (Figs. 11-25 and 11-26).

Substrate Specificities Are Only Partially Rationalized. The X-ray structures of the above three enzymes suggest the basis for their differing substrate specificities (Fig. 11-27):

1. In chymotrypsin, the bulky aromatic side chain of the preferred Phe, Trp, or Tyr residue that contributes the carbonyl group of the scissile peptide fits snugly into a slitlike hydrophobic pocket located near the catalytic groups.
2. In trypsin, the residue corresponding to chymotrypsin Ser 189, which lies at the bottom of the binding pocket, is the anionic residue Asp. The cationic side chains of trypsin's preferred residues, Arg and Lys, can therefore form ion pairs with this Asp residue. The rest of chymotrypsin's specificity pocket is preserved in trypsin so that it can accommodate the bulky side chains of Arg and Lys.
3. Elastase is so named because it rapidly hydrolyzes the otherwise nearly indigestible Ala, Gly, and Val–rich protein **elastin** (a major connective tissue component). Elastase's binding pocket is largely occluded by the side chains of Val and Thr residues that replace the Gly residues lining the specificity pockets in both chymotrypsin and trypsin. Consequently elastase, whose substrate-binding site is better described as merely a depression, specifically cleaves peptide bonds after small neutral residues, particularly Ala. In contrast, chymotrypsin and trypsin hydrolyze such peptide bonds extremely slowly because these small substrates cannot be sufficiently immobilized on the enzyme surface for efficient catalysis to occur.

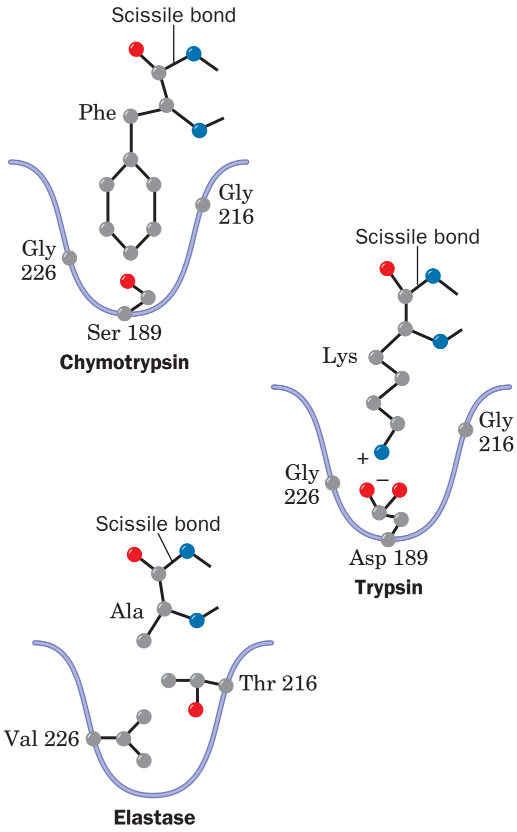

■ **Figure 11-27** | **Specificity pockets of three serine proteases.** The side chains of key residues that determine the size and nature of the specificity pocket are shown along with a representative substrate for each enzyme. Chymotrypsin prefers to cleave peptide bonds following large hydrophobic side chains; trypsin prefers Lys or Arg; and elastase prefers Ala, Gly, or Val. [After a drawing in Branden, C. and Tooze, J., *Introduction to Protein Structure* (2nd ed.), Garland Publishing, p. 213 (1999).]

Despite the foregoing, changing trypsin's Asp 189 to Ser by site-directed mutagenesis (Section 3-5D) does not switch its specificity to that of chymotrypsin but instead yields a poor, nonspecific protease. Replacing additional residues in trypsin's specificity pocket with those of chymotrypsin fails to significantly improve this catalytic activity. However, trypsin is converted to a reasonably active chymotrypsin-like enzyme when two surface loops that connect the walls of the specificity pocket (residues 185–188 and 221–225) are also replaced by those of chymotrypsin. These loops, which are conserved in each enzyme, are apparently necessary not for substrate binding per se but for properly positioning the scissile bond. These results highlight an important caveat for genetic engineers: Enzymes are so exquisitely tailored to their functions that they often respond to mutagenic tinkering in unexpected ways.

Serine Proteases Exhibit Divergent and Convergent Evolution. We have seen that sequence and structural similarities among proteins reveal their evolutionary relationships (Sections 5-4 and 6-2D). *The great similarities among chymotrypsin, trypsin, and elastase indicate that these proteins arose through duplications of an ancestral serine protease gene followed by the divergent evolution of the resulting enzymes.* Indeed, the close structural resemblance of these pancreatic enzymes to certain bacterial proteases indicates that the primordial trypsin gene arose before the divergence of prokaryotes and eukaryotes.

There are several serine proteases whose primary and tertiary structures bear no discernible relationship to each other or to chymotrypsin. Nevertheless, these proteins also contain catalytic triads at their active sites whose structures closely resemble that of chymotrypsin. These enzymes include **subtilisin,** an endopeptidase that was originally isolated from *Bacillus subtilis,* and wheat germ **serine carboxypeptidase II,** an exopeptidase. Since the orders of the corresponding active site residues in the amino acid sequences of these serine proteases are quite different (Fig. 11-28), it seems highly improbable that they could have evolved from a common ancestor protein. These enzymes apparently constitute a remarkable example of **convergent evolution:** *Nature seems to have independently discovered the same catalytic mechanism several times.*

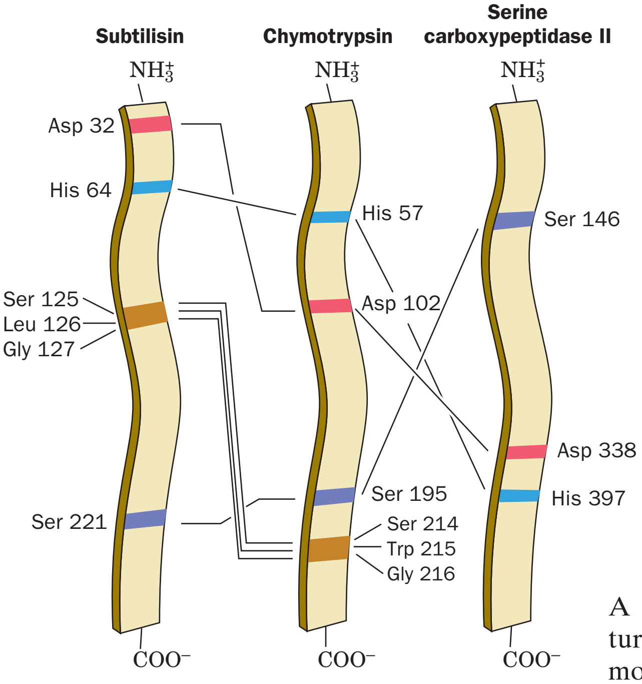

Figure 11-28 | Diagram indicating the relative positions of the active site residues of three unrelated serine proteases. The catalytic triads in subtilisin, chymotrypsin, and serine carboxypeptidase II each consist of Ser, His, and Asp residues. The peptide backbones of Ser 214, Trp 215, and Gly 216 in chymotrypsin, and their counterparts in subtilisin, participate in substrate-binding interactions. [After Robertus, J.D., Alden, R.A., Birktoft, J.J., Kraut, J., Powers, J.C., and Wilcox, P.E., *Biochemistry* **11,** 2449 (1972).] **See Kinemage Exercise 10-2.**

C | Serine Proteases Use Several Catalytic Mechanisms

A catalytic mechanism based on considerable chemical and structural data has been formulated and is given here in terms of chymotrypsin (Fig. 11-29), although it applies to all serine proteases and certain other hydrolytic enzymes:

1. After chymotrypsin has bound a substrate, Ser 195 nucleophilically attacks the scissile peptide's carbonyl group to form the **tetrahedral intermediate,** which resembles the reaction's transition state (covalent catalysis). X-Ray studies indicate that Ser 195 is ideally positioned to carry out this nucleophilic attack (proximity and orientation effects). This nucleophilic attack involves transfer of a proton to the imidazole ring of His 57, thereby forming an imidazolium ion (general base catalysis). This process is aided by the polarizing effect of the unsolvated carboxylate ion of Asp 102, which is hydrogen bonded to His 57 (electrostatic catalysis). The tetrahedral intermediate has a well-defined,

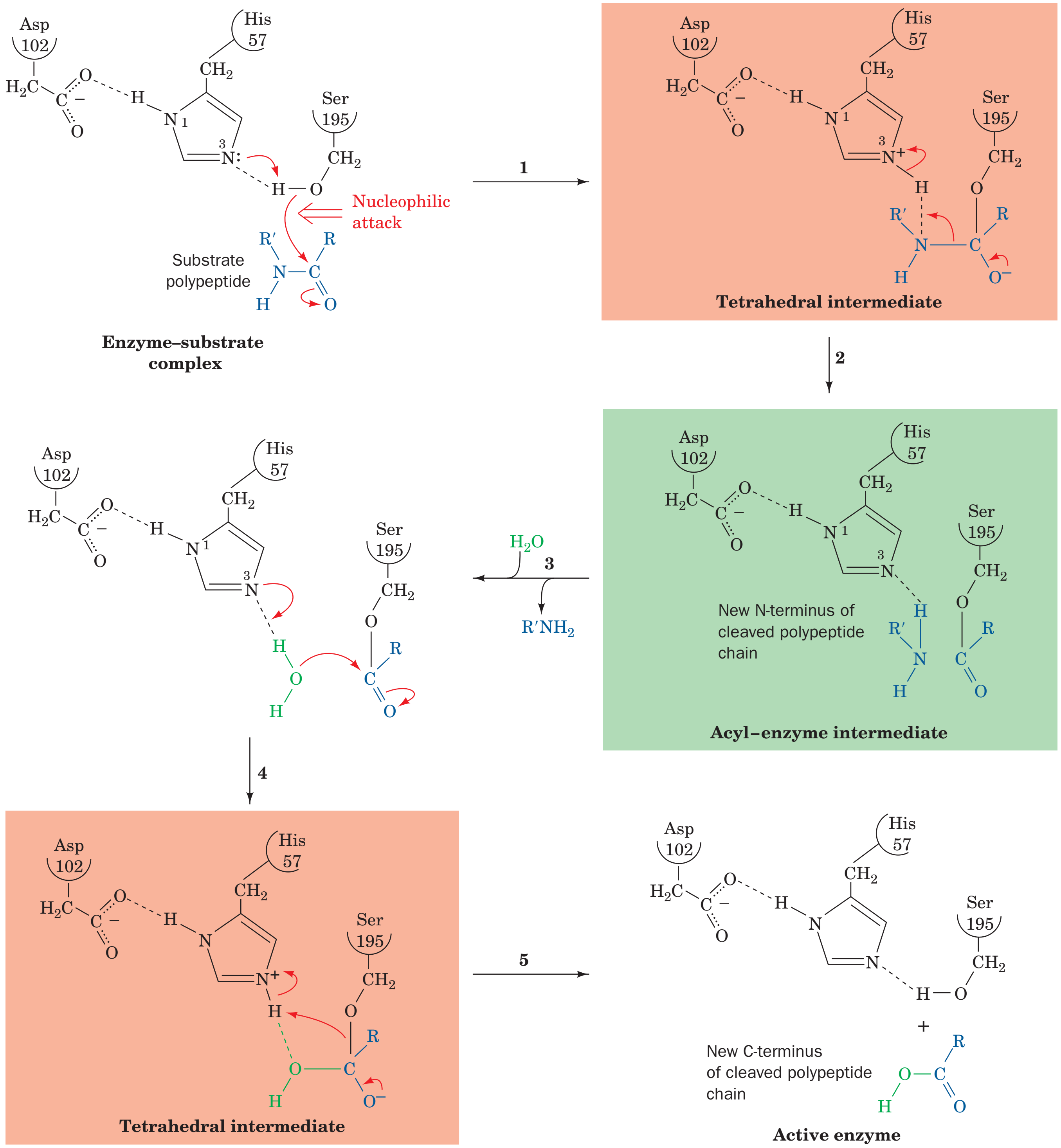
Asp 102
His 57
Ser 195
Nucleophilic attack
Substrate polypeptide
Enzyme–substrate complex
1
Tetrahedral intermediate
2
Acyl–enzyme intermediate
New N-terminus of cleaved polypeptide chain
H_2O
3
$R'NH_2$
4
Tetrahedral intermediate
5
New C-terminus of cleaved polypeptide chain
Active enzyme

■ **Figure 11-29 | The catalytic mechanism of the serine proteases.** The reaction involves (**1**) the nucleophilic attack of the active site Ser on the carbonyl carbon atom of the scissile peptide bond to form the tetrahedral intermediate; (**2**) the decomposition of the tetrahedral intermediate to the acyl–enzyme intermediate through general acid catalysis by the active site Asp-polarized His; (**3**) loss of the amine product and its replacement by a water molecule; (**4**) the reversal of Step 2 to form a second tetrahedral intermediate; and (**5**) the reversal of Step 1 to yield the reaction's carboxyl product and the active enzyme.

although transient, existence. We shall see that *much of chymotrypsin's catalytic power derives from its preferential binding of the transition state leading to this intermediate (transition state binding catalysis).*

See Guided Exploration 10
The catalytic mechanism of serine proteases.

2. The tetrahedral intermediate decomposes to the **acyl–enzyme intermediate** under the driving force of proton donation from N3 of His 57 (general acid catalysis) facilitated by the polarizing effect of Asp 102 on His 57 (electrostatic catalysis).
3. The amine leaving group ($R'NH_2$, the new N-terminal portion of the cleaved polypeptide chain) is released from the enzyme and replaced by water from the solvent.
4. The acyl–enzyme intermediate, which is highly susceptible to hydrolytic cleavage, adds water by the reversal of Step 2, yielding a second tetrahedral intermediate.
5. The reversal of Step 1 yields the carboxylate product (the new C-terminal portion of the cleaved polypeptide chain), thereby regenerating the active enzyme. In this process, water is the attacking nucleophile and Ser 195 is the leaving group.

Serine Proteases Preferentially Bind the Transition State. Detailed comparisons of the X-ray structures of several serine protease–inhibitor complexes have revealed a further structural basis for catalysis in these enzymes (Fig. 11-30):

1. The conformational distortion that occurs with the formation of the tetrahedral intermediate causes the now anionic carbonyl oxygen of the scissile peptide to move deeper into the active site so as to occupy a previously unoccupied position called the **oxyanion hole.**
2. There, it forms two hydrogen bonds with the enzyme that cannot form when the carbonyl group is in its normal trigonal conformation. The two enzymatic hydrogen bond donors were first noted by Joseph Kraut to occupy corresponding positions in chymotrypsin and subtilisin. He proposed the existence of the oxyanion hole on the basis of the premise that convergent evolution had made the active sites of these unrelated enzymes functionally identical.

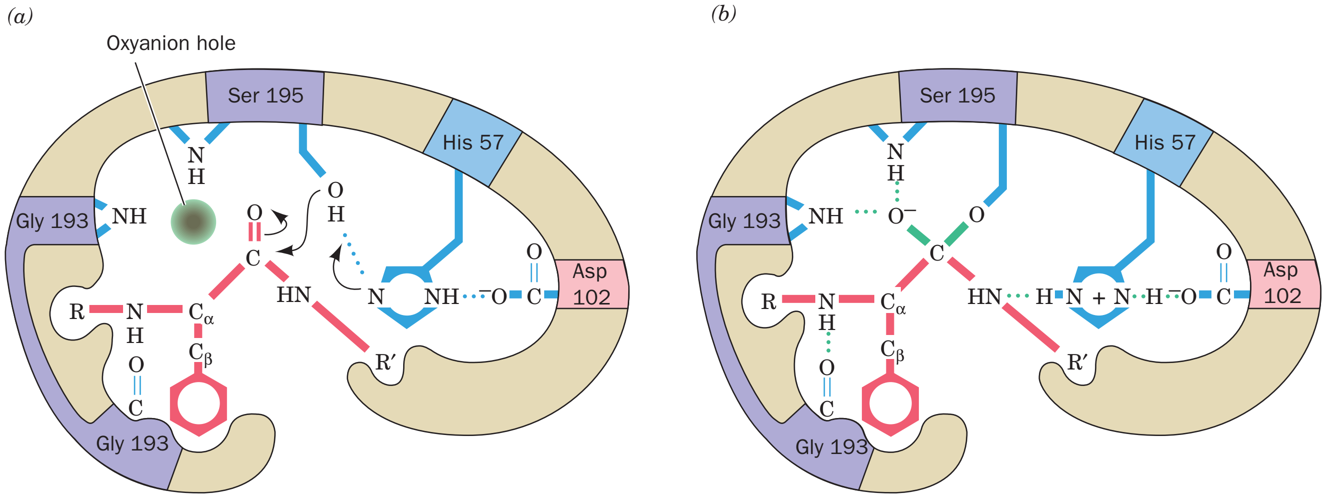

Figure 11-30 | Transition state stabilization in the serine proteases. (*a*) When the substrate binds to the enzyme, the trigonal carbonyl carbon of the scissile peptide is conformationally constrained from binding in the oxyanion hole (*upper left*). (*b*) In the tetrahedral intermediate, the now charged carbonyl oxygen of the scissile peptide (the oxyanion) enters the oxyanion hole and hydrogen bonds to the backbone NH groups of Gly 193 and Ser 195. The consequent conformational distortion permits the NH group of the residue preceding the scissile peptide bond to form an otherwise unsatisfied hydrogen bond to Gly 193. Serine proteases therefore preferentially bind the tetrahedral intermediate. [After Robertus, J.D., Kraut, J., Alden, R.A., and Birktoft, J.J., *Biochemistry* **11,** 4302 (1972).] **See Kinemage Exercise 10-3.**

3. The tetrahedral distortion, moreover, permits the formation of an otherwise unsatisfied hydrogen bond between the enzyme and the backbone NH group of the residue preceding the scissile peptide bond.

This preferential binding of the transition state (or the tetrahedral intermediate) over the enzyme–substrate complex or the acyl–enzyme intermediate is responsible for much of the catalytic efficiency of serine proteases. Thus, mutating any or all of the residues in chymotrypsin's catalytic triad yields enzymes that still enhance proteolysis by $\sim 5 \times 10^4$-fold over the uncatalyzed reaction (versus a rate enhancement of $\sim 10^{10}$ for the native enzyme). Similarly, the reason that DIPF is such an effective inhibitor of serine proteases is because its tetrahedral phosphate group makes this compound a transition state analog.

Low-Barrier Hydrogen Bonds May Stabilize the Transition State. The transition state of the chymotrypsin reaction is stabilized not just through the formation of additional hydrogen bonds in the oxyanion hole but possibly also by the formation of an unusually strong hydrogen bond. Proton transfers between hydrogen bonded groups (D—H···A) occur at physiologically reasonable rates only when the pK of the proton donor is no more than 2 or 3 pH units greater than that of the protonated form of the proton acceptor. However, when the pK's of the hydrogen bonding donor (D) and acceptor (A) groups are nearly equal, the distinction between them breaks down: *The hydrogen atom becomes more or less equally shared between them* (D···H···A). Such **low-barrier hydrogen bonds (LBHBs)** are unusually short and strong. Their free energies, as measured in the gas phase, are as high as -40 to -80 kJ · mol^{-1} (versus -12 to -30 kJ · mol^{-1} for normal hydrogen bonds) and they exhibit a D···A bond length of <2.55 Å for O—H···O and <2.65 Å for N—H···O (versus 2.8 to 3.1 Å for normal hydrogen bonds).

LBHBs are unlikely to exist in dilute aqueous solution because water molecules, which are excellent hydrogen bond donors and acceptors, effectively compete with D—H and A for hydrogen bonding sites. However, LBHBs may exist in the nonaqueous active sites of enzymes. In fact, experimental evidence indicates that in the serine protease catalytic triad, the pK's of the protonated His and Asp are nearly equal, and the hydrogen bond between His and Asp has an unusually short N···O distance of 2.62 Å with the H atom nearly centered between the N and O atoms. These findings are consistent with the formation of an LBHB in the transition state. This suggests that the enzyme uses the "strategy" of converting a weak hydrogen bond in the initial enzyme–substrate complex to a strong hydrogen bond in the transition state, thereby facilitating proton transfer while applying the difference in the free energy between the normal and low-barrier hydrogen bonds to preferentially binding the transition state.

Although several studies have revealed the existence of unusually short hydrogen bonds in enzyme active sites, it is far more difficult to demonstrate experimentally that they are unusually strong, as LBHBs are predicted to be. In fact, several studies of the strengths of unusually short hydrogen bonds in organic model compounds in nonaqueous solutions suggest that these hydrogen bonds are not unusually strong. Consequently, a lively debate has ensued as to the catalytic significance of LBHBs. However, if enzymes do not form LBHBs, it remains to be explained how the conjugate base of an acidic group (e.g., Asp 102) partially abstracts a proton from a far more basic group (e.g., His 57), a feature of numerous enzyme mechanisms.

The Tetrahedral Intermediate Resembles the Complex of Trypsin with Trypsin Inhibitor. Perhaps the most convincing structural evidence for the existence of the tetrahedral intermediate was provided by Robert Huber in

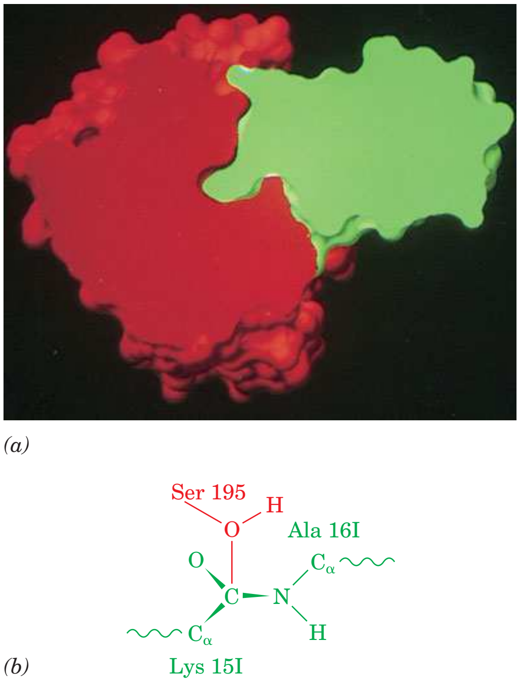

Figure 11-31 | The trypsin–BPTI complex. (*a*) The X-ray structure is shown as a computer-generated cutaway drawing indicating how trypsin (*red*) binds BPTI (*green*). The green protrusion extending into the red cavity near the center of the figure represents the inhibitor's Lys 15 side chain occupying trypsin's specificity pocket. Note the close complementary fit of the two proteins. [Courtesy of Michael Connolly, New York University.] (*b*) Trypsin Ser 195 is in closer-than-van der Waals contact with the carbonyl carbon of BPTI's scissile peptide, which is pyramidally distorted toward Ser 195. The normal proteolytic reaction is apparently arrested somewhere along the reaction coordinate preceding the tetrahedral intermediate. **See Kinemage Exercise 10-1.**

an X-ray study of the complex between **bovine pancreatic trypsin inhibitor (BPTI)** and trypsin. The 58-residue BPTI binds to the active site region of trypsin to form a complex with a tightly packed interface and a network of hydrogen-bonded cross-links. This interaction prevents any trypsin that is prematurely activated in the pancreas from digesting that organ (Section 11-5D). The complex's 10^{13} M^{-1} association constant, among the largest of any known protein–protein interaction, emphasizes BPTI's physiological importance.

The portion of BPTI in contact with the trypsin active site resembles bound substrate. A specific Lys side chain of BPTI occupies the trypsin specificity pocket (Fig. 11-31*a*), and the inhibitor's Lys-Ala peptide bond is positioned as if it were the scissile peptide bond (Fig. 11-31*b*). What is most remarkable about the BPTI–trypsin complex is that its conformation is well along the reaction coordinate toward the tetrahedral intermediate: The side chain oxygen of trypsin Ser 195, the active Ser, is in closer-than-van der Waals contact (2.6 Å) with the pyramidally distorted carbonyl carbon of BPTI's "scissile" peptide. However, the proteolytic reaction cannot proceed past this point because of the rigidity of the complex and because it is so tightly sealed that the leaving group cannot leave and water cannot enter the reaction site.

Protease inhibitors are common in nature, where they have protective and regulatory functions. For example, certain plants release protease inhibitors in response to insect bites, thereby causing the offending insect to starve by inactivating its digestive enzymes. Protease inhibitors constitute ~10% of the blood plasma proteins. For instance, **α_1-proteinase inhibitor,** which is secreted by the liver, inhibits **leukocyte elastase** (leukocytes are white blood cells; the action of leukocyte elastase is thought to be part of the inflammatory process). Pathological variants of α_1-proteinase inhibitor with reduced activity are associated with **pulmonary emphysema,** a degenerative disease of the lungs resulting from the hydrolysis of its elastic fibers. Smokers also suffer from reduced activity of their α_1-proteinase inhibitor because smoking oxidizes a required Met residue.

The Tetrahedral Intermediate Has Been Directly Observed. Because the tetrahedral intermediate resembles the transition state of the serine protease reaction, it is thought to be short-lived and unstable. However, a series of X-ray structures of porcine pancreatic elastase with a peptide substrate have shown the progress of the reaction from the acyl–enzyme intermediate stage to the release of product. This second phase of the proteolysis reaction includes a tetrahedral intermediate (Fig. 11-29).

This acyl–enzyme complex, which is stable at pH 5.0, exhibits the expected structure, with the substrate's C-terminal Ile residue covalently linked via an ester bond to Ser 195 (Fig. 11-32*a*). In this first view of a serine protease acyl–enzyme intermediate, the acyl group is fully planar, with no distortion toward a tetrahedral geometry. A water molecule is located near the intermediate's ester bond, hydrogen-bonded to His 57, where it appears poised to nucleophilically attack the ester linkage. At pH 5.0, His 57 is protonated and acts as a hydrogen bond donor to water (it cannot function as a base catalyst at this pH).

The hydrolytic reaction was triggered by deprotonation of His 57, accomplished by immersing the acyl–enzyme crystal in a solution of pH 9.0. After a period of 1 or 2 minutes, the crystals were frozen in liquid nitrogen to halt the reaction so that the X-ray structure of the enzyme complex could be determined (Box 11-2). In this way, the tetrahedral intermediate was trapped and observed (Fig. 11-32*b*).

During formation of the tetrahedral intermediate, the oxyanion hole does not undergo any change in its structure, but the peptide substrate

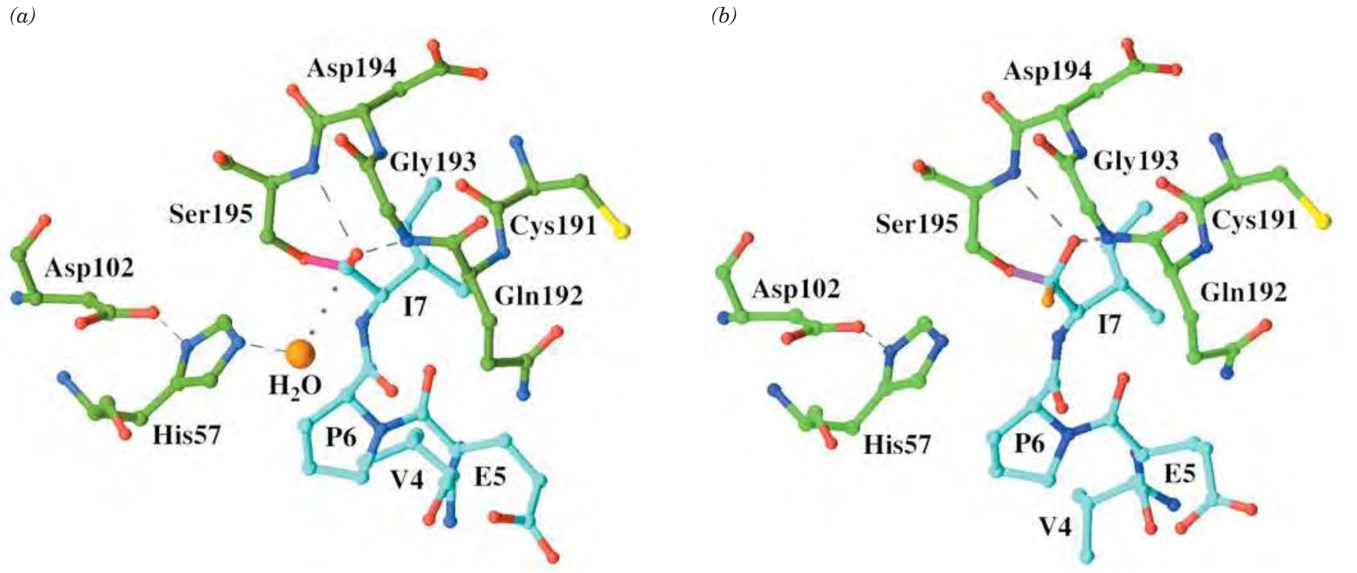

Figure 11-32 | Structure of the acyl–enzyme and tetrahedral intermediates. Porcine pancreatic elastase was incubated with a heptapeptide substrate (YPFVEPI, using the one-letter code). Only residues 4–7 are visible. The protease residues are specified by the three-letter code. Atoms are colored according to type with elastase C green, substrate C cyan, N blue, O red, and S yellow. (*a*) At pH 5.0, a covalent bond (*magenta*) links the Ser 195 O atom to the C-terminal (I7) C atom of the substrate. A water molecule (*orange sphere*) appears poised to nucleophilically attack the acyl–enzyme's carbonyl C atom. The dashed lines represent catalytically important hydrogen bonds, and the dotted line indicates the trajectory that the water molecule presumably follows in nucleophilically attacking the acyl group's carbonyl C atom. (*b*) When the complex is brought to pH 9.0 and then rapidly frozen, the water molecule becomes a hydroxyl substituent (*orange*) to the carbonyl C atom, thereby yielding the tetrahedral intermediate, which resembles the transition state. [Based on X-ray structures by Christopher Schofield and Janos Hadju, University of Oxford, U.K. PDBids (*a*) 1HAX and (*b*) 1HAZ.]

moves within its binding pocket and becomes distorted toward a tetrahedral geometry. The tetrahedral intermediate has the expected shape, similar to known transition state analog inhibitors. However, it does not bind so tightly to the amide group of the oxyanion hole (Fig. 11-30) that it would not be able to subsequently dissociate.

D | Zymogens Are Inactive Enzyme Precursors

Proteolytic enzymes are usually biosynthesized as somewhat larger inactive precursors known as **zymogens** (enzyme precursors, in general, are known as **proenzymes**). In the case of digestive enzymes, the reason for this is clear: If these enzymes were synthesized in their active forms, they would digest the tissues that synthesized them. Indeed, **acute pancreatitis,** a painful and sometimes fatal condition that can be precipitated by pancreatic trauma, is characterized by the premature activation of the digestive enzymes synthesized by that organ.

The activation of **trypsinogen,** the zymogen of trypsin, occurs when trypsinogen enters the duodenum from the pancreas. **Enteropeptidase,** a serine protease whose secretion from the duodenal mucosa is under hormonal control, excises the N-terminal hexapeptide from trypsinogen by specifically cleaving its Lys 15–Ile 16 peptide bond (Fig. 11-33). Since this activating cleavage occurs at a trypsin-sensitive site (recall that trypsin cleaves after Arg and Lys residues), the small amount of trypsin produced by enteropeptidase also catalyzes trypsinogen activation, generating even more trypsin, etc. Thus, trypsinogen activation is said to be **autocatalytic.**

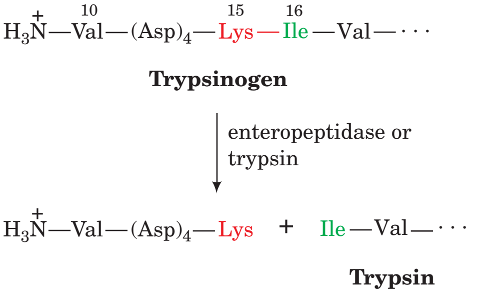

$$\mathrm{H_3\overset{+}{N}{-}\overset{10}{Val}{-}(Asp)_4{-}\overset{15}{Lys}{-}\overset{16}{Ile}{-}Val{-}\cdots}$$

Trypsinogen

enteropeptidase or trypsin

$$\mathrm{H_3\overset{+}{N}{-}Val{-}(Asp)_4{-}Lys \quad + \quad Ile{-}Val{-}\cdots}$$

Trypsin

Figure 11-33 | The activation of trypsinogen to trypsin. Proteolytic excision of the N-terminal hexapeptide is catalyzed by either enteropeptidase or trypsin. The chymotrypsinogen residue-numbering system is used here; that is, Val 10 is actually trypsinogen's N-terminus and Ile 16 is trypsin's N-terminus.

BOX 11-4 BIOCHEMISTRY IN HEALTH AND DISEASE

The Blood Coagulation Cascade

When a blood vessel is damaged, a clot forms as a result of the aggregation of platelets (small enucleated blood cells) and the formation of an insoluble **fibrin** network that traps additional blood cells.

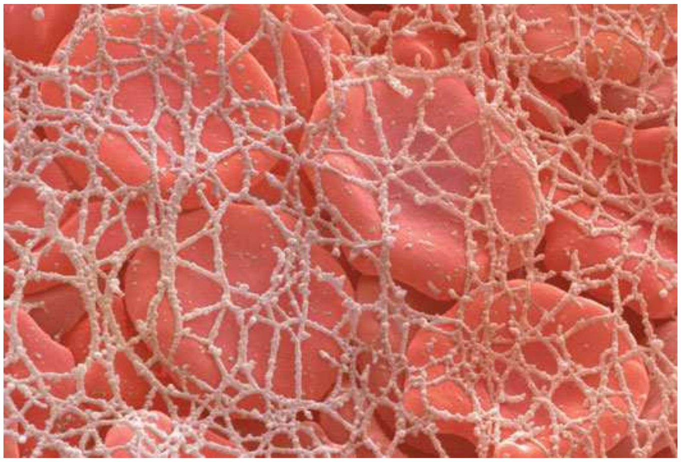

[Andrew Syred/Photo Researchers.]

Fibrin is produced from the soluble circulating protein **fibrinogen** through the action of the serine protease **thrombin.** Thrombin is the last in a series of coagulation enzymes that are sequentially activated by proteolysis of their zymogen forms. The overall process is known as the **coagulation cascade,** although experimental evidence shows that the pathway is not strictly linear, as the waterfall analogy might suggest.

The various components of the coagulation cascade, which include enzymes as well as nonenzymatic protein cofactors, are assigned Roman numerals, largely for historical reasons that do not reflect their order of action *in vivo.* The suffix *a* denotes an active factor. The catalytic domains of the coagulation proteases resemble trypsin in sequence and mechanism but are much more specific for their substrates. Additional domains mediate interactions with cofactors and help anchor the proteins to the platelet membrane, which serves as a stage for many of the coagulation reactions.

Coagulation is initiated when a membrane protein **(tissue factor)** exposed to the bloodstream by tissue damage forms a complex with circulating **factor VII** or VIIa (factor VIIa is generated from factor VII by trace amounts of other coagulation proteases, including factor VIIa itself). The tissue factor–VIIa complex proteolytically converts the zymogen **factor X** to factor Xa. Factor Xa then converts **prothrombin** to thrombin, which subsequently generates fibrin from fibrinogen. The tissue factor–dependent steps of coagulation are known as the **extrinsic pathway** because the source of tissue factor is extravascular. The extrinsic pathway is quickly dampened through the action of a protein that inhibits factor VII once factor Xa has been generated.

Sustained thrombin activation requires the activity of the **intrinsic pathway** (so named because all its components are present in the circulation). The intrinsic pathway is stimulated by the tissue factor–VIIa complex, which converts **factor IX** to its active form, factor IXa. The ensuing thrombin activates a number of components of the intrinsic pathway, including **factor XI,** a protease that activates factor IX, to maintain coagulation in the absence of tissue factor or factor VIIa. Thrombin also activates **factors V** and **VIII,** which are cofactors rather than proteases. Factor Va promotes prothrombin activation by factor Xa by as much as 20,000-fold, and factor VIIIa promotes factor X activation by factor IXa by a similar amount. Thus, thrombin promotes its own activation through a feedback mechanism that amplifies the preceding steps of the cascade. **Factor XIII** is also activated by thrombin. Factor XIIIa, which is not a serine protease, chemically cross-links fibrin molecules through formation of peptide bonds between glutamate and lysine side chains, which forms a strong fibrin network.

The intrinsic pathway of coagulation can be triggered by exposure to negatively charged surfaces such as glass. Consequently, blood clots when it is collected in a clean glass test tube. In the absence of tissue factor, a fibrin clot may not appear for several minutes, but when tissue factor is present, a clot forms within a few seconds. This suggests that rapid blood clotting *in vivo* requires tissue

Chymotrypsinogen is then activated by trypsin-catalyzed cleavage of its Arg 15–Ile 16 peptide bond.

Proelastase, the zymogen of elastase, is activated by a single tryptic cleavage that excises a short N-terminal peptide. Trypsin also activates pancreatic **procarboxypeptidases A** and **B** and **prophospholipase $\mathbf{A_2}$** (Section 9-1C). The autocatalytic nature of trypsinogen activation and the fact that trypsin activates other hydrolytic enzymes makes it essential that trypsinogen not be activated in the pancreas. We have seen that the all but irreversible binding of trypsin inhibitors such as BPTI to trypsin is a defense against trypsinogen's inappropriate activation.

Sequential proenzyme activation makes it possible to quickly generate large quantities of active enzymes in response to diverse physiological factor as well as the proteins of the intrinsic pathway. Additional evidence for the importance of the extrinsic pathway is that individuals who are deficient in factor VII tend to bleed excessively. Abnormal bleeding also results from congenital defects in factor VIII **(hemophilia a)** or factor IX **(hemophilia b).**

The sequential activation of zymogens in the coagulation cascade leads to a burst of thrombin activity, since trace amounts of factors VIIa, IXa, and Xa can activate much larger amounts of their respective substrates. The potential for amplification in the coagulation cascade is reflected in the plasma concentrations of the coagulation proteins (see table).

Plasma Concentrations of Some Human Coagulation Factors

Factor	Concentration (μM)[a]
XI	0.06
IX	0.09
VII	0.01
X	0.18
Prothrombin	1.39
Fibrinogen	8.82

[a] Concentrations calculated from data in High, K.A. and Roberts, H.R. (Eds.), *Molecular Basis of Thrombosis and Hemostasis,* Marcel Dekker (1995).

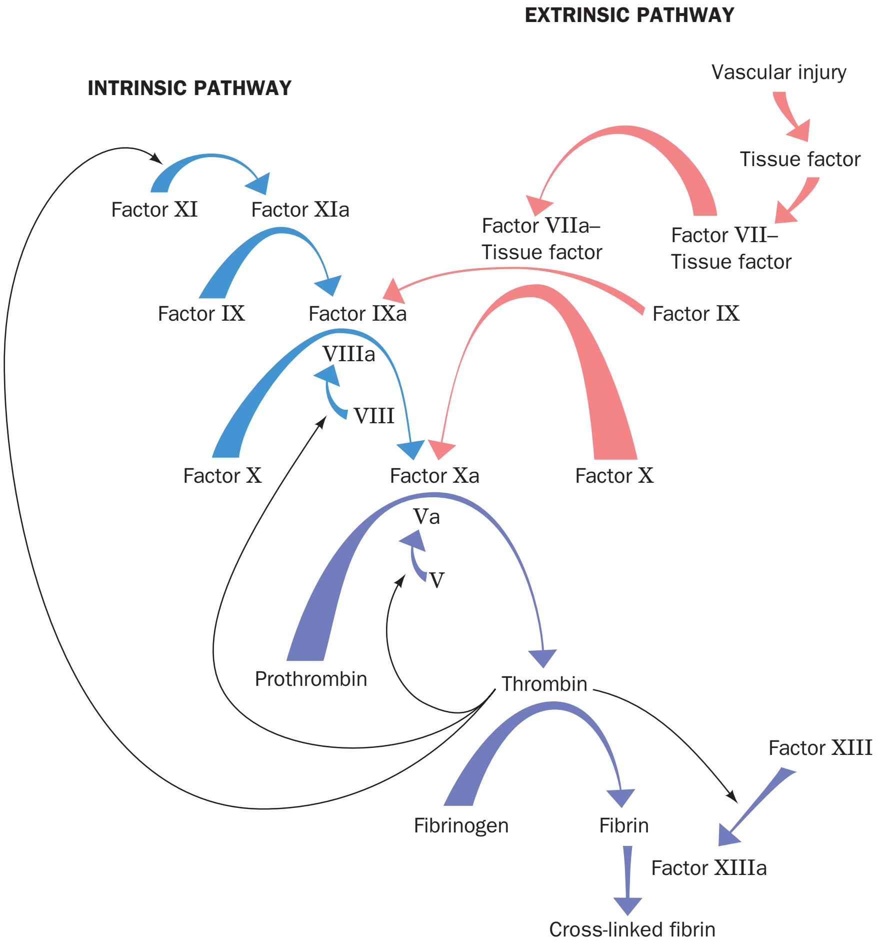
EXTRINSIC PATHWAY
INTRINSIC PATHWAY
Vascular injury
Tissue factor
Factor XI
Factor XIa
Factor VIIa–
Tissue factor
Factor VII–
Tissue factor
Factor IX
Factor IXa
Factor IX
VIIIa
VIII
Factor X
Factor Xa
Factor X
Va
V
Prothrombin
Thrombin
Factor XIII
Fibrinogen
Fibrin
Factor XIIIa
Cross-linked fibrin

[Figure adapted from Davie, E.W., *Thromb. Haemost.* **74,** 2 (1995).]

Perhaps not surprisingly, thrombin eventually triggers mechanisms that shut down clot formation, thereby limiting the duration of the clotting process and hence the extent of the clot. Such control of clotting is of extreme physiological importance since the formation of even one inappropriate blood clot within an individual's lifetime may have fatal consequences.

signals. For example, the serine proteases that lead to blood clotting are synthesized as zymogens by the liver and circulate until they are activated by injury to a blood vessel (Box 11-4).

Zymogens Have Distorted Active Sites. Since the zymogens of trypsin, chymotrypsin, and elastase have all their catalytic residues, why aren't they enzymatically active? Comparisons of the X-ray structures of trypsinogen with that of trypsin, and of chymotrypsinogen with that of chymotrypsin, show that on activation, the newly liberated N-terminal Ile 16 residue moves from the surface of the protein to an internal position, where its free cationic amino group forms an ion pair with the invariant anionic Asp 194, which is close to the catalytic triad (Fig. 11-26). Without this conformational change, the enzyme cannot properly bind its substrate or stabilize the tetrahedral intermediate because its specificity pocket and oxyanion hole are improperly formed. This provides further structural evidence favoring the role of preferential transition state binding in the catalytic mechanism of serine proteases. Nevertheless, because their catalytic triads are structurally intact, the zymogens of serine proteases actually have low levels of enzymatic activity, an observation that was made only after the above structural comparisons suggested that this might be the case.

CHECK YOUR UNDERSTANDING

Summarize the roles of the residues that make up the catalytic triad of serine proteases.

What is the function of the oxyanion hole?

What are the advantages of synthesizing proteases as zymogens?

SUMMARY

1. Enzymes, almost all of which are proteins, are grouped into six mechanistic classes.
2. Enzymes accelerate reactions by factors of up to at least 10^{15}.
3. The substrate specificity of an enzyme depends on the geometric and electronic character of its active site.
4. Some enzymes catalyze reactions with the assistance of metal ion cofactors or organic coenzymes that function as reversibly bound cosubstrates or as permanently associated prosthetic groups. Many coenzymes are derived from vitamins.
5. Enzymes catalyze reactions by decreasing the activation free energy, $\Delta G^{\ddagger}$, which is the free energy required to reach the transition state, the point of highest free energy in the reaction.
6. Enzymes use the same catalytic mechanisms employed by chemical catalysts, including general acid and general base catalysis, covalent catalysis, and metal ion catalysis.
7. The arrangement of functional groups in an enzyme active site allows catalysis by proximity and orientation effects as well as electrostatic catalysis.
8. A particularly important mechanism of enzyme-mediated catalysis is the preferential binding of the transition state of the catalyzed reaction.
9. In the catalytic mechanism of lysozyme, Glu 35 in its protonated form acts as an acid catalyst to cleave the polysaccharide substrate between its D and E rings, and Asp 52 in its anionic state forms a covalent bond to C1 of the D ring. The reaction is facilitated by the distortion of residue D to the planar half-chair conformation, which resembles the reaction's oxonium ion transition state.
10. Serine proteases contain a Ser–His–Asp catalytic triad near a binding pocket that helps determine the enzymes' substrate specificity.
11. Catalysis in the serine proteases occurs through acid–base catalysis, covalent catalysis, proximity and orientation effects, electrostatic catalysis, and by preferential transition state binding in the oxyanion hole.
12. Synthesis of pancreatic proteases as inactive zymogens protects the pancreas from self-digestion. Zymogens are activated by specific proteolytic cleavages.

KEY TERMS

active site	**323**
substrate	**324**
EC classification	**324**
induced fit	**325**
prochirality	**325**
cofactor	**326**
coenzyme	**327**
cosubstrate	**327**
prosthetic group	**327**
holoenzyme	**327**
apoenzyme	**327**
transition state	**328**
$\Delta G^{\ddagger}$	**328**
rate-determining step	**329**
general acid catalysis	**331**
general base catalysis	**331**
covalent catalysis	**333**
metalloenzyme	**335**
electrostatic catalysis	**337**
transition state analog	**339**
oxonium ion	**344**
serine protease	**347**
affinity labeling	**348**
catalytic triad	**351**
convergent evolution	**352**
tetrahedral intermediate	**352**
acyl–enzyme intermediate	**354**
oxyanion hole	**354**
low-barrier hydrogen bond	**355**
zymogen	**357**

PROBLEMS

1. Choose the best description of an enzyme:

   (a) It allows a chemical reaction to proceed extremely fast.

   (b) It increases the rate at which a chemical reaction approaches equilibrium relative to its uncatalyzed rate.

   (c) It makes a reaction thermodynamically favorable.

2. Which type of enzyme (Table 11-2) catalyzes the following reactions?

   (a)

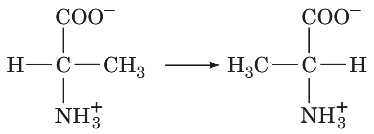

$$\mathrm{H{-}}\underset{\mathrm{NH_3^+}}{\overset{\mathrm{COO^-}}{\mathrm{C}}}\mathrm{{-}CH_3} \longrightarrow \mathrm{H_3C{-}}\underset{\mathrm{NH_3^+}}{\overset{\mathrm{COO^-}}{\mathrm{C}}}\mathrm{{-}H}$$

(b)

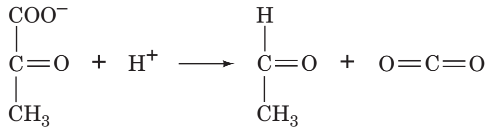

$$\mathrm{CH_3{-}C({=}O){-}COO^-} + \mathrm{H^+} \longrightarrow \mathrm{CH_3{-}C({=}O){-}H} + \mathrm{O{=}C{=}O}$$

(c)

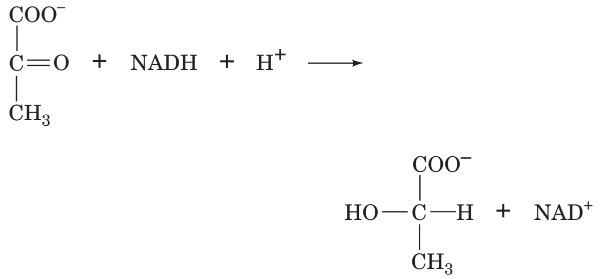

$$\mathrm{CH_3{-}C({=}O){-}COO^-} + \mathrm{NADH} + \mathrm{H^+} \longrightarrow \mathrm{HO{-}C(H)(CH_3){-}COO^-} + \mathrm{NAD^+}$$

(d)

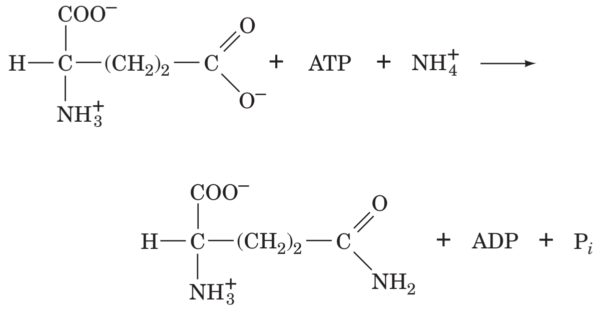

$$\mathrm{H{-}C(COO^-)(NH_3^+){-}(CH_2)_2{-}C({=}O){-}O^-} + \mathrm{ATP} + \mathrm{NH_4^+} \longrightarrow \mathrm{H{-}C(COO^-)(NH_3^+){-}(CH_2)_2{-}C({=}O){-}NH_2} + \mathrm{ADP} + \mathrm{P}_i$$

3. What is the relationship between the rate of an enzyme-catalyzed reaction and the rate of the corresponding uncatalyzed reaction? Do enzymes enhance the rates of slow uncatalyzed reactions as much as they enhance the rates of fast uncatalyzed reactions?

4. On the free energy diagram shown, label the intermediate(s) and transition state(s). Is the reaction thermodynamically favorable?

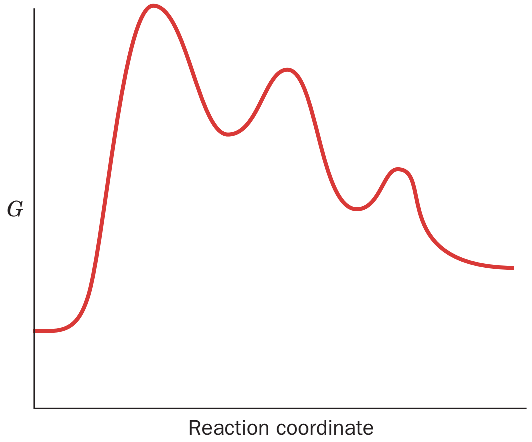

5. Draw a transition state diagram of (a) a nonenzymatic reaction and the corresponding enzyme-catalyzed reaction in which (b) S binds loosely to the enzyme and (c) S binds very tightly to the enzyme. Compare $\Delta G^{\ddagger}$ for each case. Why is tight binding of S not advantageous?

6. Approximately how much does staphylococcal nuclease (Table 11-1) decrease the activation free energy ($\Delta G^{\ddagger}$) of its reaction (the hydrolysis of a phosphodiester bond) at 25°C?

7. Studies at different pH's show that an enzyme has two catalytically important residues whose pK's are ~4 and ~10. Chemical modification experiments indicate that a Glu and a Lys residue are essential for activity. Match the residues to their pK's and explain whether they are likely to act as acid or base catalysts.

8. The covalent catalytic mechanism of an enzyme depends on a single active site Cys whose pK is 8. A mutation in a nearby residue alters the microenvironment so that this pK increases to 10. Would the mutation cause the reaction rate to increase or decrease? Explain.

9. Explain why RNase A cannot catalyze the hydrolysis of DNA.

10. Suggest a transition state analog for proline racemase that differs from those discussed in the text. Justify your suggestion.

11. Wolfenden has stated that it is meaningless to distinguish between the "binding sites" and the "catalytic sites" of enzymes. Explain.

12. Explain why lysozyme cleaves the artificial substrate $(\mathrm{NAG})_4$ ~4000 times more slowly than it cleaves $(\mathrm{NAG})_6$.

13. Lysozyme residues Asp 101 and Arg 114 are required for efficient catalysis, although they are located at some distance from the active site Glu 35 and Asp 52. Substituting Ala for either Asp 101 or Arg 114 does not significantly alter the enzyme's tertiary structure, but it significantly reduces its catalytic activity. Explain.

14. Design a chloromethylketone inhibitor of elastase.

15. Under certain conditions, peptide bond formation rather than peptide bond hydrolysis is thermodynamically favorable. Would you expect chymotrypsin to catalyze peptide bond formation?

16. Diagram the hydrogen-bonding interactions of the catalytic triad His–Lys–Ser during catalysis in a hypothetical hydrolytic enzyme.

17. The comparison of the active site geometries of chymotrypsin and subtilisin under the assumption that their similarities have catalytic significance has led to greater mechanistic understanding of both these enzymes. Discuss the validity of this strategy.

18. Predict the effect of mutating Asp 102 of trypsin to Asn (a) on substrate binding and (b) on catalysis.

19. A genetic defect in coagulation factor IX causes hemophilia b, a disease characterized by a tendency to bleed profusely after very minor trauma. However, a genetic defect in coagulation factor XI has only mild clinical symptoms. Explain this discrepancy in terms of the mechanism for activation of coagulation proteases shown in Box 11-4.

20. Why is the broad substrate specificity of chymotrypsin advantageous *in vivo*? Why would this be a disadvantage for some other proteases?

21. Tofu (bean curd), a high-protein soybean product, is prepared in such a way as to remove the trypsin inhibitor present in soybeans. Explain the reason(s) for this treatment.

CASE STUDIES

Case Study 11 (available at www.wiley.com/college/voet)

Nonenzymatic Deamidation of Asparagine and Glutamine Residues in Proteins

Focus concept: Factors influencing nonenzymatic hydrolytic deamidation of Asn and Gln residues in proteins are examined and possible mechanisms for the reactions are proposed.

Prerequisites: Chapters 5 and 11

- Protein analytical methods, particularly isoelectric focusing
- Enzyme mechanisms, especially proteases such as papain and chymotrypsin

REFERENCES

General

Benkovic, S.J. and Hammes-Schiffer, S., A perspective on enzyme catalysis, *Science* **301,** 1196–1202 (2003). [Includes a history of some of the theories and experiments on catalysis.]

Bruice, T.C. and Benkovic, S.J., Chemical basis for enzyme catalysis, *Biochemistry* **39,** 6267–6274 (2000).

Gerlt, J.A., Protein engineering to study enzyme catalytic mechanisms, *Curr. Opin. Struct. Biol.* **4,** 593–600 (1994). [Describes how information can be gained from mutagenesis and structural analysis of enzymes.]

Hackney, D.D., Binding energy and catalysis, *in* Sigman, D.S. and Boyer, P.D. (Eds.), *The Enzymes* (3rd ed.), Vol. 19, pp. 1–36, Academic Press (1990).

Kraut, J., How do enzymes work? *Science* **242,** 533–540 (1988). [A brief and very readable review of transition state theory and applications.]

Schramm, V.L., Enzymatic transition states and transition state analogues, *Curr. Opin. Struct. Biol.* **15,** 604–613 (2005).

Tipton, K.F., The naming of parts, *Trends Biochem. Sci.* **18,** 113–115 (1993). [A discussion of the advantages of a consistent naming scheme for enzymes and the difficulties of formulating one.]

Lysozyme

Kirby, A.J., The lysozyme mechanism sorted—after 50 years, *Nature Struct. Biol.* **8,** 737–739 (2001). [Briefly summarizes the theoretical and experimental evidence for a covalent intermediate in the lysozyme mechanism.]

McKenzie, H.A. and White, F.H., Jr., Lysozyme and α-lactalbumin: Structure, function and interrelationships, *Adv. Protein Chem.* **41,** 173–315 (1991).

Strynadka, N.C.J. and James, M.N.G., Lysozyme revisited: crystallographic evidence for distortion of an *N*-acetylmuramic acid residue bound in site D, *J. Mol. Biol.* **220,** 401–424 (1991).

Serine Proteases

Cleland, W.W., Frey, P.A., and Gerlt, J.A., The low barrier hydrogen bond in enzymatic catalysis, *J. Biol. Chem.* **273,** 25529–25532 (1998).

Davie, E.W., Biochemical and molecular aspects of the coagulation cascade, *Thromb. Haemost*. **74,** 1–6 (1995). [A brief review by one of the pioneers of the cascade hypothesis.]

Fersht, A., *Structure and Mechanism in Protein Science.* Freeman (1999). [Includes detailed reaction mechanisms for chymotrypsin and other enzymes.]

Perona, J.J. and Craik, C.S., Evolutionary divergence of substrate specificity within the chymotrypsin-like protease fold, *J. Biol. Chem.* **272,** 29987–29990 (1997). [Summarizes research identifying the structural basis of substrate specificity in chymotrypsin and related enzymes.]

Radisky, E.S., Lee, J.M., Lu, C-J.K., and Koshland, D.E., Jr., Insights into the serine protease mechanism from atomic resolution structures of trypsin reaction intermediates, *Proc. Natl. Acad. Sci.* **103,** 6835–6840 (2006). [Superpositions of X-ray structures representing the enzyme–substrate complex, tetrahedral intermediate, and acyl–enzyme intermediate illustrate the progress of the reaction.]

Wilmouth, R.C., Edman, K., Neutze, R., Wright, P.A., Clifton, I.J., Schneider, T.R., Schofield, C.J., and Hajdu, J., X-Ray snapshots of serine protease catalysis reveal a tetrahedral intermediate, *Nature Struct. Biol.* **8,** 689–694 (2001). [Reports the first structural evidence for a tetrahedral intermediate in the hydrolysis reaction catalyzed by a serine protease.]

12

Enzyme Kinetics, Inhibition, and Control

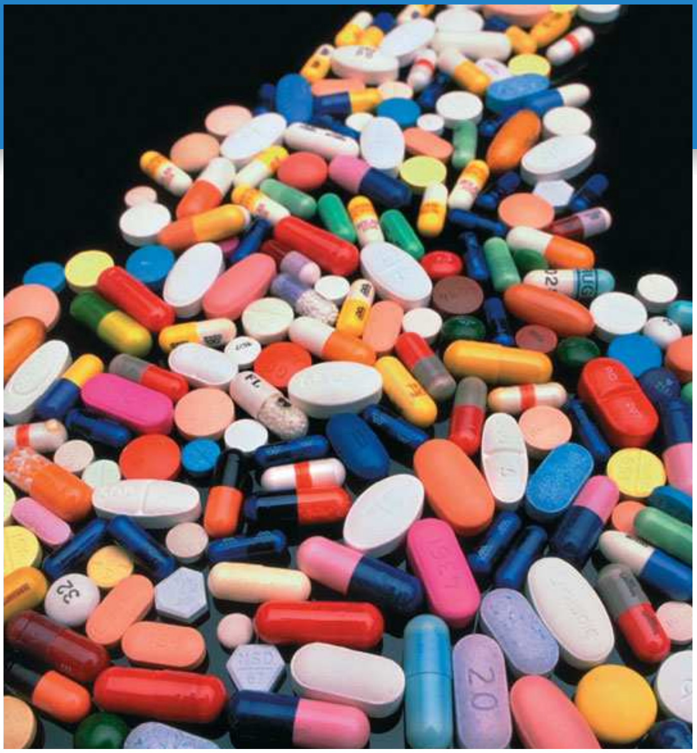

Many natural and synthetic substances are known to inhibit the activities of specific enzymes. The study of inhibitor–enzyme interactions, as quantified through enzyme kinetics, is a mainstay of modern drug development. [Larry Kolvoord/The Image Works.]

CHAPTER CONTENTS

1 Reaction Kinetics
  - A. Chemical Kinetics Is Described by Rate Equations
  - B. Enzyme Kinetics Often Follows the Michaelis–Menten Equation
  - C. Kinetic Data Can Provide Values of $V_{\max}$ and K_M
  - D. Bisubstrate Reactions Follow One of Several Rate Equations

2 Enzyme Inhibition
  - A. Competitive Inhibition Involves Inhibitor Binding at an Enzyme's Substrate Binding Site
  - B. Uncompetitive Inhibition Involves Inhibitor Binding to the Enzyme–Substrate Complex
  - C. Mixed Inhibition Involves Inhibitor Binding to Both the Free Enzyme and the Enzyme–Substrate Complex

3 Control of Enzyme Activity
  - A. Allosteric Control Involves Binding at a Site Other than the Active Site
  - B. Control by Covalent Modification Usually Involves Protein Phosphorylation

4 Drug Design
  - A. Drug Discovery Employs a Variety of Techniques
  - B. A Drug's Bioavailability Depends on How It Is Absorbed and Transported in the Body
  - C. Clinical Trials Test for Efficacy and Safety
  - D. Cytochromes P450 Are Often Implicated in Adverse Drug Reactions

MEDIA RESOURCES

(available at www.wiley.com/college/voet)

Guided Exploration 11. Michaelis–Menten kinetics, Lineweaver–Burk plots, and enzyme inhibition
Interactive Exercise 9. HIV protease
Animated Figure 12-2. Progress curves for enzyme-catalyzed reaction
Animated Figure 12-3. Plot of initial velocity versus substrate concentration
Animated Figure 12-4. Double-reciprocal (Lineweaver–Burk) plot
Animated Figure 12-7. Lineweaver–Burk plot of competitive inhibition
Animated Figure 12-8. Lineweaver–Burk plot of uncompetitive inhibition
Animated Figure 12-9. Lineweaver–Burk plot of mixed inhibition
Animated Figure 12-10. Plot of v_o versus [aspartate] for ATCase
Kinemage 11-1. Structure of ATCase
Kinemage 11-2. Conformational changes in ATCase
Kinemage 14-1. Glycogen phosphorylase
Kinemage 14-2 and 14-3. Conformational changes in glycogen phosphorylase
Case Study 7. A Storage Protein from Seeds of *Brassica nigra* Is a Serine Protease Inhibitor
Case Study 12. Production of Methanol in Ripening Fruit
Case Study 13. Inhibition of Alcohol Dehydrogenase
Case Study 15. Site-Directed Mutagenesis of Creatine Kinase
Case Study 19. Purification of Rat Kidney Sphingosine Kinase
Bioinformatics Exercise Chapter 12. Enzyme Inhibitors and Rational Drug Design

Early enzymologists, often working with crude preparations of yeast or liver cells, could do little more than observe the conversion of substrates to products catalyzed by as yet unpurified enzymes. Measuring the rates of such reactions therefore came to be a powerful tool for characterizing enzyme activity. The application of simple mathematical models to enzyme activity under varying laboratory conditions, and in the presence of competing substrates or enzyme inhibitors, made it possible to deduce the probable physiological functions and regulatory mechanisms of various enzymes.

The study of enzymatic reaction rates, or **enzyme kinetics,** is no less important now than it was early in the twentieth century. In many cases, the rate of a reaction and how the rate changes in response to different conditions reveal the path followed by the reactants and are therefore indicative of the reaction mechanism. Kinetic data, combined with detailed information about an enzyme's structure and its catalytic mechanisms, provide some of the most powerful clues to the enzyme's biological function and may suggest ways to modify it for therapeutic purposes.

We begin our consideration of enzyme kinetics by reviewing chemical kinetics. Following that, we derive the basic equations of enzyme kinetics and describe the effects of inhibitors on enzymes. We also consider some examples of enzyme control that highlight several aspects of enzyme function. Finally, we describe some practical applications of enzyme inhibition, the development of enzyme inhibitors as drugs.

1 Reaction Kinetics

LEARNING OBJECTIVES

- Understand that rate equations describe the progress of first-order and second-order reactions.
- Understand how the Michaelis–Menten equation relates the initial velocity of a reaction to the maximal reaction velocity and the Michaelis constant for a particular enzyme and substrate.
- Understand that a Lineweaver–Burk plot can be used to present kinetic data and to calculate values for K_M and $V_{\max}$.
- Understand that bisubstrate reactions can occur by an Ordered or Random sequential mechanism or by a Ping Pong mechanism.

Kinetic measurements of enzymatically catalyzed reactions are among the most powerful techniques for elucidating the catalytic mechanisms of enzymes. Enzyme kinetics is a branch of chemical kinetics, so we begin this section by reviewing the principles of chemical kinetics.

A | Chemical Kinetics Is Described by Rate Equations

A reaction of overall stoichiometry

$$\mathrm{A} \longrightarrow \mathrm{P}$$

where A represents reactants and P represents products, may actually occur through a sequence of **elementary reactions** (simple molecular processes) such as

$$\mathrm{A} \longrightarrow \mathrm{I}_1 \longrightarrow \mathrm{I}_2 \longrightarrow \mathrm{P}$$

Here, I_1 and I_2 symbolize **intermediates** in the reaction. Each elementary reaction can be characterized with respect to the number of reacting species and the rate at which they interact. *Descriptions of each elementary reaction collectively constitute the mechanistic description of the overall reaction process.* Even a complicated enzyme-catalyzed reaction can be analyzed in terms of its component elementary reactions.

Reaction Order Indicates the Number of Molecules Participating in an Elementary Reaction. At constant temperature, *the rate of an elementary reaction is proportional to the frequency with which the reacting molecules come together.* The proportionality constant is known as a **rate constant** and is symbolized ***k*.** For the elementary reaction A → P, the instantaneous rate of appearance of product or disappearance of reactant, which is called the **velocity (*v*)** of the reaction, is

$$v = \frac{d[\mathrm{P}]}{dt} = -\frac{d[\mathrm{A}]}{dt} = k[\mathrm{A}] \qquad [12\text{-}1]$$

In other words, the reaction velocity at any time point is proportional to the concentration of the reactant A. This is an example of a **first-order reaction.** Since the velocity has units of molar per second ($\mathrm{M \cdot s^{-1}}$), the first-order rate constant must have units of reciprocal seconds (s^{-1}). *The* ***reaction order*** *of an elementary reaction corresponds to the* ***molecularity*** *of the reaction, which is the number of molecules that must simultaneously collide to generate a product.* Thus, a first-order elementary reaction is a **unimolecular** reaction.

Consider the elementary reaction $2A \rightarrow P$. This **bimolecular** reaction is a **second-order reaction,** and its instantaneous velocity is described by

$$v = -\frac{d[A]}{dt} = k[A]^2 \qquad [12\text{-}2]$$

In this case, the reaction velocity is proportional to the square of the concentration of A, and the second-order rate constant k has units of $M^{-1} \cdot s^{-1}$.

The bimolecular reaction $A + B \rightarrow P$ is also a second-order reaction with an instantaneous velocity described by

$$v = -\frac{d[A]}{dt} = -\frac{d[B]}{dt} = k[A][B] \qquad [12\text{-}3]$$

Here, the reaction is said to be first order in [A] and first order in [B] (see Sample Calculation 12-1). Unimolecular and bimolecular reactions are common. **Termolecular** reactions are unusual because the simultaneous collision of three molecules is a rare event. Fourth- and higher-order reactions are unknown.

SAMPLE CALCULATION 12-1

Determine the velocity of the elementary reaction $X + Y \rightarrow Z$ when the sample contains 3 μM X and 5 μM Y and k for the reaction is 400 $M^{-1} \cdot s^{-1}$.

Use Equation 12-3 and make sure that all units are consistent:

$$\begin{aligned} v &= k[X][Y] \\ &= (400\ M^{-1} \cdot s^{-1})(3\ \mu M)(5\ \mu M) \\ &= (400\ M^{-1} \cdot s^{-1})(3 \times 10^{-6}\ M)(5 \times 10^{-6}\ M) \\ &= 6 \times 10^{-9}\ M \cdot s^{-1} \\ &= 6\ nM \cdot s^{-1} \end{aligned}$$

A Rate Equation Indicates the Progress of a Reaction as a Function of Time.

A **rate equation** can be derived from the equations that describe the instantaneous reaction velocity. Thus, a first-order rate equation is obtained by rearranging Eq. 12-1

$$\frac{d[A]}{[A]} = d\ln[A] = -k\,dt \qquad [12\text{-}4]$$

and integrating it from $[A]_o$, the initial concentration of A, to [A], the concentration of A at time t:

$$\int_{[A]_o}^{[A]} d\ln[A] = -k\int_0^t dt \qquad [12\text{-}5]$$

This results in

$$\boxed{\ln[A] = \ln[A]_o - kt} \qquad [12\text{-}6]$$

or, taking the antilog of both sides,

$$[A] = [A]_o e^{-kt} \qquad [12\text{-}7]$$

Equation 12-6 is a linear equation of the form $y = mx + b$ and can be plotted as in Fig. 12-1. Therefore, if a reaction is first order, a plot of ln[A] versus t will yield a straight line whose slope is $-k$ (the negative of the first-order rate constant) and whose intercept on the ln[A] axis is $\ln[A]_o$.

One of the hallmarks of a first-order reaction is that *the time for half of the reactant initially present to decompose, its* ***half-time*** *or* ***half-life,*** $t_{1/2}$, *is a constant and hence independent of the initial concentration of the reactant.* This is easily demonstrated by substituting the relationship $[A] = [A]_o/2$ when $t = t_{1/2}$ into Eq. 12-6 and rearranging:

$$\ln\left(\frac{[A]_o/2}{[A]_o}\right) = -kt_{1/2} \qquad [12\text{-}8]$$

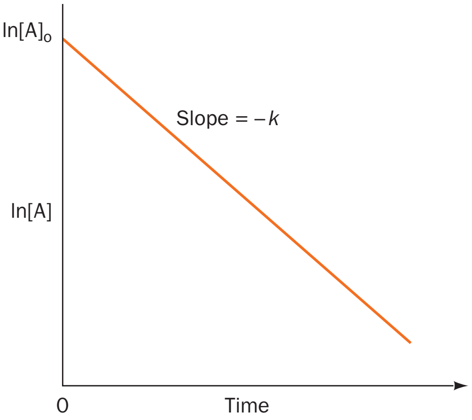

Figure 12-1 | A plot of a first-order rate equation. The slope of the line obtained when ln[A] is plotted against time gives the rate constant k.

SAMPLE CALCULATION 12-2

The decay of a hypothetical radioisotope has a rate constant of $0.01\ \text{s}^{-1}$. How much time is required for half of a 1-g sample of the isotope to decay?

The units of the rate constant indicate a first-order process. Thus, the half-life is independent of concentration. The half-life of the isotope (the half-time for its decay) is given by Eq. 12-9:

$$t_{1/2} = \frac{\ln 2}{k} = \frac{0.693}{0.01\ \text{s}^{-1}} = 69.3\ \text{s}$$

Thus

$$t_{1/2} = \frac{\ln 2}{k} = \frac{0.693}{k} \qquad [12\text{-}9]$$

Substances that are inherently unstable, such as radioactive nuclei, decompose through first-order reactions (Box 12-1 and Sample Calculation 12-2).

In a second-order reaction with one type of reactant, $2\text{A} \rightarrow \text{P}$, the variation of [A] with time is quite different from that in a first-order reaction. Rearranging Eq. 12-2 and integrating it over the same limits used for the first-order reaction yields

$$\int_{[\text{A}]_o}^{[\text{A}]} -\frac{d[\text{A}]}{[\text{A}]^2} = k\int_0^t dt \qquad [12\text{-}10]$$

so that

$$\boxed{\frac{1}{[\text{A}]} = \frac{1}{[\text{A}]_o} + kt} \qquad [12\text{-}11]$$

Equation 12-11 is a linear equation in terms of the variables $1/[\text{A}]$ and t. *The half-time for a second-order reaction is expressed* $t_{1/2} = 1/k[\text{A}]_o$ *and therefore, in contrast to a first-order reaction, depends on the initial reactant concentration.* Equations 12-6 and 12-11 may be used to distinguish a first-order from a second-order reaction by plotting $\ln[\text{A}]$ versus t and $1/[\text{A}]$ versus t and observing which, if any, of these plots is linear.

To experimentally determine the rate constant for the second-order reaction $\text{A} + \text{B} \rightarrow \text{P}$, it is often convenient to increase the concentration of one reactant relative to the other, for example, $[\text{B}] \gg [\text{A}]$. Under these conditions, [B] does not change significantly over the course of the reaction. The reaction rate therefore depends only on [A], the concentration of the reactant that is present in limited amounts. Hence, the reaction appears to be first order with respect to A and is therefore said to be a **pseudo-first-order reaction.** The reaction is first order with respect to B when $[\text{A}] \gg [\text{B}]$.

See Guided Exploration 11
Michaelis–Menten kinetics, Lineweaver–Burk plots, and enzyme inhibition.

B | Enzyme Kinetics Often Follows the Michaelis–Menten Equation

Enzymes catalyze a tremendous variety of reactions using different combinations of five basic catalytic mechanisms (Section 11-3). Some enzymes act on only a single substrate molecule; others act on two or more different substrate molecules whose order of binding may or may not be obligatory. Some enzymes form covalently bound intermediate complexes with their substrates; others do not. *Yet all enzymes can be analyzed such that their reaction rates as well as their overall efficiency can be quantified.*

The study of enzyme kinetics began in 1902 when Adrian Brown investigated the rate of hydrolysis of sucrose by the yeast enzyme **β-fructofuranosidase:**

$$\text{Sucrose} + \text{H}_2\text{O} \longrightarrow \text{glucose} + \text{fructose}$$

Brown found that when the sucrose concentration is much higher than that of the enzyme, the reaction rate becomes independent of the sucrose concentration; that is, the rate is **zeroth order** with respect to sucrose. He therefore proposed that the overall reaction is composed of two elementary reactions in which the substrate forms a complex with the enzyme that subsequently decomposes to products, regenerating enzyme:

$$\text{E} + \text{S} \underset{k_{-1}}{\overset{k_1}{\rightleftharpoons}} \text{ES} \xrightarrow{k_2} \text{P} + \text{E} \qquad [12\text{-}12]$$

BOX 12-1 PERSPECTIVES IN BIOCHEMISTRY

Isotopic Labeling

In the laboratory, it is often useful to label large or small molecules so that they can be easily detected after chromatographic or electrophoretic separation or in various binding assays. One of the most common labeling techniques is to attach a radioactive isotope to a molecule or to synthesize the molecule so that it contains a radioactive isotope in place of a normally occurring isotope. Molecules labeled in this way can be detected in solution or in solid form by measuring the radioactivity emitted by the label. This method is more sensitive than spectroscopic measurements, and it is often easier to carry out than more laborious assays based on chemical or biological activities. Metabolites labeled with NMR-active isotopes such as ^{13}C can also be detected in living tissues by NMR techniques.

Some of the most common radioactive isotopes **(radionuclides)** used in biochemistry are listed below, along with their half-lives and the type of radioactivity emitted by the spontaneously disintegrating atomic nuclei.

Radionuclide	Half-life	Type of Radiation[a]
^{3}H	12 years	β
^{14}C	5715 years	β
^{24}Na	15 hours	β
^{32}P	14 days	β
^{35}S	87 days	β
^{40}K	1.25×10^{9} years	β
^{45}Ca	163 days	β
^{125}I	59 days	γ
^{131}I	8 days	β, γ

[a] β particles are emitted electrons, and γ rays are emitted photons.

Nucleic acids can be easily labeled by attaching a terminal nucleotide that contains ^{32}P in place of the normal nonradioactive ^{31}P. Proteins can be labeled by chemically or enzymatically linking ^{125}I to a Tyr residue. Assays for cell growth and division often measure the uptake of ^{3}H-labeled **thymidine** (thymidine is incorporated exclusively into DNA). Protein synthesis is similarly monitored by the appearance of ^{35}S-labeled Met in proteins. Of course, the choice of a particular isotopic label also depends on the time course of the experiment and the method for detecting radioactivity.

A **Geiger counter,** which electronically detects the ionization of a gas caused by the passage of radiation, is not sensitive enough to detect low-energy emitters such as ^{3}H and ^{14}C. This limitation is circumvented through **liquid scintillation counting.** In this technique, a β-emitting sample is dissolved in a solvent that contains a fluorescent molecule. The β particles excite this fluor, thereby causing it to emit light that can then be optically detected. Radioactive substances that emit γ rays are detected by **scintillation counters** when the γ rays dislodge electrons from a crystal of NaI in the counter. These electrons induce fluorescence that is measured. In **autoradiography,** a radioactive substance immobilized in an agarose or polyacrylamide gel is detected by laying X-ray film over the sample followed by incubation and development of the film (dark areas on the developed film correspond to areas exposed to radioactivity). Thin sections of tissue can also be prepared for **microradiography** by covering them with a layer of photographic emulsion and examining the developed emulsion under a microscope (see figure). Instruments that electronically measure radioactivity in solid samples without the use of film **(phosphorimagers)** offer the advantage of digitized results and multiple exposure times (in contrast, film can be developed only once).

The use of radioactive isotopes as molecular labels is not without drawbacks. First and foremost is the danger of working with potentially mutagenic materials (irradiation can cause DNA damage). In addition, radioactive laboratory materials (samples as well as glassware) must be disposed of properly or the resulting contamination can cause errors in subsequent measurements of radioactivity as well as a health hazard. Scintillation fluid presents a particular problem for disposal because of the large volumes required (it also consists largely of organic solvents). The preceding table reveals that while disposal of short-lived radionuclides (such as ^{32}P, ^{35}S, and ^{125}I) can be accomplished mainly by storing the material until the radioactivity has decayed to insignificant levels, the safe disposal of long-lived species (such as ^{3}H and ^{14}C) is a problem that is unlikely to vanish any time soon. This is one reason why molecular labeling techniques that rely on chemical tags or fluorescent compounds have become popular.

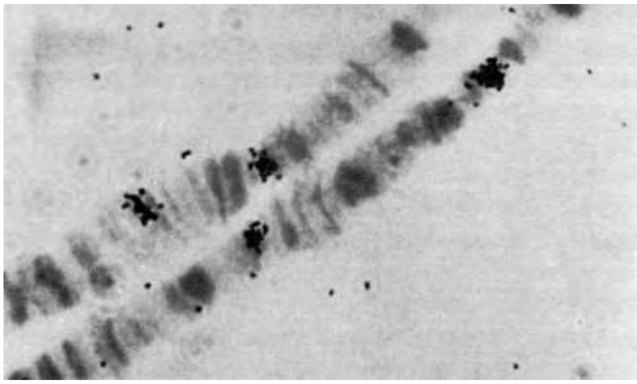

In this autoradiogram, a radioactive RNA probe has hybridized with specific sites in *Drosophila* polytene chromosomes. The black dots reveal the sites where radioactive decay has occurred. [From Loughney, K., Kreber, R., and Ganetzky, B., *Cell* **58,** 1143 (1989), by permission of Cell Press.]

Here E, S, ES, and P symbolize the enzyme, substrate, **enzyme–substrate complex,** and products, respectively. According to this model, when the substrate concentration becomes high enough to entirely convert the enzyme to the ES form, the second step of the reaction becomes rate limiting and the overall reaction rate becomes insensitive to further increases in substrate concentration.

Each of the elementary reactions that make up the above enzymatic reaction is characterized by a rate constant: $\boldsymbol{k_1}$ and $\boldsymbol{k_{-1}}$ are the forward and reverse rate constants for formation of the ES complex (the first reaction), and $\boldsymbol{k_2}$ is the rate constant for the decomposition of ES to P (the second reaction). Here we assume, for the sake of mathematical simplicity, that the second reaction is irreversible; that is, no P is converted back to S.

The Michaelis–Menten Equation Assumes that ES Maintains a Steady State. The Michaelis–Menten equation describes the rate of the enzymatic reaction represented by Eq. 12-12 as a function of substrate concentration. In this kinetic scheme, the formation of product from ES is a first-order process. Thus, the rate of formation of product can be expressed as the product of the rate constant of the reaction yielding product and the concentration of its immediately preceding intermediate. The general expression for the velocity (rate) of Reaction 12-12 is therefore

$$v = \frac{d[\mathrm{P}]}{dt} = k_2[\mathrm{ES}] \tag{12-13}$$

The overall rate of production of ES is the difference between the rates of the elementary reactions leading to its appearance and those resulting in its disappearance:

$$\frac{d[\mathrm{ES}]}{dt} = k_1[\mathrm{E}][\mathrm{S}] - k_{-1}[\mathrm{ES}] - k_2[\mathrm{ES}] \tag{12-14}$$

This equation cannot be explicitly integrated, however, without simplifying assumptions. Two possibilities are

1. ***Assumption of equilibrium.*** In 1913, Leonor Michaelis and Maud Menten, building on the work of Victor Henri, assumed that $k_{-1} \gg k_2$, so that the first step of the reaction reaches equilibrium:

$$K_S = \frac{k_{-1}}{k_1} = \frac{[\mathrm{E}][\mathrm{S}]}{[\mathrm{ES}]} \tag{12-15}$$

Here K_S is the dissociation constant of the first step in the enzymatic reaction. With this assumption, Eq. 12-14 can be integrated. Although this assumption is often not correct, in recognition of the importance of this pioneering work, the enzyme–substrate complex, ES, is known as the **Michaelis complex.**

2. ***Assumption of steady state.*** Figure 12-2 illustrates the progress curves of the various participants in Reaction 12-12 under the physiologically common condition that substrate is in great excess over enzyme ([S] ≫ [E]). With the exception of the initial stage of the reaction, which is usually over within milliseconds of mixing E and S, [ES] remains approximately constant until the substrate is nearly exhausted. Hence, the rate of synthesis of ES must equal its rate of consumption over most of the course of the reaction. In other words, ES maintains a **steady state** and [ES] can be treated as having a constant value:

$$\frac{d[\mathrm{ES}]}{dt} = 0 \tag{12-16}$$

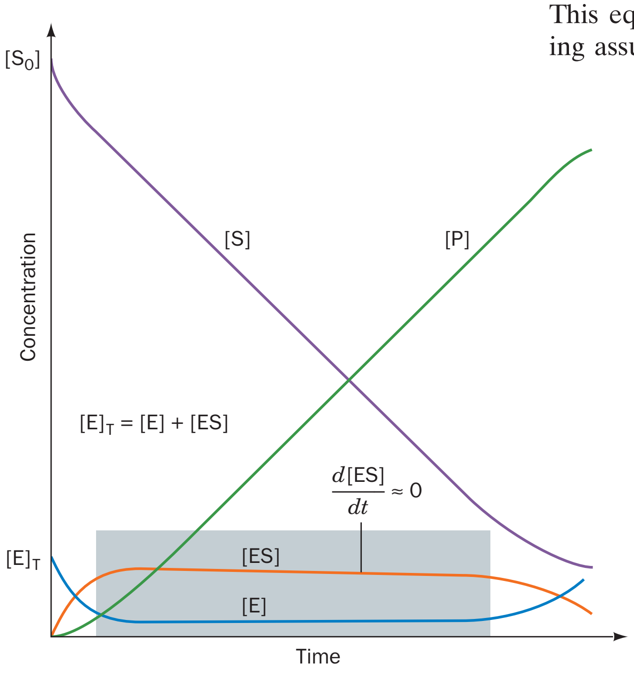

■ **Figure 12-2 | The progress curves for a simple enzyme-catalyzed reaction.** With the exception of the initial phase of the reaction (before the shaded block), the slopes of the progress curves for [E] and [ES] are essentially zero as long as [S] ≫ [E] (within the shaded block). [After Segel, I.H., *Enzyme Kinetics,* p. 27, Wiley (1993).] **See the Animated Figures.**

BOX 12-2 **PATHWAYS OF DISCOVERY**

J.B.S. Haldane and Enzyme Action

J.B.S. Haldane (1892–1964)

John Burdon Sanderson Haldane, the son of a prominent physiologist, was a gifted scientist and writer whose major contributions include the application of mathematics to areas of biology such as genetics and enzyme kinetics. As a scientist as well as a philosopher, he was aware of developments in relativity theory and quantum mechanics and was influenced by a practical philosophy that the natural world obeyed the laws of logic and arithmetic.

When Haldane published his book *Enzymes* in 1930, the idea that enzymes are proteins, rather than small catalysts surrounded by an amorphous protein "colloid," was still controversial. However, even in the absence of structural information, scientists such as Leonor Michaelis and Maud Menten had already applied the principles of thermodynamics to derive some basic equations related to enzyme kinetics. Michaelis and Menten proposed in 1913 that during a reaction, an enzyme and its substrate are in equilibrium with a complex of enzyme and substrate. In 1925, Haldane argued that this was not strictly true, since some enzyme–substrate complex does not dissociate to free enzyme and substrate but instead goes on to form product. When the enzyme and substrate are first mixed together, the concentration of the enzyme–substrate complex increases, but after a time the concentration of the complex levels off because the complex is constantly forming and breaking down to generate product. This principle, the so-called steady state assumption, underlies modern theories of enzyme activity.

Even without knowing what enzymes were made of, Haldane showed great insight in proposing that an enzyme could catalyze a reaction by bringing its substrates into a strained or out-of-equilibrium arrangement. This idea refined Emil Fischer's earlier lock-and-key simile (and was later elaborated further by Linus Pauling). Haldane's idea of strain was not fully appreciated until around 1970, after the X-ray structures of several enzymes, including lysozyme and chymotrypsin (Chapter 11), had been examined.

In addition to his work in enzymology, Haldane articulated the role of genes in heredity and formulated mathematical estimates of mutation rates—many years before the nature of genes or the structure of DNA were known. However, in addition to being a theorist, Haldane was an experimentalist who frequently performed unpleasant or dangerous experiments on himself. For example, he ingested sodium bicarbonate and ammonium chloride in order to investigate their effect on breathing rate. Beyond the laboratory, Haldane was well-known for his efforts to popularize science. In *Daedalus, or, Science and the Future,* Haldane commented on the status of various branches of science circa 1924 and speculated about future developments. His thoughts and his persona are believed to have inspired various plots and characters in other writers' works of science fiction.

Briggs, G.E. and Haldane, J.B.S., A note on the kinetics of enzyme action, *Biochem. J.* **19,** 339 (1925).

This so-called **steady state assumption,** a more general condition than that of equilibrium, was first proposed in 1925 by George E. Briggs and John B.S. Haldane (Box 12-2).

In order to be useful, kinetic expressions for overall reactions must be formulated in terms of experimentally measurable quantities. The quantities [ES] and [E] are not, in general, directly measurable, but the total enzyme concentration

$$[\mathrm{E}]_\mathrm{T} = [\mathrm{E}] + [\mathrm{ES}] \qquad [12\text{-}17]$$

is usually readily determined. The rate equation for the overall enzymatic reaction as a function of [S] and [E] can then be derived. First, Eq. 12-14 is combined with the steady state assumption (Eq. 12-16) to give

$$k_1[\mathrm{E}][\mathrm{S}] = k_{-1}[\mathrm{ES}] + k_2[\mathrm{ES}] \qquad [12\text{-}18]$$

Letting $[\mathrm{E}] = [\mathrm{E}]_\mathrm{T} - [\mathrm{ES}]$ and rearranging yields

$$\frac{([\mathrm{E}]_\mathrm{T} - [\mathrm{ES}])[\mathrm{S}]}{[\mathrm{ES}]} = \frac{k_{-1} + k_2}{k_1} \qquad [12\text{-}19]$$

The **Michaelis constant, K_M,** is defined as

$$K_M = \frac{k_{-1} + k_2}{k_1} \qquad [12\text{-}20]$$

so Eq. 12-19 can then be rearranged to give

$$K_M[\mathrm{ES}] = ([\mathrm{E}]_\mathrm{T} - [\mathrm{ES}])[\mathrm{S}] \qquad [12\text{-}21]$$

Solving for [ES],

$$[\mathrm{ES}] = \frac{[\mathrm{E}]_\mathrm{T}[\mathrm{S}]}{K_M + [\mathrm{S}]} \qquad [12\text{-}22]$$

The expression for the **initial velocity (v_o)** of the reaction, the velocity (Eq. 12-13) at $t = 0$, thereby becomes

$$v_o = \left(\frac{d[\mathrm{P}]}{dt}\right)_{t=0} = k_2[\mathrm{ES}] = \frac{k_2[\mathrm{E}]_\mathrm{T}[\mathrm{S}]}{K_M + [\mathrm{S}]} \qquad [12\text{-}23]$$

Both $[\mathrm{E}]_\mathrm{T}$ and [S] are experimentally measurable quantities. In order to meet the conditions of the steady state assumption, the concentration of the substrate must be much greater than the concentration of the enzyme, which allows each enzyme molecule to repeatedly bind a molecule of substrate and convert it to product, so that [ES] is constant. The use of the initial velocity (operationally taken as the velocity measured before more than ~10% of the substrate has been converted to product)—rather than just the velocity—minimizes such complicating factors as the effects of reversible reactions, inhibition of the enzyme by its product(s), and progressive inactivation of the enzyme. (This is also why the rate of the reverse reaction in Eq. 12-12 can be assumed to be zero.)

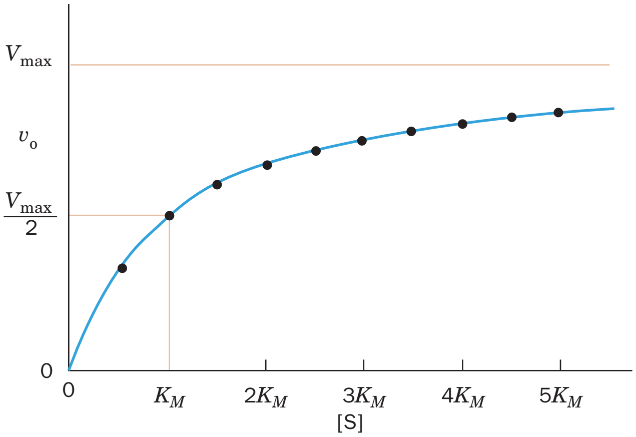

Figure 12-3 | A plot of the initial velocity v_o of a simple enzymatic reaction versus the substrate concentration [S]. Points are plotted in $0.5K_M$ intervals of substrate concentration between $0.5K_M$ and $5K_M$. **See the Animated Figures.**

The **maximal velocity** of a reaction, V_{max}, occurs at high substrate concentrations when the enzyme is **saturated,** that is, when it is entirely in the ES form:

$$V_{max} = k_2[\mathrm{E}]_\mathrm{T} \qquad [12\text{-}24]$$

Therefore, combining Eqs. 12-23 and 12-24, we obtain

$$\boxed{v_o = \frac{V_{max}[\mathrm{S}]}{K_M + [\mathrm{S}]}} \qquad [12\text{-}25]$$

This expression, the **Michaelis–Menten equation,** *is the basic equation of enzyme kinetics.* It describes a rectangular hyperbola such as that plotted in Fig. 12-3. The saturation function for oxygen binding to myoglobin (Eq. 7-6) has the same algebraic form.

The Michaelis Constant Has a Simple Operational Definition. At the substrate concentration at which $[\mathrm{S}] = K_M$, Eq. 12-25 yields $v_o = V_{max}/2$ so that K_M *is the substrate concentration at which the reaction velocity is half-maximal.* Therefore, if an enzyme has a small value of K_M, it achieves maximal catalytic efficiency at low substrate concentrations.

The K_M is unique for each enzyme–substrate pair: Different substrates that react with a given enzyme do so with different K_M values. Likewise, different enzymes that act on the same substrate have different K_M values. The magnitude of K_M varies widely with the identity of the enzyme and the nature of the substrate (Table 12-1). It is also a function of temperature and pH. The Michaelis constant (Eq. 12-20) can be expressed as

$$K_M = \frac{k_{-1}}{k_1} + \frac{k_2}{k_1} = K_\mathrm{S} + \frac{k_2}{k_1} \qquad [12\text{-}26]$$

Since K_S is the dissociation constant of the Michaelis complex (Eq. 12-15),

Table 12-1 The Values of K_M, k_{cat}, and k_{cat}/K_M for Some Enzymes and Substrates

Enzyme	Substrate	K_M (M)	k_{cat} (s^{-1})	k_{cat}/K_M ($\text{M}^{-1} \cdot \text{s}^{-1}$)
Acetylcholinesterase	Acetylcholine	9.5×10^{-5}	1.4×10^{4}	1.5×10^{8}
Carbonic anhydrase	CO_2	1.2×10^{-2}	1.0×10^{6}	8.3×10^{7}
	HCO_3^-	2.6×10^{-2}	4.0×10^{5}	1.5×10^{7}
Catalase	H_2O_2	2.5×10^{-2}	1.0×10^{7}	4.0×10^{8}
Chymotrypsin	*N*-Acetylglycine ethyl ester	4.4×10^{-1}	5.1×10^{-2}	1.2×10^{-1}
	N-Acetylvaline ethyl ester	8.8×10^{-2}	1.7×10^{-1}	1.9
	N-Acetyltyrosine ethyl ester	6.6×10^{-4}	1.9×10^{2}	2.9×10^{5}
Fumarase	Fumarate	5.0×10^{-6}	8.0×10^{2}	1.6×10^{8}
	Malate	2.5×10^{-5}	9.0×10^{2}	3.6×10^{7}
Urease	Urea	2.5×10^{-2}	1.0×10^{4}	4.0×10^{5}

as K_S decreases, the enzyme's affinity for substrate increases. K_M is therefore also a measure of the affinity of the enzyme for its substrate, provided k_2/k_1 is small compared to K_S, that is, $k_2 < k_{-1}$ so that the ES → P reaction proceeds more slowly than ES reverts to E + S.

k_{cat}/K_M Is a Measure of Catalytic Efficiency. We can define the **catalytic constant, k_{cat},** of an enzyme as

$$k_{\text{cat}} = \frac{V_{\max}}{[\text{E}]_T} \qquad [12\text{-}27]$$

This quantity is also known as the **turnover number** of an enzyme because it is the number of reaction processes (turnovers) that each active site catalyzes per unit time. The turnover numbers for a selection of enzymes are given in Table 12-l. Note that these quantities vary by over eight orders of magnitude. Equation 12-24 indicates that for a simple system, such as the Michaelis–Menten model reaction (Eq. 12-12), $k_{\text{cat}} = k_2$. For enzymes with more complicated mechanisms (e.g., multiple substrates or multiple reaction intermediates), k_{cat} may be a function of several rate constants. Note that whereas k_{cat} is a constant, $V_{\max}$ depends on the concentration of the enzyme present in the experimental system. $V_{\max}$ increases as $[\text{E}]_T$ increases.

When $[\text{S}] \ll K_M$, very little ES is formed. Consequently, $[\text{E}] \approx [\text{E}]_T$, so Eq. 12-23 reduces to a second-order rate equation:

$$v_o \approx \left(\frac{k_2}{K_M}\right)[\text{E}]_T[\text{S}] \approx \left(\frac{k_{\text{cat}}}{K_M}\right)[\text{E}][\text{S}] \qquad [12\text{-}28]$$

Here, **k_{cat}/K_M** is the apparent second-order rate constant of the enzymatic reaction; the rate of the reaction varies directly with how often enzyme and substrate encounter one another in solution. *The quantity k_{cat}/K_M is therefore a measure of an enzyme's catalytic efficiency.*

There is an upper limit to the value of k_{cat}/K_M: It can be no greater than k_1; that is, the decomposition of ES to E + P can occur no more frequently than E and S come together to form ES. The most efficient enzymes have k_{cat}/K_M values near the **diffusion-controlled limit** of 10^8 to 10^9 $\text{M}^{-1} \cdot \text{s}^{-1}$. These enzymes catalyze a reaction almost every time they encounter a substrate molecule and hence have achieved a state of virtual catalytic

BOX 12-3 **PERSPECTIVES IN BIOCHEMISTRY**

Kinetics and Transition State Theory

How is the rate of a reaction related to its activation energy (Section 11-2)? Consider a bimolecular reaction that proceeds along the following pathway:

$$\mathrm{A} + \mathrm{B} \overset{K^{\ddagger}}{\rightleftharpoons} \mathrm{X}^{\ddagger} \xrightarrow{k'} \mathrm{P} + \mathrm{Q}$$

where $\mathrm{X}^{\ddagger}$ represents the transition state. The rate of the reaction can be expressed as

$$\frac{d[\mathrm{P}]}{dt} = k[\mathrm{A}][\mathrm{B}] = k'[\mathrm{X}^{\ddagger}] \qquad \text{[12-A]}$$

where k is the ordinary rate constant of the elementary reaction and k' is the rate constant for the decomposition of $\mathrm{X}^{\ddagger}$ to products.

Although $\mathrm{X}^{\ddagger}$ is unstable, it is assumed to be in rapid equilibrium with the reactants; that is,

$$K^{\ddagger} = \frac{[\mathrm{X}^{\ddagger}]}{[\mathrm{A}][\mathrm{B}]} \qquad \text{[12-B]}$$

where $K^{\ddagger}$ is an equilibrium constant. This central assumption of transition state theory permits the powerful formalism of thermodynamics to be applied to the theory of reaction rates.

Since $K^{\ddagger}$ is an equilibrium constant, it can be expressed as

$$-RT \ln K^{\ddagger} = \Delta G^{\ddagger} \qquad \text{[12-C]}$$

where T is the absolute temperature and R ($8.3145\ \mathrm{J \cdot K^{-1} \cdot mol^{-1}}$) is the gas constant (this relationship between equilibrium constants and free energy is derived in Section 1-3D). Combining the three preceding equations yields

$$\frac{d[\mathrm{P}]}{dt} = k' e^{-\Delta G^{\ddagger}/RT}[\mathrm{A}][\mathrm{B}] \qquad \text{[12-D]}$$

This equation indicates that the rate of a reaction not only depends on the concentrations of its reactants, but also decreases exponentially with $\Delta G^{\ddagger}$. Thus, *the larger the difference between the free energy of the transition state and that of the reactants (the free energy of activation), that is, the less stable the transition state, the slower the reaction proceeds.*

We must now evaluate k', the rate at which $\mathrm{X}^{\ddagger}$ decomposes. The transition state structure is held together by a bond that is assumed to be so weak that it flies apart during its first vibrational excursion. Therefore, k' is expressed

$$k' = \kappa\nu \qquad \text{[12-E]}$$

where ν is the vibrational frequency of the bond that breaks as $\mathrm{X}^{\ddagger}$ decomposes to products, and κ, the **transmission coefficient,** is the probability that the breakdown of $\mathrm{X}^{\ddagger}$ will be in the direction of product formation rather than back to reactants. For most spontaneous reactions, κ is assumed to be 1.0 (although this number, which must be between 0 and 1, can rarely be calculated with confidence).

Planck's law states that

$$\nu = \varepsilon/h \qquad \text{[12-F]}$$

where, in this case, ε is the average energy of the vibration that leads to the decomposition of $\mathrm{X}^{\ddagger}$, and h ($6.6261 \times 10^{-34}\ \mathrm{J \cdot s}$) is **Planck's constant.** Statistical mechanics tells us that at a temperature T, the classical energy of an oscillator is

$$\varepsilon = k_{\mathrm{B}}T \qquad \text{[12-G]}$$

where k_{B} ($1.3807 \times 10^{-23}\ \mathrm{J \cdot K^{-1}}$) is the **Boltzmann constant** and $k_{\mathrm{B}}T$ is essentially the available thermal energy. Combining Eqs. 12-E through 12-G gives

$$k' = \frac{k_{\mathrm{B}}T}{h} \qquad \text{[12-H]}$$

Thus, combining Eqs. 12-A, 12-D, and 12-H yields the expression for the rate constant of the elementary reaction:

$$k = \frac{k_{\mathrm{B}}T}{h} e^{-\Delta G^{\ddagger}/RT} \qquad \text{[12-I]}$$

This equation indicates that as the temperature rises, so that there is increased thermal energy available to drive the reacting complex over the activation barrier ($\Delta G^{\ddagger}$), the reaction speeds up.

perfection. The relationship between the catalytic rate and the thermodynamics of the transition state can now be appreciated (Box 12-3).

C | Kinetic Data Can Provide Values of $V_{\max}$ and K_M

There are several methods for determining the values of the parameters of the Michaelis–Menten equation (i.e., $V_{\max}$ and K_M). At very high values of [S], the initial velocity, v_{o}, asymptotically approaches $V_{\max}$ (see Sample Calculation 12-3). In practice, however, it is very difficult to assess $V_{\max}$ accurately from direct plots of v_{o} versus [S] such as Fig. 12-3, because, even at substrate concentrations as high as $[\mathrm{S}] = 10\ K_M$, Eq. 12-25

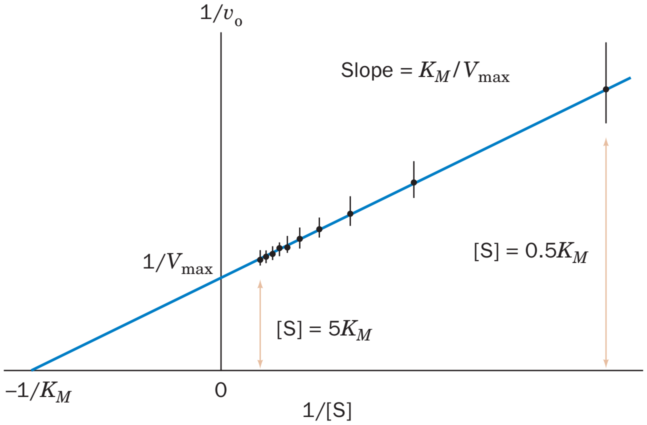

Figure 12-4 | A double-reciprocal (Lineweaver–Burk) plot. The error bars represent $\pm 0.05V_{max}$. The indicated points are the same as those in Fig. 12-3. Note the large effect of small errors at small [S] (large 1/[S]) and the crowding together of points at large [S]. **See the Animated Figures.**

indicates that v_o is only 91% of V_{max}, so that the value of V_{max} will almost certainly be underestimated.

A better method for determining the values of V_{max} and K_M, which was formulated by Hans Lineweaver and Dean Burk, uses the reciprocal of the Michaelis–Menten equation (Eq. 12-25):

$$\boxed{\frac{1}{v_o} = \left(\frac{K_M}{V_{max}}\right)\frac{1}{[S]} + \frac{1}{V_{max}}} \qquad [12\text{-}29]$$

This is a linear equation in $1/v_o$ and 1/[S]. If these quantities are plotted to obtain the so-called **Lineweaver–Burk** or **double-reciprocal plot,** the slope of the line is K_M/V_{max}, the $1/v_o$ intercept is $1/V_{max}$, and the extrapolated 1/[S] intercept is $-1/K_M$ (Fig. 12-4 and Sample Calculation 12-4).

SAMPLE CALCULATION 12-3

An enzyme-catalyzed reaction has a K_M of 1 mM and a V_{max} of 5 nM · s^{-1}. What is the reaction velocity when the substrate concentration is (a) 0.25 mM, (b) 1.5 mM, or (c) 10 mM?

Use the Michaelis–Menten equation (Eq. 12-25):

$$\text{(a)}\ v_o = \frac{(5\ \text{nM}\cdot\text{s}^{-1})(0.25\ \text{mM})}{(1\ \text{mM}) + (0.25\ \text{mM})} = \frac{1.25}{1.25}\ \text{nM}\cdot\text{s}^{-1} = 1\ \text{nM}\cdot\text{s}^{-1}$$

$$\text{(b)}\ v_o = \frac{(5\ \text{nM}\cdot\text{s}^{-1})(1.5\ \text{mM})}{(1\ \text{mM}) + (1.5\ \text{mM})} = \frac{7.5}{2.5}\ \text{nM}\cdot\text{s}^{-1} = 3\ \text{nM}\cdot\text{s}^{-1}$$

$$\text{(c)}\ v_o = \frac{(5\ \text{nM}\cdot\text{s}^{-1})(10\ \text{mM})}{(1\ \text{mM}) + (10\ \text{mM})} = \frac{50}{11}\ \text{nM}\cdot\text{s}^{-1} = 4.5\ \text{nM}\cdot\text{s}^{-1}$$

Note: When units in the numerator and denominator cancel it is unnecessary to convert them to standard units before performing the calculation.

SAMPLE CALCULATION 12-4

Determine K_M and V_{max} for an enzyme from the following data using Eq. 12-29:

[S] (mM)	v_o (μM · s^{-1})
1	2.5
2	4.0
5	6.3
10	7.6
20	9.0

First, convert the data to reciprocal form (1/[S] in units of mM^{-1}, and $1/v_o$ in units of μM^{-1} · s). Next, make a plot of $1/v_o$ versus 1/[S]. The *x*- and *y*-intercepts can be estimated by extrapolation of the straight line or can be calculated by linear regression. According to Eq. 12-29 and Fig. 12-4, the *y*-intercept, which has a value of ~0.1 μM^{-1} · s, is equivalent to $1/V_{max}$, so V_{max} (the reciprocal of the *y*-intercept) is 10 μM · s^{-1}. The *x*-intercept, −0.33 mM^{-1}, is equivalent to $-1/K_M$, so K_M (the negative reciprocal of the *x*-intercept) is equal to 3.0 mM.

As can be seen in Fig. 12-3, the best estimates of kinetic parameters are obtained by collecting data over a range of [S] from ~0.5 K_M to ~5 K_M. Thus, a disadvantage of the Lineweaver–Burk plots is that most experimental measurements of [S] are crowded onto the left side of the graph (Fig. 12-4). Moreover, for small values of [S], small errors in v_o lead to large errors in $1/v_o$ and hence to large errors in K_M and V_{max}.

Several other types of plots, each with its advantages and disadvantages, can also be used to determine K_M and V_{max} from kinetic data. However, kinetic data are now commonly analyzed by computer using mathematically sophisticated statistical treatments. Nevertheless, Lineweaver–Burk plots are valuable for the visual presentation of kinetic data.

Steady State Kinetics Cannot Unambiguously Establish a Reaction Mechanism. Although steady state kinetics provides valuable information about the rates of buildup and breakdown of ES, it provides little insight as to the nature of ES. Thus, an enzymatic reaction may, in reality, pass through several more or less stable intermediate states such as

$$\mathrm{E + S \rightleftharpoons ES \rightleftharpoons EX \rightleftharpoons EP \rightleftharpoons E + P}$$

or take a more complex path such as

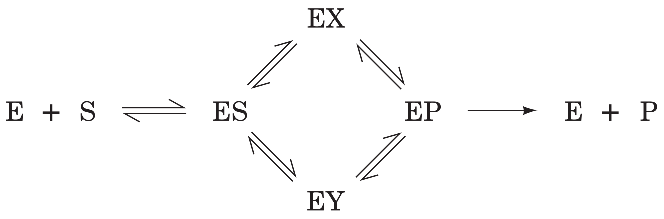

Unfortunately, steady state kinetic measurements are incapable of revealing the number of intermediates in an enzyme-catalyzed reaction. Thus, such measurements of a multistep reaction can be likened to a "black box" containing a system of water pipes with one inlet and one drain:

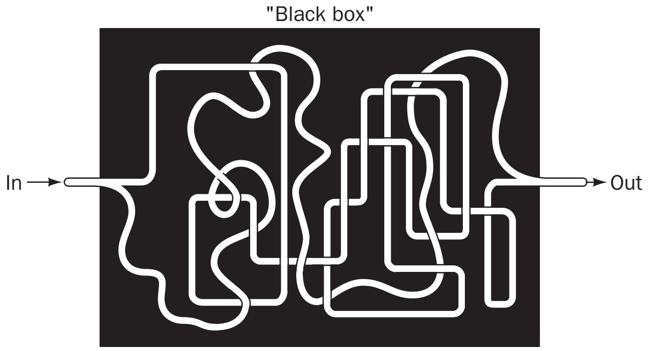

At steady state, that is, after the pipes have filled with water, the relationship between input pressure and output flow can be measured. However, such measurements yield no information concerning the detailed construction of the plumbing connecting the inlet to the drain. This would require additional information, such as opening the box and tracing the pipes. Likewise, steady state kinetic measurements can provide a phenomenological description of enzymatic behavior, but the nature of the intermediates remains indeterminate. The existence of intermediates must be verified independently, for example, by identifying them through the use of spectroscopic techniques.

The foregoing highlights a central principle of enzymology: *The steady state kinetic analysis of a reaction cannot unambiguously establish its mechanism.* This is because no matter how simple, elegant, or rational a postulated mechanism, there are an infinite number of alternative mechanisms that can also account for the kinetic data. Usually, it is the simpler mechanism that turns out to be correct, but this is not always the case. However, *if kinetic data are not compatible with a given mechanism, then that mechanism must be rejected.* Therefore, although kinetics cannot be used to establish a mechanism unambiguously without confirming data, such as the physical demonstration of an intermediate's existence, the steady state kinetic analysis of a reaction is of great value because it can be used to eliminate proposed mechanisms.

D | Bisubstrate Reactions Follow One of Several Rate Equations

We have heretofore been concerned with simple, single-substrate reactions that obey the Michaelis–Menten model (Reaction 12-12). Yet, enzymatic reactions requiring multiple substrates and yielding multiple products are far more common. Indeed, those involving two substrates and yielding two products

$$A + B \overset{E}{\rightleftharpoons} P + Q$$

account for ~60% of known biochemical reactions. Almost all of these so-called **bisubstrate reactions** are either transfer reactions in which the enzyme catalyzes the transfer of a specific functional group, X, from one of the substrates to the other:

$$P{-}X + B \overset{E}{\rightleftharpoons} P + B{-}X$$

or oxidation–reduction reactions in which reducing equivalents are transferred between the two substrates. For example, the hydrolysis of a peptide bond by trypsin (Section 11-5) is the transfer of the peptide carbonyl group from the peptide nitrogen atom to water (Fig. 12-5*a*), whereas in the alcohol dehydrogenase reaction (Section 11-1B), a hydride ion is formally transferred from ethanol to NAD$^+$ (Fig. 12-5*b*). Although bisubstrate reactions could, in principle, occur through a vast variety of mechanisms, only a few types are commonly observed.

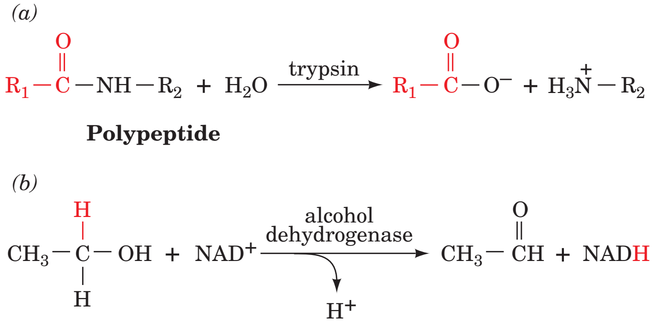

Figure 12-5 | Some bisubstrate reactions. (*a*) In the peptide hydrolysis reaction catalyzed by trypsin, the peptide carbonyl group, with its pendent polypeptide chain, R_1, is transferred from the peptide nitrogen atom to a water molecule. (*b*) In the alcohol dehydrogenase reaction, a hydride ion is formally transferred from ethanol to NAD$^+$.

Sequential Reactions Occur via Single Displacements. *Reactions in which all substrates must combine with the enzyme before a reaction can occur and products be released are known as* ***sequential reactions.*** In such reactions, the group being transferred, X, is directly passed from A (=P—X) to B, yielding P and Q (=B—X). Hence, such reactions are also called **single-displacement reactions.**

Sequential reactions can be subclassified into those with a compulsory order of substrate addition to the enzyme, which are said to have an **Ordered mechanism,** and those with no preference for the order of substrate addition, which are described as having a **Random mechanism.** In the Ordered mechanism, the binding of the first substrate is apparently required for the enzyme to form the binding site for the second substrate, whereas in the Random mechanism, both binding sites are present on the free enzyme.

In a notation developed by W.W. Cleland, substrates are designated by the letters A and B in the order that they add to the enzyme, products are designated by P and Q in the order that they leave the enzyme, the enzyme is represented by a horizontal line, and successive additions of substrates and releases of products are denoted by vertical arrows. An

Ordered bisubstrate reaction is thereby diagrammed:

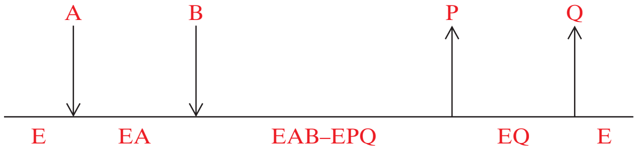

where A and B are said to be the **leading** and **following** substrates, respectively. Many NAD^+- and $NADP^+$-requiring dehydrogenases follow an Ordered bisubstrate mechanism in which the coenzyme is the leading substrate.

A Random bisubstrate reaction is diagrammed:

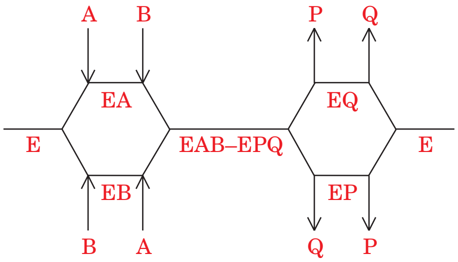

Some dehydrogenases and **kinases** operate through Random bisubstrate mechanisms (kinases are enzymes that transfer phosphoryl groups from ATP to other compounds or vice versa).

Ping Pong Reactions Occur via Double Displacements. *Group-transfer reactions in which one or more products are released before all substrates have been added are known as* ***Ping Pong reactions.*** The Ping Pong bisubstrate reaction is represented by

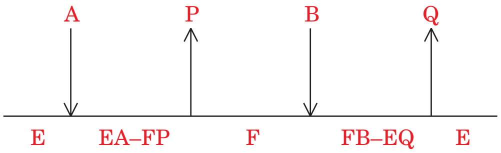

Here, a functional group X of the first substrate A (= P—X) is displaced from the substrate by the enzyme E to yield the first product P and a stable enzyme form F (= E—X) in which X is tightly (often covalently) bound to the enzyme (Ping). In the second stage of the reaction, X is displaced from the enzyme by the second substrate B to yield the second product Q (= B—X), thereby regenerating the original form of the enzyme, E (Pong). Such reactions are therefore also known as **double-displacement reactions.** *Note that in Ping Pong reactions, the substrates A and B do not encounter one another on the surface of the enzyme.* Many enzymes, including trypsin (in which F is the acyl–enzyme intermediate; Section 11-5), transaminases, and some flavoenzymes, react with Ping Pong mechanisms.

Bisubstrate Mechanisms Can Be Distinguished by Kinetic Measurements. The rate equations that describe the foregoing bisubstrate mechanisms are considerably more complicated than the equation for a single-substrate reaction. In fact, the equations for bisubstrate mechanisms (which are beyond the scope of this text) contain as many as four kinetic constants versus two (V_{max} and K_M) for the Michaelis–Menten equation. Nevertheless, steady state kinetic measurements can be used to distinguish among the various bisubstrate mechanisms.

■ CHECK YOUR UNDERSTANDING

Write the rate equations for a first-order and a second-order reaction.
What are the differences between instantaneous velocity, initial velocity, and maximal velocity for an enzymatic reaction?
Derive the Michaelis–Menten equation.
What do the values of K_M and k_{cat}/K_M reveal about an enzyme?
Write the Lineweaver–Burk (double-reciprocal) equation and describe the features of a Lineweaver–Burk plot.
Use Cleland notation to describe Ordered and Random sequential reactions and a Ping Pong reaction.

2 Enzyme Inhibition

LEARNING OBJECTIVE

- Understand that competitive, uncompetitive, and mixed enzyme inhibitors interact with the enzyme and/or the enzyme–substrate complex to alter its K_M and/or $V_{\max}$ values.

Many substances alter the activity of an enzyme by combining with it in a way that influences the binding of substrate and/or its turnover number. *Substances that reduce an enzyme's activity in this way are known as* ***inhibitors.*** A large part of the modern pharmaceutical arsenal consists of enzyme inhibitors. For example, AIDS is treated almost exclusively with drugs that inhibit the activities of certain viral enzymes.

Inhibitors act through a variety of mechanisms. Irreversible enzyme inhibitors, or **inactivators,** bind to the enzyme so tightly that they permanently block the enzyme's activity. Reagents that chemically modify specific amino acid residues can act as inactivators. For example, the compounds used to identify the catalytic Ser and His residues of serine proteases (Section 11-5A) are inactivators of these enzymes.

Reversible enzyme inhibitors diminish an enzyme's activity by interacting reversibly with it. Some enzyme inhibitors are substances that structurally resemble their enzyme's substrates but either do not react or react very slowly. These substances are commonly used to probe the chemical and conformational nature of an enzyme's active site in an effort to elucidate the enzyme's catalytic mechanism. Other inhibitors affect catalytic activity without interfering with substrate binding. Many do both. In this section, we discuss several of the simplest mechanisms for reversible inhibition and their effects on the kinetic behavior of enzymes that follow the Michaelis–Menten model. As in the preceding discussion, we will base our analysis on a simple one-substrate reaction model.

A | Competitive Inhibition Involves Inhibitor Binding at an Enzyme's Substrate Binding Site

A substance that competes directly with a normal substrate for an enzyme's substrate-binding site is known as a **competitive inhibitor.** Such an inhibitor usually resembles the substrate so that it specifically binds to the active site but differs from the substrate so that it cannot react as the substrate does. For example, **succinate dehydrogenase,** a citric acid cycle enzyme that converts **succinate** to **fumarate** (Section 17-3F), is competitively inhibited by **malonate,** which structurally resembles succinate but cannot be dehydrogenated:

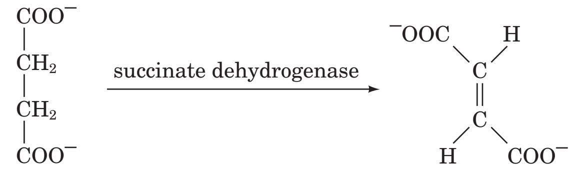

Succinate **Fumarate**

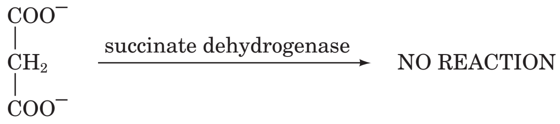

Malonate

The effectiveness of malonate as a competitive inhibitor of succinate dehydrogenase strongly suggests that the enzyme's substrate-binding site is designed to bind both of the substrate's carboxylate groups, presumably through the influence of appropriately placed positively charged residues.

Similar principles are responsible for **product inhibition.** In this phenomenon, a product of the reaction, which necessarily is able to bind to the enzyme's active site, may accumulate and compete with substrate for binding to the enzyme in subsequent catalytic cycles. Product inhibition is one way in which the cell controls the activities of its enzymes (Section 12-3).

Transition state analogs are particularly effective inhibitors. This is because effective catalysis depends on the enzyme's ability to bind to and stabilize the reaction's transition state (Section 11-3E). A compound that mimics the transition state exploits these binding interactions in ways that a substrate analog cannot. For example, **adenosine deaminase** converts the nucleoside adenosine to inosine as follows:

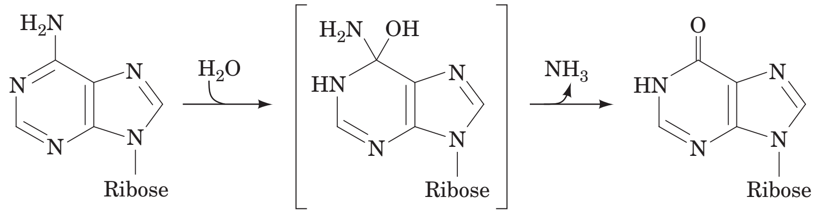

Adenosine **Inosine**

The K_M of the enzyme for the substrate adenosine is 3×10^{-5} M. The product inosine acts as an inhibitor of the reaction, with an **inhibition constant** (**K_I,** the dissociation constant for enzyme–inhibitor binding; see below) of 3×10^{-4} M. However, a transition state analog,

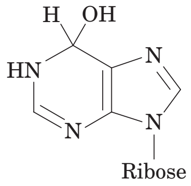

1,6-Dihydroinosine

inhibits the reaction with a K_I of 1.5×10^{-13} M.

The Degree of Competitive Inhibition Varies with the Fraction of Enzyme That Has Bound Inhibitor. The general model for competitive inhibition is given by the following reaction scheme:

$$\begin{tikzcd}
E + S \arrow[r, shift left, "k_1"] & ES \arrow[l, shift left, "k_{-1}"] \arrow[r, "k_2"] & P + E \\
+ & & \\
I \arrow[d, shift left] & & \\
EI + S \arrow[u, shift left, "K_I"] \arrow[r] & \text{NO REACTION} &
\end{tikzcd}$$

Here, I is the inhibitor, EI is the catalytically inactive enzyme–inhibitor complex, and it is assumed that the inhibitor binds reversibly to the enzyme and is in rapid equilibrium with it so that

$$K_I = \frac{[E][I]}{[EI]} \tag{12-30}$$

A competitive inhibitor therefore reduces the concentration of free enzyme available for substrate binding.

The Michaelis–Menten equation for a competitively inhibited reaction is derived as before (Section 12-1B), but with an additional term to account for the fraction of $[E]_T$ that binds to I to form EI ($[E]_T = [E] + [ES] + [EI]$). The resulting equation,

$$v_o = \frac{V_{max}[S]}{\alpha K_M + [S]} \qquad [12\text{-}31]$$

is the Michaelis–Menten equation that has been modified by a factor, α, which is defined as

$$\alpha = 1 + \frac{[I]}{K_I} \qquad [12\text{-}32]$$

Note that α, a function of the inhibitor's concentration and its affinity for the enzyme, cannot be less than 1. Comparison of Eqs. 12-25 and 12-31 indicates that $K_M^{app} = \alpha K_M$, where $\boldsymbol{K_M^{app}}$ is the apparent K_M, that is, the K_M value that would be measured in the absence of the knowledge that inhibitor is present. Figure 12-6 shows the hyperbolic plots of Eq. 12-31 for increasing values of α. The presence of I makes [S] appear to be less than it really is (makes K_M appear to be larger than it really is), a consequence of the binding of I and S to E being mutually exclusive. However, increasing [S] can overwhelm a competitive inhibitor. In fact, α *is the factor by which [S] must be increased in order to overcome the effect of the presence of inhibitor.* As [S] approaches infinity, v_o approaches V_{max} for any value of α (that is, for any concentration of inhibitor). Thus, the inhibitor does not affect the enzyme's turnover number.

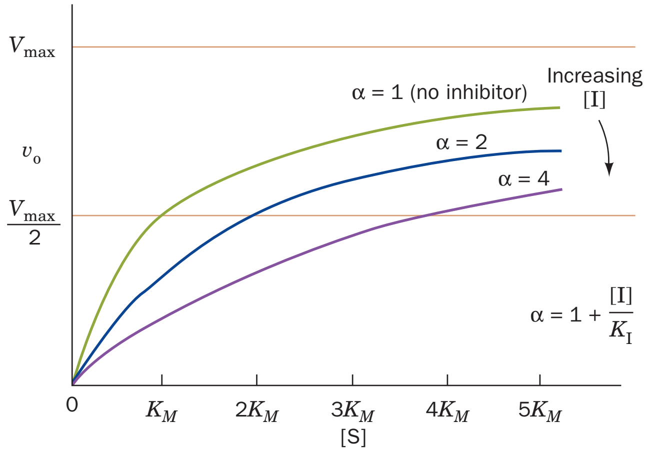

Figure 12-6 | A plot of v_o versus [S] for a Michaelis–Menten reaction in the presence of different concentrations of a competitive inhibitor.

Competitive inhibition is the principle behind the use of ethanol to treat methanol poisoning. Methanol itself is only mildly toxic. However, the liver enzyme alcohol dehydrogenase converts methanol to the highly toxic formaldehyde, only small amounts of which cause blindness and death. Ethanol competes with methanol for binding to the active site of liver alcohol dehydrogenase, thereby slowing the production of formaldehyde from methanol (the ethanol is converted to the readily metabolized acetaldehyde):

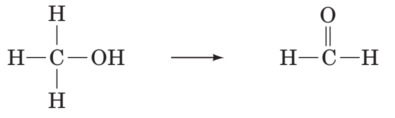

$$\mathrm{H{-}\overset{H}{\underset{H}{C}}{-}OH} \longrightarrow \mathrm{H{-}\overset{O}{\overset{\|}{C}}{-}H}$$

Methanol **Formaldehyde**

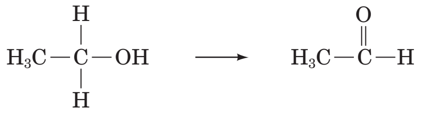

$$\mathrm{H_3C{-}\overset{H}{\underset{H}{C}}{-}OH} \longrightarrow \mathrm{H_3C{-}\overset{O}{\overset{\|}{C}}{-}H}$$

Ethanol **Acetaldehyde**

Thus, through the administration of ethanol, a large portion of the methanol will be harmlessly excreted from the body in the urine before it can be converted to formaldehyde. The same principle underlies the use of ethanol to treat antifreeze (ethylene glycol, $HOCH_2CH_2OH$) poisoning, which, due to its sweet taste, often afflicts cats and dogs.

SAMPLE CALCULATION 12-5

An enzyme has a K_M of 8 μM in the absence of a competitive inhibitor and a K_M^{app} of 12 μM in the presence of 3 μM of the inhibitor. Calculate K_I.

First calculate the value of α when K_M = 8 μM and K_M^{app} = 12 μM:

$$K_M^{\text{app}} = \alpha K_M$$

$$\alpha = \frac{K_M^{\text{app}}}{K_M}$$

$$\alpha = \frac{12\ \mu\text{M}}{8\ \mu\text{M}} = 1.5$$

Next, calculate K_I from Eq. 12-32:

$$\alpha = 1 + \frac{[\text{I}]}{K_I}$$

$$K_I = \frac{[\text{I}]}{\alpha - 1}$$

$$K_I = \frac{3\ \mu\text{M}}{1.5 - 1} = 6\ \mu\text{M}$$

K_I Can Be Measured. Recasting Eq. 12-31 in the double-reciprocal form yields

$$\frac{1}{v_o} = \left(\frac{\alpha K_M}{V_{\max}}\right)\frac{1}{[\text{S}]} + \frac{1}{V_{\max}} \qquad [12\text{-}33]$$

A plot of this equation is linear and has a slope of $\alpha K_M/V_{\max}$, a 1/[S] intercept of $-1/\alpha K_M$, and a $1/v_o$ intercept of $1/V_{\max}$ (Fig. 12-7). The double-reciprocal plots for a competitive inhibitor at various concentrations of I intersect at $1/V_{\max}$ on the $1/v_o$ axis, a property that is diagnostic of competitive inhibition.

The value of K_I for a competitive inhibitor can be determined from the plot of $K_M^{\text{app}} = (1 + [\text{I}]/K_I)K_M$ versus [I]; its intercept on the [I] axis is $-K_I$. K_I can also be calculated from Eq. 12-32 if $K_M^{\text{app}} = \alpha K_M$ is determined at a known [I] for an enzyme of known K_M (see Sample Calculation 12-5). Comparing the K_I values of competitive inhibitors with different structures can provide information about the binding properties of an enzyme's active site and hence its catalytic mechanism. For example, to ascertain the importance of the various segments of an ATP molecule

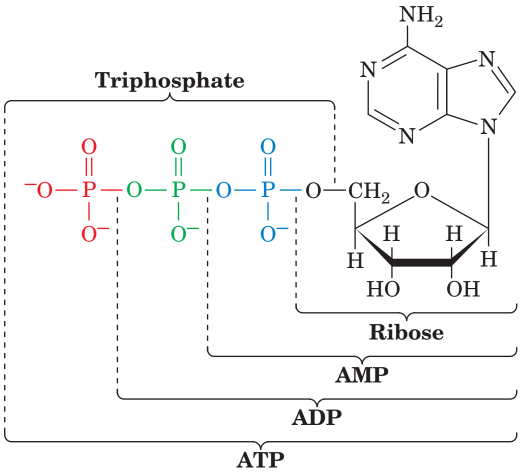

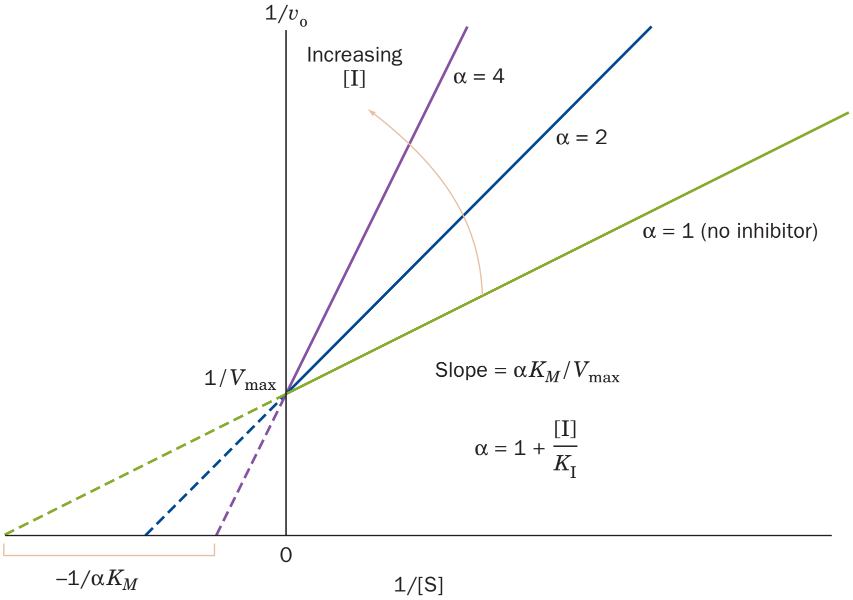

■ **Figure 12-7 | A Lineweaver–Burk plot of the competitively inhibited Michaelis–Menten enzyme described by Fig. 12-6.** Note that all lines intersect on the $1/v_o$ axis at $1/V_{\max}$. The varying slopes indicate the effect of the inhibitor on $\alpha K_M = K_M^{\text{app}}$. **See the Animated Figures.**

for binding to the active site of an ATP-requiring enzyme, one might determine the K_I, say, for ADP, AMP, ribose, triphosphate, etc. Since many of these ATP components are unreactive, inhibition studies are the most convenient method of monitoring their binding to the enzyme.

Competitive inhibition studies are also used to determine the affinities of transition state analogs for an enzyme's active site (Section 11-3E). For example, the HIV protease inhibitors (Box 12-4) have been designed to mimic the enzyme's transition state and thus bind to the enzyme with high affinity. Inhibitor studies are the mainstays of such drug development, as is described in Section 12-4.

B | Uncompetitive Inhibition Involves Inhibitor Binding to the Enzyme–Substrate Complex

In **uncompetitive inhibition,** the inhibitor binds directly to the enzyme–substrate complex but not to the free enzyme:

$$\begin{tikzcd}
\mathrm{E} + \mathrm{S} \arrow[r, shift left, "k_1"] & \mathrm{ES} \arrow[l, shift left, "k_{-1}"] \arrow[r, "k_2"] & \mathrm{P} + \mathrm{E} \\
& + & \\
& \mathrm{I} \arrow[d, shift left] & \\
& \mathrm{ESI} \arrow[u, shift left, "K'_{\mathrm{I}}"] \arrow[r] & \text{NO REACTION}
\end{tikzcd}$$

In this case, the inhibitor binding step has the dissociation constant

$$K'_{\mathrm{I}} = \frac{[\mathrm{ES}][\mathrm{I}]}{[\mathrm{ESI}]} \qquad [12\text{-}34]$$

The binding of uncompetitive inhibitor, which need not resemble substrate, presumably *distorts the active site, thereby rendering the enzyme catalytically inactive*.

The Michaelis–Menten equation for uncompetitive inhibition and the equation for its double-reciprocal plot are given in Table 12-2. The double-

Table 12-2 Effects of Inhibitors on Michaelis–Menten Reactions[a]

Type of Inhibition	Michaelis–Menten Equation	Lineweaver–Burk Equation	Effect of Inhibitor
None	$v_o = \dfrac{V_{\max}[\mathrm{S}]}{K_M + [\mathrm{S}]}$	$\dfrac{1}{v_o} = \dfrac{K_M}{V_{\max}}\dfrac{1}{[\mathrm{S}]} + \dfrac{1}{V_{\max}}$	None
Competitive	$v_o = \dfrac{V_{\max}[\mathrm{S}]}{\alpha K_M + [\mathrm{S}]}$	$\dfrac{1}{v_o} = \dfrac{\alpha K_M}{V_{\max}}\dfrac{1}{[\mathrm{S}]} + \dfrac{1}{V_{\max}}$	Increases K_M^{app}
Uncompetitive	$v_o = \dfrac{V_{\max}[\mathrm{S}]}{K_M + \alpha'[\mathrm{S}]} = \dfrac{(V_{\max}/\alpha')[\mathrm{S}]}{K_M/\alpha' + [\mathrm{S}]}$	$\dfrac{1}{v_o} = \dfrac{K_M}{V_{\max}}\dfrac{1}{[\mathrm{S}]} + \dfrac{\alpha'}{V_{\max}}$	Decreases K_M^{app} and $V_{\max}^{\mathrm{app}}$
Mixed (noncompetitive)	$v_o = \dfrac{V_{\max}[\mathrm{S}]}{\alpha K_M + \alpha'[\mathrm{S}]} = \dfrac{(V_{\max}/\alpha')[\mathrm{S}]}{(\alpha/\alpha')K_M + [\mathrm{S}]}$	$\dfrac{1}{v_o} = \dfrac{\alpha K_M}{V_{\max}}\dfrac{1}{[\mathrm{S}]} + \dfrac{\alpha'}{V_{\max}}$	Decreases $V_{\max}^{\mathrm{app}}$; may increase or decrease K_M^{app}

[a] $\alpha = 1 + \dfrac{[\mathrm{I}]}{K_{\mathrm{I}}}$ and $\alpha' = 1 + \dfrac{[\mathrm{I}]}{K'_{\mathrm{I}}}$

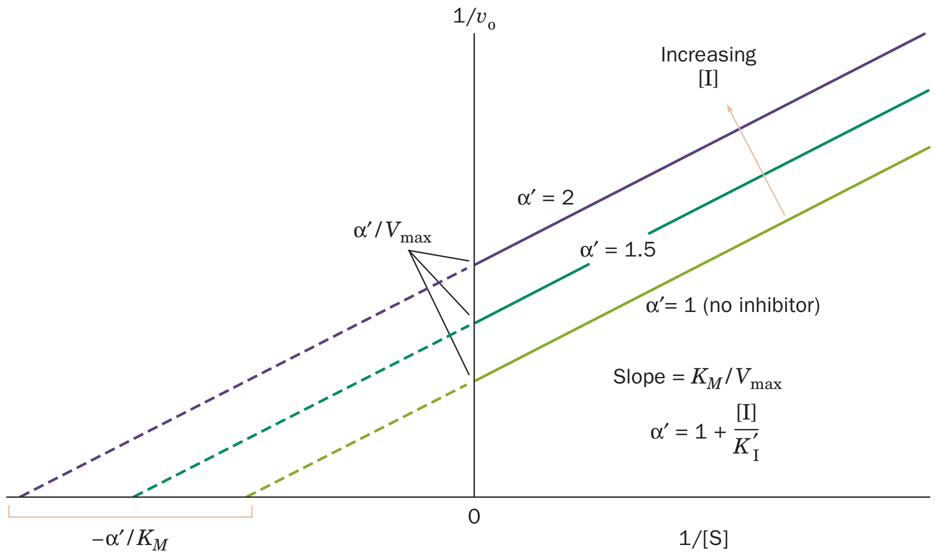

Figure 12-8 | A Lineweaver–Burk plot of a Michaelis–Menten enzyme in the presence of an uncompetitive inhibitor. Note that all lines have identical slopes of $K_M/V_{\max}$. **See the Animated Figures.**

reciprocal plot consists of a family of parallel lines (Fig. 12-8) with slope $K_M/V_{\max}$, $1/v_o$ intercepts of $\alpha'/V_{\max}$, and $1/[S]$ intercepts of $-\alpha'/K_M$. Note that in uncompetitive inhibition, both $K_M^{\text{app}} = K_M/\alpha'$ and $V_{\max}^{\text{app}} = V_{\max}/\alpha'$ are decreased, but that $K_M^{\text{app}}/V_{\max}^{\text{app}} = K_M/V_{\max}$. In contrast to the case for competitive inhibition, adding substrate does not reverse the effect of an uncompetitive inhibitor because the binding of substrate does not interfere with the binding of uncompetitive inhibitor.

Uncompetitive inhibition requires that the inhibitor affect the catalytic function of the enzyme but not its substrate binding. This is difficult to envision for single-substrate enzymes. In actuality, uncompetitive inhibition is significant only for multisubstrate enzymes.

C | Mixed Inhibition Involves Inhibitor Binding to Both the Free Enzyme and the Enzyme–Substrate Complex

Many reversible inhibitors interact with the enzyme in a way that affects substrate binding as well as catalytic activity. In other words, both the enzyme and the enzyme–substrate complex bind inhibitor, resulting in the following model:

$$\begin{tikzcd}
E + S \arrow[r, shift left, "k_1"] \arrow[d, phantom, "+"] & ES \arrow[l, shift left, "k_{-1}"] \arrow[r, "k_2"] \arrow[d, phantom, "+"] & P + E \\
I \arrow[d, shift left, "K_I"'] & I \arrow[d, shift left, "K'_I"'] & \\
EI \arrow[u, shift left] & ESI \arrow[u, shift left] \arrow[r] & \text{NO REACTION}
\end{tikzcd}$$

This phenomenon is known as **mixed inhibition** (alternatively, **noncompetitive inhibition**). Presumably, *a mixed inhibitor binds to enzyme sites that participate in both substrate binding and catalysis.* For example, metal ions, which do not compete directly with substrates for binding to an enzyme active site, as do competitive inhibitors, may act as mixed inhibitors. The two dissociation constants for inhibitor binding

$$K_I = \frac{[E][I]}{[EI]} \quad \text{and} \quad K_I' = \frac{[ES][I]}{[ESI]} \qquad [12\text{-}35]$$

are not necessarily equivalent.

The Michaelis–Menten equation and the corresponding double-reciprocal equation for mixed inhibition are given in Table 12-2. As in uncompetitive inhibition, the apparent values of K_M and $V_{\max}$ are modulated by the presence of inhibitor. The name *mixed inhibition* arises from the fact that the denominator of the Michaelis–Menten equation has the factor α multiplying K_M as in competitive inhibition and the factor α' multiplying [S] as in uncompetitive inhibition. Thus $K_M^{\text{app}} = (\alpha/\alpha')K_M$ and $V_{\max}^{\text{app}} = V_{\max}/\alpha'$.

Depending on the relative values of α and α' (and hence K_I and K_I'), K_M^{app} may increase (as in competitive inhibition) or decrease. If the enzyme and enzyme–substrate complex bind I with equal affinity, then $\alpha = \alpha'$ and the K_M^{app} value is unchanged from the K_M for the reaction in the absence of inhibitor. In this case, only $V_{\max}$ is affected, a phenomenon that is named **pure noncompetitive inhibition.**

Double-reciprocal plots for mixed inhibition consist of lines that have the slope $\alpha K_M/V_{\max}$, a $1/v_o$ intercept of $\alpha'/V_{\max}$, and a 1/[S] intercept of $-\alpha'/\alpha K_M$ (Fig. 12-9). The lines for increasing values of [I] (representing increasing saturation of E and ES with I) intersect to the left of the $1/v_o$ axis. For pure noncompetitive inhibition, the lines intersect on the 1/[S] axis at $-1/K_M$. As with uncompetitive inhibition, substrate binding does not reverse the effects of mixed inhibition.

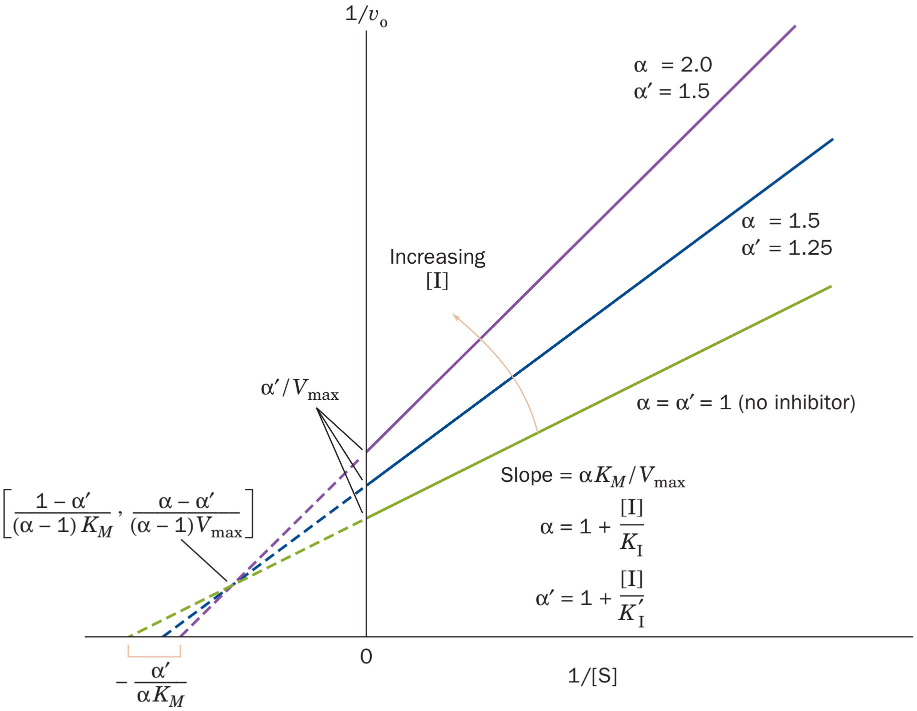

■ **Figure 12-9 | A Lineweaver–Burk plot of a Michaelis–Menten enzyme in the presence of a mixed inhibitor.** Note that the lines all intersect to the left of the $1/v_o$ axis. The coordinates of the intersection point are given in brackets. When $K_I = K_I'$ ($\alpha = \alpha'$), the lines intersect on the 1/[S] axis at $-1/K_M$. **See the Animated Figures.**

BOX 12-4 BIOCHEMISTRY IN HEALTH AND DISEASE

HIV Enzyme Inhibitors

The **human immunodeficiency virus (HIV)** causes **acquired immunodeficiency syndrome (AIDS)** by infecting and destroying the host's immune system. In the first steps of infection, HIV attaches to a target cell and injects its genetic material (which is RNA rather than DNA) into the host cell. The viral RNA is transcribed into DNA by a viral enzyme called **reverse transcriptase** (Box 25-2). After this DNA is integrated into the host's genome, the cell can produce more viral RNA and proteins for packaging it into new viral particles.

Most of the viral proteins are synthesized as parts of larger polypeptide precursors known as **polyproteins.** Consequently, proteolytic processing by the virally encoded **HIV protease** to release these viral proteins is necessary for viral reproduction. In the absence of an effective vaccine for HIV, efforts to prevent and treat AIDS have led to the development of compounds that inhibit HIV reverse transcriptase and HIV protease.

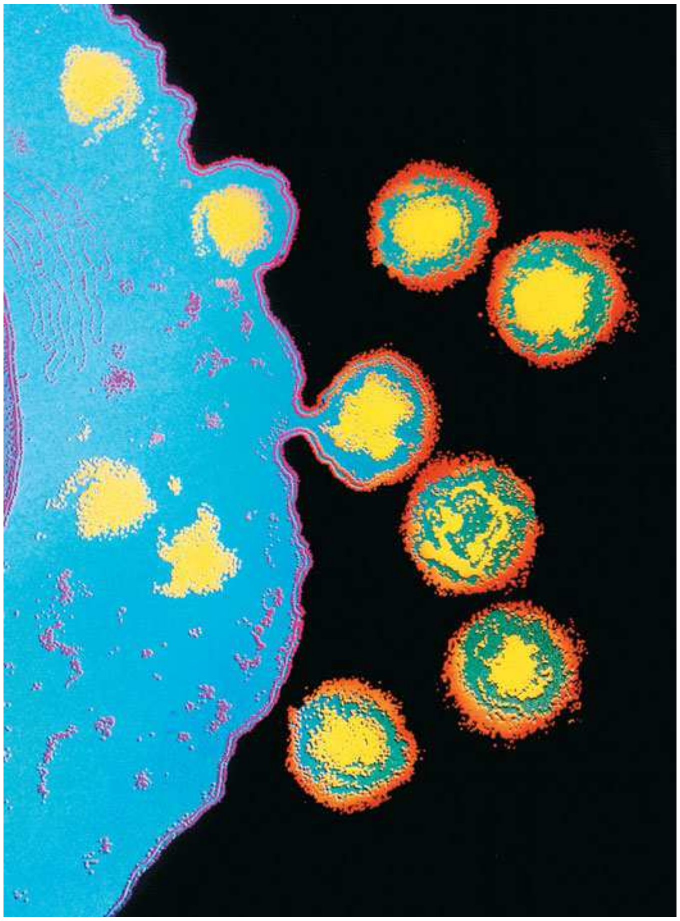

HIV particles budding from a lymphocyte. [© Chris Bjomberg/Photo Researchers.]

Several inhibitors of reverse transcriptase have been developed. The archetype is **AZT (3′-azido-3′-deoxythymidine; Zidovudine),** which is taken up by cells, phosphorylated, and incorporated into the DNA chains synthesized from the HIV template by reverse transcriptase. Because AZT lacks a 3′-OH group, it cannot support further polynucleotide chain elongation and therefore terminates DNA synthesis (Section 3-4C). Most cellular DNA polymerases have a low affinity for phosphorylated AZT, but reverse transcriptase has a high affinity for this drug, which makes AZT effective against viral replication. Other nucleoside analogs that are used to treat HIV infection are **2′,3′-dideoxycytidine (ddC, Zalcitabine)** and **2′,3′-dideoxyinosine** (**ddI, Didanosine;** inosine nucleotides are metabolically converted to adenosine and guanosine nucleotides), which also act as chain terminators. Nonnucleoside compounds such as **nevirapine** do not bind to the reverse transcriptase active site but instead bind to a hydrophobic pocket elsewhere on the enzyme.

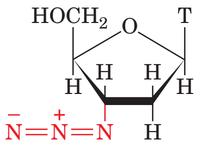

3′-Azido-3′-deoxythymidine (AZT; Zidovudine)

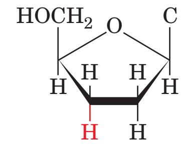

2′,3′-Dideoxycytidine (ddC, Zalcitabine)

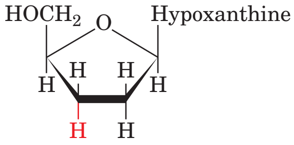

2′,3′-Dideoxyinosine (ddI, Didanosine)

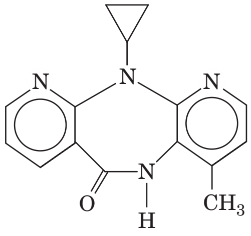

Nevirapine

HIV protease is a homodimer of 99-residue subunits. Mechanistically, it is a so-called **aspartic protease,** a family of proteases that includes **pepsin** (the gastric protease that operates at low pH). Comparisons among the active sites of the aspartic proteases were instrumental in designing HIV protease inhibitors. HIV protease cleaves a number of specific peptide bonds, including Phe–Pro and Tyr–Pro peptide bonds in its physiological substrates, the HIV proteins. Inhibitors based on these sequences should therefore selectively inhibit the viral protease. The **peptidomimetic** (peptide-imitating) drugs ritonavir and saquinavir contain phenyl and other bulky groups that bind in the HIV protease active site. Of perhaps even greater importance, these drugs have the geometry of the catalyzed

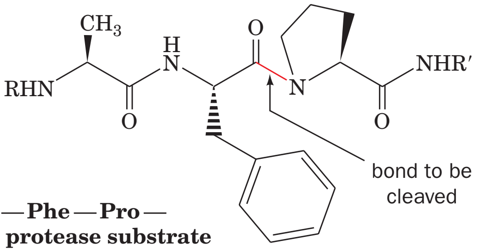

—Phe—Pro—
HIV protease substrate

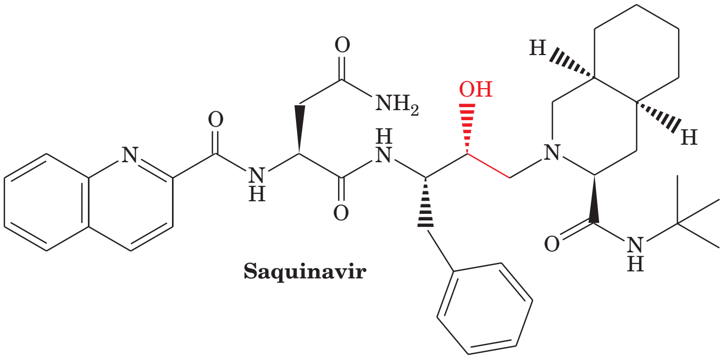

Saquinavir

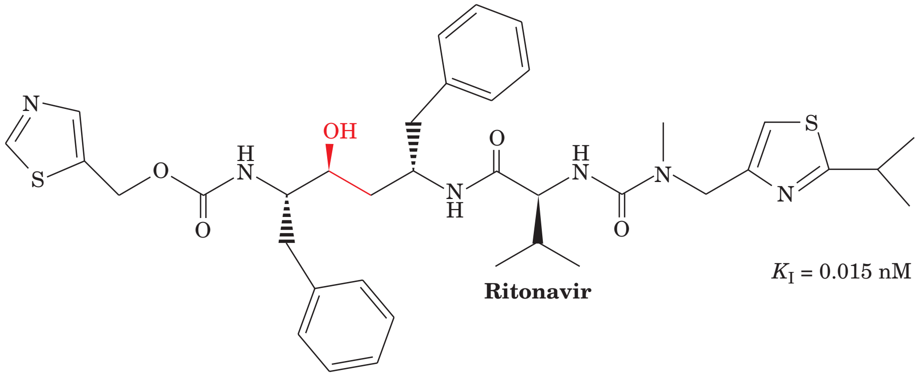

Ritonavir

reaction's tetrahedral transition state (*red*). The enzyme's peptide substrate is shown for comparison. **See Interactive Exercise 9.**

The efficacy of anti-HIV agents, like that of many drugs, is limited by their side effects. Despite their preference for viral enzymes, anti-HIV drugs also interfere with normal cellular processes. For example, the inhibition of DNA synthesis by reverse transcriptase inhibitors in rapidly dividing cells, such as the bone marrow cells that give rise to erythrocytes, can lead to severe anemia. Other side effects include nausea, kidney stones, and rashes. Side effects are particularly problematic in HIV infection, because drugs must be taken several times daily for many years, if not for a lifetime.

Acquired resistance also limits the effectiveness of antiviral drugs. This is a significant problem in HIV infection because the error-prone reverse transcriptase allows HIV to mutate rapidly. Numerous mutations in HIV are known to be associated with drug resistance.

In the case of HIV infection, it seems unlikely that a single drug will prove to be a "magic bullet," in part because HIV infects many cell types, but mostly because of its ability to rapidly evolve resistance against any one drug. The outstanding success of anti-HIV therapy rests on combination therapy, in which several different drugs are administered simultaneously. This successfully keeps AIDS at bay by reducing levels of HIV, in some cases to undetectable levels, thereby reducing the probability that HIV will evolve a drug-resistant variant. The advantages of using an inhibitor "cocktail" containing inhibitors of reverse transcriptase and HIV protease include (1) decreasing the likelihood that a viral strain will simultaneously develop resistance to every compound in the mix and (2) decreasing the doses and hence the side effects of the individual compounds.

The kinetics of an enzyme inactivator (an irreversible inhibitor) resembles that of a pure noncompetitive inhibitor because the inactivator reduces the concentration of functional enzyme at all substrate concentrations. Consequently, $V_{\max}$ decreases and K_M is unchanged. The double-reciprocal plots for irreversible inactivation therefore resemble those for pure noncompetitive inhibition (the lines intersect on the 1/[S] axis).

■ CHECK YOUR UNDERSTANDING

What distinguishes an inhibitor from an inactivator?

Describe the effects of competitive, uncompetitive, and mixed inhibitors on K_M and $V_{\max}$.

3 Control of Enzyme Activity

LEARNING OBJECTIVES

- Understand that allosteric effectors bind to multisubunit enzymes such as aspartate transcarbamoylase, thereby inducing cooperative conformational changes that alter the enzyme's catalytic activity.
- Understand that phosphorylation and dephosphorylation of an enzyme such as glycogen phosphorylase can control its activity by shifting the equilibrium between more active and less active conformations.

An organism must be able to control the catalytic activities of its component enzymes so that it can coordinate its numerous metabolic processes, respond to changes in its environment, and grow and differentiate, all in an orderly manner. There are two ways that this may occur:

1. ***Control of enzyme availability.*** The amount of a given enzyme in a cell depends on both its rate of synthesis and its rate of degradation. Each of these rates is directly controlled by the cell and is subject to dramatic changes over time spans of minutes (in bacteria) to hours (in higher organisms).
2. ***Control of enzyme activity.*** An enzyme's catalytic activity can be directly controlled through structural alterations that influence the enzyme's substrate-binding affinity or turnover number. Just as hemoglobin's oxygen affinity is allosterically regulated by the binding of ligands such as O_2, CO_2, H^+, and BPG (Section 7-1D), an enzyme's substrate-binding affinity may likewise vary with the binding of small molecules, called **allosteric effectors.** *Allosteric mechanisms can cause large changes in enzymatic activity.* The activities of many enzymes are similarly controlled by **covalent modification,** usually phosphorylation and dephosphorylation of specific Ser, Thr, or Tyr residues.

In the following sections we discuss the control of enzyme activity by allosteric interactions and covalent modification.

A | Allosteric Control Involves Binding at a Site Other than the Active Site

In this section we examine allosteric control of enzymatic activity by considering one example—**aspartate transcarbamoylase (ATCase)** from *E. coli.* Other allosteric enzymes are discussed in later chapters.

The Feedback Inhibition of ATCase Regulates Pyrimidine Synthesis. Aspartate transcarbamoylase catalyzes the formation of ***N*-carbamoyl aspartate** from **carbamoyl phosphate** and aspartate:

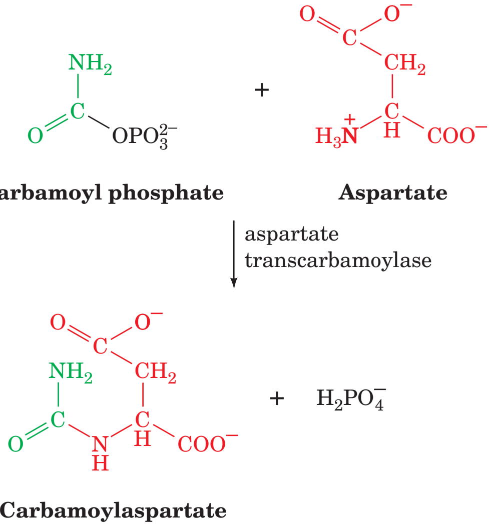

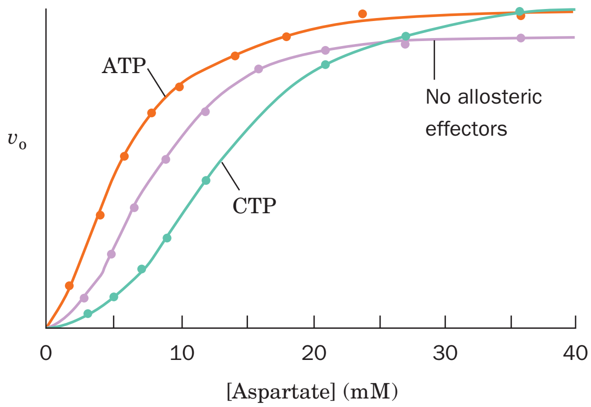

Figure 12-10 | Plot of v_o versus [aspartate] for the ATCase reaction. Reaction velocity was measured in the absence of allosteric effectors, in the presence of 0.4 mM CTP (an inhibitor), and in the presence of 2.0 mM ATP (an activator). [After Kantrowitz, E.R., Pastra-Landis, S.C., and Lipscomb, W.N., *Trends Biochem. Sci.* **5,** 125 (1980).] **See the Animated Figures.**

This reaction is the first step unique to the biosynthesis of pyrimidines (Section 23-2A). The allosteric behavior of *E. coli* ATCase has been investigated by John Gerhart and Howard Schachman, who demonstrated that both of its substrates bind cooperatively to the enzyme. Moreover, ATCase is allosterically inhibited by **cytidine triphosphate (CTP),** a pyrimidine nucleotide, and is allosterically activated by adenosine triphosphate (ATP), a purine nucleotide.

The v_o versus [S] curve for ATCase (Fig. 12-10) is sigmoidal, rather than hyperbolic as it is in enzymes that follow the Michaelis–Menten model. This is consistent with cooperative substrate binding (recall that hemoglobin's O_2-binding curve is also sigmoidal; Fig. 7-6). ATCase's allosteric effectors shift the entire curve to the right or the left: At a given substrate concentration, CTP decreases the enzyme's catalytic rate, whereas ATP increases it.

CTP, which is a product of the pyrimidine biosynthetic pathway, is an example of a **feedback inhibitor,** since *it inhibits an earlier step in its own biosynthesis* (Fig. 12-11). Thus, when CTP levels are high, CTP binds to ATCase, thereby reducing the rate of CTP synthesis. Conversely, when cellular [CTP] decreases, CTP dissociates from ATCase and CTP synthesis accelerates.

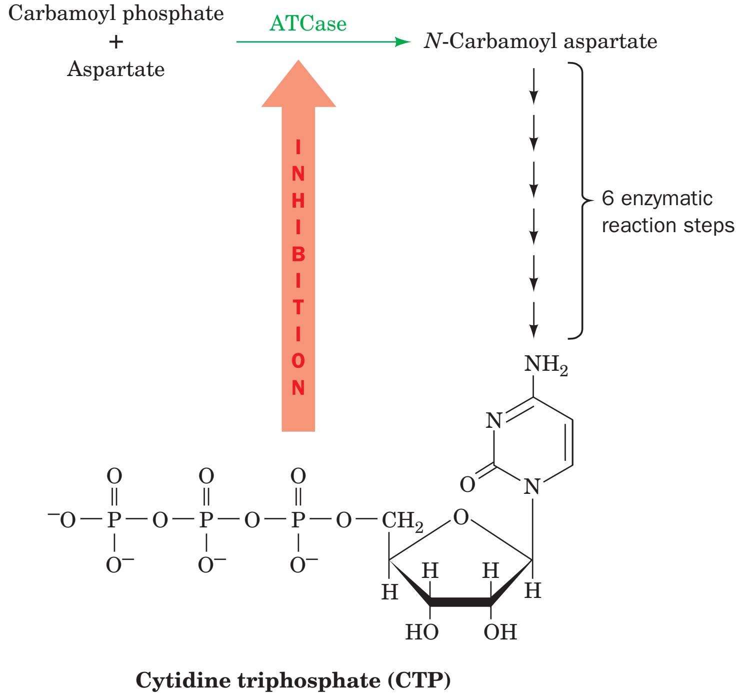

Figure 12-11 | A schematic representation of the pyrimidine biosynthesis pathway. CTP, the end product of the pathway, inhibits ATCase, which catalyzes the pathway's first step.

The metabolic significance of the ATP activation of ATCase is that it tends to coordinate the rates of synthesis of purine and pyrimidine nucleotides, which are required in roughly equal amounts in nucleic acid biosynthesis. For instance, if the ATP concentration is much greater than that of CTP, ATCase is activated to synthesize pyrimidine nucleotides until the concentrations of ATP and CTP become balanced. Conversely, if the CTP concentration is greater than that of ATP, CTP inhibition of ATCase permits purine nucleotide biosynthesis to balance the ATP and CTP concentrations.

Allosteric Changes Alter ATCase's Substrate-Binding Sites. *E. coli* ATCase (300 kD) has the subunit composition c_6r_6, where c and r represent its catalytic and regulatory subunits. The X-ray structure of ATCase (Fig. 12-12), determined by William Lipscomb, reveals that the catalytic subunits are arranged as two sets of trimers (c_3) in complex with three sets of regulatory dimers (r_2). Each regulatory dimer joins two catalytic subunits in different c_3 trimers.

The isolated catalytic trimers are catalytically active, have a maximum catalytic rate greater than that of intact ATCase, exhibit a noncooperative (hyperbolic) substrate saturation curve, and are unaffected by the presence of ATP or CTP. The isolated regulatory dimers bind the allosteric effectors but are devoid of enzymatic activity. Evidently, *the regulatory subunits allosterically reduce the activity of the catalytic subunits in the intact enzyme.*

As allosteric theory predicts (Section 7-1D), the activator ATP preferentially binds to ATCase's active (R or high substrate affinity) state, whereas the inhibitor CTP preferentially binds to the enzyme's inactive (T or low substrate affinity) state. Similarly, the unreactive bisubstrate analog ***N*-(phosphonacetyl)-L-aspartate (PALA)**

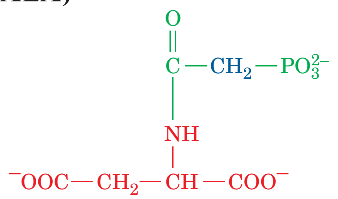

***N*-(Phosphonacetyl)-L-aspartate (PALA)**

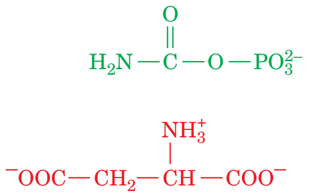

Carbamoyl phosphate
+
Aspartate

binds tightly to R-state but not to T-state ATCase.

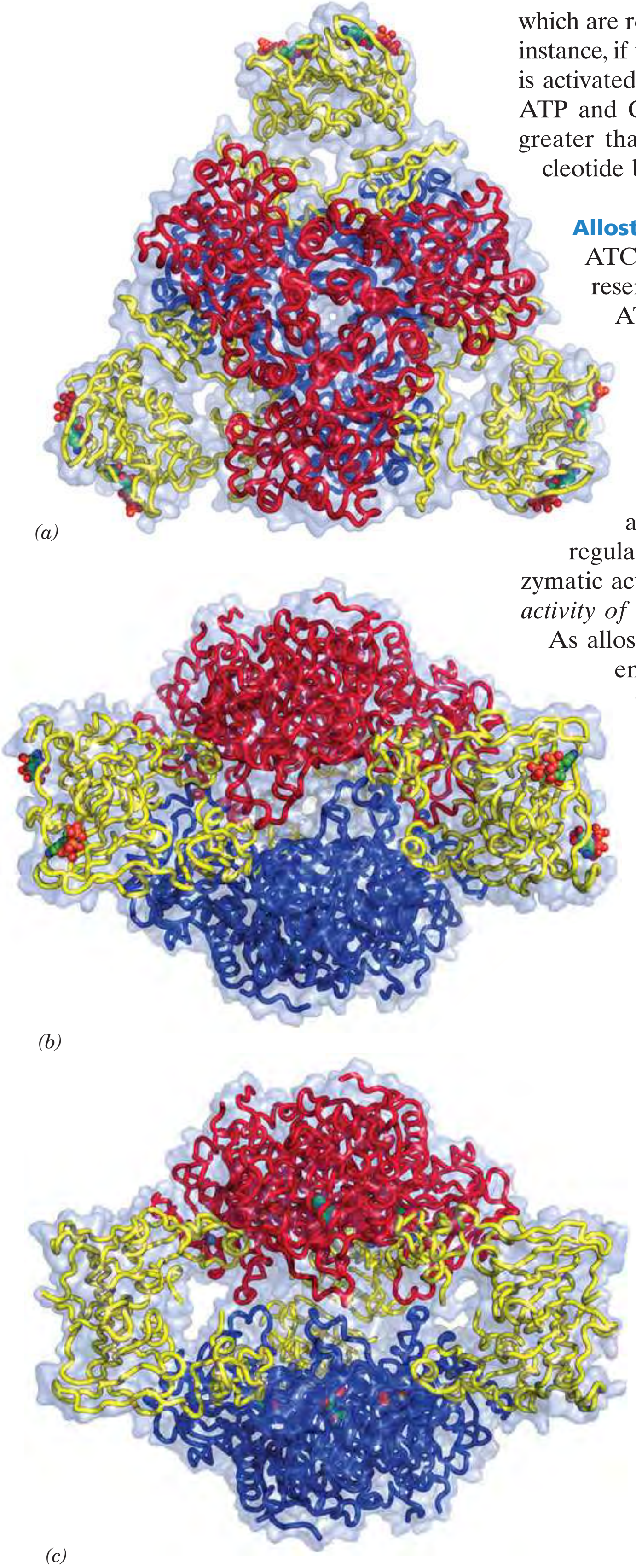

Figure 12-12 | X-Ray structure of ATCase from *E. coli*. The T-state enzyme in complex with CTP is viewed (*a*) along the protein's molecular threefold axis of symmetry and (*b*) along a molecular twofold axis of symmetry perpendicular to the view in Part *a*. The polypeptide chains are drawn in worm form embedded in their transparent molecular surface. The regulatory dimers (*yellow*) join the upper catalytic trimer (*red*) to the lower catalytic trimer (*blue*). CTP is drawn in space-filling form colored according to atom type (C green, O red, N blue, and P orange). (*c*) The R-state enzyme in complex with PALA viewed as in Part *b*. PALA (which is bound to the *c* subunits but largely obscured here) is drawn in space-filling form. Note how the rotation of the regulatory dimers in the T → R transition causes the catalytic trimers to move apart along the threefold axis. [Based on X-ray structures by William Lipscomb, Harvard University. PDBids 5AT1 and 8ATC.] **See Kinemage Exercise 11-1.**

X-Ray structures have been determined for the T-state ATCase–CTP complex and the R-state ATCase–PALA complex (as a rule, unreactive substrate analogs, such as PALA, form complexes with an enzyme that are more amenable to structural analysis than complexes of the enzyme with rapidly reacting substrates; Box 11-2). Structural studies reveal that in the T → R transition, the enzyme's catalytic trimers separate along the molecular threefold axis by ~11 Å and reorient around this axis relative to each other by 12° (Fig. 12-12*b,c*). In addition, the regulatory dimers rotate clockwise by 15° around their twofold axes and separate by ~4 Å along the threefold axis. Such large quaternary shifts are reminiscent of those in hemoglobin (Section 7-3A).

Each catalytic subunit of ATCase consists of a carbamoyl phosphate–binding domain and an aspartate-binding domain. The binding of PALA to the enzyme, which presumably mimics the binding of both substrates, induces a conformational change that swings the two domains together such that their two bound substrates can react to form product (Fig. 12-13). The conformational changes—movements of up to 8 Å for some residues—in a single catalytic subunit trigger ATCase's T → R quaternary shift. ATCase's tertiary and quaternary shifts are tightly coupled (i.e., ATCase closely follows the symmetry model of allosterism; Section 7-1D). *The*

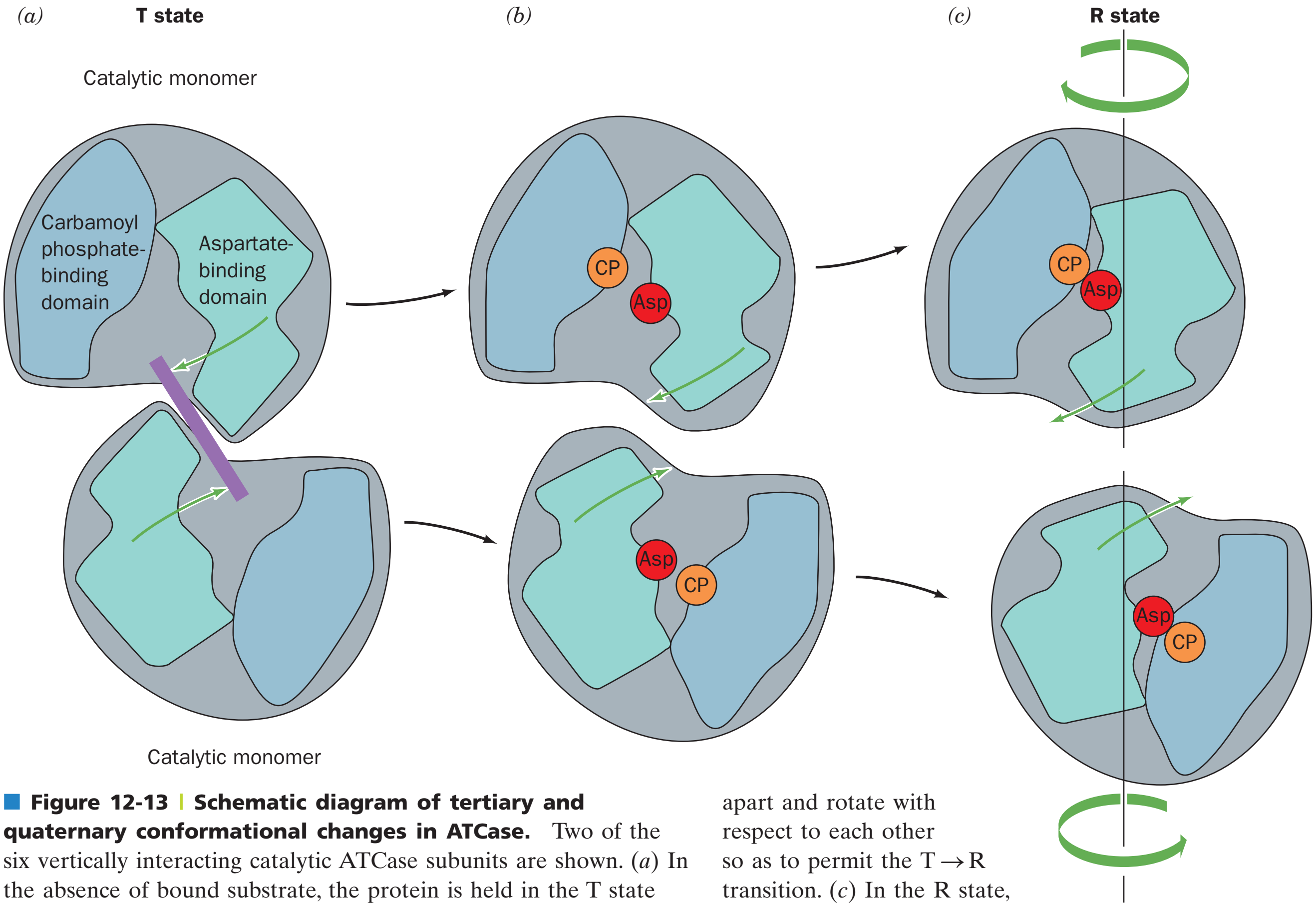

■ **Figure 12-13 | Schematic diagram of tertiary and quaternary conformational changes in ATCase.** Two of the six vertically interacting catalytic ATCase subunits are shown. (*a*) In the absence of bound substrate, the protein is held in the T state because the motions that bring together the two domains of each subunit (*green arrows*) are prevented by steric interference (*purple bar*) between the contacting aspartic acid–binding domains. (*b*) The binding of carbamoyl phosphate (CP) followed by aspartic acid (Asp) to their respective binding sites causes the subunits to move apart and rotate with respect to each other so as to permit the T → R transition. (*c*) In the R state, the two domains of each subunit come together to promote the reaction of their bound substrates to form products. [Illustration, Irving Geis/Geis Archives Trust. Copyright Howard Hughes Medical Institute. Reproduced with permission.] **See Kinemage Exercises 11-1 and 11-2.**

binding of substrate to one catalytic subunit therefore increases the substrate-binding affinity and catalytic activity of the other five catalytic subunits and hence accounts for the enzyme's cooperative substrate binding.

The Binding of Allosteric Modifiers Causes Structural Changes in ATCase. The structural basis for the effects of CTP and ATP on ATCase activity has been partially unveiled. Both the inhibitor CTP and the activator ATP bind to the same site on the outer edge of the regulatory subunit, about 60 Å away from the nearest catalytic site. CTP binds preferentially to the T state, increasing its stability, whereas ATP binds preferentially to the R state, increasing its stability.

The binding of CTP and ATP to their less favored enzyme states also has structural consequences. When CTP binds to R-state ATCase, it induces a contraction in the regulatory dimer that causes the catalytic trimers to come together by 0.5 Å (become more T-like, that is, less active). This, in turn, reorients key residues in the enzyme's active sites, thereby decreasing the enzyme's catalytic activity. ATP has essentially opposite effects when binding to the T-state enzyme: It causes the catalytic trimers to move apart by 0.4 Å (become more R-like, that is, more active), thereby reorienting key residues in the enzyme's active sites so as to increase the enzyme's catalytic activity.

Allosteric Transitions in Other Enzymes Often Resemble Those of Hemoglobin and ATCase. Allosteric enzymes are widely distributed in nature and tend to occupy key regulatory positions in metabolic pathways. Such enzymes are almost always symmetrical proteins containing at least two subunits, in which quaternary structural changes communicate binding and catalytic effects among all active sites in the enzyme. The quaternary shifts are primarily rotations of subunits relative to one another. Secondary structures are largely preserved in T → R transitions, which is probably important for mechanically transmitting allosteric effects over distances of tens of angstroms.

B | Control by Covalent Modification Usually Involves Protein Phosphorylation

In addition to allosteric interactions, many enzymes may be subject to control by covalent modification. In eukaryotes, by far the most common such modification is phosphorylation and dephosphorylation (the attachment and removal of a phosphoryl group) of the hydroxyl group of a Ser, Thr, or Tyr residue.

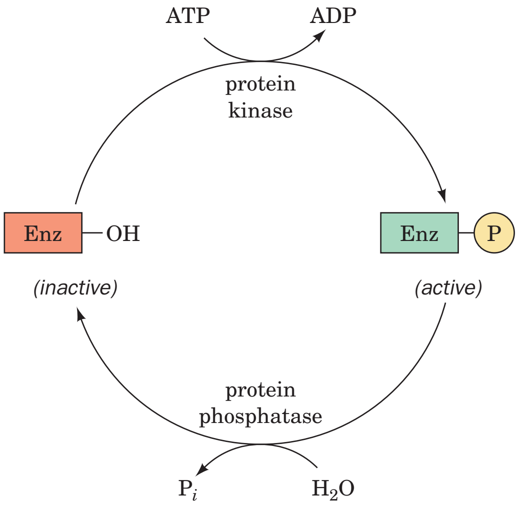

Such enzymatic modification/demodification processes, which are catalyzed by enzymes known as **protein kinases** and **protein phosphatases,** alter the activities of the modified proteins. Indeed, ~30% of human proteins, which collectively participate in nearly all biological processes, are subject to control by reversible phosphorylation.

As an example of an enzyme whose activity is controlled by covalent modification, let us consider **glycogen phosphorylase** (or simply **phosphorylase**), which catalyzes the **phosphorolysis** (bond cleavage by the substitution of a phosphate group) of glycogen [the starchlike polysaccharide that consists mainly of α(1→4)-linked glucose residues; Section 8-2C] to yield **glucose-1-phosphate (G1P):**

$$\underset{(n\text{ residues})}{\text{Glycogen}} + \text{P}_i \rightleftharpoons \underset{(n-1\text{ residues})}{\text{glycogen}} + \text{G1P}$$

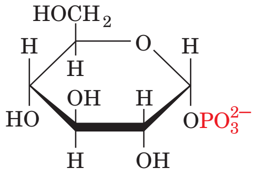

Glucose-1-phosphate (G1P)

This is the rate-controlling step in the metabolic pathway of glycogen breakdown, an important supplier of fuel for metabolic activities (Section 16-1).

Mammals express three **isozymes** (catalytically and structurally similar but genetically distinct enzymes from the same organism; also called **isoforms**) of glycogen phosphorylase, those from muscle, brain, and liver. Muscle glycogen phosphorylase, which we discuss here, is a dimer of identical 842-residue subunits. It is regulated both by allosteric interactions and by phosphorylation/dephosphorylation. The phosphorylated form of the enzyme, **phosphorylase *a*,** has a phosphoryl group esterified to its Ser 14. The dephospho form is called **phosphorylase *b*.**

The X-ray structures of phosphorylase *a* and phosphorylase *b*, which were respectively determined by Robert Fletterick and Louise Johnson, are similar. Both have a large N-terminal domain (484 residues; the largest known domain) and a smaller C-terminal domain (Fig. 12-14). The N-terminal domain contains the phosphorylation site (Ser 14), an allosteric effector site, a glycogen-binding site (called the glycogen storage site), and all the intersubunit contacts in the dimer. The enzyme's active site is located at the center of the subunit.

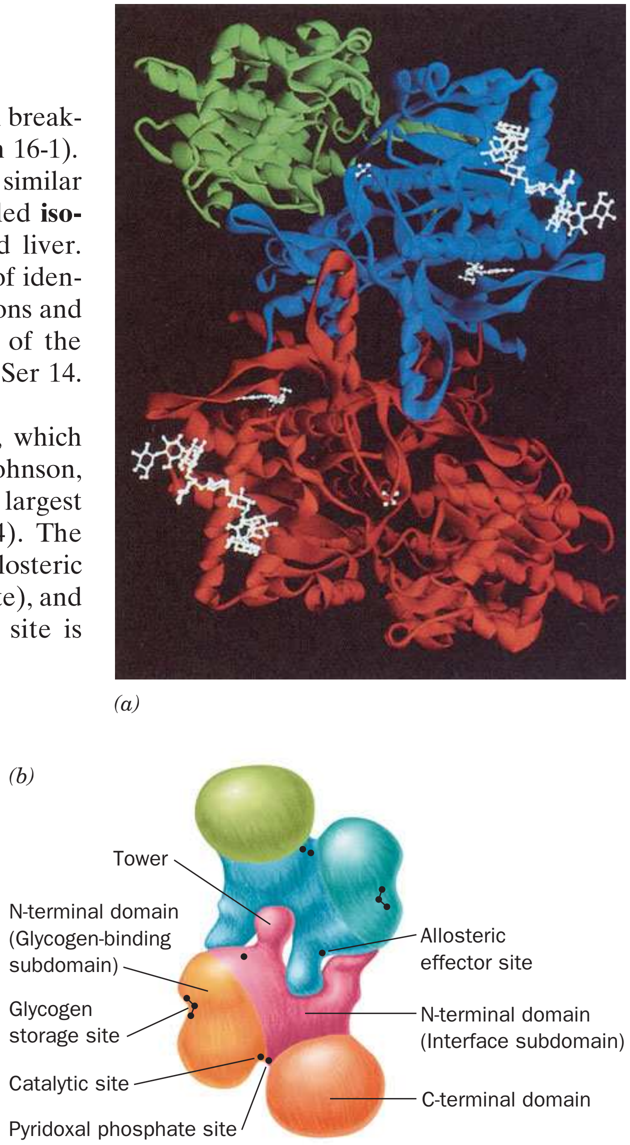

Figure 12-14 | **X-Ray structure of rabbit muscle glycogen phosphorylase.** (*a*) Ribbon diagram of the phosphorylase *a* dimer viewed along its molecular twofold axis of symmetry. The bottom subunit is colored orange, and the top subunit's N-terminal and C-terminal domains are colored blue and green, respectively. The various bound ligands are white: The phosphate group at the center of each subunit marks the enzyme's catalytic site; maltoheptose (a glucose heptamer) is bound at each glycogen storage site; and the AMPs at the "back" of the protein identify the allosteric effector sites. [Courtesy of Stephen Sprang, University of Texas Southwestern Medical Center.] (*b*) An interpretive drawing of the structure in Part *a* showing the enzyme's various ligand-binding sites. **See Kinemage Exercise 14-1.**

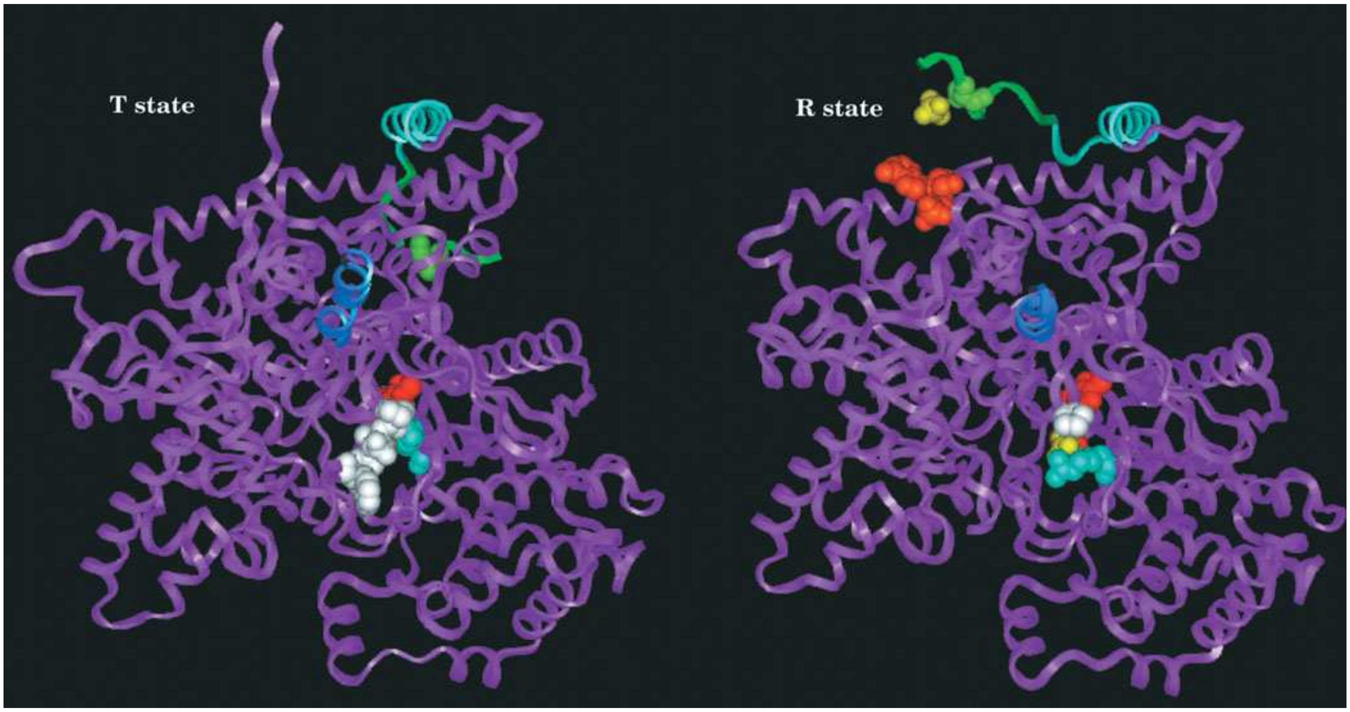

■ **Figure 12-15 | Conformational changes in glycogen phosphorylase.** One subunit of the dimeric phosphorylase *b* is shown (*left*) in the T state in the absence of allosteric effectors and (*right*) in the R state with bound AMP. The view is of the lower (*orange*) subunit in Fig. 12-14 as seen from the top of the page. The tower helix is blue, the N-terminal helix is cyan, and the N-terminal residues that change conformation on AMP binding are green. Of the groups that are shown in space-filling representation, Ser 14, the phosphorylation site, is light green; AMP is orange; the active site PLP (a prosthetic group) is red; the Arg 569 side chain, which reorients in the T → R transition so as to interact with the substrate phosphate, is cyan; loop residues 282 to 284, which in the R state are mostly disordered and hence not seen, are white; and the phosphates, both at the active site and at the R state Ser 14 phosphorylation site (not present in phosphorylase *b* but shown for position), are yellow. [X-Ray structure coordinates courtesy of Stephan Sprang, University of Texas Southwest Medical Center.] **See Kinemage Exercises 14-2 and 14-3.**

Phosphorylation and Dephosphorylation Can Alter Enzymatic Activity in a Manner That Resembles Allosteric Control. Glycogen phosphorylase has two conformational states, the enzymatically active R state and the enzymatically inactive T state (Fig. 12-15). The T-state enzyme is inactive because it has a malformed active site and a surface loop (residues 282–284) that blocks substrate access to its binding site. In contrast, in the R-state enzyme, the side chain of Arg 569 has reoriented so as to bind the substrate phosphate ion and the 282–284 loop no longer blocks the active site, thereby permitting the enzyme to bind substrate and efficiently catalyze the phosphorolysis of glycogen.

The phosphorylation of Ser 14 promotes phosphorylase's T (inactive) → R (active) conformational change. Moreover, these different enzymatic forms respond to different allosteric effectors (Fig. 12-16). Thus ATP and **glucose-6-phosphate [G6P;** to which the G1P product of the glycogen phosphorylase reaction is converted (Section 16-1C)] preferentially bind to the T state of phosphorylase *b* and, in doing so, inactivate the enzyme, whereas AMP preferentially binds to the R state of phosphorylase *b* and hence activates it. In contrast, phosphorylase *a*'s only allosteric effector is glucose, which binds to the enzyme's T state and inactivates the enzyme. Note that ATP, G6P, and glucose are present in relatively high concentrations in muscle under conditions of low exertion, a state when

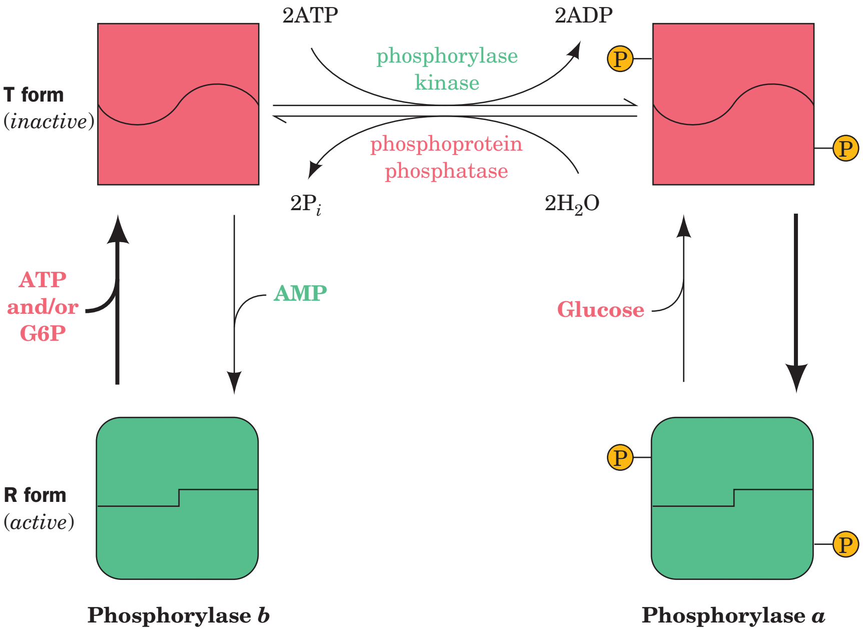

Figure 12-16 | The control of glycogen phosphorylase activity. The enzyme may assume the enzymatically inactive T conformation (*above*) or the catalytically active R form (*below*). The conformation of phosphorylase *b* is allosterically controlled by the effectors AMP, ATP, and G6P and is mostly in the T state under physiological conditions. In contrast, the phosphorylated form of the enzyme, phosphorylase *a,* is unresponsive to these effectors and is mostly in the R state unless there is a high level of glucose. Thus, under usual physiological conditions, the enzymatic activity of glycogen phosphorylase is largely determined by its rates of phosphorylation and dephosphorylation.

glycogen breakdown would be superfluous, whereas AMP is present in relatively high concentration in muscles under conditions of high exertion, a state when the G1P product of the phosphorylase reaction helps fuel muscle contraction.

The phosphate group, with its double negative charge (a property not shared with naturally occurring amino acid residues) and its covalent attachment to a protein, can induce dramatic conformational changes. In phosphorylase *a*, the Ser 14 phosphate group forms ion pairs with two cationic Arg side chains, thereby linking the active site, the subunit interface, and the N-terminal region, the latter having undergone a large conformational shift from its position in the T-state enzyme (Fig. 12-15). These binding interactions cause glycogen phosphorylase's tower helices (Figs. 12-14 and 12-15) to tilt and pull apart so as to pack more favorably, which in turn triggers a quaternary T → R transition, which largely consists of an ~10° relative rotation of the two subunits. *Thus the Ser 14–phosphate group functions as a sort of internal allosteric effector that shifts the enzyme's* $T \rightleftharpoons R$ *equilibrium in favor of the R state.*

Cascades of Protein Kinases Enable Sensitive Responses to Metabolic Needs. The enzymes that catalyze the phosphorylation and dephosphorylation of glycogen phosphorylase are named **phosphorylase kinase** and **phosphoprotein phosphatase** (Fig. 12-16). The activities of these latter enzymes are themselves controlled, both allosterically and by phosphorylation/dephosphorylation. Thus, as we shall see in Section 13-2, sequences of protein kinases and protein phosphatases, both linked in cascade fashion (i.e., protein kinase X phosphorylates protein kinase Y, which phosphorylates protein kinase Z), have far greater capacities for signal amplification (a small fractional change in effector concentration causing a larger fractional change in enzyme activity) and flexibility in response to a greater number of allosteric effectors (the activity of each protein in the cascade may be influenced by different sets of effectors) than does a simple allosteric enzyme. Indeed, just such cascades permit glycogen phosphorylase to respond with great sensitivity to the metabolic needs of the organism.

CHECK YOUR UNDERSTANDING

Explain the structural basis for cooperative substrate binding and allosteric control in ATCase.

Describe how phosphorylation and dephosphorylation control the activity of glycogen phosphorylase.

LEARNING OBJECTIVES

- Understand that structure-based design and combinatorial chemistry approaches are used to discover new drugs.
- Understand that a drug's interactions with the body determine its bioavailability.
- Understand that a drug's effectiveness and safety are tested in clinical trials.
- Understand that cytochrome P450 may modify a drug to alter its bioavailability or toxicity.

4 Drug Design

The use of drugs to treat various maladies has a long history, but the modern pharmaceutical industry, which is based on science (rather than tradition or superstition), is a product of the twentieth century. For example, at the beginning of the twentieth century, only a handful of drugs, apart from folk medicines, were known, including **digitalis,** a heart stimulant from the foxglove plant (Box 10-3); **quinine** (Fig. 12-17), obtained from the bark and roots of the *Cinchona* tree, which was used to treat malaria; and mercury, which was used to treat syphilis—a cure that was often worse than the disease. Almost all drugs in use today were discovered and developed in the past three decades. The majority of drugs act by modifying the activity of a receptor protein, with enzyme inhibitors constituting the second largest class of drugs. Indeed, the techniques of enzyme kinetics have proved to be invaluable for evaluating drug candidates.

A | Drug Discovery Employs a Variety of Techniques

How are new drugs discovered? Nearly all drugs that have been in use for over a decade were discovered by screening large numbers of compounds—either synthetic compounds or those derived from natural products (often plants used in folk remedies). Initial screening involves *in vitro* assessment of, for example, the degree of binding of a drug candidate to an enzyme that is implicated in a disease of interest, that is, determining its K_I value. Later, as the number of drug candidates is winnowed down, more sensitive screens such as testing in animals are employed.

A drug candidate that exhibits a desired effect is called a **lead compound.** A good lead compound binds to its target protein with a dissociation constant (for an enzyme, an inhibition constant) of less than 1 μM. Such a high affinity is necessary to minimize a drug's less specific binding to other macromolecules in the body and to ensure that only low doses of the drug need be taken.

A lead compound is used as a point of departure to design more efficacious compounds. Even minor modifications to a drug candidate can result in major changes in its pharmacological properties. Thus, substitution of methyl, chloro, hydroxyl, or benzyl groups at various places on a lead

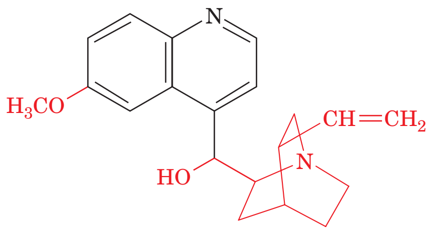

Quinine

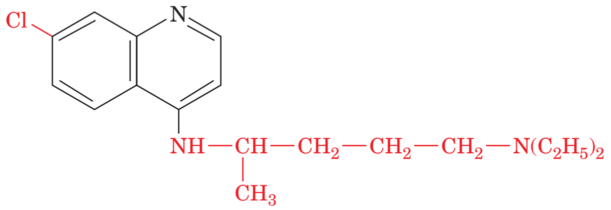

Chloroquine

Figure 12-17 | Quinine and chloroquine. These two compounds, which share a quinoline ring system, are effective antimalarial agents. The *Plasmodium* parasite multiplies within red blood cells, where it proteolyzes hemoglobin to meet its nutritional needs. This process releases heme, which in its soluble form is toxic to the parasite. The parasite sequesters the heme in a crystalline (nontoxic) form. Quinine and chloroquine pass through cell membranes and inhibit heme crystallization in the parasite.

compound may improve its action. For most drugs in use today, 5000 to 10,000 related compounds were typically synthesized and tested. Drug development is a systematic and iterative process in which the most promising derivatives of the lead compound serve as the starting points for the next round of derivatization and testing.

Structure-Based Drug Design Accelerates Drug Discovery. Since the mid 1980s, dramatic advances in the speed and precision with which a macromolecular structure can be determined by X-ray crystallography and NMR (Section 6-2A) have enabled **structure-based drug design,** a process that greatly reduces the number of compounds that need be synthesized in a drug discovery program. As its name implies, structure-based drug design (also called **rational drug design**) uses the structure of a receptor or enzyme in complex with a drug candidate to guide the development of more efficacious compounds. Such a structure will reveal, for example, the positions of the hydrogen bonding donors and acceptors in the binding site as well as cavities in the binding site into which substituents might be placed on a drug candidate to increase its binding affinity. These direct visualization techniques are usually supplemented with molecular modeling tools such as the computation of the minimum energy conformation of a proposed derivative, quantum mechanical calculations that determine its charge distribution and hence how it would interact electrostatically with the protein, and docking simulations in which an inhibitor candidate is computationally modeled into the binding site on the receptor to assess potential interactions. A structure-based approach was used to develop the analgesics (pain relievers) Celebrex and Vioxx (Section 20-6C) and to develop drugs to treat HIV infection (Box 12-4).

Combinatorial Chemistry and High-Throughput Screening Are Useful Drug Discovery Tools. As structure-based methods were developed, it appeared that they would become the dominant mode of drug discovery. However, the recent advent of **combinatorial chemistry** techniques to rapidly and inexpensively synthesize large numbers of related compounds combined with the development of robotic **high-throughput screening** techniques has caused the drug discovery "pendulum" to again swing toward the "make-many-compounds-and-see-what-they-do" approach. If a lead compound can be synthesized in a stepwise manner from several smaller modules, then the substituents on each of these modules can be varied in parallel to produce a library of related compounds (Fig. 12-18).

A variety of synthetic techniques have been developed that permit the combinatorial synthesis of thousands of related compounds in a single procedure. Thus, whereas investigations into the importance of a hydrophobic group at a particular position in a lead compound might previously have prompted the individual syntheses of only the ethyl, propyl, and benzyl derivatives of the compound, the use of combinatorial synthesis would

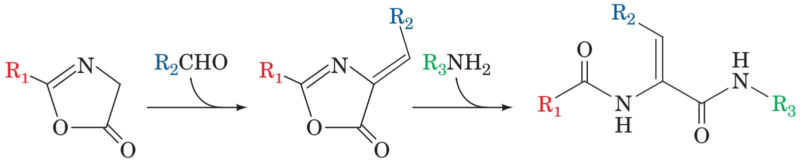

■ **Figure 12-18** | **The combinatorial synthesis of arylidene diamides.** If ten different variants of each R group are used in the synthesis, then 1000 different derivatives will be synthesized.

permit the generation of perhaps 100 different groups at that position. This would far more effectively map out the potential range of the substituent and possibly identify an unexpectedly active analog.

B | A Drug's Bioavailability Depends on How It Is Absorbed and Transported in the Body

The *in vitro* development of an effective drug candidate is only the first step in the drug development process. *Besides causing the desired response in its isolated target protein, a useful drug must be delivered in sufficiently high concentration to this protein where it resides in the human body.* For example, a drug that is administered orally (the most convenient route) must surmount a series of formidable barriers: (1) The drug must be chemically stable in the highly acidic environment of the stomach and must not be degraded by digestive enzymes; (2) it must be absorbed from the gastrointestinal tract into the bloodstream, that is, it must pass through several cell membranes; (3) it must not bind too tightly to other substances in the body (e.g., lipophilic substances tend to be absorbed by certain plasma proteins and by fat tissue); (4) it must survive derivatization by the battery of enzymes, mainly in the liver, that detoxify **xenobiotics** (foreign compounds; note that the intestinal blood flow drains directly into the liver via the portal vein so that the liver processes all orally ingested substances before they reach the rest of the body); (5) it must avoid rapid excretion by the kidneys; (6) it must pass from the capillaries to its target tissue; (7) if it is targeted to the brain, it must cross the **blood–brain barrier,** which blocks the passage of most polar substances; and (8) if it is targeted to an intracellular protein, it must pass through the plasma membrane and possibly one or more intracellular membranes.

The ways in which a drug interacts with the barriers listed above is known as its **pharmacokinetics.** Thus, the **bioavailability** of a drug (the extent to which it reaches its site of action, which is usually taken to be the systemic circulation) depends on both the dose given and its pharmacokinetics. *The most effective drugs are usually a compromise; they are neither too lipophilic nor too hydrophilic.* In addition, their pK values are usually in the range 6 to 8 so that they can readily assume both their ionized and unionized forms at physiological pH's. This permits them to cross cell membranes in their unionized form and to bind to their target protein in their ionized form.

C | Clinical Trials Test for Efficacy and Safety

Above all else, a successful drug candidate must be safe and efficacious in humans. Tests for these properties are initially carried out in animals, but since humans and animals often react quite differently to a drug, it must ultimately be tested in humans through **clinical trials.** In the United States, clinical trials are monitored by the Food and Drug Administration (FDA) and have three increasingly detailed (and expensive) phases:

Phase I. This phase is primarily designed to test the safety of a drug candidate but is also used to determine its dosage range and the optimal dosage method (e.g., oral versus injected) and frequency. It is usually carried out on a small number (20–100) of normal, healthy volunteers, but in the case of a drug candidate known to be highly toxic (e.g., a cancer chemotherapeutic agent), it is carried out on volunteer patients with the target disease.

Phase II. This phase mainly tests the efficacy of the drug against the target disease in 100 to 500 volunteer patients but also refines the dosage range and checks for side effects. The effects of the drug candidate are usually assessed via **single blind tests,** procedures in which the patient is unaware of whether he or she has received the drug or a control substance. Usually the control substance is a **placebo** (an inert substance with the same physical appearance, taste, etc., as the drug being tested) but, in the case of a life-threatening disease, it is an ethical necessity that the control substance be the best available treatment against the disease.

Phase III. This phase monitors adverse reactions from long-term use as well as confirming efficacy in 1000 to 5000 patients. It pits the drug candidate against control substances through the statistical analysis of carefully designed **double blind tests,** procedures in which neither the patients nor the clinical investigators know whether a given patient has received the drug or a control substance. This is done to minimize bias in the subjective judgments the investigators must make.

Currently, only about 5 drug candidates in 5000 that enter preclinical trials reach clinical trials. Of these, only one, on average, is ultimately approved for clinical use, with the majority failing in Phase II trials. In recent years, the preclinical portion of a drug discovery process has averaged ~3 years to complete, whereas successful clinical trials have usually required an additional 7 to 10 years. These successive stages of the drug discovery process are increasingly expensive so that successfully bringing a drug to market costs, on average, around $300 million.

The most time-consuming and expensive aspect of a drug development program is identifying a drug candidate's rare adverse reactions. Nevertheless, it is not an uncommon experience for a drug to be brought to market only to be withdrawn some months or years later when it is found to have caused unanticipated life-threatening side effects in as few as 1 in 10,000 individuals (the post-marketing surveillance of a drug is known as its Phase IV clinical trial). For example, in 1997, the FDA withdrew its approval of the drug **fenfluramine (fen),**

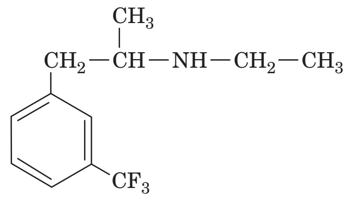

Fenfluramine

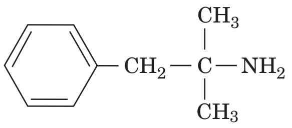

Phentermine

which it had approved in 1973 for use as an appetite suppressant in short-term (a few weeks) weight-loss programs. Fenfluramine had become widely prescribed, often for extended periods, together with another appetite suppressant, **phentermine** (**phen;** approved in 1959), a combination known as **fen-phen** (although the FDA had not approved of the use of the two drugs in combination, once it approves a drug for some purpose, a physician may prescribe it for any other purpose). The withdrawal of fenfluramine was prompted by over 100 reports of heart valve damage in individuals (mostly women) who had taken fen-phen for an average of 12 months (phentermine was not withdrawn because the evidence indicated that fenfluramine was the responsible agent). This rare side effect had not been observed in the clinical trials of fenfluramine, in part because it is such an unusual type of drug reaction that it had not been screened for.

More recently (2004), the widely prescribed analgesic Vioxx was withdrawn from use due to its previously undetected cardiac side effects, although the closely related analgesic Celebrex remains available (Section 20-6C).

D | Cytochromes P450 Are Often Implicated in Adverse Drug Reactions

Why is it that a drug that is well tolerated by the majority of patients can pose a danger to others? *Differences in reactions to drugs arise from genetic differences among individuals as well as differences in their disease states, other drugs they are taking, age, sex, and environmental factors.* The **cytochromes P450,** which function in large part to detoxify xenobiotics and which participate in the metabolic clearance of the majority of drugs in use, provide instructive examples of these phenomena.

The cytochromes P450 constitute a superfamily of heme-containing enzymes that occur in nearly all living organisms, from bacteria to mammals [their name arises from the characteristic 450-nm peak in their absorption spectra when reacted in their Fe(II) state with CO]. The human genome encodes 57 isozymes of cytochrome P450, around one-third of which occur in the liver (P450 isozymes are named by the letters "CYP" followed by a number designating its family, an uppercase letter designating its subfamily, and often another number; e.g., CYP2D6). These **monooxygenases** (Fig. 12-19), which in animals are embedded in the endoplasmic reticulum membrane, catalyze reactions of the sort

$$\mathrm{RH} + \mathrm{O_2} + 2\,\mathrm{H^+} + 2\,e^- \rightarrow \mathrm{ROH} + \mathrm{H_2O}$$

The electrons (e^-) are supplied by NADPH, which passes them to cytochrome P450's heme prosthetic group via the intermediacy of the enzyme **NADPH-P450 reductase.** Here RH represents a wide variety of usually lipophilic compounds for which the different cytochromes P450 are specific. They include polycyclic aromatic hydrocarbons [PAHs; frequently carcinogenic (cancer-causing) compounds that are present in tobacco smoke, broiled meats, and other pyrolysis products], polycyclic biphenyls (PCBs; which were widely used in electrical insulators and as plasticizers and are also carcinogenic), steroids (in whose syntheses cytochromes P450 participate), and many different types of drugs. The xenobiotics are thereby converted to a more water-soluble form, which aids in their excretion by the kidneys. Moreover, the newly generated hydroxyl groups are often enzymatically conjugated (covalently linked) to polar substances such as glucuronic acid (Section 8-1C), glycine, sulfate, and acetate, which further enhances aqueous solubility. The many types of cytochromes P450 in animals, which have different substrate specificities (although these specificities tend to be broad and hence often overlap), are thought to have arisen in response to the numerous toxins that plants produce, presumably to discourage animals from eating them (other P450s function to catalyze specific biosynthetic reactions).

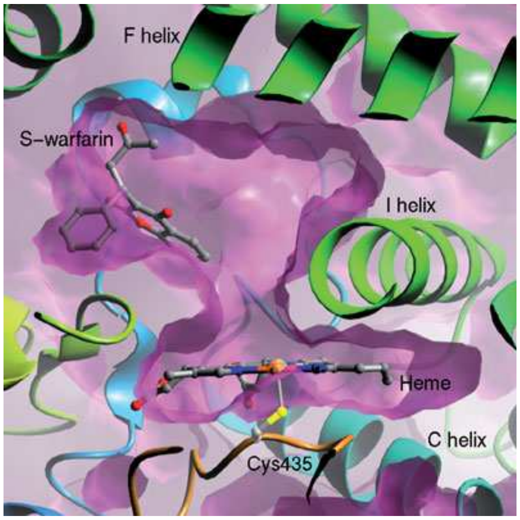

■ **Figure 12-19 | X-Ray structure of the human cytochrome P450 CYP2C9 in complex with the blood clotting inhibitor warfarin (Coumadin).** A cutaway diagram of the enzyme's active site region drawn with its surface purple and with its polypeptide backbone in ribbon form colored in rainbow order from N-terminus (*blue*) to C-terminus (*red*). The heme (seen edgewise), the Cys side chain that axially ligands the heme Fe atom, and the warfarin are shown in ball-and-stick form with C gray, N blue, O red, S yellow, and Fe orange. [Image courtesy of Astex Therapeutics Limited. PDBid 1OG5.]

***Drug–drug interactions** are often mediated by cytochromes P450.* For example, if drug A is metabolized by or otherwise inhibits a cytochrome P450 isozyme that metabolizes drug B, then coadministering drugs A and B will cause the bioavailability of drug B to increase above the value it would have had if it alone had been administered. This phenomenon is of particular concern if drug B has a low **therapeutic index** (the ratio of the dose of the drug that produces toxicity to that which produces the desired effect). Conversely, if, as is often the case, drug A induces the increased expression of the cytochrome P450 isozyme that metabolizes it and drug B, then coadministering drugs A and B will reduce drug B's bioavailability, a phenomenon that was first noted when certain antibiotics caused oral contraceptives to lose their efficacy. Moreover, if drug B is metabolized to a toxic product, its increased rate of reaction may result in an adverse reaction. Environmental pollutants such as PAHs and PCBs are also known to induce the expression of specific cytochrome P450 isozymes and thereby alter the rates at which certain drugs are metabolized. Finally, some of these same effects may occur in patients with liver disease, as well as arising from age-based, gender-based, and individual differences in liver physiology.

Although many cytochromes P450 presumably evolved to detoxify and/or help eliminate harmful substances, in several cases they have been shown to participate in converting relatively innocuous compounds to toxic agents. For example, **acetaminophen** (Fig. 12-20), a widely used analgesic and antipyretic (fever reducer) is quite safe when taken in therapeutic doses (1.2 g/day for an adult) but, in large doses (>10 g), is highly toxic. This is because, in therapeutic amounts, 95% of the acetaminophen present is enzymatically glucuronidated or sulfated at its —OH group to the

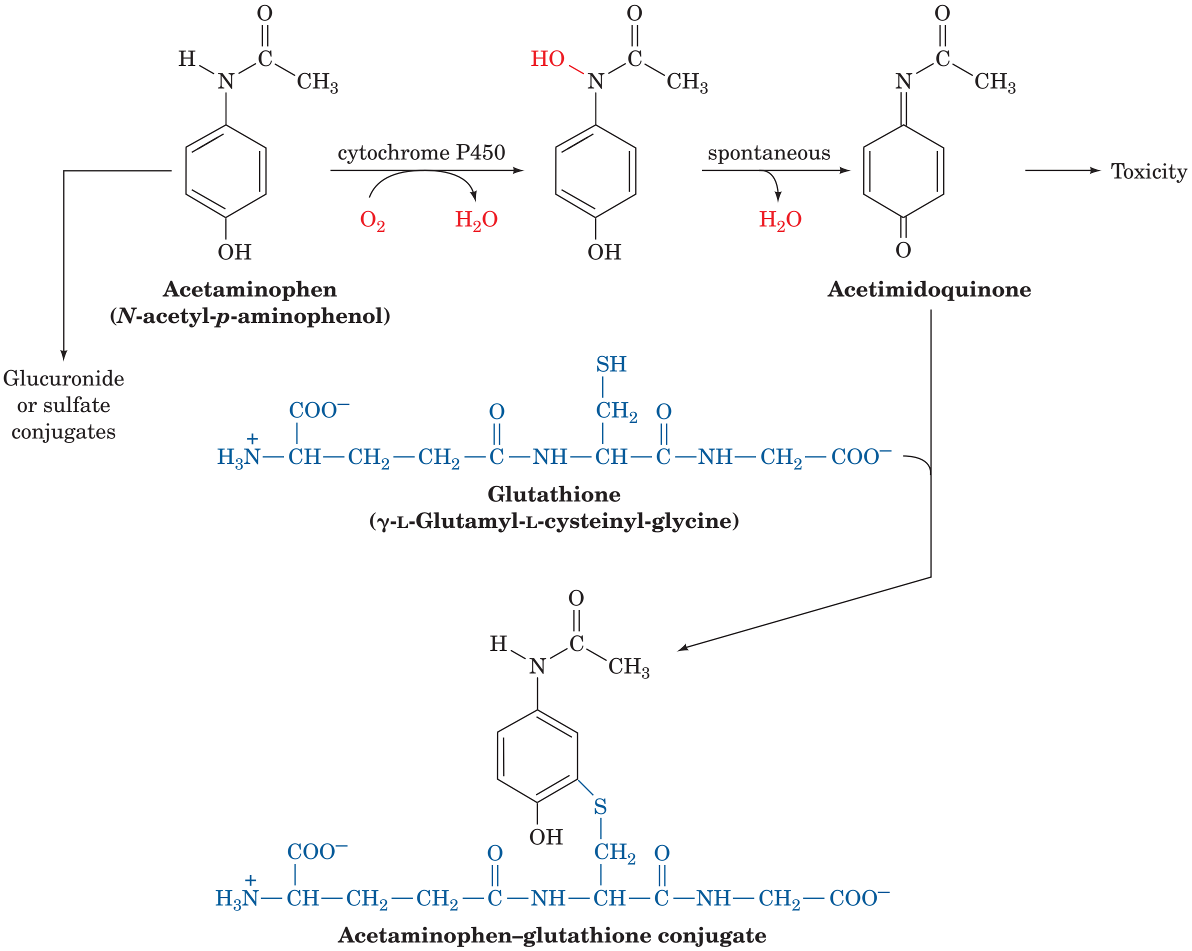
cytochrome P450
O_2
H_2O
spontaneous
H_2O
Toxicity
Acetaminophen
(*N*-acetyl-*p*-aminophenol)
Acetimidoquinone
Glucuronide or sulfate conjugates
Glutathione
(γ-L-Glutamyl-L-cysteinyl-glycine)
Acetaminophen–glutathione conjugate

Figure 12-20 | The metabolic reactions of acetaminophen. An overdose of acetaminophen leads to the buildup of acetimidoquinone, which is toxic.

corresponding conjugates, which are readily excreted. The remaining 5% is converted, through the action of a cytochrome P450 (CYP2E1), to **acetimidoquinone** (Fig. 12-20), which is then conjugated with glutathione (Section 4-3B). However, when acetaminophen is taken in large amounts, the glucuronidation and sulfation pathways become saturated and hence the cytochrome P450-mediated pathway becomes increasingly important. If hepatic (liver) glutathione is depleted faster than it can be replaced, acetimidoquinone, a reactive compound, instead conjugates with the sulfhydryl groups of cellular proteins resulting in often fatal hepatotoxicity.

Many of the cytochromes P450 in humans are unusually **polymorphic,** that is, there are several common alleles (variants) of the genes encoding each of these enzymes in the human population. Alleles that cause diminished, enhanced, and qualitatively altered rates of drug metabolism have been characterized for many of the cytochromes P450. The distributions of these various alleles differs markedly among ethnic groups and hence probably arose to permit each group to cope with the toxins in its particular diet.

Polymorphism in a given cytochrome P450 results in differences between individuals in the rates at which they metabolize certain drugs. For instance, in cases in which a cytochrome P450 variant has absent or diminished activity, otherwise standard doses of a drug that the enzyme normally metabolizes may cause the bioavailability of the drug to reach toxic levels. Conversely, if a particular P450 enzyme has enhanced activity (usually because the gene encoding it has been duplicated one or more times), higher than normal doses of a drug that the enzyme metabolizes would have to be administered to obtain the required therapeutic effect. However, if the drug is metabolized to a toxic product, this may result in an adverse reaction. Several known P450 variants have altered substrate specificities and hence produce unusual metabolites, which also may cause harmful side effects.

Experience has amply demonstrated that *there is no such thing as a drug that is entirely free of adverse reactions.* However, as the enzymes and their variants that participate in drug metabolism are characterized and as rapid and inexpensive genotyping methods are developed, it is becoming possible to tailor drug treatment to an individual's genetic makeup rather than to the population as a whole. This rapidly developing area of study is called **pharmacogenomics.**

CHECK YOUR UNDERSTANDING

Compare structure-based drug design and combinatorial chemistry as tools for developing drug candidates.
List the factors that influence a drug's bioavailability.
Summarize the purpose of phases I through III of a clinical trial.
Indicate how drugs that are well tolerated by the majority of the population cause adverse reactions in certain individuals.

SUMMARY

1. Elementary chemical reactions may be first order, second order, or, rarely, third order. In each case, a rate equation describes the progress of the reaction as a function of time.
2. The Michaelis–Menten equation describes the relationship between initial reaction velocity and substrate concentration under steady state conditions.
3. K_M is the substrate concentration at which the reaction velocity is half-maximal. The value of k_{cat}/K_M indicates an enzyme's catalytic efficiency.
4. Kinetic data can be plotted in double-reciprocal form to determine K_M and V_{max}.
5. Bisubstrate reactions are classified as sequential (single displacement) or Ping Pong (double displacement). A sequential reaction may proceed by an Ordered or Random mechanism.
6. Reversible inhibitors reduce an enzyme's activity by binding to the substrate-binding site (competitive inhibition), to the enzyme–substrate complex (uncompetitive inhibition), or to both the enzyme and the enzyme–substrate complex (mixed inhibition).
7. Enzyme activity may be controlled by allosteric effectors.
8. The activity of ATCase is increased by ATP and decreased by CTP, which alter the conformation of the catalytic sites by stabilizing the R and the T states of the enzyme, respectively.
9. Enzyme activity may be controlled by covalent modification.

10. The enzymatic activity of glycogen phosphorylase is controlled by its phosphorylation/dephosphorylation as well as by the influence of allosteric effectors.

11. An enzyme inhibitor can be developed for use as a drug through structure-based and/or combinatorial methods. It must then be tested for safety and efficacy in clinical trials. Adverse reactions to drugs and drug–drug interactions are often mediated by a cytochrome P450.

KEY TERMS

elementary reaction	**364**
k	**364**
v	**364**
first-order reaction	**364**
reaction order	**365**
molecularity	**365**
second-order reaction	**365**
rate equation	**365**
$t_{1/2}$	**365**
pseudo-first-order reaction	**366**
zero-order reaction	**366**
radionuclide	**367**
autoradiography	**367**
ES complex	**368**
k_{-1}	**368**
k_2	**368**
Michaelis complex	**368**
steady state	**368**
steady state assumption	**369**
K_M	**369**
v_o	**370**
V_{max}	**370**
enzyme saturation	**370**
Michaelis–Menten equation	**370**
k_{cat}	**371**
turnover number	**371**
k_{cat}/K_M	**371**
diffusion-controlled limit	**371**
Lineweaver–Burk (double-reciprocal) plot	**373**
sequential reaction	**375**
single-displacement reaction	**375**
Ordered mechanism	**375**
Random mechanism	**375**
Ping Pong reaction	**376**
double-displacement reaction	**376**
inhibitor	**377**
inactivator	**377**
competitive inhibition	**377**
product inhibition	**378**
transition state analog	**378**
K_I	**378**
K_M^{app}	**379**
uncompetitive inhibition	**381**
V_{max}^{app}	**381**
mixed (noncompetitive) inhibition	**382**
allosteric effector	**386**
covalent modification	**386**
feedback inhibitor	**387**
protein kinase	**391**
protein phosphatase	**391**
isozyme (isoform)	**391**
lead compound	**394**
structure-based (rational) drug design	**395**
combinatorial chemistry	**395**
xenobiotic	**396**
pharmacokinetics	**396**
bioavailability	**396**
clinical trial	**396**
cytochrome P450	**398**
drug–drug interaction	**398**
therapeutic index	**398**
pharmacogenomics	**400**

PROBLEMS

1. Consider the nonenzymatic elementary reaction $A \rightarrow B$. When the concentration of A is 20 mM, the reaction velocity is measured as 5 μM B produced per minute. (a) Calculate the rate constant for this reaction. (b) What is the molecularity of the reaction?

2. If there are 10 μmol of the radioactive isotope ^{32}P (half-life 14 days) at $t = 0$, how much ^{32}P will remain at (a) 7 days, (b) 14 days, (c) 21 days, and (d) 70 days?

3. The hypothetical elementary reaction $2A \rightarrow B + C$ has a rate constant of $10^{-6}\ M^{-1} \cdot s^{-1}$. What is the reaction velocity when the concentration of A is 10 mM?

4. For each reaction below, determine whether the reaction is first order or second order and calculate the rate constant.

Time (s)	Reaction A reactant (mM)	Reaction B reactant (mM)
0	6.2	5.4
1	3.1	4.6
2	2.1	3.9
3	1.6	3.2
4	1.3	2.7
5	1.1	2.3

5. For an enzymatic reaction, draw curves that show the appropriate relationships between the variables in each plot below.

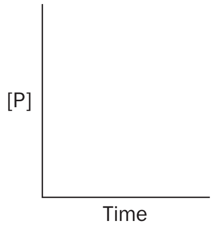

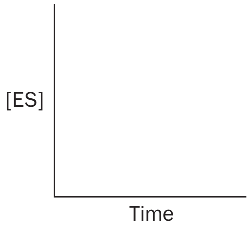

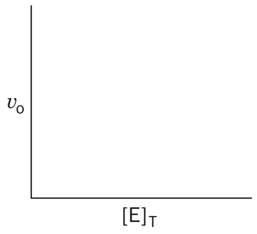

6. Explain why it is usually easier to calculate an enzyme's reaction velocity from the rate of appearance of product rather than the rate of disappearance of a substrate.

7. At what concentration of S (expressed as a multiple of K_M) will $v_o = 0.95V_{max}$?

8. Identify the enzymes in Table 12-1 whose catalytic efficiencies are near the diffusion-controlled limit.

9. Explain why each of the following data sets from a Lineweaver–Burk plot are not individually ideal for determining K_M for an enzyme-catalyzed reaction that follows Michaelis–Menten kinetics.

Set A	**1/[S] ($\mathbf{mM^{-1}}$)**	**$1/v_o$ ($\mathbf{\mu M^{-1} \cdot s}$)**
	0.5	2.4
	1.0	2.6
	1.5	2.9
	2.0	3.1

Set B	**1/[S] ($\mathbf{mM^{-1}}$)**	**$1/v_o$ ($\mathbf{\mu M^{-1} \cdot s}$)**
	8	5.9
	10	6.8
	12	7.8
	14	8.7

10. Calculate K_M and V_{max} from the following data:

[S] (μM)	**v_o ($\mathbf{mM \cdot s^{-1}}$)**
0.1	0.34
0.2	0.53
0.4	0.74
0.8	0.91
1.6	1.04

11. You are trying to determine the K_M for an enzyme. Due to a lab mishap, you have only two usable data points:

Substrate concentration (μM)	**Reaction velocity ($\mathbf{\mu M \cdot s^{-1}}$)**
1	5
100	50

Use these data to calculate an approximate value for K_M. Is this value likely to be an overestimate or an underestimate of the true value? Explain.

12. You are attempting to determine K_M by measuring the reaction velocity at different substrate concentrations, but you do not realize that the substrate tends to precipitate under the experimental conditions you have chosen. How would this affect your measurement of K_M?

13. You are constructing a velocity versus [substrate] curve for an enzyme whose K_M is believed to be about 2 μM. The enzyme concentration is 200 nM and the substrate concentrations range from 0.1 μM to 10 μM. What is wrong with this experimental setup and how could you fix it?

14. Is it necessary for measurements of reaction velocity to be expressed in units of concentration per time ($M \cdot s^{-1}$, for example) in order to calculate an enzyme's K_M?

15. Is it necessary to know $[E]_T$ in order to determine (a) K_M, (b) V_{max}, or (c) k_{cat}?

16. The K_M for the reaction of chymotrypsin with *N*-acetylvaline ethyl ester is 8.8×10^{-2} M, and the K_M for the reaction of chymotrypsin with *N*-acetyltyrosine ethyl ester is 6.6×10^{-4} M. (a) Which substrate has the higher apparent affinity for the enzyme? (b) Which substrate is likely to give a higher value for V_{max}?

17. Enzyme A catalyzes the reaction $S \rightarrow P$ and has a K_M of 50 μM and a V_{max} of 100 $nM \cdot s^{-1}$. Enzyme B catalyzes the reaction $S \rightarrow Q$ and has a K_M of 5 mM and a V_{max} of 120 $nM \cdot s^{-1}$. When 100 μM of S is added to a mixture containing equivalent amounts of enzymes A and B, after one minute which reaction product will be more abundant: P or Q?

18. In a bisubstrate reaction, a small amount of the first product P is isotopically labeled (P*) and added to the enzyme and the first substrate A. No B or Q is present. Will A (= P—X) become isotopically labeled (A*) if the reaction follows (a) a Ping Pong mechanism or (b) a Sequential mechanism?

19. Determine the type of inhibition of an enzymatic reaction from the following data collected in the presence and absence of the inhibitor.

[S] (mM)	**v_o ($\mathbf{mM \cdot min^{-1}}$)**	**v_o with I present ($\mathbf{mM \cdot min^{-1}}$)**
1	1.3	0.8
2	2.0	1.2
4	2.8	1.7
8	3.6	2.2
12	4.0	2.4

20. Estimate K_I for a competitive inhibitor when [I] = 5 mM gives an apparent value of K_M that is three times the K_M for the uninhibited reaction.

21. For an enzyme-catalyzed reaction, the presence of 5 nM of a reversible inhibitor yields a V_{max} value that is 80% of the value in the absence of the inhibitor. The K_M value is unchanged. (a) What type of inhibition is likely occurring? (b) What proportion of the enzyme molecules have bound inhibitor? (c) Calculate the inhibition constant.

22. How would diisopropylphosphofluoridate (DIPF; Section 11-5A) affect the apparent K_M and V_{max} of a sample of chymotrypsin?

23. Based on some preliminary measurements, you suspect that a sample of enzyme contains an irreversible enzyme inhibitor. You decide to dilute the sample 100-fold and remeasure the enzyme's activity. What would your results show if the inhibitor in the sample is (a) irreversible or (b) reversible?

24. Enzyme X and enzyme Y catalyze the same reaction and exhibit the v_o versus [S] curves shown below. Which enzyme is more efficient at low [S]? Which is more efficient at high [S]?

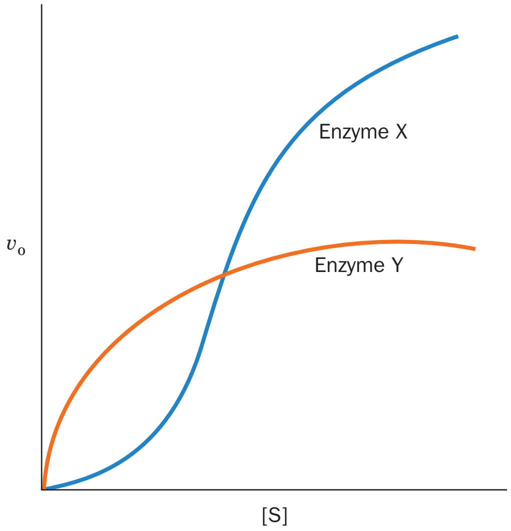

25. Sphingosine-1-phosphate (SPP) is important for cell survival. The synthesis of SPP from sphingosine and ATP is catalyzed by the enzyme sphingosine kinase. An understanding of the kinetics of the sphingosine kinase reaction may be important in the development of drugs to treat cancer. The velocity of the sphingosine kinase reaction was measured in the presence and absence of *threo*-sphingosine, a stereoisomer of sphingosine that inhibits the enzyme. The results are shown below.

[Sphingosine] (μM)	**v_o (mg · min^{-1}) (no inhibitor)**	**v_o (mg · min^{-1}) (with *threo*-sphingosine)**
2.5	32.3	8.5
3.5	40	11.5
5	50.8	14.6
10	72	25.4
20	87.7	43.9
50	115.4	70.8

Construct a Lineweaver–Burk plot to answer the following questions:

(a) What are the apparent K_M and V_{max} values in the presence and absence of the inhibitor?

(b) What kind of an inhibitor is *threo*-sphingosine? Explain.

CASE STUDIES

Case 7
A Storage Protein from Seeds of* Brassica nigra *Is a Serine Protease Inhibitor

Focus concept: Purification of a novel seed storage protein allows sequence analysis and determination of the protein's secondary and tertiary structure.

Prerequisites: Chapters 5, 11, and 12

- Protein purification techniques, particularly gel filtration and dialysis
- Protein sequencing using Edman degradation and overlapping peptides
- Structure and mechanism of serine proteases
- Reversible inhibition of enzymes

Case 12
Production of Methanol in Ripening Fruit

Focus concept: The link between the production of methanol in ripening fruit and the activity of pectin methylesterase, the enzyme responsible for methanol production, is examined in wild-type and transgenic tomato fruit.

Prerequisite: Chapter 12

- Enzyme kinetics and inhibition

Case 13
Inhibition of Alcohol Dehydrogenase

Focus concept: The inhibition of the alcohol dehydrogenase by a formamide compound is examined.

Prerequisite: Chapter 12

- Principles of enzyme kinetics
- Identification of inhibition via Lineweaver–Burk plots

Case 15
Site-Directed Mutagenesis of Creatine Kinase

Focus concept: Site-directed mutagenesis is used to create mutant creatine kinase enzymes so that the role of a single reactive cysteine in binding and catalysis can be assessed.

Prerequisites: Chapters 4, 6, 11, and 12

- Amino acid structure
- Protein architecture
- Enzyme kinetics and inhibition
- Basic enzyme mechanisms

Case 19
Purification of Rat Kidney Sphingosine Kinase

Focus concept: The purification and kinetic analysis of an enzyme that produces a product important in cell survival is the focus of this study.

Prerequisites: Chapters 5 and 12

- Protein purification techniques and protein analytical methods
- Basic enzyme kinetics

BIOINFORMATICS EXERCISES

Bioinformatics Exercises are available at www.wiley.com/college/voet.

Chapter 12
Enzyme Inhibitors and Rational Drug Design

1. **Dihydrofolate Reductase.** Examine the structure of an enzyme with an inhibitor bound to it.
2. **HIV Protease.** Compare the structures of complexes containing HIV protease and an inhibitor.
3. **Pharmacogenomics and Single Nucleotide Polymorphisms.** Use online databases to find information on cytochrome P450 polymorphisms.

REFERENCES

Kinetics

Cornish-Bowden, A., *Fundamentals of Enzyme Kinetics* (revised ed.), Portland Press (1995). [A lucid and detailed account of enzyme kinetics.]

Fersht, A., *Structure and Mechanism in Protein Science: A Guide to Enzyme Catalysis and Protein Folding,* W.H. Freeman (1999).

Gutfreund, H., *Kinetics for the Life Sciences: Receptors, Transmitters, and Catalysts,* Cambridge University Press (1995).

Segel, I.H., *Enzyme Kinetics,* Wiley-Interscience (1993). [A detailed and understandable treatise providing full explanations of many aspects of enzyme kinetics.]

Allosteric Control and Control by Covalent Modification

Jin, L., Stec, B., Lipscomb, W.N., and Kantrowitz, E.R., Insights into the mechanisms of catalysis and heterotropic regulation of *Escherichia coli* aspartate transcarbamoylase based upon a structure of the enzyme complexed with the bisubstrate analogue *N*-phosphonacetyl-L-aspartate at 2.1Å, *Proteins* **37,** 729–742 (1999).

Johnson, L.N. and Lewis, R.J., Structural basis for control by phosphorylation, *Chem. Rev.* **101,** 2209–2242 (2001).

Lipscomb, W.N., Structure and function of allosteric enzymes, *Chemtracts—Biochem. Mol. Biol.* **2,** 1–15 (1991).

Perutz, M., *Mechanisms of Cooperativity and Allosteric Regulation in Proteins,* Cambridge University Press (1990).

Drug Design

Furge, L.L. and Guengerich, F.P., Cytochrome P450 enzymes in drug metabolism and chemical toxicology, *Biochem. Mol. Biol. Educ.* **34,** 66–74 (2006).

Jorgenson, W.L., The many roles of computation in drug discovery, *Science* **303,** 1813–1818 (2004).

Ohlstein, E.H., Ruffolo, R.R., Jr., and Elliott, J.D., Drug discovery in the next millennium, *Annu. Rev. Pharmacol. Toxicol.* **40,** 177–191 (2000).

Smith, D.A. and van der Waterbeemd, H., Pharmacokinetics and metabolism in early drug design, *Curr. Opin. Chem. Biol.* **3,** 373–378 (1999).

Williams, P.A., Cosme, J., Ward, A., Angove, H.C., Vinkovic, D.M., and Jhoti, H., Crystal structure of human cytochrome P450 2C9 with bound warfarin, *Nature* **424,** 464–468 (2003).

White, R.E., High-throughput screening in drug metabolism and pharmokinetic support of drug discovery, *Annu. Rev. Pharmacol. Toxicol.* **40,** 133–157 (2000).

Wlodawer, A. and Vondrasek, J., Inhibitors of HIV-1 protease: A major success of structure-assisted drug design, *Annu. Rev. Biophys. Biomol. Struct.* **27,** 249–284 (1998). [Reviews the development of some HIV-1 protease inhibitors.]

13

Biochemical Signaling

A cell must have an appropriate receptor to recognize and respond to a chemical signal produced by another cell. [Grant V. Faint/Digital Vision/Getty Images]

CHAPTER CONTENTS

1 Hormones
- **A.** Pancreatic Islet Hormones Control Fuel Metabolism
- **B.** Epinephrine and Norepinephrine Prepare the Body for Action
- **C.** Steroid Hormones Regulate a Wide Variety of Metabolic and Sexual Processes
- **D.** Growth Hormone Binds to Receptors in Muscle, Bone, and Cartilage

2 Receptor Tyrosine Kinases
- **A.** Receptor Tyrosine Kinases Transmit Signals across the Cell Membrane
- **B.** Kinase Cascades Relay Signals to the Nucleus
- **C.** Some Receptors Are Associated with Nonreceptor Tyrosine Kinases
- **D.** Protein Phosphatases Are Signaling Proteins in Their Own Right

3 Heterotrimeric G Proteins
- **A.** G Protein–Coupled Receptors Contain Seven Transmembrane Helices
- **B.** Heterotrimeric G Proteins Dissociate on Activation
- **C.** Adenylate Cyclase Synthesizes cAMP to Activate Protein Kinase A
- **D.** Phosphodiesterases Limit Second Messenger Activity

4 The Phosphoinositide Pathway
- **A.** Ligand Binding Results in the Cytoplasmic Release of the Second Messengers IP_3 and Ca^{2+}
- **B.** Calmodulin Is a Ca^{2+}-Activated Switch
- **C.** DAG Is a Lipid-Soluble Second Messenger That Activates Protein Kinase C
- **D.** Epilog: Complex Systems Have Emergent Properties

MEDIA RESOURCES

(available at www.wiley.com/college/voet)
Guided Exploration 12. Hormone signaling by the receptor tyrosine kinase system
Guided Exploration 13. Hormone signaling by the adenylate cyclase system
Interactive Exercise 10. X-Ray structure of human growth hormone (hGH)
Interactive Exercise 11. Tyrosine kinase domain of insulin receptor
Interactive Exercise 12. A heterotrimeric G protein
Interactive Exercise 13. C subunit of protein kinase A
Animated Figure 13-7. The Ras signaling cascade
Animated Figure 13-24. The phosphoinositide signaling system
Kinemage 15. cAMP-dependent protein kinase (PKA)
Kinemage 16-1. The structure of calmodulin
Kinemage 16-2. Calmodulin complex with target polypeptide

Living things coordinate their activities at every level of their organization through complex biochemical signaling systems. Intercellular signals are mediated by chemical messengers known as **hormones** and, in higher animals, by neuronally transmitted electrochemical impulses. Intracellular communications are maintained by the synthesis or alteration of a great variety of different substances that are often integral components of the processes they control. For example, metabolic pathways, as we have seen (Section 12-3), are regulated by the feedback control of allosteric enzymes by metabolites in those pathways or by the covalent modification of the enzymes. In this chapter we consider the nature of chemical signals and how the signals are transmitted.

In general, every signaling pathway consists of a ***receptor protein*** *that specifically binds a hormone or other ligand, a mechanism for transmitting the ligand-binding event to the cell interior, and a series of intracellular responses that may involve the synthesis of a* ***second messenger*** *and/or* *chemical changes catalyzed by **kinases** and **phosphatases.** These pathways often involve **enzyme cascades,** in which a succession of events that each depend on the previous one amplifies the signal.*

We begin by discussing the functions of some representative human hormone systems. We then discuss the three major pathways whereby intercellular signals are converted (transduced) to intracellular signals: those that (1) involve receptor tyrosine kinases, (2) utilize heterotrimeric G proteins, and (3) employ phosphoinositide cascades. Neurotransmission is discussed in Section 10-2C.

LEARNING OBJECTIVES

- Understand the general functions of hormones produced by the pancreas, adrenal cortex, and adrenal medulla.
- Understand that a hormone's effects depend on the presence of a specific cellular receptor, the tissue distribution of the receptor, and the receptor's sensitivity to agonists and antagonists.
- Understand that hormone binding induces changes in the receptor, such as dimerization.

1 Hormones

In higher animals, specialized ductless **endocrine glands** (Fig. 13-1) synthesize **endocrine hormones** that they release into the bloodstream in response to external stimuli. These hormones are thereby carried to their target cells

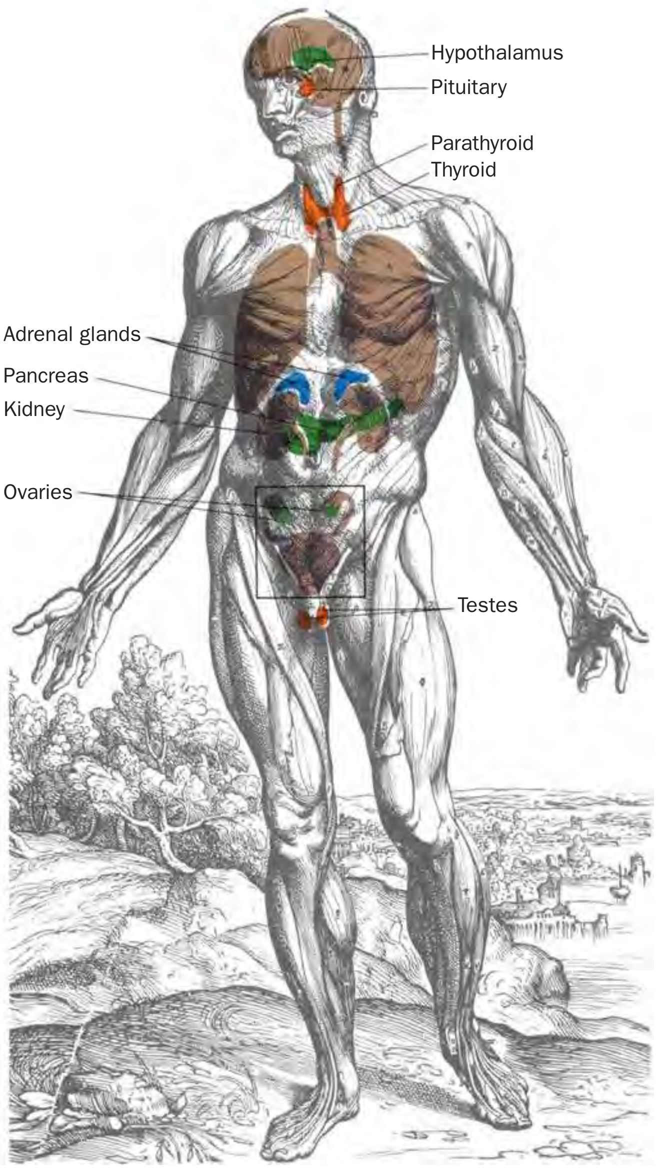

Figure 13-1 | The major glands of the human endocrine system. Other tissues, such as the intestines, also secrete endocrine hormones.

(Fig. 13-2) in which they elicit a response. The human endocrine system secretes a wide variety of hormones that enable the body to:

1. Maintain **homeostasis** (a steady state; e.g., insulin and glucagon maintain the blood glucose level within rigid limits during feast or famine).
2. Respond to a wide variety of external stimuli (such as the preparation for "fight or flight" by epinephrine and norepinephrine).
3. Follow various cyclic and developmental programs (for instance, sex hormones regulate sexual differentiation, maturation, the menstrual cycle, and pregnancy).

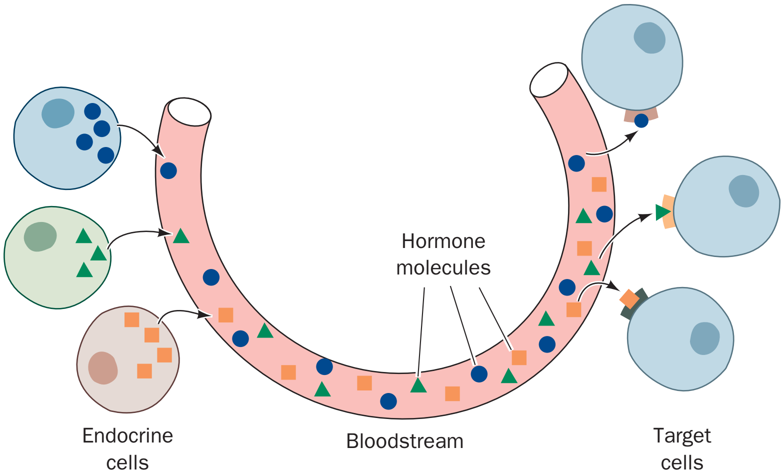

Figure 13-2 | **Endocrine signaling.** Hormones produced by endocrine cells reach their target cells via the bloodstream. Only cells that display the appropriate receptors can respond to the hormones.

Most hormones are either polypeptides, amino acid derivatives, or steroids, although there are important exceptions to this generalization. In any case, *only those cells with a specific receptor for a given hormone will respond to its presence even though nearly all cells in the body may be exposed to the hormone.* Hormonal messages are therefore quite specifically addressed.

Although we discuss specific hormones and their function in many other chapters, in this section we outline the activities of hormones produced by some representative endocrine glands. These glands are not just a collection of independent secretory organs but form a complex and highly interdependent control network. Indeed, the secretion of many hormones is under feedback control through the secretion of other hormones to which the original hormone-secreting gland responds. The concentrations of circulating hormones are typically measured using the radioimmunoassay developed by Rosalyn Yalow (Box 13-1).

A | Pancreatic Islet Hormones Control Fuel Metabolism

The pancreas is a large glandular organ, the bulk of which is an **exocrine gland** dedicated to producing digestive enzymes—such as trypsin, chymotrypsin, RNase A, α-amylase, and phospholipase A_2—that are secreted via the pancreatic duct into the small intestine. However, ~1 to 2% of pancreatic tissue consists of scattered clumps of cells known as **islets of Langerhans,** which comprise an endocrine gland that functions to maintain energy homeostasis. Pancreatic islets contain three types of cells, each of which secretes a characteristic polypeptide hormone:

1. The α cells secrete **glucagon** (29 residues).
2. The β cells secrete insulin (51 residues; Fig. 5-1).
3. The δ cells secrete **somatostatin** (14 residues).

Insulin, which is secreted in response to high blood glucose levels, primarily functions to stimulate muscle, liver, and adipose cells to store glucose for later use by synthesizing glycogen, protein, and fat (Section 22-2). Glucagon, which is secreted in response to low blood glucose, has essentially the opposite effects: It stimulates the liver to release glucose through the breakdown of glycogen (**glycogenolysis;** Section 16-1) and the synthesis of glucose from noncarbohydrate precursors (**gluconeogenesis,** Section 16-4). It also stimulates adipose tissue to release fatty acids through lipolysis. Somatostatin, which is also secreted by the hypothalamus, inhibits the release of insulin and glucagon from their islet cells.

BOX 13-1 PATHWAYS OF DISCOVERY

Rosalyn Yalow and the Radioimmunoassay (RIA)

Rosalyn Yalow (1921–)

Rosalyn Sussman Yalow was born on July 19, 1921, in New York City. Neither of her parents had the advantage of a high school education but there was never a doubt that their two children would make it through college. While Rosalyn was at Hunter, the college for women in New York City's college system (now the City University of New York), Eve Curie had just published the biography of her mother, Madame Marie Curie, a "must-read" for every aspiring female scientist. Rosalyn's goal at that time was achieving a career in physics. Despite suggestions from her family that becoming an elementary school teacher would be more practical, she persisted.

In 1941, after graduating from college, Yalow received an offer of a teaching assistantship in physics at the University of Illinois in Champaign–Urbana. At the first meeting of the faculty of the College of Engineering, she discovered that she was the only woman among its 400 members. The dean of the faculty congratulated her on her achievement and told her she was the first woman there since 1917. The draft of young men into the armed forces, even before America entered World War II, had made possible her entrance into graduate school. On the first day of graduate school she met Aaron Yalow, who was also beginning graduate study in physics at Illinois and who in 1943 was to become her husband.

In January 1945, Yalow received a Ph.D. in nuclear physics and returned to New York as assistant engineer at the Federal Telecommunications Laboratory—its only woman engineer. In 1946, she returned to Hunter College to teach physics, not to women but to returning veterans in a preengineering program. During that time she became interested in the medical aspects of radioisotopes. She joined the Bronx Veterans Administration (VA) as a part-time consultant in December 1947. Even while teaching full-time at Hunter, she equipped and developed the Radioisotope Service at the VA hospital and initiated a variety of research projects with several physicians. In January 1950, Yalow chose to leave teaching and join the VA full time. That spring, Dr. Solomon A. Berson joined the Service and began a 22-year partnership that lasted until his death in 1972.

In their joint studies, Yalow and Berson concentrated on the application of isotopes to clinical problems such as hormone analysis. At the time, insulin was the hormone most readily available in a highly purified form. In studying the reaction of insulin with antibodies, Yalow and Berson recognized that they had a tool with the potential for measuring the concentration of insulin in a complex mixture such as blood. By 1959, they had developed a practical method for quantifying insulin in human plasma, the **radioimmunoassay (RIA).** RIA is now used to measure hundreds of substances of biological interest.

The serum concentrations of insulin and other hormones are extremely low, generally between 10^{-12} and 10^{-7} M, so they usually must be measured by indirect means. In RIAs, the unknown concentration of a hormone, H, is determined by measuring how much of a known amount of the radioactively labeled hormone, H*, binds to a fixed quantity of anti-H antibody in the presence of H. This competition reaction is easily calibrated by constructing a standard curve indicating how much H* binds to the antibody as a function of [H]. The high binding affinity and specificity of antibodies for their ligands gives RIAs the advantages of great sensitivity and specificity.

By 1977, Yalow's hospital was affiliated with the Mount Sinai School of Medicine, and Yalow held the title of Distinguished Service Professor. She is a member of the National Academy of Sciences and has received numerous awards and honors, including the 1977 Nobel Prize in Physiology or Medicine (Berson died before this Nobel prize was awarded and so could not share the prize) and the 1988 National Medal of Science. "The excitement of learning separates youth from old age," Rosalyn Yalow has said. "As long as you're learning, you're not old."*

Mostly abridged from Rosalyn Yalow's autobiography, *Les Prix Nobel. The Nobel Prizes 1977,* Wilhelm Odelberg (Ed.), Nobel Foundation, 1978.

*From *O, The Oprah Magazine,* January 1, 2005.

Polypeptide hormones, like other proteins destined for secretion, are ribosomally synthesized as prohormones, processed in the rough endoplasmic reticulum and Golgi apparatus to form the mature hormone, and then packaged in secretory granules to await the signal for their release by exocytosis (Sections 9-4D–F). The most potent physiological stimuli for the release of insulin and glucagon are, respectively, high and low blood glucose concentrations so that islet cells act as the body's primary glucose sensors. However, the release of the hormones is also influenced by the autonomic (involuntary) nervous system and by hormones secreted by the gastrointestinal tract.

B | Epinephrine and Norepinephrine Prepare the Body for Action

The **adrenal glands** consist of two distinct types of tissue: the **medulla** (core), which is really an extension of the sympathetic nervous system (a part of the autonomic nervous system), and the more typically glandular **cortex** (outer layer). Here we consider the hormones of the adrenal medulla; those of the cortex are discussed in the following section.

The adrenal medulla synthesizes two hormonally active ***catecholamines*** *(amine-containing derivatives of* ***catechol,*** *1,2-dihydroxybenzene):* ***norepinephrine (noradrenalin)*** *and its methyl derivative* ***epinephrine (adrenalin;*** *at right***).** These hormones are synthesized from tyrosine as is described in Section 21-6B and stored in granules to await their exocytotic release under the control of the sympathetic nervous system.

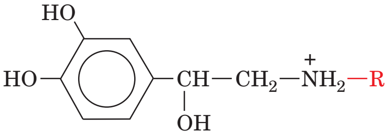

$R = H$ **Norepinephrine (noradrenalin)**

$R = CH_3$ **Epinephrine (adrenalin)**

The biological effects of catecholamines are mediated by two classes of plasma membrane receptors, the α- and **β-adrenoreceptors** (also known as **adrenergic receptors**). These transmembrane glycoproteins were originally identified on the basis of their varying responses to certain **agonists** (substances that bind to a receptor so as to evoke a response) and **antagonists** (substances that bind to a receptor but fail to elicit a response, thereby blocking agonist action). The β- but not the α-adrenoreceptors, for example, are stimulated by **isoproterenol** but blocked by **propranolol,** whereas α- but not β-adrenoreceptors are blocked by **phentolamine.**

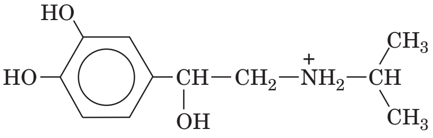

Isoproterenol

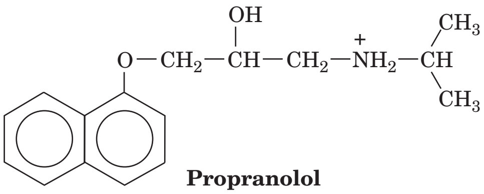

Propranolol

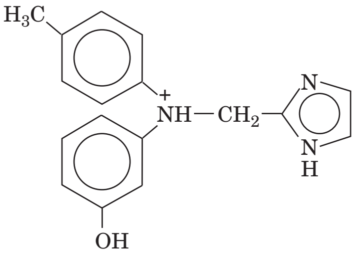

Phentolamine

The α- and β-adrenoreceptors, which occur on separate tissues in mammals, generally respond differently and often oppositely to catecholamines. For instance, β-adrenoreceptors stimulate glycogenolysis and gluconeogenesis in liver (Sections 16-1 and 16-4), glycogenolysis in skeletal muscle, lipolysis in adipose tissue, the relaxation of smooth (involuntary) muscle in the bronchi and in the blood vessels supplying the skeletal (voluntary) muscles, and increased heart action. In contrast, α-adrenoreceptors stimulate smooth muscle contraction in blood vessels supplying peripheral organs such as skin and kidney, smooth muscle relaxation in the gastrointestinal tract, and blood platelet aggregation. *Most* *of these diverse effects are directed toward a common end: the mobilization of energy resources and their shunting to where they are most needed to prepare the body for action.*

The tissue distributions of the α- and β-adrenoreceptors and their varying responses to different agonists and antagonists have important therapeutic consequences. For example, propranolol is used to treat high blood pressure and protects against heart attacks, whereas epinephrine's bronchodilator effects make it clinically useful in the treatment of **asthma,** a breathing disorder caused by the inappropriate contraction of bronchial smooth muscle.

C | Steroid Hormones Regulate a Wide Variety of Metabolic and Sexual Processes

The adrenal cortex produces at least 50 different ***adrenocortical steroids.*** These have been classified according to the physiological responses they evoke (Section 9-1E):

1. The **glucocorticoids** affect carbohydrate, protein, and lipid metabolism in a manner nearly opposite to that of insulin and influence a wide variety of other vital functions, including inflammatory reactions and the capacity to cope with stress.
2. The **mineralocorticoids** largely function to regulate the excretion of salt and water by the kidneys.
3. The **androgens** and **estrogens** affect sexual development and function. They are made in larger quantities by the gonads.

Glucocorticoids, the most common of which is **cortisol** (also known as **hydrocortisone**), and the mineralocorticoids, the most common of which is **aldosterone,** are all C_{21} compounds (Fig. 9-11).

Steroids, being water insoluble, are transported in the blood in complex with the glycoprotein **transcortin** and, to a lesser extent, with albumin. The steroids spontaneously pass through the membranes of their target cells to the cytosol, where they bind to their cognate **steroid receptors.** The steroid–receptor complexes then migrate to the cell nucleus, where they function as transcription factors to induce, or in some cases repress, the transcription of specific genes (Section 28-3B). In this way, the glucocorticoids and the mineralocorticoids influence the expression of numerous metabolic enzymes in their respective target tissues. Thyroid hormones, which are also nonpolar, function similarly. However, as we shall see in the following sections, all other hormones act less directly in that they bind to their cognate cell-surface receptors and thereby trigger complex cascades of events within cells that ultimately influence transcription as well as other cellular processes.

Gonadal Steroids Mediate Sexual Development and Function. *The* ***gonads*** *(testes in males, ovaries in females), in addition to producing sperm or ova, secrete steroid hormones (androgens and estrogens) that regulate sexual differentiation, the expression of secondary sex characteristics, and sexual behavior patterns.* Although testes and ovaries both synthesize androgens and estrogens, the testes predominantly secrete androgens, which are therefore known as **male sex hormones,** whereas ovaries produce mostly estrogens, which are consequently termed **female sex hormones.**

Androgens, of which **testosterone** (Fig. 9-11) is prototypic, lack the C_2 substituent at C17 that occurs in glucocorticoids and are therefore C_{19} compounds. Estrogens, such as **β-estradiol** (Fig. 9-11), resemble androgens but lack a C10 methyl group because they have an aromatic A ring and are therefore C_{18} compounds. Interestingly, testosterone is an intermediate in estrogen biosynthesis. Another class of ovarian steroids, C_{21} compounds called **progestins,** help mediate the menstrual cycle and pregnancy.

Androgens that promote muscle growth are known as **anabolic steroids.** Many individuals have taken anabolic steroids, both natural and synthetic, in an effort to enhance their athletic performance or for cosmetic reasons. However, because these substances and their metabolic products interact with the various steroid receptors, their use may cause adverse side effects including cardiovascular disease, the development of breast tissue in males, masculinization in females, temporary infertility in both sexes, and, in adolescents, stunted growth due to accelerated bone maturation and precocious and/or exaggerated sexual development. Consequently, anabolic steroids have been classified as controlled substances and, to prevent an unfair advantage over those not taking them, their use by competitive athletes has been banned.

Sexual Differentiation Is Both Hormonally and Genetically Controlled. What factors control sexual differentiation? If the gonads of an embryonic male mammal are surgically removed, that individual will become a phenotypic female. Evidently, *mammals are programmed to develop as females unless embryonically subjected to the influence of testicular hormones.* Indeed, genetic males with absent or nonfunctional cytosolic androgen receptors are phenotypic females, a condition named **testicular feminization.** Curiously, estrogens appear to play no part in embryonic female sexual development, although they are essential for female sexual maturation and function.

Normal individuals have either the XY (male) or the XX (female) genotypes. However, those with the abnormal genotypes XXY **(Klinefelter's syndrome)** and X0 (only one sex chromosome; **Turner's syndrome**) are, respectively, phenotypic males and phenotypic females, although both are sterile. Apparently, *the normal Y chromosome confers the male phenotype, whereas its absence results in the female phenotype.*

D | Growth Hormone Binds to Receptors in Muscle, Bone, and Cartilage

Growth hormone (GH), a 19-residue polypeptide, is produced by the anterior lobe of the pituitary gland. Its binding to receptors directly stimulates growth and metabolism in muscle, bone, and cartilage cells. GH also acts indirectly by stimulating the liver to produce additional growth factors.

Overproduction of GH, usually a consequence of a pituitary tumor, results in excessive growth. If this condition commences while the skeleton is still growing, that is, before its growth plates have ossified, then this excessive growth is of normal proportions over the entire body, resulting in **gigantism.** Moreover, since excessive GH inhibits the testosterone production necessary for growth plate ossification, such "giants" continue growing throughout their abnormally short lives. If, however, the skeleton has already matured, GH stimulates only the growth of soft tissues, resulting in enlarged hands and feet and thickened facial features, a condition named **acromegaly.** The opposite problem, GH deficiency, which results in insufficient growth **(dwarfism),** can be treated before skeletal maturity by regular injections of human GH (**hGH;** animal GH is ineffective in humans).

Since hGH was, at first, available only from the pituitaries of cadavers, it was in very short supply. Now, however, hGH can be synthesized in

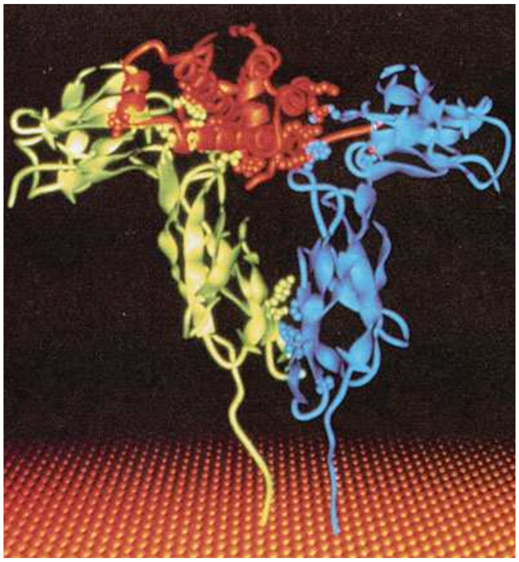

Figure 13-3 | X-Ray structure of human growth hormone (hGH) in complex with two molecules of its receptor's extracellular domain (hGHbp). The proteins are shown in ribbon form, with the two hGHbp molecules, which together bind one molecule of hGH, green and blue and with the hGH red. The side chains involved in intersubunit interactions are shown in space-filling form. The orange pebbled surface represents the cell membrane through which the C-terminal ends of the hGHbp molecules are shown penetrating as they do in the intact hGH receptor. [Courtesy of Abraham de Vos and Anthony Kossiakoff Genentech Inc., South San Francisco, California.] **See Interactive Exercise 10.**

virtually unlimited amounts via recombinant DNA techniques (Section 3-5D). Indeed, hGH has been taken by individuals to increase their athletic prowess, although there is no clear evidence that it does so. However, because of its adverse side effects, which include high blood pressure, joint and muscle pain, and acromegaly, as well as to eliminate any unfair competitive advantages in athletes, its nonmedical use is prohibited.

The GH Receptor Dimerizes on Hormone Binding. The 620-residue GH receptor is a member of a large family of structurally related proteins. These receptors consist of an N-terminal extracellular ligand-binding domain, a single transmembrane segment that is almost certainly helical, and a C-terminal cytoplasmic domain that is not homologous within the superfamily but in many cases contains a tyrosine kinase function (Section 13-2A).

The X-ray structure of hGH in complex with the extracellular domain of its binding protein **(hGHbp)** reveals that the complex consists of two molecules of hGHbp bound to a single hGH molecule (Fig. 13-3). hGH, like many other protein growth factors, consists largely of a four-helix bundle. Each hGHbp molecule consists of two structurally homologous domains, each of which forms a topologically identical sandwich of a three- and a four-stranded antiparallel β sheet that resembles the immunoglobulin fold (Section 7-3B).

The two hGHbp molecules bind to hGH with near twofold symmetry about an axis that is roughly perpendicular to the helical axes of the hGH four-helix bundle and, presumably, to the plane of the cell membrane to which the intact hGH receptor is anchored (Fig. 13-3). The C-terminal domains of the two hGHbp molecules are almost parallel and in contact with one another. Intriguingly, the two hGHbp molecules use essentially the same residues to bind to sites that are on opposite sides of hGH's four-helix bundle and which have no structural similarity.

The ligand-induced dimerization of hGHbp has important implications for the mechanism of ***signal transduction.*** The dimerization, which does not occur in the absence of hGH, apparently brings together the intact receptors' intracellular domains in a way that activates an effector protein such as a tyrosine kinase. Indeed, hGH mutants that cannot induce receptor dimerization are biologically inactive. Numerous other protein growth factors also induce the dimerization of their receptors.

CHECK YOUR UNDERSTANDING

List some of the physiological effects of insulin, glucagon, norepinephrine, glucocorticoids, mineralocorticoids, gonadal steroids, and growth hormone.
What are some dangers of nonmedical use of steroids and growth hormone?
Describe the general properties of hormone receptors.
What is the significance of dimerization of the GH receptor?

2 Receptor Tyrosine Kinases

LEARNING OBJECTIVES

- Understand that dimerization and autophosphorylation allow receptor tyrosine kinases to become active as protein tyrosine kinases.
- Understand that adaptor proteins containing SH2 and SH3 domains can link an RTK with G proteins and additional kinases that operate as a cascade.
- Understand that some receptors act via associated nonreceptor tyrosine kinases.
- Understand that protein phosphorylation participates in signaling pathways by removing phosphoryl groups from receptors and target proteins.

We have seen (Section 12-3B) that the activities of many enzymes are controlled by their covalent modification, mainly the phosphorylation of Ser and Thr residues. A similar process forms the basis of one of the major intracellular signaling systems, the ATP-dependent phosphorylation of Tyr side chains by **protein tyrosine kinases (PTKs):**

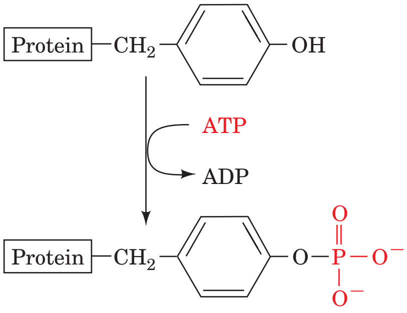

Phospho-Tyr residues mediate protein–protein interactions that are involved in numerous cell functions. Consequently, the PTKs play a central role in signal transduction, regulation of central metabolic pathways, cell cycle control, and cell growth and differentiation. In this section, we discuss the proteins that participate in this signaling system and how their activities are orchestrated to transmit signals within the cell.

A | Receptor Tyrosine Kinases Transmit Signals across the Cell Membrane

The first step in all biochemical signaling pathways is the binding of a ***ligand*** *to its receptor protein.* Box 13-2 discusses how receptor–ligand interactions are quantitated. Insulin and many other polypeptide growth factors bind to receptors whose C-terminal domains have tyrosine kinase activity. Such **receptor tyrosine kinases (RTKs)** typically contain only a single transmembrane segment and are monomers in the unliganded state. These structural features make it unlikely that ligand binding to an extracellular domain manifests itself as a conformational change in an intracellular domain (such a conformational shift seems more likely to occur in receptors with multiple transmembrane segments). Indeed, the most common mechanism for activating RTKs appears to be ligand-induced dimerization of receptor proteins as is the case with the growth hormone receptor (Section 13-1D; although it lacks tyrosine kinase activity). The insulin receptor is unusual in that it is a dimer in the unliganded state. In this case, ligand binding apparently induces a conformational change in the receptor.

See Guided Exploration 12
Mechanisms of hormone signaling involving the receptor tyrosine kinase system.

Autophosphorylation Activates Receptor Tyrosine Kinases. When an RTK dimerizes (or its conformation changes on ligand binding, in the case of the insulin receptor), its cytoplasmic protein tyrosine kinase (PTK) domains are brought close together so that they cross-phosphorylate each other on specific Tyr residues. *This* ***autophosphorylation*** *activates the PTK so that it can phosphorylate other protein substrates.*

How does autophosphorylation activate the PTK activity of the insulin receptor? The human protein is synthesized as a single 1382-residue precursor peptide that is proteolytically processed to yield the disulfide-linked α and β subunits of the mature receptor (Fig. 13-4). Insulin binds to the receptor's α subunits, which are entirely extracellular, whereas the β subunit contains a PTK domain on its intracellular side.

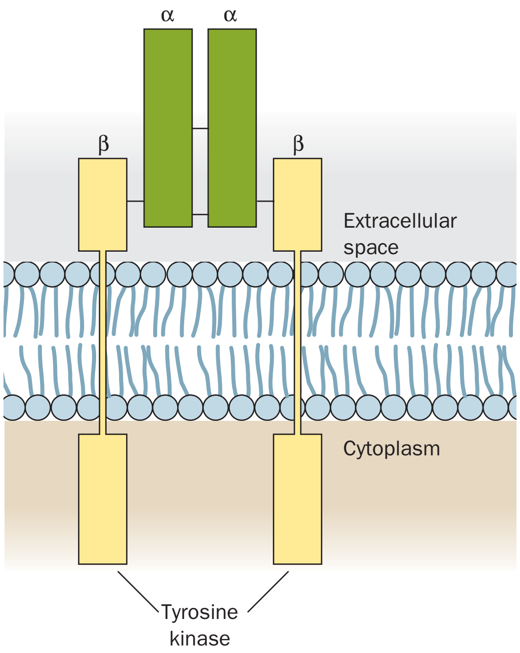

Figure 13-4 | Schematic diagram of the insulin receptor. The subunits of the $\alpha_2\beta_2$ heterotetramer are linked by disulfide bonds (short horizontal bars). The extracellular 731-residue α subunits form the insulin-binding site. The cytoplasmic portions of the 620-residue β subunits are tyrosine kinases that are activated by insulin binding.

BOX 13-2 PERSPECTIVES IN BIOCHEMISTRY

Receptor–Ligand Binding Can Be Quantitated

Receptors, like other proteins, bind their corresponding ligands according to the laws of mass action:

$$\mathrm{R} + \mathrm{L} \rightleftharpoons \mathrm{R \cdot L}$$

Here R and L represent receptor and ligand, and the reaction's dissociation constant is expressed:

$$K_L = \frac{[\mathrm{R}][\mathrm{L}]}{[\mathrm{R \cdot L}]} = \frac{([\mathrm{R}]_T - [\mathrm{R \cdot L}])[\mathrm{L}]}{[\mathrm{R \cdot L}]} \qquad [13\text{-}1]$$

where the total receptor concentration, $[\mathrm{R}]_T$, is equal to $[\mathrm{R}] + [\mathrm{R \cdot L}]$. Equation 13-1 may be rearranged to a form analogous to the Michaelis–Menten equation of enzyme kinetics (Section 12-1B):

$$Y = \frac{[\mathrm{R \cdot L}]}{[\mathrm{R}]_T} = \frac{[\mathrm{L}]}{K_L + [\mathrm{L}]} \qquad [13\text{-}2]$$

where Y is the fractional occupation of the ligand-binding sites. Equation 13-2 represents a hyperbolic curve (Fig. 1*a*) in which K_L may be operationally defined as the ligand concentration at which the receptor is half-maximally occupied by ligand.

Although K_L and $[\mathrm{R}]_T$ may, in principle, be determined from an analysis of a hyperbolic plot such as Fig. 1*a*, the analysis of a linear form of the equation is a more common procedure. Equation 13-1 may be rearranged to

$$\frac{[\mathrm{R \cdot L}]}{[\mathrm{L}]} = \frac{([\mathrm{R}]_T - [\mathrm{R \cdot L}])}{K_L} \qquad [13\text{-}3]$$

Now, in keeping with customary receptor-binding nomenclature, let us redefine $[\mathrm{R \cdot L}]$ as B (for bound ligand), $[\mathrm{L}]$ as F (for free ligand), and $[\mathrm{R}]_T$ as $\mathrm{B_{max}}$. Then Eq. 13-3 becomes

$$\frac{\mathrm{B}}{\mathrm{F}} = \frac{(\mathrm{B_{max}} - \mathrm{B})}{K_L} \qquad [13\text{-}4]$$

A plot of B/F versus B, which is known as a **Scatchard plot** (after George Scatchard, its originator), therefore yields a straight line of slope $-1/K_L$ whose intercept on the B axis is $\mathrm{B_{max}}$ (Fig. 1*b*). Here, both B and F may be determined by filter-binding assays as follows. Most receptors are insoluble membrane-bound proteins and may therefore be separated from soluble free ligand by filtration (receptors that have been solubilized may be separated from free ligand by filtration, for example, through nitrocellulose since proteins nonspecifically bind to nitrocellulose). Hence, by using radioactively labeled ligand, the values of B and F ($[\mathrm{R \cdot L}]$ and $[\mathrm{L}]$) may be determined, respectively, from the radioactivity on the filter and that remaining in solution. The rate of $\mathrm{R \cdot L}$ dissociation is generally so slow (half-times of minutes to hours) as to cause insignificant errors when the filter is washed to remove residual free ligand.

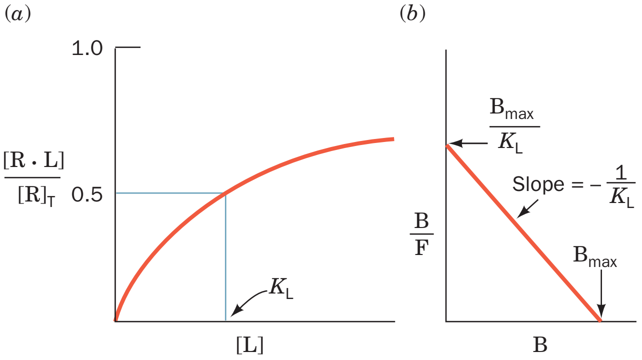

Figure 1 The binding of ligand to receptor. (*a*) A hyperbolic plot. (*b*) A Scatchard plot. Here, $\mathrm{B} = [\mathrm{R \cdot L}]$, $\mathrm{F} = [\mathrm{L}]$, and $\mathrm{B_{max}} = [\mathrm{R}]_T$.

Once the receptor-binding parameters for one ligand have been determined, the dissociation constant of other ligands for the same ligand-binding site may be determined through competitive-binding studies. The model describing this competitive binding is analogous to the competitive inhibition of a Michaelis–Menten enzyme (Section 12-2A):

$$\begin{tikzcd}
\mathrm{R + L} \arrow[r, shift left, "K_L"] & \mathrm{R \cdot L} \arrow[l, shift left] \\
+\ \mathrm{I} \arrow[d, shift left] & \\
\mathrm{R \cdot I + L} \arrow[u, shift left, "K_I"] \arrow[r] & \text{No binding}
\end{tikzcd}$$

where I is the competing ligand whose dissociation constant with the receptor is expressed:

$$K_I = \frac{[\mathrm{R}][\mathrm{I}]}{[\mathrm{R \cdot I}]} \qquad [13\text{-}5]$$

Thus, in direct analogy with the derivation of the equation describing competitive inhibition:

$$[\mathrm{R \cdot L}] = \frac{[\mathrm{R}]_T[\mathrm{L}]}{K_L\left(1 + \dfrac{[\mathrm{I}]}{K_I}\right) + [\mathrm{L}]} \qquad [13\text{-}6]$$

The relative affinities of a ligand and an inhibitor may therefore be determined by dividing Eq. 13-6 in the presence of inhibitor with that in the absence of inhibitor:

$$\frac{[\mathrm{R \cdot L}]_I}{[\mathrm{R \cdot L}]_0} = \frac{K_L + [\mathrm{L}]}{K_L\left(1 + \dfrac{[\mathrm{I}]}{K_I}\right) + [\mathrm{L}]} \qquad [13\text{-}7]$$

When this ratio is 0.5 (50% inhibition), the competitor concentration is referred to as $[\mathrm{I}_{50}]$. Thus, solving Eq. 13-7 for K_I at 50% inhibition:

$$K_I = \frac{[\mathrm{I}_{50}]}{1 + \dfrac{[\mathrm{L}]}{K_L}} \qquad [13\text{-}8]$$

The X-ray structure of the β subunit's 306-residue PTK domain (Fig. 13-5*a*) reveals a deeply clefted bilobal protein whose N-terminal domain consists of a five-stranded β sheet and an α helix and whose larger C-terminal domain is mainly α helical. This structure, as we shall repeatedly see, is typical of the large family of protein kinases, enzymes that phosphorylate the OH groups of Tyr residues and/or Ser and Thr residues. Indeed, the human genome encodes 90 PTKs and 388 protein Ser/Thr kinases (representing >2% of human genes) that collectively phosphorylate an estimated one-third of the proteins in human cells. In doing so, they play key roles in the signaling pathways by which many hormones, growth factors, neurotransmitters, and toxins affect the functions of their target cells.

In the X-ray structure of the insulin receptor PTK domain (Fig. 13-5*a*), the nonhydrolyzable ATP analog **adenosine-5′-(β,γ-imido)triphosphate** (**AMPPNP;** alternatively **ADPNP;** *at right*) is bound in the cleft between the protein domains. There, its γ-phosphate group is in close juxtaposition to the OH group of the target Tyr residue in the 18-residue substrate peptide that is also bound to the protein. Three of the PTK's Tyr residues, all of which are located on its C-terminal domain, are phosphorylated.

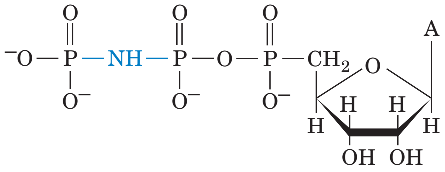

Adenosine-5′-(β,γ-imido)triphosphate (AMPPNP)

Comparison of this X-ray structure with that of the unphosphorylated and uncomplexed protein indicates that on ligand binding and

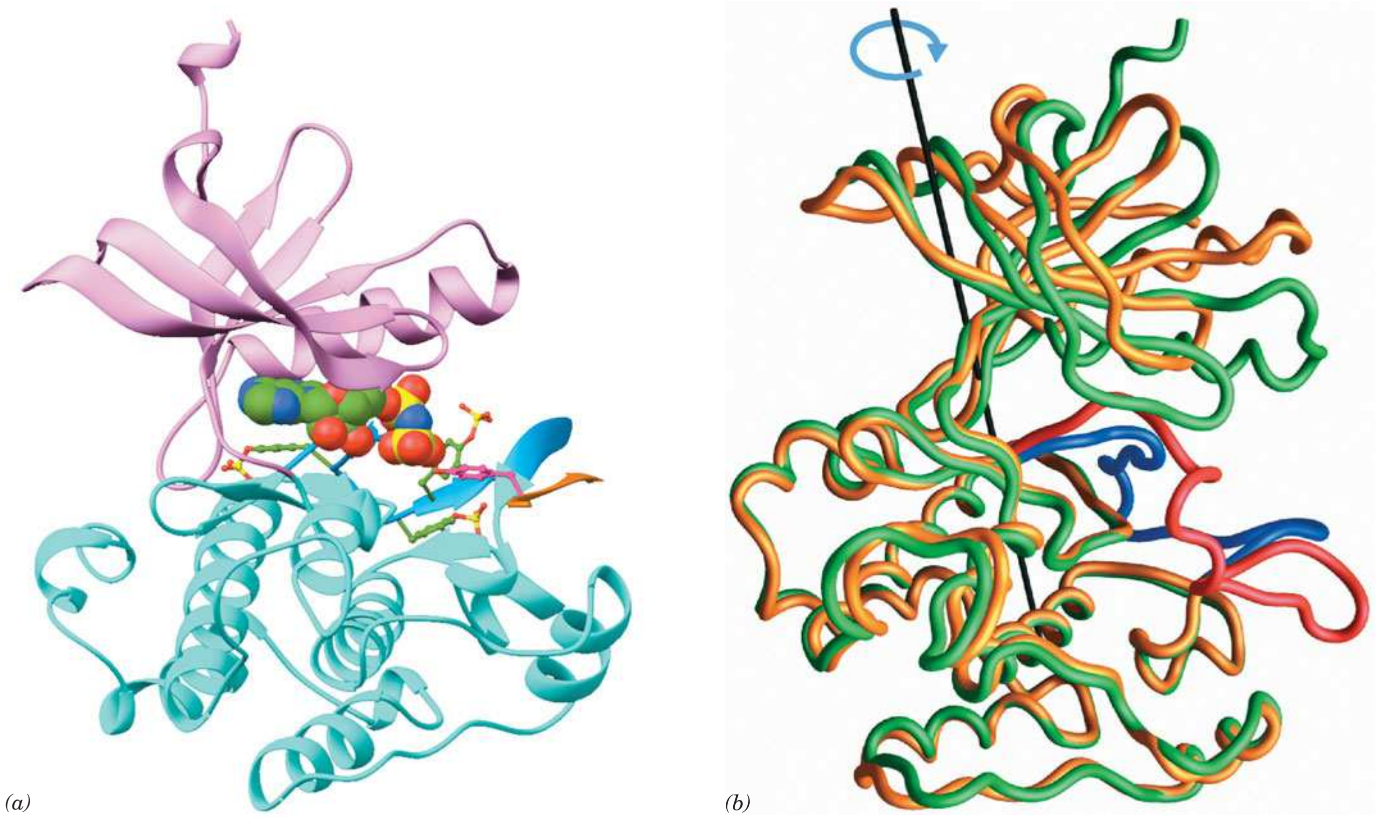

■ **Figure 13-5 | X-Ray structure of the tyrosine kinase domain of the insulin receptor.** (*a*) The tyrosine kinase domain is shown in the "standard" protein kinase orientation with its N-terminal domain lavender, its C-terminal domain cyan, and its activation loop light blue. Its three phosphorylated Tyr side chains are shown in ball-and-stick form with C green, N blue, O red, and P yellow. The ATP analog AMPPNP is shown in space-filling form. The substrate polypeptide is orange (only six of its residues are visible) and its phosphorylatable Tyr residue is shown with C magenta and O red. (*b*) The polypeptide backbones of the phosphorylated and unphosphorylated forms of the insulin receptor tyrosine kinase domain are shown superimposed on their C-terminal lobes. The phosphorylated protein is green with its activation loop blue, and the unphosphorylated protein is yellow with its activation loop red. The blue arrow and black axis indicate the rotation required to align the two N-terminal lobes. [Part *a* based on an X-ray structure by and Part *b* courtesy of Stevan Hubbard, New York University Medical School. PDBids 1IR3 and 1IRK.] **See Interactive Exercise 11.**

phosphorylation, the PTK's N-terminal lobe undergoes a nearly rigid 21° rotation relative to the C-terminal lobe (Fig. 13-5*b*). This dramatic conformational change closes the active site cleft, presumably positioning critical residues for substrate binding and catalysis. The three phospho-Tyr residues are all located on the protein's so-called activation loop. The unphosphorylated activation loop threads through the PTK active site so as to prevent the binding of both ATP and protein substrates. On phosphorylation, however, the activation loop changes its conformation such that it does not occlude the active site (Fig. 13-5*b*) but instead forms part of the substrate recognition site. In fact, the PTK activity of the insulin receptor increases with the degree of phosphorylation of its three autophosphorylatable Tyr residues.

Nearly all known PTKs have between one and three autophosphorylatable Tyr residues in their activation loops, which assume similar conformations in all phosphorylated PTKs of known structure. Moreover, many activated PTKs also phosphorylate the opposing RTK at cytoplasmic Tyr residues outside of its PTK domain. The specificity of PTKs for phosphorylating Tyr rather than Ser or Thr is explained by the observation that the side chain of Tyr, but not those of Ser or Thr, is long enough to reach the active site.

B | Kinase Cascades Relay Signals to the Nucleus

Although certain autophosphorylated RTKs directly phosphorylate their ultimate target proteins, many do not do so. How, then, are these target proteins activated? The answer, as we shall see, is through a highly diverse and complicated set of interconnected signaling pathways involving cascades of associating proteins.

SH2 Domains Bind Phospho-Tyr Residues. The main substrates of the insulin receptor tyrosine kinase are known as **insulin receptor substrates 1** and **2 (IRS-1** and **IRS-2).** When phosphorylated, these proteins can interact with yet another set of proteins that contain one or two conserved ~100-residue modules known as **Src homology 2 (SH2) domains** [because they are similar to the sequence of a domain in the protein named **Src** (pronounced "sarc")]. SH2 domains bind phospho-Tyr residues with high affinity but do not bind the far more abundant phospho-Ser and phospho-Thr residues. This specificity has a simple explanation. X-Ray structural studies reveal that phospho-Tyr interacts with an Arg at the bottom of a deep pocket (Fig. 13-6). The side chains of Ser and Thr are too short to interact with this residue.

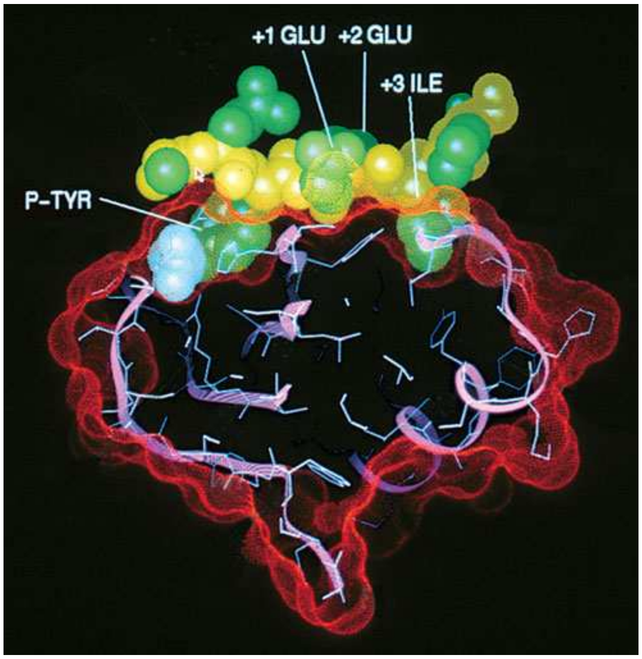

■ **Figure 13-6 | X-Ray structure of the Src SH2 domain.** An 11-residue polypeptide containing the protein's phospho-Tyr-Glu-Glu-Ile target tetrapeptide is bound to the SH2 domain. In this cutaway view, the protein surface is represented by red dots, the protein backbone (*pink*) is shown in ribbon form with its side chains in stick form, and the bound polypeptide's N-terminal 8-residue segment is shown in space-filling form with its backbone yellow, its side chains green, and its phosphate group white. [Courtesy of John Kuriyan, The Rockefeller University.]

The SH2-containing proteins that interact with the IRSs and other substrates have varied functions: Some are kinases, some are phosphatases, and some are GTPases that are therefore known as **G proteins** (Section 13-3B). To further complicate matters, IRS-1 is subject to serine phosphorylation, which attenuates the effects of insulin-stimulated tyrosine phosphorylation.

Activated RTKs Indirectly Activate the G Protein Ras. Molecular genetic analysis of signaling in a variety of distantly related organisms revealed a remarkably conserved pathway that regulates such essential functions as cell growth and differentiation. Briefly, growth factor binding to its cognate RTK activates a monomeric G protein (GTPase) named **Ras** that is anchored to the inner surface of the plasma membrane by prenylation (Section 9-3B). Activated Ras, as we shall see below, then activates a **kinase cascade** that relays the signal to the transcriptional apparatus in the nucleus.

SH3 Domains Bind Pro-Rich Sequences. The binding of a growth factor to its RTK leads to autophosphorylation of the RTK, which then interacts with an SH2-containing protein (Fig. 13-7, *left*). Many proteins that contain SH2 domains also have one or more unrelated 50- to 75-residue **SH3 domains.** SH3 domains, which bind Pro-rich sequences of 9 or 10

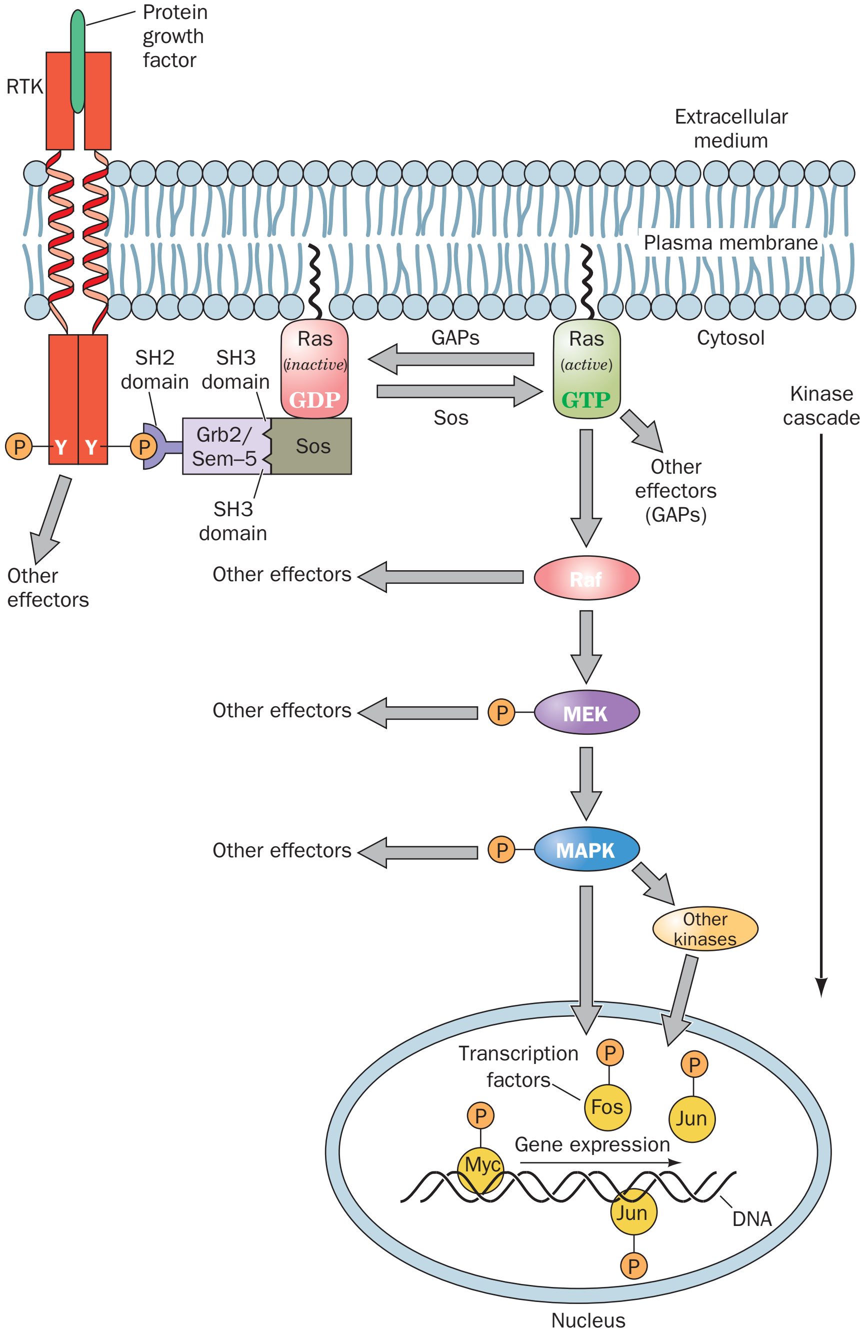
Protein growth factor
RTK
Extracellular medium
Plasma membrane
Cytosol
GAPs
Sos
Ras (inactive) GDP
Ras (active) GTP
SH2 domain
SH3 domain
P
Y
Y
P
Grb2/ Sem–5
Sos
SH3 domain
Other effectors
Other effectors (GAPs)
Kinase cascade
Other effectors
Raf
Other effectors
P
MEK
Other effectors
P
MAPK
Other kinases
Transcription factors
P
Fos
P
Jun
P
Myc
Gene expression
Jun
P
DNA
Nucleus

Figure 13-7 | **The Ras signaling cascade.** RTK binding to its cognate growth factor induces the autophosphorylation of the RTK's cytosolic domain. Grb2/Sem-5 binds to the resulting phospho-Tyr–containing peptide segment via its SH2 domain and simultaneously binds to Pro-rich segments on Sos via its two SH3 domains. This activates Sos to exchange Ras's bound GDP for GTP, which activates Ras to bind to Raf. Then, in a so-called kinase cascade, Raf, a Ser/Thr kinase, phosphorylates MEK, which in turn phosphorylates MAPK, which then migrates to the nucleus, where it phosphorylates transcription factors such as Fos, Jun, and Myc, thereby modulating gene expression. Ras is inactivated by GTP hydrolysis, a process that is accelerated by GTPase-activating proteins (GAPs). The kinase cascade eventually returns to its resting state through the action of protein phosphatases (Section 13-2D). [After Egan, S.E. and Weinberg, R.A., *Nature* **365,** 782 (1993).] **See the Animated Figures.**

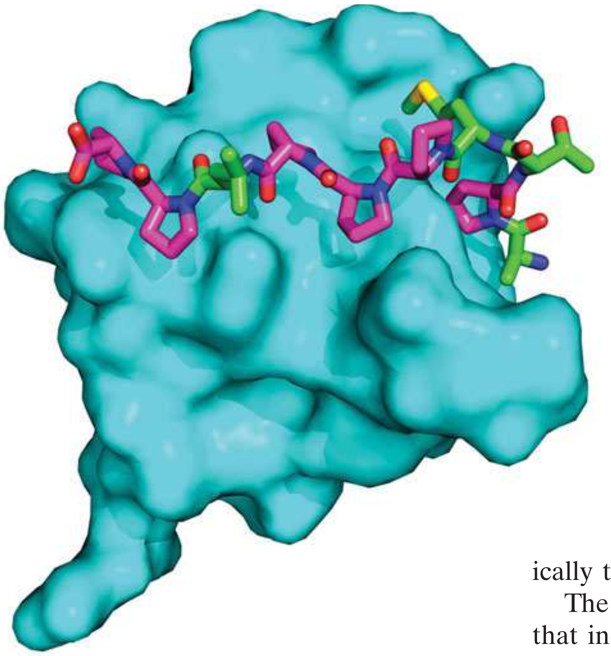

■ **Figure 13-8 | X-Ray structure of the SH3 domain from Ab1 protein in complex with its 10-residue target Pro-rich polypeptide (APTMPPPLPP).** The protein is represented by its surface diagram (*cyan*) and the peptide is drawn in stick form with Pro C magenta, other C green, N blue, O red, and S yellow. [Based on an X-ray structure by Andrea Musacchio, European Molecular Biology Laboratory, Heidelberg, Germany. PDBid 1ABO.]

residues (Fig. 13-8), are also present in some proteins that lack SH2 domains. Both types of domains mediate the interactions between kinases and regulatory proteins. In the signaling cascade shown in Fig. 13-7, a 217-residue mammalian protein known as **Grb2** (**Sem-5** in the nematode worm *Caenorhabditis elegans*), which consists almost entirely of an SH2 domain flanked by two SH3 domains (Fig. 13-9), forms a complex with the 1596-residue **Sos protein.** Sos contains a Pro-rich sequence that binds specifically to SH3 domains.

The Grb2–Sos complex bridges the activated RTK and Ras in a way that induces Ras to release its bound GDP and replace it with GTP. Ras tightly binds both GTP and GDP and hence must interact with Sos to exchange the nucleotides. Sos is therefore known as a **guanine nucleotide exchange factor (GEF).** Most G proteins, as we shall see, have a corresponding GEF. *Because only the Ras · GTP complex is capable of further relaying the signal from an activated RTK, the exchange of GDP for GTP activates Ras.*

The X-ray structure of Grb2 (Fig. 13-9) suggests that its SH2 domain is flexibly linked to its two SH3 domains. How does the binding of such a pliable **adaptor** (a linker that lacks enzymatic activity) to a phosphorylated RTK cause Sos to activate Ras? Grb2 and Sos bind one another so tightly that they are essentially permanently associated in the cell. Hence, when Grb2 binds to a phosphorylated RTK, it recruits Sos to the inner surface of the plasma membrane, where the increased local concentration of Sos causes it to more readily bind to the membrane-anchored Ras and thus act as a GEF.

GAPs Accelerate the GTPase Activities of G Proteins. Ras is an enzyme that catalyzes the hydrolysis of its bound GTP to GDP + P_i, thereby limiting the magnitude of the cell's response to the growth factor. Yet, Ras by itself hydrolyzes only two to three GTPs per minute, too slowly for effective signal transduction (for a signal to be more than a one-time switch, there must be a mechanism for turning it off as well as on). This led to the discovery of a 120-kD **GTPase-activating protein (GAP)** named **RasGAP** that, on binding Ras · GTP, accelerates the rate of GTP hydrolysis by a factor of 10^5. Most G proteins also have a corresponding GAP.

The mechanism whereby RasGAP activates the GTPase activity of Ras was revealed by the X-ray structure of the 334-residue

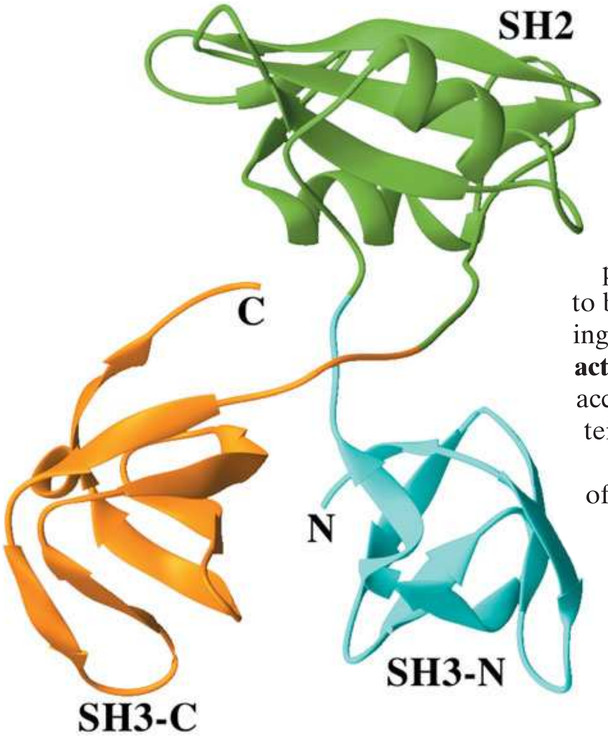

■ **Figure 13-9 | X-Ray structure of Grb2.** Its SH2 domain (*green*) is linked to its flanking SH3 domains (*cyan and orange*) via apparently unstructured and hence flexible four-residue linkers. [Based on an X-ray structure by Arnaud Ducruix, Université de Paris-Sud, Gif sur Yvette Cedex, France. PDBid 1GRI.]

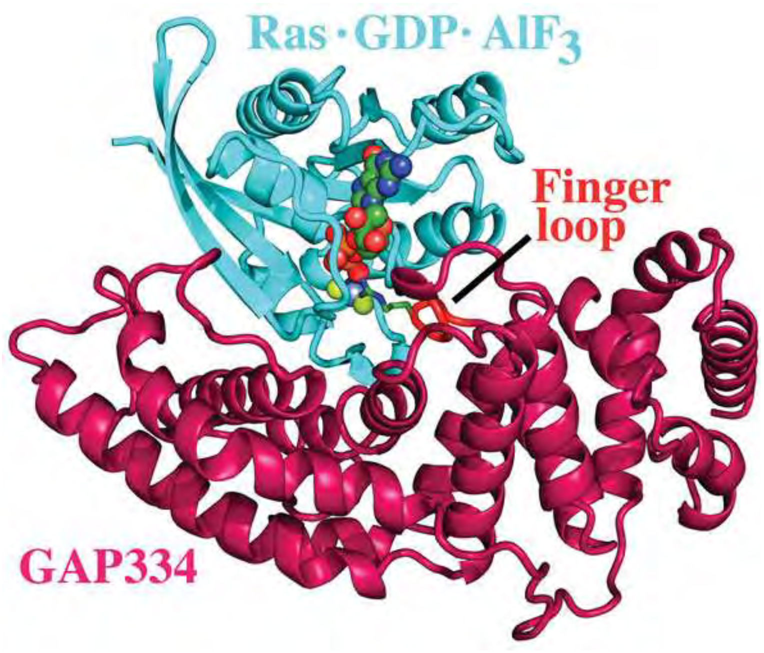

Figure 13-10 | X-Ray structure of the GAP334·Ras·GDP·AlF$_3$ complex. Ras and GAP334 are cyan and magenta with the finger loop of GAP334 red. The GDP and AlF$_3$ are drawn in space-filling form with C green, N blue, O red, F light green, and Al light blue. The side chain of Arg 789, which is drawn in stick form, extends from the finger loop. Note how it interacts with both the AlF$_3$ and the β phosphate group of the GDP. [Based on an X-ray structure by Alfred Wittinghofer, Max-Planck-Institut für Molekulare Physiologie, Dortmund, Germany. PDBid 1WQ1.]

GTPase-activating domain of RasGAP (GAP334) bound to Ras in its complex with GDP and AlF$_3$ (Fig. 13-10). GAP334 interacts with Ras over an extensive surface. The AlF$_3$, which has trigonal planar geometry, binds to Ras at the expected position of GTP's γ phosphate group with the Al atom opposite a bound water molecule that presumably would be the attacking nucleophile in the GTPase reaction. Since Al—F and P—O bonds have similar lengths, the GDP–AlF$_3$–H$_2$O assembly resembles the GTPase reaction's expected transition state with the AlF$_3$ mimicking the planar PO$_3$ group.

GAP334 binds to Ras with GAP334's so-called finger loop inserted into the Ras active site such that the finger loop's Arg 789 side chain interacts with both the Ras-bound GDP's β phosphate and the AlF$_3$ (Fig. 13-10). In Ras · GTP, this Arg side chain would be in an excellent position to stabilize the developing negative charge in the GTPase reaction's transition state. Indeed, catalytically more efficient G proteins contain an Arg residue that occupies a nearly identical position.

A Kinase Cascade Completes the Signaling Pathway. The signaling pathway downstream of Ras consists of a linear cascade of protein kinases (Fig. 13-7, *right*). The Ser/Thr kinase **Raf,** which is activated by direct interaction with Ras · GTP, phosphorylates a protein alternatively known as **MEK** or **MAP kinase kinase,** thereby activating it as a kinase. Activated MEK phosphorylates a family of proteins variously termed **mitogen-activated protein kinases (MAPKs)** or **extracellular-signal-regulated kinases (ERKs).** A MAPK must be phosphorylated at both its Thr and Tyr residues in the sequence Thr-Glu-Tyr for full activity. MEK (which stands for *M*AP kinase/*E*RK kinase-activating *k*inase) catalyzes both phosphorylations; it is therefore a protein Ser/Thr kinase as well as a protein Tyr kinase.

The activated MAP kinases migrate from the cytosol to the nucleus, where they phosphorylate a variety of proteins, including **Fos, Jun,** and **Myc.** These proteins are **transcription factors** (proteins that induce the transcription of their target genes; Section 28-3B): In their activated forms they stimulate various genes to produce the effects commissioned by the extracellular presence of the growth factor that initiated the signaling cascade. When insulin activates the Ras signaling pathway, the result is an increase in protein synthesis that supports cell growth and differentiation, a response consistent with insulin's function as a signal of fuel abundance. Variant proteins encoded by **oncogenes** subvert such signaling pathways so as to induce uncontrolled cell growth (Box 13-3).

The advantage of a kinase cascade is that *a small signal can be amplified manyfold inside the cell.* In addition, phosphorylation of more than one target protein can lead to the simultaneous activation of several intracellular processes. Thus as we shall see (Section 22-2), insulin signaling mediates changes in vesicle trafficking, enzyme activation, and gene expression.

Scaffold Proteins Organize and Position Protein Kinases. Eukaryotic cells contain numerous different MAPK signaling cascades, each with a characteristic set of component kinases, which in mammals comprise at least 12 MAP kinases, 7 MAP kinase kinases (MKKs), and 14 MAP kinase kinase kinases (MKKKs; Fig. 13-11). Although each MAPK is activated by a specific MKK, a given MKK can be activated by more than one MKKK. Moreover, several pathways may be activated by a single

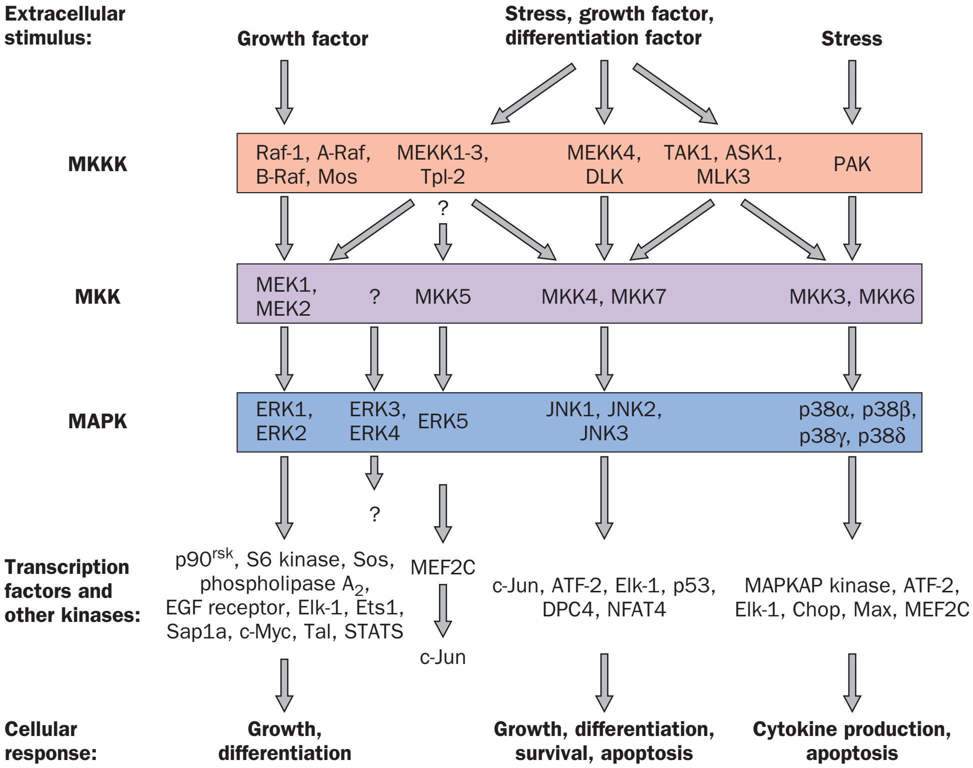
Extracellular stimulus:
Growth factor
Stress, growth factor, differentiation factor
Stress
MKKK
Raf-1, A-Raf, B-Raf, Mos
MEKK1-3, Tpl-2
MEKK4, DLK
TAK1, ASK1, MLK3
PAK
?
MKK
MEK1, MEK2
?
MKK5
MKK4, MKK7
MKK3, MKK6
MAPK
ERK1, ERK2
ERK3, ERK4
ERK5
JNK1, JNK2, JNK3
p38α, p38β, p38γ, p38δ
?
Transcription factors and other kinases:
p90rsk, S6 kinase, Sos, phospholipase A2, EGF receptor, Elk-1, Ets1, Sap1a, c-Myc, Tal, STATS
MEF2C
c-Jun
c-Jun, ATF-2, Elk-1, p53, DPC4, NFAT4
MAPKAP kinase, ATF-2, Elk-1, Chop, Max, MEF2C
Cellular response:
Growth, differentiation
Growth, differentiation, survival, apoptosis
Cytokine production, apoptosis

■ **Figure 13-11 | MAP kinase cascades in mammalian cells.** Each MAP kinase cascade consists of an MKKK, an MKK, and a MAPK. Various external stimuli may each activate one or more MKKKs, which in turn may activate one or more MKKs. However, the MKKs are relatively specific for their target MAPKs. The activated MAPKs phosphorylate specific transcription factors (e.g., **Elk-1, Ets-1, p53, NFAT4,** and **Max**), which are then translocated to the nucleus, as well as specific kinases (e.g., **p90^{rsk}, S6 kinase,** and **MAPKAP kinase**). The resulting activated transcription factors and kinases then induce cellular responses such as growth, differentiation, and **apoptosis** (programmed cell death; Section 28-4C). [After Garrington, T.P. and Johnson, G.L., *Curr. Opin. Cell Biol.* **11,** 212 (1999).]

BOX 13-3 BIOCHEMISTRY IN HEALTH AND DISEASE

Oncogenes and Cancer

The growth and differentiation of cells in the body are normally strictly controlled. Thus, with few exceptions (e.g., blood-forming cells and hair follicles), cells in the adult body are largely quiescent. However, for a variety of reasons, a cell may be made to proliferate uncontrollably to form a tumor.

Malignant tumors (cancers) grow in an invasive manner and are almost invariably life threatening. They are responsible for 20% of the mortalities in the United States.

Among the many causes of cancer are viruses that carry **oncogenes** (Greek: *onkos,* mass or tumor). For example, the **Rous sarcoma virus (RSV),** which induces the formation of **sarcomas** (cancers arising from connective tissues) in chickens, contains four genes. Three of the genes are essential for viral replication, whereas the fourth, **v-*src*** (v for viral, *src* for sarcoma), an oncogene, induces tumor formation. What is the origin of v-*src,* and how does it function? Hybridization studies by Michael Bishop and Harold Varmus in 1976 led to the remarkable discovery that uninfected chicken cells contain a gene, **c-*src*** (c for cellular), that is homologous to v-*src* and that is highly conserved in a wide variety of eukaryotes, suggesting that it is an essential cellular gene. Apparently, v-*src* was originally acquired from a cellular source by a non-tumor-forming ancestor of RSV. Both v-*src* and c-*src* encode a 60-kD tyrosine kinase. However, whereas the activity of c-*src* is strictly regulated, that of v-*src* is under no such control and hence its presence maintains the host cell in a proliferative state. Since cells are not killed by an RSV infection, this presumably enhances the viral replication rate.

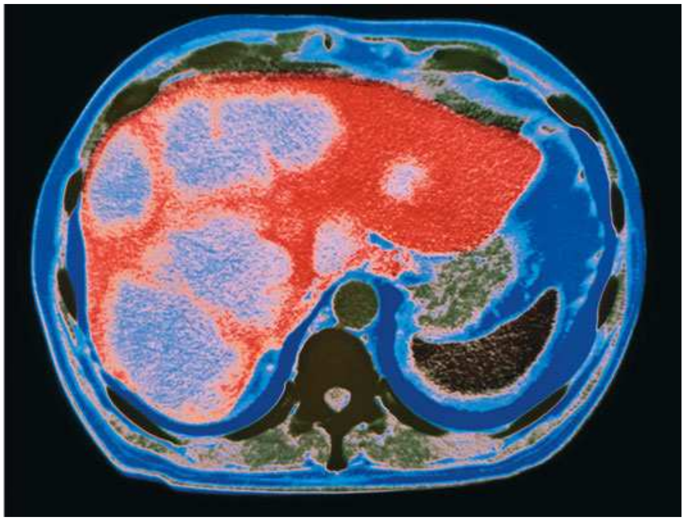

An X-ray–based false-color image showing an axial section through a human abdomen that has cancer of the liver. The liver is the large red mass occupying much of the abdomen; the light patches on the liver are cancerous tumors. A vertebra (*dark green*) can be seen at the lower center of the image. [Salisbury/Photo Researchers.]

Other oncogenes have been similarly linked to processes that regulate cell growth. For example, the **v-*erbB*** oncogene specifies a truncated version of the **epidermal growth factor (EGF) receptor,** which lacks the EGF-binding domain but retains its transmembrane segment and its tyrosine kinase domain. This kinase phosphorylates its target proteins in the absence of an extracellular signal, thereby driving uncontrolled cell proliferation.

The **v-*ras*** oncogene encodes a 21-kD protein, **v-Ras,** that resembles cellular Ras but hydrolyzes GTP much more slowly. The reduced braking effect of GTP hydrolysis on the rate of protein phosphorylation leads to increased activation of the kinases downstream of Ras (Fig. 13-7).

The transcription factors that respond to Ras-mediated signaling (e.g., Fos and Jun) are also encoded by **proto-oncogenes,** the normal cellular analogs of oncogenes. The viral genes **v-*fos*** and **v-*jun*** encode proteins that are nearly identical to their cellular counterparts and mimic their effects on host cells but in an uncontrolled fashion.

Oncogenes are not necessarily of viral origin. Indeed, few human cancers are caused by viruses. Rather, they are caused by proto-oncogenes that have mutated to form oncogenes. For example, a mutation in the **c-*ras*** gene, which converts Gly 12 of Ras to Val, reduces Ras's GTPase activity without affecting its ability to stimulate protein phosphorylation. This prolongs the time that Ras is in the "on" state, thereby inducing uncontrolled cell proliferation. In fact, oncogenic versions of c-*ras* are among the most commonly implicated oncogenes in human cancers.

To date, over 50 oncogenes have been identified. The subversive effects of oncogene products arise through their differences from the corresponding normal cellular proteins: They may have different rates of synthesis and/or degradation; they may have altered cellular functions; or they may resist control by cellular regulatory mechanisms. However, in order for a normal cell to undergo a **malignant transformation** (become a cancer cell), it must undergo several (an average of five) independent oncogenic events. This is a reflection of the complexity of cellular signaling networks (cells respond to a variety of hormones, growth factors, and transcription factors in partially overlapping ways) and explains why the incidence of cancer increases with age.

type of receptor. How then does a cell prevent inappropriate **cross talk** between closely related signaling pathways? One way that this occurs is through the use of **scaffold proteins** that bind some or all of the component protein kinases of a particular signaling cascade so as to ensure that the protein kinases of a given pathway interact only with one another. In addition, a scaffold protein can control the subcellular location of its associated kinases.

The first known scaffold protein was discovered through the genetic analysis of a MAP kinase cascade in yeast, which demonstrated that this protein, **Ste5p,** binds the MKKK, MKK, and MAPK components of the pathway and that, *in vivo,* the scaffold's absence inactivates the pathway. Evidently, the interactions between successive kinase components of this MAP kinase cascade are, by themselves, insufficient for signal transmission.

C | Some Receptors Are Associated with Nonreceptor Tyrosine Kinases

Many cell-surface receptors are not members of the receptor families that we have discussed so far and do not respond to ligand binding by autophosphorylation. These include the receptors for growth hormone (Fig. 13-3), the **cytokines** (protein growth factors that regulate the differentiation, proliferation, and activities of numerous types of cells, most conspicuously blood cells), the **interferons** (protein growth factors that stimulate antiviral defenses), and **T cell receptors** [which control the proliferation of immune system cells known as T lymphocytes (T cells); Section 7-3]. *Ligand binding induces these* ***tyrosine kinase–associated receptors*** *to dimerize (and, in some cases, to trimerize), often with different types of subunits, in a way that activates associated* ***nonreceptor tyrosine kinases (NRTKs).***

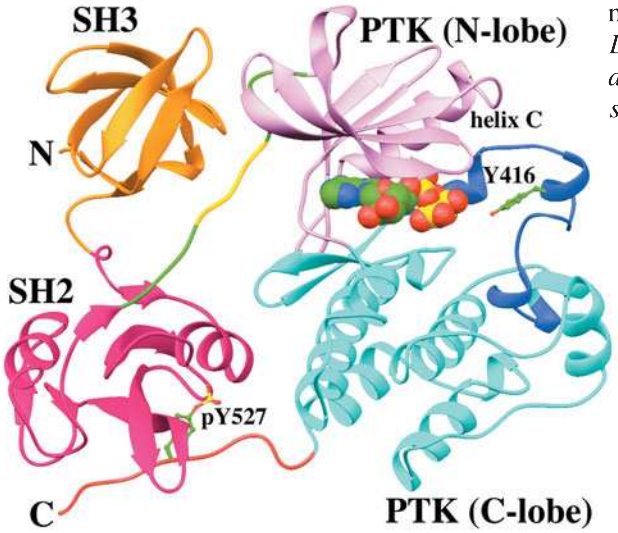

Figure 13-12 | X-Ray structure of Src·AMPPNP lacking its N-terminal domain and with Tyr 527 phosphorylated. The protein is oriented such that its PTK domain is seen in "standard" view (compare it with Fig. 13-5*a*). The SH3 domain is orange, the SH2 domain is magenta, the linker joining the SH2 domain to the PTK domain is green with residues 249 to 253, which interact with the SH3 domain, yellow, the N-terminal lobe of the PTK domain is lavender, its C-terminal lobe is cyan with its activation loop light blue, and its C-terminal tail is red. The AMPPNP is shown in space-filling form and Y416 and pY527 are shown in ball-and-stick form, all with C green, N blue, O red, and P yellow. [Based on an X-ray structure by Stephen Harrison and Michael Eck, Harvard Medical School. PDBid 2SRC.]

The Structure of Src Reveals Its Autoinhibitory Mechanism. Many of the NRTKs that are activated by tyrosine kinase–associated receptors belong to the **Src family,** which contains at least nine members including Src, **Fyn,** and **Lck.** Most of these ~530-residue membrane-anchored (by myristoylation) proteins have both an SH2 and an SH3 domain and all have a PTK domain. Hence, a Src-related kinase may also be activated by association with an autophosphorylated RTK. Although Src-related kinases are each associated with different receptors, they phosphorylate overlapping sets of target proteins. This complex web of interactions explains why different ligands often activate some of the same signaling pathways.

Src consists of, from N- to C-terminus, a myristoylated N-terminal "unique" domain that differs among Src family members, an SH3 domain, an SH2 domain, a PTK domain, and a short C-terminal tail. Phosphorylation of Tyr 416 in the PTK's activation loop activates Src, whereas phosphorylation of Tyr 527 in its C-terminal tail deactivates it. *In vivo,* Src is phosphorylated at either Tyr 416 or Tyr 527, but not at both. The dephosphorylation of Tyr 527 or the binding of external ligands to the SH2 or the SH3 domain activates Src, a state that is then maintained by the autophosphorylation of Tyr 416. When Tyr 527 is phosphorylated and no activating phosphopeptides are available, Src's SH2 and SH3 domains function to deactivate its PTK domain; that is, Src is then autoinhibited.

The X-ray structure of Src·AMPPNP lacking its N-terminal domain and with Tyr 527 phosphorylated reveals the structural basis of Src autoinhibition (Fig. 13-12). As biochemical studies had previously shown, the SH2 domain binds phospho-Tyr 527, which occurs in the sequence pYNPG rather than the pYEEI sequence characteristic of high-affinity Src SH2 target peptides. Although the pYNP segment binds to SH2 as does the pYEE segment in Fig. 13-6, the succeeding residues are poorly ordered in the X-ray structure and, moreover, the SH2 pocket in which the Ile side chain of pYEEI binds is unoccupied. Apparently, the phospho-Tyr 527–containing peptide segment binds to the Src SH2 domain with reduced affinity relative to its target peptides.

The SH3 domain binds to the linker connecting the SH3 domain to the N-terminal lobe of the PTK domain. Residues 249 to 253 of the linker bind to the SH3 domain in much the same way as do SH3's Pro-rich target peptides (Fig. 13-8). However, the only Pro in this segment is residue 250. The polar side chain of Gln 253, which occupies the position of the second Pro in SH3's normal Pro-X-X-Pro target sequence, does not enter the hydrophobic binding pocket that this second Pro would occupy (Fig. 13-8) and hence the path of the peptide deviates from that of Pro-rich target peptides at this point. Apparently, this interaction is also weaker than those with Src's SH3 target peptides.

Src's SH2 and SH3 domains bind the PTK domain on the side opposite its active site. How, then, does the conformation shown in Fig. 13-12 inhibit the PTK's activity? The two lobes of Src's PTK domain are, for the most part, closely superimposable on their counterparts in the PTK domains of phosphorylated and hence activated protein kinases (e.g., Fig. 13-5*a*). However, Src helix C (the only helix in the PTK's N-terminal lobe) is displaced from the interface between the N- and C-terminal lobes relative to its position in other activated protein kinases. Helix C contains the

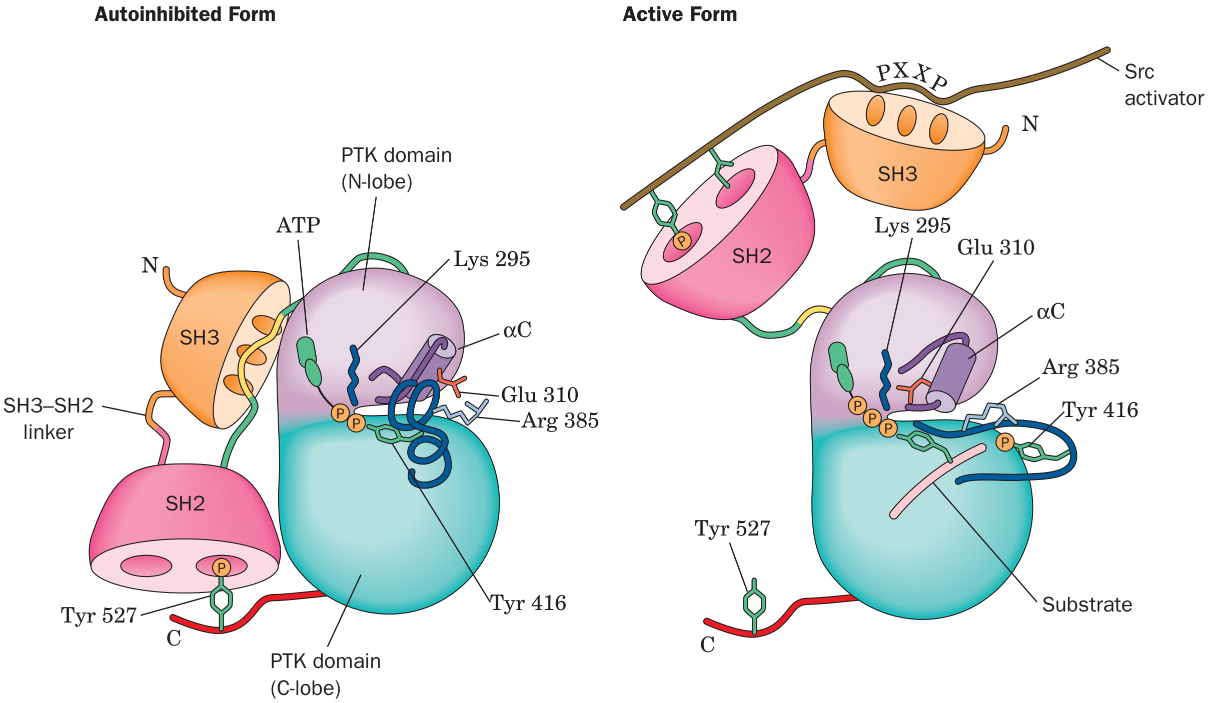

■ **Figure 13-13** | **Schematic model of Src activation.** In the autoinhibited form (*left*), the SH2 domain (*magenta*) binds to phospho-Tyr 527, and the SH3 domain (*orange*) binds to an internal Pro-containing segment (*yellow*). Glu 310 forms a salt bridge to Arg 385, the partially helical activation loop (*blue*) blocks the active site, and Tyr 416 is buried. In the active form (*right*), the SH2 and SH3 domains bind to a Src activator, Tyr 527 is dephosphorylated, the activation loop has undergone a conformational change to expose Tyr 416 to phosphorylation, Glu 310 forms a salt bridge with Lys 295, and phospho-Tyr 416 forms a salt bridge with Arg 385. The coloring scheme and viewpoint largely match those in Fig. 13-12. [After Young, M.A., Gonfloni, F., Superti-Furga, G., Roux, B., and Kuriyan, J., *Cell* **105,** 116 (2001).]

conserved residue Glu 310 (using Src numbering), which in other activated protein kinases projects into the catalytic cleft where it forms a salt bridge with Lys 295, an important ligand of the substrate ATP's α and β phosphates. In inactive Src, Glu 310 forms an alternative salt bridge with Arg 385, and Lys 295 instead interacts with Asp 404. In activated Lck, Arg 385 forms a salt bridge with phospho-Tyr 416.

The foregoing structural observations suggest the following scenario for Src activation (Fig 13-13):

1. The dephosphorylation of Tyr 527 and/or the binding of the SH2 and/or SH3 domains to their target peptides (for which SH2 and SH3 have greater affinity than their internal Src-binding sites) releases these domains from their PTK-bound positions shown in Fig. 13-12, thus relaxing conformational constraints on the PTK domain. This allows the PTK's active site cleft to open, thereby disrupting the structure of its partially helical activation loop (which occupies a blocking position in the active site cleft; Fig. 13-12) so as to expose Tyr 416 to autophosphorylation.
2. The resulting phospho-Tyr 416 forms a salt bridge with Arg 385, which sterically requires the structural reorganization of the activation loop to its active, nonblocking conformation. The consequent rupture of the Glu 310—Arg 385 salt bridge frees helix C to assume its active orientation which, in turn, allows Glu 310 to form its catalytically important salt bridge to Lys 295, thereby activating the Src PTK activity.

PTKs Are Targets of Anticancer Drugs. The hallmark of **chronic myelogenous leukemia (CML)** is a specific chromosomal translocation forming the so-called **Philadelphia chromosome** in which the *Abl* gene (which encodes the NRTK **Abl**) is fused with the *Bcr* gene (which encodes the protein Ser/Thr kinase **Bcr**). The Abl portion of the resulting Bcr–Abl fusion protein is constitutively activated (that is, continuously, without regulation), probably because its Bcr portion oligomerizes. Hematopoietic stem cells (from which all blood cells are descended) bearing the Philadelphia chromosome are therefore primed to develop CML (malignancy requires several independent genetic alterations; Box 13-3). Without a bone marrow transplant (a high-risk procedure that is unavailable to most individuals due to the lack of a suitable donor), CML is invariably fatal with an average survival time of ~6 years.

An inhibitor of Abl would be expected to prevent the proliferation of, and even kill, CML cells. However, to be an effective anti-CML agent, such a substance must not inhibit other protein kinases because this would almost certainly cause serious side effects. Derivatives of 2-phenylaminopyrimidine bind to Abl with exceptionally high affinity and specificity. One such derivative, **imatinib** (trade name **Gleevec**),

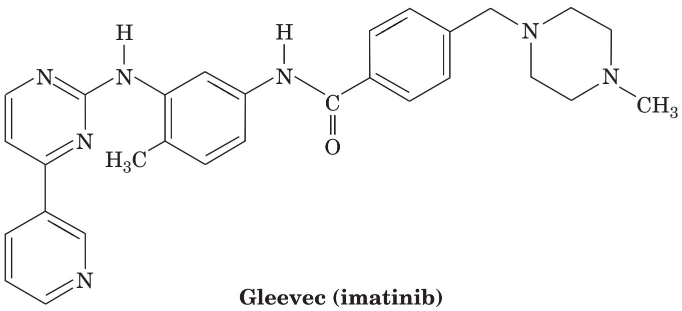

Gleevec (imatinib)

which was developed by Brian Druker and Nicholas Lydon, has caused the remission of symptoms in >90% of CML patients with almost no serious side effects. This unprecedented performance occurs, in part, because Gleevec does not bind to other protein kinases.

Abl resembles Src but lacks Src's C-terminal regulatory phosphorylation site (Figs. 13-12 and 13). The X-ray structure of Abl's PTK domain in complex with a truncated form of Gleevec, determined by John Kuriyan (Fig. 13-14), reveals, as expected, that the drug binds in Abl's ATP-binding site. Abl thereby adopts an inactive conformation in which its activation loop, which is not phosphorylated, assumes an autoinhibitory conformation.

Gleevec was the first of several 2-phenylaminopyrimidine derivatives, which inhibit specific protein kinases, to be approved by the FDA for clinical use against certain cancers. In addition, several monoclonal antibodies (Box 7-5) that bind to specific PTKs or their ligands are in clinical use as anticancer agents [e.g., **trastuzumab** (trade name **Herceptin**), which is effective against breast cancers that overexpress the RTK named **HER2;** Box 7-5]. Such receptor-targeted therapies hold enormous promise for controlling, if not curing, cancers by specifically targeting the aberrant proteins that cause the cancers. In contrast, most chemotherapeutic agents that are presently in use indiscriminately kill fast-growing cells and hence tend to have debilitating side effects.

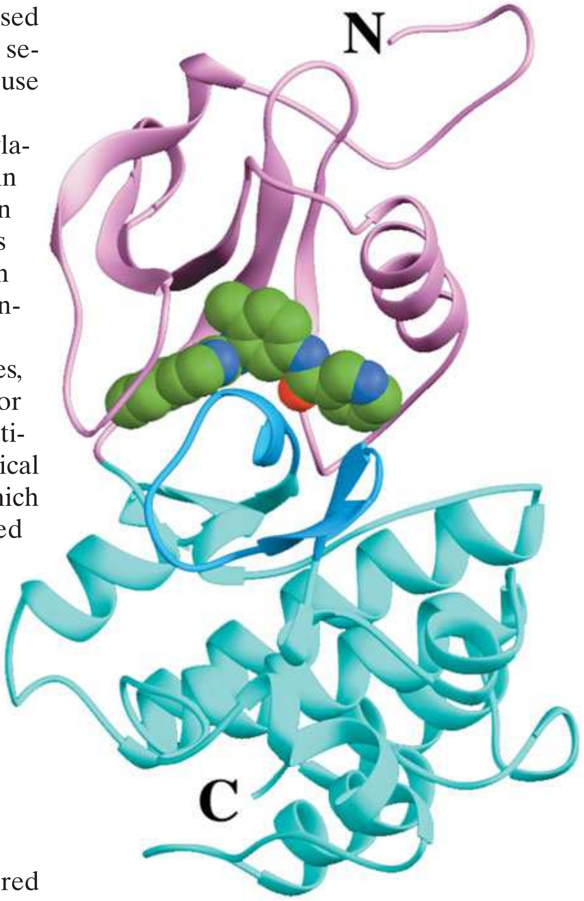

Figure 13-14 | X-Ray structure of the Abl PTK domain in complex with a truncated derivative of Gleevec. The protein is viewed from the right of the "standard" view of protein kinases (e.g., Figs. 13-5*a* and 13-12), with its N-terminal lobe lavender, its C-terminal lobe cyan, and its activation loop light blue. The truncated Gleevec, which occupies the PTK's ATP-binding site, is shown in space-filling form with C green, N blue, and O red. [Based on an X-ray structure by John Kuriyan, The Rockefeller University. PDBid 1FPU.]

D | Protein Phosphatases Are Signaling Proteins in Their Own Right

Intracellular signals must be "turned off" after the system has delivered its message so that the system can transmit future messages. In the case of protein kinases, their activities are balanced by the activities of **protein phosphatases** that hydrolyze the phosphoryl groups attached to Ser, Thr, or Tyr side chains and thereby limit the effects of the signal that activated the kinase. Although protein kinases have traditionally garnered more attention, mammalian cells express a large number of protein phosphatases with substrate specificities comparable to those of kinases.

Protein Tyrosine Phosphatases Are Multidomain Proteins. The enzymes that dephosphorylate Tyr residues, the **protein tyrosine phosphatases (PTPs),** are not just simple housekeeping enzymes but are important signal transducers. These enzymes, 107 of which are encoded by the human genome, are members of four families. Each tyrosine phosphatase contains at least one conserved ~240-residue phosphatase domain that has the 11-residue signature sequence [(I/V)HCXAGXGR(S/T)G], the so-called CX_5R motif, which contains the enzyme's catalytically essential Cys and Arg residues. During the hydrolysis reaction, the phosphoryl group is transferred from the tyrosyl residue of the substrate protein to the essential Cys on the enzyme, forming a covalent Cys–phosphate intermediate that is subsequently hydrolyzed.

Some tyrosine phosphatases are constructed much like the receptor tyrosine kinases; that is, they have an extracellular domain, a single transmembrane helix, and a cytoplasmic domain consisting of a catalytically active PTP domain that, in most cases, is followed by a second PTP domain with little or no catalytic activity. These inactive PTP domains are, nevertheless, highly conserved, which suggests that they have an important although as yet unknown function. Biochemical and structural analyses indicate that ligand-induced dimerization of a receptor-like PTP reduces its catalytic activity, probably by blocking its active sites.

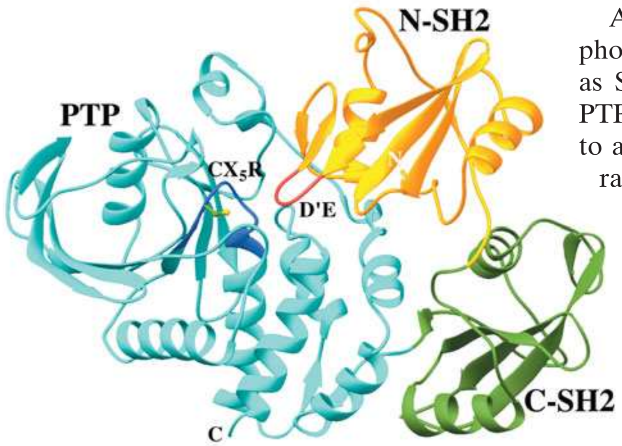

Figure 13-15 | X-Ray structure of the protein tyrosine phosphatase SHP-2. Its N-SH2 domain is gold with its D′E loop red, its C-SH2 domain is green, and its PTP domain is cyan with its 11-residue CX_5R motif blue. The side chain of the catalytically essential Cys residue is shown in ball-and-stick form with C green and S yellow. [Based on an X-ray structure by Michael Eck and Steven Shoelson, Harvard Medical School. PDBid 2SHP.]

A second group of PTPs, intracellular PTPs, contain only one tyrosine phosphatase domain, which is flanked by regions containing motifs, such as SH2 domains, that participate in protein–protein interactions. The PTP known as **SHP-2,** which is expressed in all mammalian cells, binds to a variety of phosphorylated (that is, ligand-activated) RTKs. The X-ray structure of SHP-2 lacking its C-terminal tail reveals two SH2 domains, followed by a tyrosine phosphatase domain (Fig. 13-15). The N-terminal SH2 domain (N-SH2) functions as an autoinhibitor by inserting a protein loop (labeled D′E in Fig. 13-15) into the PTP's 9-Å-deep catalytic cleft. When N-SH2 recognizes and binds a phospho-Tyr group on a substrate protein, its conformation changes, unmasking the PTP catalytic site so that the phosphatase can hydrolyze another phospho-Tyr group on the target protein (activated RTKs typically bear multiple phosphorylated Tyr residues).

The active site cleft of intracellular tyrosine phosphatases such as SHP-2 is too deep to cleave phospho-Ser/Thr side chains. However, the active site pockets of a third group of PTPs, the so-called **dual-specificity tyrosine phosphatases,** are sufficiently shallow to bind both phospho-Tyr and phospho-Ser/Thr residues.

Bubonic Plague Virulence Requires a PTP. Bacteria lack PTKs and hence do not synthesize phospho-Tyr residues. Nevertheless, PTPs are expressed by bacteria of the genus *Yersinia,* most notably *Yersinia pestis,* the pathogen that causes **bubonic plague** (the flea-transmitted "Black Death," which, since the sixth century, has been responsible for an estimated 200 million human deaths including about one-third of the European population in the years 1347–1350). The *Y. pestis* PTP, **YopH,** which is required for bacterial virulence, is far more catalytically active than other known PTPs. Hence, when *Yersinia* injects YopH into a cell, the cell's phospho-Tyr-containing proteins are catastrophically dephosphorylated. Although YopH and mammalian PTPs are only ~15% identical in sequence, they share a set of invariant residues and have similar X-ray structures. This suggests that an ancestral *Yersinia* acquired a PTP gene from a eukaryote.

Protein Ser/Thr Phosphatases Participate in Numerous Regulatory Processes. The **protein Ser/Thr phosphatases** in mammalian cells belong to two protein families: the **PPP family** and the **PPM family.** The PPP and PPM families are unrelated to each other or to the PTPs. X-Ray structures have shown that PPP catalytic centers each contain an Fe^{2+} (or possibly an Fe^{3+}) ion and a Zn^{2+} (or possibly an Mn^{2+}) ion, whereas PPM catalytic centers each contain two Mn^{2+} ions. These binuclear metal ion centers nucleophilically activate water molecules to dephosphorylate substrates in a single reaction step.

The PPP family member named **phosphoprotein phosphatase-1 (PP1),** as we shall see, plays an important role in regulating glycogen metabolism (Section 16-3B). The PPP member known as **PP2A** participates in a wide variety of regulatory processes including those governing metabolism, DNA replication, transcription, and development. PP2A is a heterotrimer that consists of a scaffold (A) subunit that binds both a catalytic (C) subunit and a regulatory (B) subunit. The A subunit, which consists of 15 imperfect tandem repeats of a 39-residue sequence termed HEAT (because it occurs in proteins named *H*untingtin, *E*F3, *A* subunit of PP2A, and *T*OR1), has a remarkable structure in which its HEAT repeats are joined in a horseshoe-shaped solenoidal arrangement (Fig. 13-16*a*).

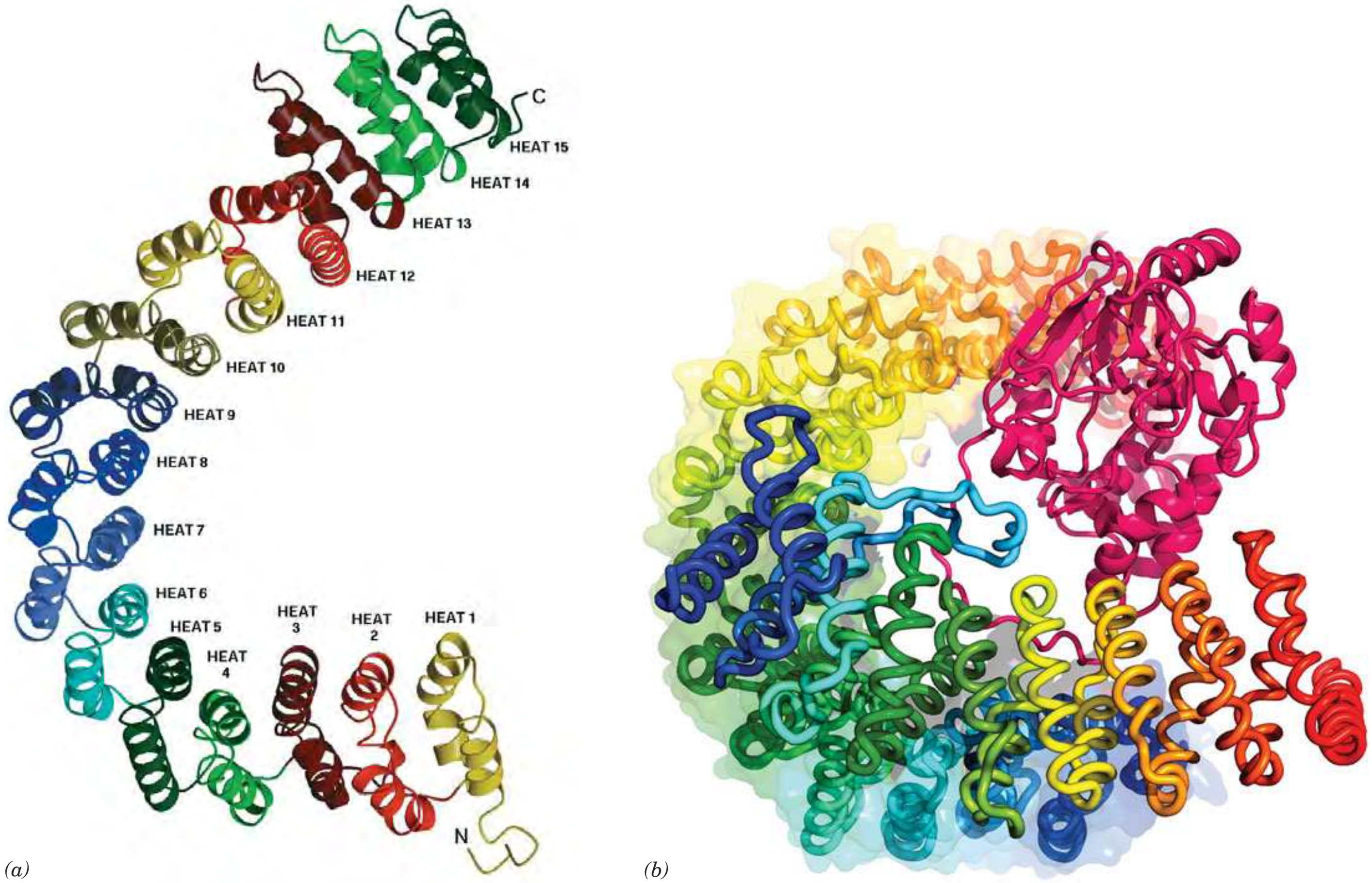

Figure 13-16 | X-Ray structure of protein phosphatase PP2A. (*a*) The structure of an isolated scaffold (A) subunit. HEAT repeats, which are drawn here in different colors, each consist of two antiparallel helices joined by a short linker. These stack on one another with their corresponding helices nearly parallel to form an ~100-Å-long right-handed superhelix (helix of helices) with a hooklike shape. [Courtesy of Bostjan Kobe, St. Vincent's Institute of Medical Research, Fitzroy, Victoria, Australia. X-Ray structure by David Barford, University of Oxford, U.K. PDBid 1B3U.] (*b*) The structure of a PP2A heterotrimer viewed with the scaffold subunit oriented approximately as in Part *a*. Here the scaffold (A; 589 residues) and regulatory (B; 449 residues) subunits are drawn in worm form, each colored in rainbow order from its N-terminus (*blue*) to its C-terminus (*red*). In addition, the A subunit is embedded in its transparent molecular surface. The catalytic (C; 309 residues) subunit (*magenta*) is drawn in ribbon form. Note the close structural resemblance of the A and B subunits. [Based on an X-ray structure by Yigong Shi, Princeton University. PDBid 2NPP.]

The X-ray structure of a PP2A **holoenzyme** (complete enzyme; Fig 13-16*b*) reveals, unexpectedly, that its regulatory subunit consists of 8 tandem HEAT-like repeats arranged like those of the A subunit, despite their lack of sequence similarity. The C subunit binds to the A subunit's concave surface along a ridge of conserved hydrophobic side chains spanning HEAT repeats 11 to 15. The regulatory subunit similarly interacts with the A subunit's HEAT repeats 2 to 8 and also binds to the C subunit via a ridge spanning its own HEAT-like repeats 6 to 8. The highly acidic, convex side of the regulatory subunit (lower part of Fig. 13-16*b*) is thereby left unoccupied, which suggests that it interacts with substrate proteins.

PP2A's catalytic and scaffold subunits both have two isoforms, and there are 16 isoforms of the regulatory subunit. This results in an enormous panoply of enzymes that are targeted to different phosphoproteins in distinct subcellular sites during different developmental stages. This complexity is a major cause of our limited understanding of how PP2A carries out its diverse cellular functions, even though it comprises between 0.3 and 1% of cellular proteins.

The PPP family also includes **calcineurin** (also called **PP2B**), a Ser/Thr phosphatase that is activated by Ca^{2+}. Calcineurin plays an essential role in T cell proliferation. It is inhibited by the action of drugs such as **cyclosporin A,** which is used clinically to suppress immune system function following organ transplantation.

CHECK YOUR UNDERSTANDING

Describe how an RTK becomes an active PTK.

Summarize the roles of SH2 and SH3 domains, Ras, GTP, and protein kinases in transmitting a signal from an RTK to a transcription factor.

What is the advantage of a pathway involving sequential kinase activation?

Describe how SH2 and SH3 domains and Tyr phosphorylation influence PTK activity.

Explain what protein phosphatases do and why they exist as multidomain or multisubunit proteins.

3 Heterotrimeric G Proteins

LEARNING OBJECTIVES

- Understand that G protein–coupled receptors contain seven membrane-spanning helices.
- Understand that ligand binding to a GPCR induces the α subunit of the associated G protein to exchange GDP for GTP and dissociate from the β and γ subunits.
- Understand that adenylate cyclase is activated to produce cAMP, which in turn activates protein kinase A.
- Understand that signaling activity is limited through the action of phosphodiesterases that act on cAMP and cGMP.

The second major class of signal transduction pathways that we shall discuss involves **heterotrimeric G proteins.** These proteins are members of the superfamily of regulatory GTPases that are collectively known as G proteins, which, as we have seen, are named for their ability to bind the guanine nucleotides GTP and GDP and hydrolyze GTP to GDP and P_i. The monomeric G proteins are essential for a wide variety of processes, including signal transduction (e.g., Ras; Section 13-2B), vesicle trafficking (Section 9-4E), the growth of actin microfilaments (Section 7-2C), translation (as ribosomal accessory factors; Section 27-4), and protein targeting [as components of the signal recognition particle (SRP) and the SRP receptor; Section 9-4D]. The many G proteins share common structural motifs that bind guanine nucleotides and catalyze the hydrolysis of GTP.

Many heterotrimeric G proteins participate in signal transduction systems that consist of three major components:

1. **G protein–coupled receptors (GPCRs),** transmembrane proteins that bind their corresponding ligand (e.g., a hormone) on their extracellular side, which induces a conformational change on their cytoplasmic side.
2. Heterotrimeric G proteins, which are anchored to the cytoplasmic side of the plasma membrane and which are activated by a GPCR when it binds its corresponding ligand.
3. **Adenylate cyclase (AC),** a transmembrane enzyme that is activated (or in some cases inhibited) by activated heterotrimeric G proteins.

Activated AC catalyzes the synthesis of **adenosine-3′,5′-cyclic monophosphate (3′,5′-cyclic AMP or cAMP)** from ATP.

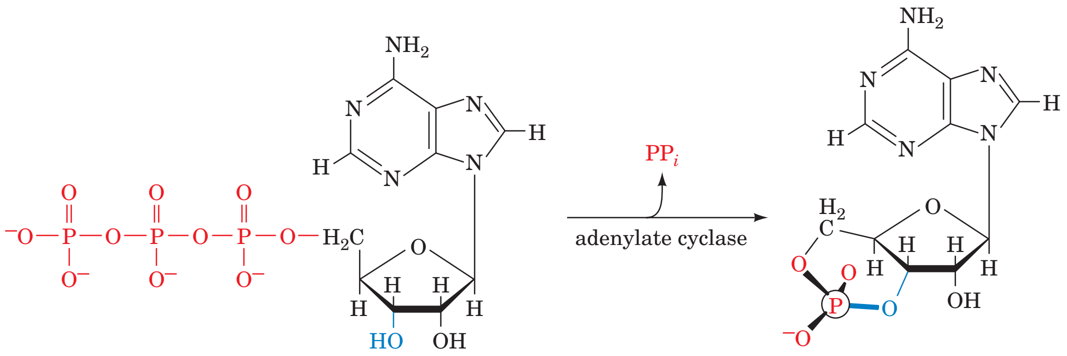

ATP

3′,5′-Cyclic AMP (cAMP)

The cAMP, in turn, binds to a variety of proteins so as to activate numerous cellular processes. Thus, as Earl Sutherland first showed, *cAMP is a*

second messenger, *that is, it intracellularly transmits the signal originated by the extracellular ligand.*

What are the mechanisms through which the binding of ligand to an extracellular receptor induces AC to synthesize cAMP in the cytosol? In answering this question we shall see that the signaling system outlined above has a surprising complexity that endows it with immense capacity for both signal amplification and regulatory flexibility.

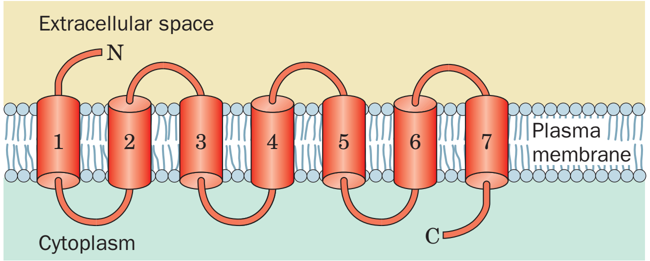

Figure 13-17 | General structure of a G protein–coupled receptor (GPCR).

A | G Protein–Coupled Receptors Contain Seven Transmembrane Helices

The G protein–coupled receptors include the glucagon receptor, the β-adrenoreceptor (to which epinephrine binds; Section 13-1B), and a host of other proteins that bind peptide hormones, odorant (having an odor) and tastant (having a taste) molecules, eicosanoids (Section 9-1F), and other compounds. All of these receptors are integral membrane proteins with seven transmembrane α helices (Fig. 13-17). The mammalian genome is estimated to contain over 1000 different GPCRs (>4% of its ~23,000 genes). The importance of these receptors is also evident in the fact that some 60% of the therapeutic drugs presently in use target specific GPCRs.

The first and, as yet, the only GPCR to be structurally characterized at the atomic level is **rhodopsin,** a light-sensing protein in the retina. Rhodopsin consists of the 348-residue protein **opsin** and the covalently linked chromophore retinal (Fig. 13-18), which is similarly linked to the homologous protein bacteriorhodopsin (Section 9-3A). The absorption of a photon causes the rhodopsin-bound retinal to isomerize from its ground-state 11-cis form to its all-trans form. The isomerization causes opsin to undergo a transient conformational change that activates its associated heterotrimeric G protein.

The transmembrane helices of GPCRs are generally uniform in size: 20 to 27 residues, which is sufficient to span a lipid bilayer. However, their N- and C-terminal segments and the loops connecting their transmembrane helices vary widely in length. These are the portions of the protein that bind ligands (on the extracellular side) and heterotrimeric G proteins (on the cytoplasmic side). Rhodopsin is posttranslationally modified by *N*-linked oligosaccharides, two of which are positioned on extracellular loops, and palmitoyl groups, at least one of which interacts with membrane lipids.

GPCRs function much like allosteric proteins such as hemoglobin (Section 7-1). *By alternating between two discrete conformations, one with ligand bound and one without, the receptor can transmit an extracellular signal to the cell interior.* This model of receptor action

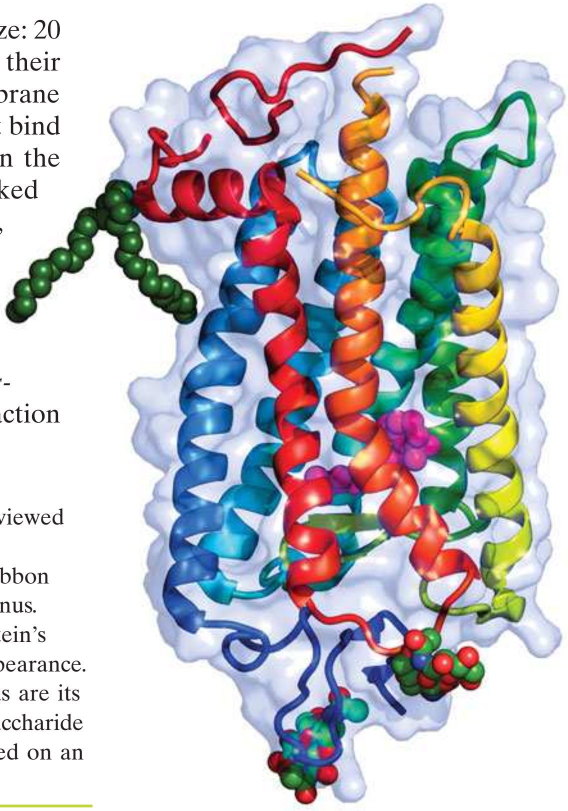

Figure 13-18 | X-Ray structure of bovine rhodopsin. The structure is viewed parallel to the plane of the membrane with the cytoplasm above. The protein is represented by its transparent molecular surface with its polypeptide chain in ribbon form colored in rainbow order from blue at its N-terminus to red at its C-terminus. Note its bundle of seven nearly parallel transmembrane helices. Two of the protein's cytoplasmic loops are partially disordered, which results in their fragmented appearance. The protein's retinal prosthetic group (*magenta*) is drawn in space-filling form as are its two covalently linked palmitoyl groups (*dark green*) and its two *N*-linked oligosaccharide groups (colored according to atom type with C green, N blue, and O red). [Based on an X-ray structure by Ronald Stenkamp, University of Washington. PDBid 1HZX.]

is similar to the operation of membrane transport proteins (e.g., Fig. 10-13); in fact, some membrane-bound receptors are ion channels that switch between the open and closed conformations in response to ligand binding.

Receptors Are Subject to Desensitization. A hallmark of biological signaling systems is that they adapt to long-term stimuli by reducing their response to them, a process named **desensitization.** *These signaling systems therefore respond to changes in stimulation levels rather than to their absolute values.* In the case of the β-adrenoreceptor, continuous exposure to epinephrine leads to the phosphorylation of one or more of the receptor's Ser residues. This phosphorylation, which is catalyzed by a specific kinase that acts on the hormone–receptor complex but not on the receptor alone, reduces the receptor's affinity for epinephrine. If the epinephrine level is reduced, the receptor is slowly dephosphorylated, eventually restoring the cell's initial epinephrine sensitivity.

B | Heterotrimeric G Proteins Dissociate on Activation

Heterotrimeric G proteins, as their name implies, are G proteins that consist of an α, β, and γ subunit (45, 37, and 9 kD, respectively). The X-ray structures of entire heterotrimeric G proteins were independently determined by Alfred Gilman and Stephan Sprang (Fig. 13-19) and by Heidi Hamm and Paul Sigler. The large α subunit, designated G_α, consists of two domains connected by two polypeptide linkers (Fig. 13-19*a*): (1) a highly conserved GTPase domain that is structurally similar to those in monomeric G proteins such as Ras and hence is known as a Ras-like domain, and (2) a

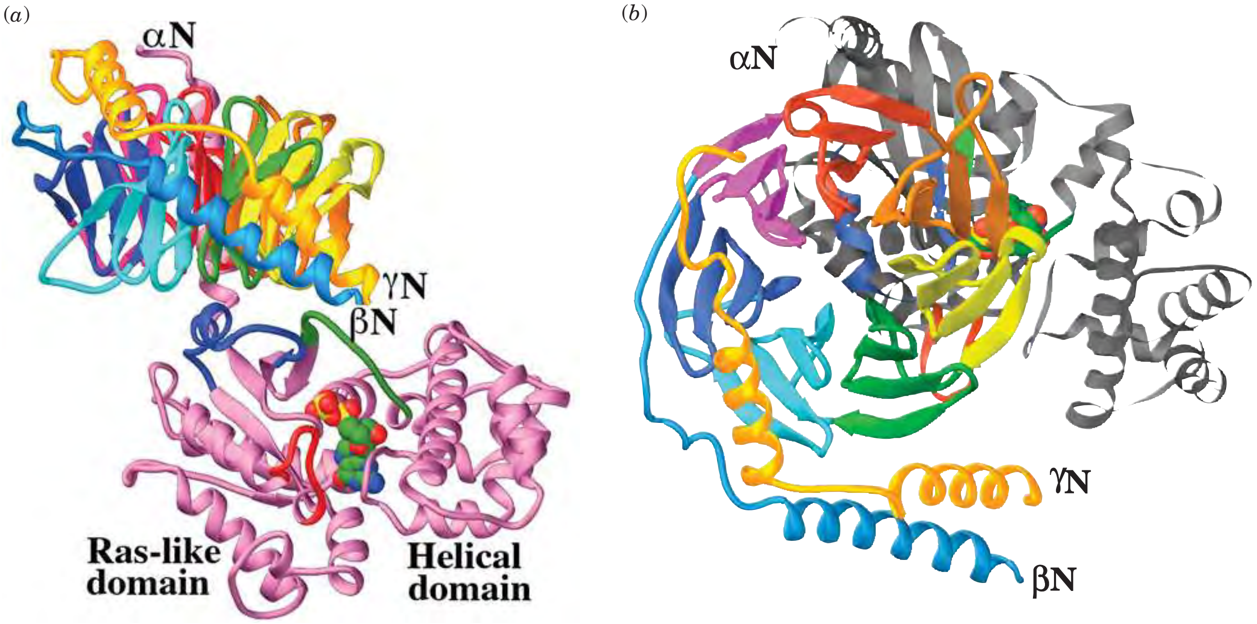

Figure 13-19 | X-Ray structure of a heterotrimeric G protein. (*a*) The G_α subunit is violet with the segments known as Switch I, II, and III green, blue, and red, respectively. A bound GDP is shown in space-filling form with C green, N blue, O red, and P yellow. The G_β subunit's N-terminal segment is light blue and each blade of its β-propeller has a different color. The G_γ subunit is gold. The plasma membrane is probably at the top of the drawing, as inferred from the positions of the N terminus of G_α and the neighboring C terminus of G_γ, which are lipid-linked *in vivo,* although the orientation of the protein relative to the membrane is unknown. (*b*) View related to that in Part *a* by a 90° rotation about the horizontal axis, that is, looking from the general direction of the plasma membrane. The protein is colored as in Part *a* except that the G_α subunit is mainly gray. [Based on an X-ray structure by Alfred Gilman and Stephan Sprang, University of Texas Southwestern Medical Center. PDBid 1GP2.] **See Interactive Exercise 12.**

helical domain that is unique to heterotrimeric G proteins. The Ras-like domain contains the guanine nucleotide–binding site in a deep cleft and is anchored to the membrane by a myristoyl or palmitoyl group, or both, covalently attached near the protein's N-terminus. The G_β subunit, which is anchored to the membrane via prenylation of its C-terminus, consists of an N-terminal helical domain followed by a C-terminal domain comprising seven 4-stranded antiparallel β sheets arranged like the blades of a propeller—a so-called **β propeller** (Fig. 13-19*b*). The G_γ subunit consists mainly of two helical segments joined by a polypeptide link (Fig. 13-19*b*). It is closely associated with G_β along its entire extended length through mainly hydrophobic interactions. G_γ binds to G_β with such high affinity that they dissociate only under denaturing conditions. Consequently, we shall henceforth refer to their complex as $G_{\beta\gamma}$.

In its unactivated state, a heterotrimeric G protein maintains its heterotrimeric state and its G_α subunit binds GDP. However, *the binding of such a* $G_\alpha \cdot GDP–G_{\beta\gamma}$ *complex to its cognate GPCR in complex with its ligand induces the* G_α *subunit to exchange its bound GDP for GTP.* Thus, the ligand–GPCR complex functions as the G_α subunit's guanine nucleotide exchange factor (GEF).

When GTP is bound to G_α, its γ phosphate group promotes conformational changes in three of G_α's so-called **switch regions** (Fig. 13-19*a*), *causing* G_α *to dissociate from* $G_{\beta\gamma}$. This occurs because the binding of GTP's γ phosphoryl group and the binding of $G_{\beta\gamma}$ to G_α are mutually exclusive; the γ phosphoryl group hydrogen-bonds with side chains in Switches I and II so as to prevent the segments from interacting with the loops and turns at the bottom of G_β's β-propeller. Switches I and II have counterparts in other G proteins of known structure. Comparison of the X-ray structures of the $G_\alpha \cdot GDP–G_{\beta\gamma}$ complex and $G_{\beta\gamma}$ alone indicates that the structure of $G_{\beta\gamma}$ is unchanged by its association with $G_\alpha \cdot GDP$. Nevertheless, both G_α and $G_{\beta\gamma}$ are active in signal transduction; they interact with additional cellular components, as we discuss below.

The effect of G protein activation is short-lived, because G_α is also a GTPase that catalyzes the hydrolysis of its bound GTP to GDP + P_i, although at the relatively sluggish rate of 2 to 3 min^{-1}. GTP hydrolysis causes the heterotrimeric G protein to reassemble as the inactive $G_\alpha \cdot GDP–G_{\beta\gamma}$ complex. This prevents a runaway response to ligand binding to a GPCR.

Heterotrimeric G Proteins Activate Other Proteins. A mammalian cell can contain numerous different kinds of heterotrimeric G proteins, since there are 20 different α subunits, 6 different β subunits, and 12 different γ subunits. This heterozygosity presumably permits various cell types to respond in different ways to a variety of stimuli.

One of the major targets of the heterotrimeric G protein system is the enzyme adenylate cyclase (described more fully in the next section). For example, when a $G_\alpha \cdot GTP$ complex dissociates from $G_{\beta\gamma}$, it may bind with high affinity to AC, thereby activating the enzyme. Such a G_α protein is known as a stimulatory G protein, $\mathbf{G_{s\alpha}}$. Other G_α proteins, known as inhibitory G proteins, $\mathbf{G_{i\alpha}}$, inhibit AC activity. The heterotrimeric $\mathbf{G_s}$ and $\mathbf{G_i}$ proteins, which differ in their α subunits, may actually contain the same β and γ subunits. Other types of heterotrimeric G proteins—acting through their G_α or $G_{\beta\gamma}$ units—stimulate the opening of ion channels, participate in the phosphoinositide signaling system (Section 13-4), activate phosphodiesterases, and activate protein kinases.

Because a single ligand–receptor interaction can activate more than one G protein, this step of the signal transduction pathway serves to amplify the original extracellular signal. In addition, several types of ligand–receptor complexes may activate the same G protein so that different extracellular signals elicit the same cellular response.

C | Adenylate Cyclase Synthesizes cAMP to Activate Protein Kinase A

See Guided Exploration 13
Mechanisms of hormone signaling involving the adenylate cyclase system.

Mammals have 10 different isoforms of adenylate cyclase, which are each expressed in a tissue-specific manner and differ in their regulatory properties. These ~120-kD transmembrane glycoproteins each consist of a small N-terminal domain (N), followed by two repeats of a unit consisting of a transmembrane domain (M) followed by two consecutive cytoplasmic domains (C), thus forming the sequence $NM_1C_{1a}C_{1b}M_2C_{2a}C_{2b}$ (Fig. 13-20). The 40% identical C_{1a} and C_{2a} domains associate to form the enzyme's catalytic core, whereas C_{1b}, as well as C_{1a} and C_{2a}, bind regulatory molecules. For example, $G_{s\alpha}$ binds to C_{2a} to activate AC, and $G_{i\alpha}$ binds to C_{1a} to inhibit the enzyme. Other regulators of AC activity include Ca^{2+} and certain Ser/Thr protein kinases. Clearly, *cells can adjust their cAMP levels in response to a great variety of stimuli.*

The structure of intact adenylate cyclase is not known, but X-ray structural studies of the catalytic domains indicate that $G_{s\alpha} \cdot GTP$ binds to the $C_{1a} \cdot C_{2a}$ complex via its Switch II region. This binding alters the orientation of the C_{1a} and C_{2a} domains so as to position their catalytic residues for the efficient conversion of ATP to cAMP. When $G_{s\alpha}$ hydrolyzes its bound GTP, its Switch II region reorients so that it can no longer bind to C_{2a}, and the adenylate cyclase reverts to its inactive conformation.

Protein Kinase A Is Activated by Binding Four cAMP. cAMP is a polar, freely diffusing second messenger. In eukaryotic cells, its main target is **protein kinase A (PKA;** also known as **cAMP-dependent protein kinase** or **cAPK),** an enzyme that phosphorylates specific Ser or Thr residues of numerous cellular proteins. These proteins all contain a consensus kinase-recognition sequence, Arg-Arg-X-Ser/Thr-Y, where Ser/Thr is the phospho-

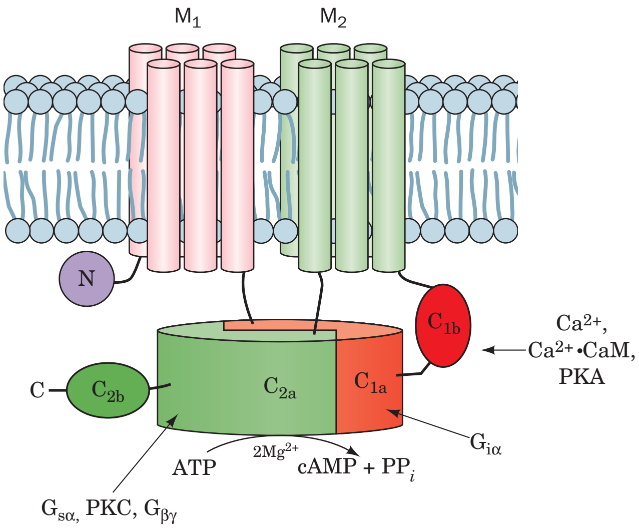

Figure 13-20 | Schematic diagram of a typical mammalian adenylate cyclase. The M_1 and M_2 domains are each predicted to contain six transmembrane helices. C_{1a} and C_{2a} form the enzyme's pseudosymmetric catalytic core. The domains with which various regulatory proteins are known to interact are indicated. [After Tesmer, J.J.G. and Sprang, S.R., *Curr. Opin. Struct. Biol.* **8,** 713 (1998).]

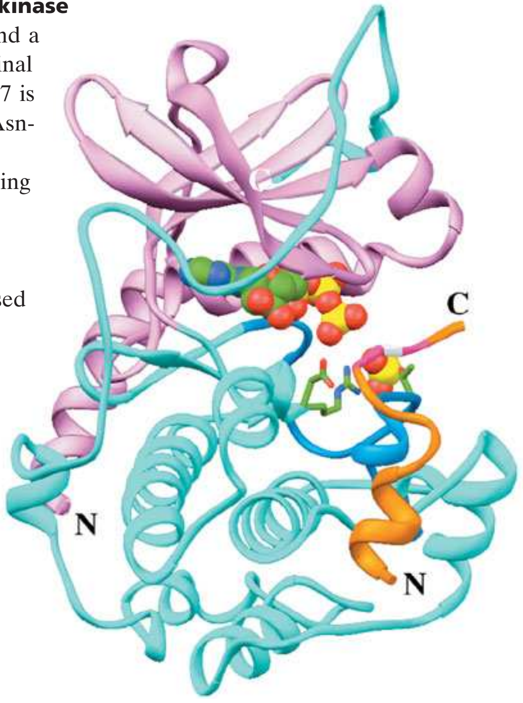

Figure 13-21 | X-Ray structure of the catalytic (C) subunit of mouse protein kinase A (PKA). The protein, which is shown in its "standard" view, is in complex with ATP and a 20-residue peptide segment of a naturally occurring protein kinase inhibitor. The N-terminal domain is pink, the C-terminal domain is cyan, and the activation loop containing Thr 197 is light blue. The polypeptide inhibitor is orange and its pseudo-target sequence, Arg-Arg-Asn-Ala-Ile, is magenta (the Ala, which replaces the Ser or Thr of a true substrate, is white). The substrate ATP and the phosphoryl group of phospho-Thr 197 are shown in space-filling form and the side chains of the catalytically essential Arg 165, Asp 166, and Thr 197 are shown in stick form, all colored according to atom type (C green, N blue, O red, and P yellow). Note that the inhibitor's pseudo-target sequence is close to ATP's γ phosphate group, the group that the enzyme transfers to the Ser or Thr of the target sequence. [Based on an X-ray structure by Susan Taylor and Janusz Sowadski, University of California at San Diego. PDBid 1ATP.] **See Interactive Exercise 13 and Kinemage Exercise 15.**

rylation site, X is any small residue, and Y is a large hydrophobic residue.

In the absence of cAMP, PKA is an inactive heterotetramer of two regulatory and two catalytic subunits, R_2C_2. The cAMP binds to the regulatory subunits to cause the dissociation of active catalytic monomers:

$$\underset{(inactive)}{R_2C_2} + 4\ \text{cAMP} \rightleftharpoons \underset{(active)}{2C} + R_2(\text{cAMP})_4$$

The intracellular concentration of cAMP therefore determines the fraction of PKA in its active form and thus the rate at which it phosphorylates its substrates.

The X-ray structure of the 350-residue C subunit of mouse PKA in complex with ATP and a 20-residue inhibitor peptide, which was determined by Susan Taylor and Janusz Sowadski, is shown in Fig. 13-21. The C subunit closely resembles other protein kinases of known structure (e.g., Figs. 13-5*a* and 13-12). In the PKA structure, the deep cleft between the lobes is occupied by ATP and a segment of the inhibitor peptide that resembles the 5-residue consensus sequence for phosphorylation except that the phosphorylated Ser/Thr is replaced by Ala. Thr 197, which is part of the activation loop, must be phosphorylated for maximal activity. The phosphoryl group at Thr 197 interacts with Arg 165, a conserved catalytic residue that is adjacent to Asp 166, the catalytic base that activates the substrate protein's target Ser/Thr hydroxyl group for phosphorylation. Thus, the phosphoryl group at PKA's Thr 197 functions to properly orient its active site residues.

The R subunit of protein kinase A competitively inhibits its C subunit. The R subunit has a well-defined structure containing two homologous cAMP-binding domains, A and B, and a so-called **autoinhibitor segment** (Fig. 13-22). In the inactive R_2C_2 complex, the autoinhibitor segment, which resembles the C subunit's substrate, binds in the C subunit's active site (as does the inhibitory peptide in Fig. 13-21) so as to block substrate binding. Each R subunit cooperatively binds two cAMPs. When the B domain lacks bound cAMP, it masks the A domain so as to prevent it from binding cAMP. However, the binding of cAMP to the B domain triggers

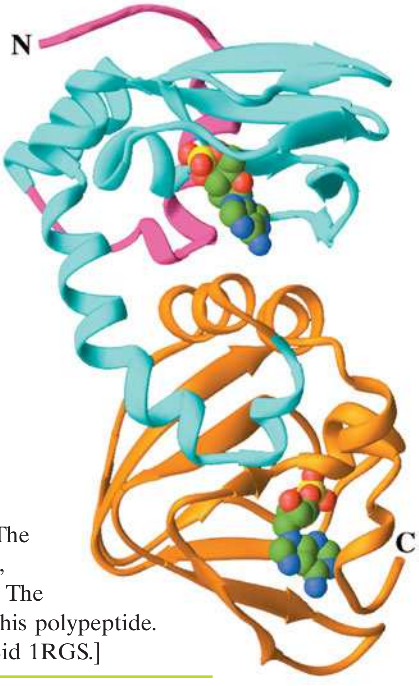

Figure 13-22 | X-Ray structure of the regulatory (R) subunit of bovine protein kinase A (PKA) in complex with cAMP. Domain A is cyan and domain B is orange. The cAMP molecules are shown in space-filling form colored according to atom type (C green, N blue, O red, and P yellow). The region containing the autoinhibitor segment is magenta. The N-terminal 91 residues of the R subunit, which mediate its dimerization, are absent from this polypeptide. [Based on an X-ray structure by Susan Taylor, University of California at San Diego. PDBid 1RGS.]

a conformational change that permits the A domain to bind cAMP, which in turn releases the now-active C subunits from the complex.

The targets of PKA include enzymes involved in glycogen metabolism. For example, when epinephrine binds to the β-adrenoreceptor of a muscle cell, the sequential activation of a heterotrimeric G protein, adenylate cyclase, and PKA leads to the activation of glycogen phosphorylase, thereby making glucose-6-phosphate available for glycolysis in a "fight-or-flight" response (Section 16-3).

Each step of a signal transduction pathway can potentially be regulated, so *the nature and magnitude of the cellular response ultimately reflect the presence and degree of activation or inhibition of all the preceding components of the pathway.* For example, the adenylate cyclase signaling pathway can be limited or reversed through ligand activation of a receptor coupled to an inhibitory G protein. The activity of the cAMP second messenger can be attenuated by the action of phosphodiesterases that hydrolyze cAMP to AMP (see below). In addition, reactions catalyzed by PKA are reversed by protein Ser/Thr phosphatases (Section 13-2D). Some of these features of the adenylate cyclase signaling pathway are illustrated in Fig. 13-23. Many drugs and toxins exert their effects by modifying components of the adenylate cyclase system (Box 13-4).

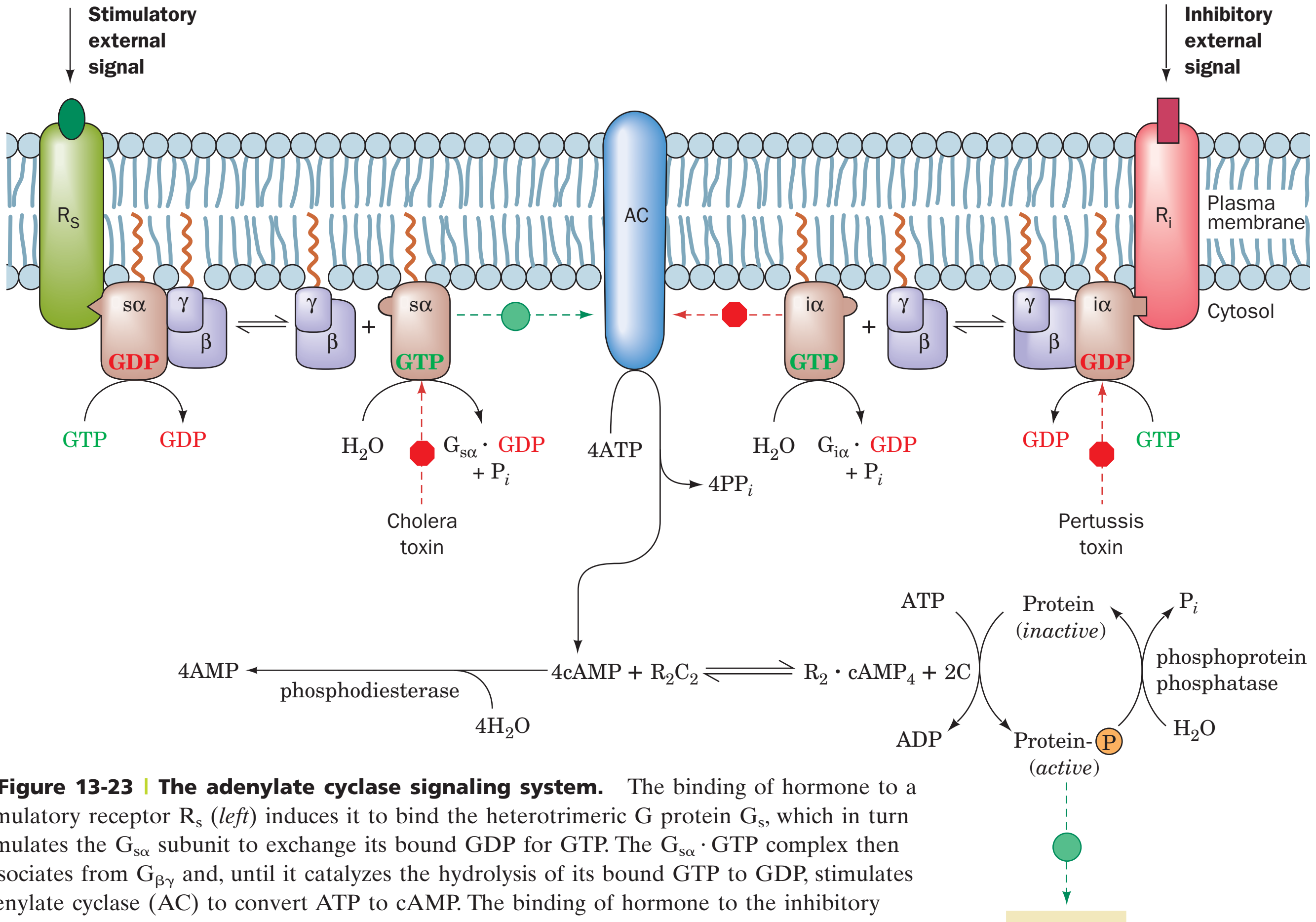
Stimulatory external signal
Inhibitory external signal
R_s
AC
R_i
Plasma membrane
Cytosol
sα
γ
β
GDP
+
GTP
iα
GTP
GDP
H_2O
$G_{s\alpha} \cdot$ GDP $+ P_i$
4ATP
$4PP_i$
H_2O
$G_{i\alpha} \cdot$ GDP $+ P_i$
GDP
GTP
Cholera toxin
Pertussis toxin
4AMP
phosphodiesterase
$4H_2O$
$4cAMP + R_2C_2 \rightleftharpoons R_2 \cdot cAMP_4 + 2C$
ATP
ADP
Protein (inactive)
Protein-P (active)
P_i
phosphoprotein phosphatase
H_2O
Cellular response

■ **Figure 13-23** | **The adenylate cyclase signaling system.** The binding of hormone to a stimulatory receptor R_s (*left*) induces it to bind the heterotrimeric G protein G_s, which in turn stimulates the $G_{s\alpha}$ subunit to exchange its bound GDP for GTP. The $G_{s\alpha} \cdot$ GTP complex then dissociates from $G_{\beta\gamma}$ and, until it catalyzes the hydrolysis of its bound GTP to GDP, stimulates adenylate cyclase (AC) to convert ATP to cAMP. The binding of hormone to the inhibitory receptor R_i (*right*) triggers an almost identical chain of events except that the presence of the $G_{i\alpha} \cdot$ GTP complex inhibits adenylate cyclase. R_2C_2 represents protein kinase A (PKA) whose catalytic subunit C, when activated by the dissociation of the regulatory dimer as $R_2 \cdot cAMP_4$, activates various cellular proteins by catalyzing their phosphorylation. The sites of action of certain toxins are indicated.

D | Phosphodiesterases Limit Second Messenger Activity

In any chemically based signaling system, the signal molecule must eventually be eliminated in order to control the amplitude and duration of the signal and to prevent interference with the reception of subsequent signals. In

BOX 13-4 BIOCHEMISTRY IN HEALTH AND DISEASE

Drugs and Toxins That Affect Cell Signaling

Complex processes such as the adenylate cyclase signaling system can be sabotaged by a variety of agents. For example, the methylated purine derivatives **caffeine** (an ingredient of coffee and tea), **theophylline** (an asthma treatment), and **theobromine** (found in chocolate) are stimulants because they antagonize adenosine receptors that act through inhibitory G proteins. This antagonism results in an increase in cAMP concentration.

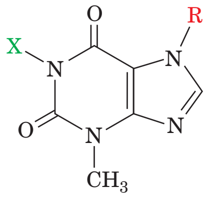

R = CH_3	X = CH_3	**Caffeine (1,3,7-trimethylxanthine)**
R = H	X = CH_3	**Theophylline (1,3-dimethylxanthine)**
R = CH_3	X = H	**Theobromine (1,7-dimethylxanthine)**

Deadlier effects result from certain bacterial toxins that interfere with heterotrimeric G protein function. The toxin released by *Vibrio cholerae* (the bacterium causing cholera) triggers massive fluid loss of over a liter per hour from diarrhea. Victims die from dehydration unless their lost water and salts are replaced. **Cholera toxin,** an 87-kD protein of subunit composition AB_5, binds to ganglioside G_{M1} (Fig. 9-9) on the surface of intestinal cells via its B subunits. This permits the toxin to enter the cell, probably via receptor-mediated endocytosis, where an ~195-residue proteolytic fragment of its A subunit is released. This fragment catalyzes the transfer of the ADP–ribose unit from NAD$^+$ to a specific Arg side chain of $G_{s\alpha}$ (*below*).

ADP-ribosylated $G_{s\alpha} \cdot GTP$ can activate adenylate cyclase but cannot hydrolyze its bound GTP (Fig. 13-23). As a consequence, the adenylate cyclase is locked in its active state and cellular cAMP levels increase ~100-fold. Intestinal cells, which normally respond to small increases in cAMP by secreting digestive fluid (an HCO_3^--rich salt solution), pour out enormous quantities of this fluid in response to the elevated cAMP concentrations.

Other bacterial toxins act similarly. Certain strains of *E. coli* cause a diarrheal disease similar to but less serious than cholera through their production of **heat-labile enterotoxin,** a protein that is closely similar to cholera toxin (their A and B subunits are >80% identical) and has the same mechanism of action. **Pertussis toxin** [secreted by *Bordetella pertussis,* the bacterium that causes **pertussis** (whooping cough), which is responsible for ~400,000 infant deaths per year worldwide] is an AB_5 protein homologous to cholera toxin that ADP-ribosylates a specific Cys residue of $G_{i\alpha}$. The modified $G_{i\alpha}$ cannot exchange its bound GDP for GTP and therefore cannot inhibit adenylate cyclase (Fig. 13-23).

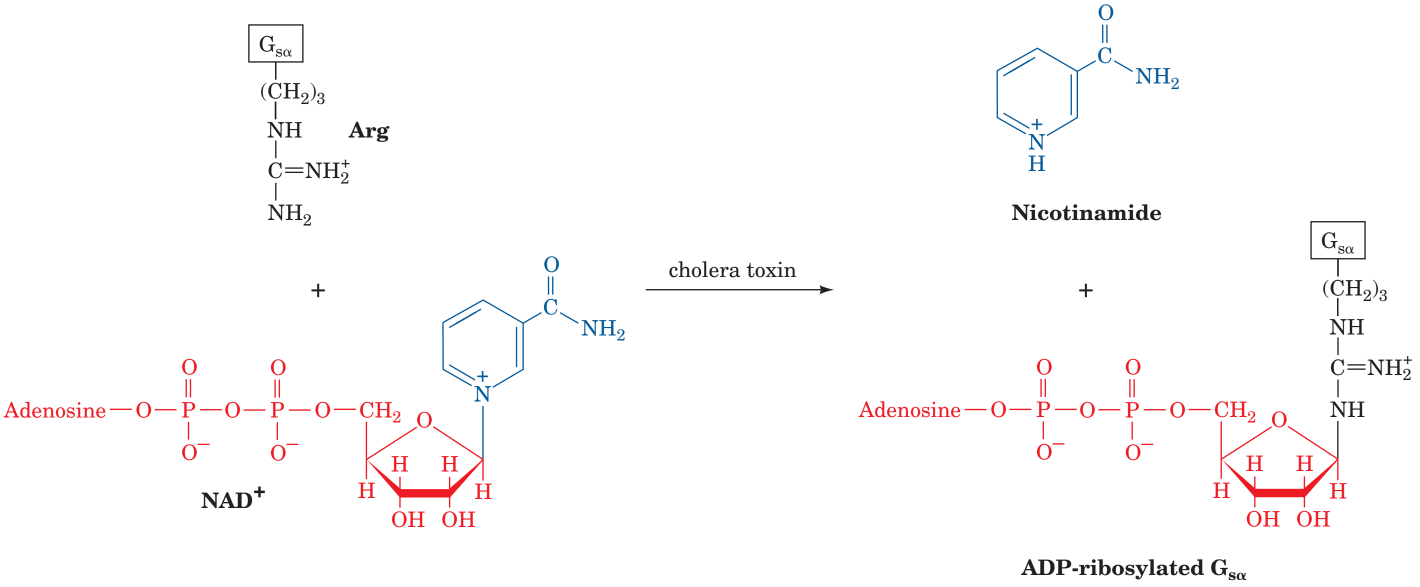

the case of cAMP, this second messenger is hydrolyzed to AMP by enzymes known as **cAMP-phosphodiesterases (cAMP-PDEs).**

The PDE superfamily, which includes both cAMP-PDEs and **cGMP-PDEs** (**cGMP** is the guanine analog of cAMP), is encoded in mammals by at least 20 different genes grouped into 11 families (PDE1 through PDE11). These are functionally distinguished by their substrate specificities (for cAMP, cGMP, or both) and kinetic properties, their responses (or lack of them) to various activators and inhibitors (see below), and their tissue, cellular, and subcellular distributions. The PDEs have characteristic modular architectures with a conserved ~270-residue catalytic domain near their C-termini and widely divergent regulatory domains or motifs, usually in their N-terminal portions. Some PDEs are membrane-anchored, whereas others are cytosolic.

PDE activity, as might be expected, is elaborately controlled. Depending on its isoform, a PDE may be activated by one or more of a variety of agents, including Ca^{2+} ion and phosphorylation by PKA and **insulin-stimulated protein kinase.** Phosphorylated PDEs are dephosphorylated by a variety of protein phosphatases. Thus, the PDEs provide a means for cross talk between cAMP-based signaling systems and those using other types of signals.

PDEs are inhibited by a variety of drugs that influence such widely divergent disorders as asthma, congestive heart failure, depression, erectile dysfunction, inflammation, and retinal degeneration. **Sildenafil** (trade name **Viagra**), a compound used to treat erectile dysfunction, specifically inhibits PDE5, which hydrolyzes only cGMP. Sexual stimulation in males causes penile nerves to release nitric oxide (NO), which activates **guanylate cyclase** to produce cGMP from GTP. The cGMP induces vascular smooth muscle relaxation in the penis, thereby increasing the inflow of blood, which results in an erection. This cGMP is eventually hydrolyzed by PDE5. Sildenafil is therefore an effective treatment in men who produce insufficient NO and hence cGMP to otherwise generate a satisfactory erection.

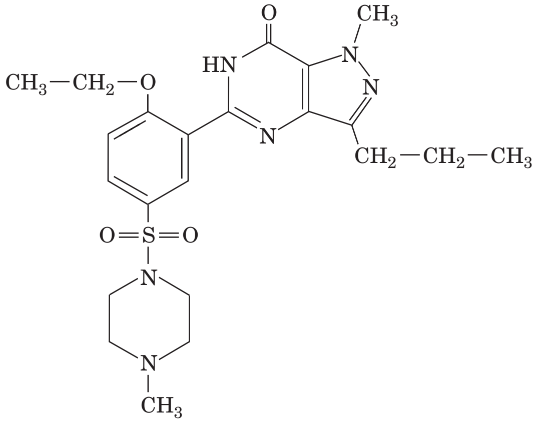

Sildenafil (Viagra)

CHECK YOUR UNDERSTANDING

Summarize the steps of signal transduction from a GPCR to phosphorylation of target proteins by PKA.

Describe how G proteins are activated and inactivated.

What is the purpose of a second messenger such as cAMP?

Why does the adenylate cyclase signaling system include phosphodiesterases?

4 The Phosphoinositide Pathway

LEARNING OBJECTIVES

- Understand that signal transduction via the phosphoinositide pathway generates the second messenger inositol trisphosphate, which triggers Ca^{2+} release, and diacylglycerol, which activates protein kinase C.
- Understand that in the presence of Ca^{2+}, calmodulin binds and activates its target proteins.
- Understand that a hormone can activate multiple signal transduction pathways to elicit a variety of intracellular responses.

A discussion of signal transduction pathways would not be complete without the **phosphoinositide pathway,** which mediates the effects of a variety of hormones. This signaling pathway requires a receptor with seven transmembrane segments, a heterotrimeric G protein, a specific kinase, and a phosphorylated glycerophospholipid that is a minor component of the plasma membrane's inner leaflet. It involves the production of three second messengers, **inositol-1,4,5-trisphosphate** (IP_3), Ca^{2+}, and **1,2-diacylglycerol (DAG).**

A | Ligand Binding Results in the Cytoplasmic Release of the Second Messengers IP_3 and Ca^{2+}

Ligand binding to its receptor, such as epinephrine binding to the α_1-adrenoreceptor, activates a heterotrimeric G protein, G_q, whose membrane-anchored α subunit in complex with GTP diffuses laterally along the plasma membrane to activate the membrane-bound enzyme **phospholipase C** (**PLC;** Fig. 13-24, *upper left*). Activated PLC catalyzes the hydrolysis of **phosphatidylinositol-4,5-bisphosphate (PIP_2)** at its glycero-phospho bond (Section 9-1C), yielding inositol-1,4,5-trisphosphate (IP_3) and 1,2-

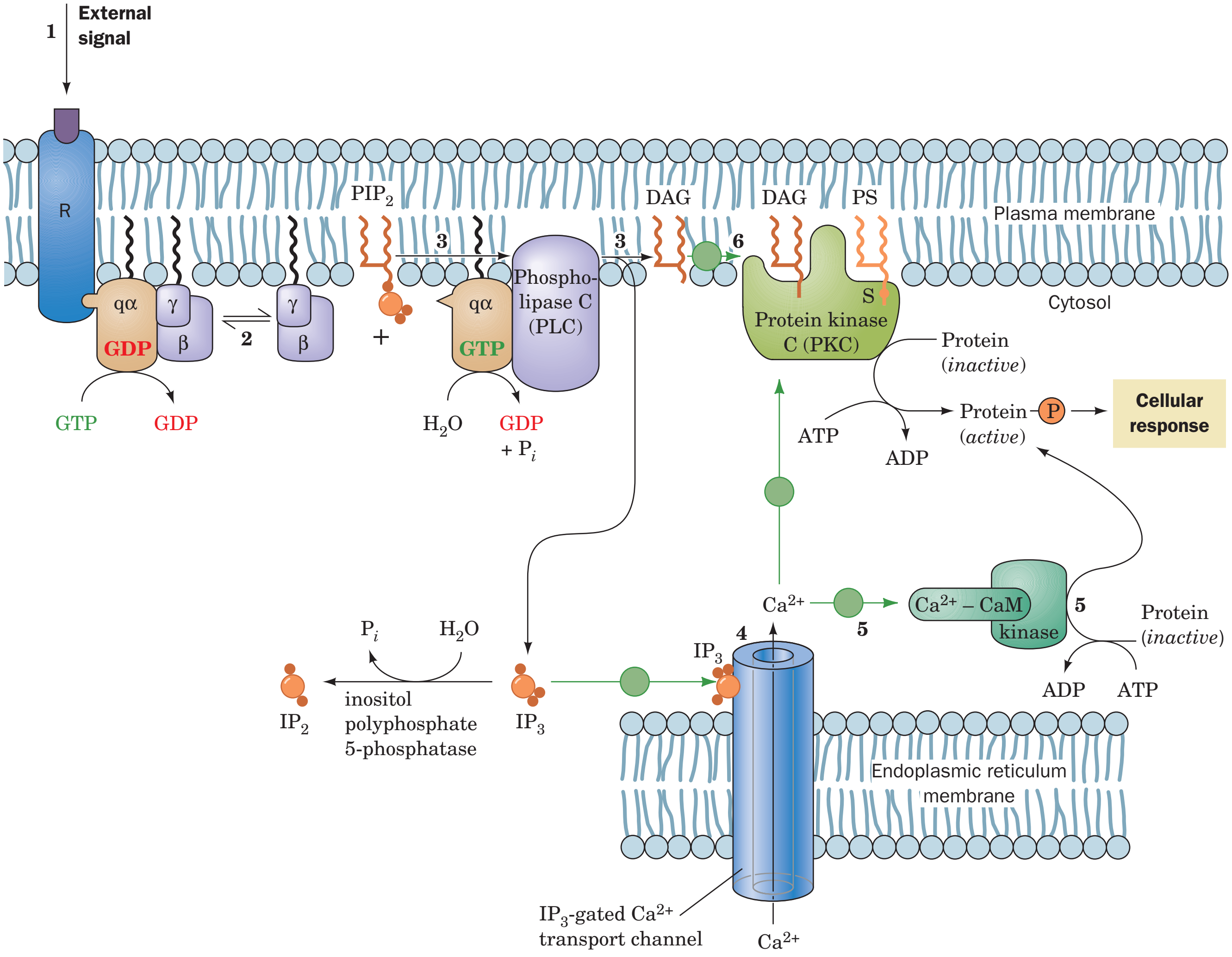

1
External signal
R
PIP2
DAG
DAG
PS
Plasma membrane
3
3
6
qα
γ
GDP
β
2
γ
β
+
qα
GTP
Phospho-lipase C (PLC)
S
Protein kinase C (PKC)
Cytosol
Protein (inactive)
Protein–P
(active)
Cellular response
ATP
ADP
GTP
GDP
H2O
GDP + Pi
Ca2+
5
Ca2+ – CaM kinase
5
Protein (inactive)
ADP
ATP
Pi
H2O
IP3
4
IP2
inositol polyphosphate 5-phosphatase
IP3
Endoplasmic reticulum membrane
IP3-gated Ca2+ transport channel
Ca2+

■ **Figure 13-24 | The phosphoinositide signaling system.** Ligand binding to a cell-surface receptor R (**1**) activates phospholipase C through the heterotrimeric G protein G_q (**2**). Phospholipase C catalyzes the hydrolysis of PIP_2 to IP_3 and DAG (**3**). The water-soluble IP_3 stimulates the release of Ca^{2+} sequestered in the endoplasmic reticulum (**4**), which in turn activates numerous cellular processes through the intermediacy of calmodulin (CaM; **5**). The nonpolar DAG remains associated with the membrane, where it activates protein kinase C (PKC) to phosphorylate and thereby modulate the activities of a number of cellular proteins (**6**). PKC activation also requires the presence of the membrane lipid phosphatidylserine (PS) and Ca^{2+}. **See the Animated Figures.**

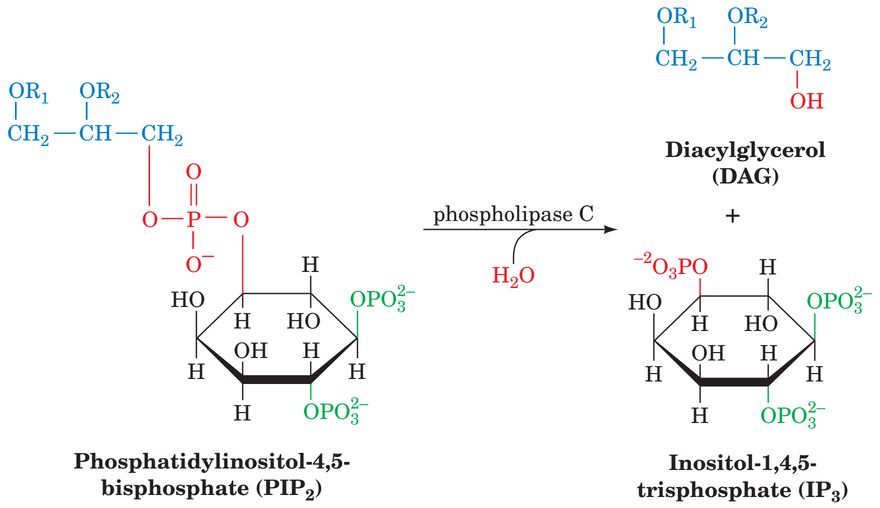

■ **Figure 13-25 | Phosphatidylinositol-4,5-bisphosphate (PIP_2) and its hydrolysis products.** PIP_2 is cleaved by phospholipase C to produce diacylglycerol (DAG) and inositol-1,4,5-trisphosphate (IP_3), both of which are second messengers. (The *bis* and *tris* prefixes denote, respectively, two and three phosphoryl groups that are linked separately to the inositol; in di- and triphosphates, the phosphoryl groups are linked sequentially.)

diacylglycerol (DAG; Fig. 13-25). PLC, which in mammals is actually a set of 11 isozymes, has a hydrophobic ridge consisting of three protein loops that is postulated to penetrate into the membrane's nonpolar region during catalysis. This would explain how the enzyme can catalyze hydrolysis of the membrane-bound PIP_2, leaving the DAG product associated with the membrane.

The Charged IP_3 Molecule Is a Water-Soluble Second Messenger. The hydrolysis of PIP_2 sets in motion both cytoplasmic and membrane-bound events. While DAG acts as a second messenger in the membrane (Section 13-4C), IP_3 diffuses through the cytoplasm to the endoplasmic reticulum (ER). There, it binds to and induces the opening of a Ca^{2+} transport channel (an example of a receptor that is also an ion channel), thereby allowing the efflux of Ca^{2+} from the ER. This causes the cytosolic $[Ca^{2+}]$ to increase from ~0.1 μM to as much as 10 mM, which triggers such diverse cellular processes as glucose mobilization and muscle contraction through the intermediacy of the Ca^{2+}-binding protein **calmodulin** (see below) and its homologs. The ER contains embedded Ca^{2+}–ATPases that actively pump Ca^{2+} from the cytosol back into the ER (Section 10-3B) so that in the absence of IP_3, the cytosolic $[Ca^{2+}]$ rapidly returns to its resting level.

B | Calmodulin Is a Ca^{2+}-Activated Switch

Calmodulin **(CaM)** is a ubiquitous, eukaryotic Ca^{2+}-binding protein that participates in numerous cellular regulatory processes. In some of these, CaM functions as a free-floating monomeric protein, whereas in others it is a subunit of a larger protein. The X-ray structure of this highly conserved 148-residue protein has a curious dumbbell-like shape in which two structurally similar globular domains are connected by a seven-turn α helix (Fig. 13-26). Note the close structural resemblance between CaM and the Ca^{2+}-binding TnC subunit of the muscle protein troponin (Fig. 7-31).

CaM's two globular domains each contain two high-affinity Ca^{2+}-binding sites. The Ca^{2+} ion in each of these sites is octahedrally coordinated by oxygen atoms from the backbone and side chains as well as from a protein-associated water molecule. Each of the Ca^{2+}-binding sites is formed by nearly superimposable helix–loop–helix motifs known as **EF hands** (Fig. 13-27) that form the Ca^{2+}-binding sites in numerous other Ca^{2+}-binding proteins of known structure.

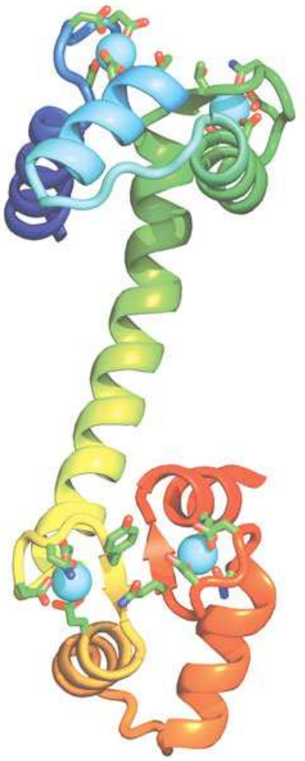

■ **Figure 13-26 | X-Ray structure of rat testis calmodulin.** This monomeric 148-residue protein, which is colored in rainbow order from N-terminus (*blue*) to C-terminus (*red*), contains two remarkably similar globular domains separated by a seven-turn α helix. The two Ca^{2+} ions bound to each domain are represented by cyan spheres. The side chains liganding the Ca^{2+} ions are drawn in stick form colored according to atom type (C green, N blue, and O red). [Based on an X-ray structure by Charles Bugg, University of Alabama at Birmingham. PDBid 3CLN.] **See Kinemage Exercise 16-1.**

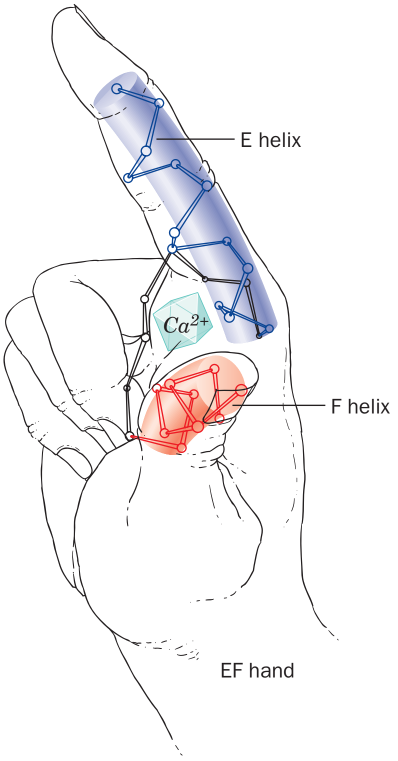

■ **Figure 13-27 | The EF hand.** The Ca^{2+}-binding sites in many proteins that sense the level of Ca^{2+} are formed by helix–loop–helix motifs named EF hands. [After Kretsinger, R.H., *Annu. Rev. Biochem.* **45,** 241 (1976).] **See Kinemage Exercise 16-1.**

Ca^{2+}–CaM Activates Its Target Proteins via an Intrasteric Mechanism. The binding of Ca^{2+} to either domain of CaM induces a conformational change in that domain, which exposes an otherwise buried Met-rich hydrophobic patch. This patch, in turn, binds with high affinity to the CaM-binding domains of numerous Ca^{2+}-regulated protein kinases (see below). These CaM-binding domains have little mutual sequence homology but are all basic amphiphilic α helices.

Despite uncomplexed CaM's extended appearance (Fig. 13-26), a variety of studies indicate that both of its globular domains bind to a single target helix. This was confirmed by the NMR structure (Fig. 13-28) of $(Ca^{2+})_4$–CaM in complex with its 26-residue CaM-binding target polypeptide from skeletal muscle **myosin light chain kinase** (**MLCK;** a homolog of the PKA C subunit, which phosphorylates and thereby activates the light chains of the muscle protein myosin; Section 7-2A). Thus, CaM's central α helix serves as a flexible tether rather than a rigid spacer, a property that probably extends the range of sequences to which CaM can bind. Indeed, both of CaM's globular domains are required for CaM to activate its targets: CaM domains that have been separated by proteolytic cleavage bind to their target peptides but do not cause enzyme activation.

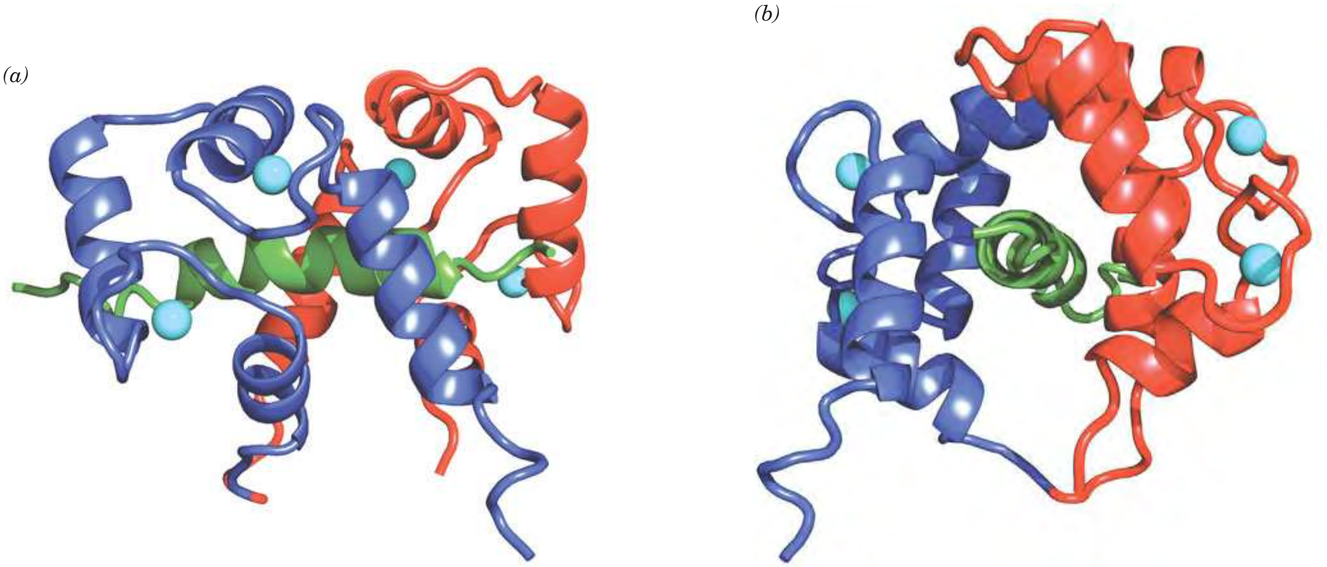

■ **Figure 13-28 | NMR structure of calmodulin in complex with a target polypeptide.** The N-terminal domain of CaM (from the fruit fly *Drosophila melanogaster*) is blue, its C-terminal domain is red, the 26-residue target polypeptide, which is from rabbit skeletal muscle myosin light chain kinase (MLCK), is green, and the Ca^{2+} ions are represented by cyan spheres. (*a*) A view of the complex in which the N-terminus of the target polypeptide is on the right. (*b*) The perpendicular view as seen from the right side of the structure shown in Part *a.* In both views, the pseudo-twofold axis relating the N- and C-terminal domains of CaM is approximately vertical. Note how the segment that joins the two domains is unwound and bent (bottom loop in Part *b*) so that CaM forms a globular protein that largely encloses the helical target polypeptide within a hydrophobic tunnel in a manner resembling two hands holding a rope. [Based on an NMR structure by Marius Clore, Angela Gronenborn, and Ad Bax, NIH. PDBid 2BBM.] **See Kinemage Exercise 16-2.**

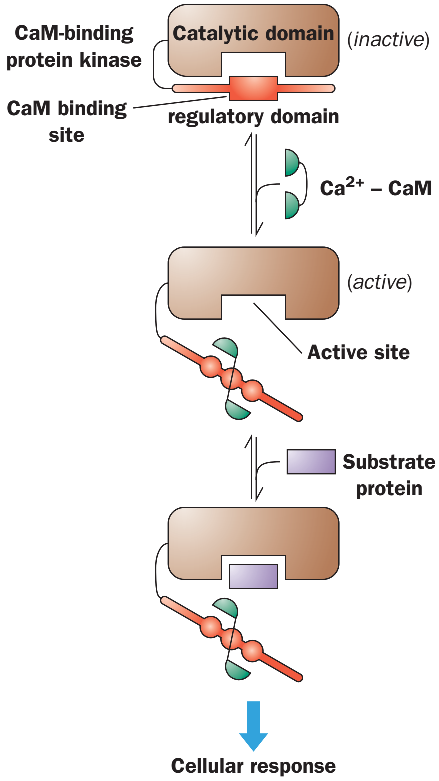

Figure 13-29 | A schematic diagram of the Ca^{2+}–CaM-dependent activation of protein kinases. Autoinhibited kinases have an N- or C-terminal “pseudosubstrate” sequence (*red*) that binds at or near the enzyme’s active site (*brown*) so as to inhibit its function. The autoinhibitory segment is in close proximity with or overlaps a Ca^{2+}–CaM binding sequence. Consequently, Ca^{2+}–CaM (*green*) binds to the sequence so as to extract it from the enzyme’s active site, thereby activating the enzyme to phosphorylate other proteins (*purple*). [After Crivici, A. and Ikura, M., *Annu. Rev. Biophys. Biomol. Struct.* **24,** 88 (1995).]

How does Ca^{2+}–CaM activate its target protein kinases? MLCK contains a C-terminal segment whose sequence resembles that of MLCK’s target polypeptide on the light chain of myosin but lacks a phosphorylation site. A model of MLCK, based on the X-ray structure of the 30% identical C subunit of PKA, strongly suggests that this autoinhibitor peptide inactivates MLCK by binding in its active site. Indeed, the excision of MLCK’s autoinhibitor peptide by limited proteolysis permanently activates the enzyme. MLCK’s CaM-binding segment overlaps the autoinhibitor peptide. Thus, *the binding of Ca^{2+}–CaM to this peptide segment extracts the autoinhibitor from MLCK’s active site, thereby activating the enzyme* (Fig. 13-29).

Ca^{2+}–CaM’s other target proteins are presumably activated in the same way. In fact, the X-ray structures of several homologous protein kinases support this so-called **intrasteric mechanism.** While the details of binding of the autoinhibitory sequence differ for each of the protein kinases, the general mode of autoinhibition and activation by Ca^{2+}–CaM is the same.

PKA’s R subunit, as we have seen (Section 13-3C), contains a similar autoinhibitory sequence adjacent to its two tandem cAMP-binding domains. In this case, however, the autoinhibitory peptide is allosterically ejected from the C subunit’s active site by the binding of cAMP to the R subunit (which lacks a Ca^{2+}–CaM-binding site).

C | DAG Is a Lipid-Soluble Second Messenger That Activates Protein Kinase C

The second product of the phospholipase C reaction, diacylglycerol (DAG), is a lipid-soluble second messenger. It therefore remains embedded in the plasma membrane, where it activates the membrane-bound **protein kinase C (PKC)** to phosphorylate and thereby modulate the activities of several different cellular proteins (Fig. 13-24, *right*). Multiple PKC enzymes are known; they differ in tissue expression, intracellular location, and their requirement for the DAG that activates them. PKC is a phosphorylated, cytosolic protein in its resting state. DAG increases the membrane affinity of PKC and also helps stabilize its active conformation. The catalytic activities of PKC and PKA are similar: Both kinases phosphorylate Ser and Thr residues.

The X-ray structure of a DAG-bound segment of PKC shows that the 50-residue motif is largely knit together by two Zn^{2+} ions, each of which is tetrahedrally liganded by one His and three Cys side chains (Fig. 13-30). A DAG analog, **phorbol-13-acetate,**

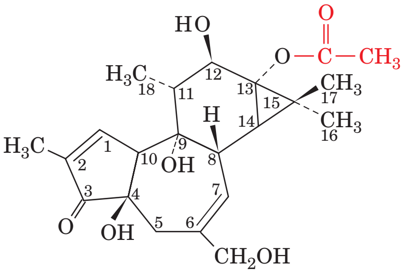

Phorbol-13-acetate

binds in a narrow groove between two long nonpolar loops. Very few soluble proteins have such a large continuous nonpolar region, suggesting that this portion of PKC inserts into the membrane. Full activation of PKC requires phosphatidylserine (which is present only in the cytoplasmic leaflet of the plasma membrane) and, in some cases, Ca^{2+} ion (presumably made available through the action of the IP_3 second messenger). Like other signaling systems, the phosphoinositide system is limited by the destruction of its second messengers, for example, through the action of **inositol polyphosphate 5-phosphatase** (Fig. 13-24, *lower left*).

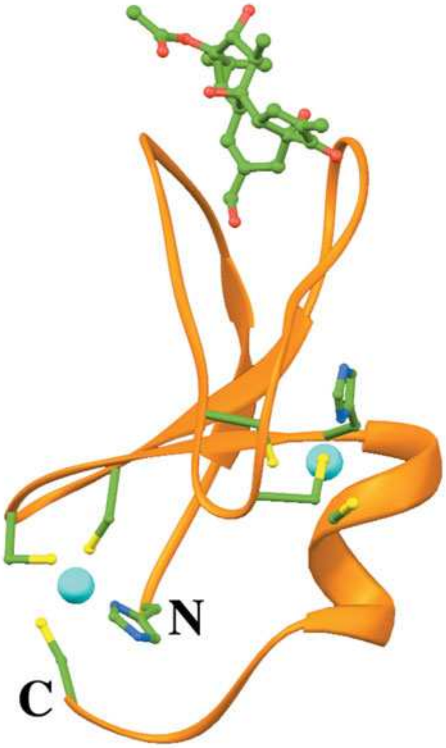

Figure 13-30 | X-Ray structure of a portion of protein kinase C in complex with phorbol-13-acetate. The protein tetrahedrally ligands two Zn^{2+} ions (*cyan spheres*), each via His and Cys side chains (shown in ball-and-stick form). Phorbol-13-acetate (*top*), which mimics the natural diacylglycerol ligand, binds between two nonpolar protein loops. Atoms are colored according to type with C green, N blue, O red, and S yellow. [Based on an X-ray structure by James Hurley, NIH. PDBid 1PTR.]

PLC Acts on Several Phospholipids to Release Different Second Messengers. Choline-containing phospholipids hydrolyzed by phospholipase C yield DAGs that differ from those released from PIP_2 and exert different effects on PKC. Another lipid second messenger, sphingosine released from sphingolipids, inhibits PKC.

The phosphoinositide signaling pathway in some cells yields a DAG that is predominantly l-stearoyl-2-arachidonoyl-glycerol. This molecule is further degraded to yield arachidonate, the precursor of the bioactive eicosanoids (prostaglandins and thromboxanes; Section 20-6C), and hence the phosphoinositide pathway yields up to four different second messengers. In other cells, IP_3 and diacylglycerol are rapidly recycled to re-form PIP_2 in the inner leaflet of the membrane. Some receptor tyrosine kinases activate an isoform of phospholipase C that contains two SH2 domains. This is another example of cross talk, the interactions of different signal transduction pathways.

D | Epilog: Complex Systems Have Emergent Properties

Complex systems are, by definition, difficult to understand and substantiate. Familiar examples include the earth's weather system, the economies of large countries, the ecologies of even small areas, and the human brain. Biological signal transduction systems, as is amply evident from a reading of this chapter, are complex systems. Thus, a hormonal signal is typically transduced through several intracellular signaling pathways, each of which consists of numerous components, many of which interact with components of other signaling pathways. For example, the **insulin signaling system** (Fig. 13-31), although not yet fully elucidated, is clearly highly complex. Upon binding insulin, the insulin receptor autophosphorylates itself at several Tyr residues (Section 13-2A) and then Tyr-phosphorylates its target proteins, thereby activating several signaling pathways that control a diverse array of effects:

1. Phosphorylation of the adaptor protein **Shc,** which generates a binding site for Grb2's SH2 domain, results in stimulation of a MAP kinase cascade (Section 13-2B), ultimately affecting growth and differentiation.
2. Phosphorylation of **Gab-1 (Grb2-associated binder-1)** similarly activates the MAP kinase cascade.
3. Phosphorylation of insulin receptor substrate (IRS) proteins (Section 13-2A) activates enzymes known as a **phosphoinositide 3-kinases (PI3Ks).** These enzymes add a phosphoryl group to the 3′-OH group of a phosphatidylinositol, often the 4,5-bisphosphate shown in Fig. 13-25. The 3-phosphorylated lipid activates **phosphoinositide-dependent protein kinase-1 (PDK1)** that in turn initiates cascades leading to glycogen synthesis (Section 16-3C) and the translocation of the glucose transporter GLUT4 to the surface of insulin-responsive cells (Section 22-2), as well as affecting cell growth and differentiation.
4. Phosphorylation of the **APS/Cbl** complex (APS for *A*daptor protein containing *p*lekstrin homology and *S*rc homology-2 domains; Cbl is an SH2/SH3-binding docking protein that is a proto-oncogene product) leads to the stimulation of **TC10** (a monomeric G protein) and to the PI3K-independent regulation of glucose transport involving the participation of lipid rafts and caveolae (Section 9-4C).

Thus, by activating multiple pathways, a hormone such as insulin can trigger a variety of physiological effects that would not be possible in a one hormone–one target regulatory system.

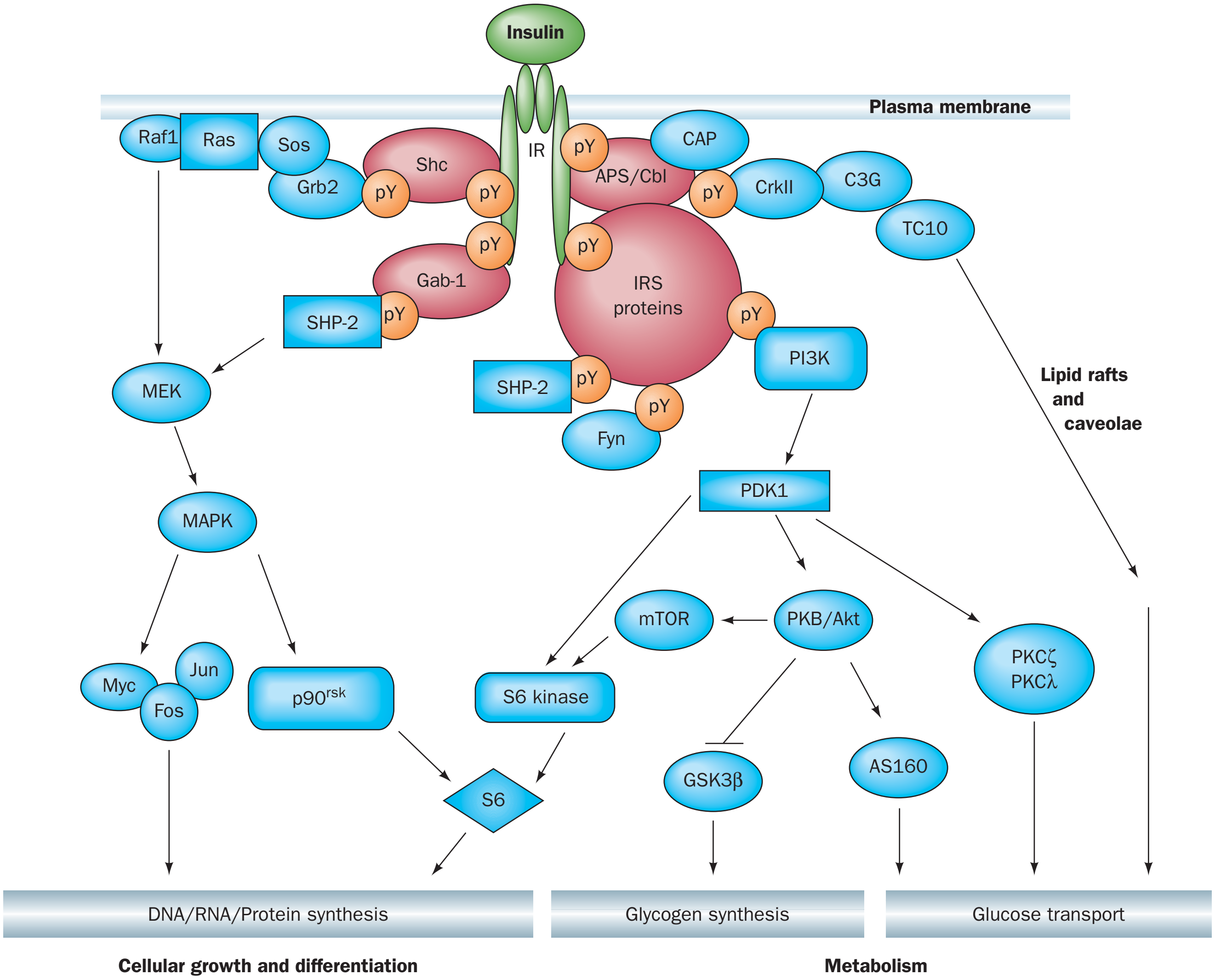
Insulin
Plasma membrane
IR
Raf1
Ras
Sos
Grb2
Shc
pY
Gab-1
SHP-2
APS/Cbl
CAP
CrkII
C3G
TC10
IRS proteins
PI3K
SHP-2
Fyn
MEK
MAPK
PDK1
Lipid rafts and caveolae
mTOR
PKB/Akt
PKCζ
PKCλ
Myc
Jun
Fos
p90rsk
S6 kinase
S6
GSK3β
AS160
DNA/RNA/Protein synthesis
Glycogen synthesis
Glucose transport
Cellular growth and differentiation
Metabolism

Figure 13-31 | **Insulin signal transduction.** The binding of insulin to the insulin receptor **(IR)** induces tyrosine phosphorylations (pY) that lead to the activation of the MAPK and PI3K phosphorylation cascades as well as a lipid raft and caveolae-associated regulation process. The MAPK cascade regulates the expression of genes involved in cellular growth and differentiation. The PI3K cascade leads to changes in the phosphorylation states of several enzymes, so as to stimulate glycogen synthesis as well as other metabolic pathways. The PI3K cascade also participates in the control of vesicle trafficking, leading to the translocation of the GLUT4 glucose transporter to the cell surface and thus increasing the rate of glucose transport into the cell. Glucose transport control is also exerted by the APS/Cbl system in a PI3K-independent manner involving lipid rafts and caveolae (Section 9-4C). Other symbols: Myc, Fos, and Jun (transcription factors), SHP-2 (an SH2-containing PTP), **CAP** (Cbl-associated protein), **C3G** [a guanine nucleotide exchange factor (GEF)], **CrkII** (an SH2/SH3-containing adaptor protein), PDK1 (phosphoinositide-dependent protein kinase-1), **PKB (protein kinase B,** also named **Akt), GSK3β (glycogen synthase-3β,** which is inhibited by phosphorylation by PKB), **mTOR** (for *m*ammalian *t*arget *o*f *r*apamycin, a PI3K-related protein kinase; **rapamycin** is an immunosuppressant), **S6** (a protein subunit of the eukaryotic ribosome's small subunit whose phosphorylation stimulates translation), and PKCζ and PKCλ (atypical isoforms of protein kinase C). [After Zick, Y., *Trends Cell Biol.* **11,** 437 (2001).]

Understanding a Complex System Requires an Integrative Approach.

The predominant approach in science is reductionist: the effort to understand a system in terms of its component parts. Thus chemists and biochemists explain the properties of molecules in terms of the properties of their component atoms, cell biologists explain the nature of cells in terms of the properties of their component macromolecules, and biologists explain the characteristics of multicellular organisms in terms of the

BOX 13-5 BIOCHEMISTRY IN HEALTH AND DISEASE

Anthrax

Anthrax is a bacterial disease that is widespread among herbivorous animals. It is rare in humans but potentially deadly, leading to its exploitation as an agent of biological warfare. The effectiveness of anthrax as a weapon was first confirmed through the accidental release of anthrax spores from a laboratory in the Soviet Union in 1979, when 68 people died.

Bacillus anthracis is a nonmotile aerobic bacterium that quickly dies outside of host tissues. However, it forms spores, particles about 1 μm in diameter, that can survive for decades. Such spores are naturally present in soils worldwide and are ingested by herbivores. The mechanism whereby the spores germinate to form full-sized bacterial cells is not well understood. If released into the air, the odorless and invisible spores can travel long distances and easily find their way indoors. The spores can cause inhalation anthrax in humans, although it is an extremely rare disease. Consequently, a cluster of inhalation anthrax cases almost certainly indicates that the spores have been specifically targeted to humans, for example, in letters or packages. As events in the United States in 2001 have shown, spores from one piece of mail can easily infect many individuals.

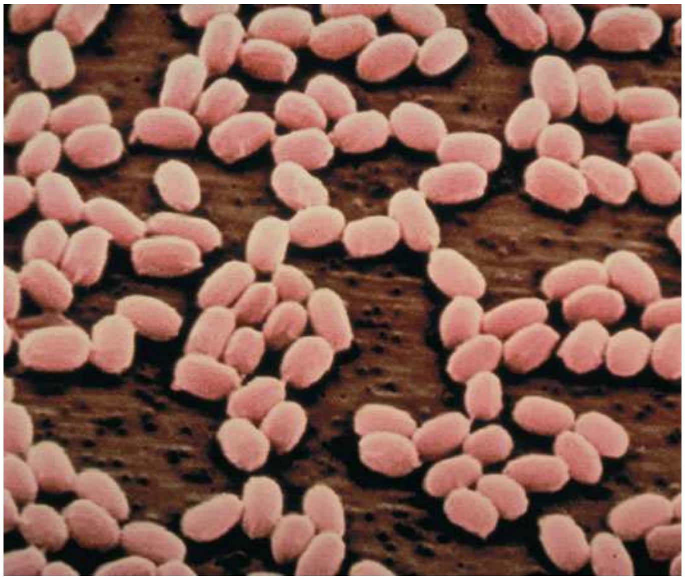

Anthrax spores. [© A. Dowsett/Photo Researchers.]

Historically, anthrax infections in humans have been of the cutaneous variety and are easily recognized by the black skin lesions that result (the word anthrax is derived from the Greek *anthrakis,* coal). Cutaneous anthrax, which is fatal in ~20% of cases, was understood to be an occupational hazard for woolsorters and others who worked with animal hides. However, inhalation anthrax is nearly always fatal. This is because the early symptoms of inhalation anthrax are nonspecific and resemble the flu, whereas the later stages of the disease, even with antibiotic treatment, are rapidly fatal, with an average interval of only 3 days between the onset of symptoms and death.

Like many deadly microbes, *B. anthracis* synthesizes a toxin (see below) that is particularly lethal to cells of the immune system. Thus, the toxin prevents the immune system from destroying the bacteria. Early identification of anthrax infection—or even just exposure—is essential to prevent death. Most naturally occurring strains of *B. anthracis* are sensitive to penicillin, but it is feared that "weaponized" anthrax may have been engineered for resistance to common antibiotics. The drug of choice is therefore the newer, broad-spectrum antibiotic **ciprofloxacin** (which inhibits DNA gyrase, a bacterial enzyme that helps maintain the proper degree of DNA supercoiling; Section 24-1D and Box 24-2). Treatment for about 60 days is required to prevent infection by spores that have delayed germination. The good news is that anthrax, unlike smallpox and bubonic plague, for example, is not highly contagious.

The Anthrax Toxin Includes Edema Factor and Lethal Factor. Even if *B. anthracis* cells can be eliminated, the toxins they have already synthesized continue to damage the host, which is why antibiotic treatment beginning in the later stages of anthrax infection does not prevent a fatal outcome. Anthrax toxin consists of three proteins that act in concert: **protective antigen (PA), edema factor (EF),** and **lethal factor (LF).** PA, which is named for its use in vaccines, is a 735-residue protein that binds to a host cell-surface protein. The receptor is a 368-residue membrane

properties of their component cells. However, complex systems have **emergent properties** that are not readily predicted from an understanding of their component parts (i.e., the whole is greater than the sum of its parts). Indeed, life itself is an emergent property that arises from the numerous chemical reactions that occur in a cell.

In order to elucidate the emergent properties of a complex system, an integrative approach is required. For signal transduction systems, such an approach would entail determining how each of the components of each signaling pathway in a cell interacts with all of the other such components under the conditions that each of these components experiences within its protein with a single bilayer-spanning α helix. Its normal cellular function is not known. After PA has bound, a cell-surface protease cleaves it, and its N-terminal fragment diffuses away. The remaining membrane-bound portions of PA form a heptameric complex that can bind the other two toxin proteins, EF and LF. The resulting toxin complex is then internalized by receptor-mediated endocytosis (Section 20-1B), following which EF and LF enter the cytosol.

EF is an adenylate cyclase that interferes with normal intracellular signaling, especially in cells such as macrophages, whose functions include the engulfment and destruction of pathogenic bacteria. *The toxic effects of EF may reflect the ability of the resulting increased concentrations of cAMP to inhibit a cellular signaling pathway necessary to maintain an effective immune response*. EF also upsets water homeostasis and hence is responsible for the massive edema (abnormal buildup of intercellular fluid) seen in cutaneous anthrax infection.

The mechanism of EF action is notable because it requires the host protein calmodulin (bacteria lack calmodulin, so this feature may protect *B. anthracis* from its own toxin). Calmodulin (Figs. 13-26 and 13-28) binds to EF by wrapping around it. This induces a conformational change that stabilizes the substrate-binding site of its adenylate cyclase function, thereby activating it. In addition, the bound calmodulin can no longer carry out its normal cellular duties, which include activating certain cAMP-phosphodiesterases (Section 13-3D). Thus, by "soaking up" calmodulin, EF enhances its ability to produce cAMP.

The other component of the anthrax toxin, LF, is a relatively large (776-residue) protease. Its X-ray structure reveals that it consists of four domains (*right*). Domain I binds to the protective antigen. Domain II resembles another bacterial toxin but has a mutated and nonfunctional active site. Domain III appears to be a duplicated version of Domain II. Domains II and III function to hold the substrate for Domain IV, which is a protease with an active site Zn^{2+} ion. The sequence of Domain IV exhibits no homology to known zinc proteases; its activity was identified on the basis of its three-dimensional structure and the position of its catalytic Zn^{2+} ion.

The substrates for lethal factor are the members of the mitogen-activated protein kinase kinase (MAPKK) family (e.g., MEK; Fig. 13-11). LF is an extremely specific protease because it interacts extensively with its substrates: The substrate-binding groove extends for about 40 Å and accommodates a 16-residue sequence of a MAPKK. Cleavage of the kinase by LF excises its docking sequence for downstream MAPKs and thereby blocks its signaling activity. Low levels of LF, which occur early in *B. anthracis* infection, inhibit the ability of macrophages to release inflammatory mediators such as cytokines and nitric oxide (Section 21-6C). This has the effect of reducing or delaying an immune response to the bacteria. Later in infection, when concentrations of the toxin are high, LF triggers macrophage lysis, causing the sudden release of inflammatory mediators. This results in massive **septic shock** (an immune system overreaction to bacterial infection resulting in a catastrophic reduction in blood pressure), the direct cause of death.

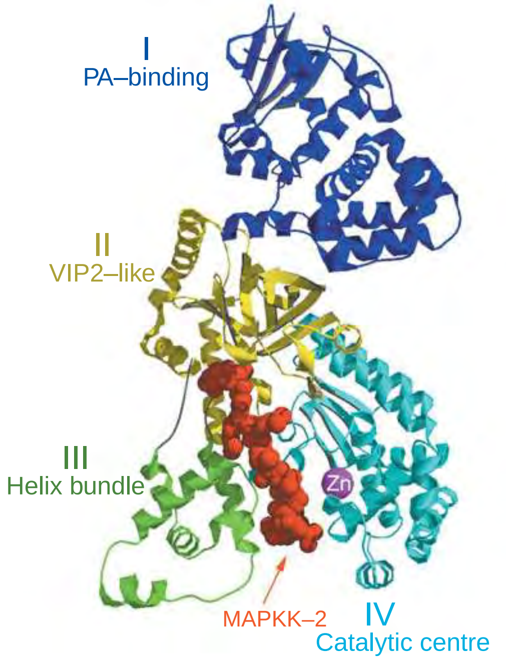

X-Ray structure of anthrax lethal factor. [Courtesy of Robert Liddington, The Burnham Institute, La Jolla, California. PDBid 1J7N.]

local environment. Yet, existing techniques for doing so are crude at best. Moreover, these systems are by no means static but vary, over multiple time scales, in response to cellular and organismal programs. Consequently, the means for understanding the holistic performance of cellular signal transduction systems are only in their earliest stages of development. Such an understanding is likely to have important biomedical consequences since many diseases, including cancer, diabetes, and a variety of neurological disorders, are caused by malfunctions of signal transduction systems. Similarly, during *Bacillus anthracis* infection, the anthrax toxin interferes with more than one signaling pathway (Box 13-5).

CHECK YOUR UNDERSTANDING

Describe how ligand binding to a receptor leads to the production of IP_3 and DAG and the release of Ca^{2+}.

How does calmodulin activate target proteins?

How is protein kinase C activated?

SUMMARY

1. Hormones produced by endocrine glands and other tissues regulate such diverse physiological processes as fuel metabolism (insulin and glucagon), fight-or-flight responses (epinephrine), sexual development (steroids), and growth (growth hormone).
2. Hormone signals interact with target tissues by binding to receptors that transduce the signal to the interior of the cell.
3. On ligand binding, receptor tyrosine kinases such as the insulin receptor undergo autophosphorylation. This activates them to phosphorylate their target proteins, in some cases triggering a kinase cascade.
4. The effects of protein kinases are reversed by the activity of protein phosphatases.
5. The G protein–coupled receptors (GPCRs) have seven transmembrane helices and, on ligand binding, activate an associated heterotrimeric G protein. The G_α and $G_{\beta\gamma}$ units may activate or inhibit targets such as adenylate cyclase, which produces the cAMP activator of protein kinase A (PKA).
6. In the phosphoinositide pathway, hormone binding leads to the hydrolysis of phosphatidylinositol-4,5-bisphosphate (PIP_2) to yield inositol-1,4,5-trisphosphate (IP_3), which opens Ca^{2+} channels, and diacylglycerol (DAG), which activates protein kinase C (PKC).

KEY TERMS

Term	Page
hormone	**405**
receptor	**405**
homeostasis	**407**
adrenoreceptor	**409**
agonist	**409**
antagonist	**409**
signal transduction	**412**
ligand	**413**
receptor tyrosine kinase	**413**
autophosphorylation	**413**
G protein	**416**
kinase cascade	**417**
GEF	**418**
GAP	**418**
oncogene	**420**
cross talk	**421**
nonreceptor tyrosine kinase	**422**
protein phosphatase	**425**
GPCR	**428**
second messenger	**429**
desensitization	**430**
heterotrimeric G protein	**430**
phosphoinositide pathway	**436**
calmodulin	**438**
emergent properties	**444**

PROBLEMS

1. Would the following alterations to Src be oncogenic? Explain. (a) The deletion or inactivation of the SH3 domain. (b) The mutation of Tyr 416 to Phe. (c) The mutation of Tyr 527 to Phe. (d) The replacement of Src residues 249 to 253 with the sequence APTMP.
2. A growth factor that acts through a receptor tyrosine kinase stimulates cell division. Predict the effect of a viral protein that inhibits the corresponding protein tyrosine phosphatase.
3. Retroviruses bearing oncogenes will infect cells from their corresponding host animal but will usually not transform them. Yet, these retroviruses will readily transform immortalized cells derived from the same organism. Explain.
4. How does the presence of the poorly hydrolyzable GTP analog **GTPγS** (in which an O atom on the terminal phosphate is replaced by an S atom) affect cAMP production by adenylate cyclase?
5. Explain why mutations of the Arg residue in $G_{s\alpha}$ that is ADP-ribosylated by cholera toxin are oncogenic mutations. Why doesn't cholera toxin cause cancer?
6. Phosphatidylethanolamine and PIP_2 containing identical fatty acyl residues can be hydrolyzed with the same efficiency by a certain phospholipase C. Will the hydrolysis products of the two lipids have the same effect on protein kinase C? Explain.
7. Why does pertussis toxin appear to inhibit certain isozymes of PLC? Identify those isozymes.
8. PKC's autoinhibitory pseudosubstrate occurs at its N-terminus, whereas that of MLCK occurs at its C-terminus (Fig. 13-29). To further investigate this phenomenon, a colleague proposes to construct a PKC with its pseudosubstrate attached to the protein's C-terminus with a sufficiently long linker so that the pseudosubstrate could bind in the enzyme's active site. Would you expect this variant PKC to be activatable? Explain.
9. Diacylglycerol is a substrate for the enzyme diacylglycerol kinase.
   (a) What is the product of this reaction?
   (b) Explain why activation of diacylglycerol kinase would limit signaling by the phosphoinositide pathway.
10. Lithium ion, which is used to treat bipolar disorder, interferes with the phosphoinositide signaling pathway by inhibiting enzymes such as inositol monophosphatase and inositol polyphosphate 1-phosphatase. Predict the effect of Li^+ on the supply of cellular inositol, a precursor of phosphatidylinositol and PIP_2.

REFERENCES

Alonso, A., et al., Protein tyrosine phosphatases in the human genome, *Cell* **117,** 699–711 (2004).

Baselga, J., Targeting tyrosine kinases in cancer: The second wave, *Science* **312,** 1175–1178 (2006).

Carrasco, S. and Mérida, I., Diacylglycerol, when simplicity becomes complex, *Trends Biochem. Sci.* **32,** 27–36 (2007). [Reviews diacylglycerol-based signaling.]

Chang, L. and Karin, M., Mammalian MAP kinase signaling cascades, *Nature* **410,** 37–40 (2001).

Cho, U.S. and Xu, W., Crystal structure of a protein phosphatase 2A heterotrimeric holoenzyme, *Nature* **445,** 53–57 (2007); *and* Xu, Y., Xing, Y., Chen, Y., Chao, Y., Lin, Z., Fan, E., Yu, J., Stack, S., Jeffrey, P., and Shi, Y., Structure of the protein phosphatase 2A holoenzyme, *Cell* **127,** 1239–1251 (2006).

Di Paolo, G. and De Camilli, P., Phosphoinositides in cell regulation and membrane dynamics, *Nature* **443,** 651–657 (2006).

Murphy, L.O. and Blenis, J., MAPK signal specificity: the right place at the right time, *Trends Biochem. Sci.* **31,** 268–275 (2006).

Neves, S.R., Ram, P.T., and Iyengar, R., G protein pathways, *Science* **296,** 1636–1639 (2002). [A brief introduction to the four families of G proteins.]

Pawson, T. and Scott, J.D., Protein phosphorylation in signaling—50 years and counting, *Trends Biochem. Sci.* **30,** 286–290 (2005).

Science's Signal Transduction Knowledge Environment (STKE). http://stke.sciencemag.org/. [A database on signaling molecules and their relationships to each other. Full access to the database requires an individual or institutional subscription.]

Yaffe, M.B., Phosphotyrosine-binding domains in signal transduction, *Nature Rev. Mol. Cell Biol.* **3,** 177–186 (2002).

14

Introduction to Metabolism

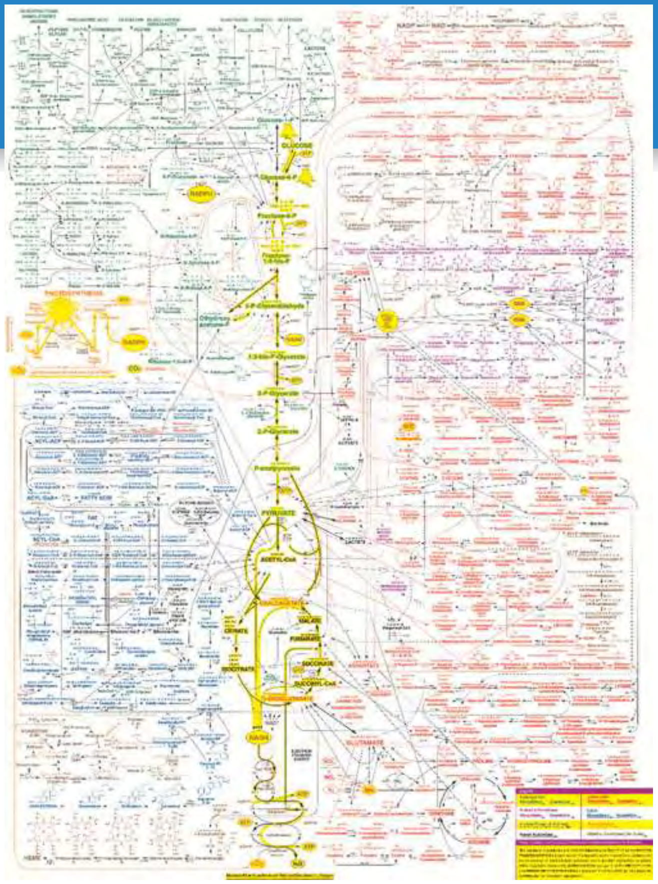

The processes by which biological molecules are broken down and resynthesized form a complex, yet highly regulated, network of interdependent enzymatic reactions that are collectively known as life. [Designed by Donald E. Nicholson, Department of Biochemistry and Molecular Biology, The University of Leeds, England, and Sigma.]

CHAPTER CONTENTS

1 Overview of Metabolism
- **A.** Nutrition Involves Food Intake and Use
- **B.** Vitamins and Minerals Assist Metabolic Reactions
- **C.** Metabolic Pathways Consist of Series of Enzymatic Reactions
- **D.** Thermodynamics Dictates the Direction and Regulatory Capacity of Metabolic Pathways
- **E.** Metabolic Flux Must Be Controlled

2 "High-Energy" Compounds
- **A.** ATP Has a High Phosphoryl Group-Transfer Potential
- **B.** Coupled Reactions Drive Endergonic Processes
- **C.** Some Other Phosphorylated Compounds Have High Phosphoryl Group-Transfer Potentials
- **D.** Thioesters Are Energy-Rich Compounds

3 Oxidation–Reduction Reactions
- **A.** NAD^+ and FAD Are Electron Carriers
- **B.** The Nernst Equation Describes Oxidation–Reduction Reactions
- **C.** Spontaneity Can Be Determined by Measuring Reduction Potential Differences

4 Experimental Approaches to the Study of Metabolism
- **A.** Labeled Metabolites Can Be Traced
- **B.** Studying Metabolic Pathways Often Involves Perturbing the System
- **C.** Systems Biology Has Entered the Study of Metabolism

MEDIA RESOURCES

(available at www.wiley.com/college/voet)

Interactive Exercise 14. Conformational changes in *E. coli* adenylate kinase

Case Study 16. Allosteric Regulation of ATCase

Bioinformatics Exercises Chapter 14: Metabolic Enzymes, Microarrays, and Proteomics

Understanding the chemical compositions and three-dimensional structures of biological molecules is not sufficient to understand how they are assembled into organisms or how they function to sustain life. We must therefore examine the reactions in which biological molecules are built and broken down. We must also consider how free energy is consumed in building cellular materials and carrying out cellular work and how free energy is generated from organic or other sources. **Metabolism,** the overall process through which living systems acquire and use free energy to carry out their various functions, is traditionally divided into two parts:

1. **Catabolism,** or degradation, in which nutrients and cell constituents are broken down to salvage their components and/or to generate energy.
2. **Anabolism,** or biosynthesis, in which biomolecules are synthesized from simpler components.

In general, catabolic reactions carry out the exergonic oxidation of nutrient molecules. The free energy thereby released is used to drive such endergonic processes as anabolic reactions, the performance of mechanical work, and the active transport of molecules against concentration gradients. Exergonic and endergonic processes are often coupled through the intermediate synthesis of a "high-energy" compound such as ATP. This simple principle underlies many of the chemical reactions presented in the following chapters. In this chapter, we introduce the general features of metabolic reactions and the roles of ATP and other compounds as energy carriers. Because many metabolic reactions are also oxidation–reduction reactions, we review the thermodynamics of these processes. Finally, we examine some approaches to studying metabolic reactions.

1 Overview of Metabolism

A bewildering array of chemical reactions occur in any living cell. Yet the principles that govern metabolism are the same in all organisms, a result of their common evolutionary origin and the constraints of the laws of thermodynamics. In fact, many of the specific reactions of metabolism are common to all organisms, with variations due primarily to differences in the source of the free energy that supports them.

LEARNING OBJECTIVES

- Understand that different organisms use different strategies for capturing free energy from their environment and can be classified by their requirement for oxygen.
- Understand that mammalian nutrition involves the intake of proteins, carbohydrates, lipids, vitamins, minerals, and water.
- Appreciate the importance of thermodynamics in determining the direction and regulatory capabilities of metabolic pathways.
- Understand the mechanisms by which metabolic flux is controlled.

A | Nutrition Involves Food Intake and Use

Nutrition, the intake and utilization of food, affects health, development, and performance. Food supplies the energy that powers life processes and provides the raw materials to build and repair body tissues. The nutritional requirements of an organism reflect its source of metabolic energy. For example, some prokaryotes are **autotrophs** (Greek: *autos,* self + *trophos,* feeder), which can synthesize all their cellular constituents from simple molecules such as H_2O, CO_2, NH_3, and H_2S. There are two possible free energy sources for this process. **Chemolithotrophs** (Greek: *lithos,* stone) obtain their energy through the oxidation of inorganic compounds such as NH_3, H_2S, or even Fe^{2+}:

$$2\ NH_3 + 4\ O_2 \rightarrow 2\ HNO_3 + 2\ H_2O$$

$$H_2S + 2\ O_2 \rightarrow H_2SO_4$$

$$4\ FeCO_3 + O_2 + 6\ H_2O \rightarrow 4\ Fe(OH)_3 + 4\ CO_2$$

Photoautotrophs do so via photosynthesis, a process in which light energy powers the transfer of electrons from inorganic donors to CO_2 to produce carbohydrates, $(CH_2O)_n$, which are later oxidized to release free energy. **Heterotrophs** (Greek: *hetero,* other) obtain free energy through the oxidation of organic compounds (carbohydrates, lipids, and proteins) and hence ultimately depend on autotrophs and/or phototrophs for those substances.

Organisms can be further classified by the identity of the oxidizing agent for nutrient breakdown. **Obligate aerobes** (which include animals) must use O_2, whereas **anaerobes** employ oxidizing agents such as sulfate or nitrate. **Facultative anaerobes,** such as *E. coli,* can grow in either the presence or the absence of O_2. **Obligate anaerobes,** in contrast, are poisoned by the presence of O_2. Their metabolisms are thought to resemble those of the earliest life-forms, which arose over 3.5 billion years ago when the earth's atmosphere lacked O_2. Most of our discussion of metabolism will focus on aerobic processes.

Animals are obligate **aerobic** heterotrophs, whose nutrition depends on a balanced intake of the **macronutrients** proteins, carbohydrates, and lipids. These are broken down by the digestive system to their component amino

Table 14-1 Characteristics of Common Vitamins

Vitamin	Coenzyme Product	Reaction Mediated	Human Deficiency Disease
Water-Soluble			
Biotin	Biocytin	Carboxylation	[a]
Pantothenic acid	Coenzyme A	Acyl transfer	[a]
Cobalamin (B_{12})	Cobalamin coenzymes	Alkylation	Pernicious anemia
Riboflavin (B_2)	Flavin coenzymes	Oxidation–reduction	[a]
—	Lipoic acid	Acyl transfer	[a]
Nicotinamide (niacin)	Nicotinamide coenzymes	Oxidation–reduction	Pellagra
Pyridoxine (B_6)	Pyridoxal phosphate	Amino group transfer	[a]
Folic acid	Tetrahydrofolate	One-carbon group transfer	Megaloblastic anemia
Thiamine (B_1)	Thiamine pyrophosphate	Aldehyde transfer	Beriberi
Ascorbic acid (C)	Ascorbate	Hydroxylation	Scurvy
Fat-Soluble			
Vitamin A		Vision	Night blindness
Vitamin D		Ca^{2+} absorption	Rickets
Vitamin E		Antioxidant	[a]
Vitamin K		Blood clotting	Hemorrhage

[a] No specific name; deficiency in humans is rare or unobserved.

Table 14-2 Major Essential Minerals and Trace Elements

Major Minerals	Trace Elements
Sodium	Iron
Potassium	Copper
Chlorine	Zinc
Calcium	Selenium
Phosphorus	Iodine
Magnesium	Chromium
Sulfur	Fluorine

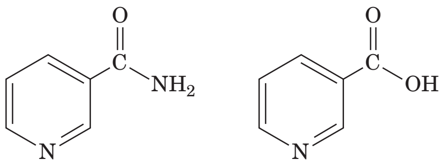

Nicotinamide (niacinamide)

Nicotinic acid (niacin)

Figure 14-1 | The structures of nicotinamide and nicotinic acid. These vitamins form the redox-active components of the nicotinamide coenzymes NAD^+ and $NADP^+$ (compare with Fig. 11-4).

acids, monosaccharides, fatty acids, and glycerol, the major nutrients involved in cellular metabolism, which are then transported by the circulatory system to the tissues. The metabolic utilization of the latter substances also requires the intake of O_2 and water, as well as **micronutrients** composed of **vitamins** and **minerals.**

B | Vitamins and Minerals Assist Metabolic Reactions

Vitamins are organic molecules that an animal is unable to synthesize and must therefore obtain from its diet. Vitamins can be divided into two groups, **water-soluble vitamins** and **fat-soluble vitamins.** Table 14-1 lists many common vitamins and the types of reactions or processes in which they participate (we shall consider the structures of these substances and their reaction mechanisms in the appropriate sections of the text).

Table 14-2 lists the essential minerals and trace elements necessary for metabolism. They participate in metabolic processes in many ways. Mg^{2+}, for example, is involved in nearly all reactions that involve ATP and other nucleotides, including the synthesis of DNA, RNA, and proteins. Zn^{2+} is a cofactor in a variety of enzymatic reactions including that catalyzed by carbonic anhydrase (Section 11-3C). Ca^{2+}, in addition to being the major mineral component of bones and teeth, is a vital participant in signal transduction processes (Section 13-4).

Most Water-Soluble Vitamins Are Converted to Coenzymes. Many coenzymes (Section 11-1C) were discovered as growth factors for microorganisms or as substances that cure nutritional deficiency diseases in humans and/or animals. For example, the NAD^+ component **nicotinamide,** or its carboxylic acid analog **nicotinic acid** (**niacin;** Fig. 14-1), relieves the ultimately fatal dietary deficiency disease in humans known as **pellagra.** The symptoms of pellagra include diarrhea, dermatitis, and dementia.

The water-soluble vitamins in the human diet are all coenzyme precursors. In contrast, the fat-soluble vitamins, with the exception of vitamin K (Section 9-1F), are not components of coenzymes, although they are also required in small amounts in the diets of many higher animals. The distant ancestors of humans probably had the ability to synthesize the various vitamins, as do many modern plants and microorganisms. Yet since vitamins are normally available in the diets of animals, which all eat other organisms, or are synthesized by the bacteria that normally inhabit their digestive systems, it seems likely that the superfluous cellular machinery to synthesize them was lost through evolution. For example, vitamin C (ascorbic acid) is required in the diets of only humans, apes, and guinea pigs (Section 6-1C and Box 6-2) because, in what is apparently a recent evolutionary loss, they lack a key enzyme for ascorbic acid biosynthesis.

C | Metabolic Pathways Consist of Series of Enzymatic Reactions

Metabolic pathways are series of connected enzymatic reactions that produce specific products. Their reactants, intermediates, and products are referred to as **metabolites.** There are around 4000 known metabolic reactions, each catalyzed by a distinct enzyme. The types of enzymes and metabolites in a given cell vary with the identity of the organism, the cell type, its nutritional status, and its developmental stage. Many metabolic pathways are branched and interconnected, so delineating a pathway from a network of thousands of reactions is somewhat arbitrary and is driven by tradition as much as by chemical logic.

In general, degradative and biosynthetic pathways are related as follows (Fig. 14-2): In degradative pathways, the major nutrients, referred to as complex metabolites, are exergonically broken down into simpler products. The free energy released in the degradative process is conserved by the synthesis of ATP from ADP + P_i or by the reduction of the coenzyme $NADP^+$ (Fig. 11-4) to NADPH. ATP and NADPH are the major free energy sources for biosynthetic reactions. We shall consider the thermodynamic properties of ATP and NADPH later in this chapter.

A striking characteristic of degradative metabolism is that *the pathways for the catabolism of a large number of diverse substances (carbohydrates, lipids, and proteins) converge on a few common intermediates*, in many cases, a two-carbon acetyl unit linked to **coenzyme A** to form **acetyl-coenzyme A**

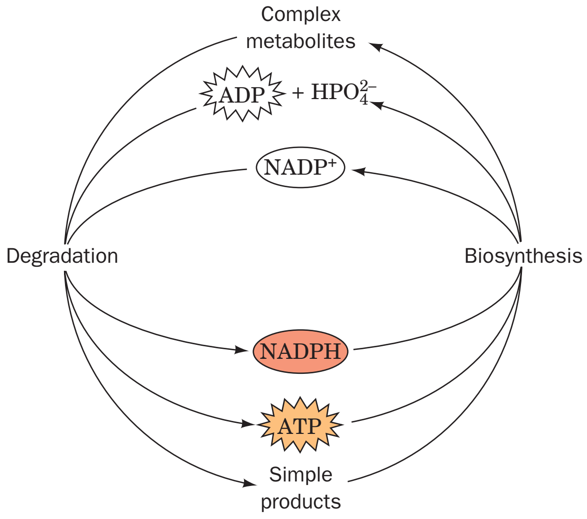

■ **Figure 14-2 | Roles of ATP and $NADP^+$ in metabolism.** ATP and NADPH, generated through the degradation of complex metabolites such as carbohydrates, lipids, and proteins, are sources of free energy for biosynthetic and other reactions.

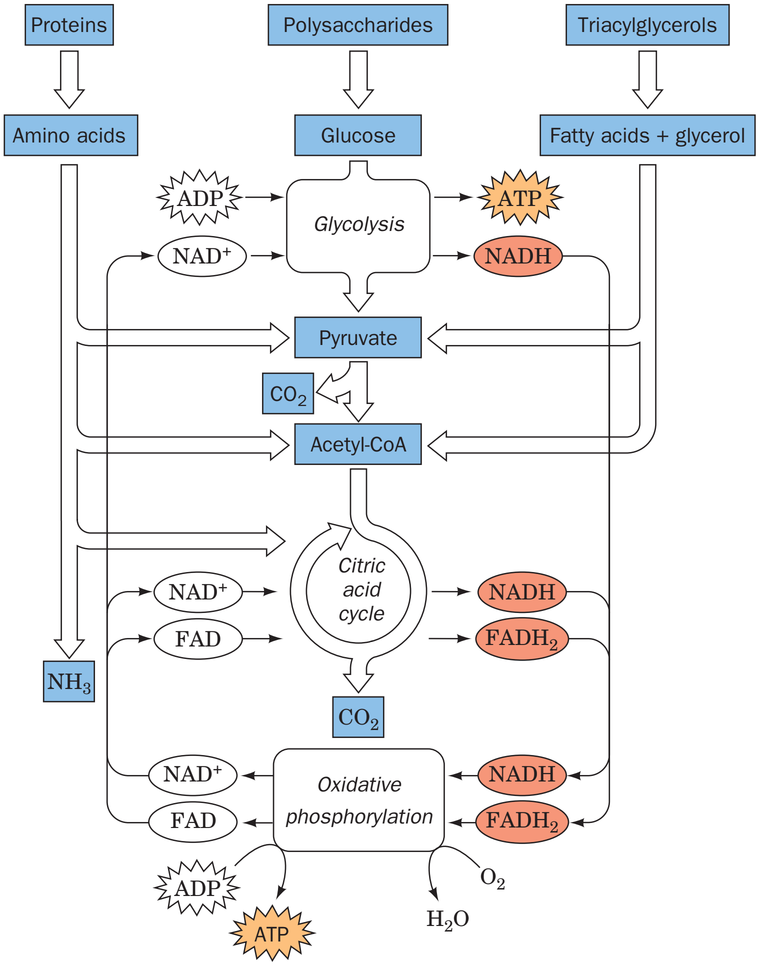
Proteins
Polysaccharides
Triacylglycerols
Amino acids
Glucose
Fatty acids + glycerol
ADP
ATP
Glycolysis
NAD+
NADH
Pyruvate
CO2
Acetyl-CoA
Citric acid cycle
NAD+
NADH
FAD
FADH2
NH3
CO2
NAD+
NADH
Oxidative phosphorylation
FAD
FADH2
ADP
ATP
O2
H2O

■ **Figure 14-3 | Overview of catabolism.** Complex metabolites such as carbohydrates, proteins, and lipids are degraded first to their monomeric units, chiefly glucose, amino acids, fatty acids, and glycerol, and then to the common intermediate, acetyl-CoA. The acetyl group is oxidized to CO_2 via the citric acid cycle with concomitant reduction of NAD^+ and FAD. Reoxidation of NADH and $FADH_2$ by O_2 during electron transport and oxidative phosphorylation yields H_2O and ATP.

(**acetyl-CoA;** Section 14-2D). These intermediates are then further metabolized in a central oxidative pathway. Figure 14-3 outlines the breakdown of various foodstuffs to their monomeric units and then to acetyl-CoA. This is followed by the oxidation of the acetyl carbons to CO_2 by the **citric acid cycle** (Chapter 17). When one substance is **oxidized** (loses electrons), another must be **reduced** (gain electrons; Box 14-1). The citric acid cycle thus produces the reduced coenzymes **NADH** and **$FADH_2$** (Section 14-3A), which then pass their electrons to O_2 to produce H_2O in the processes of **electron transport** and **oxidative phosphorylation** (Chapter 18).

Biosynthetic pathways carry out the opposite process. *Relatively few metabolites serve as starting materials for a host of varied products.* In the next several chapters, we discuss many catabolic and anabolic pathways in detail.

Enzymes Catalyze the Reactions of Metabolic Pathways. With a few exceptions, the interconversions of metabolites in degradative and biosynthetic pathways are catalyzed by enzymes. In the absence of enzymes, the reactions would occur far too slowly to support life. In addition, the specificity of enzymes guarantees the efficiency of metabolic reactions by preventing the formation of useless or toxic by-products. Most importantly, enzymes provide a mechanism for coupling an endergonic chemical reaction (which would not occur on its own) with an energetically favorable reaction, as discussed below.

BOX 14-1 PERSPECTIVES IN BIOCHEMISTRY

Oxidation States of Carbon

The carbon atoms in biological molecules can assume different oxidation states depending on the atom to which they are bonded. For example, a carbon atom bonded to less electronegative hydrogen atoms is more reduced than a carbon atom bonded to highly electronegative oxygen atoms.

The simplest way to determine the oxidation number (and hence the oxidation state) of a particular carbon atom is to examine each of its bonds and assign the electrons to the more electronegative atom. In a C—O bond, both electrons "belong" to O; in a C—H bond, both electrons "belong" to C; and in a C—C bond, each carbon "owns" one electron. An atom's oxidation number is the number of valence electrons on the free atom (4 for carbon) minus the number of its lone pair and assigned electrons. For example, the oxidation number of carbon in CO_2 is $4 - (0 + 0) = +4$, and the oxidation number of carbon in CH_4 is $4 - (0 + 8) = -4$, Keep in mind, however, that oxidation numbers are only accounting devices; actual atomic charges are much closer to neutrality.

The following compounds are listed according to the oxidation state of the highlighted carbon atom. In general, the more oxidized compounds have fewer electrons per C atom and are richer in oxygen, and the more reduced compounds have more electrons per C atom and are richer in hydrogen. But note that not all reduction events (gain of electrons) or oxidation events (loss of electrons) are associated with bonding to oxygen. For example, when an alkane is converted to an alkene, the formation of a carbon–carbon double bond involves the loss of electrons and therefore is an oxidation reaction although no oxygen is involved. Knowing the oxidation number of a carbon atom is seldom required. However, it is useful to be able to determine whether the oxidation state of a given atom increases or decreases during a chemical reaction.

Compound	Formula	Oxidation Number
Carbon dioxide	$O{=}C{=}O$	4 (most oxidized)
Acetic acid	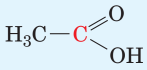	3
Carbon monoxide	$:C{\equiv}O:$	2
Formic acid	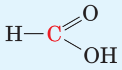	2
Acetone	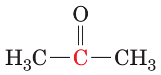 $H_3C-\overset{\overset{O}{\Vert}}{C}-CH_3$	2
Acetaldehyde	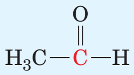 $H_3C-\overset{\overset{O}{\Vert}}{C}-H$	1
Formaldehyde	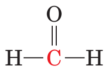 $H-\overset{\overset{O}{\Vert}}{C}-H$	0
Acetylene	$HC{\equiv}CH$	−1
Ethanol	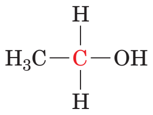 $H_3C-\underset{\underset{H}{\vert}}{\overset{\overset{H}{\vert}}{C}}-OH$	−1
Ethene	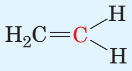	−2
Ethane	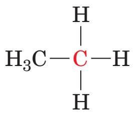 $H_3C-\underset{\underset{H}{\vert}}{\overset{\overset{H}{\vert}}{C}}-H$	−3
Methane	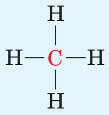 $H-\underset{\underset{H}{\vert}}{\overset{\overset{H}{\vert}}{C}}-H$	−4 (least oxidized)

We will see examples of reactions catalyzed by all six classes of enzymes introduced in Section 11-1A. These reactions fall into four major types: **oxidations and reductions** (catalyzed by oxidoreductases), **group-transfer reactions** (catalyzed by transferases and hydrolases), **eliminations, isomerizations, and rearrangements** (catalyzed by isomerases and mutases), and **reactions that make or break carbon–carbon bonds** (catalyzed by hydrolases, lyases, and ligases). Details about the enzymes that catalyze individual steps of metabolic pathways are available from Internet-accessible databases (Box 14-2).

Metabolic Pathways Occur in Specific Cellular Locations. The compartmentation of the eukaryotic cytoplasm allows different metabolic pathways to operate in different locations. For example, electron transport and oxidative phosphorylation occur in the mitochondria, whereas **glycolysis** (a carbohydrate degradation pathway) and fatty acid biosynthesis occur in

BOX 14-2 **PERSPECTIVES IN BIOCHEMISTRY**

Mapping Metabolic Pathways

The task of cataloging all the enzymatic reactions that occur in a given organism is formidable and, in many cases, far from complete. However, the metabolic reactions that constitute the major catabolic and anabolic pathways can be organized in a diagram. Typically, the structures or names of the intermediates are shown, and details about the enzymes that catalyze their interconversions can be called up. The following figure, which diagrams a portion of the photosynthetic pathway in plants, shows the interconversions of several three- and four-carbon compounds. The boxes represent enzymes, identified by their EC number (Section 11-1A).

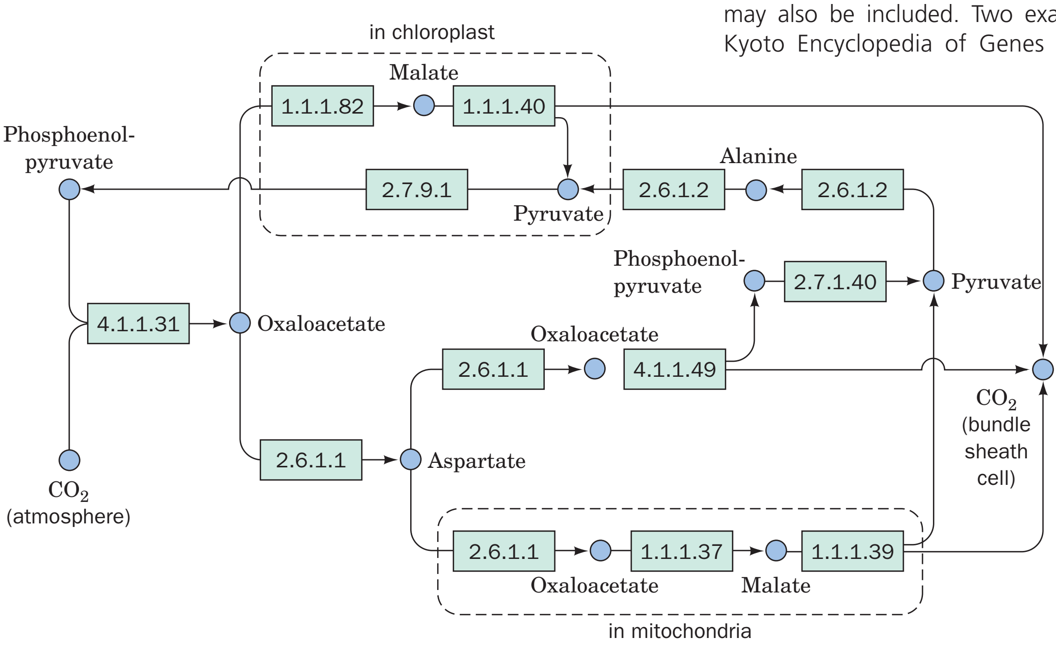

[Redrawn from the Kyoto Encyclopedia of Genes and Genomes (KEGG) Metabolic Pathways: http://www.genome.jp/kegg/metabolism.html.]

Various Internet-accessible databases contain "universal" maps of all possible metabolic reactions or more specialized maps devoted to a single species or focused on a specific pathway. Such databases may link individual enzymes in a pathway to gene sequences and to the three-dimensional structures of the proteins, if known. Information about an enzyme's activators and inhibitors may also be included. Two examples of such databases are the Kyoto Encyclopedia of Genes and Genomes (KEGG) Metabolic Pathways: www.genome.jp/kegg/metabolism.html; and BRENDA (BRaunschweig ENzyme DAtabase): www.brenda.uni-koeln.de/.

Understanding the chemical logic of metabolic pathways requires more than listing the substrates and products of each step. The ability to recognize the types of reactions that occur in a pathway provides insights into the overall metabolic capabilities of an organism and makes it easier to see the similarities and differences between pathways. At a deeper level, understanding the mechanisms and regulation of metabolic enzymes may lead to advances in treating metabolic and other diseases.

the cytosol. Table 14-3 lists the major metabolic features of eukaryotic organelles. Metabolic processes in prokaryotes, which lack organelles, may be localized to particular areas of the cytosol.

The synthesis of metabolites in specific membrane-bounded compartments in eukaryotic cells requires mechanisms to transport these substances between compartments. Accordingly, transport proteins (Chapter 10) are essential components of many metabolic processes. For example, a transport protein is required to move ATP, which is generated in the mitochondria, to the cytosol, where most of it is consumed (Section 18-1).

In multicellular organisms, compartmentation is carried a step further to the level of tissues and organs. The mammalian liver, for example, is largely responsible for the synthesis of glucose from noncarbohydrate precursors (**gluconeogenesis;** Section 16-4) so as to maintain a relatively constant level of glucose in the circulation, whereas adipose tissue is specialized for storage of triacylglycerols. The interdependence of the metabolic functions of the various organs is the subject of Chapter 22.

Table 14-3 Metabolic Functions of Eukaryotic Organelles

Organelle	**Major functions**
Mitochondrion	Citric acid cycle, electron transport and oxidative phosphorylation, fatty acid oxidation, amino acid breakdown
Cytosol	Glycolysis, pentose phosphate pathway, fatty acid biosynthesis, many reactions of gluconeogenesis
Lysosome	Enzymatic digestion of cell components and ingested matter
Nucleus	DNA replication and transcription, RNA processing
Golgi apparatus	Posttranslational processing of membrane and secretory proteins; formation of plasma membrane and secretory vesicles
Rough endoplasmic reticulum	Synthesis of membrane-bound and secretory proteins
Smooth endoplasmic reticulum	Lipid and steroid biosynthesis
Peroxisome (glyoxysome in plants)	Oxidative reactions catalyzed by amino acid oxidases and catalase; glyoxylate cycle reactions in plants

An intriguing manifestation of specialization of tissues and subcellular compartments is the existence of **isozymes,** enzymes that catalyze the same reaction but are encoded by different genes and have different kinetic or regulatory properties. For example, we have seen that mammals have three isozymes of glycogen phosphorylase, those expressed in muscle, brain, and liver (Section 12-3B). Similarly, vertebrates possess two homologs of the enzyme **lactate dehydrogenase:** the M type, which predominates in tissues subject to anaerobic conditions such as skeletal muscle and liver, and the H type, which predominates in aerobic tissues such as heart muscle. Lactate dehydrogenase catalyzes the interconversion of **pyruvate,** a product of glycolysis, and **lactate** (Section 15-3A). The M-type isozyme appears mainly to function in the reduction by NADH of pyruvate to lactate, whereas the H-type enzyme appears to be better adapted to catalyze the reverse reaction. The existence of isozymes allows for the testing of various illnesses. For example, heart attacks cause the death of heart muscle cells, which consequently rupture and release H-type LDH into the blood. A blood test indicating the presence of H-type LDH is therefore diagnostic of a heart attack.

D | Thermodynamics Dictates the Direction and Regulatory Capacity of Metabolic Pathways

Knowing the location of a metabolic pathway and enumerating its substrates and products does not necessarily reveal how that pathway functions as part of a larger network of interrelated biochemical processes. It is also necessary to appreciate how fast end product can be generated by the pathway as well as how pathway activity is regulated as the cell's needs change. Conclusions about a pathway's output and its potential for regulation can be gleaned from information about the thermodynamics of each enzyme-catalyzed step.

SAMPLE CALCULATION 14-1

Calculate the equilibrium constant for the hydrolysis of glucose-1-phosphate at 37°C. $\Delta G^{\circ\prime}$ for the reaction

$$\text{Glucose-1-phosphate} + H_2O \rightarrow \text{glucose} + P_i$$

is $-20.9\ \text{kJ}\cdot\text{mol}^{-1}$ (Table 14-4). At equilibrium, $\Delta G = 0$ and Eq. 14-1 becomes

$$\Delta G^{\circ\prime} = -RT\ln K \qquad \text{(Eq. 14-2)}$$

Therefore,

$$K = e^{-\Delta G^{\circ\prime}/RT}$$
$$K = e^{-(-20{,}900\ \text{J}\cdot\text{mol}^{-1})/(8.3145\ \text{J}\cdot\text{K}^{-1}\cdot\text{mol}^{-1})(310\ \text{K})}$$
$$K = 3.3 \times 10^3$$

Recall from Section 1-3D that the free energy change (ΔG) of a biochemical process, such as the reaction

$$A + B \rightleftharpoons C + D$$

is related to the standard free energy change ($\Delta G^{\circ\prime}$) and the concentrations of the reactants and products (Eq. 1-15):

$$\Delta G = \Delta G^{\circ\prime} + RT\ln\left(\frac{[C][D]}{[A][B]}\right) \qquad [14\text{-}1]$$

At equilibrium $\Delta G = 0$, and the equation becomes

$$\Delta G^{\circ\prime} = -RT\ln K_{eq} \qquad [14\text{-}2]$$

Thus, the value of $\Delta G^{\circ\prime}$ can be calculated from the equilibrium constant and vice versa (see Sample Calculation 14-1).

When the reactants are present at values close to their equilibrium values, $[C]_{eq}[D]_{eq}/[A]_{eq}[B]_{eq} \approx K_{eq}$, and $\Delta G \approx 0$. This is the case for many metabolic reactions, which are said to be **near-equilibrium reactions.** Because their ΔG values are close to zero, they can be relatively easily reversed by changing the ratio of products to reactants. When the reactants are in excess of their equilibrium concentrations, the net reaction proceeds in the forward direction until the excess reactants have been converted to products and equilibrium is attained. Conversely, when products are in excess, the net reaction proceeds in the reverse direction so as to convert products to reactants until the equilibrium concentration ratio is again achieved. *Enzymes that catalyze near-equilibrium reactions tend to act quickly to restore equilibrium concentrations, and the net rates of such reactions are effectively controlled by the relative concentrations of substrates and products.*

Other metabolic reactions function far from equilibrium; that is, they are irreversible. This is because an enzyme catalyzing such a reaction has insufficient catalytic activity (the rate of the reaction it catalyzes is too slow) to allow the reaction to come to equilibrium under physiological conditions. Reactants therefore accumulate in large excess of their equilibrium amounts, making $\Delta G \ll 0$. Changes in substrate concentrations therefore have relatively little effect on the rate of an irreversible reaction; the enzyme is essentially saturated. Only changes in the activity of the enzyme, through allosteric interactions, for example, can significantly alter the rate. The enzyme is therefore analogous to a dam on a river: *It controls the flow of substrate through the reaction by varying its activity, much as a dam controls the flow of a river by varying the opening of its floodgates.*

Understanding the **flux** (rate of flow) of metabolites through a metabolic pathway requires knowledge of which reactions are functioning near equilibrium and which are far from it. Most enzymes in a metabolic pathway operate near equilibrium and therefore have net rates that vary with their substrate concentrations. However, certain enzymes that operate far from equilibrium are strategically located in metabolic pathways. This has several important implications:

1. ***Metabolic pathways are irreversible.*** A highly exergonic reaction (one with $\Delta G \ll 0$) is irreversible; that is, it goes to completion. If such a reaction is part of a multistep pathway, it confers directionality on the pathway; that is, it makes the entire pathway irreversible.
2. ***Every metabolic pathway has a first committed step.*** Although most reactions in a metabolic pathway function close to equilibrium, there is generally an irreversible (exergonic) reaction early in the pathway

that "commits" its product to continue down the pathway (likewise, water that has gone over a dam cannot spontaneously return).

3. ***Catabolic and anabolic pathways differ.*** If a metabolite is converted to another metabolite by an exergonic process, free energy must be supplied to convert the second metabolite back to the first. This energetically "uphill" process requires a different pathway for at least one of the reaction steps.

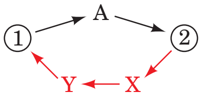

The existence of independent interconversion routes, as we shall see, is an important property of metabolic pathways because it allows independent control of the two processes. If metabolite 2 is required by the cell, it is necessary to "turn off" the pathway from 2 to 1 while "turning on" the pathway from 1 to 2. Such independent control would be impossible without different pathways.

E | Metabolic Flux Must Be Controlled

Living organisms are thermodynamically open systems that tend to maintain a steady state rather than reaching equilibrium (Section 1-3E). This is strikingly demonstrated by the observation that, over a 40-year time span, a normal human adult consumes literally tons of nutrients and imbibes over 20,000 L of water but does so without major weight change. *The flux of intermediates through a metabolic pathway in a steady state is more or less constant; that is, the rates of synthesis and breakdown of each pathway intermediate maintain it at a constant concentration.* A steady state far from equilibrium is thermodynamically efficient, because only a nonequilibrium process ($\Delta G \neq 0$) can perform useful work. Indeed, living systems that have reached equilibrium are dead.

Since a metabolic pathway is a series of enzyme-catalyzed reactions, it is easiest to describe the flux of metabolites through the pathway by considering its reaction steps individually. The flux of metabolites, J, through each reaction step is the rate of the forward reaction, v_f, less that of the reverse reaction, v_r:

$$J = v_f - v_r \qquad [14\text{-}3]$$

At equilibrium, by definition, there is no flux ($J = 0$), although v_f and v_r may be quite large. In reactions that are far from equilibrium, $v_f \gg v_r$, the flux is essentially equal to the rate of the forward reaction ($J \approx v_f$).

For the pathway as a whole, flux is set by the rate-determining step of the pathway. By definition, this step is the pathway's slowest step, which is often the first committed step of the pathway. In some pathways, flux control is distributed over several enzymes, all of which help determine the overall rate of flow of metabolites through the pathway. Because a rate-determining step is slow relative to other steps in the pathway, its product is removed by succeeding steps in the pathway before it can equilibrate with reactant. Thus, *the rate-determining step functions far from equilibrium and has a large negative free energy change*. In an analogous manner, a dam creates a difference in water levels between its upstream and downstream sides, and a large negative free energy change results from the hydrostatic pressure difference. The dam can release water to generate electricity, varying the water flow according to the need for electrical power.

Reactions that function near equilibrium respond rapidly to changes in substrate concentration. For example, upon a sudden increase in the concentration of a reactant for a near-equilibrium reaction, the enzyme catalyzing it would increase the net reaction rate so as to rapidly achieve the new equilibrium level. Thus, a series of near-equilibrium reactions downstream from the rate-determining step all have the same flux. Likewise, the flux of water in a river is the same at all points downstream from a dam.

In practice, it is often possible to identify flux control points for a pathway by identifying reactions that have large negative free energy changes. The relative insensitivity of the rates of these nonequilibrium reactions to variations in the concentrations of their substrates permits the establishment of a steady state flux of metabolites through the pathway. Of course, flux through a pathway must vary in response to the organism's requirements so as to reach a new steady state. Altering the rates of the rate-determining steps can alter the flux of material through the entire pathway, often by an order of magnitude or more.

Cells use several mechanisms to control flux through the rate-determining steps of metabolic pathways:

1. ***Allosteric control.*** Many enzymes are allosterically regulated (Section 12-3A) by effectors that are often substrates, products, or coenzymes of the pathway but not necessarily of the enzyme in question. For example, in negative feedback regulation, the product of a pathway inhibits an earlier step in the pathway:

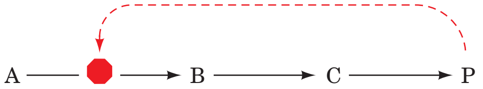

Thus, as we have seen, CTP, a product of pyrimidine biosynthesis, inhibits ATCase, which catalyzes the rate-determining step in the pathway (Fig. 12-11).

2. ***Covalent modification.*** Many enzymes that control pathway fluxes have specific sites that may be enzymatically phosphorylated and dephosphorylated (Section 12-3B) or covalently modified in some other way. Such enzymatic modification processes, which are themselves subject to control by external signals such as hormones (Section 13-1), greatly alter the activities of the modified enzymes. The signaling methods involved in such flux control mechanisms are discussed in Chapter 13.

3. ***Substrate cycles.*** If v_f and v_r represent the rates of two opposing nonequilibrium reactions that are catalyzed by different enzymes, v_f and v_r may be independently varied.

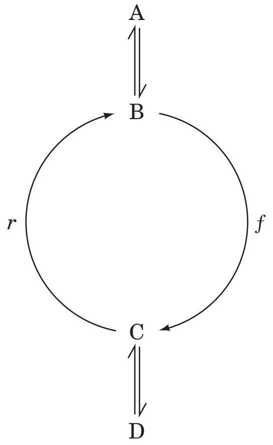

For example, flux ($v_f - v_r$) can be increased not just by accelerating the forward reaction but by slowing the reverse reaction. The flux through such a **substrate cycle,** as we shall see in Section 15-4, is more sensitive to the concentrations of allosteric effectors than is the flux through a single unopposed nonequilibrium reaction.

4. ***Genetic control.*** Enzyme concentrations, and hence enzyme activities, may be altered by protein synthesis in response to metabolic needs. With the sequencing of entire genomes, the genetic response of an organism to environmental changes has become a major field of study. **Transcriptomics** (the study of the entire collection of RNA transcribed by a cell) and **proteomics** (the study of the complete set of proteins synthesized by a cell in response to changing conditions) are part of the emerging field of **systems biology** (Section 14-4C). Mechanisms of genetic control of enzyme concentrations are a major concern of Part V of this text.

Mechanisms 1 to 3 can respond rapidly (within seconds or minutes) to external stimuli and are therefore classified as "short-term" control mechanisms. Mechanism 4 responds more slowly to changing conditions (within hours or days in higher organisms) and is therefore regarded as a "long-term" control mechanism.

Control of most metabolic pathways involves several nonequilibrium steps. Hence, the flux of material through a pathway that supplies intermediates for use by an organism may depend on multiple effectors whose relative importance reflects the overall metabolic demands of the organism at a given time. Thus, a metabolic pathway is part of a **supply–demand process.**

CHECK YOUR UNDERSTANDING

Describe the differences between autotrophs and heterotrophs.
List the categories of macronutrients and micronutrients required for mammalian metabolism.
Describe the roles of vitamins and minerals in nutrition.
Explain the metabolic significance of reactions that function near equilibrium and reactions that function far from equilibrium.
Discuss the mechanisms by which the flux through a metabolic pathway can be controlled.

2 "High-Energy" Compounds

LEARNING OBJECTIVES

- Understand that organisms capture the free energy released on degradation of nutrients as "high-energy" compounds such as ATP, whose subsequent breakdown is used to power otherwise endergonic reactions.
- Understand that "high-energy" usually means high free energy of hydrolysis or oxidation.
- Understand that phosphoryl groups are transferred from compounds with high phosphoryl group-transfer potentials to those with low phosphoryl group-transfer potentials.
- Understand that the thioester bond in acetyl-CoA is a "high-energy" bond.

The complete oxidation of a metabolic fuel such as glucose

$$C_6H_{12}O_6 + 6\,O_2 \longrightarrow 6\,CO_2 + 6\,H_2O$$

releases considerable energy ($\Delta G^{\circ\prime} = -2850\ \text{kJ}\cdot\text{mol}^{-1}$). The complete oxidation of palmitate, a typical fatty acid,

$$C_{16}H_{32}O_2 + 23\,O_2 \longrightarrow 16\,CO_2 + 16\,H_2O$$

is even more exergonic ($\Delta G^{\circ\prime} = -9781\ \text{kJ}\cdot\text{mol}^{-1}$). Oxidative metabolism proceeds in a stepwise fashion, so the released free energy can be recovered in a manageable form at each exergonic step of the overall process. *These "packets" of energy are conserved by the synthesis of a few types of* ***"high-energy" intermediates*** *whose subsequent exergonic breakdown drives endergonic processes.* These intermediates therefore form a sort of free energy "currency" through which free energy–producing reactions such as glucose oxidation or fatty acid oxidation "pay for" the free energy–consuming processes in biological systems (Box 14-3).

The cell uses several forms of energy currency, including phosphorylated compounds such as the nucleotide ATP (the cell's primary energy currency), compounds that contain thioester bonds, and reduced coenzymes such as NADH. Each of these represents a source of free energy that the cell can use in various ways, including the synthesis of ATP. We will first examine ATP and then discuss the properties of other forms of energy currency.

BOX 14-3 PATHWAYS OF DISCOVERY

Fritz Lipmann and “High-Energy” Compounds

Fritz Albert Lipmann (1899–1986)

Among the many scientists who fled Europe for the United States in the 1930s was Fritz Lipmann, a German-born physician-turned-biochemist. During the first part of the twentieth century, scientists were primarily interested in the structures and compositions of biological molecules, and not much was known about their biosynthesis. Lipmann’s contribution to this field centers on his understanding of “energy-rich” phosphates and other “active” compounds.

Lipmann began his research career by studying creatine phosphate, a compound that could provide energy for muscle contraction. He, like many of his contemporaries, was puzzled by the absence of an obvious link between this phosphorylated compound and the known metabolic activity of a contracting muscle, namely, converting glucose to lactate. One link was discovered by Otto Warburg (Box 15-1), who showed that one of the steps of glycolysis was accompanied by the incorporation of inorganic phosphate. The resulting acyl phosphate (1,3-bisphosphoglycerate) could then react with ADP to form ATP.

Lipmann wondered whether other phosphorylated compounds might behave in a similar manner. Because the purification of such labile (prone to degradation) compounds from whole cells was impractical, Lipmann synthesized them himself. He was able to show that cell extracts used synthetic acetyl phosphate to produce ATP. Lipmann went on to propose that cells contain two classes of phosphorylated compounds, which he termed “energy-poor” and “energy-rich,” by which he meant compounds with low and high negative free energies of hydrolysis (the “squiggle,” ~, which is still used, was his symbol for an “energy-rich” bond). Lipmann described a sort of “phosphate current” in which photosynthesis or breakdown of food molecules generates “energy-rich” phosphates that lead to the synthesis of ATP. The ATP, in turn, can power mechanical work such as muscle contraction or drive biosynthetic reactions.

Until this point (1941), biochemists studying biosynthetic processes were largely limited to working with whole animals or relatively intact tissue slices. Lipmann’s insight regarding the role of ATP freed researchers from their cumbersome and poorly reproducible experimental systems. Biochemists could simply add ATP to their cell-free preparations to reconstitute the biosynthetic process.

Lipmann was intrigued by the discovery that a two-carbon group, an “active acetate,” served as a precursor for the synthesis of fatty acids and steroids. Was acetyl phosphate also the “active acetate”? This proved not to be the case, although Lipmann was able to show that the addition of a two-carbon unit to another molecule (acetylation) required acetate, ATP, and a heat-stable factor present in pigeon liver extracts. He isolated and determined the structure of this factor, which he named coenzyme A. For this seminal discovery, Lipmann was awarded the 1953 Nobel Prize for Physiology or Medicine.

Even after “high-energy” thioesters (as in acetyl-CoA) came on the scene, Lipmann remained a staunch advocate of “high-energy” phosphates. For example, he realized that carbamoyl phosphate ($H_2N—COO—PO_3^{2-}$) could function as an “active” carbamoyl group donor in biosynthetic reactions. He also helped identify more obscure compounds, mixed anhydrides between phosphate and sulfate, as “active” sulfates that function as sulfate group donors.

Kleinkauf, H., von Döhren, H., and Jaenicke, L. (Eds.), *The Roots of Modern Biochemistry. Fritz Lipmann’s Squiggle and Its Consequences,* Walter de Gruyter (1988).

A | ATP Has a High Phosphoryl Group-Transfer Potential

The “high-energy” intermediate adenosine triphosphate (ATP; Fig. 14-4) occurs in all known life-forms. ATP consists of an **adenosine** moiety (adenine + ribose) to which three phosphoryl ($—PO_3^{2-}$) groups are sequentially linked via a **phosphoester** bond followed by two **phosphoanhydride** bonds.

The biological importance of ATP rests in the large free energy change that accompanies cleavage of its phosphoanhydride bonds. This occurs when either a phosphoryl group is transferred to another compound,

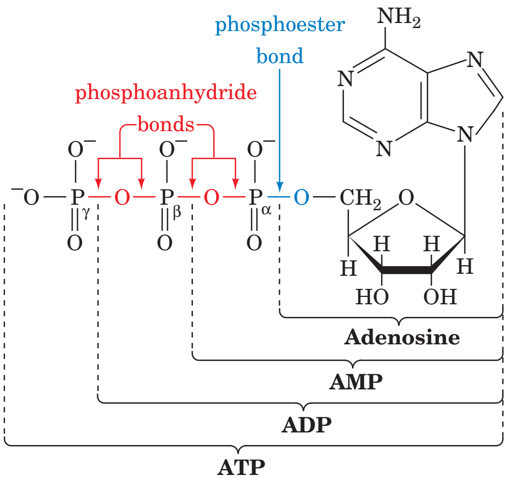

Figure 14-4 | The structure of ATP indicating its relationship to ADP, AMP, and adenosine. The phosphoryl groups, starting from AMP, are referred to as the α-, β-, and γ-phosphates. Note the differences between phosphoester and phosphoanhydride bonds.

leaving ADP, or a nucleotidyl (AMP) group is transferred, leaving **pyrophosphate** ($P_2O_7^{4-}$; **PP_i**). When the acceptor is water, the process is known as hydrolysis:

$$\text{ATP} + H_2O \rightleftharpoons \text{ADP} + P_i$$
$$\text{ATP} + H_2O \rightleftharpoons \text{AMP} + PP_i$$

Most biological group-transfer reactions involve acceptors other than water. However, knowing the free energy of hydrolysis of various phosphoryl compounds allows us to calculate the free energy of transfer of phosphoryl groups to other acceptors by determining the difference in free energy of hydrolysis of the phosphoryl donor and acceptor.

The $\Delta G^{\circ\prime}$ values for hydrolysis of several phosphorylated compounds of biochemical importance are tabulated in Table 14-4. The negatives of these values are often referred to as **phosphoryl group-transfer potentials;** they are a measure of the tendency of phosphorylated compounds to transfer their phosphoryl groups to water. Note that ATP has an intermediate phosphate group-transfer potential. Under standard conditions, the compounds above ATP in Table 14-4 can spontaneously transfer a phosphoryl group to ADP to form ATP, which can, in turn, spontaneously transfer a phosphoryl group to the appropriate groups to form the compounds listed below it. Note that a favorable free energy change for a reaction does not indicate how quickly the reaction occurs. Despite their high group-transfer potentials, ATP and related phosphoryl compounds are **kinetically stable** and do not react at a significant rate unless acted upon by an appropriate enzyme.

What Is the Nature of the “Energy” in “High-Energy” Compounds?

Bonds whose hydrolysis proceeds with large negative values of $\Delta G^{\circ\prime}$ (customarily more than $-25\ \text{kJ}\cdot\text{mol}^{-1}$) are often referred to as **“high-energy” bonds** or **“energy-rich” bonds** and are frequently symbolized by the squiggle (~). Thus, ATP can be represented as AR—P~P~P, where A, R, and P symbolize adenyl, ribosyl, and phosphoryl groups, respectively. Yet the phosphoester bond joining the adenosyl group of ATP to its α-phosphoryl group appears to be not greatly different in electronic character from the “high-energy” bonds bridging its α- and β- and its β- and γ-phosphoryl groups. In fact, none of these bonds has any unusual properties, so the term “high-energy” bond is somewhat of a misnomer (in any case, it should not be confused with the term “bond energy,” which is defined as the energy required to break, not hydrolyze, a covalent bond). Why, then, are the phosphoryl group-transfer reactions of ATP so exergonic? Several factors appear to be responsible for the “high-energy” character of phosphoanhydride bonds such as those in ATP (Fig. 14-5):

1. The resonance stabilization of a phosphoanhydride bond is less than that of its hydrolysis products. This is because a phosphoanhydride’s two strongly electron-withdrawing groups must compete for the lone pairs of electrons of its bridging oxygen atom, whereas this competition is absent in the hydrolysis products. In other words, the electronic requirements of the phosphoryl groups are less satisfied in a phosphoanhydride than in its hydrolysis products.
2. Of perhaps greater importance is the destabilizing effect of the electrostatic repulsions between the charged groups of a phosphoanhydride compared to those of its hydrolysis products. In the physiological pH range, ATP has three to four negative charges whose mutual electrostatic repulsions are partially relieved by ATP hydrolysis.

Table 14-4 Standard Free Energies of Phosphate Hydrolysis of Some Compounds of Biological Interest

Compound	$\Delta G^{\circ\prime}$ (kJ · mol^{-1})
Phosphoenolpyruvate	−61.9
1,3-Bisphosphoglycerate	−49.4
ATP (→ AMP + PP_i)	−45.6
Acetyl phosphate	−43.1
Phosphocreatine	−43.1
ATP (→ ADP + P_i)	−30.5
Glucose-1-phosphate	−20.9
PP_i	−19.2
Fructose-6-phosphate	−13.8
Glucose-6-phosphate	−13.8
Glycerol-3-phosphate	−9.2

Source: Mostly from Jencks, W.P., *in* Fasman, G.D. (Ed.), *Handbook of Biochemistry and Molecular Biology* (3rd ed.), Physical and Chemical Data, Vol. I, pp. 296–304, CRC Press (1976).

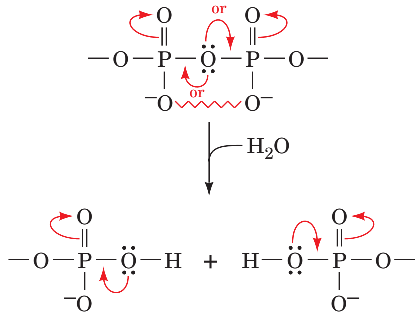

Figure 14-5 | **Resonance and electrostatic stabilization in a phosphoanhydride and its hydrolytic products.** The competing resonances (*curved arrows* from the central O) and charge–charge repulsions (*zigzag lines*) between phosphoryl groups decrease the stability of a phosphoanhydride relative to its hydrolysis products.

BOX 14-4 PERSPECTIVES IN BIOCHEMISTRY

ATP and ΔG

The standard conditions reflected in $\Delta G^{\circ\prime}$ values never occur in living organisms. Furthermore, other compounds that are present at high concentrations and that can potentially interact with the substrates and products of a metabolic reaction may dramatically affect ΔG values. For example, Mg^{2+} ions in cells partially neutralize the negative charges on the phosphate groups in ATP and its hydrolysis products, thereby diminishing the electrostatic repulsions that make ATP hydrolysis so exergonic. Similarly, changes in pH alter the ionic character of phosphorylated compounds and therefore alter their free energies.

In a given cell, the concentrations of many ions, coenzymes, and metabolites vary with both location and time, often by several orders of magnitude. Intracellular ATP concentrations are maintained within a relatively narrow range, usually 2–10 mM, but the concentrations of ADP and P_i are more variable. Consider a typical cell with $[ATP] = 3.0$ mM, $[ADP] = 0.8$ mM, and $[P_i] = 4.0$ mM. Using Eq. 14-1, the actual free energy of ATP hydrolysis at 37°C is calculated as follows.

$$\begin{aligned}\Delta G &= \Delta G^{\circ\prime} + RT\ln\left(\frac{[\mathrm{ADP}][\mathrm{P}_i]}{[\mathrm{ATP}]}\right)\\ &= -30.5\ \mathrm{kJ\cdot mol^{-1}} + (8.3145\ \mathrm{J\cdot K^{-1}\cdot mol^{-1}})(310\ \mathrm{K})\\ &\quad \ln\left(\frac{(0.8\times10^{-3}\ \mathrm{M})(4.0\times10^{-3}\ \mathrm{M})}{(3.0\times10^{-3}\ \mathrm{M})}\right)\\ &= -30.5\ \mathrm{kJ\cdot mol^{-1}} - 17.6\ \mathrm{kJ\cdot mol^{-1}}\\ &= -48.1\ \mathrm{kJ\cdot mol^{-1}}\end{aligned}$$

This value is even greater than the standard free energy of ATP hydrolysis. However, because of the difficulty in accurately measuring the concentrations of particular chemical species in a cell or organelle, the ΔG's for most *in vivo* reactions are little more than estimates. For the sake of consistency, we shall, for the most part, use $\Delta G^{\circ\prime}$ values in this textbook.

---

3. Another destabilizing influence, which is difficult to assess, is the smaller solvation energy of a phosphoanhydride compared to that of its hydrolysis products. Some estimates suggest that this factor provides the dominant thermodynamic driving force for the hydrolysis of phosphoanhydrides.

Of course, the free energy change for any reaction, including phosphoryl group transfer from a "high-energy" compound, depends in part on the concentrations of the reactants and products (Eq. 14-1). Furthermore, because ATP and its hydrolysis products are ions, ΔG also depends on pH and ionic strength (Box 14-4).

B | Coupled Reactions Drive Endergonic Processes

The exergonic reactions of "high-energy" compounds can be coupled to endergonic processes to drive them to completion. The thermodynamic explanation for the coupling of an exergonic and an endergonic process is based on the additivity of free energy. Consider the following two-step reaction pathway:

$$(1)\quad \mathrm{A} + \mathrm{B} \rightleftharpoons \mathrm{C} + \mathrm{D} \qquad \Delta G_1$$

$$(2)\quad \mathrm{D} + \mathrm{E} \rightleftharpoons \mathrm{F} + \mathrm{G} \qquad \Delta G_2$$

If $\Delta G_1 \geq 0$, Reaction 1 will not occur spontaneously. However, if ΔG_2 is sufficiently exergonic so that $\Delta G_1 + \Delta G_2 < 0$, then although the equilibrium concentration of D in Reaction 1 will be relatively small, it will be larger than that in Reaction 2. As Reaction 2 converts D to products, Reaction 1 will operate in the forward direction to replenish the equilibrium concentration of D. The highly exergonic Reaction 2 therefore "drives" or "pulls" the endergonic Reaction 1, and the two reactions are said to be coupled through their common intermediate, D. That these

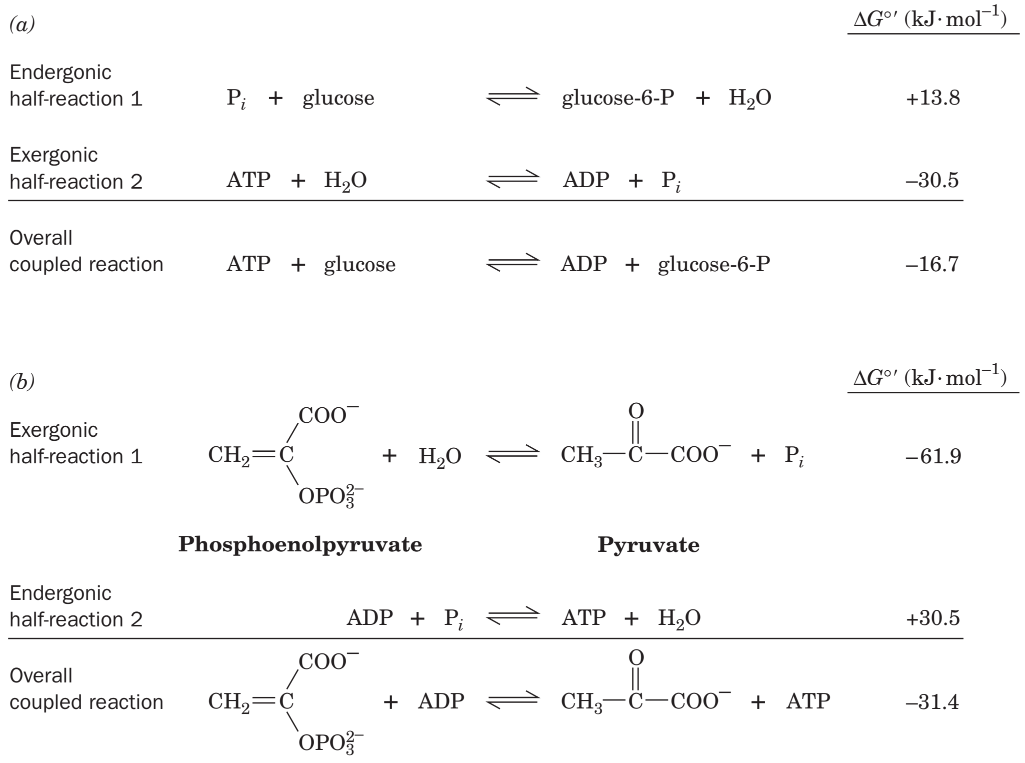
(a)
ΔG°′ (kJ·mol⁻¹)
Endergonic half-reaction 1
P_i + glucose ⇌ glucose-6-P + H₂O
+13.8
Exergonic half-reaction 2
ATP + H₂O ⇌ ADP + P_i
–30.5
Overall coupled reaction
ATP + glucose ⇌ ADP + glucose-6-P
–16.7
(b)
ΔG°′ (kJ·mol⁻¹)
Exergonic half-reaction 1
–61.9
Phosphoenolpyruvate
Pyruvate
Endergonic half-reaction 2
ADP + P_i ⇌ ATP + H₂O
+30.5
Overall coupled reaction
–31.4

Figure 14-6 | **Some coupled reactions involving ATP.** (*a*) The phosphorylation of glucose to form glucose-6-phosphate and ADP. (*b*) The phosphorylation of ADP by phosphoenolpyruvate to form ATP and pyruvate. Each reaction has been conceptually decomposed into a direct phosphorylation step (half-reaction 1) and a step in which ATP is hydrolyzed (half-reaction 2). Both half-reactions proceed in the direction that makes the overall reaction exergonic ($\Delta G < 0$).

coupled reactions proceed spontaneously can also be seen by summing Reactions 1 and 2 to yield the overall reaction

$$(1 + 2) \quad \mathrm{A + B + E \rightleftharpoons C + F + G} \qquad \Delta G_3$$

where $\Delta G_3 = \Delta G_1 + \Delta G_2 < 0$. *As long as the overall pathway is exergonic, it will operate in the forward direction.*

To illustrate this concept, let us consider two examples of phosphoryl group-transfer reactions. The initial step in the metabolism of glucose is its conversion to **glucose-6-phosphate** (Section 15-2A). Yet the direct reaction of glucose and P_i is thermodynamically unfavorable ($\Delta G°' = +13.8\ \mathrm{kJ \cdot mol^{-1}}$; Fig. 14-6*a*). In cells, however, this reaction is coupled to the exergonic cleavage of ATP (for ATP hydrolysis, $\Delta G°' = -30.5\ \mathrm{kJ \cdot mol^{-1}}$), so the overall reaction is thermodynamically favorable ($\Delta G°' = +13.8 - 30.5 = -16.7\ \mathrm{kJ \cdot mol^{-1}}$). ATP can be similarly regenerated ($\Delta G°' = +30.5\ \mathrm{kJ \cdot mol^{-1}}$) by coupling its synthesis from ADP and P_i to the even more exergonic cleavage of **phosphoenolpyruvate** ($\Delta G°' = -61.9\ \mathrm{kJ \cdot mol^{-1}}$; Fig. 14-6*b* and Section 15-2J).

Note that the half-reactions shown in Fig. 14-6 do not actually occur as written in an enzyme active site. **Hexokinase,** the enzyme that catalyzes the formation of glucose-6-phosphate (Fig. 14-6*a*), does not catalyze ATP hydrolysis but instead catalyzes the transfer of a phosphoryl group from ATP directly to glucose. Likewise, **pyruvate kinase,** the enzyme that catalyzes the reaction shown in Fig. 14-6*b*, does not add a free phosphoryl group to ADP but transfers a phosphoryl group from phosphoenolpyruvate to ADP to form ATP.

Phosphoanhydride Hydrolysis Drives Some Biochemical Processes. The free energy of the phosphoanhydride bonds of "high-energy" compounds such as ATP can be used to drive reactions even when the phosphoryl groups are not transferred to another organic compound. For example, ATP hydrolysis (i.e., phosphoryl group transfer directly to H_2O) provides the free energy for the operation of molecular chaperones (Section 6-5B), muscle contraction (Section 7-2B), and transmembrane active transport (Section 10-3). In these processes, proteins undergo conformational changes in response to binding ATP. *The exergonic hydrolysis of ATP and release of ADP and P_i renders these changes irreversible and thereby drives the processes forward*. GTP hydrolysis functions similarly to drive some of the reactions of signal transduction (Section 13-3B) and protein synthesis (Section 27-4).

In the absence of an appropriate enzyme, phosphoanhydride bonds are stable; that is, they hydrolyze quite slowly, despite the large amount of free energy released by these reactions. This is because these hydrolysis reactions have unusually high free energies of activation ($\Delta G^{\ddagger}$; Section 11-2). Consequently, *ATP hydrolysis is thermodynamically favored but kinetically disfavored*. For example, consider the reaction of glucose with ATP that yields glucose-6-phosphate (Fig. 14-6*a*). $\Delta G^{\ddagger}$ for the nonenzymatic transfer of a phosphoryl group from ATP to glucose is greater than that for ATP hydrolysis, so the hydrolysis reaction predominates (although neither reaction occurs at a biologically significant rate). However, in the presence of the appropriate enzyme, **hexokinase** (Section 15-2A), glucose-6-phosphate is formed far more rapidly than ATP is hydrolyzed. This is because the catalytic influence of the enzyme reduces the activation energy for phosphoryl group transfer from ATP to glucose to less than the activation energy for ATP hydrolysis. This example underscores the point that even a thermodynamically favored reaction ($\Delta G < 0$) may not occur in a living system in the absence of a specific enzyme that catalyzes the reaction (i.e., lowers $\Delta G^{\ddagger}$ to increase the rate of product formation; Box 12-3).

Inorganic Pyrophosphatase Catalyzes Additional Phosphoanhydride Bond Cleavage. Although many reactions involving ATP yield ADP and P_i **(orthophosphate cleavage),** others yield AMP and PP_i **(pyrophosphate cleavage).** In these latter cases, the PP_i is rapidly hydrolyzed to 2 P_i by **inorganic pyrophosphatase** ($\Delta G^{\circ\prime} = -19.2 \text{ kJ} \cdot \text{mol}^{-1}$) so that *the pyrophosphate cleavage of ATP ultimately consumes two "high-energy" phosphoanhydride bonds.* The attachment of amino acids to tRNA molecules for protein synthesis is an example of this phenomenon (Fig. 14-7 and Section 27-2B). The two steps of the reaction are readily reversible because the free energies of hydrolysis of the bonds formed are comparable to that of ATP hydrolysis. The overall reaction is driven to completion by the irreversible hydrolysis of PP_i. Nucleic acid biosynthesis from nucleoside triphosphates also releases PP_i (Sections 25-1 and 26-1). The standard free energy changes of these reactions are around 0, so the subsequent hydrolysis of PP_i is also essential for the synthesis of nucleic acids.

C | Some Other Phosphorylated Compounds Have High Phosphoryl Group-Transfer Potentials

"High-energy" compounds other than ATP are essential for energy metabolism, in part because they help maintain a relatively constant level of cellular ATP. *ATP is continually being hydrolyzed and regenerated*. Indeed, experimental evidence indicates that the metabolic half-life of an ATP

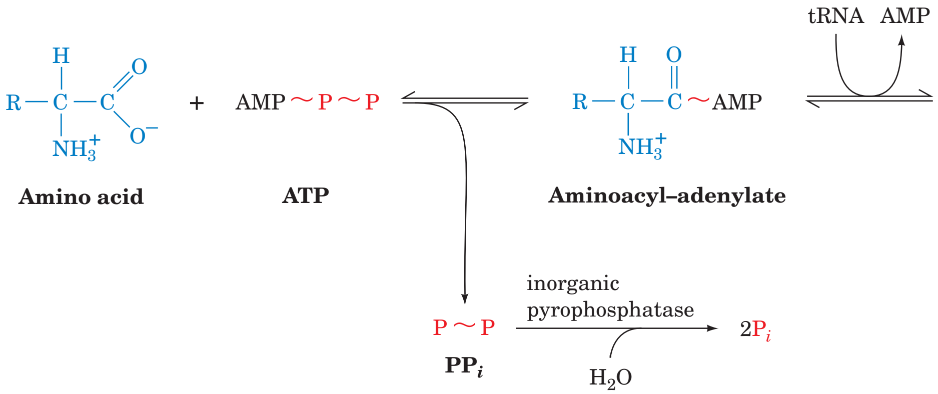

■ **Figure 14-7** | **Pyrophosphate cleavage in the synthesis of an aminoacyl–tRNA.** In the first reaction step, the amino acid is **adenylylated** by ATP. In the second step, a tRNA molecule displaces the AMP moiety to form an aminoacyl–tRNA. The exergonic hydrolysis of pyrophosphate ($\Delta G°' = -19.2 \text{ kJ} \cdot \text{mol}^{-1}$) drives the reaction forward.

molecule varies from seconds to minutes depending on the cell type and its metabolic activity. For instance, brain cells have only a few seconds supply of ATP (which partly accounts for the rapid deterioration of brain tissue by oxygen deprivation). An average person at rest consumes and regenerates ATP at a rate of ~3 mol (1.5 kg) per hour and as much as an order of magnitude faster during strenuous activity.

Just as ATP drives endergonic reactions through the exergonic process of phosphoryl group transfer and phosphoanhydride hydrolysis, *ATP itself can be regenerated by coupling its formation to a more highly exergonic metabolic process*. As Table 14-4 indicates, in the thermodynamic hierarchy of phosphoryl-transfer agents, ATP occupies the middle rank. ATP can therefore be formed from ADP by direct transfer of a phosphoryl group from a "high-energy" compound (e.g., phosphoenolpyruvate; Fig. 14-6*b* and Section 15-2J). Such a reaction is referred to as a **substrate-level phosphorylation.** Other mechanisms generate ATP indirectly, using the energy supplied by transmembrane proton concentration gradients. In oxidative metabolism, this process is called **oxidative phosphorylation** (Section 18-3), whereas in photosynthesis, it is termed **photophosphorylation** (Section 19-2D).

The flow of energy from "high-energy" phosphate compounds to ATP and from ATP to "low-energy" phosphate compounds is diagrammed in Fig. 14-8. These reactions are catalyzed by enzymes known as **kinases,** which transfer phosphoryl groups from ATP to other compounds or from phosphorylated compounds to ADP. We shall revisit these processes in our discussions of carbohydrate metabolism in Chapters 15 and 16.

The compounds whose phosphoryl group-transfer potentials are greater than that of ATP have additional stabilizing effects. For example, the hydrolysis of **acyl phosphates** (mixed phosphoric–carboxylic anhydrides), such as **acetyl phosphate** and **1,3-bisphosphoglycerate,**

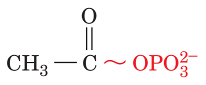
$$CH_3-\overset{\overset{\displaystyle O}{\|}}{C}\sim OPO_3^{2-}$$

Acetyl phosphate

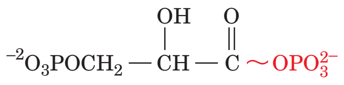
$$^{-2}O_3POCH_2-\overset{\overset{\displaystyle OH}{|}}{CH}-\overset{\overset{\displaystyle O}{\|}}{C}\sim OPO_3^{2-}$$

1,3-Bisphosphoglycerate

is driven by the same competing resonance and differential solvation effects that influence the hydrolysis of phosphoanhydrides (Fig. 14-5). Apparently, these effects are more pronounced for acyl phosphates than for phosphoanhydrides, as the rankings in Table 14-4 indicate.

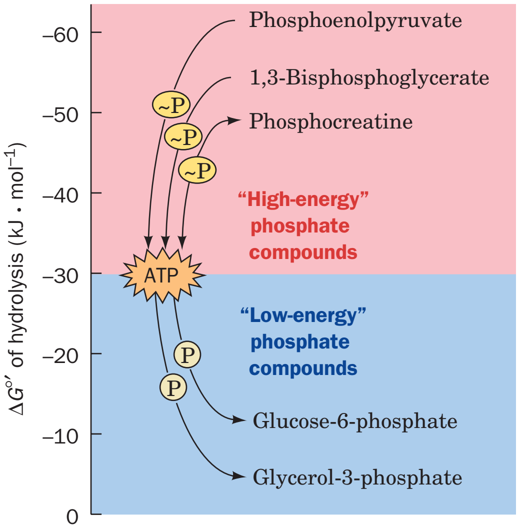

■ **Figure 14-8** | **Position of ATP relative to "high-energy" and "low-energy" phosphate compounds.** Phosphoryl groups flow from the "high-energy" donors, via the ATP–ADP system, to "low-energy" acceptors.

In contrast, compounds such as glucose-6-phosphate and **glycerol-3-phosphate,**

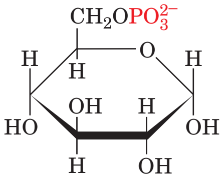

α-D-Glucose-6-phosphate

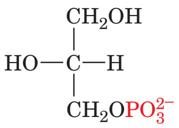

L-Glycerol-3-phosphate

which are below ATP in Table 14-4, have no significantly different resonance stabilization or charge separation compared to their hydrolysis products. Their free energies of hydrolysis are therefore much less than those of the preceding "high-energy" compounds.

The high phosphoryl group-transfer potentials of **phosphoguanidines,** such as **phosphocreatine** and **phosphoarginine,** largely result from the competing resonances in the **guanidino** group, which are even more pronounced than they are in the phosphate group of phosphoanhydrides:

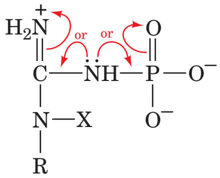

$R = CH_2—CO_2^-;\ X = CH_3$ **Phosphocreatine**

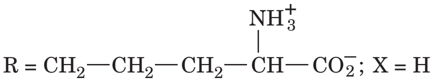

$$R = CH_2—CH_2—CH_2—\overset{\overset{NH_3^+}{|}}{C}H—CO_2^-;\ X = H$$

Phosphoarginine

Consequently, phosphocreatine can transfer its phosphoryl group to ADP to form ATP.

Phosphocreatine Provides a "High-Energy" Reservoir for ATP Formation. Muscle and nerve cells, which have a high ATP turnover, rely on phosphoguanidines to regenerate ATP rapidly. In vertebrates, phosphocreatine is synthesized by the reversible phosphorylation of creatine by ATP catalyzed by **creatine kinase:**

$$\text{ATP} + \text{creatine} \rightleftharpoons \text{phosphocreatine} + \text{ADP}$$
$$\Delta G°' = +12.6\ \text{kJ} \cdot \text{mol}^{-1}$$

Note that this reaction is endergonic under standard conditions; however, *the intracellular concentrations of its reactants and products are such that it operates close to equilibrium* ($\Delta G \approx 0$). Accordingly, when the cell is in a resting state, so that [ATP] is relatively high, the reaction proceeds with net synthesis of phosphocreatine, whereas at times of high metabolic activity, when [ATP] is low, the equilibrium shifts so as to yield net synthesis of ATP from phosphocreatine and ADP. *Phosphocreatine thereby acts as an ATP "buffer" in cells that contain creatine kinase.* A resting vertebrate skeletal muscle normally has sufficient phosphocreatine to supply its free energy needs for several minutes (but for only a few seconds at maximum exertion). In the muscles of some invertebrates, such as lobsters, phosphoarginine performs the same function. These phosphoguanidines are collectively named **phosphagens.**

Nucleoside Triphosphates Are Freely Interconverted. Many biosynthetic processes, such as the synthesis of proteins and nucleic acids, require nucleoside triphosphates other than ATP. For example, RNA synthesis requires the ribonucleotides CTP, GTP, and UTP, along with ATP, and DNA synthesis requires dCTP, dGTP, dTTP, and dATP (Section 3-1). All these nucleoside triphosphates **(NTPs)** are synthesized from ATP and the corresponding nucleoside diphosphate **(NDP)** in a reaction catalyzed by the nonspecific enzyme **nucleoside diphosphate kinase:**

$$\text{ATP} + \text{NDP} \rightleftharpoons \text{ADP} + \text{NTP}$$

The $\Delta G°'$ values for these reactions are nearly 0, as might be expected from the structural similarities among the NTPs. These reactions are driven by the depletion of the NTPs through their exergonic utilization in subsequent reactions.

Other kinases reversibly convert nucleoside monophosphates to their diphosphate forms at the expense of ATP. One of these phosphoryl group-transfer reactions is catalyzed by **adenylate kinase:**

$$\text{AMP} + \text{ATP} \rightleftharpoons 2\ \text{ADP}$$

This enzyme is present in all tissues, where it functions to maintain equilibrium concentrations of the three nucleotides. When AMP accumulates, it is converted to ADP, which can be used to synthesize ATP through substrate-level phosphorylation, oxidative phosphorylation, or photophosphorylation. The reverse reaction helps restore cellular ATP as rapid consumption of ATP increases the level of ADP.

The X-ray structure of adenylate kinase, determined by Georg Schulz, reveals that, in the reaction catalyzed by the enzyme, two ~30-residue domains of the enzyme close over the substrates (Fig. 14-9), thereby tightly binding them and preventing water from entering the active site (which would lead to hydrolysis rather than phosphoryl group transfer). The movement of one of the domains depends on the presence of four invariant charged residues. Interactions between those groups and the bound substrates apparently trigger the rearrangements around the substrate-binding site (Fig. 14-9*b*).

Once the adenylate kinase reaction is complete, the tightly bound products must be rapidly released to maintain the enzyme's catalytic efficiency. Yet since the reaction is energetically neutral (the net number of phosphoanhydride bonds is unchanged), another source of free energy is required for rapid product release. Comparison of the X-ray structures of unliganded adenylate kinase and adenylate kinase in complex with the bisubstrate model compound **Ap$_5$A** (AMP and ATP connected by a fifth phosphate) show how the enzyme avoids the kinetic trap of tight-binding substrates and products: On binding substrate, a portion of the protein

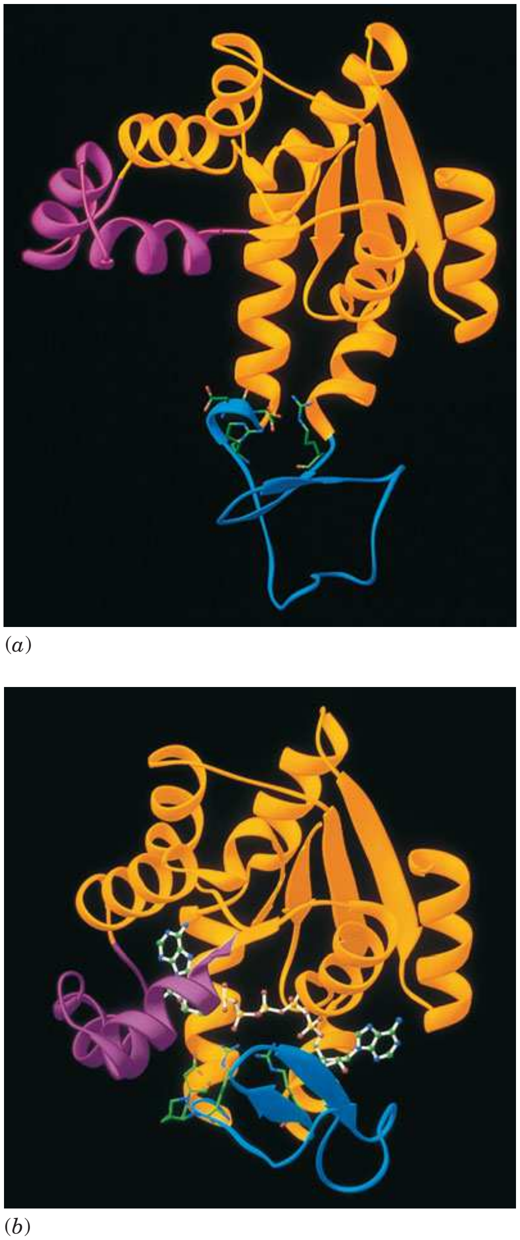

Figure 14-9 | Conformational changes in *E. coli* adenylate kinase on binding substrate. (*a*) The unliganded enzyme. (*b*) The enzyme with the bound bisubstrate analog Ap$_5$A. The Ap$_5$A is shown in ball-and-stick form (C green, N blue, O red, and P yellow). Several of the protein's side chains that have been implicated in substrate binding are shown in stick form. The protein's magenta and blue domains undergo extensive conformational changes on ligand binding, whereas the remainder of the protein (*gold*), whose orientation is the same in *a* and *b*, largely maintains its conformation. [Based on X-ray structures by Georg Schulz, Institut für Organische Chemie und Biochemie, Freiburg, Germany. PDBids (*a*) 4AKE and (*b*) 1AKE.] **See Interactive Exercises 14.**

remote from the active site increases its chain mobility and thereby consumes some of the free energy of substrate binding. The region "resolidifies" when the binding site is opened and the products are released. This mechanism is thought to act as an "energetic counterweight" to help adenylate kinase maintain a high reaction rate.

D | Thioesters Are Energy-Rich Compounds

The ubiquity of phosphorylated compounds in metabolism is consistent with their early evolutionary appearance. Yet phosphate is (and was) scarce in the abiotic world, which suggests that other kinds of molecules might have served as energy-rich compounds even before metabolic pathways became specialized for phosphorylated compounds. One candidate for a primitive "high-energy" compound is the **thioester,** which offers as its main recommendation its occurrence in the central metabolic pathways of all known organisms. Notably, the thioester bond is involved in substrate-level phosphorylation, an ATP-generating process that is independent of—and presumably arose before—oxidative phosphorylation.

The thioester bond appears in modern metabolic pathways as a reaction intermediate (involving a Cys residue in an enzyme active site) and in the form of acetyl-CoA (Fig. 14-10), the common product of carbohydrate, fatty acid, and amino acid catabolism. **Coenzyme A (CoASH or CoA)** consists of a β-mercaptoethylamine group bonded through an amide linkage to the vitamin **pantothenic acid,** which, in turn, is attached to a 3′-phosphoadenosine moiety via a pyrophosphate bridge. The acetyl group of acetyl-CoA is bonded as a thioester to the sulfhydryl portion of the

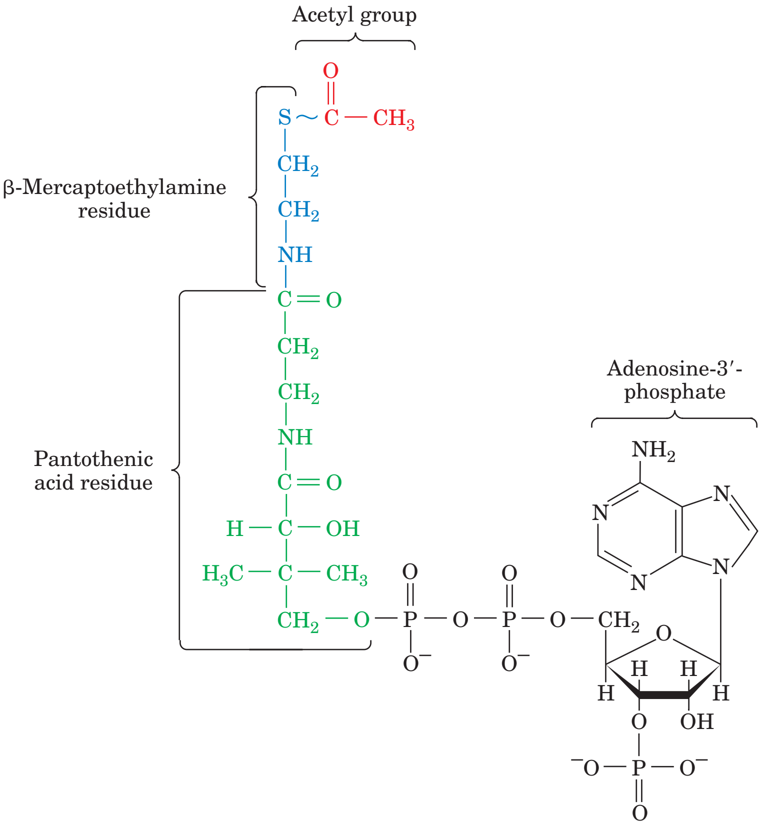

Acetyl-coenzyme A (acetyl-CoA)

■ **Figure 14-10 | The chemical structure of acetyl-CoA.** The thioester bond is drawn with a ~ to indicate that it is a "high-energy" bond (has a high negative free energy of hydrolysis). In CoA, the acetyl group is replaced by hydrogen.

β-mercaptoethylamine group. *CoA thereby functions as a carrier of acetyl and other acyl groups (the A of CoA stands for "Acetylation")*. Thioesters also take the form of acyl chains bonded to a phosphopantetheine residue that is linked to a Ser OH group in a protein (Section 20-4C) rather than to 3′-phospho-AMP, as in CoA.

Acetyl-CoA is a "high-energy" compound. The $\Delta G^{\circ\prime}$ for the hydrolysis of its thioester bond is $-31.5\ \text{kJ} \cdot \text{mol}^{-1}$, which makes this reaction slightly ($1\ \text{kJ} \cdot \text{mol}^{-1}$) more exergonic than ATP hydrolysis. The hydrolysis of thioesters is more exergonic than that of ordinary esters because the thioester is less stabilized by resonance. This destabilization is a result of the large atomic radius of S, which reduces the electronic overlap between C and S compared to that between C and O.

The formation of a thioester bond in a metabolic intermediate conserves a portion of the free energy of oxidation of a metabolic fuel. That free energy can then be used to drive an exergonic process. In the citric acid cycle, for example, cleavage of a thioester **(succinyl-CoA)** releases sufficient free energy to synthesize GTP from GDP and P_i (Section 17-3E).

CHECK YOUR UNDERSTANDING

Why is ATP a "high-energy" compound?
Describe the ways an exergonic process can drive an endergonic process.
Explain how cellular ATP is replenished.
Why is a thioester bond a "high-energy" bond?

3 Oxidation–Reduction Reactions

LEARNING OBJECTIVES

- Understand the role of NAD$^+$ and FAD in metabolism.
- Understand that the Nernst equation describes the thermodynamics of oxidation–reduction reactions.
- Understand that the reduction potential describes the tendency for an oxidized compound to gain electrons (become reduced); the change in reduction potential for a reaction describes the tendency for a given oxidized compound to accept electrons from a given reduced compound.
- Appreciate that free energy and reduction potential are negatively related: the greater the reduction potential, the more negative the free energy and the more spontaneous the reaction.

As metabolic fuels are oxidized to CO_2, electrons are transferred to molecular carriers that, in aerobic organisms, ultimately transfer the electrons to molecular oxygen. The process of electron transport results in a transmembrane proton concentration gradient that drives ATP synthesis (oxidative phosphorylation; Section 18-3). Even obligate anaerobes, which do not carry out oxidative phosphorylation, rely on the oxidation of substrates to drive ATP synthesis. In fact, oxidation–reduction reactions (also known as **redox reactions**) supply living things with most of their free energy. In this section, we examine the thermodynamic basis for the conservation of free energy during substrate oxidation.

A | NAD$^+$ and FAD Are Electron Carriers

Two of the most widely occurring electron carriers are the nucleotide coenzymes nicotinamide adenine dinucleotide (NAD$^+$) and **flavin adenine dinucleotide (FAD).** The nicotinamide portion of NAD$^+$ (and its phosphorylated counterpart NADP$^+$; Fig. 11-4) is the site of reversible reduction, which formally occurs as the transfer of a hydride ion (H$^-$; a proton with two electrons) as indicated in Fig. 14-11. The terminal electron acceptor in

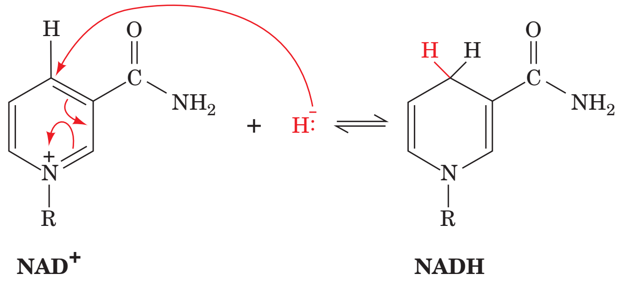

Figure 14-11 | Reduction of NAD$^+$ to NADH. R represents the ribose–pyrophosphoryl–adenosine portion of the coenzyme. Only the nicotinamide ring is affected by reduction, which is formally represented here as occurring by hydride transfer.

Figure 14-12 | Flavin adenine dinucleotide (FAD). Adenosine (*red*) is linked to **riboflavin** (*black*) by a pyrophosphoryl group (*green*). The riboflavin portion of FAD is also known as **vitamin B_2.**

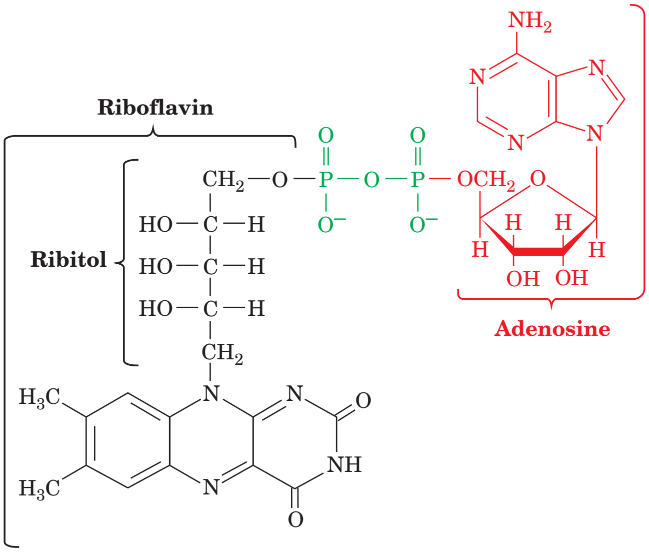
Riboflavin
Ribitol
Adenosine
NH_2
N
N
N
N
O
O
CH_2—O—P—O—P—OCH_2
O^-
O^-
HO—C—H
HO—C—H
HO—C—H
CH_2
H H
H H
OH OH
H_3C
H_3C
N
N
N
O
NH
O

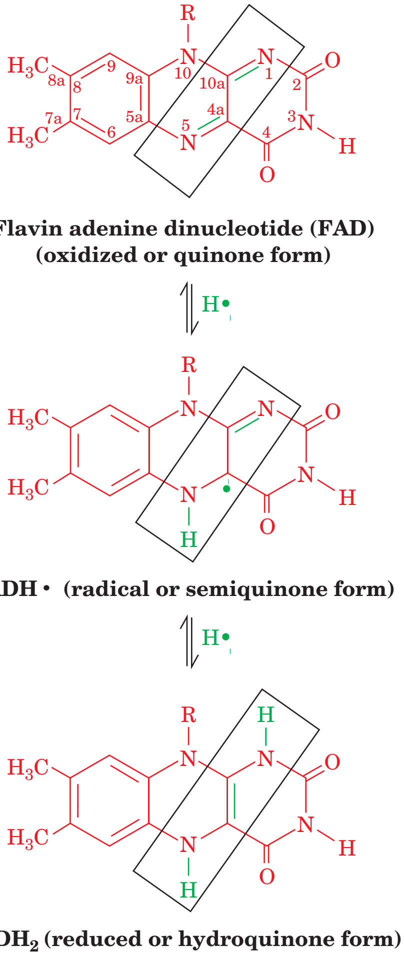
R
H_3C
H_3C
8a
8
9
9a
10
10a
1
2
3
4
4a
5
5a
6
7
7a
N
N
N
O
O
H
Flavin adenine dinucleotide (FAD)
(oxidized or quinone form)
H•
FADH • (radical or semiquinone form)
H•
$FADH_2$ (reduced or hydroquinone form)

Figure 14-13 | Reduction of FAD to $FADH_2$. R represents the ribitol–pyrophosphoryl–adenosine portion of the coenzyme. The conjugated ring system of FAD undergoes two sequential one-electron reductions or a two-electron transfer that bypasses the **semiquinone** state.

aerobic organisms, O_2, can accept only unpaired electrons; that is, electrons must be transferred to O_2 one at a time. Electrons that are removed from metabolites as pairs (e.g., with the two-electron reduction of NAD^+) must be transferred to other carriers that can undergo both two-electron and one-electron redox reactions. FAD (Fig. 14-12) is such a coenzyme.

The conjugated ring system of FAD can accept one or two electrons to produce the stable radical (semiquinone) FADH· or the fully reduced (hydroquinone) $FADH_2$ (Fig. 14-13). The change in the electronic state of the ring system on reduction is reflected in a color change from brilliant yellow (in FAD) to pale yellow (in $FADH_2$). The metabolic functions of NAD^+ and FAD demand that they undergo reversible reduction so that they can accept electrons, pass them on to other electron carriers, and thereby be regenerated to participate in additional cycles of oxidation and reduction.

Humans cannot synthesize the flavin moiety of FAD but, rather, must obtain it from their diets, for example, in the form of riboflavin (vitamin B_2; Fig. 14-12). Nevertheless, riboflavin deficiency is quite rare in humans, in part because of the tight binding of flavin prosthetic groups to their apoenzymes. The symptoms of riboflavin deficiency, which are associated with general malnutrition or bizarre diets, include an inflamed tongue, lesions in the corner of the mouth, and dermatitis.

B | The Nernst Equation Describes Oxidation–Reduction Reactions

Oxidation–reduction reactions resemble other types of group-transfer reactions except that the "groups" transferred are electrons, which are passed from an **electron donor (reductant** or **reducing agent)** to an **electron acceptor (oxidant** or **oxidizing agent).**

For example, in the reaction

$$Fe^{3+} + Cu^{+} \rightleftharpoons Fe^{2+} + Cu^{2+}$$

Cu^+, the reductant, is oxidized to Cu^{2+} while Fe^{3+}, the oxidant, is reduced to Fe^{2+}.

Redox reactions can be divided into two **half-reactions,** such as

$$Fe^{3+} + e^{-} \rightleftharpoons Fe^{2+} \qquad \text{(reduction)}$$
$$Cu^{+} \rightleftharpoons Cu^{2+} + e^{-} \qquad \text{(oxidation)}$$

whose sum is the whole reaction above. These particular half-reactions occur during the oxidation of cytochrome *c* oxidase in the mitochondrion (Section 18-2F). Note that for electrons to be transferred, both half-reactions must occur simultaneously. In fact, the electrons are the two half-reactions' common intermediate.

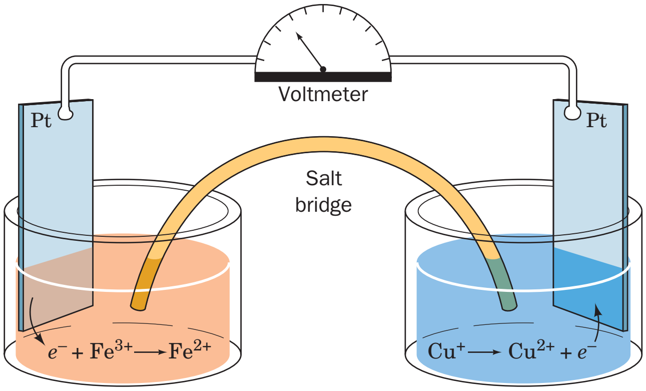
Voltmeter
Pt
Pt
Salt bridge
$e^- + \mathrm{Fe}^{3+} \longrightarrow \mathrm{Fe}^{2+}$
$\mathrm{Cu}^+ \longrightarrow \mathrm{Cu}^{2+} + e^-$

Figure 14-14 | An electrochemical cell. The half-cell undergoing oxidation (here $\mathrm{Cu}^+ \rightarrow \mathrm{Cu}^{2+} + e^-$) passes the liberated electrons through the wire to the half-cell undergoing reduction (here $e^- + \mathrm{Fe}^{3+} \rightarrow \mathrm{Fe}^{2+}$). Electroneutrality in the two half-cells is maintained by the transfer of ions through the electrolyte-containing salt bridge.

A half-reaction consists of an electron donor and its conjugate electron acceptor; in the oxidative half-reaction shown above, Cu^+ is the electron donor and Cu^{2+} is its conjugate electron acceptor. Together these constitute a **redox couple** or **conjugate redox pair** analogous to a conjugate acid–base pair (HA and A^-; Section 2-2B). An important difference between redox pairs and acid–base pairs, however, is that *the two half-reactions of a redox reaction, each consisting of a conjugate redox pair, can be physically separated to form an* ***electrochemical cell*** (Fig. 14-14). In such a device, each half-reaction takes place in its separate **half-cell,** and electrons are passed between half-cells as an electric current in the wire connecting their two electrodes. A salt bridge is necessary to complete the electrical circuit by providing a conduit for ions to migrate and thereby maintain electrical neutrality.

The free energy of an oxidation–reduction reaction is particularly easy to determine by simply measuring the voltage difference between its two half-cells. Consider the general reaction

$$\mathrm{A}_{\mathrm{ox}}^{n+} + \mathrm{B}_{\mathrm{red}} \rightleftharpoons \mathrm{A}_{\mathrm{red}} + \mathrm{B}_{\mathrm{ox}}^{n+}$$

in which n electrons per mole of reactants are transferred from reductant ($\mathrm{B}_{\mathrm{red}}$) to oxidant ($\mathrm{A}_{\mathrm{ox}}^{n+}$). The free energy of this reaction is expressed as

$$\Delta G = \Delta G^{\circ\prime} + RT\ln\left(\frac{[\mathrm{A}_{\mathrm{red}}][\mathrm{B}_{\mathrm{ox}}^{n+}]}{[\mathrm{A}_{\mathrm{ox}}^{n+}][\mathrm{B}_{\mathrm{red}}]}\right) \qquad [14\text{-}4]$$

Under reversible conditions,

$$\Delta G = -w' = -w_{\mathrm{el}} \qquad [14\text{-}5]$$

where w' is non-pressure–volume work. In this case, w' is equivalent to w_{el}, the electrical work required to transfer the n moles of electrons through the **electrical potential difference, $\Delta\mathscr{E}$** [where the units of $\mathscr{E}$ are volts (V), the number of joules (J) of work required to transfer 1 coulomb (C) of charge]. This, according to the laws of electrostatics, is

$$w_{\mathrm{el}} = n\mathscr{F}\Delta\mathscr{E} \qquad [14\text{-}6]$$

where $\mathscr{F}$**, the faraday,** is the electrical charge of 1 mol of electrons ($1\ \mathscr{F} = 96{,}485\ \mathrm{C \cdot mol^{-1}} = 96{,}485\ \mathrm{J \cdot V^{-1} \cdot mol^{-1}}$), and n is the number of moles of electrons transferred per mole of reactant converted. Thus, substituting Eq. 14-6 into Eq. 14-5,

$$\Delta G = -n\mathscr{F}\Delta\mathscr{E} \qquad [14\text{-}7]$$

Combining Eqs. 14-4 and 14-7, and making the analogous substitution for $\Delta G^{\circ\prime}$, yields the **Nernst equation:**

$$\boxed{\Delta\mathscr{E} = \Delta\mathscr{E}^{\circ\prime} - \frac{RT}{n\mathscr{F}}\ln\left(\frac{[\mathrm{A}_{\mathrm{red}}][\mathrm{B}_{\mathrm{ox}}^{n+}]}{[\mathrm{A}_{\mathrm{ox}}^{n+}][\mathrm{B}_{\mathrm{red}}]}\right)} \qquad [14\text{-}8]$$

which was originally formulated in 1881 by Walther Nernst. Here $\mathscr{E}$ is the

reduction potential, the tendency for a substance to undergo reduction (gain electrons). $\Delta\mathscr{E}$, the **electromotive force (emf),** can be described as the "electron pressure" that the electrochemical cell exerts. The quantity $\mathscr{E}°$, the reduction potential when all components are in their standard states, is called the **standard reduction potential.** If these standard states refer to biochemical standard states (Section 1-3D), then $\mathscr{E}°$ is replaced by $\boldsymbol{\mathscr{E}°'}$**.** Note that a positive $\Delta\mathscr{E}$ in Eq. 14-7 results in a negative ΔG; in other words, *a positive* $\Delta\mathscr{E}$ *indicates a spontaneous reaction, one that can do work*.

C | Spontaneity Can Be Determined by Measuring Reduction Potential Differences

Equation 14-7 shows that the free energy change of a redox reaction can be determined by directly measuring its change in reduction potential with a voltmeter (Fig. 14-14). Such measurements make it possible to determine the order of spontaneous electron transfers among a set of electron carriers such as those of the electron-transport pathway that mediates oxidative phosphorylation in cells.

Any redox reaction can be divided into its component half-reactions:

$$A_{ox}^{n+} + ne^- \rightleftharpoons A_{red}$$
$$B_{ox}^{n+} + ne^- \rightleftharpoons B_{red}$$

where, by convention, both half-reactions are written as reductions. These half-reactions can be assigned reduction potentials, $\mathscr{E}_A$ and $\mathscr{E}_B$, in accordance with the Nernst equation:

$$\mathscr{E}_A = \mathscr{E}_A^{\circ\prime} - \frac{RT}{n\mathscr{F}}\ln\left(\frac{[A_{red}]}{[A_{ox}^{n+}]}\right) \qquad [14\text{-}9]$$

$$\mathscr{E}_B = \mathscr{E}_B^{\circ\prime} - \frac{RT}{n\mathscr{F}}\ln\left(\frac{[B_{red}]}{[B_{ox}^{n+}]}\right) \qquad [14\text{-}10]$$

For the overall redox reaction involving the two half-reactions, the difference in reduction potential, $\Delta\mathscr{E}°'$, is defined as

$$\Delta\mathscr{E}^{\circ\prime} = \mathscr{E}^{\circ\prime}_{(e^-\text{ acceptor})} - \mathscr{E}^{\circ\prime}_{(e^-\text{ donor})} \qquad [14\text{-}11]$$

Thus, when the reaction proceeds with A as the electron acceptor and B as the electron donor, $\Delta\mathscr{E}^{\circ\prime} = \mathscr{E}_A^{\circ\prime} - \mathscr{E}_B^{\circ\prime}$, and $\Delta\mathscr{E} = \mathscr{E}_A - \mathscr{E}_B$.

Standard Reduction Potentials Are Used to Compare Electron Affinities. Reduction potentials, like free energies, must be defined with respect to some arbitrary standard, in this case, the hydrogen half-reaction

$$2H^+ + 2e^- \rightleftharpoons H_2(g)$$

in which H^+ is in equilibrium with $H_2(g)$ that is in contact with a Pt electrode. This half-cell is arbitrarily assigned a standard reduction potential $\mathscr{E}°$ of 0 V ($1V = 1\ J \cdot C^{-1}$) at pH 0, 25°C, and 1 atm. Under the biochemical convention, where the standard state is pH 7.0, the hydrogen half-reaction has a standard reduction potential $\mathscr{E}°'$ of -0.421 V.

When $\Delta\mathscr{E}$ is positive, ΔG is negative (Eq. 14-7), indicating a spontaneous process. In combining two half-reactions under standard conditions, the direction of spontaneity therefore involves the reduction of the redox couple with the more positive standard reduction potential. In other words, *the more positive the standard reduction potential, the higher the* *affinity of the redox couple's oxidized form for electrons, that is, the greater the tendency for the redox couple's oxidized form to accept electrons and thus become reduced.*

Biochemical Half-Reactions Are Physiologically Significant. The biochemical standard reduction potentials ($\mathscr{E}^{\circ\prime}$) of some biochemically important half-reactions are listed in Table 14-5. The oxidized form of a redox couple with a large positive standard reduction potential has a high affinity for electrons and is a strong electron acceptor (oxidizing agent), whereas its conjugate reductant is a weak electron donor (reducing agent). For example, O_2 is the strongest oxidizing agent in Table 14-5, whereas H_2O, which tightly holds its electrons, is the table's weakest reducing agent. The converse is true of half-reactions with large negative standard reduction potentials.

Since electrons spontaneously flow from low to high reduction potentials, they are transferred, under standard conditions, from the reduced

Table 14-5 Standard Reduction Potentials of Some Biochemically Important Half-Reactions

Half-Reaction	**$\mathscr{E}^{\circ\prime}$ (V)**
$\frac{1}{2}O_2 + 2H^+ + 2e^- \rightleftharpoons H_2O$	0.815
$NO_3^- + 2\,H^+ + 2\,e^- \rightleftharpoons NO_2^- + H_2O$	0.42
Cytochrome a_3 (Fe^{3+}) + e^- $\rightleftharpoons$ cytochrome a_3 (Fe^{2+})	0.385
$O_2(g) + 2\,H^+ + 2\,e^- \rightleftharpoons H_2O_2$	0.295
Cytochrome *a* (Fe^{3+}) + e^- $\rightleftharpoons$ cytochrome *a* (Fe^{2+})	0.29
Cytochrome *c* (Fe^{3+}) + e^- $\rightleftharpoons$ cytochrome *c* (Fe^{2+})	0.235
Cytochrome c_1 (Fe^{3+}) + e^- $\rightleftharpoons$ cytochrome c_1 (Fe^{2+})	0.22
Cytochrome *b* (Fe^{3+}) + e^- $\rightleftharpoons$ cytochrome *b* (Fe^{2+}) (*mitochondrial*)	0.077
Ubiquinone + 2 H^+ + 2 e^- $\rightleftharpoons$ ubiquinol	0.045
Fumarate$^-$ + 2 H^+ + 2 e^- $\rightleftharpoons$ succinate$^-$	0.031
FAD + 2 H^+ + 2 e^- $\rightleftharpoons$ $FADH_2$ (*in flavoproteins*)	~0.
Oxaloacetate$^-$ + 2 H^+ + 2 e^- $\rightleftharpoons$ malate$^-$	−0.166
Pyruvate$^-$ + 2 H^+ + 2 e^- $\rightleftharpoons$ lactate$^-$	−0.185
Acetaldehyde + 2 H^+ + 2 e^- $\rightleftharpoons$ ethanol	−0.197
FAD + 2 H^+ + 2 e^- $\rightleftharpoons$ $FADH_2$ (*free coenzyme*)	−0.219
$S + 2\,H^+ + 2\,e^- \rightleftharpoons H_2S$	−0.23
Lipoic acid + 2 H^+ + 2 e^- $\rightleftharpoons$ dihydrolipoic acid	−0.29
$NAD^+ + H^+ + 2\,e^- \rightleftharpoons NADH$	−0.315
$NADP^+ + H^+ + 2\,e^- \rightleftharpoons NADPH$	−0.320
Cysteine disulfide + 2 H^+ + 2 e^- $\rightleftharpoons$ 2 cysteine	−0.340
Acetoacetate$^-$ + 2 H^+ + 2 e^- $\rightleftharpoons$ β-hydroxybutyrate$^-$	−0.346
$H^+ + e^- \rightleftharpoons \frac{1}{2}H_2$	−0.421
$SO_4^{2-} + 2\,H^+ + 2\,e^- \rightleftharpoons SO_3^{2-} + H_2O$	−0.515
Acetate$^-$ + 3 H^+ + 2 e^- $\rightleftharpoons$ acetaldehyde + H_2O	−0.581

Source: Mostly from Loach, P.A., *In* Fasman, G.D. (Ed.), *Handbook of Biochemistry and Molecular Biology* (3rd ed.), Physical and Chemical Data, Vol. I, pp. 123–130, CRC Press (1976).

SAMPLE CALCULATION 14-2

Calculate $\Delta G^{\circ\prime}$ for the oxidation of NADH by FAD.

Combining the relevant half-reactions gives

$$\text{NADH} + \text{FAD} + \text{H}^+ \rightarrow \text{NAD}^+ + \text{FADH}_2$$

Next, calculate the electromotive force ($\Delta\mathscr{E}^{\circ\prime}$) from the standard reduction potentials given in Table 14-5, using one of the following methods.

Method 1
According to Eq. 14-11,

$$\Delta\mathscr{E}^{\circ\prime} = \mathscr{E}^{\circ\prime}_{(e^-\text{ acceptor})} - \mathscr{E}^{\circ\prime}_{(e^-\text{ donor})}$$

Since FAD ($\mathscr{E}^{\circ\prime} = -0.219$ V) is the electron acceptor, and NADH ($\mathscr{E}^{\circ\prime} = -0.315$ V) is the electron donor,

$$\Delta\mathscr{E}^{\circ\prime} = (-0.219\text{ V}) - (-0.315\text{ V}) = +0.096\text{ V}$$

Method 2
Write the net reaction as a sum of the two relevant half-reactions. For FAD, the half-reaction is the same as the reductive half-reaction given in Table 14-5, and its $\mathscr{E}^{\circ\prime}$ value is −0.219 V. For NADH, which undergoes oxidation rather than reduction, the half-reaction is the reverse of the one given in Table 14-5, and its $\mathscr{E}^{\circ\prime}$ value is +0.315 V, the reverse of the reduction potential given in the table. The two half-reactions are added to give the net oxidation–reduction reaction, and the $\mathscr{E}^{\circ\prime}$ values are also added:

$$\begin{array}{ll}
\text{FAD} + 2\,\text{H}^+ + 2\,e^- \rightarrow \text{FADH}_2 & \mathscr{E}^{\circ\prime} = -0.219\text{ V} \\
\text{NADH} \rightarrow \text{NAD}^+ + \text{H}^+ + 2\,e^- & \mathscr{E}^{\circ\prime} = +0.315\text{ V} \\
\hline
\text{NADH} + \text{FAD} + \text{H}^+ \rightarrow \text{NAD}^+ + \text{FADH}_2 & \Delta\mathscr{E}^{\circ\prime} = +0.096\text{ V}
\end{array}$$

Next, use Eq. 14-7 to calculate $\Delta G^{\circ\prime}$. Because two moles of electrons are transferred for every mole of NADH oxidized to NAD^+, $n = 2$.

$$\Delta G^{\circ\prime} = -n\mathscr{F}\Delta\mathscr{E}^{\circ\prime}$$
$$\Delta G^{\circ\prime} = -(2)(96{,}485\text{ J}\cdot\text{V}^{-1}\cdot\text{mol}^{-1})(0.096\text{ V}) = -18.5\text{ bJ}$$

products in any half-reaction in Table 14-5 to the oxidized reactants of any half-reaction above it (see Sample Calculation 14-2). However, such a reaction may not occur at a measurable rate in the absence of a suitable enzyme. Note that Fe^{3+} ions of the various cytochromes listed in Table 14-5 have significantly different reduction potentials. This indicates that *the protein components of redox enzymes play active roles in electron-transfer reactions by modulating the reduction potentials of their bound redox-active centers*.

Electron-transfer reactions are of great biological importance. For example, in the mitochondrial electron-transport chain (Section 18-2), electrons are passed from NADH along a series of electron acceptors of increasing reduction potential (including FAD and others listed in Table 14-5) to O_2. ATP is generated from ADP and P_i by coupling its synthesis to this free energy cascade. *NADH thereby functions as an energy-rich electron-transfer coenzyme*. In fact, the oxidation by O_2 of one NADH to NAD^+ supplies sufficient free energy to generate almost three ATPs. NAD^+ is an electron acceptor in many exergonic metabolite oxidations. In serving as the electron donor in ATP synthesis, it fulfills its cyclic role as a free energy conduit in a manner analogous to ATP (Fig. 14-8).

■ CHECK YOUR UNDERSTANDING

What is the metabolic role of reduced coenzymes?
Explain the terms of the Nernst equation.
How is $\Delta\mathscr{E}$ related to ΔG?

4 Experimental Approaches to the Study of Metabolism

LEARNING OBJECTIVES

- Understand that metabolic pathways are often studied by tracing labeled metabolites and perturbing the system so that intermediates accumulate.
- Understand how DNA microarrays and proteomics techniques are used to determine the genetic expression of metabolic enzymes.

A metabolic pathway can be understood at several levels:

1. In terms of the sequence of reactions by which a specific nutrient is converted to end products, and the energetics of the conversions.
2. In terms of the mechanisms by which each intermediate is converted to its successor. Such an analysis requires the isolation and characterization of the specific enzymes that catalyze each reaction.
3. In terms of the control mechanisms that regulate the flow of metabolites through the pathway. These mechanisms include the interorgan relationships that adjust metabolic activity to the needs of the entire organism.

Elucidating a metabolic pathway on all these levels is a complex process, often requiring contributions from a variety of disciplines.

The outlines of the major metabolic pathways have been known for decades, although in many cases, the enzymology behind various steps of the pathways remains unclear. Likewise, the mechanisms that regulate pathway activity under different physiological conditions are not entirely understood. These areas are of great interest because of their potential to yield information that could be useful in improving human health and curing metabolic diseases. In addition, the unexplored metabolisms of unusual organisms, including recently discovered "extremophiles," hold the promise of novel biological materials and enzymatic processes that can be exploited for the environmentally sensitive production of industrial materials, foods, and therapeutic drugs.

Early metabolic studies used whole organisms, often yeast, but also mammals. For example, Frederick Banting and Charles Best established the role of the pancreas in diabetes in 1921; they surgically removed that organ from dogs and observed that the animals then developed the disease (Box 22-1). Techniques for studying metabolic processes have since become more refined, progressing from whole-organ preparations and thin tissue slices to cultured cells and isolated organelles. The most recent approaches include identifying active genes and cataloguing their protein products.

A Labeled Metabolites Can Be Traced

A metabolic pathway in which one compound is converted to another can be followed by tracing a specifically labeled metabolite. Franz Knoop formulated this technique in 1904 to study fatty acid oxidation. He fed dogs fatty acids chemically labeled with phenyl groups and isolated the phenyl-substituted end products from the dogs' urine. From the differences in these products, depending on whether the phenyl-substituted starting material contained odd or even numbers of carbon atoms, Knoop deduced that fatty acids are degraded in two-carbon units (Section 20-2).

Chemical labeling has the disadvantage that the chemical properties of labeled metabolites differ from those of normal metabolites. This problem is largely eliminated by labeling molecules with isotopes. *The fate of an isotopically labeled atom in a metabolite can therefore be elucidated by following its progress through the metabolic pathway of interest.* The advent of isotopic labeling and tracing techniques in the 1940s revolutionized the study of metabolism.

One of the early advances in metabolic understanding resulting from the use of isotopic tracers was the demonstration, by David Shemin and David Rittenberg in 1945, that the nitrogen atoms of heme (Fig. 7-2) are derived from glycine rather than from ammonia, glutamic acid, proline, or leucine (Section 21-6A). They showed this by feeding rats the ^{15}N-labeled nutrients, isolating the heme in their blood, and analyzing it by mass spectrometry for ^{15}N content. Only when the rats were fed [^{15}N]glycine did the heme contain ^{15}N. This technique was also used with the radioactive isotope ^{14}C to demonstrate that all of cholesterol's carbon atoms are derived from acetyl-CoA (Section 20-7A). Radioactive isotopes (Box 12-1) have become virtually indispensable for establishing the metabolic origins of complex metabolites.

Another method for tracing the fates of labeled metabolites is nuclear magnetic resonance (NMR), which detects specific isotopes, including ^{1}H, ^{13}C, ^{15}N, and ^{31}P, by their characteristic nuclear spins. Since the NMR spectrum of a particular nucleus varies with its immediate environment, it is possible to identify the peaks corresponding to specific atoms even in relatively complex mixtures. The development of magnets large enough to accommodate animals and humans, and to localize spectra to specific organs, has made it possible to study metabolic pathways noninvasively by NMR techniques. For example, ^{31}P NMR can be used to study energy metabolism in muscle by monitoring the levels of phosphorylated compounds such as ATP, ADP, and phosphocreatine.

Isotopically labeling specific atoms of metabolites with ^{13}C (which is only 1.10% naturally abundant) permits the metabolic progress of the labeled atoms to be followed by ^{13}C NMR. Figure 14-15 shows *in vivo* ^{13}C NMR spectra of a rat liver before and after an injection of D-[1-^{13}C]

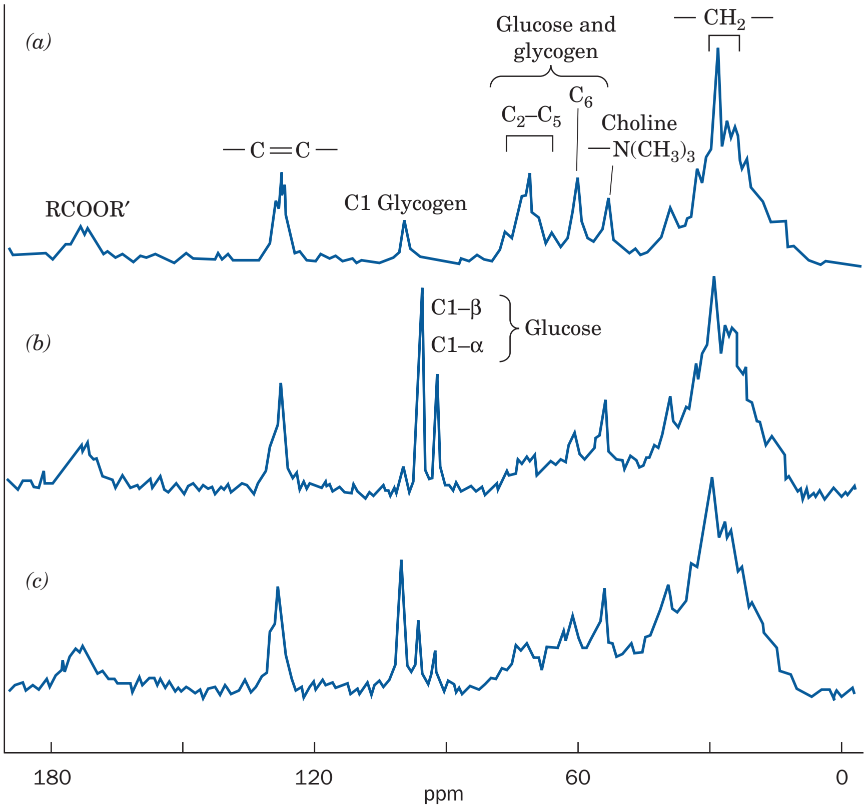

Figure 14-15 | The conversion of [1-^{13}C]glucose to glycogen as observed by localized *in vivo* ^{13}C NMR. (*a*) The natural abundance ^{13}C NMR spectrum of the liver of a live rat. Note the resonance corresponding to C1 of glycogen. (*b*) The ^{13}C NMR spectrum of the liver of the same rat ~5 min after it was intravenously injected with 100 mg of [1-^{13}C]glucose (90% enriched). The resonances of the C1 atom of both the α and β anomers of glucose are clearly distinguishable from each other and from the resonance of the C1 atom of glycogen. (*c*) The ^{13}C NMR spectrum of the liver of the same rat ~30 min after the [1-^{13}C]glucose injection. The C1 resonances of both the α- and β-glucose anomers are much reduced while the C1 resonance of glycogen has increased. [After Reo, N.V., Siegfried, B.A., and Acherman, J.J.H., *J. Biol. Chem.* **259,** 13665 (1984).]

glucose. The ^{13}C can be seen entering the liver and then being incorporated into glycogen (the storage form of glucose; Section 16-2).

B | Studying Metabolic Pathways Often Involves Perturbing the System

Many of the techniques used to elucidate the intermediates and enzymes of metabolic pathways involve perturbing the system in some way and observing how this affects the activity of the pathway. One way to perturb a pathway is to add certain substances, called **metabolic inhibitors,** that block the pathway at specific points, thereby causing the preceding intermediates to build up. This approach was used in elucidating the conversion of glucose to ethanol in yeast by glycolysis (Section 15-2). Similarly, the addition of substances that block electron transfer at different sites was used to deduce the sequence of electron carriers in the mitochondrial electron-transport chain (Section 18-2B).

Genetic Defects Also Cause Metabolic Intermediates to Accumulate. Archibald Garrod's realization, in the early 1900s, that human genetic diseases are the consequence of deficiencies in specific enzymes also contributed to the elucidation of metabolic pathways. For example, upon the ingestion of either phenylalanine or tyrosine, individuals with the largely harmless inherited condition known as **alcaptonuria,** but not normal subjects, excrete **homogentisic acid** in their urine (Box 21-2). This is because the liver of alcaptonurics lacks an enzyme that catalyzes the breakdown of homogentisic acid (Fig. 14-16).

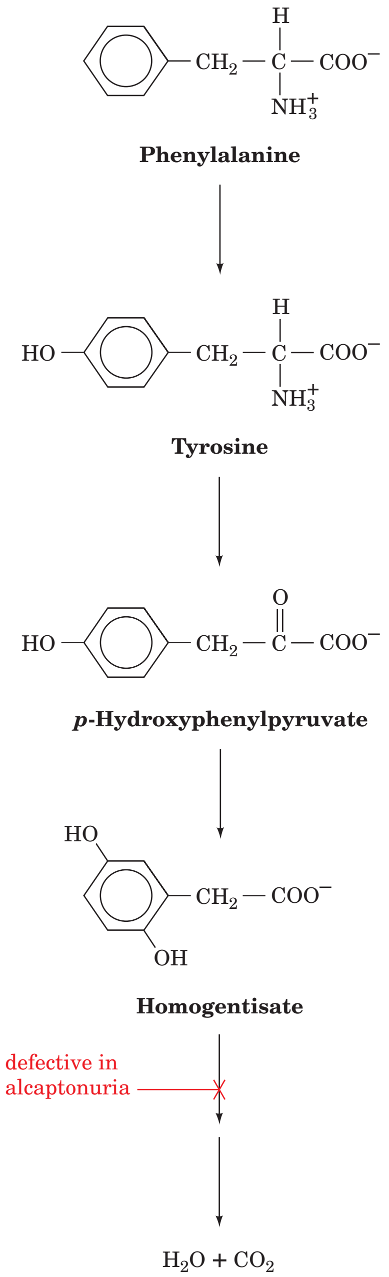

Figure 14-16 | Pathway for phenylalanine degradation. Alcaptonurics lack the enzyme that breaks down homogentisate; therefore, this intermediate accumulates and is excreted in the urine.

Genetic Manipulation Alters Metabolic Processes. Early studies of metabolism led to the astounding discovery that *the basic metabolic pathways in most organisms are essentially identical*. This metabolic uniformity has greatly facilitated the study of metabolic reactions. Thus, although a mutation that inactivates or deletes an enzyme in a pathway of interest may be unknown in higher organisms, it can be readily generated in a rapidly reproducing microorganism through the use of **mutagens** (chemical agents that induce genetic changes; Section 25-4A), X-rays, or, more recently, through genetic engineering techniques (Section 3-5). The desired mutants, which cannot synthesize the pathway's end product, can be identified by their requirement for that product in their culture medium.

Higher organisms that have been engineered to lack particular genes (i.e., gene "knockouts"; Section 3-5D) are useful, particularly in cases in which the absence of a single gene product results in a metabolic defect but is not lethal. Genetic engineering techniques have advanced to the point that it is possible to selectively "knock out" a gene only in a particular tissue. This approach is necessary in cases in which a gene product is required for development and therefore cannot be entirely deleted. In the opposite approach, techniques for constructing transgenic animals make it possible to express genes in tissues in which they were not originally present.

C | Systems Biology Has Entered the Study of Metabolism

Metabolism has traditionally been studied by hypothesis-driven research: isolating individual enzymes and metabolites and assembling them into metabolic pathways as guided by experimentally testable hypotheses. A new approach, **systems biology,** has emerged with the advent of complete

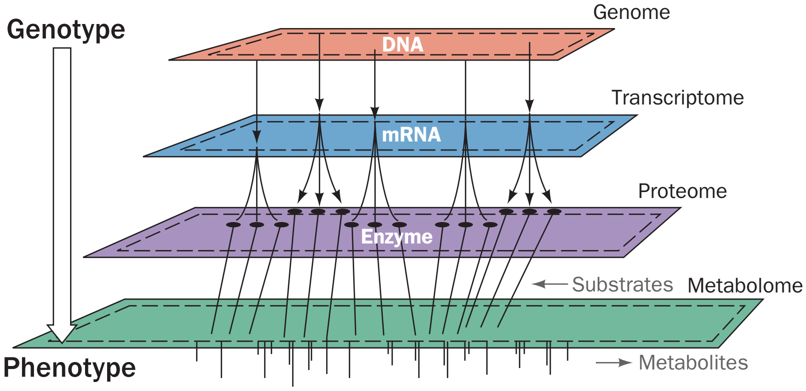

■ **Figure 14-17 | The relationship between genotype and phenotype.** The path from genetic information (genotype) to metabolic function (phenotype) has several steps. Portions of the genome are transcribed to produce the transcriptome, which directs the synthesis of the proteome, whose various activities are responsible for synthesizing and degrading the components of the metabolome.

genome sequences, the development of rapid and sensitive techniques for analyzing large numbers of gene transcripts, proteins, and metabolites all at once, and the development of new computational and mathematical tools. Systems biology is discovery-based: collecting and integrating enormous amounts of data in searchable databases so that the properties and dynamics of entire biological networks can be analyzed. As a result, our understanding of the path from genotype to phenotype has expanded. In addition to the central dogma (Section 3-3B) that a single gene composed of DNA is transcribed to mRNA which is translated to a single protein that influences metabolism, we are increasingly taking into account the **genome, transcriptome, proteome,** and **metabolome** and their interrelationships (Fig. 14-17). The term **bibliome** (Greek: *biblion,* book) has even been coined to denote the systematic incorporation of pre-existing information about reaction mechanisms and metabolic pathways (such as the one shown in Box 14-2). In the following paragraphs we discuss some of these emerging technologies and new fields of study.

Genomics Examines the Entire Complement of an Organism's DNA Sequences. The overall metabolic capabilities of an organism are encoded by its genome (its entire complement of genes). In theory, it should be possible to reconstruct a cell's metabolic activities from its DNA sequences. At present, this can be done only in a general sense. For example, the sequenced genome of *Vibrio cholerae,* the bacterium that causes cholera, reveals a large repertoire of genes encoding transport proteins and enzymes for catabolizing a wide range of nutrients. This is consistent with the complicated lifestyle of *V. cholerae,* which can live on its own, in association with zooplankton, or in the human gastrointestinal tract (where it causes cholera). Of course, a simple catalog of an organism's genes does not reveal how the genes function. Thus, some genes are expressed continuously at high levels, whereas others are expressed rarely, for example, only when the organism encounters a particular metabolite.

The Transcriptome Includes All the RNAs Transcribed by a Cell. Creating an accurate picture of gene expression is the goal of **transcriptomics,** the study of a cell's transcriptome (which, in analogy with the word "genome," is the entire collection of RNAs that the cell transcribes). Identifying and quantifying all the transcripts from a single cell type reveals which genes are active. Cells transcribe thousands of genes at once so this study requires the use of new techniques, including DNA microarray technology.

DNA Microarrays Help Create an Accurate Picture of Gene Expression. **DNA microarrays** or **DNA chips** are made by depositing numerous (up to several hundred thousand) different DNA segments of known gene sequences in a precise array on a solid support such as a coated glass surface. These DNAs are often PCR-amplified cDNA clones derived from mRNAs (PCR is discussed in Section 3-5C) or their robotically synthesized counterparts. The mRNAs extracted from cells, tissues, or other biological sources grown under differing conditions are then reverse-transcribed to cDNA, labeled with a fluorescent dye (a different color for each growth condition), and allowed to hybridize with the DNAs on the DNA microarray. After the unhybridized cDNA is washed away, the resulting fluorescence intensity and color at each site on the DNA microarray indicates how much cDNA (and therefore how much mRNA) has bound to a particular complementary DNA sequence for each growth condition. Figure 14-18 shows a DNA chip that demonstrates the change in yeast gene expression when yeast grown on glucose have depleted their glucose supply.

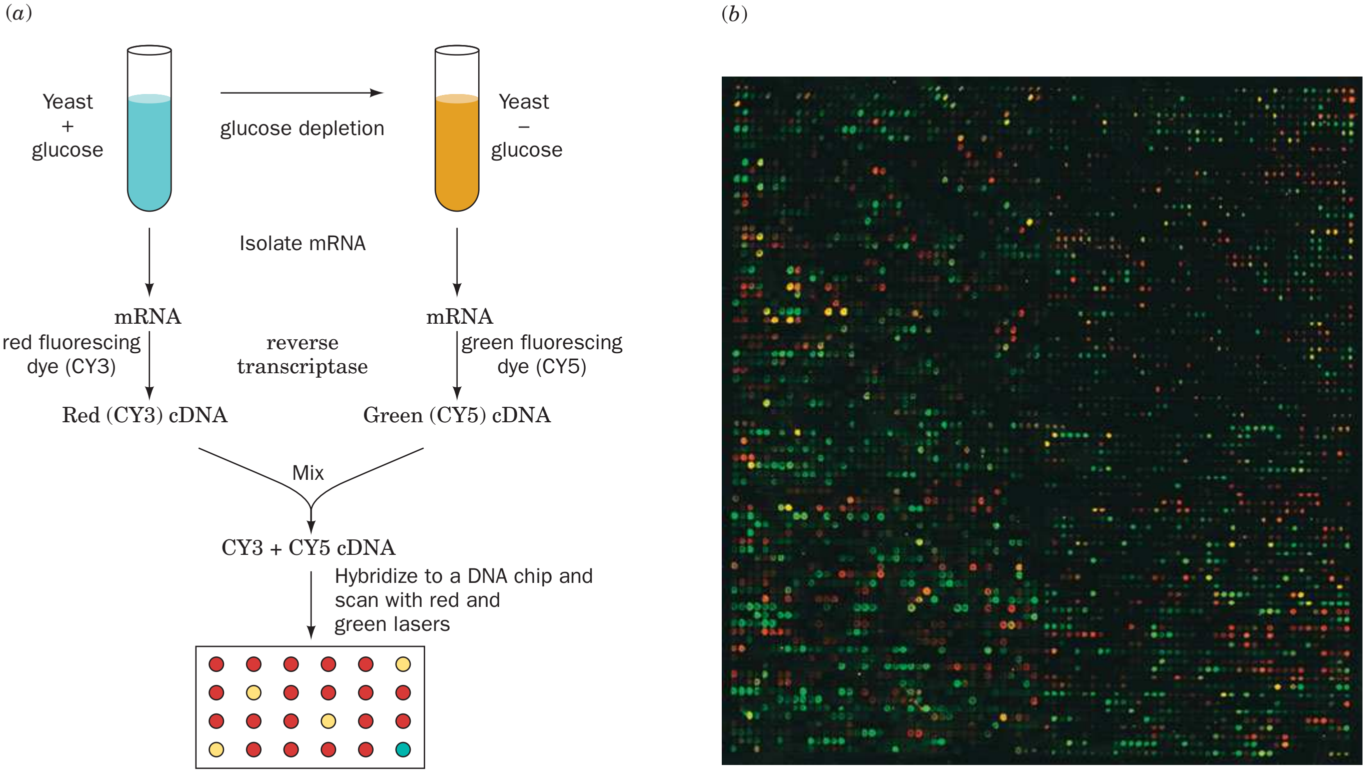

■ **Figure 14-18 | DNA chips.** (*a*) Schematic diagram indicating how DNA chips are used. (*b*) This ~6000-gene array contains most of the genes from baker's yeast, one per spot. The chip had been hybridized to the cDNAs derived from mRNAs extracted from yeast. The cDNAs derived from cells that were grown in glucose were labeled with a red-fluorescing dye, whereas the cDNAs derived from cells harvested after glucose depletion were labeled with a green-fluorescing dye. The cDNAs were mixed before hybridization. The red and green spots, respectively, reveal those genes that are transcriptionally activated by the presence or absence of glucose, whereas the yellow spots (*red plus green*) indicate genes whose expression is unaffected by the level of glucose. [Courtesy of Patrick Brown, Stanford University School of Medicine.]

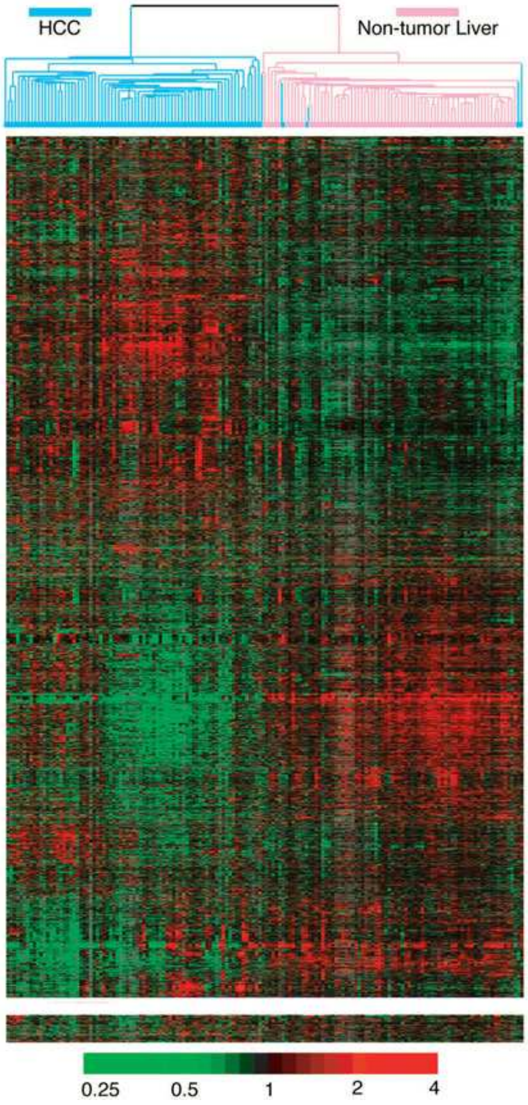

Figure 14-19 | The relative transcriptional activities of the genes in hepatocellular carcinoma (HCC) tumors as determined using DNA microarrays. The data are presented in matrix form with each column representing one of 156 tissue samples [82 HCC tumors (the most common human liver cancer and among the five leading causes of cancer deaths in the world) and 74 nontumor liver tissues] and each row representing one of 3180 genes (those of the ~17,400 genes on the DNA microarray with the greatest variation in transcriptional activity among the various tissue samples). The data are arranged so as to group the genes as well as the tissue samples on the basis of similarities of their expression patterns. The color of each cell indicates the expression level of the corresponding gene in the corresponding tissue relative to its mean expression level in all the tissue samples with bright red, black, and bright green indicating expression levels of 4, 1, and 1/4 times that of the mean for that gene (as indicated on the scale below). The dendrogram at the top of the matrix indicates the similarities in expression patterns among the various tissue samples. [Courtesy of David Botstein and Patrick Brown, Stanford University School of Medicine.]

Differences in the expression of particular genes have been correlated with many developmental processes or growth patterns. For example, DNA microarrays have been used to profile the patterns of gene expression in tumor cells because different types of tumors synthesize different types and amounts of proteins (Fig. 14-19). This information is useful in choosing how best to treat a cancer.

Proteomics Studies All the Cell's Proteins. Unfortunately, the correlation between the amount of a particular mRNA and the amount of its protein product is imperfect. This is because the various mRNAs and their corresponding proteins are synthesized and degraded at different rates. Furthermore, many proteins are posttranslationally modified, sometimes in several different ways (e.g., by phosphorylation or glycosylation). Consequently, the number of unique proteins in a cell exceeds the number of unique mRNAs.

A more reliable way than transcriptomics to assess gene expression is to examine a cell's proteome, the complete set of proteins that the cell synthesizes. This **proteomics** approach requires that the proteins first be separated, usually by two-dimensional (2D) gel electrophoresis (a technique that separates proteins by isoelectric point in one direction and by mass in the perpendicular direction; Section 5-2D). Individual proteins are then identified by using tandem mass spectrometry to obtain amino acid sequence information (Section 5-3D) and correlating it with protein sequence databases. Because many peptides are generated from a single protein, the technique enables the redundant and unambiguous identification of that protein from the database. In this way we can catalogue all the proteins that are contained in a cell or tissue under a given set of conditions.

Can we compare all the proteins synthesized by a cell under two different sets of conditions as is done for mRNA? The answer is yes, by using different isotopically labeled reagents that are either contained in the growth medium (e.g., deuterated amino acids) or that are reacted with the cell extract. One technique for labeling cellular proteins uses **isotope-coded affinity tags (ICAT),** which are analogous to the different fluorescent dyes that label cDNA.

An ICAT contains three functional elements: an iodoacetyl group to react with cysteine residues, a linker that contains either 8 hydrogen (light) or 8 deuterium (heavy) atoms, and **biotin,** a coenzyme (Section 16-4A)

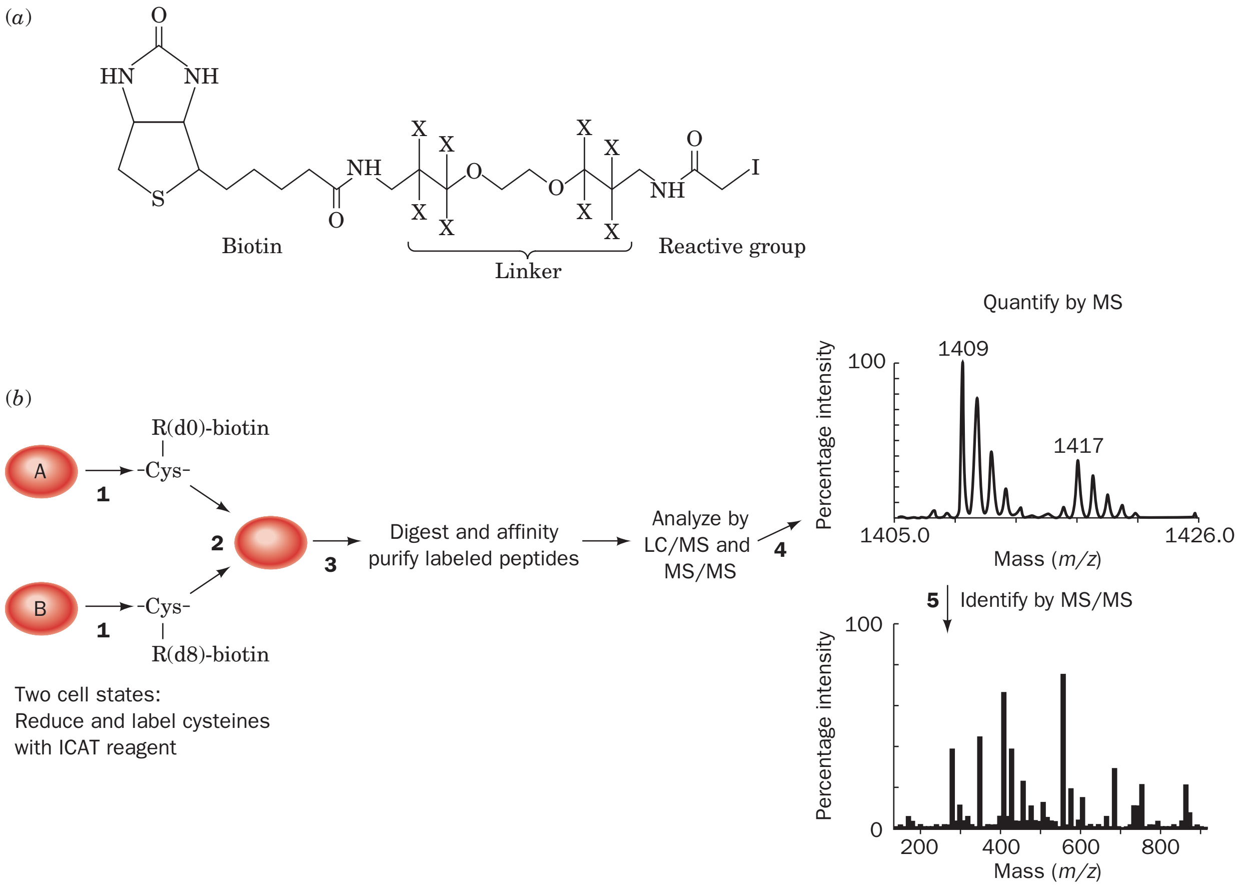
(a)
O
HN
NH
S
O
NH
X
X
X
X
O
O
X
X
X
X
O
NH
I
Biotin
Linker
Reactive group
(b)
R(d0)-biotin
A
-Cys-
1
2
3
Digest and affinity purify labeled peptides
Analyze by LC/MS and MS/MS
4
B
-Cys-
1
R(d8)-biotin
Two cell states: Reduce and label cysteines with ICAT reagent
Quantify by MS
Percentage intensity
100
1409
1417
1405.0
1426.0
Mass (m/z)
5
Identify by MS/MS
Percentage intensity
100
0
200
400
600
800
Mass (m/z)

Figure 14-20 | The isotope-coded affinity tag (ICAT) method for quantitative proteome analysis. (*a*) An example of an ICAT reagent that contains an iodoacetyl reactive group, a linker, and a biotin residue. X denotes the position of hydrogen (d0) or deuterium (d8). (*b*) The ICAT strategy for differential labeling of proteins expressed by cells under two different sets of conditions. (**1**) Proteins from States A and B are treated with light (d0) or heavy (d8) versions of the ICAT reagent. (**2**) The labeled protein mixtures are combined. (**3**) The labeled proteins are digested with trypsin to form Cys-containing labeled peptides. These peptides are then purified by biotin/avidin affinity chromatography. The purified peptides are analyzed by mass spectrometry in two ways: (**4**) Liquid chromatography followed by mass spectrometry (LC/MS) is used to quantitate the peptides. The ratio of the signal intensities from the corresponding light and heavy peptides indicates the relative peptide abundance in the two mixtures. (**5**) Tandem mass spectrometry (MS/MS) is used to determine the amino acid sequence of each peptide and identify the protein from which it is derived by comparing the peptide's sequence to those in a database of all known proteins.

that is also used as a biotechnology tool because of its extremely tight binding to the protein **avidin** ($K = 10^{-15}$ M; Fig. 14-20*a*). Avidin is immobilized on a chromatographic resin so that the ICAT-labeled peptides can be isolated by biotin/avidin affinity chromatography (Section 5-2C).

The ICAT procedure is illustrated in Fig. 14-20*b*. Two protein mixtures representing two different growth conditions are treated with light (d0) or heavy (d8) versions of the ICAT reagent. The labeled protein mixtures are then combined and digested with trypsin to form Cys-containing labeled peptides, which are then purified by biotin/avidin affinity chromatography. Individual peptides are separated by liquid chromatography and detected by mass spectrometry (LC/MS). The ratio of the intensities of the light and heavy peptide signals indicates the relative peptide abundance in the two samples. Tandem mass spectrometry (MS/MS) is then used to sequence each peptide and determine its identity. This method was used to identify many of the yeast proteins whose mRNA concentrations increased or decreased when glucose was depleted from the growth medium (Fig. 14-18*b*). A hope for the future is that samples from diseased and normal subjects can be compared in this manner to find previously undetected disease markers that would allow early diagnosis of various diseases.

Metabolomics Analyzes All of a Cell's Metabolites. In order to describe a cell's functional state (its phenotype) we need, in addition to the cell's genome, transcriptome, and proteome, a quantitative description of all of the metabolites it contains under a given set of conditions, its metabolome. However, a cell or tissue contains thousands of metabolites with vastly different properties, so that identifying and quantifying all these substances is a daunting task, requiring many different analytical tools. Consequently, this huge undertaking is often subdivided. For example, **lipidomics** is the subsection of **metabolomics** aimed at characterizing all lipids in a cell under a particular set of conditions, including how these lipids influence membrane structure, cell signaling, gene expression, cell–cell interactions, and so on.

A recently constructed model of the human metabolome—based on 1496 protein-encoding genes (open reading frames or ORFs), 2004 proteins, 2766 metabolites, and 3311 metabolic and transport reactions—has been used to simulate 288 known metabolic functions in a variety of cell and tissue types. This ***in silico*** (computerized) model is expected to provide a framework for future advances in human systems biology.

CHECK YOUR UNDERSTANDING

How are isotopically labeled compounds used to study metabolism?

Describe how information about an organism's genome can be used to assess and manipulate its metabolic activities.

What is the difference between hypothesis-driven research and discovery-based research?

Describe the "central dogma" in the "-omics" era.

SUMMARY

1. The free energy released from catabolic oxidation reactions is used to drive endergonic anabolic reactions.
2. Nutrition is the intake and utilization of food to supply free energy and raw materials.
3. Heterotrophic organisms obtain their free energy from compounds synthesized by chemolithotrophic or photoautotrophic organisms.
4. Food contains proteins, carbohydrates, fats, water, vitamins, and minerals.
5. Metabolic pathways are sequences of enzyme-catalyzed reactions that occur in different cellular locations.
6. Near-equilibrium reactions are freely reversible, whereas reactions that function far from equilibrium serve as regulatory points and render metabolic pathways irreversible.
7. Flux through a metabolic pathway is controlled by regulating the activities of the enzymes that catalyze its rate-determining steps.
8. The free energy of the "high-energy" compound ATP is made available through cleavage of one or both of its phosphoanhydride bonds.
9. An exergonic reaction such as ATP or PP_i hydrolysis can be coupled to an endergonic reaction to make it more favorable.
10. Substrate-level phosphorylation is the synthesis of ATP from ADP by phosphoryl group transfer from another compound.
11. The common product of carbohydrate, lipid, and protein catabolism, acetyl-CoA, is a "high-energy" thioester.
12. The coenzymes NAD^+ and FAD are reversibly reduced during the oxidation of metabolites.
13. The Nernst equation relates the electromotive force of a redox reaction to the standard reduction potentials and concentrations of the electron donors and acceptors.
14. Electrons flow spontaneously from the reduced member of a redox couple with the more negative reduction potential to the oxidized member of a redox couple with the more positive reduction potential.
15. Studies of metabolic pathways determine the order of metabolic transformations, their enzymatic mechanisms, their regulation, and their relationships to metabolic processes in other tissues.
16. Metabolic pathways are studied using isotopic tracers, enzyme inhibitors, natural and engineered mutations, DNA microarrays, and proteomics techniques.
17. Systems biology endeavors to quantitatively describe the properties and dynamics of biological networks as a whole through the integration of genomic, transcriptomic, proteomic, and metabolomic information.

KEY TERMS

metabolism **448**
catabolism **448**
anabolism **448**
nutrition **449**
autotroph **449**
chemolithotroph **449**
photoautotroph **449**
heterotroph **449**
aerobic **449**
anaerobic **449**
macronutrient **449**
micronutrient **450**
vitamin **450**
mineral **450**
metabolite **451**
oxidation **453**
reduction **453**
isozyme **455**
near-equilibrium reaction **456**
flux **456**
substrate cycle **459**
"high-energy" intermediate **461**
orthophosphate cleavage **464**
pyrophosphate cleavage **464**
substrate-level phosphorylation **465**
oxidative phosphorylation **465**
photophosphorylation **465**
kinase **465**
phosphagen **466**
reducing agent **470**
oxidizing agent **470**
half-reaction **470**
redox couple **471**
conjugate redox pair **471**
electrochemical cell **471**
$\Delta\mathscr{E}$ **471**
$\mathscr{F}$ **471**
Nernst equation **471**
$\mathscr{E}^{\circ\prime}$ **472**
systems biology **477**
genomics **478**
transcriptomics **478**
DNA microarray **479**
proteomics **480**
metabolomics **482**
in silico **482**

PROBLEMS

1. Rank the following compounds in order of increasing oxidation state.

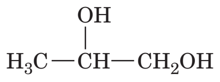
$H_3C{-}\overset{\overset{\displaystyle OH}{|}}{C}H{-}CH_2OH$

A

$^{-}OOC{-}CH_2{-}COO^{-}$

B

$H_3C{-}CH_2{-}CH_3$

C

$H_3C{-}CH{=}CH_2$

D

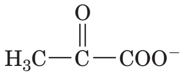
$H_3C{-}\overset{\overset{\displaystyle O}{\|}}{C}{-}COO^{-}$

E

2. A certain metabolic reaction takes the form A → B. Its standard free energy change is 7.5 kJ·mol^{-1}. (a) Calculate the equilibrium constant for the reaction at 25°C. (b) Calculate ΔG at 37°C when the concentration of A is 0.5 mM and the concentration of B is 0.1 mM. Is the reaction spontaneous under these conditions? (c) How might the reaction proceed in the cell?

3. Choose the best definition for a near-equilibrium reaction:
   (a) always operates with a favorable free energy change.
   (b) has a free energy change near zero.
   (c) is usually a control point in a metabolic pathway.
   (d) operates very slowly *in vivo*.

4. Assuming 100% efficiency of energy conservation, how many moles of ATP can be synthesized under standard conditions by the complete oxidation of (a) 1 mol of glucose and (b) 1 mol of palmitate?

5. Does the magnitude of the free energy change for ATP hydrolysis increase or decrease as the pH increases from 5 to 6?

6. The reaction for "activation" of a fatty acid ($RCOO^-$),

$$\text{ATP} + \text{CoA} + \text{RCOO}^- \rightleftharpoons \text{RCO—CoA} + \text{AMP} + \text{PP}_i$$

has $\Delta G^{\circ\prime} = +4.6\ \text{kJ}\cdot\text{mol}^{-1}$. What is the thermodynamic driving force for this reaction?

7. Predict whether creatine kinase will operate in the direction of ATP synthesis or phosphocreatine synthesis at 25°C when [ATP] = 4 mM, [ADP] = 0.15 mM, [phosphocreatine] = 2.5 mM, and [creatine] = 1 mM.

8. If intracellular [ATP] = 5 mM, [ADP] = 0.5 mM, and [P$_i$] = 1.0 mM, calculate the concentration of AMP at pH 7 and 25°C under the condition that the adenylate kinase reaction is at equilibrium.

9. List the following substances in order of their increasing oxidizing power: (a) acetoacetate, (b) cytochrome *b* (Fe^{3+}), (c) NAD^+, (d) SO_4^{2-}, and (e) pyruvate.

10. Write a balanced equation for the oxidation of ubiquinol by cytochrome *c*. Calculate $\Delta G^{\circ\prime}$ and $\Delta\mathscr{E}^{\circ\prime}$ for the reaction.

11. Under standard conditions, will the following reactions proceed spontaneously as written?
    (a) $\text{Fumarate} + \text{NADH} + \text{H}^+ \rightleftharpoons \text{succinate} + \text{NAD}^+$
    (b) $\text{Cyto } a\ (\text{Fe}^{2+}) + \text{cyto } b\ (\text{Fe}^{3+}) \rightleftharpoons \text{cyto } a\ (\text{Fe}^{3+}) + \text{cyto } b\ (\text{Fe}^{2+})$

12. Under standard conditions, is the oxidation of free $FADH_2$ by ubiquinone sufficiently exergonic to drive the synthesis of ATP?

13. A hypothetical three-step metabolic pathway consists of intermediates W, X, Y, and Z and enzymes A, B, and C. Deduce the order of the enzymatic steps in the pathway from the following information:
    1. Compound Q, a metabolic inhibitor of enzyme B, causes Z to build up.
    2. A mutant in enzyme C requires Y for growth.
    3. An inhibitor of enzyme A causes W, Y, and Z to accumulate.
    4. Compound P, a metabolic inhibitor of enzyme C, causes W and Z to build up.

14. A certain metabolic pathway can be diagrammed as

$$\mathrm{A} \xrightarrow{\mathrm{X}} \mathrm{B} \xrightarrow{\mathrm{Y}} \mathrm{C} \xrightarrow{\mathrm{Z}} \mathrm{D}$$

where A, B, C, and D are the intermediates, and X, Y, and Z are the enzymes that catalyze the reactions. The physiological free energy changes for the reactions are

X	$-0.2\ \mathrm{kJ \cdot mol^{-1}}$
Y	$-12.3\ \mathrm{kJ \cdot mol^{-1}}$
Z	$-1.2\ \mathrm{kJ \cdot mol^{-1}}$

(a) Which reaction is likely to be a major regulatory point for the pathway? (b) If your answer in Part a was in fact the case, in the presence of an inhibitor that blocks the activity of enzyme Z, would the concentrations of A, B, C, and D increase, decrease, or not be affected?

CASE STUDY

Case 16

Allosteric Regulation of ATCase

Focus concept: An enzyme involved in nucleotide synthesis is subject to regulation by a variety of combinations of nucleotides.

Prerequisites: Chapters 7, 12, and 14

- Properties of allosteric enzymes
- Basic mechanisms involving regulation of metabolic pathways

BIOINFORMATICS EXERCISES

Bioinformatics Exercises are available at www.wiley.com/college/voet.

Chapter 14

Metabolic Enzymes, Microarrays, and Proteomics

1. **Metabolic Enzymes.** Use the KEGG and Enzyme Structure databases to obtain information about dihydrofolate reductase.
2. **Microarrays.** Learn about microarray technology and its use in studying disease.
3. **Proteomics.** Review some methods and their limitations.
4. **Two-Dimensional Gel Electrophoresis.** Obtain data about dihydrofolate reductase from the Swiss-2DPAGE resource.

REFERENCES

Aebersold, R., Quantitative proteome analysis: Methods and applications, *J. Infectious Diseases*, **182** (supplement 2), S315–S320 (2003).

Alberty, R.A., Calculating apparent equilibrium constants of enzyme-catalyzed reactions at pH 7, *Biochem. Ed*. **28,** 12–17 (2000).

Campbell, A.M. and Heyer, L.J., *Discovering Genomics, Proteomics and Bioinformatics*. 2nd Ed., Pearson Benjamin Cummings, New York (2007). [An interactive introduction to these subjects.]

Duarte, N.C., Becker, S.A., Jamshidi, N., Thiele, I., Mo, M.L., Vo, T.D., Srivas, R., and Palsson, B. Ø., Global reconstruction of the human metabolic network based on genomic and bibliomic data, *Proc. Natl. Acad. Sci*, **104,** 1777–1782 (2007).

Go, V.L.W., Nguyen, C.T.H., Harris, D.M., and Lee, W.-N.P., Nutrient–gene interaction: Metabolic genotype–phenotype relationship, *J. Nutrition*, **135,** 2016s–3020s (2005).

Hanson, R.W., The role of ATP in metabolism, *Biochem. Ed*. **17,** 86–92 (1989). [Provides an excellent explanation of why ATP is an energy transducer rather than an energy store.]

Schena, M., *Microarray Analysis,* Wiley-Liss (2003).

Schulman, R.G. and Rothman, D.L., ^{13}C NMR of intermediary metabolism: Implications for systematic physiology, *Annu. Rev. Physiol*. **63,** 15–48 (2001).

Scriver, C.R., Beaudet, A.L., Sly, W.S., and Valle, D., (Eds.), *The Metabolic and Molecular Bases of Inherited Disease* (8th ed.), McGraw-Hill (2001). [Most chapters in this encyclopedic work include a review of a normal metabolic process that is disrupted by disease.]

Smolin, L.A. and Grosvenor, M.B, *Nutrition: Science and Applications*, Wiley (2008). [A good text for those interested in pursuing nutritional aspects of metabolism].

Westheimer, F.H., Why nature chose phosphates, *Science* **235,** 1173–1178 (1987).

Young, R., Biomedical discovery with DNA arrays, *Cell* **102,** 9–15 (2000).

Xia, Y., Yu, H., Jansen, R., Seringhaus, M., Baxter, S., Greenbaum, D., Zhao, H., and Gerstein, M., Analyzing cellular biochemistry in terms of molecular networks, *Annu. Rev. Biochem.* **73,** 1051–1087 (2004).

15

Glucose Catabolism

308
107
1
3
72

During a short race, for example, of 100 to 200 m, a major source of power for a runner's muscles is the free energy produced through anaerobic glycolysis, a catabolic pathway that breaks down carbohydrates and produces ATP but does not depend on the presence of oxygen. Even under aerobic conditions, glycolysis is the major starting point for carbohydrate metabolism. [AFLO Foto/Alamy Images.]

CHAPTER CONTENTS

1 Overview of Glycolysis
2 The Reactions of Glycolysis
  A. Hexokinase Uses the First ATP
  B. Phosphoglucose Isomerase Converts Glucose-6-Phosphate to Fructose-6-Phosphate
  C. Phosphofructokinase Uses the Second ATP
  D. Aldolase Converts a 6-Carbon Compound to Two 3-Carbon Compounds
  E. Triose Phosphate Isomerase Interconverts Dihydroxyacetone Phosphate and Glyceraldehyde-3-Phosphate
  F. Glyceraldehyde-3-Phosphate Dehydrogenase Forms the First "High-Energy" Intermediate
  G. Phosphoglycerate Kinase Generates the First ATP
  H. Phosphoglycerate Mutase Interconverts 3-Phosphoglycerate and 2-Phosphoglycerate
  I. Enolase Forms the Second "High-Energy" Intermediate
  J. Pyruvate Kinase Generates the Second ATP
3 Fermentation: The Anaerobic Fate of Pyruvate
  A. Homolactic Fermentation Converts Pyruvate to Lactate
  B. Alcoholic Fermentation Converts Pyruvate to Ethanol and CO_2
  C. Fermentation Is Energetically Favorable
4 Regulation of Glycolysis
  A. Phosphofructokinase Is the Major Flux-Controlling Enzyme of Glycolysis in Muscle
  B. Substrate Cycling Fine-Tunes Flux Control
5 Metabolism of Hexoses Other than Glucose
  A. Fructose Is Converted to Fructose-6-Phosphate or Glyceraldehyde-3-Phosphate
  B. Galactose Is Converted to Glucose-6-Phosphate
  C. Mannose Is Converted to Fructose-6-Phosphate
6 The Pentose Phosphate Pathway
  A. Oxidative Reactions Produce NADPH in Stage 1
  B. Isomerization and Epimerization of Ribulose-5-Phosphate Occur in Stage 2
  C. Stage 3 Involves Carbon–Carbon Bond Cleavage and Formation
  D. The Pentose Phosphate Pathway Must Be Regulated

MEDIA RESOURCES

(available at www.wiley.com/college/voet)
Guided Exploration 14. Glycolysis overview
Interactive Exercise 15. Conformational changes in yeast hexokinase
Interactive Exercise 16. Yeast TIM in complex with 2-phosphoglycolate
Interactive Exercise 17. TPP binding to pyruvate decarboxylase
Animated Figure 15-1. Overview of glycolysis
Animated Figure 15-5. Mechanism of aldolase
Animated Figure 15-9. Mechanism of GAPDH
Animated Figure 15-23. PFK activity versus F6P concentration
Kinemages 12-1, 12-2. Triose phosphate isomerase
Kinemage 13-1. Phosphofructokinase
Kinemage 13-2. Allosteric changes in phosphofructokinase
Case Study 18. Purification of Phosphofructokinase 1-C
Case Study 20. NAD^+-Dependent Glyceraldehyde-3-Phosphate Dehydrogenase from *Thermoproteus tenax*

Glucose is a major source of metabolic energy in many cells. The fermentation (anaerobic breakdown) of glucose to ethanol and CO_2 by yeast has been exploited for many centuries in baking and winemaking. However, scientific investigation of the chemistry of this catabolic pathway began only in the mid-nineteenth century, with the experiments of Louis Pasteur and others. Nearly a century would pass before the complete pathway was elucidated. During that interval, several important features of the pathway came to light:

1. In 1905, Arthur Harden and William Young discovered that phosphate is required for glucose fermentation.
2. Certain reagents, such as iodoacetic acid and fluoride ion, inhibit the formation of pathway products, thereby causing pathway intermediates to accumulate. Different substances caused the buildup of different intermediates and thereby revealed the sequence of molecular interconversions.

3. Studies of how different organisms break down glucose indicated that, with few exceptions, all of them do so the same way.

The efforts of many investigators came to fruition in 1940, when the complete pathway of glucose breakdown was described. This pathway, which is named **glycolysis** (Greek: *glykus,* sweet + *lysis,* loosening), is alternately known as the **Embden–Meyerhof–Parnas pathway** to commemorate the work of Gustav Embden, Otto Meyerhof, and Jacob Parnas in its elucidation. The discovery of glycolysis came at a time when other significant inroads were being made in the area of metabolism (Box 15-1).

Glycolysis, which is probably the most completely understood biochemical pathway, is a sequence of 10 enzymatic reactions in which one molecule of glucose is converted to two molecules of the three-carbon compound pyruvate with the concomitant generation of 2 ATP. It plays a key role in energy metabolism by providing a significant portion of the free energy used by most organisms and by preparing glucose and other compounds for further oxidative degradation. Thus, it is fitting that we begin our discussion of specific metabolic pathways by considering glycolysis. We shall examine the sequence of reactions by which glucose is degraded, along with some of the relevant enzyme mechanisms. We will then examine the features that influence glycolytic flux and the ultimate fate of its products. Finally, we will discuss the catabolism of other hexoses and the **pentose phosphate pathway,** an alternative pathway for glucose catabolism that functions to provide biosynthetic precursors.

1 Overview of Glycolysis

LEARNING OBJECTIVES

- Understand that glycolysis involves the breakdown of glucose to pyruvate while using the free energy released in the process to synthesize ATP from ADP and P_i.
- Understand that the 10-reaction sequence of glycolysis is divided into two stages: energy investment and energy recovery.

Before beginning our detailed discussion of glycolysis, let us first take a moment to survey the overall pathway as it fits in with animal metabolism as a whole. Glucose usually appears in the blood as a result of the breakdown of polysaccharides (e.g., liver glycogen or dietary starch and glycogen) or from its synthesis from noncarbohydrate precursors (**gluconeogenesis;** Section 16-4). Glucose enters most cells by a specific carrier that transports it from the exterior of the cell into the cytosol (Section 10-2E). The enzymes of glycolysis are located in the cytosol, where they are only loosely associated, if at all, with each other or with other cell structures.

Glycolysis converts glucose to two C_3 units (pyruvate). The free energy released in the process is harvested to synthesize ATP from ADP and P_i. Thus, glycolysis is a pathway of chemically coupled phosphorylation reactions (Section 14-2B). The 10 reactions of glycolysis are diagrammed in Fig. 15-1. Note that ATP is used early in the pathway to synthesize phosphorylated compounds (Reactions 1 and 3) but is later resynthesized twice over (Reactions 7 and 10). Glycolysis can therefore be divided into two stages:

Stage I Energy investment (Reactions 1–5). In this preparatory stage, the hexose glucose is phosphorylated and cleaved to yield two molecules of the triose **glyceraldehyde-3-phosphate.** This process consumes 2 ATP.

Figure 15-1 | (*opposite*) **Glycolysis.** In its first stage (Reactions 1–5), one molecule of glucose is converted to two glyceraldehyde-3-phosphate molecules in a series of reactions that consumes 2 ATP. In the second stage of glycolysis (Reactions 6–10), the two glyceraldehyde-3-phosphate molecules are converted to two pyruvate molecules, generating 4 ATP and 2 NADH. **See the Animated Figures.**

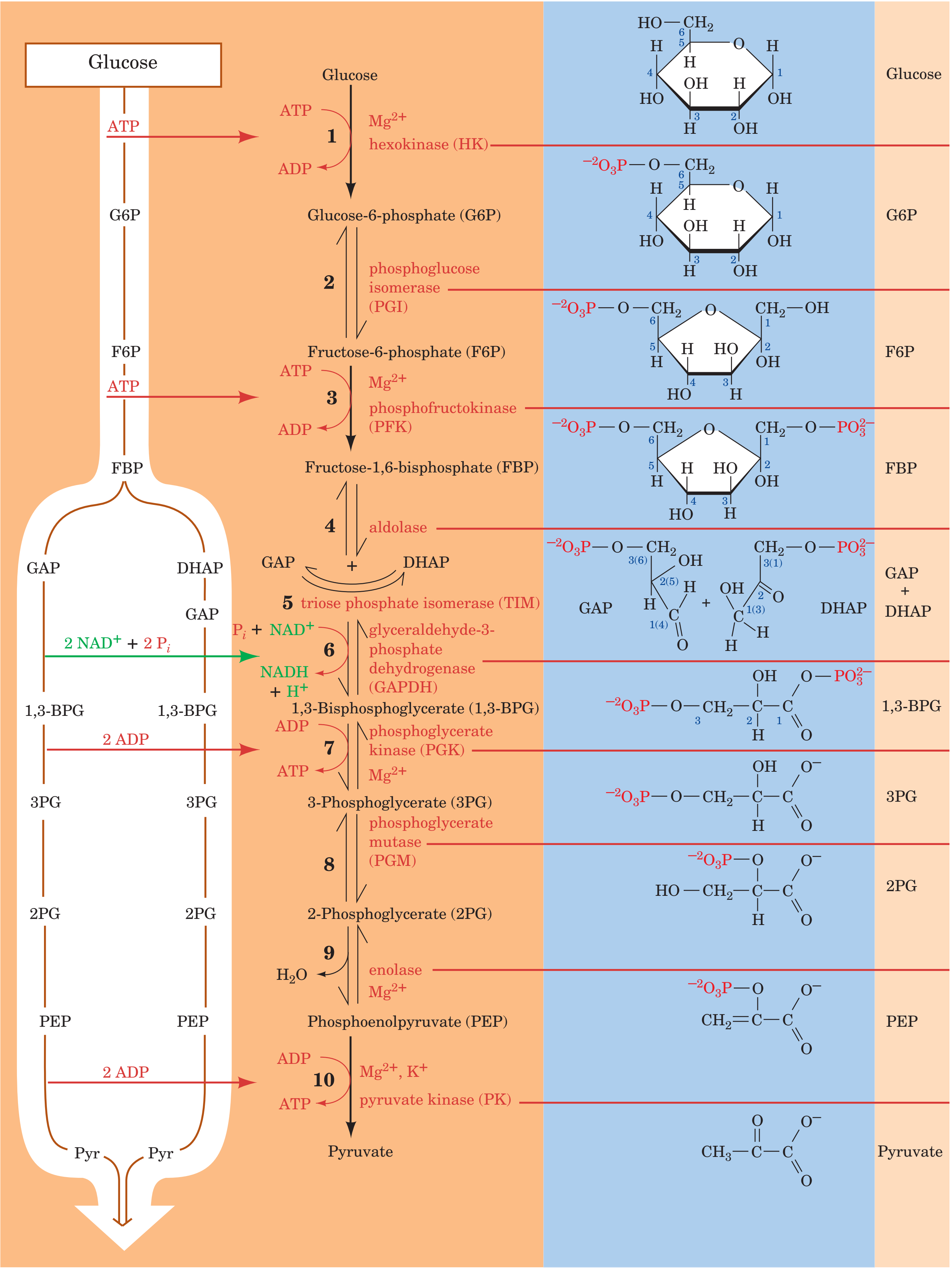
Glucose
ATP
G6P
F6P
ATP
FBP
GAP
DHAP
GAP
2 NAD⁺ + 2 Pᵢ
1,3-BPG
1,3-BPG
2 ADP
3PG
3PG
2PG
2PG
PEP
PEP
2 ADP
Pyr
Pyr
Glucose
ATP
1
Mg²⁺
hexokinase (HK)
ADP
Glucose-6-phosphate (G6P)
2
phosphoglucose isomerase (PGI)
Fructose-6-phosphate (F6P)
ATP
3
Mg²⁺
phosphofructokinase (PFK)
ADP
Fructose-1,6-bisphosphate (FBP)
4
aldolase
GAP
+
DHAP
5 triose phosphate isomerase (TIM)
Pᵢ + NAD⁺
6
glyceraldehyde-3-phosphate dehydrogenase (GAPDH)
NADH + H⁺
1,3-Bisphosphoglycerate (1,3-BPG)
ADP
7
phosphoglycerate kinase (PGK)
ATP
Mg²⁺
3-Phosphoglycerate (3PG)
8
phosphoglycerate mutase (PGM)
2-Phosphoglycerate (2PG)
9
H₂O
enolase
Mg²⁺
Phosphoenolpyruvate (PEP)
ADP
10
Mg²⁺, K⁺
pyruvate kinase (PK)
ATP
Pyruvate
GAP
DHAP
Glucose
G6P
F6P
FBP
GAP + DHAP
1,3-BPG
3PG
2PG
PEP
Pyruvate

BOX 15-1 **PATHWAYS OF DISCOVERY**

Otto Warburg and Studies of Metabolism

Otto Warburg (1883–1970)

One of the great figures in biochemistry—by virtue of his own contributions and his influence on younger researchers—is the German biochemist Otto Warburg. His long career spanned a period during which studies of whole organisms and crude extracts gave way to molecular explanations of biological structure and function. Like others of his generation, he earned a doctorate in chemistry at an early age and went on to obtain a medical degree, although he spent the remainder of his career in scientific research rather than in patient care. He became interested primarily in three subjects related to the chemistry of oxygen and carbon dioxide: respiration, photosynthesis, and cancer.

One of Warburg's first accomplishments was to develop a technique for studying metabolic reactions in thin slices of animal tissue. This method produced more reliable results than the alternative practice of chopping or mincing tissues (such manipulations tend to release lysosomal enzymes that degrade enzymes and other macromolecules). Warburg was also largely responsible for refining manometry, the measurement of gas pressure, as a technique for analyzing the consumption and production of O_2 and CO_2 by living tissues.

Warburg received a Nobel prize in 1931 for his discovery of the catalytic role of iron porphyrins (heme groups) in biological oxidation (the subject was the reaction carried out by the enzyme complex now known as cytochrome oxidase; Section 18-2F). Warburg also identified nicotinamide as an active part of some enzymes. In 1944, he was offered a second Nobel prize for his work with enzymes, but he was unable to accept the award, owing to Hitler's decree that Germans could not accept Nobel prizes. In fact, Warburg's apparent allegiance to the Nazi regime incensed some of his colleagues in other countries and may have contributed to their resistance to some of his more controversial scientific pronouncements. In any case, Warburg was not known for his warm personality. He was never a teacher and tended to recruit younger research assistants who were expected to move on after a few years.

In addition to the techniques he developed, which were widely adopted, and a number of insights into enzyme action, Warburg formulated some wide-reaching theories about the growth of cancer cells. He showed that cancer cells could live and develop even in the absence of oxygen. Moreover, he came to believe that anaerobiosis triggered the development of cancer, and he rejected the notion that viruses could cause cancer, a principle that had already been demonstrated in animals but not in humans. In the eyes of many, Warburg was guilty of equating the absence of evidence with the evidence of absence in the matter of virus-induced human cancer. Nevertheless, Warburg's observations of cancer cell metabolism, which is generally characterized by a high rate of glycolysis, were sound. Even today, the oddities of tumor metabolism offer opportunities for chemotherapy. Warburg's dedication to his research in cancer and other areas is revealed by the fact that he continued working in his laboratory until just a few days before his death at age 87.

Warburg, O., On the origin of cancer cells, *Science* **123,** 309–314 (1956).

Stage II Energy recovery (Reactions 6–10). The two molecules of glyceraldehyde-3-phosphate are converted to pyruvate, with concomitant generation of 4 ATP. Glycolysis therefore has a net "profit" of 2 ATP per glucose: Stage I consumes 2 ATP; Stage II produces 4 ATP.

The phosphoryl groups that are initially transferred from ATP to the hexose do not immediately result in "high-energy" compounds. However, subsequent enzymatic transformations convert these "low-energy" products to compounds with high phosphoryl group-transfer potentials, which are capable of phosphorylating ADP to form ATP. The overall reaction is

$$\text{Glucose} + 2\,\text{NAD}^+ + 2\,\text{ADP} + 2\,\text{P}_i \longrightarrow 2\,\text{pyruvate} + 2\,\text{NADH} + 2\,\text{ATP} + 2\,\text{H}_2\text{O} + 4\,\text{H}^+$$

Hence, the NADH formed in the process must be continually reoxidized to keep the pathway supplied with its primary oxidizing agent, NAD^+. In Section 15-3, we shall examine how organisms do so under aerobic or anaerobic conditions.

■ **CHECK YOUR UNDERSTANDING**

How many ATP are invested and how many are recovered from each molecule of glucose that follows the glycolytic pathway?

2 The Reactions of Glycolysis

See Guided Exploration 14
Glycolysis overview

LEARNING OBJECTIVES

- Understand the chemical logic and the types of reactions that act in sequence to convert glucose to pyruvate.
- Understand the catalytic mechanisms of the enzymes involved, and how amino acid side chains, coenzymes, and cofactors participate.
- Understand how chemical coupling of endergonic and exergonic reactions is used to generate ATP during glycolysis.

In this section, we examine the reactions of glycolysis more closely, describing the properties of the individual enzymes and their mechanisms. As we study the individual glycolytic enzymes, we shall encounter many of the catalytic mechanisms described in Section 11-3.

A | Hexokinase Uses the First ATP

Reaction 1 of glycolysis is the transfer of a phosphoryl group from ATP to glucose to form **glucose-6-phosphate (G6P)** in a reaction catalyzed by **hexokinase.**

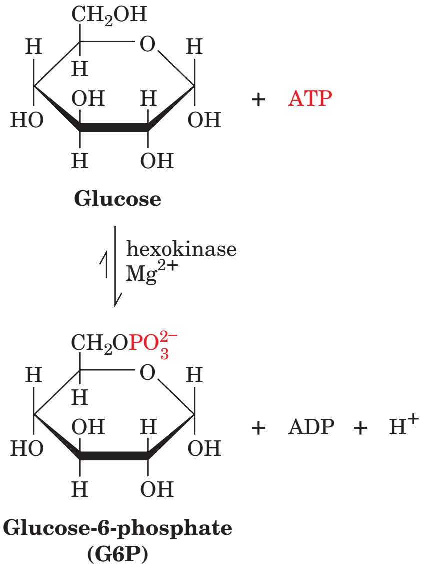

A kinase is an enzyme that transfers phosphoryl groups between ATP and a metabolite (Section 14-2C). The metabolite that serves as the phosphoryl group acceptor is indicated in the prefix of the kinase name. Hexokinase is a ubiquitous, relatively nonspecific enzyme that catalyzes the phosphorylation of hexoses such as D-glucose, D-mannose, and D-fructose. Liver cells also contain the isozyme **glucokinase,** which catalyzes the same reaction but which is primarily involved in maintaining blood glucose levels (Section 22-1D).

The second substrate for hexokinase, as for other kinases, is an Mg^{2+}–ATP complex. In fact, uncomplexed ATP is a potent competitive inhibitor of hexokinase. Although we do not always explicitly mention the participation of Mg^{2+}, it is essential for kinase activity. The Mg^{2+} shields the negative charges of the ATP's α- and β- or β- and γ-phosphate oxygen atoms, making the γ-phosphorus atom more accessible for nucleophilic attack by the C6-OH group of glucose:

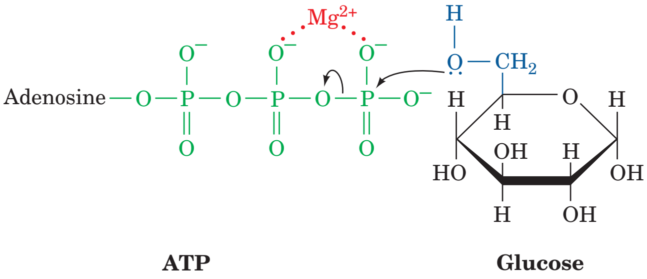

Comparison of the X-ray structures of yeast hexokinase and the glucose–hexokinase complex indicates that *glucose induces a large conformational change in hexokinase* (Fig. 15-2). The two lobes that form its active site cleft swing together by up to 8 Å so as to engulf the glucose in a manner that suggests the closing of jaws. *This movement places the ATP close to the —C6H_2OH group of glucose and excludes water from the active site (catalysis by proximity effects;* Section 11-3D). If the catalytic and reacting groups were in the proper position for reaction while the enzyme was in the open position (Fig. 15-2*a*), ATP hydrolysis (i.e., phosphoryl group transfer to water, which is thermodynamically favored; Fig. 14-6*a*) would almost certainly be the dominant reaction.

Clearly, the substrate-induced conformational change in hexokinase is responsible for the enzyme's specificity. In addition, the active site polarity is reduced by exclusion of water, thereby expediting the nucleophilic reaction process. Other kinases have the same deeply clefted structure as hexokinase and undergo conformational changes on binding their substrates (e.g., adenylate kinase; Fig. 14-9).

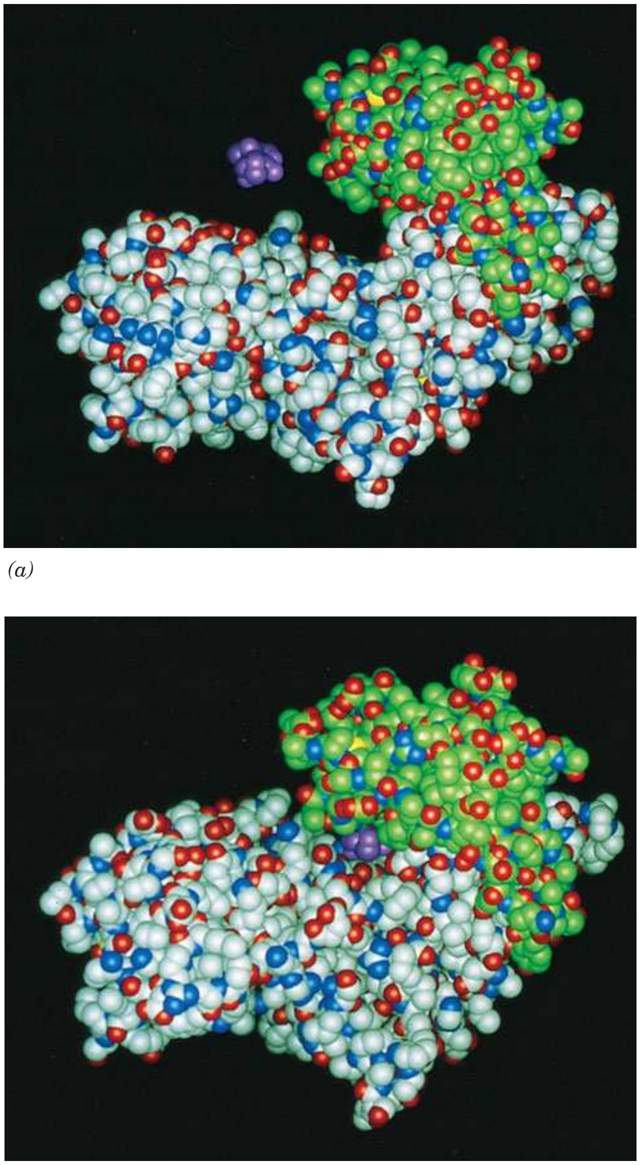
(*a*)

(*b*)

Figure 15-2 | Substrate-induced conformational changes in yeast hexokinase. (*a*) Space-filling model of a hexokinase subunit showing the prominent bilobal appearance of the free enzyme (the C atoms in the small lobe are shaded green, and those in the large lobe are light gray; the N and O atoms are blue and red). (*b*) Model of the hexokinase complex with glucose (*purple*). The lobes have swung together to engulf the substrate. [Based on X-ray structures by Thomas Steitz, Yale University. PDBids (*a*) 2YHX and (*b*) 1HKG.] **See Interactive Exercise 15.**

B | Phosphoglucose Isomerase Converts Glucose-6-Phosphate to Fructose-6-Phosphate

Reaction 2 of glycolysis is the conversion of G6P to **fructose-6-phosphate (F6P)** by **phosphoglucose isomerase (PGI).**

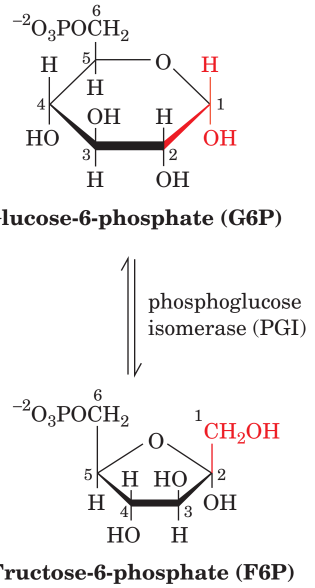

Glucose-6-phosphate (G6P)

Fructose-6-phosphate (F6P)

This is the isomerization of an aldose to a ketose.

Since G6P and F6P both exist predominantly in their cyclic forms, the reaction requires ring opening followed by isomerization and subsequent ring closure (the interconversions of cyclic and linear forms of hexoses are shown in Fig. 8-3).

A proposed reaction mechanism for the PGI reaction involves general acid–base catalysis by the enzyme (Fig. 15-3):

Step 1 The substrate binds.

Step 2 An enzymatic acid, probably the ε-amino group of a conserved Lys residue, catalyzes ring opening.

Step 3 A base, thought to be a conserved His residue, abstracts the

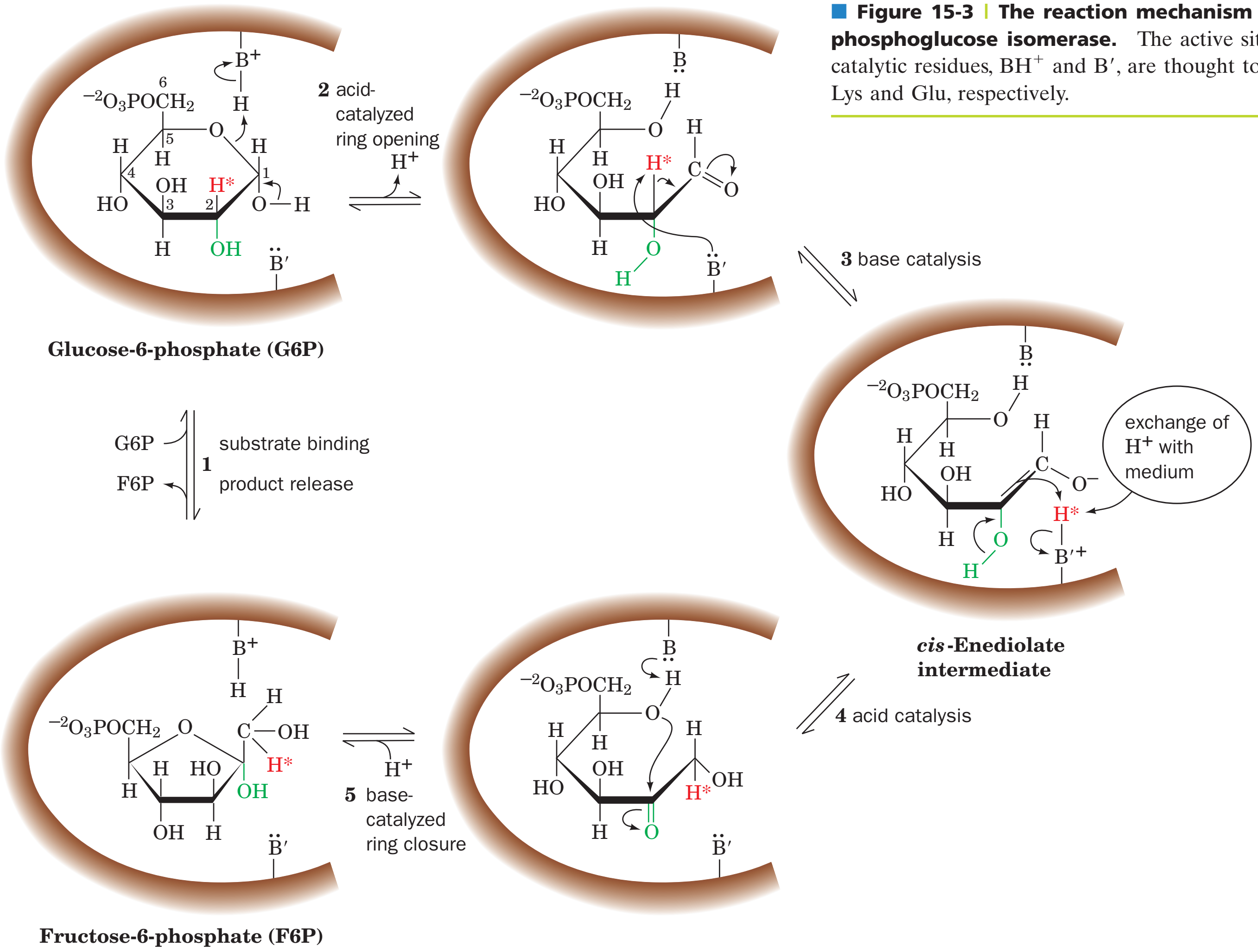
2 acid-catalyzed ring opening
H^+
3 base catalysis
exchange of H^+ with medium
4 acid catalysis
5 base-catalyzed ring closure
1 substrate binding
product release
G6P
F6P
Glucose-6-phosphate (G6P)
cis-Enediolate intermediate
Fructose-6-phosphate (F6P)
B^+
B
B′
B'^+
H*
$^{-2}O_3POCH_2$

Figure 15-3 | The reaction mechanism of phosphoglucose isomerase. The active site catalytic residues, BH^+ and B′, are thought to be Lys and Glu, respectively.

acidic proton from C2 to form a *cis*-enediolate intermediate (the proton is acidic because it is α to a carbonyl group).

Step 4 The proton is replaced on C1 in an overall proton transfer. Protons abstracted by bases rapidly exchange with solvent protons. Nevertheless, Irwin Rose confirmed this step by demonstrating that 2-[^{3}H]G6P is occasionally converted to 1-[^{3}H]F6P by intramolecular proton transfer before the ^{3}H has had a chance to exchange with the medium.

Step 5 The ring closes to form the product, which is subsequently released to yield free enzyme, thereby completing the catalytic cycle.

C | Phosphofructokinase Uses the Second ATP

In Reaction 3 of glycolysis, **phosphofructokinase (PFK)** phosphorylates F6P to yield **fructose-1,6-bisphosphate** (**FBP** or **F1,6P;** *at right*). (The product is a *bis*phosphate rather than a *di*phosphate because its two phosphate groups are not attached directly to each other.)

The PFK reaction is similar to the hexokinase reaction. The enzyme catalyzes the nucleophilic attack by the C1-OH group of F6P on the electrophilic γ-phosphorus atom of the Mg^{2+}–ATP complex.

Phosphofructokinase plays a central role in control of glycolysis because it catalyzes one of the pathway's rate-determining reactions. In many organisms, the

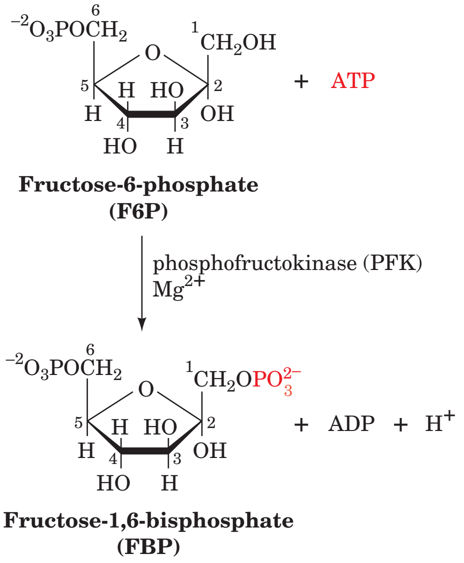
$^{-2}O_3POCH_2$
$^1CH_2OH$
+ ATP
Fructose-6-phosphate (F6P)
phosphofructokinase (PFK)
Mg^{2+}
$^1CH_2OPO_3^{2-}$
+ ADP + H^+
Fructose-1,6-bisphosphate (FBP)

activity of PFK is enhanced allosterically by several substances, including AMP, and inhibited allosterically by several other substances, including ATP and citrate. The regulatory properties of PFK are examined in Section 15-4A.

D | Aldolase Converts a 6-Carbon Compound to Two 3-Carbon Compounds

Aldolase catalyzes Reaction 4 of glycolysis, the cleavage of FBP to form the two trioses **glyceraldehyde-3-phosphate (GAP)** and **dihydroxyacetone phosphate (DHAP):**

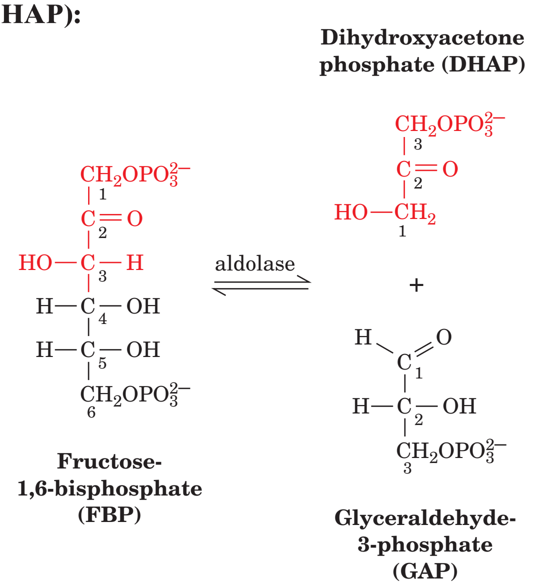
Dihydroxyacetone phosphate (DHAP)
$CH_2OPO_3^{2-}$
C=O
HO—CH₂
aldolase
+
H
O
C
H—C—OH
$CH_2OPO_3^{2-}$
HO—C—H
H—C—OH
H—C—OH
1
2
3
4
5
6
Fructose-1,6-bisphosphate (FBP)
Glyceraldehyde-3-phosphate (GAP)

Note that at this point in the pathway, the atom numbering system changes. Atoms 1, 2, and 3 of glucose become atoms 3, 2, and 1 of DHAP, thus reversing order. Atoms 4, 5, and 6 become atoms 1, 2, and 3 of GAP.

Reaction 4 is an **aldol cleavage (retro aldol condensation)** whose nonenzymatic base-catalyzed mechanism is shown in Fig. 15-4. The **enolate** intermediate is stabilized by resonance, as a result of the electron-withdrawing character of the carbonyl oxygen atom. Note that aldol cleavage between C3 and C4 of FBP requires a carbonyl at C2 and a hydroxyl at C4. Hence, the "logic" of Reaction 2 in the glycolytic pathway, the isomerization of G6P to F6P, is clear. Aldol cleavage of G6P would yield products of unequal carbon chain length, while *aldol cleavage of FBP results in two interconvertible C_3 compounds that can therefore enter a common degradative pathway.*

Aldol cleavage is catalyzed by stabilizing its enolate intermediate through increased electron delocalization. In animals and plants, the reaction occurs as follows (Fig. 15-5):

Step 1 Substrate binding.

Step 2 Reaction of the FBP carbonyl group with the ε-amino group of

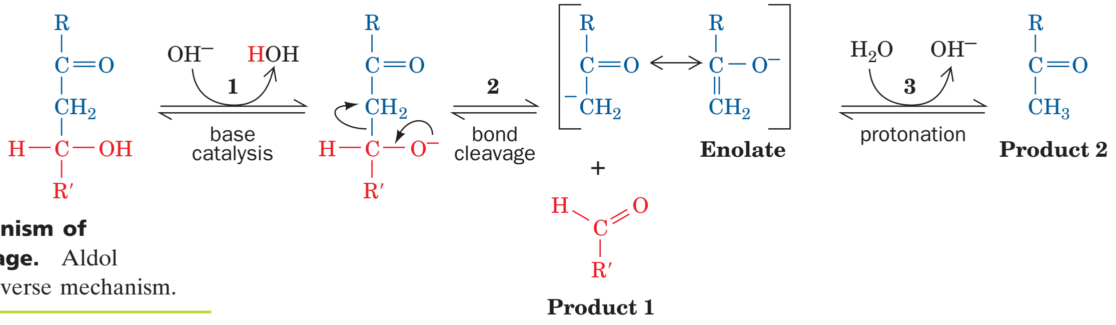
R
C=O
CH₂
H—C—OH
R′
OH⁻
HOH
1
base catalysis
C=O
CH₂
H—C—O⁻
2
bond cleavage
C—O⁻
⁻CH₂
Enolate
+
H
O
C
Product 1
H₂O
OH⁻
3
protonation
CH₃
Product 2

Figure 15-4 | The mechanism of base-catalyzed aldol cleavage. Aldol condensation occurs by the reverse mechanism.

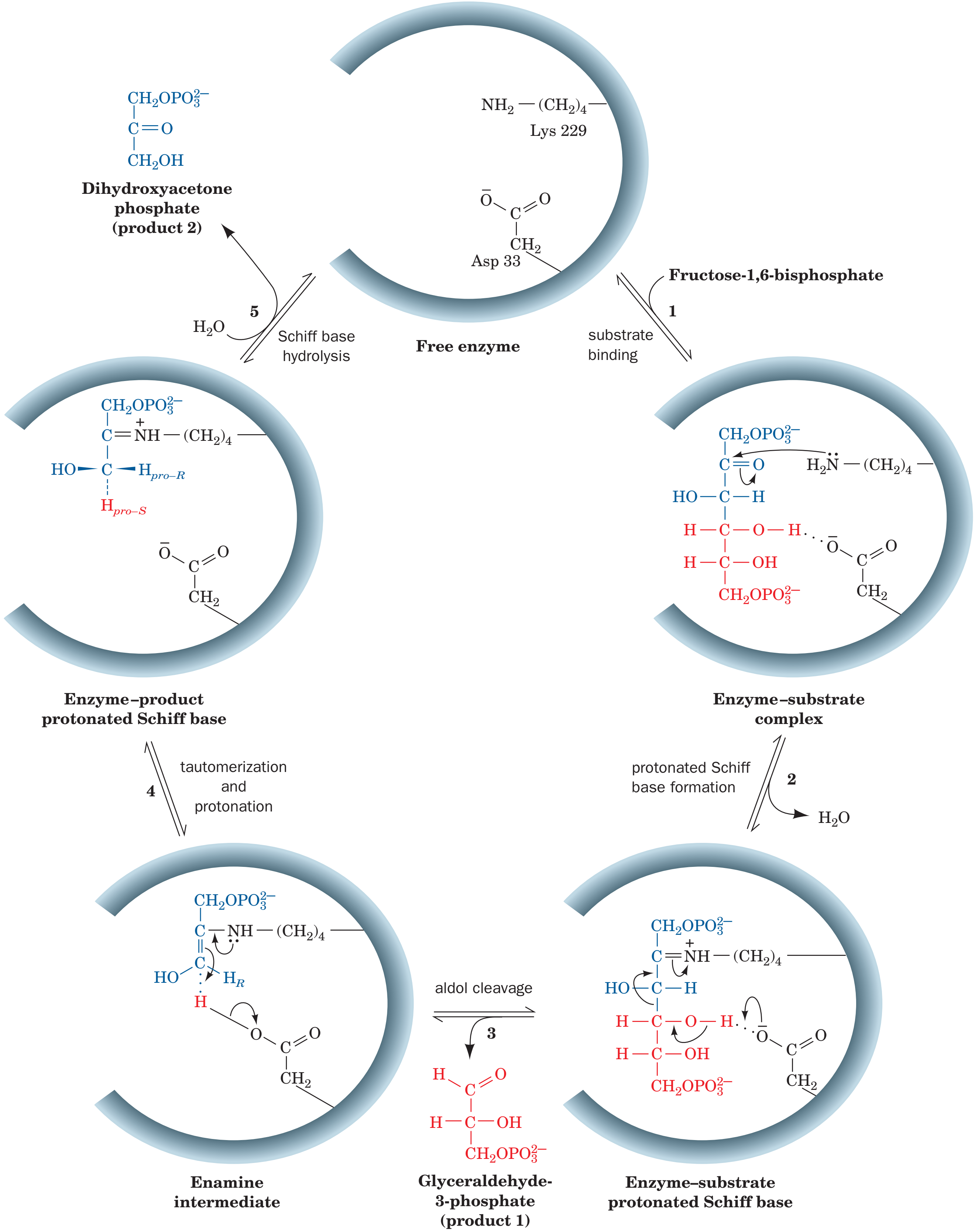
Dihydroxyacetone phosphate (product 2)
Free enzyme
Lys 229
Asp 33
Fructose-1,6-bisphosphate
1
substrate binding
5
Schiff base hydrolysis
Enzyme–product protonated Schiff base
Enzyme–substrate complex
4
tautomerization and protonation
2
protonated Schiff base formation
aldol cleavage
3
Enamine intermediate
Glyceraldehyde-3-phosphate (product 1)
Enzyme–substrate protonated Schiff base

■ **Figure 15-5** | **The enzymatic mechanism of aldolase.** The reaction involves (**1**) substrate binding; (**2**) Schiff base (imine) formation between the enzyme's active site Lys residue and the open-chain form of FBP; (**3**) aldol cleavage to form an enamine intermediate of the enzyme and DHAP, with release of GAP; (**4**) tautomerization and protonation to the iminium form of the Schiff base; and (**5**) hydrolysis of the Schiff base with release of DHAP. **See the Animated Figures.**

the active site Lys to form an iminium cation, that is, a protonated Schiff base.

Step 3 C3—C4 bond cleavage resulting in enamine formation and the release of GAP. The iminium ion is a better electron-withdrawing group than the oxygen atom of the precursor carbonyl group. Thus, catalysis occurs because the enamine intermediate (Fig. 15-5, Step 3) is more stable than the corresponding enolate intermediate of the base-catalyzed aldol cleavage reaction (Fig. 15-4, Step 2).

Step 4 Protonation of the enamine to an iminium cation.

Step 5 Hydrolysis of the iminium cation to release DHAP, with regeneration of the free enzyme.

E | Triose Phosphate Isomerase Interconverts Dihydroxyacetone Phosphate and Glyceraldehyde-3-Phosphate

Only one of the products of the aldol cleavage reaction, GAP, continues along the glycolytic pathway (Fig. 15-1). However, DHAP and GAP are ketose–aldose isomers (like F6P and G6P). They are interconverted by an isomerization reaction with an **enediol** (or **enediolate**) **intermediate. Triose phosphate isomerase (TIM)** catalyzes this process in Reaction 5 of glycolysis, the final reaction of Stage I:

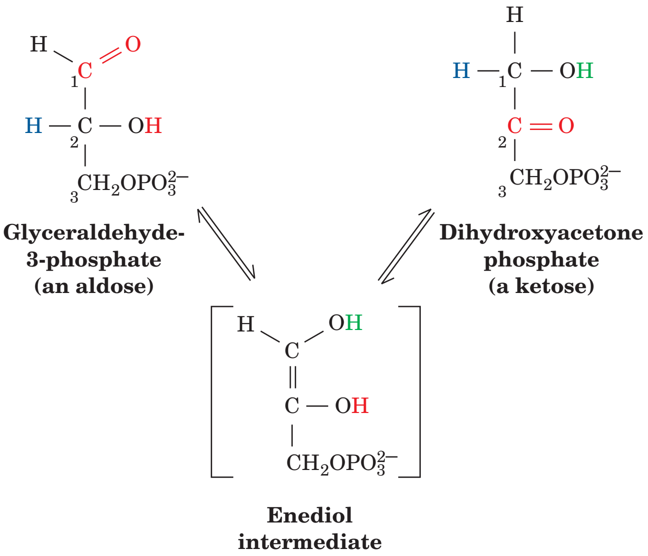
H
O
C
1
H — C — OH
2
3 CH₂OPO₃²⁻
Glyceraldehyde-3-phosphate (an aldose)
H
H — C — OH
1
C = O
2
3 CH₂OPO₃²⁻
Dihydroxyacetone phosphate (a ketose)
H
OH
C
C — OH
CH₂OPO₃²⁻
Enediol intermediate

Support for this reaction scheme comes from the use of the transition state analogs **phosphoglycohydroxamate** and **2-phosphoglycolate,** stable compounds whose geometry resembles that of the proposed enediol or enediolate intermediate:

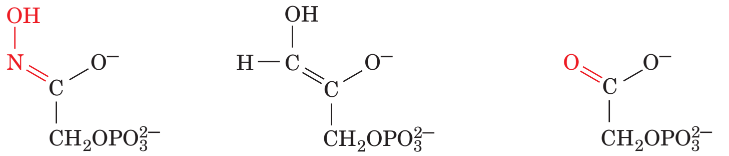
OH
N
C
O⁻
CH₂OPO₃²⁻
OH
H — C
C
O⁻
CH₂OPO₃²⁻
O
C
O⁻
CH₂OPO₃²⁻

Phosphoglycohydroxamate **Proposed enediolate intermediate** **2-Phosphoglycolate**

Enzymes catalyze reactions by binding the transition state complex more tightly than the substrate (Section 11-3E), and, in fact, phosphoglycohydroxamate and 2-phosphoglycolate bind 155- and 100-fold more tightly to TIM than does either GAP or DHAP.

Glu 165 and His 95 Act as General Acids and Bases. Mechanistic considerations suggest that the conversion of GAP to the enediol intermediate is catalyzed by a general base, which abstracts a proton from C2 of GAP, and by a general acid, which protonates its carbonyl oxygen atom. X-Ray studies reveal that the Glu 165 side chain of TIM is ideally situated to abstract the C2 proton from GAP (Fig. 15-6). In fact, the mutagenic replacement of Glu 165 by Asp, which X-ray studies show withdraws the carboxylate group only ~1 Å farther away from the substrate than its position in the wild-type enzyme, reduces TIM's catalytic activity 1000-fold. X-Ray studies similarly indicate that His 95 is hydrogen bonded to and hence is properly positioned to protonate GAP's carbonyl oxygen. The positively charged side chain of Lys 12 is thought to electrostatically stabilize the negatively charged transition state in the reaction. In the conversion of the enediol intermediate to DHAP, Glu 165 acts as a general acid to protonate C1 and His 95 acts as a general base to abstract the proton from the OH group, thereby restoring the catalytic groups to their initial protonation states.

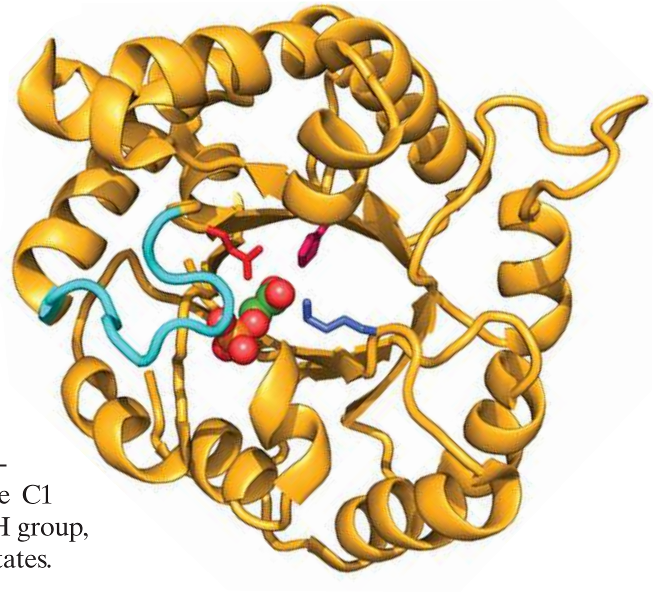

Figure 15-6 | Ribbon diagram of yeast TIM in complex with its transition state analog 2-phosphoglycolate. A single subunit of this homodimeric enzyme is viewed roughly along the axis of its α/β barrel. The enzyme's flexible loop is cyan, and the side chains of the catalytic Lys, His, and Glu residues are purple, magenta, and red, respectively. The 2-phosphoglycolate is represented by a space-filling model colored according to atom type (C, green; O, red; P, orange). [Based on an X-ray structure by Gregory Petsko, Brandeis University. PDBid 2YPI.] **See Interactive Exercise 16 and Kinemage Exercises 12-1 and 12-2.**

A Flexible Loop Closes over the Active Site. The comparison of the X-ray structure of TIM (Fig. 6-30*c*) with that of the enzyme–2-phosphoglycolate complex reveals that when substrate binds to TIM, a conserved 10-residue loop closes over the active site like a hinged lid, in a movement that involves main chain shifts of >7 Å (Fig. 15-6). A four-residue segment of the loop makes a hydrogen bond with the phosphate group of the substrate. Mutagenic excision of these four residues does not significantly distort the protein, so substrate binding is not greatly impaired. However, the catalytic power of the mutant enzyme is reduced 10^5-fold, and it only weakly binds phosphoglycohydroxamate. Evidently, loop closure preferentially stabilizes the enzymatic reaction's enediol-like transition state.

Loop closure in the TIM reaction also supplies a striking example of the so-called **stereoelectronic control** that enzymes can exert on a reaction. In solution, the enediol intermediate readily breaks down with the elimination of the phosphate at C3 to form the toxic compound **methylglyoxal:**

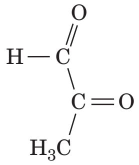

Methylglyoxal

On the enzyme's surface, however, that reaction is prevented because the phosphate group is held by the flexible loop in a position that disfavors phosphate elimination. In the mutant enzyme lacking the flexible loop, the enediol is able to escape: ~85% of the enediol intermediate is released into solution where it rapidly decomposes to methylglyoxal and P_i. Thus, the flexible loop closure assures that substrate is efficiently transformed to product.

α/β Barrel Enzymes May Have Evolved by Divergent Evolution. TIM was the first protein found to contain an α/β barrel (also known as a TIM barrel), a cylinder of eight parallel β strands surrounded by eight parallel α helices (Fig. 6-30*c*). This striking structural motif has since been found in numerous different proteins, essentially all of which are enzymes (including the glycolytic enzymes aldolase, enolase, and pyruvate kinase). Intriguingly, the active sites of nearly all known α/β barrel enzymes are located in the mouth of the barrel at the end that contains the C-terminal ends of the β strands, although there is no obvious structural rationale for this. Despite the fact that few of these proteins exhibit significant sequence similarity, it has been postulated that all of them have evolved from a common ancestor (divergent evolution). However, it has also been argued that the α/β barrel is a particularly stable arrangement that nature has independently discovered on several occasions (convergent evolution).

Triose Phosphate Isomerase Is a Catalytically Perfect Enzyme. Jeremy Knowles has demonstrated that TIM has achieved **catalytic perfection.** This means that the rate of the bimolecular reaction between enzyme and substrate is diffusion controlled, so product formation occurs as rapidly as enzyme and substrate can collide in solution. Any increase in TIM's catalytic efficiency therefore would not increase its reaction rate.

GAP and DHAP are interconverted so efficiently that the concentrations of the two metabolites are maintained at their equilibrium values: $K = [\text{GAP}]/[\text{DHAP}] = 4.73 \times 10^{-2}$. At equilibrium, $[\text{DHAP}] \gg [\text{GAP}]$. However, under the steady state conditions in a cell, GAP is consumed in the succeeding reactions of the glycolytic pathway. *As GAP is siphoned off in this manner, more DHAP is converted to GAP to maintain the equilibrium ratio.* In effect, DHAP follows GAP into the second stage of glycolysis, so a single pathway accounts for the metabolism of both products of the aldolase reaction.

Taking Stock of Glycolysis So Far. At this point in the glycolytic pathway, one molecule of glucose has been transformed into two molecules of GAP. This completes the first stage of glycolysis (Fig. 15-7). Note that 2 ATP have been consumed in generating the phosphorylated intermediates. This energy investment has not yet paid off, but with a little chemical artistry, the "low-energy" GAP can be converted to "high-energy" compounds whose free energies of hydrolysis can be coupled to ATP synthesis in the second stage of glycolysis.

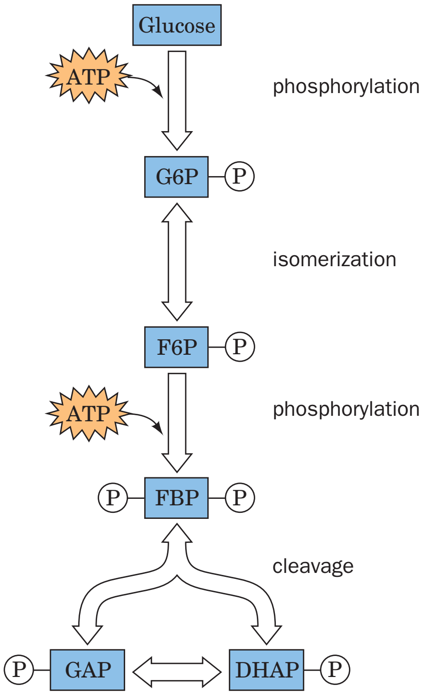

■ **Figure 15-7 | Schematic diagram of the first stage of glycolysis.** In this series of five reactions, a hexose is phosphorylated, isomerized, phosphorylated again, and then cleaved to two interconvertible triose phosphates. Two ATP are consumed in the process.

F | Glyceraldehyde-3-Phosphate Dehydrogenase Forms the First "High-Energy" Intermediate

Reaction 6 of glycolysis is the oxidation and phosphorylation of GAP by NAD^+ and P_i as catalyzed by **glyceraldehyde-3-phosphate dehydrogenase** (**GAPDH;** *at right*; Fig. 6-31). This is the first instance of the chemical artistry alluded to above. *In this reaction, aldehyde oxidation, an exergonic reaction, drives the synthesis of the "high-energy" acyl phosphate **1, 3-bisphosphoglycerate (1,3-BPG).*** Recall that acyl phosphates are compounds with high phosphoryl group-transfer potential (Section 14-2C).

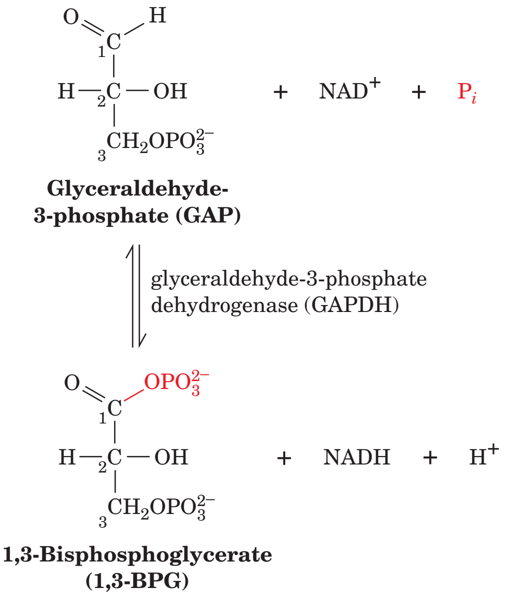

O
H
1
C
H
2
C
OH
3
$CH_2OPO_3^{2-}$
+ NAD^+ + P_i
Glyceraldehyde-3-phosphate (GAP)
glyceraldehyde-3-phosphate dehydrogenase (GAPDH)
O
OPO_3^{2-}
1
C
H
2
C
OH
3
$CH_2OPO_3^{2-}$
+ NADH + H^+
1,3-Bisphosphoglycerate (1,3-BPG)

Several key enzymological experiments have contributed to the elucidation of the GAPDH reaction mechanism:

1. GAPDH is inactivated by alkylation with stoichiometric amounts of iodoacetate. The presence of **carboxymethylcysteine** in the hydrolysate of the resulting alkylated enzyme (Fig. 15-8*a*) suggests that GAPDH has an active site Cys sulfhydryl group.
2. GAPDH quantitatively transfers ^3H from C1 of GAP to NAD^+ (Fig. 15-8*b*), thereby establishing that this reaction occurs via direct hydride transfer.
3. GAPDH catalyzes exchange of ^{32}P between P_i and the product analog **acetyl phosphate** (Fig. 15-8*c*). Such isotope exchange reactions are indicative of an acyl–enzyme intermediate; that is, the acetyl group forms

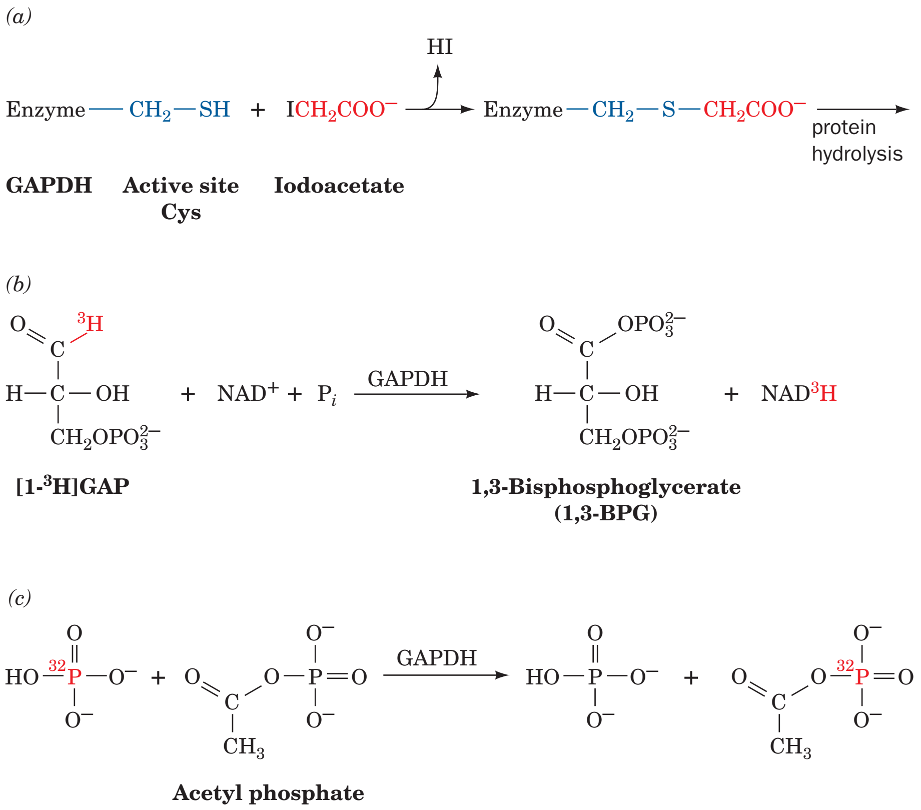

(a)
Enzyme
CH_2
SH
+
ICH_2COO^-
HI
Enzyme
CH_2
S
CH_2COO^-
protein hydrolysis
NH_3^+
CH
CH_2
S
CH_2COO^-
COO^-
+ Other amino acids
GAPDH
Active site Cys
Iodoacetate
Carboxy-methylcysteine
(b)
O
^3H
C
H
C
OH
$CH_2OPO_3^{2-}$
+ NAD^+ + P_i
GAPDH
O
OPO_3^{2-}
C
H
C
OH
$CH_2OPO_3^{2-}$
+ NAD^3H
$[1\text{-}^3H]GAP$
1,3-Bisphosphoglycerate (1,3-BPG)
(c)
O
HO
^{32}P
O^-
O^-
+
O
C
CH_3
O
P
O
O^-
O^-
GAPDH
HO
P
O^-
O
O^-
+
O
C
CH_3
O
^{32}P
O
O^-
O^-
Acetyl phosphate

Figure 15-8 | Reactions that were used to elucidate the enzymatic mechanism of GAPDH. (*a*) The reaction of iodoacetate with an active site Cys residue. (*b*) Quantitative tritium transfer from substrate to NAD^+. (*c*) The enzyme-catalyzed exchange of ^{32}P from phosphate to acetyl phosphate.

a covalent complex with the enzyme, similar to the acyl–enzyme intermediate in the serine protease reaction mechanism (Section 11-5C).

David Trentham has proposed a mechanism for GAPDH based on this information and the results of kinetic studies (Fig. 15-9):

Step 1 GAP binds to the enzyme.

Step 2 The essential sulfhydryl group, acting as a nucleophile, attacks the aldehyde to form a **thiohemiacetal.**

Step 3 The thiohemiacetal undergoes oxidation to an **acyl thioester** by direct hydride transfer to NAD^+. This intermediate, which has been isolated, has a large free energy of hydrolysis. Thus, *the energy of aldehyde oxidation has not been dissipated but has been conserved through the synthesis of the thioester and the reduction of* NAD^+ *to NADH.*

Step 4 P_i binds to the enzyme–thioester–NADH complex.

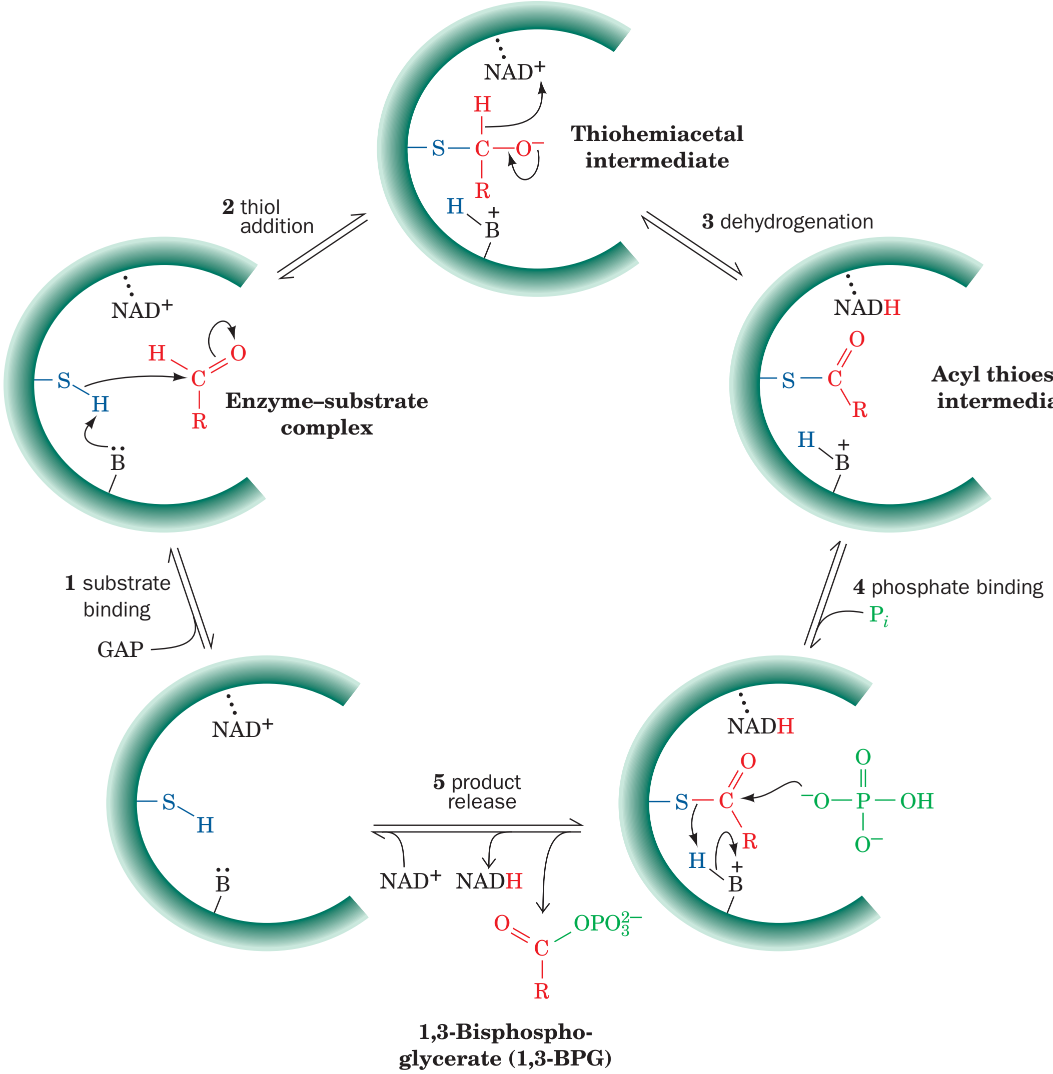
NAD+
H
S
C
O−
R
H
B
Thiohemiacetal intermediate
2 thiol addition
3 dehydrogenation
NAD+
H
O
C
S
H
R
B
Enzyme–substrate complex
NADH
O
S
C
R
H
B
Acyl thioester intermediate
1 substrate binding
GAP
4 phosphate binding
Pi
NAD+
S
H
B
5 product release
NAD+
NADH
O
C
OPO3 2−
R
NADH
O
S
C
R
H
B
O
−O
P
OH
O−
1,3-Bisphosphoglycerate (1,3-BPG)

■ **Figure 15-9 | The enzymatic mechanism of GAPDH.** (**1**) GAP binds to the enzyme; (**2**) the active site sulfhydryl group forms a thiohemiacetal with the substrate; (**3**) NAD^+ oxidizes the thiohemiacetal to a thioester; (**4**) P_i binds to the enzyme; and (**5**) P_i attacks the thioester, forming the acyl phosphate product, 1,3-BPG, which dissociates from the enzyme followed by the replacement of the newly formed NADH by NAD^+, thereby regenerating the active enzyme. **See the Animated Figures.**

Step 5 The thioester intermediate undergoes nucleophilic attack by P_i to form the "high-energy" mixed anhydride 1,3-BPG, which then dissociates from the enzyme followed by replacement of NADH by another molecule of NAD^+ to regenerate the active enzyme.

G | Phosphoglycerate Kinase Generates the First ATP

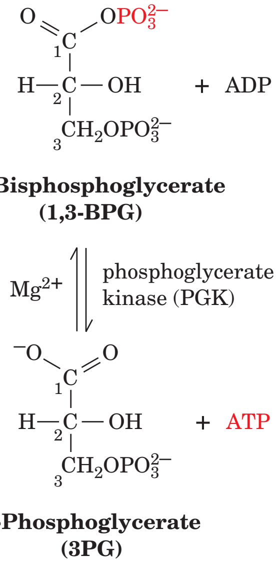

1,3-Bisphosphoglycerate (1,3-BPG)

3-Phosphoglycerate (3PG)

Reaction 7 of the glycolytic pathway yields ATP together with **3-phosphoglycerate (3PG)** in a reaction catalyzed by **phosphoglycerate kinase (PGK;** *at right*). (Note that this enzyme is called a "kinase" because the reverse reaction is phosphoryl group transfer from ATP to 3PG.)

PGK (Fig. 15-10) is conspicuously bilobal in appearance. The Mg^{2+}–ADP-binding site is located on one domain, ~10 Å from the 1,3-BPG-binding site, which is on the other domain. Physical measurements suggest that, on substrate binding, the two domains of PGK swing together to permit the substrates to react in a water-free environment, as occurs in hexokinase (Section 15-2A). Indeed, the appearance of PGK is remarkably similar to that of hexokinase (Fig. 15-2), although the structures of the proteins are otherwise unrelated.

The GAPDH and PGK Reactions Are Coupled. As described in Section 14-2B, a slightly unfavorable reaction can be coupled to a highly favorable reaction so that both reactions proceed in the forward direction. In the case of the sixth and seventh reactions of glycolysis, *1,3-BPG is the common intermediate whose consumption in the PGK reaction "pulls" the GAPDH reaction forward.* The energetics of the overall reaction pair are

$$\begin{array}{ll} \text{GAP} + \text{P}_i + \text{NAD}^+ \longrightarrow \text{1,3-BPG} + \text{NADH} & \Delta G^{\circ\prime} = +6.7\ \text{kJ}\cdot\text{mol}^{-1} \\ \text{1,3-BPG} + \text{ADP} \longrightarrow \text{3PG} + \text{ATP} & \Delta G^{\circ\prime} = -18.8\ \text{kJ}\cdot\text{mol}^{-1} \\ \hline \text{GAP} + \text{P}_i + \text{NAD}^+ + \text{ADP} \longrightarrow \text{3PG} + \text{NADH} + \text{ATP} & \\ & \Delta G^{\circ\prime} = -12.1\ \text{kJ}\cdot\text{mol}^{-1} \end{array}$$

Although the GAPDH reaction is endergonic, the strongly exergonic nature of the transfer of a phosphoryl group from 1,3-BPG to ADP makes the overall synthesis of NADH and ATP from GAP, P_i, NAD^+, and ADP favorable. *This production of ATP, which does not involve O_2, is an example of substrate-level phosphorylation.* The subsequent oxidation of the NADH produced in this reaction by O_2 generates additional ATP by oxidative phosphorylation, as we shall see in Section 18-3.

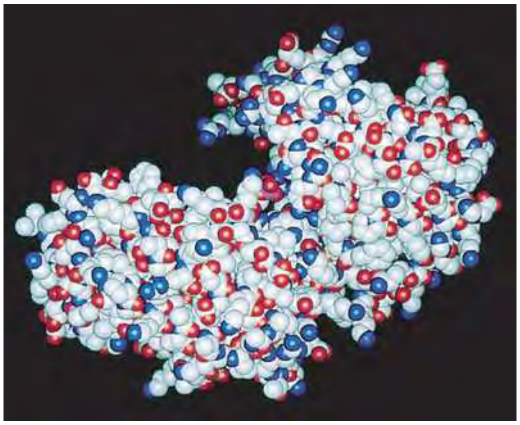

Figure 15-10 | A space-filling model of yeast phosphoglycerate kinase. The substrate-binding site is at the bottom of a deep cleft between the two lobes of the protein. This site is marked by the P atom (*magenta*) of 3PG. Compare this structure with that of hexokinase (Fig. 15-2*a*). [Based on an X-ray structure by Herman Watson, University of Bristol, U.K. PDBid 3PGK.]

H | Phosphoglycerate Mutase Interconverts 3-Phosphoglycerate and 2-Phosphoglycerate

In Reaction 8 of glycolysis, 3PG is converted to **2-phosphoglycerate (2PG)** by **phosphoglycerate mutase (PGM):**

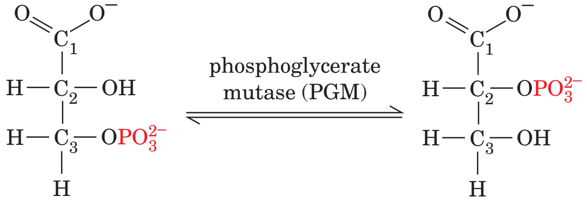

3-Phosphoglycerate (3PG)

2-Phosphoglycerate (2PG)

A **mutase** catalyzes the transfer of a functional group from one position to another on a molecule. This more or less energetically neutral reaction is necessary preparation for the next reaction in glycolysis, which generates a “high-energy” phosphoryl compound.

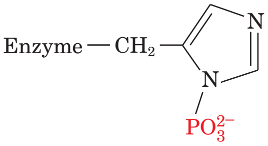

Phospho-His residue

At first sight, the reaction catalyzed by phosphoglycerate appears to be a simple intramolecular phosphoryl group transfer. This is not the case, however. The active enzyme has a phosphoryl group at its active site, attached to His 8 *(at left)*. The phosphoryl group is transferred to the substrate to form a bisphospho intermediate. This intermediate then rephosphorylates the enzyme to form the product and regenerate the active phosphoenzyme. The enzyme’s X-ray structure shows the proximity of His 8 to the substrate (Fig. 15-11).

Catalysis by phosphoglycerate mutase occurs as follows (Fig. 15-12):

Step 1 3PG binds to the phosphoenzyme in which His 8 is phosphorylated.

Step 2 The enzyme’s phosphoryl group is transferred to the substrate, resulting in an intermediate 2,3-bisphosphoglycerate–enzyme complex.

Steps 3 and 4 The complex decomposes to form the product 2PG and regenerate the phosphoenzyme.

The phosphoryl group of 3PG therefore ends up on C2 of the next 3PG to undergo reaction.

Occasionally, 2,3-bisphosphoglycerate (2,3-BPG) formed in Step 2 of the reaction dissociates from the dephosphoenzyme, leaving it in an inactive form. Trace amounts of 2,3-BPG must therefore always be available to regenerate the active phosphoenzyme by the reverse reaction. 2,3-BPG also specifically binds to deoxyhemoglobin, thereby decreasing its oxygen affinity (Section 7-1D). Consequently, erythrocytes require much more 2,3-BPG (5 mM) than the trace amounts that are used to prime phosphoglycerate mutase (Box 15-2).

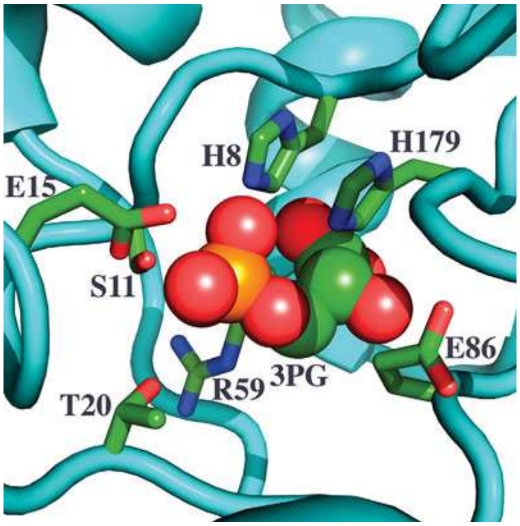

Figure 15-11 | The active site region of yeast phosphoglycerate mutase (dephospho form). The substrate, 3PG, binds to an ionic pocket. His 8 is phosphorylated in the active enzyme. [Based on an X-ray structure by Herman Watson, University of Bristol, U.K. PDBid 3PGM.]

I Enolase Forms the Second “High-Energy” Intermediate

In Reaction 9 of glycolysis, 2PG is dehydrated to **phosphoenolpyruvate (PEP)** in a reaction catalyzed by **enolase:**

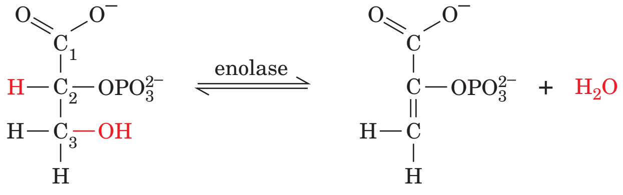

2-Phosphoglycerate (2PG)

Phosphoenolpyruvate (PEP)

The enzyme forms a complex with a divalent cation such as Mg^{2+} before the substrate binds. Fluoride ion inhibits glycolysis by blocking enolase activity (F^- was one of the metabolic inhibitors used in elucidating the glycolytic pathway). In the presence of P_i, F^- blocks substrate binding to enolase by forming a bound complex with Mg^{2+} at the enzyme’s active site. Enolase’s substrate, 2PG, therefore builds up, and, through the action of PGM, 3PG also builds up.

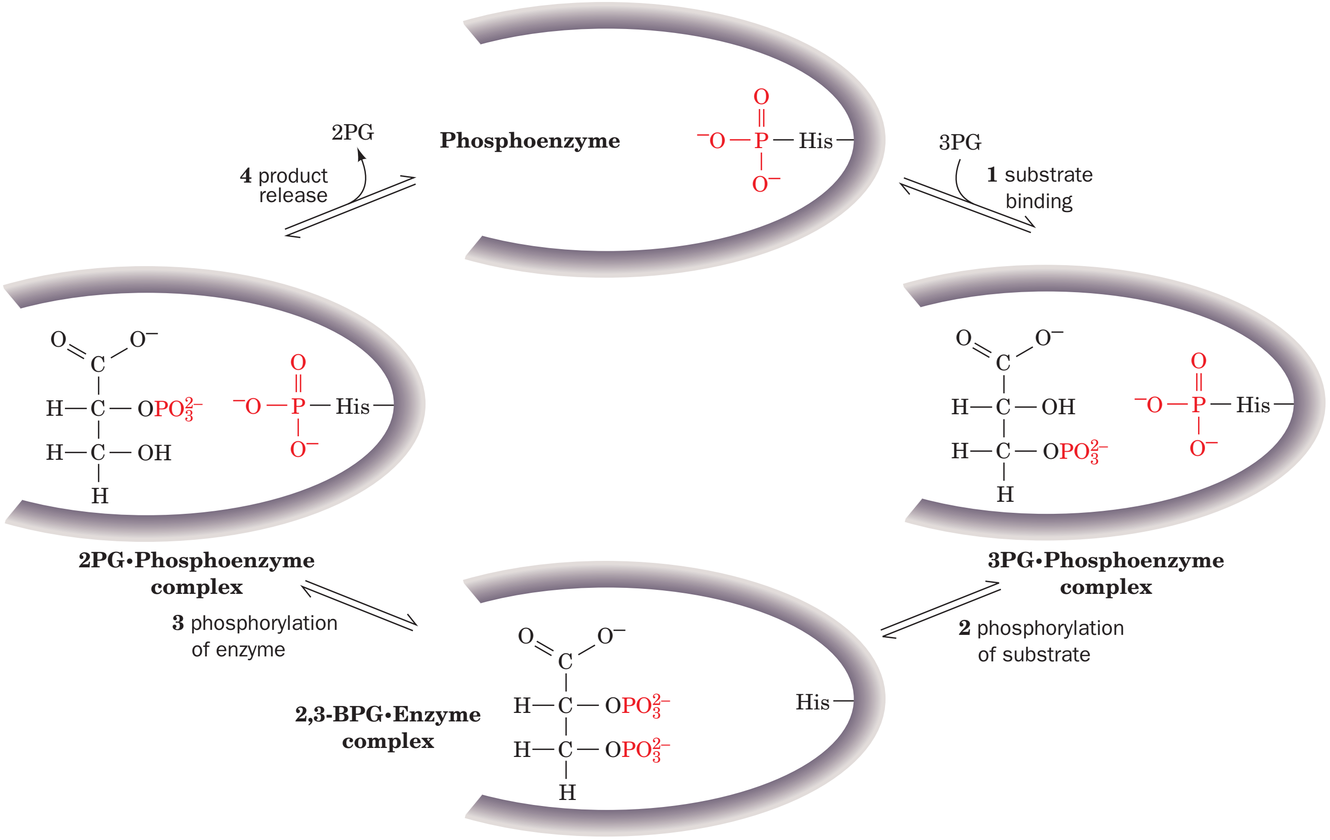
2PG
4 product release
Phosphoenzyme
O
⁻O—P—His
O⁻
3PG
1 substrate binding
O O⁻
C
H—C—OPO$_3^{2-}$
H—C—OH
H
⁻O—P—His
2PG•Phosphoenzyme complex
H—C—OH
H—C—OPO$_3^{2-}$
3PG•Phosphoenzyme complex
3 phosphorylation of enzyme
2 phosphorylation of substrate
2,3-BPG•Enzyme complex
H—C—OPO$_3^{2-}$
H—C—OPO$_3^{2-}$
His

■ **Figure 15-12** | **A proposed reaction mechanism for phosphoglycerate mutase.** The active form of the enzyme contains a phospho-His residue at the active site. (**1**) Formation of an enzyme–substrate complex; (**2**) transfer of the enzyme-bound phosphoryl group to the substrate; (**3**) rephosphorylation of the enzyme by the other phosphoryl group of the substrate; and (**4**) release of product, regenerating the active phosphoenzyme.

J | Pyruvate Kinase Generates the Second ATP

In Reaction 10 of glycolysis, its final reaction, **pyruvate kinase (PK)** couples the free energy of PEP cleavage to the synthesis of ATP during the formation of pyruvate:

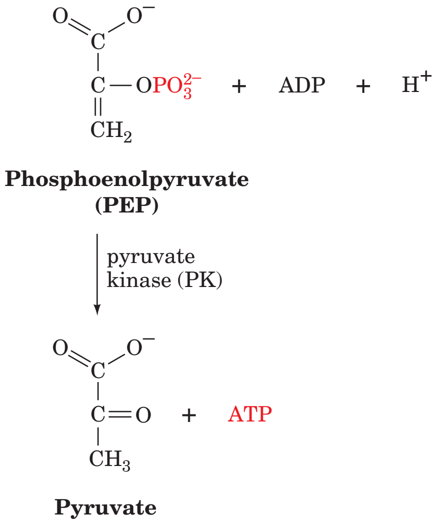
O O⁻
C
C—OPO$_3^{2-}$
CH$_2$
+ ADP + H$^+$
Phosphoenolpyruvate (PEP)
pyruvate kinase (PK)
O O⁻
C
C=O
CH$_3$
+ ATP
Pyruvate

BOX 15-2 PERSPECTIVES IN BIOCHEMISTRY

Synthesis of 2,3-Bisphosphoglycerate in Erythrocytes and Its Effect on the Oxygen Carrying Capacity of the Blood

The specific binding of 2,3-bisphosphoglycerate (2,3-BPG) to deoxyhemoglobin decreases the oxygen affinity of hemoglobin (Section 7-1D). Erythrocytes synthesize and degrade 2,3-BPG by a detour from the glycolytic pathway.

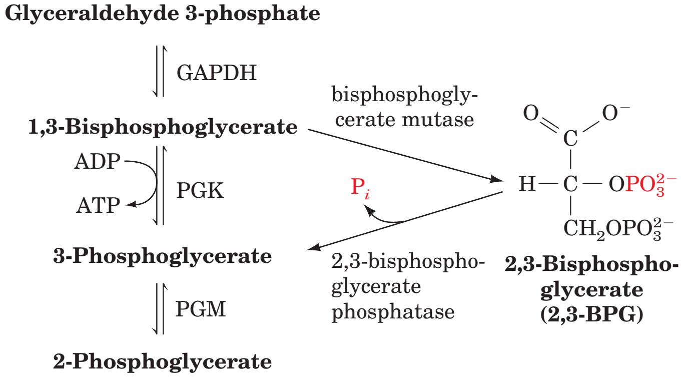
Glyceraldehyde 3-phosphate
GAPDH
1,3-Bisphosphoglycerate
ADP
ATP
PGK
3-Phosphoglycerate
PGM
2-Phosphoglycerate
bisphosphoglycerate mutase
P_i
2,3-bisphosphoglycerate phosphatase
O
O⁻
C
H
C
OPO_3^{2-}
$CH_2OPO_3^{2-}$
2,3-Bisphosphoglycerate (2,3-BPG)

Bisphosphoglycerate mutase catalyzes the transfer of a phosphoryl group from C1 to C2 of 1,3-BPG. The resulting 2,3-BPG is hydrolyzed to 3PG by **2,3-bisphosphoglycerate phosphatase.** The 3PG then continues through the glycolytic pathway.

The level of available 2,3-BPG regulates hemoglobin's oxygen affinity. Consequently, inherited defects of glycolysis in erythrocytes alter the ability of the blood to carry oxygen as is indicated by the oxygen-saturation curve of its hemoglobin.

For example, in hexokinase-deficient erythrocytes, the concentrations of all the glycolytic intermediates are low (since hexokinase catalyzes the first step of glycolysis), thereby resulting in a diminished 2,3-BPG concentration and an increased hemoglobin oxygen affinity (*green curve*). Conversely, a deficiency in pyruvate kinase (which catalyzes the final reaction of glycolysis; Fig. 15-1) decreases hemoglobin's oxygen affinity (*purple curve*) through an increase in 2,3-BPG concentration resulting from this blockade. Thus, although erythrocytes, which lack nuclei and other organelles, have only a minimal metabolism, this metabolism is physiologically significant.

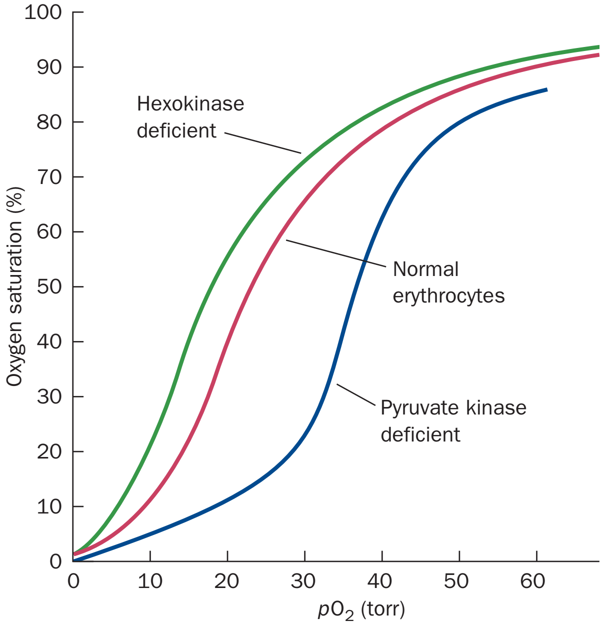

[Oxygen-saturation curves after Delivoria-Papadopoulos, M., Oski, F.A., and Gottlieb, A.J., *Science* **165,** 601 (1969).]

The PK reaction, which requires both monovalent (K^+) and divalent (Mg^{2+}) cations, occurs as follows (Fig. 15-13):

Step 1 A β-phosphoryl oxygen of ADP nucleophilically attacks the PEP phosphorus atom, thereby displacing **enolpyruvate** and forming ATP.

Step 2 Enolpyruvate tautomerizes to pyruvate.

The PK reaction is highly exergonic, supplying more than enough free energy to drive ATP synthesis (another example of substrate-level phosphorylation). At this point, the "logic" of the enolase reaction becomes clear. The standard free energy of hydrolysis of 2PG is only $-16\ \text{kJ}\cdot\text{mol}^{-1}$, which is insufficient to drive ATP synthesis from ADP ($\Delta G^{\circ\prime} = 30.5\ \text{kJ}\cdot\text{mol}^{-1}$). However, the dehydration of 2PG results in the formation of a "high-energy" compound capable of such synthesis. *The high*

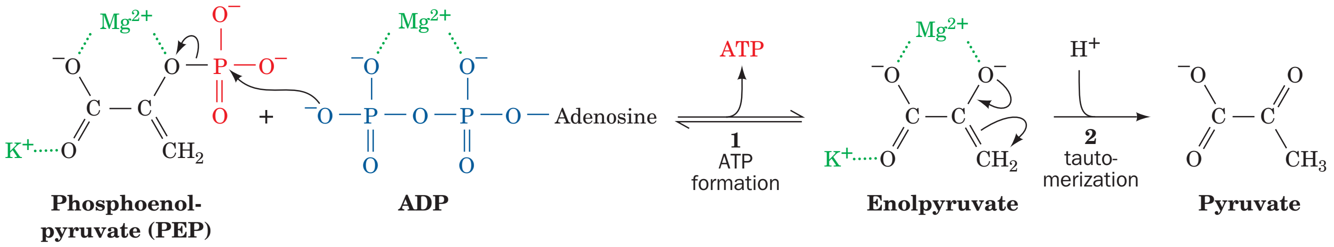
Mg2+
O−
ADP
Adenosine
ATP
1
ATP formation
H+
2
tauto-merization
K+
CH2
CH3
Phosphoenol-pyruvate (PEP)
ADP
Enolpyruvate
Pyruvate

Figure 15-13 | Figure 15-13 The mechanism of the reaction catalyzed by pyruvate kinase. (**1**) Nucleophilic attack of an ADP β-phosphoryl oxygen atom on the phosphorus atom of PEP to form ATP and enolpyruvate; and (**2**) tautomerization of enolpyruvate to pyruvate.

phosphoryl group-transfer potential of PEP reflects the large release of free energy on converting the product enolpyruvate to its keto tautomer. Consider the hydrolysis of PEP as a two-step reaction (Fig. 15-14). The tautomerization step supplies considerably more free energy than the phosphoryl group transfer step.

Assessing Stage II of Glycolysis. The energy investment of the first stage of glycolysis (2 ATP consumed) is doubly repaid in the second stage of glycolysis because two phosphorylated C_3 units are transformed to two

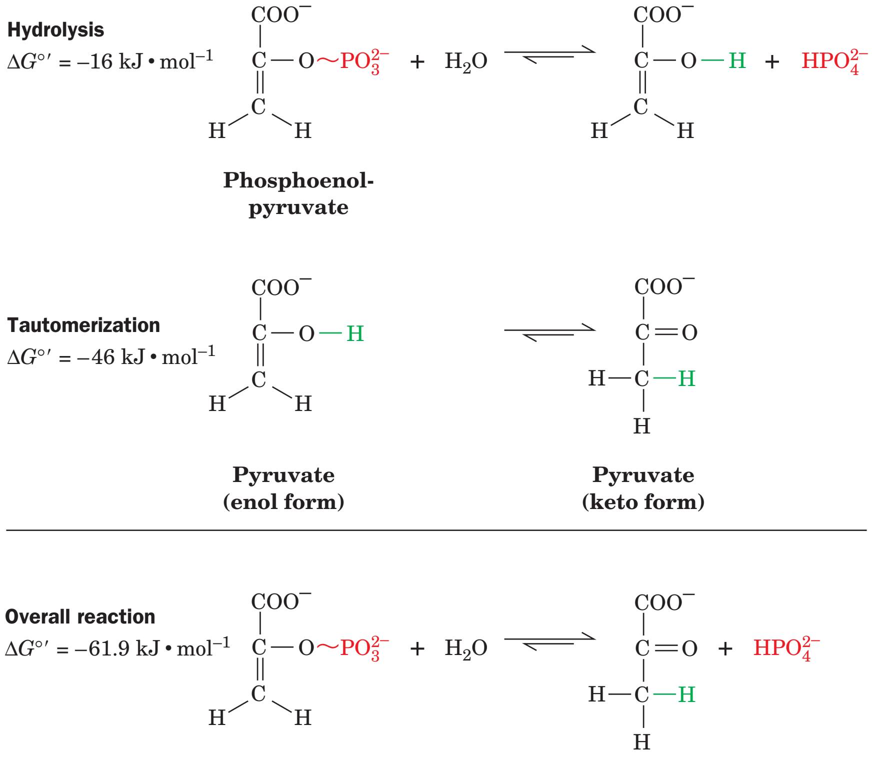
Hydrolysis
ΔG°′ = −16 kJ • mol−1
Phosphoenol-pyruvate
Tautomerization
ΔG°′ = −46 kJ • mol−1
Pyruvate (enol form)
Pyruvate (keto form)
Overall reaction
ΔG°′ = −61.9 kJ • mol−1

Figure 15-14 | The hydrolysis of PEP. The reaction is broken down into two steps, hydrolysis and tautomerization. The overall $\Delta G°'$ value is much more negative than that required to provide the $\Delta G°'$ for ATP synthesis from ADP and P_i.

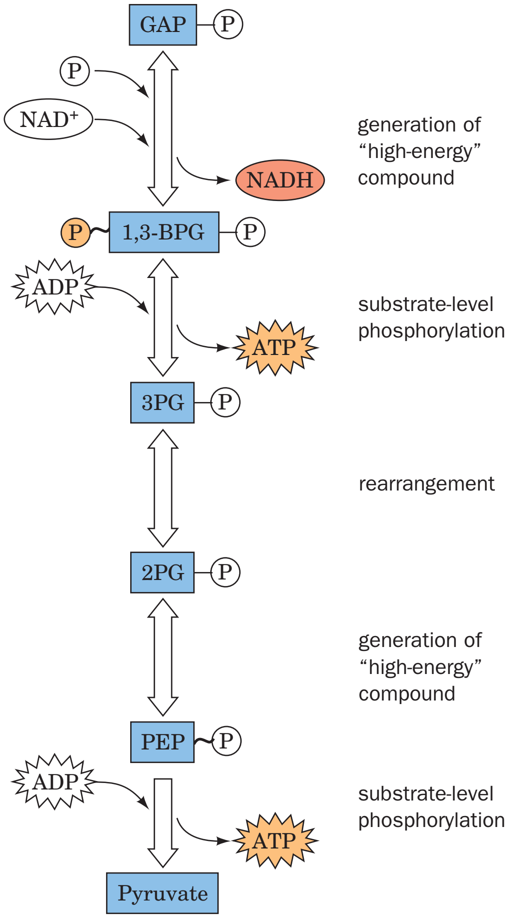
GAP
P
P
NAD+
NADH
generation of "high-energy" compound
P
1,3-BPG
P
ADP
ATP
substrate-level phosphorylation
3PG
P
rearrangement
2PG
P
generation of "high-energy" compound
PEP
P
ADP
ATP
substrate-level phosphorylation
Pyruvate

Figure 15-15 | Schematic diagram of the second stage of glycolysis. In this series of five reactions, GAP undergoes phosphorylation and oxidation, followed by molecular rearrangements so that both phosphoryl groups have sufficient free energy to be transferred to ADP to produce ATP. Two molecules of GAP are converted to pyruvate for every molecule of glucose that enters Stage I of glycolysis.

pyruvates with the coupled synthesis of 4 ATP. This process is shown schematically in Fig. 15-15.

The overall reaction of glycolysis, as we have seen, is

$$\text{Glucose} + 2\,\text{NAD}^+ + 2\,\text{ADP} + 2\,\text{P}_i \longrightarrow 2\,\text{pyruvate} + 2\,\text{NADH} + 2\,\text{ATP} + 2\,\text{H}_2\text{O} + 4\,\text{H}^+$$

Let us consider each of the three products of glycolysis:

1. ***ATP.*** The initial investment of 2 ATP per glucose in Stage I and the subsequent generation of 4 ATP by substrate-level phosphorylation (two for each GAP that proceeds through Stage II) gives a net yield of 2 ATP per glucose. In some tissues and organisms for which glucose is the primary metabolic fuel, ATP produced by glycolysis satisfies most of the cell's energy needs. For example, the parasitic protozoans *Trypanosoma* and *Leishmania* (which are the causes of several human diseases, including **African sleeping sickness** and **leishmaniasis**) rely almost entirely on glycolysis. Some of the glycolytic enzymes in these organisms differ structurally from their mammalian counterparts, which makes them attractive targets for rational drug design (Section 12-4).
2. ***NADH.*** During its catabolism by the glycolytic pathway, glucose is oxidized to the extent that two NAD^+ are reduced to two NADH. As described in Section 14-3C, reduced coenzymes such as NADH represent a source of free energy than can be recovered by their subsequent oxidation. Under aerobic conditions, electrons pass from reduced coenzymes through a series of electron carriers to the final oxidizing agent, O_2, in a process known as **electron transport** (Section 18-2). The free energy of electron transport drives the synthesis of ATP from ADP (oxidative phosphorylation; Section 18-3). In aerobic organisms, this sequence of events also serves to regenerate oxidized NAD^+ that can participate in further rounds of catalysis mediated by GAPDH. Under anaerobic conditions, NADH must be reoxidized by other means in order to keep the glycolytic pathway supplied with NAD^+ (Section 15-3).
3. ***Pyruvate.*** The two pyruvate molecules produced through the partial oxidation of each glucose are still relatively reduced molecules. Under aerobic conditions, complete oxidation of the pyruvate carbon atoms to CO_2 is mediated by the citric acid cycle (Chapter 17). The energy released in that process drives the synthesis of much more ATP than is generated by the limited oxidation of glucose by the glycolytic pathway alone. In anaerobic metabolism, pyruvate is metabolized to a lesser extent to regenerate NAD^+, as we shall see in the following section.

CHECK YOUR UNDERSTANDING

Write the reactions of glycolysis, showing the structural formulas of the intermediates and the names of the enzymes that catalyze the reactions.

What compounds with high phosphate group-transfer potential are synthesized during glycolysis?

What is the fate of the electrons obtained from the partial oxidation of glucose during glycolysis?

3 Fermentation: The Anaerobic Fate of Pyruvate

LEARNING OBJECTIVES

- Understand that NADH must be reoxidized for glycolysis to continue.
- Understand that the anaerobic reoxidation of NADH occurs by different paths in different organisms.
- Understand how various coenzymes and cofactors participate in the different types of fermentation.

The three common metabolic fates of pyruvate produced by glycolysis are outlined in Fig. 15-16.

1. *Under aerobic conditions, the pyruvate is completely oxidized via the citric acid cycle to CO_2 and H_2O.*
2. *Under anaerobic conditions, pyruvate must be converted to a reduced end product in order to reoxidize the NADH produced by the GAPDH reaction.* This occurs in two ways:
   - **(a)** Under anaerobic conditions in muscle, pyruvate is reduced to **lactate** to regenerate NAD^+ in a process known as **homolactic fermentation** (a fermentation is an anaerobic biological reaction process).
   - **(b)** In yeast, pyruvate is decarboxylated to yield CO_2 and **acetaldehyde,** which is then reduced by NADH to yield NAD^+ and ethanol. This process is known as **alcoholic fermentation.**

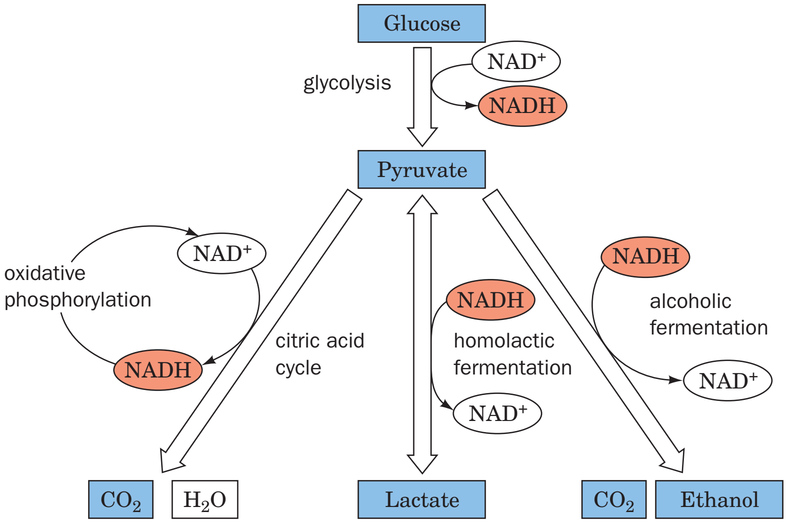
Glucose
glycolysis
NAD+
NADH
Pyruvate
oxidative phosphorylation
NAD+
NADH
citric acid cycle
NADH
homolactic fermentation
NAD+
NADH
alcoholic fermentation
NAD+
CO2
H2O
Lactate
CO2
Ethanol

Figure 15-16 | Metabolic fate of pyruvate. Under aerobic conditions (*left*), the pyruvate carbons are oxidized to CO_2 by the citric acid cycle and the electrons are eventually transferred to O_2 to yield H_2O in oxidative phosphorylation. Under anaerobic conditions in muscle, pyruvate is reversibly converted to lactate (*middle*), whereas in yeast, it is converted to CO_2 and ethanol (*right*).

Thus, in aerobic glycolysis, NADH acts as a "high-energy" compound, whereas in anaerobic glycolysis, its free energy of oxidation is dissipated as heat.

A | Homolactic Fermentation Converts Pyruvate to Lactate

In muscle, during vigorous activity, when the demand for ATP is high and oxygen is in short supply, ATP is largely synthesized via anaerobic glycolysis, which rapidly generates ATP, rather than through the slower process of oxidative phosphorylation. Under these conditions, **lactate dehydrogenase (LDH)** catalyzes the oxidation of NADH by pyruvate to yield NAD^+ and lactate:

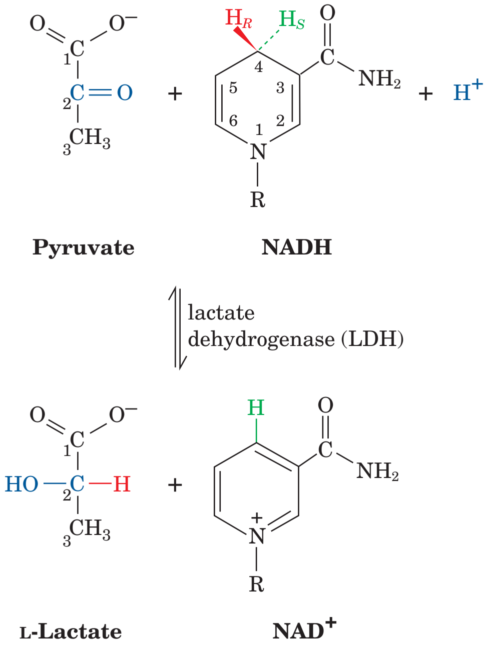
Pyruvate
NADH
H+
lactate dehydrogenase (LDH)
L-Lactate
NAD+

This reaction is often classified as Reaction 11 of glycolysis. The lactate dehydrogenase reaction is freely reversible, so *pyruvate and lactate concentrations are readily equilibrated.*

In the proposed mechanism for pyruvate reduction by LDH, a hydride ion is stereospecifically transferred from C4 of NADH to C2 of pyruvate with concomitant transfer of a proton from the imidazolium moiety of His 195:

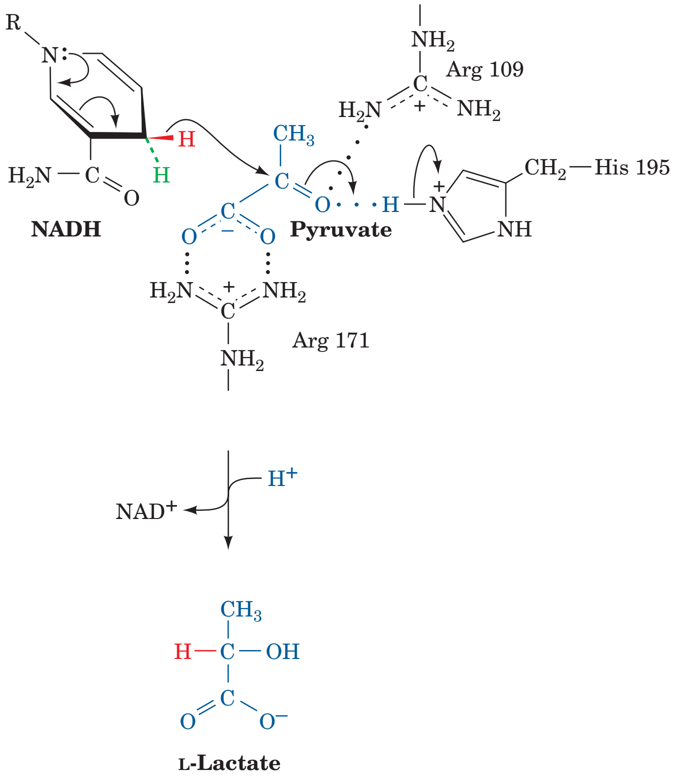

Both His 195 and Arg 171 interact electrostatically with the substrate to orient pyruvate (or lactate, in the reverse reaction) in the enzyme active site.

The overall process of anaerobic glycolysis in muscle can be represented as

$$\text{Glucose} + 2\,\text{ADP} + 2\,\text{P}_i \rightarrow 2\,\text{lactate} + 2\,\text{ATP} + 2\,\text{H}_2\text{O} + 2\,\text{H}^+$$

Lactate represents a sort of dead end for anaerobic glucose metabolism. The lactate can either be exported from the cell or converted back to pyruvate. Much of the lactate produced in skeletal muscle cells is carried by the blood to the liver, where it is used to synthesize glucose (Section 22-1F).

Contrary to widely held belief, it is not lactate buildup in the muscle per se that causes muscle fatigue and soreness but the accumulation of glycolytically generated acid (muscles can maintain their workload in the presence of high lactate concentrations if the pH is kept constant).

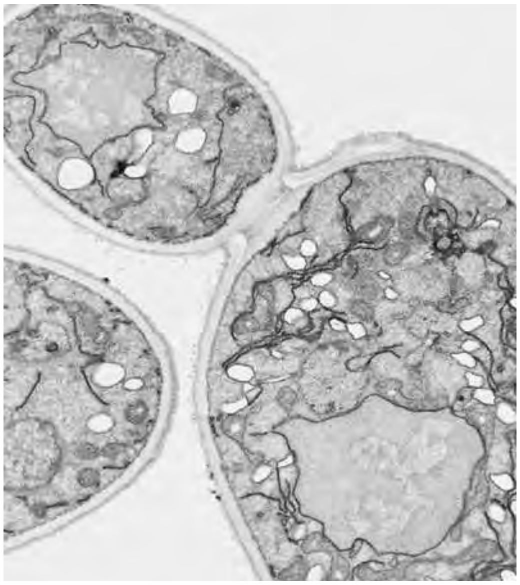

Figure 15-17 | An electron micrograph of yeast cells. [Biophoto Associates Photo Researchers.]

B | Alcoholic Fermentation Converts Pyruvate to Ethanol and CO_2

Under anaerobic conditions in yeast, NAD^+ for glycolysis is regenerated in a process that has been valued for thousands of years: the conversion of pyruvate to ethanol and CO_2. Ethanol is, of course, the active ingredient of wine and spirits; CO_2 so produced leavens bread.

Yeast (Fig. 15-17) produces ethanol and CO_2 via two consecutive reactions (Fig. 15-18):

1. The decarboxylation of pyruvate to form acetaldehyde and CO_2 as catalyzed by **pyruvate decarboxylase** (an enzyme not present in animals).

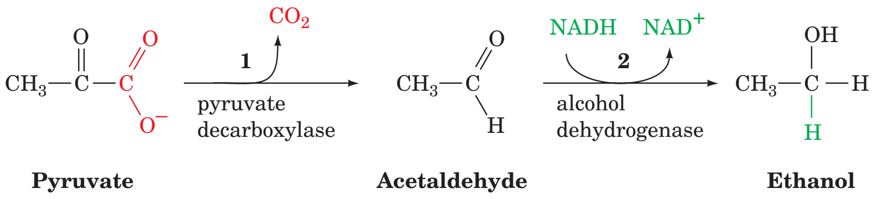

Figure 15-18 | **The two reactions of alcoholic fermentation.** (**1**) Decarboxylation of pyruvate to form acetaldehyde; and (**2**) reduction of acetaldehyde to ethanol by NADH.

2. The reduction of acetaldehyde to ethanol by NADH as catalyzed by alcohol dehydrogenase (Section 11-1C), thereby regenerating NAD$^+$ for use in the GAPDH reaction of glycolysis.

TPP Is an Essential Cofactor of Pyruvate Decarboxylase. Pyruvate decarboxylase contains the coenzyme **thiamine pyrophosphate (TPP;** also called **thiamin diphosphate, ThDP):**

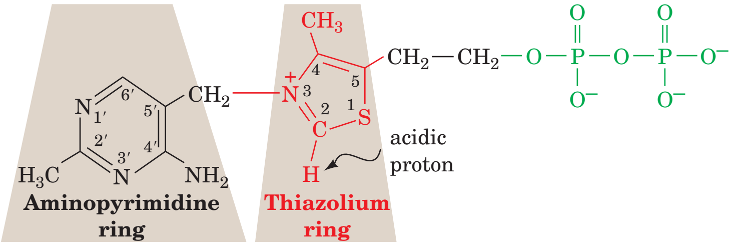

Thiamine pyrophosphate (TPP)

TPP, which is synthesized from thiamine **(vitamin B$_1$)**, binds tightly but noncovalently to pyruvate decarboxylase (Fig. 15-19).

The enzyme uses TPP because uncatalyzed decarboxylation of an α-keto acid such as pyruvate requires the buildup of negative charge on the carbonyl carbon atom in the transition state, an unstable situation:

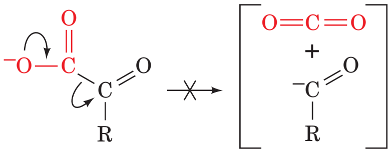

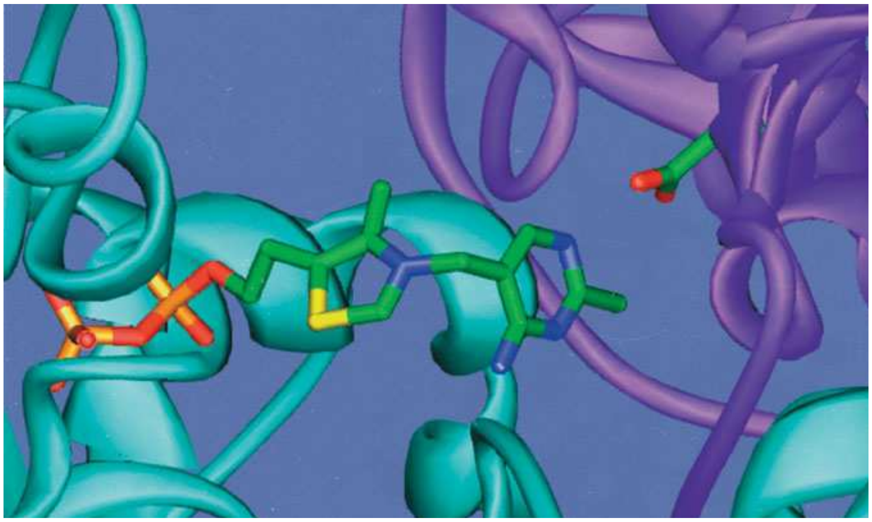

Figure 15-19 | **TPP binding to pyruvate decarboxylase from *Saccharomyces uvarum* (brewer's yeast).** The TPP and the side chain of Glu 51 are shown in stick form with C green, N blue, O red, S yellow, and P orange. The TPP binds in a cavity situated between the dimer's two subunits (*cyan and magenta*) where it hydrogen bonds to Glu 51. [Based on an X-ray structure by William Furey and Martin Sax, Veterans Administration Medical Center and University of Pittsburgh. PDBid 1PYD.] **See Interactive Exercise 17.**

This transition state can be stabilized by delocalizing the developing negative charge into a suitable "electron sink." The amino acid residues of proteins function poorly in this capacity but TPP does so easily.

*TPP's catalytically active functional group is the **thiazolium ring.*** The C2-H atom of this group is relatively acidic because of the adjacent positively charged quaternary nitrogen atom, which electrostatically stabilizes the carbanion formed when the proton dissociates. This dipolar carbanion (or **ylid**) is the active form of the coenzyme. Pyruvate decarboxylase operates as follows (Fig. 15-20):

Step 1 Nucleophilic attack by the ylid form of TPP on the carbonyl carbon of pyruvate.

Step 2 Departure of CO_2 to generate a resonance-stabilized carbanion adduct in which the thiazolium ring of the coenzyme acts as an electron sink.

Step 3 Protonation of the carbanion.

Step 4 Elimination of the TPP ylid to form acetaldehyde and regenerate the active enzyme.

This mechanism has been corroborated by the isolation of the **hydroxyethylthiamine pyrophosphate** intermediate.

Vitamin B_1 Deficiency Causes Beriberi. The ability of TPP's thiazolium ring to add to carbonyl groups and act as an electron sink makes it the coenzyme most utilized in α-keto acid decarboxylation reactions. Such

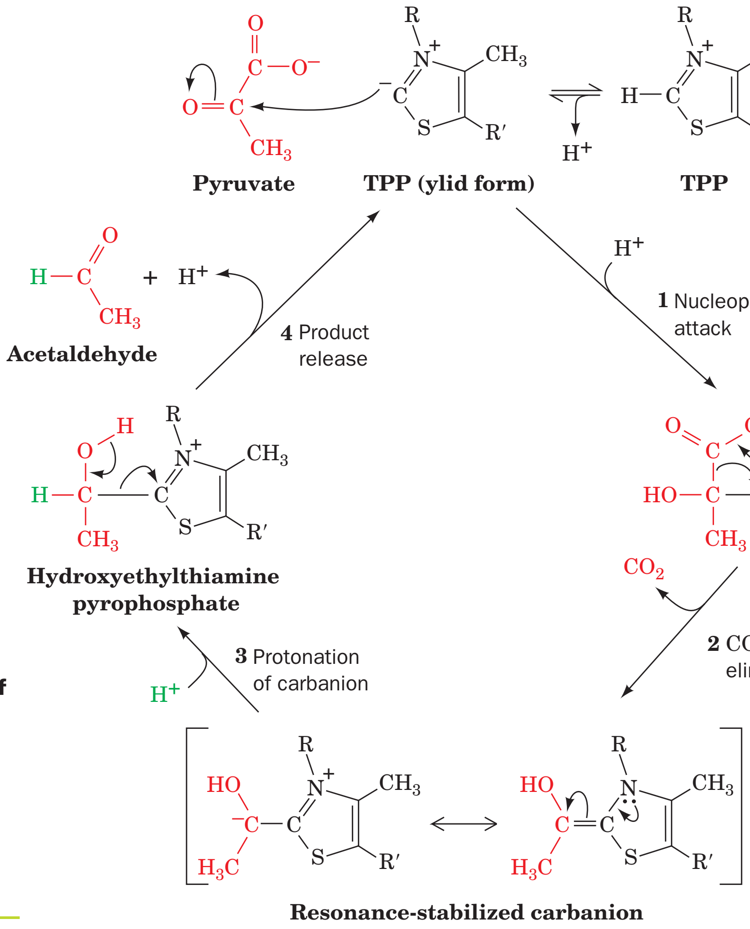
Pyruvate
TPP (ylid form)
TPP
H+
1 Nucleophilic attack
2 CO2 elimination
CO2
Resonance-stabilized carbanion
3 Protonation of carbanion
H+
Hydroxyethylthiamine pyrophosphate
4 Product release
Acetaldehyde
H+
R
R'
CH3

Figure 15-20 | The reaction mechanism of pyruvate decarboxylase. (**1**) Nucleophilic attack by the ylid form of TPP on the carbonyl carbon of pyruvate; (**2**) departure of CO_2 to generate a resonance-stabilized carbanion; (**3**) protonation of the carbanion; and (**4**) elimination of the TPP ylid and release of product.

reactions occur in all organisms, not just yeast. Consequently, thiamine (vitamin B_1), which is neither synthesized nor stored in significant quantities by the tissues of most vertebrates, is required in their diets. Thiamine deficiency in humans results in an ultimately fatal condition known as **beriberi** (Singhalese for weakness) that is characterized by neurological disturbances causing pain, paralysis, and atrophy (wasting) of the limbs and/or edema (accumulation of fluid in tissues and body cavities). Beriberi was particularly prevalent in the late eighteenth and early nineteenth centuries in the rice-consuming areas of Asia after the introduction of steam-powered milling machines that polished the rice grains to remove their coarse but thiamine-containing outer layers (the previously used milling procedures were less efficient and hence left sufficient thiamine on the grains). Parboiling rice before milling, a process common in India, causes the rice kernels to absorb nutrients from their outer layers, thereby decreasing the incidence of beriberi. Once thiamine deficiency was recognized as the cause of beriberi, enrichment procedures were instituted so that today it has ceased to be a problem except in areas undergoing famine. However, beriberi occasionally develops in alcoholics due to their penchant for drinking but not eating.

Reduction of Acetaldehyde and Regeneration of NAD^+. Yeast alcohol dehydrogenase **(YADH)**, the enzyme that converts acetaldehyde to ethanol, is a tetramer, each subunit of which binds one Zn^{2+} ion. The Zn^{2+} polarizes the carbonyl group of acetaldehyde to stabilize the developing negative charge in the transition state of the reaction *(at right)*. This facilitates the stereospecific transfer of a hydrogen from NADH to acetaldehyde.

Mammalian liver alcohol dehydrogenase **(LADH)** metabolizes the alcohols anaerobically produced by the intestinal flora as well as those from external sources (the direction of the alcohol dehydrogenase reaction varies with the relative concentrations of ethanol and acetaldehyde). Mammalian LADH is a dimer with significant amino acid sequence similarity to YADH, although LADH subunits each contain a second Zn^{2+} ion that presumably has a structural role.

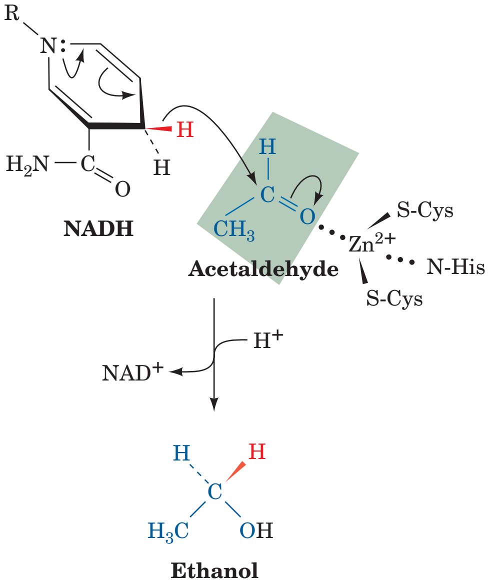

C | Fermentation Is Energetically Favorable

Thermodynamics permits us to dissect the process of fermentation into its component parts and to account for the free energy changes that occur. This enables us to calculate the efficiency with which the free energy of glucose catabolism is used in the synthesis of ATP. For homolactic fermentation,

$$\text{Glucose} \longrightarrow 2\text{ lactate} + 2\text{ H}^+ \qquad \Delta G^{\circ\prime} = -196\text{ kJ}\cdot\text{mol}^{-1}$$

For alcoholic fermentation,

$$\text{Glucose} \longrightarrow 2\text{ CO}_2 + 2\text{ ethanol} \qquad \Delta G^{\circ\prime} = -235\text{ kJ}\cdot\text{mol}^{-1}$$

Each of these processes is coupled to the net formation of 2 ATP, which requires $\Delta G^{\circ\prime} = +61\text{ kJ}\cdot\text{mol}^{-1}$ of glucose consumed. Dividing $\Delta G^{\circ\prime}$ of ATP formation by that of lactate formation indicates that homolactic fermentation is 31% "efficient"; that is, 31% of the free energy released by the process under standard biochemical conditions is sequestered in the form of ATP. The rest is dissipated as heat, thereby making the process irreversible. Likewise, alcoholic fermentation is 26% efficient under biochemical standard state conditions. *Under physiological conditions, where the concentrations of reactants and products differ from those of the standard state, these reactions have thermodynamic efficiencies of >50%.*

BOX 15-3 **PERSPECTIVES IN BIOCHEMISTRY**

Glycolytic ATP Production in Muscle

Skeletal muscle consists of both **slow-twitch** (Type I) and **fast-twitch** (Type II) **fibers.** Fast-twitch fibers, so called because they predominate in muscles capable of short bursts of rapid activity, are nearly devoid of mitochondria (where oxidative phosphorylation occurs). Consequently, they must obtain nearly all of their ATP through anaerobic glycolysis, for which they have a particularly large capacity. Muscles designed to contract slowly and steadily, in contrast, are enriched in slow-twitch fibers that are rich in mitochondria and obtain most of their ATP through oxidative phosphorylation.

Fast- and slow-twitch fibers were originally known as white and red fibers, respectively, because otherwise pale-colored muscle tissue, when enriched with mitochondria, takes on the red color characteristic of their heme-containing cytochromes. However, fiber color is an imperfect indictor of muscle physiology.

In a familiar example, the flight muscles of migratory birds such as ducks and geese, which need a continuous energy supply, are rich in slow-twitch fibers. Therefore, these birds have dark breast meat. In contrast, the flight muscles of less ambitious fliers, such as chickens and turkeys, which are used only for short bursts (often to escape danger), consist mainly of fast-twitch fibers that form white meat. In humans, the muscles of sprinters are relatively rich in fast-twitch fibers, whereas distance runners have a greater proportion of slow-twitch fibers (although their muscles have the same color).

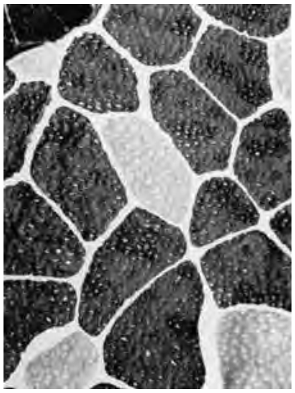

slow-twitch muscle fiber

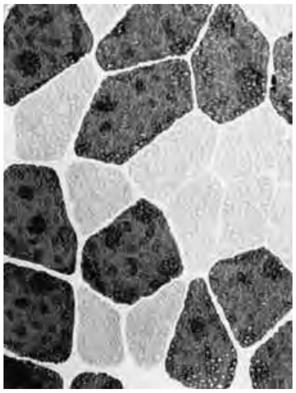

fast-twitch muscle fiber

[Photo of muscle courtesy of J.D. MacDougall, McMaster University, Canada.]

Anaerobic fermentation uses glucose in a profligate manner compared to oxidative phosphorylation: Fermentation results in the production of 2 ATP per glucose, whereas oxidative phosphorylation yields up to 32 ATP per glucose (Section 18-3C). This accounts for Pasteur's observation that yeast consume far more sugar when growing anaerobically than when growing aerobically (the **Pasteur effect**). However, *the rate of ATP production by anaerobic glycolysis can be up to 100 times faster than that of oxidative phosphorylation. Consequently, when tissues such as muscle are rapidly consuming ATP, they regenerate it almost entirely by anaerobic glycolysis.* (Homolactic fermentation does not really "waste" glucose since the lactate can be aerobically reconverted to glucose by the liver; Section 22-1F.) Certain muscles are specialized for the rapid production of ATP by glycolysis (Box 15-3).

CHECK YOUR UNDERSTANDING

Describe the three possible fates of pyruvate.

Compare the ATP yields and rates of ATP production for anaerobic and aerobic degradation of glucose.

4 Regulation of Glycolysis

LEARNING OBJECTIVES

- Understand that enzymes that function with large negative free energy changes are candidates for flux-control points.
- Understand that phosphofructokinase, the major regulatory point for glycolysis in muscle, is controlled by allosteric interactions.
- Understand that substrate cycling allows the rate of glycolysis to respond rapidly to changing needs.

Under steady state conditions, glycolysis operates continuously in most tissues, although the glycolytic flux must vary to meet the needs of the organism. Elucidation of the flux control mechanisms of a given pathway, such as glycolysis, commonly involves three steps:

1. Identification of the rate-determining step(s) of the pathway by measuring the *in vivo* ΔG for each reaction. Enzymes that operate far from equilibrium are potential control points (Section 14-1D).
2. *In vitro* identification of allosteric modifiers of the enzymes catalyzing the rate-determining reactions. The mechanisms by which these

Table 15-1 $\Delta G^{\circ\prime}$ and ΔG for the Reactions of Glycolysis in Heart Muscle[a]

Reaction	Enzyme	$\Delta G^{\circ\prime}$ ($kJ \cdot mol^{-1}$)	ΔG ($kJ \cdot mol^{-1}$)
1	Hexokinase	−20.9	−27.2
2	PGI	+2.2	−1.4
3	PFK	−17.2	−25.9
4	Aldolase	+22.8	−5.9
5	TIM	+7.9	~0
6 + 7	GAPDH + PGK	−16.7	−1.1
8	PGM	+4.7	−0.6
9	Enolase	−3.2	−2.4
10	PK	−23.0	−13.9

[a] Calculated from data in Newsholme, E.A. and Start, C., *Regulation in Metabolism,* p. 97, Wiley (1973).

compounds act are determined from their effects on the enzymes' kinetics.

3. Measurement of the *in vivo* levels of the proposed regulators under various conditions to establish whether the concentration changes are consistent with the proposed control mechanism.

Let us examine the thermodynamics of glycolysis in muscle tissue with an eye toward understanding its control mechanisms (keep in mind that different tissues control glycolysis in different ways). Table 15-1 lists the standard free energy changes ($\Delta G^{\circ\prime}$) and the actual physiological free energy change (ΔG) associated with each reaction in the pathway. It is important to realize that the free energy changes associated with the reactions under standard conditions may differ dramatically from the actual values *in vivo.*

Only three reactions of glycolysis, those catalyzed by hexokinase, phosphofructokinase, and pyruvate kinase, function with large negative free energy changes in heart muscle under physiological conditions (Fig. 15-21). These nonequilibrium reactions of glycolysis are candidates for flux-control points. The other glycolytic reactions function near equilibrium: Their forward and reverse rates are much faster than the actual flux through the pathway. Consequently, these equilibrium reactions are very sensitive to changes in the concentration of pathway intermediates and readily accommodate changes in flux generated at the rate-determining step(s) of the pathway.

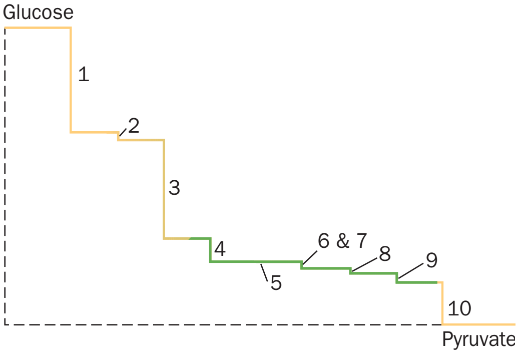

Figure 15-21 | Diagram of free energy changes in glycolysis. This "waterfall" diagram illustrates the actual free energy changes for the glycolytic reactions in heart muscle (Table 15-1). Reactions 1, 3, and 10 are irreversible. The other reactions operate near equilibrium and can mediate flux in either direction.

A | Phosphofructokinase Is the Major Flux-Controlling Enzyme of Glycolysis in Muscle

In vitro studies of hexokinase, phosphofructokinase, and pyruvate kinase indicate that each is controlled by a variety of compounds. Yet when the G6P source for glycolysis is glycogen, rather than glucose, as is often the case in skeletal muscle, the hexokinase reaction is not required (Section 16-1). Pyruvate kinase catalyzes the last reaction of glycolysis and is therefore unlikely to be the primary point for regulating flux through the entire pathway. Evidently, PFK, an elaborately regulated enzyme functioning far from equilibrium, is the major control point for glycolysis in muscle under most conditions.

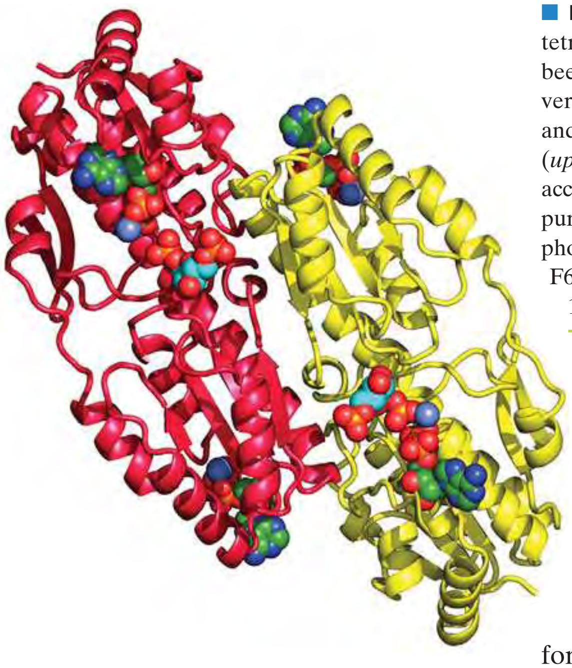

■ **Figure 15-22 | X-Ray structure of PFK from *E. coli.*** Two subunits of the tetrameric enzyme are shown in ribbon form (the other two subunits, which have been omitted for clarity, are related to those shown by a twofold rotation about the vertical axis). Each subunit binds its products, FBP (*near the center of each subunit*) and Mg^{2+}–ADP (*lower right and upper left*), together with its activator Mg^{2+}–ADP (*upper right and lower left, in the rear*), all in space-filling form with atoms colored according to type (ADP C green, FBP C cyan, N blue, O red, P orange, and Mg purple). Note the close proximity of the product ADP's β-phosphate group to the phosphoryl group at FBP's 1-position, the group that PFK transfers from ATP to F6P. [Based on an X-ray structure by Philip Evans, Cambridge University. PDBid 1PFK.] **See Kinemage Exercise 13-1.**

PFK (Fig. 15-22) is a tetrameric enzyme with two conformational states, R and T, that are in equilibrium. ATP is both a substrate and an allosteric inhibitor of phosphofructokinase. Other compounds, including ADP, AMP, and **fructose-2,6-bisphosphate (F2,6P),** reverse the inhibitory effects of ATP and are therefore activators of PFK. Each PFK subunit has two binding sites for ATP: a substrate site and an inhibitor site. The substrate site binds ATP equally well in either conformation, but the inhibitor site binds ATP almost exclusively in the T state. The other substrate of PFK, F6P, preferentially binds to the R state. Consequently, at high concentrations, ATP acts as an allosteric inhibitor of PFK by binding to the T state, thereby shifting the $T \rightleftharpoons R$ equilibrium in favor of the T state and thus decreasing PFK's affinity for F6P (this is similar to the action of 2,3-BPG in decreasing the affinity of hemoglobin for O_2; Section 7-1D).

In graphical terms, high concentrations of ATP shift the curve of PFK activity versus [F6P] to the right and make it even more sigmoidal (cooperative) (Fig. 15-23). For example, when [F6P] = 0.5 mM (the dashed line in Fig. 15-23), the enzyme is nearly maximally active, but in the presence of 1 mM ATP, the activity drops to 15% of its original level, a nearly sevenfold decrease. An activator such as AMP or ADP counters the effect of ATP by binding to R-state PFK, thereby shifting the $T \rightleftharpoons R$ equilibrium toward the R state. (Actually, the most potent allosteric effector of PFK is F2,6P, which we discuss in Section 16-4C.)

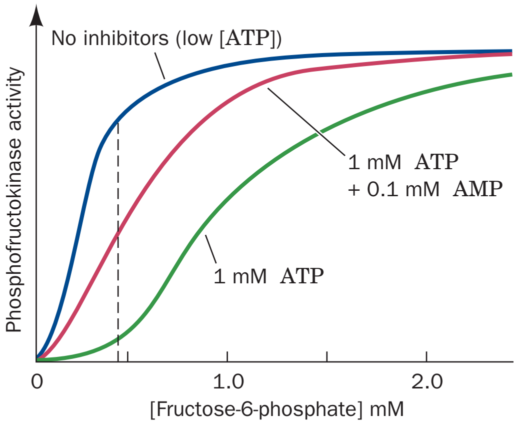

■ **Figure 15-23 | PFK activity versus F6P concentration.** The various conditions are as follows: purple, no inhibitors or activators; green, 1 mM ATP; and red, 1 mM ATP + 0.1 mM AMP. [After data from Mansour, T.E. and Ahlfors, C.E., *J. Biol. Chem.* **243,** 2523–2533 (1968).] **See the Animated Figures.**

Allosterism in Phosphofructokinase Involves Arg and Glu Side Chains. The X-ray structures of PFK from several organisms have been determined in both the R and the T states by Philip Evans. The R state of PFK is stabilized by the binding of its substrate F6P. In the R state of *Bacillus stearothermophilus* PFK, the side chain of Arg 162 forms an ion pair with the phosphoryl group of an F6P bound in the active site of another subunit (Fig. 15-24). However, Arg 162 is located at the end of a helical turn that unwinds on transition to the T state. The positively charged side chain of Arg 162 thereby swings away and is replaced by the negatively charged side chain of Glu 161. As a consequence, the doubly negative phosphoryl group of F6P has a greatly diminished affinity for the T-state enzyme. The unwinding of this helical turn, which is obligatory for the R → T transition, is prevented by the binding of the activator ADP to its effector site on the enzyme. Presumably, ATP can bind to this site only when the helical turn is in its unwound conformation (the T state).

AMP Overcomes the ATP Inhibition of PFK. Direct allosteric regulation of PFK by ATP may at first appear to be the means by which

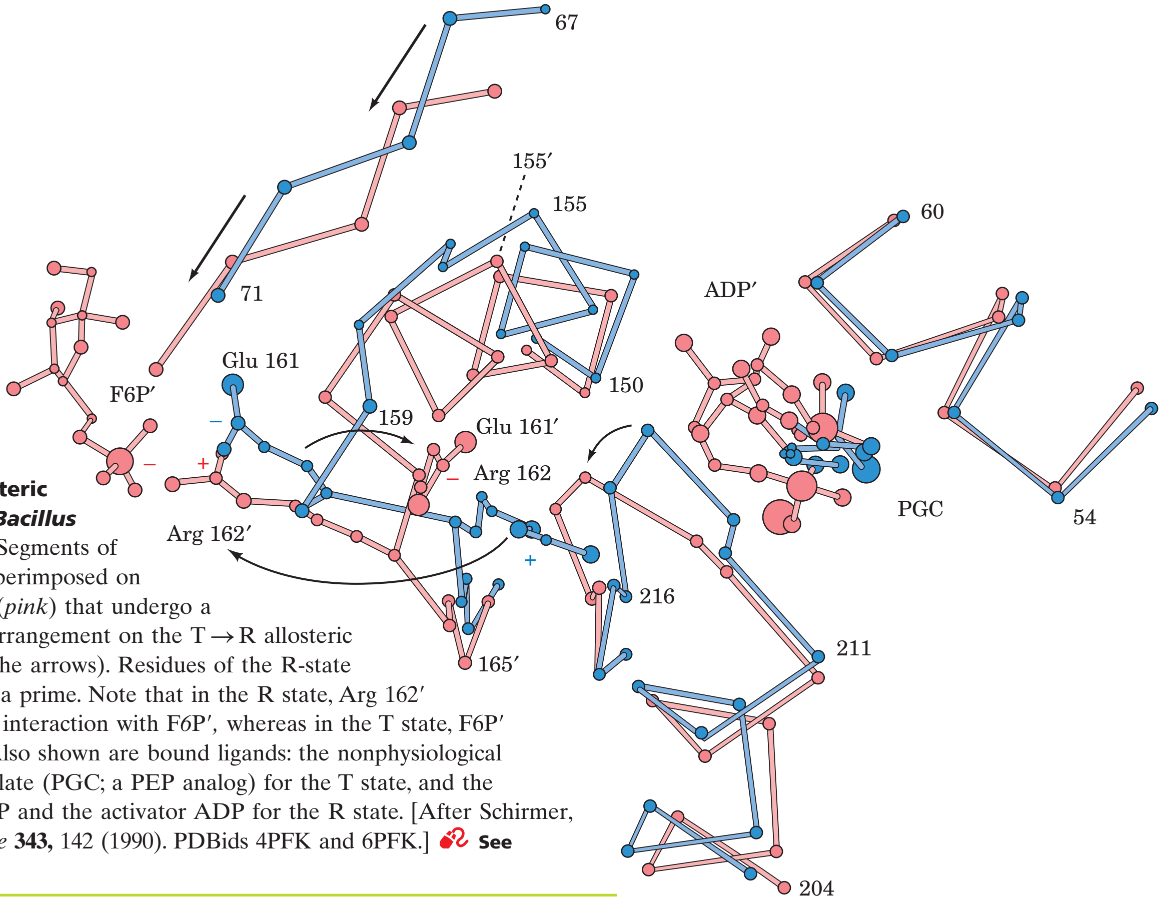

Figure 15-24 | Allosteric changes in PFK from *Bacillus stearothermophilus*. Segments of the T state (*blue*) are superimposed on segments of the R state (*pink*) that undergo a large conformational rearrangement on the T → R allosteric transition (indicated by the arrows). Residues of the R-state structure are marked by a prime. Note that in the R state, Arg 162′ forms an attractive ionic interaction with F6P′, whereas in the T state, F6P′ is repelled by Glu 161. Also shown are bound ligands: the nonphysiological inhibitor 2-phosphoglycolate (PGC; a PEP analog) for the T state, and the cooperative substrate F6P and the activator ADP for the R state. [After Schirmer, T. and Evans, P.R., *Nature* **343,** 142 (1990). PDBids 4PFK and 6PFK.] **See Kinemage Exercise 13-2.**

glycolytic flux is controlled. After all, when [ATP] is high as a result of low metabolic demand, PFK is inhibited and flux through glycolysis is low; conversely when [ATP] is low, flux through the pathway is high and ATP is synthesized to replenish the pool. Consideration of the physiological variation in ATP concentration, however, indicates that the situation must be more complex. The metabolic flux through glycolysis may vary by 100-fold or more, depending on the metabolic demand for ATP. However, *measurements of [ATP] in vivo at various levels of metabolic activity indicate that [ATP] varies <10% between rest and vigorous exertion.* Yet there is no known allosteric mechanism that can account for a 100-fold change in flux of a nonequilibrium reaction with only a 10% change in effector concentration. Thus, some other mechanism(s) must be responsible for controlling glycolytic flux.

The inhibition of PFK by ATP is relieved by AMP as well as ADP. This results from AMP's preferential binding to the R state of PFK. If a PFK solution containing 1 mM ATP and 0.5 mM F6P is brought to 0.1 mM in AMP, the activity of PFK rises from 15 to 50% of its maximal activity, a threefold increase (Fig. 15-23).

The [ATP] decreases by only 10% in going from a resting state to one of vigorous activity because it is buffered by the action of two enzymes: creatine kinase and adenylate kinase (Section 14-2C). Adenylate kinase catalyzes the reaction

$$2\,\text{ADP} \rightleftharpoons \text{ATP} + \text{AMP} \qquad K = \frac{[\text{ATP}][\text{AMP}]}{[\text{ADP}]^2} = 0.44$$

which rapidly equilibrates the ADP resulting from ATP hydrolysis in muscle contraction with ATP and AMP.

In muscle, [ATP] is ~50 times greater than [AMP] and ~10 times greater than [ADP]. Consequently, *a change in [ATP] from, for example, 1 to 0.9 mM, a 10% decrease, can result in a 100% increase in [ADP] (from 0.1 to 0.2 mM) as a result of the adenylate kinase reaction, and a >400% increase in [AMP] (from 0.02 to ~0.1 mM).* Therefore, a metabolic signal consisting of a decrease in [ATP] too small to relieve PFK inhibition is amplified significantly by the adenylate kinase reaction, which increases [AMP] by an amount that produces a much larger increase in PFK activity.

B | Substrate Cycling Fine-Tunes Flux Control

Even a finely tuned allosteric mechanism like that of PFK can account for only a fraction of the 100-fold alterations in glycolytic flux. Additional control may be achieved by substrate cycling. Recall from Section 14-1D that only a near-equilibrium reaction can undergo large changes in flux because, in a near-equilibrium reaction, $v_f - v_r \approx 0$ (where v_f and v_r are the forward and reverse reaction rates) and hence a small change in v_f will result in a large fractional change in $v_f - v_r$. However, this is not the case for the PFK reaction because, for such nonequilibrium reactions, v_r is negligible.

Nevertheless, *such equilibrium-like conditions may be imposed on a nonequilibrium reaction if a second enzyme (or series of enzymes) catalyzes the regeneration of its substrate from its product in a thermodynamically favorable manner.* This can be diagrammed as

$$\begin{tikzcd}
\mathrm{A} \arrow[r, bend left, "f"] & \mathrm{B} \arrow[l, bend left, "r"]
\end{tikzcd}$$

Since two different enzymes catalyze the forward (f) and reverse (r) reactions, v_f and v_r may be independently varied and v_r is no longer negligible compared to v_f. Note that the forward process (e.g., formation of FBP from F6P) and the reverse process (e.g., breakdown of FBP to F6P) *must* be carried out by different enzymes since the laws of thermodynamics would otherwise be violated (i.e., for a single reaction, the forward and reverse reactions cannot simultaneously be favorable).

Under physiological conditions, the reaction catalyzed by PFK:

$$\text{F6P} + \text{ATP} \longrightarrow \text{FBP} + \text{ADP}$$

is highly exergonic ($\Delta G = -25.9\ \text{kJ}\cdot\text{mol}^{-1}$). Consequently, the back reaction has a negligible rate compared to the forward reaction. **Fructose-1,6-bisphosphatase (FBPase),** however, which is present in many mammalian tissues (and which is an essential enzyme in gluconeogenesis; Section 16-4B), catalyzes the exergonic hydrolysis of FBP ($\Delta G = -8.6\ \text{kJ}\cdot\text{mol}^{-1}$).

$$\text{FBP} + \text{H}_2\text{O} \longrightarrow \text{F6P} + \text{P}_i$$

Note that the combined reactions catalyzed by PFK and FBPase result in net ATP hydrolysis:

$$\text{ATP} + \text{H}_2\text{O} \rightleftharpoons \text{ADP} + \text{P}_i$$

Such a set of opposing reactions (Section 14-1E) is known as a **substrate cycle** because it cycles a substrate to an intermediate and back again. When this set of reactions was discovered, it was referred to as a **futile cycle** since its net result seemed to be the useless consumption of ATP.

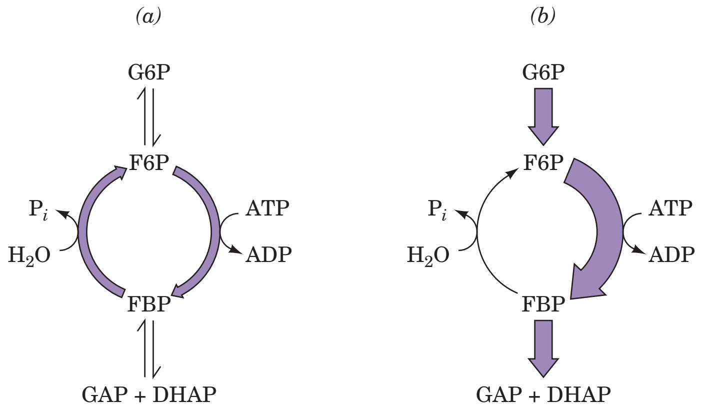

Figure 15-25 | Substrate cycling in the regulation of PFK. (*a*) In resting muscle, both enzymes in the F6P/FBP substrate cycle are active, and glycolytic flux is low. (*b*) In active muscle, PFK activity increases while FBPase activity decreases. This dramatically increases the flux through PFK and therefore results in high glycolytic flux.

Eric Newsholme has proposed that substrate cycles are not at all "futile" but, rather, have a regulatory function. *The combined effects of allosteric effectors on the opposing reactions of a substrate cycle can produce a much greater fractional effect on pathway flux* ($v_f - v_r$) *than is possible through allosteric regulation of a single enzyme.* For example, the allosteric effector F2,6P activates the PFK reaction while inhibiting the FBPase reaction (this regulatory mechanism is important for balancing glycolysis and gluconeogenesis in liver cells; Section 16-4C).

Substrate cycling does not increase the maximum flux through a pathway. On the contrary, it functions to decrease the minimum flux. In a sense, the substrate is put into a "holding pattern." In the PFK/FBPase example (Fig. 15-25), the cycling of substrate appears to be the energetic "price" that a muscle must pay to be able to change rapidly from a resting state (where $v_f - v_r$ is small), in which substrate cycling is maximal, to one of sustained high activity (where $v_f - v_r$ is large). The rate of substrate cycling itself may be under hormonal or neuronal control so as to increase the sensitivity of the metabolic system under conditions when high activity (fight or flight) is anticipated.

Substrate cycling and other mechanisms that control PFK activity *in vivo* are part of larger systems that regulate all the cell's metabolic activities. At one time, it was believed that because PFK is the controlling enzyme of glycolysis, increasing its level of expression via genetic engineering would increase flux through glycolysis. However, this is not the case, because the *activity* of PFK, whatever its concentration, is ultimately controlled by factors that reflect the cell's demand for the products supplied by glycolysis and all other metabolic pathways.

Substrate Cycling Is Related to Thermogenesis and Obesity. Many animals, including adult humans, are thought to generate much of their body heat, particularly when it is cold, through substrate cycling in muscle and liver, a process known as **nonshivering thermogenesis** (the muscle contractions of shivering or any other movement also produce heat). Substrate cycling is stimulated by thyroid hormones (which stimulate metabolism in most tissues) as is indicated, for example, by the observation that rats lacking a functional thyroid gland do not survive at 5°C. Chronically obese individuals tend to have lower than normal metabolic rates, which is probably due, in part, to a reduced rate of nonshivering thermogenesis. Such individuals therefore tend to be cold sensitive. Indeed, whereas normal individuals increase their rate of thyroid hormone activation on exposure to cold, genetically obese animals and obese humans fail to do so.

CHECK YOUR UNDERSTANDING

Which glycolytic enzymes are potential control points?
Describe the mechanisms that control phosphofructokinase activity.
What is the metabolic advantage of a substrate cycle?

5 Metabolism of Hexoses Other than Glucose

LEARNING OBJECTIVE

- Understand that the commonly available hexoses are converted to glycolytic intermediates for further metabolism.

Together with glucose, the hexoses fructose, galactose, and mannose are prominent metabolic fuels. After digestion, these monosaccharides enter the bloodstream, which carries them to various tissues. Fructose, galactose, and mannose are converted to glycolytic intermediates that are then metabolized by the glycolytic pathway (Fig. 15-26).

A | Fructose Is Converted to Fructose-6-Phosphate or Glyceraldehyde-3-Phosphate

Fructose is a major fuel source in diets that contain large amounts of fruit or sucrose (a disaccharide of fructose and glucose; Section 8-2A). There are two pathways for the metabolism of fructose; one occurs in muscle and the other occurs in liver. This dichotomy results from the different enzymes present in these tissues.

Fructose metabolism in muscle differs little from that of glucose. Hexokinase (Section 15-2A), which converts glucose to G6P, also phosphorylates fructose, yielding F6P (Fig. 15-27, *left*). The entry of fructose into glycolysis therefore involves only one reaction step.

Liver contains a hexokinase known as **glucokinase,** which has a low affinity for hexoses, including fructose (Section 22-1D). Fructose metabolism in liver must therefore differ from that in muscle. In fact, liver converts fructose to glycolytic intermediates through a pathway that involves seven enzymes (Fig. 15-27, *right*):

1. **Fructokinase** catalyzes the phosphorylation of fructose by ATP at C1 to form **fructose-1-phosphate.** Neither hexokinase nor PFK can phosphorylate fructose-1-phosphate at C6 to form the glycolytic intermediate FBP.
2. Aldolase (Section 15-2D) has several isozymic forms. Muscle contains Type A aldolase, which is specific for FBP. Liver, however, contains Type B aldolase, for which fructose-1-phosphate is also a substrate (Type B aldolase is sometimes called **fructose-1-phosphate aldolase**). In liver, fructose-1-phosphate therefore undergoes an aldol cleavage:

$$\text{Fructose-1-phosphate} \rightleftharpoons \text{dihydroxyacetone phosphate} + \text{glyceraldehyde}$$

3. Direct phosphorylation of **glyceraldehyde** by ATP through the action of **glyceraldehyde kinase** forms the glycolytic intermediate GAP.

4–7. Alternatively, glyceraldehyde is converted to the glycolytic intermediate DHAP by its NADH-dependent reduction to glycerol as catalyzed by alcohol dehydrogenase (Reaction 4), phosphorylation to **glycerol-3-phosphate** through the action of **glycerol kinase** (Reaction 5), and NAD^+-dependent reoxidation to DHAP catalyzed by **glycerol phosphate dehydrogenase** (Reaction 6). The DHAP is then converted to GAP by triose phosphate isomerase (Reaction 7).

The two pathways leading from glyceraldehyde to GAP have the same net cost: Both consume ATP, and although NADH is oxidized in Reaction 4, it is reduced again in Reaction 6. The longer pathway, however, produces glycerol-3-phosphate, which (along with DHAP) can become the glycerol backbone of glycerophospholipids and triacylglycerols (Section 20-6A).

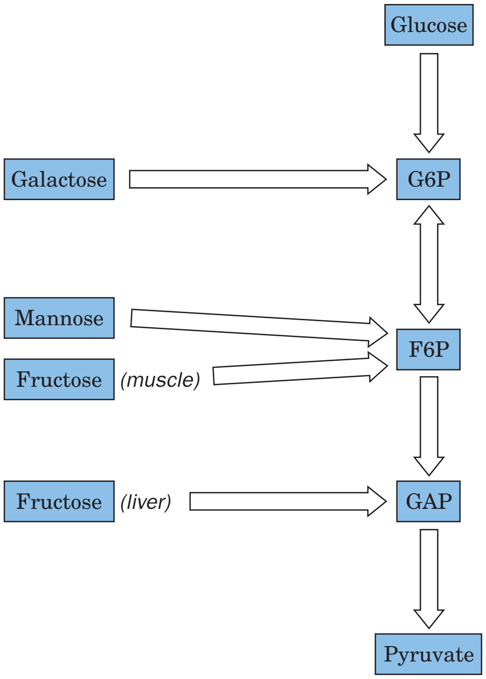

Figure 15-26 | Entry of other hexoses into glycolysis. Fructose (in muscle) and mannose are converted to F6P; liver fructose is converted to GAP; and galactose is converted to G6P.

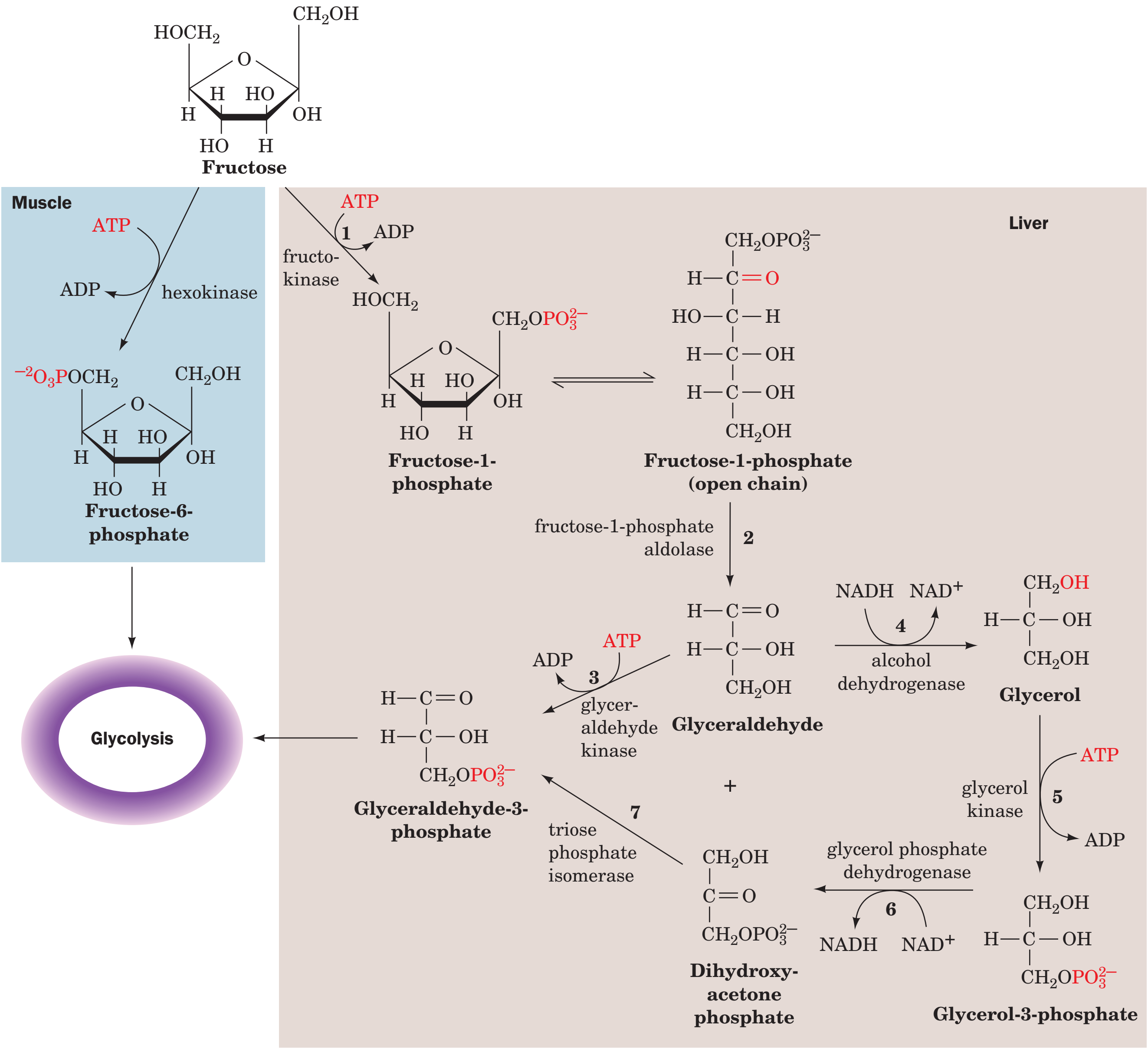

Fructose
Muscle
ATP
ADP
hexokinase
Fructose-6-phosphate
Glycolysis
Liver
ATP
1
ADP
fructokinase
Fructose-1-phosphate
Fructose-1-phosphate (open chain)
fructose-1-phosphate aldolase
2
Glyceraldehyde
NADH
NAD+
4
alcohol dehydrogenase
Glycerol
ATP
ADP
3
glyceraldehyde kinase
Glyceraldehyde-3-phosphate
+
glycerol kinase
5
ATP
ADP
7
triose phosphate isomerase
glycerol phosphate dehydrogenase
6
NADH
NAD+
Dihydroxyacetone phosphate
Glycerol-3-phosphate

Figure 15-27 | The metabolism of fructose. In muscle (*left*), the conversion of fructose to the glycolytic intermediate F6P involves only one enzyme, hexokinase. In liver (*right*), seven enzymes participate in the conversion of fructose to glycolytic intermediates: (**1**) fructokinase, (**2**) fructose-1-phosphate aldolase, (**3**) glyceraldehyde kinase, (**4**) alcohol dehydrogenase, (**5**) glycerol kinase, (**6**) glycerol phosphate dehydrogenase, and (**7**) triose phosphate isomerase.

Is Excess Fructose Harmful? The consumption of fructose in the United States has increased at least 10-fold in the last quarter century, in large part due to the use of high-fructose corn syrup as a sweetener in soft drinks and other foods. Fructose has a sweeter taste than sucrose (Box 8-2) and is inexpensive to produce. One possible hazard of excessive fructose intake is that fructose catabolism in liver bypasses the PFK-catalyzed step of glycolysis and thereby avoids a major metabolic control point. This could potentially disrupt fuel metabolism so that glycolytic flux is directed toward lipid synthesis in the absence of a need for ATP production. This hypothesis suggests a link between the increase in both fructose consumption and the recently increasing incidence of obesity in the United States.

At the opposite extreme are individuals with **fructose intolerance,** which results from a deficiency in Type B aldolase. In the absence of the aldolase, fructose-1-phosphate may accumulate enough to deplete the liver's store of P_i. Under these conditions, [ATP] drops, which causes liver damage. In addition, the increased [fructose-1-phosphate] inhibits both **glycogen phosphorylase** (an essential enzyme in the breakdown of glycogen to glucose; Section 16-1A) and fructose-1,6-bisphosphatase (an essential enzyme in gluconeogenesis; Section 16-4B), thereby causing severe **hypoglycemia** (low levels of blood glucose), which can reach life-threatening proportions. However, fructose intolerance is self-limiting: Individuals with the condition rapidly develop a strong distaste for anything sweet.

B | Galactose Is Converted to Glucose-6-Phosphate

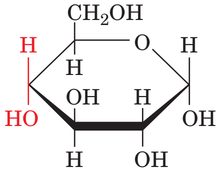

α-D-Glucose

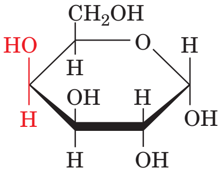

α-D-Galactose

Galactose is obtained from the hydrolysis of lactose (a disaccharide of galactose and glucose; Section 8-2A) in dairy products. Galactose and glucose (*at left*) are epimers that differ only in their configuration at C4. Although hexokinase phosphorylates glucose, fructose, and mannose, it does not recognize galactose. An epimerization reaction must therefore occur before galactose enters glycolysis. This reaction takes place after the conversion of galactose to its **uridine diphosphate** derivative (the role of UDP–sugars and other nucleotidyl–sugars is discussed in more detail in Section 16-5). The entire pathway converting galactose to a glycolytic intermediate requires four reactions (Fig. 15-28):

1. Galactose is phosphorylated at C1 by ATP in a reaction catalyzed by **galactokinase.**
2. **Galactose-1-phosphate uridylyl transferase** transfers the uridylyl group of UDP–glucose to **galactose-1-phosphate** to yield **glucose-1-phosphate (G1P)** and **UDP–galactose** by the reversible cleavage of UDP–glucose's pyrophosphoryl bond.
3. **UDP–galactose-4-epimerase** converts UDP–galactose back to UDP–glucose. This enzyme has an associated NAD^+, which suggests that the reaction involves the sequential oxidation and reduction of the hexose C4 atom:

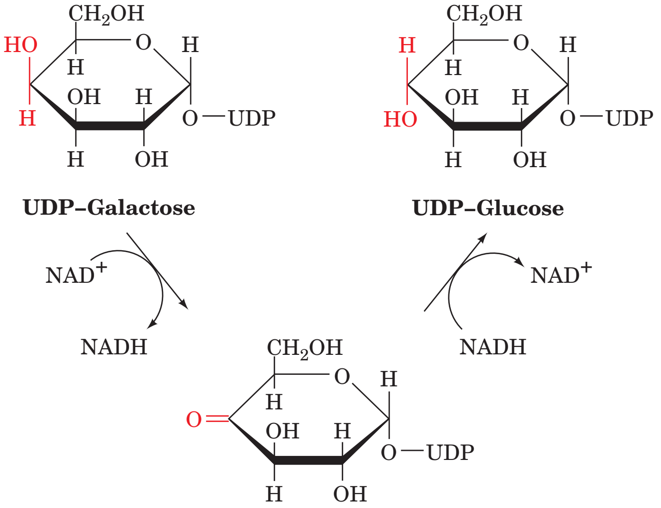

4. G1P is converted to the glycolytic intermediate G6P by the action of **phosphoglucomutase** (Section 16-1C).

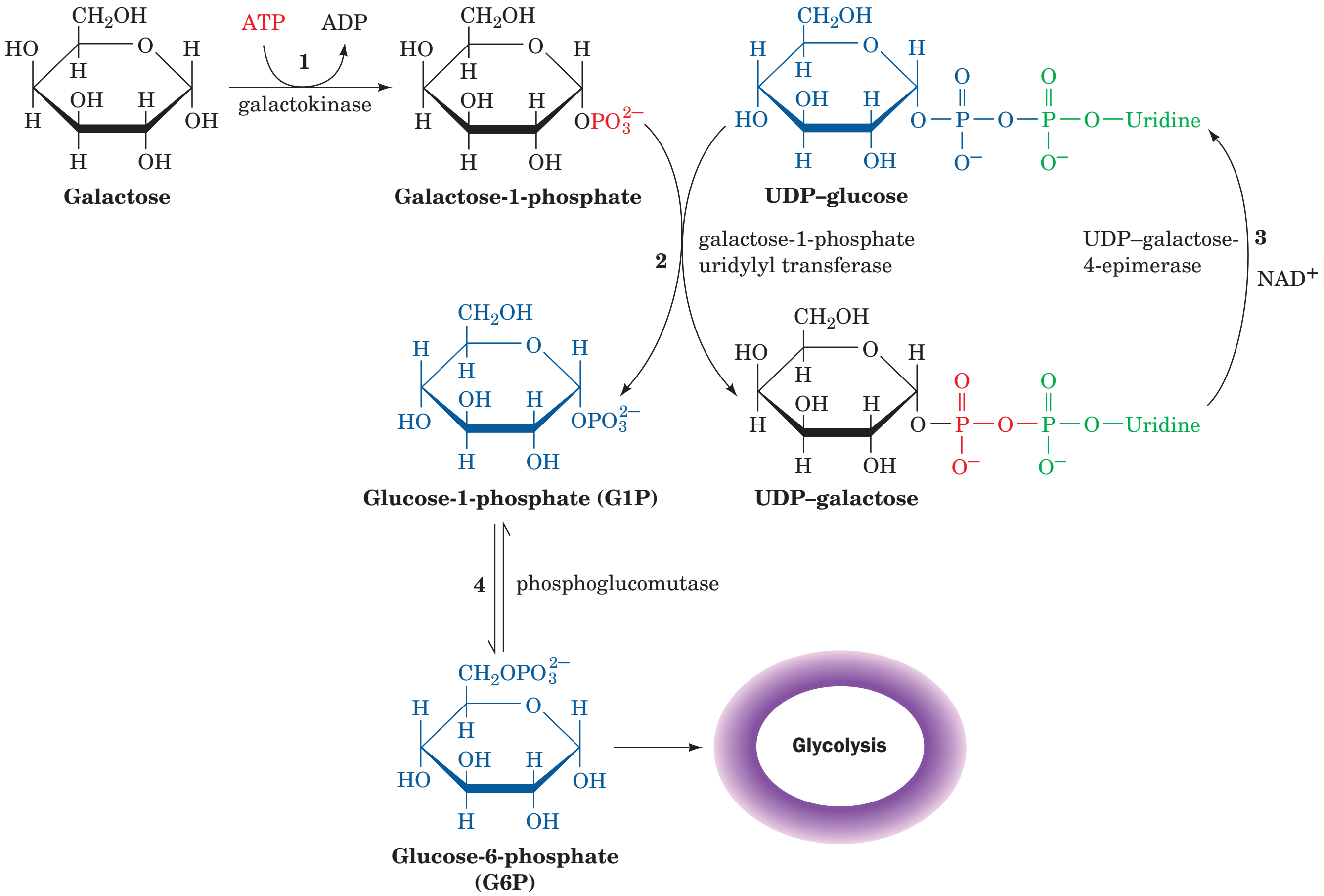

Galactose
ATP
ADP
1
galactokinase
Galactose-1-phosphate
UDP–glucose
2
galactose-1-phosphate uridylyl transferase
UDP–galactose-4-epimerase
3
NAD+
Glucose-1-phosphate (G1P)
UDP–galactose
4
phosphoglucomutase
Glucose-6-phosphate (G6P)
Glycolysis
Uridine

■ **Figure 15-28 | The metabolism of galactose.** Four enzymes participate in the conversion of galactose to the glycolytic intermediate G6P: (**1**) galactokinase, (**2**) galactose-1-phosphate uridylyl transferase, (**3**) UDP–galactose-4-epimerase, and (**4**) phosphoglucomutase.

Individuals with Galactosemia Cannot Metabolize Galactose.

Galactosemia is a genetic disease characterized by the inability to convert galactose to glucose. Its symptoms include failure to thrive, mental retardation, and, in some instances, death from liver damage. Most cases of galactosemia involve a deficiency in the enzyme catalyzing Reaction 2 of the interconversion, galactose-1-phosphate uridylyl transferase. Formation of UDP–galactose from galactose-1-phosphate is thus prevented, leading to a buildup of toxic metabolic by-products. For example, the increased galactose concentration in the blood results in a higher galactose concentration in the lens of the eye, where the sugar is reduced to **galactitol:**

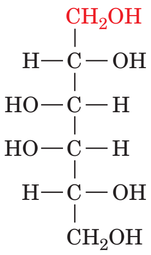

Galactitol

The presence of this sugar alcohol in the lens eventually causes cataract formation (clouding of the lens).

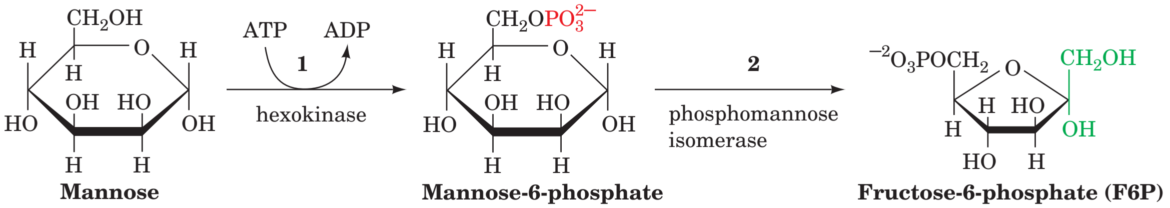

Figure 15-29 | The metabolism of mannose. Two enzymes are required to convert mannose to the glycolytic intermediate F6P: (**1**) hexokinase and (**2**) phosphomannose isomerase.

Galactosemia is treated by a galactose-free diet. Except for the mental retardation, this reverses all symptoms of the disease. The galactosyl units that are essential for the synthesis of glycoproteins (Section 8-3C) and glycolipids (Section 9-1D) can be synthesized from glucose by a reversal of the epimerase reaction. These syntheses therefore do not require dietary galactose.

C | Mannose Is Converted to Fructose-6-Phosphate

Mannose, a product of digestion of polysaccharides and glycoproteins, is the C2 epimer of glucose:

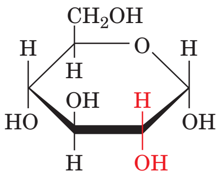

α-D-Glucose

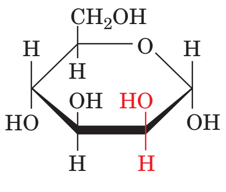

α-D-Mannose

Mannose enters the glycolytic pathway after its conversion to F6P via a two-reaction pathway (Fig. 15-29):

1. Hexokinase recognizes mannose and converts it to **mannose-6-phosphate.**
2. **Phosphomannose isomerase** then converts this aldose to the glycolytic intermediate F6P in a reaction whose mechanism resembles that of phosphoglucose isomerase (Section 15-2B).

CHECK YOUR UNDERSTANDING

Describe how fructose, galactose, and mannose enter the glycolytic pathway.

6 The Pentose Phosphate Pathway

LEARNING OBJECTIVES

- Understand that the pentose phosphate pathway consists of three stages, in which NADPH is produced, pentoses undergo isomerization, and glycolytic intermediates are recovered.
- Understand that the pathway provides NADPH for reductive biosynthesis and ribose-5-phosphate for nucleotide biosynthesis in the quantities that the cell requires.

ATP is the cell's "energy currency"; its exergonic cleavage is coupled to many otherwise endergonic cell functions. *Cells also have a second currency, reducing power.* Many endergonic reactions, notably the reductive biosynthesis of fatty acids (Section 20-4) and cholesterol (Section 20-7A), require NADPH in addition to ATP. Despite their close chemical resemblance, *NADPH and NADH are not metabolically interchangeable.* Whereas NADH uses the free energy of metabolite oxidation to synthesize ATP (oxidative phosphorylation), NADPH uses the free energy of metabolite oxidation for reductive biosynthesis. This differentiation is possible because the dehydrogenases involved in oxidative and reductive metabolism are highly specific for their respective coenzymes. Indeed, cells normally maintain their $[NAD^+]/[NADH]$ ratio near 1000, which favors metabolite oxidation, while keeping their [NADP$^+$]/[NADPH] ratio near 0.01, which favors reductive biosynthesis.

NADPH is generated by the oxidation of glucose-6-phosphate via an alternative pathway to glycolysis, the pentose phosphate pathway (also called the **hexose monophosphate shunt;** Fig. 15-30). Tissues most heavily involved in lipid biosynthesis (liver, mammary gland, adipose tissue, and

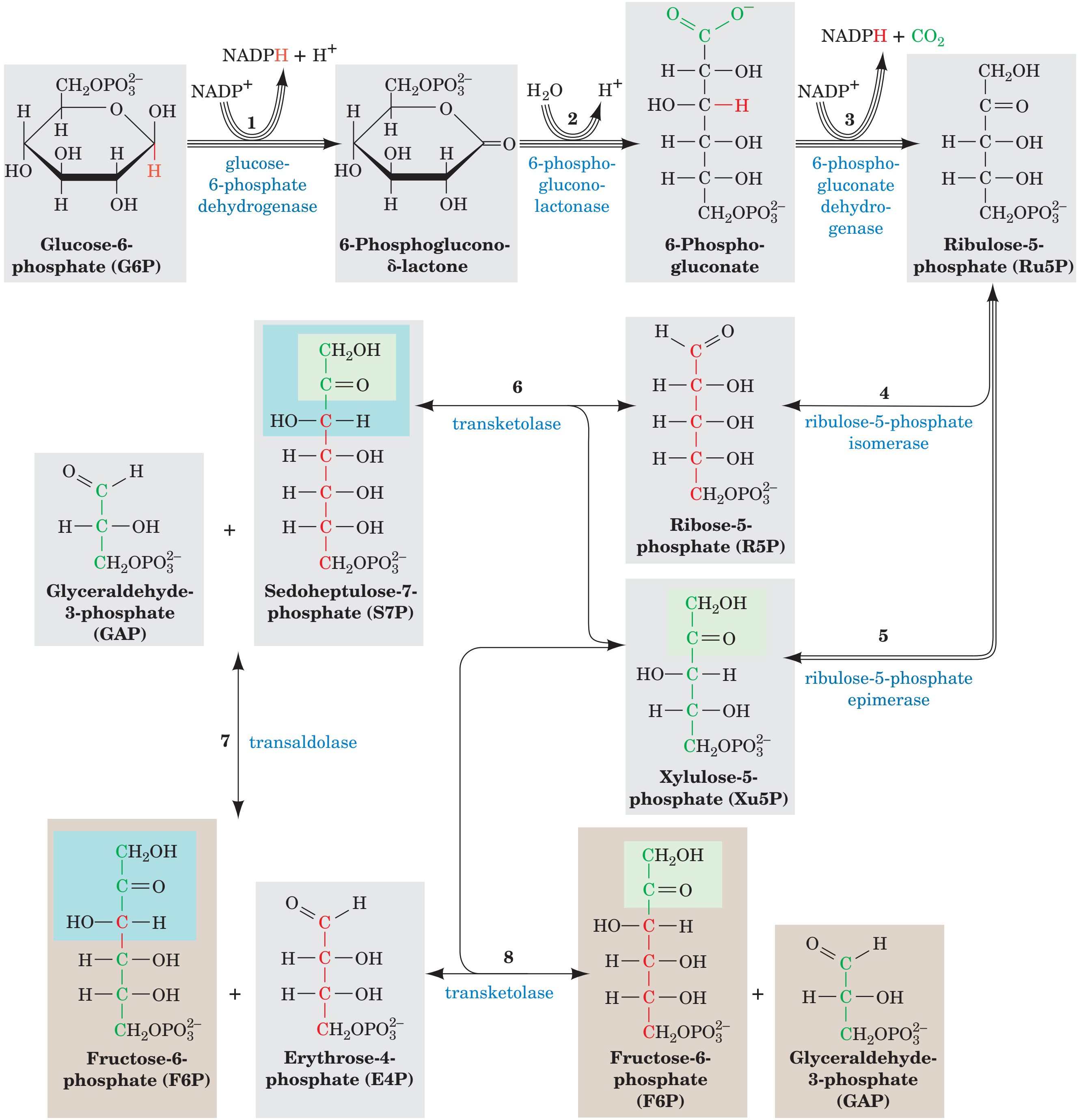
Glucose-6-phosphate (G6P)
NADP+
NADPH + H+
1
glucose-6-phosphate dehydrogenase
6-Phosphoglucono-δ-lactone
H2O
H+
2
6-phosphogluconolactonase
6-Phosphogluconate
NADP+
NADPH + CO2
3
6-phosphogluconate dehydrogenase
Ribulose-5-phosphate (Ru5P)
4
ribulose-5-phosphate isomerase
Ribose-5-phosphate (R5P)
5
ribulose-5-phosphate epimerase
Xylulose-5-phosphate (Xu5P)
6
transketolase
Glyceraldehyde-3-phosphate (GAP)
+
Sedoheptulose-7-phosphate (S7P)
7
transaldolase
Fructose-6-phosphate (F6P)
+
Erythrose-4-phosphate (E4P)
8
transketolase
Fructose-6-phosphate (F6P)
+
Glyceraldehyde-3-phosphate (GAP)

■ **Figure 15-30 | The pentose phosphate pathway.** The number of lines in an arrow represents the number of molecules reacting in one turn of the pathway so as to convert 3 G6P to 3 CO_2, 2 F6P, and 1 GAP. For the sake of clarity, sugars from Reaction 3 onward are shown in their linear forms. The carbon skeleton of R5P and the atoms derived from it are drawn in red, and those from Xu5P are drawn in green. The C_2 units transferred by transketolase are shaded in green, and the C_3 units transferred by transaldolase are shaded in blue. Double-headed arrows indicate reversible reactions.

adrenal cortex) are rich in pentose phosphate pathway enzymes. Indeed, some 30% of the glucose oxidation in liver occurs via the pentose phosphate pathway rather than glycolysis.

The overall reaction of the pentose phosphate pathway is

$$3\ \text{G6P} + 6\ \text{NADP}^+ + 3\ \text{H}_2\text{O} \rightleftharpoons 6\ \text{NADPH} + 6\ \text{H}^+ + 3\ \text{CO}_2 + 2\ \text{F6P} + \text{GAP}$$

However, the pathway can be considered to have three stages:

Stage 1 Oxidative reactions (Fig. 15-30, Reactions 1–3), which yield NADPH and **ribulose-5-phosphate (Ru5P):**

$$3\ \text{G6P} + 6\ \text{NADP}^+ + 3\ \text{H}_2\text{O} \longrightarrow 6\ \text{NADPH} + 6\ \text{H}^+ + 3\ \text{CO}_2 + 3\ \text{Ru5P}$$

Stage 2 Isomerization and epimerization reactions (Fig. 15-30, Reactions 4 and 5), which transform Ru5P either to **ribose-5-phosphate (R5P)** or to **xylulose-5-phosphate (Xu5P):**

$$3\ \text{Ru5P} \rightleftharpoons \text{R5P} + 2\ \text{Xu5P}$$

Stage 3 A series of C—C bond cleavage and formation reactions (Fig. 15-30, Reactions 6–8) that convert two molecules of Xu5P and one molecule of R5P to two molecules of F6P and one molecule of GAP.

The reactions of Stages 2 and 3 are freely reversible, so the products of the pathway vary with the needs of the cell (see below). In this section, we discuss the three stages of the pentose phosphate pathway and how the pathway is controlled.

A | Oxidative Reactions Produce NADPH in Stage 1

G6P is considered the starting point of the pentose phosphate pathway. This metabolite may arise through the action of hexokinase on glucose (Reaction 1 of glycolysis; Section 15-2A) or from glycogen breakdown (which produces G6P directly; Section 16-1). Only the first three reactions of the pentose phosphate pathway are involved in NADPH production (Fig. 15-30):

1. **Glucose-6-phosphate dehydrogenase (G6PD)** catalyzes net transfer of a hydride ion to NADP$^+$ from C1 of G6P to form **6-phosphoglucono-δ-lactone:**

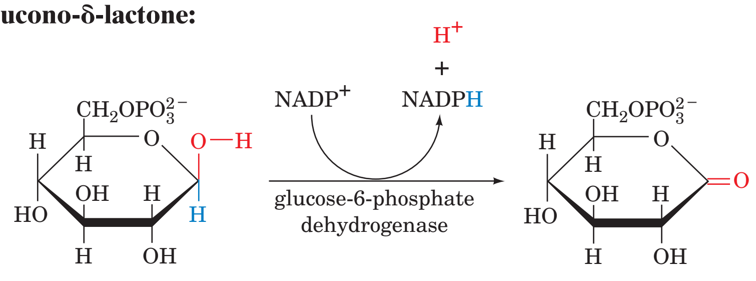

G6P

6-Phosphoglucono-δ-lactone

G6P, a cyclic hemiacetal with C1 in the aldehyde oxidation state, is thereby oxidized to a cyclic ester (lactone). The enzyme is specific for NADP$^+$ and is strongly inhibited by NADPH.

2. **6-Phosphogluconolactonase** increases the rate of hydrolysis of 6-phosphoglucono-δ-lactone to **6-phosphogluconate** (the nonenzymatic reaction occurs at a significant rate).

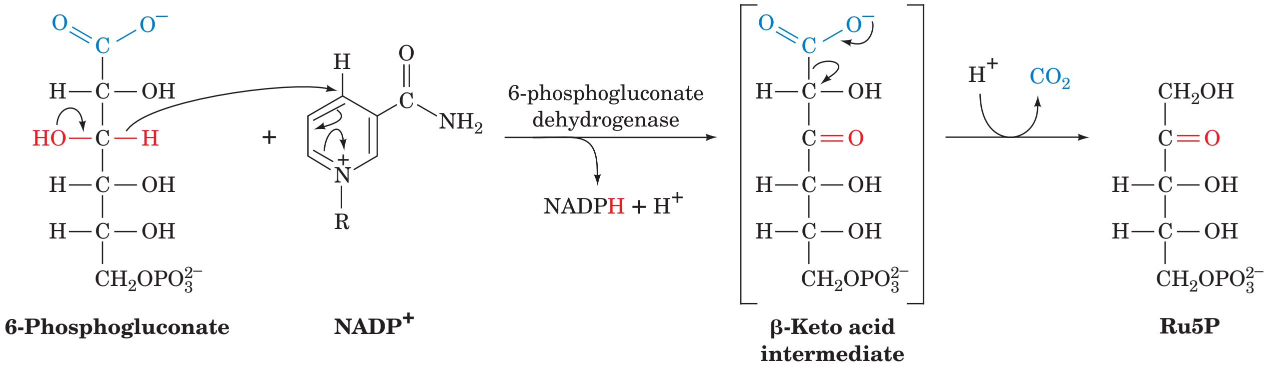

Figure 15-31 | **The 6-phosphogluconate dehydrogenase reaction.** Oxidation of the OH group forms an easily decarboxylated β-keto acid (although the proposed intermediate has not been isolated).

3. **6-Phosphogluconate dehydrogenase** catalyzes the oxidative decarboxylation of 6-phosphogluconate, a β-hydroxy acid, to Ru5P and CO_2 (Fig. 15-31). This reaction is thought to proceed via the formation of a β-keto acid intermediate. The keto group presumably facilitates decarboxylation by acting as an electron sink.

Formation of Ru5P completes the oxidative portion of the pentose phosphate pathway. *It generates two molecules of NADPH for each molecule of G6P that enters the pathway.*

B | Isomerization and Epimerization of Ribulose-5-Phosphate Occur in Stage 2

Ru5P is converted to R5P by **ribulose-5-phosphate isomerase** (Fig. 15-30, Reaction 4) or to Xu5P by **ribulose-5-phosphate epimerase** (Fig. 15-30, Reaction 5). These isomerization and epimerization reactions, like the reaction catalyzed by triose phosphate isomerase (Section 15-2E), are thought to occur via enediolate intermediates.

The relative amounts of R5P and Xu5P produced from Ru5P depend on the needs of the cell. For example, R5P is an essential precursor in the biosynthesis of nucleotides (Chapter 23). Accordingly, R5P production is relatively high (in fact, the entire pentose phosphate pathway activity may be elevated) in rapidly dividing cells, in which the rate of DNA synthesis is increased. If the pathway is being used solely for NADPH production, Xu5P and R5P are produced in a 2:1 ratio for conversion to glycolytic intermediates in the third stage of the pentose phosphate pathway as is discussed below.

C | Stage 3 Involves Carbon–Carbon Bond Cleavage and Formation

How is a five-carbon sugar transformed to a six-carbon sugar such as F6P? The rearrangements of carbon atoms in the third stage of the pentose phosphate pathway are easier to follow by considering the stoichiometry of the pathway. Every three G6P molecules that enter the pathway yield three Ru5P molecules in Stage 1. These three pentoses are then converted to one R5P and two Xu5P (Fig. 15-30, Reactions 4 and 5). The conversion of these three C_5 sugars to two C_6 sugars and one C_3 sugar involves a remarkable "juggling act" catalyzed by two enzymes, **transaldolase** and **transketolase.** These enzymes have mechanisms that involve the generation of stabilized carbanions and their addition to the electrophilic centers of aldehydes.

Transketolase Catalyzes the Transfer of C_2 Units. Transketolase, which has a thiamine pyrophosphate cofactor (TPP; Section 15-3B), catalyzes the transfer of a C_2 unit from Xu5P to R5P, yielding GAP and **sedoheptulose-7-phosphate (S7P;** Fig. 15-30, Reaction 6). The reaction intermediate is a covalent adduct between Xu5P and TPP (Fig. 15-32). The X-ray structure of the dimeric enzyme shows that the TPP binds in a deep cleft between the subunits so that residues from both subunits participate in its binding, just as in pyruvate decarboxylase (another TPP-requiring enzyme; Fig. 15-19). In fact, the structures are so similar that the enzymes likely diverged from a common ancestor.

Transaldolase Catalyzes the Transfer of C_3 Units. Transaldolase catalyzes the transfer of a C_3 unit from S7P to GAP yielding **erythrose-4-phosphate (E4P)** and F6P (Fig. 15-30, Reaction 7). The reaction occurs by aldol cleavage (Section 15-2D), which begins with the formation of a Schiff base between an ε-amino group of an essential Lys residue and the carbonyl group of S7P (Fig. 15-33).

A Second Transketolase Reaction Yields Glyceraldehyde-3-Phosphate and a Second Fructose-6-Phosphate Molecule. In a second transketolase reaction, a C_2 unit is transferred from a second molecule of Xu5P to E4P to form GAP and another molecule of F6P (Fig. 15-30, Reaction 8). The third stage of the pentose phosphate pathway thus transforms two molecules of Xu5P and one of R5P to two molecules of F6P and one molecule of GAP. These carbon skeleton transformations (Fig. 15-30, Reactions 6–8) are summarized in Fig. 15-34.

D | The Pentose Phosphate Pathway Must Be Regulated

The principal products of the pentose phosphate pathway are R5P and NADPH. The transaldolase and transketolase reactions convert excess R5P to glycolytic intermediates when the metabolic need for NADPH exceeds that of R5P in nucleotide biosynthesis. The resulting GAP and F6P can be consumed through glycolysis and oxidative phosphorylation or recycled by gluconeogenesis (Section 16-4) to form G6P.

When the need for R5P outstrips the need for NADPH, F6P and GAP can be diverted from the glycolytic pathway for use in the synthesis of R5P by reversal of the transaldolase and transketolase reactions. The relationship between glycolysis and the pentose phosphate pathway is diagrammed in Fig. 15-35.

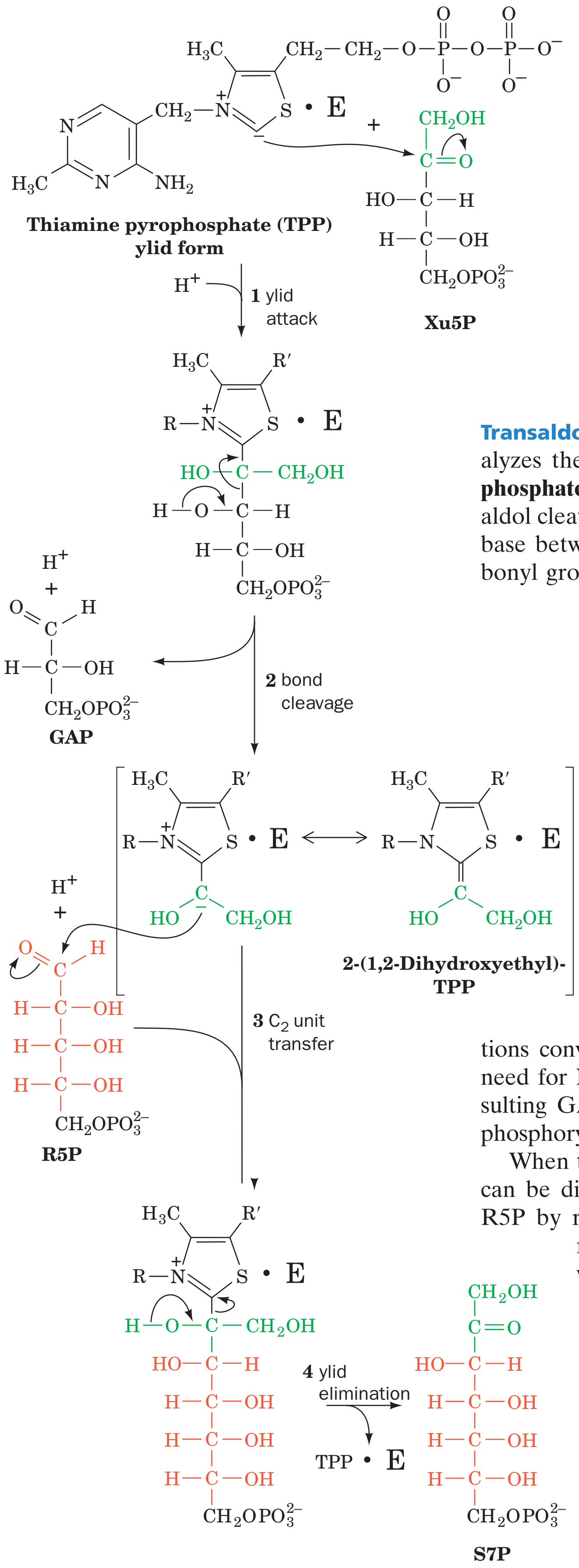

Figure 15-32 | Mechanism of transketolase. Transketolase (represented by E) uses the coenzyme TPP to stabilize the carbanion formed on cleavage of the C2—C3 bond of Xu5P. The reaction occurs as follows: (**1**) The TPP ylid attacks the carbonyl group of the Xu5P; (**2**) C2—C3 bond cleavage yields GAP and enzyme-bound 2-(1,2-dihydroxyethyl)-TPP, a resonance-stabilized carbanion; (**3**) the C2 carbanion attacks the aldehyde carbon of R5P to form an S7P–TPP adduct; (**4**) TPP is eliminated, yielding S7P and the regenerated TPP–enzyme.

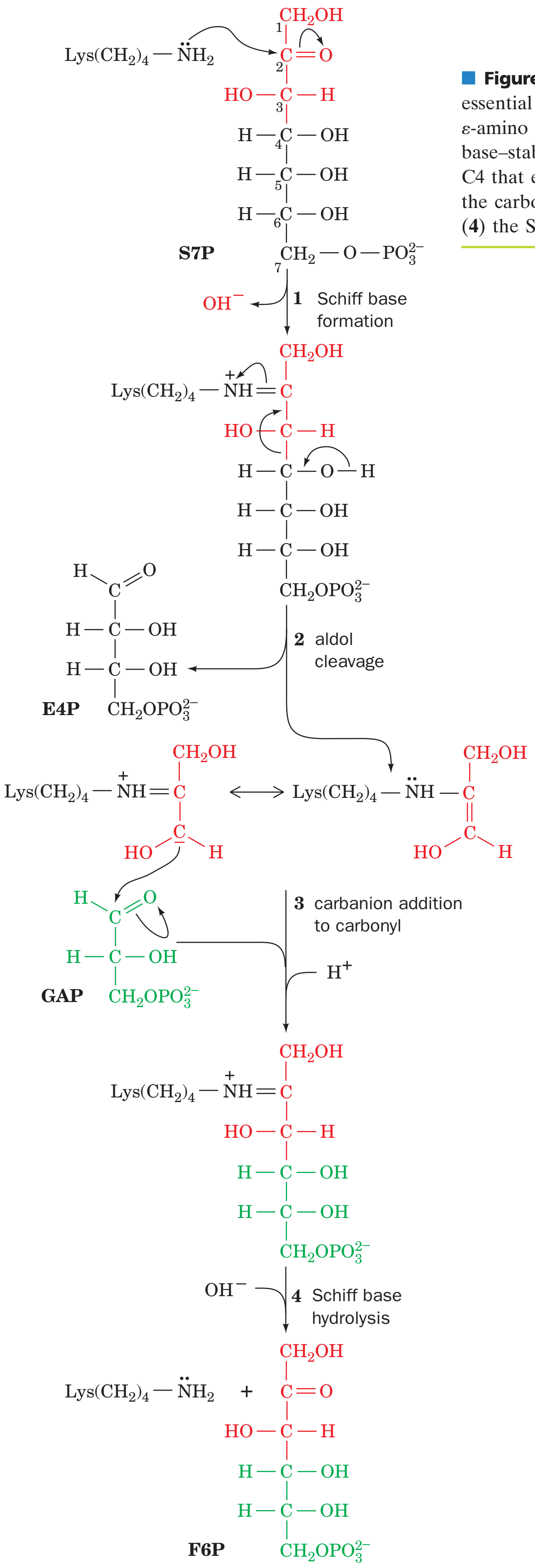

Lys(CH₂)₄—NH₂
1
2
3
4
5
6
7
S7P
OH⁻
1 Schiff base formation
Lys(CH₂)₄—NH=C
2 aldol cleavage
E4P
Lys(CH₂)₄—NH—C
3 carbanion addition to carbonyl
GAP
H⁺
OH⁻
4 Schiff base hydrolysis
Lys(CH₂)₄—NH₂ +
F6P

Figure 15-33 | Mechanism of transaldolase. Transaldolase contains an essential Lys residue that facilitates an aldol cleavage reaction as follows: (**1**) The ε-amino group of Lys forms a Schiff base with the carbonyl group of S7P; (**2**) a Schiff base–stabilized C3 carbanion is formed in an aldol cleavage reaction between C3 and C4 that eliminates E4P; (**3**) the enzyme-bound resonance-stabilized carbanion adds to the carbonyl C atom of GAP, forming F6P linked to the enzyme via a Schiff base; (**4**) the Schiff base hydrolyzes, regenerating active enzyme and releasing F6P.

$$\begin{array}{lll}
(\mathbf{6}) & C_5 + C_5 \rightleftharpoons C_7 + C_3 \\
(\mathbf{7}) & C_7 + C_3 \rightleftharpoons C_6 + C_4 \\
(\mathbf{8}) & \underline{C_5 + C_4 \rightleftharpoons C_6 + C_3} \\
(\text{Sum}) & 3\,C_5 \rightleftharpoons 2\,C_6 + C_3
\end{array}$$

Figure 15-34 | Summary of carbon skeleton rearrangements in the pentose phosphate pathway. A series of carbon–carbon bond formations and cleavages convert three C_5 sugars to two C_6 and one C_3 sugar. The number to the left of each reaction is keyed to the corresponding reaction in Fig. 15-30.

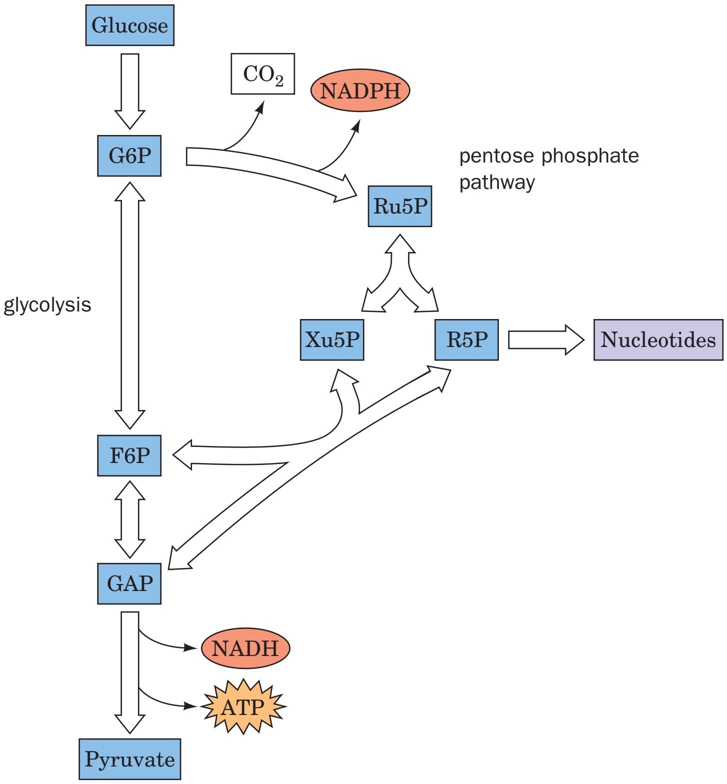

Glucose
G6P
CO₂
NADPH
pentose phosphate pathway
Ru5P
glycolysis
Xu5P
R5P
Nucleotides
F6P
GAP
NADH
ATP
Pyruvate

Figure 15-35 | Relationship between glycolysis and the pentose phosphate pathway. The pentose phosphate pathway, which begins with G6P produced in Step 1 of glycolysis, generates NADPH for use in reductive reactions and R5P for nucleotide synthesis. Excess R5P is converted to glycolytic intermediates by a sequence of reactions that can operate in reverse to generate additional R5P, if needed.

BOX 15-4 **BIOCHEMISTRY IN HEALTH AND DISEASE**

Glucose-6-Phosphate Dehydrogenase Deficiency

NADPH is required for several reductive processes in addition to biosynthesis. For example, erythrocytes require a plentiful supply of reduced **glutathione (GSH)**, a Cys-containing tripeptide (Section 4-3B).

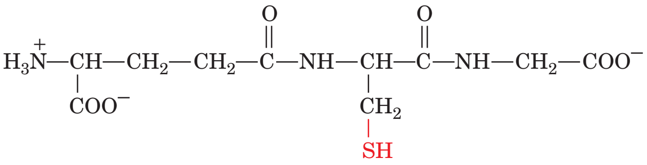

$$\mathrm{H_3\overset{+}{N}{-}\underset{\displaystyle COO^-}{CH}{-}CH_2{-}CH_2{-}\overset{\displaystyle O}{\overset{\|}{C}}{-}NH{-}\underset{\underset{\displaystyle SH}{CH_2}}{CH}{-}\overset{\displaystyle O}{\overset{\|}{C}}{-}NH{-}CH_2{-}COO^-}$$

Glutathione (GSH)
(γ-L-glutamyl-L-cysteinylglycine)

A major function of GSH in the erythrocyte is to reductively eliminate H_2O_2 and organic hydroperoxides, which are reactive oxygen metabolites that can irreversibly damage hemoglobin and cleave the C—C bonds in the phospholipid tails of cell membranes. The unchecked buildup of peroxides results in premature cell lysis. Peroxides are eliminated by reaction with glutathione, catalyzed by **glutathione peroxidase:**

$$2\,\mathrm{GSH} + \underset{\textbf{Organic hydroperoxide}}{\mathrm{R{-}O{-}O{-}H}} \xrightarrow{\text{glutathione peroxidase}} \mathrm{GSSG} + \mathrm{ROH} + \mathrm{H_2O}$$

GSSG represents oxidized glutathione (two GSH molecules linked through a disulfide bond between their sulfhydryl groups). Reduced GSH is subsequently regenerated by the reduction of GSSG by NADPH as catalyzed by **glutathione reductase:**

$$\mathrm{GSSG} + \mathrm{NADPH} + \mathrm{H^+} \xrightarrow{\text{glutathione reductase}} 2\,\mathrm{GSH} + \mathrm{NADP^+}$$

A steady supply of NADPH is therefore vital for erythrocyte integrity.

The erythrocytes in individuals who are deficient in glucose-6-phosphate dehydrogenase (G6PD) are particularly sensitive to oxidative damage, although clinical symptoms may be absent. This enzyme deficiency, which is common in African, Asian, and Mediterranean populations, came to light through investigations of the hemolytic anemia that is induced in these individuals when they ingest drugs such as the antimalarial compound **primaquine** or eat **fava beans** (**broad beans,** *Vicia faba*), a staple Middle Eastern vegetable. Primaquine stimulates peroxide formation, thereby increasing the demand for NADPH to a level that the mutant cells cannot meet. Certain toxic glycosides present in small amounts in fava beans have the same effect, producing a condition known as **favism.**

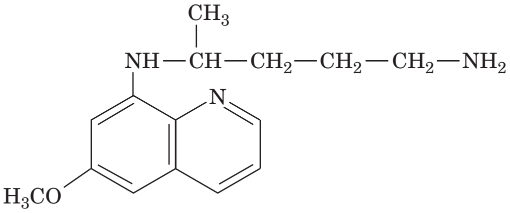

Primaquine

Flux through the pentose phosphate pathway and thus the rate of NADPH production is controlled by the rate of the glucose-6-phosphate dehydrogenase reaction (Fig. 15-30, Reaction 1). The activity of the enzyme, which catalyzes the pathway's first committed step ($\Delta G = -17.6\ \mathrm{kJ \cdot mol^{-1}}$ in liver), is regulated by the $NADP^+$ concentration (i.e., regulation by substrate availability). When the cell consumes NADPH, the $NADP^+$ concentration rises, increasing the rate of the G6PD reaction and thereby stimulating NADPH regeneration. In some tissues, the amount of enzyme synthesized also appears to be under hormonal control. A deficiency in G6PD is the most common clinically significant enzyme defect of the pentose phosphate pathway (Box 15-4).

■ CHECK YOUR UNDERSTANDING

Summarize the reactions of each stage of the pentose phosphate pathway.

How does flux through the pentose phosphate pathway change in response to the need for NADPH or ribose-5-phosphate?

The major reason for low enzymatic activity in affected cells appears to be an accelerated rate of breakdown of the mutant enzyme. This explains why patients with relatively mild forms of G6PD deficiency react to primaquine with hemolytic anemia but recover within a week despite continued primaquine treatment. Mature erythrocytes lack a nucleus and protein synthesizing machinery and therefore cannot synthesize new enzyme molecules to replace degraded ones (they likewise cannot synthesize new membrane components, which is why they are so sensitive to membrane damage in the first place). The initial primaquine treatments result in the lysis of old red blood cells whose defective G6PD has been largely degraded. Lysis products stimulate the release of young cells that contain more enzyme and are therefore better able to cope with primaquine stress.

It is estimated that ~400 million people are deficient in G6PD, which makes this condition the most common human enzyme deficiency. Indeed, ~400 G6PD variants have been reported and at least 125 of them have been characterized at the molecular level. G6PD is active in a dimer–tetramer equilibrium. Many of the mutation sites in individuals with the most severe G6PD deficiency are at the dimer interface, shifting the equilibrium toward the inactive and unstable monomer.

The high prevalence of defective G6PD in malarial areas of the world suggests that such mutations confer resistance to the malarial parasite, *Plasmodium falciparum.* Indeed, erythrocytes with G6PD deficiency appear to be less suitable hosts for plasmodia than normal cells. Thus, like the sickle-cell trait (Section 7-1E), *a defective G6PD confers a selective advantage on individuals living where malaria is endemic.*

The G6PD deficiency primarily affects erythrocytes, in which the lack of a nucleus prevents replacement of the unstable mutant enzyme. However, the importance of NADPH in cells other than erythrocytes has been demonstrated through the development of mice in which the G6PD gene has been knocked out. All the cells in these animals are extremely sensitive to oxidative stress, even though they contain other mechanisms for eliminating reactive oxygen species.

Photo of red blood cells showing intracellular *Plasmodium falciparum* (the malaria parasite). [© Dr. Gopal Murti/Photo Researchers, Inc.]

SUMMARY

1. Glycolysis is a sequence of 10 enzyme-catalyzed reactions by which one molecule of glucose is converted to two molecules of pyruvate, with the net production of 2 ATP and the reduction of 2 NAD^+ to 2 NADH.
2. In the first stage of glycolysis, glucose is phosphorylated by hexokinase, isomerized by phosphoglucose isomerase (PGI), phosphorylated by phosphofructokinase (PFK), and cleaved by aldolase to yield the trioses glyceraldehyde-3-phosphate (GAP) and dihydroxyacetone phosphate (DHAP), which are interconverted by triose phosphate isomerase (TIM). These reactions consume 2 ATP per glucose.
3. In the second stage of glycolysis, GAP is oxidatively phosphorylated by glyceraldehyde-3-phosphate dehydrogenase (GAPDH), dephosphorylated by phosphoglycerate kinase (PGK) to produce ATP, isomerized by phosphoglycerate mutase (PGM), dehydrated by enolase, and dephosphorylated by pyruvate kinase to produce a second ATP and pyruvate. This stage produces 4 ATP per glucose for a net yield of 2 ATP per glucose.
4. Under anaerobic conditions, pyruvate is reduced to regenerate NAD^+ for glycolysis. In homolactic fermentation, pyruvate is reversibly reduced to lactate.
5. In alcoholic fermentation, pyruvate is decarboxylated by a thiamine pyrophosphate (TPP)-dependent mechanism, and the resulting acetaldehyde is reduced to ethanol.
6. The glycolytic reactions catalyzed by hexokinase, phosphofructokinase, and pyruvate kinase are metabolically irreversible.

7. Phosphofructokinase is the primary flux control point for glycolysis. ATP inhibition of this allosteric enzyme is relieved by AMP and ADP, whose concentrations change more dramatically than those of ATP.
8. The opposing reactions of the fructose-6-phosphate (F6P)/fructose-1,6-bisphosphate (FBP) substrate cycle allow large changes in glycolytic flux.
9. Fructose, galactose, and mannose are enzymatically converted to glycolytic intermediates for catabolism.
10. In the pentose phosphate pathway, glucose-6-phosphate (G6P) is oxidized and decarboxylated to produce two NADPH, CO_2, and ribulose-5-phosphate (Ru5P).
11. Depending on the cell's needs, ribulose-5-phosphate may be isomerized to ribose-5-phosphate (R5P) for nucleotide synthesis or converted, via ribose-5-phosphate and xylulose-5-phosphate (Xu5P), to fructose-6-phosphate and glyceraldehyde-3-phosphate, which can re-enter the glycolytic pathway.

KEY TERMS

glycolysis **486**
pentose phosphate pathway **486**
aldol cleavage **492**
enediol intermediate **495**
catalytic perfection **496**
mutase **500**
homolactic fermentation **505**
alcoholic fermentation **505**
TPP **507**
Pasteur effect **510**
substrate cycle **514**

PROBLEMS

1. Which of the 10 reactions of glycolysis are (a) phosphorylations, (b) isomerizations, (c) oxidation–reductions, (d) dehydrations, and (e) carbon–carbon bond cleavages?
2. The aldolase reaction can proceed in reverse as an enzymatic aldol condensation. If the enzyme were not stereospecific, how many different products would be obtained?
3. Bacterial aldolase does not form a Schiff base with the substrate. Instead, it has a divalent Zn^{2+} ion in the active site. How does the ion facilitate the aldolase reaction?
4. Arsenate (AsO_4^{3-}), a structural analog of phosphate, can act as a substrate for any reaction in which phosphate is a substrate. Arsenate esters, unlike phosphate esters, are kinetically as well as thermodynamically unstable and hydrolyze almost instantaneously. Write a balanced overall equation for the conversion of glucose to pyruvate in the presence of ATP, ADP, NAD^+, and either (a) phosphate or (b) arsenate. (c) Why is arsenate a poison?
5. Draw the enediolate intermediates of the ribulose-5-phosphate isomerase reaction (Ru5P → R5P) and the ribulose-5-phosphate epimerase reaction (Ru5P → Xu5P).
6. (a) Why is it possible for the ΔG values in Table 15-1 to differ from the $\Delta G^{\circ\prime}$ values? (b) If a reaction has a $\Delta G^{\circ\prime}$ value of at least $-30.5\ \text{kJ} \cdot \text{mol}^{-1}$, sufficient to drive the synthesis of ATP ($\Delta G^{\circ\prime} = 30.5\ \text{kJ} \cdot \text{mol}^{-1}$), can it still drive the synthesis of ATP *in vivo* when its ΔG is only $-10\ \text{kJ} \cdot \text{mol}^{-1}$? Explain.
7. $\Delta G^{\circ\prime}$ for the aldolase reaction is $22.8\ \text{kJ} \cdot \text{mol}^{-1}$. In the cell at 37°C, [DHAP]/[GAP] = 5.5. Calculate the equilibrium ratio of [FBP]/[GAP] when [GAP] = 10^{-4} M.
8. The half-reactions involved in the lactate dehydrogenase (LDH) reaction and their standard reduction potentials are

$$\text{Pyruvate} + 2\,H^+ + 2\,e^- \longrightarrow \text{lactate} \qquad \mathcal{E}^{\circ\prime} = -0.185\ \text{V}$$

$$NAD^+ + 2\,H^+ + 2\,e^- \longrightarrow NADH + H^+ \qquad \mathcal{E}^{\circ\prime} = -0.315\ \text{V}$$

Calculate ΔG at pH 7.0 for the LDH-catalyzed reduction of pyruvate under the following conditions:

(a) [lactate]/[pyruvate] = 1 and [NAD^+]/[NADH] = 1
(b) [lactate]/[pyruvate] = 160 and [NAD^+]/[NADH] = 160
(c) [lactate]/[pyruvate] = 1000 and [NAD^+]/[NADH] = 1000
(d) Discuss the effect of the concentration ratios in parts a–c on the direction of the reaction.

9. Although it is not the primary flux-control point for glycolysis, pyruvate kinase is subject to allosteric regulation. (a) What is the metabolic importance of regulating flux through the pyruvate kinase reaction? (b) What is the advantage of activating pyruvate kinase with fructose-1,6-bisphosphate?
10. Compare the ATP yield of three glucose molecules that enter glycolysis and are converted to pyruvate with that of three glucose molecules that proceed through the pentose phosphate pathway such that their carbon skeletons (as two F6P and one GAP) re-enter glycolysis and are metabolized to pyruvate.
11. If G6P is labeled at its C2 position, where will the label appear in the products of the pentose phosphate pathway?
12. (a) Describe the lengths of the products of the transketolase reaction when the two substrates are both five-carbon sugars. (b) Describe the products of the reaction when the substrates are a five-carbon aldose and a six-carbon ketose. Does it matter which of the substrates binds to the enzyme first?
13. Explain why some tissues continue to produce CO_2 in the presence of high concentrations of fluoride ion, which inhibits glycolysis.
14. The catalytic behavior of liver and brain phosphofructokinase-1 (PFK-1) was observed in the presence of AMP, phosphate, and fructose-2,6-bisphosphate. The following table lists the concentrations of each effector required to achieve 50% of the maximal velocity. Compare the response of the two isozymes to the

three effectors and discuss the possible implications of their different responses.

PFK-1 isozyme	[Phosphate]	[AMP]	[F2,6P]
Liver	200 μM	10 μM	0.05 μM
Brain	350 μM	75 μM	4.5 μM

15. Some bacteria catabolize glucose by the Entner–Doudoroff pathway, a variant of glycolysis in which glucose-6-phosphate is converted to 6-phosphogluconate (as in the pentose phosphate pathway) and then to **2-keto-3-deoxy-6-phosphogluconate (KDPG).**

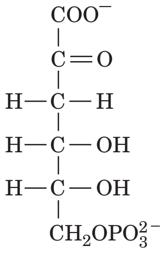

KDPG

Next, an aldolase acts on KDPG. (a) Draw the structures of the products of the KDPG aldolase reaction. (b) Describe how these reaction products are further metabolized by glycolytic enzymes. (c) What is the ATP yield when glucose is metabolized to pyruvate by the Entner–Doudoroff pathway? How does this compare to the ATP yield of glycolysis?

CASE STUDIES

Case 18 (available at www.wiley.com/college/voet)

Purification of Phosphofructokinase 1-C

Focus concept: The purification of the C isozyme of PFK-1 is presented and the kinetic properties of the purified enzyme are examined.

Prerequisites: Chapters 5, 12, and 15

- Protein purification techniques
- Enzyme kinetics and inhibition
- The glycolytic pathway

Case 20

NAD$^+$-Dependent Glyceraldehyde-3-Phosphate Dehydrogenase from *Thermoproteus tenax*

Focus concept: Glycolytic enzymes from *T. tenax* are regulated in an unusual manner.

Prerequisites: Chapters 7, 12, and 15

- The glycolytic pathway
- Enzyme kinetics and inhibition
- The cooperative nature of regulated enzymes

REFERENCES

Berstein, B.E., Michels, P.A.M., and Hol, W.G.J., Synergistic effects of substrate-induced conformational changes in phosphoglycerate activation, *Nature* **385,** 275–278 (1997).

Dalby, A., Dauter, Z., and Littlechild, J.A., Crystal structure of human muscle aldolase complexed with fructose 1,6-bisphosphate: Mechanistic implications, *Protein Science* **8,** 291–297 (1999).

Depre, C., Rider, M.H., and Hue, L., Mechanisms of control of heart glycolysis, *Eur. J. Biochem.* **258,** 277–290 (1998). [Discusses how the control of glycolysis in heart muscle is distributed among several enzymes, transporters, and other pathways.]

Frey, P.A., The Leloir pathway: a mechanistic imperative for three enzymes to change the stereochemical configuration of a single carbon in galactose, *FASEB J.* **10,** 461–470 (1996).

Gefflaut, T., Blonski, C., Perie, J., and Wilson, M., Class I aldolases: substrate specificity, mechanism, inhibitors and structural aspects, *Prog. Biophys. Molec. Biol.* **63,** 301–340 (1995).

Hofmeyr, J.-H.S. and Cornish-Bowden, A., Regulating the cellular economy of supply and demand, *FEBS Lett.* **476,** 47–51 (2000).

Lindqvist, Y. and Schneider, G., Thiamin diphosphate dependent enzymes: transketolase, pyruvate oxidase and pyruvate decarboxylase, *Curr. Opin. Struct. Biol.* **3,** 896–901 (1993).

Muirhead, H. and Watson, H., Glycolytic enzymes; from hexose to pyruvate, *Curr. Opin. Struct. Biol.* **2,** 870–876 (1992). [A brief summary of the structures of glycolytic enzymes.]

Schirmer, T. and Evans, P.R., Structural basis of the allosteric behaviour of phosphofructokinase, *Nature* **343,** 140–145 (1990).

Scriver, C.R., Beaudet, A., Sly, W.S., and Valle, D. (Eds.), *The Metabolic and Molecular Bases of Inherited Disease* (8th ed.), pp. 4517–4553, McGraw-Hill (2001). [Chapters 70 and 72 discuss fructose and galactose metabolism and their genetic disorders. Chapter 179 discusses glucose-6-phosphate dehydrogenase deficiency.]

16

Glycogen Metabolism and Gluconeogenesis

The muscles of animals contain glycogen, a storage form of the metabolic fuel glucose. In living animals, the balance between glycogen synthesis and utilization is carefully regulated. Measurement of glycogen levels in lobster has been used to determine environmental conditions, since animals that have been undernourished or stressed have depleted glycogen stores. [Andrew J. Martinez/Photo Researchers.]

CHAPTER CONTENTS

1 Glycogen Breakdown
- **A.** Glycogen Phosphorylase Degrades Glycogen to Glucose-1-Phosphate
- **B.** Glycogen Debranching Enzyme Acts as a Glucosyltransferase
- **C.** Phosphoglucomutase Interconverts Glucose-1-Phosphate and Glucose-6-Phosphate

2 Glycogen Synthesis
- **A.** UDP–Glucose Pyrophosphorylase Activates Glucosyl Units
- **B.** Glycogen Synthase Extends Glycogen Chains
- **C.** Glycogen Branching Enzyme Transfers Seven-Residue Glycogen Segments

3 Control of Glycogen Metabolism
- **A.** Glycogen Phosphorylase and Glycogen Synthase Are under Allosteric Control
- **B.** Glycogen Phosphorylase and Glycogen Synthase Undergo Control by Covalent Modification
- **C.** Glycogen Metabolism Is Subject to Hormonal Control

4 Gluconeogenesis
- **A.** Pyruvate Is Converted to Phosphoenolpyruvate in Two Steps
- **B.** Hydrolysis Reactions Bypass Irreversible Glycolytic Reactions
- **C.** Gluconeogenesis and Glycolysis Are Independently Regulated

5 Other Carbohydrate Biosynthetic Pathways

MEDIA RESOURCES

(available at www.wiley.com/college/voet)

Guided Exploration 15. Control of glycogen metabolism
Animated Figure 16-1. Overview of glucose metabolism
Animated Figure 16-13. Major phosphorylation and dephosphorylation systems in glycogen metabolism
Animated Figure 16-15. Comparison of gluconeogenesis and glycolysis
Animated Figure 16-20. Transport of PEP and oxaloacetate from mitochondrion to cytosol
Animated Figure 16-27. Pathway for dolichol-PP-oligosaccharide synthesis
Case Study 22. Carrier-Mediated Uptake of Lactate in Rat Hepatocytes
Case Study 26. The Role of Specific Amino Acids in the Peptide Hormone Glucagon in Receptor Binding and Signal Transduction

Glycogen (in animals, fungi, and bacteria) and starch (in plants) can function to stockpile glucose for later metabolic use. In animals, a constant supply of glucose is essential for tissues such as the brain and red blood cells, which depend almost entirely on glucose as an energy source (other tissues can also oxidize fatty acids for energy; Section 20-2). The mobilization of glucose from glycogen stores, primarily in the liver, provides a constant supply of glucose (~5 mM in blood) to all tissues. When glucose is plentiful, such as immediately after a meal, glycogen synthesis accelerates. Yet the liver's capacity to store glycogen is sufficient to supply the brain with glucose for about half a day. Under fasting conditions, most of the body's glucose needs are met by **gluconeogenesis** (literally, new glucose synthesis) from noncarbohydrate precursors such as amino acids. Not surprisingly, the regulation of glucose synthesis, storage, mobilization, and catabolism by glycolysis (Section 15-2) or the pentose

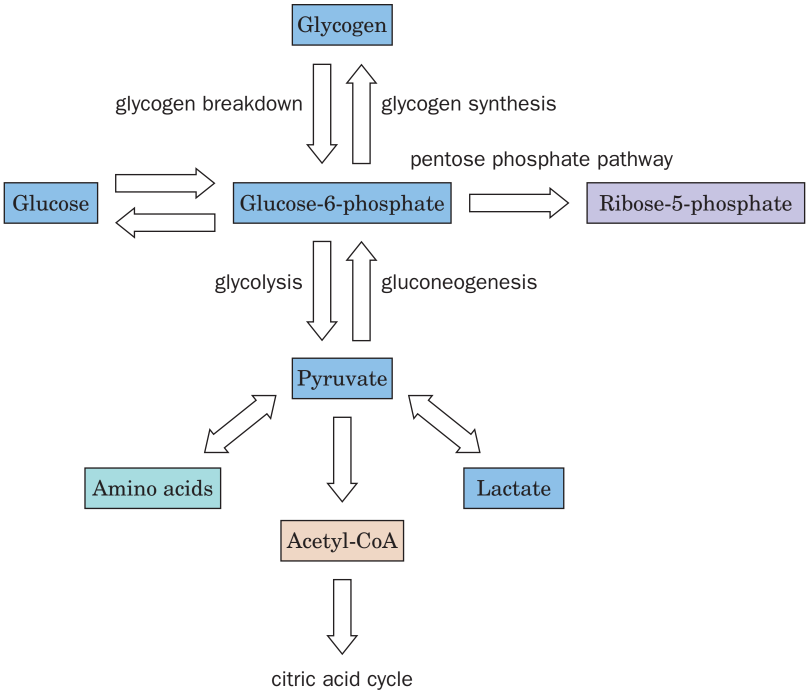

■ **Figure 16-1 | Overview of glucose metabolism.** Glucose-6-phosphate (G6P) is produced by the phosphorylation of free glucose, by glycogen degradation, and by gluconeogenesis. It is also a precursor for glycogen synthesis and the pentose phosphate pathway. The liver can hydrolyze G6P to glucose. Glucose is metabolized by glycolysis to pyruvate, which can be further broken down to acetyl-CoA for oxidation by the citric acid cycle. Lactate and amino acids, which are reversibly converted to pyruvate, are precursors for gluconeogenesis. **See the Animated Figures.**

phosphate pathway (Section 15-6) is elaborate and is sensitive to the immediate and long-term energy needs of the organism.

The importance of glycogen for glucose storage is plainly illustrated by the effects of deficiencies of the enzymes that release stored glucose. **McArdle's disease,** for example, is an inherited condition whose major symptom is painful muscle cramps on exertion. The muscles in afflicted individuals lack the enzyme required for glycogen breakdown to yield glucose. Although glycogen is synthesized normally, it cannot supply fuel for glycolysis to keep up with the demand for ATP.

Figure 16-1 summarizes the metabolic uses of glucose. Glucose-6-phosphate (G6P), a key branch point, is derived from free glucose through the action of hexokinase (Section 15-2A) or is the product of glycogen breakdown or gluconeogenesis. G6P has several possible fates: It can be used to synthesize glycogen; it can be catabolized via glycolysis to yield ATP and carbon atoms (as acetyl-CoA) that are further oxidized by the citric acid cycle; and it can be shunted through the pentose phosphate pathway to generate NADPH and/or ribose-5-phosphate. In the liver and kidney, G6P can be converted to glucose for export to other tissues via the bloodstream.

The opposing processes of glycogen synthesis and degradation, and of glycolysis and gluconeogenesis, are reciprocally regulated; that is, one is largely turned on while the other is largely turned off. In this chapter, we examine the enzymatic steps of glycogen metabolism and gluconeogenesis, paying particular attention to the regulatory mechanisms that ensure efficient operation of opposing metabolic pathways.

1 Glycogen Breakdown

LEARNING OBJECTIVES

- Understand that glycogen, the storage form of glucose, is a branched polymer.
- Understand that glucose mobilization in the liver involves a series of conversions from glycogen to glucose-1-phosphate to glucose-6-phosphate and finally to glucose.

Glycogen is a polymer of α(1→4)-linked D-glucose with α(1→6)-linked branches every 8–14 residues (Fig. 16-2*a,b* and Section 8-2C). Glycogen occurs as intracellular granules of 100- to 400-Å-diameter spheroidal molecules that each contain up to 120,000 glucose units (Fig. 16-2*c*). The granules are especially prominent in the cells that make the greatest use of glycogen: muscle (up to 1–2% glycogen by weight) and liver cells (up to 10% glycogen by weight; Fig. 8-11). Glycogen granules also contain the enzymes that catalyze glycogen synthesis and degradation as well as many of the proteins that regulate these processes.

Glucose units are mobilized by their sequential removal from the nonreducing ends of glycogen (the ends lacking a C1-OH group). Whereas glycogen has only one reducing end, there is a nonreducing end on every branch. *Glycogen's highly branched structure therefore permits rapid glucose mobilization through the simultaneous release of the glucose units at the end of every branch.*

Glycogen breakdown, or **glycogenolysis,** requires three enzymes:

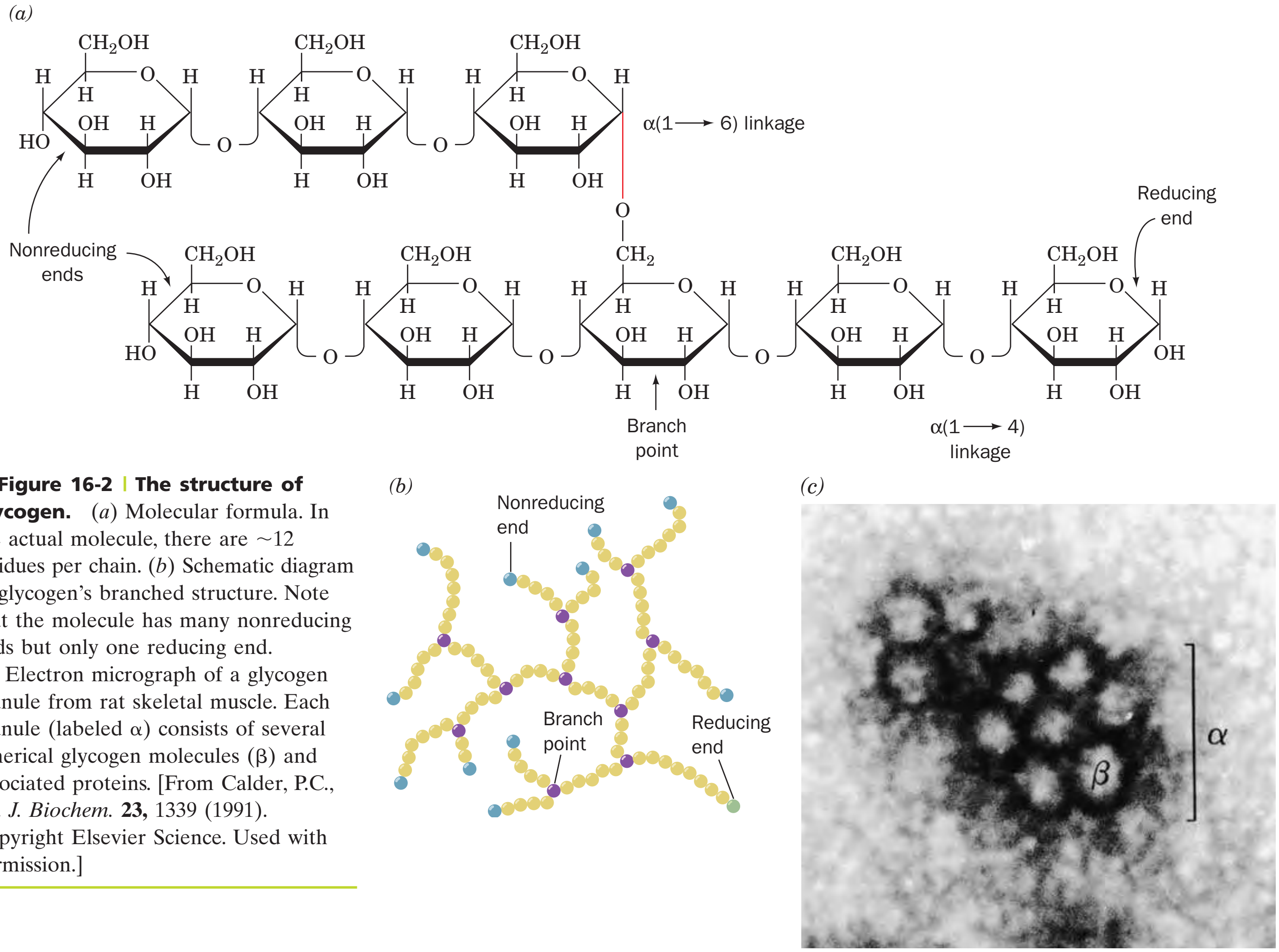

Figure 16-2 | The structure of glycogen. (*a*) Molecular formula. In the actual molecule, there are ~12 residues per chain. (*b*) Schematic diagram of glycogen's branched structure. Note that the molecule has many nonreducing ends but only one reducing end. (*c*) Electron micrograph of a glycogen granule from rat skeletal muscle. Each granule (labeled α) consists of several spherical glycogen molecules (β) and associated proteins. [From Calder, P.C., *Int. J. Biochem.* **23,** 1339 (1991). Copyright Elsevier Science. Used with permission.]

BOX 16-1 **PATHWAYS OF DISCOVERY**

Carl and Gerty Cori and Glucose Metabolism

Carl F. Cori (1896–1984)
Gerty T. Cori (1896–1957)

A lifelong collaboration commenced with the marriage of Carl and Gerty Cori in 1920. Although the Coris began their professional work in Austria, they fled the economic and social hardships of Europe in 1922 and moved to Buffalo, New York. They later made their way to Washington University School of Medicine in St. Louis, where Carl served as chair of the Pharmacology Department and, later, chair of the Biochemistry Department. Despite her role as an equal partner in their research work, Gerty officially remained a research associate.

The Coris' research focused primarily on the metabolism of glucose. One of their first discoveries was the connection between glucose metabolism in muscle and glycogen metabolism in the liver. The "Cori cycle" (Section 22-1F) describes how lactate produced by glycolysis in active muscle is transported to the liver, where it is used to synthesize glucose that is stored as glycogen until needed.

After describing the interorgan movement of glucose in intact animals, the Coris turned their attention to the metabolic fate of glucose, specifically, the intermediates and enzymes of glucose metabolism. In 1936, using a preparation of minced frog muscle, the Coris found glucose in the form of a phosphate ester (called the Cori ester, now known as glucose-1-phosphate). They traced the presence of the Cori ester to the activity of a phosphorylase (glycogen phosphorylase). This was a notable discovery, because the enzyme used phosphate, rather than water, to split glucose residues from the ends of glycogen chains. Even more remarkably, the enzyme could be made to work in reverse to elongate a glycogen polymer by adding glucose residues (from glucose-1-phosphate). For the first time, a large biological molecule could be synthesized *in vitro*.

During the 1940s, the Coris unraveled many of the secrets of glycogen phosphorylase. For example, they found that the enzyme exists in two forms, one that requires the activator AMP and one that is active in the absence of an allosteric activator. Although it was not immediately appreciated that the differences between the two forms resulted from the presence of covalently bound phosphate, this work laid the foundation for subsequent research on enzyme regulation through phosphorylation and dephosphorylation.

Carl and Gerty Cori also described phosphoglucomutase, the enzyme that converts glucose-1-phosphate to glucose-6-phosphate so that it can participate in other pathways of glucose metabolism. Over time, the Cori lab became a magnet for scientists interested in purifying and characterizing other enzymes of glucose metabolism.

Perhaps because of their experience with discrimination and—especially for Gerty—the lack of equal opportunity, the Cori lab welcomed a more diverse group of scientists than was typical of labs of that era. The Coris received the 1947 Nobel Prize in Physiology or Medicine. Several of their junior colleagues, Arthur Kornberg (see Box 25-1), Severo Ochoa, Luis Leloir, Earl Sutherland, Christian de Duve, and Edwin G. Krebs, later earned Nobel prizes of their own, quite possibly reflecting the work ethic, broad view of science and medicine, and meticulous work habits instilled by Carl and Gerty Cori.

Cori, G.T., Colowick, S.P., and Cori, C.F., The activity of the phosphorylating enzyme in muscle extracts, *J. Biol. Chem.* **127,** 771–782 (1939).

Kornberg, A., Remembering our teachers, *J. Biol. Chem. Reflections,* www.jbc.org.

1. **Glycogen phosphorylase** (or simply **phosphorylase**) catalyzes glycogen **phosphorolysis** (bond cleavage by the substitution of a phosphate group) to yield **glucose-1-phosphate (G1P):**

$$\underset{(n\text{ residues})}{\text{Glycogen}} + \text{P}_i \rightleftharpoons \underset{(n-1\text{ residues})}{\text{Glycogen}} + \text{G1P}$$

   The enzyme releases a glucose unit only if it is at least five units away from a branch point.

2. **Glycogen debranching enzyme** removes glycogen's branches, thereby making additional glucose residues accessible to glycogen phosphorylase.
3. **Phosphoglucomutase** converts G1P to G6P, which has several metabolic fates (Fig. 16-1).

Several key features of glycogen metabolism were discovered by the team of Carl and Gerty Cori (Box 16-1).

A | Glycogen Phosphorylase Degrades Glycogen to Glucose-1-Phosphate

Glycogen phosphorylase is a dimer of identical 842-residue (97-kD) subunits that catalyzes the rate-controlling step in glycogen breakdown. It is regulated both by allosteric interactions and by covalent modification (phosphorylation and dephosphorylation). Phosphorylase's allosteric inhibitors (ATP, G6P, and glucose) and its allosteric activator (AMP) interact differently with the phospho- and dephosphoenzymes, resulting in an extremely sensitive regulation process. The structure of glycogen phosphorylase as well as its regulation by phosphorylation are discussed in Section 12-3B.

An ~30-Å-long crevice on the surface of the phosphorylase monomer connects the glycogen storage site to the active site. *Since this crevice can accommodate four or five sugar residues in a chain but is too narrow to admit branched oligosaccharides, it provides a clear physical rationale for the inability of phosphorylase to cleave glycosyl residues closer than five units from a branch point.* Presumably, the glycogen storage site increases the catalytic efficiency of phosphorylase by permitting it to phosphorylyze many glucose residues on the same glycogen particle without having to dissociate and reassociate completely between catalytic cycles.

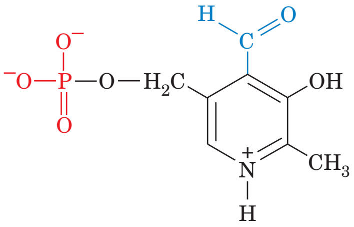

Pyridoxal-5′-phosphate (PLP)

Phosphorylase binds the cofactor **pyridoxal-5′-phosphate** (**PLP;** *at left*), which it requires for activity. This prosthetic group, a **vitamin B$_6$** derivative, is covalently linked to the enzyme via a Schiff base (imine) formed between its aldehyde group and the ε-amino group of Lys 680. PLP also occurs in a variety of enzymes involved in amino acid metabolism, where PLP's conjugated ring system functions catalytically to delocalize electrons (Sections 21-2A and 21-4A). In phosphorylase, however, only the phosphate group participates in catalysis, where it acts as a general acid–base catalyst. Phosphorolysis of glycogen proceeds by a Random mechanism (Section 12-1D) involving an enzyme · P_i · glycogen ternary complex. An oxonium ion intermediate forms during C1—O1 bond cleavage, similar to the transition state that forms in the reaction catalyzed by lysozyme (Section 11-4B). The phosphorylase reaction mechanism is diagrammed in Fig. 16-3, which shows how PLP's phosphate group functions as a general acid–base catalyst.

Glycogen Phosphorylase Undergoes Conformational Changes. The structural differences between the active (R) and inactive (T) conformations of phosphorylase (Fig. 12-15) are fairly well understood in terms of the symmetry model of allosterism (Section 7-1D). The T-state enzyme has a buried active site and hence a low affinity for its substrates, whereas the R-state enzyme has an accessible catalytic site and a high-affinity phosphate-binding site.

AMP promotes phosphorylase's T (*inactive*) → R (*active*) conformational shift by binding to the R state of the enzyme at its allosteric effector site. This conformational change results in increased access of the substrate to the active site by disordering a loop of residues (282–284) that otherwise block the active site. The conformational change also causes the Arg 569 side chain, which is located in the active site near the PLP and the P_i-binding site, to rotate in a way that increases the enzyme's binding affinity for its anionic P_i substrate (Fig. 12-15).

ATP also binds to the allosteric effector site, but in the T state, so that it inhibits rather than promotes the T → R conformational shift. This is because the β- and γ-phosphate groups of ATP prevent the alignment of

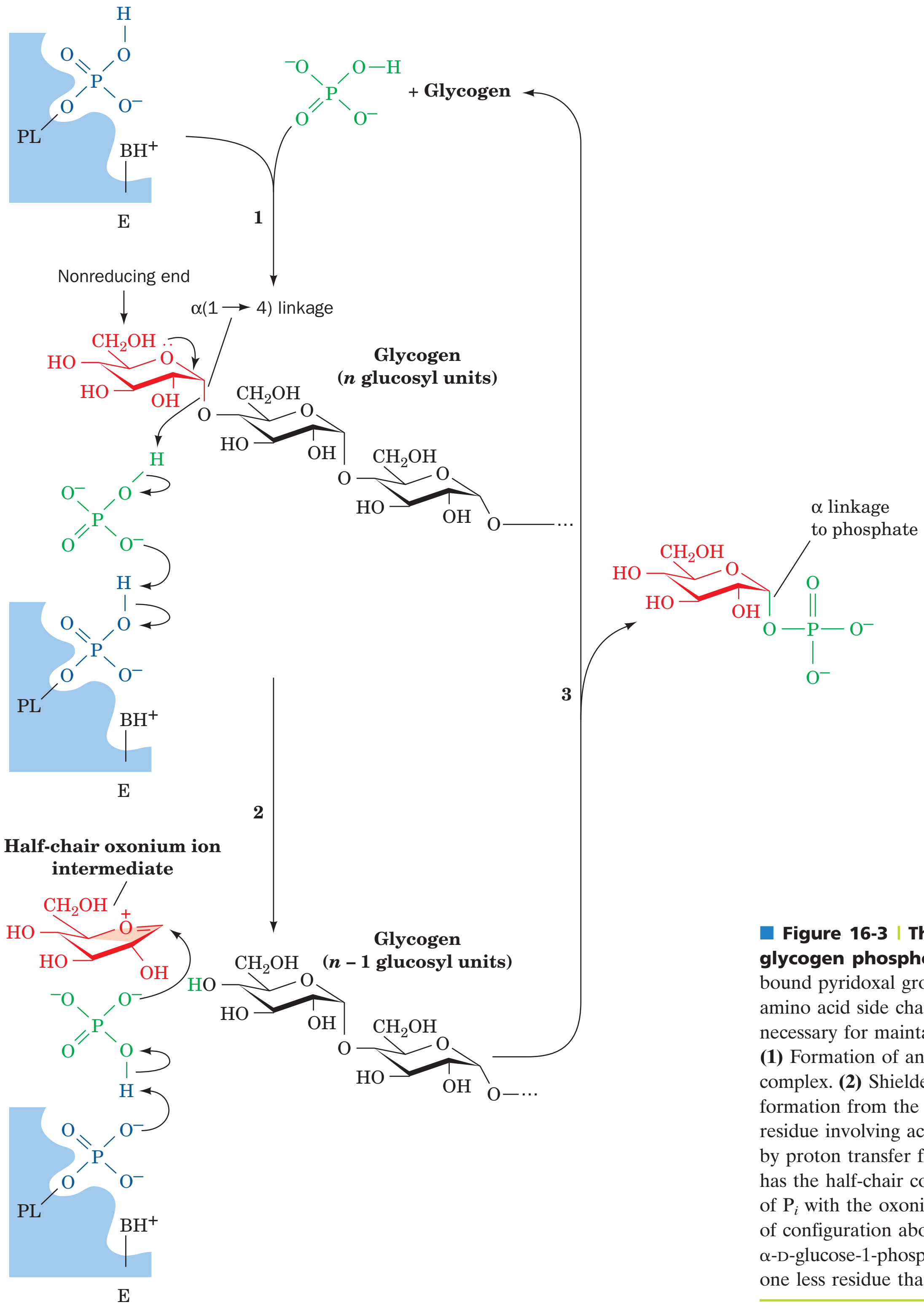
H
O
O
P
O
O⁻
PL
BH⁺
E
⁻O
O—H
P
O
O⁻
+ Glycogen
1
Nonreducing end
α(1 → 4) linkage
Glycogen
(n glucosyl units)
CH₂OH
HO
HO
OH
O
α linkage
to phosphate
3
2
Half-chair oxonium ion
intermediate
Glycogen
(n – 1 glucosyl units)

Figure 16-3 | **The reaction mechanism of glycogen phosphorylase.** PL is an enzyme-bound pyridoxal group; BH^+ is a positively charged amino acid side chain, probably that of Lys 568, necessary for maintaining PLP electrical neutrality. **(1)** Formation of an $E \cdot P_i \cdot$glycogen ternary complex. **(2)** Shielded oxonium ion intermediate formation from the α-linked terminal glucosyl residue involving acid catalysis by P_i as facilitated by proton transfer from PLP. The oxonium ion has the half-chair conformation. **(3)** Reaction of P_i with the oxonium ion with overall retention of configuration about C1 to form α-D-glucose-1-phosphate. The glycogen, which has one less residue than before, cycles back to Step 1.

its ribose and α-phosphate groups that are required for the conformational changes elicited by AMP.

Phosphorylation and dephosphorylation alter the enzymatic activity in a manner reminiscent of allosteric regulation. The phosphate group has a double negative charge (a property not shared by naturally occurring amino acid residues) and its covalent attachment to Ser 14 causes dramatic tertiary and quaternary changes as the N-terminal segment moves to allow the phospho-Ser to ion pair with two cationic Arg residues. *The presence of the Ser 14–phosphoryl group causes conformational changes similar to those triggered by AMP binding, thereby shifting the enzyme's* $T \rightleftharpoons R$ *equilibrium in favor of the R state.* This accounts for the observation that phosphorylase *b* requires AMP for activity and that the *a* form is active without AMP. We shall return to the regulation of phosphorylase activity when we discuss the mechanisms that balance glycogen synthesis against glycogen degradation (Section 16-3).

B | Glycogen Debranching Enzyme Acts as a Glucosyltransferase

Phosphorolysis proceeds along a glycogen branch until it approaches to within four or five residues of an α(1→6) branch point, leaving a "limit branch." Glycogen debranching enzyme acts as an **α(1→4) transglycosylase** (glycosyltransferase) by transferring an α(1→4)-linked trisaccharide unit from a limit branch of glycogen to the nonreducing end of another branch (Fig. 16-4). This reaction forms a new α(1→4) linkage with three more units available for phosphorylase-catalyzed phosphorolysis. The α(1→6) bond linking the remaining glycosyl residue in the branch to the main chain is hydrolyzed (not phosphorylyzed) by the same debranching enzyme to yield glucose and debranched glycogen. About 10% of the

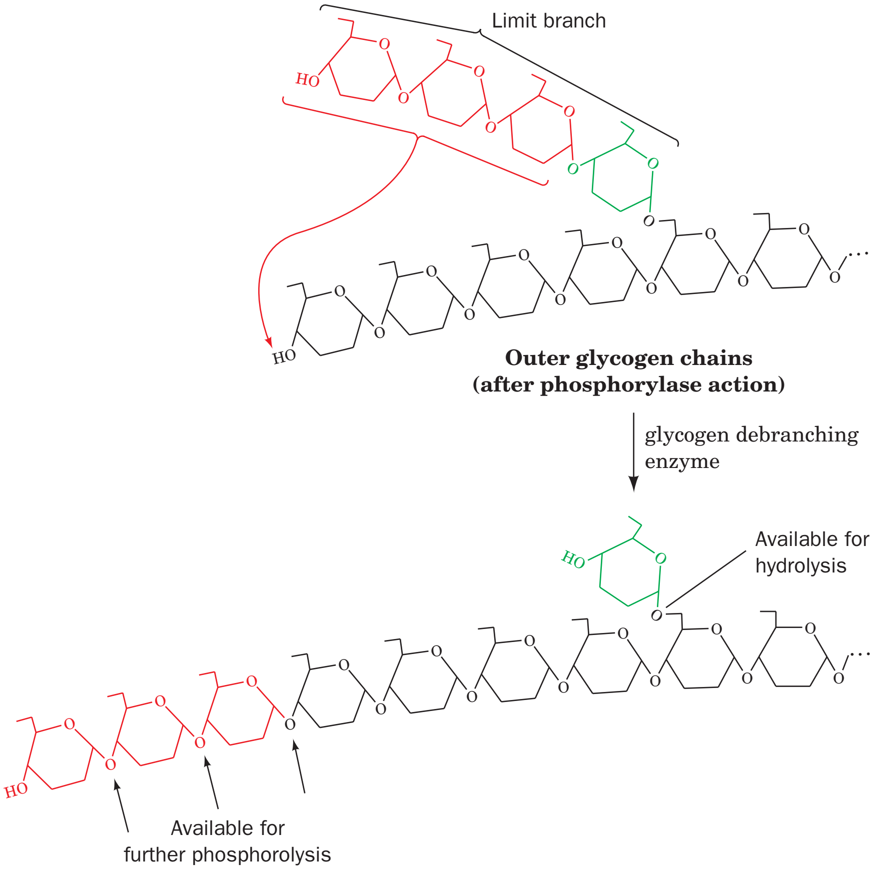
Limit branch
HO
O
HO
Outer glycogen chains
(after phosphorylase action)
glycogen debranching enzyme
HO
Available for hydrolysis
HO
Available for further phosphorolysis

Figure 16-4 | The reactions catalyzed by debranching enzyme. The enzyme transfers the terminal three α(1 → 4)-linked glucose residues from a "limit branch" of glycogen to the nonreducing end of another branch. The α(1 → 6) bond of the residue remaining at the branch point is hydrolyzed by further action of debranching enzyme to yield free glucose. The newly elongated branch is subject to degradation by glycogen phosphorylase.

residues in glycogen (those at the branch points) are therefore converted to glucose rather than G1P. *Debranching enzyme has separate active sites for the transferase and the α(1→6)-glucosidase reactions*. The presence of two independent catalytic activities on the same enzyme no doubt improves the efficiency of the debranching process.

The maximal rate of the glycogen phosphorylase reaction is much greater than that of the glycogen debranching reaction. Consequently, the outermost branches of glycogen, which constitute nearly half of its residues, are degraded in muscle in a few seconds under conditions of high metabolic demand. Glycogen degradation beyond this point requires debranching and hence occurs more slowly. This, in part, accounts for the fact that a muscle can sustain its maximum exertion for only a few seconds.

C | Phosphoglucomutase Interconverts Glucose-1-Phosphate and Glucose-6-Phosphate

Phosphorylase converts the glucosyl units of glycogen to G1P, which, in turn, is converted by phosphoglucomutase to G6P. The phosphoglucomutase reaction is similar to that catalyzed by phosphoglycerate mutase (Section 15-2H). A phosphoryl group is transferred from the active phosphoenzyme to G1P, forming **glucose-1,6-bisphosphate (G1,6P),** which then rephosphorylates the enzyme to yield G6P (Fig. 16-5; this near-equilibrium reaction also functions in reverse). An important difference between this enzyme and phosphoglycerate mutase is that the phosphoryl group in phosphoglucomutase is covalently bound to a Ser hydroxyl group rather than to a His imidazole nitrogen.

Glucose-6-Phosphatase Generates Glucose in the Liver. The G6P produced by glycogen breakdown can continue along the glycolytic pathway or the pentose phosphate pathway (note that the glucose is already phosphorylated, so that the ATP-consuming hexokinase-catalyzed phosphory-

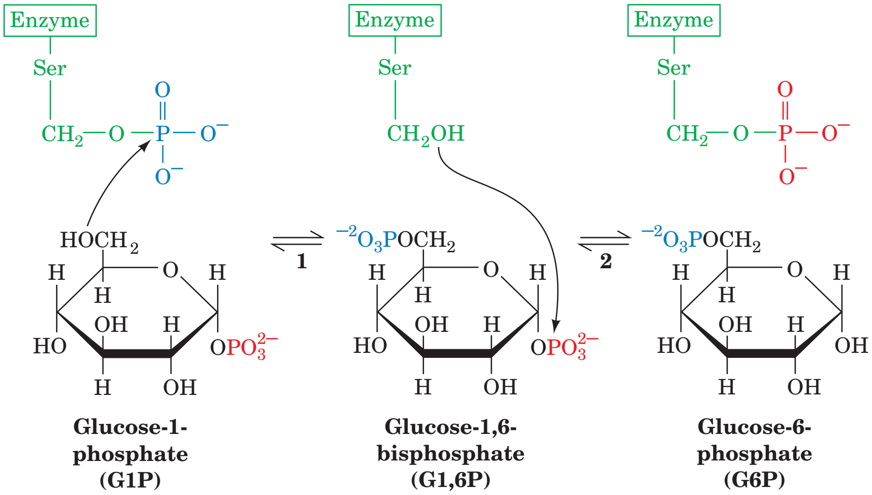
Enzyme
Ser
Enzyme
Ser
Enzyme
Ser
1
2
Glucose-1-phosphate (G1P)
Glucose-1,6-bisphosphate (G1,6P)
Glucose-6-phosphate (G6P)

■ **Figure 16-5 | The mechanism of phosphoglucomutase.** **(1)** The OH group at C6 of G1P attacks the phosphoenzyme to form a dephosphoenzyme–G1,6P intermediate. **(2)** The Ser OH group on the dephosphoenzyme attacks the phosphoryl group at C1 to regenerate the phosphoenzyme with the formation of G6P.

BOX 16-2 **BIOCHEMISTRY IN HEALTH AND DISEASE**

Glycogen Storage Diseases

Glycogen storage diseases are inherited disorders that affect glycogen metabolism, producing glycogen that is abnormal in either quantity or quality. Studies of the genetic defects that underlie these diseases have helped elucidate the complexities of glycogen metabolism (e.g., McArdle's disease). Conversely, the biochemical characterization of the pathways affected by a genetic disease often leads to useful strategies for its treatment. The table on p. 539 lists the enzyme deficiencies associated with each type of glycogen storage disease.

Glycogen storage diseases that mainly affect the liver generally produce **hepatomegaly** (enlarged liver) and **hypoglycemia** (low blood sugar), whereas glycogen storage diseases that affect the muscles cause muscle cramps and weakness. Both types of disease may also cause cardiovascular and renal disturbances.

Type I: Glucose-6-Phosphatase Deficiency (von Gierke's Disease). Glucose-6-phosphatase catalyzes the final step leading to the release of glucose into the bloodstream by the liver. Deficiency of the enzyme results in an increase of intracellular [G6P], which leads to a large accumulation of glycogen in the liver and kidney (recall that G6P activates glycogen synthase) and an inability to increase blood glucose concentration in response to the hormones glucagon or epinephrine. The symptoms of Type I glycogen storage disease include severe hepatomegaly and hypoglycemia and a general failure to thrive. Treatment of the disease has included drug-induced inhibition of glucose uptake by the liver (to increase blood [glucose]), continuous intragastric feeding overnight (again to increase blood [glucose]), surgical transposition of the portal vein, which ordinarily feeds the liver directly from the intestines (to allow this glucose-rich blood to reach peripheral tissues before it reaches the liver), and liver transplantation.

Type II: α-1,4-Glucosidase Deficiency (Pompe's Disease). α-1,4-Glucosidase deficiency is the most devastating of the glycogen storage diseases. It results in a large accumulation of glycogen of normal structure in the lysosomes of all cells and causes death by cardiorespiratory failure, usually before the age of 1 year. α-1,4-Glucosidase is not involved in the main pathways of glycogen metabolism. It occurs in lysosomes, where it hydrolyzes maltose (a glucose disaccharide) and other linear oligosaccharides, as well as the outer branches of glycogen, thereby yielding free glucose. Normally, this alternative pathway of glycogen metabolism is not quantitatively important, and its physiological significance is not known.

Type III: Amylo-1,6-Glucosidase (Debranching Enzyme) Deficiency (Cori's Disease). In Cori's disease, glycogen of abnormal structure containing very short outer chains accumulates in both liver and muscle since, in the absence of debranching enzyme, the glycogen cannot be further degraded. The resulting hypoglycemia is not as severe as in von Gierke's disease (Type I) and can be treated with frequent feedings and a high-protein diet (to offset the loss of amino acids used for gluconeogenesis). For unknown reasons, the symptoms of Cori's disease often disappear at puberty.

Type IV: Amylo-(1,4→1,6)-Transglycosylase (Branching Enzyme) Deficiency (Andersen's Disease). Andersen's disease is one of the most severe glycogen storage diseases; victims rarely survive past the age of 4 years because of liver dysfunction. Liver glycogen is present in normal concentrations, but it contains long unbranched chains that greatly reduce its solubility. The liver dysfunction may be caused by a "foreign body" immune reaction to the abnormal glycogen.

Type V: Muscle Phosphorylase Deficiency (McArdle's Disease). The symptoms of McArdle's disease, painful muscle cramps on exertion, typically do not appear until early adulthood and can be prevented by avoiding strenuous exercise. This condition affects glycogen metabolism in muscle but not in liver, which contains normal amounts of a different phosphorylase isozyme.

Type VI: Liver Phosphorylase Deficiency (Hers' Disease). Patients with a deficiency of liver glycogen phosphorylase have symptoms similar to those with mild forms of Type I glycogen storage disease. The hypoglycemia in this case results from the inability of liver glycogen phosphorylase to respond to the need for circulating glucose.

Type VII: Muscle Phosphofructokinase Deficiency (Tarui's Disease). The result of a deficiency of the glycolytic enzyme PFK in muscle is an abnormal buildup of the glycolytic metabo-

lation of glucose is bypassed). In the liver, G6P is also made available for use by other tissues. Because G6P cannot pass through the cell membrane, it is first hydrolyzed by **glucose-6-phosphatase (G6Pase):**

$$\text{G6P} + \text{H}_2\text{O} \rightarrow \text{glucose} + \text{P}_i$$

Although G6P is produced in the cytosol, G6Pase resides in the endoplasmic reticulum (ER) membrane. Consequently G6P must be imported into lites G6P and F6P. High concentrations of G6P increase the activities of glycogen synthase and UDP–glucose pyrophosphorylase (G6P is in equilibrium with G1P, a substrate for UDP–glucose pyrophosphorylase) so that glycogen accumulates in muscle. Other symptoms are similar to those of muscle phosphorylase deficiency, since PFK deficiency prevents glycolysis from keeping up with the ATP demand in contracting muscle.

Type VIII: X-Linked Phosphorylase Kinase Deficiency. Some individuals with symptoms of Type VI glycogen storage disease have normal phosphorylase enzymes but a defective phosphorylase kinase, which results in their inability to convert phosphorylase *b* to phosphorylase *a*. The α subunit of phosphorylase kinase is encoded by a gene on the X chromosome, so Type VIII disease is X-linked rather than autosomal recessive, as are the other glycogen storage diseases.

Type IX: Phosphorylase Kinase Deficiency. Phosphorylase kinase deficiency, an autosomal recessive disease, results from a mutation in one of the genes that encode the β, γ, and δ subunits of phosphorylase kinase. Because different tissues contain different phosphorylase kinase isozymes, the symptoms and severity of the disease vary according to the affected organs. Techniques for identifying genetic lesions are therefore more reliable than clinical symptoms for diagnosing a particular glycogen storage disease.

Type 0: Liver Glycogen Synthase Deficiency. Liver glycogen synthase deficiency is the only disease of glycogen metabolism in which there is a deficiency rather than an overabundance of glycogen. The activity of liver glycogen synthase is extremely low in individuals with Type 0 disease, who exhibit hyperglycemia after meals and hypoglycemia at other times. Some individuals, however, are asymptomatic, which suggests that there may be multiple forms of this autosomal recessive disorder.

Hereditary Glycogen Storage Diseases

Type	Enzyme Deficiency	Tissue	Common Name	Glycogen Structure
I	Glucose-6-phosphatase	Liver	von Gierke's disease	Normal
II	α-1,4-Glucosidase	All lysosomes	Pompe's disease	Normal
III	Amylo-1,6-glucosidase (debranching enzyme)	All organs	Cori's disease	Outer chains missing or very short
IV	Amylo-(1,4→1,6)-transglycosylase (branching enzyme)	Liver, probably all organs	Andersen's disease	Very long unbranched chains
V	Glycogen phosphorylase	Muscle	McArdle's disease	Normal
VI	Glycogen phosphorylase	Liver	Hers' disease	Normal
VII	Phosphofructokinase	Muscle	Tarui's disease	Normal
VIII	Phosphorylase kinase	Liver	X-Linked phosphorylase kinase deficiency	Normal
IX	Phosphorylase kinase	All organs		Normal
0	Glycogen synthase	Liver		Normal, deficient in quantity

the ER by a **G6P translocase** before it can be hydrolyzed. The resulting glucose and P_i are then returned to the cytosol via specific transport proteins. A defect in any of the components of this G6P hydrolysis system results in **type I glycogen storage disease** (Box 16-2). Glucose leaves the liver cell via a specific glucose transporter named **GLUT2** and is carried by the blood to other tissues. Muscle and other tissues lack G6Pase and therefore retain their G6P.

■ CHECK YOUR UNDERSTANDING

List the metabolic sources and products of G6P.

How does the structure of glycogen relate to its metabolic function?

Describe the enzymatic degradation of glycogen.

2 Glycogen Synthesis

LEARNING OBJECTIVES

- Understand that liver glycogen synthesis involves a series of conversions from glucose to glucose-6-phosphate, to UDP–glucose, and finally to glycogen.
- Understand that UPD–glucose is an activated molecule.
- Appreciate that glycogen is extended from a primer built on and by the protein glycogenin.

The $\Delta G^{\circ\prime}$ for the glycogen phosphorylase reaction is $+3.1\ \text{kJ} \cdot \text{mol}^{-1}$, but under physiological conditions, glycogen breakdown is exergonic ($\Delta G^{\circ\prime} = -5$ to $-8\ \text{kJ} \cdot \text{mol}^{-1}$). The synthesis of glycogen from G1P under physiological conditions is therefore thermodynamically unfavorable without free energy input. Consequently, *glycogen synthesis and breakdown must occur by separate pathways*. This recurrent metabolic strategy—that biosynthetic and degradative pathways of metabolism are different—is particularly important when both pathways must operate under similar physiological conditions. This situation is thermodynamically impossible if one pathway is just the reverse of the other.

It was not thermodynamics, however, that led to recognition of the separation of synthetic and degradative pathways for glycogen, but McArdle's disease. Individuals with the disease lack muscle glycogen phosphorylase activity and therefore cannot break down glycogen. Yet their muscles contain moderately high quantities of normal glycogen. Clearly, glycogen synthesis does not require glycogen phosphorylase. In this section, we describe the three enzymes that participate in glycogen synthesis: **UDP–glucose pyrophosphorylase, glycogen synthase,** and **glycogen branching enzyme.** The opposing reactions of glycogen synthesis and degradation are diagrammed in Fig. 16-6.

A | UDP–Glucose Pyrophosphorylase Activates Glucosyl Units

Since the direct conversion of G1P to glycogen and P_i is thermodynamically unfavorable (positive ΔG) under physiological conditions, glycogen biosynthesis requires an exergonic step. This is accomplished, as Luis Leloir discovered in 1957, by combining G1P with uridine triphosphate (UTP) in a reaction catalyzed by UDP–glucose pyrophosphorylase (Fig. 16-7). The product of this reaction, **uridine diphosphate glucose (UDP–glucose** or **UDPG),** is an "activated" compound that can donate a glucosyl unit to the growing glycogen chain. The formation of UDPG itself has $\Delta G^{\circ\prime} \approx 0$ (it is a phosphoanhydride exchange reaction), but the subsequent exergonic hydrolysis of PP_i by the omnipresent enzyme inorganic pyrophosphatase makes the overall reaction exergonic.

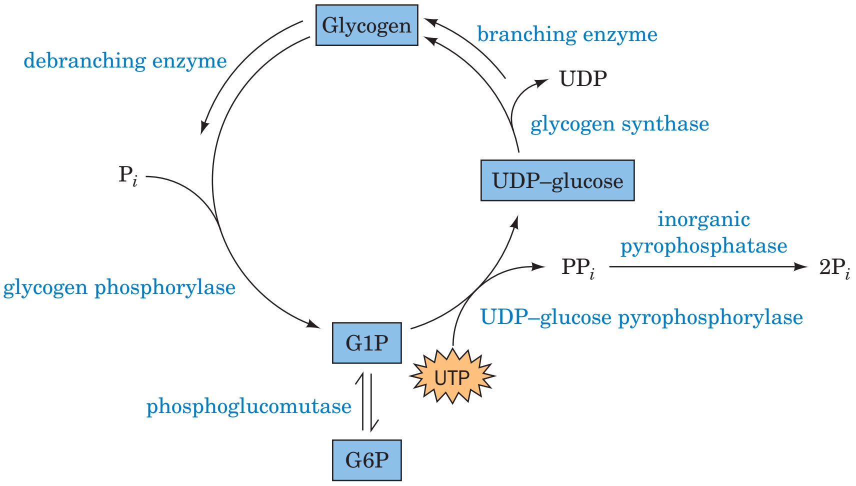

Figure 16-6 | Opposing pathways of glycogen synthesis and degradation. The exergonic process of glycogen breakdown is reversed by a process that uses UTP to generate a UDP–glucose intermediate.

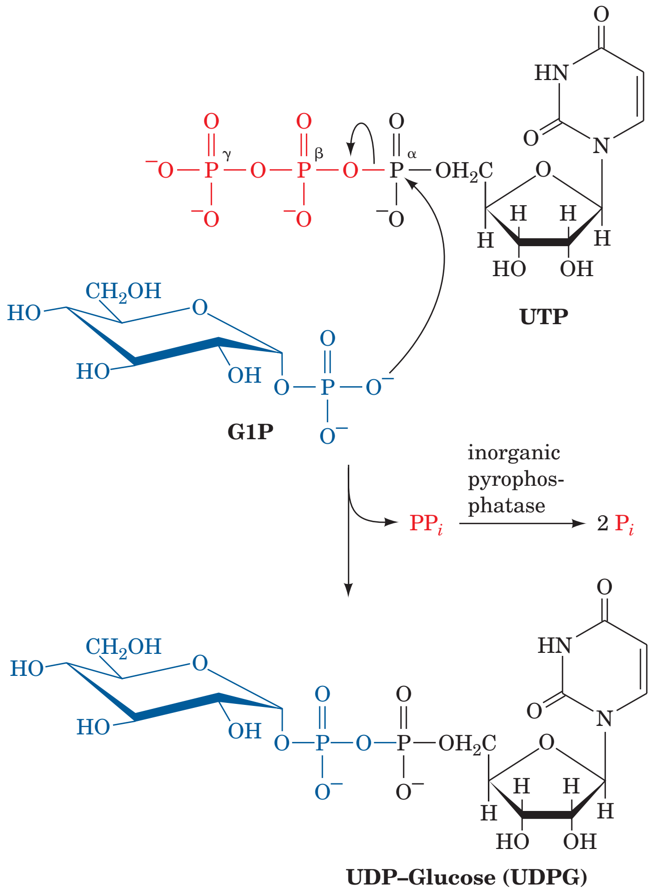

Figure 16-7 | The reaction catalyzed by UDP–glucose pyrophosphorylase. In this phosphoanhydride exchange reaction, the phosphoryl oxygen of G1P attacks the α-phosphorus atom of UTP to form UDP–glucose and PP_i. The PP_i is rapidly hydrolyzed by inorganic pyrophosphatase.

	$\Delta G^{\circ\prime}$ (kJ · mol^{-1})
$G1P + UTP \rightleftharpoons UDPG + PP_i$	~0
$H_2O + PP_i \rightarrow 2P_i$	−19.2
Overall $G1P + UTP \rightarrow UDPG + 2\ P_i$	−19.2

This is an example of the common biosynthetic strategy of cleaving a nucleoside triphosphate to form PP_i. The free energy of PP_i hydrolysis can then be used to drive an otherwise unfavorable reaction to completion (Section 14-2B); the near total elimination of the PP_i by the highly exergonic (irreversible) pyrophosphatase reaction prevents the reverse of the PP_i-producing reaction from occurring.

B | Glycogen Synthase Extends Glycogen Chains

In the next step of glycogen synthesis, the glycogen synthase reaction, the glucosyl unit of UDPG is transferred to the C4-OH group on one of glycogen's nonreducing ends to form an α(1→4) glycosidic bond. The $\Delta G^{\circ\prime}$ for the glycogen synthase reaction

$$\text{UDPG} + \underset{(n\text{ residues})}{\text{glycogen}} \longrightarrow \text{UDP} + \underset{(n+1\text{ residues})}{\text{glycogen}}$$

is -13.4 kJ · mol^{-1}, making the overall reaction spontaneous under the same conditions that glycogen breakdown by glycogen phosphorylase is also spontaneous. However, glycogen synthesis does have an energetic price. Combining the first two reactions of glycogen synthesis gives

$$\underset{(n\text{ residues})}{\text{Glycogen}} + \text{G1P} + \text{UTP} \rightarrow \underset{(n+1\text{ residues})}{\text{glycogen}} + \text{UDP} + 2\,\text{P}_i$$

Thus, *one molecule of UTP is cleaved to UDP for each glucose residue incorporated into glycogen*. The UTP is replenished through a phosphoryl-transfer reaction mediated by nucleoside diphosphate kinase (Section 14-2C):

$$\text{UDP} + \text{ATP} \rightleftharpoons \text{UTP} + \text{ADP}$$

so that UTP consumption is energetically equivalent to ATP consumption.

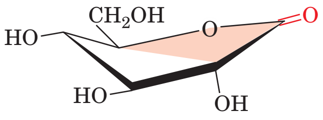

1,5-Gluconolactone

The transfer of a glucosyl unit from UDPG to a growing glycogen chain involves the formation of a glycosyl oxonium ion by the elimination of UDP, a good leaving group (Fig. 16-8). The enzyme is inhibited by **1,5-gluconolactone** *(at left)*, an analog that mimics the oxonium ion's half-chair geometry. The same analog inhibits both glycogen phosphorylase (Section 16-1A) and lysozyme (Section 11-4), which have similar mechanisms.

Human muscle glycogen synthase is a homotetramer of 737-residue subunits (the liver isozyme has 703-residue subunits). Like glycogen phosphorylase, it has two enzymatically interconvertible forms; in this case, however, the phosphorylated *b* form is less active, and the original (dephosphorylated) *a* form is more active. (Note: For enzymes subject to covalent modification, "*a*" refers to the more active form and "*b*" refers to the less active form.)

Glycogen synthase is under allosteric control; it is strongly inhibited by physiological concentrations of ATP, ADP, and P$_i$. In fact, the phosphorylated enzyme is almost totally inactive *in vivo*. The dephosphorylated enzyme, however, can be activated by G6P, so the cell's glycogen synthase activity varies with [G6P] and the fraction of the enzyme in its dephosphorylated form. The mechanistic details of the interconversion of

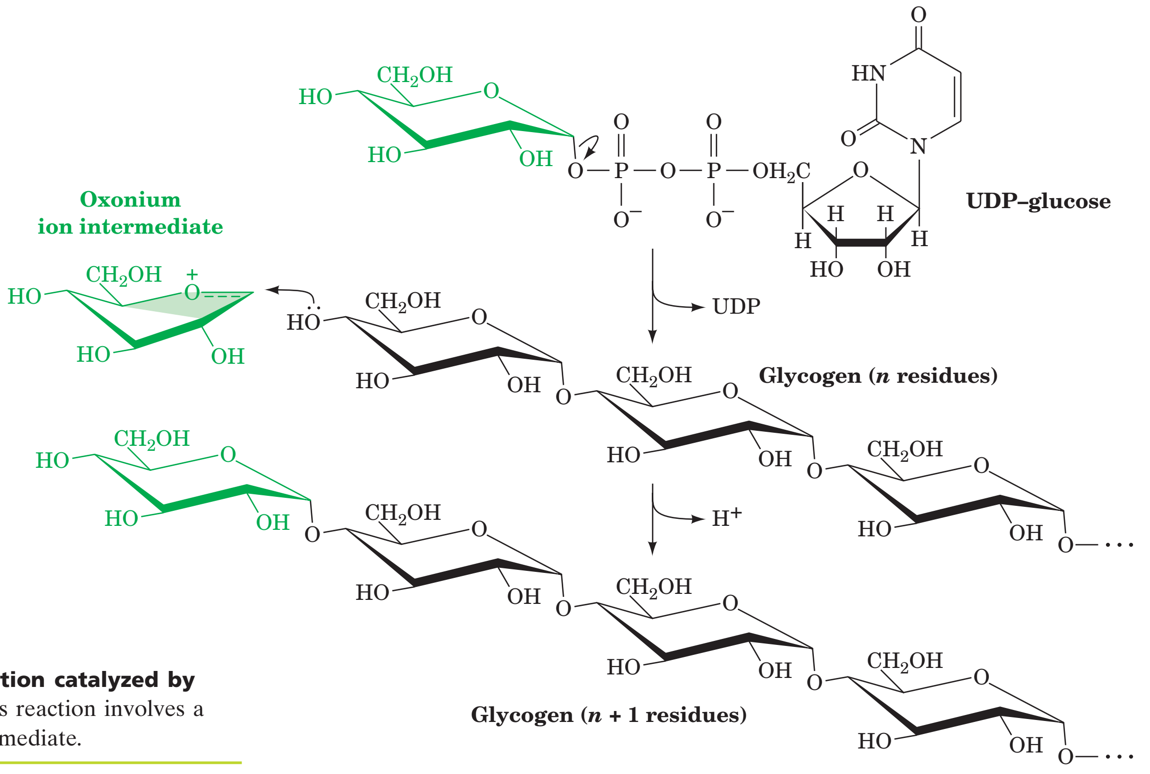

■ **Figure 16-8 | The reaction catalyzed by glycogen synthase.** This reaction involves a glucosyl oxonium ion intermediate.

phosphorylated and dephosphorylated forms of glycogen synthase are complex and are not as well understood as those of glycogen phosphorylase (for one thing, glycogen synthase has multiple phosphorylation sites). We shall discuss the regulation of glycogen synthase further in Section 16-3B.

Glycogenin Primes Glycogen Synthesis. Glycogen synthase cannot simply link together two glucose residues; it can only extend an already existing α(1→4)-linked glucan chain. How, then, is glycogen synthesis initiated? In the first step of this process, a 349-residue protein named **glycogenin,** acting as a glycosyltransferase, attaches a glucose residue donated by UDPG to the OH group of its Tyr 194. Glycogenin then extends the glucose chain by up to seven additional UDPG-donated glucose residues to form a glycogen "primer." Only at this point does glycogen synthase commence glycogen synthesis by extending the primer. Analysis of glycogen granules suggests that each glycogen molecule is associated with only one molecule each of glycogenin and glycogen synthase.

C | Glycogen Branching Enzyme Transfers Seven-Residue Glycogen Segments

Glycogen synthase generates only α(1→4) linkages to yield α-amylose. Branching to form glycogen is accomplished by a separate enzyme, **amylo-(1,4→1,6)-transglycosylase (branching enzyme),** which is distinct from glycogen debranching enzyme (Section 16-1B). A branch is created by transferring a 7-residue segment from the end of a chain to the C6-OH group of a glucose residue on the same or another glycogen chain (Fig. 16-9). Each transferred segment must come from a chain of at least 11

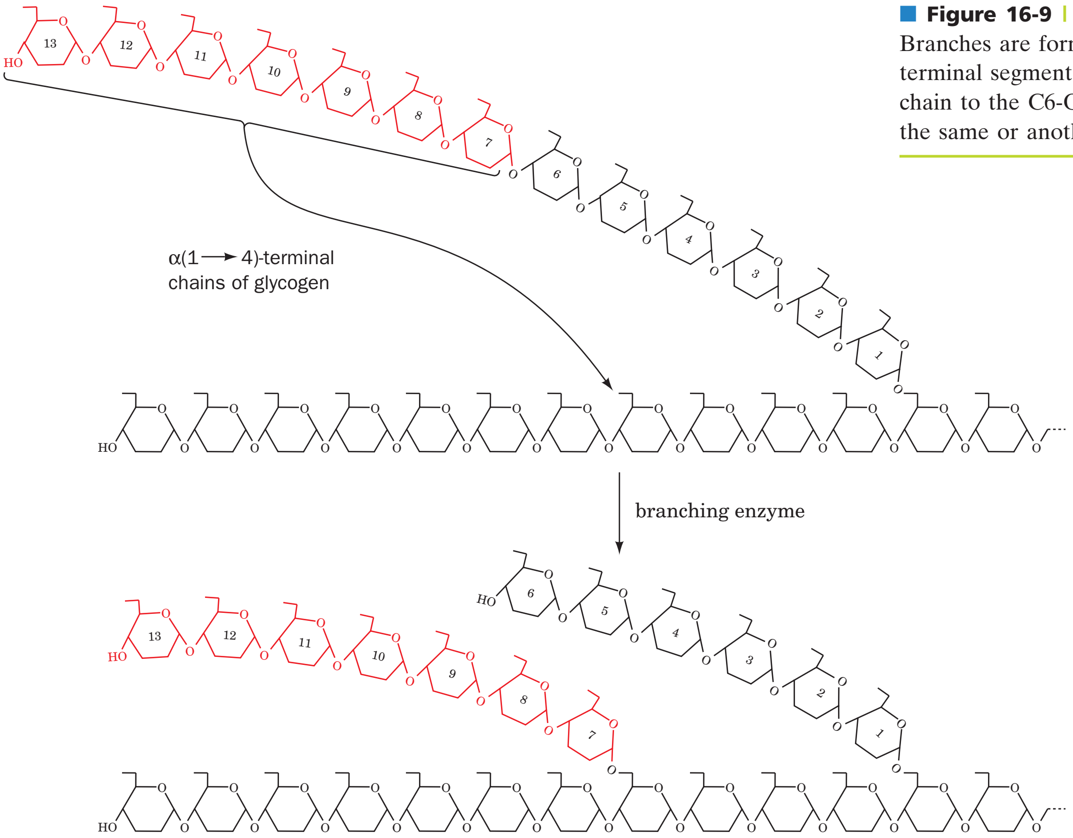

Figure 16-9 | The branching of glycogen. Branches are formed by transferring a 7-residue terminal segment from an α(1 → 4)-linked glucan chain to the C6-OH group of a glucose residue on the same or another chain.

residues, and the new branch point must be at least 4 residues away from other branch points. The branching pattern of glycogen has been optimized by evolution for the efficient storage and mobilization of glucose (Box 16-3).

■ **CHECK YOUR UNDERSTANDING**

Describe the enzymatic synthesis of glycogen.
Why must opposing biosynthetic and degradative pathways differ in at least one enzyme?

BOX 16-3 PERSPECTIVES IN BIOCHEMISTRY

Optimizing Glycogen Structure

The function of glycogen in animal cells is to store the metabolic fuel glucose and to release it rapidly when needed. Glucose must be stored as a polymer, because glucose itself could not be stored without a drastic increase in intracellular osmotic pressure (Section 2-1D). It has been estimated that the total concentration of glucose residues stored as glycogen in a liver cell is ~0.4 M, whereas the concentration of glycogen is only ~10 nM. This huge difference mitigates osmotic stress.

To fulfill its biological function, the glycogen polymer must store the largest amount of glucose in the smallest possible volume while maximizing both the amount of glucose available for release by glycogen phosphorylase and the number of nonreducing ends (to maximize the rate at which glucose residues can be mobilized). All these criteria must be met by optimizing just two variables: the degree of branching and chain length.

In a glycogen molecule, shown schematically here,

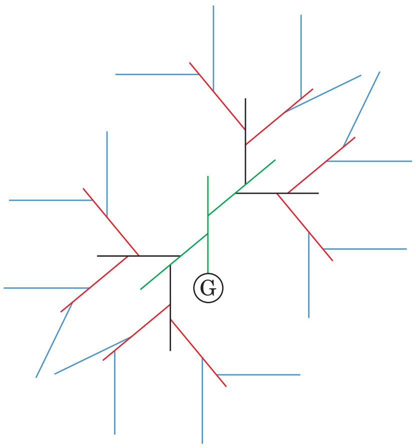

the glycogen chains, beginning with the innermost chain attached to glycogenin (G), have two branches (the outermost chains are unbranched). The entire molecule is roughly spherical and is organized in tiers. There are an estimated 12 tiers in mature glycogen (only 4 are shown above).

With two branches per chain, the number of chains in a given tier is twice the number of the preceding tier, and the outermost tier contains about half of the total glucose residues (regardless of the number of tiers). When the degree of branching increases, for example, to three branches per chain, the proportion of residues in the outermost tier increases, but so does the density of glucose residues. This severely limits the maximum size of the glycogen particle and the number of glucose residues it can accommodate. Thus, glycogen has around two branches per chain.

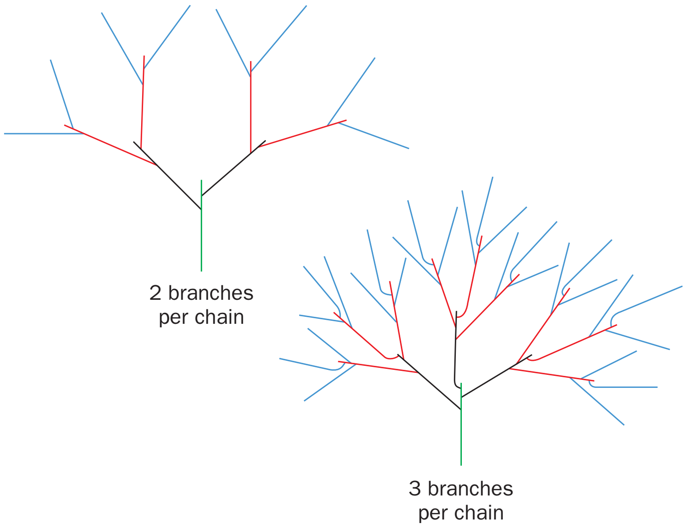

Mathematical analysis of the other variable, chain length, yields an optimal value of 13, which is in good agreement with the actual length of glycogen chains in cells (8–14 residues). Consider the two simplified glycogen molecules shown below, which contain the same number of glucose residues (the same total length of line segments) and the same branching pattern:

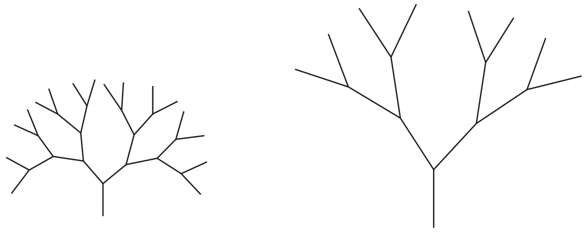

The molecule with the shorter chains packs more glucose in a given volume and has more points for phosphorylase attack, but only about half the amount of glucose can be released before debranching must occur (debranching is much slower than phosphorolysis). In the less dense molecule, the longer chains increase the number of residues that can be continuously phosphorylyzed; however, there are fewer points of attack. Thirteen residues is apparently a compromise for mobilizing the largest amount of glucose in the shortest time.

Amylopectin (Section 8-2C), which is chemically similar to glycogen, is a much larger molecule and has longer chains. Amylose lacks branches altogether. Evidently, starch, unlike glycogen, is not designed for rapid mobilization of metabolic fuel.

[Figures adapted from Meléndez-Hevia, E., Waddell, T.G., and Shelton, E.D., *Biochem. J.* **295,** 477–483 (1993).]

3 Control of Glycogen Metabolism

If glycogen synthesis and breakdown proceed simultaneously, all that is accomplished is the wasteful hydrolysis of UTP. Glycogen metabolism must therefore be controlled according to cellular needs. *The regulation of glycogen metabolism involves allosteric control as well as hormonal control by covalent modification of the pathway's regulatory enzymes.*

LEARNING OBJECTIVES

- Understand that the opposing processes of glycogen breakdown and synthesis are reciprocally regulated by allosteric interactions and covalent modification of key enzymes.
- Understand that glycogen metabolism is ultimately under hormonal control.

A | Glycogen Phosphorylase and Glycogen Synthase Are under Allosteric Control

As we saw in Sections 14-1E and 15-4B, the net flux, J, of reactants through a step in a metabolic pathway is the difference between the forward and reverse reaction velocities, v_f and v_r. However, the flux varies dramatically with substrate concentration as the reaction approaches equilibrium ($v_f \approx v_r$). The flux through a near-equilibrium reaction is therefore all but uncontrollable. *Precise flux control of a pathway is possible when an enzyme functioning far from equilibrium is opposed by a separately controlled enzyme. Then,* v_f *and* v_r *vary independently and* v_r *can be larger or smaller than* v_f*, allowing control of both rate and direction.* Exactly this situation occurs in glycogen metabolism through the opposition of the glycogen phosphorylase and glycogen synthase reactions.

Both glycogen phosphorylase and glycogen synthase are under allosteric control by effectors that include ATP, G6P, and AMP. Muscle glycogen phosphorylase is activated by AMP and inhibited by ATP and G6P. Glycogen synthase, on the other hand, is activated by G6P. This suggests that when there is high demand for ATP (low [ATP], low [G6P], and high [AMP]), glycogen phosphorylase is stimulated and glycogen synthase is inhibited, which favors glycogen breakdown. Conversely, when [ATP] and [G6P] are high, glycogen synthesis is favored.

In vivo, this allosteric scheme is superimposed on an additional control system based on covalent modification. For example, phosphorylase *a* is active even without AMP stimulation (Section 16-1A), and glycogen synthase is essentially inactive (Section 16-2B) unless it is dephosphorylated and G6P is present. *Thus, covalent modification (phosphorylation and dephosphorylation) of glycogen phosphorylase and glycogen synthase provides a more sophisticated control system that modulates the responsiveness of the enzymes to their allosteric effectors.*

B | Glycogen Phosphorylase and Glycogen Synthase Undergo Control by Covalent Modification

See Guided Exploration 15
Control of glycogen metabolism.

The interconversion of the *a* and *b* forms of glycogen synthase and glycogen phosphorylase is accomplished through enzyme-catalyzed phosphorylation and dephosphorylation (Section 12-3B), a process that is under hormonal control (Section 13-2). **Enzymatically interconvertible enzyme systems** can therefore respond to a greater number of effectors than simple allosteric systems. Furthermore, a set of kinases and phosphatases linked in cascade fashion has enormous potential for signal amplification and flexibility in response to different metabolic signals. Note that the correlation between phosphorylation and enzyme activity varies with the enzyme. For example, glycogen phosphorylase is activated by phosphorylation ($b \rightarrow a$), whereas glycogen synthase is inactivated by phosphorylation ($a \rightarrow b$). Conversely, dephosphorylation inactivates glycogen phosphorylase and activates glycogen synthase.

Glycogen Phosphorylase Is Activated by Phosphorylation. The cascade that governs the enzymatic interconversion of glycogen phosphorylase involves three enzymes (Fig. 16-10):

1. ***Phosphorylase kinase,*** which specifically phosphorylates Ser 14 of glycogen phosphorylase *b*.
2. ***Protein kinase A (PKA;*** Section 13-3C), which phosphorylates and thereby activates phosphorylase kinase.
3. ***Phosphoprotein phosphatase-1 (PP1;*** Section 13-2D), which dephosphorylates and thereby deactivates both glycogen phosphorylase *a* and phosphorylase kinase.

Phosphorylase *b* is sensitive to allosteric effectors, but phosphorylase *a* is much less so, as discussed in Section 12-3B (Fig. 12-16). In the resting cell, the concentrations of ATP and G6P are high enough to inhibit phosphorylase *b*. The level of phosphorylase activity is therefore largely determined by the fraction of enzyme present as phosphorylase *a*. The steady state fraction of phosphorylated enzyme depends on the relative activities of phosphorylase kinase, PKA, and PP1. Recall that PKA is activated by **cAMP,** a second messenger that is made by **adenylate cyclase** on hormone-stimulated activation of a heterotrimeric **G protein** (Section 13-3C). Let us examine the factors that regulate the activities of phosphorylase kinase and PP1 before we return to the regulation of glycogen synthase activity.

Phosphorylase Kinase Is Activated by Phosphorylation and by Ca^{2+}. Phosphorylase kinase is a 1300-kD protein with four nonidentical subunits, known as α, β, γ, and δ. The γ subunit contains the catalytic site, and the other three subunits have regulatory functions. *Phosphorylase kinase is maximally activated by* Ca^{2+} *and by the phosphorylation of its α and β subunits by PKA*.

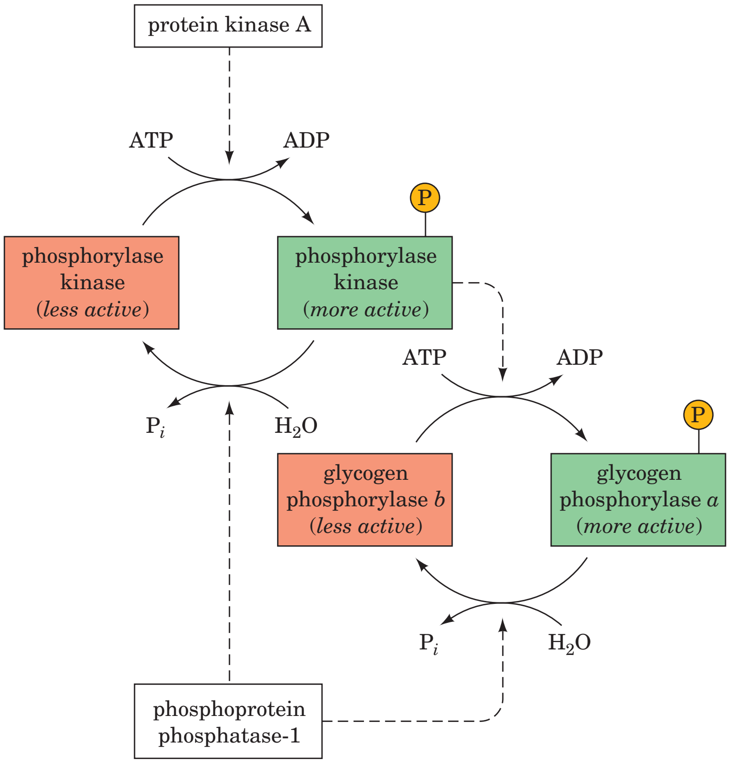
protein kinase A
ATP
ADP
P
phosphorylase kinase (less active)
phosphorylase kinase (more active)
ATP
ADP
P_i
H_2O
P
glycogen phosphorylase b (less active)
glycogen phosphorylase a (more active)
P_i
H_2O
phosphoprotein phosphatase-1

Figure 16-10 | The glycogen phosphorylase interconvertible enzyme system. Conversion of phosphorylase *b* (the less active form) to phosphorylase *a* (the more active form) is accomplished through phosphorylation catalyzed by phosphorylase kinase, which is itself subject to activation through phosphorylation by protein kinase A (PKA). Both glycogen phosphorylase *a* and phosphorylase kinase are dephosphorylated by phosphoprotein phosphatase-1.

Figure 16-11 | X-Ray structure of the γ subunit of rabbit muscle phosphorylase kinase in complex with ATP and a heptapeptide analog of the enzyme's natural substrate. The N-terminal domain is pink, the C-terminal domain is cyan, the activation loop is light blue, and the heptapeptide is orange, with its residue to be phosphorylated (Ser) white. The ATP is shown in space-filling form and the side chains of the catalytically essential Arg 148, Asp 149, and Glu 182 are shown in stick form, all colored according to atom type (C green, N blue, O red, and P yellow). Note the structural similarities and differences between this protein and other protein kinases, for example, the C subunit of protein kinase A (Fig. 13-22) and the tyrosine kinase domain of the insulin receptor (Fig. 13-5). [After an X-ray structure by Louise Johnson, Oxford University, U.K. PDBid 2PHK.]

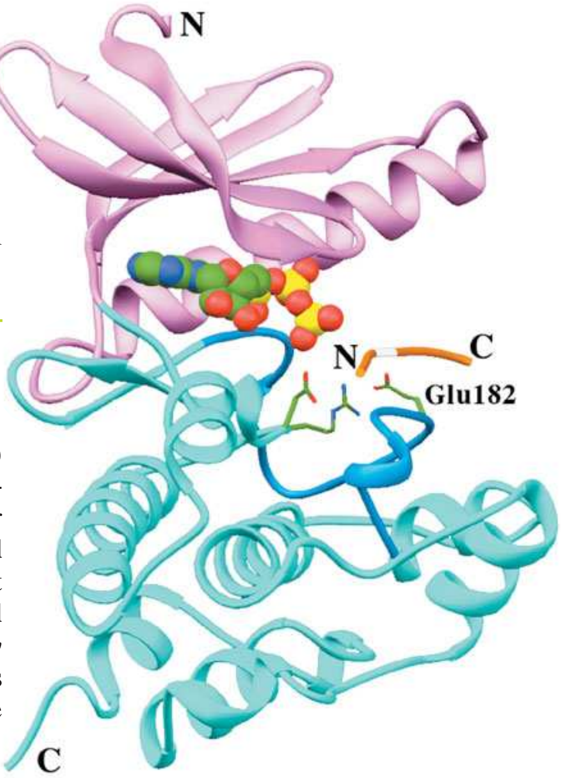

The γ subunit of phosphorylase kinase contains a 386-residue kinase domain, which is 36% identical in sequence to the PKA C subunit (Fig. 13-22) and has a similar structure (Fig. 16-11). The γ subunit is not subject to phosphorylation, as are many other protein kinases, because the Ser, Thr, or Tyr residue that is phosphorylated to activate those other kinases is replaced by a Glu residue in the γ subunit. The negative charge of the Glu is thought to mimic the presence of a phosphate group and interact with a conserved Arg residue near the active site. However, full catalytic activity of the γ subunit is prevented by an autoinhibitory C-terminal segment, which binds to and blocks the kinase's active site, much like the R subunit blocks the activity of the C subunit of protein kinase A. An inhibitory segment in the β subunit may also block the activity of the γ subunit.

Autoinhibition of phosphorylase kinase is relieved by PKA-catalyzed phosphorylation of both the α and β subunits. This presumably causes the β inhibitor segment to move aside (the way in which phosphorylation of the α subunit modulates the enzyme's behavior is not understood). However, full activity of the γ subunit also requires Ca^{2+} binding to the δ subunit, which is **calmodulin** (**CaM;** Section 13-4B; CaM functions both as a free-floating protein and as a subunit of other proteins). Ca^{2+} concentrations as low as 10^{-7} M activate phosphorylase kinase by inducing a conformational change in CaM that causes it to bind to and extract the γ subunit's autoinhibitor segment from its catalytic site.

The conversion of glycogen phosphorylase *b* to glycogen phosphorylase *a* through the action of phosphorylase kinase increases the rate of glycogen breakdown. The physiological significance of the Ca^{2+} trigger for this activation is that muscle contraction is also triggered by a transient increase in the level of cytosolic Ca^{2+} (Section 7-2B). The rate of glycogen breakdown is thereby linked to the rate of muscle contraction. This is critical because glycogen breakdown provides fuel for glycolysis to generate the ATP required for muscle contraction. Since Ca^{2+} release occurs in response to nerve impulses, whereas the phosphorylation of phosphorylase kinase ultimately occurs in response to the presence of certain hormones, these two signals act synergistically in muscle cells to stimulate glycogenolysis.

Phosphoprotein Phosphatase-1 Is Inhibited by Phosphoprotein Inhibitor-1. A steady state for many phosphorylated enzymes is maintained by a balance between phosphorylation, as catalyzed by a corresponding kinase, and hydrolytic dephosphorylation, as catalyzed by a phosphatase. Phosphoprotein phosphatase-1 (PP1) removes the phosphoryl groups from glycogen phosphorylase *a* and the α and β subunits of phosphorylase kinase (Fig. 16-10), as well as those of other proteins involved in glycogen metabolism (see below).

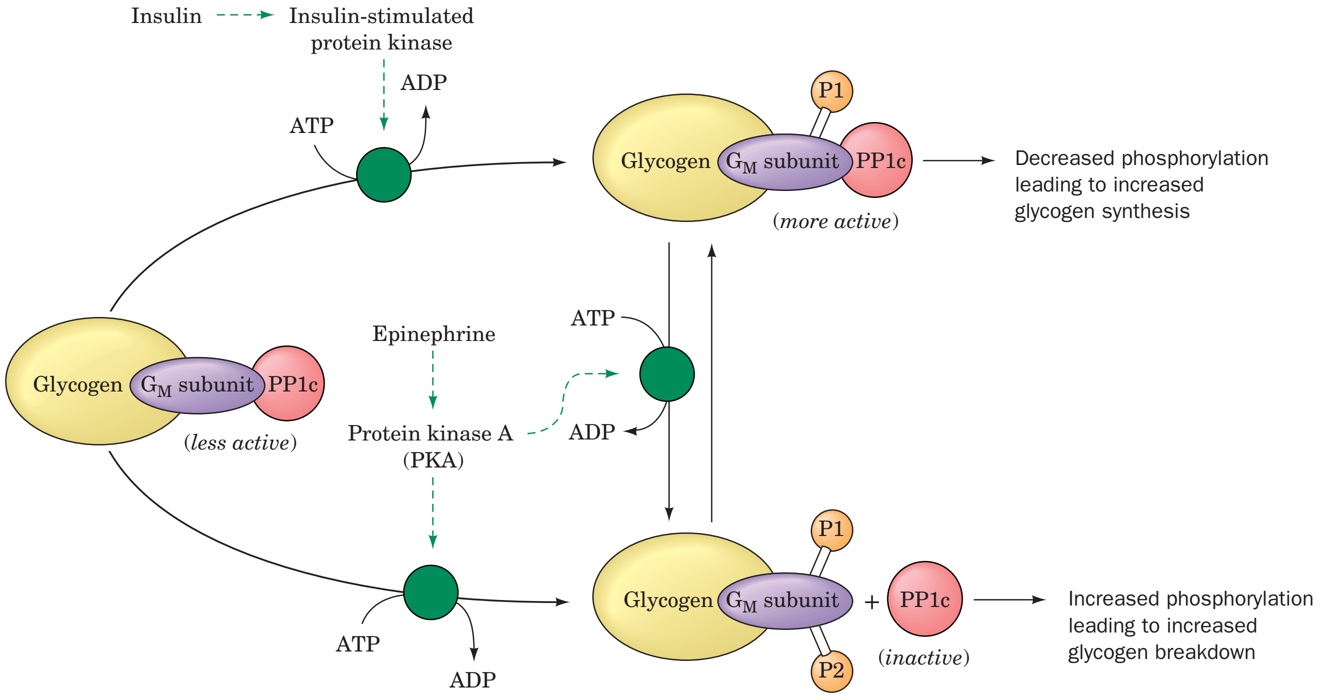
Insulin
Insulin-stimulated protein kinase
ATP
ADP
Glycogen
G_M subunit
PP1c
P1
(more active)
Decreased phosphorylation leading to increased glycogen synthesis
Glycogen
G_M subunit
PP1c
(less active)
Epinephrine
Protein kinase A (PKA)
ATP
ADP
ATP
ADP
Glycogen
G_M subunit
P1
P2
+
PP1c
(inactive)
Increased phosphorylation leading to increased glycogen breakdown

■ **Figure 16-12 | Regulation of phosphoprotein phosphatase-1 in muscle.** The antagonistic effects of insulin and epinephrine on glycogen metabolism in muscle occur through their effects on the phosphoprotein phosphatase-1 catalytic subunit, PP1c, via its glycogen-bound G_M subunit. Green circles and dashed arrows indicate activation.

PP1 is controlled differently in muscle and in liver. In muscle, the catalytic subunit of PP1 (called **PP1c**) is active only when it is bound to glycogen through its glycogen-binding **G_M subunit.** The activity of PP1c and its affinity for the G_M subunit are regulated by phosphorylation of the G_M subunit at two separate sites (Fig. 16-12). Phosphorylation of site 1 by an **insulin-stimulated protein kinase** (a homolog of PKA and the γ subunit of phosphorylase kinase) activates PP1c, whereas phosphorylation of site 2 by PKA (which can also phosphorylate site 1) causes PP1c to be released into the cytoplasm, where it cannot dephosphorylate the glycogen-bound enzymes of glycogen metabolism.

In the cytosol, phosphoprotein phosphatase-1 is also inhibited by its binding to the protein **phosphoprotein phosphatase inhibitor 1.** The latter protein provides yet another example of control by covalent modification: It too is activated by PKA and deactivated by phosphoprotein phosphatase-1 (Fig. 16-13, *lower left*). *The concentration of cAMP therefore controls the fraction of an enzyme in its phosphorylated form, not only by increasing the rate at which it is phosphorylated, but also by decreasing the rate at which it is dephosphorylated*. In the case of glycogen phosphorylase, an increase in [cAMP] not only increases the enzyme's rate of activation, but also decreases its rate of deactivation.

In liver, PP1 is also bound to glycogen, but through the intermediacy of a glycogen-binding subunit named **G_L**. In contrast to G_M, G_L is not subject to control via phosphorylation. The activity of the PP1 · G_L complex is controlled by its binding to phosphorylase *a*. Both the R and T forms of phosphorylase *a* strongly bind PP1, but only in the T state is the Ser 14 phosphoryl group accessible for hydrolysis (in the R state, the Ser 14 phosphoryl group is buried at the dimer interface; Fig. 12-15). Consequently,

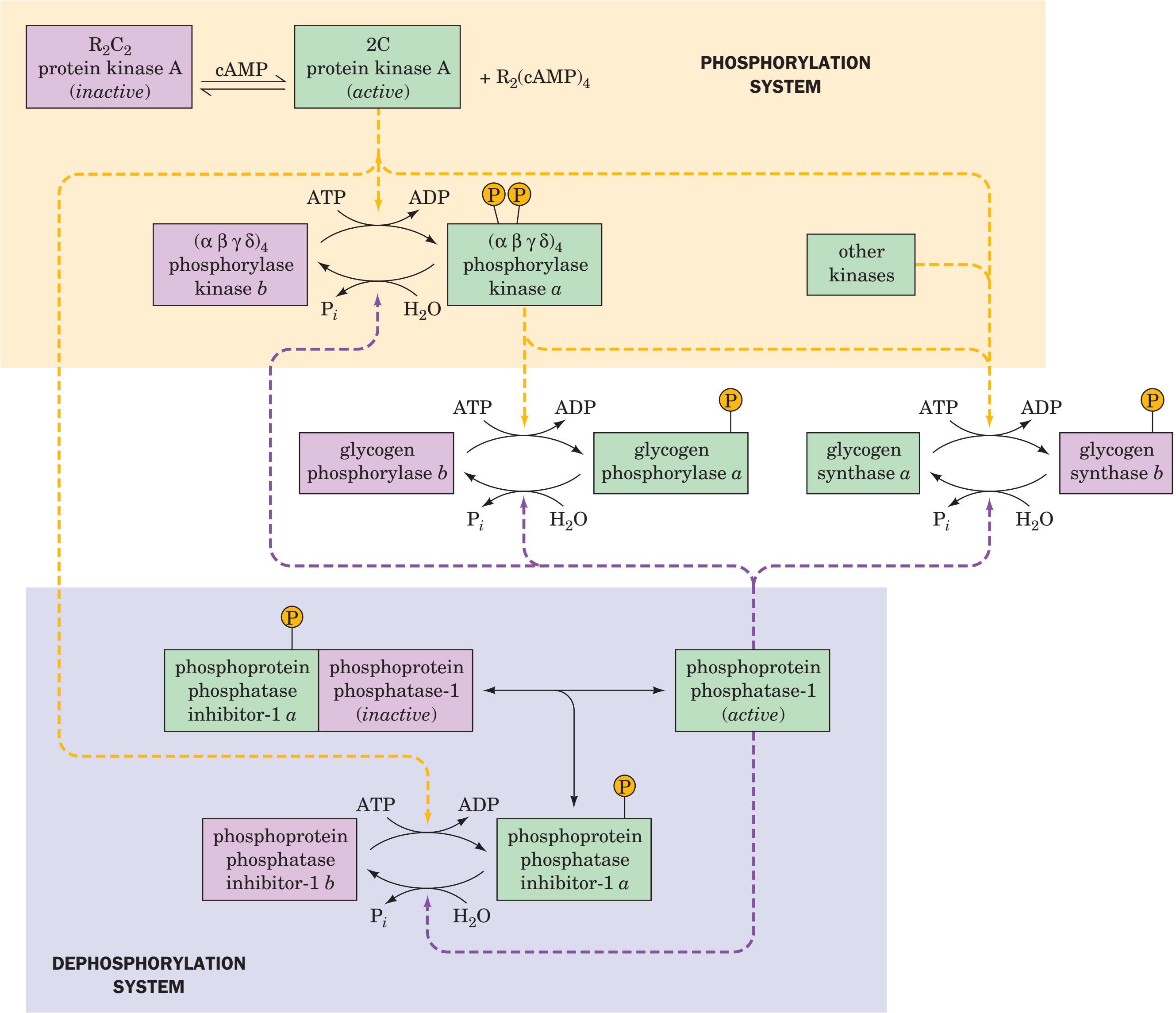
R_2C_2 protein kinase A (*inactive*)
cAMP
2C protein kinase A (*active*)
+ $R_2(cAMP)_4$
PHOSPHORYLATION SYSTEM
ATP
ADP
P P
$(\alpha\beta\gamma\delta)_4$ phosphorylase kinase *b*
$(\alpha\beta\gamma\delta)_4$ phosphorylase kinase *a*
P_i
H_2O
other kinases
ATP
ADP
P
glycogen phosphorylase *b*
glycogen phosphorylase *a*
P_i
H_2O
ATP
ADP
P
glycogen synthase *a*
glycogen synthase *b*
P_i
H_2O
P
phosphoprotein phosphatase inhibitor-1 *a*
phosphoprotein phosphatase-1 (*inactive*)
phosphoprotein phosphatase-1 (*active*)
ATP
ADP
P
phosphoprotein phosphatase inhibitor-1 *b*
phosphoprotein phosphatase inhibitor-1 *a*
P_i
H_2O
DEPHOSPHORYLATION SYSTEM

Figure 16-13 | **The major phosphorylation and dephosphorylation systems that regulate glycogen metabolism in muscle.** Activated enzymes are shaded green, and deactivated enzymes are shaded pink. Dashed arrows indicate facilitation of a phosphorylation or dephosphorylation reaction. **See the Animated Figures.**

when phosphorylase *a* is in its active R form, it effectively sequesters PP1. However, under conditions where phosphorylase *a* shifts to the T state (see below), PP1 hydrolyzes the now exposed Ser 14 phosphoryl group, thereby converting phosphorylase *a* to phosphorylase *b*, which has only a low affinity for the $PP1 \cdot G_L$ complex. One effect of phosphorylase *a* dephosphorylation, therefore, is to relieve the inhibition of PP1. Since liver cells contain 10 times more glycogen phosphorylase than PP1, the phosphatase is not released until more than ~90% of the glycogen phosphorylase is in the *b* form. Only then can PP1 dephosphorylate its other target proteins, including glycogen synthase.

Glucose is an allosteric inhibitor of phosphorylase *a* (Fig. 12-16). Consequently, when the concentration of glucose is high, phosphorylase *a* converts to its T form, thereby leading to its dephosphorylation and the dephosphorylation of glycogen synthase. Glucose is therefore thought to be important in the control of glycogen metabolism in the liver.

Glycogen Synthase Is Elaborately Regulated. Phosphorylase kinase, which activates glycogen phosphorylase, also phosphorylates and thereby inactivates glycogen synthase. Six other protein kinases, including PKA and phosphorylase kinase, are known to at least partially deactivate human muscle glycogen synthase by phosphorylating one or more of the nine Ser residues on each of its subunits (Fig. 16-13). The reason for this elaborate regulation of glycogen synthase is unclear.

The balance between net synthesis and degradation of glycogen as well as the rates of these processes depend on the relative activities of glycogen synthase and glycogen phosphorylase. To a large extent, the rates of the phosphorylation and dephosphorylation of these enzymes control glycogen synthesis and breakdown. The two processes are linked by PKA and phosphorylase kinase, which, through phosphorylation, activate glycogen phosphorylase as they inactivate glycogen synthase (Fig. 16-13). They are also linked by PP1, which in liver is inhibited by phosphorylase *a* and therefore unable to activate (dephosphorylate) glycogen synthase unless it first inactivates (also by dephosphorylation) phosphorylase *a*. Of course, control by allosteric effectors is superimposed on control by covalent modification so that, for example, the availability of the substrate G6P (which activates glycogen synthase) also influences the rate at which glucose residues are incorporated into glycogen. Inherited deficiencies of enzymes can disrupt the fine control of glycogen metabolism, leading to various diseases (Box 16-2).

C | Glycogen Metabolism Is Subject to Hormonal Control

Glycogen metabolism in the liver is largely controlled by the polypeptide hormones insulin (Fig. 5-1) and **glucagon** acting in opposition. Glucagon,

$$\text{H}_3\overset{+}{\text{N}}\text{—His—Ser—Gln—Gly—Thr—Phe—Thr—Ser—Asp—Tyr— 10}$$

$$\text{Ser—Lys—Tyr—Leu—Asp—Ser—Arg—Arg—Ala—Gln— 20}$$

$$\text{Asp—Phe—Val—Gln—Trp—Leu—Met—Asn—Thr—COO}^- \text{ 29}$$

Glucagon

like insulin, is synthesized by the pancreas in response to the concentration of glucose in the blood. In muscles and various tissues, control is exerted by insulin and by the adrenal hormones **epinephrine** and **norepinephrine** (Section 13-1B). These hormones affect metabolism in their target tissues by ultimately stimulating covalent modification (phosphorylation) of regulatory enzymes. They do so by binding to transmembrane **receptors** on the surface of cells. Different cell types have different complements of receptors and therefore respond to different sets of hormones. The responses involve the release inside the cell of molecules collectively known as **second messengers,** that is, intracellular mediators of the externally received hormonal message. Different receptors cause the release of different second messengers. cAMP, identified by Earl Sutherland in the 1950s, was the first second messenger discovered. Ca^{2+}, as released from intracellular reservoirs into the cytosol, is also a common second messenger. Receptors and second messengers are discussed in greater depth in Chapter 13.

When hormonal stimulation increases the intracellular cAMP concentration, PKA activity increases, increasing the rates of phosphorylation of many proteins and decreasing their dephosphorylation rates as well. Because of the cascade nature of the regulatory system diagrammed in Fig. 16-13, *a small change in [cAMP] results in a large change in the fraction of phosphorylated enzymes*. When a large fraction of the glycogen metabolism enzymes are phosphorylated, the metabolic flux is in the direction of glycogen breakdown, since glycogen phosphorylase is active and glycogen synthase is inactive. When [cAMP] decreases, phosphorylation rates decrease, dephosphorylation rates increase, and the fraction of enzymes in their dephospho forms increases. The resulting activation of glycogen synthase and inhibition of glycogen phosphorylase cause the flux to shift to net glycogen synthesis.

Glucagon binding to its receptor on liver cells, which generates intracellular cAMP, results in glucose mobilization from stored glycogen (Fig. 16-14). Glucagon is released from the pancreas when the concentration of circulating glucose decreases to less than ~5 mM, such as during exercise or several hours after a meal has been digested. Glucagon is therefore critical for the liver's function in supplying glucose to tissues that depend primarily on glycolysis for their energy needs. Muscle cells do not respond to glucagon because they lack the appropriate receptor.

Epinephrine and norepinephrine, which are often called the "fight or flight" hormones, are released into the bloodstream by the adrenal glands in response to stress. There are two types of receptors for these hormones: the **β-adrenoreceptor (β-adrenergic receptor),** which is linked to the adenylate

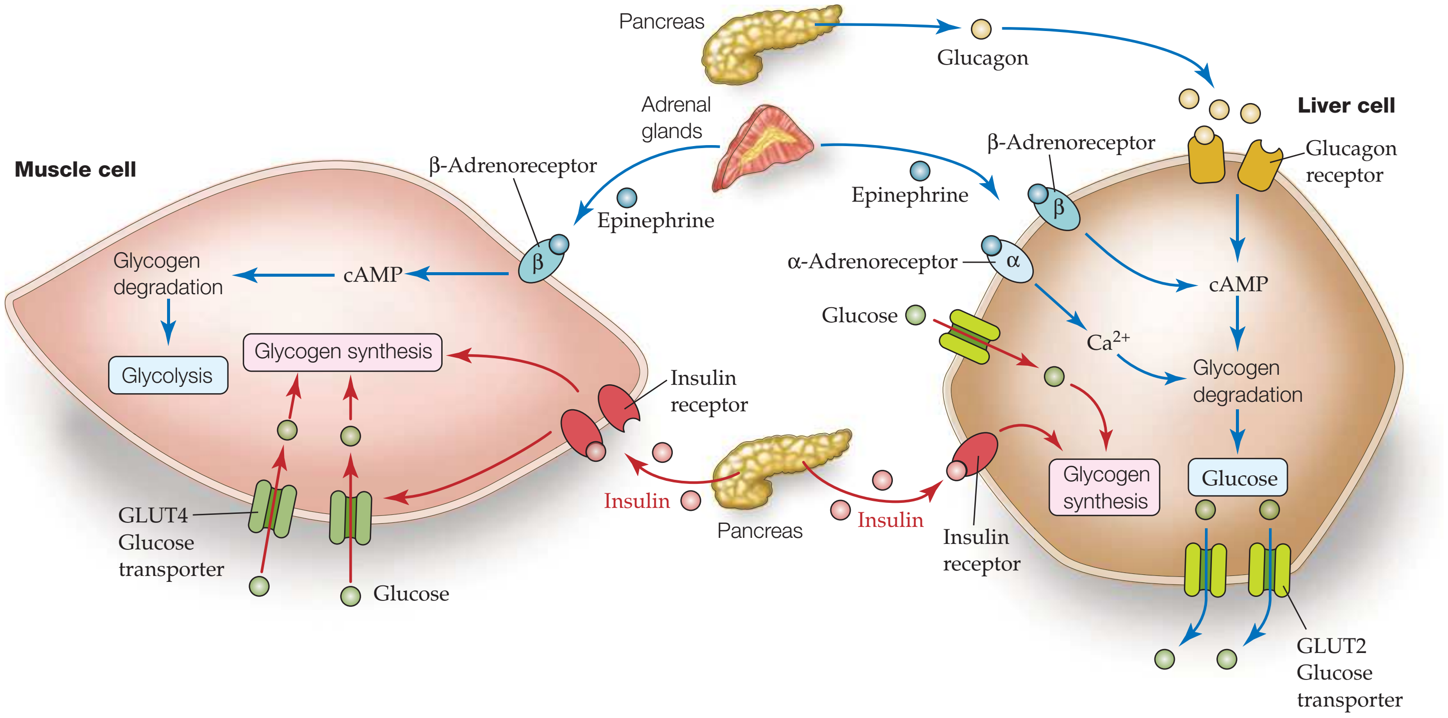
Pancreas
Glucagon
Adrenal glands
Liver cell
β-Adrenoreceptor
Glucagon receptor
Muscle cell
β-Adrenoreceptor
Epinephrine
Epinephrine
β
β
cAMP
Glycogen degradation
cAMP
α-Adrenoreceptor
α
Glucose
Ca2+
Glycolysis
Glycogen synthesis
Insulin receptor
Glycogen degradation
Glycogen synthesis
Glucose
Insulin
Pancreas
Insulin
Insulin receptor
GLUT4 Glucose transporter
Glucose
GLUT2 Glucose transporter

■ **Figure 16-14 | Hormonal control of glycogen metabolism.** Epinephrine binding to β-adrenoreceptors on liver and muscle cells increases intracellular [cAMP], which promotes glycogen degradation to G6P for glycolysis (in muscle) or to glucose for export (in liver). The liver responds similarly to glucagon. Epinephrine binding to α-adrenoreceptors on liver cells leads to increased cytosolic [Ca^{2+}], which also promotes glycogen degradation. When circulating glucose is plentiful, insulin stimulates glucose uptake and glycogen synthesis in muscle cells. The liver responds both to insulin and directly to increased glucose by increasing glycogen synthesis.

cyclase system, and the **α-adrenoreceptor (α-adrenergic receptor),** whose second messenger causes intracellular [Ca^{2+}] to increase (Section 13-4A). Muscle cells, which have the β-adrenoreceptor (Fig. 16-14), respond to epinephrine by breaking down glycogen for glycolysis, thereby generating ATP and helping the muscles cope with the stress that triggered the epinephrine release.

Liver cells respond to epinephrine directly and indirectly. Epinephrine promotes the release of glucagon from the pancreas, and glucagon binding to its receptor on liver cells stimulates glycogen breakdown as described above. Epinephrine also binds directly to both α- and β-adrenoreceptors on the surfaces of liver cells (Fig. 16-14). Binding to the β-adrenoreceptor results in increased intracellular cAMP, which leads to glycogen breakdown. Epinephrine binding to the α-adrenoreceptor stimulates an increase in intracellular [Ca^{2+}], which reinforces the cells' response to cAMP (recall that phosphorylase kinase, which activates glycogen phosphorylase and inactivates glycogen synthase, is fully active only when phosphorylated and in the presence of increased [Ca^{2+}]). In addition, glycogen synthase is inactivated through phosphorylation catalyzed by several Ca^{2+}-dependent protein kinases.

Insulin and Epinephrine Are Antagonists. Insulin is released from the pancreas in response to high levels of circulating glucose (e.g., immediately after a meal). Hormonal stimulation by insulin increases the rate of glucose transport into the many types of cells that have both insulin receptors and insulin sensitive glucose transporters called GLUT4 on their surfaces (e.g., muscle and fat cells, but not liver and brain cells). In addition, [cAMP] decreases, causing glycogen metabolism to shift from glycogen breakdown to glycogen synthesis (Fig. 16-14). The mechanism of insulin action is very complex (Sections 13-4D and 22-2), but one of its target enzymes appears to be PP1. As outlined in Fig. 16-12, insulin activates insulin-stimulated protein kinase in muscle to phosphorylate site 1 on the glycogen-binding G_M subunit of PP1 so as to activate this protein and thus dephosphorylate the enzymes of glycogen metabolism. The storage of glucose as glycogen is thereby promoted through the inhibition of glycogen breakdown and the stimulation of glycogen synthesis.

In liver, insulin stimulates glycogen synthesis as a result of the inhibition of **glycogen synthase kinase 3β:** (**GSK3β:** Fig. 13-31). This action decreases the phosphorylation of glycogen synthase, thus increasing its activity. In addition, it is thought that glucose itself, may be a messenger to which glycogen metabolism system responds. *Glucose inhibits phosphorylase* a *by binding to the enzyme's inactive T state and thereby shifting the T* $\rightleftharpoons$ *R equilibrium toward the T state* (Fig. 12-16). This conformational shift exposes the Ser 14 phosphoryl group to dephosphorylation. An increase in glucose concentration therefore promotes inactivation of glycogen phosphorylase *a* through its conversion to phosphorylase *b*. The subsequent release of phosphoprotein phosphatase-1 activates glycogen synthase. Thus when glucose is plentiful, the liver can store the excess as glycogen.

■ **CHECK YOUR UNDERSTANDING**

Why does a phosphorylation/dephosphorylation system allow more sensitive regulation of a metabolic process than a simple allosteric system?

How does regulation of glycogen metabolism differ between liver and muscle?

4 Gluconeogenesis

LEARNING OBJECTIVES

- Appreciate that glucose can be synthesized from lactate, pyruvate, and amino acids.
- Understand that gluconeogenesis is mostly the reverse of glycolysis with the few endergonic reactions bypassed by hydrolysis.
- Understand that glycolysis and gluconeogenesis must be reciprocally regulated.

When dietary sources of glucose are not available and when the liver has exhausted its supply of glycogen, glucose is synthesized from noncarbohydrate precursors by **gluconeogenesis.** In fact, gluconeogenesis provides a substantial fraction of the glucose produced in fasting humans, even within a few hours of eating. Gluconeogenesis occurs in liver and, to a lesser extent, in kidney.

The noncarbohydrate precursors that can be converted to glucose include the glycolysis products lactate and pyruvate, citric acid cycle intermediates,

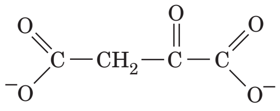

Oxaloacetate

and the carbon skeletons of most amino acids. First, however, all these substances must be converted to the four-carbon compound **oxaloacetate** *(at right)*, which itself is a citric acid cycle intermediate (Section 17-1). The only amino acids that cannot be converted to oxaloacetate in animals are leucine and lysine because their breakdown yields only acetyl-CoA (Section 21-4E) and because *there is no pathway in animals for the net conversion of acetyl-CoA to oxaloacetate*. Likewise, fatty acids cannot serve as glucose precursors in animals because most fatty acids are degraded completely to acetyl-CoA (Section 20-2). However, fatty acid breakdown generates much of the ATP that powers gluconeogenesis.

For convenience, we consider gluconeogenesis to be the pathway by which pyruvate is converted to glucose. Most of the reactions of gluconeogenesis are glycolytic reactions that proceed in reverse (Fig. 16-15).

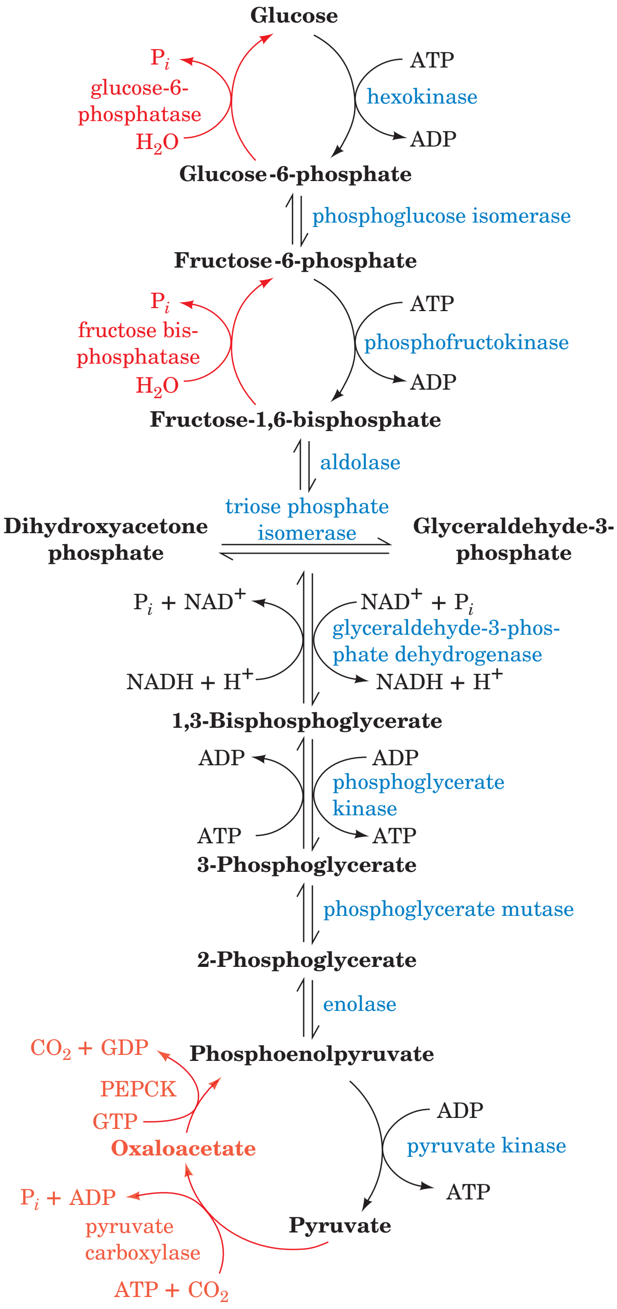
Glucose
P_i
glucose-6-phosphatase
H_2O
ATP
hexokinase
ADP
Glucose-6-phosphate
phosphoglucose isomerase
Fructose-6-phosphate
P_i
fructose bisphosphatase
H_2O
ATP
phosphofructokinase
ADP
Fructose-1,6-bisphosphate
aldolase
Dihydroxyacetone phosphate
triose phosphate isomerase
Glyceraldehyde-3-phosphate
P_i + NAD^+
NADH + H^+
NAD^+ + P_i
glyceraldehyde-3-phosphate dehydrogenase
NADH + H^+
1,3-Bisphosphoglycerate
ADP
ATP
ADP
phosphoglycerate kinase
ATP
3-Phosphoglycerate
phosphoglycerate mutase
2-Phosphoglycerate
enolase
CO_2 + GDP
Phosphoenolpyruvate
PEPCK
GTP
Oxaloacetate
ADP
pyruvate kinase
ATP
P_i + ADP
pyruvate carboxylase
Pyruvate
ATP + CO_2

Figure 16-15 | Comparison of the pathways of gluconeogenesis and glycolysis. The red arrows represent the steps that are catalyzed by different enzymes in gluconeogenesis. The other seven reaction steps of gluconeogenesis are catalyzed by glycolytic enzymes that function near equilibrium. **See the Animated Figures.**

However, the glycolytic enzymes hexokinase, phosphofructokinase, and pyruvate kinase catalyze reactions with large negative free energy changes. These reactions must therefore be replaced in gluconeogenesis by reactions that make glucose synthesis thermodynamically favorable.

A | Pyruvate Is Converted to Phosphoenolpyruvate in Two Steps

We begin our examination of the reactions unique to gluconeogenesis with the conversion of pyruvate to phosphoenolpyruvate (PEP). Because this step is the reverse of the highly exergonic reaction catalyzed by pyruvate kinase (Section 15-2J), it requires free energy input. This is accomplished by first converting the pyruvate to oxaloacetate. Oxaloacetate is a "high-energy" intermediate because its exergonic decarboxylation provides the free energy necessary for PEP synthesis. The process requires two enzymes (Fig. 16-16):

1. **Pyruvate carboxylase** catalyzes the ATP-driven formation of oxaloacetate from pyruvate and HCO_3^-.
2. **PEP Carboxykinase (PEPCK)** converts oxaloacetate to PEP in a reaction that uses GTP as a phosphoryl-group donor.

Pyruvate Carboxylase Has a Biotin Prosthetic Group. Pyruvate carboxylase is a tetrameric protein of identical ~1160-residue subunits, each of which has a **biotin** prosthetic group. Biotin (Fig. 16-17*a*) functions as a CO_2 carrier by forming a carboxyl substituent at its **ureido group** (Fig. 16-17*b*). Biotin is covalently bound to an enzyme Lys residue to form a **biocytin** (alternatively, **biotinyllysine**) residue (Fig. 16-17*b*). The biotin ring system is therefore at the end of a 14-Å-long flexible arm. Biotin, which was first identified in 1935 as a growth factor in yeast, is an essential human nutrient. Its nutritional deficiency is rare, however, because it occurs in many foods and is synthesized by intestinal bacteria.

The pyruvate carboxylase reaction occurs in two phases (Fig. 16-18):

Phase I The cleavage of ATP to ADP acts to dehydrate bicarbonate via the formation of a "high-energy" carboxyphosphate intermediate. The reaction of the resulting CO_2 with biotin is exergonic. The biotin-bound carboxyl group is therefore "activated" relative to bicarbonate and can be transferred to another molecule without further free energy input.

Phase II The activated carboxyl group is transferred from carboxybiotin to pyruvate in a three-step reaction to form oxaloacetate.

These two reaction phases occur on different subsites of the same enzyme; the 14-Å arm of biocytin transfers the biotin ring between the two sites.

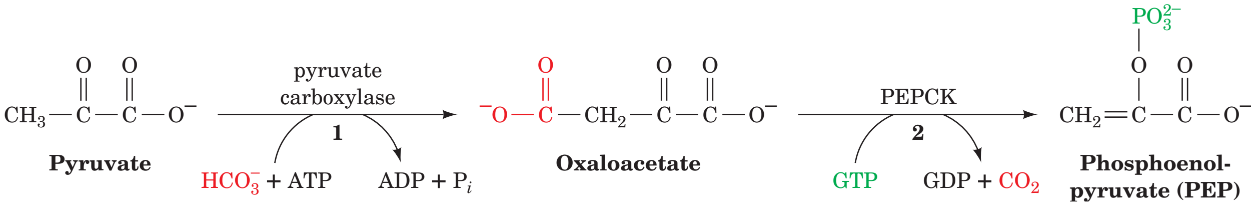

Figure 16-16 | The conversion of pyruvate to phosphoenolpyruvate (PEP). This process requires **(1)** pyruvate carboxylase to convert pyruvate to oxaloacetate and **(2)** PEP carboxykinase (PEPCK) to convert oxaloacetate to PEP.

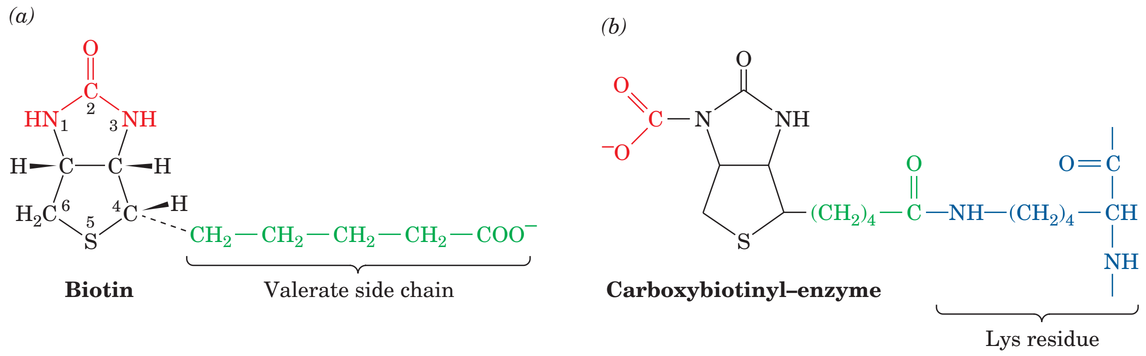
(a)
HN
NH
H
H
H_2C
S
C
O
1
2
3
4
5
6
$CH_2—CH_2—CH_2—CH_2—COO^-$
Biotin
Valerate side chain
(b)
$(CH_2)_4$
C
NH—$(CH_2)_4$—CH
O=C
NH
Carboxybiotinyl–enzyme
Lys residue

■ **Figure 16-17 | Biotin and carboxybiotinyl–enzyme.** (*a*) Biotin consists of an imidazoline ring that is cis-fused to a tetrahydrothiophene ring bearing a valerate side chain. Positions 1, 2, and 3 constitute a ureido group. (*b*) Biotin is covalently attached to carboxylases by an amide linkage between its valeryl carboxyl group and an ε-amino group of an enzyme Lys side chain. The carboxybiotinyl–enzyme forms when N1 of the biotin ureido group is carboxylated.

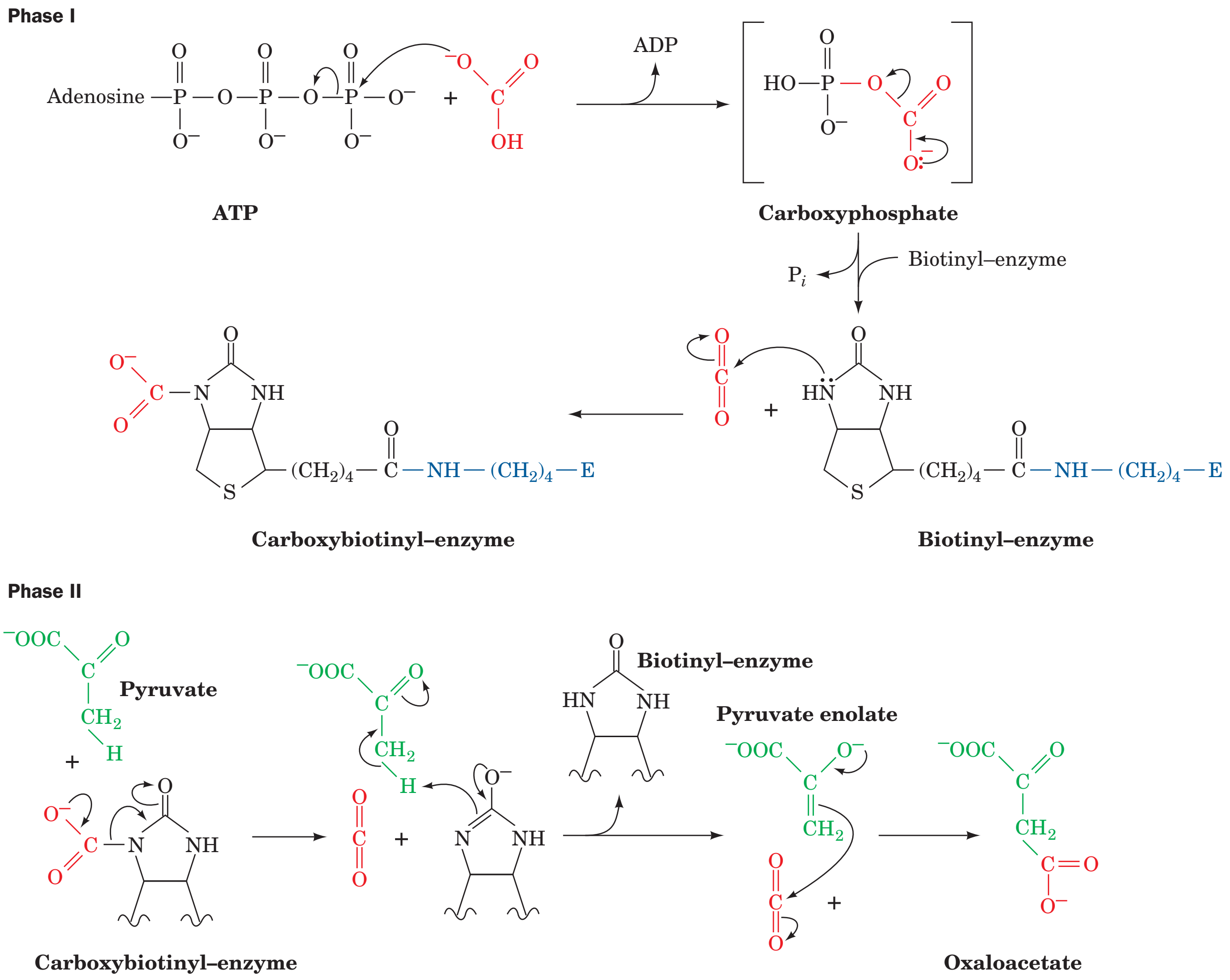
Phase I
Adenosine
OH
ADP
HO
ATP
Carboxyphosphate
P_i
Biotinyl–enzyme
HN
NH
$(CH_2)_4$
C
NH—$(CH_2)_4$—E
Carboxybiotinyl–enzyme
Biotinyl–enzyme
Phase II
^-OOC
CH_2
H
Pyruvate
Biotinyl–enzyme
Pyruvate enolate
Carboxybiotinyl–enzyme
Oxaloacetate

■ **Figure 16-18 | The two-phase reaction mechanism of pyruvate carboxylase.** Phase I is a three-step reaction in which carboxyphosphate is formed from bicarbonate and ATP, followed by the generation of CO_2, which then carboxylates biotin. Phase II is a three-step reaction in which CO_2 is produced at the active site via the elimination of the biotinyl–enzyme, which accepts a proton from pyruvate to generate pyruvate enolate. This enolate, in turn, nucleophilically attacks the CO_2, yielding oxaloacetate. [After Knowles, J.R., *Annu. Rev. Biochem.* **58,** 217 (1989).]

Oxaloacetate is both a precursor for gluconeogenesis and an intermediate of the citric acid cycle (Section 17-3). When the citric acid cycle substrate acetyl-CoA accumulates, it allosterically activates pyruvate carboxylase, thereby increasing the amount of oxaloacetate that can participate in the citric acid cycle. When citric acid cycle activity is low, oxaloacetate instead enters the gluconeogenic pathway.

PEP Carboxykinase Catalyzes the Formation of PEP. PEPCK, a monomeric ~610-residue enzyme, catalyzes the GTP-requiring decarboxylation/phosphorylation of oxaloacetate to form PEP and GDP (Fig. 16-19). Note that the CO_2 that carboxylates pyruvate to yield oxaloacetate is eliminated in the formation of PEP. The favorable decarboxylation reaction drives the formation of the enol that GTP phosphorylates. *Oxaloacetate can therefore be considered as "activated" pyruvate, with CO_2 and biotin facilitating the activation at the expense of ATP.*

Gluconeogenesis Requires Metabolite Transport between Mitochondria and Cytosol. The generation of oxaloacetate from pyruvate or citric acid cycle intermediates occurs only in the mitochondrion, whereas the enzymes that convert PEP to glucose are cytosolic. The cellular location of PEPCK varies: In some species, it is mitochondrial; in some, it is cytosolic; and in some (including humans) it is equally distributed between the two compartments. In order for gluconeogenesis to occur, either oxaloacetate must leave the mitochondrion for conversion to PEP or the PEP formed there must enter the cytosol.

PEP is transported across the mitochondrial membrane by specific membrane transport proteins. There is, however, no such transport system for oxaloacetate. *In species with cytosolic PEPCK, oxaloacetate must first be converted either to aspartate* (Fig. 16-20, Route 1) *or to* ***malate*** (Fig. 16-20, Route 2), for which mitochondrial transport systems exist. The difference between the two routes involves the transport of NADH **reducing equivalents** (in the transport of reducing equivalents, the electrons—but not the electron carrier—cross the membrane). The **malate dehydrogenase** route (Route 2) results in the transport of reducing equivalents from the mitochondrion to the cytosol, since it uses mitochondrial NADH and produces cytosolic NADH. The **aspartate aminotransferase** route (Route 1) does not involve NADH. Cytosolic NADH is required for gluconeogenesis, so, under most conditions, the route through malate is a necessity. However, when the gluconeogenic precursor is lactate, its oxidation to pyruvate generates cytosolic NADH, and either transport system can then be used. All the reactions shown in Fig. 16-20 are freely reversible, so that

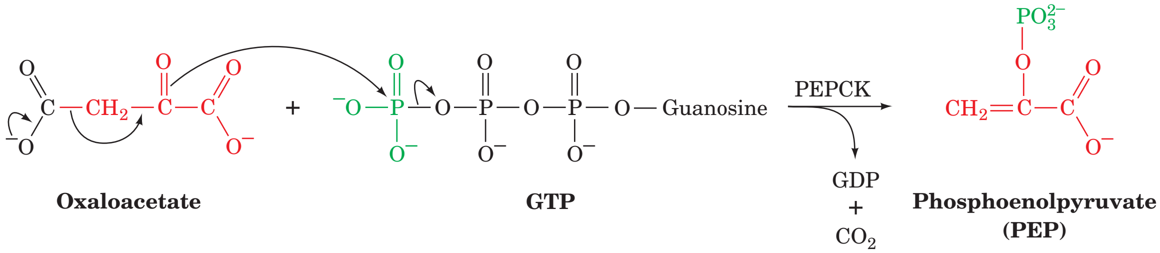

Figure 16-19 | The PEPCK mechanism. Decarboxylation of oxaloacetate (a β-keto acid) forms a resonance-stabilized enolate anion whose oxygen atom attacks the γ-phosphoryl group of GTP, forming PEP and GDP.

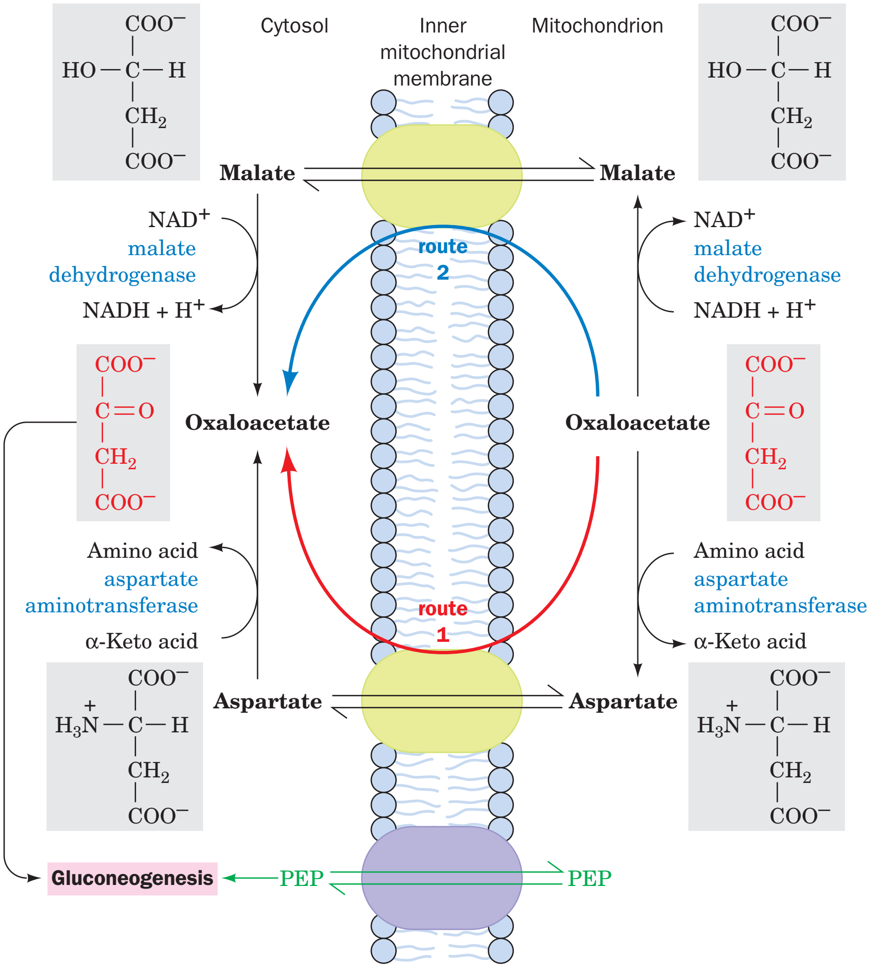
Cytosol
Inner mitochondrial membrane
Mitochondrion
Malate
Malate
NAD+
malate dehydrogenase
NADH + H+
route 2
Oxaloacetate
Oxaloacetate
Amino acid
aspartate aminotransferase
α-Keto acid
route 1
Aspartate
Aspartate
Gluconeogenesis
PEP
PEP

■ **Figure 16-20 | The transport of PEP and oxaloacetate from the mitochondrion to the cytosol.** PEP is directly transported between the compartments. Oxaloacetate, however, must first be converted to either aspartate through the action of aspartate aminotransferase (Route 1) or to malate by malate dehydrogenase (Route 2). Route 2 involves the mitochondrial oxidation of NADH followed by the cytosolic reduction of NAD^+ and therefore also transfers NADH reducing equivalents from the mitochondrion to the cytosol. **See the Animated Figures.**

under appropriate conditions, the malate–aspartate shuttle system also operates to transport NADH reducing equivalents into the mitochondrion for oxidative phosphorylation (Section 18-1B). Liver has a variation of Route 1 in which aspartate entering the cytosol is deaminated via the urea cycle before undergoing a series of reactions that yield oxaloacetate (Section 21-3A).

B | Hydrolytic Reactions Bypass Irreversible Glycolytic Reactions

The route from PEP to fructose-1,6-bisphosphate (FBP) is catalyzed by the enzymes of glycolysis operating in reverse. However, *the glycolytic reactions catalyzed by phosphofructokinase (PFK) and hexokinase are endergonic in the gluconeogenesis direction and hence must be bypassed by different gluconeogenic enzymes.* FBP is hydrolyzed by **fructose-1,6-bisphosphatase (FBPase).** The resulting fructose-6-phosphate (F6P) is isomerized to G6P, which is then hydrolyzed by glucose-6-phosphatase, the same enzyme that converts glycogen-derived G6P to glucose (Section 16-1C) and which is present only in liver and kidney. Note that these two hydrolytic reactions release P_i rather than reversing the ATP → ADP reactions that occur at this point in the glycolytic pathway.

The net energetic cost of converting two pyruvate molecules to one glucose molecule by gluconeogenesis is six ATP equivalents: two each at the steps catalyzed by pyruvate carboxylase, PEPCK, and phosphoglycerate kinase. Since the energetic profit of converting one glucose molecule to two pyruvate molecules via glycolysis is two ATP, (Section 15-1), the energetic cost of the futile cycle in which glucose is converted to pyruvate and then resynthesized is four ATP equivalents. Such free energy losses are the thermodynamic price that must be paid to maintain the independent regulation of two opposing pathways.

Although glucose is considered the endpoint of the gluconeogenic pathway, it is possible for pathway intermediates to be directed elsewhere, for example, through the transketolase and transaldolase reactions of the pentose phosphate pathway (Section 15-6C) to produce ribose-5-phosphate. The G6P produced by gluconeogenesis may not be hydrolyzed to glucose but may instead be converted to G1P for incorporation into glycogen.

C | Gluconeogenesis and Glycolysis Are Independently Regulated

The opposing pathways of gluconeogenesis and glycolysis, like glycogen synthesis and degradation, do not proceed simultaneously *in vivo*. Instead, the pathways are reciprocally regulated to meet the needs of the organism. There are three substrate cycles and therefore three potential points for regulating glycolytic versus gluconeogenic flux (Fig. 16-21).

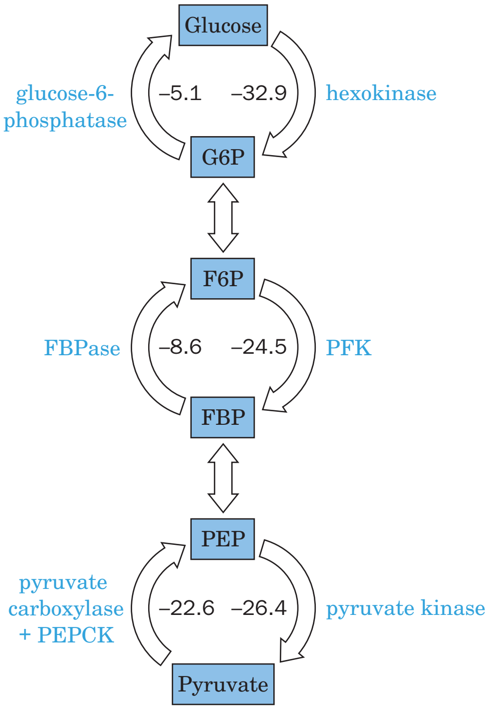

Figure 16-21 | Substrate cycles in glucose metabolism. The interconversions of glucose and G6P, F6P and FBP, and PEP and pyruvate are catalyzed by different enzymes in the forward and reverse directions so that all reactions are exergonic (the ΔG values for the reactions in liver are given in $kJ \cdot mol^{-1}$). [ΔG's obtained from Newsholme, E.A. and Leech, A.R., *Biochemistry for the Medical Sciences,* p. 448, Wiley (1983).]

Fructose-2,6-Bisphosphate Activates Phosphofructokinase and Inhibits Fructose-1,6-Bisphosphatase. The net flux through the substrate cycle created by the opposing actions of PFK and FBPase (described in Section 15-4B) is determined by the concentration of fructose-2,6-bisphosphate (F2,6P).

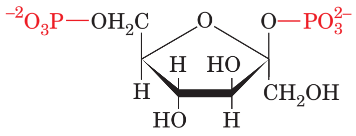

β-D-Fructose-2,6-bisphosphate (F2,6P)

F2,6P, which is not a glycolytic intermediate, is an extremely potent allosteric activator of PFK and an inhibitor of FBPase.

The concentration of F2,6P in the cell depends on the balance between its rates of synthesis and degradation by **phosphofructokinase-2 (PFK-2)** and **fructose bisphosphatase-2 (FBPase-2),** respectively (Fig. 16-22). These enzyme activities are located on different domains of the same ~100-kD homodimeric protein. The bifunctional enzyme is regulated by a variety of allosteric effectors and by phosphorylation and dephosphorylation as catalyzed by PKA and a phosphoprotein phosphatase. Thus, the balance between gluconeogenesis and glycolysis is under hormonal control.

For example, when [glucose] is low, glucagon stimulates the production of cAMP in liver cells. This activates PKA to phosphorylate the bifunctional enzyme at a specific Ser residue, which inactivates the enzyme's PFK-2 activity and activates its FBPase-2 activity. The net result is a decrease in [F2,6P], which shifts the balance between the PFK and FBPase reactions in favor of FBP hydrolysis and hence increases gluconeogenic flux (Fig. 16-23). The concurrent increases in gluconeogenesis and glycogen breakdown allow the liver to release glucose into the circulation. Conversely, when the blood [glucose] is high, cAMP levels decrease, and the resulting increase in [F2,6P] promotes glycolysis.

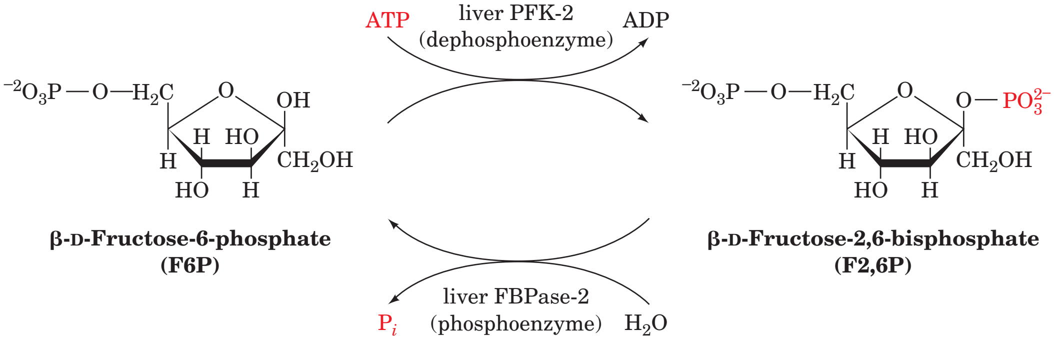
ATP
liver PFK-2
(dephosphoenzyme)
ADP
β-D-Fructose-6-phosphate
(F6P)
β-D-Fructose-2,6-bisphosphate
(F2,6P)
liver FBPase-2
(phosphoenzyme)
P_i
H_2O

Figure 16-22 | The formation and degradation of β-D-fructose-2,6-bisphosphate (F2,6P). The enzymatic activities of phosphofructokinase-2 (PFK-2) and fructose bisphosphatase-2 (FBPase-2) occur on different domains of the same protein molecule. The phosphorylation of the liver enzyme inactivates PFK-2 while activating FBPase-2.

In muscle, which is not a gluconeogenic tissue, the F2,6P control system functions quite differently from that in liver due to the presence of different PFK-2/FBPase-2 isozymes. For example, hormones that stimulate glycogen breakdown in heart muscle lead to phosphorylation of a site on the bifunctional enzyme that activates rather than inhibits PFK-2. The resulting increase in F2,6P stimulates glycolysis so that glycogen breakdown and glycolysis are coordinated. The skeletal muscle isozyme lacks a phosphorylation site altogether and is therefore not subject to cAMP-dependent control.

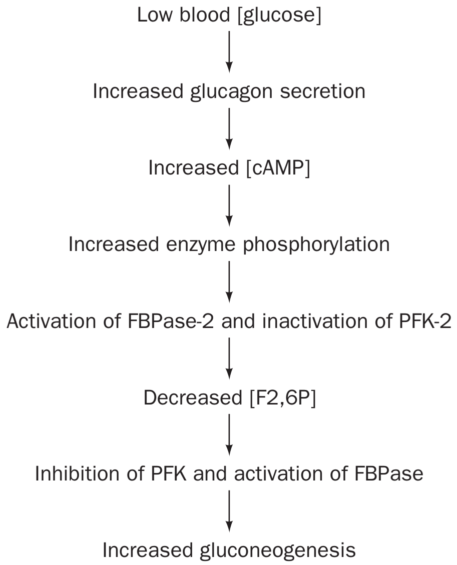
Low blood [glucose]
Increased glucagon secretion
Increased [cAMP]
Increased enzyme phosphorylation
Activation of FBPase-2 and inactivation of PFK-2
Decreased [F2,6P]
Inhibition of PFK and activation of FBPase
Increased gluconeogenesis

Figure 16-23 | Sequence of metabolic events linking low blood [glucose] to gluconeogenesis in liver.

Other Allosteric Effectors Influence Gluconeogenic Flux. Acetyl-CoA activates pyruvate carboxylase (Section 16-4A), but there are no known allosteric effectors of PEPCK, which together with pyruvate carboxylase reverses the pyruvate kinase reaction. Pyruvate kinase, however, is allosterically inhibited in the liver by alanine, a major gluconeogenic precursor. Alanine is converted to pyruvate by the transfer of its amino group to an α-keto acid to yield a new amino acid and the α-keto acid pyruvate, a process termed **transamination** (which is discussed in Section 21-2A). Liver pyruvate kinase is also inactivated by phosphorylation, further increasing gluconeogenic flux. Since phosphorylation also activates glycogen phosphorylase, the pathways of gluconeogenesis and glycogen breakdown both flow toward G6P, which is converted to glucose for export from the liver.

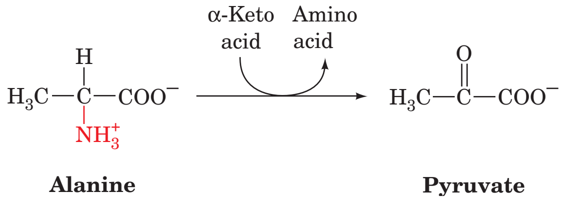
α-Keto
acid
Amino
acid
Alanine
Pyruvate

The activity of hexokinase (or glucokinase, the liver isozyme) is also controlled, as we shall see in Section 22-1D. The activity of glucose-6-phosphatase is controlled as well but this process is complex and poorly understood.

The regulation of glucose metabolism occurs not only through allosteric effectors, but also through long-term changes in the amounts of enzymes synthesized. Pancreatic and adrenal hormones influence the rates of transcription and the stabilities of the mRNAs encoding many of the regulatory proteins of glucose metabolism. For example, insulin inhibits transcription of the gene for PEPCK, whereas high concentrations of intracellular cAMP promote the transcription of the genes for PEPCK, FBPase, and glucose-6-phosphatase, and repress transcription of the genes for glucokinase, PFK, and the PFK-2/FBPase-2 bifunctional enzyme.

CHECK YOUR UNDERSTANDING

Describe the reactions of gluconeogenesis.
Why is the malate–aspartate shuttle system important for gluconeogenesis?
Describe the role of fructose-2,6-bisphosphate in regulating gluconeogenesis.

LEARNING OBJECTIVE

- Understand that the formation of glycosidic bonds in carbohydrates requires the energy of activated nucleotide sugars.

5 Other Carbohydrate Biosynthetic Pathways

The liver, by virtue of its mass and its metabolic machinery, is primarily responsible for maintaining a constant level of glucose in the circulation. Glucose produced by gluconeogenesis or from glycogen breakdown is released from the liver for use by other tissues as an energy source. Of course, glucose has other uses in the liver and elsewhere, for example, in the synthesis of lactose (Box 16-4).

Nucleotide Sugars Power the Formation of Glycosidic Bonds. Glucose and other monosaccharides (principally mannose, *N*-acetylglucosamine, fucose, galactose, *N*-acetylneuraminic acid, and *N*-acetylgalactosamine) occur in glycoproteins and glycolipids. Formation of the glycosidic bonds that link sugars to each other and to other molecules requires free energy input under physiological conditions ($\Delta G^{\circ\prime} = 16\ \text{kJ} \cdot \text{mol}^{-1}$). This free energy, as we

BOX 16-4 PERSPECTIVES IN BIOCHEMISTRY

Lactose Synthesis

Like sucrose in plants, lactose is a disaccharide that is synthesized for later use as a metabolic fuel, in this case, after digestion by very young mammals. Lactose, or milk sugar, is produced in the mammary gland by **lactose synthase.** In this reaction, the donor sugar is UDP–galactose, which is formed by the epimerization of UDP–glucose (Fig. 15-28). The acceptor sugar is glucose:

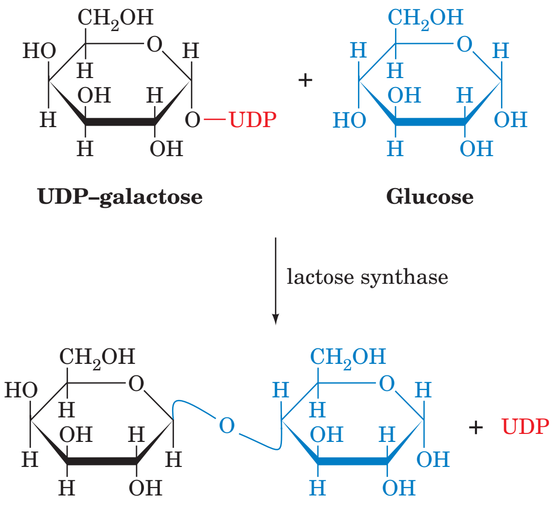

Lactose
[β-galactosyl-(1⟶4)-glucose]

Thus, both saccharide units of lactose are ultimately derived from glucose.

Lactose synthase consists of two subunits:

1. **Galactosyltransferase,** the catalytic subunit, occurs in many tissues, where it catalyzes the reaction of UDP–galactose and *N*-acetylglucosamine to yield ***N*-acetyllactosamine,** a constituent of many complex oligosaccharides.

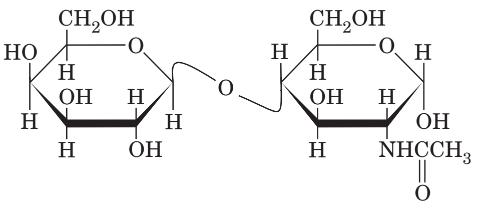

***N*-Acetyllactosamine**

2. **α-Lactalbumin,** a mammary gland protein with no catalytic activity, alters the specificity of galactosyltransferase so that it uses glucose as an acceptor, rather than *N*-acetylglucosamine, to form lactose instead of *N*-acetyllactosamine.

Synthesis of α-lactalbumin, whose sequence is ~37% identical to that of lysozyme (which also participates in reactions involving sugars), is triggered by hormonal changes at parturition (birth), thereby promoting lactose synthesis for milk production.

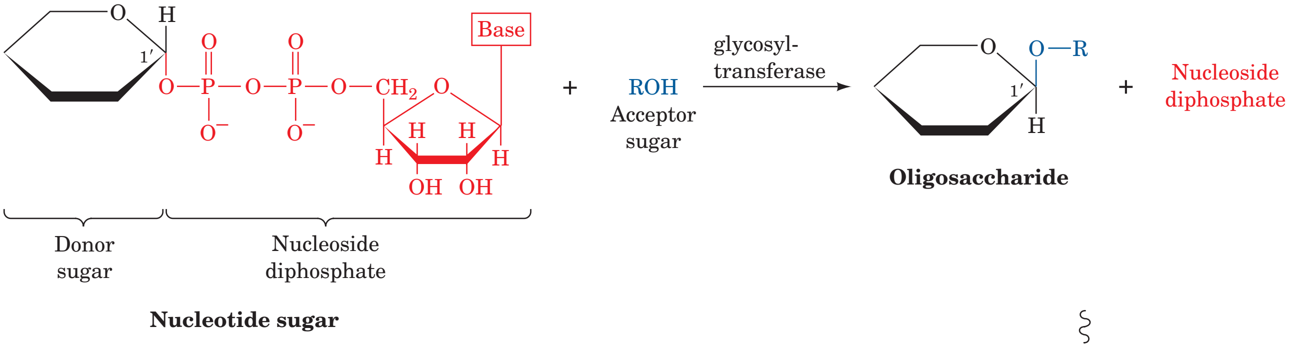

H
1′
O
Base
H
H
H
H
OH OH
+
ROH
Acceptor sugar
glycosyl-transferase
O—R
1′
H
+
Nucleoside diphosphate
Oligosaccharide
Donor sugar
Nucleoside diphosphate
Nucleotide sugar

Figure 16-24 | **Role of nucleotide sugars.** These compounds are the glycosyl donors in oligosaccharide biosynthetic reactions as catalyzed by glycosyltransferases.

have seen in glycogen synthesis (Section 16-2A), is acquired through the synthesis of a **nucleotide sugar** from a nucleoside triphosphate and a monosaccharide, thereby releasing PP_i, whose exergonic hydrolysis drives the reaction. The nucleoside diphosphate at the sugar's anomeric carbon atom is a good leaving group and thereby facilitates formation of a glycosidic bond to a second sugar in a reaction catalyzed by a glycosyltransferase (Fig. 16-24). In mammals, most glycosyl groups are donated by UDP–sugars, but fucose and mannose are carried by GDP, and sialic acid by CMP. In plants, starch is built from glucose units donated by **ADP–glucose,** and cellulose synthesis relies on ADP–glucose or **CDP–glucose.**

O-Linked Oligosaccharides Are Posttranslationally Formed.

Nucleotide sugars are the donors in the synthesis of *O*-linked oligosaccharides and in the processing of the *N*-linked oligosaccharides of glycoproteins (Section 8-3C). *O*-Linked oligosaccharides are synthesized in the Golgi apparatus by the serial addition of monosaccharide units to a completed polypeptide chain (Fig. 16-25). Synthesis begins with the transfer, as catalyzed by **GalNAc transferase,** of *N*-acetylgalactosamine (GalNAc) from UDP–GalNAc to a Ser or Thr residue on the polypeptide. The location of the glycosylation site is thought to be specified only by the secondary or tertiary structure of the polypeptide. Glycosylation continues with the stepwise addition of sugars such as galactose, sialic acid, *N*-acetylglucosamine, and fucose. In each case, the sugar residue is transferred from its nucleotide sugar derivative by a corresponding glycosyltransferase.

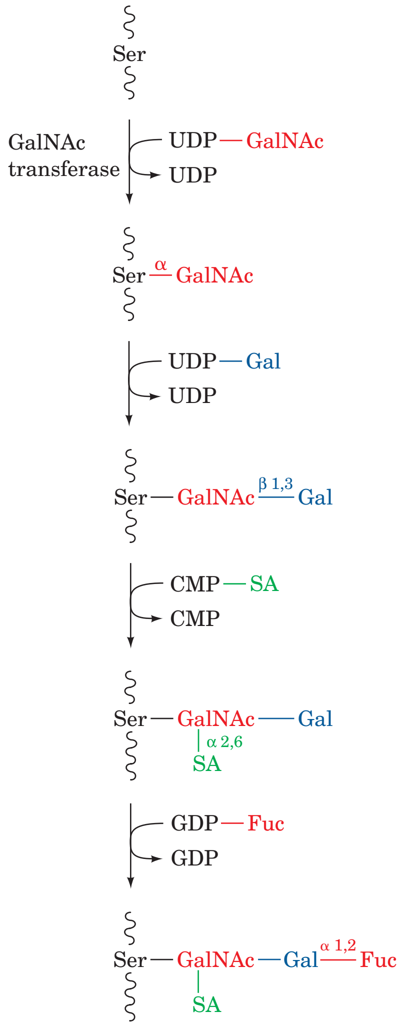

Ser
GalNAc transferase
UDP—GalNAc
UDP
Ser α GalNAc
UDP—Gal
UDP
Ser—GalNAc β 1,3 Gal
CMP—SA
CMP
Ser—GalNAc—Gal
α 2,6
SA
GDP—Fuc
GDP
Ser—GalNAc—Gal α 1,2 Fuc
SA

Figure 16-25 | **Synthesis of an *O*-linked oligosaccharide chain.** This pathway shows the proposed steps in the assembly of a carbohydrate moiety in canine submaxillary mucin. SA is sialic acid.

N-Linked Oligosaccharides Are Constructed on Dolichol Carriers.

The synthesis of *N*-linked oligosaccharides is more complicated than that of *O*-linked oligosaccharides. In the early stages of *N*-linked oligosaccharide synthesis, sugar residues are sequentially added to a lipid carrier, **dolichol pyrophosphate** (Fig. 16-26). **Dolichol** is a long-chain polyisoprenoid containing 17 to 21 isoprene units in animals and 14 to 24 units in fungi and

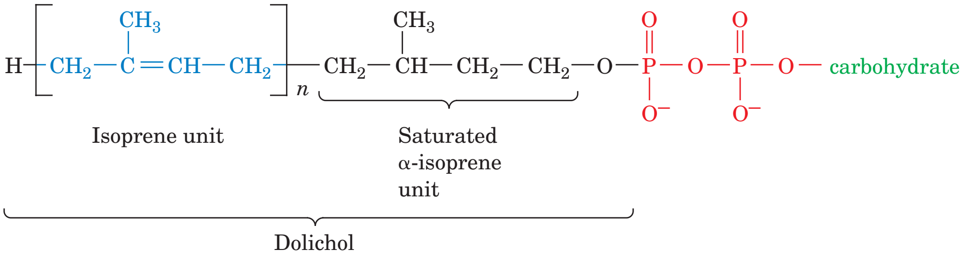

$$\mathrm{H}\left[\mathrm{CH_2-\overset{CH_3}{\overset{|}{C}}=CH-CH_2}\right]_n\mathrm{-CH_2-\overset{CH_3}{\overset{|}{C}H}-CH_2-CH_2-O-\underset{O^-}{\underset{|}{\overset{O}{\overset{\|}{P}}}}-O-\underset{O^-}{\underset{|}{\overset{O}{\overset{\|}{P}}}}-O-carbohydrate}$$

Isoprene unit
Saturated α-isoprene unit
Dolichol

Figure 16-26 | **Dolichol pyrophosphate glycoside.** The carbohydrate precursors of *N*-linked glycosides are synthesized as oligosaccharides attached to dolichol, a long-chain polyisoprenol (n = 14–24) in which the α-isoprene unit is saturated.

plants. It anchors the growing oligosaccharide to the endoplasmic reticulum membrane, where the initial glycosylation reactions take place.

Although nucleotide sugars are the most common monosaccharide donors in glycosyltransferase reactions, several mannosyl and glucosyl residues are transferred to growing dolichol-PP-oligosaccharides from their corresponding dolichol-P derivatives. Dolichol phosphate "activates" a sugar residue for subsequent transfer, as does a nucleoside diphosphate.

The construction of an *N*-linked oligosaccharide begins, as is described in Section 8-3C, by the synthesis of an oligosaccharide with the composition (N-acetylglucosamine)$_2$(mannose)$_9$(glucose)$_3$. This occurs on a dolichol carrier in a 12-step process catalyzed by a series of specific glycosyltransferases (Fig. 16-27). Note that some of these reactions take place

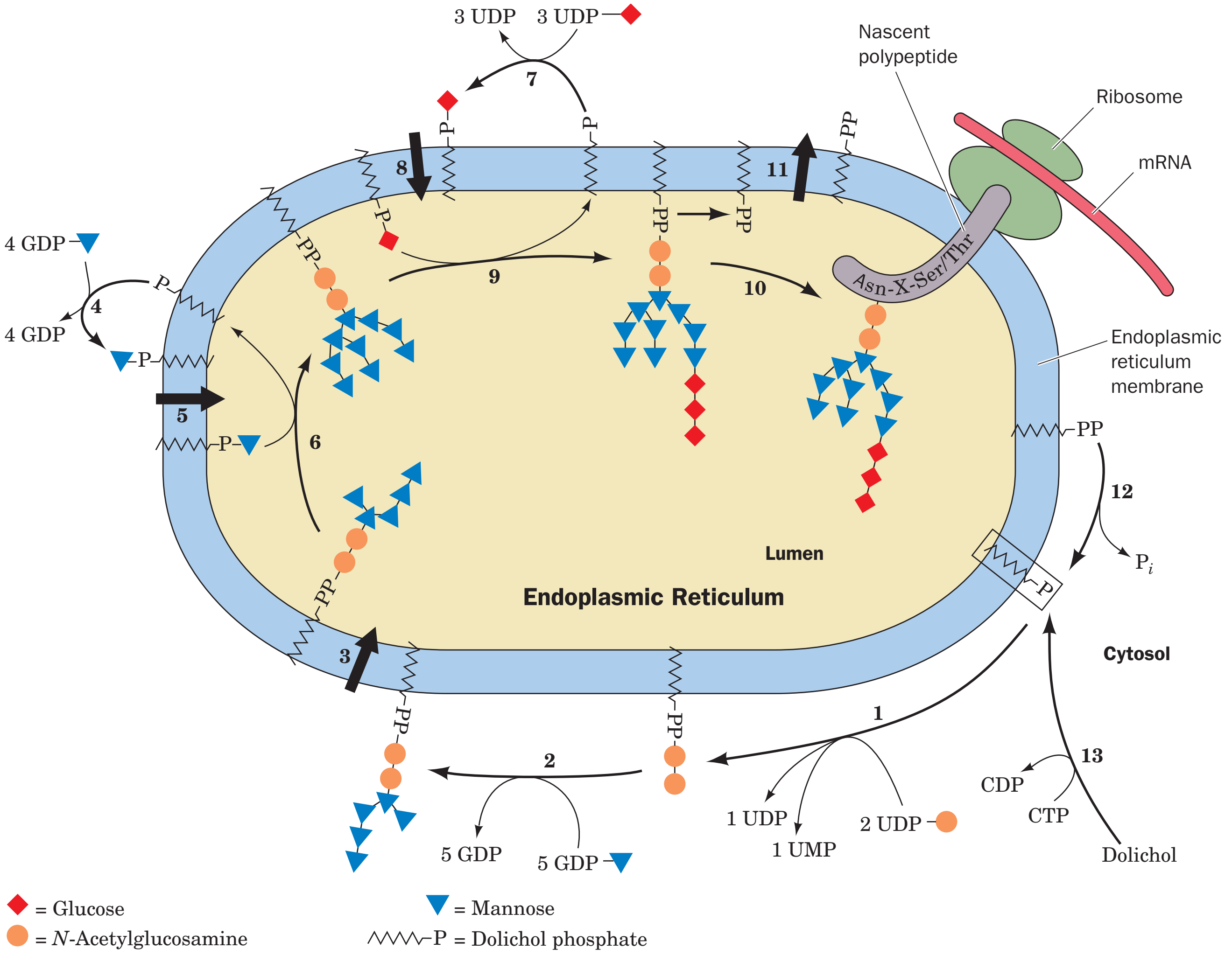
3 UDP
3 UDP
7
Nascent polypeptide
Ribosome
mRNA
8
11
P
PP
4 GDP
4
4 GDP
P
9
10
Asn-X-Ser/Thr
Endoplasmic reticulum membrane
5
6
PP
12
P_i
Lumen
Endoplasmic Reticulum
Cytosol
3
1
2
13
CDP
CTP
1 UDP
1 UMP
2 UDP
5 GDP
5 GDP
Dolichol
= Glucose
= N-Acetylglucosamine
= Mannose
= Dolichol phosphate

Figure 16-27 | **The pathway of dolichol-PP-oligosaccharide synthesis.** **(1)** Addition of *N*-acetylglucosamine-1-P and a second *N*-acetylglucosamine to dolichol-P. **(2)** Addition of five mannosyl residues from GDP–mannose in reactions catalyzed by five different mannosyltransferases. **(3)** Membrane translocation of dolichol-PP-(N-acetylglucosamine)$_2$(mannose)$_5$ to the lumen of the endoplasmic reticulum (ER). **(4)** Cytosolic synthesis of dolichol-P-mannose from GDP–mannose and dolichol-P. **(5)** Membrane translocation of dolichol-P-mannose to the lumen of the ER. **(6)** Addition of four mannosyl residues from dolichol-P-mannose in reactions catalyzed by four different mannosyltransferases. **(7)** Cytosolic synthesis of dolichol-P-glucose from UDPG and dolichol-P. **(8)** Membrane translocation of dolichol-P-glucose to the lumen of the ER. **(9)** Addition of three glucosyl residues from dolichol-P-glucose. **(10)** Transfer of the oligosaccharide from dolichol-PP to the polypeptide chain at an Asn residue in the sequence Asn-X-Ser/Thr, releasing dolichol-PP. **(11)** Translocation of dolichol-PP to the cytoplasmic surface of the ER membrane. **(12)** Hydrolysis of dolichol-PP to dolichol-P. **(13)** Dolichol-P can also be formed by phosphorylation of dolichol by CTP. [Modified from Abeijon, C. and Hirschberg, C.B., *Trends Biochem. Sci.* **17,** 34 (1992).] **See the Animated Figures.**

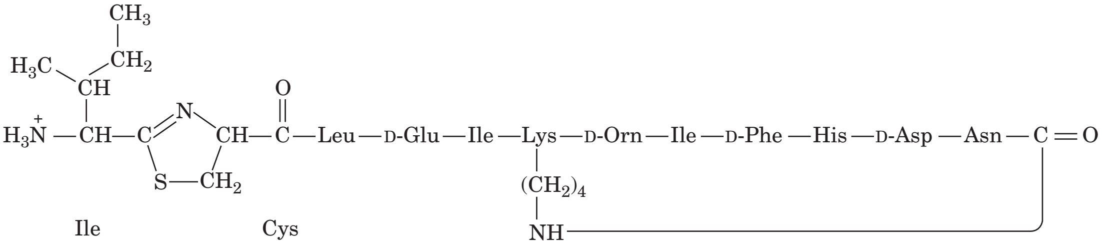

Bacitracin

Figure 16-28 | The chemical structure of bacitracin. Note that this dodecapeptide has four D-amino acid residues and two unusual intrachain linkages. "Orn" represents the nonstandard amino acid ornithine (Fig. 21-9).

on the lumenal surface of the endoplasmic reticulum, whereas others occur on its cytoplasmic surface. Hence, on four occasions (Reactions 3, 5, 8, and 11 in Fig. 16-27), dolichol and its attached hydrophilic group are translocated, via unknown mechanisms, across the endoplasmic reticulum membrane. In the final steps of the process, the oligosaccharide is transferred to the Asn residue in a segment of sequence Asn-X-Ser/Thr (where X is any residue except Pro and possibly Asp) on a growing polypeptide chain. The resulting dolichol pyrophosphate is hydrolyzed to dolichol phosphate and P_i, a process similar to the pyrophosphatase cleavage of PP_i to 2 P_i. Further processing of the oligosaccharide takes place, as described in Section 8-3C, first in the endoplasmic reticulum and then in the Golgi apparatus (Fig. 8-19), where certain monosaccharide residues are trimmed away by specific glycosylases and others are added by specific nucleotide sugar–requiring glycosyltransferases.

Bacitracin Interferes with the Dephosphorylation of Dolichol Pyrophosphate. A number of compounds block the actions of specific glycosylation enzymes, including **bacitracin** (Fig. 16-28), a cyclic polypeptide that is a widely used antibiotic. Bacitracin forms a complex with dolichol pyrophosphate that inhibits its dephosphorylation (Fig. 16-27, Reaction 12), thereby preventing the synthesis of glycoproteins from dolichol-linked oligosaccharide precursors. Bacitracin is clinically useful because it inhibits bacterial cell wall synthesis (which also involves dolichol-linked oligosaccharides) but does not affect animal cells since it cannot cross cell membranes (bacterial cell wall synthesis is an extracellular process).

CHECK YOUR UNDERSTANDING

Explain the group transfer reaction of glycosidic bond formation by describing the attacking nucleophile, the atom attacked, and the leaving group.

SUMMARY

1. Glycogen breakdown requires three enzymes. Glycogen phosphorylase converts the glucosyl units at the nonreducing ends of glycogen to glucose-1-phosphate (G1P). Debranching enzyme transfers an α(1→4)-linked trisaccharide to a nonreducing end and hydrolyzes the α(1→6) linkage. Phosphoglucomutase converts G1P to glucose-6-phosphate (G6P). In liver, G6P is hydrolyzed by glucose-6-phosphatase to glucose for export to the tissues.
2. Glycogen synthesis requires a different pathway in which G1P is activated by reaction with UTP to form UDP–glucose. Glycogen synthase adds glucosyl units to the nonreducing ends of a growing glycogen molecule that has been primed by glycogenin. Branching enzyme removes an α(1→4)-linked 7-residue segment and reattaches it through an α(1→6) linkage to form a branched chain.
3. Glycogen metabolism is controlled in part by allosteric effectors such as AMP, ATP, and G6P. Covalent modification of glycogen phosphorylase and glycogen synthase shifts their $T \rightleftharpoons R$ equilibria and therefore alters their sensitivity to allosteric effectors.
4. The ratio of phosphorylase *a* (more active) to phosphorylase *b* (less active) depends on the activity of phosphorylase kinase, which is regulated by the activity of protein kinase A (PKA), a cAMP-dependent enzyme, and on the activity of phosphoprotein phosphatase-1 (PP1). Glycogen phosphory-

lase is activated by phosphorylation, whereas glycogen synthase is activated by dephosphorylation.

5. Hormones such as glucagon, epinephrine, and insulin control glycogen metabolism. Hormone signals that generate cAMP as a second messenger or that elevate intracellular Ca^{2+}, which binds to the calmodulin subunit of phosphorylase kinase, promote glycogen breakdown. Insulin stimulates glycogen synthesis in part by activating phosphoprotein phosphatase-1.
6. Compounds that can be converted to oxaloacetate can subsequently be converted to glucose. The conversion of pyruvate to glucose by gluconeogenesis requires enzymes that bypass the three exergonic steps of glycolysis: Pyruvate carboxylase and PEP carboxykinase (PEPCK) bypass pyruvate kinase, fructose-1,6-bisphosphatase (FBPase) bypasses phosphofructokinase, and glucose-6-phosphatase bypasses hexokinase.
7. Gluconeogenesis is regulated by changes in enzyme synthesis and by allosteric effectors, including fructose-2,6-bisphosphate (F2,6P), which inhibits FBPase and activates phosphofructokinase (PFK) and whose synthesis depends on the phosphorylation state of the bifunctional enzyme phosphofructokinase-2/fructose bisphosphatase-2 (PFK-2/FBPase-2).
8. Formation of glycosidic bonds requires nucleotide sugars.

KEY TERMS

glycogenolysis **532**
phosphorolysis **533**
debranching **533**
glycogen storage disease **538**
nucleotide sugar **561**
interconvertible enzyme **545**
gluconeogenesis **552**
reducing equivalent **556**
dolichol **561**

PROBLEMS

1. Indicate the energy yield or cost, in ATP equivalents, for the following processes:
   (a) glycogen (3 residues) → 6 pyruvate
   (b) 3 glucose → 6 pyruvate
   (c) 6 pyruvate → 3 glucose
2. Write the balanced equation for (a) the sequential conversion of glucose to pyruvate and of pyruvate to glucose and (b) the catabolism of six molecules of G6P by the pentose phosphate pathway followed by conversion of ribulose-5-phosphate back to G6P by gluconeogenesis.
3. Phosphoglucokinase catalyzes the phosphorylation of the C6-OH group of G1P. Why is this enzyme important for the normal function of phosphoglucomutase?
4. The free energy of hydrolysis of an $\alpha(1 \rightarrow 4)$ glycosidic bond is $-15.5\ \text{kJ} \cdot \text{mol}^{-1}$, whereas that of an $\alpha(1 \rightarrow 6)$ glycosidic bond is $-7.1\ \text{kJ} \cdot \text{mol}^{-1}$. Use these data to explain why glycogen debranching includes three reactions [breaking and reforming $\alpha(1 \rightarrow 4)$ bonds and hydrolyzing $\alpha(1 \rightarrow 6)$ bonds], whereas glycogen branching requires only two reactions [breaking $\alpha(1 \rightarrow 4)$ bonds and forming $\alpha(1 \rightarrow 6)$ bonds].
5. Calculations based on the volume of a glucose residue and the branching pattern of cellular glycogen indicate that a glycogen molecule could have up to 28 branching tiers before becoming impossibly dense. What are the advantages of such a molecule and why is it not found *in vivo*?
6. One molecule of dietary glucose can be oxidized through glycolysis and the citric acid cycle to generate a maximum of 32 molecules of ATP. Calculate the fraction of this energy that is lost when the glucose is stored as glycogen before it is catabolized.
7. Glucose binds to glycogen phosphorylase and competitively inhibits the enzyme. What is the physiological advantage of this?
8. Many diabetics do not respond to insulin because of a deficiency of insulin receptors on their cells. How does this affect (a) the levels of circulating glucose immediately after a meal and (b) the rate of glycogen synthesis in muscle?
9. Glucose-6-phosphatase is located inside the endoplasmic reticulum. Describe the probable symptoms of a defect in G6P transport across the endoplasmic reticulum membrane.
10. Individuals with McArdle's disease often experience a "second wind" resulting from cardiovascular adjustments that allow glucose mobilized from liver glycogen to fuel muscle contraction. Explain why the amount of ATP derived in the muscle from circulating glucose is less than the amount of ATP that would be obtained by mobilizing the same amount of glucose from muscle glycogen.
11. A sample of glycogen from a patient with liver disease is incubated with P_i, normal glycogen phosphorylase, and normal debranching enzyme. The ratio of G1P to glucose formed in the reaction mixture is 100. What is the patient's most probable enzymatic deficiency?

CASE STUDIES

Case 22 (available at www.wiley.com/college/voet)
Carrier-Mediated Uptake of Lactate in Rat Hepatocytes

Focus concept: The structural characteristics of the lactate transport protein in hepatocytes are determined.

Prerequisites: Chapters 10, 15, and 16

- Transport proteins
- Major carbohydrate metabolic pathways including glycolysis and gluconeogenesis

Case 26
The Role of Specific Amino Acids in the Peptide Hormone Glucagon in Receptor Binding and Signal Transduction

Focus concept: Amino acid side chains important in glucagon binding and signal transduction are identified.

Prerequisites Chapters: 4, 13, and 16

- Amino acid structure
- Signal transduction via G proteins

SELECTED READINGS

Bollen, M., Keppens, S., and Stalmans, W., Specific features of glycogen metabolism in the liver, *Biochem. J*. **336,** 19–31 (1998). [Describes the activities of the enzymes involved in glycogen synthesis and degradation and discusses the mechanisms for regulating the processes.]

Brosnan, J.T., Comments on metabolic needs for glucose and the role of gluconeogenesis, *Eur. J. Clin. Nutr.* **53,** S107–S111 (1999). [A very readable review that discusses possible reasons why carbohydrates are used universally as metabolic fuels and why glucose is stored as glycogen.]

Browner, M.F. and Fletterick, R.J., Phosphorylase: a biological transducer, *Trends Biochem. Sci*. **17,** 66–71 (1992).

Burda, P. and Aebi, M., The dolichol pathway of N-linked glycosylation, *Biochim. Biophys. Acta* **1426,** 239–257 (1999).

Chen, Y.-T., Glycogen storage diseases, *in* Scriver, C.R., Beaudet, A.L., Sly, W.S., and Valle, D. (Eds.), *The Metabolic and Molecular Bases of Inherited Disease* (8th ed.), pp. 1521–1552, McGraw-Hill (2001). [Begins with a review of glycogen metabolism.]

Croniger, C.M., Olswang, Y., Reshef, L., Kalhan, S.C., Tilghman, S.M., and Hanson, R.W., Phosphoenolpyruvate carboxykinase revisited. Insights into its metabolic role, *Biochem. Mol. Biol. Educ*. **30,** 14–20 (2002); *and* Croniger, C.M., Chakravarty, K., Olswang, Y., Cassuto, H., Reshef, L., and Hanson, R.W., Phosphoenolpyruvate carboxykinase revisited. II. Control of PEPCK-C gene expression, *Biochem. Mol. Biol. Educ*. **30,** 353–362 (2002).

Meléndez-Hevia, E., Waddell, T.G., and Shelton, E.D., Optimization of molecular design in the evolution of metabolism: the glycogen molecule, *Biochem. J*. **295,** 477–483 (1993).

Nordlie, R.C., Foster, J.D., and Lange, A.J., Regulation of glucose production by the liver, *Annu. Rev. Nutr*. **19,** 379–406 (1999).

Okar, D.A., Manzano, À., Navarro-Sabatè, A., Riera, L., Bartrons, R., and Lange, A.J., PFK-2/FBPase-2: Maker and breaker of the essential biofactor fructose-2,6-bisphosphate, *Trends Biochem. Sci.* **26,** 30–35 (2001).

Roach, P.J. and Skurat, A.V., Self-glucosylating initiator proteins and their role in glycogen biosynthesis, *Prog. Nucleic Acid Res. Mol. Biol*. **57,** 289–316 (1997). [Discusses glycogenin.]

Whelan, W.J., Why the linkage of glycogen to glycogenin was so hard to determine. *Biochem. Mol. Biol. Educ.* **35,** 313–315 (2007).

17

Citric Acid Cycle

The synthesis and degradation of numerous biological materials depends on the flow of molecules and energy through the citric acid cycle, which has been likened to a metabolic water wheel. [Al Zwiazek/SUPERSTOCK.]

CHAPTER CONTENTS

1 Overview of the Citric Acid Cycle
2 Synthesis of Acetyl-Coenzyme A
  A. Pyruvate Dehydrogenase Is a Multienzyme Complex
  B. The Pyruvate Dehydrogenase Complex Catalyzes Five Reactions
3 Enzymes of the Citric Acid Cycle
  A. Citrate Synthase Joins an Acetyl Group to Oxaloacetate
  B. Aconitase Interconverts Citrate and Isocitrate
  C. NAD^+-Dependent Isocitrate Dehydrogenase Releases CO_2
  D. α-Ketoglutarate Dehydrogenase Resembles Pyruvate Dehydrogenase
  E. Succinyl-CoA Synthetase Produces GTP
  F. Succinate Dehydrogenase Generates $FADH_2$
  G. Fumarase Produces Malate
  H. Malate Dehydrogenase Regenerates Oxaloacetate
4 Regulation of the Citric Acid Cycle
  A. Pyruvate Dehydrogenase Is Regulated by Product Inhibition and Covalent Modification
  B. Three Enzymes Control the Rate of the Citric Acid Cycle
5 Reactions Related to the Citric Acid Cycle
  A. Other Pathways Use Citric Acid Cycle Intermediates
  B. Some Reactions Replenish Citric Acid Cycle Intermediates
  C. The Glyoxylate Cycle Shares Some Steps with the Citric Acid Cycle

MEDIA RESOURCES

(available at www.wiley.com/college/voet)
Guided Exploration 16. Citric acid cycle overview
Interactive Exercise 18. Conformational changes in citrate synthase
Animated Figure 17-1. Overview of oxidative fuel metabolism
Animated Figure 17-2. Reactions of the citric acid cycle
Animated Figure 17-16. Regulation of the citric acid cycle
Animated Figure 17-17. Amphibolic functions of the citric acid cycle
Case Study 21. Characterization of Pyruvate Carboxylase from *Methanobacterium thermoautotrophicum*

In the preceding two chapters, we examined the catabolism of glucose and its biosynthesis, storage, and mobilization. Although glucose is a source of energy for nearly all cells, it is not the only metabolic fuel, nor is glycolysis the only energy-yielding catabolic pathway. Cells that rely exclusively on glycolysis to meet their energy requirements actually waste most of the chemical potential energy of carbohydrates. When glucose is converted to lactate or ethanol, a relatively reduced product leaves the cell. If the end product of glycolysis is instead further oxidized, the cell can recover considerably more energy.

The oxidation of an organic compound requires an electron acceptor, such as NO_3^-, SO_4^{2-}, Fe^{3+}, or O_2, all of which are exploited as oxidants in different organisms. In aerobic organisms, the electrons produced by oxidative metabolism are ultimately transferred to O_2. Oxidation of metabolic fuels is carried out by the citric acid cycle, a sequence of reactions that arose sometime after levels of atmospheric oxygen became significant, about 3 billion years ago. As the reduced carbon atoms of metabolic fuels are oxidized to CO_2, electrons are transferred to electron carriers that are subsequently reoxidized by O_2. In this chapter, we examine the oxidation reactions of the citric acid cycle itself. In the following chapter, we examine the fate of the electrons and see how their energy is used to drive the synthesis of ATP.

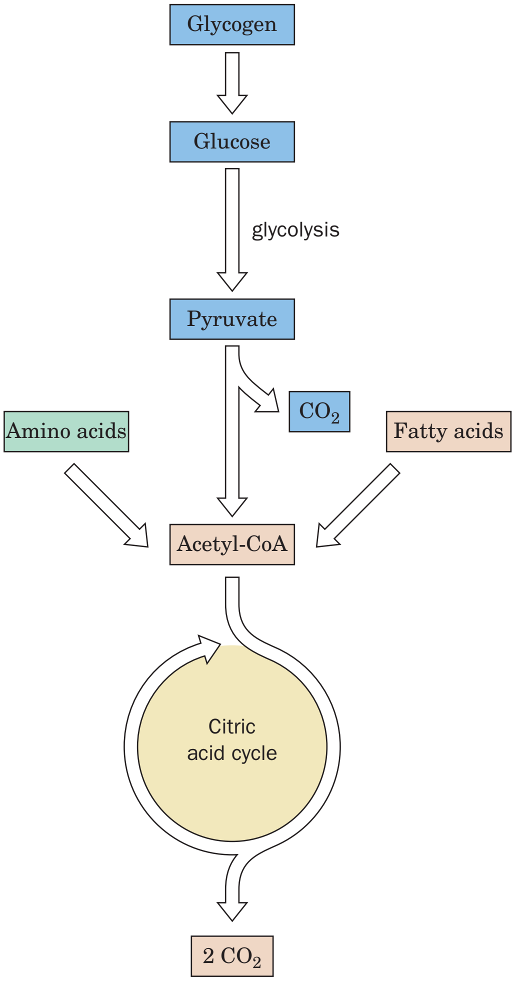

■ **Figure 17-1 | Overview of oxidative fuel metabolism.** Acetyl groups derived from carbohydrates, amino acids, and fatty acids enter the citric acid cycle, where they are oxidized to CO_2. **See the Animated Figures.**

It is sometimes convenient to think of the citric acid cycle as an addendum to glycolysis. Pyruvate derived from glucose can be split into CO_2 and a two-carbon fragment that enters the cycle for oxidation as acetyl-CoA (Fig. 17-1). However, it is really misleading to think of the citric acid cycle as merely a continuation of carbohydrate catabolism. *The citric acid cycle is a central pathway for recovering energy from several metabolic fuels, including carbohydrates, fatty acids, and amino acids, that are broken down to acetyl-CoA for oxidation.* In fact, under some conditions, the principal function of the citric acid cycle is to recover energy from fatty acids. We shall also see that the citric acid cycle supplies the reactants for a variety of biosynthetic pathways.

We begin this chapter with an overview of the citric acid cycle. Next, we explore how acetyl-CoA, its starting compound, is formed from pyruvate. After discussing the reactions catalyzed by each of the enzymes of the cycle, we consider the regulation of these enzymes. Finally, we examine the links between citric acid cycle intermediates and other metabolic processes.

1 Overview of the Citric Acid Cycle

LEARNING OBJECTIVE

- Understand that the citric acid cycle is a multistep catalytic process that converts acetyl groups derived from carbohydrates, fatty acids, and amino acids to CO_2, and produces NADH, $FADH_2$, and GTP.

See Guided Exploration 16
Citric Cycle Overview

The **citric acid cycle** (Fig. 17-2) is an ingenious series of eight reactions that oxidizes the acetyl group of acetyl-CoA to two molecules of CO_2 in a manner that conserves the liberated free energy in the reduced compounds NADH and $FADH_2$. The cycle is named after the product of its first reaction, **citrate.** One complete round of the cycle yields two molecules of CO_2, three NADH, one $FADH_2$, and one “high-energy” compound (GTP or ATP).

The citric acid cycle first came to light in the 1930s, when Hans Krebs, building on the work of others, proposed a circular reaction scheme for the interconversion of certain compounds containing two or three carboxylic acid groups (that is, di- and tricarboxylates). At the time, many of the citric acid cycle intermediates were already well known as plant products: **citrate** from citrus fruit, **aconitate** from monkshood (*Aconitum*), **succinate** from amber (*Succinum*), **fumarate** from the herb *Fumaria,* and **malate** from apple (*Malus*). Two other intermediates, **α-ketoglutarate** and **oxaloacetate,** are known by their chemical names because they were synthesized before they were identified in living organisms. Krebs was the first to show how the metabolism of these compounds was linked to the oxidation of metabolic fuels. His discovery of the citric acid cycle, in 1937, ranks as one of the most important achievements of metabolic chemistry (Box 17-1). Although the enzymes and intermediates of the citric acid cycle are now well established, many investigators continue to explore the molecular mechanisms of the enzymes and how the enzymes are regulated for optimal performance under varying metabolic conditions in different organisms.

Before we examine each of the reactions in detail, we should emphasize some general features of the citric acid cycle:

1. The circular pathway, which is also called the **Krebs cycle** or the **tricarboxylic acid (TCA) cycle,** oxidizes acetyl groups from many

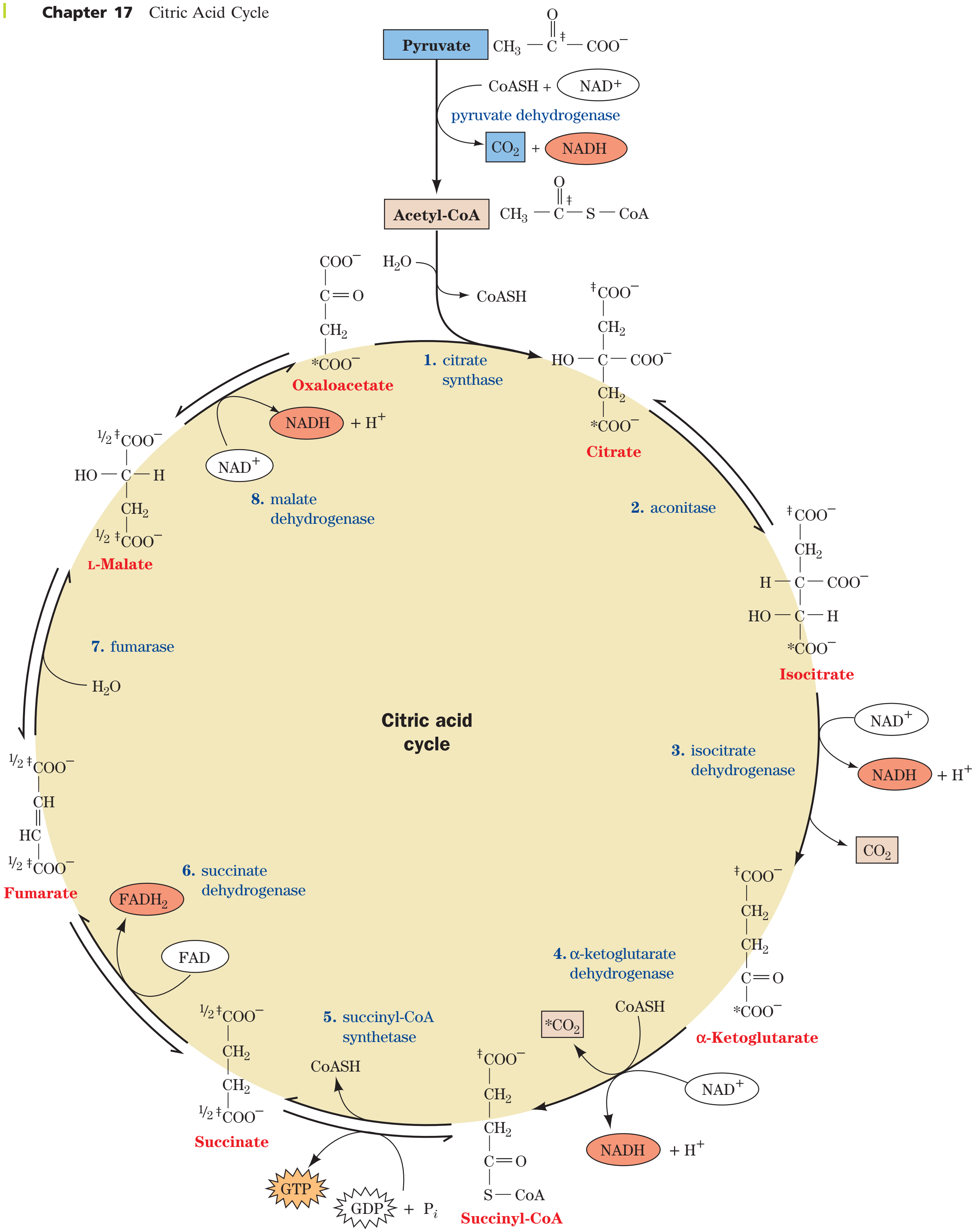
Pyruvate
CoASH + NAD+
pyruvate dehydrogenase
CO2 + NADH
Acetyl-CoA
H2O
CoASH
1. citrate synthase
Citrate
2. aconitase
Isocitrate
3. isocitrate dehydrogenase
NAD+
NADH + H+
CO2
α-Ketoglutarate
4. α-ketoglutarate dehydrogenase
CoASH
*CO2
NAD+
NADH + H+
Succinyl-CoA
5. succinyl-CoA synthetase
CoASH
GTP
GDP + Pi
Succinate
6. succinate dehydrogenase
FAD
FADH2
Fumarate
7. fumarase
H2O
L-Malate
8. malate dehydrogenase
NAD+
NADH + H+
Oxaloacetate
Citric acid cycle

■ **Figure 17-2 | The reactions of the citric acid cycle.** The reactants and products of this catalytic cycle are boxed. The pyruvate → acetyl-CoA reaction (*top*) supplies the cycle's substrate via carbohydrate metabolism but is not considered to be part of the cycle. An isotopic label at C4 of oxaloacetate (*) becomes C1 of α-ketoglutarate and is released as CO_2 in Reaction 4. An isotopic label at C1 of acetyl-CoA (‡) becomes C5 of α-ketoglutarate and is scrambled in Reaction 5 between C1 and C4 of succinate (½‡). **See the Animated Figures.**

BOX 17-1 **PATHWAYS OF DISCOVERY**

Hans Krebs and the Citric Acid Cycle

Hans Krebs (1900–1981)

Hans Krebs worked in Otto Warburg's laboratory from 1926 until 1930 and later declared that he had learned more from Warburg (see Box 15-1) than from any other teacher. Krebs applied Warburg's tissue-slice technique to the study of biosynthetic reactions (Warburg himself was interested primarily in oxidative and degradative reactions). Over a period of years, Krebs investigated synthetic pathways for urea, uric acid, and purines as well as oxidative pathways. He was forced to leave his native Germany for England in 1933, but unlike many other German emigrant scientists, he was able to bring much of his laboratory equipment with him. In England, Krebs continued to work on a series of metabolic reactions that he named the citric acid cycle.

The cycle was discovered not through sudden inspiration but through a series of careful experiments spanning the years 1932 to 1937. Krebs became interested in the "combustion" phase of fuel use, namely, what occurs after the fermentation of glucose to lactate. Until the 1930s, the mechanism of glucose oxidation and its relationship to cellular respiration (oxygen uptake) was a mystery. Krebs understood that the stoichiometry of the overall process (glucose + 6 $O_2 \rightarrow 6\ CO_2 + 6\ H_2O$) required a multistep pathway. He was also aware that other researchers had examined the ability of muscle tissue to rapidly oxidize various dicarboxylates (α-ketoglutarate, succinate, and malate) and a tricarboxylate (citrate), but none of these substances had a clear relationship to any foodstuffs.

In 1935, Albert Szent-Györgyi found that cellular respiration was dramatically accelerated by small amounts of succinate, fumarate, malate, or oxaloacetate. In fact, the addition of any of these compounds stimulated O_2 uptake and CO_2 production far in excess of what would be expected for their oxidation. In other words, the compounds acted catalytically to boost the combustion of other compounds in the cell. At about the same time, Carl Martius and Franz Knoop showed that citrate could be converted to α-ketoglutarate. Soon, Krebs had an entire sequence of reactions for converting citrate to oxaloacetate: citrate → aconitate → isocitrate → α-ketoglutarate → succinate → fumarate → malate → oxaloacetate. However, in order for this sequence of reactions to work catalytically, it must repeatedly return to its starting point; that is, the first compound must be regenerated. And there was still no obvious link to glucose metabolism!

Krebs believed that citrate and the other intermediates were involved in glucose combustion because they appeared to burn at the same rate as foodstuffs and were the only substances that did so. In addition, earlier work had shown that the three-carbon compound malonate not only blocks the conversion of succinate to fumarate, it blocks all combustion by living cells. In 1937, Martius and Knoop provided Krebs with a key piece of information: oxaloacetate and pyruvate could be converted to citrate in the presence of hydrogen peroxide.

Krebs now had the missing link: Pyruvate is a product of glucose metabolism, and its reaction with oxaloacetate to form citrate closed off the linear series of reactions to form a cycle. The idea of a circular pathway was not new to Krebs. He and Kurt Henseleit had elucidated the four-step urea cycle in 1932 (Section 21-3). Krebs quickly showed that the reaction of pyruvate with oxaloacetate to form citrate took place in living tissue and that the rates of citrate synthesis and breakdown were high enough to account for the observed fuel combustion in a variety of tissue types.

Remarkably, Krebs' initial report on the citric acid cycle was rejected by *Nature,* a leading journal, before being accepted for publication in the less prestigious *Enzymologia.* In his report, Krebs established the major outlines of the pathway, although some details were later revised. For example, the mechanism of citrate formation (which involves acetyl-CoA rather than pyruvate) and the participation of succinyl-CoA in the cycle were not immediately appreciated. Coenzyme A was not discovered until 1945, and only in 1951 was acetyl-CoA shown to be the intermediate that condenses with oxaloacetate to form citrate. Work by Krebs and others established that the citric acid cycle plays a major role in the oxidation of amino acids and fatty acids. In fact, the pathway accounts for approximately two-thirds of the energy derived from metabolic fuels. Krebs also recognized the role of the citric acid cycle in supplying precursors for synthetic reactions.

[Krebs, H.A. and Johnson, W.A., The role of citric acid in intermediate metabolism in animal tissues, *Enzymologia* **4,** 148–156 (1937).]

sources, not just pyruvate. Because it accounts for the major portion of carbohydrate, fatty acid, and amino acid oxidation, the citric acid cycle is often considered the "hub" of cellular metabolism.

2. The net reaction of the citric acid cycle is

$$3\,NAD^+ + FAD + GDP + P_i + \text{acetyl–CoA} \longrightarrow$$
$$3\,NADH + FADH_2 + GTP + CoA + 2\,CO_2$$

The oxaloacetate that is consumed in the first step of the citric acid cycle is regenerated in the last step of the cycle. Thus, *the citric acid* *cycle acts as a multistep catalyst that can oxidize an unlimited number of acetyl groups.*

3. In eukaryotes, all the enzymes of the citric acid cycle are located in the mitochondria, so all substrates, including NAD^+ and GDP, must be generated in the mitochondria or be transported into mitochondria from the cytosol. Similarly, all the products of the citric acid cycle must be consumed in the mitochondria or transported into the cytosol.
4. The carbon atoms of the two molecules of CO_2 produced in one round of the cycle are not the two carbons of the acetyl group that began the round (Fig. 17-2). These acetyl carbon atoms are lost in subsequent rounds of the cycle. However, the net effect of each round of the cycle is the oxidation of one acetyl group to 2 CO_2.
5. Citric acid cycle intermediates are precursors for the biosynthesis of other compounds (e.g., oxaloacetate for gluconeogenesis; Section 16-4).
6. The oxidation of an acetyl group to 2 CO_2 requires the transfer of four pairs of electrons. The reduction of 3 NAD^+ to 3 NADH accounts for three pairs of electrons; the reduction of FAD to $FADH_2$ accounts for the fourth pair. Much of the free energy of oxidation of the acetyl group is conserved in these reduced coenzymes. Energy is also recovered as GTP (or ATP). In Section 18-3C, we shall see that approximately 10 ATP are formed when the four pairs of electrons are eventually transferred to O_2.

■ CHECK YOUR UNDERSTANDING

Explain why the citric acid cycle is considered to be the hub of cellular metabolism.

What are the substrates and products of the net reaction corresponding to one turn of the citric acid cycle?

2 Synthesis of Acetyl-Coenzyme A

LEARNING OBJECTIVE

- Understand that pyruvate dehydrogenase is a multienzyme complex that catalyzes a five-part reaction in which pyruvate releases CO_2 and the remaining acetyl group becomes linked to coenzyme A.

Acetyl groups enter the citric acid cycle as part of the "high-energy" compound acetyl-CoA (recall that thioesters have high free energies of hydrolysis; Section 14-2D). Although acetyl-CoA can also be derived from fatty acids (Section 20-2) and some amino acids (Section 21-4), we shall focus here on the production of acetyl-CoA from pyruvate derived from carbohydrates.

As we saw in Section 15-3, the end product of glycolysis under anaerobic conditions is lactate or ethanol. However, under aerobic conditions, when the NADH generated by glycolysis is reoxidized in the mitochondria, the final product is pyruvate. A transport protein imports pyruvate along with H^+ (i.e., a pyruvate–H^+ symport) into the mitochondrion for further oxidation.

A | Pyruvate Dehydrogenase Is a Multienzyme Complex

Multienzyme complexes are groups of noncovalently associated enzymes that catalyze two or more sequential steps in a metabolic pathway. Virtually all organisms contain multienzyme complexes, which represent a step forward in the evolution of catalytic efficiency because they offer the following advantages:

1. Enzymatic reaction rates are limited by the frequency with which enzymes collide with their substrates (Section 11-3D). When a series of reactions occurs within a multienzyme complex, the distance that substrates must diffuse between active sites is minimized, thereby enhancing the reaction rate.
2. The channeling of metabolic intermediates between successive enzymes in a metabolic pathway reduces the opportunity for these

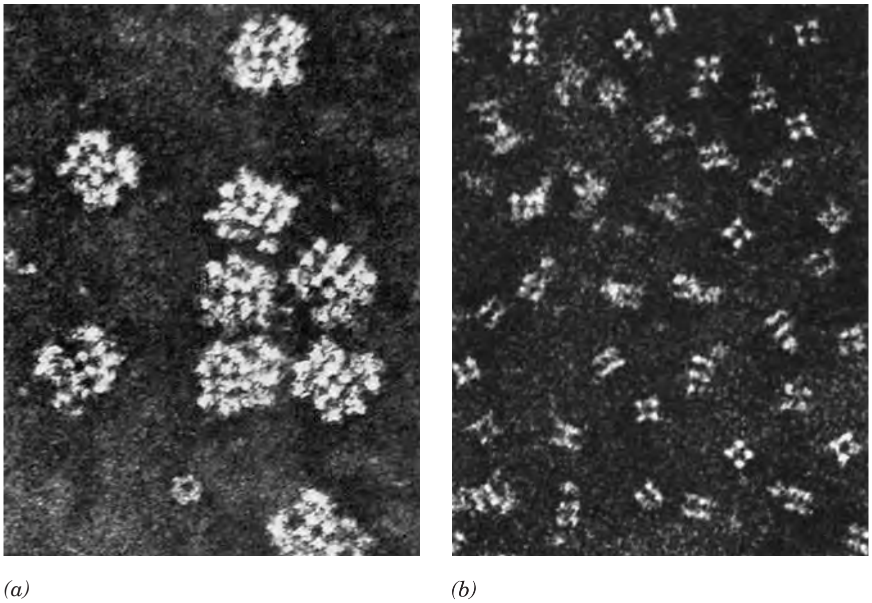

Figure 17-3 | Electron micrographs of the *E. coli* pyruvate dehydrogenase multienzyme complex. (*a*) The intact complex. (*b*) The dihydrolipoyl transacetylase (E_2) core complex. [Courtesy of Lester Reed, University of Texas at Austin.]

intermediates to react with other molecules, thereby minimizing side reactions.

3. The reactions catalyzed by a multienzyme complex can be coordinately controlled.

Acetyl-CoA is formed from pyruvate through oxidative decarboxylation by a multienzyme complex named **pyruvate dehydrogenase.** This complex contains multiple copies of three enzymes: **pyruvate dehydrogenase (E_1), dihydrolipoyl transacetylase (E_2),** and **dihydrolipoyl dehydrogenase (E_3).**

The *E. coli* pyruvate dehydrogenase complex is an ~4600-kD particle with a diameter of about 300 Å (Fig. 17-3*a*). The core of the particle is made of 24 E_2 proteins arranged in a cube (Figs. 17-3*b* and 4*a*), which is surrounded by 24 E_1 proteins and 12 E_3 proteins (Fig. 17-4*b,c*). In mammals, yeast, and some bacteria, the pyruvate dehydrogenase complex is even larger and more complicated, although it catalyzes the same reactions using homologous enzymes and similar mechanisms. In these ~10,000-kD complexes, which are among the largest known multifunctional particles in cells, the E_2 core consists of 60 subunits arranged with

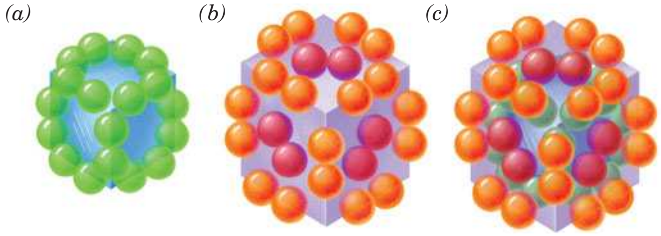

Figure 17-4 | Structural organization of the *E. coli* pyruvate dehydrogenase multienzyme complex. (*a*) The dihydrolipoyl transacetylase (E_2) core. The 24 E_2 proteins (*green spheres*) associate as trimers at the corners of a cube. (*b*) The 24 pyruvate dehydrogenase (E_1) proteins (*orange spheres*) form dimers that associate with the E_2 core (*shaded cube*) along its 12 edges. The 12 dihydrolipoyl dehydrogenase (E_3) proteins (*purple spheres*) form dimers that attach to the six faces of the E_2 cube. (*c*) Parts *a* and *b* combined form the entire 60-subunit complex.

dodecahedral symmetry [Fig. 17-5; a dodecahedron is a regular polyhedron with *I* symmetry (Fig. 6-34*c*) that has 20 vertices and 12 pentagonal faces] surrounded by a shell consisting of ~45 E_1 $\alpha_2\beta_2$ heterotetramers and ~9 E_3 homodimers. E_1 and E_3 competitively bind to mutually exclusive sites on E_2 in a random distribution. Mammalian complexes, in addition, contain ~12 copies. of **E_3 binding protein,** which facilitates the binding of E_3 to the E_2 core, and several copies of a kinase and a phosphatase that function to regulate the activity of the complex (Section 17-4A).

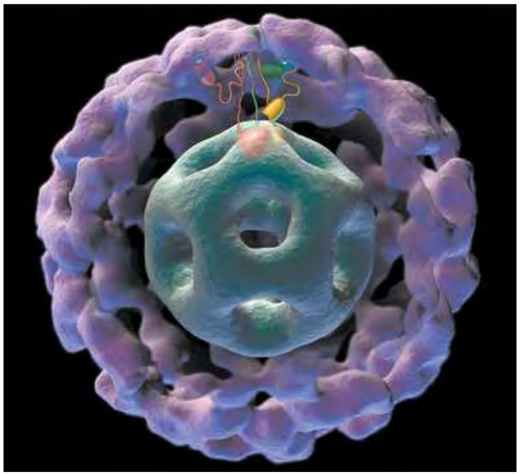

Figure 17-5 | Model of the *Bacillus stearothermophilus* pyruvate dehydrogenase complex. This ~500-Å-diameter cutaway surface diagram is based on cryoelectron microscopic images of a complex consisting of a core of 60 E_2 subunits (*gray-green*) surrounded by an outer shell of 60 E_1 subunits (*purple*) separated by an ~90-Å-wide annular gap. Three full-length E_2 subunits are schematically represented in red, green, and yellow to indicate their catalytic domains (embedded in the E_2 core), their peripheral subunit-binding domains (embedded in the E_3 shell) that bind the E_1 (and E_3) subunits, and their lipoyl domains, all connected by flexible polypeptide linkers (Section 17-2B). Here the red lipoyl domain is shown visiting an E_1 active site (*white dot*), whereas the green and yellow lipoyl domains occupy intermediate positions in the annular region between the E_2 core and E_1 shell. In a normal pyruvate dehydrogenase complex, E_3 subunits would take the place of some of the E_1 subunits. Indeed, a complex of 60 E_3 subunits and 60 E_2 subunits closely resembles the E_1E_2 complex. [Courtesy of Jacqueline Milne, National Institutes of Health, Bethesda, MD.]

B | The Pyruvate Dehydrogenase Complex Catalyzes Five Reactions

The pyruvate dehydrogenase complex catalyzes five sequential reactions with the overall stoichiometry

$$\text{Pyruvate} + \text{CoA} + \text{NAD}^+ \longrightarrow \text{acetyl-CoA} + \text{CO}_2 + \text{NADH}$$

Five different coenzymes are required: thiamine pyrophosphate (TPP; Section 15-3B), **lipoamide,** coenzyme A (Fig. 14-10), FAD (Fig. 14-12), and NAD^+ (Fig. 11-4). The coenzymes and their mechanistic functions are listed in Table 17-1. The sequence of reactions catalyzed by the pyruvate dehydrogenase complex is as follows (Fig. 17-6):

1. Pyruvate dehydrogenase (E_1), a TPP-requiring enzyme, decarboxylates pyruvate with the formation of a hydroxyethyl-TPP intermediate:

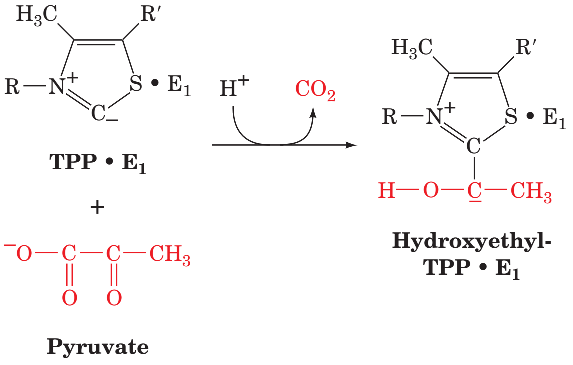

Table 17-1 The Coenzymes and Prosthetic Groups of Pyruvate Dehydrogenase

Cofactor	Location	Function
Thiamine pyrophosphate (TPP)	Bound to E_1	Decarboxylates pyruvate yielding a hydroxyethyl-TPP carbanion
Lipoic acid	Covalently linked to a Lys on E_2 (lipoamide)	Accepts the hydroxyethyl carbanion from TPP as an acetyl group
Coenzyme A (CoA)	Substrate for E_2	Accepts the acetyl group from lipoamide
Flavin adenine dinucleotide (FAD)	Bound to E_3	Reduced by lipoamide
Nicotinamide adenine dinucleotide (NAD^+)	Substrate for E_3	Reduced by FADH_2

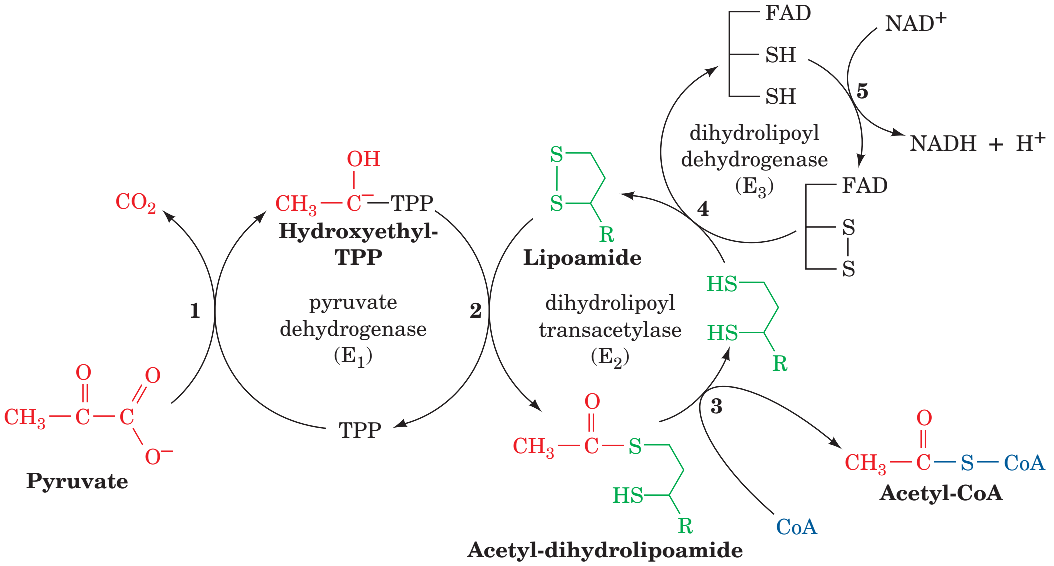
FAD
SH
SH
NAD+
5
NADH + H+
dihydrolipoyl
dehydrogenase
(E3)
FAD
S
S
4
OH
CH3—C—TPP
Hydroxyethyl-
TPP
CO2
S
S
R
Lipoamide
HS
HS
R
1
pyruvate
dehydrogenase
(E1)
2
dihydrolipoyl
transacetylase
(E2)
O
O
CH3—C—C
O−
Pyruvate
TPP
3
O
CH3—C—S
HS
R
Acetyl-dihydrolipoamide
CoA
O
CH3—C—S—CoA
Acetyl-CoA

Figure 17-6 | The five reactions of the pyruvate dehydrogenase multienzyme complex. E_1 (pyruvate dehydrogenase) contains TPP and catalyzes Reactions 1 and 2. E_2 (dihydrolipoyl transacetylase) contains lipoamide and catalyzes Reaction 3. E_3 (dihydrolipoyl dehydrogenase) contains FAD and a redox-active disulfide and catalyzes Reactions 4 and 5.

This reaction is identical to that catalyzed by yeast pyruvate decarboxylase (Fig. 15-20). Recall (Section 15-3B) that the ability of TPP's thiazolium ring to add to carbonyl groups and act as an electron sink makes it the coenzyme most utilized in α-keto acid decarboxylation reactions.

2. The hydroxyethyl group is transferred to the next enzyme, dihydrolipoyl transacetylase (E_2), which contains a lipoamide group. Lipoamide consists of **lipoic acid** linked via an amide bond to the ε-amino group of a Lys residue (Fig. 17-7). The reactive center of lipoamide is a cyclic disulfide that can be reversibly reduced to yield **dihydrolipoamide.** The hydroxyethyl group derived from pyruvate

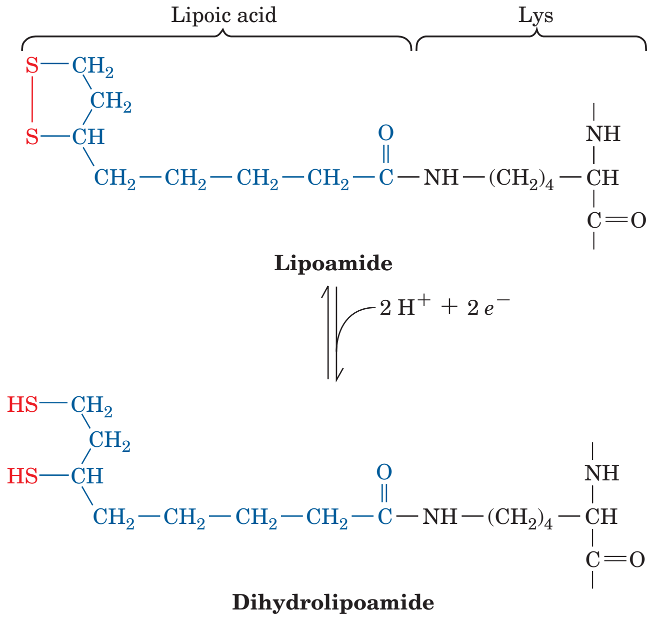
Lipoic acid
Lys
S—CH2
CH2
S—CH
O
NH
CH2—CH2—CH2—CH2—C—NH—(CH2)4—CH
C=O
Lipoamide
2 H+ + 2 e−
HS—CH2
CH2
HS—CH
O
NH
CH2—CH2—CH2—CH2—C—NH—(CH2)4—CH
C=O
Dihydrolipoamide

Figure 17-7 | Interconversion of lipoamide and dihydrolipoamide. Lipoamide consists of lipoic acid covalently joined to the ε-amino group of a Lys residue via an amide bond.

attacks the lipoamide disulfide, and TPP is eliminated. The hydroxyethyl carbanion is thereby oxidized to an acetyl group as the lipoamide disulfide is reduced:

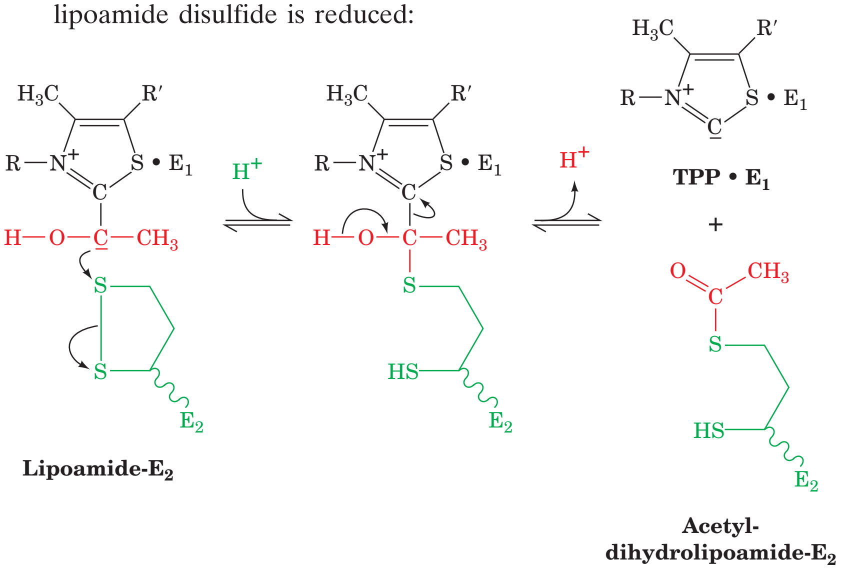
H_3C
R'
R—N
S • E_1
C
H—O—C—CH_3
S
S
E_2
H^+
H^+
HS
TPP • E_1
+
O
CH_3
C
S
HS
E_2
Lipoamide-E_2
Acetyl-dihydrolipoamide-E_2

3. E_2 then catalyzes a transesterification reaction in which the acetyl group is transferred to CoA, yielding acetyl-CoA and dihydrolipoamide-E_2:

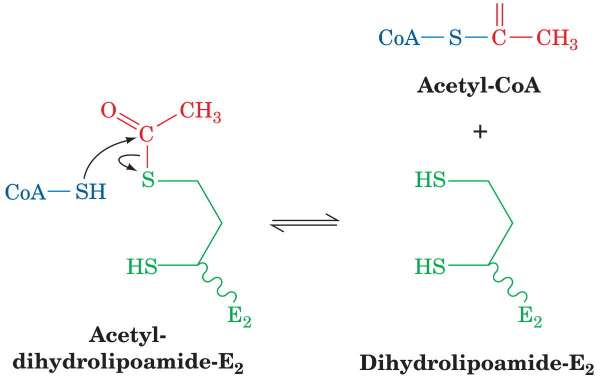
CoA—S—C—CH_3
O
Acetyl-CoA
+
CoA—SH
O
CH_3
C
S
HS
HS
HS
E_2
E_2
Acetyl-dihydrolipoamide-E_2
Dihydrolipoamide-E_2

4. Acetyl-CoA has now been formed, but the lipoamide group of E_2 must be regenerated. Dihydrolipoyl dehydrogenase (E_3) reoxidizes dihydrolipoamide to complete the catalytic cycle of E_2. Oxidized E_3 contains a reactive Cys—Cys disulfide group and a tightly bound FAD. The oxidation of dihydrolipoamide is a disulfide interchange reaction:

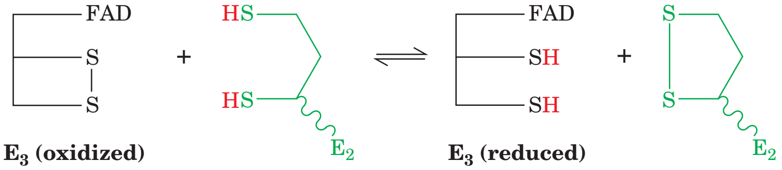
FAD
S
S
+
HS
HS
E_2
FAD
SH
SH
+
S
S
E_2
E_3 (oxidized)
E_3 (reduced)

5. Finally, reduced E_3 is reoxidized. The sulfhydryl groups are reoxidized by a mechanism in which FAD funnels electrons to NAD^+ yielding NADH:

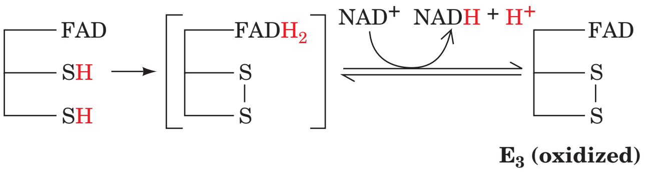
FAD
SH
SH
$FADH_2$
S
S
NAD^+
NADH + H^+
FAD
S
S
E_3 (oxidized)

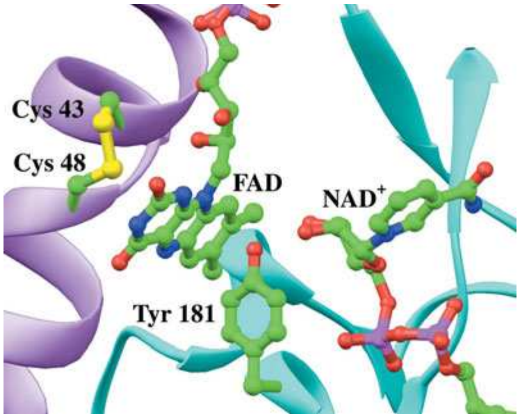

■ **Figure 17-8 | Active site of dihydrolipoamide dehydrogenase (E_3).** In this X-ray structure of the enzyme from *Pseudomonas putida,* the redox-active portions of the bound NAD$^+$ and FAD cofactors, the side chains of Cys 43 and Cys 48 forming the redox-active disulfide bond, and the side chain of Tyr 181 are shown in ball-and-stick form with C green, N blue, O red, P magenta, and S yellow. Note that the side chain of Tyr 181 is interposed between the flavin and the nicotinamide rings. [Based on an X-ray structure by Wim Hol, University of Washington. PDBid 1LVL.]

The X-ray structure of dihydrolipoyl dehydrogenase together with mechanistic information indicate that the reaction catalyzed by dihydrolipoamide dehydrogenase (E_3) is more complex than Reactions 4 and 5 in Fig. 17-6 suggest. The enzyme's redox-active disulfide bond occurs between Cys 43 and Cys 48, which reside on a highly conserved segment of the enzyme's polypeptide chain. The disulfide bond links successive turns in a distorted segment of an α helix (in an undistorted helix, the C_α atoms of Cys 43 and Cys 48 would be too far apart to permit the disulfide bond to form). The enzyme's flavin group is almost completely buried in the protein, which prevents the surrounding solution from interfering with the electron-transfer reaction catalyzed by the enzyme. The nicotinamide ring of NAD$^+$ binds on the side of the flavin opposite the disulfide. In the absence of NAD$^+$, the phenol side chain of Tyr 181 covers the nicotinamide-binding pocket so as to shield the flavin from contact with the solution (Fig. 17-8). The Tyr side chain apparently moves aside to allow the nicotinamide ring to bind near the flavin ring.

FAD prosthetic groups in proteins have reduction potentials of around 0 V (Table 14-5), which makes $FADH_2$ unsuitable for donating electrons to NAD$^+$($\mathscr{E}^{\circ\prime} = -0.315$ V). Evidence suggests that the FAD group in dihydrolipoamide dehydrogenase never becomes fully reduced as $FADH_2$. Due to the precise positioning of the flavin and nicotinamide ring, electrons are rapidly transferred from the enzyme disulfide through FAD to NAD$^+$, so a reduced flavin anion ($FADH^-$) has but a transient existence. Thus, *FAD appears to function more as an electron conduit than as a source or sink of electrons.*

A Swinging Arm Transfers Intermediates. How are reaction intermediates channeled between E_2 (the core of the pyruvate dehydrogenase complex) and the E_1 and E_3 proteins on the outside? The key is the lipoamide group of E_2. The lipoic acid residue and the side chain of the Lys residue to which it is attached have a combined length of about 14 Å. This **lipoyllysyl arm** (*at right*) apparently acts as a long tether that swings the disulfide group from E_1 (where it picks up a hydroxyethyl group), to the E_2 active site (where the hydroxyethyl group is transferred to form acetyl-CoA), and from there to E_3 (where the reduced disulfide is reoxidized). The domains of E_2 that carry the lipoyllysyl arms are linked to the rest of the E_2 protein by a highly flexible Pro- and Ala-rich segment that contributes to the mobility of the lipoyllysyl arm. Because of the flexibility and reach of the lipoyllysyl arms, one E_1 protein can acetylate numerous E_2 proteins, and one E_3 protein can reoxidize

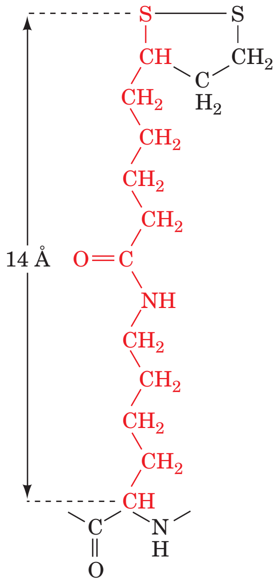

Lipoyllysyl arm (fully extended)

BOX 17-2 BIOCHEMISTRY IN HEALTH AND DISEASE

Arsenic Poisoning

The toxicity of arsenic has been known since ancient times. As(III) compounds such as **arsenite** (AsO_3^{3-}) and **organic arsenicals** are toxic because they bind to sulfhydryl compounds (including lipoamide) that can form bidentate adducts:

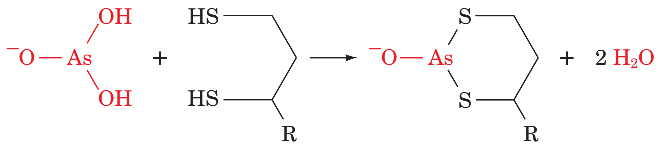

Arsenite **Dihydrolipoamide**

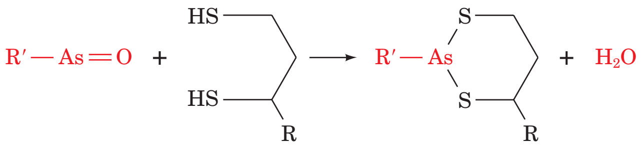

Organic arsenical

The inactivation of lipoamide-containing enzymes by arsenite, especially the pyruvate dehydrogenase and α-ketoglutarate dehydrogenase complexes, brings respiration to a halt. However, organic arsenicals are more toxic to microorganisms than they are to humans, apparently because of differences in the sensitivities of their various enzymes to the compounds. This differential toxicity is the basis for the early twentieth century use of organic arsenicals in the treatment of **syphilis** (a bacterial disease) and trypanosomiasis (a parasitic disease). These compounds were actually the first antibiotics, although, not surprisingly, they produced severe side effects.

Arsenic is often suspected as a poison in untimely deaths. It was long thought that Napoleon Bonaparte died from arsenic poisoning while in exile on the island of St. Helena, a suspicion that is strongly supported by the recent finding that a lock of his hair contains high levels of arsenic. But was it murder or environmental pollution? Arsenic-containing dyes were used in wallpaper at the time, and it was eventually determined that in damp weather, fungi convert the arsenic to a volatile compound. Surviving samples of the wallpaper from Napoleon's room in fact contain arsenic. Napoleon's arsenic poisoning may therefore have been unintentional.

Napoleon Bonaparte [© Victoria and Albert Museum/Art Resource.]

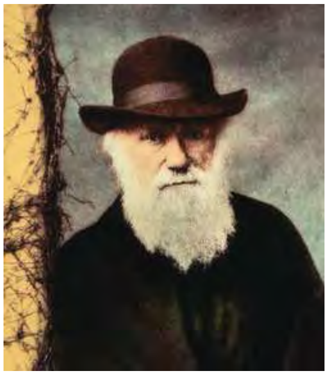

Charles Darwin [© Photo Researchers.]

Charles Darwin may also have been an unwitting victim of chronic arsenic poisoning. In the years following his epic voyage on the *Beagle,* Darwin was plagued by eczema, vertigo, headaches, gout, and nausea—all symptoms of arsenic poisoning. Fowler's solution, a widely used nineteenth century "tonic," contained 10 mg of arsenite per mL. Many individuals, quite possibly Darwin himself, took this "medication" for years.

several dihydrolipoamide groups. The lipoyllysyl arms probably protrude into the space between the E_2 core and the E_1E_3 outer shell (Fig. 17-5) and swing around in order to "visit" the active sites of E_1, E_2, and E_3. The entire pyruvate dehydrogenase complex can be inactivated by the reaction of the lipoamide group with certain arsenic-containing compounds (see Box 17-2).

CHECK YOUR UNDERSTANDING

Describe the five reactions of the pyruvate dehydrogenase multienzyme complex.

3 Enzymes of the Citric Acid Cycle

LEARNING OBJECTIVE

- Become familiar with the reactions catalyzed by the eight enzymes of the citric acid cycle, including those that generate CO_2, GTP, and the reduced coenzymes NADH and $FADH_2$.

In this section, we discuss the eight enzymes of the citric acid cycle. The elucidation of the mechanisms for each of these enzymes is the result of an enormous amount of experimental work. Even so, there remain questions about the mechanistic details of the enzymes and their regulatory properties.

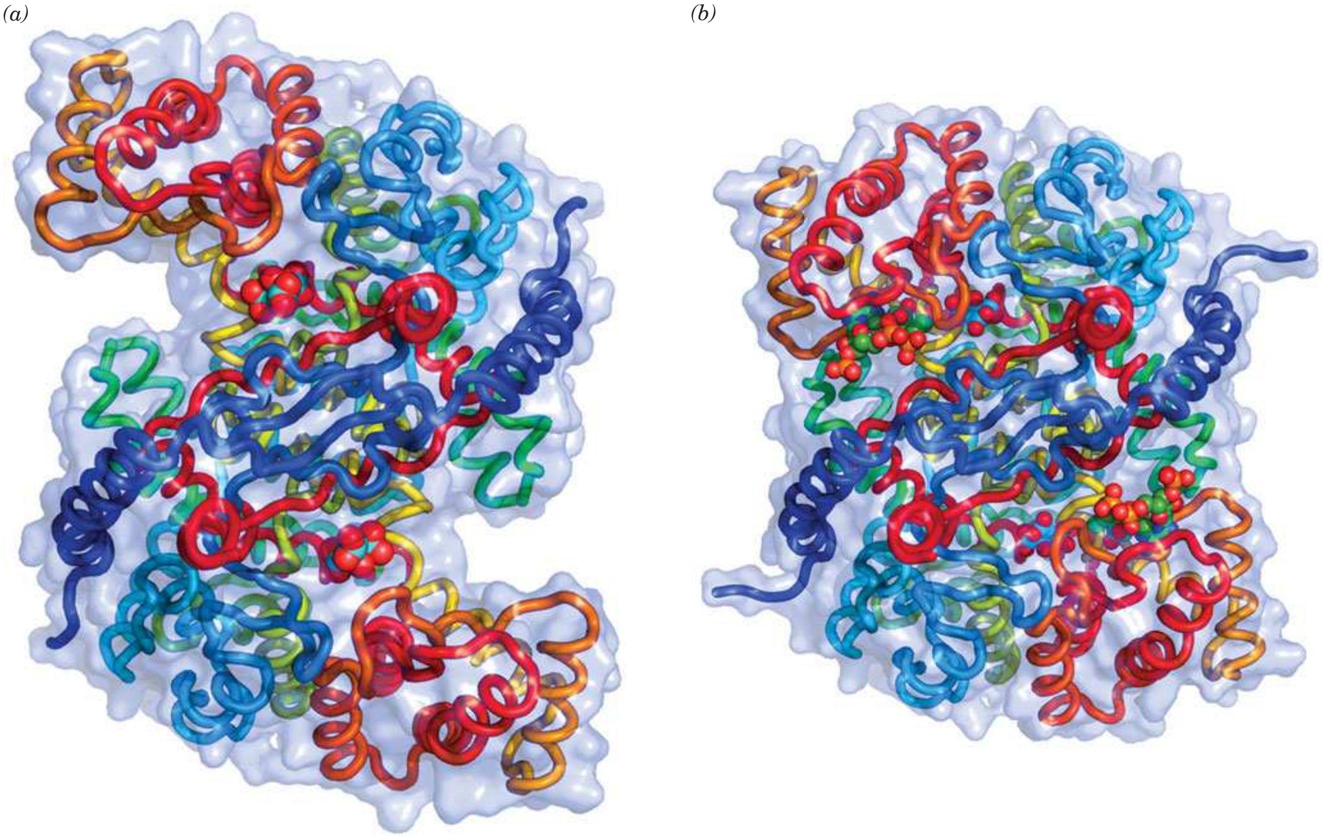

■ **Figure 17-9** | **Conformational changes in citrate synthase.** (*a*) The open conformation. (*b*) The closed, substrate-binding conformation. In both forms, the homodimeric protein is viewed along its twofold axis and is represented by its transparent molecular surface with its polypeptide chains drawn in worm form colored in rainbow order from blue at their N-termini to red at their C-termini. The reaction product citrate, which is bound to both enzymatic forms, and coenzyme A, which is also bound to the closed form, are shown in space-filling form with citrate C cyan, CoA C green, N blue, O red, and P orange. The large conformational shift between the open and closed forms entails 18° rotations of the small domains (*upper left and lower right)* relative to the large domains, resulting in relative interatomic movements of up to 15 Å. [Based on X-ray structures by James Remington and Robert Huber, Max-Planck-Institut für Biochemie, Martinsried, Germany. PDBids 1CTS and 2CTS.] **See Interactive Exercise 18.**

A | Citrate Synthase Joins an Acetyl Group to Oxaloacetate

Citrate synthase catalyzes the condensation of acetyl-CoA and oxaloacetate. This initial reaction of the citric acid cycle is the point at which carbon atoms (from carbohydrates, fatty acids, and amino acids) are "fed into the furnace" as acetyl-CoA. The citrate synthase reaction proceeds with an Ordered Sequential kinetic mechanism in which oxaloacetate binds before acetyl-CoA.

X-Ray studies show that the free enzyme (a homodimer) is in an "open" form, with two domains that form a cleft containing the substrate-binding site (Fig. 17-9*a*). When substrate binds, the smaller domain undergoes a remarkable 18° rotation, which closes the cleft (Fig. 17-9*b*). The existence of the "open" and "closed" forms explains the enzyme's Ordered Sequential kinetic behavior. *The conformational change generates the acetyl-CoA binding site and seals the oxaloacetate binding site so that solvent cannot reach the bound substrate.* We have seen similar conformational changes in adenylate kinase (Fig. 14-9) and hexokinase (Fig. 15-2), which prevent ATP hydrolysis.

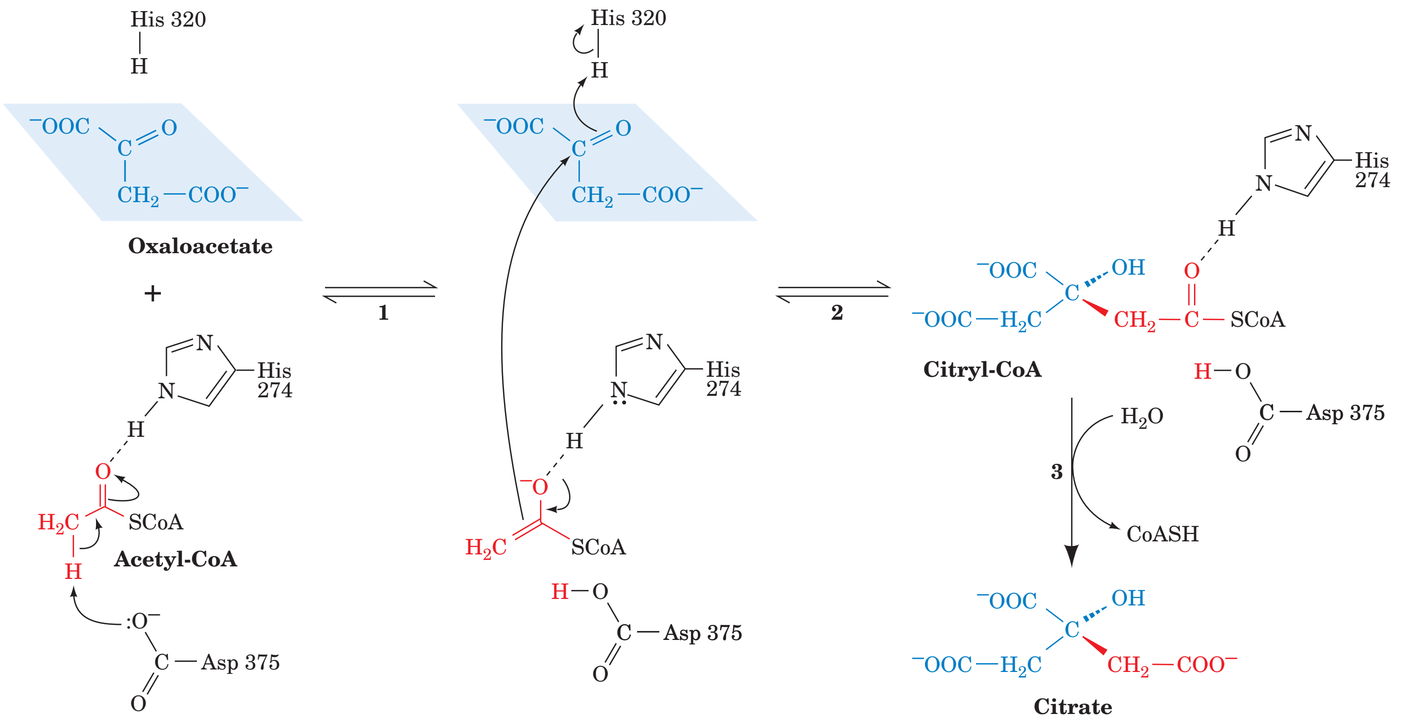
His 320
H
⁻OOC
C=O
CH₂—COO⁻
Oxaloacetate
+
N
His 274
H
O
H₂C
SCoA
Acetyl-CoA
H
:O⁻
C—Asp 375
O
1
His 320
H
⁻OOC
C=O
CH₂—COO⁻
N
His 274
H
⁻O
H₂C
SCoA
H—O
C—Asp 375
O
2
N
His 274
H
⁻OOC
OH
O
⁻OOC—H₂C
C
CH₂—C—SCoA
Citryl-CoA
H—O
C—Asp 375
O
3
H₂O
CoASH
⁻OOC
OH
⁻OOC—H₂C
C
CH₂—COO⁻
Citrate

Figure 17-10 | The mechanism of the citrate synthase reaction. His 274 and His 320 in their neutral forms and Asp 375 have been implicated as general acid–base catalysts. The rate-limiting step (**1**) is the formation of the acetyl-CoA enolate, which is stabilized by a hydrogen bond to the His 274. (**2**) The acetyl-CoA enolate then nucleophilically attacks oxaloacetate's carbonyl carbon. (**3**) The resulting intermediate, citryl-CoA, is hydrolyzed to yield citrate and CoA. [Mostly after Remington, *J.S., Curr. Opin. Struct. Biol.* **2,** 732 (1992).]

In the reaction mechanism proposed by James Remington, three ionizable side chains of citrate synthase participate in catalysis (Fig. 17-10):

1. The enol of acetyl-CoA is generated in the rate-limiting step of the reaction when Asp 375 (a base) removes a proton from the methyl group. His 274 forms a hydrogen bond with the enolate oxygen.
2. **Citryl-CoA** is formed in a concerted acid–base catalyzed step, in which the acetyl-CoA enolate (a nucleophile) attacks oxaloacetate. His 320 (an acid) donates a proton to oxaloacetate's carbonyl group. The citryl-CoA intermediate remains bound to the enzyme. Citrate synthase is one of the few enzymes that can directly form a carbon–carbon bond without the assistance of a metal ion cofactor.
3. Citryl-CoA is hydrolyzed to citrate and CoA. This hydrolysis provides the reaction's thermodynamic driving force ($\Delta G^{\circ\prime} = -31.5\ \text{kJ}\cdot\text{mol}^{-1}$). We shall see later why this reaction requires such a large, seemingly wasteful, expenditure of free energy.

B | Aconitase Interconverts Citrate and Isocitrate

Aconitase catalyzes the reversible isomerization of citrate and **isocitrate,** with ***cis*-aconitate** as an intermediate:

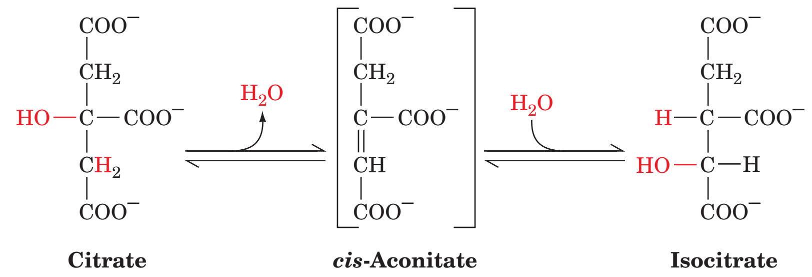
COO⁻
CH₂
HO—C—COO⁻
CH₂
COO⁻
Citrate
H₂O
COO⁻
CH₂
C—COO⁻
CH
COO⁻
cis-Aconitate
H₂O
COO⁻
CH₂
H—C—COO⁻
HO—C—H
COO⁻
Isocitrate

The reaction begins with a dehydration step in which a proton and an OH group are removed. Since citrate has two carboxymethyl groups substituent to its central C atom, it is prochiral rather than chiral. Thus, although water might conceivably be eliminated from either of the two carboxymethyl arms, aconitase removes water only from citrate's lower (*pro-R*) arm (i.e., such that the product molecule has the *R* configuration; Box 4-2).

Aconitase contains a **[4Fe–4S] iron–sulfur cluster** (an arrangement of four iron atoms and four sulfur atoms, Section 18-2C) that presumably coordinates the OH group of citrate to facilitate its elimination. Iron–sulfur clusters normally participate in redox processes; aconitase is an intriguing exception.

The second stage of the aconitase reaction is rehydration of the double bond of *cis*-aconitate to form isocitrate. Although addition of water across the double bond of *cis*-aconitate could potentially yield four stereoisomers, aconitase catalyzes the stereospecific addition of OH^- and H^+ to produce only one isocitrate stereoisomer. The ability of an enzyme to differentiate its substrate's *pro-R* and *pro-S* groups was not appreciated until 1948, when Alexander Ogston pointed out that aconitase can distinguish between the two $—CH_2COO^-$ groups of citrate when it is bound to the enzyme (Section 11-1B).

C | NAD^+-Dependent Isocitrate Dehydrogenase Releases CO_2

Isocitrate dehydrogenase catalyzes the oxidative decarboxylation of isocitrate to α-ketoglutarate. This reaction produces the first CO_2 and NADH of the citric acid cycle. Note that this CO_2 began the citric acid cycle as a component of oxaloacetate, not of acetyl-CoA (Fig. 17-2). (Mammalian tissues also contain an isocitrate dehydrogenase isozyme that uses $NADP^+$ as a cofactor.)

NAD^+-dependent isocitrate dehydrogenase, which also requires a Mn^{2+} or Mg^{2+} cofactor, catalyzes the oxidation of a secondary alcohol (isocitrate) to a ketone **(oxalosuccinate)** followed by the decarboxylation of the carboxyl group β to the ketone (Fig. 17-11). Mn^{2+} helps polarize the newly formed carbonyl group. The isocitrate dehydrogenase reaction mechanism is similar to that of phosphogluconate dehydrogenase in the pentose phosphate pathway (Section 15-6A).

The oxalosuccinate intermediate of the isocitrate dehydrogenase reaction exists only transiently, and its existence was therefore difficult to confirm. However, an enzymatic reaction can be slowed by mutating catalytically important residues—in this case, Tyr 160 and Lys 230—to

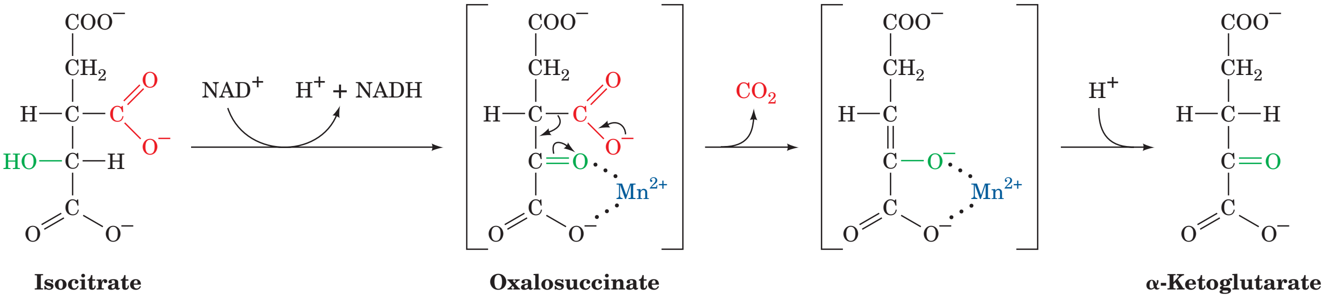

Figure 17-11 | The reaction mechanism of isocitrate dehydrogenase. Oxalosuccinate is shown in brackets because it does not dissociate from the enzyme.

create kinetic "bottlenecks" so that reaction intermediates accumulate. Accordingly, crystals of the mutant isocitrate dehydrogenase were exposed to the substrate isocitrate and immediately visualized via X-ray crystallography using rapid measurement techniques that require the highly intense X-rays generated by a synchrotron. These studies revealed the oxalosuccinate intermediate in the active site of the enzyme.

D | α-Ketoglutarate Dehydrogenase Resembles Pyruvate Dehydrogenase

α-Ketoglutarate dehydrogenase catalyzes the oxidative decarboxylation of an α-keto acid (α-ketoglutarate). This reaction produces the second CO_2 and NADH of the citric acid cycle:

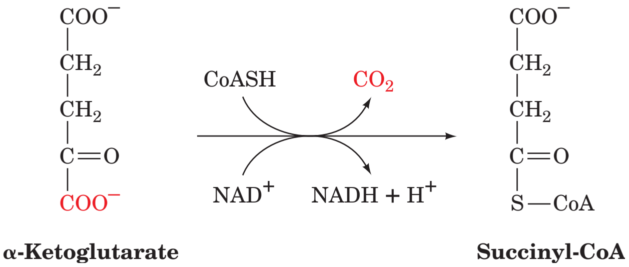

Again, this CO_2 entered the citric acid cycle as a component of oxaloacetate rather than of acetyl-CoA (Fig. 17-2). Thus, although each round of the citric acid cycle oxidizes two C atoms to CO_2, the C atoms of the entering acetyl groups are not oxidized to CO_2 until subsequent rounds of the cycle.

The α-ketoglutarate dehydrogenase reaction chemically resembles the reaction catalyzed by the pyruvate dehydrogenase multienzyme complex. α-Ketoglutarate dehydrogenase is a multienzyme complex containing **α-ketoglutarate dehydrogenase (E_1), dihydrolipoyl transsuccinylase (E_2),** and **dihydrolipoyl dehydrogenase (E_3).** Indeed, this E_3 is identical to the E_3 of the pyruvate dehydrogenase complex (a third member of the **2-keto acid dehydrogenase** family of multienzyme complexes is **branched-chain α-keto acid dehydrogenase,** which participates in the degradation of isoleucine, leucine, and valine; Section 21-4). The reactions catalyzed by the α-ketoglutarate dehydrogenase complex occur by mechanisms identical to those of the pyruvate dehydrogenase complex. Again, the product is a "high-energy" thioester, in this case, **succinyl-CoA.**

E | Succinyl-CoA Synthetase Produces GTP

Succinyl-CoA synthetase (also called **succinate thiokinase**) couples the cleavage of the "high-energy" succinyl-CoA to the synthesis of a "high-energy" nucleoside triphosphate (both names for the enzyme reflect the reverse reaction). Mammalian enzymes usually synthesize GTP from GDP + P_i, whereas plant and bacterial enzymes usually synthesize ATP from ADP + P_i. These reactions are nevertheless energetically equivalent since ATP and GTP are rapidly interconverted through the action of nucleoside diphosphate kinase (Section 14-2C):

$$\text{GTP} + \text{ADP} \rightleftharpoons \text{GDP} + \text{ATP} \qquad \Delta G^{\circ\prime} = 0$$

How does succinyl-CoA synthetase couple the exergonic cleavage of succinyl-CoA ($\Delta G^{\circ\prime} = -32.6 \text{ kJ} \cdot \text{mol}^{-1}$) to the endergonic formation of a nucleoside triphosphate ($\Delta G^{\circ\prime} = 30.5 \text{ kJ} \cdot \text{mol}^{-1}$) from the corresponding nucleoside diphosphate and P_i? This question was answered by an experiment with isotopically labeled ADP. In the absence of succinyl-CoA, the spinach enzyme catalyzes the transfer of the γ-phosphoryl group from ATP to [^{14}C]ADP, producing [^{14}C]ATP. Such an isotope-exchange reaction suggests the participation of a phosphoryl-enzyme intermediate that mediates the reaction sequence

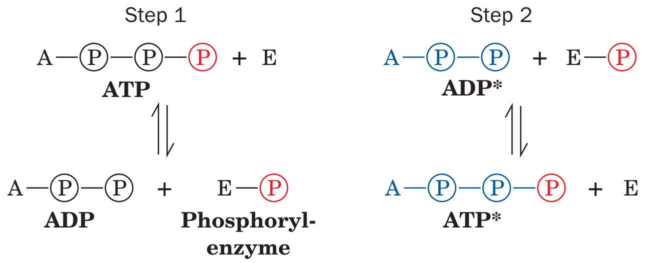
Step 1
A—Ⓟ—Ⓟ—Ⓟ + E
ATP
A—Ⓟ—Ⓟ + E—Ⓟ
ADP
Phosphoryl-enzyme
Step 2
A—Ⓟ—Ⓟ + E—Ⓟ
ADP*
A—Ⓟ—Ⓟ—Ⓟ + E
ATP*

This information led to the isolation of a kinetically active phosphoryl-enzyme in which the phosphoryl group is covalently linked to the N3 position of a His residue. A three-step mechanism for succinyl-CoA synthetase is shown in Fig. 17-12.

1. Succinyl-CoA reacts with P_i to form **succinyl-phosphate** and CoA.
2. The phosphoryl group is then transferred from succinyl-phosphate to a His residue on the enzyme, releasing succinate.
3. The phosphoryl group on the enzyme is transferred to GDP, forming GTP.

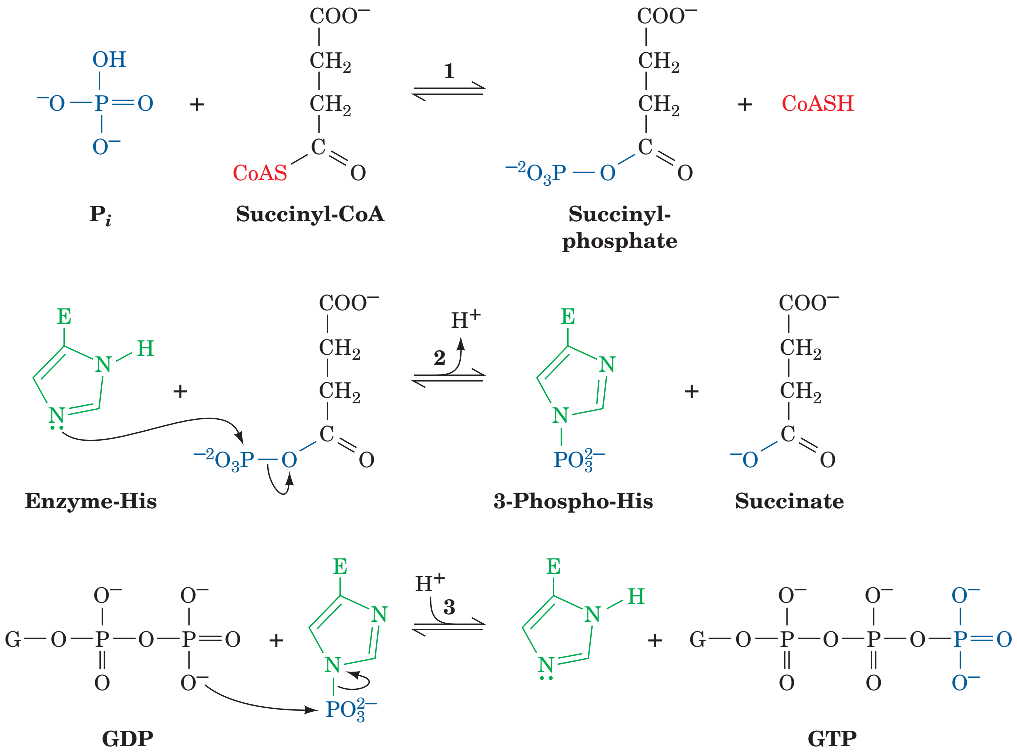
OH
⁻O—P=O
O⁻
P$_i$
COO⁻
CH$_2$
CH$_2$
C
CoAS
O
Succinyl-CoA
1
Succinyl-phosphate
$^{-2}O_3P$—O
CoASH
E
N
H
N
Enzyme-His
H⁺
2
3-Phospho-His
PO$_3^{2-}$
⁻O
Succinate
G—O—P—O—P=O
GDP
H⁺
3
GTP

■ **Figure 17-12 | The reaction catalyzed by succinyl-CoA synthetase.** (**1**) Formation of succinyl-phosphate, a "high-energy" acyl phosphate. (**2**) Formation of phosphoryl-His, a "high-energy" intermediate. (**3**) Transfer of the phosphoryl group to GDP, forming GTP.

Note that in each of these steps, *the energy of succinyl-CoA is conserved through the formation of "high-energy" compounds: first, succinyl-phosphate, then a 3-phospho-His residue, and finally GTP.* The process is reminiscent of passing a hot potato. The reaction catalyzed by succinyl-CoA synthetase is another example of substrate-level phosphorylation (ATP synthesis that does not directly depend on the presence of oxygen).

By this point in the citric acid cycle, one acetyl equivalent has been completely oxidized to two CO_2. Two NADH and one GTP (equivalent to one ATP) have also been generated. In order to complete the cycle, succinate must be converted back to oxaloacetate. This is accomplished by the cycle's remaining three reactions.

F | Succinate Dehydrogenase Generates $FADH_2$

Succinate dehydrogenase catalyzes the stereospecific dehydrogenation of succinate to fumarate:

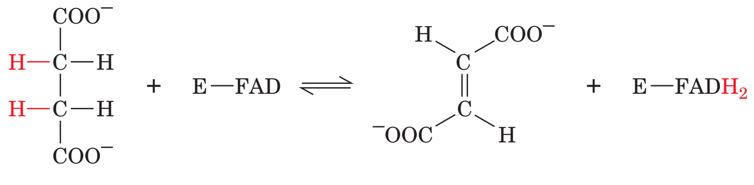

Succinate **Fumarate**

This enzyme is strongly inhibited by malonate,

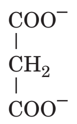
Malonate

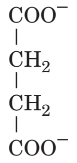
Succinate

a structural analog of succinate and a classic example of a competitive inhibitor. When Krebs was formulating his theory of the citric acid cycle, the inhibition of cellular respiration by malonate provided one of the clues that succinate plays a catalytic role in oxidizing substrates and is not just another substrate.

Succinate dehydrogenase contains an FAD prosthetic group that is covalently linked to the enzyme via a His residue (Fig. 17-13; in most other FAD-containing enzymes, the FAD is held tightly but noncovalently). In general, FAD functions biochemically to oxidize alkanes (such as succinate) to alkenes (such as fumarate), whereas NAD^+ participates in the more exergonic oxidation of alcohols to aldehydes or ketones (e.g., in the reaction catalyzed by isocitrate dehydrogenase). The dehydrogenation of succinate produces $FADH_2$, which must be reoxidized before succinate dehydrogenase can undertake another catalytic cycle. The reoxidation of $FADH_2$ occurs when its electrons are passed to the mitochondrial electron transport chain, which we shall examine in Section 18-2. Succinate dehydrogenase is the only membrane-bound enzyme of the citric acid cycle (the others are components of the mitochondrial matrix), so it is positioned to funnel electrons directly into the electron transport machinery of the mitochondrial membrane.

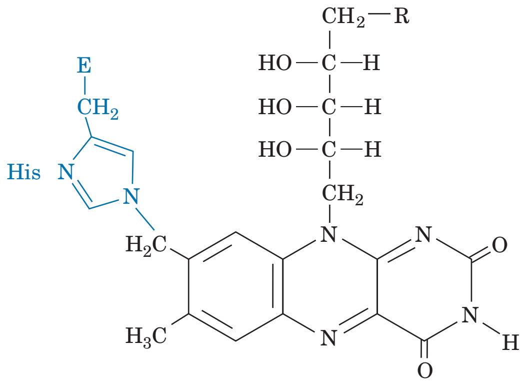

FAD

Figure 17-13 | The covalent attachment of FAD to a His residue of succinate dehydrogenase. R represents the ADP moiety.

G | Fumarase Produces Malate

Fumarase (fumarate hydratase) catalyzes the hydration of the double bond of fumarate to form malate. The hydration reaction proceeds via a carbanion transition state. OH^- addition occurs before H^+ addition:

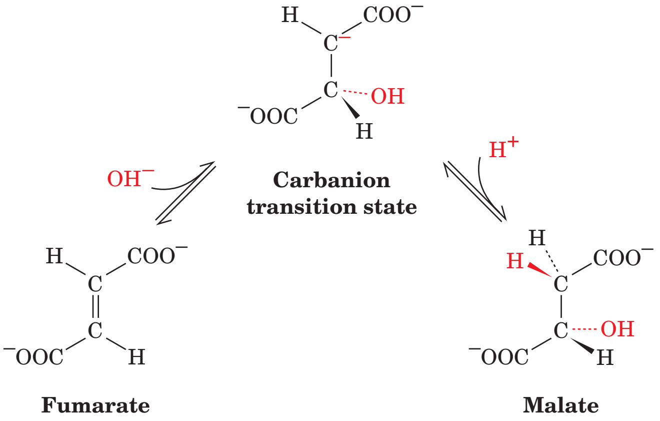

H | Malate Dehydrogenase Regenerates Oxaloacetate

Malate dehydrogenase catalyzes the final reaction of the citric acid cycle, the regeneration of oxaloacetate. The hydroxyl group of malate is oxidized in an NAD^+-dependent reaction:

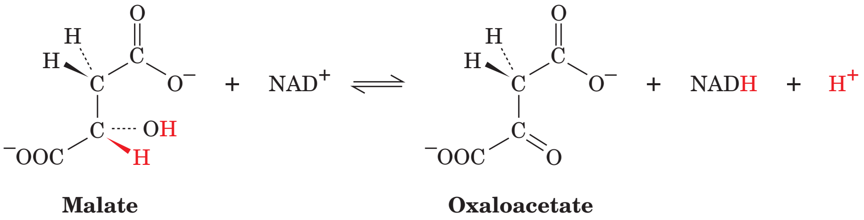

Transfer of the hydride ion to NAD^+ occurs by the same mechanism used for hydride ion transfer in lactate dehydrogenase and alcohol dehydrogenase (Section 15-3). X-Ray crystallographic comparisons of the NAD^+-binding domains of these three enzymes indicate that they are remarkably similar, consistent with the proposal that all NAD^+-binding domains evolved from a common ancestor.

The $\Delta G^{\circ\prime}$ value for the malate dehydrogenase reaction is $+29.7\ \text{kJ}\cdot\text{mol}^{-1}$; therefore, the concentration of oxaloacetate at equilibrium (and under cellular conditions) is very low relative to malate. Recall, however, that the reaction catalyzed by citrate synthase, the first reaction of the citric acid cycle, is highly exergonic ($\Delta G^{\circ\prime} = -31.5\ \text{kJ}\cdot\text{mol}^{-1}$) because of the cleavage of the thioester bond of citryl-CoA. We can now understand the necessity for such a seemingly wasteful process. It allows citrate formation to be exergonic even at the low oxaloacetate concentrations present in cells and thus helps keep the citric acid cycle rolling.

■ CHECK YOUR UNDERSTANDING

Draw the structures of the eight intermediates of the citric acid cycle and name the enzymes that catalyze their interconversions.

Which steps of the citric acid cycle release CO_2 as a product? Which steps produce NADH or $FADH_2$? Which step produces GTP?

Write the net equations for oxidation of pyruvate, the acetyl group of acetyl-CoA, and glucose to CO_2 and H_2O.

4 Regulation of the Citric Acid Cycle

The capacity of the citric acid cycle to generate energy for cellular needs is closely regulated. The availability of substrates, the need for citric acid cycle intermediates as biosynthetic precursors, and the demand for ATP all influence the operation of the cycle. There is some evidence that the

LEARNING OBJECTIVE

- Understand how the need for energy regulates the citric acid cycle capacity at the pyruvate dehydrogenase step and at the three rate-controlling steps of the cycle.

enzymes of the citric acid cycle are physically associated, which might contribute to their coordinated regulation. Before we examine the various mechanisms for regulating the citric acid cycle, let us briefly consider the energy-generating capacity of the cycle.

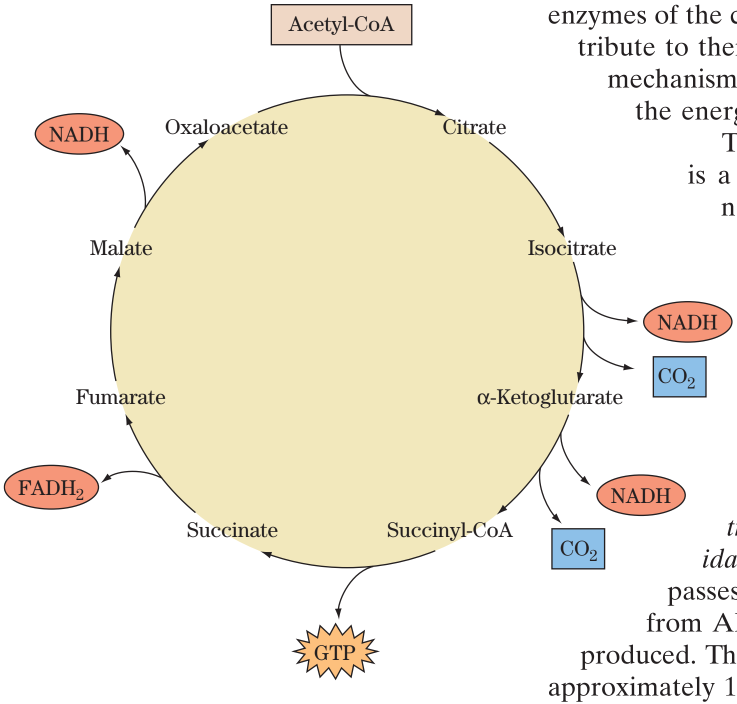

Figure 17-14 | Products of the citric acid cycle. For every two carbons that are oxidized to CO_2, electrons are recovered in the form of three NADH and one $FADH_2$. One GTP (or ATP) is also produced.

The oxidation of one acetyl group to two molecules of CO_2 is a four-electron pair process (but keep in mind that it is not the carbon atoms of the incoming acetyl group that are oxidized). For every acetyl-CoA that enters the cycle, three molecules of NAD^+ are reduced to NADH, which accounts for three of the electron pairs, and one molecule of FAD is reduced to $FADH_2$, which accounts for the fourth electron pair. In addition, one GTP (or ATP) is produced (Fig. 17-14).

The electrons carried by NADH and $FADH_2$ are funneled into the electron-transport chain, which culminates with the reduction of O_2 to H_2O. The energy of electron transport is conserved in the synthesis of ATP by oxidative phosphorylation (Section 18-3). For every NADH that passes its electrons on, approximately 2.5 ATP are produced from ADP + P_i. For every $FADH_2$, approximately 1.5 ATP are produced. Thus, one turn of the citric acid cycle ultimately generates approximately 10 ATP. We will see in Section 18-3C why these values are only approximations.

When glucose is converted to two molecules of pyruvate by glycolysis, two molecules of ATP are generated and two molecules of NAD^+ are reduced (Section 15-1). The NADH molecules yield approximately 5 molecules of ATP on passing their electrons to the electron-transport chain. When the two pyruvate molecules are converted to two acetyl-CoA by the pyruvate dehydrogenase complex, the two molecules of NADH produced in that process also eventually give rise to ~5 ATP. Two turns of the citric acid cycle (one for each acetyl group) generate ~20 ATP. Thus, one molecule of glucose can potentially yield ~32 molecules of ATP under aerobic conditions, when the citric acid cycle is operating. In contrast, only 2 molecules of ATP are produced per glucose molecule under anaerobic conditions.

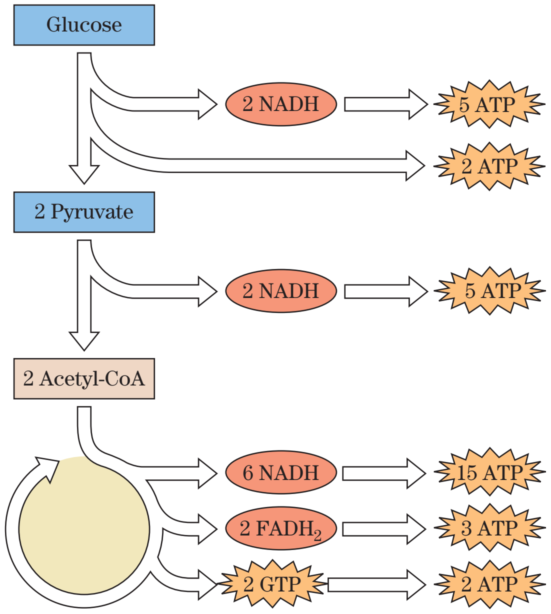

A | Pyruvate Dehydrogenase Is Regulated by Product Inhibition and Covalent Modification

Given the large amount of ATP that can potentially be generated from carbohydrate catabolism via the citric acid cycle, it is not surprising that the entry of acetyl units derived from carbohydrate sources is regulated. The decarboxylation of pyruvate by the pyruvate dehydrogenase complex is irreversible, and since there are no other pathways in mammals for the synthesis of acetyl-CoA from pyruvate, it is crucial that the reaction be precisely controlled. Two regulatory systems are used:

1. ***Product inhibition by NADH and acetyl-CoA.*** These compounds compete with NAD^+ and CoA for binding sites on their respective enzymes. They also drive the reversible transacetylase (E_2) and dihydrolipoyl dehydrogenase (E_3) reactions backward (Fig. 17-6). High $[NADH]/[NAD^+]$ and [acetyl-CoA]/[CoA] ratios therefore maintain E_2 in the acetylated form, incapable of accepting the hydroxyethyl group from the TPP on E_1. This, in turn, ties up the TPP on the E_1 subunit in its hydroxyethyl form, decreasing the rate of pyruvate decarboxylation.
2. ***Covalent modification by phosphorylation/dephosphorylation of E_1.*** In eukaryotes, the products of the pyruvate dehydrogenase reaction, NADH and acetyl-CoA, also activate the pyruvate dehydrogenase kinase associated with the enzyme complex. The resulting phosphorylation of a specific dehydrogenase Ser residue inactivates the pyruvate dehydrogenase complex (Fig. 17-15). Insulin, the hormone that signals fuel abundance, reverses the inactivation by activating pyruvate dehydrogenase phosphatase, which removes the phosphate groups from pyruvate dehydrogenase. Recall that insulin also activates glycogen synthesis by activating phosphoprotein phosphatase (Section 16-3B). Thus, in response to increases in blood [glucose], insulin promotes the synthesis of acetyl-CoA as well as glycogen.

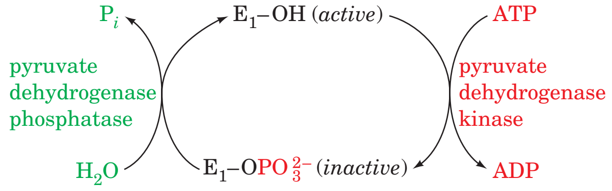
P_i
E_1–OH (*active*)
ATP
pyruvate dehydrogenase phosphatase
pyruvate dehydrogenase kinase
H_2O
E_1–OPO_3^{2-} (*inactive*)
ADP

Figure 17-15 | Covalent modification of eukaryotic pyruvate dehydrogenase. E_1 is inactivated by the specific phosphorylation of one of its Ser residues in a reaction catalyzed by pyruvate dehydrogenase kinase. This phosphoryl group is hydrolyzed through the action of pyruvate dehydrogenase phosphatase, thereby reactivating E_1.

Other regulators of the pyruvate dehydrogenase system include pyruvate and ADP, which inhibit pyruvate dehydrogenase kinase, and Ca^{2+}, which inhibits pyruvate dehydrogenase kinase and activates pyruvate dehydrogenase phosphatase. In contrast to the glycogen metabolism control system (Section 16-3B), pyruvate dehydrogenase activity is unaffected by cAMP.

B | Three Enzymes Control the Rate of the Citric Acid Cycle

To understand how a metabolic pathway is controlled, we must identify the enzymes that catalyze its rate-determining steps, the *in vitro* effectors of the enzymes, and the *in vivo* concentrations of these substances. *A proposed mechanism of flux control must operate within the physiological concentration range of the effector.*

Identifying the rate-determining steps of the citric acid cycle is more difficult than it is for glycolysis because most of the cycle's metabolites are present in both mitochondria and cytosol and we do not know their distribution between these two compartments (recall that identifying a pathway's rate-determining steps requires determining the ΔG of each of its reactions from the concentrations of its substrates and products). However, we shall assume that the compartments are in equilibrium and use the total cell concentrations of these substances to estimate their

Table 17-2 Standard Free Energy Changes ($\Delta G^{\circ\prime}$) and Physiological Free Energy Changes (ΔG) of Citric Acid Cycle Reactions

Reaction	Enzyme	$\Delta G^{\circ\prime}$ ($\text{kJ} \cdot \text{mol}^{-1}$)	ΔG ($\text{kJ} \cdot \text{mol}^{-1}$)
1	Citrate synthase	−31.5	Negative
2	Aconitase	~5	~0
3	Isocitrate dehydrogenase	−21	Negative
4	α-Ketoglutarate dehydrogenase	−33	Negative
5	Succinyl-CoA synthetase	−2.1	~0
6	Succinate dehydrogenase	+6	~0
7	Fumarase	−3.4	~0
8	Malate dehydrogenase	+29.7	~0

mitochondrial concentrations. Table 17-2 gives the standard free energy changes for the eight citric acid cycle enzymes and estimates of the physiological free energy changes for the reactions in heart muscle or liver tissue. We can see that *three of the enzymes are likely to function far from equilibrium under physiological conditions (negative ΔG): citrate synthase, NAD$^+$-dependent isocitrate dehydrogenase, and α-ketoglutarate dehydrogenase.* These are therefore the rate-determining enzymes of the cycle.

In heart muscle, where the citric acid cycle is active, the flux of metabolites through the citric acid cycle is proportional to the rate of cellular oxygen consumption. *Because oxygen consumption, NADH reoxidation, and ATP production are tightly coupled (Section 18-3), the citric acid cycle must be regulated by feedback mechanisms that coordinate NADH production with energy expenditure.* Unlike the rate-limiting enzymes of glycolysis and glycogen metabolism, which regulate flux by elaborate systems of allosteric control, substrate cycles, and covalent modification, the regulatory enzymes of the citric acid cycle seem to control flux primarily by three simple mechanisms: (1) substrate availability, (2) product inhibition, and (3) competitive feedback inhibition by intermediates further along the cycle. Some of the major regulatory mechanisms are diagramed in Fig. 17-16. There is no single flux-control point in the citric acid cycle; rather, flux control is distributed among several enzymes.

Perhaps the most crucial regulators of the citric acid cycle are its substrates, acetyl-CoA and oxaloacetate, and its product, NADH. Both acetyl-CoA and oxaloacetate are present in mitochondria at concentrations that do not saturate citrate synthase. The metabolic flux through the enzyme therefore varies with substrate concentration and is controlled by substrate availability. We have already seen that the production of acetyl-CoA from pyruvate is regulated by the activity of pyruvate dehydrogenase. The concentration of oxaloacetate, which is in equilibrium with malate, fluctuates with the [NADH]/[NAD$^+$] ratio according to the equilibrium expression

$$K = \frac{[\text{oxaloacetate}][\text{NADH}]}{[\text{malate}][\text{NAD}^+]}$$

If, for example, the muscle workload and respiration rate increase, mitochondrial [NADH] decreases. The consequent increase in [oxaloacetate] stimulates the citrate synthase reaction, which controls the rate of citrate formation.

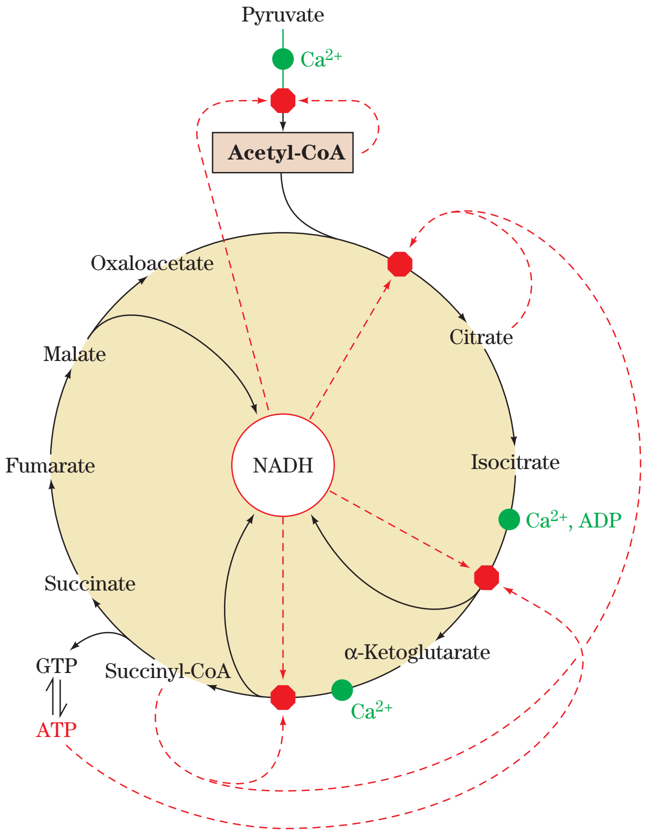

Figure 17-16 | Regulation of the citric acid cycle. This diagram of the citric acid cycle, which includes the pyruvate dehydrogenase reaction, indicates points of inhibition (*red octagons*) and the pathway intermediates that function as inhibitors (*dashed red arrows*). ADP and Ca^{2+} (*green dots*) are activators. **See the Animated Figures.**

Aconitase functions close to equilibrium, so the rate of citrate consumption depends on the activity of NAD^+-dependent isocitrate dehydrogenase, which is strongly inhibited *in vitro* by its product NADH. Citrate synthase is also inhibited by NADH but is less sensitive than isocitrate dehydrogenase to changes in [NADH].

Other instances of product inhibition in the citric acid cycle are the inhibition of citrate synthase by citrate (citrate competes with oxaloacetate) and the inhibition of α-ketoglutarate dehydrogenase by NADH and succinyl-CoA. Succinyl-CoA also competes with acetyl-CoA in the citrate synthase reaction (competitive feedback inhibition). This interlocking system helps keep the citric acid cycle coordinately regulated and the concentrations of its intermediates within reasonable bounds.

Additional Regulatory Mechanisms. *In vitro* studies of citric acid cycle enzymes have identified a few allosteric activators and inhibitors. ADP is an allosteric activator of isocitrate dehydrogenase, whereas ATP inhibits the enzyme. Ca^{2+}, in addition to its many other cellular functions, regulates the citric acid cycle at several points. It activates pyruvate dehydrogenase phosphatase (Fig. 17-15), which in turn activates the pyruvate dehydrogenase complex to produce acetyl-CoA. Ca^{2+} also activates both isocitrate dehydrogenase and α-ketoglutarate dehydrogenase (Fig. 17-16). Thus Ca^{2+}, the signal that stimulates muscle contraction, also stimulates the production of the ATP to fuel it.

CHECK YOUR UNDERSTANDING

Which steps of the citric acid cycle regulate flux through the cycle?

Describe the role of Ca^{2+}, acetyl-CoA, and NADH in regulating pyruvate dehydrogenase and the citric acid cycle.

5 Reactions Related to the Citric Acid Cycle

LEARNING OBJECTIVES

- Understand that the citric acid cycle provides metabolites for other pathways and can be replenished by other pathways.
- Understand that some organisms use the glyoxylate cycle, a variant of the citric acid cycle, for the net conversion of acetyl-CoA to oxaloacetate.

At first glance, a metabolic pathway appears to be either catabolic, with the release and conservation of free energy, or anabolic, with a requirement for free energy. The citric acid cycle is catabolic, of course, because it involves degradation and is a major free-energy conservation system in most organisms. Cycle intermediates are required in only catalytic amounts to maintain the degradative function of the cycle. However, several biosynthetic pathways use citric acid cycle intermediates as starting materials for anabolic reactions. The citric acid cycle is therefore **amphibolic** (both anabolic and catabolic). In this section, we examine some of the reactions that feed intermediates into the citric acid cycle or draw them off; we also examine the **glyoxylate cycle,** a variation of the citric acid cycle that occurs only in plants and converts acetyl-CoA to oxaloacetate. Some of the reactions that use and replenish citric acid cycle intermediates are summarized in Fig. 17-17.

A | Other Pathways Use Citric Acid Cycle Intermediates

Reactions that utilize and therefore drain citric acid cycle intermediates are called **cataplerotic reactions** (emptying; Greek: *cata,* down + *plerotikos,* to fill). These reactions serve not only to synthesize important products but also to avoid the inappropriate buildup of citric acid cycle intermediates in the mitochondrion, for example, when there is a high rate of breakdown of amino acids to citric acid cycle intermediates. Cataplerotic reactions occur in the following pathways:

1. **Glucose biosynthesis** (gluconeogenesis) utilizes oxaloacetate (Section 16-4). Because gluconeogenesis takes place in the cytosol, oxaloacetate must be converted to malate or aspartate for transport

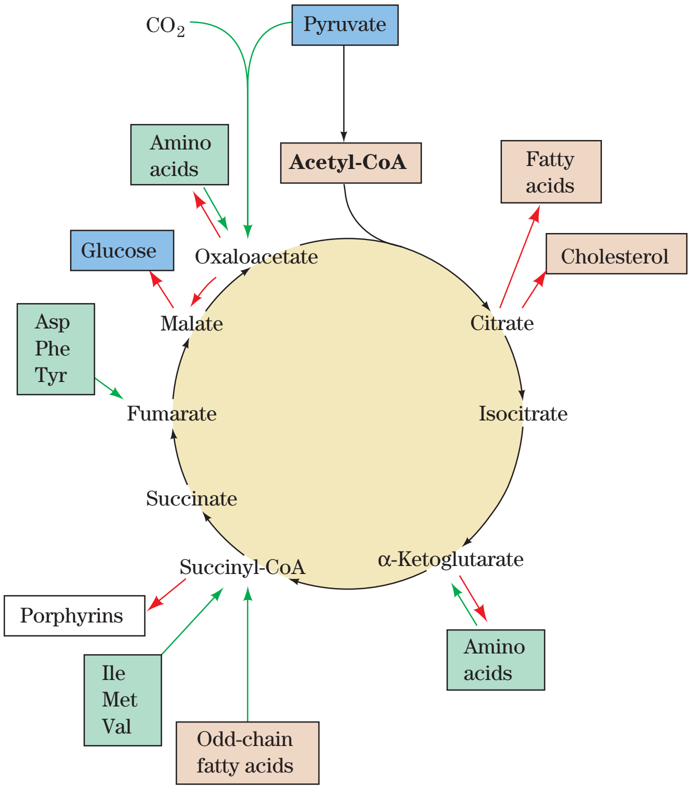

Figure 17-17 | Amphibolic functions of the citric acid cycle. The diagram indicates the positions at which intermediates are drawn off by cataplerotic reactions for use in anabolic pathways (*red arrows*) and the points where anaplerotic reactions replenish cycle intermediates (*green arrows*). Reactions involving amino acid transamination and deamination are reversible, so their direction varies with metabolic demand. **See the Animated Figures.**

out of the mitochondrion (Fig. 16-20). Since the citric acid cycle is a cyclical pathway, any of its intermediates can be converted to oxaloacetate and used for gluconeogenesis.

2. **Fatty acid biosynthesis** is a cytosolic process that requires acetyl-CoA. Acetyl-CoA is generated in the mitochondrion and is not transported across the mitochondrial membrane. *Cytosolic acetyl-CoA is therefore generated by the breakdown of citrate, which can cross the membrane, in a reaction catalyzed by* ***ATP-citrate lyase*** (Section 20-4A). This reaction uses the free energy of ATP to "undo" the citrate synthase reaction:

$$\text{ATP} + \text{citrate} + \text{CoA} \longrightarrow \text{ADP} + \text{P}_i + \text{oxaloacetate} + \text{acetyl–CoA}$$

3. **Amino acid biosynthesis** uses α-ketoglutarate and oxaloacetate as starting materials. For example, α-ketoglutarate is converted to glutamate by reductive amination catalyzed by a **glutamate dehydrogenase** that utilizes either NADH or NADPH:

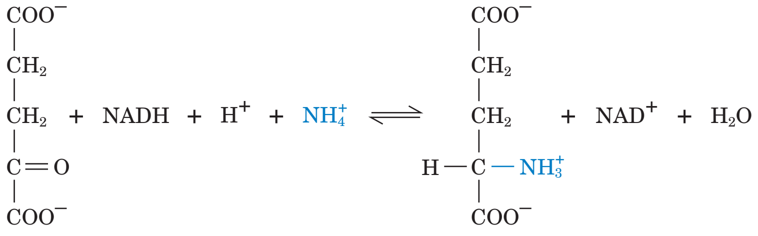

α-Ketoglutarate **Glutamate**

Oxaloacetate undergoes transamination with alanine to produce aspartate and pyruvate (Section 21-2A):

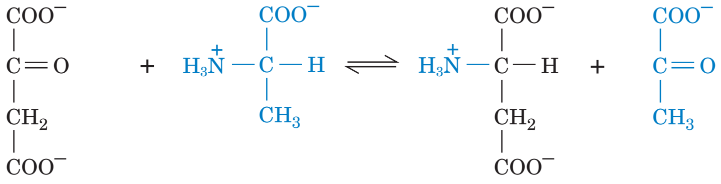

Oxaloacetate **Alanine** **Aspartate** **Pyruvate**

B | Some Reactions Replenish Citric Acid Cycle Intermediates

In aerobic organisms, the citric acid cycle is the major source of free energy, and hence the catabolic function of the citric acid cycle cannot be interrupted: Cycle intermediates that have been siphoned off must be replenished. The replenishing reactions are called **anaplerotic reactions** (filling up; Greek: *ana,* up + *plerotikos,* to fill). The most important of these reactions is catalyzed by pyruvate carboxylase, which produces oxaloacetate from pyruvate:

$$\text{Pyruvate} + \text{CO}_2 + \text{ATP} + \text{H}_2\text{O} \longrightarrow \text{oxaloacetate} + \text{ADP} + \text{P}_i$$

(This is also one of the first steps of gluconeogenesis; Section 16-4A). Pyruvate carboxylase "senses" the need for more citric acid cycle intermediates through its activator, acetyl-CoA. *Any decrease in the rate of the cycle caused by insufficient oxaloacetate or other intermediates allows the concentration of acetyl-CoA to rise.* This activates pyruvate carboxylase, which replenishes oxaloacetate. The reactions of the citric acid cycle convert the oxaloacetate to citrate, α-ketoglutarate, succinyl-CoA, and so on, until all the intermediates are restored to appropriate levels.

An increase in the concentrations of citric acid cycle intermediates supports increased flux of acetyl groups through the cycle. For example, flux through the citric acid cycle may increase as much as 60- to 100-fold in muscle cells during intense exercise. Not all of this increase is due to elevated concentrations of cycle intermediates (which only increase about fourfold), because other regulatory mechanisms (as described in Section 17-4B) also promote flux through the rate-controlling steps of the cycle.

During exercise, some of the pyruvate generated by increased glycolytic flux is directed toward oxaloacetate synthesis as catalyzed by pyruvate carboxylase. Pyruvate can also accept an amino group from glutamate (a transamination reaction) to generate alanine (the amino acid counterpart of pyruvate) and the citric acid cycle intermediate α-ketoglutarate (the ketone counterpart of glutamate). Both of these mechanisms help the citric acid cycle efficiently catabolize the acetyl groups derived—also from pyruvate—by the reactions of the pyruvate dehydrogenase complex.

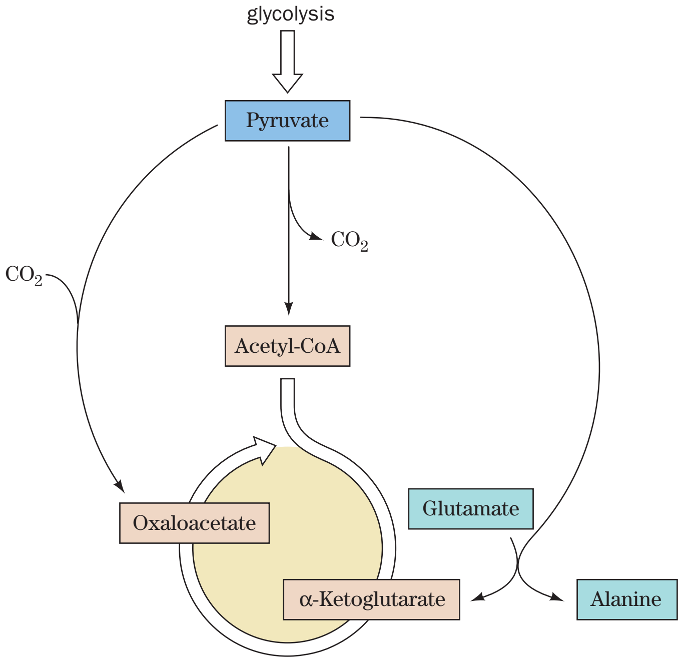

The end result is increased production of ATP to power muscle contraction.

Other metabolites that feed into the citric acid cycle are succinyl-CoA, a product of the degradation of odd-chain fatty acids (Section 20-2E) and certain amino acids (Section 21-4), and α-ketoglutarate and oxaloacetate, which are formed by the reversible transamination of certain amino acids, as indicated above. The links between the citric acid cycle and other metabolic pathways offer some clues to its evolution (Box 17-3).

C | The Glyoxylate Cycle Shares Some Steps with the Citric Acid Cycle

Plants, bacteria, and fungi, but not animals, possess enzymes that mediate the net conversion of acetyl-CoA to oxaloacetate, which can be used for gluconeogenesis. In plants, these enzymes constitute the glyoxylate cycle (Fig. 17-18), which operates in two cellular compartments: the mitochondrion and the **glyoxysome,** a membrane-bounded plant organelle that is a specialized peroxisome. Most of the enzymes of the glyoxylate cycle are the same as those of the citric acid cycle.

The glyoxylate cycle consists of five reactions (Fig. 17-18):

Reactions 1 and 2. Glyoxysomal oxaloacetate is condensed with acetyl-CoA to form citrate, which is isomerized to isocitrate as in the citric acid cycle. Since the glyoxysome contains no aconitase, Reaction 2 presumably takes place in the cytosol.

Reaction 3. Glyoxysomal **isocitrate lyase** cleaves the isocitrate to succinate and **glyoxylate** (hence the cycle's name).

Reaction 4. **Malate synthase,** a glyoxysomal enzyme, condenses glyoxylate with a second molecule of acetyl-CoA to form malate.

Reaction 5. Glyoxysomal malate dehydrogenase catalyzes the oxidation of malate to oxaloacetate by NAD^+.

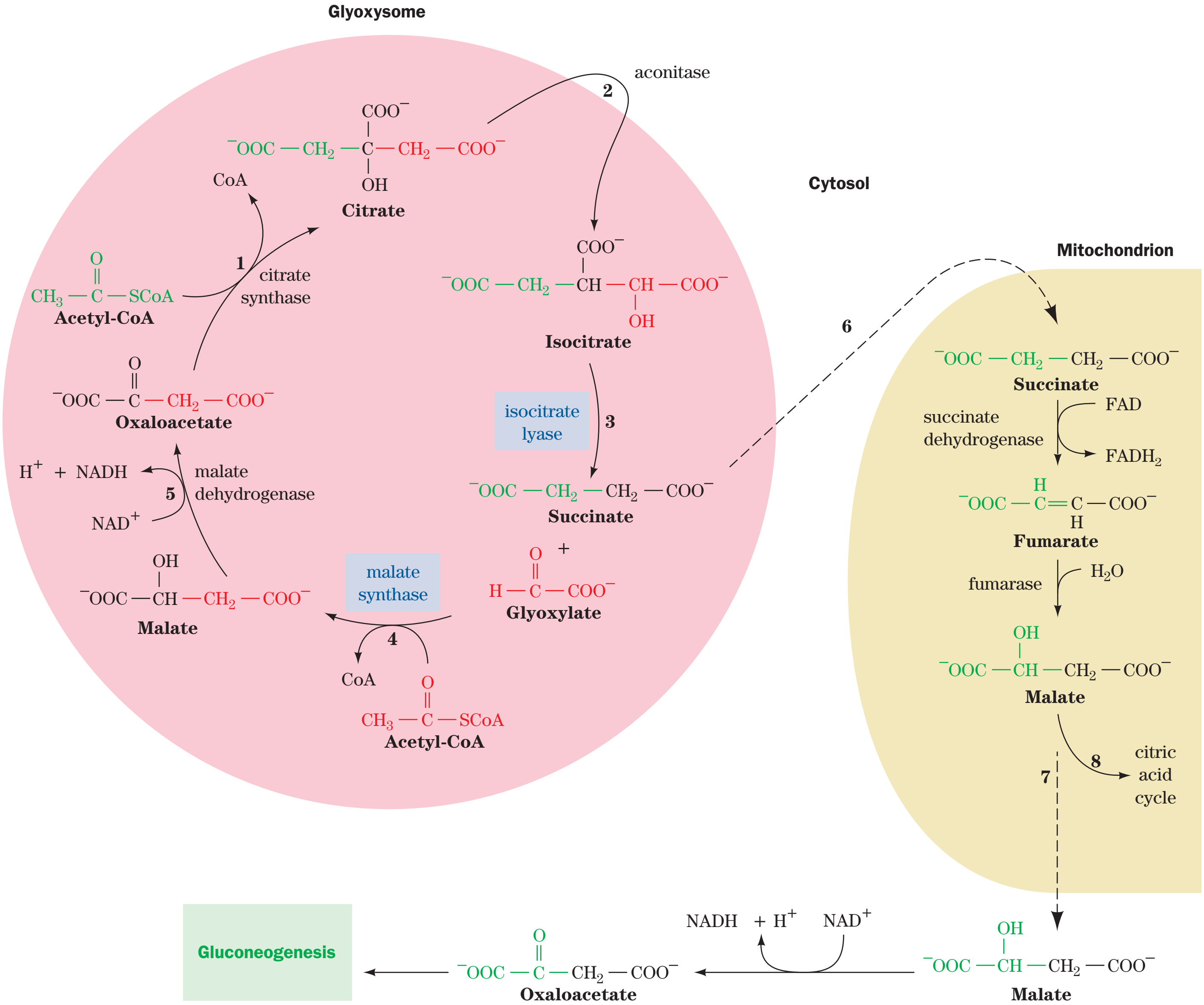
Glyoxysome
Cytosol
Mitochondrion
aconitase
2
Citrate
CoA
1
citrate synthase
Acetyl-CoA
Isocitrate
Oxaloacetate
isocitrate lyase
3
Succinate
H⁺ + NADH
NAD⁺
5
malate dehydrogenase
Malate
malate synthase
4
CoA
Glyoxylate
Acetyl-CoA
6
Succinate
succinate dehydrogenase
FAD
FADH₂
Fumarate
fumarase
H₂O
Malate
7
8
citric acid cycle
Gluconeogenesis
Oxaloacetate
NADH + H⁺
NAD⁺
Malate

■ **Figure 17-18 | The glyoxylate cycle.** The cycle results in the net conversion of two acetyl-CoA to succinate in the glyoxysome, which can be converted to malate in the mitochondrion for use in gluconeogenesis. Isocitrate lyase and malate synthase, enzymes unique to glyoxysomes (which occur only in plants), are boxed in blue. (**1**) Glyoxysomal citrate synthase catalyzes the condensation of oxaloacetate with acetyl-CoA to form citrate. (**2**) Cytosolic aconitase catalyzes the conversion of citrate to isocitrate. (**3**) Isocitrate lyase catalyzes the cleavage of isocitrate to succinate and glyoxylate. (**4**) Malate synthase catalyzes the condensation of glyoxylate with acetyl-CoA to form malate. (**5**) Glyoxysomal malate dehydrogenase catalyzes the oxidation of malate to oxaloacetate, completing the cycle. (**6**) Succinate is transported to the mitochondrion, where it is converted to malate via the citric acid cycle. (**7**) Malate is transported to the cytosol, where malate dehydrogenase catalyzes its oxidation to oxaloacetate, which can then be used in gluconeogenesis. (**8**) Alternatively, malate can continue in the citric acid cycle, making the glyoxylate cycle anaplerotic.

BOX 17-3 **PERSPECTIVES IN BIOCHEMISTRY**

Evolution of the Citric Acid Cycle

The citric acid cycle is ubiquitous in aerobic organisms and plays a central role in energy metabolism in these cells. However, an eight-step catalytic cycle such as the citric acid cycle is unlikely to have arisen all at once and must have evolved from a simpler set of enzyme-catalyzed reactions. Clues to its origins can be found by examining the metabolism of cells that resemble early life-forms. Such organisms emerged before significant quantities of atmospheric oxygen became available some 3 billion years ago. These cells may have used sulfur as their ultimate oxidizing agent, reducing it to H_2S. Their modern-day counterparts are anaerobic autotrophs that harvest free energy by pathways that are independent of the pathways that oxidize carbon-containing compounds. These organisms therefore do not use the citric acid cycle to generate reduced cofactors that are subsequently oxidized by molecular oxygen. However, all organisms must synthesize the small molecules from which they can build proteins, nucleic acids, carbohydrates, and lipids.

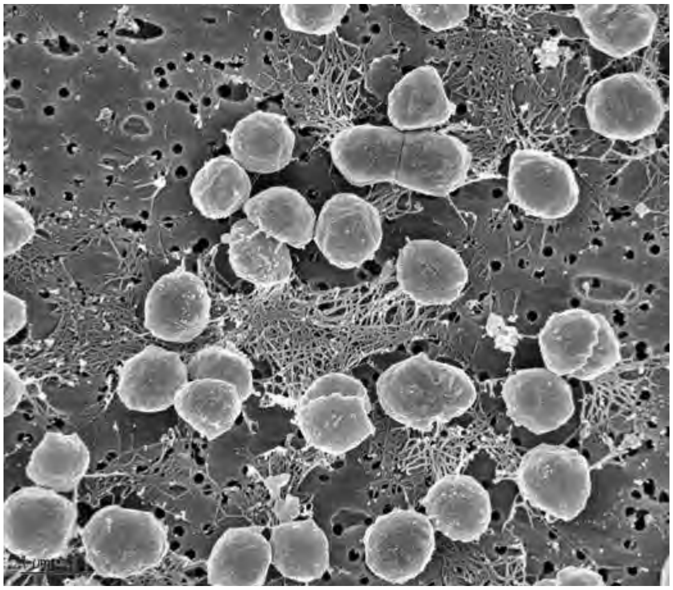

Methanococcus jannaschii, an organism without a citric acid cycle. [Courtesy of B. Boonyaratanakornkit, D.S. Clark, and G. Vrdoljak, University of California at Berkeley.]

The task of divining an organism's metabolic capabilities has been facilitated through bioinformatics. By comparing the sequences of prokaryotic genomes and assigning functions to various homologous genes, it is possible to reconstruct the central metabolic pathways for the organisms. This approach has been fruitful because many "housekeeping" genes, which encode enzymes that make free energy and molecular building blocks available to the cell, are highly conserved among different species and hence are relatively easy to recognize.

Genomic analysis reveals that many prokaryotes lack the citric acid cycle. However, these organisms do contain genes for some citric acid cycle enzymes. The last four reactions of the cycle, leading from succinate to oxaloacetate, appear to be the most highly conserved. This pathway fragment constitutes a mechanism for accepting electrons that are released during sugar fermentation. For example, the reverse of this pathway could regenerate NAD^+ from the NADH produced by the glyceraldehyde-3-phosphate dehydrogenase step of glycolysis.

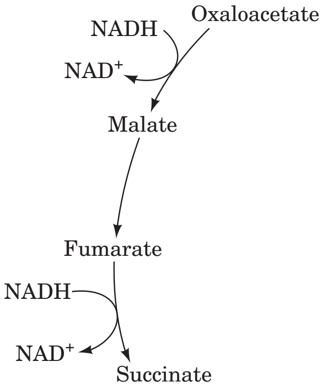

The glyoxylate cycle therefore results in the net conversion of two acetyl-CoA to succinate instead of to four molecules of CO_2 as would occur in the citric acid cycle. The succinate produced in Reaction 3 is transported to the mitochondrion where it enters the citric acid cycle and is converted to malate, which has two alternative fates: (1) It can be converted to oxaloacetate in the mitochondrion, continuing the citric acid cycle and thereby making the glyoxylate cycle an anaplerotic process (Section 17-5B); or (2) it can be transported to the cytosol, where it is converted to oxaloacetate for entry into gluconeogenesis.

The overall reaction of the glyoxylate cycle can be considered to be the formation of oxaloacetate from two molecules of acetyl-CoA:

$$2\ \text{Acetyl-CoA} + 2\,\text{NAD}^+ + \text{FAD} \longrightarrow \text{oxaloacetate} + 2\,\text{CoA} + 2\,\text{NADH} + \text{FADH}_2 + 2\,\text{H}^+$$

The resulting succinate could then be used as a starting material for the biosynthesis of other compounds.

Many archaeal cells have a **pyruvate:ferredoxin oxidoreductase** that converts pyruvate to acetyl-CoA (but without producing NADH). In a primitive cell, the resulting acetyl groups could have condensed with oxaloacetate (by the action of a citrate synthase), eventually giving rise to an oxidative sequence of reactions resembling the first few steps of the modern citric acid cycle.

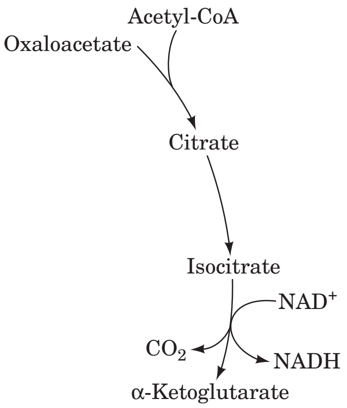

The α-ketoglutarate produced in this way can be converted to glutamate and other amino acids.

The reductive and oxidative branches of the citric acid cycle outlined so far function in modern bacterial cells such as *E. coli* cells when they are growing anaerobically, suggesting that similar pathways could have filled the metabolic needs of early cells. The evolution of a complete citric acid cycle in which the two branches are linked and both proceed in an oxidative direction (clockwise) would have required an enzyme such as α-ketoglutarate:ferredoxin reductase (a homolog of pyruvate:ferredoxin oxidoreductase) to link α-ketoglutarate and succinate.

Interestingly, a primitive citric acid cycle that operated in the reverse (counterclockwise) direction could have provided a route for fixing CO_2 (that is, incorporating CO_2 into biological molecules).

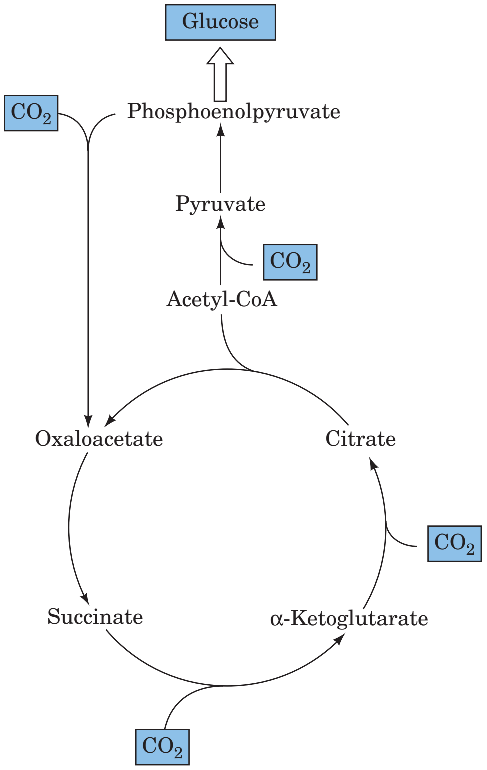

The genes encoding enzymes that catalyze the steps of such a pathway have been identified in several modern autotrophic bacteria. This reductive pathway, which occurs in some deeply rooted archaeal species, possibly predates the CO_2-fixing pathway used in some photosynthetic bacteria and in the chloroplasts of green plants (Section 19-3A).

Isocitrate lyase and malate synthase occur only in plants. These enzymes enable germinating seeds to convert their stored triacylglycerols, through acetyl-CoA, to glucose. It had long been assumed that this was a requirement of germination. However, a mutant of *Arabidopsis thaliana* (an oilseed plant) lacking isocitrate lyase, and hence unable to convert lipids to carbohydrate, nevertheless germinated. This process was only inhibited when the mutant plants were subjected to low light conditions. Therefore, it now appears that the glyoxylate cycle's importance in seedling growth is its anaplerotic function in providing four-carbon units to the citric acid cycle, which can then oxidize the triacylglycerol-derived acetyl-CoA.

Organisms that lack the glyoxylate pathway cannot undertake the net synthesis of glucose from acetyl-CoA. This is the reason humans cannot convert fats (that is, fatty acids, which are catabolized to acetyl-CoA) to carbohydrates (that is, glucose).

Some human pathogens use the glyoxylate cycle, sometimes to great advantage. For example, *Mycobacterium tuberculosis*, which causes tuberculosis, can persist for years in the lung without being attacked by the immune system. During this period, the bacterium subsists largely on lipids, using the citric acid cycle to produce precursors for amino acid synthesis and using the glyoxylate cycle to produce carbohydrate precursors. Drugs that are designed to inhibit the bacterial isocitrate lyase can therefore potentially limit the pathogen's survival. The virulence of the yeast *Candida albicans*, which often infects immunosuppressed individuals, may also depend on activation of the glyoxylate cycle when the yeast cells take up residence inside macrophages.

CHECK YOUR UNDERSTANDING

Explain how a catalytic cycle can supply precursors for other metabolic pathways without depleting its own intermediates.

Describe the reactions of the glyoxylate cycle.

SUMMARY

1. The eight enzymes of the citric acid cycle function in a multistep catalytic cycle to oxidize an acetyl group to two CO_2 molecules with the concomitant generation of three NADH, one $FADH_2$, and one GTP. The free energy released when the reduced coenzymes ultimately reduce O_2 is used to generate ATP.
2. Acetyl groups enter the citric acid cycle as acetyl-CoA. The pyruvate dehydrogenase multienzyme complex, which contains three types of enzymes and five types of coenzymes, generates acetyl-CoA from the glycolytic product pyruvate. The lipoyllysyl arm of E_2 acts as a tether that swings reactive groups between enzymes in the complex.
3. Citrate synthase catalyzes the condensation of acetyl-CoA and oxaloacetate in a highly exergonic reaction.
4. Aconitase catalyzes the isomerization of citrate to isocitrate, and isocitrate dehydrogenase catalyzes the oxidative decarboxylation of isocitrate to α-ketoglutarate to produce the citric acid cycle's first CO_2 and NADH.
5. α-Ketoglutarate dehydrogenase catalyzes the oxidative decarboxylation of α-ketoglutarate to produce succinyl-CoA and the citric acid cycle's second CO_2 and NADH.
6. Succinyl-CoA synthetase couples the cleavage of succinyl-CoA to the synthesis of GTP (or in some organisms, ATP) via a phosphoryl-enzyme intermediate.
7. The citric acid cycle's remaining three reactions, catalyzed by succinate dehydrogenase, fumarase, and malate dehydrogenase, regenerate oxaloacetate to continue the citric acid cycle.
8. Entry of glucose-derived acetyl-CoA into the citric acid cycle is regulated at the pyruvate dehydrogenase step by product inhibition (by NADH and acetyl-CoA) and by covalent modification.
9. The citric acid cycle itself is regulated at the steps catalyzed by citrate synthase, NAD^+-dependent isocitrate dehydrogenase, and α-ketoglutarate dehydrogenase. Regulation is accomplished mainly by substrate availability, product inhibition, and feedback inhibition.
10. Cataplerotic reactions deplete citric acid cycle intermediates. Some citric acid cycle intermediates are substrates for gluconeogenesis, fatty acid biosynthesis, and amino acid biosynthesis.
11. Anaplerotic reactions such as the pyruvate carboxylase reaction replenish citric acid cycle intermediates.
12. The glyoxylate cycle, which operates only in plants, bacteria, and fungi, requires the glyoxysomal enzymes isocitrate lyase and malate synthase. This variation of the citric acid cycle permits net synthesis of glucose from acetyl-CoA.

KEY TERMS

citric acid cycle **567**	lipoyllysyl arm **575**	glyoxylate cycle **588**	anaplerotic reaction **589**
multienzyme complex **570**	amphibolic pathway **588**	cataplerotic reaction **588**	glyoxysome **590**

PROBLEMS

1. (a) Explain why obligate anaerobes contain some citric acid cycle enzymes. (b) Why don't these organisms have a complete citric acid cycle?

2. The first organisms on earth may have been chemoautotrophs in which the citric acid cycle operated in reverse to "fix" atmospheric CO_2 in organic compounds. Complete a catalytic cycle that begins with the hypothetical overall reaction succinate + 2 $CO_2 \rightarrow$ citrate.

3. Which one of the five steps of the pyruvate dehydrogenase complex reaction is most likely to be metabolically irreversible? Explain.

4. Explain why an individual with a deficiency of pyruvate

dehydrogenase phosphatase (PDP) is unable to tolerate exercise.

5. The CO_2 produced in one round of the citric acid cycle does not originate in the acetyl carbons that entered that round. (a) If acetyl-CoA is labeled with ^{14}C at its carbonyl carbon, how many rounds of the cycle are required before $^{14}CO_2$ is released? (b) How many rounds are required if acetyl-CoA is labeled at its methyl group?
6. Explain why metabolic acidosis (Box 2-1) may result from the accumulation of some citric acid cycle intermediates.
7. The branched-chain α-keto acid dehydrogenase complex, which participates in amino acid catabolism, contains the same three types of enzymes as are in the pyruvate dehydrogenase and the α-ketoglutarate dehydrogenase complexes. Draw the reaction product when valine is deaminated as in the glutamate $\rightleftharpoons$ α-ketoglutarate reaction (Section 17-5A) and then is acted on by the branched-chain α-keto acid dehydrogenase.
8. Refer to Table 14-5 to explain why FAD rather than NAD^+ is used in the succinate dehydrogenase reaction.
9. Malonate is a competitive inhibitor of succinate in the succinate dehydrogenase reaction. Explain why increasing the oxaloacetate concentration can overcome malonate inhibition.
10. Why is it advantageous for citrate, the product of Reaction 1 of the citric acid cycle, to inhibit phosphofructokinase, which catalyzes the third reaction of glycolysis?
11. Anaplerotic reactions permit the citric acid cycle to supply intermediates to biosynthetic pathways while maintaining the proper levels of cycle intermediates. Write the equation for the net synthesis of citrate from pyruvate.
12. Many amino acids are broken down to intermediates of the citric acid cycle. (a) Why can't these amino acid "remnants" be directly oxidized to CO_2 by the citric acid cycle? (b) Explain why amino acids that are broken down to pyruvate can be completely oxidized by the citric acid cycle.
13. Certain microorganisms with an incomplete citric acid cycle decarboxylate α-ketoglutarate to produce **succinate semialdehyde.** A dehydrogenase then converts succinate semialdehyde to succinate.

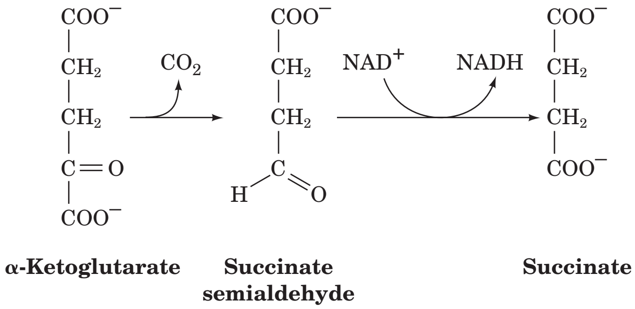

These reactions can be combined with other standard citric acid cycle reactions to create a pathway from citrate to oxaloacetate. Compare the ATP and reduced cofactor yield of the standard and alternate pathways.

14. Given the following information, calculate the physiological ΔG of the isocitrate dehydrogenase reaction at 25°C and pH 7.0: $[NAD^+]/[NADH] = 8$, $[\alpha\text{-ketoglutarate}] = 0.1$ mM, and $[\text{isocitrate}] = 0.02$ mM. Assume standard conditions for CO_2 ($\Delta G^{\circ\prime}$ is given in Table 17-2). Is this reaction a likely site for metabolic control?
15. Although animals cannot synthesize glucose from acetyl-CoA, if a rat is fed ^{14}C-labeled acetate, some of the label appears in glycogen extracted from its muscles. Explain.

CASE STUDY

Case 21 (available at www.wiley.com/college/voet)
Characterization of Pyruvate Carboxylase from Methanobacterium thermoautotrophicum

Focus concept: Pyruvate carboxylase is discovered in a bacterium that was previously thought not to contain the enzyme.

Prerequisite: Chapter 17

- Citric acid cycle reactions and associated anaplerotic reactions
- Glyoxylate cycle reactions

REFERENCES

Eastmond, P.J. and Graham, I.A., Re-examining the role of the glyoxylate cycle in oilseeds, *Trends Plant Sci.* **6,** 72–77 (2001).

Huynen M.A., Dandekar, T., and Bork, P., Variation and evolution of the citric-acid cycle: a genomic perspective, *Trends Microbiol.* **7,** 281–291 (1999). [Discusses how genome studies can allow reconstruction of metabolic pathways, even when some enzymes appear to be missing.]

Milne, J.L.S., Wu, X., Borgnia, M.J., Lengyel, J.S., Brooks, B.R., Shi, D., Perham, R.N., and Subramaniam, S., Molecular structure of a 9-MDa icosahedral pyruvate dehydrogenase subcomplex containing the E_2 and E_3 enzymes using cryoelectron microscopy, *J. Biol. Chem.* **281,** 4364–4370 (2006).

Owen, O.E., Kalhan, S.C., and Hanson, R.W., The key role of anaplerosis and cataplerosis for citric acid cycle function, *J. Biol. Chem.* **277,** 30409–30412 (2002). [Describes the influx (anaplerosis) and efflux (cataplerosis) of citric acid cycle intermediates in different organ systems.]

Perham, R.N., Swinging arms and swinging domains in multifunctional enzymes: catalytic machines for multistep reactions, *Annu. Rev. Biochem.* 69, 961–1004 (2000). [An authoritative review on multienzyme complexes.]

18

Electron Transport and Oxidative Phosphorylation

A resting human body consumes approximately 420 kilojoules of energy per hour, a power requirement that is only slightly greater than that of a 100-watt lightbulb. The body's energy needs are largely met by the electrochemical events in mitochondria, which support a relatively modest voltage of approximately 0.2 V (a household power outlet in the United States supplies 110 V) but a current of about 500 amps, representing the transmembrane movement of approximately 3×10^{21} protons per second. It is this movement that powers ATP synthesis. [Image State/Alamy Images.]

CHAPTER CONTENTS

1 The Mitochondrion
  - **A.** Mitochondria Contain a Highly Folded Inner Membrane
  - **B.** Ions and Metabolites Enter Mitochondria via Transporters

2 Electron Transport
  - **A.** Electron Transport Is an Exergonic Process
  - **B.** Electron Carriers Operate in Sequence
  - **C.** Complex I Accepts Electrons from NADH
  - **D.** Complex II Contributes Electrons to Coenzyme Q
  - **E.** Complex III Translocates Protons via the Q Cycle
  - **F.** Complex IV Reduces Oxygen to Water

3 Oxidative Phosphorylation
  - **A.** The Chemiosmotic Theory Links Electron Transport to ATP Synthesis
  - **B.** ATP Synthase Is Driven by the Flow of Protons
  - **C.** The P/O Ratio Relates the Amount of ATP Synthesized to the Amount of Oxygen Reduced
  - **D.** Oxidative Phosphorylation Can be Uncoupled from Electron Transport

4 Control of Oxidative Metabolism
  - **A.** The Rate of Oxidative Phosphorylation Depends on the ATP and NADH Concentrations
  - **B.** Aerobic Metabolism Has Some Disadvantages

MEDIA RESOURCES

(available at www.wiley.com/college/voet)
Guided Exploration 17. Electron transport and oxidative phosphorylation overview
Guided Exploration 18. The Q cycle
Guided Exploration 19. F_1F_0-ATP synthase and the binding change mechanism
Interactive Exercise 19. Complex III
Interactive Exercise 20. Cytochrome *c* residues involved in intermolecular complex formation
Interactive Exercise 21. Bovine heart cytochrome *c* oxidase
Interactive Exercise 22. F_1-ATP synthase
Animated Figure 18-8. The mitochondrial electron transport chain
Animated Figure 18-20. Coupling of electron transport and ATP synthesis
Animated Figure 18-24. The binding change mechanism of ATP synthesis
Animated Figure 18-29. Coordinated control of glycolysis and the citric acid cycle
Kinemage 5. Cytochrome *c*
Case Study 24. Uncoupling Proteins in Plants
Case Study 27. Regulation of Sugar and Alcohol Metabolism in *Saccharomyces cerevisiae*
Case Study 33. Modification of Subunit c from Bovine Mitochondrial ATPase

Aerobic organisms consume oxygen and generate carbon dioxide in the process of oxidizing metabolic fuels. The complete oxidation of glucose ($C_6H_{12}O_6$), for example, by molecular oxygen

$$C_6H_{12}O_6 + 6\,O_2 \longrightarrow 6\,CO_2 + 6\,H_2O$$

can be broken down into two half-reactions that the metabolic machinery carries out. In the first, glucose carbon atoms are oxidized:

$$C_6H_{12}O_6 + 6\,H_2O \longrightarrow 6\,CO_2 + 24\,H^+ + 24\,e^-$$

and in the second, molecular oxygen is reduced:

$$6\,O_2 + 24\,H^+ + 24\,e^- \longrightarrow 12\,H_2O$$

We have already seen that the first half-reaction is mediated by the enzymatic reactions of glycolysis and the citric acid cycle (the breakdown of fatty acids—the other major type of metabolic fuel—also requires the citric acid cycle). In this chapter, we describe the pathway by which the electrons from reduced fuel molecules are transferred to molecular oxygen in eukaryotes. We also examine how the energy of fuel oxidation is conserved and used to synthesize ATP.

As we have seen, the 12 electron pairs released during glucose oxidation are not transferred directly to O_2. Rather, they are transferred to the coenzymes NAD^+ and FAD to form 10 NADH and 2 $FADH_2$ (Fig. 18-1) in the reactions catalyzed by the glycolytic enzyme glyceraldehyde-3-phosphate dehydrogenase (Section 15-2F), pyruvate dehydrogenase (Section 17-2B), and the citric acid cycle enzymes isocitrate dehydrogenase, α-ketoglutarate dehydrogenase, succinate dehydrogenase, and malate dehydrogenase (Section 17-3). *The electrons then pass into the **mitochondrial electron-transport chain,** a system of linked electron carriers.* The following events occur during the electron-transport process:

1. By transferring their electrons to other substances, the NADH and $FADH_2$ are reoxidized to NAD^+ and FAD so that they can participate in additional substrate oxidation reactions.
2. The transferred electrons participate in the sequential oxidation–reduction of multiple **redox centers** (groups that undergo oxidation–reduction reactions) in four enzyme complexes before reducing O_2 to H_2O.
3. During electron transfer, protons are expelled from the mitochondrion, producing a proton gradient across the mitochondrial membrane. *The free energy stored in this electrochemical gradient drives the synthesis of ATP from ADP and P_i through **oxidative phosphorylation.***

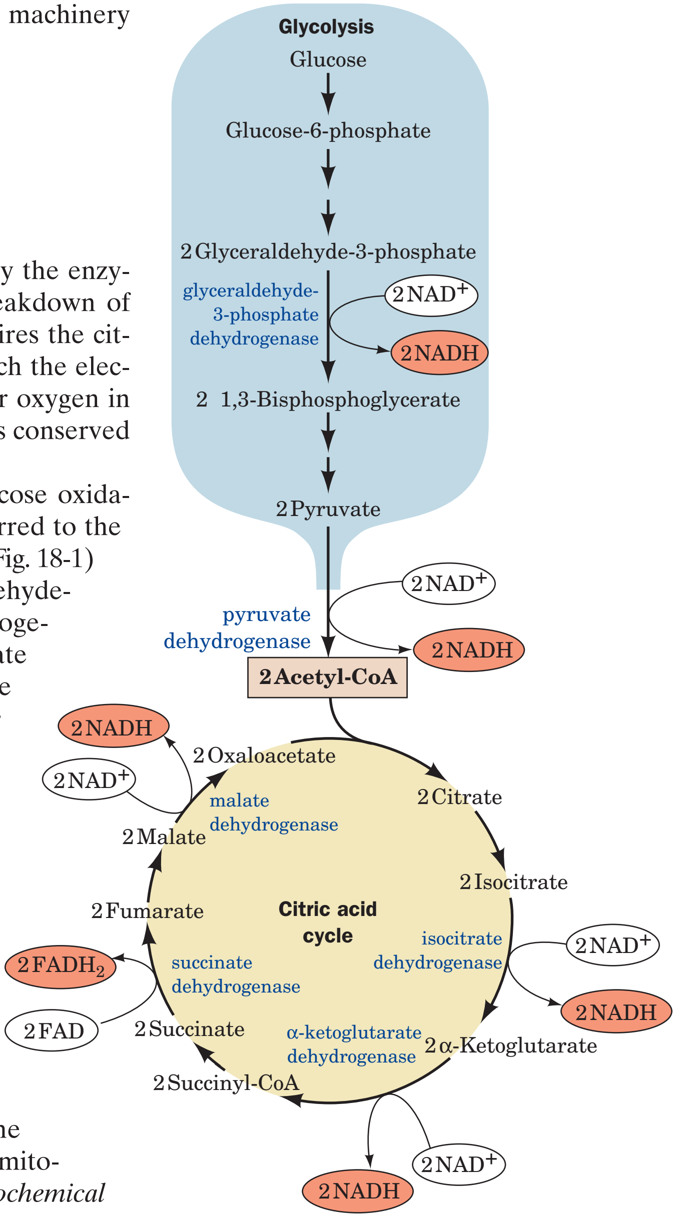
Glycolysis
Glucose
Glucose-6-phosphate
2 Glyceraldehyde-3-phosphate
glyceraldehyde-3-phosphate dehydrogenase
2 NAD+
2 NADH
2 1,3-Bisphosphoglycerate
2 Pyruvate
2 NAD+
pyruvate dehydrogenase
2 NADH
2 Acetyl-CoA
2 NADH
2 Oxaloacetate
2 NAD+
malate dehydrogenase
2 Citrate
2 Malate
2 Isocitrate
2 Fumarate
Citric acid cycle
isocitrate dehydrogenase
2 NAD+
2 FADH2
succinate dehydrogenase
2 NADH
2 FAD
2 Succinate
α-ketoglutarate dehydrogenase
2 α-Ketoglutarate
2 Succinyl-CoA
2 NAD+
2 NADH

Figure 18-1 | **The sites of electron transfer that form NADH and $FADH_2$ in glycolysis and the citric acid cycle.**

1 The Mitochondrion

The mitochondrion (Greek: *mitos,* thread + *chondros,* granule) is the site of eukaryotic oxidative metabolism. Mitochondria contain pyruvate dehydrogenase, the citric acid cycle enzymes, the enzymes catalyzing fatty acid oxidation (Section 20-2), and the enzymes and redox proteins involved in electron transport and oxidative phosphorylation. It is therefore with good reason that the mitochondrion is often described as the cell's "power plant."

LEARNING OBJECTIVES

- Understand that a highly folded inner membrane separates the mitochondrial matrix from the outer membrane.
- Understand that transport proteins are required to import reducing equivalents, ADP, and P_i into the mitochondria.

A | Mitochondria Contain a Highly Folded Inner Membrane

Mitochondria vary in size and shape, depending on their source and metabolic state, but they are often ellipsoidal with dimensions of around 0.5 × 1.0 μm, about the size of a bacterium. A eukaryotic cell typically contains

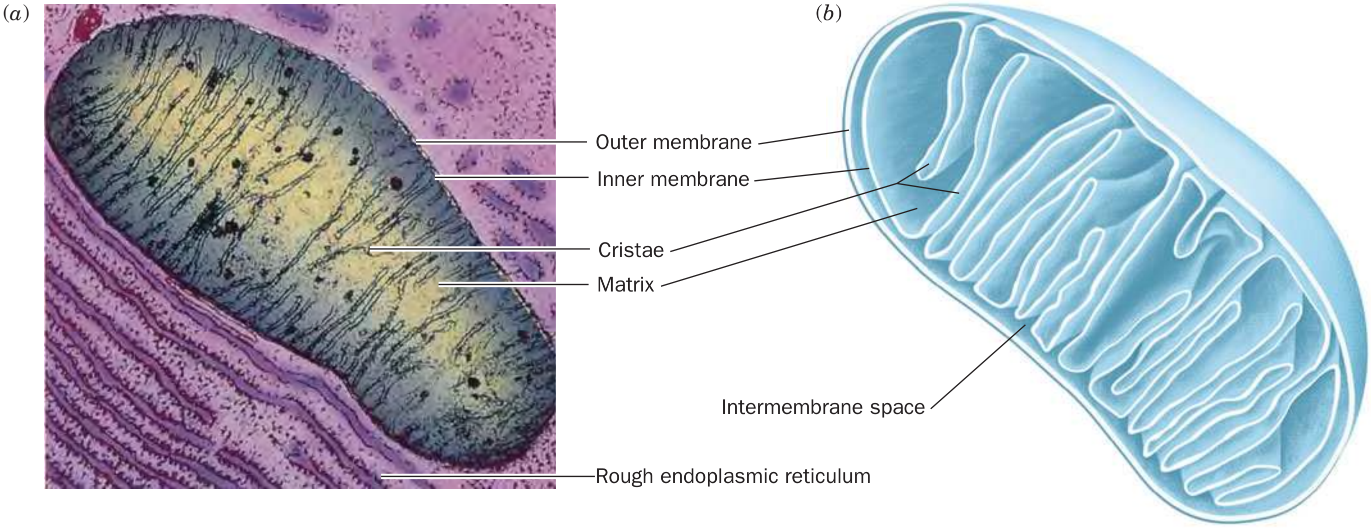

■ **Figure 18-2 | The mitochondrion.** (*a*) An electron micrograph of an animal mitochondrion. [© K.R. Porter/Photo Researchers.] (*b*) Cutaway diagram of a mitochondrion.

~2000 mitochondria, which occupy roughly one-fifth of its total cell volume. A mitochondrion is bounded by a smooth outer membrane and contains an extensively invaginated inner membrane (Fig. 18-2). The number of invaginations, called **cristae** (Latin: crests), reflects the respiratory activity of the cell. The proteins mediating electron transport and oxidative phosphorylation are bound in the inner mitochondrial membrane, so the respiration rate varies with membrane surface area.

The inner membrane divides the mitochondrion into two compartments, the **intermembrane space** and the internal **matrix.** The matrix is a gel-like solution that contains extremely high concentrations of the soluble enzymes of oxidative metabolism as well as substrates, nucleotide cofactors, and inorganic ions. The matrix also contains the mitochondrial genetic machinery—DNA, RNA, and ribosomes—that generates several (but by no means all) mitochondrial proteins.

Two-dimensional electron micrographs of mitochondria such as Fig. 18-2*a* suggest that mitochondria are discrete kidney-shaped organelles. In fact, some mitochondria adopt a tubular shape that extends throughout the cytosol. Furthermore, mitochondria are highly variable structures. For example, the cristae may not resemble baffles and the intercristal spaces may not communicate freely with the mitochondrion's intermembrane space. Electron microscopy–based three-dimensional image reconstruction methods have revealed that cristae can range in shape from simple tubular entities to more complicated lamellar assemblies that merge with the inner membrane via narrow tubular structures (Fig. 18-3). Evidently, cristae form microcompartments that restrict the diffusion of substrates and ions between the intercristal and intermembrane spaces. This has important functional implications because it would result in a locally greater pH gradient across cristal membranes than across inner membranes that are not part of cristae, thereby significantly influencing the rate of oxidative phosphorylation (Section 18-3).

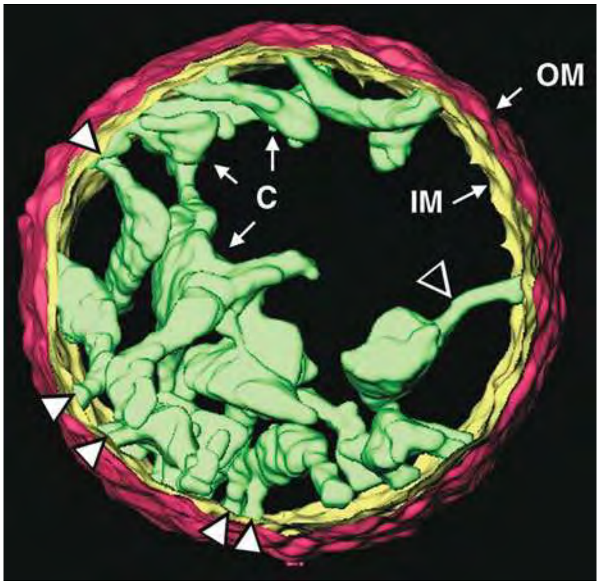

■ **Figure 18-3 | Electron microscopy–based three-dimensional image reconstruction of a rat liver mitochondrion.** The outer membrane (OM) is red, the inner membrane (IM) is yellow, and the cristae (C) are green. The arrowheads point to tubular regions of the cristae that connect them to the inner membrane and to each other. [Courtesy of Carmen Mannella, Wadsworth Center, Albany, New York.]

B | Ions and Metabolites Enter Mitochondria via Transporters

Like bacterial outer membranes, the outer mitochondrial membrane contains porins, proteins that permit the free diffusion of molecules of up to 10 kD (Section 10-2B). *The intermembrane space is therefore equivalent to the cytosol in its concentrations of metabolites and ions.* The inner membrane, which is ~75% protein by mass, is considerably richer in proteins than is the outer membrane (Fig. 18-4). It is freely permeable only to O_2, CO_2, and H_2O and contains, in addition to respiratory chain proteins, numerous transport proteins that control the passage of metabolites such as ATP, ADP, pyruvate, Ca^{2+}, and phosphate. *The controlled impermeability of the inner mitochondrial membrane to most ions and metabolites permits the generation of ion gradients across this barrier and results in the compartmentalization of metabolic functions between cytosol and mitochondria.*

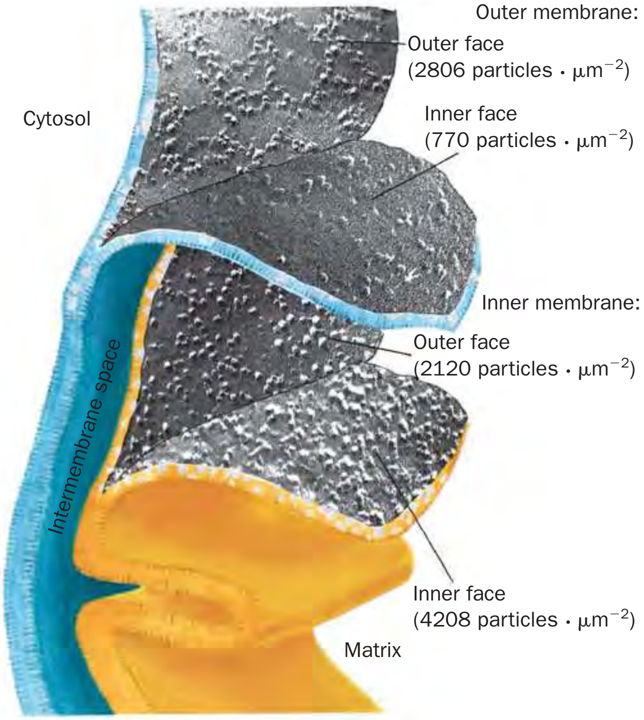

Outer membrane:
Outer face
(2806 particles · μm^{-2})
Cytosol
Inner face
(770 particles · μm^{-2})
Inner membrane:
Outer face
(2120 particles · μm^{-2})
Intermembrane space
Inner face
(4208 particles · μm^{-2})
Matrix

Figure 18-4 | Electron micrographs of the inner and outer mitochondrial membranes that have been split to expose the inner surfaces of their bilayer leaflets. Note that the inner membrane contains about twice the density of embedded particles as does the outer membrane. The particles are the portions of integral membrane proteins that were exposed when the bilayers were split. [Courtesy of Lester Packer, University of California at Berkeley.]

Cytosolic Reducing Equivalents Are "Transported" into Mitochondria. The NADH produced in the cytosol by glycolysis must gain access to the mitochondrial electron-transport chain for aerobic oxidation. However, the inner mitochondrial membrane lacks an NADH transport protein. *Only the electrons from cytosolic NADH are transported into the mitochondrion by one of several ingenious "shuttle" systems.* We have already discussed the **malate–aspartate shuttle** (Fig. 16-20), in which, when run in reverse, cytosolic oxaloacetate is reduced to malate for transport into the mitochondrion. When malate is reoxidized in the matrix, it gives up the reducing equivalents that originated in the cytosol.

In the **glycerophosphate shuttle** (Fig. 18-5) of insect flight muscle (the tissue with the largest known sustained power output—about the same power-to-weight ratio as a small automobile engine), **3-phosphoglycerol dehydrogenase** catalyzes the oxidation of cytosolic NADH by dihydroxyacetone phosphate to yield NAD^+, which re-enters glycolysis. The electrons of the resulting **3-phosphoglycerol** are transferred to **flavoprotein dehydrogenase** to form $FADH_2$. This enzyme, which is situated on the inner mitochondrial membrane's outer surface, supplies electrons directly to the electron-transport chain (Section 18-2D).

A Translocator Exchanges ADP and ATP. Most of the ATP generated in the **mitochondrial matrix** through oxidative phosphorylation is used in the cytosol. The inner mitochondrial membrane contains an **ADP–ATP translocator** (also called the

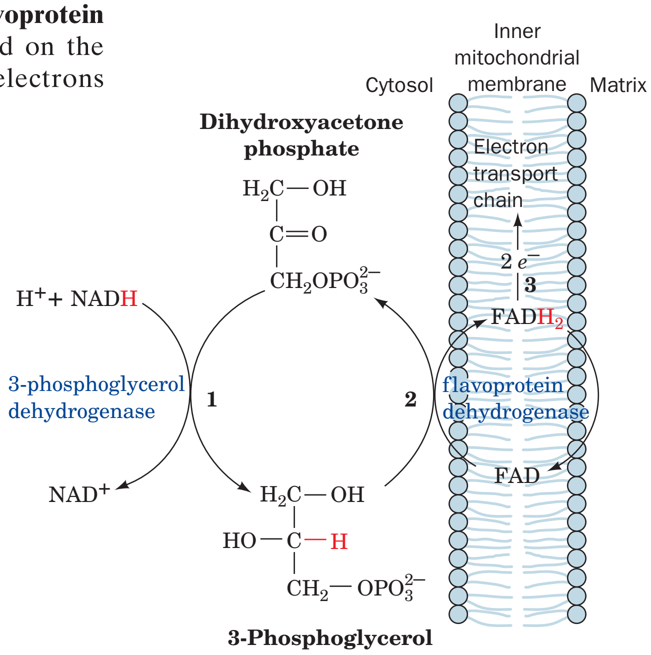

Inner mitochondrial membrane
Cytosol
Matrix
Dihydroxyacetone phosphate
H_2C-OH
$C=O$
$CH_2OPO_3^{2-}$
Electron transport chain
$2e^-$
3
$FADH_2$
$H^+ + NADH$
3-phosphoglycerol dehydrogenase
1
2
flavoprotein dehydrogenase
NAD^+
FAD
H_2C-OH
$HO-C-H$
$CH_2-OPO_3^{2-}$
3-Phosphoglycerol

Figure 18-5 | The glycerophosphate shuttle. The electrons of cytosolic NADH are transported to the mitochondrial electron-transport chain in three steps (shown in red as hydride transfers): (**1**) Cytosolic oxidation of NADH by dihydroxyacetone phosphate catalyzed by 3-phosphoglycerol dehydrogenase. (**2**) Oxidation of 3-phosphoglycerol by flavoprotein dehydrogenase with reduction of FAD to $FADH_2$. (**3**) Reoxidation of $FADH_2$ with passage of electrons into the electron-transport chain.

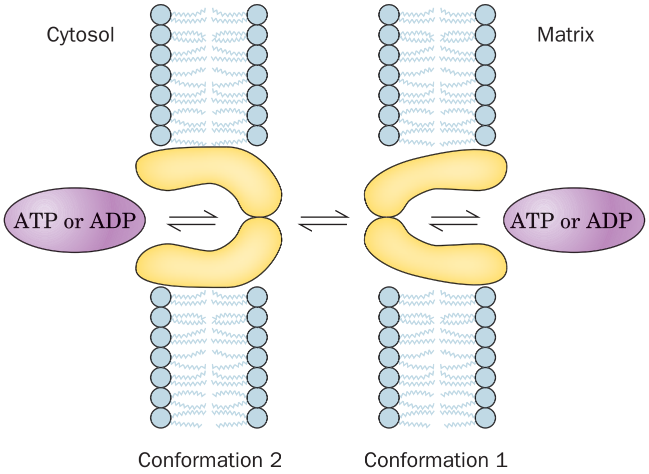

Figure 18-6 | Conformational mechanism of the ADP–ATP translocator. An adenine nucleotide–binding site located in the intersubunit contact area of the translocator dimer is alternately exposed to the two sides of the membrane.

adenine nucleotide translocase) that transports ATP out of the matrix in exchange for ADP produced in the cytosol by ATP hydrolysis.

The ADP–ATP translocator, a dimer of identical 30-kD subunits, has one binding site for which ADP and ATP compete. It has two major conformations: one with its ATP–ADP-binding site facing the inside of the mitochondrion, and the other with the site facing outward (Fig. 18-6). The translocator must bind ligand to change from one conformation to the other at a physiologically reasonable rate. Thus it functions as an exchanger by importing one ADP for every ATP that is exported. In this respect, it differs from the glucose transporter (Fig. 10-13), which can change its conformation in the absence of ligand. Note that the export of ATP (net charge -4) and the import of ADP (net charge -3) results in the export of one negative charge per transport cycle. This **electrogenic** antiport is driven by the membrane potential difference, $\Delta\Psi$, across the inner mitochondrial membrane (positive outside), which is a consequence of the transmembrane proton gradient.

Phosphate Must Be Imported into the Mitochondrion. ATP is synthesized from ADP + P_i in the mitochondrion but is utilized in the cytosol. The P_i is returned to the mitochondrion by the **phosphate carrier,** an electroneutral P_i–H symport that is driven by ΔpH. The transmembrane proton gradient generated by the electron-transport machinery of the inner mitochondrial membrane thus not only provides the thermodynamic driving force for ATP synthesis (Section 18-3), it also motivates the transport of the raw materials—ADP and P_i—required for the process.

CHECK YOUR UNDERSTANDING

Describe how shuttle systems transport reducing equivalents into the mitochondria.

Explain how the free energy of the proton gradient drives the transport of ATP, ADP, and P_i.

2 Electron Transport

LEARNING OBJECTIVES

- Understand that the free energy of electron transport from NADH to O_2 can drive the synthesis of approximately 2.5 ATP.
- Understand that electron carriers are arranged so that electrons travel from Complexes I and II via coenzyme Q to Complex III, and from there via cytochrome *c* to Complex IV.
- Understand the reactions catalyzed by Complexes I, III, and IV, and their mechanisms of proton translocation.

The electron carriers that ferry electrons from NADH and $FADH_2$ to O_2 are associated with the inner mitochondrial membrane. Some of these redox centers are mobile, and others are components of integral membrane protein complexes. The sequence of electron carriers roughly reflects their relative reduction potentials, so that the overall process of electron transport is exergonic. We begin this section by examining the thermodynamics of electron transport. We then consider the molecular characteristics of the various electron carriers.

A | Electron Transport Is an Exergonic Process

We can estimate the thermodynamic efficiency of electron transport by inspecting the standard reduction potentials of the redox centers. As we saw in our thermodynamic considerations of oxidation–reduction reactions (Section 14-3), an oxidized substrate's affinity for electrons increases with its standard reduction potential, $\mathscr{E}^{\circ\prime}$ (Table 14-5 lists the standard reduction potentials of some biologically important half-reactions). The standard reduction potential difference, $\Delta\mathscr{E}^{\circ\prime}$, for a redox reaction involving any two half-reactions is expressed

$$\Delta\mathscr{E}^{\circ\prime} = \mathscr{E}^{\circ\prime}_{(e^-\,acceptor)} - \mathscr{E}^{\circ\prime}_{(e^-\,donor)}$$

For the reaction that occurs in mitochondria, that is, the oxidation of NADH by O_2, the half-reactions are

$$\text{NAD}^+ + \text{H}^+ + 2\,e^- \rightleftharpoons \text{NADH} \qquad \mathscr{E}^{\circ\prime} = -0.315\text{ V}$$

and

$$\tfrac{1}{2}\,\text{O}_2 + 2\,\text{H}^+ + 2\,e^- \rightleftharpoons \text{H}_2\text{O} \qquad \mathscr{E}^{\circ\prime} = 0.815\text{ V}$$

Since the O_2/H_2O half-reaction has the greater standard reduction potential and therefore the higher affinity for electrons, the NADH half-reaction is reversed so that NADH is the electron donor in this couple and O_2 the electron acceptor. The overall reaction is

$$\tfrac{1}{2}\,\text{O}_2 + \text{NADH} + \text{H}^+ \rightleftharpoons \text{H}_2\text{O} + \text{NAD}^+$$

so that

$$\Delta\mathscr{E}^{\circ\prime} = 0.815\text{ V} - (-0.315\text{ V}) = 1.130\text{ V}$$

The standard free energy change for the reaction can then be calculated from Eq. 14-7:

$$\Delta G^{\circ\prime} = -n\mathscr{F}\Delta\mathscr{E}^{\circ\prime}$$

For NADH oxidation, $\Delta G^{\circ\prime} = -218\text{ kJ}\cdot\text{mol}^{-1}$. In other words, the oxidation of 1 mol of NADH by O_2 (the transfer of 2 mol e^-) under standard biochemical conditions is associated with the release of 218 kJ of free energy.

Because the standard free energy required to synthesize 1 mol of ATP from ADP + P_i is 30.5 kJ · mol^{-1}, the oxidation of NADH by O_2 is theoretically able to drive the formation of several moles of ATP. In mitochondria, the coupling of NADH oxidation to ATP synthesis is achieved by an electron-transport chain in which electrons pass through three protein complexes. *This allows the overall free energy change to be broken into three smaller parcels, each of which contributes to ATP synthesis by oxidative phosphorylation. Oxidation of one NADH results in the synthesis of approximately 2.5 ATP* (we shall see later why the relationship is not strictly stoichiometric). The thermodynamic efficiency of oxidative phosphorylation is therefore $2.5 \times 30.5\text{ kJ}\cdot\text{mol}^{-1} \times 100/218\text{ kJ}\cdot\text{mol}^{-1} = 35\%$ under standard biochemical conditions. However, under physiological conditions in active mitochondria (where the reactant and product concentrations as well as the pH deviate from standard conditions), this thermodynamic efficiency is thought to be ~70%. In comparison, the energy efficiency of a typical automobile engine is <30%.

B | Electron Carriers Operate in Sequence

See Guided Exploration 17
Electron transport and oxidative phosphorylation overview.

Oxidation of NADH and $FADH_2$ is carried out by the electron-transport chain, a set of protein complexes containing redox centers with progressively greater affinities for electrons (increasing standard reduction potentials). Electrons travel through this chain from lower to higher standard reduction potentials (Fig. 18-7). Electrons are carried from **Complexes I** and **II** to **Complex III** by **coenzyme Q** (**CoQ** or **ubiquinone;** so named because of its ubiquity in respiring organisms), and from Complex III to **Complex IV** by the peripheral membrane protein **cytochrome *c*.**

Complex I catalyzes oxidation of NADH by CoQ:

$$\text{NADH} + \text{CoQ}\ (oxidized) \rightarrow \text{NAD}^+ + \text{CoQ}\ (reduced)$$
$$\Delta\mathscr{E}^{\circ\prime} = 0.360\ \text{V} \qquad \Delta G^{\circ\prime} = -69.5\ \text{kJ}\cdot\text{mol}^{-1}$$

Complex III catalyzes oxidation of CoQ (reduced) by cytochrome c:

$$\text{CoQ}\ (reduced) + 2\ \text{cytochrome}\ c\ (oxidized) \rightarrow \text{CoQ}\ (oxidized) + 2\ \text{cytochrome}\ c\ (reduced)$$
$$\Delta\mathscr{E}^{\circ\prime} = 0.190\ \text{V} \qquad \Delta G^{\circ\prime} = -36.7\ \text{kJ}\cdot\text{mol}^{-1}$$

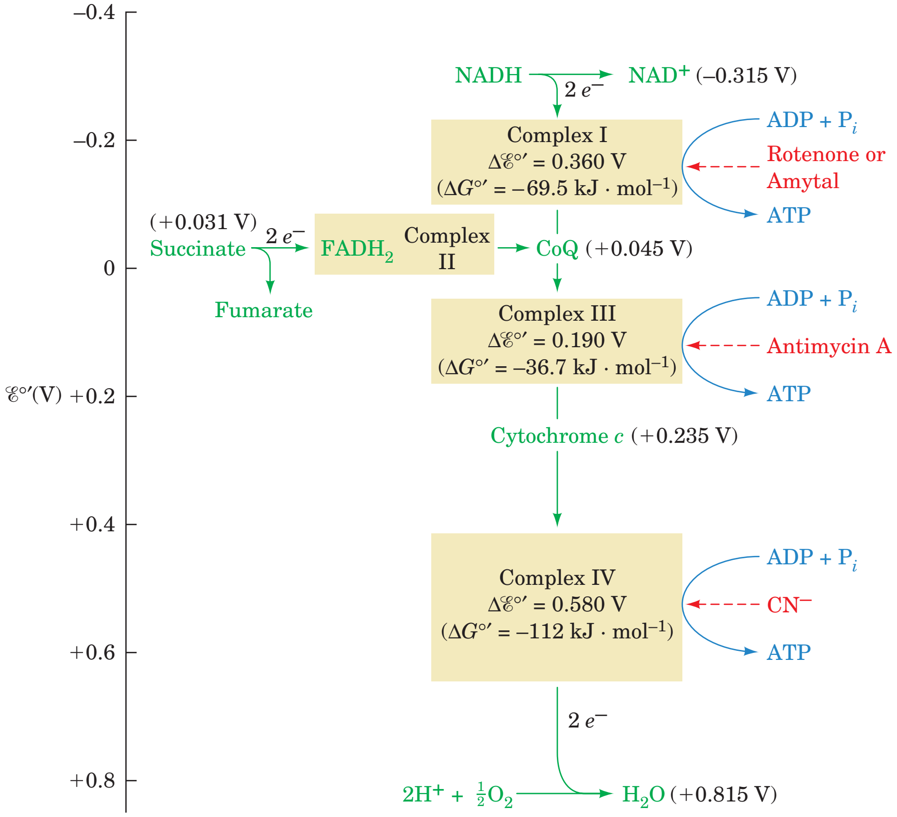

−0.4
−0.2
0
$\mathscr{E}^{\circ\prime}$(V) +0.2
+0.4
+0.6
+0.8
NADH
2 e^-
NAD^+ (−0.315 V)
Complex I
$\Delta\mathscr{E}^{\circ\prime}$ = 0.360 V
($\Delta G^{\circ\prime}$ = −69.5 kJ · mol^{-1})
ADP + P_i
Rotenone or Amytal
ATP
(+0.031 V)
Succinate
2 e^-
Fumarate
$FADH_2$
Complex II
CoQ (+0.045 V)
Complex III
$\Delta\mathscr{E}^{\circ\prime}$ = 0.190 V
($\Delta G^{\circ\prime}$ = −36.7 kJ · mol^{-1})
ADP + P_i
Antimycin A
ATP
Cytochrome *c* (+0.235 V)
Complex IV
$\Delta\mathscr{E}^{\circ\prime}$ = 0.580 V
($\Delta G^{\circ\prime}$ = −112 kJ · mol^{-1})
ADP + P_i
CN^-
ATP
2 e^-
$2H^+ + \frac{1}{2}O_2$
H_2O (+0.815 V)

Figure 18-7 | Overview of electron transport in the mitochondrion. The standard reduction potentials of its most mobile components (*green*) are indicated, as are the points where sufficient free energy is released to synthesize ATP (*blue*) and the sites of action of several respiratory inhibitors (*red*). Complexes I, III, and IV do not directly synthesize ATP but sequester the free energy necessary to do so by pumping protons outside the mitochondrion to form a proton gradient.

Complex IV catalyzes oxidation of reduced cytochrome c by O_2, the terminal electron acceptor of the electron-transport process:

$$2\text{ Cytochrome } c\ (\textit{reduced}) + \tfrac{1}{2}\,O_2 \rightarrow 2\text{ cytochrome } c\ (\textit{oxidized}) + H_2O$$
$$\Delta\mathcal{E}^{\circ\prime} = 0.580\text{ V} \qquad \Delta G^{\circ\prime} = -112\text{ kJ}\cdot\text{mol}^{-1}$$

As an electron pair successively traverses Complexes I, III, and IV, sufficient free energy is released at each step to power ATP synthesis.

Complex II catalyzes the oxidation of $FADH_2$ by CoQ:

$$FADH_2 + \text{CoQ}\ (\textit{oxidized}) \rightarrow \text{FAD} + \text{CoQ}\ (\textit{reduced})$$
$$\Delta\mathcal{E}^{\circ\prime} = 0.085\text{ V} \qquad \Delta G^{\circ\prime} = -16.4\text{ kJ}\cdot\text{mol}^{-1}$$

This redox reaction does not release sufficient free energy to synthesize ATP; it functions only to inject the electrons from $FADH_2$ into the electron-transport chain.

Inhibitors Reveal the Workings of the Electron-Transport Chain. The sequence of events in electron transport was elucidated largely through the use of specific inhibitors and later corroborated by measurements of the standard reduction potentials of the redox components. The rate at which O_2 is consumed by a suspension of mitochondria is a sensitive measure of the activity of the electron-transport chain. Compounds that inhibit electron transport, as judged by their effect on O_2 consumption, include **rotenone** (a plant toxin used by Amazonian Indians to poison fish and which is also used as an insecticide), **amytal** (a barbiturate), **antimycin A** (an antibiotic), and **cyanide.**

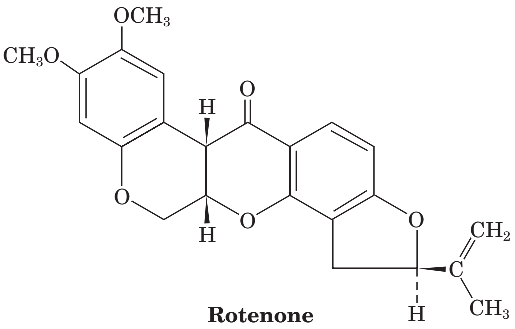

Rotenone

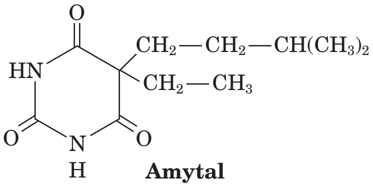

Amytal

$^{-}C\equiv N$

Cyanide

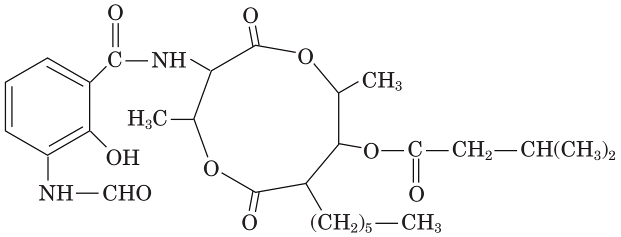

Antimycin A

Adding rotenone or amytal to a suspension of mitochondria blocks electron transport in Complex I; antimycin A blocks Complex III, and CN^- blocks electron transport in Complex IV (Fig. 18-7). Each of these inhibitors also halts O_2 consumption. Oxygen consumption resumes following addition of a substance whose electrons enter the electron-transport chain "downstream" of the block. For example, the addition of succinate to rotenone-blocked mitochondria restores electron transport and O_2 consumption. Experiments with inhibitors of electron transport thus reveal the points of entry of electrons from various substrates.

Each of the four respiratory complexes of the electron-transport chain consists of several protein components that are associated with a variety of redox-active prosthetic groups with successively increasing reduction

Table 18-1 Reduction Potentials of Electron-Transport Chain Components in Resting Mitochondria

Component	$\mathcal{E}^{\circ\prime}$ (V)
NADH	−0.315
Complex I (NADH–CoQ oxidoreductase; ~900 kD, 46 subunits):	
FMN	−0.340
[2Fe–2S]N1a	−0.380
[2Fe–2S]N1b	−0.250
[4Fe–4S]N3, 4, 5, 6a, 6b, 7	−0.250
[4Fe–4S]N2	−0.100
Succinate	0.031
Complex II (succinate–CoQ oxidoreductase; ~120 kD, 4 subunits):	
FAD	−0.040
[2Fe–2S]	−0.030
[4Fe–4S]	−0.245
[3Fe–4S]	0.060
Heme b_{560}	−0.080
Coenzyme Q	0.045
Complex III (CoQ–cytochrome *c* oxidoreductase; ~450 kD, 9–11 subunits):	
Heme b_H (b_{562})	0.030
Heme b_L (b_{566})	−0.030
[2Fe–2S]	0.280
Heme c_1	0.215
Cytochrome *c*	0.235
Complex IV (cytochrome *c* oxidase; ~410 kD, 8–13 subunits):	
Heme *a*	0.210
Cu_A	0.245
Cu_B	0.340
Heme a_3	0.385
O_2	0.815

Source: Mainly Wilson, D.F., Erecinska, M., and Dutton, P.L., *Annu. Rev. Biophys. Bioeng.* **3,** 205 and 208 (1974); *and* Wilson, D.F., *in* Bittar, E.E. (Ed.), *Membrane Structure and Function,* Vol. 1, p. 160, Wiley (1980).

potentials (Table 18-1). The complexes are all laterally mobile within the inner mitochondrial membrane and may associate to form "supercomplexes" with variable composition. In the following sections, we examine the structures of Complexes I through IV and the molecules that transfer electrons between them. Their relationships are summarized in Fig. 18-8.

C | Complex I Accepts Electrons from NADH

Complex I **(NADH–coenzyme Q oxidoreductase),** which passes electrons from NADH to CoQ, may be the largest protein complex in the inner mitochondrial membrane, containing, in mammals, 46 subunits with a total mass of ~900 kD. Electron microscopy shows an L-shaped protein with one arm embedded in the inner mitochondrial membrane and the other extending into the matrix (Fig. 18-9).

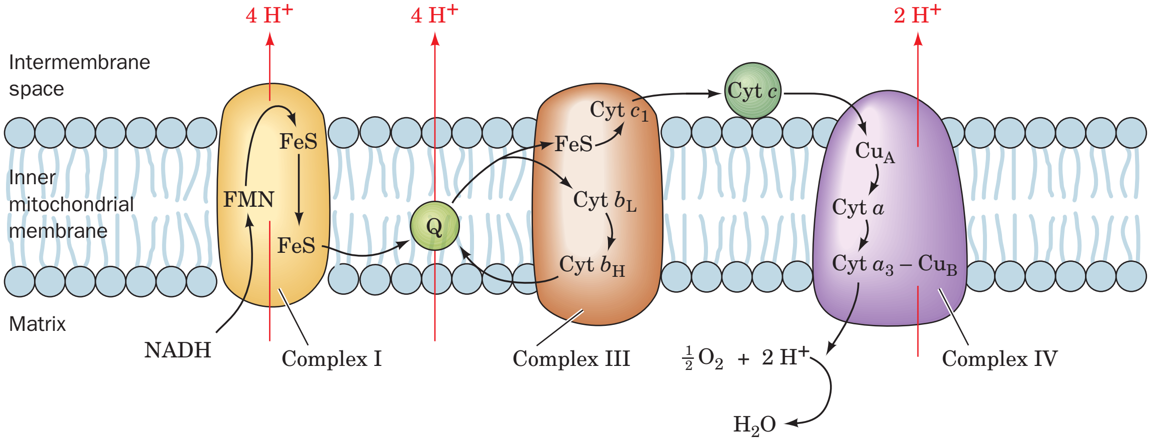
4 H+
4 H+
2 H+
Intermembrane space
Inner mitochondrial membrane
Matrix
FeS
FMN
FeS
NADH
Complex I
Q
Cyt c
Cyt c_1
FeS
Cyt b_L
Cyt b_H
Complex III
Cu_A
Cyt a
Cyt $a_3 - Cu_B$
Complex IV
$\frac{1}{2}O_2$ + 2 H+
H_2O

Figure 18-8 | The mitochondrial electron-transport chain. This diagram indicates the pathways of electron transfer (*black*) and proton translocation (*red*). Electrons are transferred between Complexes I and III by the membrane-soluble coenzyme Q (Q) and between Complexes III and IV by the peripheral membrane protein cytochrome *c*. Complex II (not shown) transfers electrons from succinate to coenzyme Q. **See the Animated Figures.**

Complex I Contains Multiple Coenzymes. Complex I contains one molecule of **flavin mononucleotide** (**FMN,** a redox-active prosthetic group that differs from FAD only by the absence of the AMP group) and eight or nine **iron–sulfur clusters.** Iron–sulfur clusters occur as the prosthetic groups of **iron–sulfur proteins** (also called **nonheme iron proteins**). The two most common types, designated **[2Fe–2S]** and **[4Fe–4S] clusters** *(at right)* consist of equal numbers of iron and sulfide ions and are both coordinated to four protein Cys sulfhydryl groups. Note that the Fe atoms in both types of clusters are each coordinated by four S atoms, which are more or less tetrahedrally disposed around the Fe.

Iron–sulfur clusters can undergo one-electron oxidation and reduction. *The oxidized and reduced states of all iron–sulfur clusters differ by one formal charge regardless of their number of Fe atoms.* This is because the Fe atoms in each cluster form a conjugated system and thus can have oxidation states between the normal +2 and +3 values for individual Fe ions.

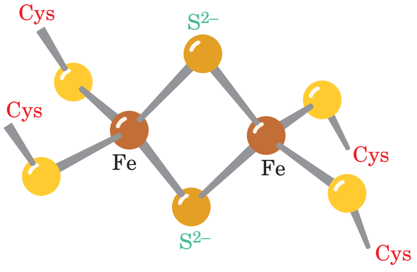
Cys
S^{2-}
Cys
Fe
Fe
Cys
S^{2-}
Cys

[2Fe–2S]

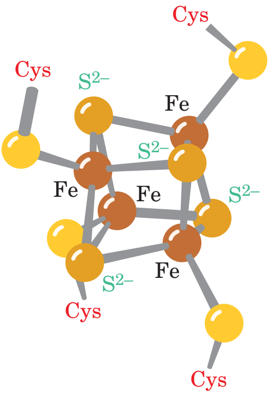
Cys
Cys
S^{2-}
Fe
S^{2-}
Fe
Fe
S^{2-}
S^{2-}
Fe
Cys
Cys

[4Fe–4S]

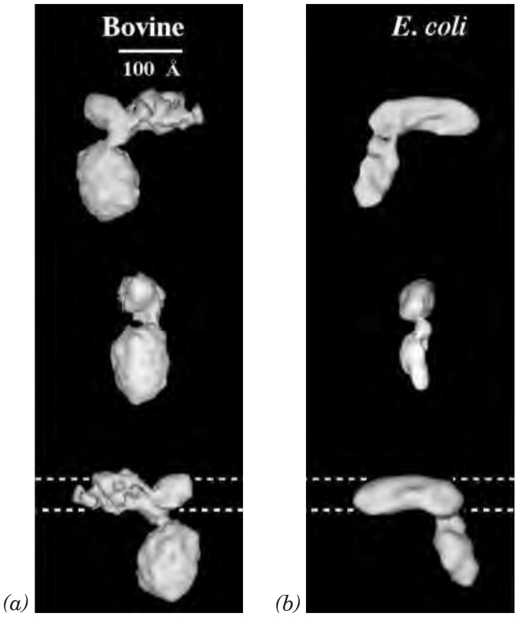
Bovine
100 Å
E. coli
(a)
(b)

Figure 18-9 | Cryoelectron microscopy–based images of Complex I. The structures from (*a*) bovine heart mitochondria and (*b*) *E. coli* were determined at 22 and 34 Å resolution, respectively. Successive views, top to bottom, are rotated by 90° about the vertical axis. The boundaries of the lipid bilayer in which the complex is immersed are indicated by the dashed lines. The vertical arm, which contains the electron-transport groups, protrudes into the mitochondrial matrix or bacterial cytoplasm. [Courtesy of Nikolaus Grigorieff, Brandeis University. The *E. coli* structure was determined by Vincent Guénebaut and Kevin Leonard, European Molecular Biology Laboratory, Heidelberg, Germany.]

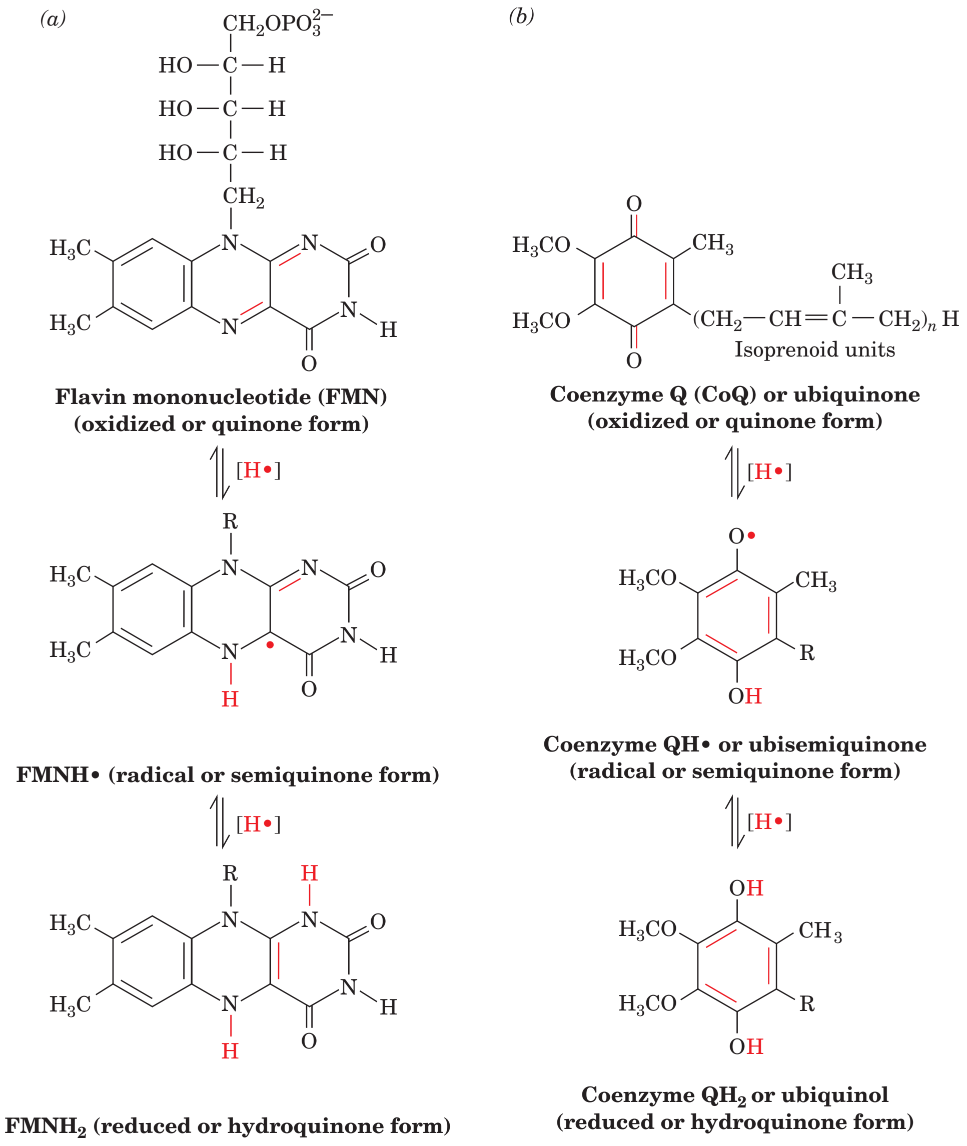
(a)
(b)
Flavin mononucleotide (FMN) (oxidized or quinone form)
Coenzyme Q (CoQ) or ubiquinone (oxidized or quinone form)
Isoprenoid units
[H•]
FMNH• (radical or semiquinone form)
Coenzyme QH• or ubisemiquinone (radical or semiquinone form)
[H•]
FMNH$_2$ (reduced or hydroquinone form)
Coenzyme QH$_2$ or ubiquinol (reduced or hydroquinone form)

Figure 18-10 | The oxidation states of FMN and coenzyme Q. Both (*a*) FMN and (*b*) coenzyme Q form stable semiquinone free-radical states.

FMN and CoQ can each adopt three oxidation states (Fig. 18-10). They are capable of accepting and donating either one or two electrons because their semiquinone forms are stable (these semiquinones are stable **free radicals,** molecules with an unpaired electron). FMN is tightly bound to proteins; however, CoQ has a hydrophobic tail that makes it soluble in the inner mitochondrial membrane's lipid bilayer. In mammals, this tail consists of 10 C_5 isoprenoid units (Section 9-1F) and hence the coenzyme is designated **Q_{10}.** In other organisms, CoQ may have only 6 **(Q_6)** or 8 **(Q_8)** isoprenoid units.

Electrons Follow a Multistep Path through Complex I. Complex I from *Thermus thermophilus* consists of 14 subunits with an aggregate molecular mass of 550 kD. The X-ray structure of its 8-subunit hydrophilic (extramembranous) arm, determined by Leonid Sazanov, reveals that this minimal model of Complex I is a Y-shaped assembly that is 140 Å high (Fig. 18-11*a*). This subcomplex contains all of the enzyme's redox centers: an FMN, seven [4Fe–4S] clusters, and two [2Fe–2S] clusters. The FMN is located at the end of a solvent-exposed cavity that presumably forms the

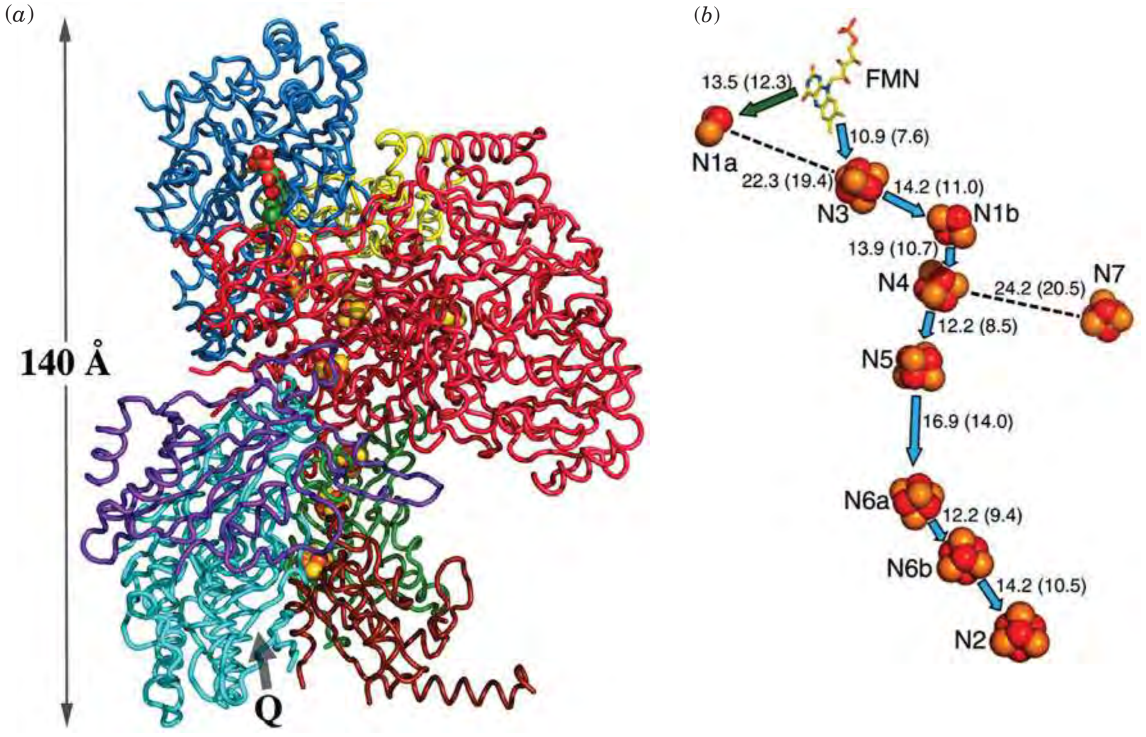

■ **Figure 18-11 | X-ray structure of the hydrophilic domain of Complex I from *Thermus thermophilus.*** (*a*) Side view with the transmembrane arm presumably beneath and extending to the right (upside down relative to Fig. 18-9*b, lower structure*). The eight subunits are drawn in worm form in different colors. The FMN (*upper left*) and the nine iron–sulfur clusters are shown in space-filling form with C green, N blue, O red, P orange, S yellow, and Fe red-brown. The likely CoQ-binding site (Q) is indicated by a gray arrow. (*b*) The arrangement of redox groups viewed similarly to Part *a*. The FMN (stick model with C yellow) and the two [Fe–S] and seven [4Fe–4S] clusters (space-filling models) are shown together with their center-to-center distances in angstroms (shortest edge-to-edge distances are indicated in parentheses). Blue arrows represent the main path of electrons after their transfer from NADH to FMN. [Part *a* based on an X-ray structure by and Part *b* courtesy of Leonid Sazanov, Medical Research Council, Cambridge, U.K. PDBid 2FUG.]

NADH-binding site. The CoQ-binding site appears to be in a cavity near the end of a chain of [4Fe–4S] clusters that is located at the presumed interface with Complex I's membrane-embedded arm.

The transit of electrons from NADH to CoQ presumably occurs by a stepwise mechanism, according to the reduction potential of the various redox centers in Complex I (Table 18-1). This process involves the transient reduction of each group as it binds electrons and its reoxidation when it passes the electrons to the next group. The spatial arrangement of the groups indicates the likely path of the electrons (Fig. 18-11*b*). Note that redox centers do not need to come into contact in order to transfer an electron. An electron's quantum mechanical properties enable it to quickly "tunnel" (jump) between protein-embedded redox groups that are separated by less than ~14 Å. Because electron transfer rates decrease exponentially with the distance between redox centers (they exhibit an ~10-fold decrease for each 1.7 Å increase in distance), electron transfers over distances longer than ~14 Å always involve chains of redox centers.

NADH can participate in only a two-electron transfer reaction. In contrast, the cytochromes of Complex III (see below), to which reduced CoQ passes its electrons, are capable of only one-electron reactions. *FMN and CoQ, which can transfer one or two electrons at a time, therefore provide an electron conduit between the two-electron donor NADH and the one-electron acceptors, the cytochromes.*

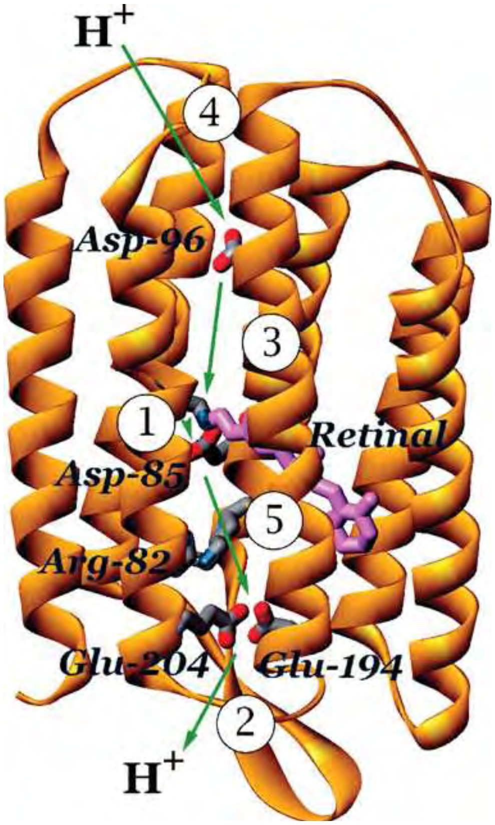

■ **Figure 18-12 | Proton translocation in bacteriorhodopsin.** The retinal prosthetic group in Schiff base linkage to Lys 216 of the seven-transmembrane helix protein is shown in purple. The side chains of amino acids that participate in light-driven proton translocation are shown in stick form with C gray, N blue, and O red. The arrows with their associated numbers indicate the order of proton-transfer steps during the photochemical cycle: (**1**) deprotonation of the Schiff base and protonation of Asp 85; (**2**) proton release to the extracellular surface; (**3**) reprotonation of the Schiff base and deprotonation of Asp 96; (**4**) reprotonation of Asp 96 from the cytoplasmic surface; and (**5**) deprotonation of Asp 85 and reprotonation of the proton release site. [Courtesy of Janos Lanyi, University of California at Irvine. PDBid 1C3W.]

Complex I Translocates Four Protons. *As electrons are transferred between the redox centers of Complex I, four protons are translocated from the matrix to the intermembrane space.* The fate of protons donated by NADH is uncertain: They may be among those pumped across the membrane or used in the reduction of CoQ to its hydroquinone form, $CoQH_2$. Proton pumping in Complex I is apparently driven by conformational changes induced by changes in the redox state of the protein. These conformational changes alter the p*K* values of ionizable side chains so that protons are taken up or released as electrons are transferred. Coupling between electron transport and proton pumping is not well understood because the redox groups are all located in the hydrophilic arm of Complex I (Fig. 18-11), whereas proton transport necessarily occurs across the membrane-embedded arm.

Because a proton is simply an atomic nucleus, it cannot be transported across a membrane in the same way as ions such as Na^+ and K^+. However, a proton can be translocated by "hopping" along a chain of hydrogen-bonded groups in a transmembrane channel, just as it "jumps" between hydrogen-bonded water molecules in solution (Fig. 2-15). Such an arrangement of hydrogen-bonded groups in the protein has been described as a **proton wire** and may include water molecules. Presumably, Complex I includes a proton wire that pumps four protons across the membrane for every pair of electrons that passes from NADH to CoQ.

Bacteriorhodopsin Is a Model Proton Pump. A useful model for proton-translocating complexes is bacteriorhodopsin, an integral membrane protein from *Halobacterium salinarium* that contains seven transmembrane helical segments surrounding a central polar channel (Fig. 9-22). Bacteriorhodopsin is a light-driven proton pump: It obtains the free energy required for pumping protons through the absorbance of light by its retinal prosthetic group. The retinal is linked to the protein via a protonated Schiff base to the side chain of Lys 216.

On absorbing light, the all-*trans*-retinal isomerizes to its 13-*cis* configuration:

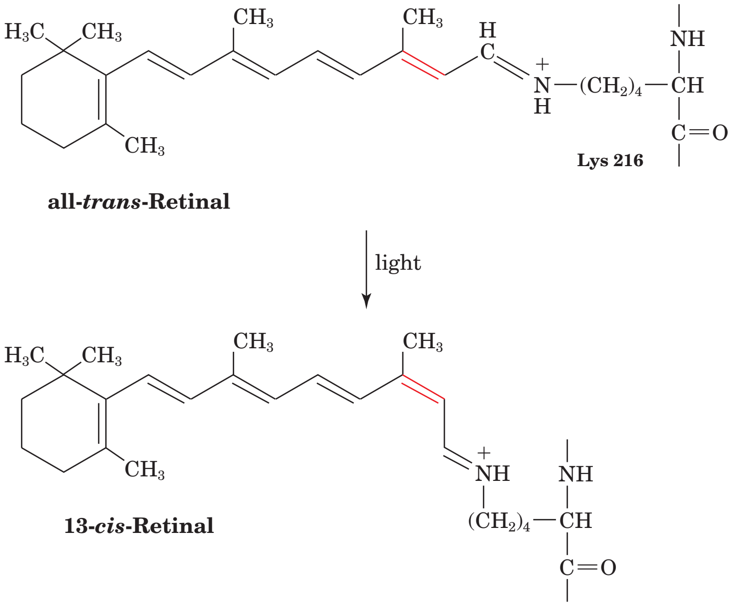

This structural change initiates a sequence of protein conformational adjustments that restore the system to its ground state over a period of ~10 ms. These conformational changes alter the p*K*'s of several amino acid side chains (Fig. 18-12). Specifically, the p*K* of Asp 85 increases so that it can receive a proton from the Schiff base. Asp 85 then transfers the proton to the extracellular medium via a hydrogen-bonded network that includes Arg 82, Glu 194, Glu 204, and several water molecules. Water molecules also move into position to form a hydrogen-bonded network that reprotonates the Schiff base with an intracellular proton via Asp 96, whose p*K* decreases. The net result is that a proton appears to move from the cytosol to the cell exterior (the proton that leaves the cytosol is not the same proton that enters the extracellular space).

The various amino acid side chains involved in proton transport in bacteriorhodopsin move by ~1 Å or less, but this is enough to alter their p*K* values and to sequentially make and break hydrogen bonds so as to allow a proton to pass along the proton wire. The vectorial (one-way) nature of this process arises from the unidirectional series of conformational changes made by the photoexcited retinal as it relaxes to its ground state. Electron transfers between the various redox cofactors of Complex I likely motivate a similar sequence of conformational and p*K* changes.

D | Complex II Contributes Electrons to Coenzyme Q

Complex II **(succinate–coenzyme Q oxidoreductase),** which contains the citric acid cycle enzyme succinate dehydrogenase (Section 17-3F), passes electrons from succinate to CoQ. Its redox groups include succinate dehydrogenase's covalently bound FAD (Fig. 17-13) to which electrons are initially passed, one [4Fe–4S] cluster, a [3Fe–4S] cluster (essentially a [4Fe–4S] complex that lacks one Fe atom), one [2Fe–2S] cluster, and one **cytochrome b_{560}** (cytochromes are discussed in Box 18-1).

The free energy for electron transfer from succinate to CoQ (Fig. 18-7) is insufficient to drive ATP synthesis. The complex is nevertheless important because it allows relatively high-potential electrons to enter the electron-transport chain by bypassing Complex I.

Note that Complexes I and II, despite their names, do not operate in series. But both accomplish the same result: the transfer of electrons to CoQ from reduced substrates (NADH or succinate). *CoQ, which diffuses in the lipid bilayer among the respiratory complexes, therefore serves as a sort of collection point for electrons.* As we shall see in Section 20-2C, the first step in fatty acid oxidation generates electrons that enter the electron-transport chain at the level of CoQ. CoQ also collects electrons from the $FADH_2$ produced by the glycerophosphate shuttle (Fig. 18-5).

Complex II Contains a Linear Chain of Redox Cofactors. The X-ray structures of mitochondrial Complex II and the closely related *E. coli* Complex II have been determined (Fig. 18-13). The *E. coli* Complex II is a 360-kD mushroom-shaped homotrimer

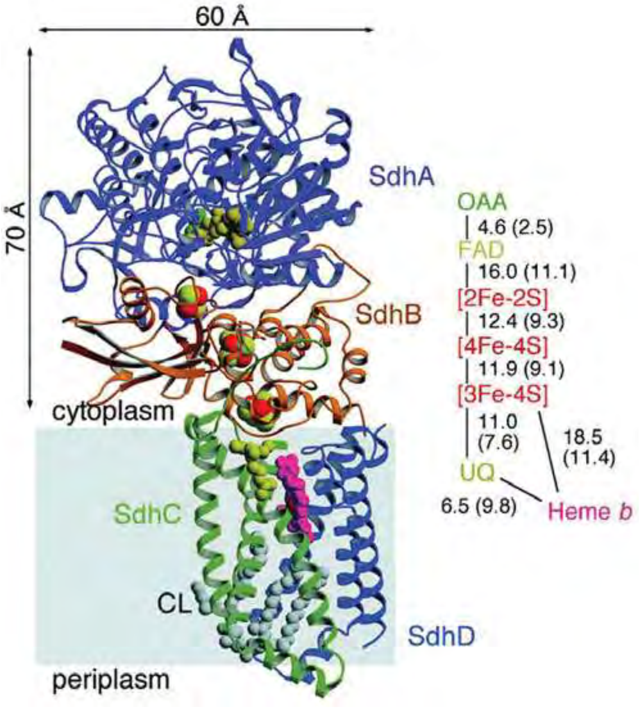

■ **Figure 18-13** | **X-Ray structure of *E. coli* Complex II.** A protomer of the trimeric complex as viewed parallel to the membrane with the cytoplasm above. SdhA, SdhB, SdhC, and SdhD are respectively purple, brown, green, and blue. The bound oxaloacetate inhibitor (OAA; *dark green*), the FAD (*yellow-green*), the Fe–S clusters (*Fe red and S green*), the ubiquinone (*green*), and the heme *b* (*magenta*) are drawn in space-filling form as are bound cardiolipin (CL) molecules (*gray*). The center-to-center and edge-to-edge (in parentheses) distances in angstroms between redox centers are shown. The inferred position of the membrane is indicated by the light blue shading. [Courtesy of So Iwata, Imperial College London, U.K. PDBid 1NEK.]

BOX 18-1 **PERSPECTIVES IN BIOCHEMISTRY**

Cytochromes Are Electron-Transport Heme Proteins

Cytochromes, whose function was elucidated in 1925 by David Keilin, are redox-active proteins that occur in all organisms except a few types of obligate anaerobes. These proteins contain heme groups that alternate between their Fe(II) and Fe(III) oxidation states during electron transport.

The heme groups of the reduced Fe(II) cytochromes have prominent visible absorption spectra consisting of three peaks: the α, β, and γ **(Soret)** bands. The spectrum for cytochrome *c* is shown in Fig. *a*.

The wavelength of the α peak, which varies characteristically with the reduced cytochrome species (it is absent in oxidized cytochromes), is used to differentiate the various cytochromes in mitochondrial membranes (*top right of Fig. a and Fig. b*).

Each group of cytochromes contains a differently substituted heme group coordinated with the redox-active iron atom. The *b*-type cytochromes contain **protoporphyrin IX,** which also occurs in myoglobin and hemoglobin (Section 7-1A). The heme group of *c*-type cytochromes differs from protoporphyrin IX in that its vinyl groups have added Cys sulfhydryls across their double bonds to form thioether linkages to the protein. Heme *a* contains a long hydrophobic tail of isoprene units attached to the porphyrin, as well as a formyl group in place of a methyl substituent in hemes *b* and *c*. The

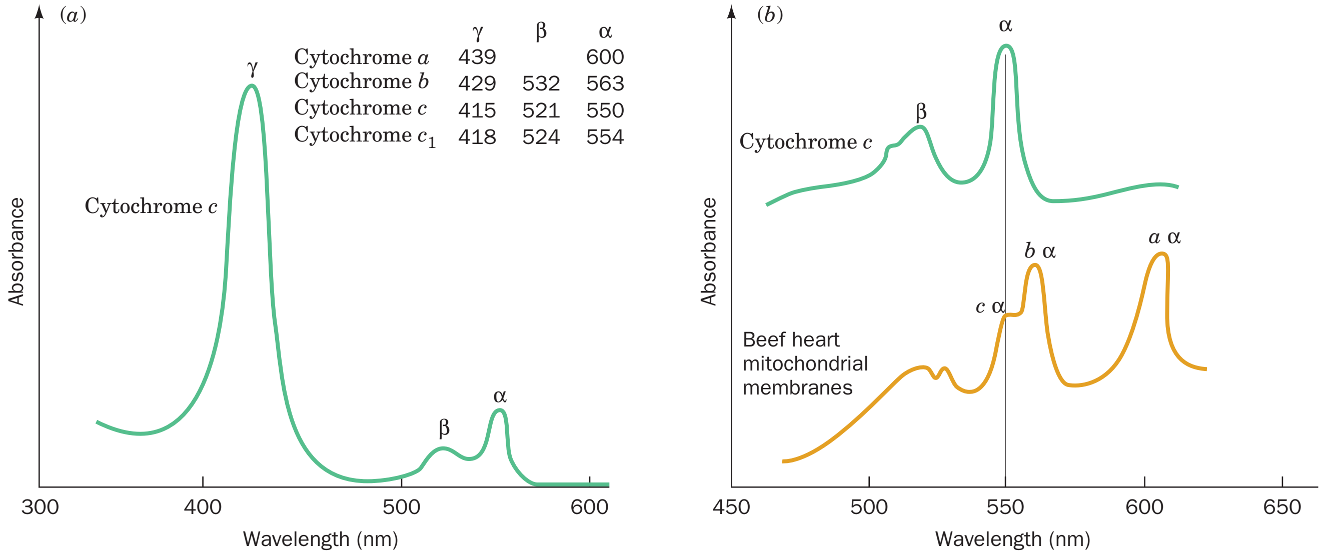

	γ	β	α
Cytochrome *a*	439		600
Cytochrome *b*	429	532	563
Cytochrome *c*	415	521	550
Cytochrome c_1	418	524	554

whose protomers each consist of two hydrophilic subunits, a flavoprotein **(SdhA)** and an iron–sulfur subunit **(SdhB),** that occupy the cytoplasm (the equivalent of the mitochondrial matrix), and two hydrophobic membrane-anchor subunits, **SdhC** and **SdhD,** which each have three transmembrane helices and which collectively bind one *b*-type heme and one ubiquinone. SdhA binds both the substrate (whose binding site is occupied by the inhibitor oxaloacetate in the X-ray structure) and the FAD prosthetic group, whereas SdhB binds the complex's three iron–sulfur clusters. The substrate- and ubiquinone-binding sites are connected by a >40-Å-long chain of redox centers with the sequence substrate–FAD—[2Fe–2S]—[4Fe–4S]—[3Fe–4S]—Q (top to bottom in Fig. 18-13). The heme *b*, which is not located in this direct electron-transfer pathway, apparently fine-tunes the system's electronic properties so as to suppress axial ligands of the heme iron also vary with the cytochrome type. In cytochromes *a* and *b*, both ligands are His residues, whereas in cytochromes *c*, one is His and the other is the S atom of Met.

Within each group of cytochromes, different heme group environments may be characterized by slightly different α peak wavelengths. For this reason, it is convenient to identify cytochromes by the wavelength (in nm) at which its α band absorbance is maximal (e.g., cytochrome b_{560} in Complex II). Cytochromes are also identified nondescriptively with either numbers or letters.

Reduced heme groups are highly reactive entities; they can transfer electrons over distances of 10 to 20 Å at physiologically significant rates. Hence cytochromes, in a *sense*, have the opposite function of enzymes: Instead of persuading unreactive substrates to react, they must prevent their hemes from transferring electrons nonspecifically to other cellular components. This, no doubt, is why these hemes are almost entirely enveloped by protein. However, cytochromes must also provide a path for electron transfer to an appropriate partner. Since electron transfer occurs far more efficiently through bonds than through space, protein structure appears to be an important determinant of the rate of electron transfer between proteins.

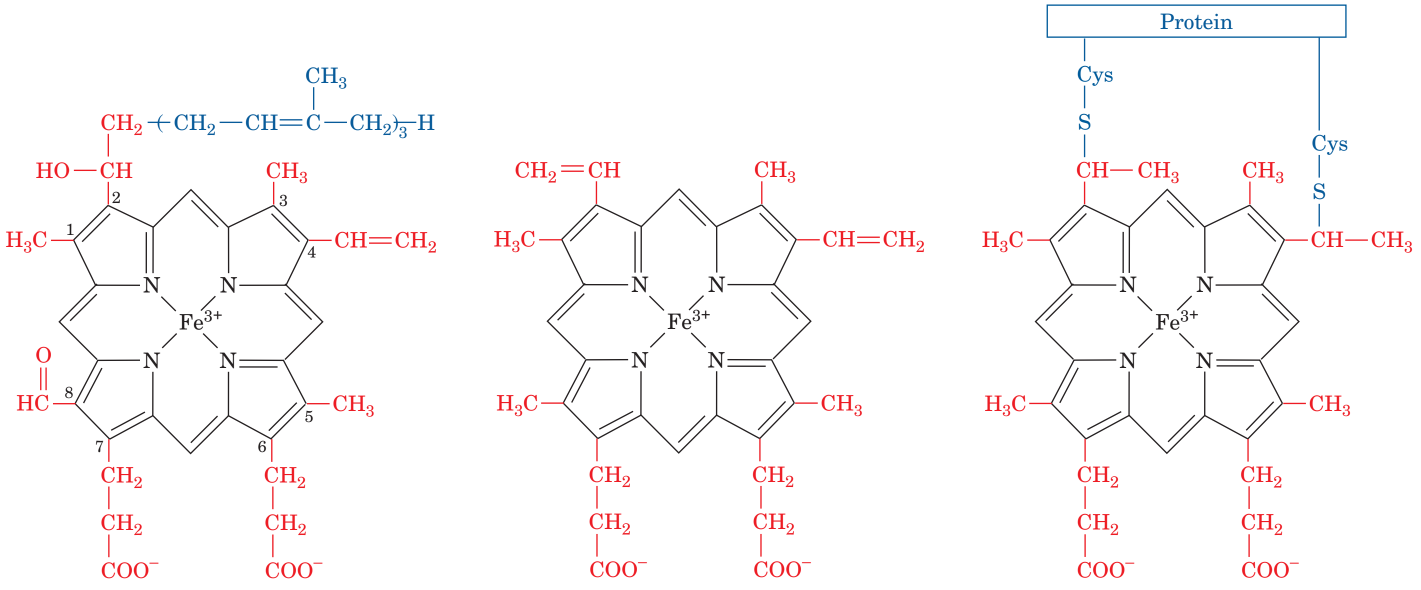

Heme *a*

Heme *b*
(iron–protoporphyrin IX)

Heme *c*

side reactions that form damaging **reactive oxygen species** such as H_2O_2 (Section 18-4B). The [2Fe–2S] cluster labeled N1a in Complex I (Fig. 18-11*b*) may have a similar role.

E | Complex III Translocates Protons via the Q Cycle

Complex III (also known as **coenzyme Q–cytochrome *c* oxidoreductase** or **cytochrome *bc*$_1$**) passes electrons from reduced CoQ to cytochrome *c*. It contains two ***b*-type cytochromes,** one **cytochrome *c*$_1$,** and one [2Fe–2S] cluster in which one of the Fe atoms is coordinated by two His residues rather than two Cys residues (and which is known as a **Rieske center** after its discoverer, John Rieske). Complex III from yeast mitochondria is a 419-kD homodimer with 9 subunits (11 in the 485-kD bovine heart

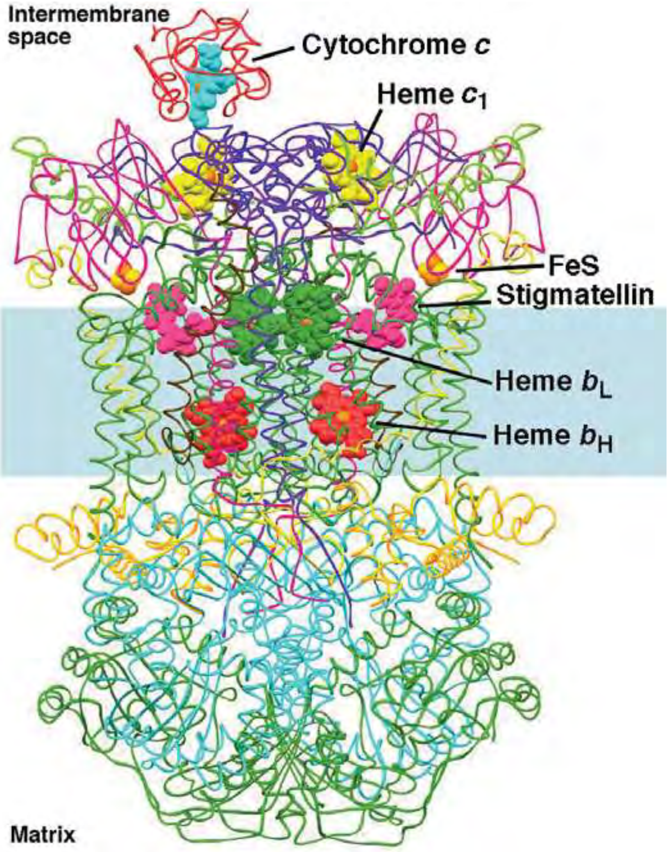

Figure 18-14 | X-Ray structure of yeast Complex III in complex with cytochrome *c* and the inhibitor stigmatellin. The homodimeric complex is viewed from within the plane of the membrane with the intermembrane space above. The nine different subunits in each protomer, which collectively have 12 transmembrane helices, are differently colored with cytochrome *b* green, cytochrome c_1 purple, the ISP magenta, and cytochrome *c* red. The four different heme groups, the [2Fe–2S] cluster, and stigmatellin are drawn in space-filling form in different colors but with all Fe atoms orange. The inferred position of the membrane is indicated by the blue shading. Note that only one cytochrome *c* is bound to the homodimeric Complex III. [Based on an X-ray structure by Carola Hunte, Max Planck Institute for Biophysics, Frankfurt am Main, Germany. PDBid 1KYO.] **See Interactive Exercise 19.**

mitochondrial Complex III). Its X-ray structure (Fig. 18-14) reveals a pear-shaped dimer whose widest part extends ~75 Å into the mitochondrial matrix. The ~40-Å-thick transmembrane portion consists of 12 transmembrane helices per protomer (14 in bovine heart Complex III), most of which are tilted with respect to the plane of the membrane. Eight of these helices belong to the **cytochrome *b*** subunit, which binds both *b*-type cytochrome hemes, $\boldsymbol{b_{562}}$ (or $\boldsymbol{b_H}$**,** for high potential, which lies near the matrix) and $\boldsymbol{b_{566}}$ (or $\boldsymbol{b_L}$**,** for low potential, which lies near the intermembrane space). The cytochrome c_1 subunit is anchored by a single transmembrane helix, with its globular head, which contains a *c*-type heme, extending into the intermembrane space. The **iron–sulfur protein (ISP),** which contains the Rieske center, is similarly anchored by a single transmembrane helix and extends into the intermembrane space. The two ISPs of the dimeric complex are intertwined so that the [2Fe–2S] cluster in the ISP of one protomer interacts with the cytochrome *b* and cytochrome c_1 subunits of the other protomer.

See Guided Exploration 18
The Q cycle.

Electrons from Coenzyme Q Follow Two Paths. Complex III functions to permit one molecule of $CoQH_2$, a two-electron carrier, to reduce two molecules of cytochrome *c*, a one-electron carrier. This occurs by a surprising bifurcation of the flow of electrons from $CoQH_2$ to cytochrome c_1 and to cytochrome *b* (in which the flow is cyclic). It is this so-called **Q cycle** that permits Complex III to pump protons from the matrix to the intermembrane space.

The essence of the Q cycle is that *$CoQH_2$ undergoes a two-cycle reoxidation in which the semiquinone, $CoQ^{\overline{\cdot}}$, is a stable intermediate.* This involves two independent binding sites for coenzyme Q: Q_o, which binds $CoQH_2$ and is located between the Rieske [2Fe–2S] center and heme b_L in proximity to the intermembrane space; and Q_i, which binds both $\text{CoQ}^{-\cdot}$ and CoQ and is located near heme b_H in proximity to the matrix. In the first cycle (Fig. 18-15, *top*), CoQH_2 from Complex I (**1** and **2**) binds to the Q_o site, where it transfers one of its electrons to the ISP (**3**), releasing its two protons into the intermembrane space and yielding $\text{CoQ}^{-\cdot}$. The ISP goes on to reduce cytochrome c_1, whereas the $\text{CoQ}^{-\cdot}$ transfers its remaining electron to cytochrome b_L (**4**), yielding fully oxidized CoQ. Cytochrome b_L then reduces cytochrome b_H (**6**). The CoQ from Step 4 is released from the Q_o site and rebinds to the Q_i site (**5**), where it picks up the electron from cytochrome b_H (**7**), reverting to the semiquinone form, $\text{CoQ}^{-\cdot}$. Thus, the reaction for this first cycle is

$$\text{CoQH}_2 + \text{cytochrome } c_1\,(\text{Fe}^{3+}) \rightarrow$$
$$\text{CoQ}^{-\cdot} + \text{cytochrome } c_1\,(\text{Fe}^{2+}) + 2\,\text{H}^+\ (\textit{intermembrane})$$

In the second cycle (Fig. 18-15, *bottom*), another CoQH_2 from Complex I repeats Steps 1 through 6: One electron reduces the ISP and then cytochrome c_1, and the other electron sequentially reduces cytochrome b_L

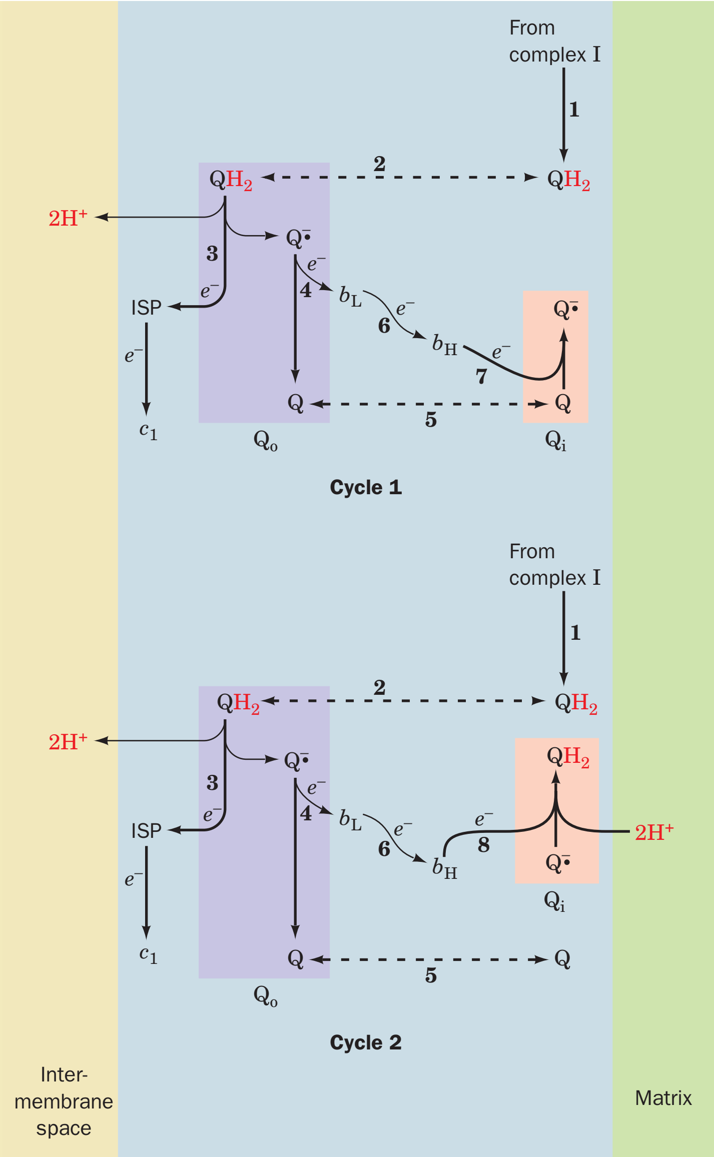

Cycle 1

Cycle 2

Figure 18-15 | **The Q cycle.** The Q cycle, which is mediated by Complex III, results in the translocation of H^+ from the matrix to the intermembrane space as driven by the transport of electrons from cytochrome *b* to cytochrome *c*. The overall cycle is actually two cycles, the first requiring Reactions 1 through 7 and the second requiring Reactions 1 through 6 and 8. (**1**) Coenzyme QH_2 is supplied by Complex I on the matrix side of the membrane. (**2**) QH_2 diffuses to the cytosolic side of the membrane, where it binds in the Q_o site on the cytochrome *b* subunit of Complex III. (**3**) QH_2 reduces the Rieske iron–sulfur protein (ISP), forming $\text{Q}^{-\cdot}$ semiquinone and releasing 2 H^+. The ISP goes on to reduce heme c_1. (**4**) $\text{Q}^{-\cdot}$ reduces heme b_L to form coenzyme Q. (**5**) Q diffuses to the matrix side, where, in Cycle 1 only, it binds in the Q_i site on cytochrome *b*. (**6**) Heme b_L reduces heme b_H. (**7,** Cycle 1 only) Q is reduced to $\text{Q}^{-\cdot}$ by heme b_H. (**8,** Cycle 2 only) $\text{Q}^{-\cdot}$ bound in the Q_i site is reduced to QH_2 by heme b_H. The net reaction is the transfer of two electrons from QH_2 to cytochrome c_1 and the translocation of four protons from the matrix to the intermembrane space [After Trumpower, B.L., *J. Biol. Chem.* **265,** 11410 (1990).]

and then cytochrome b_H. This second electron then reduces the $CoQ^{\overline{\cdot}}$ at the Q_i site produced in the first cycle (**8**), yielding $CoQH_2$. The protons consumed in this last step originate in the mitochondrial matrix. The reaction for the second cycle is therefore

$$\begin{aligned}&CoQH_2 + CoQ^{\overline{\cdot}} + \text{cytochrome } c_1\,(Fe^{3+}) + 2\,H^+\,(\textit{matrix}) \rightarrow \\ &\qquad CoQ + CoQH_2 + \text{cytochrome } c_1\,(Fe^{2+}) + 2\,H^+\,(\textit{intermembrane})\end{aligned}$$

For every two $CoQH_2$ that enter the Q cycle, one $CoQH_2$ is regenerated. The combination of both cycles, in which two electrons are transferred from $CoQH_2$ to cytochrome c_1, results in the overall reaction

$$\begin{aligned}&CoQH_2 + 2\,\text{cytochrome } c_1\,(Fe^{3+}) + 2\,H^+\,(\textit{matrix}) \rightarrow \\ &\qquad CoQ + 2\,\text{cytochrome } c_1\,(Fe^{2+}) + 4\,H^+\,(\textit{intermembrane})\end{aligned}$$

How does the structure of Complex III support the operation of the Q cycle? First, X-ray studies provide direct evidence for the independent existence of the Q_o and Q_i sites. The antifungal agent **stigmatellin,**

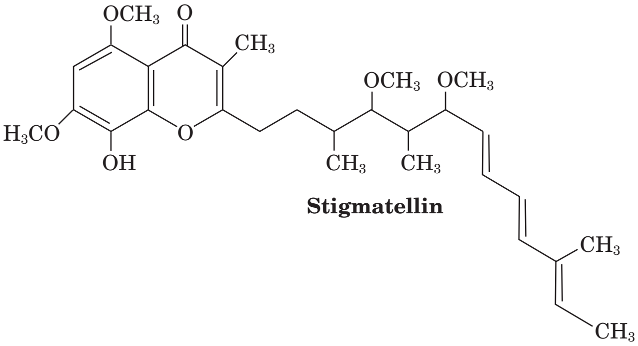

Stigmatellin

which is known to inhibit electron flow from $CoQH_2$ to the ISP and to heme b_L (Steps 3 and 4 of both cycles), binds in a pocket within cytochrome *b* midway between the iron positions of the Rieske [2Fe–2S] center and heme b_L. Thus, this binding pocket is likely to overlap the Q_o site. Similarly, antimycin A (Section 18-2B), which has been shown to block electron flow from heme b_H to CoQ or $CoQ^{\overline{\cdot}}$ (Step 7 of Cycle 1 and Step 8 of Cycle 2), binds in a pocket near heme b_H, thereby identifying this pocket as site Q_i.

The circuitous route of electron transfer in Complex III is tied to the ability of coenzyme Q to diffuse within the hydrophobic core of the membrane in order to bind to both the Q_o and Q_i sites. In fact, the mitochondrial membrane likely contains a pool of CoQ, $CoQ^{\overline{\cdot}}$, and $CoQH_2$, so that the ubiquinone molecule released from the Q_o site may not be the same one that rebinds to the Q_i site in Cycle 1 (Fig. 18-15).

X-Ray structures of cytochrome bc_1 also explain why Q_o-bound $CoQ^{\overline{\cdot}}$ exclusively reduces heme b_L rather than the Rieske [2Fe–2S] cluster of the ISP, despite the greater reduction potential difference ($\Delta\mathscr{E}$) favoring the latter reaction (Table 18-1). The globular domain of the ISP can swing via an ~20-Å hinge motion between the Q_o site and cytochrome c_1. *Consequently, the ISP acquires an electron from $CoQH_2$ in the Q_o site and mechanically delivers it to the heme c_1 group.* The $CoQ^{\overline{\cdot}}$ product cannot reduce the ISP (after it has reduced cytochrome c_1) because the ISP has moved too far away for this to occur.

The net reaction for the Q cycle indicates that *when $CoQH_2$ is oxidized, two reduced cytochrome c molecules and four protons appear on the outer side of the membrane.* Proton transport by the Q cycle thus differs from the proton-pumping mechanism of Complexes I and IV (see below): In the Q cycle, a redox center itself (CoQ) is the proton carrier.

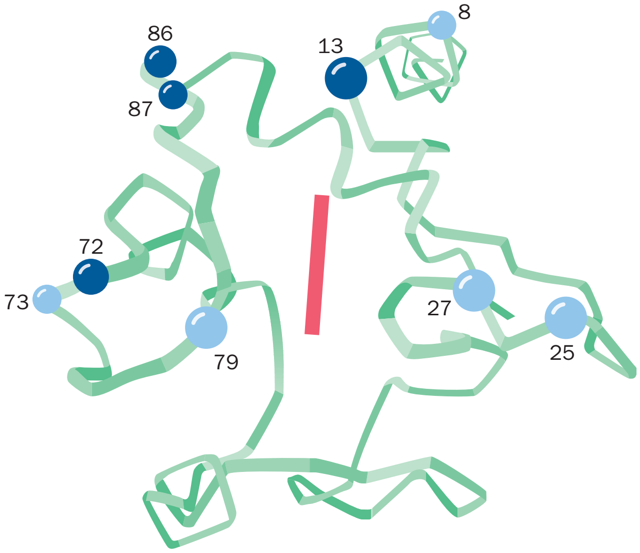

Figure 18-16 | Ribbon diagram of cytochrome *c* showing the Lys residues involved in intermolecular complex formation. Dark and light blue balls, respectively, mark the position of Lys residues whose ε-amino groups are strongly and less strongly protected by cytochrome c_1 or cytochrome c oxidase against acetylation. Note that these Lys residues form a ring around the heme (*solid bar*) on one face of the protein. [After Mathews, F.S., *Prog. Biophys. Mol. Biol.* **45,** 45 (1986).] **See Interactive Exercise 20 and Kinemage Exercise 5.**

Cytochrome *c* Is a Soluble Electron Carrier. The electrons that flow to cytochrome c_1 are transferred to cytochrome c, which, unlike the other cytochromes of the respiratory electron-transport chain, is a peripheral membrane protein. It shuttles electrons between Complexes III and IV on the outer surface of the inner mitochondrial membrane. The evolution and structure of cytochrome c are discussed in Sections 5-4A and 6-2D. Several highy conserved Lys residues in cytochrome c lie in a ring around the exposed edge of its otherwise buried heme group (Fig. 18-16). These positively charged residues constitute binding sites for complementary negatively charged groups on cytochrome c_1 and cytochrome c oxidase. Such interactions presumably serve to align redox groups for optimal electron transfer.

The X-ray structure shown in Fig. 18-14 reveals that the association between cytochrome bc_1 and cytochrome c is particularly tenuous, because its interfacial area (880 Å^2) is significantly less than that exhibited by protein–protein complexes known to have low stability (typically < 1600 Å^2). Such a small interface is well suited for fast binding and release. This interface involves only two cytochrome c Lys residues, Lys 86 and Lys 79, which respectively contact Glu 235 and Ala 164 of cytochrome c_1. Other pairs of charged and often conserved residues surround the contact site but they are not close enough for direct polar interactions. Perhaps these interactions are mediated by water molecules that are not seen in the X-ray structure. The closest approach between the heme groups of the contacting proteins is 4.5 Å between atoms of their respective vinyl side chains, which accounts for the rapid rate of electron transfer between the two redox centers.

F | Complex IV Reduces Oxygen to Water

Cytochrome *c* oxidase (Complex IV) catalyzes the one-electron oxidations of four consecutive reduced cytochrome c molecules and the concomitant four-electron reduction of one O_2 molecule:

$$4\,\text{Cytochrome } c\,(\text{Fe}^{2+}) + 4\,\text{H}^+ + \text{O}_2 \rightarrow 4\,\text{cytochrome } c\,(\text{Fe}^{3+}) + 2\,\text{H}_2\text{O}$$

Mammalian Complex IV is an ~410-kD homodimer whose component protomers are each composed of 13 subunits. The X-ray structure of

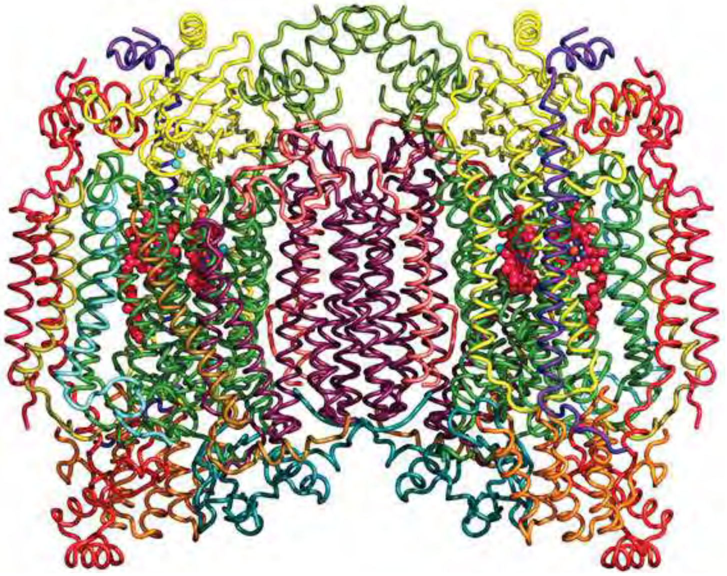

Figure 18-17 | X-Ray structure of the bovine heart cytochrome *c* oxidase homodimer. The homodimeric complex is viewed from within the plane of the membrane with the intermembrane space at the top. The 13 different subunits in each protomer, which collectively have 28 transmembrane helices, are differently colored. The protein's bound heme groups and Cu ions are drawn in space-filling form with C magenta, N blue, O red, Fe orange, and Cu cyan. [Based on an X-ray structure by Shinya Yoshikawa, Himeji Institute of Technology, Hyogo, Japan. PDBid 1V54.] **See Interactive Exercise 21.**

Complex IV from bovine heart mitochondria, determined by Shinya Yoshikawa, reveals that ten of its subunits are transmembrane proteins that contain a total of 28 membrane-spanning α helices (Fig. 18-17). The core of Complex IV consists of its three largest and most hydrophobic subunits, I, II, and III (green, yellow, and purple in Fig. 18-17), which are encoded by mitochondrial DNA (the remaining subunits are nuclearly encoded and must be transported into the mitochondrion). A concave area on the surface of the protein that faces the intermembrane space contains numerous acidic amino acids that can potentially interact with the ring of Lys residues on cytochrome *c,* the electron donor for Complex IV.

Complex IV contains four redox centers: **cytochrome *a*, cytochrome a_3,** a copper atom known as **$\mathbf{Cu_B}$,** and a pair of copper atoms known as the **$\mathbf{Cu_A}$ center** (Fig. 18-18). The Cu_A center, which is bound to Subunit II, lies 8 Å above the membrane surface. Its two copper ions are bridged by the sulfur atoms of two Cys residues, giving it a geometry similar to that of a [2Fe–2S] cluster. The other redox groups—Cu_B and cytochromes *a* and a_3—all bind to Subunit I and lie ~13 Å below the membrane surface.

Spectroscopic studies have shown that electron transfer in Complex IV is linear, proceeding from cytochrome *c* to the Cu_A center, then to heme *a*, and finally to heme a_3 and Cu_B. The Fe of heme a_3 lies only 4.9 Å from Cu_B; these redox groups really form a single binuclear complex. Electrons

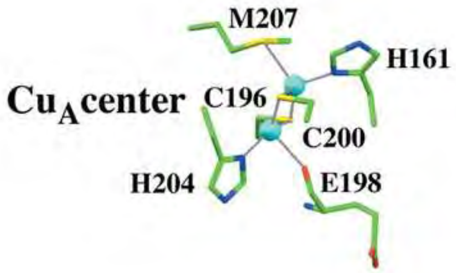

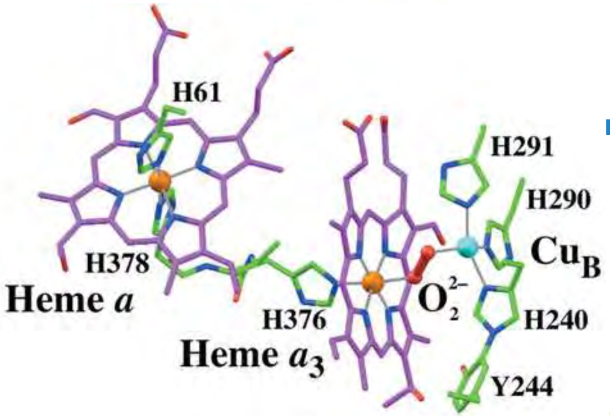

Figure 18-18 | The redox centers of bovine heart cytochrome *c* oxidase. The view is similar to that in Fig. 18-17. The Fe and Cu ions are represented by orange and cyan spheres. Their liganding heme and protein groups are drawn in stick form colored according to atom type (heme C magenta, protein C green, N blue, O red, and S yellow). The peroxy group that bridges the Cu_B and heme a_3 Fe ions is shown in ball-and-stick form in red. Coordination bonds are drawn as gray lines. Note that the side chains of His 240 and Tyr 244 are joined by a covalent bond (*lower right*). [Based on an X-ray structure by Shinya Yoshikawa, Himeji Institute of Technology, Hyogo, Japan. PDBid 2OCC.]

appear to travel between the redox centers of Complex IV via a hydrogen-bonded network, involving amino acid side chains, the polypeptide backbone, and the propionate side chains of the heme groups.

Cytochrome *c* Oxidase Catalyzes a Four-Electron Redox Reaction. The reduction of O_2 to 2 H_2O by cytochrome *c* oxidase takes place at the cytochrome a_3–Cu_B binuclear complex and requires the nearly simultaneous input of four electrons. However, the fully reduced Fe(II)–Cu(I) binuclear complex can readily contribute only three electrons to its bound O_2 in reaching its fully oxidized Fe(IV)–Cu(II) state [cytochrome a_3 assumes its Fe(IV) or **ferryl** oxidation state during the reduction of O_2; see below]. What is the source of the fourth electron?

X-Ray structures of cytochrome *c* oxidase clearly indicate that the His 240 ligand of Cu_B is covalently bonded to the side chain of a conserved Tyr residue (Tyr 244; Fig. 18-18, *lower right*). This places the Tyr phenolic —OH group close to the heme a_3–ligated O_2 such that *Tyr 244 can supply the fourth electron by transiently forming a tyrosyl radical* (TyrO·). Tyrosyl radicals have been implicated in several other enzyme-mediated redox processes, including the generation of O_2 from H_2O in photosynthesis (Section 19-2C) and in the **ribonucleotide reductase** reaction (which converts NDP to dNDP; Section 23-3A). In cytochrome *c* oxidase, the Tyr phenolic —OH group is within hydrogen-bonding distance of the enzyme-bound O_2 and hence is a likely H^+ donor during O—O bond cleavage. The formation of the covalent cross-link is expected to lower both the reduction potential and the p*K* of Tyr 244, thereby facilitating both radical formation and proton donation.

A proposed reaction sequence for cytochrome *c* oxidase, which was elucidated through the use of a variety of spectroscopic techniques, is shown in Fig. 18-19:

1 and 2. The oxidized binuclear complex $[\text{Fe(III)}_{a3}\text{—OH}^-\ \text{Cu(II)}_\text{B}]$ is reduced to its $[\text{Fe(II)}_{a3}\ \text{Cu(I)}_\text{B}]$ state by two consecutive one-electron transfers from cytochrome *c* via cytochrome *a* and Cu_A. A proton from the matrix is concomitantly acquired and an H_2O is released in this process. Tyr 244 (Y—OH) is in its phenolic state.

3. O_2 binds to the reduced binuclear complex so as to ligand its Fe(II)_{a3} atom. It binds to the heme with much the same configuration it has in oxymyoglobin (Fig. 7-3).

4. Internal electron redistribution rapidly yields the oxyferryl complex $[\text{Fe(IV)}{=}\text{O}^{2-}\ \text{HO}^-\text{—Cu(II)}]$ in which Tyr 244 has donated an electron and a proton to the complex and thereby assumed its neutral radical state (Y—O·). This is known as compound P because it was once thought to be a peroxy compound.

5. A third one-electron transfer from cytochrome *c* together with the acquisition of two protons reconverts Tyr 244 to its phenolic state, yielding compound F (for ferryl) and releasing an H_2O.

6. A fourth and final electron transfer and proton acquisition yields the oxidized $[\text{Fe(III)}_{a3}\text{—OH}^-\ \text{Cu(II)}_\text{B}]$ complex, thereby completing the catalytic cycle.

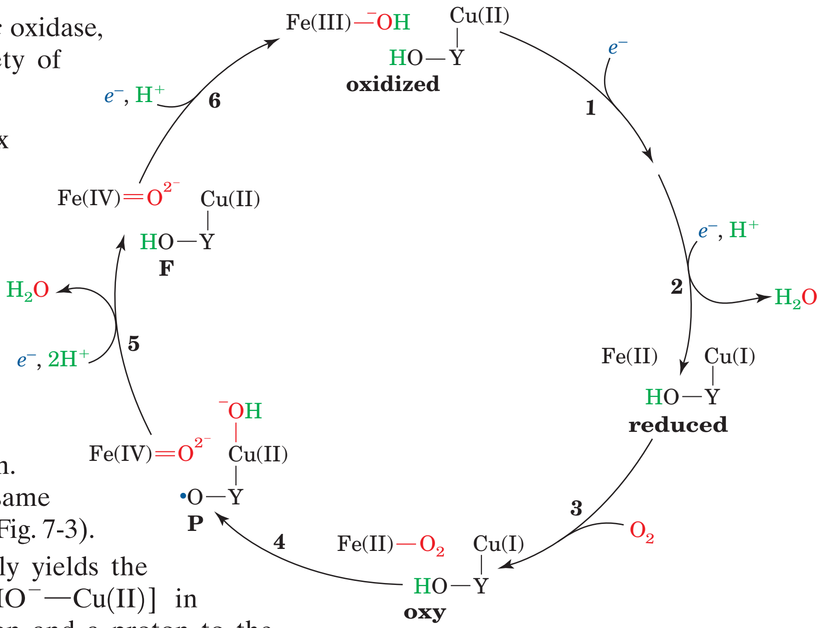

Figure 18-19 | Proposed reaction sequence for cytochrome *c* oxidase. A total of four electrons ultimately donated by four cytochrome *c* molecules, together with four protons, are required to reduce O_2 to H_2O at the cytochrome a_3–Cu_B binuclear complex. The numbered steps are discussed in the text. The entire reaction is extremely fast; it goes to completion in ~1 ms at room temperature. [Modified from Babcock, G.T., *Proc. Natl. Acad. Sci.* **96,** 12971 (1999).]

Cytochrome *c* Oxidase Has Two Proton-Translocating Channels. The reaction catalyzed by cytochrome *c* oxidase contributes to the transmembrane proton gradient in two ways. First, four so-called **chemical** or **scalar** protons are taken up from the matrix during the reduction of O_2 by cytochrome *c* oxidase to yield 2 H_2O, thereby depleting the matrix $[H^+]$. Second, the four-electron reduction reaction is coupled to the translocation of four so-called **pumped** or **vectorial** protons from the matrix to the intermembrane space. Note that for each turnover of the enzyme,

$$8\,H^+_{matrix} + O_2 + 4\text{ cytochrome } c\,(Fe^{2+}) \rightarrow 4\text{ cytochrome } c\,(Fe^{3+}) + 2\,H_2O + 4\,H^+_{intermembrane}$$

a total of eight positive charges are lost from the matrix, thus contributing to the membrane potential difference that drives ATP synthesis (Section 18-3).

X-Ray structures of cytochrome *c* oxidase reveal the presence of two channels that lead from the matrix to the vicinity of the O_2-reducing center, which could potentially transport protons via a proton wire mechanism. The **K-channel** (so named because it contains an essential Lys residue) leads from the matrix side of the protein to Tyr 244, the residue that forms a free radical as described above. Since this channel does not appear to be connected to the intermembrane space, it is thought to supply the chemical protons for O_2 reduction. The **D-channel** (named for a key Asp residue) extends from the matrix to the vicinity of the heme a_3–Cu_B center, where it connects to the so-called **exit channel,** which communicates with the intermembrane space. Apparently, the D-channel, in series with the exit channel, functions to pump vectorial protons from the matrix to the intermembrane space. Moreover, the D-channel also functions as a conduit for the chemical protons that are required for the second part of the reaction cycle (steps 5 and 6 of Fig. 18-19). Despite the foregoing, the mechanism that couples O_2 reduction to proton pumping in Complex IV remains an enigma.

■ **CHECK YOUR UNDERSTANDING**

Describe the route followed by electrons from glucose to O_2.

Discuss why several ATP molecules can be synthesized from the free energy released by electron transport from NADH to O_2.

Position the four electron-transport complexes on a graph showing their relative reduction potentials, and indicate the path of electron flow.

List the types of prosthetic groups in Complexes I, II, III, and IV and state whether they are one- or two-electron carriers.

Describe the different mechanisms for translocating protons during electron transport.

3 Oxidative Phosphorylation

LEARNING OBJECTIVES

- Understand that the chemiosmotic theory invokes a proton gradient to link electron transport to ATP synthesis.
- Understand that ATP synthase consists of an F_1 component that catalyzes ATP synthesis by a binding change mechanism, and an F_0 component that includes a *c*-ring whose rotation is driven by the dissapation of the proton gradient and drives conformational changes in the F_1 component.
- Understand that for every two electrons that enter the electron-transport chain as NADH and reduce one oxygen atom, approximately 2.5 ATP molecules are produced, giving a P/O ratio of 2.5.
- Understand that agents that dissipate the proton gradient can uncouple electron transport and ATP synthesis.

The endergonic synthesis of ATP from ADP and P_i in mitochondria is catalyzed by an **ATP synthase** (also known as **Complex V**) that is driven by the electron-transport process. *The free energy released by electron transport through Complexes I–IV must be conserved in a form that the ATP synthase can use.* Such energy conservation is referred to as **energy coupling.**

The physical characterization of energy coupling proved to be surprisingly elusive; many sensible and often ingenious ideas failed to withstand the test of experimental scrutiny. For example, one theory—now abandoned—was that electron transport yields a "high-energy" intermediate, such as phosphoenolpyruvate (PEP) in glycolysis (Section 15-2J), whose subsequent breakdown drives ATP synthesis. No such intermediate has ever been identified. In fact, ATP synthesis is coupled to electron transport through the formation of a transmembrane proton gradient during electron transport by Complexes I, III, and IV. In this section, we explore this coupling mechanism and the operation of ATP synthase.

A | The Chemiosmotic Theory Links Electron Transport to ATP Synthesis

The **chemiosmotic theory,** proposed in 1961 by Peter Mitchell, spurred considerable controversy before becoming widely accepted (Box 18-2). Mitchell's theory states that *the free energy of electron transport is conserved*

BOX 18-2 **PATHWAYS OF DISCOVERY**

Peter Mitchell and the Chemiosmotic Theory

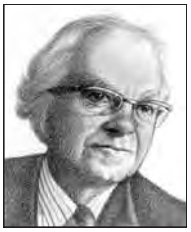

Peter Mitchell (1920–1992)

One of the most dramatic paradigm shifts in biochemistry came about through the work of Peter Mitchell, whose chemiosmotic hypothesis linked biological electron transport to ATP synthesis. Mitchell was primarily a theoretical biochemist, although he also generated experimental data to support his hypothesis. He once compared the human mind to a garden planted with facts and ideas that are constantly being rearranged. However, he promoted his own ideas, which were highly controversial, with great tenacity and very little flexibility.

Mitchell graduated from the University of Cambridge in 1942 and conducted research there, laying the groundwork for the chemiosmotic theory. Mitchell continued his work after 1955 at the University of Edinburgh. He was captivated by the idea of compartmentation in living cells and by the vectorial, or one-way, aspect of metabolic processes. Initially, he chose to study phosphate transport in bacteria because this process was linked both to metabolism and to transmembrane transport. He realized that the vectorial nature of membrane transport must be due to the presence of membrane-associated systems that were driven by chemical forces.

Mitchell also became interested in the respiratory chain, an idea formulated by David Keilin at Cambridge, because this too was a clearly vectorial biological phenomenon. Mitchell reasoned that there must be enzymes that, like transporters, convert a substrate on one side of a membrane to a product on the other side. Other researchers had already discovered that the activity of the respiratory chain generated a pH gradient. Mitchell's genius was to explain how this pH gradient could drive ATP synthesis. In his seminal paper of 1961, Mitchell proposed that the respiratory chain, associated with the cristae in the mitochondrion, generates a protonmotive force due to electrical and pH differences across the membrane. This force drives an ATPase, working in reverse, to catalyze the condensation of phosphate with ADP to produce ATP.

Mitchell's hypothesis, elegant as it was, met strong resistance from other biochemists for several reasons. First, chemiosmosis was a theoretical notion without direct experimental evidence. Second, the study of oxidative phosphorylation was dominated by a few powerful laboratories that were not inclined to welcome new theories. In particular, metabolic studies since the mid-1940s had been focused on the activities of soluble enzymes. Mitchell's theory was not a product of this classic biochemical approach but instead came through an understanding of membrane physiology. Furthermore, the prevailing theories about the connection between electron transport and ATP synthesis centered on a phosphorylated compound as a high-energy intermediate. Fritz Lipmann (Box 14-3) had proposed that a high-energy phosphate group might become attached to some component of the respiratory chain. This hypothesis was later amended to invoke a soluble phosphorylated intermediate. The search for the elusive compound lasted some 20 years, and the investment of time and money may have made some researchers hesitant to abandon this theory in favor of Mitchell's seemingly outrageous proposal. In the meantime, a third theory was proposed, in which electron transport was coupled to ATP synthesis through protein conformational changes, with the observed pH gradient presumed to be simply a by-product of this process.

Mitchell's chemiosmotic hypothesis did not garner significant support until about 10 years after its publication. During this period of sometimes acrimonious debate, Mitchell became ill, moved to Cornwall, and renovated a manor house, part of which became a private laboratory, known as Glynn Research, that was funded by Mitchell's family fortune. Here, he and his lifelong collaborator, Jennifer Moyle, produced experimental evidence to support the chemiosmotic theory. Ultimately, Mitchell was proven correct by other researchers who demonstrated the proton-pumping activity of purified mitochondrial components reconstituted in liposomes. Mitchell was awarded a Nobel Prize in Chemistry in 1978.

Mitchell succeeded in changing the prevailing views of a central feature of aerobic metabolism, although it was a long battle. He later expressed sadness that his work was taken for granted, as if it had been "self-evident from the beginning." Oddly, Mitchell stubbornly resisted altering any of his own ideas. For example, he never wavered in his belief that protons participate directly in ADP phosphorylation in the active site of ATP synthase. And for many years, Mitchell refused to acknowledge proton pumping (as we now know occurs in Complexes I and IV). Instead, he insisted that the source of the proton gradient was a "redox loop" in which two electrons are transferred from the positive to the negative side of the membrane and combine with two protons to reduce a quinone to a quinol. The quinol then diffuses back across the bilayer to be reoxidized at the positive side, where the protons are released. The redox loop mechanism, which requires two "active sites," does occur during the Q cycle in mitochondrial Complex III and in certain bacterial systems, but it cannot account for the entire protonmotive force that is the heart of the chemiosmotic mechanism.

Mitchell, P., Coupling of phosphorylation to electron and hydrogen transfer by a chemiosmotic type of mechanism, *Nature* **191,** 144–148 (1961).

Prebble, J., Peter Mitchell and the ox phos wars, *Trends Biochem. Sci.* **27,** 209–212 (2002).

by pumping H^+ from the mitochondrial matrix to the intermembrane space to create an electrochemical H^+ gradient across the inner mitochondrial membrane. The electrochemical potential of this gradient is harnessed to synthesize

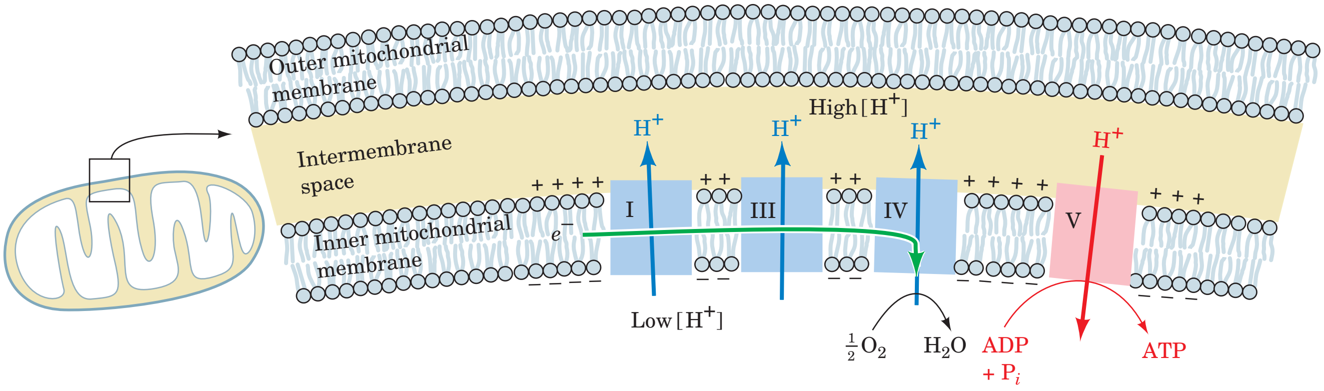

Figure 18-20 | The coupling of electron transport and ATP synthesis. Electron transport (*green arrow*) generates a proton electrochemical gradient across the inner mitochondrial membrane. H$^+$ is pumped out of the mitochondrion during electron transport (*blue arrows*) and its exergonic return powers the synthesis of ATP (*red arrows*). Note that the intermembrane space is topologically equivalent to the cytosol because the outer mitochondrial membrane is permeable to H$^+$. **See the Animated Figures.**

ATP (Fig. 18-20). Several key observations are explained by the chemiosmotic theory:

1. Oxidative phosphorylation requires an intact inner mitochondrial membrane.
2. The inner mitochondrial membrane is impermeable to ions such as H$^+$, OH$^-$, K$^+$, and Cl$^-$, whose free diffusion would discharge an electrochemical gradient.
3. Electron transport results in the transport of H$^+$ out of intact mitochondria (the intermembrane space is equivalent to the cytosol), thereby creating a measurable electrochemical gradient across the inner mitochondrial membrane.
4. Compounds that increase the permeability of the inner mitochondrial membrane to protons, and thereby dissipate the electrochemical gradient, allow electron transport (from NADH and succinate oxidation) to continue but inhibit ATP synthesis; that is, they "uncouple" electron transport from oxidative phosphorylation. Conversely, increasing the acidity outside the inner mitochondrial membrane stimulates ATP synthesis.

An entirely analogous process occurs in bacteria, whose electron-transporting machinery is located in their plasma membranes (Box 18-3).

Electron Transport Generates a Proton Gradient. *Electron transport, as we have seen, causes Complexes I, III, and IV to transport protons across the inner mitochondrial membrane from the matrix, a region of low [H$^+$], to the intermembrane space (which is in contact with the cytosol), a region of high [H$^+$]* (Fig. 18-8). The free energy sequestered by the resulting electrochemical gradient (also called the **protonmotive force; pmf**) powers ATP synthesis.

The free energy change of transporting a proton from one side of the membrane to the other has a chemical as well as an electrical component, since H$^+$ is an ion (Section 10-1). ΔG is therefore expressed by Eq. 10-3, which in terms of pH is

$$\Delta G = 2.3\,RT[\text{pH}\,(\textit{side 1}) - \text{pH}\,(\textit{side 2})] + Z\mathcal{F}\Delta\Psi \qquad [18\text{-}1]$$

where Z is the charge on the proton (including sign), $\mathcal{F}$ is the Faraday constant, and $\Delta\Psi$ is the membrane potential. The sign convention for $\Delta\Psi$ is

BOX 18-3 **PERSPECTIVES IN BIOCHEMISTRY**

Bacterial Electron Transport and Oxidative Phosphorylation

It comes as no surprise that aerobic bacteria (such as those pictured below), whose ancestors gave rise to mitochondria, use similar machinery to oxidize reduced coenzymes and conserve their energy in ATP synthesis. In bacteria, the components of the respiratory electron-transport chain are located in the plasma membrane, and protons are pumped from the cytosol to the outside of the plasma membrane. Protons flow back into the cell via an ATP synthase, whose catalytic component is oriented toward the cytosol. This is exactly the arrangement expected if bacteria and mitochondria are evolutionarily related.

The oxidation of $CoQH_2$ is universal in aerobic organisms. In mitochondria, CoQ collects electrons donated by NADH (via Complex I), succinate (via Complex II), and fatty acids. In aerobic bacteria, CoQ is the collection point for electrons extracted by dehydrogenases specific for a wide variety of substrates. In bacteria, as in mitochondria, electrons flow from CoQ through cytochrome-based oxidoreductases before reaching O_2 (*below, right*). In some species, two protein complexes (analogous to mitochondrial Complexes III and IV) carry out this process. In other species, including *E. coli,* a single type of enzyme, **quinol oxidase,** uses the electrons donated by CoQ to reduce O_2.

The advantage of a multicomplex electron-transport pathway is that it affords more opportunities for proton translocation across the bacterial membrane, so the ATP yield per electron is greater. However, the shorter electron-transport pathways may confer a selective advantage in the presence of toxins that inactivate the bacterial counterpart of mitochondrial Complex III. Multiple routes for electron transport probably also allow bacteria to adjust oxidative phosphorylation to the availability of different energy sources and to balance ATP synthesis against the regeneration of various reduced coenzymes. For example, in facultative anaerobic bacteria (which can grow in either the absence or presence of O_2), when energy needs are met through anaerobic fermentation, electron transport can be adjusted to regenerate NAD^+ without synthesizing ATP by oxidative phosphorylation.

A variety of cytochrome-containing protein complexes occur in bacterial plasma membranes. Some of these proteins represent more streamlined versions of the mitochondrial complexes since they lack the additional subunits encoded by the nuclear genome of eukaryotes. However, this is not a universal feature of respiratory complexes, and many bacterial proteins (e.g., **cytochrome *d***) have no counterparts encoded by either the mitochondrial or nuclear genomes.

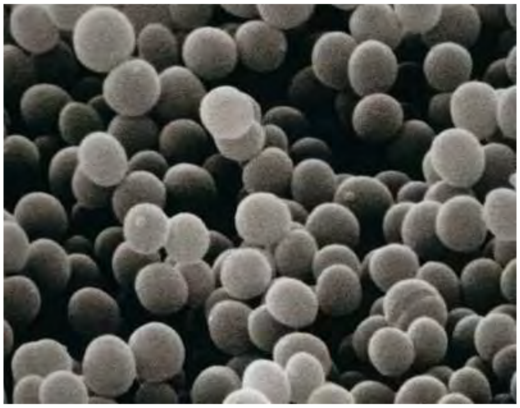

Staphylococcus aureus. [© Tony Brain/Photo Researchers.]

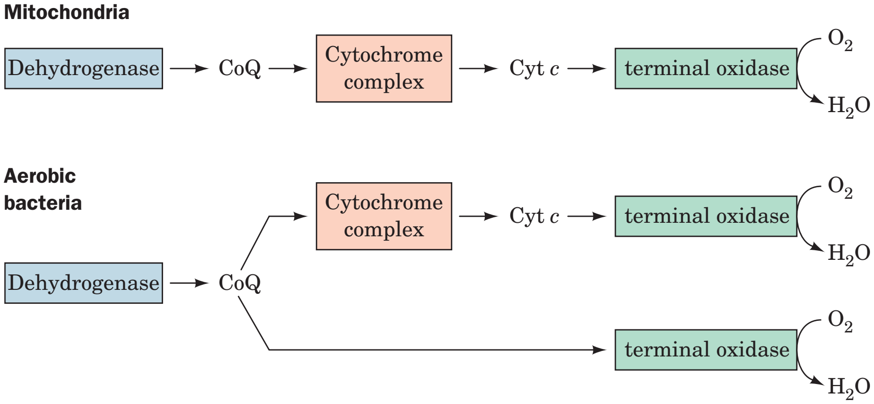

that when a proton is transported from a negative region to a positive region, $\Delta\Psi$ is positive. Since the pH outside the mitochondrion (*side 2*) is less than the pH of the matrix (*side 1*), *the export of protons from the mitochondrial matrix (against the proton gradient) is an endergonic process.*

The measured membrane potential across the inner membrane of a liver mitochondrion, for example, is 0.168 V (inside negative). The pH of its matrix is 0.75 units higher than that of its intermembrane space. ΔG for proton transport out of this mitochondrial matrix is therefore $21.5 \text{ kJ} \cdot \text{mol}^{-1}$. Because formation of the proton gradient is an endergonic process, discharge of the gradient is exergonic. This free energy is harnessed by ATP synthase to drive the phosphorylation of ADP.

An ATP molecule's estimated physiological free energy of synthesis, around +40 to +50 kJ · mol^{-1}, is too large for ATP synthesis to be driven by the passage of a single proton back into the mitochondrial matrix; at least two protons are required. In fact, most experimental measurements (which are difficult to precisely quantitate) indicate that around three protons are required per ATP synthesized.

B | ATP Synthase Is Driven by the Flow of Protons

ATP synthase, also known as **proton-pumping ATP synthase** and **F_1F_0-ATPase,** is a multisubunit transmembrane protein with a total molecular mass of 450 kD. Efraim Racker discovered that mitochondrial ATP synthase is composed of two functional units, **F_0** and **F_1.** F_0 is a water-insoluble transmembrane protein containing as many as eight different types of subunits. F_1 is a water-soluble peripheral membrane protein, composed of five types of subunits, that is easily and reversibly dissociated from F_0 by treatment with urea. Solubilized F_1 hydrolyzes ATP but cannot synthesize it (hence the name ATPase).

Electron micrographs of the inner mitochondrial membrane reveal that its matrix surface is studded with molecules of ATP synthase whose F_1 component is connected to the membrane-embedded F_0 component by a protein stalk, thereby giving F_1 a lollipop-like appearance (Fig. 18-21*a*). Similar entities have been observed lining the inner surface of the bacterial plasma membrane and in chloroplasts (Section 19-2D). Higher resolution cryoelectron micrography-based images of the ATP synthase from bovine heart mitochondria reveal that its F_1 and F_0 components are joined by both an ~50-Å-long central stalk and a less substantial peripherally located connector (Fig. 18-21*b*).

The F_1 Component Has Pseudo-Threefold Symmetry. The F_1 component of mitochondrial ATP synthase has the subunit composition $\alpha_3\beta_3\gamma\delta\varepsilon$. The X-ray structure of the 3440-residue (371-kD) F_1 subunit from bovine heart mitochondria, determined by John Walker and Andrew Leslie, reveals that it consists of an 80-Å-high and 100-Å-wide spheroid that is mounted on a 30-Å-long stem (Fig. 18-22*a*). The α and β subunits, which are 20% identical in sequence and have nearly identical folds, are arranged alternately, like the segments of an orange, around the upper portion of a 90-Å-long α helix formed by the C-terminal segment of the γ subunit (Fig. 18-22*b*). The lower portion of the helix forms an antiparallel coiled coil

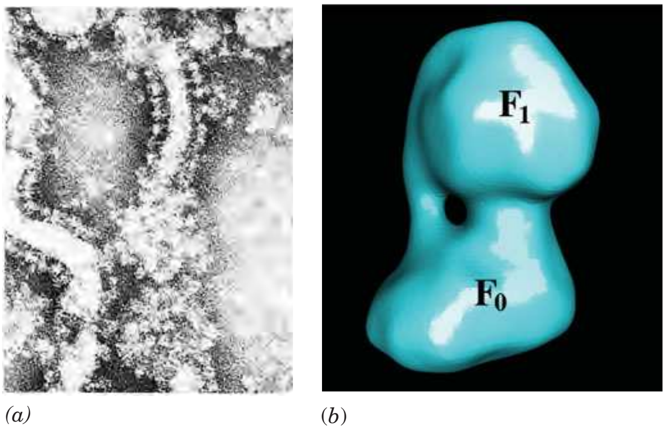

(*a*) (*b*)

■ **Figure 18-21 | Structure of ATP synthase.** (*a*) An electron micrograph of cristae from a mitochondrion showing their F_1 "lollipops" projecting into the matrix. [From Parsons, D.F., *Science* **140,** 985 (1963). Copyright © 1963 American Association for the Advancement of Science. Used by permission.] (*b*) Cryoelectron microscopy–based image of F_1F_0-ATPase from bovine heart mitochondria. [Courtesy of John Rubinstein, University of Toronto, Canada, and John Walker and Richard Henderson, MRC Laboratory of Molecular Biology, Cambridge, U.K.]

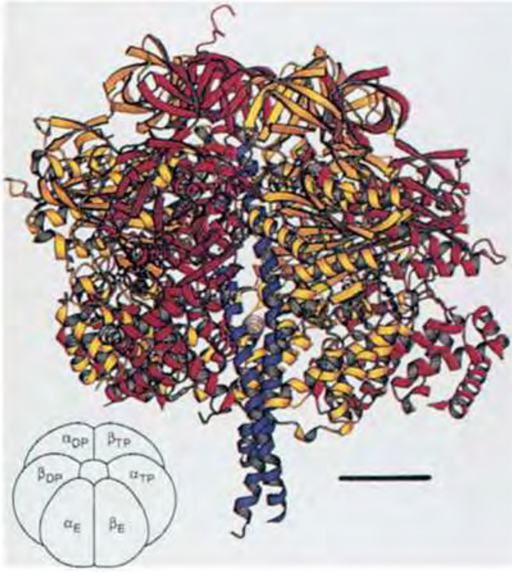

(a)

Figure 18-22 | X-Ray structure of F_1-ATP synthase from bovine heart mitochondria. (*a*) A ribbon diagram in which the α, β, and γ subunits are red, yellow, and blue, respectively. The inset drawing indicates the orientation of these subunits in this view. The bar is 20 Å long. (*b*) Cross section through the electron density map of the protein (the α and β subunits are blue, and the γ subunit is orange). The superimposed C_α backbones of these subunits are yellow, and a bound AMPPNP is represented in space-filling form (C yellow, N blue, O red). (*c*) Pseudosymmetrical arrangement of the $\alpha_3\beta_3$ assembly as viewed from the top of Parts *a* and *b*. The surface is colored according to its electrical potential, with positive potentials blue, negative potentials red, and neutral potentials white. Note the absence of charge on the inner surface of this sleeve. The portion of the γ subunit's C-terminal helix that contacts the sleeve is similarly devoid of charge. [From Abrahams, J.P., Leslie, A.G.W., Lutter, R., and Walker, J.E., *Nature* **370,** 623 and 627 (1994). PDBid 1BMF.] **See Interactive Exercise 22.**

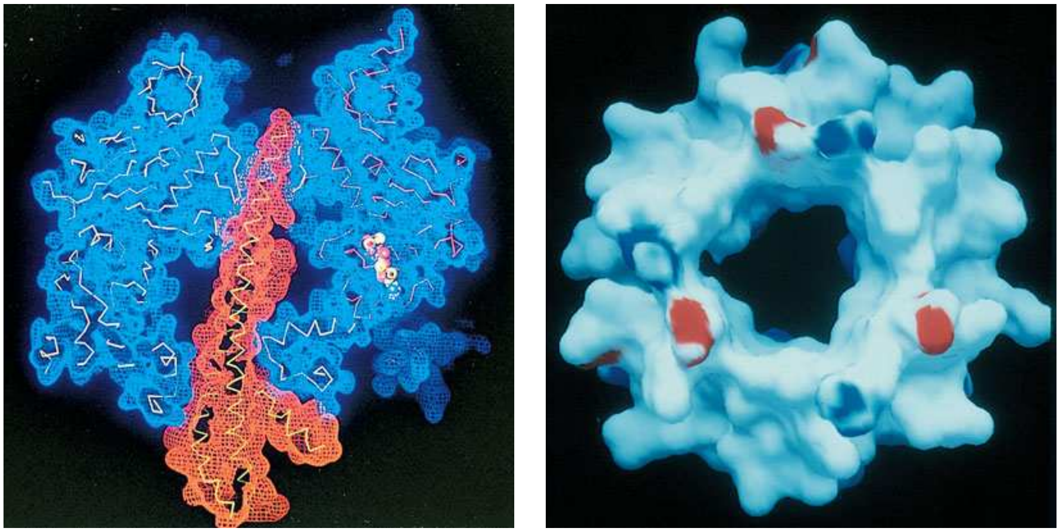

(b) *(c)*

with the N-terminal segment of the γ subunit. This coiled coil, along with the δ and ε subunits that are wrapped around it, links F_1 to F_0.

The cyclic arrangement and structural similarities of F_1's α and β subunits give it both pseudo-threefold and pseudo-sixfold rotational symmetry (Fig. 18-22*c*). Nevertheless, the protein is asymmetric due to the presence of the γ subunit but, more importantly, because each pair of α and β subunits adopts a different conformation, each with a different substrate affinity. Thus one β subunit (designated β_{TP} in Fig. 18-22*a*) binds a molecule of the nonhydrolyzable ATP analog AMPPNP, the second (β_{DP}) binds ADP, and the third (β_E) has an empty and distorted binding site. Only the β subunits catalyze the ATP synthesis reaction although the α subunits also bind AMPPNP.

The F_0 Component Includes a Transmembrane Ring. The F_0 component of bacterial and mitochondrial F_1F_0-ATPases consists of multiple

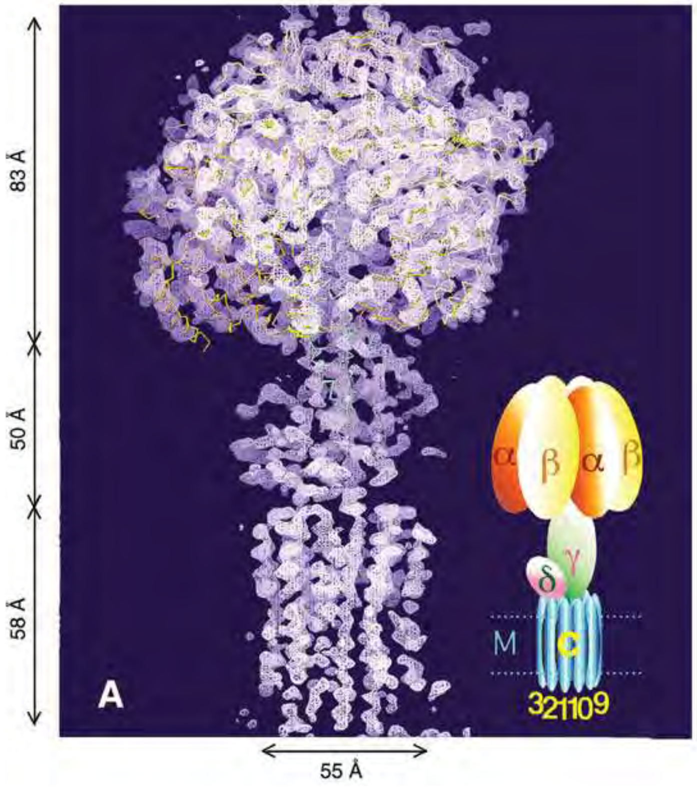

Figure 18-23 | X-Ray structure of the yeast mitochondrial F_1–c_{10} complex. This low-resolution (3.9 Å) electron density map (*pink*) shows the complex as viewed from within the inner mitochondrial membrane with the matrix above. The C_α backbone of bovine F_1 (with α orange, β yellow, and γ green) is superimposed on the electron density map. The inset indicates the location of the subunits of the complex, with the dashed lines indicating the presumed position of the inner mitochondrial membrane (M) and with the *c* subunits numbered. [Courtesy of Andrew Leslie and John Walker, Medical Research Council, Cambridge, U.K. PDBid 1QO1.]

subunits. In *E. coli,* three transmembrane subunits—*a*, *b*, and *c*—form an $a_1b_2c_{9-12}$ complex. Mitochondrial F_0 contains additional subunits whose functions are unclear. The *c* subunits, each of which contains two α helices, associate to form a ring that is embedded in the membrane.

A low-resolution X-ray structure of yeast F_1 in complex with its *c*-ring oligomer (Fig. 18-23) reveals that its α and β subunits have conformations and bound nucleotides similar to those in bovine F_1 (Fig. 18-22). The yeast *c* oligomer consists of 10 subunits (a number which may differ from that in *E. coli*) that associate side by side so as to form two concentric rings of α helices. Modeling studies indicate that the δ subunit contacts both the base of the γ subunit and the *c*-ring, forming a footlike interface between F_0 and F_1 such that about two-thirds of the top surface of the *c*-ring contacts the base of the F_1 stalk (Fig. 18-23).

The sequence of the *a* subunit suggests that this highly hydrophobic 271-residue protein forms five transmembrane helices. The 156-residue *b* subunit consists of a single transmembrane helix anchoring a polar domain that homodimerizes to form a parallel α-helical coiled coil that extends from the periphery of the *c*-ring into the matrix where it contacts the $\delta\alpha_3\beta_3$ assembly (the peripherally located connector in Fig. 18-21*b*).

See Guided Exploration 19
F_1F_0-ATP synthase and the binding change mechanism.

ATP Is Synthesized by the Binding Change Mechanism. The mechanism of ATP synthesis by proton-translocating ATP synthase can be conceptually broken down into three phases:

1. Translocation of protons carried out by F_0.
2. Catalysis of formation of the phosphoanhydride bond of ATP carried out by F_1.
3. Coupling of the dissipation of the proton gradient with ATP synthesis, which requires interaction of F_1 and F_0.

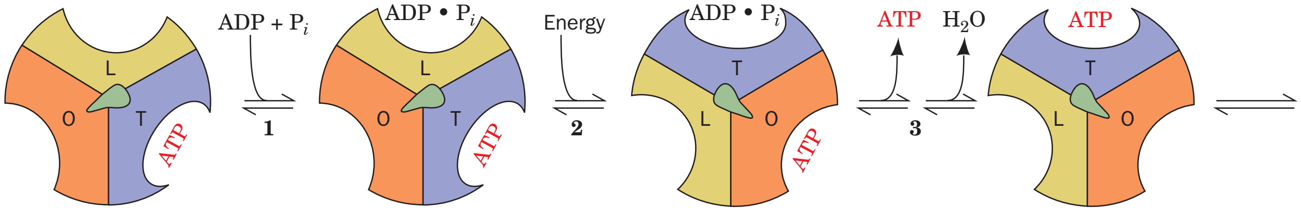

■ **Figure 18-24 | The binding change mechanism for ATP synthase.** F_1 has three chemically identical but conformationally distinct interacting αβ protomers: O, the open conformation, has very low affinity for ligands and is catalytically inactive; L binds ligands loosely and is catalytically inactive; T binds ligands tightly and is catalytically active. ATP synthesis occurs in three steps: (**1**) ADP and P_i bind to site L. (**2**) An energy-dependent conformational change converts binding site L to T, T to O, and O to L. (**3**) ATP is synthesized at site T and ATP is released from site O. The enzyme returns to its initial state after two more passes of this reaction sequence. The free energy that drives the conformational change is transmitted to the catalytic $\alpha_3\beta_3$ assembly via the rotation of the γδ assembly (γε in *E. coli*), here represented by the centrally located asymmetric object (*green*). [After Cross, R.L., *Annu. Rev. Biochem.* **50,** 687 (1980).] **See the Animated Figures.**

Considerable evidence supports a mechanism for ATP formation proposed by Paul Boyer. According to this **binding change mechanism,** F_1 has three interacting catalytic protomers (αβ units), each in a different conformational state: one that binds substrates and products loosely (L state), one that binds them tightly (T state), and one that does not bind them at all (open or O state). *The free energy released on proton translocation is harnessed to interconvert these three states.* The phosphoanhydride bond of ATP is synthesized only in the T state, and ATP is released only in the O state. The reaction involves three steps (Fig. 18-24):

1. ADP and P_i bind to the loose (L) binding site (β_{DP} in Fig. 18-22*a*).
2. A free energy–driven conformational change converts the L site to a tight (T) binding site (β_{TP}) that catalyzes the formation of ATP. This step also involves conformational changes of the other two protomers that convert the ATP-containing T site to an open (O) site (β_E) and convert the O site to an L site.
3. ATP is synthesized at the T site on one subunit while ATP dissociates from the O site on another subunit. The reaction forming ATP is essentially at equilibrium under the conditions at the enzyme's active site. The free energy supplied by the proton flow primarily facilitates the release of the newly synthesized ATP from the enzyme; that is, it drives the T → O transition, thereby disrupting the enzyme–ATP interactions that had previously promoted the spontaneous formation of ATP from ADP + P_i in the T site.

How is the free energy of proton transfer coupled to the synthesis of ATP? The cyclic nature of the binding change mechanism led Boyer to propose that *the binding changes are driven by the rotation of the catalytic assembly,* $\alpha_3\beta_3$, *with respect to other portions of the F_1F_0-ATPase.* This hypothesis is supported by the X-ray structure of F_1. Thus, the closely fitting nearly circular arrangement of the α and β subunits' inner surface about the γ subunit's helical C-terminus is reminiscent of a cylindrical bearing rotating in a sleeve (Figs. 18-22*b,c*). Indeed, the contacting hydrophobic surfaces in this assembly are devoid of the hydrogen-bonding and ionic interactions that would interfere with their free rotation (Fig. 18-22*c*); that is, the bearing and sleeve appear to be "lubricated." Moreover, the central cavity in the $\alpha_3\beta_3$ assembly (Fig. 18-22*b*) would permit the passage of the γ subunit's N-terminal helix within the core of this particle during rotation. Finally, the conformational differences between F_1's three catalytic sites appear to be correlated with the position of the γ subunit. *Apparently the γ subunit, which rotates within the fixed $\alpha_3\beta_3$ assembly, acts as a molecular camshaft in linking the proton gradient–driven F_0 engine to the conformational changes in the catalytic sites of F_1.*

The F_1F_0-ATPase Is a Rotary Engine. The proposed rotation of the $\alpha_3\beta_3$ assembly with respect to the γ subunit engendered by the binding change mechanism has led to the model of the F_1F_0-ATPase diagrammed in Fig. 18-25. A rotational engine must have both a rotor (which rotates) and a stator (which is stationary). In the F_1F_0-ATPase, the rotor is proposed to be an assembly of the *c*-ring with the γ and (*E. coli*) ε subunits, whereas the ab_2 unit and the (*E. coli*) δ subunit together with the $\alpha_3\beta_3$ spheroid form the stator. The rotation of the *c*-ring in the membrane relative to the stationary *a* subunit is driven by the migration of protons from the outside to the inside as we discuss below (here "outside" refers to the mitochondrial intermembrane space or the bacterial exterior, whereas "inside" refers to the mitochondrial matrix or the bacterial cytoplasm). The $b_2\delta$ assembly presumably functions to hold the $\alpha_3\beta_3$ spheroid in position while the γ subunit rotates inside it.

In the model for proton-driven rotation of the F_0 subunit that is diagrammed in Fig. 18-25, protons from the outside enter a hydrophilic channel between the *a* subunit and the *c*-ring, where they bind to a *c* subunit. The *c*-ring then rotates nearly a full turn (while protons bind to successive *c* subunits as they pass this input channel) until the subunit reaches a second hydrophilic channel between the *a* subunit and the *c*-ring that opens into the inside, where the proton is released (in an alternative

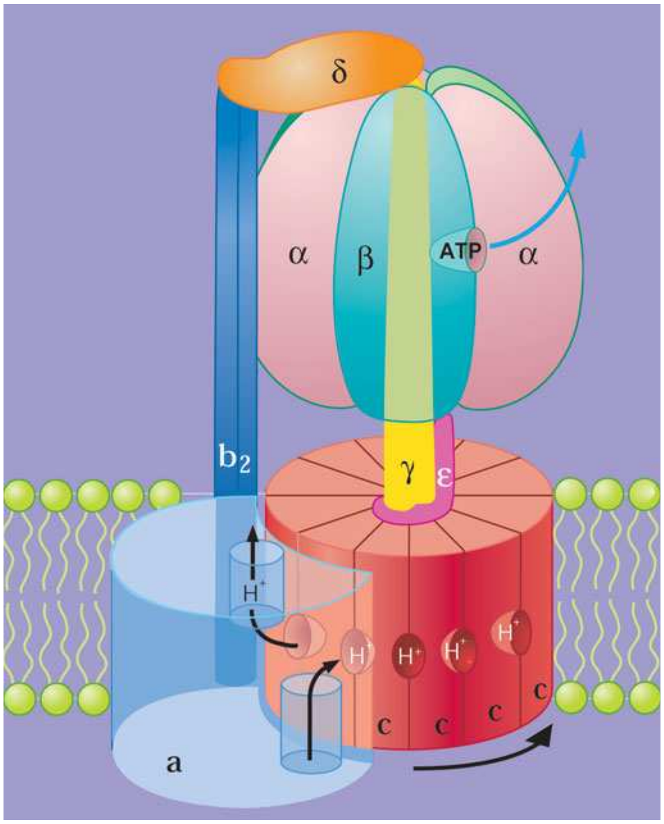

■ **Figure 18-25 | Model of the *E. coli* F_1F_0-ATPase.** The $\gamma\varepsilon-c_{12}$ ring complex is the rotor and the ab_2–$\alpha_3\beta_3\delta$ complex is the stator. Rotational motion is imparted to the rotor by the passage of protons from the outside (periplasmic space, *bottom*) to the inside (cytoplasm, *top*). Protons entering from the outside bind to a *c* subunit where it interacts with the *a* subunit, and exit to the inside after the *c*-ring has made a nearly full rotation as indicated (*black arrows*), so that the *c* subunit again contacts the *a* subunit. The $b_2\delta$ complex presumably functions to prevent the $\alpha_3\beta_3$ assembly from rotating with the γ subunit. Note that the *E. coli* ε subunit is the homolog of the mitochondrial δ subunit, the *E. coli* δ subunit is the homolog of the mitochondrial subunit known as **OSCP,** and the mitochondrial ε subunit has no counterpart in either bacterial or chloroplast ATP synthases. [Courtesy of Richard Cross, State University of New York, Syracuse, New York.]

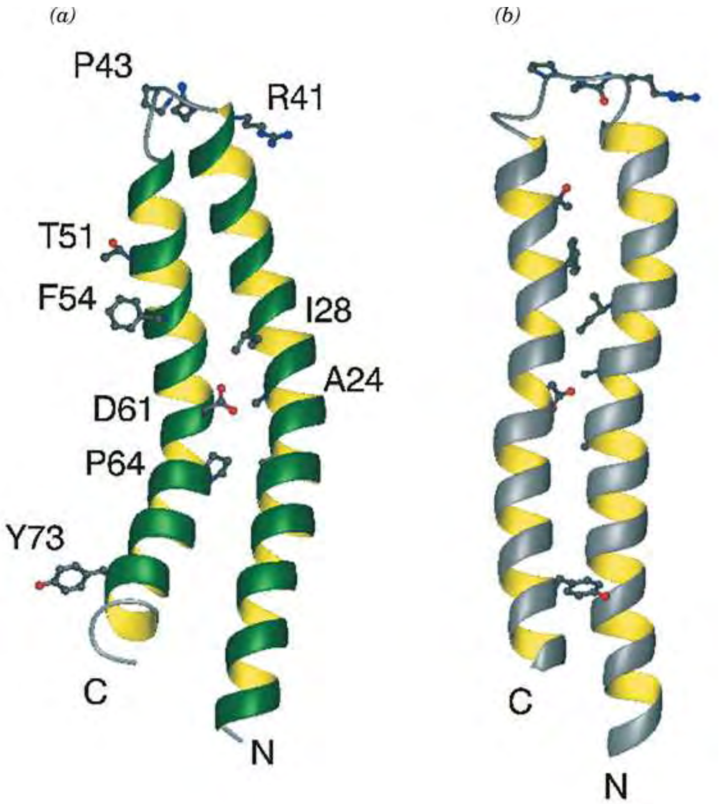

Figure 18-26 | **NMR structure of the *c* subunit of *E. coli* F_1F_0-ATPase.** (*a*) At pH 8, Asp 61 (D61) is deprotonated. (*b*) At pH 5, D61 is protonated. Selected side chains are shown to aid in the comparison of the two structures. Note that the C-terminal helix in the pH 8 structure is rotated 140° clockwise, as viewed from the top of the drawing, relative to that in the pH 5 structure. [Courtesy of Mark Girvin, Albert Einstein College of Medicine. PDBid 1COV.]

model, the protons are released through putative channels between the C-terminal helices of adjacent *c* subunits, channels that are occluded when the *a* and *c* subunits are in contact). Thus, the F_1F_0-ATPase, which generates 3 ATP per turn and (at least in yeast) has 10 *c* subunits in its F_0 assembly, ideally forms 3/10 = 0.3 ATP for every proton it passes from outside to inside.

How does the passage of protons through this system induce the rotation of the *c*-ring and hence the synthesis of ATP? Each *c* subunit consists of two α helices of different lengths that are connected by a four-residue polar loop and arranged in an antiparallel coiled coil. Protons most likely bind to Asp 61 of each *c* subunit, an invariant residue whose protonation and deprotonation alter the subunit's conformation (Fig. 18-26). Evidently, when a *c* subunit binds a proton as it passes the input channel, its conformation changes, which causes it to mechanically push against the *a* subunit so as to induce the *c*-ring to rotate in the direction indicated in Fig. 18-25. This process is augmented by the interaction between Asp 61 on the *c* subunit and the invariant Arg 210 on the *a* subunit. These two residues have been shown to become juxtaposed at some point during the *c*-ring's rotation cycle. It has therefore been proposed that the electrostatic attraction between the cationic Arg 210 and the anionic Asp 61 helps rotate the *c*-ring so as to bring the two residues into opposition but, as this occurs,

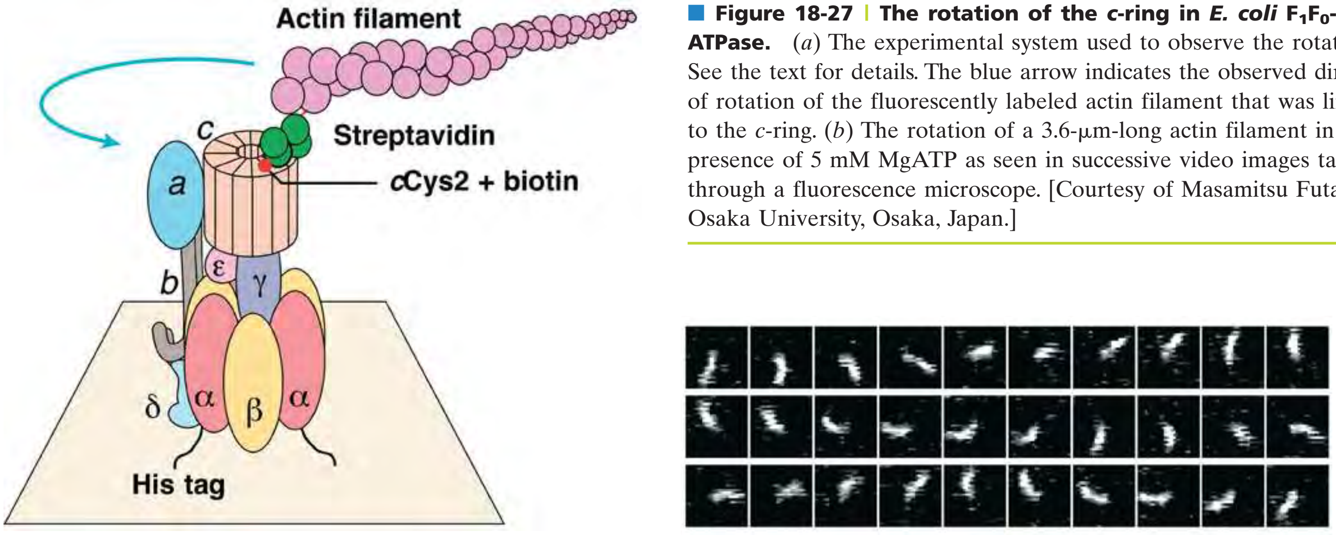

(*a*) (*b*)

Figure 18-27 | The rotation of the *c*-ring in *E. coli* F_1F_0-ATPase. (*a*) The experimental system used to observe the rotation. See the text for details. The blue arrow indicates the observed direction of rotation of the fluorescently labeled actin filament that was linked to the *c*-ring. (*b*) The rotation of a 3.6-μm-long actin filament in the presence of 5 mM MgATP as seen in successive video images taken through a fluorescence microscope. [Courtesy of Masamitsu Futai, Osaka University, Osaka, Japan.]

Asp 61 becomes protonated, thereby forcing the *c*-ring to continue its rotation.

The rotation of the γε–*c*-ring rotor with respect to the ab_2–$\alpha_3\beta_3\delta$ stator has been ingeniously demonstrated by Masamitsu Futai (Fig. 18-27*a*). The $\alpha_3\beta_3$ spheroid of *E. coli* F_1F_0-ATPase was fixed, head down, to a glass surface as follows. Six consecutive His residues (a so-called **His tag**) were mutagenically appended to the N-terminus of the α subunit, which is located at the top of the $\alpha_3\beta_3$ spheroid as it is drawn in Fig. 18-22*a*. The His-tagged assembly was applied to a glass surface coated with horseradish peroxidase (which, like most proteins, sticks to glass) conjugated with **Ni^{2+}-nitriloacetic acid** [Ni^{2+}-$N(CH_2COOH)_3$, which tightly binds His tags], thereby binding the F_1F_0-ATPase to the surface with its F_0 side facing away from the surface. The Glu 2 residues of this assembly's *c* subunits, which are located on the side of the *c*-ring facing away from F_1, had been mutagenically replaced by Cys residues, which were then covalently linked to biotin (Section 16-4A). A fluorescently labeled and biotinylated (at one end) filament of the muscle protein **actin** (Section 7-2C) was then attached to the *c* subunit through the addition of a bridging molecule of **streptavidin,** a bacterial protein that avidly binds biotin to each of four binding sites.

The *E. coli* F_1F_0-ATPase can work in reverse, that is, it can pump protons from the inside to the outside at the expense of ATP hydrolysis (this enables the bacterium to maintain its proton gradient under anaerobic conditions, which it uses to drive various processes). Thus, the foregoing preparation was observed under a fluorescence microscope as a 5 mM MgATP solution was infused over it. *Many of the actin filaments were seen to rotate (Fig. 18-27b), and always in a counterclockwise direction when viewed looking down on the glass surface (from the outside).* This would permit the γ subunit to sequentially interact with the β subunits in the direction

$$\beta_E(\text{O-state}) \rightarrow \beta_{DP}(\text{L-state}) \rightarrow \beta_{TP}(\text{T-state})$$

(Figs. 18-22*a* and 18-24), the direction expected for ATP hydrolysis. Similar experiments revealed that the γ subunit rotates mostly in increments of 120°. Presumably, electrostatic interactions between the γ and β subunits of F_1 act as a catch that temporarily holds the γ subunit in place. As the *c*-ring rotates, strain builds up and causes the γ subunit to snap to the next β subunit. In addition, when a magnetic bead was instead attached to the γ subunit of immobilized F_1-ATPase and an external magnetic field was rotated in the clockwise direction so as to force the γ subunit to follow, ATP was synthesized from ADP + P_i.

C The P/O Ratio Relates the Amount of ATP Synthesized to the Amount of Oxygen Reduced

ATP synthesis is tightly coupled to the proton gradient; that is, ATP synthesis requires the discharge of the proton gradient, and the proton gradient cannot be discharged without the synthesis of ATP. The proton gradient is established through the activity of the electron-transporting complexes of the inner mitochondrial membrane. Therefore, it is possible to express the amount of ATP synthesized in terms of substrate molecules oxidized. Experiments with isolated mitochondria show that the oxidation of NADH is associated with the synthesis of approximately 3 ATP, and the oxidation of $FADH_2$ with approximately 2 ATP. Oxidation of the nonphysiological compound **tetramethyl-*p*-phenylenediamine,**

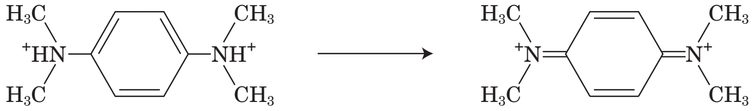

Tetramethyl-*p*-phenylenediamine (TMPD), reduced form

TMPD, oxidized form

which donates an electron pair directly to Complex IV, yields approximately 1 ATP. These stoichiometric relationships are called **P/O ratios** because they relate the amount of ATP synthesized (P) to the amount of oxygen reduced (O).

Experimentally determined P/O ratios are compatible with the chemiosmotic theory and the known structure of ATP synthase. The flow of two electrons through Complexes I, III, and IV results in the translocation of 10 protons into the intermembrane space (Fig. 18-8). Influx of these 10 protons through the F_1F_0-ATPase, which contains 10 *c* subunits in eukaryotes (Fig. 18-23), results in one complete rotation of the *c*-ring–γ subunit rotor relative to the $\alpha_3\beta_3$ spheroid, enough to drive the synthesis of ~3 ATP. Electrons that enter the electron-transport chain as $FADH_2$ at Complex II bypass Complex I and therefore lead to the transmembrane movement of only 6 protons, enough to synthesize ~2 ATP (corresponding to approximately two-thirds of a full rotation of the ATP synthase rotary engine). The transit of two electrons through Complex IV alone contributes 2 protons to the gradient, enough for ~1 ATP (around one-third of a rotation).

In actively respiring mitochondria, *P/O ratios are almost certainly not integral numbers.* This is also consistent with the chemiosmotic theory. Oxidation of a physiological substrate contributes to the transmembrane proton gradient at several points, but the gradient is tapped at only a single point, the F_1F_0-ATPase. Therefore, the number of protons translocated out of the mitochondrion by any component of the electron-transport chain need not be an integral multiple of the number of protons required to synthesize ATP from ADP + P_i. Moreover, the proton gradient is dissipated to some extent by the nonspecific leakage of protons back into the matrix and by the consumption of protons for other purposes, such as the transport of P_i into the matrix (Section 18-1B). Taking P_i transport into account gives a stoichiometry of four protons consumed per ATP synthesized from ADP + P_i. Thus, as Peter Hinkle has experimentally demonstrated, the P/O ratios above are actually closer to 2.5, 1.5, and 1. Consequently, the number of ATPs that are synthesized per molecule of glucose oxidized is 2.5 ATP/NADH × 10 NADH/glucose + 1.5 ATP/$FADH_2$ × 2 $FADH_2$/glucose + 2 ATP/glucose from the citric acid cycle + 2 ATP/glucose from glycolysis = 32 ATP/glucose.

D | Oxidative Phosphorylation Can Be Uncoupled from Electron Transport

Electron transport (the oxidation of NADH and $FADH_2$ by O_2) and oxidative phosphorylation (the proton gradient–driven synthesis of ATP) are normally tightly coupled. *This coupling depends on the impermeability of the inner mitochondrial membrane, which allows an electrochemical gradient to be established across the membrane by H^+ translocation during electron transport.* Virtually the only way for H^+ to re-enter the matrix is through the F_0 portion of ATP synthase. In the resting state, when oxidative phosphorylation is minimal, the electrochemical gradient across the inner mitochondrial membrane builds up to the extent that it prevents further proton pumping and therefore inhibits electron transport. When ATP synthesis increases, the electrochemical gradient dissipates, allowing electron transport to resume.

Over the years, compounds such as **2,4-dinitrophenol (DNP)** have been found to "uncouple" electron transport and ATP synthesis. DNP is a lipophilic weak acid that readily passes through membranes in its neutral, protonated state. In a pH gradient, it binds protons on the acidic side of the membrane, diffuses through the membrane, and releases the protons on the membrane's alkaline side, thereby acting as a proton-transporting ionophore (Section 10-2A) and dissipating the gradient (Fig. 18-28). The chemiosmotic theory provides a rationale for understanding the action of such **uncouplers.** *The presence in the inner mitochondrial membrane of an agent that increases its permeability to H^+ uncouples oxidative phosphorylation from electron transport by providing a route for the dissipation of the proton electrochemical gradient that does not require ATP synthesis.* Uncoupling therefore allows electron transport to proceed

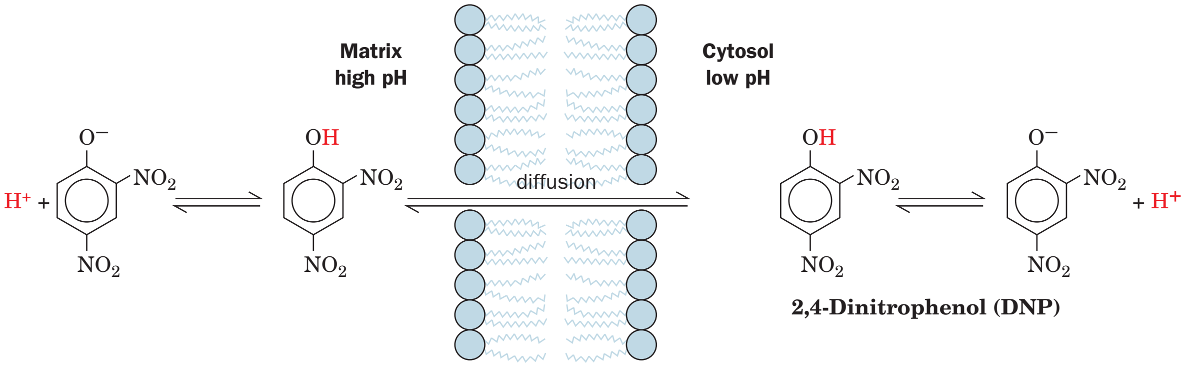

Figure 18-28 | Action of 2,4-dinitrophenol. A proton-transporting ionophore such as DNP uncouples oxidative phosphorylation from electron transport by discharging the electrochemical proton gradient generated by electron transport.

unchecked even when ATP synthesis is inhibited. Consequently, in the 1920s, DNP was used as a "diet pill," a practice that was effective in inducing weight loss but often caused fatal side effects. Under physiological conditions, *the dissipation of an electrochemical* H^+ *gradient, which is generated by electron transport and uncoupled from ATP synthesis, produces heat* (see Box 18-4).

CHECK YOUR UNDERSTANDING

Summarize the chemiosmotic theory.
Describe the overall structure of the F_1 and F_0 components of ATP synthase.
Summarize the steps of the binding change mechanism.
Describe how protons move from the intermembrane space into the matrix. How is proton translocation linked to ATP synthesis?
Explain why the P/O ratio for a given substrate is not necessarily an integer.
Explain how oxidative phosphorylation is linked to electron transport and how the two processes can be uncoupled.

4 Control of Oxidative Metabolism

LEARNING OBJECTIVES

- Understand that the rate of oxidative phosphorylation is coordinated with the cell's other oxidative pathways.
- Understand that although aerobic metabolism is efficient, it leads to the production of reactive oxygen species.

An adult woman requires some 1500 to 1800 kcal (6300–7500 kJ) of metabolic energy per day. This corresponds to the free energy of hydrolysis of over 200 mol of ATP to ADP and P_i. Yet the total amount of ATP present in the body at any one time is <0.1 mol; obviously, this sparse supply of ATP must be continually recycled. As we have seen, when carbohydrates serve as the energy supply and aerobic conditions prevail, this recycling involves glycogenolysis, glycolysis, the citric acid cycle, and oxidative phosphorylation.

Of course, the need for ATP is not constant. There is a 100-fold change in the rate of ATP consumption between sleep and vigorous activity. *The activities of the pathways that produce ATP are under strict coordinated control so that ATP is never produced more rapidly than necessary.* We have already discussed the control mechanisms of glycolysis, glycogenolysis, and the citric acid cycle (Sections 15-4, 16-3, and 17-4). In this section, we discuss the mechanisms that control the rate of oxidative phosphorylation.

A The Rate of Oxidative Phosphorylation Depends on the ATP and NADH Concentrations

In our discussions of metabolic pathways, we have seen that most of their reactions function close to equilibrium. The few irreversible reactions constitute potential control points of the pathways and usually are catalyzed by regulatory enzymes that are under allosteric control. In the case of oxidative phosphorylation, the pathway from NADH to cytochrome *c* functions near equilibrium:

$$\tfrac{1}{2}\,\text{NADH} + \text{cytochrome } c\,(\text{Fe}^{3+}) + \text{ADP} + \text{P}_i \rightleftharpoons \tfrac{1}{2}\,\text{NAD}^+ + \text{cytochrome } c\,(\text{Fe}^{2+}) + \text{ATP} \qquad \Delta G' \approx 0$$

and hence

$$K_{\text{eq}} = \left(\frac{[\text{NAD}^+]}{[\text{NADH}]}\right)^{1/2} \frac{[c^{2+}]}{[c^{3+}]} \frac{[\text{ATP}]}{[\text{ADP}][\text{P}_i]}$$

This pathway is therefore readily reversed by the addition of its product, ATP. However, *the cytochrome c oxidase reaction (the terminal step of the electron-transport chain) is irreversible and is therefore a potential control site.* Cytochrome *c* oxidase, in contrast to most regulatory enzyme systems, appears to be controlled primarily by the availability of one of its substrates, reduced cytochrome *c* (c^{2+}). Since c^{2+} is in equilibrium with the rest of the coupled oxidative phosphorylation system, the concentration of c^{2+} ultimately depends on the intramitochondrial ratios of [NADH]/[NAD$^+$] and [ATP]/[ADP][P$_i$] (the latter quantity is known as the **ATP mass action ratio**). We can see, by rearranging the foregoing equilibrium expression,

$$\frac{[c^{2+}]}{[c^{3+}]} = \left(\frac{[\text{NADH}]}{[\text{NAD}^+]}\right)^{1/2} \frac{[\text{ADP}][\text{P}_i]}{[\text{ATP}]} K_{\text{eq}}$$

BOX 18-4 PERSPECTIVES IN BIOCHEMISTRY

Uncoupling in Brown Adipose Tissue Generates Heat

Heat generation is the physiological function of **brown adipose tissue (brown fat).** This tissue is unlike typical (white) adipose tissue in that it contains numerous mitochondria whose cytochromes cause its brown color. Newborn mammals that lack fur, such as humans, as well as hibernating mammals, all contain brown fat in their neck and upper back that generates heat by **nonshivering thermogenesis.** Other sources of heat are the ATP hydrolysis that occurs during muscle contraction (in shivering or any other movement) and the operation of ATP-hydrolyzing substrate cycles (see Section 15-4B).

[© K.M. Highfill/Photo Researchers.]

The mechanism of heat generation in brown fat involves the regulated uncoupling of oxidative phosphorylation. Brown fat mitochondria contain a proton channel known as **uncoupling protein** (**UCP1,** also called **thermogenin;** see below). In cold-adapted animals, UCP1 constitutes up to 15% of the protein in the inner mitochondrial membranes of brown fat. The flow of protons through UCP1 is inhibited by physiological concentrations of purine nucleotides (ADP, ATP, GDP, GTP), but this inhibition can be overcome by free fatty acids.

Thermogenesis in brown fat mitochondria is under hormonal control (see dia-

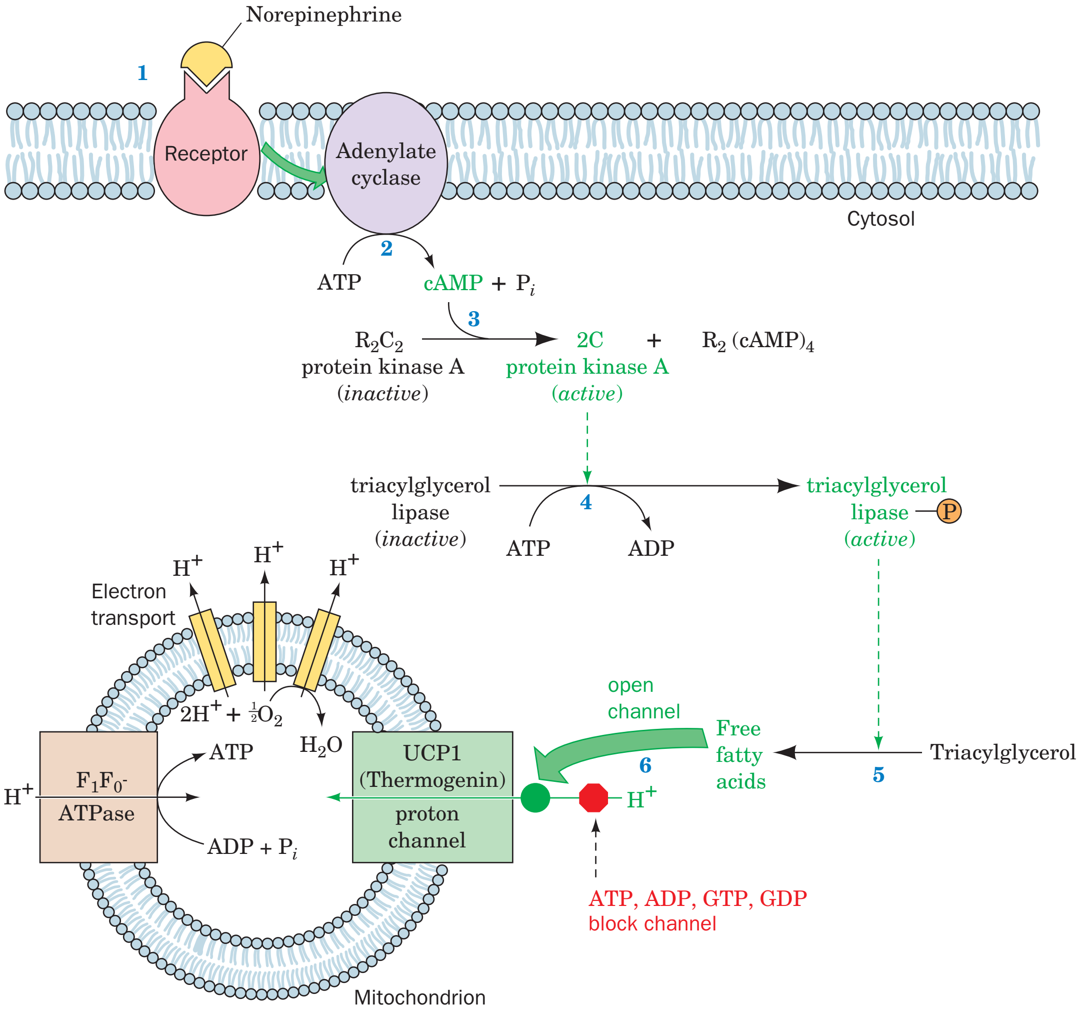
Norepinephrine
1
Receptor
Adenylate cyclase
Cytosol
2
ATP
cAMP + P_i
3
R_2C_2 protein kinase A (*inactive*)
2C protein kinase A (*active*)
+
R_2 (cAMP)$_4$
triacylglycerol lipase (*inactive*)
4
ATP
ADP
triacylglycerol lipase (*active*)
P
H^+
H^+
H^+
Electron transport
$2H^+ + \frac{1}{2}O_2$
H_2O
H^+
F_1F_0-ATPase
ATP
ADP + P_i
UCP1 (Thermogenin) proton channel
open channel
6
Free fatty acids
5
Triacylglycerol
H^+
ATP, ADP, GTP, GDP block channel
Mitochondrion

Mechanism of hormonally induced uncoupling of oxidative phosphorylation in brown fat mitochondria.

gram). Norepinephrine (**1;** noradrenaline) induces the production of the second messenger cAMP (**2**) and thereby activates protein kinase A (**3;** Section 13-3C). The kinase then activates **hormone-sensitive triacylglycerol lipase** (**4**) by phosphorylating it. The activated lipase hydrolyzes triacylglycerols (**5**) to yield free fatty acids that counteract the inhibitory effect of the purine nucleotides on UCP1 (**6**). The resulting flow of protons through UCP1 dissipates the proton gradient across the inner mitochondrial membrane. This allows substrate oxidation to proceed (and generate heat) without the synthesis of ATP.

Adult humans lack brown fat, but the mitochondria of ordinary adipose tissue and muscle appear to contain uncoupling proteins known as **UCP2** and **UCP3.** These proteins may help regulate metabolic rates, and variations in UCP levels or activity might explain why some people seem to have a "fast" or "slow" metabolism. UCPs are being studied as targets for treating obesity, since increasing the activity of UCPs could uncouple respiration from ATP synthesis, thus permitting stored metabolic fuels (especially fat) to be metabolized.

Uncoupling proteins may also play a role in maintaining body temperature, and their function may not be limited to the animal kingdom. Some plants express uncoupling proteins in response to cold stress or to increase flower temperature, possibly to enhance the vaporization of scent to attract pollinators.

that the higher the [NADH]/[NAD$^+$] ratio and the lower the ATP mass action ratio, the higher the concentration of reduced cytochrome *c* and thus the higher the cytochrome *c* oxidase activity.

How is this system affected by changes in physical activity? In an individual at rest, the rate of ATP hydrolysis to ADP and P_i is minimal and the ATP mass action ratio is high; the concentration of reduced cytochrome *c* is therefore low and the rate of oxidative phosphorylation is minimal. Increased activity results in hydrolysis of ATP to ADP and P_i, thereby decreasing the ATP mass action ratio and increasing the concentration of reduced cytochrome *c*. This results in an increase in the rate of electron transport and ADP phosphorylation.

The concentrations of ATP, ADP, and P_i in the mitochondrial matrix depend on the activities of the transport proteins that import these substances from the cytosol. Thus, the ADP–ATP translocator and the P_i transporter may play a part in regulating oxidative phosphorylation. There is also some evidence that Ca^{2+} stimulates the electron-transport complexes and possibly ATP synthase itself. This is consistent with the many other instances in which Ca^{2+} directly stimulates oxidative metabolic processes.

Mitochondria contain an 84-residue protein, called **IF_1** that functions to regulate ATP synthase. In actively respiring mitochondria, in which the matrix pH is relatively high, IF_1 exists as an inactive tetramer. However, below pH 6.5, the protein dissociates into dimers and in this form inhibits the ATPase activity of the F_1 component by binding to the interface between its α_{DP} and β_{DP} subunits so as to trap the ATP bound to the β_{DP} subunit. This appears to be a mechanism to prevent ATP hydrolysis when respiratory activity (and therefore the proton gradient) is temporarily interrupted by lack of O_2. Otherwise, the F_1F_0-ATPase would reverse its direction of rotation as driven by the hydrolysis of ATP (then generated by glycolysis), thus depriving the cell of its remaining energy resources.

Pathways of Oxidative Metabolism Are Coordinately Controlled. The primary sources of the electrons that enter the mitochondrial electron-transport chain are glycolysis, fatty acid degradation, and the citric acid cycle. For example, 10 molecules of NAD$^+$ are converted to NADH per molecule of glucose oxidized (Fig. 18-1). Not surprisingly, the control of glycolysis and the citric acid cycle is coordinated with the demand for oxidative phosphorylation. An adequate supply of electrons to feed the electron-transport chain is provided by regulation of the control points of glycolysis and the citric acid cycle (phosphofructokinase, pyruvate dehydrogenase, citrate synthase, isocitrate dehydrogenase, and α-ketoglutarate dehydrogenase) by adenine nucleotides or NADH or both, as well as by certain metabolites (Fig. 18-29).

One particularly interesting regulatory effect is the inhibition of phosphofructokinase (PFK) by citrate. When demand for ATP decreases, [ATP] increases and [ADP] decreases. Because isocitrate dehydrogenase is activated by ADP and α-ketoglutarate dehydrogenase is inhibited by ATP, the citric acid cycle slows down. This causes the citrate concentration to build up. Citrate leaves the mitochondrion via a specific transport system and, *once in the cytosol, acts to restrain further carbohydrate breakdown by inhibiting PFK.* The citrate concentration also builds up when the acetyl-CoA concentration increases, which occurs, as we shall see in Chapter 20, during the oxidation of fatty acids. The inhibition of glycolysis by fatty acid oxidation is called the **glucose–fatty acid cycle** or **Randle cycle** (after its discoverer, Phillip Randle) although it is not, in fact, a cycle. The Randle cycle allows fatty acids to be utilized as the major fuel for oxidative metabolism in heart muscle, while conserving glucose for organs such as the brain, which require it.

B | Aerobic Metabolism Has Some Disadvantages

Not all organisms carry out oxidative phosphorylation. However, those that do are able to extract considerably more energy from a given amount of a metabolic fuel. This principle is illustrated by the Pasteur effect (Section 15-3C): When anaerobically growing yeast are exposed to oxygen, their glucose consumption drops precipitously. An analogous effect is observed in mammalian muscle; the concentration of lactic acid (the anaerobic product of muscle glycolysis; Section 15-3A) drops dramatically when cells switch to aerobic metabolism. These effects are easily understood by examining the stoichiometries of anaerobic and aerobic breakdown of glucose (Section 17-4):

Anaerobic glycolysis:

$$C_6H_{12}O_6 + 2\,ADP + 2\,P_i \rightarrow 2\,\text{lactate} + 2\,H^+ + 2\,H_2O + 2\,ATP$$

Aerobic metabolism of glucose:

$$C_6H_{12}O_6 + 32\,ADP + 32\,P_i + 6\,O_2 \rightarrow 6\,CO_2 + 38\,H_2O + 32\,ATP$$

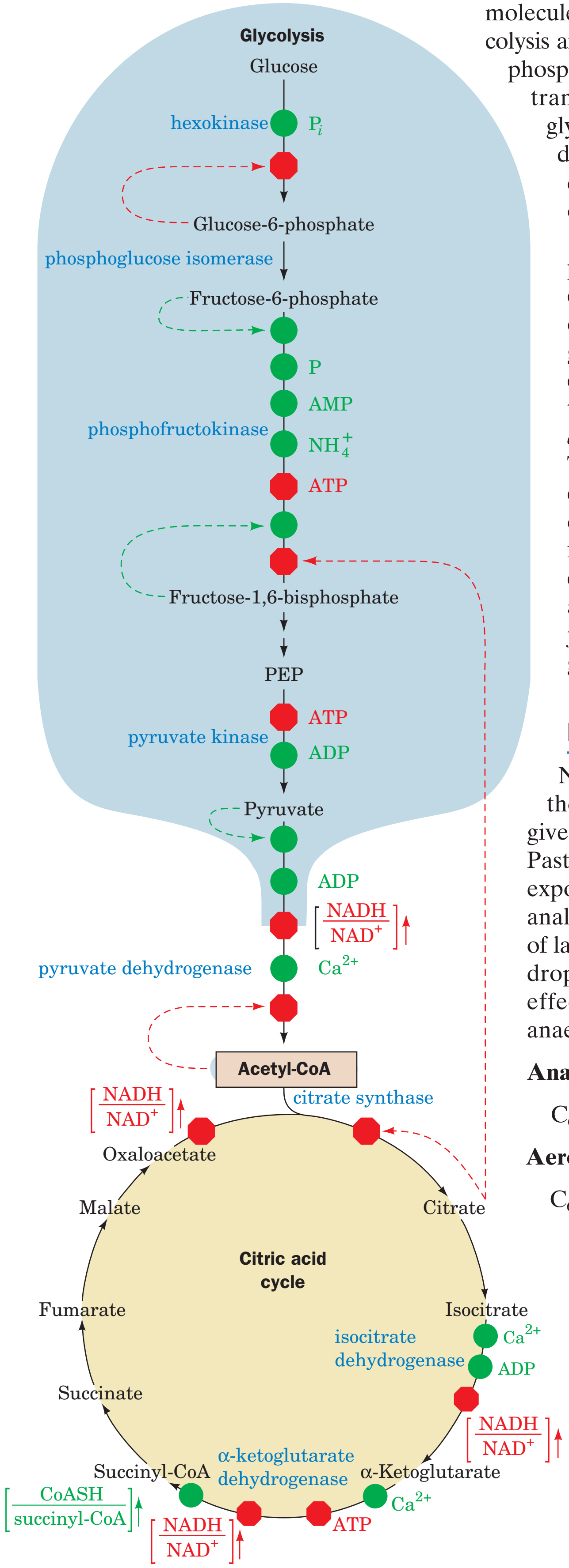
Glycolysis
Glucose
hexokinase
P_i
Glucose-6-phosphate
phosphoglucose isomerase
Fructose-6-phosphate
P
AMP
phosphofructokinase
NH_4^+
ATP
Fructose-1,6-bisphosphate
PEP
ATP
pyruvate kinase
ADP
Pyruvate
ADP
$\left[\frac{NADH}{NAD^+}\right]\uparrow$
pyruvate dehydrogenase
Ca^{2+}
Acetyl-CoA
$\left[\frac{NADH}{NAD^+}\right]\uparrow$
citrate synthase
Oxaloacetate
Malate
Citrate
Citric acid cycle
Fumarate
Isocitrate
isocitrate dehydrogenase
Ca^{2+}
ADP
Succinate
$\left[\frac{NADH}{NAD^+}\right]\uparrow$
α-ketoglutarate dehydrogenase
Succinyl-CoA
α-Ketoglutarate
$\left[\frac{CoASH}{succinyl\text{-}CoA}\right]\uparrow$
$\left[\frac{NADH}{NAD^+}\right]\uparrow$
ATP
Ca^{2+}

Figure 18-29 | The coordinated control of glycolysis and the citric acid cycle. The diagram shows the effects of ATP, ADP, AMP, P_i, Ca^{2+}, and the $[NADH]/[NAD^+]$ ratio (the vertical arrows indicate increases in this ratio). Here a green dot signifies activation and a red octagon represents inhibition. [After Newsholme, E.A. and Leech, A.R., *Biochemistry for the Medical Sciences,* pp. 316, 320, Wiley (1983).]

See the Animated Figures.

BOX 18-5 **BIOCHEMISTRY IN HEALTH AND DISEASE**

Oxygen Deprivation in Heart Attack and Stroke

As outlined in Box 7-1, organisms larger than 1 mm thick require circulatory systems to deliver nutrients to cells and dispose of cellular wastes. In addition, the circulatory fluid in most larger organisms contains proteins specialized for oxygen transport (e.g., hemoglobin). The sophistication of oxygen-delivery systems and their elaborate regulation are consistent with their essential nature and their long period of evolution.

What happens during oxygen deprivation? Consider two common causes of human death, **myocardial infarction** (heart attack) and **stroke,** which result from interruption of the blood (O_2) supply to a portion of the heart or the brain, respectively. In the absence of O_2, a cell, which must then rely only on glycolysis for ATP production, rapidly depletes its stores of phosphocreatine (a source of rapid ATP production; Section 14-2C) and glycogen. As the rate of ATP production falls below the level required by membrane ion pumps for maintaining proper intracellular ion concentrations, osmotic balance is disrupted so that the cell and its membrane-enveloped organelles begin to swell. The resulting overstretched membranes become permeable, thereby leaking their enclosed contents. For this reason, a useful diagnostic criterion for myocardial infarction is the presence in the blood of heart-specific enzymes, such as the H-type isozyme of lactate dehydrogenase (Section 14-1C), which leak out of necrotic (dead) heart tissue. Moreover, the decreased intracellular pH that accompanies anaerobic glycolysis (because of lactic acid production) permits the released lysosomal enzymes (which are active only at acidic pH) to degrade the cell contents. Thus, O_2 deprivation leads not only to cessation of cellular activity but to irreversible cell damage and cell death. Rapidly respiring tissues, such as the heart and brain, are particularly susceptible to damage by oxygen deprivation.

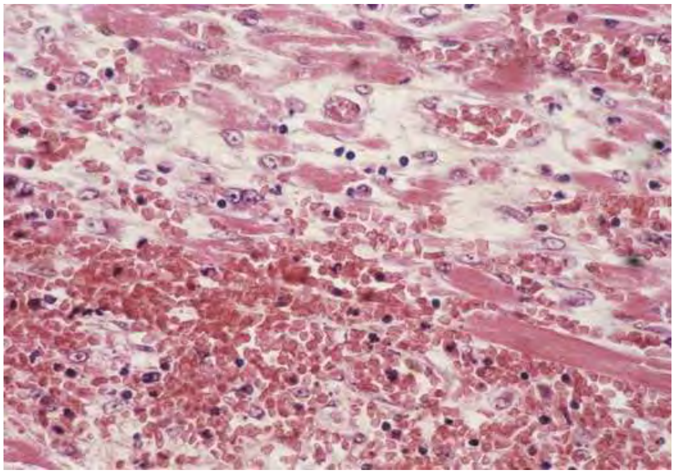

Necrotic tissue resulting from a heart attack. [© CNRI/Photo Researchers.]

Thus, *aerobic metabolism is up to 16 times more efficient than anaerobic glycolysis in producing ATP.*

Aerobic metabolism has its drawbacks, however. Many organisms and tissues depend exclusively on aerobic metabolism and suffer irreversible damage during oxygen deprivation (Box 18-5). Oxidative metabolism is also accompanied by the production of low levels of reactive oxygen metabolites that, over time, may damage cellular components. Evidently, the organisms that have existed during the last 3 billion years (the period in which the earth's atmosphere has contained significant amounts of O_2) exhibit physiological and biochemical adaptations that permit them to take advantage of the oxidizing power of O_2 while minimizing the potential dangers of oxygen itself.

Partial Oxygen Reduction Produces Reactive Oxygen Species (ROS). Although the four-electron reduction of O_2 by cytochrome c oxidase is nearly always orchestrated with great rapidity and precision, *O_2 is occasionally only partially reduced, yielding oxygen species that readily react with a variety of cellular components.* The best known reactive oxygen species is the **superoxide radical:**

$$O_2 + e^- \rightarrow O_2^- \cdot$$

Superoxide radical is a precursor of other reactive species. Protonation of $O_2^- \cdot$ yields $HO_2\cdot$, a much stronger oxidant than $O_2^- \cdot$. The most potent oxygen species in biological systems is probably the hydroxyl radical, which forms from the relatively harmless hydrogen peroxide (H_2O_2):

$$H_2O_2 + Fe^{2+} \rightarrow \cdot OH + OH^- + Fe^{3+}$$

The hydroxyl radical also forms through the reaction of superoxide with H_2O_2:

$$O_2^- \cdot \ + H_2O_2 \rightarrow O_2 + H_2O + \cdot OH$$

Although most free radicals are extremely short-lived (the half-life of $O_2^- \cdot$ is 1×10^{-6} s, and that of $\cdot OH$ is 1×10^{-9} s), they readily extract electrons from other molecules, converting them to free radicals and thereby initiating a chain reaction.

The random nature of free-radical attacks makes it difficult to characterize their reaction products, but all classes of biological molecules are susceptible to oxidative damage caused by free radicals. The oxidation of polyunsaturated lipids in cells may disrupt the structures of biological membranes, and oxidative damage to DNA may result in point mutations. Enzyme function may also be compromised through radical reactions with amino acid side chains. Because the mitochondrion is the site of the bulk of the cell's oxidative metabolism, its lipids, DNA, and proteins probably bear the brunt of free radical–related damage.

Several degenerative diseases, including **Parkinson's, Alzheimer's,** and **Huntington's diseases,** are associated with oxidative damage to mitochondria. Such observations have led to the free-radical theory of aging, which holds that *free-radical reactions arising during the course of normal oxidative metabolism are at least partially responsible for the aging process.* In fact, individuals with congenital defects in their mitochondrial DNA suffer from a variety of symptoms typical of old age, including neuromotor difficulties, deafness, and dementia. Their genetic defects may make their mitochondria all the more susceptible to the reactive oxygen species generated by the electron-transport machinery.

Cells Are Equipped with Antioxidant Mechanisms. **Antioxidants** destroy oxidative free radicals such as $O_2^- \cdot$ and $\cdot OH$. In 1969, Irwin Fridovich discovered that the enzyme **superoxide dismutase (SOD),** which is present in nearly all cells, catalyzes the conversion of $O_2^- \cdot$ to H_2O_2.

$$2\,O_2^- \cdot + 2\,H^+ \rightarrow H_2O_2 + O_2$$

Mitochondrial and bacterial SOD are both Mn-containing tetramers; eukaryotic cytosolic SOD is a dimer containing copper and zinc ions. The rate of nonenzymatic superoxide breakdown is $\sim 2 \times 10^5\, M^{-1} \cdot s^{-1}$, whereas the rate of the Cu,Zn-SOD–catalyzed reaction is $\sim 2 \times 10^9\, M^{-1} \cdot s^{-1}$. This rate enhancement, which is close to the diffusion-controlled limit (Section 12-1B), is apparently accomplished by electrostatic guidance of the negatively charged superoxide substrate into the enzyme's active site (Fig. 18-30). The active-site Cu ion lies at the bottom of a deep pocket in each enzyme subunit. A hydrogen-bonded network of Glu 123, Glu 133, Lys 136, and Thr 137 at the entrance to the pocket facilitates the diffusion of $O_2^- \cdot$ to a site between the Cu ion and Arg 143.

SOD is considered a first-line defense against reactive oxygen species. The H_2O_2 produced in the reaction, which can potentially react to yield other reactive oxygen species, is degraded to water and oxygen by enzymes such as **catalase,** which catalyzes the reaction

$$2\,H_2O_2 \rightarrow 2\,H_2O + O_2$$

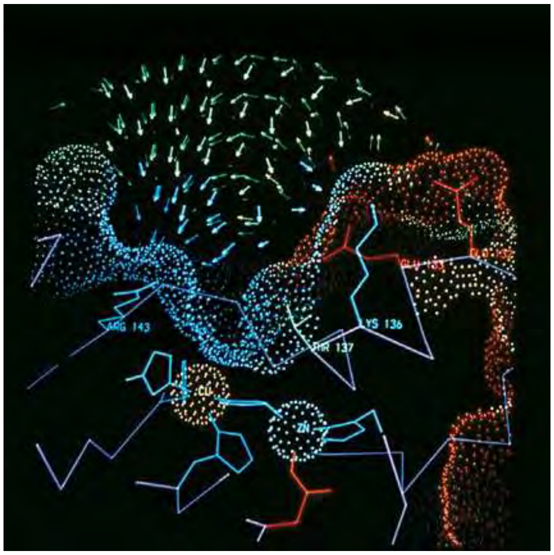

Figure 18-30 Electrostatic effects in human Cu,Zn-superoxide dismutase. In this cross section of the active site channel of Cu,Zn-SOD, the molecular surface is represented by a dot surface that is colored according to charge: red, most negative; yellow, negative; green, neutral; light blue, positive; dark blue, most positive. The electrostatic field vectors are represented by similarly colored arrows. The Cu and Zn ions at the active site are represented by orange and silver dotted spheres. The $O_2^-\cdot$-binding site is located between the Cu ion and the side chain of Arg 143. [Courtesy of Elizabeth Getzoff, The Scripps Research Institute, La Jolla, California.]

and glutathione peroxidase (Box 15-4), which uses glutathione (GSH) as the reducing agent:

$$2\ \text{GSH} + \text{H}_2\text{O}_2 \rightarrow \text{GSSG} + 2\ \text{H}_2\text{O}$$

The latter enzyme also catalyzes the breakdown of organic hydroperoxides. Some types of glutathione peroxidase require Se for activity; this is one reason why Se appears to have antioxidant activity.

Other potential antioxidants are plant-derived compounds such as ascorbate (vitamin C; Section 6-1C) and α-tocopherol (vitamin E; Section 9-1F). These compounds may help protect plants from oxidative damage during photosynthesis, a process in which H_2O is oxidized to O_2. Their efficacy as antioxidants in humans, however, is disputed.

CHECK YOUR UNDERSTANDING

What control mechanisms link glycolysis, the citric acid cycle, and oxidative phosphorylation?

Describe the advantages and disadvantages of oxygen-based metabolism.

SUMMARY

1. Electrons from the reduced coenzymes NADH and $FADH_2$ pass through a series of redox centers in the electron-transport chain before reducing O_2. During electron transfer, protons are translocated out of the mitochondrion to form an electrochemical gradient whose free energy drives ATP synthesis.
2. The mitochondrion contains soluble and membrane-bound enzymes for oxidative metabolism. Reducing equivalents are imported from the cytosol via a shuttle system. Specific transporters mediate the transmembrane movements of ADP, ATP, and P_i.
3. Electrons flow from redox centers with more negative reduction potentials to those with more positive reduction potentials. Inhibitors have been used to reveal the sequence of electron carriers and the points of entry of electrons into the electron-transport chain.
4. Electron transport is mediated by one-electron carriers (Fe–S clusters, cytochromes, and Cu ions) and two-electron carriers (CoQ, FMN, FAD).
5. Complex I transfers two electrons from NADH to CoQ while translocating four protons to the intermembrane space.
6. Complex II transfers electrons from succinate through FAD to CoQ.
7. Complex III transfers two electrons from $CoQH_2$ to two molecules of cytochrome *c*. The concomitant operation of the Q cycle translocates four protons to the intermembrane space.
8. Complex IV reduces O_2 to 2 H_2O using four electrons donated by four cytochrome *c* and four protons from the matrix. Two protons are translocated to the intermembrane space for every two electrons that reduce oxygen.
9. As explained by the chemiosmotic theory, protons translocated into the intermembrane space during electron transport through Complexes I, III, and IV establish an electrochemical gradient across the inner mitochondrial membrane.
10. The influx of protons through the F_0 component of ATP synthase (F_1F_0-ATPase) drives its F_1 component to synthesize ATP from ADP + P_i via the binding change mechanism, a process that is mechanically driven by the F_0-mediated rotation of F_1's γ subunit with respect to its catalytic $\alpha_3\beta_3$ assembly.
11. The P/O ratio, the number of ATPs synthesized per oxygen reduced, need not be an integral number.

12. Agents that discharge the proton gradient can uncouple oxidative phosphorylation from electron transport.
13. Oxidative phosphorylation is controlled by the ratio [NADH]/[NAD^+] and by the ATP mass action ratio. Glycolysis and the citric acid cycle are coordinately regulated according to the need for oxidative phosphorylation.
14. Aerobic metabolism is more efficient than anaerobic metabolism. However, aerobic organisms must guard against damage caused by reactive oxygen species.

KEY TERMS

redox center **597**
cristae **598**
intermembrane space **598**
mitochondrial matrix **599**
malate–aspartate shuttle **599**
glycerophosphate shuttle **599**
ADP–ATP translocator **599**
electrogenic transport **600**
coenzyme Q (ubiquinone) **602**
iron–sulfur protein **605**
free radical **606**
proton wire **608**
cytochrome **609**
Q cycle **612**
energy coupling **618**
chemiosmotic theory **618**
protonmotive force (pmf) **620**
F_1F_0-ATPase **622**
binding change mechanism **625**
P/O ratio **629**
uncoupler **630**
ATP mass action ratio **631**
glucose–fatty acid cycle **634**
superoxide radical **635**
antioxidant **636**

PROBLEMS

1. Explain why a liver cell mitochondrion contains fewer cristae than a mitochondrion from a heart muscle cell.
2. How many ATPs are synthesized for every cytoplasmic NADH that participates in the glycerophosphate shuttle in insect flight muscle? How does this compare to the ATP yield when NADH reducing equivalents are transferred into the matrix via the malate–aspartate shuttle?
3. Calculate $\Delta G°'$ for the oxidation of free $FADH_2$ by O_2. What is the maximum number of ATPs that can be synthesized, assuming standard conditions and 100% conservation of energy?
4. The O_2-consumption curve of a dilute, well-buffered suspension of mitochondria containing an excess of ADP and P_i takes the form

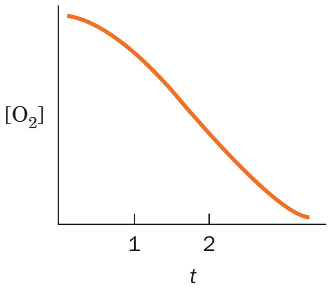

Sketch the curves obtained when (a) amytal is added at time $t = 1$; (b) amytal is added at $t = 1$ and succinate is added at $t = 2$; (c) CN^- is added at $t = 1$ and succinate is added at $t = 2$; (d) oligomycin (which binds to F_0 and prevents ATP synthesis) is added at $t = 1$ and DNP is added at $t = 2$.

5. Why is it possible for electrons to flow from a redox center with a more positive $\mathscr{E}°'$ to one with a more negative $\mathscr{E}°'$ within an electron-transfer complex?
6. Bombarding a suspension of mitochondria with high-frequency sound waves (**sonication**) produces **submitochondrial particles** derived from the inner mitochondrial membrane. These membranous vesicles seal inside out, so that the intermembrane space of the mitochondrion becomes the lumen of the submitochondrial particle. (a) Diagram the process of electron transfer and oxidative phosphorylation in these particles. (b) Assuming all the substrates for oxidative phosphorylation are present in excess, does ATP synthesis increase or decrease with an increase in the pH of the fluid in which the submitochondrial particles are suspended?
7. The difference in pH between the internal and external surfaces of the inner mitochondrial membrane is 1.4 pH units (external side acidic). If the membrane potential is 0.06 V (inside negative), what is the free energy released on transporting 1 mol of protons back across the membrane? How many protons must be transported to provide enough free energy for the synthesis of 1 mol of ATP (assuming standard biochemical conditions)?
8. Consider the mitochondrial ADP–ATP translocator and the P_i-H^+ symport protein. (a) How do the activities of the two transporters affect the electrochemical gradient across the mitochondrial membrane? (b) What thermodynamic force drives the two transport systems?
9. Dicyclohexylcarbodiimide (DCCD) is a reagent that reacts with Asp or Glu residues.

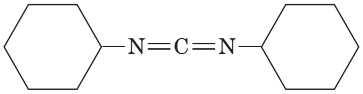

Dicyclohexylcarbodiimide (DCCD)

Explain why the reaction of DCCD with the c subunits of F_1F_0-ATPase blocks its ATP-synthesizing activity.

10. How do the P/O ratios for NADH differ in ATP synthases that contain 9 and 12 c subunits?
11. Explain why compounds such as DNP increase metabolic rates.

12. What is the advantage of hormones activating a lipase to stimulate nonshivering thermogenesis in brown fat rather than activating UCP1 directly (see Box 18-4)?
13. Describe the changes in $[NADH]/[NAD^+]$ and $[ATP]/[ADP]$ that occur during the switch from anaerobic to aerobic metabolism. How do these ratios influence the activity of glycolysis and the citric acid cycle?
14. Activated neutrophils and macrophages (types of white blood cells) fight invading bacteria by releasing superoxide. These cells contain an **NADPH oxidase** that catalyzes the reaction

$$2\,O_2 + NADPH \rightarrow 2\,O_2^{-}\cdot \; + NADP^+ + H^+$$

Explain why flux through the glucose-6-phosphate dehydrogenase reaction increases in these cells.

CASE STUDIES

Case 24 (available at www.wiley.com/college/voet)
Uncoupling Proteins in Plants

Focus concept: Uncoupling proteins in plants uncouple oxidative phosphorylation in order to generate heat in the developing plant.

Prerequisite: Chapter 18

- Electron transport and oxidative phosphorylation
- Mechanisms of uncoupling agents, such as 2,4-dinitrophenol

Case 27
Regulation of Sugar and Alcohol Metabolism in Saccharomyces cerevisiae

Focus concept: The regulation of carbohydrate metabolic pathways in yeast serves as a good model for regulation of the same pathways in multicellular organisms.

Prerequisites: Chapters 15, 16, 17, and 18

- The major pathways associated with carbohydrate metabolism, including glycolysis, the citric acid cycle, oxidative phosphorylation, pentose phosphate pathway and gluconeogenesis
- The various fates of pyruvate via alcoholic fermentation and aerobic respiration

Case 33
Modification of Subunit c from Bovine Mitochondrial ATPase

Focus concept: Modification of Lys 43 in the mitochondrial ATPase, once thought to be the structural basis of Batten disease, has been found in bovine mitochondria, indicating that this modification is completely normal.

Prerequisites: Chapters 5 and 18

- Mechanism of ATP synthesis in oxidative phosphorylation
- Protein structure/function relationships

REFERENCES

Beinert, H., Holm, R.H., and Münck, E., Iron-sulfur clusters: Nature's modular, multipurpose structures, *Science* **277,** 653–659 (1997).

Boyer, P.D., Catalytic site forms and controls in ATP synthase catalysis, *Biochim. Biophys. Acta* **1458,** 252–262 (2000). [A description of the steps of ATP synthesis and hydrolysis, along with experimental evidence and alternative explanations, by the author of the binding change mechanism.]

Crofts, A.R., The cytochrome bc_1 complex: Function in the context of structure, *Annu. Rev. Physiol.* **66,** 689–733 (2004).

Frey, T.G. and Mannella, C.A., The internal structure of mitochondria, *Trends Biochem. Sci.* **23,** 319–324 (2000).

Hinkle, P.C., P/O ratios of mitochondrial oxidative phosphorylation, *Biochim. Biophys. Acta* **1706,** 1–11 (2005).

Hosler, J.P., Ferguson-Miller, S., and Mills, D.A., Energy transduction: Proton transfer through the respiratory complexes, *Annu. Rev. Biochem.* **75,** 165–187 (2006). [A review that focuses on cytochrome *c* oxidase.]

Kühlbrandt, W., Bacteriorhodopsin—the movie, *Nature* **406,** 569– 570 (2000).

Lange, C. and Hunte, C., Crystal structure of the yeast cytochrome bc_1 complex with its bound substrate cytochrome *c, Proc. Natl. Acad. Sci.* **99,** 2800–2805 (2002).

Lanyi, J.K., Bacteriorhodopsin, *Annu. Rev. Physiol.* **66,** 665–688 (2004).

Nicholls, D.G. and Ferguson, S.J., *Bioenergetics 3,* Academic Press (2002). [An authoritative monograph devoted almost entirely to the mechanism of oxidative phosphorylation and the techniques used to elucidate it.]

Noji, H. and Yoshida, M., The rotary machine in the cell, ATP synthase, *J. Biol. Chem.* **276,** 1665–1668 (2001).

Pebay-Peyroula, E., Dahout-Gonzalez, C., Kahn, R., Trézéguet, V., Lauquin, G.J.-M., and Brandolin, G., Structure of mitochondrial ADP/ATP carrier in complex with carboxyatractyloside, *Nature* **426,** 39–44 (2003). [Reports the 2.2-Å-resolution structure of the bovine carrier monomer and proposes a mechanism in which conformational changes in each monomer of the dimeric complex allow simultaneous transport of ADP into and ATP out of the matrix.]

Sazanov, L.A. and Hinchcliffe, P., Structure of the hydrophilic domain of respiratory Complex I from *Thermus thermophilus, Science* **311,** 1430–1436 (2006).

Schultz, B.E. and Chan, S.I., Structures and proton-pumping strategies of mitochondrial respiratory enzymes, *Annu. Rev. Biophys. Biomol. Struct.* **30,** 23–65 (2001).

Stock, D., Gibbons, C., Arechaga, I., Leslie, A.G.W., and Walker, J.E., The rotary mechanism of ATP synthase, *Curr. Opin. Struct. Biol.* **10,** 692–679 (2000).

Walker, J.E. (Ed.), The Mechanism of F_1F_0-ATPase, *Biochim. Biophys. Acta* **1458,** 221–514 (2002). [A series of authoritative reviews.]

Yankovskaya, V., Horsefield, R., Törnroth, S., Luna-Chavez, C., Miyoshi, H., Léger, C., Byrne, B., Cecchini, G., and Iwata, S., Architecture of succinate dehydrogenase and reactive oxygen species generation, *Science* **299,** 700–704 (2003). [X-Ray structure of *E. coli* Complex II.]

19

Photosynthesis

Plants, such as these trees, can survive literally on water, air, and light. They oxidize H_2O to O_2 and convert CO_2 from air into carbohydrates in a process that is driven by light. [Michael Busselle/Stone/Getty Images.]

CHAPTER CONTENTS

1 Chloroplasts
- **A.** The Light Reactions Take Place in the Thylakoid Membrane
- **B.** Pigment Molecules Absorb Light

2 The Light Reactions
- **A.** Light Energy Is Transformed to Chemical Energy
- **B.** Electron Transport in Photosynthetic Bacteria Follows a Circular Path
- **C.** Two-Center Electron Transport Is a Linear Pathway That Produces O_2 and NADPH
- **D.** The Proton Gradient Drives ATP Synthesis by Photophosphorylation

3 The Dark Reactions
- **A.** The Calvin Cycle Fixes CO_2
- **B.** Calvin Cycle Products Are Converted to Starch, Sucrose, and Cellulose
- **C.** The Calvin Cycle Is Controlled Indirectly by Light
- **D.** Photorespiration Competes with Photosynthesis

MEDIA RESOURCES

(available at www.wiley.com/college/voet)
Guided Exploration 20. Two-center photosynthesis (Z-scheme) overview
Interactive Exercise 23. Light-harvesting complex LH-2
Interactive Exercise 24. *Rb. sphaeroides* reaction center
Interactive Exercise 25. Ferredoxin
Interactive Exercise 26. Ferredoxin–$NADP^+$ reductase
Animated Figure 19-6. Electronic states of chlorophyll
Animated Figure 19-26. The Calvin cycle
Animated Figure 19-28. Mechanism of RuBP carboxylase
Kinemage 8-2. Photosynthetic reaction center

The notion that plants obtain nourishment from such insubstantial things as light and air was not validated until the eighteenth century. Evidence that plants produce a vital substance—O_2—was not obtained until Joseph Priestly noted that the air in a jar in which a candle had burnt out could be "restored" by introducing a small plant into the jar. In the presence of sunlight, plants and cyanobacteria consume CO_2 and H_2O and produce O_2 and "fixed" carbon in the form of carbohydrate:

$$CO_2 + H_2O \xrightarrow{\text{light}} (CH_2O) + O_2$$

Photosynthesis, in which light energy drives the reduction of carbon, is essentially the reverse of oxidative carbohydrate metabolism. Photosynthetically produced carbohydrates therefore serve as an energy source for the organism that produces them as well as for nonphotosynthetic organisms that directly or indirectly consume photosynthetic organisms. It is estimated that photosynthesis annually fixes $\sim 10^{11}$ tons of carbon, which represents the storage of over 10^{18} kJ of energy. The process by which light energy is converted to chemical energy has its roots early in evolution, and its complexity is consistent with its long history. Our discussion focuses first on purple photosynthetic bacteria, because of the relative simplicity of their photosynthetic machinery, and then on plants, whose chloroplasts are the site of photosynthesis.

Early in the twentieth century, it was mistakenly thought that light absorbed by photosynthetic pigments directly reduced CO_2, which then combined with water to form carbohydrate. In fact, photosynthesis in plants is a two-stage process in which light energy is harnessed to oxidize H_2O:

$$2\,H_2O \xrightarrow{\text{light}} O_2 + 4\,[H\cdot]$$

The electrons thereby obtained subsequently reduce CO_2:

$$4\,[H\cdot] + CO_2 \rightarrow (CH_2O) + H_2O$$

The two stages of photosynthesis are traditionally referred to as the **light reactions** and **dark reactions:**

1. In the light reactions, specialized pigment molecules capture light energy and are thereby oxidized. A series of electron-transfer reactions, which culminate with the reduction of $NADP^+$ to NADPH, generate a transmembrane proton gradient whose energy is tapped to synthesize ATP from ADP + P_i. The oxidized pigment molecules are reduced by H_2O, thereby generating O_2.
2. The dark reactions use NADPH and ATP to reduce CO_2 and incorporate it into the three-carbon precursors of carbohydrates.

As we shall see, both processes occur in the light and are therefore better described as light-dependent and light-independent reactions. After describing the chloroplast and its contents, we shall consider the light reactions and dark reactions in turn.

1 Chloroplasts

The site of photosynthesis in eukaryotes (algae and higher plants) is the ***chloroplast.*** Cells contain 1 to 1000 chloroplasts, which vary considerably in size and shape but are typically ~5-μm-long ellipsoids. These organelles presumably evolved from photosynthetic bacteria.

LEARNING OBJECTIVE

- Understand that visible light is absorbed by pigment molecules, some arranged in light-harvesting complexes in the thylakoid membrane.

A | The Light Reactions Take Place in the Thylakoid Membrane

Like mitochondria, which they resemble in many ways, chloroplasts have a highly permeable outer membrane and a nearly impermeable inner membrane separated by a narrow intermembrane space (Fig. 19-1). The inner membrane encloses the **stroma,** a concentrated solution of enzymes,

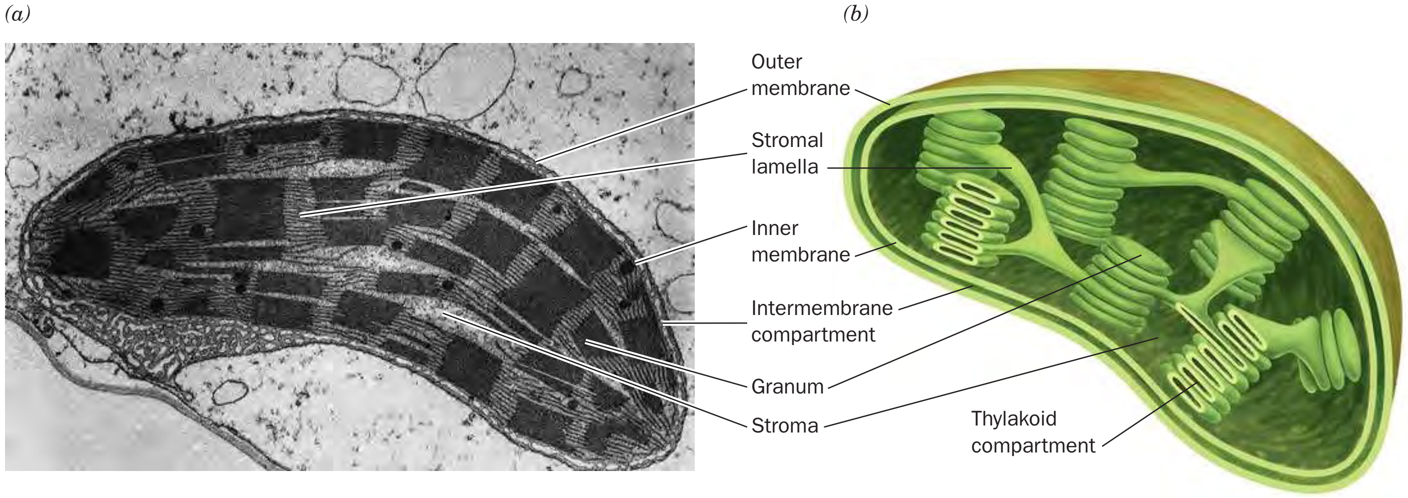

Figure 19-1 | Chloroplast from corn. (*a*) An electron micrograph. [Courtesy of T. Elliot Weier.] (*b*) Schematic diagram.

including those required for carbohydrate synthesis. The stroma also contains the DNA, RNA, and ribosomes involved in the synthesis of several chloroplast proteins.

The stroma, in turn, surrounds a third membranous compartment, the **thylakoid** (Greek: *thylakos,* a sac or pouch). The thylakoid is probably a single highly folded vesicle, although in most organisms it appears to consist of stacks of disklike sacs named **grana,** which are interconnected by unstacked **stromal lamellae.** A chloroplast usually contains 10 to 100 grana. Thylakoid membranes arise from invaginations in the inner membrane of developing chloroplasts and therefore resemble mitochondrial cristae. The thylakoid membrane contains protein complexes involved in harvesting light energy, transporting electrons, and synthesizing ATP. In photosynthetic bacteria, the machinery for the light reactions is located in the plasma membrane, which often forms invaginations or multilamellar structures that resemble grana.

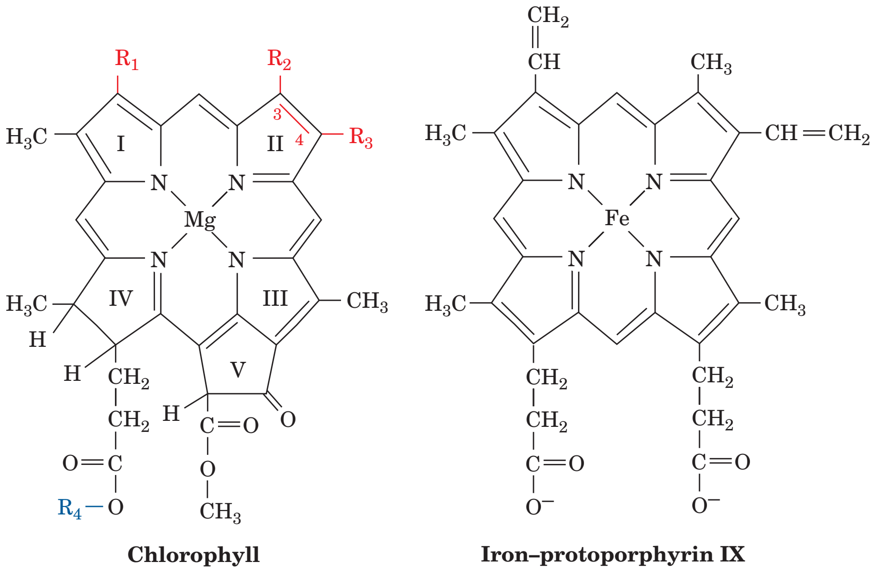

Chlorophyll **Iron–protoporphyrin IX**

	R_1	R_2	R_3	R_4
Chlorophyll *a*	$-CH{=}CH_2$	$-CH_3$	$-CH_2-CH_3$	P
Chlorophyll *b*	$-CH{=}CH_2$	$-\overset{\overset{\displaystyle O}{\|}}{C}-H$	$-CH_2-CH_3$	P
Bacteriochlorophyll *a*	$-\overset{\overset{\displaystyle O}{\|}}{C}-CH_3$	$-CH_3$[a]	$-CH_2-CH_3$[a]	P or G
Bacteriochlorophyll *b*	$-\overset{\overset{\displaystyle O}{\|}}{C}-CH_3$	$-CH_3$[a]	$=CH-CH_3$[a]	P

[a] No double bond between positions C3 and C4.

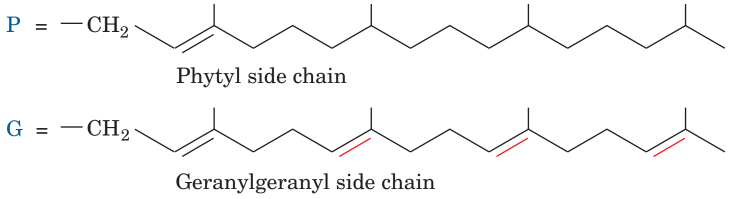

Phytyl side chain

Geranylgeranyl side chain

Figure 19-2 | Chlorophyll structures. The molecular formulas of chlorophylls *a* and *b* and bacteriochlorophylls *a* and *b* are compared to that of iron–protoporphyrin IX (heme). The isoprenoid phytyl and geranylgeranyl tails presumably increase the chlorophylls' solubility in nonpolar media.

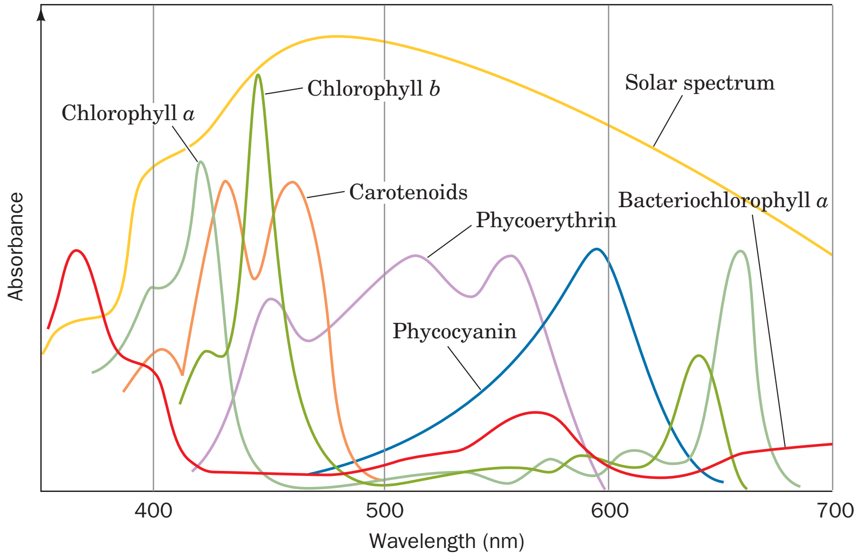

■ **Figure 19-3 | Absorption spectra of various photosynthetic pigments.** The chlorophylls have two absorption bands, one in the red (long wavelength) and one in the blue (short wavelength). Phycoerythrin absorbs blue and green light, whereas phycocyanin absorbs yellow light. Together, these pigments absorb most of the visible light in the solar spectrum. [After a drawing by Govindjee, University of Illinois.]

B | Pigment Molecules Absorb Light

The principal photoreceptor in photosynthesis is **chlorophyll.** This cyclic tetrapyrrole, like the heme group of globins and cytochromes (Section 7-1A and Box 18-1), is derived biosynthetically from protoporphyrin IX. Chlorophyll molecules, however, differ from heme in several respects (Fig. 19-2). In chlorophyll, the central metal ion is Mg^{2+} rather than Fe(II) or Fe(III), and a cyclopentanone ring, Ring V, is fused to pyrrole Ring III. The major chlorophyll forms in plants and cyanobacteria, **chlorophyll *a* (Chl *a*)** and **chlorophyll *b* (Chl *b*),** and the major forms in photosynthetic bacteria, **bacteriochlorophyll *a* (BChl *a*)** and **bacteriochlorophyll *b* (BChl *b*),** also differ from heme and from each other in the degree of saturation of Rings II and IV and in the substituents of Rings I, II, and IV.

The highly conjugated chlorophyll molecules, along with other photosynthetic pigments, strongly absorb visible light (the most intense form of the solar radiation reaching the earth's surface; Fig. 19-3). The relatively small chemical differences among the various chlorophylls greatly affect their absorption spectra.

Light-Harvesting Complexes Contain Multiple Pigments. The primary reactions of photosynthesis, as is explained in Section 19-2B, take place at **photosynthetic reaction centers.** *Yet photosynthetic assemblies contain far more chlorophyll molecules than are contained in reaction centers.* This is because most chlorophyll molecules do not participate directly in photochemical reactions but function to gather light; that is, *they act as light-harvesting antennas.* These **antenna chlorophylls** pass the energy of absorbed **photons** (units of light) from molecule to molecule until it reaches a photosynthetic reaction center (Fig. 19-4).

Transfer of energy from the antenna system to a reaction center **(RC)** occurs in $<10^{-10}$ s with an efficiency of $>90\%$. This high efficiency

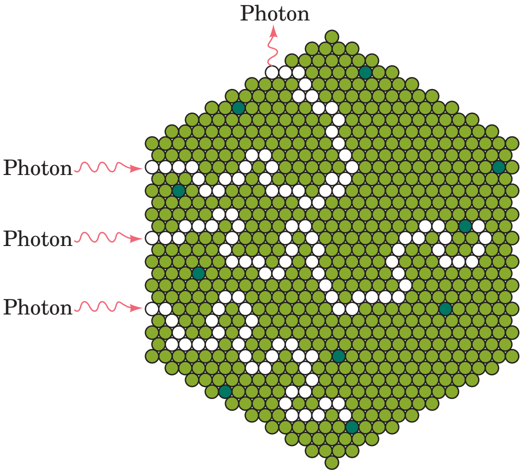

■ **Figure 19-4 | Flow of energy through a photosynthetic antenna complex.** The energy of an absorbed photon randomly migrates among the molecules of the antenna complex (*light green circles*) until it reaches a reaction center chlorophyll (*dark green circles*) or, less frequently, is re-emitted (fluorescence).

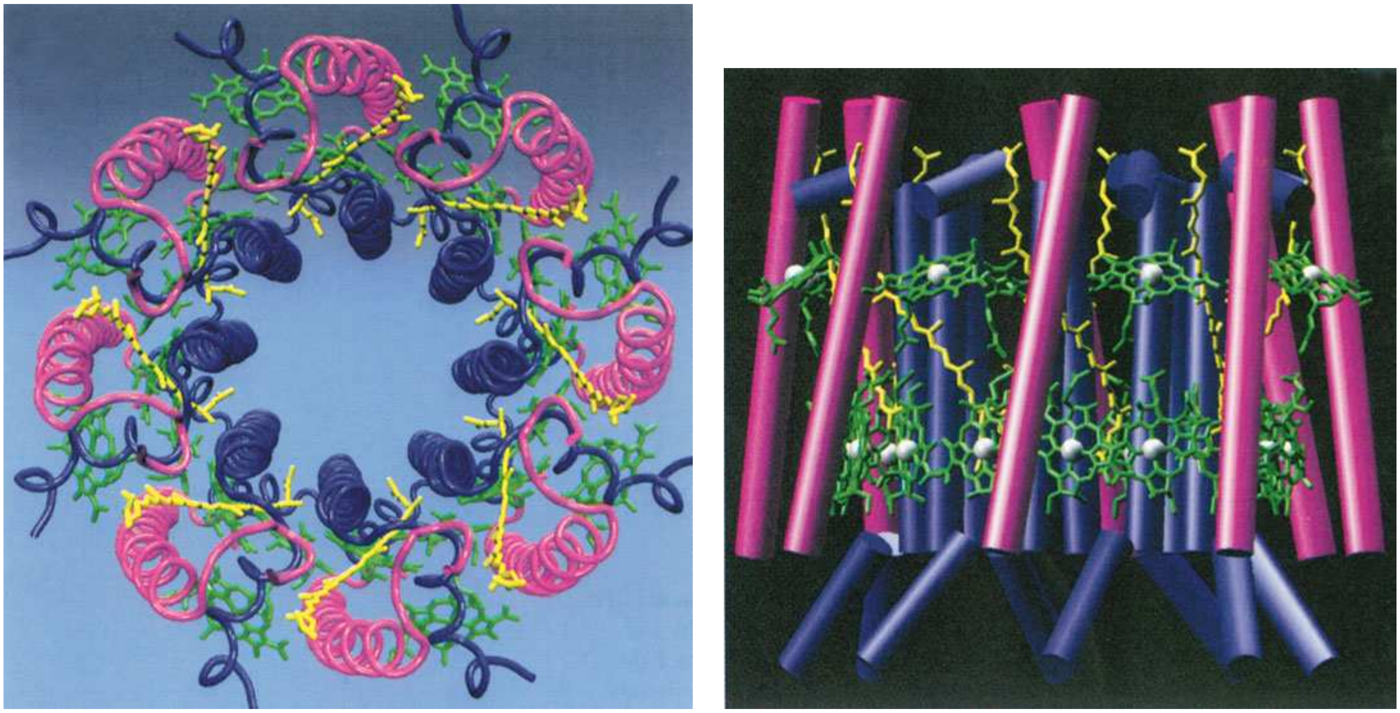
(a)
(b)

■ **Figure 19-5 | X-Ray structure of the light-harvesting complex LH-2 from *Rs. molischianum.*** (*a*) View perpendicular to the photosynthetic membrane showing that the α subunits (*blue;* 56 residues) and the β subunits (*magenta;* 45 residues), as represented by their C_α backbones, are arranged in two concentric eightfold symmetric rings. Twenty-four bacteriochlorophyll *a* (BChl *a; green*) and eight **lycopene** (a carotenoid; *yellow*) molecules are sandwiched between the protein rings. (*b*) View from the plane of the membrane, using the same colors as in Part *a,* in which the α-helical portions of the proteins are represented by cylinders and the Mg^{2+} ions are represented by white spheres. Note that eight of the BChl *a* molecules are bound near the top of the complex with their ring systems nearly parallel to the plane of the membrane, whereas the remaining sixteen BChl *a* molecules are bound near the bottom of the complex with their ring systems approximately perpendicular to the plane of the membrane. This arrangement, together with that of the lycopene molecules, presumably optimizes the light-absorbing and excitation-transmitting capability of the antenna system. [Courtesy of Juergen Koepke and Hartmut Michel, Max-Planck Institut für Biochemie, Germany. PDBid 1LGH.] **See Interactive Exercise 23.**

depends on the chlorophyll molecules having appropriate spacings and relative orientations. Even in bright sunlight, an RC directly intercepts only ~1 photon per second, a metabolically insignificant rate. Hence, a complex of antenna pigments, or **light-harvesting complex (LHC),** is essential.

LHCs consist of arrays of membrane-bound hydrophobic proteins that each contain numerous, often symmetrically arranged pigment molecules. For example, **LH-2** from the purple photosynthetic bacterium *Rhodospirillum molischianum* is an integral membrane protein that consists of eight α subunits and eight β subunits arranged in two eightfold symmetric concentric rings between which are sandwiched 32 pigment molecules (Fig. 19-5). Other LHCs vary widely in their structure and complement of light-harvesting pigments. The number and arrangement of pigment molecules in each LHC have presumably been optimized for efficient energy transfer throughout the LHC. Indeed, the ring of 16 BChl *a* molecules in LH-2 (lower part of Fig. 19-5*b*) are so strongly coupled that they absorb radiation almost as a single unit.

Most LHCs contain other light-absorbing substances besides chlorophyll. These **accessory pigments** "fill in" the absorption spectra of the antenna complexes, covering the spectral regions where chlorophylls do not absorb strongly (Fig. 19-3). For example, **carotenoids,** which are linear polyenes such as **β-carotene,**

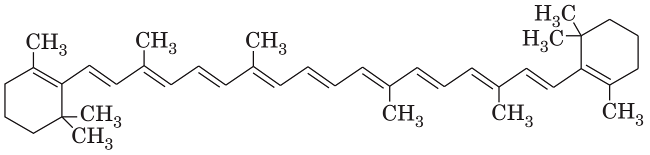

β-Carotene

are components of all green plants and many photosynthetic bacteria and are therefore the most common accessory pigments. They are largely responsible for the brilliant fall colors of deciduous trees as well as for the orange color of carrots (after which they are named).

Water-dwelling photosynthetic organisms, which carry out nearly half of the photosynthesis on earth, additionally contain other types of accessory pigments. This is because light outside the wavelengths 450 to 550 nm (blue and green light) is absorbed almost completely by passage through more than 10 m of water. In red algae and cyanobacteria, Chl *a* therefore is replaced as an antenna pigment by a set of linear tetrapyrroles, notably the red **phycoerythrobilin** and the blue **phycocyanobilin** (their spectra are shown in Fig. 19-3).

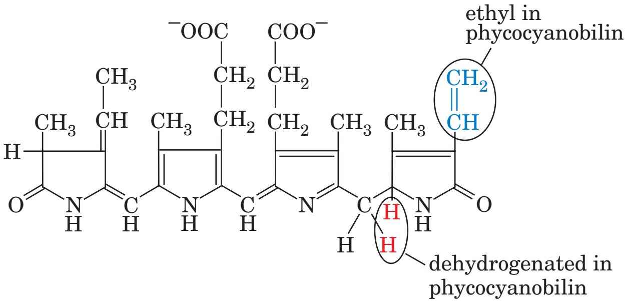

ethyl in phycocyanobilin

dehydrogenated in phycocyanobilin

Phycoerythrobilin and phycocyanobilin

CHECK YOUR UNDERSTANDING

Describe the structure of the chloroplast.

Why do photosynthetic organisms contain several types of pigment molecules?

What is the function of light-harvesting complexes?

2 The Light Reactions

LEARNING OBJECTIVES

- Understand that light energy can be dissipated by internal conversion, fluorescence, exciton transfer, or photooxidation.
- Understand the sequence of photooxidation and electron transfer in the purple bacterial photosynthetic reaction center.
- Understand that Photosystem II reduces its photooxidized special pair with electrons derived from water.
- Understand that electrons traveling from Photosystem II through the cytochrome b_6f complex undergo a Q cycle that generates a transmembrane proton gradient.
- Understand that electrons liberated by photooxidation of Photosystem I reduce $NADP^+$ or contribute to the proton gradient.
- Understand that ATP is produced by photophosphorylation.

Photosynthesis is a process in which electrons from excited chlorophyll molecules are passed through a series of acceptors that convert electronic energy to chemical energy. We can thus ask two questions: (1) What is the mechanism of energy transduction; and (2) How do photooxidized chlorophyll molecules regain their lost electrons?

A | Light Energy Is Transformed to Chemical Energy

Electromagnetic radiation is propagated as discrete **quanta** (photons) whose energy E is given by **Planck's law:**

$$E = h\nu = \frac{hc}{\lambda}$$

where h is **Planck's constant** ($6.626 \times 10^{-34}\ \text{J} \cdot \text{s}$), c is the speed of light ($2.998 \times 10^{8}\ \text{m} \cdot \text{s}^{-1}$ in vacuum), ν is the frequency of the radiation, and λ is its wavelength.

When a molecule absorbs a photon, one of its electrons is promoted from its ground (lowest energy) state molecular orbital to one of higher energy. However, *a given molecule can absorb photons of only certain wavelengths because, as is required by the law of conservation of energy, the energy difference between the two states must exactly match the energy of the absorbed photon.*

An electronically excited molecule can dissipate its excitation energy in several ways (Fig. 19-6):

1. **Internal conversion,** a common mode of decay in which electronic energy is converted to the kinetic energy of molecular motion, that is, to heat. Many molecules relax in this manner to their ground states. Chlorophyll molecules, however, usually relax only to their lowest excited states. Consequently, the photosynthetically applicable excitation energy of a chlorophyll molecule that has absorbed a photon in its short-wavelength band, which corresponds to its second excited state, is no different than if it had absorbed a photon in its less energetic long-wavelength band.
2. **Fluorescence,** in which an electronically excited molecule decays to its ground state by emitting a photon. A fluorescently emitted photon generally has a longer wavelength (lower energy) than that initially absorbed. Fluorescence accounts for the dissipation of only 3 to 6% of the light energy absorbed by living plants.
3. **Exciton transfer** (also known as **resonance energy transfer**), in which an excited molecule directly transfers its excitation energy to nearby unexcited molecules with similar electronic properties. This process

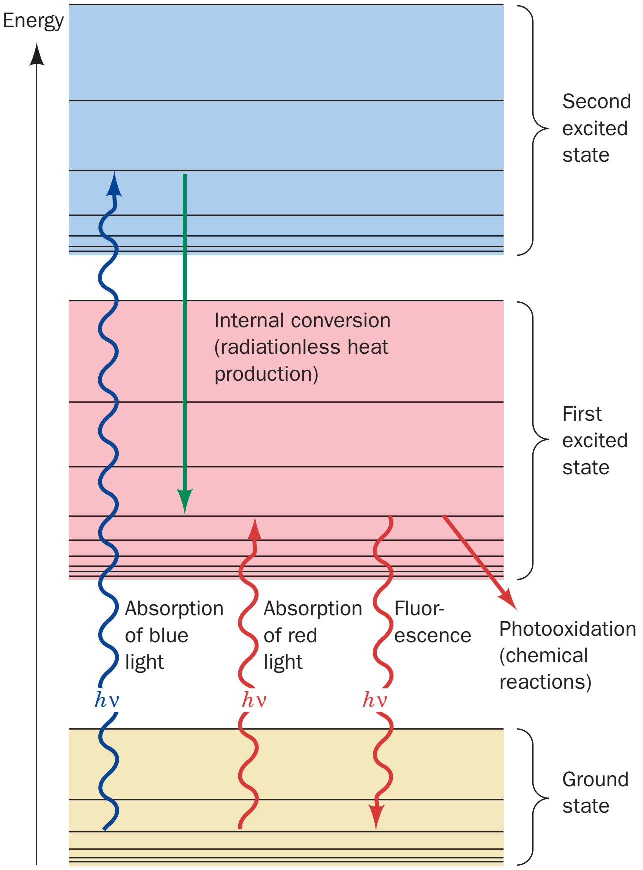
Energy
Second excited state
Internal conversion (radiationless heat production)
First excited state
Absorption of blue light
Absorption of red light
Fluorescence
Photooxidation (chemical reactions)
$h\nu$
$h\nu$
$h\nu$
Ground state

■ **Figure 19-6 | An energy diagram indicating the electronic states of chlorophyll and their most important modes of interconversion.** The wiggly arrows represent the absorption of photons or their fluorescent emission. Excitation energy may also be dissipated in radiationless processes such as internal conversion (heat production) and chemical reactions. **See the Animated Figures.**

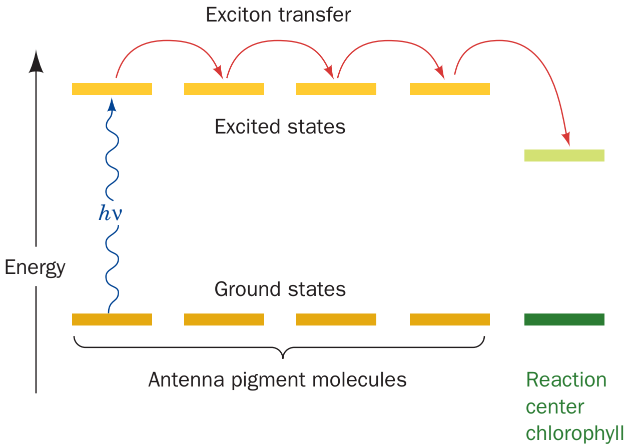

Figure 19-7 | Excitation energy trapping by the photosynthetic reaction center. Light energy that has been passed among pigment molecules by exciton transfer is trapped by the reaction center chlorophyll because its lowest excited state has a lower energy than those of the antenna pigment molecules.

occurs through interactions between the molecular orbitals of the participating molecules. *Light energy is funneled to RCs through exciton transfer among antenna pigments.* The energy (excitation) is trapped at the RC chlorophylls because they have slightly lower excited state energies than the antenna chlorophylls (Fig. 19-7). This energy difference is lost as heat.

4. **Photooxidation,** in which a light-excited donor molecule is oxidized by transferring an electron to an acceptor molecule, which is thereby reduced. This process occurs because the transferred electron is less tightly bound to the donor in its excited state than it is in the ground state. In photosynthesis, excited chlorophyll (Chl*) is such a donor. *The energy of the absorbed photon is thereby chemically transferred to the photosynthetic reaction system.* Photooxidized chlorophyll, Chl^+, a cationic free radical, eventually returns to its reduced state by oxidizing some other molecule.

B | Electron Transport in Photosynthetic Bacteria Follows a Circular Path

In purple photosynthetic bacteria, a membrane-bound bacteriochlorophyll complex undergoes photooxidation when illuminated with red light. The excited electron is transferred along a series of carriers until it returns to the original bacteriochlorophyll complex. During the electron-transfer process, cytoplasmic protons are translocated across the plasma membrane. Dissipation of the resulting proton gradient drives ATP synthesis. The relatively simple RC of purple photosynthetic bacteria **(PbRC)** illustrates some general principles of the photochemical events that occur in the more complicated photosynthetic apparatus of plants and cyanobacteria (Section 19-2C).

The PbRC Is a Transmembrane Protein. The RCs from several species of purple photosynthetic bacteria each contain three hydrophobic subunits known as H, L, and M. The L and M subunits collectively bind four molecules of bacteriochlorophyll, two molecules of **bacteriopheophytin** (**BPheo;** bacteriochlorophyll in which the Mg^{2+} ion is replaced by two protons), one Fe(II) ion, and two molecules of the redox coenzyme ubiquinone (Fig. 18-10*b*) or one molecule of ubiquinone and one of the related **menaquinone:**

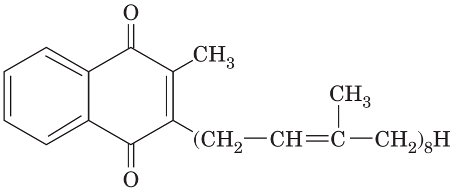

Menaquinone

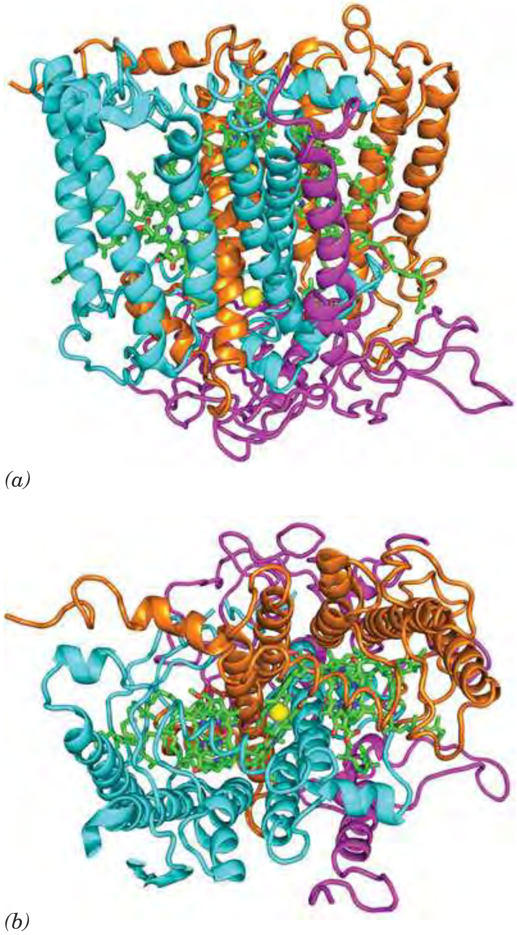

■ **Figure 19-8** | **X-Ray structure of the photosynthetic reaction center from *Rb. sphaeroides*.** *(a)* The H, M, and L subunits of this protein, as viewed from within the plane of the plasma membrane (cytoplasm below) are magenta, cyan, and orange, respectively. The prosthetic groups are drawn in stick form with C green, N blue, and O red. The Fe(II) atom is represented by a yellow sphere. The 11 largely vertical helices that form the central portion of the protein constitute its transmembrane region. *(b)* View from the extracellular side of the membrane. Note how the transmembrane portions of the M and L subunits are related by a pseudo-twofold axis passing through the Fe(II) ion and that the prosthetic groups are sandwiched between these two subunits. [Based on an X-ray structure by Marianne Schiffer, Argonne National Laboratory. PDBid 2RCR.] **See Interactive Exercise 24 and Kinemage Exercise 8-2.**

The PbRC from *Rhodobacter (Rb.) sphaeroides* is a transmembrane protein with 11 membrane-spanning helices (Fig. 19-8). The disposition of prosthetic groups in the homologous protein from *Rhodopseudomonas* (*Rps.) viridis* is shown in Fig. 19-9. *The most striking aspect of the PbRC is that these groups are arranged with nearly perfect twofold symmetry.* Two of the BChl molecules, the so-called **special pair,** are closely associated; they are nearly parallel and have an Mg—Mg distance of ~7 Å. The special pair is named for the wavelength (in nanometers) at which its absorbance maximally decreases upon photooxidation [**P870** or **P960** depending on whether it consists of Bchl *a* or BChl *b;* photosynthetic bacteria tend to inhabit murky stagnant ponds where visible light (400–800 nm) does not penetrate; they require a near infrared–absorbing species of chlorophyll]. Each member of the special pair, here P960, contacts another BChl molecule that, in turn, associates with a BPheo molecule. The menaquinone is close to the L subunit BPheo (Fig. 19-9, *right*), whereas the ubiquinone associates with the M subunit BPheo *b* (Fig. 19-9, *left*). The Fe(II) is positioned between the menaquinone and the ubiquinone rings. Curiously, the two symmetry-related sets of prosthetic groups are not functionally equivalent; electrons are almost exclusively transferred through the L subunit (the right sides of Figs. 19-8 and 19-9). This effect is generally attributed to subtle structural and electronic differences between the L and M subunits.

Photon Absorption Rapidly Photooxidizes the Special Pair. The photochemical events mediated by the PbRC occur as follows:

1. The primary photochemical event of bacterial photosynthesis is the absorption of a photon by the special pair (e.g., P960). The excited electron is delocalized over both its BChl molecules.
2. P960*, the excited state of P960, has but a fleeting existence. Within ~3 picoseconds (ps; 10^{-12} s), P960* transfers an electron to the BPheo on the right in Fig. 19-9 to yield P960$^+$ BPheo b^- (the intervening BChl group probably plays a role in conveying electrons, although it is not itself reduced; it is therefore known as the **accessory BChl**).
3. During the next 200 ps, the electron migrates to the menaquinone (or, in many species, the second ubiquinone), designated Q_A, to form

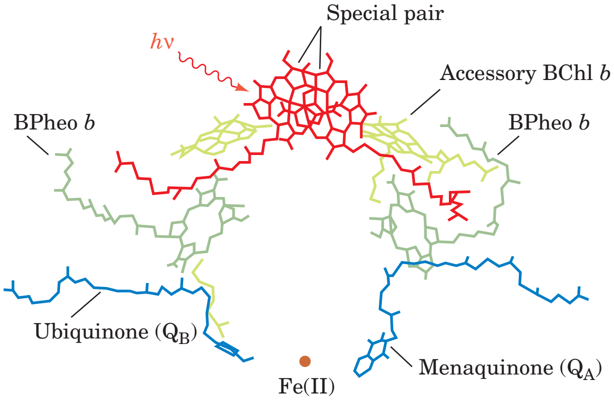

■ **Figure 19-9** | **Disposition of prosthetic groups in the photosynthetic reaction center of *Rps. viridis*.** Note that their rings, but not their aliphatic side chains, are arranged with close to twofold symmetry. The prosthetic groups bound by the L subunit are on the right and those bound by the M subunit are on the left. Photons are absorbed by the special pair of BChl *b* molecules (*red*). **See Kinemage Exercise 8-2.**

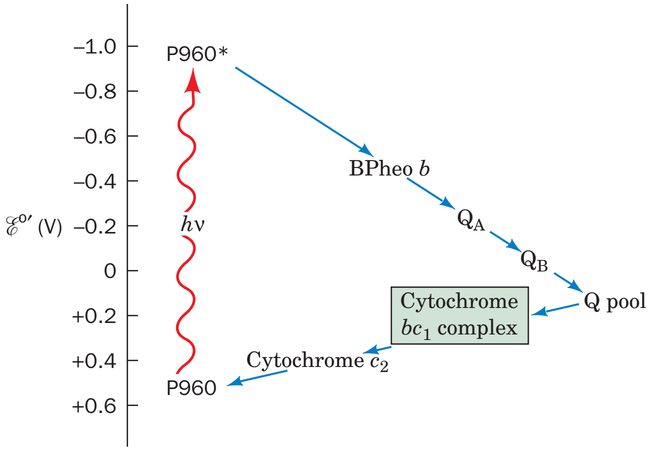

Figure 19-10 | **The photosynthetic electron-transport system of purple photosynthetic bacteria.** Electrons liberated by the absorption of photons by P960 pass through BPheo *b* and Q_A before reaching Q_B, which exchanges with a pool of free ubiquinone. Electrons from QH_2 pass through cytochrome bc_1 to cytochrome c_2, which then reduces $P960^+$. Note that two photons are required for the two-electron reduction of Q to QH_2 and that cytochrome c_2 carries one electron at a time back to the PbRC. The overall process is essentially irreversible because electrons are transferred to progressively lower energy states (more positive standard reduction potentials).

> the anionic semiquinone radical $Q_A^{-}\cdot$. All these electron transfers, as diagrammed in Fig. 19-10, are to progressively lower energy states, which makes this process all but irreversible.

Rapid removal of the excited electron from the vicinity of $P960^+$ is an essential feature of the PbRC; this prevents return of the electron to $P960^+$, which would lead to the wasteful internal conversion of its excitation energy to heat. In fact, *electron transfer in the PbRC is so efficient that its overall* ***quantum yield*** *(ratio of molecules reacted to photons absorbed) is virtually 100%.* No man-made device has yet approached this level of efficiency.

Electrons Are Returned to the Photooxidized Special Pair via an Electron-Transport Chain. $Q_A^{-}\cdot$, which occupies a hydrophobic pocket in the PbRC, transfers its excited electron to the more solvent-exposed ubiquinone, Q_B, to form $Q_B^{-}\cdot$ (the Fe ion positioned between Q_A and Q_B does not directly participate in these redox reactions). Q_A never becomes fully reduced; it shuttles between its oxidized and semiquinone forms.

When the PbRC is again excited, it transfers a second electron to $Q_B^{-}\cdot$ to form the fully reduced Q_B^{2-}. This anionic quinol takes up two protons from the cytoplasmic side of the plasma membrane to form Q_BH_2. Thus, *Q_B is a molecular transducer that converts two light-driven one-electron excitations to a two-electron chemical reduction.*

The electrons taken up by Q_BH_2 are eventually returned to $P960^+$ via an electron-transport chain (Fig. 19-10). The details of this process are species-dependent. The available redox carriers include a membrane-bound pool of ubiquinone molecules, a **cytochrome *bc*$_1$ complex,** and **cytochrome *c*$_2$** (whose structure is drawn in Fig. 6-32*b*). The electron-transport pathway leads from Q_BH_2 through the ubiquinone pool, with which Q_BH_2 exchanges, to cytochrome bc_1, and then to cytochrome c_2. The reduced cytochrome c_2, which closely resembles mitochondrial cytochrome *c,* carries an electron back to $P960^+$. The PbRC is thereby reduced and prepared to absorb another photon.

Since electron transport in purple photosynthetic bacteria is a cyclic process (Fig. 19-10), *it results in no net oxidation–reduction.* However, when QH_2 transfers its electrons to cytochrome bc_1, its protons are translocated across the plasma membrane. Cytochrome bc_1 is a transmembrane protein complex containing a [2Fe–2S] iron–sulfur protein, cytochrome c_1, and a cytochrome *b* that contains two hemes, b_H and b_L (H and L for high and low potential). Note that cytochrome bc_1 is strikingly similar to the proton-translocating Complex III of mitochondria (which is also called cytochrome bc_1; Section 18-2E). In fact, electron transfer from QH_2 (a two-electron carrier) to the one-electron acceptor cytochrome c_2 occurs in a two-stage Q cycle, exactly as occurs in mitochondrial electron transport (Fig. 18-15). The net result is that for every two electrons transferred from QH_2 to cytochrome c_2, four protons enter the periplasmic space. Thus, photon absorption by the PbRC generates a transmembrane H^+ gradient. Light-dependent synthesis of ATP is driven by the dissipation of this gradient (Section 19-2D).

C | Two-Center Electron Transport Is a Linear Pathway That Produces O_2 and NADPH

In plants and cyanobacteria, *photosynthesis is a noncyclic process that uses the reducing power generated by the light-driven oxidation of H_2O to produce NADPH.* This multistep process involves two photosynthetic reaction centers (RCs) that each bear considerable resemblance to PbRCs. These RCs are **photosystem II (PSII),** which oxidizes H_2O, and **photosystem I (PSI),** which reduces $NADP^+$. Each photosystem is independently activated by light, with electrons flowing from PSII to PSI. *PSII and PSI therefore operate in electrical series to couple H_2O oxidation with $NADP^+$ reduction.* Evidence for the existence of two photosystems came from observations that in the presence of both red light (which activates only PSI) and yellow-green light (which also activates PSII), plants produce O_2 (i.e., oxidize H_2O) at a greater rate than the sum of the rates for each light acting alone. The herbicide **3-(3,4-dichlorophenyl)-1,1-dimethylurea (DCMU)**

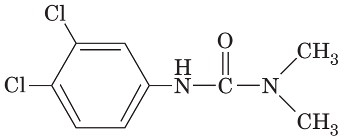

3-(3,4-Dichlorophenyl)-1,1-dimethylurea (DCMU)

blocks electron flow from PSII to PSI so that even with adequate illumination (i.e., activation of both PSI and PSII), PSI is not supplied with electrons, PSII cannot be reoxidized, and photosynthetic oxygen production ceases.

The pathway of electron transport in the chloroplast is more elaborate than in photosynthetic bacteria. *The components involved in electron transport from H_2O to NADPH are largely organized into three thylakoid membrane-bound particles (Fig. 19-11): PSII, a* ***cytochrome b_6f complex,*** *and PSI.* Electrons are transferred between these complexes via mobile electron carriers, much as occurs in the respiratory electron-transport

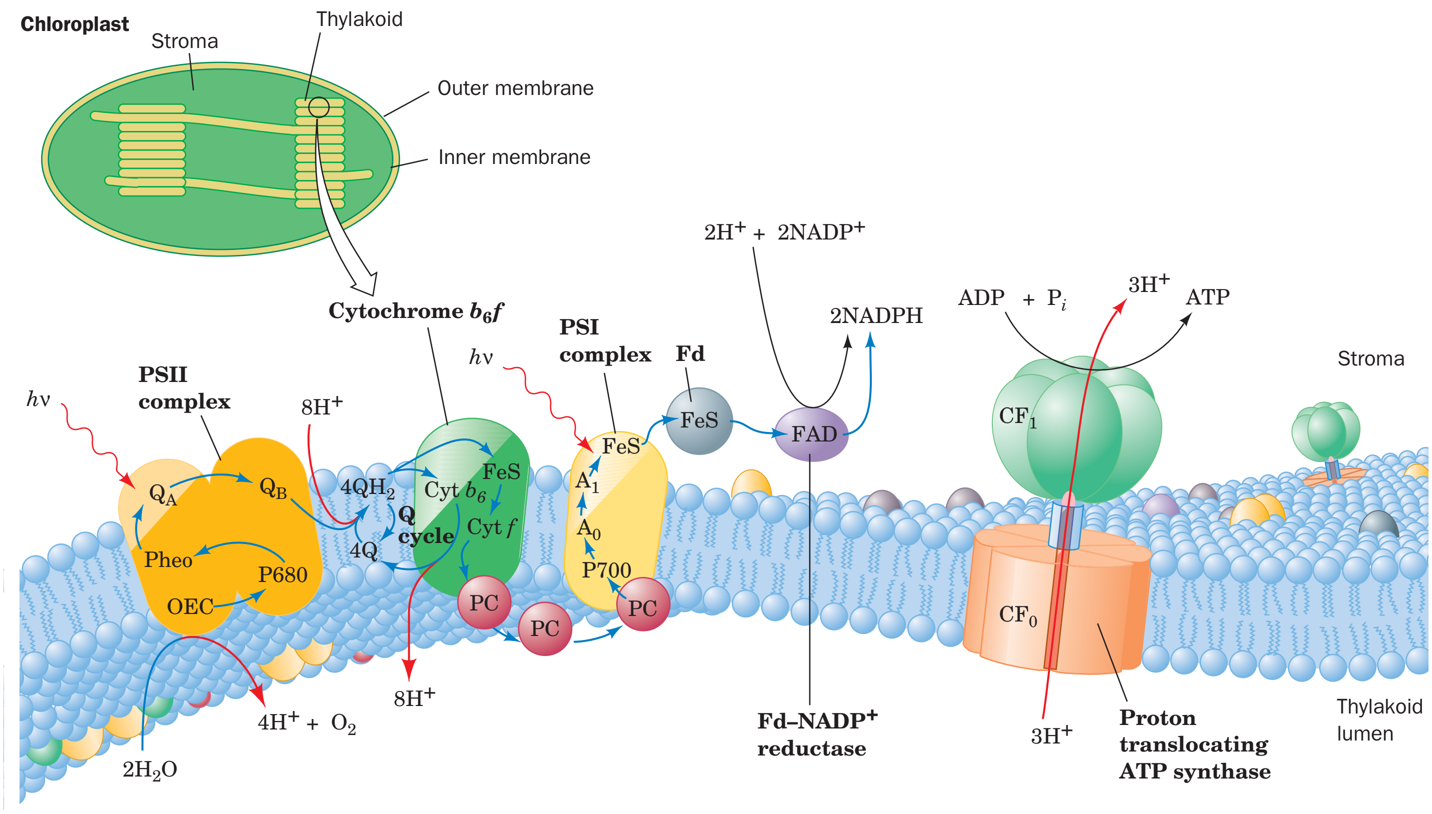
Chloroplast
Stroma
Thylakoid
Outer membrane
Inner membrane
Cytochrome b_6f
2H+ + 2NADP+
2NADPH
ADP + P_i
3H+
ATP
Stroma
$h\nu$
PSII complex
8H+
$h\nu$
PSI complex
Fd
FeS
FAD
CF_1
Q_A
Q_B
$4QH_2$
Cyt b_6
FeS
Q cycle
Cyt f
A_1
A_0
FeS
Pheo
P680
4Q
P700
OEC
PC
PC
PC
CF_0
4H+ + O_2
8H+
$2H_2O$
Fd–NADP+ reductase
3H+
Proton translocating ATP synthase
Thylakoid lumen

Figure 19-11 | **A model of the thylakoid membrane.** The electron-transport system consists of three protein complexes: PSII, the cytochrome b_6f complex, and PSI, which are electrically "connected" by the diffusion of the electron carriers plastoquinone (Q) and plastocyanin (PC). Light-driven transport of electrons (*blue arrows*) from H_2O to $NADP^+$ motivates the transport of protons (*red arrows*) into the thylakoid lumen. Additional protons are split off from water by the oxygen-evolving center (OEC), yielding O_2. The resulting proton gradient powers the synthesis of ATP by the CF_1CF_0 proton-translocating ATP synthase. The membrane also contains light-harvesting complexes (not shown) whose component pigments transfer their excitations to PSII and PSI. Fd represents ferredoxin. [After Ort, D.R. and Good, N.E., *Trends Biochem. Sci.* **13**, 469 (1988).]

chain. The ubiquinone analog **plastoquinone (Q),** via its reduction to **plastoquinol (QH_2),**

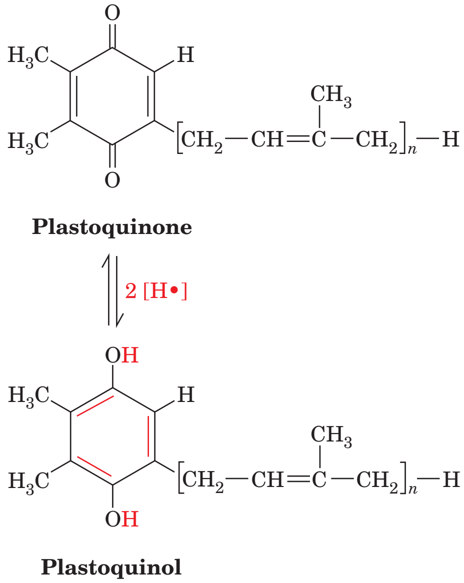
O
H_3C
H
CH_3
H_3C
$[CH_2-CH=C-CH_2]_n-H$
O
Plastoquinone
2 [H•]
OH
H_3C
H
CH_3
H_3C
$[CH_2-CH=C-CH_2]_n-H$
OH
Plastoquinol

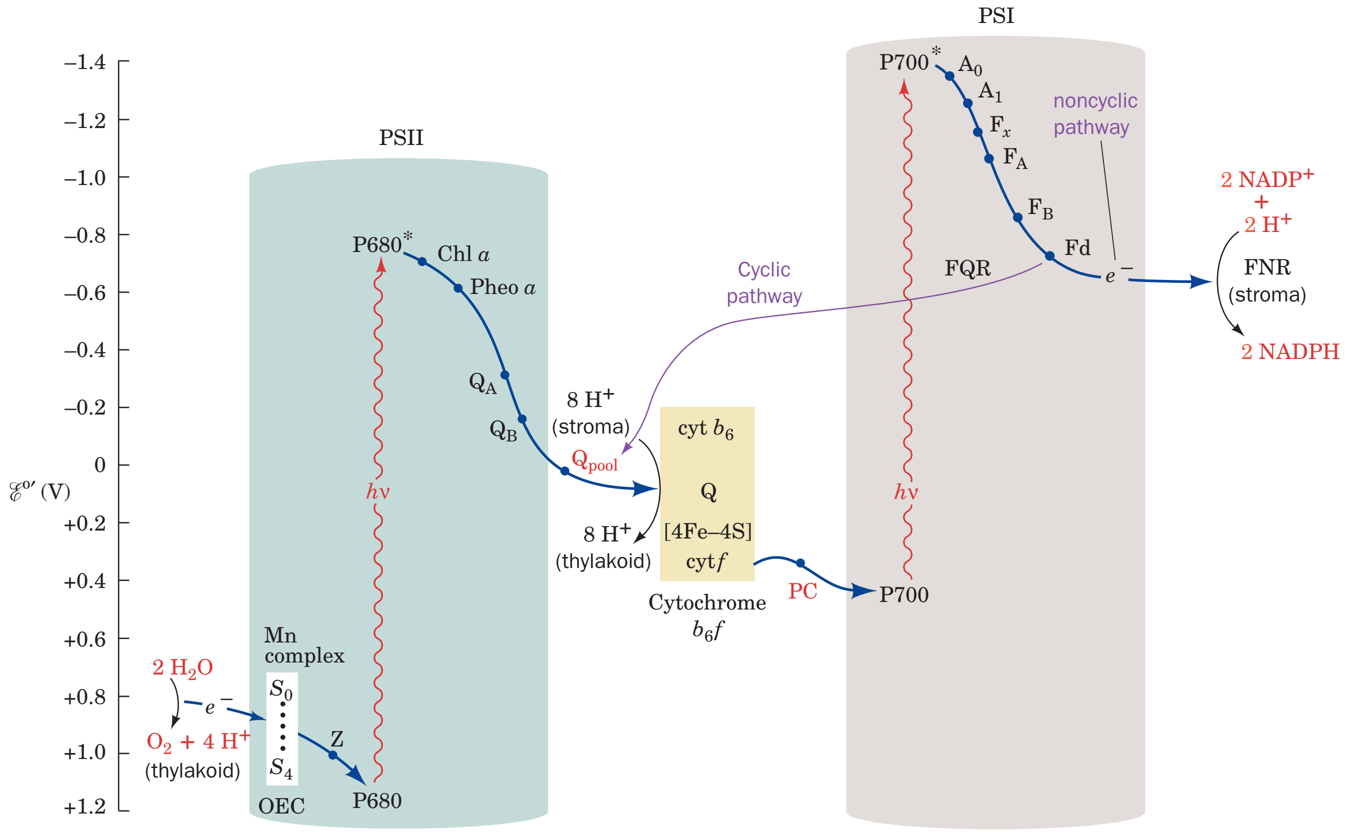
PSI
PSII
−1.4
−1.2
−1.0
−0.8
−0.6
−0.4
−0.2
0
+0.2
+0.4
+0.6
+0.8
+1.0
+1.2
$\mathscr{E}^{\circ\prime}$ (V)
P680*
Chl a
Pheo a
Q_A
Q_B
$h\nu$
8 H⁺
(stroma)
Q_{pool}
8 H⁺
(thylakoid)
cyt b_6
Q
[4Fe–4S]
cyt$f$
Cytochrome
b_6f
PC
Cyclic
pathway
Mn
complex
$2\ H_2O$
e^-
$O_2 + 4\ H^+$
(thylakoid)
S_0
S_4
Z
OEC
P680
P700*
A_0
A_1
F_x
F_A
F_B
Fd
FQR
noncyclic
pathway
e^-
$h\nu$
P700
2 NADP⁺
+
2 H⁺
FNR
(stroma)
2 NADPH

Figure 19-12 | The Z-scheme of photosynthesis. Electrons ejected from P680 in PSII by the absorption of photons are replaced with electrons abstracted from H_2O by an Mn-containing complex (the oxygen-evolving center; OEC), thereby forming O_2 and 4 H^+. Each ejected electron passes through a chain of electron carriers to a pool of plastoquinone molecules (Q_{pool}). The resulting plastoquinol, in turn, reduces the cytochrome b_6f complex (*yellow box*) with the concomitant translocation of protons into the thylakoid lumen. Cytochrome b_6f then transfers the electrons to plastocyanin (PC). The plastocyanin regenerates photooxidized P700 in PSI. The electron ejected from P700, through the intermediacy of a chain of electron carriers, reduces $NADP^+$ to NADPH in noncyclic electron transport. Alternatively, the electron may return to the cytochrome b_6f complex in a cyclic process that translocates additional protons into the thylakoid lumen. The reduction potentials increase downward so that electrons flow spontaneously in this direction.

links PSII to the cytochrome b_6f complex, which, in turn, interacts with PSI through the mobile peripheral membrane protein **plastocyanin (PC).** Electrons eventually reach **ferredoxin–NADP⁺ reductase (FNR),** where they are used to reduce $NADP^+$. The oxidation of water and the passage of electrons through a Q cycle generate a transmembrane proton gradient, with the greater $[H^+]$ in the thylakoid lumen. The free energy of this proton gradient is tapped by chloroplast ATP synthase.

See Guided Exploration 20
Two-center photosynthesis (Z-scheme) overview.

The various prosthetic groups of the photosynthetic apparatus of plants can be arranged in a diagram known as the **Z-scheme** (Fig. 19-12). As in other electron-transport systems, electrons flow from low to high reduction potentials. The zigzag nature of the Z-scheme reflects the two loci for photochemical events (one at PSII, one at PSI) that are required to drive electrons from H_2O to $NADP^+$.

PSII Resembles the PbRC. PSII from the thermophilic cyanobacterium *Thermosynechococcus elongatus* consists of 19 subunits, 14 of which occupy the photosynthetic membrane. These transmembrane subunits include the reaction center proteins **D1 (PsbA)** and **D2 (PsbD),** the chlorophyll-

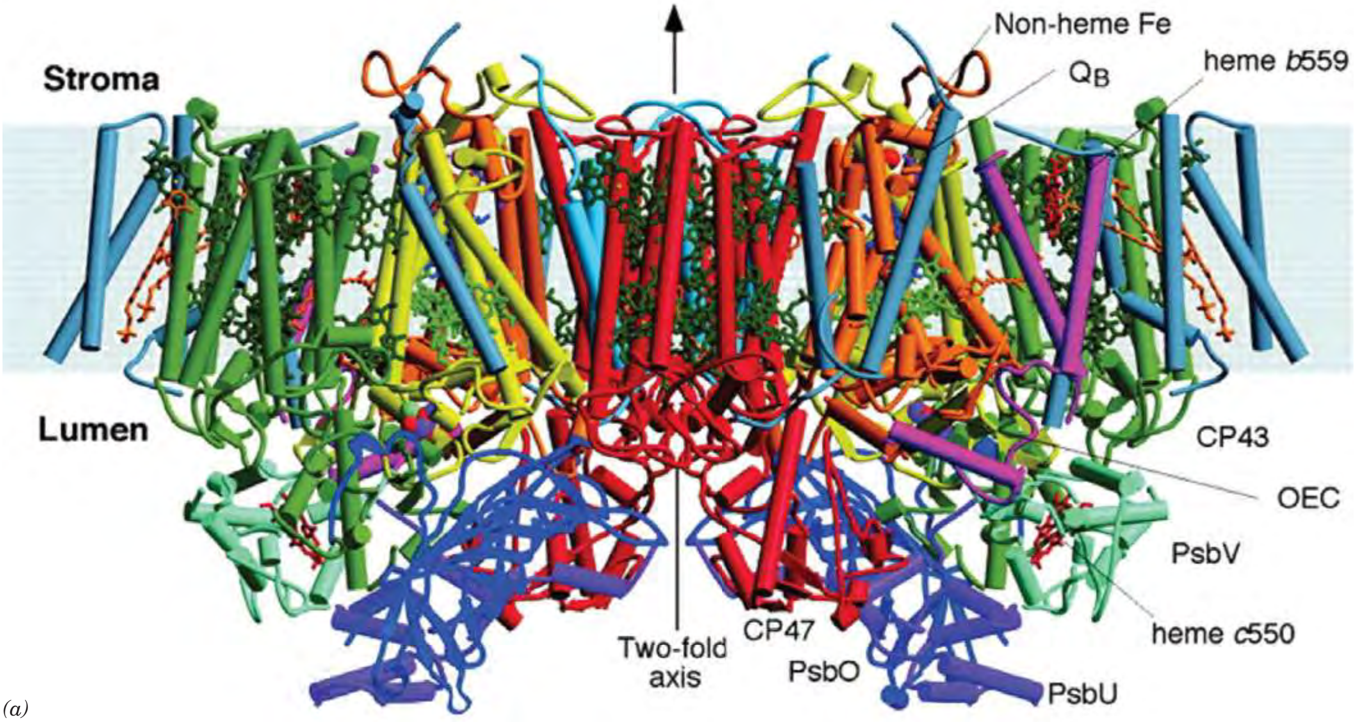

(a)

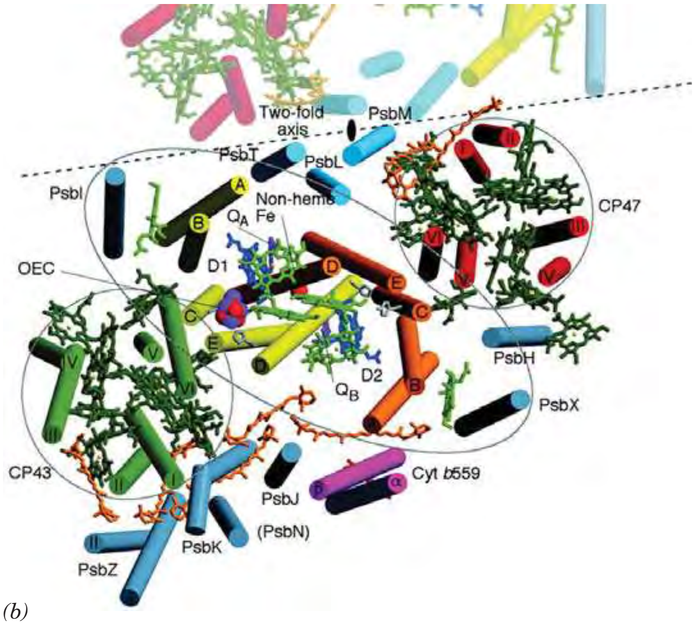

(b)

Figure 19-13 | X-Ray structure of PSII from *T. elongatus*. The PSII dimer is viewed from within the plane of the membrane. Its transmembrane subunits include D1 (*yellow*), D2 (*orange*), CP47 (*red*), CP43 (*green*), and cytochrome b_{559} (*magenta*). Other transmembrane subunits are colored light blue and blue-gray. Its extrinsic proteins are PsbO (*dark blue*), PsbU (*purple*), and PsbV (*light green*). The various cofactors are drawn in stick form with the chlorophylls of the D1/D2 reaction center light green, those of the antenna complexes dark green, pheophytins dark blue, hemes red, β-carotenes orange, Q_A and Q_B purple, and the nonheme Fe represented by a red sphere. The inferred position of the membrane is indicated by the light blue band. (*b*) View of a PSII protomer perpendicular to the membrane from the thylakoid lumen showing only the transmembrane portions of the complex and colored as in Part *a*. A portion of the other protomer in the PSII dimer is shown in muted colors with the dashed line indicating the region of monomer–monomer interactions. The pseudo-twofold axis, which is perpendicular to the membrane and passes through the nonheme Fe, relates the transmembrane helices of the D1/D2 heterodimer, CP43 and CP47, and PsbI and PsbX as emphasized by the black lines encircling these subunits. [Courtesy of James Barber and So Iwata, Imperial College London, U.K. PDBid 1S5L.]

containing inner-antenna subunits **CP43 (PsbC)** and **CP47 (PsbB),** and **cytochrome b_{559}.** The X-ray structure of this PSII (Fig. 19-13), determined by James Barber and So Iwata, reveals that this ~340-kD protein is a symmetric dimer, whose protomeric units each contain 35 transmembrane helices. Each protomer, which has pseudo-twofold symmetry, binds 36 Chl *a*'s, 2 **pheophytin *a*'s** (**Pheo *a*'s;** Chl *a* with its Mg^{2+} replaced by two protons), 1 heme *b,* 1 heme *c,* 2 plastoquinones, 1 nonheme Fe, 7 all-trans carotenoids presumed to be β-carotene, 2 HCO_3^- ions, and 1 Mn_4CaO_4 complex known as the **oxygen-evolving center (OEC).** In higher plants, the

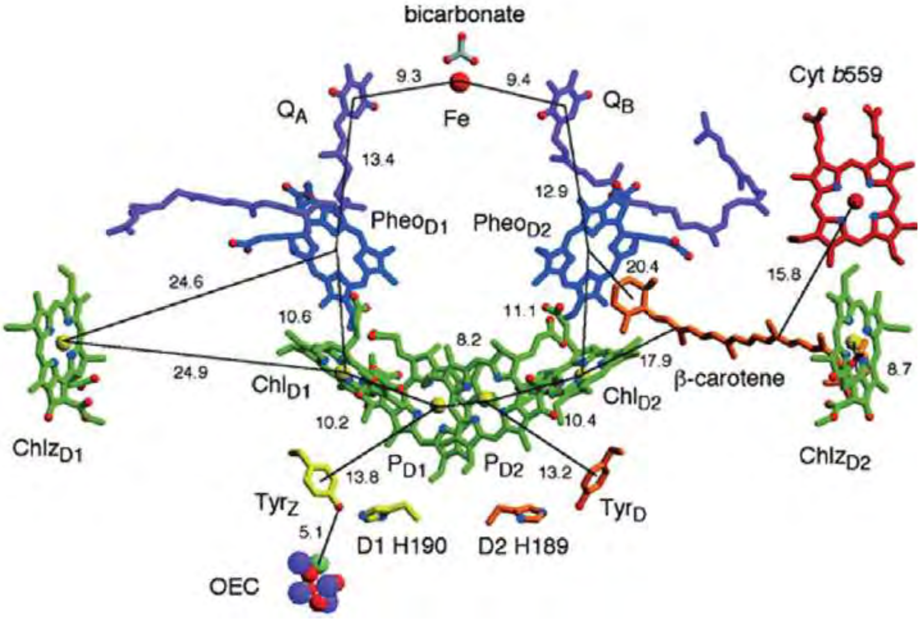

Figure 19-14 | The arrangement of electron-transfer cofactors in PSII from *T. elongatus.* The complex is viewed along the membrane plane with the thylakoid lumen below. The cofactors are colored as in Fig. 19-13 but with Mg^{2+} yellow, N blue, and O red. The phytyl tails of the chlorophylls and pheophytins have been removed for clarity. The side chains of Tyr_Z (D1 Tyr 161) and D1 His 190 are yellow, and those of Tyr_D (D2 Tyr 160) and D2 His 189 are orange. The OEC is drawn in space-filling form with Mn purple, Ca^{2+} cyan, and O red. The numbers indicate the center-to-center distances, in angstroms, between the cofactors spanned by the accompanying thin black lines. Compare this figure to Fig. 19-9 (which is drawn upside down relative to this figure). [Courtesy of James Barber and So Iwata, Imperial College London, U.K. PDBid 1S5L.]

PSII protomer contains ~25 subunits and forms a ~1000-kD transmembrane supercomplex with several antenna proteins. The arrangement of the 5 transmembrane helices in both D1 and D2 resembles that in the L and M subunits of the PbRC (Fig. 19-8). Indeed, these two sets of subunits have similar sequences, thereby indicating that they arose from a common ancestor.

The cofactors of PSII's RC (Fig. 19-14) are organized similarly to those of the bacterial system (Fig. 19-9): They have essentially the same components (with Chl *a,* Pheo *a,* and plastoquinone replacing BChl *b,* BPheo *b,* and menaquinone, respectively) and are symmetrically organized along the complex's pseudo-twofold axis. The two Chl *a* rings labeled P_{D1} and P_{D2} in Fig. 19-14 are positioned analogously to the BChl *b*'s of P960's "special pair" and are therefore presumed to form PSII's primary electron donor, **P680** (named after the wavelength at which its absorbance maximally decreases on photooxidation). The electron ejected from P680 follows a similar asymmetric course as that in the PbRC even though the two systems operate over different ranges of reduction potential (compare Figs. 19-10 and 19-12). As indicated in the central part of Fig. 19-12, the electron is transferred to a molecule of Pheo *a* ($Pheo_{D1}$ in Fig. 19-14), probably via a Chl *a* molecule (Chl_{D1}), and then to a bound plastoquinone (Q_A). The electron is subsequently transferred to a second plastoquinone molecule, Q_B, which after it receives a second electron in a like manner takes up two protons at the stromal (cytoplasmic in cyanobacteria) surface of the thylakoid membrane. The resulting plastoquinol, Q_BH_2, then exchanges with a membrane-bound pool of plastoquinone molecules. DCMU as well as many other commonly used herbicides compete with plastoquinone for the Q_B-binding site on PSII, which explains how they inhibit photosynthesis.

O_2 Is Generated by a Five-Stage Water-Splitting Reaction. The electron ejected by photooxidation of P680 is replaced by an electron derived from H_2O via the OEC. The OEC of PSII is also known as the **water-splitting enzyme** because it breaks down two water molecules to O_2, four protons, and four electrons. Insight into this process was garnered by

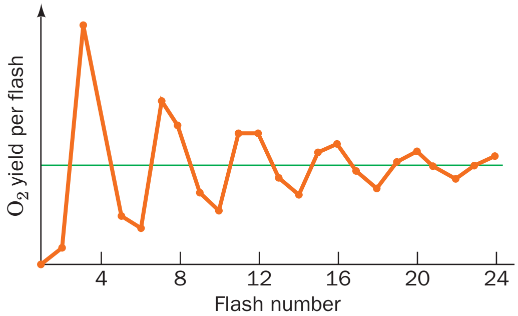

Figure 19-15 | **The O_2 yield per flash in dark-adapted spinach chloroplasts.** Note that the yield peaks on the third flash and then on every fourth flash thereafter until the curve eventually damps out to its average value. [After Forbush, B., Kok, B., and McGloin, M.P., *Photochem. Photobiol.* **14,** 309 (1971).]

Pierre Joliet and Bessel Kok, who analyzed the production of O_2 by dark-adapted chloroplasts that were exposed to a series of short flashes of light. O_2 was evolved with a peculiar oscillatory pattern (Fig. 19-15). There is virtually no O_2 evolved by the first two flashes. The third flash results in the maximum O_2 yield. Thereafter, the amount of O_2 produced peaks with every fourth flash until the oscillations damp out to a steady state. This periodicity indicates that each OEC must undergo four light-dependent reactions—that is, four electron transfers—before releasing O_2.

The OEC is thought to cycle through five different states, S_0 through S_4 (Fig. 19-16). O_2 is released in the transition between S_4 and S_0. The observation that O_2 evolution peaks at the third rather than the fourth flash indicates that the OEC's resting state is predominantly S_1 rather than S_0. The oscillations gradually damp out because a small fraction of the RCs fail to be excited or become doubly excited by a given flash of light, so that the RCs eventually lose synchrony. The complete reaction sequence releases a total of four water-derived protons into the inner thylakoid space in a stepwise manner. These protons contribute to the transmembrane proton gradient.

Since the OEC abstracts electrons from H_2O, its five states must have extraordinarily high reduction potentials (recall from Table 14-5 that the O_2/H_2O half-reaction has a standard reduction potential of 0.815 V). PSII must also stabilize the highly reactive intermediates for extended periods (as much as minutes) in close proximity to water.

The OEC, which is located at the lumenal surface of the D1 subunit (Fig. 19-14), is a Mn_4CaO_4 or Mn_4CaO_5 complex in which the O atoms bridge neighboring Mn atoms. The structure of the OEC remains elusive due to PSII's relatively poorly resolved X-ray structures and the observation that the OEC decomposes when illuminated with X-rays at the intensities used in X-ray structure determinations. However, the use of X-ray spectroscopy techniques of lower intensity that are sensitive to bond lengths have led to the formulation of several related models for the OEC that are compatible with the X-ray structure of PSII. One of these models is shown in Fig. 19-17.

The water-splitting reaction is driven by the excitation of the PSII RC. A variety of evidence indicates that the Mn ions in the OEC's various *S* states (Fig. 19-16) cycle through specific combinations of Mn(II), Mn(III), Mn(IV), and Mn(V) while abstracting protons and electrons from two H_2O molecules to yield O_2, which is released into the thylakoid lumen. However, the mechanism whereby this occurs, that is, the nature of the five *S* states, remains unknown due to the lack of structural information concerning these states.

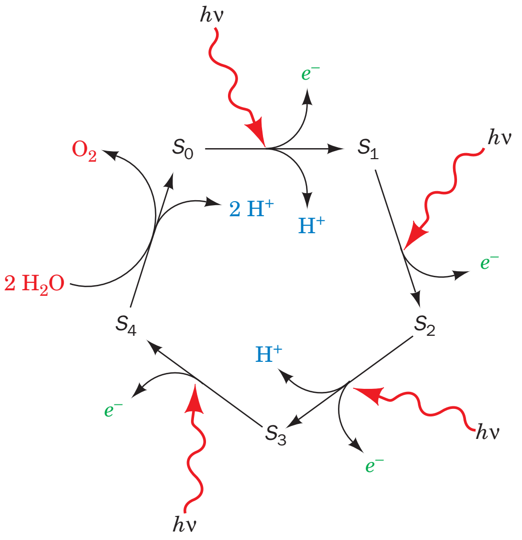

Figure 19-16 | **The schematic mechanism of O_2 generation in chloroplasts.** Four electrons are stripped, one at a time, in light-driven reactions ($S_0 \rightarrow S_4$), from two bound H_2O molecules. In the recovery step ($S_4 \rightarrow S_0$), which is light independent, O_2 is released and two more H_2O molecules are bound. Three of these five steps release protons into the thylakoid lumen.

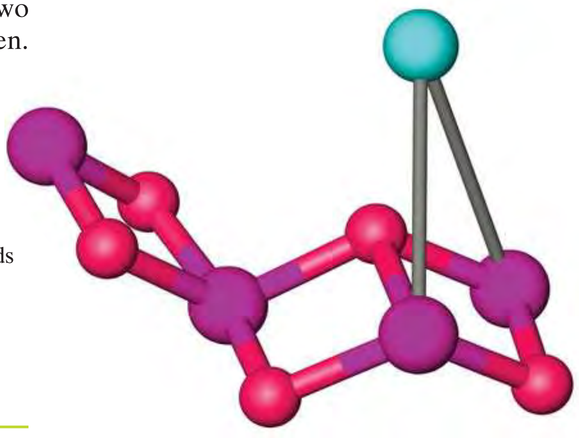

Figure 19-17 | **A model of the OEC.** This Mn_4CaO_5 complex is shown in ball-and-stick form with Mn ions magenta, the Ca^{2+} ion cyan, and O red. The bonds between the Ca and Mn ions are drawn in gray to indicate that the position of the Ca ion is relatively poorly defined. Presumably, numerous protein side chains and water molecules ligand the Ca and Mn ions. Several related models are also compatible with the structural data. [Based on a model by Vittal Yachandra, Lawrence Berkeley National Laboratory, Berkeley, CA.]

The electrons abstracted from water by the OEC are relayed, one at a time, to P680$^+$ by an entity originally named Z (Fig. 19-12). Spectroscopic measurements have identified Z as a transient neutral tyrosyl radical (TyrO·) located on D1 Tyr 161 (known as Tyr$_Z$), which is situated between the OEC and P680 (Fig. 19-14). Recall that a tyrosyl radical has also been implicated in the reduction of O_2 to 2 H_2O by cytochrome *c* oxidase (Complex IV) in the respiratory electron transport chain (Section 18-2F).

Electron Transport through the Cytochrome *b*$_6$*f* Complex Generates a Proton Gradient. From the plastoquinone pool, electrons pass through the cytochrome *b*$_6$*f* complex. This integral membrane assembly resembles cytochrome *bc*$_1$, its purple bacterial counterpart (Section 19-2B), as well as Complex III of the mitochondrial electron-transport chain (Section 18-2E). Electron flow through the cytochrome *b*$_6$*f* complex occurs through a Q cycle (Fig. 18-15). Accordingly, two protons are translocated across the thylakoid membrane for every electron transported. The four electrons abstracted from 2 H_2O by the OEC therefore lead to the translocation of eight H$^+$ from the stroma to the thylakoid lumen. *Electron transport via the cytochrome b*$_6$*f complex generates much of the electrochemical proton gradient that drives the synthesis of ATP in chloroplasts.*

The X-ray structure of cytochrome *b*$_6$*f* (Fig. 19-18) was independently determined by Janet Smith and William Cramer and by Jean-Luc Polpot and Daniel Picot. Cytochrome *b*$_6$*f* is a dimer of ~109-kD protomers, each containing four large subunits (18–32 kD) that have counterparts in cytochrome *bc*$_1$: **cytochrome *b*$_6$,** a homolog of the N-terminal half of cytochrome *b;* **subunit IV,** a homolog of the C-terminal half of cytochrome *b;* **cytochrome**

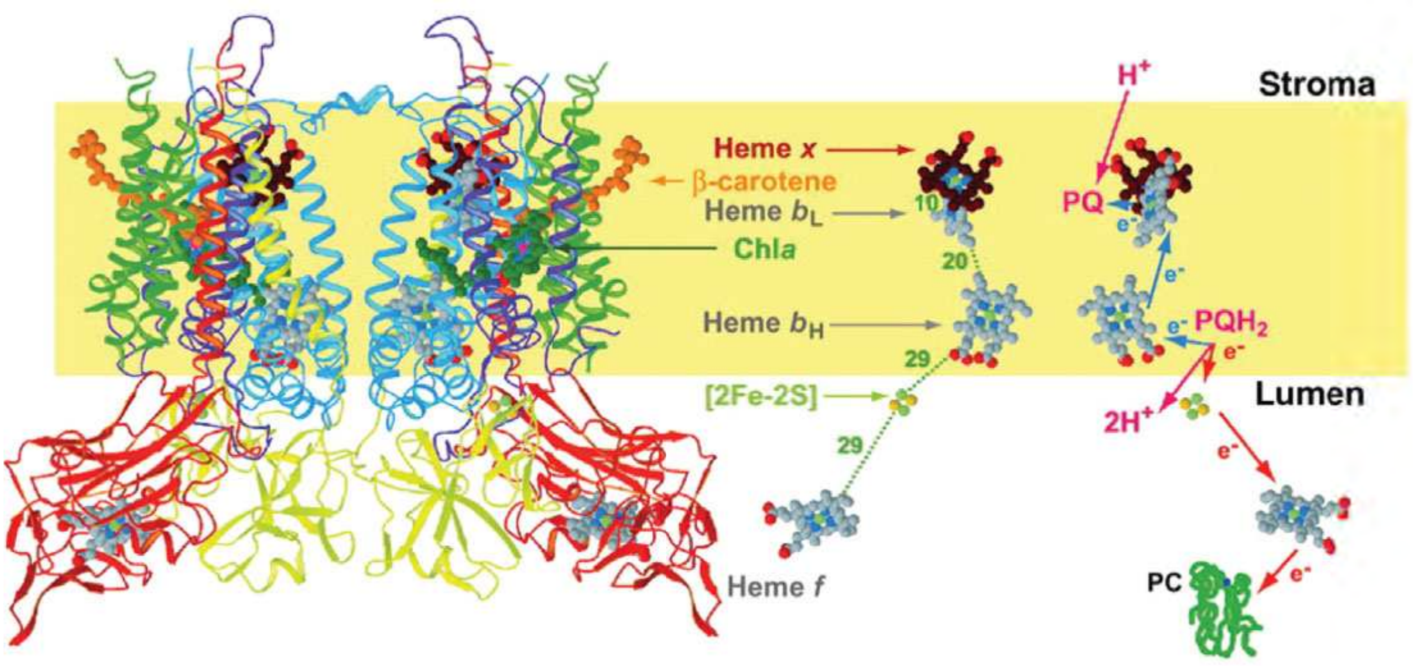

Figure 19-18 | X-Ray structure of the cytochrome *b*$_6$*f* complex from the thermophilic cyanobacterium *Mastigocladus laminosus.* A ribbon diagram of the dimeric complex is drawn on the left with cytochrome *b*$_6$ blue, subunit IV purple, cytochrome *f* red, the iron–sulfur protein (ISP) yellow, and the other subunits green. The inferred position of the lipid bilayer is indicated by a yellow band. Compare this figure to Fig. 18-14 (which is upside down relative to this figure). The paths of electron and proton transfer through the complex and the distances, in angstroms, between redox centers are shown on the right. [Modified from a drawing by William A. Cramer and Janet Smith, Purdue University. PDBid 1UM3.]

f (*f* for *feuille,* French for leaf), a *c*-type cytochrome that is a functional analog of cytochrome c_1, although the two are unrelated in structure or sequence; and a Rieske iron–sulfur protein (ISP), which is also present in cytochrome bc_1. In addition, cytochrome b_6f has four small hydrophobic subunits that have no equivalents in cytochrome bc_1. Each protomer contains 13 transmembrane helices, four in cytochrome b_6, three in subunit IV, and one each in the remaining subunits. Cytochrome b_6f binds cofactors that are the equivalents of all of those in cytochrome bc_1: **heme *f*,** a *c*-type heme bound by cytochrome *f;* a [2Fe–2S] cluster bound by the ISP; hemes b_H and b_L; a plastoquinone molecule that occupies either the Q_i site (the quinone-binding site at which fully reduced quinone is regenerated during the Q cycle; Section 18-2E) or the Q_o site. In addition, cytochrome b_6f binds several cofactors that have no counterparts in cytochrome bc_1: a Chl *a,* a β-carotene, and, unexpectedly, a novel heme named **heme *x*** (alternatively, **heme c_i**), which is covalently linked to the protein via a single thioether bond to Cys 35 of cytochrome b_6, and whose only axial ligand is a water molecule (compare with hemes *a, b,* and *c* in Box 18-1).

Plastocyanin Transports Electrons from Cytochrome b_6f to PSI. Electron transfer between cytochrome *f,* the terminal electron carrier of the cytochrome b_6f complex, and PSI is mediated by plastocyanin (PC), a peripheral membrane protein located on the thylakoid lumenal surface (Fig. 19-11). The Cu-containing redox center of this mobile monomer cycles between its Cu(I) and Cu(II) oxidation states. The X-ray structure of PC from poplar leaves shows that the Cu atom is coordinated with distorted tetrahedral geometry by a Cys, a Met, and two His residues (Fig. 19-19). Cu(II) complexes with four ligands normally adopt a square planar coordination geometry, whereas those of Cu(I) are usually tetrahedral. Evidently, the strain of Cu(II)'s protein-imposed tetrahedral coordination in PC promotes its reduction to Cu(I). This hypothesis accounts for PC's high standard reduction potential (0.370 V) compared to that of the normal Cu(II)/Cu(I) half-reaction (0.158 V) and illustrates how proteins can modulate the reduction potentials of their redox centers. In the case of plastocyanin, this facilitates electron transfer from the cytochrome b_6f complex to PSI.

The structures of cytochrome *f* and PC suggest how these proteins associate. Cytochrome *f*'s Lys 187, a member of a conserved group of five positively charged residues on the protein's surface, can be cross-linked to Asp 44 on PC, which occupies a conserved negatively charged surface patch. Quite possibly the two proteins associate through electrostatic interactions, much like PC's functional analog cytochrome *c* interacts with its redox partners in the mitochondrial electron-transport chain (Section 18-2E).

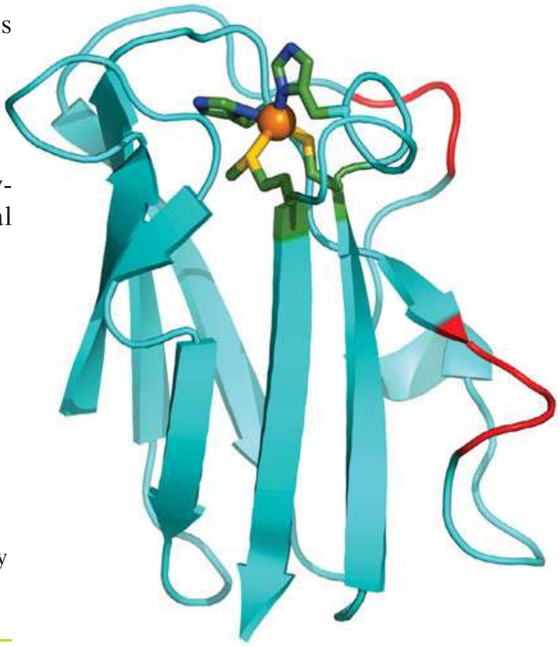

■ **Figure 19-19** | **X-Ray structure of plastocyanin (PC) from poplar leaves.** This 99-residue monomeric protein, a member of the family of **blue copper proteins,** folds into a β sandwich. Its Cu atom (*orange sphere*), which alternates between its Cu(I) and Cu(II) oxidation states, is tetrahedrally coordinated by the side chains of His 37, Cys 84, His 87, and Met 92, which are shown in stick form with their C, N, and S atoms green, blue, and yellow. Seven conserved Asp and Glu residues that form a negatively charged patch on the protein's surface are red. [Based on an X-ray structure by Mitchell Guss and Hans Freeman, University of Sydney, Australia. PDBid 1PLC.]

The PSI RC Resembles Both the PSII RC and the PbRC. Cyanobacterial PSIs are trimers of protomers that each consist of at least 11 different protein subunits coordinating >100 cofactors. The X-ray structure of PSI from *T. elongatus* (Fig. 19-20), determined by Wolfram Saenger, reveals that each of its 356-kD protomers contains nine transmembrane subunits **(PsaA, PsbB, PsaF, PsaI–M,** and **PsaX)** and three stromal (cytoplasmic in cyanobacteria) subunits **(PsaC–E),** which collectively bind 127 cofactors that comprise 30% of PSI's mass. The cofactors forming the PSI RC are all bound by the homologous subunits PsaA (755 residues) and PsaB (740 residues), whose 11 transmembrane helices each are arranged in a manner resembling those in the L and M subunits of the PbRC (Fig. 19-8) and the D1 and D2 subunits of PSII (Fig. 19-13), thus supporting the notion that all RCs arose from a common ancestor. PsaA and PsaB, together with other transmembrane subunits, also bind the cofactors of the core antenna system (see below).

Figure 19-21 indicates that PSI's RC consists of 6 Chl *a*'s and two molecules of **phylloquinone,**

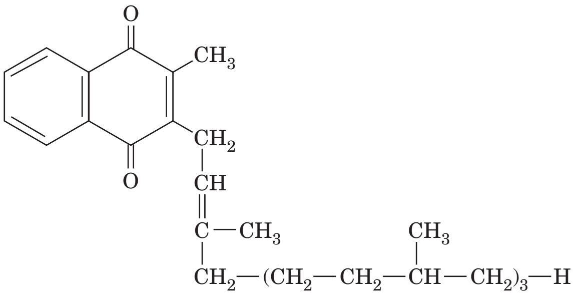

Phylloquinone

which has the same phytyl side chain as do chlorophylls (Fig. 19-2), all arranged in two pseudosymmetrically related branches, followed by three [4Fe–4S] clusters. The primary electron donor of this system, **P700,** consists of a pair of parallel Chl *a*'s, A1 and B1, whose Mg^{2+} ions are separated by 6.3 Å, and thus resembles the "special pair" in the PbRC. A1 is followed in the left branch of Fig. 19-21 by two more Chl *a* rings, B2 and A3, and B1 is followed by A2 and B3 in the right branch. One or both of the third pair of Chl *a* molecules, A3 and B3, probably form the spectroscopically identified primary electron acceptor A_0 (right side of Fig. 19-12). The Mg^{2+} ions of A3 and B3 are each axially liganded by the S atoms of a Met residue rather than by His side chains (thereby forming the only known biological examples of Mg^{2+}—S coordination). Electrons are passed from A3 and B3 to the phylloquinones, Q_K-A and Q_K-B, which almost certainly correspond to the spectroscopically identified electron acceptor A_1. Spectroscopic investigations indicate that, in contrast to the case for the PbRC, electrons pass through both branches of the PSI RC, although at different rates. Indeed, the PSI RC is most closely related to the RC of **green sulfur bacteria** (a second class of photosynthetic bacteria), which is a true homodimer.

Up until this point, PSI's RC resembles those of PSII and purple photosynthetic bacteria. However, rather than the reduced forms of either Q_K-A or Q_K-B dissociating from PSI, both of these quinones directly pass their photoexcited electron to a chain of three spectroscopically identified [4Fe–4S] clusters designated F_X, F_A, and F_B (right side of Fig. 19-12). F_X, which lies on the pseudo-twofold axis relating PsaA and PsaB, is coordinated by two Cys residues from each of these subunits. F_A and F_B are

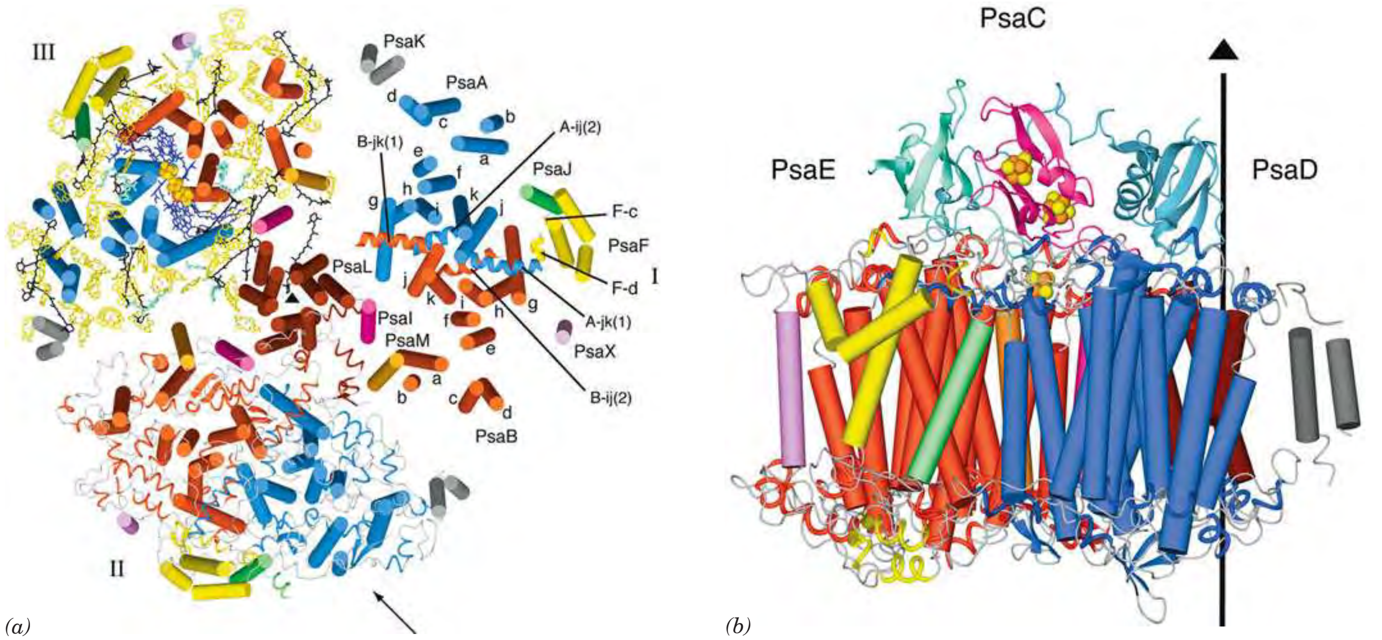

■ **Figure 19-20** | **X-Ray structure of PSI from *T. elongatus.*** (*a*) View of the trimeric complex perpendicular to the membrane from its stromal side. The stromal subunits have been removed for clarity. PSI's threefold axis of symmetry is represented by the small black triangle. Different structural elements are shown for each of the three protomers (I, II, and III). I shows the arrangement of transmembrane helices (*cylinders*), which are differently colored for each subunit. The transmembrane helices of both PsaA (*blue*) and PsaB (*red*) are named a through k from their N- to C-termini. The six helices in extramembranous loop regions are drawn as spirals. II shows the transmembrane helices as cylinders with the stromal and lumenal loop regions drawn in ribbon form. III shows the transmembrane helices as cylinders together with all cofactors. The RC Chl *a*'s and quinones, drawn in stick form, are blue, the Fe and S atoms of the [4Fe–4S] clusters are drawn as orange and yellow spheres, the antenna system Chl *a*'s (whose side chains have been removed for clarity) are yellow, the carotenoids are black, and the bound lipids are light green. (*b*) One protomer as viewed parallel to the membrane along the arrow in Part *a* with the stroma above. The transmembrane subunits are colored as in Part *a* with the stromal subunits PsaC, PsaD, and PsaE pink, cyan, and light green. The vertical line and triangle mark the trimer's threefold axis of symmetry. [Courtesy of Wolfram Saenger, Freie Universität Berlin, Germany. PDBid 1JB0.]

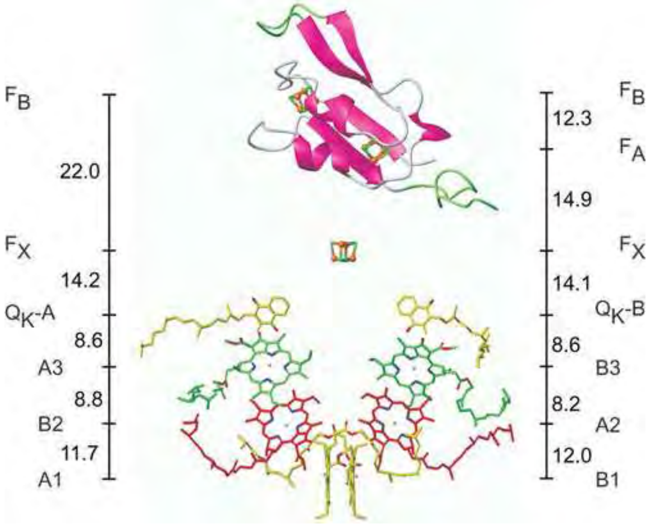

■ **Figure 19-21** | **The cofactors of the PSI RC and PsaC as viewed parallel to the membrane plane with the stroma above.** The Chl *a* and phylloquinone molecules are arranged in two pseudosymmetric branches. The Chl *a*'s are labeled A or B to indicate that their Mg^{2+} ions are liganded by the side chains of PsaA or PsaB, respectively. The phylloquinones are named Q_K-A and Q_K-B. PsaC is shown in ribbon form with those portions resembling segments in bacterial 2[4Fe–4S] ferredoxins pink and with insertions and extensions green. The three [4Fe–4S] clusters are shown in ball-and-stick form and are labeled according to their spectroscopic identities F_X, F_A, and F_B. The center-to-center distances between cofactors (*vertical black lines*) are given in angstroms. Compare this figure with Figs. 19-9 and 19-14. [Courtesy of Wolfram Saenger, Freie Universität Berlin, Germany. PDBid 1JB0.]

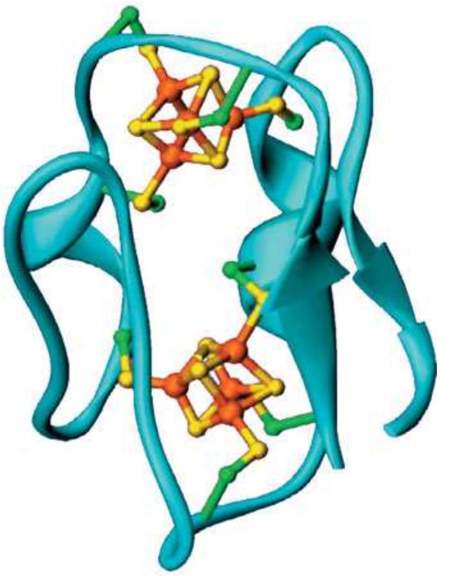

Figure 19-22 | **X-Ray structure of ferredoxin from *Peptococcus aerogenes*.** This monomeric 54-residue protein contains two [4Fe–4S] clusters. The C_β atoms of the four Cys residues liganding each cluster are green, the Fe atoms are orange, and the S atoms are yellow. [Based on an X-ray structure by Elinor Adman, Larry Sieker, and Lyle Jensen, University of Washington. PDBid 1FDX.] **See Interactive Exercise 25.**

bound to the stromal subunit PsaC, which structurally resembles bacterial ferredoxins that contain two [4Fe–4S] clusters (Fig. 19-22). The observation that both branches of PSI's electron-transfer pathways are active, in contrast to only one active branch in PSII and the PbRC, is rationalized by the observation that the two quinones at the ends of each branch are functionally equivalent in PSI but functionally different in PSII and the PbRC.

PSI's core antenna system consists of 90 Chl *a* molecules and 22 carotenoids (Fig. 19-20*a*). The spatial distribution of these antenna Chl *a*'s resembles that in the core antenna subunits CP43 and CP47 of PSII (Fig. 19-13). Indeed, the N-terminal domains of PsaA and PsaB are similar in sequence to those of CP43 and CP47 and fold into similar structures containing six transmembrane helices each. The carotenoids, which are mostly β-carotenes, are deeply buried in the membrane, where they are in van der Waals contact with Chl *a* rings. This permits efficient energy transfer from photoexcited carotenoids to Chl *a*.

PSIs from higher plants are monomers rather than trimers as are cyanobacterial PSIs. Nevertheless, the X-ray structure of PSI from peas reveals that the positions and orientations of the chlorophylls in both species of PSIs are nearly identical, a remarkable finding considering the >1 billion years since chloroplasts diverged from their cyanobacterial ancestors. However, pea PSI has four antenna proteins not present in cyanobacterial PSI that are arranged in a crescent-shaped transmembrane belt around one side of its RC and which collectively bind 56 chlorophyll molecules.

PSI-Activated Electrons May Reduce $NADP^+$ or Motivate Proton Gradient Formation. *Electrons ejected from F_B in PSI may follow either of two alternative pathways* (Fig. 19-12):

1. Most electrons follow a noncyclic pathway by reducing an ~100-residue, [2Fe–2S]-containing, soluble protein called **ferredoxin (Fd)** that is located in the stroma. Reduced Fd, in turn, reduces $NADP^+$ in a reaction mediated by the ~310-residue, monomeric, FAD-containing ferredoxin–$NADP^+$ reductase (FNR, Fig. 19-23) to yield the final product of the chloroplast light reactions, NADPH. Two reduced Fd molecules successively deliver one electron each to the FAD of FNR, which thereby sequentially assumes the neutral semiquinone and fully reduced states before transferring the two electrons and a proton to the $NADP^+$ via what is formally a hydride ion transfer.
2. Some electrons are returned from PSI, via cytochrome b_6, to the plastoquinone pool, thereby traversing a cyclic pathway that translocates protons across the thylakoid membrane. A mechanism that has been proposed for this process is that Fd transfers an electron to heme *x* of cytochrome b_6 (Fig. 19-18)

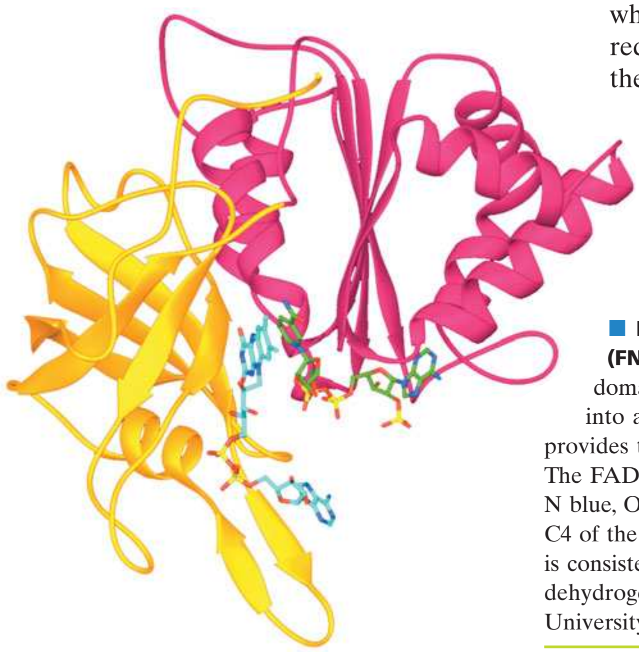

Figure 19-23 | **X-Ray structure of pea ferredoxin–$NADP^+$ reductase (FNR) in complex with FAD and $NADP^+$.** This 308-residue protein has two domains: The N-terminal domain (*gold*), which forms the FAD-binding site, folds into an antiparallel β barrel, whereas the C-terminal domain (*magenta*), which provides the $NADP^+$-binding site, forms a dinucleotide-binding fold (Section 6-2C). The FAD and $NADP^+$ are shown in stick form with $NADP^+$ C green, FAD C cyan, N blue, O red, and P yellow. The flavin and nicotinamide rings are in opposition with C4 of the nicotinamide ring and C5 of the flavin ring 3.0 Å apart, an arrangement that is consistent with direct hydride transfer as also occurs in dihydrolipoyl dehydrogenase (Fig. 17-8). [Based on an X-ray structure by Andrew Karplus, Cornell University. PDBid 1QFY.] **See Interactive Exercise 26.**

rather than to FNR. Since heme *x* contacts heme b_L at the periphery of cytochrome b_6f's Q_i site, an electron injected into heme *x* would be expected to reduce plastoquinone via a Q cycle-like mechanism (Fig. 18-15). Note that the cyclic pathway is independent of the action of PSII and hence does not result in the evolution of O_2. This accounts for the observation that chloroplasts absorb more than eight photons per O_2 molecule evolved.

The cyclic electron flow presumably functions to increase the amount of ATP produced relative to that of NADPH and thus permits the cell to adjust the relative amounts of the two substances produced according to its needs. However, the mechanism that apportions electrons between the cyclic and noncyclic pathways is unknown. Fine-tuning of the light reactions also depends on the segregation of PSI and PSII in distinct portions of the thylakoid membrane (Box 19-1).

D | The Proton Gradient Drives ATP Synthesis by Photophosphorylation

Chloroplasts generate ATP in much the same way as mitochondria, that is, by coupling the dissipation of a proton gradient to the enzymatic synthesis of ATP (Section 18-3). This light-dependent process is known as **photophosphorylation.** Like oxidative phosphorylation, it requires an intact thylakoid membrane and can be uncoupled from light-driven electron transport by compounds such as 2,4-dinitrophenol (Fig. 18-28).

Electron micrographs of thylakoid membrane stromal surfaces and bacterial plasma membrane inner surfaces reveal lollipop-shaped structures (Fig. 19-24). These closely resemble the F_1 units of the proton-translocating ATP synthase in mitochondria (Fig. 18-21*a*). In fact, the chloroplast ATP synthase, which is also known as the $\mathbf{CF_1CF_0}$ complex (C for chloroplast), is remarkably similar to the mitochondrial F_1F_0 complex. For example,

1. Both the F_0 and the CF_0 units are hydrophobic transmembrane proteins that contain a proton-translocating channel.
2. Both the F_1 and the CF_1 units are hydrophilic peripheral membrane proteins of subunit composition $\alpha_3\beta_3\gamma\delta\varepsilon$, of which β is a reversible ATPase.
3. Both ATP synthases are inhibited by oligomycin and by dicyclohexylcarbodiimide (DCCD).

Clearly, proton-translocating ATP synthase must have evolved very early in the history of cellular life. Note, however, that whereas chloroplast ATP synthase translocates protons out of the thylakoid space into the stroma (Fig. 19-11), mitochondrial ATP synthase conducts them from the intermembrane space into the matrix space (Fig. 18-20). This is because the stroma is topologically analogous to the mitochondrial matrix.

Photosynthesis with Noncyclic Electron Transport Produces Around One ATP per Absorbed Photon. At saturating light intensities, chloroplasts generate proton gradients of ~3.5 pH units across their thylakoid membranes as a result of two processes:

1. The evolution of a molecule of O_2 from two H_2O molecules releases four protons into the thylakoid lumen.
2. The transport of the liberated four electrons through the cytochrome b_6f complex occurs with the translocation of eight protons from the stroma to the thylakoid lumen.

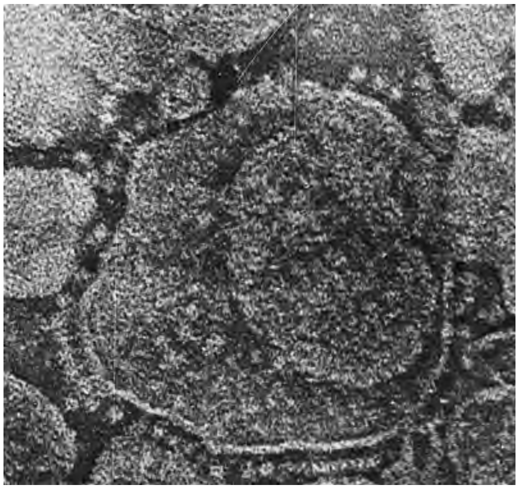

Figure 19-24 | Electron micrograph of thylakoids showing the CF_1 "lollipops" of their ATP synthases projecting from their stromal surfaces. Compare this with Fig. 18-21*a*. [Courtesy of Peter Hinkle, Cornell University.]

BOX 19-1 **PERSPECTIVES IN BIOCHEMISTRY**

Segregation of PSI and PSII

Electron microscopy has revealed that the protein complexes of the thylakoid membrane have characteristic distributions (*see figure*).

1. PSI occurs mainly in the unstacked stromal lamellae, in contact with the stroma, where it has access to $NADP^+$.
2. PSII is located almost exclusively between the closely stacked grana, out of direct contact with the stroma.
3. Cytochrome b_6f is uniformly distributed throughout the membrane.

The high mobilities of plastoquinone and plastocyanin, the electron carriers that shuttle electrons between these particles, permit photosynthesis to proceed at a reasonable rate.

What function is served by the segregation of PSI and PSII? If these two photosystems were in close proximity, the higher excitation energy of PSII (P680 versus P700) would cause it to pass a large fraction of its absorbed photons to PSI via exciton transfer; that is, PSII would act as a light-harvesting antenna for PSI. The separation of the particles by around 100 Å eliminates this difficulty.

The physical separation of PSI and PSII also permits the chloroplast to respond to changes in illumination. The relative amounts of light absorbed by the two photosystems vary with how the light-harvesting complexes are distributed between the stacked and unstacked portions of the thylakoid membrane. Under high illumination (normally direct sunlight, which contains a high proportion of short-wavelength blue light), PSII absorbs more light than PSI. PSI is then unable to take up electrons as fast as PSII can supply them, so the plastoquinone is predominantly in its reduced state. The reduced plastoquinone activates a protein kinase to phosphorylate specific Thr residues of the LHCs, which, in response, migrate to the unstacked regions of the thylakoid membrane, where they associate with PSI. A greater fraction of the incident light is thereby funneled to PSI.

Under low illumination (normally shady light, which contains a high proportion of long-wavelength red light), PSI takes up electrons faster than PSII can provide them so that plastoquinone predominantly assumes its oxidized form. The LHCs are consequently dephosphorylated and migrate to the stacked portions of the thylakoid membrane, where they associate with PSII. The chloroplast therefore maintains the balance between its two photosystems by a light-activated feedback mechanism.

[Figure based on Anderson, J.M. and Anderson, B., *Trends Biochem. Sci.* **7,** 291 (1982).]

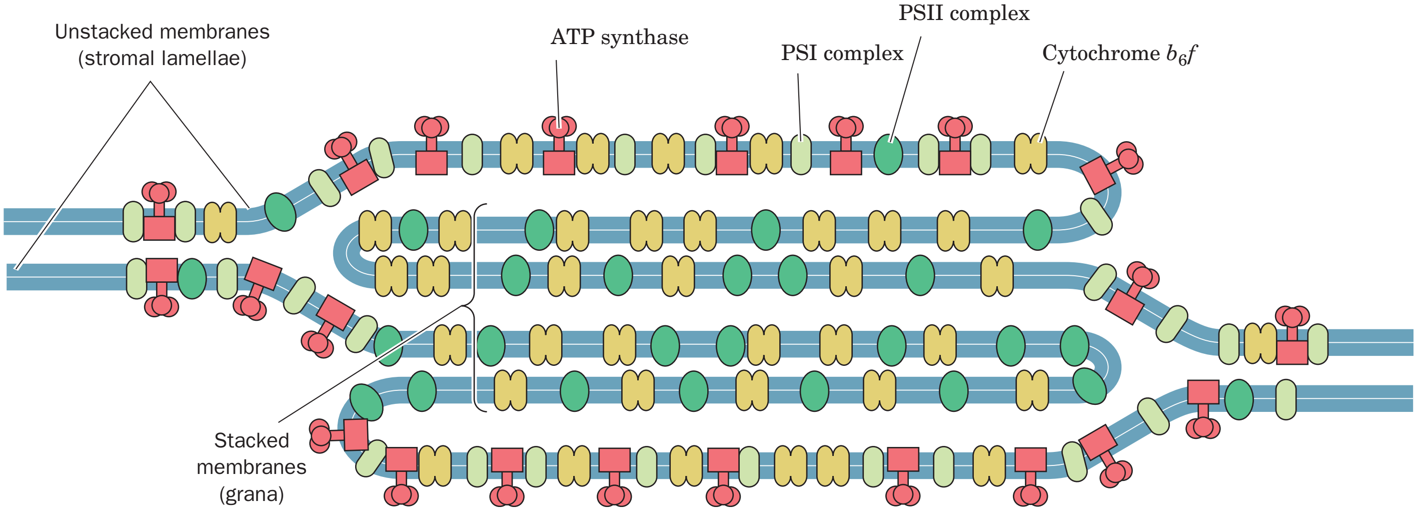
Unstacked membranes (stromal lamellae)
ATP synthase
PSII complex
PSI complex
Cytochrome b_6f
Stacked membranes (grana)

Altogether, ~12 protons enter the lumen per molecule of O_2 produced by noncyclic electron transport.

The thylakoid membrane, in contrast to the inner mitochondrial membrane, is permeable to ions such as Mg^{2+} and Cl^-. Translocation of protons and electrons across the thylakoid membrane is consequently accompanied by the passage of these ions so as to maintain electrical neutrality (Mg^{2+} out and Cl^- in). This all but eliminates the membrane potential. *The electrochemical gradient in chloroplasts is therefore almost entirely a result of the pH (concentration) gradient.*

Chloroplast ATP synthase, according to most estimates, produces one ATP for every three protons it transports from the thylakoid lumen to the stroma. Noncyclic electron transport in chloroplasts therefore results in the production of $\sim 12/3 = 4$ molecules of ATP per molecule of O_2 evolved (cyclic electron transport generates more ATP because more protons are translocated to the thylakoid lumen via the Q cycle mediated by cytochrome b_6f).

Noncyclic electron transport, of course, also yields NADPH (2 NADPH for every 4 electrons liberated from 2 H_2O by the OEC). Each NADPH has the free energy to produce 2.5 ATP (Section 18-3C; although NADPH is not used to drive ATP synthesis), for a total of 5 more ATP equivalents per O_2 produced. Consequently, a total of 9 ATP equivalents are generated per O_2 produced. A minimum of two photons is required for each electron traversing the system from H_2O to NADPH, that is, eight photons per O_2 produced. This is confirmed by experimental measurements which indicate that plants and algae require 8 to 10 photons of visible light to produce one molecule of O_2. Thus, the overall efficiency of the light reactions is 9 ATP/8–10 photons, or approximately one ATP per absorbed photon.

■ CHECK YOUR UNDERSTANDING

How do molecules dissipate absorbed light energy?
Explain why electron transport in purple photosynthetic bacteria follows a circular path.
Describe the effect of photooxidation of the redox reactions summarized in the Z-scheme.
What is the importance of the water-splitting reaction for photosynthesis?
What are the implications of cyclic and noncyclic electron transfer in PSI?
Compare and contrast photophosphorylation and oxidative phosphorylation.

3 The Dark Reactions

In the previous section we saw how plants harness light energy to generate ATP and NADPH. In this section we discuss how these products are used to synthesize carbohydrates and other substances from CO_2.

LEARNING OBJECTIVES

- Understand that the Calvin cycle carboxylates a pentose, converts the products to glyceraldehyde-3-phosphate, and regenerates the pentose, using the ATP and NADPH produced by the light reactions.
- Understand that the products of the Calvin cycle are converted to carbohydrates (glucose polymers).
- Understand that the Calvin cycle enzymes are more reactive in the light.
- Understand that plants undergo photorespiration, which consumes O_2 and generates CO_2.

A | The Calvin Cycle Fixes CO_2

The metabolic pathway by which plants incorporate CO_2 into carbohydrates was elucidated between 1946 and 1953 by Melvin Calvin, James Bassham, and Andrew Benson. They did so by tracing the metabolic fate of the radioactive label from $^{14}CO_2$ in cultures of algal cells. Some of Calvin's earliest experiments indicated that algae exposed to $^{14}CO_2$ for a minute or more synthesize a complex mixture of labeled metabolites, including sugars and amino acids. Analysis of the algae within 5 s of their exposure to $^{14}CO_2$, however, showed that *the first stable radioactive compound formed is **3-phosphoglycerate (3PG),** which is initially labeled only in its carboxyl group*. This result immediately suggested that the 3PG was formed by the carboxylation of a C_2 compound. Yet no such precursor was found. The actual carboxylation reaction involves a pentose derived from **ribulose-5-phosphate (Ru5P):**

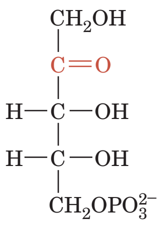

$$\begin{array}{c} CH_2OH \\ | \\ C{=}O \\ | \\ H{-}C{-}OH \\ | \\ H{-}C{-}OH \\ | \\ CH_2OPO_3^{2-} \end{array}$$

Ribulose-5-phosphate (Ru5P)

The resulting C_6 product splits into two C_3 compounds, both of which turn out to be 3PG. ATP and NADPH, the products of the light reactions, are required to convert 3PG to glyceraldehyde-3-phosphate (GAP), which is

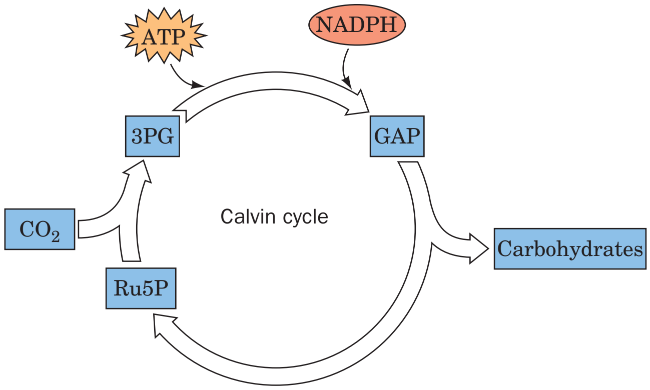

Figure 19-25 | Overview of the dark reactions. The products of the light reactions, ATP and NADPH, are consumed in converting CO_2 into carbohydrates in a process called the Calvin cycle.

used to synthesize carbohydrates as well as re-form Ru5P (Fig. 19-25). The entire pathway, which involves the carboxylation of a pentose, the formation of carbohydrate products, and the regeneration of the pentose, is known as the **Calvin cycle** or the **reductive pentose phosphate cycle.**

During the search for the carboxylation substrate, several other photosynthetic intermediates had been identified and their labeling patterns elucidated. For example, the hexose fructose-1,6-bisphosphate (FBP) is initially labeled only at its C3 and C4 positions but later becomes labeled to a lesser degree at its other atoms. A consideration of the flow of labeled carbon through the various tetrose, pentose, hexose, and heptose phosphates led, in what is a milestone of metabolic biochemistry, to the deduction of the Calvin cycle as is diagrammed in Fig. 19-26. The existence of many of its postulated reactions was eventually confirmed by *in vitro* studies using purified enzymes.

The Calvin Cycle Generates GAP from CO_2 via a Two-Stage Process. The Calvin cycle can be considered to have two stages:

Stage 1. The production phase (top line of Fig. 19-26), in which three molecules of Ru5P react with three molecules of CO_2 to yield six molecules of glyceraldehyde-3-phosphate (GAP) at the expense of nine ATP and six NADPH molecules. *The cyclic nature of the entire pathway makes this process equivalent to the synthesis of one GAP from three CO_2 molecules.* At this point, GAP can be bled off from the cycle for use in biosynthesis.

Stage 2. The recovery phase (bottom lines of Fig. 19-26), in which the carbon atoms of the remaining five GAPs are shuffled in a remarkable series of reactions, similar to those of the pentose phosphate pathway (Section 15-6), to re-form the three Ru5Ps with which the cycle began. This stage can be conceptually

Figure 19-26 | (*Opposite*) The Calvin cycle. The number of lines in an arrow indicates the number of molecules reacting in that step for a single turn of the cycle that converts three CO_2 molecules to one GAP molecule. For the sake of clarity, the sugars are all shown in their linear forms, although the hexoses and heptoses predominantly exist in their cyclic forms. The ^{14}C-labeling patterns generated in one turn of the cycle through the use of $^{14}CO_2$ are indicated in red. Note that two of the product Ru5Ps are labeled only at C3, whereas the third Ru5P is equally labeled at C1, C2, and C3. **See the Animated Figures.**

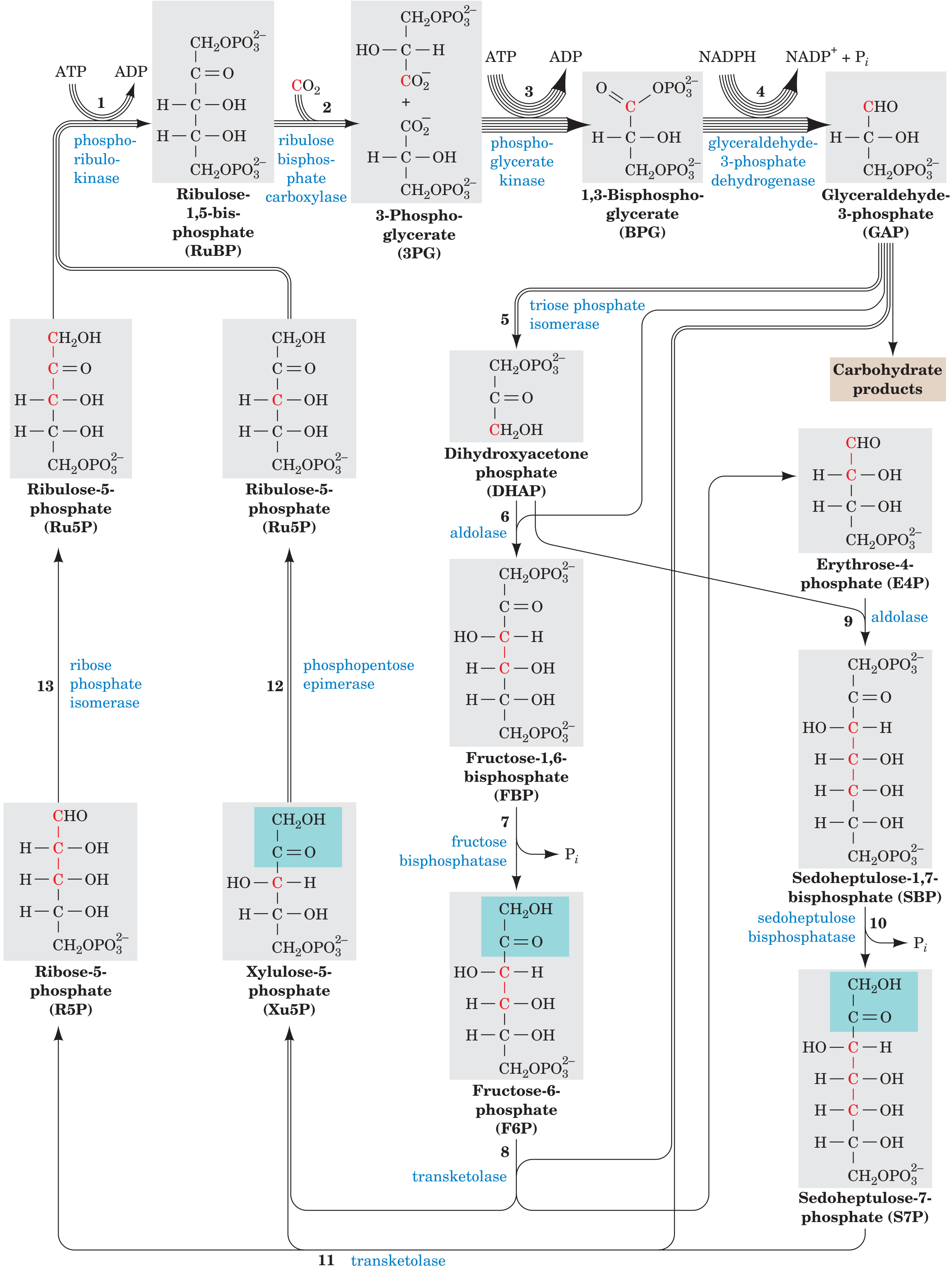
ATP
ADP
1
phospho-ribulo-kinase
Ribulose-1,5-bis-phosphate (RuBP)
CO2
2
ribulose bisphos-phate carboxylase
3-Phospho-glycerate (3PG)
ATP
ADP
3
phospho-glycerate kinase
1,3-Bisphospho-glycerate (BPG)
NADPH
NADP+ + Pi
4
glyceraldehyde-3-phosphate dehydrogenase
Glyceraldehyde-3-phosphate (GAP)
Carbohydrate products
5
triose phosphate isomerase
Dihydroxyacetone phosphate (DHAP)
6
aldolase
Fructose-1,6-bisphosphate (FBP)
7
fructose bisphosphatase
Pi
Fructose-6-phosphate (F6P)
8
transketolase
Erythrose-4-phosphate (E4P)
9
aldolase
Sedoheptulose-1,7-bisphosphate (SBP)
sedoheptulose bisphosphatase
10
Pi
Sedoheptulose-7-phosphate (S7P)
11
transketolase
Ribose-5-phosphate (R5P)
13
ribose phosphate isomerase
Ribulose-5-phosphate (Ru5P)
Xylulose-5-phosphate (Xu5P)
12
phosphopentose epimerase
Ribulose-5-phosphate (Ru5P)

decomposed into four sets of reactions (with the numbers keyed to the corresponding reactions in Fig. 19-26):

6. $C_3 + C_3 \rightarrow C_6$
8. $C_3 + C_6 \rightarrow C_5 + C_4$
9. $C_3 + C_4 \rightarrow C_7$
11. $C_3 + C_7 \rightarrow C_5 + C_5$

The overall stoichiometry for this process is therefore

$$5\ C_3 \longrightarrow 3\ C_5$$

Note that this stage of the Calvin cycle occurs without further input of free energy (ATP) or reducing equivalents (NADPH).

The first reaction of the Calvin cycle is the phosphorylation of Ru5P by **phosphoribulokinase** to form **ribulose-1,5-bisphosphate (RuBP).** Following the carboxylation of RuBP (Reaction 2; discussed below), the resulting 3PG is converted first to 1,3-bisphosphoglycerate (BPG) and then to GAP. This latter sequence is the reverse of two consecutive glycolytic reactions (Section 15-2G and 15-2F) except that the Calvin cycle reaction uses NADPH rather than NADH.

The second stage of the Calvin cycle begins with the reverse of a familiar glycolytic reaction, the isomerization of GAP to dihydroxyacetone phosphate (DHAP) by triose phosphate isomerase (Section 15-2E). Following this, DHAP is directed along two analogous paths: Reactions 6 to 8 or Reactions 9 to 11. Reactions 6 and 9 are aldolase-catalyzed aldol condensations in which DHAP is linked to an aldehyde. Reaction 6 is also the reverse of a glycolytic reaction (Section 15-2D). Reactions 7 and 10 are phosphate hydrolysis reactions that are catalyzed, respectively, by fructose bisphosphatase (FBPase; Section 15-4B) and **sedoheptulose bisphosphatase (SBPase).** The remaining Calvin cycle reactions are catalyzed by enzymes that also participate in the pentose phosphate pathway. In Reactions 8 and 11, both catalyzed by transketolase, a C_2 keto unit (shaded green in Fig. 19-26) is transferred from a ketose to GAP to form xylulose-5-phosphate (Xu5P), leaving the aldoses erythrose-4-phosphate (E4P) in Reaction 8 and ribose-5-phosphate (R5P) in Reaction 11. The E4P produced by Reaction 8 feeds into Reaction 9. The Xu5Ps produced by Reactions 8 and 11 are converted to Ru5P by **phosphopentose epimerase** in Reaction 12. The R5P from Reaction 11 is also converted to Ru5P by **ribose phosphate isomerase** in Reaction 13, thereby completing a turn of the Calvin cycle. Only 3 of the 11 Calvin cycle enzymes—phosphoribulokinase, the carboxylation enzyme ribulose bisphosphate carboxylase, and SBPase—have no equivalents in animal tissues.

RuBP Carboxylase Catalyzes CO_2 Fixation. The enzyme that catalyzes CO_2 fixation, ribulose bisphosphate carboxylase **(RuBP carboxylase),** is arguably the world's most important enzyme since nearly all life on earth ultimately depends on its action. This protein, presumably as a consequence of its low catalytic efficiency ($k_{cat} \approx 3\ s^{-1}$), accounts for up to 50% of leaf proteins and is therefore the most abundant protein in the biosphere. RuBP carboxylase from higher plants and most photosynthetic microorganisms consists of eight large (L) subunits (477 residues in tobacco leaves) encoded by chloroplast DNA, and eight small (S) subunits (123 residues) specified by a nuclear gene (the RuBP carboxylase from certain photosynthetic bacteria is an L_2 dimer whose L subunit has 28% sequence identity with and is structurally similar to that of the L_8S_8 enzyme). X-Ray

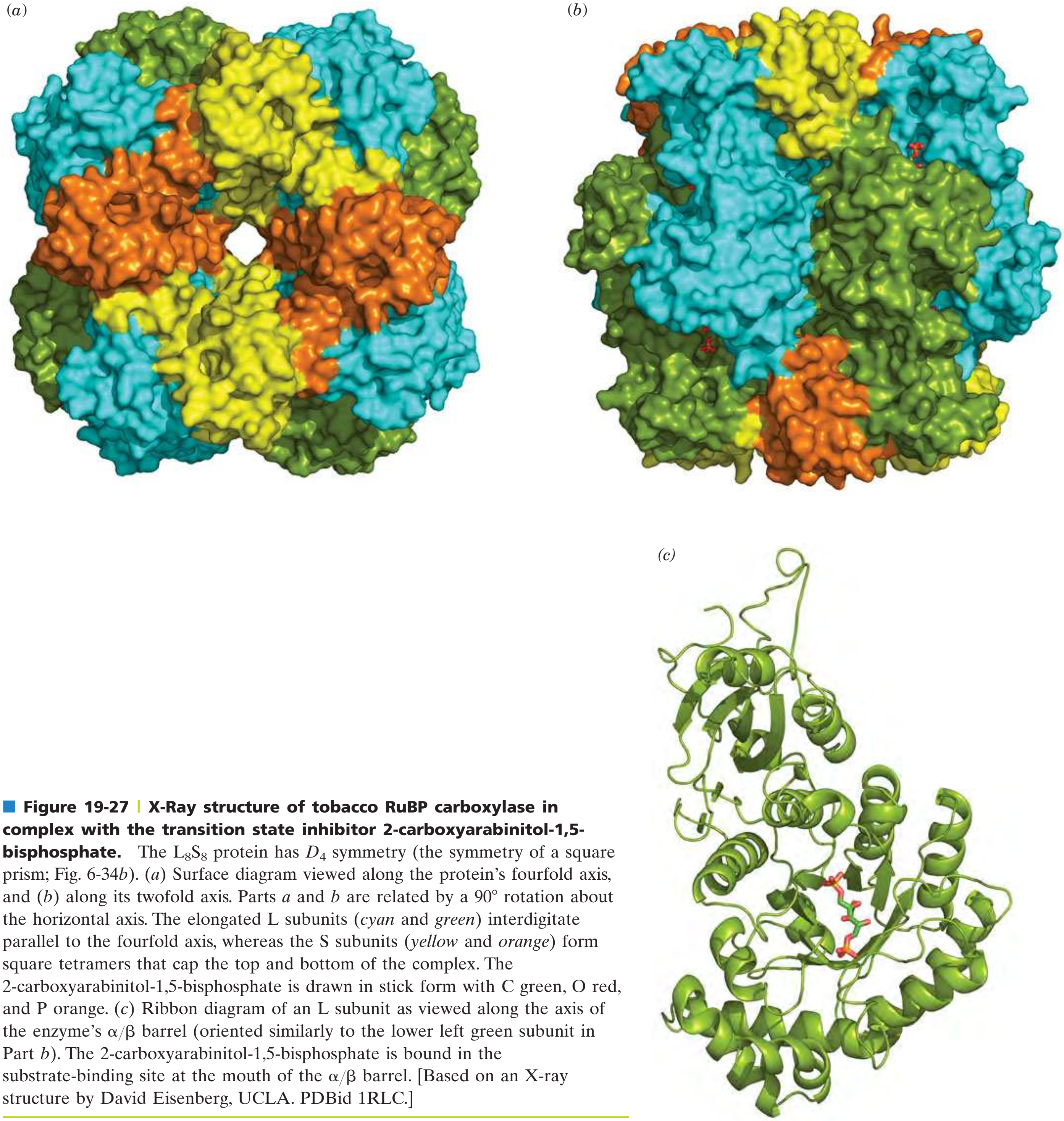

Figure 19-27 | X-Ray structure of tobacco RuBP carboxylase in complex with the transition state inhibitor 2-carboxyarabinitol-1,5-bisphosphate. The L_8S_8 protein has D_4 symmetry (the symmetry of a square prism; Fig. 6-34*b*). (*a*) Surface diagram viewed along the protein's fourfold axis, and (*b*) along its twofold axis. Parts *a* and *b* are related by a 90° rotation about the horizontal axis. The elongated L subunits (*cyan* and *green*) interdigitate parallel to the fourfold axis, whereas the S subunits (*yellow* and *orange*) form square tetramers that cap the top and bottom of the complex. The 2-carboxyarabinitol-1,5-bisphosphate is drawn in stick form with C green, O red, and P orange. (*c*) Ribbon diagram of an L subunit as viewed along the axis of the enzyme's α/β barrel (oriented similarly to the lower left green subunit in Part *b*). The 2-carboxyarabinitol-1,5-bisphosphate is bound in the substrate-binding site at the mouth of the α/β barrel. [Based on an X-ray structure by David Eisenberg, UCLA. PDBid 1RLC.]

studies by Carl-Ivar Brändén and by David Eisenberg demonstrated that the L_8S_8 enzyme has the symmetry of a square prism (Fig. 19-27*a*). The L subunit is made of a β sheet domain and an α/β barrel domain that contains the enzyme's catalytic site (Fig. 19-27*c*). The function of the S subunit is unknown; attempts to show that is has a regulatory role, in analogy with other enzymes, have been unsuccessful.

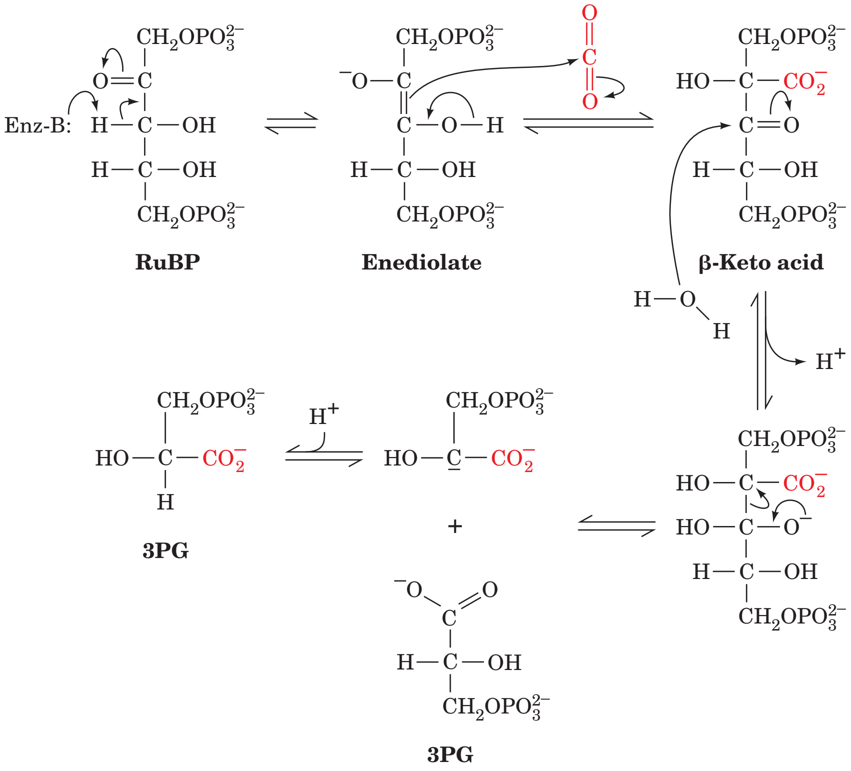

■ **Figure 19-28 | Mechanism of the RuBP carboxylase reaction.** The reaction proceeds via an enediolate intermediate that nucleophilically attacks CO_2 to form a β-keto acid. This intermediate reacts with water to yield two molecules of 3PG. **See the Animated Figures.**

The accepted mechanism of RuBP carboxylase, which was largely formulated by Calvin, is indicated in Fig. 19-28. Abstraction of the C3 proton of RuBP, the reaction's rate-determining step, generates an enediolate that nucleophilically attacks CO_2. The resulting β-keto acid is rapidly attacked at its C3 position by H_2O to yield an adduct that splits, by a reaction similar to aldol cleavage, to yield the two product 3PG molecules. *The driving force for the overall reaction, which is highly exergonic ($\Delta G^{\circ\prime} = -35.1\ kJ \cdot mol^{-1}$), is provided by the cleavage of the β-keto acid intermediate to yield an additional resonance-stabilized carboxylate group.*

RuBP carboxylase activity requires Mg^{2+}, which probably stabilizes developing negative charges during catalysis. The Mg^{2+} is, in part, bound to the enzyme by a catalytically important carbamate group (—NH—COO^-) that is generated by the reaction of a nonsubstrate CO_2 with the ε-amino group of Lys 201. This essential reaction is catalyzed *in vivo* by the enzyme **RuBP carboxylase activase** in an ATP-driven process.

B | Calvin Cycle Products Are Converted to Starch, Sucrose, and Cellulose

The overall stoichiometry of the Calvin cycle is

$$3\ CO_2 + 9\ ATP + 6\ NADPH \rightarrow GAP + 9\ ADP + 8\ P_i + 6\ NADP^+$$

GAP, the primary product of photosynthesis, is used in a variety of biosynthetic pathways, both inside and outside the chloroplast. For example, it can be converted to fructose-6-phosphate by the further action of Calvin cycle enzymes and then to glucose-1-phosphate (G1P) by phosphoglucose isomerase and phosphoglucomutase (Section 16-1C). *G1P is the precursor of the higher order carbohydrates characteristic of plants.*

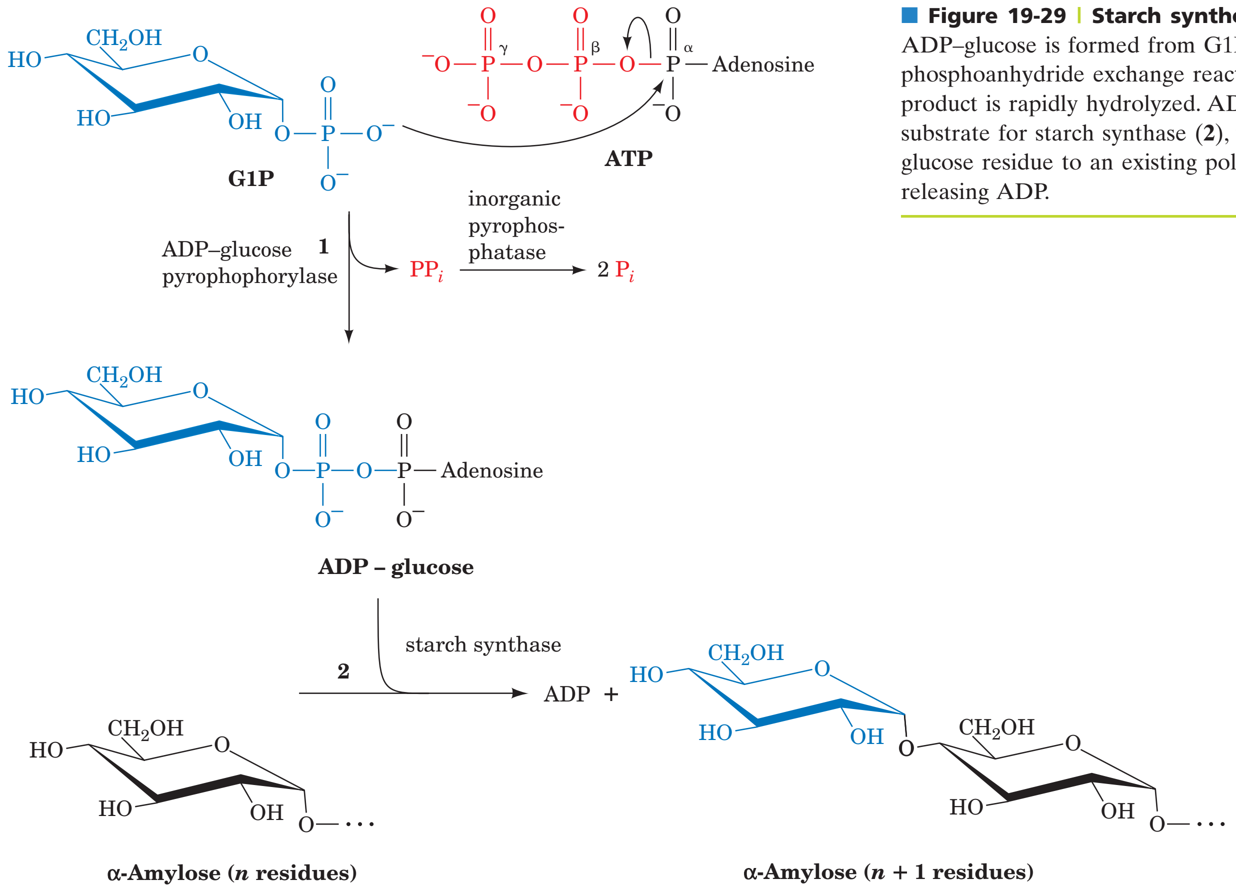
G1P
ATP
γ
β
α
Adenosine
ADP–glucose pyrophosphorylase
1
inorganic pyrophosphatase
PP_i
2 P_i
ADP – glucose
starch synthase
2
ADP +
α-Amylose (*n* residues)
α-Amylose (*n* + 1 residues)

Figure 19-29 | Starch synthesis. ADP–glucose is formed from G1P and ATP in a phosphoanhydride exchange reaction (**1**). The PP_i product is rapidly hydrolyzed. ADP–glucose is the substrate for starch synthase (**2**), which adds the glucose residue to an existing polysaccharide, releasing ADP.

The polysaccharide α-amylose, a major component of starch (Section 8-2C), is synthesized in the chloroplast stroma as a temporary storage depot for glucose units. It is also synthesized as a long-term storage molecule elsewhere in the plant, including leaves, seeds, and roots. G1P is first activated by its reaction with ATP to form ADP–glucose as catalyzed by **ADP–glucose pyrophosphorylase. Starch synthase** then transfers the glucose residue to the nonreducing end of an α-amylose molecule, forming a new glycosidic linkage (Fig. 19-29). The overall reaction is driven by the exergonic hydrolysis of the PP_i released in the formation of ADP–glucose. A similar reaction sequence occurs in glycogen synthesis, which uses UDP–glucose (Section 16-2).

Sucrose, a disaccharide of glucose and fructose (Section 8-2A), is the major transport sugar for delivering carbohydrates to nonphotosynthesizing cells and hence is the major photosynthetic product of green leaves. Since sucrose is synthesized in the cytosol, either glyceraldehyde-3-phosphate or dihydroxyacetone phosphate is transported out of the chloroplast by an antiporter that exchanges phosphate for a triose phosphate. Two trioses combine to form fructose-6-phosphate (F6P) and subsequently glucose-1-phosphate (G1P), which is then activated by UTP to form UDP–glucose. Next, sucrose-6-phosphate is produced in a reaction catalyzed by **sucrose-phosphate synthase.** Finally, sucrose-6-phosphate is hydrolyzed by **sucrose-phosphate phosphatase** to yield sucrose *(at right)*, which is then exported to other plant tissues.

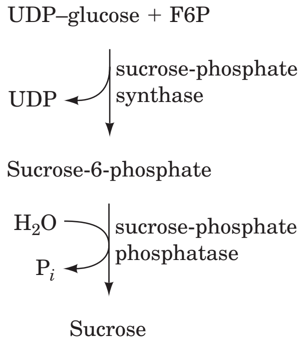
UDP–glucose + F6P
UDP
sucrose-phosphate synthase
Sucrose-6-phosphate
H_2O
P_i
sucrose-phosphate phosphatase
Sucrose

Cellulose, which consists of long chains of β(1→4)-linked glucose units and is the major polysaccharide of plants, is also synthesized from UDP–glucose. Plant cell walls consist of almost-crystalline cables containing ~36 cellulose chains, all embedded in an amorphous matrix of other polysaccharides and lignin (Section 8-2B). Unlike starch in plants or glycogen in mammals, cellulose is synthesized by multisubunit enzyme complexes in the plant plasma membrane and extruded into the extracellular space.

C | The Calvin Cycle Is Controlled Indirectly by Light

During the day, plants satisfy their energy needs via the light and dark reactions of photosynthesis. At night, however, like other organisms, they must use their nutritional reserves to generate ATP and NADPH through glycolysis, oxidative phosphorylation, and the pentose phosphate pathway. Since the stroma contains the enzymes of glycolysis and the pentose phosphate pathway as well as those of the Calvin cycle, *plants must have a light-sensitive control mechanism to prevent the Calvin cycle from consuming this catabolically produced ATP and NADPH in a wasteful futile cycle.*

As we have seen, the control of flux in a metabolic pathway occurs at enzymatic steps that are far from equilibrium (large negative value of ΔG). Inspection of Table 19-1 indicates that the three best candidates for flux control in the Calvin cycle are the reactions catalyzed by RuBP carboxylase, FBPase, and SBPase (Reactions 2, 7, and 10 of Fig. 19-26). In fact, the catalytic efficiencies of the three enzymes all vary *in vivo* with the level of illumination.

Table 19-1 Standard and Physiological Free Energy Changes for the Reactions of the Calvin Cycle

Step[a]	Enzyme	$\Delta G°'$ (kJ · mol^{-1})	ΔG (kJ · mol^{-1})
1	Phosphoribulokinase	−21.8	−15.9
2	Ribulose bisphosphate carboxylase	−35.1	−41.0
3 + 4	Phosphoglycerate kinase + glyceraldehyde-3-phosphate dehydrogenase	+18.0	−6.7
5	Triose phosphate isomerase	−7.5	−0.8
6	Aldolase	−21.8	−1.7
7	Fructose bisphosphatase	−14.2	−27.2
8	Transketolase	+6.3	−3.8
9	Aldolase	−23.4	−0.8
10	Sedoheptulose bisphosphatase	−14.2	−29.7
11	Transketolase	+0.4	−5.9
12	Phosphopentose epimerase	+0.8	−0.4
13	Ribose phosphate isomerase	+2.1	−0.4

[a] Refer to Fig. 19-26.

Source: Bassham, J.A. and Buchanan, B.B., *in* Govindjee (Ed.), *Photosynthesis,* Vol. II, p. 155, Academic Press (1982).

The activity of RuBP carboxylase responds to three light-dependent factors:

1. pH. On illumination, the pH of the stroma increases from ~7.0 to ~8.0 as protons are pumped from the stroma into the thylakoid lumen. RuBP carboxylase has a sharp pH optimum near pH 8.0.
2. [Mg^{2+}]. Recall that the light-induced influx of protons to the thylakoid lumen is accompanied by the efflux of Mg^{2+} to the stroma (Section 19-2D). This Mg^{2+} stimulates RuBP carboxylase.
3. The transition state analog **2-carboxyarabinitol-1-phosphate (CA1P).**

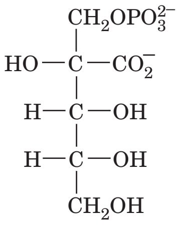

2-Carboxyarabinitol-
1-phosphate
(CA1P)

Many plants synthesize this compound, which inhibits RuBP carboxylase, only in the dark. RuBP carboxylase activase facilitates the release of the tight-binding CA1P from RuBP carboxylase as well as catalyzing its carbamoylation (Section 19-3A).

FBPase and SBPase are also activated by increased pH and [Mg^{2+}], and by NADPH as well. The action of these factors is complemented by a second regulatory system that responds to the redox potential of the stroma. **Thioredoxin,** an ~105-residue protein that occurs in many types of cells, contains a reversibly reducible disulfide group. Reduced thioredoxin activates both FBPase and SBPase by a disulfide interchange reaction (Fig. 19-30). The redox level of thioredoxin is maintained by a second disulfide-containing enzyme, **ferredoxin–thioredoxin reductase,** which directly responds to the redox state of the soluble ferredoxin in the stroma. This in turn varies with the illumination level. The thioredoxin system also deactivates phosphofructokinase (PFK), the main flux-generating enzyme of glycolysis (Section 15-4A). Thus, in plants, *light stimulates the Calvin cycle while deactivating glycolysis, whereas darkness has the opposite effect* (that is, the so-called dark reactions do not occur in the dark).

D | Photorespiration Competes with Photosynthesis

It has been known since the 1960s that *illuminated plants consume O_2 and evolve CO_2 in a pathway distinct from oxidative phosphorylation. In fact, at low CO_2 and high O_2 levels, this **photorespiration** process can outstrip photosynthetic CO_2 fixation.* The basis of photorespiration was unexpected: *O_2 competes with CO_2 as a substrate for RuBP carboxylase* (RuBP carboxylase

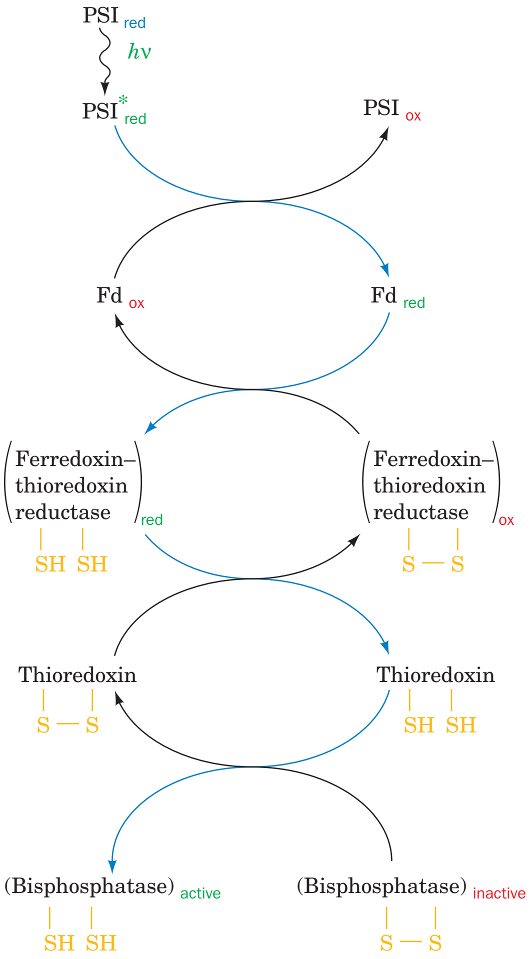

■ **Figure 19-30 | The light-activation mechanism of FBPase and SBPase.** Photoactivated PSI reduces soluble ferredoxin (Fd), which reduces ferredoxin–thioredoxin reductase, which, in turn, reduces the disulfide linkage of thioredoxin. Reduced thioredoxin reacts with the inactive bisphosphatases by disulfide interchange, thereby activating these flux-controlling Calvin cycle enzymes.

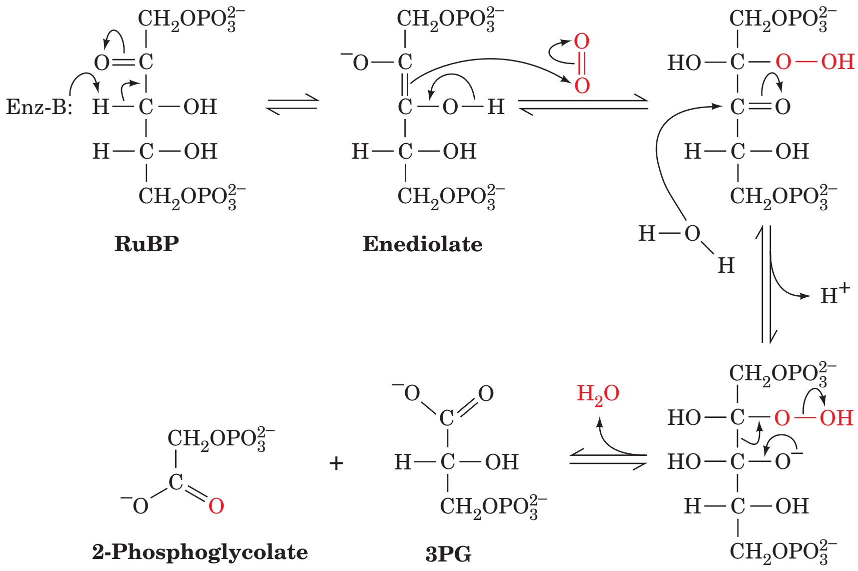

■ **Figure 19-31 | Probable mechanism of the oxygenase reaction catalyzed by RuBP carboxylase–oxygenase.** Note the similarity of this mechanism to that of the carboxylase reaction catalyzed by the same enzyme (Fig. 19-28).

is therefore also called **RuBP carboxylase–oxygenase** or **RuBisCO**). In the oxygenase reaction, O_2 reacts with the enzyme's other substrate, RuBP, to form 3PG and **2-phosphoglycolate** (Fig. 19-31). The 2-phosphoglycolate is hydrolyzed to **glycolate** by **phosphoglycolate phosphatase** and, as described below, is partially oxidized to yield CO_2 by a series of enzymatic reactions that occur in the **peroxisome** and the mitochondrion. Thus, photorespiration is a seemingly wasteful process that undoes some of the work of photosynthesis. In this section we discuss the biochemical basis of photorespiration and how certain plants manage to evade its deleterious effects.

Photorespiration Dissipates ATP and NADPH. The photorespiration pathway is outlined in Fig. 19-32. Glycolate is exported from the chloroplast to the peroxisome (also called the glyoxysome; Section 17-5C), where it is oxidized by **glycolate oxidase** to glyoxylate and H_2O_2. The H_2O_2, a potentially harmful oxidizing agent, is converted to H_2O and O_2 by the heme-containing enzyme catalase (Section 18-4B). The glyoxylate can be converted to glycine in a transamination reaction, as is discussed in Section 21-2A, and exported to the mitochondrion. There, two molecules of glycine are converted to one molecule of serine and one of CO_2. *This is the origin of the CO_2 generated by photorespiration.* The serine is transported back to the peroxisome, where a transamination reaction converts it to **hydroxypyruvate.** This substance is reduced to **glycerate** and phosphorylated in the cytosol to 3PG, which re-enters the chloroplast and is reconverted to RuBP in the Calvin cycle. *The net result of this complex photorespiration cycle is that some of the ATP and NADPH generated by the light reactions is uselessly dissipated.*

Although photorespiration has no known metabolic function, the RuBP carboxylases from the great variety of photosynthetic organisms so far tested all exhibit oxygenase activity. Yet, over the eons, the forces of evolution must have optimized the function of this important enzyme. Photorespiration may confer a selective advantage by protecting the photosynthetic apparatus from photooxidative damage when insufficient CO_2 is available to otherwise dissipate its absorbed light energy. This hypothesis is supported by the observation that when chloroplasts or leaf cells are brightly illuminated in the absence of both CO_2 and O_2, their photosynthetic capacity is rapidly and irreversibly lost.

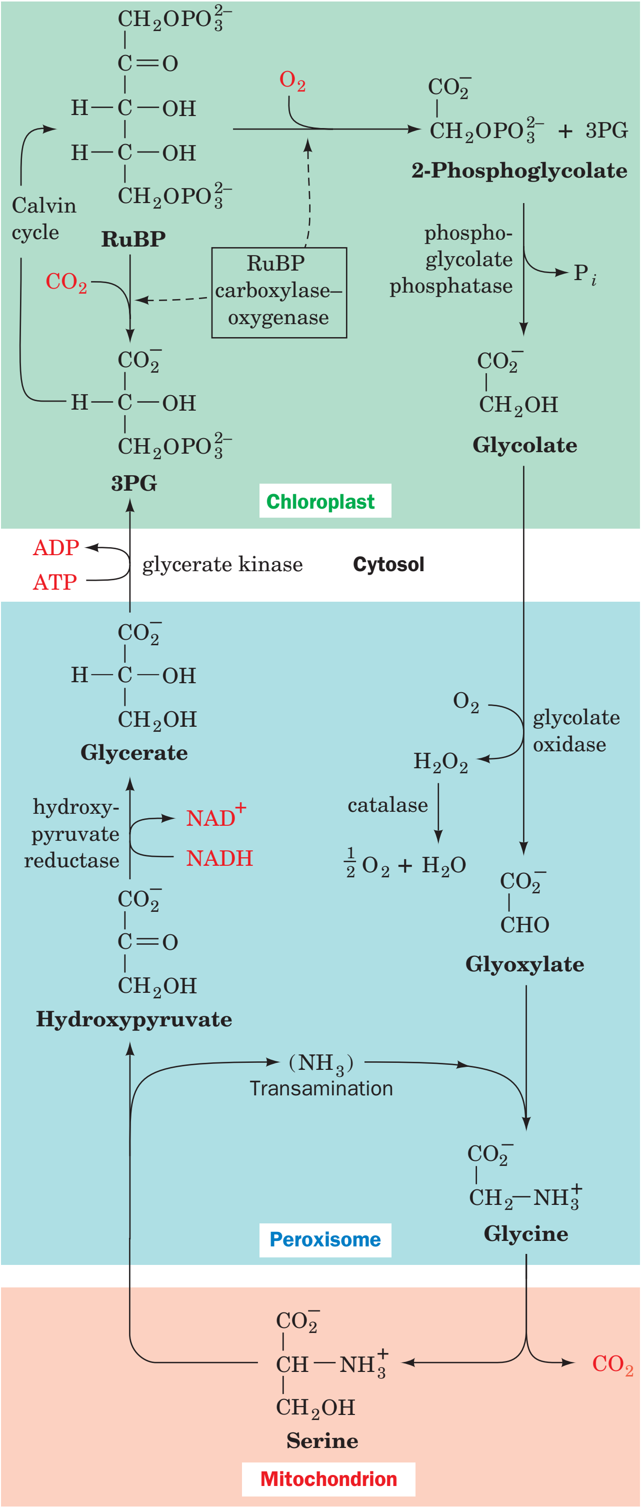
$CH_2OPO_3^{2-}$
$C{=}O$
$H{-}C{-}OH$
$H{-}C{-}OH$
$CH_2OPO_3^{2-}$
RuBP
Calvin cycle
O_2
CO_2^-
$CH_2OPO_3^{2-}$ + 3PG
2-Phosphoglycolate
RuBP carboxylase–oxygenase
CO_2
CO_2^-
$H{-}C{-}OH$
$CH_2OPO_3^{2-}$
3PG
phospho-glycolate phosphatase
P_i
CO_2^-
CH_2OH
Glycolate
Chloroplast
ADP
ATP
glycerate kinase
Cytosol
CO_2^-
$H{-}C{-}OH$
CH_2OH
Glycerate
O_2
glycolate oxidase
H_2O_2
catalase
$\frac{1}{2}O_2 + H_2O$
hydroxy-pyruvate reductase
NAD^+
NADH
CO_2^-
$C{=}O$
CH_2OH
Hydroxypyruvate
CO_2^-
CHO
Glyoxylate
(NH_3)
Transamination
CO_2^-
$CH_2{-}NH_3^+$
Glycine
Peroxisome
CO_2^-
$CH{-}NH_3^+$
CH_2OH
Serine
CO_2
Mitochondrion

Figure 19-32 | Photorespiration. This pathway metabolizes the phosphoglycolate produced by the RuBP carboxylase–catalyzed oxidation of RuBP. The reactions occur, as indicated, in the chloroplast, the peroxisome, the mitochondrion, and the cytosol. Note that two glycines are required to form serine + CO_2.

C_4 Plants Concentrate CO_2. On a hot, bright day, when photosynthesis has depleted the level of CO_2 at the chloroplast and raised that of O_2, the rate of photorespiration approaches the rate of photosynthesis. This phenomenon is a major limitation on the growth of many plants (and is therefore an important agricultural problem that is being attacked through genetic engineering studies—none of which has yet been successful). However, *certain species of plants, such as sugarcane, corn, and most important weeds, have a*

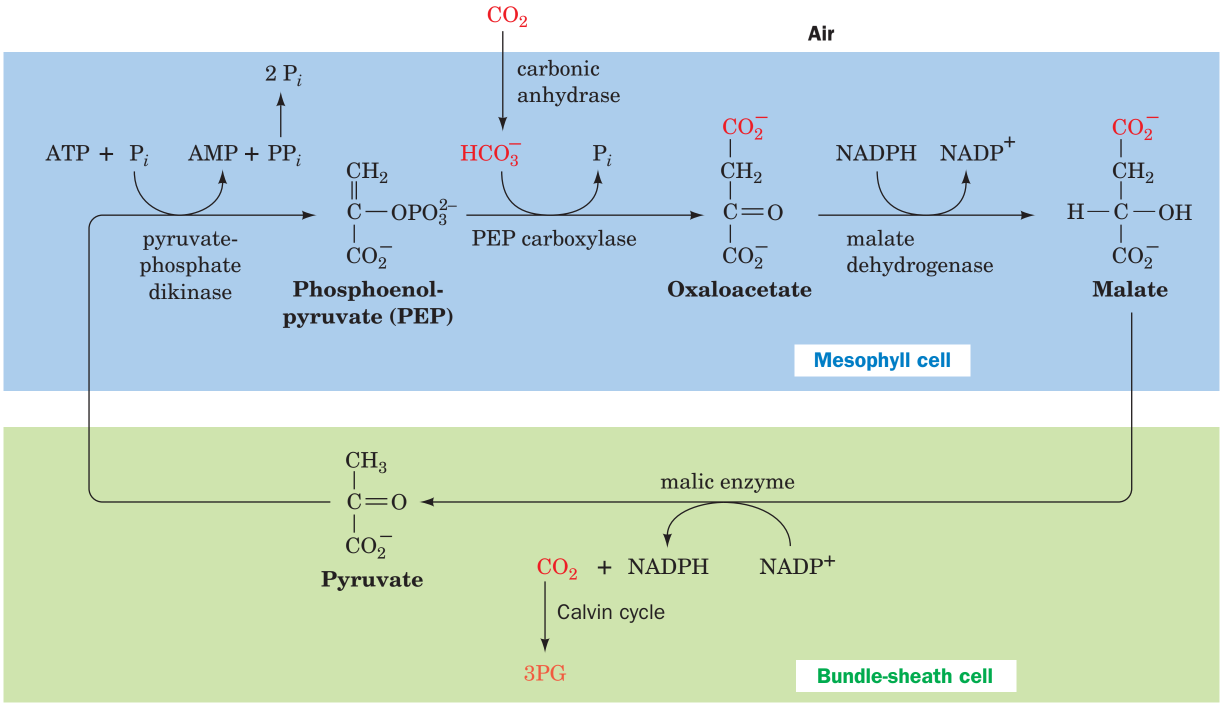
CO2
Air
2 Pi
carbonic anhydrase
ATP + Pi
AMP + PPi
HCO3−
Pi
CO2−
CH2
C=O
CO2−
NADPH
NADP+
CH2
C—OPO3 2−
CO2−
H—C—OH
pyruvate-phosphate dikinase
PEP carboxylase
malate dehydrogenase
Phosphoenol-pyruvate (PEP)
Oxaloacetate
Malate
Mesophyll cell
CH3
C=O
CO2−
malic enzyme
Pyruvate
CO2 + NADPH
NADP+
Calvin cycle
3PG
Bundle-sheath cell

Figure 19-33 | The C_4 pathway. CO_2 is concentrated in the mesophyll cells and transported to the bundle-sheath cells for entry into the Calvin cycle.

metabolic cycle that concentrates CO_2 in their photosynthetic cells, thereby almost totally preventing photorespiration. The leaves of plants that have this so-called **C_4 cycle** have a characteristic anatomy. Their fine veins are concentrically surrounded by a single layer of so-called **bundle-sheath cells,** which in turn are surrounded by a layer of **mesophyll cells.**

The C_4 cycle (Fig. 19-33) was elucidated in the 1960s by Marshall Hatch and Rodger Slack. It begins when mesophyll cells, which lack RuBP carboxylase, take up atmospheric CO_2 by condensing it as HCO_3^- with phosphoenolpyruvate (PEP) to yield oxaloacetate. The oxaloacetate is reduced by NADPH to malate, which is exported to the bundle-sheath cells (the name C_4 refers to these four-carbon acids). There, the malate is oxidatively decarboxylated by NADP to form CO_2, pyruvate, and NADPH. The CO_2, which has been concentrated by this process, enters the Calvin cycle. The pyruvate is returned to the mesophyll cells, where it is phosphorylated to regenerate PEP. The enzyme that mediates this reaction, **pyruvate-phosphate dikinase,** has the unusual action of simultaneously phosphorylating pyruvate and P_i with ATP's β and γ phosphoryl groups, respectively. *The C_4 pathway thereby concentrates CO_2 in the bundle-sheath cells at the expense of 2 ATP equivalents. Consequently, photosynthesis in C_4 plants consumes a total of 5 ATP per CO_2 fixed versus the 3 ATP required by the Calvin cycle alone.*

C_4 plants occur largely in tropical regions because they grow faster under hot and sunny conditions than other, so-called **C_3 plants** (so named because they initially fix CO_2 in the form of three-carbon acids). In cooler climates, where photorespiration is less of a burden, C_3 plants have the advantage because they require less energy to fix CO_2.

CAM Plants Store CO_2 through a Variant of the C_4 Cycle. A variant of the C_4 cycle that separates CO_2 acquisition and the Calvin cycle in time rather than in space occurs in many desert-dwelling succulent plants. If these plants opened their stomata (pores in the leaves) by day to acquire CO_2, as most plants do, they would lose unacceptable amounts of water by evaporation. To minimize this loss, these succulents absorb CO_2 only at night and use the reactions of the C_4 pathway (Fig. 19-33) to store it as malate. This process is known as **crassulacean acid metabolism (CAM),** so named because it was first discovered in plants of the family Crassulaceae. The large amount of PEP necessary to store a day's supply of CO_2 is obtained by the breakdown of starch via glycolysis. During the course of the day, the malate is broken down to CO_2, which enters the Calvin cycle, and pyruvate, which is used to resynthesize starch. CAM plants are thus able to carry out photosynthesis with minimal water loss.

■ CHECK YOUR UNDERSTANDING

Explain the relationship between the light and dark reactions.
Summarize the two stages of the Calvin cycle.
Describe how GAP produced by the Calvin cycle is converted to sucrose, starch, and cellulose.
How do pH, Mg^{2+}, and ferredoxin link the light reactions with control of the Calvin cycle?
How do plants minimize photorespiration?

SUMMARY

1. Photosynthesis is the process whereby light energy drives the reduction of CO_2 to yield carbohydrates. In plants and cyanobacteria, photosynthesis oxidizes water to O_2.
2. In plants, the photosynthetic machinery consists of protein complexes embedded in the thylakoid membrane and enzymes dissolved in the stroma of chloroplasts.
3. Chlorophyll and other light-absorbing pigments are organized in light-harvesting complexes that funnel light energy to photosynthetic reaction centers (RCs).
4. The purple bacterial photosynthetic reaction center (PbRC) undergoes photooxidation when it absorbs a photon. The excited electron passes through a series of electron carriers before reducing ubiquinone. The reduced ubiquinone is reoxidized by cytochrome bc_1, which in the process translocates four protons from the cytosol to the periplasmic space via a Q cycle. The electron is then returned to the PbRC via an electron-transport chain resulting in no net oxidation–reduction.
5. In plants and cyanobacteria, photosystems I and II (PSI and PSII) operate in electrical series in an arrangement known as the Z-scheme. The oxidation of water by the Mn-containing oxygen-evolving center (OEC) is driven by the photooxidation of PSII.
6. The electrons released by the photooxidation of PSII are transferred, via plastoquinone, to the cytochrome b_6f complex, which mediates a proton-translocating Q cycle while passing the electrons to plastocyanin.
7. The photooxidation of PSI drives the electrons obtained from plastocyanin to ferredoxin and then to $NADP^+$ to produce NADPH. In cyclic electron flow, however, electrons return to cytochrome b_6f, thereby bypassing the need for PSII photooxidation.
8. The reaction centers of the PbRC, PSII, and PSI have similar structures and mechanisms and therefore appear to have arisen from a common ancestor.
9. In photophosphorylation, the protons released by the oxidation of H_2O and proton translocation into the thylakoid lumen generate a transmembrane proton gradient that is tapped by chloroplast ATP synthase to drive the phosphorylation of ADP. A similar process occurs in purple photosynthetic bacteria.
10. The dark reactions use the ATP and NADPH produced in the light reactions to power the synthesis of carbohydrates from CO_2. In the first phase of the Calvin cycle, CO_2 reacts with ribulose-1,5-bisphosphate (RuBP) to ultimately yield glyceraldehyde-3-phosphate (GAP). The remaining reactions of the cycle regenerate the RuBP acceptor of CO_2.
11. RuBP carboxylase, the key enzyme of the dark reactions, is regulated by pH, $[Mg^{2+}]$, and the inhibitory compound 2-carboxyarabinitol-1-phosphate (CA1P). The two bisphosphatases of the Calvin cycle are controlled by the redox state of the chloroplast via disulfide interchange reactions mediated in part by thioredoxin.
12. Photorespiration, in which plants consume O_2 and evolve CO_2, uses the ATP and NADPH produced by the light reactions. C_4 plants minimize the oxygenase activity of RuBP carboxylase (RuBisCO) by concentrating CO_2 in their photosynthetic cells. CAM plants use a related mechanism to conserve water.

KEY TERMS

photosynthesis **640**
light reactions **641**
dark reactions **641**
stroma **641**
thylakoid **642**
grana **642**
stromal lamella **642**
photosynthetic reaction center **643**
antenna chlorophyll **643**
photon **643**
LHC **644**
accessory pigment **644**
Planck's law **645**
internal conversion **646**
fluorescence **646**
exciton transfer (resonance energy transfer) **646**
photooxidation **647**
special pair **648**
Z-scheme **652**
photophosphorylation **661**
Calvin cycle **664**
photorespiration **671**
C_4 plant **674**
C_3 plant **674**
CAM **675**

PROBLEMS

1. The "red tide" is a massive proliferation of certain algal species that causes seawater to become visibly red. Describe the spectral characteristics of the dominant photosynthetic pigments in the algae.
2. The net equation for oxidative phosphorylation can be written as

$$2\,\text{NADH} + 2\,\text{H}^+ + \text{O}_2 \rightarrow 2\,\text{H}_2\text{O} + 2\,\text{NAD}^+$$

Write an analogous equation for the light reactions of photosynthesis.

3. The three electron-transporting complexes of the thylakoid membrane can be called plastocyanin–ferredoxin oxidoreductase, plastoquinone–plastocyanin oxidoreductase, and water–plastoquinone oxidoreductase. What are the common names of these enzymes and in what order do they act?
4. $H_2{}^{18}O$ is added to a suspension of chloroplasts capable of photosynthesis. Where does the label appear when the suspension is exposed to sunlight?
5. (a) Calculate the energy of one mole of photons of red light ($\lambda = 700$ nm). (b) How many moles of ATP could theoretically be synthesized using this energy?
6. (a) Calculate $\Delta\mathscr{E}^{\circ\prime}$ and $\Delta G^{\circ\prime}$ for the light reactions in plants, that is, the four-electron oxidation of H_2O by $NADP^+$. (b) Use the solution of Problem 19-5 to calculate how many moles of photons of red light ($\lambda = 700$ nm) are theoretically required to drive this process. (c) How many moles of photons of UV light ($\lambda = 220$ nm) would be required?
7. Describe the functional similarities between the purple bacterial photosynthetic reaction center and PSI.
8. Why is it possible for chloroplasts to absorb much more than 8–10 photons per O_2 molecule evolved?
9. Under conditions of very high light intensity, excess absorbed solar energy is dissipated by the action of photoprotective proteins in the thylakoid membrane. (a) Explain why it is advantageous for these proteins to be activated by buildup of the proton gradient across the membrane. (b) Which of the mechanisms for dissipating light energy shown in Fig. 19-6 would best protect the photosystems from excess light energy?
10. Predict the effect of an uncoupler such as dinitrophenol (Fig. 18-28) on production of (a) ATP and (b) NADPH in a chloroplast.
11. Describe the effects of an increase in oxygen pressure on the dark reactions of photosynthesis.
12. Chloroplasts are illuminated until the levels of the Calvin cycle intermediates reach a steady state. The light is then turned off. How do the levels of RuBP and 3PG vary after this point?
13. Calculate the energy cost of the Calvin cycle combined with glycolysis and oxidative phosphorylation, that is, the ratio of the energy spent synthesizing starch from CO_2 and photosynthetically produced NADPH and ATP to the energy generated by the complete oxidation of starch. Assume that each NADPH is energetically equivalent to 2.5 ATP and that starch biosynthesis and breakdown are mechanistically identical to glycogen synthesis and breakdown.
14. The leaves of some species of desert plants taste sour in the early morning, but, as the day wears on, they become tasteless and then bitter. Explain.

REFERENCES

Ben-Shem, A., Frolow, F., and Nelson, N., Crystal structure of plant Photosystem I, *Nature* **426,** 630–635 (2003).

Blankenship, R.E., *Molecular Mechanisms of Photosynthesis,* Blackwell Science (2002).

Chitnis, P.R., Photosystem I: Function and physiology, *Annu. Rev. Plant Physiol. Plant Biol.* **52,** 593–626 (2001).

Ferreira, K.N., Iverson, T.M., Maghlaoui, K., Barber, J., and Iwata, S., Architecture of the photosynthetic oxygen-evolving center, *Science* **303,** 1831–1838 (2004); *and* Loll, B., Kern, J., Saenger, W., Zouni, A., and Biesiadka, J., Towards complete cofactor arrangement in the 3.0 Å resolution structure of photosystem II, *Nature* **438,** 1040–1044 (2005). [The X-ray structure of PSII.]

Heathcote, P., Fyfe, P.K., and Jones, M.R., Reaction centres: the structure and evolution of biological solar power, *Trends Biochem. Sci.* **27,** 79–87 (2002).

Jordan, P., Fromme, P., Witt, H.T., Klukas, O., Saenger, W., and Krauss, N., Three-dimensional structure of cyanobacterial photosystem I at 2.5 Å resolution, *Nature* **411,** 909–917 (2001).

Koepke, J., Hu, X., Muenke, C., Schulen, K., and Michel, H., The crystal structure of the light-harvesting complex II (B800–850) from *Rhodospirillum molischianum, Structure* **4,** 581–597 (1996).

Kurisu, G., Zhang, H., Smith, J.L., and Cramer, W.A., Structure of the cytochrome b_6f complex of oxygenic photosynthesis: Tuning the cavity, *Science* **302,** 1009–1014 (2003); *and* Stroebel, D., Choquet, Y., Popot, J.-L., and Picot, D., An atypical haem in the cytochrome b_6f complex, *Nature* **426,** 413–418 (2003).

Spreitzer, R.J. and Salvucci, M.E., Rubisco: structure, regulatory interactions, and possibilities for a better enzyme, *Annu. Rev. Plant Biochem.* **53,** 449–475 (2002).

Yano, J., et al., Where water is oxidized to dioxygen: Structure of the photosynthetic Mn_4Ca cluster, *Science* **314,** 821–825 (2006).

20

Lipid Metabolism

Lipids act as an organism's major storage form of metabolic energy. In hibernating mammals, such as this marmot, these fat reserves are synthesized during the warmer months and are oxidized during the winter to keep the animal alive. [Jeff Foote/Bruce Coleman, Inc.]

■ CHAPTER CONTENTS

1 Lipid Digestion, Absorption, and Transport
  - **A.** Triacylglycerols Are Digested before They Are Absorbed
  - **B.** Lipids Are Transported as Lipoproteins

2 Fatty Acid Oxidation
  - **A.** Fatty Acids Are Activated by Their Attachment to Coenzyme A
  - **B.** Carnitine Carries Acyl Groups across the Mitochondrial Membrane
  - **C.** β Oxidation Degrades Fatty Acids to Acetyl-CoA
  - **D.** Oxidation of Unsaturated Fatty Acids Requires Additional Enzymes
  - **E.** Oxidation of Odd-Chain Fatty Acids Yields Propionyl-CoA
  - **F.** Peroxisomal β Oxidation Differs from Mitochondrial β Oxidation

3 Ketone Bodies

4 Fatty Acid Biosynthesis
  - **A.** Mitochondrial Acetyl-CoA Must Be Transported into the Cytosol
  - **B.** Acetyl-CoA Carboxylase Produces Malonyl-CoA
  - **C.** Fatty Acid Synthase Catalyzes Seven Reactions
  - **D.** Fatty Acids May Be Elongated and Desaturated
  - **E.** Fatty Acids Are Esterified to Form Triacylglycerols

5 Regulation of Fatty Acid Metabolism

6 Synthesis of Other Lipids
  - **A.** Glycerophospholipids Are Built from Intermediates of Triacylglycerol Synthesis
  - **B.** Sphingolipids Are Built from Palmitoyl-CoA and Serine
  - **C.** C_{20} Fatty Acids Are the Precursors of Prostaglandins

7 Cholesterol Metabolism
  - **A.** Cholesterol Is Synthesized from Acetyl-CoA
  - **B.** HMG-CoA Reductase Controls the Rate of Cholesterol Synthesis
  - **C.** Abnormal Cholesterol Transport Leads to Atherosclerosis

■ MEDIA RESOURCES

(available at www.wiley.com/college/voet)

Interactive Exercise 27. Active site of medium-chain acyl-CoA dehydrogenase

Interactive Exercise 28. X-Ray structure of methylmalonyl-CoA mutase

Animated Figure 20-8. Receptor-mediated endocytosis

Animated Figure 20-12. β-oxidation pathway of fatty acyl-CoA

Animated Figure 20-23. Comparison of fatty acid β oxidation and fatty acid biosynthesis

Animated Figure 20-26. Reaction sequence for biosynthesis of fatty acids

Case Study 23. The Role of Uncoupling Proteins in Obesity

Most cells contain a wide variety of lipids, but many of these structurally distinct molecules are functionally similar. For example, most cells can tolerate variations in the lipid composition of their membranes, provided that membrane fluidity, which is largely a property of their component fatty acid chains, is maintained (Section 9-2B).

Even greater variation is exhibited in the cellular content of lipids stored as energy reserves. Triacylglycerol stores are built up and gradually depleted in response to changing physiological demands. The camel's hump is a well-known example of a fat depot that supplies energy (the catabolism of the fat also generates water). Other organisms that undergo dramatic changes in body fat content are hibernating mammals and birds that migrate long distances without refueling. Lipid metabolism in those cases is notable for the sheer amount of material that flows through the few relatively simple biosynthetic and degradative pathways.

In this chapter, we acknowledge the central function of lipids in energy metabolism by first examining the absorption and transport of their component fatty acids and the oxidation of fatty acids to produce energy. The second part of this chapter examines the synthesis of fatty acids and other lipids, including glycerophospholipids, sphingolipids, and cholesterol.

1 Lipid Digestion, Absorption, and Transport

LEARNING OBJECTIVES

- Understand that triacylglycerols are broken down by lipases, and the products are absorbed by the intestine.
- Understand that lipoproteins transport lipids between the intestines, liver, and other tissues.

Triacylglycerols (also called fats or triglycerides) constitute ~90% of dietary lipids and are the major form of metabolic energy storage in humans. Triacylglycerols consist of glycerol triesters of fatty acids such as palmitic and oleic acids

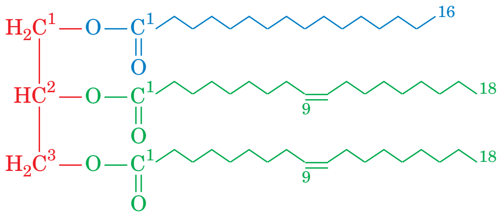

1-Palmitoyl-2,3-dioleoyl-glycerol

(the names and structural formulas of some biologically common fatty acids are listed in Table 9-1). The mechanisms for digesting, absorbing, and transporting triacylglycerols from the intestine to the tissues must accommodate their inherent hydrophobicity.

A | Triacylglycerols Are Digested before They Are Absorbed

Since triacylglycerols are water insoluble, whereas digestive enzymes are water soluble, triacylglycerol digestion takes place at lipid–water interfaces. The rate of triacylglycerol digestion therefore depends on the surface area of the interface, which is greatly increased by the churning peristaltic movements of the intestine combined with the emulsifying action of **bile acids.** The bile acids (also called **bile salts**) are amphipathic detergent-like molecules that act to solubilize fat globules. Bile acids are cholesterol derivatives that are synthesized by the liver and secreted as glycine or **taurine** conjugates (Fig. 20-1) into the gallbladder for storage. From there, they are secreted into the small intestine, where lipid digestion and absorption mainly take place.

Lipases Act at the Lipid–Water Interface. Pancreatic **lipase (triacylglycerol lipase)** catalyzes the hydrolysis of triacylglycerols at their 1 and

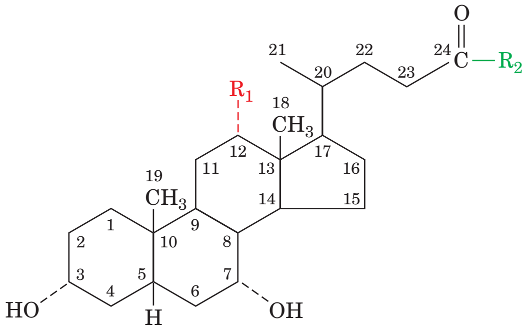

	$R_1 = OH$	$R_1 = H$
$R_2 = OH$	**Cholic acid**	**Chenodeoxycholic acid**
$R_2 = NH{-}CH_2{-}COOH$	**Glycocholic acid**	**Glycochenodeoxycholic acid**
$R_2 = NH{-}CH_2{-}CH_2{-}SO_3H$	**Taurocholic acid**	**Taurochenodeoxycholic acid**

Figure 20-1 | Structures of the major bile acids and their glycine and taurine conjugates.

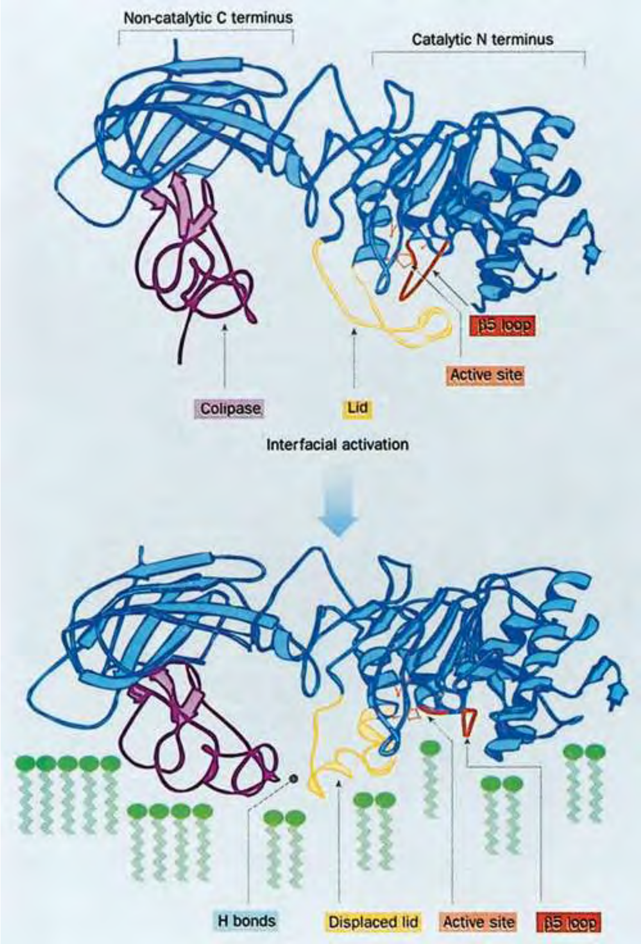

Figure 20-2 | The mechanism of interfacial activation of triacylglycerol lipase. The enzyme is in complex with procolipase (the precursor of colipase; *magenta*). On binding to a phospholipid micelle (*green*), the 25-residue lid (*yellow*) covering the enzyme's active site (*tan*) changes conformation so as to expose its hydrophobic residues, thereby uncovering the active site. This causes the 10-residue β5 loop (*brown*) to move aside in a way that forms the enzyme's oxyanion hole. The procolipase also changes its conformation so as to hydrogen bond to the "open" lid, thereby stabilizing it in that conformation and, together with lipase, forming an extended hydrophobic surface. [From *Nature* **362,** 793 (1993). Reproduced with permission. PDBid 1LPA.]

3 positions to form sequentially **1,2-diacylglycerols** and **2-acylglycerols,** together with the Na^+ and K^+ salts of fatty acids (soaps). The enzymatic activity of pancreatic lipase greatly increases when it contacts the lipid–water interface, a phenomenon known as **interfacial activation.** Binding to the lipid–water interface requires mixed micelles of phosphatidylcholine and bile acids, as well as pancreatic **colipase,** a 90-residue protein that forms a 1:1 complex with lipase. The X-ray structures, determined by Christian Cambillau, of pancreatic lipase–colipase complexes reveal the structural basis of the interfacial activation of lipase as well as how colipase and micelles help lipase bind to the lipid–water interface (Fig. 20-2).

The active site of the 449-residue pancreatic lipase, which is contained in the enzyme's N-terminal domain (residues 1–336), contains a catalytic triad that closely resembles that in serine proteases (Section 11-5B; recall that ester hydrolysis is mechanistically similar to peptide hydrolysis). In the absence of lipid micelles, lipase's active site is covered by a 25-residue helical "lid." However, in the presence of the micelles, the lid undergoes a complex structural reorganization that exposes the active site. Simultaneously, a 10-residue loop, called the β5 loop, changes conformation in a way that forms the active enzyme's oxyanion hole and generates a hydrophobic surface near the entrance to the active site.

Colipase binds to the C-terminal domain of lipase (residues 337–449) such that the hydrophobic tips of its three loops extend from the complex.

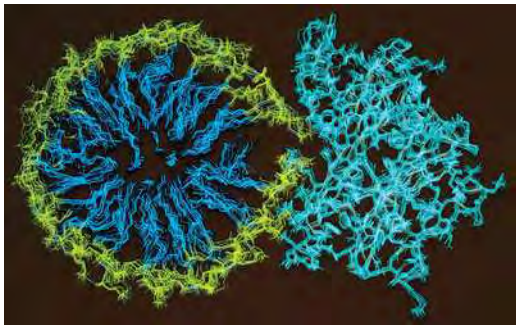

(*a*)

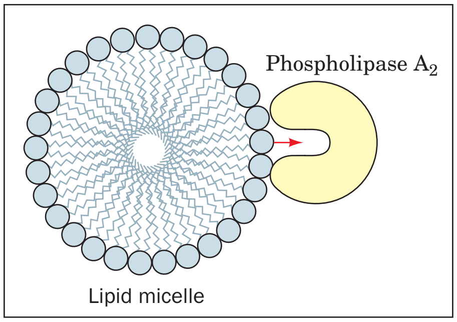

(*b*)

■ **Figure 20-3 | Substrate binding to phospholipase A_2.** (*a*) Hypothetical model of phospholipase A_2 in complex with a micelle of lysophosphatidylethanolamine as shown in cross section. The protein is drawn in cyan, the phospholipid head groups are yellow, and their hydrocarbon tails are blue. The calculated atomic motions of the assembly are indicated through a series of superimposed images taken at 5-ps intervals. [Courtesy of Raymond Salemme, E. I. du Pont de Nemours & Company.] (*b*) Schematic diagram of a phospholipid contained in a micelle entering the hydrophobic phospholipid channel in phospholipase A_2 (*red arrow*).

This creates a continuous hydrophobic plateau, extending >50 Å past the lipase active site, that presumably helps bind the complex to the lipid surface. Colipase also forms three hydrogen bonds to the opened lid, thereby stabilizing it in that conformation.

Other lipases, such as phospholipase A_2 (Fig. 9-6), also preferentially catalyze reactions at interfaces. Instead of changing its conformation, however, phospholipase A_2 contains a hydrophobic channel that provides the substrate with direct access from the phospholipid aggregate (micelle or membrane) surface to the bound enzyme's active site (Fig. 20-3). Hence, on leaving its micelle to bind to the enzyme, the substrate need not become solvated and then desolvated. In contrast, soluble and dispersed phospholipids must first surmount those significant kinetic barriers in order to bind to the enzyme.

Bile Acids and Fatty Acid–Binding Protein Facilitate the Intestinal Absorption of Lipids. The mixture of fatty acids and mono- and diacylglycerols produced by lipid digestion is absorbed by the cells lining the small intestine (the intestinal **mucosa**). *Bile acids not only aid lipid digestion; they are essential for the absorption of the digestion products.* The micelles formed by the bile acids take up the nonpolar lipid degradation products so as to permit their transport across the unstirred aqueous boundary layer at the intestinal wall. The importance of this process is demonstrated in individuals with obstructed bile ducts: They absorb little of their ingested lipids but, rather, eliminate them in hydrolyzed form in their feces. Bile acids are likewise required for the efficient intestinal absorption of the lipid-soluble vitamins A, D, E, and K.

Inside the intestinal cells, fatty acids form complexes with **intestinal fatty acid–binding protein (I-FABP),** a cytoplasmic protein that increases the effective solubility of these water-insoluble substances and also protects the cell from their detergent-like effects. The X-ray structure of rat I-FABP, determined by James Sacchettini, shows that this monomeric, 131-residue protein consists largely of 10 antiparallel β strands stacked in two approximately orthogonal β sheets (Fig. 20-4). A fatty acid molecule occupies a gap between two of the β strands, lying between the β sheets so that it is more or less parallel to the gapped β strands (a structure that has been dubbed a "β-clam"). The fatty acid's carboxyl group interacts with Arg 106, Gln 115, and two bound water molecules, whereas its tail is encased by the side chains of several hydrophobic, mostly aromatic residues.

B | Lipids Are Transported as Lipoproteins

The fatty acid products of lipid digestion that are absorbed by the intestinal mucosa make their way to other tissues for catabolism or storage. But because they are only sparingly soluble in aqueous solution, lipids are transported by the circulation in complex with proteins.

Lipoproteins Are Complexes of Lipid and Protein. ***Lipoproteins*** *are globular micelle-like particles that consist of a nonpolar core of triacylglycerols*

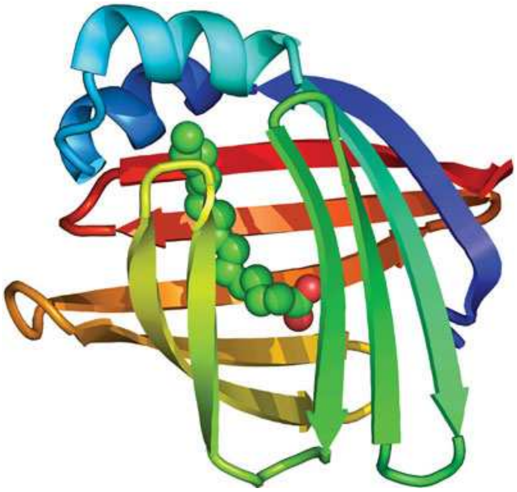

■ **Figure 20-4 | X-Ray structure of rat intestinal fatty acid–binding protein in complex with palmitate.** The protein is colored in rainbow order from its N-terminus (*blue*) to its C-terminus (*red*). The palmitate is drawn in spacefilling form with C green and O red. [Based on an X-ray structure by James Sacchettini, Texas A&M University. PDBid 2IFB.]

Table 20-1 Characteristics of the Major Classes of Lipoproteins in Human Plasma

	Chylomicrons	VLDL	IDL	LDL	HDL
Density ($g \cdot cm^{-3}$)	<0.95	<1.006	1.006–1.019	1.019–1.063	1.063–1.210
Particle diameter (Å)	750–12,000	300–800	250–350	180–250	50–120
Particle mass (kD)	400,000	10,000–80,000	5000–10,000	2300	175–360
% Protein[a]	1.5–2.5	5–10	15–20	20–25	40–55
% Phospholipids[a]	7–9	15–20	22	15–20	20–35
% Free cholesterol[a]	1–3	5–10	8	7–10	3–4
% Triacylglycerols[b]	84–89	50–65	22	7–10	3–5
% Cholesteryl esters[b]	3–5	10–15	30	35–40	12
Major apolipoproteins	A-I, A-II, B-48, C-I, C-II, C-III, E	B-100, C-I, C-II, C-III, E	B-100, C-I, C-II, C-III, E	B-100	A-I, A-II, C-I, C-II, C-III, D, E

[a] Surface components.
[b] Core lipids.

and cholesteryl esters surrounded by an amphiphilic coating of protein, phospholipid, and cholesterol. There are five classes of lipoproteins (Table 20-1), which vary in composition and physiological function.

Intestinal mucosal cells convert dietary fatty acids to triacylglycerols and package them, along with dietary cholesterol, into lipoproteins called **chylomicrons.** These particles are released into the intestinal lymph and are transported through the lymphatic vessels before draining into the large veins. The bloodstream then delivers chylomicrons throughout the body. Other lipoproteins known as **very low density lipoproteins (VLDL), intermediate density lipoproteins (IDL),** and **low density lipoproteins (LDL)** are synthesized by the liver to transport endogenous (internally produced) triacylglycerols and cholesterol from the liver to the tissues. **High density lipoproteins (HDL)** transport cholesterol and other lipids from the tissues back to the liver.

Each lipoprotein contains just enough protein, phospholipid, and cholesterol to form an ~20-Å-thick monolayer of these substances on the particle surface (Fig. 20-5). Lipoprotein densities increase with decreasing particle diameter because the density of their outer coating is greater than that of their inner core. Thus, the HDL, which are the most dense of the lipoproteins, are also the smallest.

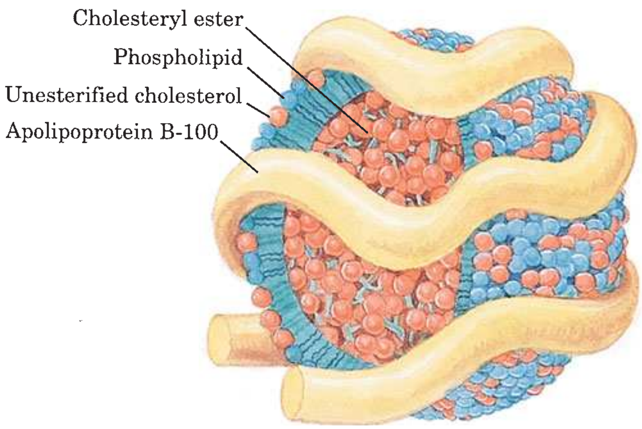

Figure 20-5 | Diagram of LDL, the major cholesterol carrier of the bloodstream. This spheroidal particle consists of some 1500 cholesteryl ester molecules surrounded by an amphiphilic coat of ~800 phospholipid molecules, ~500 cholesterol molecules, and a single 4536-residue molecule of apolipoprotein B-100.

Apolipoproteins Coat Lipoprotein Surfaces. The protein components of lipoproteins are known as **apolipoproteins** or just **apoproteins.** At least nine apolipoproteins are distributed in different amounts in the human lipoproteins (Table 20-1). For example, LDL contain **apolipoprotein B-100 (apoB-100).** This protein, a 4536-residue monomer (and thus one of the largest monomeric proteins known), has a hydrophobicity approaching that of integral membrane proteins. Each LDL particle contains only one molecule of apoB-100, which appears to cover at least half of the particle surface (Fig. 20-5).

Unlike apoB-100, the other apolipoproteins are water soluble and associate rather weakly with lipoproteins. These apolipoproteins also have a high helix content, which increases when they are incorporated into lipoproteins. Contact with a hydrophobic surface apparently favors formation of helices, which satisfy the hydrogen bonding potential of the protein's polar backbone groups. In addition, *the helices in apolipoproteins have hydrophilic and hydrophobic side chains on opposite sides of the helical cylinder, suggesting that lipoprotein α helices are amphipathic and float on phospholipid surfaces, much like logs on water.* The charged head groups of the lipids presumably bind to oppositely charged residues on the helix while the first few methylene groups of their fatty acyl chains associate with the nonpolar face of the helix.

Apolipoprotein A-I (apoA-I), which occurs in chylomicrons and HDL, is a 243-residue, 29-kD polypeptide. It consists largely of tandem 22-residue segments of similar sequence. The X-ray structure of a truncated apolipoprotein A-I (lacking residues 1–43) reveals that the polypeptide chain forms a pseudocontinuous α helix that is punctuated by kinks at Pro residues spaced about every 22 residues. Four monomers associate to form the structure shown in Fig. 20-6*a*. The size and twisted elliptical shape of this complex seem ideal for wrapping around an HDL particle. Figure 20-6*b* contains a helical wheel representation of a portion of apoA-I, illustrating the amphipathic nature of the helix.

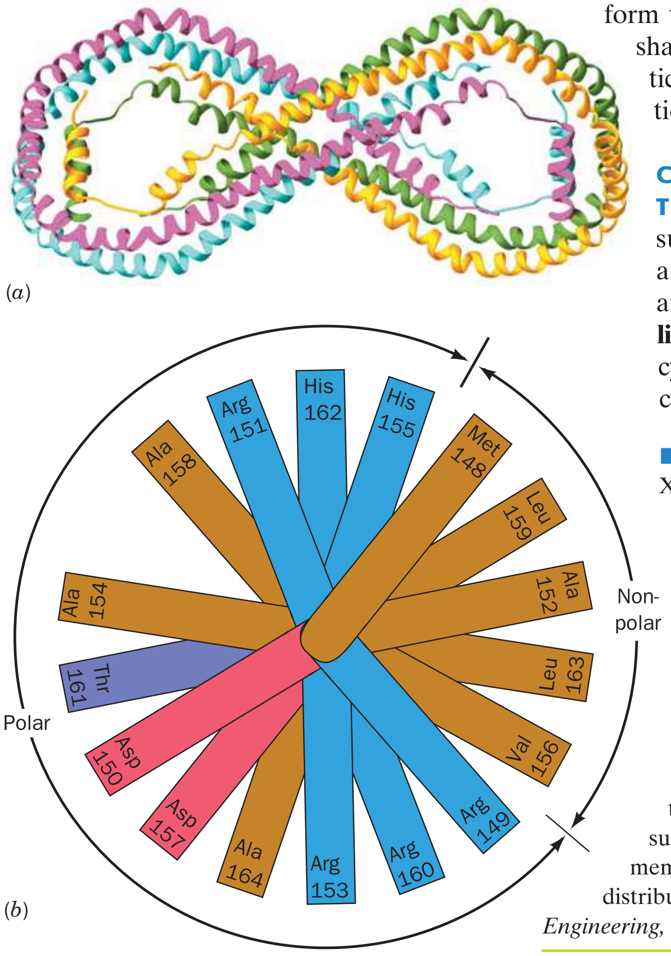

■ **Figure 20-6 | Structure of human apolipoprotein A-I.** (*a*) The X-ray structure of this D_2-symmetric homotetramer with its four subunits, which lack their N-terminal 43 residues, drawn in different colors. The complex, which has a twisted ellipsoidal shape, is viewed along one of its twofold axes. [Based on an X-ray structure by David Borhani, Southern Research Institute, Birmingham, Alabama, and Christie Brouillette, University of Alabama Medical Center, Birmingham, Alabama. PDBid 1AV1.] (*b*) A helical wheel projection of the amphipathic α helix constituting residues 148 to 164 of apolipoprotein A-I (in a helical wheel representation, the side chain positions are projected down the helix axis onto a plane). Note the segregation of nonpolar and polar residues to different sides of the helix as well as the segregation of the basic residues to the outer edges of the polar surface, where they can interact with the anionic head groups of membrane lipids. Other apolipoprotein helices have similar polarity distributions. [After Kaiser, E.T., *in* Oxender, D.L. and Fox, C.F. (Eds.), *Protein Engineering,* p. 194, Liss (1987).]

Chylomicrons Are Delipidated in the Capillaries of Peripheral Tissues. Chylomicrons adhere to binding sites on the inner surface (endothelium) of the capillaries in skeletal muscle and adipose tissue. The chylomicron's component triacylglycerols are hydrolyzed through the action of the extracellular enzyme **lipoprotein lipase.** The tissues then take up the liberated monoacylglycerol and fatty acids. The chylomicrons shrink as their triacylglycerols are progressively hydrolyzed until they are reduced to

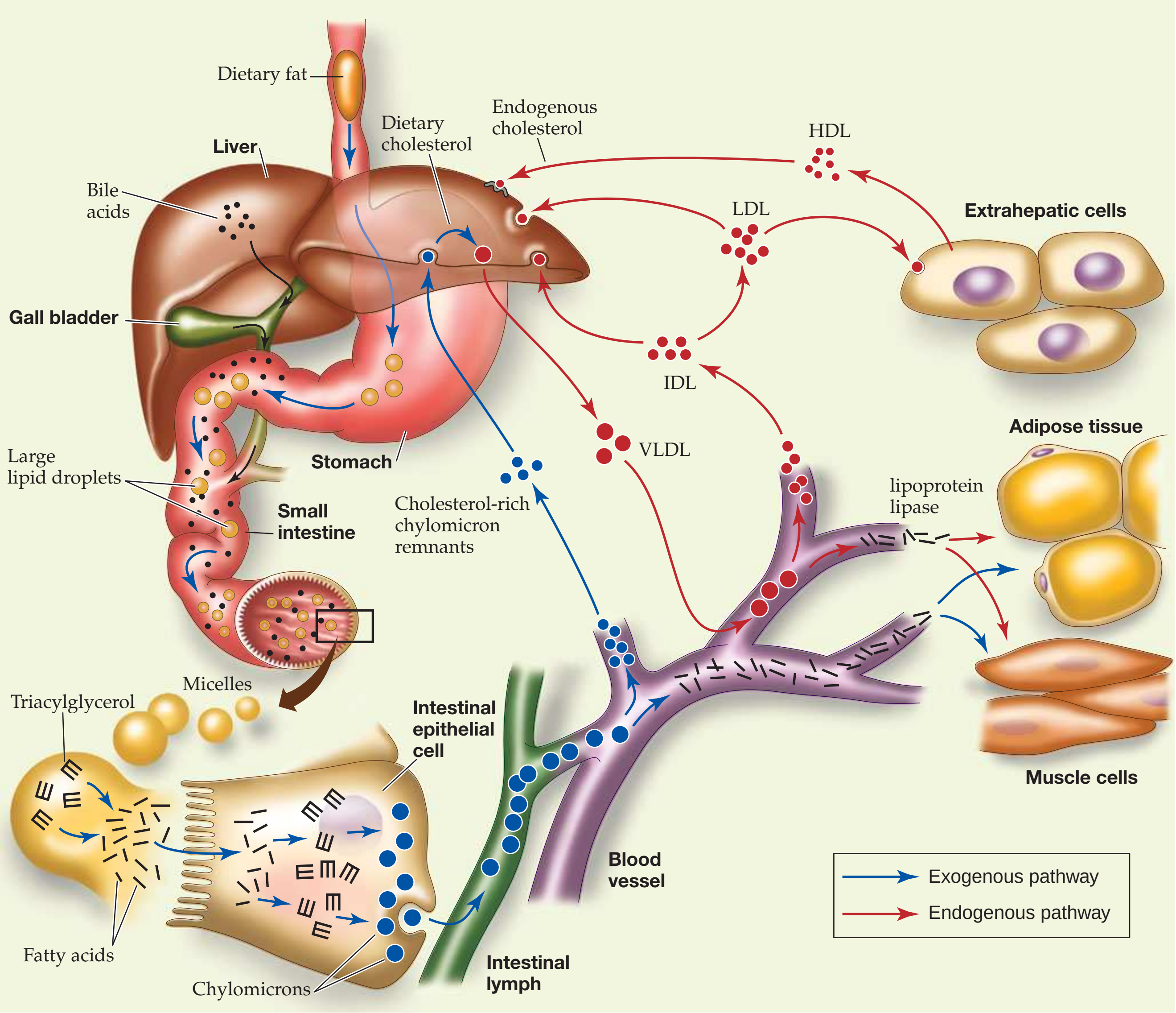
Dietary fat
Liver
Dietary cholesterol
Endogenous cholesterol
HDL
Bile acids
LDL
Extrahepatic cells
Gall bladder
IDL
Adipose tissue
VLDL
Large lipid droplets
Stomach
lipoprotein lipase
Small intestine
Cholesterol-rich chylomicron remnants
Micelles
Triacylglycerol
Intestinal epithelial cell
Muscle cells
Blood vessel
Exogenous pathway
Endogenous pathway
Fatty acids
Chylomicrons
Intestinal lymph

■ **Figure 20-7** | **Plasma triacylglycerol and cholesterol transport in humans.**

cholesterol-enriched **chylomicron remnants.** The remnants dissociate from the capillary endothelium and re-enter the circulation to be taken up by the liver. *Chylomicrons therefore deliver dietary triacylglycerols to muscle and adipose tissue, and dietary cholesterol to the liver* (Fig. 20-7, *blue arrows*).

VLDL Are Gradually Degraded. Very low density lipoproteins (VLDL), which transport endogenous triacylglycerols and cholesterol, are also degraded by lipoprotein lipase in the capillaries of adipose tissue and muscle (Fig. 20-7, *red arrows*). The released fatty acids are taken up by the cells and oxidized for energy or used to resynthesize triacylglycerols. The glycerol backbone of triacylglycerols is transported to the liver or kidneys and converted to the glycolytic intermediate dihydroxyacetone phosphate. Oxidation of this three-carbon unit, however, yields only a small fraction of the energy available from oxidizing the three fatty acyl chains of a triacylglycerol.

After giving up their triacylglycerols, the VLDL remnants, which have also lost some of their apolipoproteins, appear in the circulation first as IDL and then as LDL. About half of the VLDL, after degradation to IDL and LDL, are taken up by the liver.

Cells Take Up LDL by Receptor-Mediated Endocytosis. Animal cells acquire cholesterol, an essential component of cell membranes (Section 9-2B), either by synthesizing it or by taking up LDL, which are rich in cholesterol and cholesteryl esters. The latter process, as Michael Brown and Joseph Goldstein have demonstrated, occurs by **receptor-mediated endocytosis** (engulfment) of the LDL (Fig. 20-8). The LDL particles are sequestered by **LDL receptors,** cell-surface transmembrane glycoproteins

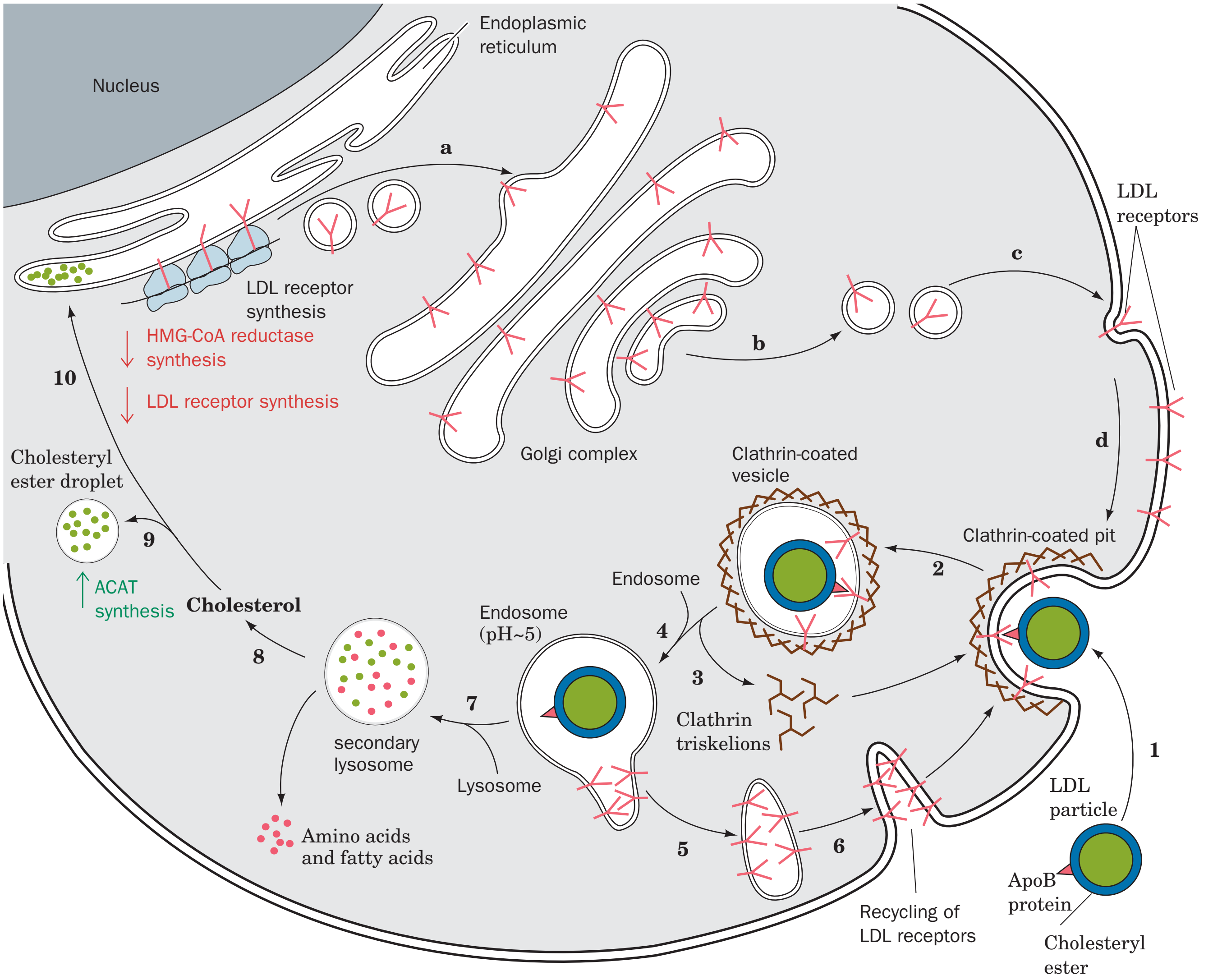

Endoplasmic reticulum
Nucleus
a
LDL receptors
c
LDL receptor synthesis
HMG-CoA reductase synthesis
b
10
LDL receptor synthesis
d
Cholesteryl ester droplet
Golgi complex
Clathrin-coated vesicle
9
Clathrin-coated pit
ACAT synthesis
Cholesterol
Endosome
2
Endosome (pH~5)
4
8
3
7
Clathrin triskelions
1
secondary lysosome
Lysosome
LDL particle
Amino acids and fatty acids
5
6
ApoB protein
Recycling of LDL receptors
Cholesteryl ester

■ **Figure 20-8 | Receptor-mediated endocytosis of LDL.** LDL receptor is synthesized on the endoplasmic reticulum (**a**), processed in the Golgi apparatus (**b**), and inserted into the plasma membrane (**c**), where it becomes a component of clathrin-coated pits (**d**). The apolipoprotein B-100 (apoB-100) component of LDL specifically binds to LDL receptors on clathrin-coated pits (**1**). These bud into the cell (**2**) to form clathrin-coated vesicles, whose clathrin coats depolymerize to form triskelions (**3**), which are recycled to the cell surface. The uncoated vesicles fuse with vesicles called endosomes (**4**), which have an internal pH of ~5.0. The acidity induces the LDL particle to dissociate from its receptor. The LDL accumulates in the vesicular portion of the endosome, whereas the LDL receptors concentrate in the membrane of an attached tubular structure, which then separates from the endosome (**5**) and subsequently recycles the LDL receptors to the plasma membrane (**6**). The vesicular portion of the endosome fuses with a lysosome (**7**), yielding a **secondary lysosome** wherein the apoB-100 component of the LDL and the cholesteryl esters are hydrolyzed. This releases cholesterol (**8**), which either is converted to cholesteryl esters through the action of **acyl-CoA:cholesterol acyltransferase (ACAT)** and sequestered in a droplet (**9**) or proceeds to the endoplasmic reticulum (**10**). Increased cholesterol concentration in the endoplasmic reticulum decreases the rate of synthesis of **HMG-CoA reductase** (the enzyme that catalyzes the rate-limiting step of cholesterol biosynthesis; Section 20-7B) and LDL receptors (*down arrows*), while increasing that of ACAT (*up arrow*). [After Brown, M.S. and Goldstein, J.L., *Curr. Top. Cell. Reg.* **26,** 7 (1985).] **See the Animated Figures.**

that specifically bind apoB-100. LDL receptors cluster into **clathrin-coated pits,** which gather the cell-surface receptors that are destined for endocytosis while excluding other cell-surface proteins. The coated pits invaginate from the plasma membrane to form **clathrin-coated vesicles** (Section 9-4E). Then, after divesting themselves of their clathrin coats, the vesicles fuse with vesicles known as **endosomes,** whose internal pH is ~5.0. Under these conditions, the LDL particle dissociates from its receptor. The receptors are recycled back to the cell surface, while the endosome with its enclosed LDL fuses with a lysosome. In the lysosome, LDL's apoB-100 is rapidly degraded to its component amino acids, and the cholesteryl esters are hydrolyzed to yield cholesterol and fatty acids.

Receptor-mediated endocytosis is a general mechanism whereby cells take up large molecules, each through a corresponding specific receptor. Many cell-surface receptors recycle between the plasma membrane and the endosomal compartment as does the LDL receptor, even in the absence of ligand. The LDL receptor cycles in and out of the cell membrane about every 10 minutes. New receptors are synthesized on the endoplasmic reticulum and travel via vesicles through the Golgi complex to the cell surface (Fig. 20-8; Section 9-4E). The intracellular concentration of free cholesterol controls the rate of LDL receptor synthesis (Section 20-7). However, defects in the LDL receptor system lead to abnormally high levels of circulating cholesterol with the attendant increased risk of heart disease.

HDL Transport Cholesterol from the Tissues to the Liver. HDL have essentially the opposite function of LDL: *They remove cholesterol from the tissues.* HDL are assembled in the plasma from components largely obtained through the degradation of other lipoproteins. *A circulating HDL particle acquires its cholesterol by extracting it from cell-surface membranes.* The cholesterol is then converted to cholesteryl esters by the HDL-associated enzyme **lecithin–cholesterol acyltransferase (LCAT),** which is activated by apoA-I. HDL therefore function as cholesterol scavengers.

The liver is the only organ capable of disposing of significant quantities of cholesterol (by its conversion to bile acids; Fig. 20-1). About half of the VLDL, after their degradation to IDL and LDL, are taken up by the liver via LDL receptor-mediated endocytosis (Fig. 20-7). However, liver cells take up HDL by an entirely different mechanism: Rather than being engulfed and degraded, an HDL particle binds to a cell-surface receptor named **SR-BI** (for *s*cavenger *r*eceptor class *B* type *I*) and selectively transfers its component lipids to the cell. The lipid-depleted HDL particle then dissociates from the cell and re-enters the circulation.

CHECK YOUR UNDERSTANDING

Explain the purpose of bile acids, colipase, and fatty acid–binding protein in the digestion and absorption of lipids.

Describe the roles of the various lipoproteins in transporting triacylglycerols and cholesterol.

2 Fatty Acid Oxidation

LEARNING OBJECTIVES

- Understand that fatty acids are linked to CoA in an ATP-dependent reaction.
- Understand how fatty acyl groups are transported into the mitochondrion for oxidation.
- Understand that each round of β oxidation produces $FADH_2$, NADH, and acetyl-CoA.
- Understand that additional enzymes are required to oxidize unsaturated fatty acids.
- Understand that the propionyl-CoA produced by the oxidation of odd-chain fatty acids is converted to succinyl-CoA.
- Understand that peroxisomes oxidize long-chain fatty acids, producing H_2O_2.

The triacylglycerols stored in adipocytes are mobilized in times of metabolic need by the action of **hormone-sensitive lipase** (Section 20-5). The free fatty acids are released into the bloodstream, where they bind to albumin, a soluble 66-kD monomeric protein. In the absence of albumin, the maximum solubility of fatty acids is $\sim 10^{-6}$ M; the effective solubility of fatty acids in complex with albumin is as high as 2 mM. Nevertheless, those rare individuals with **analbuminemia** (severely depressed levels of albumin) suffer no apparent adverse symptoms; evidently, their fatty acids are transported in complex with other serum proteins.

Fatty acids are catabolized by an oxidative process that releases free energy. The biochemical strategy of fatty acid oxidation was understood long before the oxidative enzymes were purified. In 1904, Franz Knoop, in the first use of chemical labels to trace metabolic pathways, fed dogs

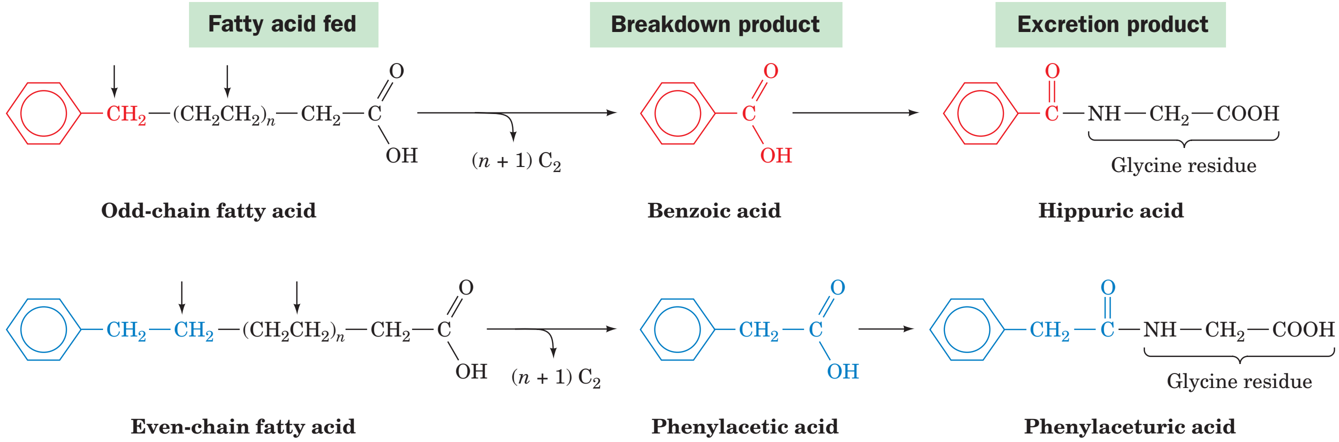

Figure 20-9 | Franz Knoop's classic experiment indicating that fatty acids are metabolically oxidized at their β-carbon atom. ω-Phenyl-labeled fatty acids containing an odd number of carbon atoms are oxidized to the phenyl-labeled C_1 product, benzoic acid, whereas those with an even number of carbon atoms are oxidized to the phenyl-labeled C_2 product, phenylacetic acid. These products are excreted as their respective glycine amides, hippuric and phenylaceturic acids. The vertical arrows indicate the deduced sites of carbon oxidation. The intermediate C_2 products are oxidized to CO_2 and H_2O and were therefore not isolated.

fatty acids labeled at their ω (last) carbon atom by a benzene ring and isolated the phenyl-containing metabolic products from their urine. Dogs fed labeled odd-chain fatty acids excreted **hippuric acid,** the glycine amide of **benzoic acid,** whereas those fed labeled even-chain fatty acids excreted **phenylaceturic acid,** the glycine amide of **phenylacetic acid** (Fig. 20-9). Knoop therefore deduced that fatty acids are progressively degraded by two-carbon units and that this process involves the oxidation of the carbon atom β to the carboxyl group. Otherwise, the phenylacetic acid would be further oxidized to benzoic acid. Knoop's **β oxidation** hypothesis was only confirmed in the 1950s. The β-oxidation pathway is a series of enzyme-catalyzed reactions that operates in a repetitive fashion to progressively degrade fatty acids by removing two-carbon units.

A | Fatty Acids Are Activated by Their Attachment to Coenzyme A

Before fatty acids can be oxidized, they must be "primed" for reaction in an ATP-dependent acylation reaction to form fatty acyl-CoA. The activation process is catalyzed by a family of at least three **acyl-CoA synthetases** (also called **thiokinases**) that differ in their chain-length specificities. These enzymes, which are associated with either the endoplasmic reticulum or the outer mitochondrial membrane, all catalyze the reaction

$$\text{Fatty acid} + \text{CoA} + \text{ATP} \rightleftharpoons \text{acyl-CoA} + \text{AMP} + \text{PP}_i$$

This reaction proceeds via an acyladenylate mixed anhydride intermediate that is attacked by the sulfhydryl group of CoA to form the thioester product (Fig. 20-10), thereby preserving the free energy of ATP hydrolysis in the "high-energy" thioester bond (Section 14-2D). The overall reaction is driven to completion by the exergonic hydrolysis of pyrophosphate catalyzed by inorganic pyrophosphatase.

B | Carnitine Carries Acyl Groups across the Mitochondrial Membrane

Although fatty acids are activated for oxidation in the cytosol, they are oxidized in the mitochondrion, as Eugene Kennedy and Albert Lehninger

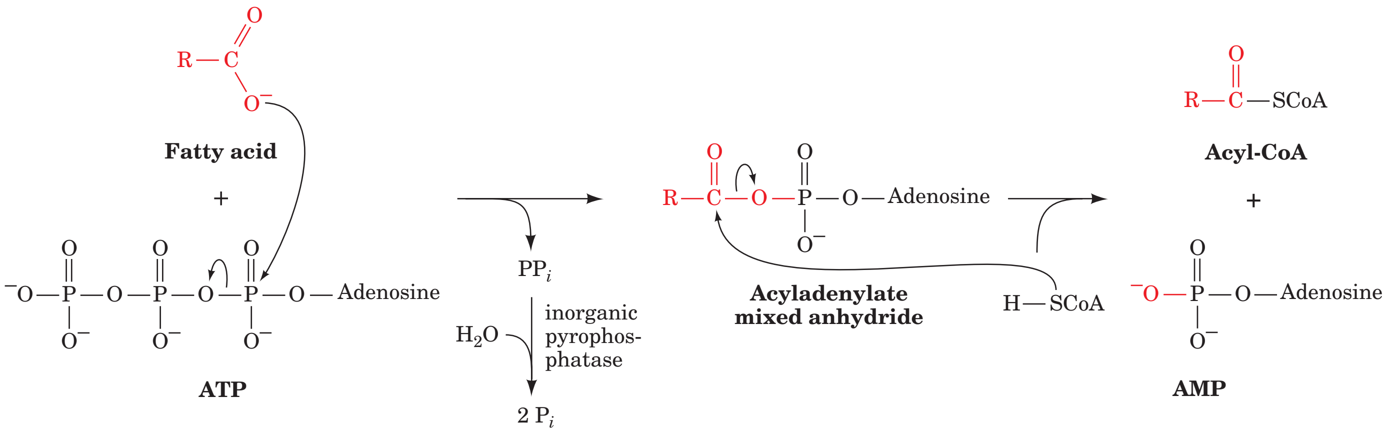
Fatty acid
ATP
PP_i
inorganic pyrophosphatase
H_2O
2 P_i
Acyladenylate mixed anhydride
H—SCoA
Acyl-CoA
AMP
Adenosine

■ **Figure 20-10 | The mechanism of fatty acid activation catalyzed by acyl-CoA synthetase.** Formation of acyl-CoA involves an intermediate acyladenylate mixed anhydride.

established in 1950. We must therefore consider how fatty acyl-CoA is transported across the inner mitochondrial membrane. A long-chain fatty acyl-CoA cannot directly cross the inner mitochondrial membrane. Instead, its acyl portion is first transferred to **carnitine,** a compound that occurs in both plant and animal tissues.

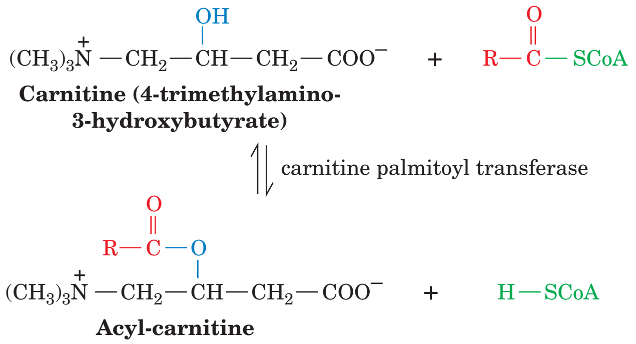
Carnitine (4-trimethylamino-3-hydroxybutyrate)
carnitine palmitoyl transferase
Acyl-carnitine
H—SCoA

This transesterification reaction has an equilibrium constant close to 1, which indicates that the *O*-acyl bond of **acyl-carnitine** has a free energy of hydrolysis similar to that of acyl-CoA's thioester bond. **Carnitine palmitoyl transferases I** and **II,** which can transfer a variety of acyl groups (not just palmitoyl groups), are located, respectively, on the external and internal surfaces of the inner mitochondrial membrane. The translocation process itself is mediated by a specific carrier protein that transports acyl-carnitine into the mitochondrion while transporting free carnitine in the opposite direction. The acyl-CoA transport system is diagrammed in Fig. 20-11.

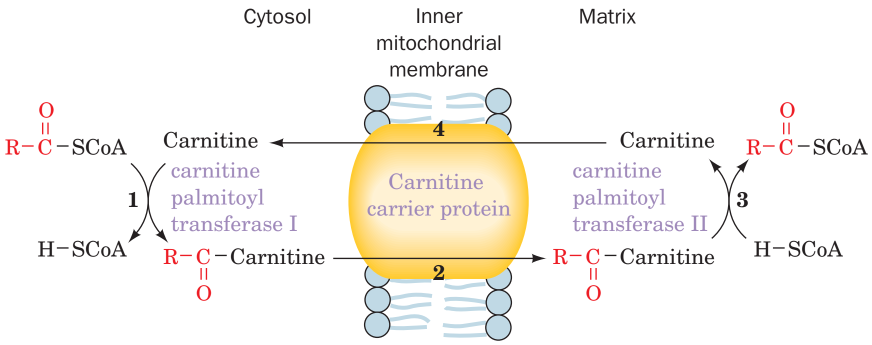
Cytosol
Inner mitochondrial membrane
Matrix
R−C−SCoA
Carnitine
carnitine palmitoyl transferase I
1
H−SCoA
R−C−Carnitine
4
Carnitine carrier protein
2
Carnitine
carnitine palmitoyl transferase II
3
R−C−SCoA
R−C−Carnitine
H−SCoA

■ **Figure 20-11 | The transport of fatty acids into the mitochondrion.** (**1**) The acyl group of a cytosolic acyl-CoA is transferred to carnitine, thereby releasing the CoA to its cytosolic pool. (**2**) The resulting acyl-carnitine is transported into the mitochondrial matrix by the carrier protein. (**3**) The acyl group is transferred to a CoA molecule from the mitochondrial pool. (**4**) The product carnitine is returned to the cytosol.

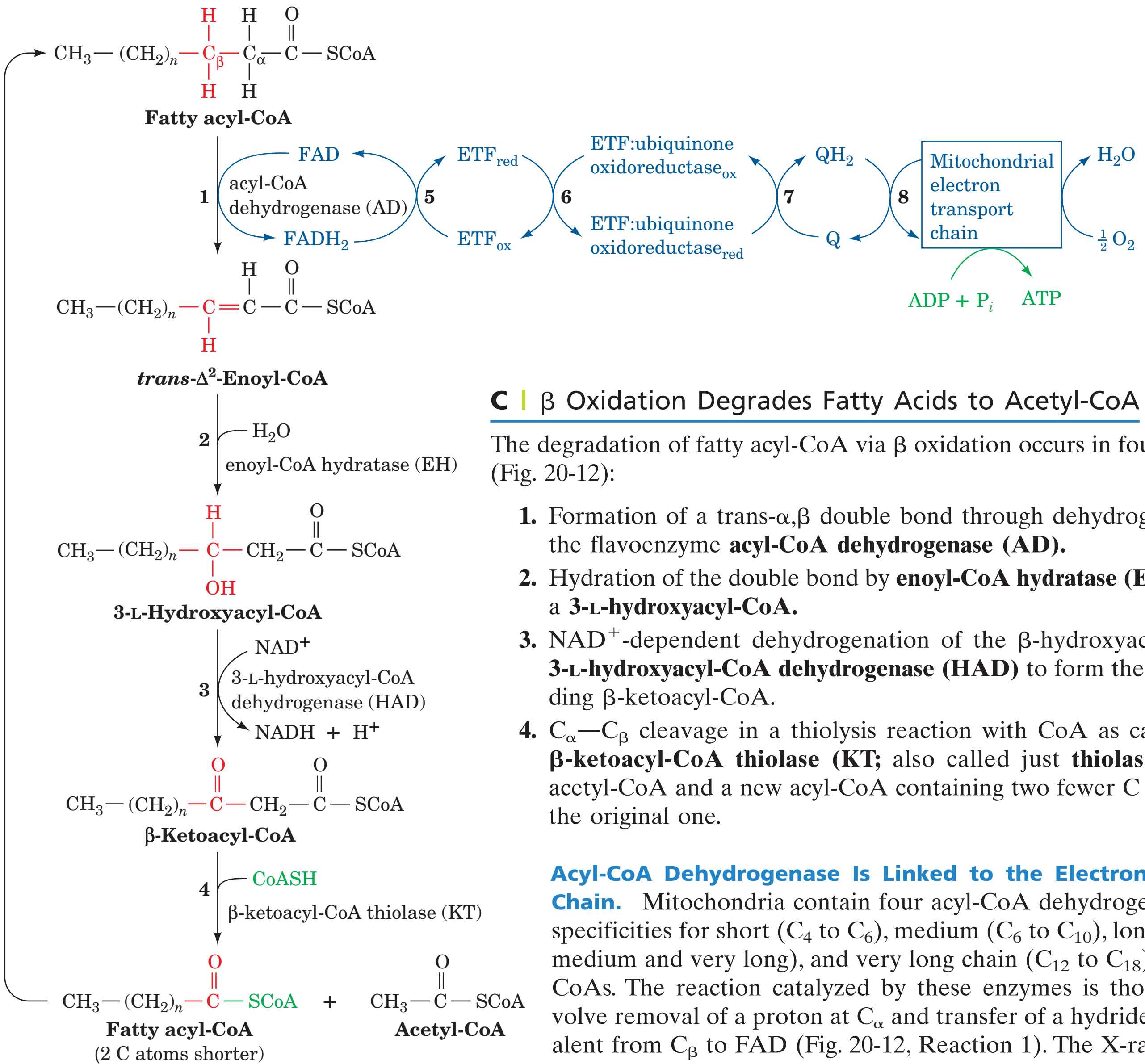
Fatty acyl-CoA
1
acyl-CoA dehydrogenase (AD)
FAD
FADH2
5
ETFred
ETFox
6
ETF:ubiquinone oxidoreductaseox
ETF:ubiquinone oxidoreductasered
7
QH2
Q
8
Mitochondrial electron transport chain
H2O
½ O2
ADP + Pi
ATP
trans-Δ2-Enoyl-CoA
2
H2O
enoyl-CoA hydratase (EH)
3-L-Hydroxyacyl-CoA
3
NAD+
3-L-hydroxyacyl-CoA dehydrogenase (HAD)
NADH + H+
β-Ketoacyl-CoA
4
CoASH
β-ketoacyl-CoA thiolase (KT)
Fatty acyl-CoA (2 C atoms shorter)
+
Acetyl-CoA

Figure 20-12 | The β-oxidation pathway of fatty acyl-CoA. See the Animated Figures.

C | β Oxidation Degrades Fatty Acids to Acetyl-CoA

The degradation of fatty acyl-CoA via β oxidation occurs in four reactions (Fig. 20-12):

1. Formation of a trans-α,β double bond through dehydrogenation by the flavoenzyme **acyl-CoA dehydrogenase (AD).**
2. Hydration of the double bond by **enoyl-CoA hydratase (EH)** to form a **3-L-hydroxyacyl-CoA.**
3. NAD^+-dependent dehydrogenation of the β-hydroxyacyl-CoA by **3-L-hydroxyacyl-CoA dehydrogenase (HAD)** to form the corresponding β-ketoacyl-CoA.
4. C_α—C_β cleavage in a thiolysis reaction with CoA as catalyzed by **β-ketoacyl-CoA thiolase (KT;** also called just **thiolase)** to form acetyl-CoA and a new acyl-CoA containing two fewer C atoms than the original one.

Acyl-CoA Dehydrogenase Is Linked to the Electron-Transport Chain. Mitochondria contain four acyl-CoA dehydrogenases, with specificities for short (C_4 to C_6), medium (C_6 to C_{10}), long (between medium and very long), and very long chain (C_{12} to C_{18}) fatty acyl-CoAs. The reaction catalyzed by these enzymes is thought to involve removal of a proton at C_α and transfer of a hydride ion equivalent from C_β to FAD (Fig. 20-12, Reaction 1). The X-ray structure of **medium-chain acyl-CoA dehydrogenase (MCAD)** in complex with **octanoyl-CoA,** determined by Jung-Ja Kim, clearly shows how the enzyme orients a basic group (Glu 376), the substrate C_α—C_β bond, and the FAD prosthetic group for reaction (Fig. 20-13).

A deficiency of MCAD has been identified in ~10% of cases of **sudden infant death syndrome (SIDS).** Glucose is the principal metabolic fuel just after eating, but when the glucose level later decreases, the rate of fatty acid oxidation must correspondingly increase. The sudden death of infants lacking MCAD may be caused by the imbalance between glucose and fatty acid oxidation.

The $FADH_2$ resulting from the oxidation of the fatty acyl-CoA substrate is reoxidized by the mitochondrial electron-transport chain through a series of electron-transfer reactions. **Electron-transfer flavoprotein (ETF)** transfers an electron pair from $FADH_2$ to the flavo-iron–sulfur protein **ETF:ubiquinone oxidoreductase,** which in turn transfers an electron pair to the mitochondrial electron-transport chain by reducing coenzyme Q (CoQ; Fig. 20-12, Reactions 5–8). Reduction of O_2 to H_2O by the electron-transport chain beginning at the CoQ stage results in the synthesis of approximately 1.5 ATP per electron pair transferred (Section 18-3C).

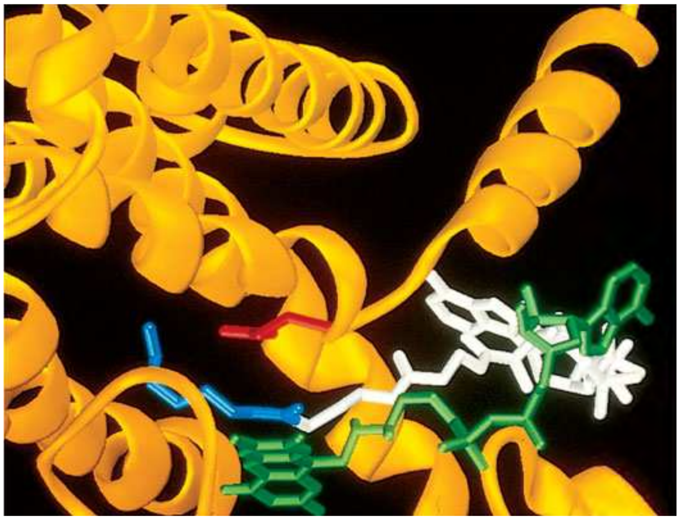

Figure 20-13 | Ribbon diagram of the active site region of medium-chain acyl-CoA dehydrogenase. The enzyme, from pig liver mitochondria, is a tetramer of identical 385-residue subunits, each of which binds an FAD prosthetic group (*green*) and an octanoyl-CoA substrate (whose octanoyl and CoA moieties are blue and white) in largely extended conformations. The octanoyl-CoA binds such that its C_α—C_β bond is sandwiched between the carboxylate group of Glu 376 (*red*) and the flavin ring (*green*), consistent with the proposal that Glu 376 is the general base that abstracts the α proton in the α,β dehydrogenation reaction catalyzed by the enzyme. [Based on an X-ray structure by Jung-Ja Kim, Medical College of Wisconsin. PDBid 3MDE.] **See Interactive Exercise 27.**

Long-Chain Enoyl-CoAs Are Converted to Acetyl-CoA and a Shorter Acyl-CoA by Mitochondrial Trifunctional Protein. The product of acyl-CoA dehydrogenases are 2-enoyl-CoAs. Depending on their chain lengths, their processing is continued by one of three systems (Fig. 20-12): the short chain, medium chain, or long chain 2-enoyl-CoA hydratases (EHs), hydroxyacyl-CoA dehydrogenases (HADs), and 3-ketoacyl-CoA thiolases (KTs). The long chain (LC) versions of these enzymes are contained on one $\alpha_4\beta_4$ heterooctameric, trifunctional protein, located in the inner mitochondrial membrane. LCEH and LCHAD are contained on the α subunits while LCKT is located on the β subunits. The protein is therefore both a multifunctional protein (more than one enzyme activity on a single polypeptide chain) and a multienzyme complex (a complex of polypeptides catalyzing more than one reaction). The advantage of such a trifunctional enzyme is the ability to channel the intermediates toward the final product. Indeed, no long-chain hydroxyacyl-CoA or ketoacyl-CoA intermediates are released into solution by this system.

The Thiolase Reaction Occurs via Claisen Ester Cleavage. The fourth step of β oxidation is the thiolase reaction (Fig. 20-12, Reaction 4), which yields acetyl-CoA and a new acyl-CoA that is two carbon atoms shorter than the one that began the cycle (Fig. 20-14):

1. An active site thiol group adds to the β-keto group of the substrate acyl-CoA.
2. Carbon–carbon bond cleavage yields a thioester between the acyl-CoA substrate and the active site thiol group, together with an acetyl-CoA carbanion intermediate that is stabilized by electron withdrawal into the thioester's carbonyl group. This type of reaction is known as a Claisen ester cleavage (the reverse of a Claisen condensation). The citric acid cycle enzyme citrate synthase also catalyzes a reaction that involves a stabilized acetyl-CoA carbanion intermediate (Section 17-3A).

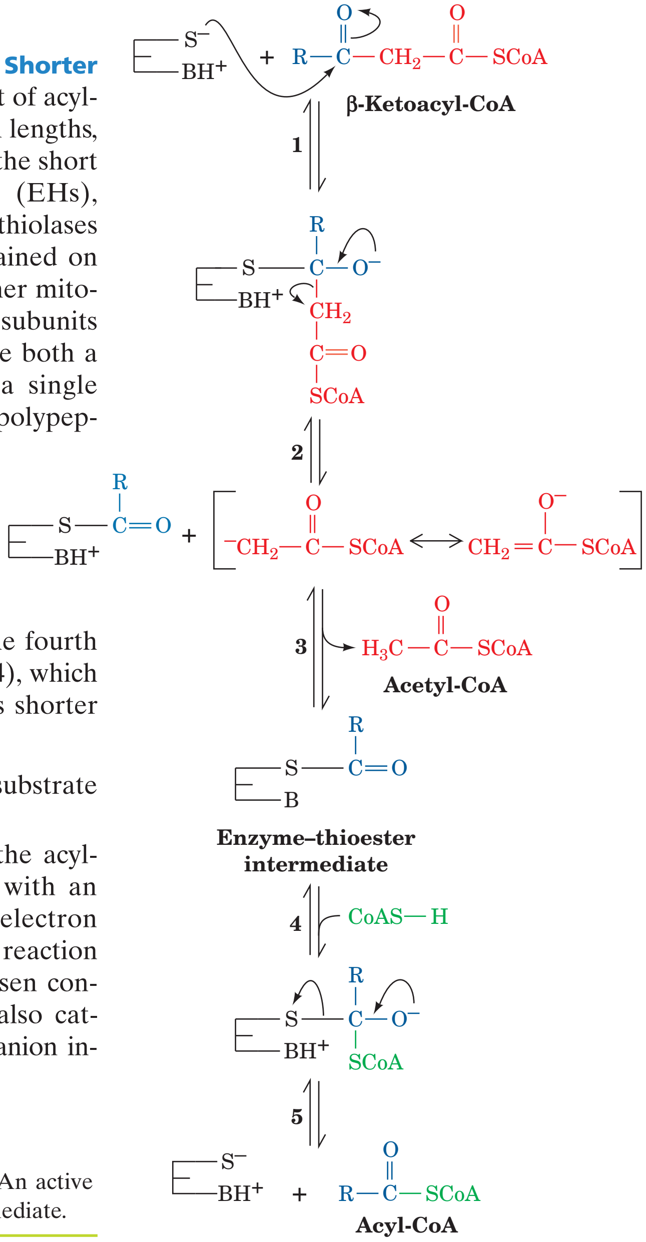

Figure 20-14 | Mechanism of action of β-ketoacyl-CoA thiolase. An active site Cys residue participates in the formation of an enzyme–thioester intermediate.

3. An enzyme acidic group protonates the acetyl-CoA carbanion, yielding acetyl-CoA.

4 and 5. Finally, CoA displaces the enzyme thiol group from the enzyme–thioester intermediate, yielding an acyl-CoA that is shortened by two C atoms.

Fatty Acid Oxidation Is Highly Exergonic. The function of fatty acid oxidation is, of course, to generate metabolic energy. Each round of β oxidation produces one NADH, one $FADH_2$, and one acetyl-CoA. Oxidation of acetyl-CoA via the citric acid cycle generates an additional $FADH_2$ and 3 NADH, which are reoxidized through oxidative phosphorylation to form ATP. Complete oxidation of a fatty acid molecule is therefore a highly exergonic process that yields numerous ATPs. For example, oxidation of palmitoyl-CoA (which has a C_{16} fatty acyl group) involves seven rounds of β oxidation, yielding 7 $FADH_2$, 7 NADH, and 8 acetyl-CoA. Oxidation of the 8 acetyl-CoA, in turn, yields 8 GTP, 24 NADH, and 8 $FADH_2$. Since oxidative phosphorylation of the 31 NADH molecules yields 77.5 ATP and that of the 15 $FADH_2$ yields 22.5 ATP, subtracting the 2 ATP equivalents required for fatty acyl-CoA formation (Section 20-2A), *the oxidation of one palmitate molecule has a net yield of 106 ATP.*

D | Oxidation of Unsaturated Fatty Acids Requires Additional Enzymes

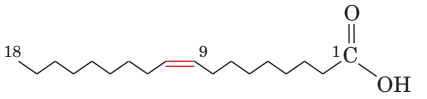

Oleic acid
(9-*cis*-octadecenoic acid)

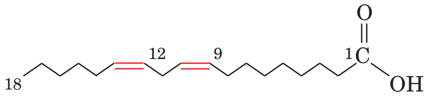

Linoleic acid
(9,12-*cis*-octadecadienoic acid)

Almost all unsaturated fatty acids of biological origin contain only cis double bonds, which most often begin between C9 and C10 (referred to as a Δ^9 or 9-double bond; Table 9-1). Additional double bonds, if any, occur at three-carbon intervals and are therefore never conjugated. Two examples of unsaturated fatty acids are oleic acid and linoleic acid (*at left*).

Note that one of the double bonds in linoleic acid is at an odd-numbered carbon atom and the other is at an even-numbered carbon atom. The double bonds in fatty acids such as linoleic acid pose three problems for the β-oxidation pathway that are solved through the actions of four additional enzymes (Fig. 20-15).

Problem 1: **A β,γ Double Bond.** The first enzymatic difficulty occurs after the third round of β oxidation: The resulting cis-β,γ double bond–containing enoyl-CoA is not a substrate for enoyl-CoA hydratase. **Enoyl-CoA isomerase,** however, converts the cis-Δ^3 double bond to the trans-Δ^2 form. The Δ^2 compound is the normal substrate of enoyl-CoA hydratase, so β oxidation can continue.

Problem 2: **A Δ^4 Double Bond Inhibits Enoyl-CoA Hydratase.** The next difficulty arises in the fifth round of β oxidation: The presence of a double bond at an even-numbered carbon atom results in the formation of 2,4-dienoyl-CoA, which is a poor substrate for enoyl-CoA hydratase. However, NADPH-dependent **2,4-dienoyl-CoA reductase** reduces the Δ^4 double bond. The *E. coli* reductase produces *trans*-2-enoyl-CoA, a normal substrate of β oxidation. The mammalian reductase, however, yields *trans*-3-enoyl-CoA, which, to proceed along the β-oxidation pathway, must first be isomerized to *trans*-2-enoyl-CoA by **3,2-enoyl-CoA isomerase.**

Problem 3: **The Unanticipated Isomerization of 2,5-Enoyl-CoA by 3,2-Enoyl-CoA Isomerase.** Mammalian 3,2-enoyl-CoA isomerase catalyzes a reversible reaction that interconverts Δ^2

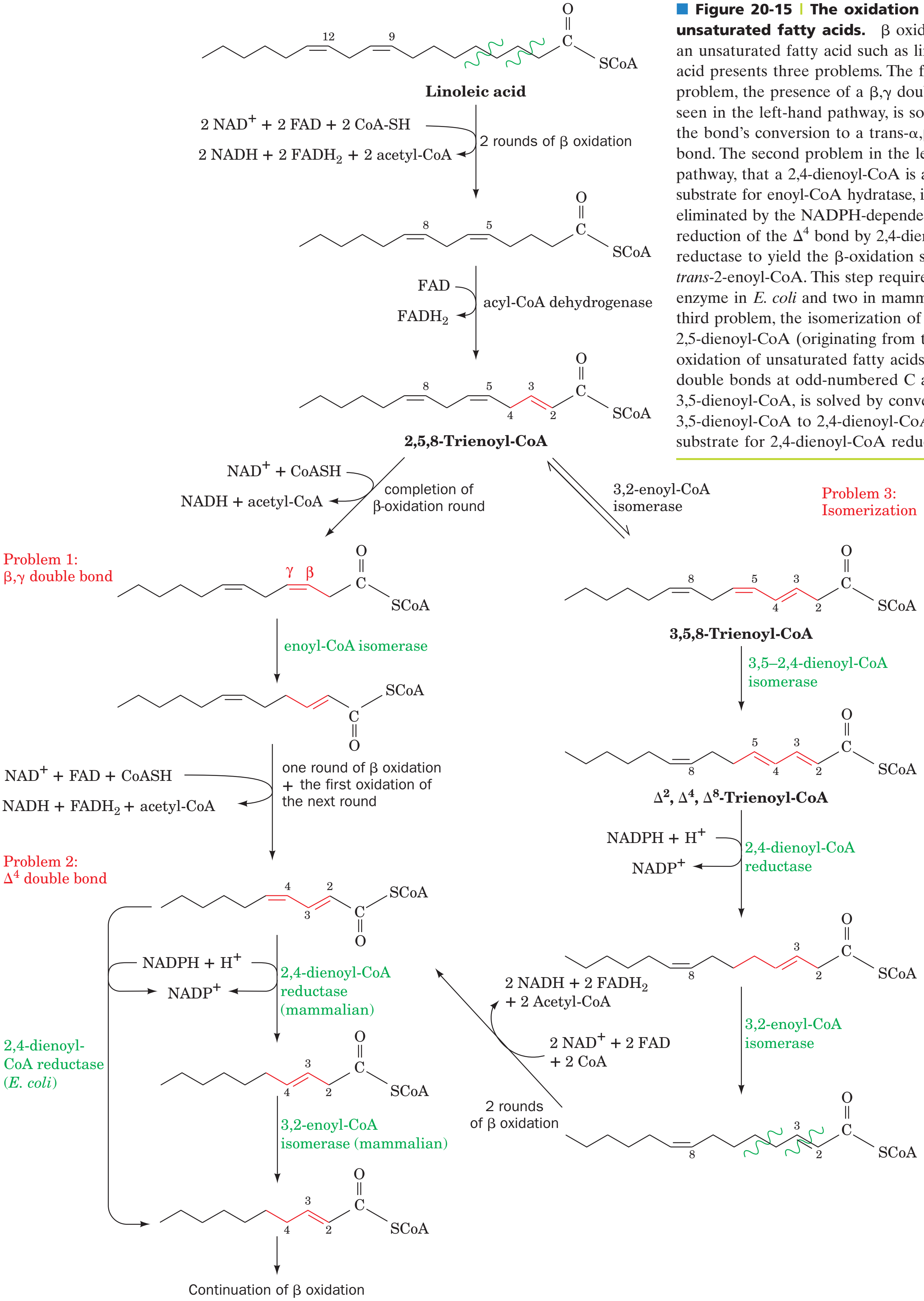

12
9
O
C
SCoA
Linoleic acid
2 NAD$^+$ + 2 FAD + 2 CoA-SH
2 NADH + 2 FADH$_2$ + 2 acetyl-CoA
2 rounds of β oxidation
8
5
FAD
FADH$_2$
acyl-CoA dehydrogenase
3
4
2
2,5,8-Trienoyl-CoA
NAD$^+$ + CoASH
NADH + acetyl-CoA
completion of β-oxidation round
3,2-enoyl-CoA isomerase
Problem 3: Isomerization
Problem 1: β,γ double bond
γ β
enoyl-CoA isomerase
3,5,8-Trienoyl-CoA
3,5–2,4-dienoyl-CoA isomerase
NAD$^+$ + FAD + CoASH
NADH + FADH$_2$ + acetyl-CoA
one round of β oxidation + the first oxidation of the next round
Δ^2, Δ^4, Δ^8-Trienoyl-CoA
NADPH + H$^+$
NADP$^+$
2,4-dienoyl-CoA reductase
Problem 2: Δ^4 double bond
NADPH + H$^+$
NADP$^+$
2,4-dienoyl-CoA reductase (mammalian)
2 NADH + 2 FADH$_2$ + 2 Acetyl-CoA
2 NAD$^+$ + 2 FAD + 2 CoA
2,4-dienoyl-CoA reductase (*E. coli*)
3,2-enoyl-CoA isomerase
3,2-enoyl-CoA isomerase (mammalian)
2 rounds of β oxidation
Continuation of β oxidation

Figure 20-15 | The oxidation of unsaturated fatty acids. β oxidation of an unsaturated fatty acid such as linoleic acid presents three problems. The first problem, the presence of a β,γ double bond, seen in the left-hand pathway, is solved by the bond's conversion to a trans-α,β double bond. The second problem in the left-hand pathway, that a 2,4-dienoyl-CoA is a poor substrate for enoyl-CoA hydratase, is eliminated by the NADPH-dependent reduction of the Δ^4 bond by 2,4-dienoyl-CoA reductase to yield the β-oxidation substrate *trans*-2-enoyl-CoA. This step requires one enzyme in *E. coli* and two in mammals. The third problem, the isomerization of 2,5-dienoyl-CoA (originating from the oxidation of unsaturated fatty acids with double bonds at odd-numbered C atoms) to 3,5-dienoyl-CoA, is solved by converting the 3,5-dienoyl-CoA to 2,4-dienoyl-CoA, a substrate for 2,4-dienoyl-CoA reductase.

and Δ^3 double bonds. A carbonyl group is stabilized by being conjugated to a Δ^2 double bond. However, the presence of a Δ^5 double bond (originating from an unsaturated fatty acid with a double bond at an odd-numbered C atom such as the Δ^9 double bond of linoleic acid) is likewise stabilized by being conjugated with a Δ^3 double bond. If a 2,5-enoyl-CoA is converted by 3,2-enoyl-CoA isomerase to 3,5-enoyl CoA, which occurs up to 20% of the time, another enzyme is necessary to continue the oxidation: **3,5–2,4-Dienoyl-CoA isomerase** isomerizes the 3,5 diene to a 2,4 diene, which is then reduced by 2,4-dienoyl-CoA reductase and isomerized by 3,2-enoyl-CoA isomerase as in Problem 2 above. After two more rounds of β oxidation, the cis-Δ^4 double bond originating from the cis-Δ^{12} double bond of linoleic acid is also dealt with as in Problem 2.

E | Oxidation of Odd-Chain Fatty Acids Yields Propionyl-CoA

Most fatty acids, for reasons explained in Section 20-4, have even numbers of carbon atoms and are therefore completely converted to acetyl-CoA. Some plants and marine organisms, however, synthesize fatty acids with an odd number of carbon atoms. *The final round of β oxidation of these fatty acids yields propionyl-CoA, which is converted to succinyl-CoA for entry into the citric acid cycle.* Propionate and propionyl-CoA are also produced by the oxidation of the amino acids isoleucine, valine, and methionine (Section 21-4D).

The conversion of propionyl-CoA to succinyl-CoA involves three enzymes (Fig. 20-16):

1. The first reaction, catalyzed by **propionyl-CoA carboxylase,** requires a biotin prosthetic group and is driven by the hydrolysis of ATP to ADP + P_i. The reaction resembles that of pyruvate carboxylase (Fig. 16-18).
2. The (*S*)-methylmalonyl-CoA product of the carboxylase reaction is converted to the *R* form by **methylmalonyl-CoA racemase.**
3. (*R*)-Methylmalonyl-CoA is a substrate for **methylmalonyl-CoA mutase,** which catalyzes an unusual carbon skeleton rearrangement.

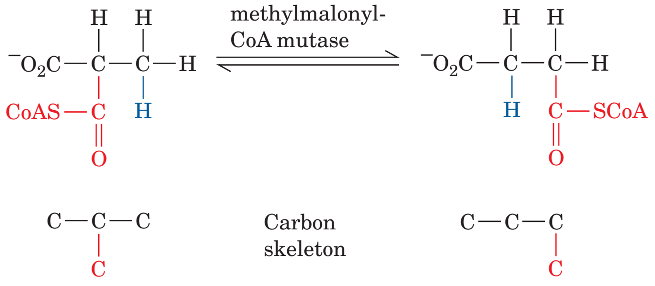

(*R*)-Methylmalonyl-CoA **Succinyl-CoA**

Methylmalonyl-CoA mutase uses a **5′-deoxyadenosylcobalamin** prosthetic group (**AdoCbl;** also called coenzyme B_{12}, a derivative of **cobalamin,** or **vitamin B_{12};** Box 20-1). Dorothy Hodgkin determined the structure of this complex molecule (Fig. 20-17) in 1956 through X-ray crystallographic analysis combined with chemical degradation studies, a landmark achievement (Box 20-2).

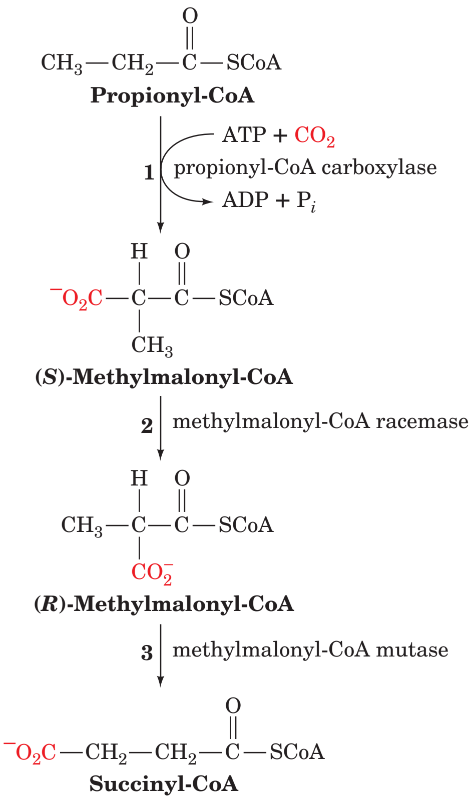

Figure 20-16 | Conversion of propionyl-CoA to succinyl-CoA.

5′-Deoxyadenosylcobalamin contains a hemelike **corrin** ring whose four pyrrole N atoms each ligand a six-coordinate Co ion. The fifth Co ligand is an N atom of a **5,6-dimethylbenzimidazole (DMB)** nucleotide that is covalently linked to the corrin D ring. The sixth ligand is a 5′-deoxyadenosyl group in which the deoxyribose C5′ atom forms a covalent C—Co bond, *one of only two carbon–metal bonds known in biology* (the other is a C—Ni bond in the bacterial enzyme **carbon monoxide dehydrogenase**). In some cobalamin-dependent enzymes, the sixth ligand instead is a CH_3 group that likewise forms a C—Co bond. There are only about a dozen known cobalamin-dependent enzymes, which catalyze molecular rearrangements or methyl-group transfer reactions.

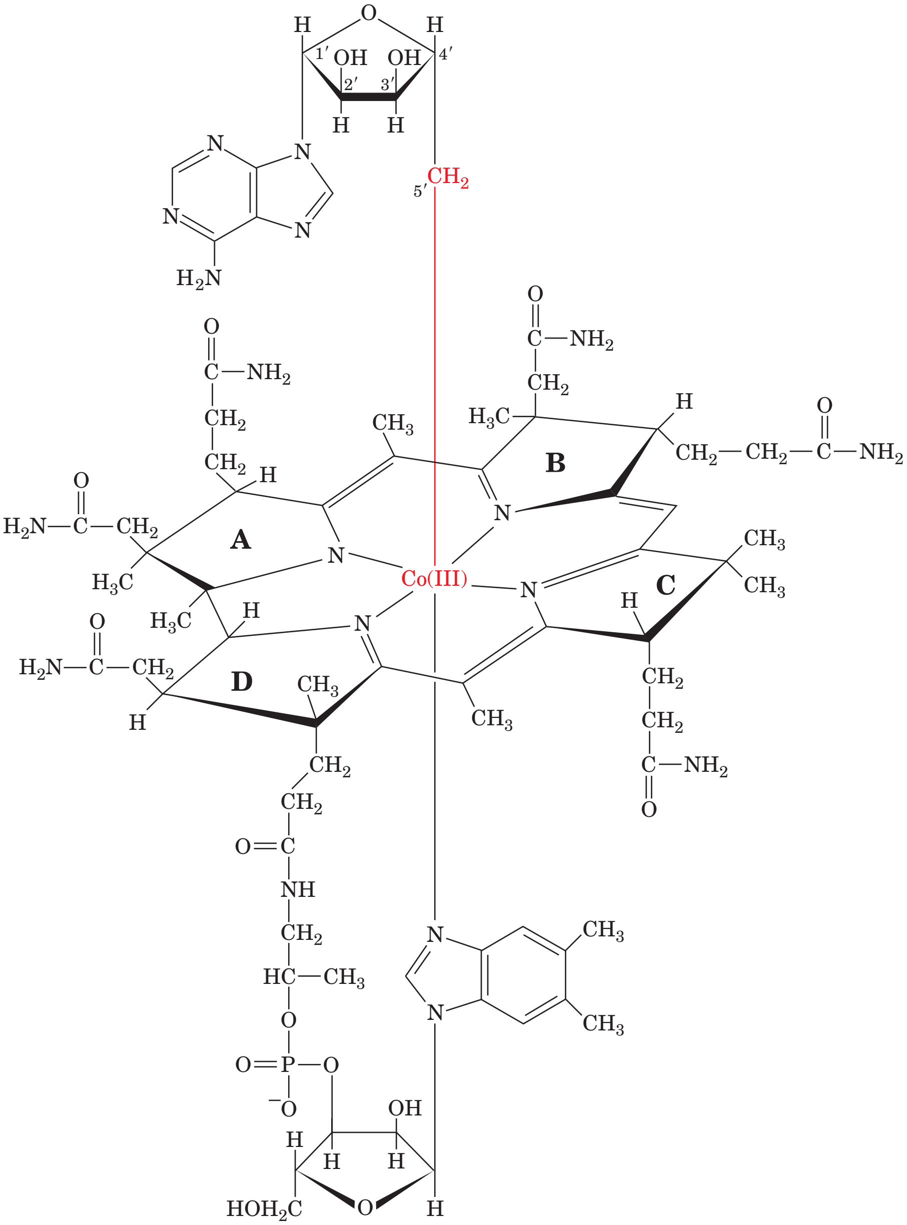

H
O
H
1′
OH
OH
4′
2′
3′
H
H
N
N
5′
CH2
N
N
H2N
O
C—NH2
CH2
O
C—NH2
CH2
H
O
CH3
H3C
CH2—CH2—C—NH2
CH2
CH2
H
B
O
H2N—C—CH2
N
CH3
A
N
H3C
Co(III)
N
C
CH3
O
H3C
H
N
H
H2N—C—CH2
D
CH3
H
CH3
CH2
CH2
CH2
C—NH2
CH2
O
O=C
NH
CH2
N
CH3
HC—CH3
N
O
CH3
O=P—O
−O
OH
H
H
H
HOH2C
O
H

5′-Deoxyadenosylcobalamin (coenzyme B_{12})

Figure 20-17 | Structure of 5′-deoxyadenosylcobalamin.

Methylmalonyl-CoA Mutase Has a Unique α/β Barrel. The X-ray structure of methylmalonyl-CoA mutase from *Propionibacterium shermanii,* an αβ heterodimer, in complex with the substrate analog **2-carboxypropyl-CoA** (which lacks methylmalonyl-CoA's thioester oxygen atom) was determined by Philip Evans. Its AdoCbl cofactor is sandwiched between the catalytically active α subunit's two domains: a 559-residue N-terminal α/β barrel (TIM barrel, the most common enzymatic motif; Sections 6-2C and 15-2) and a 169-residue C-terminal α/β domain that resembles a Rossmann fold (Section 6-2C). The structure of the α/β barrel contains several surprising features (Fig. 20-18):

1. The active sites of nearly all α/β barrel enzymes are located at the C-terminal ends of the barrel's β strands. In methylmalonyl-CoA mutase, however, the AdoCbl is packed against the N-terminal ends of the barrel's β strands.
2. In free AdoCbl, the Co atom is axially liganded by an N atom of its DMB group and by the adenosyl residue's 5′-CH_2 group (Fig. 20-17). In the enzyme, however, the DMB has swung aside to bind in a separate pocket and has been replaced by the side chain of His 610 from the C-terminal domain. The adenosyl group is not visible in the structure due to disorder and hence has probably also swung aside.
3. In nearly all other α/β barrel–containing enzymes, the center of the barrel is occluded by large, often branched, hydrophobic side chains. In methylmalonyl-CoA mutase, however, the 2-carboxypropyl-CoA's pantetheine group binds in a narrow tunnel along the center of the α/β barrel so as to put the methylmalonyl group of an intact substrate in close proximity to the unliganded face of the cobalamin ring. This tunnel provides the only direct access to the active site cavity, thereby protecting the reactive free radical intermediates that are produced in the catalytic reaction from side reactions (see below). The tunnel is lined by small hydrophilic residues (Ser and Thr).

Methylmalonyl-CoA mutase's substrate-binding mode resembles that of several other AdoCbl-containing enzymes of known structure, which are collectively unique among α/β barrel–containing enzymes.

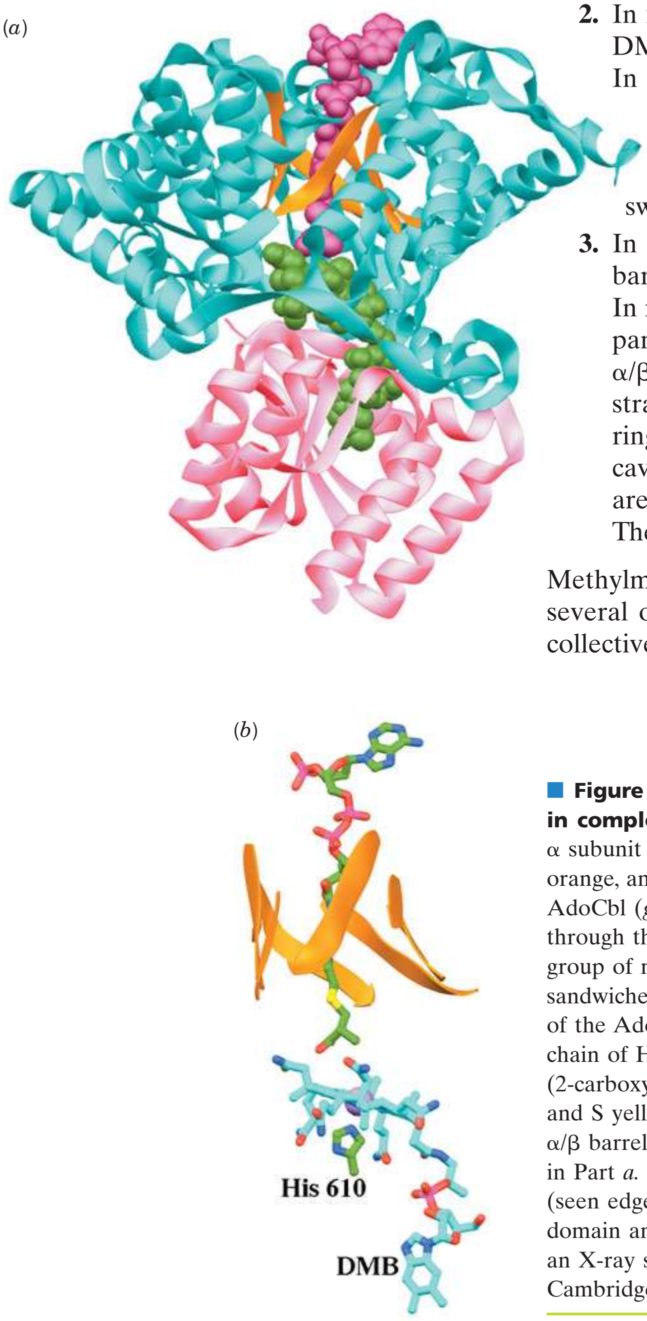

Figure 20-18 | X-Ray structure of *P. shermanii* methylmalonyl-CoA mutase in complex with 2-carboxypropyl-CoA and AdoCbl. (*a*) The catalytically active α subunit in which the N-terminal domain is cyan, the β strands of its α/β barrel are orange, and the C-terminal domain is pink. The 2-carboxypropyl-CoA (*magenta*) and AdoCbl (*green*) are drawn in space-filling form. The 2-carboxypropyl-CoA passes through the center of the α/β barrel and is oriented such that the methylmalonyl group of methylmalonyl-CoA would contact the corrin ring of the AdoCbl, which is sandwiched between the enzyme's N- and C-terminal domains. (*b*) The arrangement of the AdoCbl and 2-carboxypropyl-CoA molecules which, together with the side chain of His 610, are represented in stick form colored according to atom type (2-carboxypropyl-CoA and His C green, AdoCbl C cyan, N blue, O red, P magenta, and S yellow). The corrin ring's Co atom is represented by a lavender sphere and the α/β barrel's β strands are represented by orange ribbons. The view is similar to that in Part *a.* Note that the DMB group (*bottom*) has swung away from the corrin ring (seen edgewise) to be replaced by the side chain of His 610 from the C-terminal domain and that the 5′-deoxyadenosyl group is unseen (due to disorder). [Based on an X-ray structure by Philip Evans, MRC Laboratory of Molecular Biology, Cambridge, U.K. PDBid 7REQ.] **See Interactive Exercise 28.**

Methylmalonyl-CoA Mutase Stabilizes and Protects Free Radical Intermediates. The proposed methylmalonyl-CoA mutase reaction mechanism (Fig. 20-19) begins with the **homolytic cleavage** of the cobalamin C—Co bond; in other words, the C and Co atoms each acquire one of the electrons that formed the cleaved electron pair bond. (Note that a homolytic cleavage reaction is unusual in biology; most other biological bond-cleavage reactions occur via **heterolytic cleavage** in which the electron

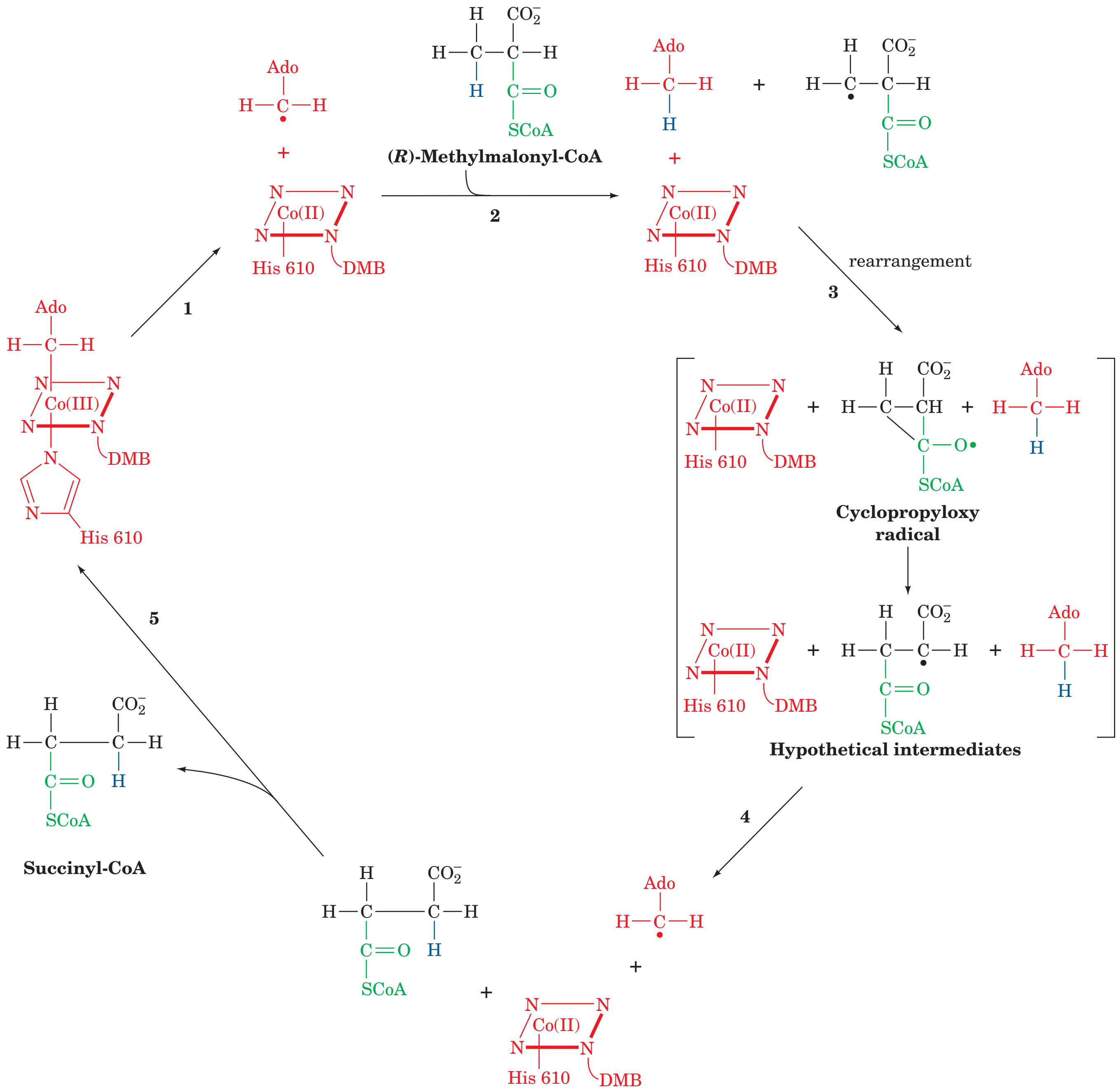

Ado
Co(III)
DMB
His 610
1
Co(II)
(*R*)-Methylmalonyl-CoA
2
rearrangement
3
Cyclopropyloxy radical
Hypothetical intermediates
4
5
Succinyl-CoA
SCoA

■ **Figure 20-19 | Proposed mechanism of methylmalonyl-CoA mutase.** (**1**) The homolytic cleavage of the C—Co(III) bond yields a 5′-deoxyadenosyl (Ado) radical and cobalamin in its Co(II) oxidation state. (**2**) The 5′-deoxyadenosyl radical abstracts a hydrogen atom from methylmalonyl-CoA, thereby generating a methylmalonyl-CoA radical. (**3**) Carbon skeleton rearrangement yields a succinyl-CoA radical via a proposed cyclopropyloxy radical intermediate. (**4**) The succinyl-CoA radical abstracts a hydrogen atom from 5′-deoxyadenosine to regenerate the 5′-deoxyadenosyl radical. (**5**) The release of succinyl-CoA re-forms the coenzyme.

BOX 20-1 **BIOCHEMISTRY IN HEALTH AND DISEASE**

Vitamin B_{12} Deficiency

The existence of vitamin B_{12} came to light in 1926 when George Minot and William Murphy discovered that **pernicious anemia,** an often fatal disease of the elderly characterized by decreased numbers of red blood cells, low hemoglobin levels, and progressive neurological deterioration, can be treated by the daily consumption of large amounts of raw liver. Nevertheless, the antipernicious anemia factor—vitamin B_{12}—was not isolated until 1948.

Vitamin B_{12} is synthesized by neither plants nor animals but only by a few species of bacteria. Herbivores obtain their vitamin B_{12} from the bacteria that inhabit their gut (in fact, some animals, such as rabbits, must periodically eat some of their feces to obtain sufficient amounts of this essential substance). Humans, however, obtain almost all their vitamin B_{12} directly from their diet, particularly from meat. In the intestine, the glycoprotein **intrinsic factor,** which is secreted by the stomach, specifically binds vitamin B_{12}, and the protein–vitamin complex is absorbed via a receptor in the intestinal mucosa. The complex dissociates and the liberated vitamin B_{12} is transported to the bloodstream. At least three different plasma proteins, called **transcobalamins,** bind the vitamin and facilitate its uptake by the tissues.

Pernicious anemia is not usually a dietary deficiency disease but, rather, results from insufficient secretion of intrinsic factor. The normal human requirement for cobalamin is very small, $\sim 3\ \mu g \cdot day^{-1}$, and the liver stores a 3- to 5-year supply of the vitamin. This accounts for the insidious onset of pernicious anemia and the fact that true dietary deficiency of vitamin B_{12}, even among strict vegetarians, is extremely rare.

pair forming the cleaved bond is fully acquired by one of the separating atoms.) The Co ion therefore alternates between its Co(III) and Co(II) oxidation states and hence *functions as a reversible free radical generator.* The C—Co(III) bond is well suited to this function because it is inherently weak (dissociation energy 109 $kJ \cdot mol^{-1}$) and is further weakened through steric interactions with the enzyme.

Spectroscopic measurements indicate that the Co atom in methylmalonyl-CoA mutase is in the Co(II) state, thereby confirming that it has no sixth ligand (as occurs during its catalytic cycle; Fig. 20-19). Protein-induced strain makes the His N—Co bond extremely long (2.5 Å versus 1.9–2.0 Å in various other B_{12}-containing structures), stabilizing the Co(II) species relative to Co(III) and thereby favoring the formation of the adenosyl radical. This radical abstracts a hydrogen atom from the methylmalonyl-CoA substrate, thereby facilitating its rearrangement to succinyl-CoA through the intermediate formation of a cyclopropyloxy radical.

Succinyl-CoA Is Not Directly Consumed by the Citric Acid Cycle. Methylmalonyl-CoA mutase catalyzes the conversion of a metabolite to a citric acid cycle intermediate other than acetyl-CoA. However, such C_4 intermediates are actually catalysts, not substrates, of the citric acid cycle. *In order for succinyl-CoA to undergo net oxidation by the citric acid cycle, it must first be converted to pyruvate and thence to acetyl-CoA.* This is accomplished by converting succinyl-CoA to malate (Reactions 5–7 of the citric acid cycle; Fig. 17-2) followed by its transport to the cytosol and oxidative decarboxylation to pyruvate and CO_2 by **malic enzyme**

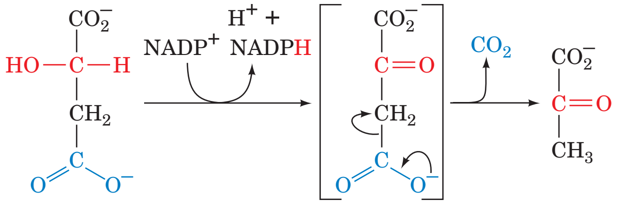

BOX 20-2 **PATHWAYS OF DISCOVERY**

Dorothy Crowfoot Hodgkin and the Structure of Vitamin B_{12}

Dorothy Crowfoot Hodgkin (1910–1994)

The third woman to receive a Nobel Prize in Chemistry, after Marie Curie in 1911 and her daughter Irene Joliot-Curie in 1935, was Dorothy Crowfoot Hodgkin, who received the award in 1964 for determining the structures of biological molecules by X-ray crystallography. Hodgkin's career as a scientist is notable not only for her accomplishments—elucidating the structures of sterols, penicillin, vitamin B_{12}, and insulin—but also for her contributions to the methodology of X-ray crystallography.

Hodgkin's fascination with crystals reportedly began at age 10 with a simple experiment involving alum. Her scientific tendencies were encouraged by her parents, particularly her mother, who was an accomplished amateur botanist. Hodgkin attributed her independent spirit to the fact that her parents were absent for long periods, as her father worked as an archaeologist in Egypt and the Middle East.

Hodgkin's formal training in crystallography took place at Oxford during her undergraduate years and continued as she earned a doctorate under the guidance of J.D. Bernal at Cambridge. Unlike many of his colleagues at the time, Bernal was generous in giving credit to his junior associates. Consequently, Hodgkin received recognition along with Bernal in 1934 when they reported the first X-ray diffraction pattern of a protein, pepsin. Bernal and Hodgkin had thereby shown that proteins are not amorphous colloids but have discrete structures. They also advanced the field of macromolecular crystallography by noting the necessity of examining crystals surrounded by their mother liquor (the solution from which the molecules crystallize) rather than air-dried, as was standard procedure at the time.

After returning to Oxford, Hodgkin established her own laboratory, a challenging task for someone striking out in a new field, and even more difficult for a woman trying to balance work with marriage and motherhood in the late 1930s. At Oxford, Hodgkin undertook studies of crystallized cholesterol and other steroids, showing that calculations based on X-ray diffraction in three rather than two dimensions could disclose considerable information about molecular structure, including the stereochemistry of each carbon atom. Hodgkin also began studying crystals of insulin, although an atomic model of the 777-atom protein took 34 years to complete (the sequence of insulin, determined by Frederick Sanger, was not known until 1955; Box 5-1). During World War II, Hodgkin turned her attention to the structure of penicillin and used X-ray crystallography to elucidate its unexpected ring structure (three carbons and a nitrogen; Box 8-3). This discovery helped pave the way for the synthesis of penicillin and its derivatives. Hodgkin's work also marked the beginning of an electronic age in biochemical research, as she used one of the first analog computers from IBM to help with the required calculations.

In 1955, a visitor brought Hodgkin crystals of cyanocobalamin, whose deep-red color may have enticed Hodgkin to immediately examine their X-ray diffraction. The cobalamin structure, four times larger than that of penicillin, had not yet yielded its structural secrets to conventional chemical approaches. Hodgkin's success in determining the structure of cobalamin was the result of experience as well as intuition. She was reportedly able to discern features of molecular structure simply by examining the diffraction pattern. However, she also took advantage of powerful computers available to her collaborator Kenneth Trueblood in Los Angeles, who, due to the great distance between them, communicated with her through letters and telegrams. Hodgkin bravely decided to use the cobalt atom naturally present in cobalamin to solve the "phase problem" that prevented the straightforward determination of X-ray structures (Box 7-2). Although others believed that the cobalt atom would not scatter X-rays strongly enough relative to the lighter atoms in the structure, Hodgkin was able to derive the necessary phase information and thus was spared having to produce cobalamin crystals containing a heavier atom.

Hodgkin and her collaborators identified the unusual porphyrin structure of cyanocobalamin, in which rings A and D are directly linked and ring A is fully saturated (Fig. 20-17). They subsequently identified cobalamin, with its Co—C bond, as the first known biological organometallic compound. Hodgkin later determined the structure of the physiological form of vitamin B_{12}, adenosylcobalamin, in 1961. Now that the structure of the vitamin was known, it could be synthesized and used to treat pernicious anemia (Box 20-1). In addition to its obvious implications for human health, Hodgkin's work with cobalamin encouraged other researchers to pursue the structures of large compounds previously thought to be too complicated for crystallographic analysis. Hodgkin herself finally completed a three-dimensional model of insulin in 1969.

After receiving the Nobel prize in 1964, along with many other honors, Hodgkin became increasingly involved in international organizations, including the International Union of Crystallography and other groups dedicated to promoting scientific cooperation as a means for decreasing international tensions during the Cold War. Her own laboratory over the years hosted scientists from around the globe. By the end of her life, her efforts to foster international goodwill were no less notable than her accomplishments as a crystallographer.

Ferry, G., *Dorothy Hodgkin: A Life,* Cold Spring Harbor Laboratory Press (2000).

Hodgkin, D.C., Kamper, J., Mackay, M., Pickworth, J., Trueblood, K.N. and White, J.G., Structure of vitamin B-12, *Nature* **178,** 64 (1956).

(this enzyme also functions in the C_4 cycle of photosynthesis; Fig. 19-33). Pyruvate is then completely oxidized via pyruvate dehydrogenase and the citric acid cycle.

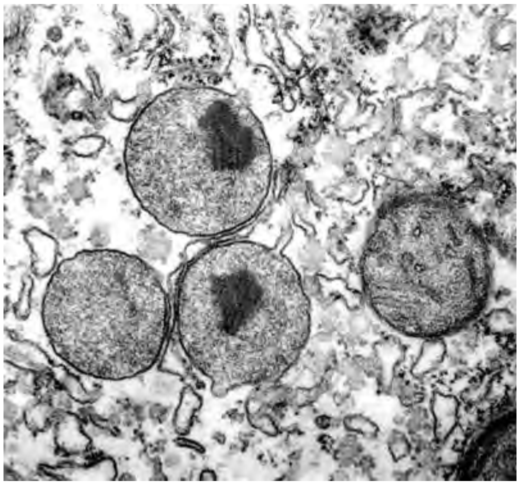

Figure 20-20 | Peroxisomes. These membrane-bounded organelles perform a variety of metabolic functions, including the oxidation of very long chain fatty acids. [© Donald Fawcett/Visuals Unlimited.]

F | Peroxisomal β Oxidation Differs from Mitochondrial β Oxidation

In mammalian cells, the bulk of β oxidation occurs in the mitochondria, but peroxisomes (Fig. 20-20) also oxidize fatty acids, particularly those with very long chains or branched chains. In plants, fatty acid oxidation occurs exclusively in the peroxisomes and glyoxysomes (which are specialized peroxisomes). In addition to lipid catabolism, mammalian peroxisomes participate in the synthesis of certain lipids, including bile acids. A variety of human diseases result from defects in peroxisomal enzymes or proteins that transport intermediates across the peroxisomal membrane.

Peroxisomal β oxidation, which differs only slightly from mitochondrial β oxidation, shortens very long chain fatty acids (>22 carbon atoms), which are then fully degraded by the mitochondrial pathway. Very long chain fatty acids are transported into the peroxisomes by a mechanism that does not require carnitine, and are activated by a long chain acyl-CoA synthetase. Peroxisomal β oxidation results in the same chemical changes to fatty acids as in the mitochondrial pathway but requires only three enzymes:

1. **Acyl-CoA oxidase** catalyzes the reaction

$$\text{Fatty acyl-CoA} + O_2 \rightarrow \textit{trans}\text{-}\Delta^2\text{-enoyl-CoA} + H_2O_2$$

   The enzyme uses an FAD cofactor, but the abstracted electrons are transferred directly to O_2 rather than passing through the electron-transport chain with its concomitant oxidative phosphorylation (Fig. 20-12, Reactions 5–8). Peroxisomal fatty acid oxidation therefore generates two fewer ATP per C_2 cycle than mitochondrial fatty acid oxidation. Catalase converts the H_2O_2 produced in the oxidase reaction to $H_2O + O_2$.
2. Peroxisomal enoyl-CoA hydratase and 3-L-hydroxyacyl-CoA dehydrogenase activities occur on a single polypeptide. The reactions catalyzed are identical to those of the mitochondrial system (Fig. 20-12, Reactions 2 and 3).
3. Peroxisomal thiolase catalyzes the final step of oxidation. This enzyme is almost inactive with acyl-CoAs of length C_8 or less, so peroxisomes incompletely oxidize fatty acids.

The peroxisome contains both a carnitine acetyltransferase and a transferase specific for longer chain acyl groups. Acyl-CoAs that have been chain-shortened by peroxisomal β oxidation are thereby converted to their carnitine esters. These substances, for the most part, passively diffuse out of the peroxisome to the mitochondrion, where they are oxidized further.

CHECK YOUR UNDERSTANDING

Describe the activation and transport of a cytosolic fatty acid into the mitochondrion for degradation.

Summarize the chemical reactions that occur in each round of β oxidation. How is ATP recovered from the products of β oxidation?

What additional steps are required to oxidized unsaturated and odd-chain fatty acids?

Describe the differences between peroxisomal and mitochondrial β oxidation.

3 Ketone Bodies

LEARNING OBJECTIVE

- Understand that acetyl-CoA may be reversibly converted to ketone bodies to be used as fuel by other tissues.

The acetyl-CoA produced by oxidation of fatty acids can be further oxidized via the citric acid cycle. In liver mitochondria, however, a significant fraction of this acetyl-CoA has another fate. By a process known as **ketogenesis,** acetyl-CoA is converted to **acetoacetate** or **D-β-hydroxybutyrate.** These compounds together with acetone are somewhat inaccurately referred to as **ketone bodies:**

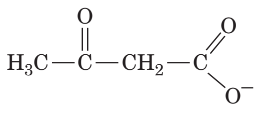

Acetoacetate

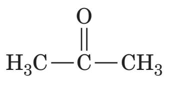

Acetone

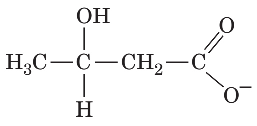

D-β-Hydroxybutyrate

Ketone bodies are important metabolic fuels for many peripheral tissues, particularly heart and skeletal muscle. The brain, under normal circumstances, uses only glucose as its energy source (fatty acids are unable to pass through the blood–brain barrier), but during starvation, the small, water-soluble ketone bodies become the brain's major fuel source (Section 22-4A).

Acetoacetate formation occurs in three reactions (Fig. 20-21):

1. Two molecules of acetyl-CoA are condensed to **acetoacetyl-CoA** by thiolase (also called **acetyl-CoA acetyltransferase**) working in the reverse direction from the way it does in the final step of β oxidation (Fig. 20-12, Reaction 4).
2. Condensation of the acetoacetyl-CoA with a third acetyl-CoA by **HMG-CoA synthase** forms **β-hydroxy-β-methylglutaryl-CoA (HMG-CoA).** The mechanism of this reaction resembles the reverse of the thiolase reaction (Fig. 20-14) in that an active site thiol group forms an acyl-thioester intermediate.
3. HMG-CoA is degraded to acetoacetate and acetyl-CoA in a mixed aldol–Claisen ester cleavage by **HMG-CoA lyase.** The mechanism of this reaction is analogous to the reverse of the citrate synthase reaction (Fig. 17-10). HMG-CoA is also a precursor in cholesterol biosynthesis (Section 20-7A). HMG-CoA lyase is present only in liver mitochondria and therefore does not interfere with cholesterol synthesis in the cytoplasm.

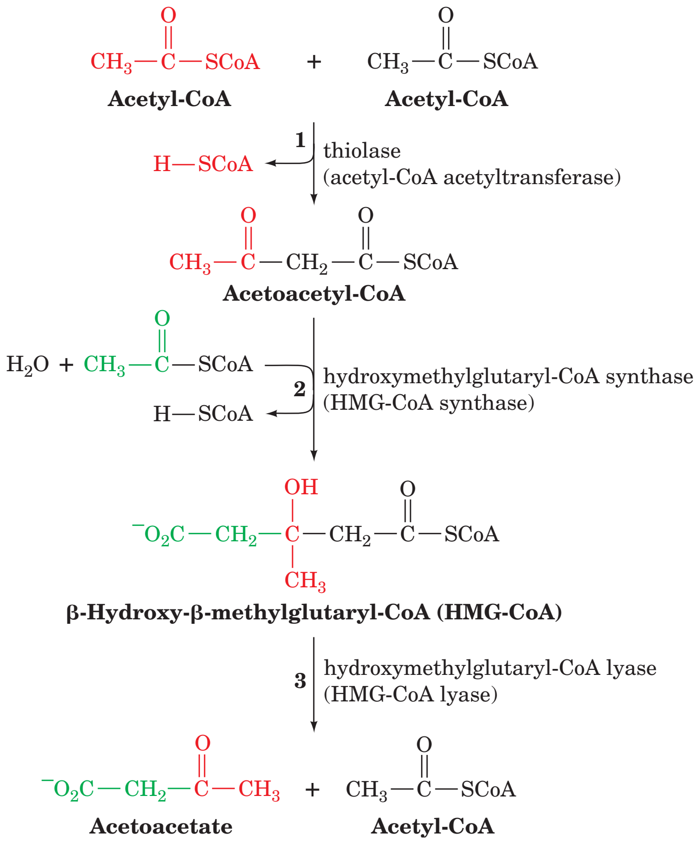

Acetyl-CoA
Acetyl-CoA
1
thiolase
(acetyl-CoA acetyltransferase)
H—SCoA
Acetoacetyl-CoA
H₂O
2
hydroxymethylglutaryl-CoA synthase
(HMG-CoA synthase)
H—SCoA
β-Hydroxy-β-methylglutaryl-CoA (HMG-CoA)
3
hydroxymethylglutaryl-CoA lyase
(HMG-CoA lyase)
Acetoacetate
Acetyl-CoA

Figure 20-21 | **Ketogenesis.** Acetoacetate is formed from acetyl-CoA in three steps. (**1**) Two molecules of acetyl-CoA condense to form acetoacetyl-CoA. (**2**) A Claisen ester condensation of the acetoacetyl-CoA with a third acetyl-CoA forms β-hydroxy-β-methylglutaryl-CoA (HMG-CoA). (**3**) HMG-CoA is degraded to acetoacetate and acetyl-CoA in a mixed aldol–Claisen ester cleavage.

Acetoacetate may be reduced to D-β-hydroxybutyrate by **β-hydroxybutyrate dehydrogenase:**

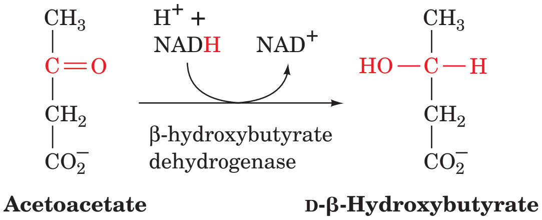
CH_3
C=O
CH_2
CO_2^-
H^+ +
NADH
NAD^+
β-hydroxybutyrate
dehydrogenase
CH_3
HO—C—H
CH_2
CO_2^-
Acetoacetate
D-β-Hydroxybutyrate

Acetoacetate, a β-keto acid, also undergoes relatively facile nonenzymatic decarboxylation to acetone and CO_2. Indeed, in individuals with **ketosis,** a pathological condition in which acetoacetate is produced faster than it is metabolized (a symptom of diabetes; Section 22-4B), the breath has the characteristic sweet smell of acetone.

The liver releases acetoacetate and β-hydroxybutyrate, which are carried by the bloodstream to the peripheral tissues for use as alternative fuels. There, these products are converted to two acetyl-CoA as is diagrammed in Fig. 20-22. Succinyl-CoA, which acts as the CoA donor in this process, can also be converted to succinate with the coupled synthesis of GTP in the succinyl-CoA synthetase reaction of the citric acid cycle (Section 17-3E). The "activation" of acetoacetate bypasses this step and therefore "costs" the free energy of GTP hydrolysis.

■ **CHECK YOUR UNDERSTANDING**

How are ketone bodies synthesized and degraded?

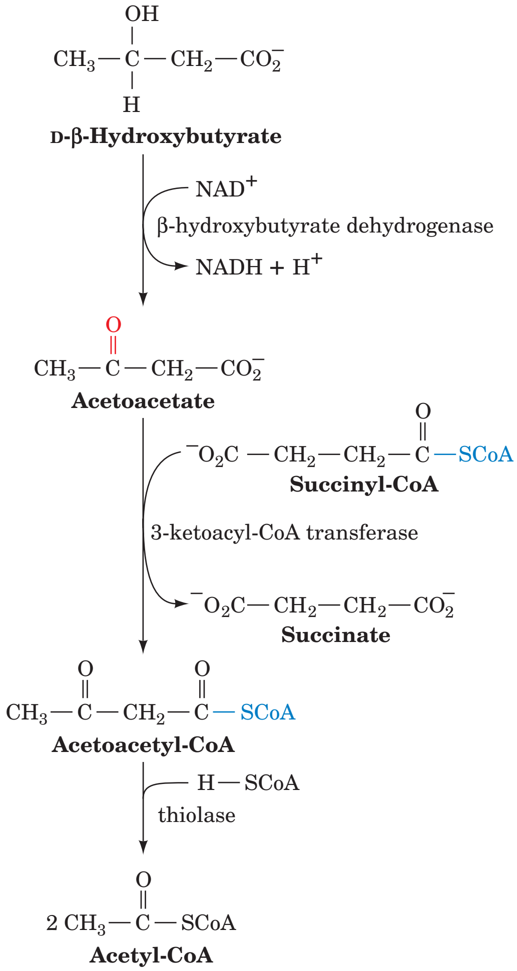
OH
CH_3—C—CH_2—CO_2^-
H
D-β-Hydroxybutyrate
NAD^+
β-hydroxybutyrate dehydrogenase
NADH + H^+
O
CH_3—C—CH_2—CO_2^-
Acetoacetate
O
^-O_2C—CH_2—CH_2—C—SCoA
Succinyl-CoA
3-ketoacyl-CoA transferase
^-O_2C—CH_2—CH_2—CO_2^-
Succinate
O
O
CH_3—C—CH_2—C—SCoA
Acetoacetyl-CoA
H—SCoA
thiolase
O
2 CH_3—C—SCoA
Acetyl-CoA

■ **Figure 20-22 | Metabolic conversion of ketone bodies to acetyl-CoA.**

4 Fatty Acid Biosynthesis

Fatty acid biosynthesis occurs through condensation of C_2 units, the reverse of the β-oxidation process. Through isotopic labeling techniques, David Rittenberg and Konrad Bloch demonstrated, in 1945, that these condensation units are derived from acetic acid. Subsequent research showed that both acetyl-CoA and bicarbonate are required, and that a C_3 unit, **malonyl-CoA,** is an intermediate of fatty acid biosynthesis.

The pathway of fatty acid synthesis differs from that of fatty acid oxidation. This situation, as we saw in Section 16-3, is typical of opposing biosynthetic and degradative pathways because it permits them both to be thermodynamically favorable and independently regulated under similar physiological conditions. Figure 20-23 outlines fatty acid oxidation and synthesis with emphasis on the differences between these pathways, including the cellular locations of the pathways, the redox coenzymes, and the manner in which C_2 units are removed or added to the fatty acyl chain.

LEARNING OBJECTIVES

- Understand that acetyl-CoA is transported into the cytosol for fatty acid synthesis.
- Understand that fatty acid synthesis begins with the carboxylation of acetyl-CoA.
- Understand that fatty acid synthase carries out seven reactions and lengthens a fatty acid two carbons at a time.
- Understand that elongases and desaturases may modify fatty acids.
- Understand that triacylglycerols are synthesized from glycerol and fatty acids.

A | Mitochondrial Acetyl-CoA Must Be Transported into the Cytosol

Acetyl-CoA, the starting material for fatty acid synthesis, is generated in the mitochondrion by the oxidative decarboxylation of pyruvate as catalyzed by pyruvate dehydrogenase (Section 17-2B) as well as by the oxidation of fatty acids. When the demand for ATP is low, so that the oxidation of acetyl-CoA via the citric acid cycle and oxidative phosphorylation is minimal, this mitochondrial acetyl-CoA may be stored for future use as fat. Fatty acid biosynthesis occurs in the cytosol, however, and the

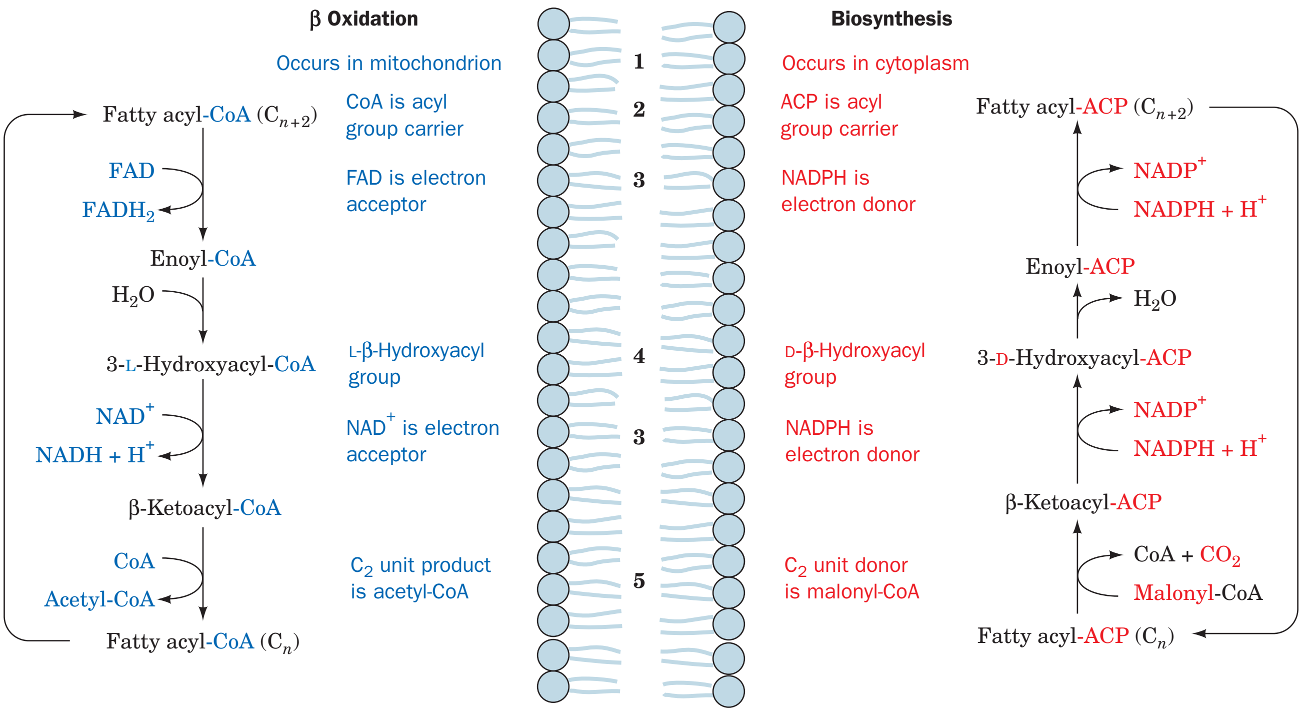
β Oxidation
Occurs in mitochondrion
Fatty acyl-CoA (C_{n+2})
CoA is acyl group carrier
FAD
$FADH_2$
FAD is electron acceptor
Enoyl-CoA
H_2O
3-L-Hydroxyacyl-CoA
L-β-Hydroxyacyl group
NAD^+
NADH + H^+
NAD^+ is electron acceptor
β-Ketoacyl-CoA
CoA
Acetyl-CoA
C_2 unit product is acetyl-CoA
Fatty acyl-CoA (C_n)
1
2
3
4
3
5
Biosynthesis
Occurs in cytoplasm
ACP is acyl group carrier
Fatty acyl-ACP (C_{n+2})
NADPH is electron donor
$NADP^+$
NADPH + H^+
Enoyl-ACP
H_2O
D-β-Hydroxyacyl group
3-D-Hydroxyacyl-ACP
NADPH is electron donor
$NADP^+$
NADPH + H^+
β-Ketoacyl-ACP
C_2 unit donor is malonyl-CoA
CoA + CO_2
Malonyl-CoA
Fatty acyl-ACP (C_n)

Figure 20-23 | Comparison of fatty acid β oxidation and fatty acid biosynthesis. Differences occur in (**1**) cellular location, (**2**) acyl group carrier, (**3**) electron acceptor/donor, (**4**) stereochemistry of the hydration/dehydration reaction, and (**5**) the form in which C_2 units are produced/donated. **See the Animated Figures.**

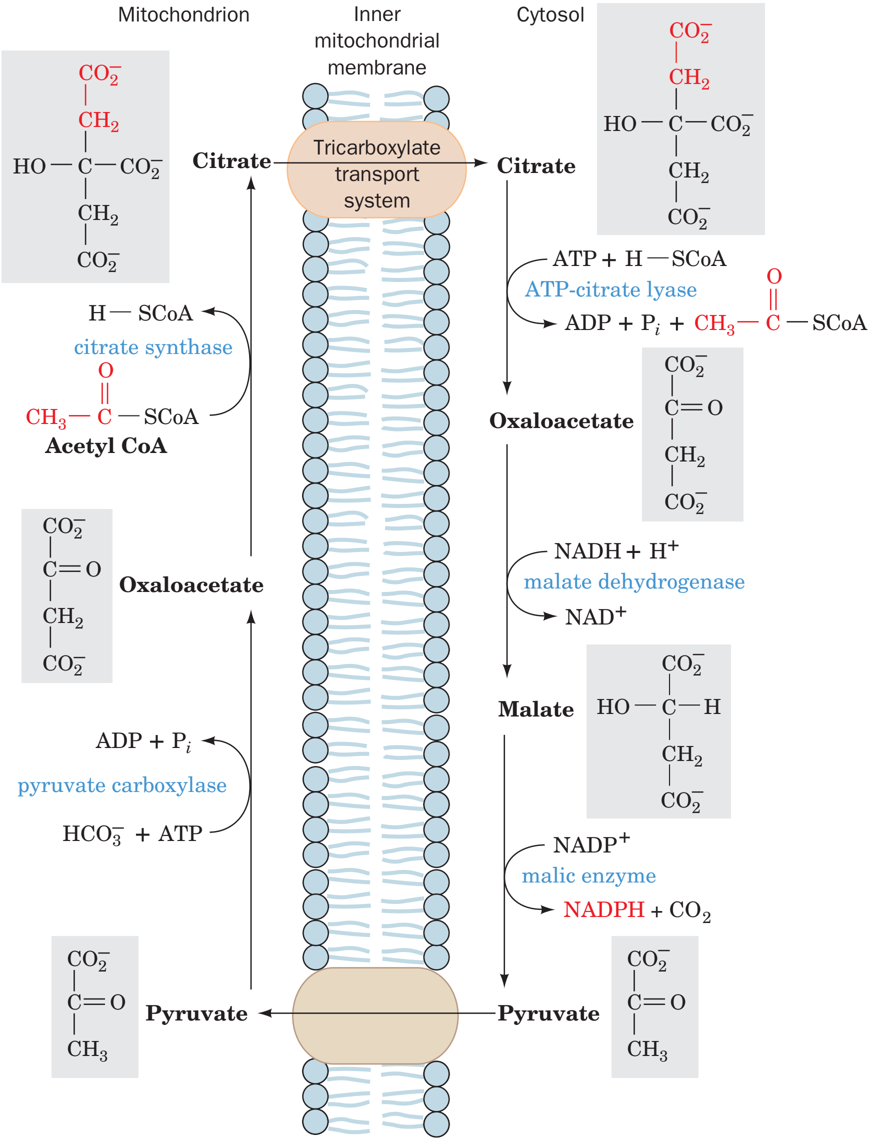
Mitochondrion
Inner mitochondrial membrane
Cytosol
Tricarboxylate transport system
Citrate
Citrate
H—SCoA
citrate synthase
CH3—C(=O)—SCoA
Acetyl CoA
ATP + H—SCoA
ATP-citrate lyase
ADP + Pi + CH3—C(=O)—SCoA
Oxaloacetate
Oxaloacetate
NADH + H+
malate dehydrogenase
NAD+
Malate
ADP + Pi
pyruvate carboxylase
HCO3− + ATP
NADP+
malic enzyme
NADPH + CO2
Pyruvate
Pyruvate
HO—C—CO2−
HO—C—H
C=O
CH2
CH3
CO2−

Figure 20-24 | The tricarboxylate transport system. The overall effect of this sequence of reactions is the transfer of acetyl groups from the mitochondrion to the cytosol.

mitochondrial membrane is essentially impermeable to acetyl-CoA. *Acetyl-CoA enters the cytosol in the form of citrate via the* ***tricarboxylate transport system*** (Fig. 20-24). **ATP-citrate lyase** then catalyzes the reaction

$$\text{Citrate} + \text{CoA} + \text{ATP} \rightarrow \text{acetyl-CoA} + \text{oxaloacetate} + \text{ADP} + P_i$$

which resembles the reverse of the citrate synthase reaction (Fig. 17-10) except that ATP hydrolysis is required to drive the synthesis of the thioester bond. Oxaloacetate is then reduced to malate by malate dehydrogenase. Malate is oxidatively decarboxylated to pyruvate by malic enzyme and returned in this form to the mitochondrion. This reaction involves the reoxidation of malate to oxaloacetate, a β-keto acid, which is then decarboxylated, a reaction reminiscent of the isocitrate dehydrogenase reaction in the citric acid cycle (Section 17-3C). The NADPH produced is used in the reductive reactions of fatty acid biosynthesis.

B | Acetyl-CoA Carboxylase Produces Malonyl-CoA

Acetyl-CoA carboxylase (ACC) catalyzes the first committed step of fatty acid biosynthesis and one of its rate-controlling steps. The mechanism of this biotin-dependent enzyme is similar to those of propionyl-CoA carboxylase (Section 20-2E) and pyruvate carboxylase (Fig. 16-18). The reaction occurs in two steps, a CO_2 activation and a carboxylation:

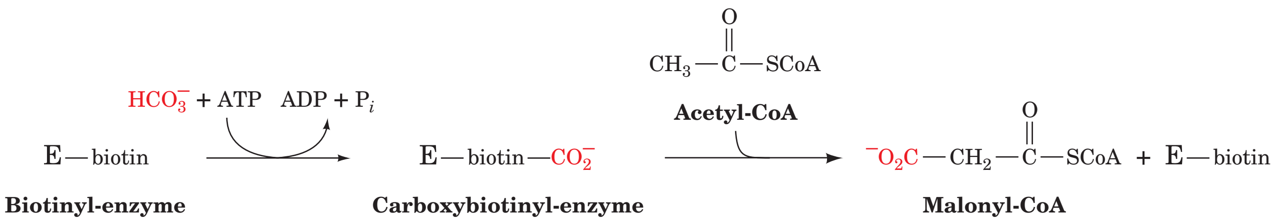

The result is a three-carbon (malonyl) group linked as a thioester to CoA.

Mammalian acetyl-CoA carboxylase, a 230-kD polypeptide, is subject to allosteric and hormonal control. For example, citrate stimulates acetyl-CoA carboxylase and long chain fatty acyl-CoAs are feedback inhibitors of the enzyme. Fine-tuning of enzyme activity is accomplished through covalent modification. Acetyl-CoA carboxylase is a substrate for several kinases. It has six phosphorylation sites, but phosphorylation of only one (Ser 79) is clearly associated with enzyme inactivation. Ser 79 is phosphorylated by **AMP-dependent protein kinase (AMPK)** in a cAMP-independent pathway. However, glucagon as well as epinephrine, which act through protein kinase A (PKA; Section 16-3B), promote the phosphorylation of Ser 79, possibly by inhibiting its dephosphorylation (recall that this occurs in glycogen metabolism when the PKA-mediated phosphorylation of phosphoprotein phosphatase inhibitor-1 inhibits dephosphorylation; Fig. 16-13). Insulin, on the other hand, stimulates dephosphorylation of acetyl-CoA carboxylase and thereby activates the enzyme.

Mammalian Acetyl-CoA Carboxylase Has Two Major Isoforms. There are two major isoforms of ACC. **α-ACC** occurs in adipose tissue and **β-ACC** occurs in tissues that oxidize but do not synthesize fatty acids, such as heart muscle. Tissues that both synthesize and oxidize fatty acids, such as liver, contain both isoforms, which are homologous although the genes encoding them are located on different chromosomes. What is the function of β-ACC? The product of the ACC-catalyzed reaction, malonyl-CoA, strongly inhibits the mitochondrial import of fatty acyl-CoA for fatty acid oxidation, the major control point for this process. Thus it appears that β-ACC has a regulatory function (Section 20-5).

The *E. coli* acetyl-CoA carboxylase, which is a multisubunit protein, is regulated by guanine nucleotides so that fatty acid synthesis is coordinated with cell growth. In prokaryotes, fatty acids serve primarily as phospholipid precursors, since these organisms do not synthesize triacylglycerols for energy storage.

C | Fatty Acid Synthase Catalyzes Seven Reactions

The synthesis of fatty acids, mainly palmitic acid, from acetyl-CoA and malonyl-CoA involves seven enzymatic reactions. These reactions were first studied in cell-free extracts of *E. coli,* in which they are catalyzed by independent enzymes. Individual enzymes with these activities also occur in chloroplasts (plant fatty acid synthesis does not occur in the cytosol). In yeast, **fatty acid synthase** is a cytosolic, 2500-kD multifunctional enzyme with the composition $\alpha_6\beta_6$, whereas in animals it is a 534-kD multifunctional enzyme consisting of two identical polypeptide chains. Presumably, such proteins evolved by the joining of previously independent genes for the enzymes.

Although fatty acid synthesis begins with the synthesis of a CoA ester, malonyl-CoA, the growing fatty acid is anchored to **acyl-carrier protein**

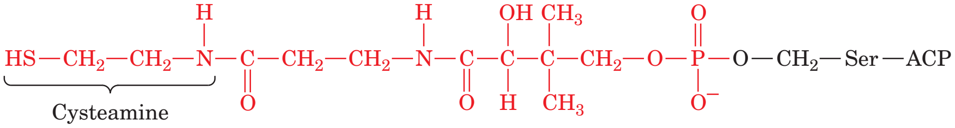

Phosphopantetheine prosthetic group of ACP

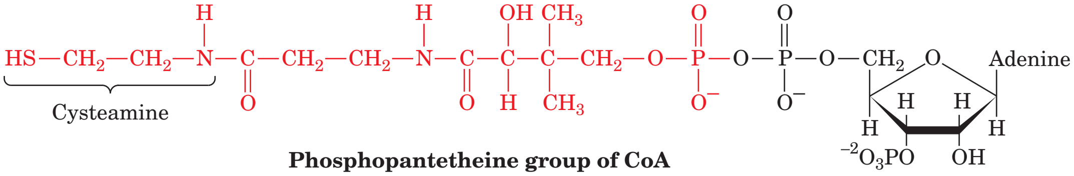

Phosphopantetheine group of CoA

Figure 20-25 | The phosphopantetheine group in acyl-carrier protein (ACP) and in CoA.

(**ACP;** Fig. 20-25). ACP, like CoA, contains a phosphopantetheine group that forms a thioester with an acyl group. The phosphopantetheine phosphoryl group is esterified with a Ser OH group of ACP, whereas in CoA it is linked to AMP. In *E. coli,* ACP is a 10-kD polypeptide, whereas in animals it is part of the multifunctional fatty acid synthase.

The reactions catalyzed by mammalian fatty acid synthase are diagrammed in Fig. 20-26:

1. These are priming reactions in which the synthase is "loaded" with the precursors for the condensation reaction. In mammals, **malonyl/acetyl-CoA-ACP transacylase (MAT)** catalyzes two similar reactions at a single active site: An acetyl group originally linked as a thioester in acetyl-CoA is transferred to ACP **(1a),** and a malonyl group is transferred from malonyl-CoA to ACP **(1b).**
2. The **β-ketoacyl-ACP synthase (KS;** also known as **condensing enzyme)** first transfers the acetyl group from ACP to an enzyme Cys residue **(2a).** In the condensation reaction **(2b),** the malonyl-ACP is decarboxylated, and the resulting carbanion attacks the acetyl-thioester to form a four-carbon acetoacetyl-ACP. The decarboxylation reaction drives the condensation reaction:

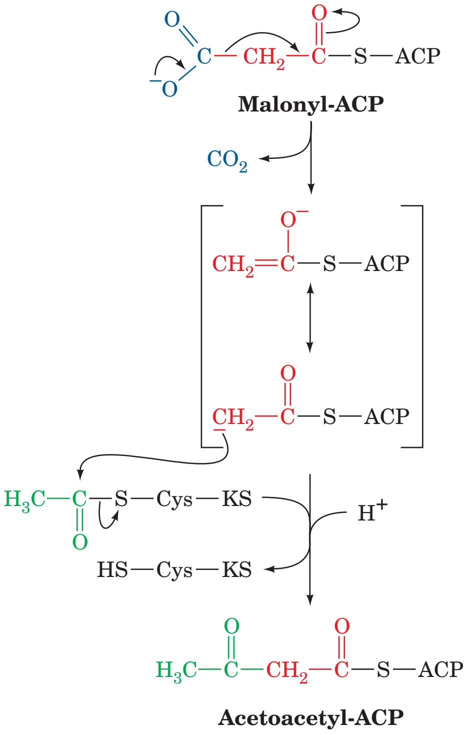

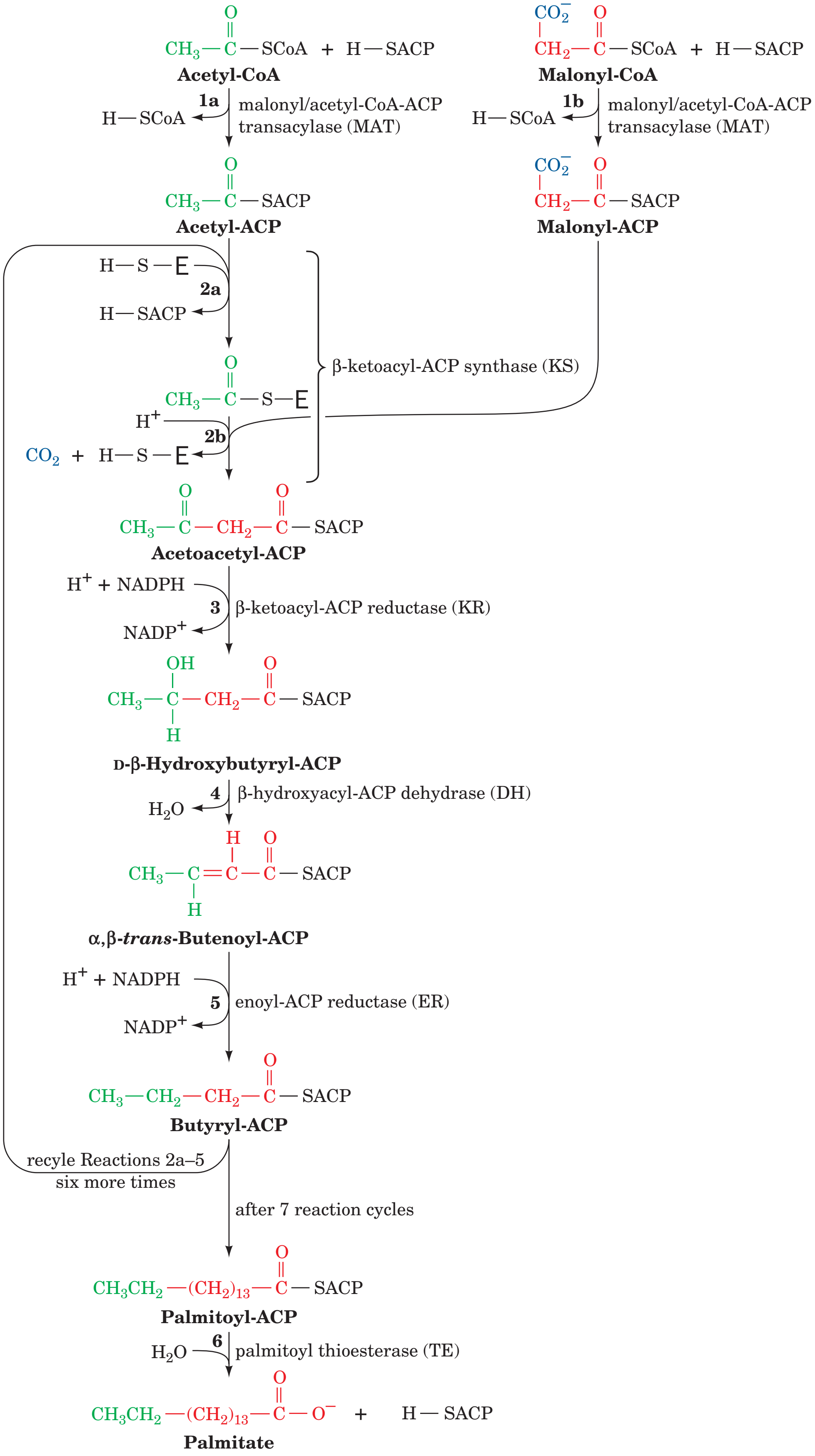
CH₃—C(=O)—SCoA + H—SACP
Acetyl-CoA
CO₂⁻—CH₂—C(=O)—SCoA + H—SACP
Malonyl-CoA
1a
H—SCoA
malonyl/acetyl-CoA-ACP transacylase (MAT)
1b
H—SCoA
malonyl/acetyl-CoA-ACP transacylase (MAT)
CH₃—C(=O)—SACP
Acetyl-ACP
CO₂⁻—CH₂—C(=O)—SACP
Malonyl-ACP
H—S—E
2a
H—SACP
CH₃—C(=O)—S—E
β-ketoacyl-ACP synthase (KS)
H⁺
2b
CO₂ + H—S—E
CH₃—C(=O)—CH₂—C(=O)—SACP
Acetoacetyl-ACP
H⁺ + NADPH
3
NADP⁺
β-ketoacyl-ACP reductase (KR)
CH₃—C(OH)(H)—CH₂—C(=O)—SACP
D-β-Hydroxybutyryl-ACP
4
H₂O
β-hydroxyacyl-ACP dehydrase (DH)
CH₃—C(H)=C(H)—C(=O)—SACP
α,β-trans-Butenoyl-ACP
H⁺ + NADPH
5
NADP⁺
enoyl-ACP reductase (ER)
CH₃—CH₂—CH₂—C(=O)—SACP
Butyryl-ACP
recyle Reactions 2a–5 six more times
after 7 reaction cycles
CH₃CH₂—(CH₂)₁₃—C(=O)—SACP
Palmitoyl-ACP
H₂O
6
palmitoyl thioesterase (TE)
CH₃CH₂—(CH₂)₁₃—C(=O)—O⁻ + H—SACP
Palmitate

Figure 20-26 | Reaction sequence for the biosynthesis of fatty acids. In forming palmitate, the pathway is repeated for seven cycles of C_2 elongation followed by a final hydrolysis step. **See the Animated Figures.**

3–5. Two reductions and a dehydration convert the β-keto group to an alkyl group. The coenzyme in both reductive steps is NADPH. In β oxidation, the analogs of Reactions 3 and 5, respectively, use NAD^+ and FAD (Fig. 20-12, Reactions 3 and 1). Moreover, Reaction 4 requires a D-β-hydroxyacyl substrate, whereas the analogous reaction in β oxidation forms the corresponding L isomer.

At this point, the acyl group, originally an acetyl group, has been elongated by a C_2 unit. This butyryl group is then transferred from ACP to the Cys—SH of the enzyme (a repeat of Reaction 2a) so that it can be extended by additional rounds of the fatty acid synthase reaction sequence. Note that the malonyl-CoA synthesized by the acetyl-CoA carboxylase reaction is decarboxylated in the condensation reaction. The formation of a C—C bond is an endergonic process requiring an activated precursor. Malonyl-ACP is a β-keto ester whose exergonic decarboxylation yields the acetyl-ACP carbanion required for C—C bond formation. The free energy required for the overall reaction is supplied by the ATP hydrolysis in the acetyl-CoA carboxylase reaction, which generates the malonyl-CoA precursor of malonyl-ACP. This carboxylation–decarboxylation sequence is similar to the activation of pyruvate to oxaloacetate for conversion to phosphoenolpyruvate in gluconeogenesis (Section 16-4A).

In each reaction cycle, the ACP is "reloaded" with a malonyl group, and the acyl chain grows by two carbon atoms. Note that each new acetyl unit donated by malonyl-CoA adds to the growing acyl chain at its point of attachment to the enzyme. Thus, the fatty acid grows from its thioester end, not from its methyl end (likewise, fatty acids are catabolized from their thioester ends).

Seven cycles of elongation are required to form **palmitoyl-ACP.** The thioester bond is then hydrolyzed by **palmitoyl thioesterase** (**TE;** Fig. 20-26, Reaction 6), yielding palmitate, the normal product of the fatty acid synthase pathway, and regenerating the enzyme for a new round of synthesis.

The stoichiometry of palmitate synthesis is therefore

$$\begin{aligned}&\text{Acetyl-CoA} + 7\ \text{malonyl-CoA} + 14\ \text{NADPH} + 7\ \text{H}^+ \rightarrow \\ &\qquad \text{palmitate} + 7\ \text{CO}_2 + 14\ \text{NADP}^+ + 8\ \text{CoA} + 6\ \text{H}_2\text{O}\end{aligned}$$

Since the 7 malonyl-CoA are derived from acetyl-CoA as follows:

$$\begin{aligned}&7\ \text{Acetyl-CoA} + 7\ \text{CO}_2 + 7\ \text{ATP} \rightarrow \\ &\qquad 7\ \text{malonyl-CoA} + 7\ \text{ADP} + 7\ \text{P}_i + 7\ \text{H}^+\end{aligned}$$

the overall stoichiometry for palmitate biosynthesis is

$$\begin{aligned}&8\ \text{Acetyl-CoA} + 14\ \text{NADPH} + 7\ \text{ATP} \rightarrow \\ &\qquad \text{palmitate} + 14\ \text{NADP}^+ + 8\ \text{CoA} + 6\ \text{H}_2\text{O} + 7\ \text{ADP} + 7\ \text{P}_i\end{aligned}$$

The Two Halves of Fatty Acid Synthase Operate in Concert. In animals, the seven reactions of fatty acid synthesis are localized to six discrete active sites (MAT carries out two reactions, 1a and 1b). The enzymatic activities are arranged along the polypeptide chain as indicated in Fig. 20-27*a*. Several other enzymes exhibit similar multifunctionality, but none has as many separate catalytic activities as animal fatty acid synthase. A model of the structure of fatty acid synthase is shown in Fig. 20-27*b*. The two subunits form an asymmetric X with two reaction chambers, each defined by a full set of catalytic domains.

The condensation reaction (2b) requires the juxtaposition of the sulfhydryl group of an ACP phosphopantetheine and the active site Cys

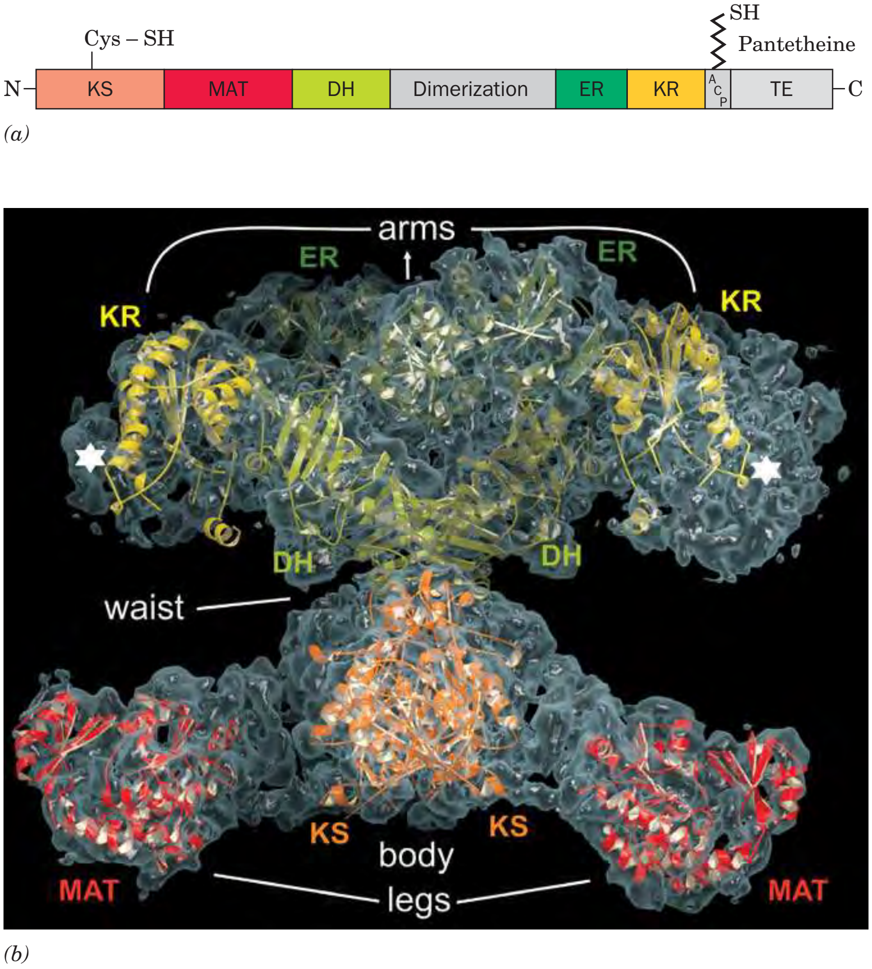

Figure 20-27 | Structure of mammalian fatty acid synthase. (*a*) Order of enzymatic activities along the polypeptide chain. The abbreviations for each enzyme activity are given in Fig. 20-26. (*b*) X-ray structure of porcine fatty acid synthase at low 4.5 (Å) resolution. Models of each catalytic domain, based on the high resolution structures of the homologous bacterial enzymes, were fitted to the electron density and colored as in Part *a*. White stars represent the likely location of ACP and the TE domain. [Courtesy of Nenad Ban and Tim Maier, Swiss Federal Institute of Technology. PDBid 2CF2.]

residue, which are located at opposite ends of the fatty acid synthase monomer. Experiments with fatty acid synthase mutants indicate that these groups can interact in the monomer. However, in native fatty acid synthase, which is a dimer, the interacting groups more often belong to different monomers. This suggests that the adjacent arms and legs in the structure shown in Fig. 20-27*b* belong to different subunits. Presumably, the arms and legs flex up and down, allowing the long, flexible phosphopantetheine chain of ACP to transport the substrate between the various catalytic sites. The flexible lipoyllysyl arms of the pyruvate dehydrogenase multienzyme complex (Section 17-2B) perform a similar function in that enzyme. Because fatty acid synthase is a dimer, two fatty acids can be synthesized simultaneously.

In well-nourished individuals, fatty acid synthesis proceeds at a low rate. However, certain tissues, particularly malignancies, express high levels of fatty acid synthase and produce fatty acids at a high rate. Consequently, inhibitors of fatty acid synthase may act as anticancer agents. One widely used antibacterial agent is actually an inhibitor of bacterial fatty acid synthesis (Box 20-3).

D | Fatty Acids May Be Elongated and Desaturated

Palmitate, a saturated C_{16} fatty acid, is converted to longer chain saturated and unsaturated fatty acids through the actions of **elongases** and **desaturases.** Elongases are present in both the mitochondria and the endoplasmic

BOX 20-3 PERSPECTIVES IN BIOCHEMISTRY

Triclosan: An Inhibitor of Fatty Acid Synthesis

Many cosmetics, toothpastes, antiseptic soaps, and even plastic toys and kitchenware contain the compound 5-chloro-2-(2,4-dichlorophenoxy)phenol, better known as triclosan:

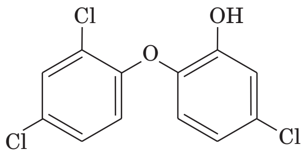

Triclosan

This compound has been used for over 30 years as an antibacterial agent, although its mechanism of action was not understood until recently.

[S.T. Yiap/Alamy Images.]

Triclosan was long believed to act as a general microbicide, which meant that it killed nonspecifically, much like household bleach or ultraviolet light. Such nonspecific microbicides are effective because it is difficult for bacteria to evolve specific resistance mechanisms. However, triclosan actually operates more like an antibiotic with a specific biochemical target, in this case, one of the enzymes of fatty acid synthesis (in bacteria, the enzymes are separate proteins, not part of a multifunctional fatty acid synthase). *In bacteria, triclosan inhibits enoyl-ACP reductase* (which catalyzes Step 5 as shown in Fig. 20-26).

The enzyme's natural substrate has a K_M of about 22 μM, but the dissociation constant for the inhibitor is 20 to 40 pM, indicating extremely tight binding. In the active site, one of the phenyl rings of triclosan, whose structure mimics the structure of the reaction intermediate, stacks on top of the nicotinamide ring of the NADPH cofactor. Triclosan also binds through van der Waals interactions and hydrogen bonds with amino acid residues in the active site. Some *E. coli* strains that are resistant to triclosan have mutations in one of these contact residues.

The specific action of triclosan as an inhibitor of a fatty acid synthesis enzyme and the existence of resistant bacterial strains indicate that triclosan is subject to the same drawbacks as other antibiotics, namely, the eventual emergence of resistance through gene mutation. The widespread use of triclosan in the home and workplace increases the chances for resistance genes to spread. It is probably only a matter of time before resistance genes are ubiquitous, rendering triclosan useless as an antimicrobial agent.

reticulum, but the mechanisms of elongation at the two sites differ. Mitochondrial elongation (a process independent of the fatty acid synthase pathway in the cytosol) occurs by the successive addition and reduction of acetyl units in a reversal of fatty acid oxidation; the only chemical difference between these two pathways occurs in the final reduction step in which NADPH takes the place of $FADH_2$ as the terminal redox coenzyme (Fig. 20-28). Elongation in the endoplasmic reticulum involves the successive condensations of malonyl-CoA with acyl-CoA. These reactions are each followed by NADPH-dependent reductions similar to those catalyzed by fatty acid synthase, the only difference being that the fatty acid is elongated as its CoA derivative rather than as its ACP derivative.

Unsaturated fatty acids are produced by **terminal desaturases.** Mammalian systems contain four terminal desaturases of broad chain-length specificities designated **Δ^9-, Δ^6-, Δ^5-, and Δ^4-fatty acyl-CoA desaturases.** These nonheme iron–containing enzymes catalyze the general reaction

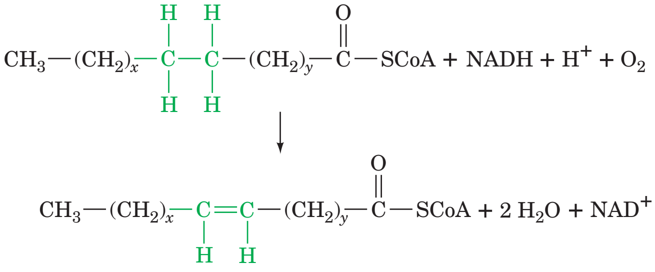

$$CH_3-(CH_2)_x-\underset{H}{\overset{H}{C}}-\underset{H}{\overset{H}{C}}-(CH_2)_y-\overset{O}{\overset{\|}{C}}-SCoA + NADH + H^+ + O_2$$
$$\downarrow$$
$$CH_3-(CH_2)_x-\underset{H}{C}=\underset{H}{C}-(CH_2)_y-\overset{O}{\overset{\|}{C}}-SCoA + 2\,H_2O + NAD^+$$

where x is at least five and where $(CH_2)_x$ can contain one or more double bonds. The $(CH_2)_y$ portion of the substrate is always saturated. Double bonds are inserted between existing double bonds in the $(CH_2)_x$ portion of the substrate and the CoA group such that the new double bond is three carbon atoms closer to the CoA group than the next double bond (not conjugated to an existing double bond) and, in animals, never at positions beyond C9.

Certain Polyunsaturated Fatty Acids Must Be Obtained in the Diet. A variety of unsaturated fatty acids can be synthesized by combinations of elongation and desaturation reactions. However, since palmitic acid is the shortest available fatty acid in animals, the above rules preclude the formation of the Δ^{12} double bond of linoleic acid ($\Delta^{9,12}$-octadecadienoic acid; a polyunsaturated fatty acid), a required precursor of **prostaglandins** and other **eicosanoids** (Section 9-1F). *Linoleic acid must consequently be obtained in the diet (ultimately from plants that have Δ^{12}- and Δ^{15}-desaturases) and is therefore an **essential fatty acid.*** Indeed, animals maintained on a fat-free diet develop an ultimately fatal condition that is initially characterized by poor growth, poor wound healing, and dermatitis. Linoleic acid is also an important constituent of epidermal sphingolipids that function as the skin's water permeability barrier: Animals deprived of linoleic acid must drink far more water than those with an adequate diet.

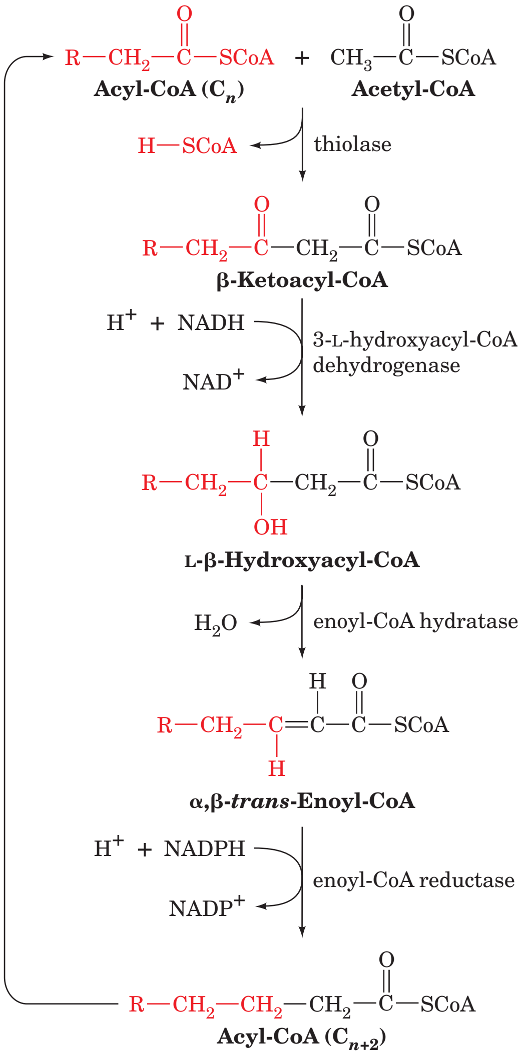

Acyl-CoA (C_n)
Acetyl-CoA
H—SCoA
thiolase
β-Ketoacyl-CoA
H^+ + NADH
NAD^+
3-L-hydroxyacyl-CoA dehydrogenase
L-β-Hydroxyacyl-CoA
H_2O
enoyl-CoA hydratase
α,β-*trans*-Enoyl-CoA
H^+ + NADPH
$NADP^+$
enoyl-CoA reductase
Acyl-CoA (C_{n+2})

Figure 20-28 | Mitochondrial fatty acid elongation. This process is the reverse of fatty acid oxidation (Fig. 20-12) except that the final reaction employs NADPH rather than $FADH_2$ as its redox coenzyme.

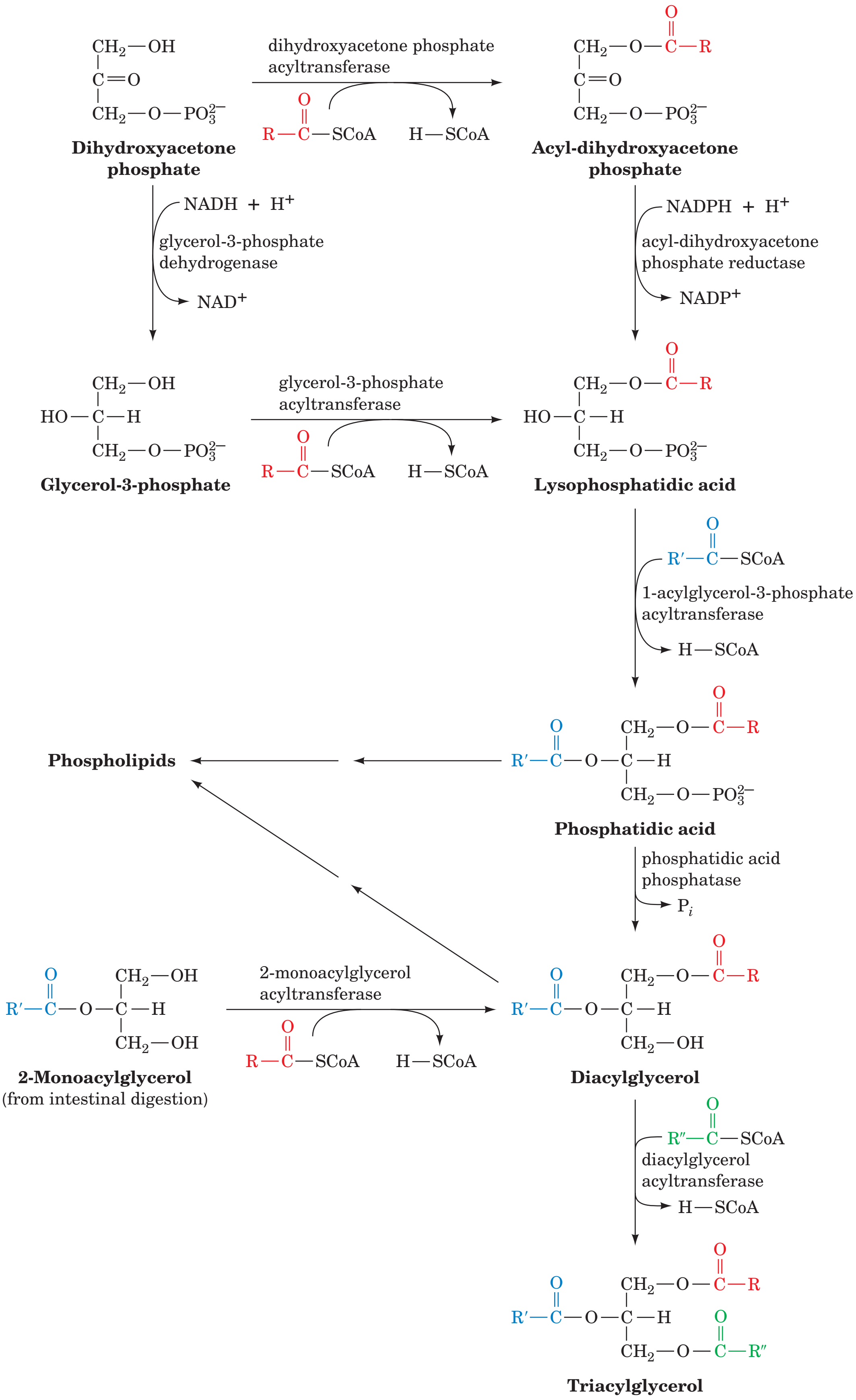
Dihydroxyacetone phosphate
dihydroxyacetone phosphate acyltransferase
R—C(=O)—SCoA
H—SCoA
Acyl-dihydroxyacetone phosphate
NADH + H+
glycerol-3-phosphate dehydrogenase
NAD+
NADPH + H+
acyl-dihydroxyacetone phosphate reductase
NADP+
Glycerol-3-phosphate
glycerol-3-phosphate acyltransferase
R—C(=O)—SCoA
H—SCoA
Lysophosphatidic acid
R′—C(=O)—SCoA
1-acylglycerol-3-phosphate acyltransferase
H—SCoA
Phospholipids
Phosphatidic acid
phosphatidic acid phosphatase
Pi
2-Monoacylglycerol
(from intestinal digestion)
2-monoacylglycerol acyltransferase
R—C(=O)—SCoA
H—SCoA
Diacylglycerol
R″—C(=O)—SCoA
diacylglycerol acyltransferase
H—SCoA
Triacylglycerol

Figure 20-29 | **The reactions of triacylglycerol biosynthesis.**

E | Fatty Acids Are Esterified to Form Triacylglycerols

Triacylglycerols are synthesized from fatty acyl-CoA esters and glycerol-3-phosphate or dihydroxyacetone phosphate (Fig. 20-29, *opposite*). The initial step in this process is catalyzed either by **glycerol-3-phosphate acyltransferase** in mitochondria and the endoplasmic reticulum, or by **dihydroxyacetone phosphate acyltransferase** in the endoplasmic reticulum or peroxisomes. In the latter case, the product acyl-dihydroxyacetone phosphate is reduced to the corresponding **lysophosphatidic acid** by an NADPH-dependent reductase. The lysophosphatidic acid is converted to a triacylglycerol by the successive actions of **1-acylglycerol-3-phosphate acyltransferase, phosphatidic acid phosphatase,** and **diacylglycerol acyltransferase.** The intermediate phosphatidic acid and 1,2-diacylglycerol can also be converted to phospholipids by the pathways described in Section 20-6A. The acyltransferases are not completely specific for particular fatty acyl-CoAs, either in chain length or degree of unsaturation, but in human adipose tissue triacylglycerols, palmitate tends to be concentrated at position 1 and oleate at position 2.

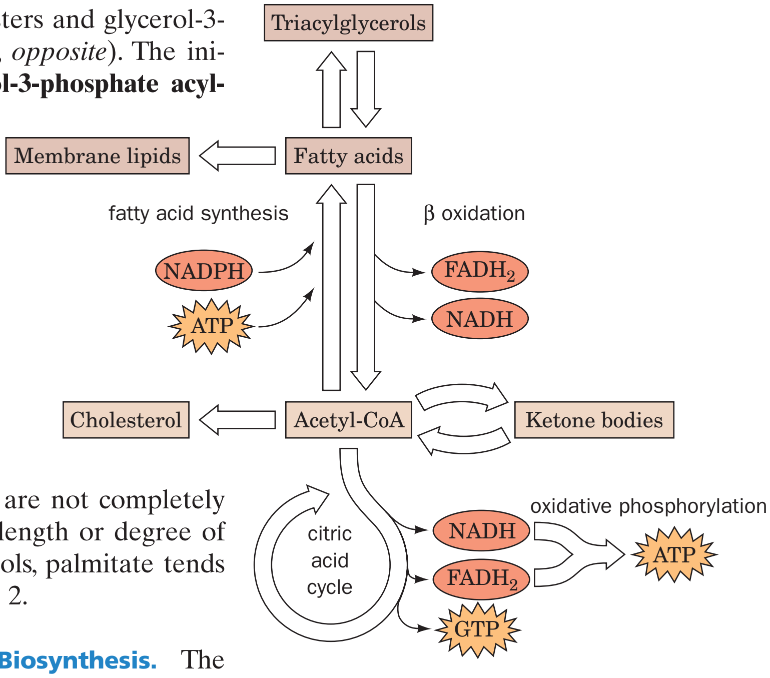

■ **Figure 20-30 | A summary of lipid metabolism.**

Glyceroneogenesis Is Important for Triacylglycerol Biosynthesis. The dihydroxyacetone phosphate used to make glycerol-3-phosphate for triacylglycerol synthesis comes either from glucose via the glycolytic pathway (Fig. 15-1) or from oxaloacetate via an abbreviated version of gluconeogenesis (Fig. 16-15) termed **glyceroneogenesis.** Glyceroneogenesis is necessary in times of starvation, since approximately 30% of the fatty acids that enter the liver during a fast are re-esterified to triacylglycerol and exported in VLDL (Section 20-1). Adipocytes also carry out glyceroneogenesis in times of starvation. They do not carry out gluconeogenesis but contain the gluconeogenic enzyme phosphoenolpyruvate carboxykinase (PEPCK), which is upregulated when the glucose concentration is low, and participates in the glyceroneogenesis required for triacylglycerol biosynthesis.

At this point, we can appreciate how triacylglycerols synthesized from fatty acids built from two-carbon acetyl units can be broken back down into acetyl units. In the liver, the resulting acetyl-CoA may be shunted to the formation of ketone bodies and later converted back to acetyl-CoA by another tissue. The acetyl-CoA can then either be used to build fatty acids that are stored as triacylglycerols or be oxidized by the citric acid cycle to generate considerable ATP by oxidative phosphorylation. As we shall see, the flux of material in the direction of triacylglycerol synthesis or triacylglycerol degradation depends on the metabolic energy needs of the organism and the need for synthesis of other compounds, such as membrane lipids (Section 20-6) and cholesterol (Section 20-7A). These key features of lipid metabolism are summarized in Fig. 20-30.

■ **CHECK YOUR UNDERSTANDING**

Compare the shuttle systems for transporting fatty acids into the mitochondria and acetyl-CoA into the cytosol.
Describe the reactions that produce and consume malonyl-CoA during fatty acid synthesis.
Summarize the reactions catalyzed by fatty acid synthase and compare them to the reactions of fatty acid oxidation.
What is the purpose of elongases and desaturases?
Describe how newly made fatty acids are incorporated into triacylglycerols.

5 Regulation of Fatty Acid Metabolism

LEARNING OBJECTIVE

- Understand the hormonal and cellular factors that regulate fatty acid oxidation and synthesis.

Discussions of metabolic control are usually concerned with the regulation of metabolite flow through a pathway in response to the differing energy needs and dietary states of an organism. In mammals, glycogen and triacylglycerols serve as primary fuels for energy-requiring processes and are synthesized in times of plenty for future use. *Synthesis and breakdown of* *glycogen and triacylglycerols are processes that concern the whole organism, with its organs and tissues forming an interdependent network connected by the bloodstream.* The blood carries the metabolites responsible for energy production: triacylglycerols in the form of chylomicrons and VLDL, fatty acids as their albumin complexes, ketone bodies, amino acids, lactate, and glucose. As in glycogen metabolism (Section 16-3), *hormones such as insulin and glucagon regulate the rates of the opposing pathways of lipid metabolism and thereby control whether fatty acids will be oxidized or synthesized.* The major control mechanisms are summarized in Fig. 20-31.

Fatty acid oxidation is regulated largely by the concentration of fatty acids in the blood, which is, in turn, controlled by the hydrolysis rate of triacylglycerols in adipose tissue by **hormone-sensitive triacylglycerol lipase.** This enzyme is so named because it is susceptible to regulation by phosphorylation and dephosphorylation in response to hormonally controlled cAMP levels. Glucagon, epinephrine, and norepinephrine, which are released in times of metabolic need, increase adipose tissue cAMP concentrations. cAMP allosterically activates PKA (Fig. 13-3C), which in turn phosphorylates certain enzymes. Phosphorylation activates hormone-sensitive lipase, thereby stimulating lipolysis in adipose tissue, raising blood fatty acid levels, and ultimately activating the β-oxidation pathway in other tissues such as liver and muscle. In liver, this process leads to the production of ketone bodies that are secreted into the bloodstream for use as an alternative fuel to glucose by peripheral tissues. PKA also inactivates acetyl-CoA carboxylase (Section 20-4B), so *cAMP-dependent phosphorylation simultaneously stimulates fatty acid oxidation and inhibits fatty acid synthesis.*

Insulin, a pancreatic hormone released in response to high blood glucose concentrations (the fed state), has the opposite effect of glucagon and epinephrine: It stimulates the formation of glycogen and triacylglycerols. Insulin decreases cAMP levels, leading to the dephosphorylation and thus the inactivation of hormone-sensitive lipase. This reduces the amount of fatty acid available for oxidation. Insulin also activates acetyl-CoA carboxylase (Section 20-4B). *The glucagon:insulin ratio therefore determines the rate and direction of fatty acid metabolism.*

Another mechanism that inhibits fatty acid oxidation when fatty acid synthesis is stimulated is the inhibition of carnitine palmitoyl transferase I by malonyl-CoA. This inhibition keeps the newly synthesized fatty acids out of the mitochondria (Section 20-2B) and thus away from the β-oxidation system. In fact, heart muscle, an oxidative tissue that does not carry out fatty acid biosynthesis, contains an isoform of acetyl-CoA carboxylase, β-ACC (Section 20-4B), whose sole function appears to be the synthesis of malonyl-CoA to regulate fatty acid oxidation.

AMP-dependent protein kinase (AMPK), which phosphorylates (inactivates) ACC, may itself be an important regulator of fatty acid metabolism. The enzyme is activated by AMP and inhibited by ATP and thus has been proposed to serve as a fuel gauge for the cell. When ATP levels are high, signaling the fed and rested state, this kinase is inhibited, allowing ACC to become dephosphorylated (activated) so as to stimulate malonyl-CoA production for fatty acid synthesis in adipose tissue and for inhibition of fatty acid oxidation in muscle cells. When activity levels increase, causing ATP levels to decrease with a concomitant increase in AMP levels, AMPK is activated to phosphorylate (inactivate) ACC. The resulting decrease in malonyl-CoA levels causes fatty acid biosynthesis to decrease in adipose tissue while fatty acid oxidation increases in muscle to provide the ATP for continued activity.

Factors such as substrate availability, allosteric interactions, and covalent modification (phosphorylation) control enzyme activity with response

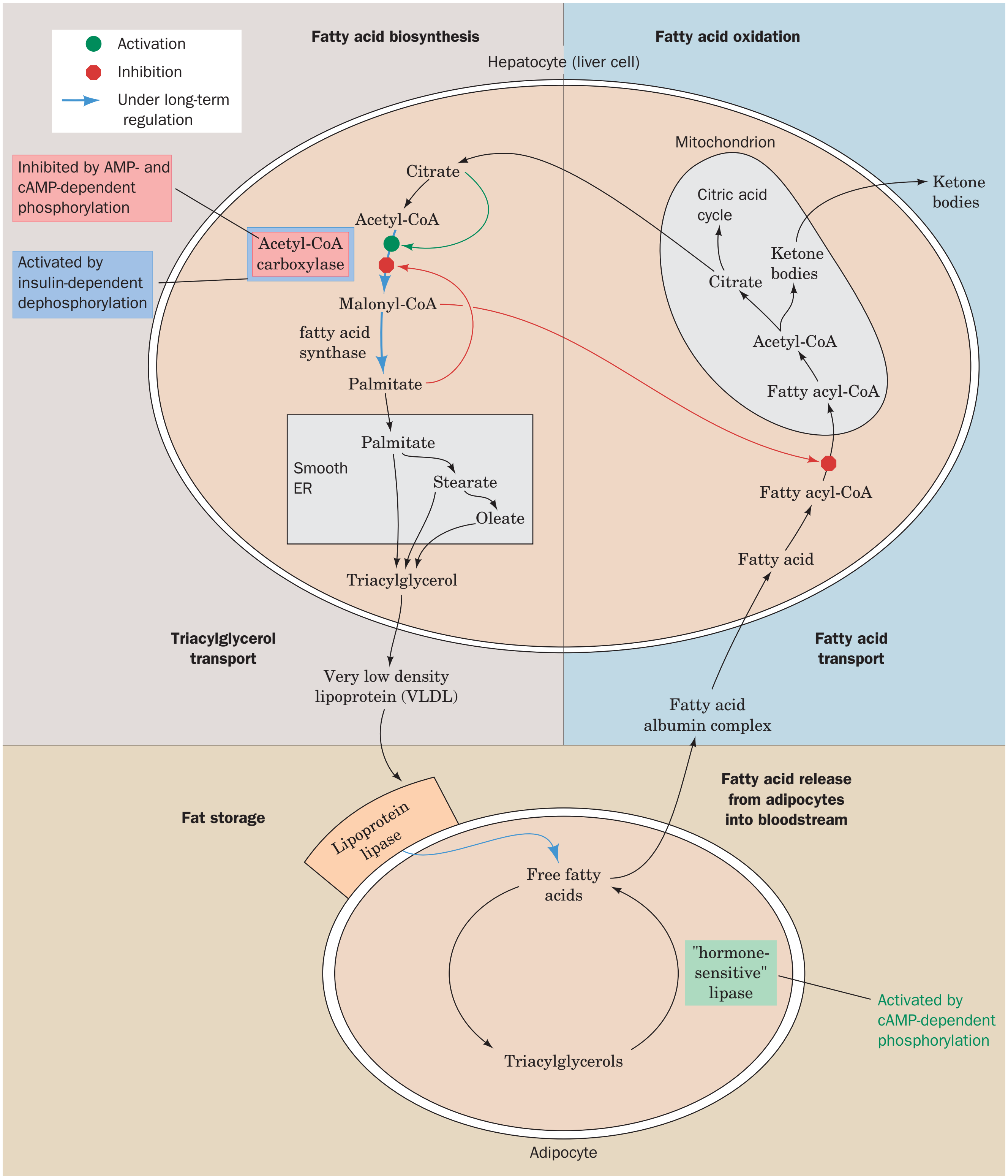
Activation
Inhibition
Under long-term regulation
Fatty acid biosynthesis
Fatty acid oxidation
Hepatocyte (liver cell)
Inhibited by AMP- and cAMP-dependent phosphorylation
Activated by insulin-dependent dephosphorylation
Citrate
Acetyl-CoA
Acetyl-CoA carboxylase
Malonyl-CoA
fatty acid synthase
Palmitate
Smooth ER
Palmitate
Stearate
Oleate
Triacylglycerol
Mitochondrion
Citric acid cycle
Citrate
Ketone bodies
Acetyl-CoA
Fatty acyl-CoA
Ketone bodies
Fatty acyl-CoA
Fatty acid
Triacylglycerol transport
Very low density lipoprotein (VLDL)
Fatty acid transport
Fatty acid albumin complex
Fat storage
Lipoprotein lipase
Fatty acid release from adipocytes into bloodstream
Free fatty acids
"hormone-sensitive" lipase
Activated by cAMP-dependent phosphorylation
Triacylglycerols
Adipocyte

Figure 20-31 | **Sites of regulation of fatty acid metabolism.**

times of minutes or less. Such **short-term regulation** is complemented by **long-term regulation,** which requires hours or days and governs a pathway's regulatory enzyme by altering the amount of enzyme present.

This is accomplished through changes in the rates of protein synthesis and/or breakdown.

The long-term regulation of lipid metabolism includes stimulation by insulin and inhibition by starvation of the synthesis of acetyl-CoA carboxylase and fatty acid synthase. The amount of adipose tissue lipoprotein lipase, the enzyme that initiates the entry of lipoprotein-packaged fatty acids into adipose tissue for storage (Section 20-1B), is also increased by insulin and decreased by starvation. Thus, an abundance of glucose, reflected in the level of insulin, promotes fatty acid synthesis and the storage of fatty acids by adipocytes, whereas starvation, when glucose is unavailable, decreases fatty acid synthesis and the uptake of fatty acids by adipocytes.

CHECK YOUR UNDERSTANDING

Describe the major mechanisms of regulating fatty acid metabolism in humans.

6 Synthesis of Other Lipids

LEARNING OBJECTIVES

- Understand that triacylglycerol precursors are used to synthesize glycerophospholipids.
- Understand that sphingolipids are synthesized from palmitoyl-CoA and serine.
- Understand that prostaglandin synthesis from arachidonate can be blocked by drugs.

Fatty acids are the precursors not just of triacylglycerols but of a variety of other compounds, including membrane lipids and certain signaling molecules. Most membrane lipids are dual-tailed amphipathic molecules composed of either 1,2-diacylglycerol or *N*-acylsphingosine (ceramide) linked to a polar head group that is either a carbohydrate or a phosphate ester (Fig. 20-32). In this section, we describe the biosynthesis of these complex lipids from their simpler components. These lipids are synthesized in membranes, mostly on the cytosolic face of the endoplasmic reticulum, and from there are transported in vesicles to their final cellular destinations (Section 9-4E). Arachidonate groups released from membrane lipids give rise to prostaglandins of various types.

A | Glycerophospholipids Are Built from Intermediates of Triacylglycerol Synthesis

Glycerophospholipids have significant asymmetry in their C1- and C2-linked fatty acyl groups: C1 substituents are mostly saturated fatty acids, whereas those at C2 are by and large unsaturated fatty acids.

Activated Head Groups or Activated Lipids Are Used to Synthesize Diacylglycerophospholipids. The triacylglycerol precursors 1,2-diacylglycerol and phosphatidic acid are also the precursors of glycerophospholipids (Fig. 20-29). The polar head groups of glycerophospholipids are

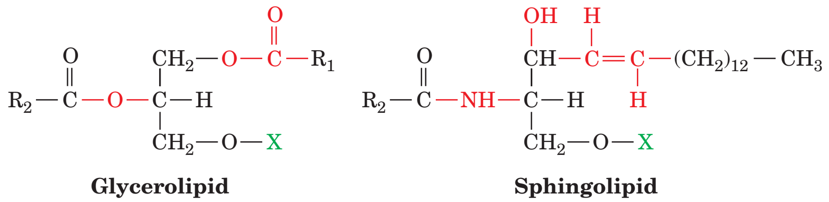

X = H	**1,2-Diacylglycerol**	***N*-Acylsphingosine (ceramide)**
X = Carbohydrate	**Glyceroglycolipid**	**Sphingoglycolipid (glycosphingolipid)**
X = Phosphate ester	**Glycerophospholipid**	**Sphingophospholipid**

Figure 20-32 | Glycerolipids and sphingolipids. The structures of the common head groups, X, are presented in Table 9-2. Plant membranes are particularly rich in glyceroglycolipids.

Figure 20-33 | Biosynthesis of phosphatidylethanolamine and phosphatidylcholine. In mammals, CDP–ethanolamine and CDP–choline are the precursors of the head groups.

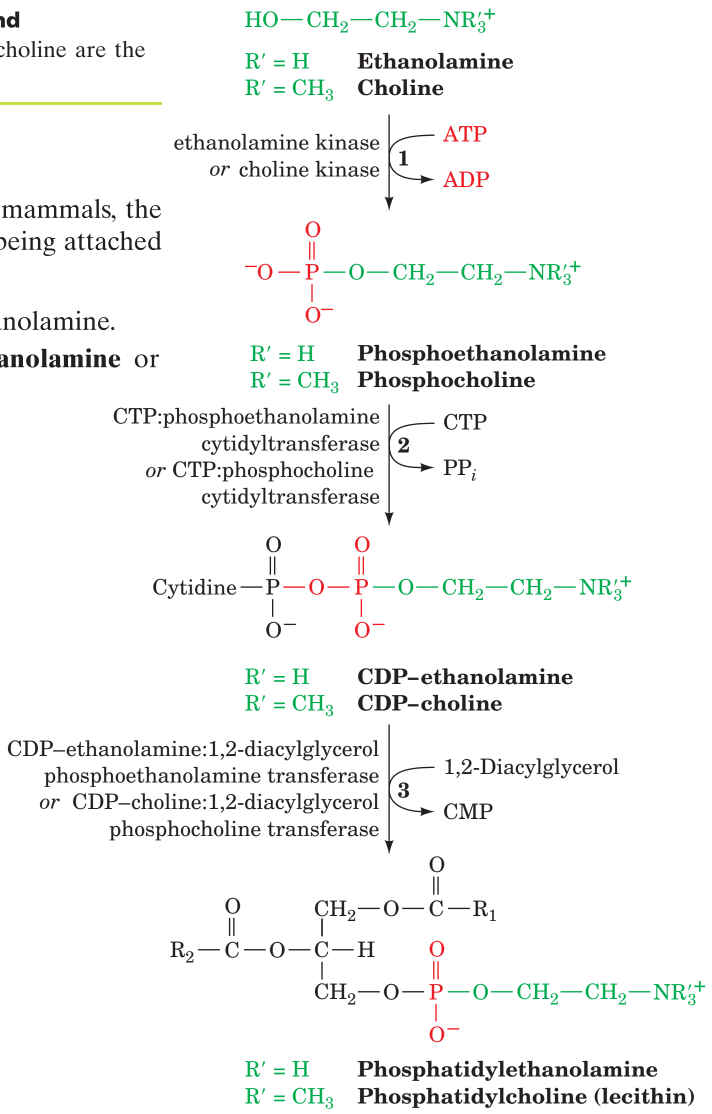
HO—CH₂—CH₂—NR′₃⁺
R′ = H Ethanolamine
R′ = CH₃ Choline
ethanolamine kinase
or choline kinase
1
ATP
ADP
Phosphoethanolamine
Phosphocholine
CTP:phosphoethanolamine cytidyltransferase
or CTP:phosphocholine cytidyltransferase
2
CTP
PPᵢ
Cytidine
CDP–ethanolamine
CDP–choline
CDP–ethanolamine:1,2-diacylglycerol phosphoethanolamine transferase
or CDP–choline:1,2-diacylglycerol phosphocholine transferase
3
1,2-Diacylglycerol
CMP
Phosphatidylethanolamine
Phosphatidylcholine (lecithin)

linked to C3 of the glycerol via a phosphodiester bond. In mammals, the head groups **ethanolamine** and **choline** are activated before being attached to the lipid (Fig. 20-33):

1. ATP phosphorylates the OH group of choline or ethanolamine.
2. The phosphoryl group of the resulting **phosphoethanolamine** or **phosphocholine** then attacks CTP, displacing PP_i, to form the corresponding CDP derivatives, which are activated phosphate esters of the polar head group.
3. The C3-OH group of 1,2-diacylglycerol attacks the phosphoryl group of the activated CDP–ethanolamine or CDP–choline, displacing CMP to yield the corresponding glycerophospholipid.

In liver, phosphatidylethanolamine can also be converted to phosphatidylcholine by the addition of methyl groups.

Phosphatidylserine is synthesized from phosphatidylethanolamine by a head group exchange reaction catalyzed by **phosphatidylethanolamine serine transferase** in which serine's OH group attacks the donor's phosphoryl group. The original head group is then eliminated, forming phosphatidylserine:

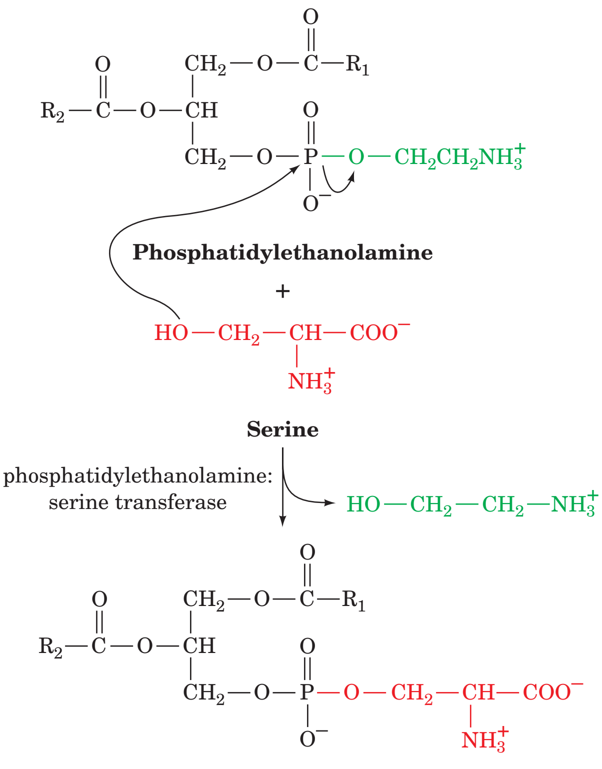
Phosphatidylethanolamine
+
Serine
phosphatidylethanolamine:
serine transferase
HO—CH₂—CH₂—NH₃⁺

Phosphatidylserine

In the synthesis of **phosphatidylinositol** and **phosphatidylglycerol,** the hydrophobic tail is activated rather than the polar head group.

Phosphatidic acid, the precursor of 1,2-diacylglycerol (Fig. 20-29), attacks the α-phosphoryl group of CTP to form the activated **CDP–diacylglycerol** and PP_i (Fig. 20-34). Phosphatidylinositol results from the attack of inositol on CDP–diacylglycerol. Phosphatidylglycerol is formed in two reactions: (1) attack of the C1-OH group of glycerol-3-phosphate on CDP–diacylglycerol, yielding **phosphatidylglycerol phosphate;** and (2) hydrolysis of the phosphoryl group to form phosphatidylglycerol.

Cardiolipin forms by the condensation of two molecules of phosphatidylglycerol with the elimination of one molecule of glycerol:

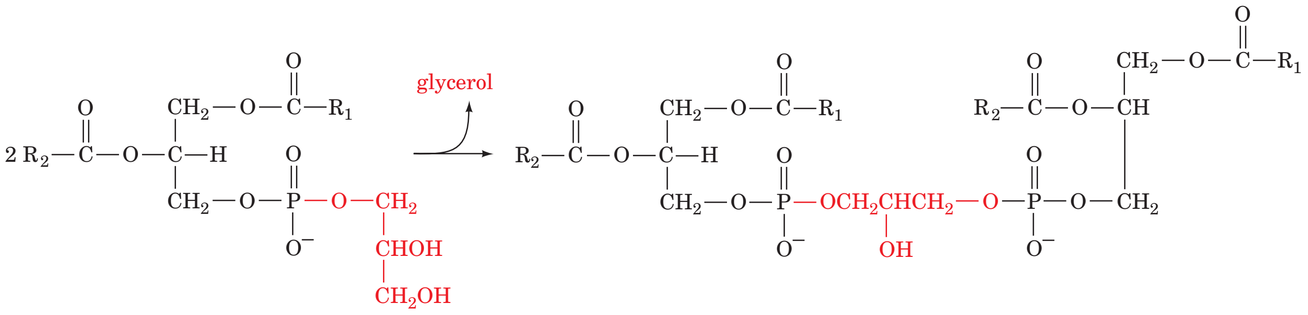

Phosphatidylglycerol **Cardiolipin**

Enzymes that synthesize phosphatidic acid have a general preference for saturated fatty acids at C1 and for unsaturated fatty acids at C2. Yet this general preference cannot account, for example, for the observations that ~80% of brain phosphatidylinositol has a stearoyl group (18:0) at C1 and an arachidonoyl group (20:4) at C2, and that ~40% of lung phosphatidylcholine has palmitoyl groups (16:0) at both positions (the latter substance is the major component of the surfactant that prevents the lung from collapsing when air is expelled; its deficiency in premature infants is responsible for respiratory distress syndrome; see Box 9-1). *William Lands showed that such side chain specificity results from "remodeling" reactions in which specific acyl groups of individual glycerophospholipids are exchanged by specific phospholipases and acyltransferases.*

Glycerophospholipids Include the Plasmalogens and Alkylacylglycerophospholipids. Eukaryotic membranes contain significant amounts of two other types of glycerophospholipids: **plasmalogens,** which contain a hydrocarbon chain linked to glycerol C1 via a vinyl ether linkage, and **alkylacylglycerophospholipids,** in which the alkyl substituent at glycerol C1 is attached via an ether linkage.

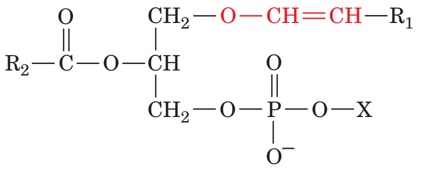

A plasmalogen

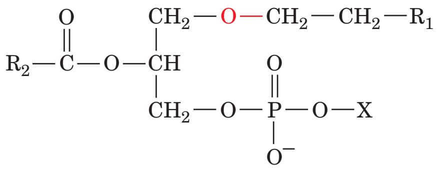

An alkylacylglycerophospholipid

About 20% of mammalian glycerophospholipids are plasmalogens, but the exact percentage varies both among species and among tissues within a given organism. For example, plasmalogens account for only 0.8% of the phospholipids in human liver but 23% of those in human nervous tissue. The alkylacylglycerophospholipids are much less abundant than the

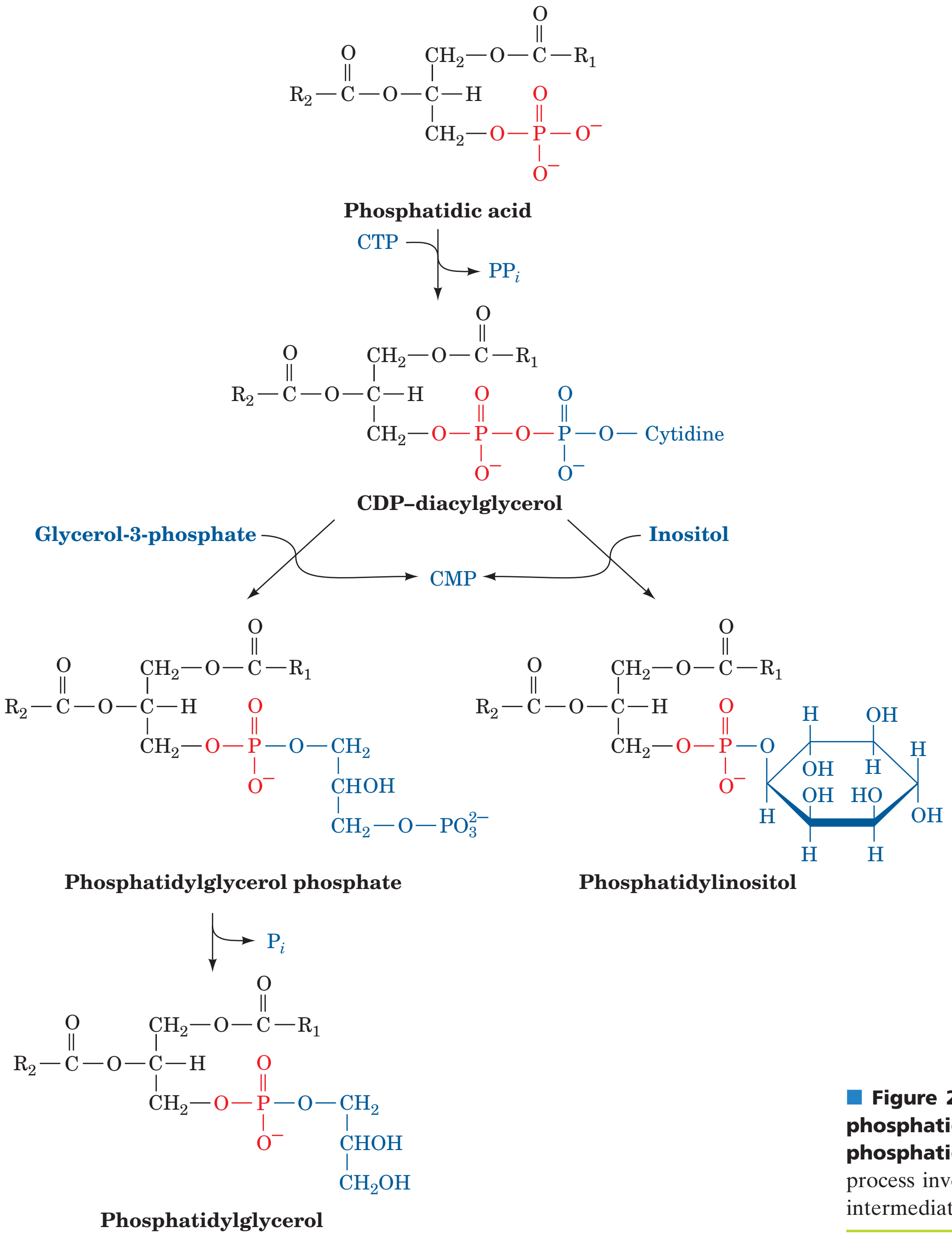
Phosphatidic acid
CTP
PP$_i$
CDP–diacylglycerol
Cytidine
Glycerol-3-phosphate
Inositol
CMP
Phosphatidylglycerol phosphate
Phosphatidylinositol
P$_i$
Phosphatidylglycerol

■ **Figure 20-34 | Biosynthesis of phosphatidylinositol and phosphatidylglycerol.** In mammals, this process involves a CDP–diacylglycerol intermediate.

plasmalogens. The biosynthetic pathway for these lipids yields the alkylacylglycerophospholipid, and this ether is then oxidized to a vinyl ether by the action of a desaturase to yield the plasmalogen.

B | Sphingolipids Are Built from Palmitoyl-CoA and Serine

Most sphingolipids are **sphingoglycolipids;** that is, their polar head groups consist of carbohydrate units. **Cerebrosides** are ceramide monosaccharides, whereas **gangliosides** are sialic acid–containing ceramide oligosaccharides (Section 9-1D). These lipids are synthesized by attaching carbohydrate units to the C1-OH group of ceramide (*N*-acylsphingosine).

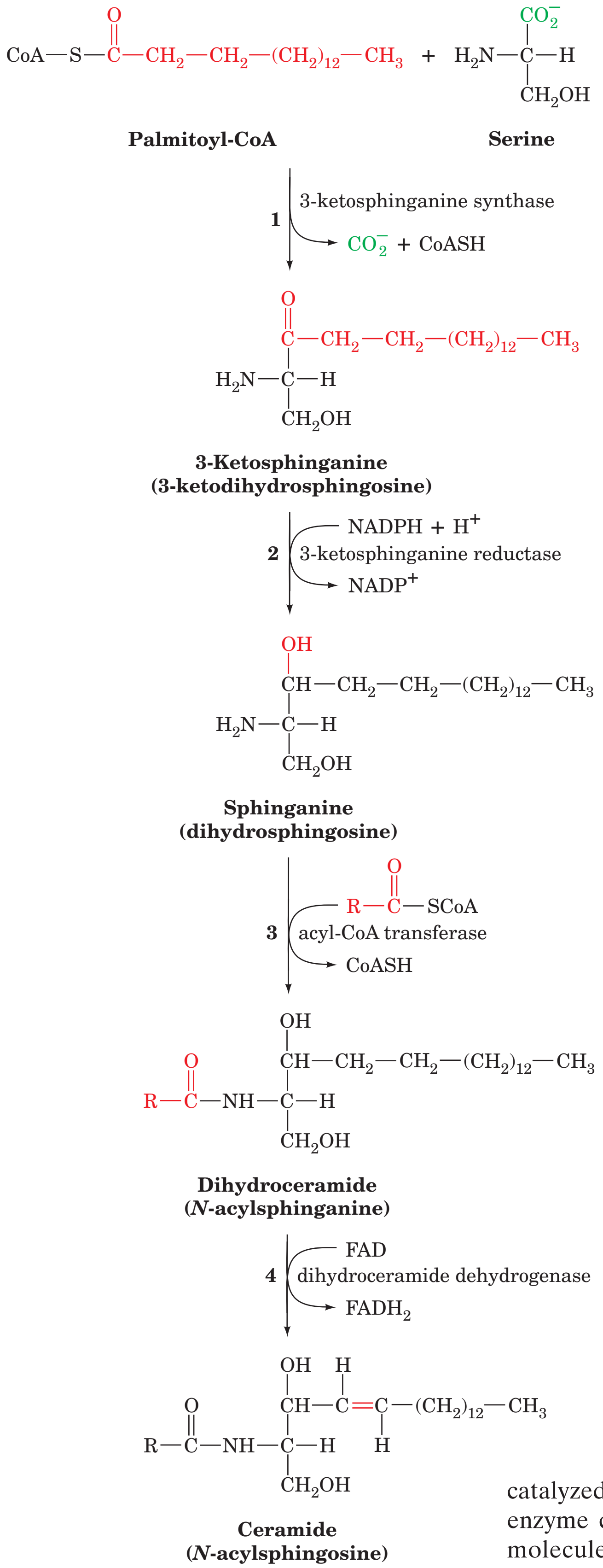
CoA—S—C(=O)—CH₂—CH₂—(CH₂)₁₂—CH₃
+
H₂N—C(CO₂⁻)—H, CH₂OH
Palmitoyl-CoA
Serine
1
3-ketosphinganine synthase
CO₂⁻ + CoASH
3-Ketosphinganine
(3-ketodihydrosphingosine)
2
NADPH + H⁺
3-ketosphinganine reductase
NADP⁺
Sphinganine
(dihydrosphingosine)
3
R—C(=O)—SCoA
acyl-CoA transferase
CoASH
Dihydroceramide
(N-acylsphinganine)
4
FAD
dihydroceramide dehydrogenase
FADH₂
Ceramide
(N-acylsphingosine)

■ **Figure 20-35 | Biosynthesis of ceramide (*N*-acylsphingosine).**

N-Acylsphingosine is synthesized in four reactions from the precursors palmitoyl-CoA and serine (Fig. 20-35):

1. **3-Ketosphinganine synthase** catalyzes condensation of palmitoyl-CoA with serine, yielding **3-ketosphinganine.**
2. **3-Ketosphinganine reductase** catalyzes the NADPH-dependent reduction of 3-ketosphinganine's keto group to form **sphinganine (dihydrosphingosine).**
3. **Dihydroceramide** is formed by transfer of an acyl group from an acyl-CoA to sphinganine's 2-amino group, forming an amide bond.
4. **Dihydroceramide dehydrogenase** converts dihydroceramide to ceramide by an FAD-dependent oxidation reaction.

The nonglycosylated lipid sphingomyelin, an important structural lipid of nerve cell membranes,

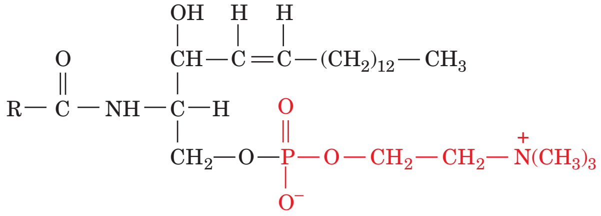

Sphingomyelin

is the product of a reaction in which phosphatidylcholine donates its phosphocholine group to the C1-OH group of *N*-acylsphingosine.

Cerebrosides, which are most commonly 1-β-galactoceramide or 1-β-glucoceramide, are synthesized from ceramide by the addition of the glycosyl unit from the corresponding UDP–hexose to ceramide's C1-OH group. The more elaborate oligosaccharide head groups of gangliosides (Fig. 9-9) are constructed through the action of a series of glycosyltransferases. Defects in the pathways for degrading these complex lipids are responsible for certain **lipid storage diseases** (Box 20-4).

C | C_{20} Fatty Acids Are the Precursors of Prostaglandins

Prostaglandins and related compounds (Fig. 9-12) are derivatives of C_{20} fatty acids such as arachidonate, which is released from membrane phospholipids in response to hormones and other signals. The functions of prostaglandins vary in a tissue-specific manner, but several of them trigger pain, fever, or inflammation. The production of prostaglandins begins with the formation of a cyclopentane ring in the linear fatty acid, as catalyzed by **prostaglandin H_2 synthase** (Fig. 20-36). This heme-containing enzyme contains two catalytic activities: a **cyclooxygenase** that adds two molecules of O_2 to arachidonate, and a **peroxidase** that converts the resulting hydroperoxy group to an OH group. The enzyme is commonly called **COX,** after its cyclooxygenase activity (not to be confused with cytochrome *c* oxidase, which is also called COX).

Figure 20-36 | The prostaglandin H_2 synthase reaction. A cyclooxygenase activity (**1**) catalyzes the additions and rearrangements that generate the cyclopentane ring. The enzyme's peroxidase activity (**2**) converts the peroxide intermediate to prostaglandin H_2 (PGH_2), which is the precursor of other prostaglandins.

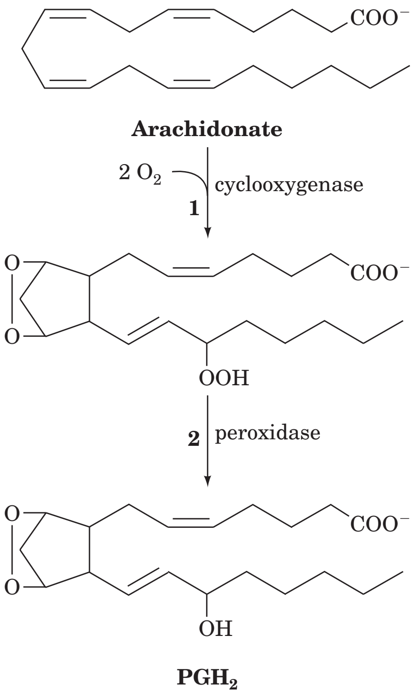

The use of **aspirin** as an analgesic (pain-relieving), antipyretic (fever-reducing), and anti-inflammatory agent has been widespread since the nineteenth century. Yet it was not until 1971 that John Vane discovered its mechanism of action: Aspirin inhibits the synthesis of prostaglandins by acetylating a specific Ser residue of prostaglandin H_2 synthase, which prevents arachidonate from reaching the cyclooxygenase active site. Other **nonsteroidal anti-inflammatory drugs (NSAIDs)** such as **ibuprofen** and **acetaminophen** noncovalently bind to the enzyme so as to similarly block its active site.

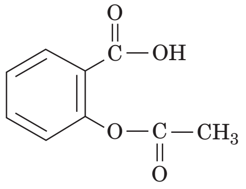

Aspirin (acetylsalicylic acid)

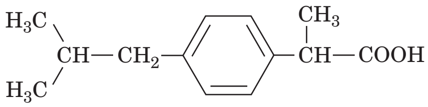

Ibuprofen

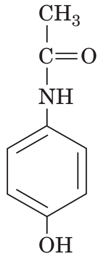

Acetaminophen

COX-2 Inhibitors Lack the Side Effects of Other NSAIDs. Prostaglandin H_2 synthase has two isoforms, **COX-1** and **COX-2,** that share a high degree (60%) of sequence identity and structural homology. COX-1 is constitutively (without regulation) expressed in most, if not all, mammalian tissues, thereby supporting levels of prostaglandin synthesis necessary to maintain organ and tissue homeostasis. In contrast, COX-2 is only expressed in certain tissues in response to inflammatory stimuli and hence is responsible for the elevated prostaglandin levels that cause inflammation.

Aspirin and ibuprofen are relatively nonspecific and therefore can have adverse side effects (e.g., gastrointestinal ulceration) when used to treat inflammation or fever. A structure-based drug design program (Section 12-4) was therefore instituted to create inhibitors that would target COX-2 but not COX-1. The three-dimensional structures of COX-1 and COX-2 are almost identical. However, their amino acid differences make COX-2's active site channel ~20% larger in volume than that of COX-1. Chemists therefore synthesized inhibitors, collectively known as **coxibs,** that could enter the COX-2 channel but are excluded from that of COX-1. Two of these inhibitors, **rofecoxib (Vioxx)** and **celecoxib (Celebrex)** *(at right)*, became major drugs for the treatment of inflammatory diseases such as arthritis because they lack the major side effects of the nonspecific NSAIDs. However, in 2004, Vioxx was withdrawn from the market because of unanticipated cardiac side effects.

Interestingly, acetaminophen, the most commonly used analgesic/antipyretic, binds poorly to both COX-1 and COX-2 and is not (despite its inclusion in this category) an anti-inflammatory agent. Its mechanism of action remained a mystery until Daniel Simmons' recent discovery of a third COX isozyme, **COX-3,** which is expressed at high levels in the central nervous system and is apparently the target of drugs that decrease pain and fever.

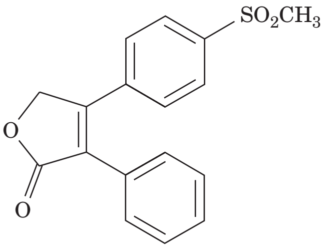

Rofecoxib (Vioxx)

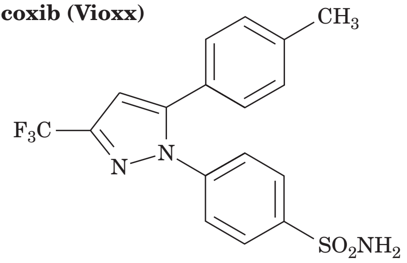

Celecoxib (Celebrex)

CHECK YOUR UNDERSTANDING

Explain how glycerophospholipids are synthesized by activating either the head group or the lipid tail.

Describe the biosynthesis of ceramide, sphingomyelin, and cerebrosides.

Explain the action of drugs such as aspirin, NSAIDs, and coxibs.

BOX 20-4 BIOCHEMISTRY IN HEALTH AND DISEASE

Sphingolipid Degradation and Lipid Storage Diseases

Sphingoglycolipids are lysosomally degraded by a series of enzymatically mediated hydrolytic reactions. Below is shown the pathway for the degradation of ganglioside G_{M1} and a related globoside and sulfatide. The abbreviations for the monosaccharide residues are Gal, galactose; GalNAc, *N*-acetylgalactosamine; Glc, glucose; NANA, *N*-acetylneuraminic acid (sialic acid). Cer represents ceramide.

A hereditary defect in one of these enzymes (indicated by a red bar) results in a **sphingolipid storage disease.** The substrate of the missing enzyme therefore accumulates, often with disastrous consequences. In many cases, affected individuals suffer from mental retardation and die in infancy or early childhood. One of the most common lipid storage diseases is **Tay–Sachs disease,** an autosomal recessive deficiency in **hexosaminidase A,** which

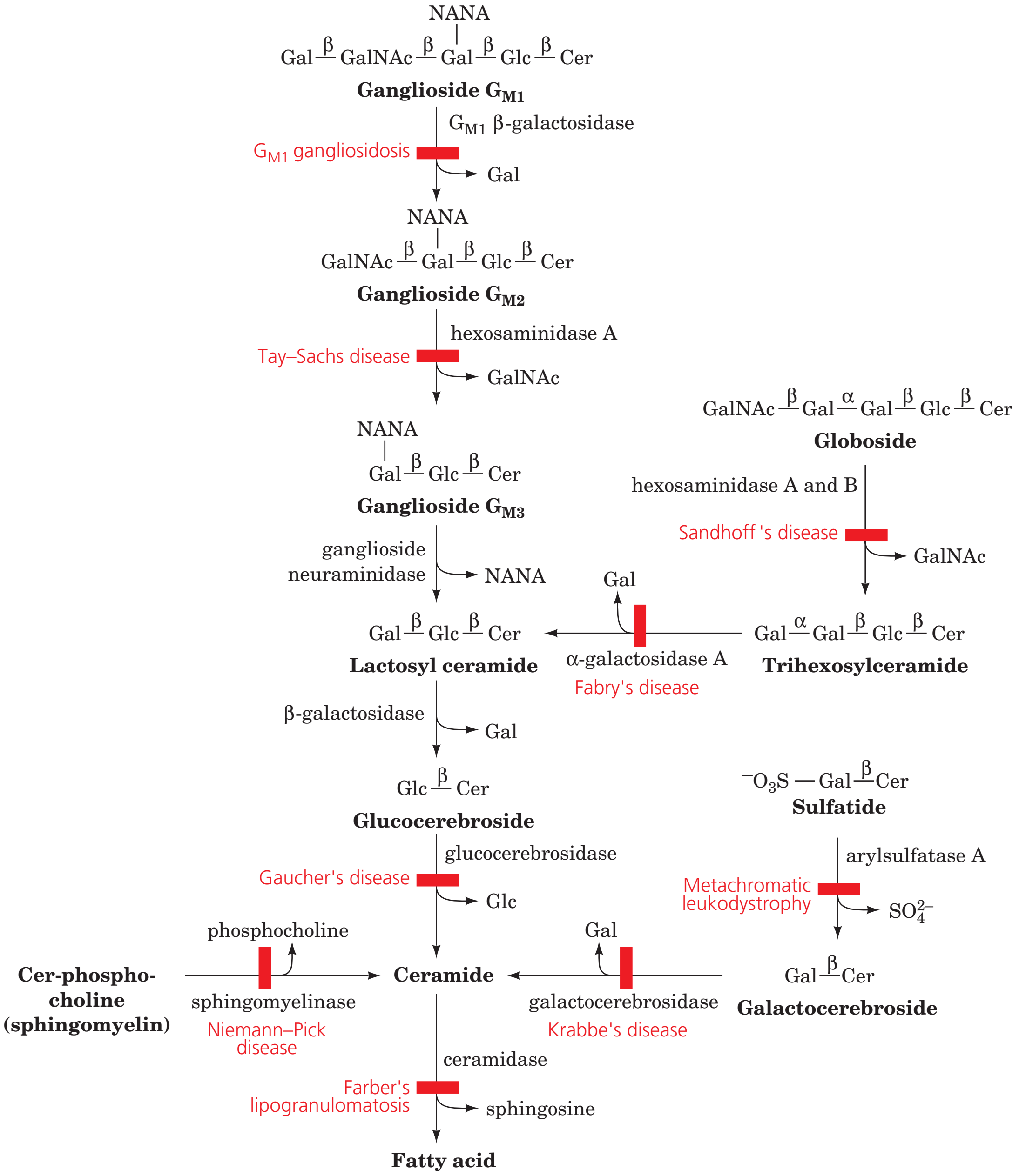
NANA
Gal β GalNAc β Gal β Glc β Cer
Ganglioside G$_{M1}$
G$_{M1}$ β-galactosidase
G$_{M1}$ gangliosidosis
Gal
NANA
GalNAc β Gal β Glc β Cer
Ganglioside G$_{M2}$
hexosaminidase A
Tay–Sachs disease
GalNAc
GalNAc β Gal α Gal β Glc β Cer
Globoside
NANA
Gal β Glc β Cer
Ganglioside G$_{M3}$
hexosaminidase A and B
Sandhoff 's disease
GalNAc
ganglioside neuraminidase
NANA
Gal
Gal β Glc β Cer
Lactosyl ceramide
α-galactosidase A
Fabry's disease
Gal α Gal β Glc β Cer
Trihexosylceramide
β-galactosidase
Gal
Glc β Cer
Glucocerebroside
$^{-}$O$_3$S — Gal β Cer
Sulfatide
glucocerebrosidase
Gaucher's disease
Glc
arylsulfatase A
Metachromatic leukodystrophy
SO$_4^{2-}$
phosphocholine
Gal
Cer-phospho-choline (sphingomyelin)
sphingomyelinase
Niemann–Pick disease
Ceramide
galactocerebrosidase
Krabbe's disease
Gal β Cer
Galactocerebroside
ceramidase
Farber's lipogranulomatosis
sphingosine
Fatty acid

hydrolyzes *N*-acetylgalactosamine from ganglioside G_{M2}. The absence of hexosaminidase A activity results in the accumulation of G_{M2} as shell-like inclusions in neuronal cells as shown below:

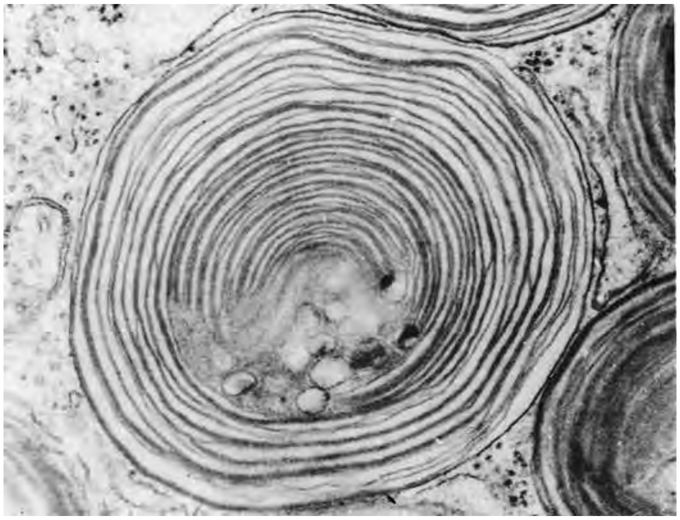

[Photo courtesy of John S. O'Brien, University of California at San Diego.]

Although infants born with Tay–Sachs disease at first appear normal, by ~1 year of age, when sufficient G_{M2} has accumulated to interfere with neuronal function, they become progressively weaker, retarded, and blinded until they die, usually by the age of 3 years. It is possible, however, to screen potential carriers of the disease by a simple serum assay for hexosaminidase A.

Experiments using a mouse model of Tay–Sachs disease suggest that G_{M2} accumulation can be reduced by inhibiting its synthesis. This is accomplished in mice by administering the imino sugar ***N*-butyldeoxynojirimycin,**

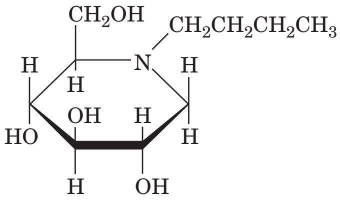

***N*-Butyldeoxynojirimycin**

which inhibits the glycosyltransferase in the first step of glucoceramide synthesis. Similar "substrate deprivation" approaches may be effective in treating other lipid storage diseases, particularly when the defective but essential enzyme has some residual activity.

7 Cholesterol Metabolism

Cholesterol is a vital constituent of cell membranes and the precursor of steroid hormones and bile acids. It is clearly essential to life, yet its deposition in arteries is associated with cardiovascular disease and stroke, two leading causes of death in humans. *In a healthy organism, an intricate balance is maintained between the biosynthesis, utilization, and transport of cholesterol, keeping its harmful deposition to a minimum.* In this section, we study the pathways of cholesterol biosynthesis and transport and how they are controlled.

LEARNING OBJECTIVES

- Understand that acetyl-CoA is converted to cholesterol.
- Understand how cholesterol synthesis is regulated by the amount of HMG-CoA reductase.
- Understand that the LDL receptor keeps circulating cholesterol low.

A | Cholesterol Is Synthesized from Acetyl-CoA

Cholesterol biosynthesis follows a lengthy pathway, first outlined by Konrad Bloch, in which acetate (from acetyl-CoA) is converted to **isoprene units** that have the carbon skeleton of **isoprene:**

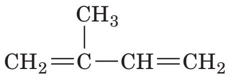

$$CH_2{=}\overset{\overset{\displaystyle CH_3}{|}}{C}{-}CH{=}CH_2$$

Isoprene
(2-methyl-1,3-butadiene)

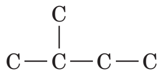

$$C{-}\overset{\overset{\displaystyle C}{|}}{C}{-}C{-}C$$

An isoprene unit

The isoprene units then condense to form a linear molecule with 30 carbons that cyclizes to form the four-ring structure of cholesterol.

HMG-CoA Is a Key Cholesterol Precursor. Acetyl-CoA is converted to isoprene units by a series of reactions that begins with formation of hydroxymethylglutaryl-CoA (HMG-CoA; this compound is also an intermediate in ketone body synthesis; Fig. 20-21). HMG-CoA synthesis requires thiolase and HMG-CoA synthase. In mitochondria, these two enzymes form HMG-CoA for ketone body synthesis. Cytosolic isozymes of these two proteins generate the HMG-CoA that is used in cholesterol biosynthesis. Four additional reactions convert HMG-CoA to the isoprenoid intermediate **isopentenyl pyrophosphate** (Fig. 20-37):

1. The CoA thioester group of HMG-CoA is reduced to an alcohol in an NADPH-dependent four-electron reduction catalyzed by **HMG-CoA reductase,** yielding **mevalonate,** a C_6 compound. This is the rate-determining step of cholesterol biosynthesis.
2. The new OH group is phosphorylated by **mevalonate-5-phosphotransferase.**
3. The phosphate group is converted to a pyrophosphate by **phosphomevalonate kinase.**
4. The molecule undergoes an ATP-dependent decarboxylation–dehydration reaction catalyzed by **pyrophosphomevalonate decarboxylase:**

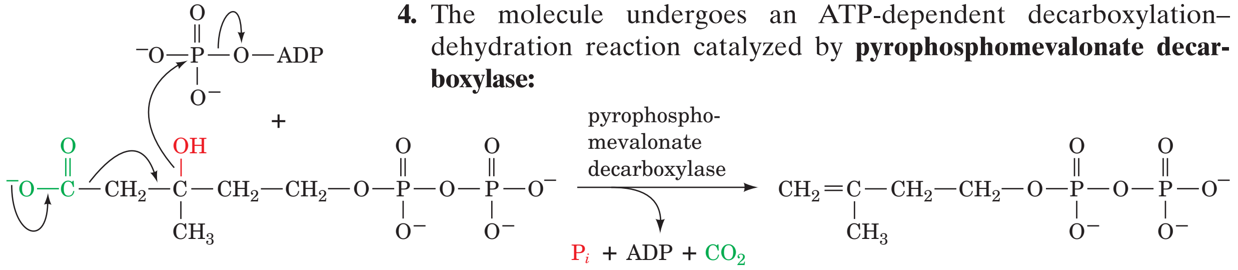

5-Pyrophosphomevalonate

Isopentenyl pyrophosphate

Squalene Is Formed by the Condensation of Six Isoprene Units. Isopentenyl pyrophosphate is converted to **dimethylallyl pyrophosphate** by **isopentenyl pyrophosphate isomerase.**

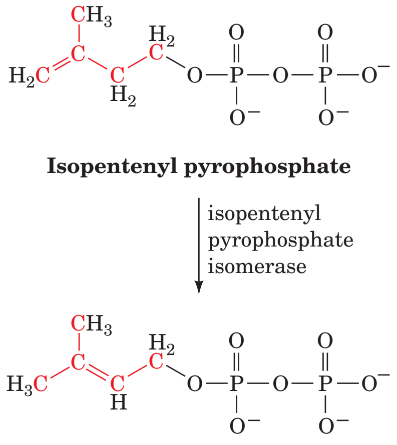

Isopentenyl pyrophosphate

Dimethylallyl pyrophosphate

Four isopentenyl pyrophosphates and two dimethylallyl pyrophosphates condense to form the C_{30} cholesterol precursor **squalene** in three reactions catalyzed by two enzymes (Fig. 20-38):

1. **Prenyltransferase** catalyzes the head-to-tail condensation of

dimethylallyl pyrophosphate and isopentenyl pyrophosphate to yield the C_{10} compound **geranyl pyrophosphate.**

2. Prenyltransferase catalyzes a second head-to-tail condensation of geranyl pyrophosphate and isopentenyl pyrophosphate to yield the C_{15} compound **farnesyl pyrophosphate.** The prenyltransferase

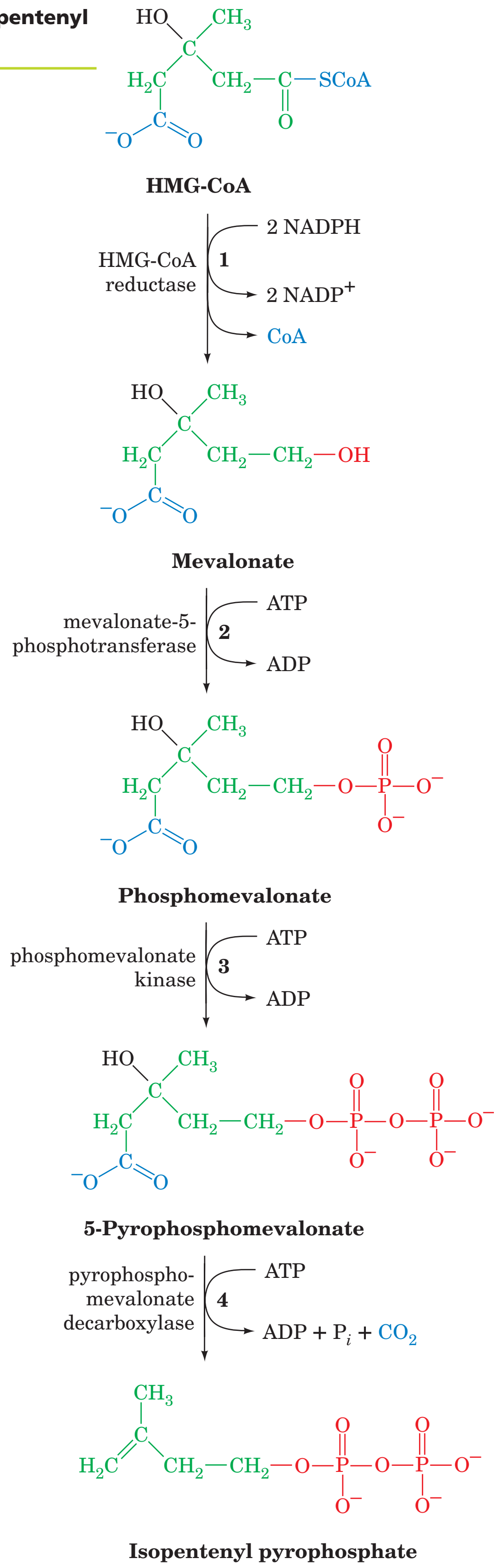
HMG-CoA
HMG-CoA reductase
1
2 NADPH
2 NADP+
CoA
Mevalonate
mevalonate-5-phosphotransferase
2
ATP
ADP
Phosphomevalonate
phosphomevalonate kinase
3
ATP
ADP
5-Pyrophosphomevalonate
pyrophosphomevalonate decarboxylase
4
ATP
ADP + Pi + CO2
Isopentenyl pyrophosphate

■ **Figure 20-37 | Formation of isopentenyl pyrophosphate from HMG-CoA.**

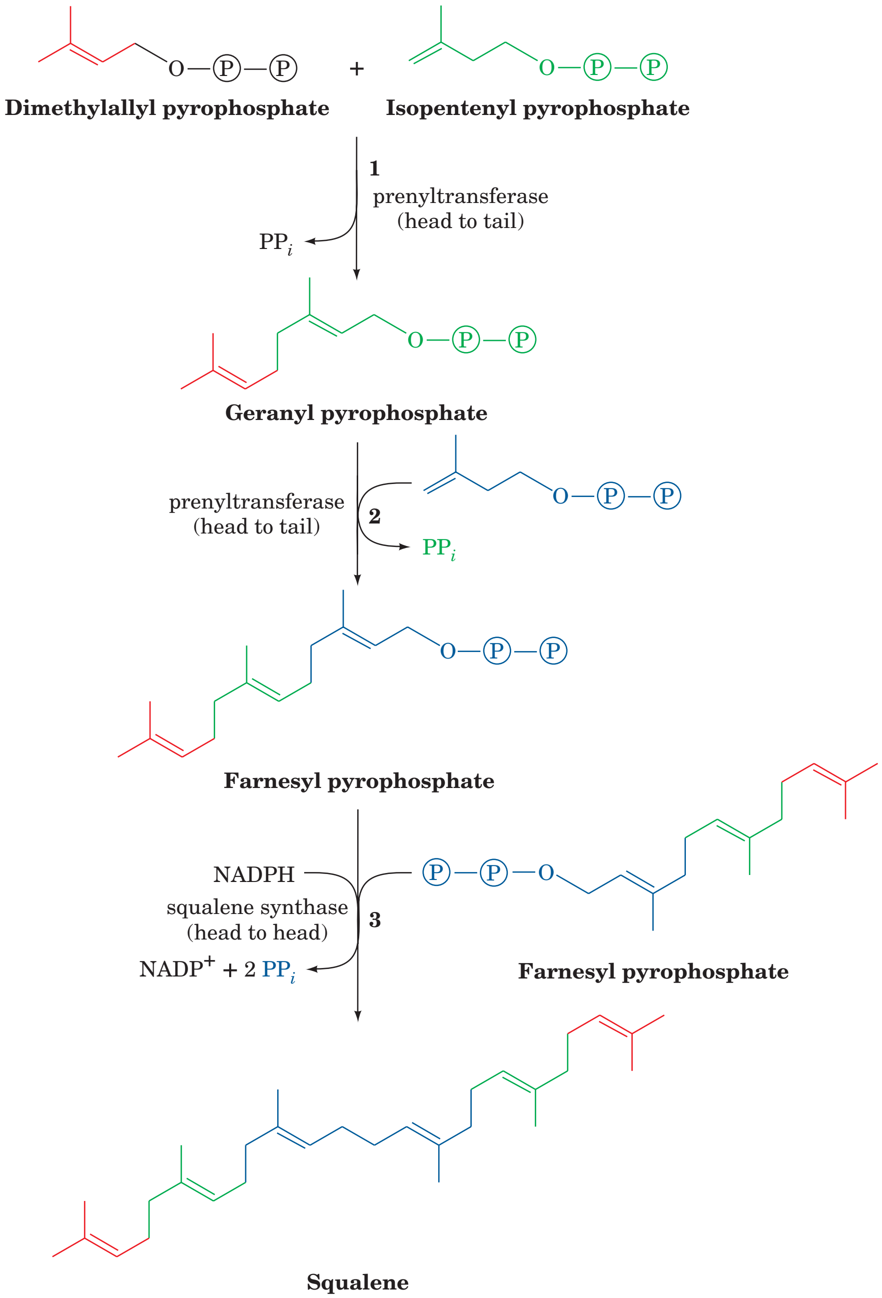
Dimethylallyl pyrophosphate
+
Isopentenyl pyrophosphate
1
prenyltransferase (head to tail)
PPi
Geranyl pyrophosphate
prenyltransferase (head to tail)
2
PPi
Farnesyl pyrophosphate
NADPH
squalene synthase (head to head)
3
NADP+ + 2 PPi
Farnesyl pyrophosphate
Squalene

■ **Figure 20-38 | Formation of squalene from isopentenyl pyrophosphate and dimethylallyl pyrophosphate.** The pathway involves two head-to-tail condensations catalyzed by prenyltransferase and a head-to-head condensation catalyzed by squalene synthase.

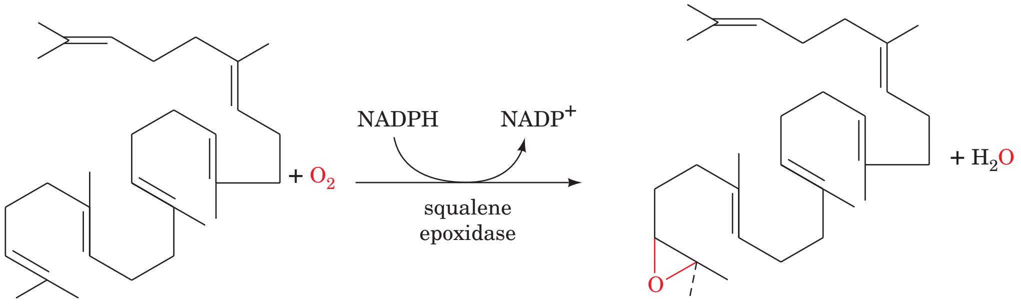

Squalene **2,3-Oxidosqualene**

Figure 20-39 | The squalene epoxidase reaction.

catalyzes an S_N1 reaction to form a carbocation intermediate with an ionization–condensation–elimination mechanism:

Ionization–condensation–elimination

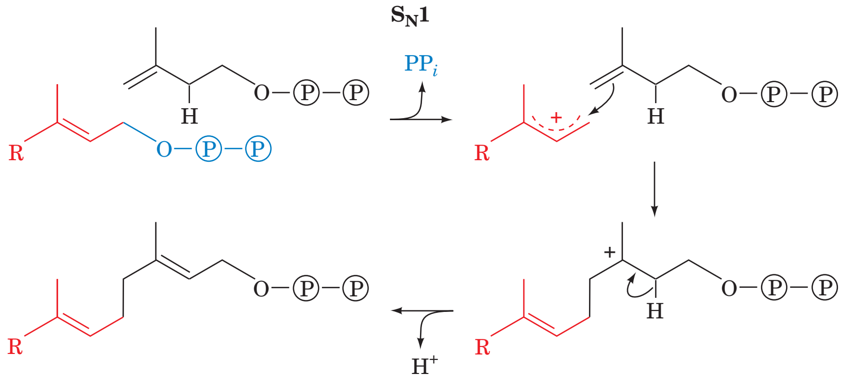

3. **Squalene synthase** then catalyzes the head-to-head condensation of two farnesyl pyrophosphate molecules to form squalene.

Farnesyl pyrophosphate is also the precursor of other isoprenoid compounds in mammals, including ubiquinone (Section 9-1F) and the isoprenoid tails of some lipid-linked membrane proteins (Section 9-3B).

Squalene Cyclization Eventually Yields Cholesterol. Squalene, a linear hydrocarbon, cyclizes to form the tetracyclic steroid skeleton in two steps. **Squalene epoxidase** catalyzes oxidation of squalene to form **2,3-oxidosqualene** (Fig. 20-39). **Oxidosqualene cyclase** converts this epoxide to the steroid **lanosterol.** The reaction is a chemically complex process involving cyclization of 2,3-oxidosqualene to a **protosterol** cation and rearrangement of the cation to lanosterol by a series of 1,2 hydride and methyl shifts (Fig. 20-40).

Conversion of lanosterol to cholesterol

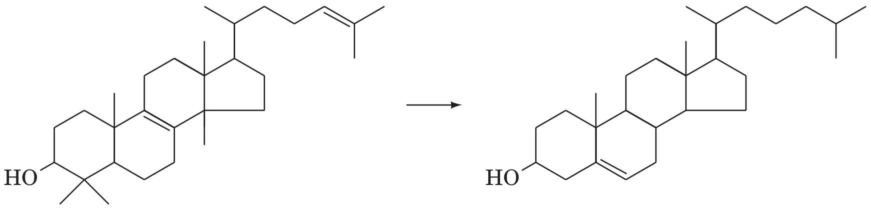

Lanosterol **Cholesterol**

is a 19-step process that involves an oxidation and the loss of three methyl groups. The enzymes required for this process are embedded in the endoplasmic reticulum membrane.

Uses of Cholesterol. Cholesterol is the precursor of steroid hormones such as cortisol, androgens, and estrogens (Section 9-1E). The liver converts cholesterol to bile acids (Fig. 20-1), which act as emulsifying agents in the digestion and absorption of fats (Section 20-1A). An efficient recycling system allows the bile acids to re-enter the bloodstream and return to the liver for reuse several times each day. The bile acids that escape this recycling are further metabolized by intestinal microorganisms and excreted. *This is the only route for cholesterol excretion.*

Cholesterol synthesized by the liver may be esterified by **acyl-CoA: cholesterol acyltransferase (ACAT)** to form cholesteryl esters.

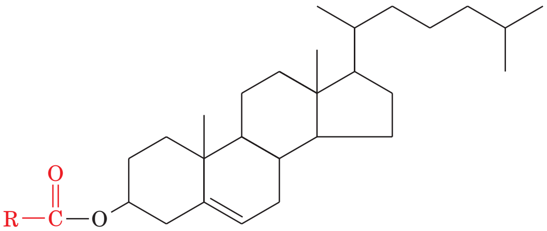

Cholesteryl ester

These highly hydrophobic compounds are transported throughout the body in lipoprotein complexes (Section 20-1B).

B | HMG-CoA Reductase Controls the Rate of Cholesterol Synthesis

HMG-CoA reductase, which catalyzes the rate-limiting step of cholesterol biosynthesis (Fig. 20-37), is the pathway's main regulatory site. The enzyme is subject to short-term control by competitive inhibition, allosteric effects, and covalent modification involving reversible phosphorylation. Like glycogen phosphorylase, glycogen synthase, and other enzymes, HMG-CoA reductase exists in interconvertible more active and less active forms. When phosphorylated at Ser 871, the enzyme is less active. Phosphorylation is carried out by AMP-dependent protein kinase (AMPK), the same enzyme that inactivates acetyl-CoA carboxylase (Section 20-4B). It appears that this control mechanism conserves energy when ATP levels fall and AMP levels rise, by generally inhibiting biosynthetic pathways.

The primary regulatory mechanism for HMG-CoA reductase activity is long-term feedback control of the amount of enzyme present in the cell. The amount of enzyme can rise as much as 200-fold, due to an increase in enzyme synthesis combined with a decrease in its degradation. In fact, cholesterol itself regulates the expression of the HMG-CoA reductase gene along with more than 20 other genes involved in its biosynthesis and uptake, including the gene encoding the LDL receptor. These genes all contain a specific recognition sequence called a **sterol regulatory element** (**SRE;** control of eukaryotic gene expression is discussed in detail in Chapter 28). The transcription of these genes, as Brown and Goldstein elucidated, requires the binding to their SRE of a portion of **sterol regulatory element binding protein (SREBP).** However, when cholesterol levels are sufficiently high, SREBP resides in the endoplasmic reticulum (ER) membrane as an inactive 1160-residue precursor that binds to **SREBP cleavage-activating protein (SCAP).** SCAP is an ~1276-residue intracellular

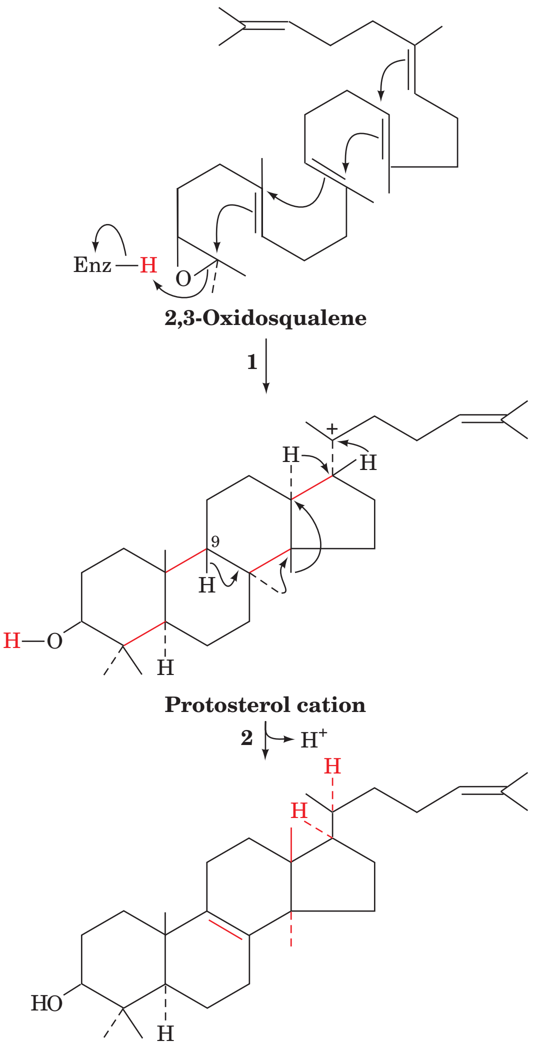

Figure 20-40 | The oxidosqualene cyclase reaction. (**1**) 2,3-Oxidosqualene is cyclized to the protosterol cation in a process that is initiated by the enzyme-mediated protonation of the squalene epoxide oxygen. The opening of the epoxide leaves an electron-deficient center whose migration drives the series of cyclizations that form the protosterol cation. (**2**) A series of methyl and hydride migrations followed by the elimination of a proton from C9 of the sterol to form a double bond ultimately yields neutral lanosterol.

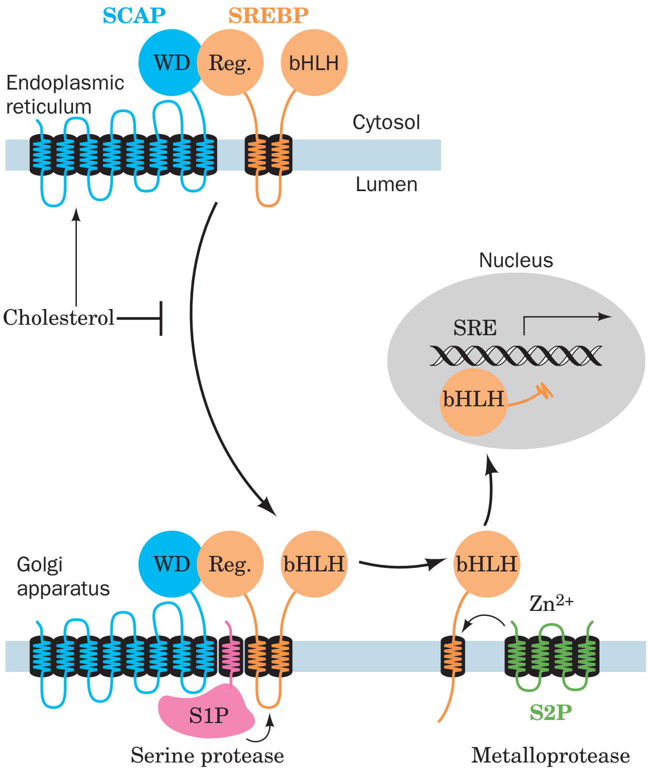

Figure 20-41 | The cholesterol-mediated proteolytic activation of SREBP. When cholesterol levels in the cell are high, the SREBP–SCAP complex resides in the ER. When cholesterol levels are low, SCAP escorts SREBP via membranous vesicles to the Golgi apparatus, where SREBP undergoes sequential proteolytic cleavage by the membrane-bound proteases S1P and S2P. This releases SREBP's N-terminal domain, which enters the nucleus where it binds to the SREs of its target genes, thereby inducing their transcription. [After Goldstein, J., Rawson, R.B., and Brown, M., *Arch. Biochem. Biophys.* **397,** 139 (2002).]

cholesterol sensor that contains two domains: an N-terminal transmembrane domain called the **sterol-sensing domain** that interacts with sterols, and a C-terminal domain containing five copies of a protein–protein interaction motif known as a **WD repeat** that interacts with the C-terminal so-called regulatory domain of SREBP (Fig. 20-41). When cholesterol in the ER membrane is depleted, SCAP changes conformation and escorts its bound SREPB to the Golgi apparatus via membranous vesicles. SREBP is then sequentially cleaved by two Golgi proteases: **site-1 protease (S1P),** a serine protease that cleaves SREBP only when it is associated with SCAP, and **site-2 protease (S2P),** a zinc metalloprotease that cleaves SREBP at a peptide bond exposed by the S1P cleavage. This results in the release of the active fragment, a soluble 480-residue protein that travels to the nucleus, where it activates the transcription of genes containing an SRE by binding to the SRE via a DNA-binding motif known as a **basic helix–loop–helix** (**bHLH;** Section 24-4C; Fig. 20-41). The cholesterol level in the cell thereby rises until SCAP no longer induces the translocation of SREBP to the Golgi apparatus, a classic case of feedback inhibition.

Statins Inhibit HMG-CoA Reductase. High levels of circulating cholesterol, a condition known as **hypercholesterolemia,** can be treated with drugs called **statins** that inhibit HMG-CoA reductase (Fig. 20-42). These compounds all contain an HMG-like group that acts as a competitive inhibitor of HMG-CoA binding to the enzyme. The statins bind extremely tightly, with K_I values in the nanomolar range, whereas the substrate, HMG-CoA, has a K_M of ~4 μM.

The X-ray structures of HMG-CoA reductase in its complexes with six different statins reveal that the bulky hydrophobic groups of the inhibitors play a major role in interfering with enzyme activity. The HMG-CoA reductase active site normally accommodates NADPH as well as the pantothenate portion of CoA. Statin binding does not interfere with NADPH

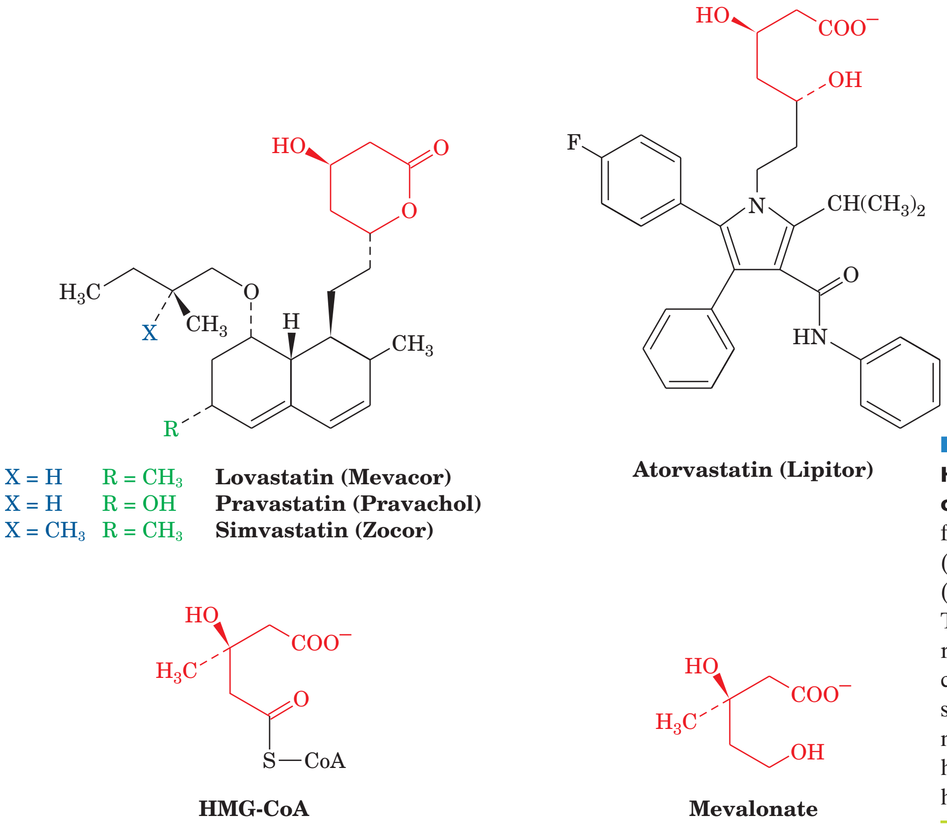

X = H	R = CH_3	**Lovastatin (Mevacor)**
X = H	R = OH	**Pravastatin (Pravachol)**
X = CH_3	R = CH_3	**Simvastatin (Zocor)**

Atorvastatin (Lipitor)

HMG-CoA

Mevalonate

Figure 20-42 | Competitive inhibitors of HMG-CoA reductase used for the treatment of hypercholesterolemia. The molecular formulas of lovastatin (Mevacor), pravastatin (Pravachol), simvastatin (Zocor), and atorvastatin (Lipitor), which are known as statins, are given. The structures of HMG-CoA and the HMG-CoA reductase product mevalonate are shown for comparison. Note that lovastatin, pravastatin, and simvastatin are lactones whereas atorvastatin and mevalonate are hydroxy acids. The lactones are hydrolyzed enzymatically *in vivo* to the active hydroxy-acid forms.

binding. However, the enzyme alters its conformation in order to accommodate the large hydrophobic groups of the statins. It appears that these inhibitors exploit the inherent flexibility of the enzyme. Furthermore, despite the structural variation among the different statins, they all experience extensive van der Waals contacts with the enzyme. *This high degree of complementarity between the statins and the active site, a result of the enzyme's flexibility, accounts for the extremely low inhibition constants.*

The initial decreased cellular cholesterol supply caused by the presence of statins is met by the induction of the LDL receptor and HMG-CoA reductase (Sections 20-1B and 20-7C; Fig. 20-8) so that at the new steady state, the HMG-CoA level is almost that of the predrug state. However, the increased number of LDL receptors causes increased removal from the blood of both LDL and IDL (the apoB-100 containing precursor to LDL), decreasing serum LDL-cholesterol levels appreciably.

C | Abnormal Cholesterol Transport Leads to Atherosclerosis

As mentioned above, cellular cholesterol concentrations depend not only on the rate of cholesterol synthesis but also on the ability of cells to absorb cholesterol from circulating lipoproteins (Section 20-1B). The role of lipoproteins in cholesterol metabolism has been studied extensively because an elevated cholesterol level in the blood, primarily in the form of LDL, is a strong risk factor for cardiovascular disease.

Atherosclerosis Results from Accumulation of Lipid in Vessel Walls. Approximately half of all deaths in the United States are linked to the vascular disease **atherosclerosis** (Greek: *athera,* mush + *sclerosis,* hardness). Atherosclerosis is a slow progressive disease that begins with the deposition

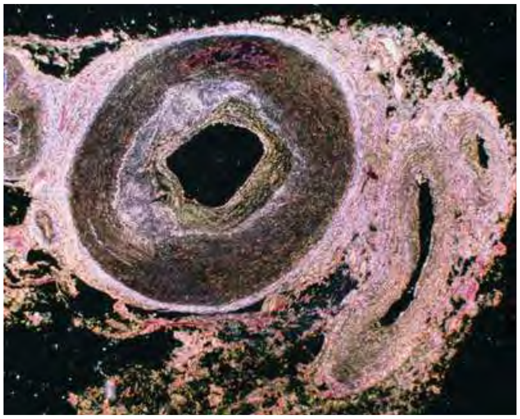

Figure 20-43 | An atherosclerotic plaque in a coronary artery. The vessel wall is dramatically thickened as a result of lipid accumulation and activation of inflammatory processes. [© Eye of Science/Photo Researchers.]

of lipids in the walls of large blood vessels, particularly the coronary arteries. The initial event appears to be the association of lipoproteins with vessel wall proteoglycans (Section 8-3A). The trapped lipids trigger inflammation by inducing the endothelial cells lining the vessels to express adhesion molecules specific for monocytes, a type of white blood cell. Once these cells burrow into the vessel wall, they differentiate into macrophages that take up the accumulated lipids, becoming so engorged that they are known as "foam cells." Macrophages do not normally take up lipids but do so when the lipids are oxidized, as apparently occurs when LDL particles are trapped for an extended period in blood vessel walls. Factors released by the foam cells, and possibly the oxidized lipids themselves, recruit more white blood cells, perpetuating a state of inflammation.

The damaged vessel wall forms a **plaque** with a core of cholesterol, cholesteryl esters, and remnants of dead macrophages, surrounded by proliferating smooth muscle cells that may undergo calcification, as occurs in bone formation (hence the "hardening" of the arteries). Although a very large plaque can occlude the lumen of the artery (Fig. 20-43), blood flow is usually not completely blocked unless the plaque ruptures. This triggers formation of a blood clot that can prevent circulation to the heart, causing **myocardial infarction** (heart attack). Stoppage of blood flow to the brain causes **stroke.**

The development of atherosclerosis is strongly correlated with the concentration of circulating LDL (often referred to as "bad cholesterol"). Some high-fat diets may contribute to atherosclerosis by boosting LDL levels, but genetic factors and infection also increase the risk of atherosclerosis. Smoking contributes to the disease because cigarette smoke oxidizes LDL, which promotes their uptake by macrophages. Atherosclerosis is less likely to occur in individuals who maintain low total cholesterol levels in their blood and who have high levels of HDL (or "good cholesterol"). These lipoproteins transport excess cholesterol to the liver for disposal as bile acids. Women have more HDL than men and a lower risk of heart disease. Statins also reduce the risk of cardiovascular disease by decreasing blood cholesterol levels (Section 20-7B).

LDL Receptor Deficiency Causes Hypercholesterolemia. LDL receptors clearly play an important role in the maintenance of plasma LDL levels. Circulating LDL and IDL (which both contain apolipoproteins that specifically bind to the LDL receptor) re-enter the liver through receptor-mediated endocytosis (Fig. 20-8). *Individuals with the inherited disease **familial hypercholesterolemia (FH)** are deficient in functional LDL receptors.* FH homozygotes, who lack the receptors entirely, have such high levels of cholesterol-rich LDL in their plasma that their cholesterol levels are three to five times greater than the average level of ~200 mg/dL. This situation results in the deposition of cholesterol in their skin and tendons as yellow nodules known as **xanthomas.** However, far greater damage is caused by the development of atherosclerosis, which causes death from heart attacks as early as age 5. FH heterozygotes (about 1 person in 500) have about half the normal number of functional LDL receptors and exhibit plasma LDL levels of about twice the average. They typically develop symptoms of cardiovascular disease after age 30.

The long-term ingestion of a high-fat/high-cholesterol diet has an effect similar to although not as extreme as FH. Cholesterol regulates the synthesis of the LDL receptor by the same mechanism that regulates HMG-CoA reductase synthesis (Section 20-7A). Consequently, high intracellular concentrations of cholesterol suppress LDL receptor synthesis so that more LDL particles remain in the circulation. Excessive dietary cholesterol,

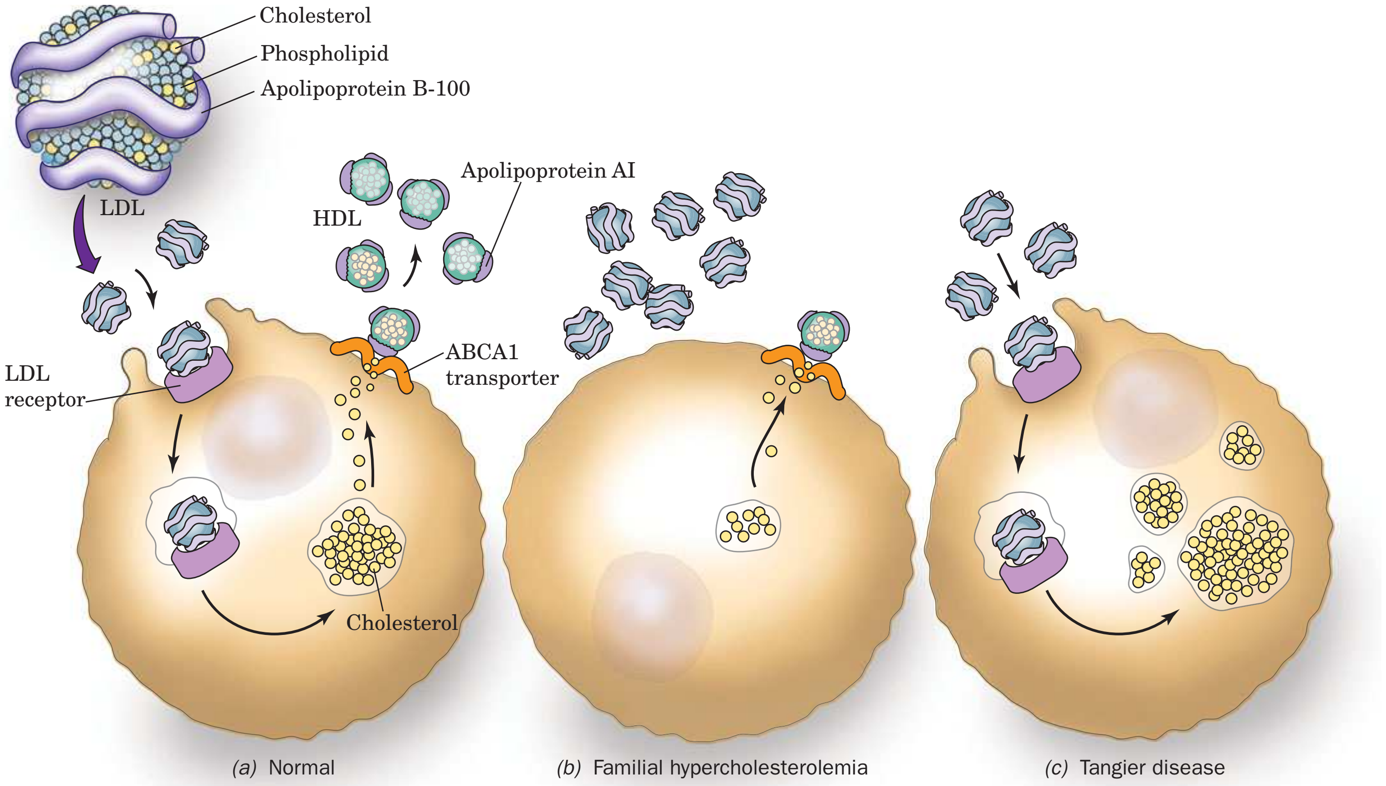

(a) Normal *(b)* Familial hypercholesterolemia *(c)* Tangier disease

■ **Figure 20-44 | The role of LDL and HDL in cholesterol metabolism.** (*a*) Cells acquire cholesterol and cholesteryl esters via endocytosis of LDL as mediated by the LDL receptor (*purple*). Cholesterol efflux to form HDL is assisted by the ABCA1 transporter (*orange*). (*b*) In familial hypercholesterolemia, a lack of functional LDL receptors results in high levels of circulating LDL. (*c*) In Tangier disease, cells become laden with cholesterol and cholesteryl esters and few HDL are formed because efflux is prevented due to lack of functional ABCA1.

delivered to the tissues via chylomicrons, therefore contributes to high plasma LDL levels.

Cholesterol Efflux from Cells. Most cells do not consume cholesterol by converting it to steroid hormones or bile acids, for example, but all cells require cholesterol to maintain membrane fluidity. Cholesterol in excess of this requirement can be esterified by the action of ACAT and stored as cholesteryl esters in intracellular deposits. Cholesterol can also be eliminated from cells by a mechanism illuminated through studies of individuals with **Tangier disease.** In this recessive inherited disorder, almost no HDL are produced, because cells have a defective transport protein, known as **ATP-cassette binding protein A1 (ABCA1).**

In normal individuals, ABCA1 apparently acts as a flipase (Section 9-4C) to transfer cholesterol, cholesteryl esters, and other lipids from the inner to the outer leaflet of the plasma membrane, from which they can be captured by apolipoprotein A-I to form HDL. Cells lacking ABCA1 are unable to offload cholesterol and accumulate cholesteryl esters in the cytoplasm. Macrophages thus engorged with lipids contribute to the development of atherosclerosis, so that individuals with Tangier disease exhibit symptoms similar to those with FH. The functions of the LDL receptor and ABCA1 in cholesterol homeostasis are presented schematically in Fig. 20-44.

■ **CHECK YOUR UNDERSTANDING**

Describe the types of reactions required to produce a molecule of cholesterol.

How does cholesterol control its own synthesis?

What do familial hypercholesterolemia and Tangier disease reveal about the development of atherosclerosis?

SUMMARY

1. Triacylglycerol digestion depends on the emulsifying activity of bile acids and the activation of lipases at the lipid–water interface.
2. Lipoproteins, complexes of nonpolar lipids surrounded by a coat of amphipathic lipids and apolipoproteins, transport lipids in the bloodstream. Cells take up cholesterol and other lipids by the receptor-mediated endocytosis of LDL.
3. Fatty acid oxidation begins with the activation of the acyl group by formation of a thioester with CoA. The acyl group is transferred to carnitine for transport into the mitochondria, where it is re-esterified to CoA.
4. β oxidation occurs in four reactions: (1) formation of an α,β double bond, (2) hydration of the double bond, (3) dehydrogenation to form a β-ketoacyl-CoA, and (4) thiolysis by CoA to produce acetyl-CoA and an acyl-CoA shortened by two carbons. This process is repeated until fatty acids with even numbers of carbon atoms are converted to acetyl-CoA and the fatty acids with odd numbers of carbon atoms are converted to acetyl-CoA and one molecule of propionyl-CoA. The acetyl-CoA is oxidized by the citric acid cycle and oxidative phosphorylation to generate ATP.
5. The oxidation of unsaturated fatty acids requires an isomerase to convert Δ^3 double bonds to Δ^2 double bonds and a reductase to remove Δ^4 double bonds. The oxidation of odd-chain fatty acids yields propionyl-CoA, which is converted to succinyl-CoA through a cobalamin (B_{12})-dependent pathway. Very long chain fatty acids are partially oxidized by a three-enzyme system in peroxisomes.
6. The liver uses acetyl-CoA to synthesize the ketone bodies acetoacetate and β-hydroxybutyrate, which are released into the bloodstream. Tissues that use these ketone bodies for fuel convert them back to acetyl-CoA.
7. In fatty acid synthesis, mitochondrial acetyl-CoA is shuttled to the cytosol via the tricarboxylate transport system and activated to malonyl-CoA by the action of acetyl-CoA carboxylase.
8. A series of seven enzymatic activities, which in mammals are contained in a multifunctional homodimeric enzyme, extend acyl-ACP chains by two carbons at a time. An enzyme-bound acyl group and malonyl-ACP condense to form a β-ketoacyl intermediate and CO_2. Two reductions and a dehydration yield an acyl-ACP in a series of reactions that resemble the reverse of β oxidation but are catalyzed by separate enzymes in the cytosol. Palmitate (C_{16}), the normal product of fatty acid biosynthesis, is synthesized in seven such reaction cycles and is then cleaved from ACP by a thioesterase.
9. Other fatty acids are synthesized from palmitate through the action of elongases and desaturases. Human triacylglycerols synthesized from fatty acyl-CoA and glycerol-3-phosphate or dihydroxyacetone phosphate tend to contain saturated fatty acids at C1 and unsaturated fatty acids at C2.
10. The opposing pathways of fatty acid degradation and synthesis are hormonally regulated. Glucagon and epinephrine activate hormone-sensitive lipase in adipose tissue, thereby increasing the supply of fatty acids for oxidation in other tissues, and inactivate acetyl-CoA carboxylase. Insulin has the opposite effect. Insulin also regulates the levels of acetyl-CoA carboxylase and fatty acid synthase by controlling their rates of synthesis.
11. Mammalian phosphatidylethanolamine and phosphatidylcholine are synthesized from 1,2-diacylglycerol and CDP derivatives of the head groups. Phosphatidylinositol, phosphatidylglycerol, and cardiolipin syntheses begin with CDP–diacylglycerol.
12. Sphingoglycolipids are synthesized from ceramide (*N*-acylsphingosine, a derivative of palmitate and serine) by the addition of glycosyl units donated by nucleotide sugars.
13. Arachidonate is the precursor of prostaglandins. Certain drugs, including aspirin, block prostaglandin synthesis by inhibiting cyclooxygenase.
14. Cholesterol is synthesized from acetyl units that pass through HMG-CoA and mevalonate intermediates on the way to being converted to a C_5 isoprene unit. Six isoprene units condense to form the C_{30} compound squalene, which cyclizes to yield lanosterol, the steroid precursor of cholesterol.
15. A cholesterol sensing system in the endoplasmic reticulum regulates the synthesis of HMG-CoA reductase and LDL receptor in the cell. HMG-CoA reductase is sensitive to statin drugs.
16. Hypercholesterolemia, associated with certain genetic defects or a high-cholesterol diet, contributes to the development of atherosclerosis.

KEY TERMS

interfacial activation	**679**
chylomicron	**681**
VLDL	**681**
IDL	**681**
LDL	**681**
HDL	**681**
apolipoprotein	**682**
receptor-mediated endocytosis	**684**
β oxidation	**686**
homolytic cleavage	**695**
heterolytic cleavage	**695**
ketogenesis	**698**
ketosis	**700**
acyl-carrier protein	**703**
elongase	**707**
desaturase	**707**
essential fatty acid	**709**
hormone-sensitive lipase	**712**
lipid storage disease	**718**
hypercholesterolemia	**726**
atherosclerosis	**727**

PROBLEMS

1. Explain why individuals with a hereditary deficiency of carnitine palmitoyl transferase II have muscle weakness. Why are these symptoms more severe during fasting?
2. The removal of fatty acids from triacylglycerols leaves glycerol. Show how the actions of glycerol kinase and glycerol-

3-phosphate dehydrogenase on glycerol produce an intermediate of glycolysis.

3. The first three steps of β oxidation (Fig. 20-12) chemically resemble three successive steps of the citric acid cycle. Which steps are these?
4. Certain branched-chain fatty acids such as **pristanic acid**

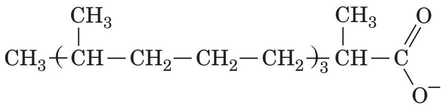

$$CH_3\left(\overset{\displaystyle CH_3}{\overset{|}{C}}H-CH_2-CH_2-CH_2\right)_3\overset{\displaystyle CH_3}{\overset{|}{C}}H-\underset{\displaystyle O^-}{\overset{\displaystyle O\,/\!/}{C}}$$

Pristanic acid

can undergo β oxidation. (a) How many cycles of β oxidation are required to completely degrade this fatty acid? (b) How many C_2 (acetyl-CoA), C_3 (propionyl-CoA), and C_4 (methylpropionyl-CoA) products are obtained?

5. Why are unsaturated fats preferable to saturated fats for an individual whose caloric intake must be limited?
6. Explain why the degradation of odd-chain fatty acids can boost the activity of the citric acid cycle.
7. The complete combustion of palmitate and glucose yields $9781\ kJ \cdot mol^{-1}$ and $2850\ kJ \cdot mol^{-1}$ of free energy, respectively. Compare these values to the free energy (as ATP) obtained though cellular catabolism of palmitate and glucose. Which process is more efficient?
8. Why is it important that liver cells lack 3-ketoacyl-CoA transferase (Fig. 20-22)?
9. The tricarboxylate transport system supplies cytosolic acetyl-CoA for palmitate synthesis. What percentage of the NADPH required for palmitate synthesis is thereby provided?
10. On what carbon atoms does the $^{14}CO_2$ used to synthesize malonyl-CoA from acetyl-CoA appear in palmitate?
11. Explain why adipocytes need glucose as well as fatty acids in order to synthesize triacylglycerols.
12. Is the fatty acid shown below likely to be synthesized in animals? Explain.

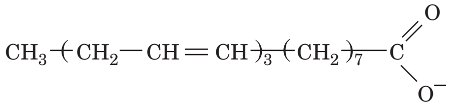

$$CH_3\left(CH_2-CH=CH\right)_3\left(CH_2\right)_7-\underset{\displaystyle O^-}{\overset{\displaystyle O\,/\!/}{C}}$$

13. Compare the energy cost, in ATP equivalents, of synthesizing stearate from mitochondrial acetyl-CoA to the energy recovered by degrading stearate (a) to acetyl-CoA and (b) to CO_2.
14. An animal is fed palmitate with a ^{14}C-labeled carboxyl group. (a) Under ketogenic conditions, where would the label appear in acetoacetate? (b) Under conditions of membrane lipid synthesis, where would the label appear in sphinganine?
15. Hypercholesterolemic individuals taking statins are sometimes advised to take supplements of coenzyme Q. Explain.

CASE STUDY

Case 23 (available at www.wiley.com/college/voet).

The Role of Uncoupling Proteins in Obesity

Focus concept: The properties of adipose tissue factors that uncouple oxidative phosphorylation are discussed, and possible links between uncoupling proteins and obesity are examined.

Prerequisites: Chapters 18 and 20

- Electron transport and oxidative phosphorylation
- Mechanisms of uncoupling agents, such as 2,4-dinitrophenol
- Fatty acid oxidation

REFERENCES

Lipoproteins

Ajees, A.A., Anantharamaiah, G.M., Mishra, V.K., Hussain, M.M., and Murthy, H.M.K., Crystal structure of human apolipoprotein A-I: Insights into its protective effect against cardiovascular diseases, *Proc. Natl. Acad. Sci.* **103,** 2126–2131 (2006).

Fatty Acid Metabolism

Bartlett, K. and Eaton, S., Mitochondrial β-oxidation, *Eur. J. Biochem.* **271,** 462–469 (2004). [Discusses the reactions and enzymes of mitochondrial β oxidation as well as their regulation.]

Kent, C., Eukaryotic phospholipid synthesis, *Annu. Rev. Biochem.* **64,** 315–342 (1995).

Kim, J.-J.P. and Battaile, K.P., Burning fat: the structural basis of fatty acid β-oxidation, *Curr. Opin. Struct. Biol.* **12,** 721–728 (2002).

Maier, T., Jenni, S., and Ban, N., Architecture of mammalian fatty acid synthase at 4.5 Å resolution, *Science* **311,** 1258–1262 (2006).

Marsh, E.N.G. and Drennan, C.L., Adenosylcobalamin-dependent isomerases: new insights into structure and mechanism, *Curr. Opin. Chem. Biol.* **5,** 499–505 (2001).

Metabolism of Other Lipids

Kurumbail, R.G., Kiefer, J.R., and Marnett, L.J., Cyclooxygenase enzymes: catalysis and inhibition, *Curr. Opin. Struct. Biol.* **11,** 752–760 (2001).

Scriver, C.R., Beaudet, A.C., Sly, W.S., and Valle, D. (Eds.), *The Metabolic and Molecular Bases of Inherited Disease* (8th ed.), McGraw-Hill (2001). [Volumes 2 and 3 contain numerous chapters on defects in lipid metabolism.]

Cholesterol Metabolism

Ikonen, E., Mechanisms for cellular cholesterol transport: defects and human disease, *Physiol. Rev.* **86,** 1237–1261 (2006).

Istvan, E.S. and Deisenhofer, J., Structural mechanism for statin inhibition of HMG-CoA reductase, *Science* **292,** 1160–1164 (2001).

Steinberg, D., Atherogenesis in perspective: hypercholesterolemia and inflammation as partners in crime, *Nature Medicine* **8,** 1211–1216 (2002). [Summarizes current hypotheses linking cholesterol levels to the development of atherosclerosis.]

21

Amino Acid Metabolism

All organisms need a source of nitrogen. Complex metabolic pathways convert a few nitrogen-containing compounds into many others, including amino acids for protein synthesis. These green bean plants grow in symbiotic association with microorganisms that make nitrogen available to them; other crops require a nitrogen-containing fertilizer. [Maurice Nimmo/Corbis Images.]

CHAPTER CONTENTS

1 Protein Degradation
- **A.** Lysosomes Degrade Many Proteins
- **B.** Ubiquitin Marks Proteins for Degradation
- **C.** The Proteasome Unfolds and Hydrolyzes Ubiquitinated Polypeptides

2 Amino Acid Deamination
- **A.** Transaminases Use PLP to Transfer Amino Groups
- **B.** Glutamate Can Be Oxidatively Deaminated

3 The Urea Cycle
- **A.** Five Enzymes Carry Out the Urea Cycle
- **B.** The Urea Cycle Is Regulated by Substrate Availability

4 Breakdown of Amino Acids
- **A.** Alanine, Cysteine, Glycine, Serine, and Threonine Are Degraded to Pyruvate
- **B.** Asparagine and Aspartate Are Degraded to Oxaloacetate
- **C.** Arginine, Glutamate, Glutamine, Histidine, and Proline Are Degraded to α-Ketoglutarate
- **D.** Isoleucine, Methionine, and Valine Are Degraded to Succinyl-CoA
- **E.** Leucine and Lysine Are Degraded Only to Acetyl-CoA and/or Acetoacetate
- **F.** Tryptophan Is Degraded to Alanine and Acetoacetate
- **G.** Phenylalanine and Tyrosine Are Degraded to Fumarate and Acetoacetate

5 Amino Acid Biosynthesis
- **A.** Nonessential Amino Acids Are Synthesized from Common Metabolites
- **B.** Plants and Microorganisms Synthesize the Essential Amino Acids

6 Other Products of Amino Acid Metabolism
- **A.** Heme Is Synthesized from Glycine and Succinyl-CoA
- **B.** Amino Acids Are Precursors of Physiologically Active Amines
- **C.** Nitric Oxide Is Derived from Arginine

7 Nitrogen Fixation
- **A.** Nitrogenase Reduces N_2 to NH_3
- **B.** Fixed Nitrogen Is Assimilated into Biological Molecules

MEDIA RESOURCES

(available at www.wiley.com/college/voet)
Interactive Exercise 29. Ubiquitin
Interactive Exercise 30. The bifunctional enzyme tryptophan synthase
Interactive Exercise 31. *A. vinelandii* nitrogenase
Animated Figure 21-8. Mechanism of PLP-dependent transamination
Animated Figure 21-9. The urea cycle

The metabolism of amino acids comprises a wide array of synthetic and degradative reactions by which amino acids are assembled as precursors of polypeptides or other compounds and broken down to recover metabolic energy. The chemical transformations of amino acids are distinct from those of carbohydrates or lipids in that they involve the element nitrogen. We must therefore examine the origin of nitrogen in biological systems and its disposal.

The bulk of the cell's amino acids are incorporated into proteins, which are continuously being synthesized and degraded. Aside from this dynamic pool of polymerized amino acids, there is no true storage form of amino acids analogous to glycogen or triacylglycerols. Mammals synthesize certain amino acids and obtain the rest from their diets. *Excess dietary amino acids are not simply excreted but are converted to common metabolites that are precursors of glucose, fatty acids, and ketone bodies and are therefore metabolic fuels.*

In this chapter, we consider the pathways of amino acid metabolism, beginning with the degradation of proteins and the **deamination** (amino group removal) of their component amino acids. We then examine the incorporation of nitrogen into urea for excretion. Next, we examine the pathways by which the carbon skeletons of individual amino acids are broken down and synthesized. We conclude with a brief examination of some other biosynthetic pathways involving amino acids and **nitrogen fixation,** a process that converts atmospheric N_2 to a biologically useful form.

1 Protein Degradation

LEARNING OBJECTIVES

- Understand that proteins to be degraded are taken up by lysosomes or conjugated to the protein ubiquitin.
- Understand that the proteasome unfolds ubiquitinated proteins in an ATP-dependent fashion and degrades them.

The components of living cells are constantly turning over. Proteins have lifetimes that range from as short as a few minutes to weeks or more. In any case, *cells continuously synthesize proteins from and degrade them to amino acids.* This seemingly wasteful process has three functions: (1) to store nutrients in the form of proteins and to break them down in times of metabolic need, processes that are most significant in muscle tissue; (2) to eliminate abnormal proteins whose accumulation would be harmful to the cell; and (3) to permit the regulation of cellular metabolism by eliminating superfluous enzymes and regulatory proteins. *Controlling a protein's rate of degradation is therefore as important to the cellular and organismal economy as is controlling its rate of synthesis.*

The half-lives of different enzymes in a given tissue vary substantially, as is indicated for rat liver in Table 21-1. Remarkably, *the most rapidly degraded enzymes all occupy important metabolic control points, whereas the relatively stable enzymes have nearly constant catalytic activities under all physiological conditions.* The susceptibilities of enzymes to degradation have evidently evolved along with their catalytic and allosteric properties so that cells can efficiently respond to environmental changes and metabolic requirements. The rate of protein degradation in a cell also varies with its nutritional and hormonal state. For example, under conditions of nutritional deprivation, cells increase their rate of protein degradation so as to provide the necessary nutrients for indispensable metabolic processes.

A | Lysosomes Degrade Many Proteins

Lysosomes contain ~50 hydrolytic enzymes, including a variety of proteases known as **cathepsins.** The lysosome maintains an internal pH of ~5, and its enzymes have acidic pH optima. This situation presumably protects the cell against accidental lysosomal leakage since lysosomal enzymes are largely inactive at cytosolic pH's.

Lysosomes degrade substances that the cell takes up via endocytosis (Section 20-1B). They also recycle intracellular constituents that are enclosed within vacuoles that fuse with lysosomes. *In well-nourished cells, lysosomal protein degradation is nonselective.* In starving cells, however, this degradation would deplete essential enzymes and regulatory proteins. Lysosomes therefore also have a selective pathway, which is activated only after a prolonged fast, that imports and degrades cytosolic proteins containing the pentapeptide Lys-Phe-Glu-Arg-Gln (KFERQ) or a closely related sequence. Such **KFERQ proteins** are selectively lost from tissues that atrophy in response to fasting (e.g., liver and kidney) but not from tissues that do not do so (e.g., brain and testes). Many normal and pathological processes are associated with increased lysosomal activity, for example, the muscle wastage caused by disuse, denervation, or traumatic injury. The regression of the uterus after childbirth, when the muscular organ reduces its mass from 2 kg to 50 g in nine days, is a striking example of this process. Many chronic inflammatory diseases such as **rheumatoid arthritis** involve the extracellular release of lysosomal enzymes, which break down surrounding tissues.

Table 21-1 Half-Lives of Some Rat Liver Enzymes

Enzyme	Half-Life (*h*)
Short-Lived Enzymes	
Ornithine decarboxylase	0.2
RNA polymerase I	1.3
Tyrosine aminotransferase	2.0
Serine dehydratase	4.0
PEP carboxylase	5.0
Long-Lived Enzymes	
Aldolase	118
GAPDH	130
Cytochrome *b*	130
LDH	130
Cytochrome *c*	150

Source: Dice, J.F. and Goldberg, A.L., *Arch. Biochem. Biophys.* **170,** 214 (1975).

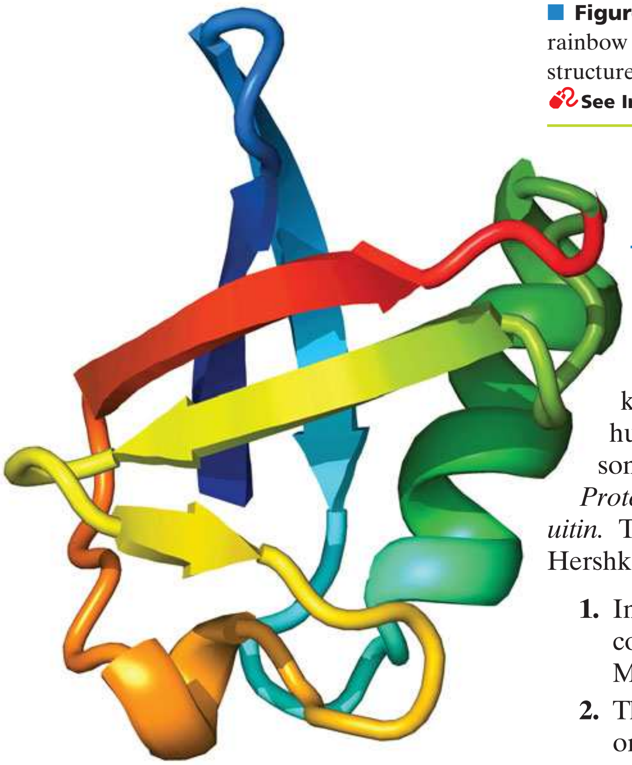

■ **Figure 21-1 | X-Ray structure of ubiquitin.** The polypeptide is colored in rainbow order from its N-terminus (*blue*) to its C-terminus (*red*). [Based on an X-ray structure by Charles Bugg, University of Alabama at Birmingham. PDBid 1UBQ.]

See Interactive Exercise 29.

B | Ubiquitin Marks Proteins for Degradation

Protein breakdown in eukaryotic cells also occurs in an ATP-requiring process that is independent of lysosomes. This process involves **ubiquitin** (Fig. 21-1), a 76-residue monomeric protein named for its ubiquity and abundance. It is one of the most highly conserved eukaryotic proteins known (it is identical in such diverse organisms as humans, trout, and *Drosophila*), suggesting that it is uniquely suited for some essential cellular function(s).

Proteins are marked for degradation by covalently linking them to ubiquitin. This process occurs in three steps elucidated notably by Avram Hershko, Aaron Ciechanover, and Irwin Rose (Fig. 21-2):

1. In an ATP-requiring reaction, ubiquitin's terminal carboxyl group is conjugated, via a thioester bond, to **ubiquitin-activating enzyme (E1).** Most organisms have only one type of E1.
2. The ubiquitin is then transferred to a specific Cys sulfhydryl group on one of numerous homologous proteins named **ubiquitin-conjugating enzymes** (**E2s;** 11 in yeast and >20 in mammals). The various E2s are characterized by a $\sim$150-residue catalytic core containing the active site Cys.
3. **Ubiquitin-protein ligase (E3)** transfers the activated ubiquitin from E2 to a Lys ε-amino group of a previously bound protein, thereby forming an **isopeptide bond.** Cells contain many species of E3s, each of which mediates the ubiquitination (alternatively, ubiquitylation) of a specific set of proteins and thereby marks them for degradation. Each E3 is served by one or a few specific E2s. The known E3s are members of two unrelated families, those containing a **HECT** domain (HECT for *h*omologous to *E*6AP *C*-*t*erminus) and those containing a so-called **RING finger** (RING for *r*eally *i*nteresting *n*ew *g*ene), although some E2s react well with members of both families.

In order for a protein to be efficiently degraded, it must be linked to a chain of at least four tandemly linked ubiquitin molecules in which Lys 48 of each ubiquitin forms an isopeptide bond with the C-terminal carboxyl group of the following ubiquitin. These **polyubiquitin** chains may contain 50 or more ubiquitin units. Ubiquitinated proteins are dynamic entities, with ubiquitin molecules being rapidly attached and removed (the latter by **ubiquitin isopeptidases**).

The Ubiquitin System Has Both Housekeeping and Regulatory Functions. Until the mid-1990s, it appeared that the ubiquitin system functioned mainly in a "housekeeping" capacity to maintain the proper

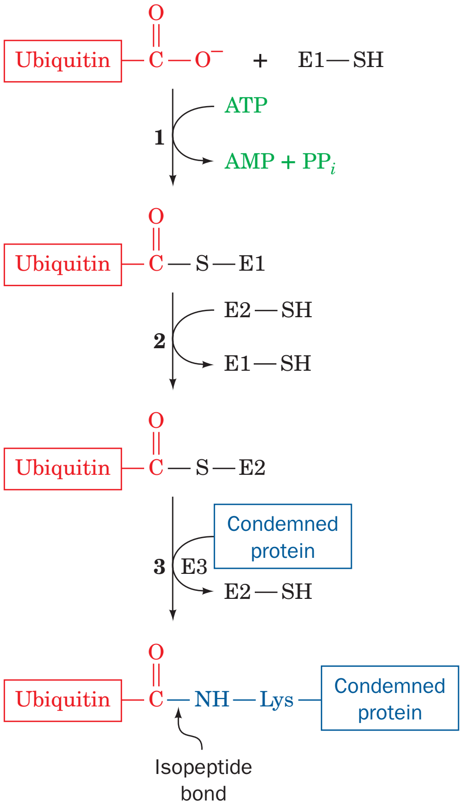

■ **Figure 21-2 | Reactions involved in protein ubiquitination.** Ubiquitin's terminal carboxyl group is first joined, via a thioester linkage, to E1 in a reaction driven by ATP hydrolysis. The activated ubiquitin is subsequently transferred to a sulfhydryl group of an E2 and then, in a reaction catalyzed by E3, to a Lys ε-amino group on a condemned protein, thereby marking the protein for proteolytic degradation.

balance among metabolic proteins and to eliminate damaged proteins. Indeed, as Alexander Varshavsky discovered, the half-lives of many cytoplasmic proteins vary with the identities of their N-terminal residues via the so-called **N-end rule:** Proteins with the "destabilizing" N-terminal residues Asp, Arg, Leu, Lys, and Phe have half-lives of only 2 to 3 minutes, whereas those with the "stabilizing" N-terminal residues Ala, Gly, Met, Ser, Thr, and Val have half-lives of >10 hours in prokaryotes and >20 hours in eukaryotes. The N-end rule applies in both eukaryotes and prokaryotes, which suggests the system that selects proteins for degradation is conserved in eukaryotes and prokaryotes, even though prokaryotes lack ubiquitin.

In eukaryotes, the N-end rule results from the actions of a RING finger E3 named **E3α** whose ubiquitination signals are the destabilizing N-terminal residues. However, it is now clear that the ubiquitin system is far more sophisticated than a simple garbage disposal system. Thus, the growing list of known E3s have a variety of ubiquitination signals that often occur on a quite limited range of target proteins, many of which have regulatory functions. For example, it has long been known that proteins with segments rich in Pro (P), Glu (E), Ser (S), and Thr (T), the so-called **PEST proteins,** are rapidly degraded. It is now realized that this is because these PEST elements often contain phosphorylation sites that target their proteins for ubiquitination. The resulting destruction of these regulatory proteins, of course, has important regulatory consequences. Interestingly, reversible **monoubiquitination** controls the activities of certain proteins rather than their degradation, in much the same way that phosphorylation and dephosphorylation alter protein activity (Section 12-3B).

C | The Proteasome Unfolds and Hydrolyzes Ubiquitinated Polypeptides

Ubiquitinated proteins are proteolytically degraded in an ATP-dependent process mediated by a large (~2100 kD, 26S) multiprotein complex named the **26S proteasome** (Fig. 21-3). The 26S proteasome consists of a hollow cylindrical core, known as the **20S proteasome,** which is covered at each end by a **19S cap.** [The quantities "26S," "20S," and "19S" refer to the corresponding particles' **sedimentation coefficients** in units of **Svedbergs** (**S;** 1 S = 10^{-13} s), which indicate the rate at which they sediment (move) in an ultracentrifuge. A particle's sedimentation coefficient increases with its mass but other quantities are also involved. Consequently, the sedimentation coefficient of a complex of particles (e.g., that of the 26S proteasome) is not equal to the sum of the sedimentation coefficients of its components (e.g., those of the 20S proteasome and the two 19S caps).]

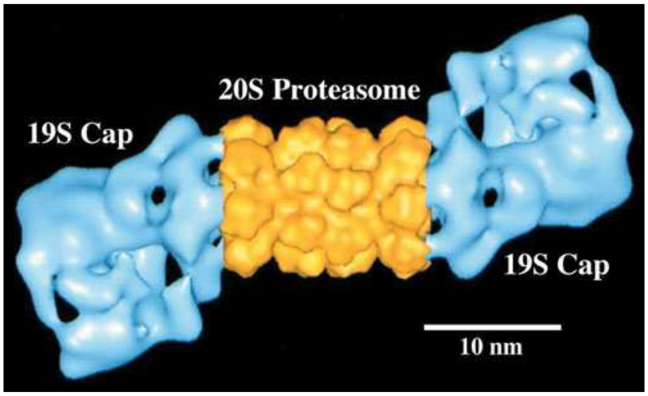

Figure 21-3 | Electron microscopy–based image of the *Drosophila melanogaster* 26S proteasome. The complex is around 450 × 190 Å. The central portion of the twofold symmetric multiprotein complex (*yellow*), the 20S proteasome, consists of four stacked seven-membered rings of subunits that form a hollow barrel in which the proteolysis of ubiquitin-linked proteins occurs. The 19S caps (*blue*), which may attach to one or both ends of the 20S proteasome, control the access of condemned proteins to the 20S proteasome (see text). [Courtesy of Wolfgang Baumeister, Max-Planck-Institut für Biochemie, Martinsried, Germany.]

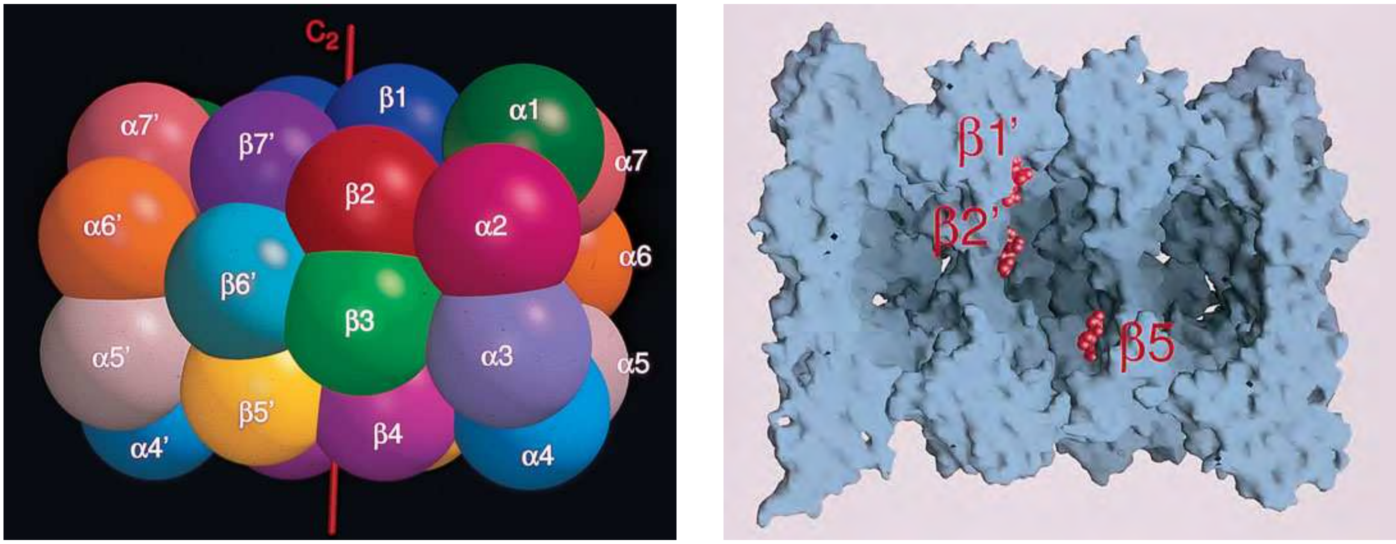

(*a*)

(*b*)

Figure 21-4 | X-Ray structure of the yeast 20S proteasome. (*a*) The arrangement of the 28 subunits shown as spheres. Four rings of seven subunits each are stacked to form a barrel (the ends of the barrel are at the right and left) with the α-type and β-type subunits forming the outer and inner rings, respectively. The complex's twofold (C_2) axis of symmetry is represented by the vertical red line. (*b*) Surface view of the proteasome core cut along its cylindrical axis. Three bound protease inhibitor molecules marking the three active β subunits are shown in red as space-filling models. [Courtesy of Robert Huber, Max-Planck-Institut für Biochemie, Martinsried, Germany. PDBid 1RYP.]

The yeast 20S proteasome, which is closely similar to other eukaryotic 20S proteasomes, is composed of seven different types of α-like subunits and seven different types of β-like subunits. The X-ray structure of this enormous (6182-residue, ~670-kD) protein complex, determined by Robert Huber, reveals that it consists of four stacked rings of subunits with its outer and inner rings, respectively, consisting of seven different α-type subunits and seven different β-type subunits (Fig. 21-4*a*). The various α-type subunits have folds that are similar to one another and to the various β-type subunits. Consequently, this 28-subunit complex has exact twofold rotational symmetry relating the two pairs of rings, but only pseudo-sevenfold rotational symmetry relating the subunits within each ring. The 20S proteasome's hollow core consists of three large chambers (Fig. 21-4*b*): Two are located at the interfaces between adjoining rings of α and β subunits, with the third, larger chamber centrally located between the two rings of β subunits.

Although the α-type subunits and the β-type subunits are structurally similar, only three of the β-type subunits have proteolytic activity. The X-ray structure together with enzymological studies reveal that the three active sites catalyze peptide bond hydrolysis via a novel mechanism in which the β subunits' N-terminal Thr residues function as catalytic nucleophiles. The active sites are located inside the central chamber of the 20S proteasome, thereby preventing this omnivorous protein-dismantling machine from indiscriminately hydrolyzing the proteins in its vicinity. It appears that polypeptide substrates must enter the central chamber of the barrel through the narrow axially located apertures in the α rings that are lined with hydrophobic residues so that only unfolded proteins can enter the central chamber. Nevertheless, in the X-ray structure of the yeast 20S proteasome (Fig. 21-4*b*), these apertures are blocked by a plug formed by the interdigitation of the α subunit's N-terminal tails.

The three active β-type subunits have different substrate specificities, cleaving after acidic residues (the β1 subunit), basic residues (the β2 subunit), and hydrophobic residues (the β5 subunit). As a result, the 20S proteasome cleaves its polypeptide substrates into ~8-residue fragments, which then diffuse out of the proteasome. Cytosolic peptidases degrade the peptides to their component amino acids. The ubiquitin molecules attached to the target protein are not degraded, however, but are returned to the cell and reused.

19S Caps Control the Access of Ubiquitinated Proteins to the 20S Proteasome. The 20S proteasome probably does not exist alone *in vivo;* it is most often in complex with two 19S caps that recognize ubiquitinated proteins, unfold them, and feed them into the 20S proteasome in an ATP-dependent manner. The 19S cap, which consists of ~18 different subunits, is poorly characterized due in large part to its low intrinsic stability. Its so-called base complex consists of 9 different subunits, 6 of which are ATPases that form a ring that abuts the α ring of the 20S proteasome (Fig. 21-3). Cecile Pickart demonstrated, via cross-linking experiments, that one of these ATPases, named **S6′,** contacts the polyubiquitin signal that targets a condemned protein to the 26S proteasome. This suggests that the recognition of the polyubiquitin chain as well as substrate protein unfolding are ATP-driven processes. Moreover, the ring of ATPases must open the otherwise closed axial aperture of the 20S proteasome so as to permit the entry of the unfolded substrate protein.

Eight additional subunits form the so-called lid complex, the portion of the 19S cap that is more distant from the 20S proteasome. The functions of the lid subunits are largely unknown, although a truncated 26S proteasome that lacks the lid subunits is unable to degrade polyubiquitinated substrates. Several other subunits may be transiently associated with the 19S cap and/or with the 20S proteasome.

Eubacteria Also Contain Self-Compartmentalized Proteases. Although 20S proteasomes occur in all eukaryotes and archaebacteria yet examined, they are absent in nearly all eubacteria (which provides further evidence that eukaryotes arose from archaea; Fig. 1-9). Nevertheless, eubacteria have ATP-dependent proteolytic assemblies that share a barrel-shaped architecture with proteasomes and carry out similar functions. For example, in *E. coli,* two proteins known as **Lon** and **Clp** carry out up to 80% of the bacterium's protein degradation. Thus, *all cells appear to contain proteases whose active sites are only available from the inner cavity of a hollow particle to which access is controlled.* These so-called **self-compartmentalized proteases** appear to have arisen early in the history of cellular life, before the advent of eukaryotic membrane-bound organelles such as the lysosome, which similarly carry out degradative processes in a way that protects the cell contents from indiscriminant destruction.

Clp protease consists of two components, the proteolytically active **ClpP** and one of several ATPases, which in *E. coli* are **ClpA** and **ClpX.** The X-ray structure of ClpP reveals that it oligomerizes to form a hollow barrel ~90 Å long and wide that consists of two back-to-back sevenfold symmetric rings of 193-residue subunits and thereby has the same rotational symmetry as does the 20S proteasome (Fig. 21-5). Nevertheless, the ClpP subunit has a novel fold that is entirely different from that of the 20S proteasome's homologous α and β subunits. The ClpP active site, which is only exposed on

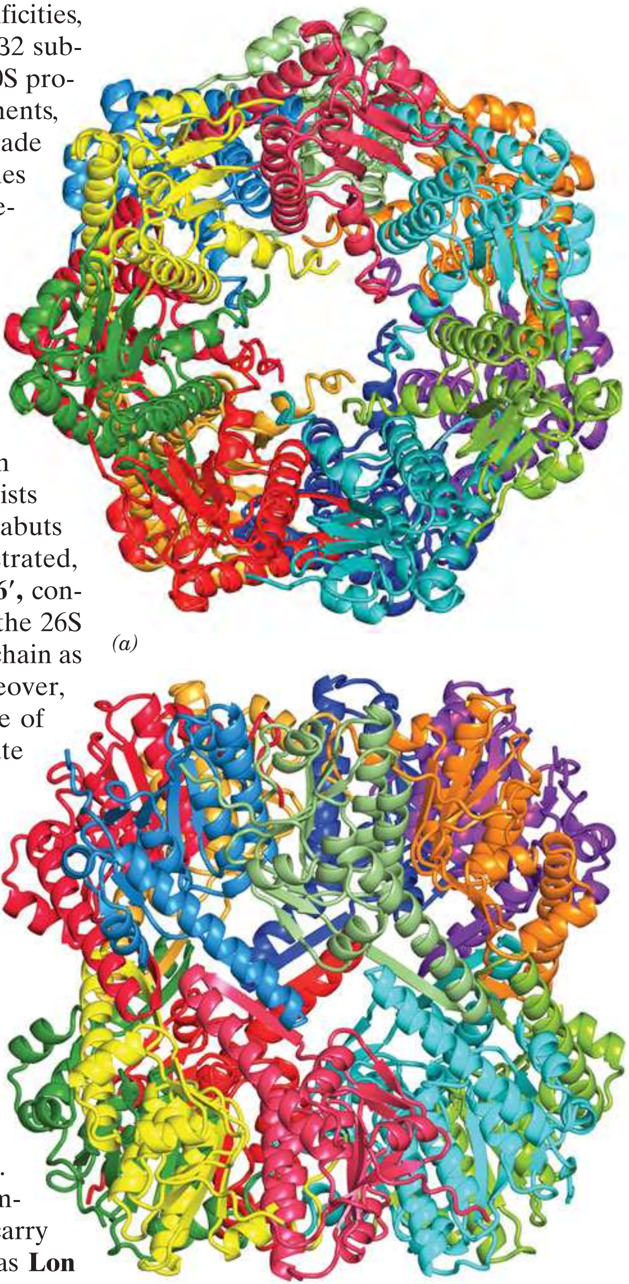

Figure 21-5 | X-Ray structure of *E. coli* ClpP. This complex of 14 identical subunits has D_7 symmetry (the symmetry of a heptagonal prism; Section 6-3). (*a*) View along the protein's sevenfold axis with each of its subunits differently colored. (*b*) View along the protein's twofold axis (rotated 90° about a horizontal axis with respect to Part *a*). [Based on an X-ray structure by John Flannagan, Brookhaven National Laboratory, Upton, New York. PDBid 1TYF.]

the inside of the barrel, contains a catalytic triad composed of its Ser 97, His 122, and Asp 171, and hence is a serine protease (Fig. 11-26).

CHECK YOUR UNDERSTANDING

What is the role of the lysosome in degrading extracellular and intracellular proteins?

Describe the pathway for proteasome-mediated protein degradation, including the roles of ubiquitin and ATP.

2 Amino Acid Deamination

LEARNING OBJECTIVES

- Understand that transamination interconverts an amino acid and an α-keto acid.
- Understand that oxidative deamination of glutamate releases ammonia for disposal.

Free amino acids originate from the degradation of cellular proteins and from the digestion of dietary proteins. The gastric protease **pepsin,** the pancreatic enzymes trypsin, chymotrypsin, and elastase (discussed in Sections 5-3B and 11-5), and a host of other endo- and exopeptidases degrade polypeptides to oligopeptides and amino acids. These substances are absorbed by the intestinal mucosa and transported via the bloodstream to be absorbed by other tissues.

The further degradation of amino acids takes place intracellularly and includes a step in which the α-amino group is removed. In many cases, the amino group is converted to ammonia, which is then incorporated into urea for excretion (Section 21-3). The remaining carbon skeleton (α-keto acid) of the amino acid can be broken down to other compounds (Section 21-4). This metabolic theme is outlined in Fig. 21-6.

A | Transaminases Use PLP to Transfer Amino Groups

Most amino acids are deaminated by **transamination,** the transfer of their amino group to an α-keto acid to yield the α-keto acid of the original amino acid and a new amino acid. The predominant amino group acceptor is α-ketoglutarate, producing glutamate and the new α-keto acid:

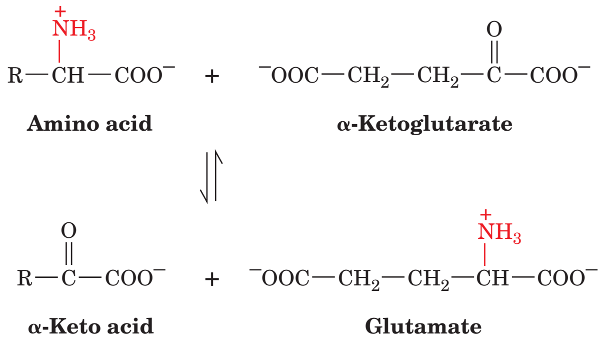

$$\mathrm{R{-}\overset{\overset{+}{N}H_3}{\overset{|}{C}H}{-}COO^- \;+\; {}^-OOC{-}CH_2{-}CH_2{-}\overset{O}{\overset{\|}{C}}{-}COO^- \;\rightleftharpoons\; R{-}\overset{O}{\overset{\|}{C}}{-}COO^- \;+\; {}^-OOC{-}CH_2{-}CH_2{-}\overset{\overset{+}{N}H_3}{\overset{|}{C}H}{-}COO^-}$$

Glutamate's amino group, in turn, can be transferred to oxaloacetate in a second transamination reaction, yielding aspartate and reforming α-ketoglutarate:

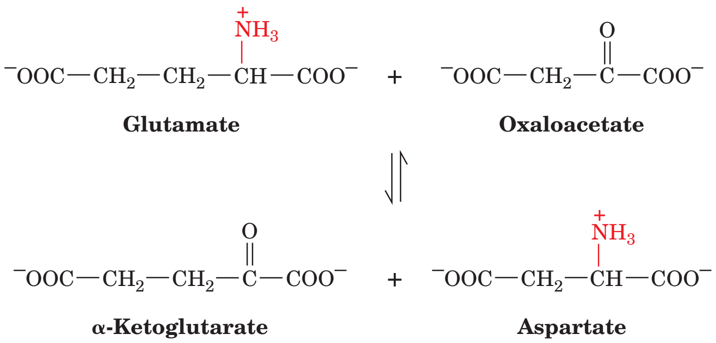

$$\mathrm{{}^-OOC{-}CH_2{-}CH_2{-}\overset{\overset{+}{N}H_3}{\overset{|}{C}H}{-}COO^- \;+\; {}^-OOC{-}CH_2{-}\overset{O}{\overset{\|}{C}}{-}COO^- \;\rightleftharpoons\; {}^-OOC{-}CH_2{-}CH_2{-}\overset{O}{\overset{\|}{C}}{-}COO^- \;+\; {}^-OOC{-}CH_2{-}\overset{\overset{+}{N}H_3}{\overset{|}{C}H}{-}COO^-}$$

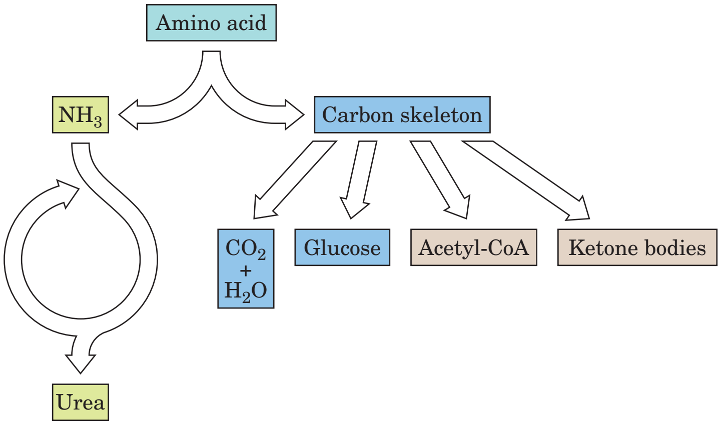
Amino acid
NH_3
Carbon skeleton
CO_2 + H_2O
Glucose
Acetyl-CoA
Ketone bodies
Urea

Figure 21-6 | Overview of amino acid catabolism. The amino group is removed and incorporated into urea for disposal. The remaining carbon skeleton (α-keto acid) can be broken down to CO_2 and H_2O or converted to glucose, acetyl-CoA, or ketone bodies.

The enzymes that catalyze transamination, called **aminotransferases** or **transaminases,** require the coenzyme **pyridoxal-5′-phosphate** (**PLP;** Fig. 21-7*a*). PLP is a derivative of **pyridoxine** (**vitamin B_6;** Fig. 21-7*b*). The coenzyme is covalently attached to the enzyme via a Schiff base (imine) linkage formed by the condensation of its aldehyde group with the ε-amino group of an enzyme Lys residue (Fig. 21-7*c*). The Schiff base, which is conjugated

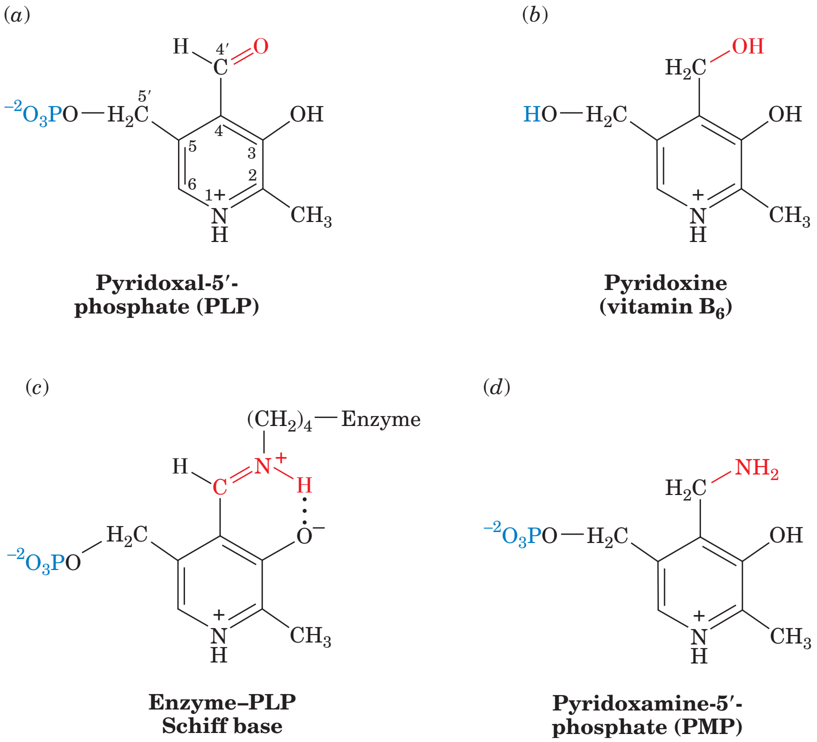
(*a*)
H
4′
O
C
5′
$^{-2}O_3PO—H_2C$
OH
4
5
3
2
6
1+
N
H
CH_3
(*b*)
H_2C
OH
$HO—H_2C$
OH
+
N
H
CH_3
(*c*)
$(CH_2)_4$—Enzyme
H
C
N^+
H
H_2C
O^-
$^{-2}O_3PO$
+
N
H
CH_3
(*d*)
H_2C
NH_2
$^{-2}O_3PO—H_2C$
OH
+
N
H
CH_3

Pyridoxal-5′-phosphate (PLP)

Pyridoxine (vitamin B_6)

Enzyme–PLP Schiff base

Pyridoxamine-5′-phosphate (PMP)

Figure 21-7 | Forms of pyridoxal-5′-phosphate. (*a*) The coenzyme pyridoxal-5′-phosphate (PLP). (*b*) Pyridoxine (vitamin B_6). (*c*) The Schiff base that forms between PLP and an enzyme ε-amino group. (*d*) Pyridoxamine-5′-phosphate (PMP).

to the pyridinium ring, is the center of the coenzyme's activity. When PLP accepts the amino group from an amino acid as described below, it becomes **pyridoxamine-5′-phosphate** (**PMP;** Fig. 21-7*d*).

Esmond Snell, Alexander Braunstein, and David Metzler demonstrated that the aminotransferase reaction occurs via a Ping Pong mechanism (Section 12-1D) whose two stages consist of three steps each (Fig. 21-8):

Stage I Converts an Amino Acid to a Keto Acid.

1. The amino acid's nucleophilic amino group attacks the enzyme–PLP Schiff base carbon atom in a **transimination** reaction to form an amino acid–PLP Schiff base (an aldimine), with concomitant release of the enzyme's Lys amino group. This Lys is then free to act as a general base at the active site.
2. The amino acid–PLP Schiff base tautomerizes to an α-keto acid–PMP Schiff base (a ketimine) by the active site Lys–catalyzed removal of the amino acid α-hydrogen and protonation of PLP atom C4′ via a resonance-stabilized carbanion intermediate. This resonance stabilization facilitates the cleavage of the C_α—H bond.
3. The α-keto acid–PMP Schiff base is hydrolyzed to PMP and an α-keto acid.

Stage II Converts an α-Keto Acid to an Amino Acid. To complete the aminotransferase's catalytic cycle, the coenzyme must be converted from PMP back to the enzyme–PLP Schiff base. This involves the same three steps as above, but in reverse order:

3′. PMP reacts with an α-keto acid to form a Schiff base.

2′. The α-keto acid–PMP Schiff base tautomerizes to form an amino acid–PLP Schiff base.

1′. The ε-amino group of the active site Lys residue attacks the amino acid–PLP Schiff base in a transimination reaction to regenerate the active enzyme–PLP Schiff base and release the newly formed amino acid.

Note that removal of the substrate amino acid's amino group produces a resonance-stabilized C_α carbanion whose electrons are delocalized all the way to the coenzyme's protonated pyridinium nitrogen atom; that is, *PLP functions as an electron sink.* For transamination reactions, this electron-withdrawing capacity facilitates removal of the α proton (*a* bond cleavage, top right of Fig. 21-8) during tautomerization. PLP functions similarly in enzymatic reactions involving *b* and *c* bond cleavage.

Aminotransferases differ in their specificity for amino acid substrates in the first stage of the transamination reaction, thereby producing the correspondingly different α-keto acid products. Most aminotransferases, however, accept only α-ketoglutarate or (to a lesser extent) oxaloacetate as the α-keto acid substrate in the second stage of the reaction, thereby yielding glutamate or aspartate as their only amino acid product. *The amino groups from most amino acids are consequently funneled into the formation of glutamate and aspartate.* The transaminase reaction is freely reversible, so transaminases participate in pathways for amino acid synthesis as well as degradation. Lysine is the only amino acid that is not transaminated.

The presence of transaminases in muscle and liver cells makes them useful markers of tissue damage. Assays of the enzymes' activities in the

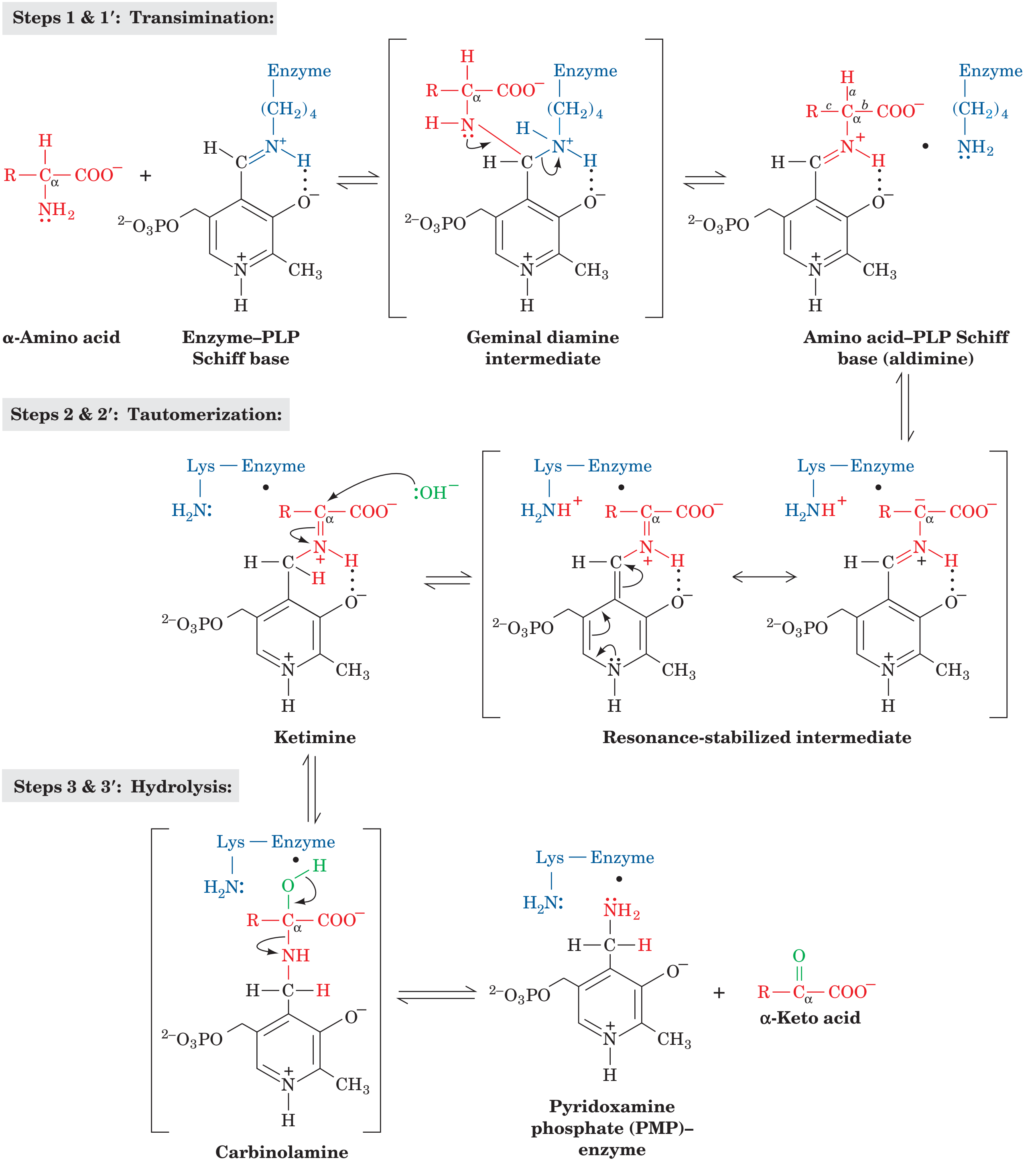
Steps 1 & 1′: Transimination:
α-Amino acid
Enzyme–PLP Schiff base
Geminal diamine intermediate
Amino acid–PLP Schiff base (aldimine)
Steps 2 & 2′: Tautomerization:
Ketimine
Resonance-stabilized intermediate
Steps 3 & 3′: Hydrolysis:
Carbinolamine
Pyridoxamine phosphate (PMP)–enzyme
α-Keto acid
Enzyme
Lys — Enzyme
$(CH_2)_4$
H_2N:
H_2NH^+
:OH^-
$^{2-}O_3PO$
CH_3
COO^-
Cα

■ **Figure 21-8 | The mechanism of PLP-dependent enzyme-catalyzed transamination.** The first stage of the reaction, in which the α-amino group of an amino acid is transferred to PLP yielding an α-keto acid and PMP, consists of three steps: (**1**) transimination, (**2**) tautomerization, in which the Lys released during the transimination reaction acts as a general acid–base catalyst, and (**3**) hydrolysis. The second stage of the reaction, in which the amino group of PMP is transferred to a different α-keto acid to yield a new α-amino acid and PLP, is essentially the reverse of the first stage: Steps 3′, 2′, and 1′ are, respectively, the reverse of Steps 3, 2, and 1. **See the Animated Figures.**

blood are the basis of the commonly used clinical measurements known as **SGOT (serum glutamate-oxaloacetate transaminase,** also known as **aspartate transaminase, AST)** and **SGPT (serum glutamate-pyruvate transaminase,** or **alanine transaminase, ALT).** The concentrations of these enzymes in the blood increase after a heart attack, when damaged heart muscle leaks its intracellular contents. Liver damage is also monitored by SGOT and SGPT levels.

B | Glutamate Can Be Oxidatively Deaminated

Transamination, of course, does not result in any net deamination. Glutamate, however, can be oxidatively deaminated by **glutamate dehydrogenase (GDH),** yielding ammonia and regenerating α-ketoglutarate for use in additional transamination reactions.

Glutamate dehydrogenase, a mitochondrial enzyme, is the only known enzyme that can accept either NAD^+ or $NADP^+$ as its redox coenzyme. Oxidation is thought to occur with transfer of a hydride ion from glutamate's C_α to $NAD(P)^+$, thereby forming α-iminoglutarate, which is hydrolyzed to α-ketoglutarate and ammonium ion:

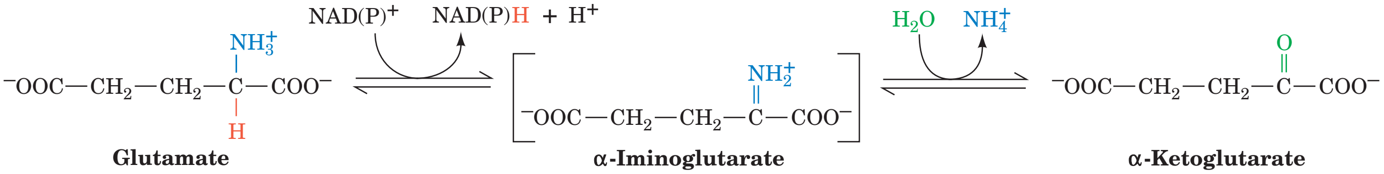

The enzyme is allosterically inhibited by GTP and NADH (signaling abundant metabolic energy) and activated by ADP and NAD^+ (signaling the need to generate ATP). Because the product of the reaction, α-ketoglutarate, is an intermediate of the citric acid cycle, activation of glutamate dehydrogenase can stimulate flux through the citric acid cycle, leading to increased ATP production by oxidative phosphorylation.

The equilibrium position of the glutamate dehydrogenase reaction ($\Delta G^{\circ\prime} \approx 30\ \text{kJ} \cdot \text{mol}^{-1}$) favors glutamate synthesis, the reverse of the reaction written above. At one time, it was believed that this reaction represented a route for the body to remove free ammonia, which is toxic at high concentrations. Under physiological conditions, the enzyme was thought to function close to equilibrium so changes in ammonia concentration could, in principle, cause a shift in equilibrium toward glutamate synthesis to remove the excess ammonia. However, a form of hyperinsulinism that is characterized by hypoglycemia and **hyperammonemia** (**HI/HA;** hyperammonemia is elevated levels of ammonia in the blood) is caused by mutations in GDH resulting in decreased sensitivity to GTP inhibition and therefore increased GDH activity. Since HI/HA patients have increased GDH activity but higher levels of NH_3 than normal, this accepted role of GDH functioning close to equilibrium and preventing ammonia toxicity cannot be correct. Indeed, if GDH functioned close to equilibrium, changes in its activity resulting from allosteric interactions would not result in significant flux changes (recall that enzymes controlling flux must function far from equilibrium).

The ammonia liberated in the GDH reaction as written above is eventually excreted in the form of urea. Thus, *the glutamate dehydrogenase reaction functions to eliminate amino groups from amino acids that undergo transamination reactions with α-ketoglutarate.*

■ CHECK YOUR UNDERSTANDING

Describe how α-ketoglutarate and oxaloacetate participate in amino acid catabolism.

Summarize the reactions that release an amino acid's amino group as ammonia.

3 The Urea Cycle

LEARNING OBJECTIVES

- Understand that five reactions incorporate ammonia and an amino group into urea.
- Understand that the rate of the urea cycle changes with the rate of amino acid breakdown.

Living organisms excrete the excess nitrogen arising from the metabolic breakdown of amino acids in one of three ways. Many aquatic animals simply excrete ammonia. Where water is less plentiful, however, processes have evolved that convert ammonia to less toxic waste products that require less water for excretion. One such product is urea, which is produced by most terrestrial vertebrates; another is **uric acid,** which is excreted by birds and terrestrial reptiles:

NH_3

Ammonia

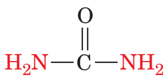

$$H_2N-\overset{\displaystyle O}{\overset{\|}{C}}-NH_2$$

Urea

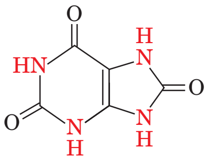

Uric acid

In this section, we focus our attention on urea formation. Uric acid biosynthesis is discussed in Section 23-4.

Urea is synthesized in the liver by the enzymes of the **urea cycle.** It is then secreted into the bloodstream and sequestered by the kidneys for excretion in the urine. The urea cycle was outlined in 1932 by Hans Krebs and Kurt Henseleit (the first known metabolic cycle; Krebs did not elucidate the citric acid cycle until 1937; Box 17-1). Its individual reactions were later described in detail by Sarah Ratner and Philip Cohen. The overall urea cycle reaction is

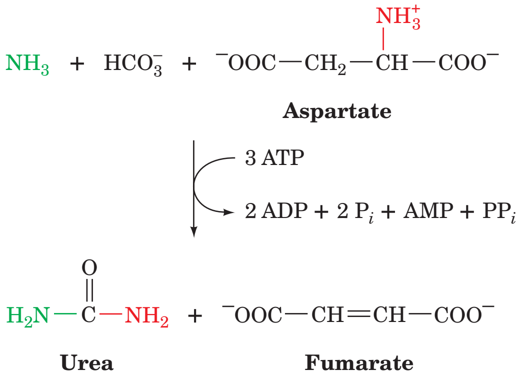

$$NH_3 + HCO_3^- + {}^-OOC-CH_2-\overset{\displaystyle NH_3^+}{\overset{|}{C}H}-COO^-$$

Aspartate

$$\xrightarrow[\text{2 ADP + 2 P}_i\text{ + AMP + PP}_i]{\text{3 ATP}}$$

$$H_2N-\overset{\displaystyle O}{\overset{\|}{C}}-NH_2 + {}^-OOC-CH=CH-COO^-$$

Urea **Fumarate**

Thus, urea's two nitrogen atoms are contributed by ammonia and aspartate, whereas its carbon atom comes from HCO_3^-.

A | Five Enzymes Carry Out the Urea Cycle

Five enzymatic reactions are involved in the urea cycle, two of which are mitochondrial and three cytosolic (Fig. 21-9).

1. Carbamoyl Phosphate Synthetase Acquires the First Urea Nitrogen Atom. **Carbamoyl phosphate synthetase (CPS)** is technically not a member of the urea cycle. It catalyzes the condensation and activation of NH_3 and HCO_3^- to form **carbamoyl phosphate,** the first of the cycle's two nitrogen-containing substrates, with the concomitant cleavage of 2 ATP. Eukaryotes have two forms of CPS: Mitochondrial **CPS I** uses ammonia

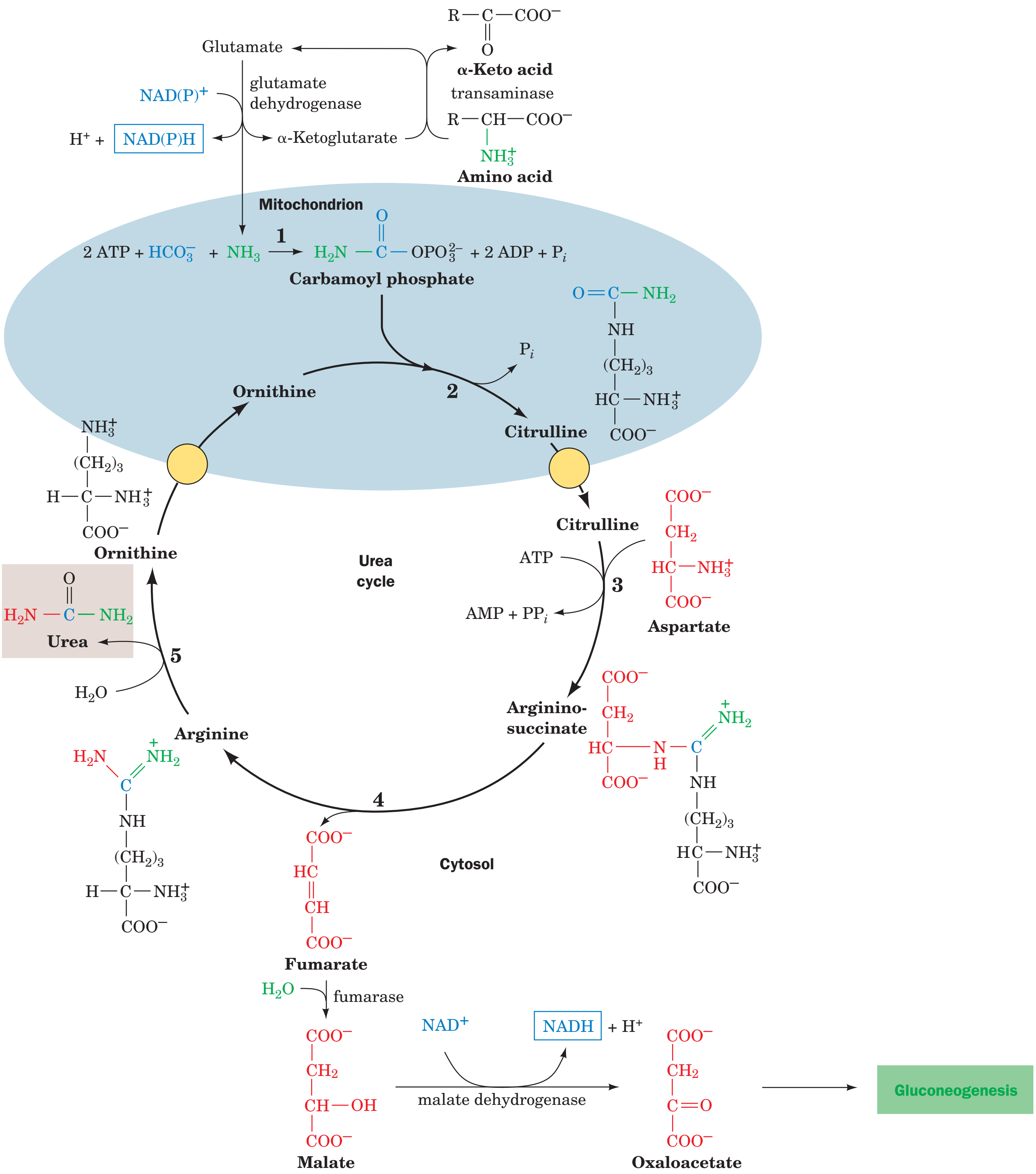
Glutamate
α-Keto acid
transaminase
Amino acid
glutamate dehydrogenase
NAD(P)+
H+ + NAD(P)H
α-Ketoglutarate
Mitochondrion
2 ATP + HCO3− + NH3
1
Carbamoyl phosphate
+ 2 ADP + Pi
Pi
2
Ornithine
Citrulline
Citrulline
ATP
3
AMP + PPi
Aspartate
Argininosuccinate
Urea cycle
4
Arginine
5
Urea
H2O
Ornithine
Fumarate
Cytosol
H2O
fumarase
Malate
NAD+
NADH + H+
malate dehydrogenase
Oxaloacetate
Gluconeogenesis

Figure 21-9 | The urea cycle. Five enzymes participate in the urea cycle: (**1**) carbamoyl phosphate synthetase, (**2**) ornithine transcarbamoylase, (**3**) argininosuccinate synthetase, (**4**) argininosuccinase, and (**5**) arginase. Enzymes 1 and 2 are mitochondrial and enzymes 3–5 are cytosolic. Ornithine and citrulline must therefore be transported across the mitochondrial membrane by specific transport systems (*yellow circles*). The urea amino groups arise from the deamination of amino acids. One amino group (*green*) originates as ammonia that is generated by the glutamate dehydrogenase reaction (*top*). The other amino group (*red*) is obtained from aspartate (*right*), which is formed via the transamination of oxaloacetate by an amino acid. The fumarate product of Reaction 4 is converted to the gluconeogenic precursor oxaloacetate by the action of cytosolic fumarase and malate dehydrogenase (*bottom*). **See the Animated Figures.**

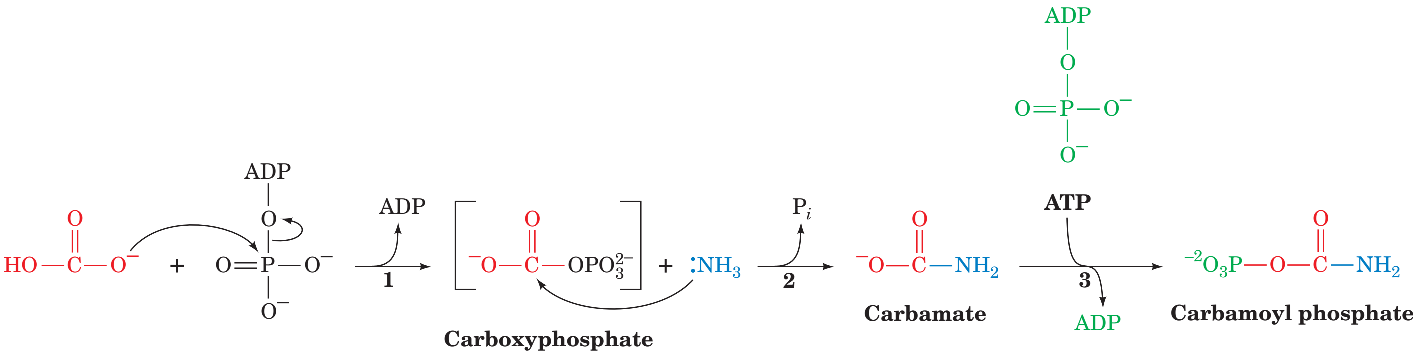

Figure 21-10 | **The mechanism of action of CPS I.** (**1**) Phosphorylation activates HCO_3^- to form the intermediate carboxyphosphate. (**2**) NH_3 attacks carboxyphosphate to form carbamate. (**3**) ATP phosphorylates carbamate, yielding carbamoyl phosphate.

as its nitrogen donor and participates in urea biosynthesis, whereas cytosolic **CPS II** uses glutamine as its nitrogen donor and is involved in pyrimidine biosynthesis (Section 23-2A). CPS I catalyzes an essentially irreversible reaction that is the rate-limiting step of the urea cycle (Fig. 21-10):

1. ATP activates HCO_3^- to form **carboxyphosphate** and ADP.
2. Ammonia attacks carboxyphosphate, displacing the phosphate to form **carbamate** and P_i.
3. A second ATP phosphorylates carbamate to form carbamoyl phosphate and ADP.

In *E. coli*, a single CPS with the subunit structure $(\alpha\beta)_4$ generates carbamoyl phosphate, using glutamine as its nitrogen donor. The enzyme's small subunit is a **glutaminase** that hydrolyzes glutamine, and its large subunit catalyzes Reactions 1, 2, and 3 of Fig. 21-10. The X-ray structure of *E. coli* CPS, determined by Hazel Holden and Ivan Rayment, reveals the astonishing fact that although the three active sites are widely separated in space, they are connected by a narrow 96-Å-long tunnel that runs nearly the entire length of the protein molecule (Fig. 21-11). The NH_3 produced by the glutaminase active site travels ~45 Å in order to react with carboxyphosphate. The resulting carbamate then travels ~35 Å to reach the carbamoyl phosphate synthesis site. This phenomenon, in which the intermediate of two reactions is directly transferred from one enzyme active site to another, is called **channeling.**

Channeling increases the rate of a metabolic pathway by preventing the loss of its intermediate products as well as protecting the intermediates from degradation. Channeling is critical for CPS because the intermediates carboxyphosphate and carbamate are extremely reactive, having half-lives of 28 and 70 ms, respectively, at neutral pH. Also, channeling allows the local concentration of NH_3 to reach a higher value than is present in the cellular

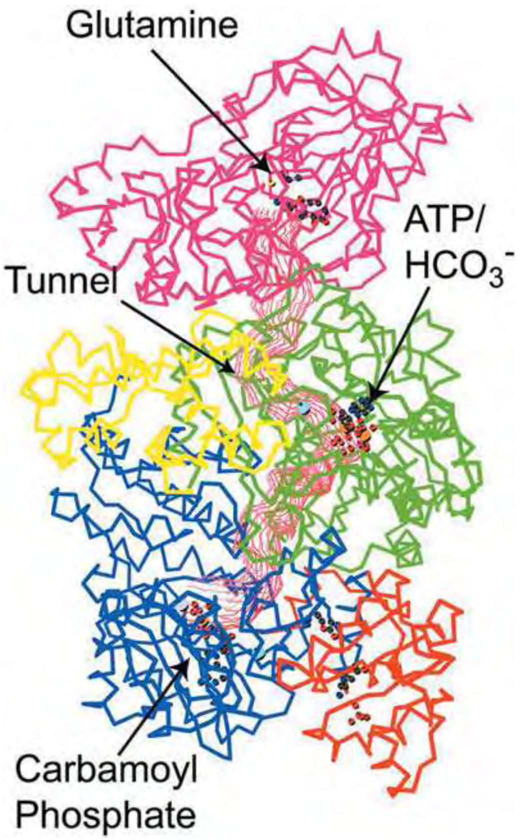

Figure 21-11 | **X-Ray structure of *E. coli* carbamoyl phosphate synthetase.** The protein is represented by its C_α backbone. The small subunit (*magenta*) contains the glutamine-binding site where NH_3 is produced. The large subunit consists of several domains (*green, yellow, blue, and orange*) and contains the other two active sites. The 96-Å-long tunnel connecting the three active sites is outlined in red. [Courtesy of Hazel Holden and Ivan Rayment, University of Wisconsin. PDBid 1JDB.]

medium. We shall encounter several other examples of channeling in our studies of metabolic enzymes, but the CPS tunnel is among the longest known.

2. Carbamoylation of Ornithine Produces Citrulline. **Ornithine transcarbamoylase** transfers the carbamoyl group of carbamoyl phosphate to **ornithine,** yielding **citrulline** (Fig. 21-9, Reaction 2). Note that both of the latter compounds are "nonstandard" α-amino acids that do not occur in proteins. The transcarbamoylase reaction occurs in the mitochondrion, so ornithine, which is produced in the cytosol, must enter the mitochondrion via a specific transport system. Likewise, since the remaining urea cycle reactions occur in the cytosol, citrulline must be exported from the mitochondrion.

3. Argininosuccinate Synthetase Acquires the Second Urea Nitrogen Atom. Urea's second nitrogen atom is introduced by the condensation of citrulline's ureido group with an aspartate amino group by **argininosuccinate synthetase** (Fig. 21-12). ATP activates the ureido oxygen atom as a leaving group through formation of a citrullyl–AMP intermediate, and AMP is subsequently displaced by the aspartate amino group. The PP_i formed in the reaction is hydrolyzed to 2 P_i, so the reaction consumes two ATP equivalents.

4. Argininosuccinase Produces Fumarate and Arginine. With the formation of argininosuccinate, all of the urea molecule components have been assembled. However, the amino group donated by aspartate is still attached to the aspartate carbon skeleton. This situation is remedied by the **argininosuccinase**-catalyzed elimination of fumarate, leaving arginine (Fig. 21-9, Reaction 4). Arginine is urea's immediate precursor. The fumarate produced in the argininosuccinase reaction is converted to oxaloacetate by the action of fumarase and malate dehydrogenase. These two reactions are the same as those that occur in the citric acid cycle, although they take place in the cytosol rather than in the mitochondrion. The oxaloacetate is then used for gluconeogenesis (Section 16-4).

5. Arginase Releases Urea. The urea cycle's final reaction is the **arginase**-catalyzed hydrolysis of arginine to yield urea and regenerate ornithine (Fig. 21-9, Reaction 5). Ornithine is then returned to the mitochondrion for another round of the cycle.

The urea cycle thus converts two amino groups, one from ammonia and one from aspartate, and a carbon atom from HCO_3^- to the relatively nontoxic product, urea, at the cost of four "high-energy" phosphate bonds. The energy spent is more than recovered, however, by the oxidation of the

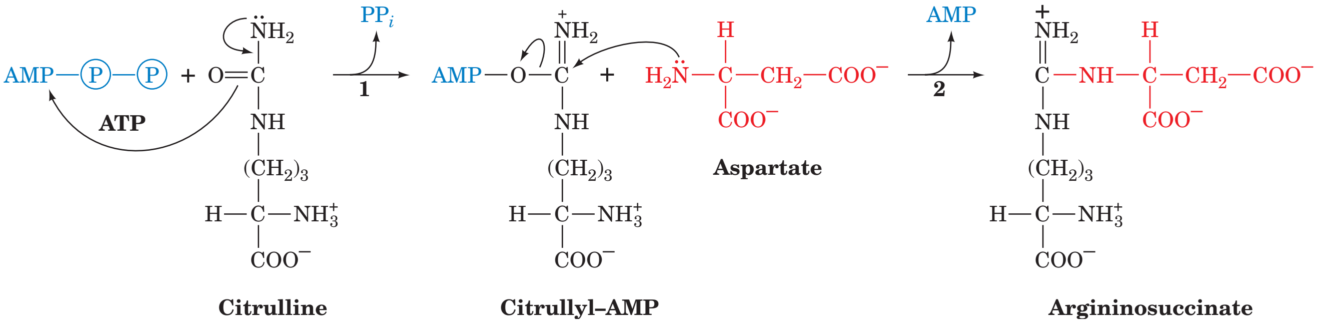

Figure 21-12 | The mechanism of action of argininosuccinate synthetase. (**1**) The formation of citrullyl–AMP activates the ureido oxygen of citrulline. (**2**) The α-amino group of aspartate displaces AMP.

carbon skeletons of the amino acids that have donated their amino groups, via transamination, to glutamate and aspartate. Indeed, half the oxygen that the liver consumes is used to provide this energy.

B | The Urea Cycle Is Regulated by Substrate Availability

Carbamoyl phosphate synthetase I, which catalyzes the first committed step of the urea cycle, is allosterically activated by ***N*-acetylglutamate** *(at right)*. This metabolite is synthesized from glutamate and acetyl-CoA by ***N*-acetylglutamate synthase.** When amino acid breakdown rates increase, the concentration of glutamate increases as a result of transamination. The increased glutamate stimulates *N*-acetylglutamate synthesis. The resulting activation of carbamoyl phosphate synthetase increases the rate of urea production. Thus, the excess nitrogen produced by amino acid breakdown is efficiently excreted. Note that the urea cycle, like gluconeogenesis (Section 16-4) and ketogenesis (Section 20-3), is a pathway that occurs in the liver but serves the needs of the body as a whole.

The remaining enzymes of the urea cycle are controlled by the concentrations of their substrates. In individuals with inherited deficiencies in urea cycle enzymes other than arginase, the corresponding substrate builds up, increasing the rate of the deficient reaction so that the rate of urea production is normal (the total lack of a urea cycle enzyme, however, is lethal). The anomalous substrate buildup is not without cost, however. The substrate concentrations become elevated all the way back up the cycle to ammonia, resulting in hyperammonemia. Although the root cause of ammonia toxicity is not completely understood, it is clear that the brain is particularly sensitive to high ammonia concentrations (symptoms of urea cycle enzyme deficiencies include mental retardation and lethargy).

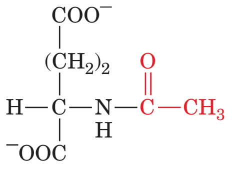
COO⁻
(CH₂)₂
O
H—C—N—C—CH₃
H
⁻OOC

***N*-Acetylglutamate**

CHECK YOUR UNDERSTANDING

Summarize the steps of the urea cycle. How do the amino groups of amino acids enter the cycle?

How is the rate of amino acid deamination linked to the rate of the urea cycle?

LEARNING OBJECTIVE

- Understand that amino acids are broken down to seven metabolic intermediates that are glucogenic, ketogenic, or both.

4 Breakdown of Amino Acids

Amino acids are degraded to compounds that can be metabolized to CO_2 and H_2O or used in gluconeogenesis. Indeed, oxidative breakdown of amino acids typically accounts for 10 to 15% of the metabolic energy generated by animals. In this section we consider how the carbon skeletons of the 20 "standard" amino acids are catabolized. We shall not describe in detail all of the many reactions involved. Rather, we shall consider how the pathways are organized and focus on a few reactions of chemical and/or medical interest.

"Standard" amino acids are degraded to one of seven metabolic intermediates: pyruvate, α-ketoglutarate, succinyl-CoA, fumarate, oxaloacetate, acetyl-CoA, or acetoacetate (Fig. 21-13). The amino acids can therefore be divided into two groups based on their catabolic pathways:

1. **Glucogenic amino acids,** which are degraded to pyruvate, α-ketoglutarate, succinyl-CoA, fumarate, or oxaloacetate and are therefore glucose precursors (Section 16-4).
2. **Ketogenic amino acids,** which are broken down to

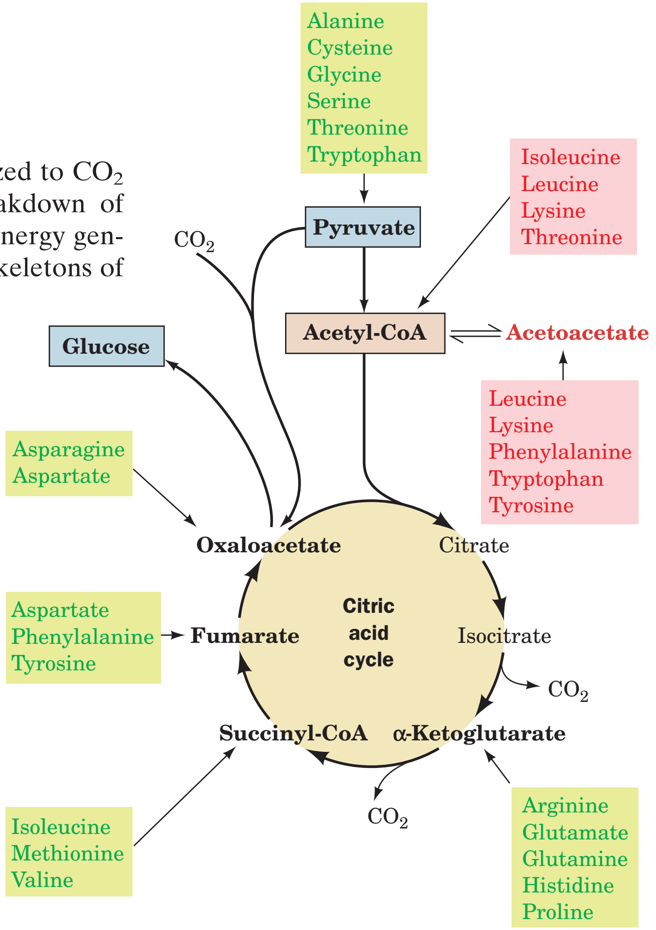
Alanine
Cysteine
Glycine
Serine
Threonine
Tryptophan
Isoleucine
Leucine
Lysine
Threonine
CO₂
Pyruvate
Glucose
Acetyl-CoA
Acetoacetate
Leucine
Lysine
Phenylalanine
Tryptophan
Tyrosine
Asparagine
Aspartate
Oxaloacetate
Citrate
Citric acid cycle
Aspartate
Phenylalanine
Tyrosine
Fumarate
Isocitrate
CO₂
Succinyl-CoA
α-Ketoglutarate
CO₂
Isoleucine
Methionine
Valine
Arginine
Glutamate
Glutamine
Histidine
Proline

Figure 21-13 | Degradation of amino acids to one of seven common metabolic intermediates. Glucogenic and ketogenic degradations are indicated in green and red, respectively.

acetyl-CoA or acetoacetate and can thus be converted to fatty acids or ketone bodies (Section 20-3).

Some amino acids are precursors of both carbohydrates and ketone bodies. Since animals lack any metabolic pathways for the net conversion of acetyl-CoA or acetoacetate to gluconeogenic precursors, *no net synthesis of carbohydrates is possible from the purely ketogenic amino acids Lys and Leu.*

In studying the specific pathways of amino acid breakdown, we shall organize the amino acids into groups that are degraded to each of the seven metabolites mentioned above.

A | Alanine, Cysteine, Glycine, Serine, and Threonine Are Degraded to Pyruvate

Five amino acids—alanine, cysteine, glycine, serine, and threonine—are broken down to yield pyruvate (Fig. 21-14). Alanine is straightforwardly transaminated to pyruvate. Serine is converted to pyruvate through dehydration by **serine dehydratase.** This PLP-dependent enzyme, like the

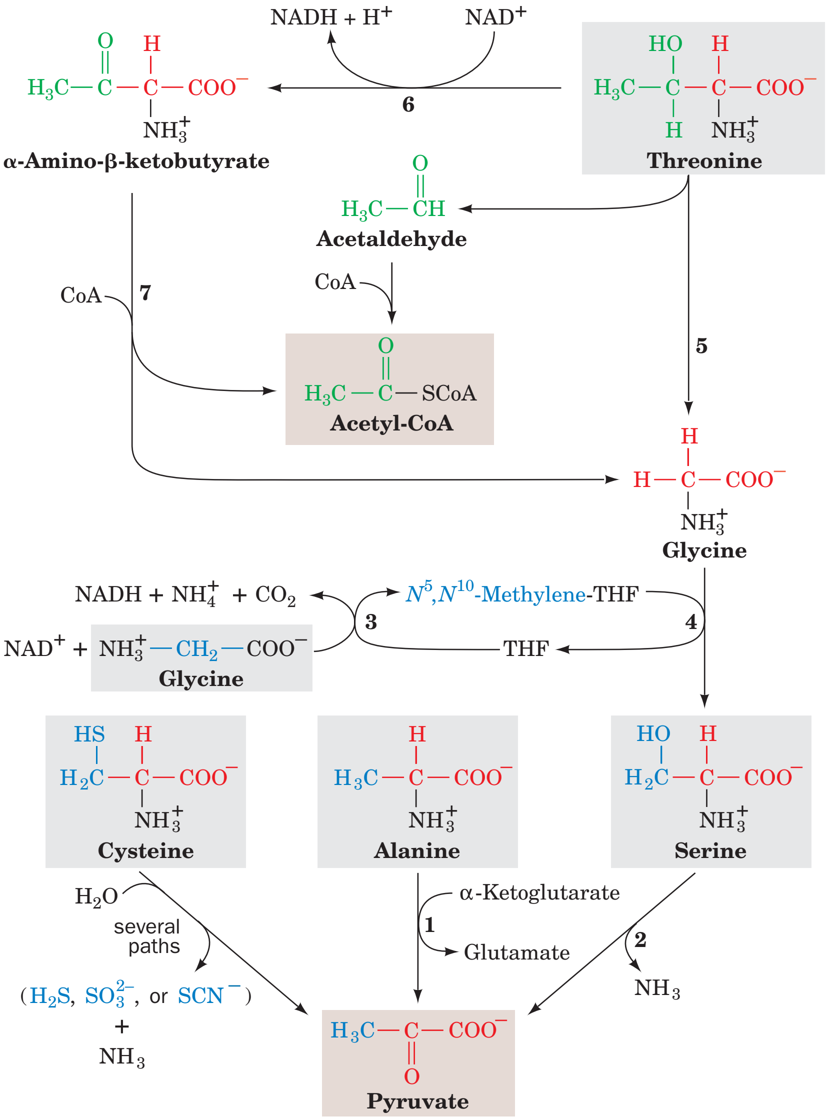

NADH + H⁺
NAD⁺
6
α-Amino-β-ketobutyrate
Threonine
Acetaldehyde
CoA
7
CoA
5
Acetyl-CoA
Glycine
NADH + NH₄⁺ + CO₂
N⁵,N¹⁰-Methylene-THF
3
4
NAD⁺ + NH₃⁺—CH₂—COO⁻
THF
Glycine
Cysteine
Alanine
Serine
H₂O
several paths
(H₂S, SO₃²⁻, or SCN⁻)
+
NH₃
α-Ketoglutarate
1
Glutamate
2
NH₃
Pyruvate

■ **Figure 21-14 | The pathways converting alanine, cysteine, glycine, serine, and threonine to pyruvate.** The enzymes involved are (**1**) alanine aminotransferase, (**2**) serine dehydratase, (**3**) glycine cleavage system, (**4** and **5**) serine hydroxymethyltransferase, (**6**) threonine dehydrogenase, and (**7**) α-amino-β-ketobutyrate lyase.

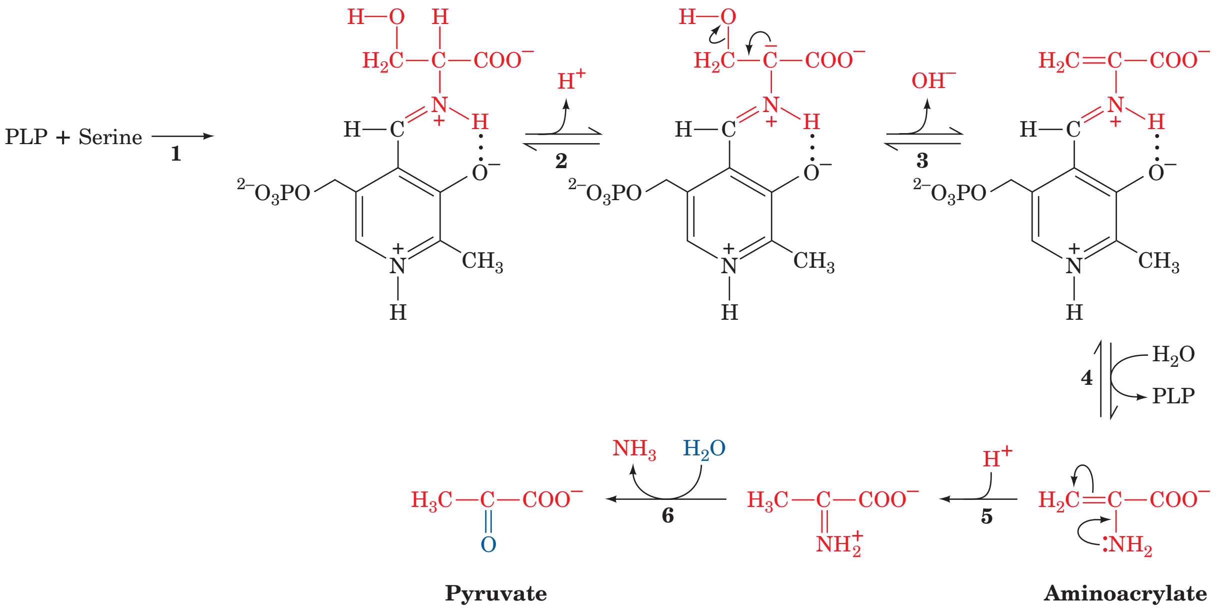

Figure 21-15 | **The serine dehydratase reaction.** This PLP-dependent enzyme catalyzes the elimination of water from serine in six steps: (**1**) formation of a serine–PLP Schiff base, (**2**) removal of the α-H atom of serine to form a resonance-stabilized carbanion, (**3**) β elimination of OH^-, (**4**) hydrolysis of the Schiff base to yield the PLP–enzyme and aminoacrylate, (**5**) nonenzymatic tautomerization to the imine, and (**6**) nonenzymatic hydrolysis to form pyruvate and ammonia.

aminotransferases (Section 21-2A), forms a PLP–amino acid Schiff base which facilitates the removal of the amino acid's α-hydrogen atom. In the serine dehydratase reaction, however, the C_α carbanion breaks down with the elimination of the amino acid's C_β OH, rather than with tautomerization (Fig. 21-8, Step 2), so that the substrate undergoes α,β elimination of H_2O rather than deamination (Fig. 21-15). The product of the dehydration, the enamine **aminoacrylate,** tautomerizes nonenzymatically to the corresponding imine, which spontaneously hydrolyzes to pyruvate and ammonia.

Cysteine can be converted to pyruvate via several routes in which the sulfhydryl group is released as H_2S, SO_3^{2-}, or SCN^-.

Glycine is converted to pyruvate by first being converted to serine by the enzyme **serine hydroxymethyltransferase,** another PLP-containing enzyme (Fig. 21-14, Reaction 4). This enzyme uses ***N*⁵,*N*¹⁰-methylenetetrahydrofolate (*N*⁵,*N*¹⁰-methylene-THF)** as a one-carbon donor (the structure and chemistry of THF cofactors are described in Section 21-4D). The methylene group of the THF cofactor is obtained from a second glycine in Reaction 3 of Fig. 21-14, which is catalyzed by the **glycine cleavage system** (called the **glycine decarboxylase multienzyme system** in plants). This enzyme is a multiprotein complex that resembles pyruvate dehydrogenase (Section 17-2). The glycine cleavage system mediates the major route of glycine degradation in mammalian tissues. An inherited deficiency of the glycine cleavage system causes the disease **nonketotic hyperglycinemia,** which is characterized by mental retardation and accumulation of large amounts of glycine in body fluids.

Threonine is both glucogenic and ketogenic since it generates both pyruvate and acetyl-CoA. Its major route of breakdown is through **threonine dehydrogenase** (Fig. 21-14, Reaction 6), producing **α-amino-β-ketobutyrate,** which is converted to acetyl-CoA and glycine by **α-amino-β-ketobutyrate lyase** (Fig. 21-14, Reaction 7). The glycine can be converted, through serine, to pyruvate.

Serine Hydroxymethyltransferase Catalyzes PLP-Dependent C_α—C_β Bond Formation and Cleavage. Threonine can also be converted directly to glycine and acetaldehyde (which is subsequently oxidized to acetyl-CoA) via Reaction 5 of Fig. 21-14, which breaks threonine's C_α—C_β bond. This PLP-dependent reaction is catalyzed by serine hydroxymethyltransferase, the same enzyme that adds a hydroxymethyl group to glycine to produce serine (Fig. 21-14, Reaction 4). In the glycine → serine reaction, the amino acid's C_α—H bond is cleaved (as occurs in transamination; Fig. 21-8) and a C_α—C_β bond is formed. In contrast, the degradation of threonine to glycine by serine hydroxymethyltransferase acts in reverse, beginning with C_α—C_β bond cleavage:

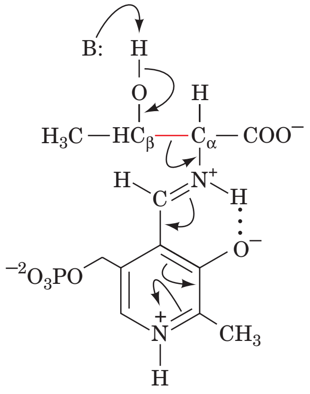

With the cleavage of any of the bonds to C_α, the PLP group delocalizes the electrons of the resulting carbanion. This feature of PLP action is the key to understanding how the same amino acid–PLP Schiff base can undergo cleavage of different bonds to C_α in different enzymes (bonds *a, b,* or *c* in the upper right of Fig. 21-8). The bond that is cleaved is the one that lies in the plane perpendicular to that of the π-orbital system of the PLP (Fig. 21-16). This arrangement allows the PLP π-orbital system to overlap the bonding orbital containing the electron pair being delocalized. Any other geometry would

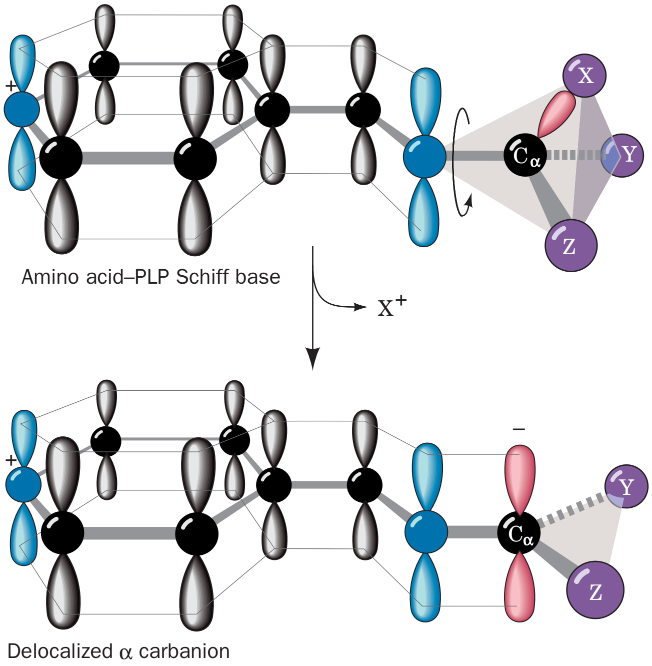

Figure 21-16 | The π-orbital framework of a PLP–amino acid Schiff base. The bond from X to C_α is in a plane perpendicular to the plane of the PLP π-orbital system (*top*) and is therefore labile. The broken bond's electron pair (*bottom*) is delocalized over the conjugated molecule.

reduce or even eliminate this orbital overlap (the newly formed double bond would be twisted out of planarity) yielding a higher energy arrangement. Different bonds to C_α can be positioned for cleavage by rotation around the C_α—N bond. Evidently, *each enzyme binds its amino acid–PLP Schiff base adduct with the appropriate geometry for bond cleavage.*

B | Asparagine and Aspartate Are Degraded to Oxaloacetate

Transamination of aspartate leads directly to oxaloacetate:

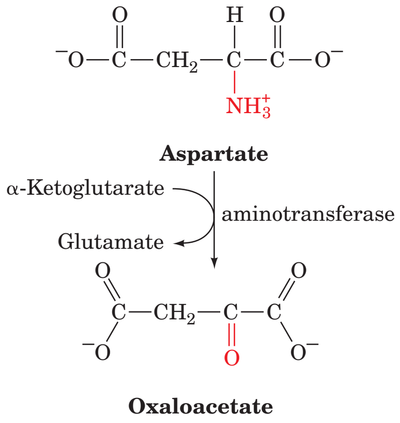

Asparagine is also converted to oxaloacetate in this manner after its hydrolysis to aspartate by **L-asparaginase:**

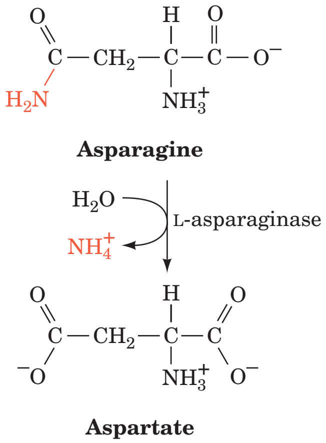

Interestingly, L-asparaginase is an effective chemotherapeutic agent in the treatment of cancers that must obtain asparagine from the blood, particularly **acute lymphoblastic leukemia.**

C | Arginine, Glutamate, Glutamine, Histidine, and Proline Are Degraded to α-Ketoglutarate

Arginine, glutamine, histidine, and proline are all degraded by conversion to glutamate (Fig. 21-17), which in turn is oxidized to α-ketoglutarate by glutamate dehydrogenase (Section 21-2B). Conversion of glutamine to glutamate involves only one reaction: hydrolysis by **glutaminase.** In the kidney, the action of glutaminase produces ammonia, which combines with a proton to form the ammonium ion (NH_4^+) and is excreted. During metabolic acidosis (Box 2-1), kidney glutaminase helps eliminate excess acid. Although free NH_3 in the blood could serve the same acid-absorbing purpose, ammonia is toxic. It is therefore converted to glutamine by glutamine synthetase in the liver (Section 21-5A). Glutamine therefore acts as an ammonia transport system between the liver, where much of it is synthesized, and the kidneys, where it is hydrolyzed by glutaminase.

Histidine's conversion to glutamate is more complicated: It is nonoxidatively deaminated, then it is hydrated, and its imidazole ring is cleaved to form ***N*-formiminoglutamate.** The formimino group is then transferred to tetrahydrofolate, forming glutamate and ***N*^{5}-formimino-tetrahydrofolate** (Section 21-4D). Both arginine and proline are converted to glutamate through the intermediate formation of **glutamate-5-semialdehyde.**

Figure 21-17 | The degradation of arginine, glutamate, glutamine, histidine, and proline to α-ketoglutarate. The enzymes catalyzing the reactions are (**1**) glutamate dehydrogenase, (**2**) glutaminase, (**3**) arginase, (**4**) ornithine-δ-aminotransferase, (**5**) glutamate-5-semialdehyde dehydrogenase, (**6**) proline oxidase, (**7**) spontaneous, (**8**) histidine ammonia lyase, (**9**) urocanate hydratase, (**10**) imidazolone propionase, and (**11**) glutamate formiminotransferase.

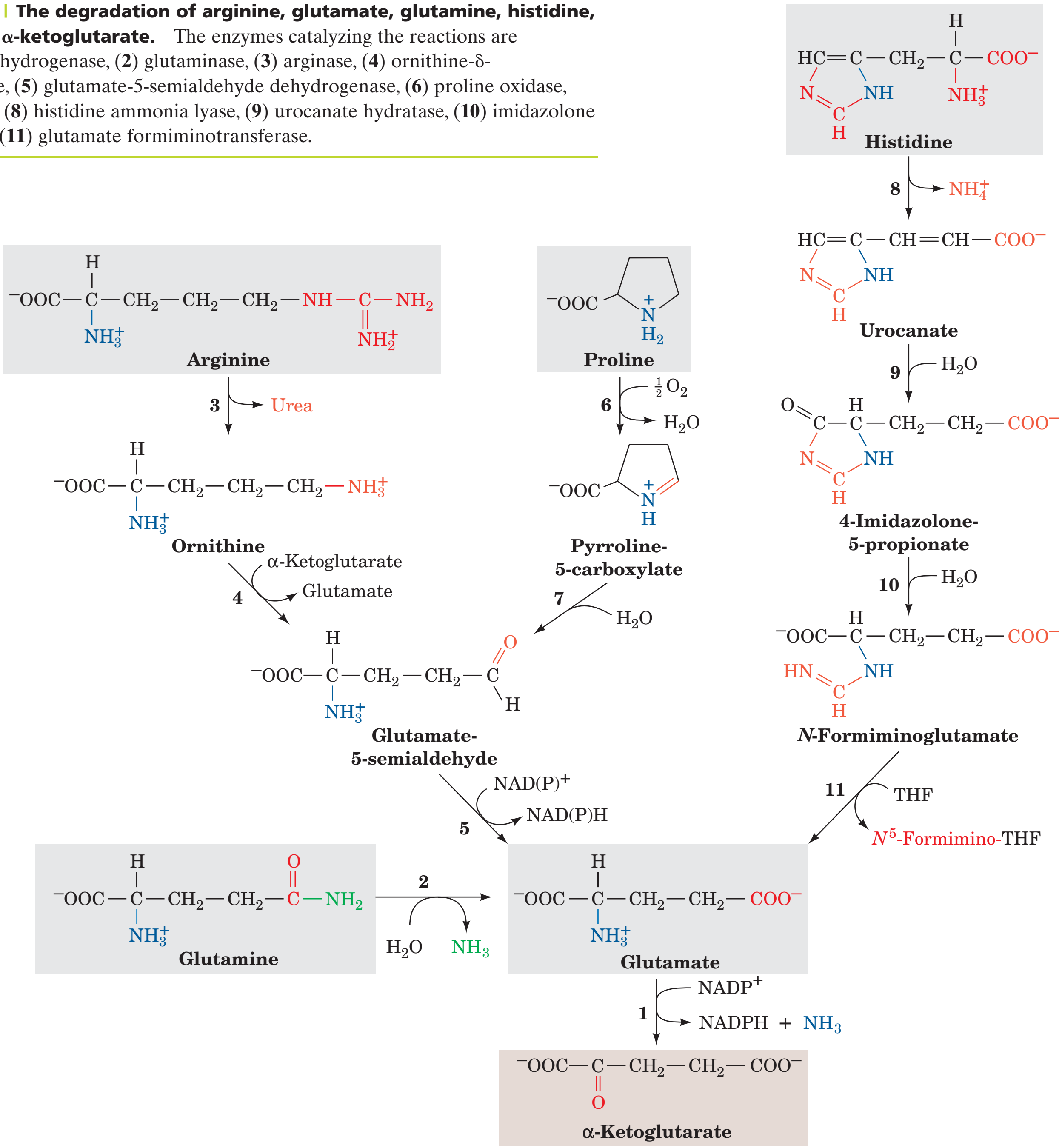
Histidine
8
NH_4^+
Urocanate
9
H_2O
4-Imidazolone-5-propionate
10
H_2O
N-Formiminoglutamate
11
THF
N^5-Formimino-THF
Arginine
3
Urea
Ornithine
α-Ketoglutarate
Glutamate
4
Proline
6
$\frac{1}{2}O_2$
H_2O
Pyrroline-5-carboxylate
7
H_2O
Glutamate-5-semialdehyde
$NAD(P)^+$
NAD(P)H
5
Glutamine
2
H_2O
NH_3
Glutamate
1
$NADP^+$
NADPH + NH_3
α-Ketoglutarate

D | Isoleucine, Methionine, and Valine Are Degraded to Succinyl-CoA

Isoleucine, methionine, and valine have complex degradative pathways that all yield propionyl-CoA, which is also a product of odd-chain fatty acid degradation. Propionyl-CoA is converted to succinyl-CoA by a series of reactions requiring biotin and coenzyme B_{12} (Section 20-2E).

Methionine Breakdown Involves Synthesis of *S*-Adenosylmethionine and Cysteine. Methionine degradation (Fig. 21-18) begins with its reaction with ATP to form ***S*-adenosylmethionine (SAM;** alternatively **AdoMet).** *This sulfonium ion's highly reactive methyl group makes it an important biological methylating agent.* For instance, SAM is the methyl donor

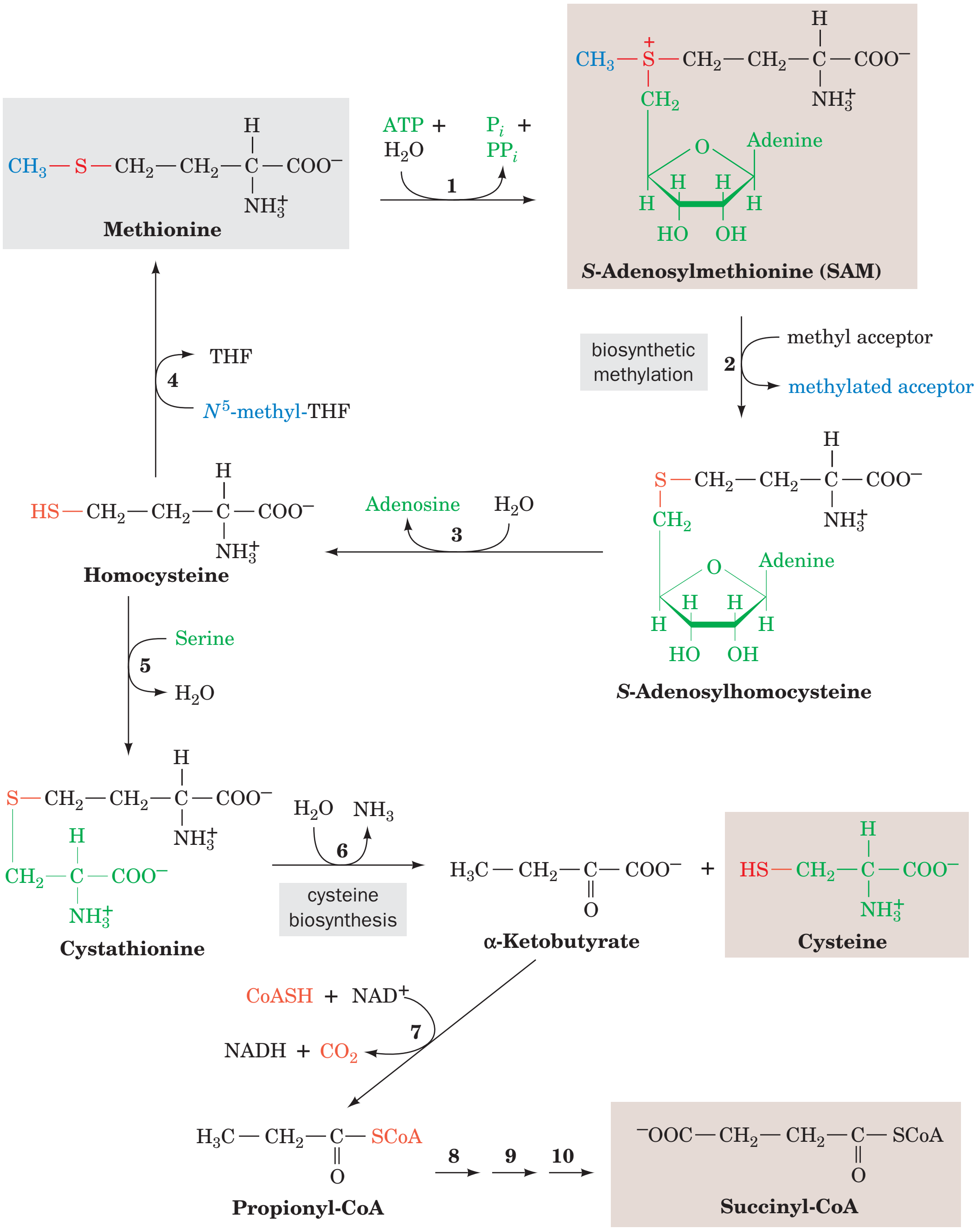

Methionine
ATP + H2O
Pi + PPi
1
S-Adenosylmethionine (SAM)
Adenine
biosynthetic methylation
2
methyl acceptor
methylated acceptor
THF
4
N5-methyl-THF
Homocysteine
Adenosine
H2O
3
S-Adenosylhomocysteine
Serine
5
H2O
Cystathionine
H2O NH3
6
cysteine biosynthesis
α-Ketobutyrate
Cysteine
CoASH + NAD+
7
NADH + CO2
Propionyl-CoA
8 9 10
Succinyl-CoA

Figure 21-18 | Methionine degradation. This pathway yields cysteine and succinyl-CoA. The enzymes are (**1**) methionine adenosyltransferase in a reaction that yields the biological methylating agent *S*-adenosylmethionine (SAM), (**2**) methyltransferase, (**3**) adenosylhomocysteinase, (**4**) methionine synthase (a coenzyme B_{12}–dependent enzyme), (**5**) cystathionine β-synthase (a PLP-dependent enzyme), (**6**) cystathionine γ-lyase, (**7**) α-keto acid dehydrogenase, (**8**) propionyl-CoA carboxylase, (**9**) methylmalonyl-CoA racemase, and (**10**) methylmalonyl-CoA mutase (a coenzyme B_{12}–dependent enzyme). Reactions 8–10 are discussed in Section 20-2E.

in the synthesis of phosphatidylcholine from phosphatidylethanolamine (Section 20-6A).

Donation of a methyl group from SAM leaves ***S*-adenosylhomocysteine,** which is then hydrolyzed to adenosine and **homocysteine.** The homocysteine can be methylated to re-form methionine via a reaction in which ***N*^{5}-methyltetrahydrofolate** (see below) is the methyl donor. Alternatively, the homocysteine can combine with serine to yield **cystathionine,** which subsequently forms cysteine (cysteine biosynthesis) and **α-ketobutyrate.** The α-ketobutyrate continues along the degradative pathway to propionyl-CoA and then succinyl-CoA. High homocysteine levels are associated with disease (Box 21-1).

Tetrahydrofolates Are One-Carbon Carriers. Many biosynthetic processes involve the addition of a C_1 unit to a metabolic precursor. In most carboxylation reactions (e.g., pyruvate carboxylase; Fig. 16-18), the enzyme uses a biotin cofactor. In some reactions, *S*-adenosylmethionine (Fig. 21-18) functions as a methylating agent. However, tetrahydrofolate (THF) is more versatile than either of those cofactors because it can transfer C_1 units in several oxidation states.

THF is a 6-methylpterin derivative linked in sequence to a ***p*-aminobenzoic acid** and a Glu residue:

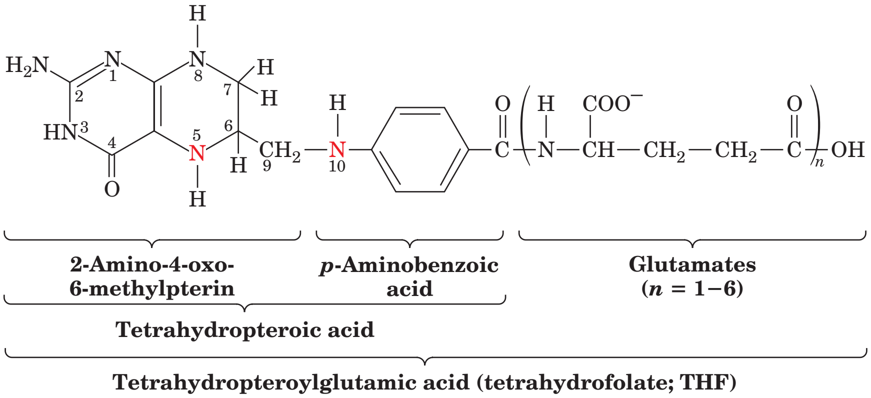
H₂N
HN
O
H
H
H
H
H
CH₂
H
N
O
H
COO⁻
CH
CH₂
CH₂
C
O
OH
n
1
2
3
4
5
6
7
8
9
10
2-Amino-4-oxo-6-methylpterin
p-Aminobenzoic acid
Glutamates (n = 1–6)
Tetrahydropteroic acid
Tetrahydropteroylglutamic acid (tetrahydrofolate; THF)

Up to five additional Glu residues are linked to the first glutamate via isopeptide bonds to form a polyglutamyl tail. THF is derived from the vitamin **folic acid** (Latin: *folium,* leaf), a doubly oxidized form of THF that must be enzymatically reduced before it becomes an active coenzyme (Fig. 21-19). Both reductions are catalyzed by **dihydrofolate reductase (DHFR).**

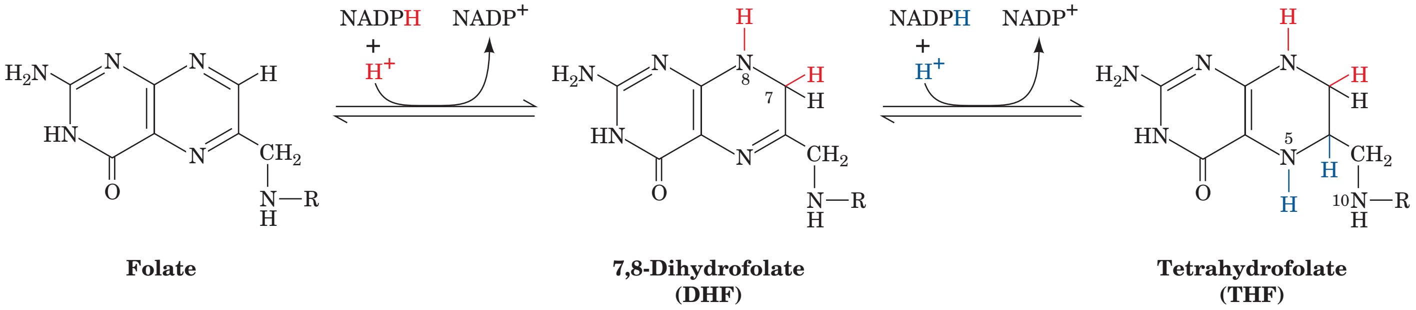
NADPH + H⁺
NADP⁺
NADPH + H⁺
NADP⁺
H₂N
HN
O
CH₂
N—R
H
5
7
8
10
Folate
7,8-Dihydrofolate (DHF)
Tetrahydrofolate (THF)

■ **Figure 21-19 | The two-stage reduction of folate to THF.** Both reactions are catalyzed by dihydrofolate reductase.

BOX 21-1 BIOCHEMISTRY IN HEALTH AND DISEASE

Homocysteine, a Marker of Disease

The cellular level of homocysteine depends on its rate of synthesis through methylation reactions utilizing SAM (Fig. 21-18, Reactions 2 and 3) and its rate of utilization through remethylation to form methionine (Fig. 21-18, Reaction 4) and reaction with serine to form cystathionine in the cysteine biosynthetic pathway (Fig. 21-18, Reaction 5). An increase in homocysteine levels leads to **hyperhomocysteinemia,** elevated concentrations of homocysteine in the blood, which is associated with cardiovascular disease. The link was first discovered in individuals with **homocysteinuria,** a disorder in which excess homocysteine is excreted in the urine. These individuals develop atherosclerosis as children, possibly because homocysteine causes oxidative damage to the walls of blood vessels even in the absence of elevated LDL levels (Section 20-7C).

Hyperhomocysteinemia is also associated with **neural tube defects,** the cause of a variety of severe birth defects including **spina bifida** (defects in the spinal column that often result in paralysis) and **anencephaly** (the invariably fatal failure of the brain to develop, which is the leading cause of infant death due to congenital anomalies). Hyperhomocysteinemia is readily controlled by ingesting the vitamin precursors of the coenzymes that participate in homocysteine breakdown, namely, B_6 (pyridoxine, the PLP precursor; Fig. 21-7), B_{12} (Fig. 20-17), and folate (Section 21-4D). Folate, especially, alleviates hyperhomocysteinemia; its administration to pregnant women dramatically reduces the incidence of neural tube defects in newborns. Because neural tube development is one of the earliest steps of embryogenesis, women of childbearing age are encouraged to consume adequate amounts of folate even before they become pregnant.

Around 10% of the population is homozygous for an Ala → Val mutation in **N^5,N^{10}-methylene-tetrahydrofolate reductase (MTHFR),** which catalyzes the conversion of N^5,N^{10}-methylene-THF to N^5-methyl-THF (Fig. 21-20, *top center*). This reaction generates the N^5-methyl-THF required to convert homocysteine to methionine (Fig. 21-18, Reaction 4). The mutation does not affect the enzyme's reaction kinetics but instead increases the rate at which its essential flavin cofactor dissociates. Folate derivatives that bind to the enzyme decrease the rate of flavin loss, thus increasing the enzyme's overall activity and decreasing the homocysteine concentration. The prevalence of the MTHFR mutation in the human population suggests that it has (or once had) some selective advantage; however, this is as yet a matter of speculation.

Mammals cannot synthesize folic acid, so it must be provided in the diet or by intestinal microorganisms.

C_1 units are covalently attached to THF at positions N5, N10, or both N5 and N10. These C_1 units, which may be at the oxidation levels of formate, formaldehyde, or methanol (Table 21-2), are all interconvertible by enzymatic redox reactions (Fig. 21-20).

THF acquires C_1 units in the conversion of serine to glycine by serine hydroxymethyltransferase (the reverse of Reaction 4, Fig. 21-14), in the cleavage of glycine (Fig. 21-14, Reaction 3), and in histidine breakdown (Fig. 21-17, Reaction 11). The C_1 units carried by THF are used in the synthesis of thymine nucleotides (Section 23-3B) and in the synthesis of methionine from homocysteine (Fig. 21-18). By promoting the latter process, supplemental folate helps prevent diseases associated with abnormally high levels of homocysteine (Box 21-1).

Table 21-2 Oxidation Levels of C_1 Groups Carried by THF

Oxidation Level	Group Carried	THF Derivative(s)
Methanol	Methyl ($—CH_3$)	N^5-Methyl-THF
Formaldehyde	Methylene ($—CH_2—$)	N^5,N^{10}-Methylene-THF
Formate	Formyl ($—CH{=}O$)	N^5-Formyl-THF, N^{10}-formyl-THF
	Formimino ($—CH{=}NH$)	N^5-Formimino-THF
	Methenyl ($—CH{=}$)	N^5,N^{10}-Methenyl-THF

Figure 21-20 | Interconversion of the C_1 units carried by THF.

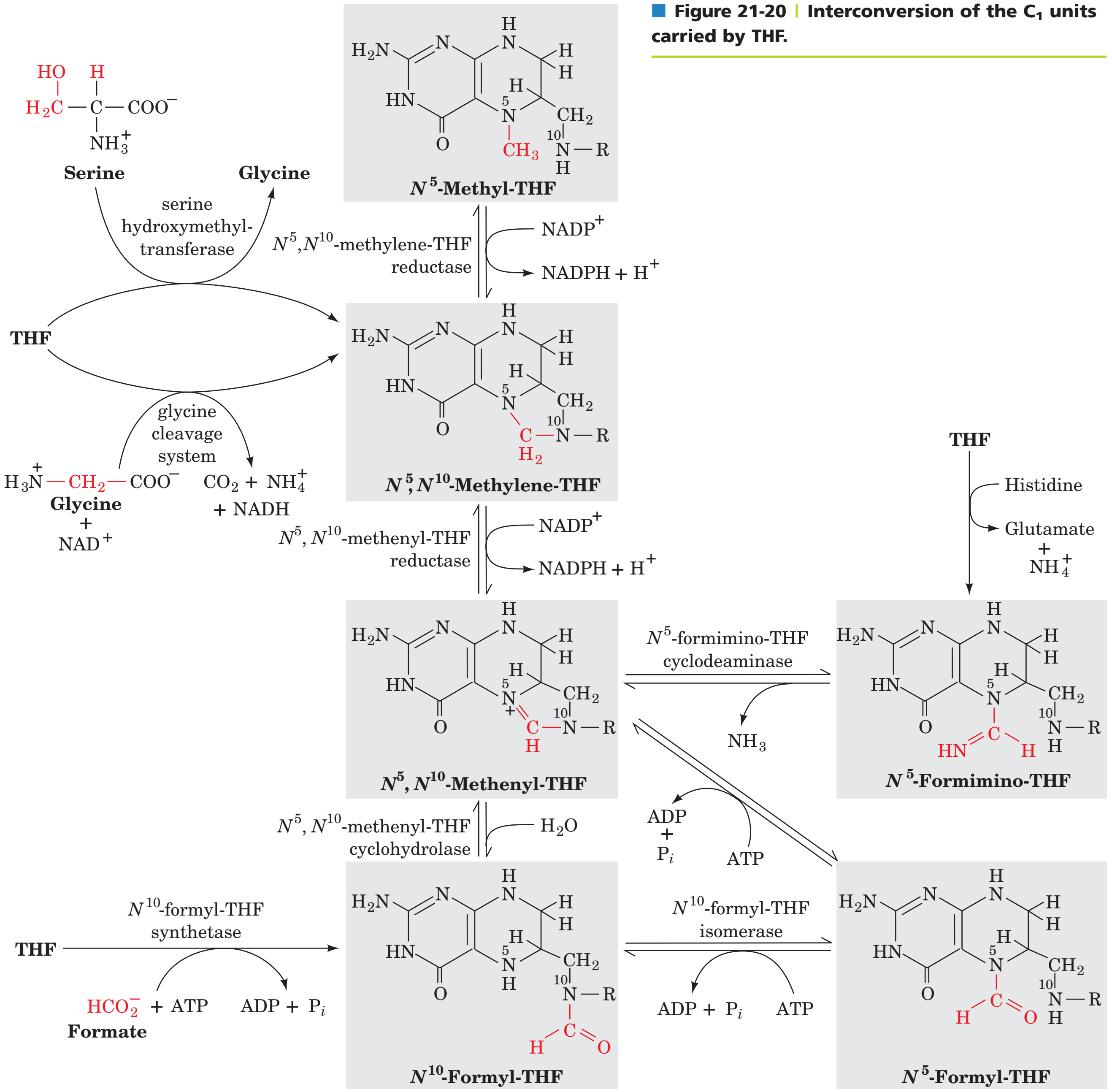
Serine
Glycine
serine hydroxymethyl-transferase
THF
glycine cleavage system
Glycine + NAD+
CO2 + NH4+ + NADH
N5-Methyl-THF
N5,N10-methylene-THF reductase
NADP+
NADPH + H+
N5,N10-Methylene-THF
N5,N10-methenyl-THF reductase
NADP+
NADPH + H+
N5,N10-Methenyl-THF
THF
Histidine
Glutamate + NH4+
N5-formimino-THF cyclodeaminase
NH3
N5-Formimino-THF
N5,N10-methenyl-THF cyclohydrolase
H2O
ADP + Pi
ATP
N10-formyl-THF synthetase
THF
HCO2− + ATP
Formate
ADP + Pi
N10-Formyl-THF
N10-formyl-THF isomerase
ADP + Pi
ATP
N5-Formyl-THF

Sulfonamides (sulfa drugs) such as **sulfanilamide** are antibiotics that are structural analogs of the *p*-aminobenzoic acid constituent of THF:

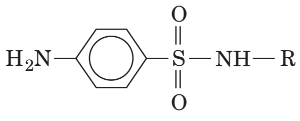
Sulfonamides
(R = H, sulfanilamide)

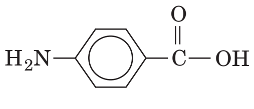
***p*-Aminobenzoic acid**

They competitively inhibit bacterial synthesis of THF at the *p*-aminobenzoic acid incorporation step, thereby blocking THF-requiring reactions. The inability of mammals to synthesize folic acid leaves them unaffected by sulfonamides, which accounts for the medical utility of these widely used antibacterial agents.

Branched-Chain Amino Acid Degradation Involves Acyl-CoA Oxidation. Degradation of the branched-chain amino acids isoleucine, leucine, and valine begins with three reactions that employ common enzymes (Fig. 21-21):

1. Transamination to the corresponding α-keto acid.
2. Oxidative decarboxylation to the corresponding acyl-CoA.
3. Dehydrogenation by FAD to form a double bond.

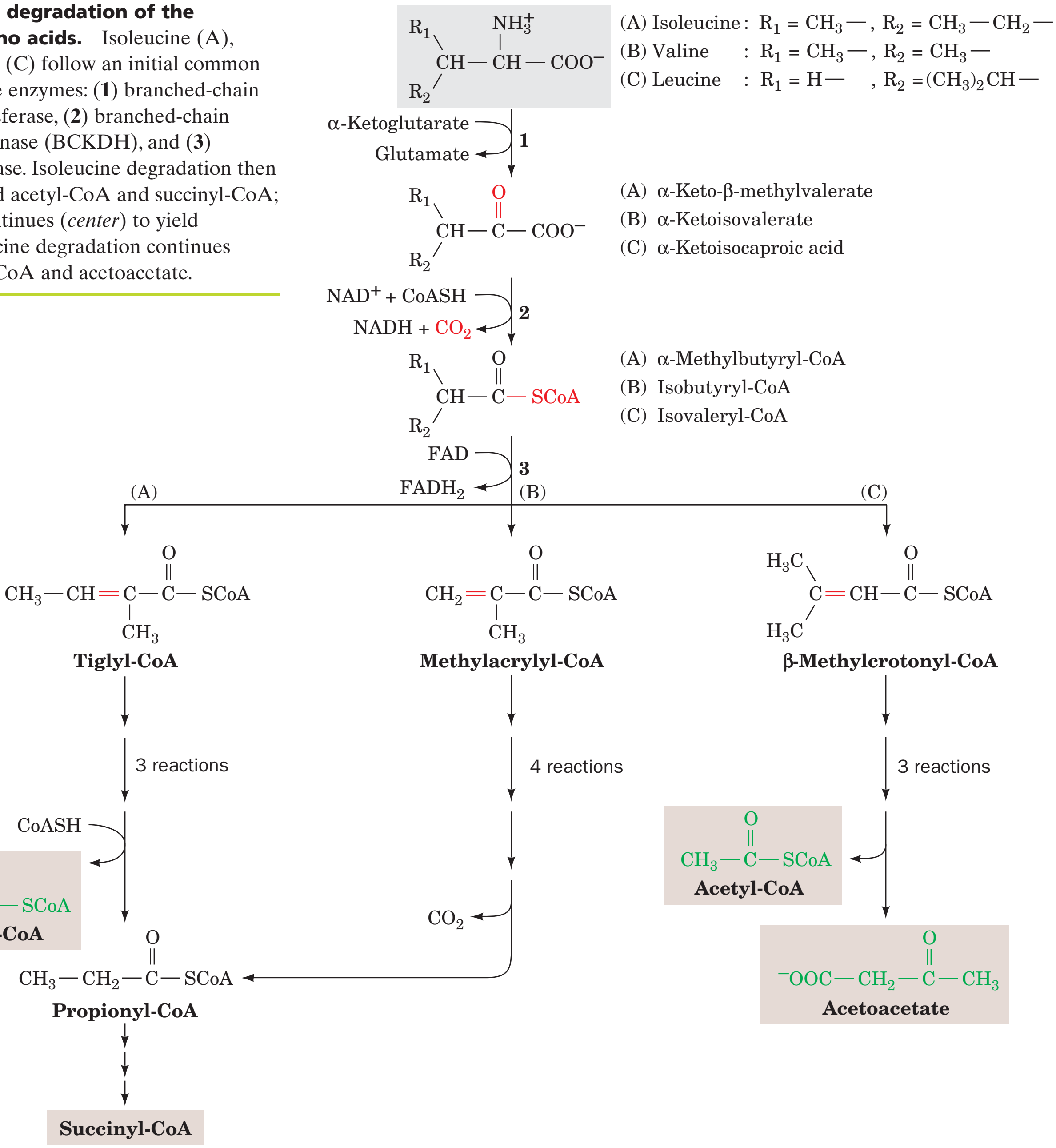

R_1, R_2, CH—CH—COO⁻, NH_3^+
(A) Isoleucine : $R_1 = CH_3$—, $R_2 = CH_3—CH_2$—
(B) Valine : $R_1 = CH_3$—, $R_2 = CH_3$—
(C) Leucine : $R_1 = H$—, $R_2 = (CH_3)_2CH$—
α-Ketoglutarate
Glutamate
1
(A) α-Keto-β-methylvalerate
(B) α-Ketoisovalerate
(C) α-Ketoisocaproic acid
NAD^+ + CoASH
NADH + CO_2
2
(A) α-Methylbutyryl-CoA
(B) Isobutyryl-CoA
(C) Isovaleryl-CoA
FAD
$FADH_2$
3
(A)
(B)
(C)
Tiglyl-CoA
Methylacrylyl-CoA
β-Methylcrotonyl-CoA
3 reactions
4 reactions
3 reactions
CoASH
Acetyl-CoA
CO_2
Acetyl-CoA
Propionyl-CoA
Acetoacetate
Succinyl-CoA

Figure 21-21 | The degradation of the branched-chain amino acids. Isoleucine (A), valine (B), and leucine (C) follow an initial common pathway utilizing three enzymes: (**1**) branched-chain amino acid aminotransferase, (**2**) branched-chain α-keto acid dehydrogenase (BCKDH), and (**3**) acyl-CoA dehydrogenase. Isoleucine degradation then continues (*left*) to yield acetyl-CoA and succinyl-CoA; valine degradation continues (*center*) to yield succinyl-CoA; and leucine degradation continues (*right*) to yield acetyl-CoA and acetoacetate.

The remaining reactions of the isoleucine degradation pathway are analogous to those of fatty acid oxidation (Section 20-2C), thereby yielding acetyl-CoA and propionyl-CoA, which is subsequently converted via three reactions to succinyl-CoA. The degradation of valine, which contains one less carbon than isoleucine, yields CO_2 and propionyl-CoA, which is then converted to succinyl-CoA. The further degradation of leucine, which yields acetoacetate instead of propionyl-CoA, is considered in Section 21-4E.

Branched-chain α-keto acid dehydrogenase (BCKDH), which catalyzes Reaction 2 of Fig. 21-21, is a multienzyme complex that closely resembles the pyruvate dehydrogenase and α-ketoglutarate dehydrogenase complexes (Sections 17-2 and 17-3D). Indeed, all three multienzyme complexes share a common subunit, E_3 (dihydrolipoamide dehydrogenase), and employ the coenzymes TPP, lipoamide, and FAD in addition to their terminal oxidizing agent, NAD^+.

A genetic deficiency in BCKDH causes **maple syrup urine disease,** so named because the consequent buildup of branched-chain α-keto acids imparts the urine with the characteristic odor of maple syrup. Unless promptly treated by a diet low in branched-chain amino acids, maple syrup urine disease is rapidly fatal.

E | Leucine and Lysine Are Degraded Only to Acetyl-CoA and/or Acetoacetate

Leucine degradation begins in the same manner as isoleucine and valine degradation (Fig. 21-21), but the dehydrogenated CoA adduct β-methylcrotonyl-CoA is converted to acetyl-CoA and acetoacetate, a ketone body.

The predominant pathway for lysine degradation in mammalian liver produces acetoacetate and 2 CO_2 via the initial formation of the α-ketoglutarate–lysine adduct **saccharopine** (Fig. 21-22). This pathway is worth examining in detail because we have encountered 7 of its 11 reactions in other pathways. Reaction 4 is a PLP-dependent transamination. Reaction 5 is the oxidative decarboxylation of an α-keto acid by a multienzyme complex similar to pyruvate dehydrogenase (Section 17-2). Reactions 6, 8, and 9 are standard reactions of fatty acyl-CoA oxidation: dehydrogenation by FAD, hydration, and dehydrogenation by NAD^+. Reactions 10 and 11 are standard reactions in ketone body formation. Two moles of CO_2 are produced at Reactions 5 and 7 of the pathway.

The saccharopine pathway is thought to predominate in mammals because a genetic defect in the enzyme that catalyzes Reaction 1 in the sequence results in **hyperlysinemia** and **hyperlysinuria** (elevated levels of lysine in the blood and urine, respectively) along with mental and physical retardation. This is yet another example of how the study of rare inherited disorders has helped to trace metabolic pathways.

F | Tryptophan Is Degraded to Alanine and Acetoacetate

The complexity of the major tryptophan degradation pathway (outlined in Fig. 21-23) precludes a detailed discussion of all its reactions. However, one reaction is of particular interest: The fourth reaction is catalyzed by **kynureninase,** whose PLP group facilitates cleavage of the C_β—C_γ bond to release alanine. The kynureninase reaction follows the same initial steps as transamination (Fig. 21-8), but an enzyme nucleophilic group then attacks C_γ of the resonance-stabilized intermediate, resulting in C_β—C_γ bond cleavage. The remainder of the tryptophan skeleton is converted in five

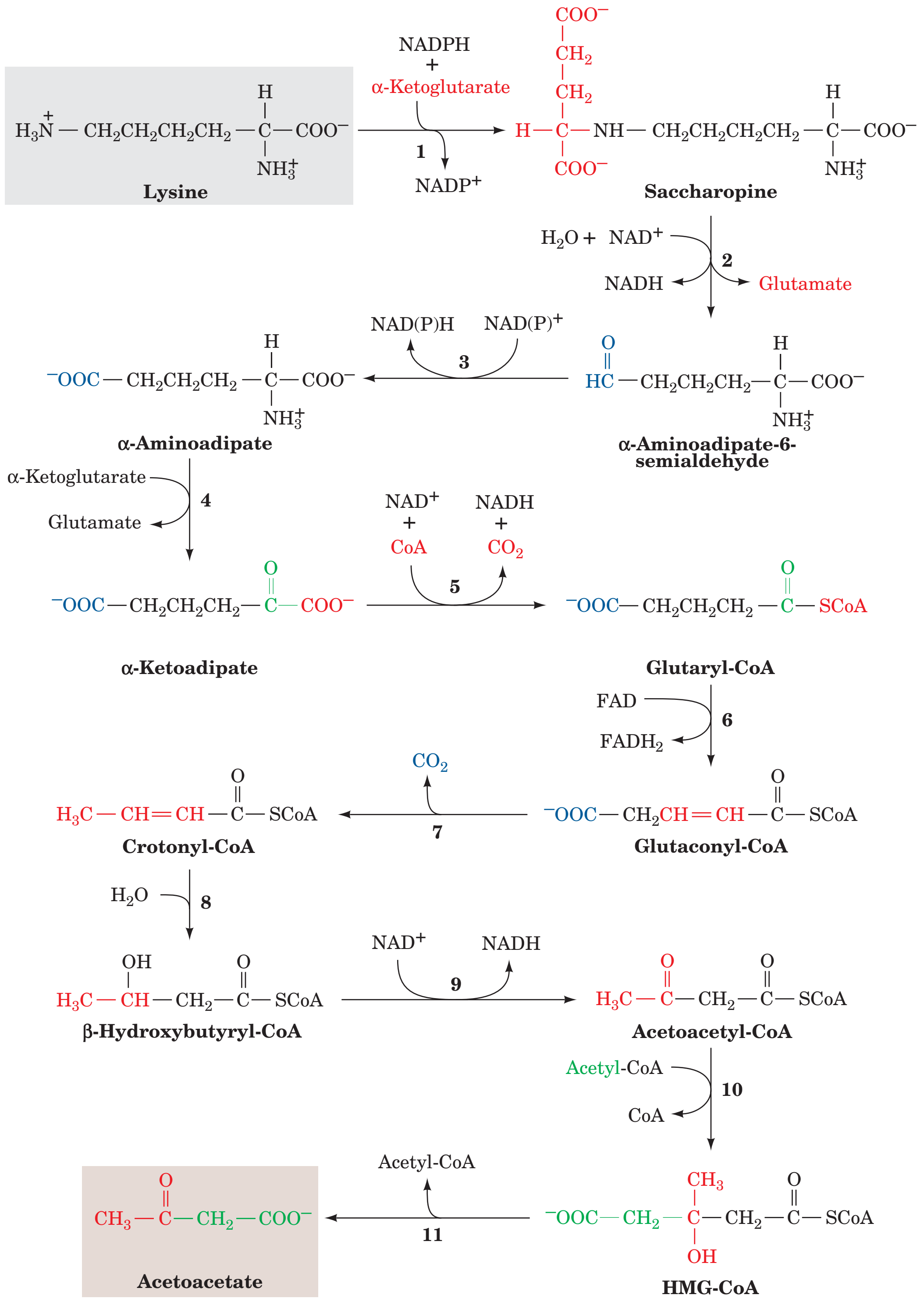
Lysine
NADPH
+
α-Ketoglutarate
1
NADP+
Saccharopine
H2O + NAD+
NADH
2
Glutamate
α-Aminoadipate-6-semialdehyde
NAD(P)H
NAD(P)+
3
α-Aminoadipate
α-Ketoglutarate
Glutamate
4
α-Ketoadipate
NAD+ + CoA
NADH + CO2
5
Glutaryl-CoA
FAD
FADH2
6
Glutaconyl-CoA
CO2
7
Crotonyl-CoA
H2O
8
β-Hydroxybutyryl-CoA
NAD+
NADH
9
Acetoacetyl-CoA
Acetyl-CoA
CoA
10
HMG-CoA
Acetyl-CoA
11
Acetoacetate

Figure 21-22 | The pathway of lysine degradation in mammalian liver. The enzymes are (**1**) saccharopine dehydrogenase ($NADP^+$, lysine forming), (**2**) saccharopine dehydrogenase (NAD^+, glutamate forming), (**3**) aminoadipate semialdehyde dehydrogenase, (**4**) aminoadipate aminotransferase (a PLP-dependent enzyme), (**5**) α-keto acid dehydrogenase, (**6**) glutaryl-CoA dehydrogenase, (**7**) decarboxylase, (**8**) enoyl-CoA hydratase, (**9**) β-hydroxyacyl-CoA dehydrogenase, (**10**) HMG-CoA synthase, and (**11**) HMG-CoA lyase. Reactions 10 and 11 are discussed in Section 20-3.

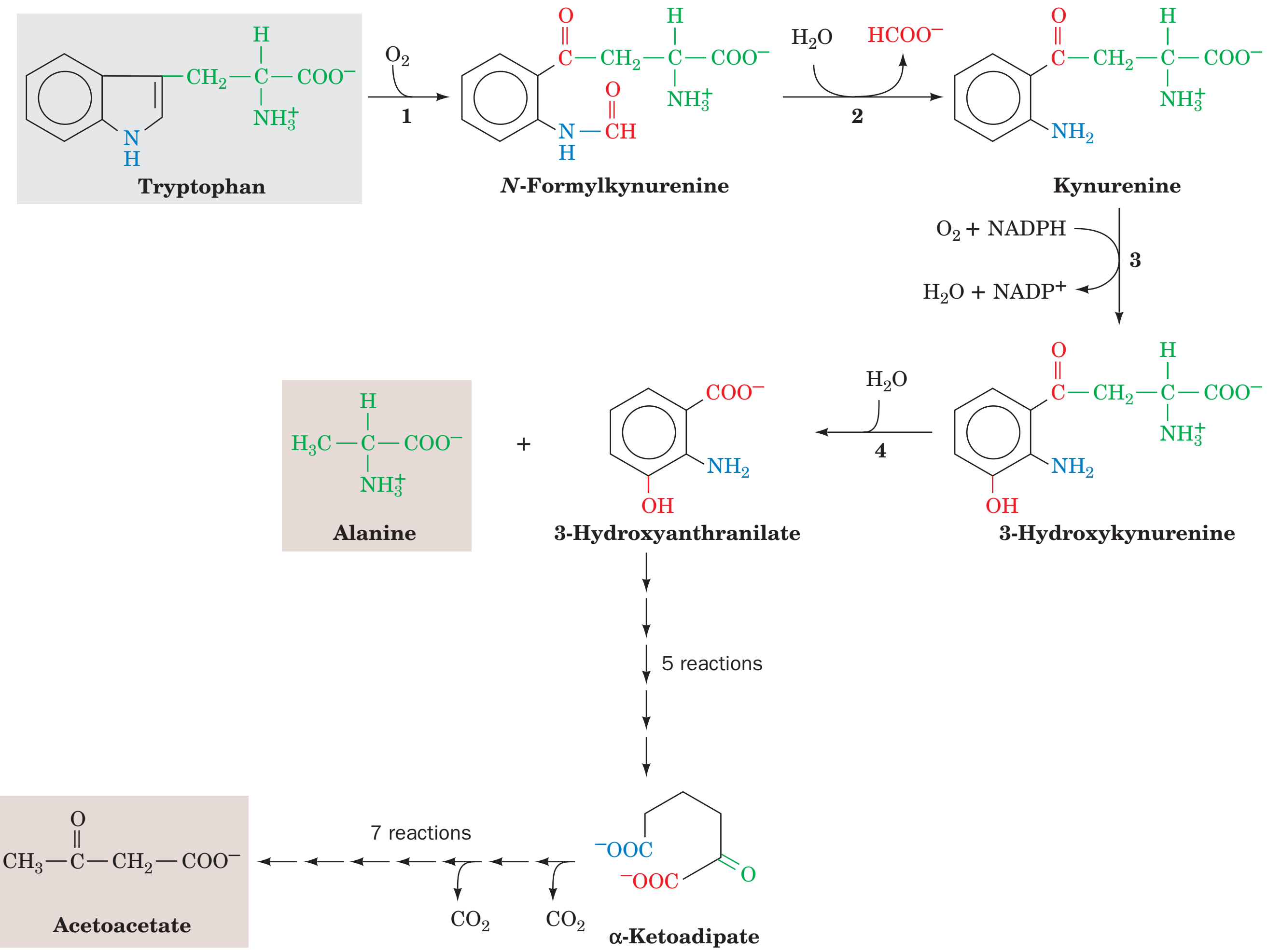
Tryptophan
O_2
1
N-Formylkynurenine
H_2O
$HCOO^-$
2
Kynurenine
O_2 + NADPH
H_2O + $NADP^+$
3
3-Hydroxykynurenine
H_2O
4
3-Hydroxyanthranilate
+
Alanine
5 reactions
α-Ketoadipate
7 reactions
CO_2
CO_2
Acetoacetate

Figure 21-23 | The pathway of tryptophan degradation. The enzymatic reactions shown are (**1**) tryptophan-2,3-dioxygenase, (**2**) formamidase, (**3**) kynurenine-3-monooxygenase, and (**4**) kynureninase (a PLP-dependent enzyme). Five reactions convert 3-hydroxyanthranilate to α-ketoadipate, which is converted to acetyl-CoA and acetoacetate in seven reactions as shown in Fig. 21-22, Reactions 5–11.

reactions to α-ketoadipate, which is also an intermediate in lysine degradation. α-Ketoadipate is broken down to 2 CO_2 and acetoacetate in seven reactions, as shown in Fig. 21-22.

G | Phenylalanine and Tyrosine Are Degraded to Fumarate and Acetoacetate

Since the first reaction in phenylalanine degradation is its hydroxylation to tyrosine, a single pathway (Fig. 21-24) is responsible for the breakdown of both of these amino acids. The final products of the six-reaction degradation are fumarate, a citric acid cycle intermediate, and acetoacetate, a ketone body. Defects in the enzymes that catalyze Reactions 1 and 4 cause disease (Box 21-2).

Pterins Are Redox Cofactors. The hydroxylation of phenylalanine by the Fe(III)-containing enzyme **phenylalanine hydroxylase** (Fig. 21-24, Reaction 1) requires the cofactor **biopterin,** a **pterin** derivative. Pterins are compounds that contain the **pteridine** ring (Fig. 21-25). Note the resemblance

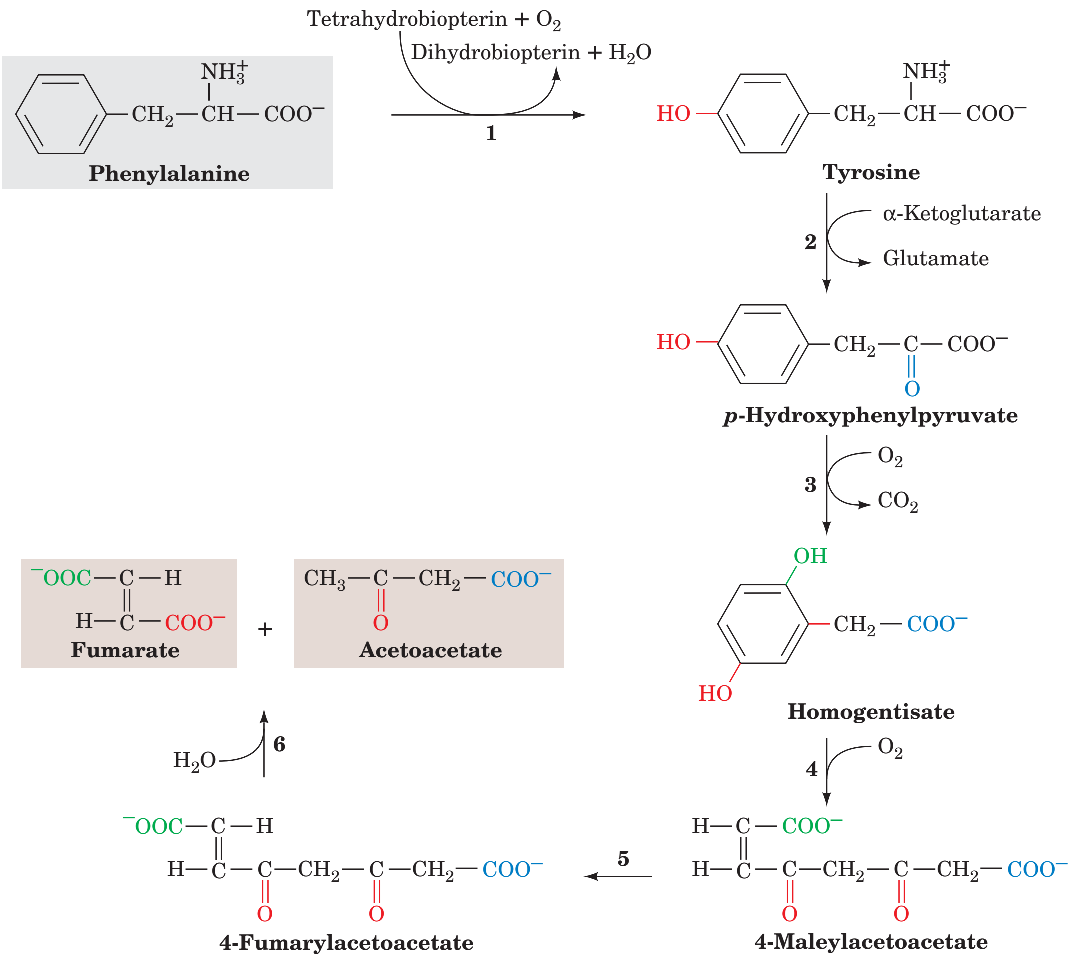
Phenylalanine
Tetrahydrobiopterin + O_2
Dihydrobiopterin + H_2O
1
Tyrosine
2
α-Ketoglutarate
Glutamate
p-Hydroxyphenylpyruvate
3
O_2
CO_2
Homogentisate
4
O_2
4-Maleylacetoacetate
5
4-Fumarylacetoacetate
6
H_2O
Fumarate
+
Acetoacetate

Figure 21-24 | **The pathway of phenylalanine degradation.** The enzymes involved are (**1**) phenylalanine hydroxylase, (**2**) aminotransferase, (**3**) *p*-hydroxyphenylpyruvate dioxygenase, (**4**) homogentisate dioxygenase, (**5**) maleylacetoacetate isomerase, and (**6**) fumarylacetoacetase.

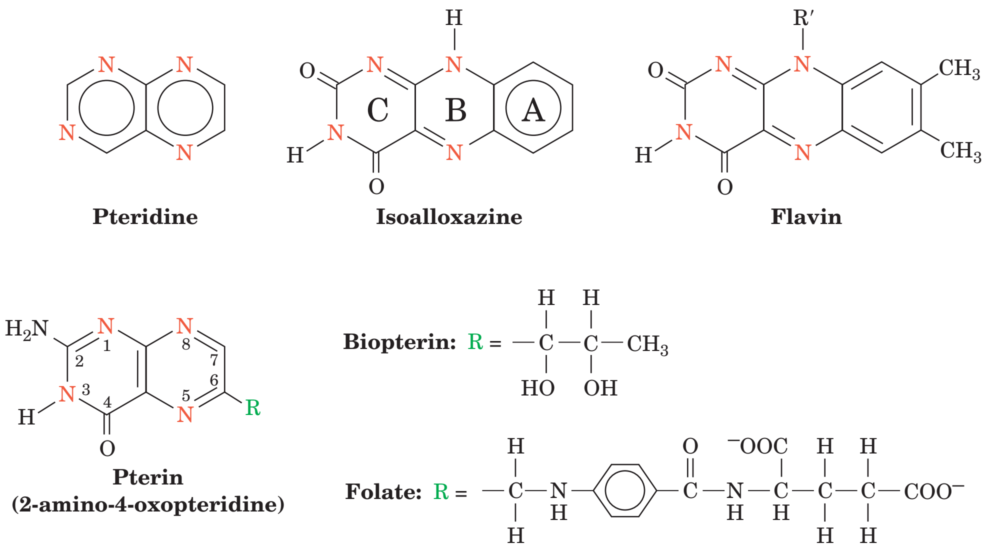
Pteridine
Isoalloxazine
C
B
A
Flavin
Pterin
(2-amino-4-oxopteridine)
Biopterin: R =
Folate: R =

Figure 21-25 | **The pteridine ring nucleus of biopterin and folate.** Note the similar structures of pteridine and the isoalloxazine ring of flavin coenzymes.

BOX 21-2 **BIOCHEMISTRY IN HEALTH AND DISEASE**

Phenylketonuria and Alcaptonuria Result from Defects in Phenylalanine Degradation

Archibald Garrod realized in the early 1900s that human genetic diseases result from specific enzyme deficiencies. We have repeatedly seen how this realization has contributed to the elucidation of metabolic pathways. The first such disease Garrod recognized was **alcaptonuria,** which results in the excretion of large quantities of **homogentisic acid** (Section 14-4). This condition results from deficiency of **homogentisate dioxygenase** (Fig. 21-24, Reaction 4). Alcaptonurics suffer no ill effects other than arthritis later in life (although their urine darkens alarmingly on exposure to air because of the rapid oxidation of the homogentisate they excrete).

Individuals suffering from **phenylketonuria (PKU)** are not so fortunate. Severe mental retardation occurs within a few months of birth if the disease is not detected and treated immediately. PKU is caused by the inability to hydroxylate phenylalanine (Fig. 21-24, Reaction 1) and therefore results in increased blood levels of phenylalanine **(hyperphenylalaninemia).** The excess phenylalanine is transaminated to **phenylpyruvate** by an otherwise minor pathway. The "spillover" of phenylpyruvate (a phenylketone) into the urine was the first observation connected with the disease and gave the disease its name. All babies born in the United States are now screened for PKU immediately after birth by testing for elevated levels of phenylalanine in the blood.

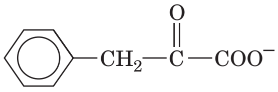

Phenylpyruvate

Classical PKU results from a deficiency in phenylalanine hydroxylase. When this was established in 1947, it was the first inborn error of metabolism whose basic biochemical defect had been identified. Since all of the tyrosine breakdown enzymes are normal, treatment consists in providing the patient with a low-phenylalanine diet and monitoring the blood level of phenylalanine to ensure that it remains within normal limits for the first 5 to 10 years of life (the adverse effects of hyperphenylalaninemia seem to disappear after that age). **Aspartame (NutraSweet),** an often used sweetening ingredient in diet soft drinks and many other dietetic food products, is Asp-Phe-methyl ester (Box 8-2) and is therefore a source of dietary phenylalanine. Consequently, a warning label for phenylketonurics appears on all those products.

Phenylalanine hydroxylase deficiency also accounts for another common symptom of PKU: Its victims have lighter hair and skin color than their siblings. This is because elevated phenylalanine levels inhibit tyrosine hydroxylation, the first reaction in the formation of the skin pigment **melanin** (Fig. 21-39).

Other variants of hyperphenylalaninemia have been discovered since the introduction of infant screening techniques. These are caused by deficiencies in the enzymes catalyzing the formation or regeneration of 5,6,7,8-tetrahydrobiopterin, the phenylalanine hydroxylase cofactor (Fig. 21-26).

---

between the pteridine ring and the isoalloxazine ring of the flavin coenzymes (Fig. 14-12); the positions of the nitrogen atoms in pteridine are identical to those of the B and C rings of isoalloxazine. Folate derivatives also contain the pterin ring (Section 21-4D).

Pterins, like flavins, participate in biological oxidations. The active form of biopterin is the fully reduced form, **5,6,7,8-tetrahydrobiopterin.** It is produced from **7,8-dihydrobiopterin** and NADPH, in what may be considered a priming reaction, by dihydrofolate reductase (Fig. 21-26), which simultaneously reduces dihydrofolate to tetrahydrofolate (Fig. 21-19). In the phenylalanine hydroxylase reaction, 5,6,7,8-tetrahydrobiopterin is hydroxylated to **pterin-4a-carbinolamine** (Fig. 21-26), which is then converted to 7,8-dihydrobiopterin **(quinoid form)** by **pterin-4a-carbinolamine dehydratase.** This quinoid is subsequently reduced by the NAD(P)H-requiring enzyme **dihydropteridine reductase** to regenerate the active cofactor. Although dihydrofolate reductase and dihydropteridine reductase produce the same product, they use different tautomers of the substrate.

■ CHECK YOUR UNDERSTANDING

Describe the two general metabolic fates of the carbon skeletons of amino acids.

List the seven metabolites that represent the end products of amino acid catabolism.

Describe the roles of the cofactors pyridoxal-5′-phosphate, tetrahydrofolate, and tetrahydrobiopterin in the catabolism of amino acids.

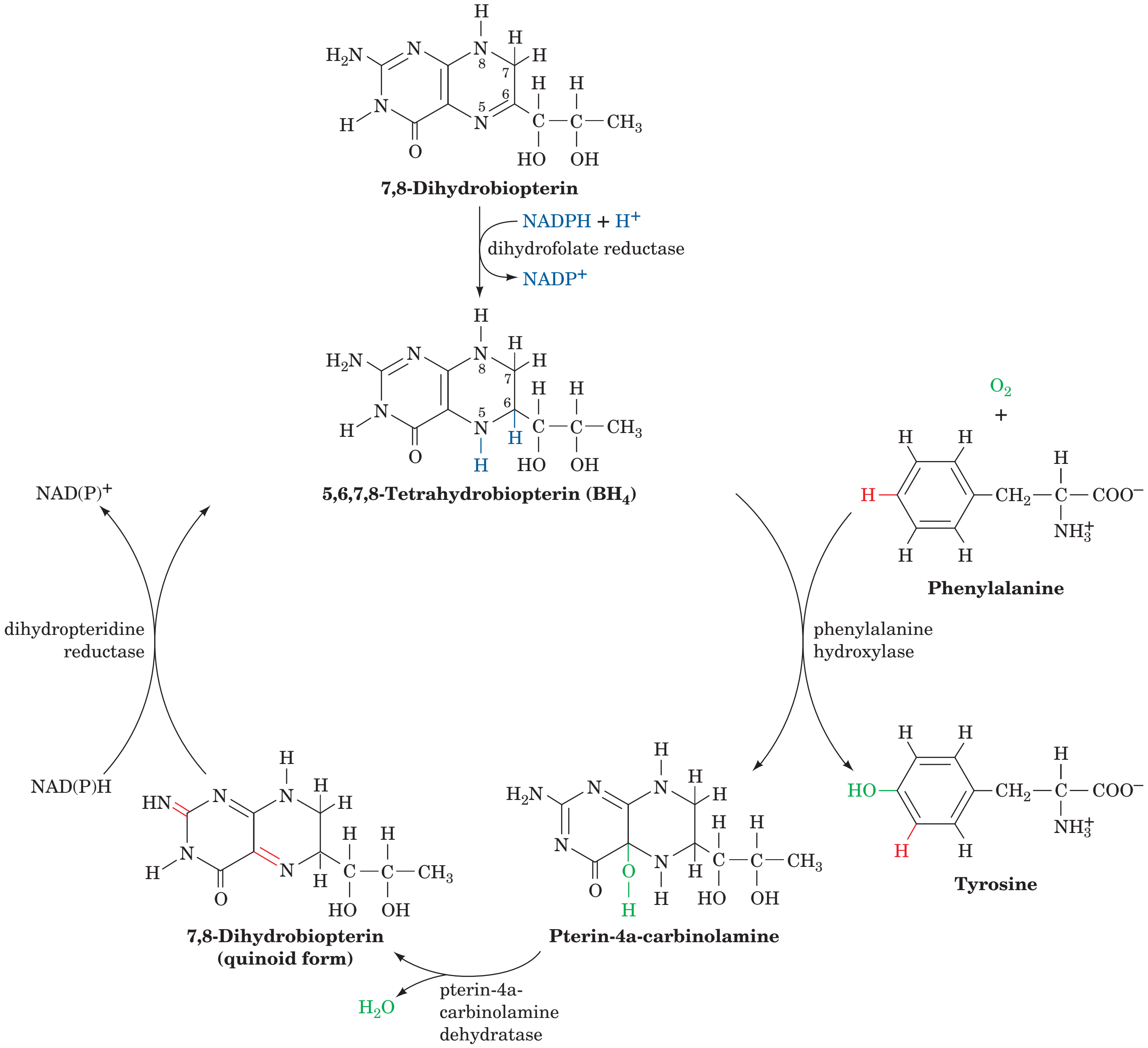
7,8-Dihydrobiopterin
NADPH + H+
dihydrofolate reductase
NADP+
5,6,7,8-Tetrahydrobiopterin (BH4)
O2
+
Phenylalanine
phenylalanine hydroxylase
Tyrosine
Pterin-4a-carbinolamine
pterin-4a-carbinolamine dehydratase
H2O
7,8-Dihydrobiopterin (quinoid form)
NAD(P)H
dihydropteridine reductase
NAD(P)+

■ **Figure 21-26** | **The formation, utilization, and regeneration of 5,6,7,8-tetrahydrobiopterin in the phenylalanine hydroxylase reaction.**

5 Amino Acid Biosynthesis

Many amino acids are synthesized by pathways that are present only in plants and microorganisms. Since mammals must obtain these amino acids in their diets, these substances are known as **essential amino acids.** The other amino acids, which can be synthesized by mammals from common intermediates, are termed **nonessential amino acids.** Their α-keto acid carbon skeletons are converted to amino acids by transamination reactions (Section 21-2A) utilizing the preformed α-amino nitrogen of another

LEARNING OBJECTIVES

- Understand that some amino acids are synthesized in one or a few steps from common metabolites.
- Understand that the essential amino acids are mostly derived from other amino acids and glucose metabolites.

Table 21-3 Essential and Nonessential Amino Acids in Humans

Essential	Nonessential
Arginine[a]	Alanine
Histidine	Asparagine
Isoleucine	Aspartate
Leucine	Cysteine
Lysine	Glutamate
Methionine	Glutamine
Phenylalanine	Glycine
Threonine	Proline
Tryptophan	Serine
Valine	Tyrosine

[a] Although mammals synthesize arginine, they cleave most of it to form urea (Section 21-3A).

amino acid, usually glutamate. Although it was originally presumed that glutamate can be synthesized from ammonia and α-ketoglutarate by GDH acting in reverse, it now appears that the predominant physiological direction of this enzyme is glutamate breakdown (Section 21-2B). Consequently, *preformed α-amino nitrogen should also be considered to be an essential nutrient.* In this context, it is interesting to note that, in addition to the four well-known taste receptors, those for sweet, sour, salty, and bitter tastes, a fifth taste receptor has recently been characterized, that for the meaty taste of **monosodium glutamate (MSG),** which is known as **umami** (a Japanese name).

The essential and nonessential amino acids for humans are listed in Table 21-3. Arginine is classified as essential, even though it is synthesized by the urea cycle (Section 21-3A), because it is required in greater amounts than can be produced by that route during the normal growth and development of children (but not adults). The essential amino acids occur in animal and vegetable proteins. Different proteins, however, contain different proportions of the essential amino acids. Milk proteins, for example, contain them all in the proportions required for proper human nutrition. Bean protein, on the other hand, contains an abundance of lysine but is deficient in methionine, whereas wheat is deficient in lysine but contains ample methionine. A balanced protein diet therefore must contain a variety of different protein sources that complement each other to supply the proper proportions of all the essential amino acids.

In this section we study the pathways involved in the formation of the nonessential amino acids. We also briefly consider such pathways for the essential amino acids as they occur in plants and microorganisms. Keep in mind that *there is considerable variation in these pathways among different species. In contrast, the basic pathways of carbohydrate and lipid metabolism are all but universal.*

A | Nonessential Amino Acids Are Synthesized from Common Metabolites

All the nonessential amino acids except tyrosine are synthesized by simple pathways leading from one of four common metabolic intermediates: pyruvate, oxaloacetate, α-ketoglutarate, and 3-phosphoglycerate. Tyrosine, which is really misclassified as being nonessential, is synthesized by the one-step hydroxylation of the essential amino acid phenylalanine (Fig. 21-24). Indeed, the dietary requirement for phenylalanine reflects the need for tyrosine as well. The presence of dietary tyrosine therefore decreases the need for phenylalanine.

Alanine, Asparagine, Aspartate, Glutamate, and Glutamine Are Synthesized from Pyruvate, Oxaloacetate, and α-Ketoglutarate. Pyruvate, oxaloacetate, and α-ketoglutarate are the α-keto acids (the so-called carbon skeletons) that correspond to alanine, aspartate, and glutamate, respectively. Indeed, the synthesis of each of these amino acids is a one-step transamination reaction (Fig. 21-27, Reactions 1–3). The ultimate source of the α-amino group in these transamination reactions is glutamate, which is synthesized in microorganisms, plants, and lower eukaryotes by glutamate synthase (Section 21-7), an enzyme that is absent in vertebrates.

Asparagine and glutamine are, respectively, synthesized from aspartate and glutamate by ATP-dependent amidation. In the **glutamine synthetase** reaction (Fig. 21-27, Reaction 5), glutamate is first activated by reaction

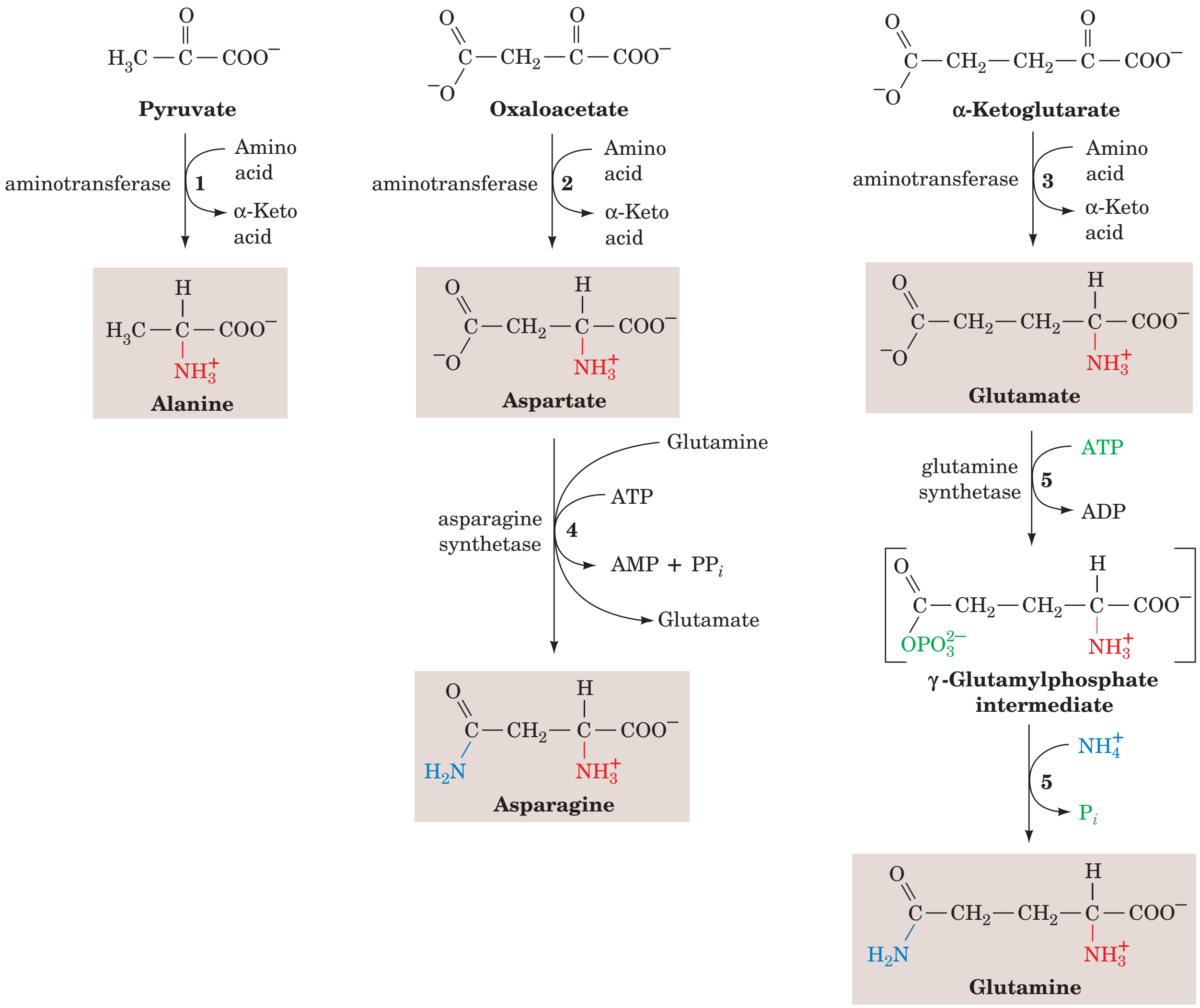
Pyruvate
Oxaloacetate
α-Ketoglutarate
aminotransferase
Amino acid
α-Keto acid
1
2
3
Alanine
Aspartate
Glutamate
Glutamine
ATP
asparagine synthetase
4
AMP + PP$_i$
Glutamate
glutamine synthetase
5
ADP
γ-Glutamylphosphate intermediate
NH$_4^+$
P$_i$
Asparagine
Glutamine

■ **Figure 21-27** | **The syntheses of alanine, aspartate, glutamate, asparagine, and glutamine.** These reactions involve, respectively, transamination of (**1**) pyruvate, (**2**) oxaloacetate, and (**3**) α-ketoglutarate, and amidation of (**4**) aspartate and (**5**) glutamate.

with ATP to form a **γ-glutamylphosphate** intermediate. NH_4^+ then displaces the phosphate group to produce glutamine. Curiously, aspartate amidation by **asparagine synthetase** to form asparagine follows a different route; it uses glutamine as its amino group donor and cleaves ATP to AMP + PP_i (Fig. 21-27, Reaction 4).

Glutamine Synthetase Is a Central Control Point in Nitrogen Metabolism. Glutamine is the amino group donor in the formation of many biosynthetic products as well as being a storage form of ammonia. The control of glutamine synthetase is therefore vital for regulating nitrogen metabolism. Mammalian glutamine synthetases are activated by α-ketoglutarate, the product of glutamate's oxidative deamination (Section 21-2B). This control presumably helps prevent the accumulation of the ammonia produced by that reaction.

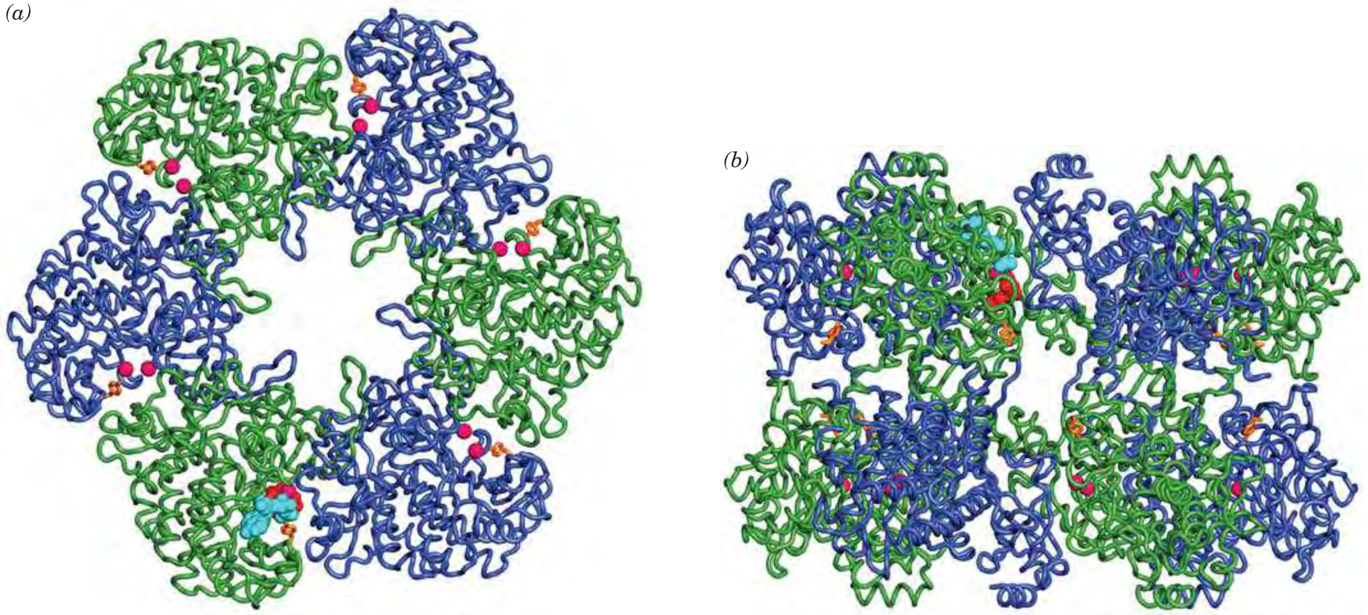

■ **Figure 21-28 | X-Ray structure of glutamine synthetase from the bacterium *Salmonella typhimurium.*** The enzyme consists of 12 identical subunits, here drawn in worm form, arranged with D_6 symmetry (the symmetry of a hexagonal prism). (*a*) View down the sixfold axis of symmetry showing only the six subunits of the upper ring in alternating blue and green. The subunits of the lower ring are roughly directly below those of the upper ring. A pair of Mn^{2+} ions (*magenta spheres*) that occupy the positions of the Mg^{2+} ions required for enzymatic activity are bound in each active site. Each adenylylation site, Tyr 397 (*orange*), lies between two subunits. Also drawn in one active site are ADP (*cyan*) and phosphinothricin (*red*), a competitive inhibitor of glutamate. (*b*) Side view along one of the twofold axes showing only the eight nearest subunits. The sixfold axis is vertical in this view. [Based on an X-ray structure by David Eisenberg, UCLA. PDBid 1FPY.]

Bacterial glutamine synthetase, as Earl Stadtman showed, has a much more elaborate control system. This enzyme, which consists of 12 identical 469-residue subunits arranged at the corners of a hexagonal prism (Fig. 21-28), is regulated by several allosteric effectors as well as by covalent modification. Several aspects of its control system bear note. *Nine allosteric feedback inhibitors, each with its own binding site, control the activity of bacterial glutamine synthetase in a cumulative manner.* Six of the effectors—histidine, tryptophan, carbamoyl phosphate (as synthesized by carbamoyl phosphate synthetase), glucosamine-6-phosphate, AMP, and CTP—are all end products of pathways leading from glutamine. The other three—alanine, serine, and glycine—reflect the cell's nitrogen level.

E. coli glutamine synthetase is covalently modified by **adenylylation** (addition of an AMP group) of a specific Tyr residue (Fig. 21-29). The enzyme's susceptibility to cumulative feedback inhibition increases, and its activity therefore decreases, with its degree of adenylylation. The level of adenylylation is controlled by a complex metabolic cascade that is conceptually similar to that controlling glycogen phosphorylase (Section 16-3B). Both adenylylation and deadenylylation of glutamine synthetase are catalyzed by **adenylyltransferase** in complex with a tetrameric regulatory protein, $\mathbf{P_{II}}$**.** This complex deadenylylates glutamine synthetase when P_{II} is **uridylylated** (also at a Tyr residue) and adenylylates glutamine synthetase when P_{II} lacks UMP residues. The level of P_{II} uridylylation, in turn, depends on the relative levels of two enzymatic activities located on the same protein: a **uridylyltransferase** that uridylylates P_{II} and a **uridylyl-removing**

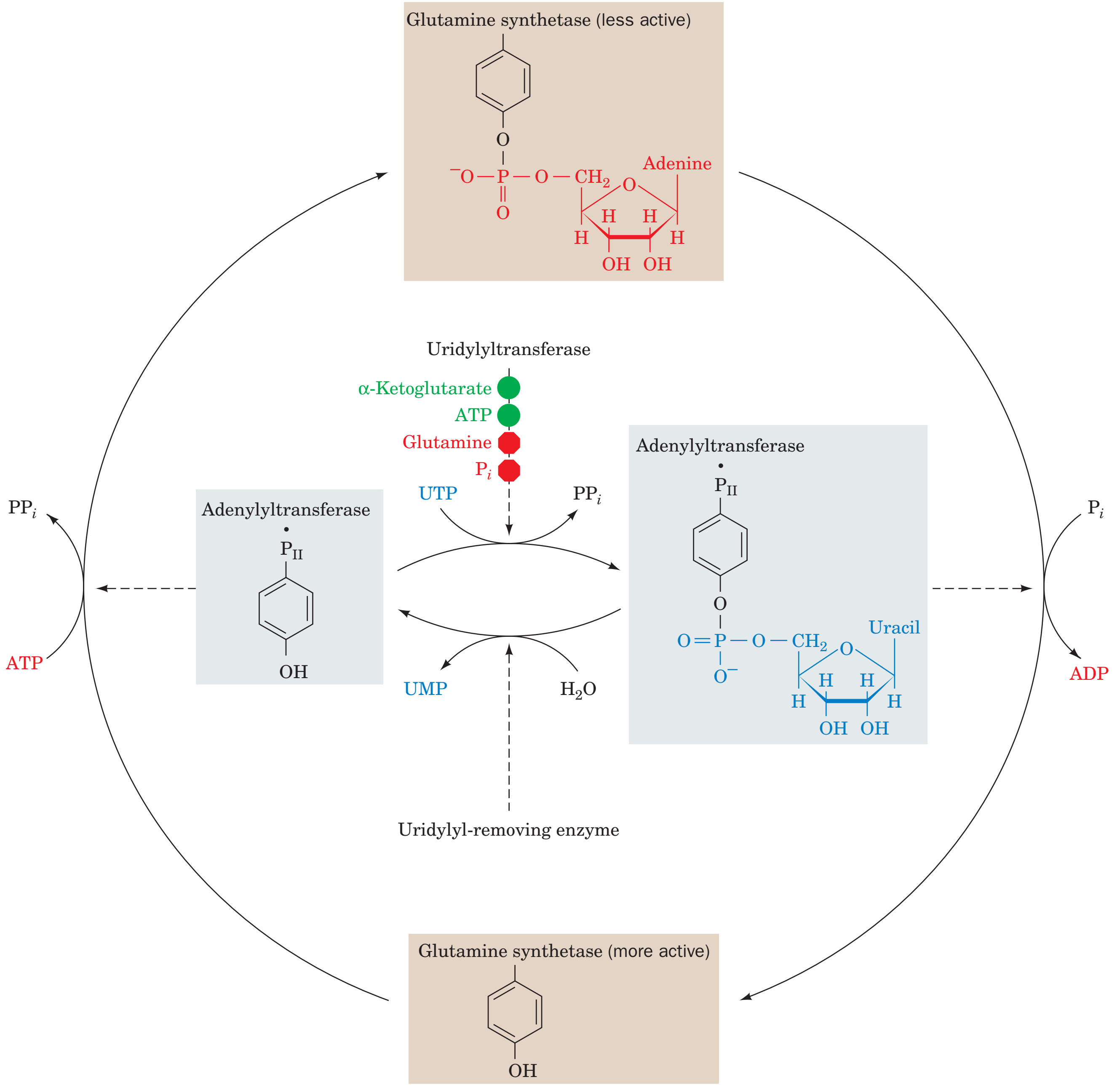
Glutamine synthetase (less active)
O
$^{-}O-P-O-CH_2$
O
Adenine
H H
H H
OH OH
Uridylyltransferase
α-Ketoglutarate
ATP
Glutamine
P_i
UTP
PP_i
Adenylyltransferase • P_{II}
OH
Adenylyltransferase • P_{II}
O
$O=P-O-CH_2$
O^-
Uracil
H H
H H
OH OH
UMP
H_2O
Uridylyl-removing enzyme
PP_i
ATP
P_i
ADP
Glutamine synthetase (more active)
OH

Figure 21-29 | The regulation of bacterial glutamine synthetase. The adenylylation/deadenylylation of a specific Tyr residue is controlled by the level of uridylylation of a specific adenylyltransferase·P_{II} Tyr residue. This uridylylation level, in turn, is controlled by the relative activities of uridylyltransferase, which is sensitive to the levels of a variety of nitrogen metabolites, and uridylyl-removing enzyme, whose activity is independent of those metabolite levels.

enzyme that hydrolytically excises the attached UMP groups of P_{II}. The uridylyltransferase is activated by α-ketoglutarate and ATP and inhibited by glutamine and P_i, whereas uridylyl-removing enzyme is insensitive to those metabolites. This intricate metabolic cascade therefore renders the activity of *E. coli* glutamine synthetase extremely responsive to the cell's nitrogen requirements.

Glutamate Is the Precursor of Proline, Ornithine, and Arginine. Conversion of glutamate to proline (Fig. 21-30, Reactions 1–4) involves the reduction of the γ-carboxyl group to an aldehyde followed by the formation of an internal Schiff base whose further reduction yields proline. Reduction of the glutamate γ-carboxyl group to an aldehyde is an endergonic process that is facilitated by first phosphorylating the carboxyl group in a reaction catalyzed by **γ-glutamyl kinase.** The unstable product, **glutamate-5-phosphate,** has not been isolated from reaction mixtures but is presumed to be the substrate for the reduction that follows. The resulting **glutamate-5-semialdehyde** (which is also a product of arginine and

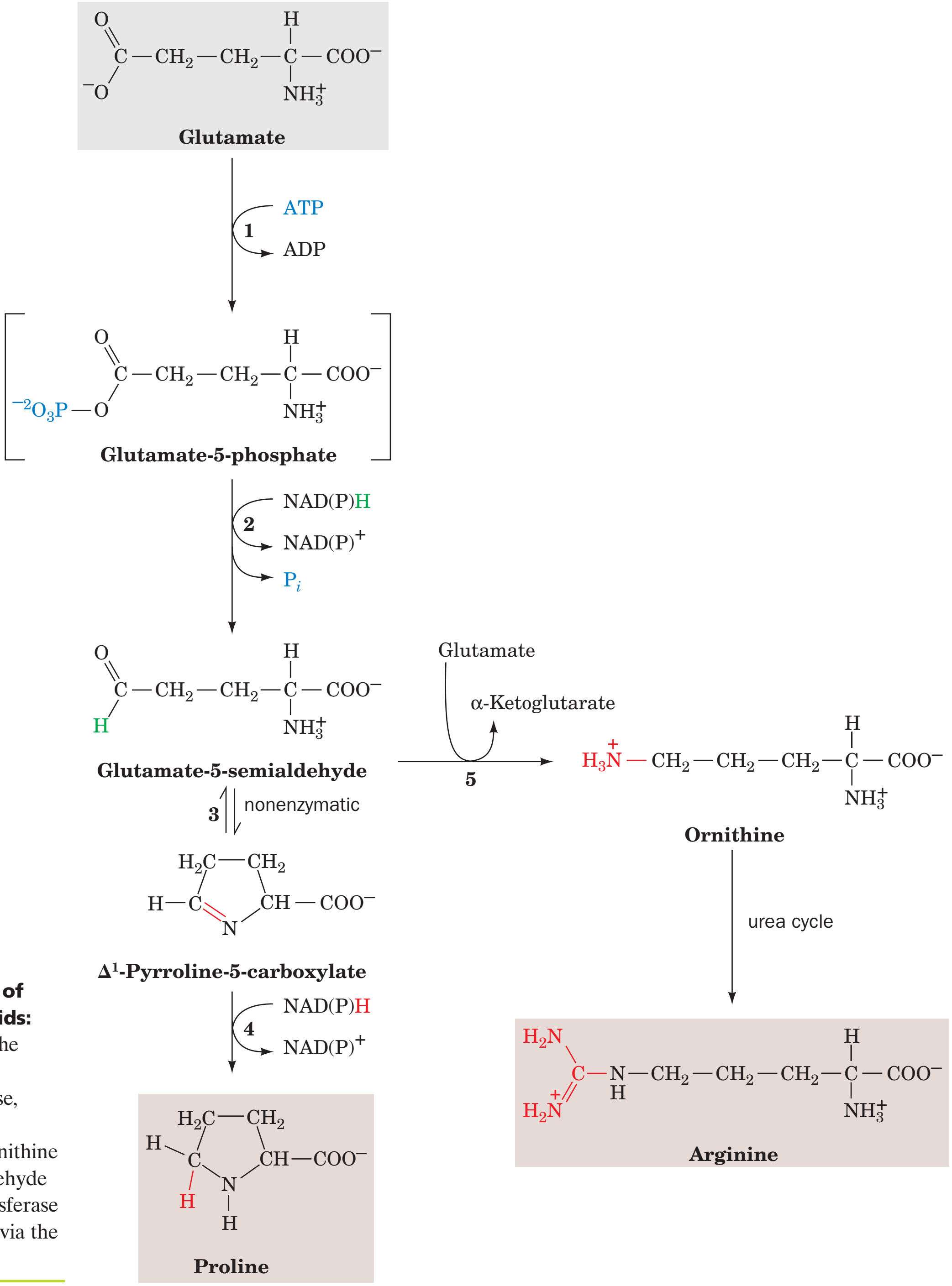
Glutamate
ATP
1
ADP
Glutamate-5-phosphate
NAD(P)H
2
NAD(P)+
Pi
Glutamate-5-semialdehyde
3
nonenzymatic
Δ1-Pyrroline-5-carboxylate
NAD(P)H
4
NAD(P)+
Proline
Glutamate
α-Ketoglutarate
5
Ornithine
urea cycle
Arginine

Figure 21-30 | The biosynthesis of the glutamate family of amino acids: arginine, ornithine, and proline. The catalysts for proline biosynthesis are (**1**) γ-glutamyl kinase, (**2**) dehydrogenase, (**3**) nonenzymatic, and (**4**) pyrroline-5-carboxylate reductase. In mammals, ornithine is produced from glutamate-5-semialdehyde by the action of ornithine-δ-aminotransferase (**5**). Ornithine is converted to arginine via the urea cycle (Section 21-3A).

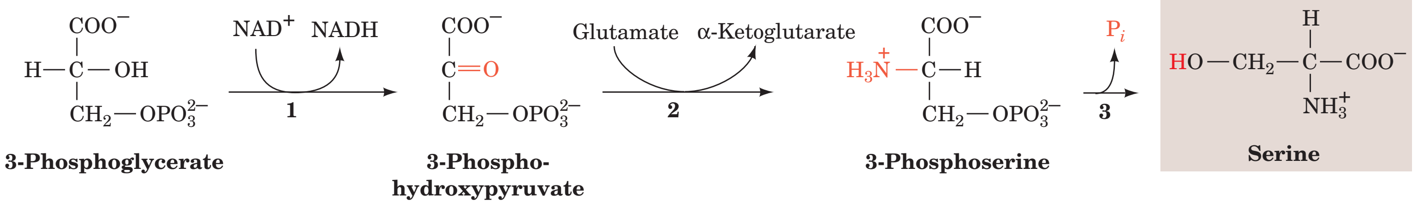

Figure 21-31 | The conversion of 3-phosphoglycerate to serine. The pathway enzymes are (**1**) 3-phosphoglycerate dehydrogenase, (**2**) a PLP-dependent aminotransferase, and (**3**) phosphoserine phosphatase.

proline degradation; Fig. 21-17) cyclizes spontaneously to form the internal Schiff base **Δ^1-pyrroline-5-carboxylate.** The final reduction to proline is catalyzed by **pyrroline-5-carboxylate reductase.** Whether the enzyme requires NADH or NADPH is unclear.

In humans, a three-step pathway leads from glutamate to ornithine via a branch from proline biosynthesis after Step 2 (Fig. 21-30). Glutamate-5-semialdehyde, which is in equilibrium with Δ^1-pyrroline-5-carboxylate, is directly transaminated to yield ornithine in a reaction catalyzed by **ornithine-δ-amino transferase** (Fig. 21-30, Reaction 5). Ornithine is converted to arginine by the reactions of the urea cycle (Fig. 21-9).

Serine, Cysteine, and Glycine Are Derived from 3-Phosphoglycerate.

Serine is formed from the glycolytic intermediate 3-phosphoglycerate in a three-reaction pathway (Fig. 21-31):

1. Conversion of 3-phosphoglycerate's 2-OH group to a ketone, yielding **3-phosphohydroxypyruvate,** serine's phosphorylated keto acid analog.
2. Transamination of 3-phosphohydroxypyruvate to phosphoserine.
3. Hydrolysis of phosphoserine to serine.

Serine participates in glycine synthesis in two ways:

1. Direct conversion of serine to glycine by serine hydroxymethyltransferase in a reaction that also yields N^5,N^{10}-methylene-THF (Fig. 21-14, Reaction 4 in reverse).
2. Condensation of the N^5,N^{10}-methylene-THF with CO_2 and NH_4^+ by glycine synthase (Fig. 21-14, Reaction 3 in reverse).

In animals, cysteine is synthesized from serine and homocysteine, a breakdown product of methionine (Fig. 21-18, Reactions 5 and 6). Homocysteine combines with serine to yield cystathionine, which subsequently forms cysteine and α-ketobutyrate. Since cysteine's sulfhydryl group is derived from the essential amino acid methionine, cysteine can be considered to be an essential amino acid.

B | Plants and Microorganisms Synthesize the Essential Amino Acids

Essential amino acids, like nonessential amino acids, are synthesized from familiar metabolic precursors. Their synthetic pathways are present only in microorganisms and plants, however, and usually involve more steps than those of the nonessential amino acids. The enzymes that synthesize essential amino acids were apparently lost early in animal evolution, possibly because of the ready availability of these amino acids in the diet. We shall focus on only a few of the many reactions in the biosynthesis of essential amino acids.

Lysine, Methionine, and Threonine Are Synthesized from Aspartate. In bacteria, aspartate is the common precursor of lysine, methionine, and threonine (Fig. 21-32). The biosyntheses of these essential amino acids all begin with the **aspartokinase**-catalyzed phosphorylation of aspartate to yield **aspartyl-β-phosphate.** We have seen that the control of metabolic pathways commonly occurs at the first committed step of the pathway. One might therefore expect lysine, methionine, and threonine biosynthesis to be controlled as a group. Each of these pathways is, in fact, independently controlled. *E. coli* has three isozymes of aspartokinase that respond differently to the three amino acids in terms both of feedback inhibition of enzyme activity and repression of enzyme synthesis. In addition, the pathway direction is controlled by feedback inhibition at the branch points by the amino acid products of the branches.

Methionine synthase (alternatively **homocysteine methyltransferase**) catalyzes the methylation of homocysteine to form methionine using N^5-methyl-THF as its methyl group donor (Reaction 4 in both Figs. 21-18 and 21-32). Methionine synthase is the only coenzyme B_{12}–associated enzyme in mammals besides methylmalonyl-CoA mutase (Section 20-2E). However, the coenzyme B_{12}'s Co ion in methionine synthase is axially liganded by a methyl group to form **methylcobalamin** rather than by a 5′-adenosyl group

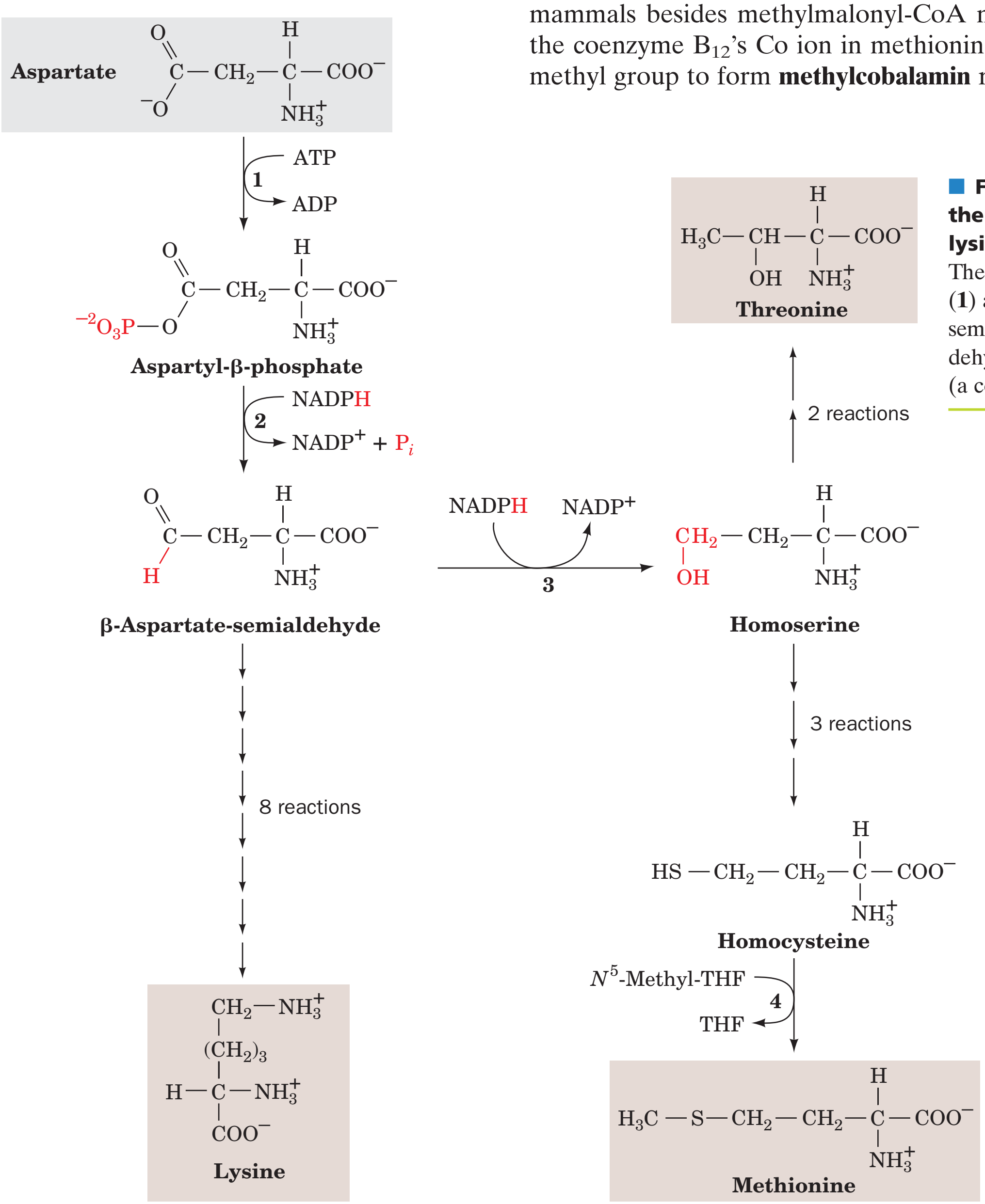
Aspartate
ATP
1
ADP
Aspartyl-β-phosphate
NADPH
2
NADP+ + Pi
β-Aspartate-semialdehyde
NADPH
NADP+
3
Homoserine
2 reactions
Threonine
3 reactions
Homocysteine
N5-Methyl-THF
4
THF
Methionine
8 reactions
Lysine

Figure 21-32 | The biosynthesis of the aspartate family of amino acids: lysine, methionine, and threonine. The pathway enzymes shown are (**1**) aspartokinase, (**2**) β-aspartate semialdehyde dehydrogenase, (**3**) homoserine dehydrogenase, and (**4**) methionine synthase (a coenzyme B_{12}–dependent enzyme).

as in methylmalonyl-CoA mutase (Fig. 20-17). In mammals, the primary function of methionine synthase is not *de novo* methionine synthesis, as Met is an essential amino acid. Instead, it functions in the cyclic synthesis of SAM for use in biological methylations (Fig. 21-18).

Leucine, Isoleucine, and Valine Are Derived from Pyruvate. Valine and isoleucine follow the same biosynthetic pathway utilizing pyruvate as a starting reactant, the only difference being in the first step of the series (Fig. 21-33). In this thiamine pyrophosphate–dependent reaction, which resembles those catalyzed by pyruvate decarboxylase (Fig. 15-20) and transketolase (Fig. 15-32), pyruvate forms an adduct with TPP that is

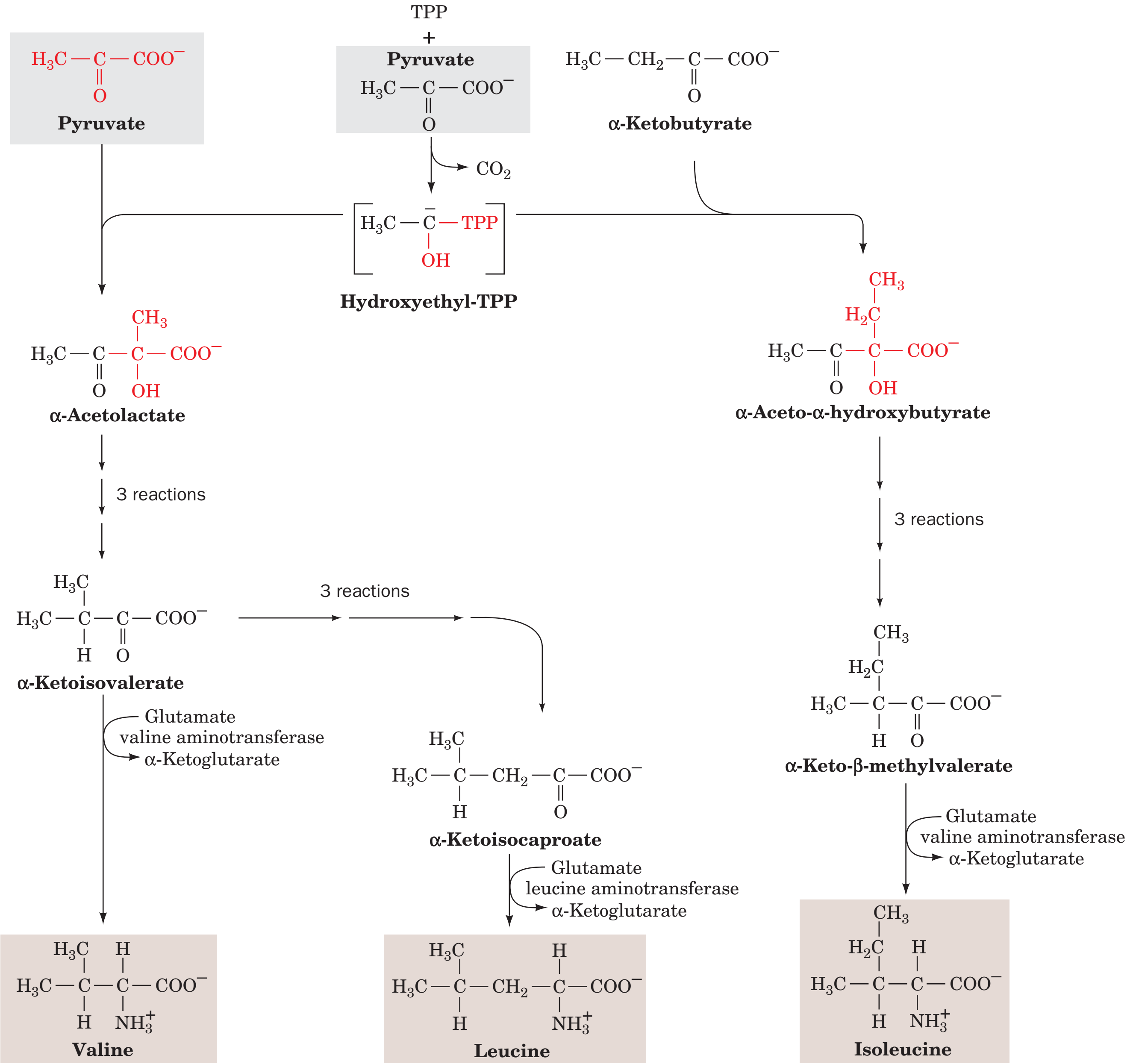
TPP
+
Pyruvate
Pyruvate
α-Ketobutyrate
CO₂
Hydroxyethyl-TPP
α-Acetolactate
α-Aceto-α-hydroxybutyrate
3 reactions
3 reactions
3 reactions
α-Ketoisovalerate
α-Ketoisocaproate
α-Keto-β-methylvalerate
Glutamate
valine aminotransferase
α-Ketoglutarate
Glutamate
leucine aminotransferase
α-Ketoglutarate
Glutamate
valine aminotransferase
α-Ketoglutarate
Valine
Leucine
Isoleucine

Figure 21-33 | The biosynthesis of the pyruvate family of amino acids: isoleucine, leucine, and valine. The first enzyme, **acetolactate synthase** (a TPP enzyme), catalyzes two reactions, one leading to valine and leucine, and the other to isoleucine. Note also that **valine aminotransferase** catalyzes the formation of both valine and isoleucine from their respective α-keto acids.

decarboxylated to hydroxyethyl-TPP. This resonance-stabilized carbanion adds either to the keto group of a second pyruvate to form **acetolactate** on the way to valine, or to the keto group of **α-ketobutyrate** to form **α-aceto-α-hydroxybutyrate** on the way to isoleucine. The leucine biosynthetic pathway

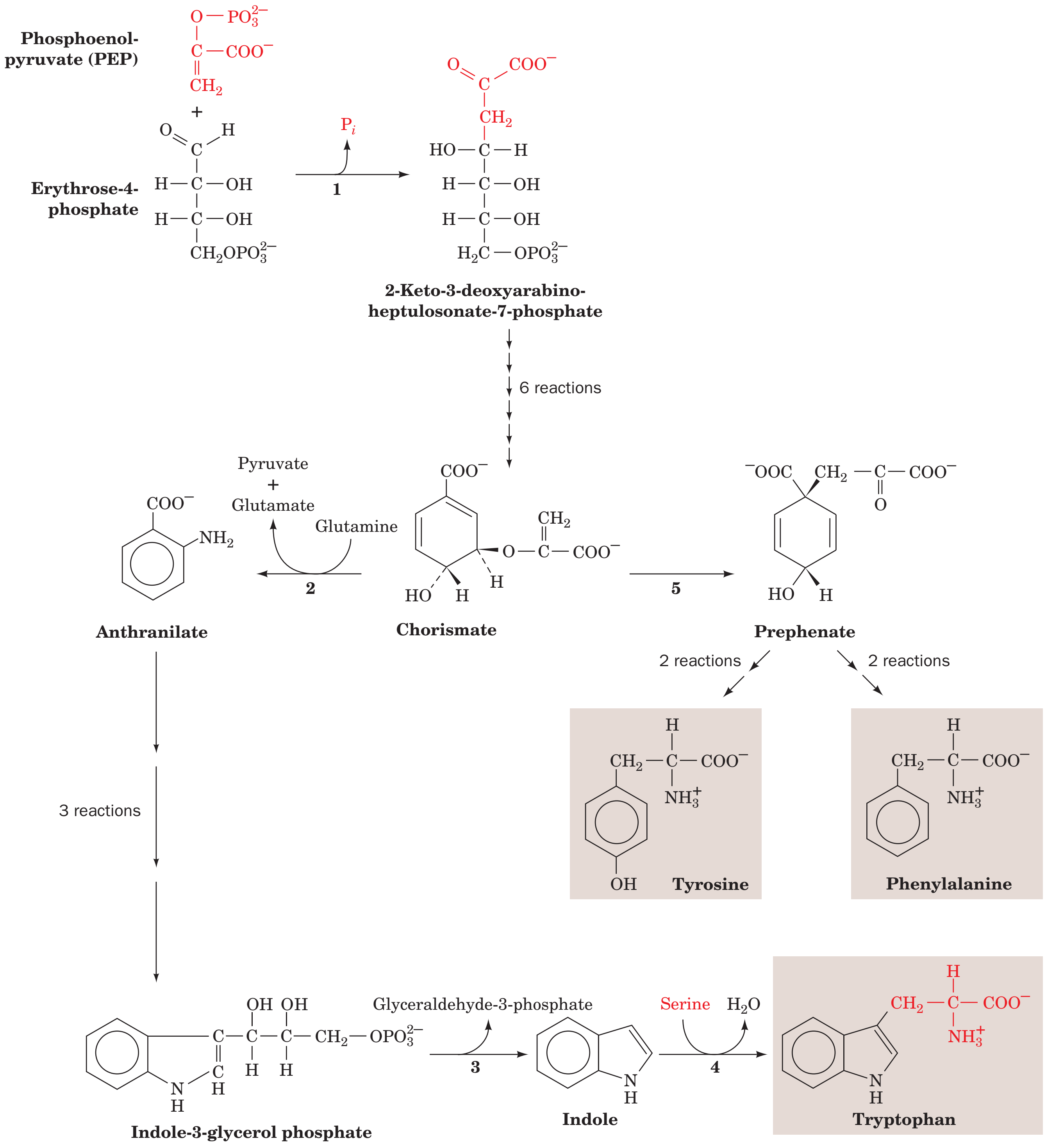
Phosphoenol-pyruvate (PEP)
Erythrose-4-phosphate
P_i
1
2-Keto-3-deoxyarabino-heptulosonate-7-phosphate
6 reactions
Pyruvate + Glutamate
Glutamine
2
Anthranilate
Chorismate
5
Prephenate
2 reactions
2 reactions
Tyrosine
Phenylalanine
3 reactions
Glyceraldehyde-3-phosphate
3
Serine
H_2O
4
Indole-3-glycerol phosphate
Indole
Tryptophan

■ **Figure 21-34 | The biosynthesis of phenylalanine, tryptophan, and tyrosine.** The enzymes shown are (**1**) 2-keto-3-deoxy-D-arabinoheptulosonate-7-phosphate synthase, (**2**) anthranilate synthase, (**3**) tryptophan synthase, α subunit, (**4**) tryptophan synthase, β subunit (a PLP-dependent enzyme), and (**5**) chorismate mutase.

branches off from the valine pathway. The final step in each of the three pathways, which begin with pyruvate rather than an amino acid, is the PLP-dependent transfer of an amino group from glutamate to form the amino acid.

The Aromatic Amino Acids Phenylalanine, Tyrosine, and Tryptophan Are Synthesized from Glucose Derivatives. The precursors of the aromatic amino acids are the glycolytic intermediate phosphoenolpyruvate (PEP) and erythrose-4-phosphate (an intermediate in the pentose phosphate pathway; Fig. 15-30). Their condensation forms **2-keto-3-deoxy-D-arabinoheptulosonate-7-phosphate** (Fig. 21-34). This C_7 compound cyclizes and is ultimately converted to **chorismate,** the branch point for tryptophan synthesis. Chorismate is converted to either **anthranilate** and then to tryptophan, or to **prephenate** and on to tyrosine or phenylalanine. Although mammals synthesize tyrosine by the hydroxylation of phenylalanine (Fig. 21-24), many microorganisms synthesize it directly from prephenate. The last step in the synthesis of tyrosine and phenylalanine is the addition of an amino group through transamination. In tryptophan synthesis, the amino group is part of the serine molecule that is added to **indole.**

Indole Is Channeled between Two Active Sites in Tryptophan Synthase. The final two reactions of tryptophan biosynthesis (Reactions 3 and 4 in Fig. 21-34) are both catalyzed by **tryptophan synthase:**

1. The α subunit (268 residues) of this $\alpha_2\beta_2$ bifunctional enzyme cleaves **indole-3-glycerol phosphate,** yielding indole and glyceraldehyde-3-phosphate.
2. The β subunit (396 residues) joins indole with serine in a PLP-dependent reaction to form tryptophan.

Either subunit alone is enzymatically active, but when they are joined in the $\alpha_2\beta_2$ tetramer, the rates of both reactions and their substrate affinities increase by 1 to 2 orders of magnitude. Indole, the intermediate product, does not appear free in solution because it is channeled between the two subunits.

The X-ray structure of tryptophan synthase from *Salmonella typhimurium,* determined by Craig Hyde, Edith Miles, and David Davies, reveals that the protein forms a 150-Å-long, twofold symmetric α-β-β-α complex in which the active sites of neighboring α and β subunits are separated by ~25 Å (Fig. 21-35). *These active sites are joined by a solvent-filled tunnel that is wide enough to permit the*

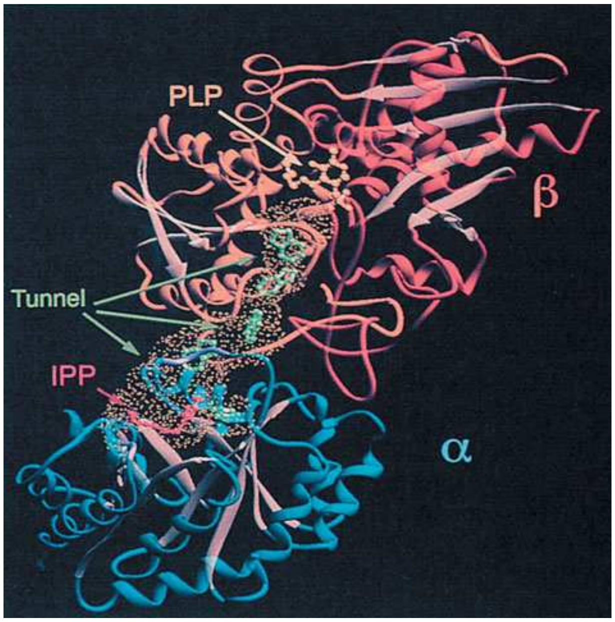

Figure 21-35 | **A ribbon diagram of the bifunctional enzyme tryptophan synthase from *S. typhimurium*.** Only one $\alpha\beta$ protomer of the bifunctional $\alpha\beta\beta\alpha$ heterotetramer is shown. The α subunit is blue, the β subunit's N-terminal domain is orange, its C-terminal domain is red-orange, and all β sheets are tan. The active site of the α subunit is located by its bound competitive inhibitor, **indolepropanol phosphate** (IPP; *red ball-and-stick model*), whereas that of the β subunit is marked by its PLP coenzyme (*yellow ball-and-stick model*). The solvent-accessible surface of the ~25-Å-long tunnel connecting the α and β active sites is outlined by yellow dots. Several indole molecules (*green ball-and-stick models*) have been modeled into the tunnel to show that it is wide enough for indole to pass from one active site to the other. [Courtesy of Craig Hyde, Edith Miles, and David Davies, NIH.]

See Interactive Exercise 30.

passage of the intermediate substrate, indole. This structure, the first in which a tunnel connecting two active sites was observed, suggests the following series of events: The indole-3-glycerol phosphate substrate binds to the α subunit through an opening into its active site, its "front door," and the glyceraldehyde-3-phosphate product leaves via the same route. Similarly, the β subunit active site has a "front door" opening to the solvent through which serine enters and tryptophan leaves. Both active sites also have "back doors" that are connected by the tunnel. *The indole intermediate presumably diffuses between the two active sites via the tunnel and hence does not escape to the solvent.* Channeling may be particularly important for indole since this nonpolar molecule otherwise can escape the bacterial cell by diffusing through its plasma and outer membranes.

In order for channeling to increase tryptophan synthase's catalytic efficiency, (1) its connected active sites must be coupled such that their catalyzed reactions occur in phase, and (2) after substrate has bound to the α subunit, its active site ("front door") must close off to ensure that the product indole passes through the tunnel ("back door") to the β subunit rather than escaping into solution. A variety of experimental evidence indicates that this series of events is facilitated through allosteric signals derived from covalent transformations at the β subunit's active site. These switch the enzyme between an open, low-activity conformation to which substrates bind, and a closed, high-activity conformation from which indole cannot escape.

Histidine Biosynthesis Includes an Intermediate in Nucleotide Biosynthesis. Five of histidine's six C atoms are derived from **5-phosphoribosyl-α-pyrophosphate** (**PRPP;** Fig. 21-36), a phospho-sugar intermediate that is also involved in the biosynthesis of purine and pyrimidine nucleotides (Sections 23-1A and 23-2A). The histidine's sixth carbon originates from ATP. The ATP atoms that are not incorporated into histidine are eliminated as **5-aminoimidazole-4-carboxamide ribonucleotide** (Fig. 21-36, Reaction 2), which is also an intermediate in purine biosynthesis.

The unusual biosynthesis of histidine from a purine (**N^1-5′-phosphoribosyl ATP,** the product of Reaction 1 in Fig. 21-36) has been cited as evidence supporting the hypothesis that life was originally RNA-based. His residues, as we have seen, are often components of enzyme active sites, where they act as nucleophiles and/or general acid–base catalysts. The discovery that RNA can have catalytic properties therefore suggests that the imidazole moiety of purines plays a similar role in RNA enzymes. This further suggests that the histidine biosynthetic pathway is a "fossil" of the transition to more efficient protein-based life-forms.

■ CHECK YOUR UNDERSTANDING

What are the metabolic precursors of the nonessential amino acids?

List the compounds that are used to synthesize the essential amino acids in plants and microorganisms.

LEARNING OBJECTIVES

- Understand that heme is synthesized from glycine and succinyl-CoA and is degraded to a variety of colored compounds for excretion.
- Understand that the synthesis of bioactive amines begins with amino acid decarboxylation.
- Understand that arginine gives rise to the gas nitric oxide.

6 Other Products of Amino Acid Metabolism

Certain amino acids, in addition to their major function as protein building blocks, are essential precursors of a variety of important biomolecules, including nucleotides and nucleotide coenzymes, heme, and various hormones and neurotransmitters. In this section, we consider the pathways leading to some of these substances. The biosynthesis of nucleotides is considered in Chapter 23.

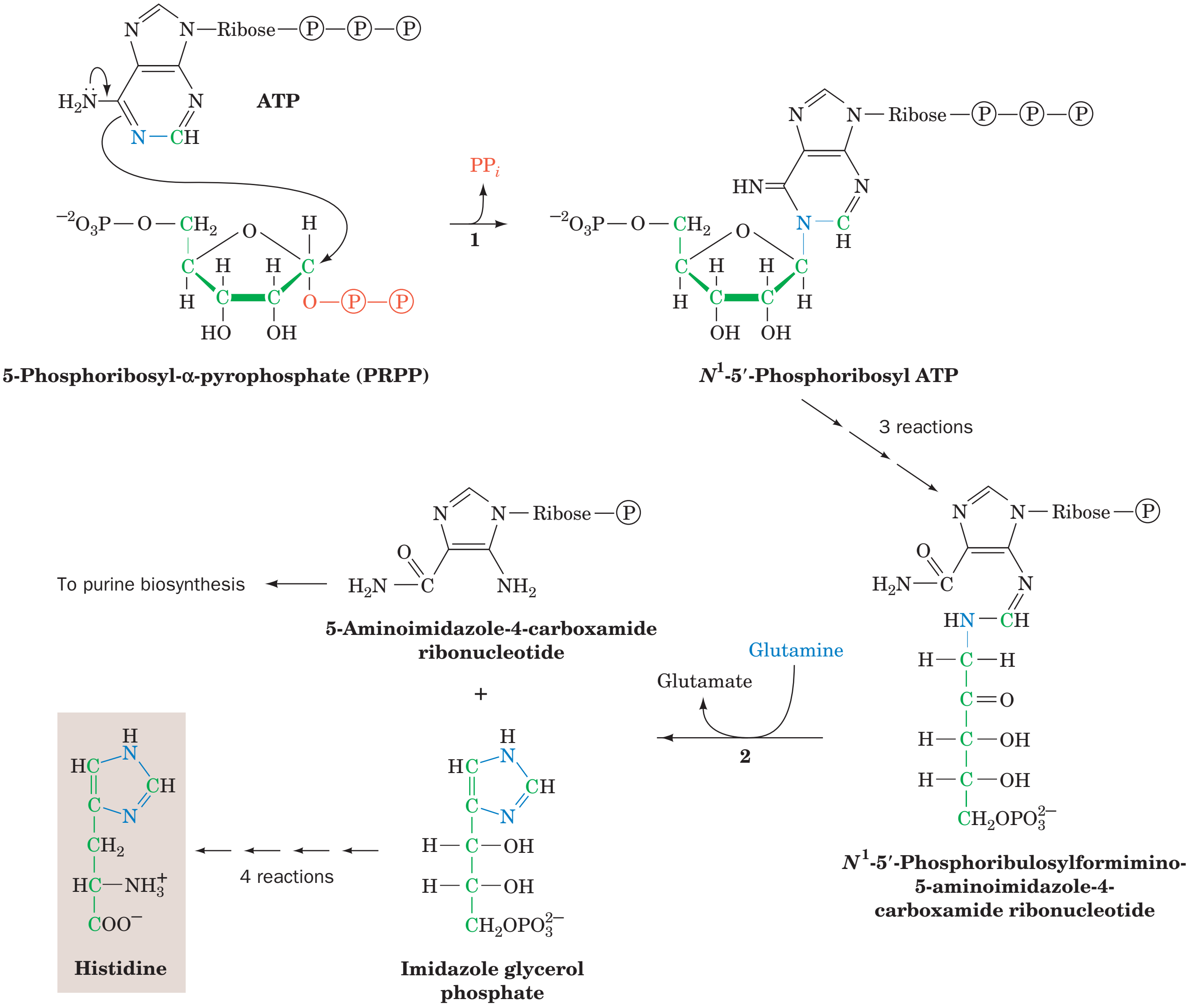
ATP
PP$_i$
1
5-Phosphoribosyl-α-pyrophosphate (PRPP)
N^1-5′-Phosphoribosyl ATP
3 reactions
N^1-5′-Phosphoribulosylformimino-5-aminoimidazole-4-carboxamide ribonucleotide
Glutamine
Glutamate
2
To purine biosynthesis
5-Aminoimidazole-4-carboxamide ribonucleotide
+
Imidazole glycerol phosphate
4 reactions
Histidine

Figure 21-36 | The biosynthesis of histidine. The enzymes shown are (**1**) ATP phosphoribosyltransferase and (**2**) glutamine amidotransferase.

A | Heme Is Synthesized from Glycine and Succinyl-CoA

Heme, as we have seen, is an Fe-containing prosthetic group that is an essential component of many proteins, notably hemoglobin, myoglobin, and the cytochromes. The initial reactions of heme biosynthesis are common to the formation of other tetrapyrroles including chlorophyll in plants and bacteria (Fig. 19-2) and coenzyme B_{12} in bacteria (Fig. 20-17).

Elucidation of the heme biosynthetic pathway involved some interesting detective work. David Shemin and David Rittenberg, who were among the first to use isotopic tracers in the elucidation of metabolic pathways, demonstrated, in 1945, that *all of heme's C and N atoms can be derived from acetate and glycine.* Heme biosynthesis takes place partly in the mitochondrion and

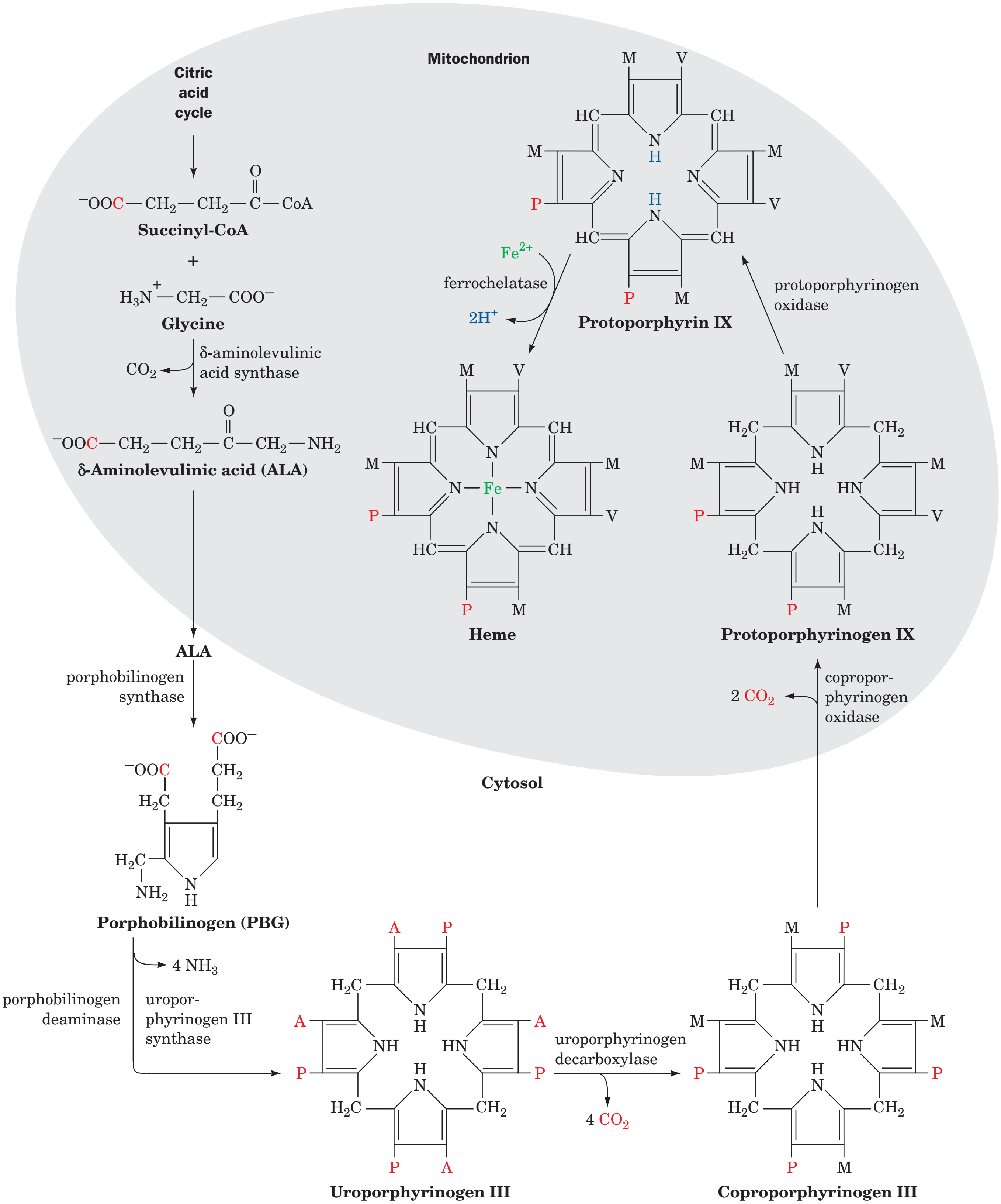
Mitochondrion
Citric acid cycle
⁻OOC—CH₂—CH₂—C(=O)—CoA
Succinyl-CoA
+
H₃N⁺—CH₂—COO⁻
Glycine
δ-aminolevulinic acid synthase
CO₂
⁻OOC—CH₂—CH₂—C(=O)—CH₂—NH₂
δ-Aminolevulinic acid (ALA)
ALA
porphobilinogen synthase
Porphobilinogen (PBG)
4 NH₃
porphobilinogen deaminase
uroporphyrinogen III synthase
Uroporphyrinogen III
uroporphyrinogen decarboxylase
4 CO₂
Coproporphyrinogen III
2 CO₂
coproporphyrinogen oxidase
Protoporphyrinogen IX
protoporphyrinogen oxidase
Protoporphyrin IX
Fe²⁺
ferrochelatase
2H⁺
Heme
Cytosol

Figure 21-37 | **The pathway of heme biosynthesis.** δ-Aminolevulinic acid (ALA) is synthesized in the mitochondrion from succinyl-CoA and glycine by ALA synthase. ALA is transported to the cytosol, where two molecules condense to form PBG, four molecules of which condense to form a porphyrin ring. The next three reactions involve oxidation of the pyrrole ring substituents, yielding protoporphyrinogen IX, which is transported back into the mitochondrion during its formation. After oxidation of the methylene groups, ferrochelatase catalyzes the insertion of Fe^{2+} to yield heme. A, P, M, and V, respectively, represent acetyl, propionyl, methyl, and vinyl (—CH=CH_2) groups. C atoms originating as the carboxyl group of acetate are red.

partly in the cytosol (Fig. 21-37; *opposite*). Mitochondrial acetate is metabolized via the citric acid cycle to succinyl-CoA, which condenses with glycine in a reaction that produces CO_2 and **δ-aminolevulinic acid (ALA).** ALA is transported to the cytosol, where it combines with a second ALA to yield **porphobilinogen (PBG).** The reaction is catalyzed by the Zn-requiring enzyme **porphobilinogen synthase.**

Inhibition of PBG synthase by lead is one of the major manifestations of acute lead poisoning. Indeed, it has been suggested that the accumulation, in the blood, of ALA, which resembles the neurotransmitter **γ-aminobutyric acid** (Section 21-6B), is responsible for the psychosis that often accompanies lead poisoning.

The next phase of heme biosynthesis is the condensation of four PBG molecules to form **uroporphyrinogen III,** the porphyrin nucleus, in a series of reactions catalyzed by **porphobilinogen deaminase** (also called **uroporphyrinogen synthase**) and **uroporphyrinogen III cosynthase.** The initial product, **hydroxymethylbilane,**

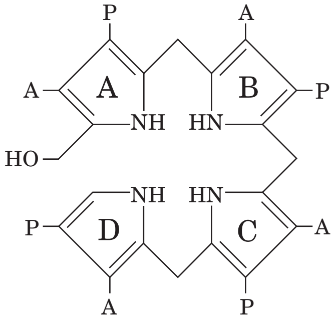

A = acetyl

P = propionyl

Hydroxymethylbilane

is a linear tetrapyrrole that cyclizes. **Protoporphyrin IX,** to which Fe is added to form heme, is produced from uroporphyrinogen III in a series of reactions catalyzed by (1) **uroporphyrinogen decarboxylase,** which decarboxylates all four acetate side chains (A) to form methyl groups (M); (2) **coproporphyrinogen oxidase,** which oxidatively decarboxylates two of the propionate side chains (P) to vinyl groups (V); and (3) **protoporphyrinogen oxidase,** which oxidizes the methylene groups linking the pyrrole rings to methenyl groups. During the coproporphyrinogen oxidase reaction, the porphyrin is transported back into the mitochondrion. In the final reaction of heme biosynthesis, **ferrochelatase** inserts Fe(II) into protoporphyrin IX.

The Liver and Erythroid Cells Regulate Heme Biosynthesis. The two major sites of heme biosynthesis are erythroid cells, which synthesize ~85% of the body's heme groups, and the liver, which synthesizes most of the remainder. In liver, the level of heme synthesis must be adjusted according to metabolic conditions. For example, the synthesis of the heme-containing cytochromes P450 (Section 12-4D) fluctuates with the need for detoxification. In contrast, heme synthesis in erythroid cells is a one-time event; heme and protein synthesis cease when the cell matures, so that the hemoglobin must last the erythrocyte's lifetime (~120 days).

In liver, the main control target in heme biosynthesis is ALA synthase, the enzyme catalyzing the pathway's first committed step. Heme, or its Fe(III) oxidation product **hemin,** controls this enzyme's activity through feedback inhibition, inhibition of the transport of ALA synthase from its site of synthesis in the cytosol to its reaction site in the mitochondrion (Fig. 21-37), and repression of ALA synthase synthesis.

BOX 21-3 BIOCHEMISTRY IN HEALTH AND DISEASE

The Porphyrias

Defects in heme biosynthesis in liver or erythroid cells result in the accumulation of porphyrin and/or its precursors and are therefore known as porphyrias. Two such defects are known to affect erythroid cells: uroporphyrinogen III cosynthase deficiency **(congenital erythropoietic porphyria)** and ferrochelatase deficiency **(erythropoietic protoporphyria).** The former results in accumulation of uroporphyrinogen derivatives. Excretion of those compounds colors the urine red; their deposition in the teeth turns them reddish brown; and their accumulation in the skin renders it extremely photosensitive, so that it ulcerates and forms disfiguring scars. Increased hair growth is also observed in afflicted individuals; fine hair may cover much of the face and extremities. These symptoms have prompted speculation that the werewolf legend has a biochemical basis.

The most common porphyria that primarily affects liver is porphobilinogen deaminase deficiency **(acute intermittent porphyria).** This disease is marked by intermittent attacks of abdominal pain and neurological dysfunction. Excessive amounts of ALA and PBG are excreted in the urine during and after such attacks. The urine may become red resulting from the excretion of excess porphyrins synthesized from PBG in nonhepatic cells, although the skin does not become unusually photosensitive. King George III, who ruled England during the American Revolution, and who has been widely portrayed as being mad, in fact, had attacks characteristic of acute intermittent porphyria; he was reported to have urine the color of port wine, and had several descendants who were diagnosed as having the disease. American history might have been quite different had George III not inherited that metabolic defect.

In erythroid cells, heme exerts quite a different effect on its biosynthesis. Heme induces, rather than represses, protein synthesis in **reticulocytes** (immature erythrocytes). Although the vast majority of the protein synthesized by reticulocytes is globin, heme may also induce these cells to synthesize the enzymes of heme biosynthesis. Moreover, the rate-determining steps of heme biosynthesis in erythroid cells may be the ferrochelatase and porphobilinogen deaminase reactions rather than the ALA synthase reaction. This is consistent with the supposition that when erythroid heme biosynthesis is "switched on," all of its steps function at their maximal rates rather than any one step limiting the flow through the pathway. Heme-stimulated synthesis of globin also ensures that heme and globin are synthesized in the correct ratio for assembly into hemoglobin (Section 28-3C). Genetic defects in heme biosynthesis cause conditions known as **porphyrias** (Box 21-3).

Heme Degradation Products Are Excreted. At the end of their lifetime, red cells are removed from the circulation and their components degraded. Heme catabolism (Fig. 21-38) begins with oxidative cleavage, by heme oxygenase, of the porphyrin between rings A and B to form **biliverdin,** a green linear tetrapyrrole. Biliverdin's central methenyl bridge (between rings C and D) is then reduced to form the red-orange **bilirubin.** The changing colors of a healing bruise are a visible manifestation of heme degradation.

In the reaction forming biliverdin, the methenyl bridge carbon between rings A and B is released as CO, which is a tenacious heme ligand (with 200-fold greater affinity for hemoglobin than O_2; Section 7-1A). Consequently, $\sim$1% of hemoglobin's binding sites are blocked by CO even in the absence of air pollution.

The highly lipophilic bilirubin is insoluble in aqueous solutions. Like other lipophilic metabolites, such as free fatty acids, it is transported in the blood in complex with serum albumin. Bilirubin derivatives are secreted in the bile and for the most part are further degraded by bacterial enzymes in the large intestine. Some of the resulting **urobilinogen** is reabsorbed and transported via the bloodstream to the kidney, where it is converted to the yellow **urobilin** and excreted, thus giving urine its characteristic color. Most

Figure 21-38 | Pathway for heme degradation. M, V, P, and E represent methyl, vinyl, propionyl, and ethyl groups.

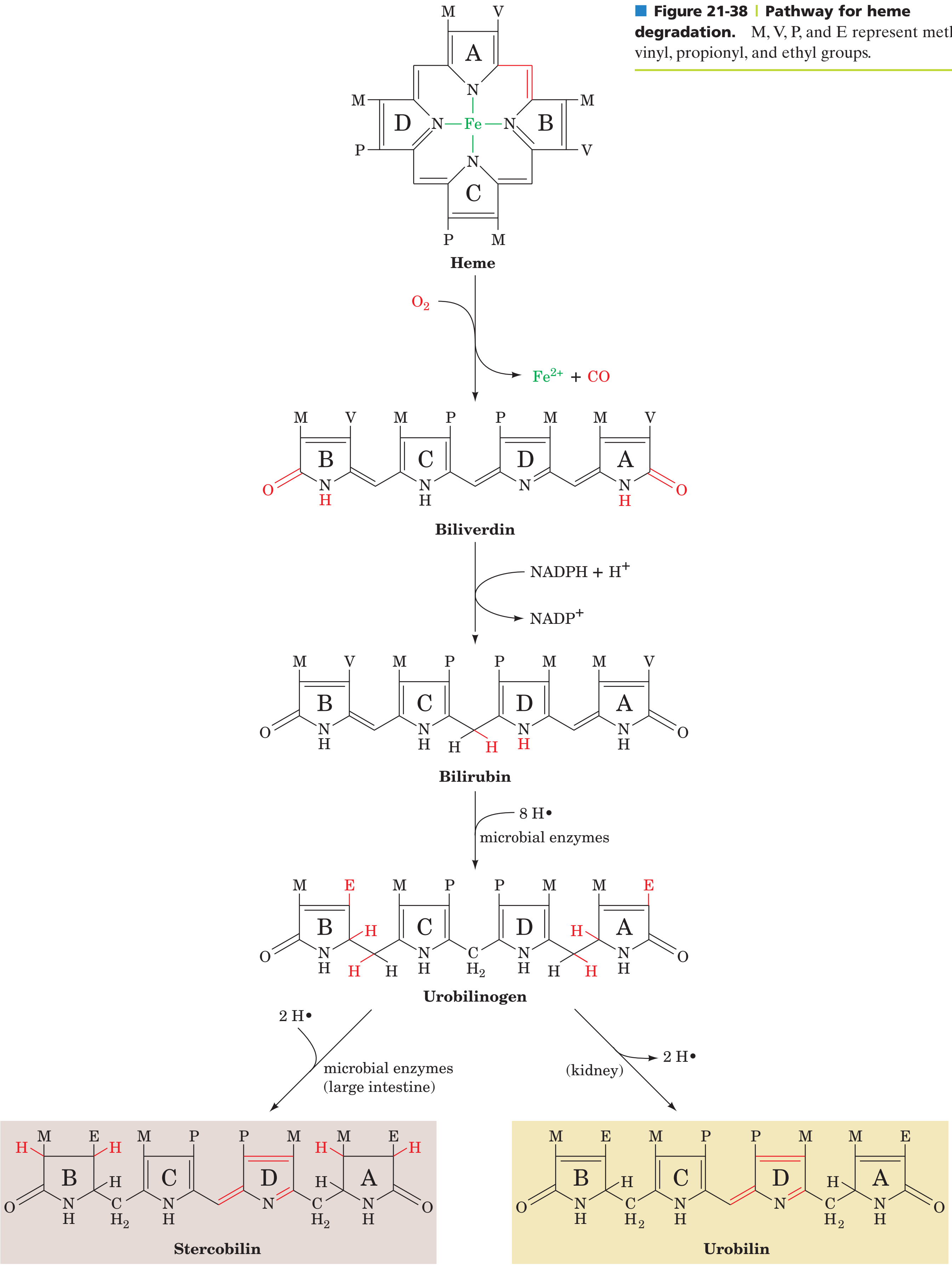
Heme
Fe
A
B
C
D
M
V
P
O_2
Fe^{2+} + CO
Biliverdin
NADPH + H^+
$NADP^+$
Bilirubin
8 H•
microbial enzymes
E
Urobilinogen
2 H•
microbial enzymes
(large intestine)
(kidney)
2 H•
Stercobilin
Urobilin

urobilinogen, however, is microbially converted to the deeply red-brown **stercobilin,** the major pigment of feces.

When the blood contains excessive amounts of bilirubin, the deposition of this highly insoluble substance colors the skin and the whites of the eyes yellow. This condition, called **jaundice** (French: *jaune,* yellow), signals either an abnormally high rate of red cell destruction, liver dysfunction, or bile duct obstruction. Newborn infants, particularly when premature, often become jaundiced because they lack an enzyme that degrades bilirubin. Jaundiced infants are treated by bathing them with light from a fluorescent lamp; this photochemically converts bilirubin to more soluble isomers that the infant can degrade and excrete.

B | Amino Acids Are Precursors of Physiologically Active Amines

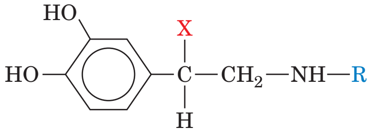

X = OH, R = CH_3 **Epinephrine (Adrenalin)**
X = OH, R = H **Norepinephrine**
X = H, R = H **Dopamine**

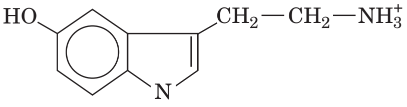

Serotonin (5-hydroxytryptamine)

$^{-}OOC-CH_2-CH_2-CH_2-NH_3^+$

γ-Aminobutyric acid (GABA)

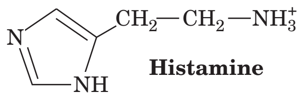

Histamine

Epinephrine (adrenaline), norepinephrine, dopamine, serotonin (5-hydroxytryptamine), γ-aminobutyric acid (GABA), and **histamine** *(at left)* are hormones and/or neurotransmitters derived from amino acids. Epinephrine, as we have seen, activates muscle adenylate cyclase, thereby stimulating glycogen breakdown (Section 16-3B); deficiency in dopamine production is associated with **Parkinson's disease,** a degenerative condition causing "shaking palsy"; serotonin causes smooth muscle contraction; GABA is one of the brain's major inhibitory neurotransmitters; and histamine is involved in allergic responses (as allergy sufferers who take antihistamines will realize), as well as in the control of acid secretion by the stomach.

The biosynthesis of each of these physiologically active amines involves decarboxylation of the corresponding precursor amino acid. Amino acid decarboxylases are PLP-dependent enzymes that form a PLP–Schiff base with the substrate so as to stabilize (by delocalization) the C_α carbanion formed on C_α—COO^- bond cleavage (Section 21-2A):

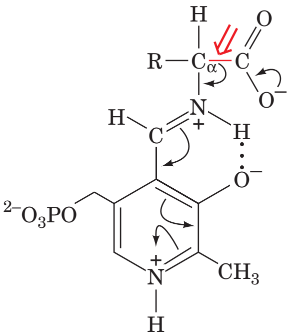

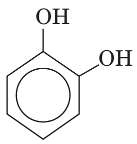

Catechol

Formation of histamine (from histidine) and formation of GABA (from glutamate) are one-step processes; the synthesis of serotonin from tryptophan requires a hydroxylation step as well as decarboxylation. The various **catecholamines**—dopamine, norepinephrine, and epinephrine—are related to **catechol** *(at left)* and are sequentially synthesized from tyrosine (Fig. 21-39):

1. Tyrosine is hydroxylated to **3,4-dihydroxyphenylalanine (L-DOPA)** in a reaction that requires 5,6,7,8-tetrahydrobiopterin (Fig. 21-26).
2. L-DOPA is decarboxylated to dopamine.
3. A second hydroxylation yields norepinephrine.
4. Methylation of norepinephrine's amino group by *S*-adenosylmethionine (Fig. 21-18) produces epinephrine.

The specific catecholamine that a cell produces depends on which enzymes of the pathway are present. In adrenal medulla, for example, epinephrine is

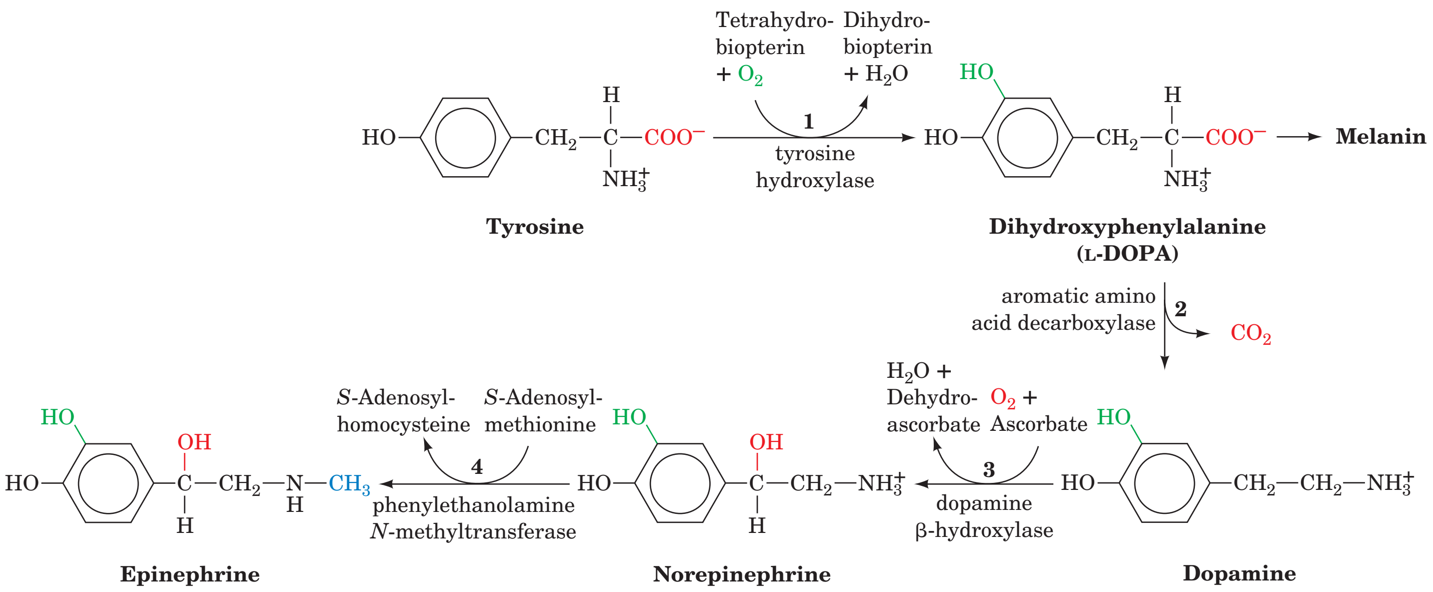
Tetrahydro-biopterin + O₂
Dihydro-biopterin + H₂O
1
tyrosine hydroxylase
Tyrosine
Dihydroxyphenylalanine (L-DOPA)
Melanin
aromatic amino acid decarboxylase
2
CO₂
H₂O + Dehydro-ascorbate
O₂ + Ascorbate
3
dopamine β-hydroxylase
Dopamine
Norepinephrine
S-Adenosyl-homocysteine
S-Adenosyl-methionine
4
phenylethanolamine N-methyltransferase
Epinephrine

Figure 21-39 | The sequential synthesis of L-DOPA, dopamine, norepinephrine, and epinephrine from tyrosine. L-DOPA is also the precursor of the skin pigment melanin.

the predominant product. In some areas of the brain, norepinephrine is more common. In other areas, the pathway stops at dopamine. In melanocytes, L-DOPA is the precursor of red and black melanins, which are irregular cross-linked polymers that give hair and skin much of their color.

C | Nitric Oxide Is Derived from Arginine

Arginine is the precursor of a substance that was originally called **endothelium-derived relaxing factor (EDRF)** because it was synthesized by vascular endothelial cells and caused the underlying smooth muscle to relax. The signal for vasodilation was not a peptide, as expected, but the stable free radical gas **nitric oxide, NO.** The identification of NO as a vasodilator came in part from studies that identified NO as the decomposition product that mediates the vasodilating effects of compounds such as **nitroglycerin** *(at right)*. Nitroglycerin is often administered to individuals suffering from **angina pectoris,** a disease caused by insufficient blood flow to the heart muscle, to rapidly but temporarily relieve their chest pain.

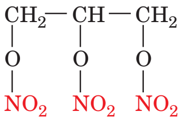

Nitroglycerin

The reaction that converts arginine to NO and citrulline is catalyzed by **nitric oxide synthase (NOS):**

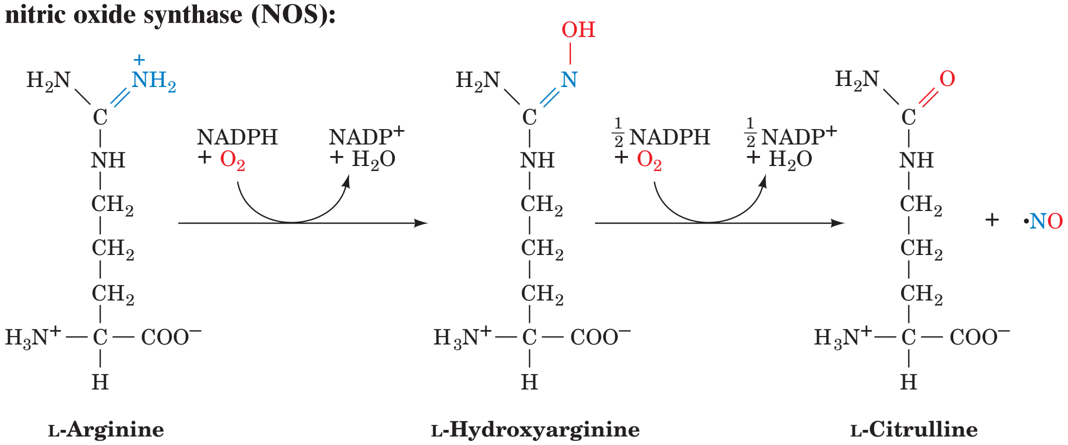
NADPH + O₂
NADP⁺ + H₂O
½ NADPH + O₂
½ NADP⁺ + H₂O
+ •NO
L-Arginine
L-Hydroxyarginine
L-Citrulline

The reaction proceeds via an enzyme-bound hydroxyarginine intermediate and requires an array of redox coenzymes. NOS is a homodimeric protein of 125- to 160-kD subunits, and each subunit contains one FMN, one FAD, one tetrahydrobiopterin (Fig. 21-26), and one Fe(III)-heme. These cofactors facilitate the five-electron oxidation of arginine to produce NO.

Because NO is a gas, it rapidly diffuses across cell membranes, although its high reactivity (half-life ~5 s) prevents it from acting much further than ~1 mm from its site of synthesis. NO is produced by endothelial cells in response to a wide variety of agents and physiological conditions. Neuronal cells also synthesize NO (neuronal NOS is ~55% homologous to endothelial NOS). This endothelium-independent NO synthesis induces the dilation of cerebral and other arteries and is responsible for penile erection. The brain contains more NOS than any other tissue in the body, suggesting that NO is essential for the function of the central nervous system. A third type of NOS is found in leukocytes (white blood cells). These cells produce NO as part of their cytotoxic arsenal. NO combines with superoxide (Section 18-4B) to produce the highly reactive hydroxyl radical (·OH), which kills invading bacteria. The sustained release of NO has been implicated in **endotoxic shock** (an often fatal immune system overreaction to bacterial infection), in inflammation-related tissue damage, and in the damage to neurons in the vicinity of but not directly killed by a stroke (which often does greater harm than the stroke itself).

CHECK YOUR UNDERSTANDING

List the starting materials and end products of heme metabolism.

Identify the amino acids that give rise to catecholamines, serotonin, GABA, and histamine.

What are the substrates and products of the nitric oxide synthase reaction?

7 Nitrogen Fixation

LEARNING OBJECTIVES

- Understand that the reduction of N_2 to NH_3 by nitrogenase is an energetically costly process.
- Understand how ammonia is incorporated into amino acids.

The most prominent chemical elements in living systems are O, H, C, N, and P. The elements O, H, and P occur widely in metabolically available forms (H_2O, O_2, and P_i). However, the major forms of C and N, CO_2 and N_2, are extremely stable (unreactive); for example, the N≡N triple bond has a bond energy of 945 $kJ \cdot mol^{-1}$ (versus 351 $kJ \cdot mol^{-1}$ for a C—O single bond). CO_2, with minor exceptions, is metabolized (fixed) only by photosynthetic organisms (Chapter 19). *N_2 fixation is even less common; this element is converted to metabolically useful forms by only a few strains of bacteria, called* ***diazotrophs.*** These organisms include certain marine cyanobacteria and bacteria that colonize the root nodules of legumes (plants belonging to the pea family, including beans, clover, and alfalfa; Fig. 21-40). Once N_2 is fixed, the nitrogen is **assimilated** (incorporated) into biological molecules as amino groups that can then be transferred to other molecules. In this section we examine the processes of nitrogen fixation and nitrogen assimilation.

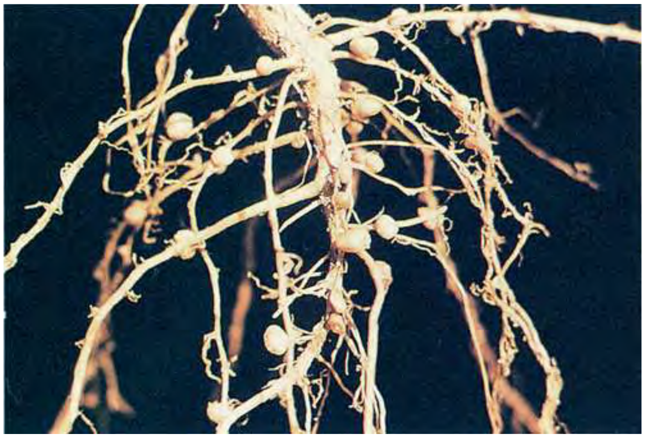

Figure 21-40 | Root nodules of a pea plant. Bacteria of the genus *Rhizobium,* which carry out nitrogen fixation, live symbiotically with the root nodules of such legumes. [Vu/Cabisco/Visuals Unlimited.]

A | Nitrogenase Reduces N_2 to NH_3

Diazotrophs produce the enzyme **nitrogenase,** which catalyzes the reduction of N_2 to NH_3:

$$N_2 + 8\,H^+ + 8\,e^- + 16\,\text{ATP} + 16\,H_2O \rightarrow 2\,NH_3 + H_2 + 16\,\text{ADP} + 16\,P_i$$

In legumes, this nitrogen-fixing system produces more metabolically useful nitrogen than the legume needs; the excess is excreted into the soil, enriching it. It is therefore common agricultural practice to plant a field with alfalfa every few years to build up the supply of usable nitrogen in the soil for later use in growing other crops.

Nitrogenase Contains Novel Redox Centers. **Nitrogenase,** which catalyzes the reduction of N_2 to NH_3, is a complex of two proteins:

1. The **Fe-protein,** a homodimer that contains one [4Fe–4S] cluster and two ATP-binding sites.
2. The **MoFe-protein,** an $\alpha_2\beta_2$ heterotetramer that contains Fe and Mo.

The X-ray structure of *Azotobacter vinelandii* nitrogenase in complex with the inhibitor $\text{ADP} \cdot \text{AlF}_4^-$ (which mimics the transition state in ATP hydrolysis), determined by Douglas Rees, reveals that each MoFe-protein associates with two molecules of Fe-protein (Fig. 21-41).

Each Fe-protein dimer's single [4Fe–4S] cluster is located in a solvent-exposed cleft between the two subunits and is symmetrically linked to Cys 97 and Cys 132 from both subunits such that an Fe-protein resembles

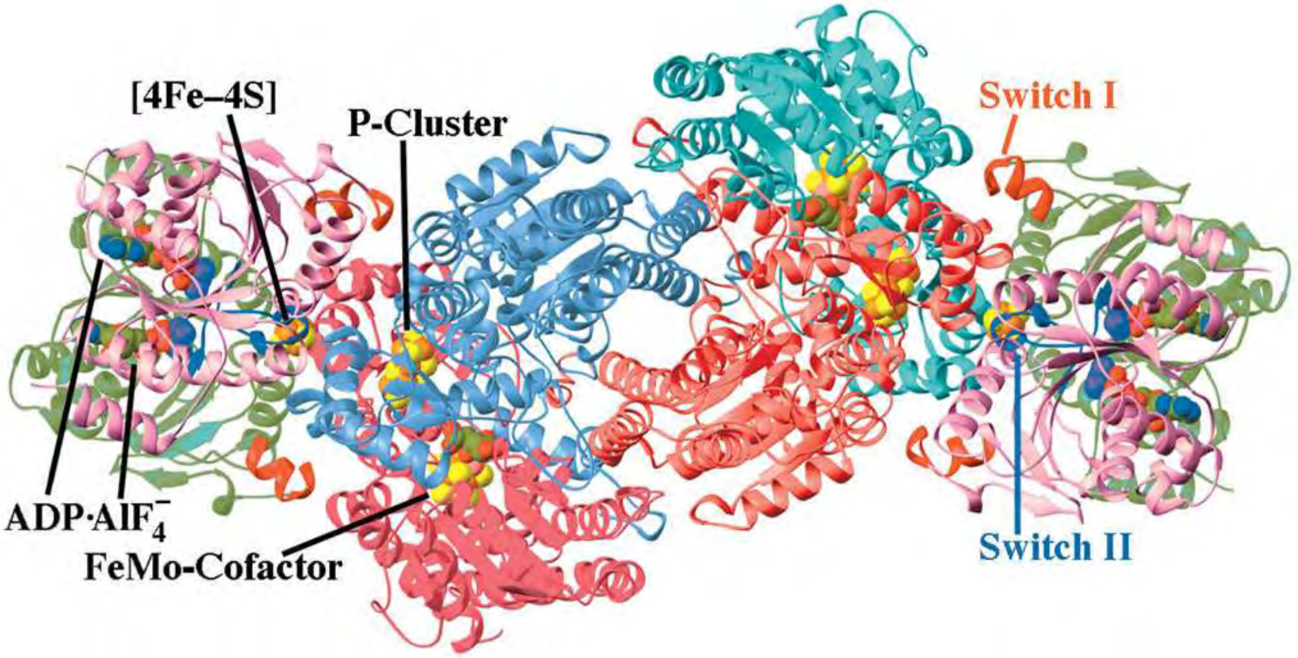

Figure 21-41 | X-Ray structure of the *A. vinelandii* nitrogenase in complex with $\text{ADP} \cdot \text{AlF}_4^-$. The enzyme, which is viewed along its molecular twofold axis, is an $(\alpha\beta\gamma_2)_2$ heterooctamer in which the β-α-α-β assembly, the MoFe-protein, is flanked by two γ_2 Fe-proteins whose 289-residue subunits are related by local twofold symmetry. The homologous α subunits (*cyan and red;* 491 residues) and β subunits (*light red and light blue;* 522 residues) are related by pseudo-twofold symmetry. The two γ subunits forming each Fe-protein (*pink and green with their Switch I and Switch II segments red and blue*) bind to the MoFe-protein with the twofold axis relating them coincident with the pseudo-twofold axis relating the MoFe-protein's α and β subunits. The $\text{ADP} \cdot \text{AlF}_4^-$, [4Fe–4S] cluster, FeMo-cofactor, and P-cluster are drawn in space-filling form with C green, N blue, O red, S yellow, Fe orange, Mo pink, and the AlF_4^- ion purple. [Based on an X-ray structure by Douglas Rees, California Institute of Technology. PDBid 1N2C.] **See Interactive Exercise 31.**

an "iron butterfly" with the [4Fe–4S] cluster at its head. Its nucleotide-binding sites are located at the interface between its two subunits.

The MoFe-protein's α and β subunits assume similar folds and extensively associate to form a pseudo-twofold symmetric αβ dimer, two of which more loosely associate to form the twofold symmetric $\alpha_2\beta_2$ tetramer (Fig. 21-41). Each αβ dimer has two bound redox centers:

1. The **P-cluster** (Figs. 21-42*a,b*), which consists of two [4Fe–3S] clusters linked through an additional sulfide ion forming the eighth corner of both of the clusters to make cubane-like structures, and bridged by two Cys thiol ligands, each coordinating one Fe from each cluster. Four additional Cys thiols coordinate the remaining four Fe atoms. The positions of two of the Fe atoms in one of the [4Fe–3S] clusters change on oxidation, rupturing the bonds from these Fe atoms to the linking sulfide ion. These bonds are replaced in the oxidized state by a Ser oxygen ligand to one of the Fe atoms, and by a bond to the amide N of a Cys from the other Fe atom.
2. The **FeMo-cofactor** (Fig. 21-42*c*), which consists of a [4Fe–3S] cluster and a [1Mo–3Fe–3S] cluster bridged by three sulfide ions. The FeMo-cofactor's Mo atom is approximately octahedrally coordinated by three cofactor sulfurs, a His imidazole nitrogen, and two oxygens from a bound **homocitrate** ion:

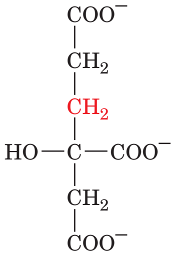

$$\begin{array}{c} \mathrm{COO^-} \\ | \\ \mathrm{CH_2} \\ | \\ \mathrm{CH_2} \\ | \\ \mathrm{HO{-}C{-}COO^-} \\ | \\ \mathrm{CH_2} \\ | \\ \mathrm{COO^-} \end{array}$$

Homocitrate

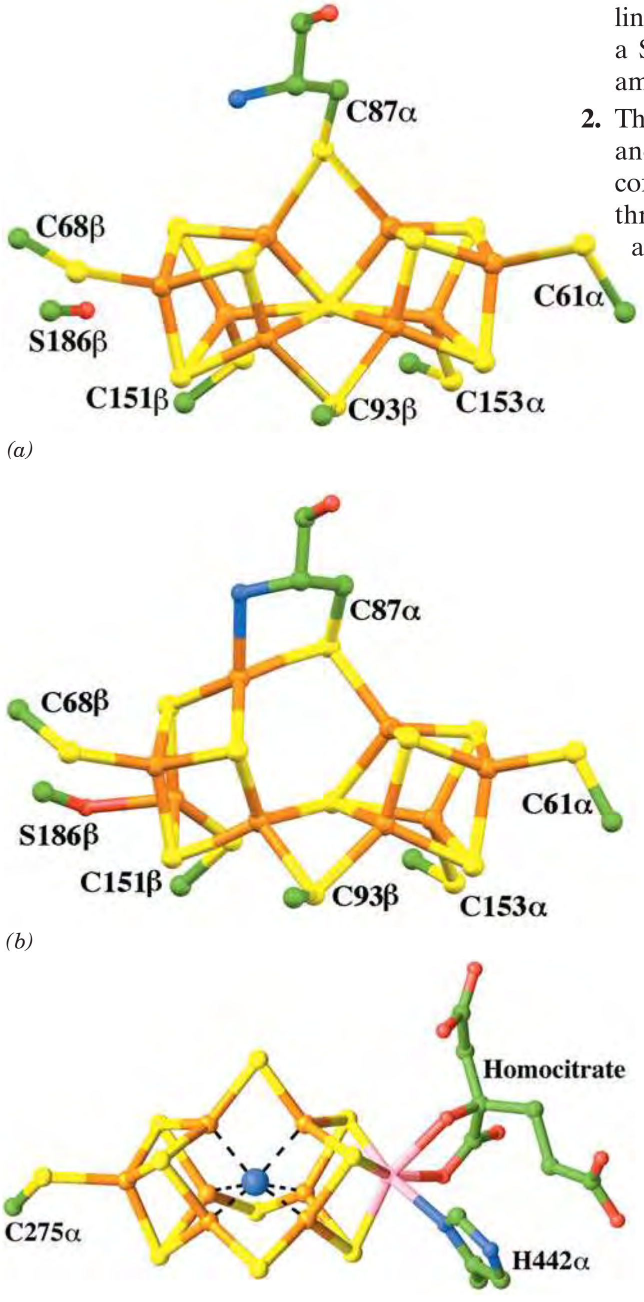

Figure 21-42 | The prosthetic groups of the nitrogenase MoFe-protein. The molecules are drawn in ball-and-stick form with C green, N blue, O red, S yellow, Fe orange, and Mo pink. (*a*) The reduced *Klebsiella pneumoniae* P-cluster. It consists of two [4Fe–3S] complexes linked by an additional sulfide ion forming the eighth corner of each cubane-like structure, and bridged by two Cys thiol ligands, each coordinating one Fe from each cluster. Four additional Cys thiols coordinate the remaining four Fe atoms. (*b*) The 2-electron-oxidized *K. pneumoniae* P-cluster. In comparison with the reduced complex in Part *a,* two of the Fe—S bonds from the centrally located sulfide ion that bridges the two [4Fe–3S] clusters have been replaced by ligands from the Cys 87α amide N and the Ser 186β side chain O yielding a [4Fe–3S] cluster (*left*) and a [4Fe–4S] cluster (*right*) that remain linked by a direct Fe—S bond and two bridging Cys thiols. (*c*) The *A. vinelandii* FeMo-cofactor. It consists of a [4Fe–3S] cluster and a [1Mo–3Fe–3S] cluster that are bridged by three sulfide ions. The FeMo-cofactor is linked to the protein by only two ligands at its opposite ends, one from His 442α to the Mo atom and the other from Cys 275α to an Fe atom. The Mo atom is additionally doubly liganded by homocitrate. What is most likely an N atom (*blue sphere*) is liganded to the FeMo-cluster's six central Fe atoms (*dashed black lines*). [Parts *a* and *b* based on X-ray structures by David Lawson, John Innes Centre, Norwich, U.K. Part *c* based on an X-ray structure by Douglas Rees, California Institute of Technology. PDBids (*a*) 1QGU, (*b*) 1QH1, and (*c*) 1M1N.]

(an essential component of the FeMo-cofactor). The FeMo-cofactor contains a central cavity that a high-resolution X-ray structure of *A. vinelandii* MoFe-protein, also determined by Rees, reveals contains what most probably is a nitrogen atom (although a C or an O atom cannot be ruled out). This putative N atom is liganded to the FeMo-cofactor's central six Fe atoms such that it completes the approximate tetrahedral coordination environment of each of the Fe atoms.

ATP Hydrolysis Triggers Conformational Changes in Nitrogenase. Nitrogen fixation by nitrogenase requires a source of electrons. These are generated either oxidatively or photosynthetically, depending on the organism. The electrons are transferred to **ferredoxin,** a [4Fe–4S]-containing electron carrier that transfers an electron to the Fe-protein of nitrogenase, beginning the nitrogen fixation process (Fig. 21-43).

The transfer of electrons during the nitrogenase reaction requires ATP-dependent protein conformational changes and the dissociation of the Fe-protein from the MoFe-protein after each electron transfer. During the reaction cycle, two molecules of ATP bind to the Fe-protein and are hydrolyzed as an electron passes to the MoFe-protein. ATP hydrolysis induces a conformational change in the Fe-protein that alters its redox potential from −0.29 to −0.40 V, making the electron capable of N_2 reduction ($\mathscr{E}^{\circ\prime}$ for the reaction $N_2 + 6\,H^+ + 6\,e^- \rightleftharpoons 2\,NH_3$ is −0.34 V).

How are events at the ATP-binding site linked to electron transfer? ATP hydrolysis occurs at a significant rate only when the Fe-protein is in complex with the MoFe-protein (and, of course, electron transfer can occur only when the two proteins are associated). Intriguingly, the binding of $ADP \cdot AlF_4^-$ to the Fe-protein induces conformational changes in two regions of the Fe-protein, designated Switch I and Switch II (Fig. 21-41), that are homologous to segments of signal-transducing G proteins in which nucleotide hydrolysis is coupled to protein conformational changes (Section 13-3B). At Switch I, these conformational changes affect the interactions between the Fe-protein and the MoFe-protein, whereas at Switch II they affect the environment of the [4Fe–4S] cluster. X-Ray structures of the Fe-protein alone and with bound ADP or ATP indicate that ATP hydrolysis triggers a structural change including rotation of the two Fe-protein subunits by about 13° toward each other. This conformational change brings the [4Fe–4S] cluster closer to the P-cluster of the adjacent MoFe-protein (from 18 to 14 Å apart), thereby promoting electron transfer from the Fe-protein to the MoFe-protein.

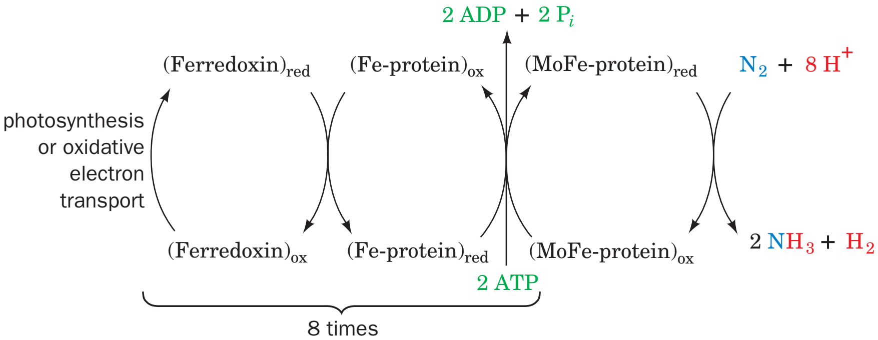

Figure 21-43 | **The flow of electrons in the nitrogenase-catalyzed reduction of N_2.**

Kinetic studies of nitrogenase indicate that the rate-limiting step of N_2 reduction is the dissociation of the Fe-protein from the MoFe-protein. If the Fe-protein functions in the same way as a G protein, then nucleotide hydrolysis might trigger its dissociation from the MoFe-protein. Reassociation could occur when the ADP exits the active site and is replaced by ATP. ATP hydrolysis would not occur again until the Fe-protein was docked with the MoFe-protein and poised to transfer electrons.

N_2 Reduction Is Energetically Costly. The actual reduction of N_2 occurs on the MoFe-protein in three discrete steps, each involving an electron pair:

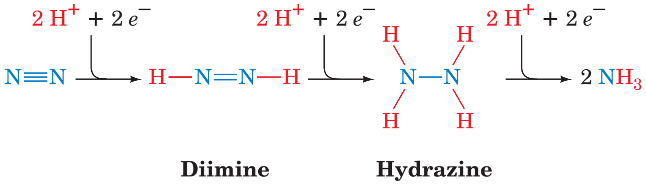

An electron transfer must occur six times per N_2 molecule fixed, so a total of 12 ATP are required to fix one N_2 molecule. However, nitrogenase also reduces H_2O to H_2, which in turn reacts with **diimine** to re-form N_2.

$$HN{=}NH + H_2 \rightarrow N_2 + 2\,H_2$$

This futile cycle is favored when the ATP level is low and/or the reduction of the Fe-protein is sluggish. Even when ATP is plentiful, however, the cycle cannot be suppressed beyond about one H_2 molecule produced per N_2 reduced and hence appears to be a requirement for the nitrogenase reaction. The total cost of N_2 reduction is therefore 8 electrons transferred and 16 ATP hydrolyzed. Under cellular conditions, the cost is closer to 20–30 ATP. Consequently, nitrogen fixation is an energetically expensive process.

Although atmospheric N_2 is the ultimate nitrogen source for all living things, most plants do not support the symbiotic growth of nitrogen-fixing bacteria. They must therefore depend on a source of "prefixed" nitrogen such as nitrate or ammonia. These nutrients come from lightning discharges (the source of ~10% of naturally fixed N_2), decaying organic matter in the soil, or from fertilizer applied to it (~50% of the nitrogen fixed is now generated by the **Haber-Bosch process,** which is used in the industrial production of ammonia from N_2 and H_2). One major long-term goal of genetic engineering is to induce agriculturally useful nonleguminous plants to fix their own nitrogen. This would free farmers, particularly those in developing countries, from either purchasing fertilizers, periodically letting their fields lie fallow (giving legumes the opportunity to grow), or following the slash-and-burn techniques that are rapidly destroying the world's tropical forests.

B | Fixed Nitrogen Is Assimilated into Biological Molecules

After atmospheric N_2 has been converted to a biologically useful form (e.g., ammonia), it must be assimilated into a cell's biomolecules. Once nitrogen has been introduced into an amino acid, the amino group can be transferred to other compounds by transamination. Because most organisms do not fix nitrogen and hence must rely on prefixed nitrogen, nitrogen assimilation reactions are critical for conserving this essential element.

We have already considered the reaction catalyzed by glutamine synthetase (Section 21-5A), which in microorganisms represents a metabolic entry point for fixed nitrogen (in animals, this reaction helps "mop up" excess ammonia). The glutamine synthetase reaction requires the nitrogen-containing compound glutamate as a substrate. So what is the source of the amino group in glutamate? In bacteria and plants, but not animals, the enzyme **glutamate synthase** converts α-ketoglutarate and glutamine to two molecules of glutamate:

$$\alpha\text{-Ketoglutarate} + \text{glutamine} + \text{NADPH} + \text{H}^+ \rightarrow 2\ \text{glutamate} + \text{NADP}^+$$

This reductive amination reaction requires electrons from NADPH and takes place at three distinct active sites in the $\alpha_2\beta_2$ heterotetramer (Fig. 21-44). X-Ray structures of the enzyme reveal that the substrate-binding sites are widely separated. As a result, the ammonia that is transferred from glutamine to α-ketoglutarate must travel through a 31-Å-long tunnel in the protein. This channeling probably helps prevent the loss of NH_3 to the cytosol and maintains this intermediate in its more reactive deprotonated state (in the cytosol, NH_3 would immediately acquire a proton to become NH_4^+). Furthermore, the tunnel is blocked by the side chains of several residues and opens only when α-ketoglutarate is bound to the enzyme and NADPH is available. This mechanism apparently prevents the wasteful hydrolysis of glutamine.

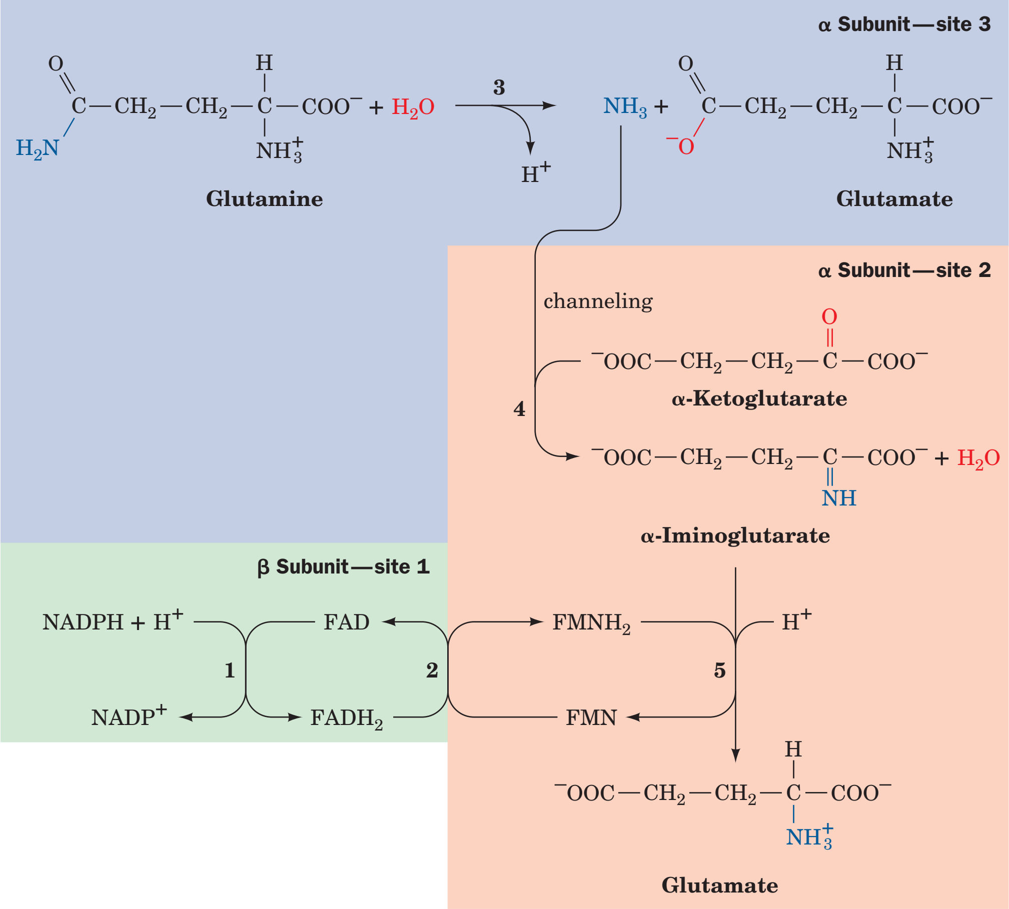

Figure 21-44 | The glutamate synthase reaction. (**1**) Electrons are transferred from NADPH to FAD at active site 1 on the β subunit to yield $FADH_2$. (**2**) Electrons travel from the $FADH_2$ to FMN at site 2 on an α subunit to yield $FMNH_2$. (**3**) Glutamine is hydrolyzed to glutamate and ammonia at site 3. (**4**) The ammonia produced in Step 3 moves to site 2 by channeling, where it reacts with α-ketoglutarate. (**5**) The α-iminoglutarate product is reduced by $FMNH_2$ to form glutamate.

The net result of the glutamine synthetase and glutamate synthase reactions is

$$\alpha\text{-Ketoglutarate} + NH_4^+ + NADPH + ATP \rightarrow \text{glutamate} + NADP^+ + ADP + P_i$$

Thus, *the combined action of these two enzymes assimilates fixed nitrogen (NH_4^+) into an organic compound (α-ketoglutarate) to produce an amino acid (glutamate)*. Once the nitrogen is assimilated as glutamate, it can be used in the synthesis of other amino acids by transamination.

The Nitrogen Cycle Describes the Interconversion of Nitrogen in the Biosphere. The ammonia produced by the nitrogenase reaction and incorporated into amino acids is eventually recycled in the biosphere as described by the **nitrogen cycle** (Fig. 21-45). Nitrate is produced by certain bacteria that oxidize NH_3 to NO_2^- and then NO_3^-, a process called **nitrification.** Still other organisms convert nitrate back to N_2, which is known as **denitrification.** In addition, nitrate is reduced to NH_3 by plants, fungi, and many bacteria, a process called **ammonification** in which **nitrate reductase** catalyzes the two-electron reduction of nitrate to nitrite (NO_2^-):

$$NO_3^- + 2\,H^+ + 2\,e^- \longrightarrow NO_2^- + H_2O$$

and then **nitrite reductase** converts nitrite to ammonia,

$$NO_2^- + 7\,H^+ + 6\,e^- \longrightarrow NH_3 + 2\,H_2O$$

The direct anaerobic oxidation of NH_3 back to N_2 without the intermediacy of nitrate, the reverse of nitrogen fixation, has recently been discovered in certain bacteria.

■ CHECK YOUR UNDERSTANDING

Summarize the mechanistic role of ATP in nitrogen fixation.

Describe the reactions that assimilate NH_3 into amino acids.

How is fixed nitrogen recycled in the biosphere?

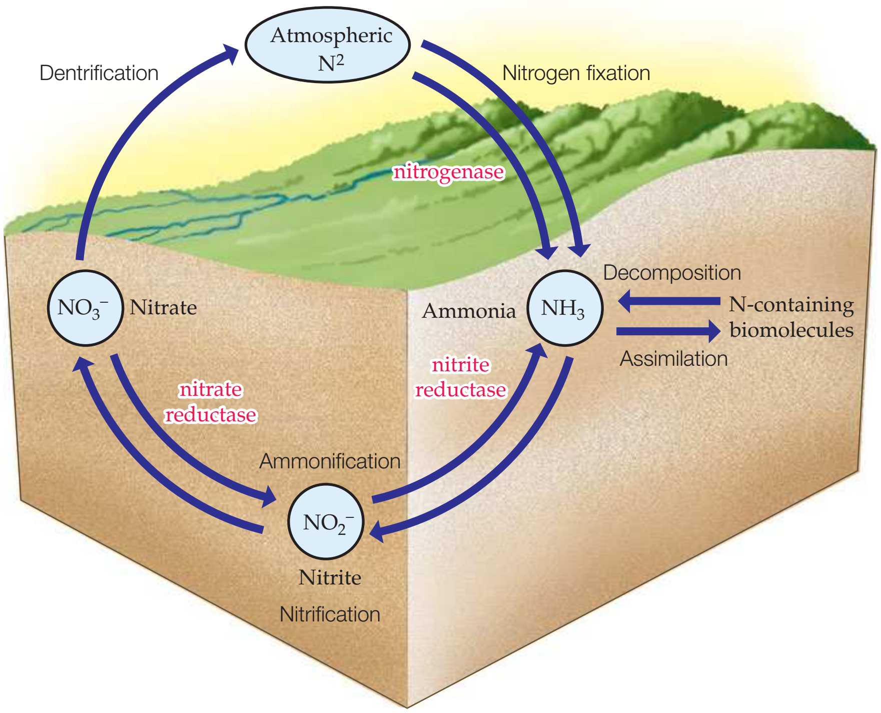
Atmospheric N^2
Dentrification
Nitrogen fixation
nitrogenase
Decomposition
NO_3^-
Nitrate
Ammonia
NH_3
N-containing biomolecules
Assimilation
nitrate reductase
nitrite reductase
Ammonification
NO_2^-
Nitrite
Nitrification

■ **Figure 21-45 | The nitrogen cycle.** Nitrogen fixation by nitrogenase converts N_2 to the biologically useful ammonia ion. Nitrate can also be converted to ammonia by the sequential actions of nitrate reductase and nitrite reductase. Ammonia is transformed to N_2 by nitrification followed by denitrification. Ammonia may be assimilated into nitrogen-containing biomolecules, which may be decomposed back to ammonia.

SUMMARY

1. Intracellular proteins are degraded by lysosomal proteases or, after being ubiquitinated, by the action of proteasomes.
2. The degradation of an amino acid almost always begins with the removal of its amino group in a PLP-facilitated transamination reaction.
3. In the urea cycle, a nitrogen atom from ammonia (a product of the oxidative deamination of glutamate) and a nitrogen atom from aspartate combine with HCO_3^- to form urea for excretion. The rate-limiting step of the process is catalyzed by carbamoyl phosphate synthetase.
4. The 20 "standard" amino acids are degraded to compounds that give rise either to glucose or to ketone bodies or fatty acids: pyruvate, α-ketoglutarate, succinyl-CoA, fumarate, oxaloacetate, acetyl-CoA, or acetoacetate.
5. The nonessential amino acids are synthesized in simple pathways from pyruvate, oxaloacetate, α-ketoglutarate, and 3-phosphoglycerate. The pathways for the syntheses of essential amino acids are more complicated and vary among organisms.
6. Amino acids are the precursors of various biomolecules. Heme is synthesized from glycine and acetate. Various hormones and neurotransmitters are synthesized by the decarboxylation and hydroxylation of histidine, glutamate, tryptophan, and tyrosine. The five-electron oxidation of arginine yields the bioactive stable radical nitric oxide.
7. Nitrogen fixation in bacteria, which requires 8 electrons and at least 16 ATP, is catalyzed by nitrogenase, a multisubunit protein with redox centers containing Fe, S, and Mo. Fixed nitrogen is incorporated into amino acids via the glutamine synthetase and glutamate synthase reactions.

KEY TERMS

ubiquitin	**734**
isopeptide bond	**734**
N-end rule	**735**
proteasome	**735**
sedimentation coefficient	**735**
transamination	**738**
PLP	**739**
deamination	**742**
hyperammonemia	**742**
urea cycle	**743**
channeling	**745**
glucogenic amino acid	**747**
ketogenic amino acid	**747**
THF	**749**
SAM	**753**
biopterin	**760**
essential amino acid	**763**
nonessential amino acid	**763**
adenylylation	**766**
uridylylation	**766**
porphyria	**778**
jaundice	**780**
catecholamine	**780**
nitrogen fixation	**782**
nitrogen assimilation	**782**

PROBLEMS

1. Explain why protein degradation by proteasomes requires ATP even though proteolysis is an exergonic process.
2. Explain why the symptoms of a partial deficiency in a urea cycle enzyme can be attenuated by a low-protein diet.
3. Production of the enzymes that catalyze the reactions of the urea cycle can increase or decrease according to the metabolic needs of the organism. High levels of these enzymes are associated with high-protein diets as well as starvation. Explain this apparent paradox.
4. Which three mammalian enzymes can potentially react with and thereby decrease the concentration of free NH_4^+?
5. *Helicobacter pylori,* the bacterium responsible for gastric ulcers, can survive in the stomach (where the pH is as low as 1.5) in part because it synthesizes large amounts of the enzyme urease. (a) Write the reaction for urea hydrolysis by urease. (b) Explain why this reaction could help establish a more hospitable environment for *H. pylori,* which tolerates acid but prefers to grow at near-neutral pH.
6. In the degradation pathway for isoleucine (Fig. 21-21), draw the reactions that convert tiglyl-CoA to acetyl-CoA and propionyl-CoA.
7. Draw the amino acid–Schiff base that forms in the breakdown of 3-hydroxykynurenine to form 3-hydroxyanthranilate in the tryptophan degradation pathway (Fig. 21-23, Reaction 4) and indicate which bond is to be cleaved.
8. Which of the 20 "standard" amino acids are (a) purely glucogenic, (b) purely ketogenic, and (c) both glucogenic and ketogenic?
9. Alanine, cysteine, glycine, serine, and threonine are amino acids whose breakdown yields pyruvate. Which, if any, of the remaining 15 amino acids also do so?
10. What are the metabolic consequences of a defective uridylyl-removing enzyme in *E. coli?*
11. Many of the most widely used herbicides inhibit the synthesis of aromatic amino acids. Explain why these compounds are safe to use near animals.
12. One of the symptoms of **kwashiorkor,** the dietary protein deficiency disease in children, is the depigmentation of the skin and hair. Explain the biochemical basis of this symptom.

REFERENCES

Protein Degradation

Groll, M. and Clausen, M., Molecular shredders: How proteasomes fulfill their roles. *Curr. Opin. Struct. Biol.* **13,** 665–673 (2003).

Hartmann-Peterson, R., Seeger, M., and Gordon, C., Transferring substrates to the 26S proteasome, *Trends Biochem. Sci.* **28,** 26–31 (2003).

Varshavsky, A., Regulated protein degradation, *Trends Biochem. Sci.* **30,** 283–286 (2005).

Urea Cycle

Withers, P.C., Urea: Diverse functions of a 'waste product,' *Clin. Exp. Pharm. Physiol.* **25,** 722–727 (1998). [Discusses the various roles of urea, contrasting it with ammonia with respect to toxicity, acid–base balance, and nitrogen transport.]

Amino Acid Catabolism and Synthesis

Brosnan, J.T., Glutamate, at the interface between amino acid and carbohydrate metabolism, *J. Nutr.* **130,** 988S–990S (2000). [Summarizes the metabolic roles of glutamate as a fuel and as a participant in deamination and transamination reactions.]

Eisenberg, D., Gill, H.S., Pfluegl, M.U., and Rotstein, S.H., Structure–function relationships of glutamine synthetases, *Biochim. Biophys. Acta* **1477,** 122–145 (2000).

Eliot, A.C. and Kirsch, J.F., Pyridoxal phosphate enzymes, *Annu. Rev. Biochem.* **73,** 383–415 (2004).

Huang, X., Holden, H.M., and Raushel, F.M., Channeling of substrates and intermediates in enzyme-catalyzed reactions, *Annu. Rev. Biochem.* **70,** 149–180 (2001).

Katagiri, M. and Nakamura, M., Animals are dependent on preformed α-amino nitrogen as an essential nutrient, *Life* **53,** 125–129 (2002).

Medina, M.Á., Urdiales, J.L., and Amores-Sánchez, M.I., Roles of homocysteine in cell metabolism: Old and new functions, *Eur. J. Biochem.* **268,** 3871–3882 (2001).

Scriver, C.R., Beaudet, A.L., Sly, S.S., and Vale, D. (Eds.), *Metabolic and Molecular Bases of Inherited Disease* (8th ed.), McGraw-Hill (2001). [Volume 2, Part 8 contains numerous chapters on amino acid metabolism and its defects.]

Nitrogen Fixation

Howard, J.B. and Rees, D.C., How many metals does it take to fix N_2? A mechanistic overview of biological nitrogen fixation, *Proc. Natl. Acad. Sci.* **103,** 17088–17093 (2006).

Igarashi, R.Y. and Seefeldt, L.C., Nitrogen fixation: The mechanism of Mo-dependent nitrogenase, *Crit. Rev. Biochem. Mol. Biol.* **38,** 351–384 (2003).

Jang, S.B., Seefeldt, L.C., and Peters, J.W., Insights into nucleotide signal transduction in nitrogenase: structure of an iron protein with MgADP, *Biochemistry* **39,** 14745–14752 (2000).

22

Mammalian Fuel Metabolism: Integration and Regulation

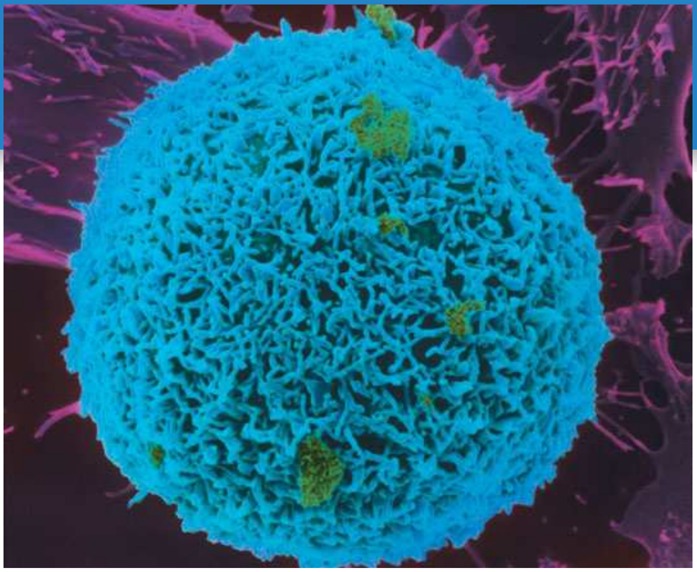

Hepatocytes (liver cells) carry out a great variety of metabolic processes. How are the specialized activities of hepatocytes and other types of cells coordinated for maximum metabolic efficiency and adaptability? How does faulty regulation result in disease? [CAMR/A.B. Dowsett/Photo Researchers.]

MEDIA RESOURCES

(available at www.wiley.com/college/voet)

Interactive Exercise 32. Human leptin

Animated Figure 22-6. The Cori cycle

Animated Figure 22-7. The glucose–alanine cycle

Animated Figure 22-8. GLUT4 activity

Case Study 25. Glycogen Storage Diseases

Case Study 28. The Bacterium *Helicobacter pylori* and Peptic Ulcers

Case Study 30. Phenylketonuria

CHAPTER CONTENTS

1 Organ Specialization
  - **A.** The Brain Requires a Steady Supply of Glucose
  - **B.** Muscle Utilizes Glucose, Fatty Acids, and Ketone Bodies
  - **C.** Adipose Tissue Stores and Releases Fatty Acids and Hormones
  - **D.** Liver Is the Body's Central Metabolic Clearinghouse
  - **E.** Kidney Filters Wastes and Maintains Blood pH
  - **F.** Blood Transports Metabolites in Interorgan Metabolic Pathways

2 Hormonal Control of Fuel Metabolism

3 Metabolic Homeostasis: The Regulation of Energy Metabolism, Appetite, and Body Weight
  - **A.** AMP-Dependent Protein Kinase Is the Cell's Fuel Gauge
  - **B.** Adiponectin Regulates AMPK Activity
  - **C.** Leptin Is a Satiety Hormone
  - **D.** Ghrelin and $\text{PYY}_{3\text{–}36}$ Act as Short-Term Regulators of Appetite
  - **E.** Energy Expenditure Can Be Controlled by Adaptive Thermogenesis

4 Disturbances in Fuel Metabolism
  - **A.** Starvation Leads to Metabolic Adjustments
  - **B.** Diabetes Mellitus Is Characterized by High Blood Glucose Levels
  - **C.** Obesity Is Usually Caused by Excessive Food Intake

In even the simplest prokaryotic cell, metabolic processes must be coordinated so that opposing pathways do not operate simultaneously and so that the organism can respond to changing external conditions such as the availability of nutrients. In addition, the organism's metabolic activities must meet the demands set by genetically programmed growth and reproduction. The challenges of coordinating energy acquisition and expenditure are markedly more complex in multicellular organisms, in which individual cells must cooperate. In animals and plants, this task is simplified by the division of metabolic labor among tissues.

In animals, the interconnectedness of various tissues is ensured by neuronal circuits and by hormones. Such regulatory systems do not simply switch cells on and off but elicit an almost infinite array of responses. The exact response of a cell to a given regulatory signal depends on the cell's ability to recognize the signal and on the presence of synergistic or antagonistic signals.

Our examination of mammalian carbohydrate, lipid, and amino acid metabolism (Chapters 15–21) would be incomplete without a discussion of how such processes are coordinated at the molecular level and how their malfunctions produce disease. In this chapter, we summarize the specialized metabolism of different organs and the pathways that link them. We also examine the mechanisms by which extracellular hormones influence intracellular events. We conclude with a discussion of disruptions in mammalian fuel metabolism.

1 Organ Specialization

LEARNING OBJECTIVES

- Review and integrate the oxidative and biosynthetic metabolic pathways.
- Understand the roles of the brain, muscle, adipose tissue, liver, and kidney in maintaining health.
- Understand that several metabolic processes require cooperation among organs.

Many of the metabolic pathways discussed so far have to do with the oxidation of metabolic fuels for the production of ATP. These pathways, which encompass the synthesis and breakdown of glucose, fatty acids, and amino acids, are summarized in Fig. 22-1.

1. **Glycolysis.** The metabolic degradation of glucose begins with its conversion to two molecules of pyruvate with the net generation of two molecules of ATP (Section 15-1).
2. **Gluconeogenesis.** Mammals can synthesize glucose from a variety of precursors, such as pyruvate, via a series of reactions that largely reverse the path of glycolysis (Section 16-4).

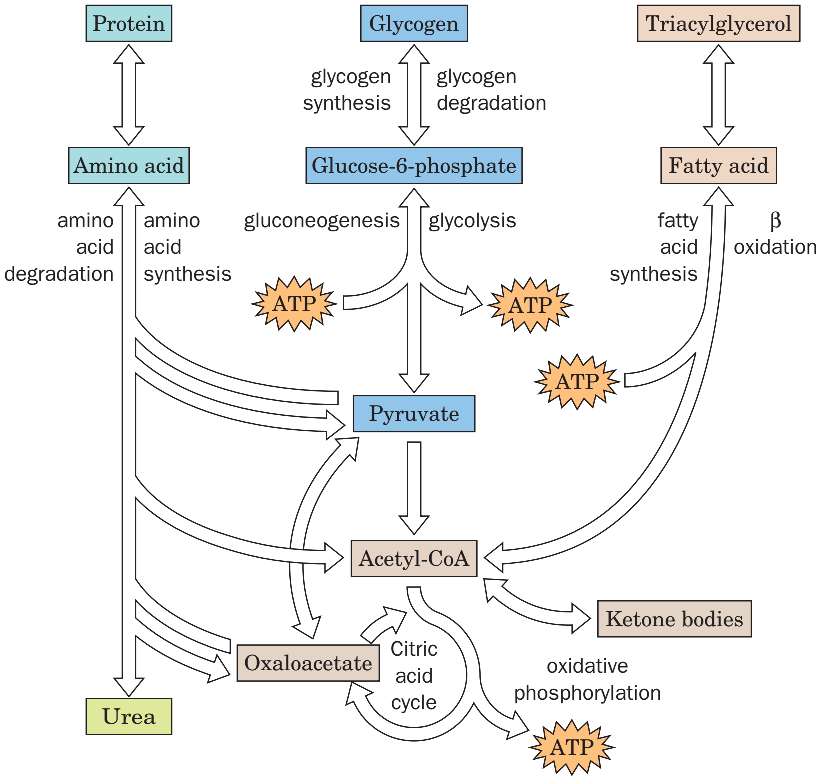
Protein
Glycogen
Triacylglycerol
glycogen synthesis
glycogen degradation
Amino acid
Glucose-6-phosphate
Fatty acid
amino acid degradation
amino acid synthesis
gluconeogenesis
glycolysis
fatty acid synthesis
β oxidation
ATP
ATP
ATP
Pyruvate
Acetyl-CoA
Ketone bodies
Oxaloacetate
Citric acid cycle
oxidative phosphorylation
ATP
Urea

Figure 22-1 | The major pathways of fuel metabolism in mammals. Proteins, glycogen, and triacylglycerols are built up from and broken down to smaller units: amino acids, glucose-6-phosphate, and fatty acids. Oxidation of those fuels yields metabolic energy in the form of ATP. Pyruvate (a product of glucose and amino acid degradation) and acetyl-CoA (a product of glucose, amino acid, and fatty acid degradation) occupy central positions in mammalian fuel metabolism. Compounds that give rise to pyruvate, such as oxaloacetate, can be used for gluconeogenesis; acetyl-CoA can give rise to ketone bodies but not glucose. Not all the pathways shown here occur in all cells or occur simultaneously in a given cell.

3. **Glycogen degradation and synthesis.** The opposing processes catalyzed by glycogen phosphorylase and glycogen synthase are reciprocally regulated by hormonally controlled phosphorylation and dephosphorylation (Section 16-3).
4. **Fatty acid synthesis and degradation.** Fatty acids are broken down through β oxidation to form acetyl-CoA (Section 20-2), which, through its conversion to malonyl-CoA, is also the substrate for fatty acid synthesis (Section 20-4).
5. **The citric acid cycle.** The citric acid cycle (Section 17-1) oxidizes acetyl-CoA to CO_2 and H_2O with the concomitant production of reduced coenzymes whose reoxidation drives ATP synthesis. Many glucogenic amino acids can be oxidized via the citric acid cycle following their breakdown to one of its intermediates (Section 21-4), which, in turn, are broken down to pyruvate and then to acetyl-CoA, the cycle's only substrate.
6. **Oxidative phosphorylation.** This mitochondrial pathway couples the oxidation of NADH and $FADH_2$ produced by glycolysis, β oxidation, and the citric acid cycle to the phosphorylation of ADP (Section 18-3).
7. **Amino acid synthesis and degradation.** Excess amino acids are degraded to metabolic intermediates of glycolysis and the citric acid cycle (Section 21-4). The amino group is disposed of through urea synthesis (Section 21-3). Nonessential amino acids are synthesized via pathways that begin with common metabolites (Section 21-5A).

Two compounds lie at the crossroads of the major metabolic pathways: acetyl-CoA and pyruvate (Fig. 22-1). Acetyl-CoA is the common degradation product of glucose, fatty acids, and ketogenic amino acids. Its acetyl group can be oxidized to CO_2 and H_2O via the citric acid cycle and oxidative phosphorylation or used to synthesize ketone bodies or fatty acids. Pyruvate is the product of glycolysis and the breakdown of glucogenic amino acids. It can be oxidatively decarboxylated to yield acetyl-CoA, thereby committing its atoms either to oxidation or to the biosynthesis of fatty acids. Alternatively, pyruvate can be carboxylated via the pyruvate carboxylase reaction to form oxaloacetate, which can either replenish citric acid cycle intermediates or give rise to glucose or certain amino acids.

Only a few tissues, such as liver, can carry out all the reactions shown in Fig. 22-1, and in a given cell only a small portion of all possible metabolic reactions occur at a significant rate. The flux through any sequence of reactions depends on the presence of the appropriate enzyme catalysts and on the organism's need for the reaction products.

We shall consider the metabolism of five mammalian organs: brain, muscle, adipose tissue, liver, and kidney. Metabolites flow between these organs in well-defined pathways in which flux varies with the nutritional state of the animal (Fig. 22-2). For example, immediately following a meal, glucose, amino acids, and fatty acids are directly available from the intestine. Later, when those fuels have been exhausted, the liver supplies other tissues with glucose and ketone bodies, whereas adipose tissue provides them with fatty acids. All these organs are connected via the bloodstream.

A | The Brain Requires a Steady Supply of Glucose

Brain tissue has a remarkably high respiration rate. Although the human brain constitutes only ~2% of the adult body mass, it is responsible for ~20% of its resting O_2 consumption. Most of the brain's energy production

Figure 22-2 | The metabolic interrelationships among brain, adipose tissue, muscle, liver, and kidney. The red arrows indicate pathways that predominate in the well-fed state.

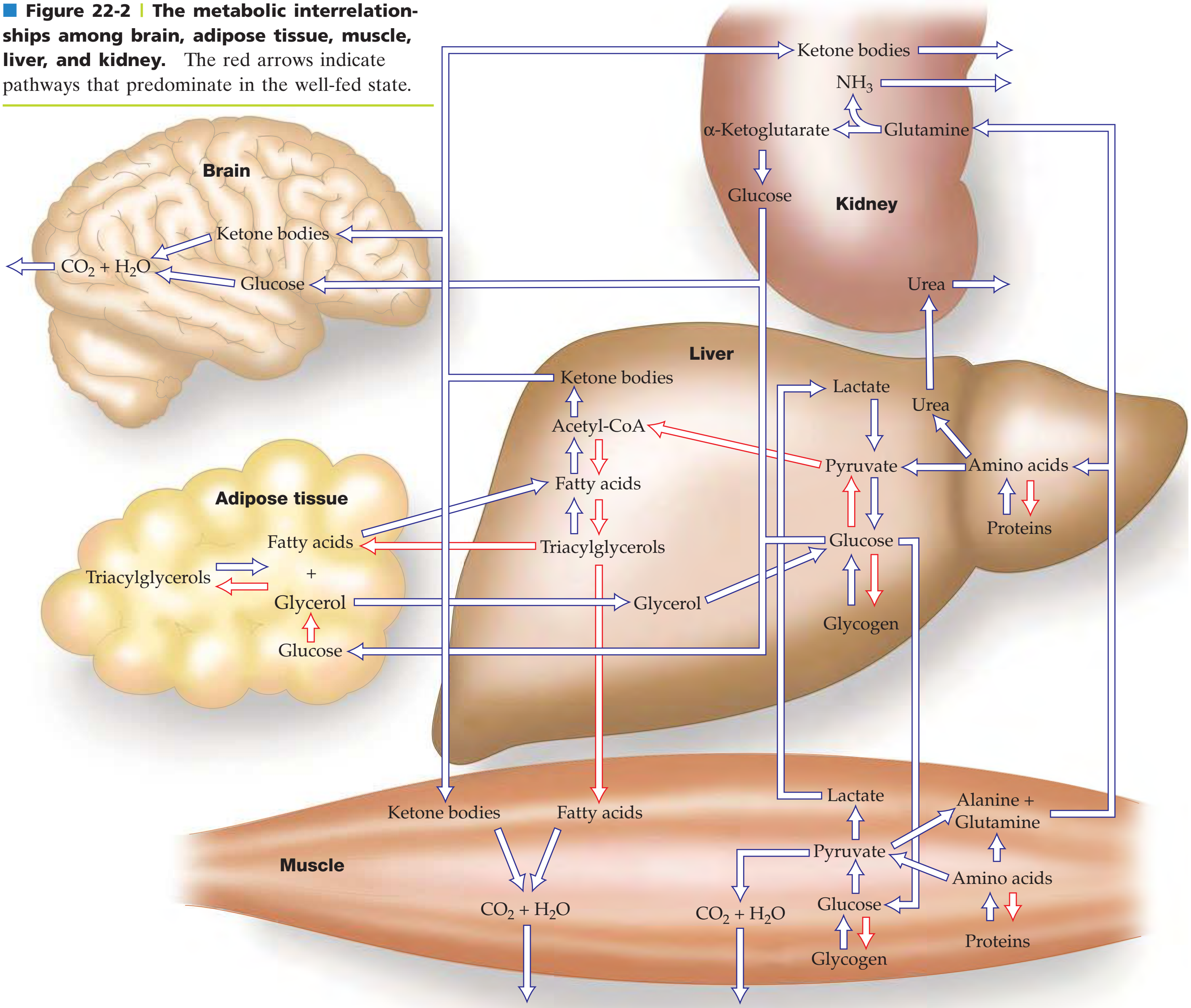
Ketone bodies
NH_3
α-Ketoglutarate
Glutamine
Glucose
Kidney
Urea
Brain
Ketone bodies
$CO_2 + H_2O$
Glucose
Liver
Ketone bodies
Lactate
Urea
Acetyl-CoA
Pyruvate
Amino acids
Fatty acids
Proteins
Adipose tissue
Fatty acids
Triacylglycerols
Glucose
Triacylglycerols
+
Glycerol
Glycerol
Glycogen
Glucose
Ketone bodies
Fatty acids
Lactate
Alanine + Glutamine
Muscle
Pyruvate
Amino acids
$CO_2 + H_2O$
$CO_2 + H_2O$
Glucose
Proteins
Glycogen

powers the plasma membrane (Na^+–K^+)–ATPase (Section 10-3A), which maintains the membrane potential required for nerve impulse transmission.

Under usual conditions, glucose is the brain's primary fuel (although during an extended fast, the brain gradually switches to ketone bodies; Section 22-4A). Since brain cells store very little glycogen, *they require a steady supply of glucose from the blood.* A blood glucose concentration of less than half the normal value of ~5 mM results in brain dysfunction. Levels much below this result in coma, irreversible damage, and ultimately death.

B | Muscle Utilizes Glucose, Fatty Acids, and Ketone Bodies

Muscle's major fuels are glucose (from glycogen), fatty acids, and ketone bodies. Rested, well-fed muscle synthesizes a glycogen store comprising 1 to 2% of its mass. Although triacylglycerols are a more efficient form of energy storage (Section 9-1B), the metabolic effort of synthesizing glycogen is cost-effective because glycogen can be mobilized more rapidly than fat and because glucose can be metabolized anaerobically, whereas fatty acids cannot.

In muscle, glycogen is converted to glucose-6-phosphate (G6P) for entry into glycolysis. Muscle cannot export glucose, however, because it lacks glucose-6-phosphatase. Furthermore, although muscle can synthesize glycogen from glucose, it does not participate in gluconeogenesis because it lacks the required enzymatic machinery. Consequently, *muscle carbohydrate metabolism serves only muscle.*

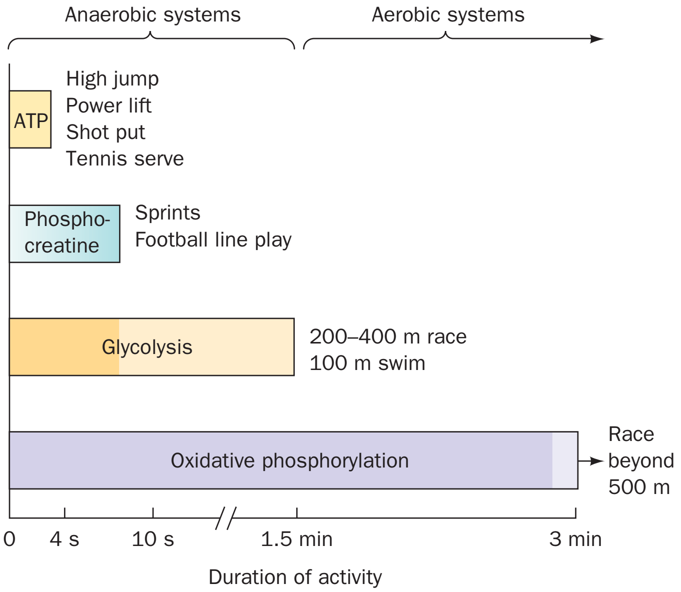

Figure 22-3 | Source of ATP during exercise in humans. The supply of endogenous ATP is extended for a few seconds by phosphocreatine, after which anaerobic glycolysis generates ATP. The shift from anaerobic to aerobic metabolism (oxidative phosphorylation) occurs after about 90 sec, or slightly later in trained athletes. [Adapted from McArdle, W.D., Katch, F.I., and Katch, V.L., *Exercise Physiology,* 2nd ed., Lea & Febiger (1986), p. 348.]

Muscle Contraction Is Anaerobic under Conditions of High Exertion. Muscle contraction is driven by ATP hydrolysis (Section 7-2) and therefore requires either an aerobic or an anaerobic ATP regeneration system. Respiration (the citric acid cycle and oxidative phosphorylation) is the body's major source of ATP resupply. Skeletal muscle at rest uses ~30% of the O_2 consumed by the human body. A muscle's respiration rate may increase in response to a heavy workload by as much as 25-fold. Yet, its rate of ATP hydrolysis can increase by a much greater amount. The ATP is initially regenerated by the reaction of phosphocreatine with ADP (Section 14-2C):

$$\text{Phosphocreatine} + \text{ADP} \rightleftharpoons \text{creatine} + \text{ATP}$$

(phosphocreatine is resynthesized in resting muscle by the reversal of this reaction). Under conditions of maximum exertion, however, such as during a sprint, a muscle has only about a 4-s supply of phosphocreatine. It must then shift to ATP production via glycolysis of G6P, a process whose maximum flux greatly exceeds those of the citric acid cycle and oxidative phosphorylation. Much of the G6P is therefore degraded anaerobically to lactate (Section 15-3A). As we shall see in Section 22-1F, export of lactate relieves much of the muscle's respiratory burden. Muscle fatigue, which occurs after ~20 s of maximal exertion, is not caused by exhaustion of the muscle's glycogen supply but by the drop in pH that results from the buildup of lactate (Section 15-3A). This phenomenon may be an adaptation that prevents muscle cells from committing suicide by fully depleting their ATP supply. Exercise lasting more than a minute or two is fueled primarily by oxidative phosphorylation, which generates ATP more slowly but much more efficiently than glycolysis alone. The source of ATP during exercise of varying duration is summarized in Fig. 22-3.

The Heart Is Largely Aerobic. The heart is a muscular organ that acts continuously rather than intermittently. Therefore, heart muscle relies entirely on aerobic metabolism and is richly endowed with mitochondria; they occupy up to 40% of its cytoplasmic space. The heart can metabolize fatty acids, ketone bodies, glucose, pyruvate, and lactate. Fatty acids are the resting heart's fuel of choice, but during heavy work, the heart greatly increases its consumption of glucose, which is derived mostly from its relatively limited glycogen store.

C | Adipose Tissue Stores and Releases Fatty Acids and Hormones

The function of adipose tissue is to store and release fatty acids as needed for fuel as well as to secrete hormones involved in regulating metabolism. Adipose tissue is widely distributed throughout the body but occurs most prominently under the skin, in the abdominal cavity, and in skeletal muscle. The adipose tissue of a normal 70-kg man contains ~15 kg of fat. This amount represents some 590,000 kJ of energy (141,000 dieter's Calories), which is sufficient to maintain life for ~3 months.

Adipose tissue obtains most of its fatty acids for storage from circulating lipoproteins as described in Section 20-1B. Fatty acids are activated by the formation of the corresponding fatty acyl-CoA and then esterified with glycerol-3-phosphate to form the stored triacylglycerols. The glycerol-3-phosphate arises from the reduction of dihydroxyacetone phosphate, which must be glycolytically generated from glucose.

In times of metabolic need, adipocytes hydrolyze triacylglycerols to fatty acids and glycerol through the action of hormone-sensitive lipase (Section 20-5). If glycerol-3-phosphate is abundant, many of the fatty acids so formed are reesterified to triacylglycerols. If glycerol-3-phosphate is in short supply, the fatty acids are released into the bloodstream. Thus, *fatty acid mobilization depends in part on the rate of glucose uptake since glucose is the precursor of glycerol-3-phosphate.* Metabolic need is signaled directly by a decrease in [glucose] as well as by hormonal stimulation.

D | Liver Is the Body's Central Metabolic Clearinghouse

The liver maintains the proper levels of circulating fuels for use by the brain, muscles, and other tissues. It is uniquely situated to carry out this task because all the nutrients absorbed by the intestines except fatty acids are released into the portal vein, which drains directly into the liver.

Glucokinase Converts Blood Glucose to Glucose-6-Phosphate. *One of the liver's major functions is to act as a blood glucose "buffer."* It does so by taking up and releasing glucose in response to hormones and to the concentration of glucose itself. After a carbohydrate-containing meal, when the blood glucose concentration reaches ~6 mM, the liver takes up glucose by converting it to G6P. This reaction is catalyzed by **glucokinase,** a liver isozyme of hexokinase. The hexokinases in most cells obey Michaelis–Menten kinetics, have a high glucose affinity ($K_M < 0.1$ mM), and are inhibited by their reaction product (G6P). Glucokinase, in contrast, has much lower glucose affinity (reaching half-maximal velocity at ~5 mM) and displays sigmoidal kinetics. Consequently, *glucokinase activity increases rapidly with blood [glucose] over the normal physiological range* (Fig. 22-4). Glucokinase, moreover, is not inhibited by physiological concentrations of G6P. Therefore, the higher the blood [glucose], the faster the liver converts glucose to G6P. At low blood [glucose], the liver does not compete with other tissues for the available glucose, whereas at high blood [glucose], when the glucose needs of those tissues are met, the liver can take up the excess glucose at a rate roughly proportional to the blood glucose concentration.

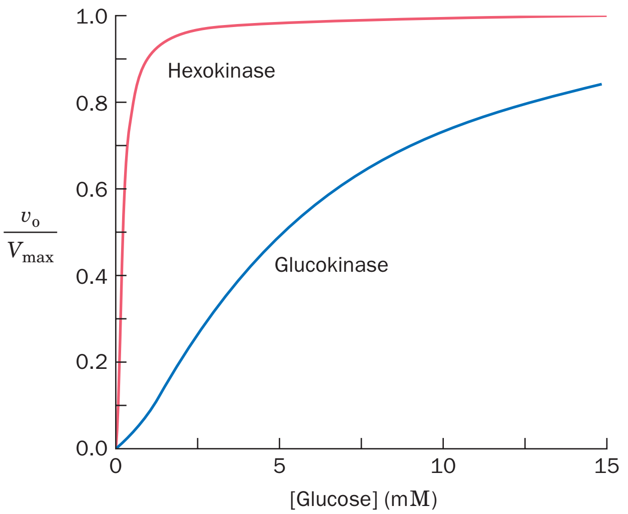

■ **Figure 22-4 | Relative enzymatic activities of hexokinase and glucokinase over the physiological blood glucose range.** Glucokinase has much lower affinity for glucose ($K_M \approx 5$ mM) than does hexokinase ($K_M =$ 0.1 mM) and exhibits sigmoidal rather than hyperbolic variation with [glucose]. [The glucokinase curve was generated using the Hill equation (Eq. 7-8) with $K = 10$ mM and $n = 1.5$ as obtained from Cardenas, M.L., Rabajille, E., and Niemeyer, H., *Eur. J. Biochem.* **145,** 163–171 (1984).]

Glucokinase is a monomeric enzyme, so its sigmoidal kinetic behavior is somewhat puzzling (models of allosteric interactions do not explain cooperative behavior in a monomeric protein; Section 7-1D). Glucokinase is subject to metabolic control, however. Emile Van Schaftingen has isolated a **glucokinase regulatory protein** from rat liver, which, in the presence of the glycolytic intermediate fructose-6-phosphate (F6P), is a competitive inhibitor of glucokinase. Since F6P and the glucokinase product G6P are equilibrated in liver cells by phosphoglucose isomerase, glucokinase is, in effect, inhibited by its product. Fructose-1-phosphate (F1P), an intermediate in liver fructose metabolism (Section 15-5A), overcomes this inhibition. Since fructose is normally available only from dietary sources, fructose may be the signal that triggers the uptake of dietary glucose by the liver.

Glucose-6-Phosphate Is at the Crossroads of Carbohydrate Metabolism. G6P has several alternative fates in the liver, depending on the glucose demand (Fig. 22-5):

1. G6P can be converted to glucose, by the action of glucose-6-phosphatase, for transport via the bloodstream to the peripheral organs. This occurs only when the blood [glucose] drops below ~5 mM. During exercise or fasting, low concentrations of blood glucose cause the pancreas to secrete glucagon. Glucagon receptors on the liver cell surface respond by activating adenylate cyclase. The resulting increase in intracellular [cAMP] triggers glycogen breakdown (Section 16-3).
2. G6P can be converted to glycogen (Section 16-2) when the body's demand for glucose is low.
3. G6P can be converted to acetyl-CoA via glycolysis and the action of pyruvate dehydrogenase. This glucose-derived acetyl-CoA, if it is not oxidized via the citric acid cycle and oxidative phosphorylation to generate ATP, can be used to synthesize fatty acids (Section 20-4), phospholipids (Section 20-6), and cholesterol (Section 20-7A).
4. G6P can be degraded via the pentose phosphate pathway (Section 15-6) to generate the NADPH required for the biosynthesis of fatty acids and other compounds.

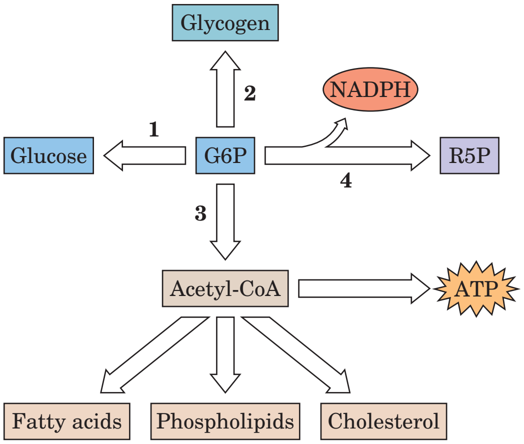

Figure 22-5 | Metabolic fate of glucose-6-phosphate (G6P) in liver. G6P can be converted (**1**) to glucose for export or (**2**) to glycogen for storage. Acetyl-CoA derived from G6P degradation (**3**) is the starting material for lipid biosynthesis. It is also consumed in generating ATP by respiration. Degradation of G6P via the pentose phosphate pathway (**4**) yields NADPH.

The Liver Can Synthesize or Degrade Triacylglycerols. Fatty acids are also subject to alternative metabolic fates in the liver. When the demand for metabolic fuels is high, fatty acids are degraded to acetyl-CoA and then to ketone bodies for export to the peripheral tissues. The liver itself cannot use ketone bodies as fuel, because liver cells lack 3-ketoacyl-CoA transferase, an enzyme required to convert ketone bodies back to acetyl-CoA (Section 20-3). Fatty acids rather than glucose or ketone bodies are therefore the liver's major acetyl-CoA source under conditions of high metabolic demand. The liver generates its ATP from this acetyl-CoA through the citric acid cycle and oxidative phosphorylation.

When the demand for metabolic fuels is low, fatty acids are incorporated into triacylglycerols that are secreted into the bloodstream as VLDL for uptake by adipose tissue. Fatty acids are also incorporated into phospholipids (Section 20-6). Under these conditions, fatty acids synthesized in the liver are not oxidized to acetyl-CoA because fatty acid synthesis (in the cytosol) is separated from fatty acid oxidation (in the mitochondria) and because malonyl-CoA, an intermediate in fatty acid synthesis, inhibits the transport of fatty acids into the mitochondria.

Amino Acids Are Metabolic Fuels. The liver degrades amino acids to a variety of metabolic intermediates that can be completely oxidized to CO_2 and H_2O or converted to glucose or ketone bodies (Section 21-4). Oxidation of amino acids provides a significant fraction of metabolic energy immediately after a meal, when amino acids are present in relatively high concentrations in the blood. During a fast, when other fuels become scarce, glucose is produced from amino acids arising mostly from muscle protein degradation to alanine and glutamine. Thus, *proteins, in addition to their structural and functional roles, are important fuel reserves.*

E | Kidney Filters Wastes and Maintains Blood pH

The kidney filters urea and other waste products from the blood while it recovers important metabolites such as glucose. In addition, the kidney maintains the blood's pH by regenerating depleted blood buffers such as bicarbonate (lost by the exhalation of CO_2) and by excreting excess H^+ together with the conjugate bases of excess metabolic acids such as the ketone bodies acetoacetate and β-hydroxybutyrate. Protons are also excreted in the form of NH_4^+ with the ammonia derived from glutamine or glutamate. The remaining amino acid skeleton, α-ketoglutarate, can be converted to glucose by gluconeogenesis (the kidney is the only tissue besides liver that can undertake glucose synthesis). During starvation, the kidneys generate as much as 50% of the body's glucose supply.

F | Blood Transports Metabolites in Interorgan Metabolic Pathways

The ability of the liver to supply other tissues with glucose or ketone bodies, or the ability of adipocytes to make fatty acids available to other tissues, depends, of course, on the circulatory system, which transports metabolic fuels, intermediates, and waste products among tissues. In addition, several important metabolic pathways are composed of reactions occurring in multiple tissues. In this section, we describe two well-known interorgan pathways.

Glucose and Lactate Are Transported in the Cori Cycle. The ATP that powers muscle contraction is generated through oxidative phosphorylation (in mitochondrion-rich slow-twitch muscle fibers; Box 15-3) or by rapid catabolism of glucose to lactate (in fast-twitch muscle fibers). Slow-twitch fibers also produce lactate when ATP demand exceeds oxidative flux. The lactate is transferred via the bloodstream to the liver, where it is reconverted to pyruvate by lactate dehydrogenase and then to glucose by gluconeogenesis. Thus, liver and muscle are linked by the bloodstream in a metabolic cycle known as the **Cori cycle** (Fig. 22-6) in honor of Carl and Gerty Cori (Box 16-1), who first described it.

The ATP-consuming glycolysis/gluconeogenesis cycle would be a futile cycle if it occurred within a single cell. In this case, the two halves of the pathway occur in different organs. Liver ATP is used to resynthesize glucose from lactate produced in muscle. The resynthesized glucose returns to the muscle, where it may be stored as glycogen or catabolized immediately to generate ATP for muscle contraction.

The ATP consumed by the liver during the operation of the Cori cycle is regenerated by oxidative phosphorylation. After vigorous exertion, it may take at least 30 min for the oxygen consumption rate to decrease to its resting level. The elevated O_2 consumption pays off the **oxygen debt** created by the demand for ATP to drive gluconeogenesis.

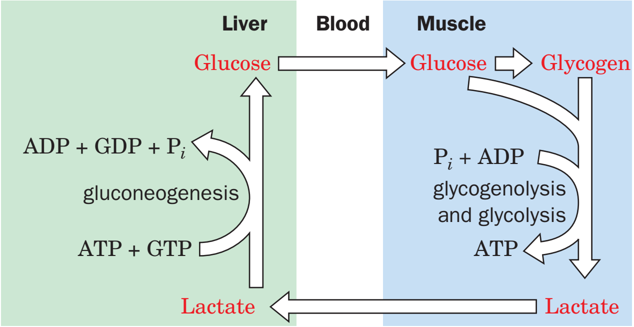

Figure 22-6 | The Cori cycle. Lactate produced by muscle glycolysis is transported by the bloodstream to the liver, where it is converted to glucose by gluconeogenesis. The bloodstream carries the glucose back to the muscle, where it may be stored as glycogen. **See the Animated Figures.**

The Glucose–Alanine Cycle Transfers Alanine to the Liver. In a pathway similar to the Cori cycle, alanine rather than lactate travels from muscle to the liver. In muscle, certain aminotransferases use pyruvate as

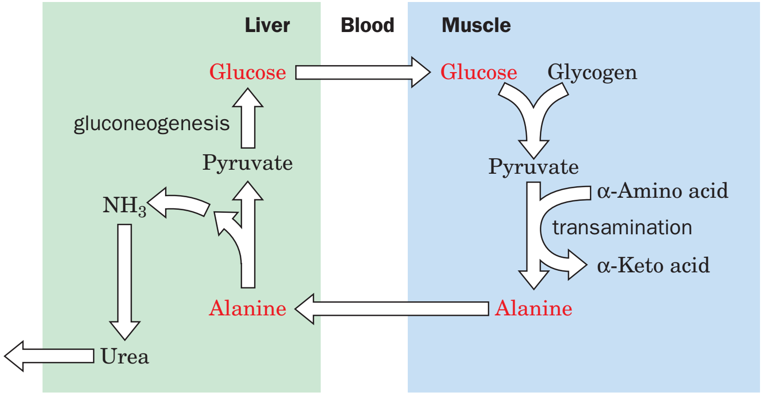

Figure 22-7 | The glucose–alanine cycle. Pyruvate produced by muscle glycolysis is the amino-group acceptor for muscle aminotransferases. The resulting alanine is transported by the bloodstream to the liver, where it is converted back to pyruvate (its amino group is disposed of via urea synthesis). The pyruvate is a substrate for gluconeogenesis, and the bloodstream carries the resulting glucose back to the muscles. **See the Animated Figures.**

their α-keto acid substrate rather than α-ketoglutarate or oxaloacetate (Section 21-2A):

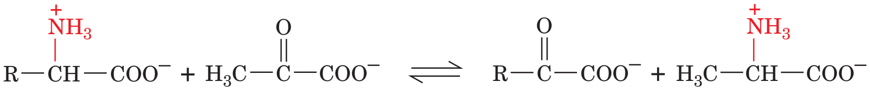

$$\underset{\textbf{Amino acid}}{R{-}\overset{\overset{+}{N}H_3}{\overset{|}{C}H}{-}COO^-} + \underset{\textbf{Pyruvate}}{H_3C{-}\overset{O}{\overset{\|}{C}}{-}COO^-} \rightleftharpoons \underset{\textbf{α-Keto acid}}{R{-}\overset{O}{\overset{\|}{C}}{-}COO^-} + \underset{\textbf{Alanine}}{H_3C{-}\overset{\overset{+}{N}H_3}{\overset{|}{C}H}{-}COO^-}$$

The product amino acid, alanine, is released into the bloodstream and transported to the liver, where it undergoes transamination back to pyruvate. This pyruvate is a substrate for gluconeogenesis, and the resulting glucose can be returned to the muscles to be glycolytically degraded. This is the **glucose–alanine cycle** (Fig. 22-7). The amino group carried by alanine ends up in either ammonia or aspartate and can be used for urea biosynthesis (which occurs only in the liver). Thus, *the glucose–alanine cycle is a mechanism for transporting nitrogen from muscle to liver.*

During fasting, the glucose formed in the liver by this route is also used by other tissues, breaking the cycle. Because the pyruvate originates from muscle protein degradation, muscle supplies glucose to other tissues even though it does not carry out gluconeogenesis.

CHECK YOUR UNDERSTANDING

Summarize the major features of fuel metabolism in the brain, muscle, adipose tissue, liver, and kidney.
Explain why the high K_M of glucokinase is important for the role of the liver in buffering blood glucose.
Describe the conditions under which the Cori cycle and the glucose–alanine cycle operate.

2 Hormonal Control of Fuel Metabolism

LEARNING OBJECTIVE

- Understand the roles of insulin, glucagon, and the catecholamines in coordinating metabolism in different tissues.

Multicellular organisms coordinate their activities at every level of their organization through complex signaling systems (Chapter 13). Most cells in a multicellular organism will not even take up fuel for growth and metabolism without first receiving a signal to do so. The human endocrine system responds to the needs of an organism by secreting a wide variety of hormones that enable the body to maintain **homeostasis,** respond to external stimuli, and follow various developmental programs.

We have already discussed steroid hormones (Section 9-1E), the peptide hormones insulin and glucagon (Sections 13-1A, 13-4D, and 16-3C), and the catecholamines epinephrine and norepinephrine (Sections 13-1B, 16-3C, and 21-6B). With the exception of steroids, which can diffuse through cell membranes and interact directly with intracellular components (and which we discuss further in Section 28-3B), these extracellular signals must first bind to a cell-surface receptor. In this section, we review the action of hormones synthesized by the pancreas and adrenal glands, since these play the largest roles in regulating the metabolism of fuels in various mammalian tissues. We will also review the receptors and pathways by which these hormones exert their effects on cells.

Insulin Release Is Triggered by Glucose. The pancreas responds to increases in the concentration of blood glucose by secreting insulin, which therefore serves as a signal for plentiful metabolic fuel. Pancreatic β cells are most sensitive to glucose at concentrations of 5.5 to 6.0 mM (normal blood glucose concentrations range from 3.6 to 5.8 mM). There is no evidence for a cell-surface glucose "receptor" that might relay a signal to the secretory machinery in the β cell. In fact, glucose enters β cells via passive transport, and its metabolism generates the signal for insulin secretion.

The rate-limiting step of glucose metabolism in β cells is the reaction catalyzed by glucokinase (the same enzyme that occurs in hepatocytes). Consequently, glucokinase is considered the β cell's glucose "sensor." Glucokinase's G6P product is not used to synthesize glycogen, and the activity of the pentose phosphate pathway is minor. Furthermore, lactate dehydrogenase activity is low. As a result, essentially all the G6P produced in β cells is degraded to pyruvate and then converted to acetyl-CoA for oxidation by the citric acid cycle. This one-way, linear catabolic pathway for glucose directly links the β cell's rate of oxidative phosphorylation to the amount of available glucose. By mechanisms that are not entirely understood, the overall level of the β cell's respiratory activity regulates insulin synthesis and secretion.

Insulin Promotes Fuel Storage in Muscle and Adipose Tissue. Insulin signaling is very complex (Fig. 13-31). It acts as the primary regulator of blood glucose concentration by promoting glucose uptake in muscles and adipose tissue and by inhibiting hepatic glucose production. Insulin also stimulates cell growth and differentiation by increasing the synthesis of glycogen, proteins, and triacylglycerols.

Muscle cells and adipocytes express an insulin-sensitive glucose transporter known as **GLUT4.** Insulin stimulates GLUT4 activity. Such an increase can occur through an increase in the intrinsic activity of the transporter molecules, but in the case of GLUT4, the increase is accomplished through the appearance of additional transporter molecules in the plasma membrane (Fig. 22-8). In the absence of insulin, GLUT4 is localized in intracellular vesicles and tubular structures. Insulin promotes the fusion of these vesicles to the plasma membrane in a process that is mediated by SNAREs (Section 9-4F). GLUT4 appears on the cell surface only a few minutes after insulin stimulation. GLUT4 has a relatively low K_M for glucose (2–5 mM), so cells containing this transporter can rapidly take up glucose from the blood. On insulin withdrawal, the glucose transporters are gradually sequestered through endocytosis.

The insulin-dependent GLUT4 transport system allows muscle and adipose tissue to quickly stockpile metabolic fuel immediately after a meal. Tissues such as the brain, which uses glucose almost exclusively as a fuel, constitutively express an insulin-insensitive glucose transporter. Consequently, the central nervous system does not experience large fluctuations in glucose absorption. Significantly, the liver also lacks GLUT4 and therefore does not respond to increases in insulin levels by increasing its rate of glucose uptake.

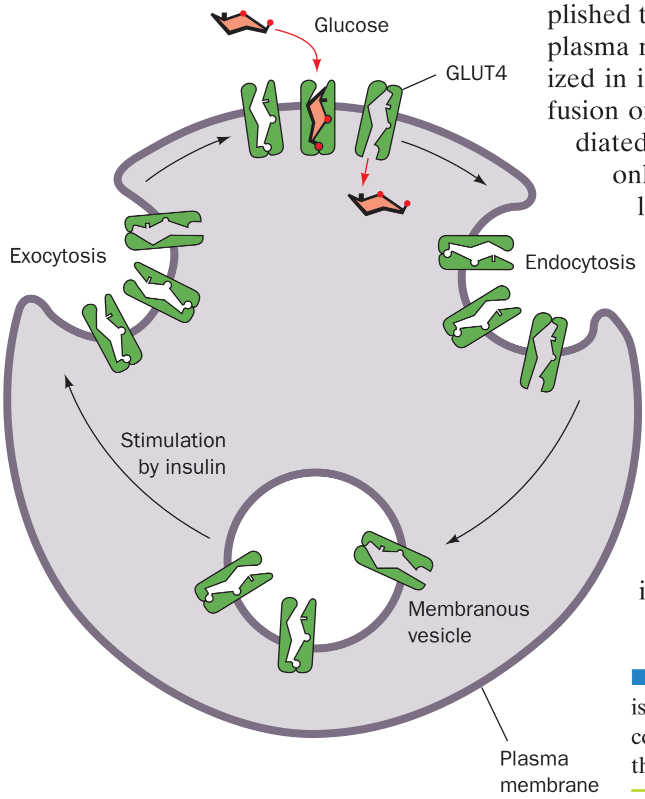

Figure 22-8 | GLUT4 activity. Glucose uptake in muscle and fat cells is regulated by the insulin-stimulated exocytosis of membranous vesicles containing GLUT4 (*left*). On insulin withdrawal, the process reverses itself through endocytosis (*right*). **See the Animated Figures.**

Once glucose enters cells, it can be used to synthesize glycogen (in muscle) and triacylglycerols (in adipocytes; the glucose must first be metabolized to acetyl-CoA for fatty acid synthesis). Insulin specifically promotes those metabolic activities. As discussed in Section 16-3, insulin activates glycogen synthase by promoting its dephosphorylation. In adipocytes, insulin activates the pyruvate dehydrogenase complex (by activating the associated phosphatase; Section 17-4A), and it activates acetyl-CoA carboxylase and increases levels of fatty acid synthase (Section 20-5). At the same time, insulin inhibits lipolysis by inhibiting hormone-sensitive lipase.

Insulin Blocks Liver Gluconeogenesis and Glycogenolysis. Although the liver does not respond to insulin by increasing its rate of uptake of glucose, insulin binding to its receptor on hepatocytes has several consequences. The inactivation of phosphorylase kinase decreases the rate of glycogenolysis, and the activation of glycogen synthase promotes glycogen synthesis. Insulin also inhibits transcription of the genes encoding the gluconeogenic enzymes phosphoenolpyruvate carboxykinase, fructose-1,6-bisphosphatase, and glucose-6-phosphatase (Section 16-4) and stimulates transcription of the genes for the glycolytic enzymes glucokinase and pyruvate kinase. The expression of lipogenic enzymes such as acetyl-CoA carboxylase and fatty acid synthase also increases. The result of these regulatory changes is that *the liver stores glucose (as glycogen and as triacylglycerols) rather than producing glucose by glycogenolysis or gluconeogenesis.* The major metabolic effects of insulin are summarized in Table 22-1.

Glucagon and Catecholamines Counter the Effects of Insulin. As we discussed in Section 16-3C, the peptide hormone glucagon activates a series of intracellular events that lead to glycogenolysis in the liver. This control mechanism helps make glucose available to other tissues when the concentration of circulating glucose drops. Muscle cells, which lack a glucagon receptor and cannot respond directly to the hormone, benefit indirectly from the glucose released by the liver. Glucagon also stimulates fatty acid mobilization from adipose tissue by activating hormone-sensitive lipase.

The catecholamines elicit responses similar to glucagon's. Epinephrine and norepinephrine, which are released during times of stress, bind to two different types of receptors (Section 13-1B): the β-adrenoreceptor, which is linked to the adenylate cyclase system (Fig. 13-23), and the α-adrenoreceptor, whose second messenger, inositol-1,4,5-trisphosphate (IP_3; Section 13-4A), causes intracellular Ca^{2+} concentrations to increase.

Liver cells respond to epinephrine directly and indirectly. Epinephrine promotes the release of glucagon from the pancreas, and glucagon binding to its receptor on liver cells stimulates glycogen breakdown. Epinephrine also binds directly to both α- and β-adrenoreceptors on the surfaces of

Table 22-1 Hormonal Effects on Fuel Metabolism

Tissue	Insulin	Glucagon	Epinephrine
Muscle	↑ Glucose uptake ↑ Glycogen synthesis	No effect	↑ Glycogenolysis
Adipose tissue	↑ Glucose uptake ↑ Lipogenesis ↓ Lipolysis	↑ Lipolysis	↑ Lipolysis
Liver	↑ Glycogen synthesis ↑ Lipogenesis ↓ Gluconeogenesis	↓ Glycogen synthesis ↑ Glycogenolysis	↓ Glycogen synthesis ↑ Glycogenolysis ↑ Gluconeogenesis

liver cells (Fig. 16-14b, *right*). Binding to the β-adrenoreceptor results in increased intracellular cAMP, which leads to glycogen breakdown and gluconeogenesis. Epinephrine binding to the α-adrenoreceptor stimulates an increase in intracellular [Ca^{2+}], which reinforces the cells' response to cAMP (recall that phosphorylase kinase, which activates glycogen phosphorylase and inactivates glycogen synthase, is fully active only when phosphorylated and in the presence of increased [Ca^{2+}]; Section 16-3B). In addition, glycogen synthase is inactivated through phosphorylation catalyzed by several Ca^{2+}-dependent protein kinases.

Epinephrine binding to the β-adrenoreceptor on muscle cells similarly promotes glycogen degradation, thereby mobilizing glucose that can be metabolized by glycolysis to produce ATP. In adipose tissue, epinephrine binding to several α- and β-type adrenoreceptors leads to activation of hormone-sensitive lipase, which results in the mobilization of fatty acids that can be used as fuels by other tissues. In addition, epinephrine stimulates smooth muscle relaxation in the bronchi and blood vessels supplying skeletal muscle, while it stimulates constriction of the blood vessels that

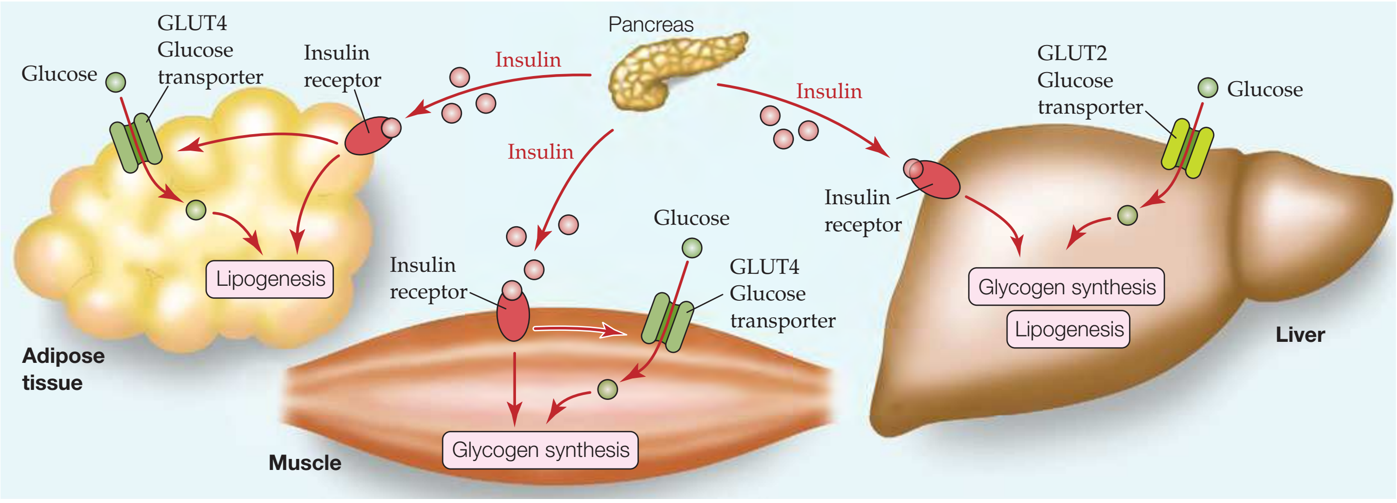
Pancreas
Insulin
Insulin
Insulin
GLUT4
Glucose
transporter
Glucose
Insulin
receptor
Lipogenesis
Adipose
tissue
Insulin
receptor
Glucose
GLUT4
Glucose
transporter
Glycogen synthesis
Muscle
GLUT2
Glucose
transporter
Glucose
Insulin
receptor
Glycogen synthesis
Lipogenesis
Liver

(*a*) Fed state

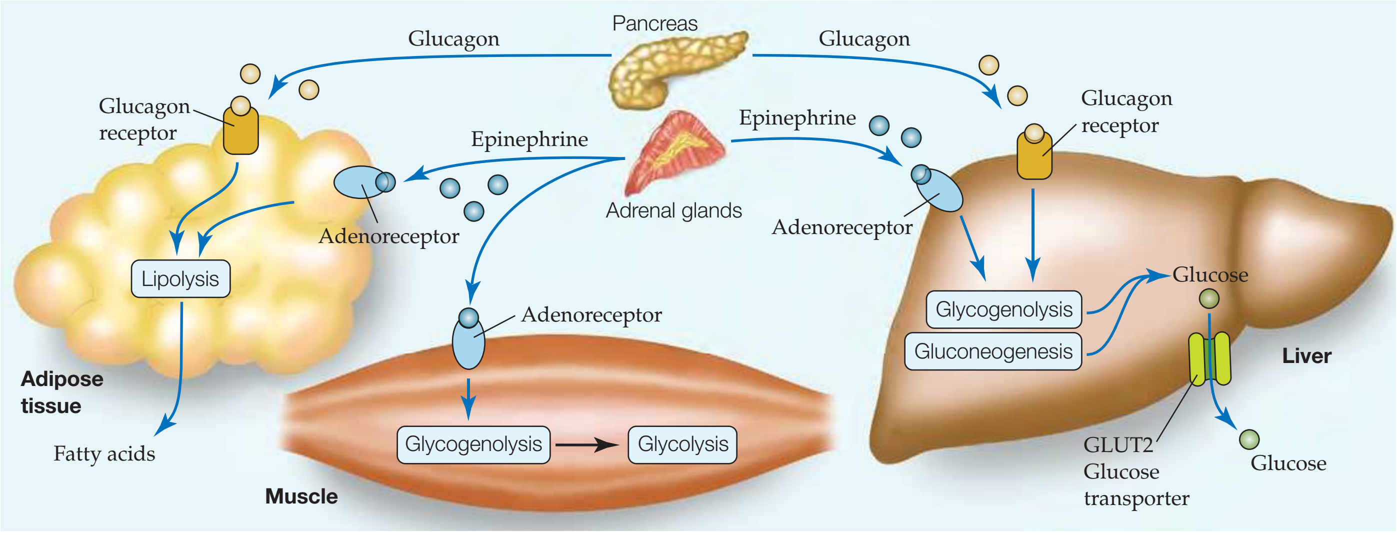
Pancreas
Glucagon
Glucagon
Glucagon
receptor
Epinephrine
Epinephrine
Adrenal glands
Adenoreceptor
Adenoreceptor
Adenoreceptor
Lipolysis
Adipose
tissue
Fatty acids
Glycogenolysis
Glycolysis
Muscle
Glucagon
receptor
Glycogenolysis
Gluconeogenesis
Glucose
Liver
GLUT2
Glucose
transporter
Glucose

(*b*) Fasted state/stress

Figure 22-9 | Overview of hormonal control of fuel metabolism. (*a*) Immediately after a meal, when glucose and fatty acids are abundant, insulin signals tissues to store fuel as glycogen and triacylglycerols. Insulin also stimulates tissues other than liver to take up glucose via the GLUT4 transporter. (*b*) When dietary fuels are not available, glucagon stimulates the liver to release glucose and adipose tissue to release fatty acids. During stress, epinephrine elicits similar responses.

supply skin and other peripheral organs. Together, these physiological changes prepare the body for sudden action by mobilizing energy reserves and directing them where they are needed. The major responses to glucagon and epinephrine are summarized in Table 22-1, and the metabolic effects of insulin, glucagon, and epinephrine under different conditions are presented schematically in Fig. 22-9 (*opposite*).

Several Types of Receptors and Biochemical Signaling Pathways Participate in Metabolic Regulation. As described in Chapter 13, every signaling pathway consists of a receptor, a mechanism for transmitting the ligand-binding event to the cell interior, and a series of intracellular responses that may involve a second messenger and/or chemical changes catalyzed by kinases and phosphatases. There are three major signal transduction pathways: those involving receptor tyrosine kinases associated with the Ras signaling cascade (Section 13-2), those in which adenylate cyclase generates cAMP (3′,5′-cyclic AMP) as a second messenger (Section 13-3), and those involving phosphoinositide cleavage by phospholipase C (PKC), with inositol-1,4,5-trisphosphate (IP_3) and 1,2-diacylglycerol (DAG), as well as Ca^{2+}, as second messengers (Section 13-4). Both second messenger systems involve G protein–coupled receptors (Section 13-3). The major G protein activating adenylate cyclase is G_s, and the major G protein activating phospholipase C is G_q. Figure 22-10 is a composite of the three signaling systems.

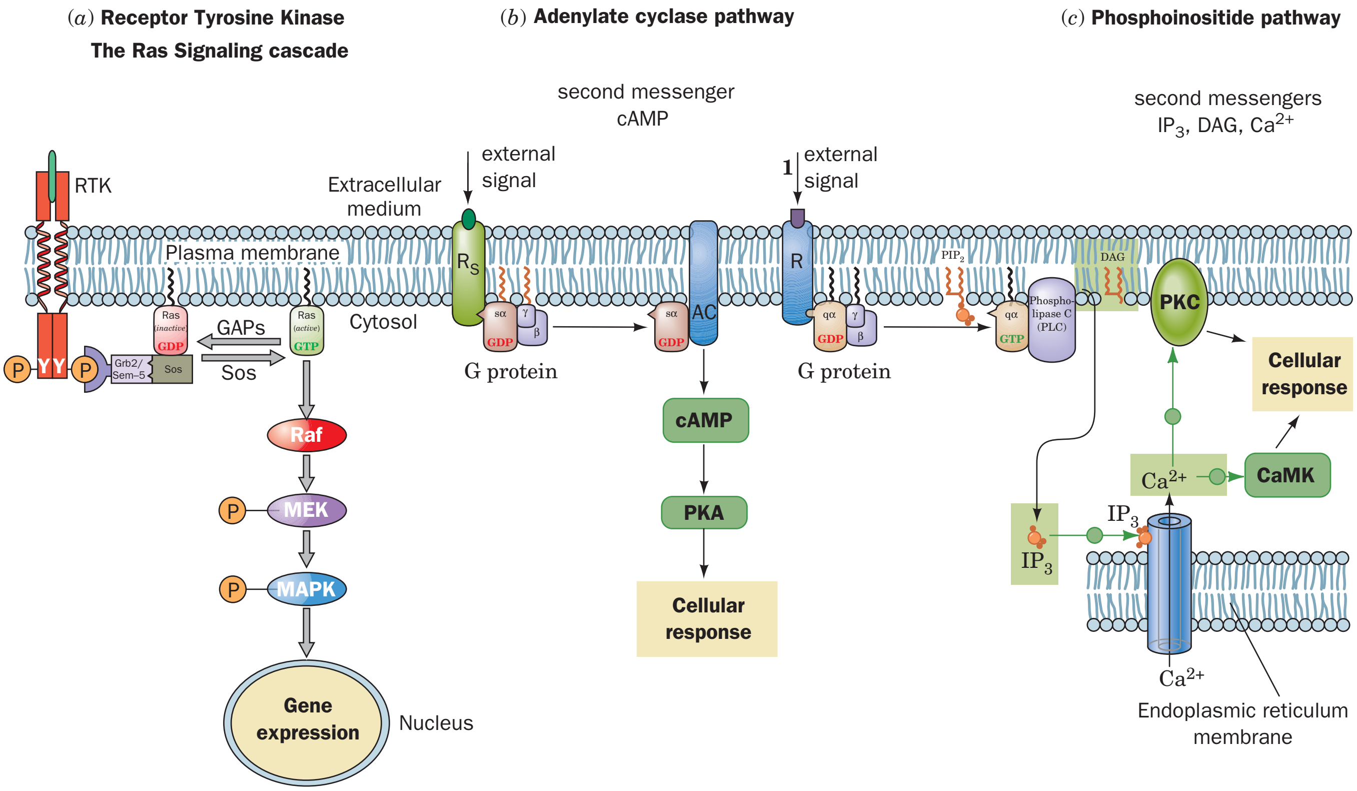
(a) Receptor Tyrosine Kinase
The Ras Signaling cascade
(b) Adenylate cyclase pathway
(c) Phosphoinositide pathway
second messenger
cAMP
second messengers
IP3, DAG, Ca2+
RTK
Extracellular
medium
external
signal
1
external
signal
Plasma membrane
Rs
R
PIP2
DAG
Ras
(inactive)
GDP
Ras
(active)
GTP
GAPs
Sos
Cytosol
P
YY
P
Grb2/
Sem–5
Sos
sα
γ
β
GDP
sα
GDP
AC
qα
γ
β
GDP
qα
GTP
Phospho-
lipase C
(PLC)
PKC
G protein
G protein
Raf
P
MEK
P
MAPK
Gene
expression
Nucleus
cAMP
PKA
Cellular
response
Cellular
response
Ca2+
CaMK
IP3
IP3
Ca2+
Endoplasmic reticulum
membrane

■ **Figure 22-10 | Overview of the major signal transduction pathways.** (*a*) The binding of a ligand to a receptor tyrosine kinase initiates the Ras signaling cascade of phosphorylations, which leads to changes in gene expression. (*b*) The binding of a ligand to its corresponding G protein–coupled receptor stimulates (or in some cases inhibits) adenylate cyclase to synthesize the second messenger cAMP. The cAMP, in turn, activates protein kinase A (PKA) to phosphorylate its target proteins, leading to a cellular response. (*c*) The binding of a ligand to its corresponding G_q protein–coupled receptor initiates the phosphoinositide pathway, which activates phospholipase C (PLC) to hydrolyze the membrane lipid PIP_2 to the second messengers IP_3 and DAG. IP_3 causes the release of Ca^{2+} from mitochondria, DAG activates protein kinase C (PKC), and Ca^{2+} activates both PKC and Ca^{2+}–calmodulin-dependent protein kinase (CaMK). The phosphorylation of target proteins by PKC and CaMK leads to cellular responses.

The hormones described above and in Section 13-1, as well as many other hormones, growth factors, and other signaling molecules, use these signal-transduction pathways to set in motion a series of biochemical reactions that produce biological responses such as altered metabolism, cell differentiation, or cell growth and division. The exact nature of the response depends on many factors. Cells respond to a hormone, generally referred to as a ligand, only if they display the appropriate receptor. Specific intracellular responses are modulated by the number, type, and cellular locations of the elements of the signaling systems. Furthermore, a given cell typically contains receptors for many different ligands, so the response to one particular ligand may depend on the level of engagement of the other ligands with the cell's signal-transduction machinery. As a result, *cells can react to discrete signals or combinations of signals with variations in the magnitude and duration of the cellular response.*

■ CHECK YOUR UNDERSTANDING

Summarize the roles of insulin, glucagon, and epinephrine in regulating mammalian fuel metabolism.

3 Metabolic Homeostasis: The Regulation of Energy Metabolism, Appetite, and Body Weight

LEARNING OBJECTIVES

- Understand the role of AMP-dependent protein kinase as the cell's fuel gauge.
- Understand that the adipose tissue hormones adiponectin and leptin are involved in controlling energy balance.
- Understand that appetite is regulated by several hormones secreted by adipose tissue and the gut.
- Understand that energy expenditure must be balanced with energy intake.

The complexity of the mechanisms that regulate mammalian fuel metabolism permit the body to respond efficiently to changing energy demands and to accommodate changes in the availability of various fuels, maintaining reasonable **metabolic homeostasis** (balance between energy inflow and output). This balance depends on the interactions of many factors. In this section we discuss some of the participants in this complex network regulating energy expenditure, appetite, and body weight.

A | AMP-Dependent Protein Kinase Is the Cell's Fuel Gauge

All of the metabolic pathways discussed above are affected in one way or another by the need for ATP, as is indicated by the cell's AMP-to-ATP ratio (Section 15-4A). Several enzymes are either activated or inhibited allosterically by AMP, and several others are phosphorylated by **AMP-dependent protein kinase (AMPK),** a major regulator of metabolic homeostasis. *AMPK activates metabolic breakdown pathways that generate ATP while inhibiting biosynthetic pathways so as to conserve ATP for more vital processes.* AMPK is an $\alpha\beta\gamma$ heterotrimer found in all eukaryotic organisms from yeast to humans. The α subunit contains a protein kinase domain, and the γ subunit contains sites for allosteric activation by AMP and inhibition by ATP. Like other protein kinases, AMPK's kinase domain must be phosphorylated for activity. Binding of AMP to the γ subunit causes a conformational change that exposes Thr 172 in the activation loop of the α subunit, promoting its phosphorylation and increasing its activity at least 100-fold. AMP can activate the phosphorylated enzyme up to 5-fold more. The major kinase that phosphorylates AMPK is named **LKB1.** The specific knockout of LKB1 in mouse liver results in the loss of the phosphorylated form of AMPK.

AMPK Activates Glycolysis in Ischemic Cardiac Muscle. AMPK's targets include the heart isozyme of the bifunctional enzyme PFK-2/FBPase-2, which controls the fructose-2,6-bisphosphate (F2,6P) concentration (Section 16-4C). The phosphorylation of this isozyme activates the PFK-2 activity, increasing [F2,6P], which in turn activates PFK-1 and glycolysis. Consequently, in blood-starved (ischemic) heart muscle cells, when there is insufficient oxygen for oxidative phosphorylation to maintain adequate concentrations of ATP, the resulting AMP buildup causes the cells to switch to anaerobic glycolysis for ATP production.

AMPK Inhibits Lipogenesis and Gluconeogenesis in Liver. AMPK-mediated phosphorylation also inhibits acetyl-CoA carboxylase (ACC, which catalyzes the first committed step of fatty acid synthesis; Section 20-4B), hydroxymethylglutaryl-CoA reductase (HMG-CoA reductase, which catalyzes the rate-determining step in cholesterol biosynthesis; Section 20-7B), and glycogen synthase (which catalyzes the rate-limiting reaction in glycogen synthesis; Section 16-2B). Consequently, when the rate of ATP production is inadequate, these biosynthetic pathways are turned off, thereby conserving ATP for the most vital cellular functions.

AMPK Promotes Fatty Acid Oxidation and Glucose Uptake in Skeletal Muscle. The inhibition of ACC results in a decrease in the concentration of malonyl-CoA, the starting material for fatty acid biosynthesis. Malonyl-CoA has an additional role, however. It is an inhibitor of carnitine palmitoyl transferase I (Section 20-5), which is required to transfer cytosolic palmitoyl-CoA into the mitochondria for oxidation. The decrease in malonyl-CoA concentration therefore allows more palmitoyl-CoA to be oxidized. AMPK also increases the expression of both GLUT1 and GLUT4 on muscle cell surfaces, facilitating the insulin-independent entry of glucose into these cells.

AMPK Inhibits Lipolysis in Adipocytes. AMPK phosphorylates hormone-sensitive triacylglycerol lipase in adipose tissue (Section 20-5). This phosphorylation inhibits rather than activates the enzyme, in part by preventing the relocation of the enzyme to the lipid droplet, the cellular location of lipolysis. As a result, fewer triacylglycerols are broken down so that fewer fatty acids are exported to the bloodstream. The major effects of AMPK activation on glucose and lipid metabolism in liver, skeletal muscle, heart muscle, and adipose tissue are diagrammed in Fig. 22-11.

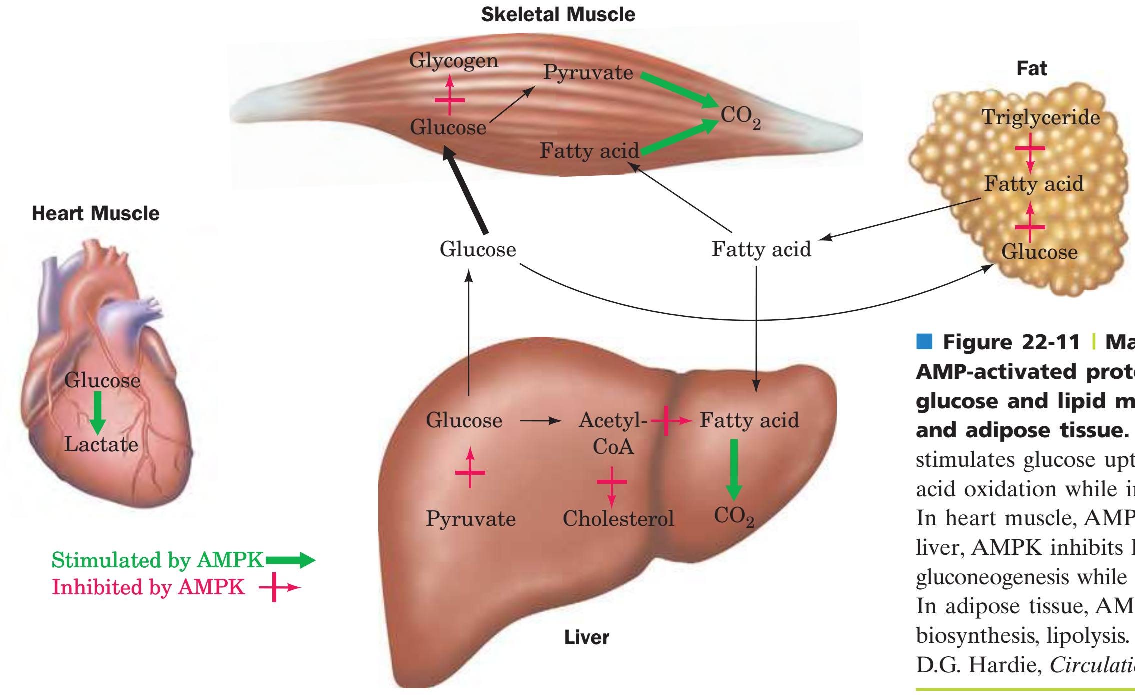

Figure 22-11 | Major effects of AMP-activated protein kinase (AMPK) on glucose and lipid metabolism in liver, muscle, and adipose tissue. In skeletal muscle, AMPK stimulates glucose uptake and glucose and fatty acid oxidation while inhibiting glycogen synthesis. In heart muscle, AMPK stimulates glycolysis. In liver, AMPK inhibits lipid biosynthesis and gluconeogenesis while activating fatty acid oxidation. In adipose tissue, AMPK inhibits fatty acid biosynthesis, lipolysis. [After M.C. Towler and D.G. Hardie, *Circulation Res.* **100,** 328 (2007).]

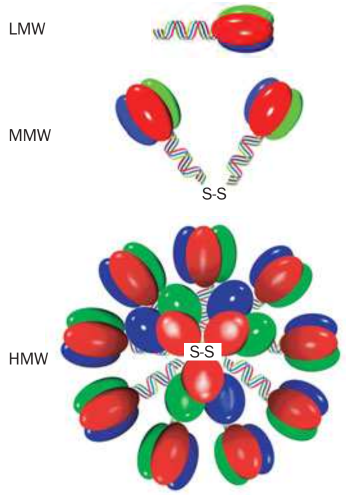

■ **Figure 22-12 | Adiponectin trimers, hexamers, and multimers.** These complexes are referred to as low molecular weight (LMW), medium molecular weight (MMW), and high molecular weight (HMW) forms. [After Kadowaki, T. and Yamauchi, T., *Endocrine Rev.* **26**, 439 (2005).]

B | Adiponectin Regulates AMPK Activity

Adiponectin is a 247-residue protein hormone, secreted exclusively by adipocytes, that helps regulate energy homeostasis and glucose and lipid metabolism by controlling AMPK activity. Its monomers consist of an N-terminal collagen-like domain and a C-terminal globular domain. Adiponectin occurs in the bloodstream in several forms: a low molecular weight (LMW) trimer formed by the coiling of its collagen-like domains into a triple helix (Section 6-1C) as well as hexamers (MMW) and multimers (HMW) that form disulfide–cross-linked bouquets (Fig. 22-12). In addition, globular adiponectin, formed by the cleavage of the collagen-like domain to release globular monomers, occurs in lower concentrations.

The binding of adiponectin to **adiponectin receptors,** which occur on the surfaces of both liver and muscle cells, acts to increase the phosphorylation and activity of AMPK. This, as we have seen (Section 22-3A), inhibits gluconeogenesis and stimulates fatty acid oxidation in liver and stimulates glucose uptake and glucose and fatty acid oxidation in muscle. All of these effects act to increase insulin sensitivity, in part because adiponectin and insulin elicit similar responses in tissues such as liver. Decreased adiponectin is associated with insulin resistance (Section 22-4B). Paradoxically, the blood concentration of adiponectin, which is secreted by adipocytes, decreases with increased amounts of adipose tissue. This may be because increased adipose tissue is also associated with increased production of **tumor necrosis factor-α,** a protein growth factor that decreases both the expression and secretion of adiponectin from adipose tissue.

C | Leptin Is a Satiety Hormone

Leptin (Greek: *leptos,* thin) is a 146-residue polypeptide that is normally produced by adipocytes (Fig. 22-13). It was discovered by studying genetically obese mice. Most animals, including humans, tend to have stable

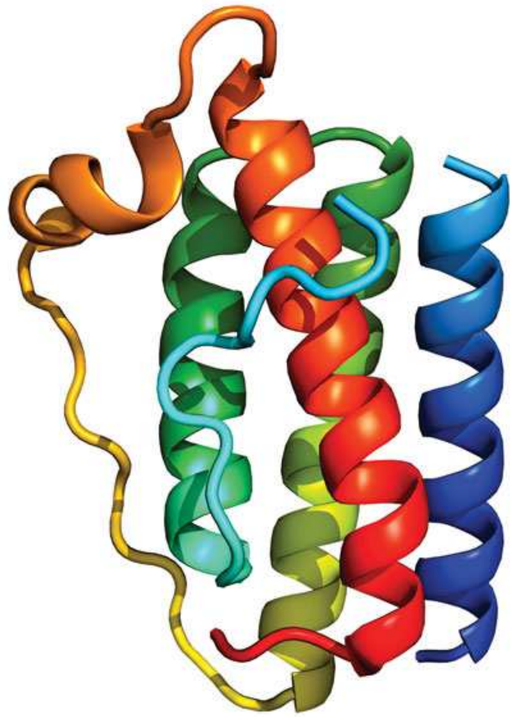

■ **Figure 22-13 | X-Ray structure of human leptin-E100.** This mutant form of leptin (Trp 100 → Glu) has comparable biological activity to the wild-type protein but crystallizes more readily. The protein, which is colored in rainbow order from its N-terminus (*blue*) to its C-terminus (*red*), forms a four-helix bundle as do many protein growth factors (e.g., human growth hormone; Fig. 13-3). Residues 25 to 38 are not visible in the X-ray structure. [Based on an X-ray structure by Faming Zhang, Eli Lilly & Co., Indianapolis, Indiana. PDBid 1AX8.] **See Interactive Exercise 32.**

weights; that is, if they are given free access to food, they eat just enough to maintain their "set-point" weight. However, a strain of mice that are homozygous for defects in the *obese* gene (known as *ob/ob* mice) are over twice the weight of normal (*OB/OB*) mice (Fig. 22-14) and overeat when given access to unlimited quantities of food. The *OB* gene encodes leptin. When leptin is injected into *ob/ob* mice, they eat less and lose weight. Leptin has therefore been considered a "satiety" signal that affects the appetite control system of the brain. Leptin also causes higher energy expenditure.

The simple genetic basis for obesity in *ob/ob* mice does not appear to apply to most obese humans. Leptin levels in humans increase with the percentage of body fat, consistent with the synthesis of leptin by adipocytes. Thus, obesity in humans is apparently the result not of faulty leptin production but of leptin resistance, perhaps due to a decrease in the level of a leptin receptor in the brain or the saturation of the receptor that transports leptin across the blood–brain barrier into the central nervous system.

A diminished response to leptin leads to high concentrations of **neuropeptide Y,**

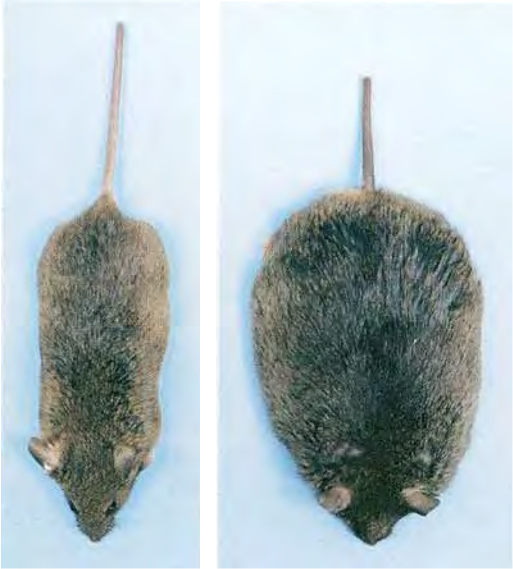

Figure 22-14 | Normal (*OB/OB, left*) and obese (*ob/ob, right*) mice. [Courtesy of Richard D. Palmiter, University of Washington.]

$$\overset{1}{\text{Tyr}}\text{—Pro—Ser—Lys—Pro—Asp—Asn—Pro—Gly—}\overset{10}{\text{Glu}}\text{—Asp—Ala—}$$

$$\text{Pro—Ala—Glu—Asp—Met—Ala—Arg—}\overset{20}{\text{Tyr}}\text{—Tyr—Ser—Ala—Leu—}$$

$$\text{Arg—His—Tyr—Ile—Asn—}\overset{30}{\text{Leu}}\text{—Ile—Thr—Arg—Gln—Arg—}\overset{36}{\text{Tyr}}\text{—NH}_2$$

Neuropeptide Y
(The C-terminal carboxyl is amidated.)

a 36-residue peptide released by the **hypothalamus,** a part of the brain that controls many physiological functions. Neuropeptide Y stimulates appetite, which in turn leads to fat accumulation. Both leptin and insulin, when bound to their respective receptors in the hypothalamus, inhibit neuropeptide Y secretion.

D | Ghrelin and $PYY_{3–36}$ Act as Short-Term Regulators of Appetite

It is not surprising that fuel metabolism, body weight, and appetite are linked. In addition to leptin, insulin, and neuropeptide Y, other peptide hormones are known to be involved in appetite control. For example, **ghrelin** is an appetite-stimulating peptide secreted by the empty stomach.

$$\text{Gly—Ser—X—Phe—Leu—Ser—Pro—Glu—His—}\overset{10}{\text{Gln}}\text{—}$$

$$\text{Arg—Val—Gln—Gln—Arg—Lys—Glu—Ser—Lys—}\overset{20}{\text{Lys}}\text{—}$$

$$\text{Pro—Pro—Ala—Lys—Leu—Gln—Pro—}\overset{28}{\text{Arg}}$$

Ghrelin
(X = Ser modified with *n*-octanoic acid)

Ghrelin appears to boost levels of neuropeptide Y, and most likely is part of a short-term appetite-control system, since ghrelin levels fluctuate on the order of hours, increasing before meals and decreasing immediately afterward.

The gastrointestinal tract secretes an appetite-suppressing hormone called **PYY$_{3\text{–}36}$:**

$$\begin{array}{l}
\overset{3}{\text{Ile}}\text{—Lys—Pro—Glu—Ala—Pro—Gly—}\overset{10}{\text{Glu}}\text{—} \\[1em]
\text{Asp—Ala—Ser—Pro—Glu—Glu—Leu—Asn—Arg—}\overset{20}{\text{Tyr}}\text{—} \\[1em]
\text{Tyr—Ala—Ser—Leu—Arg—His—Tyr—Leu—Asn—}\overset{30}{\text{Leu}}\text{—} \\[1em]
\text{Val—Thr—Arg—Gln—Arg—}\overset{36}{\text{Tyr}}
\end{array}$$

PYY$_{3\text{–}36}$

In animals and humans, an infusion of this peptide decreases food intake by inhibiting neuropeptide Y secretion. In summary, ghrelin stimulates appetite while leptin, insulin, and PYY$_{3\text{–}36}$ all suppress it by regulating the secretion of neuropeptide Y from the hypothalamus.

E | Energy Expenditure Can Be Controlled by Adaptive Thermogenesis

The nutritional calories contained in food are utilized by an organism either in the performance of work or in the release of heat. Excess fuel is stored as glycogen or fat for future use. In well-balanced individuals, the storage of excess fuel remains constant over many years. However, when fuel consumed consistently outpaces energy expenditures, obesity results.

The body has several mechanisms for guarding against obesity. One of them, discussed above, is appetite control. Another is **diet-induced thermogenesis,** a form of adaptive thermogenesis (heat production in response to environmental stress). We have already discussed adaptive thermogenesis in response to cold, which is accomplished in rodents and newborn humans by the uncoupling of oxidative phosphorylation in brown adipose tissue (Box 18-4). The mechanism of this thermogenesis involves release of norepinephrine from the brain in response to cold and its binding to β-adrenoreceptors on brown adipose tissue, which is followed by an increase in cAMP that triggers an enzymatic phosphorylation cascade leading to the activation of hormone-sensitive lipase. The increase in the concentration of free fatty acids provides fuel for oxidation and leads to the opening of a proton channel called uncoupling protein 1 (UCP1; alternatively, thermogenin) in the inner mitochondrial membrane. The opening of UCP1 dissipates the electrochemical gradient generated by electron transport (Section 18-2) and thereby uncouples electron transport from oxidative phosphorylation. The consequent continuation of oxidation without ATP synthesis generates heat.

While it is clear from metabolic measurements that a high energy intake increases thermogenesis, the cause of this increase in adult humans is unclear and is under active investigation. Adult humans have little brown adipose tissue, where UCP1-mediated thermogenesis occurs. However, homologs of the UCP1 are known (Box 18-4): **UCP2** is present in many tissues, including white adipose tissue, and its synthesis is induced by leptin. **UCP3** occurs in muscle (as well as in brown adipose tissue) and could be significant because skeletal muscle represents up to 40% of total body weight and has high mitochondrial capacity. However, it has yet to be demonstrated that UCP3 in muscle is involved in diet-induced thermogenesis.

■ CHECK YOUR UNDERSTANDING

Why is AMPK called the cell's fuel gauge?
Compare the roles of leptin, ghrelin, insulin, and PYY in controlling appetite.
How does thermogenesis help prevent obesity?

4 Disturbances in Fuel Metabolism

The complex systems that regulate fuel metabolism can malfunction, producing acute or chronic diseases of variable severity. Considerable effort has been directed at elucidating the molecular basis of conditions such as diabetes and obesity, both of which are essentially disorders of fuel metabolism. In this section, we examine the metabolic changes that occur in starvation, diabetes, and obesity.

LEARNING OBJECTIVES

- Understand that the body adapts metabolically to both dietary deficiency and excess.
- Understand that diabetes may be caused by either insufficient production of insulin (type I) or an insensitivity to its presence (type II).
- Understand that obesity may result from improper regulation of appetite or energy expenditure.

A | Starvation Leads to Metabolic Adjustments

Because humans do not eat continuously, the disposition of dietary fuels and the mobilization of fuel stores shifts dramatically during the few hours between meals. Yet humans can survive fasts of up to a few months by adjusting their fuel metabolism. Such metabolic flexibility certainly evolved before modern humans became accustomed to thrice-daily meals.

Absorbed Fuels Are Allocated Immediately. When a meal is digested, nutrients are broken down to small, usually monomeric, units for absorption by the intestinal mucosa. From there, the products of digestion pass through the circulation to the rest of the body. Dietary proteins, for example, are broken down to amino acids for absorption. The small intestine uses amino acids for fuel, but most travel to the liver via the portal vein. There, they are used for protein synthesis or, if present in excess, oxidized to produce energy or converted to glycogen for storage. They may also be converted to glucose or triacylglycerols for export, depending on conditions. There is no dedicated storage depot for amino acids; whatever the liver does not metabolize circulates to peripheral tissues to be catabolized or used for protein synthesis.

Dietary carbohydrates, like proteins, are degraded in the intestine, and the absorbed monomeric products (e.g., glucose derived from dietary starch) are delivered to the liver via the portal vein. As much as one-third of the dietary glucose is immediately converted to glycogen in the liver; at least half of the remainder is converted to glycogen in muscle cells, and the rest is oxidized by these and other tissues for immediate energy needs. Excess glucose is converted to triacylglycerol in the liver and exported for storage in adipose tissue. Both glucose uptake and glycogen and fatty acid biosynthesis are stimulated by insulin, whose concentration in the blood increases in response to high blood [glucose].

Dietary fatty acids are packaged as triacylglycerols in chylomicrons (Section 20-1), which circulate first in the lymph and then in the bloodstream and therefore are not delivered directly to the liver as are absorbed amino acids and carbohydrates. Instead, a significant portion of the dietary fatty acids are taken up by adipose tissue. Lipoprotein lipase first hydrolyzes the triacylglycerols, and the released fatty acids are absorbed and reesterified in the adipocytes.

Blood Glucose Remains Nearly Constant. As tissues take up and metabolize glucose, blood [glucose] drops, thereby causing the pancreatic α cells to release glucagon. This hormone stimulates glycogen breakdown and the release of glucose from the liver. It also promotes gluconeogenesis from amino acids and lactate. *The reciprocal effects of insulin and glucagon, which both respond to and regulate blood [glucose], ensure that the concentration of glucose available to extrahepatic tissues remains relatively constant.*

Table 22-2 Fuel Reserves for a Normal 70-kg Man

Fuel	Mass (kg)	Calories[a]
Tissues		
Fat (adipose triacylglycerols)	15	141,000
Protein (mainly muscle)	6	24,000
Glycogen (muscle)	0.150	600
Glycogen (liver)	0.075	300
Circulating fuels		
Glucose (extracellular fluid)	0.020	80
Free fatty acids (plasma)	0.0003	3
Triacylglycerols (plasma)	0.003	30
Total		***166,000***

[a] 1 (dieter's) Calorie = 1 kcal = 4.184 kJ.

Source: Cahill, G.E., Jr., *New Engl. J. Med.* **282,** 669 (1970).

However, the body stores less than a day's supply of carbohydrate (Table 22-2). After an overnight fast, the combination of increased glucagon secretion and decreased insulin secretion promotes the mobilization of fatty acids from adipose tissue (Section 20-5). The diminished insulin also decreases glucose uptake by muscle tissue. Muscles therefore switch from glucose to fatty acid metabolism for energy production. This adaptation spares glucose for use by tissues, such as the brain, that cannot utilize fatty acids.

Gluconeogenesis Supplies Glucose during Starvation. After a lengthy fast, the liver's store of glycogen becomes depleted (Fig. 22-15). Under these conditions, the rate of gluconeogenesis increases. Gluconeogenesis supplies ~96% of the glucose produced by the liver after 40 hours of fasting. The kidney also is active in gluconeogenesis under these conditions. In animals, glucose cannot be synthesized from fatty acids. This is because neither pyruvate nor oxaloacetate, the precursors of glucose in gluconeogenesis, can be synthesized in a net manner from acetyl-CoA. During starvation, glucose must therefore be synthesized from the glycerol product of triacylglycerol breakdown and, more importantly, from the amino acids derived from the proteolytic degradation of proteins, the major source of which is muscle. The breakdown of muscle cannot continue indefinitely, however, since loss of muscle mass would eventually prevent an animal from moving about in search of food. The organism must therefore make alternate metabolic arrangements.

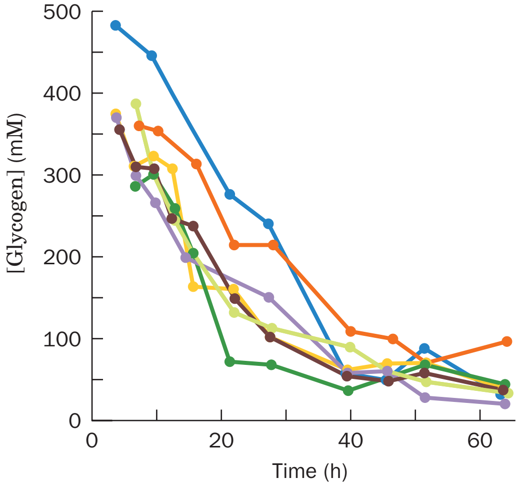

Figure 22-15 | Liver glycogen depletion during fasting. The liver glycogen content in seven subjects was measured using ^{13}C NMR over the course of a 64-hour fast. [After Rothman, D.L., Magnusson, I., Katz, L.D., Shulman, R.G., and Shulman, G.I., *Science* **254,** 575 (1991).]

Ketone Bodies Become a Major Energy Source during Starvation. After several days of starvation, the liver directs acetyl-CoA, which is derived from fatty acid β oxidation, to the synthesis of ketone bodies (Section 20-3). These fuels are then released into the blood. The brain gradually adapts to using ketone bodies as fuel through the synthesis of the appropriate enzymes: After a 3-day fast, only about one-third of the brain's energy requirements are satisfied by ketone bodies, and after 40 days of starvation, ~70% of its energy needs are so met. The rate of muscle breakdown during prolonged starvation consequently decreases to ~25% of its rate after a several-day fast. *The survival time of a starving individual therefore depends much more on the size of fat reserves than on muscle mass.* Indeed, highly obese individuals can survive a year or more without eating (and have done so in clinically supervised weight-reduction programs).

Caloric Restriction May Increase Longevity. Caloric restriction is a modified form of starvation whereby energy intake is reduced 30–40%, while micronutrient (vitamin and mineral) levels are maintained. Rodents kept on such a diet live up to 50% longer than rodents on normal diets. The lifespans of a large range of organisms from yeast to primates are similarly extended. Considerable research effort is being expended to determine the biochemical basis of these observations.

B | Diabetes Mellitus Is Characterized by High Blood Glucose Levels

In the disease **diabetes mellitus** (often called just **diabetes**), which is the third leading cause of death in the United States after heart disease and cancer, insulin either is not secreted in sufficient amounts or does not efficiently stimulate its target cells. As a consequence, blood glucose levels become so elevated that the glucose "spills over" into the urine, providing a convenient diagnostic test for the disease. Yet, despite these high blood glucose levels, cells "starve" since insulin-stimulated glucose entry into cells is impaired. Triacylglycerol hydrolysis, fatty acid oxidation, gluconeogenesis, and ketone body formation are accelerated and, in a condition known as **ketosis,** ketone body levels in the blood become abnormally high. Since ketone bodies are acids, their high concentration puts a strain on the buffering capacity of the blood and on the kidney, which controls blood pH by excreting the excess H^+ into the urine. This H^+ excretion is accompanied by NH_4^+, Na^+, K^+, P_i, and H_2O excretion, causing severe dehydration (excessive thirst is a classic symptom of diabetes) and a decrease in blood volume—ultimately life-threatening situations.

There are two major forms of diabetes mellitus:

1. **Insulin-dependent** or **juvenile-onset diabetes mellitus,** which most often strikes suddenly in childhood.
2. **Non-insulin-dependent** or **maturity-onset diabetes mellitus,** which usually develops gradually after the age of 40.

Insulin-Dependent Diabetes Is Caused by a Deficiency of Pancreatic β Cells. In insulin-dependent (type I) diabetes mellitus, insulin is absent or nearly so because the pancreas lacks or has defective β cells. This condition usually results from an autoimmune response that selectively destroys pancreatic β cells. Individuals with insulin-dependent diabetes, as Frederick Banting and Charles Best first demonstrated in 1921 (Box 22-1), require daily insulin injections to survive and must follow carefully balanced diet and exercise regimens. Their lifespans are, nevertheless, reduced by up to one-third as a result of degenerative complications such as kidney malfunction, nerve impairment, and cardiovascular disease that apparently arise from the imprecise metabolic control provided by periodic insulin injections. The **hyperglycemia** (high blood [glucose]) of diabetes mellitus also leads to blindness through retinal degeneration and the glucosylation of lens proteins, which causes cataracts (Fig. 22-16).

The usually rapid onset of the symptoms of insulin-dependent diabetes had suggested that the autoimmune attack on the pancreatic β cells is of short duration. Typically, however, the disease develops over several years as the immune system slowly destroys the β cells. Only when

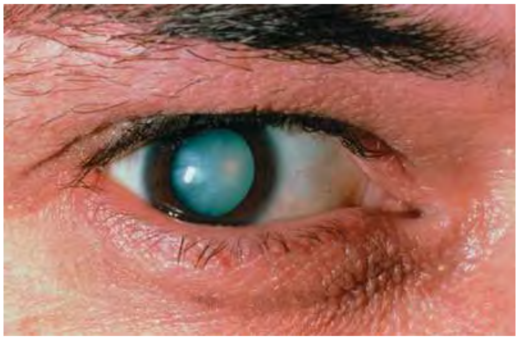

■ **Figure 22-16 | Photo of a diabetic cataract.** The accumulation of glucose in the lens leads to swelling and precipitation of lens proteins. The resulting opacification causes blurred vision and ultimately complete loss of sight. [© Sue Ford/Photo Researchers.]

BOX 22-1 **PATHWAYS OF DISCOVERY**

Frederick Banting and Charles Best and the Discovery of Insulin

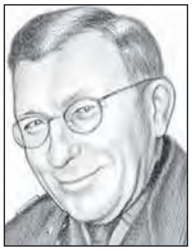

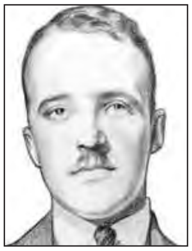

Frederick Banting (1891–1941)
Charles Best (1899–1978)

One of the most celebrated clinical research stories is the discovery and therapeutic use of insulin, the hormone missing in type I diabetes. Since the end of the nineteenth century, clinical scientists understood that there was a connection between diabetes and secretions from the pancreas, specifically, from the clumps of cells known as the islets of Langerhans. Several unsuccessful attempts were made to extract the secretions. In 1920, Frederick Banting, reading an account of such work, wondered whether an active extract could be purified if the pancreatic ducts, which collect potentially destructive digestive enzymes, were first ligated (closed off).

Banting, a young surgeon whose medical practice had not yet gotten off the ground, was working as a demonstrator at the University of Western Ontario. He took his idea to John J.R. Macleod, the head of the Department of Physiology at the University of Toronto. A skeptical Macleod gave Banting the use of laboratory space for the summer of 1921, access to experimental dogs, and the help of assistant Charles Best. Banting, despite his medical training and experience with the Canadian Army Medical Service, was not much of an experimentalist. Best, however, had just completed a degree in physiology and biochemistry and had already worked as an assistant to Macleod. Best quickly learned surgical techniques from Banting, as Banting picked up analytical techniques, such as measuring sugar levels in dogs' blood and urine, from Best.

Banting's and Best's experimental protocol required pancreatectomized dogs, but the surgery was difficult, and many dogs died of infection (it was rumored that strays from the streets of Toronto were gathered as replacements). Successfully pancreatectomized dogs, who developed the fatal symptoms of diabetes, were injected with a pancreatic extract that Banting and Best named insulin, after the Latin word *insula* (island). Finally, at the end of July, Banting and Best achieved their desired result, when the insulin injection dramatically reduced the dog's blood sugar level. The experiment was repeated, with similar results, in other dogs.

Although Banting's temporary position was to have been terminated at the end of the summer, his results were promising enough to secure him additional funding, the supervision of a more enthusiastic Macleod, and the continued assistance of Best, who had originally intended to work with Banting for only 2 months. By fall, Banting's and Best's success at prolonging the lives of diabetic dogs was putting enormous pressure on their ability to produce insulin in large amounts and of consistent purity. Assistance was offered by James Collip, a biochemist on sabbatical leave from the University of Alberta. Collip's insulin preparations, which were made without any clue as to the proteinaceous nature of the hormone, proved good enough for experimental use in humans. At that time, a diagnosis of diabetes was a virtual death sentence, with the only treatment being a severely limited diet that probably extended life for only a few months (many patients died of malnutrition).

In January 1923, Banting injected Collip's extract into Leonard Thompson, a 14-year-old diabetic who was near death. Thompson's blood sugar level immediately returned to normal, and his strength increased. Such a dramatic clinical outcome did not go unnoticed, and within months, Banting opened a clinic to begin treating diabetics desperate for a treatment that restored their hopes for a near-normal life. He enlisted the help of the Connaught Antitoxin Laboratories at the University of Toronto and the Eli Lilly Pharmaceutical Company to produce insulin on a scale suitable for clinical testing. Best, just 23, was put in charge of insulin production for all of Canada. It eventually became clear that Banting's original assumption—that the presence of digestive enzymes compromised the purification of insulin—was mistaken, and insulin could be successfully isolated from an intact pancreas.

Amid some controversy, the 1923 Nobel Prize for Physiology or Medicine was awarded to Banting and Macleod. Banting, annoyed by the omission of Best, split his share of the prize with his assistant. Macleod, who had not offered much support during the initial research, split his share with Collip. Banting subsequently held a variety of administrative posts and pursued research in silicosis, but he never accomplished much. He was killed in a plane crash en route to Britain for a wartime mission in 1941. Best, who replaced Macleod as head of physiology at the age of 29, continued his research into the biological action of insulin. He also supervised efforts to purify the anticoagulant glycosaminoglycan heparin and to produce dried human serum for medical use by the military.

Banting, F.G. and Best, C.H., The internal secretion of the pancreas, *J. Lab. Clin. Med.* **7,** 251–266 (1922).

>80% of these cells have been eliminated do the classic symptoms of diabetes suddenly emerge. Consequently, one of the most successful treatments for insulin-dependent diabetes is a β-cell transplant, a procedure that became possible with the development of relatively benign immunosuppressive drugs.

Non-Insulin-Dependent Diabetes May Be Caused by a Deficiency of Insulin Receptors or Insulin Signal Transduction. Non-insulin-dependent (type II) diabetes mellitus, which accounts for over 90% of the diagnosed cases of diabetes and affects 18% of the population over 65 years of age, usually occurs in obese individuals with a genetic predisposition for the condition. These individuals have normal or even greatly elevated insulin levels, but their cells are not responsive to insulin and are therefore said to be **insulin resistant.** As a result, blood glucose concentrations are much higher than normal, particularly after a meal (Fig. 22-17).

The hyperglycemia that accompanies insulin resistance induces the pancreatic β cells to increase their production of insulin. Yet the high basal level of insulin secretion diminishes the ability of the β cells to respond to further increases in blood glucose. Consequently, the hyperglycemia and its attendant complications tend to worsen over time.

A small percentage of cases of type II diabetes result from mutations in the insulin receptor that affect its insulin-binding ability or tyrosine kinase activity. However, a clear genetic cause has not been identified in the vast majority of cases. It is therefore likely that many factors play a role in the development of the disease. For example, the increased insulin production resulting from overeating may eventually suppress the synthesis of insulin receptors. This hypothesis accounts for the observation that diet alone often decreases the severity of the disease.

Another hypothesis, put forward by Gerald Shulman, is that the elevated concentration of free fatty acids in the blood caused by obesity decreases insulin signal transduction. This high concentration ultimately results in an activation of a PKC isoform that phosphorylates insulin receptor substrates (IRSs) on Ser and Thr, thereby inhibiting the Tyr phosphorylation that activates them. The failure to activate IRSs decreases the cell's response to insulin (Fig. 13-31).

Other treatments for non-insulin-dependent diabetes are drugs such as **metformin** and the **thiazolidinediones (TZDs)** (*at right*), which decrease insulin resistance by either suppressing glucose release by the liver (metformin) or promoting insulin-stimulated glucose disposal in muscle (TZDs). The drugs act by increasing AMPK activity but by different mechanisms. TZDs cause a large increase in the AMP-to-ATP ratio in muscle

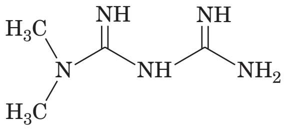

Metformin

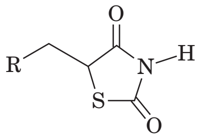

A thiazolidinedione (TZD)

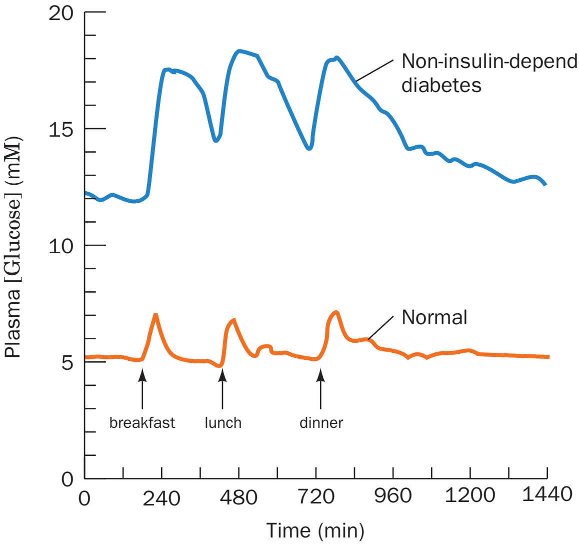

■ **Figure 22-17 | Twenty-four-hour plasma glucose profiles in normal and non-insulin-dependent diabetic subjects.** The basal level of glucose and the peaks following meals are higher in the diabetic individuals. [After Bell, G.I., Pilkis, S.J., Weber, I.T., and Polonsky, K.S., *Annu. Rev. Physiol.* **58,** 178 (1996).]

cells, with the expected concomitant increase in AMPK phosphorylation and activity. Metformin, however, increases AMPK phosphorylation and activity without changing the AMP-to-ATP ratio. In both cases, the increase in AMPK activity decreases gluconeogenesis in liver and increases glucose utilization in muscle (Fig. 22-11). In addition, the TZDs decrease insulin resistance by binding to and activating a transcription factor known as a **peroxisome proliferator–activated receptor-γ (PPAR-γ),** primarily in adipose tissue. Among other things, PPAR-γ activation induces the synthesis of adiponectin (Section 22-3B), which leads to an increase in AMPK activity. In adipose tissue, AMPK action leads to a decrease in lipolysis and fatty acid export, decreasing the concentration of free fatty acids in the blood and therefore decreasing insulin resistance (see above).

Rodent adipocytes secrete a 108-residue polypeptide hormone called **resistin.** The hormone is named for its ability to block the action of insulin on adipocytes. In fact, resistin production is decreased by TZDs, a feature that led to its discovery. Overproduction of resistin was proposed to contribute to the development of non-insulin-dependent diabetes. However, an interesting divergence between rodents and humans is that in humans, resistin is produced by macrophages and its role in human metabolic regulation is therefore unclear.

C | Obesity Is Usually Caused by Excessive Food Intake

The human body regulates glycogen and protein levels within relatively narrow limits, but fat reserves, which are much larger, can become enormous. The accumulation of fatty acids as triacylglycerols in adipose tissue is largely a result of excess fat or carbohydrate intake compared to energy expenditure. Fat synthesis from carbohydrates occurs when the carbohydrate intake is high enough that glycogen stores, to which excess carbohydrate is normally directed, approach their maximum capacity.

A chronic imbalance between fat and carbohydrate consumption and utilization increases the mass of adipose tissue through an increase in the number of adipocytes or their size (once formed, adipocytes are not lost, although their size may increase or decrease). The increase in adipose tissue mass increases the pool of fatty acids that can be mobilized to generate metabolic energy. Eventually, a steady state is achieved in which the mass of adipose tissue no longer increases and fat storage is balanced by fat mobilization. This phenomenon explains in part the high incidence of obesity in affluent societies, where fat- and carbohydrate-rich foods are plentiful and physical activity is not a requirement for survival. Considerable evidence suggests that behavior (e.g., eating habits and levels of physical activity) influences an individual's body composition. Yet, as we have seen (Section 22-3), some cases of obesity are also the result of innate disturbances in an individual's capacity to metabolize fuels.

The hormonal mechanisms that contribute to obesity and its attendant health problems, such as diabetes, may have conferred a selective advantage in premodern times. For example, the ability to gain weight easily would have protected against famine. One theory proposes that as humans evolved, the regulation of fuel metabolism was geared toward overeating large quantities of food when available, thereby obtaining essential nutrients while storing excess nonessential energy as fat for use during famine. In modern cultures in which famines are rare and nutritious food is readily available, human genetic heritage has apparently contributed to an epidemic of obesity: An estimated 30% of U.S. adults are obese and another 35% are overweight.

Obesity Is a Contributing Factor in Metabolic Syndrome. **Metabolic syndrome** is a disturbance in metabolism characterized by insulin resistance, inflammation, and a predisposition to several disorders including type 2 diabetes, hypertension, and atherosclerosis. Those disorders are accompanied by an increase in coronary heart disease. Obesity, physical inactivity, and possibly genetic determinants have been implicated in its occurrence, which affects as many as 65 million people in the United States alone. Exercise, calorie/weight reduction, adiponectin, leptin, metformin, and TZDs have all been successfully used to treat metabolic syndrome. All of these increase AMPK activity, making AMPK a promising target for drug development.

CHECK YOUR UNDERSTANDING

Describe the metabolic changes that occur during starvation.

Distinguish insulin-dependent and non-insulin-dependent diabetes mellitus.

How is obesity related to non-insulin-dependent diabetes mellitus?

SUMMARY

1. The pathways for the synthesis and degradation of the major metabolic fuels (glucose, fatty acids, and amino acids) converge on acetyl-CoA and pyruvate. In mammals, flux through these pathways is tissue specific.
2. The brain uses glucose as its primary metabolic fuel. Muscle can oxidize a variety of fuels but depends on anaerobic glycolysis for maximum exertion. Adipose tissue stores excess fatty acids as triacylglycerols and mobilizes them as needed.
3. The liver maintains the concentrations of circulating fuels. The action of glucokinase allows liver to take up excess glucose, which can then be directed to several metabolic fates. The liver also converts fatty acids to ketone bodies and metabolizes amino acids derived from the diet or from protein breakdown. Both the liver and kidney carry out gluconeogenesis.
4. The Cori cycle and the glucose–alanine cycle are multiorgan pathways through which the liver and muscle exchange metabolic intermediates.
5. Hormones such as insulin, glucagon, and epinephrine transmit regulatory signals to target tissues by binding to receptors that transduce the signal to responses in the interior of the cell. Insulin promotes fuel storage, and glucagon and epinephrine mobilize stored fuels.
6. AMP-dependent protein kinase (AMPK), the cell's fuel gauge, senses the cell's need for ATP and activates metabolic breakdown pathways while inhibiting biosynthetic pathways.
7. Adiponectin, an adipocyte hormone that increases insulin sensitivity, acts by activating AMPK.
8. Appetite is controlled in the hypothalamus by the hormones leptin, insulin, ghrelin, and PYY.
9. During starvation, when dietary fuels are unavailable, the liver releases glucose first by glycogen breakdown and then by gluconeogenesis from amino acid precursors. Eventually, ketone bodies supplied by fatty acid breakdown meet most of the body's energy needs.
10. Diabetes mellitus causes hyperglycemia and other physiological difficulties resulting from destruction of insulin-producing pancreatic β cells or from insulin resistance (from loss of receptors or their insensitivity to insulin).
11. Obesity, an imbalance between food intake and energy expenditure, may result from abnormal regulation by peptide hormones produced in different tissues.
12. Metabolic syndrome is caused by obesity, physical inactivity, and possibly genetic determinants.

KEY TERMS

Cori cycle	**798**
oxygen debt	**798**
glucose–alanine cycle	**799**
homeostasis	**799**
diet-induced thermogenesis	**808**
diabetes	**811**
ketosis	**811**
hyperglycemia	**811**
insulin resistance	**813**
metabolic syndrome	**815**

PROBLEMS

1. Predict the effect of an overdose of insulin on brain function in a normal person.
2. Why would oxidative metabolism, which generates ATP, cease when a cell's ATP supply is exhausted?
3. The passive glucose transporter, called GLUT1 (Fig. 10-13), is present in the membranes of many cells, but not in the liver. Instead, liver cells express the GLUT2 transporter, which exhibits different transport kinetics. (a) Given what you know

about the role of the liver in buffering blood glucose, compare the K_M values of GLUT1 and GLUT2. (b) Explain why a deficiency of GLUT2 produces symptoms resembling those of Type I glycogen storage disease (Box 16-2).

4. Pancreatic β cells express a receptor for fatty acids. Fatty acid binding to this protein appears to stimulate insulin secretion. (a) Does this phenomenon make metabolic sense? (b) Fatty acids appear to stimulate insulin secretion to a much greater extent when glucose is also present. Why is this significant?
5. Adaptation to high altitude includes increases in GLUT1 and phosphofructokinase in muscle. Explain why this would be advantageous.
6. Individuals with a deficiency of medium chain acyl-CoA dehydrogenase (MCAD) tend to develop nonketotic hypoglycemia. Explain why this defect makes them unable to undertake (a) ketogenesis and (b) gluconeogenesis.
7. Would you expect insulin to increase or decrease the activity of the enzyme ATP-citrate lyase?
8. Explain why insulin is required for adipocytes to synthesize triacylglycerols from fatty acids.
9. Experienced runners know that it is poor practice to ingest large amounts of glucose immediately before running a marathon. What is the metabolic basis for this apparent paradox?
10. After several days of starvation, the capacity of the liver to metabolize acetyl-CoA via the citric acid cycle is greatly diminished. Explain.
11. If the circulatory system of an *ob*/*ob* mouse is surgically joined to that of a normal mouse, what will be the effect on the appetite and weight of the *ob*/*ob* mouse?
12. Why can adipose tissue be considered to be an endocrine organ?
13. In experiments to test the appetite-suppressing effects of PYY_{3-36}, why must the hormone be administered intravenously rather than orally?
14. High concentrations of free fatty acids in the blood are known to cause insulin resistance in muscle, but only after 5 hours. This suggests that a metabolite of the fatty acids may be responsible for this phenomenon. It is also known that an isoform of protein kinase C is activated during the process and that high concentrations of free fatty acids result in intramuscular accumulation of triacylglycerols. With this information, review the mechanism of activation of PKC and the pathway of triacylglycerol biosynthesis and suggest a metabolite that may be responsible for PKC activation.
15. Discuss, in molecular terms, how physical inactivity might lead to insulin resistance.

CASE STUDIES

Case 25 (available at www.wiley.com/college/voet)
Glycogen Storage Diseases

Focus concept: Disturbances in glycogen utilization result if an enzyme involved in glycogen synthesis or degradation is missing.

Prerequisites: Chapters 16 and 22

- Glycogen synthesis and degradation pathways
- The link between glycogen metabolism and fat metabolism

Case 28
The Bacterium Helicobacter pylori and Peptic Ulcers

Focus concept: The entire genome of *Helicobacter pylori* has been sequenced. This allows biochemists to examine the organism's proteins in detail. In this case, mechanisms employed by *Helicobacter pylori* that permit it to survive in the acidic environment of the stomach are examined.

Prerequisites: Chapters 6 and 15–22

- Protein structure and function
- Basic metabolic pathways up through amino acid metabolism

Case 30
Phenylketonuria

Focus concept: The characteristics of phenylalanine hydroxylase, the enzyme missing in persons afflicted with the genetic disorder phenylketonuria (PKU), are examined.

Prerequisites: Chapters 21 and 22

- Amino acid synthesis and degradation pathways
- Integration of amino acid metabolic pathways with carbohydrate metabolic pathways

REFERENCES

Bollen, M., Keppens, S., and Stalmans, W., Specific features of glycogen metabolism in the liver, *Biochem. J.* **336,** 19–31 (1998).

Huang, H. and Czech, M.P., The GLUT4 glucose transporter**,** *Cell Metabolism* **5,** 237–252 (2007).

Kadowaki, T. and Yamauchi, T., Adiponectin and adiponectin receptors, *Endocrine Rev.* **26**, 439–451 (2005).

Obesity, *Science* **299,** 845–860 (2003). [A series of informative reports on the origins and treatments of obesity.]

Saltiel, A.R. and Kahn, C.R., Insulin signaling and the regulation of glucose and lipid metabolism, *Nature* **414,** 799–806 (2001). [Summarizes the mechanisms of insulin action and insulin resistance.]

Spiegelman, B.M. and Flier, J.S., Obesity and the regulation of energy balance, *Cell* **104,** 531–543 (2001).

Towler, M.C. and Hardie, D.G., AMP-Activated protein kinase in metabolic control and insulin signaling, *Circulation Res.* **100,** 328–341 (2007).

23

Nucleotide Metabolism

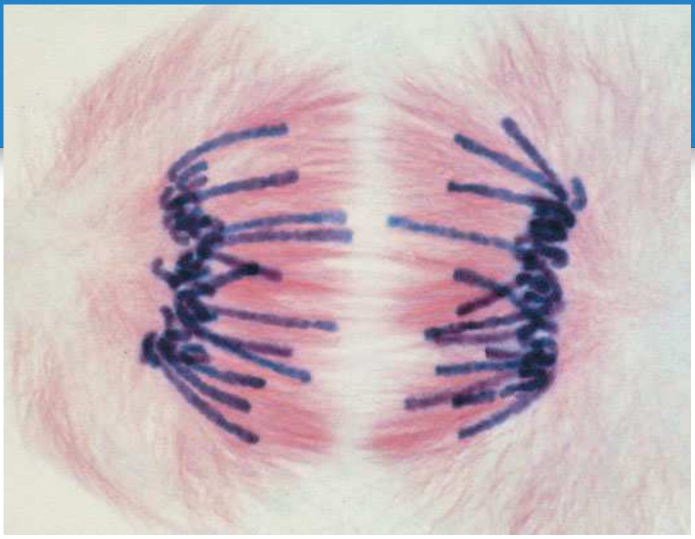

The synthesis of two complete sets of chromosomes requires large amounts of newly synthesized nucleotides. During cell division (mitosis), sets of identical chromosomes (purple) are pulled apart. [Courtesy of Andrew Bajer, University of Oregon.]

■ CHAPTER CONTENTS

1 Synthesis of Purine Ribonucleotides
- **A.** Purine Synthesis Yields Inosine Monophosphate
- **B.** IMP Is Converted to Adenine and Guanine Ribonucleotides
- **C.** Purine Nucleotide Biosynthesis Is Regulated at Several Steps
- **D.** Purines Can Be Salvaged

2 Synthesis of Pyrimidine Ribonucleotides
- **A.** UMP Is Synthesized in Six Steps
- **B.** UMP Is Converted to UTP and CTP
- **C.** Pyrimidine Nucleotide Biosynthesis Is Regulated at ATCase or Carbamoyl Phosphate Synthetase II

3 Formation of Deoxyribonucleotides
- **A.** Ribonucleotide Reductase Converts Ribonucleotides to Deoxyribonucleotides
- **B.** dUMP Is Methylated to Form Thymine

4 Nucleotide Degradation
- **A.** Purine Catabolism Yields Uric Acid
- **B.** Some Animals Degrade Uric Acid
- **C.** Pyrimidines Are Broken Down to Malonyl-CoA and Methylmalonyl-CoA

■ MEDIA RESOURCES

(available at www.wiley.com/college/voet)
Interactive Exercise 33. *E. coli* ribonucleotide reductase
Interactive Exercise 34. Human dihydrofolate reductase
Interactive Exercise 35. Murine adenosine deaminase
Animated Figure 23-1. Metabolic pathway for *de novo* biosynthesis of IMP
Animated Figure 23-4. Control of purine biosynthesis pathway
Animated Figure 23-5. The *de novo* synthesis of UMP
Animated Figure 23-8. Regulation of pyrimidine biosynthesis

Nucleotides are phosphate esters of a pentose (ribose or deoxyribose) in which a purine or pyrimidine base is linked to C1′ of the sugar (Section 3-1). Nucleoside triphosphates are the monomeric units that act as precursors of nucleic acids; nucleotides also perform a wide range of other biochemical functions. For example, we have seen how the cleavage of "high-energy" compounds such as ATP provides the free energy that makes various reactions thermodynamically favorable. We have also seen that nucleotides are components of some of the central cofactors of metabolism, including FAD, NAD^+, and coenzyme A. The importance of nucleotides in cellular metabolism is indicated by the observation that nearly all cells can synthesize them both *de novo* (anew) and from the degradation products of nucleic acids. However, unlike carbohydrates, amino acids, and fatty acids, nucleotides do not provide a significant source of metabolic energy.

In this chapter, we consider the nature of the nucleotide biosynthetic pathways. In doing so, we shall examine how they are regulated and the consequences of their blockade, both by genetic defects and through the administration of chemotherapeutic agents. We then discuss how nucleotides are degraded. In following the general chemical themes of nucleotide metabolism, we shall break our discussion into sections on purines, pyrimidines, and deoxynucleotides (including thymidylate). The structures and nomenclature of the major purines and pyrimidines are given in Table 3-1.

1 Synthesis of Purine Ribonucleotides

LEARNING OBJECTIVES

- Understand that IMP is synthesized through the assembly of a purine base on ribose-5-phosphate.
- Understand that kinases convert IMP-derived AMP and GMP to ATP and GTP.
- Understand the mechanisms that regulate purine nucleotide synthesis.
- Understand that salvage reactions convert purines to their nucleotide forms.

In 1948, John Buchanan obtained the first clues to the *de novo* synthesis of purine nucleotides by feeding a variety of isotopically labeled compounds to pigeons and chemically determining the positions of the labeled atoms in their excreted **uric acid** (a purine; *at right*). The results of his studies demonstrated that N1 of purines arises from the amino group of aspartate; C2 and C8 originate from formate; N3 and N9 are contributed by the amide group of glutamine; C4, C5, and N7 are derived from glycine (strongly suggesting that this molecule is wholly incorporated into the purine ring); and C6 comes from HCO_3^-.

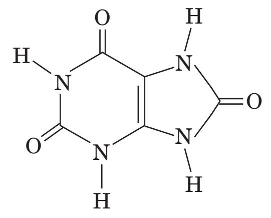

Uric acid

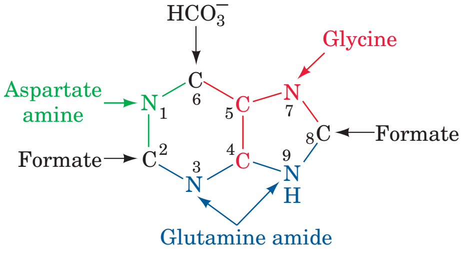

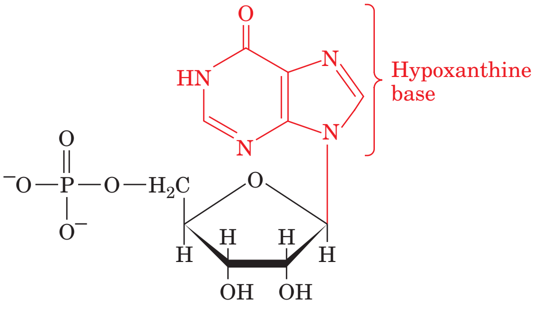

Inosine monophosphate (IMP)

The actual pathway by which these precursors are incorporated into the purine ring was elucidated in subsequent investigations performed largely by Buchanan and G. Robert Greenberg. The initially synthesized purine derivative is **inosine monophosphate (IMP,** *at left*), the nucleotide of the base **hypoxanthine.** IMP is the precursor of both AMP and GMP. Thus, contrary to expectation, *purines are initially formed as ribonucleotides rather than as free bases*. Additional studies have demonstrated that such widely divergent organisms as *E. coli,* yeast, pigeons, and humans have virtually identical pathways for the biosynthesis of purine nucleotides, thereby further demonstrating the biochemical unity of life.

A | Purine Synthesis Yields Inosine Monophosphate

IMP is synthesized in a pathway composed of 11 reactions (Fig. 23-1):

1. **Activation of ribose-5-phosphate.** The starting material for purine biosynthesis is α-D-ribose-5-phosphate, a product of the pentose phosphate pathway (Section 15-6). In the first step of purine biosynthesis, **ribose phosphate pyrophosphokinase** activates the ribose by reacting it with ATP to form **5-phosphoribosyl-α-pyrophosphate (PRPP).** This compound is also a precursor in the biosynthesis of pyrimidine nucleotides (Section 23-2A) and the amino acids histidine and tryptophan (Section 21-5B). As is expected for an enzyme at such an important biosynthetic crossroads, the activity of ribose phosphate pyrophosphokinase is precisely regulated.
2. **Acquisition of purine atom N9.** In the first reaction unique to purine biosynthesis, **amidophosphoribosyl transferase** catalyzes the displacement of PRPP's pyrophosphate group by glutamine's amide nitrogen. The reaction occurs with inversion of the α configuration at C1 of PRPP, thereby forming **β-5-phosphoribosylamine** and establishing the anomeric form of the future nucleotide. The reaction, which is driven to completion by the subsequent hydrolysis of the released PP_i, is the pathway's flux-controlling step.

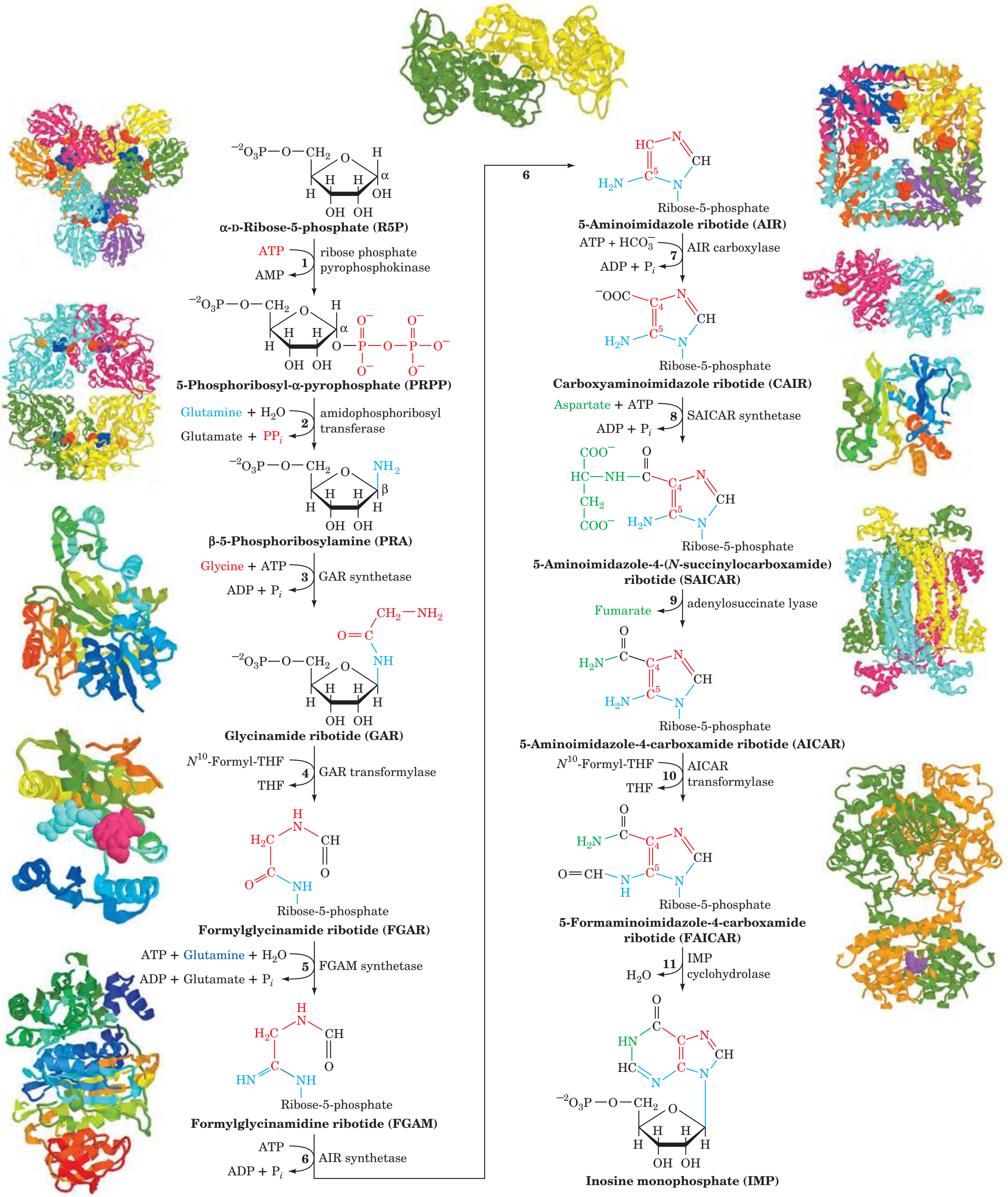

α-D-Ribose-5-phosphate (R5P)
ATP
AMP
1
ribose phosphate pyrophosphokinase
5-Phosphoribosyl-α-pyrophosphate (PRPP)
Glutamine + H2O
Glutamate + PPi
2
amidophosphoribosyl transferase
β-5-Phosphoribosylamine (PRA)
Glycine + ATP
ADP + Pi
3
GAR synthetase
Glycinamide ribotide (GAR)
N10-Formyl-THF
THF
4
GAR transformylase
Formylglycinamide ribotide (FGAR)
ATP + Glutamine + H2O
ADP + Glutamate + Pi
5
FGAM synthetase
Formylglycinamidine ribotide (FGAM)
ATP
ADP + Pi
6
AIR synthetase
6
5-Aminoimidazole ribotide (AIR)
ATP + HCO3−
ADP + Pi
7
AIR carboxylase
Carboxyaminoimidazole ribotide (CAIR)
Aspartate + ATP
ADP + Pi
8
SAICAR synthetase
5-Aminoimidazole-4-(N-succinylocarboxamide) ribotide (SAICAR)
Fumarate
9
adenylosuccinate lyase
5-Aminoimidazole-4-carboxamide ribotide (AICAR)
N10-Formyl-THF
THF
10
AICAR transformylase
5-Formaminoimidazole-4-carboxamide ribotide (FAICAR)
H2O
11
IMP cyclohydrolase
Inosine monophosphate (IMP)
Ribose-5-phosphate

Figure 23-1 | **The metabolic pathway for the *de novo* biosynthesis of IMP.** Here the purine residue is built up on a ribose ring in 11 enzyme-catalyzed reactions. The X-ray structures for all the enzymes are shown to the outside of the corresponding reaction arrow. The peptide chains of monomeric enzymes are color-ramped from N-terminus (*blue*) to C-terminus (*red*). The oligomeric enzymes, all of which consist of identical polypeptide chains, are viewed along a rotation axis with their various chains differently colored. Bound ligands are shown in space-filling form. [PDBids: enzyme 1, 1DKU; enzyme 2, 1AO0; enzyme 3, 1GSO; enzyme 4, 1CDE; enzyme 5, 1VK3; enzyme 6, 1CLI; enzyme 7, 1D7A (PurE) and 1B6S (PurK); enzyme 8, 1A48; enzyme 9, 1C3U; enzymes 10 and 11, 1G8M.] **See the Animated Figures.**

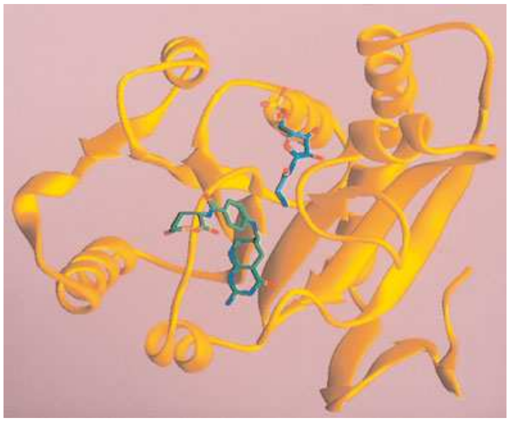

Figure 23-2 | X-Ray structure of GAR transformylase in complex with GAR and 5dTHF. The C atoms of GAR (*upper right*) and 5dTHF (*lower left*) are cyan and green, whereas their N, C, and P atoms are blue, red, and yellow, respectively. Note the proximity of GAR to 5dTHF. [Based on an X-ray structure by Robert Almassy, Agouron Pharmaceuticals, San Diego, California. PDBid 1CDE.]

3. **Acquisition of purine atoms C4, C5, and N7.** Glycine's carboxyl group forms an amide with the amino group of phosphoribosylamine, yielding **glycinamide ribotide (GAR).** This reaction is reversible, despite its concomitant hydrolysis of ATP to ADP + P_i. It is the only step of the purine biosynthetic pathway in which more than one purine ring atom is acquired.
4. **Acquisition of purine atom C8.** GAR's free α-amino group is formylated to yield **formylglycinamide ribotide (FGAR).** The formyl donor in the reaction is N^{10}-formyltetrahydrofolate (N^{10}-formyl-THF), a coenzyme that transfers C_1 units (THF cofactors are described in Section 21-4D). The X-ray structure of the enzyme catalyzing the reaction, **GAR transformylase,** in complex with GAR and the THF analog **5-deazatetrahydrofolate (5dTHF)** was determined by Robert Almassy (Fig. 23-2). Note the proximity of the GAR amino group to N10 of 5dTHF. This supports enzymatic studies suggesting that the GAR transformylase reaction proceeds via the nucleophilic attack of the GAR amine group on the formyl carbon of N^{10}-formyl-THF to yield a tetrahedral intermediate.
5. **Acquisition of purine atom N3.** The amide amino group of a second glutamine is transferred to the growing purine ring to form **formylglycinamidine ribotide (FGAM).** This reaction is driven by the coupled hydrolysis of ATP to ADP + P_i.
6. **Formation of the purine imidazole ring.** The purine imidazole ring is closed in an ATP-requiring intramolecular condensation that yields **5-aminoimidazole ribotide (AIR).** The aromatization of the imidazole ring is facilitated by the tautomeric shift of the reactant from its imine to its enamine form.
7. **Acquisition of C6.** Purine C6 is introduced as HCO_3^- (CO_2) in a reaction catalyzed by **AIR carboxylase** that yields **carboxyaminoimidazole ribotide (CAIR).** In yeast, plants, and most prokaryotes (including *E. coli*), AIR carboxylase consists of two proteins called **PurE** and **PurK.** Although PurE alone can catalyze the carboxylation reaction, its K_M for HCO_3^- is ~110 mM, so the reaction would require an unphysiologically high HCO_3^- concentration (~100 mM) to proceed. PurK decreases the HCO_3^- concentration required for the PurE reaction by >1000-fold but at the expense of ATP hydrolysis.
8. **Acquisition of N1.** Purine atom N1 is contributed by aspartate in an amide-forming condensation reaction yielding **5-aminoimidazole-4-(*N*-succinylocarboxamide) ribotide (SACAIR).** This reaction, which is driven by the hydrolysis of ATP, chemically resembles Reaction 3.
9. **Elimination of fumarate.** SACAIR is cleaved with the release of fumarate, yielding **5-aminoimidazole-4-carboxamide ribotide (AICAR).** Reactions 8 and 9 chemically resemble the reactions in the urea cycle in which citrulline is aminated to form arginine (Section 21-3A). In both pathways, aspartate's amino group is transferred to an acceptor through an ATP-driven coupling reaction followed by the elimination of the aspartate carbon skeleton as fumarate.
10. **Acquisition of C2.** The final purine ring atom is acquired through formylation by N^{10}-formyl-THF, yielding **5-formaminoimidazole-4-carboxamide ribotide (FAICAR).** This reaction and Reaction 4 of purine biosynthesis are inhibited indirectly by **sulfonamides,** structural analogs of the *p*-aminobenzoic acid constituent of THF (Section 21-4D).
11. **Cyclization to form IMP.** The final reaction in the purine biosynthetic pathway, ring closure to form IMP, occurs through the

elimination of water. In contrast to Reaction 6, the cyclization that forms the imidazole ring, this reaction does not require ATP hydrolysis.

In animals, Reactions 10 and 11 are catalyzed by a bifunctional enzyme, as are Reactions 7 and 8. Reactions 3, 4, and 6 also take place on a single protein. *The intermediate products of these multifunctional enzymes are not readily released to the medium but are channeled to the succeeding enzymatic activities of the pathway.* As in the reactions catalyzed by the pyruvate dehydrogenase complex (Section 17-2), fatty acid synthase (Section 20-4C), bacterial glutamate synthase (Section 21-7), and tryptophan synthase (Section 21-5B), channeling in the nucleotide synthetic pathways increases the overall rate of these multistep processes and protects intermediates from degradation by other cellular enzymes.

B | IMP Is Converted to Adenine and Guanine Ribonucleotides

IMP does not accumulate in the cell but is rapidly converted to AMP and GMP. AMP, which differs from IMP only in the replacement of its 6-keto group by an amino group, is synthesized in a two-reaction pathway (Fig. 23-3, *left*). In the first reaction, aspartate's amino group is linked to

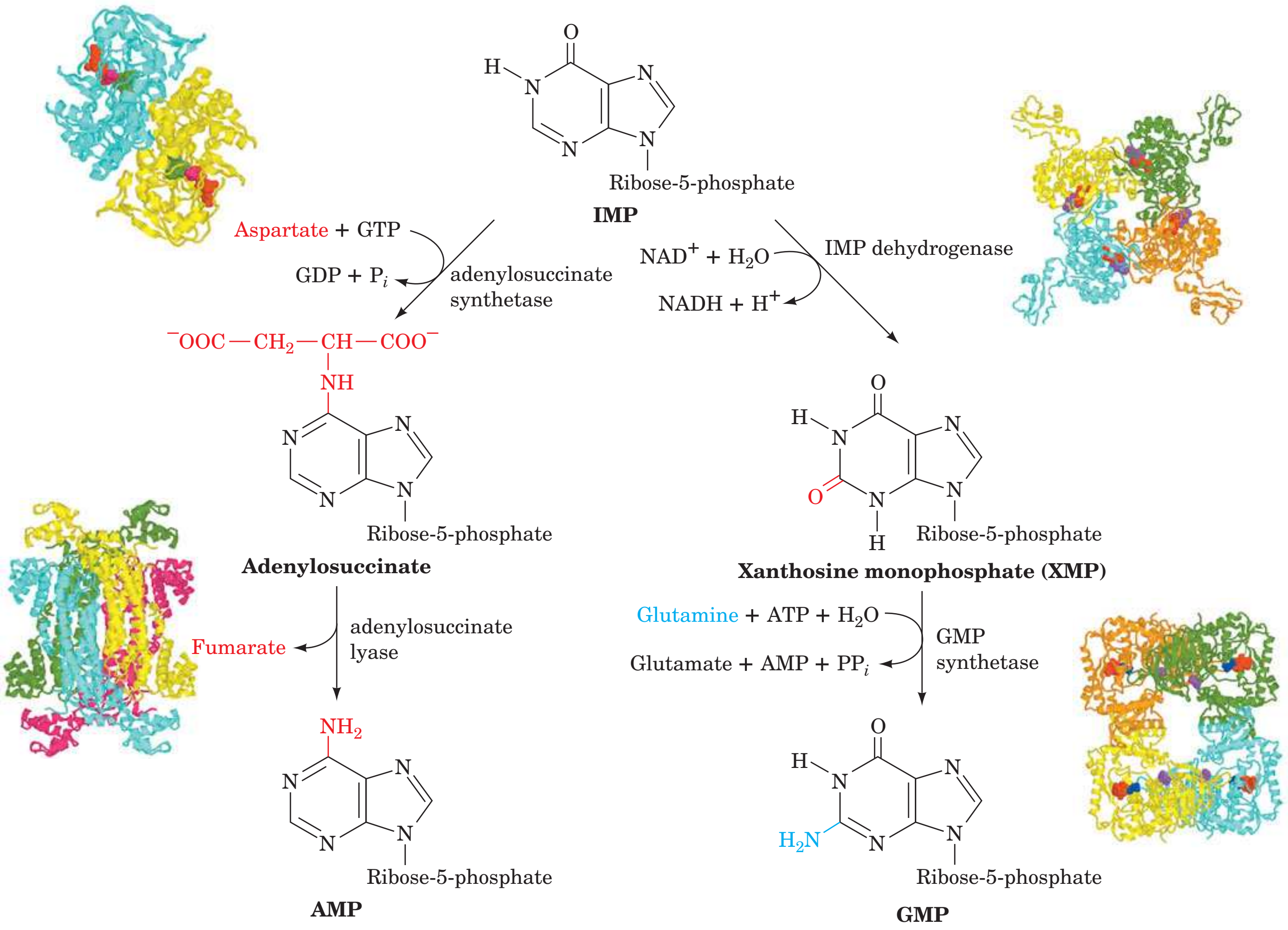
Ribose-5-phosphate
IMP
Aspartate + GTP
GDP + P$_i$
adenylosuccinate synthetase
NAD$^+$ + H$_2$O
NADH + H$^+$
IMP dehydrogenase
$^-$OOC—CH$_2$—CH—COO$^-$
NH
Ribose-5-phosphate
Adenylosuccinate
Ribose-5-phosphate
Xanthosine monophosphate (XMP)
Fumarate
adenylosuccinate lyase
Glutamine + ATP + H$_2$O
Glutamate + AMP + PP$_i$
GMP synthetase
NH$_2$
H$_2$N
Ribose-5-phosphate
AMP
Ribose-5-phosphate
GMP

Figure 23-3 | Conversion of IMP to AMP or GMP in separate two-reaction pathways. The X-ray structures of the homo-oligomeric enzymes catalyzing the reactions are shown as is described in the legend for Fig. 23-1. [PDBids: adenylosuccinate synthetase, 1G1M; adenylosuccinate lyase, 1C3U; IMP dehydrogenase, 1JR1; GMP synthetase, 1GPM.]

IMP in a reaction powered by the hydrolysis of GTP to GDP + P_i to yield **adenylosuccinate.** In the second reaction, **adenylosuccinate lyase** eliminates fumarate from adenylosuccinate to form AMP. The same enzyme catalyzes Reaction 9 of the IMP pathway (Fig. 23-1). Both reactions add a nitrogen with the elimination of fumarate.

GMP is also synthesized from IMP in a two-reaction pathway (Fig. 23-3, *right*). In the first reaction, IMP is dehydrogenated via the reduction of NAD^+ to form **xanthosine monophosphate (XMP;** the ribonucleotide of the base **xanthine).** XMP is then converted to GMP by the transfer of the glutamine amide nitrogen in a reaction driven by the hydrolysis of ATP to AMP + PP_i (and subsequently to 2 P_i). In B and T lymphocytes, which mediate the immune response, IMP dehydrogenase activity is high in order to supply the guanosine the cells need for proliferation. The fungal compound **mycophenolic acid** (*at left*) inhibits the enzyme and is used as an immunosuppressant following kidney transplants.

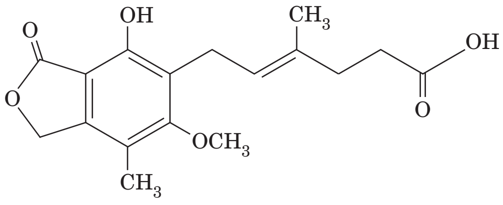

Mycophenolic acid

Nucleoside Diphosphates and Triphosphates Are Synthesized by the Phosphorylation of Nucleoside Monophosphates. *In order to participate in nucleic acid synthesis, nucleoside monophosphates must first be converted to the corresponding nucleoside triphosphates.* First, nucleoside diphosphates are synthesized from the corresponding nucleoside monophosphates by base-specific **nucleoside monophosphate kinases.** For example, adenylate kinase (Section 14-2C) catalyzes the phosphorylation of AMP to ADP:

$$\text{AMP} + \text{ATP} \rightleftharpoons 2\ \text{ADP}$$

Similarly, GDP is produced by **guanylate kinase:**

$$\text{GMP} + \text{ATP} \rightleftharpoons \text{GDP} + \text{ADP}$$

These nucleoside monophosphate kinases do not discriminate between ribose and deoxyribose in the substrate.

Nucleoside diphosphates are converted to the corresponding triphosphates by **nucleoside diphosphate kinase;** for instance,

$$\text{GDP} + \text{ATP} \rightleftharpoons \text{GTP} + \text{ADP}$$

Although the reaction is written with ATP as the phosphoryl donor, this enzyme exhibits no preference for the bases of its substrates or for ribose over deoxyribose. Furthermore, the nucleoside diphosphate kinase reaction, as might be expected from the nearly identical structures of its substrates and products, normally operates close to equilibrium ($\Delta G \approx 0$). ADP is, of course, also converted to ATP by a variety of energy-releasing reactions such as those of glycolysis and oxidative phosphorylation. Indeed, it is those reactions that ultimately drive the foregoing kinase reactions.

C | Purine Nucleotide Biosynthesis Is Regulated at Several Steps

The pathways synthesizing IMP, ATP, and GTP are individually regulated in most cells so as to control the total amounts of purine nucleotides available for nucleic acid synthesis, as well as the relative amounts of ATP and GTP. This control network is diagrammed in Fig. 23-4.

The IMP pathway is regulated at its first two reactions: those catalyzing the synthesis of PRPP and 5-phosphoribosylamine. Ribose phosphate pyrophosphokinase, the enzyme catalyzing Reaction 1 of the IMP pathway (Fig. 23-1), is inhibited by both ADP and GDP. Amidophosphoribosyl transferase, the enzyme catalyzing the first committed step of the IMP

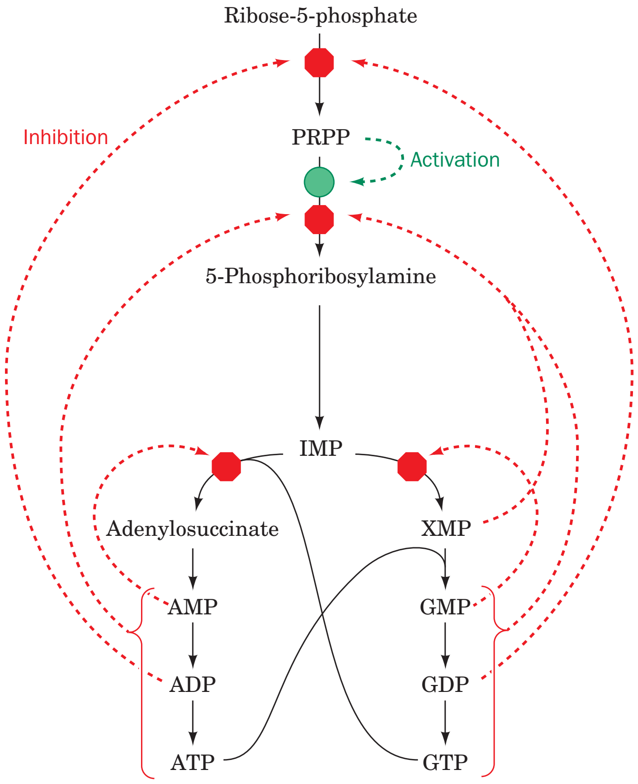

Figure 23-4 | Control of the purine biosynthesis pathway. Red octagons and green circles indicate control points. Feedback inhibition is indicated by dashed red arrows, and feedforward activation is represented by a dashed green arrow. **See the Animated Figures.**

pathway (Reaction 2) is likewise subject to feedback inhibition. In this case, the enzyme binds ATP, ADP, and AMP at one inhibitory site and GTP, GDP, and GMP at another. *The rate of IMP production is therefore independently but synergistically controlled by the levels of adenine nucleotides and guanine nucleotides.* Moreover, amidophosphoribosyl transferase is allosterically stimulated by PRPP **(feedforward activation).**

A second level of regulation occurs immediately below the branch point leading from IMP to AMP and GMP. AMP and GMP are each competitive inhibitors of IMP in their own synthesis, which prevents excessive buildup of the pathway products. In addition, the rates of adenine and guanine nucleotide synthesis are coordinated. Recall that GTP powers the synthesis of AMP from IMP, whereas ATP powers the synthesis of GMP from IMP (Fig. 23-3). This reciprocity balances the production of AMP and GMP (which are required in roughly equal amounts in nucleic acid biosynthesis): *The rate of synthesis of GMP increases with [ATP], whereas that of AMP increases with [GTP].*

D | Purines Can Be Salvaged

In most cells, the turnover of nucleic acids, particularly some types of RNA, releases adenine, guanine, and hypoxanthine (Section 23-4A). These free purines are reconverted to their corresponding nucleotides through **salvage pathways.** In contrast to the *de novo* purine nucleotide synthetic pathway, which is virtually identical in all cells, salvage pathways are diverse in character and distribution. In mammals, purines are mostly salvaged by two different enzymes. **Adenine phosphoribosyltransferase (APRT)** mediates AMP formation using PRPP:

$$\text{Adenine} + \text{PRPP} \rightleftharpoons \text{AMP} + \text{PP}_i$$

Hypoxanthine–guanine phosphoribosyltransferase (HGPRT) catalyzes the analogous reaction for both hypoxanthine and guanine:

$$\text{Hypoxanthine} + \text{PRPP} \rightleftharpoons \text{IMP} + \text{PP}_i$$
$$\text{Guanine} + \text{PRPP} \rightleftharpoons \text{GMP} + \text{PP}_i$$

Lesch–Nyhan Syndrome Results from HGPRT Deficiency. The symptoms of **Lesch–Nyhan syndrome,** which is caused by a severe HGPRT deficiency, indicate that purine salvage reactions have functions other than conservation of the energy required for *de novo* purine biosynthesis. This sex-linked congenital defect (it affects mostly males) results in excessive uric acid production (uric acid is a purine degradation product; Section 23-4A) and neurological abnormalities such as spasticity, mental retardation, and highly aggressive and destructive behavior, including a bizarre compulsion toward self-mutilation. For example, many children with Lesch–Nyhan syndrome have such an irresistible urge to bite their lips and fingers that they must be restrained. If the restraints are removed, communicative patients will plead that the restraints be replaced, even as they attempt to injure themselves.

The excessive uric acid production in patients with Lesch–Nyhan syndrome is readily explained. The lack of HGPRT activity leads to an accumulation of the PRPP that would normally be used to salvage hypoxanthine and guanine. The excess PRPP activates amidophosphoribosyl transferase (which catalyzes Reaction 2 of the IMP biosynthetic pathway), thereby greatly accelerating the synthesis of purine nucleotides and thus the formation of their degradation product, uric acid. Yet the physiological basis of the associated neurological abnormalities remains obscure. That a defect in a single enzyme can cause such profound but well-defined behavioral changes nevertheless has important neurophysiological implications.

CHECK YOUR UNDERSTANDING

List the starting materials and cofactors required for IMP biosynthesis.

Describe the reactions that convert IMP to ATP and GTP.

How do guanine and adenine nucleotides inhibit their own synthesis?

Describe how free purines are converted back to nucleotides.

2 Synthesis of Pyrimidine Ribonucleotides

LEARNING OBJECTIVES

- Understand that UMP is synthesized as a pyrimidine base to which ribose-5-phosphate is added.
- Understand that CTP and UTP are derived from UMP.
- Understand what steps are the major control points for pyrimidine nucleotide synthesis.

The biosynthesis of pyrimidines is simpler than that of purines. Isotopic labeling experiments have shown that atoms N1, C4, C5, and C6 of the pyrimidine ring are all derived from aspartic acid, C2 arises from HCO_3^-, and N3 is contributed by glutamine.

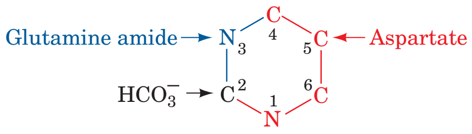

A | UMP Is Synthesized in Six Steps

UMP, which is also the precursor of CMP, is synthesized in a six-reaction pathway (Fig. 23-5). In contrast to purine nucleotide synthesis, the pyrimidine ring is coupled to the ribose-5-phosphate moiety *after* the ring has been synthesized.

1. **Synthesis of carbamoyl phosphate.** The first reaction of pyrimidine biosynthesis is the synthesis of **carbamoyl phosphate** from HCO_3^- and the amide nitrogen of glutamine by the cytosolic enzyme **carbamoyl phosphate synthetase II.** This reaction consumes two molecules of ATP: One provides a phosphate group and the other energizes the reaction. Carbamoyl phosphate is also synthesized in the urea cycle (Section 21-3A). In that reaction, catalyzed by the

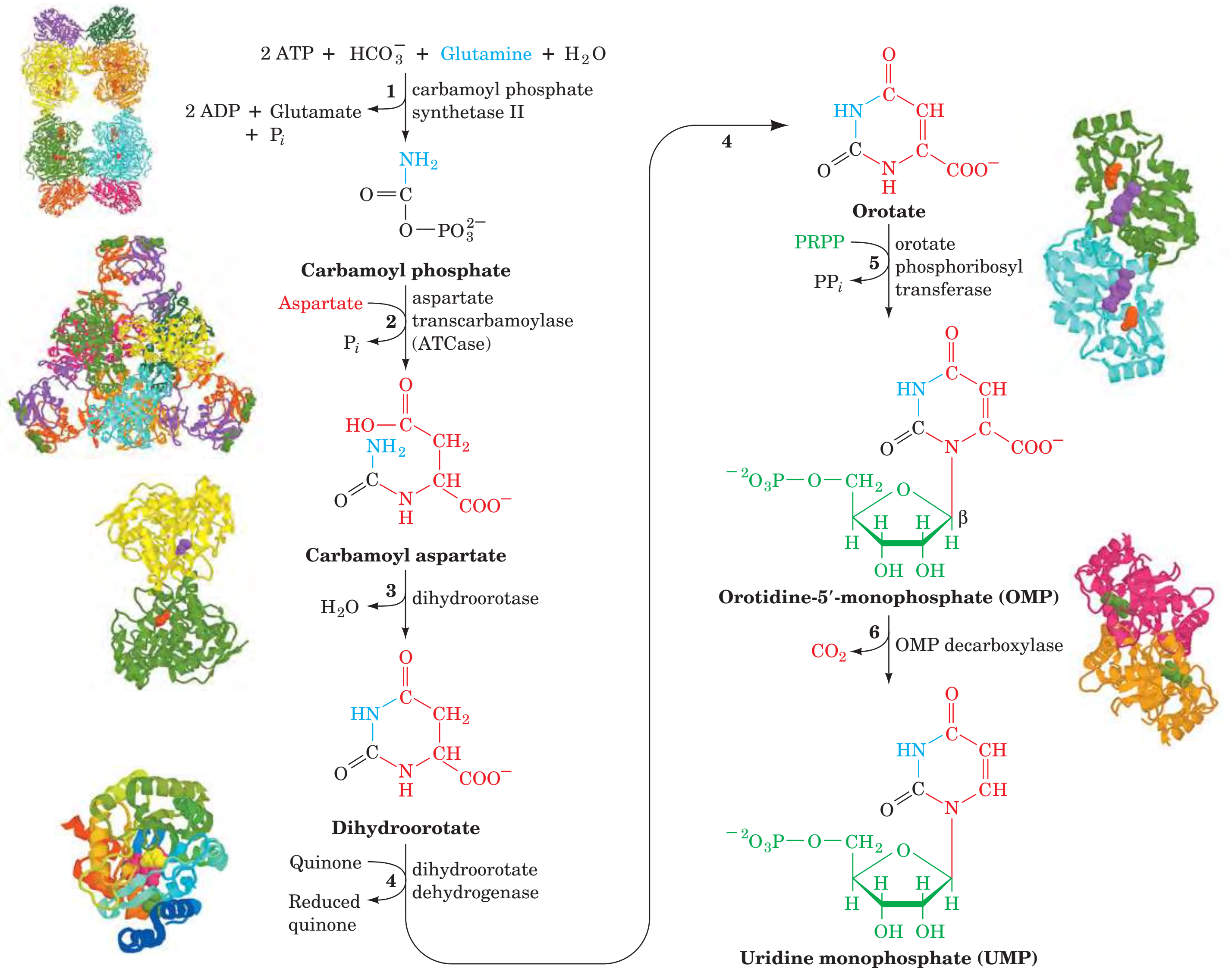
2 ATP + HCO$_3^-$ + Glutamine + H$_2$O
1
carbamoyl phosphate synthetase II
2 ADP + Glutamate + P$_i$
Carbamoyl phosphate
Aspartate
2
aspartate transcarbamoylase (ATCase)
P$_i$
Carbamoyl aspartate
3
dihydroorotase
H$_2$O
Dihydroorotate
Quinone
4
dihydroorotate dehydrogenase
Reduced quinone
4
Orotate
PRPP
5
orotate phosphoribosyl transferase
PP$_i$
β
Orotidine-5′-monophosphate (OMP)
6
OMP decarboxylase
CO$_2$
Uridine monophosphate (UMP)

■ **Figure 23-5** | **The *de novo* synthesis of UMP.** The X-ray structures of the six enzymes catalyzing the reactions are shown as is described in the legend for Fig. 23-1. [PDBids: enzyme 1, 1BXR; enzyme 2, 5AT1; enzyme 3, 1J79; enzyme 4, 1D3H; enzyme 5, 1OPR; enzyme 6, 1DBT.] **See the Animated Figures.**

mitochondrial enzyme carbamoyl phosphate synthetase I, ammonia is the nitrogen source.

2. **Synthesis of carbamoyl aspartate.** Condensation of carbamoyl phosphate with aspartate to form **carbamoyl aspartate** is catalyzed by **aspartate transcarbamoylase (ATCase).** This reaction proceeds without ATP hydrolysis because carbamoyl phosphate is already "activated." The structure and regulation of *E. coli* ATCase are discussed in Section 12-3.
3. **Ring closure to form dihydroorotate.** The third reaction of the pathway is an intramolecular condensation catalyzed by **dihydroorotase** to yield **dihydroorotate.**
4. **Oxidation of dihydroorotate.** Dihydroorotate is irreversibly oxidized to **orotate** by **dihydroorotate dehydrogenase.** The eukaryotic enzyme, which contains FMN and nonheme Fe, is located on the outer surface

of the inner mitochondrial membrane, where quinones supply its oxidizing power. The other five enzymes of pyrimidine nucleotide biosynthesis are cytosolic in animal cells. Inhibition of dihydroorotate dehydrogenase blocks pyrimidine synthesis in T lymphocytes, thereby attenuating the autoimmune disease rheumatoid arthritis.

5. **Acquisition of the ribose phosphate moiety.** Orotate reacts with PRPP to yield **orotidine-5′-monophosphate (OMP)** in a reaction catalyzed by **orotate phosphoribosyl transferase.** The reaction, which is driven by the hydrolysis of the eliminated PP_i, fixes the anomeric form of pyrimidine nucleotides in the β configuration. Orotate phosphoribosyl transferase also salvages other pyrimidine bases, such as uracil and cytosine, by converting them to their corresponding nucleotides.
6. **Decarboxylation to form UMP.** The final reaction of the pathway is the decarboxylation of OMP by **OMP decarboxylase (ODCase)** to form UMP. ODCase enhances the rate (k_{cat}/K_M) by a factor of 2×10^{23} over that of the uncatalyzed reaction, making it the most catalytically proficient enzyme known. Nevertheless, the reaction requires no cofactors to help stabilize its putative carbanion intermediate. Although the mechanism of the ODCase reaction is not fully understood, the removal of OMP's phosphate group, which is quite distant from the C6 carboxyl group, deceases the reaction rate by a factor of 7×10^7, thus providing a striking example of how binding energy can be applied to catalysis (preferential transition state binding).

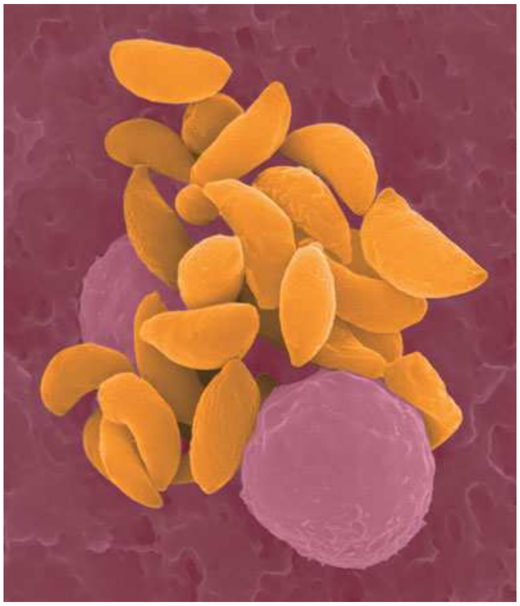

Figure 23-6 | ***Toxoplasma gondii.*** This intracellular parasite (*yellow*) causes toxoplasmosis. [© Dennis Kunkel/Phototake.]

In bacteria, the six enzymes of UMP biosynthesis occur as independent proteins. In animals, however, as Mary Ellen Jones demonstrated, the first three enzymatic activities of the pathway—carbamoyl phosphate synthetase II, ATCase, and dihydroorotase—occur on a single 210-kD polypeptide chain.

The pyrimidine biosynthetic pathway is a target for antiparasitic drugs. For example, the parasite *Toxoplasma gondii* (Fig. 23-6), which infects most mammals, causes **toxoplasmosis,** a disease whose complications include blindness, neurological dysfunction, and death in immunocompromised individuals (e.g., those with AIDS). Most parasites have evolved to take advantage of nutrients supplied by their hosts, but *T. gondii* is unable to meet its needs exclusively through nucleotide salvage pathways and retains the ability to synthesize uracil *de novo.* Drugs that target the parasite's carbamoyl phosphate synthetase II (an enzyme whose structure and kinetics distinguish it from its mammalian counterpart) could therefore prevent *T. gondii* growth. Moreover, there is evidence that *T. gondii* strains that have been engineered to lack carbamoyl phosphate synthetase II are avirulent and could be useful as vaccines in humans and livestock.

B | UMP Is Converted to UTP and CTP

The synthesis of UTP from UMP is analogous to the synthesis of purine nucleoside triphosphates (Section 23-1B). The process occurs by the sequential actions of a nucleoside monophosphate kinase and nucleoside diphosphate kinase:

$$\text{UMP} + \text{ATP} \rightleftharpoons \text{UDP} + \text{ADP}$$
$$\text{UDP} + \text{ATP} \rightleftharpoons \text{UTP} + \text{ADP}$$

CTP is formed by amination of UTP by **CTP synthetase** (Fig. 23-7). In animals, the amino group is donated by glutamine, whereas in bacteria it is supplied directly by ammonia.

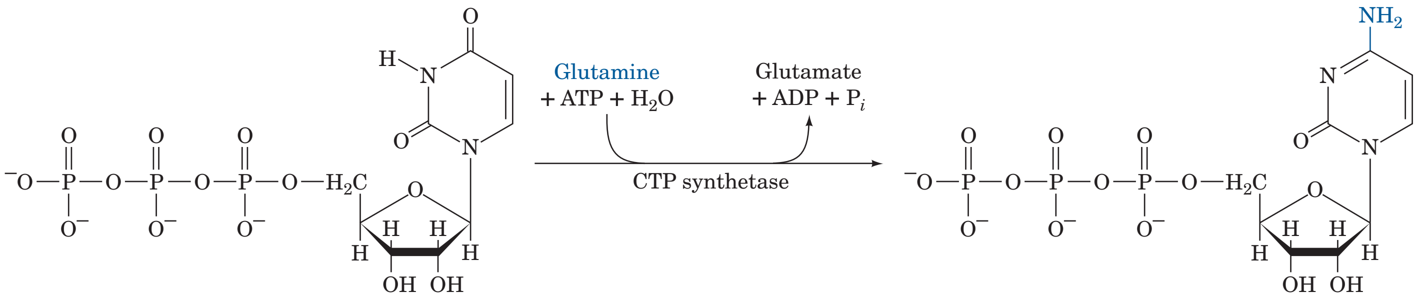
Glutamine
+ ATP + H_2O
Glutamate
+ ADP + P_i
CTP synthetase

UTP

CTP

Figure 23-7 | The synthesis of CTP from UTP.

C | Pyrimidine Nucleotide Biosynthesis Is Regulated at ATCase or Carbamoyl Phosphate Synthetase II

In bacteria, the pyrimidine biosynthetic pathway is primarily regulated at Reaction 2, the ATCase reaction (Fig. 23-8*a*). In *E. coli,* control is exerted through the allosteric stimulation of ATCase by ATP and its inhibition by CTP (Section 12-3). In many bacteria, however, UTP is the major ATCase inhibitor.

In animals, ATCase is not a regulatory enzyme. Rather, pyrimidine biosynthesis is controlled by the activity of carbamoyl phosphate

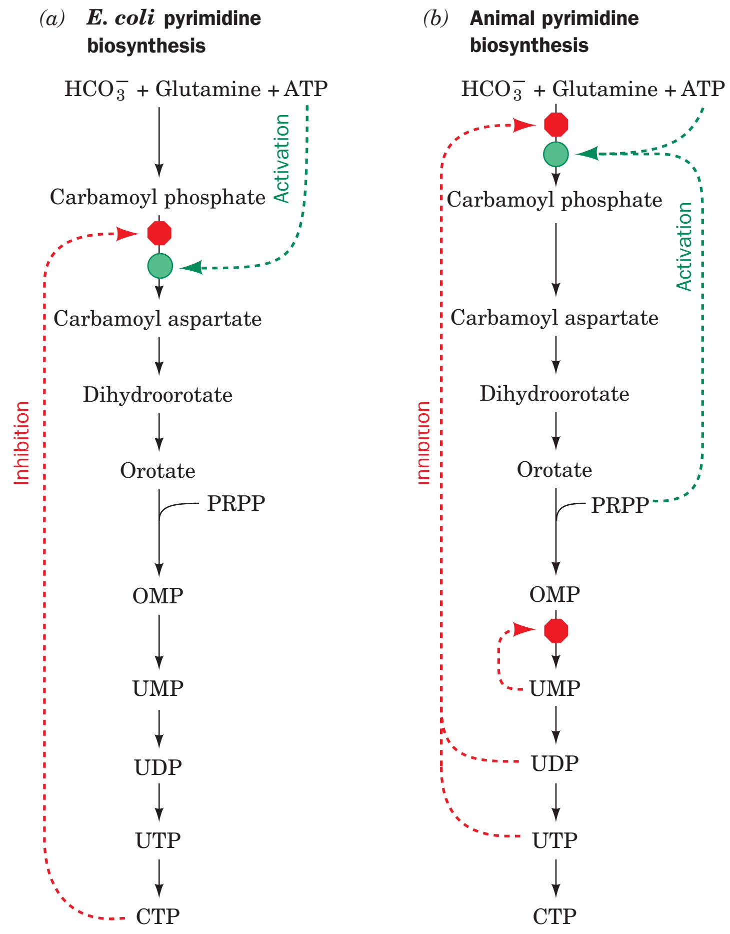
(*a*) ***E. coli*** **pyrimidine biosynthesis**

(*b*) **Animal pyrimidine biosynthesis**

HCO_3^- + Glutamine + ATP
Activation
Carbamoyl phosphate
Carbamoyl aspartate
Dihydroorotate
Orotate
PRPP
OMP
UMP
UDP
UTP
CTP
Inhibition
HCO_3^- + Glutamine + ATP
Carbamoyl phosphate
Activation
Carbamoyl aspartate
Dihydroorotate
Orotate
PRPP
OMP
UMP
UDP
UTP
CTP
Inhibition

Figure 23-8 | Regulation of pyrimidine biosynthesis. The control networks are shown for (*a*) *E. coli* and (*b*) animals. Red octagons and green circles indicate control points. Feedback inhibition is represented by dashed red arrows, and activation is indicated by dashed green arrows. **See the Animated Figures.**

synthetase II, which is inhibited by UDP and UTP and activated by ATP and PRPP (Fig. 23-8*b*). A second level of control in the mammalian pathway occurs at OMP decarboxylase, for which UMP and to a lesser extent CMP are competitive inhibitors. In all organisms, the rate of OMP production varies with the availability of its precursor, PRPP. Recall that the PRPP level depends on the activity of ribose phosphate pyrophosphokinase (Fig. 23-1, Reaction 1), which is inhibited by ADP and GDP (Section 23-1C).

Orotic Aciduria Results from an Inherited Enzyme Deficiency. **Orotic aciduria,** an inherited human disease, is characterized by the urinary excretion of large amounts of orotic acid, retarded growth, and severe anemia. It results from a deficiency in the bifunctional enzyme catalyzing Reactions 5 and 6 of pyrimidine nucleotide biosynthesis. Consideration of the biochemistry of this situation led to its effective treatment: the administration of uridine and/or cytidine. The UMP formed through the phosphorylation of the nucleosides, besides replacing that normally synthesized, inhibits carbamoyl phosphate synthetase II so as to attenuate the rate of orotic acid synthesis. No other genetic deficiency in pyrimidine nucleotide biosynthesis is known in humans, presumably because such defects are lethal *in utero*.

■ CHECK YOUR UNDERSTANDING

Compare the pathways of purine and pyrimidine nucleotide synthesis with respect to (a) precursors, (b) energy cost, (c) acquisition of the ribose moiety, and (d) number of enzymatic steps.

How are CTP and UTP derived from UMP?

How does regulation of pyrimidine synthesis differ in bacteria and animals?

3 Formation of Deoxyribonucleotides

LEARNING OBJECTIVES

- Understand that ribonucleotide reductase uses a free radical mechanism to convert ribonucleotides to deoxyribonucleotides.
- Understand that thymidylate synthase transfers a methyl group to dUMP to form thymine.

DNA differs chemically from RNA in two major respects: (1) Its nucleotides contain 2′-deoxyribose residues rather than ribose residues, and (2) it contains the base thymine (5-methyluracil) rather than uracil. In this section, we consider the biosynthesis of these DNA components.

A | Ribonucleotide Reductase Converts Ribonucleotides to Deoxyribonucleotides

Deoxyribonucleotides are synthesized from their corresponding ribonucleotides by the reduction of their C2′ position rather than by their de novo synthesis from deoxyribose-containing precursors.

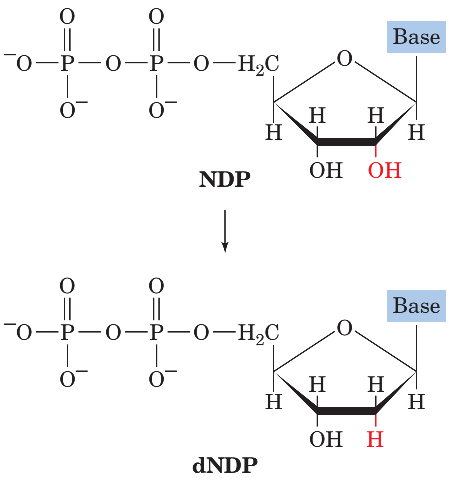

Enzymes that catalyze the formation of deoxyribonucleotides by the reduction of the corresponding ribonucleotides are named **ribonucleotide reductases (RNRs).** There are three classes of RNRs, which differ in their prosthetic groups, although they all replace the 2′-OH group of ribose with

H via a free-radical mechanism. We shall discuss the mechanism of the so-called Class I RNRs, which contain an Fe prosthetic group and which occur in most eukaryotes and aerobic prokaryotes.

Class I RNRs reduce ribonucleoside diphosphates (NDPs) to the corresponding deoxyribonucleoside diphosphates (dNDPs). *E. coli* ribonucleotide reductase, as Peter Reichard demonstrated, is mainly present *in vitro* as a heterotetramer that can be decomposed to two catalytically inactive homodimers, $R1_2$ and $R2_2$ (Fig. 23-9*a*). Each R1 subunit contains a substrate-binding site that includes several redox-active thiol groups. The R1 subunits also contain three effector-binding sites that control the enzyme's catalytic activity as well as its substrate specificity (see below).

The X-ray structure of $R2_2$ (Fig. 23-9*b*), which was determined by Hans Eklund, reveals that the subunits are bundles of eight unusually long helices. Each subunit contains a novel binuclear Fe(III) prosthetic group whose Fe(III) ions are liganded by a variety of groups including an O^{2-} ion (Fig. 23-9*c*). The Fe(III) complex interacts with Tyr 122 to form an

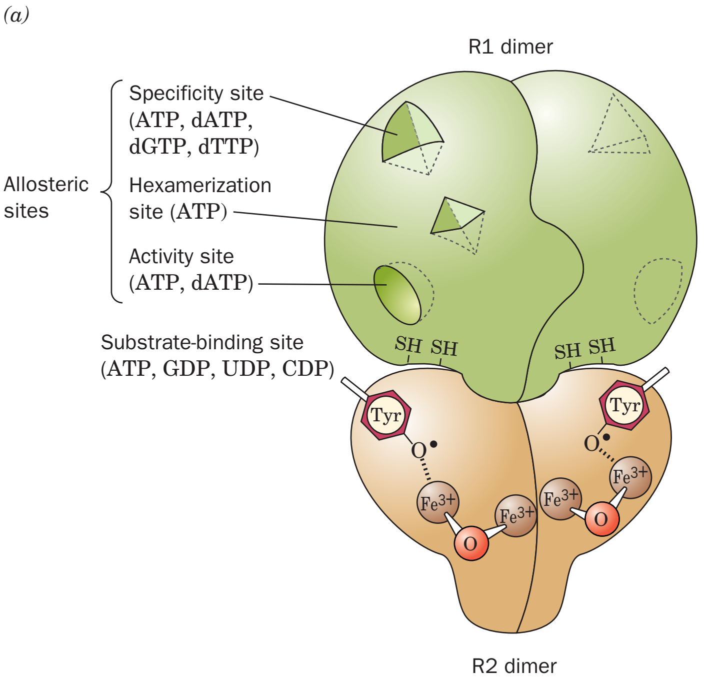
(a)
R1 dimer
Allosteric sites
Specificity site (ATP, dATP, dGTP, dTTP)
Hexamerization site (ATP)
Activity site (ATP, dATP)
Substrate-binding site (ATP, GDP, UDP, CDP)
SH SH
SH SH
Tyr
Tyr
O•
O•
Fe3+
Fe3+
Fe3+
Fe3+
O
O
R2 dimer

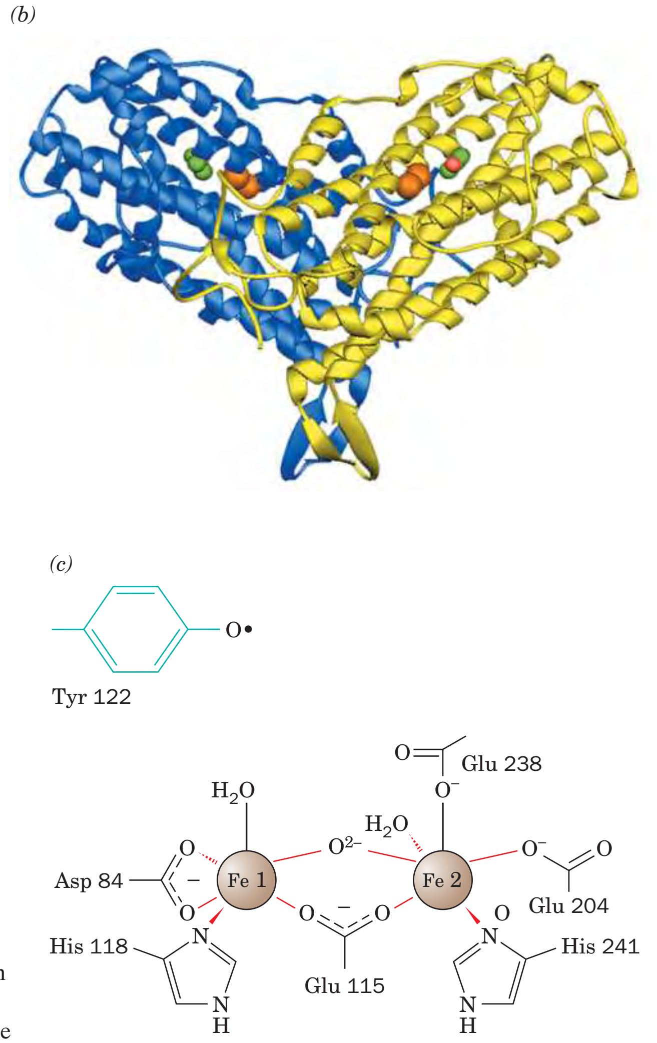
(b)
(c)
O•
Tyr 122
O
Glu 238
O⁻
H2O
H2O
O2–
O
Asp 84
Fe 1
Fe 2
O⁻
O
Glu 204
O
O
O
O
His 118
N
N
H
Glu 115
N
N
H
His 241

■ **Figure 23-9** | **Class I ribonucleotide reductase from *E. coli.*** (*a*) Schematic diagram of the quaternary structure. The enzyme consists of two identical pairs of subunits, $R1_2$ and $R2_2$. Each R2 subunit contains a binuclear Fe(III) complex that generates a phenoxy radical at Tyr 122. The R1 subunits each contain three different allosteric effector sites and five catalytically important Cys residues. The enzyme's two active sites occur at the interface between the R1 and R2 subunits. (*b*) A ribbon diagram of $R2_2$ viewed perpendicularly to its twofold axis with the subunits drawn in blue and yellow. The Fe(III) ions are represented by orange spheres, and the radical-harboring Tyr 122 side chains are shown in space-filling representation with their C and O atoms green and red. (*c*) The binuclear Fe(III) complex of R2. Each Fe(III) ion is octahedrally coordinated by a His N atom and five O atoms, including those of the O^{2-} ion and the Glu carboxyl group that bridges the two Fe(III) ions. [Part *b* based on an X-ray structure by Hans Eklund, Swedish University of Agricultural Sciences, Uppsala, Sweden. PDBid 1RIB.] **See Interactive Exercise 33.**

unusual tyrosyl free radical. Tyrosine radicals also take part in the reactions catalyzed by cytochrome *c* oxidase (Section 18-2F) and plant Photosystem II (Section 19-2C).

JoAnne Stubbe has proposed the following catalytic mechanism for *E. coli* ribonucleotide reductase (Fig. 23-10):

1. Ribonucleotide reductase's free radical (X·) abstracts an H atom from C3′ of the substrate in the reaction's rate-determining step.

2 and 3. Acid-catalyzed cleavage of the C2′—OH bond releases H_2O to yield a radical–cation intermediate. The C3′-OH group's unshared electron pair stabilizes the C2′ cation. This accounts for the radical's catalytic role.

4. The radical–cation intermediate is reduced by the enzyme's redox-active sulfhydryl pair to yield a 3′-deoxynucleotide radical and a protein disulfide group (this group must eventually be reduced to regenerate the enzyme's activity).

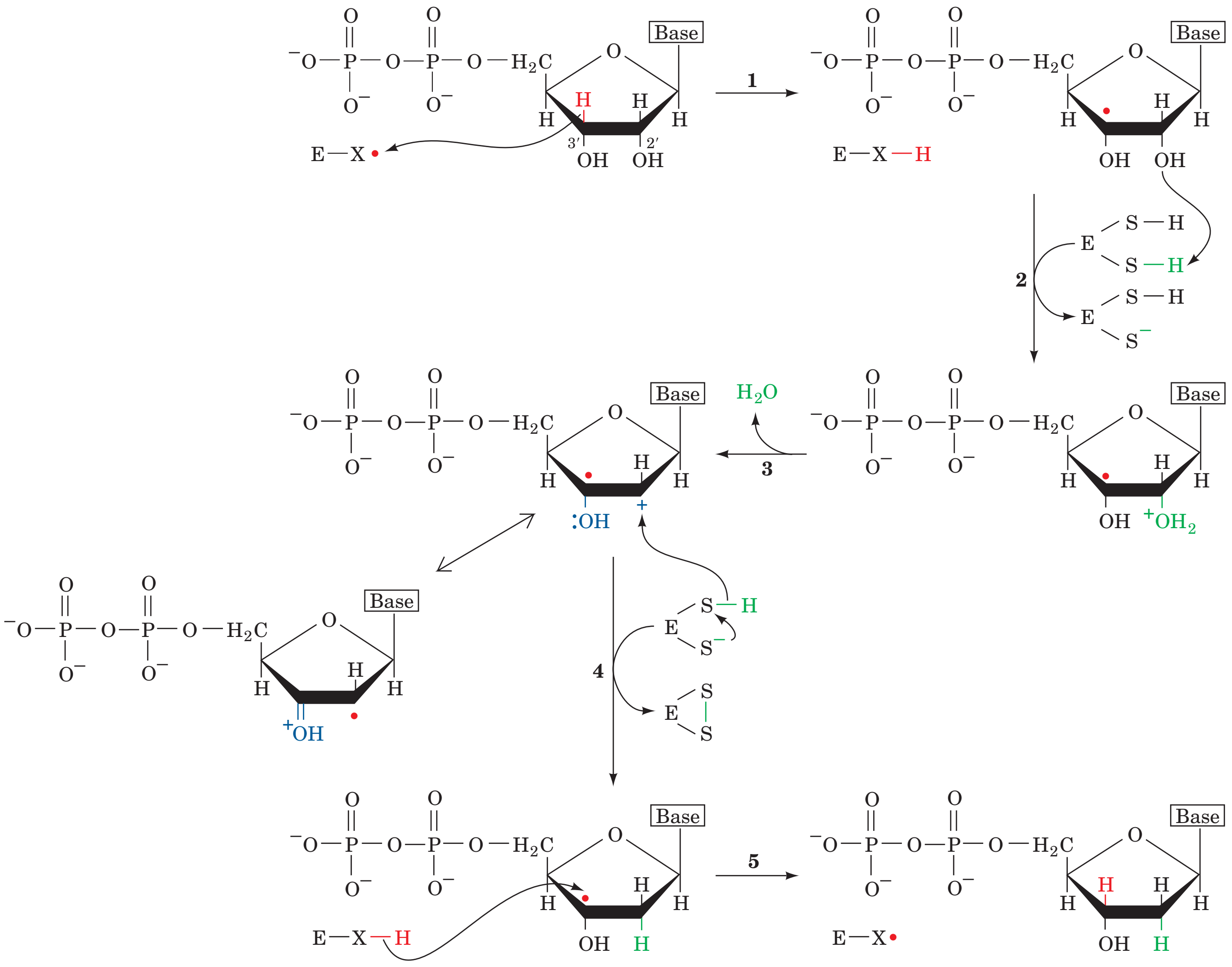

■ Figure 23-10 | Enzymatic mechanism of ribonucleotide reductase. The reaction occurs via a free radical–mediated process in which reducing equivalents are supplied by the formation of an enzyme disulfide bond. [After Stubbe, J.A., *J. Biol. Chem.* **265,** 5330 (1990).]

5. The 3′ radical abstracts an H atom from the protein to yield the product deoxynucleoside diphosphate and restore the enzyme to its radical state.

The Tyr 122 radical in R2 is buried 10 Å beneath the surface of the protein, too far for the enzyme's catalytic site to abstract an electron directly from the substrate. Evidently, the protein mediates electron transfer from this tyrosyl radical to another group that is closer to the substrate, probably the thiyl radical (—S·) form of Cys 439 in R1 (represented as X· in Fig. 23-10). Two other R1 Cys residues probably form the redox-active sulfhydryl pair that directly reduces the substrate. The resulting disulfide bond is reduced via disulfide interchange with yet two other Cys residues, which are positioned to accept electrons from external reducing agents to regenerate the active enzyme. Thus, each R1 subunit contains at least five Cys residues that chemically participate in nucleotide reduction.

The Inability of Oxidized Ribonucleotide Reductase to Bind Substrate Serves an Essential Protective Function. Comparison of the X-ray structures of reduced R1 (in which the redox-active Cys 225 and Cys 462 residues are in their SH forms) and oxidized R1 (in which Cys 225 and Cys 462 are disulfide-linked) reveals that Cys 462 in reduced R1 has rotated away from its position in oxidized R1 to become buried in a hydrophobic pocket, whereas Cys 225 moves into the region formerly occupied by Cys 462. The distance between the formerly disulfide-linked S atoms thereby increases from 2.0 Å to 5.7 Å. These movements are accompanied by small shifts of the surrounding polypeptide chain. R1 Cys 225 in oxidized ribonucleotide reductase prevents the binding of substrate through steric interference of its S atom with the substrate NDP's O2′ atom.

The inability of oxidized ribonucleotide reductase to bind substrate has functional significance. In the absence of substrate, the enzyme's free radical is stored in the interior of the R2 subunit, close to its dinuclear iron center. When substrate is bound, the radical is presumably transferred to it via a series of protein side chains in both R2 and R1. If the substrate is unable to properly react after accepting this free radical, as would be the case if the enzyme were in its oxidized state, the free radical could potentially destroy both the substrate and the enzyme. Thus, *an important role of the enzyme is to control the release of the radical's powerful oxidizing capability. It does so in part by preventing the binding of substrate while the enzyme is in its oxidized form.*

Thioredoxin Reduces Ribonucleotide Reductase. *The final step in the ribonucleotide reductase catalytic cycle is reduction of the enzyme's newly formed disulfide bond to re-form its redox-active sulfhydryl pair.* One of the enzyme's physiological reducing agents is **thioredoxin,** a ubiquitous monomeric protein with a pair of neighboring Cys residues (and which also participates in regulating the Calvin cycle; Section 19-3C). Thioredoxin reduces oxidized ribonucleotide reductase via disulfide interchange.

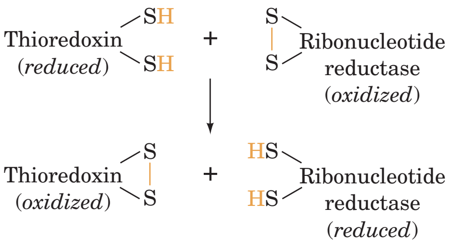

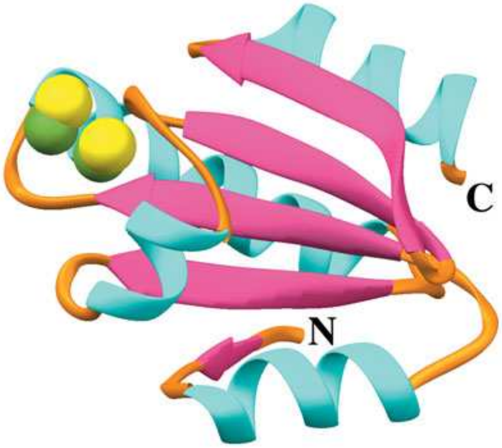

Figure 23-11 | **X-Ray structure of human thioredoxin in its reduced (sulfhydryl) state.** The backbone of the 105-residue monomer is colored according to secondary structure with helices cyan, sheets magenta, and the remaining portions orange. The side chains of the redox-active Cys residues are shown in space-filling form with C green and S yellow. [Based on an X-ray structure by William Montfort, University of Arizona. PDBid 1ERT.]

The X-ray structure of thioredoxin (Fig. 23-11) reveals that its redox-active disulfide group is located on a molecular protrusion, making the protein the only known example of a "male" enzyme.

Oxidized thioredoxin is, in turn, reduced in a reaction mediated by **thioredoxin reductase,** which contains redox-active thiol groups and an FAD prosthetic group. This enzyme is a homolog of glutathione reductase (Box 15-4) and lipoamide dehydrogenase (Section 17-2B) and catalyzes a similar reaction: the NADPH-mediated reduction of a substrate disulfide bond. NADPH therefore serves as the terminal reducing agent in the ribonucleotide reductase–catalyzed reduction of NDPs to dNDPs (Fig. 23-12).

Ribonucleotide Reductase Is Regulated by a Complex Feedback Network. The synthesis of the four dNTPs in the amounts required for DNA synthesis is accomplished through feedback control. Maintaining the proper intracellular ratios of dNTPs is essential for normal growth. Indeed, *a deficiency of any dNTP is lethal, whereas an excess is mutagenic because the probability that a given dNTP will be erroneously incorporated into a growing DNA strand increases with its concentration relative to those of the other dNTPs.*

The activities of both *E. coli* and mammalian ribonucleotide reductases are remarkably responsive to the levels of nucleotides in the cell.

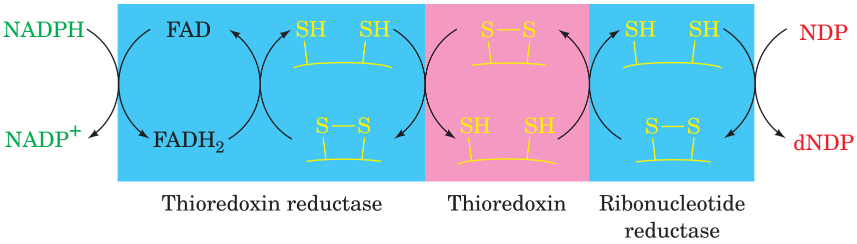

Figure 23-12 | **An electron-transfer pathway for nucleoside diphosphate (NDP) reduction.** NADPH provides the reducing equivalents for the process through the intermediacy of thioredoxin reductase, thioredoxin, and ribonucleotide reductase.

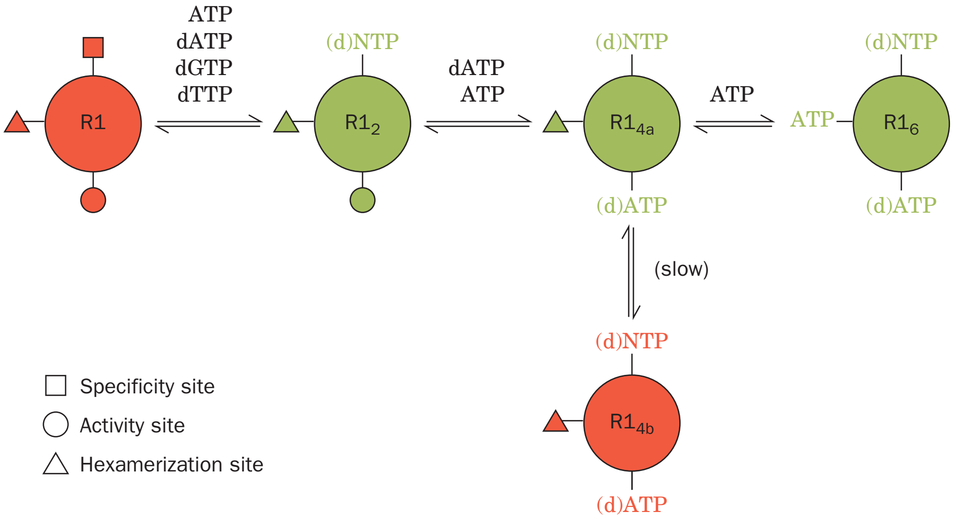

Figure 23-13 | Regulation of ribonucleotide reductase. Allosteric regulators alter the state of oligomerization. States shown in green have high activity, and states shown in red have little or no activity. R2 has been omitted for simplicity. [After Kashlan, O.B., Scott, C.P., Lear, J.D., and Cooperman, B.S., *Biochemistry* **41,** 461 (2002).]

For example, ATP induces the reduction of CDP and UDP; dTTP induces the reduction of GDP and inhibits the reduction of CDP and UDP; and dATP inhibits the reduction of all NDPs. Barry Cooperman has shown that the catalytic activity of mouse ribonucleotide reductase varies with its state of oligomerization, which in turn is governed by the binding of nucleotide effectors to three independent allosteric sites on R1 (Fig. 23-9*a*): (1) the specificity site, which binds ATP, dATP, dGTP, and dTTP; (2) the activity site, which binds ATP and dATP; and (3) the hexamerization site, which binds only ATP. Cooperman's model for the allosteric regulation of Class I ribonucleotide reductase, which quantitatively accounts for the enzyme's regulatory properties, has the following features (Fig. 23-13):

1. The binding of ATP, dATP, dGTP, or dTTP to the specificity site induces the catalytically inactive R1 monomers to form a catalytically active dimer, $R1_2$.
2. The binding of dATP or ATP to the activity site causes the dimers to form tetramers, $R1_{4a}$, that slowly but reversibly change conformation to a catalytically inactive state, $R1_{4b}$.
3. The binding of ATP to the hexamerization site induces the tetramers to further aggregate to form catalytically active hexamers, $R1_6$, the enzyme's major active form.

The concentration of ATP in a cell is such that, *in vivo,* R1 is almost entirely in its tetrameric or hexameric forms. As a consequence, ATP couples the overall rate of DNA synthesis to the cell's energy state.

dNTPs Are Produced by Phosphorylation of dNDPs. *The final step in the production of all dNTPs is the phosphorylation of the corresponding dNDPs:*

$$\text{dNDP} + \text{ATP} \rightleftharpoons \text{dNTP} + \text{ADP}$$

This reaction is catalyzed by nucleoside diphosphate kinase, the same enzyme that phosphorylates NDPs (Section 23-1B). As before, the reaction is written with ATP as the phosphoryl donor, although any NTP or dNTP can function in that capacity.

B | dUMP Is Methylated to Form Thymine

The dTMP component of DNA is synthesized by methylation of dUMP. The dUMP is generated through the hydrolysis of dUTP by **dUTP diphosphohydrolase (dUTPase):**

$$\text{dUTP} + H_2O \rightarrow \text{dUMP} + \text{PP}_i$$

dTMP, once it is formed, is phosphorylated to form dTTP. The apparent reason for the energetically wasteful process of dephosphorylating dUTP and rephosphorylating dTMP is that cells must minimize their concentration of dUTP in order to prevent incorporation of uracil into their DNA (the enzyme system that synthesizes DNA from dNTPs does not efficiently discriminate between dUTP and dTTP; Section 25-2A).

Human dUTPase is a homotrimer of 141-residue subunits. Its X-ray structure, determined by John Tainer, reveals the basis for the enzyme's exquisite specificity for dUTP. Each subunit binds dUTP in a snug-fitting cavity that sterically excludes thymine's C5 methyl group via the side chains of conserved residues (Fig. 23-14*a*). The enzyme differentiates uracil from the similarly shaped cytosine via a set of hydrogen bonds that in part mimic adenine's base pairing interactions (Fig. 23-14*b*). The 2′-OH group of ribose is likewise sterically excluded by the side chain of a conserved Tyr.

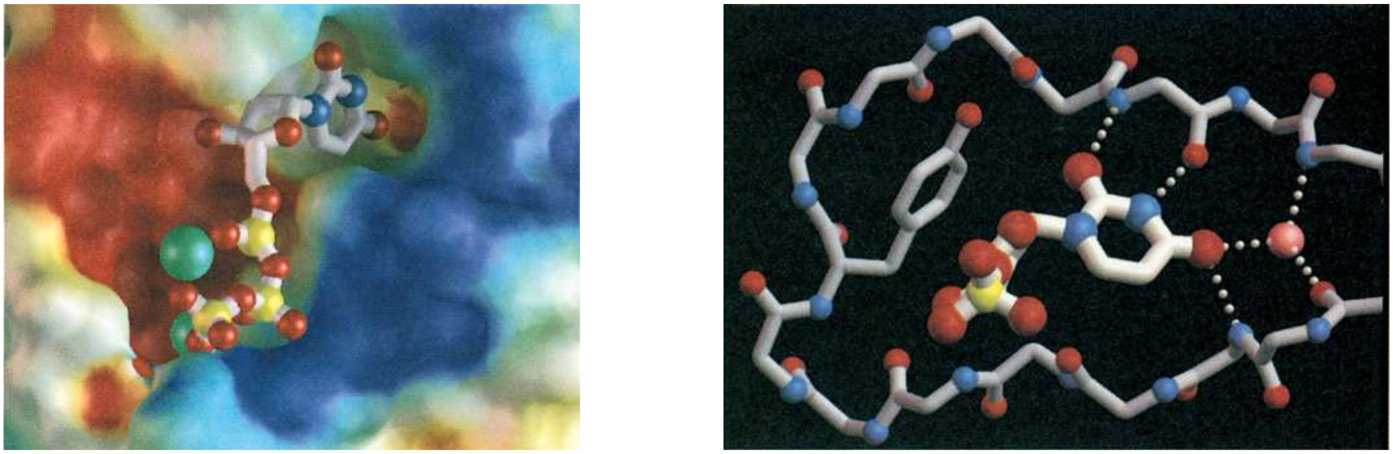

Figure 23-14 | X-Ray structure of human dUTPase. (*a*) The active site region of dUTPase in complex with dUTP. The protein is represented by its molecular surface colored according to its electrostatic potential (negative, red; positive, blue; and near neutral, white). The dUTP is shown in ball-and-stick form with its N, O, and P atoms blue, red, and yellow. Mg^{2+} ions that have been modeled into the structure are represented by green spheres. Note the complementary fit of the uracil ring into its binding pocket, particularly the close contacts that discriminate against a methyl group on C5 of the pyrimidine ring and a 2′-OH group on the ribose ring. (*b*) The binding site of dUMP, showing the hydrogen bonding system responsible for the enzyme's specific binding of a uracil ring. The dUMP and the polypeptide backbone binding it are shown in ball-and-stick form with atoms colored as in Part *a;* hydrogen bonds are indicated by white dotted lines; and a conserved water molecule is represented by a pink sphere. The side chain of a conserved Tyr is tightly packed against the ribose ring so as to discriminate against the presence of a 2′-OH group. [Courtesy of John Tainer and Clifford Mol, The Scripps Research Institute, La Jolla, California.]

Thymidylate Synthase. Thymidylate (dTMP) is synthesized from dUMP by **thymidylate synthase** with N^5,N^{10}-methylenetetrahydrofolate (N^5,N^{10}-methylene-THF) as the methyl donor:

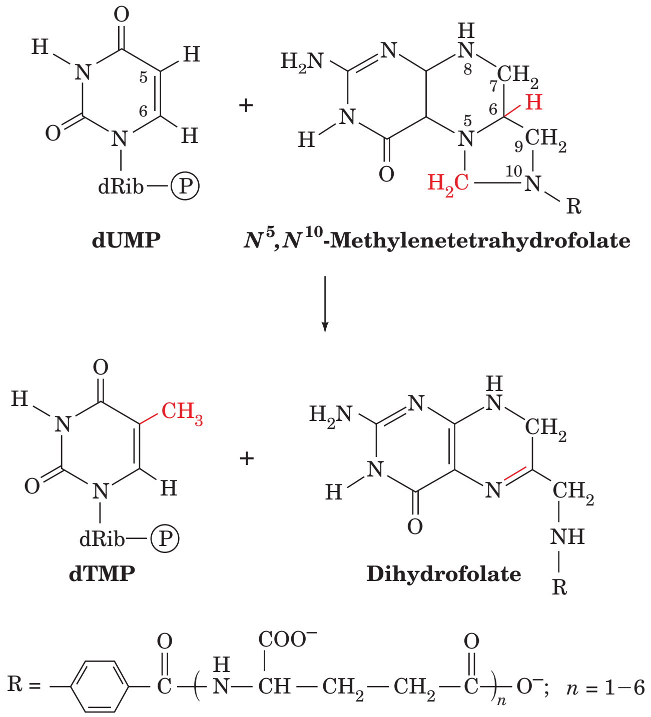

Note that the transferred methylene group (in which the carbon has the oxidation state of formaldehyde) is reduced to a methyl group (which has the oxidation state of methanol) at the expense of the oxidation of the THF cofactor to **dihydrofolate (DHF).**

Thymidylate synthase, a highly conserved 65-kD homodimeric protein, follows a mechanistic scheme proposed by Daniel Santi (Fig. 23-15):

1. An enzyme nucleophile, identified as the thiolate group of Cys 146, attacks C6 of dUMP to form a covalent adduct.
2. C5 of the resulting enolate ion attacks the CH_2 group of the iminium cation in equilibrium with N^5,N^{10}-methylene-THF to form an enzyme–dUMP–THF ternary covalent complex.
3. An enzyme base abstracts the acidic proton at the C5 position of the enzyme-bound dUMP, forming an exocyclic methylene group and eliminating the THF cofactor. The abstracted proton subsequently exchanges with solvent.
4. The redox change occurs via the migration of the C6-H atom of THF as a hydride ion to the exocyclic methylene group, converting it to a methyl group and yielding DHF. This reduction promotes the displacement of the Cys thiolate group from the intermediate to release product, dTMP, and re-form the active enzyme.

Tetrahydrofolate Is Regenerated in Two Reactions. *The thymidylate synthase reaction is biochemically unique in that it oxidizes THF to DHF; no other enzymatic reaction employing a THF cofactor alters this coenzyme's net oxidation state.* The DHF product of the thymidylate

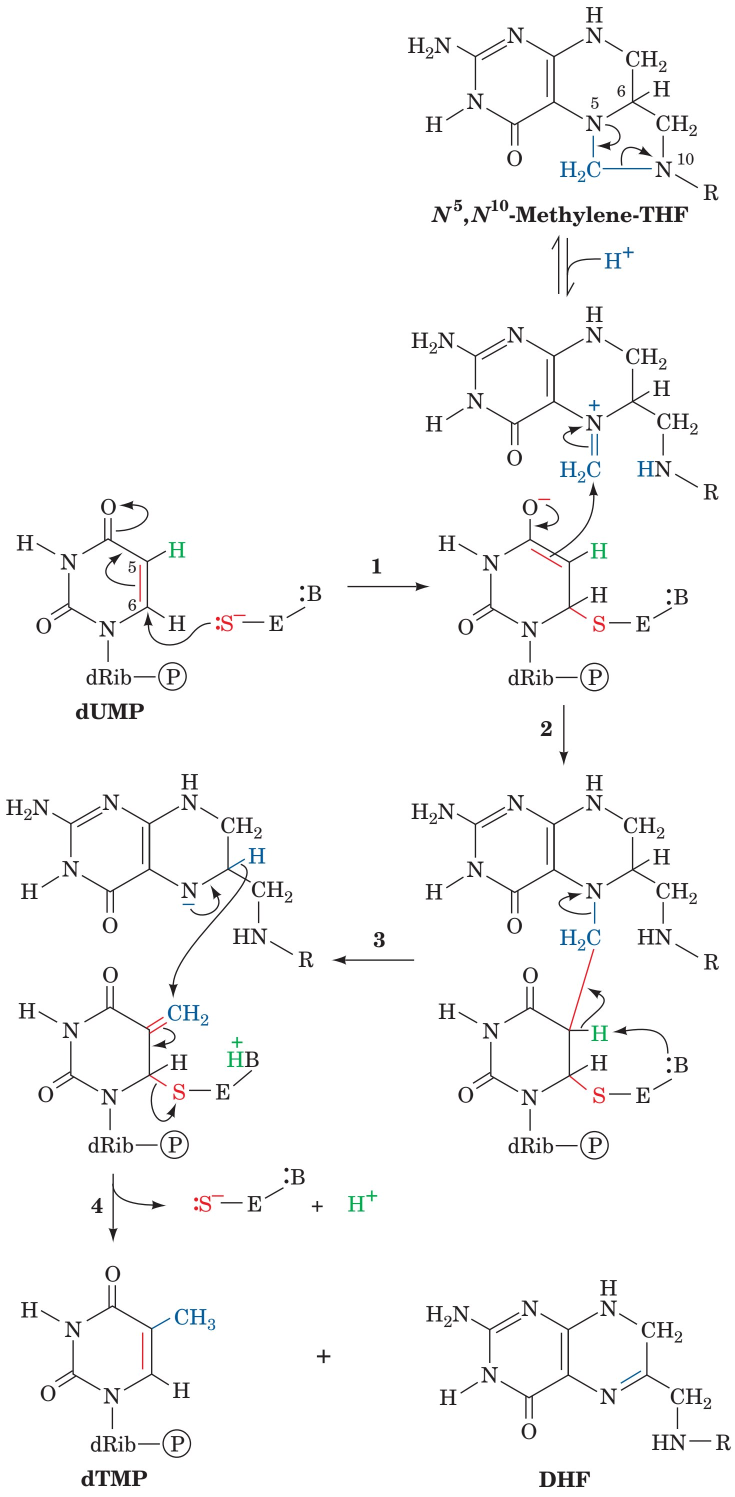

Figure 23-15 | Catalytic mechanism of thymidylate synthase. The methyl group is supplied by N^5,N^{10}-methylene-THF, which is concomitantly oxidized to dihydrofolate.

synthase reaction is recycled back to N^5,N^{10}-methylene-THF through two sequential reactions (Fig. 23-16):

1. DHF is reduced to THF by NADPH as catalyzed by **dihydrofolate reductase** (**DHFR;** Fig. 23-17). Although in most organisms DHFR is a monomeric, monofunctional enzyme, in protozoa and some

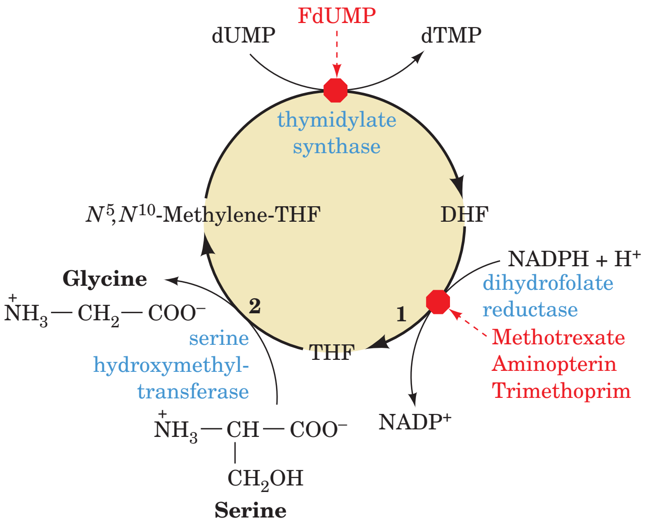
FdUMP
dUMP
dTMP
thymidylate synthase
N^5,N^{10}-Methylene-THF
DHF
NADPH + H$^+$
dihydrofolate reductase
Glycine
$\overset{+}{N}H_3—CH_2—COO^-$
2
1
serine hydroxymethyl-transferase
THF
Methotrexate
Aminopterin
Trimethoprim
$\overset{+}{N}H_3—CH—COO^-$
CH_2OH
NADP$^+$
Serine

■ **Figure 23-16 | Regeneration of N^5,N^{10}-methylenetetrahydrofolate.** The DHF product of the thymidylate synthase reaction is converted back to N^5,N^{10}-methylene-THF by the sequential actions of **(1)** dihydrofolate reductase and **(2)** serine hydroxymethyltransferase. The sites of action of some inhibitors are indicated by red octagons. Thymidylate synthase is inhibited by FdUMP, whereas dihydrofolate reductase is inhibited by the antifolates methotrexate, aminopterin, and trimethoprim (Box 23-1).

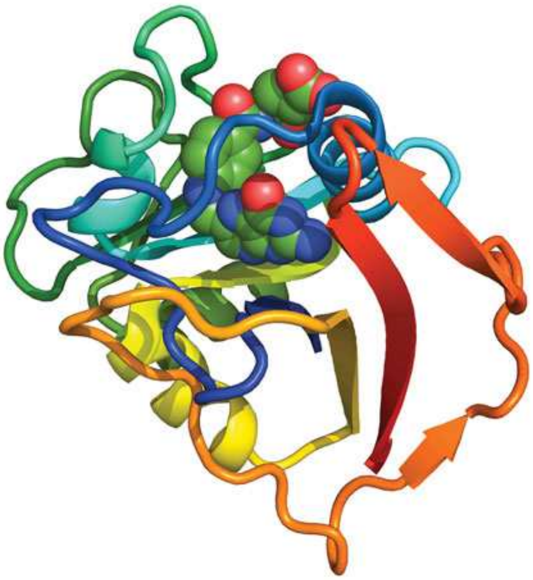

■ **Figure 23-17 | X-Ray structure of human dihydrofolate reductase in complex with folic acid.** The polypeptide is colored in rainbow order from its N-terminus (*blue*) to its C-terminus (*red*). The folic acid is drawn in space-filling form with C green, N blue, and O red. [Based on an X-ray structure by Joseph Kraut, University of California at San Diego. PDBid 1DHF.] **See Interactive Exercise 34.**

plants DHFR and thymidylate synthase occur on the same polypeptide chain to form a bifunctional enzyme that has been shown to channel DHF from its thymidylate synthase to its DHFR active sites.

2. Serine hydroxymethyltransferase (Section 21-4A) transfers the hydroxymethyl group of serine to THF yielding N^5,N^{10}-methylene-THF and glycine.

Inhibition of thymidylate synthase or DHFR blocks dTMP synthesis and is therefore the basis of cancer chemotherapies (Box 23-1).

■ CHECK YOUR UNDERSTANDING

Describe the production of dNTPs from their corresponding NDPs.

Describe the roles of dUTPase, thymidylate synthase, and dihydrofolate reductase in the synthesis of dTMP.

BOX 23-1 **BIOCHEMISTRY IN HEALTH AND DISEASE**

Inhibition of Thymidylate Synthesis in Cancer Therapy

dTMP synthesis is a critical process for rapidly proliferating cells, such as cancer cells, which require a steady supply of dTMP for DNA synthesis. Interruption of dTMP synthesis can therefore kill those cells. Most normal mammalian cells, which grow slowly if at all, require less dTMP and so are less sensitive to agents that inhibit thymidylate synthase or dihydrofolate reductase (notable exceptions are the bone marrow cells that constitute the blood-forming tissue and much of the immune system, the intestinal mucosa, and hair follicles).

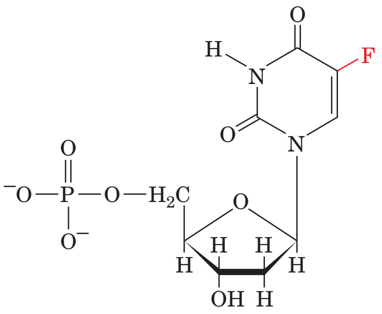

5-Fluorodeoxyuridylate (FdUMP)

5-Fluorodeoxyuridylate (FdUMP) is an irreversible inhibitor of thymidylate synthase. This substance, like dUMP, binds to the enzyme (an F atom is not much larger than an H atom) and undergoes the first two steps of the normal enzymatic reaction (Fig. 23-15). In Step 3, however, the enzyme cannot abstract the F atom as F$^+$ (F is the most electronegative element) so that the enzyme is frozen in an enzyme–FdUMP–THF ternary covalent complex.

The X-ray structure of the covalent thymidylate synthase–FdUMP–THF ternary complex has been determined. The enzyme's active site region is shown (*lower left*) with the polypeptide chain colored in rainbow order from its N-terminus (*blue*) to its C-terminus (*red*). The FdUMP, THF, and Cys 146 side chain are drawn in stick form colored according to atom type (FdUMP C cyan, THF and Cys C green, N blue, O red, F magenta, P orange, S yellow). The C5 and C6 atoms of FdUMP form covalent bonds with the CH$_2$ group substituent to N5 of THF and the S atom of Cys 146.

Enzyme inhibitors, such as FdUMP, that inactivate an enzyme only after undergoing part or all of the normal catalytic reaction are called **mechanism-based inhibitors** (alternatively, **suicide substrates** because they cause the enzyme to "commit suicide"). Because of their extremely high specificity, mechanism-based inhibitors are among the most useful therapeutic agents.

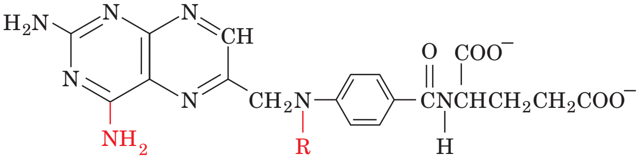

R = H **Aminopterin**
R = CH$_3$ **Methotrexate (amethopterin)**

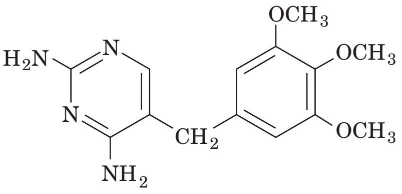

Trimethoprim

Inhibition of DHFR blocks dTMP synthesis as well as all other THF-dependent biological reactions, because the THF converted to DHF by the thymidylate synthase reaction cannot be regenerated. **Methotrexate (amethopterin), aminopterin,** and trimethoprim are DHF analogs that competitively although nearly irreversibly bind to DHFR with an ~1000-fold greater affinity than does DHF. These **antifolates** (substances that interfere with the action of folate cofactors) are effective anticancer agents, particularly against childhood leukemias. In fact, a successful chemotherapeutic strategy is to treat a cancer victim with a lethal dose of methotrexate and some hours later "rescue" the patient (but hopefully not the cancer) by administering massive doses of 5-formyl-THF and/or thymidine. Trimethoprim binds much more tightly to bacterial DHFRs than to those of mammals and is therefore a clinically useful antibacterial agent.

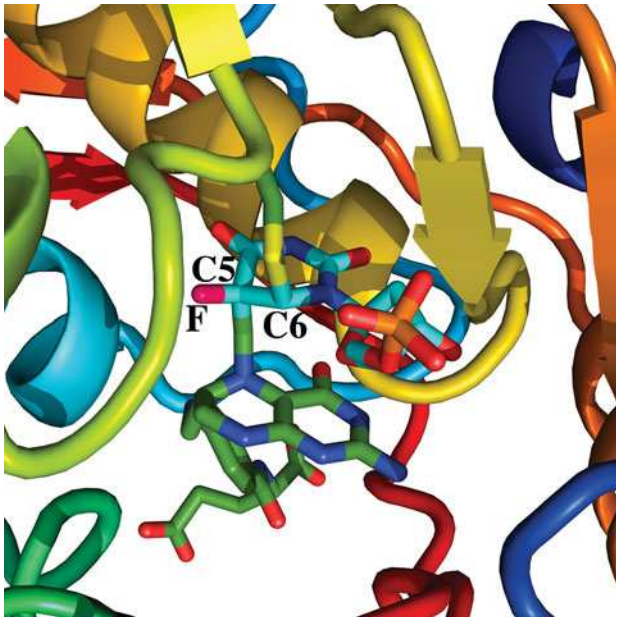

[Based on an X-ray structure by William Montfort, University of Arizona. PDBid 1TSN.]

4 Nucleotide Degradation

LEARNING OBJECTIVES

- Understand that purines are broken down to uric acid.
- Understand that uric acid may be further catabolized.
- Understand that pyrimidines are converted to CoA derivatives.

Most foodstuffs, being of cellular origin, contain nucleic acids. Dietary nucleic acids survive the acidic medium of the stomach; they are degraded to their component nucleotides, mainly in the intestine, by pancreatic nucleases and intestinal phosphodiesterases. The ionic nucleotides, which cannot pass through cell membranes, are then hydrolyzed to nucleosides by a variety of group-specific nucleotidases and nonspecific phosphatases. Nucleosides may be directly absorbed by the intestinal mucosa or further degraded to free bases and ribose or ribose-1-phosphate through the action of **nucleosidases** and **nucleoside phosphorylases:**

$$\text{Nucleoside} + \text{H}_2\text{O} \xrightarrow{\text{nucleosidase}} \text{base} + \text{ribose}$$

$$\text{Nucleoside} + \text{P}_i \xrightarrow[\text{}]{\substack{\text{nucleoside}\\ \text{phosphorylase}}} \text{base} + \text{ribose-1-P}$$

Radioactive labeling experiments have demonstrated that only a small fraction of the bases of ingested nucleic acids are incorporated into tissue nucleic acids. Evidently, *the de novo pathways of nucleotide biosynthesis largely satisfy an organism's need for nucleotides.* Consequently, ingested bases are mostly degraded and excreted. Cellular nucleic acids are also subject to degradation as part of the continual turnover of nearly all cellular components. In this section, we outline these catabolic pathways and discuss the consequences of several of their inherited defects. A summary of nucleotide metabolism is shown in Fig. 23-18.

A | Purine Catabolism Yields Uric Acid

The major pathways of purine nucleotide and deoxynucleotide catabolism in animals are diagrammed in Fig. 23-19. The pathways in other organisms differ somewhat, but all the pathways lead to uric acid. Of course, the pathway intermediates may be directed to purine nucleotide synthesis via

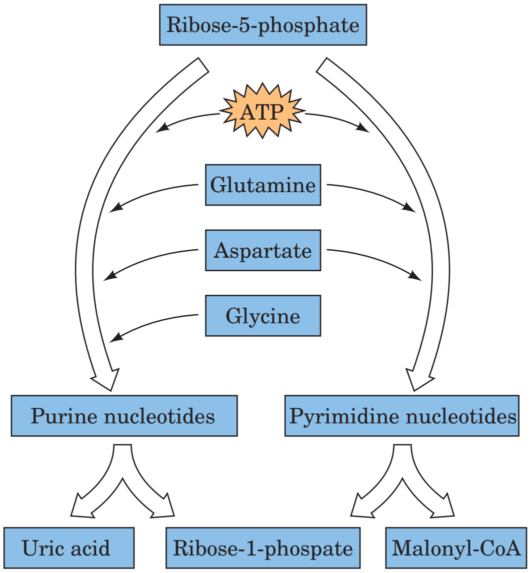

Figure 23-18 | Summary of nucleotide metabolism. Nucleotides are synthesized from amino acids and ribose-5-phosphate by pathways in which the base is built onto the sugar (purine synthesis) or the sugar is added to the base (pyrimidine synthesis). Nucleotide catabolism yields a derivative of the base and releases the sugar as ribose-1-phosphate.

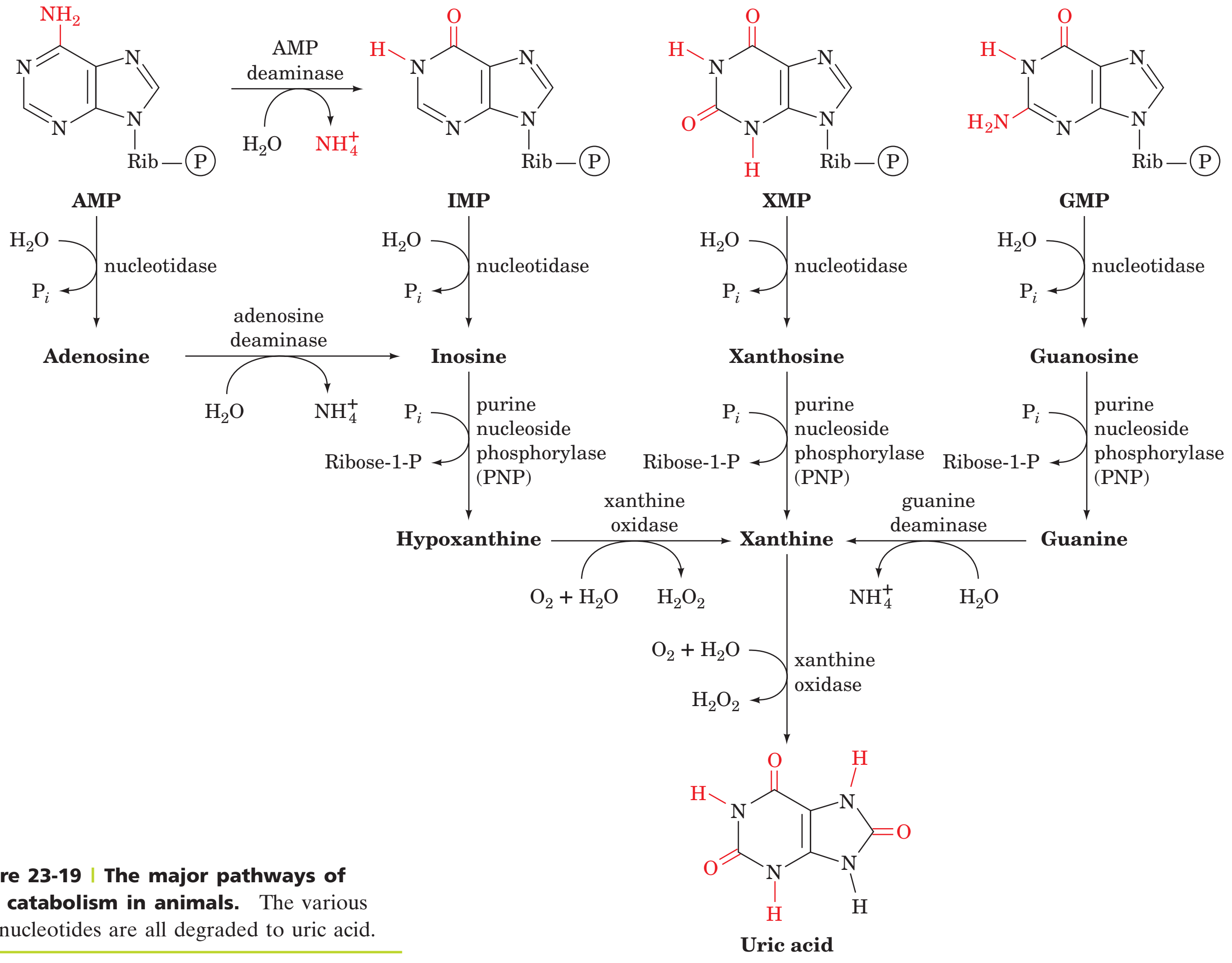
AMP
AMP deaminase
H2O
NH4+
IMP
XMP
GMP
Rib — P
H2O
Pi
nucleotidase
Adenosine
adenosine deaminase
Inosine
Xanthosine
Guanosine
purine nucleoside phosphorylase (PNP)
Ribose-1-P
Hypoxanthine
xanthine oxidase
O2 + H2O
H2O2
Xanthine
guanine deaminase
Guanine
Uric acid

Figure 23-19 | The major pathways of purine catabolism in animals. The various purine nucleotides are all degraded to uric acid.

salvage reactions. In addition, ribose-1-phosphate, a product of the reaction catalyzed by **purine nucleoside phosphorylase (PNP),** is a precursor of PRPP.

Adenosine and deoxyadenosine are not degraded by mammalian PNP. Rather, adenine nucleosides and nucleotides are deaminated by **adenosine deaminase (ADA)** and **AMP deaminase** to their corresponding inosine derivatives, which can then be further degraded.

ADA is an eight-stranded α/β barrel (Fig. 23-20) with its active site in a pocket at the C-terminal end of the β barrel, as in nearly all known α/β barrel enzymes. A catalytically essential zinc ion is bound in the deepest part of the active site pocket. Mutations that affect the active site of ADA selectively kill lymphocytes, causing **severe combined immunodeficiency**

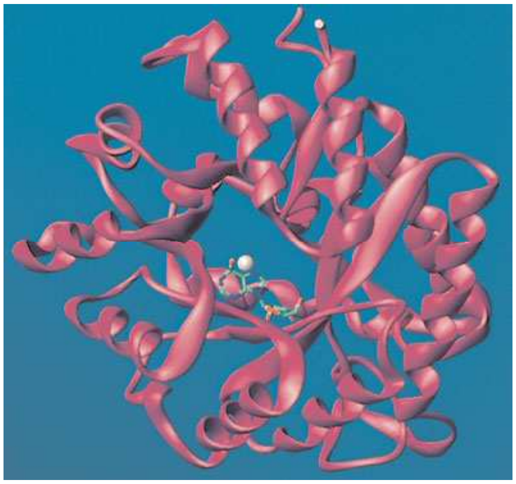

Figure 23-20 | X-Ray structure of murine adenosine deaminase. The enzyme is viewed approximately down the axis of its α/β barrel from the N-terminal ends of its β strands. A transition state analog, **6-hydroxyl-1,6-dihydropurine ribonucleoside (HDPR),** is shown in skeletal form with its C, N, and O atoms green, blue, and red. The enzyme-bound Zn^{2+} ion, which is coordinated by HDPR's 6-hydroxyl group, is represented by a silver sphere. [Based on an X-ray structure by Florante Quiocho, Baylor College of Medicine. PDBid 1ADA.] **See Interactive Exercise 35.**

disease (SCID). Without special protective measures, the disease is invariably fatal in infancy because of overwhelming infection.

Biochemical considerations provide a plausible explanation of SCID's etiology (causes). In the absence of active ADA, deoxyadenosine is phosphorylated to yield levels of dATP that are 50-fold greater than normal. This high concentration of dATP inhibits ribonucleotide reductase (Section 23-3A), thereby preventing the synthesis of the other dNTPs, choking off DNA synthesis and thus cell proliferation. The tissue-specific effect of ADA deficiency on the immune system can be explained by the observation that lymphoid tissue is particularly active in deoxyadenosine phosphorylation. ADA deficiency was one of the first genetic diseases to be successfully treated by gene therapy.

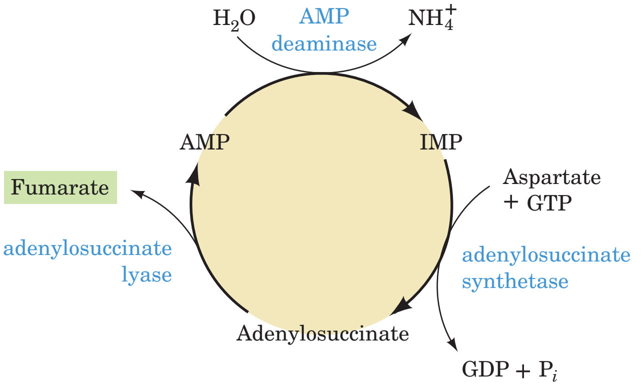

Net: H_2O + Aspartate + GTP $\longrightarrow$ NH_4^+ + GDP + P_i + fumarate

Figure 23-21 | **The purine nucleotide cycle.** This pathway functions in muscle to prime the citric acid cycle by generating fumarate.

The Purine Nucleotide Cycle Generates Fumarate. The deamination of AMP to IMP, when combined with the synthesis of AMP from IMP (Fig. 23-3, *left*), has the net effect of deaminating aspartate to yield fumarate (Fig. 23-21). John Lowenstein demonstrated that this **purine nucleotide cycle** has an important metabolic role in skeletal muscle. An increase in muscle activity requires an increase in the activity of the citric acid cycle. This process usually occurs through the generation of additional citric acid cycle intermediates (Section 17-5B). Muscles, however, lack most of the enzymes that catalyze these anaplerotic (filling up) reactions in other tissues. Instead, muscle replenishes its citric acid cycle intermediates with fumarate generated in the purine nucleotide cycle.

The importance of the purine nucleotide cycle in muscle metabolism is indicated by the observation that the activities of the three enzymes involved are all severalfold higher in muscle than in other tissues. In fact, individuals with an inherited deficiency in muscle AMP deaminase **(myoadenylate deaminase deficiency)** are easily fatigued and usually suffer from cramps after exercise.

Xanthine Oxidase Is a Mini-Electron-Transport System. **Xanthine oxidase (XO)** converts hypoxanthine (the base of IMP) to xanthine, and xanthine to uric acid (Fig. 23-19, *bottom*). The reaction product is an enol (which has a p*K* of 5.4; hence the name uric *acid*). The enol tautomerizes to the more stable keto form:

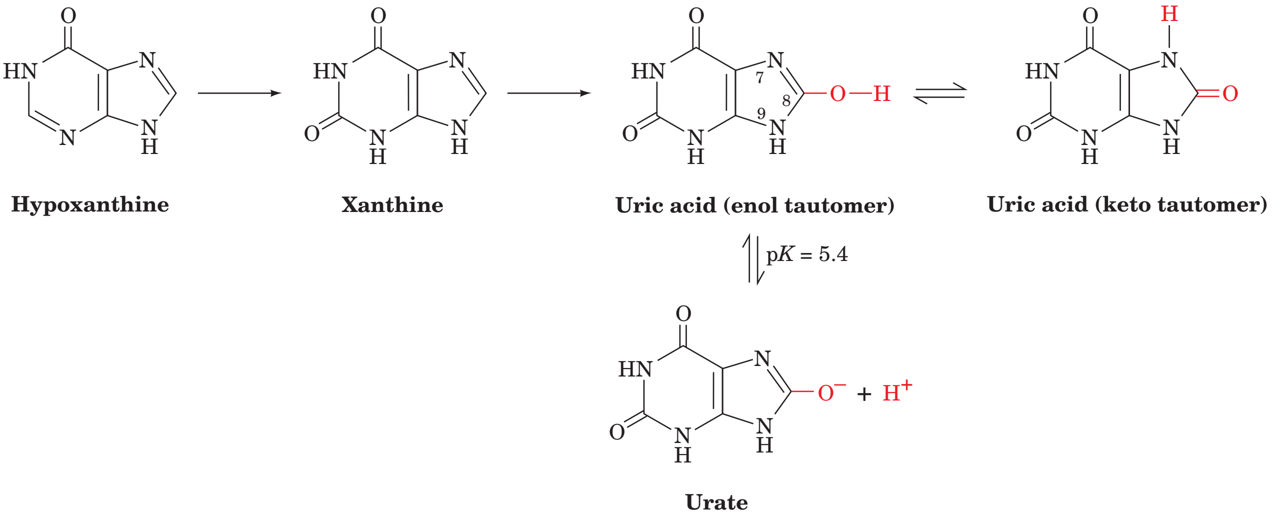

In mammals, xanthine oxidase occurs almost exclusively in the liver and the small intestinal mucosa. It is a dimeric protein of identical 130-kD subunits, each of which contains an entire "zoo" of electron-transfer agents: an FAD, a Mo complex that cycles between its Mo(VI) and Mo(IV) oxidation states, and two different Fe—S clusters. The final electron acceptor is O_2, which is converted to H_2O_2, a potentially harmful oxidizing agent (Section 18-4B) that is subsequently converted to H_2O and O_2 by catalase.

B | Some Animals Degrade Uric Acid

In humans and other primates, the final product of purine degradation is uric acid, which is excreted in the urine. The same is true in birds, terrestrial

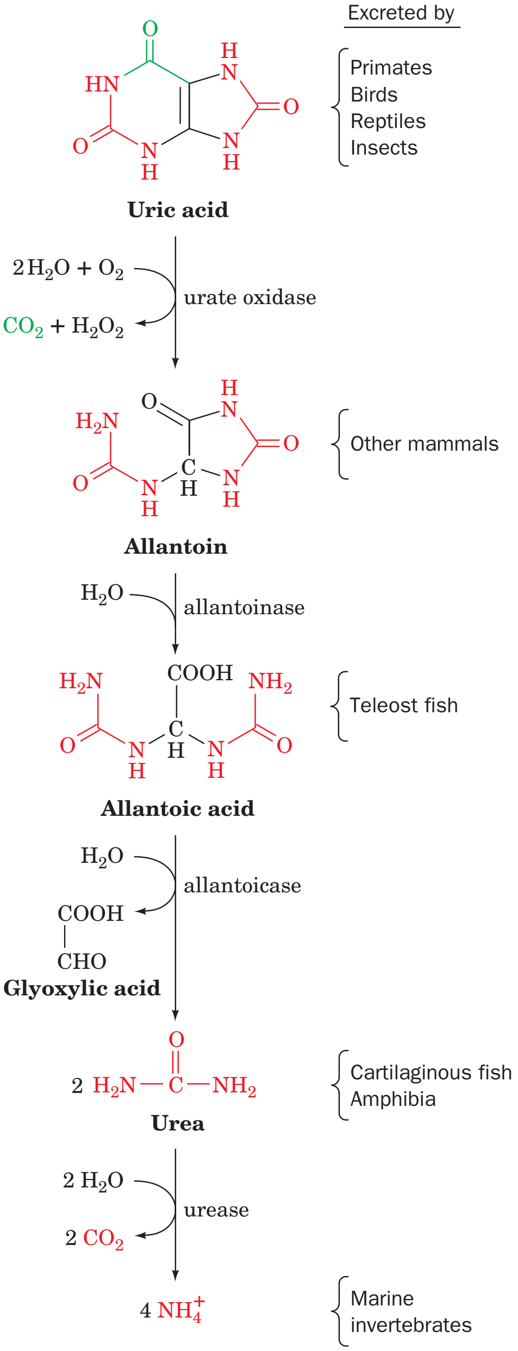
Excreted by
Primates
Birds
Reptiles
Insects
Uric acid
$2H_2O + O_2$
$CO_2 + H_2O_2$
urate oxidase
Other mammals
Allantoin
H_2O
allantoinase
Teleost fish
Allantoic acid
H_2O
allantoicase
COOH
CHO
Glyoxylic acid
$2\ H_2N—C—NH_2$
Urea
Cartilaginous fish
Amphibia
$2\ H_2O$
$2\ CO_2$
urease
$4\ NH_4^+$
Marine invertebrates

Figure 23-22 | Degradation of uric acid to ammonia. The process is arrested at different stages in the indicated species, and the resulting nitrogen-containing product is excreted.

reptiles, and many insects, but those organisms, which do not excrete urea, also catabolize their excess amino acid nitrogen to uric acid via purine biosynthesis. This complicated system of nitrogen excretion has a straightforward function: *It conserves water.* Uric acid is only sparingly soluble in water, so its excretion as a paste of uric acid crystals is accompanied by very little water. In contrast, the excretion of an equivalent amount of the much more water-soluble urea osmotically sequesters a significant amount of water.

In all other organisms, uric acid is further processed before excretion (Fig. 23-22). Mammals other than primates oxidize it to their excretory product, **allantoin,** in a reaction catalyzed by the Cu-containing enzyme **urate oxidase.** A further degradation product, **allantoic acid,** is excreted by teleost (bony) fish. Cartilaginous fish and amphibia further degrade allantoic acid to urea prior to excretion. Finally, marine invertebrates decompose urea to NH_4^+.

Gout Is Caused by an Excess of Uric Acid. **Gout** is a disease characterized by elevated levels of uric acid in body fluids. Its most common manifestation is excruciatingly painful arthritic joint inflammation of sudden onset, most often of the big toe (Fig. 23-23), caused by deposition of nearly insoluble crystals of sodium urate. Sodium urate and/or uric acid may also precipitate in the kidneys and ureters as stones, resulting in renal damage and urinary tract obstruction.

Gout, which affects ~3 per 1000 persons, predominantly males, has been traditionally, although inaccurately, associated with overindulgent eating and drinking. The probable origin of this association is that in previous centuries, when wine was often contaminated with lead during its manufacture and storage, heavy drinking resulted in chronic lead poisoning that, among other things, decreases the kidney's ability to excrete uric acid.

The most prevalent cause of gout is impaired uric acid excretion (although usually for reasons other than lead poisoning). Gout may also result from a number of metabolic insufficiencies, most of which are not well characterized. One well-understood cause is HGPRT deficiency (Lesch–Nyhan syndrome in severe cases), which leads to excessive uric acid production through PRPP accumulation (Section 23-1D).

Gout can be treated by administering the xanthine oxidase inhibitor **allopurinol** (*at right*)**,** a hypoxanthine analog with interchanged N7 and C8 positions. Xanthine oxidase hydroxylates allopurinol, as it does hypoxanthine, yielding **alloxanthine** (*at right*), which remains tightly bound to the reduced form of the enzyme, thereby inactivating it. Allopurinol consequently

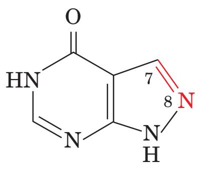

Allopurinol

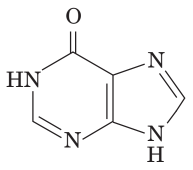

Hypoxanthine

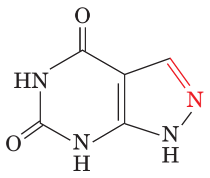

Alloxanthine

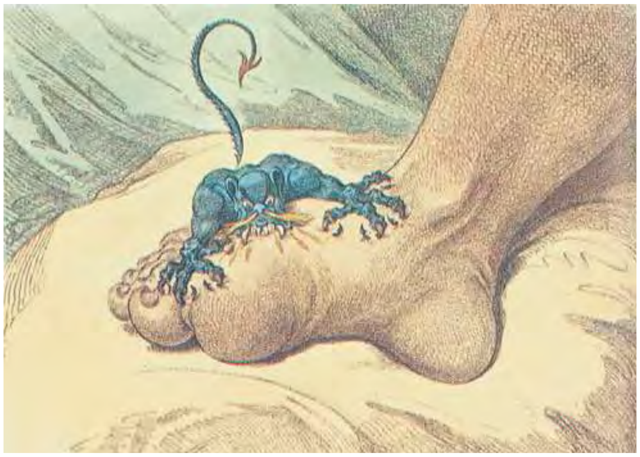

■ **Figure 23-23** | ***The Gout,* a cartoon by James Gillray (1799).** [Courtesy of Yale University Medical Historical Library.]

BOX 23-2 PATHWAYS OF DISCOVERY

Gertrude Elion and Purine Derivatives

Gertrude Elion (1918–1999)

Gertrude Elion's choice of career was made at age 15 when she graduated from high school in New York City. As she watched her grandfather suffer and die from stomach cancer, she decided to dedicate herself to finding a cure for cancer. When she enrolled at Hunter College the next fall, she began to study chemistry. Despite her academic accomplishments, she was unable to obtain a scholarship for graduate school and spent the next two years as a teacher and lab assistant. She eventually obtained a Master of Science degree in 1941.

After discovering that working in an industrial chemistry laboratory was boring, Elion obtained a position with George Hitchings at the pharmaceutical company Burroughs Wellcome. There, she found an intellectually stimulating environment where she was able to expand her understanding of chemistry as well as pharmacology, immunology, and other fields. Although she ultimately received numerous honorary degrees, Elion never formally earned a doctoral degree; after several years of attending classes at night, she was forced to choose between her work with Hitchings, which she loved, and full-time study. Fortunately for science, Elion kept her job and significantly advanced the development of drugs for cancer, gout, organ transplants, and infectious diseases.

Hitchings asked Elion to investigate purine metabolism, with the idea that disrupting a cell's supply of nucleotides could interfere with its ability to synthesize DNA. Ideally, compounds that blocked DNA synthesis would disable rapidly growing cancer cells, bacteria, and viruses, without affecting normal cells. Without knowing the structures of the relevant enzymes, or even of DNA, Elion and her colleagues used a simple bacterial growth assay to investigate the ability of various purine derivatives to act as "antimetabolites."

Elion's first clinical success was **6-mercaptopurine,** which was used to treat leukemia in children. Many patients showed a dramatic recovery, but to Elion's dismay they often relapsed and later died. Their initial improvement, however, confirmed Elion's belief that interfering with nucleotide metabolism was a sound therapeutic strategy.

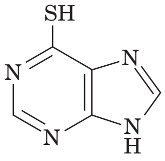

6-Mereaptopurine

A related compound, **azathioprine,** is converted to 6-mercaptopurine intracellularly. It turned out to be effective not as an anticancer drug but as an inhibitor of the immune response. This drug helped solve the problem of rejection in organ transplants and was used for the first successful human kidney transplant in 1961.

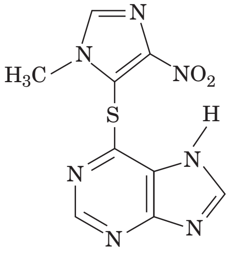

Azathioprine

Studies aimed at improving the effectiveness of purine derivatives by preventing their degradation by xanthine oxidase led to the discovery of allopurinol (Section 23-4B), which is still used to treat gout and some parasitic diseases. Elion also helped develop the antibacterial agent trimethoprim (Box 23-1) and the widely used antiviral drug acyclovir (Zovir).

After Hitchings' retirement, Elion became head of the Department of Experimental Therapy in 1967. Although she formally retired in 1983, Elion's line of research continued to bear fruit with the development of azidothymidine (AZT; Box 12-4), a nucleoside analog that was the sole drug that was effective for treating AIDS until 1991 and is still in use.

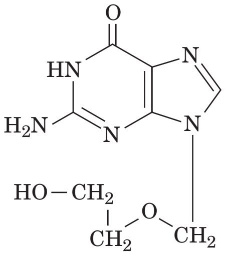

Acyclovir

Elion, together with Hitchings and James Black [who discovered cimetidine (Tagamet), the first drug to inhibit stomach acid secretion, and propranolol (Inderol), which is widely used in the treatment of high blood pressure], was awarded the Nobel Prize for Physiology or Medicine in 1988, a rare accomplishment for a scientist in the pharmaceutical industry. It was her research, which was based on an understanding of nucleotide metabolism, rather than her ability to simply synthesize novel compounds, that merited recognition.

Elion, G.B., Hitchings, G.H., and Vanderwerff, H., Antagonists of nucleic acid derivatives. VI. Purines, *J. Biol. Chem.* **192,** 505–518 (1951).

Elion, G.B., Kovensky, A., and Hitchings, G.H., Metabolic studies of allopurinol, an inhibitor of xanthine oxidase, *Biochem. Pharmacol.* **15,** 863–880 (1966).

alleviates the symptoms of gout by decreasing the rate of uric acid production while increasing the levels of the more soluble hypoxanthine and xanthine. Although allopurinol controls the gouty symptoms of Lesch–Nyhan syndrome, it has no effect on its neurological symptoms. Allopurinol, along with several other notable purine derivatives, was developed by the chemist Gertrude Elion (Box 23-2).

C | Pyrimidines Are Broken Down to Malonyl-CoA and Methylmalonyl-CoA

Animal cells degrade pyrimidine nucleotides to their component bases (Fig. 23-24, *top*). The reactions, like those of purine nucleotides, occur through dephosphorylation, deamination, and glycosidic bond cleavages. The resulting uracil and thymine are then broken down in the liver through reduction (Fig. 23-24, *middle*) rather than by oxidation as occurs in purine catabolism. The end products of pyrimidine catabolism, **β-alanine** and **β-aminoisobutyrate,** are amino acids and are metabolized as such. They are converted, through transamination and activation reactions, to malonyl-CoA and methylmalonyl-CoA (Fig. 23-24, *bottom left*). Malonyl-CoA is a

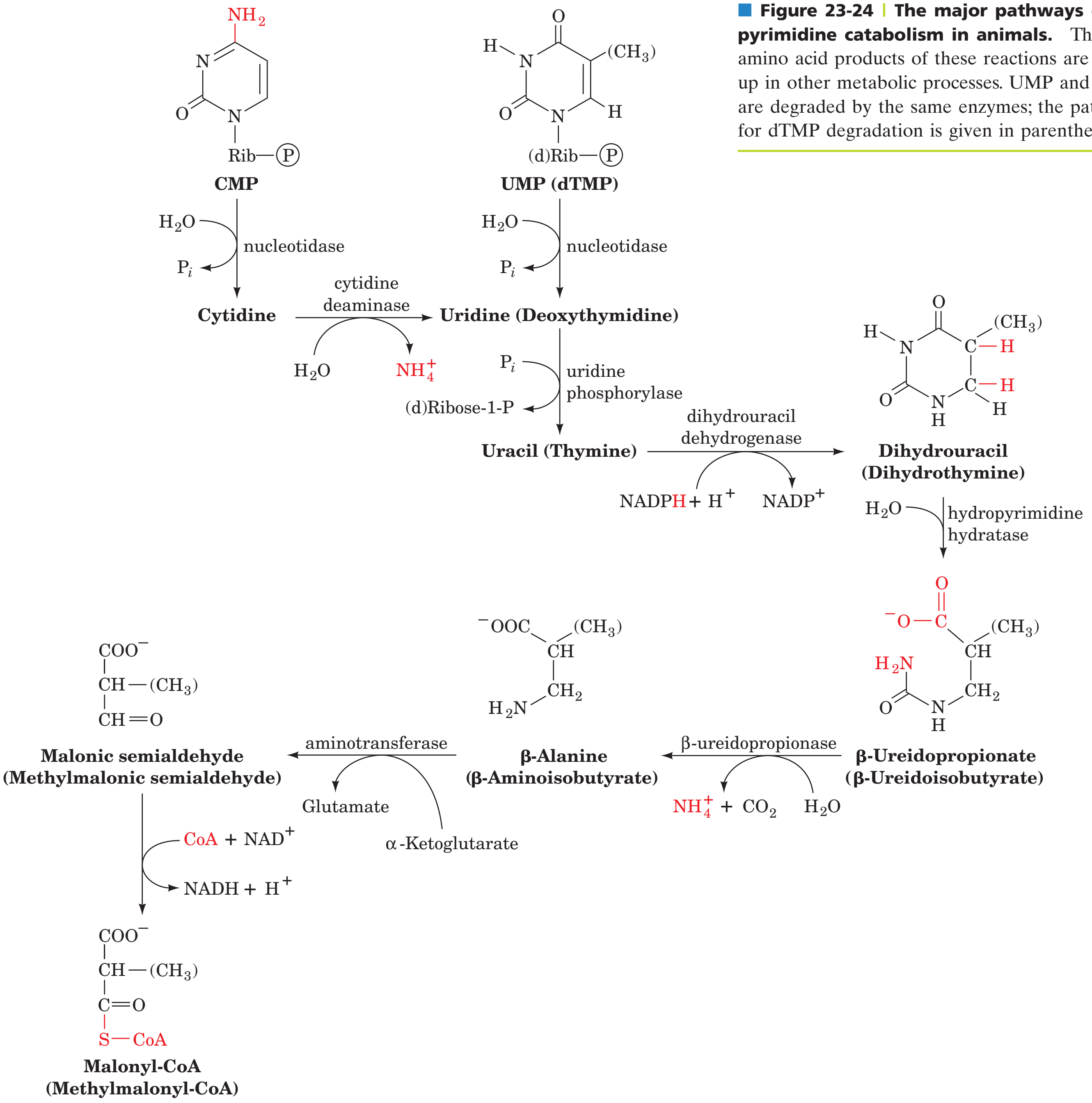

NH2
CMP
Rib—P
UMP (dTMP)
(d)Rib—P
(CH3)
H2O
Pi
nucleotidase
Cytidine
cytidine deaminase
NH4+
Uridine (Deoxythymidine)
uridine phosphorylase
(d)Ribose-1-P
Uracil (Thymine)
dihydrouracil dehydrogenase
NADPH + H+
NADP+
Dihydrouracil (Dihydrothymine)
hydropyrimidine hydratase
β-Ureidopropionate (β-Ureidoisobutyrate)
β-ureidopropionase
NH4+ + CO2
β-Alanine (β-Aminoisobutyrate)
aminotransferase
Glutamate
α-Ketoglutarate
Malonic semialdehyde (Methylmalonic semialdehyde)
CoA + NAD+
NADH + H+
Malonyl-CoA (Methylmalonyl-CoA)

■ **Figure 23-24 | The major pathways of pyrimidine catabolism in animals.** The amino acid products of these reactions are taken up in other metabolic processes. UMP and dTMP are degraded by the same enzymes; the pathway for dTMP degradation is given in parentheses.

precursor of fatty acid synthesis (Fig. 20-26), and methylmalonyl-CoA is converted to the citric acid cycle intermediate succinyl-CoA (Fig. 20-16). Thus, *to a limited extent, catabolism of pyrimidine nucleotides contributes to the energy metabolism of the cell.*

CHECK YOUR UNDERSTANDING

What compounds are produced by the degradation of purines and pyrimidines?

Describe how purine catabolism is related to SCID, muscle function, and gout.

SUMMARY

1. The purine nucleotide IMP is synthesized in 11 steps from ribose-5-phosphate, aspartate, fumarate, glutamine, glycine, and HCO_3^-. Purine nucleotide synthesis is regulated at its first and second steps.
2. IMP is the precursor of AMP and GMP, which are phosphorylated to produce the corresponding di- and triphosphates.
3. The pyrimidine nucleotide UMP is synthesized from 5-phosphoribosyl pyrophosphate, aspartate, glutamine, and HCO_3^- in six reactions. UMP is converted to UTP and CTP by phosphorylation and amination.
4. Pyrimidine nucleotide synthesis is regulated in bacteria at the ATCase step and in animals at the step catalyzed by carbamoyl phosphate synthetase II.
5. Deoxyribonucleoside diphosphates are synthesized from the corresponding NDPs by the action of ribonucleotide reductase, which contains a binuclear Fe(III) prosthetic group, a tyrosyl radical, and several redox-active sulfhydryl groups. Enzyme activity is regenerated through disulfide interchange with thioredoxin.
6. Ribonucleotide reductase is regulated by allosteric effectors, which ensure that deoxynucleotides are synthesized in the amounts required for DNA synthesis.
7. dTMP is synthesized from dUMP by thymidylate synthase. The dihydrofolate produced in the reaction is converted back to tetrahydrofolate by dihydrofolate reductase (DHFR).
8. Purine nucleotides are degraded by nucleosidases and purine nucleoside phosphorylase (PNP). Adenine nucleotides are deaminated by adenosine deaminase and AMP deaminase. The synthesis and degradation of AMP in the purine nucleotide cycle yield the citric acid cycle intermediate fumarate in muscles. Xanthine oxidase catalyzes the oxidation of hypoxanthine to xanthine and of xanthine to uric acid.
9. In primates, birds, reptiles, and insects, the final product of purine degradation is uric acid, which is excreted. Other organisms degrade urate further.
10. Pyrimidines are broken down to intermediates of fatty acid metabolism.

KEY TERMS

PRPP	**818**
feedforward activation	**823**
salvage pathway	**823**
mechanism-based inhibitor	**838**
purine nucleotide cycle	**841**

PROBLEMS

1. Calculate the cost, in ATP equivalents, of synthesizing *de novo* (a) IMP, (b) AMP, and (c) CTP. Assume all substrates (e.g., ribose-5-phosphate and glutamine) and cofactors are available.
2. Certain glutamine analogs irreversibly inactivate enzymes that bind glutamine. Identify the nucleotide biosynthetic intermediates that accumulate in the presence of those compounds.
3. Rats are given cytidine that is ^{14}C-labeled at both its base and ribose components. Their DNA is then extracted and degraded with nucleases. Describe the labeling pattern of the recovered deoxycytidylate residues if deoxycytidylate production in the cell followed a pathway in which (a) intact CDP is reduced to dCDP, and (b) CDP is broken down to cytosine and ribose before reduction.
4. Explain why hydroxyurea,

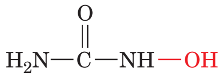

$$H_2N{-}\overset{\overset{\displaystyle O}{\|}}{C}{-}NH{-}OH$$

Hydroxyurea

which destroys tyrosyl radicals, is useful as an antitumor agent.

5. Why is dATP toxic to mammalian cells?

6. Why do individuals who are undergoing chemotherapy with FdUMP or methotrexate often temporarily go bald?
7. Normal cells die in a nutrient medium containing thymidine and methotrexate, whereas mutant cells defective in thymidylate synthase survive and grow. Explain.
8. Explain why methotrexate inhibits the synthesis of histidine and methionine.
9. Some microorganisms lack DHFR activity, but their thymidylate synthase has an FAD cofactor. What is the function of the FAD?
10. Explain whether the following are mechanism-based inhibitors: (a) trimethoprim with bacterial dihydrofolate reductase, and (b) allopurinol with xanthine oxidase.
11. Why does von Gierke's glycogen storage disease (Box 16-2) cause symptoms of gout?
12. In animals, one pathway for NAD^+ synthesis begins with nicotinamide. Draw the structures generated by the reactions shown.

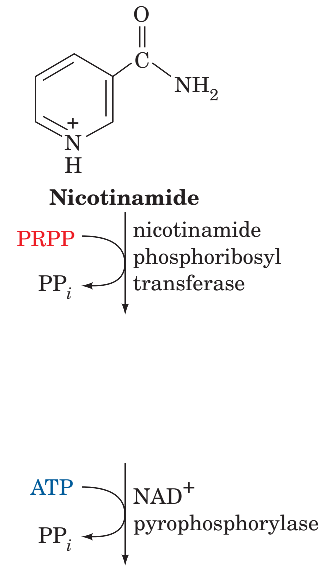
O
C
NH_2
+
N
H
Nicotinamide
PRPP
PP_i
nicotinamide phosphoribosyl transferase
ATP
PP_i
NAD^+ pyrophosphorylase

REFERENCES

Carreras, C.W. and Santi, D.V., The catalytic mechanism and structure of thymidylate synthase, *Annu. Rev. Biochem.* **64,** 721–762 (1995).

Finer-Moore, J.S., Santi, D.V., and Stroud, R.M., Lessons and conclusions from dissecting the mechanism of a bisubstrate enzyme: thymidylate synthase mutagenesis, function, and structure, *Biochemistry* **42,** 248–256 (2003).

Greasley, S.E., Horton, P., Ramcharan, J., Beardsley, G.P., Benkovic, S.J., and Wilson, I.A., Crystal structure of a bifunctional transformylase and cyclohydrolase enzyme in purine biosynthesis, *Nature Struct. Biol.* **8,** 402–406 (2001).

Kappock, T.J., Ealick, S.E., and Stubbe, J., Modular evolution of the purine biosynthetic pathway, *Curr. Opin. Chem. Biol.* **4,** 567–572 (2000).

Liu, S., Neidhardt, E.A., Grossman, T.H., Ocain, T., and Clardy, J., Structures of human dihydroorotate dehydrogenase in complex with antiproliferative agents, *Structure* **8,** 25–33 (1999).

Scriver, C.R., Beaudet, A.L., Sly, W.S., and Valle, D. (Eds.), *The Metabolic and Molecular Bases of Inherited Disease* (8th ed.), Chapters 106–114, McGraw-Hill (2001). [These chapters describe normal and abnormal pathways of nucleotide metabolism.]

Stubbe, J., Ge, J., and Yee, C.S., The evolution of ribonucleotide reduction revisited, *Trends Biochem. Sci.* **26,** 93–99 (2001).

24

Nucleic Acid Structure

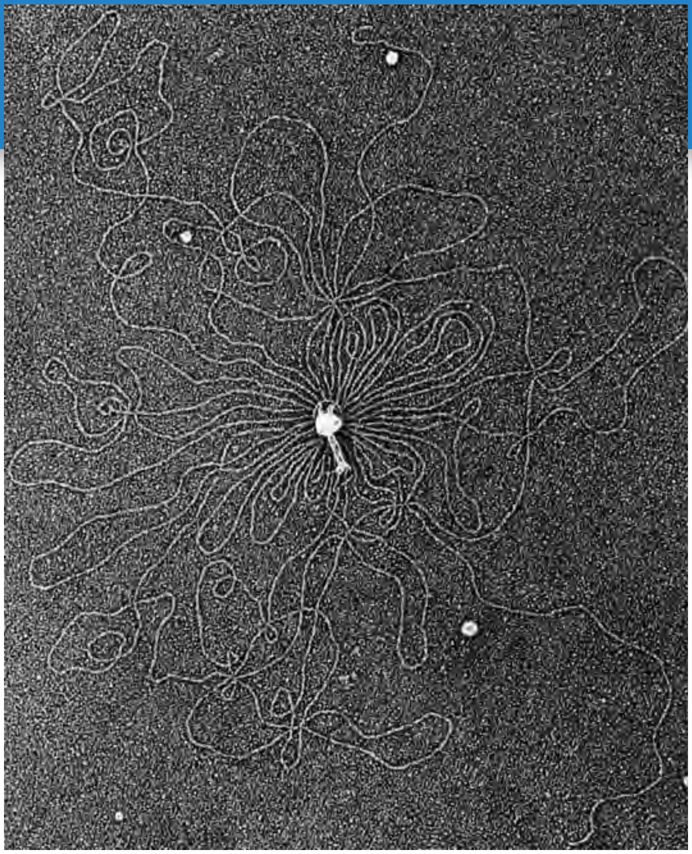

DNA molecules, such as that spilling out of the osmotically lysed bacteriophage T2 shown here, are enormous. A cell must be able to efficiently package and safely store its DNA. However, despite DNA's highly condensed structure, a cell must be able to read and interpret the meaning of the encoded genetic information. [From Kleinschmidt, A.K., Lang, D., Jacherts, D., and Zahn, R.K., *Biochimica et Biophysica Acta,* **61,** 861 (1962), Elsevier.]

CHAPTER CONTENTS

1 The DNA Helix
- **A.** DNA Can Adopt Different Conformations
- **B.** DNA Has Limited Flexibility
- **C.** DNA Can Be Supercoiled
- **D.** Topoisomerases Alter DNA Supercoiling

2 Forces Stabilizing Nucleic Acid Structures
- **A.** DNA Can Undergo Denaturation and Renaturation
- **B.** Nucleic Acids Are Stabilized by Base Pairing, Stacking, and Ionic Interactions
- **C.** RNA Structures Are Highly Variable

3 Fractionation of Nucleic Acids
- **A.** Nucleic Acids Can Be Purified by Chromatography
- **B.** Electrophoresis Separates Nucleic Acids by Size

4 DNA–Protein Interactions
- **A.** Restriction Endonucleases Distort DNA on Binding
- **B.** Prokaryotic Repressors Often Include a DNA-Binding Helix
- **C.** Eukaryotic Transcription Factors May Include Zinc Fingers or Leucine Zippers

5 Eukaryotic Chromosome Structure
- **A.** Histones Are Positively Charged
- **B.** DNA Coils around Histones to Form Nucleosomes
- **C.** Chromatin Forms Higher-Order Structures

MEDIA RESOURCES

(available at www.wiley.com/college/voet)

Guided Exploration 21. DNA structures
Guided Exploration 22. DNA supercoiling
Guided Exploration 23. Transcription factor–DNA interactions
Guided Exploration 24. Nucleosome structure
Interactive Exercise 36. An RNA–DNA helix
Interactive Exercise 37. Yeast topoisomerase II
Interactive Exercise 38. A hammerhead ribozyme
Interactive Exercise 39. A portion of phage 434 repressor in complex with target DNA
Interactive Exercise 40. *E. coli trp* repressor–operator complex
Interactive Exercise 41. *E. coli met* repressor–operator complex
Interactive Exercise 42. A three–zinc finger segment of Zif268 in complex with DNA
Interactive Exercise 43. GAL4 DNA-binding domain in complex with DNA
Interactive Exercise 44. GCN4 bZIP region in complex with DNA
Interactive Exercise 45. Max binding to DNA
Animated Figure 24-19. UV absorbance spectra of native and heat-denatured DNA
Animated Figure 24-20. Example of DNA melting curve
Kinemage 17-1, 17-4, 17-5, 17-6. Structure of A, B, Z DNA
Kinemage 17-2. Watson–Crick base pairs
Kinemage 17-3. Nucleotide sugar conformations
Kinemage 18-1. *Eco*RI endonuclease in complex with DNA
Kinemage 18-2. *Eco*RV endonuclease in complex with DNA
Kinemage 19. 434 phage repressor in complex with DNA
Kinemage 20. GCN4 leucine zipper motif
Case Study 31. Hyperactive DNase I Variants: A Treatment for Cystic Fibrosis

In every organism, the ultimate source of biological information is nucleic acid. The shapes and activities of individual cells are, to a large extent, determined by genetic instructions contained in DNA (or RNA, in some viruses). According to the central dogma of molecular biology (Section 3-3B), sequences of nucleotide bases in DNA encode the amino acid sequences of proteins. Many of the cell's proteins are enzymes that carry out the metabolic processes we have discussed in Chapters 15–23. Other proteins have a structural or regulatory role or participate in maintaining and transmitting genetic information.

Two kinds of nucleic acids, DNA and RNA, store information and make it available to the cell. The structures of these molecules are consistent with the following:

1. Genetic information must be stored in a form that is manageable in size and stable over a long period.
2. Genetic information must be decoded—often many times—in order to be used. **Transcription** is the process by which nucleotide sequences in DNA are copied onto RNA so that they can direct protein synthesis, a process known as **translation.**
3. Information contained in DNA or RNA must be accessible to proteins and other nucleic acids. These agents must recognize nucleic acids (in many cases, in a sequence-specific fashion) and bind to them in a way that alters their function.
4. The progeny of an organism must be equipped with the same set of instructions as in the parent. Thus, DNA is **replicated** (an exact copy made) so that each daughter cell receives the same information.

As we shall see, many cellular components are required to execute all the functions of nucleic acids. Yet nucleic acids are hardly inert "read-only" entities. RNA in particular, owing to its single-stranded nature, is a dynamic molecule that provides structural scaffolding as well as catalytic proficiency in a number of processes that decode genetic information. In this chapter, we shall focus on the structural properties of nucleic acids, including their interactions with proteins, that allow them to carry out their duties. In subsequent chapters, we shall examine the processes of replication (Chapter 25), transcription (Chapter 26), and translation (Chapter 27).

1 The DNA Helix

We begin our discussion of nucleic acid structure by examining the various forms of DNA, with an eye toward understanding how this molecule safeguards genetic information while leaving it accessible for replication and transcription.

LEARNING OBJECTIVES

- Understand that a DNA helix can have the A, B, or Z conformation.
- Understand that the conformational freedom of the glycosidic bond, the ribose ring, and the sugar–phosphate backbone is limited.
- Understand the nature of supercoiling.
- Understand that topoisomerases cut one (type I) or both (type II) strands of DNA to add or remove supercoils.

See Guided Exploration 21
DNA structures.

A | DNA Can Adopt Different Conformations

DNA is a two-stranded polymer of deoxynucleotides linked by phosphodiester bonds (Figs. 3-3 and 3-8). The biologically most common form of DNA is known as **B-DNA,** which has the structural features first noted by James Watson and Francis Crick together with Rosalind Franklin and others (Section 3-2B and Box 24-1):

1. The two antiparallel polynucleotide strands wind in a right-handed manner around a common axis to produce an ~20-Å-diameter double helix.

BOX 24-1 **PATHWAYS OF DISCOVERY**

Rosalind Franklin and the Structure of DNA

Rosalind Franklin (1920–1958)

James Watson and Francis Crick were the first to publish an accurate model of the structure of DNA. This seminal discovery was not only based on their own insights but, like all scientific discoveries, built on the work of others. One of the major contributors to this process was Rosalind Franklin, who was probably never fully aware of her role in this discovery and did not share the 1962 Nobel Prize in Physiology or Medicine awarded to Watson, Crick, and Maurice Wilkins.

Franklin was born in England in an intellectually oriented and well-to-do family. She excelled in mathematics, and although career opportunities for women with her talents were few, she obtained a doctorate in physical chemistry at the University of Cambridge in 1945. From 1947 to 1950 she worked in a French government laboratory, where she became an authority in applying X-ray diffraction techniques to imperfectly crystalline substances such as coal; her numerous publications on the structures of coal and other forms of carbon changed the way that these substances were viewed.

In 1951, she returned to England at the invitation of John Randall, the head of the Medical Research Council's (MRC's) Biophysics Research Unit at King's College London, to investigate the structure of DNA. Randall had indicated to Franklin that she would be given an independent position, whereas Wilkins, who had been working on DNA at King's for some time, was given the impression that Franklin would be working under his direction. That misunderstanding, together with their sharply contrasting personalities (Franklin was quick, assertive, and confrontational, whereas Wilkins was deliberate, shy, and indirect), led to a falling out between the two such that they were barely on speaking terms. Hence, they worked independently. Some popular accounts of Franklin's life and work have implied that the atmosphere at King's College was inhospitable to women, but Franklin's correspondence as well as first-hand accounts indicate that the atmosphere was in fact congenial. Still, she was unhappy at King's, apparently for personal reasons, and in the spring of 1953, departed for Birkbeck College in London. There, until her untimely death of ovarian cancer in 1958, she carried out groundbreaking investigations on the structures of viruses.

Early in her tenure at King's, Franklin discovered, through the analysis of X-ray fiber diffraction patterns, that DNA (which she obtained from Wilkins, who had gotten it from Rudoph Signer in Switzerland) exists in two distinct conformations, which she called the A and B forms. Prior to this discovery, the X-ray diffraction patterns of DNA that had been obtained were confusing because they were of mixtures of the A and B forms. Through careful control of the humidity, Franklin obtained an X-ray fiber diffraction photograph of B-DNA of unprecedented clarity (Fig. 3-5) that strikingly indicated the DNA's helical character. Analysis of the photograph permitted Franklin to determine that B-DNA is double helical, it has a diameter of 20 Å, and each turn of the helix is 34 Å long and contains 10 base pairs, each separated by 3.4 Å. Further analysis suggested that the hydrophilic sugar–phosphate chains were on the outside of the helix and the relatively hydrophobic bases were on the inside. Although Franklin was aware of Chargaff's rules (Section 3-2A) and Jerry Donohue's work concerning the tautomeric forms of the bases (Section 3-2B), she did not deduce the existence of base pairs in double-stranded DNA.

In January 1953, Wilkins showed Franklin's X-ray photograph of B-DNA to Watson, when he visited King's College. Moreover, in February 1953, Max Perutz (Box 7-2), Crick's thesis advisor at Cambridge University, showed Watson and Crick his copy of the 1952 Report of the MRC, which summarized the work of all of its principal investigators, including that of Franklin. Within a week (and after 13 months of inactivity on the project), Watson and Crick began building a model of DNA with a backbone structure compatible with Franklin's data [in earlier modeling attempts, they had placed the bases on the outside of the helix (as did a model published by Linus Pauling; Box 6-1) because they assumed that the bases could transmit genetic information only if they were externally accessible]. On several occasions Crick acknowledged that Franklin's findings were crucial to this enterprise.

Watson and Crick published their model of B-DNA in *Nature* in April 1953. This paper was followed, back-to-back, by papers by Wilkins and by Franklin on their structural studies of DNA. Franklin's manuscript had been written in March 1953, before she knew about Watson and Crick's work. The only change that Franklin made to her manuscript when she became aware of Watson and Crick's model was the addition of a single sentence, "Thus our general ideas are not inconsistent with the model proposed by Watson and Crick in the preceding communication." She was apparently unaware that the Watson–Crick model was, to a significant extent, based on her work. Since Watson and Crick did not acknowledge Franklin in their 1953 *Nature* paper, her paper was widely taken as data that supported the Watson–Crick model rather than being an important element in its formulation. Only after her death did Watson and Crick indicate the crucial role of Franklin's contributions.

Interestingly, Watson, Crick, and Franklin developed a close friendship. Starting in 1954 they maintained a correspondence and commented on each other's work. In the summer of 1954, Watson offered to drive Franklin across the United States from Woods Hole, Massachusetts, to her destination at Caltech, where he was also going. In the spring of 1956, she toured Spain with Crick and his wife Odile and, later, stayed with them at their house in Cambridge when she was recovering from her treatments for ovarian cancer.

If Watson and Crick had not formulated their model of B-DNA, would Franklin, who had a distaste for speculative modeling, have eventually done so? We, of course, shall never know. And, had she lived, would Franklin have received the Nobel prize together with Watson, Crick, and Wilkins? (The prize cannot be awarded posthumously.) Those who argue that she was an indispensable participant in the discovery process would say yes. However, the Nobel committee typically awards those who initiate the research (i.e., Wilkins), and the prize cannot be shared by more than three individuals.

Franklin, R.E. and Gosling, R.G., Molecular configuration in sodium thymonucleate, *Nature* **171,** 740–741 (1953).

Maddox, B., *Rosalind Franklin: The Dark Lady of DNA,* HarperCollins (2002).

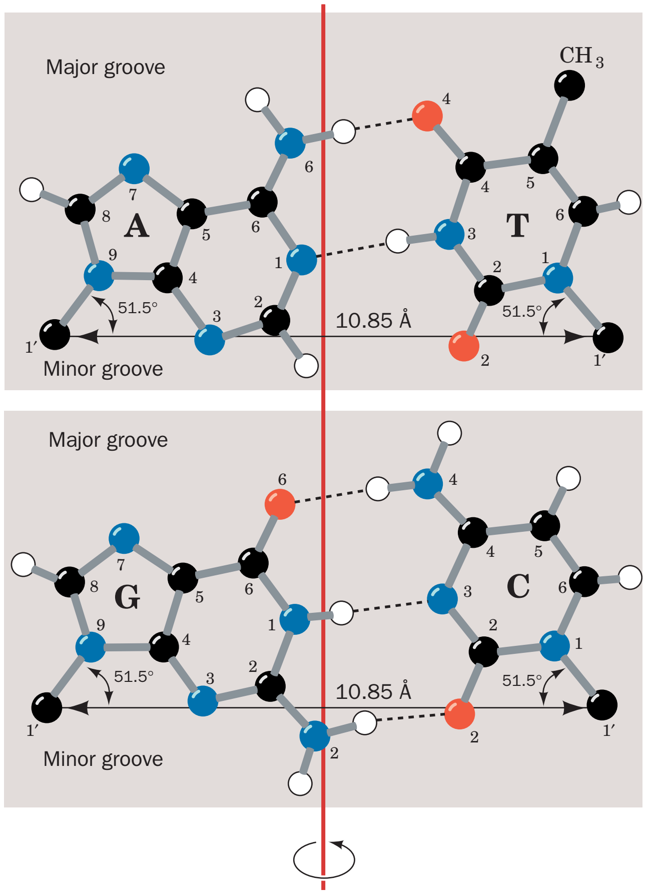

Figure 24-1 | The Watson–Crick base pairs. The line joining the C1′ atoms is the same length in both A · T and G · C base pairs and makes equal angles with the glycosidic bonds to the bases. This gives DNA a series of pseudo-twofold symmetry axes that pass through the center of each base pair (*red line*) and are perpendicular to the helix axis. [After Arnott, S., Dover, S.D., and Wonacott, A.J., *Acta Cryst.* **B25,** 2196 (1969).]

See Kinemage Exercise 17-2.

2. The planes of the nucleotide bases, which form hydrogen-bonded pairs, are nearly perpendicular to the helix axis. In B-DNA, the bases occupy the core of the helix while the sugar–phosphate backbones wind around the outside, forming the major and minor grooves. Only the edges of the base pairs are exposed to solvent.
3. Each base pair has approximately the same width (Fig. 24-1), which accounts for the near-perfect symmetry of the DNA molecule, regardless of base composition. A · T and G · C base pairs are interchangeable: *They can replace each other in the double helix without altering the positions of the sugar–phosphate backbones' C1′ atoms.* Likewise, the partners of a Watson–Crick base pair can be switched (i.e., by changing a G · C to a C · G or an A · T to a T · A). In contrast, any other combination of bases would significantly distort the double helix.
4. The "ideal" B-DNA helix has 10 base pairs (bp) per turn (a helical twist of 36° per bp) and, since the aromatic bases have van der Waals thicknesses of 3.4 Å and are partially stacked on each other, the helix has a pitch (rise per turn) of 34 Å.

Double-helical DNA can assume several distinct structures depending on the solvent composition and base sequence. The major structural variants of DNA are **A-DNA** and **Z-DNA.** The geometries of these molecules are summarized in Table 24-1 and Fig. 24-2.

A-DNA's Base Pairs Are Inclined to the Helix Axis. Under dehydrating conditions, B-DNA undergoes a reversible conformational change to

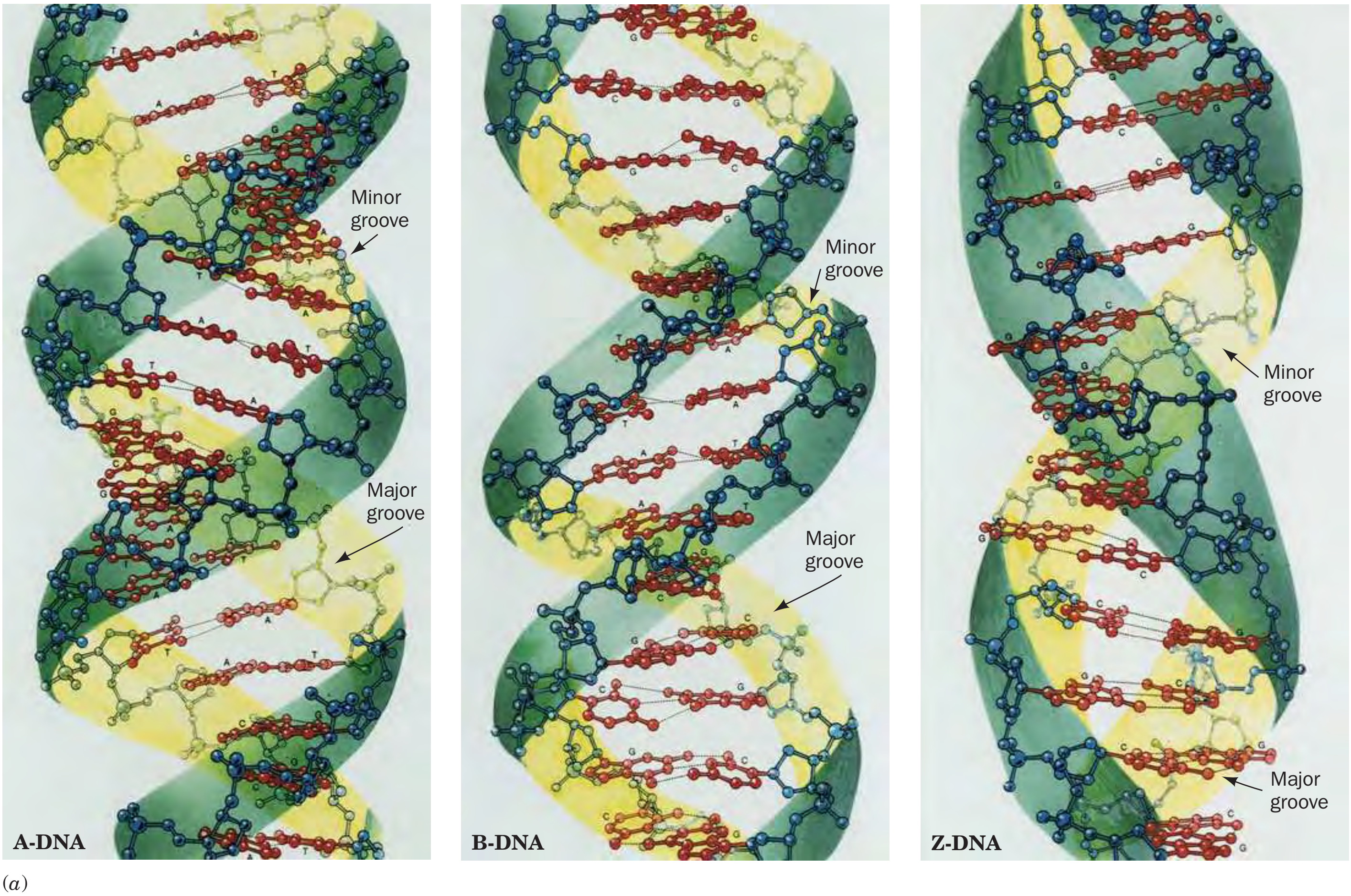

Figure 24-2 | Structures of A-, B-, and Z-DNA. (*a*) View perpendicular to the helix axis. The sugar–phosphate backbones are outlined by a green ribbon and the bases are red. (*b*) (*Opposite*) Space-filling models colored according to type with C green, N blue, O red, and P orange, respectively. H atoms have been omitted for clarity. (*c*) (*Opposite*) View down the helix axis. The ribose ring O atoms are red and the nearest base is white. [Based on structures by A-DNA: Olga Kennard, Dov Rabinovitch, Zippora Shakked, and Mysore Viswamitra, Cambridge University, U.K., Nucleic Acid Database ID ADH010; B-DNA: Richard Dickerson and Horace Drew, Caltech, PDBid 1BNA; and Z-DNA: Andrew Wang and Alexander Rich, MIT, PDBid 2DCG. Illustrations in Parts *a* and *c*, Irving Geis/Geis Archives Trust. Copyright Howard Hughes Medical Institute. Reproduced with permission. Model coordinates for Part *b* generated by Helen Berman, Rutgers University.] **See Kinemage Exercises 17-1, 17-4, 17-5, and 17-6.**

Table 24-1 Structural Features of Ideal A-, B-, and Z-DNA

	A	B	Z
Helical sense	Right handed	Right handed	Left handed
Diameter	~26 Å	~20 Å	~18 Å
Base pairs per helical turn	11.6	10	12 (6 dimers)
Helical twist per base pair	31°	36°	60° (per dimer)
Helix pitch (rise per turn)	34 Å	34 Å	44 Å
Helix rise per base pair	2.9 Å	3.4 Å	7.4 Å per dimer
Base tilt normal to the helix axis	20°	6°	7°
Major groove	Narrow and deep	Wide and deep	Flat
Minor groove	Wide and shallow	Narrow and deep	Narrow and deep
Sugar pucker	C3′-*endo*	C2′-*endo*	C2′-*endo* for pyrimidines; C3′-*endo* for purines
Glycosidic bond conformation	Anti	Anti	Anti for pyrimidines; syn for purines

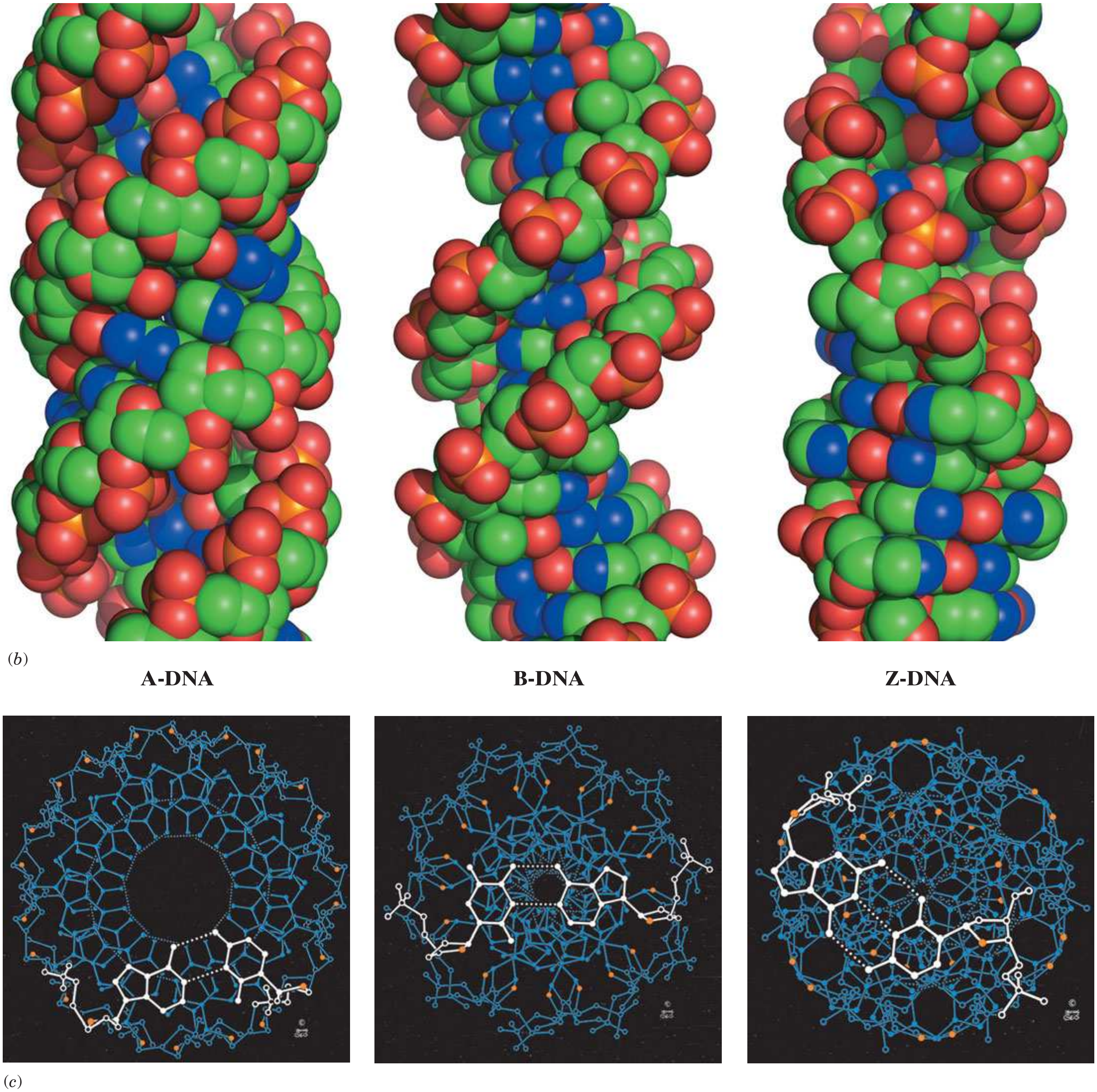

Figure 24-2 | (*Continued*)

A-DNA, which forms a wider and flatter right-handed helix than does B-DNA. A-DNA has 11.6 bp per turn and a pitch of 34 Å, which gives it an axial hole (Fig. 24-2*c, left*). A-DNA's most striking feature, however, is that the planes of its base pairs are tilted 20° with respect to the helix axis. Since the axis does not pass through its base pairs, A-DNA has a deep major groove and a very shallow minor groove; it can be described as a flat ribbon wound around a 6-Å-diameter cylindrical hole.

Z-DNA Forms a Left-Handed Helix. Occasionally, a familiar system exhibits quite unexpected properties. Over 25 years after the discovery of the Watson–Crick DNA structure, the crystal structure determination of d(CGCGCG) by Andrew Wang and Alexander Rich revealed, quite surprisingly, that this self-complementary sequence formed a left-handed double helix. This helix, which was dubbed Z-DNA, has 12 Watson–Crick base pairs per turn, a pitch of 44 Å, a deep minor groove, and no discernible major groove. Z-DNA therefore resembles a left-handed drill bit in appearance (Fig. 24-2, *right*).

Fiber diffraction and NMR studies have shown that complementary polynucleotides with alternating purines and pyrimidines, such as poly d(GC) · poly d(GC) or poly d(AC) · poly d(GT), assume the Z conformation at high salt concentrations. The salt stabilizes Z-DNA relative to B-DNA by reducing the electrostatic repulsions between closest approaching phosphate groups on opposite strands (which are 8 Å apart in Z-DNA and 12 Å apart in B-DNA).

Does Z-DNA have a biological function? The discovery of Z-DNA-binding proteins strongly suggests that Z-DNA does exist *in vivo*. Rich has determined the X-ray structure of a Z-DNA-binding domain named **Zα** in complex with DNA. One Zα domain binds to each strand of Z-DNA via hydrogen bonds and ionic interactions between polar and basic side chains and the sugar–phosphate backbone of the DNA; none of the DNA's bases participate in these associations (Fig. 24-3). The protein's DNA-binding surface is complementary in shape to the Z-DNA and is positively charged, as is expected for a protein that interacts with closely spaced anionic phosphate groups. Sequences capable of forming Z-DNA frequently occur near the start of genes, and the reversible conversion of B-DNA to Z-DNA at these sites may play a role in the control of transcription.

RNA Can Form an A Helix. Double-stranded RNA is the genetic material of certain viruses, but it is synthesized only as a single strand. Nevertheless, single-stranded RNA can fold back on itself so that complementary sequences base-pair to form double-stranded stems with single-stranded loops (Fig. 3-9). Moreover, short segments of double-stranded RNA have been implicated in the control of gene expression (Section 28-3C). Double-stranded RNA is unable to assume a B-DNA-like conformation because of steric clashes involving its 2′-OH groups. Rather, it usually assumes a conformation resembling A-DNA (Fig. 24-2) that ideally has

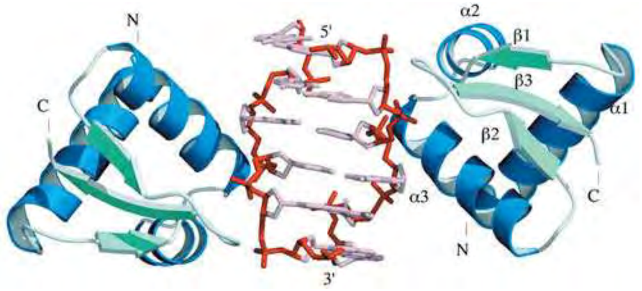

Figure 24-3 | X-Ray structure of Zα in complex with Z-DNA. The DNA sequence d(CGCGCG) is shown in stick form with its backbone red. The Zα domains are drawn with α helices blue and β sheets light green. Note that each Zα domain contacts only one strand of Z-DNA and that none of the bases of the Z-DNA interacts directly with the protein. [Courtesy of Alexander Rich, MIT. PDBid 1QBJ.]

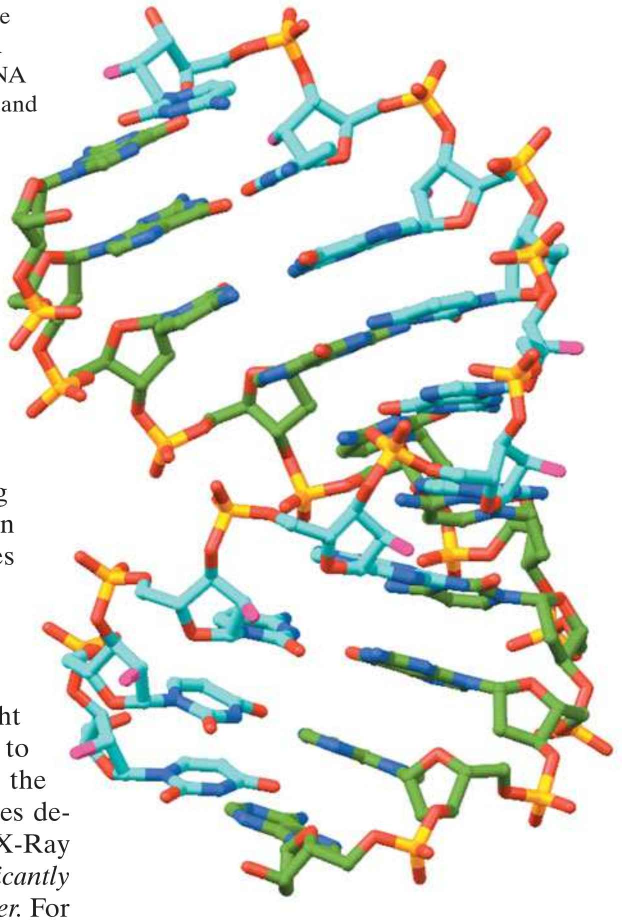

Figure 24-4 **X-Ray structure of a 10-bp RNA–DNA hybrid helix.** The complex consists of the RNA UUCGGGCGCC that is base paired to its DNA complement. The structure is shown in stick form with RNA C atoms cyan, DNA C atoms green, N blue, O red except for RNA O2′ atoms, which are magenta, and P gold. [Based on an X-ray structure by Nancy Horton and Barry Finzel, Pharmacia & Upjohn, Inc., Kalamazoo, Michigan. PDBid 1FIX.] **See Interactive Exercise 36.**

11.0 bp per helical turn, a pitch of 30.9 Å, and base pairs that, on average, are inclined to the helix axis by 16.7°.

Hybrid double helices, which consist of one strand each of RNA and DNA, also have an A-DNA-like conformation (Fig. 24-4), although hybrid helices also have B-DNA-like qualities in that their overall conformation is intermediate to those of A-DNA and B-DNA. Short stretches of RNA–DNA hybrid helices occur during the initiation of DNA replication by small segments of RNA (Section 25-1) and during the transcription of RNA on DNA templates (Section 26-1C).

B | DNA Has Limited Flexibility

The structurally distinct A, B, and Z forms of DNA are not thought to freely interconvert *in vivo.* Rather, the transition from one form to another requires unusual physical conditions (e.g., dehydration) or the influence of DNA-binding proteins. In addition, real DNA molecules deviate from the ideal structures described in the preceding section. X-Ray structures of B-DNA segments reveal that *individual residues significantly depart from the average conformation in a sequence-dependent manner.* For example, the helical twist per base pair may range from 26° to 43°. Each base pair can also deviate from its ideal conformation by rolling or twisting like the blade of a propeller. Such conformational variation appears to be important for the sequence-specific recognition of DNA by the proteins that process genetic information.

B-DNA molecules, which are 20 Å thick and many times as long, are not perfectly rigid rods. In fact, it is imperative that these molecules be somewhat flexible so that they can be packaged in cells. DNA helices can adopt different degrees of curvature ranging from gentle arcs to sharp bends. The more severe distortions from linearity generally occur in response to the binding of specific proteins.

Bond Rotation Is Hindered. The conformation of a nucleotide unit, as Fig. 24-5 indicates, is specified by the six torsion angles of the sugar–phosphate backbone and the torsion angle describing the orientation of the base around the glycosidic bond (the bond joining C1′ to the base). It would seem that these seven degrees of freedom per nucleotide would render polynucleotides highly flexible. Yet these torsion angles are subject to a variety of internal constraints that greatly restrict their rotational freedom.

The rotation of a base around its glycosidic bond (angle χ) is greatly hindered. Purine residues have two sterically permissible orientations known as the **syn** (Greek: with) and **anti** (Greek: against) conformations

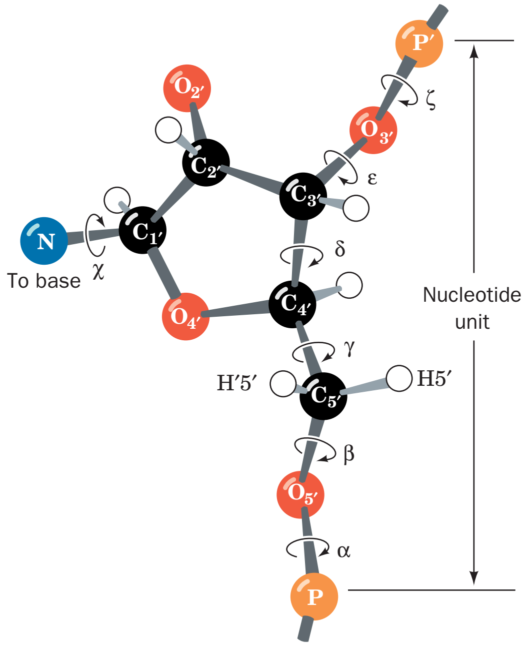

Figure 24-5 **The seven torsion angles that determine the conformation of a nucleotide unit.**

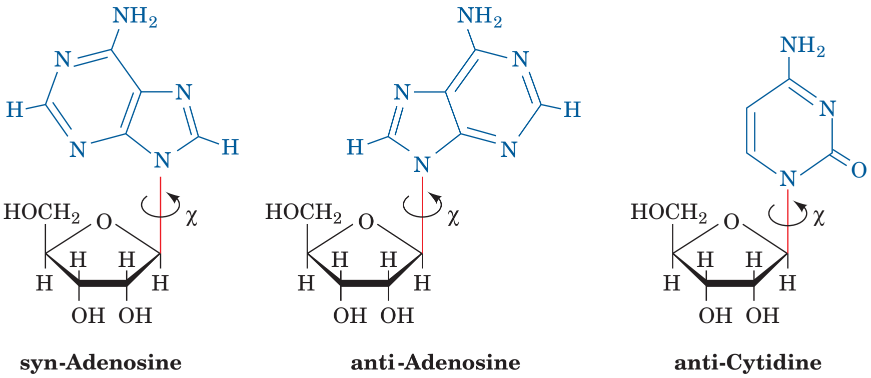

■ **Figure 24-6 | The sterically allowed orientations of purine and pyrimidine bases with respect to their attached ribose units.** In B-DNA, the nucleotide residues all have the anti conformation.

(Fig. 24-6). Only the anti conformation of pyrimidines is stable, because, in the syn conformation, the sugar residue sterically interferes with the pyrimidine's C2 substituent. *In most double-helical nucleic acids, all bases are in the anti conformation.* The exception is Z-DNA (Section 24-1A), in which the alternating pyrimidine and purine residues are anti and syn, respectively (this is one reason why the repeating unit of Z-DNA is a dinucleotide).

The flexibility of the ribose ring itself is also limited. The vertex angles of a regular pentagon are 108°, a value quite close to the tetrahedral angle (109.5°), so one might expect the ribofuranose ring to be nearly flat. However, the ring substituents are eclipsed when the ring is planar. To relieve this crowding, which occurs even between hydrogen atoms, the ring puckers; that is, it becomes slightly nonplanar. In the great majority of known nucleoside and nucleotide X-ray structures, four of the ring atoms are coplanar to within a few hundredths of an angstrom and the remaining atom is out of this plane by several tenths of an angstrom. The out-of-plane atom is almost always C2′ or C3′ (Fig. 24-7). The two most common ribose conformations are known as **C3′-*endo*** and **C2′-*endo;*** "*endo*"

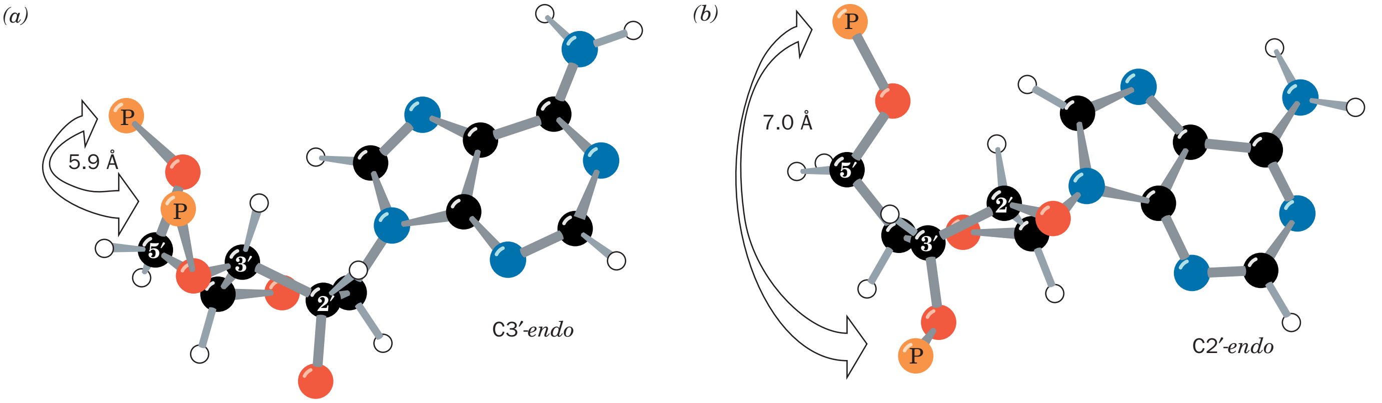

■ **Figure 24-7 | Nucleotide sugar conformations.** (*a*) The C3′-*endo* conformation (C3′ is displaced to the same side of the ring as C5′), which occurs in A-RNA. (*b*) The C2′-*endo* conformation, which occurs in B-DNA. The distances between adjacent P atoms in the sugar–phosphate backbone are indicated. [After Saenger, W., *Principles of Nucleic Acid Structure,* p. 237, Springer-Verlag (1983).] **See Kinemage Exercise 17-3.**

(Greek: *endon,* within) indicates that the displaced atom is on the same side of the ring as C5′, whereas "*exo*" (Greek: *exo,* out of) indicates displacement toward the opposite side of the ring from C5′.

The ribose pucker is conformationally important in nucleic acids because it governs the relative orientations of the phosphate substituents to each ribose residue. In fact, B-DNA has the C2′-*endo* conformation, whereas A-DNA is C3′-*endo.* In Z-DNA, the purine nucleotides are all C3′-*endo* and the pyrimidine nucleotides are C2′-*endo.*

The Sugar–Phosphate Backbone Is Conformationally Constrained. Finally, if the torsion angles of the sugar–phosphate chain (angles α to ζ in Fig. 24-5) were completely free to rotate, there could probably be no stable nucleic acid structure. However, these angles are actually quite restricted. This is because of noncovalent interactions between the ribose ring and the phosphate groups and, in polynucleotides, steric interferences between residues. The overall result is that *the sugar–phosphate chains of the double helix are stiff, although the sugar–phosphate conformational angles are reasonably strain-free.*

C | DNA Can Be Supercoiled

See Guided Exploration 22
DNA supercoiling.

The chromosomes of many viruses and bacteria are circular molecules of duplex DNA. In electron micrographs (e.g., Fig. 24-8), some of these molecules have a peculiar twisted appearance, a phenomenon known as **supercoiling** or **superhelicity.** Supercoiled DNA molecules are more compact than "relaxed" molecules with the same number of nucleotides. This has important consequences for packaging DNA in cells (Section 24-5) and for the unwinding events that occur as part of DNA replication and RNA transcription.

Superhelix Topology Can Be Simply Described. Consider a double-helical DNA molecule in which each of its polynucleotide strands forms a covalently closed circle, thus forming a circular duplex molecule. A geometric property of such an assembly is that *its number of coils cannot be altered without first cleaving at least one of its strands.* You can easily demonstrate this with a buckled belt in which each edge of the belt

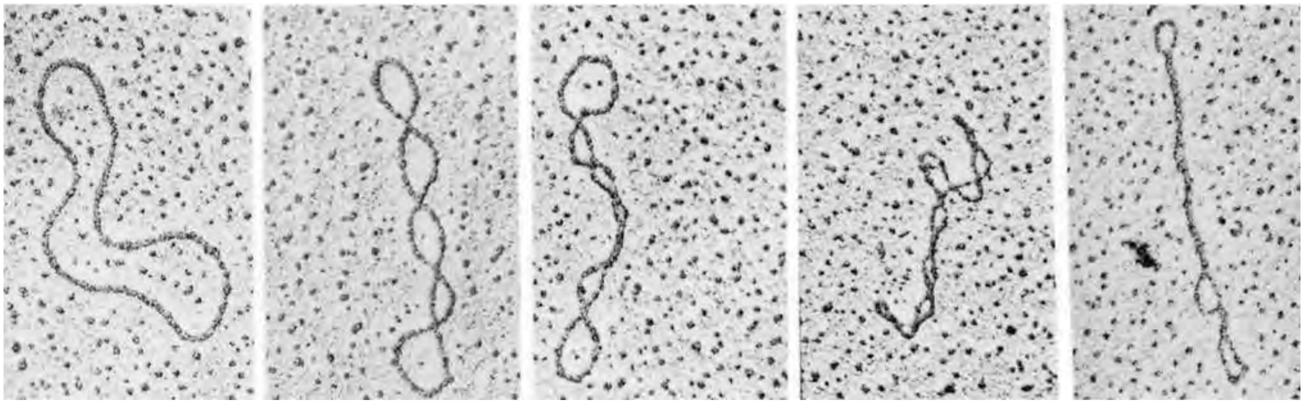

■ **Figure 24-8 | Electron micrographs of circular duplex DNAs.** Their conformations vary from no supercoiling (*left*) to tightly supercoiled (*right*). [Electron micrographs by Laurien Polder. From Kornberg, A. and Baker, T.A., *DNA Replication* (2nd ed.), p. 36, W.H. Freeman (1992). Used by permission.]

represents a strand of DNA. The number of times the belt is twisted before it is buckled cannot be changed without unbuckling the belt (cutting a polynucleotide strand).

This phenomenon is mathematically expressed

$$L = T + W \qquad [24\text{-}1]$$

in which:

1. ***L*, the linking number,** is the number of times that one DNA strand winds around the other. This integer quantity is most easily counted when the molecule is made to lie flat on a plane. The linking number cannot be changed by twisting or distorting the molecule, as long as both its polynucleotide strands remain covalently intact.
2. ***T*, the twist,** is the number of complete revolutions that one polynucleotide strand makes around the duplex axis. By convention, T is positive for right-handed duplex turns so that, for B-DNA, the twist is normally the number of base pairs divided by 10.4 (the observed number of base pairs per turn of the B-DNA double helix in aqueous solution).
3. ***W*, the writhing number,** is the number of turns that the duplex axis makes around the superhelix axis. *It is a measure of the DNA's superhelicity.* The difference between writhing and twisting is illustrated in Fig. 24-9. When a circular DNA is constrained to lie in a plane, $W = 0$.

The two DNA conformations diagrammed on the right of Fig. 24-10 are topologically equivalent; that is, they have the same linking number, L, but differ in their twists and writhing numbers (topology is the study of the geometric properties of objects that are unaltered by deformation but not by cutting).

Since L is a constant in an intact duplex DNA circle, for every new double-helical twist, ΔT, there must be an equal and opposite superhelical twist; that is, $\Delta W = -\Delta T$. For example, a closed circular DNA without supercoils (Fig. 24-10, *upper right*) can be converted to a negatively supercoiled conformation (Fig. 24-10, *lower right*) by winding the duplex helix the same number of positive (right-handed) turns.

Supercoiled DNA Is Relaxed by Nicking One Strand. Supercoiled DNA may be converted to **relaxed circles** (as appears in the leftmost panel of Fig. 24-8) by treatment with **pancreatic DNase I,** an **endonuclease** (an

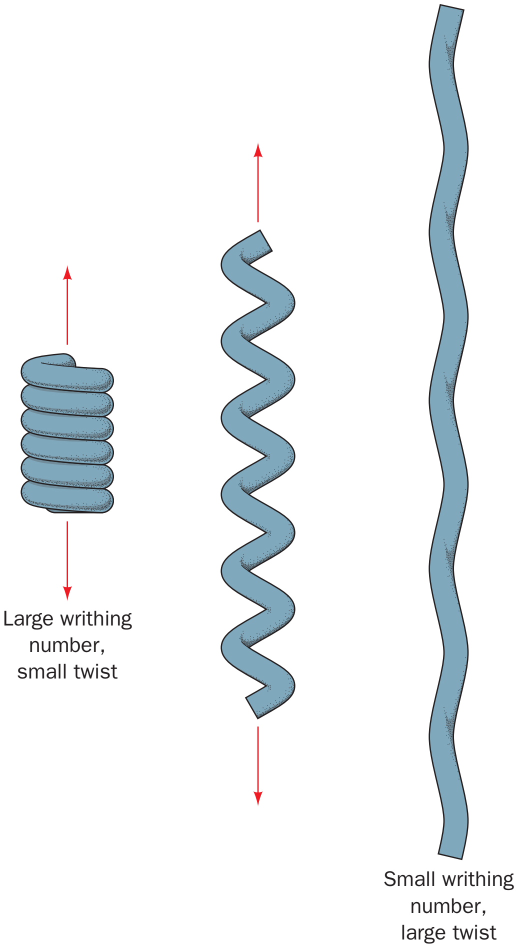
Large writhing number, small twist
Small writhing number, large twist

Figure 24-9 | The difference between writhing and twist as demonstrated by a coiled spring or telephone cord. In its relaxed state (*left*), the spring or cord is in a helical form that has a large writhing number and a small twist. As the coil is pulled out (*center*) until it is nearly straight (*right*), its writhing number becomes small and its twist becomes large.

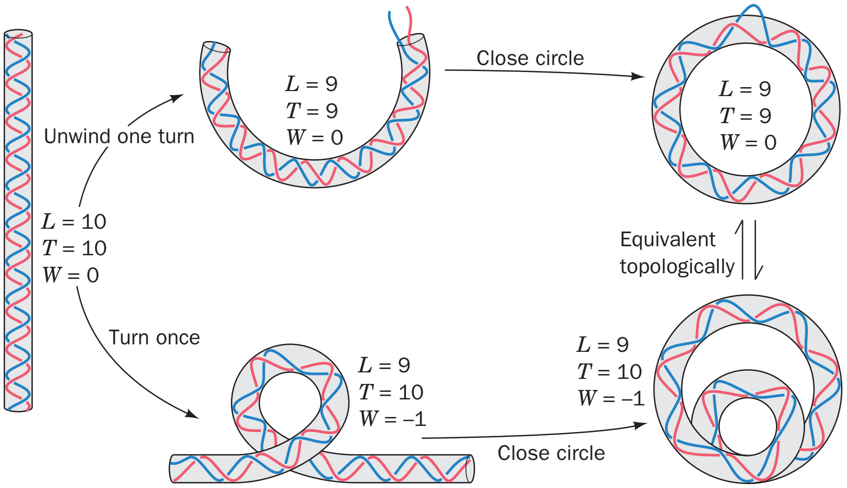

Figure 24-10 | Two ways of introducing one supercoil into a DNA that has 10 duplex turns. The two closed circular forms shown (*right*) are topologically equivalent; that is, they are interconvertible without breaking any covalent bonds. The linking number L, twist T, and writhing number W are indicated for each form. Strictly speaking, the linking number is defined only for a covalently closed circle.

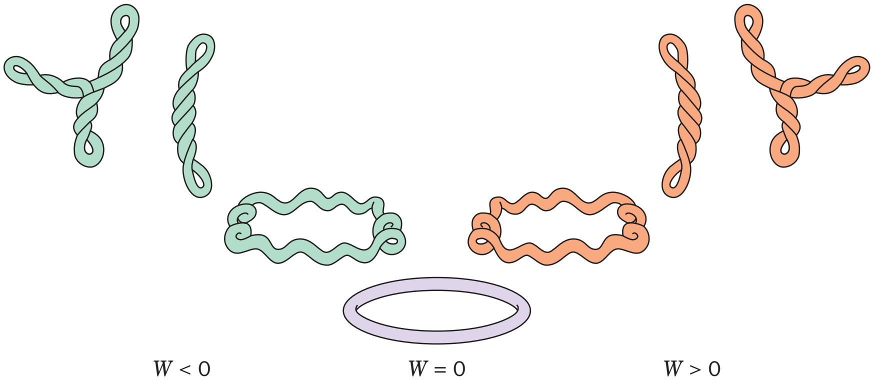

Figure 24-11 | Progressive unwinding of a negatively supercoiled DNA molecule. As the double helix in a negatively supercoiled circle ($W < 0$) is unwound without breaking covalent bonds (T decreases), W increases until it reaches 0. Further unwinding of the double helix then causes the DNA to supercoil in the opposite direction, yielding a positively coiled superhelix ($W > 0$).

enzyme that cleaves phosphodiester bonds within a polynucleotide strand), which cleaves only one strand of a duplex DNA. *One single-strand nick is sufficient to relax a supercoiled DNA.* This is because the sugar–phosphate chain opposite the nick is free to swivel about its backbone bonds (Fig. 24-5) so as to change the molecule's linking number and thereby alter its superhelicity. Supercoiling builds up elastic strain in a DNA circle, much as it does in a rubber band. This is why the relaxed state of a DNA circle is not supercoiled.

Naturally Occurring DNA Circles Are Underwound. The linking numbers of natural DNA circles are less than those of their corresponding relaxed circles; that is, they are underwound. However, because DNA tends to adopt an overall conformation that maintains its normal twist of 1 turn/10.4 bp, the molecule is negatively supercoiled ($W < 0$; Fig. 24-11, *left*). If the duplex is unwound (if T decreases), then W increases (L must remain constant). At first, this reduces the superhelicity of an underwound circle. However, with continued unwinding, the value of W passes through zero (a relaxed circle; Fig. 24-11, *center*) and then becomes positive, yielding a positively coiled superhelix (Fig. 24-11, *right*).

D | Topoisomerases Alter DNA Supercoiling

DNA functions normally only if it is in the proper topological state. In such basic biological processes as replication and transcription, complementary polynucleotide strands must separate. The negative supercoiling of naturally occurring DNAs in both prokaryotes and eukaryotes promotes such separations since it tends to unwind the duplex helix (an increase in W must be accompanied by a decrease in T). *If DNA lacks the proper superhelical tension, the above vital processes cannot occur.*

The supercoiling of DNA is controlled by a remarkable group of enzymes known as **topoisomerases.** They are so named because they alter the topological state (linking number) of circular DNA but not its covalent structure. There are two classes of topoisomerases in prokaryotes and eukaryotes:

1. **Type I topoisomerases** act by creating transient single-strand breaks in DNA. Type I enzymes are further classified as **type IA** and **type IB topoisomerases,** which differ in sequence and reaction mechanism.
2. **Type II topoisomerases** act by making transient double-strand breaks in DNA.

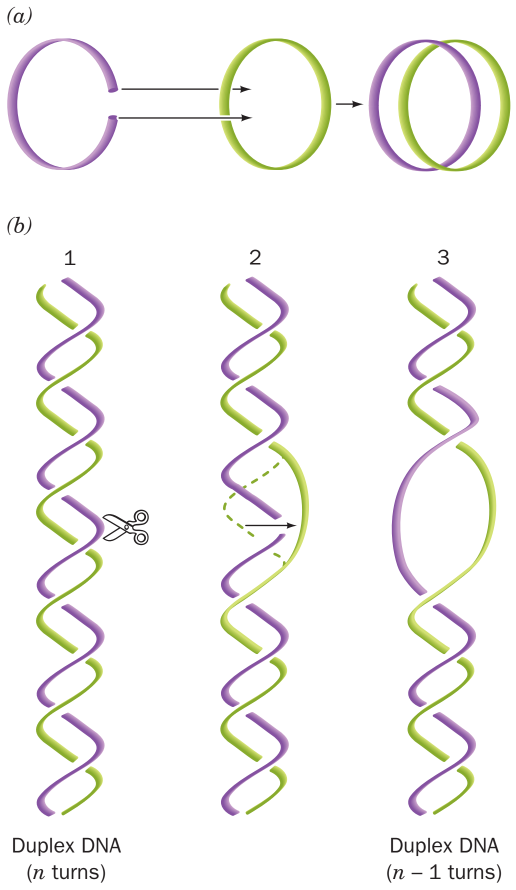

Figure 24-12 | Type IA topoisomerase action. By cutting a single-stranded DNA, passing a loop of a second strand through the break, and then resealing the break, a type IA topoisomerase can (*a*) catenate two single-stranded circles or (*b*) unwind duplex DNA by one turn.

Type IA Topoisomerases Relax Negatively Supercoiled DNA. *Type I topoisomerases catalyze the relaxation of supercoiled DNA by changing the linking number in increments of one.* Type IA enzymes, which are present in all cells, relax only negatively supercoiled DNA. A clue to the mechanism of type IA topoisomerases was provided by the observation that they reversibly **catenate** (interlink) single-stranded circles (Fig. 24-12*a*). Apparently the enzyme operates by cutting a single strand, passing a single-strand loop through the resulting gap, and then resealing the break (Fig. 24-12*b*). For negatively supercoiled DNA, this increases the linking number and makes the writhing number more positive (fewer negative supercoils). The process can be repeated until all of the supercoils have been removed ($W = 0$). This **strand-passage** mechanism is supported by the observation that the denaturation of type IA topoisomerase that has been incubated with single-stranded circular DNA yields a linear DNA that has its 5′-terminal phosphoryl group linked to the enzyme via a phospho-Tyr diester linkage:

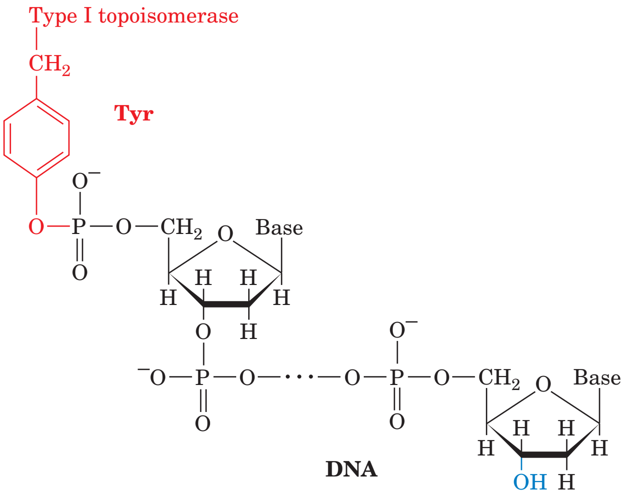

Formation of the covalent enzyme–DNA intermediate conserves the free energy of the cleaved phosphodiester bond so that no free energy input is needed to later reseal the nick in the DNA.

E. coli **topoisomerase III,** a type IA enzyme, is a 659-residue monomer. The X-ray structure of its catalytically inactive Y328F mutant in complex with the single-stranded octanucleotide d(CGCAACTT) was determined by Alfonso Mondragón. The enzyme folds into four domains that enclose an ~20 by 28 Å hole which is large enough to contain duplex DNA and which is lined with numerous Arg and Lys residues (Fig. 24-13). The octanucleotide binds in a groove that is also lined with Arg and Lys side chains with its sugar–phosphate backbone in contact with the protein and with most of its bases exposed for possible base pairing. This single-stranded DNA assumes a B-DNA-like conformation even though its complementary strand would be sterically excluded from the groove. The DNA strand is oriented with its 3′ end near the active site where, if the mutant Phe 328 were the wild-type Tyr, its side chain would be properly positioned to nucleophilically attack the phosphate group bridging the DNA's C-6 and T-7 nucleotides to form a 5′-phospho-Tyr linkage with T-7 and release C-6 with a free 3′-OH. This structure suggests the mechanism for the type IA topoisomerase-catalyzed strand-passage reaction that is diagrammed in Fig. 24-14.

Type IB Topoisomerases Relax Supercoiled DNA via Controlled Rotation. Type IB topoisomerases can relax both negative and positive supercoils. In doing so, they transiently cleave one strand of a duplex DNA

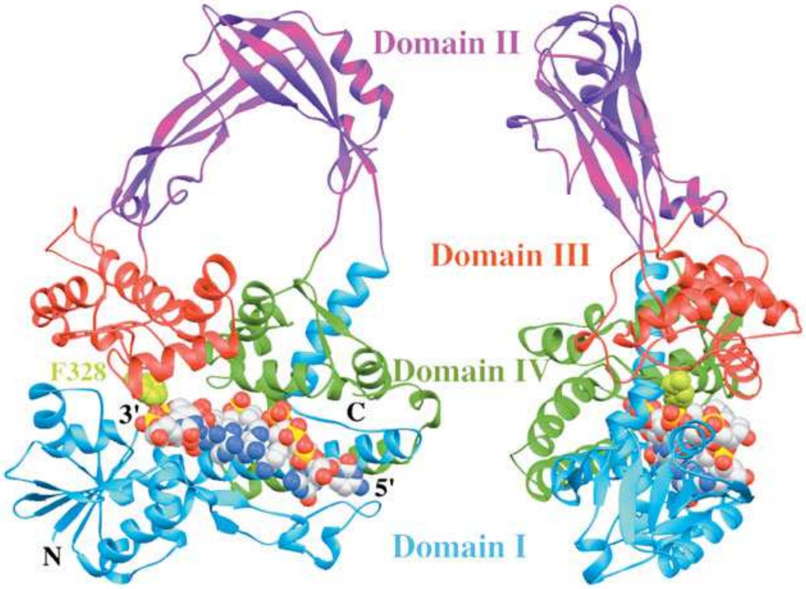

Figure 24-13 | X-Ray structure of the Y328F mutant of *E. coli* topoisomerase III in complex with the single-stranded octanucleotide d(CGCAACTT). The protein's four domains are drawn in different colors and the two views shown are related by a 90° rotation about a vertical axis. The DNA is drawn in space-filling form with C white, N blue, O red, and P yellow. This type IA topoisomerase's active site is marked by the side chain of Phe 328, which is shown in space-filling form in yellow-green. [Based on an X-ray structure by Alfonso Mondragón, Northwestern University. PDBid 1I7D.]

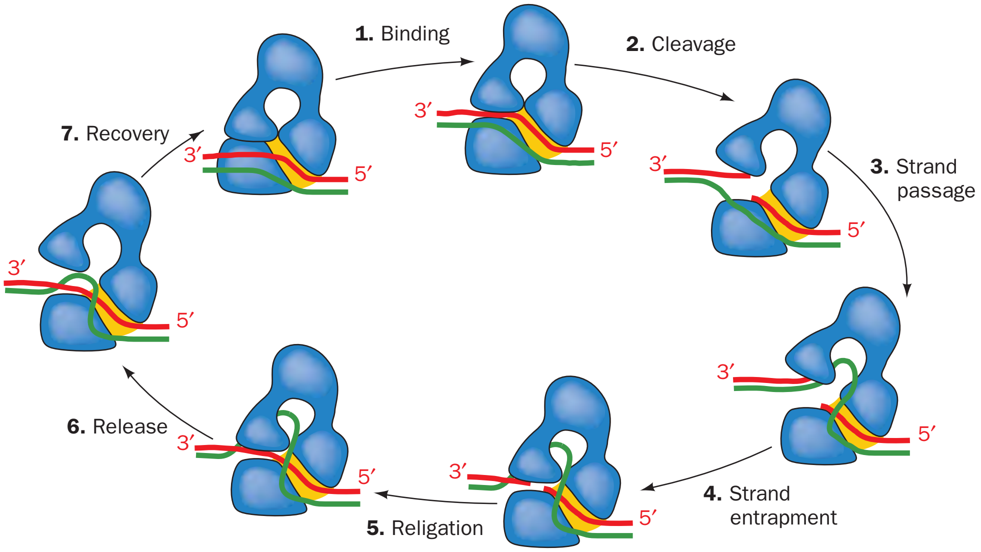

Figure 24-14 | Proposed mechanism for type IA topoisomerases. The enzyme is shown in blue with the yellow patch representing the binding groove for single-stranded (ss) DNA. The two DNA strands, which are drawn in red and green, could represent the two strands of a covalently closed circular duplex or two ss circles. **(1)** The enzyme recognizes a ss region of the DNA, here the red strand, and binds it in its binding groove. This is followed by or occurs simultaneously with the opening of a gap between domains I and III. **(2)** The DNA is cleaved, with the newly formed 5′ end becoming covalently linked to the active site Tyr and the segment with the newly formed 3′ end remaining tightly but noncovalently bound in the binding groove. **(3)** The unbroken (*green*) strand is passed through the opening formed by the cleaved (*red*) strand to enter the protein's central hole. **(4)** The unbroken strand is trapped by the partial closing of the gap. **(5)** The two cleaved ends of the red strand are rejoined in what is probably a reversal of the cleavage reaction. **(6)** The gap between domains I and III reopens to permit the escape of the red strand, yielding the reaction product in which the green strand has been passed through a transient break in the red strand. **(7)** The enzyme returns to its initial state. If the two strands form a negatively supercoiled duplex DNA, its linking number, L, has increased by 1; if they are separate ss circles, they have been catenated or decatenated. For negatively supercoiled duplex DNA, this process can be repeated until all of its supercoils have been removed ($W = 0$). [After a drawing by Alfonso Mondragón, Northwestern University.]

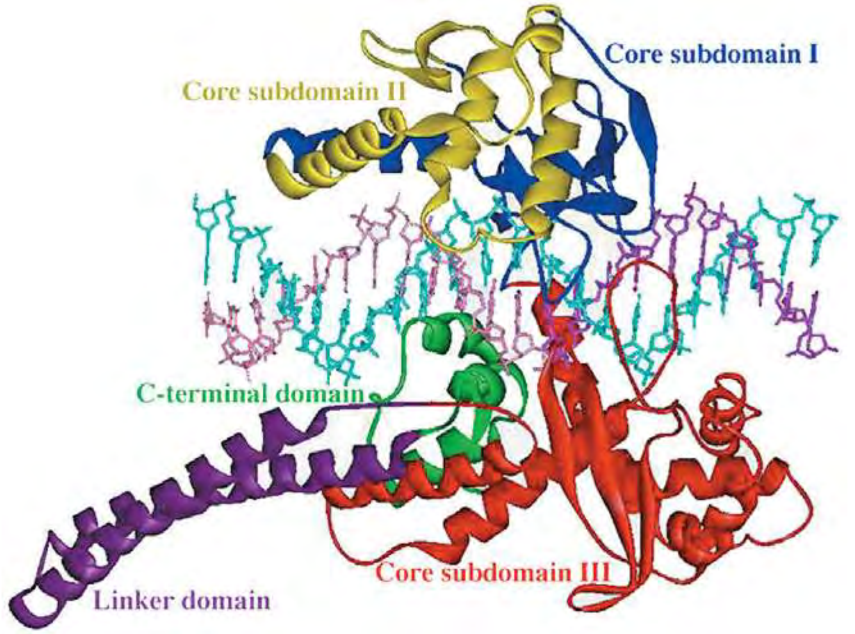

Figure 24-15 | X-Ray structure of the Y723F mutant of human topoisomerase I in complex with a 22-bp duplex DNA. This type IB topoisomerase consists of several domains and subdomains that are drawn here in different colors. Tyr 723 is on the C-terminal domain (*green*). The DNA's uncleaved strand is cyan, and the upstream and downstream portions of the scissile strand are magenta and pink, respectively. [Courtesy of Wim Hol, University of Washington. PDBid 1A36.]

through the nucleophilic attack of an active site Tyr on a DNA P atom to yield a 3′-linked phospho-Tyr intermediate and a free 5′-OH group on the succeeding nucleotide (in contrast to the 5′-linked phospho-Tyr and free 3′-OH group formed by type IA topoisomerases). The X-ray structure of the catalytically inactive Y723F mutant of human **topoisomerase I,** a type IB topoisomerase, in complex with a 22-bp duplex DNA was determined by Wim Hol. The core domain of the bilobal protein is wrapped around the DNA in a tight embrace (Fig. 24-15). If the mutant Phe 723 were the wild-type Tyr, its OH group would be ideally positioned to nucleophilically attack the P on the scissile P—O5′ bond so as to form a covalent linkage with the 3′ end of the cleaved strand. The protein interacts to a much greater extent with the five base pairs of the DNA's "downstream" segment (which would contain the cleaved strand's newly formed 5′ end) than it does with the base pairs of the DNA's "upstream" segment (to which Tyr 723 would be covalently linked), and in both cases it does so in a largely sequence-independent manner.

Topoisomerase I does not appear sterically capable of unwinding supercoiled DNA via the strand-passage mechanism that type IA topoisomerases follow (Fig. 24-14). Rather, it is likely that topoisomerase I relaxes DNA supercoils by permitting the cleaved duplex DNA's loosely held downstream segment to rotate relative to the tightly held upstream segment. This rotation can only occur about the sugar–phosphate bonds in the uncleaved strand (α, β, γ, ε, and ζ in Fig. 24-5) that are opposite the cleavage site because the cleavage frees those bonds to rotate. In support of this mechanism, the protein region surrounding the downstream segment contains 16 conserved, positively charged residues that form a ring about the duplex DNA, which apparently holds the DNA but not in any specific orientation. Nevertheless, the downstream segment is unlikely to rotate freely because the cavity containing it is shaped so as to interact with the downstream segment during some portions of its rotation. Hence, type IB topoisomerases are said to mediate a **controlled rotation** mechanism in relaxing supercoiled DNA. This unwinding is driven by the superhelical tension in the DNA and hence requires no other energy input.

Eventually, the DNA is religated by a reversal of the cleavage reaction and the now less supercoiled DNA is released.

Type II Topoisomerases Hydrolyze ATP. Type II topoisomerases are multimeric enzymes that require ATP hydrolysis to complete a reaction cycle in which two DNA strands are cleaved, duplex DNA is passed through the break, and the break is resealed. Type II topoisomerases therefore change the linking number in increments of two rather than one, as in type I topoisomerases. Both prokaryotic and eukaryotic type II enzymes relax negative and positive supercoils, but only the prokaryotic enzyme (also known as **DNA gyrase**) can introduce negative supercoils. The negative supercoils in eukaryotic chromosomes result primarily from its packaging in nucleosomes (Section 24-5B) rather than from topoisomerase action.

Type II topoisomerases superficially resemble the type I enzymes: They have a pair of catalytic Tyr residues, which form transient covalent intermediates with the 5′ ends of duplex DNA. They thereby mediate the cleavage of the two DNA strands at staggered sites to produce 4-nucleotide "sticky ends." Stephen Harrison and James Wang determined the X-ray structure of a large homodimeric fragment of yeast **topoisomerase II,** a type II topoisomerase, that can cleave duplex DNA but cannot transport it through the break because it lacks the intact protein's N-terminal ATPase domain. The heart-shaped dimer has a triangular hole that is 55 Å wide at its base and 60 Å high (Fig. 24-16), far larger than the diameter of B-DNA. The two active-site Tyr residues are located 27 Å apart, so they must move a considerable distance to link to the 5′ ends of a cleaved duplex DNA.

A proposed mechanism for type II topoisomerases, based on this X-ray structure, is diagrammed in Fig. 24-17. The DNA to be cleaved first binds to the enzyme and is clamped in place. In the presence of ATP, the bound

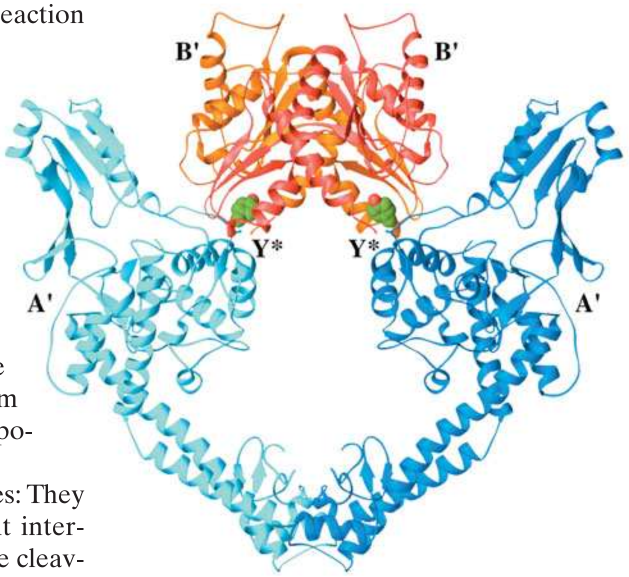

Figure 24-16 | **X-Ray structure of yeast topoisomerase II.** This homodimeric type II enzyme (residues 410–1202 of the 1429-residue protein) is viewed with its twofold axis vertical. The A′ and B′ subfragments of one subunit are blue and red, and those of the other subunit are cyan and orange. The active-site Tyr side chains (Y*) are shown in space-filling form with C green and O red. [Based on an X-ray structure by James Berger, Stephen Harrison, and James Wang, Harvard University. PDBid 1BGW.] **See Interactive Exercise 37.**

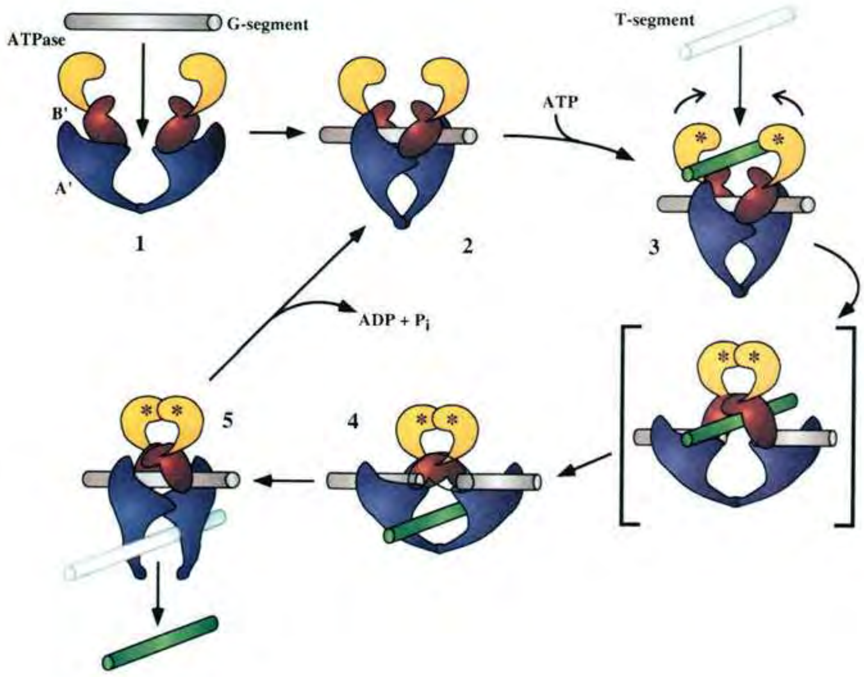

Figure 24-17 | **Proposed mechanism for Type II topoisomerase.** The protein's ATPase, B′, and A′ domains are colored yellow, red, and purple. **(1)** An unliganded enzyme binds duplex DNA (the so-called G-segment; *gray*), and a conformational change **(2)** clamps the DNA in place. **(3)** ATP binding (represented by asterisks) promotes cleavage of the G-segment DNA so that another duplex DNA (the T-segment; *green*) can pass into the central hole of the enzyme **(4)**. This DNA transport step is shown as proceeding through a hypothetical intermediate drawn inside square brackets. The G-segment is then resealed **(5)**, and the T-segment exits the enzyme. ATP hydrolysis and release regenerate state **2.** [Courtesy of Stephen Harrison and James Wang, Harvard University.]

DNA is cleaved and a second duplex DNA is passed through the opening into the central hole of the protein. The cleaved DNA is then resealed and the transported DNA exits the complex at a point opposite its point of entry. ATP hydrolysis to ADP + P_i prepares the enzyme for an additional catalytic cycle. The importance of topoisomerases in maintaining DNA in its proper topological state is indicated by the fact that many antibiotics and chemotherapeutic agents are inhibitors of topoisomerases (Box 24-2).

CHECK YOUR UNDERSTANDING

Describe the structural differences between A-, B-, and Z-DNA, including handedness, diameter, and presence of grooves.
How do the structures of RNA and DNA differ?
Explain why most nucleotides adopt the anti conformation.
In what nucleic acid conformation(s) does the ribose pucker with C2′ *endo*? C3′ *endo*?
Summarize the relationship between linking number, twist, and writhing number.
How do type IA, type IB, and type II topoisomerases alter DNA topology?

2 Forces Stabilizing Nucleic Acid Structures

LEARNING OBJECTIVES

- Understand that DNA can be denatured by heating and renatured through annealing.
- Understand that a double-stranded nucleic acid structure is stabilized by hydrogen bonding between base pairs, by stacking interactions, and by ionic interactions.
- Understand that RNA assumes more varied shapes than DNA and in some cases has catalytic activity.

DNA does not exhibit the structural complexity of proteins because it has only a limited repertoire of secondary structures and no comparable tertiary or quaternary structures. This is perhaps to be expected since the 20 amino acid residues of proteins have a far greater range of chemical and physical properties than do the four DNA bases. Nevertheless, many RNAs have well-defined tertiary structures. In this section, we examine the forces that determine the structures of nucleic acids.

A | DNA Can Undergo Denaturation and Renaturation

When a solution of duplex DNA is heated above a characteristic temperature, its native structure collapses and its two complementary strands separate and assume random conformations (Fig. 24-18). The denaturation process is accompanied by a qualitative change in the DNA's physical properties. For example, the characteristic high viscosity of native DNA solutions, which arises from the resistance to deformation of its rigid and rodlike duplex molecules, drastically decreases when the DNA decomposes to the conformationally flexible single chains. Likewise, DNA's ultraviolet absorbance, which is almost entirely due to its aromatic bases, increases by ~40% on denaturation (Fig. 24-19) as a consequence of the disruption of the electronic interactions among neighboring bases. The increase in absorbance is known as the **hyperchromic effect.**

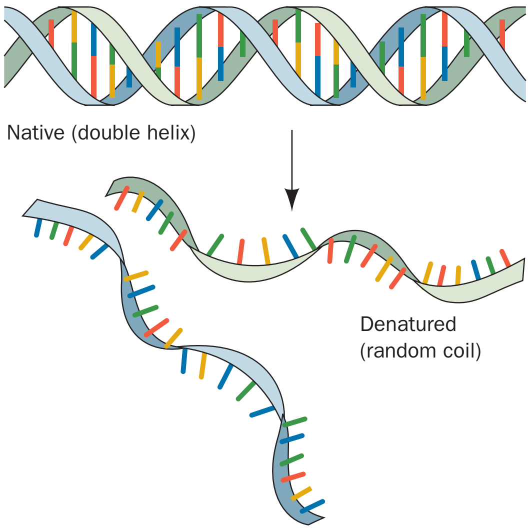

Figure 24-18 | A schematic representation of DNA denaturation.

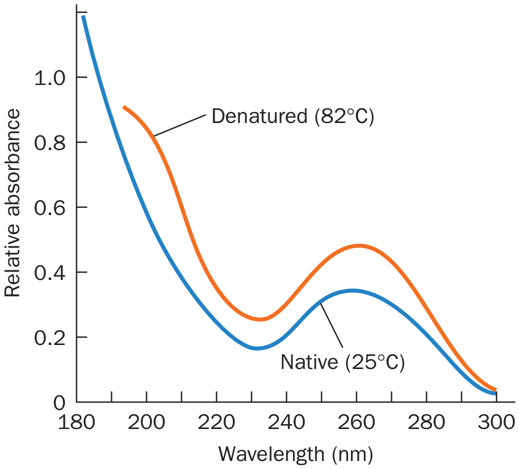

Figure 24-19 | The UV absorbance spectra of native and heat-denatured *E. coli* DNA. Note that denaturation does not change the general shape of the absorbance curve but only increases its intensity. [After Voet, D., Gratzer, W.B., Cox, R.A., and Doty, P., *Biopolymers* **1,** 205 (1963).] **See the Animated Figures.**

BOX 24-2 **BIOCHEMISTRY IN HEALTH AND DISEASE**

Inhibitors of Topoisomerases as Antibiotics and Anticancer Chemotherapeutic Agents

Type II topoisomerases are inhibited by a variety of compounds. For example, **ciprofloxacin** and **novobiocin** (*below*) specifically inhibit DNA gyrase but not eukaryotic topoisomerase II and are therefore antibiotics. In fact, ciprofloxacin is the most efficacious oral antibiotic presently in clinical use (e.g., it is the preferred antibiotic in the treatment of anthrax). In contrast, novobiocin's adverse side effects and the rapid generation of bacterial resistance to its presence have resulted in the discontinuation of its use in the treatment of human infections. A number of substances, including **doxorubicin** and **etoposide,** inhibit eukaryotic type II topoisomerases and are therefore widely used in cancer chemotherapy.

Different type II topoisomerase inhibitors act in one of two ways. Many of these agents, including novobiocin, inhibit their target enzyme's ATPase activity. They therefore kill cells by blocking topoisomerase activity, which results in the arrest of DNA replication and RNA transcription since the cell can no longer control the level of supercoiling in its DNA. However, other substances, including ciprofloxacin, doxorubicin, and etoposide, enhance the rate at which their target type II topoisomerases cleave double-stranded DNA and/or reduce the rate at which the breaks are resealed. Consequently, these substances induce higher than normal levels of transient protein-bridged breaks in the DNA of treated cells. The protein bridges are easily ruptured by the passage of the replication and transcription machinery, thereby rendering the breaks permanent. Although all cells have extensive enzymatic machinery for repairing damaged DNA (Section 25-5), a sufficiently high level of DNA damage can overwhelm the repair mechanisms and trigger cell death. Consequently, since rapidly replicating cells such as cancer cells have elevated levels of type II topoisomerases, they are far more likely to incur lethal DNA damage through the inhibition of their type II topoisomerases than are slow-growing or quiescent cells.

Camptothecin and its derivatives, the only known inhibitors of type IB topoisomerases, act by prolonging the lifetime of the covalent enzyme–DNA intermediate. These substances bind to the complex between the ends of the severed DNA strand, positioning the 5′-OH groups over 4.5 Å away from the phosphate groups that must be reattached in the religation reaction. Because the nicked DNA cannot be replicated, camptothecin prevents the proliferation of rapidly growing cells such as cancer cells and hence is a potent anticancer agent.

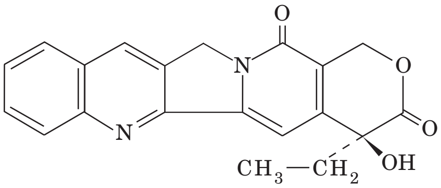

Camptothecin

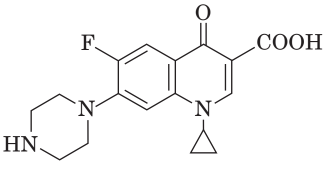

Ciprofloxacin

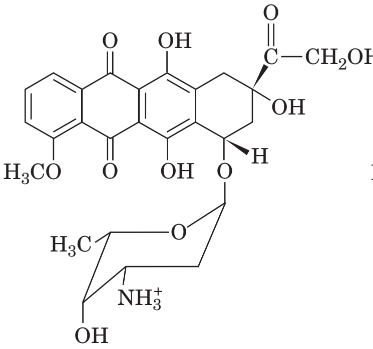

Doxorubicin

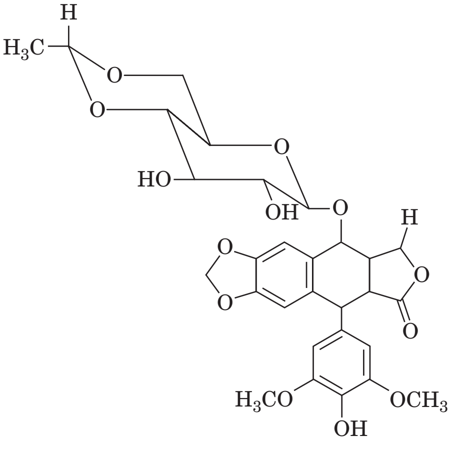

Etoposide

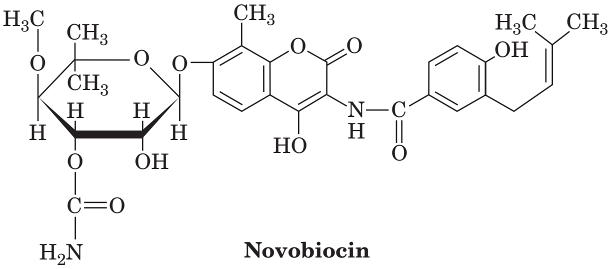

Novobiocin

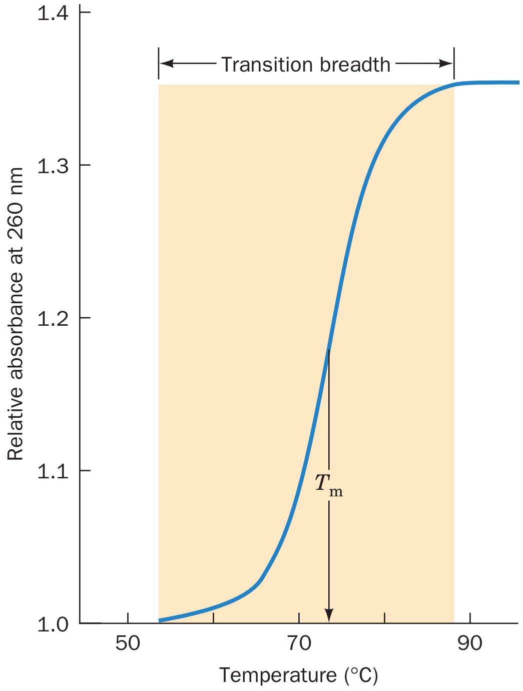

Figure 24-20 | An example of a DNA melting curve. The relative absorbance is the ratio of the absorbance (customarily measured at 260 nm) at the indicated temperature to that at 25°C. The melting temperature, T_m, is the temperature at which half of the maximum absorbance increase is attained. **See the Animated Figures.**

Monitoring the changes in absorbance at a single wavelength (usually 260 nm) as the temperature increases reveals that the increase in absorbance occurs over a narrow temperature range (Fig. 24-20). This indicates that *the denaturation of DNA is a cooperative phenomenon in which the collapse of one part of the structure destabilizes the remainder.* In analogy with the melting of a solid, Fig. 24-20 is referred to as a **melting curve,** and the temperature at its midpoint is defined as its **melting temperature, T_m.**

The stability of the DNA double helix, and hence its T_m, depends on several factors, including the nature of the solvent, the identities and concentrations of the ions in solution, and the pH. T_m also increases linearly with the mole fraction of G · C base pairs, although this is not, as one might expect, entirely because G · C base pairs contain one more hydrogen bond than A · T base pairs (see below).

DNA Can Be Renatured by Cooling. If a solution of denatured DNA is rapidly cooled below its T_m, the resulting DNA will be only partially base-paired (Fig. 24-21), because the complementary strands will not have had sufficient time to find each other before the randomly base-paired structure becomes effectively "frozen in." If, however, the temperature is maintained ~25°C below the T_m, enough thermal energy is available for short base-paired regions to rearrange by melting and re-forming. Under such **annealing** conditions, as Julius Marmur discovered in 1960, denatured DNA eventually completely renatures. Likewise, complementary strands of RNA and DNA, in a process known as **hybridization,** form RNA–DNA hybrid double helices that are only slightly less stable than the corresponding DNA double helices.

B | Nucleic Acids Are Stabilized by Base Pairing, Stacking, and Ionic Interactions

Base pairing is apparently a "glue" that holds together double-stranded nucleic acids, although other intramolecular forces help shape nucleic acid structures. Only **Watson–Crick base pairs** normally occur in DNA structures, but other hydrogen-bonded base pairs are known, particularly in RNA (Fig. 24-22). For example, in some A · T base pairs, adenine N7 is the hydrogen bond acceptor (**Hoogsteen** geometry; Fig. 24-22*a*) rather than N1 (Watson–Crick geometry; Fig. 24-1).

Observations of DNA structures indicate that *Watson–Crick geometry is the most stable mode of base pairing in the double helix, even though non-Watson–Crick base pairs are theoretically possible.* Initially, it was believed that the geometrical constraints of the double helix precluded other types of base pairing. Recall that because A · T, T · A, G · C, and C · G base pairs are

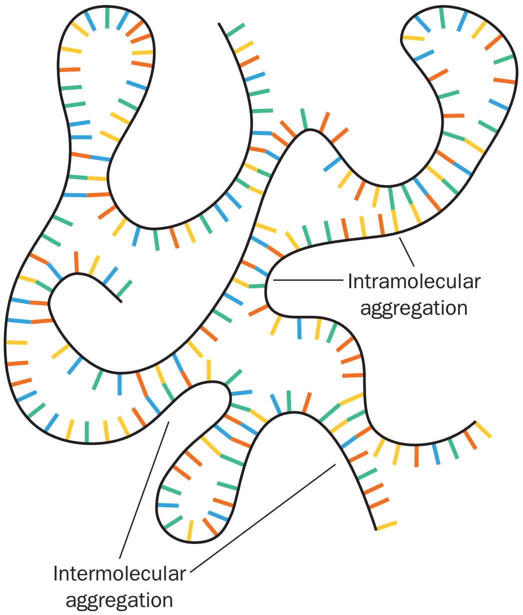

Figure 24-21 | Partially renatured DNA. This schematic representation shows the imperfectly base-paired structures assumed by DNA that has been heat-denatured and then rapidly cooled. Note that both intramolecular and intermolecular aggregation can occur.

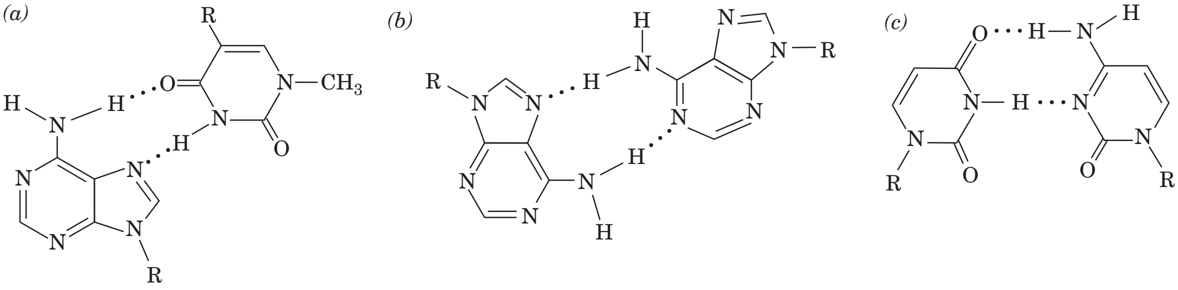

■ **Figure 24-22** | **Some non-Watson–Crick base pairs.** (*a*) Hoogsteen pairing between adenine and thymine residues. (*b*) An A · A base pair. (*c*) A U · C base pair. (R represents ribose-5-phosphate). Compare these base pairs to those shown in Fig. 24-1.

geometrically similar, they can be interchanged without altering the conformation of the sugar–phosphate chains. However, experimental measurements show that a major reason that other base pairs do not appear in the double helix is that *Watson–Crick base pairs have an intrinsic stability that non-Watson–Crick base pairs lack; that is, the bases in a Watson–Crick pair have a higher mutual affinity than those in a non-Watson–Crick pair.* Nevertheless, as we shall see, the double-helical segments of many RNAs contain unusual base pairs, such as G · U, that help stabilize their tertiary structures.

Hydrogen Bonds Only Weakly Stabilize Nucleic Acid Structures. It is clear that hydrogen bonding is required for the specificity of base pairing in DNA. Yet, as is also true for proteins (Section 6-4A), *hydrogen bonding contributes little to the stability of nucleic acid structures.* This is because, on denaturation, the hydrogen bonds between the base pairs of a native nucleic acid are replaced by energetically similar hydrogen bonds between the bases and water. Other types of forces must therefore play an important role in stabilizing nucleic acid structures.

Stacking Interactions Result from Hydrophobic Forces. Purines and pyrimidines tend to form extended stacks of planar parallel molecules. This has been observed in the structures of nucleic acids (Fig. 24-2*c*) and in the structures of crystallized nucleic acid bases (e.g., Fig. 24-23). These **stacking interactions** are a form of van der Waals interaction (Section 2-1A).

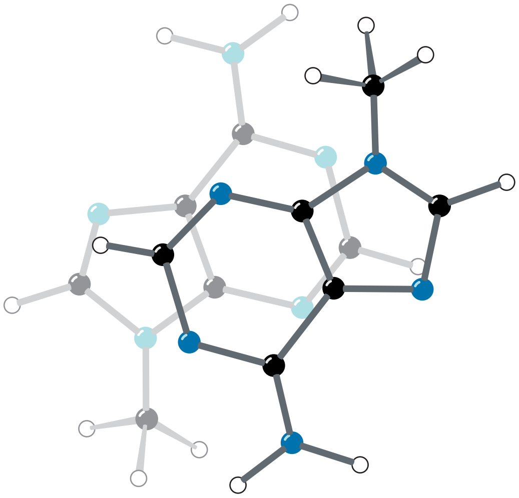

■ **Figure 24-23** | **The stacking of adenine rings in the X-ray structure of 9-methyladenine.** The partial overlap of the rings is typical of the association between bases in crystal structures and in double-helical nucleic acids. [After Stewart, R.F. and Jensen, L.H., *J. Chem. Phys.* **40,** 2071 (1964).]

Table 24-2 Stacking Energies for the Ten Possible Dimers in B-DNA

Stacked Dimer	Stacking Energy ($kJ \cdot mol^{-1}$)
C · G G · C	−61.0
C · G A · T	−44.0
C · G T · A	−41.0
G · C C · G	−40.5
G · C G · C	−34.6
G · C A · T	−28.4
T · A A · T	−27.5
G · C T · A	−27.5
A · T A · T	−22.5
A · T T · A	−16.0

Source: Ornstein, R.L., Rein, R., Breen, D.L., and MacElroy, R.D., *Biopolymers* **17,** 2356 (1978).

Interactions between stacked G and C bases are greater than those between stacked A and T bases (Table 24-2), which largely accounts for the greater thermal stability of DNAs with a high G + C content. Note also that differing sets of base pairs in a stack have different stacking energies. Thus, *the stacking energy of a double helix is sequence-dependent.*

One might assume that hydrophobic interactions in nucleic acids are qualitatively similar to those that stabilize protein structures. This is not the case. Recall that folded proteins are stabilized primarily by the increase in entropy of the solvent water molecules (the hydrophobic effect; Section 6-4A); in other words, protein folding is enthalpically opposed and entropically driven. In contrast, thermodynamic measurements reveal that the base stacking in nucleic acids is enthalpically driven and entropically opposed, although the theoretical basis for this observation is not well understood. The difference between hydrophobic forces in proteins and in nucleic acids may reflect the fact that nucleic acid bases are much more polar than most protein side chains (e.g., adenine versus the side chain of Phe or Leu). Whatever their origin, hydrophobic forces are of central importance in determining nucleic acid structures, as is clear from the denaturing effect of adding nonpolar solvents to aqueous solutions of DNA.

Cations Shield the Negative Charges of Nucleic Acids. Any theory of the stability of nucleic acid structures must take into account the electrostatic interactions of their charged phosphate groups. For example, the melting temperature of duplex DNA increases with the Na^+ concentration because the ions electrostatically shield the anionic phosphate groups from each other. Other monovalent cations such as Li^+ and K^+ have similar nonspecific interactions with phosphate groups. Divalent cations, such as Mg^{2+}, Mn^{2+}, and Co^{2+}, in contrast, specifically bind to phosphate groups, so *they are far more effective shielding agents for nucleic acids than are monovalent cations.* For example, an Mg^{2+} ion has an influence on the DNA double helix comparable to that of 100 to 1000 Na^+ ions. Indeed, enzymes that mediate reactions with nucleic acids or nucleotides almost always require an Mg^{2+} ion cofactor for activity. Mg^{2+} ions also play an essential role in stabilizing the complex structures assumed by many RNAs.

C | RNA Structures Are Highly Variable

The structure of RNA is stabilized by the same forces that stabilize DNA, and its conformational flexibility is limited by many of the same features that limit DNA conformation. In fact, RNA may be even more rigid than DNA owing to the presence of a greater number of water molecules that form hydrogen bonds to the 2′-OH groups of RNA. Even so, RNA comes in a greater variety of shapes and sizes than DNA and, in some cases, has catalytic activity.

RNAs May Contain Double-Stranded Segments. Bacterial ribosomes, which are two-thirds RNA and one-third protein, contain three highly conserved RNA molecules (Section 27-3). The smallest of these is the 120-nucleotide **5S RNA** [so named because it sediments in the ultracentrifuge at the rate of 5 Svedbergs (S); Section 21-1C]. 5S RNA has a secondary structure consisting of several base-paired regions connected by loops of various kinds (Fig. 24-24*a*). These structural elements can be discerned in the X-ray structure of this RNA molecule, in which the base-paired segments form mostly A-type helices (Fig. 24-24*b*). Approximately two-thirds of the bases in 5S rRNA participate in base-pairing interactions; the remaining nucleotides, which are located in loops and at the 3′ and 5′ ends,

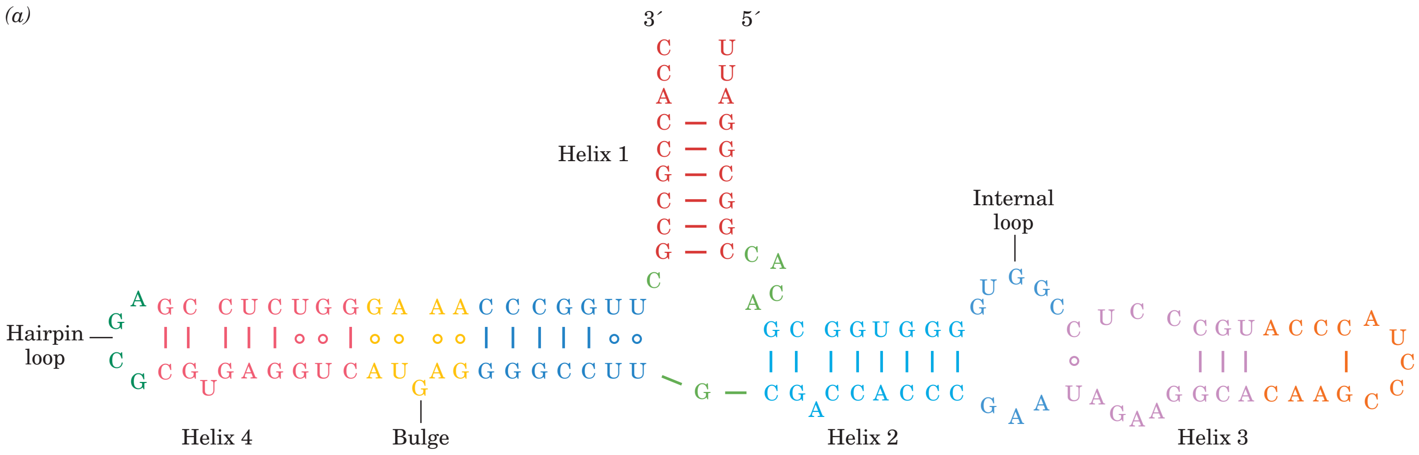

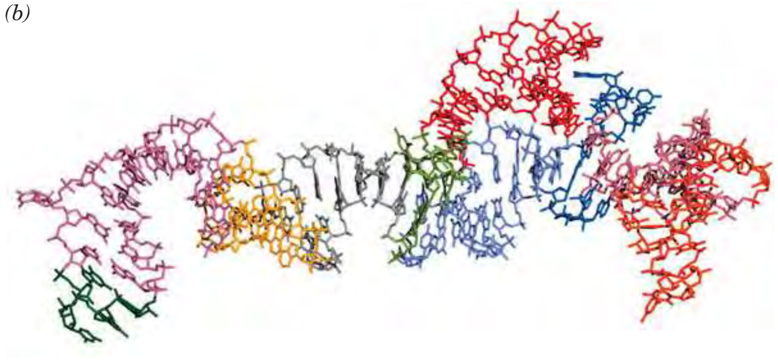

■ **Figure 24-24 | Secondary and tertiary structure of 5S RNA from *Haloarcula marismortui.*** (*a*) Secondary structure diagram. This single-stranded RNA molecule contains four double-stranded base-paired helices, as well as hairpin loops, internal loops, and bulges. The dashes indicate Watson–Crick base pairing, and circles indicate other modes of base pairing. (*b*) The X-ray structure in stick form colored according to its secondary structure as in Part *a.* [Based on an X-ray structure by Peter Moore and Thomas Steitz, Yale University. PDBid 1JJ2.]

are free to interact with ribosomal proteins or with unpaired nucleotides in other rRNA molecules.

Large RNA molecules presumably fold in stages, as do multidomain proteins (Section 6-5). RNA folding is almost certainly a cooperative process, with the rapid formation of short duplex regions preceding the collapse of the structure into its mature conformation. The complete folding process may take several minutes, it may involve relatively stable intermediates, and it may require the assistance of proteins.

RNA Molecules Are Stabilized by Stacking Interactions. The three-dimensional structure of the yeast transfer RNA that forms a covalent complex with Phe **(tRNA$^{\text{Phe}}$)** was elucidated in 1974 by Alexander Rich in collaboration with Sung-Hou Kim and, in a different crystal form, by Aaron Klug. The molecule is compact and L-shaped, with each leg of the L ~60 Å long (Fig. 24-25). The structural complexity of yeast tRNA$^{\text{Phe}}$ is reminiscent of that of a protein. Although only 42 of its 76 bases occur in double-helical stems, 71 of them participate in stacking associations.

tRNA structures are characterized by the presence of covalently modified bases and unusual base pairs, including hydrogen-bonding associations involving three bases. These tertiary interactions contribute to the compact structure of the tRNAs (tRNA structure is discussed in greater detail in Section 27-2A).

Some RNAs Are Catalysts. Although the discovery of catalytic RNA in 1982 was initially greeted with skepticism, subsequent studies have demonstrated that the catalytic potential of RNA is virtually unlimited. *At least nine naturally occurring types of catalytic RNAs have been described, and*

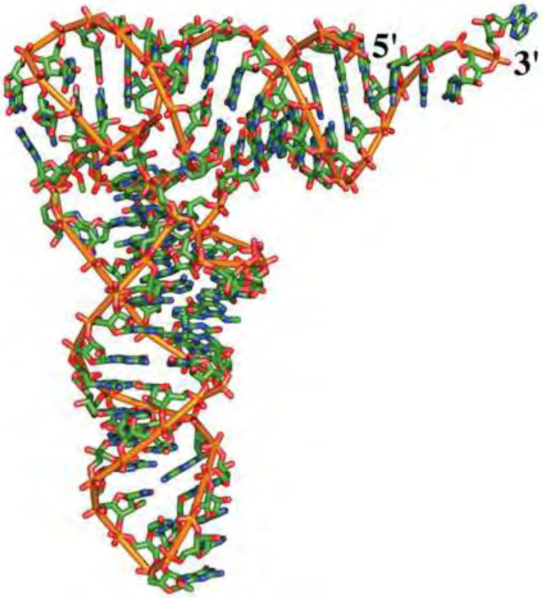

■ **Figure 24-25 | Structure of yeast tRNA$^{\text{Phe}}$.** The 76-nucleotide RNA is shown in stick form with C green, N blue, O red, and P orange and with successive P atoms linked by orange rods. Nearly all the bases are stacked, thereby stabilizing the compact structure of the tRNA. [After an X-ray structure by Alexander Rich and Sung-Hou Kim, MIT. PDBid 6TNA.]

many more ***ribozymes*** *have been developed in the laboratory.* Most naturally occurring RNA catalysts participate in aspects of RNA metabolism such as mRNA splicing (Section 26-3A) and hydrolytic RNA processing (Section 26-3B). The formation of peptide bonds during protein synthesis is catalyzed by ribosomal RNA (Section 27-4). *In vitro,* RNA molecules can catalyze some of the reactions required for their own production, such as the synthesis of glycosidic bonds and nucleotide polymerization. This functional versatility has led to the hypothesis that RNA once carried out many of the basic activities of early life, before DNA or proteins had evolved. This scenario has been dubbed the RNA world (Box 24-3).

One of the best-characterized ribozymes is the **hammerhead ribozyme,** a minimally ~40-nt molecule that participates in the replication of certain virus-like RNAs that infect plants and also occurs in schistosomes (species of parasitic flat worms). The hammerhead ribozyme catalyzes the site-specific cleavage of one of its own phosphodiester bonds. The secondary structures of the 63-nt hammerhead ribozyme from *Schistosoma mansoni,* which cleaves itself between its C-17 and C-1.1 nucleotides, has three duplex stems and a catalytic core of two nonhelical segments (Fig. 24-26*a*). The X-ray structure of this hammerhead ribozyme (Fig. 24-26*b*), determined by William Scott, reveals that it forms three A-type helices. The nucleotides in the helical stems mainly form normal Watson–Crick base pairs, whereas the various loops and bulges interact through a variety of hydrogen bonding and base stacking interactions.

The bases in the highly conserved catalytic core of the hammerhead ribozyme participate in an extensive hydrogen bonded network. This helps position C-17 such that its O2′ atom is properly oriented for nucleophilic attack on the P atom linking atom O3′ of C-17 to atom O5′ of C-1.1, so as to yield a cyclic 2′,3′-phosphodiester on C-17 together with a free 5′-OH on C-1.1. The 2'-OH of the invariant G-8 and N1 of the invariant G-12

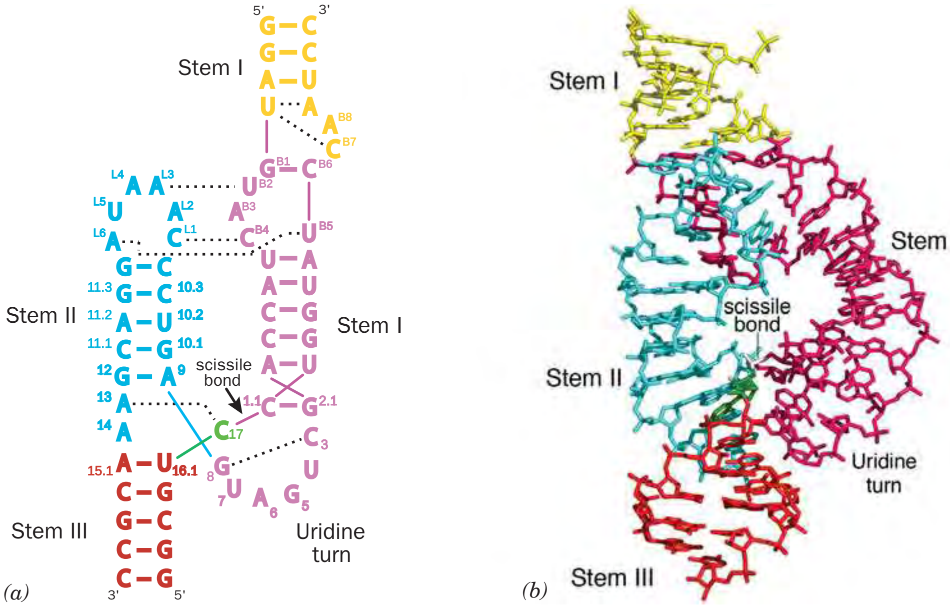

Figure 24-26 | Structure of a hammerhead ribozyme. (*a*) The sequence and schematic structural representation of the ribozyme oriented and colored to match the X-ray structure drawn in Part *b*. Base pairs are represented by colored lines and dotted lines represent tertiary interactions. Nucleotides are labeled according to the universal numbering system. (*b*) X-ray structure of the ribozyme drawn in stick form. The scissile phosphate (bridging C-17 and C-1.1) and the nucleophile (O2′ of C-17) are highlighted in white. [Courtesy of William Scott, University of California at Santa Cruz. PDBid 2GOZ.] **See Interactive Exercise 38.**

BOX 24-3 **PERSPECTIVES IN BIOCHEMISTRY**

The RNA World

The observations that nucleic acids but not proteins can direct their own synthesis, that cells contain batteries of protein-based enzymes for manipulating DNA (Chapter 25) but few for processing RNA, and that many coenzymes in biosynthetic processes and energy-harvesting pathways are ribonucleotides (e.g., ATP, NAD^+, FAD, and coenzyme A) led to the hypothesis that *RNAs were the original biological catalysts in precellular times—the so-called* ***RNA world.*** Indeed, RNA remains the carrier of genetic information in viruses with single- or double-stranded RNA genomes. The fact that RNA-based functions are distributed across all three domains of life provides additional evidence that the role of RNA in modern cells reflects its establishment very early in evolution.

Assuming that an RNA world did once exist, we must ask two questions: Why did protein catalysts take the place of most ribozymes, and why did DNA become the dominant molecule of heredity? The first question is readily answered by observing that the 20 amino acid residues of proteins contain functional groups—hydroxyl, sulfhydryl, amide, and carboxylate groups—that are lacking in RNA, whose four nucleotide residues are more uniform and less reactive. Thus, proteins probably replaced RNA as cellular workhorses by virtue of their greater chemical virtuosity. Nevertheless, RNA continues to play the dominant role in the synthesis of proteins: Ribosomes are predominantly RNA, which is now known to catalyze peptide bond formation (Section 27-4B).

As for DNA, it is more stable than RNA because RNA is highly susceptible to base-catalyzed hydrolysis by the reaction mechanism at the right. The base-induced deprotonation of the 2′-OH group facilitates its nucleophilic attack on the adjacent phosphorus atom, thereby cleaving the RNA backbone. The resulting 2′,3′-cyclic phosphate group subsequently hydrolyzes to produce a 2′- or 3′-nucleotide product (the RNase A–catalyzed hydrolysis of RNA follows a nearly identical reaction sequence but generates only 3′-nucleotides; Section 11-3A). DNA is not susceptible to such degradation because it lacks a 2′-OH group. This greater chemical stability of DNA makes it more suitable than RNA for the long-term storage of genetic information.

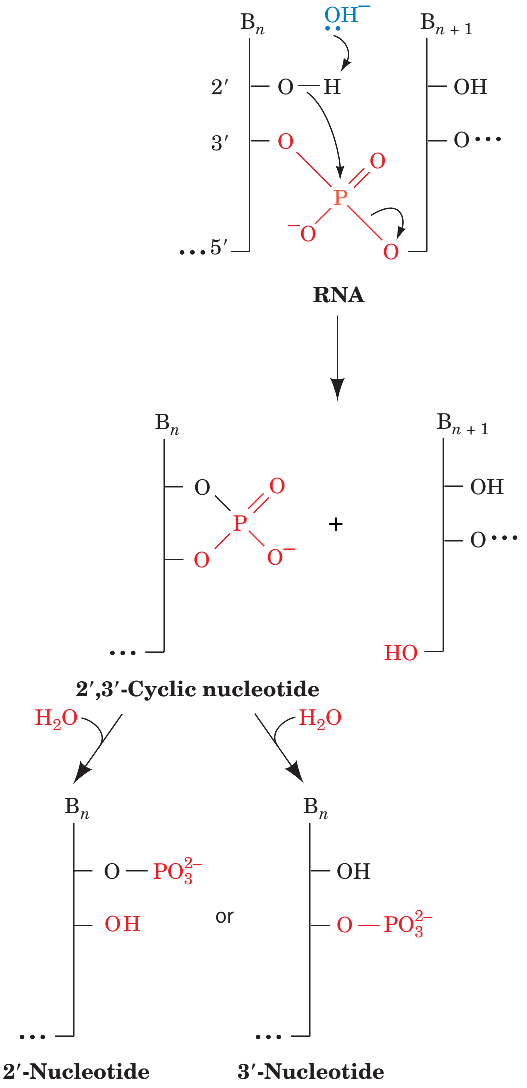

when deprotonated appear to be properly positioned to act as acid and base catalysts in this reaction. Interestingly, no metal ions are present in the ribozyme's active site region.

The hammerhead ribozyme is not a true catalyst, since it is its own substrate and hence cannot return to its original state. However, other ribozymes catalyze multiple turnovers without themselves undergoing alteration. Ribozymes are comparable to protein enzymes in their rate enhancement (10^9-fold for the hammerhead ribozyme), in their ability to use cofactors such as metal ions or imidazole groups, and in their regulation by small allosteric effectors. Although RNA molecules lack the repertoire of functional groups possessed by protein catalysts, RNA molecules can assume conformations that specifically bind substrates, orient them for reaction, and stabilize the transition state—all hallmarks of enzyme catalysts.

CHECK YOUR UNDERSTANDING

Explain the molecular events of nucleic acid denaturation and renaturation.

Describe the forces that stabilize nucleic acid structure.

What properties allow RNA molecules to act as catalysts?

3 Fractionation of Nucleic Acids

LEARNING OBJECTIVE

- Understand that nucleic acids can be fractionated on the basis of size, composition, and sequence by chromatography and electrophoresis.

In Section 5-2 we considered the most common procedures for isolating and characterizing proteins. Most of these methods, often with some modifications, are also used to fractionate nucleic acids according to size, composition, and sequence. There are also many techniques that apply only to nucleic acids. In this section, we outline some of the most useful nucleic acid fractionation procedures.

Nucleic acids in cells are invariably associated with proteins. Once cells have been broken open, their nucleic acids are usually deproteinized. This can be accomplished by shaking the protein–nucleic acid mixture with a phenol solution so that the protein precipitates and can be removed by centrifugation. Alternatively, the protein can be dissociated from the nucleic acids by detergents, guanidinium chloride, or high salt concentration, or it can be enzymatically degraded by proteases. In all cases, the nucleic acids, a mixture of RNA and DNA, can then be isolated by precipitation with ethanol. The RNA can be recovered from such precipitates by treating them with pancreatic DNase to eliminate the DNA. Conversely, the DNA can be freed of RNA by treatment with RNase.

In all these and subsequent manipulations, the nucleic acids must be protected from degradation by nucleases that occur both in the experimental material and on human hands. Nucleases can be inhibited by chelating agents such as EDTA, which sequester the divalent metal ions they require for activity. Laboratory glassware can also be autoclaved to heat-denature the nucleases. Nevertheless, nucleic acids are generally easier to handle than proteins because most lack a complex tertiary structure and are therefore relatively tolerant of extreme conditions.

A | Nucleic Acids Can Be Purified by Chromatography

Many of the chromatographic techniques that are used to separate proteins (Section 5-2C) also apply to nucleic acids. However, **hydroxyapatite,** a form of calcium phosphate [$Ca_5(PO_4)_3OH$], is particularly useful in the chromatographic purification and fractionation of DNA. Double-stranded DNA binds to hydroxyapatite more tightly than do most other molecules. Consequently, DNA can be rapidly isolated by passing a cell lysate through a hydroxyapatite column, washing the column with a phosphate buffer of concentration low enough to release only the RNA and protein, and then eluting the DNA with a concentrated phosphate solution.

Affinity chromatography is used to isolate specific nucleic acids. For example, most eukaryotic messenger RNAs (mRNAs) have a poly(A) sequence at their 3′ ends (Section 26-3A). They can be isolated on agarose or cellulose to which poly(U) is covalently attached. The poly(A) sequences specifically bind to the complementary poly(U) in high salt and at low temperature and can later be released by altering those conditions.

B | Electrophoresis Separates Nucleic Acids by Size

Nucleic acids of a given type can be separated by polyacrylamide gel electrophoresis (Section 3-4B) because their electrophoretic mobilities in such gels vary inversely with their molecular masses. However, DNAs of more than a few thousand base pairs cannot penetrate even a weakly cross-linked polyacrylamide gel and so must be separated in agarose gels. Yet conventional gel electrophoresis is limited to DNAs of $<$100,000 bp, because larger DNA molecules tend to worm their way through the agarose at a rate independent of their size. Charles Cantor and Cassandra Smith overcame this limitation by developing **pulsed-field gel electrophoresis (PFGE),** which can resolve DNAs of up to 10 million bp (6.6 million kD). In the simplest type of PFGE apparatus, the polarity of the electrodes is periodically reversed, with the duration of each pulse varying from 0.1 to 1000 s, depending on the sizes of the DNAs being separated. With each change in polarity, the migrating DNA must reorient to the new electrical field before it can resume movement. A DNA molecule may actually migrate backward for part of the time. Because small molecules reorient more quickly than large molecules, different-sized DNA molecules gradually separate (Fig. 24-27).

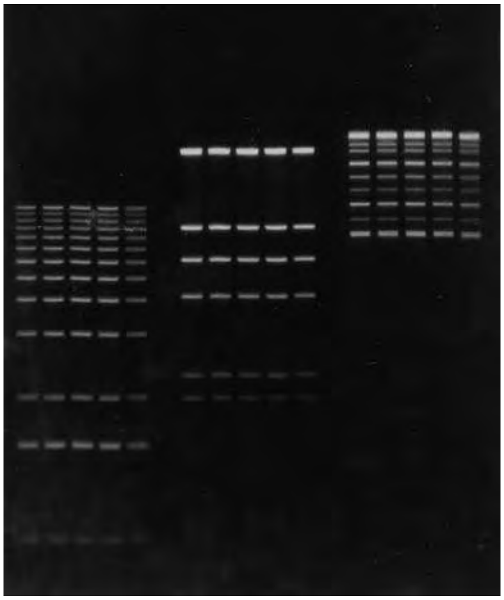

Figure 24-27 | Pulsed-field gel electrophoresis. The three samples contain DNA fragments ranging from 0.5 to 48.5 kb. The smallest (fastest migrating) molecules are at the bottom. [Courtesy of Hoefer Scientific Instruments.]

Intercalation Agents Stain Duplex DNA. The various DNA bands in a gel can be stained by planar aromatic cations such as **ethidium ion, acridine orange,** or **proflavin:**

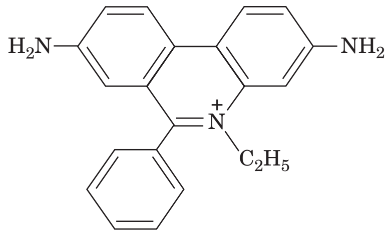

Ethidium

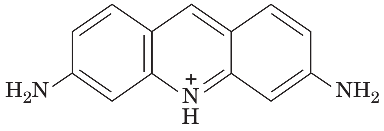

Proflavin

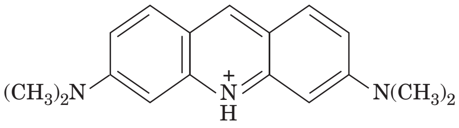

Acridine orange

The dyes bind to double-stranded DNA by **intercalation** (slipping in between the stacked bases; Fig. 24-28), where they exhibit a fluorescence under UV light that is far more intense than that of the free dye. As little as 50 ng of DNA can be detected in a gel by staining it with ethidium bromide. Single-stranded DNA and RNA also stimulate the fluorescence of ethidium but to a lesser extent than does duplex DNA.

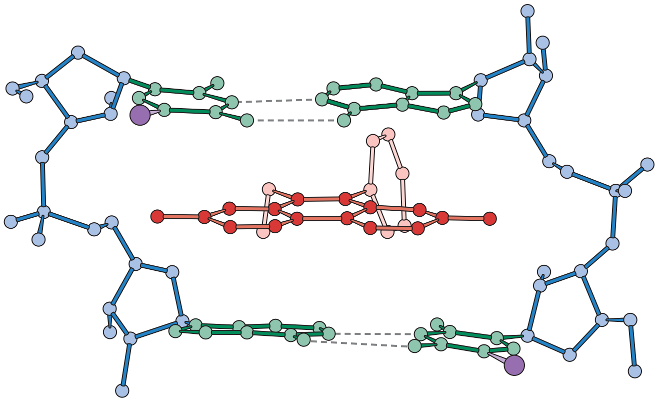

Figure 24-28 | X-Ray structure of a complex of ethidium with 5-iodo-UpA. Ethidium (*red*) intercalates between the base pairs of the double-helically paired dinucleotide and thereby provides a model of the binding of ethidium to duplex DNA. [After Tsai, C.-C., Jain, S.C., and Sobell, H.M., *Proc. Natl. Acad. Sci.* **72,** 629 (1975).]

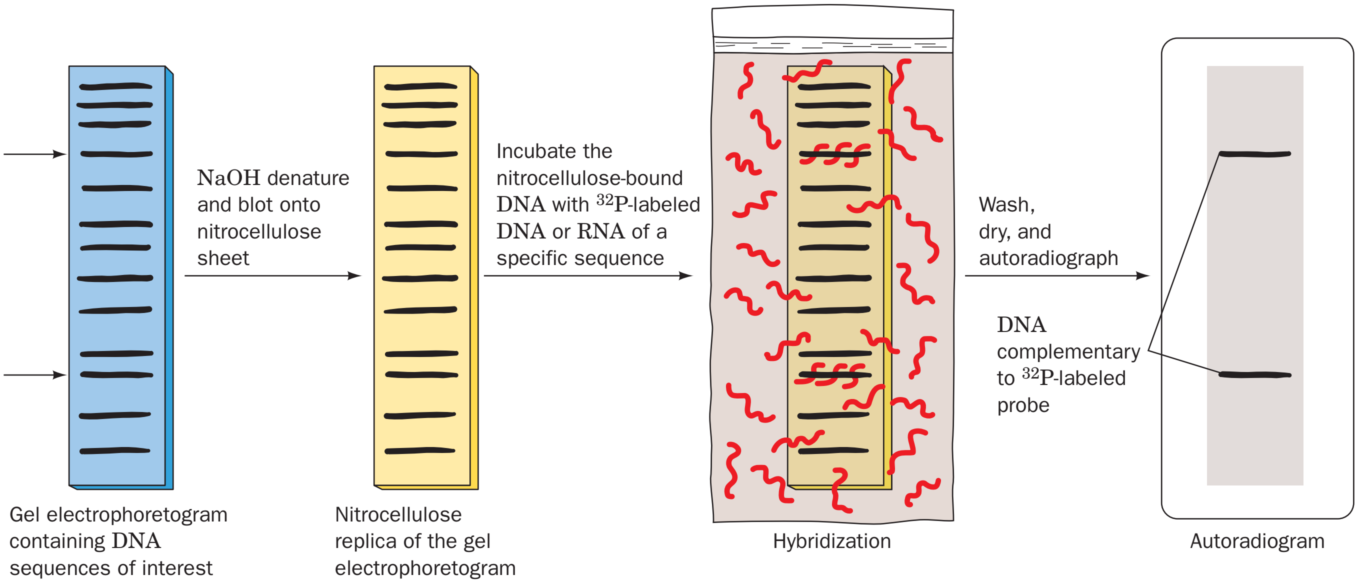
NaOH denature and blot onto nitrocellulose sheet
Incubate the nitrocellulose-bound DNA with ^{32}P-labeled DNA or RNA of a specific sequence
Wash, dry, and autoradiograph
DNA complementary to ^{32}P-labeled probe
Gel electrophoretogram containing DNA sequences of interest
Nitrocellulose replica of the gel electrophoretogram
Hybridization
Autoradiogram

Figure 24-29 | **The detection of DNAs containing specific base sequences by Southern blotting.**

Southern Blotting Identifies DNAs with Specific Sequences. DNA with a specific base sequence can be identified through a procedure developed by Edwin Southern known as **Southern blotting** (Fig. 24-29). This procedure takes advantage of the ability of nitrocellulose to tenaciously bind single-stranded but not duplex DNA. Following gel electrophoresis of double-stranded DNA, the gel is soaked in 0.5 M NaOH to convert the DNA to its single-stranded form. The gel is then overlaid by a sheet of nitrocellulose paper. Molecules in the gel are forced through the nitrocellulose by drawing out the liquid with a stack of absorbent towels compressed against the far side of the nitrocellulose, or by using an electrophoretic process **(electroblotting).** The single-stranded DNA binds to the nitrocellulose at the same position it had in the gel. After drying at 80°C, which permanently fixes the DNA in place, the nitrocellulose sheet is moistened with a minimal quantity of solution containing a ^{32}P-labeled single-stranded DNA or RNA probe that is complementary in sequence to the DNA of interest. The moistened nitrocellulose is held at a suitable renaturation temperature for several hours to permit the probe to hybridize to its target sequence(s), washed to remove the unbound radioactive probe, dried, and then autoradiographed by placing it for a time over a sheet of X-ray film. The positions of the molecules that are complementary to the radioactive probe are indicated by a blackening of the developed film.

Specific RNA sequences can be detected through a variation of the Southern blot, punningly named a **Northern blot,** in which the RNA is immobilized on nitrocellulose paper and probed with a complementary radioactive RNA or DNA. A specific protein can be analogously detected in an **immunoblot** or **Western blot** through the use of antibodies directed against the protein in a procedure similar to that used in an ELISA (Fig. 5-3).

CHECK YOUR UNDERSTANDING

Which fractionation procedures separate nucleic acids according to their binding affinity? According to their size?

LEARNING OBJECTIVES

- Understand that sequence-specific DNA-binding proteins interact with DNA via direct or indirect hydrogen bonds, van der Waals interactions, and ionic interactions.
- Understand that both the protein and the DNA may change their conformations on binding.
- Understand that DNA-binding proteins often include motifs such as the helix–turn–helix in prokaryotes, and the zinc finger and leucine zipper in eukaryotes.

4 DNA–Protein Interactions

The accessibility of genetic information depends on the ability of proteins to recognize and interact with DNA in a manner that allows the encoded information to be copied as DNA (in replication) or as RNA (in transcription). Even the most basic steps of these processes require many proteins that interact with each other and with the nucleic acids. In addition, organisms regulate the expression of most genes, which requires yet other proteins that act as repressors or activators of transcription.

Many proteins bind DNA nonspecifically, that is, without regard to the sequence of nucleotides. For example, histones (which are involved in packaging DNA; Section 24-5A) and certain DNA replication proteins (which must potentially interact with all the sequences of an organism's genome) bind to DNA primarily through interactions between protein functional groups and the sugar–phosphate backbone of DNA. Proteins that recognize specific DNA sequences presumably also bind nonspecifically but loosely to DNA so that they can scan the polynucleotide chain for their target sequences to which they then bind specifically and tightly. Most DNA–protein complexes have dissociation constants ranging from 10^{-9} to 10^{-12} M; these values represent binding that is 10^3 to 10^7 times stronger than nonspecific binding. Sequence-specific DNA–protein interactions must be extremely precise so that the proteins can exert their effects at sites selected from among—in the human genome—billions of base pairs. How do such proteins interact with their target sites on DNA?

Sequence-specific DNA-binding proteins generally do not disrupt the base pairs of the duplex DNA to which they bind. They do, however, *discriminate among the four base pairs ($A \cdot T$, $T \cdot A$, $G \cdot C$, and $C \cdot G$) according to the functional groups of the base pairs that project into DNA's major and minor grooves.* As can be seen in Fig. 24-2, these groups are more exposed in the major groove of B-DNA than in its narrower minor groove. Moreover, the major groove contains more sequence-specific functional groups than does the minor groove (Fig. 24-1). However, as revealed in a systematic survey of 129 protein–DNA complexes, only about one-third of the interactions between the binding protein and the DNA involve hydrogen bonds, either directly or via intervening water molecules. Approximately two-thirds of all interactions are van der Waals contacts. Ionic interactions with backbone phosphate groups also occur. The complementarity of the binding partners in many cases is augmented by an "induced fit" phenomenon in which the protein and the nucleic acid change their conformations for greater stability. In some cases, these changes allow the binding proteins to interact with other proteins or alter the accessibility of the DNA to other molecules. Below, we examine some examples of specific DNA–protein binding. We shall encounter many more examples of nucleic acid–protein interactions in subsequent chapters.

A | Restriction Endonucleases Distort DNA on Binding

Type II restriction endonucleases rid bacterial cells of foreign DNA by cleaving the DNA at specific sites that have not yet been methylated by the host's modification methylase (Section 3-4A). Restriction enzymes recognize palindromic DNA sequences of ~4 to 8 base pairs with such remarkable specificity that a single base change can reduce their activity by a millionfold. This degree of specificity is necessary to prevent accidental cleavage of other sites in a DNA sequence.

The X-ray structure of *Eco*RI endonuclease in complex with a segment of B-DNA containing the enzyme's recognition sequence was determined by John Rosenberg. The DNA binds in the symmetric cleft between the two identical 276-residue subunits of the dimeric enzyme (Fig. 24-30), thereby accounting for the DNA's palindromic recognition sequence. Protein binding causes the dihedral angle between the recognition sequence's central two base pairs to open up by ~50° toward the minor

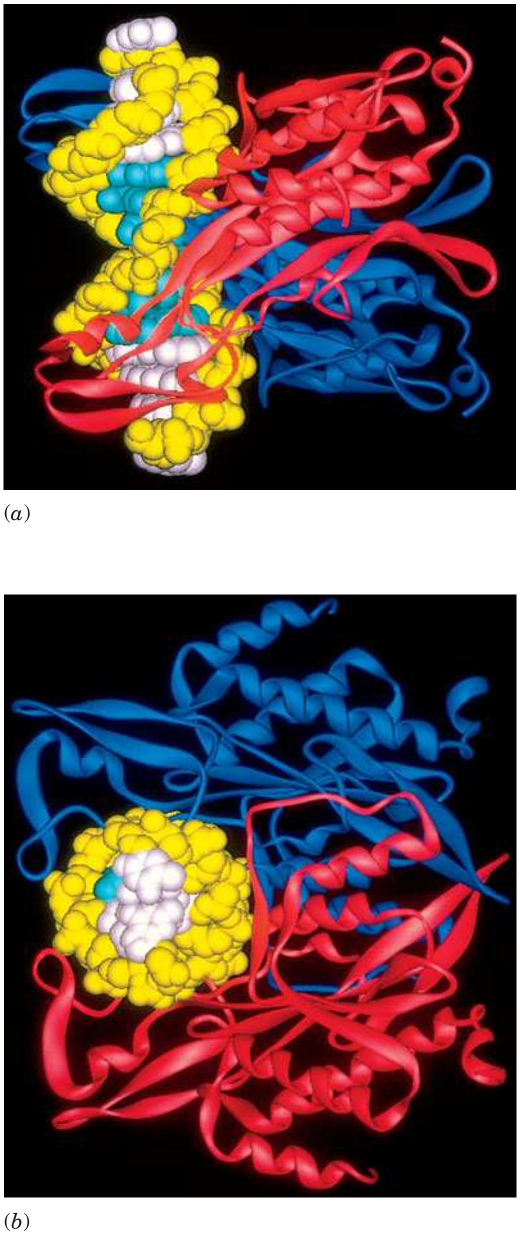

Figure 24-30 | X-Ray structure of *Eco*RI endonuclease in complex with DNA. The segment of duplex DNA has the self-complementary sequence TCGCGAATTCGCG (12 bp with an overhanging T at both 5′ ends; the enzyme's 6-bp target sequence is underlined) and is drawn as a space-filling model with its sugar–phosphate chains yellow, its recognition sequence bases cyan, and its other bases white. The protein is drawn in ribbon form with its two identical subunits red and blue. The complex is shown (*a*) with its DNA helix axis vertical and (*b*) in end view. The complex's twofold axis is horizontal and the DNA's major groove faces right (toward the protein) in both views. [Based on an X-ray structure by John Rosenberg, University of Pittsburgh. PDBid 1ERI.] **See Kinemage Exercise 18-1.**

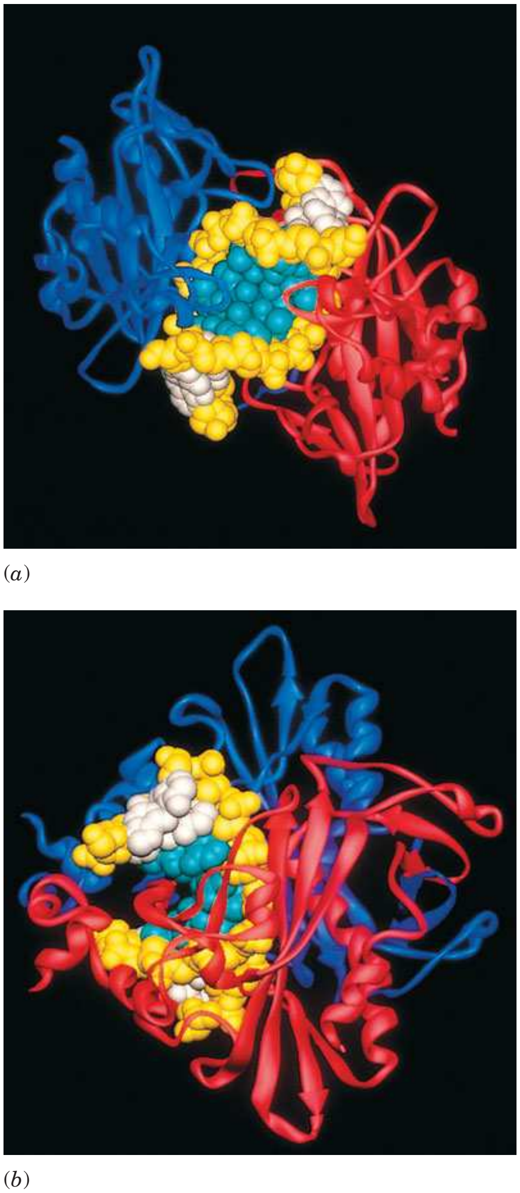

Figure 24-31 | X-Ray structure of *Eco*RV endonuclease in complex with DNA. The 10-bp segment of DNA has the self-complementary sequence GGGATATCCC (the enzyme's 6-bp target sequence is underlined). The DNA and protein are colored as in Fig. 24-30. (*a*) The complex as viewed along its twofold axis, facing the DNA's major groove. The two symmetry-related protein loops that overlie the major groove (composed of residues 182 to 186) are the only parts of the enzyme that make base-specific contacts with the DNA. (*b*) The complex as viewed from the right in Part *a* (the DNA's major groove faces left). Note how the protein kinks the DNA toward its major groove. [Based on an X-ray structure by Fritz Winkler, Hoffman-LaRoche Ltd., Basle, Switzerland. PDBid 4RVE.] **See Kinemage Exercise 18-2.**

groove. These base pairs thereby become unstacked, but the DNA remains nearly straight due to compensating bends at the adjacent base pairs. Nevertheless, this unwinds the DNA by 28° and widens the major groove by 3.5 Å at the recognition site. The N-terminal ends of a pair of parallel helices from each protein subunit are inserted into the widened major groove, where they participate in a hydrogen-bonded network with the bases of the recognition sequence. The phosphodiester cleavage points are located two bases from the center of the palindrome (Table 3-2).

Certain other restriction endonucleases, including *Eco*RV (Fig. 24-31), also induce kinks in the DNA, in some cases by opening up the minor groove and compressing the major groove. However, *complementary hydrogen bonding between the nucleotide bases and protein side chain and backbone groups, rather than the DNA distortion per se, is the primary prerequisite for the formation of a sequence-specific endonuclease–DNA complex.* For example, in the *Bam*HI–DNA complex, every potential hydrogen bond donor and acceptor in the major groove of the recognition site takes part in direct or water-mediated hydrogen bonds with the protein. No other DNA sequence could support this degree of complementarity with *Bam*HI.

See Guided Exploration 23
Transcription factor–DNA interactions.

B | Prokaryotic Repressors Often Include a DNA-Binding Helix

In prokaryotes, the expression of many genes is governed at least in part by **repressors,** proteins that bind at or near the gene so as to prevent its transcription (Section 28-2). These repressors often contain ~20-residue polypeptide segments that form a **helix–turn–helix (HTH) motif** containing two α helices that cross at an angle of ~120°. HTH motifs, which are apparently evolutionarily related, occur as components of domains that otherwise have widely varying structures, although all of them bind DNA. Note that HTH motifs are structurally stable only when they are components of larger proteins.

Like restriction endonuclease recognition sites, the sequences to which repressors bind (called **operators**) exhibit palindromic symmetry or nearly so. Typically, the repressors are dimeric, although their interactions with DNA may not be perfectly symmetrical. Binding involves interactions between the amino acid side chains extending from the second helix of the HTH motif (the "recognition" helix) and the bases and sugar–phosphate chains of the DNA.

The X-ray structure of a dimeric repressor from **bacteriophage 434** bound to its 20-bp recognition sequence was determined by Stephen Harrison. The **434 repressor** associates with the DNA in a twofold symmetric manner with a recognition helix from each subunit bound in successive turns of the DNA's major groove (Fig. 24-32). The repressor closely conforms to the DNA surface and interacts with its paired bases and sugar–phosphate chains through elaborate networks of hydrogen bonds, salt bridges, and van der Waals contacts. In the repressor–DNA complex,

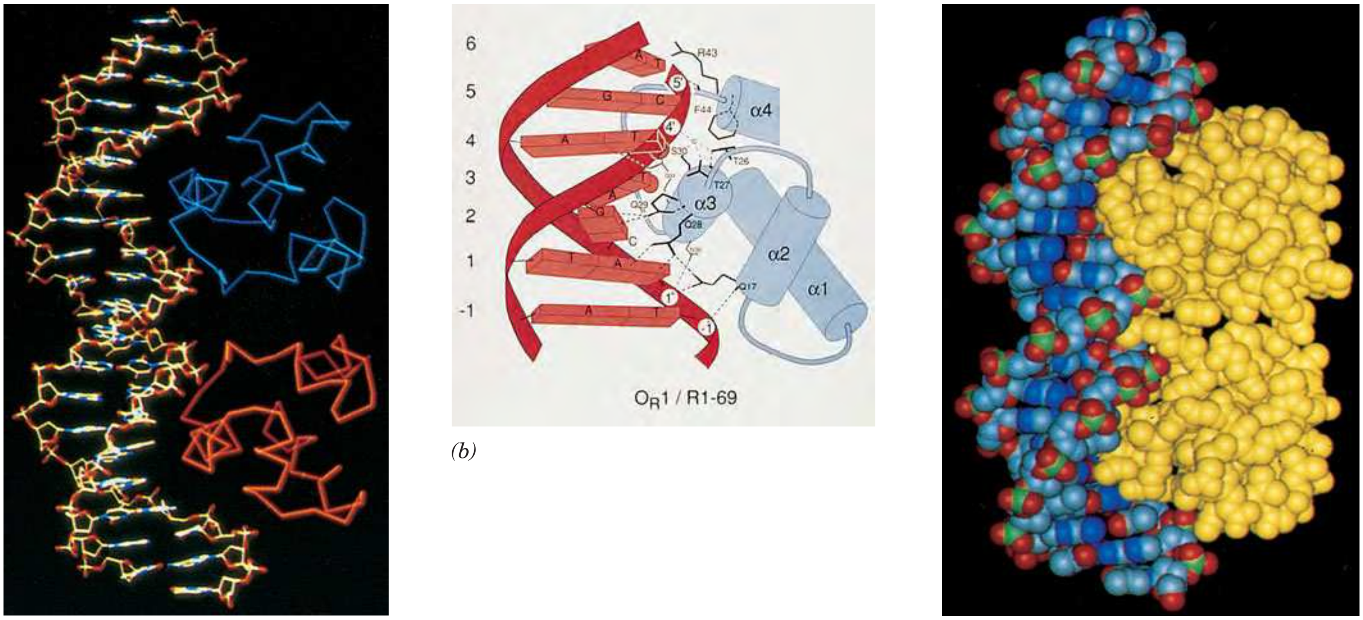

(a) *(b)* *(c)*

■ **Figure 24-32 | X-Ray structure of a portion of the 434 phage repressor in complex with its target DNA.** One strand of the 20-bp DNA (*left*) has the sequence d(TATACAAGAAAGTTTGTACT). (*a*) A skeletal model showing the DNA and the first 63 residues of the protein's two identical subunits (*blue and red,* C_α backbone only). (*b*) A schematic drawing indicating how the helix–turn–helix motif, which encompasses helices α2 and α3, interacts with the DNA. Residues are identified by single-letter codes. Short bars emanating from the polypeptide chain represent peptide NH groups, dashed lines represent hydrogen bonds, and numbered circles represent DNA phosphates. The small circle is a water molecule. (*c*) A space-filling model corresponding to Part *a*. All the protein's non-H atoms are drawn in yellow. [Courtesy of Aneel Aggarwal, John Anderson, and Stephen Harrison, Harvard University. PDBid 2OR1.] **See Interactive Exercise 39 and Kinemage Exercise 19.**

the DNA bends around the protein in an arc of radius ~65 Å, which compresses the minor groove by ~2.5 Å near its center (between the two protein monomers) and widens it by ~2.5 Å toward its ends.

The *E. coli trp* Repressor Binds DNA Indirectly. The *E. coli* ***trp*** **repressor** regulates the transcription of genes required for tryptophan biosynthesis (Section 28-2C). Paul Sigler determined the X-ray structure of the protein in complex with a DNA containing an 18-bp palindrome (of single-strand sequence TGTACTAGTTAACTAGTAC, where the *trp* repressor's target sequence is underlined) that closely resembles the *trp* operator. The homodimeric repressor protein also has HTH motifs whose recognition helices bind, as expected, in successive major grooves of the DNA, each in contact with half of the operator sequence (ACTAGT; Fig. 24-33). There are numerous hydrogen-bonding contacts between the *trp* repressor and the DNA's nonesterified phosphate oxygens.

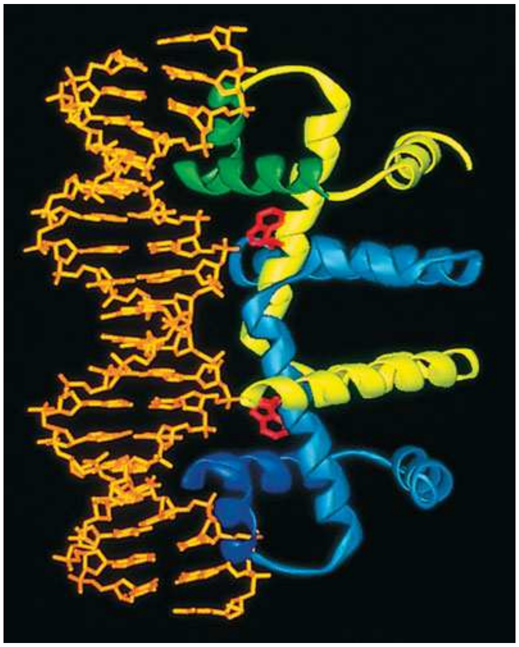

■ **Figure 24-33 | X-Ray structure of an *E. coli trp* repressor–operator complex.** The molecular twofold axis is horizontal and in the plane of the paper. The protein's two identical subunits are shown in ribbon form in green and blue with the HTH motifs more deeply colored. The 18-bp self-complementary DNA is yellow. *trp* repressor binds its operator only when L-tryptophan (*red*) is also bound. Note that the protein's recognition helices bind, as expected, in successive major grooves of the DNA but extend approximately perpendicular to the DNA helix axis, whereas those of 434 phage repressor are nearly parallel to the major grooves of its bound DNA (Fig. 24-32). [Based on an X-ray structure by Paul Sigler, Yale University. PDBid 1TRO.] **See Interactive Exercise 40.**

Astoundingly, however, there are no direct hydrogen bonds or nonpolar contacts that can explain the repressor's specificity for its operator. Rather, all but one of the side chain–base hydrogen-bonding interactions are mediated by bridging water molecules. In addition, the operator contains several base pairs that are not in contact with the repressor but whose mutation nevertheless greatly decreases repressor binding affinity. This suggests that *the operator assumes a sequence-specific conformation that makes favorable contacts with the repressor.* Other DNA sequences could conceivably assume the same conformation but at too high an energy cost to form a stable complex with the repressor. This phenomenon, in which a protein senses the base sequence of DNA through the DNA's backbone conformation and/or flexibility, is referred to as **indirect readout.** This finding puts to rest the notion that proteins recognize nucleic acid sequences exclusively via particular sets of pairings between amino acid side chains and nucleotide bases analogous to Watson–Crick base pairing.

The *met* Repressor Binds DNA via a Two-Stranded β Sheet. Simon Phillips first determined the X-ray structure of the *E. coli* ***met*** **repressor** in the absence of DNA (the *met* repressor regulates the transcription of genes involved in methionine biosynthesis). The homodimeric protein lacks an HTH motif, but model-building studies suggested that the repressor might bind to its palindromic target DNA via a symmetry-related pair of protruding α helices, reminiscent of the way the recognition helices of HTH motifs interact with DNA. However, the subsequently determined X-ray structure of the *met* repressor–operator complex showed that the protein actually binds its target DNA sequence through a pair of symmetrically related β strands (located on the opposite side of the protein from the protruding α helices) that form a two-stranded antiparallel β sheet that inserts into the DNA's major groove (Fig. 24-34). The β strands make sequence-specific contacts with the DNA via hydrogen bonding and, probably, indirect readout. This result indicates that the conclusions of even what appear to be straightforward model-building studies should be viewed with skepticism. In the case of the *met* repressor–operator

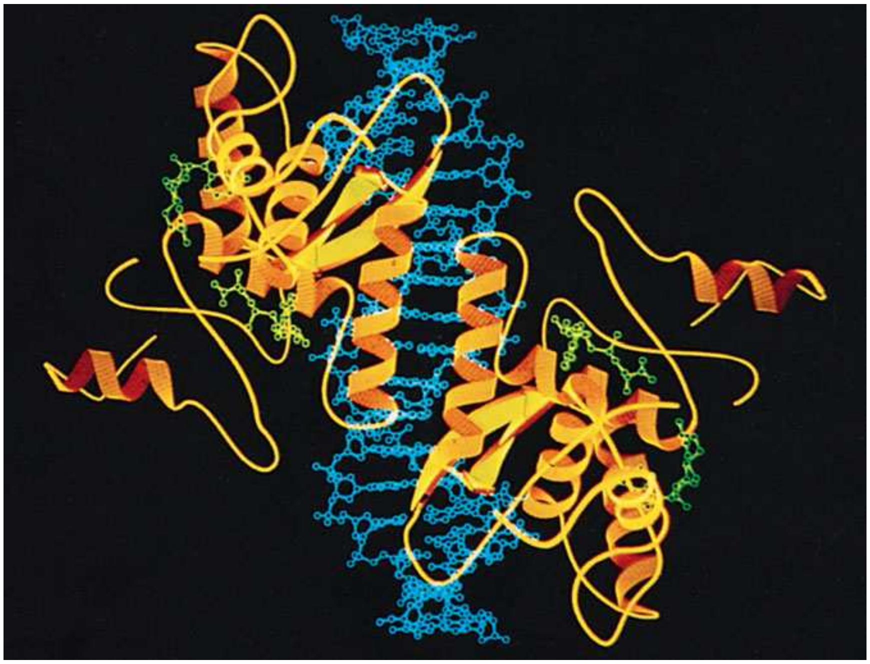

Figure 24-34 | X-Ray structure of the *E. coli met* repressor–operator complex. The 104-residue repressor subunits are shown in gold. The self-complementary 19-bp DNA is shown as a blue ball-and-stick model. The methionine derivative *S*-adenosylmethionine, shown in green, must be bound to the repressor for it to bind DNA. Note that the DNA has four bound repressor subunits: Pairs of subunits form symmetric dimers in which each subunit donates one strand of the two-stranded β sheet that is inserted in the DNA's major groove (*upper left and lower right*). Two such dimers pair across the complex's twofold axis via their antiparallel N-terminal helices, which contact each other over the DNA's minor groove. [Courtesy of Simon Phillips, University of Leeds, Leeds, U.K. PDBid 1CMA.] **See Interactive Exercise 41.**

complex, the model-building study favored the incorrect model because it could not take into account the small conformational adjustments that both the protein and the DNA make on binding one another.

C | Eukaryotic Transcription Factors May Include Zinc Fingers or Leucine Zippers

In eukaryotes, genes are selectively expressed in different cell types; this requires more complicated regulatory machinery than in prokaryotes. Prokaryotic repressors of known structure either contain an HTH motif or resemble the *met* repressor. However, eukaryotic DNA-binding proteins employ a much wider variety of structural motifs to bind DNA. A number of proteins known as **transcription factors** (Section 26-2C) promote the transcription of genes by binding to DNA sequences at or near those genes. In this section, we describe a variety of the DNA-binding motifs in eukaryotic transcription factors.

Zinc Fingers Form Compact DNA-Binding Structures. The first of the predominantly eukaryotic DNA-binding motifs, the **zinc finger,** was discovered by Klug in **transcription factor IIIA (TFIIIA)** from *Xenopus laevis* (an African clawed toad). The 344-residue TFIIIA contains nine similar, tandemly repeated, ~30-residue modules, each of which contains two invariant Cys residues and two invariant His residues. Each of these units binds a Zn^{2+} ion, which is tetrahedrally liganded by the Cys and His residues (a **Cys_2–His_2 zinc finger;** Fig. 24-35*a* and Fig. 6-37). In some zinc fingers, the two Zn^{2+}-liganding His residues are replaced by two additional Cys residues, whereas others have six Cys residues liganding two Zn^{2+} ions. Indeed, structural diversity is a hallmark of zinc finger proteins. In all cases, however, the Zn^{2+} ions appear to knit together relatively small globular domains, thereby eliminating the need for much larger hydrophobic protein cores (Section 6-4A).

The Cys_2–His_2 zinc finger contains a two-stranded antiparallel β sheet and one α helix. Three of these motifs are incorporated into a 72-residue segment of the mouse protein **Zif268,** whose X-ray structure in complex with a target DNA was elucidated by Carl Pabo (Fig. 24-35*b*). The three zinc fingers are arranged as separate domains in a C-shaped structure that fits snugly into the DNA's major groove. Each zinc finger interacts in a conformationally identical manner with successive 3-bp segments of the DNA, predominantly through hydrogen bonds between the zinc finger's α helix and one strand of the DNA. Each zinc finger

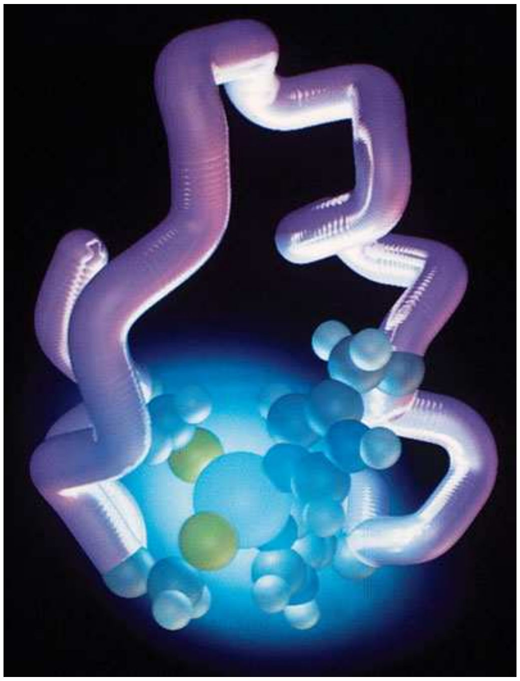
(*a*)

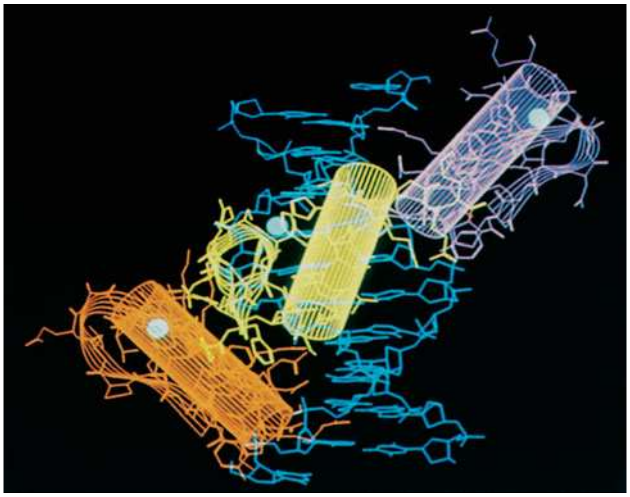
(*b*)

■ **Figure 24-35 | Cys_2–His_2 zinc finger motif.** (*a*) NMR structure of a single zinc finger from the *Xenopus* protein Xfin. The Zn^{2+} ion together with the atoms of its His and Cys ligands are represented as spheres with Zn^{2+} cyan, C gray, N blue, S yellow, and H white. [Courtesy of Michael Pique, The Scripps Research Institute, La Jolla, California. Based on an NMR structure by Peter E. Wright, The Scripps Research Institute. PDBid 1ZNF.] (*b*) X-Ray structure of a three–zinc finger segment of Zif268 in complex with a 10-bp DNA. The protein and DNA (with a single nucleotide overhang at each end) are shown in stick form, with superimposed cylinders and ribbons marking the protein's α helices and β sheets. Finger 1 is orange, finger 2 is yellow, finger 3 is pink, the DNA is blue, and the Zn^{2+} ions are represented by white spheres. Note how the N-terminal (lower) end of each zinc finger's helix extends into the DNA's major groove to contact three base pairs. [Courtesy of Carl Pabo, MIT. PDBid 1ZAA.] **See Interactive Exercise 42.**

specifically hydrogen bonds to two bases in the major groove. Interestingly, five of these six associations involve Arg–guanine pairs. In addition to these sequence-specific interactions, each zinc finger hydrogen bonds with the DNA's phosphate groups via conserved Arg and His residues.

The Cys_2–His_2 zinc finger broadly resembles the prokaryotic HTH motif as well as most other DNA-binding motifs we shall encounter (including other types of zinc fingers). All these DNA-binding motifs provide a platform for inserting an α helix into the major groove of B-DNA. However, the Cys_2–His_2 zinc fingers, unlike other DNA-binding motifs, occur as modules that each contact successive DNA segments (some transcription factors contain over 60 zinc fingers). *Such a modular system can recognize extended asymmetric base sequences.*

A binuclear **Cys_6 zinc finger** mediates the DNA binding of the yeast protein **GAL4,** a transcriptional activator of several genes that encode galactose-metabolizing enzymes. Residues 1 to 65 of this 881-residue protein include six Cys residues that collectively bind two Zn^{2+} ions (Fig. 24-36*a*). Each Zn^{2+} ion is tetrahedrally coordinated by four Cys residues, with two of these residues ligating both metal ions. GAL4 binds to its 17-bp target DNA as a symmetric dimer (Fig. 24-36*b*), although in the absence of DNA it is a monomer. Each subunit includes a compact zinc finger (residues 8–40) that binds DNA, an extended linker (residues 41–49), and an α helix (residues 50–64) that assists in GAL4 dimerization. The N-terminal helix of the zinc finger inserts into the DNA's major groove, making sequence-specific contacts with a highly conserved CCG sequence at each end of the recognition sequence. The bound DNA retains its B conformation.

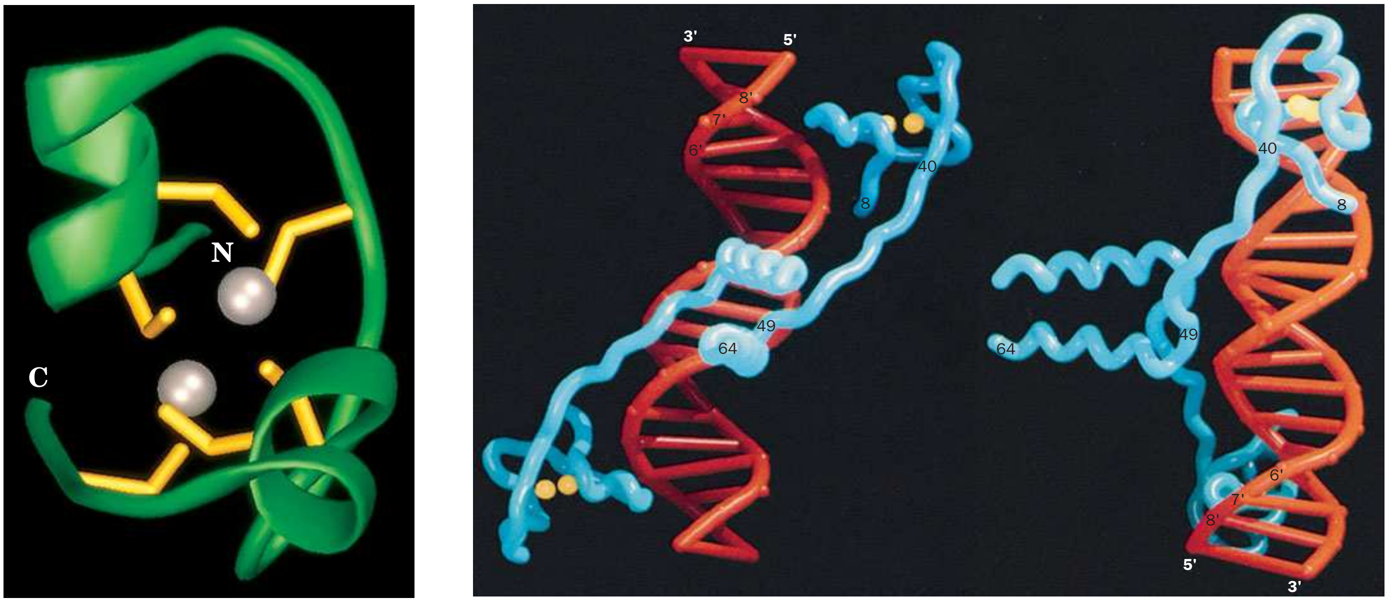

(*a*)

(*b*)

Figure 24-36 | X-Ray structure of the GAL4 DNA-binding domain in complex with DNA. (*a*) A ribbon model of the protein's zinc finger domain (residues 8–40) with its six Cys side chains in stick form (*yellow*) and its Zn^{2} ions shown as silver spheres. Compare this structure with Figs. 6-37 and 24-35*a*. (*b*) The complex of the dimeric GAL4 protein with a palindromic 19-bp DNA (except for the central base pair) containing the protein's binding sequence. The structure is shown in tube form with the DNA red, the protein backbone cyan, and the Zn^{2+} ions represented by yellow spheres. The views are along the complex's twofold axis (*left*) and turned 90° with the twofold axis horizontal (*right*). Note how the C-terminal end of each subunit's N-terminal helix extends into the DNA's major groove. [Part *b* courtesy of and Part *a* based on an X-ray structure by Ronen Marmorstein and Stephen Harrison, Harvard University. PDBid 1D66.] **See Interactive Exercise 43.**

The dimerization helices of GAL4 (center of Fig. 24-36*b*) are positioned over the minor groove of the DNA. The linkers connecting those helices to the zinc fingers wrap around the DNA, largely following its minor groove. The two symmetrically related DNA-binding zinc fingers thereby approach the major groove from opposite sides of the DNA, ~1.5 helical turns apart, rather than from the same side of the DNA, ~1 turn apart, as do HTH motifs. The resulting relatively open structure could permit other proteins to bind simultaneously to the DNA.

Some Transcription Factors Include Leucine Zippers. Segments of certain eukaryotic transcription factors, such as the yeast protein **GCN4,** contain a Leu at every seventh position. We have already seen that α helices with the seven-residue pseudorepeating sequence $(a\text{-}b\text{-}c\text{-}d\text{-}e\text{-}f\text{-}g)_n$, in which the *a* and *d* residues are hydrophobic, have a hydrophobic strip along one side that allows them to dimerize as a coiled coil (e.g., α-keratin; Section 6-1C). Steven McKnight suggested that DNA-binding proteins containing such **heptad repeats** also form coiled coils in which the Leu side chains might interdigitate, much like the teeth of a zipper (Fig. 24-37). In fact, *these* ***leucine zippers*** *mediate the dimerization of certain DNA-binding proteins but are not themselves DNA-binding motifs.*

The X-ray structure of the 33-residue polypeptide corresponding to the leucine zipper of GCN4 was determined by Peter Kim and Thomas Alber. The first 30 residues, which contain ~3.6 heptad repeats (Fig. 24-37*a*), coil into an ~8-turn α helix that dimerizes as McKnight predicted to form ~1/4 turn of a parallel left-handed coiled coil (Fig. 24-37*b*). The dimer can be envisioned as a twisted ladder whose sides consist of the helix backbones and whose rungs are formed by the interacting hydrophobic side chains. The conserved Leu residues in the heptad position *d,* which corresponds to every second rung, are not interdigitated as McKnight originally suggested, but instead make side-to-side contacts. The alternate rungs are

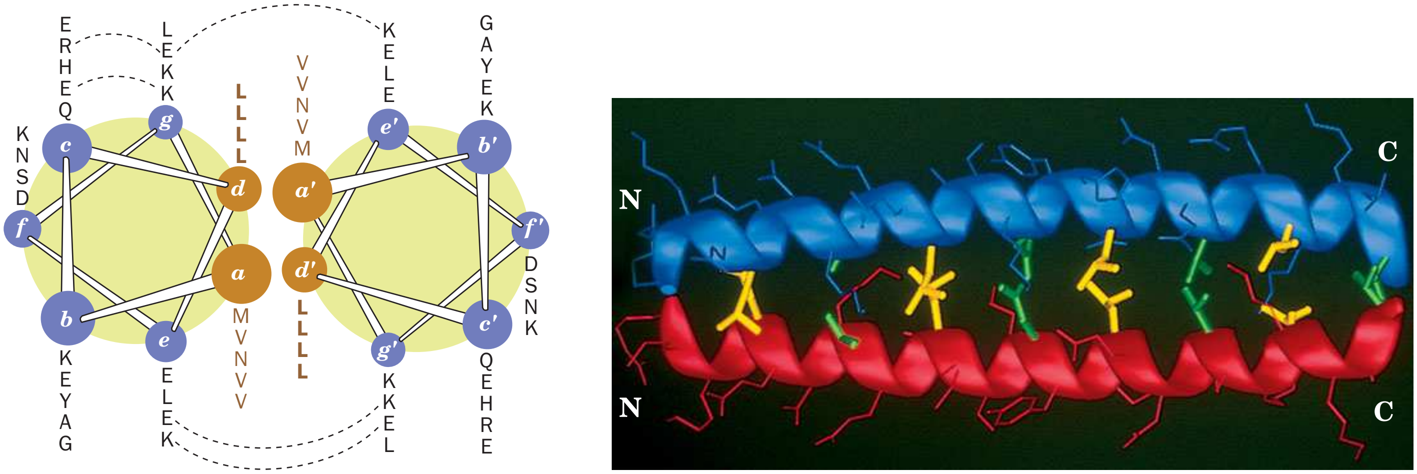

(*a*) (*b*)

Figure 24-37 | The GCN4 leucine zipper motif. (*a*) A helical wheel representation of the motif's two helices as viewed from their N-termini. The sequences of residues at each position are indicated by the adjacent column of one-letter codes. Residues that form ion pairs in the crystal structure are connected by dashed lines. Note that all residues at positions *d* and *d′* are Leu (L), those at positions *a* and *a′* are mostly Val (V), and those at other positions are mostly polar. [After O'Shea, E.K., Klemm, J.D., Kim, P.S., and Alber, T., *Science* **254,** 540 (1991).] (*b*) The X-ray structure, in side view, in which the helices are shown in ribbon form. Side chains are shown in stick form with the contacting Leu residues at positions *d* and *d′* yellow and residues at positions *a* and *a′* green. [Based on an X-ray structure by Peter Kim, MIT, and Tom Alber, University of Utah School of Medicine. PDBid 2ZTA.] **See Kinemage Exercise 20.**

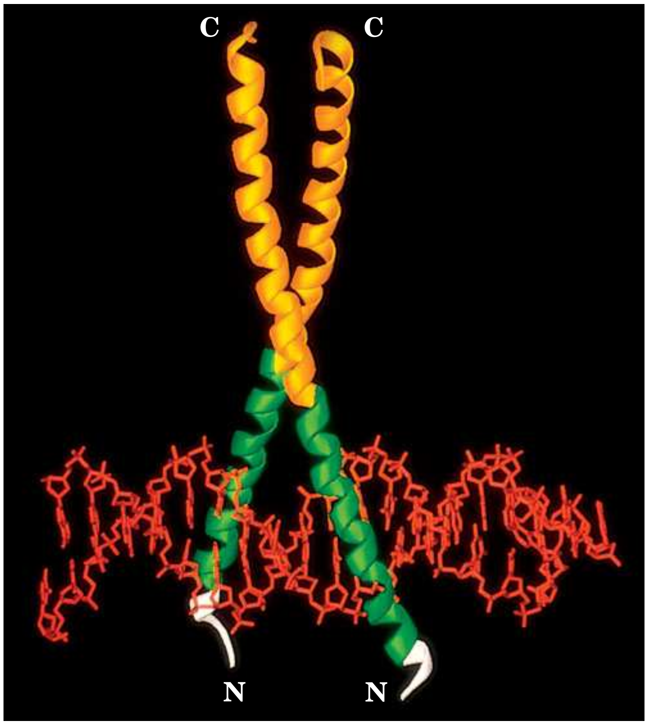

■ **Figure 24-38 | X-Ray structure of the GCN4 bZIP region in complex with its target DNA.** The DNA (*red*), shown in stick form, consists of a 19-bp segment with a single nucleotide overhang at each end and contains the protein's palindromic (except for the central base pair) 7-bp target sequence. The two identical GCN4 subunits, shown in ribbon form, each contain a continuous 52-residue α helix. At their C-terminal ends, (*yellow*), the two subunits associate in a parallel coiled coil (a leucine zipper), and at their basic regions (*green*), they smoothly diverge to each engage the DNA in its major groove at the target sequence. The N-terminal ends are white. [Based on an X-ray structure by Stephen Harrison, Harvard University. PDBid 1YSA.] **See Interactive Exercise 44.**

likewise formed by the *a* residues of the heptad repeat (which are mostly Val). These contacts form an extensive hydrophobic interface between the two helices.

In many leucine zipper–containing proteins, a DNA-binding region that is rich in basic residues is immediately N-terminal to the leucine zipper, and hence these proteins are known as **basic region leucine zipper (bZIP) proteins.** For example, in GCN4, the C-terminal 56 residues form an extended α helix. The last 25 residues of two such helices associate as a leucine zipper. The N-terminal portions of the helices smoothly diverge to bind in the major grooves on opposite sides of the DNA, thereby clamping the DNA in a sort of scissors grip (Fig. 24-38). The basic region residues that are conserved in bZIP proteins make numerous contacts with both the bases and the phosphate oxygens of their DNA target sequence without distorting its conformation.

Many eukaryotic transcription factors contain a conserved DNA-binding basic region that is immediately followed by two amphipathic helices connected by a loop to form a so-called **basic helix–loop–helix (bHLH) motif.** The basic region, together with the N-terminal portion of the first (H1) helix of the bHLH motif, binds in the major groove of its target DNA. The C-terminal (H2) helix of the bHLH motif mediates the dimerization of the protein via the formation of a coiled coil. In many proteins, the bHLH motif is continuous with a leucine zipper (Z) that presumably augments the dimerization. Thus, as is shown in Fig. 24-39 for the protein **Max,** the dimeric **bHLH/Z** protein grips the DNA in a manner reminiscent of a pair of forceps. Each basic region

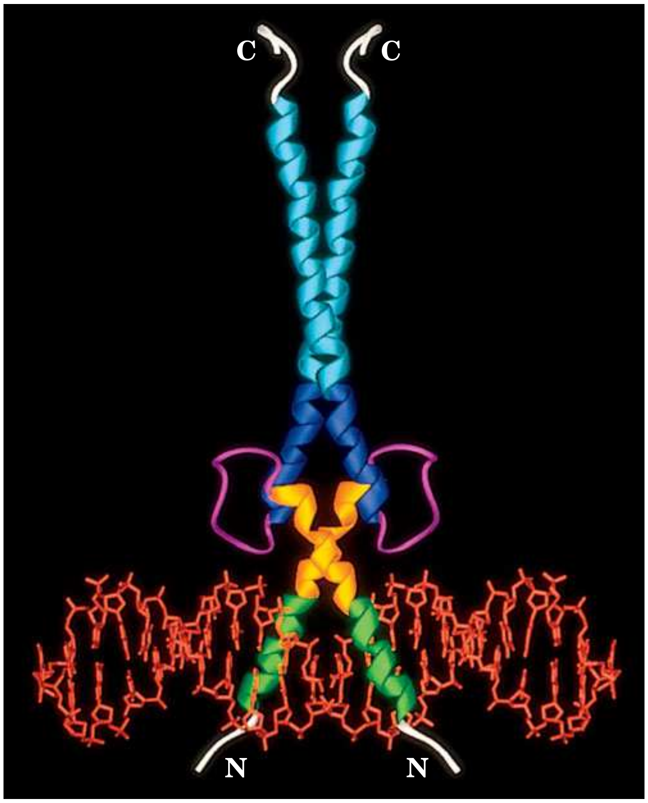

■ **Figure 24-39 | X-Ray structure of Max binding to DNA.** Residues 22–113 of the 160-residue transcription factor Max form a complex with a 22-bp DNA containing the protein's palindromic 6-bp target sequence. The DNA (*red*) is shown in stick form, and the homodimeric protein is shown in ribbon form. The protein's N-terminal basic region (*green*) forms an α helix that engages its target sequence in the DNA's major groove and then merges smoothly with the H1 helix (*yellow*) of the basic helix–loop–helix (bHLH) motif. Following the loop (*magenta*), the protein's two H2 helices (*purple*) of the bHLH motif form a short parallel four-helix bundle with the N-terminal ends of the two H1 helices. Each H2 helix then merges smoothly with the leucine zipper (Z) motif (*cyan*) to form a parallel coiled coil. The protein's N- and C-terminal ends are white. [Based on an X-ray structure by Edward Ziff and Stephen Burley, The Rockefeller University. PDBid 1AN2.] **See Interactive Exercise 45.**

contacts specific bases of the DNA as well as phosphate groups. Side chains of both the loop and the N-terminal end of the H2 helix also contact DNA phosphate groups.

■ CHECK YOUR UNDERSTANDING

Describe the types of interactions between nucleic acids and proteins.
How does the DNA binding of a zinc finger–containing transcription factor differ from that of a prokaryotic repressor?

5 Eukaryotic Chromosome Structure

LEARNING OBJECTIVES

- Understand that DNA is negatively supercoiled around a core of histone proteins to form a nucleosome.
- Understand that nucleosomes are folded into higher-order chromatin structures.

Although each base pair of B-DNA contributes only ~3.4 Å to its **contour length** (the end-to-end length of a stretched-out native molecule), DNA molecules are generally enormous (as shown on page 848). Indeed, the 23 chromosomes of the 3.2 billion-bp human genome have a total contour length of almost 1 m. One of the enduring questions of molecular biology is how such vast quantities of genetic information can be scanned and decoded in a reasonable time while stored in a small portion of the cell's volume.

The elongated shape of duplex DNA (its diameter is only 20 Å) and its relative stiffness make it susceptible to mechanical damage when outside the protective environment of the cell. For example, a *Drosophila* chromosome, if expanded by a factor of 500,000, would have the shape and some of the mechanical properties of a 6-km-long strand of uncooked spaghetti. In fact, the **shear degradation** of DNA by stirring, shaking, or pipetting a DNA solution is a standard laboratory method for preparing DNA fragments.

Prokaryotic genomes typically comprise a single circular DNA molecule. However, most eukaryotes condense and package their genome in several **chromosomes.** Each chromosome is a complex of DNA and protein, a material known as **chromatin,** and is a dynamic entity whose appearance varies dramatically with the stage of the **cell cycle** (the general sequence of events that occur in the lifetime of a eukaryotic cell; Section 28-4A). For example, chromosomes assume their most condensed forms only during the metaphase stage of cell division (Fig. 24-40). During the remainder of the cell cycle, when the DNA is transcribed and replicated, the chromosomes of most cells become so highly dispersed that they cannot be distinguished. Yet the DNA of the chromosomes is still compacted relative to its free B-helix form. Human chromosomes have contour lengths between 1.5 and 8.4 cm but in their most condensed state are only 1.3 to 10 μm long. In this section, we examine how DNA is packaged in cells to achieve that degree of condensation.

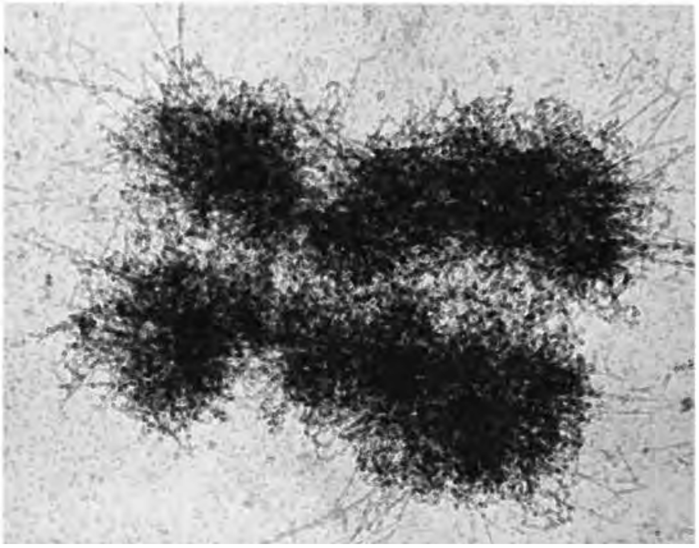

■ **Figure 24-40 | Electron micrograph of a human metaphase chromosome.** [Courtesy of Gunther Bahr, Armed Forces Institute of Pathology.]

Table 24-3 Calf Thymus Histones

Histone	Number of Residues	Mass (kD)	% Arg	% Lys
H1	215	23.0	1	29
H2A	129	14.0	9	11
H2B	125	13.8	6	16
H3	135	15.3	13	10
H4	102	11.3	14	11

A | Histones Are Positively Charged

Chromatin is about one-half protein by mass, and most of this protein consists of **histones.** To understand how DNA is packaged, we must first examine the histone proteins. The five major classes of histones, **H1, H2A, H2B, H3,** and **H4,** all have a large proportion of positively charged residues (Arg and Lys; Table 24-3). These proteins can therefore bind DNA's negatively charged phosphate groups through electrostatic interactions.

The amino acid sequences of histones H2A, H2B, H3, and H4 are remarkably conserved. For example, histones H4 from cows and peas, species that diverged 1.2 billion years ago, differ by only two conservative residue changes, which makes this protein among the most evolutionarily conserved proteins known (Section 5-4A). *Such evolutionary stability implies that the histones have critical functions to which their structures are so well tuned that they are all but intolerant to change.* The fifth histone, H1, is more variable than the other histones; we shall see below that it also has a somewhat different role.

Histones are subject to posttranslational modifications that include methylation, acetylation, and phosphorylation of specific Arg, His, Lys, Ser, and Thr residues. *These modifications, many of which are reversible, all decrease the histones' positive charges, thereby significantly altering histone–DNA interactions.* Despite the histones' great evolutionary stability, their degree of modification varies enormously with the species, the tissue, and the stage of the cell cycle. As we shall see (Section 28-3A), modification of histones has been linked to transcriptional activation. The modifications probably create new protein binding sites on the histones themselves or on the DNA with which they associate.

See Guided Exploration 24
Nucleosome structure.

B | DNA Coils around Histones to Form Nucleosomes

The first level of chromatin organization was pointed out by Roger Kornberg in 1974 from several lines of evidence:

1. Chromatin contains roughly equal numbers of histones H2A, H2B, H3, and H4, and no more than half that number of histone H1.
2. Electron micrographs of chromatin preparations at low ionic strength reveal ~100-Å-diameter particles connected by thin strands of apparently naked DNA, rather like beads on a string (Fig. 24-41).
3. Brief digestion of chromatin by **micrococcal nuclease** (which hydrolyzes double-stranded DNA) cleaves the DNA only between the above particles; apparently the particles protect the DNA closely associated with them from nuclease digestion. Gel electrophoresis indicates that each particle contains ~200 bp of DNA.

Kornberg proposed that the chromatin particles, which are called **nucleosomes,** consist of the octamer $(H2A)_2(H2B)_2(H3)_2(H4)_2$ in association with ~200 bp of DNA. The fifth histone, H1, was postulated to be associated in some other manner with the nucleosome (see below).

The Nucleosome Core Particle Contains a Histone Octamer and 146 bp of DNA. Micrococcal nuclease initially degrades chromatin to single nucleosomes in complex with histone H1. Further digestion trims away additional DNA, releasing histone H1. This leaves the so-called **nucleosome core particle,** which consists of a 146-bp strand of DNA associated with the histone octamer. A segment of **linker DNA,** the DNA that is removed by the nuclease, joins neighboring nucleosomes. Its length varies between 8 and 114 bp among organisms and tissues, although it is usually ~55 bp.

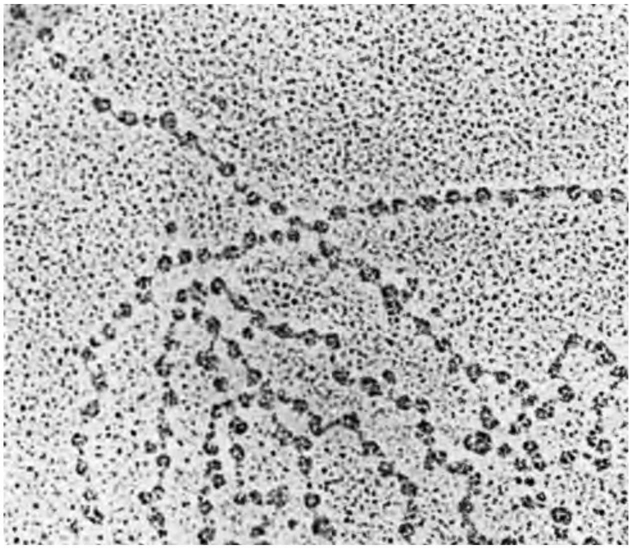

Figure 24-41 | Electron micrograph of *D. melanogaster* chromatin showing strings of closely spaced nucleosomes. [Courtesy of Oscar L. Miller, Jr., and Steven McKnight, University of Virginia.]

The X-ray structure of the nucleosome core particle, independently determined by Timothy Richmond and Gerard Bunick, reveals a nearly twofold symmetric complex in which B-DNA is wrapped around the outside of the histone octamer in 1.65 turns of a left-handed superhelix (Fig. 24-42). This is the origin of supercoiling in eukaryotic DNA. Despite having only weak sequence similarity, all four types of histones share a similar ~70-residue fold in which a long central helix is flanked on each

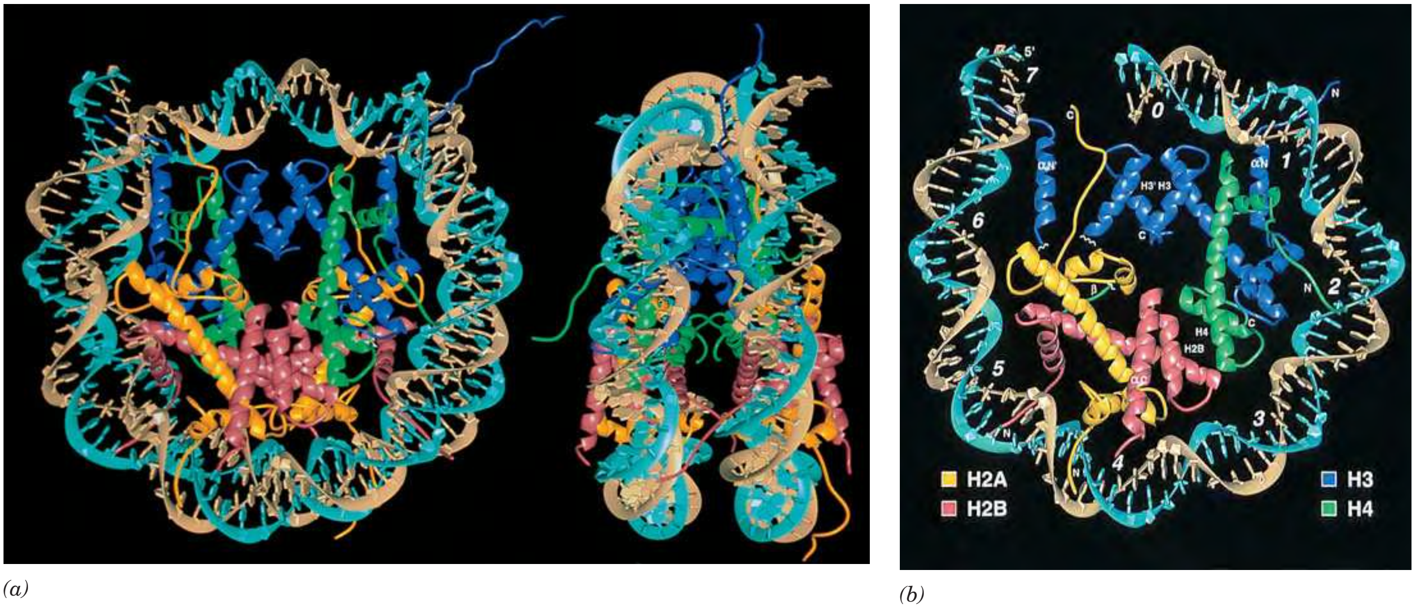

Figure 23-42 | X-Ray structure of the nucleosome core particle. (*a*) The entire core particle as viewed (*left*) along its superhelical axis and (*right*) rotated 90° about the vertical axis. The proteins of the histone octamer are drawn in ribbon form with H3 blue, H4 green, H2A yellow, and H2B red. The sugar–phosphate backbones of the 146-bp DNA are drawn as tan and turquoise ribbons whose attached bases are represented by polygons of the same color. In both views, the pseudo-twofold axis is vertical and passes through the DNA center at the top. (*b*) The top half of the nucleosome core particle as viewed in Part *a, left,* and identically colored. The numbers 0 through 7 arranged about the inside of the 73-bp DNA superhelix mark the positions of sequential double-helical turns. Those histones that are drawn in their entirety are primarily associated with this DNA segment, whereas only fragments of H3 and H2B from the other half of the particle are shown. The two four-helix bundles shown are labeled H3′ H3 and H2B H4. [Courtesy of Timothy Richmond, Eidgenössische Technische Hochschule, Zürich, Switzerland. PDBid 1AOI.]

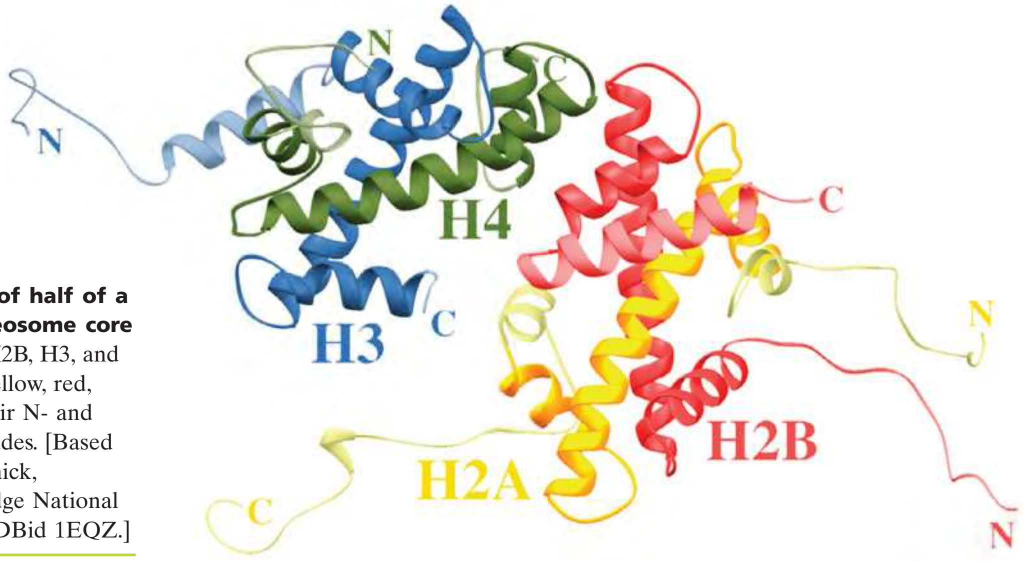

Figure 24-43 | X-Ray structure of half of a histone octamer within the nucleosome core particle. Those portions of H2A, H2B, H3, and H4 that form the histone folds are yellow, red, blue, and green, respectively, with their N- and C-terminal tails colored in lighter shades. [Based on an X-ray structure by Gerard Bunick, University of Tennessee and Oak Ridge National Laboratory, Oak Ridge, Tennessee. PDBid 1EQZ.]

side by a loop and a shorter helix (Fig. 24-43). Pairs of histones interdigitate in a sort of "molecular handshake" to form the crescent-shaped heterodimers H2A–H2B and H3–H4, each of which binds 2.5 turns of duplex DNA that curves around it in a 140° bend. The H3–H4 pairs interact, via a bundle of four helices from the two H3 histones, to form an $(H3–H4)_2$ tetramer with which each H2A–H2B pair interacts, via a similar four-helix bundle between H2B and H4, to form the histone octamer (Fig. 24-42*b*).

The histones bind exclusively to the inner face of the DNA, primarily via its sugar–phosphate backbones, through hydrogen bonds, salt bridges, and helix dipoles (their positive N-terminal ends), all interacting with phosphate oxygens, as well as through hydrophobic interactions with the deoxyribose rings. There are few contacts between the histones and the bases, in accord with the nucleosome's lack of sequence specificity. However, an Arg side chain is inserted into the DNA's minor groove at each of the 14 positions at which it faces the histone octamer. The DNA superhelix has a radius of 42 Å and a pitch (rise per turn) of 26 Å. The DNA does not follow a uniform superhelical path but, rather, is bent fairly sharply at several locations due to outward bulges of the histone core. Moreover, the DNA double helix exhibits considerable conformational variation along its length such that its twist, for example, varies from 7.5 to 15.2 bp/turn with an average value of 10.4 bp/turn (versus 10.4 bp/turn for DNA in solution). Approximately 75% of the DNA surface is accessible to solvent and hence appears to be available for interactions with DNA-binding proteins.

Linker Histones Bring Nucleosomes Together. In the micrococcal nuclease digestion of chromatin fibers, the ~200-bp DNA is first degraded to 166 bp. Then there is a pause before histone H1 is released and the DNA is further shortened to 146 bp. Since the 146-bp DNA of the core particle makes 1.65 superhelical turns, the 166-bp intermediate should make nearly two full superhelical turns, which would bring its two ends close together. Klug has proposed that histone H1 binds to nucleosomal DNA at this point, where the DNA segments enter and leave the core particle (Fig. 24-44*a*). Chromatin fibers containing H1 have closely spaced

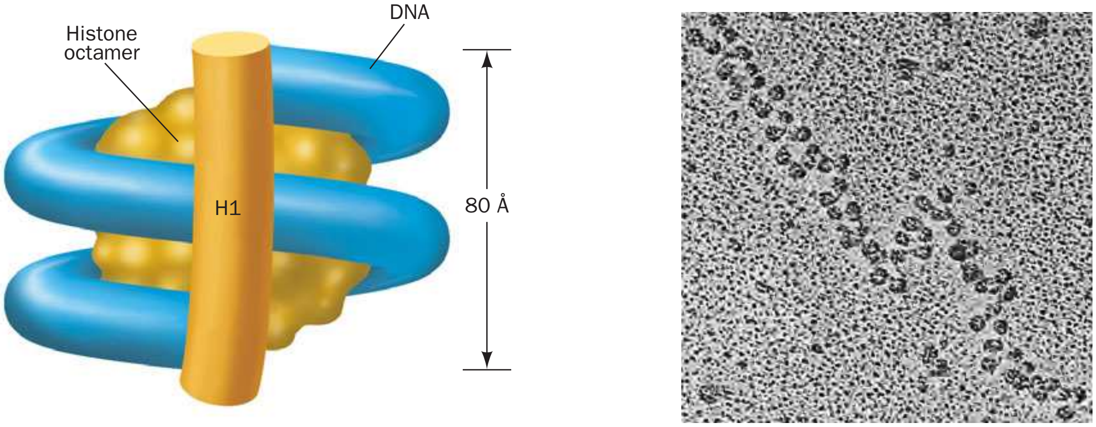

(a) *(b)*

Figure 24-44 | Binding of histone H1 to the nucleosome. (*a*) Model of histone H1 binding to the DNA of the 166-bp nucleosome. The two complete superhelical turns of the DNA (*blue*) enable H1 (*orange cylinder*) to bind to the DNA's two ends and its middle. The histone octamer is represented by the yellow central spheroid. (*b*) Electron micrograph of H1-containing chromatin. Compare this with Fig. 24–41. [Courtesy of Fritz Thoma, Eigenössiche Technische Hochschule, Zürich, Switzerland.]

nucleosomes (Fig. 24-44*b*), consistent with DNA entering and exiting the nucleosome on the same side. In H1-depleted chromatin (e.g., Fig. 24-41), the nucleosomes are more dispersed, suggesting that linker histones play a role in condensing chromatin fibers and regulating the access of other proteins to the DNA.

C | Chromatin Forms Higher-Order Structures

Winding the DNA helix around a nucleosome reduces its contour length sevenfold (the 560-Å length of 166 bp is compressed to an ~80-Å-high supercoil). Under physiological conditions, chromatin condenses further by folding in a zigzag fashion to form a helical filament with a diameter of ~30 nm. A model of this **30-nm fiber** based on the X-ray structure of a tetranucleosome, and which is consistent with cross-linking studies and electron micrographs, shows that sequential nucleosomes are rotated ~71° to each other. The nucleosomes follow a zigzag path so that all the odd-numbered nucleosomes, and all the even-numbered nucleosomes, stack next to each other (Fig. 24-45). The ~250-Å-diameter structure, in which the two stacks wind around each other in two left-handed helices, has approximately 18.9 nucleosomes per turn, covering a distance of about 316 Å along the fiber axis.

The 30-nm fiber is stabilized by interactions involving H2A–H2B dimers and histone H4. As the X-ray structure of the nucleosome shows

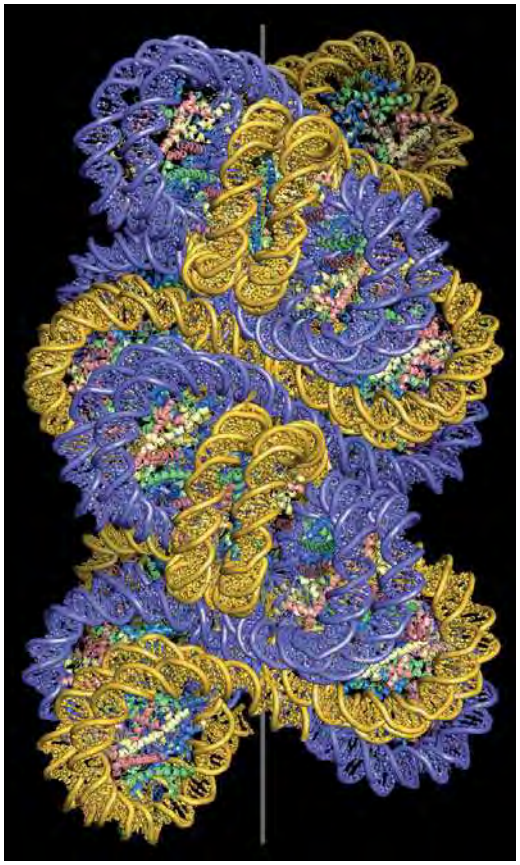

Figure 24-45 | Model of the 30-nm fiber. Sequential nucleosomes, with their DNA colored gold and purple, stack in a zigzag manner to form a double-helical structure. The fiber axis is shown as a vertical gray line. This model is based on the X-ray structure of a four-nucleosome unit in which each nucleosome consists of 147 bp of DNA plus a histone octamer (shown in ribbon form and colored blue, green, red, and yellow) and is linked to the next by 20 bp of DNA. This model does not include linker histones. [Courtesy of Timothy Richmond, Eigenössiche Techische Hochschule, Zürich, Switzerland.]

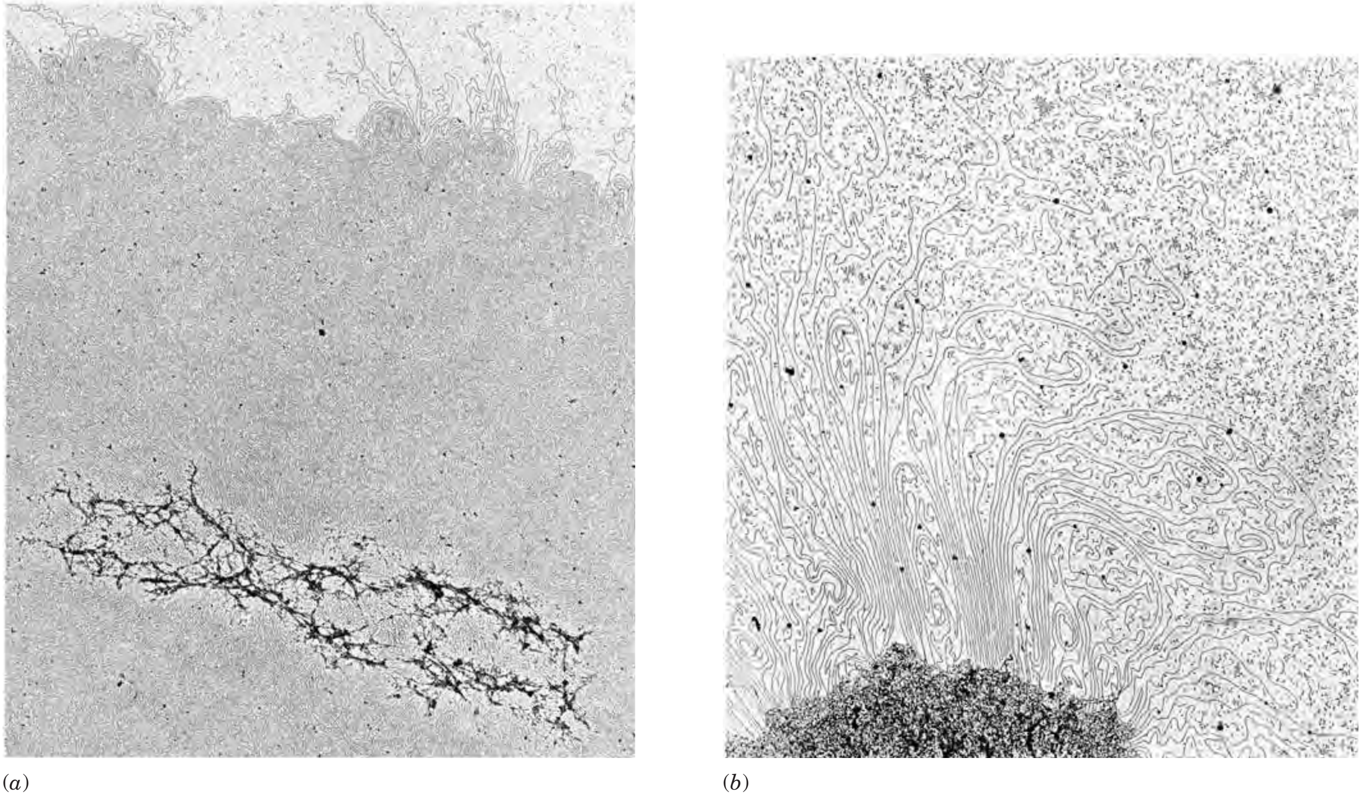
(*a*) (*b*)

■ **Figure 24-46 | Electron micrographs of a histone-depleted metaphase human chromosome.** (*a*) The fibrous central protein matrix (scaffold) anchors the surrounding DNA. (*b*) Higher magnification reveals that the DNA is attached to the scaffold in loops. [Courtesy of Ulrich Laemmli, University of Geneva, Switzerland.]

(Fig. 24-42*a*), H4's positively charged N-terminal tail can bind to an intensely negatively charged region on an exposed face of the H2A–H2B dimer in a neighboring nucleosome. Acetylation of H4's N-terminal tail reduces its positive charge and would therefore weaken this interaction. The highly basic tails of H2B and H3 also extend out from the nucleosome core (Fig. 24-42*a*). Since histone tails contain numerous acetylation sites, higher-order chromatin structure is likely to be controlled, at least in part, by the acetylation of certain histone residues but not others.

Loops of DNA Are Attached to a Scaffold. Histone-depleted metaphase chromosomes exhibit a central fibrous protein "scaffold" surrounded by an extensive halo of DNA (Fig. 24-46*a*). The strands of DNA that can be followed form loops that enter and exit the scaffold at nearly the same point (Fig. 24-46*b*). Most of these loops are 15 to 30 μm long (which corresponds to 45–90 kb), so when condensed as 30-nm filaments, they would be ~0.6 μm long. Electron micrographs of metaphase chromosomes in cross section, such as Fig. 24-47, strongly suggest that the loops of chromatin are radially arranged and would each contribute 0.3 μm to the diameter of the chromosome (a fiber must double back on itself to form a loop). These loops, along with the 0.4-μm width of the scaffold, would account for the

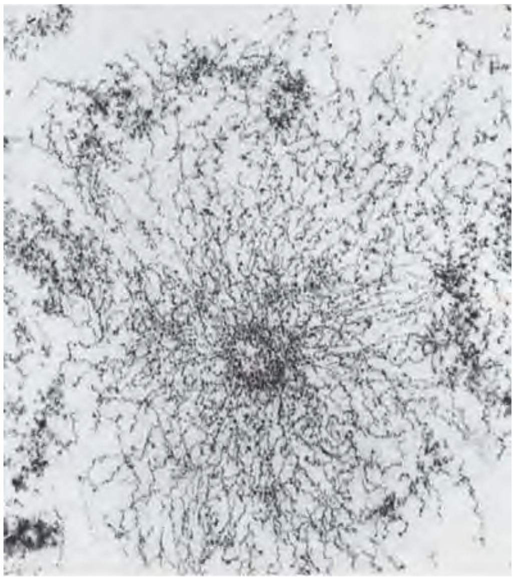
■ **Figure 24-47 | Cross section of a metaphase human chromosome.** Note the mass of chromatin fibers radially projecting from the central scaffold. [Courtesy of Ulrich Laemmli, University of Geneva, Switzerland.]

1.0-μm diameter of the metaphase chromosome. A typical human chromosome, which contains ~140 million bp and is about 6 μm long, would therefore have ~2000 radial loops. Presumably, nonhistone proteins, which constitute ~10% of the chromosomal proteins, must be involved in organizing the DNA in these higher-order structures (Fig. 24-48) and managing the interconversion of highly condensed metaphase chromosomes with the more dispersed DNA present during the rest of the cell cycle.

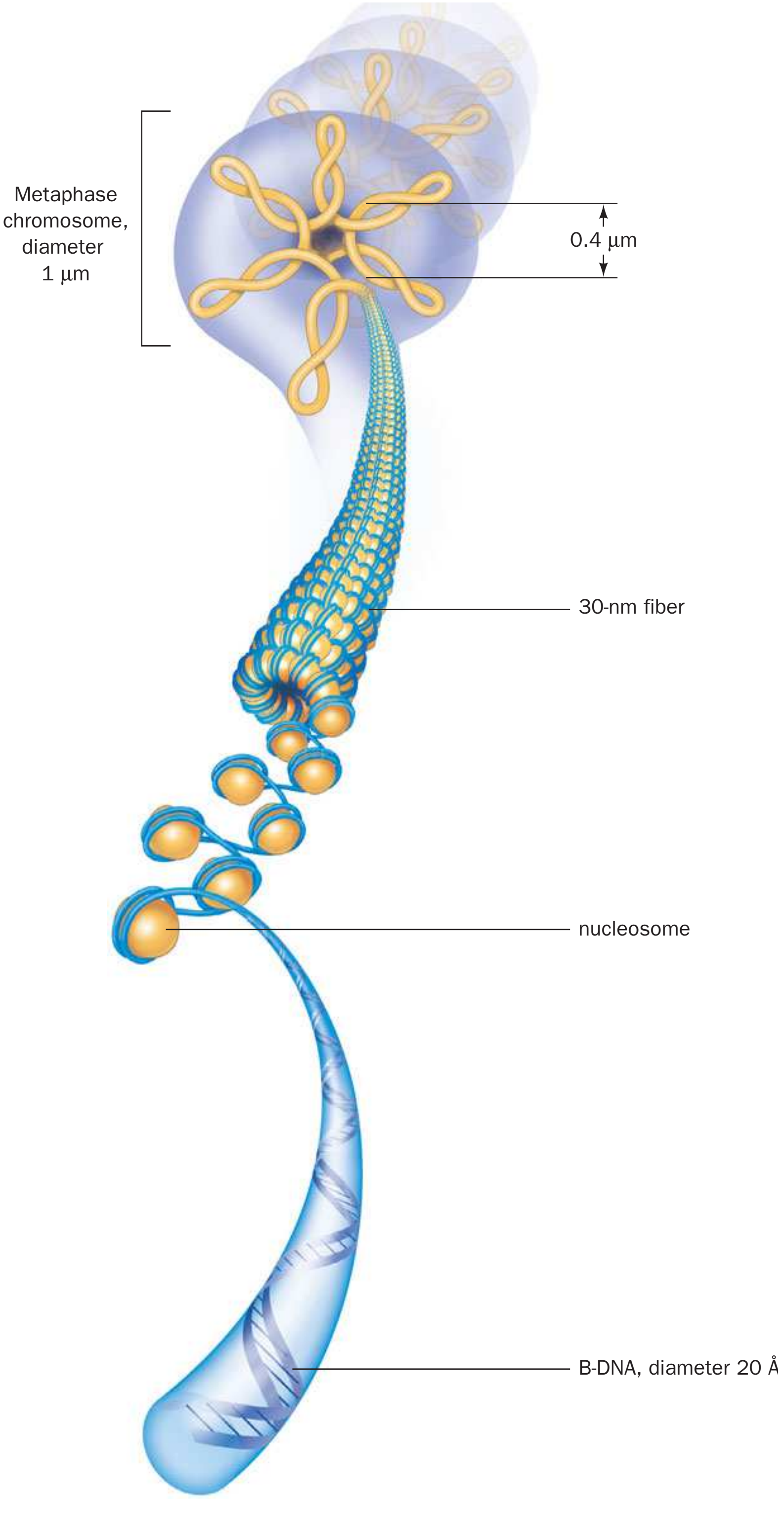

■ **Figure 24-48 | Levels of chromatin structure.** B-DNA winds around histone octamers to form nucleosomes; these fold into a 30-nm fiber. Loops of chromatin are attached to a protein scaffold to form the metaphase chromosome.

■ CHECK YOUR UNDERSTANDING

What is the role of histones in compacting DNA?

Describe the levels of DNA packaging in eukaryotic cells, from B-DNA to a metaphase chromosome.

In prokaryotes, DNA is also packaged through its association with highly basic proteins that functionally resemble histones. Nucleosome-like particles condense to form large loops that are attached to a protein scaffold, yielding a relatively compact chromosome.

SUMMARY

1. The most common form of DNA is B-DNA, which is a right-handed double helix containing A · T and G · C base pairs of similar geometry. The A-DNA helix, which also occurs in double-stranded RNA, is wider and flatter than the B-DNA helix. The left-handed Z-DNA helix may occur in sequences of alternating purines and pyrimidines.
2. The flexibility of nucleotides in nucleic acids is constrained by the allowed rotation angles around the glycosidic bond, the puckering of the ribose ring, and the torsion angles of the sugar–phosphate backbone.
3. Naturally occurring DNA is negatively supercoiled (underwound). Topoisomerases relax supercoils by cleaving one or both strands of the DNA, passing the DNA through the break (type IA and II topoisomerases) or allowing controlled rotation of the uncleaved strand (type IB topoisomerase), and resealing the broken strand(s).
4. Nucleic acids can be denatured by increasing the temperature above their T_m and renatured by lowering the temperature to ∼25°C below their T_m.
5. The structures of nucleic acids are stabilized by Watson–Crick base pairing, by hydrophobic interactions between stacked base pairs, and by divalent cations that shield adjacent phosphate groups.
6. RNA molecules assume a variety of structures consisting of double-stranded stems and single-stranded loops. Some RNAs have catalytic activity.
7. Nucleic acids are fractionated by methods similar to those used to fractionate proteins, including solubilization, affinity chromatography, and electrophoresis.
8. Sequence-specific DNA-binding proteins interact primarily with bases in the major groove and with phosphate groups through direct and indirect hydrogen bonds, van der Waals interactions, and ionic interactions. The conformations of both the protein and the DNA may change on binding.
9. Common structural motifs in DNA-binding proteins include the helix–turn–helix (HTH) motif in prokaryotic repressors, and zinc fingers, leucine zippers, and basic helix–loop–helix (bHLH) motifs in eukaryotic transcription factors.
10. The DNA of eukaryotic chromatin winds around histone octamers to form nucleosome core particles that further condense in the presence of linker histones. Additional condensation is accomplished by folding chromatin into 30-nm-diameter filaments, which are then attached in loops to a fibrous protein scaffold to form a condensed (metaphase) chromosome.

KEY TERMS

syn conformation	**856**
anti conformation	**856**
C3′-*endo*	**856**
C2′-*endo*	**856**
supercoiling	**857**
linking number	**858**
twist	**858**
writhing number	**858**
topoisomerase	**859**
hyperchromic effect	**864**
T_m	**866**
anneal	**866**
hybridization	**866**
Watson–Crick base pair	**866**
Hoogsteen base pair	**866**
stacking interactions	**867**
ribozyme	**870**
pulsed-field gel electrophoresis	**873**
intercalation agent	**873**
Southern blotting	**874**
repressor	**876**
HTH motif	**876**
operator	**876**
indirect readout	**878**
transcription factor	**879**
zinc finger	**879**
heptad repeat	**881**
leucine zipper	**881**
bHLH motif	**882**
contour length	**883**
shear degradation	**883**
chromosome	**883**
chromatin	**883**
histone	**884**
nucleosome	**884**
nucleosome core particle	**884**
linker DNA	**884**
30-nm fiber	**887**

PROBLEMS

1. Amino acid residues in proteins are each specified by three contiguous bases. What is the contour length of a segment of B-DNA that encodes a 50-kD protein? Calculate the contour length for the same gene if it assumed an A-DNA conformation.
2. Unusual bases and non-Watson–Crick base pairs frequently appear in tRNA molecules. (a) Which base is most likely to pair with hypoxanthine (Section 23-1)? Draw this base pair. (b) Draw the structure of a $G \cdot U$ base pair.
3. The ends of eukaryotic chromosomes terminate in a G-rich single-stranded overhang that can fold up on itself to form a four-stranded structure. In this structure, four guanine residues assume a hydrogen-bonded planar arrangement with an overall geometry that can be represented as

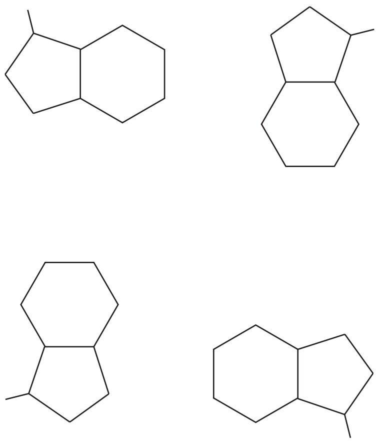

   (a) Draw the complete structure of this "G quartet," including the hydrogen bonds between the purine bases.

   (b) Show schematically how a single strand of four repeating TTAGGG sequences can fold to generate a structure with three stacked G quartets linked by TTA loops.
4. The enzyme ornithine decarboxylase generates a product that has been proposed to play a role in stabilizing compacted DNA. Draw the structure of the ornithine decarboxylase reaction product and explain how it interacts with DNA.
5. You have discovered an enzyme secreted by a particularly virulent bacterium that cleaves the C2′–C3′ bond in the deoxyribose residues of duplex DNA. What is the effect of this enzyme on supercoiled DNA?
6. A closed circular duplex DNA has a 100-bp segment of alternating C and G residues. On transfer to a high salt solution, the segment undergoes a transition from the B conformation to the Z conformation. What is the change in its linking number, writhing number, and twist?
7. Compare the melting temperature of a 1-kb segment of DNA containing 20% A residues to that of a 1-kb segment containing 30% A residues under the same conditions.
8. How is the melting curve of duplex DNA affected by (a) decreasing the ionic strength of the solution, and (b) adding a small amount of ethanol?
9. The melting curve for the polyribonucleotide poly(A) is shown below. (a) Explain why absorbance increases with increasing temperature. (b) Why does the shape of the curve differ from the one shown in Fig. 24-20?

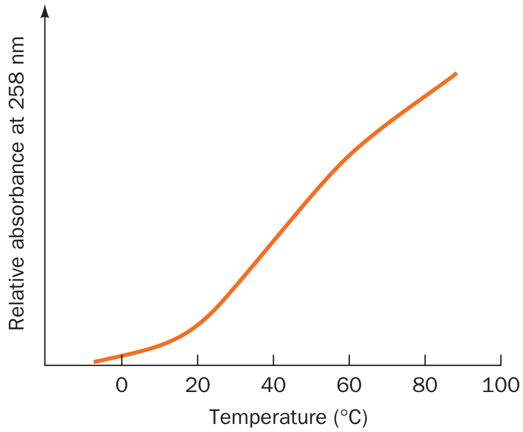

10. For the RNA sequence AUUGGCAUCCGAUAA, draw the secondary structure that maximizes its base pairing.
11. In addition to the standard base-paired helical structures (e.g., Fig. 24-2), DNA can form X-shaped hairpin structures called **cruciforms** in which most bases are involved in Watson–Crick pairs. Such structures tend to occur at sequences with inverted repeats. Draw the cruciform structure formed by the DNA sequence TCAAGTCCACGGTGGACTTGC.
12. *E. coli* ribosomes contain three RNA molecules named for their sedimentation behavior: 5S, 16S, and 23S. Draw a diagram showing the approximate positions of the three RNA species following electrophoresis.
13. What is the probability that the palindromic symmetry of the *trp* repressor target DNA sequence (Section 24-4B) is merely accidental?
14. The *E. coli* genome contains approximately 4639 kb. (a) How many copies of the 6-bp recognition sequence for the *trp* repressor would be expected to occur in the *E. coli* chromosome? (b) Explain why it would make sense for the *trp* repressor to be a dimer that recognizes two adjacent 6-bp sequences.
15. For a linear B-DNA molecule of 50,000 kb, calculate (a) the contour length, (b) the length of the DNA as packaged in nucleosomes with linker histones present, and (c) the length of the DNA in a 30-nm fiber.
16. Mouse genomic DNA is treated with a restriction endonuclease and electrophoresed in an agarose gel. A radioactive probe made from the human gene *rxr-1* is used to perform a Southern blot. The experiment was repeated three times. Explain the results of these repeated experiments:

    Experiment 1. The autoradiogram shows a large smudge at a position corresponding to the top of the lane in which the mouse DNA was electrophoresed.

    Experiment 2. The autoradiogram shows a smudge over the entire lane containing the mouse DNA.

    Experiment 3. The autoradiogram shows three bands of varying intensity.

CASE STUDY

Case 31 (available at www.wiley.com/college/voet)

Hyperactive DNase I Variants: A Treatment for Cystic Fibrosis

Focus concept: Understanding the mechanism of action of an enzyme can lead to the construction of hyperactive variant enzymes with a greater catalytic efficiency than the wild-type enzyme.

Prerequisites: Chapters 12 and 24

- Enzyme kinetics and inhibition
- DNA structure
- The hyperchromic effect
- The properties of supercoiled DNA

REFERENCES

Nucleic Acid Structure

Arnott, S., DNA polymorphism and the early history of the double helix, *Trends Biol. Sci.* **31,** 349–354 (2006).

Doudna, J.A. and Cech, T.R., The chemical repertoire of natural ribozymes, *Nature* **418,** 222–228 (2002). [Describes some of the major ribozymes and how they relate to the RNA world.]

Rich, A., The double helix: a tale of two puckers, *Nature Struct. Biol.* **10,** 247–249 (2003). [A brief history of DNA and RNA structural studies.]

Snustad, D.P. and Simmons, M.J., *Principles of Genetics,* 4th ed., Wiley (2005). [This and other textbooks review DNA structure and function.]

The double helix—50 years, *Nature* **421,** 395–453 (2003). [A supplement containing a series of articles on the historical, cultural, and scientific influences of the DNA double helix on the fiftieth anniversary of its discovery.]

Topoisomerases

Corbett, K.D. and Berger, J.M., Structure, molecular mechanisms, and evolutionary relationships in DNA topoisomerases, *Annu. Rev. Biophys. Biomol. Struct.* **33,** 95–118 (2004).

Wang, J.C., Cellular roles of DNA topoisomerases: a molecular perspective, *Nature Rev. Mol. Cell Biol.* **3,** 430–440 (2002).

Chromatin

Gruss, C. and Knippers, R., Structure of replicating chromatin, *Prog. Nucleic Acid Res. Mol. Biol.* **52,** 337–365 (1996).

Luger, K., Mäder, A.W., Richmond, R.K., Sargent, D.F., and Richmond, T.J., Crystal structure of the nucleosome core particle at 2.8 Å resolution, *Nature* **389,** 251–260 (1997); *and* Harp, J.M., Hanson, B.L., Timm, D.E., and Bunick, G.J., Asymmetries in the nucleosome core particle at 2.5 Å resolution, *Acta Cryst.* **D56,** 1513–1534 (2000).

Schalch, T., Duda, S., Sargent, D.F., and Richmond, T.J., X-Ray structure of a tetranucleosome and its implications for the chromatin fibre, *Nature* **436,** 138–141 (2005).

Widom, J., Structure, dynamics, and function of chromatin in vitro, *Annu. Rev. Biophys. Biomol. Struct.* **27,** 285–327 (1998).

DNA–Protein Interactions

Aggarwal, A.K., Structure and function of restriction endonucleases, *Curr. Opin. Struct. Biol.* **5,** 11–19 (1995).

Berg, J.M. and Shi, Y., The galvanization of biology: a growing appreciation of the roles of zinc, *Science* **271,** 1081–1085 (1996). [Summarizes different types of zinc fingers and discusses why zinc is suitable for stabilizing small protein domains.]

Ellenberger, T.E., Getting a grip on DNA recognition: structures of the basic region leucine zipper, and the basic region helix-loop-helix DNA-binding domains, *Curr. Opin. Struct. Biol.* **4,** 12–21 (1994).

Luscombe, N.M., Austin, S.E., Berman, H.M., and Thornton, J.M., An overview of the structures of protein-DNA complexes, *Genome Biol.* **1,** reviews 001.1–001.37 (2000). [This review, which contains many molecular models, is available online at http://genomebiology.com/2000/1/1/reviews/001.]

Marmorstein, R., Carey, M., Ptashne, M., and Harrison, S.C., DNA recognition by GAL4: structure of a protein–DNA complex, *Nature* **356,** 408–414 (1992).

Sarai, A. and Kono, H., Protein-DNA recognition patterns and predictions, *Annu. Rev. Biophys. Biomol. Struct.* **34,** 379–398 (2005).

Somers, W.S. and Phillips, S.E.V., Crystal structure of the *met* repressor–operator complex at 2.8 Å resolution reveals DNA recognition by β-strands, *Nature* **359,** 387–393 (1992).

25

DNA Replication, Repair, and Recombination

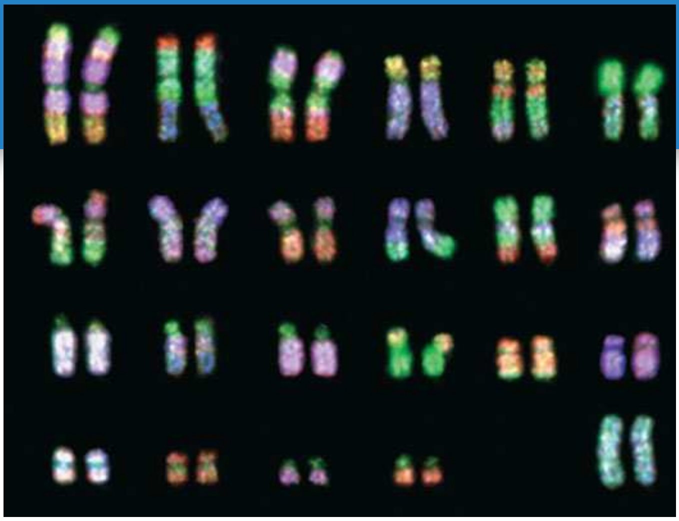

Each time a human cell divides, the DNA in each of its 46 chromosomes must be replicated rapidly and accurately. Errors that do occur may be repaired to ensure the faithful transmission of genetic information. [L. Willatt/Photo Researchers.]

■ MEDIA RESOURCES

(available at www.wiley.com/college/voet)
Guided Exploration 25. The replication of DNA in *E. coli*
Interactive Exercise 46. *E. coli* DNA Pol I Klenow fragment with double-helical DNA
Interactive Exercise 47. *E. coli* Tus in complex with Ter-containing DNA
Interactive Exercise 48. Structure of PCNA
Interactive Exercise 49. HIV reverse transcriptase
Animated Figure 25-1. Meselson and Stahl experiment
Animated Figure 25-36. Holliday model of general recombination
Case Study 32: Glucose-6-Phosphate Dehydrogenase Activity and Cell Growth

■ CHAPTER CONTENTS

1 Overview of DNA Replication
2 Prokaryotic DNA Replication
  A. DNA Polymerases Add the Correctly Paired Nucleotide
  B. Replication Initiation Requires Helicase and Primase
  B. The Leading and Lagging Strands Are Synthesized Simultaneously
  D. Replication Terminates at Specific Sites
  E. DNA Is Replicated with High Fidelity
3 Eukaryotic DNA Replication
  A. Eukaryotes Use Several DNA Polymerases
  B. Eukaryotic DNA Is Replicated from Multiple Origins
  C. Telomerase Extends Chromosome Ends
4 DNA Damage
  A. Environmental and Chemical Agents Generate Mutations
  B. Many Mutagens Are Carcinogens
5 DNA Repair
  A. Some Damage Can Be Directly Reversed
  B. Base Excision Repair Requires a Glycosylase
  C. Nucleotide Excision Repair Removes a Segment of a DNA Strand
  D. Mismatch Repair Corrects Replication Errors
  E. Some DNA Repair Mechanisms Introduce Errors
6 Recombination
  A. Homologous Recombination Involves Several Protein Complexes
  B. DNA Can Be Repaired by Recombination
  C. Transposition Rearranges Segments of DNA

Watson and Crick's seminal paper describing the DNA double helix ended with the statement: "It has not escaped our notice that the specific pairing we have postulated immediately suggests a possible copying mechanism for the genetic material." As they predicted, when DNA replicates, each polynucleotide strand acts as a template for the formation of a complementary strand through base pairing interactions. The two strands of the parent molecule must therefore separate so that a complementary daughter strand can be enzymatically synthesized on the surface of each parent strand. This results in two molecules of duplex DNA, each consisting of one polynucleotide strand from the parent molecule and a newly synthesized complementary strand (Fig. 3-11). Such a mode of replication is termed **semiconservative** (in **conservative replication,** the parental DNA would remain intact and both strands of the daughter duplex would be newly synthesized).

The semiconservative nature of DNA replication was elegantly demonstrated in 1958 by Matthew Meselson and Franklin Stahl. The density of DNA was increased by labeling it with ^{15}N, a heavy isotope of nitrogen (^{14}N is the naturally abundant isotope). This was accomplished by growing *E. coli* in a medium that contained $^{15}NH_4Cl$ as its only nitrogen source. The labeled bacteria were then abruptly transferred to a ^{14}N-containing

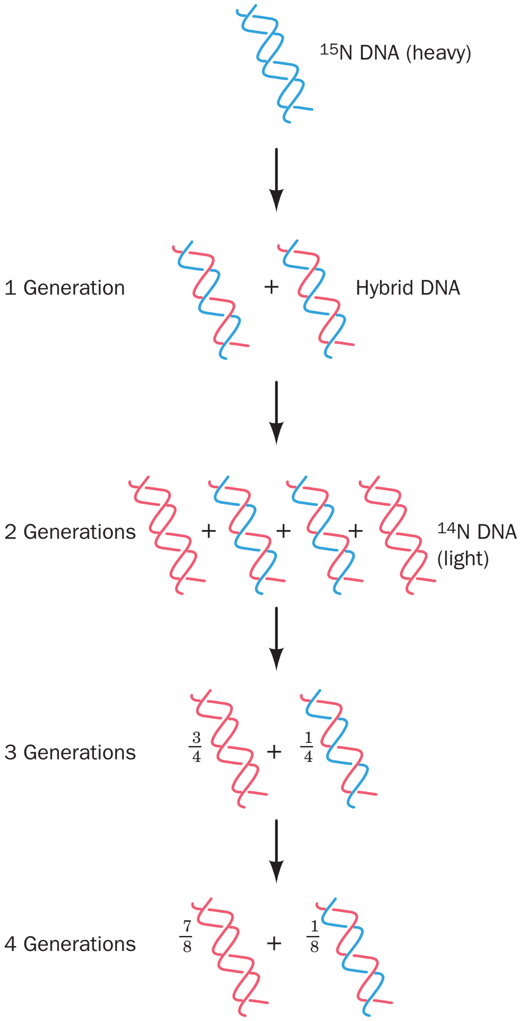

Figure 25-1 | The Meselson and Stahl experiment. Parental (^{15}N-labeled or "heavy") DNA is replicated semiconservatively so that in the first generation, DNA molecules contain one parental (*blue*) strand and one newly synthesized (*red*) strand. In succeeding generations, the proportion of ^{14}N-labeled ("light") strands increases, but hybrid molecules containing one heavy and one light strand persist. **See the Animated Figures.**

LEARNING OBJECTIVES

- Understand that DNA polymerase requires a template and primers to synthesize DNA.
- Understand that double-stranded DNA is replicated semidiscontinuously.

medium and the density of their DNA was monitored over several generations by ultracentrifugation.

Meselson and Stahl found that after one generation (one doubling of the cell population), all the DNA had a density exactly halfway between the densities of fully ^{15}N-labeled DNA and unlabeled DNA. This DNA must therefore contain equal amounts of ^{14}N and ^{15}N as is expected after one generation of semiconservative replication (Fig. 25-1). Conservative DNA replication, in contrast, would preserve the fully ^{15}N-labeled parental strand and generate an equal amount of unlabeled DNA. After two generations, half of the DNA molecules were unlabeled and the remainder were ^{14}N–^{15}N hybrids. In succeeding generations, the amount of unlabeled DNA increased relative to the amount of hybrid DNA although the hybrid never totally disappeared. This is in accord with semiconservative replication but at odds with conservative replication, in which hybrid DNA never forms.

The details of DNA replication, including the unwinding of the parental strands and the assembly of complementary strands from nucleoside triphosphates, have emerged gradually since 1958. DNA replication is far more complex than the overall chemistry of this process might suggest, in large part because replication must be extremely accurate in order to preserve the integrity of the genome from generation to generation. In this chapter, we examine the protein assemblies that mediate DNA replication in prokaryotes and eukaryotes. We also discuss the mechanisms for ensuring fidelity during replication and for correcting polymerization errors and other types of DNA damage.

1 Overview of DNA Replication

DNA is replicated by enzymes known as **DNA-directed DNA polymerases** or simply **DNA polymerases.** These enzymes use single-stranded DNA **(ssDNA)** as templates on which to catalyze the synthesis of the complementary strand from the appropriate deoxynucleoside triphosphates (Fig. 25-2). The reaction occurs through the nucleophilic attack of the growing DNA chain's 3′-OH group on the α-phosphoryl of an incoming nucleoside triphosphate. The otherwise reversible reaction is driven by the subsequent hydrolysis of the eliminated PP_i. The incoming nucleotides are selected by their ability to form Watson–Crick base pairs with the template DNA so that the newly synthesized DNA strand forms a double helix with the template strand. Nearly all known DNA polymerases can add a nucleotide only to the free 3′-OH group of a base-paired polynucleotide so that *DNA chains are extended only in the 5′ → 3′ direction.*

DNA Replication Occurs at Replication Forks. John Cairns observed DNA replication through the autoradiography of chromosomes from *E. coli* grown in a medium containing [^{3}H]thymidine. These circular chromosomes contain replication "eyes" or "bubbles" (Fig. 25-3), called **θ structures** (after their resemblance to the Greek letter theta), that form when the two parental strands of DNA separate to allow the synthesis of their complementary daughter strands. DNA replication involving θ structures is known as **θ replication.**

A branch point in a replication eye at which DNA synthesis occurs is called a **replication fork.** A replication bubble may contain one or two replication forks **(unidirectional** or **bidirectional replication).** Autoradiographic studies have demonstrated that θ replication is almost always bidirectional (Fig. 25-4). In other words, *DNA synthesis proceeds in both directions from the point where replication is initiated.*

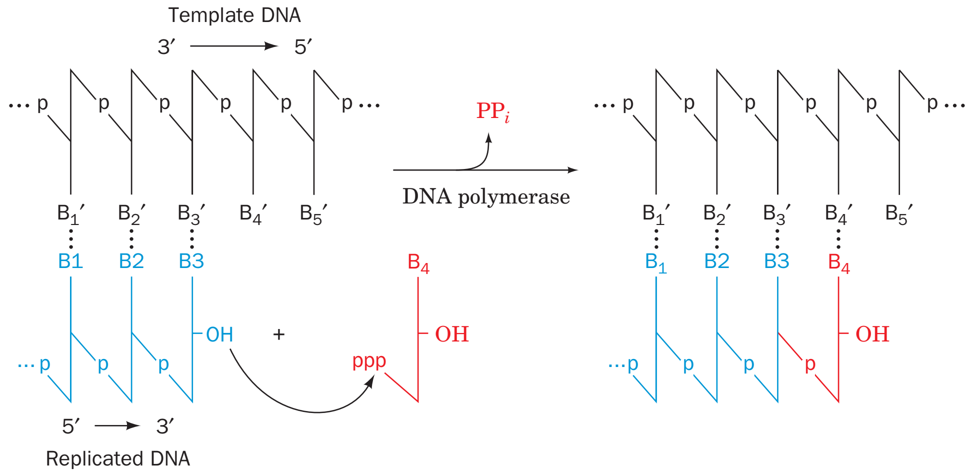
Template DNA
3′ → 5′
… p p p p p p …
B_1' B_2' B_3' B_4' B_5'
B1 B2 B3
OH
+
B_4
OH
ppp
… p p p
5′ → 3′
Replicated DNA
PP_i
DNA polymerase
… p p p p p p …
B_1' B_2' B_3' B_4' B_5'
B_1 B2 B3 B_4
OH
… p p p p

Figure 25-2 | Action of DNA polymerases. These enzymes assemble incoming deoxynucleoside triphosphates on single-stranded DNA templates. The OH group at the 3′ end of a growing polynucleotide strand is a nucleophile that attacks the α-phosphate group of an incoming dNTP that base-pairs with the template DNA strand, and hence the growing strand is elongated in its 5′ → 3′ direction. Although formation of a new phosphodiester bond is reversible, the subsequent hydrolysis of the PP_i product makes the overall reaction irreversible.

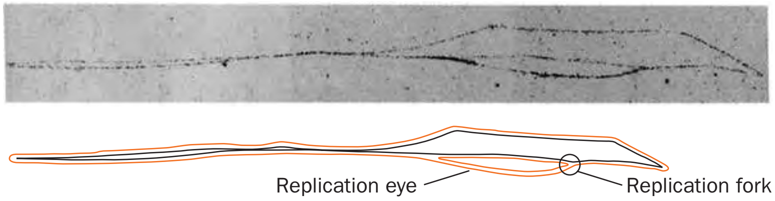
Replication eye
Replication fork

Figure 25-3 | An autoradiogram and its interpretive drawing of a replicating *E. coli* chromosome. The bacterium had been grown in a medium containing $[^3H]$thymidine, thereby labeling the subsequently synthesized DNA so that it appears as a line of dark grains in the photographic emulsion (*red lines in the drawing*). The size of the replication eye indicates that this circular chromosome is about one-eighth duplicated. [Courtesy of John Cairns, Cold Spring Harbor Laboratory.]

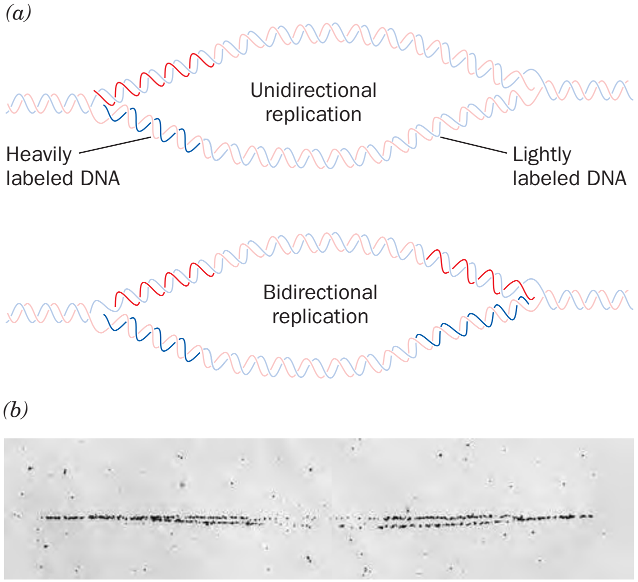
(a)
Unidirectional replication
Heavily labeled DNA
Lightly labeled DNA
Bidirectional replication
(b)

Figure 25-4 | The autoradiographic differentiation of unidirectional and bidirectional θ replication of DNA. (*a*) An organism is grown for several generations in a medium that is lightly labeled with $[^3H]$thymidine so that all of its DNA will be visible in an autoradiogram. A large amount of $[^3H]$thymidine is then added to the medium for a few seconds before the DNA is isolated **(pulse-labeling)** in order to heavily label bases near the replication fork(s). Unidirectional DNA replication will exhibit only one heavily labeled branch point, whereas bidirectional DNA replication will exhibit two such branch points. (*b*) An autoradiogram of *E. coli* DNA demonstrating that it is bidirectionally replicated. [Courtesy of David M. Prescott, University of Colorado.]

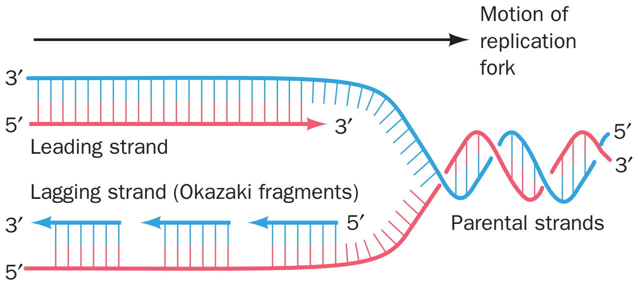
Motion of replication fork
3′
5′
3′
Leading strand
Lagging strand (Okazaki fragments)
3′
5′
5′
5′
3′
Parental strands

■ Figure 25-5 | Semidiscontinuous DNA replication. Both daughter strands (*leading strand red, lagging strand blue*) are synthesized in their 5′ → 3′ direction. The leading strand is synthesized continuously, whereas the lagging strand is synthesized discontinuously. The lagging strand segments are known as Okazaki fragments.

Replication Is Semidiscontinuous. The low-resolution images provided by autoradiograms such as Figs. 25-3 and 25-4*b* suggest that duplex DNA's two antiparallel strands are simultaneously replicated at an advancing replication fork. Yet since DNA polymerases extend DNA strands only in the 5′ → 3′ direction, how can they copy the parent strand that extends in the 5′ → 3′ direction past the replication fork? This question was answered in 1968 by Reiji Okazaki through the following experiment. If a growing *E. coli* culture is pulse labeled for 30 s with [^{3}H]thymidine, much of the radioactive and hence newly synthesized DNA consists of 1000- to 2000-nucleotide **(nt)** fragments (in eukaryotes, these so-called **Okazaki fragments** are 100–200 nt long). When the cells are transferred to an unlabeled medium after the [^{3}H]thymidine pulse, the size of the labeled fragments increases over time. *The Okazaki fragments must therefore become covalently incorporated into larger DNA molecules.*

Okazaki interpreted his experimental results in terms of the **semidiscontinuous replication** model (Fig. 25-5). The two parent strands are replicated in different ways. The newly synthesized DNA strand that extends 5′ → 3′ in the direction of replication fork movement, the **leading strand,** is continuously synthesized in its 5′ → 3′ direction as the replication fork advances. The other new strand, the **lagging strand,** is also synthesized in its 5′ → 3′ direction. However, it can only be made discontinuously, as Okazaki fragments, as single-stranded parental DNA becomes newly exposed at the replication fork. The Okazaki fragments are later covalently joined together by the enzyme **DNA ligase.**

DNA Synthesis Extends RNA Primers. Given that DNA polymerases require a free 3′-OH group to extend a DNA chain, how is DNA synthesis initiated? Careful analysis of Okazaki fragments revealed that their 5′ ends consist of RNA segments of 1 to 60 nt (the length is species dependent) that are complementary to the template DNA chain (Fig. 25-6). In *E. coli,* these **RNA primers** are synthesized by the enzyme **primase.** Multiple primers are required for lagging strand synthesis, but only one primer is required to initiate synthesis of the leading strand. Mature DNA, however, does not contain RNA. *The RNA primers are eventually replaced with DNA.*

■ CHECK YOUR UNDERSTANDING

Explain why DNA polymerase requires a template and a primer.

Why is DNA replicated semiconservatively and semidiscontinuously?

2 Prokaryotic DNA Replication

LEARNING OBJECTIVES

- Understand that DNA polymerases include 3′ → 5′ exonuclease activity and, in the case of Pol I, 5′ → 3′ exonuclease activity.
- Understand that DNA replication requires additional proteins to separate DNA strands, unwind the helix, bind to single-stranded DNA, and synthesize RNA primers.
- Understand that a sliding clamp is loaded onto the template DNA to enhance the processivity of DNA polymerase.
- Understand that complete replication of DNA requires DNA ligase, a termination factor, and topoisomerases.
- Understand that balanced nucleotide levels, the polymerase mechanism, its proofreading mechanism, and the activity of DNA repair enzymes contribute to the accuracy of DNA replication.

DNA replication involves a great variety of enzymes in addition to those mentioned above. Many of the required enzymes were first isolated from prokaryotes and are therefore better understood than their eukaryotic counterparts. Accordingly, we begin with a detailed consideration of prokaryotic DNA replication. Replication in eukaryotes is discussed in Section 25-3.

A | DNA Polymerases Add the Correctly Paired Nucleotides

In 1957, Arthur Kornberg discovered an *E. coli* enzyme that catalyzes the synthesis of DNA, based on its ability to incorporate the radioactive label from [^{14}C]thymidine triphosphate into DNA (Box 25-1). This enzyme, which is now known as **DNA polymerase I** or **Pol I,** consists of a single 928-residue polypeptide. Pol I is said to be a **processive enzyme** because

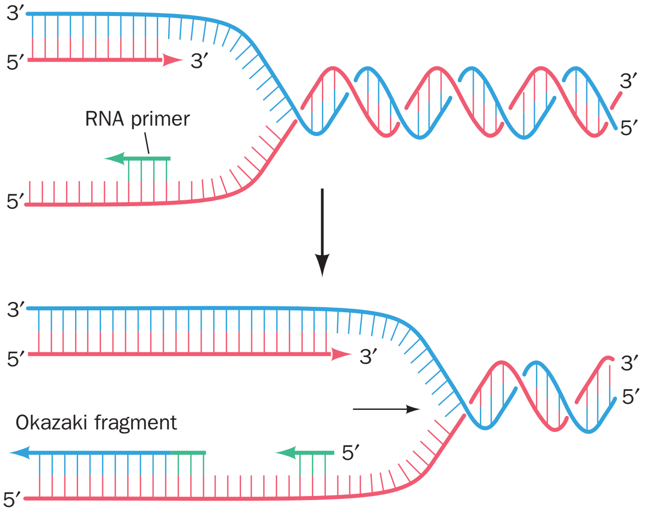

Figure 25-6 | Priming of DNA synthesis by short RNA segments. Each Okazaki fragment consists of an RNA primer (*green*) that has been extended by DNA polymerase. The RNA primer is later removed.

it catalyzes a series of successive nucleotide polymerization steps, typically 20 or more, without releasing the single-stranded template.

Pol I Has Exonuclease Activity. In addition to its polymerase activity, Pol I has two independent hydrolytic activities that occupy separate active sites: a 3′ → 5′ exonuclease and a 5′ → 3′ exonuclease. *The 3′ → 5′ exonuclease activity allows Pol I to edit its mistakes.* If Pol I erroneously incorporates a mispaired nucleotide at the end of a growing DNA chain, the polymerase activity is inhibited and the 3′ → 5′ exonuclease hydrolytically excises the offending nucleotide (Fig. 25-7). The polymerase activity then resumes DNA replication. This **proofreading** mechanism explains the high fidelity of DNA replication by Pol I.

The Pol I 5′ → 3′ exonuclease binds to duplex DNA at single-strand nicks (breaks). It cleaves the nicked DNA strand in a base-paired region

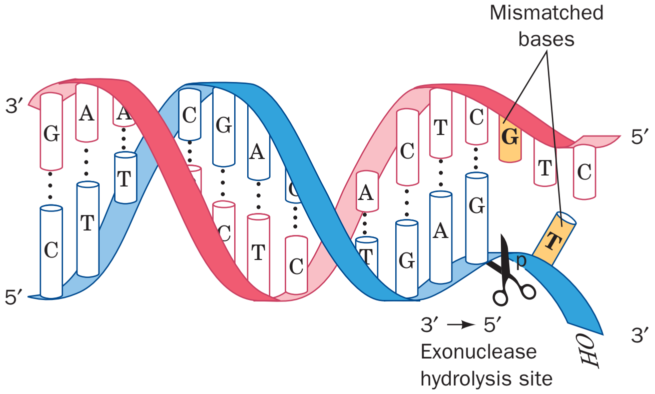

Figure 25-7 | The 3′ → 5′ exonuclease function of DNA polymerase I. This enzymatic activity excises mispaired nucleotides from the 3′ end of the growing DNA strand (*blue*).

BOX 25-1 **PATHWAYS OF DISCOVERY**

Arthur Kornberg and DNA Polymerase I

Arthur Kornberg (1918–2007)

Like a number of his contemporaries during the Great Depression, Arthur Kornberg entered medical school because of the lack of jobs in teaching or industry. He subsequently served in the U.S. Coast Guard as a ship's doctor but quickly realized that he was better suited to the laboratory than the sea. When he began his work at the National Institutes of Health in 1942, the classic studies of nutrition and vitamins were giving way to the new science of enzymology. After purifying aconitase from rat hearts, Kornberg stated that he found enzymes intoxicating. He likened purifying an enzyme to ascending an uncharted mountain, with the reward being the view from the top and the satisfaction of being the first one there.

Kornberg spent 6 months at the Cori laboratory (Box 16-1) and in 1948 began working on enzymes involved in the synthesis of nucleotide cofactors. He found that the enzyme nucleotide pyrophosphorylase catalyzed a reaction in which a nucleotide was incorporated into a coenzyme:

$$\text{Nicotinamide ribonucleotide} + \text{ATP} \rightarrow \text{NAD}^+ + \text{PP}_i$$

Next, Kornberg began to search for an enzyme that could assemble many nucleotides to make a nucleic acid chain. Some people have mistakenly assumed that Kornberg was inspired to look for DNA polymerase by the publication of the Watson–Crick model of DNA in 1953. In fact, Kornberg was following his instincts as an enzymologist, and his curiosity stemmed from his familiarity with other enzymes, including glycogen phosphorylase, which was capable of synthesizing the polymer glycogen *in vitro.* Kornberg had also experimented with enzymes involved in the synthesis of phospholipids, which—like DNA—contain phosphodiester bonds (he abandoned this line of investigation because he didn't like working with "greasy" molecules).

To purify a DNA-synthesizing enzyme, Kornberg started with extracts of fast-growing *E. coli* cells, which had replaced slower growing yeast cells as a laboratory subject. He added radioactive thymidine to the extracts and measured the production of radioactive DNA. Disappointingly, the incorporation of thymidine was extremely low, but thymidine phosphate (TMP) worked better, and thymidine triphosphate (TTP) better still. Kornberg also discovered that the amount of newly synthesized DNA increased when a small amount of DNA was included in the reaction mixture. This was not entirely unexpected, as Kornberg already knew that a small amount of glycogen could serve as a primer for additional glycogen synthesis. At first, however, Kornberg believed that the DNA added to his reaction mixture acted as a substrate for nucleases that were present in cell extracts and thereby protected the newly synthesized radioactive DNA from degradation. Later, he realized that the added DNA functioned as a template for the synthesis of a new strand and through its partial degradation also supplied the other, nonradioactive nucleotides required for polymerization. The idea of a template was, at the time, foreign to most enzymologists and other biochemists, but biologists seemed more receptive to the role of a template in DNA synthesis. For his discovery and characterization of DNA polymerase (later known as DNA polymerase I or Pol I), Kornberg was awarded the 1959 Nobel Prize in Physiology or Medicine.

Even with purified Pol I in hand, Kornberg was faced with the need to prove that the reaction product was biologically active. He therefore used Pol I to synthesize the 5386-bp DNA of bacteriophage ϕX174 on viral DNA templates and then used DNA ligase to close up the synthetic DNA molecule to yield a circular DNA that was infectious. To Kornberg's chagrin, the popular press misunderstood this work, hailing it as the creation of life in a test tube.

Kornberg later confessed that he was amazed by the virtuosity of the DNA polymerase he had isolated from *E. coli:* The enzyme could synthesize a chain of thousands of nucleotides with an accuracy that exceeded chemical predictions. However, during the 1970s, genetic studies and other evidence clearly indicated that other proteins were responsible for DNA replication in *E. coli,* and DNA polymerases II and III were soon discovered and characterized. For the next two decades, Kornberg led the effort to determine the mechanism of DNA replication. Indeed, many of the leading researchers in the field were trained in his laboratory.

Kornberg, A., Active center of DNA polymerase, *Science* **163,** 1410–1418 (1969).

Kornberg, A., *For Love of Enzymes: The Odyssey of a Biochemist,* Harvard University Press (1989). [A scientific autobiography.]

beyond the nick to excise the DNA as either mononucleotides or oligonucleotides of up to 10 residues (Fig. 25-8).

Although Pol I was the first of the *E. coli* DNA polymerases to be discovered, it is not *E. coli's* primary replicase. Rather, its most important (and only essential) function is in lagging strand synthesis, in which it removes the RNA primers and replaces them with DNA. This process involves the 5′ → 3′ exonuclease and polymerase activities of Pol I working

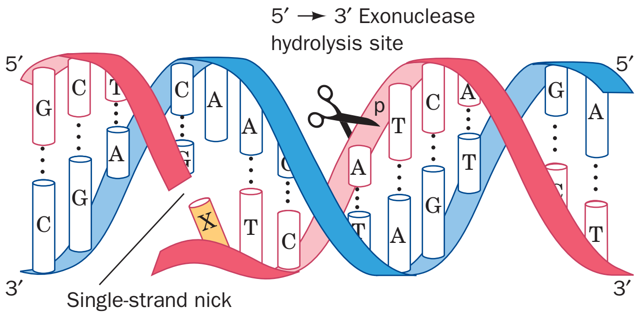

■ **Figure 25-8 | The 5′ → 3′ exonuclease function of DNA polymerase I.** This enzymatic activity excises up to 10 nucleotides from the 5′ end of a single-strand nick. The nucleotide immediately past the nick (X) may or may not be paired.

in concert to excise the ribonucleotides on the 5′ end of the single-strand nick between the new and old (previously synthesized) Okazaki fragments and to replace them with deoxynucleotides that are appended to the 3′ end of the new Okazaki fragment (Fig. 25-9). The nick is thereby translated (moved) toward the DNA strand's 3′ end, a process known as **nick translation.** When the RNA has been entirely excised, the nick is sealed by the action of DNA ligase (Section 25-2C), thereby linking the new and old Okazaki fragments.

Biochemists use nick translation to prepare radioactive DNA. Double-stranded DNA **(dsDNA)** is nicked in only a few places by treating it with small amounts of pancreatic **DNase I.** Radioactively labeled dNTPs are then added and Pol I translates the nicks, thereby replacing unlabeled deoxynucleotides with labeled deoxynucleotides.

Pol I also functions in the repair of damaged DNA. As we discuss in Section 25-5, damaged DNA is detected by a variety of DNA repair systems, many of which endonucleolytically cleave the damaged DNA on the 5′ side of the lesion. Pol I's 5′ → 3′ exonuclease activity then excises the damaged DNA while its polymerase activity fills in the resulting single-strand gap in the same way it replaces the RNA primers of Okazaki frag-

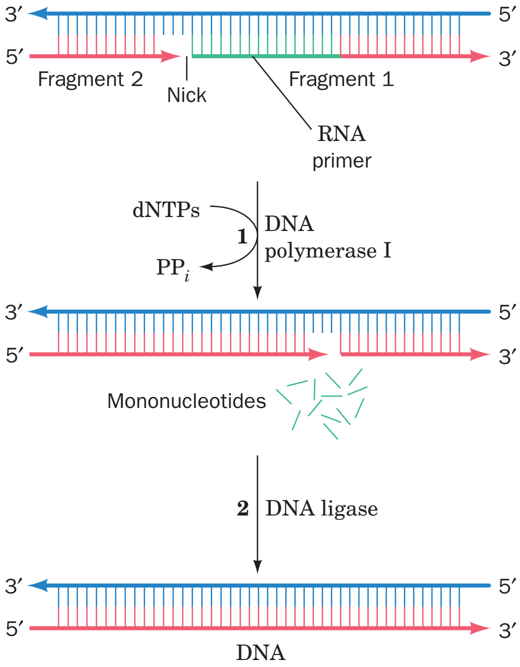

■ **Figure 25-9 | The replacement of RNA primers by DNA in lagging strand synthesis.** **(1)** The RNA primer at the 5′ end of a previously synthesized Okazaki fragment (*Fragment 1*) is excised through the action of Pol I's 5′ → 3′ exonuclease function and replaced through its polymerase function, which adds deoxynucleotides to the 3′ end of the newly synthesized Okazaki fragment (*Fragment 2*). This, in effect, translates the nick originally at the 5′ end of the RNA to the position that was occupied by its 3′ end (nick translation). **(2)** The nick is sealed by the action of DNA ligase.

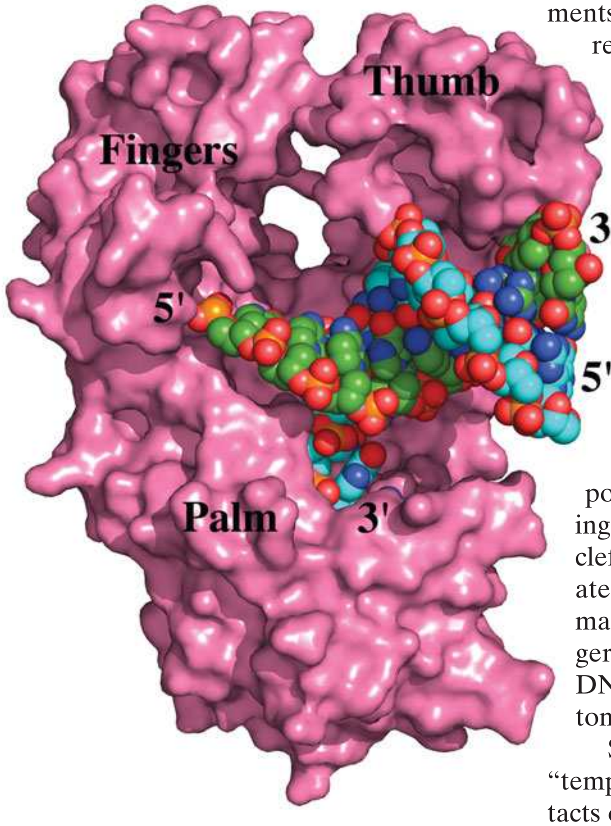

■ **Figure 25-10 | X-Ray structure of *E. coli* DNA polymerase I Klenow fragment in complex with a double-helical DNA.** The protein is represented by its surface diagram (*magenta*), and its bound DNA is drawn in space-filling form colored according to atom type with the C atoms of the 12-nt template strand green, the C atoms of the 14-nt primer strand cyan, N blue, O red, and P orange. Note that the 3′ end of the primer strand occupies the enzyme's 3′ → 5′ exonuclease site and hence this structure is a so-called editing complex. [Based on an X-ray structure by Thomas Steitz, Yale University. PDBid 1KLN.] **See Interactive Exercise 46.**

ments. Thus, Pol I has indispensable roles in *E. coli* DNA replication and repair although it is not, as was first supposed, responsible for the bulk of DNA synthesis.

The Klenow Fragment Is a Model DNA Polymerase. *E. coli* DNA polymerase I, a protein whose three enzymatic activities occupy three separate active sites, can be proteolytically cleaved to a large or **"Klenow" fragment** (residues 324–928), which contains both the polymerase and the 3′ → 5′ exonuclease activities, and a small fragment (residues 1–323), which contains the 5′ → 3′ exonuclease activity. The X-ray structure of the Klenow fragment, determined by Thomas Steitz, reveals that it consists of two domains (Fig. 25-10). The smaller domain (residues 324–517; the lower portion of the structure shown in Fig. 25-10) contains the 3′ → 5′ exonuclease site. The larger domain (residues 521–928) contains the polymerase active site at the bottom of a prominent cleft, a surprisingly large distance (~25 Å) from the 3′ → 5′ exonuclease site. The cleft, which is lined with positively charged residues, has the appropriate size and shape (~22 Å × ~30 Å) to bind a B-DNA molecule in a manner resembling a right hand grasping a rod (note the thumb, fingers, and palm structures in Fig. 25-10). The active sites of nearly all DNA and RNA polymerases of known structure are located at the bottoms of similarly shaped clefts.

Steitz cocrystallized the Klenow fragment with a short DNA "template" strand and a complementary "primer" strand. The protein contacts only the phosphate backbone of the duplex DNA, consistent with Pol I's lack of sequence specificity in binding DNA. The separation of the polymerase and 3′ → 5′ exonuclease active sites suggests that the bound DNA undergoes a large conformational shift in shuttling between the sites.

DNA Polymerase Senses Watson–Crick Base Pairs via Sequence-Independent Interactions. The C-terminal domain of the thermostable *Thermus aquaticus (Taq)* DNA polymerase I **(Klentaq1)** is 50% identical in sequence and closely similar in structure to the large domain of Klenow fragment (Klentaq1 lacks a functional 3′ → 5′ exonuclease site). Gabriel Waksman crystallized Klentaq1 in complex with a double-stranded DNA molecule with a GGAAA overhang at its 5′ end (representing a template with a complementary DNA primer). The crystals were then incubated with 2′,3′-dideoxy-CTP (ddCTP, which lacks a 3′-OH group). The X-ray structure of the crystals (Fig. 25-11*a*) reveals that a ddC residue is covalently linked to the 3′ end of the primer, where it forms a Watson–Crick pair with the G residue at the 3′ end of the overhang. Moreover, a separate ddCTP molecule (to which the primer's new 3′-terminal ddC residue is incapable of forming a covalent bond) occupies the enzyme's active site, where it forms a Watson–Crick pair with the template's next G. Clearly, Klentaq1 retains its catalytic activity in this crystal.

A DNA polymerase must distinguish correctly paired bases from mismatches and yet do so via sequence-independent interactions with the incoming dNTP. The Klentaq1 structure reveals that this occurs in an active site pocket whose shape is complementary to Watson–Crick base pairs. In addition, although the bound dsDNA is mainly in the B conformation, the 3 base pairs nearest the active site assume the A conformation, as has also been observed in the X-ray structures of several other DNA polymerases in their complexes with DNA. The resulting wider and shallower minor groove (Section 24-1A) permits protein side chains to form hydrogen bonds with the otherwise inaccessible N3 atoms of the purine bases and O2 atoms

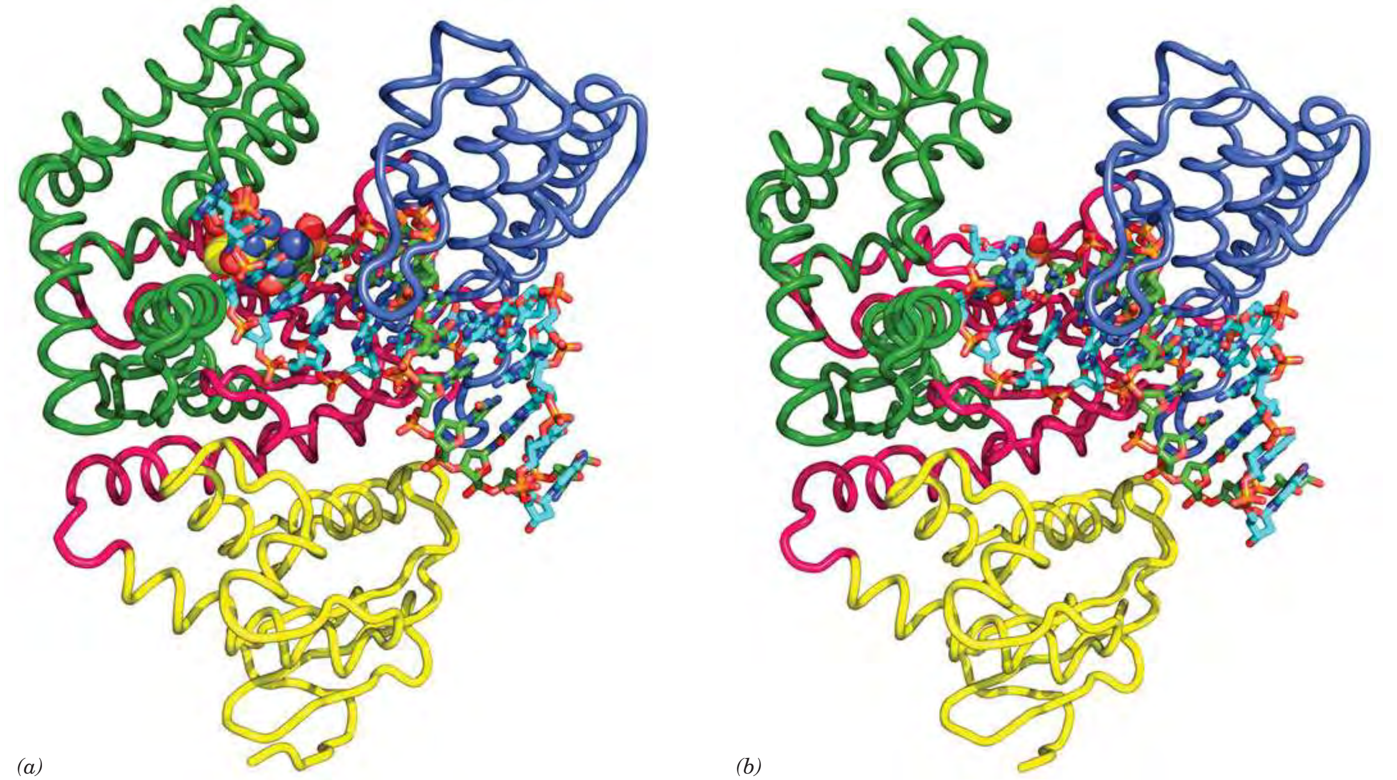

Figure 25-11 | X-Ray structure of Klentaq1 in complex with DNA in the closed and open conformations. (*a*) The closed conformation (with ddCTP). (*b*) The open conformation (ddCTP depleted). The protein, which is viewed as in Fig. 25-10, is represented in worm form with its N-terminal, palm, fingers, and thumb domains colored yellow, magenta, green, and blue, respectively. The DNA is shown in stick form, whereas the primer strand's 3′-terminal ddC residue is drawn in space-filling form as is the ddCTP in Part *a* that is base-paired with a template G residue in the enzyme's active site pocket. The atoms are colored according to type with template strand C cyan, primer strand C green, ddCTP C yellow, N blue, O red, and P orange. [Based on X-ray structures by Gabriel Waksman, Washington University School of Medicine. PDBids 3KTQ and 2KTQ.]

of the pyrimidine bases. The positions of these hydrogen bond acceptors are sequence-independent, as can be seen from an inspection of Fig. 24-1 (in contrast, the positions of the hydrogen bonding acceptors in the major groove vary with the sequence). However, with a non-Watson–Crick pairing—that is, with a mismatched dNTP in the active site—these hydrogen bonds would be greatly distorted if not completely disrupted. The polymerase also makes extensive sequence-independent hydrogen bonding and van der Waals interactions with the DNA's sugar–phosphate backbone.

After the Klentaq1 · DNA · ddCTP crystals described above were depleted of ddCTP by soaking them in a ddCTP-free solution, the enzyme's fingers domain assumed a so-called open conformation (Fig. 25-11*b*), which differs significantly from the closed conformation shown in Fig. 25-11*a*. Evidently, the fingers helices in the open conformation move toward the active site when ddCTP binds, thereby burying the nucleotide in the catalytically active closed complex. These observations are consistent with kinetic measurements indicating that the binding of the correct dNTP to Pol I induces a rate-limiting conformational change that yields a tight ternary complex. It therefore appears that the enzyme rapidly samples the available dNTPs in its open conformation, but only when it binds the correct dNTP in a Watson–Crick pairing with the template base does it form the catalytically competent closed conformation. After formation of the phosphodiester bond, a second conformational change releases the PP_i

product, and the DNA is translocated in the active site so as to position it for the next reaction cycle.

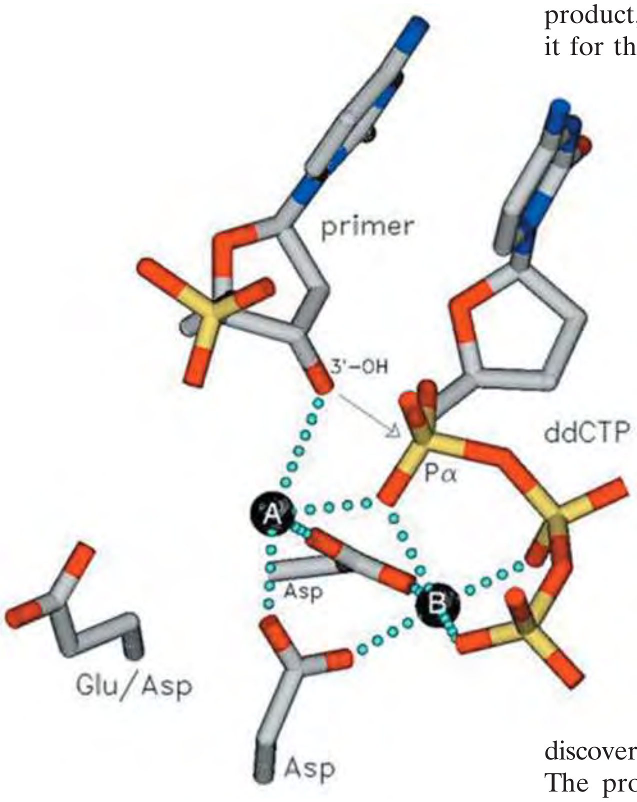

Figure 25-12 | Role of metal ions in nucleotidyl transfer. A and B represent enzyme-bound metal ions, usually Mg^{2+}, in the DNA polymerase active site. Atoms are colored according to type (C gray, N blue, O red, and P yellow), and metal ion coordination is represented by green dotted lines. Metal ion A activates the primer's 3′-OH group for nucleophilic attack (*arrow*) on the α-phosphate group of the incoming nucleotide (here, ddCTP). Metal ion B orients and electrostatically stabilizes the negatively charged triphosphate group. [Courtesy of Tom Ellenberger, Harvard Medical School.]

The DNA Polymerase Catalytic Mechanism Involves Two Metal Ions. The X-ray structures of a variety of DNA polymerases suggest that they share a common catalytic mechanism for nucleotidyl transfer. Their active sites all contain two metal ions, usually Mg^{2+}, that are liganded by two invariant Asp side chains in the palm domain (Fig. 25-12). Metal ion B is liganded by all three phosphate groups of the bound dNTP, whereas metal ion A bridges the α-phosphate group of this dNTP and the primer's 3′-OH group. Metal ion A presumably activates the primer's 3′-OH group for a nucleophilic attack on the α-phosphate group, whereas metal ion B functions to orient its bound triphosphate group and to electrostatically shield its negative charges as well as the additional negative charge on the transition state leading to the release of the PP_i ion.

DNA Polymerase III Is *E. coli's* DNA Replicase. The discovery of normally growing *E. coli* mutants that have very little (but not entirely absent) Pol I activity stimulated the search for additional DNA polymerizing activities. This effort was rewarded by the discovery of two more enzymes, designated, in the order they were discovered, **DNA polymerase II (Pol II)** and **DNA polymerase III (Pol III).** The properties of these enzymes are compared with those of Pol I in Table 25-1. Pol II and Pol III had not previously been detected because their combined activities in the assays used are normally <5% that of Pol I. Pol II participates in DNA repair; mutant cells lacking Pol II can therefore grow normally. The absence of Pol III, however, is lethal, demonstrating that it is *E. coli's* DNA replicase.

The catalytic core of Pol III consists of three subunits: α, which contains the complex's DNA polymerase activity; ε, its 3′ → 5′ exonuclease; and θ. However, at least seven other subunits (τ, γ, δ, δ′, χ, ψ, and β) combine with them to form a labile multisubunit enzyme known as the **Pol III holoenzyme.** The catalytic properties of the Pol III core resemble those of Pol I except that Pol III lacks 5′ → 3′ exonuclease activity on dsDNA. Thus, *Pol III can synthesize a DNA strand complementary to a single-stranded template and can edit the polymerization reaction to increase replication fidelity, but it cannot catalyze nick translation.*

Table 25-1 Properties of *E. coli* DNA Polymerases

	Pol I	Pol II	Pol III
Mass (kD)	103	90	130
Molecules/cell	400	?	10–20
Turnover number[a]	600	30	9000
Structural gene	*polA*	*polB*	*polC*
Conditionally lethal mutant	+	−	+
Polymerization: 5′ → 3′	+	+	+
Exonuclease: 3′ → 5′	+	+	+
Exonuclease: 5′ → 3′	+	−	−

[a] Nucleotides polymerized $\text{min}^{-1} \cdot \text{molecule}^{-1}$ at 37°C.

Source: Kornberg, A. and Baker, T.A., *DNA Replication* (2nd ed.), p. 167, Freeman (1992).

B | Replication Initiation Requires Helicase and Primase

See Guided Exploration 25
The replication of DNA in *E. coli.*

The *E. coli* chromosome is a supercoiled DNA molecule of 4.6×10^6 bp. Since DNA polymerase requires a single-stranded template, other proteins participate in DNA replication by locating the replication initiation site, unwinding the DNA, and preventing the single strands from reannealing. Replication in *E. coli* begins at a 245-bp region known as ***oriC.*** Elements of this sequence are highly conserved among gram-negative bacteria. Multiple copies of a 52-kD protein known as **DnaA** bind to *oriC* and cause ~45 bp of an AT-rich segment of the DNA to separate into single strands. This melting requires the free energy of ATP hydrolysis and is probably also facilitated by both the AT-rich nature of the DNA segment and the negative supercoiling (underwinding) of the circular DNA chromosome [the latter being generated by DNA gyrase, a type II topoisomerase (Section 24-1D) whose activity is required for prokaryotic DNA replication].

Helicases Unwind DNA. DnaA bound to *oriC* recruits two hexameric complexes of **DnaB,** one to each end of the melted region. DnaB is a **helicase** that further separates the DNA strands. Helicases are a diverse group of enzymes that unwind DNA during replication, transcription, and a variety of other processes. DnaB is one of 12 helicases expressed by *E. coli.* Helicases function by translocating along one strand of a double-helical nucleic acid so as to mechanically unwind the helix in their path, a process that is driven by the free energy of NTP hydrolysis.

E. coli DnaB, a hexamer of identical 471-residue subunits, separates the two strands of the parental DNA by translocating along the lagging strand template in the 5′ → 3′ direction, while hydrolyzing ATP (it can also use GTP and CTP but not UTP). Some helicases move in the 3′ → 5′ direction, and some are dimers rather than hexamers. The X-ray structure of a hexameric helicase from bacteriophage T7, which infects *E. coli,* reveals that the protein forms a ring with a central channel large enough to accommodate a DNA strand (Fig. 25-13). Adjacent helicase subunits have different conformations, as is also the case in the F_1F_0-ATPase (Section 18-3B). This suggests that when a helicase subunit binds and hydrolyzes an NTP, it undergoes a conformational change that alters its interaction

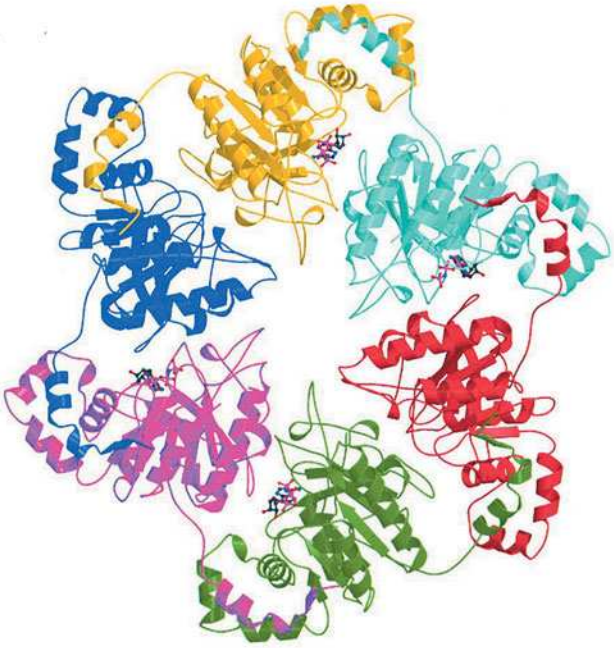

■ **Figure 25-13** | **X-Ray structure of T7 helicase.** Each subunit of the cyclic hexamer is drawn in a different color. Four bound ATP analogs are shown in ball-and-stick form. Note that the conformations of adjacent subunits are not identical. This structure is part of a larger protein complex that also contains primase activity. [Courtesy of Dale Wigley, Cancer Research U.K., London Research Institute. PDBid 1E0J.]

with the ssDNA in the center of the ring. The cumulative effect of each subunit sequentially binding NTP, hydrolyzing it, and releasing the products is that *the protein pulls itself along a DNA strand, mechanically separating the dsDNA ahead of it.*

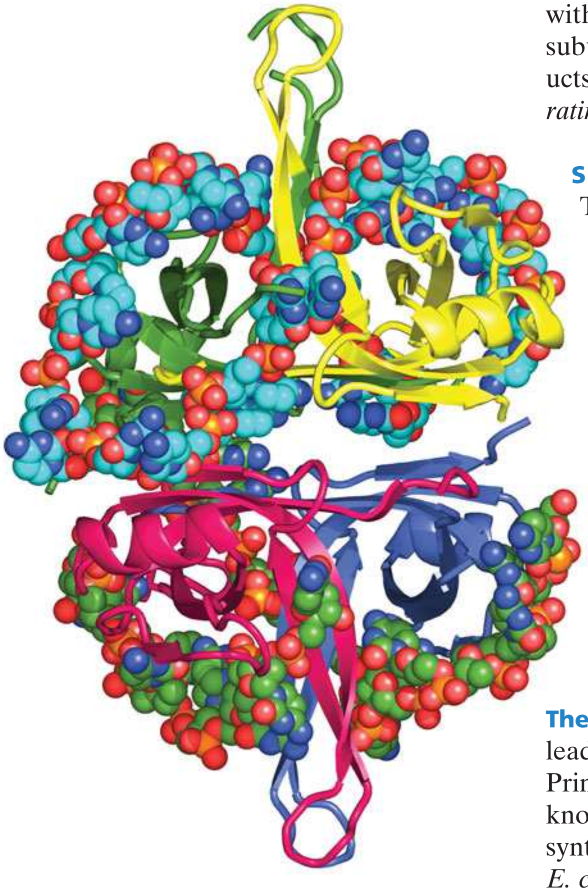

■ **Figure 25-14 | X-Ray structure of SSB in complex with dC(pC)$_{34}$.** The homotetramer, which has D_2 symmetry, is viewed along one of its twofold axes with its other twofold axes horizontal and vertical. Each of its subunits (which include the N-terminal 134 residues of the 177-residue polypeptide) are differently colored. Its two bound ssDNA molecules are drawn in space-filling form colored according to atom type with the upper strand C cyan, lower strand C green, N blue, O red, and P orange. (The lower strand is partially disordered and hence appears to consist of two fragments). [Based on an X-ray structure by Timothy Lohman and Gabriel Waksman, Washington University School of Medicine. PDBid 1EYG.]

Single-Strand Binding Protein Prevents DNA from Reannealing. The separated DNA strands behind an advancing helicase do not reanneal to form dsDNA because they become coated with **single-strand binding protein (SSB).** The SSB coat also prevents ssDNA from forming secondary structures (such as stem-loops) and protects it from nucleases. Note that the DNA must be stripped of SSB before it can be replicated by DNA polymerase.

E. coli SSB is a tetramer of 177-residue subunits that can bind to DNA in several different ways. In the major binding mode (Fig. 25-14), each U-shaped strand of ssDNA is draped across two of SSB's four subunits. This would permit an unlimited series of SSB tetramers to interact end-to-end along the length of a ssDNA. The DNA-binding cleft of SSB, which is contained in its N-terminal 115 residues, is positively charged so that the protein can interact electrostatically with DNA phosphate groups. The cleft is too narrow to accommodate dsDNA.

The Primosome Synthesizes RNA Primers. All DNA synthesis, both of leading and lagging strands, requires the prior synthesis of an RNA primer. Primer synthesis in *E. coli* is mediated by an ~600-kD protein assembly known as a **primosome,** which includes the DnaB helicase and an RNA-synthesizing **primase** called **DnaG,** as well as five other types of subunits. *E. coli* DnaG is a monomeric protein whose catalytic domain does not resemble any of the other DNA and RNA polymerases of known structure. Nevertheless, it catalyzes the same polymerization reaction (Fig. 25-2 using NTPs rather than dNTPs) to produce an RNA segment of ~11 nucleotides.

The primosome is propelled in the 5′ → 3′ direction along the DNA template for the lagging strand (i.e., toward the replication fork) in part by DnaB-catalyzed ATP hydrolysis. This motion, which displaces the SSB in its path, is opposite in direction to that of template reading during DNA chain synthesis. Consequently, the primosome reverses its migration momentarily to allow primase to synthesize an RNA primer in the 5′ → 3′ direction (Fig. 25-6).

The primosome is required to initiate each Okazaki fragment. The single RNA segment that primes the synthesis of the leading strand can be synthesized, at least *in vitro,* by either primase or **RNA polymerase** (the enzyme that synthesizes RNA transcripts from a DNA template; Section 26-1), but its rate of synthesis is greatly enhanced when both enzymes are present.

C | The Leading and Lagging Strands Are Synthesized Simultaneously

In *E. coli,* the Pol III holoenzyme catalyzes the synthesis of both the leading and lagging strands. This occurs in a single multiprotein particle, the **replisome,** which contains two Pol III enzymes. In some other prokaryotes and in eukaryotes, two different polymerases synthesize the leading and lagging strands, but like Pol III, they are part of a multiprotein replisome. *In order for the replisome to move as a single unit in the 5′ → 3′ direction along the leading strand, the lagging strand template must loop around*

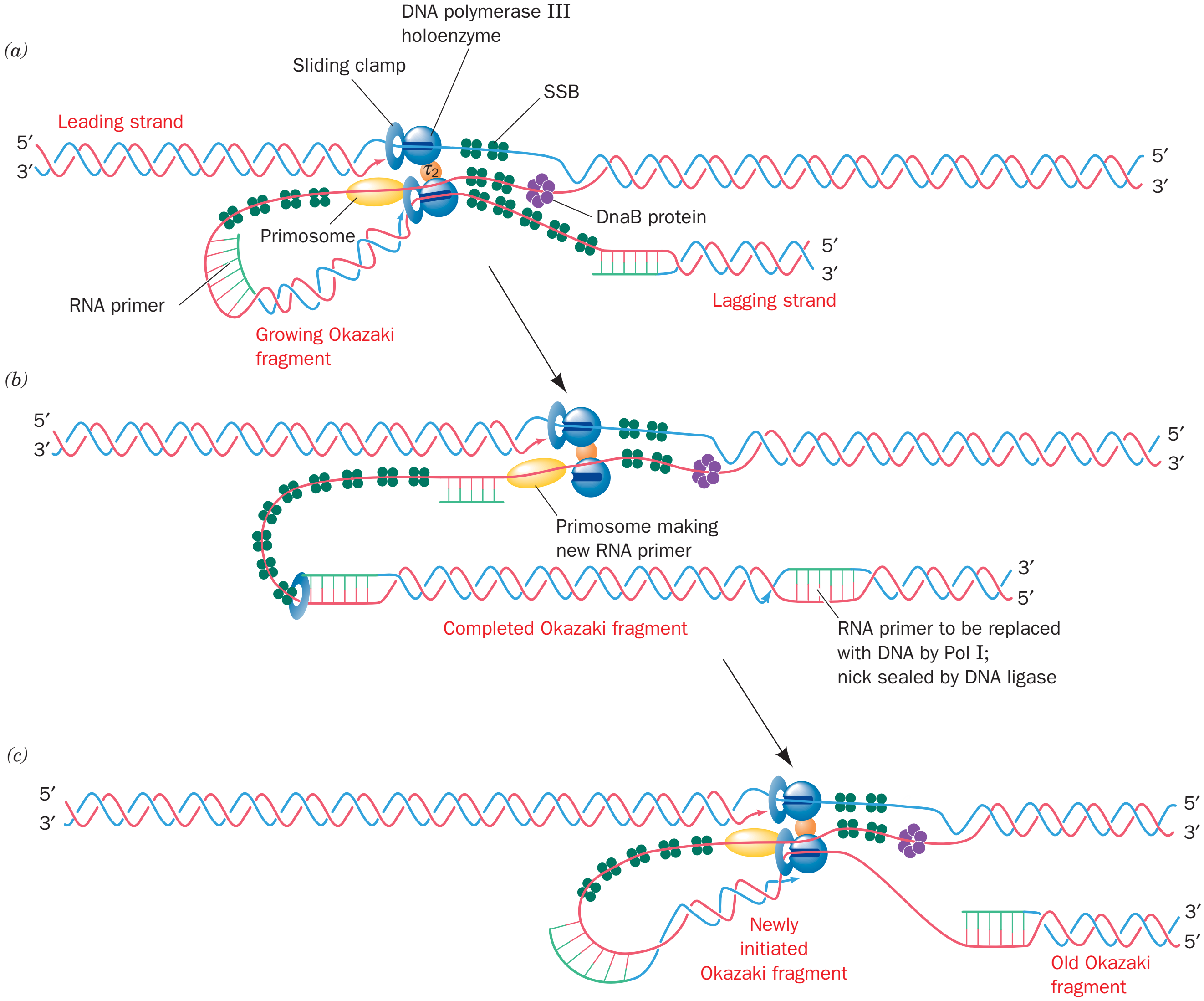
(a)
DNA polymerase III holoenzyme
Sliding clamp
SSB
Leading strand
5′
3′
τ_2
5′
3′
DnaB protein
Primosome
5′
3′
RNA primer
Lagging strand
Growing Okazaki fragment
(b)
5′
3′
5′
3′
Primosome making new RNA primer
3′
5′
Completed Okazaki fragment
RNA primer to be replaced with DNA by Pol I; nick sealed by DNA ligase
(c)
5′
3′
5′
3′
3′
5′
Newly initiated Okazaki fragment
Old Okazaki fragment

■ **Figure 25-15 | The replication of *E. coli* DNA.** (*a*) The replisome, which contains two DNA polymerase III holoenzymes, synthesizes both the leading and the lagging strands. The lagging strand template must loop around to permit the holoenzyme to extend the primed lagging strand. (*b*) The holoenzyme releases the lagging strand template when it encounters the previously synthesized Okazaki fragment. This may signal the primosome to initiate synthesis of a lagging strand RNA primer. (*c*) The holoenzyme rebinds the lagging strand template and extends the RNA primer to form a new Okazaki fragment. Note that in this model, leading strand synthesis is always ahead of lagging strand synthesis.

(Fig. 25-15). After completing the synthesis of an Okazaki fragment, the lagging strand holoenzyme relocates to a new primer near the replication fork and resumes synthesis. *The result of this process is a continuous leading strand and a series of RNA-primed Okazaki fragments separated by single-strand nicks.* The RNA primers are replaced with DNA through Pol I–catalyzed nick translation, and the nicks in the lagging strand are then sealed through the action of DNA ligase (see below).

A Sliding Clamp Promotes Pol III Processivity. The Pol III core enzyme dissociates from the template DNA after replicating only ~12 residues; that is, it has a processivity of ~12 residues. However, the Pol III holoenzyme has a processivity of >5000 residues, due to the presence of

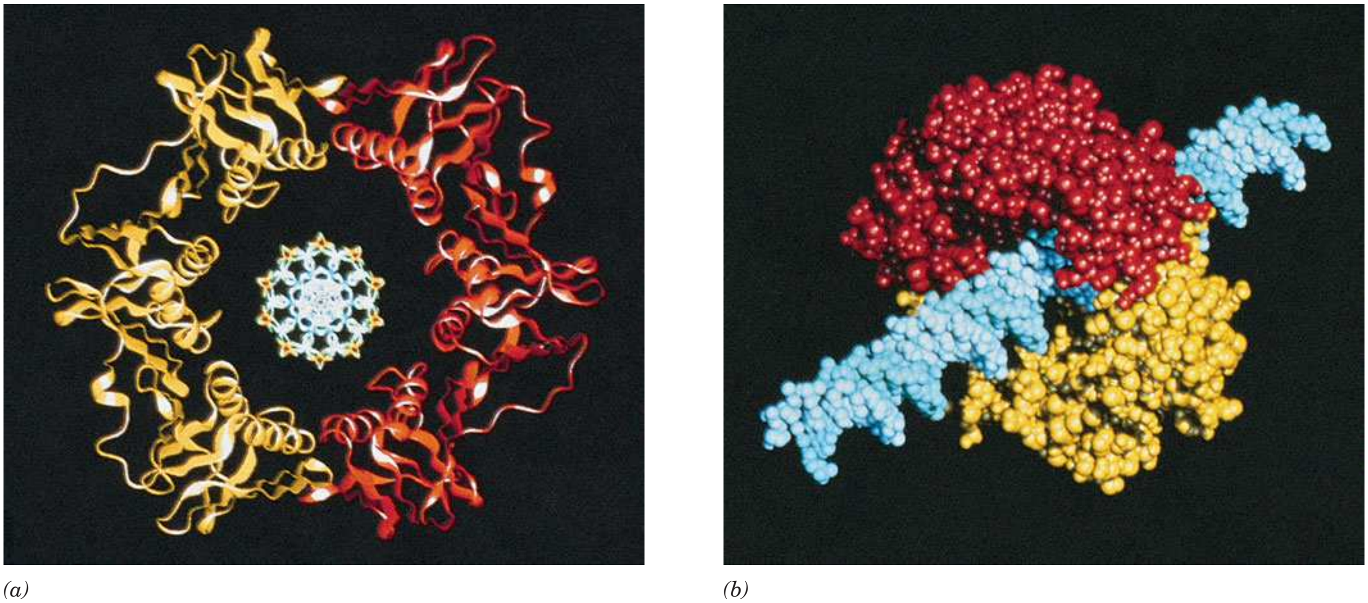
(a) (b)

Figure 25-16 | X-Ray structure of the β clamp of *E. coli* Pol III holoenzyme. (*a*) A ribbon drawing showing the two monomeric units of the dimeric protein in yellow and red as viewed along the dimer's twofold axis. A stick model of B-DNA is placed with its helix axis coincident with the protein dimer's twofold axis. (*b*) A space-filling model of the protein, colored as in Part *a,* in a hypothetical complex with B-DNA (*cyan*). [Courtesy of John Kuriyan, The Rockefeller University. PDBid 2POL.]

its **β subunit.** A β subunit bound to a cut circular DNA slides to the break and falls off. This suggests that the β subunit *forms a ring around the DNA that functions as a **sliding clamp** (alternatively, **β clamp**) that can move along it, thereby keeping the Pol III holoenzyme from diffusing away.* The β clamp also increases the rate of nucleotide polymerization.

The X-ray structure of the β clamp (Fig. 25-16), determined by John Kuriyan, reveals that it is a dimer of C-shaped monomers that form an ~80-Å-diameter donut-shaped structure. The central ~35-Å-diameter hole is larger than the 20- and 26-Å diameters of B- and A-DNAs (the hybrid helices containing RNA primers and DNA have an A-DNA-like conformation; Section 24-1A). Each β subunit forms three domains of similar structure so that the dimeric ring is a pseudo-symmetrical six-pointed star. The interior surface of the ring is positively charged, whereas its outer surface is negatively charged.

Model-building studies in which a B-DNA helix is threaded through the central hole (Fig. 25-16) indicate that the protein's α helices span the major and minor grooves of the DNA rather than entering into them as do, for example, the recognition helices of helix–turn–helix motifs (Section 24-4B). It appears that the β subunit is designed to minimize its associations with DNA. This presumably permits the protein to freely slide along the DNA helix.

E. coli DNA is replicated at a rate of ~1000 nt/s. Thus, in lagging strand synthesis, the DNA polymerase holoenzyme must be reloaded onto the template strand every second or so (Okazaki fragments are ~1000 nt long). Consequently, a new β clamp, which promotes Pol III's processivity, must be installed around the lagging strand template about once every second. The **γ complex** of the Pol III holoenzyme (subunit composition $\gamma\tau_2\delta\delta'\chi\psi$) is also known as the **clamp loader** because it opens the dimeric β clamp to load it onto the DNA template in an

ATP-dependent manner. The γ complex bridges the replisome's two Pol III cores (αεθ) via the C-terminal segments of its two τ subunits (Fig. 25-15), which also bind the DnaB helicase. This apparently allows the helicase to match the pace of the two polymerases.

Once the β clamp has been loaded onto the DNA, the Pol III core binds to the β clamp more tightly than does the γ complex, thereby displacing it and permitting processive DNA replication to occur. When the polymerase encounters the previously synthesized Okazaki fragment, that is, when the gap between the two successively synthesized Okazaki fragments has been reduced to a nick, the Pol III core releases the DNA and loses its affinity for the β clamp. However, the components of the replisome don't go far; the γ subunit and the Pol III core are held in the vicinity of the lagging strand template through their linkage to the Pol III core engaged in leading strand synthesis (which remains tethered to the DNA by its associated β clamp). Consequently, the γ complex can quickly load a new β clamp around the template DNA at the next primer so that Pol III can begin synthesizing a new Okazaki fragment. The leading-strand Pol III pauses only momentarily while the lagging-strand polymerase is repositioned.

The sliding clamp that remains around the completed Okazaki fragment probably recruits Pol I and DNA ligase so as to replace the RNA primer on the previously synthesized Okazaki fragment with DNA and seal the remaining nick. However, the sliding clamp must eventually be recycled. It was initially assumed that this was the job of the clamp loader. However, it is now clear that the release of the sliding clamp from its associated DNA is carried out by free δ subunit (the "wrench" in the clamp loader that cracks apart the β subunits forming the sliding clamp), which is synthesized in 5-fold excess over that required to populate the cell's few clamp loaders.

DNA Ligase Is Activated by NAD$^+$ or ATP.

The free energy for the DNA ligase reaction is obtained, in a species-dependent manner, through the coupled hydrolysis of either NAD$^+$ to **nicotinamide mononucleotide (NMN$^+$)** + AMP, or ATP to PP$_i$ + AMP. *E. coli* DNA ligase, a 77-kD monomer that uses NAD$^+$, catalyzes a three-step reaction (Fig. 25-17):

1. The adenylyl group of NAD$^+$ is transferred to the ε-amino group of an enzyme Lys residue to form an unusual phosphoamide adduct.
2. The adenylyl group of this activated enzyme is transferred to the 5′-phosphoryl terminus of the nick to form an adenylylated DNA. Here, AMP is linked to the 5′-nucleotide via a pyrophosphate rather than the usual phosphodiester bond.
3. DNA ligase catalyzes the formation of a phosphodiester bond by attack of the 3′-OH on the 5′-phosphoryl group, thereby sealing the nick and releasing AMP.

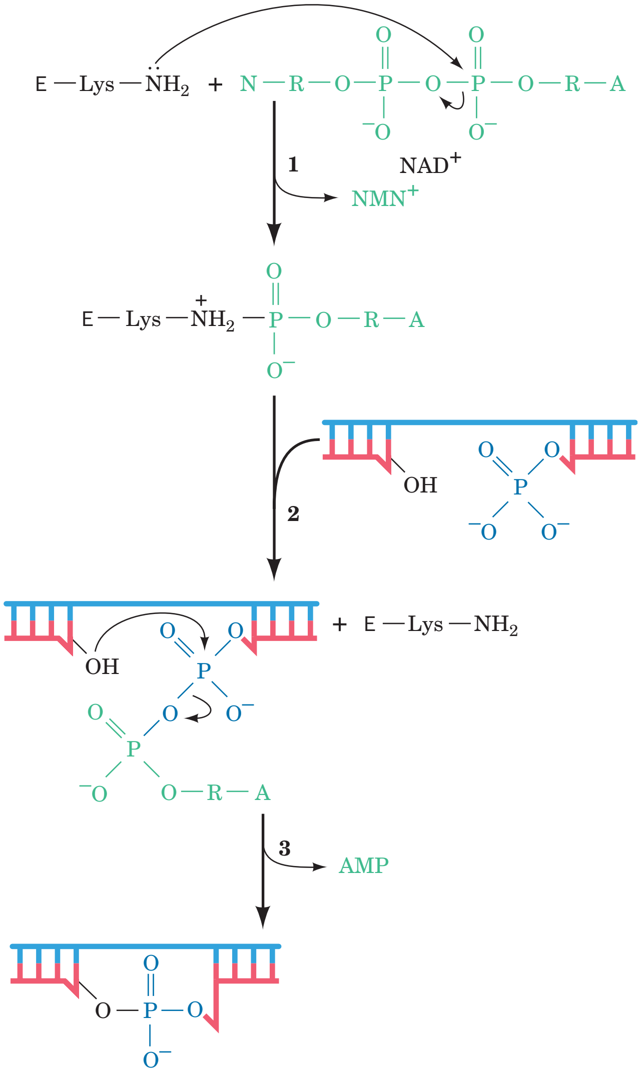

■ **Figure 25-17** | **The reactions catalyzed by *E. coli* DNA ligase.** In eukaryotic and T4 ligases, NAD$^+$ is replaced by ATP so that PP$_i$ rather than NMN$^+$ is eliminated in the first reaction step. Here A, R, and N represent the adenine, ribose, and nicotinamide residues, respectively.

ATP-requiring DNA ligases, such as those of eukaryotes, release PP_i in the first step of the reaction rather than NMN^+. The DNA ligase from the bacteriophage T4 is notable because it can link together two duplex DNAs that lack complementary single-stranded ends **(blunt end ligation)** in a reaction that is a boon to genetic engineering (Section 3-5).

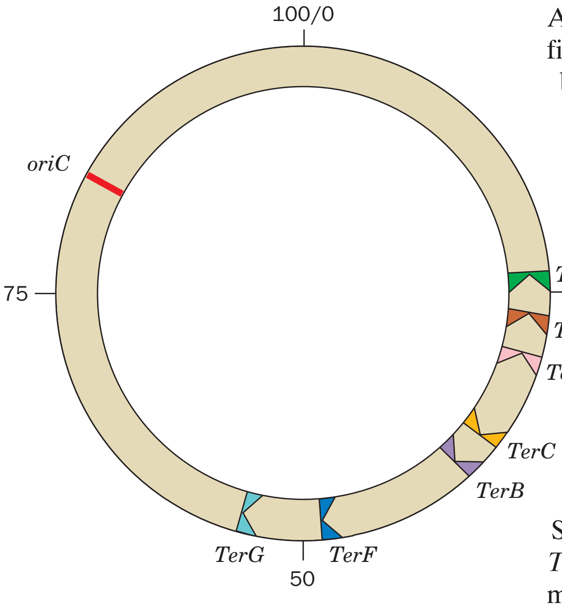

Figure 25-18 | Map of the E. coli chromosome showing the positions of the Ter sites. The *TerC, TerB, TerF,* and *TerG* sites, in combination with Tus protein, allow a counterclockwise-moving replisome to pass but not a clockwise-moving replisome. The opposite is true of the *TerA, TerD,* and *TerE* sites. Consequently, two replication forks that initiate bidirectional DNA replication at *oriC* will meet between the oppositely facing *Ter* sites.

D | Replication Terminates at Specific Sites

The *E. coli* replication terminus is a large (350-kb) region flanked by seven nearly identical nonpalindromic ~23-bp terminator sites, ***TerE, TerD,*** and ***TerA*** on one side and ***TerG, TerF, TerB,*** and ***TerC*** on the other (Fig. 25-18; note that *oriC* is directly opposite the termination region on the *E. coli* chromosome). A replication fork, traveling counterclockwise as drawn in Fig. 25-18 passes through *TerG, TerF, TerB,* and *TerC* but stops on encountering either *TerA, TerD,* or *TerE* (*TerD* and *TerE* are presumably backup sites for *TerA*). Similarly, a clockwise-traveling replication fork passes *TerE, TerD,* and *TerA* but halts at *TerC* or, failing that, *TerB, TerF,* or *TerG.* Thus, these termination sites are polar; they act as one-way valves that allow replication forks to enter the terminus region but not to leave it. *This arrangement guarantees that the two replication forks generated by bidirectional initiation at oriC will meet in the replication terminus even if one of them arrives there well ahead of its counterpart.*

The arrest of replication fork motion at *Ter* sites requires the action of **Tus protein,** a 309-residue monomer that is the product of the ***tus*** gene (for *t*erminator *u*tilization *s*ubstance). Tus protein specifically binds to a *Ter* site, where it prevents strand displacement by DnaB helicase, thereby arresting replication fork advancement.

The X-ray structure of Tus in complex with a 15-bp *Ter* fragment (Fig. 25-19) reveals that the protein forms a deep positively charged cleft in which the DNA binds. A 5-bp segment of the DNA near the side of Tus that permits the passage of the replication fork is deformed and underwound relative to canonical (normal) DNA: Its major groove is deeper,

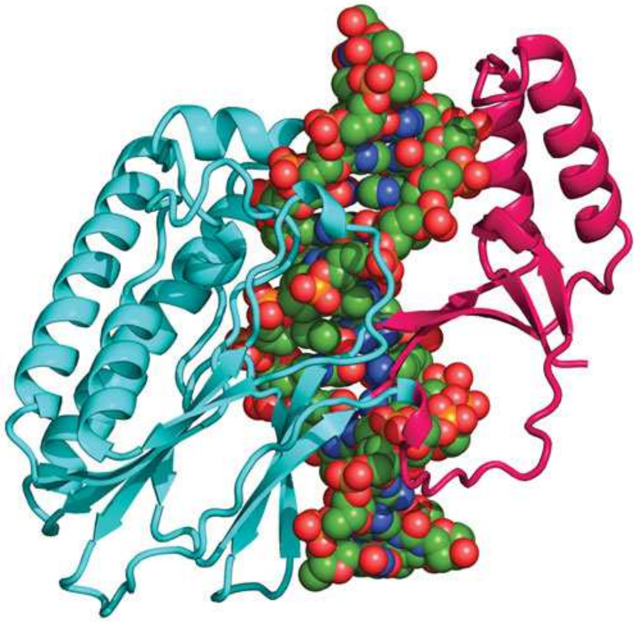

Figure 25-19 | X-Ray structure of *E. coli* Tus in complex with a 15-bp *Ter*-containing DNA. The protein is shown in ribbon form with its N- and C-terminal domains colored cyan and magenta. The DNA is drawn in space-filling form colored according to atom type (C green, N blue, O red, P orange). [Based on an X-ray structure by Kosuke Morikawa, Protein Engineering Research Institute, Osaka, Japan. PDBid 1ECR.] **See Interactive Exercise 47.**

and its minor groove is significantly expanded. Protein side chains at the bottom of the cleft penetrate the DNA's widened major groove to make sequence-specific contacts such that the protein cannot release the bound DNA without a large conformational change. Nevertheless, the mechanism through which Tus prevents replication fork advancement from one side of a *Ter* site but not the other is unclear. Curiously, however, this system is not essential for termination. When the replication terminus is deleted, replication simply stops, apparently through the collision of opposing replication forks. Nevertheless, this termination system is highly conserved in gram-negative bacteria.

The final step in *E. coli* DNA replication is the topological unlinking of the catenated (interlocked) parental DNA strands, thereby separating the two replication products. This reaction is probably catalyzed by one or more topoisomerases.

E | DNA Is Replicated with High Fidelity

Since a single polypeptide as small as the Pol I Klenow fragment can replicate DNA by itself, why does *E. coli* maintain a battery of over 20 intricately coordinated proteins to replicate its chromosome? The answer apparently is *to ensure the nearly perfect fidelity of DNA replication required to accurately transmit genetic information.*

The rates of reversion of mutant *E. coli* or T4 phages to the wild type indicates that only one mispairing occurs per 10^8 to 10^{10} base pairs replicated. This corresponds to ~1 error per 1000 bacteria per generation. Such high replication accuracy arises from four sources:

1. Cells maintain balanced levels of dNTPs through the mechanisms discussed in Sections 23-1C and 23-2C. This is important because a dNTP present at aberrantly high levels is more likely to be misincorporated and, conversely, one present at low levels is more likely to be replaced by one of the dNTPs present at higher levels.
2. The polymerase reaction itself has extraordinary fidelity because it occurs in two stages. First, the incoming dNTP base-pairs with the template while the enzyme is in an open, catalytically inactive conformation. Polymerization occurs only after the polymerase has closed around the newly formed base pair, which properly positions the catalytic residues (induced fit; Fig. 25-11). *The protein conformational change constitutes a double-check for correct Watson–Crick base pairing between the dNTP and the template.*
3. The $3' \rightarrow 5'$ exonuclease functions of Pol I and Pol III detect and eliminate the occasional errors made by their polymerase functions.
4. A remarkable set of enzyme systems in all cells repairs residual errors in the newly synthesized DNA as well as any damage that may occur after its synthesis through chemical and/or physical insults. We discuss the DNA repair systems in Section 25-5.

In addition, the inability of a DNA polymerase to initiate chain elongation without a primer increases DNA replication fidelity. The first few nucleotides of a chain are those most likely to be mispaired because of the cooperative nature of base-pairing interactions (Section 24-2). The use of RNA primers eliminates this source of error since the RNA is eventually replaced by DNA under conditions that permit more accurate base pairing.

■ CHECK YOUR UNDERSTANDING

Summarize the functions of the following proteins in *E. coli* DNA replication: DNA polymerase I, DNA polymerase III, DnaA, helicase, SSB, primase, the sliding clamp, clamp loader, DNA ligase, Tus, and topoisomerase.

How many sliding clamps and clamp-loading events are required for synthesis of the leading and lagging strands?

Explain the four factors that contribute to the high fidelity of DNA replication.

3 Eukaryotic DNA Replication

LEARNING OBJECTIVES

- Understand that eukaryotic DNA replication requires DNA polymerases with different degrees of accuracy and processivity.
- Understand that pre-replication complexes assemble at multiple origins distributed throughout the eukaryotic genome.
- Understand that telomerase uses an RNA template to extend the 3′ ends of eukaryotic chromosomes.

Eukaryotic and prokaryotic DNA replication mechanisms are remarkably similar, although the eukaryotic system is vastly more complex in terms of the amount of DNA to be replicated and the number of proteins required (estimated at >27 in yeast and mammals). Several different modes of DNA replication occur in eukaryotic cells, which contain nuclear DNA as well as mitochondrial and, in plants, chloroplast DNA. In this section, we consider some of the proteins of eukaryotic DNA replication as well as the challenge of replicating the ends of linear chromosomes.

A | Eukaryotes Use Several DNA Polymerases

Animal cells contain at least 13 distinct DNA polymerases, which have been named with Greek letters according to their order of discovery. A newer classification scheme uses sequence homology to group eukaryotic as well as prokaryotic polymerases into six families: A, B, C, D, X, and Y. In this section, we describe the three main enzymes involved in replicating eukaryotic nuclear DNA: **polymerases α, δ,** and **ε,** which are all members of the B-family of polymerases (Table 25-2).

DNA polymerase α **(pol α),** like all DNA polymerases, replicates DNA by extending a primer in the 5′ → 3′ direction under the direction of a ssDNA template. This enzyme has no exonuclease activity and therefore cannot proofread its polymerization product. Pol α is only moderately processive (polymerizing ~100 nucleotides at a time) and associates tightly with a primase, indicating that it is involved in initiating DNA replication. The pol α/primase complex synthesizes a 7- to 10-nt RNA primer and extends it by an additional 15 or so deoxynucleotides. Its lack of proofreading activity is not problematic, since the first few residues of newly synthesized DNA are typically removed and replaced along with the RNA primer.

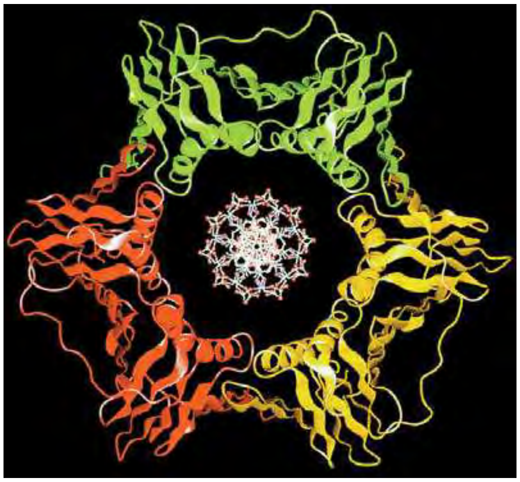

Figure 25-20 | X-Ray structure of PCNA. The three protein monomers (*red, green, and yellow*) form a threefold symmetric ring structure. A model of duplex B-DNA (viewed along its helix axis) has been placed in the center of the PCNA ring. Compare this structure to that of the β clamp of the *E. coli* Pol III holoenzyme (Fig. 25-16). [Courtesy of John Kuriyan, The Rockefeller University. PDBid 1PLQ.] **See Interactive Exercise 48.**

DNA polymerase δ **(pol δ)** does not associate with a primase and contains a 3′ → 5′ exonuclease active site. In addition, the processivity of pol δ is essentially unlimited (it can replicate the entire length of a template DNA), but only when it is in complex with a sliding-clamp protein named **proliferating cell nuclear antigen (PCNA).** The X-ray structure of PCNA (Fig. 25-20), also determined by Kuriyan, reveals that it forms a trimeric ring with almost identical structure (and presumably function) as the *E. coli* β_2 sliding clamp (Fig. 25-16). Intriguingly, PCNA and the β clamp exhibit no significant sequence identity, even when their structurally similar portions are aligned.

Pol δ in complex with PCNA is required for DNA synthesis. During replication, **RFC (replication factor C,** a clamp loader that is the eukaryotic counterpart of the *E. coli* γ complex) loads PCNA onto the template

Table 25-2 Properties of Some Eukaryotic DNA Polymerases

	α	δ	ε
3′ → 5′ Exonuclease	no	yes	yes
Associates with primase	yes	no	no
Processivity	moderate	high	high
Requires PCNA	no	yes	no

strand near the primer. This displaces pol α, allowing pol δ to bind and processively extend the new DNA strand.

DNA polymerase ε **(pol ε)** superficially resembles pol δ but is highly processive in the absence of PCNA. For this reason, and because it is essential for DNA replication, pol ε has been proposed to function as the leading-strand polymerase while pol α and pol δ cooperate to synthesize the lagging strand. However, experiments in yeast suggest that pol ε's essential function can be carried out by only the noncatalytic C-terminal half of its 256-kD catalytic subunit, which is unique among B-family DNA polymerases. It therefore appears that, at least in yeast, pol ε has an essential control function but not a catalytic function.

DNA polymerase γ (pol γ), an A-family enzyme, occurs exclusively in the mitochondrion, where it presumably replicates the mitochondrial genome. Chloroplasts contain a similar enzyme. An additional member of the polymerase family of proteins is the viral enzyme **reverse transcriptase,** an RNA-directed DNA polymerase (Box 25-2).

Additional Enzymes Participate in Eukaryotic DNA Replication. As in prokaryotic DNA replication, a helicase is required to pry apart the two template strands. In eukaryotes, this function belongs to the heterohexameric complex known as **MCM.** Single-stranded DNA becomes coated with the trimeric **RPA,** the eukaryotic equivalent of the bacterial SSB. The eukaryotic replisome also includes additional proteins that have no prokaryotic counterparts and whose functions are not yet understood.

Eukaryotes lack a nick-translating polymerase like *E. coli* Pol I. Instead, the RNA primers of Okazaki fragments are removed through the actions of two enzymes: **RNase H1** removes most of the RNA, leaving only a 5′-ribonucleotide adjacent to the DNA, which is then removed through the action of **flap endonuclease-1 (FEN1).** Yet, as we have seen, pol α extends the RNA primer by ~15 nt of DNA before it is displaced by pol δ. Since pol α lacks proofreading ability, this primer extension is more likely to contain errors than the DNA synthesized by pol δ. However, FEN1 provides what is, in effect, pol α's proofreading function: It is also an endonuclease that excises mismatch-containing oligonucleotides up to 15 nt long from the 5′ end of an annealed DNA strand. Moreover, FEN1 can make several such excisions in succession to remove more distant mismatches. The excised segment is later replaced by pol δ as it synthesizes the succeeding Okazaki fragment (Fig. 25-21).

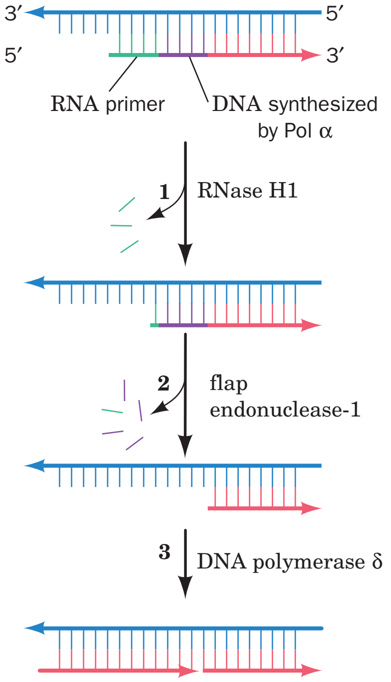

Figure 25-21 | Removal of RNA primers in eukaryotes. **(1)** RNase H1 excises all but the 5′-ribonucleotide of the RNA primer. **(2)** FEN1, a 5′ → 3′ endonuclease, then removes the remaining ribonucleotide along with a segment of adjoining DNA if it contains mismatches. **(3)** The excised nucleotides are replaced as DNA polymerase δ completes the synthesis of the next Okazaki fragment (on the left in this diagram). The nick is eventually sealed by DNA ligase.

B | Eukaryotic DNA Is Replicated from Multiple Origins

Replication fork movement in eukaryotes is ~10 times slower than in prokaryotes. Since a eukaryotic chromosome typically contains 60 times more DNA than does a prokaryotic chromosome, its bidirectional replication from a single origin, as in prokaryotes, would require ~1 month. Electron micrographs such as Fig. 25-22, however, show that *eukaryotic*

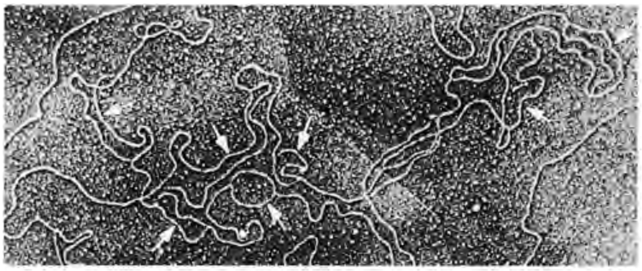

Figure 25-22 | Electron micrograph of a fragment of replicating *Drosophila* DNA. The arrows indicate the multiple replication eyes. [From Kreigstein, H.J. and Hogness, D.S., *Proc. Natl. Acad. Sci.* **71,** 136 (1974).]

BOX 25-2 PERSPECTIVES IN BIOCHEMISTRY

Reverse Transcriptase

Reverse transcriptase **(RT)** is an essential enzyme of **retroviruses,** which are RNA-containing eukaryotic viruses such as **human immunodeficiency virus** (**HIV,** the causative agent of AIDS). RT, which was independently discovered in 1970 by Howard Temin and David Baltimore, synthesizes DNA in the 5′ → 3′ direction from an RNA template. Although the activity of the enzyme was initially considered antithetical to the central dogma of molecular biology (Section 3-3B), there is no thermodynamic prohibition to the RT reaction (in fact, under certain conditions, Pol I can copy RNA templates). RT catalyzes the first step in the conversion of the virus' single-stranded RNA genome to a double-stranded DNA.

After the virus enters a cell, its RT uses the viral RNA as a template to synthesize a complementary DNA strand, yielding an RNA–DNA hybrid helix. The DNA synthesis is primed by a host cell tRNA whose 3′ end unfolds to base-pair with a complementary segment of viral RNA. The viral RNA strand is then nucleolytically degraded by an **RNase H** (an RNase activity that hydrolyzes the RNA of an RNA–DNA hybrid helix). Finally, the DNA strand acts as a template for the synthesis of its complementary DNA, yielding dsDNA that is then integrated into a host cell chromosome.

RT has been a particularly useful tool in genetic engineering because it can transcribe mRNAs to complementary strands of DNA **(cDNA).** mRNA-derived cDNAs can be used, for example, to express eukaryotic structural genes in *E. coli* (Section 3-5D). Since *E. coli* lacks the machinery to splice out introns (Section 26-3A), the use of genomic DNA to express a eukaryotic structural gene in *E. coli* would require the prior excision of its introns—a technically difficult feat.

HIV-1 reverse transcriptase is a dimeric protein whose subunits are synthesized as identical 66-kD polypeptides, known as **p66,**

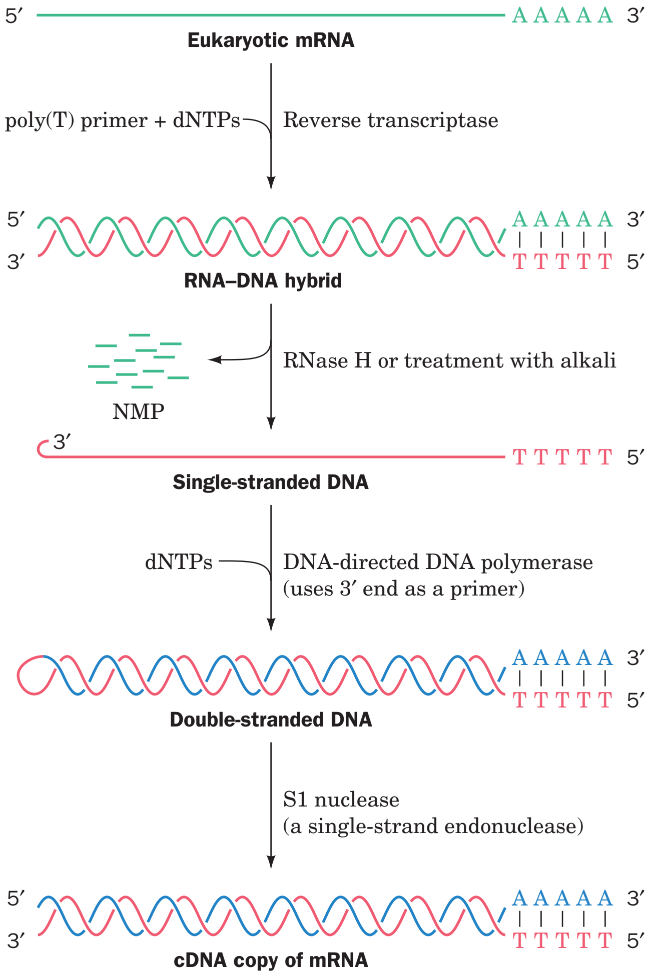

chromosomes contain multiple origins, one every 3 to 300 kb, depending on both the species and the tissue, so replication requires a few hours to complete.

In yeast, the initiation of DNA replication occurs at **autonomously replicating sequences (ARS),** which are conserved 11-bp sequences adjacent to easily unwound DNA. In mammalian genomes, replication origins do not exhibit sequence conservation, yet these sites all support the binding of a six-subunit **origin recognition complex (ORC).** Additional ATP-hydrolyzing proteins help assemble the helicase MCM. The resulting **pre-replication complex (pre-RC)** is not competent to initiate replication until it has been activated by other factors that control progress through the cell cycle (Section 28-4A). Presumably, the separate control of pre-RC assembly and activation allows cells to select replication origins before MCM unwinds the template DNA and replication commences. Once DNA synthesis is under way, no new pre-RC complexes can form, thereby ensuring that the DNA is replicated once and only once per cell cycle.

Initiation sites are uniformly distributed across the genome in early embryogenesis, when cell division is rapid. However, after cells have

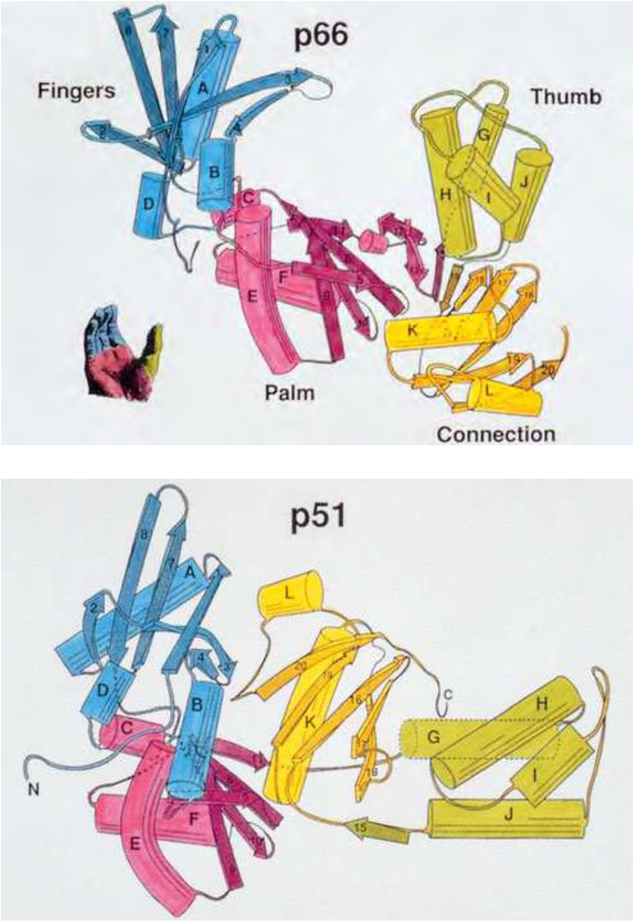

that each contain a polymerase domain and an RNase H domain. However, the RNase H domain of one of the two subunits is proteolytically excised, thereby yielding a 51-kD polypeptide named **p51.** Thus, RT is a dimer of p66 and p51.

The X-ray structure of HIV-1 RT shows that the two subunits have different structures, although each has a fingers, palm, and thumb domain as well as a "connection" domain. The RNase H domain of the p66 subunit follows the connection domain. The p66 and p51 subunits are not related by twofold molecular symmetry (a rare but not unprecedented phenomenon) but instead associate in a sort of head-to-tail arrangement. Consequently, RT has only one polymerase active site.

Reverse transcriptase lacks a proofreading exonuclease function and hence is highly error-prone. Indeed, it is HIV's capacity to rapidly evolve, even within a single host, that presents a major obstacle to the development of an anti-HIV vaccine. This rapid rate of mutation is also the main contributor to the ability of HIV to rapidly develop resistance to drugs that inhibit virally encoded enzymes, including RT. **See Interactive Exercise 49.**

[Structure of RT courtesy of Thomas Steitz, Yale University. PDBid 3HVT.]

differentiated, the distribution of replication origins changes, possibly reflecting patterns of gene expression and/or alterations in DNA packaging in different cell types.

Cytological observations indicate that the various chromosomal regions are not all replicated simultaneously. Rather, clusters of 20 to 80 adjacent **replicons** (replicating units; DNA segments that are each served by a replication origin) are activated simultaneously. New sets of replicons are activated until the entire chromosome has been replicated. DNA replication proceeds in each direction from the origin of replication until each replication fork collides with a fork from the adjacent replicon. Eukaryotes appear to lack termination sequences analogous to the *Ter* sites in *E. coli.*

Nucleosomes Reassemble behind the Replication Forks. Unlike prokaryotic DNA, eukaryotic DNA is packaged in nucleosomes (Section 24-5B). Some alteration of this structure is probably necessary for initiation, but once replication is under way, nucleosomes do not seem to impede the progress of DNA polymerases. Experiments with labeled histones indicate that nucleosomes just ahead of the replication fork disassemble and the freed histones, either individually or as dimers or tetramers, immediately reassociate with the emerging daughter duplexes. The parental histones randomly associate with the leading and lagging duplexes. DNA replication (which occurs in the nucleus) is coordinated with histone protein synthesis in the cytosol so that new histones are available in the required amounts.

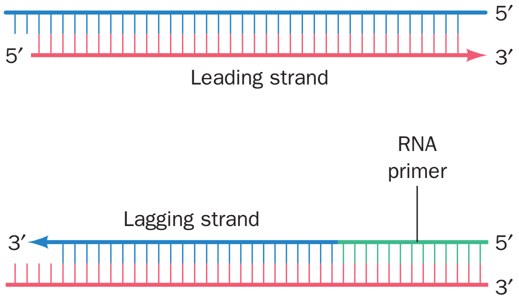

Figure 25-23 | Replication of a linear chromosome. Leading strand synthesis can proceed to the end of the chromosome (*top*). However, DNA polymerase cannot synthesize the extreme 5′ end of the lagging strand because it can only extend an RNA primer that is paired with the 3′ end of a template strand (*bottom*). Removal of the primer and degradation of the remaining single-stranded extension would cause the chromosome to shorten with each round of replication.

C | Telomerase Extends Chromosome Ends

The ends of linear chromosomes present a problem for the replication machinery. Specifically, *DNA polymerase cannot synthesize the extreme 5′ end of the lagging strand* (Fig. 25-23). Even if an RNA primer were paired with the 3′ end of the DNA template, it could not be replaced with DNA (recall that DNA polymerase operates only in the 5′ → 3′ direction; it can only extend an existing primer, and the primer must be bound to its complementary strand). Consequently, *in the absence of a mechanism for completing the lagging strand, linear chromosomes would be shortened at both ends by at least the length of an RNA primer with each round of replication.*

Telomeres Are Built from an RNA Template. The ends of eukaryotic chromosomes, the **telomeres** (Greek: *telos*, end), have an unusual structure. Telomeric DNA consists of 1000 or more tandem repeats of a short G-rich sequence (TTGGGG in the protozoan *Tetrahymena* and TTAGGG in humans) on the 3′-ending strand of each chromosome end.

Elizabeth Blackburn has shown that telomeric DNA is synthesized and maintained by an enzyme named **telomerase,** which is a **ribonucleoprotein** (a complex of protein and RNA). The RNA component (451 nt in humans) includes a segment that is complementary to the repeating telomeric sequence and acts as a template for a reaction in which nucleotides are added to the 3′ end of the DNA (Fig. 25-24, *top*). Telomerase thus functions similarly to reverse transcriptase (Box 25-2); in fact, its protein component is homologous to reverse transcriptase. Telomerase repeatedly translocates to the new 3′ end of the DNA strand, thereby adding multiple telomeric sequences to the DNA (Fig. 25-24, *bottom*). The DNA strand complementary to the telomeric G-rich strand is apparently synthesized by the normal cellular machinery for lagging strand synthesis, leaving a 100- to 300-nt single-stranded overhang on the G-rich strand.

The absence of telomerase, which allows the gradual truncation of chromosomes with each round of DNA replication, contributes to the normal senescence of cells. Conversely, enhanced telomerase activity permits the uncontrolled replication and cell growth that occur in cancer (Box 25-3).

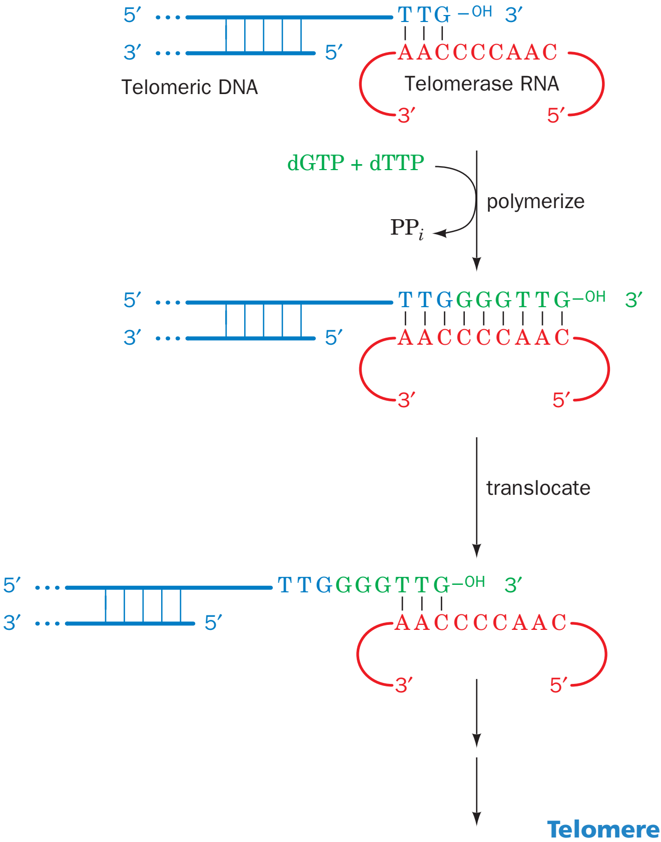

Figure 25-24 | Mechanism for the synthesis of telomeric DNA by *Tetrahymena* telomerase. The telomere's 5′-ending strand is later extended by normal lagging strand synthesis. [After Greider, C.W. and Blackburn, E.H., *Nature* **337,** 336 (1989).]

Telomeres Form G-Quartets. Guanine-rich polynucleotides are notoriously difficult to work with. This is because of their propensity to aggregate via Hoogsteen-type base pairing (Section 24-2B) to form cyclic tetramers known as **G-quartets** (Fig. 25-25*a*). Indeed, the G-rich overhanging strands of telomeres fold back on themselves to form a hairpin, two of which associate in an antiparallel fashion to form stable complexes of stacked G-quartets (Fig. 25-25*b*). Such structures presumably serve as

BOX 25-3 **BIOCHEMISTRY IN HEALTH AND DISEASE**

Telomerase, Aging, and Cancer

Without the action of telomerase, a chromosome would be shortened at both ends by at least the length of an RNA primer with every cycle of DNA replication and cell division. It was therefore initially assumed that, in the absence of active telomerase, essential genes located near the ends of chromosomes would eventually be lost, thereby killing the descendents of the originally affected cells. However, it is now evident that telomeres serve another vital chromosomal function that must be compromised before this can happen. Free DNA ends trigger DNA damage repair systems that normally function to rejoin the ends of broken chromosomes (Section 25-5E). Consequently, exposed telomeric DNA would result in the end-to-end fusion of chromosomes, a process that leads to chromosomal instability and eventual cell death (fused chromosomes often break in mitosis; their two centromeres cause them to be pulled in opposite directions). However, in a process known as **capping,** telomeric DNA is specifically bound by proteins that hide the DNA ends. There is mounting evidence that capping is a dynamic process in which the probability of a telomere spontaneously uncapping increases as telomere length decreases.

The somatic cells of multicellular organisms lack telomerase activity. This explains why such cells in culture can undergo only a limited number of doublings (20–60) before they reach **senescence** (a stage in which they cease dividing) and eventually die. Indeed, otherwise immortal *Tetrahymena* cultures with mutationally impaired telomerases exhibit characteristics reminiscent of senescent mammalian cells before dying off. Apparently, *the loss of telomerase function in somatic cells is a basis for aging in multicellular organisms.*

Despite the foregoing, there is only a weak correlation between the proliferative capacity of a cultured cell and the age of its donor. There is, however, a strong correlation between the initial telomere length in a cell and its proliferative capacity. Cells that initially have relatively short telomeres undergo significantly fewer doublings than cells with longer telomeres. Moreover, fibroblasts from individuals with **progeria** (a rare disease characterized by rapid and premature aging resulting in childhood death) have short telomeres, an observation that is consistent with their known reduced proliferative capacity in culture. In contrast, sperm (which are essentially immortal) have telomeres that do not vary in length with donor age, which indicates that telomerase is active during germ-cell growth. Likewise, those few cells in culture that become immortal (capable of unlimited proliferation) exhibit an active telomerase and a telomere of stable length, as do the cells of unicellular eukaryotes (which are also immortal).

What selective advantage might multicellular organisms gain by eliminating the telomerase activity in their somatic cells? An intriguing possibility is that cellular senescence is a mechanism that protects multicellular organisms from cancer. Indeed, cancer cells, which are immortal and grow uncontrollably, contain active telomerase. For example, the enzyme is active in ovarian cancer cells but not in normal ovarian tissue. This hypothesis makes telomerase inhibitors an attractive target for antitumor drug development.

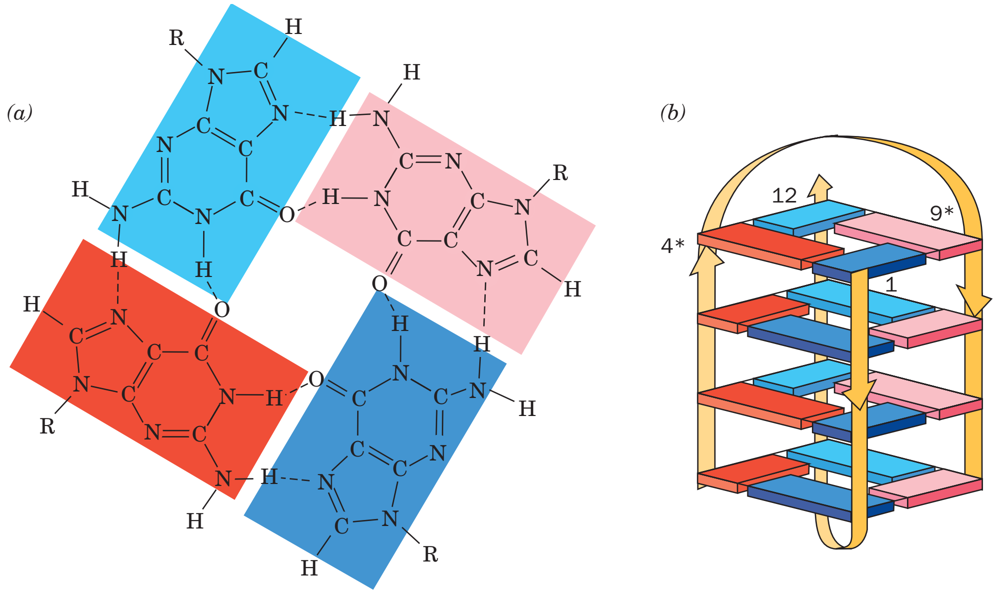

Figure 25-25 | Structure of the telomeric oligonucleotide d(GGGGTTTTGGGG). (*a*) The base-pairing interactions in the G-quartet. (*b*) Schematic diagram of the NMR structure in which the strand directions are indicated by arrows. The nucleotides are numbered 1 to 12 in one strand and 1* to 12* in the symmetry-related strand. Guanine residues G1 to G4 are represented by blue rectangles, G9 to G12 are cyan, G1* to G4* are red, and G9* to G12* are pink. [After Schultze, P., Smith, F.W., and Feigon, J., *Structure* **2,** 227 (1994). PDBid 156D.]

binding sites for capping proteins, which may help regulate telomere length and prevent activation of DNA repair mechanisms that recognize the ends of broken DNA molecules.

CHECK YOUR UNDERSTANDING

Describe how pol α, pol δ, PCNA, RNase H1, FEN1, and DNA ligase participate in eukaryotic DNA synthesis.

What is the function of the pre-replication complex?

Describe the structure, function, and synthesis of telomeres.

4 DNA Damage

LEARNING OBJECTIVES

- Understand that DNA is susceptible to damage from a variety of sources.
- Understand that mutagenicity, which is related to carcinogenicity, can be tested.

The fidelity of DNA replication carried out by DNA polymerases and their attendant proofreading functions is essential for the accurate transmission of genetic information during cell division. Yet errors in polymerization occasionally occur and, if not corrected, may alter the nucleotide sequences of genes. DNA can also be chemically altered by agents that are naturally present in the cell or in the cell's external environment.

In many cases, damaged DNA can be repaired, as discussed in Section 25-5. Severe lesions, however, may be irreversible, leading to the loss of genetic information and, often, cell death. Even when damaged DNA can be mended, the restoration may be imperfect, producing a **mutation,** a heritable alteration of genetic information. In multicellular organisms, genetic changes are usually notable only when they occur in germline cells so that the change is passed on to all the cells of the organism's offspring. Damage to the DNA of a somatic cell, in contrast, rarely has an effect beyond that cell unless the mutation contributes to a malignant transformation (cancer).

A | Environmental and Chemical Agents Generate Mutations

Environmental agents such as ultraviolet light, ionizing radiation, and certain chemical agents can physically damage DNA. For example, UV radiation (200–300 nm) promotes the formation of a cyclobutyl ring between adjacent thymine residues on the same DNA strand to form an intrastrand **thymine dimer** (Fig. 25-26). Similar cytosine and thymine–cytosine dimers also form but less frequently. Such **pyrimidine dimers** locally distort DNA's base-paired structure, interfering with transcription and replication. Ionizing radiation also damages DNA either through its direct action on the DNA molecule or indirectly by inducing the formation of free radicals, particularly the hydroxyl radical (HO·), in the surrounding aqueous medium. This can lead to strand breakage.

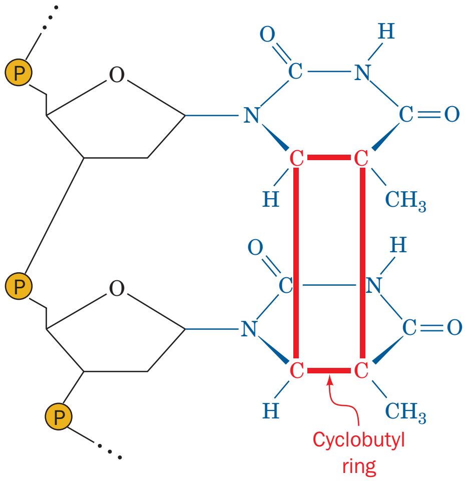

Figure 25-26 | The cyclobutylthymine dimer. The dimer forms on UV irradiation of two adjacent thymine residues on a DNA strand. The ~1.6-Å-long covalent bonds joining the thymine rings (*red*) are much shorter than the normal 3.4-Å spacing between stacked rings in B-DNA, thereby locally distorting the DNA.

The DNA damage produced by **chemical mutagens,** substances that induce mutations, falls into two major classes:

1. **Point mutations,** in which one base pair replaces another. These are subclassified as:
   (a) **Transitions,** in which one purine (or pyrimidine) is replaced by another.
   (b) **Transversions,** in which a purine is replaced by a pyrimidine or vice versa.
2. **Insertion/deletion mutations,** in which one or more nucleotide pairs are inserted in or deleted from DNA.

Point Mutations Result from Altered Bases. One cause of point mutations is treatment of DNA with nitrous acid (HNO_2), which oxidatively deaminates aromatic primary amines. Cytosine is thereby converted to uracil and adenine to the guanine-like hypoxanthine (which forms two of guanine's three hydrogen bonds with cytosine; Fig. 25-27). Hence, treatment of DNA with nitrous acid results in both $A \cdot T \rightarrow G \cdot C$ and $G \cdot C \rightarrow A \cdot T$ transitions. Despite its potential mutagenic activity, nitrite (the conjugate base of nitrous acid) is used as a preservative in prepared meats

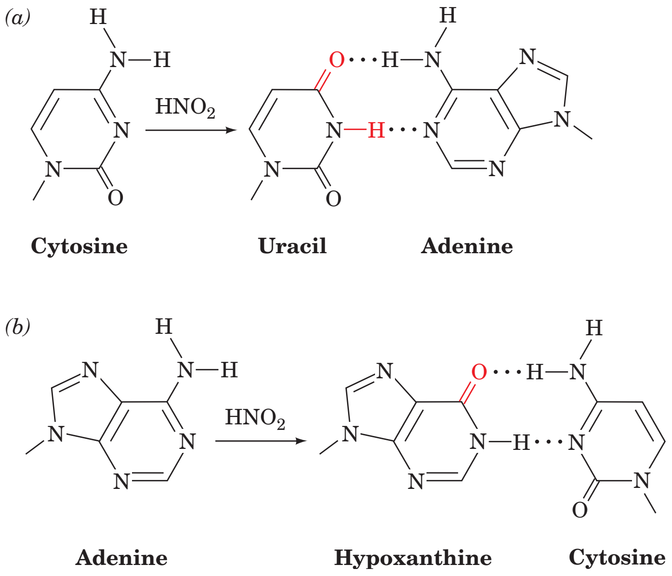

Figure 25-27 | Oxidative deamination by nitrous acid. (*a*) Cytosine is converted to uracil, which base-pairs with adenine. (*b*) Adenine is converted to hypoxanthine, a guanine derivative (it lacks guanine's 2-amino group) that base-pairs with cytosine.

such as frankfurters because it also prevents the growth of *Clostridium botulinum,* the organism that causes botulism. Base deamination reactions also occur spontaneously in the absence of nitrous acid.

Cellular metabolism itself exposes DNA to the damaging effects of reactive oxygen species (e.g., the superoxide ion $O_2^{-}\cdot$, the hydroxyl radical, and H_2O_2) that are normal by-products of oxidative metabolism (Section 18-4B). Over 100 different oxidative modifications to DNA have been catalogued. For example, guanine can be oxidized to **8-oxoguanine (oxoG):**

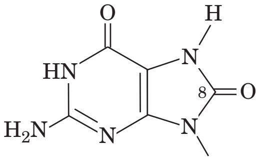

8-Oxoguanine (oxoG)

When the modified DNA strand is replicated, the oxoG can base-pair with either C or A, causing a G · C → T · A transversion.

Alkylating agents such as dimethyl sulfate, **nitrogen mustard, ethylnitrosourea,** and ***N*-methyl-*N′*-nitro-*N*-nitrosoguanidine (MNNG)**

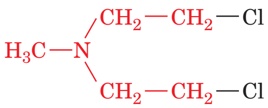

Nitrogen mustard

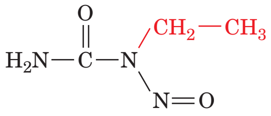

Ethylnitrosourea

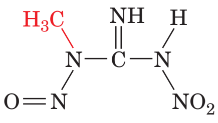

***N*-Methyl-*N′*-nitro-*N*-nitrosoguanidine (MNNG)**

can also generate transversions. For example, the exposure of DNA to MNNG yields, among other products, ***O*^{6}-methylguanine** residues (*at right*), which can base-pair with either C or T. The metabolic methylating agent *S*-adenosylmethionine (Section 21-4D) occasionally nonenzymatically

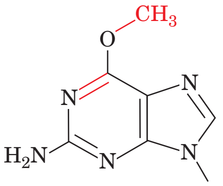

***O*^{6}-Methylguanine residue**

BOX 25-4 PERSPECTIVES IN BIOCHEMISTRY

DNA Methylation

Not all DNA modifications are detrimental. For example, the A and C residues of DNA may be methylated, in a species-specific pattern, to form ***N*^{6}-methyladenine (m^{6}A), *N*^{4}-methylcytosine (m^{4}C),** and **5-methylcytosine (m^{5}C)** residues:

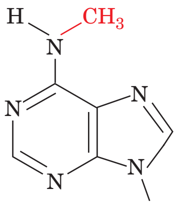

N^6-Methyladenine (m^{6}A) residue

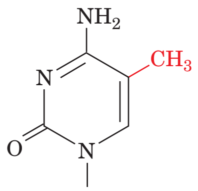

5-Methylcytosine (m^{5}C) residue

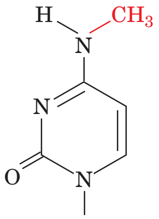

N^4-Methylcytosine (m^{4}C) residue

These methyl groups project into B-DNA's major groove, where they can interact with DNA-binding proteins. In most cells, only a few percent of the susceptible bases are methylated, although this figure rises to >30% of the C residues in some plants.

Bacterial DNAs are methylated at their own particular restriction sites by modification methylases, thereby preventing the corresponding restriction endonuclease from cleaving the DNA (Section 3-4A). Other **methyltransferases** also modify DNA bases in a sequence-specific manner. For example, in *E. coli,* the **Dam methyltransferase** methylates the A residue in all GATC sequences and the **Dcm methyltransferase** methylates both C residues in $\mathrm{CC}^{\mathrm{A}}_{\mathrm{T}}\mathrm{TGG}$ at their C5 positions. Note that both of these sequences are palindromic.

In addition to its role in restriction–modification systems, DNA methylation in prokaryotes functions most conspicuously as a marker of parental DNA in the repair of mismatched base pairs. Any replicational mispairing that has eluded the editing functions of Pol I and Pol III may still be corrected by a process known as mismatch repair (Section 25-5D). However, if this system is to correct errors rather than perpetuate them, it must distinguish the parental DNA, which has the correct base, from the daughter strand, which has the incorrect although normal base. The observation that *E. coli* cells with a deficient Dam methyltransferase have higher mutation rates than wild-type bacteria suggests how this distinction is made. A newly replicated daughter strand is undermethylated compared to the parental strand because DNA methylation lags behind DNA synthesis.

5-Methylcytosine is the only methylated base in most eukaryotic DNAs, including those of vertebrates. This modification occurs largely in the CG dinucleotide of various palindromic sequences. CG is present in the vertebrate genome at only about one-fifth its randomly expected frequency. The upstream regions of many genes, however, have normal CG frequencies and are therefore known as **CpG islands.**

There is clear evidence that *DNA methylation switches off eukaryotic gene expression, particularly when it occurs in the promoter regions upstream of a gene's transcribed sequence* (Section 28-3A). For example, globin genes are less methylated in erythroid cells than they are in nonerythroid cells and, in fact, the specific methylation of the control region in a recombinant globin gene inhibits its transcription. Moreover, the methylation pattern of a parental DNA strand directs the methylation of its daughter strand (a methylated CG sequence directs a methyltransferase to methylate its complementary CG sequence), so that the "inheritance" of a methylation pattern in a cell line permits all the cells to have the same differentiated phenotype. Variations in methylation are responsible for **genomic imprinting** in mammals, the phenomenon in which certain maternal and paternal genes are differentially expressed in the offspring (Section 28-3A).

methylates a base to form derivatives such as 3-methyladenine and 7-methylguanine residues. However, base methylations also have normal physiological functions (Box 25-4).

The alkylation of the N7 position of a purine nucleotide renders its glycosidic bond susceptible to hydrolysis, leading to loss of the base. The resulting gap in the sequence is filled in by an error-prone enzymatic repair system. Transversions arise when the missing purine is replaced by a pyrimidine. Even in the absence of alkylating agents, the glycosidic bonds of an estimated 10,000 of the 3.2 billion purine nucleotides in the human genome spontaneously hydrolyze every day.

Insertion/Deletion Mutations Are Generated by Intercalating Agents. Insertion/deletion mutations may arise from the treatment of DNA with intercalating agents such as acridine orange or proflavin (Section 24-3B). The distance between two consecutive base pairs is roughly doubled by the intercalation of such a molecule between them. The replication of this distorted DNA occasionally results in the insertion or deletion of one or more nucleotides in the newly synthesized polynucleotide. (Insertions and deletions of large segments generally arise from aberrant crossover events; Section 25-6A.)

All Mutations Are Random. The bulk of the scientific data regarding mutagenesis is that mutations, whether the result of polymerase errors, spontaneous modification, or chemical damage to DNA, occur at random. This paradigm was challenged by John Cairns, who demonstrated that bacteria unable to digest lactose preferentially acquired the mutations they needed in order to use lactose when it was the only nutrient available. This observation, which suggests that bacteria can "direct" mutations that benefit them, more likely reflects a nonspecific adaptive response in which the overall rate of mutation—useful as well as nonuseful—increases when the cells are under metabolic stress. *The hypermutable state appears to reflect the activation of error-prone DNA repair and recombination systems that are relatively inactive in normally growing cells.*

B | Many Mutagens Are Carcinogens

Not all alterations to DNA have phenotypic consequences. For example, mutations in noncoding segments of DNA are often invisible. Similarly, the redundancy of the genetic code (more than one trinucleotide may specify a particular amino acid; Section 27-1C) can mask point mutations. Even when a protein's amino acid sequence is altered, its function may be preserved if the substitution is conservative (Section 5-4A) or occurs on a surface loop. Nevertheless, even a single point mutation, if appropriately located, can irreversibly alter cellular metabolism, for example, by causing cancer. As many as 80% of human cancers may be caused by **carcinogens** that damage DNA or interfere with its replication or repair. Consequently, many mutagens are also carcinogens.

There are presently over 60,000 man-made chemicals of commercial importance, and ~1000 new ones are introduced every year. The standard animal tests for carcinogenesis, exposing rats or mice to high levels of the suspected carcinogen and checking for cancer, are expensive and require ~3 years to complete. Thus, relatively few substances have been tested in that manner. Likewise, epidemiological studies in humans are costly, time-consuming, and often inconclusive.

Bruce Ames devised a rapid and effective bacterial assay for carcinogenicity that is based on the high correlation between carcinogenesis and mutagenesis. He constructed special strains of the bacterium *Salmonella typhimurium* that are *his*$^-$ (cannot synthesize histidine and therefore cannot grow in its absence). Mutagenesis in these strains is indicated by their reversion to the *his*$^+$ phenotype. In the **Ames test,** $\sim 10^9$ test bacteria are spread on a culture plate that lacks histidine. A mutagen placed in the culture medium causes some of the *his*$^-$ bacteria to become *his*$^+$ so that they grow into visible colonies after 2 days at 37°C (Fig. 25-28). The mutagenicity of a substance is scored as the number of such colonies minus the few spontaneously revertant colonies that occur in the absence of the mutagen. Dose–response curves, which are generated by testing a given compound

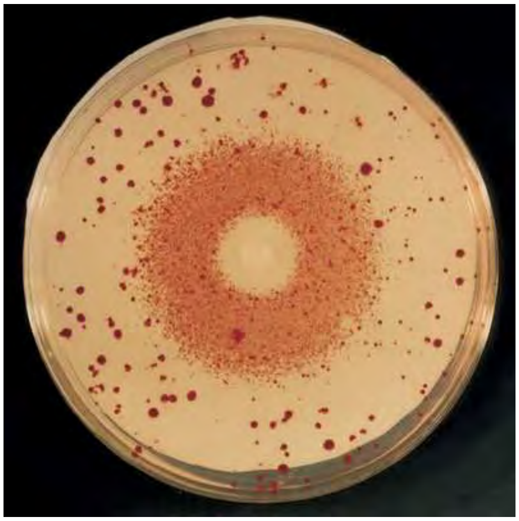

Figure 25-28 | The Ames test for mutagenesis. A filter paper disk containing a mutagen, in this case the alkylating agent ethyl methanesulfonate, is centered on a culture plate containing *his*$^-$ strains of *Salmonella typhimurium* in a medium that lacks histidine. A dense halo of revertant bacterial colonies appears around the disk from which the mutagen diffused. The larger colonies distributed around the culture plate are spontaneous revertants. The bacteria near the disk have been killed by the toxic mutagen's high concentration. [Courtesy of Raymond Devoret, Institut Curie, Orsay, France.]

at a number of concentrations, are almost always linear, indicating that *there is no threshold concentration for mutagenesis.*

About 80% of the compounds determined to be carcinogens in whole-animal experiments are also mutagenic by the Ames test. Because many noncarcinogens are converted to carcinogens in the liver or in other tissues via a variety of detoxification reactions (e.g., those catalyzed by the cytochromes P450; Section 12-4D), a small amount of rat liver homogenate is therefore included in the Ames test medium in order to approximate the effects of mammalian metabolism. Alternatively, carcinogenicity testing may be carried out using mammalian cell cultures rather than bacteria.

Several compounds to which humans had been extensively exposed that were found to be mutagenic by the Ames test were later found to be carcinogenic in animal tests. These include **tris(2,3-dibromopropyl)phosphate,** which was used as a flame retardant in children's sleepwear in the mid-1970s and can be absorbed through the skin; and **furylfuramide,** which was used in Japan in the 1960s and 1970s as an antibacterial additive in many prepared foods (and which had passed two animal tests before it was found to be mutagenic).

CHECK YOUR UNDERSTANDING

List some ways that mutations can occur.
Why is it practical to test carcinogens by a mutagenesis assay?

5 DNA Repair

LEARNING OBJECTIVES

- Understand that some DNA damage can be repaired by the action of a single enzyme.
- Understand that damaged bases can be removed and replaced by base excision repair or nucleotide excision repair.
- Understand that replication errors can be corrected by mismatch repair.
- Understand that some repair mechanisms are error-prone.

DNA damage must be repaired to maintain the integrity of genetic information. The biological importance of DNA repair is indicated by the great variety of repair mechanisms in even simple organisms such as *E. coli.* These systems include enzymes that simply reverse the chemical modification of nucleotide bases as well as more complicated multienzyme systems that depend on the inherent redundancy of the information in duplex DNA to restore the damaged molecule.

A | Some Damage Can Be Directly Reversed

Several enzymes recognize and reverse certain types of DNA damage. For example, pyrimidine dimers (Fig. 25-26) may be restored to their monomeric forms by **photoreactivation** catalyzed by light-absorbing enzymes known as **DNA photolyases.** These 55- to 65-kD monomeric enzymes are found in many prokaryotes and eukaryotes but not in humans. Photolyases contain two prosthetic groups: a light-absorbing cofactor and $FADH^-$. In the *E. coli* enzyme, the cofactor N^5,N^{10}-methenyltetrahydrofolate (Section 21-4D) absorbs UV–visible light (300–500 nm) and transfers the excitation energy to the $FADH^-$, which then transfers an electron to the pyrimidine dimer, thereby splitting it. The resulting pyrimidine anion reduces the $FADH\cdot$ to regenerate the enzyme.

E. coli DNA photolyase binds ssDNA or dsDNA without regard to base sequence. Its X-ray structure reveals its DNA-binding site to be a positively charged flat surface with a hole that has a size and polarity complementary to that of a pyrimidine dimer (Fig. 25-29). In order to bind in this

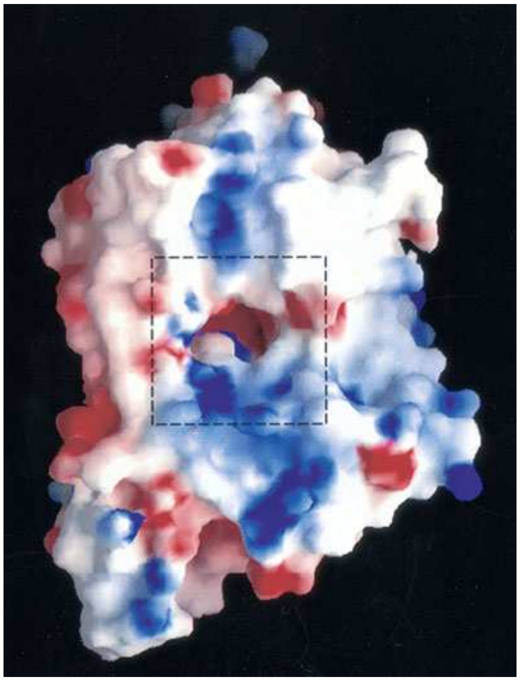

Figure 25-29 | X-Ray structure of *E. coli* DNA photolyase. The solvent-accessible surface of the enzyme is shaded according to its electrostatic potential (*blue,* most positive; *red,* most negative; and *white,* neutral). The dashed lines surround the hole in the protein surface where the pyrimidine dimer is thought to bind. [Courtesy of Johann Deisenhofer, University of Texas Southwestern Medical Center, Dallas, Texas. PDBid 1DNP.]

site and contact the isoalloxazine ring of the $FADH^-$ for electron transfer, the pyrimidine dimer must flip out of the double helix. This conformational change is probably facilitated by the relatively weak base pairing of the pyrimidine dimer and the distortion it imposes on the double helix. **Base-flipping** is a common feature of enzymes that chemically alter DNA bases as part of repair pathways or normal metabolism (e.g., cytosine methylation; Section 28-3A).

Another type of direct DNA repair is the reversal of base methylation by **alkyltransferases.** For example, O^6-methylguanine and O^6-ethylguanine lesions of DNA are repaired by **O^6-alkylguanine–DNA alkyltransferase,** which directly transfers the offending methyl or ethyl group to one of its own Cys residues. This reaction inactivates the protein, which therefore cannot be strictly classified as an enzyme. Apparently, the cost of sacrificing the alkyltransferase is justified by the highly mutagenic nature of the modified guanine residue.

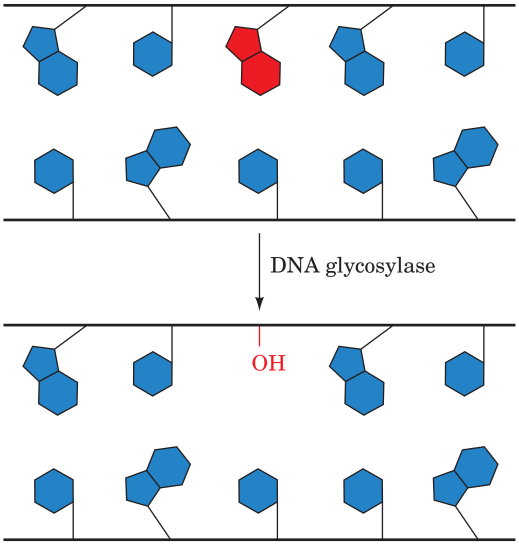

Figure 25-30 | Action of DNA glycosylases. These enzymes hydrolyze the glycosidic bond of their corresponding altered base (*red*) to yield an AP site.

B | Base Excision Repair Requires a Glycosylase

Damaged bases that cannot be directly repaired may be removed and replaced in a process known as **base excision repair (BER).** This pathway, as its name implies, begins with removal of the damaged base. Cells contain a variety of **DNA glycosylases** that each cleave the glycosidic bond of a corresponding type of altered nucleotide, leaving a deoxyribose residue with no attached base (Fig. 25-30). Such **apurinic** or **apyrimidinic sites (AP** or **abasic sites)** also result from the occasional spontaneous hydrolysis of glycosidic bonds. The deoxyribose residue is then cleaved on one side by an **AP endonuclease,** the deoxyribose and several adjacent residues are removed by the action of a cellular exonuclease (possibly associated with a DNA polymerase), and the gap is filled in and sealed by a DNA polymerase and DNA ligase.

The enzymes of BER, which correct the most frequent type of DNA damage, include a glycosylase that recognizes 8-oxoguanine and the enzyme **uracil–DNA glycosylase (UDG),** which excises uracil residues. The latter arise from cytosine deamination as well as the occasional misincorporation of uracil instead of thymine into DNA (Box 25-5).

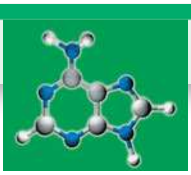

BOX 25-5 PERSPECTIVES IN BIOCHEMISTRY

Why Doesn't DNA Contain Uracil?

Three of the deoxynucleotide bases in DNA (adenine, guanine, and cytosine) also occur as ribonucleotide bases in RNA. The fourth deoxynucleotide base, thymine, is synthesized—at considerable metabolic effort (Section 23-3B)—from uracil, which occurs in RNA. Since uracil and thymine have identical base-pairing properties, why do cells bother to synthesize thymine at all?

This enigma was solved by the discovery of cytosine's penchant for conversion to uracil by deamination, either spontaneously or by reaction with nitrites (Section 25-4A). If U were a normal DNA base, the deamination of C would be highly mutagenic because there would be no indication of whether the resulting mismatched G · U base pair had initially been G · C or A · U. Since T is DNA's normal base, however, any U in DNA is almost certainly a deaminated C and can be removed by uracil–DNA glycosylase.

Uracil–DNA glycosylase also has an important function in DNA replication. dUTP, an intermediate in dTTP synthesis, is present in all cells in small amounts. DNA polymerases do not discriminate well between dUTP and dTTP, both of which can base-pair with template A's. Consequently, newly synthesized DNA contains an occasional U. These U's are rapidly replaced by T through base excision repair.

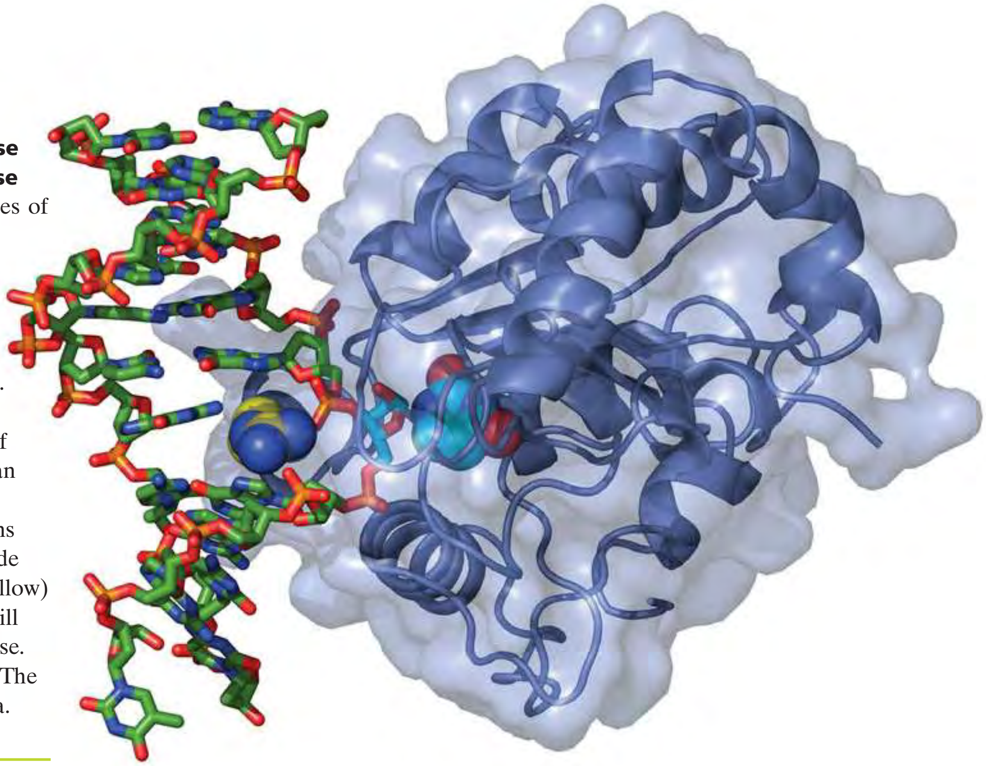

Figure 25-31 | X-Ray structure of a complex of human uracil–DNA glycosylase with a 10-bp DNA containing a U · G base pair. The protein (the C-terminal 223 residues of the 304-residue monomer) is represented by its ribbon diagram embedded in its transparent molecular surface. The DNA, viewed looking into its major groove, is drawn in stick form colored according to atom type (C green, N blue, O red, P orange). The U · G base pair's uridine nucleotide has flipped out of the double helix (to the right of the DNA) and has been hydrolyzed to yield an AP site (stick form with C cyan) and uracil (space-filling form with C cyan), which remains bound in the enzyme's binding pocket. The side chain of Arg 272 (space-filling form with C yellow) has intercalated into the DNA base stack to fill the space vacated by the flipped-out uracil base. [Based on an X-ray structure by John Tainer, The Scripps Research Institute, La Jolla, California. PDBid 4SKN.]

The X-ray structure of human UDG in complex with a 10-bp DNA containing a U · G mismatch (which forms a doubly hydrogen-bonded base pair whose shape differs from that of Watson–Crick base pairs; Section 24-1A), determined by John Tainer, reveals that the enzyme has bound the DNA with the U · G base pair's uridine nucleotide flipped out of the double helix (Fig. 25-31). Moreover, the enzyme has hydrolyzed the uridine's glycosidic bond, yielding the free uracil base and an AP site on the DNA, although both products remain bound to the enzyme. The cavity in the DNA's base stack that would otherwise be occupied by the flipped-out uracil is filled by the side chain of Arg 272, which intercalates into the DNA from its minor groove side.

How does UDG detect a base-paired uracil in the center of DNA and how does it discriminate so acutely between uracil and other bases, particularly the closely similar thymine? The X-ray structures indicate that the phosphate groups flanking the flipped-out base are 4 Å closer together than they are in B-DNA (8 Å versus 12 Å), which causes the DNA to kink by ~45° in the direction parallel to the view in Fig. 25-31. Tainer has postulated that UDG rapidly scans a DNA molecule for uracil by periodically binding to it so as to compress and thereby slightly bend the DNA backbone. The DNA bends more readily at a uracil-containing site (a U · G base pair is smaller than C · G and hence leaves a space in the base stack, whereas a U · A base pair is even weaker than T · A), permitting the enzyme to flip out the uracil by inserting Arg 272 into the minor groove. The exquisite specificity of the UDG's binding pocket for uracil prevents the binding and hydrolysis of any other base that the enzyme might have induced to flip. Thus the overall shapes of adenine and guanine exclude them from this pocket, whereas thymine's 5-methyl group is sterically blocked by the rigidly held side chain of Tyr 147. Cytosine, which has approximately the same shape as uracil, is excluded through a set of hydrogen bonds emanating from the protein that mimic those made by adenine in a Watson–Crick A · U base pair (dUTPase discriminates similarly between uracil and other bases; Fig. 23-14).

AP sites in mammalian DNA are highly cytotoxic because they irreversibly trap mammalian topoisomerase I in its covalent complex with DNA (Section 24-1D). Moreover, since the ribose at the AP site lacks a glycosidic bond, it can readily convert to its linear form (Section 8-1B), whose reactive aldehyde group can cross-link to other cell components. This rationalizes why AP sites remain tightly bound to UDG in solution. UDG activity is enhanced by AP endonuclease, the next enzyme in the base excision repair pathway, but the two enzymes do not interact in the absence of DNA. This suggests that UDG remains bound to an AP site it generated until it is displaced by the more tightly binding AP endonuclease, thereby protecting the cell from the AP site's cytotoxic effects. Its seems likely that other damage-specific DNA glycosylases function similarly.

C | Nucleotide Excision Repair Removes a Segment of a DNA Strand

All cells have a more elaborate pathway, **nucleotide excision repair (NER),** to correct pyrimidine dimers and other DNA lesions in which the bases are displaced from their normal position or have bulky substituents. The NER system appears to respond to helix distortions rather than by the recognition of any particular group. In humans, NER is the major defense against two important carcinogens, sunlight and tobacco smoke.

In *E. coli,* NER is carried out in an ATP-dependent process through the actions of the **UvrA, UvrB,** and **UvrC** proteins (the products of the *uvrA, uvrB,* and *uvrC* genes). This system, which is often referred to as the **UvrABC endonuclease** (although there is no complex that contains all three subunits), cleaves the damaged DNA strand at the seventh and at the third or fourth phosphodiester bonds from the lesion's 5′ and 3′ sides, respectively (Fig. 25-32). The excised 11- or 12-nt oligonucleotide is then

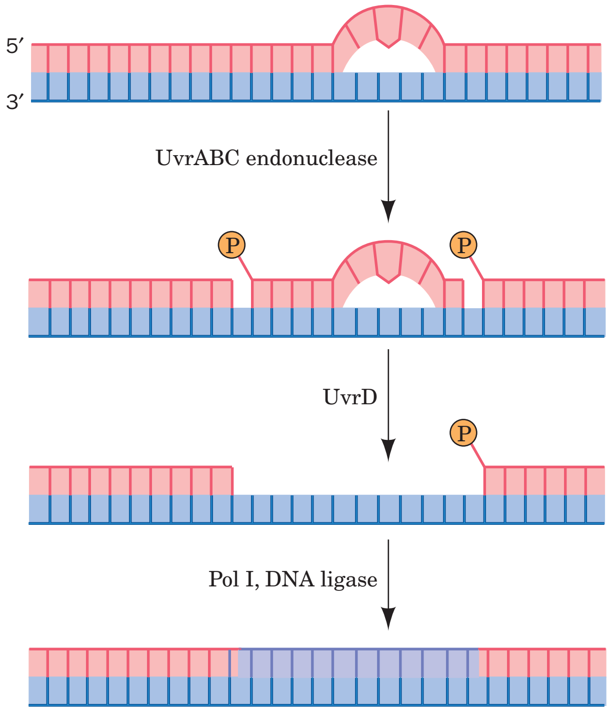

Figure 25-32 | The mechanism of nucleotide excision repair (NER) of pyrimidine dimers.

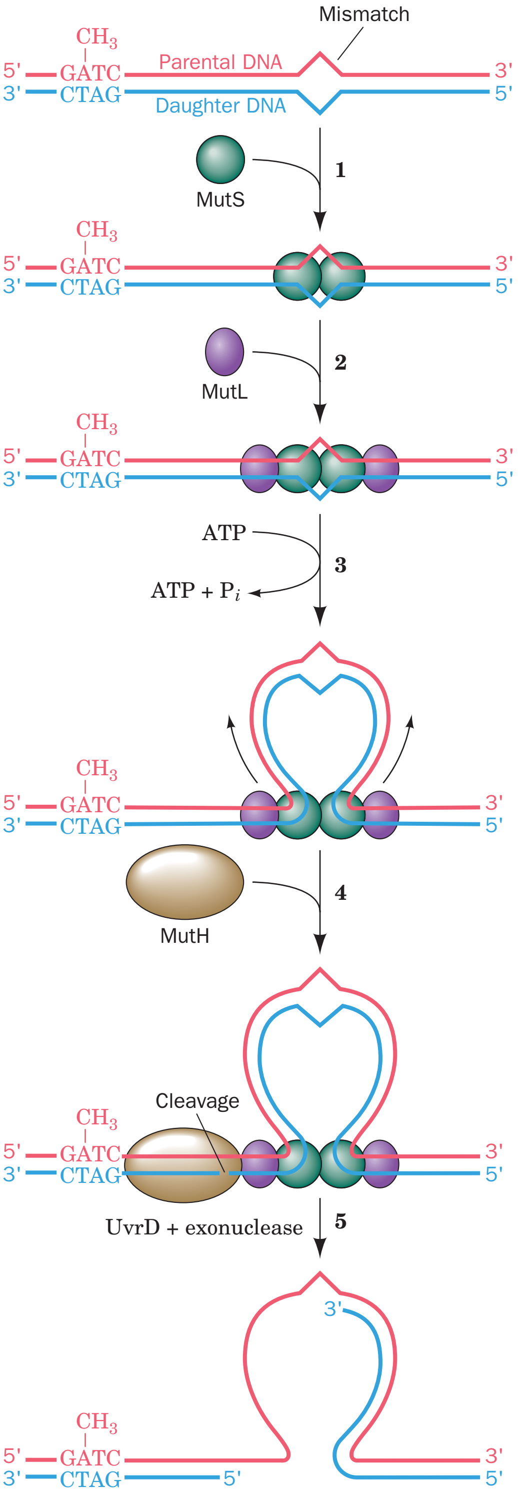

Figure 25-33 | The mechanism of mismatch repair in *E. coli*. **(1)** MutS binds. **(2)** MutL binds. **(3)** The mismatch-containing DNA loops out. **(4)** MutH endonuclease binds. **(5)** The unmethylated DNA strand containing the mismatched base is excised.

displaced by the binding of **UvrD** (also called **helicase II**) and is replaced through the actions of Pol I and DNA ligase.

Xeroderma Pigmentosum and Cockayne Syndrome Are Caused by Genetically Defective NER. In humans, NER requires at least 16 proteins and removes oligonucleotides of ~30 residues. Many of the enzymes involved in the pathway have been identified through mutations that are manifested as two genetic diseases. The inherited disease **xeroderma pigmentosum** (**XP;** Greek: *xeros,* dry + *derma,* skin) is mainly characterized by the inability of skin cells to repair UV-induced DNA lesions. Individuals suffering from this autosomal recessive condition are extremely sensitive to sunlight. During infancy they develop marked skin changes such as dryness, excessive freckling, and keratoses (a type of skin tumor; the skin of these children is described as resembling that of farmers with many years of sun exposure), together with eye damage, such as opacification and ulceration of the cornea. Moreover, they develop often fatal skin cancers at an ~2000-fold greater rate than normal and internal cancers at a 10- to 20-fold increased rate. Curiously, many individuals with XP also have a bewildering variety of seemingly unrelated symptoms including progressive neurological degeneration and developmental deficits.

Cockayne syndrome (CS), a rare inherited disease that is also associated with defective NER, arises from defects in three of the same genes that are defective in XP as well as in two additional genes. Individuals with CS are hypersensitive to UV radiation and exhibit stunted growth, neurological dysfunction due to neuron demyelination, and the appearance of premature aging but, intriguingly, have a normal incidence of skin cancer. The proteins that are defective in CS normally recognize an RNA polymerase whose progress has been halted by a damaged or distorted DNA template. In order for transcription to resume, the stalled RNA polymerase must be removed so that the DNA damage can be repaired by the NER system. In CS, the DNA cannot be repaired, which causes the cell to undergo **apoptosis** (programmed cell death; Section 28-3D). The death of transcriptionally active cells may account for the developmental symptoms of Cockayne syndrome.

D | Mismatch Repair Corrects Replication Errors

Any replicational mispairing that has eluded the editing functions of the DNA polymerases may still be corrected by a process known as **mismatch repair (MMR).** The MMR system can also correct insertions or deletions of up to four nucleotides (which arise from the slippage of one strand relative to the other in the active site of DNA polymerase). The importance of mismatch repair is indicated by the fact that defects in the human mismatch repair system result in a high incidence of cancer, most notably **hereditary nonpolyposis colorectal cancer syndrome,** which affects several organs and may be the most common inherited predisposition to cancer.

Mismatch repair in *E. coli* is carried out by three proteins (Fig. 25-33). A homodimer of **MutS** binds to a mismatched base pair, or to unpaired bases, and then binds a homodimer of **MutL.** Then, in an ATP-dependent process, the resulting MutS$_2$MutL$_2$ complex translocates along the DNA in both directions, thereby causing the duplex DNA to form a mismatch-containing loop that is closed by the MutS$_2$MutL$_2$ complex. The mismatch repair system can distinguish the two DNA strands because newly replicated DNA remains hemimethylated until methyltransferases have had sufficient time to methylate the daughter strand (Box 25-4). On encountering a hemimethylated GATC palindrome, the $MutS_2MutL_2$ complex recruits **MutH** and activates this endonuclease to make a nick on the 5′ side of the unmethylated GATC sequence. This site may be located on either side of the mismatch and over 1000 bp distant from it. The UvrD helicase, which also participates in NER, separates the parental and daughter strands. An exonuclease completely removes the defective daughter segment, which is then replaced by the action of DNA polymerase III.

Eukaryotic cells contain several homologs of MutS and MutL but not of MutH and must therefore use some other cue than methylation status to differentiate the daughter and parental strands. One possibility is that a newly synthesized daughter strand is identified by its as yet unsealed nicks.

E | Some DNA Repair Mechanisms Introduce Errors

Individuals with a variant form of XP exhibit increased rates of skin cancer even though their NER proteins are normal. The defect in this disorder has been pinpointed to an enzyme known as **DNA polymerase η (pol η)** When functioning normally, pol η can bypass DNA lesions such as UV-induced thymine dimers, incorporating two adenine bases in the new strand. Although it is useful as a translesion polymerase, pol η is relatively inaccurate and has no proofreading exonuclease activity: It inserts an incorrect base on average every 30 nucleotides.

The existence of error-prone polymerases provides a fail-safe mechanism for replicating stretches of DNA that cannot be navigated by the standard replication machinery. In fact, such alternative DNA polymerases typically outnumber the polymerases devoted to normal replication. For example, eukaryotes contain at least five such "bypass" polymerases that act with different degrees of accuracy. However, the errors generated by bypass polymerases may still be corrected by the mismatch repair system.

End-Joining Repairs Double-Strand Breaks. Both the base excision repair and nucleotide excision repair pathways act when the lesion affects only one strand of DNA. However, DNA is susceptible to double-strand breaks **(DSBs),** often caused by ionizing radiation or the free radical by-products of oxidative metabolism. Unrepaired DSBs can be lethal to cells or cause chromosomal aberrations that may lead to cancer. Hence the efficient repair of DSBs is essential for cell viability and genomic integrity.

Cells have two general mechanisms to repair DSBs: **recombination repair** and **nonhomologous end-joining (NHEJ).** Here we discuss NHEJ, a process which, as its name implies, directly rejoins DSBs. The recombination repair of DSBs is discussed in Section 25-6B.

In NHEJ, the ends of the broken DNA must be aligned, frayed ends trimmed off or filled in, and the strands ligated. The core of the end-joining machinery in eukaryotes includes the protein **Ku** (a heterodimer of homologous 70- and 83-kD subunits, **Ku70** and **Ku80**), which appears to be the cell's broken-DNA sensor. The X-ray structure of Ku in complex with a 14-bp DNA, determined by Jonathan Goldberg, reveals that the protein cradles the dsDNA segment along its entire length and encircles its central ~3 bp segment (Fig. 25-34). Ku makes no specific contacts with the DNA's bases and few with its backbone but instead fits snugly into the major and minor grooves. Ku–DNA complexes dimerize so as to align both halves of a double-strand break while leaving the strand ends accessible to nucleases, polymerases, and ligases. Nucleotide

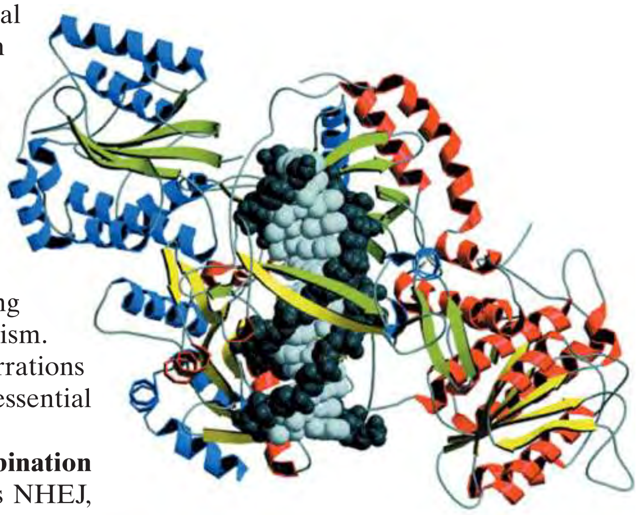

Figure 25-34 | X-Ray structure of human Ku protein in complex with a 14-bp DNA. The subunits of Ku70 (*red helices and yellow β strands*) and Ku80 (*blue helices and green β strands*) are viewed along the pseudo-twofold axis relating them. The DNA is drawn in space-filling form with its sugar–phosphate backbone dark gray and its base pairs light gray. Note that the DNA is surrounded by a ring of protein. [Courtesy of John Tainer, The Scripps Research Institute, La Jolla, California. Based on an X-ray structure by Jonathan Goldberg, Memorial Sloan-Kettering Cancer Center, New York, New York. PDBid 1JEY.]

trimming, of course, generates mutations, but an unrepaired double-strand break would be even more detrimental to the cell.

The *E. coli* SOS Response Is Mutagenic. In *E. coli,* agents that damage DNA induce a complex system of cellular changes known as the **SOS response.** Cells undergoing the SOS response cease dividing and increase their capacity to repair damaged DNA. **LexA,** a repressor, and **RecA,** a DNA-binding protein, regulate the activity of this system. (RecA is also a key player in homologous recombination, discussed in the following section, which offers a means for repairing damaged DNA after it has been replicated.) During normal growth, LexA represses SOS gene expression. However, when DNA is damaged (and cannot fully replicate), the resulting single strands bind to RecA to form a complex that activates LexA to cleave and thereby inactivate itself. The SOS genes, which include *recA* and *lexA* as well as the NER genes *uvrA* and *uvrB* (Section 25-5C), are thereby expressed. On the repair of the DNA, the DNA · RecA complex is no longer present, so the newly synthesized LexA again represses the expression of the SOS genes.

Among the 43 genes controlled by the SOS system are **DNA polymerases IV** and **V,** both of which replicate DNA with low fidelity and lack proofreading exonuclease activity. Because these translesion polymerases can synthesize DNA even when there is no information as to which bases were originally present, *the SOS repair system is error-prone and consequently mutagenic.* It is therefore a process of last resort that is initiated only ~50 min after SOS induction if the DNA has not already been repaired by other means. Hence, the SOS repair system is a testimonial to the proposition that survival with a chance of loss of function (and the possible gain of a new one) is advantageous, in the Darwinian sense, over death—although only a small fraction of cells survive this process.

■ CHECK YOUR UNDERSTANDING

What are the functions of DNA photolyases and alkyltransferases?

Describe the enzymatic activities required for base excision repair, nucleotide excision repair, and mismatch repair.

Describe why cells require error-prone repair systems such as pol η, nonhomologous end-joining, and the SOS response.

6 Recombination

LEARNING OBJECTIVES

- Understand that in homologous recombination, DNA strands cross over to exchange places.
- Understand that recombination can repair damaged replication forks and double-strand breaks.
- Understand that transposons move themselves and sometimes additional genes to new chromosomal locations.

Over the years, genetic studies have shown that genes are not immutable. In higher organisms, pairs of genes may exchange by crossing-over when homologous chromosomes are aligned (Fig. 25-35). Bacteria, which do not contain duplicate chromosomes, also have an elaborate mechanism for recombining genetic information. In addition, foreign DNA can be installed in a host's chromosome through recombination. In this section, we examine the molecular events of recombination and discuss the biochemistry of **transposons,** which are mobile genetic elements.

A | Homologous Recombination Involves Several Protein Complexes

Homologous recombination (also called **general recombination**) occurs between DNA segments with extensive homology; **site-specific recombination** occurs between two short, specific DNA sequences. The prototypical model for homologous recombination (Fig. 25-36) was proposed by Robin Holliday in 1964. The corresponding strands of two aligned homologous DNA duplexes are nicked, and the nicked strands cross over to pair with the nearly complementary strands on the homologous duplex, thereby forming a segment of **heterologous DNA,** after which the nicks are sealed (Fig. 25-36*a–e*). The crossover point is a four-stranded structure known as a **Holliday junction.** A Holliday junction has, in fact, been observed

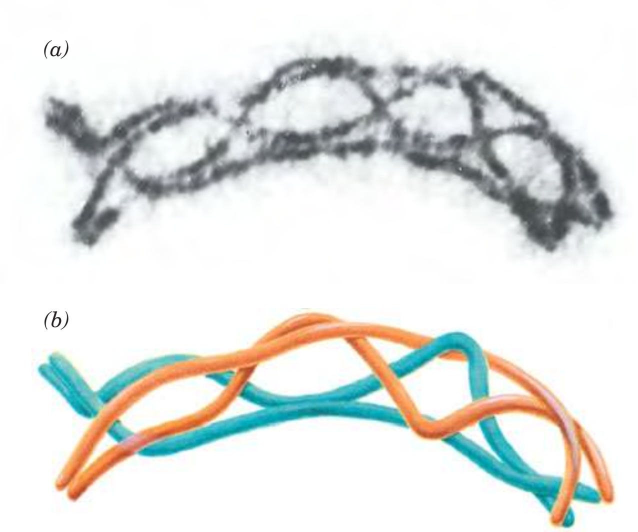

■ **Figure 25-35 | Crossing-over.** (*a*) An electron micrograph and (*b*) its interpretive drawing of two homologous pairs of chromatids during meiosis in the grasshopper *Chorthippus parallelus.* Nonsister chromatids (*different colors*) may recombine at any of the points where they cross over. [Courtesy of Bernard John, The Australian National University, Canberra, Australia.]

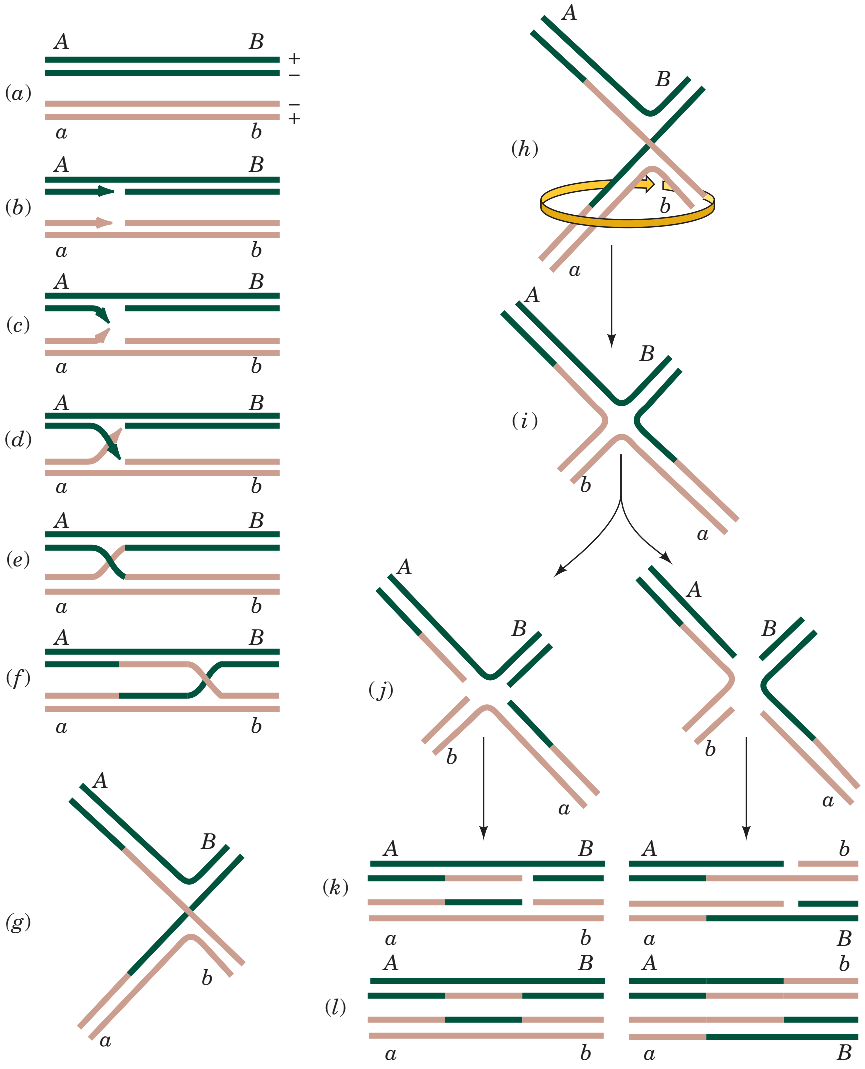

■ **Figure 25-36 | The Holliday model of general recombination between homologous DNA duplexes.** **See the Animated Figures.**

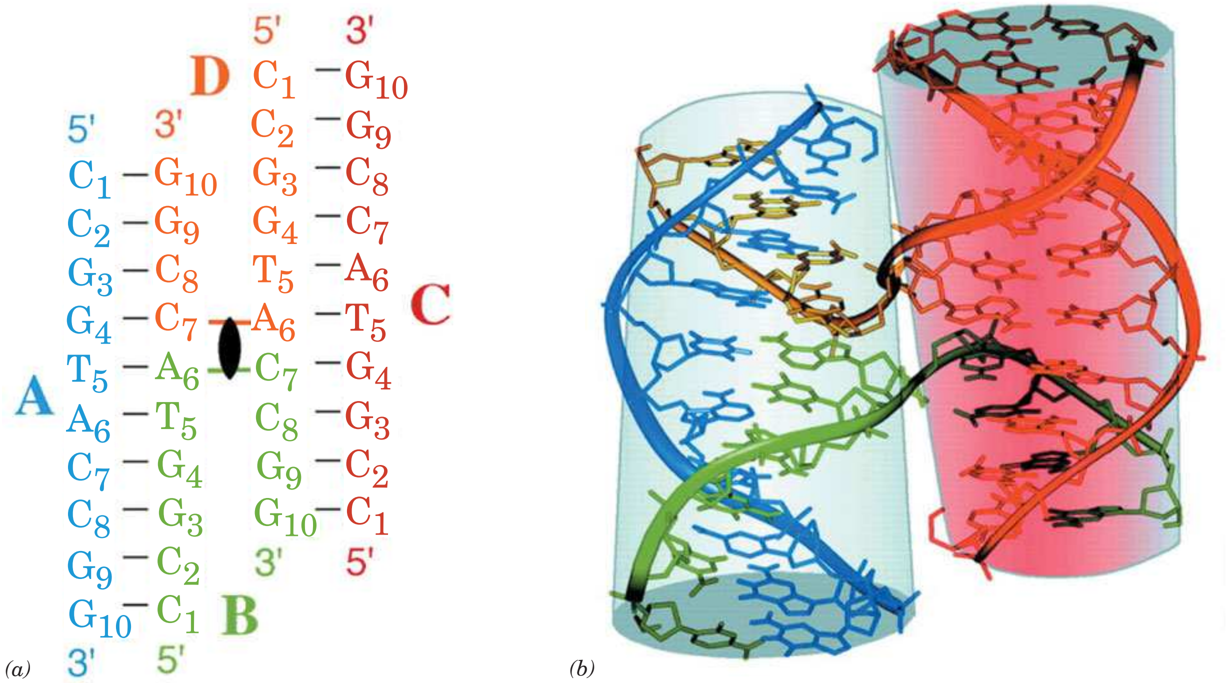

Figure 25-37 | X-Ray structure of a Holliday junction. (*a*) The secondary structure of the four-stranded Holliday junction formed by the palindromic sequence d(CCGGTACCGG) in which the four strands, A, B, C, and D, are individually colored, their nucleotides are numbered 1 to 10 from their 5′ to 3′ termini, and Watson–Crick base-pairing interactions are represented by black dashes. The twofold axis relating the two helices is represented by the black lenticular symbol. (*b*) The three-dimensional structure of the Holliday junction, as viewed along its twofold axis, in which the oligonucleotides are represented in stick form with their backbones traced by ribbons, all colored as in Part *a*. With the exception of the backbones of strands B and D at the crossovers, the two arms of this structure each form an undistorted B-DNA helix, including the stacking of the base pairs flanking the crossovers. Note that Fig. 25-36*g* is a schematic representation of this structure as viewed from the side in this drawing. [Courtesy of Shing Ho, Oregon State University. PDBid 1DCW.]

in the X-ray structure of the self-complementary d(CCGGTACCGG), determined by Shing Ho (Fig. 25-37). The crossover point can move in either direction, often thousands of nucleotides, in a process known as **branch migration** (Fig. 25-36*e* and *f*).

The Holliday junction can be "resolved" into two duplex DNAs in two equally probable ways (Fig. 25-36*g*–*l*):

1. Cleavage of the strands that did not cross over exchanges the ends of the original duplexes to form, after nick sealing, the traditional recombinant DNA molecule (right branch of Fig. 25-36*j*–*l*).
2. Cleavage of the strands that crossed over exchanges a pair of homologous single-stranded segments (left branch of Fig. 25-36*j*–*l*).

RecA Promotes Recombination in *E. coli*. The 352-residue RecA protein polymerizes on ssDNA or dsDNA that contains a single-strand gap. Electron microscopy reveals that RecA filaments bound to DNA form a right-handed helix with ~6.2 RecA monomers per turn (Fig. 25-38). Three nucleotides (or base pairs) bind to each RecA monomer so that the DNA assumes an extended conformation with ~18.6 nt (or bp) per turn (B-DNA has 10.4 bp per turn). The X-ray structure of RecA confirms that the central cavity of the RecA filament has a diameter of 25 Å, large enough to accommodate DNA.

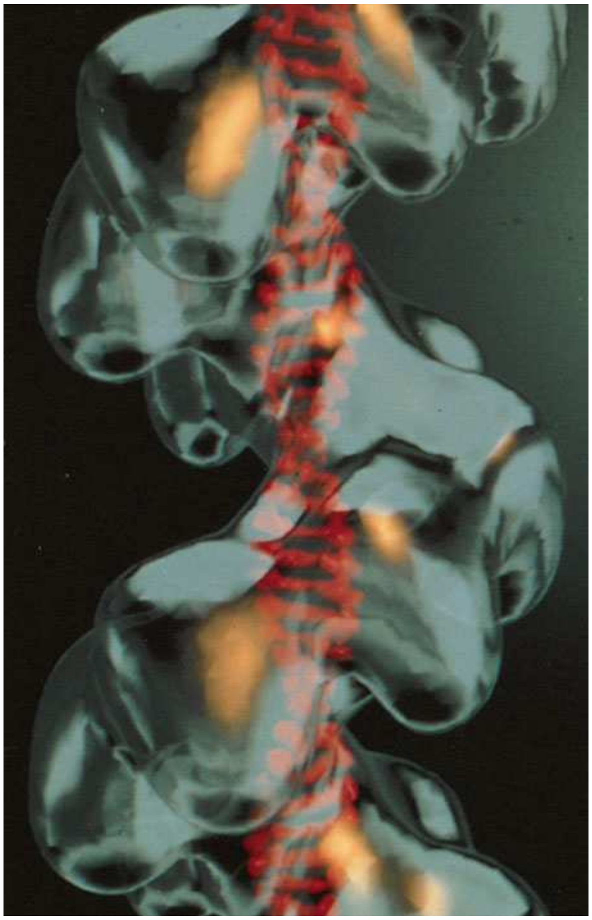

■ **Figure 25-38 | Model of a RecA–DNA complex.** In this electron microscopy–based image, the transparent surface represents an *E. coli* RecA filament. The extended and untwisted duplex DNA (*red*) has been modeled into the image. [Courtesy of Edward Egelman, University of Minnesota Medical School.]

How does RecA mediate DNA strand exchange between ssDNA and dsDNA? On encountering a duplex DNA with a strand that is complementary to its bound ssDNA, RecA partially unwinds the duplex and, in an ATP-driven reaction, exchanges the ssDNA with the corresponding strand on the dsDNA. ATP hydrolysis is thought to drive the rearrangement of a three-stranded DNA intermediate bound to the protein (Fig. 25-39) in a process that tolerates only a limited degree of mispairing. As the RecA filament rotates about its axis, the duplex DNA is spooled

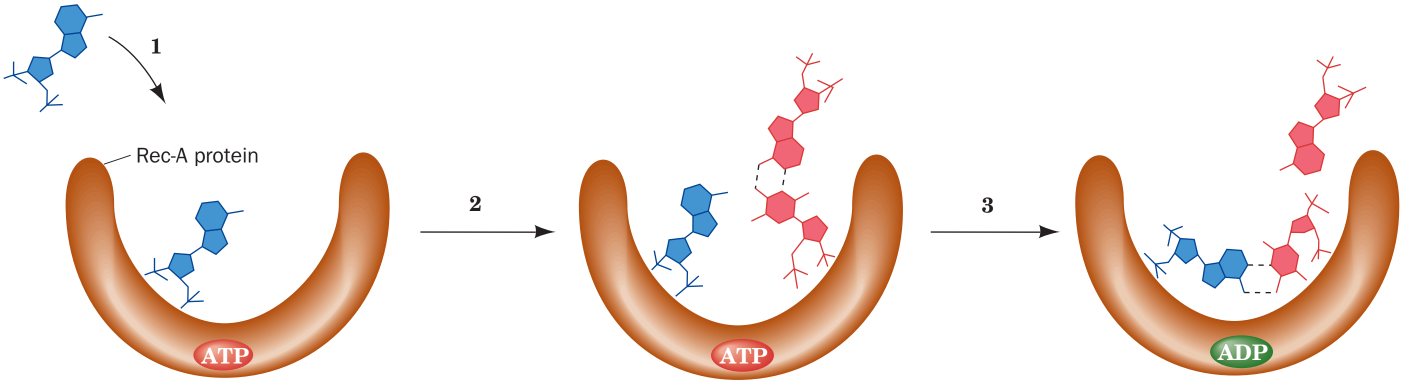

■ **Figure 25-39 | A model for RecA-mediated pairing.** **(1)** A ssDNA binds to RecA to form an initiation complex. **(2)** dsDNA binds to the initiation complex so as to transiently form a three-stranded helix. **(3)** RecA rotates the bases of the aligned homologous strands to effect strand exchange in an ATP-driven process. [After West, S.C., *Annu. Rev. Biochem.* **61,** 618 (1992).]

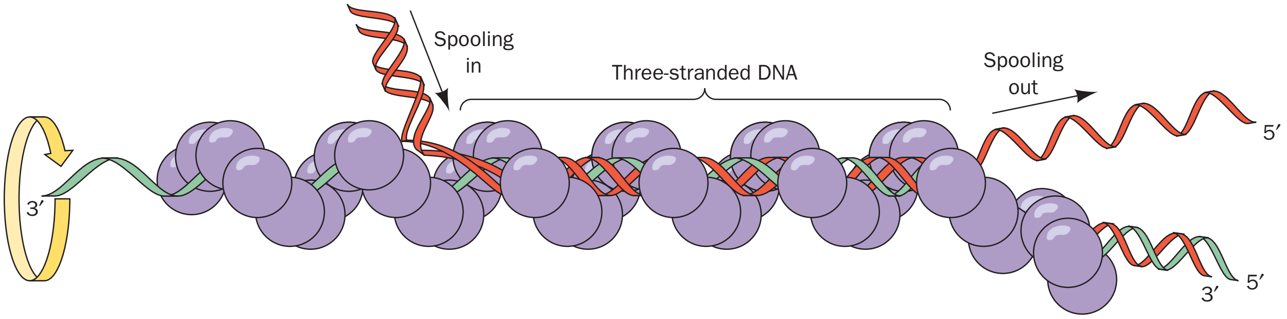

Figure 25-40 | Model for RecA-mediated strand exchange. Homologous DNA molecules are paired in advance of strand exchange in a three-stranded helix. The ATP-driven rotation of the RecA filament (*purple*) around its helix axis causes duplex DNA to be "spooled in" to the filament, left to right as drawn. [After West, S.C., *Annu. Rev. Biochem.* **61,** 617 (1992).]

in (Fig. 25-40). Two such strand-exchange processes must occur simultaneously in a Holliday junction. In eukaryotes, the protein **Rad51,** which is homologous to *E. coli* RecA, apparently functions in a similar ATP-dependent manner to mediate DNA recombination.

RecBCD Initiates Recombination by Making a Single Strand Available. The single-strand segments to which RecA binds are made by the **RecBCD** protein, the 330-kD heterotrimeric product of the SOS genes *recB, recC,* and *recD,* which has both helicase and nuclease activities (Fig. 25-41). The process begins with RecBCD binding to the end of a dsDNA and then unwinding it via its ATP-driven helicase function. As it does so, it nucleolytically degrades the unwound single strands behind it, with the 3′-ending strand being cleaved more often and hence broken down to smaller fragments than the 5′-ending strand. However, on encountering the sequence GCTGGTGG from its 3′ end (the so-called **Chi sequence,** which occurs about every 5 kb in the *E. coli* genome), it stops cleaving the 3′-ending strand and increases the rate at which it cleaves the 5′-ending strand, thereby yielding the 3′-ending single-strand segment to which RecA binds. This explains the observation that regions containing Chi sequences have elevated rates of recombination.

RecBCD can commence unwinding DNA only at a free duplex end. Such ends are not normally present in *E. coli,* which has a circular genome, but become available during recombinational processes.

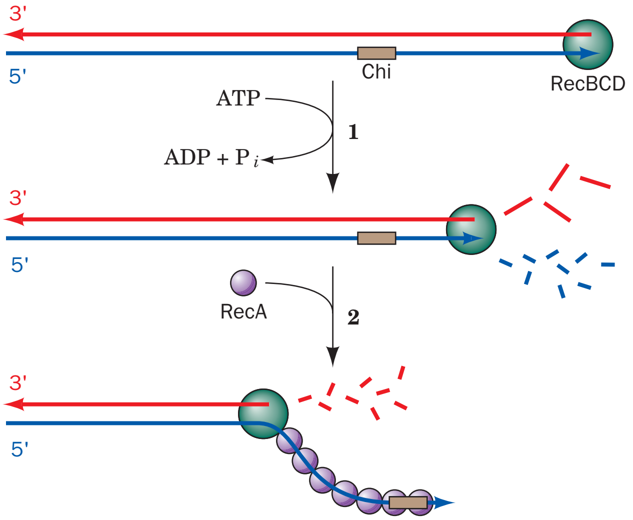

Figure 25-41 | The generation of a 3′-ending single-strand DNA segment by RecBCD to initiate recombination. (1) RecBCD binds to a free end of a dsDNA and, in an ATP-driven process, advances along the helix, unwinding the DNA and degrading the resulting single strands behind it, with the 3′-ending strand cleaved more often than the 5′-ending strand. **(2)** When RecBCD encounters a properly oriented Chi sequence, it increases the frequency at which it cleaves the 5′-ending strand but stops cleaving the 3′-ending strand, thereby generating the 3′-ending strand segment to which RecA binds.

RuvABC Mediates the Branch Migration and the Resolution of the Holliday Junction. Branch migration requires the proteins **RuvA** and **RuvB.** The X-ray structure of RuvA in complex with a Holliday junction, determined by Kosuke Morikawa, indicates that RuvA forms a homotetramer with the appearance of a four-petaled flower (C_4 symmetry) and is relatively flat ($80 \times 80 \times 45$ Å) with one face concave and the other convex (Fig. 25-42). The concave face (facing the viewer in Fig. 25-42), which is highly positively charged and is studded with numerous conserved residues, has four symmetry-related grooves that bind the Holliday junction's four arms. Four negatively charged projections or "pins" are centrally located. The repulsive forces between the pins and the Holliday junction's anionic phosphate groups probably facilitate the separation of the ssDNA segments and guide them from one double helix to another.

However, this is not the entire story. The X-ray structure of a RuvA–Holliday junction complex crystallized under different conditions than that in Fig. 25-42 resembles the complex in Fig. 25-42 but with a second RuvA tetramer in face-to-face contact with the first. Here the Holliday junction is contained in two intersecting tunnels running through the resulting D_2-symmetric RuvA octamer. In the presence of dsDNA, RuvB, an ATPase, oligomerizes to form a pseudohexameric ring with a 30-Å-diameter hole through which a dsDNA can be threaded. A model for RuvAB action, based on the X-ray structure of RuvA in complex with RuvB together with electron micrographs of the RuvAB–Holliday junction complex (Fig. 25-43*a*), places two RuvB hexamers on opposite sides of a RuvA octamer–Holliday junction complex (Fig. 25-43*b*).

The two RuvB rings were originally postulated to counterrotate as driven by ATP hydrolysis so as to screw the single strands of the vertical

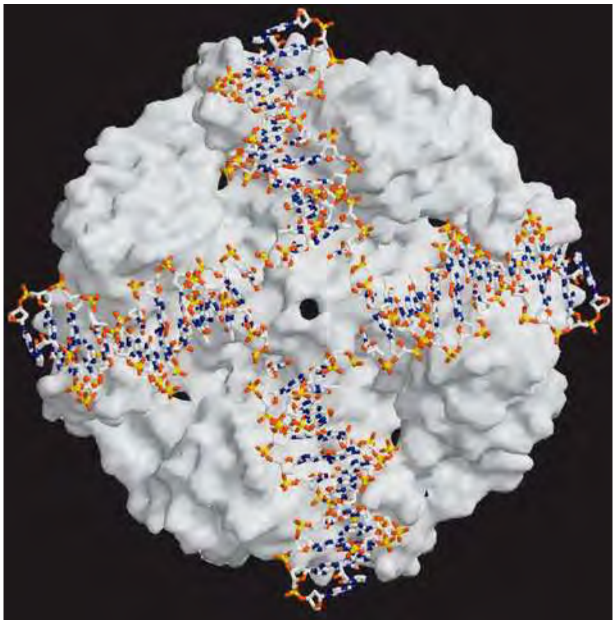

Figure 25-42 | **X-Ray structure of a RuvA–Holliday junction complex.** The protein tetramer, which is viewed along its fourfold axis, is represented by its molecular surface (*gray*). The DNA is drawn in stick form colored according to atom type (C white, N blue, O red, and P yellow). [Courtesy of Kosuke Morikawa, Biomolecular Engineering Research Institute, Osaka, Japan. PDBid 1C7Y.]

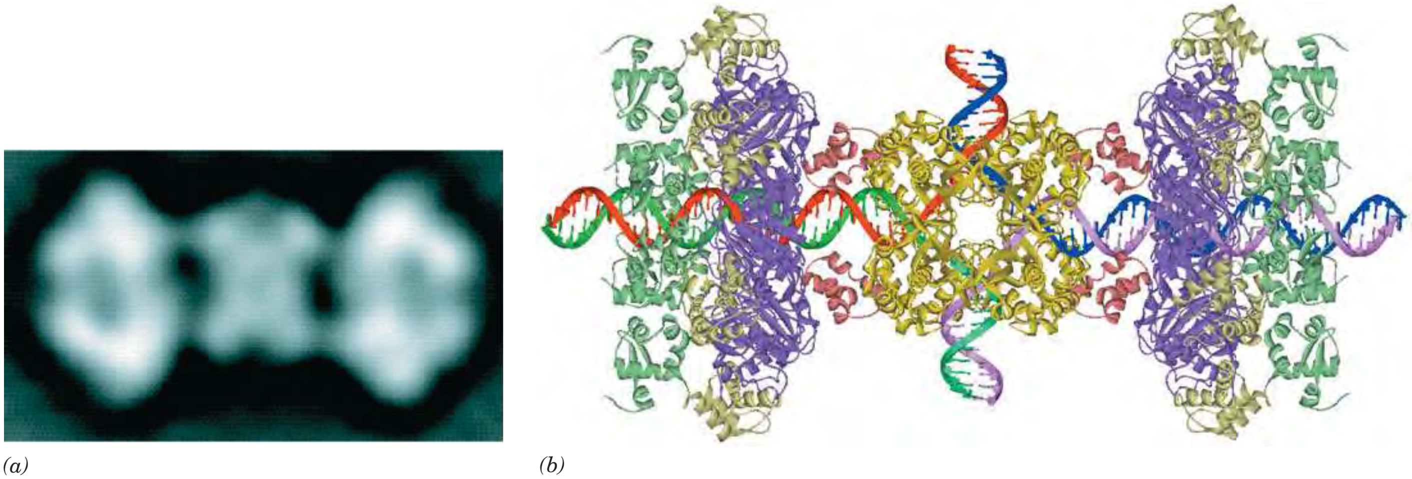

Figure 25-43 | **RuvAB–Holliday junction complex.** (*a*) An electron microscopy–based image of the complex. (*b*) A model of the complex based on fitting the X-ray structures of the RuvA octamer and the RuvB hexameric ring to the image in Part *a.* The RuvA octamer is yellow with its RuvB-contacting domains orange. The domains of the RuvB subunits are colored purple, light green, and dark green. The DNA of the Holliday junction is drawn in ladder form with its homologous red and purple strands complementary to its green and blue strands. Branch migration occurs via the ATP-driven "counterrotation" of two oppositely located dsDNA strands by their associated RuvB hexamers. This unidirectionally pumps (screws) the vertical dsDNA strands in through the center of the Holliday junction on RuvA and out through the RuvB hexamers, a process in which the strands of the vertical dsDNA separate and then rejoin, via base pairing, to form the horizontal dsDNAs. [Courtesy of Kazuhiro Yamada, Tomoko Miyata, and Kosuke Morikawa, Biomolecular Engineering Research Institute, Osaka, Japan.]

dsDNAs through the center of the junction and into the horizontal dsDNAs, thereby effecting branch migration. However, the large area of contact between RuvA and RuvB suggests that the RuvB hexamer does not rotate relative to the RuvA octamer. Instead, it appears that RuvB's DNA-contacting loops unidirectionally "walk" along the horizontal dsDNA's grooves (much like the hexagonal helicases; Section 25-2B), which screws these dsDNAs out through RuvB. This pulls the single strands of the vertical dsDNAs through the center of RuvA, where they rejoin to form the horizontal dsDNAs. The direction of branch migration depends on which pair of opposing arms of the Holliday junction the RuvB hexamers are loaded onto.

The final stage of homologous recombination is the resolution of the Holliday junction into its two homologous dsDNAs. This process is carried out by **RuvC,** a homodimeric nuclease. This requires that one of the RuvA tetramers dissociate from the complex shown in Fig. 25-43*b* to expose the Holliday junction DNA. RuvC presumably sits down on the open face of the resulting RuvA–Holliday junction complex (the side visible in Fig. 25-42) to cleave oppositely located strands at the Holliday junction (Figs. 25-36*i* and *j*). The resulting single-strand nicks are then sealed by DNA ligase (Figs. 25-36*k* and *l*).

B | DNA Can Be Repaired by Recombination

In haploid organisms such as bacteria, homologous recombination between chromosomal DNA and exogenously supplied DNA as occurs, for example, in transformation (Section 3-3A) is such a rare event that the vast majority of such cells never participate in this process. Similarly, in multicellular organisms, the only time that gene shuffling through homologous recombination occurs is during meiosis (Fig. 25-35), which takes place only in germline cells. Why then do nearly all cells have elaborate systems for mediating homologous recombination? This is because damaged replication forks occur at least once per bacterial cell generation and perhaps ten times per eukaryotic cell cycle. The underlying DNA lesions can be corrected via homologous recombination in a process named **recombination repair** [error-prone repair (Section 25-5E), which is highly mutagenic, is a process of last resort]. Indeed, the rates of synthesis of RuvA and RuvB are greatly enhanced by the SOS response. Thus, as Michael Cox pointed out, *the primary function of homologous recombination is to repair damaged replication forks.*

Recombination repair in *E. coli* occurs as follows (Fig. 25-44):

1. When a replication fork encounters an unrepaired single-strand nick or gap, the fork collapses (falls apart).
2. The repair process begins via the RecBCD + RecA–mediated invasion of the newly synthesized and undamaged 3′-ending strand into the homologous dsDNA starting at its broken end.
3. Branch migration, as mediated by RuvAB, then yields a Holliday junction, which exchanges the replication fork's 3′-ending strands.
4. RuvC then resolves the Holliday junction yielding a reconstituted replication fork ready for replication restart.

Thus, the 5′-ending strand of the nick has, in effect, become the 5′ end of an Okazaki fragment.

The final step in the recombination repair process is the restart of DNA replication. This process is, of necessity, distinct from the replication

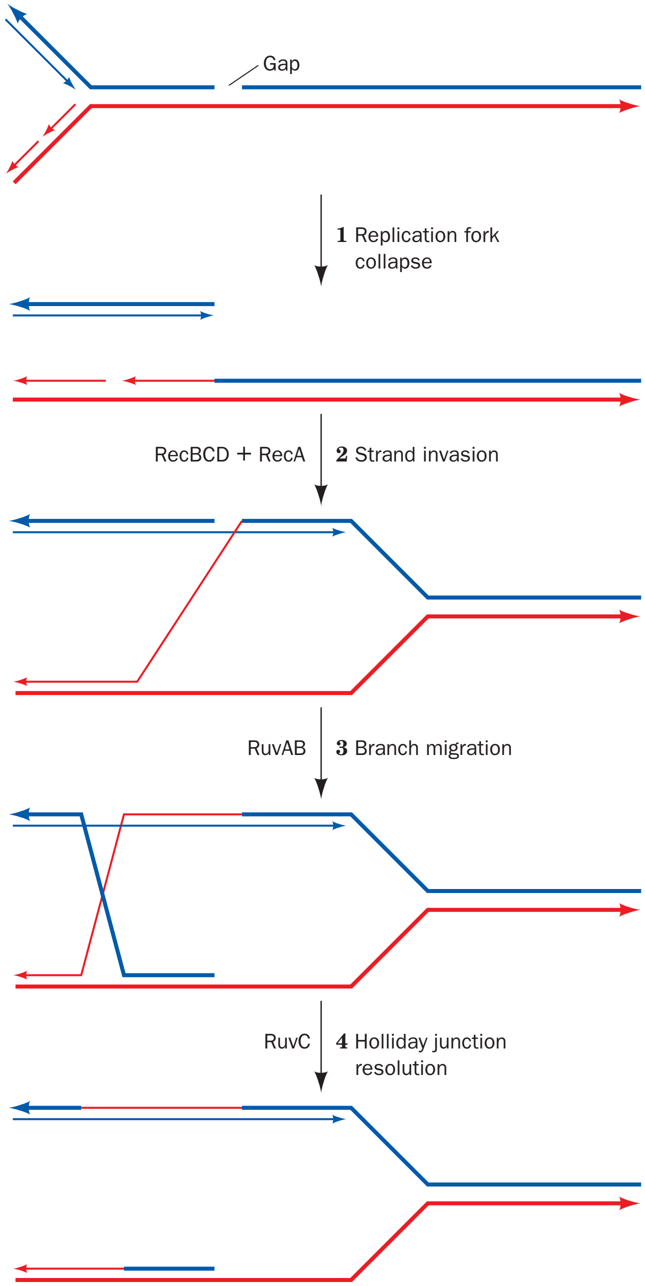
Gap
1 Replication fork collapse
RecBCD + RecA
2 Strand invasion
RuvAB
3 Branch migration
RuvC
4 Holliday junction resolution

Figure 25-44 | The recombination repair of a replication fork that has encountered a single-strand nick. Thick lines indicate parental DNA, thin lines indicate newly synthesized DNA, and the arrows point in the $5' \rightarrow 3'$ direction. [After Cox, M.M., *Annu. Rev. Genet.* **35,** 53 (2001).]

initiation that occurs at *oriC* (Section 25-2B). **Origin-independent replication restart** is mediated by a specialized seven-subunit primosome, which has therefore been named the **restart primosome.**

Recombination Repair Reconstitutes Double-Strand Breaks. We have seen that double-strand breaks (DSBs) in DNA can be rejoined, often mutagenically, by nonhomologous end-joining (NHEJ; Section 25-5E). DSBs may also be nonmutagenically repaired through a recombination repair

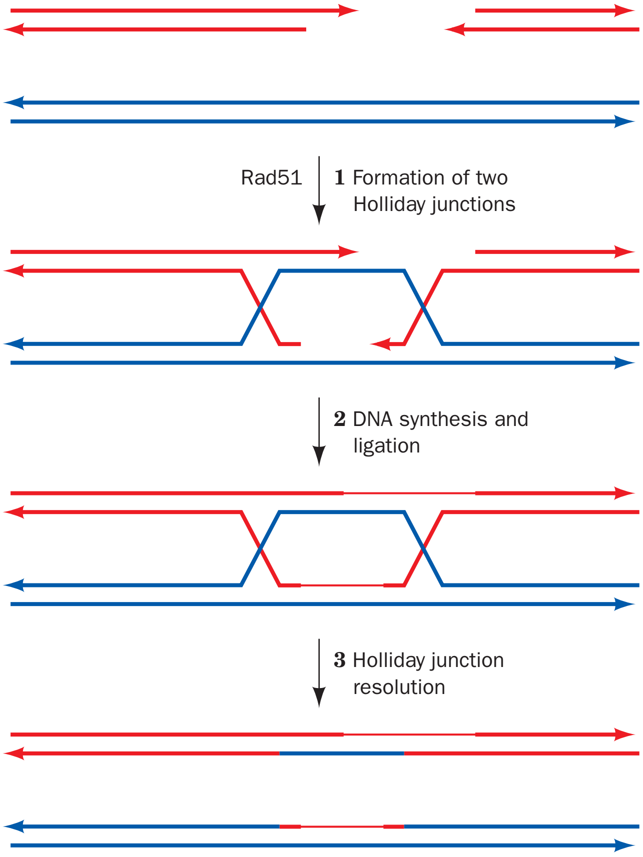
Rad51
1 Formation of two Holliday junctions
2 DNA synthesis and ligation
3 Holliday junction resolution

■ **Figure 25-45 | The repair of a double-strand break in DNA by homologous end-joining.** Thick lines indicate parental DNA, thin lines indicate newly synthesized DNA, and the arrows point in the 5′ → 3′ direction. [After Haber, J.E., *Trends Genet.* **16,** 259 (2000).]

process known as **homologous end-joining,** which occurs via two Holliday junctions (Fig. 25-45):

1. The DSB's double-stranded ends are resected to produce single-stranded ends. One of the 3′-ending strands invades the corresponding sequence of a homologous chromosome to form a Holliday junction, a process mediated by Rad51 (the eukaryotic RecA homolog). The other 3′-ending strand pairs with the displaced strand segment on the homologous chromosome to form a second Holliday junction.
2. DNA polymerase fills in the gaps, and ligase seals the joints.
3. Both Holliday junctions are resolved to yield two intact double-stranded DNAs.

Thus, the sequences that may have been lost in the formation of the DSB are copied from the homologous chromosome. Of course, a limitation of homologous end-joining, particularly in haploid cells, is that a homologous chromosomal segment may not be available.

The importance of recombination repair in humans is demonstrated by the observation that defects in the proteins **BRCA1** (1863 residues) and **BRCA2** (3418 residues), both of which interact with Rad51, are associated with a greatly increased incidence of breast, ovarian, prostate, and pancreatic cancers. Indeed, individuals with mutant *BRCA1* or *BRCA2* genes have up to an 80% lifetime risk of developing cancer.

C | Transposition Rearranges Segments of DNA

In the early 1950s, Barbara McClintock reported that the variegated pigmentation pattern of maize (Indian corn) kernels results from the action of genetic elements that can move within the maize genome. This proposal was resoundingly ignored because it was contrary to the then-held orthodoxy that chromosomes consist of genes linked in fixed order. Another 20 years were to pass before evidence of mobile genetic elements was found in another organism, *E. coli.*

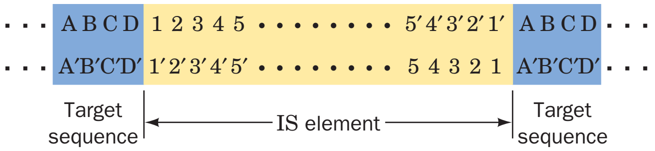

. . . A B C D 1 2 3 4 5 • • • • • • • • • 5′ 4′ 3′ 2′ 1′ A B C D . . .
. . . A′B′C′D′ 1′ 2′ 3′ 4′ 5′ • • • • • • • • • 5 4 3 2 1 A′B′C′D′ . . .
Target sequence
IS element
Target sequence

Figure 25-46 | Structure of IS elements. These and other transposons have inverted terminal repeats (*numerals*) and are flanked by direct repeats of host DNA sequences (*letters*).

Transposons Move Genes between Unrelated Sites. It is now known that **transposable elements,** or **transposons,** are common in both prokaryotes and eukaryotes, where they influence the variation of phenotypic expression over the short term and evolutionary development over the long term. Each transposon codes for the enzymes that insert it into the recipient DNA. This process differs from homologous recombination in that it requires no homology between donor and recipient DNA and occurs at a rate of only one event in every 10^4 to 10^7 cell divisions.

Prokaryotic transposons with three levels of complexity have been characterized:

1. The simplest transposons are named **insertion sequences** or **IS elements.** They are normal constituents of bacterial chromosomes and **plasmids** (autonomously replicating circular DNA molecules that usually consist of several thousand base pairs; Section 3-5A). For example, a common *E. coli* strain has eight copies of **IS1** and five copies of **IS2.** IS elements generally consist of <2000 bp, comprising a so-called **transposase** gene and, in some cases, a regulatory gene, flanked by short inverted (having opposite orientation) terminal repeats. On each side of an inserted IS element is a directly (having the same orientation) repeated segment of host DNA (Fig. 25-46). This suggests that *an IS element is inserted in the host DNA at a staggered cut that is later filled in* (Fig. 25-47). The length of the target sequence

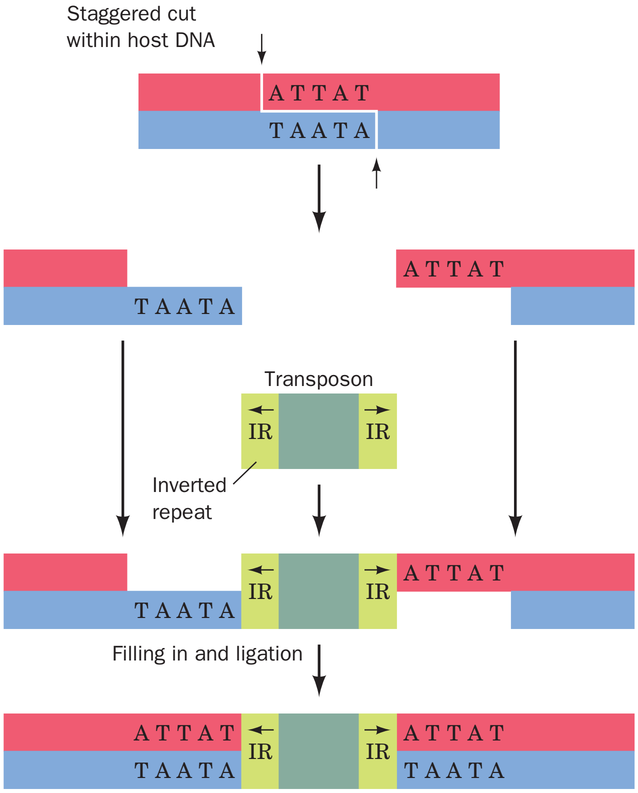

Staggered cut within host DNA
A T T A T
T A A T A
T A A T A
A T T A T
Transposon
IR
IR
Inverted repeat
T A A T A
IR
IR
A T T A T
Filling in and ligation
A T T A T
T A A T A
IR
IR
A T T A T
T A A T A

Figure 25-47 | A model for transposon insertion. A staggered cut that is later filled in generates direct repeats of the target sequence.

(most commonly 5–9 bp), but not its sequence, is characteristic of the IS element.

2. *More complex transposons carry genes not involved in the transposition process,* such as antibiotic resistance genes. For example, **Tn3** consists of 4957 bp and has inverted terminal repeats of 38 bp each.

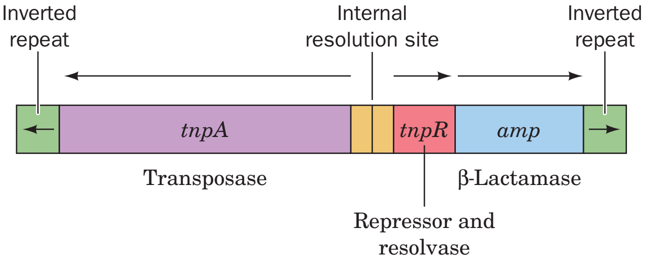

The central region of Tn3 codes for three proteins: (1) a 1015-residue transposase named **TnpA;** (2) a 185-residue protein known as **TnpR,** which represses the expression of both ***tnpA*** and ***tnpR*** and mediates the site-specific recombination reaction necessary for transposition (see below); and (3) a **β-lactamase** (encoded by ***amp***) that inactivates the antibiotic ampicillin (Box 8-3). The site-specific recombination occurs in an AT-rich region, the **internal resolution site,** between *tnpA* and *tnpR.*

3. The so-called **composite transposons** (Fig. 25-48) consist of a gene-containing central region flanked by two identical or nearly identical IS-like modules that have either the same or an inverted relative orientation. Composite transposons apparently arose by the association of two originally independent IS elements. Experiments demonstrate that *composite transposons can transpose any sequence of DNA in their central region.*

The Transposition Mechanism Involves Replication. Transposons do not simply jump from point to point within a genome, as their name implies. Instead, *the mechanism of transposition involves the replication of the transposon.* A model for the movement of a transposon between two plasmids consists of the following steps (Fig. 25-49):

1. A pair of staggered single-strand cuts (such as in Fig. 25-47) is made at the target sequence of the recipient plasmid. Similarly, single-strand cuts are made on opposite strands on either side of the transposon.
2. Each of the transposon's free ends is ligated to a protruding single strand at the insertion site. This forms a replication fork at each end of the transposon.

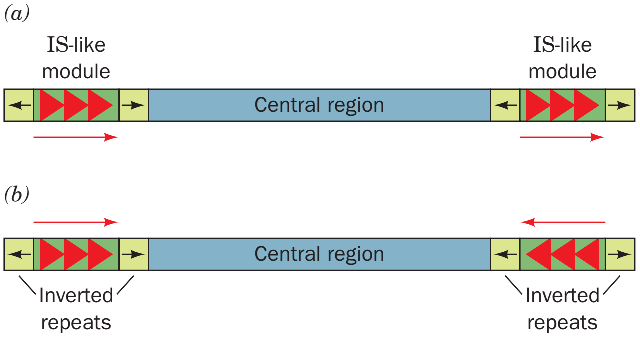

Figure 25-48 | A composite transposon. This element consists of two identical or nearly identical IS-like modules (*green*) flanking a central region carrying various genes. The IS-like modules may have either (*a*) direct or (*b*) inverted relative orientations.

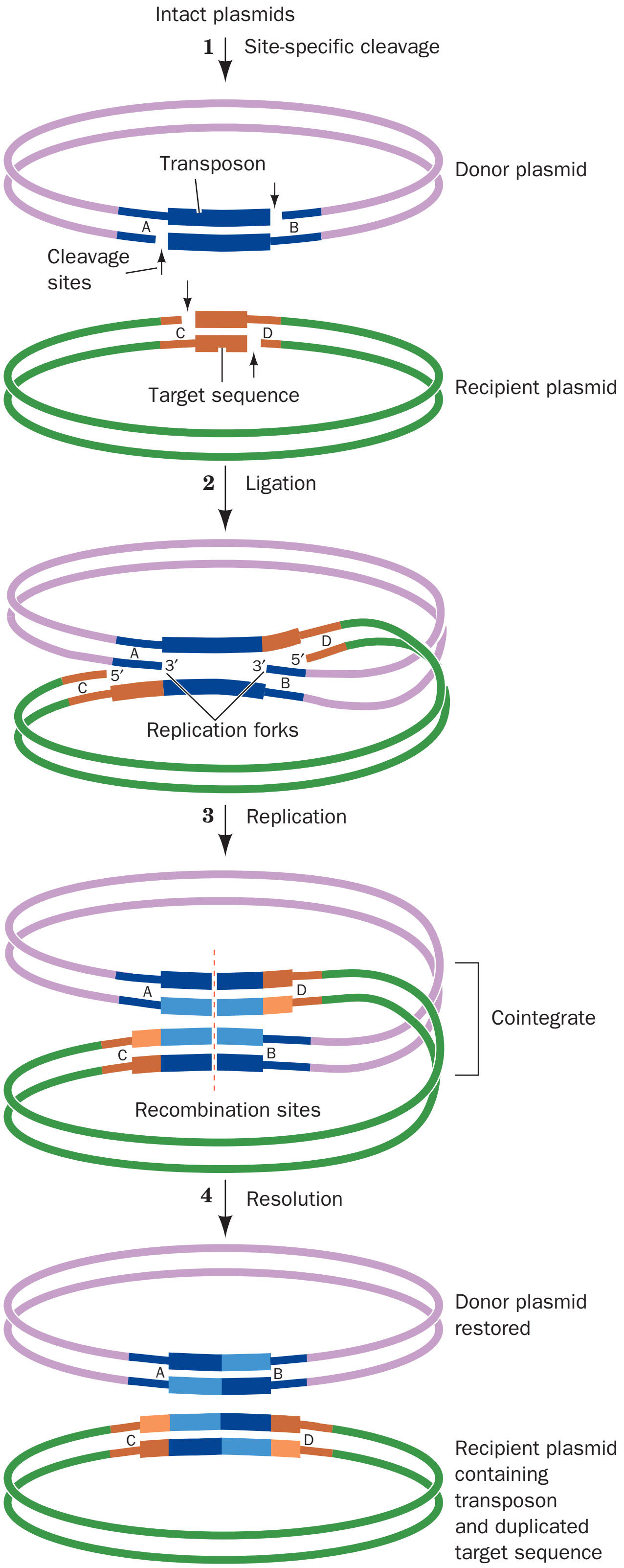
Intact plasmids
1
Site-specific cleavage
Transposon
Donor plasmid
A
B
Cleavage sites
C
D
Target sequence
Recipient plasmid
2
Ligation
A
D
5′
3′
3′
5′
C
B
Replication forks
3
Replication
A
D
C
B
Cointegrate
Recombination sites
4
Resolution
Donor plasmid restored
A
B
C
D
Recipient plasmid containing transposon and duplicated target sequence

■ **Figure 25-49 | A model for transposition involving the intermediacy of a cointegrate.** More lightly shaded bars represent newly synthesized DNA. [After Shapiro, J.A., *Proc. Natl. Acad. Sci.* **76,** 1934 (1979).]

3. The transposon is replicated, thereby yielding a **cointegrate** (the fusion of the two plasmids). Such cointegrates have been isolated.
4. Through a site-specific crossover between the internal resolution sites of the two transposons, the cointegrate is resolved into two

separate plasmids, each of which contains the transposon. This recombination process is catalyzed by a transposon-coded **resolvase** (TnpR in Tn3) rather than by RecA.

Transposition Is Responsible for Much Genetic Rearrangement. In addition to mediating their own insertion into DNA, *transposons promote inversions, deletions, and rearrangements of the host DNA.* Inversions can occur when the host DNA contains two copies of a transposon in inverted orientation. The recombination of these transposons inverts the region between them (Fig. 25-50*a*). If, instead, the two transposons have the same orientation, recombination deletes the segment between them (Fig. 25-50*b*). The deletion of a chromosomal segment in this manner, followed by its integration into the chromosome at a different site by a separate recombination event, results in chromosomal rearrangement.

Transposons can be considered nature's genetic engineering "tools." For example, the rapid evolution, since antibiotics came into common use, of plasmids that confer resistance to several antibiotics (Section 3-5A) has resulted from the accumulation of the corresponding antibiotic-resistance transposons in these plasmids. Transposon-mediated rearrangements may also have been responsible for forming new proteins by linking two formerly independent gene segments. Moreover, transposons can apparently mediate the transfer of genetic information between unrelated species.

Most Eukaryotic Transposons Resemble Retroviruses. Transposons occur in such distantly related eukaryotes as yeast, maize, fruit flies, and humans. In fact, ~3% of the human genome consists of DNA-based transposons although, in most cases, their sequences have mutated so as to render them inactive; that is, these transposons are evolutionary fossils.

Despite the foregoing, many eukaryotic transposons exhibit little similarity to those of prokaryotes. Rather, their base sequences resemble those of

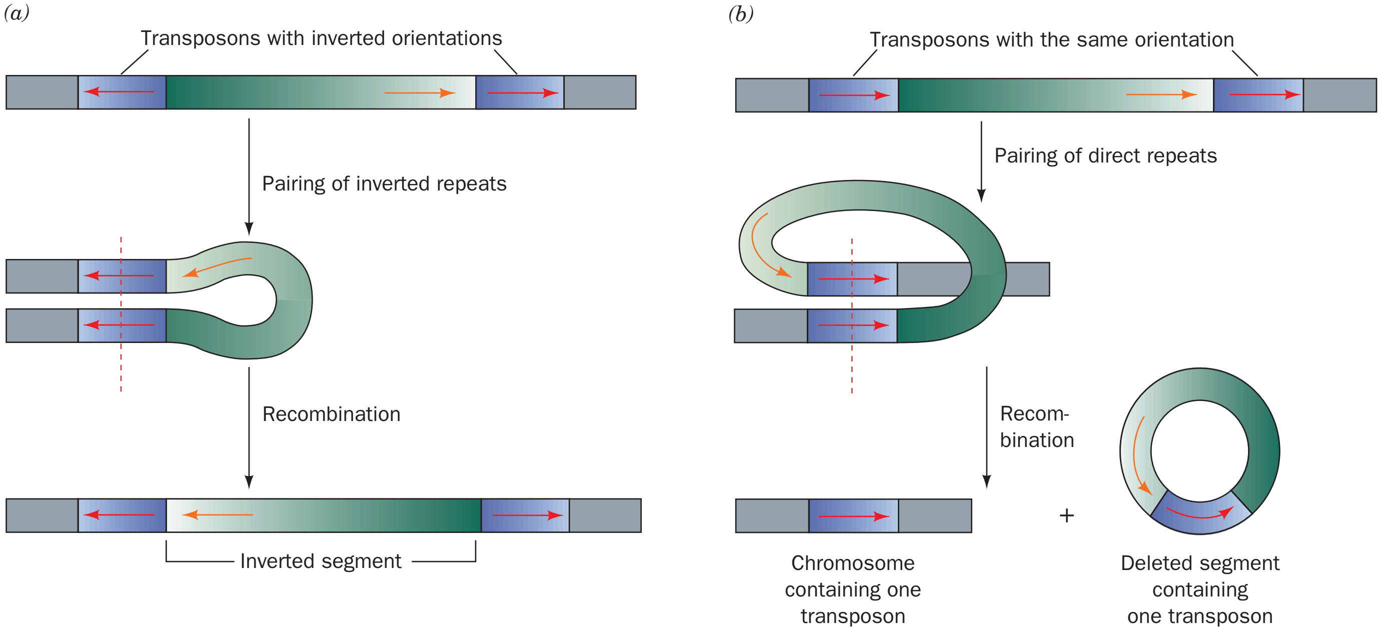
(a)
Transposons with inverted orientations
Pairing of inverted repeats
Recombination
Inverted segment
(b)
Transposons with the same orientation
Pairing of direct repeats
Recombination
+
Chromosome containing one transposon
Deleted segment containing one transposon

■ **Figure 25-50 | Chromosomal rearrangement via recombination.** (*a*) The inversion of a DNA segment between two identical transposons with inverted orientations. (*b*) The deletion of a DNA segment between two identical transposons with the same orientation.

retroviruses (Box 25-2), which suggests that these transposons are degenerate retroviruses. The transposition of these so-called **retrotransposons** occurs via a pathway that resembles the replication of retroviral DNA: (1) their transcription to RNA, (2) the reverse transcriptase–mediated copying of this RNA to cDNA, and (3) the largely random insertion of this DNA into the host organism's genome as mediated by enzymes known as **integrases** (which resemble DNA transposases in structure and mechanism).

Vertebrate genomes also contain retrotransposons that replicate via a different mechanism from that of retroviruses. A common family of these **nonviral retrotransposons** is the 6- to 8-kb **long interspersed nuclear elements (LINEs).** Around 1.4 million LINEs or LINE fragments are present in the human genome and comprise ~20% of its 3.2 billion bp. The great majority of these molecular parasites have mutated to the point of inactivity but a few still appear capable of further transposition. Indeed, several hereditary diseases are caused by the insertion of a LINE into a gene. Several other types of retrotransposons collectively comprise another 22% of the human genome, for a total of ~45% transposon content.

CHECK YOUR UNDERSTANDING

Describe the processes of strand invasion, branch migration, and resolution during homologous recombination.

What is the role of recombination in repairing damaged DNA?

How do transposons mediate genetic rearrangements?

SUMMARY

1. DNA is replicated semiconservatively through the action of DNA polymerases that use the separated parental strands as templates for the synthesis of complementary daughter strands.
2. Replication is semidiscontinuous: The leading strand is synthesized continuously while the lagging strand is synthesized as RNA-primed Okazaki fragments that are later joined.
3. *E. coli* DNA polymerase I (Pol I), which has 3′ → 5′ and 5′ → 3′ exonuclease activities in addition to its 5′ → 3′ polymerase activity, excises RNA primers and replaces them with DNA. Pol III is the primary polymerase in *E. coli.*
4. To initiate replication, parental strands are first melted apart at a specific site named *oriC* and further unwound by a helicase. Single-strand binding protein (SSB) prevents the resulting single strands from reannealing. A primase-containing primosome synthesizes an RNA primer.
5. Because DNA polymerases operate only in the 5′ → 3′ direction, the lagging strand template must loop back to the replisome, which contains two polymerases. A sliding clamp increases Pol III processivity. DNA ligase seals the nicks between Okazaki fragments. Replication proceeds until the two replication forks meet between oppositely facing *Ter* sequences.
6. The high fidelity of DNA replication is achieved by the regulation of dNTP levels, by the requirement for RNA primers, by 3′ → 5′ proofreading, and by DNA repair mechanisms.
7. Eukaryotes contain a number of DNA polymerases. Pol α extends primers, and the highly processive pol δ is the main polymerase. Eukaryotic replication has multiple origins and proceeds through nucleosomes.
8. In order to replicate the 5′ end of the lagging strand, eukaryotic chromosomes end with repeated telomeric sequences added by the ribonucleoprotein telomerase. The 3′ extension at the end of each chromosome serves as a template for primer synthesis. Somatic cells lack telomerase activity, which may prevent them from transforming to cancer cells.
9. Mutations in nucleotide sequences arise spontaneously from replication errors and from alterations triggered by agents such as UV light, radiation, and chemical mutagens. Many compounds that are mutagenic in the Ames test are also carcinogenic.
10. Some forms of DNA damage (e.g., alkylated bases and pyrimidine dimers) may be reversed in a single step. In base excision repair, a glycosylase removes damaged bases. In nucleotide excision repair, an oligonucleotide containing the lesion is removed and replaced. Repair pathways that use error-prone polymerases, nonhomologous end-joining, and the *E. coli* SOS response are mutagenic.
11. Homologous recombination, in which strands of homologous DNA segments are exchanged, involves a crossover structure (Holliday junction). Recombination requires proteins to unwind DNA, mediate strand exchange, drive branch migration, and resolve the Holliday junction. Damaged DNA can be repaired through recombination.
12. Transposons are genetic elements that move within a genome by mechanisms involving their replication. Transposons mediate rearrangement of the host DNA.

KEY TERMS

semiconservative replication	**893**
θ structure	**894**
replication fork	**894**
Okazaki fragment	**896**
semidiscontinuous replication	**896**
leading strand	**896**
lagging strand	**896**
DNA ligase	**896**
primer	**896**

processivity	**896**
proofreading	**897**
nick translation	**899**
helicase	**903**
SSB	**904**
primosome	**904**
primase	**904**
replisome	**904**
replicon	**913**
telomere	**914**
telomerase	**914**
ribonucleoprotein	**914**
G-quartet	**914**
mutation	**916**
pyrimidine dimer	**916**
mutagen	**916**
point mutation	**916**
transition	**916**
transversion	**916**
insertion/deletion mutation	**916**
carcinogen	**919**
Ames test	**919**
photoreactivation	**920**
base excision repair (BER)	**921**
DNA glycosylase	**921**
AP site	**921**
nucleotide excision repair (NER)	**923**
mismatch repair (MMR)	**924**
nonhomologous end-joining (NHEJ)	**925**
SOS response	**926**
homologous recombination	**926**
heterologous DNA	**926**
Holliday junction	**926**
branch migration	**928**
recombination repair	**932**
homologous end-joining	**934**
transposon	**935**
IS element	**935**
composite transposon	**936**
cointegrate	**937**
retrovirus	**939**
retrotransposon	**939**

PROBLEMS

1. Approximately how many Okazaki fragments are synthesized in the replication of the *E. coli* chromosome?
2. Explain why a DNA polymerase that could synthesize DNA in the 3′ → 5′ direction would have a selective disadvantage even if it had 5′ → 3′ proofreading activity.
3. You have discovered a drug that inhibits the activity of inorganic pyrophosphatase. What effect would this drug have on DNA synthesis?
4. A reaction mixture contains DNA polymerase, the four dNTPs, and one of the DNA molecules whose structure is represented below. Which reaction mixtures generate PP_i?

(a)

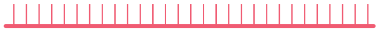

(b)

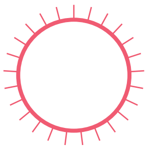

(c)

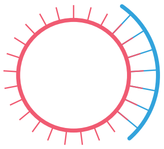

(d)

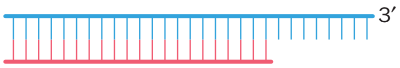

(e)

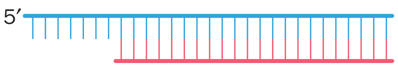

(f)

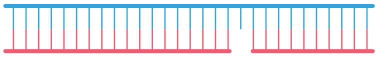

5. Why are there no Pol I mutants that completely lack 5′ → 3′ exonuclease activity?
6. Why is it advantageous to use only the Klenow fragment, rather than intact *E. coli* Pol I, in DNA sequencing reactions (Section 3-4C)?
7. *E. coli oriC* is rich in A · T base pairs. Why is this advantageous?
8. Explain why DNA gyrase is required for efficient unwinding of DNA by helicase at the replication fork.
9. Why is the observed mutation rate of *E. coli* 10^{-8} to 10^{-10} per base pair replicated, even though the error rates of Pol I and Pol III are 10^{-6} to 10^{-7} per base pair replicated?
10. Why can't a linear duplex DNA, such as that of bacteriophage T7, be fully replicated by just *E. coli*-encoded proteins?
11. The base analog **5-bromouracil (5BU),**

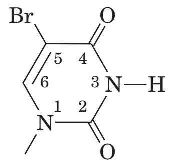

5-Bromouracil (5BU)

which sterically resembles thymine, more readily undergoes tautomerization from its keto form to its enol form than does thymine. 5BU can be incorporated into newly synthesized DNA when it pairs with adenine on the template strand. However, the enol form of 5BU can pair with guanine rather than adenine. (a) Draw the 5BU · G base pair. (b) What type of mutation results?

12. The deamination of adenine yields the base hypoxanthine, which can pair with cytosine. What type of repair system would cells most likely use to repair DNA with a deaminated adenine?
13. **Hydroxylamine** (NH_2OH) converts cytosine to the compound shown below.

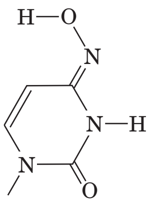

With which base does this modified cytosine pair? Does this generate a transition or a transversion mutation?

14. In eukaryotic cells, a specific triphosphatase cleaves deoxy-8-oxoguanosine triphosphate (oxo-dGTP) to oxo-dGMP + PP_i. What is the advantage of this reaction?
15. Certain sites in the *E. coli* chromosome are known as **hot spots** because they have unusually high rates of point mutations. Many of these sites contain a 5-methylcytosine residue. Explain the existence of such hot spots.
16. Predict whether loss of the following *E. coli* genes would be lethal or not: (a) *dnaB* (which encodes DnaB), (b) *polA* (which encodes Pol I), (c) *ssb,* (d) *recA.*
17. In *E. coli,* all newly synthesized DNA appears to be fragmented (an observation that could be interpreted to mean that the leading strand as well as the lagging strand is synthesized discontinuously). However, in *E. coli* mutants that are defective in uracil–DNA glycosylase, only about half the newly synthesized DNA is fragmented. Explain.
18. *E. coli* DNA polymerase V has the ability to bypass thymine dimers. However, Pol V tends to incorporate G rather than A opposite the damaged T bases. Would you expect Pol V to be more or less processive than Pol III? Explain.

CASE STUDY

Case 32 (available at www.wiley.com/college/voet)
Glucose-6-Phosphate Dehydrogenase Activity and Cell Growth

Focus concept: The activity of the pentose phosphate pathway enzyme glucose-6-phosphate dehydrogenase has been found to be important in the regulation of cell growth.

Prerequisites: Chapters 5, 13, 15, and 25

- Pentose phosphate pathway reactions
- SDS-PAGE analysis
- DNA replication
- Signal transduction pathways involving tyrosine phosphorylation

REFERENCES

DNA Replication

Autexier, C. and Lue, N.F., The structure and function of telomerase reverse transcriptase, *Annu. Rev. Biochem.* **75,** 493–517 (2006).

Blackburn, E.H., Telomere states and cell fates, *Nature* **408,** 53–56 (2000).

Bowman, G.D., Goedken, E.R., Kazmirski, S.L., O'Donnell, M., and Kuriyan, J., DNA polymerase clamp loaders and DNA replication, *FEBS Lett.* **579,** 863–867 (2005).

Caruthers, J.M. and McKay, D.B., Helicase structure and mechanism, *Curr. Opin. Struct. Biol.* **12,** 123–133 (2002).

Groth, A., Rocha, W., Verreault, A., and Almouzni, G., Chromatin challenges during DNA replication and repair, *Cell* **128,** 721–733 (2007).

Hübscher, U., Maga, G., and Spadari, S., Eukaryotic DNA polymerases, *Annu. Rev. Biochem.* **71,** 133–163 (2002).

Lansdorp, P.M., Major cutbacks at chromosome ends, *Trends Biochem. Sci.* **30,** 388–395 (2005). [Discusses normal and abnormal mechanisms for telomere shortening.]

O'Donnell, M., Replisome architecture and dynamics in *E. coli, J. Biol. Chem.* **281,** 10653–10656 (2006); *and* Johnson, A. and O'Donnell, M., Cellular DNA replicases: Components and dynamics at the replication fork, *Annu. Rev. Biochem.* **74,** 283–315 (2005).

Rothwell, P.J. and Waksman, G., Structure and mechanism of DNA polymerases, *Adv. Prot. Chem.* **71,** 401–440 (2005).

DNA Repair

Friedberg, E.C., Wagner, R., and Radman, M., Specialized DNA polymerases, cellular survival, and the genesis of mutations, *Science* **296,** 1627–1630 (2002). [Reviews the roles of error-prone DNA polymerases in DNA repair and antibody generation.]

Garber, P.M., Vidanes, G., and Toczyski, D.P., Damage in transition, *Trends Biochem. Sci.* **30,** 63–66 (2005). [Describes how broken DNA can be repaired by NHEJ or recombination.]

Rouse, J. and Jackson, S.P., Interfaces between the detection, signaling, and repair of DNA damage, *Science* **297,** 547–551 (2002). [Summarizes current understanding of how signaling pathways triggered by DNA damage lead to DNA repair.]

Sancar, A., Lindsey-Bolz, L.A., Ünsal-Kaçmaz, K., and Linn, S., Molecular mechanisms of mammalian DNA repair and the DNA damage checkpoints, *Annu. Rev. Biochem.* **73,** 39–85 (2004).

Scriver, C.R., Beaudet, A.L., Sly, W.S., and Valle, D. (Eds.), *The Metabolic and Molecular Bases of Inherited Disease* (8th ed.), Chaps. 28 and 32, McGraw-Hill (2001). [Discussions of xeroderma pigmentosum, Cockayne syndrome, and hereditary nonpolyposis colorectal cancer.]

Recombination and Transposition

Cox, M.M., Recombinational DNA repair of damaged replication forks in *Escherichia coli:* questions, *Annu. Rev. Genet.* **35,** 53–82 (2001).

Craig, N.L., Craigie, R., Gellert, M., and Lambowitz, A.M. (Eds.), *Mobile DNA II,* ASM Press (2002). [A compendium of authoritative articles.]

Kowalczykowski, S.C., Initiation of genetic recombination and recombination-dependent replication, *Trends Biochem. Sci.* **25,** 156–165 (2000). [Presents models for and describes the proteins involved in recombination/replication events in bacteria.]

West, S.C., Molecular views of recombination proteins and their control, *Nature Rev. Mol. Cell. Biol.* **4,** 435–445 (2003).

Yamada, K., Ariyoshi, M., and Morikawa, K., Three-dimensional structural views of branch migration and resolution in DNA homologous recombination, *Curr. Opin. Struct. Biol.* **14,** 130–137 (2004).

26

Transcription and RNA Processing

TTAAGCTAAACCC

Transcription is the process by which DNA directs the synthesis of a complementary strand of RNA that reflects the genetic information encoded in the DNA. In the same way, a photographic negative image is complementary to its corresponding positive image. [Pictor International/Alamy Images.]

CHAPTER CONTENTS

1 Prokaryotic RNA Transcription
- **A.** RNA Polymerase Resembles Other Polymerases
- **B.** Transcription Is Initiated at a Promoter
- **C.** The RNA Chain Grows from the 5′ to 3′ End
- **D.** Transcription Terminates at Specific Sites

2 Transcription in Eukaryotes
- **A.** Eukaryotes Have Several RNA Polymerases
- **B.** Each Polymerase Recognizes a Different Type of Promoter
- **C.** Transcription Factors Are Required to Initiate Transcription

3 Posttranscriptional Processing
- **A.** Messenger RNAs Undergo 5′ Capping, Addition of a 3′ Tail, and Splicing
- **B.** Ribosomal RNA Precursors May Be Cleaved, Modified, and Spliced
- **C.** Transfer RNAs Are Processed by Nucleotide Removal, Addition, and Modification

MEDIA RESOURCES

(available at www.wiley.com/college/voet)
Interactive Exercise 50. The RNA polymerase II elongation complex.
Interactive Exercise 51. TATA-binding protein in complex with TATA box
Interactive Exercise 52. Self-splicing group I intron from *Tetrahymena*

DNA is confined almost exclusively to the nucleus of eukaryotic cells, as shown by microscopists in the 1930s. By the 1950s, the site of protein synthesis was identified by showing that radioactively labeled amino acids that had been incorporated into proteins were associated with cytosolic RNA–protein complexes called ribosomes. Thus, *protein synthesis is not immediately directed by DNA because, at least in eukaryotes, DNA and ribosomes are never in contact.* The intermediary between DNA and the protein-biosynthesis machinery, as outlined in Francis Crick's central dogma of molecular biology (Section 3-3B), is RNA.

Cells contain three major types of RNA: **ribosomal RNA (rRNA),** which constitutes two-thirds of the ribosomal mass; **transfer RNA (tRNA),** a set of small compact molecules that deliver amino acids to the ribosomes for assembly into proteins; and **messenger RNA (mRNA),** whose nucleotide sequences direct protein synthesis. In addition, a host of other small RNA species play various roles in the regulation of gene expression and the processing of newly transcribed RNA molecules. All types of RNA can be shown to hybridize with complementary sequences on DNA from the same organism. Thus, *all cellular RNAs are transcribed from DNA templates.*

The transcription of DNA to RNA is carried out by **RNA polymerases (RNAPs)** that operate as multisubunit complexes, as do the DNA polymerases that catalyze DNA replication. In this chapter, we examine the catalytic properties of RNAPs and discuss how these proteins—unlike DNA polymerases—are targeted to specific genes. We shall also see how newly synthesized RNA is processed to become fully functional.

1 Prokaryotic RNA Transcription

RNAP, the enzyme responsible for the DNA-directed synthesis of RNA, was discovered independently in 1960 by Samuel Weiss and Jerard Hurwitz. The enzyme couples together the ribonucleoside triphosphates (NTPs) ATP, CTP, GTP, and UTP on DNA templates in a reaction that is driven by the release and subsequent hydrolysis of PP_i:

$$(\mathrm{RNA})_{n\ \mathrm{residues}} + \mathrm{NTP} \rightleftharpoons (\mathrm{RNA})_{n+1\ \mathrm{residues}} + \mathrm{PP}_i \xrightarrow{\mathrm{H_2O}} 2\,\mathrm{P}_i$$

All cells contain RNAP. In bacteria, one enzyme synthesizes all of the cell's RNA except the short RNA primers employed in DNA replication (Section 25-2B). Eukaryotic cells contain four or five RNAPs that each synthesize a different class of RNA. We shall first consider the bacterial enzyme because it is smaller and simpler than the eukaryotic enzymes.

LEARNING OBJECTIVES

- Understand that RNA polymerase has a structure and mechanism similar to those of DNA polymerases.
- Understand that bacterial transcription begins with the RNAP holoenzyme binding to a promoter to melt apart the DNA.
- Understand that as the polymerase processively extends an RNA chain, another polymerase can initiate transcription.
- Understand that transcription termination is a complex multistep process.

A | RNA Polymerase Resembles Other Polymerases

The *E. coli* RNAP **holoenzyme** is an ~449-kD protein with subunit composition $\alpha_2\beta\beta'\omega\sigma$. Once RNA synthesis has been initiated, however, the σ subunit (also called the **σ factor**) dissociates from the **core enzyme** $\alpha_2\beta\beta'\omega$, which carries out the actual polymerization process. RNAP is large enough to be clearly visible in electron micrographs (Fig. 26-1).

The X-ray structure of a related RNAP core enzyme from *Thermus aquaticus* (*Taq*), determined by Seth Darst, shows that it is shaped like a crab

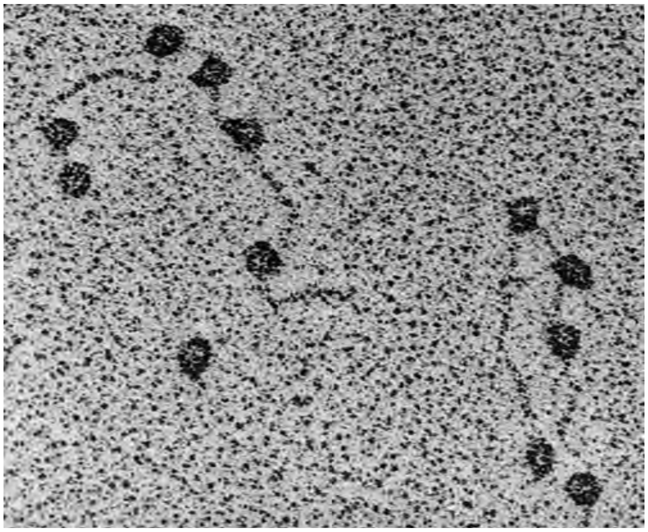

Figure 26-1 | An electron micrograph of *E. coli* RNA polymerase holoenzyme. This soluble enzyme, one of the largest known, is attached to various promoter sites on bacteriophage T7 DNA. [From Williams, R.C., *Proc. Natl. Acad. Sci.* **74,** 2313 (1977).]

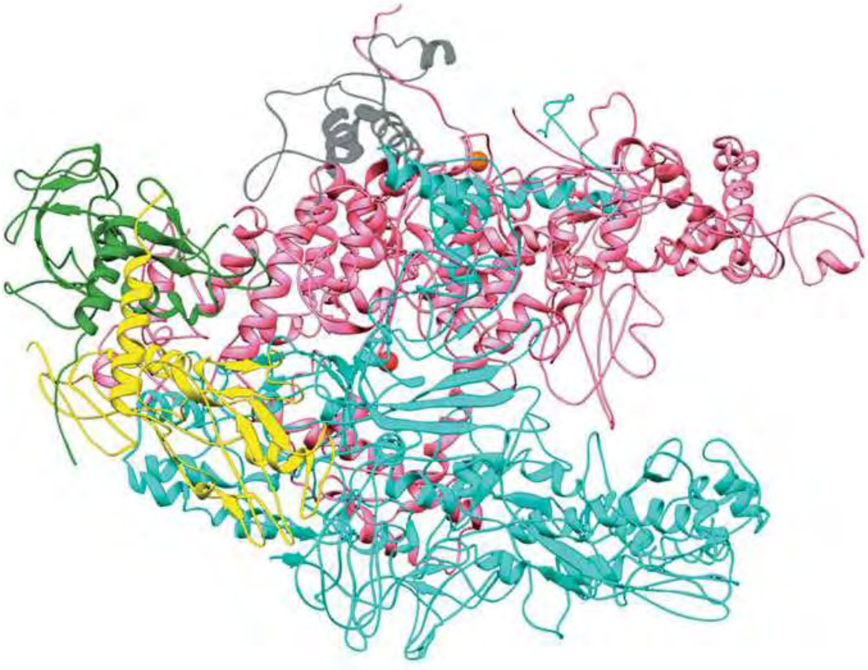

■ **Figure 26-2 | X-Ray structure of *Taq* core RNA polymerase.** The two α subunits are yellow and green, the β subunit is cyan, the β′ subunit (part of which is disordered and therefore not visible in this model) is pink, and the ω subunit is gray. Bound Mg^{2+} and Zn^{2+} ions are represented by red and orange spheres, respectively. [Based on an X-ray structure by Seth Darst, The Rockefeller University. PDBid 1HQM.]

claw whose two pincers are formed by the β and β′ subunits (Fig. 26-2). The channel or space between the pincers is ~27 Å high. The active site, which includes a Mg^{2+} ion, is located at the base of the channel. In the *Taq* holoenzyme, the σ subunit extends across the top of the core enzyme and causes the pincers to come together so as to narrow the channel between them by about 10 Å. The outer surface of the holoenzyme is almost uniformly negatively charged, whereas those surfaces presumed to interact with nucleic acids, particularly the inner walls of the channel, are positively charged.

B | Transcription Is Initiated at a Promoter

RNA synthesis is normally initiated only at specific sites on the DNA template. In contrast to replication, which requires that both strands of the chromosome be entirely copied, the regulated expression of genetic information involves much smaller, single-strand portions of the genome. The DNA strand that serves as a template during transcription is known as the **antisense** or **noncoding strand** since its sequence is complementary to that of the RNA. The other DNA strand, which has the same sequence (except for the replacement of U with T) as the transcribed RNA, is known as the **sense** or **coding strand** (Fig. 26-3). The two strands of DNA in an organism's chromosome can therefore contain different sets of genes.

Keep in mind that "gene" is a relatively loose term that refers to sequences that encode polypeptides, as well as those that correspond to the sequences of rRNA, tRNA, and other RNA species. Furthermore, a gene typically includes sequences that participate in initiating and terminating transcription (and translation) that are not actually transcribed (or translated). The expression of many genes also depends on regulatory sequences that do not directly flank the coding regions but may be located a considerable distance away.

Most protein-coding genes (called **structural genes**) in eukaryotes are transcribed individually. In prokaryotic genomes, however, genes are frequently arranged in tandem along a single DNA strand so that they can be

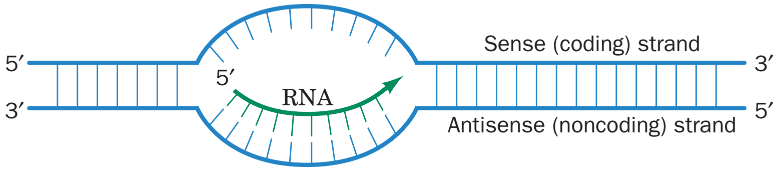

Figure 26-3 | Sense and antisense DNA strands. The template strand of duplex DNA is known as its antisense or noncoding strand. Its complementary sense or coding strand has the same nucleotide sequence and orientation as the transcribed RNA.

transcribed together. These genetic units, called **operons,** typically contain genes with related functions. For example, the three different rRNA genes of *E. coli* occur in single operons (Section 26-3B). The *E. coli* ***lac*** **operon,** whose expression is described in detail in Section 28-2A, contains three genes encoding proteins involved in lactose metabolism as well as sequences that control their transcription (Fig. 26-4). Other operons contain genes encoding proteins required for biosynthetic pathways, for example, the ***trp*** **operon,** whose six **gene products** (proteins are often referred to as gene products) catalyze tryptophan synthesis. An operon is transcribed as a single unit, giving rise to a **polycistronic mRNA** that directs the more-or-less simultaneous synthesis of each of the encoded polypeptides (the term **cistron** is a somewhat archaic synonym for gene). In contrast, eukaryotic structural genes, which are not part of operons, give rise to **monocistronic mRNAs.**

RNA Polymerase Holoenzyme Binds to Promoters. How does RNAP recognize the correct DNA strand and initiate RNA synthesis at the beginning of a gene (or operon)? *RNAP binds to its initiation sites through base sequences known as* ***promoters*** *that are recognized by the corresponding* σ *factor.* The existence of promoters was first revealed through mutations that enhanced or diminished the transcription rates of certain genes. Promoters consist of ~40-bp sequences that are located on the 5′ side of the transcription start site. By convention, the sequence of this DNA is represented by its sense (nontemplate) strand so that it will have the same sequence and directionality as the transcribed RNA. A base pair in a promoter region is assigned a negative or positive number that indicates its position, upstream or downstream in the direction of RNAP travel, from the first nucleotide that is transcribed to RNA; this start site is +1 and there is no 0. Because RNA is synthesized in the $5' \rightarrow 3'$ direction (see below), the promoter is said to lie upstream of the RNA's starting nucleotide.

The holoenzyme forms tight complexes with promoters (dissociation constant $K \approx 10^{-14}$ M). This tight binding can be demonstrated by show-

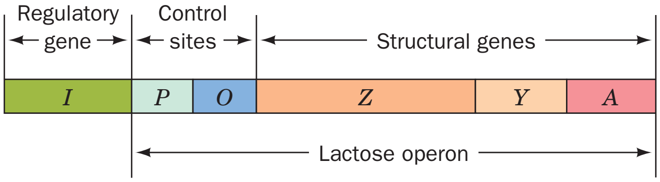

Figure 26-4 | The *E. coli lac* operon. This DNA includes genes encoding the proteins mediating lactose metabolism and the genetic sites that control their expression. The *Z*, *Y*, and *A* genes, respectively, specify the proteins **β-galactosidase** (Box 8-1)**, galactoside permease** (Section 10-3D), and **thiogalactoside transacetylase.** The closely linked regulatory gene, *I*, which is not part of the *lac* operon, encodes a repressor that inhibits transcription of the *lac* operon.

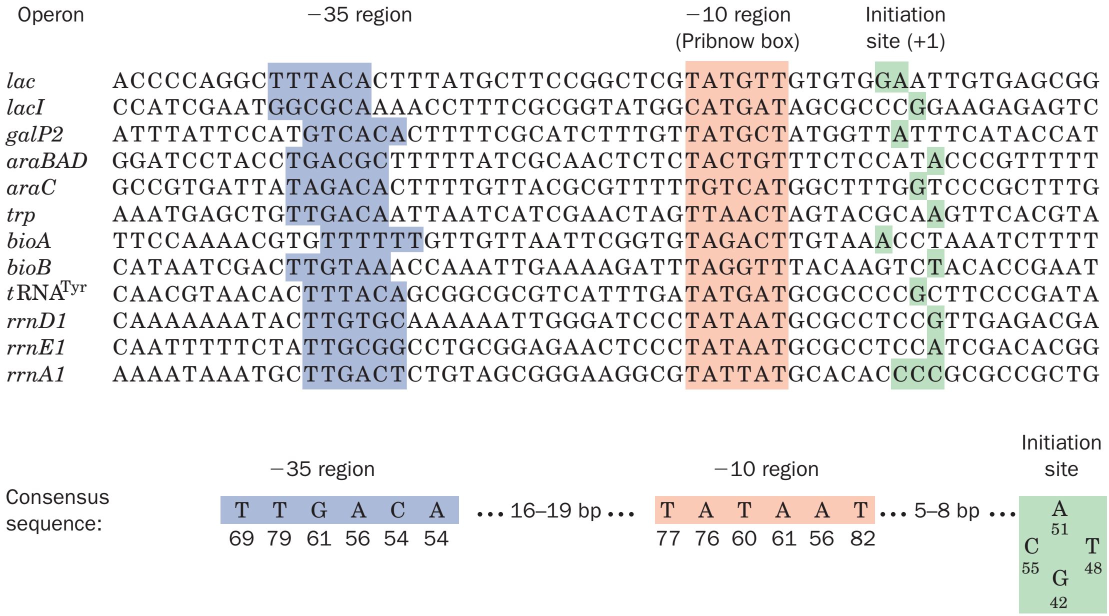
Operon
−35 region
−10 region
(Pribnow box)
Initiation
site (+1)
lac ACCCCAGGCTTTACACTTTATGCTTCCGGCTCGTATGTTGTGTGGAATTGTGAGCGG
lacI CCATCGAATGGCGCAAAACCTTTCGCGGTATGGCATGATAGCGCCCGGAAGAGAGTC
galP2 ATTTATTCCATGTCACACTTTTCGCATCTTTGTTATGCTATGGTTATTTCATACCAT
araBAD GGATCCTACCTGACGCTTTTTATCGCAACTCTCTACTGTTTCTCCATACCCGTTTTT
araC GCCGTGATTATAGACACTTTTGTTACGCGTTTTTGTCATGGCTTTGGTCCCGCTTTG
trp AAATGAGCTGTTGACAATTAATCATCGAACTAGTTAACTAGTACGCAAGTTCACGTA
bioA TTCCAAAACGTGTTTTTTGTTGTTAATTCGGTGTAGACTTGTAAACCTAAATCTTTT
bioB CATAATCGACTTGTAAACCAAATTGAAAAGATTTAGGTTTACAAGTCTACACCGAAT
tRNA^Tyr CAACGTAACACTTTACAGCGGCGTCATTTGATATGATGCGCCCCGCTTCCCGATA
rrnD1 CAAAAAAATACTTGTGCAAAAAATTGGGATCCCTATAATGCGCCTCCGTTGAGACGA
rrnE1 CAATTTTTCTATTGCGGCCTGCGGAGAACTCCCTATAATGCGCCTCCATCGACACGG
rrnA1 AAAATAAATGCTTGACTCTGTAGCGGGAAGGCGTATTATGCACACCCCGCGCCGCTG
−35 region
−10 region
Initiation
site
Consensus
sequence:
T T G A C A
69 79 61 56 54 54
... 16–19 bp ...
T A T A A T
77 76 60 61 56 82
... 5–8 bp ...
A 51
C 55
T 48
G 42

Figure 26-5 | The sense (coding) strand sequences of selected *E. coli* promoters. A 6-bp region centered around the −10 position (*red shading*) and a 6-bp sequence around the −35 region (*blue shading*) are both conserved. The transcription initiation sites (+1), which in most promoters occur at a single purine nucleotide, are shaded in green. The bottom row shows the consensus sequence of 298 *E. coli* promoters with the number below each base indicating its percentage occurrence. [After Rosenberg, M. and Court, D., *Annu. Rev. Genet.* **13,** 321–323 (1979). Consensus sequence from Lisser, D. and Margalit, H., *Nucleic Acids Res.* **21,** 1512 (1993).]

ing that the holoenzyme protects the bound DNA segments from digestion *in vitro* by the endonuclease DNase I. Sequence determinations of the protected regions from numerous *E. coli* genes have identified the "consensus" sequence of *E. coli* promoters (Fig. 26-5). Their most conserved sequence is a hexamer centered at about the −10 position (sometimes called the **Pribnow box,** after David Pribnow, who described it in 1975). It has a consensus sequence of TATAAT in which the leading TA and the final T are highly conserved. Upstream sequences around position −35 also have a region of sequence similarity, TTGACA. The initiating (+1) nucleotide, which is nearly always A or G, is centered in a poorly conserved CAT or CGT sequence. Most promoter sequences vary considerably from the consensus sequence (Fig. 26-5). Nevertheless, a mutation in one of the partially conserved regions can greatly increase or decrease a promoter's initiation efficiency. This is because *the rates at which E. coli genes are transcribed vary directly with the rates at which their promoters form stable initiation complexes with the RNAP holoenzyme.*

Initiation Requires the Formation of an Open Complex. The promoter regions in contact with the RNAP holoenzyme have been identified by a procedure named **footprinting.** In this procedure, DNA is incubated with a protein to which it binds and is then treated with an alkylation agent such as dimethyl sulfate (DMS). This results in alkylation of the DNA's bases followed by backbone cleavage at the alkylated positions. However, those portions of the DNA that bind proteins are protected from alkylation and hence cleavage. The resulting pattern of protection is called the protein's footprint. The footprint of RNAP holoenzyme indicates that it contacts the promoter primarily at its −10 and −35 regions. In some genes, additional upstream sequences may also influence RNAP binding to DNA.

DMS methylates G residues at N7 and A residues at N3 in both double- and single-stranded DNA. DMS also methylates N1 of A and N3 of C, but only if the latter positions are not involved in base-pairing interactions. The pattern of DMS methylation therefore reveals whether the DNA is single or double stranded. Footprinting studies indicate that holoenzyme binding "melts" (separates) ~11 bp of DNA (from −9 to +2). The resulting **open complex** is analogous to the region of unwound DNA at the replication origin (Section 25-2B).

The core enzyme, which does not specifically bind promoters, tightly binds duplex DNA (the complex's dissociation constant is $K \approx 5 \times 10^{-12}$ M, and its half-life is ~60 min). *The holoenzyme, in contrast, binds to nonpromoter DNA comparatively loosely* ($K \approx 10^{-7}$ M and a half-life of >1 s). Evidently, the σ subunit allows the holoenzyme to move rapidly along a DNA strand in search of the σ subunit's corresponding promoter. Once transcription has been initiated and the σ subunit jettisoned, the tight binding of the core enzyme to DNA apparently stabilizes the ternary enzyme–DNA–RNA complex.

Gene Expression Is Controlled by Different σ Factors. Because different σ factors recognize different promoters, *a cell's complement of σ factors determines which genes are transcribed.* Development and differentiation, which involve the temporally ordered expression of sets of genes, can be orchestrated through a "cascade" of σ factors. For example, infection of *Bacillus subtilis* by **bacteriophage SP01** requires the expression of different sets of phage genes at different times. The first set, known as the **early genes,** are transcribed using the bacterial σ factor. One of the early phage gene products is a σ subunit known as $\boldsymbol{\sigma^{gp28}}$, which displaces the host σ factor and thereby permits the RNAP to recognize only the phage **middle gene** promoters. The phage middle genes, in turn, specify $\boldsymbol{\sigma^{gp33/34}}$, which promotes transcription of only phage **late genes.**

Several bacteria, including *E. coli* and *Bacillus subtilis,* likewise have several different σ factors. These are not necessarily used in a sequential manner. For example, σ factors in *E. coli* that differ from its primary σ factor (which is named $\boldsymbol{\sigma^{70}}$ because its molecular mass is 70 kD) control the transcription of coordinately expressed groups of special-purpose genes whose promoters are quite different from those recognized by σ^{70}.

C | The RNA Chain Grows from the 5′ to 3′ End

Because RNA synthesis, like DNA synthesis, proceeds in the 5′ → 3′ direction (Fig. 26-6), the growing RNA molecule has a 5′-triphosphate group. Mature RNA molecules, as we shall see, may also be chemically modified at one or both ends.

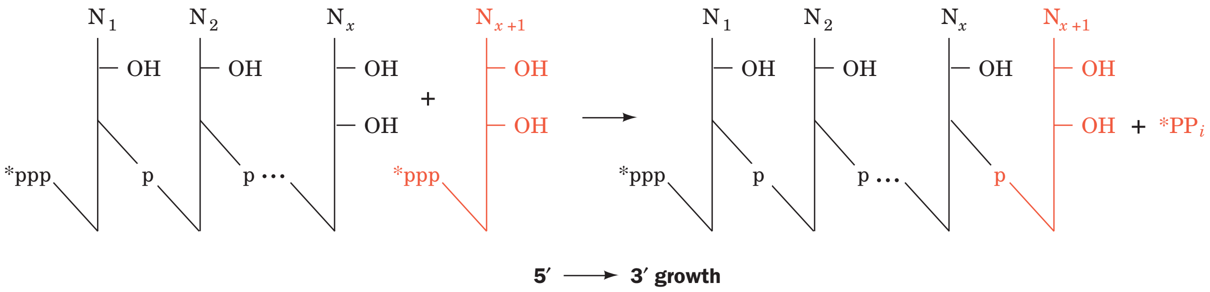

■ **Figure 26-6 | 5′ → 3′ RNA chain growth.** Nucleotides are added to the 3′ end of the growing RNA chain via attack of the 3′-OH group on the incoming nucleoside triphosphate. A radioactive label at the γ position of an NTP (indicated by an asterisk) is retained in the initial nucleotide of the RNA (the 5′ end) but is lost as PP_i during the polymerization of subsequent nucleotides.

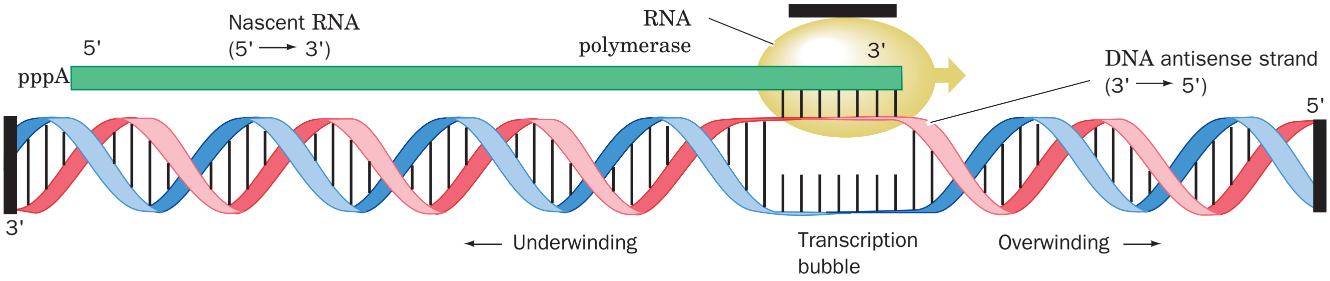

Figure 26-7 | DNA supercoiling during transcription. In the region being transcribed, the DNA double helix is unwound by about a turn to permit the DNA's antisense strand to form a short segment of DNA–RNA hybrid double helix. As the RNA polymerase advances along the DNA template (here to the right), the DNA unwinds ahead of the RNA's growing 3′ end and rewinds behind it, thereby stripping the newly synthesized RNA from the template strand. Because the ends of the DNA as well as the RNA polymerase are apparently prevented from rotating by attachments within the cell (*black bars*), the DNA becomes overwound (positively supercoiled) ahead of the advancing transcription bubble and underwound (negatively supercoiled) behind it (consider the consequences of placing your finger between the twisted DNA strands in this model and pushing toward the right). [After Futcher, B., *Trends Genet.* **4,** 272 (1988).]

A portion of the double-stranded DNA template remains opened up at the point of RNA synthesis. This allows the antisense strand to direct the synthesis of its complementary RNA strand. The RNA chain transiently forms a short length of RNA–DNA hybrid duplex. The unpaired "bubble" of DNA in the open initiation complex apparently travels along the DNA with the RNAP (Fig. 26-7).

As DNA's helical turns are pushed ahead of the advancing transcription bubble, they become more tightly wound (more positively supercoiled) while the DNA behind the bubble becomes equivalently unwound (more negatively supercoiled). This scenario is supported by the observation that the transcription of plasmids in *E. coli* induces their positive supercoiling in gyrase mutants (which cannot relax positive supercoils; Section 24-1D) and their negative supercoiling in topoisomerase I mutants (which cannot relax negative supercoils). Inappropriate superhelicity in the DNA being transcribed halts transcription. Quite possibly, the torsional tension in the DNA generated by negative superhelicity behind the transcription bubble is required to help drive the transcriptional process, whereas too much such tension prevents the opening and maintenance of the transcription bubble.

Strain that builds up in the DNA template is apparently responsible for a curious property of RNAP: It frequently releases its newly synthesized RNA after only ~9 to 11 nt have been polymerized, a process known as **abortive initiation.** When RNAP begins transcribing, it keeps its grip on the promoter (which is on the DNA's nontemplate strand). Consequently, conformational tension builds up as the template strand is pulled through the RNAP's active site, a process called **scrunching** because the resulting increased size of the transcription bubble in the downstream direction must somehow be accommodated within the RNAP. In successful initiation, the strain eventually provides enough energy to strip the promoter from the RNAP, which then continues its progress along the template. In abortive initiation, the RNAP fails to escape the promoter and instead relieves the conformational tension by releasing the newly synthesized RNA

BOX 26-1 **PERSPECTIVES IN BIOCHEMISTRY**

Collisions between DNA Polymerase and RNA Polymerase

In rapidly proliferating bacterial cells, DNA synthesis is likely to occur even as genes are being transcribed. The DNA replication machinery moves along the circular chromosome at a rate many times faster than the movement of the transcription machinery. Collisions between DNA polymerase and RNA polymerase seem unavoidable. What happens when the two enzyme complexes collide? Using *in vitro* model systems, Bruce Alberts has shown that when both enzymes are moving in the same direction, the replication fork passes the RNA polymerase without displacing it, leaving it fully competent to resume RNA chain elongation.

When the replication fork collides head-on with a transcription complex, however, the replisome pauses briefly before moving past the RNA polymerase. Surprisingly, this causes the RNA polymerase to switch its template strand. The growing RNA chain dissociates from the original template DNA strand and hybridizes with the newly synthesized daughter DNA strand of the same sequence before RNA elongation resumes.

Head-on collisions are disadvantageous because (1) replication slows when DNA polymerase pauses, and (2) dissociation of the RNA polymerase during the jump from one template strand to the other could abort the transcription process. Indeed, in many bacterial and phage genomes, the most heavily transcribed genes are oriented so that replication and transcription complexes move in the same direction. It remains to be seen whether a similar arrangement holds in eukaryotic genomes, which contain multiple replication origins and genes that are much larger than are prokaryotic genes.

fragment, thereby letting the transcription bubble relax to its normal size. The RNAP then reinitiates transcription from the +1 position.

RNA Polymerase Is Processive. Once the open complex has been formed, transcription proceeds without dissociation of the enzyme from the template. Processivity is accomplished without an obvious clamplike structure (e.g., the β clamp of *E. coli* DNA polymerase III; Fig. 25-16), although the RNAP itself apparently functions as a sliding clamp by binding tightly but flexibly to the DNA–RNA complex. In experiments in which the RNAP was immobilized and a magnetic bead was attached to the DNA, up to 180 rotations (representing nearly two thousand base pairs at 10.4 bp per turn) were observed before the polymerase slipped. Such processivity is essential, since genes are often thousands (in eukaryotes, sometimes millions) of nucleotides in length.

The tight association between RNAP and DNA and their multiple attachment sites may explain why a transcription complex does not completely dissociate from a DNA template even when transcription is interrupted by the DNA replication machinery proceeding along the same strand of DNA (see Box 26-1).

Transcription Is Rapid. In *E. coli,* the *in vivo* rate of transcription is 20 to 50 nucleotides per second at 37°C (but still several times slower than the DNA replication rate; Section 25-2C). The error frequency in RNA synthesis is one wrong base incorporated for every $\sim 10^4$ transcribed. This frequency, which is 10^4 to 10^6 times higher than that for DNA synthesis, is tolerable because most genes are repeatedly transcribed, because the genetic code contains numerous synonyms (Section 27-1C), and because amino acid substitutions in proteins are often functionally innocuous.

Once an RNAP molecule has initiated transcription and moved away from the promoter, another RNAP can follow suit. The synthesis of RNAs that are needed in large quantities, rRNAs, for example, is initiated as often as is sterically possible, about once per second. This gives rise to an

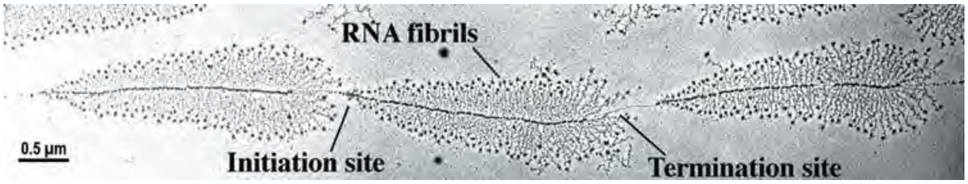

Figure 26-8 | An electron micrograph of three contiguous ribosomal genes undergoing transcription. The "arrowhead" structures result from the increasing lengths of the nascent RNA chains as the RNA polymerases synthesizing them move from the initiation site on the DNA to the termination site. [Courtesy of Ulrich Scheer, University of Würzburg, Germany.]

arrowhead appearance of the transcribed DNA (Fig. 26-8). mRNAs encoding proteins are generally synthesized at less frequent intervals, and there is enormous variation in the amounts of different polypeptides produced. For example, an *E. coli* cell may contain 10,000 copies of a ribosomal protein, whereas a regulatory protein may be present in only a few copies per cell. Many enzymes, particularly those involved in basic cellular "housekeeping" functions, are synthesized at a more or less constant rate; they are called **constitutive enzymes.** Other enzymes, termed **inducible enzymes,** are synthesized at rates that vary with the cell's circumstances. To a large extent, the regulation of gene expression relies on mechanisms that govern the rate of transcription, as we shall see in Section 28-2. The products of transcription also vary in their stabilities. Ribosomal RNA turns over much more slowly than mRNA, which is rapidly synthesized and rapidly degraded (sometimes so fast that the 5′ end of an mRNA is degraded before its 3′ end has been synthesized).

D | Transcription Terminates at Specific Sites

Electron micrographs such as Fig. 26-8 suggest that DNA contains specific sites at which transcription is terminated. The transcription termination sequences of many *E. coli* genes share two common features (Fig. 26-9*a*):

1. A series of 4 to 10 consecutive A · T base pairs, with the A's on the template strand. The transcribed RNA is terminated in or just past this sequence.
2. A G + C-rich region with a palindromic sequence that immediately precedes the series of A · T's.

The RNA transcript of this region can therefore form a self-complementary "hairpin" structure that is terminated by several U residues (Fig. 26-9*b*).

The structural stability of an RNA transcript at its terminator's G + C-rich hairpin and the weak base pairing of its oligo(U) tail to template DNA appear to be important factors in ensuring proper chain termination. The formation of the G + C-rich hairpin causes RNAP to pause for several seconds at the termination site. This probably induces a conformational change in the RNAP that permits the nontemplate DNA strand to displace the weakly bound oligo(U) tail from the template strand, thereby terminating transcription.

Despite the foregoing, experiments by Michael Chamberlin indicate that the RNA-terminator hairpin and U-rich 3′ tail do not function independently of their upstream and downstream flanking regions. Indeed, termi-

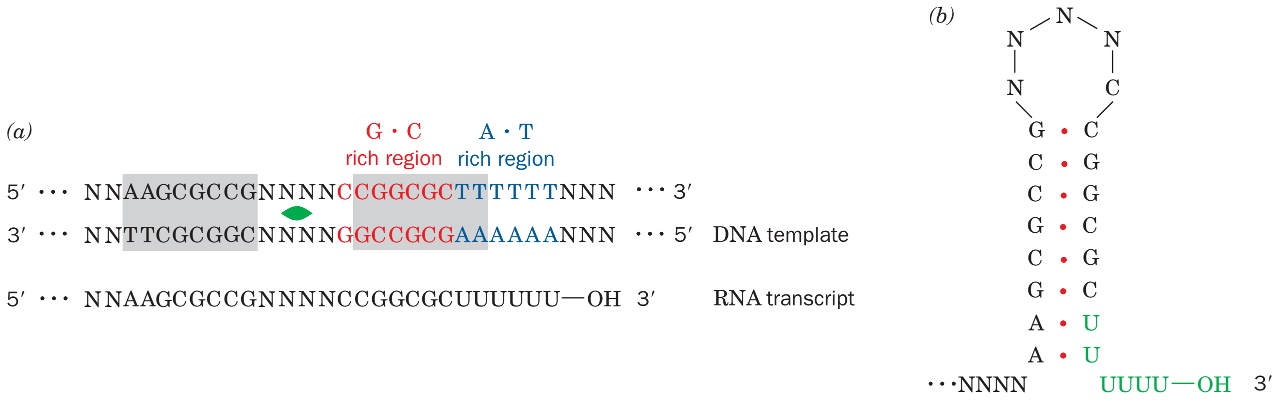

■ **Figure 26-9 | A hypothetical strong (efficient) *E. coli* terminator.** The base sequence was deduced from the sequences of several transcripts. (*a*) The DNA sequence together with its corresponding RNA. The A · T-rich and G · C-rich sequences are shown in blue and red, respectively. The twofold symmetry axis (*green symbol*) relates the flanking shaded segments that form an inverted repeat. (*b*) The RNA hairpin structure and poly(U) tail that triggers transcription termination. [After Pribnow, D., *in* Goldberger, R.F. (Ed.), *Biological Regulation and Development,* Vol. 1, p. 253, Plenum Press (1979).]

nators that lack a U-rich segment can be highly efficient when joined to the appropriate sequence immediately downstream from the termination site. Termination efficiency also varies with the concentrations of nucleoside triphosphates, with the level of supercoiling in the DNA template, with changes in the salt concentration, and with the sequence of the terminator. These results suggest that *termination is a complex multistep process.*

Termination Often Requires Rho Factor. The termination sequences described above induce the spontaneous termination of transcription. Other termination sites, however, lack any obvious similarities and are unable to form strong hairpins; *they require the action of a protein known as **Rho factor** to terminate transcription.* Rho factor, a hexamer of identical 419-residue subunits, enhances the termination efficiency of spontaneously terminating transcripts and induces termination of nonspontaneously terminating transcripts.

Several key observations have led to a model of Rho-dependent termination:

1. Rho factor is a helicase that catalyzes the unwinding of RNA–DNA and RNA–RNA double helices. This process is powered by the hydrolysis of ATP to ADP + P_i.
2. Genetic manipulations indicate that Rho-dependent termination requires a specific recognition sequence on the nascent (still being synthesized) RNA upstream of the termination site.

These observations suggest that Rho factor attaches to the RNA at its recognition sequence and then migrates along the RNA in the $5' \rightarrow 3'$ direction until it encounters an RNAP paused at the termination site (without the pause, Rho might not be able to overtake the RNAP). There, Rho unwinds the RNA–DNA duplex at the transcription bubble, thereby releasing the RNA transcript. Rho-terminated transcripts have 3′ ends that typically vary over a range of ~50 nt. This suggests that Rho gradually pries the RNA away from its template DNA rather than liberating the RNA at a specific point.

Each Rho subunit consists of two domains: Its N-terminal domain binds single-stranded polynucleotides and its C-terminal domain, which is homologous to the α and β subunits of the F_1-ATPase (Section 18-3B),

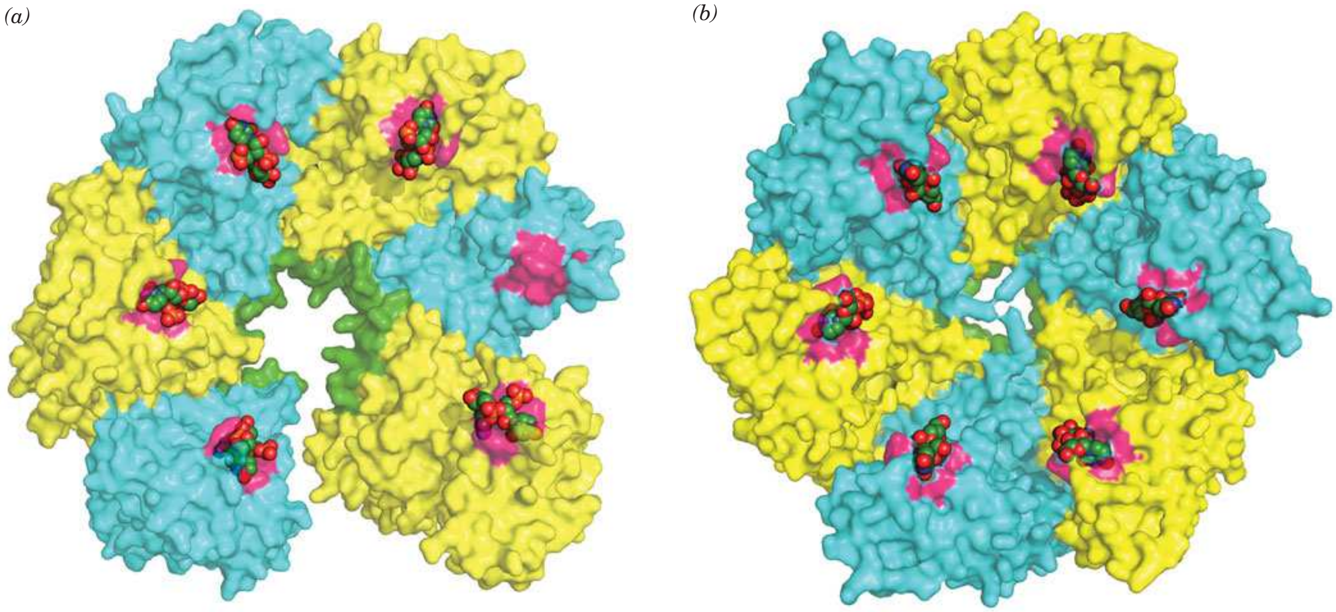

Figure 26-10 | X-Ray structures of *E. coli* Rho factor in its complexes with RNA. (*a*) A complex with an 8-nt RNA, $(CU)_4$. The semitransparent surface diagram of the Rho hexamer, with its subunits alternately colored yellow and cyan, is viewed from the top of the lock washer–shaped helix. The primary and secondary RNA-binding sites are magenta and green. The RNA, which is drawn in space-filling form and colored according atom type (C green, N blue, O red, and P orange) is only partially visible in the X-ray structure. It binds to the primary RNA-binding sites. (*b*) A complex with a 30-nt RNA, $(CU)_{15}$, viewed and colored as in Part *a*. In this complex, the six Rho subunits form a closed ring in which the subunits alternate in their conformations. [Based on X-ray structures by Emmanuel Skordalakes and James Berger, University of California at Berkeley. PDBids 1PVO and 2HT1.]

binds an NTP. The X-ray structure of Rho in complex with AMPPNP and an 8-nt RNA (Fig. 26-10*a*) reveals that Rho forms a hexameric lock washer–shaped helix that is 120 Å in diameter with an ~30-Å-diameter central hole and whose first and sixth subunits are separated by a 12-Å gap and a rise of 45 Å along the helix axis. The RNA binds along the interior of the helix to the so-called primary RNA binding sites on the N-terminal domains and to the so-called secondary RNA binding sites on the C-terminal domains. This X-ray structure represents an open state that is poised to bind mRNA that has entered its central cavity through the notch. However, in the X-ray structure of Rho in complex with a 30-nt RNA (Fig. 26-10*b*), the protein's six subunits have formed a closed ring in which alternate subunits have different conformations, that is, it is a trimer of dimers. This suggests that cycles of ATP hydrolysis causes the subunits to alternate in their conformations in a way that propels Rho along its bound RNA in the 5′ → 3′ direction.

CHECK YOUR UNDERSTANDING

Compare DNA and RNA polymerases with respect to structure, substrates, mechanism, error rate, and template specificity.
Why is it hard to precisely define "gene"?
What is the significance of the different DNA-binding properties of prokaryotic RNA polymerase core enzyme and holoenzyme?
Explain why a single gene can quickly give rise to many copies of its gene products (RNA or protein).
Describe how transcription is terminated with and without Rho factor.

2 Transcription in Eukaryotes

LEARNING OBJECTIVES

- Understand that eukaryotes use at least three RNA polymerases.
- Understand how the structure of RNAP II reflects its ability to carry out DNA-directed RNA synthesis.
- Understand that the three RNA polymerases recognize different and sometimes highly variable promoter sequences.
- Understand that a set of general transcription factors are required to initiate transcription in eukaryotes.

Although the fundamental principles of transcription are similar in prokaryotes and eukaryotes, *eukaryotic transcription is distinguished by having multiple RNAPs and by relatively complicated control sequences*. Moreover, the eukaryotic transcription machinery, as we shall see, is far more complex than that of prokaryotes, requiring well over 100 polypeptides that form assemblies with molecular masses of several million daltons to recognize the control sequences and initiate transcription.

A | Eukaryotes Have Several RNA Polymerases

Eukaryotic nuclei contain three distinct types of RNA polymerase that differ in the RNAs they synthesize:

1. **RNA polymerase I (RNAP I),** which is located in the **nucleoli** (dark-staining nuclear bodies where ribosomes are assembled; Fig. 1-8), synthesizes the precursors of most rRNAs.
2. **RNA polymerase II (RNAP II),** which occurs in the nucleoplasm, synthesizes the mRNA precursors.
3. **RNA polymerase III (RNAP III),** which also occurs in the nucleoplasm, synthesizes the precursors of 5S rRNA, the tRNAs, and a variety of other small nuclear and cytosolic RNAs.

In addition to these nuclear enzymes, eukaryotic cells contain separate mitochondrial and (in plants) chloroplast RNAPs. The essential function of RNAPs in all cells makes them attractive targets for antibiotics and other drugs (Box 26-2).

Eukaryotic RNAPs, which have molecular masses of as much as 600 kD, have considerably greater subunit complexity than the prokaryotic enzymes. Each eukaryotic RNAP contains two nonidentical "large" (>120 kD) subunits, which are homologs of the prokaryotic β and β′ subunits, and an array of up to 13 different "small" (<50 kD) subunits, two of which are homologs of the prokaryotic α subunit and one of which is a homolog of the ω subunit. Five of the small subunits, including the ω homolog, are identical in all three eukaryotic enzymes, and the α homologs are identical in RNAPs I and III.

In a crystallographic tour de force, Roger Kornberg determined the X-ray structure of yeast RNAP II (Fig. 26-11). This enzyme, as expected, resembles *Taq* RNAP (Fig. 26-2) in its overall crab claw–like shape and in

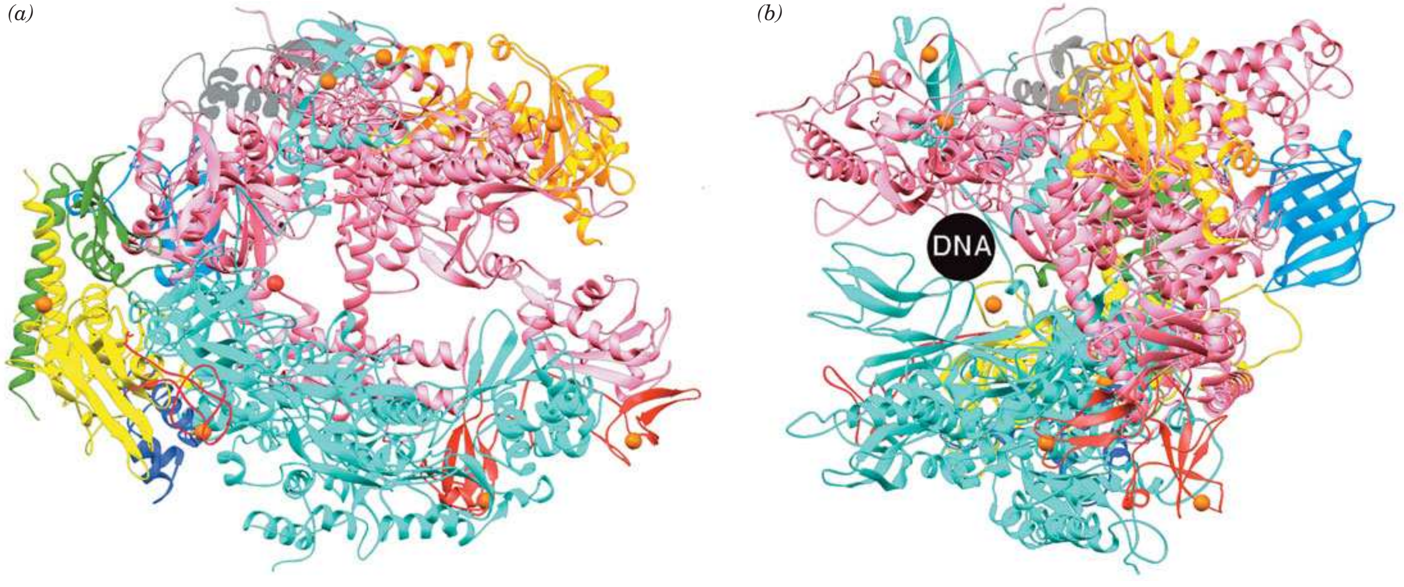

Figure 26-11 | X-Ray structure of yeast RNA polymerase II. (*a*) The enzyme is oriented similarly to the *Taq* RNAP in Fig. 26-2, and subunits that are homologous to those in *Taq* RNA polymerase are given the same colors as in Fig. 26-2. The position of an active site Mg^{2+} ion is marked by a red sphere, and eight Zn^{2+} ions are represented by orange spheres. Two nonessential polymerase subunits and the C-terminus of the β′ homolog are not visible in this structure. (*b*) View of the enzyme from the right of Part *a*, showing the DNA-binding cleft. The circle has the approximate diameter of B-DNA. [Based on an X-ray structure by Roger Kornberg, Stanford University. PDBid 1I50.]

BOX 26-2 BIOCHEMISTRY IN HEALTH AND DISEASE

Inhibitors of Transcription

A wide variety of compounds inhibit transcription in prokaryotes and eukaryotes. These agents are therefore toxic to susceptible organisms; that is, they function as antibiotics. Such compounds are also useful research tools since they arrest the transcription process at well-defined points.

Two related antibiotics, **rifamycin B,** which is produced by *Streptomyces mediterranei,* and its semisynthetic derivative **rifampicin,**

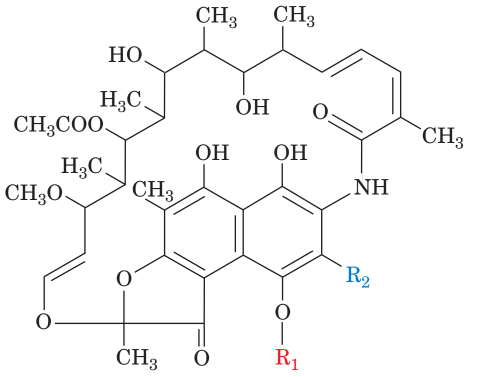

Rifamycin B $R_1 = CH_2COO^-$; $R_2 = H$

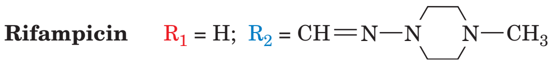

Rifampicin $R_1 = H$; $R_2 = CH{=}N{-}N\qquad N{-}CH_3$

specifically inhibit transcription by prokaryotic but not eukaryotic RNA polymerases. The selectivity and high potency of rifampicin (2×10^{-8} M results in 50% inhibition of bacterial RNA polymerase) makes it a medically useful bactericidal agent. Rifamycins inhibit neither the binding of RNA polymerase to the promoter nor the formation of the first phosphodiester bonds, but they prevent further chain elongation. The inactivated RNA polymerase remains bound to the promoter, thereby blocking initiation by uninhibited enzyme. Once RNA chain initiation has occurred, however, rifamycins have no effect on the subsequent elongation process. The rifamycins can therefore be used in the laboratory to dissect transcriptional initiation and elongation.

Actinomycin D (*at right*)**,** a useful antineoplastic (anticancer) agent produced by *Streptomyces antibioticus,* tightly binds to duplex DNA and, in doing so, strongly inhibits both transcription and DNA replication, presumably by interfering with the passage of RNA and DNA polymerases. The X-ray structure of actinomycin D in complex with an 8-bp DNA is shown opposite as two vertically stacked complexes in space-filling form, with the DNA's sugar–phosphate backbone yellow, its bases white, and the actinomycins colored according to atom type (C green, N blue, and O red). The actinomycin's phenoxazone ring system (which is visible in the lower molecule) intercalates between the DNA's base pairs, thereby unwinding the DNA helix by 23° and separating the neighboring

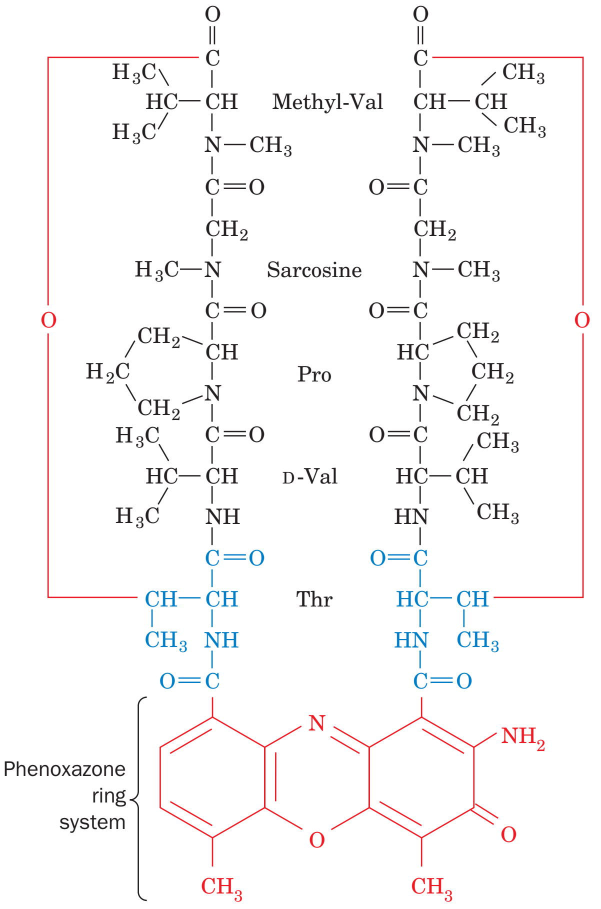

Actinomycin D

the positions and core folds of their homologous subunits, although RNAP II is somewhat larger and has several subunits that have no counterpart in *Taq* RNAP. RNAP II binds two Mg^{2+} ions at its active site in the vicinity of five conserved acidic residues, which suggests that RNAPs catalyze RNA elongation via a two-metal ion mechanism similar to that employed by DNA polymerases (Section 25-2A). As is the case with *Taq* RNAP, the surface of RNAP II is almost entirely negatively charged except for the DNA-binding cleft and the region about the active site, which are positively charged.

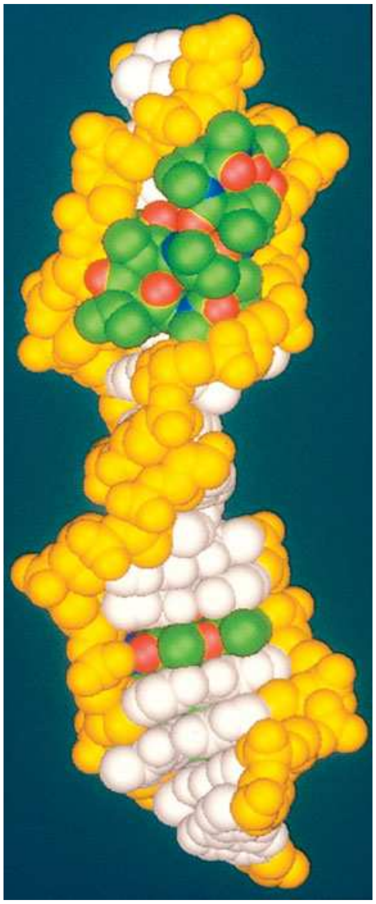

[Structure of actinomycin D–DNA complex based on an X-ray structure by Fusao Takusagawa, University of Kansas. PDBid 172D.]

base pairs by 7.0 Å. Actinomycin's chemically identical cyclic **depsipeptides** (which are seen in the upper molecule; depsipeptides have both peptide bonds and ester linkages) extend in opposite directions from the intercalation site along the minor groove of the DNA. Other intercalation agents, including ethidium and proflavin (Section 24-3B), also inhibit nucleic acid synthesis, presumably by similar mechanisms.

The poisonous mushroom *Amanita phalloides* (death cap), which is responsible for the majority of fatal mushroom poisonings in Europe, contains several types of toxic substances, including a series of unusual bicyclic octapeptides known as **amatoxins. α-Amanitin,**

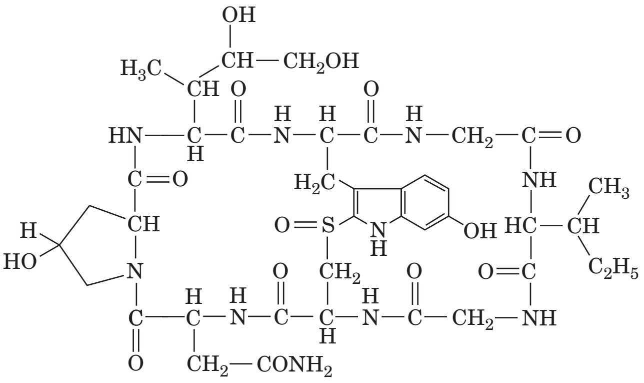

α-Amanitin

which is representative of the amatoxins, forms a tight 1:1 complex with RNAP II ($K = 10^{-8}$ M) and a looser one with RNAP III ($K = 10^{-6}$ M) so as to specifically block their elongation steps. The X-ray structure of RNAP II in complex with α-amanitin reveals that α-amanitin binds in the funnel beneath the protein's bridge helix (Fig. 26-12b) such that it interacts almost exclusively with the residues of the bridge helix and the adjacent part of Rpb1. The α-amanitin binding site is too far away from the enzyme active site to directly interfere with NTP entry or RNA synthesis, consistent with the observation that α-amanitin does not influence the affinity of RNAP II for NTPs. Most probably, α-amanitin binding impedes the conformational change of the bridge helix postulated to motivate the RNAP translocation step (Section 26-2A), which further supports this mechanism. RNAP I as well as mitochondrial, chloroplast, and prokaryotic RNA polymerases are insensitive to α-amanitin.

Despite the amatoxins' high toxicity (5–6 mg, contained in ~40 g of fresh mushrooms, is sufficient to kill a human adult), they act slowly. Death, usually from liver dysfunction, occurs no earlier than several days after mushroom ingestion (and after recovery from the effects of other mushroom toxins). This, in part, reflects the slow turnover rate of eukaryotic mRNAs and proteins.

RNAP II's **Rpb1** subunit (pink in Fig. 26-11), the homolog of the β′ subunit in prokaryotic RNAPs, has an extraordinary C-terminal domain **(CTD).** In mammals, the CTD contains 52 highly conserved repeats with the consensus sequence Pro-Thr-Ser-Pro-Ser-Tyr-Ser (26 repeats in yeast, with other eukaryotes having intermediate values). As many as 50 Ser residues in this hydroxyl-rich protein segment are subject to reversible phosphorylation. RNAP II initiates transcription only when the CTD is unphosphorylated but commences elongation only after the CTD has been phosphorylated. Charge–charge repulsions between nearby phosphate groups probably cause a highly phosphorylated CTD to project as far as 500 Å from the globular portion of the polymerase. As we shall see, the phosphorylated CTD provides the binding sites for numerous protein factors that are essential for transcription.

The RNA Polymerase Structure Explains Its Function. To produce a snapshot of RNAP II in action, Kornberg incubated the enzyme with a dsDNA molecule bearing a 3′ single-stranded tail (the template strand) together with all the NTP substrates except UTP. As a consequence, the polymerase synthesized a short (14-nt) RNA strand before pausing at the first template A residue (when the crystals of this complex were soaked in UTP, transcription resumed, demonstrating that the complex was active). The X-ray structure and a cutaway diagram of this paused RNAP II are shown in Fig. 26-12.

In the RNAP–DNA–RNA complex, a massive (~50-kD) portion of the **Rpb2** subunit (the β homolog; cyan in Fig. 26-11), named the "clamp," has swung downward over the DNA to trap it in the cleft, in large part accounting for the enzyme's essentially infinite processivity.

The DNA unwinds by three nucleotides before entering the active site (which is contained on Rpb1). Past this point, however, a portion of Rpb2 dubbed the "wall" directs the template strand out of the cleft in an ~90° turn. As a consequence, the template base at the active site (+1) points toward the floor of the active site where it can be read out by the polymerase. This base is paired with the ribonucleotide at the 3′ end of the RNA, which is positioned above a "pore" at the end of a "funnel" to the

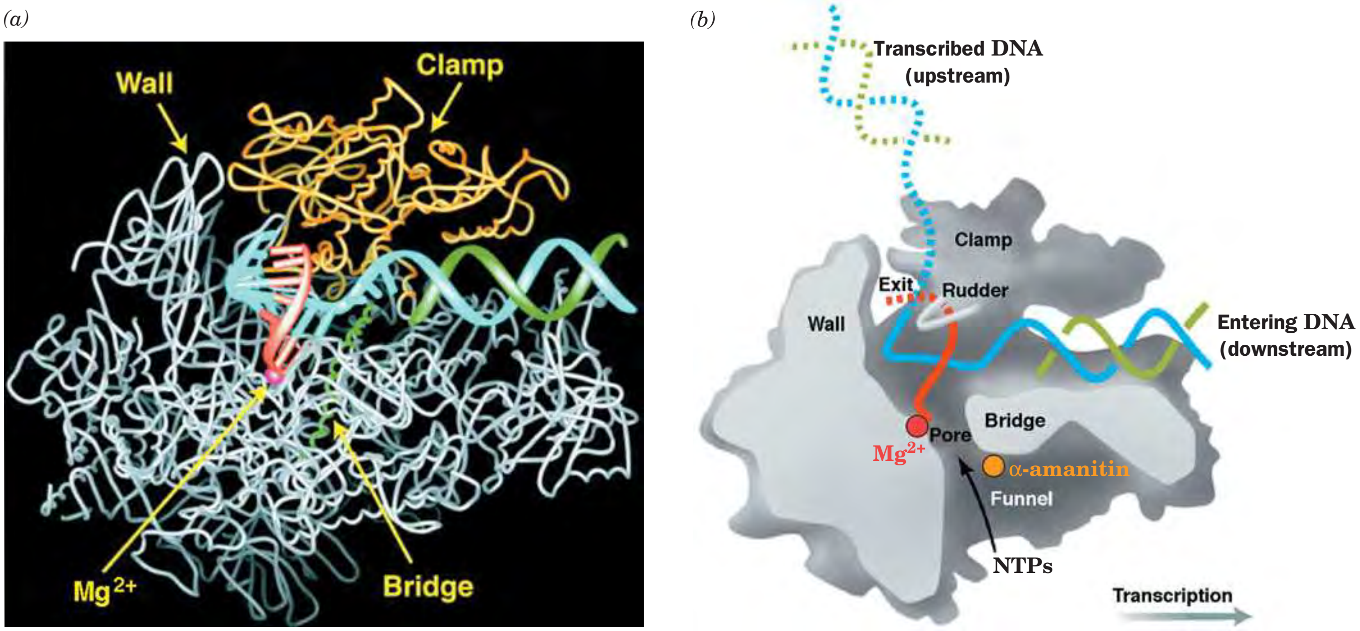

Figure 26-12 | The RNA polymerase II elongation complex. (*a*) X-Ray structure of the complex as viewed from the bottom of Fig. 26-11*a* (portions of Rpb2 that form the near side of the cleft have been removed to expose the bound RNA · DNA complex). The protein is represented by its backbone in which the clamp, which is closed over the downstream DNA duplex, is yellow, the bridge helix is green, and the remaining portions of the protein are gray. The template DNA strand (*cyan*), the nontemplate DNA strand (*green*), and the newly synthesized RNA (*red*) are drawn with their well-ordered portions in ladder form and their less ordered portions in backbone form. An active site Mg^{2+} ion is represented by a magenta sphere. (*b*) Cutaway diagram of the transcribing complex in Part *a* in which the cut surfaces of the protein are light gray, its remaining surfaces are darker gray, and several of its functionally important structural features are labeled. The DNA, RNA, and active site Mg^{2+} ion are colored as in Part *a* with portions of the DNA and RNA that are not visible in the X-ray structure represented by dashed lines. α-Amanitin (*orange ball*) is discussed in Box 26-2. [Modified from diagrams by Roger Kornberg, Stanford University. PDBid 1I6H.] **See Interactive Exercise 50.**

protein exterior through which NTPs presumably gain access to the otherwise sealed-off active site.

The hybrid helix adopts a nonstandard conformation intermediate between those of A- and B-DNAs, which is underwound relative to that in the X-ray structure of an RNA·DNA hybrid helix alone (Fig. 24-4). Nearly all contacts that the protein makes with the RNA and DNA are to their sugar–phosphate backbones; none are with the edges of their bases. The specificity of the enzyme for a ribonucleotide rather than a deoxyribonucleotide appears due to the enzyme's recognition of both the incoming ribose sugar and the RNA·DNA hybrid helix. After about one turn of hybrid helix, a loop extending from the clamp known as the "rudder" separates the RNA and template DNA strands, thereby permitting the DNA double helix to re-form as it exits the enzyme (although the unpaired 5′ tail of the nontemplate strand and the 3′ tail of the template strand are disordered in the X-ray structure).

How does RNAP translocate its bound DNA–RNA assembly at the end of each catalytic cycle? A highly conserved helical segment of Rpb1 called the "bridge" (because it bridges the two pincers forming the enzyme's cleft) nonspecifically contacts the template DNA base at the +1 position. The bridge is straight in the X-ray structures of RNAP II (Figs. 26-11*a* and 26-12*a*) but bent in the X-ray structure of *Taq* RNAP (Fig. 26-2). If the bridge helix, in fact, alternates between its straight and bent conformations, it would move by 3 to 4 Å. Kornberg has therefore speculated that translocation occurs through the bending of the bridge helix so as to push the paired nucleotides at position +1 to position −1. The recovery of the bridge helix to its straight conformation would then yield an empty site at position +1 for entry of the next NTP, thereby preparing the enzyme for a new round of nucleotide addition.

RNAP II selects its substrate ribonucleotide through a two-stage process. The incoming NTP first binds to the so-called E (for entry) site (Fig. 26-13), which exhibits no selectivity for the identity of its base. The NTP then pivots

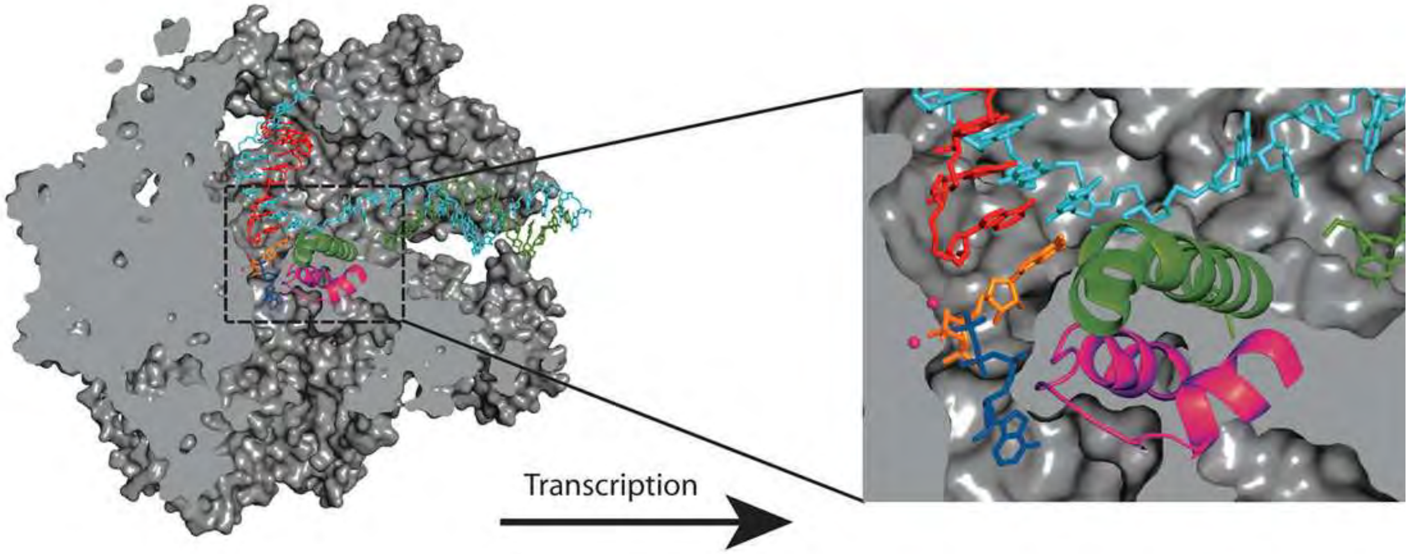

Figure 26-13 | The A and E sites and the trigger loop in RNA polymerase II. A cutaway view of the transcribing complex viewed as in Figs. 26-11*a* and 26-12. The template DNA, nontemplate DNA, newly transcribed RNA, GTP in the A site, and ATP in the E site are cyan, green, red, orange, and blue, respectively. The trigger loop is magenta, the bridge helix is green, and the two Mg^{2+} ions at the active site are represented by magenta spheres. The RNAP II surface is gray. [Courtesy of Dong Wang and Roger Kornberg, Stanford University. PDBid 2E2H.]

to enter the A (for addition) site, which accepts only an NTP that forms a Watson–Crick base pair with the template base in the +1 position. This process is mediated by the RNAP's so-called trigger loop, which swings in beneath the correctly base-paired NTP in the A site to form an extensive hydrogen-bonded network involving both the NTP and other portions of the RNAP, interactions that acutely discriminate against dNTPs.

RNAP II, like DNA polymerase I, edits its work. If a deoxynucleotide or a mispaired ribonucleotide is mistakenly incorporated into RNA, the DNA–RNA hybrid helix becomes distorted. This causes polymerization to cease, and the newly synthesized RNA backs out of the active site through the pore and funnel by which ribonucleotides enter the active site. The exposed RNA containing the error is then trimmed by a nuclease, which excises between 1 and 11 residues. Transcription may resume if the 3′ end of the truncated transcript is then repositioned at the active site.

B | Each Polymerase Recognizes a Different Type of Promoter

In eukaryotes, RNAP does not include a removable σ factor. Instead, a number of accessory proteins identify promoters and recruit RNAP to the transcription start site (as described more fully in Section 26-2C). As expected, eukaryotic promoters are more complex and diverse than prokaryotic promoters. In addition, the three eukaryotic RNAPs recognize different types of promoters.

Mammalian RNA Polymerase I Has a Bipartite Promoter. Both prokaryotic and eukaryotic genomes contain multiple copies of their rRNA genes in order to meet the enormous demand for these rRNAs (which comprise, e.g., 80% of an *E. coli* cell's RNA content). Since the numerous rRNA genes in a given eukaryotic cell have essentially identical sequences, its RNAP I recognizes only one promoter. Yet, in contrast to RNAP II and III promoters, RNAP I promoters are species specific; that is, an RNAP I recognizes only its own promoter and those of closely related species.

RNAP I promoters were identified by determining how the transcription rate of an rRNA gene is affected by a series of increasingly longer deletions approaching its transcription start site from either its upstream or its downstream side. Such studies have indicated, for example, that mammalian RNAP I requires a so-called **core promoter element,** which spans positions −31 to +6 and hence overlaps the transcribed region. However, efficient transcription also requires an **upstream promoter element,** which is located between residues −187 and −107. These elements, which are G + C-rich and ~85% identical, are bound by specific transcription factors which then recruit RNAP I to the transcription start site.

RNA Polymerase II Promoters Are Complex and Diverse. The promoters recognized by RNAP II are considerably longer and more diverse than those of prokaryotic genes. The structural genes expressed in all tissues (the housekeeping genes, which are thought to be constitutively transcribed) have GC-rich stretches of DNA located upstream from their transcription start sites. *These CpG islands (Box 25-4) function analogously to prokaryotic promoters.* On the other hand, structural genes that are selectively expressed in one or a few cell types often lack these GC-rich sequences. Instead, *they contain a core promoter of 40 to 50 nt that includes the transcription start site.* Within the core promoter for a given gene are one or more conserved elements that act—for the most part in a cooperative fashion—to direct transcription initiation.

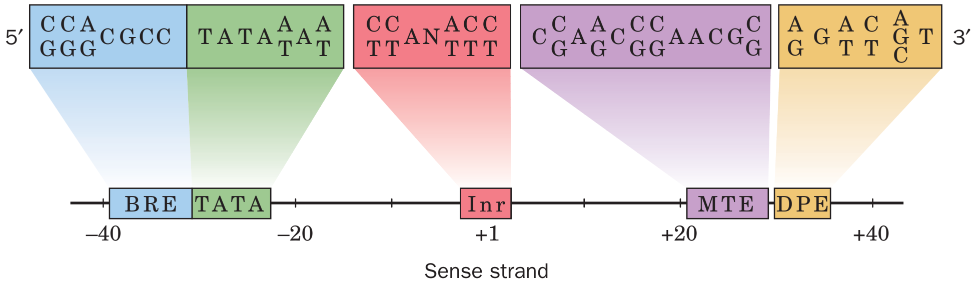

Figure 26-14 | Some core promoter sequences for RNA polymerase II. The consensus sequence of each element is given (some positions can accommodate two or more nucleotides; N represents any nucleotide). The relative positions of the elements are shown, with +1 representing the transcription start site. Note that a specific core promoter may contain all, some, or none of these motifs. The **BRE (TFII*B* *r*ecognition *e*lement)** is an upstream extension of the TATA box. The **DPE (*d*ownstream core *p*romoter *e*lement)** and the **MTE (*m*otif *t*en *e*lement)** must be accompanied by an Inr.

Among the best-known core promoter elements is the **TATA box,** an AT-rich sequence located 25 to 30 bp upstream from the transcription start site. The TATA box (consensus sequence $\mathrm{TATA}{}^{\mathrm{A}}_{\mathrm{T}}\mathrm{A}{}^{\mathrm{A}}_{\mathrm{T}}$) resembles the −10 region of a prokaryotic promoter (TATAAT), although it differs in its location relative to the transcription start site (−27 versus −10). Around two-thirds of protein-encoding genes lack a TATA box, but approximately half have a conserved 7-nt **Inr (initiator) element** that includes the initiating (+1) nucleotide. The consensus sequences and relative positions of several core promoter elements are shown in Fig. 26-14. Most of these elements have been identified from their conservation in many genes from different eukaryotic species, and their participation in RNAP II-directed transcription has been verified experimentally by mutating their sequences and/or positions and by introducing them into genes whose original core promoter elements had been deleted. None of the core promoter elements occurs in all promoters, although some general patterns are apparent; for example, core promoters that lack a TATA box use MTE or DPE, and vice versa. All of the core promoter elements, either singly or as sets, interact with their corresponding protein factors that in turn recruit RNAP II to the initiation site (Section 26-2C).

The gene region extending between about −50 and −110 also contains promoter elements. For instance, many eukaryotic structural genes have a conserved consensus sequence of CCAAT (the **CCAAT box**) located between about −70 and −90 whose alteration greatly reduces the gene's transcription rate. Evidently, *the sequences upstream of the core promoter constitute additional DNA-binding sites for proteins involved in transcription initiation.*

Enhancers Are Transcriptional Activators That Can Have Variable Positions and Orientations. *Perhaps the most surprising aspect of eukaryotic transcriptional control elements is that some of them need not have fixed positions and orientations relative to their corresponding transcribed sequences.* For example, the genome of **simian virus 40 (SV40),** in which such elements were first discovered, contains two repeated sequences of 72 bp each that are located upstream from the promoter for early gene expression. Transcription is unaffected if one of the repeats is deleted but is nearly eliminated when both are absent. The analysis of a series of SV40 mutants containing only one of the repeats demonstrated that its ability to stimulate transcription from its corresponding promoter is all but independent of its position and orientation. Indeed, transcription is unimpaired when this segment is several thousand base pairs upstream or downstream from the transcription start site. Gene segments with such properties are named **enhancers** to indicate that they differ from promoters, which are site-specific and strand-specific regarding transcription initiation.

Enhancers occur in cellular genes as well as eukaryotic viruses and are required for the full activities of their cognate promoters. Rather than interacting with RNAP II directly, *enhancers are recognized by specific transcription factors that stimulate RNAP II to bind to the corresponding but distant promoter.* This requires that the DNA between the enhancer and promoter loop around so that the transcription factor can simultaneously contact the enhancer and RNAP II at the promoter. Most cellular enhancers are associated with genes that are selectively expressed in specific tissues. It therefore seems, as we discuss in Section 28-3B, that *enhancers mediate much of the selective gene expression in eukaryotes.*

RNA Polymerase III Promoters Can Be Located Downstream from Their Transcription Start Sites. *The promoters of some genes transcribed by RNAP III are located entirely within the genes' transcribed regions.* In a gene for the 5S RNA of *Xenopus borealis,* deletions of base sequences that start from outside one or the other end of the transcribed portion of the gene prevent transcription only if they extend into the segment between nucleotides +40 and +80. This portion of the gene is effective as a promoter because it contains the binding site for a transcription factor that stimulates upstream binding of RNAP III. Further studies have shown, however, that the promoters of other RNAP III–transcribed genes lie entirely upstream of their start sites. These upstream sites also bind transcription factors that recruit RNAP III.

C | Transcription Factors Are Required to Initiate Transcription

Differentiated eukaryotic cells possess a remarkable capacity for the selective expression of specific genes. The synthesis rates of a particular protein in two cells of the same organism may differ by as much as a factor of 10^9. Thus, for example, reticulocytes (immature red blood cells) synthesize large amounts of hemoglobin but no detectable insulin, whereas the pancreatic β cells produce large quantities of insulin but no hemoglobin. In contrast, prokaryotic systems generally exhibit no more than a thousandfold range in their transcription rates so that at least a few copies of all the proteins they encode are present in any cell. Nevertheless, *the basic mechanism for initiating transcription of structural genes is the same in eukaryotes and prokaryotes: Protein factors bind selectively to the promoter regions of DNA.* With class II promoters (those transcribed by RNAP II), a complex of at least six **general transcription factors (GTFs;** Table 26-1) operate as a formal equivalent of a prokaryotic σ factor. The structures of several eukaryotic transcription factors are described in Section 24-4C.

The six GTFs, which are highly conserved from yeast to humans, are required for the synthesis of all mRNAs, even those with strong promoters. The GTFs allow a low (basal) level of transcription that can be augmented by the participation of other gene-specific factors. We will examine the action of some of those other proteins in Section 28-3. The GTFs, whose names begin with TF (for transcription factor) followed by the Roman numeral II to indicate that they are involved in transcription by RNAP II, combine with the enzyme and promoter DNA in an ordered pathway to form a **preinitiation complex (PIC).**

Table 26-1 Properties and Functions of the Eukaryotic General Transcription Factors

Factor	Number of Subunits	Mass (kD)[a]	Function
TFIID			
TBP	1	27	Bending TATA box DNA around TFIIB and RNAP II
TAFs	14	749	Promoter recognition
TFIIA	2	46	Stabilizes binding of TBP on DNA
TFIIB	1	38	Start site determination
TFIIE	2	92	Couples RNAP II–promoter interaction to recruitment of TFIIH
TFIIF	3	156	Interaction with nontemplate DNA strand
TFIIH	9	525	Promoter opening and RNAP II phosphorylation

[a] Mass data are for yeast proteins.

Source: Mainly Bushnell, D.A., Westover, K.D., Davis, R.E., and Kornberg, R.D., *Science* **303,** 983 (2004).

PIC Formation Often Begins with TATA-Binding Protein Binding to the TATA Box. As indicated in Section 26-2B, the promoters of many eukaryotic structural genes contain a TATA box at position −27. The GTFs are targeted to this and other sequences that make up the core promoter. The first transcription factor to bind to TATA box–containing promoters is the **TATA-binding protein (TBP),** which as its name indicates, binds to the TATA box and thereby helps identify the transcription start site. TBP is subsequently joined on the promoter by additional subunits to form the ∼775-kD multisubunit complex **TFIID.**

The highly conserved C-terminal domain of TBP contains two ∼40% identical direct repeats of 66 residues separated by a highly basic segment. Its X-ray structure, which was independently determined by Roger Kornberg and Stephen Burley, reveals a saddle-shaped molecule that consists of two structurally similar domains arranged with pseudo-twofold symmetry (Fig. 26-15*a*). TBP's structure suggests that it could fit snugly astride an

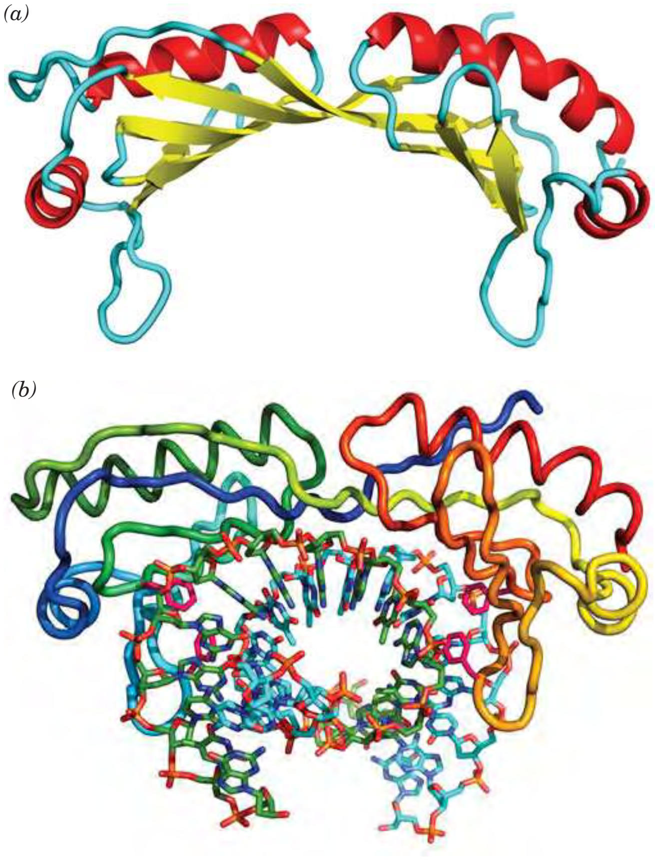

Figure 26-15 | **X-Ray structures of TATA-binding protein (TBP).** (*a*) A ribbon diagram of yeast TBP in the absence of DNA, in which α helices are red, β strands are yellow, and the remainder of the polypeptide backbone is cyan. The protein's pseudo-twofold axis of symmetry is vertical. [Based on an X-ray structure by Roger Kornberg, Stanford University. PDBid 1TBP.] (*b*) The structure of human TBP in complex with a 16-bp TATA box–containing duplex DNA. The DNA, which is largely in the B form, is drawn in stick form and colored according to atom type with sense strand C green, antisense strand C cyan, N blue, O red, and P orange. It enters its binding site with the 5′ end of the sense strand on the right and exits on the left with its helix axis nearly perpendicular to the page. The protein is drawn in worm form colored in rainbow order from its N-terminus (*blue*) to its C-terminus (*red*). The side chains of Phe residues 193, 210, 284, and 301, which induce sharp kinks in the DNA, are drawn in stick form (*magenta*). Between the kinks, which are located at each end of the TATA box, the DNA is partially unwound with the protein's eight-stranded β sheet inserted into the DNA's greatly widened minor groove. The TBP does not contact the DNA's major groove. [Based on an X-ray structure by Stephen Burley, Structural GenomiX, Inc., San Diego, California. PDBid 1CDW.] **See Interactive Exercise 51.**

undistorted B-DNA helix. However, the X-ray structures of TBP–DNA complexes, independently determined by Burley and Paul Sigler, reveal a quite different interaction. The DNA indeed binds to the concave surface of TBP but with its duplex axis nearly perpendicular rather than parallel to the saddle's cylindrical axis (Fig. 26-15*b*). The bound DNA is kinked by ~45° between the first two base pairs of the 7-bp TATA box and between its last base pair and the succeeding base pair, thereby assuming a crank-like shape. The TBP, which undergoes little conformational change on binding DNA, does so via hydrogen bonding and van der Waals interactions. The kinked and partially unwound DNA is stabilized by a wedge of two Phe side chains on each side of the saddle structure that pry apart the two base pairs flanking each kink from their minor groove sides. The bent conformation of DNA creates a stage for the assembly of other proteins to form the PIC.

TFIIA, TFIIB, and TAFs Interact with TBP and RNAP II. The other GTFs required for basal transcription assemble as is diagrammed in Fig. 26-16. The PIC requires, at a minimum, TBP, **TFIIB, TFIIE, TFIIF,** and **TFIIH.** TFIIB consists of two domains, an N-terminal domain **($TFIIB_N$),** which interacts with RNAP II, and a C-terminal domain **($TFIIB_C$),** which binds DNA and interacts with TBP. The X-ray structures of TFIIA–TBP–DNA

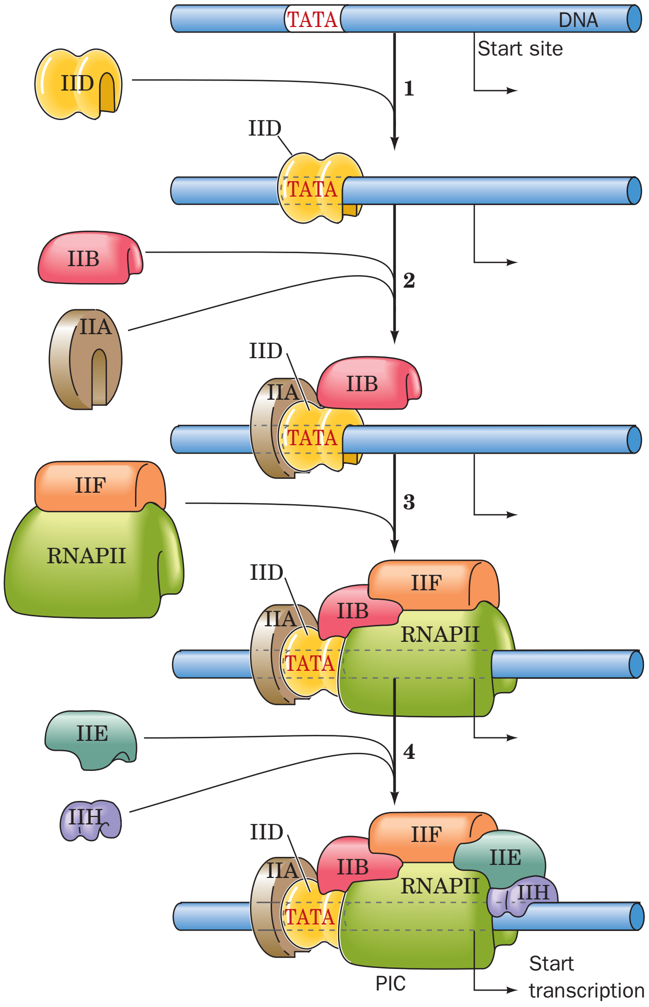

Figure 26-16 | The assembly of the preinitiation complex (PIC) on a TATA box–containing promoter. (**1**) The TBP component of TFIID binds to the TATA box of the promoter. (**2**) TFIIA and TFIIB then bind. (**3**) TFIIF binds to RNAP II and escorts it to the complex. (**4**) Finally, TFIIE and TFIIH are sequentially recruited, thereby completing the PIC. [After Zawel, L. and Reinberg, D., *Curr. Opin. Cell Biol.* **4,** 490 (1992).] **See Interactive Exercise 51.**

Figure 26-17 | Structural models for the interactions of TFIIB. (*a*) Model of the TFIIA–TBP–TFIIB_C–promoter complex based on the independently determined X-ray crystal structures of the TFIIA–TBP–promoter and TFIIB_C–TBP–promoter complexes. The DNA (*white sticks*) has been extended in both directions beyond the TATA box. The pseudosymmetrical TBP (*cyan and purple*), viewed from above, induces two sharp kinks in the DNA, giving it a cranklike shape. Both TFIIA (*yellow and green*) and TFIIB_C (*magenta and red*) interact with TBP, but each interacts with independent sites on the DNA. The transcription start site (+1) is at the left. [Courtesy of Stephen Burley, Structural GenomiX, Inc., San Diego, California. Based on PDBids 1YTF and 1VOL.] (*b*) Model of the TFIIB–TBP–RNAP II–promoter complex based on the X-ray structures of the TFIIB_N–RNAP II and TFIIB_C–TBP–promoter complexes. The view of the RNAP II is from the bottom of Fig. 26-12 after it has been turned 180° in the plane of the paper. The protein and the DNA are represented by their solvent-accessible surfaces with the protein colored gray except as indicated in the accompanying key, and the DNA colored according to atom type (C white, N blue, O red, and P yellow). The DNA has been extended by 20 bp at both ends. [Courtesy of Roger Kornberg, Stanford University. Based on PDBids 1R5U and 1VOL.]

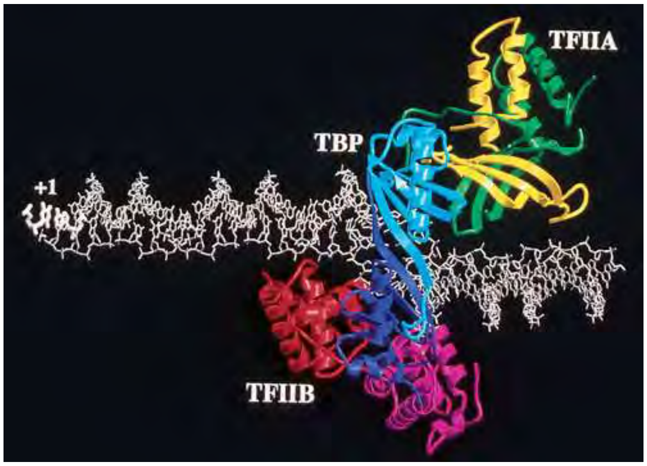

(*a*)

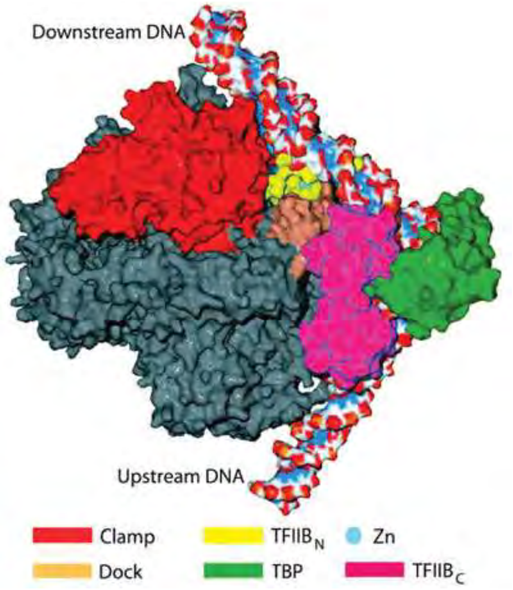

(*b*)

and TFIIB_C–TBP–DNA complexes have permitted the generation of a plausible model for the TFIIA–TFIIB_C–TBP–DNA complex (Fig. 26-17*a*). The three proteins bind to the DNA just upstream from the transcription start site, leaving ample room for additional proteins and RNAP II to bind. Since the pseudosymmetric TBP has been shown to bind to the TATA box in either orientation, it appears that base-specific interactions between TFIIB and the promoter function to position TFIIB to properly orient the TBP on the promoter.

The X-ray structure of the TFIIB_N–RNAP II complex, also determined by Kornberg, reveals that TFIIB_N contacts the "dock" domain of RNAP II near its RNA exit channel and that TFIIB_N inserts its "finger" domain into the active center of RNAP II. A model of the TFIIB–TBP–RNAP II–DNA complex based on this X-ray structure together with that of the TFIIB_C–TBP–DNA complex is shown in Fig. 26-17*b*.

The remaining components of TFIID, which are known as **TBP-associated factors (TAFs),** form a horseshoe-shaped complex to which TFIIA and TFIIB are bound (Fig. 26-18). TBP is located at the top of the cavity, and the promoter DNA passes through the cavity. Portions of 9 of the 14 known TAFs, which are highly conserved from yeast to humans, are homologous to nonlinker histones (Section 24-5A). Indeed, X-ray and other studies suggest that four of these TAFs associate to form a nucleosome-like heterooctamer. Nevertheless, it is unlikely that the DNA wraps around the TAFs as it does in a nucleosome because many of the histone residues

Figure 26-18 | Electron microscopy–based image of the human TFIID–TFIIA–TFIIB complex at 35 Å resolution. The complex consists of three domains, A, B, and C, arranged in a horseshoe shape roughly 200 Å wide, 135 Å high, and 110 Å thick. The red and green meshes indicate the positions of TFIIA and TFIIB as determined by comparison with the EM-based images of the TFIID–TFIIA complex and TFIID alone. The yellow mesh indicates the binding position of an anti-TBP antibody. [Courtesy of Eva Nogales, University of California at Berkeley.]

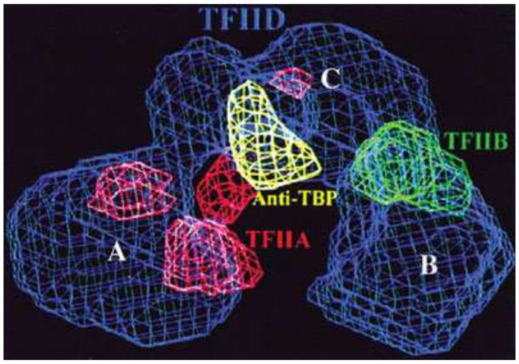

that make critical contacts with the DNA in the nucleosome have not been conserved in the histone-like TAFs.

In the final steps of PIC formation (Fig. 26-16), TFIIF recruits RNAP II to the promoter in a manner reminiscent of the way that σ factor interacts with bacterial RNAP. In fact, the second largest of TFIIF's three subunits is homologous to σ^{70}, the predominant bacterial σ factor, and, moreover, can specifically interact with bacterial RNAPs (although it does not participate in promoter recognition). Finally, TFIIE and TFIIH join the assembly. Once this complex has been assembled, the ATP-dependent helicase activity of TFIIH induces the formation of the open complex so that RNA synthesis can commence. Note that the yeast PIC, exclusive of the ~12-subunit, ~600-kD RNAP II, contains 32 subunits with an aggregate mass of 1633 kD (Table 26-1). Many of the proteins in the PIC are the targets of transcriptional regulators.

Promoters That Lack a TATA Box Also Bind TBP. Since the TATA-binding protein is a component of TFIID, a general transcription factor for RNAP II, how does the preinitiation complex form properly at TATA-less promoters? In many cases, the presence of the Inr element is sufficient to direct RNAP II to the correct start site. These systems require the participation of many of the same GTFs that initiate transcription from TATA box–containing promoters. Surprisingly, they also require TBP. This suggests that with TATA-less promoters, Inr recruits TFIID such that its component TBP binds to the −30 region in a sequence-nonspecific manner. Indeed, in Inr-containing promoters that also contain a TATA box, the two elements act synergistically to promote transcriptional initiation. Nevertheless, a mutant TBP that is defective in TATA box binding will support efficient transcription from some TATA-less promoters although not from others. This suggests that the former promoters do not require a stable interaction with TBP. Consequently, the scheme outlined in Fig. 26-16 should be taken as a flexible framework for RNAP II transcription initiation in eukaryotes, with the exact protein requirements depending on the nature of the promoter and the presence of additional protein factors.

TBP Is a Universal Transcription Factor. RNAP I and RNAP III require different sets of GTFs from each other and from RNAP II to initiate transcription at their respective promoters. This is not unexpected considering the very different organizations of these three classes of promoters (Section 26-2B). Indeed, the promoters recognized by RNAP I (class I promoters) and nearly all those recognized by RNAP III (class III promoters) lack TATA boxes. Thus, it came as a surprise when it was demonstrated that *TBP is required for initiation by both RNAP I and RNAP III.* TBP participates by combining with different sets of TAFs to form the GTFs **SLI** (with class I promoters) and **TFIIIB** (with class III promoters). As with certain class II TATA-less promoters, a TBP mutant that is defective for TATA box binding can still support *in vitro* transcriptional initiation by both RNAP I and RNAP III. Clearly, TBP, the only known universal transcription factor, is an unusually versatile protein.

Elongation Requires Different Transcription Factors. After RNAP II initiates RNA synthesis and successfully produces a short transcript, the transcription machinery undergoes a transition to the elongation mode.

The switch appears to involve phosphorylation of the C-terminal domain (CTD) of RNAP II's Rpb1 subunit. Phosphorylated RNAP II releases some of the transcription-initiating factors and advances beyond the promoter region. In fact, when RNAP II moves away from ("clears") the promoter, it leaves behind some GTFs, including TFIID. These proteins can reinitiate transcription by recruiting another RNAP II to the promoter. Consequently, *the first RNAP to transcribe a gene may act as a "pioneer" polymerase that helps pave the way for additional rounds of transcription.*

During elongation, a six-protein complex called **Elongator** binds to the phosphorylated CTD of Rpb1, taking the place of the jettisoned transcription factors. Although Elongator is not essential for transcription by RNAP II *in vitro,* its presence accelerates transcription. Interestingly, TFIIF and TFIIH remain associated with the polymerase during elongation. Well over a dozen other proteins are known to associate with an elongating RNAP II. Some of the proteins are involved in processing the nascent RNA, modifying the packaging of the DNA template, and terminating transcription.

Eukaryotes Lack Precise Transcription Termination Sites. The sequences signaling transcriptional termination in eukaryotes have not been identified. This is largely because the termination process is imprecise; that is, the primary transcripts of a given structural gene have heterogeneous 3′ sequences. *However, a precise termination site is not required because the transcript undergoes processing that includes endonucleolytic cleavage at a specific site* (see below). The endonuclease may act even while the polymerase is still transcribing, so RNA cleavage itself may signal the polymerase to stop.

CHECK YOUR UNDERSTANDING

What are the functions of the three eukaryotic RNA polymerases?
Explain the functions of RNAP II's CTD, clamp, wall, funnel, rudder, and bridge.
What are the advantages of having multiple types of promoters and enhancers?
Summarize the role of TBP in transcription initiation in eukaryotes.
Describe the assembly of the RNAP II preinitiation complex.

3 Posttranscriptional Processing

LEARNING OBJECTIVES

- Understand that eukaryotic mRNAs are modified by a 5′ cap and a 3′ poly(A) tail.
- Understand that eukaryotic genes include introns that must be spliced out by the action of snRNPs in the spliceosome.
- Understand that a single gene can generate several protein products through alternative mRNA splicing.
- Understand that prokaryotic and eukaryotic rRNA and tRNA precursors are variously processed by endonucleolytic cleavage, covalent modification, splicing, and nucleotide addition.

The immediate products of transcription, the **primary transcripts,** are not necessarily functional. In order to acquire biological activity, many of them must be specifically altered: (1) by the exo- and endonucleolytic removal of polynucleotide segments; (2) by appending nucleotide sequences to their 3′ and 5′ ends; and/or (3) by the modification of specific nucleotide residues. The three major classes of RNA—mRNA, rRNA, and tRNA—are altered in different ways in prokaryotes and in eukaryotes. In this section, we shall outline these **posttranscriptional modification** processes.

A Messenger RNAs Undergo 5′ Capping, Addition of a 3′ Tail, and Splicing

In prokaryotes, most primary mRNA transcripts are translated without further modification. Indeed, protein synthesis usually begins before transcription is complete (Section 27-4). In eukaryotes, however, mRNAs are synthesized in the cell nucleus, whereas translation occurs in the cytosol. Eukaryotic mRNA transcripts can therefore undergo extensive posttranscriptional processing while still in the nucleus.

Eukaryotic mRNAs Have 5′ Caps. *Eukaryotic mRNAs have a **cap** structure consisting of a **7-methylguanosine (m^7G)** residue joined to the*

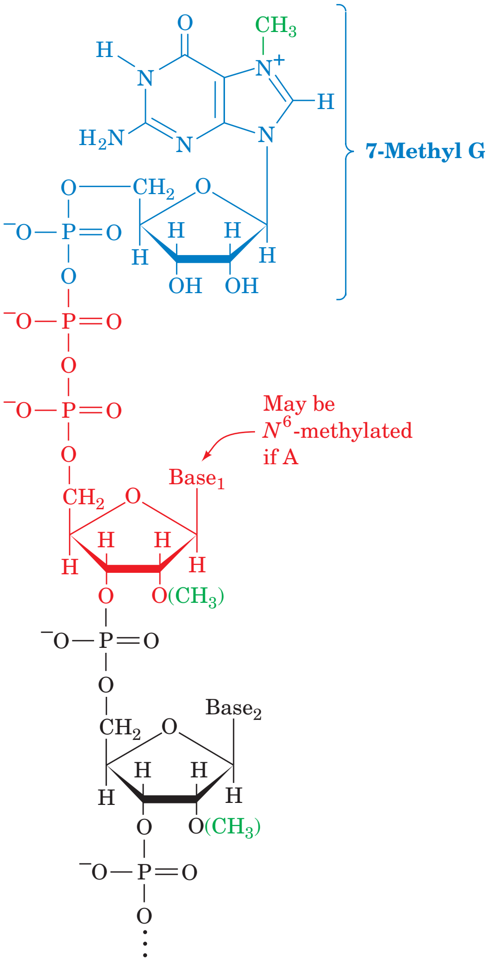

Figure 26-19 | Structure of the 5′ cap of eukaryotic mRNAs. A cap may be $O^{2'}$-methylated at the transcript's leading nucleoside (the predominant cap in multicellular organisms), at its first two nucleosides, or at neither of those positions (the predominant cap in unicellular eukaryotes). If the first nucleoside is adenosine (it is usually a purine), it may also be N^6-methylated.

transcript's initial (5′) nucleotide via a 5′–5′ triphosphate bridge (Fig. 26-19). The cap, which adds to the growing transcript when it is ~30 nt long, identifies the eukaryotic translation start site (Section 27-4A). Capping involves several enzymatic reactions: (1) the removal of the leading phosphate group from the mRNA's 5′ terminal triphosphate group by an **RNA triphosphatase;** (2) the guanylylation of the mRNA by **capping enzyme,** which requires GTP and yields the 5′–5′ triphosphate bridge and PP_i; and (3) the methylation of guanine by **guanine-7-methyltransferase,** in which the methyl group is supplied by *S*-adenosylmethionine (SAM). In addition, the cap may be $O^{2'}$-methylated at the first and second nucleotides of the transcript by a SAM-requiring **2′-*O*-methyltransferase.** Capping enzyme binds to RNAP II's phosphorylated CTD (Section 26-2A), and hence it appears that capping marks the completion of RNAP II's switch from transcription initiation to elongation. Capped mRNAs are resistant to 5′-exonucleolytic degradation.

Eukaryotic mRNAs Have Poly(A) Tails. Eukaryotic RNA transcripts have heterogeneous 3′ sequences because the transcription termination process is imprecise. *Mature eukaryotic mRNAs, however, have well-defined 3′ ends terminating in* ***poly(A) tails*** of ~250 nt (~80 nt in yeast). The poly(A) tails are enzymatically appended to the primary transcripts in two reactions:

1. A transcript is cleaved 15 to 25 nt past a highly conserved AAUAAA sequence and less than 50 nt before a less-conserved U-rich or GU-rich sequence. The precision of this cleavage reaction has apparently eliminated the need for accurate transcription termination.
2. The poly(A) tail is subsequently generated from ATP through the stepwise action of **poly(A) polymerase (PAP),** a template-independent RNA polymerase that elongates an mRNA primer with a free 3′-OH group. PAP is activated by **cleavage and polyadenylation specificity factor (CPSF)** when the latter protein recognizes the AAUAAA sequence. Once the poly(A) tail has grown to ~10 residues, the AAUAAA sequence is no longer required for further chain elongation. This suggests that CPSF becomes disengaged from its recognition site in a manner reminiscent of the way σ factor is released from the transcription initiation site during elongation of prokaryotic RNA.

CPSF binds to the phosphorylated RNAP II CTD; deleting the CTD inhibits polyadenylation. Evidently, the CTD couples polyadenylation to transcription.

PAP is part of a 500- to 1000-kD complex that also contains the proteins required for mRNA cleavage. Consequently, the cleaved transcript is polyadenylated before it can dissociate and be digested by cellular nucleases (see below). The maximum length of the poly(A) tail may be determined by the stoichiometric binding of multiple copies of **poly(A) binding protein II (PAB II).**

In vitro studies indicate that a poly(A) tail is not required for mRNA translation. Rather, the observation that an mRNA's poly(A) tail shortens as it ages in the cytosol suggests that poly(A) tails have a protective role. In fact, the only mature mRNAs that lack poly(A) tails, those encoding histones (which are required in large quantities only during the relatively short period during the cell cycle when DNA is being replicated), have cytosolic lifetimes of <30 min versus hours or days for most other mRNAs. The poly(A) tails are specifically complexed in the cytosol by **poly(A)-binding protein** (**PABP;** not related to PAB II), which organizes poly(A)-bearing mRNAs into ribonucleoprotein particles. PABP is thought to protect mRNA from degradation as is suggested, for example, by the observation that the addition of PABP to a cell-free system containing mRNA and mRNA-degrading nucleases greatly reduces the rate at which the mRNAs are degraded and the rate at which their poly(A) tails are shortened.

Eukaryotic Genes Consist of Alternating Exons and Introns. The most striking difference between eukaryotic and prokaryotic structural genes is that *the coding sequences of most eukaryotic genes are interspersed with unexpressed regions.* The primary transcripts, also called **pre-mRNAs** or **heterogeneous nuclear RNAs (hnRNAs),** are variable in length and are much larger (∼2000 to >20,000 nt) than expected from the known sizes of eukaryotic proteins. Rapid labeling experiments demonstrated that little of the hnRNA is ever transported to the cytosol; most of it is quickly degraded in the nucleus. Yet the hnRNA's 5′ caps and 3′ tails eventually appear in cytosolic mRNAs. The straightforward explanation of these observations, that pre-mRNAs are processed by the excision of internal sequences, seemed so bizarre that it came as a great surprise in 1977 when Phillip Sharp and Richard Roberts independently demonstrated that this is actually the case (Box 26-3). Thus, *pre-mRNAs are processed by the excision of nonexpressed* ***intervening sequences (introns),*** *following which the flanking* ***expressed sequences (exons)*** *are* ***spliced*** *(joined) together.*

A pre-mRNA typically contains eight introns whose aggregate length averages 4 to 10 times that of its exons. This situation is graphically illustrated in Fig. 26-20, which is an electron micrograph of chicken **ovalbumin** mRNA hybridized to the antisense (template) strand of the ovalbumin gene (ovalbumin is the major protein component of egg white). In humans, the number of introns in a gene varies from none to 234 (in the gene encoding the 34,350-residue muscle protein **titin,** the largest known single-chain protein; Section 7-2A), with intron lengths ranging from ∼65 to 2.4

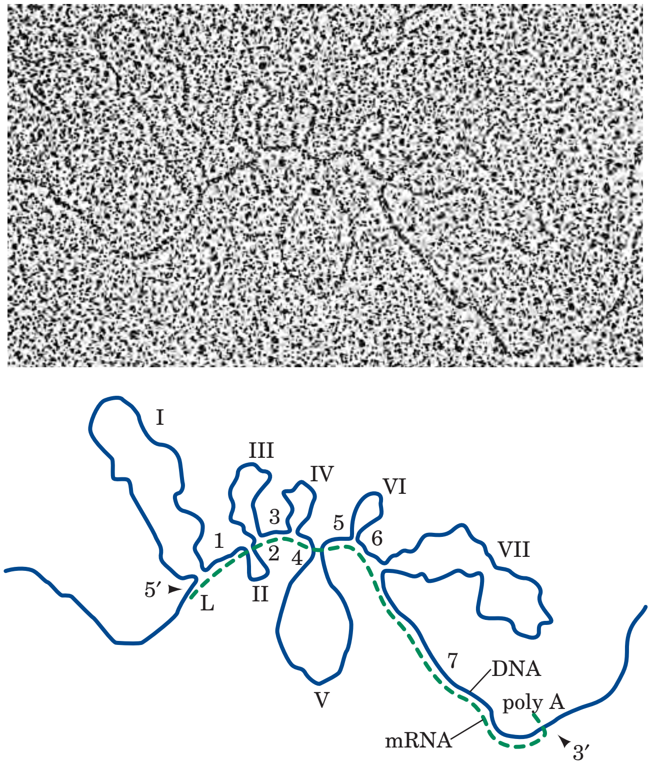

■ **Figure 26-20** | **The chicken ovalbumin gene and its mRNA.** The electron micrograph and its interpretive drawing show the hybridization of the antisense (template) strand of the chicken ovalbumin gene and its corresponding mRNA. The complementary segments of the DNA (*blue line in drawing*) and mRNA (*green dashed line*) have annealed to reveal the exon positions (*L,* 1–7). The looped-out segments (I–VII), which have no complementary sequences in the mRNA, are the introns. [From Chambon, P., *Sci. Am.* **244**(5), 61 (1981).]

BOX 26-3 **PATHWAYS OF DISCOVERY**

Richard Roberts and Phillip Sharp and the Discovery of Introns

Richard J. Roberts (1943–)
Phillip A. Sharp (1944–)

For several decades following the discovery that DNA is the genetic material in all organisms, it was believed that genes were continuous sequences of nucleic acid. A messenger RNA molecule was thought to be a faithful copy of the gene, aligning exactly with the DNA sequence. In fact, this is largely true for simple genetic systems such as bacteria and bacteriophages, which were widely used in early studies of molecular biology. However, Richard Roberts and Phillip Sharp, working independently, showed in 1977 that genes could be discontinuous. We now understand that the mRNA segments corresponding to these "split genes" must be spliced together in order for the gene to be properly expressed.

Richard Roberts began his scientific career as an organic chemist. While working on his thesis, he read a book by John Kendrew (who had determined the X-ray structure of myoglobin; Section 7-1A) and became hooked on the new field of molecular biology. His first project in the world of nucleic acids was to determine the sequence of nucleotides in a tRNA molecule. He was able to take advantage of new sequencing techniques devised by Frederick Sanger (who subsequently developed the dideoxy sequencing method; Section 3-4C). Roberts next turned his attention to restriction endonucleases. He recognized that the enzymes could be invaluable tools for cutting large DNA molecules down to size, including the adenovirus-2 genome that he began to characterize.

During roughly the same period, Phillip Sharp completed a thesis describing his use of statistical and physical theories to describe the DNA polymer. By his own admission, he was not a skilled experimenter. His outlook changed, however, when he joined a molecular biology laboratory that made extensive use of electron microscopy to examine DNA–RNA heteroduplexes. When Sharp subsequently turned to the study of eukaryotic gene expression, the only practical experimental systems were animal viruses with DNA genomes, such as adenovirus-2. Because that virus, which is a cause of the common cold, infects mammalian cells, its genes were thought to resemble those of its host.

Thus, in the mid-1970s, both Roberts (at the Cold Spring Harbor Laboratory on Long Island, New York) and Sharp (at the Massachusetts Institute of Technology) came to be mapping the adenovirus genome. They located viral genes by obtaining expressed mRNA molecules and hybridizing them to segments of the viral DNA. Sharp observed that the nuclei of virus-infected cells accumulated viral mRNAs that were not transported to the cytoplasm, and he speculated that the nuclear mRNAs were processed in order to generate the cytoplasmic mRNAs. Meanwhile, Roberts observed that "late" (mature) mRNAs began with an oligonucleotide that was not encoded in the DNA next to the main body of the mRNA.

Both scientists prepared samples in which the mRNA was allowed to hybridize with the DNA, and then visualized the hybrid by electron microscopy. The results were as exciting as they were unexpected: A single mRNA molecule hybridized with as many as four well-separated segments of the DNA molecule, so that the unpaired DNA sequences between the hybrid segments looped out (as in Fig. 26-20). The inescapable conclusion was that viral genetic information was organized discontinuously, a notion that contradicted commonly held views about the nature of genes. Nevertheless, other researchers were eager to see whether split genes occurred in other viruses and animal cells. Within a year, similar results were confirmed for a handful of other genes. Subsequent research showed that most animal genes are discontinuous. The sequences that are ultimately expressed were termed exons, and the intervening sequences that did not appear in the mature mRNA were named introns. For their discoveries of split genes, Roberts and Sharp shared the 1993 Nobel Prize in Physiology or Medicine.

The existence of split genes solved some biochemical puzzles but, as is always the case with important discoveries, introduced new ones: How are introns cut out and the remaining exons joined together? Are the same exons spliced together in all cells? Could evolution occur more rapidly through exon shuffling? Answers to these questions are still being refined.

Chow, L.T., Gelinas, R.E., Broker, T.R., and Roberts, R.J., An amazing sequence arrangement at the 5′ ends of adenovirus 2 messenger RNA, *Cell* **12,** 1–8 (1977).

Berget, S.M., Moore, C., and Sharp, P.A., Spliced segments at the 5′ terminus of adenovirus 2 late mRNA, *Proc. Natl. Acad. Sci.* **74,** 3171–3175 (1977).

million nt (in the gene encoding the muscle protein **dystrophin;** Section 7-2A) and averaging ~3500 nt (exons, in contrast, have lengths that average ~150 nt and range up to 17,106 nt in the gene encoding titin). The introns from corresponding genes in two vertebrate species rarely vary in number and position, but often differ extensively in length and sequence so as to bear little resemblance to one another.

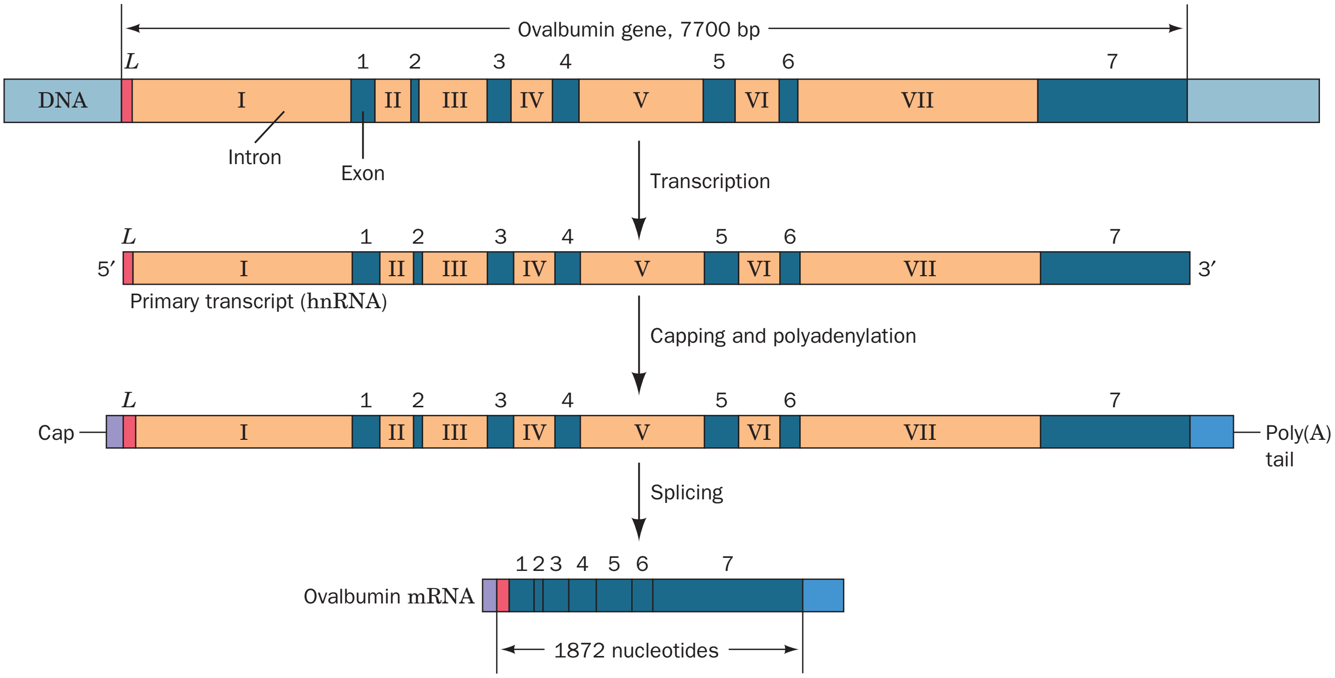
Ovalbumin gene, 7700 bp
L
1
2
3
4
5
6
7
DNA
I
II
III
IV
V
VI
VII
Intron
Exon
Transcription
5′
3′
Primary transcript (hnRNA)
Capping and polyadenylation
Cap
Poly(A) tail
Splicing
1 2 3 4 5 6 7
Ovalbumin mRNA
1872 nucleotides

Figure 26-21 | The sequence of steps in the production of mature eukaryotic mRNA. This example shows the chicken ovalbumin gene. Following transcription, the primary transcript is capped and polyadenylated. The introns are excised and the exons spliced together to form the mature mRNA. Note that capping and splicing occur cotranscriptionally, so that introns nearer the capped 5′ end may be excised before transcription of the 3′ end is complete.

The production of a translation-competent eukaryotic mRNA begins with the transcription of the entire gene, including its introns (Fig. 26-21). Capping occurs soon after initiation, and splicing commences during the elongation phase of transcription. The mature mRNA emerges only after splicing is complete and the RNA has been polyadenylated. The mRNA is then transported to the cytosol, where the ribosomes are located, for translation into protein.

Exons Are Spliced in a Two-Stage Reaction. Sequence comparisons of exon–intron junctions from a diverse group of eukaryotes indicate that they have a high degree of homology (Fig. 26-22), with most of them having an invariant GU at the intron's 5′ boundary and an invariant AG at its 3′ boundary. *These sequences are necessary and sufficient to define a*

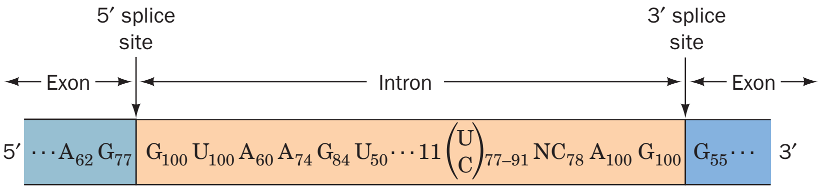
5′ splice site
3′ splice site
Exon
Intron
Exon
5′ ···A62 G77 | G100 U100 A60 A74 G84 U50 ··· 11 (U/C) 77–91 NC78 A100 G100 | G55 ··· 3′

Figure 26-22 | The consensus sequences at the exon–intron junctions of eukaryotic pre-mRNAs. The subscripts indicate the percentage of pre-mRNAs in which the specified base(s) occurs. Note that the 3′ splice site is preceded by a tract of 11 predominantly pyrimidine nucleotides. [Based on data from Padgett, R.A., Grabowski, P.J., Konarska, M.M., Seiler, S.S., and Sharp, P.A., *Annu. Rev. Biochem.* ***55,*** 1123 (1986).]

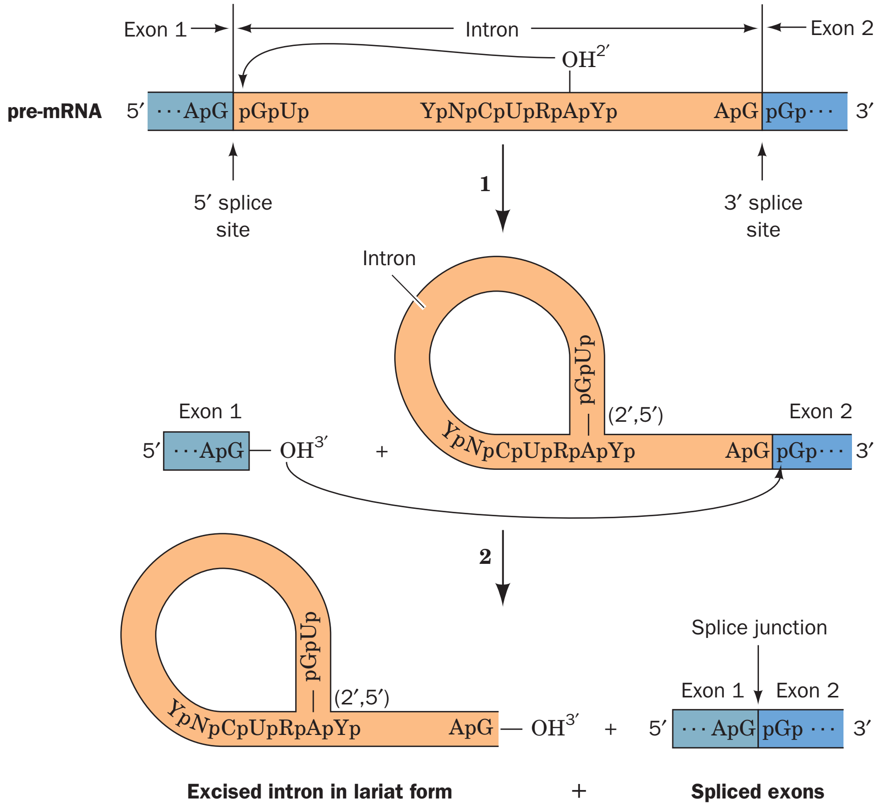

Figure 26-23 | The splicing reaction. Two transesterification reactions splice together the exons of eukaryotic pre-mRNAs. The exons and introns are drawn in blue and orange, and R and Y represent purine and pyrimidine residues. (**1**) The 2′-OH group of a specific intron A residue nucleophilically attacks the 5′-phosphate at the 5′ intron boundary to displace the 3′ end of the 5′ exon, thereby yielding a 2′,5′-phosphodiester bond and forming a lariat structure. (**2**) The liberated 3′-OH group attacks the 5′-phosphate of the 5′-terminal residue of the 3′ exon, forming a 3′,5′-phosphodiester bond, thereby displacing the intron in lariat form and splicing the two exons together.

splice junction. The splicing reaction occurs via two transesterification reactions (Fig. 26-23):

1. A 2′,5′-phosphodiester bond forms between an intron adenosine residue and the intron's 5′-terminal phosphate group. The 5′ exon is thereby released and the intron assumes a novel **lariat structure** (so called because of its shape). The adenosine at the lariat branch point is typically located in a conserved sequence 20 to 50 residues upstream of the 3′ splice site. Mutations that change this branch point A residue abolish splicing at that site.
2. The 5′ exon's free 3′-OH group displaces the 3′ end of the intron, forming a phosphodiester bond with the 5′-terminal phosphate of the 3′ exon and yielding the spliced product. The intron is thereby eliminated in its lariat form with a free 3′-OH group. Mutations that alter the conserved AG at the 3′ splice junction block this second step, although they do not interfere with lariat formation. The lariat is eventually debranched (linearized) and, *in vivo,* is rapidly degraded.

Note that the splicing process proceeds without free energy input; its transesterification reactions preserve the free energy of each cleaved phosphodiester bond through the concomitant formation of a new one. The sequences required for splicing are the short consensus sequences at the 3′ and 5′ splice sites and at the branch site. Nevertheless, these sequences are poorly conserved, and even highly sophisticated computer programs are only ~50% successful in predicting actual splice sites over apparently equally good candidates that are not.

A simplistic interpretation of Fig. 26-23 suggests that any 5′ splice site could be joined with any following 3′ splice site, thereby eliminating all the intervening exons together with the introns joining them. However, such **exon skipping** does not normally take place (but see below). Rather, all of a pre-mRNA's introns are individually excised in what appears to be a largely fixed order that more or less proceeds in the $5' \rightarrow 3'$ direction. This occurs, at least in part, because splicing occurs cotranslationally. Thus, as a newly synthesized exon emerges from an RNAP II, it is bound by splicing factors (see below) that are also bound to the RNAP II's highly phosphorylated CTD. This tethers the exon and its associated splicing machinery to the CTD so as to ensure that splicing occurs when the next exon emerges from the RNAP II.

Splicing Is Mediated by snRNPs in the Spliceosome. How are splice junctions recognized and how are the two exons to be joined brought together in the splicing process? Part of the answer to this question was established by Joan Steitz going on the assumption that one nucleic acid is best recognized by another. The eukaryotic nucleus contains numerous copies of highly conserved 60- to 300-nt RNAs called **small nuclear RNAs (snRNAs),** which form protein complexes termed **small nuclear ribonucleoproteins** (**snRNPs;** pronounced "snurps"). Steitz noted that the 5′ end of one of these snRNAs, **U1-snRNA** (which is so named because of its high uridine content), is partially complementary to the consensus sequence of 5′ splice junctions. Apparently, *U1-snRNP recognizes the 5′ splice junction.* Other snRNPs that participate in splicing are **U2-snRNP, U4–U6-snRNP** (in which the **U4-** and **U6-snRNAs** associate via base pairing), and **U5-snRNP.**

Splicing takes place in an ~60S particle dubbed the **spliceosome.** The spliceosome brings together a pre-mRNA, the snRNPs, and a variety of pre-mRNA binding proteins. The spliceosome, which consists of 5 RNAs and at least 100 polypeptides, is comparable in size and complexity to the ribosome (Section 27-3). A preassembled spliceosome appears to associate with the pre-mRNA and then undergoes significant structural changes, including rearrangement of base-paired stems among the snRNAs, as it carries out the two transesterification reactions. The U6-snRNA coordinates a catalytically essential metal ion that enhances the nucleophilicity of the attacking OH group and stabilizes the leaving group. The existence of self-splicing introns (see below) and the results of experiments with protein-free snRNAs strongly suggest that the RNA components of the spliceosome, rather than the proteins, catalyze splicing.

All four snRNPs involved in mRNA splicing contain the same so-called **snRNP core protein,** which consists of seven **Sm proteins,** named **B, D_1, D_2, D_3, E, F,** and **G proteins.** These proteins collectively bind to a conserved AAUUUGUGG sequence known as the **Sm RNA motif,** which occurs in U1-, U2-, U4-, and U5-snRNAs. The X-ray structures of the D_3B and D_1D_2 heterodimers reveal that these four proteins share a common fold, which consists of an N-terminal helix followed by a five-stranded antiparallel β sheet that is strongly bent so as to form a hydrophobic core. Model building based on these X-ray structures together with biochemical and mutagenic evidence suggest that the seven Sm proteins form a heptameric ring in which the fourth β strand of one Sm protein interacts with the fifth β strand of an adjacent Sm protein through main-chain hydrogen bonding (Fig. 26-24). The funnel-shaped central hole of the Sm ring, which is lined with positive charges, is large enough to accommodate single-stranded snRNA. This model is corroborated by the X-ray structure of an Sm-like protein from the hyperthermophilic archaebacterium *Pyrobaculum aerophilum* that forms a homoheptameric ring that is structurally similar to the heteroheptameric model. Evidently, the seven eukaryotic Sm proteins arose through a series of duplications of an archaeal Sm-like protein gene.

Mammalian U1-snRNP consists of U1-snRNA and ten proteins, namely, the seven Sm proteins that are common to all U-snRNPs as well as three

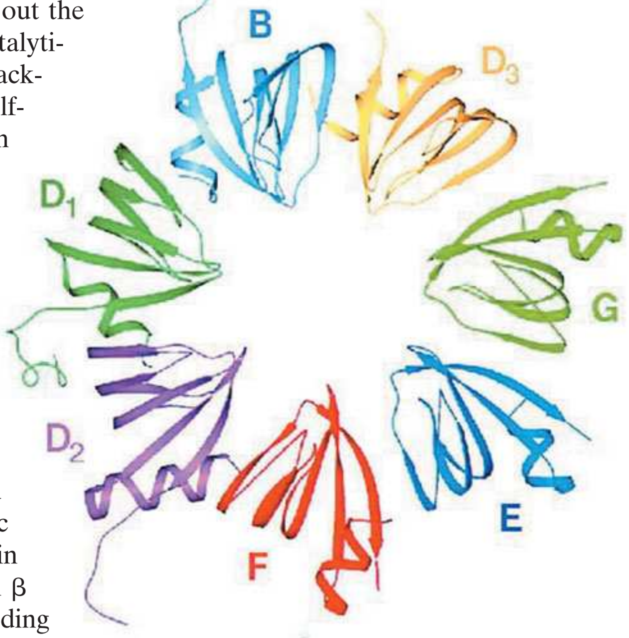

■ **Figure 26-24 | A model of the snRNP core protein.** Its seven Sm proteins, which are each differently colored, are arranged in a seven-membered ring. This heptameric ring has an outer diameter of 70 Å and a central hole with a diameter of 20 Å when only the main chain atoms are considered. [Courtesy of Kiyoshi Nagai, MRC Laboratory of Molecular Biology, Cambridge, U.K.]

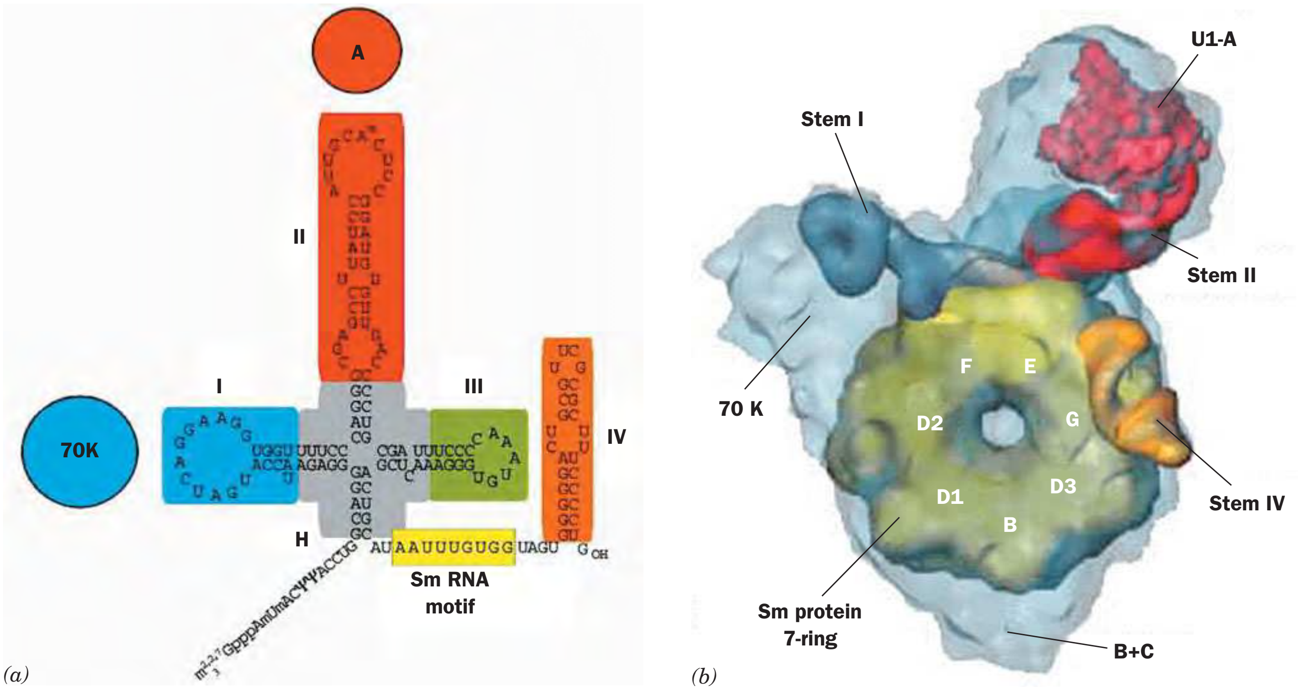

Figure 26-25 | Electron microscopy–based structure of U1-snRNP at 10 Å resolution. (*a*) The predicted secondary structure of U1-snRNA with the positions at which the proteins U1-70K and U1-A bind the RNA indicated. (*b*) The molecular outline of U1-snRNP in light gray with its component ring-shaped Sm core protein yellow (and viewed oppositely from Fig. 26-24) and U1-snRNA colored as in Part *a*. [Courtesy of Holger Stark, Max-Planck-Institut für biophysikalische Chemie, Göttingen, Germany.]

that are specific to U1-snRNP: **U1-70K, U1-A,** and **U1-C.** The predicted secondary structure of the 165-nt U1-snRNA (Fig. 26-25*a*) contains five double-helical stems, four of which come together at a four-way junction. U1-70K and U1-A bind directly to RNA stem–loops I and II, respectively, whereas U1-C is bound by other proteins.

An electron microscopy–based image of U1-snRNP (Fig. 26-25*b*), elucidated by Holger Stark and Reinhard Lührmann, contains as its most obvious feature a ring-shaped body that is 70 to 80 Å in diameter with a funnel-shaped central hole that closely matches the model of the snRNP core protein in Fig. 26-24. Proteins were assigned to U1-snRNP's various protuberances based on cross-linking and binding studies as well electron micrographs of U1-snRNP lacking U1-A or U1-70K. The positions of the U1-snRNA's various structural elements, which were identified on the basis of known protein–RNA interactions, indicate that the Sm RNA motif, in fact, passes through the central hole in the snRNP core protein.

Gene Splicing Offers Evolutionary Advantages. Analysis of the large body of known DNA sequences reveals that introns are rare in prokaryotic structural genes, uncommon in lower eukaryotes such as yeast (which has a total of 239 introns in its ~6000 genes and, with two exceptions, only one intron per polypeptide), and abundant in higher eukaryotes (the only known vertebrate structural genes lacking introns are those encoding histones and the antiviral proteins known as **interferons**). Pre-mRNA introns, as we have seen, can be quite long and many genes contain large numbers of them. Consequently, unexpressed sequences constitute ~80% of a typical vertebrate structural gene and >99% of a few of them.

The argument that introns are only molecular parasites **(junk DNA)** seems untenable since it would then be difficult to rationalize why the evolution of complex splicing machinery offered any selective advantage over the elimination of the split genes. What then is the function of gene splicing? Although, since its discovery, the significance of gene splicing has been debated, often vehemently, two important roles for it have emerged:

1. Gene splicing is an agent for rapid protein evolution. Many eukaryotic proteins consist of modules that also occur in other proteins (Section 5-4B). For example, SH2 and SH3 domains occur in many of the proteins involved in signal transduction (Section 13-2B). *It therefore appears that the genes encoding these modular proteins arose by the stepwise collection of exons that were assembled by (aberrant) recombination between their neighboring introns.*
2. Through **alternative splicing,** which we discuss below, gene splicing permits a single gene to encode several (sometimes many) proteins that may have significantly different functions.

Alternative mRNA Splicing Yields Multiple Proteins from a Single Gene. *The expression of numerous cellular genes is modulated by the selection of alternative splice sites.* Thus, genes containing multiple exons may give rise to transcripts containing mutually exclusive exons. In effect, certain exons in one type of cell may be introns in another. For example, a single rat gene encodes seven tissue-specific variants of the muscle protein **α-tropomyosin** through the selection of alternative splice sites (Fig. 26-26).

Alternative splicing occurs in all multicellular organisms and is especially prevalent in vertebrates. In fact, an estimated 60% of human structural genes are subject to alternative splicing. This helps explain the discrepancy between the ~23,000 genes identified in the human genome and

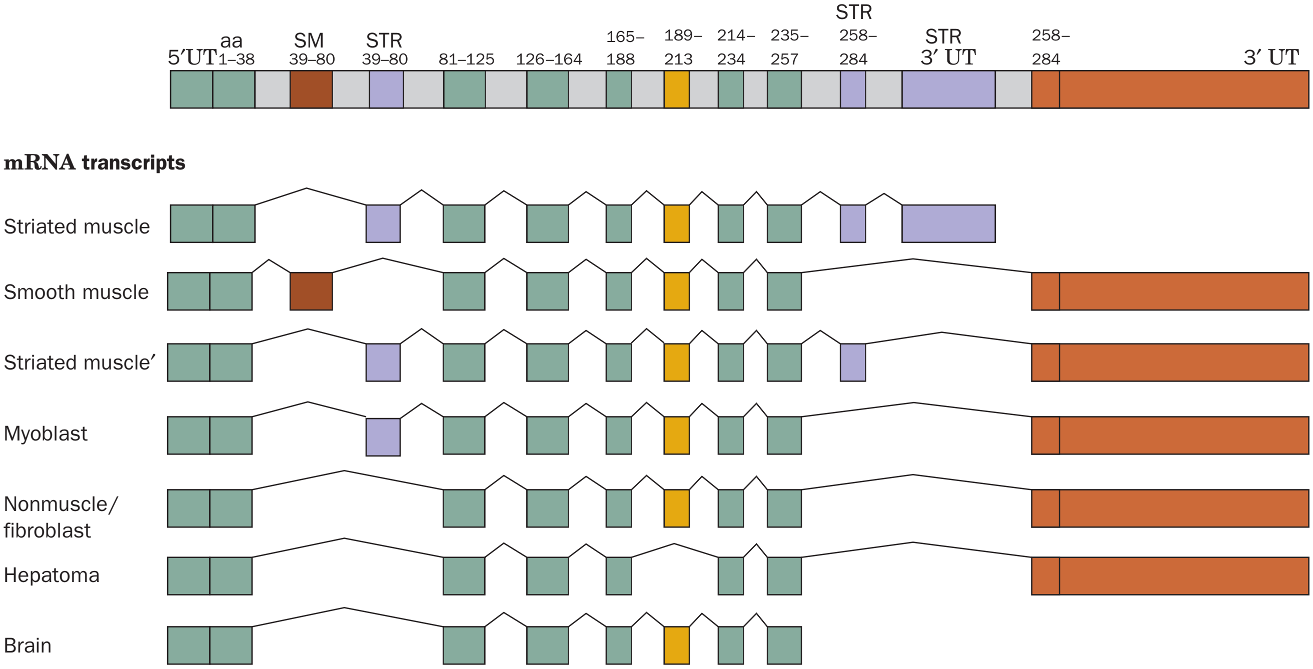

■ **Figure 26-26 | Alternative splicing in the rat α-tropomyosin gene.** Seven alternative splicing pathways give rise to cell-specific α-tropomyosin variants. The thin kinked lines indicate the positions occupied by the introns before they are spliced out to form the mature mRNAs. Tissue-specific exons are indicated together with the amino acid (aa) residues they encode: "constitutive" exons (those expressed in all tissues) are green; those expressed only in smooth muscle (SM) are dark brown; those expressed only in striated muscle (STR) are purple; and those variably expressed are yellow. Note that the smooth and striated muscle exons encoding amino acid residues 39 to 80 are mutually exclusive and, likewise, there are alternative 3′ untranslated (UT) exons. [After Breitbart, R.E., Andreadis, A., and Nadal-Ginard, B., *Annu. Rev. Biochem.* **56,** 481 (1987).]

earlier estimates that it contains over 100,000 structural genes. The variations in spliced mRNA sequences can take several different forms: Exons can be retained or skipped; introns may be excised or retained; and the positions of 5′ and 3′ splice sites can be shifted to make exons longer or shorter. Alterations in the transcriptional start site and/or the polyadenylation site can further contribute to the diversity of the mRNAs that are transcribed from a single gene. In a particularly striking example, the *Drosophila* **DSCAM** protein, which functions in neuronal development, is encoded by 24 exons of which there are 12 mutually exclusive variants of exon 4, 48 of exon 6, 33 of exon 9, and 2 of exon 17 (which are therefore known as **cassette exons**) for a total of 38,016 possible variants of the protein (compared to ~13,000 identified genes in the *Drosophila* genome). Although it is unknown whether all possible DSCAM variants are produced, experimental evidence suggests that the *Dscam* gene expresses many thousands of them. Clearly, *the number of genes in an organism's genome does not by itself provide an adequate assessment of its protein diversity.* Indeed, it has been estimated that, on average, each human structural gene encodes three different proteins.

The types of changes that alternative splicing confers on expressed proteins span the entire spectrum of protein properties and functions. Entire functional domains or even single amino acid residues may be inserted into or deleted from a protein, and the insertion of a **Stop codon** may truncate the expressed polypeptide [a codon is a 3-nt sequence that specifies an amino acid in a polypeptide; a Stop codon is a 3-nt sequence that instructs the ribosome to terminate polypeptide synthesis (Section 27-1C)]. Splice variations may, for example, control whether a protein is soluble or membrane bound, whether it is phosphorylated by a specific kinase, the subcellular location to which it is targeted, whether an enzyme binds a particular allosteric effector, or the affinity with which a receptor binds a ligand. Changes in an mRNA, particularly in its noncoding regions, may also influence the rate at which it is transcribed and its susceptibility to degradation. Since the selection of alternative splice sites is both tissue- and developmental stage-specific, splice site choice must be tightly regulated in both space and time. In fact, ~15% of human genetic diseases are caused by point mutations that result in pre-mRNA splicing defects. Some of these mutations delete functional splice sites, thereby activating nearby preexisting **cryptic splice sites.** Others generate new splice sites that are used instead of the normal ones. In addition, tumor progression is correlated with changes in levels of proteins implicated in alternative splice site selection.

How are alternative splice sites selected? One example of this process occurs in the *transformer* (*tra*) gene during sex determination in *Drosophila.* Exon 2 of *tra* pre-mRNA contains two alternative 3′ splice sites, with the proximal (close; to exon 1) site used in males and the distal (far) site used in females (Fig. 26-27). The region between the two sites contains a Stop codon with the sequence UAG. In males, the splicing factor **U2-snRNP auxiliary factor (U2AF)** binds to the proximal 3′ splice site to yield an mRNA containing the premature Stop codon, which thereby directs the synthesis of a truncated and hence nonfunctional **TRA** protein. However, in females, the proximal 3′ splice site is bound by the female-specific **SXL** protein, the product of the *sex-lethal (sxl)* gene (which is only expressed in females), so as to block the binding of U2AF, which then binds to the distal 3′ splice site, thereby inducing the expression of functional TRA protein. In females, the TRA protein directs the splicing of mRNA from another sex-determination gene, leading to production of a repressor of male-specific genes.

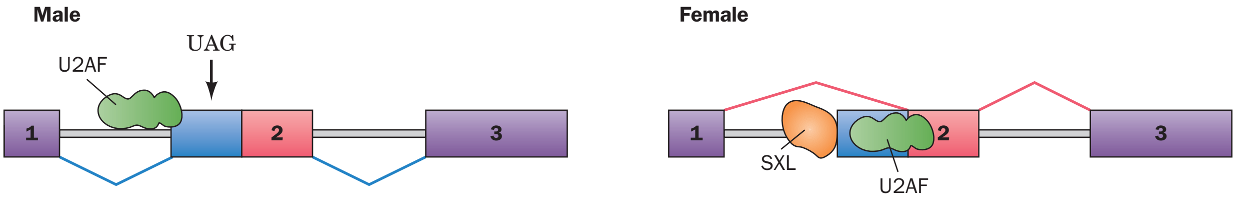

Figure 26-27 | Alternative splice site selection in the *Drosophila tra* gene. Exons of the pre-mRNA are represented by colored rectangles, and introns are shown as gray bands with those to be excised flanked by kinked lines. UAG is a Stop codon. In females, the protein SXL directs the spliceosome to the second of two possible splice sites, to generate mRNA for a full-length TRA protein. [After a drawing by Maniatis, T. and Tasic, B., *Nature* **418,** 236 (2002).]

Similar mechanisms for repressing or activating a splice site occur in vertebrates. Some of the proteins involved in splice site selection—both constitutive and alternative—belong to the family of **SR proteins** [named for the presence of numerous Ser–Arg (SR) dipeptide sequences]. These proteins bind to small (5–10 nt) **exonic splicing enhancers/silencers (ESEs/ESSs)** located in exons; such interactions help the splicing machinery distinguish true exons (which are relatively short) from the more numerous sequences within introns (which are relatively long) that happen to exhibit the consensus splice-site sequences. The SR proteins include a conserved domain structure with one or two **RNA-recognition motifs (RRM)** that bind RNA sequences, followed by an SR domain of variable length, which mediates protein–protein interactions (U2AF and TRA both contain an SR domain, but neither has an RRM and so is not considered to be an SR protein). Tissue-specific expression of SR proteins and their reversible phosphorylation undoubtedly contribute to the complex regulation of mRNA splicing.

mRNA May Be Edited. Additional posttranscriptional modifications of eukaryotic mRNAs include the methylation of certain A residues. In a few cases, mRNAs undergo **RNA editing,** which involves base changes, deletions, or insertions. In the most extreme examples of this phenomenon, which occur in the trypanosomes and related protozoa, several hundred U residues may be added and removed to produce a translatable mRNA. Not surprisingly, the mRNA editing machinery includes RNAs known as **guide RNAs (gRNAs)** that base-pair with the immature mRNA to direct its alteration.

In a few mRNAs, specific bases are chemically altered, for example, by enzyme-catalyzed deamination of C to produce U and/or deamination of A to produce inosine (which is read as G by the ribosome), a process called **substitutional editing.** For example, humans express two forms of **apolipoprotein B (apoB): apoB-48,** which is made only in the small intestine and functions in chylomicrons to transport triacylglycerols from the intestine to the liver and peripheral tissues; and **apoB-100,** which is made only in the liver and functions with VLDL, IDL, and LDL to transport cholesterol from the liver to the peripheral tissues (Table 20-1). ApoB-100 is an enormous 4536-residue protein, whereas apoB-48 consists of apoB-100's N-terminal 2152 residues and therefore lacks the C-terminal domain of apoB-100 that mediates LDL receptor binding. Although apoB-48 and apoB-100 are expressed from the same gene, the mRNAs encoding the two proteins differ by a single C → U change: The codon for Gln 2153

(CAA) in apoB-100 mRNA is, in apoB-48 mRNA, a UAA Stop codon. The enzyme that catalyzes this conversion is site-specific **cytidine deaminase.**

Substitutional editing may contribute to protein diversity. For example, *Drosophila cacophony* pre-mRNA, which encodes a voltage-gated Ca^{2+} channel subunit, contains 10 different substitutional editing sites and hence has the potential of generating $2^{10} \approx 1000$ different isoforms in the absence of alternative splicing. Substitutional editing can also generate alternative splice sites. For example, the enzyme **ADAR2** (ADAR for *a*denosine *d*eaminase *a*cting on *R*NA) edits its own pre-mRNA by converting an intronic AA dinucleotide to AI, which mimics the AG normally found at 3′ splice sites (Fig. 26-23). The consequent new splice site adds 47 nucleotides near the 5′ end of the *ADAR2* mRNA so as to generate a new translational initiation site. The resulting ADAR2 isozyme is catalytically active but is produced in smaller amounts than that from unedited transcripts, perhaps due to a less efficient translational initiation site. Thus, ADAR2 appears to regulate its own rate of expression.

B | Ribosomal RNA Precursors May Be Cleaved, Modified, and Spliced

E. coli has three types of rRNAs, the **5S, 16S,** and **23S rRNAs.** These are specified by seven operons, each of which contains one nearly identical copy of each of the three rRNA genes. The polycistronic primary transcripts of these operons are >5500 nt long and contain, in addition to the rRNAs, transcripts for as many as four tRNAs (Fig. 26-28). The steps in processing the primary transcripts to mature rRNAs were elucidated with the aid of mutants defective in one or more of the processing enzymes.

The initial processing, which yields products known as **pre-rRNAs,** commences while the primary transcript is still being synthesized. It consists of specific endonucleolytic cleavages by **RNase III, RNase P, RNase E,** and **RNase F** at the sites indicated in Fig. 26-28. The cleavage sites are probably recognized on the basis of their secondary structures.

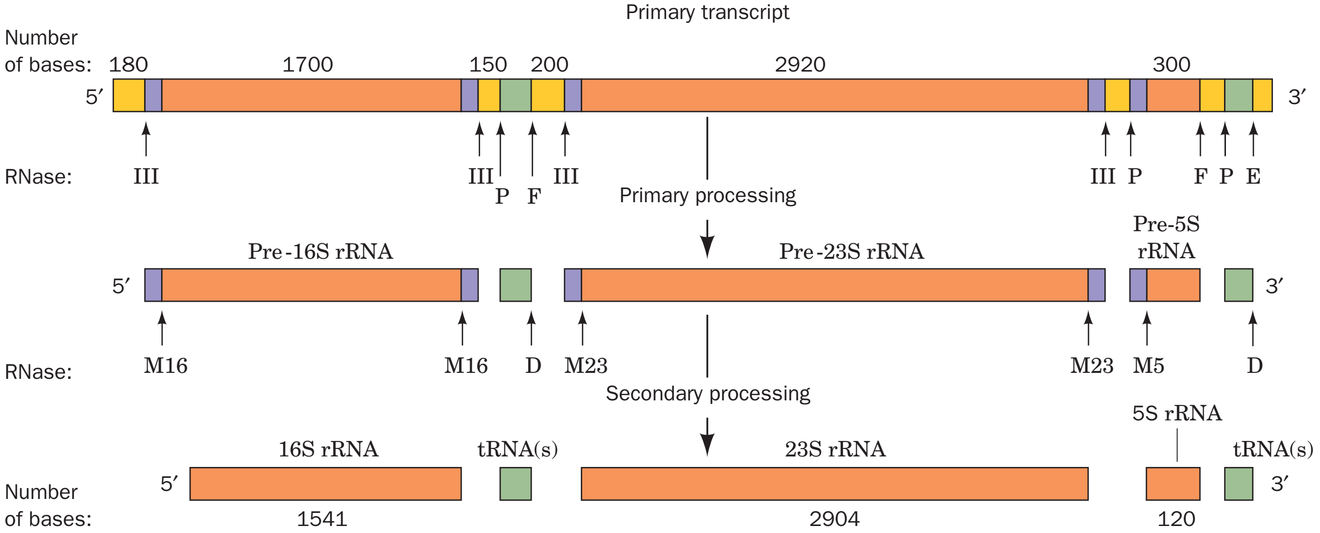

■ **Figure 26-28 | The posttranscriptional processing of *E. coli* rRNA.** The transcriptional map is shown approximately to scale. The labeled arrows indicate the positions of the various nucleolytic cuts and the nucleases that generate them. [After Apiron, D., Ghora, B.K., Plantz, G., Misra, T.K., and Gegenheimer, P., *in* Söll, D., Abelson, J.N., and Schimmel, P.R. (Eds.), *Transfer RNA: Biological Aspects,* p. 148, Cold Spring Harbor Laboratory (1980).]

The 5′ and 3′ ends of the pre-rRNAs are trimmed away in secondary processing steps through the action of **RNases D, M16, M23,** and **M5** to produce the mature rRNAs. These final cleavages occur only after the pre-rRNAs become associated with ribosomal proteins. During ribosomal assembly, specific rRNA residues are methylated, which may help protect them from inappropriate nuclease digestion.

snoRNAs Direct the Methylation of Eukaryotic rRNAs. The eukaryotic genome typically has several hundred tandemly repeated copies of rRNA genes. These genes are transcribed and processed in the nucleolus. The primary eukaryotic rRNA transcript is an ~7500-nt **45S RNA** that contains the **18S, 5.8S,** and **28S rRNAs** separated by spacer sequences:

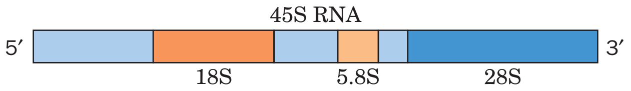

In the first stage of its processing, 45S RNA is specifically methylated at numerous sites (106 in humans) that occur mostly in its rRNA sequences. About 80% of these modifications yield ***O*$^{2'}$-methylribose** residues, and the remainder yield methylated bases such as ***N*^{6},*N*^{6}-dimethyladenine** and **2-methylguanine.** The subsequent cleavage and trimming of the 45S RNA superficially resemble those of prokaryotic rRNAs. In fact, enzymes exhibiting RNase III- and RNase P-like activities occur in eukaryotes. Eukaryotic ribosomes contain four different rRNAs (Section 27-3). The fourth type, 5S eukaryotic rRNA, is separately processed in a manner resembling that of tRNA (Section 26-3C).

The methylation sites in yeast and vertebrate rRNAs generally occur in invariant sequences, although the methylation sites do not appear to have a consensus structure that might be recognized by a single methyltransferase. How are the methylation sites targeted? Pre-rRNAs interact with members of a large family of **small nucleolar RNAs (snoRNAs).** Mammals have ~200 snoRNAs, most of which are encoded by the introns of structural genes (and hence not all excised introns are discarded). The snoRNAs, whose lengths vary from 70 to 100 nt, contain segments of 10 to 21 nt that are precisely complementary to segments of the mature rRNAs that contain *O*$^{2'}$-methylation sites. The snoRNAs appear to direct a protein complex containing a methyltransferase to the methylation site. Presumably, without the snoRNAs, the cell would need to synthesize a different methyltransferase to recognize each methylation sequence. Complexes of small RNAs and proteins also catalyze the conversion of certain rRNA uridine residues to **pseudouridine (ψ):**

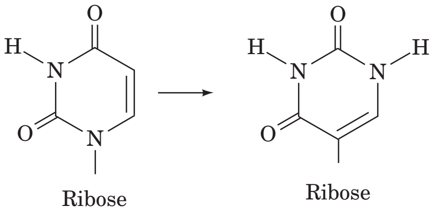

Uridine **Pseudouridine (ψ)**

Some Eukaryotic rRNAs Are Self-Splicing. A few eukaryotic rRNA genes contain introns. In fact, it was Thomas Cech's study of how these introns are spliced out that led to the astonishing discovery, in 1982, that

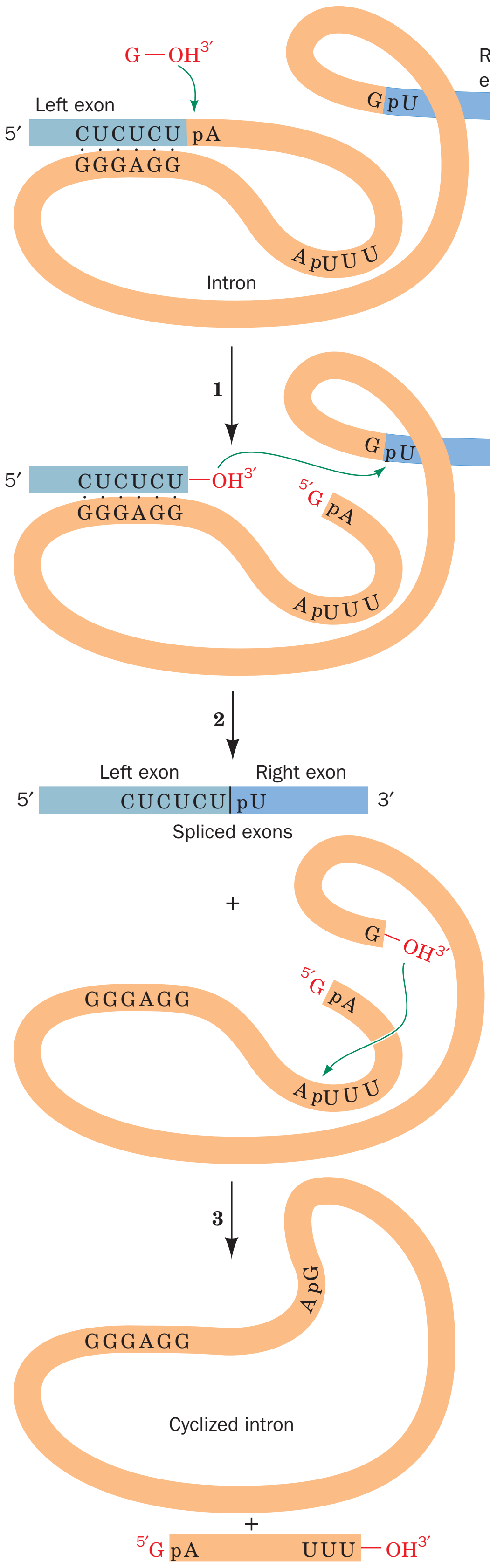

Figure 26-29 | **The sequence of reactions in the self-splicing of *Tetrahymena* pre-rRNA.** (**1**) The 3′-OH group of a guanine nucleotide attacks the intron's 5′-terminal phosphate to form a phosphodiester bond, displacing the 5′ exon. (**2**) The newly generated 3′-OH group of the 5′ exon attacks the 5′-terminal phosphate of the 3′ exon, thereby splicing the two exons and displacing the intron. (**3**) The 3′-OH group of the intron attacks the phosphate of the nucleotide that is 15 residues from the 5′ end so as to cyclize the intron and displace its 5′-terminal fragment. Throughout this process, the RNA maintains a folded, internally hydrogen-bonded conformation that permits the precise excision of the intron.

RNA can act as an enzyme (a ribozyme; Section 24-2C). Cech showed that when the isolated pre-rRNA of the ciliated protozoan *Tetrahymena thermophila* is incubated with guanosine or a free guanine nucleotide (GMP, GDP, or GTP), but in the absence of protein, its single 413-nt intron excises itself and splices together its flanking exons; that is, *the pre-rRNA is self-splicing.* The three-step reaction sequence of this process (Fig. 26-29) resembles that of mRNA splicing:

1. The 3′-OH group of the guanosine attacks the intron's 5′ end, displacing the 3′-OH group of the 5′ exon and thereby forming a new phosphodiester linkage with the 5′ end of the intron.
2. The 3′-terminal OH group of the newly liberated 5′ exon attacks the 5′-phosphate of the 3′ exon to form a new phosphodiester bond, thereby splicing together the two exons and displacing the intron.
3. The 3′-terminal OH group of the intron attacks a phosphate of the nucleotide 15 residues from the intron's end, displacing the 5′ terminal fragment and yielding the 3′ terminal fragment in cyclic form.

The self-splicing process consists of a series of transesterifications and therefore does not require free energy input.

Self-splicing RNAs that react as shown in Fig. 26-29 are known as **group I introns** and occur in the nuclei, mitochondria, and chloroplasts of diverse eukaryotes (but not vertebrates), and in some bacteria. **Group II introns,** which occur in the mitochondria and chloroplasts of fungi and plants, react via a lariat intermediate and do not require an external nucleotide. The chemical similarities of the pre-mRNA and group II intron splicing reactions therefore suggest that *spliceosomes are ribozymal systems whose RNA components have evolved from primordial self-splicing RNAs and that their protein components serve mainly to fine-tune ribozymal structure and function.* This, of course, is consistent with the hypothesis that RNAs were the original biological catalysts in precellular times (the RNA world; Box 24-3).

The *Tetrahymena* Group I Ribozyme Has a Complex Tertiary Structure.

In order to function as a catalyst, the self-splicing RNA must be able to assume a stable tertiary structure, as does a protein enzyme. The sequence of the *Tetrahymena* group I intron contains nine double-stranded segments, designated P1 through P9 (Fig. 26-30*a*). Jennifer Doudna and Cech determined the X-ray structure of the 160-nt P4–P6 domain (Fig. 26-30*b*), which contains the active site. The structure consists mostly of two coaxially stacked sets of A-RNA helices, one of 29 bp and the other of 23 bp. Extensive hydrogen bonding and Mg^{2+} ions coordinated by the oxygens of two or more phosphate groups contribute to a structure whose interior

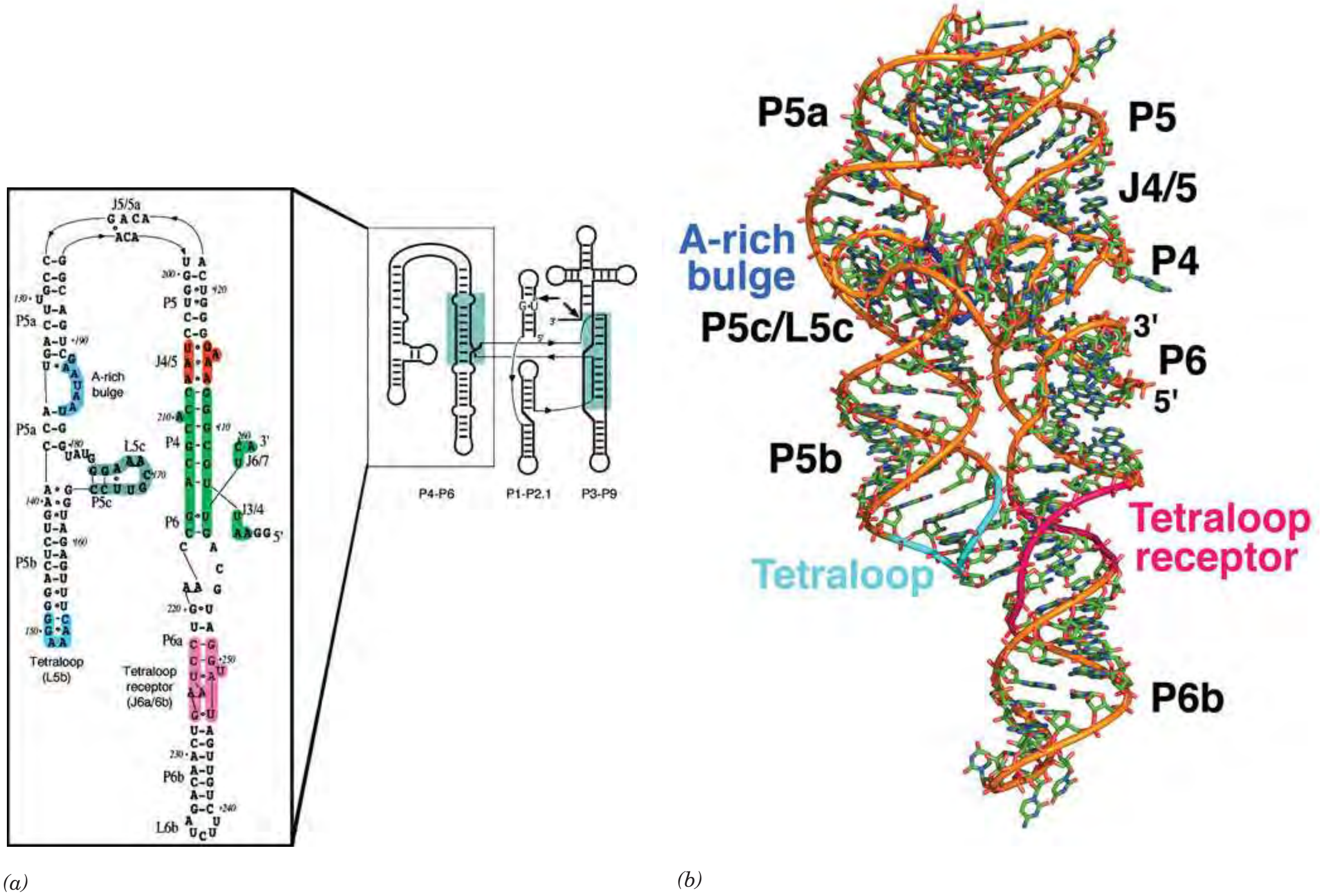

Figure 26-30 | **The self-splicing group I intron from *Tetrahymena thermophila.*** (*a*) The secondary structure of the entire 413-nt intron is shown on the right with its phylogenetically conserved catalytic core shaded in blue-green. Helical regions are numbered sequentially along the intron's sequence with P for base-*p*aired segment, J for *j*oining region, and L for *l*oop; the short arrows indicate the 5′ and 3′ splice sites. The sequence of the independently folded 160-nt P4–P6 domain is enlarged on the left. Segments of functional interest are highlighted as follows: the GAAA tetraloop is cyan; the conserved tetraloop receptor is magenta; the A-rich bulge, which is required for the proper folding of P4–P6, is blue; segments of the conserved core are green and red; and P5c is gray. Watson–Crick and non-Watson–Crick base-pairing interactions are represented by short horizontal lines and small filled circles. (*b*) The X-ray structure of P4–P6 viewed as in Part *a*. The structure is drawn in stick form with C green, N blue, O red, and P yellow. The sugar–phosphate backbone is traced by a rod that is colored as in Part *a* for the tetraloop, tetraloop receptor, and A-rich bulge and is gold elsewhere. Note the numerous interactions between the various segments of this RNA molecule. [Part *a* based on a drawing by and Part *b* based on an X-ray structure by Jennifer Doudna, Yale University. PDBid 1GID.] **See Interactive Exercise 52.**

is densely packed and solvent inaccessible, much like the interior of a protein enzyme. Of particular note are its so-called A-rich bulge, a 7-nt sequence about halfway along the short arm of the U-shaped macromolecule, and the 6-nt sequence at the tip of the short arm of the U, whose central GAAA assumes a characteristic conformation known as a **tetraloop.** In both of these substructures, the bases are splayed outward so as to stack on each other and to associate in the minor groove of specific segments of the long arm of the U via hydrogen-bonding interactions involving ribose residues as well as bases. In the interaction involving the A-rich bulge, the close packing of phosphates from adjacent helices is mediated by hydrated Mg^{2+} ions. Throughout this structure, the defining characteristic of RNA, its 2′-OH group, is both a donor and acceptor of hydrogen bonds to phosphate, bases, and other 2′-OH groups (which may explain why "deoxyribozymes" are unknown in biology, although synthetic ssDNAs with catalytic properties are known).

C | Transfer RNAs Are Processed by Nucleotide Removal, Addition, and Modification

A tRNA molecule, as discussed in Section 24-2C, consists of ~80 nucleotides, many of which are chemically modified, that assume a cloverleaf-shaped secondary structure with four base-paired stems (Fig. 26-31). The *E. coli* chromosome contains ~60 tRNA genes. Some of them are components of rRNA operons; the others are distributed, often in clusters, throughout the chromosome. The primary tRNA transcripts, which contain as many as five identical tRNA species, have extra nucleotides at the 3′ and 5′ ends of each tRNA sequence. The excision and trimming of these tRNA sequences resemble *E. coli* rRNA processing (Fig. 26-28) in that the two processes employ some of the same nucleases.

E. coli RNase P, which processes rRNA and generates the 5′ ends of tRNAs, is a particularly interesting enzyme because it is a ribozyme with a catalytically essential 377-nt (125 kD) RNA and a 119-residue (14 kD) polypeptide. At first, the RNA was believed to recognize the substrate through base pairing and thereby guide the protein subunit, which was presumed to be the nuclease, to the cleavage site. However, Sidney Altman showed that *the RNA component of RNase P is, in fact, the enzyme's catalytic subunit by demonstrating that free RNase P RNA catalyzes the cleavage of substrate RNA at high salt concentrations.* The RNase P protein, which is basic, evidently functions to electrostatically reduce the repulsions between the polyanionic ribozyme and its substrate RNAs. RNase P activity also occurs in eukaryotes, although the enzyme includes 9 or 10 protein subunits. RNase P, unlike the self-splicing introns, is a true enzyme capable of multiple turnovers. Indeed, RNase P mediates one of the two ribozymal activities that occur in all cellular life, the other being ribosomally catalyzed peptide bond formation (Section 27-4B).

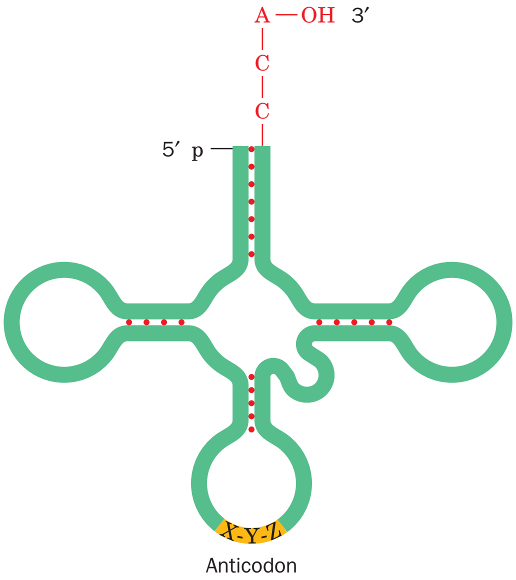

■ **Figure 26-31 | Schematic diagram of the tRNA cloverleaf secondary structure.** Each red dot indicates a base pair in the hydrogen-bonded stems. The positions of the **anticodon** (the 3-nt sequence that binds to mRNA during translation) and the 3′-terminal —CCA are indicated.

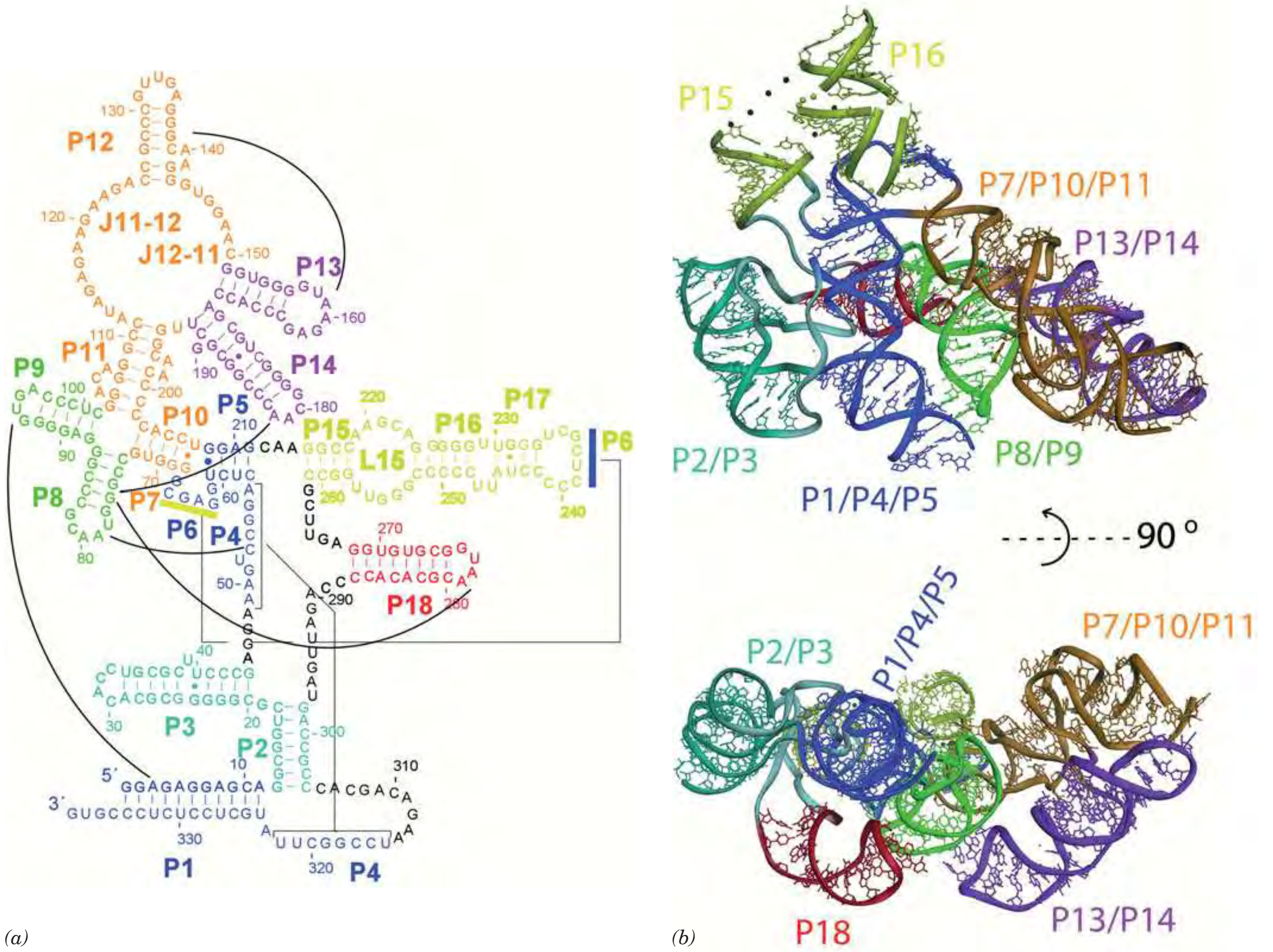

■ **Figure 26-32 | Structure of the RNA component of *T. maritima* RNase P.** (*a*) Its sequence and secondary structure. The various segments (P for paired region, J for joining region, and L for loop) are shown in different colors. The black lines indicate major interactions that are observed in the X-ray structure, and small filled circles represent non-Watson–Crick base pairs. (*b*) Its X-ray structure, which is color coded as in Part *a*. Of its 338 nucleotides 309 are visible. The lower view is related to the upper view by a 90° rotation about the horizontal axis. [Courtesy of Alfonso Mondragón, Northwestern University. PDBid 2A2E.]

The RNase P from *Thermotoga maritima* contains a 338-residue RNA whose secondary structure includes numerous base-paired stems (P1–P18; Fig. 26-32*a*). The X-ray structure of the RNA (Fig. 26-32*b*), determined by Alfonso Mondragón, consists mainly of stacked helical stems with an overall compact structure typical of protein enzymes. Biochemical studies and modeling indicate that the RNase active site lies in a cleft between the P2/P3 region (*cyan* in Fig. 26-32) and the P1/P4/P5 region (*dark blue* in Fig. 26-32). That portion of the structure encompassing P1 through P4, P9 through P11, J11-12, and J12-11 is present in all known RNase P's and hence is known as the universal minimum consensus structure. This structure was presumably present in the primordial RNase P.

Many Eukaryotic Pre-tRNAs Have Introns. Eukaryotic genomes contain from several hundred to several thousand tRNA genes. Many

■ CHECK YOUR UNDERSTANDING

Summarize the posttranscriptional modifications of eukaryotic mRNA.

What is the advantage of starting RNA processing before transcription is complete?

Discuss the advantages, in terms of protein structure and evolution, that result from alternative mRNA splicing.

Describe the modifications that occur during processing of prokaryotic and eukaryotic rRNAs and tRNAs.

eukaryotic primary tRNA transcripts, for example, that of yeast **tRNA^{Tyr}** (Fig. 26-33), contain a small intron as well as extra nucleotides at their 5′ and 3′ ends. tRNA processing therefore includes nucleolytic removal of the extra nucleotides. The three nucleotides, CCA, at the 3′ termini of all tRNAs, the sites at which amino acids are attached (Section 27-2B), are lacking in the immature tRNA transcripts. This trinucleotide is appended by the enzyme **tRNA nucleotidyltransferase,** which sequentially adds two C's and an A to tRNA using CTP and ATP as substrates (prokaryotic tRNA primary transcripts include the CCA sequence).

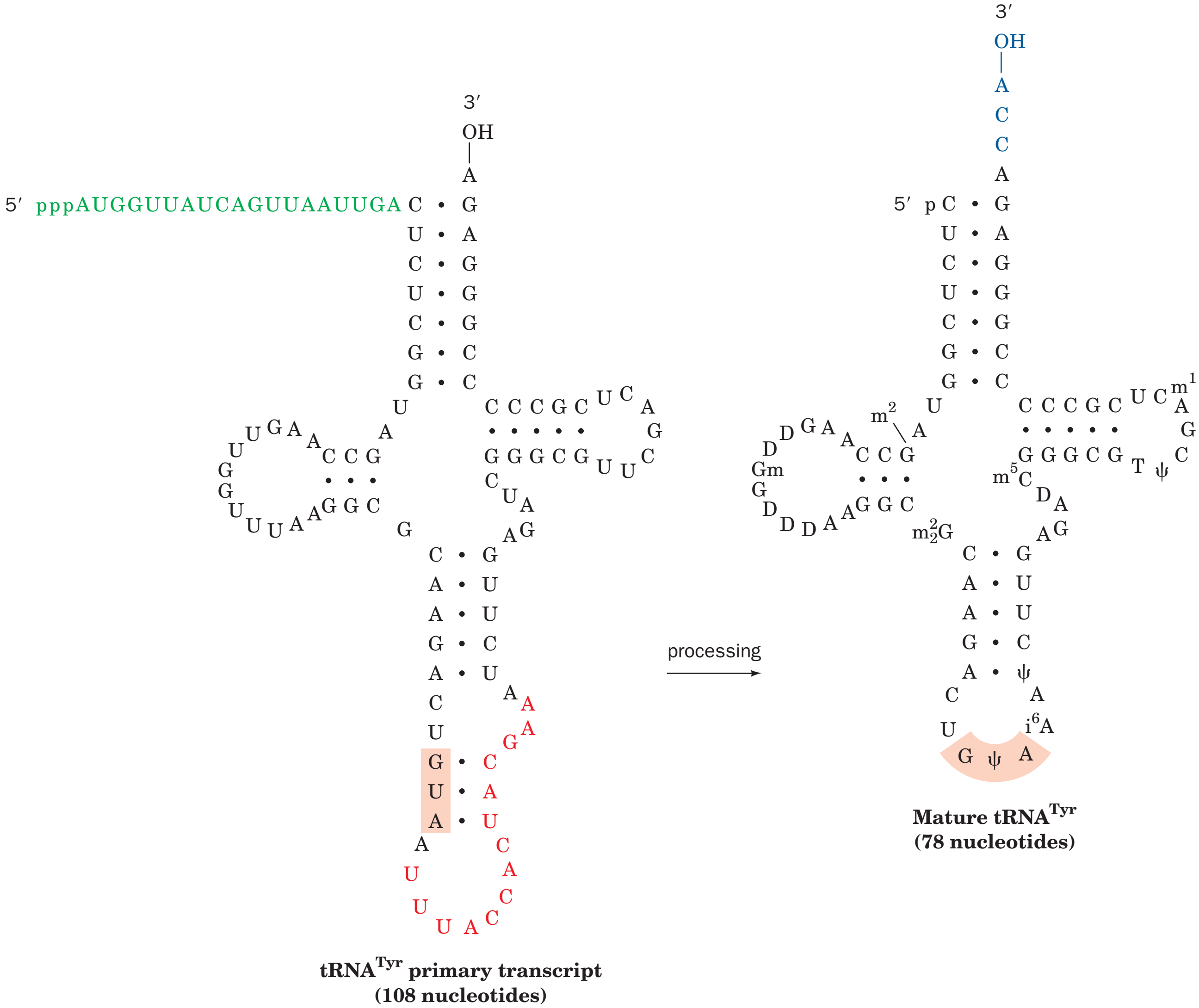

■ **Figure 26-33 | The posttranscriptional processing of yeast tRNA^{Tyr}.** A 14-nt intervening sequence (*red*) and a 19-nt 5′-terminal sequence (*green*) are excised from the primary transcript, a —CCA (*blue*) is appended to its 3′ end, and several of the bases are modified to form the mature tRNA (m^{2}G, *N*^{2}-methylguanosine; D, dihydrouridine; Gm, 2′-methylguanosine; m$_2^2$G, *N*^{2},*N*^{2}-dimethylguanosine; ψ, pseudouridine; i^{6}A, *N*^{6}-isopentenyladenosine; m^{5}C, 5-methylcytosine; m^{1}A, 1-methyladenosine; see Fig. 27-4). The anticodon is shaded. [After DeRobertis, E.M. and Olsen, M.V., *Nature* **278,** 142 (1989).]

SUMMARY

1. RNA polymerase synthesizes a polynucleotide chain from ribonucleoside triphosphates using a single strand (the antisense or noncoding strand) of DNA as a template.
2. The σ factor of *E. coli* RNA polymerase holoenzyme recognizes and binds to a promoter sequence to position the enzyme to initiate transcription.
3. RNA synthesis requires the formation of an open complex. The transcription bubble travels along the DNA as the RNA chain is elongated by the processive activity of RNA polymerase.
4. In *E. coli,* RNA synthesis is terminated in response to specific secondary structural elements in the transcript and may require the action of Rho factor.
5. Eukaryotes contain three nuclear RNA polymerases that synthesize its different types of RNAs.
6. Eukaryotic promoters are diverse: They vary in position relative to the transcription start site and may consist of multiple sequences. Enhancers form the binding sites for regulatory proteins that function as activators of transcription.
7. Basal transcription of eukaryotic genes requires six general transcription factors, including TBP, that form a preinitiation complex with RNA polymerase at the promoter. Some of these proteins remain with the polymerase when it is phosphorylated and shifts to elongation.
8. The primary transcripts of most eukaryotic structural genes are posttranscriptionally modified by the addition of a 5′ cap and a 3′ poly(A) tail. mRNAs that contain introns undergo splicing, in which the introns are excised and the flanking exons are joined together via two transesterification reactions mediated by an snRNA-containing spliceosome.
9. The processing of pre-rRNAs includes nucleolytic cleavage and snoRNA-assisted methylation. Some eukaryotic rRNA transcripts undergo splicing catalyzed by the intron itself.
10. tRNA transcripts may be processed by the addition, removal, and modification of nucleotides.

KEY TERMS

rRNA	**942**
tRNA	**942**
mRNA	**942**
RNAP	**942**
holoenzyme	**943**
σ factor	**944**
antisense strand	**944**
noncoding strand	**944**
sense strand	**944**
coding strand	**944**
structural gene	**944**
operon	**945**
polycistronic mRNA	**945**
cistron	**945**
monocistronic mRNA	**945**
promoter	**945**
Pribnow box	**946**
footprinting	**946**
open complex	**947**
constitutive enzyme	**950**
inducible enzyme	**950**
Rho factor	**951**
nucleolus	**953**
TATA box	**959**
CCAAT box	**959**
enhancer	**960**
general transcription factor	**960**
preinitiation complex	**960**
TBP	**961**
TAFs	**963**
primary transcript	**965**
posttranscriptional modification	**965**
cap	**965**
poly(A) tail	**966**
hnRNA	**967**
intron	**967**
exon	**967**
splicing	**967**
snRNA	**971**
snRNP	**971**
spliceosome	**971**
alternative splicing	**973**
RNA editing	**975**
gRNA	**975**
snoRNA	**977**
group I intron	**978**
group II intron	**978**

PROBLEMS

1. The antibiotic **cordycepin** inhibits bacterial RNA synthesis.

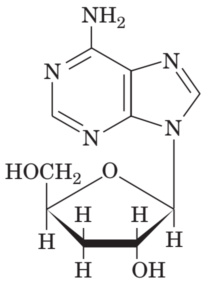

Cordycepin

(a) Of which nucleoside is cordycepin a derivative?

(b) Explain cordycepin's mechanism of action.

2. Indicate the −10 region, the −35 region, and the initiating nucleotide on the sense strand of the *E. coli* tRNA^{Tyr} promoter shown below.

5′ CAACGTAACACTTTACAGCGGCGCGTCATTTGATATGATGCGCCCCGCTTCCCGATA 3′
3′ GTTGCATTGTGAAATGTCGCCGCGCAGTAAACTATACTACGCGGGGCGAAGGGCTAT 5′

3. Design a six-residue nucleic acid probe that would hybridize with the greatest number of *E. coli* gene promoters.
4. Explain why inserting 5 bp of DNA at the −50 position of a eukaryotic gene decreases the rate of RNA polymerase II transcription initiation to a greater extent than inserting 10 bp at the same site.
5. Why does promoter efficiency tend to decrease with the number of G · C base pairs in the −10 region of a prokaryotic gene?
6. A eukaryotic ribosome contains 4 different rRNA molecules

and ~82 different proteins. Why does a cell contain many more copies of the rRNA genes than the ribosomal protein genes?

7. Design an oligonucleotide-based affinity chromatography system for purifying mature mRNAs from eukaryotic cell lysates.

8. A eukaryotic cell carrying out transcription and RNA processing is incubated with ^{32}P-labeled ATP. Where will the radioactive isotope appear in mature mRNA if the ATP is labeled at the (a) α position, (b) β position, and (c) γ position?

9. Compare DNA polymerase, RNA polymerase, poly(A) polymerase, and tRNA nucleotidyl transferase with respect to requirement for a primer, template, and substrates.

10. Explain why the active site of poly(A) polymerase is much narrower than that of DNA and RNA polymerases.

11. Explain why the $O^{2'}$-methylation of ribose residues protects rRNA from RNases.

12. Would you expect spliceosome-catalyzed intron removal to be reversible in a highly purified *in vitro* system and *in vivo?* Explain.

13. Introns in eukaryotic protein-coding genes may be quite large, but almost none are smaller than about 65 bp. What is the reason for this minimum intron size?

14. Infection with certain viruses inhibits snRNA processing in eukaryotic cells. Explain why this favors the expression of viral genes in the host cell.

REFERENCES

RNA Polymerase

Cramer, P., Multisubunit RNA polymerases, *Curr. Opin. Struct. Biol.* **12,** 89–97 (2002).

Kadonaga, K.T., The RNA polymerase II core promoter, *Annu. Rev. Biochem.* **72,** 449–479 (2003).

Marakami, K.S. and Darst, S.A., Bacterial RNA polymerases: the whole story. *Curr. Opin. Struct. Biol.* **13,** 31–39 (2003).

Shilatifard, A., Conway, R.C., and Conway, J.W., The RNA polymerase II elongation complex, *Annu. Rev. Biochem.* **72,** 693–715 (2003).

Skordalakes, E. and Berger, J.M., Structural insights into RNA-dependent ring closure and ATPase activation by the Rho termination factor, *Cell* **127,** 553–564 (2006).

Wang, D., Bushnell, D.A., Westover, K.D., Kaplan, C.D., and Kornberg, R.D., Structural basis of transcription: Role of the trigger loop in substrate specificity and catalysis, *Cell* **127,** 941–954 (2006).

RNA Processing

Black, D.L., Mechanism of alternative pre-messenger RNA splicing, *Annu. Rev. Biochem.* **72,** 291–336 (2003).

Blencoe, B.J., Alternative splicing: New insights from global analysis, *Cell* **126,** 37–47 (2006).

Decatur, W.A. and Fournier, M.J., RNA-guided nucleotide modification of ribosomal and other RNAs, *J. Biol. Chem.* **278,** 695–698 (2003).

Evans, D., Marquez, S.M., and Pace, N.R., RNase P: interface in the RNA and protein worlds, *Trends Biochem. Sci.* **31,** 333–341 (2006).

Maniatis, T. and Reed, R., An extensive network of coupling among gene expression machines, *Nature* **416,** 499–506 (2002). [Describes why efficient gene expression requires coupling between transcription and RNA processing.]

Proudfoot, N.J., Furger, A., and Dye, M.J., Integrating mRNA processing with transcription, *Cell* **108,** 501–512 (2002).

Stark, H. and Luhrmann, R., Cryo-electron microscopy of spliceosomal components, *Annu. Rev. Biophys. Biomol. Struct.* **35,** 435–457 (2006).

Vincens, Q. and Cech, T.R., Atomic level architecture of group I introns revealed, *Trends Biochem. Sci.* **31,** 41–51 (2005).

27

Protein Synthesis

Just as a printing press can generate numerous copies of a page, a ribosome, consisting of RNA as well as protein, can translate a given mRNA molecule many times to produce a large number of protein molecules. [Erich Lessing/Art Resource.]

■ CHAPTER CONTENTS

1 The Genetic Code
- **A.** Codons Are Triplets That Are Read Sequentially
- **B.** The Genetic Code Was Systematically Deciphered
- **C.** The Genetic Code Is Degenerate and Nonrandom

2 Transfer RNA and Its Aminoacylation
- **A.** All tRNAs Have a Similar Structure
- **B.** Aminoacyl–tRNA Synthetases Attach Amino Acids to tRNAs
- **C.** A tRNA May Recognize More than One Codon

3 Ribosomes
- **A.** The Prokaryotic Ribosome Consists of Two Subunits
- **B.** The Eukaryotic Ribosome Is Larger and More Complex

4 Translation
- **A.** Chain Initiation Requires an Initiator tRNA and Initiation Factors
- **B.** The Ribosome Decodes the mRNA, Catalyzes Peptide Bond Formation, Then Moves to the Next Codon
- **C.** Release Factors Terminate Translation

5 Posttranslational Processing
- **A.** Ribosome-Associated Chaperones Help Proteins Fold
- **B.** Newly Synthesized Proteins May Be Covalently Modified

■ MEDIA RESOURCES

(available at www.wiley.com/college/voet)

Guided Exploration 26. The structure of tRNA

Guided Exploration 27. The structures of aminoacyl–tRNA synthetases and their interactions with tRNAs

Guided Exploration 28. Translational initiation

Guided Exploration 29. Translational elongation

Interactive Exercise 53. Ribosomal subunits in complex with three tRNAs and an mRNA

Interactive Exercise 54. Elongation factor EF-Tu in its complexes with GDP and GMPPNP

Kinemage 21-1. Structure of yeast tRNA^{Phe}

Kinemage 21-2. Modified bases in tRNAs

Kinemage 22. Structure of GlnRS–tRNA^{Gln}–ATP

Case Study 29. Pseudovitamin D Deficiency

How is the genetic information encoded in DNA decoded? In the preceding chapter, we saw how the base sequence of DNA is transcribed into that of RNA. In this chapter, we shall consider the remainder of the decoding process by examining how the base sequences of RNAs are translated into the amino acid sequences of proteins. This second part of the central dogma of molecular biology (DNA → RNA → protein) shares a number of features with both DNA replication and transcription, the other major events of nucleic acid metabolism. First, all three processes are carried out by large, complicated protein-containing macromolecular machines whose proper functioning depends on a variety of specific and nonspecific protein–nucleic acid interactions. Accessory factors are also required for the initiation, elongation, and termination phases of these processes. Furthermore, translation, like replication and transcription, must be executed with accuracy. Although translation involves base pairing between complementary nucleotides, it is amino acids, rather than nucleotides, that are ultimately joined to generate a polymeric product. This process, like replication and transcription, is endergonic and requires the cleavage of "high-energy" phosphoanhydride bonds.

An understanding of translation requires not only a knowledge of the macromolecules that participate in polypeptide synthesis, but an appreciation for the mechanisms that produce a chain of linked amino acids in the exact order specified by mRNA. Accordingly, we begin this chapter by examining the **genetic code,** the correspondence between nucleic acid sequences and polypeptide sequences. We then consider in turn the structures and properties of tRNAs and ribosomes. Next, we examine how the translation machinery operates as a coordinated whole. Finally, we take a brief look at some posttranslational steps of protein synthesis.

1 The Genetic Code

LEARNING OBJECTIVES

- Understand that the genetic code is based on codons that are read sequentially.
- Understand that each codon represents one amino acid or a Stop signal.
- Understand that the genetic code is degenerate, nonrandom, and nearly universal.

One of the most fascinating puzzles in molecular biology is how a sequence of nucleotides composed of only four types of residues can specify the sequence of up to 20 types of amino acids in a polypeptide chain. Clearly, a one-to-one correspondence between nucleotides and amino acids is not possible. *A group of several bases, termed a* ***codon,*** *is necessary to specify a single amino acid.* A triplet code, that is, one with 3 bases per codon, is more than sufficient to specify all the amino acids since there are $4^3 = 64$ different triplets of bases. A doublet code with 2 bases per codon ($4^2 = 16$ possible doublets) would be inadequate. The triplet code allows many amino acids to be specified by more than one codon. Such a code, in a term borrowed from mathematics, is said to be **degenerate.**

How does the polypeptide-synthesizing apparatus group DNA's continuous sequences of bases into codons? For example, the code might be overlapping; that is, in the sequence

ABCDEFGHIJ · · ·

ABC might code for one amino acid, BCD for a second, CDE for a third, etc. Alternatively, the code might be nonoverlapping, so that ABC specifies one amino acid, DEF a second, GHI a third, etc. In fact, *the genetic code is a nonoverlapping, degenerate, triplet code.* A number of elegant experiments, some of which are outlined below, revealed the workings of the genetic code.

A | Codons Are Triplets That Are Read Sequentially

In genetic experiments on bacteriophage T4, Francis Crick and Sydney Brenner found that a mutation that resulted in the deletion of a nucleotide could abolish the function of a specific gene. However, a second mutation, in which a nucleotide was inserted at a different but nearby position, could restore gene function. These two mutations are said to be **suppressors** of one another; that is, they cancel each other's mutant properties. On the basis of these experiments, Crick and Brenner concluded that *the genetic code is read in a sequential manner starting from a fixed point in the gene.* The insertion or deletion of a nucleotide shifts the **reading frame** (grouping) in which succeeding nucleotides are read as codons. Insertions or deletions of nucleotides are therefore known as **frameshift mutations.**

In further experiments, Crick and Brenner found that whereas two closely spaced deletions or two closely spaced insertions could not suppress each other (restore gene function), three closely spaced deletions or insertions could do so. These observations clearly established that *the genetic code is a triplet code.*

The foregoing principles are illustrated by the following analogy. Consider a sentence (gene) in which the words (codons) each consist of three letters (bases):

THE BIG RED FOX ATE THE EGG

Here the spaces separating the words have no physical significance; they are present only to indicate the reading frame. The deletion of the fourth letter, which shifts the reading frame, changes the sentence to

THE IGR EDF OXA TET HEE GG

so that all words past the point of deletion are unintelligible (specify the wrong amino acids). An insertion of any letter, however, say an X in the ninth position,

THE IGR EDX FOX ATE THE EGG

restores the original reading frame. Consequently, only the words between the two changes (mutations) are altered. As in this example, such a sentence might still be intelligible (the gene could still specify a functional protein), particularly if the changes are close together. Two deletions or two insertions, no matter how close together, would not suppress each other but just shift the reading frame. However, three insertions, say X, Y, and Z in the fifth, eighth, and twelfth positions, respectively, would change the sentence to

THE BXI GYR EDZ FOX ATE THE EGG

which, after the third insertion, restores the original reading frame. The same would be true of three deletions. As before, if all three changes were close together, the sentence might still retain its meaning. Like this textual analogy, *the genetic code has no internal punctuation to indicate the reading frame; instead, the nucleotide sequence is read sequentially, triplet by triplet.*

Since any nucleotide sequence may have three reading frames, it is possible, at least in principle, for a polynucleotide to encode two or even three different polypeptides. In fact, some single-stranded DNA bacteriophages (which presumably must make maximal use of their small complement of DNA) contain completely overlapping genes that have different reading frames. A similar form of coding economy is exhibited by bacteria, in which the ribosomal initiation sequence of one gene in a polycistronic mRNA often overlaps the end of the preceding gene.

B | The Genetic Code Was Systematically Deciphered

In order to understand how the genetic code dictionary was elucidated, we must first review how proteins are synthesized. An mRNA does not directly recognize amino acids. Rather, *it specifically binds molecules of tRNA that each carry a corresponding amino acid* (Fig. 27-1). Each tRNA contains a trinucleotide sequence, its **anticodon,** that is complementary to an mRNA codon specifying the tRNA's amino acid. During translation, amino acids carried by tRNAs are joined together according to the order in which the tRNA anticodons bind to the mRNA codons at the ribosome (Fig. 3-14).

The genetic code could, in principle, be determined by simply comparing the base sequence of an mRNA with the amino acid sequence of the polypeptide it specifies. In the 1960s, however, techniques for isolating and sequencing mRNAs had not yet been developed. Moreover, techniques for synthesizing RNAs were quite rudimentary. They utilized **polynucleotide phosphorylase,** an enzyme from *Azotobacter vinelandii* that links together nucleotides without the use of a template.

$$(\text{RNA})_n + \text{NDP} \rightleftharpoons (\text{RNA})_{n+1} + \text{P}_i$$

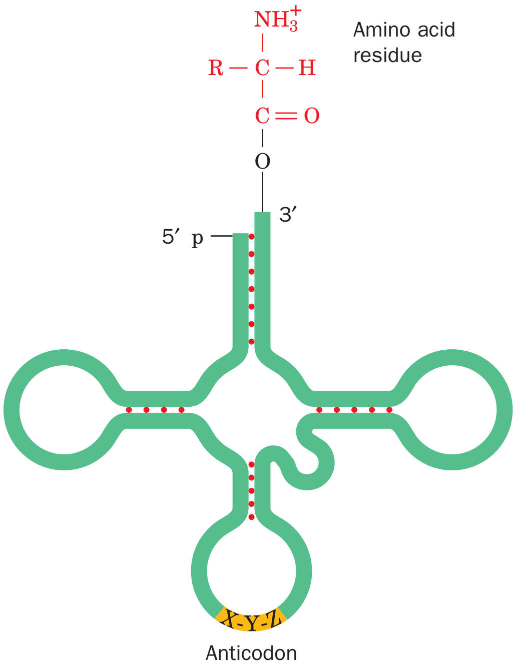

Figure 27-1 | Transfer RNA in its "cloverleaf" form. Its covalently linked amino acid residue is at the top, and its anticodon (X-Y-Z, a trinucleotide segment that base-pairs with the complementary mRNA codon during translation) is at the bottom.

Thus, the NDPs are linked together at random so that the base composition of the product RNA reflects that of the reactant NDP mixture. The elucidation of the genetic code therefore proved to be a difficult task, even with the development of cell-free translation systems.

E. coli cells that have been gently broken open and centrifuged to remove cell walls and membranes yield an extract containing DNA, mRNA, ribosomes, enzymes, and other cell constituents necessary for protein synthesis. When fortified with ATP, GTP, and amino acids, this system synthesizes small amounts of protein. A cell-free translation system, of course, produces proteins specified by the cell's DNA. Adding DNase halts protein synthesis after a few minutes because the system can no longer synthesize mRNA, and the mRNA originally present is rapidly degraded. At this point, purified mRNA or synthetic mRNA can be added to the system and the resulting polypeptide products can be subsequently recovered.

In 1961, Marshall Nirenberg and Heinrich Matthaei added the synthetic polyribonucleotide poly(U) to a cell-free translation system containing isotopically labeled amino acids and recovered a labeled poly(Phe) polypeptide. They concluded that *UUU must be the codon that specifies Phe.* Similar experiments with poly(A) and poly(C) yielded poly(Lys) and poly(Pro), respectively, thereby identifying AAA as a codon for Lys and CCC as a codon for Pro.

In another series of experiments, different trinucleotides were tested for their ability to promote tRNA binding to ribosomes. The ribosomes, with their bound tRNAs, are retained by a nitrocellulose filter, but free tRNAs are not. The bound tRNA can be identified by the radioactive amino acid attached to it. This simple binding assay revealed that, for instance, UUU stimulates the ribosomal binding of only Phe tRNA. Likewise, UUG, UGU, and GUU stimulate the binding of Leu, Cys, and Val tRNAs, respectively. Hence UUG, UGU, and GUU must be codons that specify Leu, Cys, and Val, respectively. In this way, the amino acids specified by some 50 codons were identified. For the remaining codons, the binding assay was either negative (no tRNA bound) or ambiguous.

The genetic code dictionary was completed and previous results confirmed through H. Gobind Khorana's chemical synthesis of polynucleotides with specified repeating sequences (at the time, an extremely laborious process). In a cell-free translation system, UCUCUCUC. . ., for example, is read

UCU CUC UCU CUC UCU CUC · · ·

so that it specifies a polypeptide chain of two alternating amino acid residues. This particular mRNA stimulated the production of

Ser — Leu — Ser — Leu — Ser — Leu — · · ·

since UCU codes for Ser and CUC codes for Leu.

Alternating sequences of three nucleotides, such as poly(UAC), specify three different homopolypeptides because ribosomes may initiate polypeptide synthesis on these synthetic mRNAs in any of the three possible reading frames (Fig. 27-2). Analyses of the polypeptides specified by various alternating sequences of two and three nucleotides confirmed the identify of many codons and filled out missing portions of the genetic code.

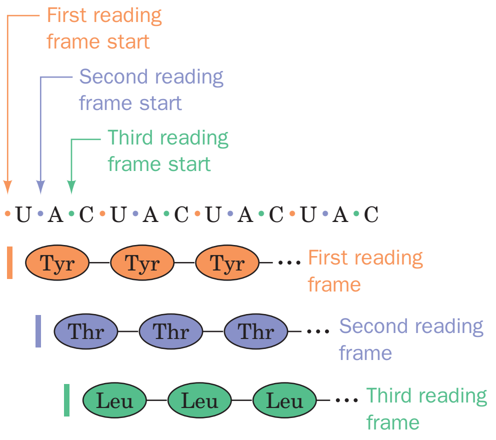
First reading frame start
Second reading frame start
Third reading frame start
U · A · C · U · A · C · U · A · C · U · A · C
Tyr
Tyr
Tyr
First reading frame
Thr
Thr
Thr
Second reading frame
Leu
Leu
Leu
Third reading frame

Figure 27-2 | The three potential reading frames of an mRNA. Each reading frame would yield a different polypeptide.

C | The Genetic Code Is Degenerate and Nonrandom

The genetic code, presented in Table 27-1, has several remarkable features:

1. *The code is highly degenerate.* Three amino acids—Arg, Leu, and Ser—are each specified by six different codons, and most of the rest are specified by either four, three, or two codons. Only Met and Trp,

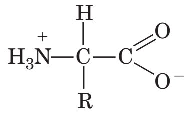

Table 27-1 The "Standard" Genetic Code[a]

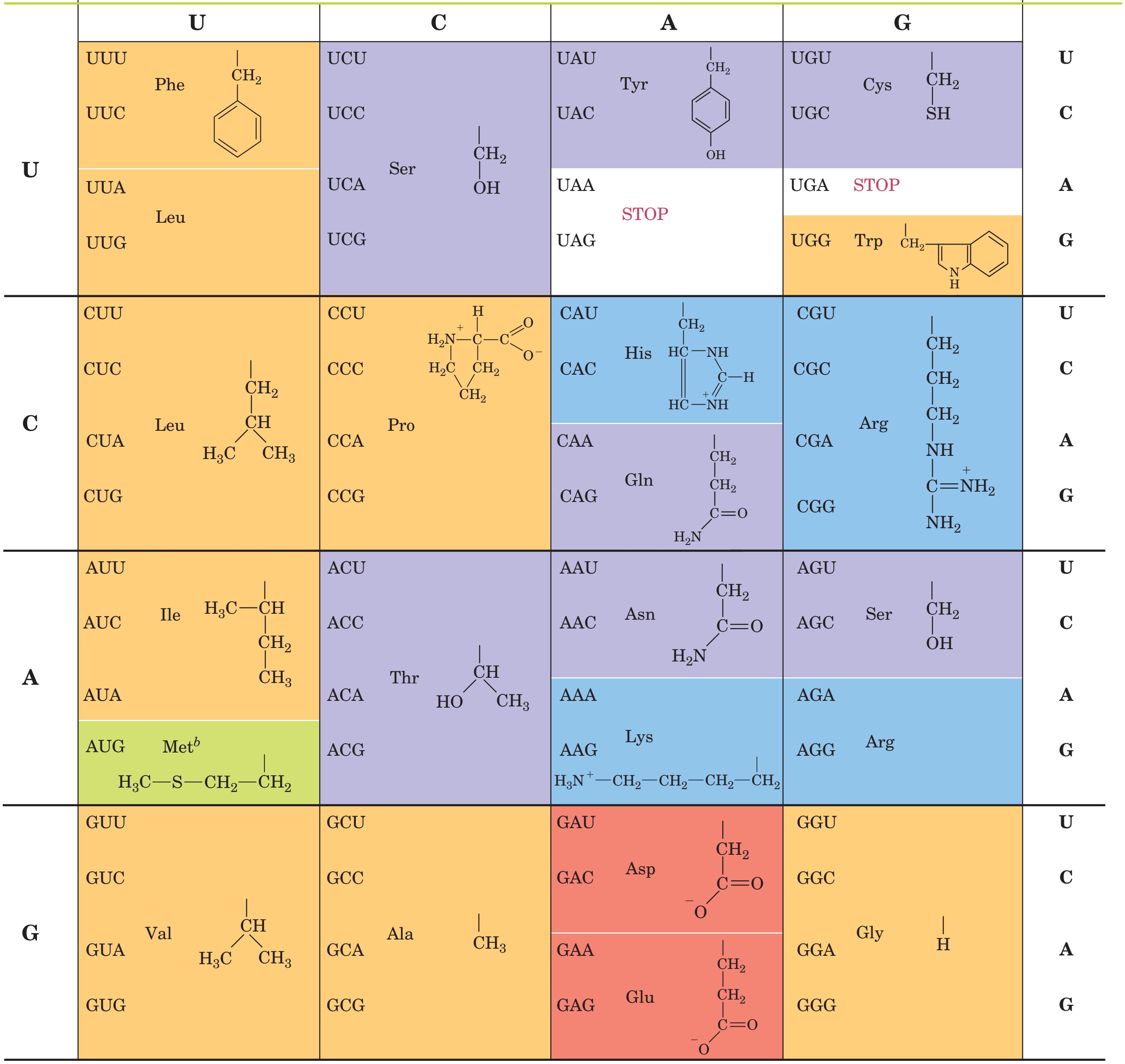

First position (5′ end)	Second position U	Second position C	Second position A	Second position G	Third position (3′ end)
U	UUU Phe	UCU Ser	UAU Tyr	UGU Cys	**U**
	UUC	UCC	UAC	UGC	**C**
	UUA Leu	UCA	UAA STOP	UGA STOP	**A**
	UUG	UCG	UAG	UGG Trp	**G**
C	CUU Leu	CCU Pro	CAU His	CGU Arg	**U**
	CUC	CCC	CAC	CGC	**C**
	CUA	CCA	CAA Gln	CGA	**A**
	CUG	CCG	CAG	CGG	**G**
A	AUU Ile	ACU Thr	AAU Asn	AGU Ser	**U**
	AUC	ACC	AAC	AGC	**C**
	AUA	ACA	AAA Lys	AGA Arg	**A**
	AUG Met[b]	ACG	AAG	AGG	**G**
G	GUU Val	GCU Ala	GAU Asp	GGU Gly	**U**
	GUC	GCC	GAC	GGC	**C**
	GUA	GCA	GAA Glu	GGA	**A**
	GUG	GCG	GAG	GGG	**G**

[a] Nonpolar amino acid residues are tan, basic residues are blue, acidic residues are red, and polar uncharged residues are purple.

[b] AUG forms part of the initiation signal as well as coding for internal Met residues.

two of the least common amino acids in proteins (Table 4-1), are represented by a single codon. Codons that specify the same amino acid are termed **synonyms.**

BOX 27-1 PERSPECTIVES IN BIOCHEMISTRY

Evolution of the Genetic Code

Because of the degeneracy of the genetic code, a point mutation in the third position of a codon seldom alters the specified amino acid. For example, a GUU → GUA transversion still codes for Val and is therefore said to be phenotypically silent. Other point mutations, even at the first or second codon positions, producing AUU (Ile) or GCU (Ala), for instance, result in the substitution of a chemically similar amino acid and may have minimal impact on the encoded protein's overall structure or function. This built-in protection against mutation may be more than accidental.

In the 1960s, the perceived universality of the genetic code led Francis Crick to propose the "frozen accident" theory, which holds that codons were allocated to different amino acids entirely by chance. Once assigned, the meaning of a codon could not change because of the high probability of disrupting the structure of the encoded protein. Thus, once established, the genetic code was thought to have ceased evolving.

However, the distribution of codons as presented in Table 27-1 suggests an alternative evolutionary history of the genetic code, in which a few simple codons corresponding to a handful of amino acids gradually became more complex. One scenario begins with an RNA-based world containing only A and U nucleotides. Uracil is almost certainly a primordial base since the pyrimidine biosynthetic pathway yields uracil nucleotides before cytosine or thymine nucleotides (Section 23-2). Adenine would have been required as uracil's complement.

Assuming that a triplet-based genetic code was established at the outset (and it is difficult to envision how any other arrangement could have given rise to the present-day triplet code), the two bases could have coded for $2^3 = 8$ amino acids. In fact, the contemporary genetic code assigns these all-U/A codons to six amino acids and a stop signal:

UUU = Phe
UUA = Leu
UAU = Tyr
AUU = Ile
AAA = Lys
AAU = Asn
AUA = Ile
UAA = Stop

The AUA codon may well have originally specified the initiating Met (now encoded by AUG), bringing the total to seven amino acids.

When G and C appeared in evolving life-forms, these nucleotides were incorporated into RNA. Codons containing three or four types of bases could specify additional amino acids, but because of selective pressure against introducing disruptive mutations into proteins, the level of codon redundancy increased. An inspection of Table 27-1 shows that triplet codons made entirely of G and C specify only four different amino acids, which is half the theoretical maximum of eight:

GGG, GGC = Gly
GCG, GCC = Ala
CGG, CGC = Arg
CCC, CCG = Pro

This nonrandom allocation of codons to amino acids argues against a completely random origin for the genetic code. The gradual introduction of two new bases (G and C) to a primitive genetic code based on U and A must have allowed greater information capacity (i.e., coding for 20 amino acids) while minimizing the rate of deleterious substitutions.

2. *The arrangement of the code table is nonrandom.* Most synonyms occupy the same box in Table 27-1; that is, they differ only in their third nucleotide. XYU and XYC always specify the same amino acid; XYA and XYG do so in all but two cases. Moreover, changes in the first codon position tend to specify similar (if not the same) amino acids, whereas codons with second position pyrimidines encode mostly hydrophobic amino acids (tan in Table 27-1), and those with second position purines encode mostly polar amino acids (blue, red, and purple in Table 27-1). These observations suggest a nonrandom origin of the genetic code and indicate that the code evolved so as to minimize the deleterious effects of mutations (see Box 27-1).
3. *UAG, UAA, and UGA are* ***Stop codons.*** These three codons (also known as **nonsense codons**) do not specify amino acids but signal the ribosome to terminate polypeptide chain elongation. UAG, UAA, and UGA are often referred to as **amber, ochre,** and **opal codons** (these names are the result of a laboratory joke: The German word for *amber* is Bernstein, the name of an individual who helped discover amber mutations, which change some other codon to UAG; *ochre* and *opal* are puns on *amber*).
4. *AUG and GUG are chain initiation codons.* The codons AUG and, less

frequently, GUG specify the starting point for polypeptide chain synthesis. However, they also specify the amino acids Met and Val, respectively, at internal positions in polypeptide chains. We shall see in Section 27-4A how ribosomes differentiate the two types of codons.

The "Standard" Genetic Code Is Not Universal. For many years, it was thought that the "standard" genetic code (that given in Table 27-1) was universal. This assumption was based in part on the observation that one kind of organism (e.g., *E. coli*) can accurately translate the genes for quite different organisms (e.g., humans). Indeed, this phenomenon is the basis of genetic engineering. DNA studies in 1981 nevertheless revealed that *the genetic codes of certain mitochondria are variants of the "standard" genetic code.* For example, in mammalian mitochondria, AUA, as well as the standard AUG, is a Met/initiation codon; UGA specifies Trp rather than "Stop"; and AGA and AGG are "Stop" rather than Arg. Apparently, mitochondria, which contain their own genes and protein-synthesizing systems, are not subject to the same evolutionary constraints as are nuclear genomes. An alternate genetic code also appears to have evolved in ciliated protozoa, which branched off very early in eukaryotic evolution. Thus, the "standard" genetic code, although very widely utilized, is not universal.

CHECK YOUR UNDERSTANDING

Why do frameshift mutations occur with the insertion or deletion of one or two, but not three, nucleotides?

Describe how the "meaning" of each codon was determined.

Explain why codons must consist of at least three nucleotides.

2 Transfer RNA and Its Aminoacylation

LEARNING OBJECTIVES

- Understand that tRNA molecules have a characteristic structure.
- Understand that an aminoacyl–tRNA synthetase charges each tRNA with the appropriate amino acid.
- Understand that the wobble hypothesis explains the ability of a tRNA to recognize more than one codon.

Cells must translate the language of RNA base sequences into the language of polypeptides. In 1955, Francis Crick hypothesized that translation occurs through the mediation of "adaptor" molecules, which we now know are tRNAs, that carry a specific amino acid and recognize the corresponding mRNA codon.

See Guided Exploration 26
The structure of tRNA.

A | All tRNAs Have a Similar Structure

In 1965, after a 7-year effort, Robert Holley reported the first known base sequence of a biologically significant nucleic acid, that of the 76-residue yeast **alanine tRNA ($\mathbf{tRNA^{Ala}}$).** Currently, the base sequences of over 7600 tRNAs from more than 200 organisms and organelles are known (most from their DNA sequences). They vary in length from 54 to 100 nucleotides (18–28 kD) although most have ~76 nucleotides.

Almost all known tRNAs can be schematically arranged in the so-called cloverleaf secondary structure (Fig. 27-3). Starting from the 5′ end, they have the following common features:

1. A 5′-terminal phosphate group.
2. A 7-bp stem that includes the 5′-terminal nucleotide and that may contain non-Watson–Crick base pairs such as G · U. This assembly is known as the **acceptor** or **amino acid stem** because the amino acid residue carried by the tRNA is covalently attached to its 3′-terminal OH group.

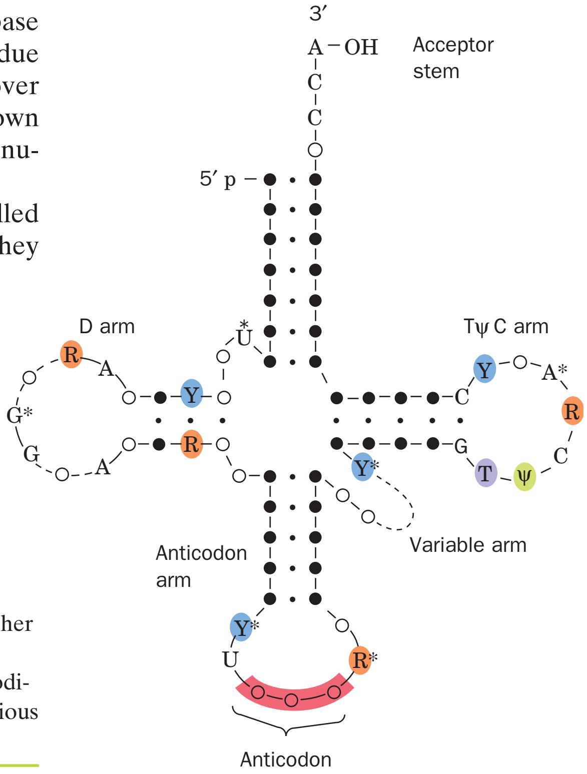

Figure 27-3 | The cloverleaf secondary structure of tRNA. Filled circles connected by dots represent Watson–Crick base pairs, and open circles indicate other bases. Invariant positions are indicated: R and Y represent invariant purines and pyrimidines, and ψ represents pseudouridine. The starred nucleotides are often modified. The D and variable arms contain different numbers of nucleotides in the various tRNAs.

3. A 3- or 4-bp stem ending in a 5- to 7-nt loop that frequently contains the modified base **dihydrouridine (D).** This stem and loop are therefore collectively termed the **D arm.**
4. A 5-bp stem ending in a loop that contains the anticodon. These features are known as the **anticodon arm.**
5. A 5-bp stem ending in a loop that usually contains the sequence TψC (where ψ is the symbol for **pseudouridine;** Section 26-3B). This assembly is called the **TψC** or **T arm.**
6. A 3′ CCA sequence with a free 3′-OH group. The —CCA may be genetically specified or enzymatically added to immature tRNA, depending on the species (Section 26-3C).

tRNAs have 15 invariant positions (always have the same base) and 8 **semi-invariant** positions (only a purine or only a pyrimidine) that occur mostly in the loop regions. The purine on the 3′ side of the anticodon is invariably modified. The site of greatest variability among the known tRNAs occurs in the so-called **variable arm.** It has from 3 to 21 nucleotides and may have a stem consisting of up to 7 bp.

tRNAs Have Numerous Modified Bases. One of the most striking characteristics of tRNAs is their large proportion, up to 25%, of posttranscriptionally modified bases. Nearly 80 such bases, found at >60 different tRNA positions, have been characterized. A few of them, together with their standard abbreviations, are indicated in Fig. 27-4. None of these modifications are essential for maintaining a tRNA's structural integrity or for its proper binding to the ribosome. However, base modifications may help promote attachment of the proper amino acid to the acceptor stem or strengthen codon–anticodon interactions.

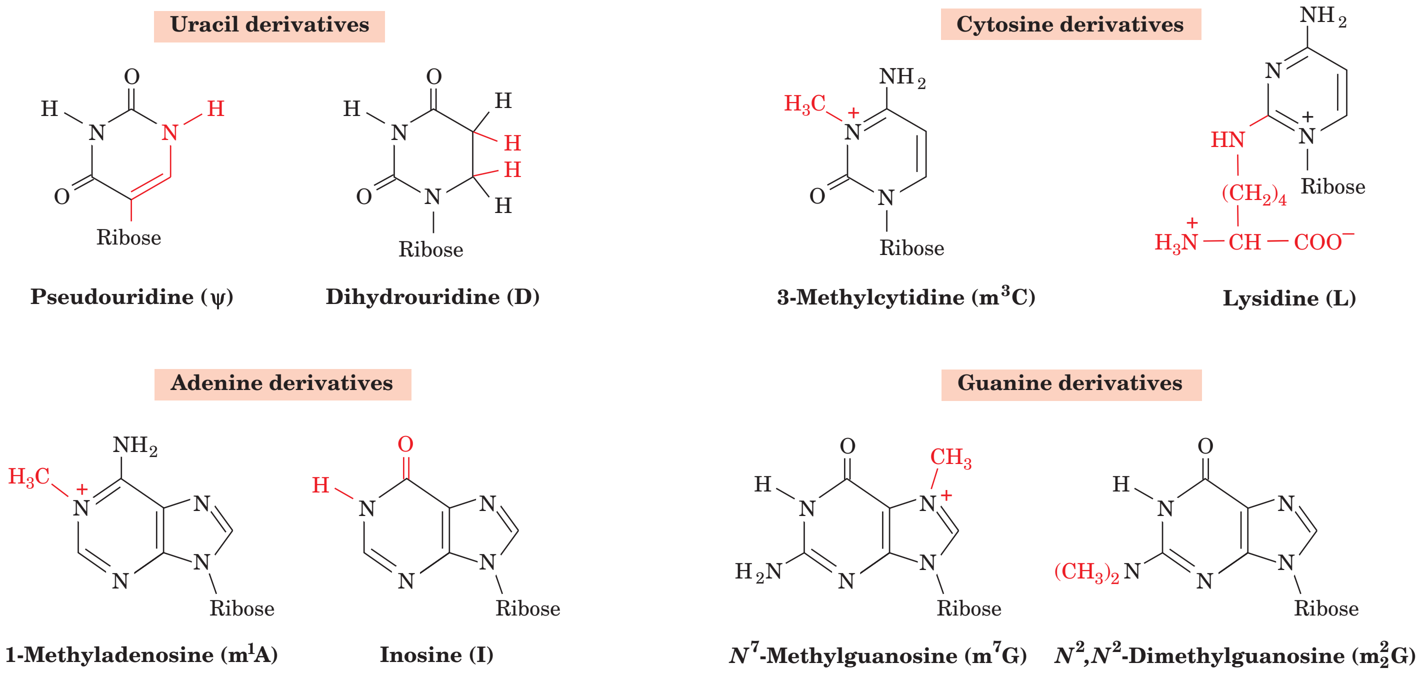

Pseudouridine (ψ) **Dihydrouridine (D)** **3-Methylcytidine (m^3C)** **Lysidine (L)**

1-Methyladenosine (m^1A) **Inosine (I)** **N^7-Methylguanosine (m^7G)** **N^2,N^2-Dimethylguanosine (m^2_2G)**

Figure 27-4 | A few of the modified nucleosides that occur in tRNAs. Note that although inosine chemically resembles guanosine, it is biochemically derived by the deamination of adenosine. Nucleosides may also be methylated at their ribose 2′ positions to form residues symbolized, for instance, by Cm, Gm, and Um. **See Kinemage Exercise 21-2.**

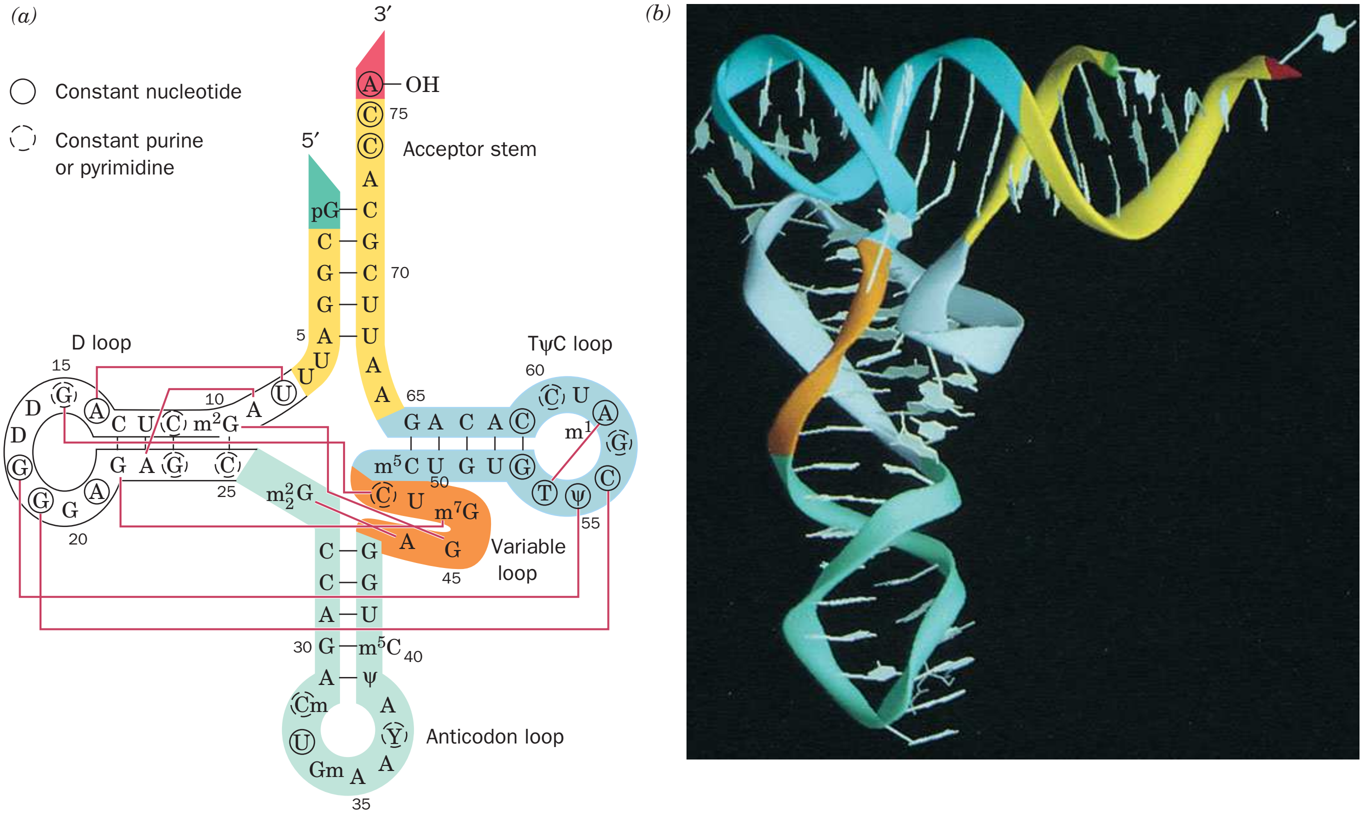

■ **Figure 27-5 | The structure of yeast tRNA^{Phe}.** (*a*) The base sequence drawn in cloverleaf form. Tertiary base-pairing interactions are represented by thin red lines connecting the participating bases. Bases that are conserved or semiconserved in all tRNAs are circled by solid and dashed lines, respectively. The 5′ terminus is colored bright green, the acceptor stem is yellow, the D arm is white, the anticodon arm is light green, the variable arm is orange, the TψC arm is cyan, and the 3′ terminus is red. (*b*) The X-ray structure drawn to show how its base-paired stems are arranged to form the L-shaped molecule. The sugar–phosphate backbone is represented by a ribbon with the same color scheme as in Part *a*. [Courtesy of Mike Carson, University of Alabama at Birmingham. PDBid 6TNA.] **See Kinemage Exercise 21-1.**

tRNA Has a Complex Tertiary Structure. As described in Section 24-2C, tRNA molecules have an L-shape in which the acceptor and T stems form one leg and the D and anticodon stems form the other (Fig. 27-5). Each leg of the L is ~60 Å long and the anticodon and amino acid acceptor sites are at opposite ends of the molecule, some 76 Å apart. The narrow 20- to 25-Å width of tRNA is essential to its biological function: During protein synthesis, three tRNA molecules must simultaneously bind in close proximity at adjacent codons on mRNA (Section 27-4B).

tRNA's complex tertiary structure is maintained by extensive stacking interactions and base pairing within and between the helical stems. Many of the tertiary base-pairing interactions are non-Watson–Crick associations. Moreover, most of the bases involved in these interactions are either invariant or semi-invariant, consistent with the notion that *all tRNAs have similar conformations.* The compact structure of yeast tRNA^{Phe} renders most of its bases inaccessible to solvent. The most notable exceptions are the anticodon bases and those of the amino acid–bearing —CCA terminus. Both of these groupings must be accessible in order to carry out their biological functions.

See Guided Exploration 27
The structures of aminoacyl–tRNA synthetases and their interactions with tRNAs.

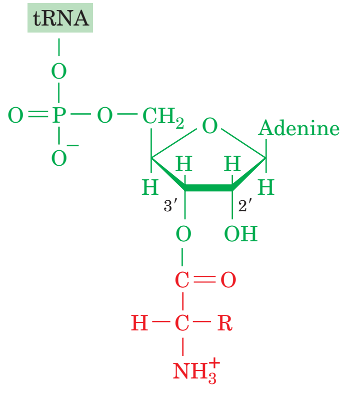

Aminoacyl–tRNA

Figure 27-6 | An aminoacyl–tRNA. The amino acid residue is esterified to the tRNA's 3′-terminal nucleotide at either its 3′-OH group, as shown here, or its 2′-OH group.

Table 27-2 Classification of *E. coli* Aminoacyl–tRNA Synthetases

Class I Amino Acid	Class II Amino Acid
Arg	Ala
Cys	Asn
Gln	Asp
Glu	Gly
Ile	His
Leu	Lys
Met	Phe
Trp	Pro
Tyr	Ser
Val	Thr

B | Aminoacyl–tRNA Synthetases Attach Amino Acids to tRNAs

Accurate translation requires two equally important recognition steps:

1. The correct amino acid must be selected for covalent attachment to a tRNA by an **aminoacyl–tRNA synthetase** (discussed below).
2. The correct **aminoacyl–tRNA (aa–tRNA)** must pair with an mRNA codon at the ribosome (discussed in Section 27-4B).

An amino acid–specific aminoacyl–tRNA synthetase **(aaRS)** appends an amino acid to the 3′-terminal ribose residue of its cognate tRNA to form an aa–tRNA (Fig. 27-6). Aminoacylation occurs in two sequential reactions that are catalyzed by a single enzyme.

1. The amino acid is first "activated" by its reaction with ATP to form an **aminoacyl–adenylate,**

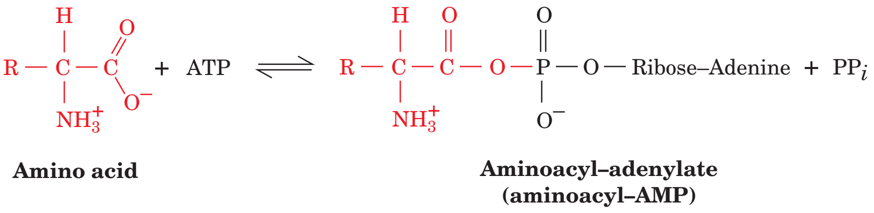

$$R-\underset{NH_3^+}{\overset{H}{C}}-C\begin{matrix}{/\!/}O\\ \backslash O^-\end{matrix} + \text{ATP} \rightleftharpoons R-\underset{NH_3^+}{\overset{H}{C}}-\overset{O}{\overset{\|}{C}}-O-\underset{O^-}{\overset{O}{\overset{\|}{P}}}-O-\text{Ribose–Adenine} + PP_i$$

which, with all but three aaRSs, can occur in the absence of tRNA. Indeed, this intermediate can be isolated, although it normally remains tightly bound to the enzyme.

2. The mixed anhydride then reacts with tRNA to form the aa–tRNA:

$$\text{Aminoacyl–AMP} + \text{tRNA} \rightleftharpoons \text{aminoacyl–tRNA} + \text{AMP}$$

The overall aminoacylation reaction

$$\text{Amino acid} + \text{tRNA} + \text{ATP} \rightarrow \text{aminoacyl–tRNA} + \text{AMP} + PP_i$$

is driven to completion by the hydrolysis of the PP_i generated in the first reaction step. The aa–tRNA product is a "high-energy" compound (Section 14-2A); for this reason, the amino acid is said to be "activated" and the tRNA is said to be "charged." Amino acid activation resembles fatty acid activation (Section 20-2A); the major difference is that tRNA is the acyl acceptor in amino acid activation whereas CoA performs this function in fatty acid activation.

There Are Two Classes of Aminoacyl–tRNA Synthetases. Most cells have at least one aaRS for each of the 20 amino acids. The similarity of the reaction catalyzed by these enzymes and the structural similarities among tRNAs suggest that all aaRSs evolved from a common ancestor and should therefore be structurally related. This is not the case. In fact, *the aaRSs form a diverse group of enzymes with different sizes and quaternary structures and little sequence similarity.* Nevertheless, these enzymes can be grouped into two classes that each have the same 10 members in nearly all organisms (Table 27-2). **Class I** and **Class II aminoacyl–tRNA synthetases** differ in several ways:

1. **Structural motifs.** The Class I enzymes share two homologous polypeptide segments that are components of a dinucleotide-binding fold (Rossmann fold, which is also present in many NAD^+- and ATP-binding proteins; Section 6-2C). The Class II synthetases

lack the foregoing sequences but have three other sequences in common.

2. **Anticodon recognition.** Many Class I aaRSs must recognize the anticodon to aminoacylate their cognate tRNAs. In contrast, several Class II enzymes do not interact with their bound tRNA's anticodon.
3. **Site of aminoacylation.** All Class I enzymes aminoacylate their bound tRNA's 3′-terminal 2′-OH group, whereas Class II enzymes charge the 3′-OH group. Nevertheless, an aminoacyl group attached at the 2′ position rapidly equilibrates between the 2′ and 3′ positions (it must be at the 3′ position to take part in protein synthesis).
4. **Amino acid specificity.** The amino acids for which the Class I synthetases are specific tend to be larger and more hydrophobic than those for Class II synthetases.

Aminoacyl–tRNA Synthetases Recognize Unique Structural Features of tRNA. How does an aaRS recognize a tRNA so that it can be charged with the proper amino acid? First, all tRNAs have similar structures, so the features that differentiate them must be subtle variations in sequence or local structure. On the other hand, since the genetic code is degenerate, more than one tRNA may carry a given amino acid. The members of each set of these so-called **isoaccepting tRNAs** must all be recognized by their cognate aaRS. Finally, the tRNA must be charged with only the amino acid that corresponds to its anticodon, and not any of the 19 other amino acids.

Clues to the specificity of synthetase–tRNA interactions have been gleaned from studies using tRNA fragments, mutationally altered tRNAs, chemical cross-linking agents, computerized sequence comparisons, and X-ray crystallography. When the experimentally determined synthetase contact sites, or identity elements, for a variety of tRNAs are mapped onto a three-dimensional model of a tRNA molecule, they cluster in the acceptor stem, the anticodon loop, and other points on the inner (concave) face of the L (Fig. 27-7). However, there appears to be little regularity in how the synthetases recognize their cognate tRNAs, and some enzyme–tRNA interactions do not involve the anticodon at all.

Synthetases that do interact with both the anticodon and the acceptor stem must have a size and structure adequate to bind both legs of the L-shaped tRNA. This is evident in the complex of *E. coli* **glutaminyl–tRNA synthetase (GlnRS)** with **tRNA$^{\text{Gln}}$** and ATP (Fig. 27-8), determined by Thomas Steitz, the first such structure to be elucidated. GlnRS, a 553-residue monomeric Class I enzyme, has an elongated shape so that it binds the anticodon near one end of the protein and the acceptor stem near the other. Genetic and biochemical data indicate that the identity elements for tRNA$^{\text{Gln}}$ include all seven bases of the anticodon loop. The bases of the anticodon itself are unstacked and splay outward so as to bind in separate recognition pockets of GlnRS.

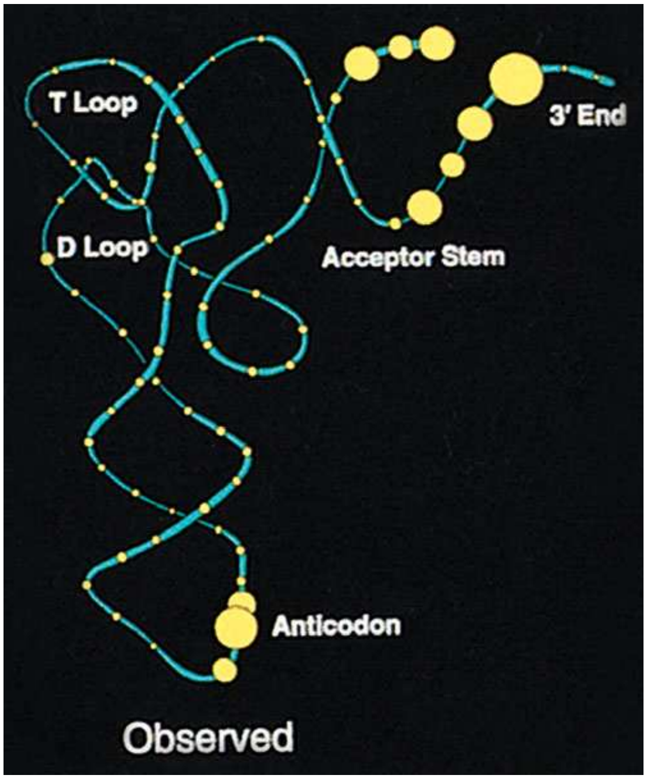

■ **Figure 27-7 | Experimentally observed identity elements of tRNAs.** The tRNA backbone is cyan, and each of its nucleotides is represented by a yellow circle whose diameter is proportional to the fraction of the various tRNA acceptor types for which the nucleotide is an identity element for aaRS recognition. [Courtesy of William McClain, University of Wisconsin.]

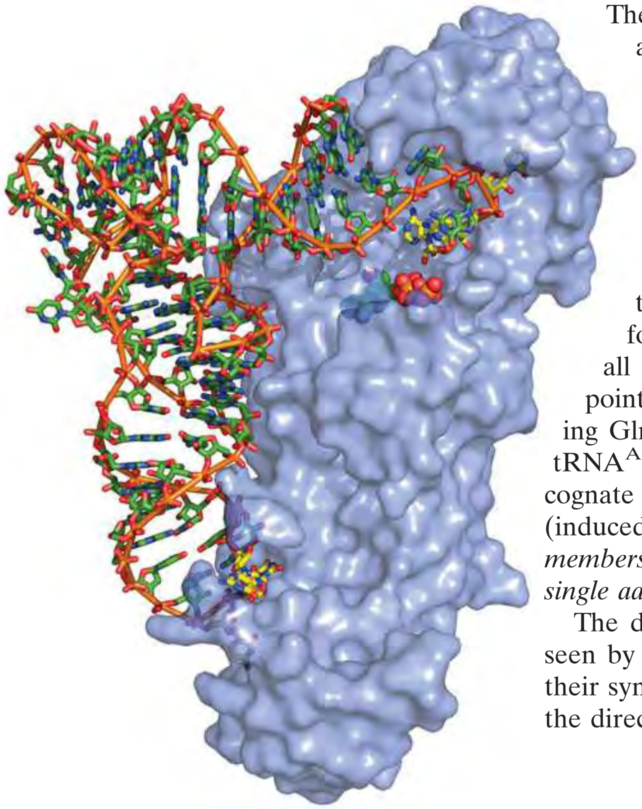

Figure 27-8 | X-Ray structure of *E. coli* GlnRS · tRNA^{Gln} · ATP. The ATP bound in the protein's active site is drawn in space-filling form with C green, N blue, O red, and P orange. The tRNA is drawn in stick form colored as the ATP but with the C atoms of the anticodon (UCG) and the 3′-CCA end yellow. An orange rod links its successive P atoms. The protein is represented by a semitransparent lavender surface diagram that reveals the buried portions of the tRNA and ATP. Note that both the 3′ end of the tRNA (*top right*) and its anticodon bases (*bottom*) are inserted into deep pockets in the protein. [Based on an X-ray structure by Thomas Steitz, Yale University. PDBid 1GTR.] **See Kinemage Exercise 22.**

The 3′ end of tRNA^{Gln} plunges deeply into a protein pocket that also binds the enzyme's ATP and glutamine substrates.

Yeast **AspRS,** a Class II enzyme, is a homodimer of 557-residue subunits. Its X-ray structure in complex with **tRNA^{Asp},** determined by Dino Moras, reveals that the protein symmetrically binds two tRNA molecules by contacting them principally at their acceptor stem and anticodon regions (Fig. 27-9). The anticodon arm of tRNA^{Asp} is bent by as much as 20 Å toward the inside of the L relative to that in the X-ray structure of uncomplexed tRNA^{Asp}, and its anticodon bases are unstacked. The hinge point for the bend is a G30 · U40 base pair in the anticodon stem (nearly all other species of tRNA contain a Watson–Crick base pair at that point). The anticodon bases of tRNA^{Gln} are also unstacked in contacting GlnRS but with a backbone conformation that differs from that in tRNA^{Asp}. Evidently, the conformation of a tRNA in complex with its cognate synthetase is dictated more by its interactions with the protein (induced fit) than by its sequence. This is perhaps one reason why *the members of each set of isoaccepting tRNAs in a cell are recognized by a single aaRS.*

The different modes of tRNA binding by GlnRS and AspRS can be seen by comparing Figs. 27-8 and 27-9. Although both tRNAs approach their synthetases along the inside of the L shapes, tRNA^{Gln} does so from the direction of the minor groove of its acceptor stem, whereas tRNA^{Asp}

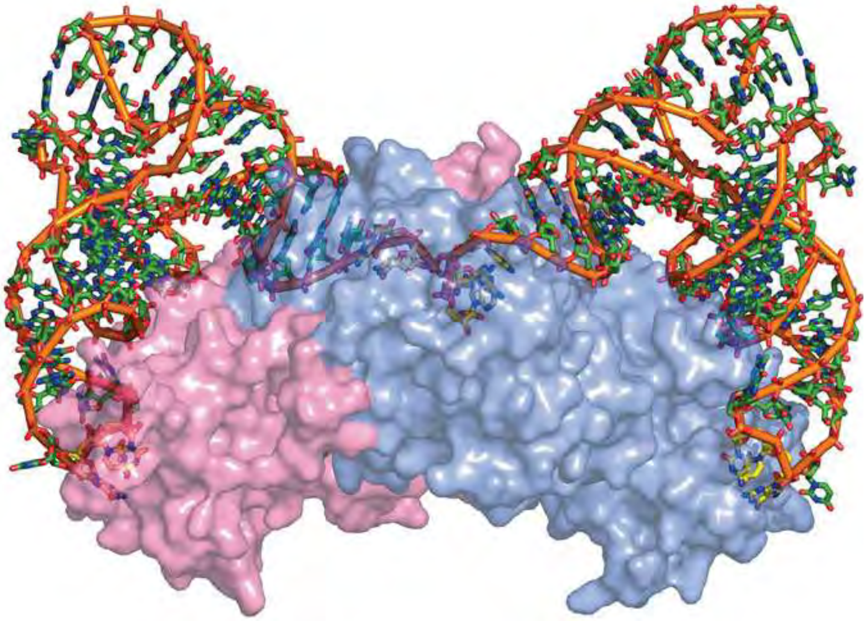

Figure 27-9 | X-Ray structure of yeast AspRS · tRNA^{Asp}. The homodimeric enzyme with its two symmetrically bound tRNAs is viewed with its twofold axis approximately vertical. The tRNAs are drawn in skeletal form colored according to atom type with the C atoms of the anticodon (GUC) and the 3′-CCA end yellow, the remaining C atoms green, N blue, O red, and P orange. An orange rod connects its successive P atoms. The two protein subunits are represented by semitransparent pink and lavender surface diagrams that reveal the buried portions of the tRNAs. [Based on an X-ray structure by Dino Moras, CNRS/INSERM/ULP, Illkirch Cédex, France. PDBid 1ASY.]

does so from the direction of its major groove. The 3′ end of tRNA$^{\text{Asp}}$ thereby continues its helical track as it plunges into AspRS's catalytic site, whereas the 3′ end of tRNA$^{\text{Gln}}$ bends backward into a hairpin turn as it enters its active site. These structural differences account for the observation that Class I and Class II enzymes aminoacylate different OH groups on the 3′ terminal ribose of tRNA.

Proofreading Enhances the Fidelity of Amino Acid Attachment to tRNA. The charging of a tRNA with its cognate amino acid is a remarkably accurate process. Experimental measurements indicate, for example, that at equal concentrations of isoleucine and valine, **IleRS** transfers ~40,000 isoleucines to tRNA$^{\text{Ile}}$ for every valine it so transfers. This high degree of accuracy is surprising because valine, which differs from isoleucine only by the lack of a single methylene group, should fit easily into the isoleucine-binding site of IleRS. The binding free energy of a methylene group is estimated to be ~12 kJ · mol^{-1}. Equation 1-16 indicates that the ratio f of the equilibrium constants, K_1 and K_2, with which two substances bind to a particular site is given by

$$f = \frac{K_1}{K_2} = \frac{e^{-\Delta G_1^{\circ\prime}/RT}}{e^{-\Delta G_2^{\circ\prime}/RT}} = e^{-\Delta\Delta G^{\circ\prime}/RT} \qquad [27\text{-}1]$$

where $\Delta\Delta G^{\circ\prime} = \Delta G_1^{\circ\prime} - \Delta G_2^{\circ\prime}$ is the difference between the free energies of binding of the two substances. It is therefore estimated that isoleucyl–tRNA synthetase could discriminate between isoleucine and valine by no more than a factor of ~100.

Paul Berg resolved this apparent paradox by demonstrating that, in the presence of tRNA$^{\text{Ile}}$, IleRS catalyzes the quantitative hydrolysis of valine–adenylate, the intermediate of the aminoacylation reaction, to valine + AMP rather than forming Val–tRNA$^{\text{Ile}}$. Thus, *isoleucyl–tRNA synthetase subjects aminoacyl–adenylates to a proofreading or editing step,* a process reminiscent of that carried out by DNA polymerase I (Section 25-2A).

IleRS has two active sites that operate as a double sieve. The first site activates isoleucine and the chemically similar valine. The second active site, which hydrolyzes aminoacylated tRNA$^{\text{Ile}}$, admits only aminoacyl groups that are smaller than isoleucine (i.e., Val–tRNA$^{\text{Ile}}$). The X-ray structure of a bacterial IleRS, a Class I enzyme, determined by Steitz, reveals that the protein contains an additional editing domain inserted into its dinucleotide-binding fold domain (Fig. 27-10). The 3′ terminus of tRNA$^{\text{Ile}}$ appears to shuttle between the aminoacylation and editing sites by a conformational change. *The combined selectivities of the aminoacylation and editing steps are responsible for the high fidelity of translation, a phenomenon that occurs at the expense of ATP hydrolysis.*

Other aminoacyl–tRNA synthetases discriminate against noncognate amino acids through a variety of noncovalent interactions. In **ValRS,** the side chain of Asp 279 protrudes into the editing active site, where it hydrogen bonds with the hydroxyl group of threonine. The isosteric (having the same shape) valine lacks this hydroxyl group and is thereby excluded from the editing pocket. **ThrRS** has the opposite problem: It must synthesize Thr–tRNA$^{\text{Thr}}$ but not Val–tRNA$^{\text{Thr}}$. Specificity is conferred by the aminoacylation site, which contains a Zn^{2+} ion that is

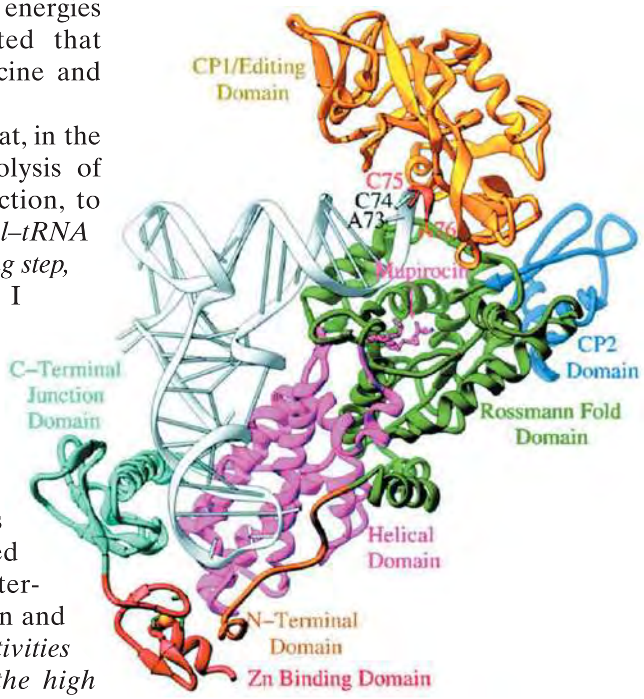

Figure 27-10 | X-Ray structure of *Staphylococcus aureus* isoleucyl–tRNA synthetase in complex with tRNA$^{\text{Ile}}$. The tRNA is white, the protein is colored by domain, and **mupirocin,** an antibiotic that binds to IleRS, is drawn in stick form in pink. The four terminal residues of the tRNA are labeled. The 3′ terminus of the tRNA is positioned near the editing active site. [Courtesy of Thomas Steitz, Yale University. PDBid 1QU2.]

coordinated by the side chain OH group of threonine. Valine cannot coordinate the Zn^{2+} in this way and hence does not undergo adenylylation by ThrRS. A separate editing site deals with misacylated Ser–$tRNA^{Thr}$. **TyrRS** distinguishes between tyrosine and phenylalanine through hydrogen bonding with tyrosine's OH group. Since no other amino acid resembles tyrosine, the enzyme can do without an editing function.

Some Organisms Lack Certain aaRSs. Many bacteria lack the expected complement of 20 aminoacyl–tRNA synthetases. For example, GlnRS is absent in gram-positive bacteria, archaebacteria, cyanobacteria, mitochondria, and chloroplasts. Instead, glutamate is linked to $tRNA^{Gln}$ by the same GluRS that synthesizes Glu–$tRNA^{Glu}$. The resulting Glu–$tRNA^{Gln}$ is then converted to Gln–$tRNA^{Gln}$ by **Glu–$tRNA^{Gln}$ amidotransferase** in an ATP-requiring reaction in which glutamine is the amide donor. Some microorganisms that lack **AsnRS** use a similar transamidation pathway for the synthesis of Asn–$tRNA^{Asn}$ from Asp–$tRNA^{Asn}$.

Certain archaebacteria lack a gene for **CysRS.** In these cells, Cys–$tRNA^{Cys}$ is produced by a ProRS (called **ProCysRS**). Despite its unusual dual specificity, ProCysRS does not generate either Cys–$tRNA^{Pro}$ or Pro–$tRNA^{Cys}$. This is because adenylylation of Pro does not require the presence of $tRNA^{Pro}$, but the activation of Cys requires $tRNA^{Cys}$. Presumably, the binding of Pro–AMP or $tRNA^{Cys}$ elicits conformational changes that are mutually exclusive.

C | A tRNA May Recognize More than One Codon

In protein synthesis, the proper tRNA is selected only through codon–anticodon interactions; the aminoacyl group does not participate in this process (this is one reason why accurate aminoacylation is critical for protein synthesis). The three nucleotides of an mRNA codon pair with the three nucleotides of a complementary tRNA anticodon in an antiparallel fashion. One might naively guess that each of the 61 codons specifying an amino acid would be read by a different tRNA. Yet even though most cells contain numerous groups of isoaccepting tRNAs, *many tRNAs bind to two or three of the codons specifying their cognate amino acids.* For example, yeast $tRNA^{Phe}$, which has the anticodon GmAA (where Gm indicates G with a 2′-methyl group), recognizes the codons UUC and UUU,

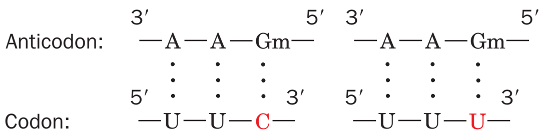

and yeast $tRNA^{Ala}$, which has the anticodon IGC (where I is inosine), recognizes the codons GCU, GCC, and GCA:

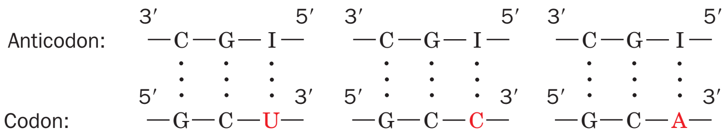

Evidently, non-Watson–Crick base pairing can occur at the third codon–anticodon position (the anticodon's first position is defined as its

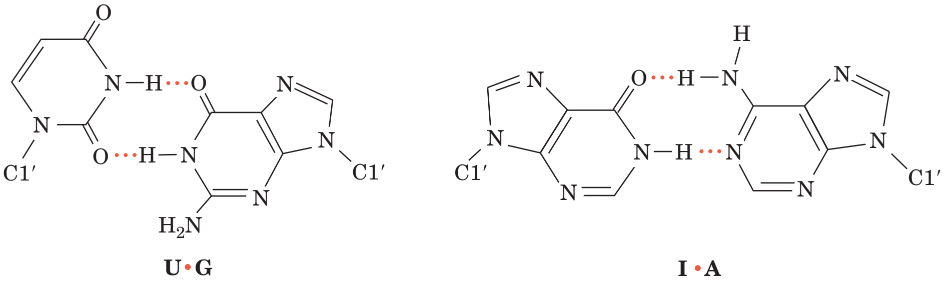

Figure 27-11 | **U • G and I • A wobble pairs.** Both have been observed in X-ray structures.

3′ nucleotide), the site of most codon degeneracy (Table 27-1). Note that the third (5′) anticodon position commonly contains a modified base such as Gm or I.

The Wobble Hypothesis Accounts for Codon Degeneracy. By combining structural insight with logical deduction, Crick proposed the **wobble hypothesis** to explain how a tRNA can recognize several degenerate codons. He assumed that *the first two codon–anticodon pairings have normal Watson–Crick geometry and that there could be a small amount of play or "wobble" in the third anticodon position to allow limited conformational adjustments in its pairing geometry.* This permits the formation of several non-Watson–Crick pairs such as U·G and I·A (Fig. 27-11). The allowed pairings for the third codon–anticodon position are listed in Table 27-3. An anticodon with C or A in its third position can potentially pair only with its Watson–Crick complementary codon (although, in fact, there is no known instance of a tRNA with an A in its third anticodon position). If U or G occupies the third anticodon position, two codons can potentially be recognized. I at the third anticodon position can pair with U, C, or A.

A consideration of the various wobble pairings indicates that at least 31 tRNAs are required to translate all 61 coding triplets of the genetic code (there are 32 tRNAs in the minimal set because translation initiation requires a separate tRNA; Section 27-4A). Most cells have >32 tRNAs, some of which have identical anticodons. In fact, mammalian cells have >150 tRNAs. Some organisms contain unique tRNAs that are charged with unusual amino acids (Box 27-2).

Table 27-3 Allowed Wobble Pairing Combinations in the Third Codon–Anticodon Position

5′-Anticodon Base	3′-Codon Base
C	G
A	U
U	A or G
G	U or C
I	U, C, or A

Frequently Used Codons Are Complementary to the Most Abundant tRNA Species. The analysis of the base sequences of several highly expressed structural genes of baker's yeast, *Saccharomyces cerevisiae,* has revealed a remarkable bias in their codon usage. Only 25 of the 61 coding triplets are commonly used. *The preferred codons are those that are most nearly complementary, in the Watson–Crick sense, to the anticodons in the most abundant species in each set of isoaccepting tRNAs.* A similar phenomenon occurs in *E. coli,* although several of its 22 preferred codons differ from those in yeast. The degree with which the preferred codons occur in a given gene is strongly correlated, in both organisms, with the gene's level of expression. This probably permits the mRNAs of proteins that are required in high abundance to be rapidly and smoothly translated.

CHECK YOUR UNDERSTANDING

Describe the major structural features of tRNA.

Why is it important for all tRNAs to have similar structures?

What features of tRNA structure are involved in recognition and aminoacylation by an aaRS?

Describe how the double-sieve mechanism of IleRS promotes accurate tRNA aminoacylation.

Explain the wobble hypothesis.

BOX 27-2 PERSPECTIVES IN BIOCHEMISTRY

Expanding the Genetic Code

It is widely stated that proteins are synthesized from 20 "standard" amino acids, but two other amino acids are known to be incorporated into proteins during translation (other nonstandard amino acid residues in proteins are the result of posttranslational modifications). In both cases, the amino acid is attached to a unique tRNA that recognizes a Stop codon.

Several enzymes in eukaryotes and prokaryotes contain the nonstandard amino acid **selenocysteine (Sec):**

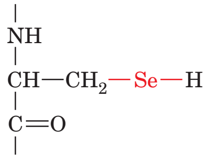

$$\begin{array}{l} | \\ \mathrm{NH} \\ | \\ \mathrm{CH{-}CH_2{-}Se{-}H} \\ | \\ \mathrm{C{=}O} \\ | \end{array}$$

The selenocysteine (Sec) residue

The Sec residues of **selenoproteins** are thought to participate in redox reactions such as those catalyzed by mammalian glutathione peroxidase (Box 15-4) and thioredoxin reductase (Section 23-3A). For this reason, selenium is an essential trace element. The human genome contains an estimated 25 selenoproteins.

Selenocysteine, sometimes called the "twenty-first amino acid," is incorporated into proteins with the aid of a tRNA that interprets the UGA Stop codon as a Sec codon. **tRNA$^{\mathbf{Sec}}$** is initially charged with serine in a reaction catalyzed by the same SerRS that charges tRNA$^{\mathrm{Ser}}$. The resulting Ser–tRNA$^{\mathrm{Sec}}$ is enzymatically selenylated to produce selenocysteinyl–tRNA$^{\mathrm{Sec}}$. Although tRNA$^{\mathrm{Sec}}$ must resemble tRNA$^{\mathrm{Ser}}$ enough to interact with the same SerRS, its acceptor stem has 8 bp (rather than 7), its D arm has a 6-bp stem and a 4-base loop (rather than a 4-bp stem and a 7–8-base loop), its TψC stem has 4 bp rather than 5, and its anticodon, UCA, recognizes a UGA Stop codon rather than a Ser codon. In addition, several of the invariant residues of other tRNAs are altered in tRNA$^{\mathrm{Sec}}$. These changes explain why tRNA$^{\mathrm{Sec}}$ is not recognized by EF-Tu · GTP, which escorts other aminoacyl–tRNAs to the ribosome (Section 27-4B). Instead, a dedicated protein (a special elongation factor) named **SELB** in complex with GTP is required to deliver Sec–tRNA$^{\mathrm{Sec}}$ to the ribosome. SELB · GTP · Sec–tRNA$^{\mathrm{Sec}}$ reads the UGA codon as "Sec" rather than "Stop," provided that the ribosomally bound mRNA has a hairpin loop on the 3′ side of the UGA specifying Sec.

The archaebacterial protein **methylamine methyltransferase** includes the amino acid **pyrrolysine (Pyl),** a lysine with its ε-nitrogen in amide linkage to a pyrroline group:

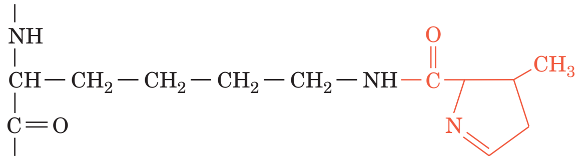

The pyrrolysine (Pyl) residue

Pyl is specified by the codon UAG (normally a Stop codon). **tRNA$^{\mathbf{Pyl}}$** differs from typical tRNAs in having an anticodon stem with 6 bp rather than 5. The tRNA is charged by a specific aminoacyl–tRNA synthetase that differs from known lysyl–tRNA synthetases. Because the PylRS readily generates Lys–tRNA$^{\mathrm{Pyl}}$, it is not clear whether the substrate for aminoacylation is lysine, which is later modified, or preformed pyrrolysine. The mRNA signals that allow UAG to be read as a Pyl codon rather than as a Stop codon have not yet been elucidated.

3 Ribosomes

LEARNING OBJECTIVES

- Understand that the ribosome consists of a large and a small subunit composed of RNA and a number of small proteins.
- Understand that the complex structure of the ribosome allows it to bind mRNA and three tRNA molecules and to carry out protein synthesis.

Ribosomes, small organelles that were once thought to be artifacts of cell disruption, were identified as the site of protein synthesis in 1955 by Paul Zamecnik, who demonstrated that ^{14}C-labeled amino acids are transiently associated with ribosomes before they appear in free proteins. The ribosome is both enormous ($\sim$2.5 $\times$ 10^6 D in bacteria and 3.9 to 4.5 $\times$ 10^6 D in eukaryotes) and complex (ribosomes contain several large RNA molecules and dozens of different proteins). This complexity is necessary for the ribosome to carry out the following vital functions:

1. The ribosome binds mRNA such that its codons can be read with high fidelity.
2. The ribosome includes specific binding sites for tRNA molecules.
3. The ribosome mediates the interactions of nonribosomal protein

factors that promote polypeptide chain initiation, elongation, and termination.

4. The ribosome catalyzes peptide bond formation.
5. The ribosome undergoes movement so that it can translate sequential codons.

In this section, we discuss the structure of the ribosome, beginning with the smaller and simpler prokaryotic ribosome and ending with the larger and more complicated eukaryotic ribosome.

A | The Prokaryotic Ribosome Consists of Two Subunits

Ribosomal components are traditionally described in terms of their rate of sedimentation in an ultracentrifuge, which correlates roughly with their size (Section 21-1B). Thus, the intact *E. coli* ribosome has a sedimentation coefficient of 70S. As James Watson discovered, the ribosome can be dissociated into two unequal subunits (Table 27-4). The small **(30S)** subunit consists of a **16S rRNA** molecule and 21 different proteins, whereas the large **(50S)** subunit contains a **5S** and a **23S rRNA** together with 31 different proteins. By convention, ribosomal proteins from the small and large subunits are designated with the prefixes S and L, respectively, followed by a number that roughly increases from the largest to the smallest. These proteins, which range in size from 46 to 557 residues, occur in only one copy per ribosome with the exception of L12, which is present in four copies. Most of these proteins, which exhibit little sequence similarity with one another, are rich in the basic amino acids Lys and Arg and contain few aromatic residues, as is expected for proteins that are closely associated with polyanionic RNA molecules. The up to 20,000 ribosomes in an *E. coli* cell account for ~80% of its RNA content and 10% of its protein.

Ribosomal RNAs Have Complicated Secondary Structures. The *E. coli* 16S rRNA, which was sequenced by Harry Noller, consists of 1542 nucleotides. A computerized search of this sequence for stable double-helical segments yielded many plausible but often mutually exclusive secondary structures. However, the comparison of the sequences of 16S rRNAs from several prokaryotes, under the assumption that their structures have been evolutionarily conserved, led to the flowerlike secondary

Table 27-4 Components of *E. coli* Ribosomes

	Ribosome	Small Subunit	Large Subunit
Sedimentation coefficient	70S	30S	50S
Mass (kD)	2520	930	1590
RNA			
Major		16S, 1542 nucleotides	23S, 2904 nucleotides
Minor			5S, 120 nucleotides
RNA mass (kD)	1664	560	1104
Proportion of mass	66%	60%	70%
Proteins		21 polypeptides	31 polypeptides
Protein mass (kD)	857	370	487
Proportion of mass	34%	40%	30%

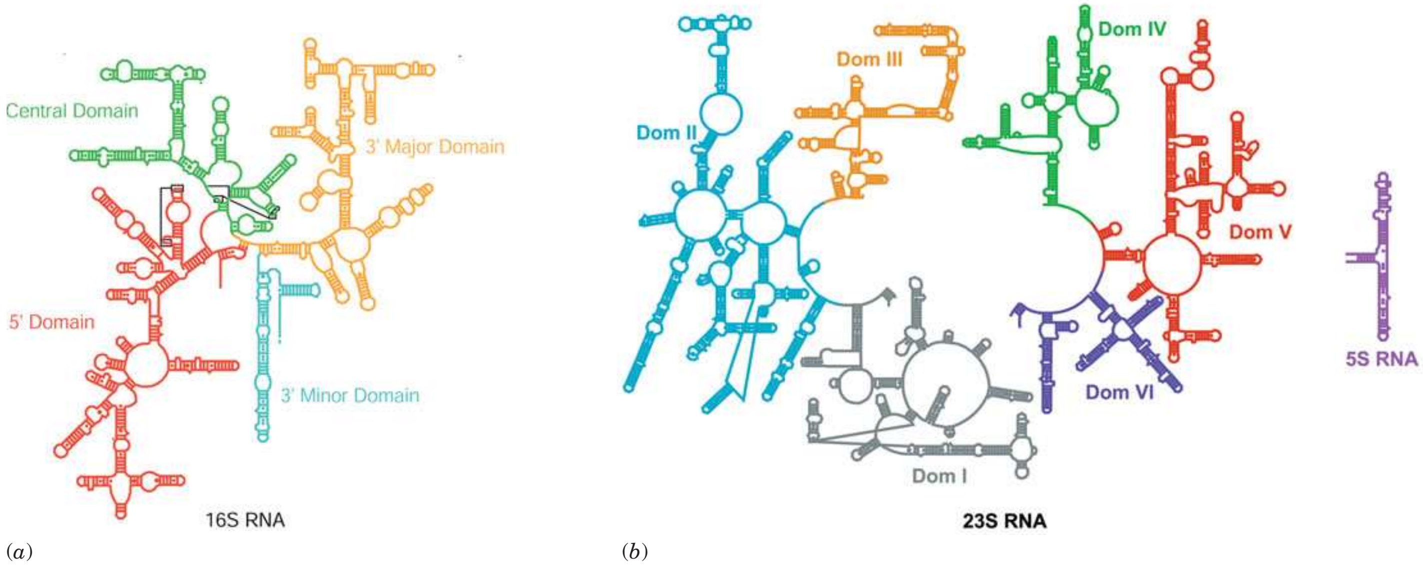

■ **Figure 27-12 | Secondary structures of the *E. coli* ribosomal RNAs.** (*a*) 16S rRNA and (*b*) 23S and 5S rRNAs. The rRNAs are colored by domain. The stems, which contain Watson–Crick base pairs, G · U base pairs, and other non-Watson–Crick base pairs, form flowerlike structures within each domain. [Courtesy of V. Ramakrishnan, MRC Laboratory of Molecular Biology, Cambridge, U.K., and Peter Moore, Yale University.]

structure for 16S rRNA seen in Fig. 27-12*a.* In this four-domain structure, which is 54% base paired, the double-helical stems tend to be short ($<$8 bp) and many of them are imperfect. The large ribosomal subunit's 5S and 23S rRNAs, which consist of 120 and 2904 nucleotides, respectively, also exhibit extensive secondary structures (Fig. 27-12*b*).

The Ribosome Has a Complex Three-Dimensional Structure. The structure of the ribosome began to come into focus through electron microscopy (EM; Fig. 27-13*a*) and later through **cryoelectron microscopy** (**cryo-EM;** Fig. 27-13*b*). In the latter technique, the sample is cooled to near liquid N_2 temperatures (-196°C) so rapidly (in a few milliseconds) that the water in the sample does not have time to crystallize but, rather, assumes a vitreous (glasslike) state. Consequently, the sample remains hydrated and hence retains its native shape to a greater extent than in conventional electron microscopy. Cryo-EM studies, carried out largely by Joachim Frank, revealed that the ribosome has an irregular shape, about 250 Å across, with numerous lobes and bulges as well as channels and tunnels.

The fine structure of the ribosome was determined by X-ray crystallography, a landmark achievement owing to the enormous size of the particle. Ribosomal subunits were first crystallized by Ada Yonath in 1980, but it took another 20 years for improvements in crystal quality and technical advances in crystallography to meet the challenge of determining the X-ray structures of these gargantuan molecular complexes. In 2000, Peter Moore and Steitz reported the X-ray structure of the ~100,000-atom 50S ribosomal subunit of the halophilic (salt-loving) bacterium *Haloarcula marismortui* at atomic (2.4 Å) resolution, and shortly thereafter V. Ramakrishnan and Yonath independently reported the X-ray structure of the 30S subunit of *T. thermophilus* at ~3 Å resolution. Since then, higher-resolution structures of the entire 70S ribosomes from *T. thermophilus* and *E. coli* have been obtained.

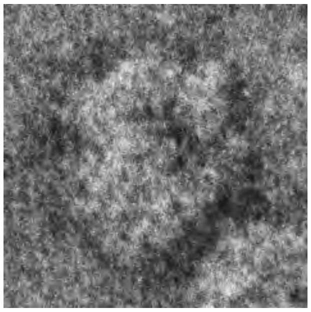
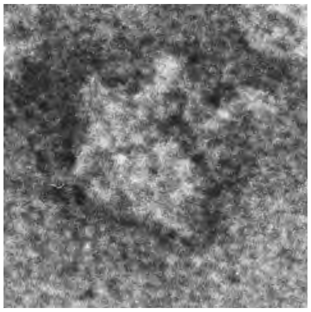
(*a*)

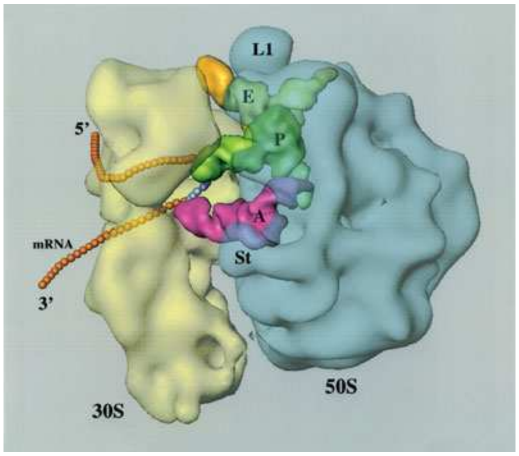

(*b*)

Figure 27-13 | Structure of the *E. coli* ribosome. (*a*) Low resolution electron micrographs. [Courtesy of James Lake, UCLA.] (*b*) Cryoelectron microscopy–based image at ~25 Å resolution. In this semitransparent three-dimensional model, the 30S subunit (*yellow*) is on the left and the 50S subunit (*cyan*) is on the right. The tRNAs that occupy the A, P, and E sites (Section 27-4B) are colored magenta, green, and gold. The inferred path of the mRNA is represented by a chain of orange beads with the six nucleotides contacting the A and P sites blue and purple, respectively. The exit of the tunnel in the 50S subunit through which the growing polypeptide chain is extruded is visible (*center right*). [Courtesy of Joachim Frank, State University of New York at Albany.]

Prokaryotic ribosomes exhibit the following architectural features:

1. Both the 16S and 23S rRNAs are assemblies of helical elements connected by loops, most of which are irregular extensions of helices (Fig. 27-14). These structures, which are in close accord with previous secondary structure predictions (Fig. 27-12), are stabilized by interactions between helices such as minor groove to minor groove packing (recall that A-form RNA has a very shallow minor groove); the insertion of a phosphate ridge into a minor groove; and the insertion of conserved adenines into minor grooves.
2. Each of the 16S rRNA’s four domains, which extend out from a central junction (Fig. 27-12*a*), forms a morphologically distinct portion of the 30S subunit (Fig. 27-14*a*). In contrast, the 23S rRNA’s six domains (Fig. 27-12*b*) are intricately intertwined in the 50S subunit

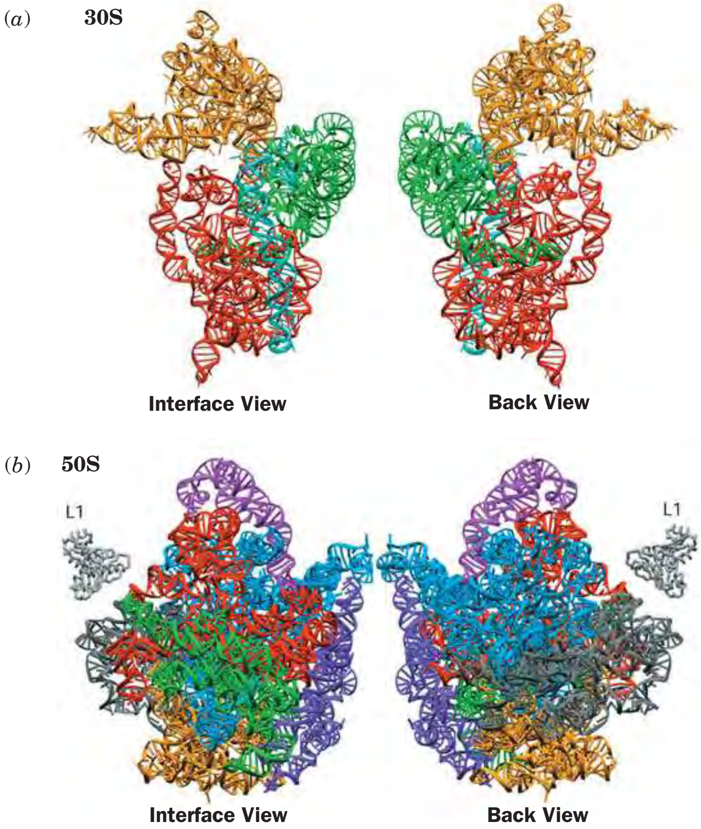

Figure 27-14 | Tertiary structures of the ribosomal RNAs. (*a*) The 16S rRNA of *T. thermophilus.* (*b*) The 23S rRNA of *H. marismortui.* The rRNAs are colored according to domain as in Fig. 27-12. The interface view of a ribosomal subunit (*left*) shows the surface that associates with the other subunit in the whole ribosome and the back view (*right*) shows the opposite (solvent-exposed) side. Note that the secondary structure domains of the 16S rRNA fold as separate tertiary structure domains, whereas in the 23S rRNA, the secondary structure domains are more intertwined. The L1 protein, part of the large subunit, is shown for purposes of orientation. [Courtesy of V. Ramakrishnan, MRC Laboratory of Molecular Biology, Cambridge, U.K., and Peter Moore, Yale University. PDBids 1J5E and 1JJ2.]

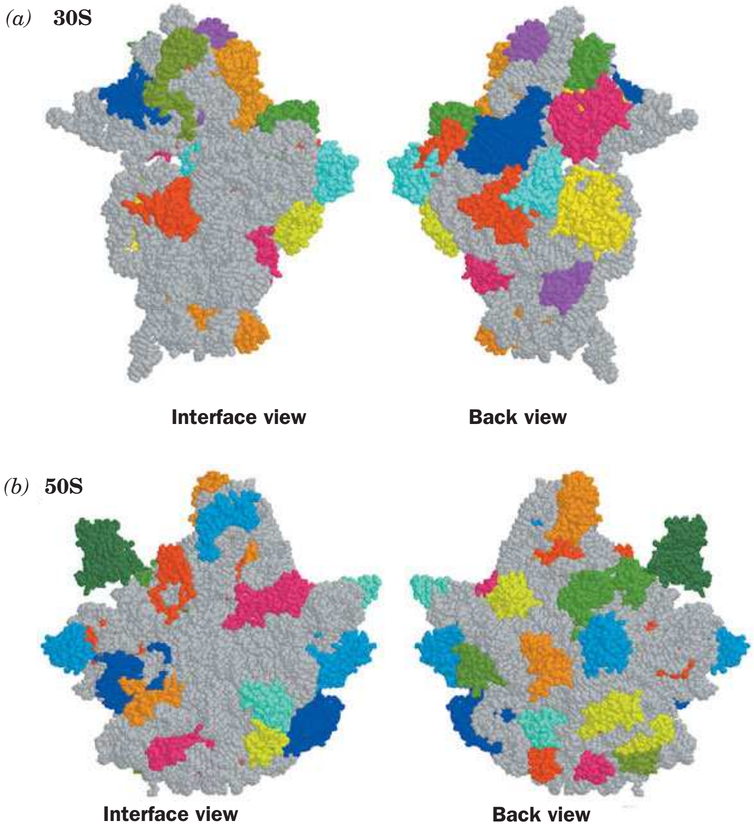

■ **Figure 27-15 | Distribution of protein and RNA in the ribosomal subunits.** (*a*) The 30S subunit of *T. thermophilus.* (*b*) The 50S subunit of *H. marismortui.* The subunits are drawn in space-filling form with their RNAs gray and their proteins in various colors. Note that the interface side of each subunit is largely free of protein. The globular portions of proteins are exposed on the surface of their associated subunit (Fig. 27-16), whereas their extended segments are largely buried in the RNA. [Part *a* based on an X-ray structure by V. Ramakrishnan, MRC Laboratory of Molecular Biology, Cambridge, U.K. Part *b* based on an X-ray structure by Peter Moore and Thomas Steitz, Yale University. PDBids 1J5E and 1JJ2.]

(Fig. 27-14*b*). Since the ribosomal proteins are embedded in the RNA (see below), this suggests that the domains of the 30S subunit can move relative to one another during protein synthesis, whereas the 50S subunit appears to be rigid.

3. The distribution of the proteins in the two ribosomal subunits is not uniform (Fig. 27-15). The vast majority of the ribosomal proteins are located on the back and sides of their subunits. In contrast, the face of each subunit that forms the interface between the two subunits, particularly those regions that bind the tRNAs and mRNA (see below), is largely devoid of proteins.
4. Most ribosomal proteins consist of a globular domain and a tail. The globular domain, when present, is located on a subunit surface (Fig. 27-15). The tail segment, which is largely devoid of secondary structure and unusually rich in basic residues, infiltrates between the RNA helices into the subunit interior (Fig. 27-16). These protein tails make far fewer base-specific interactions than do other known RNA-binding proteins. They tend to interact with the RNA through salt bridges between their positively charged side chains and the RNAs' negatively charged phosphate oxygen atoms, thereby neutralizing the repulsive charge–charge interactions between nearby RNA segments. Moreover, the sequences of these proteins' tails are more conserved than their attached globular domains. This is consistent with the hypothesis that the primordial ribosome consisted entirely of RNA (the RNA world) and that the proteins that were eventually acquired stabilized its structure and fine-tuned its function. Indeed, a comparison of Figs. 27-14 and 27-15 indicates that the structures of

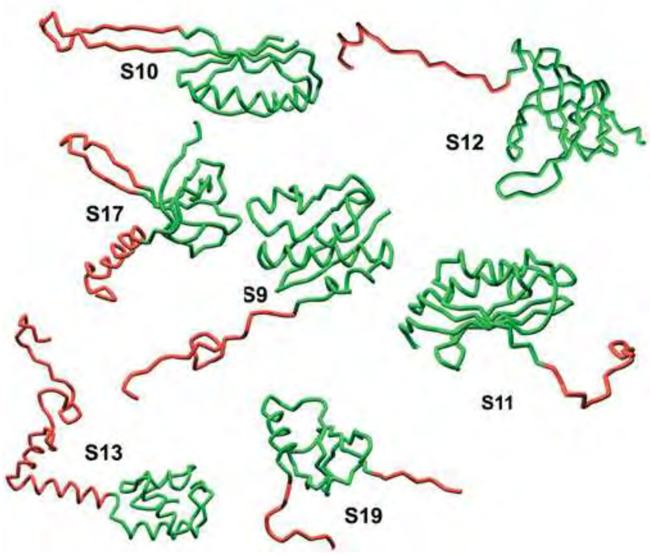

Figure 27-16 | Backbone structures of selected ribosomal proteins. Globular portions of the proteins are green, and extended segments are red. [Courtesy of V. Ramakrishnan, MRC Laboratory of Molecular Biology, Cambridge, U.K. PDBid 1J5E.]

the large and small ribosomal subunits are determined largely by their rRNA components, not their proteins.

In the intact ribosome, the large and small subunits maintain the overall shapes of the isolated subunits (Fig. 27-17). The two subunits contact each other at 12 positions via RNA–RNA, protein–protein, and RNA–protein

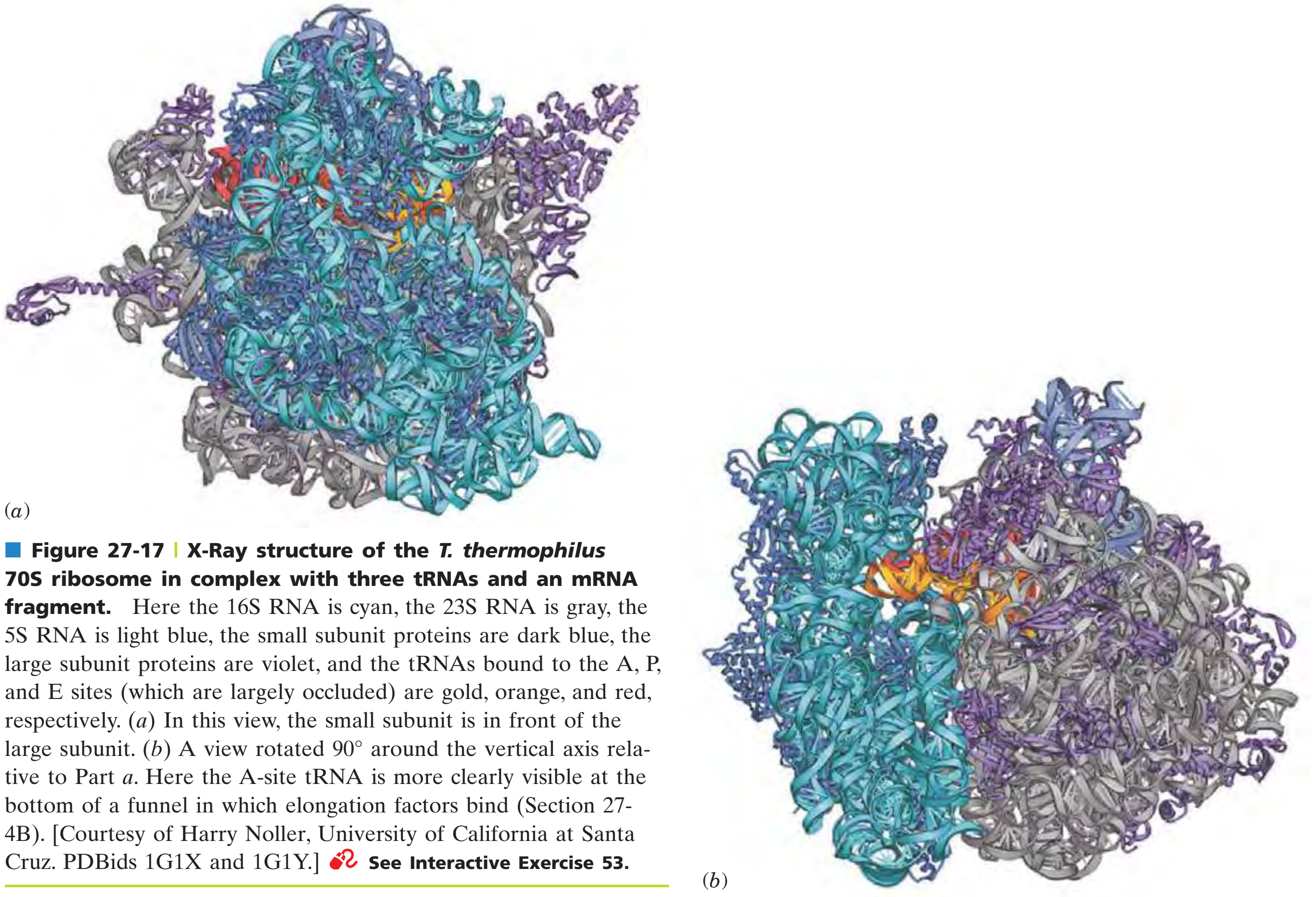

Figure 27-17 | X-Ray structure of the *T. thermophilus* 70S ribosome in complex with three tRNAs and an mRNA fragment. Here the 16S RNA is cyan, the 23S RNA is gray, the 5S RNA is light blue, the small subunit proteins are dark blue, the large subunit proteins are violet, and the tRNAs bound to the A, P, and E sites (which are largely occluded) are gold, orange, and red, respectively. (*a*) In this view, the small subunit is in front of the large subunit. (*b*) A view rotated 90° around the vertical axis relative to Part *a*. Here the A-site tRNA is more clearly visible at the bottom of a funnel in which elongation factors bind (Section 27-4B). [Courtesy of Harry Noller, University of California at Santa Cruz. PDBids 1G1X and 1G1Y.] **See Interactive Exercise 53.**

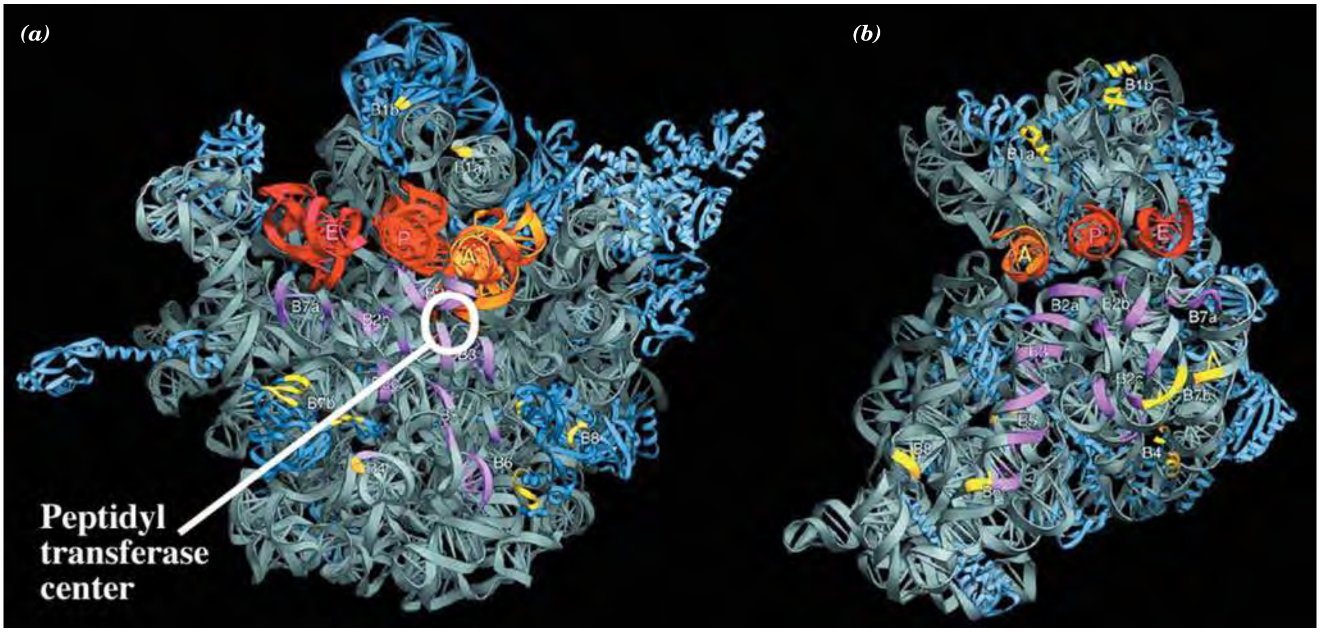

Figure 27-18 | Ribosomal subunits in the X-ray structure of the *T. thermophilus* ribosome in complex with three tRNAs and an mRNA. (*a*) Interface view of the large subunit (similar to Fig. 27-15*b, left*). (*b*) Interface view of the small subunit (similar to Fig. 27-15*a, left*). The RNA is gray with segments that participate in intersubunit contacts magenta, and the proteins are blue with segments that participate in intersubunit contacts yellow. The tRNAs bound in the A, P, and E sites are gold, orange, and red, respectively. The active site where peptide bond formation occurs is circled. [Courtesy of Harry Noller, University of California at Santa Cruz. PDBids 1GIX and 1GIY.]

bridges (Fig. 27-18). Mg^{2+} ions mediate many of these interactions. Although the bridges are essential for the stable association of the two ribosomal subunits, some of the contacts must be broken and re-formed in order to permit the ribosome to carry out the various activities of translation.

Ribosomes Have Three tRNA-Binding Sites. Ribosomes have three functionally distinct tRNA-binding sites: the **A** or **aminoacyl site** (it accommodates the incoming aminoacyl–tRNA), the **P** or **peptidyl site** (it accommodates the **peptidyl–tRNA,** the tRNA to which the growing peptide chain is attached), and the **E** or **exit site** (it accommodates a deacylated tRNA that is about to exit the ribosome). The ribosome binds all three tRNAs in a similar manner with their anticodon arms bound to the 30S subunit and their remaining portions bound to the 50S subunit. These interactions, which mainly consist of RNA–RNA contacts, are made to the tRNAs' universally conserved segments, thereby permitting the ribosome to bind different species of tRNAs in the same way. Nevertheless, the three bound tRNAs have slightly different conformations, with the A-site tRNA most closely resembling the X-ray structure of $tRNA^{Phe}$ (Fig. 27-5*b*) and the E-site tRNA most distorted.

The growing polypeptide fits into a tunnel on the 50S subunit that extends from the P site to the outer ribosomal surface (the tunnel exit is approximately in the center of the 50S subunit as is seen in Fig. 27-13*b*). The ~100-Å-long tunnel is lined with mostly hydrophilic residues and has an average diameter of ~15 Å. This is barely large enough for an α helix, so significant protein folding probably cannot occur until the polypeptide exits the ribosome.

We discuss the path of the mRNA and how it interacts with the tRNAs in Section 27-4. There we shall see that *the large subunit is mainly involved in mediating biochemical tasks such as catalyzing the reactions of polypeptide elongation, whereas the small subunit is the major actor in ribosomal recognition processes such as mRNA and tRNA binding* (although, as we have seen, the large subunit also participates in tRNA binding). We shall also see that *rRNA has the major functional role in ribosomal processes* (recall that RNA has demonstrated catalytic properties; Sections 24-2C and 26-3A).

B | The Eukaryotic Ribosome Is Larger and More Complex

Although eukaryotic and prokaryotic ribosomes resemble each other in both structure and function, they differ in nearly all details. Eukaryotic ribosomes have particle masses in the range 3.9 to 4.5 $\times$ 10^6 D and have a nominal sedimentation coefficient of 80S. They dissociate into two unequal subunits with compositions that are distinctly different from those of prokaryotes (Table 27-5; compare with Table 27-4). The small **(40S)** subunit of the rat liver cytoplasmic ribosome, the best characterized eukaryotic ribosome, consists of 33 unique polypeptides and an **18S rRNA.** Its large **(60S)** subunit contains 49 different polypeptides and three rRNAs of 28S, 5.8S, and 5S. The additional complexity of the eukaryotic ribosome relative to its prokaryotic counterpart is presumably due to the eukaryotic ribosome's additional functions: Its mechanism of translational initiation is more complex (Section 27-4A); it must be transported from the nucleus, where it is formed, to the cytoplasm, where translation occurs; and the machinery with which it participates in the secretory pathway is more complicated (Section 9-4D).

Sequence comparisons of the corresponding rRNAs from various species indicate that evolution has conserved their secondary structures rather than their base sequences (Fig. 27-12). For example, a G·C in a base-paired stem of *E. coli* 16S rRNA has been replaced by an A·U in the analogous stem of yeast 18S rRNA. The **5.8S rRNA,** which occurs in the large eukaryotic subunit in base-paired complex with the **28S rRNA,** is homologous in sequence to the 5′ end of prokaryotic 23S rRNA. Apparently 5.8S RNA arose through mutations that altered rRNA's posttranscriptional processing to produce a fourth rRNA.

Table 27-5 Components of Rat Liver Cytoplasmic Ribosomes

	Ribosome	Small Subunit	Large Subunit
Sedimentation coefficient	80S	40S	60S
Mass (kD)	4220	1400	2820
RNA			
Major		18S, 1874 nucleotides	28S, 4718 nucleotides
Minor			5.8S, 160 nucleotides 5S, 120 nucleotides
RNA mass (kD)	2520	700	1820
Proportion of mass	60%	50%	65%
Proteins		33 polypeptides	49 polypeptides
Protein mass (kD)	1700	700	1000
Proportion of mass	40%	50%	35%

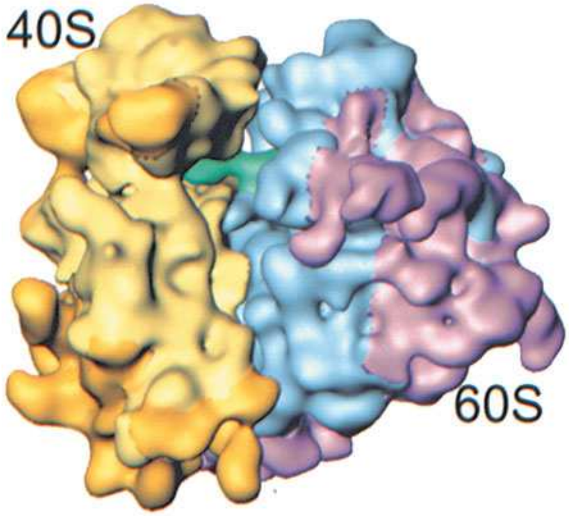

■ **Figure 27-19 | Cryo-EM–based image of the yeast 80S ribosome at 15 Å resolution.** In this side view, the small (40S) subunit is yellow, the large (60S) subunit is cyan, and the tRNA that is bound in the ribosomal P site is green. Portions of this ribosome that are not homologous to the RNA or proteins of the *E. coli* ribosome are shown in gold for the small subunit and magenta for the large subunit. [Courtesy of Joachim Frank, State University of New York at Albany.] **See Interactive Exercise 53.**

The cryo-EM–based image of the yeast 80S ribosome (Fig. 27-19), determined at 15 Å resolution by Andrej Sali, Günter Blobel, and Frank, reveals that there is a high degree of structural conservation between eukaryotic and prokaryotic ribosomes (compare Fig. 27-19 with Fig. 27-13*b*). Although the yeast 40S subunit (which consists of a 1798-nt 18S rRNA and 32 proteins) contains an additional 256 nt of RNA and 11 proteins relative to the *E. coli* 30S subunit (Table 27-4; 15 of the yeast proteins are homologous to those of *E. coli*), both exhibit similar structures. Many of the differences between these two small ribosomal subunits are accounted for by the 40S subunit's additional RNA and proteins, although their homologous portions exhibit several distinct conformational differences. Similarly, the yeast 60S subunit (which consists of an aggregate of 3671 nt and 45 proteins) structurally resembles the considerably smaller prokaryotic 50S subunit. The yeast ribosome exhibits 16 intersubunit bridges, 12 of which match the 12 that were observed in the X-ray structure of the *T. thermophilus* ribosome (Fig. 27-18), a remarkable evolutionary conservation that indicates the importance of these bridges.

■ CHECK YOUR UNDERSTANDING

Summarize the relationship between rRNA and the overall structure of the ribosome.
Describe the distribution of proteins in the ribosomal subunits.
Describe the positions and functions of the three tRNA-binding sites in the ribosome.
Describe the similarities and differences between prokaryotic and eukaryotic ribosomes.

4 Translation

LEARNING OBJECTIVES

- Understand that initiation factors help to assemble the ribosomal subunits, deliver the initiator tRNA, and in eukaryotes, locate the initiation codon.
- Understand that the ribosome selects the correct aminoacyl–tRNA, catalyzes the transpeptidation reaction, and then translocates along the mRNA during the elongation phase of protein synthesis.
- Understand that a release factor and ribosome recycling factor participate in terminating polypeptide synthesis.

In order to appreciate the manner in which the ribosome orchestrates the translation of mRNA to synthesize polypeptides, it is helpful to assimilate the following points:

1. *Polypeptide synthesis proceeds from the N-terminus to the C-terminus;* that is, a **peptidyl transferase** activity appends an incoming amino acid to a growing polypeptide's C-terminus. This was shown to be the case in 1961 by Howard Dintzis, who exposed reticulocytes (immature red blood cells) that were actively synthesizing hemoglobin to ^{3}H-labeled leucine for less time than it takes to synthesize an entire polypeptide. The extent to which the tryptic peptides from the soluble (completed) hemoglobin molecules were labeled increased with their proximity to the C-terminus (Fig. 27-20), thereby indicating that incoming amino acids are appended to the growing polypeptide's C-terminus.

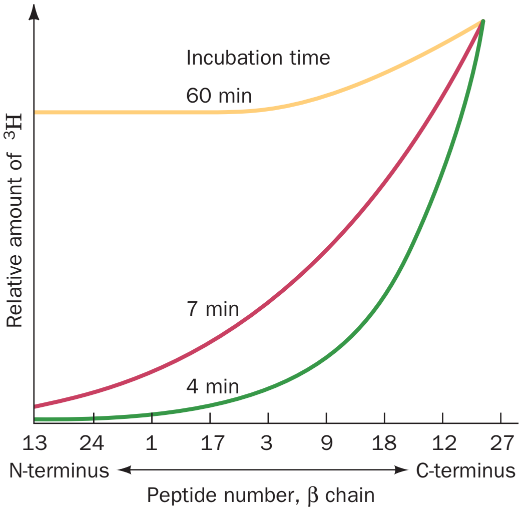

■ **Figure 27-20 | Demonstration that polypeptide synthesis proceeds from the N- to the C-terminus.** Rabbit reticulocytes were incubated with [^{3}H]leucine for the indicated times. The curves show the distribution of [^{3}H]Leu among the tryptic peptides from the β subunit of soluble rabbit hemoglobin. The numbers on the horizontal axis are peptide identifiers, arranged from the N-terminus to the C-terminus. [After Dintzis, H.M., *Proc. Natl. Acad. Sci.* **47,** 255 (1961).]

2. *Chain elongation occurs by linking the growing polypeptide to the incoming tRNA's amino acid residue.* If the growing polypeptide is released from the ribosome by treatment with high salt concentrations, its C-terminal residue is esterified to a tRNA molecule as a peptidyl–tRNA (*at right*). The nascent (growing) polypeptide must therefore grow by being transferred from the peptidyl–tRNA in the P site to the incoming aa–tRNA in the A site to form a peptidyl–tRNA with one more residue (Fig. 27-21). After the peptide bond has formed, the new peptidyl–tRNA, which now occupies the A site, is translocated to the P site so that a new aa–tRNA can enter the A site. The uncharged tRNA in the P site moves to the E site before it dissociates from the ribosome (we discuss the details of chain elongation in Section 27-4B).

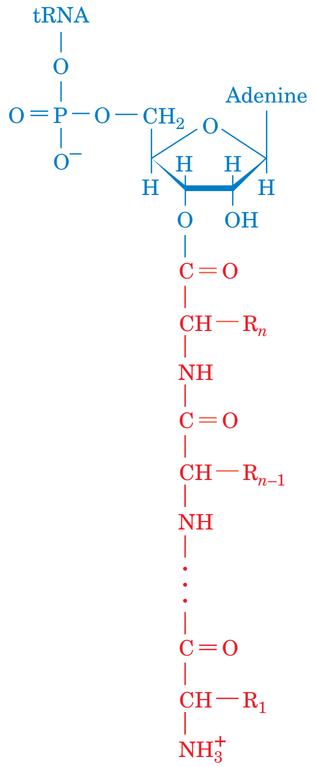

Peptidyl–tRNA

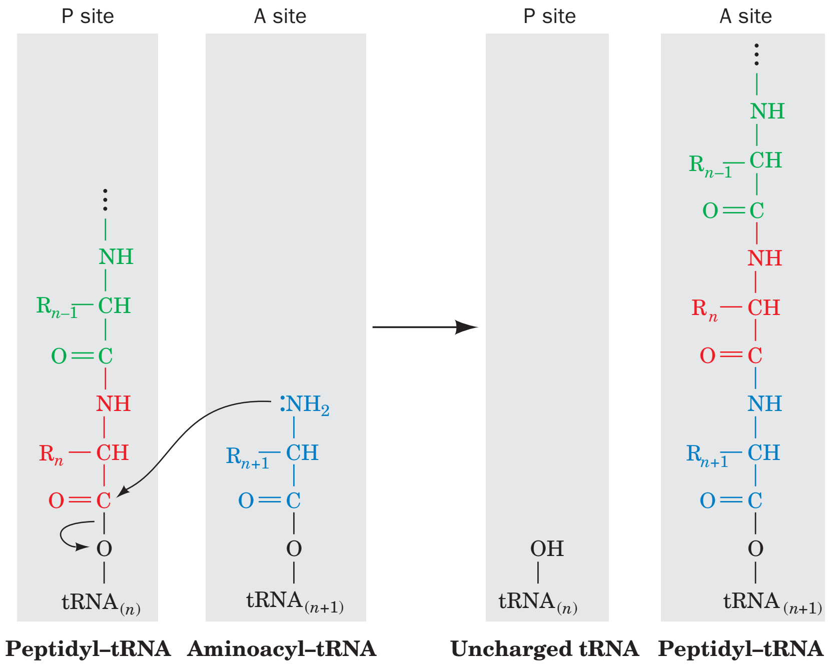

■ **Figure 27-21 | The ribosomal peptidyl transferase reaction forming a peptide bond.** The amino group of the aminoacyl–tRNA in the A site nucleophilically displaces the tRNA of the peptidyl–tRNA ester in the P site, thereby forming a new peptide bond and transferring the nascent polypeptide to the A-site tRNA.

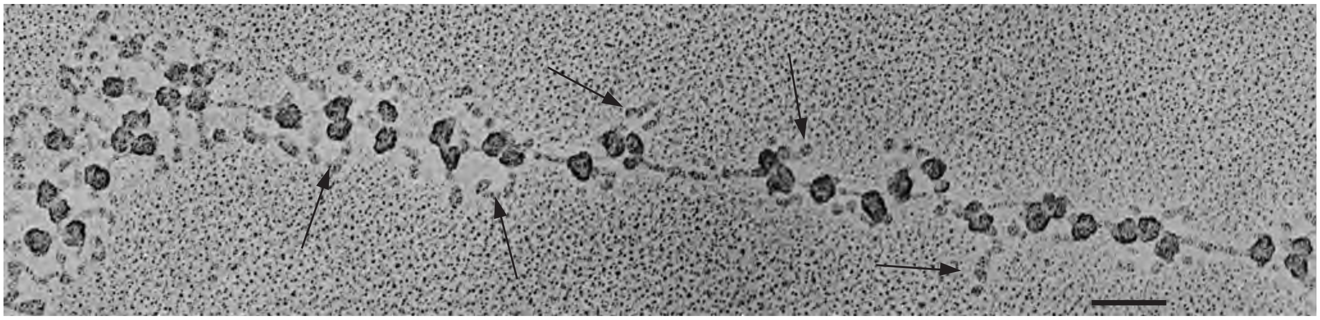

Figure 27-22 | Electron micrograph of polysomes from silk gland cells of the silkworm *Bombyx mori*. The 3′ end of the mRNA is on the left. Arrows point to the silk fibroin polypeptides. The bar represents 0.1 μm. [Courtesy of Oscar L. Miller, Jr., and Steven L. McKnight, University of Virginia.]

3. *Ribosomes read mRNA in the 5′ → 3′ direction.* This was shown through the use of a cell-free protein-synthesizing system in which the mRNA was poly(A) with a 3′-terminal C:

$$5'\ \mathrm{A{-}A{-}A{-}\cdots{-}A{-}A{-}A{-}C}\quad 3'$$

Such a system synthesizes a poly(Lys) that has a C-terminal Asn:

$$\mathrm{H_3N^+{-}Lys{-}Lys{-}Lys{-}\cdots{-}Lys{-}Lys{-}Asn{-}COO^-}$$

Together with the knowledge that AAA and AAC code for Lys and Asn (Table 27-1) and the polarity of peptide synthesis, this established that the mRNA is read in the 5′ → 3′ direction. Because mRNA is also synthesized in the 5′ → 3′ direction, prokaryotic ribosomes can commence translation as soon as a nascent mRNA emerges from RNA polymerase. This, however, is not possible in eukaryotes because the nuclear membrane separates the site of transcription (the nucleus) from the site of translation (the cytosol).

4. *Active translation occurs on polysomes.* In both prokaryotes and eukaryotes, multiple ribosomes can bind to a single mRNA transcript, giving rise to a beads-on-a-string structure called a **polyribosome** (**polysome;** Fig. 27-22). Individual ribosomes are separated by gaps of 50 to 150 Å so that they have a maximum density on the mRNA of ~1 ribosome per 80 nt. Polysomes arise because once an active ribosome has cleared its initiation site on mRNA, a second ribosome can initiate translation at that site.

See Guided Exploration 28
Translational initiation.

A | Chain Initiation Requires an Initiator tRNA and Initiation Factors

The first indication of how ribosomes initiate polypeptide synthesis was the observation that almost half of the *E. coli* proteins begin with the otherwise uncommon amino acid residue Met. In fact, the tRNA that initiates translation is a peculiar form of Met–$\mathrm{tRNA^{Met}}$ in which the Met residue is *N*-formylated:

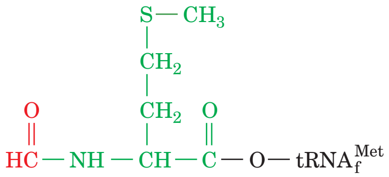

$$\mathrm{HC(=O){-}NH{-}CH(CH_2{-}CH_2{-}S{-}CH_3){-}C(=O){-}O{-}tRNA_f^{Met}}$$

***N*-Formylmethionine–$\mathrm{tRNA_f^{Met}}$**
(fMet–$\mathrm{tRNA_f^{Met}}$)

Because the ***N*-formylmethionine** residue **(fMet)** already has an amide bond, it can only be the N-terminal residue of a polypeptide. *E. coli* proteins are posttranslationally modified by deformylation of their fMet residue and, in many proteins, by the subsequent removal of the resulting N-terminal Met. This processing usually occurs on the nascent polypeptide, which accounts for the observation that mature *E. coli* proteins all lack fMet.

The tRNA that recognizes the initiation codon, **$\mathrm{tRNA}_\mathrm{f}^\mathrm{Met}$,** differs from the tRNA that carries internal Met residues, **$\mathrm{tRNA}_\mathrm{m}^\mathrm{Met}$,** although they both recognize the same AUG codon. Presumably, the conformations of these tRNAs are different enough to permit them to be distinguished in the reactions of chain initiation and elongation.

In *E. coli,* uncharged $\mathrm{tRNA}_\mathrm{f}^\mathrm{Met}$ is aminoacylated with Met by the same MetRS that charges $\mathrm{tRNA}_\mathrm{m}^\mathrm{Met}$. The resulting Met–$\mathrm{tRNA}_\mathrm{f}^\mathrm{Met}$ is specifically *N*-formylated to yield fMet–$\mathrm{tRNA}_\mathrm{f}^\mathrm{Met}$ by a transformylase that employs N^{10}-formyltetrahydrofolate (Section 21-4D) as its formyl donor. This transformylase does not recognize Met–$\mathrm{tRNA}_\mathrm{m}^\mathrm{Met}$.

Base Pairing between mRNA and the 16S rRNA Helps Select the Translation Initiation Site. AUG codes for internal Met residues as well as the initiating Met residue of a polypeptide. Moreover, mRNAs usually contain many AUGs (and GUGs) in different reading frames. Clearly, *a translation initiation site must be specified by more than just an initiation codon.*

In *E. coli,* the 16S rRNA contains a pyrimidine-rich sequence at its 3′ end. This sequence, as John Shine and Lynn Dalgarno pointed out in 1974, is partially complementary to a purine-rich tract of 3 to 10 nucleotides, the **Shine–Dalgarno sequence,** that is centered ~10 nucleotides upstream from the start codon of nearly all known prokaryotic mRNAs (Fig. 27-23). *Base-pairing interactions between an mRNA's Shine–Dalgarno sequence and the 16S rRNA apparently permit the ribosome to select the proper initiation codon.*

The X-ray structure of the 70S ribosome reveals, in agreement with Fig. 27-13*b,* that an ~30-nt segment of the mRNA is wrapped in a groove

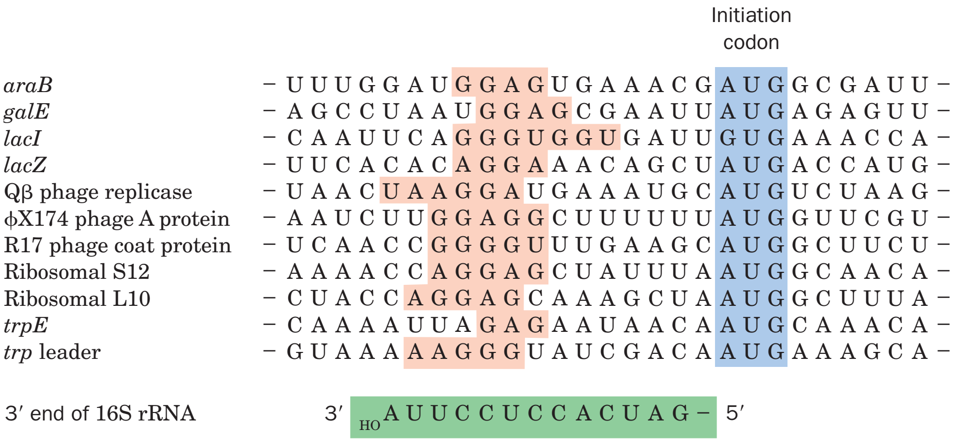
Initiation codon
araB – U U U G G A U G G A G U G A A A C G A U G G C G A U U –
galE – A G C C U A A U G G A G C G A A U U A U G A G A G U U –
lacI – C A A U U C A G G G U G G U G A U U G U G A A A C C A –
lacZ – U U C A C A C A G G A A A C A G C U A U G A C C A U G –
Qβ phage replicase – U A A C U A A G G A U G A A A U G C A U G U C U A A G –
ϕX174 phage A protein – A A U C U U G G A G G C U U U U U U A U G G U U C G U –
R17 phage coat protein – U C A A C C G G G G U U U G A A G C A U G G C U U C U –
Ribosomal S12 – A A A A C C A G G A G C U A U U U A A U G G C A A C A –
Ribosomal L10 – C U A C C A G G A G C A A A G C U A A U G G C U U U A –
trpE – C A A A A U U A G A G A A U A A C A A U G C A A A C A –
trp leader – G U A A A A A G G G U A U C G A C A A U G A A A G C A –
3′ end of 16S rRNA 3′ HO A U U C C U C C A C U A G – 5′

■ **Figure 27-23** | **Some translation initiation sequences recognized by *E. coli* ribosomes.** The RNAs are aligned according to their initiation codons (*blue shading*). Their Shine–Dalgarno sequences (*red shading*) are complementary, counting G · U pairs, to a portion of the 16S rRNA's 3′ end (*below*). [After Steitz, J.A., *in* Chambliss, G., Craven, G. R., Davies, J., Davis, K., Kahan, L., and Nomura, M. (Eds.), *Ribosomes. Structure, Function and Genetics,* pp. 481–482, University Park Press (1979).]

that encircles the neck of the 30S subunit (Fig. 27-24). The mRNA codons in the A and P sites are exposed on the interface side of the 30S subunit, whereas its 5′ and 3′ ends are bound in tunnels composed of RNA and protein. The mRNA's Shine–Dalgarno sequence, which is located near its 5′ end, is base-paired, as expected, with the 16S rRNA's anti-Shine–Dalgarno sequence, which is situated close to the E site. The proteins that in part form the tunnel through which the mRNA enters the ribosome (green in Fig. 27-24) probably function as a helicase to remove secondary structures from the mRNA that would otherwise interfere with tRNA binding.

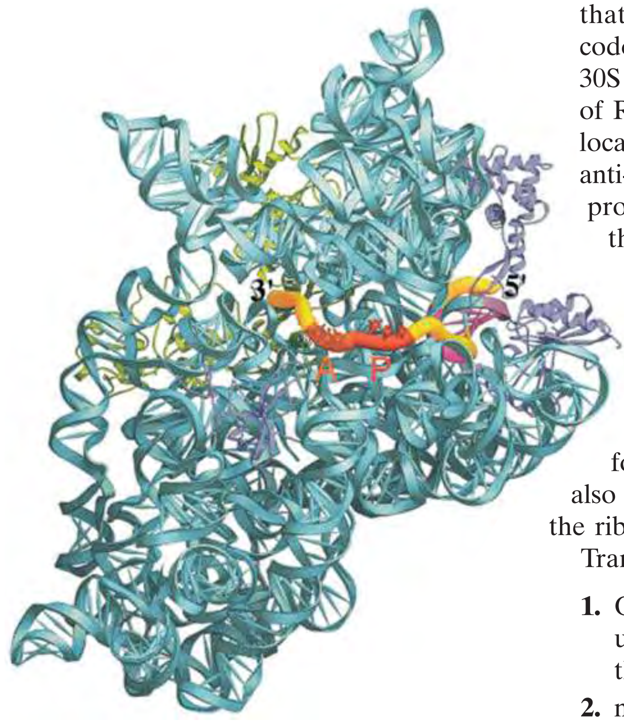

■ **Figure 27-24** | **Path of mRNA through the *T. thermophilus* 30S subunit.** The ribosomal subunit is viewed from its interface side. The 16S rRNA is cyan, the mRNA is represented in worm form with its A- and P-site codons orange and red, the Shine–Dalgarno helix (which includes a segment of 16S rRNA) magenta, and its remaining segments yellow. The ribosomal proteins that in part form the entry and exit tunnels for the mRNA are drawn in green and purple. The remaining ribosomal proteins have been omitted for clarity. [Courtesy of Gloria Culver, Iowa State University. Based on an X-ray structure by Harry Noller, University of California at Santa Cruz. PDBid 1JGO.]

Initiation Requires Soluble Protein Factors. Translation initiation in *E. coli* is a complex process in which the two ribosomal subunits and fMet–$\text{tRNA}_\text{f}^\text{Met}$ assemble on a properly aligned mRNA to form a complex that can commence chain elongation. This process also requires **initiation factors** that are not permanently associated with the ribosome, designated **IF-1, IF-2,** and **IF-3** in *E. coli* (Table 27-6).

Translation initiation in *E. coli* occurs in three stages (Fig. 27-25):

1. On completing a cycle of polypeptide synthesis, the 30S and 50S subunits remain associated as an inactive 70S ribosome. IF-3 binds to the 30S subunit so as to promote the dissociation of this complex.
2. mRNA and IF-2 in a ternary complex with GTP and fMet–$\text{tRNA}_\text{f}^\text{Met}$, along with IF-1, subsequently bind to the 30S subunit in either order. Since the ternary complex containing fMet–$\text{tRNA}_\text{f}^\text{Met}$ can bind

Table 27-6 The Soluble Protein Factors of *E. coli* Protein Synthesis

Factor	Number of Residues[a]	Function
Initiation Factors		
IF-1	71	Assists IF-3 binding
IF-2	890	Binds initiator tRNA and GTP
IF-3	180	Releases mRNA and tRNA from recycled 30S subunit and aids new mRNA binding
Elongation Factors		
EF-Tu	393	Binds aminoacyl–tRNA and GTP
EF-Ts	282	Displaces GDP from EF-Tu
EF-G	703	Promotes translocation through GTP binding and hydrolysis
Release Factors		
RF-1	360	Recognizes UAA and UAG Stop codons
RF-2	365	Recognizes UAA and UGA Stop codons
RF-3	528	Stimulates RF-1/RF-2 release via GTP hydrolysis
RRF	185	Together with EF-G, induces ribosomal dissociation to small and large subunits

[a] All *E. coli* translational factors are monomeric proteins.

to the ribosome before mRNA, fMet–$\text{tRNA}_\text{f}^\text{Met}$ binding must not be mediated by a codon–anticodon interaction; it is the only tRNA–ribosome association that does not require one, although this interaction helps bind fMet–$\text{tRNA}_\text{f}^\text{Met}$ to the ribosome. IF-1 binds in the A site, where it may prevent the inappropriate binding of a tRNA. IF-3 also functions at this stage of the initiation process by preventing the binding of tRNAs other than $\text{tRNA}_\text{f}^\text{Met}$.

3. Last, in a process that is preceded by IF-1 and IF-3 release, the 50S subunit joins the 30S initiation complex in a manner that stimulates IF-2 to hydrolyze its bound GTP to GDP + P*i*. This irreversible reaction conformationally rearranges the 30S subunit and releases IF-2 for participation in further initiation reactions.

Initiation results in the formation of an fMet–tRNA_f^{Met} · mRNA · ribosome complex in which the fMet–tRNA_f^{Met} occupies the ribosome's P site while its A site is poised to accept an incoming aa–tRNA (an arrangement analogous to that at the conclusion of a round of elongation; Section 27-4B). Note that $\text{tRNA}_\text{f}^\text{Met}$ is the only tRNA that directly enters the P site. All other tRNAs must first enter the A site during chain elongation.

Initiation in Eukaryotes Is Far More Complicated than in Prokaryotes. Ribosomal initiation in eukaryotes requires the assistance of at least 11 initiation factors (designated eIF*n;* "e" for *e*ukaryotic) that consist of 26 polypeptide chains. Nevertheless, Steps 1 and 3 of the prokaryotic process (Fig. 27-25) are superficially similar in eukaryotes. However, the way in which the mRNA's initiating codon is identified in eukaryotes is fundamentally different from that in prokaryotes.

The pairing of the initiator tRNA with the initiating AUG in the ribosomal P site begins with **eIF2,** a heterotrimer in complex with GTP, escorting the initiator tRNA to the complex of the 40S subunit with several other initiation factors, thereby forming the **43S preinitiation complex** (a process that resembles Step 2 in prokaryotic initiation but without the mRNA). The initiator tRNA is $\mathbf{tRNA_i^{Met}}$ ("i" for *i*nitiator). Its appended Met residue is not formylated as in prokaryotes. Nevertheless, both species of initiator tRNAs are readily interchangeable *in vitro.*

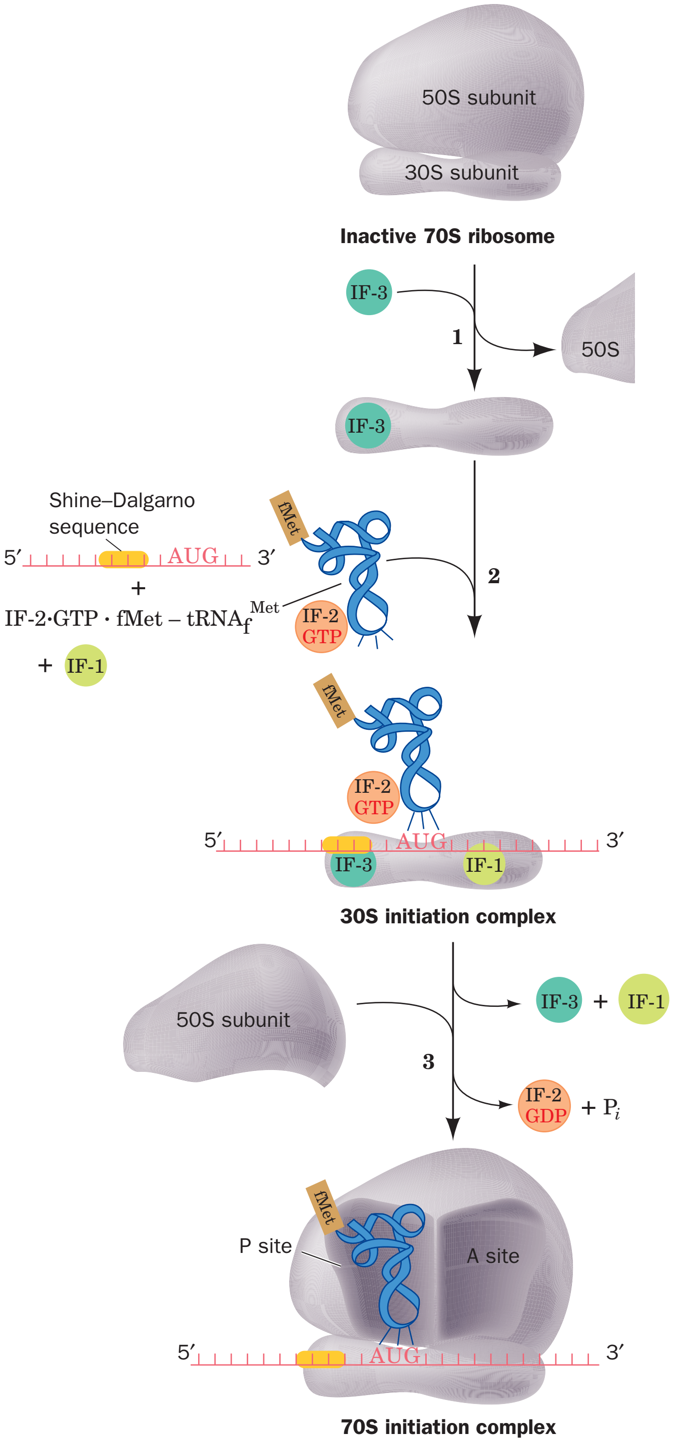

Figure 27-25 | Translation initiation pathway in *E. coli.*

Eukaryotic mRNAs lack the complementary sequences to bind to the 18S rRNA in the Shine–Dalgarno manner. Rather, they have an entirely different mechanism for recognizing the mRNA's initiating AUG codon. *Eukaryotic mRNAs, nearly all of which have a 7-methylguanosine (m^7G) cap and a poly(A) tail (Section 26-3A), are invariably monocistronic and almost always initiate translation at their leading AUG.* This AUG, which occurs at the end of a 5′-untranslated region of 50 to 70 nt, is embedded in the consensus sequence GCCRCC**AUG**G. Changes in the purine (R) 3 nt before the AUG and in the G immediately following it each reduce translational efficiency by ~10-fold. The recognition of the initiation site begins by the binding of

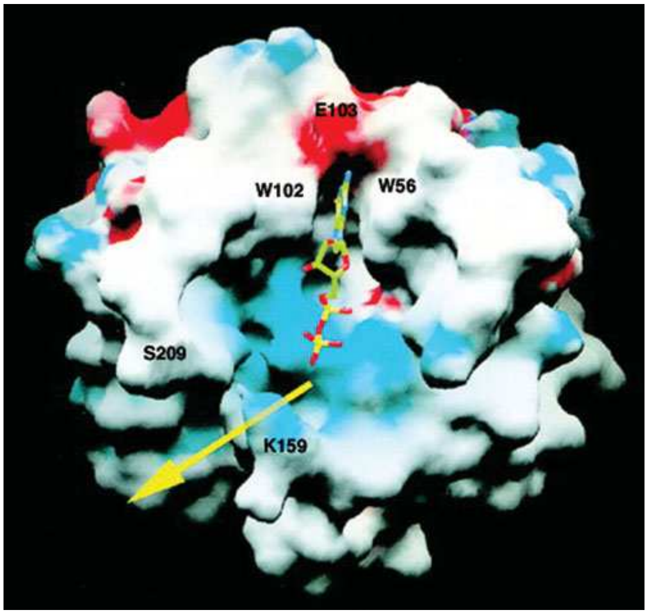

■ **Figure 27-26 | X-Ray structure of murine eIF4E in complex with the m^{7}G cap analog m^{7}GDP.** The protein is shown as its solvent-accessible surface colored according to its electrostatic potential (red negative, blue positive, and white neutral). The m^{7}GDP is drawn in stick form with C green, N blue, O red, and P yellow. The two Trp residues that bind the m^{7}G base are indicated, as are a Lys and Ser residue that flank the putative mRNA-binding cleft (*yellow arrow*). [Courtesy of Nahum Sonenberg, McGill University, Montreal, Quebec, Canada. PDBid 1EJ1.]

eIF4F to the mRNA's m^{7}G cap. eIF4F is a heterotrimeric complex of **eIF4E, eIF4G,** and **eIF4A** (all monomers), in which eIF4E (also known as **cap-binding protein**) recognizes the mRNA's m^{7}G cap and eIF4G serves as a scaffold to join eIF4E with eIF4A.

The structure of eIF4E in complex with **m^{7}GDP** reveals that the protein binds the m^{7}G base by intercalating it between two highly conserved Trp residues in a region that is adjacent to a positively charged cleft that presumably forms the mRNA-binding site (Fig. 27-26). The m^{7}G base is specifically recognized by hydrogen bonding to protein side chains in a manner reminiscent of G·C base pairing. eIF4G also binds poly(A)-binding protein (PABP; Section 26-3A), which coats the mRNA's poly(A) tail, thereby circularizing the mRNA. Although this explains the synergism between an mRNA's m^{7}G cap and its poly(A) tail in stimulating translational initiation, the function of the circle is unclear. However, an attractive hypothesis is that it enables a ribosome that has finished translating the mRNA to reinitiate translation without having to disassemble and then reassemble. Another possibility is that it prevents the translation of incomplete (broken) mRNAs.

The eIF4F–mRNA complex is subsequently joined by several additional initiation factors. The resulting complex joins the 43S preinitiation complex, which then scans down the mRNA in an ATP-driven process until it encounters the mRNA's initiating AUG codon, thereby forming the **48S initiation complex.** The recognition of the AUG occurs mainly through base pairing with the CUA anticodon on the bound Met–tRNA$_i^{Met}$, as was demonstrated by the observation that mutating this anticodon results in the recognition of the new cognate codon instead of AUG.

In the analog of Step 3 of prokaryotic initiation (Fig. 27-25), the eIF2-catalyzed hydrolysis of its bound GTP induces the release of all initiation factors from the 48S initiation complex. The resulting 40S subunit–Met–tRNA$_i^{Met}$ complex is joined by the 60S subunit in a GTP-dependent reaction mediated by **eIF5B** (a monomer and homolog of prokaryotic IF-2), thereby forming the 80S ribosomal initiation complex.

See Guided Exploration 29
Translational elongation.

B | The Ribosome Decodes the mRNA, Catalyzes Peptide Bond Formation, Then Moves to the Next Codon

Ribosomes elongate polypeptide chains in a three-stage reaction cycle (Fig. 27-27):

1. **Decoding,** in which the ribosome selects and binds an aminoacyl–tRNA whose anticodon is complementary to the mRNA codon in the A site.

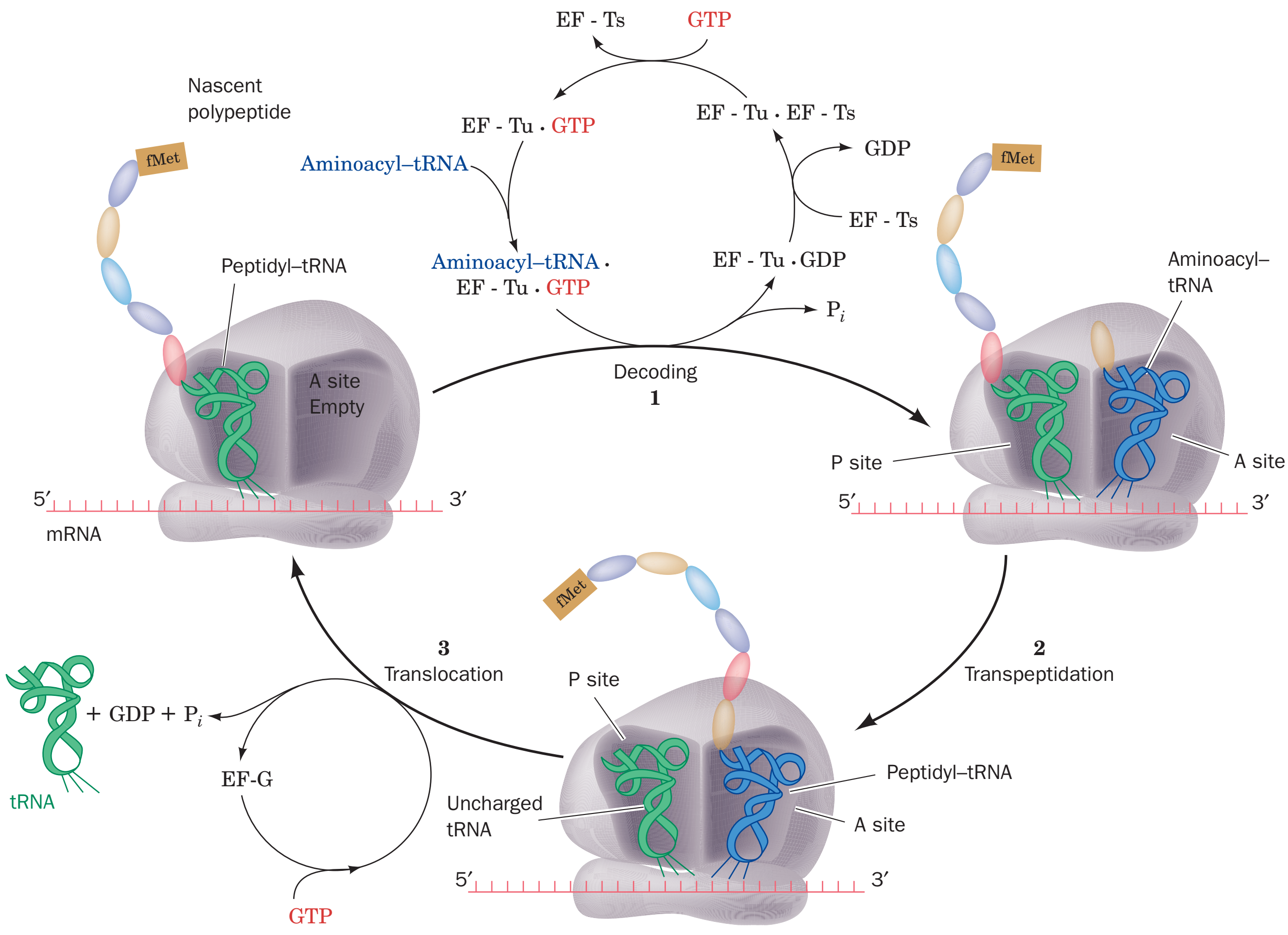
EF - Ts
GTP
Nascent polypeptide
EF - Tu · GTP
EF - Tu · EF - Ts
GDP
fMet
fMet
Aminoacyl–tRNA
EF - Ts
Peptidyl–tRNA
Aminoacyl–tRNA ·
EF - Tu · GTP
EF - Tu · GDP
Aminoacyl–tRNA
P_i
Decoding
1
A site
Empty
P site
A site
5′
3′
5′
3′
mRNA
fMet
3
Translocation
2
Transpeptidation
P site
+ GDP + P_i
EF-G
Peptidyl–tRNA
tRNA
Uncharged tRNA
A site
5′
3′
GTP

Figure 27-27 | **Elongation cycle in *E. coli* ribosomes.** The E site is not shown. Eukaryotic elongation follows a similar cycle, but EF-Tu and EF-Ts are replaced by a single multisubunit protein, eEF1, and EF-G is replaced by eEF2.

2. **Transpeptidation,** or peptide bond formation, in which the peptidyl group in the P-site tRNA is transferred to the aminoacyl group in the A site.
3. **Translocation,** in which the A-site and P-site tRNAs are respectively transferred to the P and E sites, accompanied by their bound mRNA; that is, the mRNA, together with its base-paired tRNAs, is ratcheted through the ribosome by one codon.

This process, which occurs at a rate of 10 to 20 amino acid residues per second, requires several nonribosomal proteins known as **elongation factors** (Table 27-6).

Decoding: An Aminoacyl–tRNA Binds to the Ribosomal A Site.

In the first stage of the *E. coli* elongation cycle, a binary complex of GTP and the elongation factor **EF-Tu** combines with an aa–tRNA. The resulting ternary complex binds to the ribosome. Binding of the aa–tRNA in a codon–anticodon complex to the ribosomal A site is accompanied by the hydrolysis of GTP to GDP so that EF-Tu · GDP and P_i are released. The EF-Tu · GTP complex is regenerated when GDP is displaced from EF-Tu·GDP by the elongation factor **EF-Ts,** which in turn is displaced by GTP.

Aminoacyl–tRNAs can bind to the ribosomal A site without EF-Tu but at a rate too slow to support cell growth. The importance of EF-Tu is indicated by the fact that it is the most abundant *E. coli* protein; it is present in ~100,000 copies per cell (>5% of the cell's protein), which is approximately the number of tRNA molecules in the cell. Consequently, *the cell's entire complement of aa–tRNAs is essentially sequestered by EF-Tu.*

The X-ray structure of EF-Tu in complex with Phe–tRNA^{Phe} and the nonhydrolyzable GTP analog **guanosine-5′-(β,γ-imido)triphosphate (GMPPNP;** alternatively **GDPNP),** was determined by Brian Clark and Jens Nyborg (Fig. 27-28). This complex has a corkscrew-shaped structure in which the EF-Tu and the tRNA's acceptor stem form a knoblike handle and the tRNA's anticodon helix forms the screw. The macromolecules appear to associate rather tenuously via three major regions: (1) The 3′-CCA–Phe segment of the Phe–tRNA^{Phe} binds in the cleft between domains 1 and 2 of EF-Tu · GMPPNP (the blue and green mainly helical domain and the yellow β sheet domain in Fig. 27-28); (2) the 5′-phosphate of the tRNA binds in a depression at the junction of EF-Tu's three domains; and (3) one side of the TψC stem of the tRNA makes contacts with exposed main chain and side chains of EF-Tu domain 3 (the orange β barrel–containing domain in Fig. 27-28).

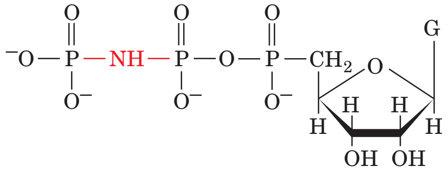

Guanosine-5′-(β,γ-imido)triphosphate (GMPPNP)

EF-Tu binds all aminoacylated tRNAs, but not uncharged tRNAs or initiator tRNAs. Evidently, the tight association of the aminoacyl group with EF-Tu greatly increases the affinity of EF-Tu for the otherwise loosely bound tRNA. $\text{tRNA}_f^{\text{Met}}$ does not bind to EF-Tu because it has a 3′ overhang of 5 nt versus 4 nt in an elongator tRNA. This, together with the formyl group attached to the fMet residue, apparently prevents fMet– $\text{tRNA}_f^{\text{Met}}$ from binding to EF-Tu, thereby explaining why the initiator tRNA never translates internal AUG codons.

EF-Tu is a G protein that undergoes a large conformational change on hydrolyzing GTP. Its N-terminal domain 1 (blue, cyan, and green in Fig. 27-28) resembles other G proteins (Sections 13-2B and 13-3B), with Switch I and Switch II regions signaling the state of the bound nucleotide (GTP or GDP). GTP hydrolysis also causes domain 1 to reorient with respect to domains

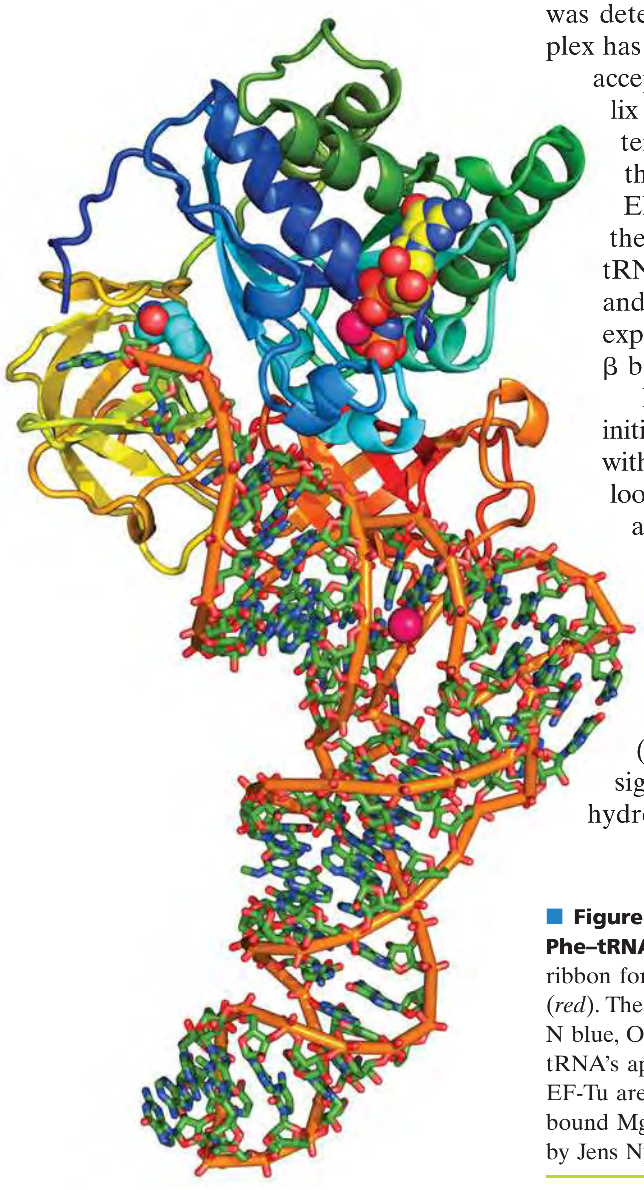

■ **Figure 27-28 | X-Ray structure of the ternary complex of yeast Phe–tRNA^{Phe}, *Thermus aquaticus* EF-Tu, and GMPPNP.** The EF-Tu is drawn in ribbon form colored in rainbow order from its N-terminus (*blue*) to its C-terminus (*red*). The tRNA is shown in stick form colored according to atom type with C green, N blue, O red, and P orange and with an orange rod linking successive P atoms. The tRNA's appended aminoacyl-Phe residue and the GMPPNP that is bound to the EF-Tu are drawn in space-filling form with C atoms cyan and yellow, respectively. Two bound Mg^{2+} ions are represented by magenta spheres. [Based on an X-ray structure by Jens Nyborg, University of Aarhus, Århus, Denmark. PDBid 1TTT.]

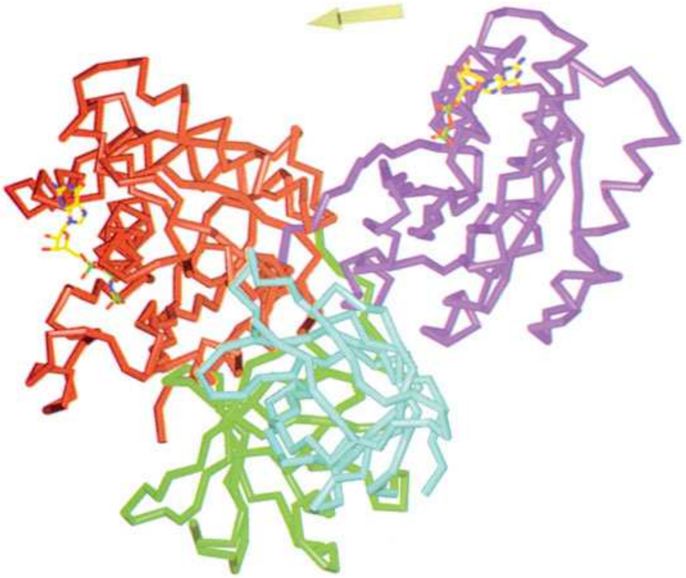

Figure 27-29 | Comparison of the X-ray structures of ribosomal elongation factor EF-Tu in its complexes with GDP and GMPPNP. The protein is represented by its Cα backbone with domain 1, its GTP-binding domain, purple in the GDP complex and red in the GMPPNP complex. Domains 2 and 3, which have the same orientation in both complexes, are green and cyan. The bound GDP and GMPPNP are shown in skeletal form with C yellow, N blue, O red, and P green. [Courtesy of Morton Kjeldgaard and Jens Nyborg, Aarhus University, Århus, Denmark. PDBid 1EFT.] **See Interactive Exercise 54.**

2 and 3 by a dramatic 91° rotation (Fig. 27-29), a conformational change that eliminates the tRNA-binding site. Since EF-Tu is a G protein, the ribosome can be classified as its GTPase-activating protein (GAP) and EF-Ts functions as its guanine nucleotide exchange factor (GEF).

The Ribosome Monitors Correct Codon–Anticodon Pairing. When EF-Tu · GTP delivers an aa–tRNA to the ribosome, it first inserts the anticodon end of the tRNA into the ribosome. The tRNA's aminoacyl end moves fully into the A site only after GTP is hydrolyzed and EF-Tu dissociates. *This multistep process allows the ribosome to verify that the aa–tRNA has correctly paired with an mRNA codon.* How does the ribosome monitor codon–anticodon pairing?

The X-ray structure of the *T. thermophilus* 30S subunit in complex with a U_6 hexanucleotide "mRNA" and a 17-nt RNA consisting of the $tRNA^{Phe}$ anticodon arm (Fig. 27-5, but with its nucleotides unmodified), determined by Ramakrishnan, reveals how an mRNA-specified tRNA initially binds to the ribosome. The codon–anticodon association is stabilized by its interactions with three universally conserved ribosomal bases, A1492, A1493, and G530 (Fig. 27-30):

1. The first codon–anticodon base pair, that between mRNA U1 and tRNA A36, is stabilized by the binding of the rRNA A1493 base in the base pair's minor groove (Fig. 27-30*a*).

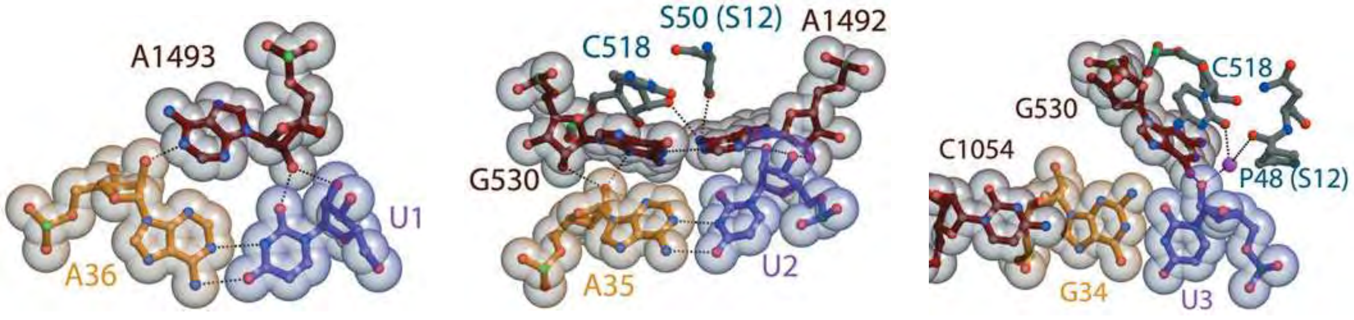

(*a*) (*b*) (*c*)

Figure 27-30 | Codon–anticodon interactions in the ribosome. The (*a*) first, (*b*) second, and (*c*) third codon–anticodon base pairs as seen in the X-ray structure of the *T. thermophilus* 30S subunit in complex with U_6 (a model mRNA) and the 17-nt anticodon arm of $tRNA^{Phe}$ (whose anticodon is GAA). The structures are drawn in ball-and-stick form embedded in their semitransparent van der Waals surfaces. Codons are purple, anticodons are yellow, and rRNA is brown or gray with non-C atoms colored according to type (N blue, O red, and P green). Protein segments are gray and Mg^{2+} ions are represented by magenta spheres. [Courtesy of V. Ramakrishnan, MRC Laboratory of Molecular Biology, Cambridge, U.K. PDBid 1IBM.]

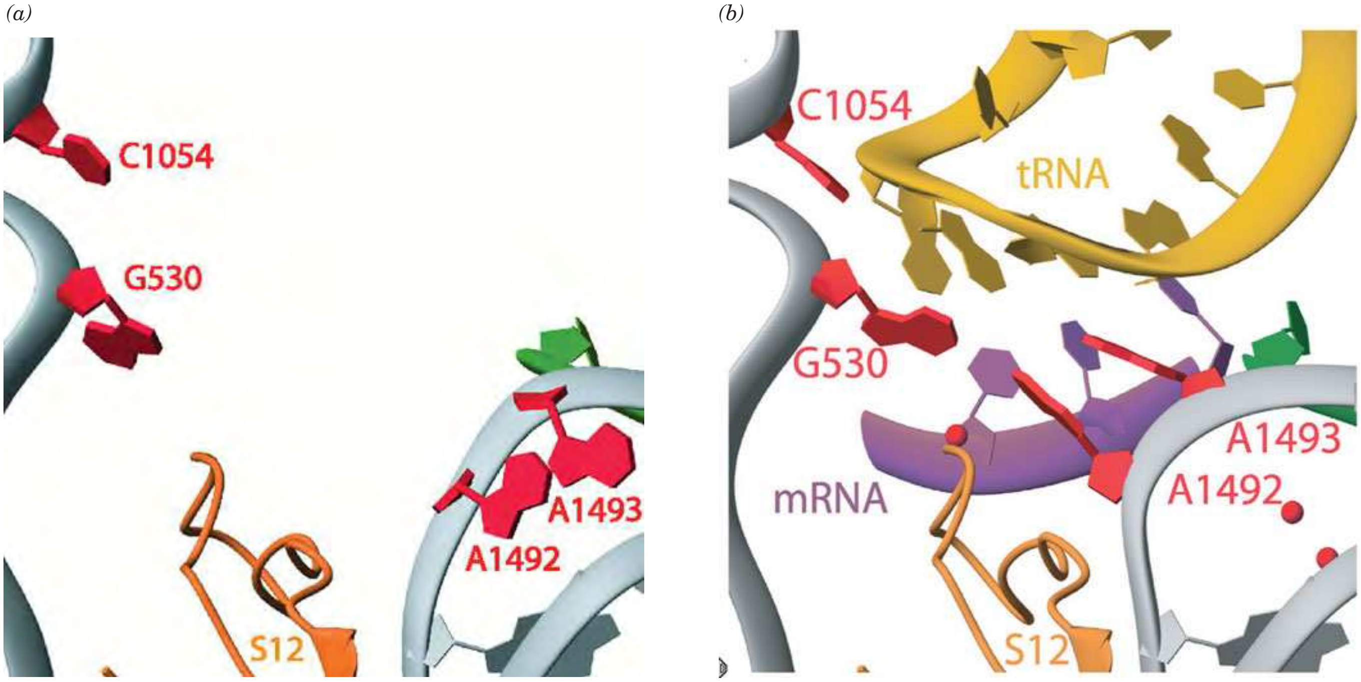

Figure 27-31 | Ribosomal decoding site. The X-ray structures of *T. thermophilus* 30S subunit (*a*) alone and (*b*) in its complex with U_6 and the anticodon stem–loop of $tRNA^{Phe}$. The RNAs are drawn as ribbons with their nucleotides in paddle form with tRNA gold, A-site mRNA purple, P-site mRNA green, rRNA gray, and nucleotides that undergo conformational changes red. Protein S12 is tan and Mg^{2+} ions are represented by red spheres. [Courtesy of V. Ramakrishnan, MRC Laboratory of Molecular Biology, Cambridge, U.K. PDBids (*a*) 1FJF and (*b*) 1IBM.]

2. The second codon–anticodon base pair, that between U2 and A35, is bolstered by A1492 and G530, which both bind in this base pair's minor groove (Fig. 27-30*b*).
3. The third codon–anticodon base pair (the wobble pair; Section 27-2C), that between U3 and G34, is reinforced through minor groove binding by G530 (Fig. 27-30*c*). The latter interaction appears to be less stringent than those in the first and second codon–anticodon positions, which is consistent with the need for the third codon–anticodon pairing to tolerate non-Watson–Crick base pairs (Section 27-2C).

Comparison of this structure with that of the 30S subunit alone reveals that the foregoing rRNA nucleotides undergo conformational changes on the formation of a codon–anticodon complex (Fig. 27-31): In the absence of tRNA, the bases of A1492 and A1493 stack in the interior of an RNA loop, whereas in the codon–anticodon complex, these bases have flipped out of the loop and the G530 base has switched from the syn to the anti conformation (Section 24-1B). These interactions enable the ribosome to monitor whether an incoming tRNA is cognate to the codon in the A site; a non-Watson–Crick base pair could not bind these ribosomal bases in the same way. Indeed, any mutation of A1492 or A1493 is lethal because pyrimidines in these positions could not reach far enough to interact with the codon–anticodon complex or G530, and because a G in either position would be unable to form the required hydrogen bonds and its N2 would be subjected to steric collisions. An incorrect codon–anticodon interaction provides insufficient free energy to bind the tRNA to the ribosome and it therefore dissociates from the ribosome, still in its ternary complex with EF-Tu and GTP.

GTP Hydrolysis by EF-Tu Is a Thermodynamic Prerequisite to Ribosomal Proofreading. An aa–tRNA is selected by the ribosome only according to its anticodon, a process that has a measured error rate of only $\sim 10^{-4}$ per residue. Yet the binding energy loss arising from a single base mismatch in a codon–anticodon interaction is estimated to be ~ 12 $\text{kJ} \cdot \text{mol}^{-1}$, which, according to Eq. 27-1, cannot account for a ribosomal decoding accuracy of less than $\sim 10^{-2}$ errors per codon. Evidently, the ribosome has some sort of proofreading mechanism that increases its overall decoding accuracy.

A proofreading step must be entirely independent of the initial selection step. Only then can the overall probability of error be equal to the product of the probabilities of error of the individual selection steps. We have seen that DNA polymerases and aminoacyl–tRNA synthetases maintain the independence of their two selection steps by carrying them out at separate active sites (Sections 25-2A and 27-2B). Yet the ribosome recognizes the incoming aa–tRNA only according to its anticodon's complementarity to the codon in the A site. Consequently, the ribosome must somehow examine this codon–anticodon interaction in two separate ways. How does this occur?

Cryo-EM studies by Frank indicate that in the ribosome · aa–tRNA · EF-Tu · GTP complex, the aa–tRNA assumes an otherwise energetically unfavorable conformation in which the anticodon arm has moved via a hinge motion toward the inside of the tRNA's L. The formation of a correct codon–anticodon complex triggers EF-Tu to hydrolyze its bound GTP and thereby dissociate from the aa–tRNA, which then assumes its energetically more favorable conformation while maintaining its codon–anticodon interaction. This movement swings the acceptor stem with its attached aminoacyl group into the peptidyl transferase center on the 50S subunit (see below). A noncognate (mispaired) aa–tRNA would presumably have insufficient strength in its codon–anticodon interaction to hold it in place during this conformational change and would therefore dissociate from the ribosome. EF-Tu's irreversible GTPase reaction must precede this proofreading step because otherwise the dissociation of a noncognate aa–tRNA (the release of its anticodon from the codon) would simply be the reverse of the initial binding step; that is, it would be part of the initial selection step rather than proofreading. *GTP hydrolysis therefore provides the second context necessary for proofreading; it is the entropic price the system must pay for accurate tRNA selection.*

Transpeptidation: The Ribosome Is a Ribozyme. In the second (transpeptidation) stage of the elongation cycle (Fig. 27-27), the peptide bond is formed through the nucleophilic displacement of the P site tRNA by the amino group of the 3′-linked aa–tRNA in the A site (Fig. 27-21). The nascent polypeptide chain is thereby lengthened at its C-terminus by one residue and transferred to the A-site tRNA. The reaction occurs without the need of activating cofactors such as ATP because the ester linkage between the nascent polypeptide and the P-site tRNA is a "high-energy" bond.

The peptidyl transferase center that catalyzes peptide bond formation is located on the large subunit and consists entirely of rRNA. Numerous observations had suggested that the ribosome is indeed a ribozyme rather than a conventional protein enzyme. For example, rRNAs are more highly conserved throughout evolution than are ribosomal proteins, and most mutations that confer resistance to antibiotics that inhibit protein synthesis occur in genes encoding rRNAs rather than ribosomal proteins. However, it was the X-ray structure of the large ribosomal subunit that unambiguously demonstrated that rRNA functions catalytically in protein synthesis. In hindsight, this seems obvious on evolutionary grounds: Since all proteins, including those associated with ribosomes, are ribosomally synthesized, the primordial ribosome must have preceded the primordial proteins and hence consisted entirely of RNA.

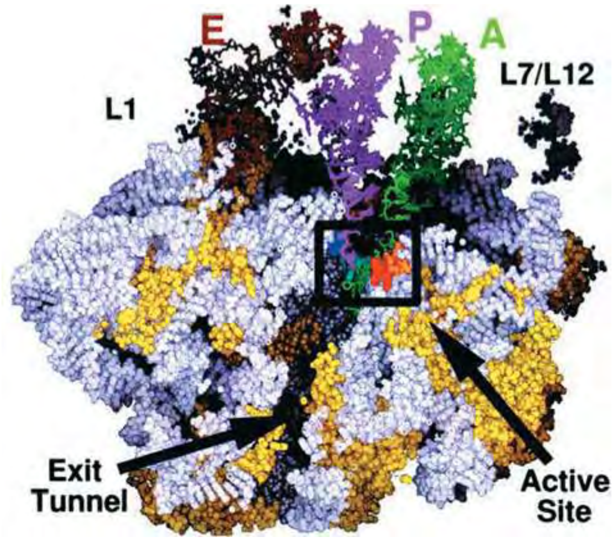

■ **Figure 27-32 | Cutaway view of the large ribosomal subunit from *H. marismortui*.** The three tRNAs are superimposed on the positions they occupy in the A, P, and E sites of the 70S ribosome. This cutaway view exposes the lumen of the peptide exit tunnel and the peptidyl transferase site (*boxed*). The complex is drawn in space-filling form with its rRNA white, its proteins yellow, the tRNAs in the A, P, and E sites green, magenta, and brown and some of the nucleotides that interact with the A-site tRNA red and orange. [Courtesy of Peter Moore and Thomas Steitz, Yale University.]

The ribosome's active site lies in a highly conserved region in domain V of the 23S rRNA (Figs. 27-12*b*, 27-18, and 27-32). The nearest protein side chain is ~18 Å away from the newly formed peptide bond, and the nearest Mg^{2+} ion is ~8.5 Å away—both too far to be involved in catalysis. Clearly, *the ribosomal transpeptidase reaction is catalyzed solely by RNA.*

The ribosomal transpeptidase reaction occurs ~10^7-fold faster than the uncatalyzed reaction. How does the ribosome catalyze this reaction? Ribosomally mediated peptide bond formation proceeds via the nucleophilic attack of the amino group on the carbonyl group of an ester to form a tetrahedral intermediate that collapses to an amide and an alcohol (Fig. 27-21). However, in the physiological pH range, the attacking amino group is predominantly in its ammonium form (RNH_3^+), which lacks the lone pair necessary to undertake a nucleophilic attack. This suggests that the transpeptidase reaction is catalyzed in part by a general base that abstracts a proton from the ammonium group to generate the required free amino group (RNH_2).

Inspection of the peptidyl transferase active site in *H. marismortui* reveals that the only basic group within 5 Å of the inferred position of the attacking amino group is atom N3 of the invariant rRNA base A2486 (A2451 in *E. coli*). It is ~3 Å from and hence hydrogen bonded to the attacking amino group (Fig. 27-33). This further suggests that the protonated A2486-N3 electrostatically stabilizes the oxyanion of the tetrahedral reaction intermediate and then donates the proton to the leaving group of the P-site tRNA to yield a 3′-OH group (general acid catalysis). However, in order for A2486-N3 to act as a general base in abstracting the proton from an ammonium group (whose p*K* is ~10), it must have a p*K* of at least 7 (recall that proton transfers between hydrogen-bonded groups occur at physiologically significant rates only when the p*K* of the proton donor is no more than 2 or 3 pH units greater than that of the proton acceptor;

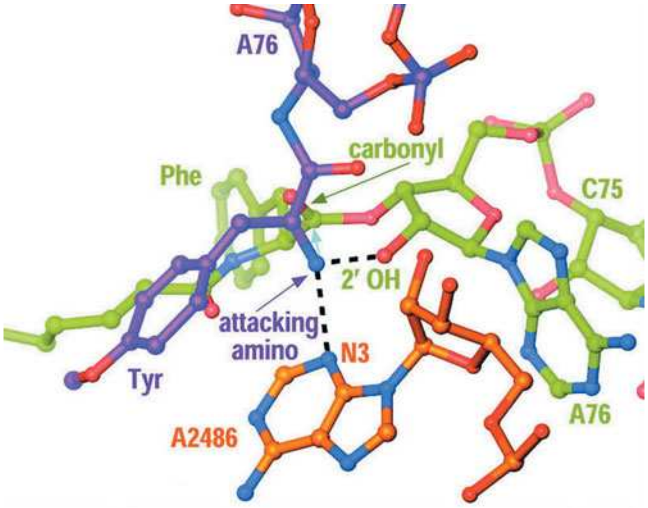

■ **Figure 27-33 | Model of the substrate complex of the 50S ribosomal subunit.** Atoms are colored according to type with the A-site substrate (Tyr–$tRNA^{Tyr}$) C purple, P-site substrate C green, 23S rRNA C orange, N blue, and O red. The attacking amino group of the A-site aminoacyl residue is held in position for nucleophilic attack (*purple arrow*) on the carbonyl C of the P-site aminoacyl ester through hydrogen bonds (*dashed black lines*) to A2486-N3 and the 2′-O of the P-site A76. [Courtesy of Peter Moore and Thomas Steitz, Yale University.]

Section 11-5C). Yet, the pK of N3 in AMP is <3.5. Moreover, the model displayed in Fig. 27-33 indicates that the tetrahedral intermediate's oxyanion would point away from and hence could not be stabilized by protonated A2486-N3.

The Ribosome Is an Entropy Trap. The resolution to this conundrum was provided by Marina Rodnina and Richard Wolfenden, who noted that the uncatalyzed reaction of esters with amines to form amides occurs quite facilely in aqueous solution. They therefore measured the rates of both uncatalyzed peptide bond formation by model compounds and peptidyl transfer by the ribosome at several different temperatures. This provided values of $\Delta\Delta H^{\ddagger}_{\text{cat}}$ and $\Delta\Delta S^{\ddagger}_{\text{cat}}$, the reaction's change in the enthalpy and entropy of activation by the ribosome relative to the uncatalyzed reaction. Here $\Delta\Delta H^{\ddagger}_{\text{cat}} - T\Delta\Delta S^{\ddagger}_{\text{cat}} = \Delta\Delta G^{\ddagger}_{\text{cat}} = \Delta G^{\ddagger}(\text{uncat}) - \Delta G^{\ddagger}(\text{cat})$, where $\Delta\Delta G^{\ddagger}_{\text{cat}}$ is the change in the reaction's free energy of activation by the ribosome relative to the uncatalyzed reaction, and $\Delta G^{\ddagger}(\text{uncat})$ and $\Delta G^{\ddagger}(\text{cat})$ are the free energies of activation of the uncatalyzed and catalyzed (ribosomal) reactions (Sections 1-3D and 11-2). The measured value of $\Delta\Delta H^{\ddagger}_{\text{cat}}$ is $-19\ \text{kJ} \cdot \text{mol}^{-1}$, a quantity that would be positive, not negative, if the ribosomal reaction had a significant component of chemical catalysis such as acid–base catalysis and/or the formation of new hydrogen bonds. In contrast, the value of $T\Delta\Delta S^{\ddagger}_{\text{cat}}$ is $+52\ \text{kJ} \cdot \text{mol}^{-1}$, which indicates that the Michaelis complex (E·S; Section 12-1B) in the ribosomal reaction is significantly more ordered relative to the transition state than is the uncatalyzed reaction. This value of $T\Delta\Delta S^{\ddagger}_{\text{cat}}$ largely accounts for the observed $\sim 10^7$-fold rate enhancement of the ribosomal reaction relative to the uncatalyzed reaction (the rate enhancement by the ribosome is given by $e^{\Delta\Delta G^{\ddagger}_{\text{cat}}/RT}$; Section 11-2). Evidently, *the ribosome enhances the rate of peptide bond formation by properly positioning and orienting its substrates and/or excluding water from the preorganized electrostatic environment of the active site (a form of reactant ordering) rather than by chemical catalysis.*

The X-ray structures of the large ribosomal subunit in complex with aminoacyl–tRNA and peptidyl–tRNA indicate that the ribosome uses an induced fit mechanism, as occurs in enzymes such as hexokinase (Section 15-2A). Conformational changes in the 23S rRNA, presumably triggered by proper binding of the aminoacyl–tRNA in the A site, orient the ester group of the peptidyl–tRNA for nucleophilic attack. In the absence of a tRNA in the A site, the peptidyl–tRNA is held in a position that prevents nucleophilic attack by water (hydrolysis, which would release the peptidyl group from the ribosome).

Translocation: The Ribosome Moves to the Next Codon. Following transpeptidation, the now uncharged P-site tRNA moves to the E site (not shown in Fig. 27-27), and the new peptidyl–tRNA in the A site, together with its bound mRNA, moves to the P site. These events, which leave the A site vacant, prepare the ribosome for the next elongation cycle. During translocation, the peptidyl–tRNA's interaction with the codon, which is no longer necessary for amino acid specification, acts as a placekeeper so that the ribosome can advance by exactly three nucleotides along the mRNA, as required to preserve the reading frame. An Mg^{2+}-stabilized kink in the mRNA between the A and P codons may help prevent slipping. Indeed, certain mutant tRNA molecules that cause frameshifting induce the ribosome to translocate by four nucleotides, thereby demonstrating that mRNA movement is directly coupled to tRNA movement.

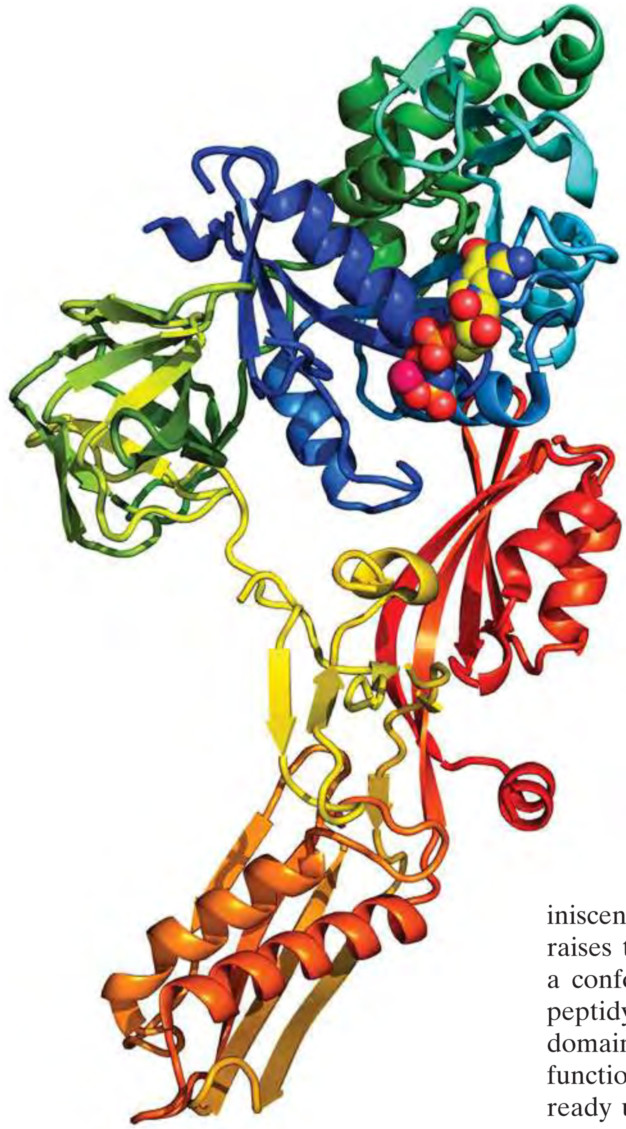

■ **Figure 27-34 | X-Ray structure of EF-G from *Thermus thermophilus* in complex with GMPPNP.** The protein is drawn in ribbon form colored in rainbow order from its N-terminus (*blue*) to its C-terminus (*red*). The GDP is drawn in space-filling form colored according to atom type with C yellow, N blue, O red, and P orange. An Mg^{2+} ion that is bound to the GMPPNP is represented by a magenta sphere. Portions of the structure are not visible. Note the remarkable resemblance in shape between this structure and that of $Phe\text{–}tRNA^{Phe} \cdot$ EF-Tu · GMPPNP (Fig. 27-28). [Based on an X-ray structure by Anders Liljas and Derek Logan, Lund University, Lund, Sweden. PDBid 2BV3.]

The translocation process requires an elongation factor, **EF-G** in *E. coli,* that binds to the ribosome together with GTP and is released only on hydrolysis of the GTP to GDP + P_i (Fig. 27-27). EF-G release is prerequisite for beginning the next elongation cycle because the ribosomal binding sites of EF-G and EF-Tu partially or completely overlap and hence their ribosomal binding is mutually exclusive. GTP hydrolysis, which precedes translocation, provides free energy for tRNA movement.

EF-G Structurally Mimics the EF-Tu · tRNA Complex. The X-ray structure of EF-G (Fig. 27-34) reveals that this protein has an elongated shape comprising five domains, the first two of which (blue through green in Fig. 27-34) are arranged similarly to the first two domains of the EF-Tu · GMPPNP complex (Fig. 27-28). Most intriguingly, the remaining three domains of EF-G (yellow, orange, and red in Fig. 27-34) have a conformation reminiscent of the shape of tRNA bound to EF-Tu. Such molecular mimicry raises the possibility that EF-G drives translocation not just by inducing a conformational change in the ribosome but by actively displacing the peptidyl–tRNA from the A site. The structural similarity between EF-G domains 3 to 5 and tRNA also suggests that in the earliest cells, whose functions were based on RNA, proteins evolved by mimicking shapes already used successfully by RNA.

Translocation Occurs Via Intermediate States. Variations in chemical footprinting patterns during the elongation cycle, together with X-ray and cryo-EM studies, indicate that the translocation of tRNA through the ribosome occurs in several discrete steps (Fig. 27-35):

1. In the **posttranslocational state,** a deacylated tRNA occupies the E site of both the 30S and 50S subunits (the E/E state), a peptidyl–tRNA occupies both P sites (the P/P state), and the A site is vacant. An aa–tRNA in complex with EF-Tu · GTP binds to the ribosome accompanied by the release of the E-site tRNA (see below). This yields a complex in which the incoming aa–tRNA is bound in the 30S subunit's A site via a codon–anticodon interaction (recall that the mRNA is bound to the 30S subunit) but with the EF-Tu · GTP preventing the entry of the tRNA's aminoacyl end into the 50S subunit's A site, an arrangement termed the A/T state (T for EF-*T*u).
2. As we discussed above, EF-Tu hydrolyzes its bound GTP to GDP + P_i and is released from the ribosome, thereby permitting the aa–tRNA to fully bind to the A site (the A/A state).
3. The transpeptidation reaction occurs, yielding the **pretranslocational state.**

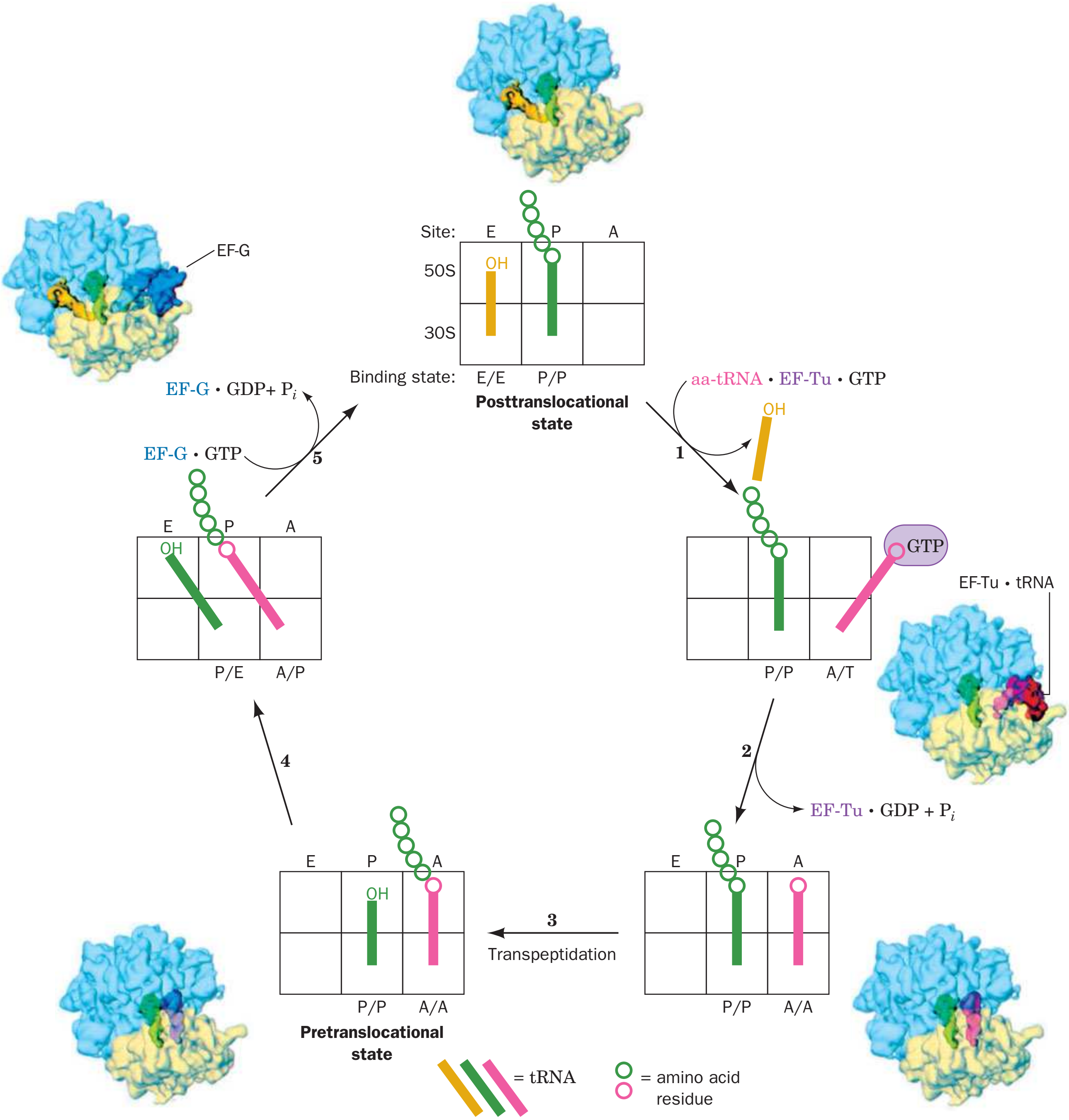
Site: E P A
50S
30S
OH
Binding state: E/E P/P
Posttranslocational state
aa-tRNA • EF-Tu • GTP
OH
1
GTP
EF-Tu • tRNA
P/P A/T
2
EF-Tu • GDP + P_i
E P A
P/P A/A
3
Transpeptidation
E P A
OH
P/P A/A
Pretranslocational state
4
E P A
OH
P/E A/P
EF-G • GTP
5
EF-G • GDP+ P_i
EF-G
= tRNA
= amino acid residue

■ Figure 27-35 | Ribosomal binding states in the elongation cycle. Note how this scheme elaborates the classical elongation cycle diagrammed in Fig. 27-27. The drawings are accompanied by 17-Å-resolution cryo-EM–based images of the *E. coli* 70S ribosome in the corresponding binding states in which the 30S subunit is transparent yellow, the 50S subunit is transparent blue, and the tRNAs and elongation factors are colored as in the drawing they accompany. [Cryo-EM images courtesy of Knud Nierhaus, Max-Planck-Institut für Molekulare Genetik, Berlin, Germany, and Joachim Frank, State University of New York at Albany.]

4. The acceptor end of the new peptidyl–tRNA shifts to the P site of the 50S subunit, while the tRNA's anticodon end remains associated with the A site of the 30S subunit (yielding the A/P state). The acceptor end of the newly deacylated tRNA simultaneously moves to the E site of the 50S subunit while its anticodon end remains associated with the P site of the 30S subunit (the P/E state).

BOX 27-3 BIOCHEMISTRY IN HEALTH AND DISEASE

The Effects of Antibiotics on Protein Synthesis

The majority of known antibiotics, including a great variety of medically useful substances, block translation. This situation is presumably a consequence of the translation machinery's enormous complexity, which makes it vulnerable to disruption in many ways. Antibiotics have also been useful in analyzing ribosomal mechanisms because the blockade of a specific function often permits its biochemical dissection into its component steps. For example, the ribosomal elongation cycle was originally characterized through the use of the antibiotic **puromycin,** which resembles the 3′ end of Tyr–tRNA:

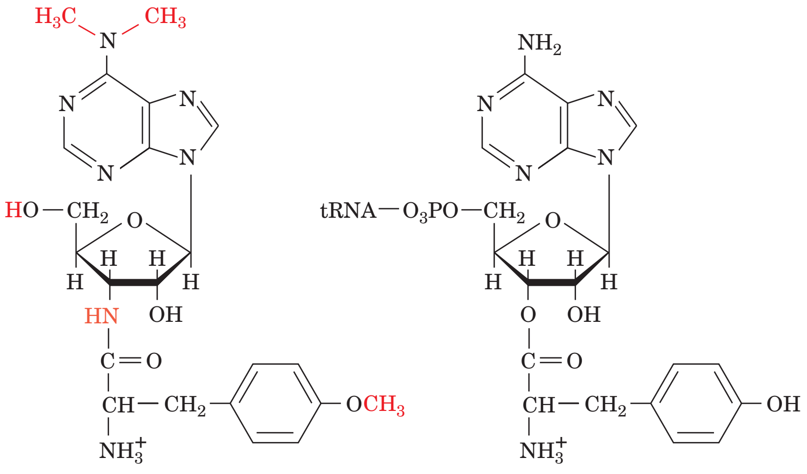

Puromycin **Tyrosyl–tRNA**

Puromycin binds to the ribosomal A site without the need of elongation factors. The transpeptidation reaction yields a peptidyl–puromycin in which puromycin's "amino acid residue" is linked to its "tRNA" via an amide rather than an ester bond. The ribosome therefore cannot catalyze further transpeptidation, and polypeptide synthesis is aborted.

Streptomycin is a medically important member of a family of antibiotics known as **aminoglycosides** that inhibit prokaryotic ribosomes in a variety of ways.

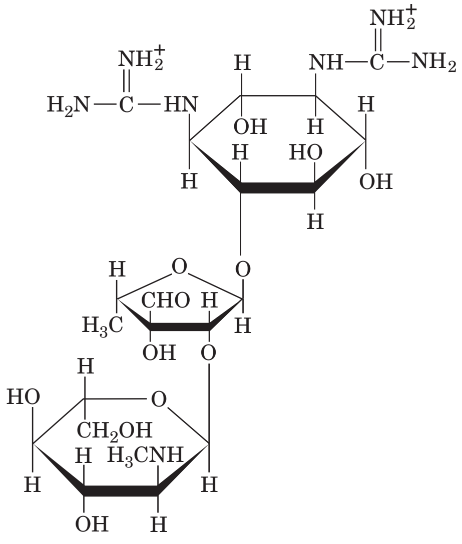

Streptomycin

At low concentrations, streptomycin induces the ribosome to characteristically misread mRNA: One pyrimidine may be mistaken for the other in the first and second codon positions, and either pyrim-

5. EF-G · GTP binding to the ribosome and the resulting GTP hydrolysis impel the anticodon ends of the two tRNAs, together with their bound mRNA, to move relative to the small ribosomal subunit such that the peptidyl–tRNA assumes the P/P state and the deacylated tRNA assumes the E/E state (the posttranslocational state), thereby completing the elongation cycle.

The binding of tRNAs to the A and E sites of the ribosome, as Knud Nierhaus has shown, exhibits negative allosteric cooperativity. In the pretranslocational state, the E site binds the newly deacylated tRNA with high affinity, whereas the now empty A site has low affinity for aa–tRNA. The binding of a new aa–tRNA · EF-Tu · GTP complex induces the ribosome to undergo a conformational change that converts the A site to a high-affinity state and the E site to a low-affinity state that consequently releases the deacylated tRNA. Thus, the E site is not simply a passive holding site for spent tRNAs but performs an essential function in the translation process.

idine may be mistaken for adenine in the first position. This inhibits the growth of susceptible cells but does not kill them. At higher concentrations, however, streptomycin prevents proper chain initiation and thereby causes cell death.

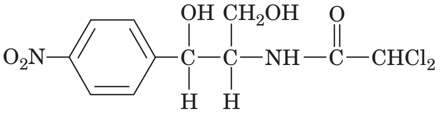

Chloramphenicol

Chloramphenicol, the first of the "broad-spectrum" antibiotics, inhibits the peptidyl transferase activity of prokaryotic ribosomes. However, its clinical uses are limited to severe infections because of its toxic side effects, which are caused in part by the chloramphenicol sensitivity of mitochondrial ribosomes. Chloramphenicol binds to the large subunit near the A site, which explains why it competes for binding with puromycin and the 3′ end of aminoacyl–tRNA but not with peptidyl–tRNAs.

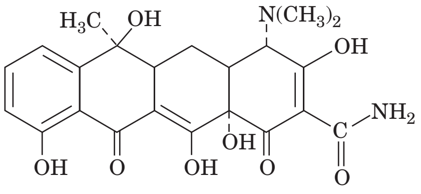

Tetracycline

Tetracycline and its derivatives are broad-spectrum antibiotics that bind to the small subunit of prokaryotic ribosomes. Tetracycline binding prevents the entry of aminoacyl–tRNAs into the A site but allows EF-Tu to hydrolyze its GTP. As a result, protein synthesis cannot proceed, and GTP hydrolysis, which occurs every time another aminoacyl–tRNA attempts to enter the ribosome, presents an enormous energetic drain on the cell.

Tetracycline-resistant bacterial strains have become quite common, thereby precipitating a serious clinical problem. Most often resistance is conferred by a decrease in bacterial cell membrane permeability to tetracycline rather than any alteration of ribosomal components that would overcome the inhibitory effect on translation.

Although it is a protein rather than a small molecule, the enzyme **ricin** can be considered an antibiotic. Ricin is an *N*-glycosidase from castor beans, the source of castor oil. The enzyme inactivates the large subunit of eukaryotic ribosomes by hydrolytically removing the adenine base of a highly conserved residue of 28S rRNA. The modified ribosome is unable to bind elongation factors, and translation ceases. Because it acts catalytically rather than stoichiometrically, a single ricin molecule can inactivate tens of thousands of ribosomes. Its deadliness in minute amounts makes ricin attractive to bioterrorists, but methods for selectively targeting ricin to particular cells, such as cancer cells, raise the possibility of its therapeutic use.

The requirement that the GTP-hydrolyzing proteins EF-Tu and EF-G alternate in their activities ensures that the ribosome cycles unidirectionally through the transpeptidation and translocation stages of translation. Translocation can occur in the absence of GTP, which indicates that the free energy of the transpeptidation reaction is sufficient to drive the entire translational process. However, the GTP hydrolysis catalyzed by EF-Tu and EF-G increases the overall rate of translation. *Because GTP hydrolysis is irreversible, the accompanying conformational changes in the ribosome are also irreversible and hence unidirectional.*

Several of the many antibiotics that disrupt ribosomal functioning are discussed in Box 27-3.

The Eukaryotic Elongation Cycle Resembles That of Prokaryotes. Elongation in eukaryotes closely resembles that in prokaryotes. In eukaryotes, the functions of EF-Tu and EF-Ts are assumed by the eukaryotic elongation factors **eEF1A** and **eEF1B.** Likewise, **eEF2** functions in a manner analogous to prokaryotic EF-G. However, the corresponding eukaryotic and prokaryotic elongation factors are not interchangeable.

C | Release Factors Terminate Translation

Polypeptide synthesis under the direction of synthetic mRNAs such as poly(U) results in a peptidyl–tRNA "stuck" in the ribosome. However, the translation of natural mRNAs, which contain the Stop codons UAA, UGA, or UAG, yields free polypeptides. In *E. coli,* the Stop codons, which normally have no corresponding tRNAs, are recognized by protein **release factors** (Table 27-6): **RF-1** recognizes UAA and UAG, whereas the 38% identical **RF-2** recognizes UAA and UGA. In eukaryotes, a single release factor, **eRF1,** recognizes all three termination codons.

Termination, like initiation and elongation, has several stages. The sequence of events in *E. coli* is diagrammed in Fig. 27-36:

1. RF-1 or RF-2 recognizes a corresponding Stop codon in the ribosome's A site.

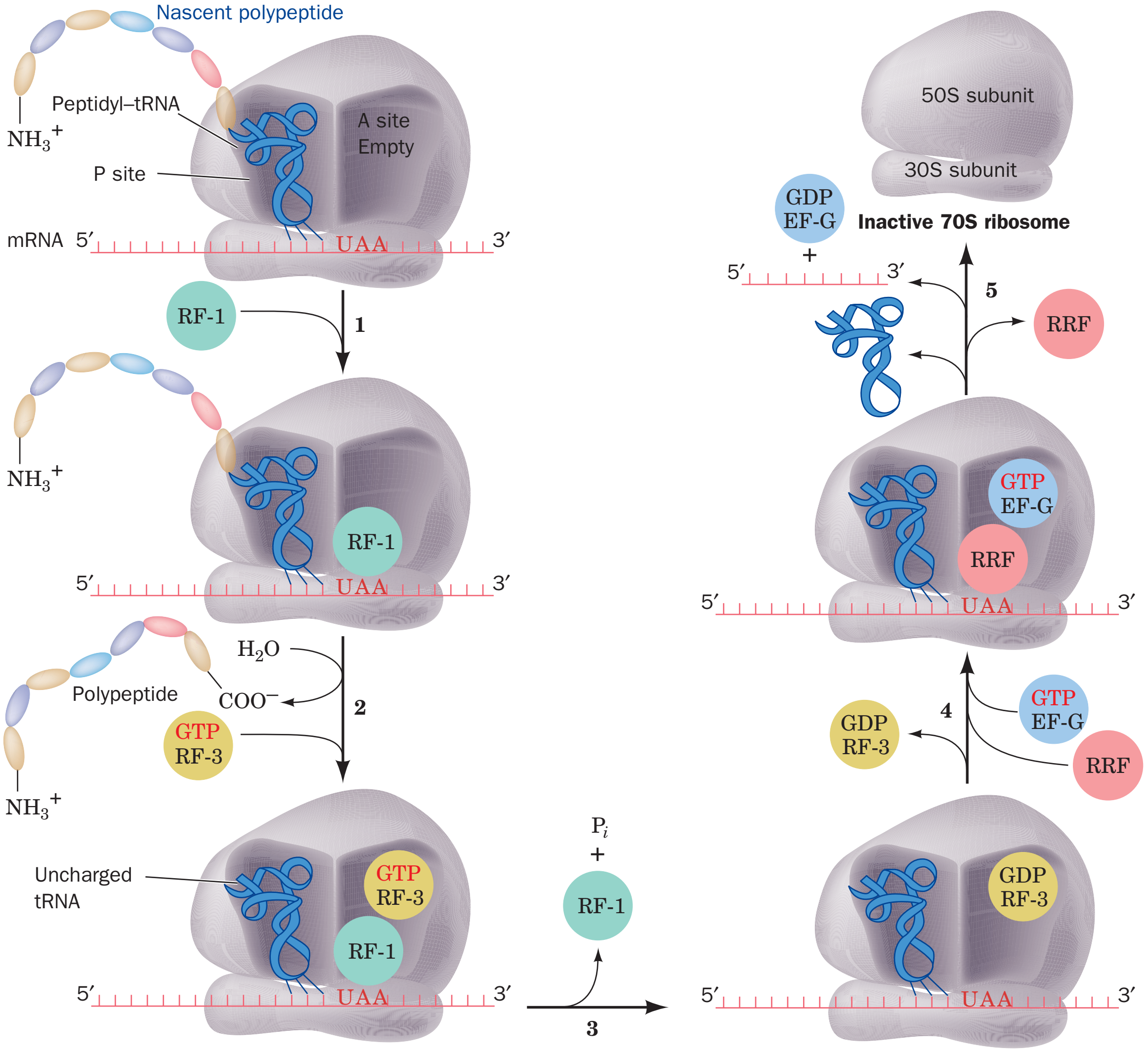

Nascent polypeptide
Peptidyl–tRNA
NH_3^+
A site
Empty
P site
mRNA 5′
UAA
3′
RF-1
1
NH_3^+
RF-1
5′
UAA
3′
H_2O
Polypeptide
COO^-
2
GTP
RF-3
NH_3^+
Uncharged
tRNA
GTP
RF-3
RF-1
5′
UAA
3′
P_i
+
RF-1
3
5′
UAA
3′
GDP
RF-3
4
GDP
RF-3
GTP
EF-G
RRF
5′
UAA
3′
GTP
EF-G
RRF
5
RRF
5′
3′
GDP
EF-G
+
Inactive 70S ribosome
50S subunit
30S subunit

■ **Figure 27-36 | The translation termination pathway in *E. coli* ribosomes.** RF-1 recognizes the Stop codons UAA and UAG, whereas RF-2 (not shown) recognizes UAA and UGA. Eukaryotic termination follows an analogous pathway but requires only a single release factor, eRF1, that recognizes all three Stop codons.

2. The release factor induces the transfer of the peptidyl group from the peptidyl–tRNA to water, rather than to another aa–tRNA, to yield an uncharged tRNA in the P site and a free polypeptide that dissociates from the ribosome.
3. A third factor, **RF-3** (**eRF** in eukaryotes), a G protein, binds to the ribosome in complex with GTP. The subsequent hydrolysis of this GTP induces the ribosome to release its bound RF-1 or RF-2.
4. The RF-3 · GDP complex is released and then **ribosome recycling factor (RRF),** which was largely characterized by Akira Kaji, binds in the A site, followed by EF-G · GTP.
5. EF-G hydrolyzes its bound GTP, which causes RRF to move to the P site and the tRNAs occupying the P and E sites (the latter not shown in Fig. 27-36) to be released. Finally, the RRF and then the EF-G · GDP and mRNA dissociate, yielding an inactive 70S ribosome ready for reinitiation (Fig. 27-25).

The release factors' functional mimicry of tRNAs suggests that they structurally resemble tRNAs. Indeed, the X-ray structures of human eRF1 (Fig. 27-37*a*) and *E. coli* RF-2 (Fig. 27-37*b*) indicate that these two unrelated proteins both structurally resemble tRNA. However, cryo-EM studies reveal that RF-2 undergoes a large conformational change on binding to the ribosome so that it no longer mimics tRNA. The X-ray structure of *Thermotoga maritima* RRF (Fig. 27-37*c*) also has an L-shaped structure that could potentially fit one of the ribosome's tRNA binding sites. However, footprinting and cryo-EM studies indicate that RRF partially occupies the A and P sites in an orientation that differs markedly from any previously observed for a tRNA. Evidently, structural mimicry can be misleading.

Nonsense Suppressors Prevent Termination. A mutation that converts an aminoacyl-coding ("sense") codon to a Stop codon is known as a **nonsense mutation** and leads to the premature termination of translation. An organism with such a mutation may be "rescued" by a second mutation in a tRNA gene that causes the tRNA to recognize a Stop (nonsense)

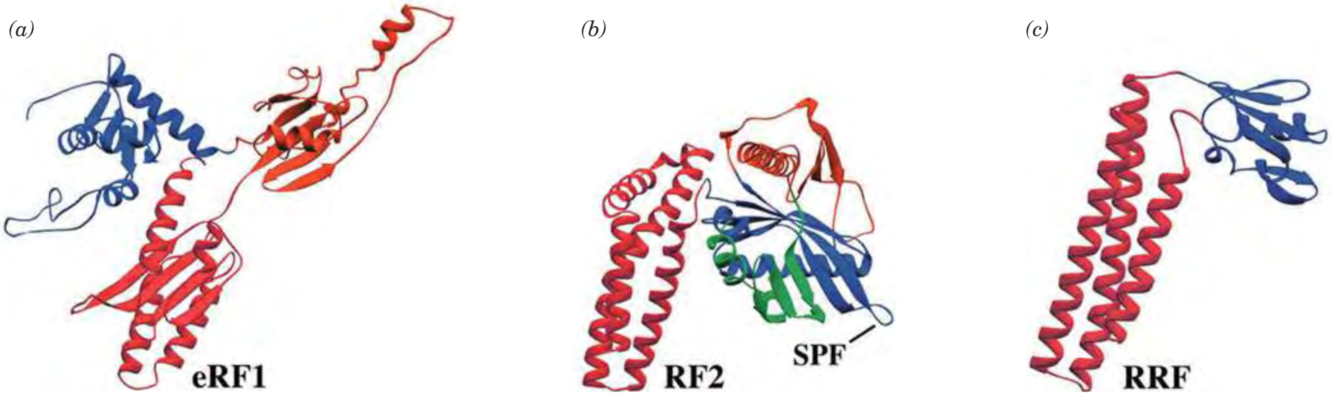

■ **Figure 27-37 | X-Ray structures of putative tRNA mimics that participate in translation termination.** (*a*) Human eRF1, (*b*) *E. coli* RF-2, and (*c*) *Thermotoga maritima* RRF (the structure of RF-1 closely resembles that of RF-2). The various domains in these proteins are differently colored with the domains that appear to mimic the tRNA anticodon stem drawn in red. The SPF tripeptide in RF-2 is believed to act as an anticodon. Compare these structures to Figs. 27-28 and 27-34. [Courtesy of V. Ramakrishnan, MRC Laboratory of Molecular Biology, Cambridge, U.K. Part *a* is based on an X-ray structure by David Barford, Institute of Cancer Research, London, U.K.; Part *b* is based on an X-ray structure by Richard Buckingham, CNRS, Paris, France, and Jens Nyborg and Morten Kjeldgaard, University of Aarhus, Århus, Denmark; and Part *c* is based on an X-ray structure by Akira Kaji, University of Pennsylvania, and Anders Liljas, Lund University, Lund, Sweden. PDBids (*a*) 1DT9, (*b*) 1GQE, and (*c*) 1DD5.]

codon. This **nonsense suppressor** tRNA carries the same amino acid as its wild-type progenitor and appends it to the growing polypeptide at the Stop codon, thereby preventing chain termination. For example, the *E. coli* **amber suppressor** known as *su*3 is a tRNA^{Tyr} whose anticodon has mutated from the wild-type GUA (which reads the Tyr codons UAU and UAC) to CUA (which recognizes the amber Stop codon UAG). An $su3^+$ *E. coli* cell with an otherwise lethal amber mutation in a gene coding for an essential protein would be viable if the replacement of the wild-type amino acid residue by Tyr does not inactivate the protein.

How do cells tolerate a mutation that both eliminates a normal tRNA and prevents the termination of polypeptide synthesis? They survive because the mutated tRNA is usually a minor member of a set of isoaccepting tRNAs and because nonsense suppressor tRNAs must compete with release factors for binding to Stop codons. Consequently, many suppressor-rescued mutants grow more slowly than wild-type cells.

CHECK YOUR UNDERSTANDING

Compare prokaryotic and eukaryotic translation initiation with respect to delivering an initiator tRNA to the ribosome and locating the initiation codon.

Summarize the roles of initiation, elongation, and release factors in translation.

Summarize the role of GTP hydrolysis in promoting the efficiency of translation initiation, decoding, translocation, and chain termination.

How does the ribosome verify correct tRNA–mRNA pairing?

5 Posttranslational Processing

LEARNING OBJECTIVES

- Understand that chaperones bind to polypeptide chains as they emerge from the ribosome.
- Understand that the polypeptide chain may be covalently modified and translocated via the secretory pathway.

The tunnel that leads from the peptidyl transferase active site to the exterior of the bacterial ribosome (Fig. 27-32) is ~100 Å long, enough to shelter a polypeptide of ~30 residues. Once it emerges from the ribosome, the polypeptide faces two challenges: how to fold properly and how to reach its final cellular destination. Both processes occur with the aid of other proteins. In addition, a nascent polypeptide may be covalently modified before it achieves its mature form. In this section we review some of the events of **posttranslational protein processing.**

A | Ribosome-Associated Chaperones Help Proteins Fold

The ribosome's peptide exit tunnel is too narrow (~15 Å wide) to permit the formation of secondary structure other than perhaps helices, so a nascent polypeptide cannot begin to fold until after it emerges from the ribosome. However, folding commences well before translation is complete. Molecular chaperones (Section 6-5B) bind to the N-terminus of nascent polypeptides to prevent their aggregation, to facilitate their folding, and to promote their proper association with other subunits.

A growing body of evidence suggests that ribosomal proteins play a role in protein folding by recruiting chaperones. For example, in *E. coli,* a protein known as **trigger factor** associates with the ribosomal protein **L23,** which is located at the outlet of the peptide exit tunnel. Trigger factor recognizes relatively short hydrophobic protein segments when they first emerge from the ribosome. **DnaK,** a member of the Hsp70 family of chaperones, together with **DnaJ,** an Hsp40 cochaperonin (Section 6-5B), can bind to and protect longer polypeptides (DnaK and DnaJ were so named because they were discovered through the isolation of mutants that do not support the growth of bacteriophage λ and hence were initially assumed to participate in DNA replication). The activities of trigger factor and DnaK/J are somewhat redundant, as *E. coli* can tolerate the deletion of either one. The loss of both, however, is lethal above 30°C and is accompanied by the massive aggregation of newly synthesized proteins. Ultimately, the chaperonins GroEL and GroES facilitate protein folding after translation termination (Section 6-5B).

The X-ray structure of *E. coli* trigger factor reveals an elongated multidomain protein that has a pronounced hydrophobic cleft along its cen-

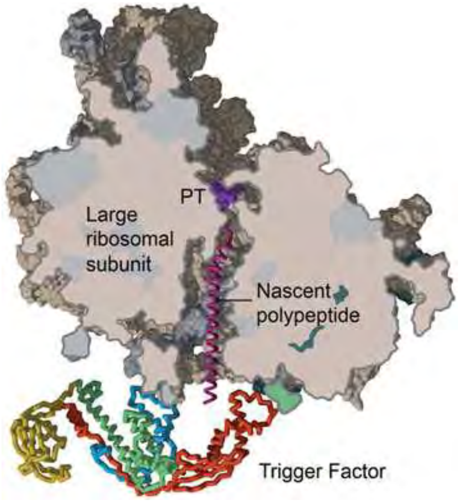

■ **Figure 27-38** | **Model of the association of trigger factor with the 50S ribosomal subunit.** The 50S subunit is shown in a cutaway view that exposes its peptide exit tunnel into which an α helix (*magenta*) extending from the peptidyl transferase center (PT) has been modeled. The ribosomal RNA is pink and the ribosomal proteins are gray. Trigger factor is drawn in worm form with its four domains colored, from N- to C-terminus, red, yellow, green, and blue. [Courtesy of Nenad Ban, Eidgenössische Technische Hochschule, Zürich, Switzerland.]

tral region. The X-ray structure of trigger factor's 144-residue ribosome-binding N-terminal domain in complex with the 50S subunit from *H. marismortui* reveals that this domain binds near the exit of the ribosome's peptide tunnel. The superposition of this N-terminal domain with that in the X-ray structure of the intact 432-residue trigger factor generated a model of the interaction of trigger factor with the 50S subunit (Fig. 27-38).

In this model, trigger factor hunches over the exit of the ribosome's peptide tunnel with its hydrophobic concave face positioned to interact with a newly synthesized polypeptide segment as it emerges from the tunnel. Moreover, fluorescence energy transfer experiments show that on binding to the ribosome, trigger factor undergoes a conformational expansion that further exposes its hydrophobic surface.

Unlike other chaperones (e.g., DnaK/J and GroEL/ES), trigger factor does not require ATP for its activation. Activated trigger factor dissociates from the ribosome after ~10 s but may remain associated with the elongating polypeptide for >30 s, during which time an additional molecule of trigger factor can bind to the ribosome and shield hydrophobic sequences farther along the polypeptide chain. Apparently, *trigger factor functions to shield hydrophobic segments of newly synthesized and hence unfolded polypeptides so as to prevent their misfolding and aggregation.* Eukaryotic cells lack a homolog of trigger factor but contain other small chaperones that may have similar functions.

B | Newly Synthesized Proteins May Be Covalently Modified

The list of known posttranslational modifications is long and includes the removal and/or derivatization of specific residues. For example, a polypeptide's N-terminal Met or fMet residue is usually excised. Other common posttranslational modifications are the hydroxylation of Pro and Lys residues in collagen (Section 6-1C), glycosylation (Sections 8-3C and 16-5), and the prenylation and fatty acylation of membrane anchored proteins (Section 9-3B). Many covalent modifications, such as phosphorylation (Section 12-3B) and palmitoylation (Section 9-3B), are reversible. Over 150 different types of side chain modifications are known; these involve all side chains except those of Ala, Ile, Leu, and Val. The functions of such modifications are varied and in many cases remain enigmatic.

A growing number of proteins are known to be ubiquitinated. Recall from Section 21-1B that the attachment of the 76-residue protein ubiquitin marks a protein for degradation by the proteasome. A similar 97-residue protein known as **small ubiquitin-related modifier (SUMO)** can be ligated to a Lys residue, as is ubiquitin, to regulate protein function. But whereas ubiquitination is usually associated with protein degradation, sumoylation appears to play a role in determining protein localization inside cells.

Proteins that are synthesized as inactive precursors, called **proproteins** or proenzymes, are activated by limited proteolysis. The zymogens of serine proteases are converted to active enzymes in that fashion (Section 11-5D).

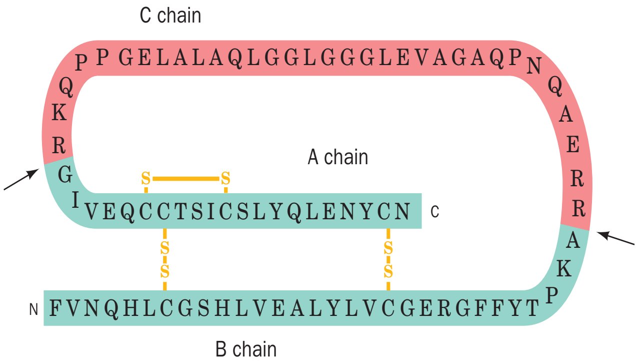
C chain
P P G E L A L A Q L G G L G G G L E V A G A Q P N
Q
K
R
Q
A
E
R
R
A chain
G
I V E Q C C T S I C S L Y Q L E N Y C N C
S S
S S
S S
A
K
P
N F V N Q H L C G S H L V E A L Y L V C G E R G F F Y T
B chain

Figure 27-39 | Conversion of proinsulin to insulin. The prohormone, with three disulfide bonds, is proteolyzed at two sites (*arrows*) to eliminate the C chain. The mature hormone insulin consists of the disulfide-linked A and B chains.

Proteins that are translocated into the endoplasmic reticulum for export from the cell typically contain a signal peptide that must be excised (Section 9-4D). Proteins bearing a signal peptide are known as **preproteins,** or **preproproteins** if they undergo additional proteolysis during their maturation. For example, the hormone insulin (Section 22-2) is synthesized as a preproprotein, which is converted to the proprotein **proinsulin,** a single 84-residue polypeptide. Proteolysis at two sites generates the mature hormone, whose A and B chains remain linked by disulfide bonds (Fig. 27-39). The 33-residue C chain is discarded.

The Signal Recognition Particle Is a Ribonucleoprotein. Many transmembrane and secretory proteins are translocated into or completely through cellular membranes [the endoplasmic reticulum (ER) in eukaryotes and the plasma membrane in prokaryotes] via a series of events known as the secretory pathway (Section 9-4D). As their N-terminal signal sequences emerge from the ribosome, these proteins associate with the signal recognition particle (SRP). Peptide chain elongation ceases on SRP binding to the ribosome but resumes after the SRP docks with its receptor on the ER membrane. The SRP then dissociates from the ribosome, allowing the nascent polypeptide to pass into or through the membrane via a protein pore called the translocon.

Like the ribosome and the spliceosome (Section 26-3A), the SRP is a ribonucleoprotein. The eukaryotic SRP contains six different polypeptides and a 300-residue RNA. The *E. coli* SRP, which consists of a single polypeptide called **Ffh** and a 114-nt RNA, appears to be a structurally minimized version of the eukaryotic SRP.

Jennifer Doudna determined the structure of the highly conserved core of the SRP, represented by the so-called M domain of Ffh and domain IV of the RNA. The 49-nt RNA segment forms a 70-Å-long double-helical rod in which the RNA chain doubles back on itself (Fig. 27-40*a*). The RNA and the protein interact mainly via a dense hydrogen-bonded network involving the RNA's unpaired bases and α helices from the protein (Fig. 27-40*b*). Ffh forms a deep groove that is lined almost entirely with hydrophobic residues, including 11 of the protein's 14 Met residues. This 15-Å-wide by 25-Å-long groove apparently binds the signal peptide as an α helix. The Met side chains, which have flexibility and polarity similar to *n*-butyl groups, provide some structural plasticity, so that *the SRP can accommodate different signal sequences as long as they are hydrophobic and form an α helix.* The sugar–phosphate backbone of the SRP RNA forms a ledge extending from the protein's hydrophobic binding groove and provides an anionic surface to bind the basic residues of the signal sequence (Fig. 9-36).

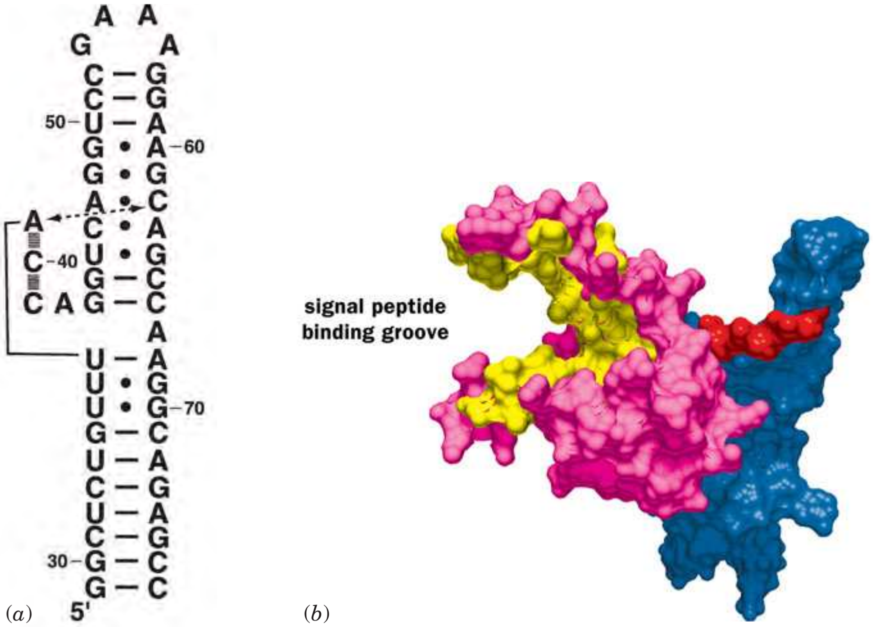

Figure 27-40 | X-Ray structure of the SRP core from *E. coli*. (*a*) The secondary structure of the 49-nt RNA. (*b*) The molecular surface of the complex oriented to show the signal peptide binding groove. The double-helical RNA is dark blue, the protein is pink, the hydrophobic residues lining the signal peptide binding groove are yellow, and the RNA's adjoining phosphate groups are red. [Courtesy of Robert Batey and Jennifer Doudna, Yale University. PDBid 1DUL.]

An atomic model of the mammalian SRP was constructed by docking the known X-ray structures of its various components into the cryo-EM–based image of the SRP bound to an 80S ribosome carrying a signal sequence. This model indicates that the complex assumes a bent conformation in which the RNA constitutes the hinges (Fig. 27-41*a*). The cryo-EM structure of the SRP in complex with the 80S ribosome (Fig. 27-41*b*) reveals that the SRP extends from the polypeptide exit channel on the 60S subunit to the intersubunit space near the A site. Structural and bio-

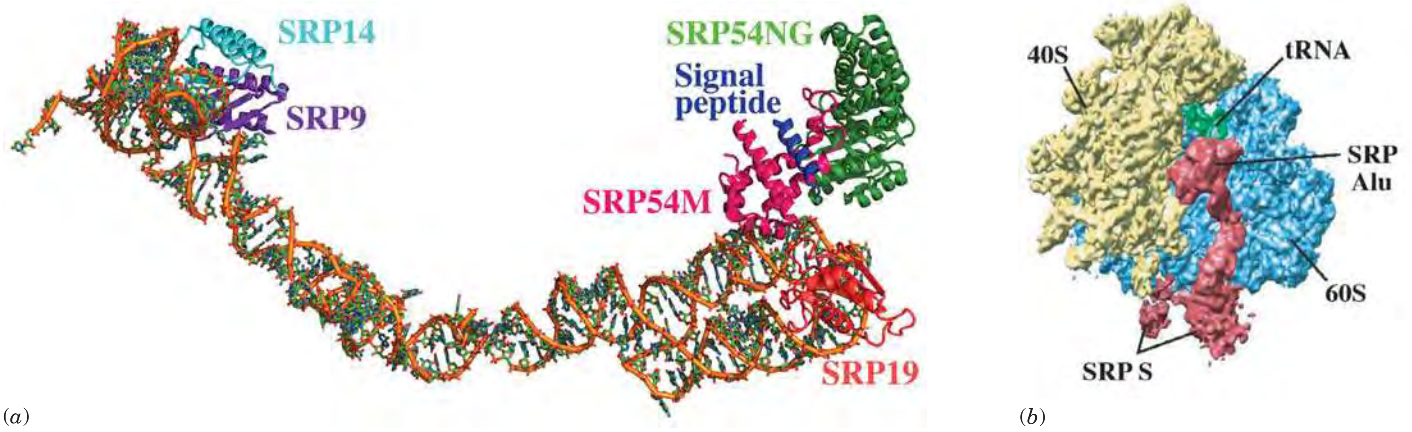

Figure 27-41 | Eukaryotic signal recognition particle. (*a*) Model of the SRP in which the RNA is drawn in stick form colored according to atom type (C green, N blue, O red, and P orange) with successive P atoms linked by orange rods. The nascent polypeptide's signal peptide (*purple*) binds to the M domain of protein SRP54 (SRP54M; SRP54 is the eukaryotic analog of *E. coli* Ffh). The remainder of SRP54 (SRP54NG) includes its GTPase domain. Proteins **SRP9** and **SRP14** and the associated RNA form the Alu domain that binds in the ribosome's intersubunit interface. [Based on a model by Joachim Frank, State University of New York at Albany, and Roland Beckmann, University of Munich, Germany. PDBid 1RY1.] (*b*) Cryo–EM-based image of the SRP bound to an 80S ribosome. The S (signal sequence–binding) domain of the SRP (*red*) interacts with the polypeptide emerging from the ribosome's exit channel, and the SRP Alu domain binds to the ribosome at the elongation factor–binding site. The small (40S) subunit is yellow, the large (60S) subunit is cyan, and a tRNA in the P site is green. [Courtesy of Roland Beckmann, University of Munich, Germany.]

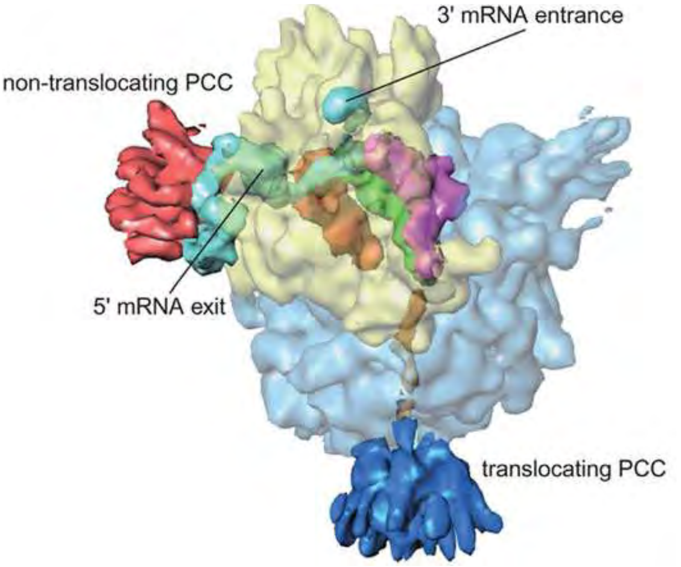

Figure 27-42 | Cryo-EM structure of the *E. coli* ribosome in complex with the translocon. The 30S subunit is yellow, the 50S subunit is light blue, the A-, P-, and E-site tRNAs are magenta, green, and orange, respectively, the mRNA is cyan, the nascent polypeptide is gold, and the translocon at the polypeptide channel exit is dark blue. The translocon contains two copies of the SecYEG complex. A second, nonfunctional PCC (*red*) is bound to the ribosome at the exit of the mRNA channel. [Courtesy of Joachim Frank, State University of New York at Albany.]

chemical studies indicate that the eukaryotic SRP first binds to the ribosome via its **SRP54** protein, the homolog of *E. coli* Ffh. This interaction involves several ribosomal proteins, including L23, to which trigger factor also binds. When an emerging signal peptide binds to the Met-rich M domain of the SRP54 protein (SRP54M), the ribonucleoprotein alters its conformation in a way that allows its other end, called the Alu domain (because it contains *Alu*-like sequences; Section 28-1C), to fit into the site on the intersubunit interface where elongation factor eEF2 (the eukaryotic counterpart of *E. coli* EF-G) also binds. This presumably interferes with the ribosomal elongation cycle (Fig. 27-27) and explains how the SRP arrests translation. The *E. coli* SRP lacks the Alu domain and therefore must suspend translation by a mechanism other than mimicry of an elongation factor.

Protein synthesis resumes after the SRP docks with its membrane receptor and its place has been taken by the translocon (also known as the **protein-conducting channel; PCC**), whose ribosomal binding site largely overlaps that of the SRP. In *E. coli,* the PCC consists of two three-protein complexes known as **SecYEG** (the structure of the largest of these, SecY, is shown in Fig. 9-37). Cryo-EM studies of ribosomes in the process of synthesizing a polypeptide containing a transmembrane segment show the translocon positioned at the polypeptide exit channel, as expected (Fig. 27-42). The translocon contacts the ribosome at three points via protein–protein and protein–rRNA interactions. An opening between the translocon and the ribosome may admit other proteins, such as trigger factor.

Glycosylation Acts as a Quality Control Mechanism. In eukaryotes, polypeptides that are translocated into the ER by the secretory pathway undergo glycosylation. The cotranslational addition of a 14-residue oligosaccharide to an Asn residue is the first step in the production of *N*-linked glycoproteins (Section 8-3C). The attachment of the oligosaccharide verifies that the protein is being successfully translocated from the cytosol to the lumen of the endoplasmic reticulum. The subsequent removal of the two terminal glucose residues allows the protein to interact with a chaperone that recognizes the partially processed oligosaccharide. The

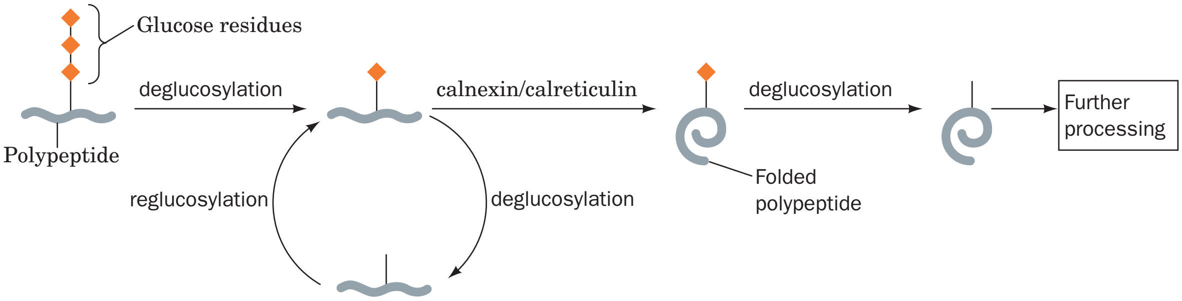

Figure 27-43 | Quality control in oligosaccharide processing. A partially processed glycoprotein bearing one terminal glucose residue can bind to the chaperones calnexin or calreticulin. The bound glycoprotein is then deglucosylated and processed further. An improperly folded glycoprotein that becomes deglucosylated is reglucosylated by an enzyme that is specific for unfolded glycoproteins. This mechanism promotes the proper folding and oligosaccharide processing of newly synthesized glycoproteins.

membrane-bound 572-residue form of the chaperone, called **calnexin,** or its soluble 400-residue homolog **calreticulin,** binds the immature (unfolded) glycoprotein to assist its folding and to protect it from degradation or premature transfer to the Golgi apparatus (where the late stages of oligosaccharide processing take place).

After the folded glycoprotein is released from calnexin/calreticulin, it proceeds through the rest of the oligosaccharide-processing pathway. A glycoprotein that is released before it has adopted its mature conformation can still undergo the next step of processing, which is the removal of another glucose residue. However, when this happens, a glycosyltransferase that recognizes only unfolded glycoproteins reattaches a glucose residue to the immature oligosaccharide. As a result, the glycoprotein can bind again to calnexin/calreticulin for another chance to fold properly (Fig. 27-43). Most glycoproteins undergo reglucosylation at least once.

CHECK YOUR UNDERSTANDING

What is the function of trigger factor? Why must the number of trigger factor molecules be at least as great as the number of ribosomes?

List some posttranslational modifications of proteins.

Describe the functions of the complexes that interact with the ribosome near its polypeptide exit channel.

SUMMARY

1. The genetic code, by which nucleic acid sequences are translated into amino acid sequences, is composed of three-nucleotide codons that do not overlap and are read sequentially by the protein-synthesizing machinery.
2. The standard genetic code of 64 codons includes numerous synonyms, three Stop codons, and one initiation codon.
3. All tRNAs have numerous chemically modified bases and a similar cloverleaf secondary structure comprising an acceptor stem, D arm, TψC arm, anticodon arm, and variable arm. The three-dimensional structures of tRNAs are likewise similar and are maintained by stacking interactions and non-Watson–Crick hydrogen-bonded cross-links.
4. Aminoacyl–tRNA synthetases (aaRSs) catalyze the ATP-dependent attachment of an amino acid to the appropriate tRNA to yield an aminoacyl–tRNA (aa–tRNA). The acceptor stem and anticodon loop are common identity elements for tRNA–aaRS interactions. The fidelity of aminoacylation is enhanced by proofreading.
5. Wobble pairing between mRNA codons and tRNA anticodons at the third position accounts for much of the degeneracy of the genetic code. Within a species, the preferred codons correspond to the most abundant species in each set of isoaccepting tRNAs.
6. Ribosomes, which are large complexes of RNA and protein, have a structure that is determined by their RNA components. A small subunit and large subunit associate to form the intact ribosome, which accommodates an aa–tRNA in the A site, a peptidyl–tRNA in the P site, and a deacylated tRNA in the E site.
7. During translation initiation, an initiator tRNA charged with fMet (in prokaryotes) or Met (in eukaryotes), an mRNA with an AUG initiation codon, and the ribosomal subunits assemble. Initiation requires GTP-hydrolyzing initiation factors. The initiating AUG codon is identified in prokaryotes via the mRNA's Shine–Dalgarno sequence. In eukaryotes it is the mRNA's initiating AUG that is identified in a complex process by its proximity to the mRNA's 5′ cap.
8. A polypeptide chain is elongated from its N- to its C-terminus. An aa–tRNA in complex with a GTP-hydrolyzing elongation factor binds to the A site, where the ribosome senses correct codon–anticodon pairing, a process whose accuracy is enhanced by proofreading. The peptidyl transferase activity of

the large subunit's RNA catalyzes the attack of the A-site bound aa–tRNA's amino group on the peptidyl–tRNA in the P site. Following transpeptidation, a second GTP-hydrolyzing elongation factor promotes the translocation of the new peptidyl–tRNA to the P site.

9. Translation termination requires release factors that recognize Stop codons.
10. As a polypeptide emerges from the ribosome, it begins to fold with the assistance of chaperones. Proteins may undergo posttranslational processing that includes proteolysis, covalent modification, translocation through a membrane, and glycosylation.

KEY TERMS

genetic code	**986**
codon	**986**
degeneracy	**986**
suppressor	**986**
reading frame	**986**
frameshift mutation	**986**
anticodon	**987**
synonym	**989**
Stop codon	**990**
acceptor stem	**991**
D arm	**992**
anticodon arm	**992**
TψC arm	**992**
variable arm	**992**
aaRS	**994**
aminoacyl–tRNA	**994**
isoaccepting tRNA	**995**
wobble hypothesis	**999**
cryoelectron microscopy	**1002**
A site	**1006**
P site	**1006**
peptidyl–tRNA	**1006**
E site	**1006**
peptidyl transferase	**1008**
polyribosome	**1010**
fMet	**1011**
Shine–Dalgarno sequence	**1011**
initiation factor	**1012**
transpeptidation	**1015**
translocation	**1015**
elongation factor	**1015**
release factor	**1026**
nonsense mutation	**1027**
nonsense suppressor	**1028**
posttranslational processing	**1028**
proprotein	**1029**
preprotein	**1030**
preproprotein	**1030**

PROBLEMS

1. Could a single nucleotide deletion restore the function of a protein-coding gene interrupted by the insertion of a 4-nt sequence? Explain.
2. List all possible codons present in a ribonucleotide polymer containing U and G in random sequence. Which amino acids are encoded by this RNA?
3. Which amino acids are specified by codons that can be changed to an amber codon by a single point mutation?
4. A double-stranded fragment of viral DNA, one of whose strands is shown below, encodes two peptides, called *vir-1* and *vir-2*. Adding this double-stranded DNA fragment to an *in vitro* transcription and translation system yields peptides of 10 residues (*vir-1*) and 5 residues (*vir-2*).

   AGATCGGATGCTCAACTATATGTGATTAACAGAGCATGCGGCATAAACT

   (a) Identify the DNA sequence that encodes each peptide.

   (b) Determine the amino acid sequence of each peptide.

   (c) In a mutant viral strain, the T at position 23 has been replaced with G. Determine the amino acid sequences of the two peptides encoded by the mutant virus.
5. The sequence of the sense strand of a mammalian gene is

   TATAATACGCGCAATACAATCTACAGCTTCGCGTA
   AATCGCAGGTAAGTTGTAATAAATATAAGTGAGT
   ATGATAGGGCTTTGGACCGATAGATGCGACCCTG
   CAGGTAAGTATAGATTAATTAAGCACAGGCATGCA
   GGGATATCCTCCAAACAGGTAAGTAACCTTACGG
   TCAATTAATTAGGCAGTAGATGAATAAACGATAT
   CGATCGGTTACAGGAGTCTGAT

   Determine the sequences of the mature RNA and the encoded protein. Assume that transcription initiates approximately 25 bp downstream of the TATAATA sequence, that each 5′ splice site has the sequence AG/GUAAGU, and that each 3′ splice site has the sequence CAG/G and the / marks the location of the splice.
6. IleRS uses a double-sieve mechanism to accurately produce Ile–tRNA^{Ile} and prevent the synthesis of Val–tRNA^{Ile}. Which other pairs of amino acids differ in structure by a single carbon and might have aaRSs that use a similar double-sieve proofreading mechanism?
7. In eukaryotes, the primary rRNA transcript is a 45S rRNA that includes the sequences of the 18S, 5.8S, and 28S rRNAs separated by short spacers. What is the advantage of this operon-like arrangement of rRNA genes?
8. Explain why the translation of a given mRNA can be inhibited by a segment of its complementary sequence, a so-called **antisense RNA.**
9. Explain the significance of the observation that peptides such as fMet-Leu-Phe "activate" the phagocytotic (particle-engulfing) functions of mammalian leukocytes (white blood cells).
10. Explain why prokaryotic ribosomes can translate a circular mRNA molecule, whereas eukaryotic ribosomes normally cannot, even in the presence of the required cofactors.
11. EF-Tu binds all aminoacyl–tRNAs with approximately equal affinity so that it can deliver them to the ribosome with the same efficiency. Based on the experimentally determined binding constants for EF-Tu and correctly charged and mischarged aminoacyl–tRNAs (see Table), explain how the tRNA–EF-Tu recognition system could prevent the incorporation of the wrong amino acid during translation.

Aminoacyl–tRNA	Dissociation Constant (nM)
Ala–$tRNA^{Ala}$	6.2
Gln–$tRNA^{Ala}$	0.05
Gln–$tRNA^{Gln}$	4.4
Ala–$tRNA^{Gln}$	260

[*Source:* LaRiviere, F.J., Wolfson, A.D., and Uhlenbeck, O.C., *Science* **294,** 167 (2001).]

12. Eukaryotic initiation factor eIF2B is a guanine nucleotide exchange factor. Explain why eIF2B would enhance the activity of eIF2.
13. The antibiotic **paromomycin** binds to a ribosome and induces the same conformational changes in 16S rRNA residues A1492 and A1493 as are induced by codon–anticodon pairing (Fig. 27-31). Propose an explanation for the antibiotic effect of paromomycin.
14. The rate of the peptidyl transferase reaction increases as the pH increases from 6 to 8. (a) Explain these results in terms of its reaction mechanism. (b) It has been proposed that residue A2486 is protonated and therefore stabilizes the tetrahedral reaction intermediate. Is this mechanistic embellishment consistent with the observed pH effect?
15. All cells contain an enzyme called **peptidyl–tRNA hydrolase,** and cells that are deficient in the enzyme grow very slowly. What is the probable function of the enzyme and why is it necessary?
16. Calculate the energy required, in ATP equivalents, to synthesize a 100-residue protein from free amino acids in *E. coli* (assume that the N-terminal Met remains attached to the polypeptide and that no ribosomal proofreading occurs).
17. Design an mRNA with the necessary prokaryotic control sites that codes for the octapeptide Lys-Pro-Ala-Gly-Thr-Glu-Asn-Ser.

CASE STUDY

Case 29 (available at www.wiley.com/college/voet)

Pseudovitamin D Deficiency

Focus concept: An apparent vitamin D deficiency is actually caused by a mutation in an enzyme leading to the vitamin's synthesis.

Prerequisites: Chapters 9 and 27

- Vitamins and coenzymes
- The genetic code

REFERENCES

Genetic code

Judson, J.F., *The Eighth Day of Creation,* Expanded edition, Part II, Cold Spring Harbor Laboratory Press (1996). [A fascinating historical narrative on the elucidation of the genetic code.]

Knight, R.D., Freeland, S.J., and Landweber, L.F., Selection, history and chemistry: the three faces of the genetic code, *Trends Biochem. Sci.* **24,** 241–247 (1999).

Transfer RNA structure and aminoacylation

Ibba, M., Becker, H.D., Stathopoulos, C., Tumbula, D.L., and Söll, D., The adaptor hypothesis revisited, *Trends Biochem. Sci.* **25,** 311–316 (1999). [Describes exceptions to the 20 aminoacyl–tRNA synthetase rule.]

Nureki, O., Vassylyev, D.G., Tateno, M., Shimada, A., Nakama, T., Fukai, S., Konno, M., Hendrickson, T.L., Schimmel, P., and Yokoyama, S., Enzyme structure with two catalytic sites for double-sieve selection of substrate, *Science* **280,** 578–582 (1998). [The X-ray structures of IleRS in complexes with isoleucine and valine.]

Ribosomes and translation

Dintzis, H.M., The wandering pathway to determining N to C synthesis of proteins, *Biochem. Mol. Biol. Educ.* **34,** 241–246 (2006). [A personal history of how the direction of polypeptide synthesis was determined.]

Green, R. and Lorsch, J.R., The path to perdition is paved with protons, *Cell* **110,** 665–668 (2002). [Discusses the difficulties in characterizing the catalytic mechanism of the ribosomal peptidyl transferase.]

Kiel, M.C., Kaji, H., and Kaji, A., Ribosome recycling, *Biochem. Mol. Biol. Educ.* **35,** 40–44 (2007).

Korostelev, A. and Noller, H.F., The ribosome in focus: new structures bring new insights, *Trends Biochem. Sci.* **32,** 434–441 (2007).

Moore, P.B. and Steitz, T.A., RNA, the first macromolecular catalyst: the ribosome is a ribozyme, *Trends Biochem. Sci.* **28,** 411–418 (2003); *and* The structural basis of large ribosomal subunit function, *Annu. Rev. Biochem.* **72,** 813–850 (2003).

Nissen, P., Kjeldgaard, M., and Nyborg, J., Macromolecular mimicry, *EMBO J.* **19,** 489–495 (2000). [Describes how translation factors and other proteins function by adopting the same structures and interacting with the same binding sites as nucleic acids.]

Ogle, J.M., Brodersen, D.E., Clemons, W.M., Jr., Tarry, M.J., Carter, A.P., and Ramakrishnan, V., Recognition of cognate transfer RNA by the 30S ribosomal subunit, *Science* **292,** 897–902 (2001). [Presents X-ray structural evidence for an rRNA sensor that verifies correct codon–anticodon pairing in the ribosome.]

Rodnina, M.V., Beringer, M., and Wintermeyer, W., How ribosomes make peptide bonds, *Trends Biochem. Sci.* **32,** 20–26 (2007).

Selmer, M., Dunham, C.M., Murphy, F.V., IV, Weixlbaumer, A., Petry, S., Kelley, A.C., Weir, J.R., and Ramakrishnan, V., Structure of the 70S ribosome complexed with mRNA and tRNA, *Science* **313,** 1935–1942 (2006); *and* Korostelev, A., Trakhanov, S., Laurberg, M., and Noller, H.F., Crystal structure of a 70S ribosome–tRNA complex reveals functional interactions and rearrangements, *Cell* **126,** 1065–1077 (2006). [Presents high resolution (3.7 and 2.8 Å) X-ray structures of the *T. thermophilus* ribosome.]

Sievers, A., Beringer, M., Rodnina, M.V., and Wolfenden, R., The ribosome as an entropy trap, *Proc. Natl. Acad. Sci.* **101,** 7897–7901 (2004).

Valle, M., Zavialov, A., Li, W., Stagg, S.M., Sengupta, J., Nielsen, R.C., Nissen, P., Harvey, S.C., Ehrenberg, M., and Frank, J., Incorporation of aminoacyl-tRNA into the ribosome as seen by cryo-electron microscopy, *Nature Struct. Biol.* **10,** 899–906 (2003).

Posttranslational processing

Halic, M., Becker, T., Pool, M.R., Spahn, C.M.T., Grassucci, R.A., Frank, J., and Beckmann, R., Structure of the signal recognition particle interacting with the elongation-arrested ribosome, *Nature* **427,** 808–814 (2004).

Hartl, F.U. and Hayer-Hartl, M., Molecular chaperones in the cytosol: from nascent chain to folded protein, *Science* **295,** 1852–1858 (2002). [Describes the structures, functions, and potential interactions of the various chaperone systems in eukaryotes, eubacteria, and archaea.]

Williams, D.B., Beyond lectins: the calnexin/calreticulin chaperone system of the endoplasmic reticulum, *J. Cell Sci.* **119,** 615–623 (2006).

28

Regulation of Gene Expression

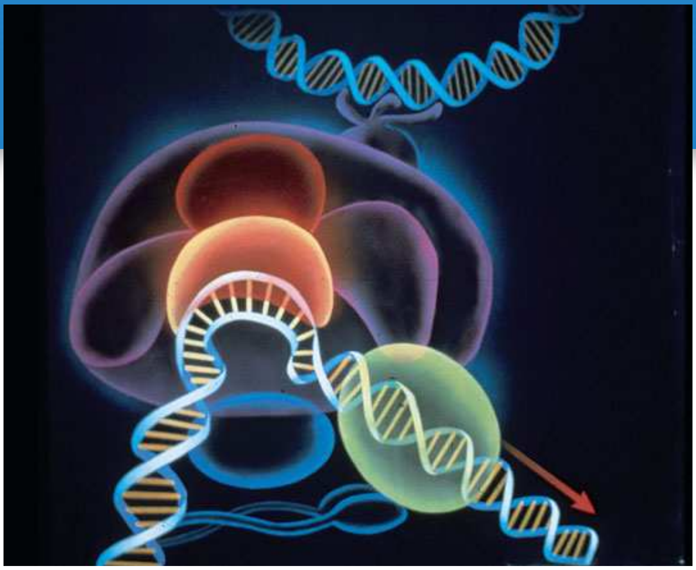

The controlled expression of genetic information requires a multitude of factors that interact specifically and nonspecifically with DNA. This painting schematically diagrams transcription factors in the preinitiation complex whose formation in eukaryotes must precede the transcription of DNA to mRNA. [Illustration, Irving Geis. Image from the Irving Geis Collection/Howard Hughes Medical Institute. Rights owned by HHMI. Reproduction by permission only.]

CHAPTER CONTENTS

1 Genome Organization
- **A.** Gene Number Varies among Organisms
- **B.** Some Genes Occur in Clusters
- **C.** Eukaryotic Genomes Contain Repetitive DNA Sequences

2 Regulation of Prokaryotic Gene Expression
- **A.** The *lac* Operon Is Controlled by a Repressor
- **B.** Catabolite-Repressed Operons Can Be Activated
- **C.** Attenuation Regulates Transcription Termination
- **D.** Riboswitches Are Metabolite-Sensing RNAs

3 Regulation of Eukaryotic Gene Expression
- **A.** Chromatin Structure Influences Gene Expression
- **B.** Eukaryotes Contain Multiple Transcriptional Activators
- **C.** Posttranscriptional Control Mechanisms Include RNA Degradation
- **D.** Antibody Diversity Results from Somatic Recombination and Hypermutation

4 The Cell Cycle, Cancer, and Apoptosis
- **A.** Progress through the Cell Cycle Is Tightly Regulated
- **B.** Tumor Suppressors Prevent Cancer
- **C.** Apoptosis Is an Orderly Process
- **D.** Development Has a Molecular Basis

MEDIA RESOURCES

(available at www.wiley.com/college/voet)

Guided Exploration 30. The regulation of gene expression by the *lac* repressor system
Interactive Exercise 55. CAP–cAMP dimer in complex with DNA
Interactive Exercise 56. Glucocorticoid receptor DNA-binding domain in complex with DNA
Interactive Exercise 57. Cdk2 phosphorylated at Thr 160
Interactive Exercise 58. DNA-binding domain of human p53 in complex with its target DNA
Interactive Exercise 59. Engrailed protein homeodomain in complex with its target DNA

The faithful replication of DNA ensures that all the descendants of a single cell contain virtually identical sets of genetic instructions. Yet individual cells may differ—sometimes dramatically—from their progenitors, depending on how those instructions are read. The **expression** of genetic information in a given cell or organism, that is, the synthesis of RNA and proteins specified by the DNA sequence, is neither random nor fully preprogrammed. Rather, *the information in an organism's genome must be tapped in an orderly fashion during development and yet must also be available to direct the organism's responses to changes in internal or external conditions.*

Much of the mystery surrounding the regulation of gene expression has to do with how genetic information is organized and how it can be located and accessed on an appropriate time scale. The complexity of the mechanisms for transcribing and translating genes suggests the potential for even more complicated systems for enhancing or inhibiting these processes. Indeed, we have already seen numerous examples of how accessory protein factors influence the rates or specificities of transcription and translation. In this chapter, we consider some additional aspects of gene expression by examining a variety of strategies used by prokaryotes and eukaryotes to control how genetic information specifies cell structures and metabolic functions.

1 Genome Organization

LEARNING OBJECTIVES

- Understand that an organism's complexity increases with the number of its genes but not the size of its genome.
- Understand that rRNA and tRNA genes occur in clusters.
- Understand that eukaryotic genomes contain segments of repetitive DNA.

Genomics, the study of organisms' genomes, was established as a discipline with the advent of techniques for rapidly sequencing enormous tracts of DNA, such as make up the chromosomes of living things. Studies that once relied on the hybridization of oligonucleotide probes to identify genes can now be conducted by comparing nucleotide sequences deposited in databases (Section 5-3E). In fact, a computerized database is the only practical format for storing the vast amount of information provided by a whole-genome sequence. Even a simplified diagram of the genome of the relatively simple bacterium *Helicobacter pylori* reveals a bewildering array of genes (Fig. 28-1). Nevertheless, the ability to sequence and map the entire genome of an organism makes it possible to draw far-reaching conclusions about how many genes an organism contains, how they are organized, and how they serve the organism.

A | Gene Number Varies among Organisms

The rough correlation between the quantity of an organism's unique genetic material (its **C value**) and the complexity of its morphology and metabolism (Table 3-3) has numerous exceptions, known as the **C-value paradox.** For example, the genomes of lungfishes are 10 to 15 times larger than those of mammals (Fig. 28-2). Some algae have genomes 10 times larger still. We know that much of this "extra" DNA is unexpressed, but its function is largely a matter of conjecture. The complete genomic sequences of numerous prokaryotes and eukaryotes, including data from

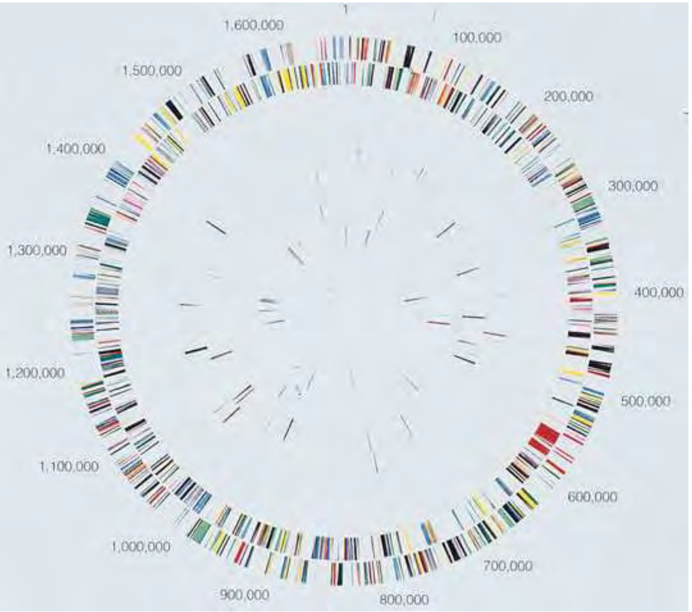

■ **Figure 28-1 | Map of the 1670-kb *H. pylori* circular chromosome.** The 1590 predicted protein-coding sequences (91% of the genome) are indicated in different colors on the two outermost rings, which represent the two DNA strands. The third and fourth rings indicate intervening sequence elements and other repeating sequences (2.3% of the genome). The fifth and sixth rings show the genes for tRNAs, rRNAs, and other small RNAs (0.7% of the genome). Intergenic sequences account for 6% of the genome. [Courtesy of J. Craig Venter, Celera Genomics, Rockville, Maryland.]

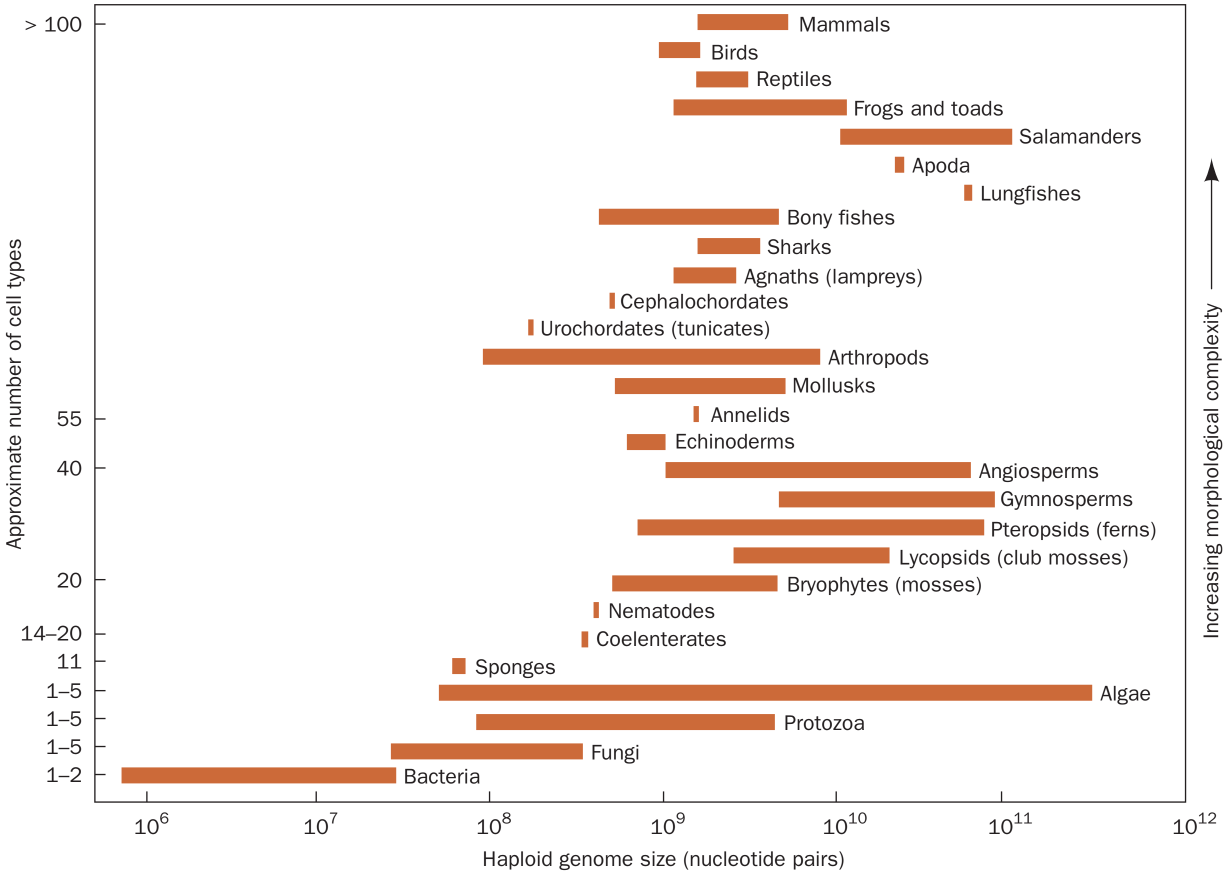

Figure 28-2 | Range of haploid genome DNA contents in various categories of organisms. The morphological complexity of the organisms, as estimated from their number of different cell types, increases from bottom to top. Haploid genome size roughly correlates with complexity; exceptions are described by the C-value paradox. [After Raff, R.A. and Kaufman, T.C., *Embryos, Genes, and Evolution,* p. 314, Macmillan (1983).]

some large complicated genomes, nevertheless indicate that *the apparent number of genes, like the overall quantity of DNA, roughly parallels the organism's complexity* (Table 28-1). Thus, humans have ~23,000 genes compared to *E. coli's* ~4300 genes.

Table 28-1 Genome Size and Gene Number in Some Organisms

Organism	Genome Size (kb)	Number of Genes
Haemophilus influenzae (bacterium)	1,830	1,740
Escherichia coli (bacterium)	4,639	4,289
Saccharomyces cerevisiae (yeast)	11,700	6,034
Caenorhabditis elegans (nematode)	97,000	19,099
Oryza sativa (rice)	390,000	~35,000
Arabidopsis thaliana (mustard weed)	117,000	~26,000
Drosophila melanogaster (fruit fly)	137,000	13,061
Mus musculus (mouse)	2,500,000	~23,000
Homo sapiens (human)	3,200,000	~23,000

Only a Small Portion of the Human Genome Encodes Proteins. About 3,000,000 kb of the 3,200,000-kb human genome has been fully sequenced (the remaining DNA includes gene-poor regions near the centromeres and telomeres). *No more than about 1.4% of the genome encodes proteins,* and the 23,000 or so protein-coding genes are distributed throughout the genome, sometimes in clusters. Identifying the genes in human or other genomes involves several approaches.

A gene can be identified by its homology to a previously described mRNA or protein sequence. A protein-coding gene may also be identified as an **open reading frame (ORF),** a sequence that is not interrupted by Stop codons and that exhibits the same codon-usage preferences as other genes in the organism. However, our incomplete knowledge of the features through which cells recognize genes, combined with the fact that human genes consist of relatively short exons (averaging ~150 nt) separated by much longer introns (averaging ~3500 nt and often much longer), has limited the success of computer-based gene identification algorithms. Such algorithms therefore rely on sequence alignments with **expressed sequence tags** (**ESTs;** cDNAs that have been reverse-transcribed from mRNAs) together with alignments with known genes from other organisms. Genes may also be revealed by the presence of a **CpG island** (Box 25-4). CpG dinucleotides are present in vertebrate genomes at only about one-fifth their randomly expected frequency (because the spontaneous deamination of m^5C yields a normal T and therefore often results in a CG → TA mutation), but they appear in clusters, or islands, at near-normal frequencies in the upstream regions of many genes (~56% of human genes).

The number of human genes is much lower than had once been predicted. The discrepancy between current estimates—some predicting <20,000 genes—and earlier estimates of as many as 140,000 protein-coding, or structural, genes is largely attributed to the high prevalence of alternative splicing (Section 26-3A). In addition, variations in posttranslational processing (Section 27-5B) mean that a given DNA sequence can give rise to several functionally distinct protein products.

The functions of many human genes have been identified through sequence comparisons at the level both of protein families and of domains (Fig. 28-3). Note that nearly 42% of these genes have unknown functions, as is likewise the case with most other genomes of known sequence, including those of prokaryotes. Genes with no known function are called **orphan genes.** Some of these sequences may represent novel genes whose protein products have not yet been discovered. Others may simply be counterparts of known genes but are too different in sequence to be recognized as such.

About three-quarters of all known human genes appear to have counterparts in other species. About one-quarter are present only in other vertebrates, and one-quarter are present in prokaryotes as well as eukaryotes. As expected, the human genome contains approximately the same number of "housekeeping" genes (genes required for the most fundamental cellular activities) as other eukaryotes. But it includes relatively more genes for vertebrate-specific activities, such as those relevant to the immune system and neuronal and hormonal signaling pathways.

A Significant Portion of the Human Genome Is Transcribed to RNA. Although the proportion of exonic DNA in the human genome is relatively small (~1.4%), as much as 60% of the genome may be transcribed. This mass of RNA includes the products of 4000 or so identified genes for tRNAs, rRNAs, and other small RNAs, as well as tens of thousands of

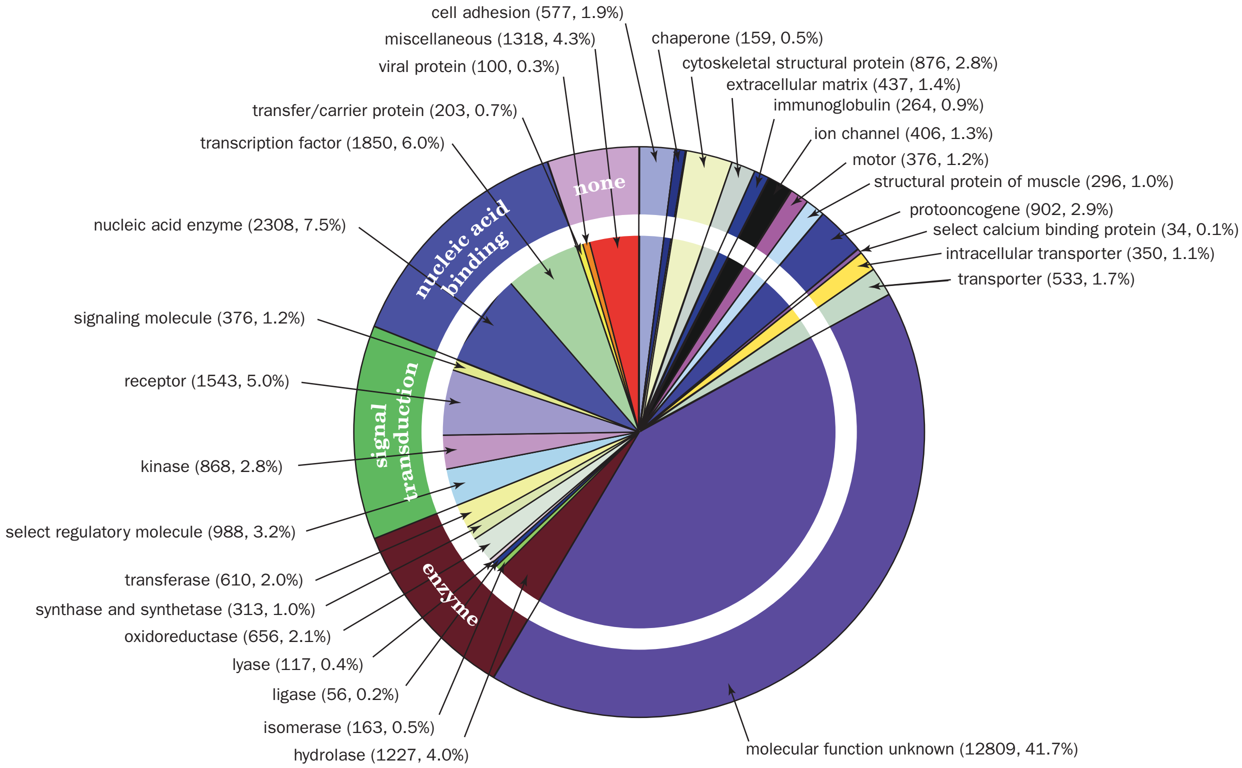

Figure 28-3 | Distribution of molecular functions of the putative structural genes in the human genome. Each wedge of the pie chart lists, in parentheses, the number and percentage of the genes assigned to the indicated category of molecular function. The outer circle indicates the general functional categories whereas the inner circle provides a more detailed breakdown of the categories. [Courtesy of J. Craig Venter, Celera Genomics, Rockville, Maryland.]

other **noncoding RNAs (ncRNAs),** many of which have no known function. Some ncRNAs are polyadenylated, as are mRNAs (Section 26-3A), but do not correspond to any known genes. One possibility is that this RNA represents transcriptional noise arising from promoter-like elements scattered throughout the genome. However, the observation that some ncRNAs exhibit conservation between species and tissue-specific splice variants suggests that such RNA performs a regulatory function.

Many Disease Genes Have Been Identified. The availability of human genomic data has facilitated the identification of sequence variants that are associated with particular diseases. Over 2000 such genes have been catalogued, including those for cystic fibrosis (see Box 3-1) and some hereditary forms of cancer. However, monogenetic diseases are relatively rare. Most diseases result from interactions among several genes and from environmental factors. One goal of genomics is to identify genetic features that can be linked to susceptibility to disease or infection. To that end, a catalog of human DNA sequence variations is being compiled as a database of **single nucleotide polymorphisms** (**SNPs;** pronounced “snips”). A SNP, or single-base difference between individuals, occurs about every 1250 bp on average. Nearly 2 million SNPs have been described. Although less than 1% of them result in protein variants, and probably fewer still have functional consequences, it is becoming increasingly apparent that SNPs are largely responsible for an individual’s susceptibility to many diseases as well as to adverse reactions to drugs (side effects; Section 12-4).

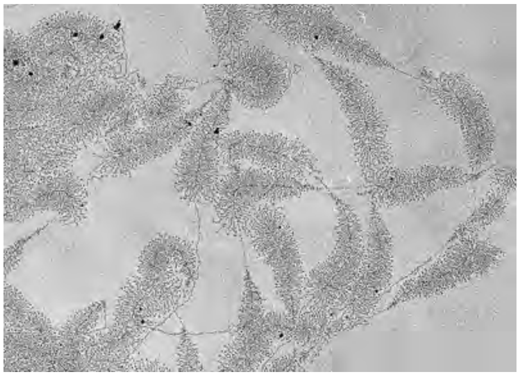

■ **Figure 28-4 | An electron micrograph of tandem arrays of actively transcribing 18S, 5.8S, and 28S rRNA genes from the newt *Notophthalmus viridescens.*** The axial fibers are DNA. The fibrillar "Christmas tree" matrices, which consist of newly synthesized RNA strands in complex with proteins, outline each transcriptional unit. Note that the longest ribonucleoprotein branches are only ~10% of the length of their corresponding DNA. Apparently, the RNA strands are compacted through secondary structure interactions and/or protein associations. The matrix-free segments of DNA are the untranscribed spacers. [Courtesy of Oscar L. Miller, Jr., and Barbara R. Beatty, University of Virginia.]

Moreover, SNPs can potentially serve as genetic markers for nearby disease-related genes.

B | Some Genes Occur in Clusters

Genes are not necessarily randomly distributed throughout an organism's genome. For example, the average gene frequency in the human genome is ~1 gene per 100 kb but ranges from 0 to 64 genes per 100 kb. Moreover, some protein-coding genes and other chromosomal elements exhibit a certain degree of organization. Prokaryotic genomes, for example, contain numerous operons, in which, as we have seen (Section 26-1B), genes with related functions (e.g., encoding the proteins involved in a particular metabolic pathway) occur close together, sometimes in the same order in which their encoded proteins act in a metabolic reaction sequence, and are transcribed onto a single polycistronic mRNA.

Gene clusters also occur in both prokaryotes and eukaryotes. Although most genes occur only once in an organism's haploid genome, genes such as those for rRNA and tRNA, whose products are required in relatively large amounts, may occur in multiple copies. As we saw in Section 26-3B, large rRNA transcripts are cleaved to yield the mature rRNA molecules. Furthermore, the transcribed blocks of 18S, 5.8S, and 28S eukaryotic rRNA genes are arranged in tandem repeats that are separated by nontranscribed spacers (Fig. 28-4). The rRNA genes, which may be distributed among several chromosomes, vary in haploid number from less than 50 to over 10,000, depending on the species. Humans, for example, have 50 to 200 blocks of rRNA genes spread over five chromosomes. tRNA genes are similarly reiterated and clustered.

Protein-coding genes almost never occur in multiple copies, presumably because the repeated translation of a few mRNA transcripts provides adequate amounts of most proteins. One exception is histone proteins, which are required in large amounts during the short time when eukaryotic DNA synthesis occurs. Not only are histone genes reiterated (up to ~100 times in *Drosophila*), they often occur as sets of each of the five different histone genes separated by nontranscribed sequences (Fig. 28-5). The gene order and the direction of transcription in these quintets are preserved over large evolutionary distances. The spacer sequences vary widely among species and, to a limited extent, among the repeating quintets within a genome. In birds and mammals, which contain 10 to 20 copies of each of the five histone genes, the genes occur in clusters but in no particular order.

Other gene clusters contain genes of similar but not identical sequence. For example, human globin genes are arranged in two clusters on separate

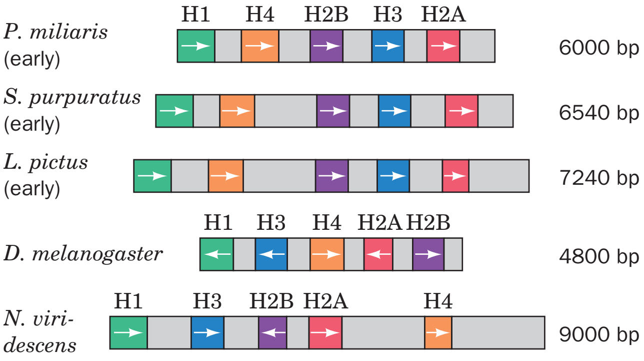

■ **Figure 28-5 | The organization and lengths of the histone gene cluster repeating units in a variety of organisms.** Coding regions are indicated in color, and spacers are gray. The arrows denote the direction of transcription (the top three organisms are distantly related sea urchins).

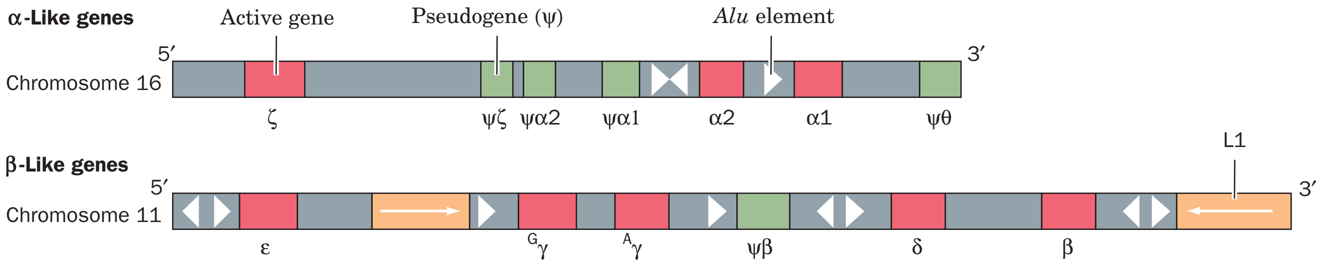

Figure 28-6 | **The organization of human globin genes.** Red boxes represent active genes; green boxes represent pseudogenes; yellow boxes represent repetitive sequences, with the arrows indicating their relative orientations; and triangles represent *Alu* elements in their relative orientations. [After Karlsson, S. and Nienhuis, A.W., *Annu. Rev. Biochem.* **54,** 1074 (1985).]

chromosomes (Fig. 28-6). The various genes are transcribed at different developmental stages. Adult hemoglobin is an $\alpha_2\beta_2$ tetramer, whereas the first hemoglobin made by the human embryo is a $\zeta_2\varepsilon_2$ tetramer in which ζ and ε are α- and β-like subunits, respectively (Fig. 28-7). At approximately 8 weeks after conception, fetal hemoglobin containing α and γ subunits appears. The γ subunit is gradually supplanted by β starting a few weeks before birth. Adult human blood normally contains ~97% $\alpha_2\beta_2$ hemoglobin, 2% $\alpha_2\delta_2$ (in which δ is a β variant), and 1% $\alpha_2\gamma_2$.

The **α-globin gene cluster** (Fig. 28-6, *top*), which spans 28 kb, contains three functional genes: the embryonic ζ gene and two slightly different α genes, α1 and α2, which encode identical polypeptides. The α cluster also contains four pseudogenes (nontranscribed relics of ancient gene duplications): ψζ, ψα2, ψα1, and ψθ. The **β-globin gene cluster** (Fig. 28-6, *bottom*), which spans >60 kb, contains five functional genes: the embryonic ε gene, the fetal genes $^G\gamma$ and $^A\gamma$ (duplicated genes encoding polypeptides that differ only by having either Gly or Ala at position 136), and the adult genes δ and β. The β-globin cluster also contains one pseudogene, ψβ. Both α and β gene clusters also include copies of **repetitive DNA sequences** (see below).

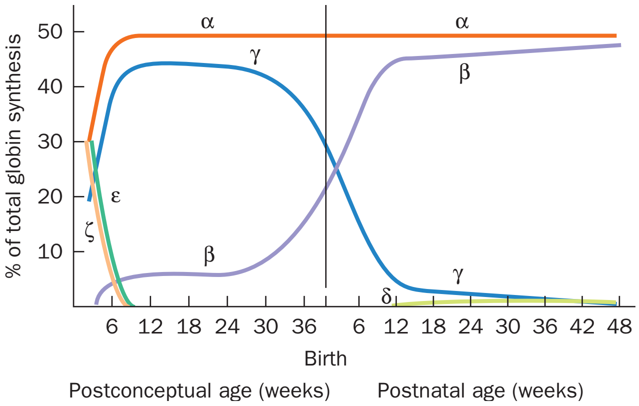

Figure 28-7 | **The progression of human globin chain synthesis with fetal development.** Note that any red blood cell contains only one type each of α- and β-like subunits. [After Weatherall, D.J. and Clegg, J.B., *The Thalassaemia Syndromes* (3rd ed.), p. 64, Blackwell Scientific Publications (1981).]

C | Eukaryotic Genomes Contain Repetitive DNA Sequences

Approximately 11% of the *E. coli* genome consists of nontranscribed regions, including the regulatory sequences that separate individual genes and sites that govern the origin and termination of replication. In addition, bacterial genomes typically contain insertion sequences (Section 25-6C) and the remnants of integrated bacteriophages.

The small sizes of prokaryotic genomes probably exert selective pressure against the accumulation of useless DNA. Eukaryotic genomes, however, which are usually much larger than prokaryotic genomes, apparently are not subject to the same selective forces. About 30% of the yeast genome consists of nonexpressed sequences, and the proportion is far greater in higher eukaryotes. Much of this DNA consists of repetitive sequences that contribute significantly to the relatively large genomes of certain plants and amphibians. Some repetitive DNA plays a structural role at the **centromeres** of eukaryotic chromosomes, the regions attached to the microtubular spindle during mitosis. These sequences may help align chromosomes and facilitate recombination. The telomeres also are composed of repeating DNA sequences (Section 25-3C). A variety of neurological

BOX 28-1 BIOCHEMISTRY IN HEALTH AND DISEASE

Trinucleotide Repeat Diseases

At least 14 human diseases are associated with repeated trinucleotides in certain genes. These **trinucleotide repeats** exhibit an unusual genetic instability: Above a threshold of about 35 to 50 copies (100–150 bp), the repeats tend to expand with successive generations. Because the overall length of the repeat typically correlates with the age of onset of the disease, descendants of an individual with a trinucleotide repeat disease tend to be more severely affected and at an earlier age. The disease is therefore said to exhibit **genetic anticipation.**

Some types of trinucleotide repeat diseases are caused by massive expansion (usually to hundreds of copies) of a trinucleotide in the noncoding region of a gene, for example, in a region upstream of the transcription start site, in a 5′ or 3′ untranslated region **(UTR),** or in an intron (see table). These expansions generally affect gene expression. For example, **myotonic dystrophy** results from aberrant expression of a protein kinase. The severity of the symptoms, progressive muscle weakness and wasting, correlate with the number of CTG repeats ($>$2000 in some cases) in its gene's 5′ UTR.

Some Diseases Associated with Trinucleotide Repeats

Disease	Repeat	Site of Repeat
Fragile X syndrome	CGG	5′ UTR
Myotonic dystrophy	CTG	Upstream region, 3′ UTR
Friedrich's ataxia	GAA	Intron
Spinobulbar muscular atrophy	CAG	Exon
Huntington's disease	CAG	Exon

Fragile X syndrome, the most common cause of mental retardation after Down's syndrome, is so named because the tip of the X chromosome's long arm is connected to the rest of the chromosome by a slender thread that is easily broken. As in many trinucleotide repeat diseases, the genetics of fragile X syndrome are bizarre. The maternal grandfathers of individuals having fragile X syndrome may be asymptomatic. Their daughters are likewise asymptomatic, but these daughters' children of either sex may have the syndrome. Evidently, the fragile X defect is activated by passage through a female.

The affected gene in fragile X syndrome, *FMR1* (for *f*ragile X *m*ental *r*etardation *1*), encodes a 632-residue RNA-binding protein named **FMRP** (for *FMR* *p*rotein), which apparently functions in the transport of certain mRNAs from the nucleus to the cytoplasm. FMRP, which is highly conserved in vertebrates, is heavily expressed in brain neurons, where a variety of evidence indicates that it participates in the proper formation and/or function of synapses. In the general population, the 5′ untranslated region of *FMR1* contains a $(CGG)_n$ sequence with n ranging from 6 to 60 (such a gene is said to be **polymorphic**). However, in individuals with fragile X syndrome, this triplet repeat has undergone an astonishing expansion to values of n ranging from $>$200 to several thousand. Moreover, these triplet repeats differ in size among siblings and often exhibit heterogeneity within an individual, suggesting that they are somatically generated.

Some trinucleotide repeat diseases result from the moderate expansion of a CAG triplet (which codes for Gln) in the protein-coding region of a gene. For example, in normal individuals, **huntingtin,** a polymorphic, $\sim$3150-residue protein of unknown function, contains a stretch of 11 to 34 consecutive Gln residues beginning 17 residues from its N-terminus. However, in **Huntington's disease (HD),** this poly(Gln) tract has expanded to between 37 and

diseases result from excessively reiterated trinucleotide sequences (see Box 28-1).

Highly Repetitive Sequences Are Tandemly Repeated Millions of Times. Nearly identical sequences up to 10 bp long that are tandemly repeated in clusters may be present at $>10^6$ copies per haploid genome. Approximately 3% of the human genome consists of **highly repetitive DNA sequences** (also known as **short tandem repeats; STRs**), with the greatest contribution (0.5%) provided by dinucleotide repeats, most frequently CA and TA. STRs appear to have arisen by template slippage during DNA replication. This occurs more frequently with short repeats, which therefore have a high degree of length polymorphism in the human population. Because the number of repeats at a given STR locus varies between individuals, analysis of STRs is widely used for DNA fingerprinting (Box 3-2).

86 repeats. Synthetic poly(Gln) aggregates as β sheets that are linked by hydrogen bonds involving both their main chain and side chain amide groups.

Individuals with HD, an autosomal dominant condition, suffer progressive choreic (jerky and disordered) movements, cognitive decline, and emotional disturbances over a 15 to 20 year course that is invariably fatal. This devastating disease typically develops late in life, around age 40, or earlier in individuals with high numbers of trinucleotide repeats. One of the hallmarks of HD, as well as of other neurodegenerative diseases such as Alzheimer's disease, is the deposition of insoluble protein aggregates in the cytosol and nuclei of neurons (Section 6-5C). The appearance of these intracellular aggregates (presumably huntingtin and/or its proteolytic products in HD) often coincides with the onset of neurological symptoms, although it is not clear whether protein aggregation directly causes neuronal death and its attendant symptoms. The long incubation period before the symptoms of HD become evident is attributed to the lengthy nucleation time for aggregate formation, much like what we have seen occurs in the formation of amyloid fibrils (Section 6-5C).

The expansion of trinucleotide repeats occurs by an unknown mechanism. One theory, that additional nucleotides are introduced by the slippage of DNA polymerases during replication, is inconsistent with the gradual accumulation of trinucleotide repeats over time in cells such as neurons that normally do not divide. Another possibility is that the additional nucleotides are introduced during DNA repair processes (which are ongoing and independent of DNA replication) and may result from hairpin formation within the trinucleotide repeat region. These intrastrand base-paired structures (*at right*) may lead to misalignment of DNA strands and the polymerization of additional nucleotides to fill in the gaps.

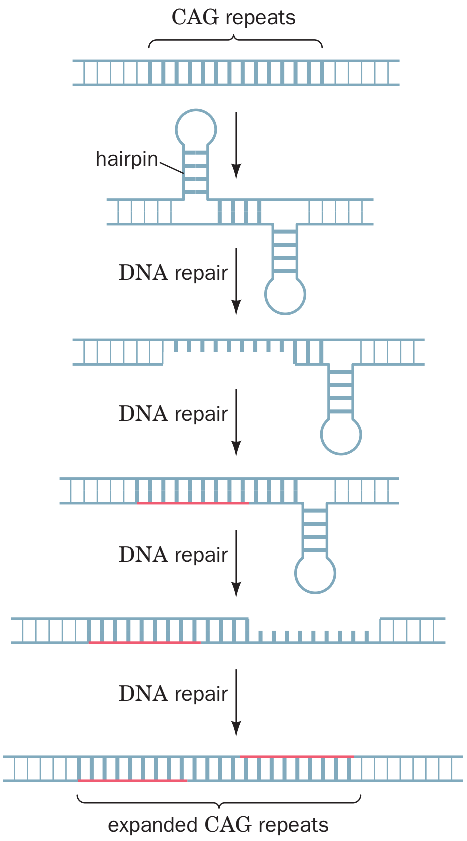

Moderately Repetitive Sequences Arise from Transposons. Moderately repetitive DNA ($<10^6$ copies per haploid genome) occurs in segments of 100 to several thousand base pairs that are interspersed with larger blocks of unique DNA. Most of the repetitive sequences are the remnants of retrotransposons (transposable elements that propagate through the intermediate synthesis of RNA; Section 25-6C). Around 42% of the human genome consists of three types of retrotransposons:

1. **Long interspersed nuclear elements (LINEs)** are 6- to 8-kb-long segments (Section 25-6C). The great majority of these have accumulated mutations that render them transcriptionally inactive.
2. **Short interspersed nuclear elements (SINEs)** consist of 100- to 400-bp elements. The most common SINEs in the human genome are members of the ***Alu* family,** which are so named because most of their ~300-bp segments contain a cleavage site for the restriction

Table 28-2 Moderately Repetitive Sequences in the Human Genome

Type of Repeat	Length (bp)	Number of Copies (× 1000)	Percentage of Genome
LINEs	6000–8000	868	20.4
SINEs	100–300	1558	13.1
LTR retrotransposons	1500–11,000	443	8.3
DNA transposons	80–3000	294	2.8
Total			44.8

Source: International Human Genome Sequencing Consortium, *Nature* **409,** 800 (2001).

endonuclease *Alu*I (AGCT; Table 3-2). The globin gene cluster contains several *Alu* elements (Fig. 28-6).

3. Retrotransposons with **long terminal repeats (LTRs).**

In addition, the human genome contains DNA transposons that resemble bacterial transposons. Overall, ~45% of the human genome consists of widely dispersed and almost entirely inactive transposable elements (Table 28-2).

No function has been unequivocally assigned to **moderately repetitive DNA,** which therefore has been termed **selfish** or **junk DNA.** This DNA apparently is a molecular parasite that, over many generations, has disseminated itself throughout the genome through transposition. The theory of natural selection suggests that the increased metabolic burden imposed by the replication of an otherwise harmless selfish DNA would eventually lead to its elimination. Yet for slowly growing eukaryotes, the relative disadvantage of replicating an additional 100 bp of selfish DNA in an ~1-billion-bp genome would be so slight that its rate of elimination would be balanced by its rate of propagation. *Because unexpressed sequences are subject to little selective pressure, they accumulate mutations at a greater rate than do expressed sequences.*

CHECK YOUR UNDERSTANDING

What are some factors that allow humans to get by with only slightly more genes than invertebrates?

What are the origins and functions of gene clusters?

Summarize the relationship between genome size, repetitive DNA, transcribed DNA, and protein-coding exons in the human genome.

2 Regulation of Prokaryotic Gene Expression

LEARNING OBJECTIVES

- Understand how the *lac* repressor prevents or allows transcription of the *lac* operon.
- Understand that cAMP stimulates transcription of catabolite-repressed operons.
- Understand how attenuation links amino acid availability to operon expression.
- Understand that a riboswitch changes its conformation to regulate gene expression.

A complete genome sequence reveals the metabolic capabilities of an organism, but *gene sequences alone do not necessarily indicate when or where the encoded molecules are produced.* The route from gene sequence to fully functional gene product offers many potential points for regulation, but *in prokaryotes, gene expression is primarily controlled at the level of transcription.* This is perhaps because prokaryotic mRNAs have lifetimes of only a few minutes, so translational control is less necessary. In this section, we examine a few well-documented examples of gene regulation in prokaryotes. In the following section, we shall consider how eukaryotic cells regulate gene expression.

See Guided Exploration 30
The regulation of gene expression by the *lac* repressor system.

A | The *lac* Operon Is Controlled by a Repressor

Bacteria adapt to their environments by producing enzymes that metabolize certain nutrients only when those substances are available. For example, *E. coli* cells grown in the absence of lactose are initially unable to metabolize the disaccharide. To do so they require two proteins: **β-galactosidase,** which catalyzes the hydrolysis of lactose to its component monosaccharides,

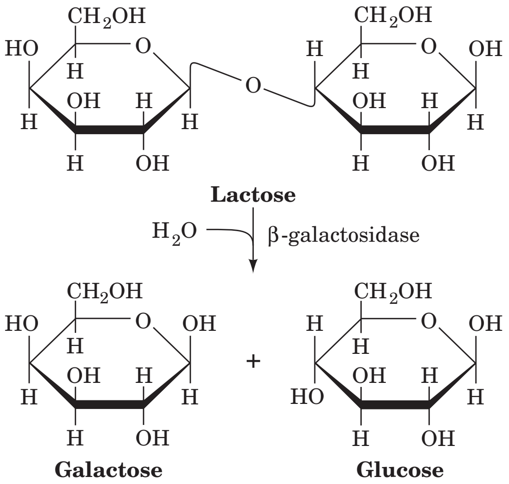

and **galactoside permease** (also known as **lactose permease;** Section 10-3D), which transports lactose into the cell. Cells grown in the absence of lactose contain only a few molecules of the proteins. Yet a few minutes after lactose is introduced into their medium, the cells increase the rate at which they synthesize the proteins by ~1000-fold and maintain that pace until lactose is no longer available. *This ability to produce a series of proteins only when the substances they metabolize are present permits the bacteria to adapt to their environment without the debilitating need to continuously synthesize large quantities of otherwise unnecessary enzymes.*

Lactose or one of its metabolic products must somehow act as an **inducer** to trigger the synthesis of the above proteins. The physiological inducer of the lactose system, the lactose isomer **1,6-allolactose,**

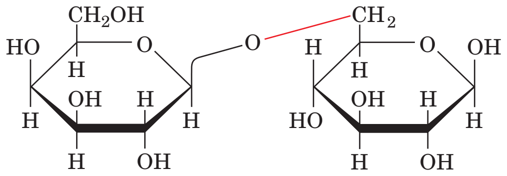

1,6-Allolactose

arises from lactose's occasional transglycosylation by β-galactosidase. Most *in vitro* studies of lactose metabolism use **isopropylthiogalactoside (IPTG),**

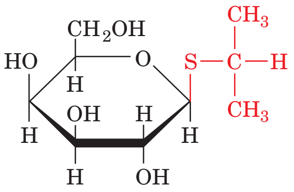

Isopropylthiogalactoside (IPTG)

a synthetic inducer that structurally resembles allolactose but is not degraded by β-galactosidase. Natural and synthetic inducers also stimulate the synthesis of **thiogalactoside transacetylase,** an enzyme whose physiological role is unknown.

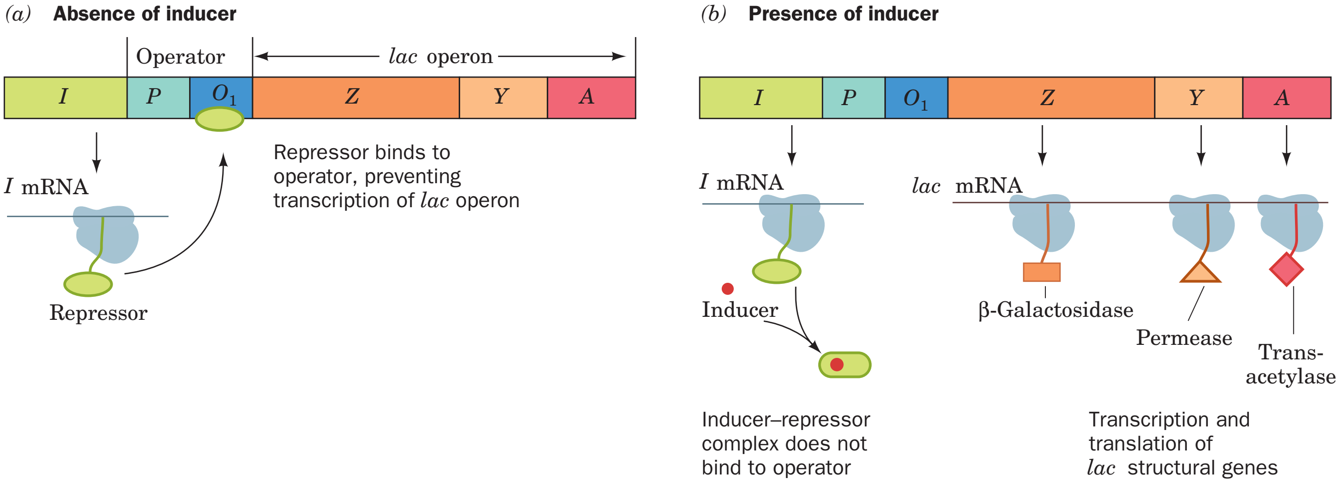
(a) Absence of inducer
Operator
lac operon
I
P
O1
Z
Y
A
I mRNA
Repressor
Repressor binds to operator, preventing transcription of lac operon
(b) Presence of inducer
I
P
O1
Z
Y
A
I mRNA
lac mRNA
Inducer
β-Galactosidase
Permease
Trans-acetylase
Inducer–repressor complex does not bind to operator
Transcription and translation of lac structural genes

■ **Figure 28-8 | The expression of the *lac* operon.** (*a*) In the absence of inducer, the repressor (the product of the *I* gene) binds to the operator (O_1), thereby preventing transcription of the *lac* operon from the promoter (*P*). (*b*) On binding inducer, the repressor dissociates from the operator, which permits the transcription and subsequent translation of the *lac* structural genes (*Z, Y,* and *A*, which respectively encode β-galactosidase, lactose permease, and thiogalactoside transacetylase).

The genes specifying β-galactosidase, galactoside permease, and thiogalactoside transacetylase, designated *Z, Y,* and *A,* respectively, are contiguously arranged in the *lac* operon (Fig. 26-4). All three structural genes are translated from a single mRNA transcript. A nearby gene, *I,* encodes the ***lac*** **repressor,** a protein that inhibits the synthesis of the three *lac* proteins.

***lac* Repressor Recognizes Operator Sequences.** The target of the *lac* repressor is a region of the *lac* operon known as its **operator,** which lies near the beginning of the β-galactosidase gene. *In the absence of inducer, lac repressor specifically binds to the operator to prevent the transcription of mRNA (Fig. 28-8a). On binding inducer, the repressor dissociates from the operator, thereby permitting the transcription and subsequent translation of the lac enzymes (Fig. 28-8b).*

The *lac* operon actually contains three operator sequences to which *lac* repressor binds with high affinity, known as O_1, O_2, and O_3. O_1, the primary repressor-binding site, was identified through its protection by *lac* repressor from nuclease digestion. The 26-bp protected sequence lies within a nearly twofold symmetrical sequence of 35 bp (Fig. 28-9). O_1 overlaps the transcription start site of the *lacZ* gene. The operator sequence O_2 is centered 401 bp downstream, fully within the *lacZ* gene, and O_3 is centered 93 bp upstream of O_1, at the end of the *lacI* gene. Genetic engineering experiments show that all three operator sequences must be present for maximum repression *in vivo*.

The observed rate constant for the binding of *lac* repressor to *lac* operator is $k \approx 10^{10}\ \text{M}^{-1} \cdot \text{s}^{-1}$. This "on" rate is much greater than that calculated for the diffusion-controlled process in solution: $k \approx 10^{7}\ \text{M}^{-1} \cdot \text{s}^{-1}$ for molecules the size of *lac* repressor. Since it is impossible for a reaction to proceed faster than its diffusion-controlled rate, *lac* repressor must not encounter operator from solution in a random three-dimensional search. Rather, it appears that *lac repressor finds its operator by nonspecifically binding to DNA and sliding along it in a far more efficient one-dimensional search.*

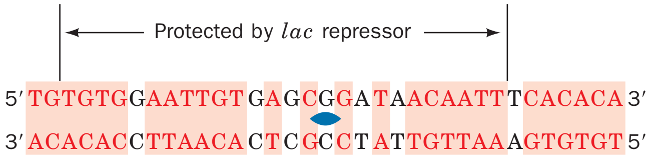
Protected by lac repressor
5′ TGTGTGGAATTGTGAGCGGATAACAATTTCACACA 3′
3′ ACACACCTTAACACTCGCCTATTGTTAAAGTGTGT 5′

■ **Figure 28-9 | The base sequence of the *lac* operator O_1.** Its symmetry-related regions, which comprise 28 of its 35 bp, are shaded in red.

lac Repressor Binds Two DNA Segments Simultaneously. The isolation of *lac* repressor, by Beno Müller-Hill and Walter Gilbert in 1966, was exceedingly difficult because the repressor constitutes only ~0.002% of the protein in wild-type *E. coli*. Molecular cloning techniques (Section 3-5) later made it possible to produce large quantities of *lac* repressor. Nevertheless, it was not until 1996 that Ponzy Lu and Mitchell Lewis reported the complete three-dimensional structure of the protein. Each 360-residue subunit of the repressor homotetramer has four functional units (Fig. 28-10):

1. An N-terminal "headpiece," which contains a helix–turn–helix (HTH) motif that resembles those in other prokaryotic DNA-binding proteins (Section 24-4B) and which specifically binds operator DNA sequences.
2. A linker, which contains a short α helix that acts as a hinge and also binds DNA. In the absence of DNA, the hinge helices of the *lac* repressor tetramer are disordered, allowing the headpieces to move freely.
3. A two-domain core, which binds inducers such as IPTG.
4. A C-terminal α helix, which is required for the quaternary structure of *lac* repressor. In the tetramer, all four C-terminal helices associate. Surprisingly, the repressor homotetramer does not exhibit the D_2 symmetry of nearly all homotetrameric proteins of known structure (three mutually perpendicular twofold axes; Section 6-3) but is instead V-shaped (with only twofold symmetry) and is therefore best considered to be a dimer of dimers (Fig. 28-11).

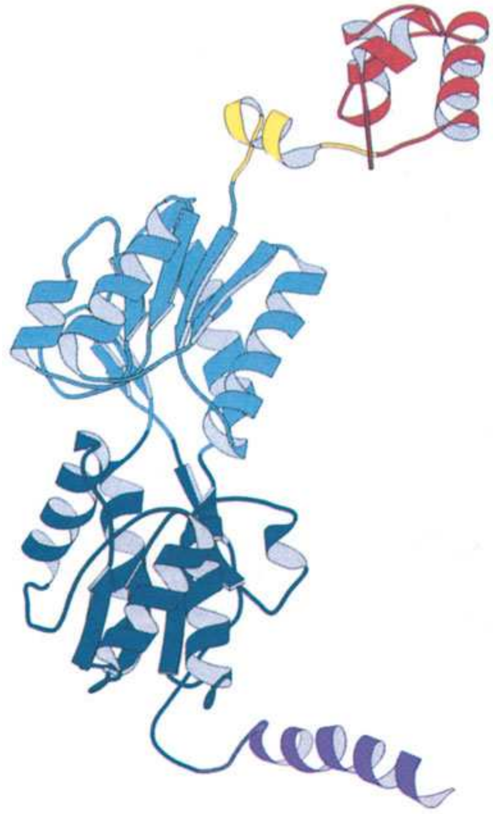

■ **Figure 28-10 | Ribbon diagram of the *lac* repressor monomer.** The DNA-binding domain containing its helix–turn–helix motif is red; the hinge helix is yellow; the inducer-binding core is light and dark blue; and the tetramerization helix is purple. [Courtesy of Ponzy Lu and Mitchell Lewis, University of Pennsylvania. PDBid 1LBG.]

The X-ray structure of a complex between *lac* repressor and a 21-bp synthetic DNA containing a high-affinity binding sequence reveals that each repressor tetramer binds two DNA segments (Fig. 28-11). The repressor's HTH motif fits snugly into the major groove, bending the DNA so that it has a radius of curvature of 60 Å. The two bound DNA segments are laterally separated by ~25 Å.

IPTG binds to the repressor core at the interface between the two domains colored light and dark blue in Fig. 28-10. This binding induces a conformational change in the repressor dimer that is communicated through the hinge helices to the headpieces. This causes the two DNA-binding domains in each dimer to separate by ~3.5 Å so that they can no longer simultaneously bind DNA, thereby causing the repressor to dissociate from the DNA.

The *lac* repressor is an allosteric protein: IPTG binding to one subunit alters the DNA-binding activity of its dimeric partner (but not of the other dimer in the repressor tetramer). Since the allosteric transition occurs within the dimer, why does full repressor activity require a tetramer? Model-building studies provide a plausible answer to this puzzle. *A lac repressor tetramer simultaneously binds to two operators so that it brings them together, forming a loop of DNA either 93 or 401 bp long, depending*

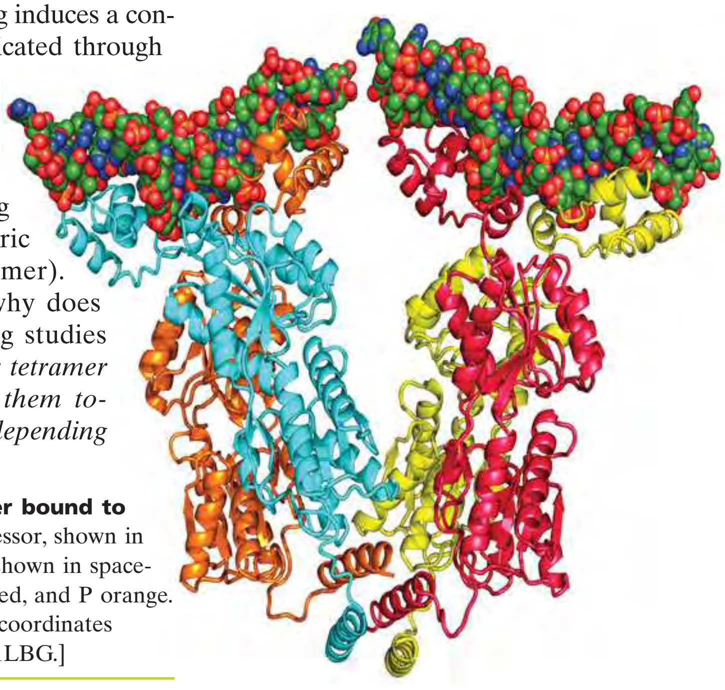

■ **Figure 28-11 | X-Ray structure of the *lac* repressor tetramer bound to two 21-bp segments of DNA.** The monomeric units of the repressor, shown in ribbon form, are drawn in different colors, and the DNA segments, shown in space-filling form, are colored according to type with C green, N blue, O red, and P orange. [Based on an X-ray structure by Ponzy Lu and Mitchell Lewis with coordinates generated by Benjamin Wieder, University of Pennsylvania. PDBid 1LBG.]

on whether the repressor binds O_1 and O_3 or O_1 and O_2. The formation of a stable looped structure may require additional DNA-binding proteins; one candidate is **CAP** (see below), a DNA-binding protein that binds to the DNA between O_1 and O_3 (Fig. 28-12). In the model shown in Fig. 28-12, the *lac* promoter is part of the looped DNA.

It was widely assumed for years that *lac* repressor simply physically obstructs the binding of RNA polymerase (RNAP) to the *lac* promoter. However, experiments have demonstrated that RNAP can bind to the promoter in the presence of the repressor but cannot properly initiate transcription. Dissociation of the repressor in response to an inducer would allow unimpeded transcription. If RNAP were already bound to the *lac* promoter, transcription could begin immediately. Nevertheless, in the model shown in Fig. 28-12, the contact surface for RNAP is on the inside of the DNA loop, which presumably would preclude the binding of RNAP. Further studies are needed to resolve this apparent contradiction.

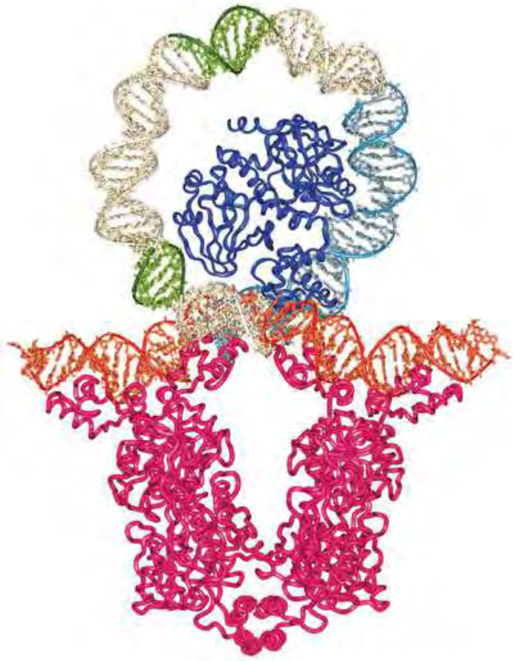

Figure 28-12 | Model of the 93-bp loop formed when the *lac* repressor tetramer binds to O_1 and O_3. The proteins are represented by their C_α backbones, and the DNA is shown in skeletal form with its sugar–phosphate backbones traced by helical ribbons. The model was constructed from the X-ray structure of *lac* repressor (*red*) in complex with two 21-bp operator DNA segments (*orange*) and the X-ray structure of CAP (*purple*) in complex with its 30-bp target DNA (*cyan*). The remainder of the DNA loop was generated by applying a smooth curvature to B-DNA (*white*) with the −10 and −35 regions of the *lac* promoter highlighted in green. [Courtesy of Ponzy Lu and Mitchell Lewis, University of Pennsylvania.]

B | Catabolite-Repressed Operons Can Be Activated

Glucose is *E. coli*'s metabolic fuel of choice; adequate amounts of glucose prevent the full expression of genes specifying proteins involved in the fermentation of numerous other catabolites, including lactose, arabinose, and galactose, even when they are present in high concentrations. This phenomenon, which is known as **catabolite repression,** prevents the wasteful duplication of energy-producing enzyme systems. Catabolite repression is overcome in the absence of glucose by a cAMP-dependent mechanism. cAMP levels are low in the presence of glucose but rise when glucose becomes scarce.

CAP–cAMP Complex Stimulates the Transcription of Catabolite-Repressed Operons. Certain *E. coli* mutants, in which the absence of glucose does not relieve catabolite repression, are missing a cAMP-binding protein that is synonymously named **catabolite gene activator protein (CAP)** or **cAMP receptor protein (CRP).** CAP is a dimeric protein of identical 210-residue subunits that undergoes a large conformational change on binding cAMP. The CAP–cAMP complex, but not CAP alone, binds to the promoter region of the *lac* operon (among others) and stimulates transcription in the absence of repressor. CAP is therefore a **positive regulator** (it turns transcription on), in contrast to *lac* repressor, which is a **negative regulator** (it turns transcription off).

How does the CAP–cAMP complex operate? The *lac* operon has a weak (low-efficiency) promoter. One possibility is that CAP–cAMP binding enhances the ability of RNAP to transcribe the *lac* operon by inducing a conformational change in the promoter DNA. In fact, the X-ray structure of CAP–cAMP in complex with a 30-bp segment of DNA, whose sequence resembles the CAP-binding site, reveals that the CAP dimer binds in successive turns of DNA's major groove via its two HTH motifs so as to bend the DNA by ~90° around the protein dimer (Fig. 28-13). The bend arises from two ~45° kinks in the DNA between the fifth and sixth bases out from the complex's twofold axis in both directions and results in a closing of the major groove and in an enormous widening of the minor groove at each kink. The distorted DNA may be a more efficient substrate for transcription initiation than linear DNA. A second possibility is that CAP–cAMP stimulates transcription initiation through direct contact with RNAP. Indeed, the CAP–cAMP binding site on the *lac* operon overlaps the *lac* promoter.

The model for *lac* repressor binding (Fig. 28-12) paradoxically includes CAP, which is an activator. This dual binding may be a mechanism for

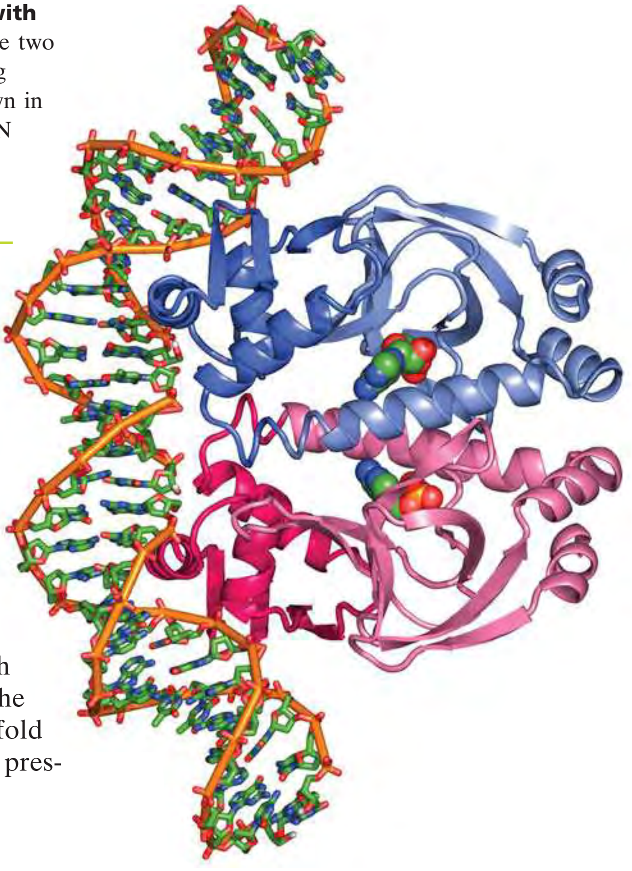

Figure 28-13 | X-Ray structure of the CAP–cAMP dimer in complex with DNA. The complex is viewed with its twofold axis of symmetry horizontal. The two subunits of the homodimeric protein are pink and blue with their DNA-binding C-terminal domains darker shades. The 30-bp self-complementary DNA is drawn in stick form and the cAMPs are drawn in space-filling form, both with C green, N blue, O red, and P orange. Successive P atoms in the DNA are connected by orange rods. [Based on an X-ray structure by Thomas Steitz, Yale University. PDBid 1CGP.] **See Interactive Exercise 55.**

conserving cellular energy in the absence of both glucose and lactose. If lactose became available, *lac* repressor would dissociate, and CAP–cAMP would be poised to promote transcription of the *lac* operon.

C | Attenuation Regulates Transcription Termination

The *E. coli* ***trp*** **operon** encodes five polypeptides (which form three enzymes) that mediate the synthesis of tryptophan from chorismate (Section 21-5B). The five *trp* operon genes (*A–E;* Fig. 28-14) are coordinately expressed under the control of the *trp* repressor, which binds L-tryptophan to form a complex that specifically binds to the *trp* operator to reduce the rate of *trp* operon transcription 70-fold (Section 24-4B). In this system, tryptophan acts as a **corepressor;** its presence prevents what would be superfluous tryptophan biosynthesis.

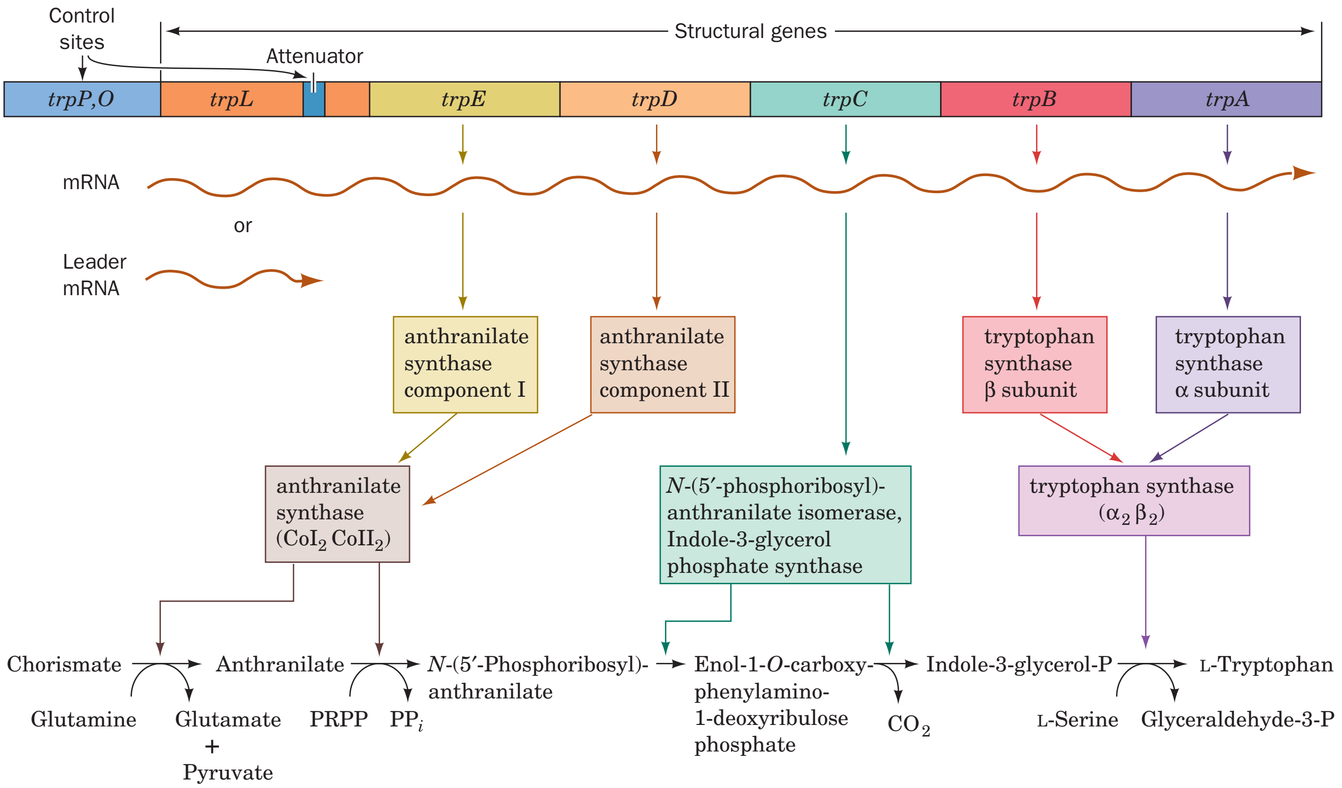
Control sites
Structural genes
Attenuator
trpP,O
trpL
trpE
trpD
trpC
trpB
trpA
mRNA
or
Leader mRNA
anthranilate synthase component I
anthranilate synthase component II
tryptophan synthase β subunit
tryptophan synthase α subunit
anthranilate synthase (CoI$_2$ CoII$_2$)
N-(5′-phosphoribosyl)-anthranilate isomerase, Indole-3-glycerol phosphate synthase
tryptophan synthase (α$_2$β$_2$)
Chorismate
Glutamine
Glutamate + Pyruvate
Anthranilate
PRPP
PP$_i$
N-(5′-Phosphoribosyl)-anthranilate
Enol-1-O-carboxyphenylamino-1-deoxyribulose phosphate
CO$_2$
Indole-3-glycerol-P
L-Serine
Glyceraldehyde-3-P
L-Tryptophan

Figure 28-14 | Genetic map of the *E. coli trp* operon indicating the enzymes it specifies and the reactions they catalyze. The gene product of *trpC* catalyzes two sequential reactions in the synthesis of tryptophan (Section 21-5B). [After Yanofsky, C., *J. Am. Med. Assoc.* **218,** 1027 (1971).]

The *trp* repressor–operator system was at first thought to fully account for the regulation of tryptophan biosynthesis in *E. coli*. However, the discovery of *trp* deletion mutants located downstream from the operator (*trpO*) that increase *trp* operon expression sixfold indicated the existence of an additional transcriptional control element. This element is located ~30 to 60 nucleotides upstream of the structural gene *trpE* in a 162-nucleotide **leader sequence** (*trpL;* Fig. 28-14).

When tryptophan is scarce, the entire 6720-nucleotide polycistronic *trp* mRNA, including the *trpL* sequence, is synthesized. When the encoded enzymes begin synthesizing tryptophan, the rate of *trp* operon transcription decreases as tryptophan binds to *trp* repressor. Of the *trp* mRNA that is transcribed, however, an increasing proportion consists of only a 140-nucleotide segment corresponding to the 5′ end of *trpL*. *The availability of tryptophan therefore results in the premature termination of trp operon transcription.* The control element responsible for this effect is consequently termed an **attenuator.**

The *trp* Attenuator's Transcription Terminator Is Masked when Tryptophan Is Scarce. The attenuator transcript contains four complementary segments that can form one of two sets of mutually exclusive base-paired hairpins (Fig. 28-15). Segments 3 and 4 together with the succeeding residues constitute a transcription terminator (Section 26-1D): a

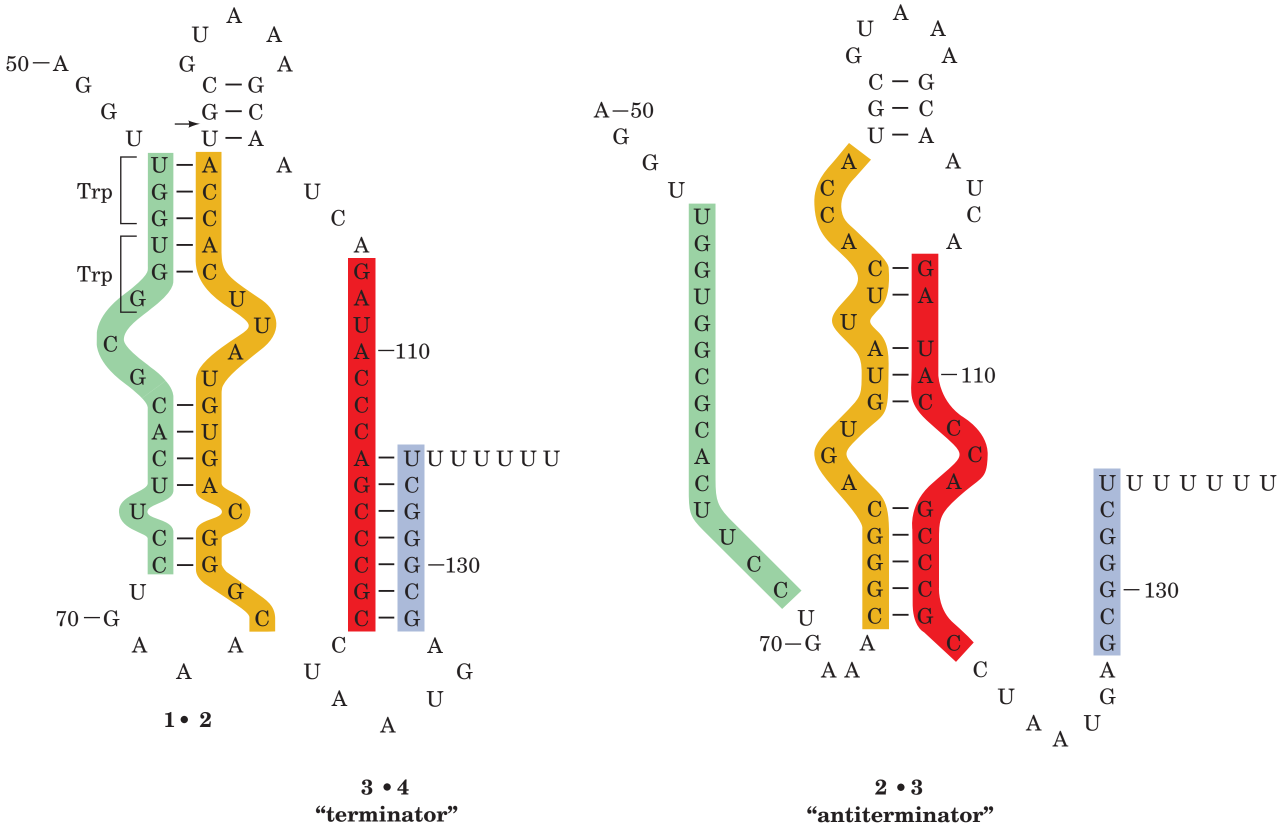

■ **Figure 28-15 | Alternative secondary structures of *trpL* mRNA.** The formation of the base-paired 2 · 3 (antiterminator) hairpin (*right*) precludes formation of the 1 · 2 and 3 · 4 (terminator) hairpins (*left*) and vice versa. Attenuation results in the premature termination of transcription immediately after nucleotide 140 when the 3 · 4 hairpin is present. The arrow indicates the mRNA site past which RNA polymerase pauses until approached by an active ribosome. [After Fisher, R.F. and Yanofsky, C., *J. Biol. Chem.* **258,** 8147 (1983).]

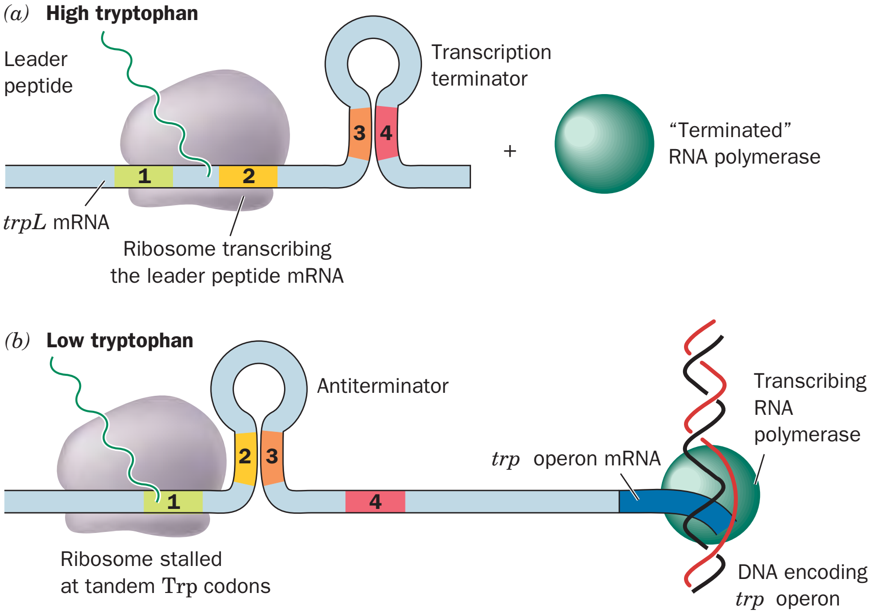

Figure 28-16 | Attenuation in the *trp* operon. (*a*) When Trp–tRNA$^{\text{Trp}}$ is abundant, the ribosome translates *trpL* mRNA. The presence of the ribosome on segment 2 prevents the formation of the base-paired 2 · 3 hairpin. The 3 · 4 hairpin, an essential component of the transcriptional terminator, can then form, thus aborting transcription. (*b*) When Trp–tRNA$^{\text{Trp}}$ is scarce, the ribosome stalls on the tandem Trp codons of segment 1. This situation permits the formation of the 2 · 3 hairpin, which precludes the formation of the 3 · 4 hairpin. RNA polymerase therefore transcribes through this unformed terminator and continues transcribing the *trp* operon.

G + C-rich hairpin followed by several sequential U's (compare with Fig. 26-9). Transcription rarely proceeds beyond this termination site unless tryptophan is in short supply.

How does a shortage of tryptophan cause transcription to proceed past the terminator? A section of the leader sequence, which includes segment 1 of the attenuator, is translated to form a 14-residue polypeptide that contains two consecutive Trp residues (Fig. 28-15, *left*). The position of this particularly rare dipeptide (~1% of the residues in *E. coli* proteins are Trp) provided an important clue to the mechanism of attenuation, as proposed by Charles Yanofsky (Fig. 28-16): An RNA polymerase that has escaped repression initiates *trp* operon transcription. Soon after the ribosomal initiation site of the *trpL* sequence has been transcribed, a ribosome attaches to it and begins translating the leader peptide. When tryptophan is abundant (i.e., there is a plentiful supply of Trp–tRNA$^{\text{Trp}}$), the ribosome follows closely behind the transcribing RNA polymerase. Indeed, RNA polymerase pauses past position 92 of the transcript and continues transcribing only on the approach of a ribosome, thereby ensuring the close coupling of transcription and translation. The progress of the ribosome prevents the formation of the 2 · 3 hairpin and permits the formation of the 3 · 4 hairpin, which terminates transcription (Fig. 28-16*a*). When tryptophan is scarce, however, the ribosome stalls at the tandem UGG codons (which specify Trp) because of the lack of Trp–tRNA$^{\text{Trp}}$. As transcription continues, the newly synthesized segments 2 and 3 form a hairpin because the stalled ribosome prevents the otherwise competitive formation of the 1 · 2 hairpin (Fig. 28-16*b*). The 3 · 4 hairpin does not form, allowing transcription to proceed past this region and into the remainder of the *trp* operon. Thus, attenuation regulates *trp* operon transcription according to the tryptophan supply.

The leader peptides of the five other amino acid–biosynthesizing operons known to be regulated by attenuation are all rich in their corresponding amino acid residues. For example, the *E. coli* ***his* operon,** which specifies enzymes synthesizing histidine, has seven tandem His residues in its 16-residue leader peptide, whereas the ***ilv* operon,** which specifies enzymes participating in isoleucine, leucine, and valine biosynthesis, has five Ile, three Leu, and six Val residues in its 32-residue leader peptide. The leader transcripts of these operons resemble that of the *trp* operon in their capacity to form two alternative secondary structures, one of which contains a trailing transcription terminator.

D | Riboswitches Are Metabolite-Sensing RNAs

We have just seen how the formation of secondary structure in a growing RNA transcript can regulate gene expression though attenuation. The conformational flexibility of mRNA also allows it to regulate genes by directly interacting with certain cellular metabolites, thereby eliminating the need for sensor proteins such as the *lac* repressor, CAP, and the *trp* repressor.

In *E. coli,* the biosynthesis of thiamine pyrophosphate (TPP; Section 15-3B) requires the action of several proteins whose levels vary according to the cell's need for TPP. In at least two of the relevant genes the untranslated regions at the 5′ end of the mRNA include a highly conserved

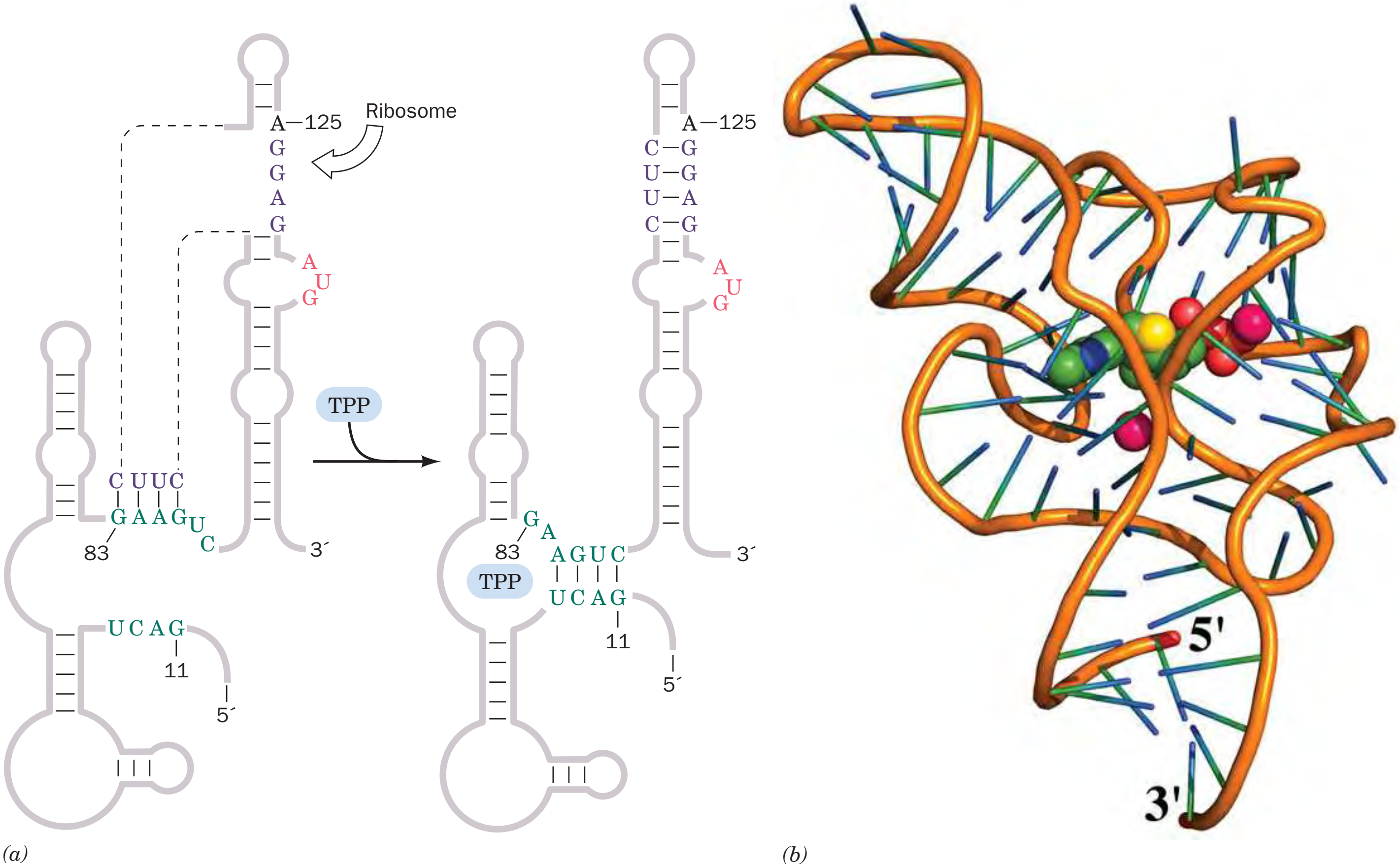

Figure 28-17 | Structure of the TPP-sensing riboswitch from *E. coli*. (*a*) The predicted secondary structure of a 165-residue segment at the 5′ end of the *thiM* gene is shown in the absence (*left*) and presence (*right*) of TPP. The TPP-binding conformation masks the Shine–Dalgarno sequence (*purple*) required by the ribosome to initiate translation at the AUG sequence (*red*) just downstream. [After Winkler, W., Nahvi, A., and Breaker, R.R., *Nature* **419,** 952 (2002).] (*b*) The X-ray structure of the riboswitch's TPP-sensing domain. The RNA is drawn in ladder form with its sugar–phosphate backbone represented by an orange rod and its bases represented by green and blue sticks. The TPP is drawn in space-filling form with C green, N blue, O red, and S yellow. Mg^{2+} ions are represented by magenta spheres. [Based on an X-ray structure by Ronald Breaker, Yale University, and Dinshaw Patel, Memorial Sloan-Kettering Cancer Center, New York, New York. PDBid 2GDI.]

sequence called the ***thi*** **box.** The susceptibility of the *thi* box to chemical or enzymatic cleavage, as Ronald Breaker showed, differs in the presence and absence of TPP, suggesting that the RNA changes its secondary structure when TPP binds to it (the binding of a metabolite by RNA is not unprecedented; synthetic oligonucleotides known as **aptamers** bind specific molecules with high specificity and affinity). The TPP-sensing mRNA element has been dubbed a **riboswitch.**

The predicted secondary structure of the TPP-sensing riboswitch and its proposed mechanism are shown in Fig. 28-17*a*. In the absence of TPP, the mRNA assumes a conformation that allows a ribosome to begin translation. In the presence of TPP, an alternative secondary structure masks its Shine–Dalgarno sequence (Section 27-4A) so that the ribosome cannot initiate the mRNA's translation. Thus, *the concentration of a metabolite can regulate the expression of genes required for its synthesis.* The X-ray structure of the 80-nt TPP-binding domain from the *E. coli* TPP-sensing riboswitch, determined by Breaker and Dinshaw Patel, reveals an intricately folded RNA that binds TPP in an extended conformation (Fig. 28-17*b*).

Nine types of bacterial riboswitches have as yet been identified, including those that regulate the expression of enzymes involved in the synthesis of coenzyme B_{12} (Fig. 20-17), riboflavin (Fig. 14-12), and *S*-adenosylmethionine (SAM; Fig. 21-18). These collectively regulate $>2\%$ of the genes in certain bacteria. In some cases, metabolite binding to the mRNA controls the formation of an internal transcription termination site so that transcription beyond this site proceeds only when the metabolite is absent. In others, a ribozyme that forms a portion of an mRNA is activated by the binding of a metabolite to self-cleave, thereby inactivating the mRNA. Plants and fungi also contain riboswitches. The fact that the interaction of riboswitches with their effectors does not require the participation of proteins suggests that they are relics of the RNA world (Box 24-3) and hence among the oldest regulatory systems.

CHECK YOUR UNDERSTANDING

What is the regulatory advantage of arranging genes in operons?

Describe the regulation of the *lac* operon by *lac* repressor and CAP.

How does the conformation of mRNA regulate gene expression by attenuation and in riboswitches?

3 Regulation of Eukaryotic Gene Expression

LEARNING OBJECTIVES

- Understand that chromatin structure, as influenced by chromatin-remodeling complexes, histone modification, and DNA methylation, controls gene expression.
- Understand that numerous proteins and DNA elements interact to regulate transcription initiation in eukaryotes.
- Understand that mRNA degradation limits gene expression.
- Understand that somatic recombination and hypermutation in immunoglobulin gene segments contributes to antibody diversity.

The general principles that govern the expression of prokaryotic genes apply also to eukaryotic genes: *The expression of specific genes may be actively inhibited or stimulated through the effects of proteins that bind to DNA or RNA.* As in prokaryotes, the majority of known regulatory mechanisms act at the level of gene transcription, but unlike prokaryotic control systems, the eukaryotic mechanisms must contend with much larger amounts of DNA that is packaged in seemingly inaccessible structures. In this section, we describe a few of the strategies whereby eukaryotic cells manage their genetic information.

A | Chromatin Structure Influences Gene Expression

The majority of DNA in multicellular organisms is not expressed. This includes the portion of the genome that does not encode protein or RNA, as well as the genes whose expression is inappropriate for a particular cell type. Although nearly all the cells in an organism contain identical sets of DNA, genes are expressed in a highly tissue-specific manner. For example, most pancreatic cells synthesize and secrete digestive enzymes, but the pancreatic islet cells synthesize insulin or glucagon instead (Section 22-2).

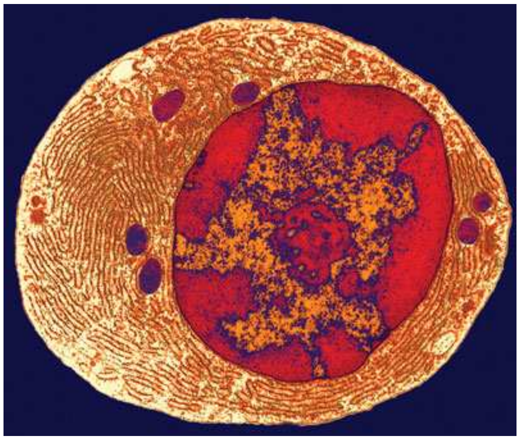

Figure 28-18 | Electron micrograph of a B lymphocyte. The large body in the center of the cell is the nucleus in which heterochromatin (*red*) adheres to the inner nuclear membrane and the transcriptionally active euchromatin (*orange*) is more centrally located. The small red body at the center of the nucleus is the nucleolus. Also note the extensive rough endoplasmic reticulum filling the cytoplasm of this antibody-producing cell (Section 7-3). Compare this figure with Fig. 1-8. [Don Fawcett/Visuals Unlimited.]

Nonexpressed DNA is typically highly condensed in a form known as **heterochromatin** (Fig. 28-18). An extreme example of this is the complete inactivation of one of the two X chromosomes in female mammals (Box 28-2). Transcriptionally active DNA, which is known as **euchromatin,** is less condensed, presumably to provide access to the transcription machinery. In fact, Harold Weintraub demonstrated that transcriptionally active chromatin is more susceptible to digestion by pancreatic DNase I than is transcriptionally inactive chromatin. Yet nuclease sensitivity apparently reflects a gene's potential for transcription rather than transcription itself.

In order for genetic information to be expressed, the transcription machinery must gain access to the DNA, which is packaged in nucleosomes (Section 24-5B). Not surprisingly, nucleosomes are not fixed structures but can undergo remodeling. In addition, histones can be covalently modified to alter their ability to interact with other cellular components.

Chromatin-Remodeling Complexes Shuffle Nucleosomes. Sequence-specific DNA-binding proteins must gain access to their target DNAs before they can bind to them. Yet nearly all DNA in eukaryotes is sequestered by nucleosomes if not by higher order chromatin. How then do the proteins that bind to DNA segments gain access to their target DNAs? The answer, which has only become apparent since the mid-1990s, is that *chromatin contains ATP-driven complexes that remodel nucleosomes,* that is, they somehow disrupt the interactions between histones and DNA in nucleosomes to make the DNA more accessible. This may cause the histone octamer to slide along the DNA strand to a new location or even relocate to a different DNA strand. Thus, *these **chromatin-remodeling complexes** impose a "fluid" state on chromatin that maintains the DNA's overall packaging but transiently exposes individual sequences to interacting factors.*

Chromatin-remodeling complexes consist of multiple subunits. The first of them to be characterized was the yeast **SWI/SNF** complex, so called because it is essential for mating type switching (SWI for *swi*tching defective) and for growth on sucrose (SNF for *s*ucrose *n*on*f*ermenter). SWI/SNF, an 1150-kD complex of 11 different types of subunits, is essential for the expression of only ~3% of yeast genes and is not required for cell viability. However, a related complex named **RSC** (for *r*emodels the *s*tructure of *c*hromatin) is ~100 times more abundant in yeast and is required for cell viability. RSC shares two subunits with SWI/SNF, and many of their remaining subunits are homologs, including their ATPase subunits. All eukaryotes contain multiple chromatin-remodeling complexes. Biochemical studies indicate that the RSC binds tightly to nucleosomes in a 1:1 complex. Indeed, cryoelectron microscopy–based images of the yeast RSC reveal that it has an irregular shape containing a large central cavity that is remarkably complementary in size and shape to a single nucleosome core particle (Fig. 28-19).

The simultaneous release of all of the many interactions holding DNA to a histone octamer would require an enormous free energy input and hence is unlikely to occur. How, then, do chromatin-remodeling complexes function? Their various ATP-hydrolyzing translocase subunits share a region of homology with helicases (Section 25-2B), although they lack helicase activity. Nevertheless, it seems plausible that, like helicases, chromatin-remodeling complexes "walk" up DNA strands as driven by ATP hydrolysis. If such a complex were somehow tethered to a histone, this would put torsional strain on the DNA in the nucleosome, thereby decreasing its local twist (DNA supercoiling is discussed in Section 24-1C). The region of decreased twist could diffuse along the DNA wrapped around the

BOX 28-2 **PERSPECTIVES IN BIOCHEMISTRY**

X Chromosome Inactivation

Female mammalian cells contain two X chromosomes, whereas male cells have one X and one Y chromosome. *Female somatic cells, however, maintain only one of their X chromosomes in a transcriptionally active state.* Consequently, both males and females make approximately equal amounts of X chromosome-encoded gene products, a phenomenon known as **dosage compensation.**

The inactive X chromosome is visible as a highly condensed and darkly staining **Barr body** at the periphery of the cell nucleus.

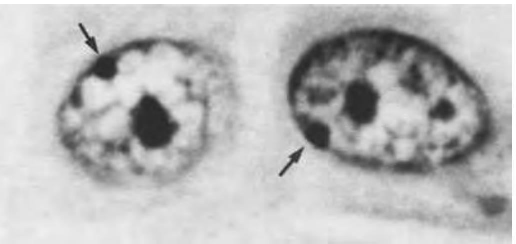

[From Moore, K.L. and Barr, M.L., *Lancet* **2,** 57 (1955).]

In marsupials (pouched mammals such as kangaroos), the Barr body is always the paternally inherited X chromosome, but in placental mammals, one randomly selected X chromosome in every somatic cell is inactivated when the embryo consists of only a few cells. The progeny of each of these cells maintain the same inactive X chromosome. Female placental animals are therefore mosaics of cloned groups of cells in which the active X chromosome is either paternally or maternally inherited. The calico cat, for example, with its patches of black and yellow fur, is almost always a female cat whose two X chromosomes specify the different coat colors.

[© Hank Delespinasse/Age Fotostock America, Inc.]

The mechanism of chromosome inactivation is only beginning to come to light. Inactivation appears to be triggered by the transcription of the ***Xist*** gene in the inactive chromosome only. The resulting *Xist* RNA coats the inactive X chromosome over its entire length but does not bind to the active X chromosome. The bound *Xist* RNA appears to recruit specific DNA-binding proteins that repress transcription, as well as variant histones. The CpG islands (Section 28-1A) within many promoters on the inactive X chromosome become methylated, probably as part of the mechanism that maintains the chromosome's inactive state in subsequent cell generations. Still, an estimated 25% of X-chromosome genes escape this repression and are expressed to some degree.

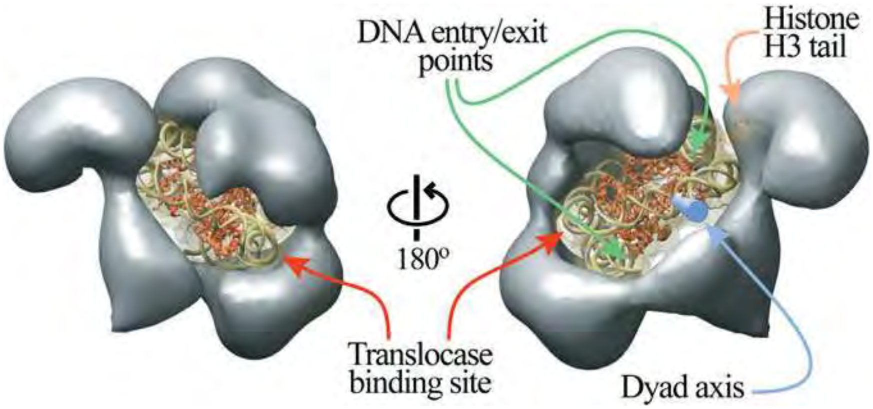

■ **Figure 28-19** | **Model of the RSC with a bound nucleosome.** The X-ray structure of the nucleosome (with the proteins shown as orange ribbons and the DNA backbone in light green) was fitted into a EM–based image of the RSC (*gray*). The two views show the back and front of the complex. The DNA's dyad (twofold) axis is represented by a blue rod, and two possible binding sites for the ATP-hydrolyzing translocase subunit are indicated. [Courtesy of Eva Nogales and Andrew Leschziner, University of California at Berkeley.]

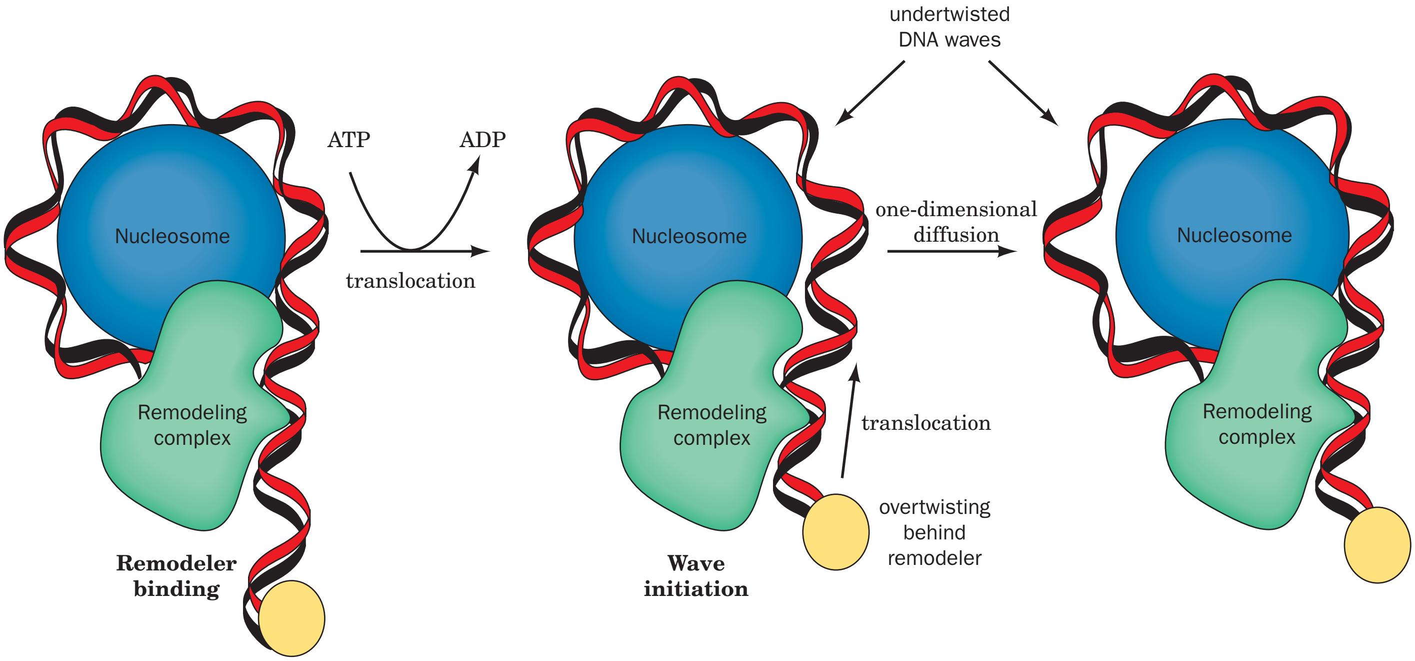

■ **Figure 28-20 | Model for nucleosome remodeling by chromatin-remodeling complexes.** The chromatin-remodeling complex (*green*) couples the free energy of ATP hydrolysis to the translocation and concomitant twisting of the DNA in the nucleosome (*blue,* only half of which is shown for clarity) as depicted by the movement of a fixed point on the DNA (*yellow ball*). This locally breaks the contacts between the histones and the DNA. The position of the undertwisted and/or bulged DNA propagates around the nucleosome in a one-dimensional wave that transiently releases the DNA from the histone as it passes with the overall effect of translocating the nucleosome along the DNA. [After a drawing by Saha, A., Wittmeyer, J., and Cairns, B.R., *Genes Dev.* **16,** 2120 (2002).]

nucleosome, thereby transiently loosening the histone octamer's grip on a segment of DNA. The torsional strain might also be partially accommodated as a writhe, which would lift a segment of DNA off the nucleosome's surface. In either case, the resulting DNA distortion could diffuse around the surface of the nucleosome in a wave that would locally and transiently release the DNA from the histone octamer as it passed (Fig. 28-20). Multiple cycles of ATP hydrolysis would send multiple DNA-loosening waves around the nucleosome, thereby sliding the nucleosome along the DNA and providing DNA-binding proteins access to the DNA.

HMG Proteins Are Architectural Proteins That Help Regulate Gene Expression. The variation of a given gene's transcriptional activity according to cell type indicates that chromosomal proteins participate in the gene activation process. Yet histones' chromosomal abundance and lack of variety make it highly unlikely that they have the specificity required for this role. Among the most common nonhistone protein components of chromatin are the members of the **high mobility group (HMG),** so named because of their high electrophoretic mobilities in polyacrylamide gels. These highly conserved, low molecular mass (<30 kD) proteins, which have the unusual amino acid composition of ~25% basic side chains and 30% acidic side chains, are relatively abundant with ~1 HMG molecule per 10 to 15 nucleosomes.

The yeast HMG protein known as **NHP6A** contains an ~80-residue structural motif called an **HMG box.** Its NMR structure in complex with DNA, determined by Juli Feigon, reveals that it causes the DNA to bend by as much as 70° toward its major groove (Fig. 28-21). Such proteins presumably facilitate the binding of other regulatory proteins to the DNA and are therefore described as **architectural proteins.** Other HMG proteins

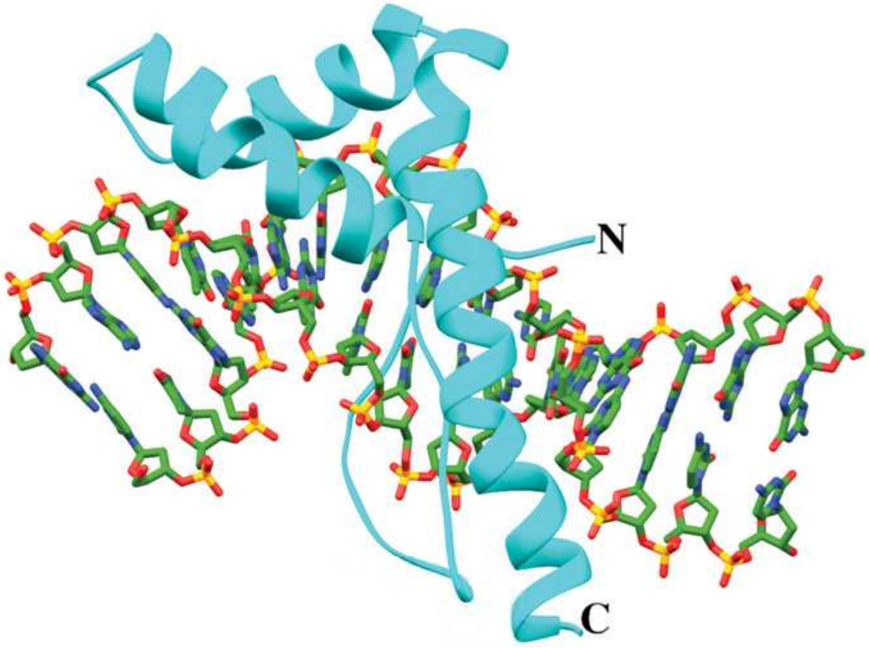

■ **Figure 28-21 | NMR structure of yeast NHP6A protein in complex with a 15-bp DNA.** The protein is drawn in ribbon form (*cyan*) and the DNA is drawn in stick form colored according to atom type (C green, N blue, O red, and P yellow). The three helices of the HMG box form an L shape, with the inside of the L inserted into the DNA's minor groove so as to bend the DNA by ~70° toward its major groove. [Based on an NMR structure by Juli Feigon, University of California at Los Angeles. PDBid 1J5N.]

differ in structure but can also alter DNA conformation by inducing it to bend, straighten, unwind, or form loops. Some HMG proteins compete with histones for DNA, thereby altering nucleosomal structure.

Histones Are Covalently Modified. The posttranslational modifications to which core histones are subject include the acetylation of specific Lys side chains, the methylation of specific Lys and Arg side chains, the phosphorylation of specific Ser and possibly Thr side chains, and the ubiquitination of specific Lys side chains (Fig. 28-22). Moreover, Lys side chains can be mono-, di-, and trimethylated and Arg side chains can be mono- and

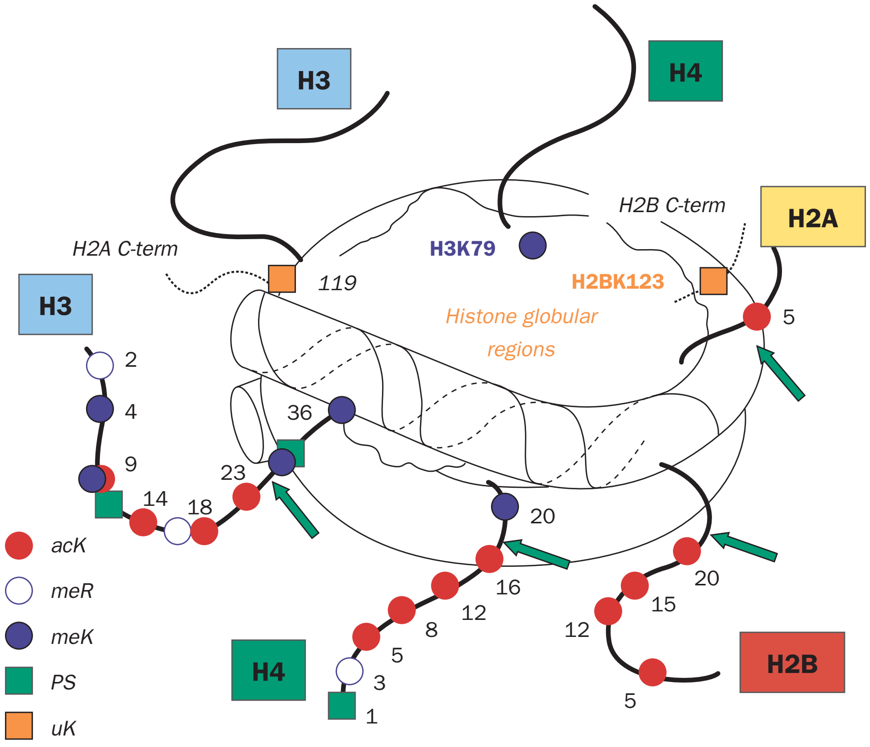

■ **Figure 28-22 | Histone modifications on the nucleosome core particle.** Posttranslational modification sites are indicated by the residue numbers and the colored symbols, which are defined in the key at the lower left (acK = acetyl-Lys, meR = methyl-Arg, meK = methyl-Lys, PS = phospho-Ser, and uK = ubiquitinated Lys). Note that H3 Lys 9 can be either methylated or acetylated. The N-terminal tail modifications are shown on only one of the two molecules of H3 and H4, and only one molecule each of H2A and H2B is shown. The C-terminal tails of one H2A and one H2B are represented by dashed lines. The green arrows indicate the sites in intact nucleosomes that are susceptible to trypsin cleavage. This cartoon summarizes data from several organisms, some of which may lack particular modifications. [Courtesy of Bryan Turner, University of Birmingham School of Medicine, U.K.]

both symmetrically and asymmetrically dimethylated. All of these modifications can be undone by the action of specific enzymes.

The core histones' N-terminal tails, as we have seen (Section 24-5C), are implicated in stabilizing the structures of both core nucleosomes and higher-order chromatin. All of the above modifications except methylations reduce (make more negative) the electronic charge of their attached side chains and hence are likely to weaken histone–DNA interactions so as to promote chromatin decondensation, although as we shall see, this is not always the case. Methyl groups, in contrast, increase the basicity and hydrophobicity of the side chains to which they are linked and hence tend to stabilize chromatin structure. Modified histone tails also interact with specific chromatin-associated nonhistone proteins in a way that changes the transcriptional accessibility of their associated genes. Internucleosome and histone–histone interactions are also likely to be affected by covalent modification of the globular cores of the histone protein, not just their tails.

The characterization of a variety of histone tail modifications led David Allis to hypothesize that *there is a* ***histone code*** *in which specific modifications evoke certain chromatin-based functions and that these modifications act sequentially or in combination to generate unique biological outcomes.* For example, uncondensed and hence transcriptionally active chromatin is associated with the acetylation of histone H3 Lys 9 and 14 and histone H4 Lys 5 and the methylation of H3 Lys 4 and H4 Arg 3; condensed and hence transcriptionally inactive chromatin is associated with the acetylation of H4 Lys 12 and the methylation of H3 Lys 9; and nucleosome deposition is associated with the phosphorylation of H3 Ser 10 and 28. It can be seen from Fig. 28-22 that there are a vast number of possible combinations of histone modifications.

Histone Acetyltransferases Are Components of Multisubunit Transcriptional Coactivators. Histone Lys side chains are acetylated in a sequence-specific manner by enzymes known as **histone acetyltransferases (HATs),** all of which employ acetyl-CoA as their acetyl group donor:

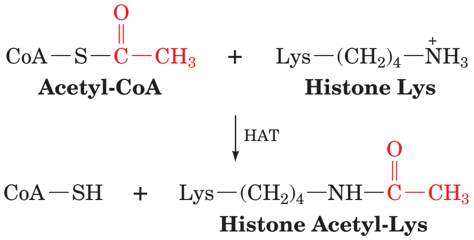

$$\underset{\textbf{Acetyl-CoA}}{\mathrm{CoA{-}S{-}\overset{O}{\overset{\|}{C}}{-}CH_3}} + \underset{\textbf{Histone Lys}}{\mathrm{Lys{-}(CH_2)_4{-}\overset{+}{N}H_3}} \xrightarrow{\text{HAT}} \mathrm{CoA{-}SH} + \underset{\textbf{Histone Acetyl-Lys}}{\mathrm{Lys{-}(CH_2)_4{-}NH{-}\overset{O}{\overset{\|}{C}}{-}CH_3}}$$

Most if not all HATs function *in vivo* as members of often large (10–20 subunits) multisubunit complexes, many of which were initially characterized as transcriptional regulators. For example, **TAF1,** the largest subunit of the general transcription factor TFIID (TAF for *T*BP-*a*ssociated *f*actor, where TBP is TATA-binding protein; Section 26-2C), is a HAT. Moreover, many **HAT complexes** share subunits. Thus, the HAT complex named **SAGA** contains **TAF5, TAF6, TAF9, TAF10,** and **TAF12** as does the **PCAF complex** with the exception that TAF5 and TAF6 are replaced in the PCAF complex by their close homologs **PAF65β** and **PAF65α.** Portions of TAF6, TAF9, and TAF12 are structural homologs of histones H3, H4, and H2B, respectively (Section 24-5). Consequently, these TAFs probably associate to form an architectural element that is common to TFIID, SAGA, and the PCAF complex and hence these complexes are likely to interact with TBP in a similar manner. The various HAT complexes presumably target their component HATs to the promoters of active genes.

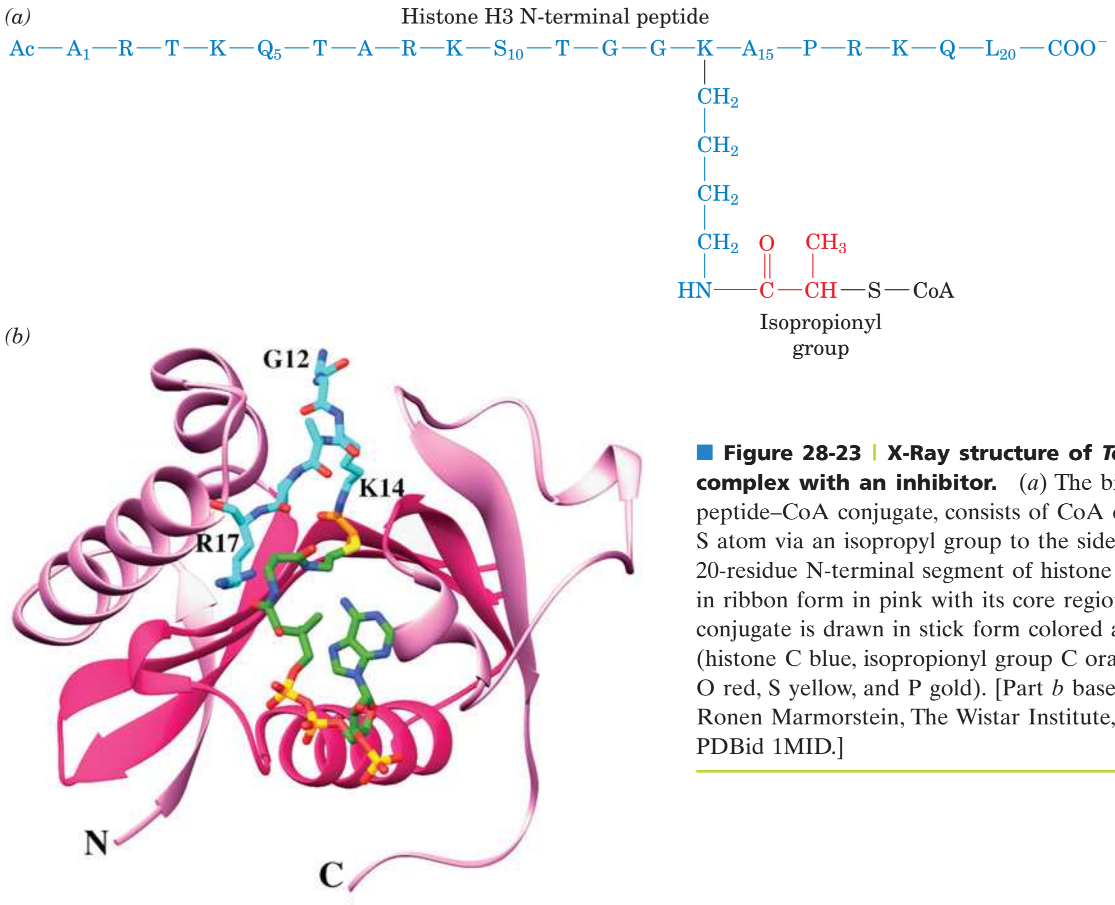
(a)
Histone H3 N-terminal peptide
Ac—A1—R—T—K—Q5—T—A—R—K—S10—T—G—G—K—A15—P—R—K—Q—L20—COO−
CH2
CH2
CH2
CH2
O
CH3
HN—C—CH—S—CoA
Isopropionyl group
(b)
G12
K14
R17
N
C

Figure 28-23 | X-Ray structure of *Tetrahymena* GCN5 in complex with an inhibitor. (*a*) The bisubstrate inhibitor, a peptide–CoA conjugate, consists of CoA covalently linked from its S atom via an isopropyl group to the side chain of Lys 14 of the 20-residue N-terminal segment of histone H3. (*b*) The protein is drawn in ribbon form in pink with its core region magenta. The peptide–CoA conjugate is drawn in stick form colored according to atom type (histone C blue, isopropionyl group C orange, CoA C green, N blue, O red, S yellow, and P gold). [Part *b* based on an X-ray structure by Ronen Marmorstein, The Wistar Institute, Philadelphia, Pennsylvania. PDBid 1MID.]

The X-ray structure of the HAT domain of *Tetrahymena thermophila* **GCN5** (residues 48–210 of the 418-residue protein) in complex with a bisubstrate inhibitor was determined by Ronen Marmorstein. The bisubstrate inhibitor (Fig. 28-23*a*) consists of CoA covalently linked from its S atom via an isopropionyl group (which mimics an acetyl group) to the side chain of Lys 14 (the acetyl group acceptor) of the 20-residue N-terminal segment of histone H3. The enzyme (Fig. 28-23*b*) is deeply clefted and contains a core region common to all HATs of known structure (magenta in Fig. 28-23*b*) that consists of a three-stranded antiparallel β sheet connected via an α helix to a fourth β strand that forms a parallel interaction with the β sheet. Only six residues of the histone tail, Gly 12 through Arg 17, are visible in the X-ray structure. The CoA moiety binds in the enzyme's cleft such that it is mainly contacted by core residues. The comparison of this structure with other GCN5-containing structures indicates that the cleft has closed down about the CoA moiety.

Bromodomains Recruit Coactivators to Acetylated Lys Residues in Histone Tails. The different patterns of histone acetylation required for different functions (the histone code) suggest that the function of histone acetylation is more complex than merely attenuating the charge–charge interactions between the cationic histone N-terminal tails and anionic DNA. In fact, there is growing evidence that specific acetylation patterns are recognized by protein modules of transcriptional **coactivators** in much the same way that specific phosphorylated sequences are recognized by protein modules such as the SH2 domain that mediates signal transduction via protein kinase cascades (Section 13-2B). Thus, nearly all HAT-associated transcriptional coactivators contain ~110-residue modules known

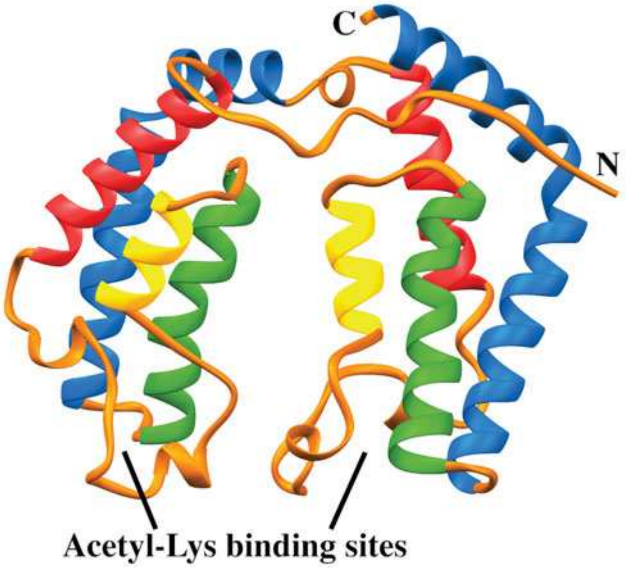

Figure 28-24 | X-Ray structure of the human TAF1 double bromodomain. Each bromodomain consists of an antiparallel four-helix bundle whose helices are colored, from N- to C-termini, red, yellow, green, and blue, with the remaining portions of the protein orange. The acetyl-Lys binding sites occupy deep hydrophobic pockets at the end of each four-helix bundle opposite its N- and C-termini. [Based on an X-ray structure by Robert Tjian, University of California at Berkeley. PDBid 1EQF.]

as **bromodomains** that specifically bind acetylated Lys residues on histones. For example, GCN5 essentially consists of a HAT domain followed by a bromodomain, whereas TAF1 consists mainly of an N-terminal kinase domain followed by a HAT domain and two tandem bromodomains.

The X-ray structure of human TAF1's double bromodomain (residues 1359–1638 of the 1872-residue protein), determined by Robert Tjian, reveals that it consists of two nearly identical antiparallel four-helix bundles (Fig. 28-24). A variety of evidence, including NMR structures of single bromodomains in complex with their target acetyl-Lys–containing peptides, indicates that the acetyl-Lys–binding site of each bromodomain occurs in a deep hydrophobic pocket that is located at the end of its four-helix bundle opposite its N- and C-termini. The double bromodomain's two binding pockets are separated by ~25 Å, which makes them ideally positioned to bind two acetyl-Lys residues that are separated by 7 or 8 residues. In fact, the N-terminal tail of histone H4 contains Lys residues at positions 5, 8, 12, and 16 (Fig. 28-22), whose acetylation is correlated with increased transcriptional activity. Moreover, the 36-residue N-terminal peptide of histone H4, when fully acetylated, binds to the TAF1 double bromodomain in 1:1 ratio with 70-fold higher affinity than to single bromodomains but fails to bind when it is unacetylated.

The foregoing structure suggests that the TAF1 bromodomains serve to target TFIID to promoters that are within or near nucleosomes [in contrast to the widely held notion that TFIID targets PICs (preinitiation complexes) to nucleosome-free regions]. Tjian has therefore postulated that the transcriptional initiation process begins with the recruitment of a HAT-containing coactivator complex by an upstream DNA-binding protein (Fig. 28-25). The HAT could then acetylate the N-terminal histone tails of nearby nucleosomes, which would recruit TFIID to an appropriately located promoter via the binding of its TAF1 bromodomains to the acetyl-Lys residues. Moreover, the TAF1 HAT activity could acetylate other nearby nucleosomes, thereby initiating a cascade of acetylation events that would render the DNA template competent for transcriptional initiation.

Histone acetylation is a reversible process. The enzymes that remove the acetyl groups from histones, the **histone deacetylases (HDACs),** promote transcriptional repression and gene silencing. Eukaryotic cells from

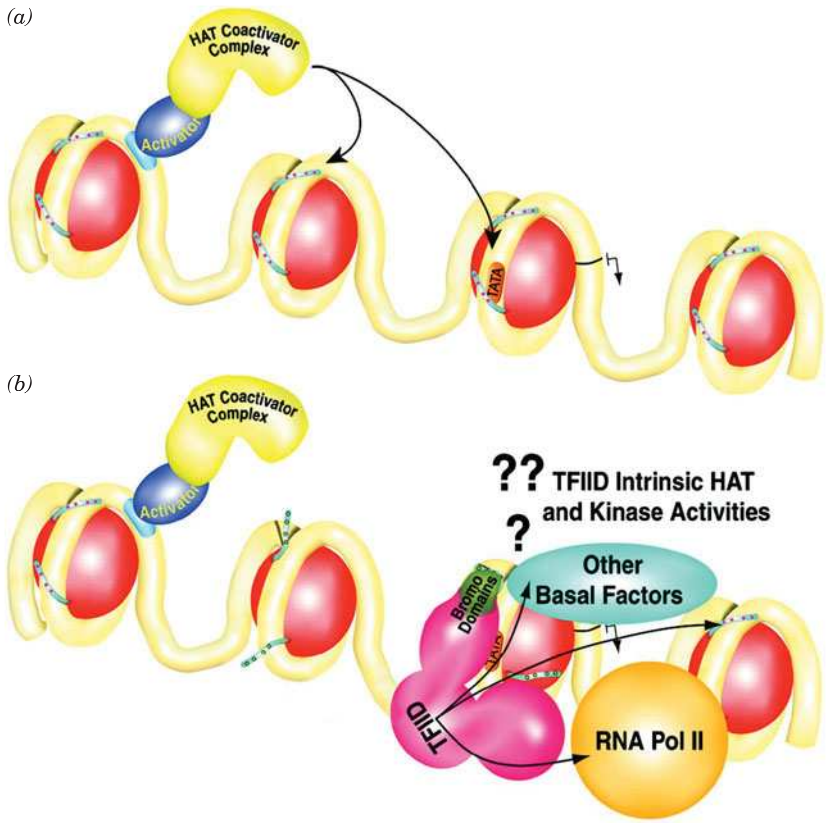

Figure 28-25 | Simplified model for the assembly of a transcriptional initiation complex on chromatin-bound templates. Here the DNA is represented by a yellow worm, the histone octamers around which the DNA wraps to form nucleosomes are shown as red spheres, and their N-terminal histone tails are drawn as short cyan rods with the red dots and small black circles representing unacetylated and acetylated Lys residues. The transcription initiation site is represented by the black ring about the DNA from which the squared-off arrow points downstream. (*a*) The process begins by the recruitment of a HAT-containing transcriptional coactivator complex (*yellow-green*) through its interactions with a DNA-binding activator protein (*purple*) that is bound to an upstream enhancer (*light blue*). The HAT coactivator complex is thereby positioned to acetylate the N-terminal tail on nearby nucleosomes (*curved arrows*). (*b*) The binding of its TAF1's bromodomains to the acetylated histone tails could then help recruit TFIID (*magenta*) to a nearby TATA box (*orange patch*). Further acetylation of nearby histone tails by the TAF1's HAT domain could help recruit other basal factors (*cyan*) and RNAP II (*orange*) to the promoter, thus stimulating PIC formation. [Modified from a drawing by Robert Tjian, University of California at Berkeley.]

yeast to humans typically contain numerous different HDACs; 10 HDACs have been identified in yeast and 17 in humans.

Histone Methylation May Silence or Activate Genes. Histone methylation at both the Lys and Arg side chains of histone H3 and H4 N-terminal tails (Fig. 28-22) tends to silence the associated genes by inducing the formation of heterochromatin, although trimethylated Lys 4 of histone H3 is associated with active genes. The enzymes mediating histone methylation, the **histone methyltransferases (HMTs),** all utilize *S*-adenosylmethionine (SAM) as their methyl donor. Thus, the lysine HMTs, the most extensively characterized HMTs, catalyze the following reaction:

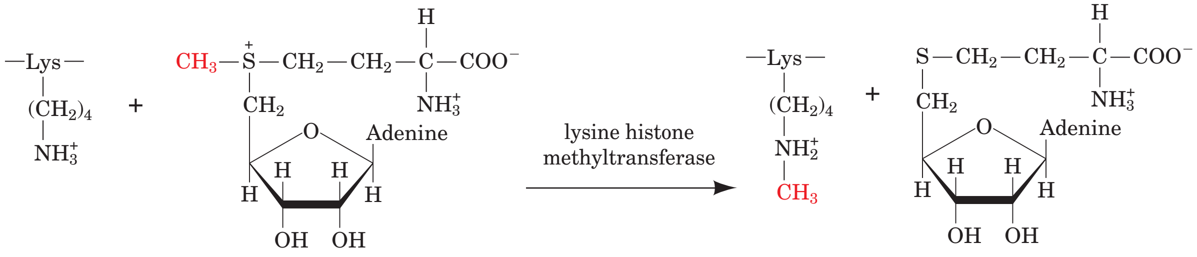

Histone Lys **S-Adenosylmethionine** **S-Adenosylhomocysteine**

These enzymes all have a so-called **SET domain,** which contains their catalytic sites.

The human lysine HMT named **SET7/9** monomethylates Lys 4 of histone H3. The X-ray structure of the SET domain of SET7/9 (residues 108–366 of the 366-residue protein) in complex with SAM and the N-terminal

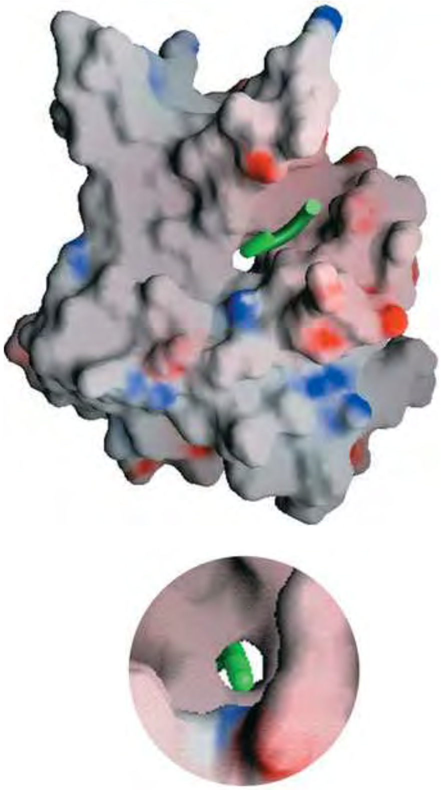

Figure 28-26 | **X-Ray structure of the human histone methyltransferase SET7/9 in complex with SAM and the histone H3 N-terminal decapeptide with its Lys 4 monomethylated.** The protein is represented by its surface diagram colored according to charge (blue most positive, red most negative, and gray neutral) and the H3 decapeptide is represented by a green ribbon. Note the narrow tunnel through the protein in which the methyl-Lys side chain is inserted. The inset below shows a close-up of this Lys access channel containing the methyl-Lys side chain (*green*) as viewed from the opposite side of the protein from the SAM-binding site. [Courtesy of Steven Gamblin, National Institute for Medical Research, London, U.K. PDBid 1O9S.]

decapeptide of histone H3 in which Lys 4 is monomethylated was determined by Steven Gamblin. Interestingly, SAM and the peptide substrate bind to opposite sides of the protein (Fig. 28-26). However, there is a narrow tunnel through the protein into which the Lys 4 side chain is inserted such that its amine group is properly positioned for methylation by SAM. The arrangement of the hydrogen bonding acceptors for the Lys amino group stabilize the methyl-Lys side chain in its observed orientation about the C_ε—N_ζ bond, thus sterically precluding the methyl-Lys group from assuming a conformation in which it could be further methylated by SAM.

Methylated histones are bound by several kinds of protein domains that recognize specific Lys residues with some preference for their mono-, di-, or trimethyl forms. The so-called **chromodomain** and the motif known as a **PHD finger** (for *p*lant *h*omeo*d*omain) both include binding sites for methylated Lys residues that can be characterized as aromatic cages (Fig. 28-27). Interestingly, the methyl-Lys binding proteins often include additional histone code–reading motifs such as a bromodomain, or a histone-modifying enzyme such as a deacetylase.

The chromodomain-containing **heterochromatin protein 1 (HP1),** which binds dimethylated H3 Lys 9, contributes to gene silencing. The bound HP1 recruits the HMT **Suv39h,** which methylates nearby nucleosomes at their H3 Lys 9 residues, thereby recruiting additional HP1, etc. This mechanism could explain why heterochromatin has a tendency to spread so as to silence neighboring genes. In transcriptionally silent chromatin, the DNA itself may also be methylated.

Figure 28-27 | **Binding sites for histone trimethyl-Lys residues.** (*a*) H3 Trimethyl-Lys 9 bound to the chromodomain of *Drosophila* heterochromatin protein 1 (HP1), and (*b*) H3 trimethyl-Lys 4 bound to a human PHD finger. The H3 trimethyl-Lys residues are drawn with C green and N blue and with the peptide backbone yellow. The aromatic side chains of HP1 and the PHD finger that cage the trimethylammonium group are drawn with C cyan, N blue, and O red. The dot surfaces delineate the van der Waals surfaces of the aromatic side chains and the trimethylammonium groups. [Part *a* based on an X-ray structure by Sepideh Khorasanizadeh, University of Virginia. PDBid 1KNE. Part *b* based on an X-ray structure by David Allis, Rockefeller University; and Dinshaw Patel, Memorial Sloan-Kettering Cancer Center, New York, New York. PDBid 2F6J.]

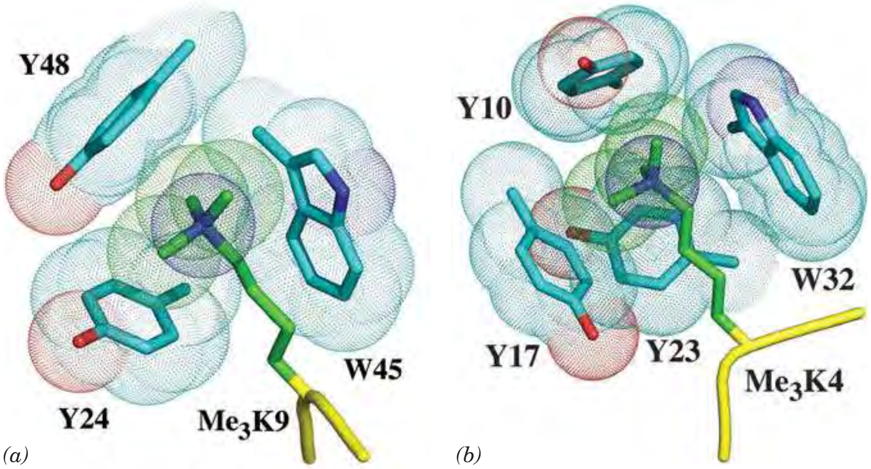

Methyltransferases Flip Their Target Bases Out of the DNA Double Helix. The methylation of DNA, as we have seen (Box 25-4), switches off eukaryotic gene expression. Eukaryotic DNAs are methylated only on their cytosine residues to form 5-methylcytosine (m^5C) residues, a modification that occurs largely on the palindromic CpG islands that commonly occur in the upstream promoter regions of genes (Section 26-2B). The enzymes that mediate these reactions, the **DNA methyltransferases (DNA MTases),** all use SAM as their methyl donor. Cells also contain **demethylases,** which catalyze the reaction

$$\text{5-Methylcytosine} + H_2O \rightarrow \text{cytosine} + HO—CH_3$$

In DNA MTase reactions, SAM reacts with the enzyme's targeted cytosine base to form a tetrahedral intermediate in which the cytosine C5 is substituted by both its original hydrogen atom and the donated methyl group. This requires that the attacking methyl group approach C5 from above or below the cytosine ring. Yet the faces of nucleic acid bases are inaccessible within the DNA double helix. Consequently, a DNA MTase must induce its target cytosine base to flip out of the double helix to where it can be methylated by SAM. Such a flipped-out intermediate is observed in the X-ray structure of the DNA MTase from *Haemophilus haemolyticus* **(M.HhaI),** determined by Richard Roberts and Xiaodong Cheng, in which the target cytosine base has been replaced by 5-fluorocytosine (Fig. 28-28). Although the normally present C5—H atom is eliminated from the

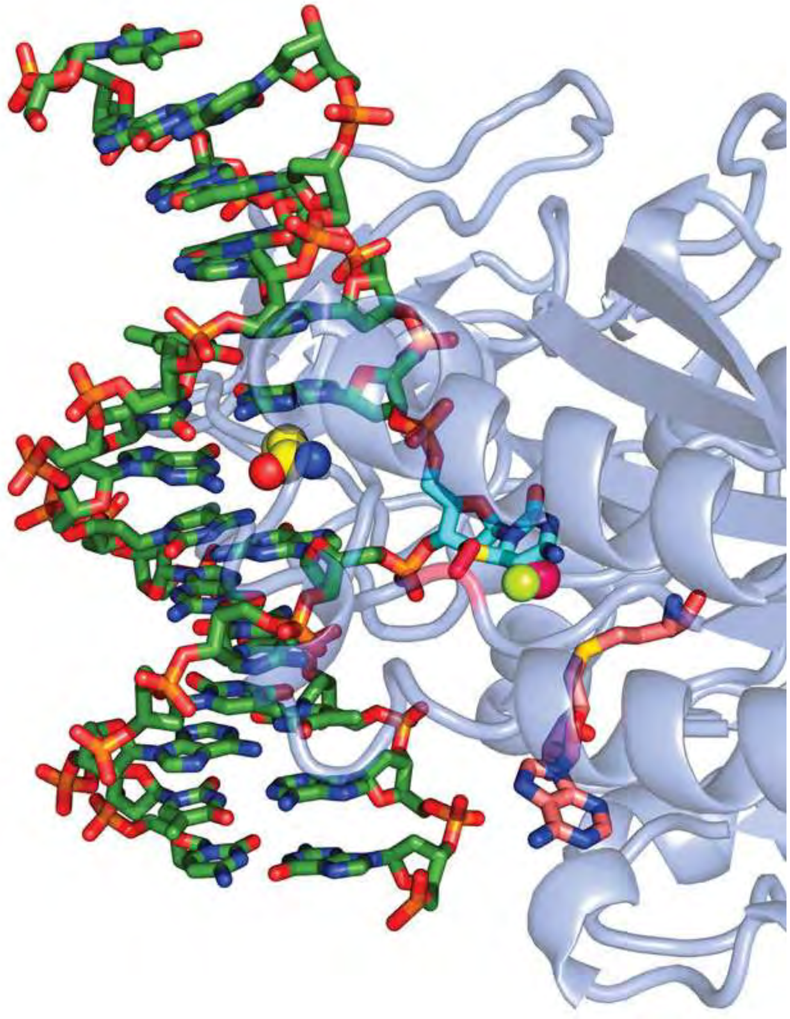

Figure 28-28 | X-Ray structure of the M.HhaI DNA methyltransferase in complex with *S*-adenosylhomocysteine and a dsDNA containing a methylated 5-fluorocytosine base at the enzyme's target site. The protein is represented by a semitransparent ribbon. The DNA is drawn in stick form colored according to atom type (C green, N blue, O red, and P orange). Its methylated 5-fluorocytidine residue (C atoms cyan) has swung out of the DNA helix into the enzyme's active site pocket, where its C6 forms a covalent bond with the S atom of an enzyme Cys residue (C atoms magenta and S yellow). The methyl group and a fluorine atom at C5 (which prevents the methylation reaction from going to completion) are represented by magenta and yellow-green spheres, respectively. The position of the flipped-out cytosine base in the DNA double helix is occupied by the side chain of a Gln residue (shown in space-filling form with C yellow), which hydrogen bonds to the "orphaned" guanine base. The *S*-adenosylmethionine, which has given up its methyl group, is drawn in stick form with its C atoms pink. [Based on an X-ray structure by Richard Roberts, New England Biolabs, Beverly, Massachusetts, and Xiaodong Cheng, Cold Spring Harbor Laboratory, Cold Spring Harbor, New York. PDBid 1MHT.]

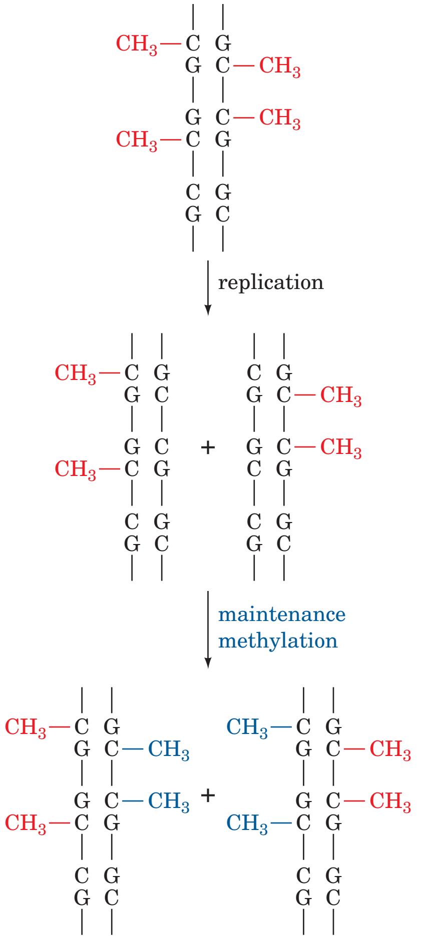

Figure 28-29 | Maintenance methylation. The pattern of methylation on a parental DNA strand induces the corresponding methylation pattern in the complementary strand. In this way, a stable methylation pattern may be maintained in a cell line.

foregoing tetrahedral intermediate as H^+ to yield the methylation reaction's m^5C product, the high electronegativity of fluorine prevents the C5—F atom from being eliminated as F^+, thereby trapping the tetrahedral intermediate on the enzyme. Certain DNA repair enzymes that act on individual DNA bases also operate by flipping their target base out the DNA helix (Section 25-5A).

DNA Methylation in Eukaryotes Is Self-Perpetuating. The palindromic nature of DNA methylation sites in eukaryotes permits the methylation pattern on a parental DNA strand to direct the generation of the same pattern in its daughter strand (Fig. 28-29). This **maintenance methylation** would result in the stable "inheritance" of a methylation pattern in a cell line and hence cause these cells to all have the same differentiated phenotype. Such changes to the genome are described as being **epigenetic** (Greek: *epi,* on or beside) because they provide an additional layer of information that specifies when and where specific portions of the otherwise fixed genome are expressed [epigenetic changes that we have already encountered are the lengthening of telomeres in germ cells (Section 25-3C) and the inactivation of a specific X chromosome in female mammals (Box 28-2)]. Epigenetic characteristics, as we shall see, are not bound by the laws of Mendelian inheritance.

There is considerable experimental evidence favoring the existence of maintenance methylation, including the observation that artificially methylated viral DNA, when taken up by eukaryotic cells, maintains its methylation pattern for at least 30 cell generations. Maintenance methylation in mammals appears to be mediated mainly by **DNMT1** protein, which has a strong preference for methylating hemimethylated substrate DNAs. In contrast, prokaryotic DNA MTases such as M.HhaI do not differentiate between hemimethylated and fully methylated substrate DNAs. The importance of maintenance methylation is demonstrated by the observation that mice that are homozygous for the deletion of the *DNMT1* gene die early in embryonic development.

The pattern of DNA methylation in mammals varies in early embryonic development. DNA methylation levels are high in mature gametes (sperm and ova) but are nearly eliminated by the time a fertilized ovum has become a **blastocyst** (a hollow ball of cells, the stage at which the embryo implants into the uterine wall; embryonic development is discussed in Section 28-4D). After that stage, however, the embryo's DNA methylation levels globally rise until, by the time the embryo has reached the developmental stage known as a **gastrula,** its DNA methylation levels have risen to adult levels, where they remain for the lifetime of the animal. This *de novo* (new) methylation appears to be mediated by two DNA MTases distinct from DNMT1 named **DNMT3a** and **DNMT3b.** An important exception to this remethylation process is that the CpG islands of germline cells (cells that give rise to sperm or ova) remain unmethylated. This ensures the faithful transmission of the CpG islands to the succeeding generation in the face of the strong mutagenic pressure of m^5C deamination (which yields T, a mutation that mismatch repair occasionally fails to correct; Box 25-5). In female mammals, the inactivation of the same X chromosome from cell generation to cell generation is, at least in part, preserved by maintenance methylation (Box 28-2).

The change in DNA methylation levels (epigenetic reprogramming) during embryonic development suggests that the pattern of genetic expression differs in embryonic and somatic cells. This explains the observed high failure rate in cloning mammals (sheep, mice, cattle, etc.) by transferring the nucleus of an adult cell into an enucleated oocyte (immature ovum). Few of these animals survive to birth, many of those that do so die shortly thereafter, and most of the ~1% that do survive have a variety of abnormalities, most prominently an unusually large size. However, the survival of any embryos at all indicates that the oocyte has the remarkable capacity to epigenetically reprogram somatic chromosomes (although it is rarely entirely successful in doing so) and that mammalian embryos are relatively tolerant of epigenetic abnormalities. Presumably, the reproductive cloning of humans from adult nuclei would result in similar abnormalities and for this reason (in addition to social and ethical prohibitions) should not be attempted.

Genomic Imprinting Results from Differential DNA Methylation. It has been known for thousands of years that maternal and paternal inheritance can differ. For example, a mule (the offspring of a mare and a male donkey) and a hinny (the offspring of a stallion and a female donkey) have obviously different physical characteristics, a hinny having shorter ears, a thicker mane and tail, and stronger legs than a mule. This is because, in mammals only, certain maternally and paternally supplied genes are differentially expressed, a phenomenon termed **genomic imprinting.** The genes that are subject to genomic imprinting are, as Rudolph Jaenisch has shown, differentially methylated in the two parents during gametogenesis, and the resulting different methylation patterns are resistant to the wave of demethylation that occurs during the formation of the blastocyst and to the wave of *de novo* methylation that occurs thereafter.

The importance of genomic imprinting is demonstrated by the observation that an embryo derived from the transplantation of two male or two female pronuclei into an ovum fails to develop (pronuclei are the nuclei of mature sperm and ova before they fuse during fertilization). Inappropriate imprinting is also associated with certain diseases. For example, **Prader-Willi syndrome (PWS),** which is characterized by the failure to thrive in infancy, small hands and feet, marked obesity, and variable mental retardation, is caused by a >5000-kb deletion in a specific region of the paternally inherited chromosome 15. In contrast, **Angelman syndrome (AS),** which is manifested by severe mental retardation, a puppetlike ataxic (uncoordinated) gait, and bouts of inappropriate laughter, is caused by a deletion of the same region from the maternally inherited chromosome 15. These syndromes are also exhibited by those rare individuals who inherit both their chromosomes 15 from their mothers for PWS and from their fathers for AS. Evidently, certain genes on the deleted chromosomal region must be paternally inherited to avoid PWS and others must be maternally inherited to avoid AS. Several other human diseases are also associated with either maternal or paternal inheritance or lack of it. Aberrant epigenetic programming may also play a role in tumor growth, as cancer cells often exhibit abnormal patterns of DNA methylation.

B | Eukaryotes Contain Multiple Transcriptional Activators

In addition to the six general transcription factors described in Section 26-2C, eukaryotic cells contain a host of other proteins that interact with DNA and/or other transcription factors to stimulate or repress the transcription of class II genes (genes that are transcribed by RNAP II). Some of these proteins bind to any available DNA containing their target sequences, whereas others must be activated and deactivated, often as part of a signal transduction pathway (Section 13-2B). These regulatory proteins are known as **activators** and **repressors,** and their target DNA sites are known as **enhancers** and **silencers,** respectively.

An enhancer typically is not essential for transcription but greatly increases its rate. Unlike promoters, which are necessarily located a short distance from the transcription start site, *enhancers (or silencers) need not have fixed positions and orientations* (Section 26-2B). For example, William Rutter linked the upstream (5′-flanking) sequences of either the insulin or the chymotrypsin gene to the sequence encoding **chloramphenicol acetyltransferase (CAT),** an easily assayed enzyme not normally present in eukaryotic cells. A plasmid containing the insulin gene sequences elicits expression of the CAT gene only when introduced into cultured cells that normally produce insulin. Likewise, the chymotrypsin recombinants are active only in chymotrypsin-producing cells. Dissection of the insulin gene control sequence indicates that the enhancer lies between positions −103 and −333 and, in insulin-producing cells only, it stimulates the transcription of the CAT gene with little regard to its position and orientation relative to the promoter. Because so many enhancers are located upstream of transcribed sequences, the proteins that bind to them are often called **upstream transcription factors.**

Upstream Transcription Factors Act Cooperatively with Each Other and the PIC. How do upstream transcription factors stimulate (or inhibit) transcription? *Evidently, when these proteins bind to their target DNA sites in the vicinity of a PIC (in some cases, many thousands of base pairs distant), they somehow activate (or repress) its component RNAP II to initiate transcription.* Transcription factors may bind cooperatively to each other and/or the PIC, thereby synergistically stimulating (or repressing) transcriptional initiation. Indeed, molecular cloning experiments indicate that many enhancers and silencers consist of segments (modules) whose individual deletion reduces but does not eliminate enhancer/silencer activity. *Such complex arrangements presumably permit transcriptional control systems to respond to a variety of stimuli in a graded manner.* In some cases, however, several transcription factors together with architectural proteins cooperatively assemble on an ~100-bp enhancer to form a multisubunit complex known as an **enhanceosome,** in which the absence of a single subunit all but eliminates its ability to stimulate transcriptional initiation at the associated promoter. Thus, enhanceosomes function more like on/off switches rather than providing a graded response. Enhanceosomes may also contain coactivators and/or corepressors, proteins that do not bind to DNA but, rather, interact with proteins that do so to activate or repress transcription.

The functional properties of many upstream transcription factors are surprisingly simple. They typically consist of (at least) two domains:

1. A DNA-binding domain that specifically binds to the protein's target DNA sequence (several such domains are described in Section 24-4C).
2. A domain containing the transcription factor's activation function. Sequence analysis indicates that many of these **activation domains** have conspicuously acidic surface regions whose negative charges, if mutationally increased or decreased, respectively raise or lower the transcription factor's activity. This suggests that the associations between these transcription factors and a PIC are mediated by relatively nonspecific electrostatic interactions rather than by conformationally more demanding hydrogen bonds. Other types of activation domains have also been characterized, including those with Gln-rich regions and those with Pro-rich regions.

The DNA-binding and activation functions of eukaryotic transcription factors can be physically separated (which is why they are thought to occur on different domains). In fact, a genetically engineered hybrid protein, containing the DNA-binding domain of one transcription factor and the activation domain of a second, activates the same genes as the first transcription factor. Moreover, it makes little functional difference as to whether the activation domain is placed on the N-terminal side of the DNA-binding domain or on its C-terminal side. This geometric permissiveness in the binding between the activation domain and its target protein is also indicated by the observation that transcription factors are largely insensitive to the orientations and positions of their corresponding enhancers relative to the transcriptional start site. Of course, *the DNA between an enhancer and its distant transcriptional start site must be looped around for an enhancer-bound transcription factor to interact with the promoter-bound PIC* (Section 26-2C).

The synergy (cooperativity) of multiple transcription factors in initiating transcription may be understood in terms of a simple recruitment model. Suppose an enhancer-bound transcription factor increases the affinity with which a PIC binds to the enhancer's associated promoter so as to increase the rate at which the PIC initiates transcription there by a factor of 10. Then, if another transcription factor binding to a different enhancer subsite likewise increases the initiation rate by a factor of 20, both transcription factors acting together will increase the initiation rate by a factor of 200. *In this way, a limited number of transcription factors can support a much larger number of transcription patterns.* Transcriptional activation, according to this model, is essentially a mass action effect: The binding of a transcription factor to an enhancer increases the transcription factor's effective concentration at the associated promoter (the DNA holds the transcription factor in the vicinity of the promoter), which consequently increases the rate at which the PIC binds to the promoter. This explains why a transcription factor that is not bound to DNA (or even lacks a DNA-binding domain) inhibits transcriptional initiation. Such unbound transcription factors compete with DNA-bound transcription factors for their target sites and thereby reduce the rate at which the PIC is recruited to the associated promoter. This phenomenon, which is known as **squelching,** is apparently why transcription factors in the nucleus are almost always bound to inhibitors unless they are actively engaged in transcriptional initiation.

Mediator Links Transcriptional Activators and RNAP II. Eukaryotic genomes encode as many as several thousand transcriptional regulators for class II genes (e.g., Fig. 28-3). However, activators fail to stimulate transcription by a reconstituted PIC *in vitro.* Evidently, an additional factor is required to do so. *Indeed, genetic studies in yeast by Roger Kornberg led him to discover an ~20-subunit, ~1000-kD complex named* ***Mediator,*** *whose presence is required for transcription from nearly all class II gene promoters in yeast.* Mediator, which is therefore considered to be a coactivator, binds to the C-terminal domain (CTD) of RNAP II's β′ subunit (Section 26-2A). Further investigations revealed that multicellular organisms contain multisubunit complexes that function similarly to yeast Mediator and which share many of their numerous subunits. Moreover, many of their subunits are related, albeit distantly, to those of yeast Mediator. *Mediators apparently function as adaptors that bridge DNA-bound transcriptional regulators and RNAP II so as to influence (induce or inhibit) the formation of a stable PIC at the associated promoter. They* *thereby function to integrate the various signals implied by the binding of these transcriptional regulators to their target DNAs.*

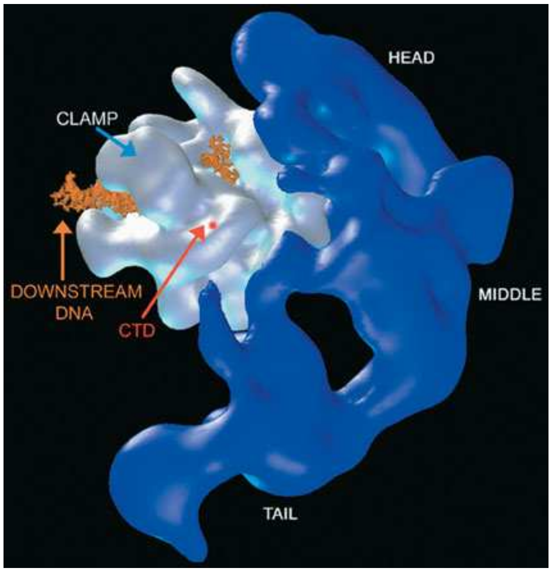

■ **Figure 28-30 | Electron microscopy–based projection of the yeast RNA polymerase II–Mediator complex at 35 Å resolution.** The head, middle, and tail domains of Mediator (*blue*) are clearly distinguishable. The independently determined EM-based image of RNAP II (*silver*) is oriented to best match the polymerase density in the lower resolution holoenzyme image. Promoter DNA (*orange*) was modeled in, based on the structure of the yeast RNAP II elongation complex (Fig. 26-12*b*). Note that the RNAP II's DNA-binding cleft remains fully accessible in the holoenzyme complex. The red dot labeled CTD indicates the position where RNAP II's C-terminal domain extends from the enzyme. [Courtesy of Francisco Asturias, The Scripps Research Institute, La Jolla, California, and Roger Kornberg, Stanford University School of Medicine.]

The EM-based image of the yeast RNAP II–Mediator complex (Fig. 28-30), determined by Kornberg and Francisco Asturias, reveals that Mediator consists of three domains known as the head, middle, and tail domains. The head domain interacts closely with the RNAP II, although >75% of RNAP II's surface remains accessible for interaction with other components of the PIC. The tail domain, however, appears not to contact RNAP II at all. Including Mediator, the transcriptional machinery for class II genes comprises nearly 60 polypeptides with an aggregate molecular mass of ~3 million D (by comparison, the eukaryotic ribosome is only slightly larger, with a molecular mass of ~4.2 million D; Table 27-5).

Insulators Limit the Effects of Enhancers and Stop Heterochromatin Spreading. Enhancers function independently of their position relative to the promoter. So what prevents an enhancer from affecting the transcription of all the genes in its chromosome? Conversely, heterochromatin, as we have seen (Section 28-3A), appears to be self-nucleating. What prevents heterochromatin from spreading into neighboring segments of euchromatin? Experiments in which DNA sequences near *Drosophila* genes were rearranged revealed that short (<2 kb) segments of DNA known as **insulators** define the boundaries of functional units for transcription. Inserting an insulator between a gene and its upstream enhancer blocks the effect of the enhancer on transcription. Insulators may also prevent heterochromatin from spreading. For example, the **HS4** insulator in the chicken β-globin gene cluster recruits HATs that acetylate H3 Lys 9 on nearby nucleosomes (which is associated with transcriptional activity), thereby blocking their methylation (which induces heterochromatin formation). The mechanism of action of insulators is enigmatic. Presumably, it is not the insulators themselves but the proteins that bind to them that form the active insulator elements. Indeed, the HAT-recruiting activity of HS4 is distinct from its enhancer-blocking function, which is mediated by the binding of an 11-zinc finger protein named **CTCF** to a different subsite of HS4 than that to which HATs bind.

Many Signal Transduction Pathways Activate Transcription Factors. A variety of signaling pathways, including some involving steroid hormones, heterotrimeric G proteins, receptor tyrosine kinases (RTKs), and phosphoinositide cascades (Chapter 13), result in the activation (or inactivation) of transcription factors. In this way, extracellular factors such as hormones can influence gene expression inside a cell. We have already seen that the Ras signaling cascade (Fig. 13-7) results in the phosphorylation of several transcription factors, including Fos, Jun, and Myc, thereby modulating their activities. The sterol regulatory element binding protein (SREBP), which regulates the expression of the genes involved in cholesterol biosynthesis by binding to their sterol regulatory elements (SREs; Section 20-7B), is also an inducible transcription factor. In the following paragraphs, we discuss two additional examples of signaling pathways that activate transcription factors.

The JAK-STAT Pathway Relays Cytokine-Based Signals. The protein growth factors that regulate the differentiation, proliferation, and activities of numerous types of cells, most conspicuously white blood cells, are known as **cytokines.** The signal that certain cytokines have been extracellularly bound by their cognate receptors is transmitted within the cell, as James Darnell elucidated, by the **JAK-STAT pathway. Cytokine receptors** form complexes with proteins of the **Janus kinase (JAK)** family of **nonreceptor tyrosine kinases (NRTKs),** so named because each of its four ~1150-residue members has two tyrosine kinase domains (Janus is the two-faced Roman god of gates and doorways), although only the C-terminal domain is functional. **STATs** (for *s*ignal *t*ransducers and *a*ctivators of *t*ranscription) comprise a family of seven ~800-residue proteins that are the only known transcription factors whose activities are regulated by Tyr phosphorylation and that have SH2 domains.

The JAK-STAT pathway functions as is diagrammed in Fig. 28-31:

1. Ligand binding induces the cytokine receptor to dimerize (or, in some cases, to trimerize or even tetramerize).
2. The cytokine receptor's two associated JAKs are thereby brought into apposition, whereon they reciprocally phosphorylate each other and then their associated receptors, a process resembling the autophosphorylation of dimerized RTKs (Section 13-2A).
3. STATs bind to the phospho-Tyr group on their cognate activated

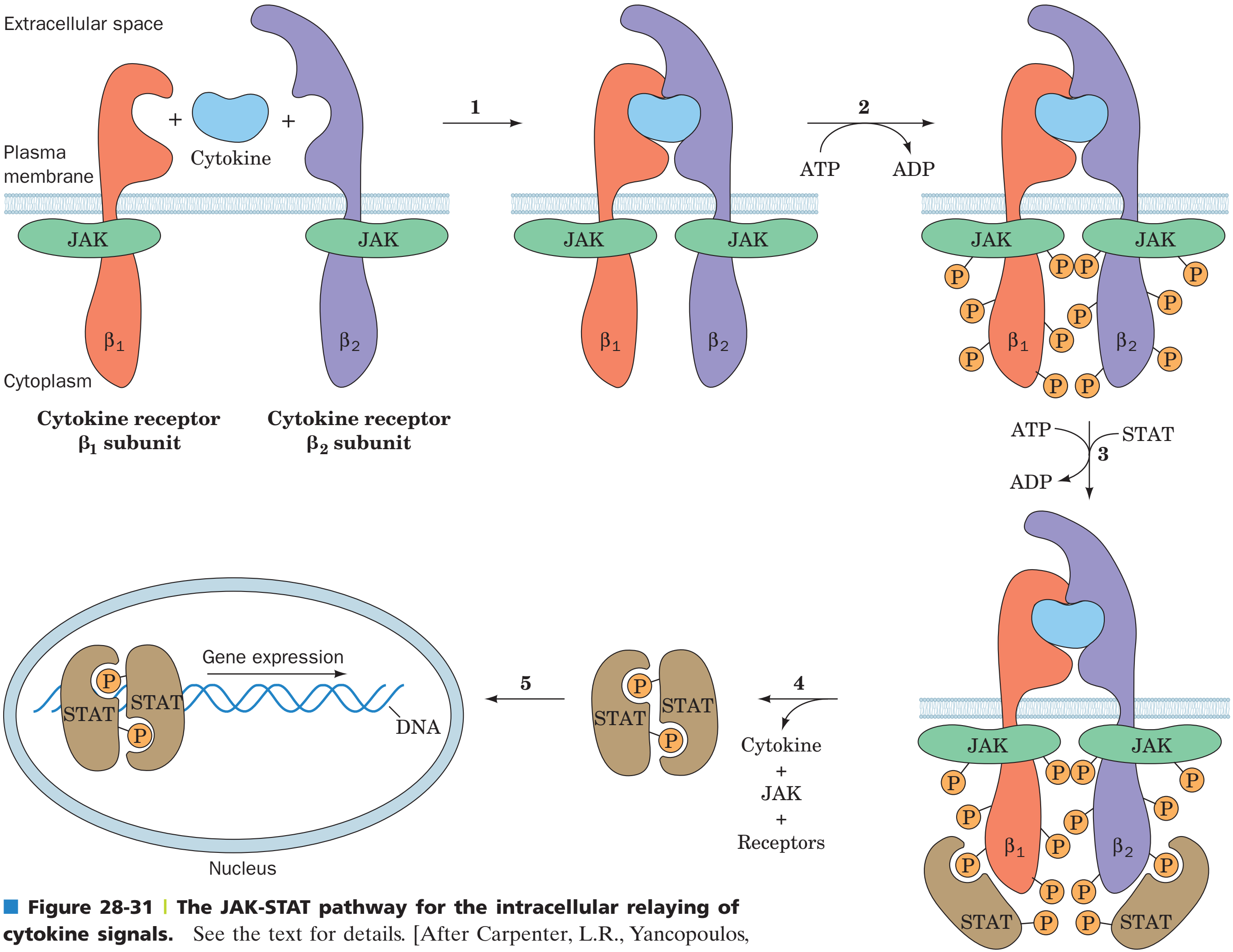
Extracellular space
Plasma membrane
Cytoplasm
+
Cytokine
+
JAK
JAK
β_1
β_2
Cytokine receptor β_1 subunit
Cytokine receptor β_2 subunit
1
2
ATP
ADP
P
3
ATP
STAT
ADP
4
Cytokine + JAK + Receptors
STAT
5
Gene expression
DNA
Nucleus

■ **Figure 28-31** | **The JAK-STAT pathway for the intracellular relaying of cytokine signals.** See the text for details. [After Carpenter, L.R., Yancopoulos, G.D., and Stahl, N., *Adv. Prot. Chem.* **52,** 109 (1999).]

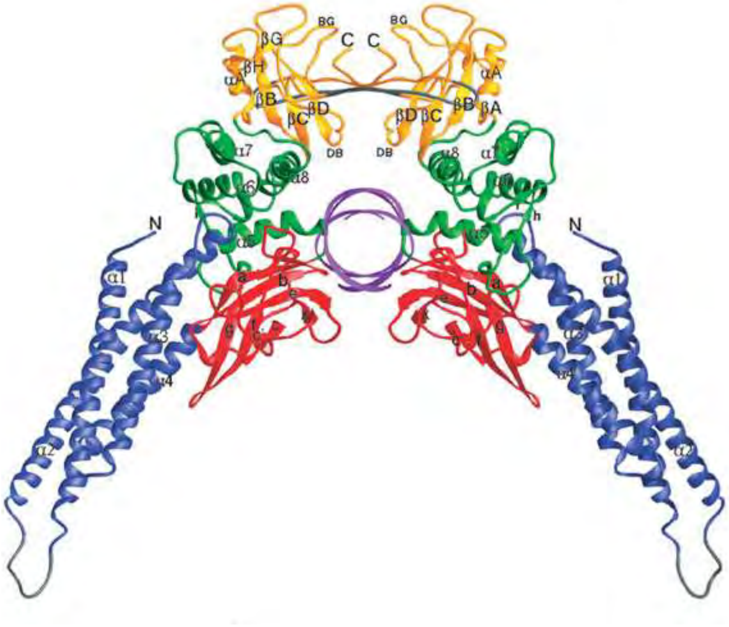

Figure 28-32 | X-Ray structure of the Stat3β homodimer bound to a 17-bp DNA containing its 9-bp target sequence. The complex is viewed along the helix axis of the DNA, which is represented by a purple ribbon. The protein's various domains are drawn in different colors. The phosphorylatable Tyr residues are located in the SH2 domains (*yellow*), which mediate the protein's dimerization. Note how the STAT dimer binds the DNA in a sort of scissors grip. [Courtesy of Christoph Müller, European Molecular Biology Laboratory, Grenoble, France. PDBid 1BG1.]

receptor via their SH2 domain and are then phosphorylated on a conserved Tyr residue by the associated JAK.

4. Following their dissociation from the receptor, the phosphorylated STATs homo- or heterodimerize via the association of their phospho-Tyr residue with the SH2 domain on the opposing subunit.
5. The STAT dimers are then translocated to the nucleus, where the now functional transcription factors specifically bind to 9-bp DNA segments with the consensus sequence TTCCGGGAA, thereby inducing the transcription of their associated genes.

Like many other components of signal transduction pathways, the STAT signal is inactivated through the action of phosphatases so that a STAT typically remains active for only a few minutes. The X-ray structure of the STAT named **Stat3β,** determined by Christoph Müller, is shown in Fig. 28-32.

Nuclear Receptors Are Activated by Hormones. The **nuclear receptor superfamily,** which occurs in animals ranging from worms to humans, is composed of >150 proteins that bind a variety of hormones including steroids (glucocorticoids, mineralocorticoids, estrogens, and androgens; Section 9-1E), **thyroid hormones** such as thyroxine (Fig. 4-15) that stimulate metabolism, and vitamin D (Section 9-1E), all of which are nonpolar molecules. The nuclear receptors, many of which activate distinct but overlapping sets of genes, share a conserved modular organization that includes, from N- to C-terminus, a poorly conserved activation domain, a highly conserved DNA-binding domain, a connecting hinge region, and a ligand-binding domain. The DNA-binding domains each contain eight Cys residues that, in groups of four, tetrahedrally coordinate two Zn^{2+} ions. Many members of the nuclear receptor superfamily recognize specific DNA segments known as **hormone response elements (HREs)** that have the half-site consensus sequences 5′-AGAACA-3′ for steroid receptors and 5′-AGGTCA-3′ for other nuclear receptors. These sequences are arranged in direct repeats (→*n*→), inverted repeats (→*n*←), and everted repeats (←*n*→), where *n* represents a 0- to 8-bp spacer (usually 1–5 bp) to whose length a specific receptor is targeted. **Steroid receptors** bind to their hormone response elements as homodimers, whereas other nuclear receptors do so as homodimers, as heterodimers, and in a few cases as monomers.

Steroid hormones, being nonpolar, readily pass through cell membranes into the cytosol or nucleus, where they bind to their receptors (although in some cases, they may also interact with cell-surface receptors). In the absence of their cognate steroid, these receptors are part of large multiprotein complexes. Steroid binding releases these receptors, whereon they dimerize and, if they are cytoplasmic, enter the nucleus, where they bind to their target HREs so as to induce, or in some cases repress, the transcription of the associated genes.

The X-ray structure of the 86-residue DNA-binding domain of rat **glucocorticoid receptor** (**GR;** which regulates carbohydrate, protein, and lipid metabolism) in complex with DNA containing two ideal 6-bp **glucocorticoid response element (GRE)** half-sites arranged in inverted repeats was determined by Paul Sigler and Keith Yamamoto (Fig. 28-33). The protein forms a symmetric dimer involving protein–protein contacts even though it exhibits no tendency to dimerize in the absence of DNA (NMR measurements indicate that the contact region is flexible in solution). Each protein subunit consists of two structurally distinct modules, each nucleated by a Zn^{2+} coordination center, that closely associate to form a compact globular fold. The C-terminal module provides the entire dimerization interface and also makes several contacts with the phosphate groups of the DNA backbone. The N-terminal module, which is also anchored to the phosphate backbone, makes all of the GR's sequence-specific interactions with the GRE via three side chains that extend from the N-terminal α helix, its recognition helix, which is inserted into the GRE's major groove.

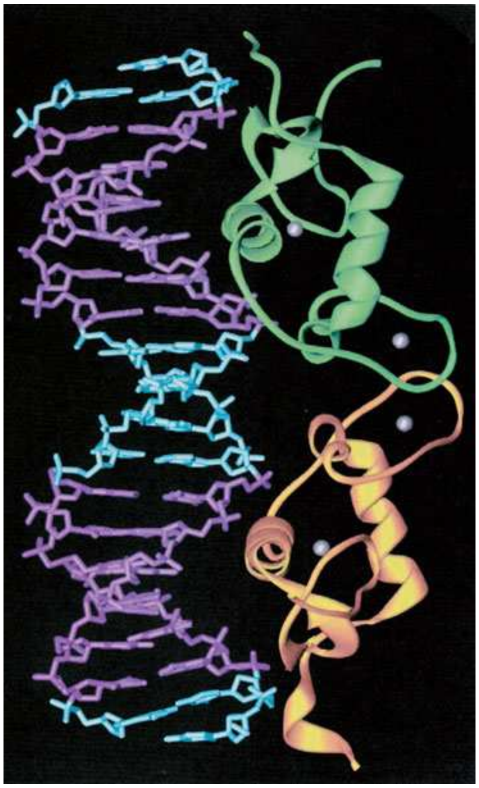

Figure 28-33 | X-Ray structure of the dimeric glucocorticoid receptor DNA-binding domain in complex with DNA. The 18-bp DNA, which has a single nucleotide overhang at each of its 5′ ends, contains two symmetrical 6-bp glucocorticoid response element half-sites (*magenta*) separated by a 4-bp spacer (*cyan*). The protein subunits, which are drawn as green and gold ribbons, each contain two zinc fingers (Section 24-4C) in which each Zn^{2+} ion (*silver spheres*) is tetrahedrally liganded by four Cys side chains. Note how the glucocorticoid receptor's two N-terminal helices are inserted into successive major grooves in a manner reminiscent of the recognition helices of prokaryotic helix–turn–helix (HTH) domains (Section 24-4B). [Based on an X-ray structure by Paul Sigler, Yale University, and Keith Yamamoto, University of California at San Francisco. PDBid 1GLU.] **See Interactive Exercise 56.**

Afterword. As we have seen, eukaryotic transcriptional initiation is an astoundingly complex process that involves large segments of DNA as well as the synergistic participation of numerous multisubunit complexes comprising several hundred often loosely or sequentially interacting polypeptides (i.e., histones, the PIC, Mediator, transcription factors, architectural factors, coactivators, corepressors, chromatin-remodeling complexes, and histone-modifying enzymes). Despite the extensive characterization of many of these factors, we are far from having a more than rudimentary understanding of how these various components interact *in vivo* to transcribe only those genes required by their cell under its particular circumstances in the appropriate amounts and with the proper timing. Nevertheless, an increase in the complexity of transcriptional regulation—rather than an increase in gene number per se—is likely to be at least partially responsible for the vast differences in morphology and behavior among nematodes, fruit flies, and humans, which have comparable numbers of genes (Table 28-1).

C | Posttranscriptional Control Mechanisms Include RNA Degradation

Although most regulation of gene expression in eukaryotes occurs at the level of transcription, additional control mechanisms act after an RNA transcript has been synthesized. In this section, we consider several of these mechanisms, including mRNA degradation, RNA interference, and control of translation initiation. We have already discussed alternative mRNA splicing (Section 26-3A) as a posttranscriptional mechanism for modulating gene expression through the selection of different exons.

mRNAs Are Degraded at Different Rates. The range of mRNA stability in eukaryotic cells, measured in half-lives, varies from a few minutes to many hours or days. The mRNA molecules themselves appear to contain elements that dictate their decay rates. These elements include the poly(A) tail, the 5′ cap, and sequences that are located within the coding region.

A major route for mRNA degradation begins with the progressive removal of its poly(A) tail, a process catalyzed by **deadenylases** that appear to be located throughout the cytosol. When the residual poly(A) tail is less than ~10 nt long and hence no longer capable of interacting with poly(A) binding protein (Section 26-3A), the mRNA becomes a substrate for a **decapping enzyme,** which hydrolytically excises the mRNA's m^7GDP cap. The resulting RNA is then degraded by exonucleases. In yeast and other cells, a decapping enzyme, 5′ → 3′ exonucleases, and accessory proteins appear to form a complex called a **processing body,** or **P body,** that may function either to degrade mRNA or to store it in an inactive form.

How does degradation of the 3′ end of the mRNA stimulate decapping at the 5′ end? *In vivo,* as we have seen (Section 27-4A), the translation initiation factor eIF4G interacts with both poly(A) binding protein and cap binding protein, thereby circularizing the mRNA so that events at the 3′ end can be coupled to events at the 5′ end.

Proteins that bind to AU-rich sequences in the 3′ untranslated region of the mRNA also appear to increase or decrease the rate of mRNA degradation, although their exact action is not understood. In some cases, RNA secondary structure and RNA-binding proteins—which may be susceptible to modification by cellular signaling pathways—play a role in regulating mRNA stability. mRNAs that cannot be translated due to the presence of a premature Stop codon are specifically targeted for degradation (Box 28-3).

BOX 28-3 PERSPECTIVES IN BIOCHEMISTRY

Nonsense-Mediated Decay

Errors during DNA replication, transcription, or mRNA splicing can give rise to a Stop codon either through substitution of one nucleotide for another or through frameshifting. "Premature" Stop codons that interrupt a coding sequence may account for as many as one-third of human genetic diseases. Interestingly, eukaryotic mRNAs with premature Stop codons rarely produce the corresponding truncated polypeptide because the mRNA is destroyed through **nonsense-mediated decay (NMD)** soon after its synthesis.

How do cells distinguish a premature Stop codon from a normal Stop codon at the end of the coding sequence? Experiments suggest that the signal for NMD depends on RNA splicing. Following intron removal, an **exon-junction protein complex (EJC)** containing splicing factors and other components remains associated with each exon–exon junction, even after the mRNA has been exported to the cytosol for translation. An EJC following a Stop codon apparently marks the transcript for destruction.

A revised model for NMD proposes that quality control occurs before the mRNA leaves the nucleus. Although the bulk of translation occurs in the cytosol, *an estimated 10 to 15% of total translation in mammalian cells takes place inside the nucleus.* During nuclear translation, a ribosome paused at a Stop codon may be converted to a "surveillance" complex that then scans the rest of the mRNA for the presence of an EJC. If an EJC is detected, the mRNA is degraded by removal of its 5′ cap and 3′ poly(A) tail and by the action of exonucleases.

Two other quality-control mechanism also depend on translation. mRNAs that lack Stop codons entirely are subject to **nonstop decay.** When the ribosome reaches the 3′ end of the defective mRNA, a protein known as **Ski7p,** which structurally resembles the release factor eRF3, binds to the A site and recruits a nuclease complex called an **exosome** to degrade the mRNA. In yeast, a mechanism known as **no-go decay** deals with mRNAs that include an obstacle such as a stable stem–loop that halts translation. In this case, the mRNA is cleaved by an endonuclease associated with the stalled ribosome.

RNA Interference Is a Type of Posttranscriptional Gene Silencing. In recent years it has become increasingly clear that noncoding RNAs can have important roles in controlling gene expression. One of the first indications of this phenomenon occurred in Richard Jorgensen's attempt to genetically engineer more vividly purple petunias by introducing extra copies of the gene that directs the synthesis of the purple pigment. Unexpectedly, the resulting transgenic plants had variegated or entirely white flowers. Apparently, the purple-making genes switched each other off. This result was at first attributed to the well-known phenomenon in which **antisense RNA** (RNA that is complementary to a portion of an mRNA) prevents the translation of the corresponding mRNA because the ribosome cannot translate double-stranded RNA. However, injecting **sense RNA** (RNA with the same sequence as the mRNA) into experimental organisms such as the nematode *C. elegans* also blocked protein production. Since the added RNA somehow interferes with gene expression, this phenomenon is known as **RNA interference (RNAi).** RNAi is now known to occur in all eukaryotes.

Further experiments by Andrew Fire and Craig Mello revealed that double-stranded RNA is even more effective than either of its component strands alone at interfering with gene expression. In fact, RNAi can be induced by just a few molecules of double-stranded RNA, indicating that RNAi is a catalytic rather than a stoichiometric phenomenon.

RNA interference is not merely an artifact of genetic engineering. In many cells, naturally occurring small RNA molecules, called **short interfering RNAs (siRNAs)** or **micro RNAs (miRNAs),** depending on their origin, down-regulate gene expression by binding to complementary mRNA molecules. Thousands of miRNAs, ranging in length from 18 to 25 nucleotides, have been identified in mammals, although their mRNA targets are only just beginning to be characterized.

Several Nucleases Participate in RNAi. Work with exogenous double-stranded RNA in *C. elegans* and *Drosophila* has led to the elucidation of the following pathway for RNAi (Fig. 28-34):

1. The trigger double-stranded RNA, as Phillip Zamore discovered, is chopped up into $\sim$21- to 23-nt fragments (that is, siRNAs), each of whose strands has a 5′ phosphate and a 2-nt overhang at its 3′ end. The cleavage reaction is catalyzed by an ATP-dependent RNase named **Dicer.** Model-building studies based on homologous RNases suggest that Dicer functions as a homodimer whose active sites are separated by a distance that corresponds to $\sim$22 nucleotides of an RNA helix.
2. An siRNA is transferred to a 250- to 500-kD enzyme complex known as the **RNA-induced silencing complex (RISC).** RISC has at least four protein components, one of which is an ATP-dependent RNA helicase that is

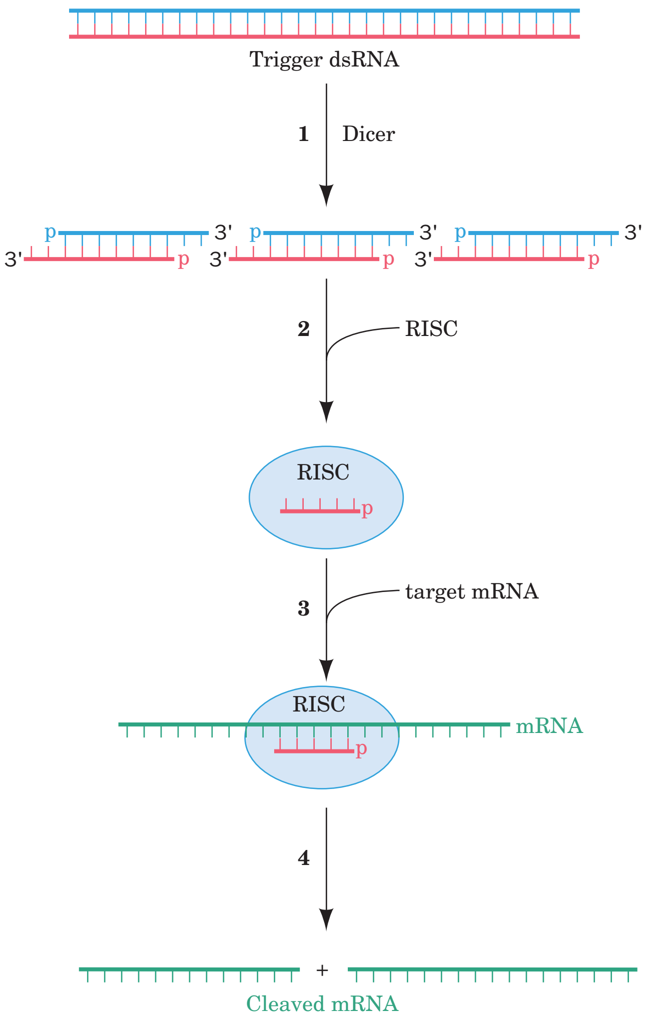

Figure 28-34 | **A mechanism of RNA interference.** See the text for details. ATP is required for Dicer-catalyzed cleavage of RNA and for RISC-associated helicase unwinding of double-stranded RNA. Depending on the species, the mRNA may not be completely degraded.

probably responsible for generating single-stranded siRNA. In some species, but apparently not in humans, the original siRNA signal is amplified by the action of an **RNA-dependent RNA polymerase.**

3. The antisense strand of the siRNA guides the RISC to an mRNA with the complementary sequence.
4. An endonuclease component of RISC cleaves the mRNA, probably opposite the bound siRNA. The cleaved mRNA is then further degraded by cellular nucleases, thereby preventing its translation.

Although the molecular machinery involved in RNAi is highly conserved from yeast to humans, variations abound, even within a single organism. For example, different Dicer enzymes can potentially generate different lengths of siRNAs, which may differ in their gene-silencing activities. The exact length of the siRNA, or the degree to which its sequence exactly complements the mRNA sequence, may determine whether a corresponding mRNA is completely degraded or just rendered nontranslatable.

The ease with which RNAi can be induced by exogenous RNAs suggests that the pathway may have arisen as a defense against viruses. In many eukaryotes, the major source of double-stranded RNA is RNA viruses, many of which encode their own RNA-dependent RNA polymerase to convert their single-stranded genome into double-stranded RNA. In fact, many plant viruses contain genes that suppress various steps of RNAi and that are therefore essential for pathogenesis.

RNAi Has Numerous Applications. RNAi has become the method of choice for "knocking out" specific genes in plants and invertebrates. For example, in *C. elegans,* RNAi has been used to systematically inactivate over 16,000 of its ~19,000 protein-coding genes in an attempt to assign a function to each gene. *C. elegans* is particularly amenable to the RNAi approach, since these worms eat *E. coli* cells, and it is relatively easy to genetically engineer the bacterial cells to express double-stranded RNA that becomes part of the worms' diet. One limitation of the RNAi method is that only gene inactivation—rather than gene activation—can be examined.

Manipulating the RNAi pathway in mammals is more difficult, mainly due to the difficulty of delivering double-stranded RNA to cells and eliciting more than transient gene silencing. To complicate matters, mammalian cells have additional pathways for dealing with foreign RNA, which result in nonspecific degradation of RNA and cessation of all translation (these responses probably also help prevent infection by RNA viruses). Nevertheless, experiments have demonstrated that it is possible to use RNAi to block the liver's inflammatory response to a hepatitis virus, at least in mice, and to prevent HIV replication in cultured human cells. One challenge for the future is to devise protocols for more specific and longer-lasting gene silencing that would make it possible to prevent viral infections or to block the effects of disease-causing mutant genes.

mRNA Translation May Be Controlled. In some cells, altering the rates of mRNA production or degradation does not provide the necessary level of control. For example, the early embryonic development of sea urchins, insects, and frogs depends on the rapid translation of mRNA that has been stockpiled in the oocyte. The mRNA is stored in inactive form in association with proteins but on fertilization becomes available for translation. This permits embryogenesis to commence immediately, without waiting for mRNAs from paternally supplied genes to be synthesized.

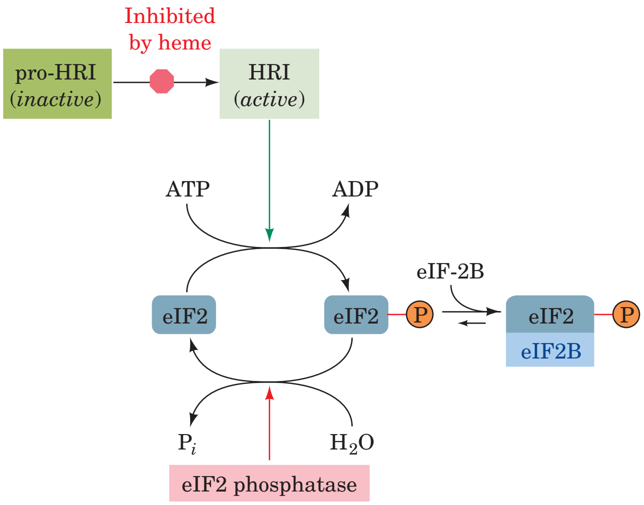

Figure 28-35 | **A model for heme-controlled protein synthesis in reticulocytes.**

Globin synthesis in reticulocytes (immature red blood cells) also proceeds rapidly, but only if heme is available. The inhibition of globin synthesis occurs at the level of translation initiation. In the absence of heme, reticulocytes accumulate a protein, **heme-regulated inhibitor (HRI).** HRI is a kinase that phosphorylates a specific Ser residue, Ser 51, on the α subunit of eIF2 (the initiation factor that delivers GTP and Met–$\text{tRNA}_\text{i}^\text{Met}$ to the ribosome; Section 27-4A).

Phosphorylated eIF2 participates in translation initiation in much the same way as unphosphorylated eIF2, but it is not regenerated normally. At the completion of the initiation process, unmodified eIF2 exchanges its bound GDP for GTP in a reaction mediated by another initiation factor, **eIF2B:**

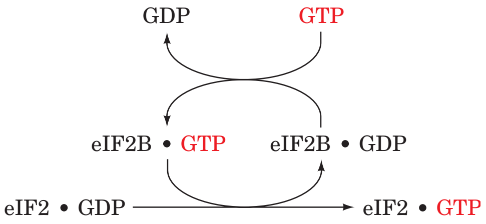

Phosphorylated eIF2 forms a much tighter complex with eIF2B than does unphosphorylated eIF2. This sequesters eIF2B (Fig. 28-35), which is present in lesser amounts than is eIF2, thereby preventing regeneration of the eIF2 · GTP required for translation.

In the presence of heme, the heme-binding sites in HRI are occupied, which inactivates the kinase. The eIF2 molecules that are already phosphorylated are reactivated through the action of **eIF2 phosphatase,** which is unaffected by heme. The reticulocyte thereby coordinates its synthesis of globin and heme.

D | Antibody Diversity Results from Somatic Recombination and Hypermutation

As described in Section 7-3B, an individual can generate an extraordinary number of different antibody molecules from a limited number of immunoglobulin gene segments. This feat is accomplished through an unusual mutation process and through **somatic recombination** in cells of the immune system. Homologous recombination (Section 25-6A), a fundamental feature of reproduction in multicellular organisms, occurs only in germline cells. The mechanism whereby a developing B lymphocyte "selects" light and heavy chain gene segments for expression is described below. Similar events occur in T lymphocytes to generate a large number of unique T cell receptors.

Immunoglobulin Chain Genes Are Assembled from Multiple Gene Segments. One of the two types of immunoglobulin light chains, the **κ chain,** is encoded by four exons (Fig. 28-36):

1. A **leader** or **L_κ segment,** which encodes a 17- to 20-residue hydrophobic signal peptide. This polypeptide directs newly synthesized κ chains to the endoplasmic reticulum and is then excised (Section 9-4D).
2. A **V_κ segment,** which encodes the first 95 residues of the κ chain's 108-residue variable region.
3. A **joining** or **J_κ segment,** which encodes the variable region's remaining 13 residues.
4. The **C_κ segment,** which encodes the κ chain's constant region.

In embryonic tissues (which do not make antibodies), these exons occur in clusters. The human κ chain gene family contains ~40 functional L_κ and V_κ segments, separated by introns, with the L_κ–V_κ units separated from each other by ~7-kb spacers. This sequence of exon pairs is followed, well downstream, by 5 J_κ segments at intervals of ~300 bp, a 2.4-kb spacer, and a single C_κ segment.

The assembly of a κ chain mRNA is a complex process involving both somatic recombination and selective mRNA splicing (Section 26-3A) over several cell generations. The first step of this process, which occurs in B cell progenitor cells, is an intrachromosomal recombination that joins an L_κ–V_κ unit to a J_κ segment and deletes the intervening DNA sequences

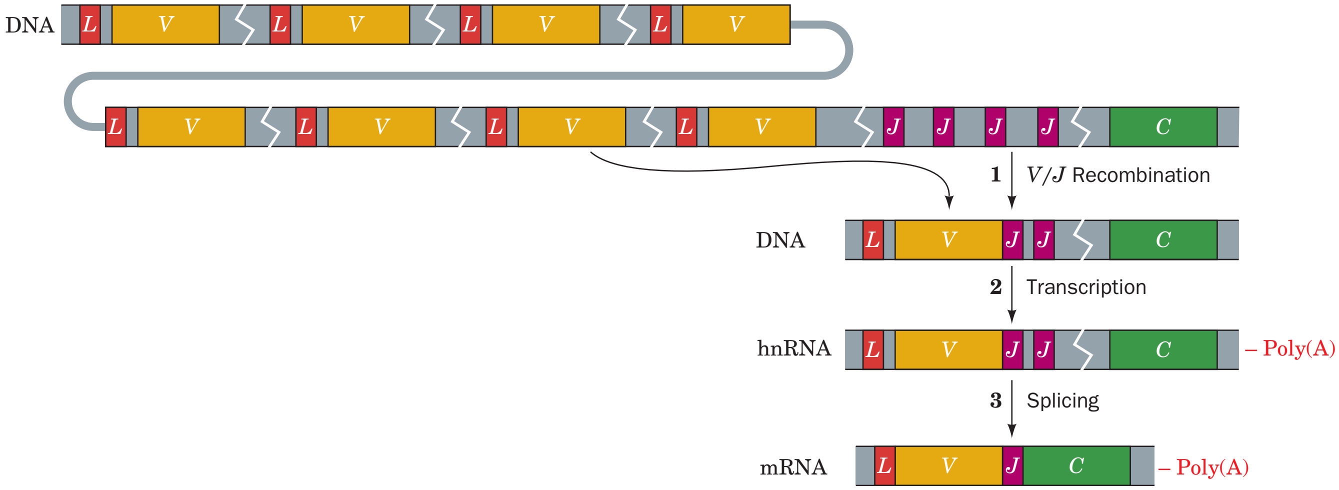

Figure 28-36 | The organization and rearrangement of the κ chain gene family in humans. The germline κ chain gene family consists of ~40 sequential pairs of L_κ and V_κ gene segments followed by 5 J_κ segments and a C_κ segment. **(1)** During lymphocyte differentiation, a single L_κ–V_κ unit is joined to a J_κ unit through somatic recombination. In the progeny B cells, the rearranged gene is transcribed **(2)** and spliced **(3)** to join the previously selected L_κ, V_κ, and J_κ exons with the C_κ exon.

(Fig. 28-36). Then, in later cell generations, the entire modified gene is transcribed and the resulting transcript is selectively spliced so as to join the L_κ–V_κ–J_κ unit to the C_κ segment. The L_κ and V_κ segments are also spliced together in this step, yielding an mRNA that encodes one of each of the four elements of a κ chain gene.

The joining of 1 of 40 functional V_κ segments to 1 of 5 J_κ segments can generate only 40 × 5 = 200 different κ chains, far less than the number observed. However, studies of many joining events involving the same V_κ and J_κ segments revealed that *the V/J recombination site is not precisely defined; the two gene segments can join at different points* (Fig. 28-37). Consequently, the amino acids specified by the codons in the vicinity of the *V*/*J* joint, which corresponds to the third hypervariable loop (Fig. 7-40), depend on which nucleotides are supplied by the germline V_κ segment and which are supplied by the germline J_κ segment. Assuming that this junctional flexibility increases the possible κ chain diversity 10-fold, the expected number of possible different κ chains is increased to around 40 × 5 × 10 = 2000.

The other type of immunoglobulin light chain, the **λ chain,** is similarly encoded by a gene family containing $\boldsymbol{L_\lambda}$, $\boldsymbol{V_\lambda}$, $\boldsymbol{J_\lambda}$, and $\boldsymbol{C_\lambda}$ segments whose recombination likewise yields a large number of possible polypeptides.

Heavy chain genes are assembled in much the same way as are light chain genes but with the additional inclusion of an ~13-bp **diversity** or ***D* segment** between their V_{H} and J_{H} segments. The human heavy chain gene family consists of clusters of ~65 different functional L_{H}–V_{H} units, ~27 *D* segments, 6 J_{H} segments, and 8 C_{H} segments (Fig. 28-38). Germline V_{H}, *D*, and J_{H} segments are joined in a particular order (*D* is joined to J_{H} before V_{H} is joined to DJ_{H}), and the joining sites are subject to the same junctional flexibility as are light chain *V*/*J* sites. Thus the number of possible different heavy chains is around $65 \times 27 \times 6 \times 8 \times 10^2 = 8.4 \times 10^6$.

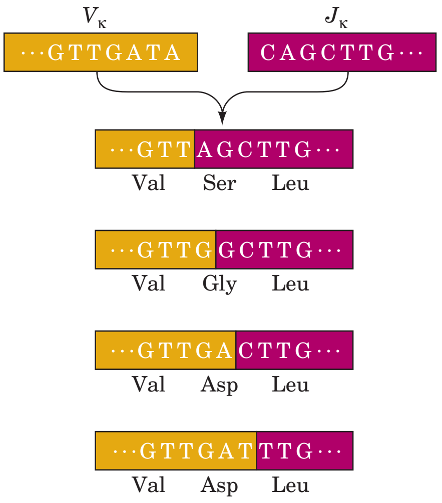

Figure 28-37 | Variation at the V_κ/J_κ joint. The point at which the V_κ and J_κ sequences somatically recombine varies by several nucleotides, thereby giving rise to different nucleotide sequences in the active κ gene. In this example of junctional flexibility, the second amino acid can be Ser, Gly, or Asp.

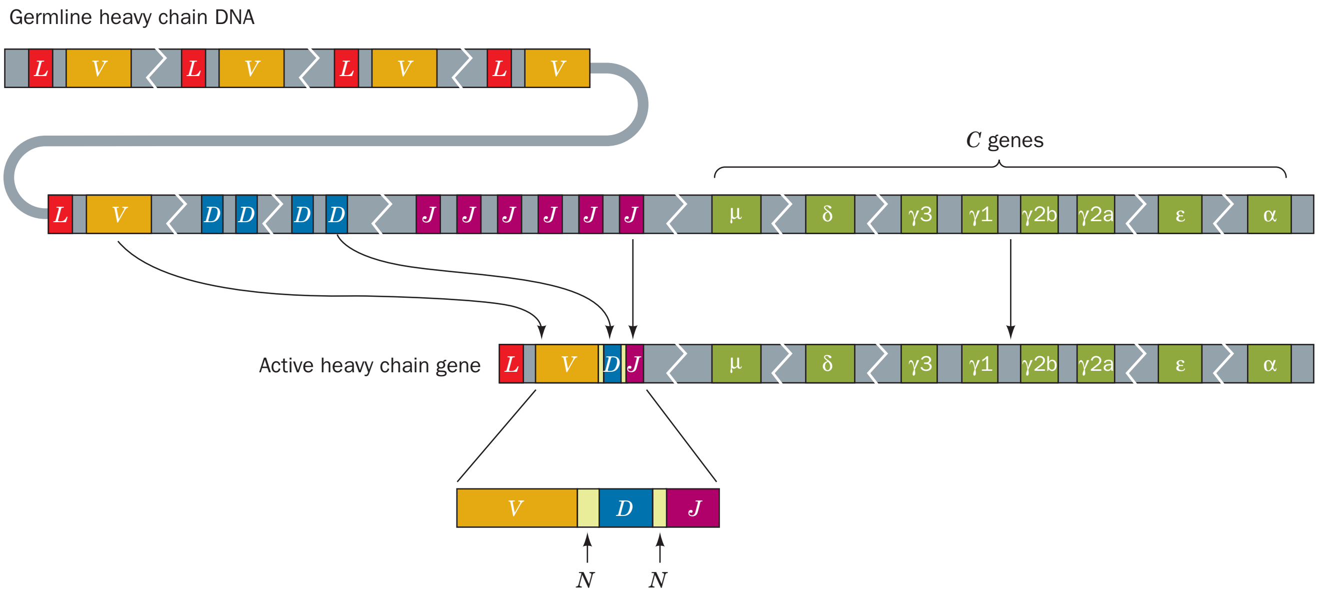

Figure 28-38 | The organization and rearrangement of the heavy chain gene family in humans. This gene family consists of ~65 sequential pairs of L_{H} and V_{H} gene segments followed by ~27 *D* segments, 6 J_{H} segments, and 8 C_{H} segments (one for each class or subclass of heavy chains; Table 7-2). During lymphocyte differentiation, an L_{H}–V_{H} unit is joined to a *D* segment and a J_{H} segment. In this process, the *D* segment becomes flanked by short stretches of random sequence called *N* regions. In the B cell and its progeny, transcription and splicing join the L_{H}–V_{H}–N–D–N–J_{H} unit to one of the 8 C_{H} gene segments.

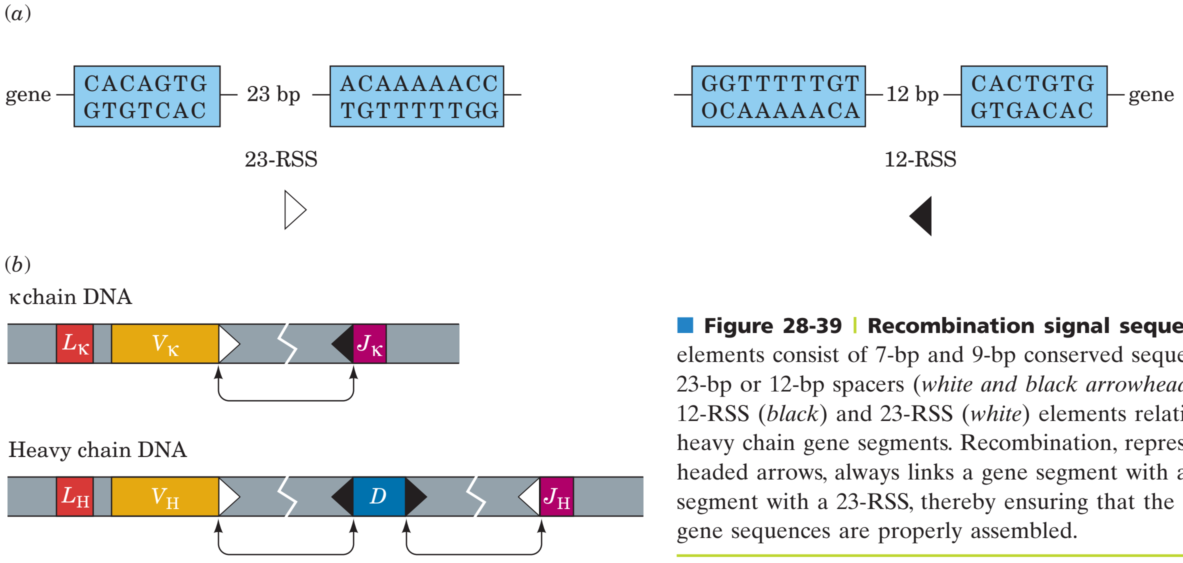

Figure 28-39 | Recombination signal sequences. (*a*) The RSS elements consist of 7-bp and 9-bp conserved sequences separated by 23-bp or 12-bp spacers (*white and black arrowheads*). (*b*) Locations of 12-RSS (*black*) and 23-RSS (*white*) elements relative to light chain and heavy chain gene segments. Recombination, represented by the double-headed arrows, always links a gene segment with a 12-RSS to a gene segment with a 23-RSS, thereby ensuring that the V_κ/J_κ and $V_H/D/J_H$ gene sequences are properly assembled.

Somatic Recombination Occurs at Specific Sequences. Highly conserved sequences flanking the *V*, *D*, and *J* gene segments act as **recombination signal sequences (RSS;** Fig. 28-39*a*). Each RSS consists of a palindromic heptamer and an AT-rich nonamer separated by either 12 bp (corresponding to ~1 turn of the DNA helix) or 23 bp (corresponding to ~2 helical turns). The recombination machinery joins a segment with a so-called 12-RSS to a segment with a 23-RSS. Because each V_κ gene segment has a 12-RSS and each J_κ segment has a 23-RSS, somatic recombination cannot join two V_κ segments or two J_κ segments. Similarly, the distribution of 12-RSS and 23-RSS elements in heavy chain gene segments is such that V_H must join to D_H, and D_H to J_H, which precludes V_H/J_H joining (Fig. 28-39*b*).

Recombination requires enzymes that are synthesized only in developing lymphocytes, as well as ubiquitous DNA repair proteins. All ***V(D)J* joining** reactions are catalyzed by an evolutionarily conserved ***V(D)J* recombinase** system. Indeed, David Baltimore discovered two proteins, **RAG1** and **RAG2** (RAG for *r*ecombination *a*ctivating *g*enes), that work in concert to recognize the RSS elements of two different gene segments, align them, and catalyze DNA cleavage. This process is assisted by HMG proteins **HMG1** and **HMG2,** which appear to bend the DNA. Under laboratory conditions, RAG1 and RAG2 can catalyze transposition, that is, the relocation of a DNA segment to another DNA molecule (Section 25-6C), consistent with the proposal that the RAG proteins originated as a transposon that appeared in vertebrates around 450 million years ago.

During recombination, the two RSS elements are neatly excised, but their adjacent coding sequences may be trimmed by nucleases and unevenly joined, thereby contributing to junctional flexibility (Fig. 28-37). The trimming and ligating reactions are not unique to lymphocytes but apparently make use of a variety of DNA repair enzymes that function in all cells (Section 25-5).

In addition, a few nucleotides may be added to the recombination joints, either as part of the DNA-repair process or, in the case of heavy chain gene assembly, by the action of the lymphocyte-specific enzyme **terminal deoxynucleotidyl transferase.** This DNA polymerase is unusual in that it does not require a template. It may add up to 15 nucleotides at the V_H/D_H and D_H/J_H joints, which, of course, greatly increases the potential for sequence diversity in the encoded variable region of the immunoglobulin chain.

Hypermutation Is a Further Source of Antibody Diversity. Despite the enormous antibody diversity generated by somatic recombination, immunoglobulins are subject to even more variation that arises as the B cells undergo cell division. The amino acid sequences of the variable regions of both heavy and light chains are more diverse than is expected from their original germline nucleotide sequences. Indeed, these regions mutate at rates of up to 10^{-3} base changes per nucleotide per cell generation, rates that are at least a millionfold higher than the rates of spontaneous mutation in other genes. B cells and/or their progenitors apparently possess enzymes that mediate this **somatic hypermutation** of immunoglobulin gene segments. The mutations, which are mostly nucleotide substitutions, occur throughout the *V*/*J* and *V*/*D*/*J* regions but are concentrated at the sequences corresponding to the three hypervariable loops of each chain. DNA sequences in other genes do not seem to be affected.

Somatic hypermutation appears to act over many cell generations after antigen stimulation. Because B cells producing antibodies with high affinity for their antigen tend to proliferate faster than B cells producing poorly binding antibodies, the pool of antibody molecules becomes exquisitely tailored to a particular antigen over time. The diversity arising from somatic recombination, with its junctional flexibility, and from hypermutation thereby permits an individual's immune system to cope, in a kind of Darwinian struggle, with the rapid mutation rates of pathogenic microorganisms.

■ CHECK YOUR UNDERSTANDING

Why is chromatin remodeling necessary for efficient gene expression?
Describe how histone modifications can affect the structure of nucleosomes and the function of transcription factors.
Summarize the role of DNA methylation in epigenetic inheritance and imprinting.
Explain why eukaryotic gene expression requires proteins in addition to the six general transcription factors.
Why is the spacing between enhancers and promoters variable?
Describe the steps of RNA interference.
Describe how antibody diversity is generated. List the responsible enzymatic activities that are unique to lymphocytes.

4 The Cell Cycle, Cancer, and Apoptosis

In addition to selecting *which* genes to express from among the thousands that are present in its genome, a cell must decide *when* to express them. Thus a cell can undertake a particular developmental program or respond effectively to changing conditions. The events of the eukaryotic cell cycle, encompassing normal and abnormal cell reproduction, as well as cell death, illustrate how particular gene products regulate a cell's activities at different times.

LEARNING OBJECTIVES

- Understand that cyclins and cyclin-dependent kinases regulate progress through the cell cycle.
- Understand that tumor suppressors such as p53 alter gene expression to arrest the cell cycle.
- Understand that apoptosis leads to cell death in response to internal or external signals.
- Understand that developmental programs are genetically controlled in a sequential fashion.

A | Progress through the Cell Cycle Is Tightly Regulated

The **cell cycle,** the general sequence of events that occur during the lifetime of a eukaryotic cell, is divided into four distinct phases (Fig. 28-40):

1. Mitosis and cell division occur during the relatively brief **M phase** (for mitosis).

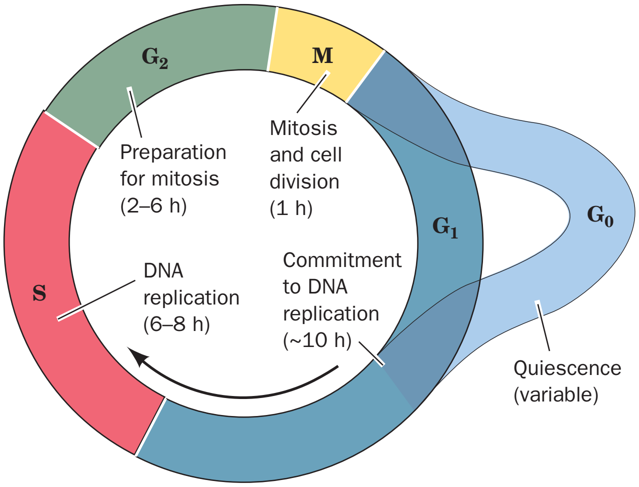
G_2
M
Preparation for mitosis (2–6 h)
Mitosis and cell division (1 h)
G_1
G_0
S
DNA replication (6–8 h)
Commitment to DNA replication (~10 h)
Quiescence (variable)

■ **Figure 28-40 | The eukaryotic cell cycle.** Cells may enter a quiescent phase (G_0) rather than continuing about the cycle.

2. This is followed by the **G_1 phase** (for gap), which covers the longest part of the cell cycle.
3. G_1 gives way to the **S phase** (for synthesis), which, in contrast to events in prokaryotes, *is the only period in the cell cycle when DNA is synthesized.*
4. During the relatively short **G_2 phase,** the now tetraploid cell prepares for mitosis. It then enters M phase once again and thereby commences a new round of the cell cycle.

The cell cycle for cells in culture typically occupies a 16- to 24-h period. In contrast, cell cycle times for the different types of cells in a multicellular organism may vary from as little as 8 h to >100 days. Most of this variation occurs in the G_1 phase. Moreover, many terminally differentiated cells, such as neurons or muscle cells, never divide; they assume a quiescent state known as the **G_0 phase.**

Progression through the cell cycle is triggered by external as well as internal signals. In addition, the cell cycle has a series of **checkpoints** that monitor its progress and the health of the cell and arrest the cell cycle if certain conditions have not been satisfied. For example, G_2 has a checkpoint that prevents the initiation of M until all of the cell's DNA has been replicated, thereby ensuring that both daughter cells will receive a full complement of DNA. Similarly, a checkpoint in M prevents mitosis until all chromosomes have properly attached to the mitotic spindle (if this were not the case, even for one chromosome, one daughter cell would lack this chromosome and the other would have two, both deleterious if not lethal conditions). Checkpoints in G_1 and S also arrest the cell cycle in response to damaged DNA so as the give the cell time to repair the damage (Section 25-5). In the cells of multicellular organisms, if after a time the checkpoint conditions have not been met, the cell may be directed to commit suicide, a process named **apoptosis** (see below), thereby preventing the proliferation of an irreparably damaged and hence dangerous (e.g., cancerous) cell.

The Activities of Cyclin-Dependent Protein Kinases Change throughout the Cell Cycle. The progression of a cell through the cell cycle is regulated by proteins known as **cyclins** and **cyclin-dependent protein kinases (Cdks).** Cyclins are so named because they are synthesized during one phase of the cell cycle and are completely degraded during a succeeding phase (protein degradation is discussed in Section 21-1). A particular cyclin specifically binds to and thereby activates its corresponding Cdk(s), which are Ser/Thr protein kinases, to phosphorylate their target nuclear proteins. These proteins, which include histone H1, several oncogene proteins (see below), and proteins involved in nuclear disassembly and cytoskeletal rearrangement, are thereby activated to carry out the processes making up that phase of the cell cycle.

The human Cdk named **Cdk2** is activated by the binding of **cyclin A** and by phosphorylation of its Thr 160 as catalyzed by **Cdk-activating kinase** (**CAK;** this kinase is itself a complex of **cyclin H** and **Cdk7**). Phosphorylation of Cdk2 residues Thr 14 and Tyr 15 negatively regulates Cdk2 activity. The X-ray structure of unphosphorylated Cdk2 in complex with ATP but in the absence of cyclin A (Fig. 28-41*a*) closely resembles that of the catalytic subunit of protein kinase A (PKA; Fig. 13-21). However, Cdk2 is inactive as a kinase in part because access of protein substrates to the γ-phosphate of the bound ATP is blocked by a 19-residue protein loop dubbed the **T loop** (which contains Thr 160). Phosphorylation

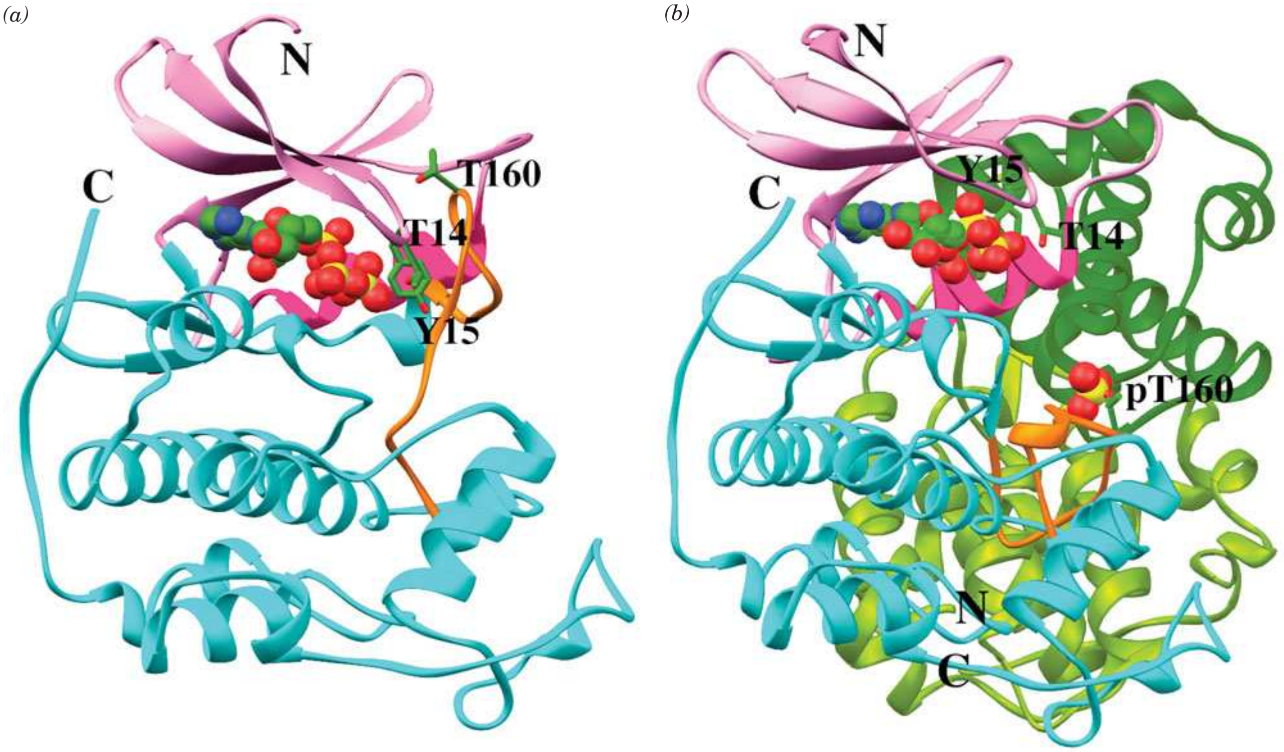

Figure 28-41 **X-Ray structure of human cyclin-dependent kinase 2 (Cdk2).** (*a*) Cdk2 in complex with ATP. The protein is shown in the "standard" protein kinase orientation with its N-terminal lobe pink, its C-terminal lobe cyan, its PSTAIRE helix (residues 45–56) magenta, and its T loop (residues 152–170) orange. The ATP is shown in space-filling form and the phosphorylatable side chains of Thr 14, Tyr 15, and Thr 160 are shown in stick form, all colored according to atom type (C green, N blue, O red, and P yellow). Compare this structure with that of protein kinase A (PKA; Fig. 13-21). [Based on an X-ray structure by Sung-Hou Kim, University of California at Berkeley. PDBid 1HCK.] (*b*) The complex of Thr 160–phosphorylated Cdk2 with cyclin A and ATP. The Cdk2 and ATP are represented as in Part *a* and viewed similarly. The cyclin A is colored light and dark green. The phosphoryl group at Thr 160 of Cdk2 is drawn in space-filling form. Note how the binding of cyclin A together with the phosphorylation of Thr 160 has caused a major structural reorganization of the T loop and the Cdk2 N-terminal lobe, including its PSTAIRE helix. Also note the different conformations of the ATP triphosphate group in the two structures. [Based on an X-ray structure by Nikola Pavletich, Memorial Sloan-Kettering Cancer Center, New York, New York. PDBid 1JST.] **See Interactive Exercise 57.**

of Thr 160 and binding of cyclin A alter the conformation of Cdk2 (Fig. 28-41*b*). In particular, the N-terminal α helix of Cdk2, which contains the PSTAIRE sequence motif characteristic of the Cdk family, rotates about its axis by 90° and moves several angstroms in order to position several residues in a catalytically active arrangement. In addition, Cdk2's T loop undergoes a dramatic reorganization, involving position shifts of up to 21 Å, that allows protein substrates access to the active site. The phosphate group on Thr 160 fits snugly into a positively charged pocket composed of three Arg residues that forms, in part, on cyclin A binding.

In addition to their control by phosphorylation/dephosphorylation and by the binding of the appropriate cyclin, *Cdk activities are regulated by* ***cyclin-dependent kinase inhibitors (CKIs),*** *which arrest the cell cycle in response to such antiproliferative signals as contact with other cells, DNA damage, terminal differentiation, and senescence (in which cell cycle arrest is permanent)*. The importance of CKIs is indicated by their frequent alterations in cancer, which is manifest as uncontrolled cell division. The pathways by which sensor proteins monitor cellular conditions and activate or inactivate Cdks are not yet fully understood. However, considerable information has been provided by studies of proteins, including p53 and pRb (see below), whose mutations are associated with loss of cell cycle control.

B | Tumor Suppressors Prevent Cancer

Individuals with the rare inherited condition known as **Li–Fraumeni syndrome** are highly susceptible to a variety of malignant tumors, particularly breast cancer, which they often develop before their thirtieth birthdays. These individuals have germline mutations in their ***p53*** gene, which suggests that its normal protein product, **p53** (a *p*olypeptide with a nominal mass of *53* kD), is a **tumor suppressor.** In other words, *p53 functions to restrain the uninhibited cell proliferation that is characteristic of cancer.* Indeed, the *p53* gene is the most commonly altered gene in human cancers; ~50% of human cancers contain a mutation in *p53,* and many other oncogenic (cancer-causing) mutations occur in genes that encode proteins that directly or indirectly interact with p53. Evidently, p53 functions as a "molecular policeman" in monitoring genome integrity.

p53 Arrests the Cell Cycle in G_2. Despite the central role of p53 in preventing tumor formation, the way it does so has only gradually come to light. p53 is specifically bound by **Mdm2** protein, a ubiquitin-protein ligase (E3) that specifically ubiquitinates p53, thereby marking it for proteolytic degradation by the proteasome (Section 21-1). Consequently, the amplification (generation of several copies) of the *mdm2* gene, which occurs in >35% of human **sarcomas** (none of which have a mutated *p53* gene; sarcomas are malignancies of connective tissues such as muscle, tendon, and bone), results in an increased rate of degradation of p53, thereby predisposing cells to malignant transformation. Thus, *an additional way that oncogenes (cancer-causing genes; Box 13-3) can cause cancer is by inactivating normal tumor suppressors.*

p53 is an efficient transcriptional activator. Indeed, all point-mutated forms of p53 that are implicated in cancer have lost their sequence-specific DNA-binding properties. How, then, does p53 function as a tumor suppressor? A clue to this riddle came from the observation that the treatment of cells with DNA-damaging ionizing radiation results in the accumulation of normal p53. This led to the discovery that the activated protein kinases **ATM** and **Chk2** both phosphorylate p53 [ATM for *a*taxia *t*elangiectasia *m*utated (**ataxia telangiectasia** is a rare genetic disease characterized by a progressive loss of motor control, growth retardation, premature aging, and a greatly increased risk of cancer); Chk for *ch*eckpoint *k*inase]. ATM and Chk2 had previously been shown to be activated by and participate in a phosphorylation cascade that induces cell cycle arrest at the G_2 checkpoint on the detection of damaged or unreplicated DNA. The phosphorylation of p53 prevents its binding by Mdm2 and hence increases the otherwise low level of p53 in the nucleus. *Although p53 does not initiate cell cycle arrest in G_2, its presence is required to prolong this process. It does so by activating the transcription of the gene encoding the cyclin-dependent kinase inhibitor (CKI) named* ***$p21^{Cip1}$,*** *which binds to several Cdk–cyclin complexes so as to inhibit both the G_1/S and G_2/M transitions.*

Cells that are irreparably damaged synthesize excessive levels of p53, which in turn induces these cells to commit suicide by activating the expression of several of the proteins that participate in apoptosis (see below). In the absence of p53 activation, cells control the level of p53 through a feedback loop in which p53 stimulates the transcription of the ***mdm2*** gene.

The X-Ray Structure of p53 Explains Its Oncogenic Mutations. p53 is a tetramer of identical 393-residue subunits, which each contain a sequence-specific DNA-binding core. The X-ray structure of this domain (residues 102–313) in complex with a 21-bp target DNA sequence, determined by Nikola Pavletich, is shown in Fig. 28-42. The p53 DNA-binding motif does not resemble any other that has previously been characterized (Sections 24-4B and 24-4C). It makes sequence-specific contacts with the bases of the DNA in its major groove (lower right of Fig. 28-42). In addition, the side chain of Arg 248 extends into the DNA's minor groove (upper right of Fig. 28-42). The protein also contacts the DNA backbone between the major and minor grooves in this region (notably with Arg 273).

The structure's most striking feature is that *its DNA-binding motif consists of conserved regions comprising the most frequently mutated residues in the >1000 p53 variants found in human tumors.* Among them are one Gly and five Arg residues (indicated in Fig. 28-42) whose mutations collectively account for over 40% of the *p53* variants in tumors. The two most frequently mutated residues, Arg 248 and Arg 273, as we saw, directly contact the DNA. The other four "mutational hotspot" residues appear to play a critical role in structurally stabilizing p53's DNA-binding surface. The relatively sparse secondary structure in the polypeptide segments forming this surface (one helix and three loops) accounts for this high mutational sensitivity: Its structural integrity mostly relies on specific side chain–side chain and side chain–backbone interactions.

p53 Is a Sensor That Integrates Information from Several Pathways. p53 may be activated by several other pathways. For example, aberrant growth signals, including those generated by oncogenic variants of Ras signaling cascade components (Fig. 13-7) such as Ras, cause the inappropriate activation of a variety of transcription factors. One of them, **Myc,** activates the transcription of the gene encoding **p14^{ARF},** which binds to Mdm2 and thereby inhibits its activity. This prevents the degradation of

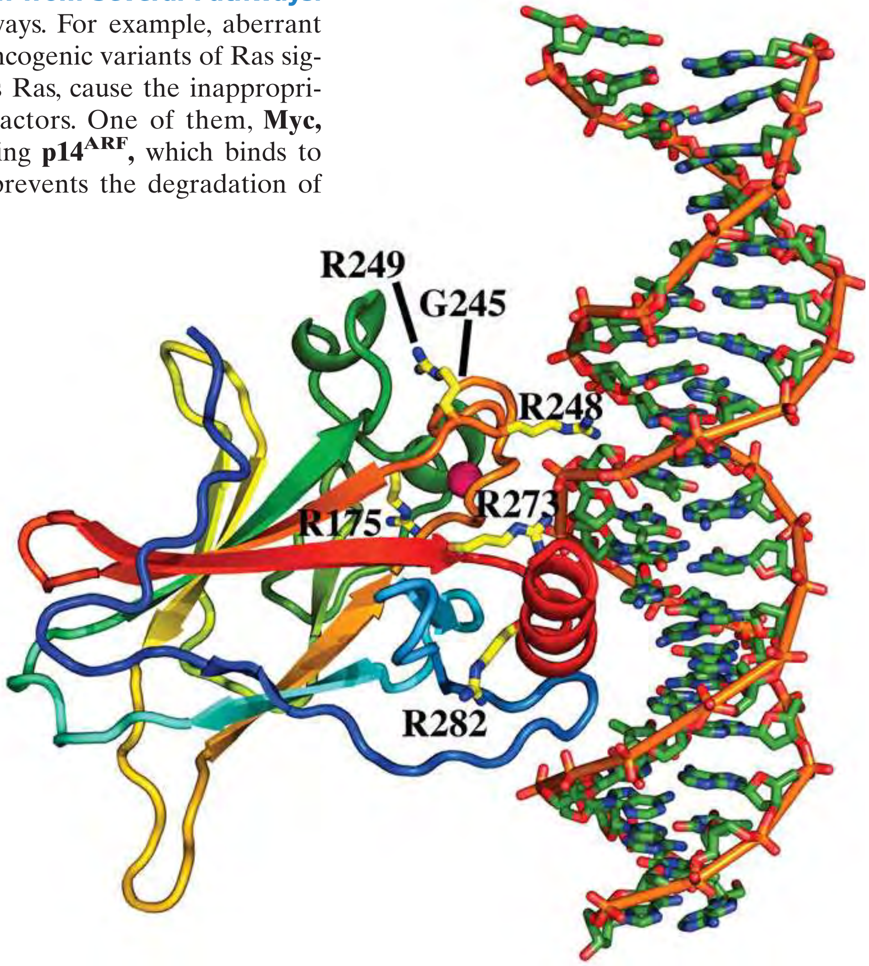

■ **Figure 28-42** | **X-Ray structure of the DNA-binding domain of human p53 in complex with its target DNA.** The DNA is drawn in stick form colored according to atom type (C green, N blue, O red, and P orange) with its successive P atoms joined by orange rods. The protein is shown in ribbon form colored in rainbow order from its N-terminus (*blue*) to its C-terminus (*red*). A tetrahedrally liganded Zn^{2+} ion is represented by a magenta sphere, and the side chains of the six most frequently mutated residues in human tumors are shown in stick form with C yellow and identified with their one-letter codes. [Based on an X-ray structure by Nikola Pavletich, Memorial Sloan-Kettering Cancer Center, New York, New York. PDBid 1TSR.] **See Interactive Exercise 58.**

p53 and hence triggers the p53-dependent transcriptional programs leading to cell cycle arrest as well as apoptosis. Evidently, $p14^{ARF}$ acts as part of a p53-dependent fail-safe system to counteract hyperproliferative signals.

A third activation pathway for p53 is induced by a wide variety of DNA-damaging chemotherapeutic agents, protein kinase inhibitors, and UV radiation. These activate a protein kinase named **ATR** to phosphorylate p53 so as to reduce its affinity for Mdm2 in much the same way as do ATM and Chk2. p53 is also subject to a rich variety of reversible post-translational modifications that markedly influence the expression of its target genes, including acetylation at several Lys residues, glycosylation, and sumoylation (Section 27-5B), in addition to its phosphorylation at multiple Ser/Thr residues and ubiquitination.

p53, as we have only glimpsed, is the recipient of a vast number of intracellular signals and, in turn, controls the activities of a large number of downstream regulators. One way to understand the operation of this highly complex and interconnected network is in analogy with the Internet. In the Internet (cell), a small number of highly connected servers or hubs ("master" proteins) transmit information to/from a large number of computers or nodes (other proteins) that directly interact with only a few other nodes (proteins). In such a network, overall performance is largely unperturbed by the inactivation of one of the nodes (other proteins). However, the inactivation of a hub ("master" protein) will greatly impact system performance. p53 is a "master" protein, that is, it is analogous to a hub. Inactivation of one of the many proteins that influences its performance or one of the many proteins whose activity it influences usually has little effect on cellular events due to the cell's redundant and highly interconnected components. However, the inactivation of p53 or several of its most closely associated proteins (e.g., Mdm2) disrupts the cell's responses to DNA damage and tumor-predisposing stresses, thereby leading to tumor formation.

Loss of pRb Protein Leads to Cancer. **Retinoblastoma,** a cancer of the developing retina that affects infants and young children, is associated with the loss of the *Rb* gene, which encodes the tumor suppressor **pRb.** This 928-residue DNA-binding protein interacts with the **E2F** family of transcription factors, which has six members in mammals. E2F proteins induce the transcription of genes that encode proteins required for entry into S phase. pRb can be phosphorylated at as many as 16 of its Ser/Thr residues by various Cdk–cyclin complexes (the various complexes phosphorylate different sets of sites on pRb). In nonproliferating cells (those in early G_1), pRb is hypophosphorylated. In that state, it binds to E2F so as to prevent it from activating transcription at the promoters to which it is bound. In response to a mitogenic signal (a signal that induces mitosis), the levels of D-type cyclins increase, which triggers phosphorylation of pRb by **Cdk4/6–cyclin D** complexes. Hyperphosphorylated pRb releases E2F, which thereupon induces the expression of genes that promote cell cycle progression, including genes for additional cyclins and Cdks. The E2F-binding site of pRb is the major site of *Rb* gene alterations in tumors.

C | Apoptosis Is an Orderly Process

Programmed cell death or **apoptosis** (Greek: falling off, as leaves from a tree), which was first described by John Kerr in the late 1960s, is a normal part of development as well as maintenance and defense of the adult animal body. For example, in many vertebrates, the digits of the developing hands and feet are initially connected by webbing that is eliminated by programmed cell death (Fig. 28-43). In the adult human body, which consists of nearly 10^{14} cells, an estimated 10^{11} cells are eliminated each day through programmed cell death (which closely matches the number of new cells produced by mitosis). The immune system eliminates virus-infected cells, in part by inducing them to undergo apoptosis, in order to prevent viral replication. Cells with irreparably damaged DNA and hence at risk for malignant transformation undergo apoptosis, thereby protecting the entire organism from cancer. In fact, as Martin Raff pointed out, *apoptosis appears to be the default option for animal cells: Unless they continually receive external hormonal and/or neuronal signals not to commit suicide, they will do so.* Thus, adult organs maintain their constant size by balancing cell proliferation with apoptosis. Not surprisingly, therefore, inappropriate apoptosis has been implicated in several neurodegenerative diseases including Alzheimer's disease (Section 6-5C), Parkinson's disease (Section 21-6B), and Huntington's disease (Box 28-1), as well as much of the damage caused by stroke and heart attack.

Apoptosis is qualitatively different from **necrosis,** the type of cell death caused by trauma (e.g., lack of oxygen, extremes of temperature, and mechanical injury). Cells undergoing necrosis essentially explode: They and their membrane-enclosed organelles swell as water rushes in through their compromised membranes, releasing lytic enzymes that digest the cell contents until the cell lyses, spilling its contents into the surrounding region (Box 18-5). The cytokines that the cell releases often induce an inflammatory response (which can damage surrounding cells). In contrast, apoptosis begins with the loss of intercellular contacts by an apparently healthy cell followed by its shrinkage, the condensation of its chromatin at the nuclear periphery, the collapse of its cytoskeleton, the dissolution of its nuclear envelope, the fragmentation of its DNA, and violent blebbing (blistering) of its plasma membrane. Eventually, the cell disintegrates into numerous membrane-enclosed **apoptotic bodies** that are phagocytosed (engulfed) by neighboring cells as well as by roving macrophages without spilling the cell contents and hence not inducing an inflammatory response.

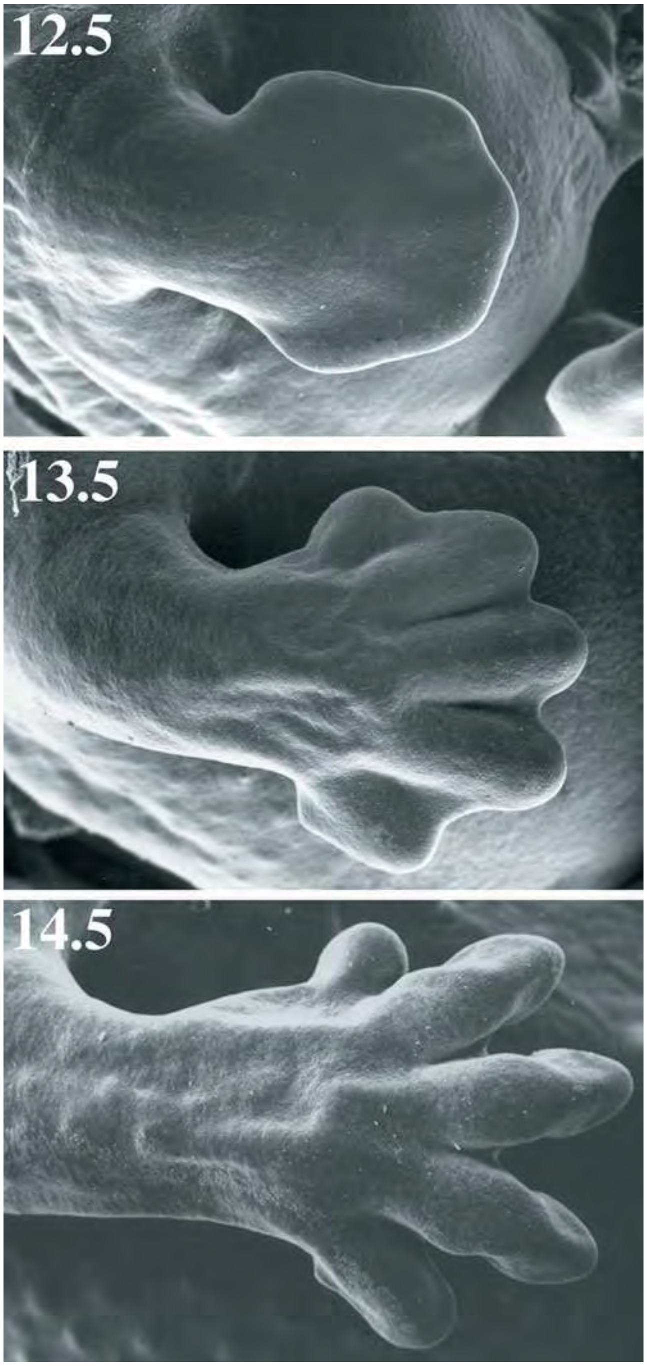

Figure 28-43 | **Programmed cell death in the embryonic mouse paw.** At day 12.5 of development, its digits are fully connected by webbing. At day 13.5, the webbing has begun to die. By day 14.5, the apoptotic process is complete. [Courtesy of Paul Martin, University College of London, U.K.]

Caspases Participate in Apoptosis. Apoptosis involves a family of proteases known as **caspases** (for *c*ysteinyl *asp*artate-specific prote*ases*), which are **cysteine proteases** whose mechanism resembles that of serine proteases (Section 11-5) but with Cys replacing the active site Ser. Caspases cleave target polypeptides after an Asp residue.

Caspases are $\alpha_2\beta_2$ heterotetramers that consist of two large α subunits (~300 residues) and two small β subunits (~100 residues). They are expressed as single-chained zymogens **(procaspases)** that are activated by proteolytic excision of their N-terminal prodomains and proteolytic separation of their α and β subunits. The activating cleavage sites all follow Asp residues and are, in fact, targets for caspases, suggesting that caspase activation may either be autocatalytic or be catalyzed by another caspase.

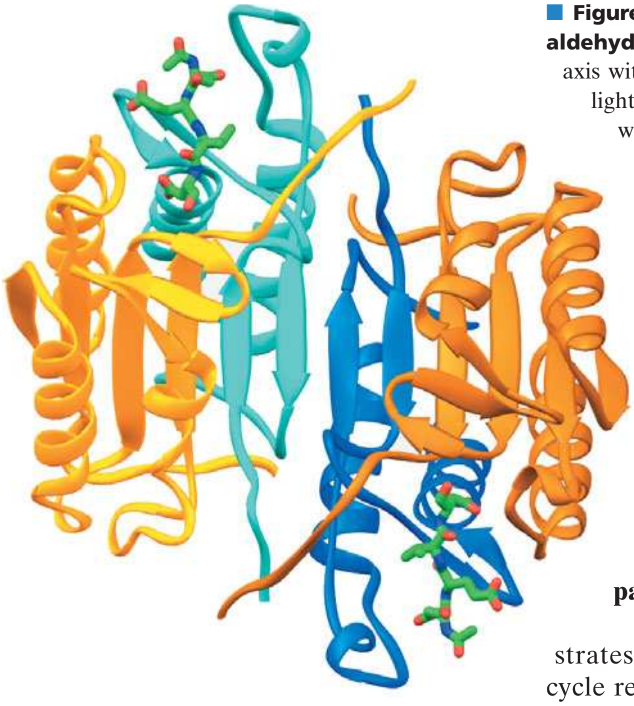

Figure 28-44 | X-Ray structure of caspase-7 in complex with a tetrapeptide aldehyde inhibitor. The $\alpha_2\beta_2$ heterotetrameric enzyme is viewed along its twofold axis with its large (α) subunits orange and gold and its small (β) subunits cyan and light blue. The acetyl-Asp-Glu-Val-Asp-CHO inhibitor is drawn in stick form with C green, N blue, and O red. [Based on an X-ray structure by Keith Wilson and Paul Charifson, Vertex Pharmaceuticals, Cambridge, Massachusetts. PDBid 1F1J.]

The X-ray structure of human **caspase-7** (Fig. 28-44), determined by Keith Wilson and Paul Charifson, reveals that each $\alpha\beta$ heterodimer contains a six-stranded β sheet flanked by five α helices that are approximately parallel to the β strands. The β sheet is continued across the enzyme's twofold axis to form a twisted 12-stranded β sheet. The active site of each $\alpha\beta$ heterodimer is located at the C-terminal ends of its parallel β strands. The structures of other caspases differ mainly in the conformations of the four loops forming their active sites. In the inactive **procaspase-7,** these loops are folded so as to obliterate the active site.

Over 60 cellular proteins have been identified as caspase substrates. These include cytoskeletal proteins, proteins involved in cell cycle regulation (including cyclin A, $p21^{Cip1}$, ATM, and pRb), proteins that participate in DNA replication, transcription factors, and proteins that participate in signal transduction. Nevertheless, how the cleavage of these numerous proteins causes the morphological changes that cells undergo during apoptosis is unclear. The induction of apoptosis also causes the rapid degradation of DNA by the action of **caspase-activated DNase.** Presumably, DNA degradation prevents the genetic transformation of other cells that subsequently phagocytose apoptotic bodies containing viral DNA or damaged chromosomal DNA.

Apoptosis Is Triggered Extracellularly or Intracellularly. *Apoptosis in a given cell may be induced either by externally supplied signals in the so-called* ***extrinsic pathway*** *(death by commission) or by the absence of external signals that inhibit apoptosis in the so-called* ***intrinsic pathway*** *(death by omission).* The extrinsic pathway is initiated by the association of a cell destined to undergo apoptosis with a cell that has selected it to do so. In what is perhaps the best characterized such pathway (Fig. 28-45), a transmembrane protein named **Fas ligand (FasL)** that projects from the plasma membrane of the inducing cell, a so-called **death ligand,** binds to a transmembrane protein known as **Fas** that projects from the plasma membrane of the apoptotic cell, a so-called **death receptor.** Fas ligand is a homotrimeric protein whose binding to three Fas molecules causes the Fas cytoplasmic domains to trimerize. The trimerized Fas recruits three molecules of a 208-residue adaptor protein named **FADD** (for *F*as-*a*ssociating *d*eath *d*omain-containing protein), which in turn recruits **procaspase-8** and **procaspase-10.** The consequent clustering of procaspase-8 and procaspase-10 results in the proteolytic autoactivation of these zymogens, thereby generating **caspases-8** and **-10,** which are termed **initiator caspases.** This is because these enzymes then activate **caspase-3,** which is known as an **effector (executioner) caspase** because its actions cause the cell to undergo apoptosis.

The intrinsic pathway for initiating apoptosis follows a slightly different route to caspase-3 activation. Most animal cells are continuously bathed in an extracellular soup, generated in part by neighboring cells, that contains

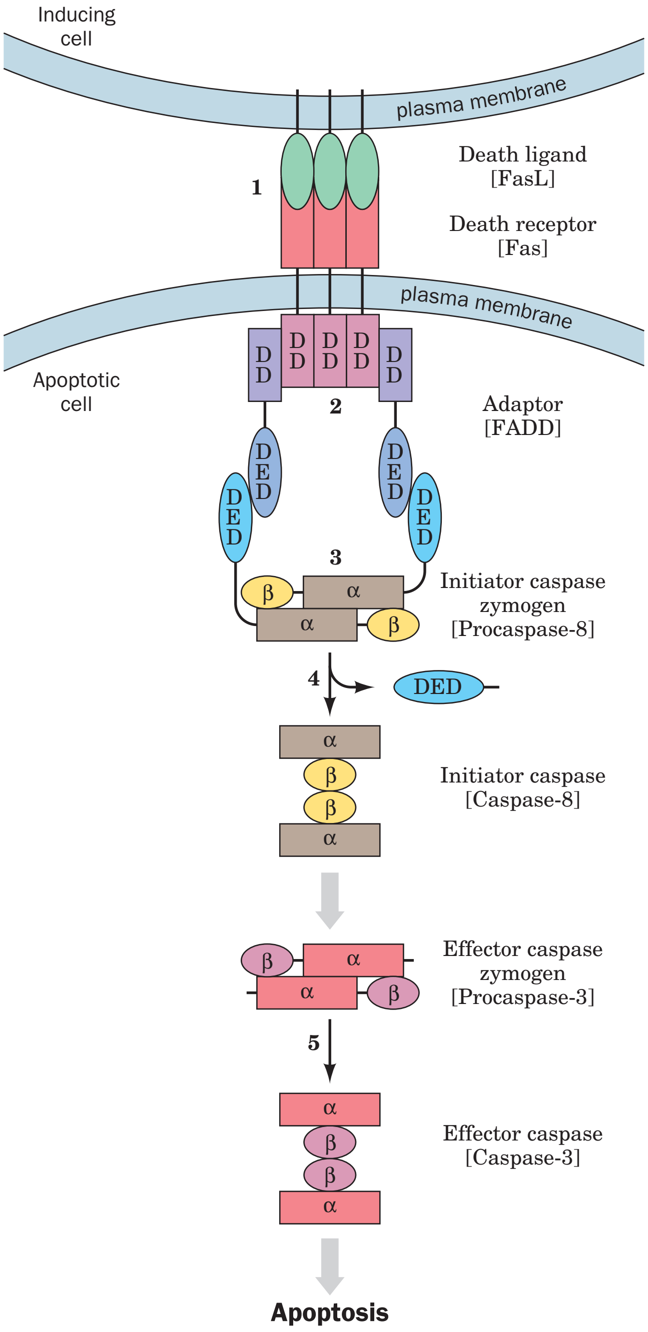
Inducing cell
plasma membrane
Death ligand [FasL]
1
Death receptor [Fas]
plasma membrane
Apoptotic cell
DD
DD
DD
DD
DD
2
Adaptor [FADD]
DED
DED
DED
DED
3
Initiator caspase zymogen [Procaspase-8]
β
α
α
β
4
DED
α
β
β
α
Initiator caspase [Caspase-8]
β
α
α
β
Effector caspase zymogen [Procaspase-3]
5
α
β
β
α
Effector caspase [Caspase-3]
Apoptosis

Figure 28-45 | **The extrinsic pathway of apoptosis.** Flat gray arrows indicate activation. **(1)** The binding of a trimeric death ligand (e.g., FasL, *green*) on the inducing cell to the death receptor (e.g., Fas, *red*) on the apoptotic cell causes the death receptor's cytoplasmic death domains (DDs) to trimerize **(2).** This recruits adaptors (e.g., FADD), which bind via their DDs to the DDs of the death receptor. The adaptors, in turn, recruit initiator procaspases (e.g., procaspase-8) via the interactions between the death effector domains (DEDs) on the adaptors and the initiator procaspases **(3),** which induces the autoactivation **(4)** of the initiator procaspases to form the corresponding heterotetrameric initiator caspases (e.g., caspase-8). **(5)** The initiator caspases then proteolytically activate effector procaspases (e.g., procaspase-3) to yield the heterotetrameric effector caspases (e.g., caspase-3), which catalyze the proteolytic cleavages resulting in apoptosis.

a wide variety of substances that regulate the cell's growth, differentiation, activity, and survival. The withdrawal of this chemical support for its survival or the loss of direct cell–cell interactions induces a cell to undergo apoptosis via the intrinsic pathway. The initial step of this pathway appears to be the activation of one or more members of the **Bcl-2** family (so named because its founding member is involved in *B c*ell *l*ymphoma). Association of certain Bcl-2 proteins with the mitochondrion causes it to release cytochrome *c* (Section 18-2E) from the intermembrane space into the cytosol. It is not clear how cytochrome *c* exits the mitochondrion. It may traverse the outer membrane via a newly formed pore or via an existing pore whose conformation is altered to accommodate the ~12-kD cytochrome, or the outer membrane may rupture as a result of Bcl-2 activity.

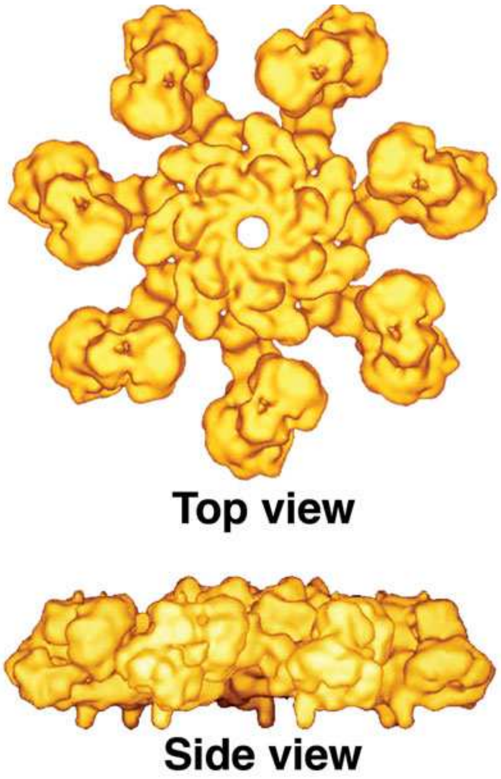

Figure 28-46 | Cryoelectron microscopy–based image of the apoptosome at 12.8 Å resolution. In its top view, the particle is viewed along its sevenfold axis of symmetry. The side view reveals the flattened nature of this ~250-Å-in-diameter wheel-shaped particle. Cytochrome *c* forms the bulge protruding from the top of the large knob at the end of every arm. [Courtesy of Christopher Akey, Boston University School of Medicine.]

The cytochrome *c* combines with a 1248-residue protein called **Apaf-1** (for *a*poptosis *p*rotease-*a*ctivating *f*actor-*1*) and ATP or dATP to form an ~1100-kD wheel-shaped complex named the **apoptosome** (Fig. 28-46). The apoptosome binds several molecules of **procaspase-9** in a manner that induces their autoactivation. The resulting **caspase-9,** still bound to the apoptosome, then activates procaspase-3 to instigate cell death.

D | Development Has a Molecular Basis

Perhaps the most awe-inspiring event in biology is the growth and development of a fertilized ovum to form an extensively differentiated multicellular organism. No outside instruction is required to do so; *fertilized ova contain all the information necessary to form complex multicellular organisms such as human beings.* Much of what we know about the molecular basis of cell differentiation is based on studies of the fruit fly *Drosophila melanogaster.* We therefore begin this section with a synopsis of *Drosophila* embryogenesis.

The *Drosophila* Embryo Is Divided into Segments. Almost immediately after the *Drosophila* egg (Fig. 28-47*a*) is laid (which, rather than the earlier fertilization, triggers development), it commences a series of rapid, synchronized nuclear divisions, one every 6 to 10 min. Here, the nuclear division process is not accompanied by the formation of new cell membranes; the nuclei continue sharing their common cytoplasm to form a so-called **syncytium** (Fig. 28-47*b*). After the eighth round of nuclear division, the ~256 nuclei begin to migrate toward the cortex (outer layer) of the egg where, by around the eleventh nuclear division, they have formed a single layer surrounding a yolk-rich core (Fig. 28-47*c;* the germ-cell progenitors, the pole cells, are set aside after the ninth division). At this stage, the mitotic cycle time begins to lengthen while the nuclear genes, which have heretofore been fully engaged in DNA replication, become transcriptionally active (a freshly laid egg contains an enormous store of mRNA that has been contributed by the developing oocyte's surrounding "nurse" cells). In the fourteenth nuclear division cycle, which lasts ~60 min, the egg's plasma membrane invaginates around each of the ~6000 nuclei to yield a cellular monolayer called a **blastoderm** (Fig. 28-47*d*). At this point, after ~2.5 h of development, transcriptional activity reaches its maximum and mitotic synchrony is lost.

During the next few hours, the embryo undergoes **gastrulation** (migration of cells to form a triple-layered structure) and organogenesis. A striking aspect of this remarkable process, in *Drosophila* as well as in higher animals, is the division of the embryo into a series of segments corresponding to the adult organism's organization (Fig. 28-47*e*). The *Drosophila* embryo has at least three segments that eventually merge to form its head (Md, Mx, and Lb for mandibulary, maxillary, and labial), three thoracic segments (T1–T3), and eight abdominal segments (A1–A8). As development continues, the embryo elongates and several of its abdominal segments fold over its thoracic segments (Fig. 28-47*f*). At this stage, the segments become subdivided into anterior (forward) and posterior (rear) compartments. The embryo then shortens and unfolds to form a larva that hatches 1 day after beginning development (Fig. 28-47*g*). Over the next 5 days, the larva feeds, grows, molts twice, pupates, and commences metamorphosis to form an adult (Fig. 28-47*h*). In the latter process, the larval epidermis is almost entirely replaced (through apoptosis) by the outgrowth of apparently undifferentiated patches of larval epithelium known as **imaginal disks** that are committed to their developmental fates as early as the blastoderm stage. These structures, which maintain the larva's segmental boundaries, form the adult's legs, wings, antennae, eyes, etc. About 10 days after commencing development, the adult emerges and, within a few hours, initiates a new reproductive cycle.

Developmental Patterns Are Genetically Mediated. What is the mechanism of embryonic pattern formation? Much of what we know about this process stems from genetic analyses of a series of bizarre mutations in three classes of *Drosophila* genes that normally specify progressively finer regions of cellular specialization in the developing embryo:

1. ***Maternal-effect genes,*** *which define the embryo's polarity,* that is, its anteroposterior (head to tail) and dorsoventral (back to belly) axes. Mutations of these genes globally alter the embryonic body pattern, producing, for example, nonviable embryos with two anterior or two posterior ends pointing in opposite directions.
2. ***Segmentation genes,*** *which specify the correct number and polarity of embryonic body segments.* Investigations by Christiane Nüsslein-Volhard and Eric Wieschaus led to their subclassification as follows:
    - (a) **Gap genes,** the first of a developing embryo's to be transcribed, are so named because their mutations result in gaps in the embryo's segmentation pattern. Embryos with defective ***hunchback (hb)*** genes, for example, lack mouthparts and thorax structures.
    - (b) **Pair-rule genes** specify the division of the embryo's broad gap domains into segments. These genes are so named because their mutations usually delete portions of every second segment.
    - (c) **Segment polarity genes** specify the polarities of the developing segments. Thus, homozygous ***engrailed (en)*** mutants lack the posterior compartment of each segment.

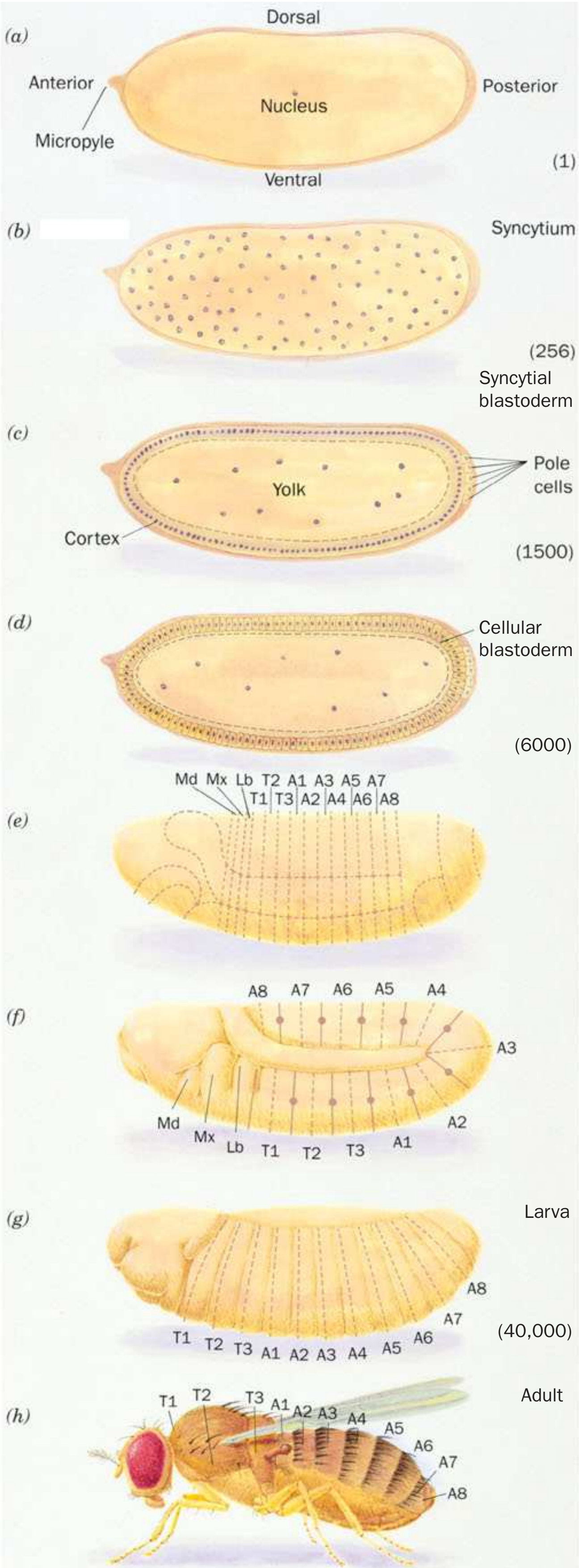

■ **Figure 28-47** | **Development in *Drosophila*.** The various stages are explained in the text. Note that the embryos and newly hatched larva are all the same size, ~0.5 mm long. The adult is, of course, much larger. The approximate numbers of cells in the early stages of development are given in parentheses.

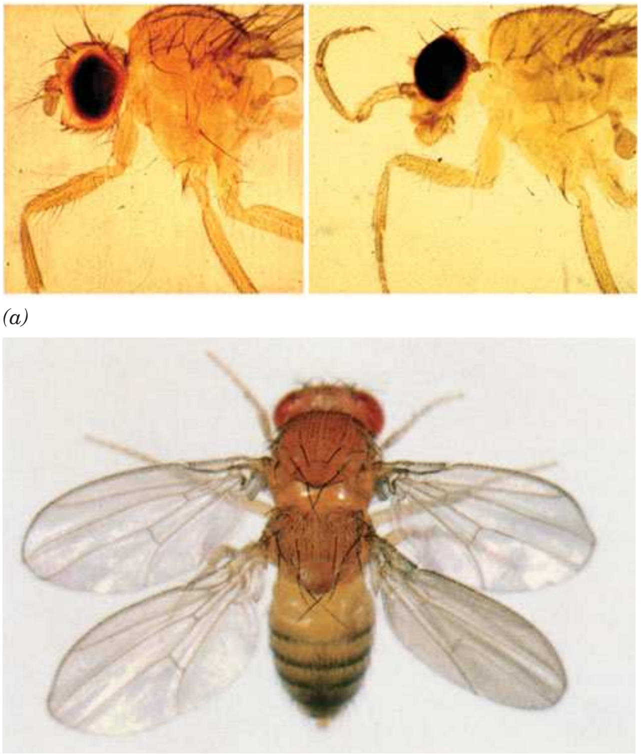

(a)

(b)

Figure 28-48 | Developmental mutants of *Drosophila*. (*a*) Head and thorax of a wild-type adult fly (*left*) and one that is homozygous for a mutant form of the homeotic *Antennapedia* (*antp*) gene (*right*). The mutant gene is inappropriately expressed in the imaginal disks that normally form antennae (where the wild-type *antp* gene is not expressed) so that they develop as the legs that normally occur only on segment T2. [Courtesy of Ginés Morata, Universidad Autónoma de Madrid, Spain.] (*b*) A four-winged *Drosophila* (it normally has two wings) that results from the presence of three mutations in the bithorax complex. These mutations cause the normally haltere-bearing segment T3 to develop as if it were the wing-bearing segment T2. [Courtesy of Edward B. Lewis, Caltech.]

3. ***Homeotic selector genes,*** *which specify segmental identity.* Mutations of homeotic selector genes transform one body part into another. For instance, ***Antennapedia*** (***antp,*** antennafoot) mutants have legs in place of antennae (Fig. 28-48*a*), whereas the mutations ***bithorax (bx), anteriorbithorax (abx),*** and ***postbithorax (pbx)*** each transform sections of halteres (vestigial wings that function as balancers), which normally occur only on segment T3, to the corresponding sections of wings, which normally occur only on segment T2 (Fig. 28-48*b*).

The properties of maternal-effect gene mutants suggest that maternal-effect genes specify substances known as ***morphogens*** *whose distributions in the egg cytoplasm define the future embryo's spatial coordinate system.* Indeed, immunofluorescence studies by Nüsslein-Volhard have demonstrated that the product of the ***bicoid (bcd)*** gene is distributed in a gradient that decreases toward the posterior end of the normal embryo (Fig. 28-49*a*), whereas embryos with *bcd*-deficient mothers lack this gradient. The gradient arises through the secretion, by ovarian nurse cells, of *bcd* mRNA into the anterior end of the oocyte during oogenesis. The ***nanos*** gene mRNA is similarly deposited near the egg's posterior pole. The *bcd* and *nanos* gene products regulate the expression of specific gap genes. Some other maternal-effect genes specify proteins that trap the localized mRNAs in their area of deposition. This explains why early embryos produced by females homozygous for maternal-effect mutations can often be "rescued" by the injection of cytoplasm, or sometimes just the mRNA, from early wild-type embryos.

The mRNA of the gap gene *hunchback (hb)* is deposited uniformly in the unfertilized egg (Fig. 28-49*a*). However, **Bicoid protein** activates the transcription of the embryonic *hb* gene, whereas **Nanos protein** inhibits the translation of *hb* mRNA. Consequently, **Hunchback protein** becomes distributed in a gradient that decreases from anterior to posterior (Fig. 28-49*b*). Footprinting studies have demonstrated that Bicoid protein binds to five homologous sites (consensus sequence TCTAATCCC) in the *hb* gene's upstream promoter region.

Hunchback protein controls the expression of several other gap genes (Fig. 28-49*c, d*): High levels of Hunchback protein induce ***giant*** expression; ***Krüppel*** (German: cripple) is expressed where the level of Hunchback protein begins to decline; ***knirps*** (German: pigmy) is expressed at even lower levels of Hunchback protein; and *giant* is again activated in regions where Hunchback protein is undetectable. These patterns of gene expression are stabilized and maintained by additional interactions. For example, **Krüppel protein** binds to the promoters of the *hb* gene, which it activates, and the *knirps* gene, which it represses. Conversely, **Knirps protein** represses the *Krüppel* gene. This mutual repression is thought to be responsible for the sharp boundaries between the various gap domains.

Pair-rule genes are expressed in sets of seven stripes, each just a few nuclei wide, along the early embryo's anterior–posterior axis (Fig. 28-50). The gap gene products directly control three **primary pair-rule genes:** ***hairy, even-skipped (eve),*** and ***runt.*** The promoters of most primary pair-rule genes consist of a series of modules, each of which contains a particular arrangement of activating and inhibitory binding sites for the various gap gene proteins. As a result, the expression of a pair-rule gene reflects

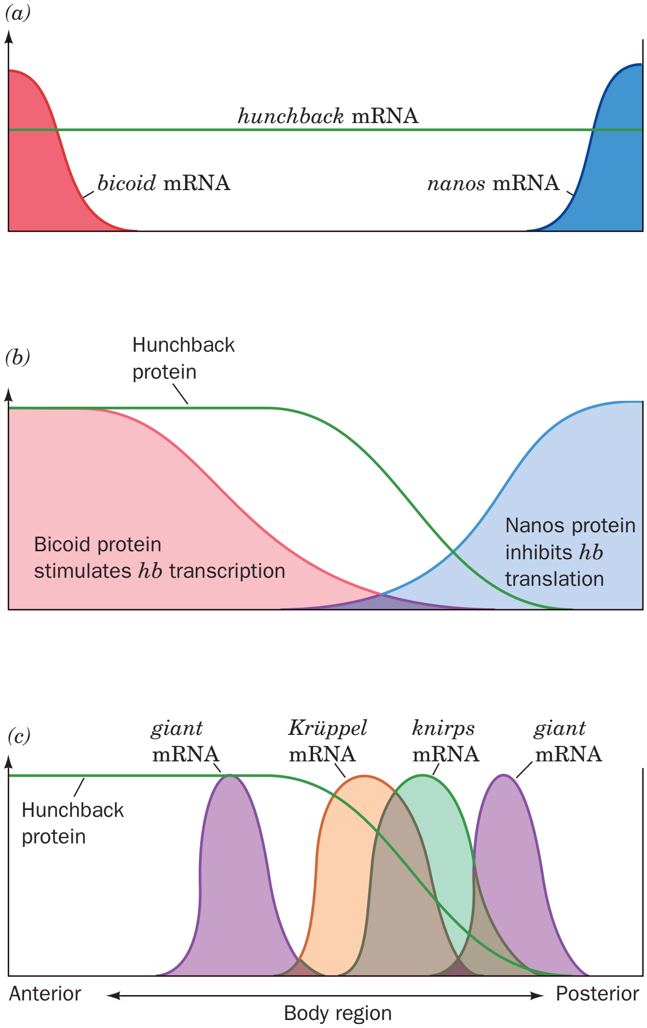

(d)

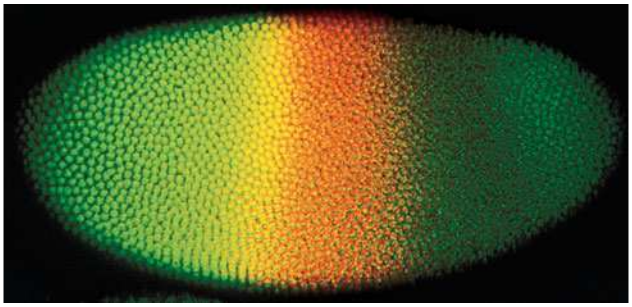

Figure 28-49 | **The formation and effects of the Hunchback protein gradient in *Drosophila* embryos.** (*a*) The unfertilized egg contains maternally supplied *bicoid* and *nanos* mRNAs placed at its anterior and posterior poles, together with a uniform distribution of *hunchback* mRNA. (*b*) On fertilization, the three mRNAs are translated. Bicoid and Nanos proteins are not bound in place as are their mRNAs and hence their gradients are broader than those of the mRNAs. Bicoid protein stimulates the translation of *hunchback* mRNA whereas Nanos protein inhibits its translation, resulting in a gradient of Hunchback protein that decreases nonlinearly from anterior to posterior. (*c*) Specific concentrations of Hunchback protein induce the transcription of the *giant, Krüppel,* and *knirps* genes. The gradient of Hunchback protein thereby specifies the positions at which the latter mRNAs are synthesized. (*d*) A photomicrograph of a *Drosophila* embryo (*anterior end left*) that has been immunofluorescently stained for both Hunchback (*green*) and Krüppel proteins (*red*). The region where the proteins overlap is yellow. [Parts *a, b,* and *c* after Gilbert, S. F., *Developmental Biology* (5th ed.), pp. 550 and 565, Sinauer Associates (1997); Part *d* courtesy of Jim Langeland, Stephen Paddock, and Sean Carroll, Howard Hughes Medical Institute, University of Wisconsin—Madison.]

the combination of gap gene proteins present, giving rise to a "zebra stripe" pattern. As with the gap genes, the patterns of expression of the primary pair-rule genes become stabilized through interactions among themselves. The primary pair-rule gene products also induce or inhibit the

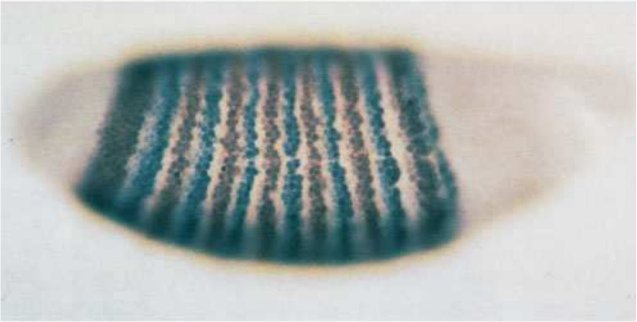

Figure 28-50 | ***Drosophila* embryos stained for pair-rule genes.** The **Fushi tarazu** protein **(Ftz)** is stained brown, and the **Eve** protein is stained gray. These proteins are each expressed in seven stripes. [Courtesy of Peter Lawrence, MRC Laboratory of Molecular Biology, Cambridge, U.K.]

expression of five **secondary pair-rule genes** including ***fushi tarazu*** (***ftz;*** Japanese for not enough segments). Thus, as Walter Gehring demonstrated, *ftz* transcripts first appear in the nuclei lining the cortical cytoplasm during the embryo's tenth nuclear division cycle. By the fourteenth division cycle, when the cellular blastoderm forms, *ftz* is expressed in a pattern of seven belts around the blastoderm, each 3 or 4 cells wide (Fig. 28-50).

The expression of eight known segment polarity genes is initiated by pair-rule gene products. For example, by the thirteenth nuclear division cycle, as Thomas Kornberg demonstrated, *engrailed (en)* transcripts become detectable but are more or less evenly distributed throughout the embryonic cortex. However, since *en* is preferentially expressed in nuclei containing high concentrations of either Eve or Ftz proteins, by the fourteenth cycle they form a striking pattern of 14 stripes around the blastoderm (half the spacing of *ftz* expression). The *en* gene product thereby induces the posterior half of each segment to develop in a different fashion from its anterior half.

Homeotic Genes Direct Development of Individual Body Parts. The structural components of developmentally analogous body parts, say *Drosophila* antennae and legs, are nearly identical; only their organizations differ (Fig. 28-51). *Consequently, developmental genes must control the pattern of structural gene expression rather than simply turning these genes on or off.*

The *Drosophila* homeotic selector genes map into two large gene families: the **bithorax complex *(BX-C)*,** which controls differentiation in the thoracic and abdominal segments, and the **antennapedia complex *(ANT-C)*,** which primarily affects head and thoracic segments. *Homozygous mutations in BX-C cause one or more segments to develop as if they were more anterior segments* (e.g., segment T3 develops as if it were segment T2; Fig. 28-48*b*). The entire deletion of *BX-C* causes all segments posterior to T2 to resemble T2; apparently T2 is the developmental "ground state" of the more distal segments. The evolution of homeotic gene families, it is

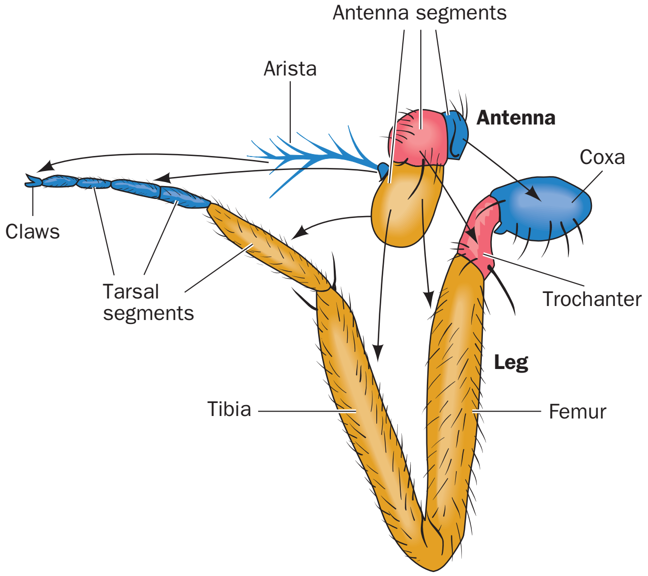

■ **Figure 28-51 | The correspondence between *Drosophila* antennae and legs.** [After Postlethwait, J.H. and Schneiderman, H.A., *Dev. Biol.* **25,** 622 (1971).]

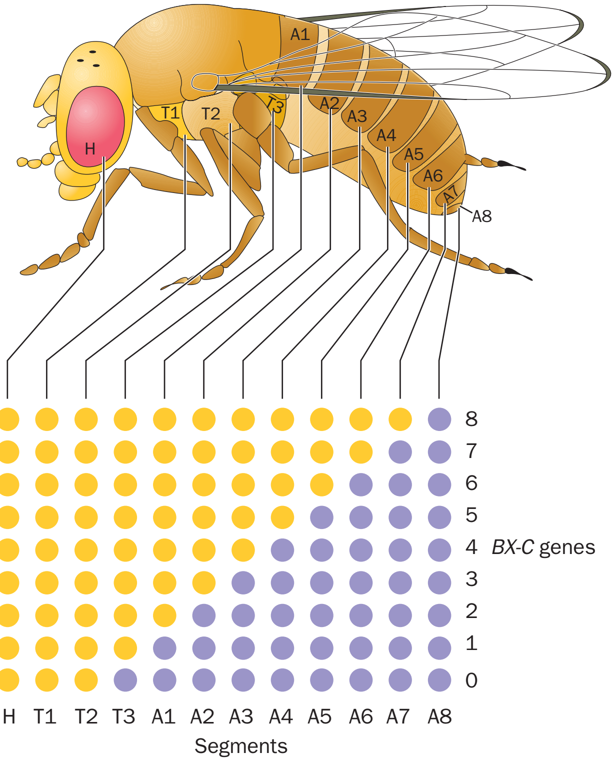

Figure 28-52 | Model for the differentiation of embryonic segments in *Drosophila*. Segments T2, T3, and A1–8, as the lower drawing indicates, are each characterized by a unique combination of active (*purple circles*) and inactive (*yellow circles*) *BX-C* "genes." These "genes" (which are really enhancer elements), here numbered 0 to 8, are thought to be sequentially activated from anterior to posterior in the embryo so that segment T2, the developmentally most primitive segment, has no active *BX-C* genes, while in segment A8, all of them are active. [After Ingham, P., *Trends Genet*. **1,** 113 (1985).]

thought, permitted arthropods (the phylum containing insects) to arise from the more primitive annelids (segmented worms) in which all segments are nearly alike.

Detailed genetic analysis of *BX-C* led Edward B. Lewis to formulate a model for segmental differentiation (Fig. 28-52): *BX-C,* Lewis proposed, contains at least one gene for each segment from T3 to A8 (numbered 0 to 8 in Fig. 28-52). Starting with segment T3, progressively more posterior segments express successively more *BX-C* genes until, in segment A8, all of these genes are expressed. Such a pattern of gene expression may result from a gradient in the concentration of a *BX-C* repressor that decreases from the anterior to the posterior end. The developmental fate of a segment is thereby determined by its position in the embryo. Subsequent sequence analysis revealed that the nine "genes" in the Lewis model are actually enhancer elements on three *BX-C* genes.

In characterizing the *Antennapedia (antp)* gene, Gehring and Matthew Scott independently discovered that *antp* cDNA hybridizes to both the *antp* and the *ftz* genes, indicating that *these genes share a common base sequence.* Subsequent experiments revealed that a similar sequence, called a **homeodomain** or **homeobox,** occurs in many *Drosophila* homeotic genes. These sequences, which are 70 to 90% identical to one another, encode even more identical 60-residue polypeptide segments.

Further hybridization studies using homeodomain probes led to the truly astonishing finding that *homeodomains are also present in the genomes of many animals.* Homeodomain-containing genes have collectively become known as ***Hox* genes.** In vertebrates, they are organized in four clusters of 9 to 11 genes, each located on a separate chromosome and spanning more than 100 kb. In contrast, *Drosophila,* as we saw, have two *Hox* clusters, whereas nematodes, which are evolutionarily more primitive than insects, have only one *Hox* cluster. The various *Hox* clusters, as well

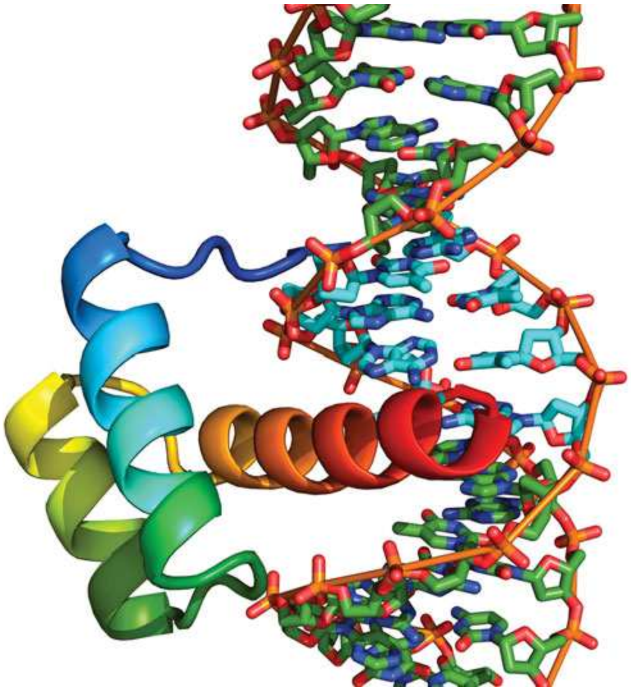

Figure 28-53 | X-Ray structure of the Engrailed protein homeodomain in complex with its target DNA. The protein is shown in ribbon form colored in rainbow order from its N-terminus (*blue*) to its C-terminus (*red*). The DNA is shown in stick form colored according to atom type (C green, N blue, O red, and P orange) with the nucleotides forming its TAAT subsite highlighted with C atoms cyan. Successive P atoms are linked by orange rods. Note that the protein's recognition helix, its C-terminal helix (*red and orange*), is bound in the DNA's major groove, and that the protein's N-terminal segment (*blue*) is inserted into the DNA's minor groove. [Based on an X-ray structure by Carl Pabo, MIT. PDBid 1HDD.] **See Interactive Exercise 59.**

as their component genes, almost certainly arose through a series of gene duplications.

***Hox* Genes Encode Transcription Factors.** Some *Hox* genes are remarkably similar; for example, the homeodomains of the *Drosophila antp* gene and the frog ***MM3* gene** encode polypeptides that have 59 of their 60 amino acids in common. Since vertebrates and invertebrates diverged over 600 million years ago, this strongly suggests that the product of the homeodomain has an essential function.

The polypeptide encoded by the homeodomain of the *Drosophila engrailed* gene specifically binds to the DNA sequences just upstream from the transcription start sites of both the *en* and the *ftz* genes. Moreover, fusing the *ftz* gene's upstream sequence to other genes imposes *ftz*'s pattern of stripes (Fig. 28-50) on the expression of these genes in *Drosophila* embryos. *These observations suggest that homeodomain-containing genes encode transcription factors that regulate the expression of other genes.*

Thomas Kornberg and Carl Pabo have determined the X-ray structure of the 61-residue homeodomain from the *Drosophila* Engrailed protein in complex with a 21-bp DNA (Fig. 28-53). The homeodomain consists largely of three α helices, the last two of which form an HTH motif that is closely superimposable on the HTH motifs of prokaryotic repressors (Section 24-4B).

Vertebrate *Hox* genes, like those of *Drosophila,* are expressed in specific patterns and at particular stages during embryogenesis. That the *Hox* genes directly specify the identities and fates of embryonic cells was shown, for example, by the following experiment. Mouse embryos were made transgenic for the *Hox-1.1* gene that had been placed under the control of a promoter that is active throughout the body even though *Hox-1.1* is normally expressed only below the neck. The resulting mice had severe craniofacial abnormalities such as a cleft palate and an extra vertebra and an intervertebral disk at the base of the skull. Some also had an extra pair of ribs in the neck region. Thus, the altered expression of the

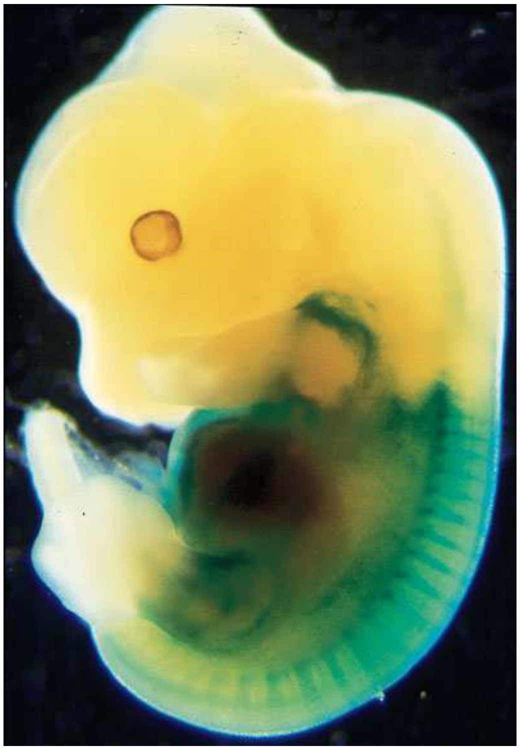

■ **Figure 28-54 | Pattern of expression of the *Hox-3.1* gene in a 12.5-day-old mouse embryo.** The protein-coding portion of the *Hox-3.1* gene was replaced by the *lacZ* gene. The regions of this transgenic embryo in which *Hox-3.1* is expressed are revealed by soaking the embryo in a buffer containing a substance (X-gal; Section 3-5A) that turns blue when hydrolyzed by the *lacZ* gene product, β-galactosidase. [Courtesy of Phillipe Brûlet, Collège de France and the Institut Pasteur, France.]

Hox-1.1 gene induced a homeotic mutation, that is, a change in the development pattern, analogous to those observed in *Drosophila* (Fig. 28-48).

Homozygotic mice whose *Hox-3.1* coding sequence has been replaced with that of *lacZ* are born alive but usually die within a few days. They exhibit skeletal deformities in their trunk regions in which several skeletal segments are transformed into the likenesses of more anterior segments. The pattern of β-galactosidase activity, as colorimetrically detected through the use of a substrate analog whose hydrolysis products are blue (Fig. 28-54), indicates that *Hox-3.1* deletion modifies the properties but not the positions of the embryonic cells that normally express *Hox-3.1*.

■ CHECK YOUR UNDERSTANDING

Summarize the stages of the cell cycle. What is the role of cyclins?

Explain how p53 and pRb suppress tumor formation.

Summarize the events of apoptosis.

Summarize the sequence of events in *Drosophila* embryogenesis and explain the functions of the substances that control these events.

SUMMARY

1. Genomic DNA sequence data reveal the total number of genes, their probable functions, and possible links to disease.
2. Certain genes are found in clusters, for example, those in bacterial operons, rRNA and tRNA genes, and eukaryotic histone genes. The human globin gene clusters contain genes expressed at different developmental stages.
3. Prokaryotic genomes contain small amounts of nontranscribed DNA, which include control regions for replication and transcription. The genomes of higher eukaryotes contain much larger proportions of nontranscribed DNA in the form of repetitive sequences, many of them the remnants of transposons.
4. Prokaryotic gene expression is controlled primarily at the level of transcription. Regulation of the *lac* operon is mediated by the binding of the *lac* repressor to its operator sequences. This binding, which prevents transcription of the operon, is reversed by the binding to the *lac* repressor of an inducer whose presence signals the availability of lactose, the substrate for the *lac* operon–encoded enzymes.
5. In catabolite repression, a complex of CAP and cAMP, which signals the scarcity of glucose, binds to its target DNA to stimulate the transcription of genes encoding proteins that participate in the metabolism of other sugars.
6. Attenuation is a mechanism whereby the translation-dependent formation of alternate mRNA secondary structures in an operon's leader sequence determines whether transcription proceeds or terminates. In a riboswitch, metabolite binding to an mRNA regulates gene expression.
7. The expression of eukaryotic genetic information involves the repositioning of nucleosomes and the covalent modification of histones as part of the histone code that is read by regulatory proteins. DNA methylation allows epigenetic inheritance.

8. In eukaryotes, activators and repressors, which bind to DNA enhancers and silencers, act cooperatively to regulate the rate of transcription initiation. Some of these transcription factors are activated by hormone signaling.
9. Eukaryotic gene expression may also be controlled by variable rates of mRNA degradation and regulation of translation initiation. RNA interference is a posttranscriptional gene silencing pathway in which double-stranded RNA directs the selective degradation of complementary mRNA.
10. Antibody diversity results from somatic recombination involving the selection of individual members of clustered gene sequences encoding the different segments of the immunoglobulin light and heavy chains. Diversity is augmented by imprecise *V/D/J* joining and by somatic hypermutation.
11. The eukaryotic cell cycle is governed by cyclin-dependent kinases, whose targets include the tumor suppressors p53 and pRb. p53 functions as a transcriptional activator that detects a variety of pathological states such as DNA damage and thereon helps maintain cell cycle arrest and, if the damage cannot be repaired, apoptosis (programmed cell death).
12. Extracellular or intracellular signals may trigger apoptosis, a cell-suicide pathway that requires the activity of various caspases.
13. The development of the *Drosophila* embryo is controlled by maternal-effect genes, which define the embryo's polarity; gap, pair-rule, and segment polarity genes, which specify the number and polarity of embryonic body segments; and homeotic selector genes (*Hox* genes), which encode transcription factors that regulate the expression of genes and therefore govern cell differentiation. *Hox* genes similarly regulate vertebrate development.

KEY TERMS

gene expression	**1037**
genomics	**1038**
C value	**1038**
C-value paradox	**1038**
ORF	**1040**
EST	**1040**
CpG island	**1040**
orphan gene	**1040**
ncRNA	**1041**
SNP	**1041**
gene cluster	**1042**
centromere	**1043**
genetic anticipation	**1044**
highly repetitive DNA	**1044**
STR	**1044**
moderately repetitive DNA	**1046**
selfish DNA	**1046**
inducer	**1047**
repressor	**1048**
operator	**1048**
catabolite repression	**1050**
corepressor	**1051**
leader sequence	**1052**
attenuation	**1053**
aptamer	**1055**
riboswitch	**1055**
heterochromatin	**1056**
euchromatin	**1056**
chromatin-remodeling complex	**1056**
Barr body	**1057**
HMG protein	**1058**
histone code	**1060**
HAT	**1060**
bromodomain	**1062**
chromodomain	**1064**
epigenetics	**1066**
imprinting	**1067**
enhancer	**1067**
silencer	**1067**
enhanceosome	**1068**
squelching	**1069**
insulator	**1070**
STAT	**1071**
hormone response element	**1072**
nonsense-mediated decay	**1074**
antisense RNA	**1075**
RNAi	**1075**
siRNA	**1075**
somatic recombination	**1078**
somatic hypermutation	**1081**
cell cycle	**1081**
cyclin	**1082**
tumor suppressor	**1084**
apoptosis	**1086**
necrosis	**1087**
caspase	**1087**
syncytium	**1090**
blastoderm	**1090**
gastrulation	**1090**
imaginal disk	**1091**
maternal-effect gene	**1091**
segmentation gene	**1091**
gap gene	**1091**
pair-rule gene	**1091**
segment polarity gene	**1091**
homeotic selector gene	**1092**
morphogen	**1092**
homeodomain	**1095**
Hox gene	**1095**

PROBLEMS

1. DNA isolated from an organism can be sheared into fragments of uniform size (~1000 bp), heated to separate the strands, then cooled to allow complementary strands to reanneal. The renaturation process can be followed over time. Explain why the renaturation of *E. coli* DNA is a monophasic process whereas the renaturation of human DNA is biphasic (an initial rapid phase followed by a slower phase).
2. Explain why the organization of genes in operons facilitates the assignment of functions to previously unidentified ORFs in a bacterial genome.
3. Explain why (a) inactivation of the O_1 sequence of the *lac* operator almost completely abolishes repression of the *lac* operon; (b) inactivation of O_2 or O_3 causes only a twofold loss in repression; and (c) inactivation of both O_2 and O_3 reduces repression ~70-fold.
4. Why do *E. coli* cells with a defective *lacZ* gene fail to show galactoside permease activity after the addition of lactose in the absence of glucose?
5. Describe the probable genetic defect that abolishes the sensitivity of the *lac* operon to the absence of glucose when other metabolic operons continue to be sensitive to the absence of glucose.
6. Why can't eukaryotic transcription be regulated by attenuation?
7. Predict the effect of deleting the leader peptide sequence on regulation of the *trp* operon.
8. Red–green color blindness is caused by an X-linked recessive genetic defect. Hence females rarely exhibit the red–green colorblind phenotype but may be carriers of the defective gene. When a narrow beam of red or green light is projected onto some areas of the retina of such a female carrier, she can readily differentiate the two colors but on other areas she has difficulty in doing so. Explain.
9. Draw the molecular formulas of the covalently modified histone side chains acetyllysine, methyllysine, and methylarginine. How do these modifications alter the chemical properties of the side chains?

10. Explain why a deficiency of the vitamin folic acid could lead to undermethylation of histones and DNA.
11. Monomethylation of histone Arg residues can be reversed by the action of a peptidylarginine deiminase, which requires water to remove the methyl group along with the imino group of Arg. Draw the structure of the resulting amino acid side chain and identify this nonstandard amino acid.
12. Why is transcriptionally active chromatin ~10 times more susceptible to cleavage by DNase I than transcriptionally silent chromatin?
13. Is it possible for a transcription enhancer to be located within the protein-coding sequence of a gene? Explain.
14. Explain why natural selection has favored the instability of RNA.
15. Explain why RNAi would be a less efficient mechanism for regulating the expression of specific genes if Dicer hydrolyzed double-stranded RNA every 11 bp rather than every 22 bp.
16. How many different heavy chain variable regions can theoretically be generated by somatic recombination in humans (ignore junctional flexibility)? If each of these heavy chains could combine with any of the ~2000 κ light chains, how many different immunoglobulins could be produced?
17. *V*/*D*/*J* recombination frequently yields a gene whose mRNA cannot be successfully translated into an immunoglobulin chain. What aspect of somatic recombination is likely to produce nonproductive gene rearrangement?
18. Why is it disadvantageous for single-celled eukaryotes such as yeast to undergo apoptosis?
19. In *Drosophila,* an *esc*$^-$ homozygote develops normally unless its mother is also an *esc*$^-$ homozygote. Explain.

REFERENCES

Genome Organization

Cummings, C.J. and Zoghbi, H.Y., Trinucleotide repeats: mechanisms and pathophysiology, *Annu. Rev. Genomics Hum. Genet.* **1,** 281–328 (2002).

Jurka, J., Repeats in genomic DNA: mining and meaning, *Curr. Opin. Struct. Biol.* **8,** 333–337 (1998). [Reviews the evolutionary history and function of repetitive DNA sequences.]

The International HapMap Consortium, The International HapMap Project, *Nature* **426,** 789–796 (2003). [Describes how patterns of single-nucleotide polymorphisms can be mapped and used as markers for genetic diseases.]

Prokaryotic Gene Expression

Bell, C.E. and Lewis, M., The Lac repressor: a second generation of structural and functional studies, *Curr. Opin Struct. Biol.* **11,** 19–25 (2001).

Kolb, A., Busby, S., Buc, H., Garges, S., and Adhya, S., Transcriptional regulation by cAMP and its receptor protein, *Annu. Rev. Biochem.* **62,** 749–795 (1993).

Tucker, B.J. and Breaker, R.R., Riboswitches as versatile control elements, *Curr. Opin. Struct. Biol.* **15,** 342–348 (2005).

Yanofsky, C., Transcription attenuation, *J. Biol. Chem.* **263,** 609–612 (1988). [A general discussion of attenuation.]

Eukaryotic Gene Expression

Agrawal, A., Eastman, Q.M., and Schatz, D.G., Transposition mediated by RAG1 and RAG2 and its implications for the evolution of the immune system, *Nature* **394,** 744–751 (1998).

Becker, P.B. and Hörz, W., ATP-dependent nucleosome remodeling, *Annu. Rev. Biochem.* **71,** 247–273 (2002).

Brivanlou, A.H. and Darnell, J.E., Jr., Signal transduction and the control of gene expression, *Science* **295,** 813–818 (2002).

Cohen, D.E. and Lee, J.T., X-Chromosome inactivation and the search for chromosome-wide silencers, *Curr. Opin. Genet. Dev.* **12,** 219–224 (2002).

Di Noia, J.M. and Neuberger, M.S. Molecular mechanisms of antibody somatic hypermutation. *Annu. Rev. Biochem.* **76,** 1–22 (2007).

Felsenfeld, G. and Groudine, M., Controlling the double helix, *Nature* **421,** 448–453 (2003). [A brief review of chromatin packaging, including histone modifications and epigenetics.]

Gilbert, S.F., *Developmental Biology* (8th ed.), Sinauer Associates (2006).

Hickman, E.S., Moroni, M.C., and Helin, K., The role of p53 and pRB in apoptosis and cancer, *Curr. Opin. Genet. Dev.* **12,** 60–66 (2002).

Iizuka, M. and Smith, M.M., Functional consequences of histone modifications, *Curr. Opin. Genet. Dev.* **13,** 154–160 (2003).

Janeway, C.A., Jr., Travers, P., Walport, M., and Shlomchik, M.J., *Immunobiology 6*: *The Immune System in Health and Disease,* Garland Science (2004).

Jiang, X. and Wang, X., Cytochrome *c*-mediated apoptosis, *Annu. Rev. Biochem.* **73,** 87–106 (2004).

Jones, P.A. and Takai, D., The role of DNA methylation in mammalian epigenetics, *Science* **293,** 1068–1070 (2001).

Kornberg, R.D., Mediator and the mechanism of transcriptional activation, *Trends Biochem. Sci.* **30,** 235–239 (2005).

Lemon, B. and Tjian, R., Orchestrated response: A symphony of transcription factors for gene control, *Genes Devel.* **14,** 2551–2569 (2000).

Lemons, D. and McGinnis, W., Genomic evolution of Hox gene clusters, *Science* **313,** 1918–1922 (2006).

Levine, M. and Tjian, R., Transcription regulation and animal diversity, *Nature* **424,** 147–151 (2003). [Discusses how multiple regulatory DNA sequences and transcription factors could account for differences in the complexity of organisms with similar numbers of genes.]

Loyola, A. and Almouzni, G., Marking histone H3 variants: How, when and why? *Trends Biochem. Sci.* **32,** 425–433 (2007).

Sen, G.L. and Blau, H.M., A brief history of RNAi: the silence of the genes, *FASEB J.* **20,** 1293–1299 (2006).

Shabbazian, M. and Grunstein, M., Functions of site-specific histone acetylation and deacetylation. *Annu. Rev. Biochem.* **76,** 75–100 (2007).

Shilatifard, A., Chromatin modifications by methylation and ubiquitination: Implication in the regulation of gene expression. *Annu. Rev. Biochem.* **75,** 243–269 (2006).

Sumner, A.T., *Chromosomes, Organization and Function,* Blackwell Science (2003).

Turner, B.M., Cellular memory and the histone code, *Cell* **111,** 285–291 (2002).

This page intentionally left blank

Solutions to Problems

CHAPTER 1

1. A Thiol (sulfhydryl) group
   B Carbonyl group
   C Amide linkage
   D Phosphoanhydride (pyrophosphoryl) linkage
   E Phosphoryl group (P_i)
   F Hydroxyl group

2. The cell membrane must be semipermeable so that the cell can retain essential compounds while allowing nutrients to enter and wastes to exit.

3. Concentration = (number of moles)/(volume)

$$\text{Volume} = (4/3)\pi r^3 = (4/3)\pi(5 \times 10^{-7}\ \text{m})^3$$
$$= 5.24 \times 10^{-19}\ \text{m}^3 = 5.24 \times 10^{-16}\ \text{L}$$

$$\text{Moles of protein} = (2\ \text{molecules})/(6.022 \times 10^{23}\ \text{molecules} \cdot \text{mol}^{-1}) = 3.32 \times 10^{-24}\ \text{mol}^{-1}$$

$$\text{Concentration} = (3.32 \times 10^{-24}\ \text{mol})/(5.24 \times 10^{-16}\ \text{L})$$
$$= 6.3 \times 10^{-9}\ \text{M} = 6.3\ \text{nM}$$

4. $$\text{Number of molecules} = (\text{molar conc.})(\text{volume})(6.022 \times 10^{23}\ \text{molecules} \cdot \text{mol}^{-1})$$
$$= (1.0 \times 10^{-3}\ \text{mol} \cdot \text{L}^{-1})(5.24 \times 10^{-16}\ \text{L})(6.022 \times 10^{23}\ \text{molecules} \cdot \text{mol}^{-1})$$
$$= 3.2 \times 10^{5}\ \text{molecules}$$

5. (a) Liquid water; (b) ice has less entropy at the lower temperature.

6. (a) Decreases; (b) increases; (c) increases; (d) no change.

7. (a) $T = 273 + 10 = 283\ \text{K}$

$$\Delta G = \Delta H - T\Delta S$$
$$\Delta G = 15\ \text{kJ} - (283\ \text{K})(0.050\ \text{kJ} \cdot \text{K}^{-1})$$
$$= 15 - 14.15\ \text{kJ} = 0.85\ \text{kJ}$$

ΔG is greater than zero, so the reaction is not spontaneous.

(b) $T = 273 + 80 = 353\ \text{K}$

$$\Delta G = \Delta H - T\Delta S$$
$$\Delta G = 15\ \text{kJ} - (353\ \text{K})(0.050\ \text{kJ} \cdot \text{K}^{-1})$$
$$= 15 - 17.65\ \text{kJ} = -2.65\ \text{kJ}$$

ΔG is less than zero, so the reaction is spontaneous.

8. $$K_{\text{eq}} = e^{-\Delta G^{\circ\prime}/RT} = e^{-(-20.900\ \text{J}\cdot\text{mol}^{-1})/(8.314\ \text{J}\cdot\text{K}^{-1}\cdot\text{mol}^{-1})(298\ \text{K})}$$
$$= 4.6 \times 10^{3}$$

9. $$\Delta G^{\circ\prime} = -RT \ln K_{\text{eq}} = -RT \ln([\text{C}][\text{D}]/[\text{A}][\text{B}])$$
$$= -(8.314\ \text{J} \cdot \text{K}^{-1} \cdot \text{mol}^{-1})(298\ \text{K})\ln[(3)(5)/(10)(15)]$$
$$= 5700\ \text{J} \cdot \text{mol}^{-1} = 5.7\ \text{kJ} \cdot \text{mol}^{-1}$$

Since $\Delta G^{\circ\prime}$ is positive, the reaction is endergonic under standard conditions.

10. From Eq. 1-17, $K_{\text{eq}} = [\text{G6P}]/[\text{G1P}] = e^{-\Delta G^{\circ\prime}/RT}$

$$[\text{G6P}]/[\text{G1P}] = e^{-(-7100\ \text{J}\cdot\text{mol}^{-1})/(8.314\ \text{J}\cdot\text{K}^{-1}\cdot\text{mol}^{-1})(298\ \text{K})}$$
$$[\text{G6P}]/[\text{G1P}] = 17.6$$
$$[\text{G1P}]/[\text{G6P}] = 0.057$$

11. $\Delta G = \Delta H - T\Delta S$

$$\Delta G = -7000\ \text{J} \cdot \text{mol}^{-1} - (298\ \text{K})(-25\ \text{J} \cdot \text{K}^{-1} \cdot \text{mol}^{-1})$$
$$\Delta G = -7000 + 7450\ \text{J} \cdot \text{mol}^{-1} = 450\ \text{J} \cdot \text{mol}^{-1}$$

The reaction is not spontaneous because $\Delta G > 0$. The temperature must be decreased in order to decrease the value of the $T\Delta S$ term.

12. In order for ΔG to have a negative value (a spontaneous reaction), $T\Delta S$ must be greater than ΔH.

$$T\Delta S > \Delta H$$
$$T > \Delta H/\Delta S$$
$$T > 7000\ \text{J} \cdot \text{mol}^{-1}/20\ \text{J} \cdot \text{K}^{-1} \cdot \text{mol}^{-1}$$
$$T > 350\ \text{K or } 77^{\circ}\text{C}$$

13. (a) False. A spontaneous reaction only occurs in one direction. (b) False. Thermodynamics does not specify the rate of a reaction. (c) True. (d) True. A reaction is spontaneous so long as $\Delta S > \Delta H/T$.

14. This strategy will NOT work because Reaction 1 has a negative enthalpy change, releasing heat, and will therefore become more favorable with decreasing temperature, whereas Reaction 2, which has a positive enthalpy change, will become less favorable. Thus decreasing the temperature will favor Reaction 1, not Reaction 2. In order to make Reaction 2 more favorable, the temperature must be raised.

To calculate the amount that the temperature must be raised, Equation 1-18 may be used as follows:

$$\ln K_{\text{eq}} = \frac{-\Delta H^{\circ}}{R}\left(\frac{1}{T}\right) + \frac{\Delta S^{\circ}}{R}$$
$$\ln \frac{K_1^{T_1}}{K_1^{T_2}} = \frac{-\Delta H_1^{\circ}}{R}\left(\frac{1}{T_1} - \frac{1}{T_2}\right)$$
$$\ln \frac{K_2^{T_1}}{K_2^{T_2}} = \frac{-\Delta H_2^{\circ}}{R}\left(\frac{1}{T_1} - \frac{1}{T_2}\right)$$

On subtraction of the previous two equations, and taking into account that $K_2^{T_1}/K_1^{T_1} = 1$, we get

$$\ln\left[\frac{K_1^{T_1}K_2^{T_2}}{K_1^{T_2}K_2^{T_1}}\right] = \ln \frac{K_2^{T_2}}{K_1^{T_2}} = \frac{\Delta H_2^{\circ} - \Delta H_1^{\circ}}{R}\left(\frac{1}{T_1} - \frac{1}{T_2}\right)$$

We would like $K_2^{T_2}/K_1^{T_2} = 10$. Substituting in all values and solving for T_2 we get

$$\ln \frac{K_2^{T_2}}{K_1^{T_2}} = \ln 10 = 2.3 = \frac{28{,}000 + 28{,}000}{8.31}\left(\frac{1}{298} - \frac{1}{T_2}\right)$$

Solving for T_2 we get

$$T_2 = \frac{1}{\dfrac{1}{298} - \dfrac{2.3 \times 8.31}{56{,}000}} = 332\ \text{K}$$

Hence to increase K_2/K_1 from 1 to 10, the temperature must be raised from 298 K to 332 K.

CHAPTER 2

1. (a) Donors: NH1, NH_2 at C2, NH9; acceptors: N3, O at C6, N7. (b) Donors: NH1, NH_2 at C4; acceptors: O at C2, N3. (c) Donors: NH_3^+ group, OH group; acceptors: COO^- group, OH group.
2. A protonated (and therefore positively charged) nitrogen would promote the separation of charge in the adjacent C—H bond so that the C would have a partial negative charge and the H would have a partial positive charge. This would make the H more likely to be donated to a hydrogen bond acceptor group.
3. From most soluble (most polar) to least soluble (least polar): c, b, e, a, d.
4. (a) Water; (b) water; (c) micelle.
5. The waxed car is a hydrophobic surface. To minimize its interaction with the hydrophobic molecules (wax), each water drop minimizes its surface area by becoming a sphere (the geometrical shape with the lowest possible ratio of surface to volume). Water does not bead on glass, because the glass presents a hydrophilic surface with which the water molecules can interact. This allows the water to spread out.
6. Water molecules move from inside the dialysis bag to the surrounding seawater by osmosis. Ions from the seawater diffuse into the dialysis bag. At equilibrium, the compositions of the solutions inside and outside the dialysis bag are identical. If the membrane were solute-impermeable, essentially all the water would leave the dialysis bag.
7. (a)

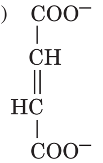

$\mathrm{^-OOC{-}CH{=}HC{-}COO^-}$

(b)

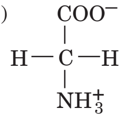

$\mathrm{H{-}\overset{\displaystyle COO^-}{\underset{\displaystyle NH_3^+}{C}}{-}H}$

(c)

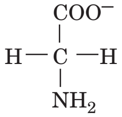

$\mathrm{H{-}\overset{\displaystyle COO^-}{\underset{\displaystyle NH_2}{C}}{-}H}$

(d)

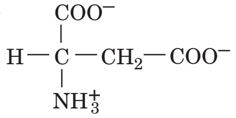

$\mathrm{H{-}\overset{\displaystyle COO^-}{\underset{\displaystyle NH_3^+}{C}}{-}CH_2{-}COO^-}$

8. (a) pH 4, NH_4^+; pH 8, NH_4^+; pH 11, NH_3.
(b) pH 4, $H_2PO_4^-$; pH 8, HPO_4^{2-}; pH 11, HPO_4^{2-}.
9. The increase in $[H^+]$ due to the addition of HCl is (50 mL)(1 mM)/(250 mL) = 0.2 mM = 2×10^{-4} M. Because the $[H^+]$ of pure water, 10^{-7} M, is relatively insignificant, the pH of the solution is equal to $-\log(2 \times 10^{-4})$ or 3.7.
10. (a) $(0.010\ \mathrm{L})(5\ \mathrm{mol \cdot L^{-1}\ NaOH})/(1\ \mathrm{L}) = 0.05\ \mathrm{M\ NaOH} \equiv 0.05\ \mathrm{M\ OH^-}$

$$[H^+] = K_w/[OH^-] = (10^{-14})/(0.05) = 2 \times 10^{-13}\ \mathrm{M}$$

$$\mathrm{pH} = -\log[H^+] = -\log(2 \times 10^{-13}) = 12.7$$

(b) $(0.020\ \mathrm{L})(5\ \mathrm{mol \cdot L^{-1}\ HCl})/(1\ \mathrm{L}) = 0.1\ \mathrm{M HCl} \equiv 0.1\ \mathrm{M\ H^+}$

Since the contribution of 0.01 L × 100 mM/(1 L) = 1 mM glycine is insignificant in the presence of 0.1 M HCl,

$$\mathrm{pH} = -\log[H^+] = -\log(0.1) = 1.0$$

(c) $\mathrm{pH} = \mathrm{p}K + \log([\mathrm{acetate}]/[\mathrm{acetic\ acid}])$

$$[\mathrm{acetate}] = (5\ \mathrm{g})(1\ \mathrm{mol}/82\ \mathrm{g})/(1\ \mathrm{L}) = 0.061\ \mathrm{M}$$

$$[\mathrm{acetic\ acid}] = (0.01\ \mathrm{L})(2\ \mathrm{mol \cdot L^{-1}})/(1\ \mathrm{L}) = 0.02\ \mathrm{M}$$

$$\mathrm{pH} = 4.76 + \log(0.061/0.02) = 4.76 + 0.48 = 5.24$$

11. The standard free energy change can be calculated using Eq. 1-16 and the value of K from Table 2-4.

$$\begin{aligned}\Delta G^{\circ\prime} &= -RT \ln K \\ &= -(8.314\ \mathrm{J \cdot K^{-1} \cdot mol^{-1}})(298\ \mathrm{K}) \ln(3.39 \times 10^{-8}) \\ &= 42{,}600\ \mathrm{J \cdot mol^{-1}} = 42.6\ \mathrm{kJ \cdot mol^{-1}}\end{aligned}$$

12. The pK corresponding to the equilibrium between $H_2PO_4^-$ (HA) and HPO_4^{2-} (A^-) is 6.82 (Table 2-4). The concentration of A^- is (50 mL)(2.0 M)/(200 mL) = 0.5 M, and the concentration of HA is (25 mL)(2.0 M)/(200 mL) = 0.25 M. Substitute these values into the Henderson–Hasselbalch equation (Eq. 2-9):

$$\mathrm{pH} = \mathrm{p}K + \log\frac{[A^-]}{[HA]}$$

$$\mathrm{pH} = 6.82 + \log\frac{0.5}{0.25}$$

$$\mathrm{pH} = 6.82 + \log 2$$

$$\mathrm{pH} = 6.82 + 0.30 = 7.12$$

13. Use the Henderson–Hasselbalch equation (Eq. 2-9) and solve for pK:

$$\mathrm{pH} = \mathrm{p}K + \log\frac{[A^-]}{[HA]}$$

$$\mathrm{p}K = \mathrm{pH} - \log\frac{[A^-]}{[HA]}$$

$$\mathrm{p}K = 6.5 - \log\frac{0.2}{0.1}$$

$$\mathrm{p}K = 6.5 - 0.3 = 6.2$$

14. Let HA = sodium succinate and A^- = disodium succinate.

$[A^-] + [HA] = 0.050\ \mathrm{M}$, so $[A^-] = 0.050\ \mathrm{M} - [HA]$

From Eq. 2-9 and Table 2-4,

$\log([A]/[HA]) = \mathrm{pH} - \mathrm{p}K = 6.0 - 5.64 = 0.36$

$[A^-]/[HA] = \mathrm{antilog}\ 0.36 = 2.29$

$(0.050\ \mathrm{M} - [HA])/[HA] = 2.29$

$[HA] = 0.015\ \mathrm{M}$

$[A^-] = 0.050\ \mathrm{M} - 0.015\ \mathrm{M} = 0.035\ \mathrm{M}$

grams of sodium succinate =

$$(0.015\ \mathrm{mol \cdot L^{-1}})(140\ \mathrm{g \cdot mol^{-1}}) \times (1\ \mathrm{L}) = 2.1\ \mathrm{g}$$

grams of disodium succinate =

$$(0.035\ \mathrm{mol \cdot L^{-1}})(162\ \mathrm{g \cdot mol^{-1}}) \times (1\ \mathrm{L}) = 5.7\ \mathrm{g}$$

15. At pH 4, essentially all the phosphoric acid is in the $H_2PO_4^-$ form, and at pH 9, essentially all is in the HPO_4^{2-} form (Fig. 2-18). Therefore, the concentration of OH^- required is equivalent to the concentration of the acid: (0.100 mol · L^{-1} phosphoric acid)(0.1 L) = 0.01 mol NaOH required = (0.01 mol)(1 L/5 mol NaOH) = 0.002 L = 2 mL.
16. (a) Succinic acid; (b) ammonia; (c) HEPES.
17. The dissociation of $TrisH^+$ to its basic form and H^+ is associated with a large, positive enthalpy change. Consequently, heat is taken up by the reactant on dissociation. When the temperature is lowered, there is less heat available for this process, shifting the equilibrium constant toward the associated form (the effect of temperature on the equilibrium constant of a reaction is given by Eq. 1-18). To avoid this problem, the buffer should be prepared at the same temperature as its planned use.

18. (a) Carboxylic acid groups are stronger acids than ammonium groups and therefore lose their protons at lower pH values. This can be seen in Fig. 2-17, where the carboxylic acid group of CH_3COOH is 50% dissociated to $CH_3COO^- + H^+$ at pH 4.7 while it is not until pH 9.25 that the ammonium ion is 50% dissociated to NH_3.

(b) $$H_3N^+CH_2COOH \rightleftharpoons H_3N^+CH_2COO^- + H^+ \rightleftharpoons H_2NCH_2COO^- + H^+$$

(c) The p*K* values of glycine's two ionizable groups are sufficiently different so that the Henderson–Hasselbalch equation (Section 2-2B) adequately describes the behavior of the solution of the diacid and the monodissociated species.

$$\mathrm{pH} = \mathrm{p}K + \log\frac{[\mathrm{A}^-]}{[\mathrm{HA}]}$$

$$2.65 = \mathrm{p}K + \log\frac{0.02}{0.01}$$

$$\mathrm{p}K = 2.65 - 0.3$$

$$\mathrm{p}K = 2.35$$

(d)

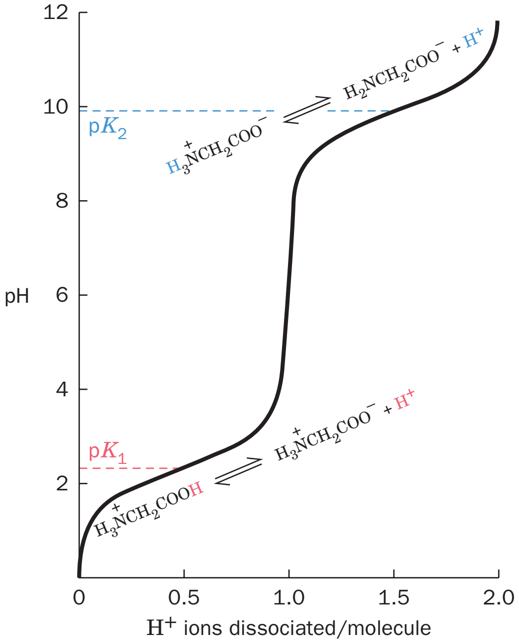

CHAPTER 3

1. (a) Yes; (b) no; (c) no; (d) yes.

2. Since the haploid genome contains 21% G, it must contain 21% C (because G = C) and 58% A + T (or 29% A and 29% T, because A = T). Each cell is diploid, containing 90,000 kb or 9×10^7 bases. Therefore,

$$\mathrm{A} = \mathrm{T} = (0.29)(9 \times 10^7) = 2.61 \times 10^7 \text{ bases}$$

$$\mathrm{C} = \mathrm{G} = (0.21)(9 \times 10^7) = 1.89 \times 10^7 \text{ bases}$$

3. The DNA contains 40 bases in all. Since G = C, there are 7 cytosine residues. The remainder (40 − 14 = 26) must be adenine and thymine. Since A = T, there are 13 adenine residues. There are no uracil residues (U is a component of RNA but not DNA).

4. (a)

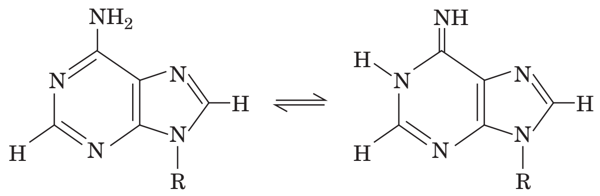

(b)

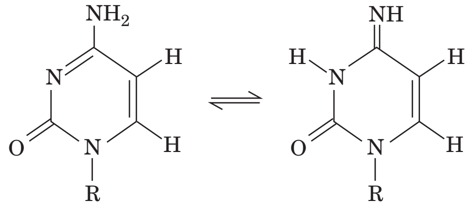

5.

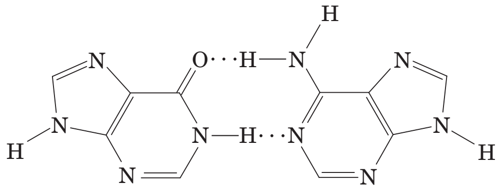

Hypoxanthine **Adenine**

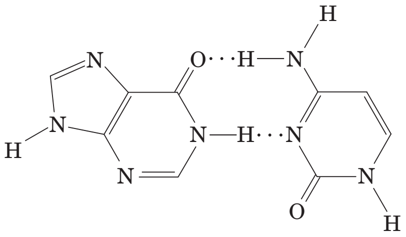

Hypoxanthine **Cytosine**

6. The high pH eliminates hydrogen bonds between bases, making it easier to separate the strands of DNA.

7. The number of possible sequences of four different nucleotides is 4^n where *n* is the number of nucleotides in the sequence. Therefore, (a) $4^1 = 4$, (b) $4^2 = 16$, (c) $4^3 = 64$, and (d) $4^4 = 256$.

8. 5′-A C G T–3′ + 5′-C G A A T C–3′
3′-T G C A G C–5′ 3′-T T A G–5′

9. (a) *Alu*I, *Eco*RV, *Hae*III, *Pvu*II; (b) *Hpa*II and *Msp*I; (c) *Bam*HI and *Bgl*II; *Hpa*II and *Taq*I; *Sal*I and *Xho*I.

10. (a) Newly synthesized chains would be terminated less frequently, so the bands representing truncated fragments on the sequencing gel would appear faint.

(b) Chain termination would occur more frequently, so longer fragments would be less abundant.

(c) The amount of DNA synthesis would decrease and the resulting gel bands would appear faint.

(d) No effect.

11. The *C. elegans* genome contains 97,000 kb, so

$$f = 5/97{,}000 = 5.2 \times 10^{-5}.$$

Using Eq. 3-2,

$$N = \log(1 - P)/\log(l - f)$$
$$N = \log(1 - 0.99)/\log(1 - 5.2 \times 10^{-5})$$
$$N = -2/(-2.24 \times 10^{-5}) = 8.91 \times 10^{4}$$

12. The desired clones are colorless when grown in the presence of ampicillin and X-gal. Nontransformed bacteria cannot grow in the presence of ampicillin, because they lack the amp^R gene carried by the plasmid. Clones transformed with the plasmid only are blue, since they have an intact *lacZ* gene and produce β-galactosidase, which cleaves the chromogenic substrate X-gal. Clones that contain the plasmid with the foreign DNA insert are colorless because the insert interrupts the *lacZ* gene.

13. (a) Only single DNA strands of variable length extending from the remaining primer would be obtained. The number of these strands would increase linearly with the number of cycles rather than geometrically.

    (b) PCR would yield a mixture of DNA segments whose lengths correspond to the distance between the position of the primer with a single binding site and the various sites where the multispecific primer binds.

    (c) The first cycle of PCR would yield only the new strand that is complementary to the intact DNA strand, since DNA synthesis cannot proceed when the template is broken. However, since the new strand has the same sequence as the broken strand, PCR can proceed normally from the second cycle on.

    (d) DNA synthesis would terminate at the breaks in the first cycle of PCR.

14. ATAGGCATAGGC and CTGACCAGCGCC.

15. (a) The genomic library contains DNA sequences corresponding to all the organism's DNA, which includes genes and nontranscribed sequences. A cDNA library represents only the DNA sequences that are transcribed into mRNA.

    (b) Different cell types express different sets of genes. Therefore, the populations of mRNA molecules used to construct the cDNA libraries also differ.

16. (a) If an individual is homozygous (has two copies of the same allele) at a locus, then only one peak will appear in the electrophoretogram (for example, the D3S1358 locus from Suspect 2).

    (b) Suspect 3, whose alleles exactly match those from the blood stain, is the most likely source of the blood.

    (c) Analysis of each of the three STR loci in this example shows a match between the sample and Suspect 3, and no matches with the other suspects. In practice, however, multiple loci are analyzed in order to minimize the probability of obtaining a match by chance.

    (d) The peak heights are lower for Suspect 1 compared to Suspect 4, suggesting that less DNA was available for PCR amplification from Suspect 1.

CHAPTER 4

1. Gly and Ala; Ser and Thr; Val, Leu, and Ile; Asn and Gln; Asp and Glu.

2. $^{+}H_3N-CH_2-CH_2-COO^{-}$

3. Hydrogen bond donors: α-amino group, amide nitrogen. Hydrogen bond acceptors: α-carboxylate group, amide carbonyl.

4.

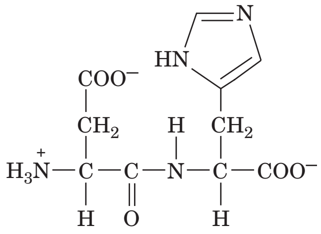

5. The first residue can be one of five residues, the second one of the remaining four, etc.

$$N = 5 \times 4 \times 3 \times 2 \times 1 = 120$$

6. (a) +1; (b) 0; (c) −1; (d) −2.

7. (a) $pI = (2.35 + 9.87)/2 = 6.11$

   (b) $pI = (6.04 + 9.33)/2 = 7.68$

   (c) $pI = (2.10 + 4.07)/2 = 3.08$

8. The polypeptide would be even less soluble than free Tyr, because most of the amino and carboxylate groups that interact with water and make Tyr at least slightly soluble are lost in forming the peptide bonds in poly(Tyr).

9.

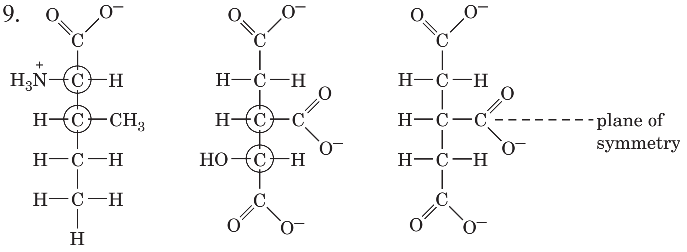

10.

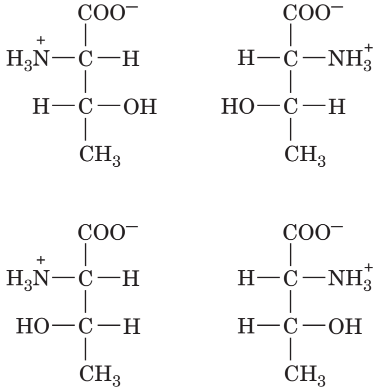

11.

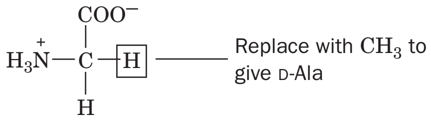

Replace with CH_3 to give D-Ala

12.

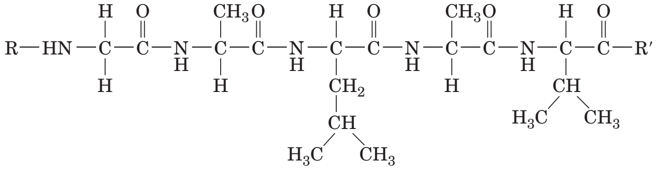

13. (2*S*,3*S*)-Isoleucine

14. (a) Glutamate; (b) aspartate

15. (a) Serine (*N*-acetylserine); (b) lysine (5-hydroxylysine); (c) methionine (*N*-formylmethionine).

16.

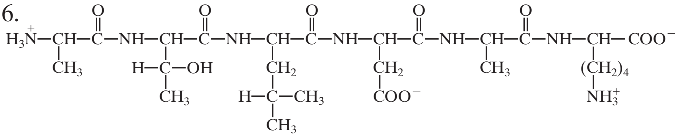

(a) The pK's of the ionizable side chains (Table 4-1) are 3.90 (Asp) and 10.54 (Lys); assume that the terminal Lys carboxyl group has a pK of 3.5 and the terminal Ala amino group has a pK of 8.0 (Section 4-1D). The pI is approximately midway between the pK's of the two ionizations involving the neutral species (the pK of Asp and the N-terminal pK):

$$pI \approx \tfrac{1}{2}(3.90 + 8.0) \approx 5.95$$

(b) The net charge at pH 7.0 is 0 (as drawn above).

17. At position A8, duck insulin has a Glu residue, whereas human insulin has a Thr residue. Since Glu is negatively charged at physiological pH and Thr is neutral, human insulin has a higher pI than duck insulin. (The other amino acids that differ between the proteins do not affect the pI because they are uncharged.)

CHAPTER 5

1. Peptide B, because it contains more Trp and other aromatic residues.

2. Since $A = \varepsilon cl$, $A = (0.4\ \text{mL}\cdot\text{mg}^{-1}\cdot\text{cm}^{-1})(2.0\ \text{mg}\cdot\text{mL}^{-1})(1\ \text{cm}) = 0.8$

3. Lowering the pH from 7.0 to 5.0 would promote the precipitation of protein Q because the protein will be least soluble when its net charge is zero (when pH = pI).

4. (a) Leu, His, Arg. (b) Lys, Val, Glu.

5. (a)

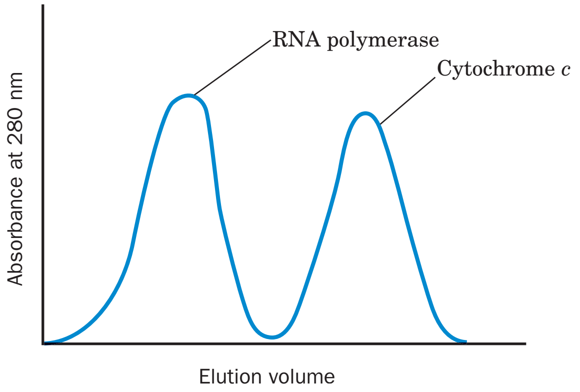

(b)

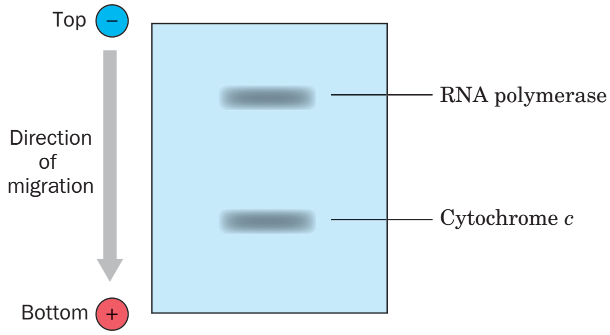

6. The protein behaves like a larger protein during gel filtration, suggesting that it has an elongated shape. The mass determined by SDS-PAGE is more accurate since the mobility of a denatured SDS-coated protein depends only on its size.

7. The protein contains two 60-kD polypeptides and two 40-kD polypeptides. Each 40-kD chain is disulfide bonded to a 60-kD chain. The 100-kD units associate noncovalently to form a protein with a molecular mass of 200 kD.

8. Because protein 1 has a greater proportion of hydrophobic residues (Ala, Ile, Pro, Val) than do proteins 2 and 3, hydrophobic interaction chromatography could be used to isolate it.

9. (a)

Purification step	mg total protein	μmol Mb	Specific activity (μmol Mb/mg total protein)	% yield	Fold purification
1. Crude extract	1550	0.75	4.8×10^{-4}	100	1
2. DEAE-cellulose chromatography	550	0.35	6.4×10^{-4}	47	1.3
3. Affinity chromatography	5.0	0.28	5.9×10^{-2}	80 from Affinity chromatography (37 overall)	123-fold overall, 92-fold from Affinity chromatography

(b) The DEAE chromatography step results in only a 47% yield, while the affinity chromatography step results in an 80% yield from the step before it. The DEAE chromatography step therefore results in the greatest loss of Mb.

(c) The DEAE chromatography step results in a 1.3-fold purification, while the affinity chromatography step results in a 92-fold purification from the previous step. The affinity chromatography step therefore results in the greatest purification of Mb.

(d) The affinity chromatography step is the best choice for a one-step purification of Mb in this example.

10. Dansyl chloride reacts with primary amino groups, including the ϵ-amino group of Lys residues.

11. (a) Gly; (b) Thr; (c) none (the N-terminal amino group is acetylated and hence unreactive with Edman's reagent)

12. Thermolysin would yield the most fragments (9) and endopeptidase V8 would yield the fewest (2).

13. (a) The positive charges are caused by the protonation of basic side chains (H, K, and R) and the N-terminal amino groups of the protein.

(b) There is 1 H, 6 K, 11 R, and 1 NH_2 at the N-terminus. Therefore, the maximum number of positive charges that can be obtained is 19.

(c) From Sample Calculation 5-1 we see that

$$M = (p_2 - 1)(p_1 - 1)/(p_2 - p_1)$$

Therefore

$$\begin{aligned} M &= (1789.2 - 1)(1590.6 - 1)/(1789.2 - 1590.6) \\ &= (1788.2)(1589.6)/198.6 \\ &= 14{,}312.8 \end{aligned}$$

(d) Peak 5 is p_1 in our calculation. From Sample Calculation 5-1,

$$p_1 = (\mathrm{M} + z)/z$$
$$1590.6 = (14312.8 + z)/z$$
$$1590.6z - z = 14312.8$$
$$z(1590.6 - 1) = 14312.8$$
$$z = 14312.8/1589.6 = 9.00$$

The charge on the fifth peak in the mass spectrum is 9.00.

14. Gln–Ala–Phe–Val–Lys–Gly–Tyr–Asn–Arg–Leu–Glu

15. Asp–Met–Leu–Phe–Met–Arg–Ala–Tyr–Gly–Asn

16. (a) There is one Met, so CNBr would produce two peptides.

(b) There are four possible sites for chymotrypsin to hydrolyze the peptide: following Phe, Tyr (twice), and Trp. This would yield five peptides.

(c) Four Cys residues form two disulfide bonds.

(d) Arbitrarily choosing one Cys residue, there are three ways it can make a disulfide bond with the remaining three Cys residues. After choosing one of them, there is only one way that the remaining two Cys residues can form a disulfide bond. Thus there are 3 × 1 = 3 possible arrangements of the disulfide bonds.

17.

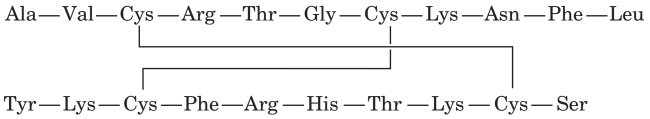
Ala—Val—Cys—Arg—Thr—Gly—Cys—Lys—Asn—Phe—Leu
Tyr—Lys—Cys—Phe—Arg—His—Thr—Lys—Cys—Ser

18. Arg–Ile–Pro–Lys–Cys–Arg–Lys–Phe–Gln–Gln–Ala–Gln–His–Leu–Arg–Ala–Cys–Gln–Gln–Trp–Leu–His–Lys–Gln–Ala–Asn–Gln–Ser–Gly–Gly–Gly–Pro–Ser

19. Because the side chain of Gly is only an H atom, it often occurs in a protein at a position where no other residue can fit. Consequently, Gly can take the place of a larger residue more easily than a larger residue, such as Val, can take the place of Gly.

20. (a) Position 6 (Gly) and Position 9 (Val) appear to be invariant.

(b) Conservative substitutions occur at Position 1 (Asp and Lys, both charged), Position 10 (Ile and Leu, similar in structure and hydrophobicity), and Position 2 (all uncharged bulky side chains). Positions 5 and 8 appear to tolerate some substitution.

(c) The most variable positions are 3, 4, and 7, where a variety of residues appear.

CHAPTER 6

1.

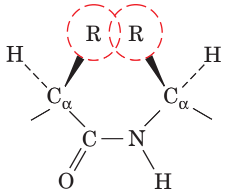

2. (a) 3.6_{13}; (b) steeper.

3. (100 residues)(1 α-helical turn/3.6 residues)

(5.1 Å/keratin turn) = 142 Å

4. (a) The first and fourth side chains of the two helices of a coiled coil form buried hydrophobic interacting surfaces, but the remaining side chains are exposed to the solvent and therefore tend to be polar or charged.

(b) Although the residues at positions 1 and 4 in both sequences are hydrophobic, Trp and Tyr are much larger than Ile and Val and would therefore not fit as well in the area of contact between the two polypeptides in a coiled coil.

5. A fibrous protein such as α keratin does not have a discrete globular core. Most of the residues in its coiled coil structure are exposed to the solvent. The exception is the strip of nonpolar side chains at the interface of the two coils.

6. The reducing conditions promote cleavage of the disulfide bonds that cross-link α keratin molecules. This helps the larvae digest the wool clothing that they eat.

7. Collagen's primary structure is its amino acid sequence, which is a repeating triplet of mostly Gly–Pro–Hyp. Its secondary structure is the left-handed helical conformation characteristic of its repeating sequence. Its tertiary structure is essentially the same as its secondary structure, since most of the protein consists of one type of secondary structure. Collagen's quaternary structure is the arrangement of its three chains in a right-handed triple helix.

8. Because collagen has such an unusual amino acid composition (almost two-thirds consists of Gly and Pro or Pro derivatives), it contains relatively fewer of the other amino acids and is therefore not as good a source of amino acids as proteins containing a greater variety of amino acids.

9. Yes, although such irregularity should not be construed as random.

10. (a) Gln; (b) Ser; (c) Ile; (d) Cys. See Table 6-1.

11. (a) C_4 and D_2; (b) C_6 and D_3.

12. (a) Phe. Ala and Phe are both hydrophobic, but Phe is much larger and might not fit as well in Val's place.

(b) Asp. Replacing a positively charged Lys residue with an oppositely charged Asp residue would be more disruptive.

(c) Glu. The amide-containing Asn would be a better substitute for Gln than the acidic Glu.

(d) His. Pro's constrained geometry is best approximated by Gly, which lacks a side chain, rather than a residue with a bulkier side chain such as His.

13. A polypeptide synthesized in a living cell has a sequence that has been optimized by natural selection so that it folds properly (with hydrophobic residues on the inside and polar residues on the outside). The random sequence of the synthetic peptide cannot direct a coherent folding process, so hydrophobic side chains on different molecules aggregate, causing the polypeptide to precipitate from solution.

14. No.

15. Hydrophobic effects, van der Waals interactions, and hydrogen bonds are destroyed during denaturation. Covalent cross-links are retained.

16. At physiological pH, the positively charged Lys side chains repel each other. Increasing the pH above the pK (>10.5) would neutralize the side chains and allow an α helix to form.

17. The molecular mass of O_2 is 32 D. Hence the ratio of the masses of hemoglobin and 4 O_2, which is equal to the ratio of their

volumes, is 65,000/(4 × 32) = 508. The 70-kg office worker has a volume of 70 kg × 1 cm^3/g × (1000 g/kg) × (1 m/100 cm)^3 = 0.070 m^3. Hence the ratio of the volumes of the office and the office worker is (4 × 4 × 3)/0.070 = 686. These ratios are similar in magnitude, which you may not have expected.

18. Peptide c is most likely to form an α helix with its three charged residues (Lys, Glu, and Arg) aligned on one face of the helix. Peptide a has adjacent basic residues (Arg and Lys), which would destabilize a helix. Peptide b contains Gly and Pro, both of which are helix-breaking (Table 6-1). The presence of Gly and Pro would also inhibit the formation of β strands, so peptide b is least likely to form a β strand.

19. In a protein crystal, the residues at the end of a polypeptide chain may experience fewer intramolecular contacts and therefore tend to be less ordered (more mobile in the crystal). If their disorder prevents them from generating a coherent diffraction pattern, it may be impossible to map their electron density.

CHAPTER 7

1.

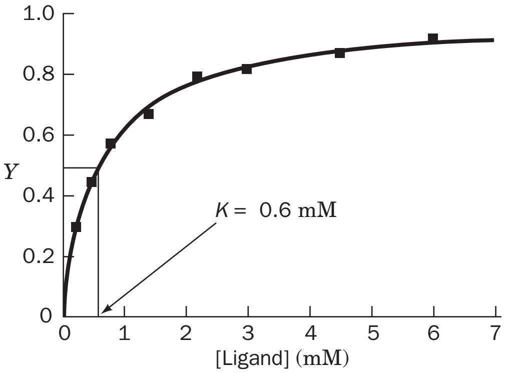

2. Set b describes sigmoidal binding to an oligomeric protein and hence represents cooperative binding.

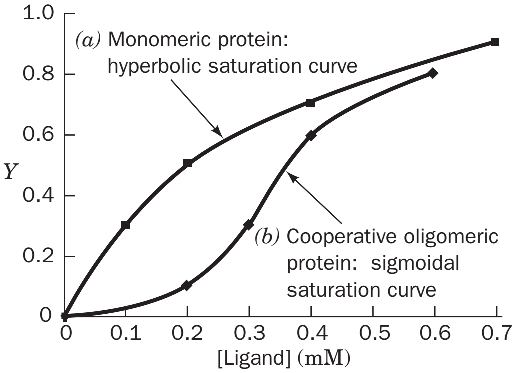

3. According to Eq. 7-6,

$$Y_{O_2} = \frac{pO_2}{K + pO_2}$$

When pO_2 = 10 torr,

$$Y_{O_2} = \frac{10}{2.8 + 10} = 0.78$$

When pO_2 = 1 torr,

$$Y_{O_2} = \frac{1}{2.8 + 1} = 0.26$$

The difference in Y_{O_2} values is 0.78 − 0.26 = 0.52. Therefore, in active muscle cells, myoglobin can transport a significant amount of O_2 by diffusion from the cell surface to the mitochondria.

4. (a) Hyperventilation eliminates CO_2, but it does not significantly affect the O_2 concentration, since the hemoglobin in arterial blood is already essentially saturated with oxygen.

   (b) The removal of CO_2 also removes protons, according to the reaction

$$H^+ + HCO_3^- \rightleftharpoons H_2O + CO_2$$

   The resulting increase in blood pH would increase the O_2 affinity of hemoglobin through the Bohr effect. The net result would be that less oxygen could be delivered to the tissues until the CO_2 balance was restored. Thus, hyperventilation has the opposite of the intended effect (note that since hyperventilation suppresses the urge to breathe, doing so may cause the diver to lose consciousness due to lack of O_2 and hence drown).

5. (a) Vitamin O is useless because the body's capacity to absorb oxygen is not limited by the amount of oxygen available but by the ability of hemoglobin to bind and transport O_2. Furthermore, oxygen is normally introduced into the body via the lungs, so it is unlikely that the gastrointestinal tract would have an efficient mechanism for extracting oxygen.

   (b) The fact that oxygen delivery in vertebrates requires a dedicated O_2-binding protein (hemoglobin) indicates that dissolved oxygen by itself cannot attain the high concentrations required. Moreover, a few drops of vitamin O would make an insignificant contribution to the amount of oxygen already present in a much larger volume of blood.

6. (a) Lower; (b) higher. The Asp 99β → His mutation of hemoglobin Yakima disrupts a hydrogen bond at the α_1–β_2 interface of the T state (Fig. 7-9*a*), causing the T ⇌ R equilibrium to shift toward R state (lower p_{50}). The Asn 102β → Thr of hemoglobin Kansas causes the opposite shift in the T ⇌ R equilibrium by abolishing an R-state hydrogen bond (Fig. 7-9*b*).

7. The increased BPG helps the remaining erythrocytes deliver O_2 to tissues. However, BPG stabilizes the T conformation of hemoglobin, so it promotes sickling and therefore aggravates the disease.

8. (a) Because the mutation destabilizes the T conformation of hemoglobin Rainier, the R (oxy) conformation is more stable. Therefore, the oxygen affinity of hemoglobin Rainier is greater than normal.

   (b) The ion pairs that normally form in deoxyhemoglobin absorb protons. The absence of these ion pairs in hemoglobin Rainier decreases the Bohr effect (in fact, the Bohr effect in hemoglobin Rainier is about half that of normal hemoglobin).

   (c) Because the R conformation of hemoglobin Rainier is more stable than the T conformation, even when the molecule is not oxygenated, O_2-binding cooperativity is reduced. The Hill coefficient of hemoglobin Rainier is therefore less than that for normal hemoglobin.

9. As the crocodile remains under water without breathing, its metabolism generates CO_2 and hence the HCO_3^- content of its

blood increases. The HCO_3^- preferentially binds to the crocodile's deoxyhemoglobin, which allosterically prompts the hemoglobin to assume the deoxy conformation and thus release its O_2. This helps the crocodile stay under water long enough to drown its prey.

10. (a)

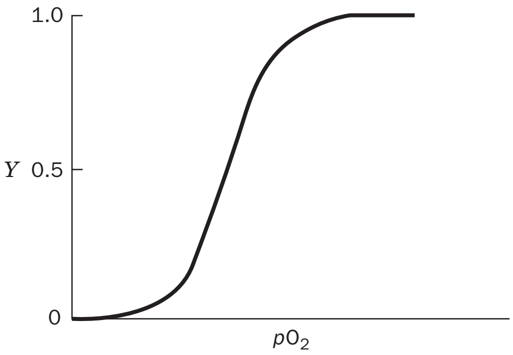

(b) The Hill coefficient most likely has a value between 1 (no cooperativity) and 2 (perfect cooperativity between the two subunits).

11. Myosin is both fibrous and globular. Its two heads are globular, with several layers of secondary structure. Its tail, however, consists of a lengthy, fibrous coiled coil.

12. Because many myosin heads bind along a thin filament where it overlaps a thick filament, and because the myosin molecules do not execute their power strokes simultaneously, the thick and thin filaments can move past each other by more than 100 Å in the interval between power strokes of an individual myosin molecule.

13. In the absence of ATP, each myosin head adopts a conformation that does not allow it to release its bound actin molecule. Consequently, thick and thin filaments form a rigid cross-linked array.

14. Microfilaments consist entirely of actin subunits that are assembled in a head-to-tail fashion so that the polarity of the subunits is preserved in the fully assembled fiber. In keratin filaments, however, successive heterodimers align in an antiparallel fashion, so that in a fully assembled intermediate filament, half the molecules are oriented in one direction and half are oriented in the opposite direction (Fig. 6-16).

15. (a) 150–200 kD; (b) 150–200 kD; (c) ~23 kD and 53–75 kD.

16. The loops are on the surface of the domain, so they can tolerate more amino acid substitutions. Amino acid changes in the β sheets would be more likely to destabilize the domain.

17. The antigenic site in the native protein usually consists of several peptide segments that are no longer contiguous when the tertiary structure of the protein is disrupted.

18. (a) Fab fragments are monovalent and therefore cannot cross-link antigens to produce a precipitate. (b) A small antigen has only one antigenic site and therefore cannot bind more than one antibody to produce a precipitate. (c) When antibody is in great excess, most antibodies that are bound to antigen bind only one per immunoglobulin molecule. When antigen is in excess, most immunoglobulins bind to two independent antigens.

CHAPTER 8

1. (a) 4; (b) 8; (c) 16.
2. (a) and (d)
3. Tagatose is derived from galactose.
4.

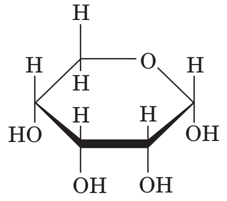
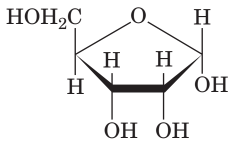

5. (a) Yes; (b) no (its symmetric halves are superimposable); (c) no.
6.

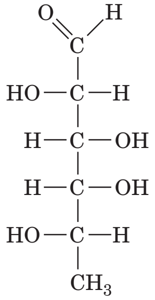

L-Fucose

L-Fucose is the 6-deoxy form of L-galactose.

7. (a) α-D-glucose-(1 → 1)-α-D-glucose or α-D-glucose-(1 → 1)-β-D-glucose. (b) The numerous hydrogen-bonding —OH groups of the disaccharide act as substitutes for water molecules.
8. 19
9.

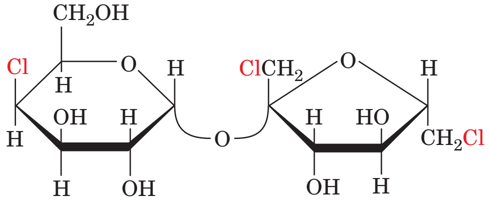

10. One
11. Amylose (it has only one nonreducing end from which glucose can be mobilized).
12. Glucosamine is a building block of certain glycosaminoglycan components of proteoglycans (Fig. 8-12). Boosting the body's supply of glucosamine might slow the progression of the disease osteoarthritis, which is characterized by the degradation of proteoglycan-rich articular (relating to a joint) cartilage.
13. −200
14.

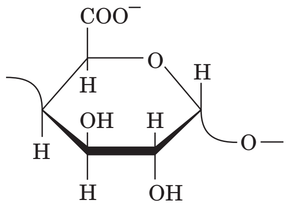

15.

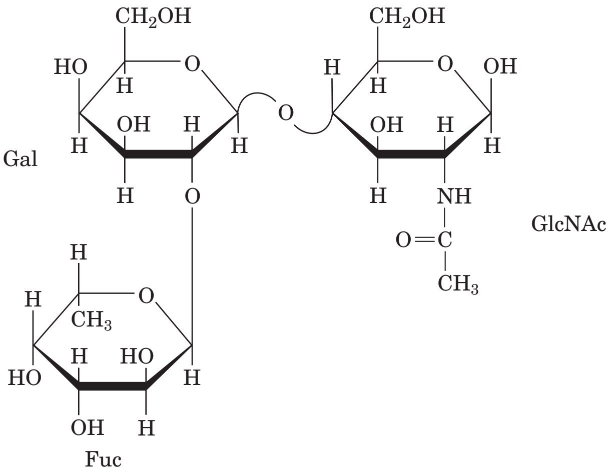

16. (a) There are four types of methylated glucose molecules, corresponding to (1) the residue at the reducing end of the glycogen molecule, (2) residues at the nonreducing ends, (3) residues at the α(1 → 6) branch points, and (4) residues from the linear α(1 → 4)-linked segments of glycogen. Type 4 is the most abundant type of residue.

(b)

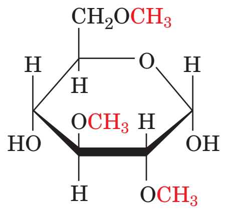

CHAPTER 9

1. *trans*-Oleic acid has a higher melting point because, in the solid state, its hydrocarbon chains pack together more tightly than those of *cis*-oleic acid.
2. Of the 4 × 4 = 16 pairs of fatty acid residues at C1 and C3, only 10 are unique because a molecule with different substituents at C1 and C3 is identical to the molecule with the reverse substitution order. However, C2 may have any of the four substituents for a total of 4 × 10 = 40 different triacylglycerols.
3. The triacylglycerol containing the stearic acid residues yields more energy since it is fully reduced.
4.

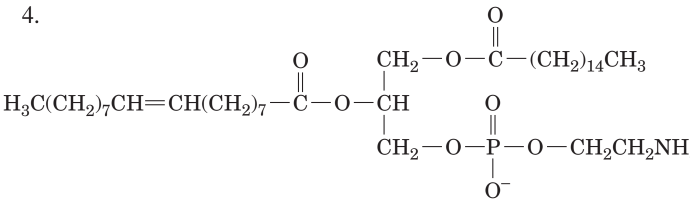

5. (a) Palmitic acid and 2-oleoyl-3-phosphatidylserine;
   (b) oleic acid and 1-palmitoyl-3-phosphatidylserine;
   (c) phosphoserine and 1-palmitoyl-2-oleoyl-glycerol;
   (d) serine and 1-palmitoyl-2-oleoyl-phosphatidic acid.
6. All except choline can form hydrogen bonds.
7. No; the two acyl chains of the "head group" are buried in the bilayer interior, leaving a head group of diphosphoglycerol.
8. Both DNA and phospholipids have exposed phosphate groups that are recognized by the antibodies.
9. Steroid hormones, which are hydrophobic, can diffuse through the cell membrane to reach their receptors.
10. Eicosanoids synthesized from arachidonic acid are necessary for intercellular communication. Cultured cells do not need such communication and therefore do not require linoleic acid.
11. Triacylglycerols lack polar head groups, so they do not orient themselves in a bilayer with their acyl chains inward and their glycerol moiety toward the surface.
12. The large oligosaccharide head groups of gangliosides would prevent efficient packing of the lipids in a bilayer.
13. (a) Saturated; (b) long-chain. By increasing the proportion of saturated and long-chain fatty acids, which have higher melting points, the bacteria can maintain constant membrane fluidity at the higher temperature.
14. (a) (1 turn/5.4 Å)(30 Å) = 5.6 turns
    (b) (3.6 residues/turn)(5.6 turns) = 20 residues
    (c) The additional residues form a helix, which partially satisfies backbone hydrogen bonding requirements, where the lipid head groups do not offer hydrogen bonding partners.
15. No. Although the β strand could span the bilayer, a single strand would be unstable because its backbone could not form the hydrogen bonds it would form with water in aqueous solution.
16. (a) Inner; (b) outer. See Fig. 9-32.
17. (a) Both the intra- and extracellular portions will be labeled. (b) Only the extracellular portion will be labeled. (c) Only the intracellular portion will be labeled.
18. The mutant signal peptidase would cleave many preproteins within their signal peptides, which often contain Leu-Leu sequences. This would not affect translocation into the ER, since signal peptidase acts after the signal peptide enters the ER lumen. Proteins lacking the Leu-Leu sequence would retain their signal peptides. These proteins, and those with abnormally cleaved signal sequences, would be more likely to fold abnormally and therefore function abnormally.
19. In order for a neuron to repeatedly release neurotransmitters, the components of its exocytotic machinery must be recycled. Following the fusion of synaptic vesicles with the plasma membrane, the four-helix SNARE complex is disassembled so that the Q-SNAREs remain in the plasma membrane while portions of the membrane containing R-SNAREs can be used to re-form synaptic vesicles. This recycling process would not be possible if the R- and Q-SNAREs remained associated, and the neuron would eventually be unable to release neurotransmitters.

CHAPTER 10

1. (a) Nonmediated; (b) mediated; (c) nonmediated; (d) mediated.
2. The less polar a substance, the faster it can diffuse through the lipid bilayer. From slowest to fastest: C, A, B.
3. $$\Delta G = RT \ln \frac{[\text{Glucose}]_{in}}{[\text{Glucose}]_{out}}$$
$$= (8.3145\ \text{J} \cdot \text{K}^{-1} \cdot \text{mol}^{-1})(298\ \text{K}) \ln \frac{(0.003)}{(0.005)}$$
$$= -1270\ \text{J} \cdot \text{mol}^{-1} = -1.27\ \text{kJ} \cdot \text{mol}^{-1}$$

4. (a)
$$\begin{aligned}\Delta G &= RT\ln([\text{Na}^+]_{in}/[\text{Na}^+]_{out})\\ &= (8.314\ \text{J}\cdot\text{K}^{-1}\cdot\text{mol}^{-1})(310\ \text{K})\\ &\quad(\ln[10\ \text{mM}/150\ \text{mM}])\\ &= (8.314)(310)(-2.71)\ \text{J}\cdot\text{mol}^{-1}\\ &= -6980\ \text{J}\cdot\text{mol}^{-1} = -7.0\ \text{kJ}\cdot\text{mol}^{-1}\end{aligned}$$
   (b)
$$\begin{aligned}\Delta G &= RT\ln([\text{Na}^+]_{in}/[\text{Na}^+]_{out}) + Z_{\text{A}}\mathcal{F}\Delta\Psi\\ &= -6980 + (1)(96{,}485\ \text{C}\cdot\text{mol}^{-1})(-0.06\ \text{J}\cdot\text{C}^{-1})\\ &= -6980\ \text{J}\cdot\text{mol}^{-1} - 5790\ \text{J}\cdot\text{mol}^{-1}\\ &= -12{,}770\ \text{J}\cdot\text{mol}^{-1} = -12.8\ \text{kJ}\cdot\text{mol}^{-1}\end{aligned}$$

5. Use Equation 10-3 and let $Z = 2$ and $T = 310$ K:

   (a)
$$\begin{aligned}\Delta G &= RT\ln\frac{[\text{Ca}^{2+}]_{in}}{[\text{Ca}^{2+}]_{out}} + Z\mathcal{F}\Delta\Psi\\ &= (8.314\ \text{J}\cdot\text{K}^{-1}\cdot\text{mol}^{-1})(310\ \text{K})\ln(10^{-7})/(10^{-3})\\ &\quad + (2)(96{,}485\ \text{J}\cdot\text{V}^{-1}\cdot\text{mol}^{-1})(-0.050\ \text{V})\\ &= -23{,}700\ \text{J}\cdot\text{mol}^{-1} - 9600\ \text{J}\cdot\text{mol}^{-1}\\ &= -33{,}300\ \text{J}\cdot\text{mol}^{-1} = -33.3\ \text{kJ}\cdot\text{mol}^{-1}\end{aligned}$$
   The negative value of ΔG indicates a thermodynamically favorable process.

   (b)
$$\begin{aligned}\Delta G &= RT\ln\frac{[\text{Ca}^{2+}]_{in}}{[\text{Ca}^{2+}]_{out}} + Z\mathcal{F}\Delta\Psi\\ &= (8.314\ \text{J}\cdot\text{K}^{-1}\cdot\text{mol}^{-1})(310\ \text{K})\ln(10^{-7})/(10^{-3})\\ &\quad + (2)(96{,}485\ \text{J}\cdot\text{V}^{-1}\cdot\text{mol}^{-1})(+0.150\ \text{V})\\ &= -23{,}700\ \text{J}\cdot\text{mol}^{-1} + 28{,}900\ \text{J}\cdot\text{mol}^{-1}\\ &= +5{,}200\ \text{J}\cdot\text{mol}^{-1} = +5.2\ \text{kJ}\cdot\text{mol}^{-1}\end{aligned}$$
   The positive value of ΔG indicates a thermodynamically unfavorable process.

6. K^+ transport ceases because the ionophore–K^+ complex cannot diffuse through the membrane when the lipids are immobilized in a gel-like state.

7. The number of ions to be transported is
$$\begin{aligned}&(10\ \text{mM})(100\ \mu\text{m}^3)(N)\\ &= (0.010\ \text{mol}\cdot\text{L}^{-1})(10^{-13}\ \text{L})(6.02\times10^{23}\ \text{ions}\cdot\text{mol}^{-1})\\ &= 6.02\times10^{8}\ \text{ions}\end{aligned}$$
   Since there are 100 ionophores, each must transport 6.02×10^6 ions. The time required is $(6.02\times10^6\ \text{ions})(1\ \text{s}/10^4\ \text{ions}) = 602\ \text{s} = 10$ min.

8. (a) The data do not indicate the involvement of a transport protein, since the rate of transport does not approach a maximum as [X] increases.

   (b) To verify that a transport protein is involved, increase [X] to demonstrate saturation of the transporter at high [X], or add a structural analog of X to compete with X for binding to the transporter, resulting in a lower flux of X.

9. In the absence of ATP, Na^+ extrusion by the (Na^+–K^+)–ATPase would cease, so no glucose could enter the cell by the Na^+–glucose symport. The glucose in the cell would then exit via the passive-mediated glucose transporter, and the cellular [glucose] would decrease until it matched the extracellular [glucose] (of course, the cell would probably osmotically burst before this could occur).

10. The hyperbolic curve for glucose transport into pericytes indicates a protein-mediated sodium-dependent process. The transport protein has binding sites for sodium ions. At low [Na^+], glucose transport is directly proportional to [Na^+]. However, at high [Na^+], all Na^+ binding sites on the transport protein are occupied, and thus glucose transport reaches a maximum velocity. Glucose transport into endothelial cells is not sodium-dependent and occurs at a high rate whether or not Na^+ is present. There is not enough information in the figure to determine whether glucose transport into endothelial cells is protein-mediated.

11. (a) No; there is no glycerol backbone.

    (b) Miltefosine is amphipathic and therefore cannot cross the parasite cell membrane by diffusion. Since it is not a normal cell component, it probably does not have a dedicated active transporter. It most likely enters the cell via a passive transport protein.

    (c) This amphipathic molecule most likely accumulates in membranes, with its hydrophobic tail buried in the bilayer and its polar head group exposed to the solvent.

    (d) The protein recognizes the phosphocholine head group, which also occurs in some sphingolipids and some glycerophospholipids. Since the protein does not bind all phospholipids or triacylglycerols, it does not recognize the hydrocarbon tail.

12. (a) A transporter similar to a porin would be inadequate since even a large β barrel would be far too small to accommodate the massive ribosome. Likewise, a transport protein with alternating conformations would not be up to the task due to its small size relative to the ribosome. In addition, neither type of protein would be suited for transporting a particle across two membranes. (In fact, ribosomes and other large particles move between the nucleus and cytoplasm via nuclear pores, which are constructed from many different proteins and form a structure that is much larger than the ribosome and spans both nuclear membranes.)

    (b) Ribosomal transport might appear to be a thermodynamically favorable process, since the concentration of ribosomes is greater in the nucleus, where they are synthesized. However, free energy would ultimately be required to establish a pore (which would span two membrane thicknesses) for the ribosome to pass through. (In fact, the nucleocytoplasmic transport of all but very small substances requires the activity of GTPases that escort particles through the nuclear pore assembly and help ensure that transport proceeds in one direction.)

13. (a) Acetylcholine binding triggers the opening of the channel, an example of a ligand-gated transport protein.

    (b) Na^+ ions flow into the muscle cell, where their concentration is low.

    (c) The influx of positive charges causes the membrane potential to increase.

14. (a) $\text{pH} = -\log[\text{H}^+] = -\log(0.15) = 0.82$

    The pH of the secreted HCl is over 6 pH units lower than the cytosolic pH, which corresponds to a [H^+] of $\sim4\times10^{-8}$ M.

    (b) $\text{CO}_2 + \text{H}_2\text{O} \rightleftharpoons \text{HCO}_3^- + \text{H}^+$

    (c)

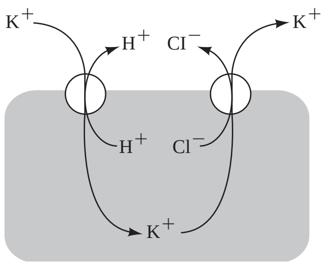

15. Overexpression of an MDR transporter would increase the ability of the cancer cell to excrete anticancer drugs. Higher concentrations of the drugs or different drugs would then be required to kill the drug-resistant cells.

CHAPTER 11

1. b
2. (a) isomerase (alanine racemase); (b) lyase (pyruvate decarboxylase); (c) oxidoreductase (lactate dehydrogenase); (d) ligase (glutamine synthetase).
3. As shown in Table 11-1, the only relationship between the rates of catalyzed and uncatalyzed reactions is that the catalyzed reaction is faster than the uncatalyzed reaction. The absolute rate of an uncatalyzed reaction does not correlate with the degree to which it is accelerated by an enzyme.
4. There are three transition states ($X^\ddagger$) and two intermediates (I). The reaction is not thermodynamically favorable because the free energy of the products is greater than that of the reactants.

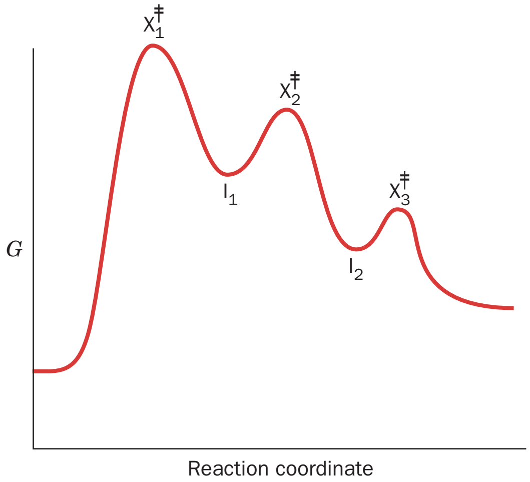

5. The tighter S binds to the enzyme, the greater the value of $\Delta G_E^\ddagger$. As $\Delta G_E^\ddagger$ approaches $\Delta G_N^\ddagger$ the rate of the enzyme-catalyzed reaction approaches the rate of the nonenzymatic reaction.

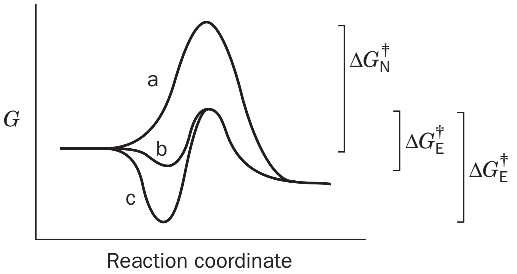

6. At 25°C, every 10-fold increase in rate corresponds to a decrease of about 5.7 $kJ \cdot mol^{-1}$ in $\Delta G^\ddagger$. For the nuclease, with a rate enhancement on the order of 10^{14}, $\Delta G^\ddagger$ is lowered about $14 \times 5.7\ kJ \cdot mol^{-1}$, or about 80 $kJ \cdot mol^{-1}$. Alternatively, since the rate enhancement, k, is given by $k = e^{\Delta\Delta G^\ddagger_{cat}/RT}$,

$$\ln k = \ln(10^{14}) = \Delta\Delta G^\ddagger_{cat}/8.3145 \times (273 + 25)$$

Hence, $\Delta\Delta G^\ddagger_{cat} = 80\ kJ \cdot mol^{-1}$.

7. Glu has a pK of ~4 and, in its ionized form, acts as a base catalyst. Lys has a pK of ~10 and, in its protonated form, acts as an acid catalyst.
8. The active form of the enzyme contains the thiolate ion. The increased pK would increase the nucleophilicity of the thiolate and thereby increase the rate of the reaction catalyzed by the active form of the enzyme. However, at physiological pH, there would be less of the active form of the enzyme and therefore the overall rate would be decreased.
9. DNA lacks the 2′-OH group required for the formation of the 2′,3′-cyclic reaction intermediate.
10. Two such analogs are

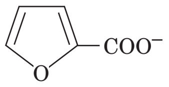

Furan-2-carboxylate

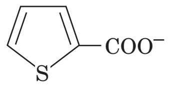

Thiophene-2-carboxylate

Both of these molecules are planar, particularly at the C atom to which the carboxylate is bonded, as is true of the transition state for the proline racemase reaction.

11. The preferential binding of the transition state to an enzyme is an important (often the most important) part of an enzyme's catalytic mechanism. Hence, the substrate-binding site is the catalytic site.
12. The lysozyme active site is arranged to cleave oligosaccharides between the fourth and fifth residues. Moreover, since the lysozyme active site can bind at least six monosaccharide units, $(NAG)_6$ would be more tightly bound to the enzyme than $(NAG)_4$, and this additional binding free energy would be applied to distorting the D ring to its half-chair conformation, thereby facilitating the reaction.
13. Asp 101 and Arg 114 form hydrogen bonds with the substrate molecule (Fig. 11-19). Ala cannot form these hydrogen bonds, so the substituted enzyme is less active.
14.

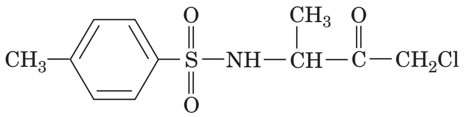

Tosyl-L-alanine chloromethylketone or

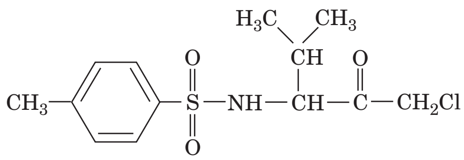

Tosyl-L-valine chloromethylketone

15. Yes. An enzyme decreases the activation energy barrier for both the forward and the reverse directions of a reaction.
16.

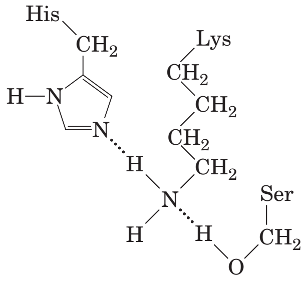

17. The observation that subtilisin and chymotrypsin are genetically

unrelated indicates that their active site geometries arose by convergent evolution. Assuming that evolution has optimized the catalytic efficiencies of these enzymes and that there is only one optimal arrangement of catalytic groups, any similarities between the active sites of subtilisin and chymotrypsin must be of catalytic significance. Conversely, any differences are unlikely to be catalytically important.

18. (a) Little or no effect; (b) catalysis would be much slower because the mutation disrupts the function of the catalytic triad.
19. Activated factor IXa leads, via several steps, to the activation of the final coagulation protease, thrombin. The absence of factor IX therefore slows the production of thrombin, delaying clot formation, and causing the bleeding of hemophilia. Although activated factor XIa also leads to thrombin production, factor XI plays no role until it is activated by thrombin itself. By this point, coagulation is already well underway, so a deficiency of factor XI does not significantly delay coagulation.
20. As a digestive enzyme, chymotrypsin's function is to indiscriminately degrade a wide variety of ingested proteins, so that their component amino acids can be recovered. Broad substrate specificity would be dangerous for a protease that functions outside of the digestive system, since it might degrade proteins other than its intended target.
21. If the soybean trypsin inhibitor were not removed from tofu, it would inhibit the trypsin in the intestine. At best, this would reduce the nutritional value of the meal by rendering its protein indigestible. It might very well also lead to intestinal upset.

CHAPTER 12

1. (a) $v = k[\text{A}]$
$k = v/[\text{A}]$
$k = (5\ \mu\text{M}\cdot\text{min}^{-1})/(20\ \text{mM})$
$= (0.005\ \text{mM}\cdot\text{min}^{-1})/(20\ \text{mM})$
$= 2.5 \times 10^{-4}\ \text{min}^{-1}$

(b) The reaction has a molecularity of 1.

2. From Eq. 12-7, $[\text{A}] = [\text{A}]_o\, e^{-kt}$. Since $t_{1/2} = 0.693/k$, $k = 0.693/14\ \text{d} = 0.05\ \text{d}^{-1}$. (a) 7 μmol; (b) 5 μmol; (c) 3.5 μmol; (d) 0.3 μmol.
3. $v = k[\text{A}]^2$
$v = (10^{-6}\ \text{M}^{-1}\cdot\text{s}^{-1})(0.010\ \text{M})(0.010\ \text{M})$
$v = 10^{-10}\ \text{M}\cdot\text{s}^{-1}$
4. For Reaction A, only a plot of 1/[reactant] versus t gives a straight line, so the reaction is second order. The slope, k, is $0.15\ \text{mM}^{-1}\cdot\text{s}^{-1}$. For Reaction B, only a plot of ln[reactant] versus t gives a straight line, so the reaction is first order. The negative of the slope, k, is $0.17\ \text{s}^{-1}$.

Time (s)	Reaction A 1/[reactant] (mM^{-1})	Reaction B ln[reactant]
0	0.16	1.69
1	0.32	1.53
2	0.48	1.36
3	0.62	1.16
4	0.77	0.99
5	0.91	0.83

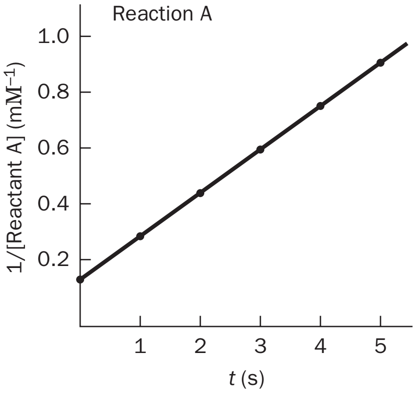

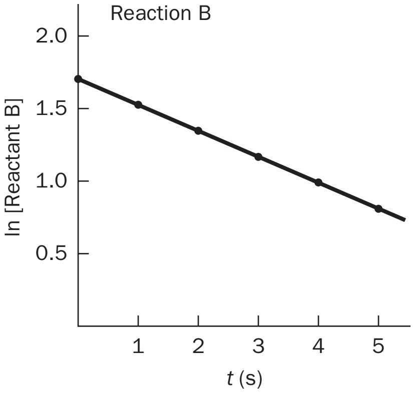

5.

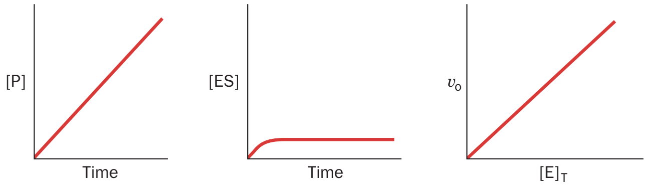

6. Enzyme activity is measured as an initial reaction velocity, the velocity before much substrate has been depleted and before much product has been generated. It is easier to measure the appearance of a small amount of product from a baseline of zero product than to measure the disappearance of a small amount of substrate against a background of a high concentration of substrate.
7. $v_o = V_{\max}[\text{S}]/(K_M + [\text{S}])$
$v_o/V_{\max} = [\text{S}]/(K_M + [\text{S}])$
$0.95 = [\text{S}]/(K_M + [\text{S}])$
$[\text{S}] = 0.95K_M + 0.95[\text{S}]$
$0.05[\text{S}] = 0.95\ K_M$
$[\text{S}] = (0.95/0.05)K_M = 19\ K_M$
8. Acetylcholinesterase, carbonic anhydrase, catalase, and fumarase.
9. Set A corresponds to $[\text{S}] > K_M$, and set B corresponds to $[\text{S}] < K_M$. Ideally, a single data set should include [S] values that are both larger and smaller than K_M.

Set A [S] (mM)	v_o ($\mu M \cdot s^{-1}$)	Set B [S] (mM)	v_o ($\mu M \cdot s^{-1}$)
2	0.42	0.12	0.17
1	0.38	0.10	0.15
0.67	0.34	0.08	0.13
0.50	0.32	0.07	0.11

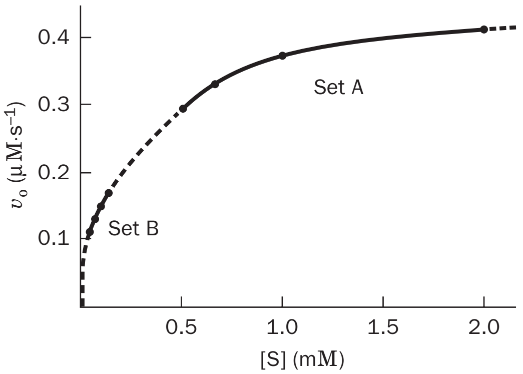

10. Construct a Lineweaver–Burk plot.

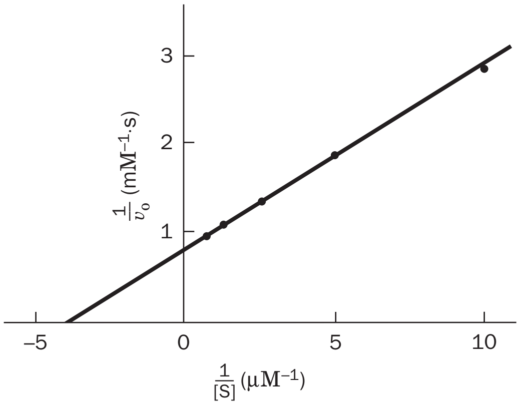

$$K_M = -1/x\text{–intercept} = -1/(-4\ \mu M^{-1}) = 0.25\ \mu M$$
$$V_{max} = 1/y\text{–intercept} = 1/(0.8\ mM^{-1} \cdot s) = 1.25\ mM \cdot s^{-1}$$

11. Comparing the two data points, since a 100-fold increase in substrate concentration only produces a 10-fold increase in reaction velocity, it appears that when [S] = 100 mM, the velocity is close to V_{max}. Therefore, assume that $V_{max} \approx 50\ \mu M \cdot s^{-1}$ and use the other data point to estimate K_M using the Michaelis–Menten equation:

$$v_o = \frac{V_{max}[S]}{K_M + [S]}$$
$$K_M + [S] = \frac{V_{max}[S]}{v_o}$$
$$K_M = \frac{V_{max}[S]}{v_o} - [S]$$
$$K_M = \frac{(50\ \mu M \cdot s^{-1})(1\ \mu M)}{(5\ \mu M \cdot s^{-1})} - (1\ \mu M) = 9\ \mu M$$

The true V_{max} must be greater than the estimated value, so the value of K_M is an underestimate of the true K_M.

12. The experimentally determined K_M would be greater than the true K_M because the actual substrate concentration is less than expected.

13. The enzyme concentration is comparable to the lowest substrate concentration and therefore does not meet the requirement that $[E] \ll [S]$. You could fix this problem by decreasing the amount of enzyme used for each measurement.

14. Velocity measurements can be made using any convenient unit of change per unit of time. K_M is, by definition, a substrate concentration (the concentration when $v_o = V_{max}/2$), so its value does not reflect how the velocity is measured.

15. (a, b) It is not necessary to know $[E]_T$. The only variables required to determine K_M and V_{max} (for example, by constructing a Lineweaver–Burk plot) are [S] and v_o. (c) The value of $[E]_T$ is required to calculate k_{cat} since $k_{cat} = V_{max}/[E]_T$.

16. (a) *N*-Acetyltyrosine ethyl ester, which has the lower value of K_M, has greater apparent affinity for chymotrypsin. (b) The value of V_{max} is not related to the value of K_M, so no conclusion can be drawn.

17. Product P will be more abundant because enzyme A has a much lower K_M for the substrate than enzyme B. Because V_{max} is approximately the same for the two enzymes, the relative efficiency of the enzymes depends almost entirely on their K_M values.

18. (a, b) A* will appear only if the reaction follows a Ping Pong mechanism, since only a double-displacement reaction can exchange an isotope from P back to A in the absence of B. Hence, in a reaction that has a sequential mechanism, A will not become isotopically labeled.

19. The lines of the double-reciprocal plots intersect to the left of the $1/v_o$ axis (on the 1/[S] axis). Hence, inhibition is mixed (with $\alpha = \alpha'$).

[S]	1/[S]	$1/v_o$	$1/v_o$ with I
1	1.00	0.7692	1.2500
2	0.50	0.5000	0.8333
4	0.25	0.3571	0.5882
8	0.125	0.2778	0.4545
12	0.083	0.2500	0.4167

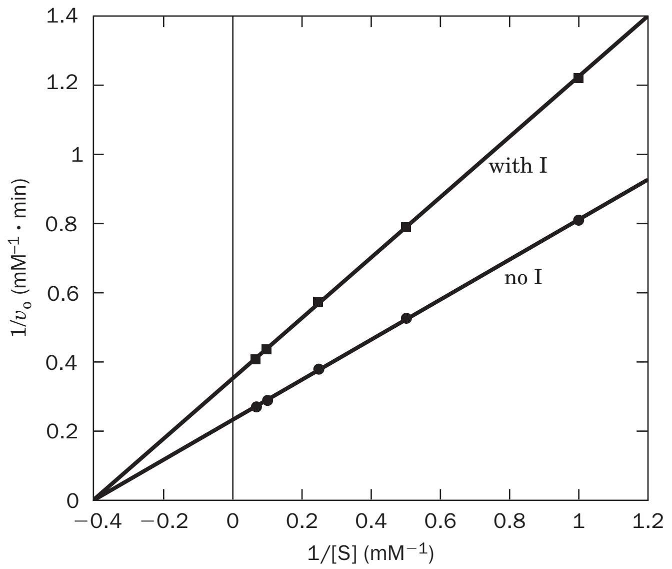

20. From Eq. 12-32, α is 3.

$$\alpha = 3 = 1 + [\mathrm{I}]/K_\mathrm{I} = 1 + 5\ \mathrm{mM}/K_\mathrm{I}$$
$$K_\mathrm{I} = 2.5\ \mathrm{mM}$$

21. (a) Inhibition is most likely mixed (noncompetitive) with $\alpha = \alpha'$ since it is reversible and only $V_{\max}$ is affected.

(b) Since $V_{\max}^{\mathrm{app}} = 0.8\,V_{\max}$, 80% of the enzyme remains uninhibited. Therefore, 20% of the enzyme molecules have bound inhibitor.

(c) As indicated in Table 12-2 for mixed inhibition, $V_{\max}^{\mathrm{app}} = V_{\max}/\alpha'$. Thus,

$$\alpha' = \frac{V_{\max}}{V_{\max}^{\mathrm{app}}} = \frac{1}{0.8} = 1.25$$

From Eq. 12-32,

$$1.25 = 1 + \frac{[\mathrm{I}]}{K_\mathrm{I}'}$$
$$K_\mathrm{I}' = \frac{5\,\mathrm{nM}}{1.25 - 1} = 20\,\mathrm{nM}$$

22. By irreversibly reacting with chymotrypsin's active site, DIPF would decrease $[\mathrm{E}]_\mathrm{T}$. The apparent $V_{\max}$ would decrease since $V_{\max} = k_{\mathrm{cat}}[\mathrm{E}]_\mathrm{T}$. K_M would not be affected since the uninhibited enzyme would bind substrate normally.

23. (a) If an irreversible inhibitor is present, the enzyme solution's activity would be exactly 100 times lower when the sample is diluted 100-fold. Dilution would not significantly change the enzyme's degree of inhibition. (b) For reversible inhibition, $K_\mathrm{I} = [\mathrm{E}][\mathrm{I}]/[\mathrm{EI}]$ so that $[\mathrm{E}]/[\mathrm{EI}] = K_\mathrm{I}/[\mathrm{I}]$. Hence, if a reversible inhibitor is present, dilution would lower the concentrations of both the enzyme and inhibitor so that the degree of dissociation of the inhibitor from the enzyme would increase. The enzyme solution's activity would therefore not be exactly 100 times less than the undiluted sample, but would be somewhat greater than that value because the proportion of uninhibited enzyme would be greater at the lower concentration.

24. Enzyme Y is more efficient at low [S]; enzyme X is more efficient at high [S].

25.

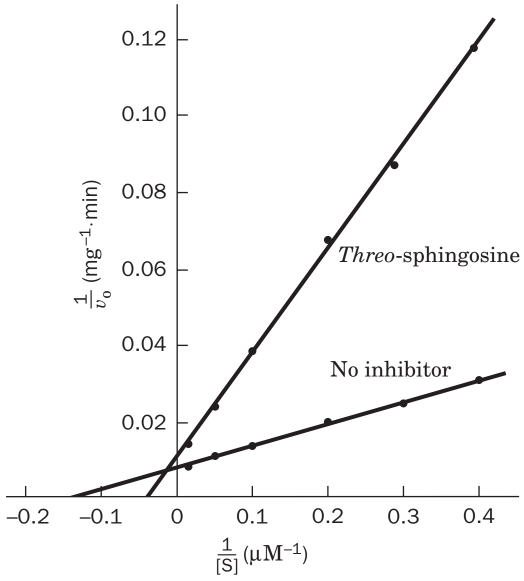

(a) K_M is determined from the x-intercept ($= -1/K_M$). In the absence of inhibitor, $K_M = 1/0.14\ \mu\mathrm{M}^{-1} = 7\ \mu\mathrm{M}$. In the presence of inhibitor, $K_M^{\mathrm{app}} = 1/0.04\ \mu\mathrm{M}^{-1} = 25\ \mu\mathrm{M}$. $V_{\max}$ is determined from the y-intercept ($= 1/V_{\max}$). In the absence of inhibitor, $V_{\max} = 1/0.008\ \mathrm{mg}^{-1}\cdot\mathrm{min} = 125\ \mathrm{mg}\cdot\mathrm{min}^{-1}$. In the presence of inhibitor, $V_{\max}^{\mathrm{app}} = 1/0.01\ \mathrm{mg}^{-1}\cdot\mathrm{min} = 100\ \mathrm{mg}\cdot\mathrm{min}^{-1}$.

(b) The lines in the double-reciprocal plots intersect very close to the $1/v_\mathrm{o}$ axis. Hence, *threo*-sphingosine is most likely a competitive inhibitor. Competitive inhibition is likely also because of the structural similarity between the inhibitor and the substrate, which allows them to compete for binding to the enzyme active site.

CHAPTER 13

1. (a) Yes, because the binding of Src's SH3 domain to the linker that connects its SH2 domain to the N-terminal lobe of its PTK domain is required for Src to maintain its autoinhibited conformation. Hence, the deletion of this SH3 domain would constitutively activate Src, thereby driving the cell with this mutation to a state of unrestrained proliferation.

(b) No, because the phosphorylation of Tyr 416 is required for the activation of Src and hence the Y416F mutation would inhibit the mutant cell's proliferation.

(c) Yes, because the phosphorylation of Tyr 527 is required for the autoinhibition of Src via the binding of its SH2 domain and hence the Y527F mutant Src would be constitutively activated.

(d) No, because replacing the wild-type Glu at position 253 of Src with Pro would make the 250 to 253 segment of Src into a normal Pro-X-X-Pro binding target for the SH3 domain, thereby stabilizing Src's autoinhibited conformation.

2. In the presence of the viral protein, the cell would undergo more cycles of cell division in response to the growth factor.

3. Cell transformation results from several genetic changes in a cell. Thus, a single oncogene supplied to an otherwise normal cell will be insufficient to transform it. However, an immortalized cell already has some of the genetic changes necessary for transformation (malignant cells are also immortal). In such cells, the additional oncogene may be all they require to complete their transformation.

4. Because the GTP analog cannot be hydrolyzed, G_α remains active. Analog binding to G_s therefore increases cAMP production. Analog binding to G_i decreases cAMP production.

5. When $\mathrm{G}_{\mathrm{s}\alpha}$ catalyzes the hydrolysis of its bound GTP to GDP + P_i, the Arg side chain that cholera toxin ADP-ribosylates functions to stabilize the transition state's developing negative charge. The ADP-ribosylated $\mathrm{G}_{\mathrm{s}\alpha}$ therefore hydrolyzes its bound GTP at a greatly reduced rate and hence remains activated far longer than normal $\mathrm{G}_{\mathrm{s}\alpha}$. Mutating this Arg will have a similar effect. Consequently, in cells in which a $\mathrm{G}_{\mathrm{s}\alpha}\cdot\mathrm{GTP}$ functions to induce cell proliferation, mutating this Arg will drive the cell into a state of unrestrained proliferation, a requirement for the malignant transformation of the cell. The gene encoding such a $\mathrm{G}_{\mathrm{s}\alpha}$ subunit is a proto-oncogene and the mutation of its Arg residue converts it to an oncogene. Cholera toxin does not

cause cancer because the $G_{s\alpha}$ it ADP-ribosylates only mediates the intestinal cell's secretion of digestive fluid, not its rate of proliferation. Moreover, cholera toxin does not pass through the intestine to the other tissues and hence does not affect other cells. However, even if it did so, its effect would only last as long as the cholera infection, whereas a mutation permanently affects the cell in which it has occurred and all its progeny.

6. No. Although the diacylglycerol second messengers are identical, phosphatidylethanolamine does not generate an IP_3 second messenger that triggers the release of Ca^{2+}, which in turn alters protein kinase C activity.
7. Pertussis toxin ADP ribosylates $G_{i\alpha}$ so as to prevent it from exchanging its bound GDP for GTP and hence from releasing $G_{\beta\gamma}$ upon interacting with its cognate activated GPCRs. The PLC-β isozymes, which are activated through their association with free $G_{\beta\gamma}$, are effectively inhibited by pertussis toxin as a consequence of the reduction in the $G_{\beta\gamma}$ concentration that it causes.
8. The C1 domain of PKC binds to membrane-bound DAG, whereas its C2 domain binds membrane-bound phosphatidylserine in a Ca^{2+}-mediated manner. The simultaneous binding of both of these domains to the membrane conformationally extracts the adjacent N-terminal pseudosubstrate from PKC's active site, thereby activating it. If the pseudosubstrate were relocated to the PKC's C-terminus, the simultaneous binding to the membrane of C1 and C2, which are on the N-terminal side of the protein kinase, would be unlikely to conformationally extract the pseudosubstrate from the protein kinase's active site. Hence the protein kinase would remain inhibited even when C1 and C2 were both bound to the membrane.
9. (a) Diacylglycerol kinase converts DAG to phosphatidic acid (Section 9-1C).

   (b) Activation of the kinase converts the nonpolar DAG to a more amphiphilic molecule that can no longer activate protein kinase C. In effect, the kinase limits the activity of one of the second messengers produced during signaling by the phosphoinositide pathway.
10. Li^+ blocks the conversion of phosphorylated inositol species to inositol, thereby preventing the recycling of IP_3 and its degradation products back to inositol. This in turn prevents the synthesis of phosphatidylinositol and PIP_2, the precursor of the IP_3 second messenger.

CHAPTER 14

1. C, D, A, E, B
2. (a) Since $\Delta G^{\circ\prime} = -RT \ln K$,

$$K = e^{-\Delta G^{\circ\prime}/RT}$$
$$K = e^{-(7500\ \mathrm{J\cdot mol^{-1}})/(8.3145\ \mathrm{J\cdot K^{-1}\cdot mol^{-1}})(298\ \mathrm{K})}$$
$$K = 0.048$$

(b) $\Delta G = \Delta G^{\circ\prime} + RT \ln \dfrac{[\mathrm{B}]}{[\mathrm{A}]}$

$$\Delta G = 7500\ \mathrm{J\cdot mol^{-1}} + (8.3145\ \mathrm{J\cdot K^{-1}\cdot mol^{-1}})(310\ \mathrm{K})\ln\frac{(0.0001)}{(0.0005)}$$
$$\Delta G = 7500\ \mathrm{J\cdot mol^{-1}} - 4150\ \mathrm{J\cdot mol^{-1}}$$
$$\Delta G = 3350\ \mathrm{J\cdot mol^{-1}} = 3.35\ \mathrm{kJ\cdot mol^{-1}}$$

The reaction is not spontaneous since $\Delta G > 0$.

(c) The reaction can proceed in the cell if the product B is the substrate for a second reaction such that the second reaction continually draws off B, causing the first reaction to continually produce more B from A.

3. b
4. The theoretical maximum yield of ATP is equivalent to ($\Delta G^{\circ\prime}$ for fuel oxidation)/($\Delta G^{\circ\prime}$ for ATP synthesis).

   (a) $(-2850\ \mathrm{kJ\cdot mol^{-1}})/(-30.5\ \mathrm{kJ\cdot mol^{-1}}) \approx 93$ ATP

   (b) $(-9781\ \mathrm{kJ\cdot mol^{-1}})/(-30.5\ \mathrm{kJ\cdot mol^{-1}}) \approx 320$ ATP
5. At pH 6, the phosphate groups are more ionized than they are at pH 5, which increases their electrostatic repulsion and therefore increases the magnitude of ΔG for hydrolysis (makes it more negative).
6. The exergonic hydrolysis of PP_i by pyrophosphatase ($\Delta G^{\circ\prime} = -19.2\ \mathrm{kJ\cdot mol^{-1}}$) drives fatty acid activation.
7. Calculating ΔG for the reaction ATP + creatine $\rightleftharpoons$ phospho-creatine + ADP, using Eq. 14-1:

$$\Delta G = \Delta G^{\circ\prime} + RT \ln\left(\frac{[\text{phosphocreatine}][\text{ADP}]}{[\text{creatine}][\text{ATP}]}\right)$$
$$= 12.6\ \mathrm{kJ\cdot mol^{-1}} + (8.3145\ \mathrm{J\cdot K^{-1}\cdot mol^{-1}})(298\ \mathrm{K}) \ln\left(\frac{(2.5\ \mathrm{mM})(0.15\ \mathrm{mM})}{(1\ \mathrm{mM})(4\ \mathrm{mM})}\right)$$
$$= 12.6\ \mathrm{kJ\cdot mol^{-1}} - 5.9\ \mathrm{kJ\cdot mol^{-1}} = 6.7\ \mathrm{kJ\cdot mol^{-1}}$$

Since $\Delta G > 0$, the reaction will proceed in the opposite direction as written above, that is, in the direction of ATP synthesis.

8. Using the data in Table 14-4, we calculate $\Delta G^{\circ\prime}$ for the adenylate kinase reaction.

	$\Delta G^{\circ\prime}$
$\mathrm{ATP + H_2O \rightarrow AMP + PP_i}$	$-45.6\ \mathrm{kJ\cdot mol^{-1}}$
$\mathrm{2\ ADP + 2\ P_i \rightarrow 2\ ATP + 2\ H_2O}$	$2 \times 30.5\ \mathrm{kJ\cdot mol^{-1}}$ $= 61.0\ \mathrm{kJ\cdot mol^{-1}}$
$\mathrm{PP_i + H_2O \rightarrow 2\ P_i}$	$-19.2\ \mathrm{kJ\cdot mol^{-1}}$
$\mathrm{2\ ADP \rightarrow ATP + AMP}$	$-3.8\ \mathrm{kJ\cdot mol^{-1}}$

Since ΔG for a reaction at equilibrium is zero, Eq. 14-1 becomes $\Delta G^{\circ\prime} = -RT \ln K_{\mathrm{eq}}$ so that $K_{\mathrm{eq}} = e^{-\Delta G^{\circ\prime}/RT}$.

$$K_{\mathrm{eq}} = \frac{[\mathrm{ATP}][\mathrm{AMP}]}{[\mathrm{ADP}]^2} = e^{-\Delta G^{\circ\prime}/RT}$$
$$[\mathrm{AMP}] = \frac{(5 \times 10^{-4}\ \mathrm{M})^2}{(5 \times 10^{-3}\ \mathrm{M})} \times e^{-(-3800\ \mathrm{J\cdot mol^{-1}})/(8.3145\ \mathrm{J\cdot K^{-1}\cdot mol^{-1}})(298\ \mathrm{K})}$$
$$[\mathrm{AMP}] = 2.3 \times 10^{-4}\ \mathrm{M} = 0.23\ \mathrm{mM}$$

9. The more positive the reduction potential, the greater the oxidizing power. From Table 14-5,

Compound	$\mathcal{E}^{\circ\prime}$ (V)
SO_4^{2-}	−0.515
Acetoacetate	−0.346
NAD^+	−0.315
Pyruvate	−0.185
Cytochrome *b* (Fe^{3+})	0.077

10. The balanced equation is

$$2 \text{ cyto } c\ (\text{Fe}^{3+}) + \text{ ubiquinol} \rightarrow 2 \text{ cyto } c\ (\text{Fe}^{2+}) + \text{ubiquinone} + 2\text{H}^+$$

Using the data in Table 14-5,

$$\Delta\mathscr{E}^{\circ\prime} = \mathscr{E}^{\circ\prime}_{(e^-\text{ acceptor})} - \mathscr{E}^{\circ\prime}_{(e^-\text{ donor})} = 0.235 \text{ V} - 0.045 \text{ V} = 0.190 \text{ V}$$

$$\Delta G^{\circ\prime} = -n\mathscr{F}\Delta\mathscr{E}^{\circ\prime} = -(2)(96{,}485 \text{ J}\cdot\text{V}^{-1}\cdot\text{mol}^{-1})(0.190 \text{ V}) = -36.7 \text{ kJ}\cdot\text{mol}^{-1}$$

11. Using the data in Table 14-5:

(a) $\Delta\mathscr{E}^{\circ\prime} = \mathscr{E}^{\circ\prime}_{(e^-\text{ acceptor})} - \mathscr{E}^{\circ\prime}_{(e^-\text{ donor})} = \mathscr{E}^{\circ\prime}_{(\text{fumarate})} - \mathscr{E}^{\circ\prime}_{(\text{NAD}^+)} = 0.031 \text{ V} - (-0.315 \text{ V}) = 0.346$ V. Because $\Delta\mathscr{E}^{\circ\prime} > 0$, $\Delta G^{\circ\prime} < 0$ and the reaction will spontaneously proceed as written.

(b) $\Delta\mathscr{E}^{\circ\prime} = \mathscr{E}^{\circ\prime}_{(e^-\text{ acceptor})} - \Delta\mathscr{E}^{\circ\prime}_{(e^-\text{ donor})} = \mathscr{E}^{\circ\prime}_{(\text{cyto } b)} - \mathscr{E}^{\circ\prime}_{(\text{cyto } a)} = 0.077 \text{ V} - (0.290 \text{ V}) = -0.213$ V. Because $\Delta\mathscr{E}^{\circ\prime} < 0$, $\Delta G^{\circ\prime} > 0$ and the reaction will spontaneously proceed in the opposite direction from that written.

12. Using the data in Table 14-5, for the oxidation of free FADH_2 ($\mathscr{E}^{\circ\prime} = -0.219$ V) by ubiquinone ($\mathscr{E}^{\circ\prime} = 0.045$ V),

$$\Delta\mathscr{E}^{\circ\prime} = \mathscr{E}^{\circ\prime}_{(\text{ubiquinone})} - \mathscr{E}^{\circ\prime}_{(\text{FADH}_2)} = (0.045 \text{ V}) - (-0.219 \text{ V}) = 0.264 \text{ V}$$

$$\Delta G^{\circ\prime} = -n\mathscr{F}\Delta\mathscr{E}^{\circ\prime} = -(2)(96{,}485 \text{ J}\cdot\text{V}^{-1}\cdot\text{mol}^{-1})(0.264 \text{ V}) = -50.9 \text{ kJ}\cdot\text{mol}^{-1}$$

This is more than enough free energy to drive the synthesis of ATP from ADP + P_i ($\Delta G^{\circ\prime} = +30.5 \text{ kJ}\cdot\text{mol}^{-1}$; Table 14.4).

13. $\text{Z} \xrightarrow{\text{B}} \text{W} \xrightarrow{\text{C}} \text{Y} \xrightarrow{\text{A}} \text{X}$

14. (a) The step catalyzed by enzyme Y is likely to be the major flux-control point, since this step operates farthest from equilibrium (it is an irreversible step). (b) Inhibition of enzyme Z would cause the concentration of D, the reaction's product, to decrease, and it would cause C, the reaction's substrate, to accumulate. The concentrations of A and B would not change because the steps catalyzed by enzymes X and Y would not be affected. The accumulated C would not be transformed back to B since the step catalyzed by enzyme Y is irreversible.

CHAPTER 15

1. (a) Reactions 1, 3, 7, and 10; (b) Reactions 2, 5, and 8; (c) Reaction 6; (d) Reaction 9; (e) Reaction 4.

2. C1 of DHAP and C1 of GAP are achiral but become chiral in FBP (as C3 and C4). There are four stereoisomeric products that differ in configuration at C3 and C4: fructose-1,6-bisphosphate, psicose-1,6-bisphosphate, tagatose-1,6-bisphosphate, and sorbose-1,6-bisphosphate (see Fig. 8-2).

3. The Zn^{2+} polarizes the carbonyl oxygen of the substrate to stabilize the enolate intermediate of the reaction.

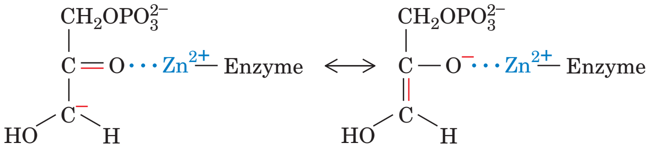

4. (a) $\text{Glucose} + 2\ \text{NAD}^+ + 2\ \text{ADP} + 2\ \text{P}_i \rightarrow 2\ \text{pyruvate} + 2\ \text{NADH} + 2\ \text{ATP} + 2\ \text{H}_2\text{O}$

(b)

$$\text{Glucose} + 2\ \text{NAD}^+ + 2\ \text{ADP} + 2\ \text{AsO}_4^{3-} \rightarrow 2\ \text{pyruvate} + 2\ \text{NADH} + 2\ \text{ADP—AsO}_3^{2-} + 2\ \text{H}_2\text{O}$$

$$\underline{2\ \text{ADP—AsO}_3^{2-} + 2\ \text{H}_2\text{O} \rightarrow 2\ \text{ADP} + 2\ \text{AsO}_4^{3-}}$$

$$\text{Overall: Glucose} + 2\ \text{NAD}^+ \rightarrow 2\ \text{pyruvate} + 2\ \text{NADH}$$

(c) Arsenate is a poison because it uncouples ATP generation from glycolysis. Consequently, glycolytic energy generation cannot occur.

5. ribulose-5-phosphate isomerase reaction:

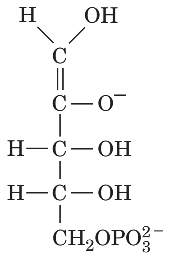

1,2-Enediolate intermediate

ribulose-5-phosphate epimerase reaction:

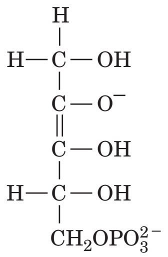

2,3-Enediolate intermediate

6. (a) ΔG values differ from $\Delta G^{\circ\prime}$ values because $\Delta G = \Delta G^{\circ\prime} + RT \ln[\text{Products}]/[\text{Reactants}]$ and cellular reactants and products are not in their standard states.

(b) Yes. The same *in vivo* conditions that decrease the magnitude of ΔG relative to $\Delta G^{\circ\prime}$ may also decrease ΔG for ATP synthesis.

7. When $[\text{GAP}] = 10^{-4}$ M, $[\text{DHAP}] = 5.5 \times 10^{-4}$ M. According to Eq. 1-17,

$$K = e^{-\Delta G^{\circ\prime}/RT}$$

$$\frac{[\text{GAP}][\text{DHAP}]}{[\text{FBP}]} = e^{-(22{,}800 \text{ J}\cdot\text{mol}^{-1})/(8.3145 \text{ J}\cdot\text{K}^{-1}\cdot\text{mol}^{-1})(310 \text{ K})}$$

$$\frac{(10^{-4})(5.5 \times 10^{-4})}{[\text{FBP}]} = 1.4 \times 10^{-4}$$

$$[\text{FBP}] = 3.8 \times 10^{-4} \text{ M}$$

$$[\text{FBP}]/[\text{GAP}] = (3.8 \times 10^{-4} \text{ M})/(10^{-4} \text{ M}) = 3.8$$

8. For the coupled reaction

$$\text{Pyruvate} + \text{NADH} + \text{H}^+ \longrightarrow \text{lactate} + \text{NAD}^+$$

$\Delta\mathscr{E}^{\circ\prime} = (-0.185 \text{ V}) - (-0.315 \text{ V}) = 0.130$ V. According to Eq. 14-8

$$\Delta\mathscr{E} = \Delta\mathscr{E}^{\circ\prime} - \frac{RT}{n\mathscr{F}} \ln\left(\frac{[\text{lactate}][\text{NAD}^+]}{[\text{pyruvate}][\text{NADH}]}\right)$$

and $\Delta G = -n\mathscr{F}\Delta\mathscr{E}$ (Eq. 14-7). Since two electrons are transferred in the above reaction, $n = 2$.

(a) $\Delta\mathscr{E} = 0.130 \text{ V} - \dfrac{RT}{nF} \ln(1) = 0.130 \text{ V}$

$$\Delta G = -(2)(96{,}485 \text{ J}\cdot\text{V}^{-1}\cdot\text{mol}^{-1})(0.130 \text{ V}) = -25.1 \text{ kJ}\cdot\text{mol}^{-1}$$

(b) $RT/n\mathscr{F} = (8.3145 \text{ J}\cdot\text{K}^{-1}\cdot\text{mol}^{-1})(298 \text{ K})/(2)(96{,}485 \text{ J}\cdot\text{V}^{-1}\cdot\text{mol}^{-1}) = 0.01284 \text{ V}$

$$\Delta\mathscr{E} = 0.130 \text{ V} - 0.01284 \text{ V} \ln(160 \times 160)$$

$$\Delta\mathscr{E} = 0.130 \text{ V} - 0.130 \text{ V} = 0$$

$$\Delta G = 0$$

(c) $\Delta\mathscr{E} = 0.130 \text{ V} - 0.01284 \text{ V} \ln(1000 \times 1000)$

$$\Delta\mathscr{E} = 0.130 \text{ V} - 0.177 \text{ V} = -0.047 \text{ V}$$

$$\Delta G = -(2)(96{,}485 \text{ J}\cdot\text{V}^{-1}\cdot\text{mol}^{-1})(-0.047 \text{ V}) = 9.1 \text{ kJ}\cdot\text{mol}^{-1}$$

(d) At the concentration ratios of Part a, ΔG is negative and the reaction proceeds as written. As [lactate]/[pyruvate] increases, the reaction ΔG increases even though $[\text{NAD}^+]/[\text{NADH}]$ also increases so that in Part b the reaction is at equilibrium ($\Delta G = 0$) and in Part c ΔG is positive and the reaction proceeds spontaneously in the opposite direction.

9. (a) Pyruvate kinase regulation is important for controlling the flux of metabolites, such as fructose (in liver), which enter glycolysis after the PFK step.

   (b) FBP is the product of the third reaction of glycolysis, so it acts as a feed-forward activator of the enzyme that catalyzes Step 10. This regulatory mechanism helps ensure that once metabolites pass the PFK step of glycolysis, they will continue through the pathway.

10. The three glucose molecules that proceed through glycolysis yield 6 ATP. The bypass through the pentose phosphate pathway results in a yield of 5 ATP.

11. The label will appear at C1 and C3 of F6P (see Fig. 15-30).

12. (a) Transketolase transfers 2-carbon units from a ketose to an aldose, so the products are a 3-carbon sugar and a 7-carbon sugar. (b) The products are a 4-carbon sugar and a 7-carbon sugar. The order of binding does matter. The ketose binds first and transfers the 2-carbon unit to the TPP on the enzyme. The aldose then binds and accepts the 2-carbon unit.

13. Even when the flux of glucose through glycolysis and hence the citric acid cycle is blocked, glucose can be oxidized by the pentose phosphate pathway, with the generation of CO_2.

14. The liver enzyme is far more sensitive than the brain enzyme to the three activators. It is possible that liver PFK-1 is subject to a greater degree of regulation than brain PFK-1. Fuel must be supplied to the brain continuously and thus glycolysis is always active, but the liver has a wide variety of physiological roles and is more likely to regulate cellular pathways.

15. (a)

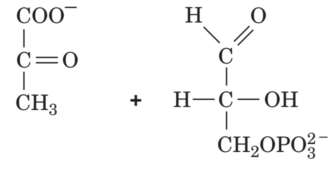

Pyruvate **GAP**

   (b) The pyruvate product of the aldolase reaction is not further modified. The GAP product is converted to pyruvate by the actions of the glycolytic enzymes glyceraldehyde-3-phosphate dehydrogenase, phosphoglycerate kinase, phosphoglycerate mutase, enolase, and pyruvate kinase.

   (c) One ATP is consumed when glucose is converted to glucose-6-phosphate. One ATP is generated by the phosphoglycerate kinase reaction and one by the pyruvate kinase reaction (these quantities are not doubled because only one three-carbon fragment of glucose follows this route), for a net yield of one ATP per glucose. The standard glycolytic pathway generates two ATP per glucose.

CHAPTER 16

1. (a) +9 ATP, (b) +6 ATP, (c) −18 ATP.

2. (a) The overall reaction for glycolysis is

$$\text{Glucose} + 2\,\text{NAD}^+ + 2\,\text{ADP} + 2\,\text{P}_i \longrightarrow 2\,\text{pyruvate} + 2\,\text{NADH} + 4\,\text{H}^+ + 2\,\text{ATP} + 2\,\text{H}_2\text{O}$$

   The overall reaction for gluconeogenesis is

$$2\,\text{Pyruvate} + 2\,\text{NADH} + 4\,\text{H}^+ + 4\,\text{ATP} + 2\,\text{GTP} + 6\,\text{H}_2\text{O} \longrightarrow \text{glucose} + 2\,\text{NAD}^+ + 4\,\text{ADP} + 2\,\text{GDP} + 6\,\text{P}_i$$

   For the two processes operating sequentially,

$$2\,\text{ATP} + 2\,\text{GTP} + 4\,\text{H}_2\text{O} \longrightarrow 2\,\text{ADP} + 2\,\text{GDP} + 4\,\text{P}_i$$

   (b) The reaction for catabolism of 6 G6P by the pentose phosphate pathway is

$$6\,\text{G6P} + 12\,\text{NADP}^+ + 6\,\text{H}_2\text{O} \longrightarrow 6\,\text{Ru5P} + 12\,\text{NADPH} + 12\,\text{H}^+ + 6\,\text{CO}_2$$

   Ru5P can be converted to G6P by transaldolase, transketolase, and gluconeogenesis:

$$6\,\text{Ru5P} + \text{H}_2\text{O} \longrightarrow 5\,\text{G6P} + \text{P}_i$$

   The net equation is therefore

$$\text{G6P} + 12\,\text{NADP}^+ + 7\,\text{H}_2\text{O} \longrightarrow 12\,\text{NADPH} + 12\,\text{H}^+ + 6\,\text{CO}_2 + \text{P}_i$$

3. Phosphoglucokinase activity generates G1,6P, which is necessary to "prime" phosphoglucomutase that has become dephosphorylated and thereby inactivated through the loss of its G1,6P reaction intermediate.

4. The overall free energy change for debranching is

Breaking $\alpha(1 \rightarrow 4)$ bond	$\Delta G^{\circ\prime} = -15.5\ \text{kJ}\cdot\text{mol}^{-1}$
Forming $\alpha(1 \rightarrow 4)$ bond	$+15.5\ \text{kJ}\cdot\text{mol}^{-1}$
Hydrolyzing $\alpha(1 \rightarrow 6)$ bond	$-7.1\ \text{kJ}\cdot\text{mol}^{-1}$
Total	$\Delta G^{\circ\prime} = -7.1\ \text{kJ}\cdot\text{mol}^{-1}$

   The overall free energy change for branching is

Breaking $\alpha(1 \rightarrow 4)$ bond	$\Delta G^{\circ\prime} = -15.5\ \text{kJ}\cdot\text{mol}^{-1}$
Forming $\alpha(1 \rightarrow 6)$ bond	$+7.1\ \text{kJ}\cdot\text{mol}^{-1}$
Total	$\Delta G^{\circ\prime} = -8.4\ \text{kJ}\cdot\text{mol}^{-1}$

   Assuming that $\Delta G^{\circ\prime}$ is close to ΔG, the sum of the two reactions of branching has $\Delta G < 0$, but debranching would be endergonic ($\Delta G > 0$) without the additional step of hydrolyzing the $\alpha(1 \rightarrow 6)$ bond to form glucose.

5. A glycogen molecule with 28 tiers would represent the most efficient arrangement for storing glucose, and its outermost tier would contain considerably more glucose residues than a glycogen molecule with only 12 tiers. However, densely packed glucose residues would be inaccessible to phosphorylase. In fact, such a dense glycogen molecule could not be synthesized because glycogen synthase and branching enzyme would have no room to operate (see Box 16-3 for a discussion of glycogen structure).

6. In the course of glucose catabolism, a detour through glycogen synthesis and glycogen breakdown begins and ends with G6P. The energy cost of this detour is 1 ATP equivalent, consumed in the UDP–glucose pyrophosphorylase step. The overall energy lost is therefore 1/32 or ~3%.

7. This mechanism allows glycogen phosphorylase activity to be regulated by the concentration of glucose so that glycogen is not broken down when glucose is already plentiful.

8. (a) Circulating [glucose] is high because cells do not respond to the insulin signal to take up glucose.

   (b) Insulin is unable to activate phosphoprotein phosphatase-1 in muscle, so glycogen synthesis is not stimulated. Moreover, glycogen synthesis is much reduced by the lack of available glucose in the cell.

9. A defect in G6P transport would have the symptoms of glucose-6-phosphatase deficiency: accumulation of glycogen and hypoglycemia.
10. The conversion of circulating glucose to lactate in the muscle generates 2 ATP. If muscle glycogen could be mobilized, the energy yield would be 3 ATP, since phosphorolysis of glycogen bypasses the hexokinase-catalyzed step that consumes ATP in the first stage of glycolysis.
11. The deficiency is in branching enzyme (Type IV glycogen storage disease). The high ratio of G1P to glucose indicates abnormally long chains of $\alpha(1 \rightarrow 4)$-linked residues with few $\alpha(1 \rightarrow 6)$-linked branch points (the normal ratio is ~10).

CHAPTER 17

1. (a) Because citric acid cycle intermediates such as citrate and succinyl-CoA are precursors for the biosynthesis of other compounds, anaerobes must be able to synthesize them.
   (b) These organisms do not need a complete citric acid cycle, which would yield reduced coenzymes that must be reoxidized.
2. Citrate can be cleaved to generate an acetyl group and oxaloacetate. The oxaloacetate can then be converted to succinate to complete the cycle.
3. The decarboxylation step is most likely to be metabolically irreversible since the CO_2 product is rapidly hydrated to bicarbonate. The reverse reaction, a carboxylation, requires the input of free energy to become favorable (Section 16-4A). The other four reactions are transfer reactions or oxidation–reduction reactions (transfer of electrons) that are more easily reversed.
4. PDP removes the phosphate group that inactivates the pyruvate dehydrogenase complex. A deficiency of PDP leads to less pyruvate dehydrogenase activity in muscle cells, making it difficult for the muscle to increase flux through the citric acid cycle in order to meet the energy demands of exercise.
5. (a) The labeled carbon becomes C4 of the succinyl moiety of succinyl-CoA. Because succinate is symmetrical, the label appears at C1 and C4 of succinate. When the resulting oxaloacetate begins the second round, the labeled carbons appear as $^{14}CO_2$ in the isocitrate dehydrogenase and the α-ketoglutarate dehydrogenase reactions (see Fig. 17-2).
   (b) The labeled carbon becomes C3 of the succinyl moiety of succinyl-CoA and hence appears at C2 and C3 of succinate, fumarate, malate, and oxaloacetate. Neither C2 nor C3 of oxaloacetate is released as CO_2 in the second round of the cycle. However, the ^{14}C label appears at C1 and C2 of the succinyl moiety of succinyl-CoA in the second round and therefore appears at all four positions of the resulting oxaloacetate. Thus, in the third round, ^{14}C is released as $^{14}CO_2$.
6. Citric acid cycle intermediates are all acids and as such represent a source of hydrogen ions that would lead to a decrease in blood pH (acidosis).
7. 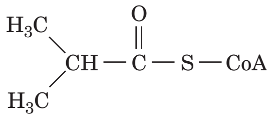

8. NAD$^+$ ($\mathscr{E}^{\circ\prime} = -0.315$ V) does not have a high enough reduction potential to support oxidation of succinate to fumarate ($\mathscr{E}^{\circ\prime} = +0.031$ V); that is, the succinate dehydrogenase reaction has insufficient free energy to reduce NAD$^+$. Enzyme-bound FAD ($\mathscr{E}^{\circ\prime} \approx 0$) is more suitable for oxidizing succinate.
9. Competitive inhibition can be overcome by adding more substrate, in this case succinate. Oxaloacetate overcomes malonate inhibition because it is converted to succinate by the reactions of the citric acid cycle.
10. The phosphofructokinase reaction is the major flux-control point for glycolysis. Inhibiting phosphofructokinase slows the entire pathway, so the production of acetyl-CoA by glycolysis followed by the pyruvate dehydrogenase complex can be decreased when the citric acid cycle is operating at maximum capacity and the citrate concentration is high. As citric acid cycle intermediates are consumed in synthetic pathways, the citrate concentration drops, relieving phosphofructokinase inhibition and allowing glycolysis to proceed in order to replenish the citric acid cycle intermediates.
11. To synthesize citrate, pyruvate must be converted to oxaloacetate by pyruvate carboxylase:

$$\text{Pyruvate} + CO_2 + \text{ATP} + H_2O \longrightarrow \text{oxaloacetate} + \text{ADP} + P_i$$

A second pyruvate is converted to acetyl-CoA by pyruvate dehydrogenase:

$$\text{Pyruvate} + \text{CoASH} + \text{NAD}^+ \longrightarrow \text{acetyl-CoA} + CO_2 + \text{NADH}$$

The acetyl-CoA then combines with oxaloacetate to produce citrate:

$$\text{Oxaloacetate} + \text{acetyl-CoA} + H_2O \longrightarrow \text{citrate} + \text{CoASH} + H^+$$

The net reaction is

$$2\ \text{Pyruvate} + \text{ATP} + \text{NAD}^+ + 2\ H_2O \longrightarrow \text{citrate} + \text{ADP} + P_i + \text{NADH} + H^+$$

12. (a) The citric acid cycle is a multistep catalyst. Degrading an amino acid to a citric acid cycle intermediate boosts the catalytic activity of the cycle but does not alter the stoichiometry of the overall reaction (acetyl-CoA → 2 CO_2). In order to undergo oxidation, the citric acid cycle intermediate must exit the cycle and be converted to acetyl-CoA to reenter the cycle as a substrate. (b) Pyruvate derived from the degradation of an amino acid can be converted to acetyl-CoA by the pyruvate dehydrogenase complex; these amino acid carbons can then be completely oxidized by the citric acid cycle.
13. The alternate pathway bypasses the succinyl-CoA synthetase reaction of the standard citric acid cycle, a step that is accompanied by the phosphorylation of ADP. The alternate pathway therefore generates one less ATP than the standard citric acid cycle. There is no difference in the number of reduced cofactors generated.
14. For the reaction isocitrate + NAD$^+$ $\rightleftharpoons$ α-ketoglutarate + NADH + CO_2 + H^+, we assume $[H^+]$ and $[CO_2] = 1$. According to Eq. 14-1,

$$\Delta G = \Delta G^{\circ\prime} + RT\ln\left(\frac{[\text{NADH}][\alpha\text{-ketoglutarate}]}{[\text{NAD}^+][\text{isocitrate}]}\right)$$

$$= -21\ \text{kJ}\cdot\text{mol}^{-1} + (8.3145\ \text{J}\cdot\text{K}\cdot\text{mol}^{-1})(298\ \text{K})\ln\left[\frac{(1)(0.1)}{(8)(0.02)}\right]$$

$$= -21\ \text{kJ}\cdot\text{mol}^{-1} - 1.16\ \text{kJ}\cdot\text{mol}^{-1} = -22.16\ \text{kJ}\cdot\text{mol}^{-1}$$

With such a large negative free energy of reaction under physiological conditions, isocitrate dehydrogenase is likely to be a metabolic control point.

15. Animals cannot carry out the net synthesis of glucose from acetyl-CoA (to which acetate is converted). However, ^{14}C-labeled acetyl-CoA enters the citric acid cycle and is converted to oxaloacetate. Some of this oxaloacetate may exchange with the cellular pool of oxaloacetate to be converted to glucose through gluconeogenesis and subsequently taken up by muscle and incorporated into glycogen.

CHAPTER 18

1. Mitochondria with more cristae have more surface area and therefore more proteins for electron transport and oxidative phosphorylation. Tissues with a high demand for ATP synthesis (such as heart) contain mitochondria with more cristae than tissues with lower demand for oxidative phosphorylation (such as liver).
2. When NADH participates in the glycerophosphate shuttle, the electrons of NADH flow to FAD and then to CoQ, bypassing Complex I. Thus, about 1.5 ATP are synthesized per NADH. About 2.5 ATP are produced when NADH participates in the malate–aspartate shuttle.
3. The relevant half-reactions (Table 14-5) are

$$\mathrm{FAD} + 2\,\mathrm{H}^+ + 2\,e^- \rightleftharpoons \mathrm{FADH_2} \qquad \mathscr{E}' = -0.219\ \mathrm{V}$$

$$\tfrac{1}{2}\mathrm{O_2} + 2\,\mathrm{H}^+ + 2\,e^- \rightleftharpoons \mathrm{H_2O} \qquad \mathscr{E}^{\circ\prime} = -0.815\ \mathrm{V}$$

Since the O_2/H_2O half-reaction has the more positive $\mathscr{E}^{\circ\prime}$, the FAD half-reaction is reversed and the overall reaction is

$$\tfrac{1}{2}\mathrm{O_2} + \mathrm{FADH_2} \rightleftharpoons \mathrm{H_2O} + \mathrm{FAD}$$

$$\Delta\mathscr{E}^{\circ\prime} = 0.815\ \mathrm{V} - (-0.219\ \mathrm{V}) = 1.034\ \mathrm{V}$$

Since $\Delta G^{\circ\prime} = -n\mathscr{F}\Delta\mathscr{E}^{\circ\prime}$,

$$\begin{aligned}\Delta G^{\circ\prime} &= -(2)(96{,}485\ \mathrm{J\cdot V^{-1}\cdot mol^{-1}})(1.034\ \mathrm{V})\\ &= -200\ \mathrm{kJ\cdot mol^{-1}}\end{aligned}$$

The maximum number of ATP that could be synthesized under standard conditions is therefore $200\ \mathrm{kJ\cdot mol^{-1}}/30.5\ \mathrm{kJ\cdot mol^{-1}} = 6.6$ mol ATP/mol $FADH_2$ oxidized by O_2.

4.

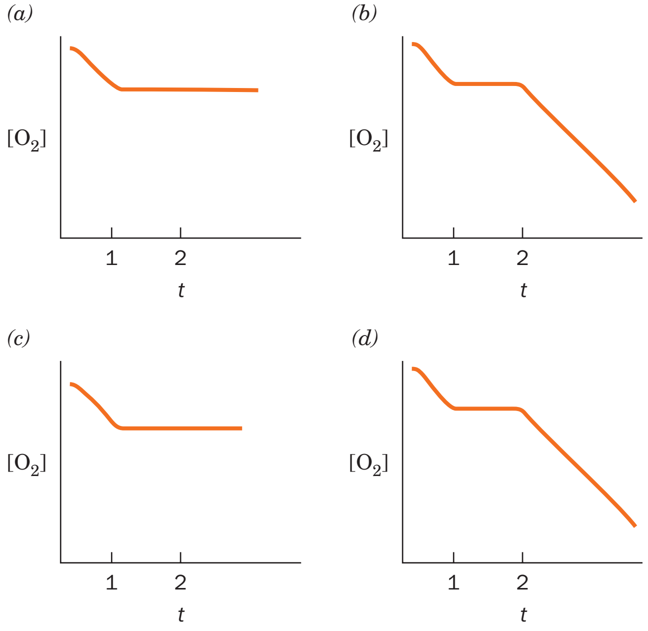

(a) O_2 consumption ceases because amytal blocks electron transport in Complex I.

(b) Electrons from succinate bypass the amytal block by entering the electron-transport chain at Complex II and thereby restore electron transport through Complexes III and IV.

(c) CN^- blocks electron transport in Complex IV, after the point of entry of succinate.

(d) Oligomycin blocks oxidative phosphorylation and hence O_2 consumption. DNP uncouples electron transport from oxidative phosphorylation and thereby permits O_2 consumption to resume.

5. $\mathscr{E}$ may differ from $\mathscr{E}^{\circ\prime}$, depending on the redox center's microenvironment and the concentrations of reactants and products. In addition, the tight coupling between successive electron transfers within a complex may "pull" electrons so that the overall process is spontaneous.
6. (a)

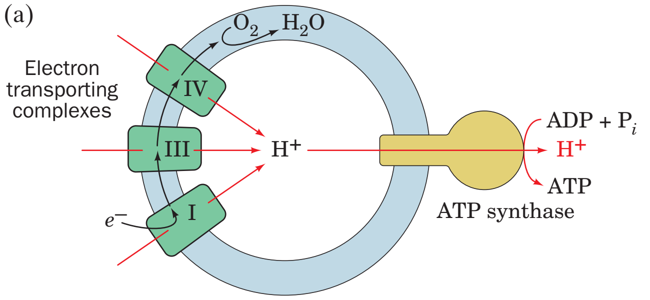

(b) An increase in external pH (decrease in $[H^+]$) increases the electrochemical potential across the mitochondrial membrane and therefore leads to an increase in ATP synthesis.

7. For the transport of a proton from outside to inside (Eq. 18-1),

$$\Delta G = 2.3RT[\mathrm{pH}\ (side\ 1) - \mathrm{pH}\ (side\ 2)] + Z\mathscr{F}\Delta\Psi$$

The difference in pH is −1.4. Since an ion is transported from the positive to the negative side of the membrane, $\Delta\Psi$ is negative.

$$\begin{aligned}\Delta G = {}&(2.3)(8.314\ \mathrm{J\cdot K^{-1}\cdot mol^{-1}})(298\ \mathrm{K})(-1.4) +\\ &(1)(96{,}485\ \mathrm{J\cdot V^{-1}\cdot mol^{-1}})(-0.06\ \mathrm{V})\end{aligned}$$

$$\Delta G = -7980\ \mathrm{J\cdot mol^{-1}} - 5790\ \mathrm{J\cdot mol^{-1}} = 13.8\ \mathrm{KJ\cdot mol^{-1}}$$

Since $\Delta G^{\circ\prime}$ for ATP synthesis is $30.5\ \mathrm{kJ\cdot mol^{-1}}$ and $30.5/13.8 = 2.2$, between two and three moles of protons must be transported to provide the free energy to synthesize one mole of ATP under standard biochemical conditions.

8. (a) The import of ADP (net charge −3) and the export of ATP (net charge −4) represents a loss of negative charge inside the mitochondria. This decreases the difference in electrical charge across the membrane, since the outside is positive due to the translocation of protons during electron transport. Consequently, the electrochemical gradient is diminished by the activity of the ADP–ATP translocator. The activity of the P_i–H^+ symport protein diminishes the proton gradient by allowing protons from the intermembrane space to re-enter the matrix.

(b) Both transport systems are driven by the free energy of the electrochemical proton gradient.

9. The protonation and subsequent deprotonation of Asp 61 of the F_1F_0-ATPase's *c* subunits induces the rotation of the *c*-ring, which in turn, mechanically drives the synthesis of ATP. DCCD

reacts with Asp 61 in a manner that prevents it from binding a proton and thereby prevents the synthesis of ATP.

10. In an ATP synthase with more *c* subunits, more proton translocation events are required to drive one complete rotation of the *c* ring. Consequently, more substrate oxidation (O_2 consumption) is required to synthesize three ATP (the yield of one cycle of the rotary engine), and the P/O ratio is lower.

11. DNP and related compounds dissipate the proton gradient required for ATP synthesis. The dissipation of this gradient decreases the rate of synthesis of ATP, decreasing the ATP mass action ratio. Decreasing this ratio relieves the inhibition of the electron transport chain, causing an increase in metabolic rate.

12. Hormones stimulate the release of fatty acids from stored triacylglycerols, which activates UCP1 and also provides the fuel whose oxidation yields electrons for the heat-generating electron transfer process. This cascade also amplifies the effect of the hormone.

13. The switch to aerobic metabolism allows ATP to be produced by oxidative phosphorylation. The phosphorylation of ADP increases the [ATP]/[ADP] ratio, which then increases the [NADH]/[NAD^+] ratio because a high ATP mass action ratio slows electron transport. The increases in [ATP] and [NADH] inhibit their target enzymes in glycolysis and the citric acid cycle (Fig. 18-29) and thereby slow those processes.

14. Glucose is shunted through the pentose phosphate pathway to provide NADPH, whose electrons are required to reduce O_2 to $O_2^{-}\cdot$.

CHAPTER 19

1. The color of the seawater indicates that the photosynthetic pigments of the algae absorb colors of visible light other than red.

2. $2\ H_2O + 2\ NADP^+ \longrightarrow 2\ NADPH + 2\ H^+ + O_2$

3. The order of action is water–plastoquinone oxidoreductase (Photosystem II), plastoquinone–plastocyanin oxidoreductase (cytochrome b_6f), and plastocyanin–ferredoxin oxidoreductase (Photosystem I).

4. The label appears as $^{18}O_2$:

$$H_2{}^{18}O + CO_2 \xrightarrow{\text{light}} (CH_2O) + {}^{18}O_2$$

5. (a) The energy per photon is $E = hc/\lambda$, so the energy per mole of photons ($\lambda = 700$ nm) is

$$\begin{aligned} E &= Nhc/\lambda \\ &= (6.022 \times 10^{23}\ \text{mol}^{-1})(6.626 \times 10^{-34}\ \text{J}\cdot\text{s}) \\ &\quad\ (2.998 \times 10^{8}\ \text{m}\cdot\text{s}^{-1})/(7 \times 10^{-7}\ \text{m}) \\ &= 1.71 \times 10^{5}\ \text{J}\cdot\text{mol}^{-1} \\ &= 171\ \text{kJ}\cdot\text{mol}^{-1} \end{aligned}$$

(b) $(171\ \text{kJ}\cdot\text{mol}^{-1})/(30.5\ \text{kJ}\cdot\text{mol}^{-1}) = 5.6$

Five moles of ATP could theoretically be synthesized (at least under standard biochemical conditions).

6. (a) The relevant half-reactions are (Table 14-5):

$$\begin{aligned} &O_2 + 4\,e^- + 4\,H^+ \rightarrow 2\,H_2O && \mathcal{E}^{\circ\prime} = 0.815\ \text{V} \\ &NADP^+ + H^+ + 2\,e^- \rightarrow NADPH && \mathcal{E}^{\circ\prime} = -0.320\ \text{V} \end{aligned}$$

The overall reaction is

$$\begin{aligned} 2\,NADP^+ + 2\,H_2O &\rightarrow 2\,NADPH + O_2 + 2\,H^+ \\ \Delta\mathcal{E}^{\circ\prime} &= -0.320\ \text{V} - (0.815\ \text{V}) = -1.135\ \text{V} \\ \Delta G^{\circ\prime} &= -n\mathcal{F}\Delta\mathcal{E}^{\circ\prime} \\ &= -(4)(96{,}485\ \text{J}\cdot\text{V}^{-1}\cdot\text{mol}^{-1})(-1.135\ \text{V}) \\ &= 438\ \text{kJ}\cdot\text{mol}^{-1} \end{aligned}$$

(b) One mole of photons of red light ($\lambda = 700$ nm) has an energy of 171 kJ. Therefore, $438/171 = 2.6$ moles of photons are theoretically required to drive the oxidation of H_2O by $NADP^+$ to form one mole of O_2.

(c) The energy of a mole of photons of UV light ($\lambda = 220$ nm) is

$$\begin{aligned} E &= Nhc/\lambda \\ &= (6.022 \times 10^{23}\ \text{mol}^{-1})(6.626 \times 10^{-34}\ \text{J}\cdot\text{s}) \\ &\quad\ (2.998 \times 10^{8}\ \text{ms}^{-1})/(2.2 \times 10^{-7}\ \text{m}) \\ &= 544\ \text{kJ}\cdot\text{mol}^{-1} \end{aligned}$$

The number of moles of 220-nm photons required to produce one mole of O_2 is $438/544 = 0.8$.

7. Both systems mediate cyclic electron flows. The photooxidized bacterial reaction center passes electrons through a series of electron carriers so that electrons return to the reaction center (e.g., $P960^+$) and restore it to its original state. During cyclic electron flow in PSI, electrons from photooxidized P700 are transferred to cytochrome b_6f and, via plastoquinone and plastocyanin, back to $P700^+$. In both cases, there is no net change in the redox state of the reaction center, but the light-driven electron movements are accompanied by the transmembrane movement of protons.

8. When cyclic electron flow occurs, photoactivation of PSI drives electron transport independently of the flow of electrons derived from water. Thus, the oxidation of H_2O by PSII is not linked to the number of photons consumed by PSI.

9. (a) The buildup of the proton gradient is indicative of a high level of activity of the photosystems. A steep gradient could therefore trigger photoprotective activity to prevent further photooxidation when the proton-translocating machinery is operating at maximal capacity. (b) Photooxidation would not be a good protective mechanism since it might interfere with the normal redox balance among the electron-carrying groups in the thylakoid membrane. Releasing the energy by exciton transfer or fluorescence (emitting light of a longer wavelength) could potentially funnel light energy back to the overactive photosystems. Dissipation of the excess energy via internal conversion to heat would be the safest mechanism, since the photosystems do not have any way to harvest thermal energy to drive chemical reactions.

10. (a) An uncoupler dissipates the transmembrane proton gradient by providing a route for proton translocation other than ATP synthase. Therefore, chloroplast ATP production would decrease. (b) The uncoupler would not affect $NADP^+$ reduction since light-driven electron transfer reactions would continue regardless of the state of the proton gradient.

11. An increase in [O_2] increases the oxygenase activity of RuBP carboxylase–oxygenase and therefore lowers the efficiency of CO_2 fixation.

12. After the light is turned off, ATP and NADPH levels fall as those substances are used up in the Calvin cycle without being replaced by the light reactions. 3PG builds up because it cannot pass through the phosphoglycerate kinase reaction in the absence of ATP. The RuBP level drops because it is consumed by the RuBP carboxylase reaction (which requires neither ATP nor NADPH) and its replenishment is blocked by the lack of ATP for the phosphoribulokinase reaction.

13. The net synthesis of 2 GAP from 6 CO_2 in the initial stage of the Calvin cycle (Fig. 19-26) consumes 18 ATP and 12 NADPH (equivalent to 30 ATP). The conversion of 2 GAP to glucose-6-phosphate (G6P) by gluconeogenesis does not require energy input (Section 16-4B), nor does the isomerization of G6P to glucose-1-phosphate (G1P). The activation of G1P to its nucleotide derivative consumes 2 ATP equivalents (Section 16-5), but ADP is released when the glucose residue is incorporated into starch. These steps represent an overall energy investment of 18 + 30 + 1 = 49 ATP.

    Starch breakdown by phosphorolysis yields G1P, whose subsequent degradation by glycolysis yields 3 ATP, 2 NADH (equivalent to 5 ATP), and 2 pyruvate. Complete oxidation of 2 pyruvate to 6 CO_2 by the pyruvate dehydrogenase reaction and the citric acid cycle (Section 17-1) yields 8 NADH (equivalent to 20 ATP), 2 $FADH_2$ (equivalent to 3 ATP), and 2 GTP (equivalent to 2 ATP). The overall ATP yield is therefore 3 + 5 + 20 + 3 + 2 = 33 ATP.

    The ratio of energy spent to energy recovered is 49/33 = 1.5.

14. These plants store CO_2 by CAM. At night, CO_2 reacts with PEP to form malate. By morning, so much malate (malic acid) has accumulated that the leaves have a sour taste. During the day, the malate is converted to pyruvate + CO_2. The leaves therefore become less acidic and hence tasteless. Late in the day, when all the malate is consumed, the leaves become slightly basic, that is, bitter.

CHAPTER 20

1. A defect in carnitine palmitoyl transferase II prevents normal transport of activated fatty acids into the mitochondria for β oxidation. Tissues such as muscle that use fatty acids as metabolic fuels therefore cannot generate ATP as needed. The problem is more severe during a fast because other fuels, such as dietary glucose, are not readily available.

2.

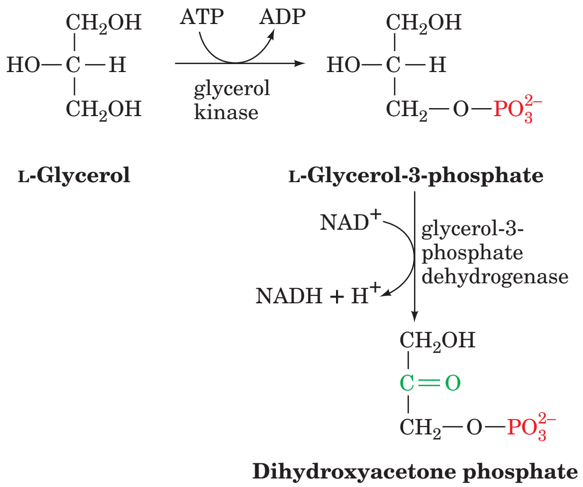

3. The first three steps of β oxidation resemble the reactions that convert succinate to oxaloacetate (Sections 17-3F to 17-3H).

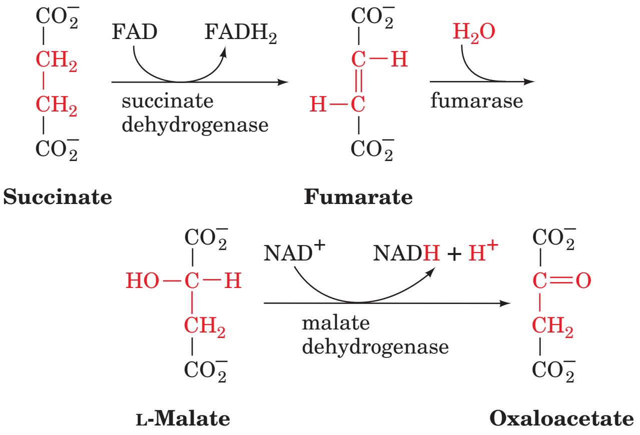

4. (a) Six cycles are required.

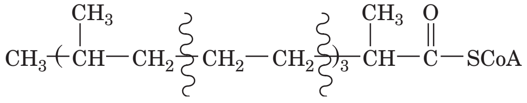

$$CH_3\text{-}\left(\overset{CH_3}{\overset{|}{CH}}-CH_2 \wr CH_2-CH_2 \wr\right)_3-\overset{CH_3}{\overset{|}{CH}}-\overset{O}{\overset{\|}{C}}-SCoA$$

   (b) 3 Acetyl-CoA, 3 propionyl-CoA, and 1 methylpropionyl-CoA.

5. There are not as many usable nutritional calories per gram in unsaturated fatty acids as there are in saturated fatty acids. This is because oxidation of fatty acids containing double bonds yields fewer reduced coenzymes whose oxidation drives the synthesis of ATP. In the oxidation of fatty acids with a double bond at an odd-numbered carbon, the enoyl-CoA isomerase reaction bypasses the acyl-CoA dehydrogenase reaction and therefore does not generate $FADH_2$ (equivalent to 1.5 ATP). A double bond at an even-numbered carbon must be reduced by NADPH (equivalent to the loss of 2.5 ATP).

6. Oxidation of odd-chain fatty acids generates succinyl-CoA, an intermediate of the citric acid cycle. Because the citric acid cycle operates as a multistep catalyst to convert acetyl groups to CO_2, increasing the concentration of a cycle intermediate can increase the catalytic activity of the cycle.

7. Palmitate oxidation produces 106 ATP and glucose catabolism produces 32 ATP (Section 17-4). Assuming a free energy cost of 30.5 $kJ \cdot mol^{-1}$ to synthesize ATP, palmitate catabolism has an efficiency of

$$106 \times 30.5/9781 \times 100 = 33\%$$

   Glucose catabolism has an efficiency of

$$32 \times 30.5/2850 \times 100 = 34\%$$

   Thus, the two processes have very nearly the same overall efficiency.

8. 3-Ketoacyl-CoA transferase is required to convert ketone bodies to acetyl-CoA. If the liver contained this enzyme, it would be unable to supply ketone bodies as fuels for other tissues.

9. Palmitate (C_{16}) synthesis requires 14 NADPH. The transport of 8 acetyl-CoA to the cytosol by the tricarboxylate transport system supplies 8 NADPH (Fig. 20-24), which represents 8/14 × 100 = 57% of the required NADPH.

10. The label does not appear in palmitate because $^{14}CO_2$ is released in Reaction 2b of fatty acid synthesis (Fig. 20-26).

11. The breakdown of glucose by glycolysis generates the dihydroxyacetone phosphate that becomes the glycerol backbone of triacylglycerols (Fig. 20-29).

12. This fatty acid **(linolenate)** cannot be synthesized by animals because it contains a double bond closer than 6 carbons from its noncarboxylate end.

13. The synthesis of stearate (18:0) from mitochondrial acetyl-CoA requires 9 ATP to transport 9 acetyl-CoA from the mitochondria to the cytosol. Seven rounds of fatty acid synthesis consume 7 ATP (in the acetyl-CoA carboxylase reaction) and 14 NADPH (equivalent to 35 ATP). Elongation of palmitate to stearate requires 1 NADH and 1 NADPH (equivalent to 5 ATP). The energy cost is therefore $9 + 7 + 35 + 5 = 56$ ATP.

    (a) The degradation of stearate to 9 acetyl-CoA consumes 2 ATP (in the acyl-CoA synthetase reaction) but generates, in eight rounds of β oxidation, 8 $FADH_2$ (equivalent to 12 ATP) and 8 NADH (equivalent to 20 ATP). Thus, the energy yield is $12 + 20 - 2 = 30$ ATP. This represents only about half of the energy consumed in synthesizing stearate (30 ATP versus 56 ATP).

    (b) The complete oxidation of the 9 acetyl-CoA to CO_2 by the citric acid cycle yields an additional 9 GTP (equivalent to 9 ATP), 27 NADH (equivalent to 67.5 ATP), and 9 $FADH_2$ (equivalent to 13.5 ATP) for a total of $30 + 9 + 67.5 + 13.5 = 120$ ATP. Thus, more than twice the energy investment of synthesizing stearate is recovered (120 ATP versus 56 ATP).

14. (a)

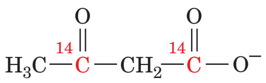

$H_3C{-}\overset{O}{\overset{\|}{^{14}C}}{-}CH_2{-}\overset{O}{\overset{\|}{^{14}C}}{-}O^-$

Acetoacetate

See Fig. 20-21.

(b)

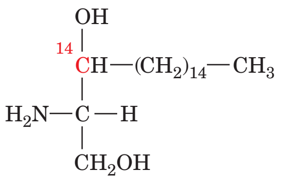

Sphinganine

See Fig. 20-35.

15. Statins inhibit the HMG-CoA reductase reaction, which produces mevalonate, a precursor of cholesterol. Although lower cholesterol levels induce the synthesis of HMG-CoA reductase to make up for the loss in activity, some decrease in activity may still be present. Because mevalonate is also the precursor of ubiquinone (coenzyme Q), supplementary ubiquinone may be necessary.

CHAPTER 21

1. Proteasome-dependent proteolysis requires ATP to activate ubiquitin in the first step of linking ubiquitin to the target protein (Fig. 21-2) and for denaturing the protein as it enters the proteasome.

2. The urea cycle transforms excess nitrogen from protein breakdown to an excretable form, urea. In a deficiency of a urea cycle enzyme, the preceding urea cycle intermediates may build up to a toxic level. A low-protein diet minimizes the amount of nitrogen that enters the urea cycle and therefore reduces the concentrations of the toxic intermediates.

3. An individual consuming a high-protein diet uses amino acids as metabolic fuels. As the amino acid skeletons are converted to glucogenic or ketogenic compounds, the amino groups are disposed of as urea, leading to increased flux through the urea cycle. During starvation, proteins (primarily from muscle) are degraded to provide precursors for gluconeogenesis. Nitrogen from these protein-derived amino acids must be eliminated, which demands a high level of urea cycle activity.

4. Glutamate dehydrogenase, glutamine synthetase, and carbamoyl phosphate synthetase.

5. (a)

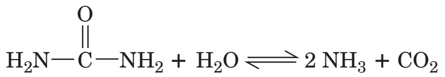

$H_2N{-}\overset{O}{\overset{\|}{C}}{-}NH_2 + H_2O \rightleftharpoons 2\,NH_3 + CO_2$

    (b) The NH_3 produced by the action of urease can combine with protons in gastric fluid to form NH_4^+. This could reduce the concentration of protons and therefore increase the pH.

6. Since the three reactions converting tiglyl-CoA to acetyl-CoA and propionyl-CoA are analogous to those of fatty acid oxidation (β oxidation; Fig. 20-12), the reactions are:

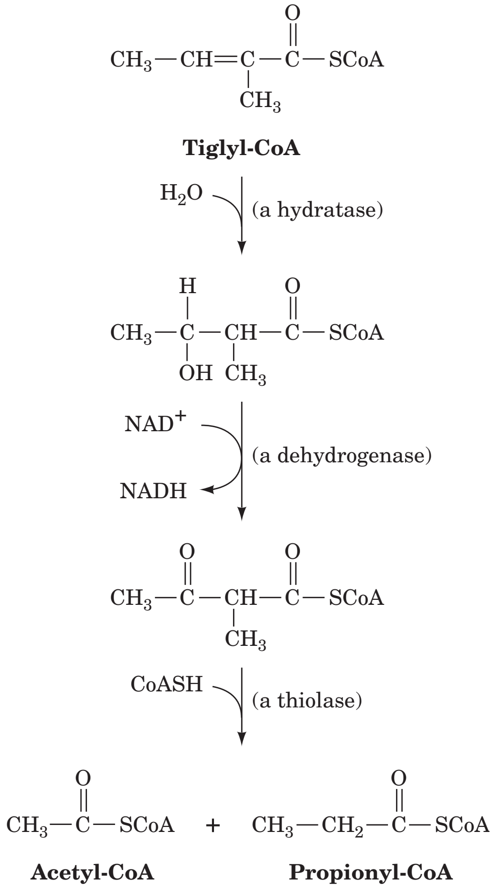

7. 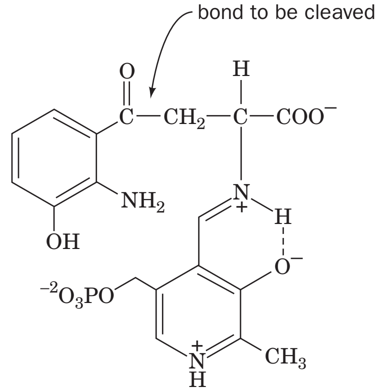

8. (a) Ala, Arg, Asn, Asp, Cys, Gln, Glu, Gly, His, Met, Pro, Ser, and Val

   (b) Leu and Lys

   (c) Ile, Phe, Thr, Trp, and Tyr

9. Tryptophan can be considered a member of this group since one of its degradation products is alanine, which is converted to pyruvate by deamination.

10. In the absence of uridylyl-removing enzyme, adenylyltransferase·P_{II} will be fully uridylylated, since there is no mechanism for removing the uridylyl groups once they are attached. Uridylylated adenylyltransferase·P_{II} adenylylates glutamine synthetase, which activates it. Hence, the defective *E. coli* cells will have a hyperactive glutamine synthetase and thus a higher than normal glutamine concentration. Reactions requiring glutamine will therefore be accelerated, thereby depleting glutamate and the citric acid cycle intermediate α-ketoglutarate. Consequently, biosynthetic reactions requiring transamination, as well as energy metabolism, will be suppressed.

11. Since only plants and microorganisms synthesize aromatic amino acids, herbicides that inhibit these pathways do not affect amino acid metabolism in animals.

12. The pigment coloring skin and hair is melanin, which is synthesized from tyrosine. When tyrosine is in short supply, as when dietary protein is not available, melanin cannot be synthesized in normal amounts, and the skin and hair become depigmented.

CHAPTER 22

1. Hyperinsulinemia would result in a decrease in blood glucose. The decrease in [glucose] for the brain would cause loss of brain function (leading to coma and death).

2. ATP generating pathways such as glycolysis and fatty acid oxidation require an initial investment of ATP (the hexokinase and phosphofructokinase steps of glycolysis and the acyl-CoA synthetase activation step that precedes β oxidation). This "priming" cannot occur when ATP has been exhausted.

3. (a) GLUT2 has a higher K_M than GLUT1 so that the rate of glucose entry into liver cells can vary directly with the concentration of glucose in the blood. A transporter with a high K_M is less likely to be saturated with its ligand and therefore would not limit the rate of transport. (b) Type I glycogen storage disease results from a deficiency of glucose-6-phosphatase so that glucose-6-phosphate produced by glycogenolysis cannot exit the cell as glucose. A defect in the glucose-transport protein GLUT2 would similarly prevent the exit of glucose (a passive transporter can operate in either direction). In both cases, the buildup of intracellular glucose-6-phosphate prevents glycogen breakdown, and glycogen accumulates.

4. (a) Because fatty acids, like glucose, are metabolic fuels, it makes sense for them to stimulate insulin release, which is a signal of abundant fuel. (b) Elevated levels of circulating fatty acids occur during an extended fast, when dietary glucose and glucose mobilized from glycogen stores are no longer available. Insulin release would be inappropriate for these conditions. A combination of abundant fatty acids and glucose, indicating the fed state, would serve as a better trigger for insulin release.

5. At high altitude, less oxygen is available for aerobic metabolism, so glycolysis, an anaerobic pathway, would become relatively more important in active muscles. An increase in GLUT1 would increase the intracellular glucose concentration, and an increase in PFK would increase the flux of glucose through the pathway.

6. (a) In the absence of MCAD, fatty acids cannot be fully oxidized to acetyl-CoA (Section 20-2C). Since ketone bodies are synthesized from acetyl-CoA (Section 20-3), ketogenesis is impaired.

   (b) In normal individuals, acetyl-CoA activates pyruvate carboxylase (Section 17-5B), which converts pyruvate to oxaloacetate. This increases the capacity of the citric acid cycle to metabolize acetyl-CoA. When glucose levels are low, the oxaloacetate is used for gluconeogenesis (Section 16-4). In MCAD deficiency, lack of fatty acid–derived acetyl-CoA keeps pyruvate carboxylase activity low, thereby limiting the synthesis of glucose and contributing to hypoglycemia.

7. Insulin activates ATP-citrate lyase, which is the enzyme that converts citrate to oxaloacetate and acetyl-CoA (Section 20-4A). The activity of this enzyme is essential for making acetyl units available for fatty acid biosynthesis in the cytosol. The acetyl units, generated from pyruvate in the mitochondria, combine with oxaloacetate to form citrate, which can then be transported from the mitochondria to the cytosol for reconversion to acetyl-CoA.

8. Insulin promotes the uptake of glucose via the increase in GLUT4 receptors on the adipocyte surface. A source of glucose is necessary to supply the glycerol-3-phosphate backbone of triacylglycerols.

9. Ingesting glucose while in the resting state causes the pancreas to release insulin. This stimulates the liver, muscle, and adipose tissue to synthesize glycogen, fat, and protein from the excess nutrients while inhibiting the breakdown of these metabolic fuels. Hence, ingesting glucose before a race will gear the runner's metabolism for resting rather than for running.

10. During starvation, the synthesis of glucose from liver oxaloacetate depletes the supply of citric acid cycle intermediates and thus decreases the ability of the liver to metabolize acetyl-CoA via the citric acid cycle.

11. The leptin produced by the normal mouse will enter the circulation of the *ob*/*ob* mouse, resulting in decreases in its appetite and weight.

12. Adipose tissue synthesizes and releases the polypeptide hormones adiponectin, leptin, and resistin.

13. Since PYY_{3-36} is a peptide hormone, it would be digested if taken orally. Introducing it directly into the bloodstream avoids degradation.

14. An intermediate in the biosynthesis of triacylglycerols is diacylglycerol (DAG), a second messenger responsible for activating PKC.

15. Physical inactivity would lead to a decreased need for ATP in muscle, which would be reflected by a decreased AMP to ATP ratio. A decrease in this ratio would lead to a decrease in AMPK activity. AMPK activity is positively associated with glucose uptake by cells due to an increase in GLUT4 activity. GLUT4 activity is also increased by insulin. A decrease in AMPK would lead to a decrease in GLUT4 activity, making insulin's job more difficult.

CHAPTER 23

1. (a) 7 ATP;
   (b) 8 ATP;
   (c) 7 ATP.

2. PRPP and FGAR accumulate because they are substrates of Reactions 2 and 5 in the IMP biosynthetic pathway (Fig. 23-1). XMP also accumulates because the GMP synthetase reaction is blocked (Fig. 23-3). Although glutamine is a substrate of carbamoyl phosphate synthetase II (the first enzyme of UMP synthesis; Fig. 23-5), the other substrates of that enzyme do not accumulate.

3. (a) The recovered deoxycytidylate would be equally labeled in its base and ribose components (i.e., the same labeling pattern as in the original cytidine). (b) The recovered deoxycytidylate would be unequally labeled in its base and ribose components because the separated ^{14}C-cytosine and ^{14}C-ribose would mix with the different-sized pools of unlabeled cellular cytosine and ribose before recombining as the deoxycytidylate that becomes incorporated into DNA. [This experiment established that deoxyribonucleotides, in fact, are synthesized from their corresponding ribonucleotides (alternative a).]

4. Hydroxyurea destroys the tyrosyl radical that is essential for the activity of ribonucleotide reductase. Tumor cells are generally fast-growing and cannot survive without this enzyme, which supplies dNTPs for nucleic acid synthesis. In contrast, most normal cells grow slowly, if at all, and hence have less need for nucleic acid synthesis.

5. dATP inhibits ribonucleotide reductase, thereby preventing the synthesis of the deoxynucleotides required for DNA synthesis.

6. FdUMP and methotrexate kill rapidly proliferating cells, such as cancer cells and those of hair follicles. Consequently, hair falls out.

7. The mutant cells grow because the medium contains the thymidine they are unable to make. Normal cells, however, continue to synthesize their own thymidine and thereby convert their limited supply of THF to DHF. The methotrexate inhibits dihydrofolate reductase, so THF cannot be regenerated. Without a supply of THF for the synthesis of nucleotides and amino acids, the cells die.

8. The synthesis of histidine and methionine requires THF. The cell's THF is converted to DHF by the thymidylate synthase reaction, but in the presence of methotrexate THF cannot be regenerated.

9. The conversion of dUMP to dTMP is a reductive methylation. In the thymidylate synthase reaction shown in Fig. 23-15, THF is oxidized to DHF, so that DHFR must subsequently reduce the DHF to THF. Organisms that lack DHFR use an alternative mechanism for converting dUMP to dTMP in which the FAD cofactor of the enzyme, rather than the folate, undergoes oxidation.

10. (a) Trimethoprim binds to bacterial dihydrofolate reductase but does not permanently inactivate the enzyme. Therefore, it is not a mechanism-based inhibitor. (b) Allopurinol is oxidized by xanthine oxidase to a product that irreversibly binds to the enzyme. It is therefore a mechanism-based inhibitor of xanthine oxidase.

11. In von Gierke's disease (glucose-6-phosphatase deficiency), glucose-6-phosphate accumulates in liver cells, thereby stimulating the pentose phosphate pathway. The resulting increase in ribose-5-phosphate production boosts the concentration of PRPP, which in turn stimulates purine biosynthesis. High levels of uric acid derived from the breakdown of these excess purines causes gout.

12.

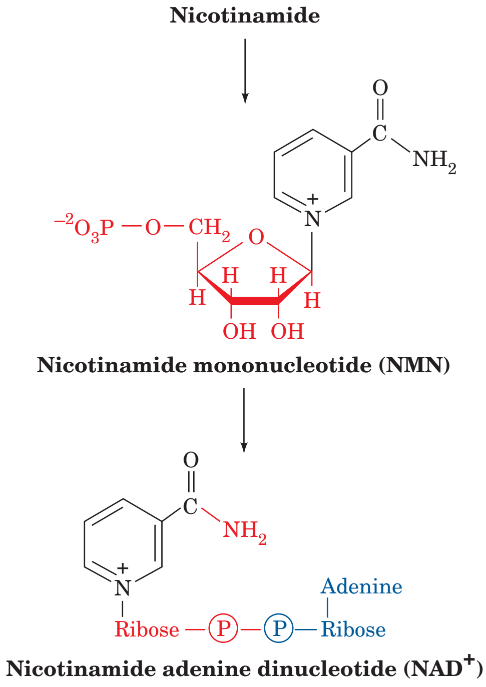

CHAPTER 24

1. Since amino acids have an average molecular mass of ~110 D, the 50-kD protein contains 50,000 D ÷ 110 D/residue = ~455 residues. These residues are encoded by 455 × 3 = 1365 nucleotides. In B-DNA, the rise per base pair is 3.4 Å, so the contour length of 1365 bp is 3.4 Å/bp × 1365 bp = 4641 Å, or

0.46 μm. In A-DNA, the contour length would be 1365 bp × 2.9 Å/bp = 3959 Å, or 0.40 μm.

2. (a) Hypoxanthine pairs with cytosine in much the same way as does guanine.

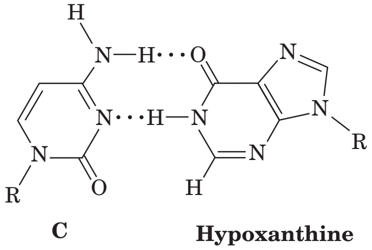

(b)

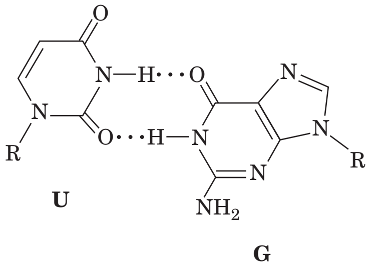

3. (a)

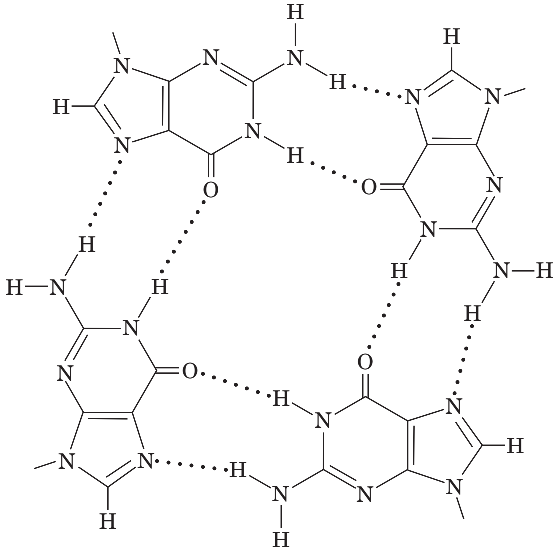

(b)

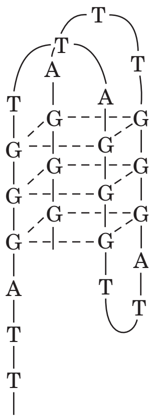

4. The decarboxylation of the amino acid ornithine, an intermediate of the urea cycle (Fig. 21-9), generates 1,4-diaminobutane (also known as putrescine).

$$^{+}H_3N\text{—}(CH_2)_4\text{—}NH_3^{+}$$

This cationic molecule interacts electrostatically with the negatively charged phosphate groups of DNA.

5. The enzyme has no effect on the supercoiling of DNA since cleaving the C2′—C3′ bond of ribose does not sever the sugar–phosphate chain of DNA.

6. In the B-DNA to Z-DNA transition, a right-handed helix with one turn per 10.4 base pairs converts to a left-handed helix with one turn per 12 base pairs. Since a right-handed duplex helix has a positive twist, the twist decreases:

$$\Delta T = -\frac{100}{10.4} + \frac{-100}{12} = -17.9 \text{ turns}$$

The linking number must remain constant ($\Delta L = 0$) since no covalent bonds are broken. Hence, the change in writhing number is $\Delta W = -\Delta T = 17.9$ turns.

7. The segment with 20% A residues (i.e., 40% A · T base pairs) contains 60% G · C base pairs and therefore melts at a higher temperature than a segment with 30% A residues (i.e., 40% G · C base pairs).

8. (a) Its T_m decreases because the charges on the phosphate groups are less shielded from each other at lower ionic strength and hence repel each other more strongly, thereby destabilizing the double helix. (b) The nonpolar solvent diminishes the hydrophobic forces that stabilize double-stranded DNA and hence lowers the T_m.

9. (a) As the temperature increases, the stacked bases melt apart so that their ultraviolet absorbance increases (the hyperchromic effect). (b) The broad shape of the poly(A) melting curve indicates noncooperative changes, as expected for a single-stranded RNA. The sharp melting curve for DNA reflects the cooperativity of strand separation.

10.

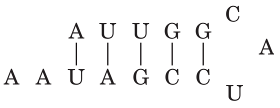

11.

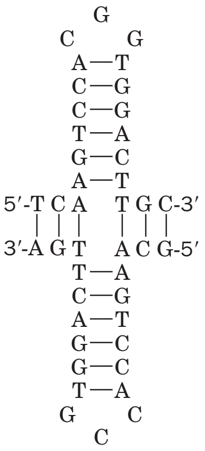

12.

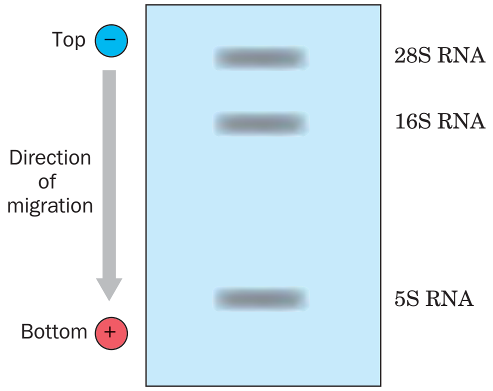

13. The target sequence consists of 6 symmetry-related base pairs. Since there are 4 possible base pairs (A · T, T · A, G · C, and C · G), the probability that any two base pairs are randomly related by symmetry is 1/4. Hence, the probability of finding all 6 pairs of base pairs by random chance is $(1/4)^6 = 2.4 \times 10^{-4}$.

14. (a) A 6-nt sequence would be expected to occur, on average, every $4^6 = 4096$ nt in single-stranded DNA. However, in double-stranded DNA, it would be expected to occur at twice this frequency, that is, every 4096/2 = 2048 bp. Thus the expected number of copies of a 6-bp sequence in the *E. coli* genome is 4,639,000 bp/2048 bp = 2265.

    (b) A 12-bp sequence would be expected to occur, on average, every $4^{12}/2 = 8{,}388{,}608$ bp, which is nearly twice as large as the number of base pairs in the *E. coli* genome. Thus the *trp* repressor is unlikely to bind specifically to any other site in the *E. coli* chromosome.

15. (a) The contour length is 5×10^7 bp × 3.4 Å/bp = 1.7×10^8 Å = 17 mm.

    (b) A nucleosome, which binds ~200 bp, compresses the DNA to an 80-Å-high supercoil. The length of the DNA is therefore (80 Å/200 bp) × (5×10^7 bp) = 2×10^7 Å = 2 mm.

    (c) In the 30-nm fiber, 18.9 nucleosomes cover 316 Å. The length of the DNA is (316 Å/18.9 nucleosomes) × (1 nucleosome/200 bp) × (5×10^7 bp) = 4.2×10^6 Å = 0.42 mm.

16. Experiment 1. The restriction enzyme failed to digest the genomic DNA, leaving the DNA too large to enter the gel during electrophoresis.

    Experiment 2. The hybridization conditions were too "relaxed," resulting in nonspecific hybridization of the probe to all the DNA fragments. This problem could be corrected by boiling the blot to remove the probe and repeating the hybridization at a higher temperature and/or lower salt concentration.

    Experiment 3. The probe hybridized with three different mouse genes. The different intensity of each band reflects the relatedness of the sequences. The most intense band is most similar to the human *rxr-1* gene, whereas the least intense band is least similar to the *rxr-1* gene.

CHAPTER 25

1. Okazaki fragments are 1000 to 2000 nt long, and the *E. coli* chromosome contains 4.6×10^6 bp. Therefore, *E. coli* chromosomal replication requires 2300 to 4600 Okazaki fragments.

2. As indicated in Fig. *a* (*below*), nucleotides would be added to a polynucleotide strand by attack of the 3′-OH of the incoming nucleotide on the 5′ triphosphate group of the growing strand with the elimination of PP_i. The hydrolytic removal of a mispaired nucleotide by the 5′ → 3′ exonuclease activity (Fig. *b, below*) would leave only an OH group or monophosphate group at the 5′ end of the DNA chain. This would require an additional activation step before further chain elongation could commence.

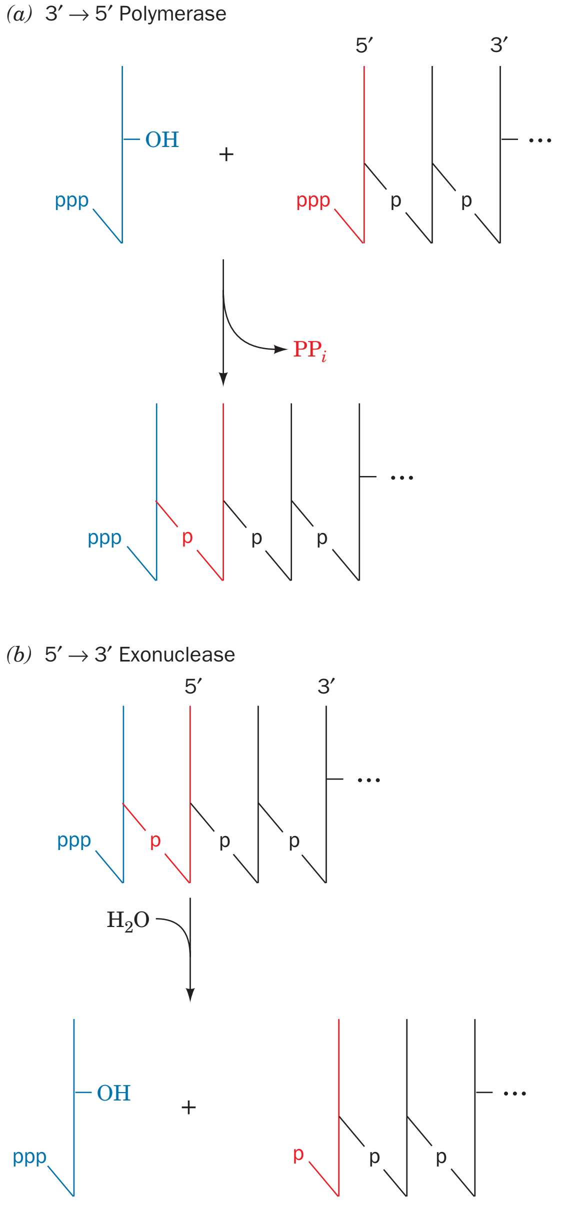

3. The drug would inhibit DNA synthesis because the polymerization reaction is accompanied by the release and hydrolysis of PP_i. Failure to hydrolyze the PP_i would remove the thermodynamic driving force for polymerization, that is, it would be reversible.

4. PP_i is the product of the polymerization reaction catalyzed by DNA polymerase. This reaction also requires a template DNA strand and a primer with a free 3′ end.

(a) There is no primer strand, so no PP_i is produced.

(b) There is no primer strand, so no PP_i is produced.

(c) PP_i is produced.

(d) No PP_i is produced because there is no 3′ end that can be extended.

(e) PP_i is produced.

(f) PP_i is produced.

5. The 5′ → 3′ exonuclease activity is essential for DNA replication because it removes RNA primers and replaces them with DNA. Absence of this activity would be lethal.

6. The Klenow fragment, which lacks 5′ → 3′ exonuclease activity (and therefore cannot catalyze nick translation), is used to ensure that all the replicated DNA chains have the same 5′ terminus, a necessity if a sequence is to be assigned according to fragment length.

7. AT-rich DNA is less stable than GC-rich DNA and therefore would more readily melt apart, a requirement for initiating replication.

8. DNA gyrase adds negative supercoils to relieve the positive supercoiling that helicase-catalyzed unwinding produces ahead of the replication fork.

9. Mismatch repair and other repair systems correct most of the errors missed by the proofreading functions of DNA polymerases.

10. The *E. coli* replication system can fully replicate only circular DNAs. Bacteria do not have a mechanism (e.g., telomerase-catalyzed extension of telomeres) for replicating the extreme 3′ ends of linear template strands.

11. (a)

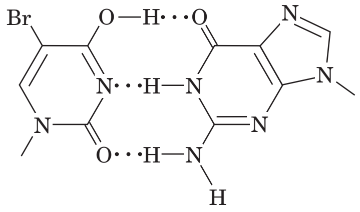

5BU (enol tautomer) **Guanine**

(b) When 5BU incorporated into DNA pairs with G, the result is an A · T → G · C transition after two more rounds of DNA replication:

$$A \cdot T \rightarrow A \cdot 5BU \rightarrow G \cdot 5BU \rightarrow G \cdot C$$

12. Base excision repair. The deaminated base can be recognized because hypoxanthine does not normally occur in DNA.

13. The cytosine derivative base-pairs with adenine, generating a C · G → T · A transition.

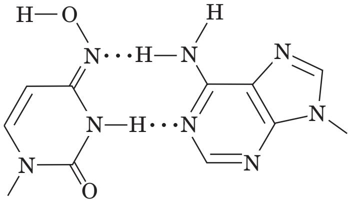

Adenine

14. The triphosphatase destroys nucleotides containing the modified base before they can be incorporated into DNA during replication.

15. When 5-methylcytosine residues deaminate, they form thymine residues.

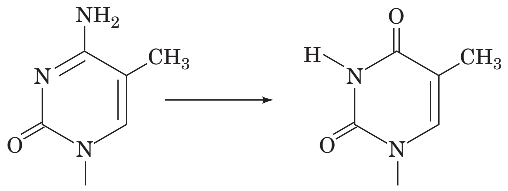

5-Methyl-C **T**

Since thymine is a normal DNA base, the repair systems cannot determine whether such a T or its opposing G is the mutated base. Consequently, only about half of the deaminated 5-methylcytosines are correctly repaired.

16. (a) Loss of the helicase DnaB, which unwinds DNA for replication, would be lethal.

(b) Loss of Pol I would prevent the excision of RNA primers and would therefore be lethal.

(c) SSB prevents reannealing of separated single strands. Loss of SSB would be lethal.

(d) RecA protein mediates the SOS response and homologous recombination. Loss of RecA would be harmful but not necessarily lethal.

17. *E. coli* contains a low concentration of dUTP, which DNA polymerase incorporates into DNA in place of dTTP. The resulting uracil bases are rapidly excised by uracil–DNA glycosylase followed by nucleotide excision repair (NER), which temporarily causes a break in the DNA chain. DNA that is isolated before DNA polymerase I and DNA ligase can complete the repair process would be fragmented. However, in the absence of a functional uracil–DNA glycosylase, the inappropriate uracil residues would remain in place, and hence leading strand DNA would be free of breaks. The lagging strand, being synthesized discontinuously, would still contain breaks, although fewer than otherwise.

18. Pol V is less processive than Pol III. When the progress of Pol III is arrested by the presence of a thymine dimer, Pol V can take over, allowing replication to continue at a high rate, although with a greater incidence of mispairings. The damage is minimal, however, since Pol V soon dissociates from the DNA, allowing the more accurate Pol III to resume replicating DNA.

CHAPTER 26

1. (a) Cordycepin is the 3′-deoxy analog of adenosine.

(b) Because it lacks a 3′-OH group, the cordycepin incorporated into a growing RNA chain cannot support further chain elongation in the 5′ → 3′ direction.

2. The top strand is the sense strand. Its TATGAT segment differs by only one base from the TATAAT consensus sequence of the promoter's −10 sequence; its TTTACA sequence differs by only one base from the TTGACA consensus sequence of the promoter's −35 sequence and is appropriately located ~25 nt to the 5′ side of the −10 sequence; and the initiating G

nucleotide is the only purine that is located ~10 nt downstream of the −10 sequence.

5′ CAACGTAACACTTTACAGCGGCGCGTCATTTGATATGATGCGCCCCGCTTCCCGATA 3′

–35 region   –10 region   start point

3. The probe should have a sequence complementary to the consensus sequence of the 6-nt Pribnow box: 5′-ATTATA-3′.

4. Promoter elements for RNA polymerase II include sequences at −27 (the TATA box) and between −50 and −100. The insertion of 10 bp would separate the promoter elements by the distance of the turn of the DNA helix, thereby diminishing the binding of proteins required for transcription initiation. However, the protein-binding sites would still be on the same side of the helix. Inserting 5 bp (half of a helical turn) would move the protein-binding sites to opposite sides of the helix, making it even more difficult to initiate transcription.

5. G · C base pairs are more stable than A · T base pairs. Hence, the more G · C base pairs that the promoter contains, the more difficult it is to form the open complex during transcription initiation.

6. Transcription of an rRNA gene yields a single rRNA molecule that is incorporated into a ribosome. In contrast, transcription of a ribosomal protein gene yields an mRNA that can be translated many times to produce many copies of its corresponding protein. The greater number of rRNA genes relative to ribosomal protein genes helps ensure the balanced synthesis of rRNA and proteins necessary for ribosome assembly.

7. The cell lysates can be applied to a column containing a matrix with immobilized poly(dT). The poly(A) tails of processed mRNAs will bind to the poly(dT) while other cellular components are washed away. The mRNAs can be eluted by decreasing the salt concentration to destabilize the A · T base pairs.

8. (a) The phosphate groups of the phosphodiester backbone of the mRNA will be labeled at all sites where α-[^{32}P]ATP is used as a substrate by RNA polymerase.

   (b) ^{32}P will appear only at the 5′ end of mRNA molecules that have A as the first residue (this residue retains its α and β phosphates). In all other cases where β-[^{32}P]ATP is used as a substrate for RNA synthesis, the β and γ phosphates are released as PP$_i$ (see Fig. 26-6).

   (c) No ^{32}P will appear in the RNA chain. During polymerization, the β and γ phosphates are released as PP$_i$. The terminal (γ) phosphate of an A residue at the 5′ end of an RNA molecule is removed during the capping process.

9. DNA polymerase needs a primer; poly(A) polymerase uses the pre-mRNA as a primer; tRNA nucleotidyl transferase uses the immature tRNA as a primer; and RNA polymerase does not require a primer. Both DNA polymerase and RNA polymerase require a DNA template, but neither poly(A) polymerase nor tRNA nucleotidyl transferase uses a template. The four polymerases use different sets of nucleotides: DNA polymerase uses all four dNTPS; RNA polymerase uses all four NTPs; poly(A) polymerase uses only ATP; and tRNA nucleotidyl transferase uses ATP and CTP.

10. The active site of poly(A) polymerase is narrower because it does not need to accommodate a template strand.

11. The mechanism of RNase hydrolysis requires a free 2′-OH group to form a 2′,3′-cyclic phosphate intermediate (Figure 11-10). Nucleotide residues lacking a 2′-OH group would therefore be resistant to RNase-catalyzed hydrolysis.

12. The mRNA splicing reaction, which requires no free energy input and results in no loss of phosphodiester bonds, is theoretically reversible *in vitro.* However, the degradation of the excised intron makes the reaction irreversible in the cell.

13. The intron must be large enough to include a spliceosome binding site(s).

14. Inhibition of snRNA processing interferes with mRNA splicing. As a result, host mRNA cannot be translated, so the host ribosomes will synthesize only viral proteins.

CHAPTER 27

1. A 4-nt insertion would add one codon and shift the gene's reading frame by one nucleotide. The proper reading frame could be restored by deleting a nucleotide. Gene function, however, would not be restored if (a) the 4-nt insertion interrupted the codon for a functionally critical amino acid; (b) the 4-nt insertion created a codon for a structure-breaking amino acid; (c) the 4-nt insertion introduced a Stop codon early in the gene; or (d) the 1-nt deletion occurred far from the 4-nt insertion so that even though the reading frame was restored, a long stretch of frame-shifted codons separated the insertion and deletion points.

2. The possible codons are UUU, UUG, UGU, GUU, UGG, GUG, GGU, and GGG. The encoded amino acids are Phe, Leu, Cys, Val, Trp, and Gly (Table 27-1).

3. An amber mutation results from any of the point mutations XAG, UXG, or UAX to UAG. The XAG codons specify Gln, Lys, and Glu; the UXG codons specify Leu, Ser, and Trp; and the UAX codons that are not Stop codons both specify Tyr. Hence some of the codons specifying these amino acids can undergo a point mutation to UAG.

4. (a) Each ORF begins with an initiation codon (ATG) and ends with a Stop codon (TGA):

   ATGCTCAACTATATGTGA encodes *vir-2* and

   ATGCCGCATGCTCTGTTAATCACATATAGTTGA
   on the complementary strand encodes *vir-1.*

   (b) *vir-1:* MPHALLITYS; *vir-2:* MLNYM.

   (c) *vir-1:* MPHALLIPYS; *vir-2:* MLNYMGLTEHAA.

5. There are four exons (the underlined bases)

   TATAATACGCGCAATACAATCTACAGCTTCGCGTA
   AATCGCAGGTAAGTTGTAATAAATATAAGTGAGT
   ATGATAGGGCTTTGGACCGATAGATGCGACCCTG
   CAGGTAAGTATAGATTAATTAAGCACAGGCATGCA
   GGGATATCCTCCAAACAGGTAAGTAACCTTACGG
   TCAATTAATTAGGCAGTAGATGAATAAACGATAT
   CGATCGGTTACAGTAGTCTGAT

   The mature mRNA, which has a 5′ cap and a 3′ poly(A) tail, therefore has the sequence

   GCGUAAAUCGUAGGCUUUGGACCGAUAG**AUG**
   CGACCCUGGAGCAUGCAGGGAUAUCCUCCAAA
   UAGCAGUAGA**UGA**AUAAACGAUAUCGAUCGG
   UUAGGU

The initiation codon and termination codon are shown in boldface. The encoded protein has the sequence

MRPWSMQGYPPNSSR

6. Gly and Ala; Val and Leu; Ser and Thr, Asn and Gln; and Asp and Glu.
7. The assembly of functional ribosomes requires equal amounts of the rRNA molecules, so it is advantageous for the cell to synthesize the rRNAs all at once.
8. Ribosomes cannot translate double-stranded RNA, so the base pairing of a complementary antisense RNA to an mRNA prevents its translation.
9. Only newly synthesized bacterial polypeptides have fMet at their N-terminus. Consequently, the appearance of fMet in a mammalian system signifies the presence of invading bacteria. Leukocytes that recognize the fMet residue can therefore combat these bacteria through phagocytosis.
10. Prokaryotic ribosomes can select an initiation codon located anywhere on the mRNA molecule as long as it lies just downstream of a Shine–Dalgarno sequence. In contrast, eukaryotic ribosomes usually select the AUG closest to the 5′ end of the mRNA. Eukaryotic ribosomes therefore cannot recognize a translation initiation site on a circular mRNA.
11. As expected, the correctly charged tRNAs (Ala–tRNA$^{\text{Ala}}$ and Gln–tRNA$^{\text{Gln}}$) bind to EF-Tu with approximately the same affinity, so they are delivered to the ribosomal A site with the same efficiency. The mischarged Ala–tRNA$^{\text{Gln}}$ binds to EF-Tu much more loosely, indicating that it may dissociate from EF-Tu before it reaches the ribosome. The mischarged Gln–tRNA$^{\text{Ala}}$ binds to EF-Tu much more tightly, indicating that EF-Tu may not be able to dissociate from it at the ribosome. These results suggest that either a higher or a lower binding affinity could affect the ability of EF-Tu to carry out its function, which would decrease the rate at which mischarged aminoacyl–tRNAs bind to the ribosomal A site during translation.
12. eIF2 is a G protein that delivers the initiator tRNA to the 40S ribosomal subunit and then hydrolyzes its bound GTP to GDP. The GEF eIF2B helps eIF2 release GDP in order to bind GTP so that it can participate in another round of translation initiation.
13. By inducing the same conformational changes that occur during correct tRNA–mRNA pairing, paromomycin can mask the presence of an incorrect codon–anticodon match. Without proofreading at the aminoacyl–tRNA binding step, the ribosome synthesizes a polypeptide with the wrong amino acids, which is likely to be nonfunctional or toxic to the cell.
14. (a) Transpeptidation involves the nucleophilic attack of the amino group of the aminoacyl–tRNA on the carbonyl carbon of the peptidyl–tRNA. As the pH increases, the amino group becomes more nucleophilic (less likely to be protonated).

    (b) As the pH increases, residue A2486 would be less likely to be protonated and therefore less likely to stabilize the negatively charged oxyanion of the tetrahedral reaction intermediate. Thus, the mechanistic embellishment is inconsistent with the observed effect.
15. The enzyme hydrolyzes peptidyl–tRNA molecules that dissociate from a ribosome before normal translation termination takes place. Because peptide synthesis is prematurely halted, the resulting polypeptide, which is still linked to tRNA, is likely to be nonfunctional. Peptidyl–tRNA hydrolase is necessary for recycling the amino acids and the tRNA.
16. Aminoacylation occurs via pyrophosphate cleavage of ATP, and hence the aminoacylation of 100 tRNAs requires 200 ATP equivalents; translation initiation requires 1 GTP (1 ATP equivalent); 99 cycles of elongation require 99 GTP (99 ATP equivalents) for EF-Tu action; 99 cycles of ribosomal translocation require 99 GTP (99 ATP equivalents) for EF-G action; and translation termination requires 1 GTP (1 ATP equivalent), bringing the total energy cost to 200 + 1 + 99 + 99 + 1 = 400 ATP equivalents.
17.

$$5'\text{-}\underbrace{\text{AGGAGCUX}_{\sim 4}}\quad \overset{\text{Start}}{{}^{\text{A}}_{\text{G}}\text{UG}}\quad \overset{\text{Lys}}{\text{AA}^{\text{A}}_{\text{G}}}\quad \overset{\text{Pro}}{\text{CCX}}\quad \overset{\text{Ala}}{\text{GCX}}\text{ -}$$

Shine–Dalgarno sequence.
3–10 base pairs with G · U's
allowed

Gly	Thr	Glu	Asn	Ser	Stop
GGX	ACX	$\text{GA}^{\text{A}}_{\text{G}}$	$\text{AA}^{\text{U}}_{\text{C}}$	UCX or $\text{AG}^{\text{U}}_{\text{C}}$	UAA UAG - 3′ UGA

CHAPTER 28

1. Virtually all the DNA sequences in *E. coli* are present as single copies, so the renaturation of *E. coli* DNA is a straightforward process of each fragment reassociating with its complementary strand. In contrast, the human genome contains many repetitive DNA sequences. The many DNA fragments containing these sequences find each other to form double-stranded regions (renature) much faster than the single-copy DNA sequences that are also present, giving rise to a biphasic renaturation curve.
2. Because genes encoding proteins with related functions often occur in operons, the identification of one or several genes in an operon may suggest functions for the remaining genes in that operon.
3. (a) O_1 is the primary repressor-binding site, so *lac* repressor cannot stably bind to the operator in its absence and repression cannot occur.

   (b) Both O_2 and O_3 are secondary repressor-binding sequences. If one is absent, the other can still function, resulting in only a small loss of repressor effectiveness.

   (c) In the absence of both O_2 and O_3, the repressor can bind only to O_1, which partially interferes with transcription but does not repress transcription as fully as when a DNA loop forms through the cooperative binding of *lac* repressor to O_1 and either O_2 or O_3.
4. In the absence of β-galactosidase (the product of the *lacZ* gene), lactose is not converted to the inducer allolactose. Consequently, *lac* enzymes, including galactoside permease, are not synthesized.
5. Since operons other than the *lac* operon maintain their sensitivity to the absence of glucose, the defect is probably not in the gene that encodes CAP. Instead, the defect is probably located in the portion of the *lac* operon that binds CAP–cAMP.
6. In eukaryotes, transcription takes place in the nucleus and translation occurs in the cytoplasm. Hence, in eukaryotes,

ribosomes are never in contact with nascent mRNAs, an essential aspect of the attenuation mechanism in prokaryotes.

7. Deletion of the leader peptide sequence from *trpL* would eliminate sequence 1 of the attenuator. Consequently, the $2 \cdot 3$ hairpin rather than the $3 \cdot 4$ terminator hairpin would form. Transcription would therefore continue into the remainder of the *trp* operon, which would then be regulated solely by *trp* repressor.

8. Red–green color blindness is conferred by a mutation in an X-linked gene so that female carriers of this condition, who do not appear to be red–green colorblind, have one wild-type gene and one mutated gene for this condition. In placental mammals such as humans, females are mosaics of clones of cells in which only one of their two X chromosomes is transcriptionally active. Hence in a female carrier of red–green color blindness, the transcriptionally active X chromosome in some of these clones will contain the wild-type gene and the others will contain the mutated gene. The former type of retinal clone is able to differentiate red and green light, whereas the latter type of retinal clone is unable to do so. Apparently, these retinal clones are small enough so that a narrow beam of light is necessary to separately interrogate them.

9.

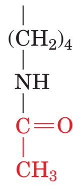

Acetyllysine

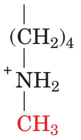

Methyllysine

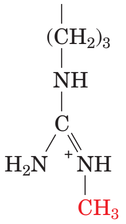

Methylarginine

In acetyllysine, the cationic side chain of Lys has been converted to a polar but uncharged side chain. In methyllysine and methylarginine, the hydrophobic methyl group partially masks the cationic character of the Lys or Arg side chain.

10. Histone and DNA methylation requires *S*-adenosylmethionine (SAM), which becomes *S*-adenosylhomocysteine after it gives up its methyl group (Fig. 21-18). *S*-Adenosylhomocysteine is converted back to methionine, the precursor of SAM, in a reaction in which the methyl group is donated by the folic acid derivative tetrahydrofolate (THF; Fig. 21-18). A shortage of this cofactor could limit cellular production of SAM, which would result in the undermethylation of histones and DNA.

11. The product is a citrulline residue (Fig. 21-9).

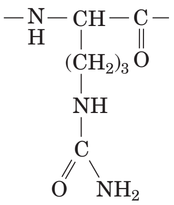

12. Transcriptionally active chromatin has a more open structure due to histone modifications that help make the DNA more accessible to transcription factors and RNA polymerase as well as nucleases.

13. A sequence located downstream of the gene's promoter (i.e., within the coding region) could regulate gene expression if it were recognized by the appropriate transcription factor such that the resulting DNA–protein complex successfully recruited RNA polymerase to the promoter.

14. The susceptibility of RNA to degradation *in vivo* makes it possible to regulate gene expression by adjusting the rate of mRNA degradation. If mRNA were very stable, it might continue to direct translation even when the cell no longer needed the encoded protein.

15. A 22-bp segment of RNA, incorporating all four nucleotides, has 4^{22} or 1.8×10^{13} possible unique sequences. An RNA half this size would have only 4^{11} or 4.2×10^{6} possible sequences. The shorter the siRNA, the greater is the probability that it could hybridize with more than one complementary mRNA, thereby making it less efficient in silencing a specific gene. (In the 3.2×10^{9}-bp human genome, a sequence of 16 bp has a high probability of randomly occurring at least once.)

16. Since there are 65 V_H, 27 D, and 6 J_H segments that can be used to assemble the coding sequence of the variable region of the heavy chain, somatic recombination could theoretically generate $65 \times 27 \times 6 = 10530$ heavy chain genes (junctional flexibility would increase this number). Since each immunoglobulin molecule contains two identical heavy chains and two identical light chains, the possible number of immunoglobulins would be $10530 \times 2000 = {\sim}21$ million.

17. The imprecise joining of V, D, and J segments, along with nucleotide addition or removal at the junction, can generate a Stop codon (yielding a truncated and hence nonfunctional immunoglobulin) or create a shift in the reading frame (yielding a misfolded and nonfunctional protein).

18. In multicellular organisms, apoptosis of damaged cells minimizes damage to the entire organism. For a single-celled organism, survival of a genetically damaged cell is preferable in a Darwinian sense to its death.

19. The *esc* gene is apparently a maternal-effect gene. Thus, the proper distribution of the *esc* gene product in the fertilized egg, which is maternally specified, is sufficient to permit normal embryonic development regardless of the embryo's genotype.

One- and Three-Letter Symbols for the Amino Acids[a]

A	Ala	Alanine
B	Asx	Asparagine or aspartic acid
C	Cys	Cysteine
D	Asp	Aspartic acid
E	Glu	Glutamic acid
F	Phe	Phenylalanine
G	Gly	Glycine
H	His	Histidine
I	Ile	Isoleucine
K	Lys	Lysine
L	Leu	Leucine
M	Met	Methionine
N	Asn	Asparagine
P	Pro	Proline
Q	Gln	Glutamine
R	Arg	Arginine
S	Ser	Serine
T	Thr	Threonine
V	Val	Valine
W	Trp	Tryptophan
Y	Tyr	Tyrosine
Z	Glx	Glutamine or glutamic acid

---

[a] The one-letter symbol for an undetermined or nonstandard amino acid is X.

Thermodynamic Constants and Conversion Factors

Joule **(J)**
$1\ \mathrm{J} = 1\ \mathrm{kg\cdot m^2\cdot s^{-2}}$ $\quad$ $1\ \mathrm{J} = 1\ \mathrm{C\cdot V}$ (coulomb volt)
$1\ \mathrm{J} = 1\ \mathrm{N\cdot m}$ (newton meter)

Calorie **(cal)**
1 cal heats 1 g of H_2O from 14.5 to 15.5°C
1 cal = 4.184 J

Large calorie **(Cal)**
1 Cal = 1 kcal $\quad$ 1 Cal = 4184 J

Avogadro's number (N)
$N = 6.0221 \times 10^{23}\ \mathrm{molecules\cdot mol^{-1}}$

Coulomb **(C)**
$1\ \mathrm{C} = 6.241 \times 10^{18}$ electron charges

Faraday **($\mathcal{F}$)**
$1\ \mathcal{F} = N$ electron charges
$1\ \mathcal{F} = 96{,}485\ \mathrm{C\cdot mol^{-1}} = 96{,}485\ \mathrm{J\cdot V^{-1}\cdot mol^{-1}}$

Kelvin temperature scale **(K)**
0 K = absolute zero $\quad$ 273.15 K = 0°C

Boltzmann constant **(k_B)**
$k_B = 1.3807 \times 10^{-23}\ \mathrm{J\cdot K^{-1}}$

Gas constant (R)
$R = Nk_B$ $\quad$ $R = 1.9872\ \mathrm{cal\cdot K^{-1}\cdot mol^{-1}}$
$R = 8.3145\ \mathrm{J\cdot K^{-1}\cdot mol^{-1}}$ $\quad$ $R = 0.08206\ \mathrm{L\cdot atm\cdot K^{-1}\cdot mol^{-1}}$

The Standard Genetic Code

First Position (5′ end)	*Second Position*				*Third Position (3′ end)*
	U	C	A	G	
U	UUU Phe	UCU Ser	UAU Tyr	UGU Cys	U
	UUC Phe	UCC Ser	UAC Tyr	UGC Cys	C
	UUA Leu	UCA Ser	UAA Stop	UGA Stop	A
	UUG Leu	UCG Ser	UAG Stop	UGG Trp	G
C	CUU Leu	CCU Pro	CAU His	CGU Arg	U
	CUC Leu	CCC Pro	CAC His	CGC Arg	C
	CUA Leu	CCA Pro	CAA Gln	CGA Arg	A
	CUG Leu	CCG Pro	CAG Gln	CGG Arg	G
A	AUU Ile	ACU Thr	AAU Asn	AGU Ser	U
	AUC Ile	ACC Thr	AAC Asn	AGC Ser	C
	AUA Ile	ACA Thr	AAA Lys	AGA Arg	A
	AUG Met[a]	ACG Thr	AAG Lys	AGG Arg	G
G	GUU Val	GCU Ala	GAU Asp	GGU Gly	U
	GUC Val	GCC Ala	GAC Asp	GGC Gly	C
	GUA Val	GCA Ala	GAA Glu	GGA Gly	A
	GUG Val	GCG Ala	GAG Glu	GGG Gly	G

[a] AUG forms part of the initiation signal as well as coding for internal Met residues.

Some Common Biochemical Abbreviations

A	adenine
aaRS	aminoacyl–tRNA synthetase
ACAT	acyl-CoA:cholesterol acyltransferase
ACP	acyl-carrier protein
ADA	adenosine deaminase
ADP	adenosine diphosphate
AIDS	acquired immunodeficiency syndrome
ALA	δ-aminolevulinic acid
AMP	adenosine monophosphate
ATCase	aspartate transcarbamoylase
ATP	adenosine triphosphate
BChl	bacteriochlorophyll
bp	base pair
BPG	D-2,3-bisphosphoglycerate
BPheo	bacteriopheophytin
BPTI	bovine pancreatic trypsin inhibitor
C	cytosine
CaM	calmodulin
CAM	crassulacean acid metabolism
cAMP	cyclic AMP
CAP	catabolite gene activator protein
CDK	cyclin-dependent protein kinase
cDNA	complementary DNA
CDP	cytidine diphosphate
CE	capillary electrophoresis
Chl	chlorophyll
CM	carboxymethyl
CMP	cytidine monophosphate
CoA or CoASH	coenzyme A
CoQ	coenzyme Q (ubiquinone)
COX	cyclooxygenase
CPS	carbamoyl phosphate synthetase
CTP	cytidine triphosphate
D	dalton
d	deoxy
DAG	1,2-diacylglycerol
DCCD	dicyclohexylcarbodiimide
dd	dideoxy
ddNTP	2′,3′-dideoxynucleoside triphosphate
DEAE	diethylaminoethyl
DHAP	dihydroxyacetone phosphate
DHF	dihydrofolate
DHFR	dihydrofolate reductase
DNA	deoxyribonucleic acid
DNP	2,4-dinitrophenol
dNTP	2′-deoxynucleoside triphosphate
E4P	erythrose-4-phosphate
EF	elongation factor
ELISA	enzyme-linked immunosorbent assay
EM	electron microscopy
emf	electromotive force
ER	endoplasmic reticulum
ESI	electrospray ionization
ETF	electron-transfer flavoprotein
F1P	fructose-1-phosphate
F2,6P	fructose-2,6-bisphosphate
F6P	fructose-6-phosphate
FAD	flavin adenine dinucleotide, oxidized form
FADH·	flavin adenine dinucleotide, radical form
$FADH_2$	flavin adenine dinucleotide, reduced form
FBP	fructose-1,6-bisphosphate
FBPase	fructose-1,6-bisphosphatase
Fd	ferredoxin
FH	familial hypercholesterolemia
fMet	*N*-formylmethionine
FMN	flavin mononucleotide
G	guanine
G1P	glucose-1-phosphate
G6P	glucose-6-phosphate
G6PD	glucose-6-phosphate dehydrogenase
GABA	γ-aminobutyric acid
Gal	galactose
GalNAc	*N*-acetylgalactosamine
GAP	glyceraldehyde-3-phosphate
GAPDH	glyceraldehyde-3-phosphate dehydrogenase
GDH	glutamate dehydrogenase
GDP	guanosine diphosphate
Glc	glucose
GlcNAc	*N*-acetylglucosamine
GMP	guanosine monophosphate
GPI	glycosylphosphatidylinositol
GSH	glutathione
GSSH	glutathione disulfide
GTF	general transcription factor
GTP	guanosine triphosphate
Hb	hemoglobin
HDL	high density lipoprotein
HIV	human immunodeficiency virus
HMG-CoA	β-hydroxy-β-methylglutaryl-CoA
hnRNA	heterogeneous nuclear RNA
HPLC	high performance liquid chromatography
Hsp	heat shock protein
HTH	helix–turn–helix
Hyl	5-hydroxylysine
Hyp	4-hydroxyproline
IDL	intermediate density lipoprotein
IF	initiation factor
IgG	immunoglobulin G
IMP	inosine monophosphate
IP_3	inositol-1,4,5-trisphosphate
IPTG	isopropylthiogalactoside
IR	infrared
IS	insertion sequence
ISP	iron–sulfur protein
kb	kilobase pair
kD	kilodalton
K_M	Michaelis constant
LDH	lactate dehydrogenase
LDL	low density lipoprotein
LHC	light-harvesting complex
MALDI	matrix-assisted desorption-ionization
Man	mannose
Mb	myoglobin

(table continued on following page)

mRNA	messenger RNA
MS	mass spectrometry
MurNAc	*N*-acetylmuramic acid
NAD$^+$	nicotinamide adenine dinucleotide, oxidized form
NADH	nicotinamide adenine dinucleotide, reduced form
NADP$^+$	nicotinamide adenine dinucleotide phosphate, oxidized form
NADPH	nicotinamide adenine dinucleotide phosphate, reduced form
NAG	*N*-acetylglucosamine
NAM	*N*-acetylmuramic acid
NANA	*N*-acetylneuraminic (sialic) acid
NDP	nucleoside diphosphate
NER	nucleotide excision repair
NeuNAc	*N*-acetylneuraminic acid
NMN	nicotanamide mononucleotide
NMR	nuclear magnetic resonance
nt	nucleotide
NTP	nucleoside triphosphate
OEC	oxygen-evolving center
OMP	orotidine monophosphate
ORF	open reading frame
P or p	phosphate
PAGE	polyacrylamide gel electrophoresis
PBG	porphobilinogen
PC	plastocyanin
PCNA	proliferating cell nuclear antigen
PCR	polymerase chain reaction
PDB	protein data bank
PDBid	PDB identification code
PDI	protein disulfide isomerase
PE	phosphatidylethanolamine
PEP	phosphoenolpyruvate
PEPCK	PEP carboxykinase
PFGE	pulsed-field gel electrophoresis
PFK	phosphofructokinase
2PG	2-phosphoglycerate
3PG	3-phosphoglycerate
PGI	phosphoglucose isomerase
PGK	phosphoglycerate kinase
PGM	phosphoglycerate mutase
Pheo	pheophytin
P$_i$	orthophosphate
PIC	preinitiation complex
PIP$_2$	phosphatidylinositol-4,5-bisphosphate
PK	pyruvate kinase
PKA	protein kinase A
PKB	protein kinase B
PKU	phenylketonuria
PLP	pyridoxal-5′-phosphate
pmf	protonmotive force
PMP	pyridoxamine-5′-phosphate
PNP	purine nucleotide phosphorylase
Pol	DNA polymerase
PP$_i$	pyrophosphate

PRPP	5-phosphoribosyl-α-pyrophosphate
PS	photosystem
PTK	protein tyrosine kinase
PTP	protein tyrosine phosphatase
Q	ubiquinone (CoQ) or plastoquinone
QH$_2$	ubiquinol or plastoquinol
r	ribo
R5P	ribose-5-phosphate
RER	rough endoplasmic reticulum
RF	release factor
RFLP	restriction fragment length polymorphism
RIA	radioimmunoassay
RNA	ribonucleic acid
RNAi	RNA interference
rRNA	ribosomal RNA
RS	aminoacyl–tRNA synthetase
RT	reverse transcriptase
RTK	receptor tyrosine kinase
Ru5P	ribulose-5-phosphate
RuBP	ribulose-1,5-bisphosphate
S	Svedberg unit
S7P	sedoheptulose-7-phosphate
SAM	*S*-adenosylmethionine
SCID	severe combined immunodeficiency disease
SDS	sodium dodecyl sulfate
SNAP	soluble NSF attachment protein
SNARE	SNAP receptor
snRNA	small nuclear RNA
snRNP	small nuclear ribonucleoprotein
SOD	superoxide dismutase
SRP	signal recognition particle
SSB	single-strand binding protein
STAT	signal transducer and activator of transcription
T	thymine
TAF	TBP-associated factor
TBP	TATA box–binding protein
TCA	tricarboxylic acid
THF	tetrahydrofolate
TIM	triose phosphate isomerase
TNBS	trinitrobenzenesulfonic acid
TPP	thiamine pyrophosphate
tRNA	transfer RNA
TTP	thymidine triphosphate
U	uracil
UDP	uridine diphosphate
UDPG	uridine diphosphate glucose
UMP	uridine monophosphate
UTP	uridine triphosphate
UV	ultraviolet
VLDL	very low density lipoprotein
$V_{\max}$	maximal velocity
XMP	xanthosine monophosphate
Xu5P	xylulose-5-phosphate
YAC	yeast artificial chromosome
YADH	yeast alcohol dehydrogenase

This page intentionally left blank

Media Resources

To accompany
FUNDAMENTALS OF BIOCHEMISTRY 3/e

WileyPLUS, along with the companion website for the book (www.wiley.com/college/voet), contain an extensive set of resources for enhancing student understanding of biochemistry. These are keyed to the text and in most cases are specifically called out with a red mouse icon.

A complete listing is available in the Guide to Media Resources starting on p. xxv at the front of the text.

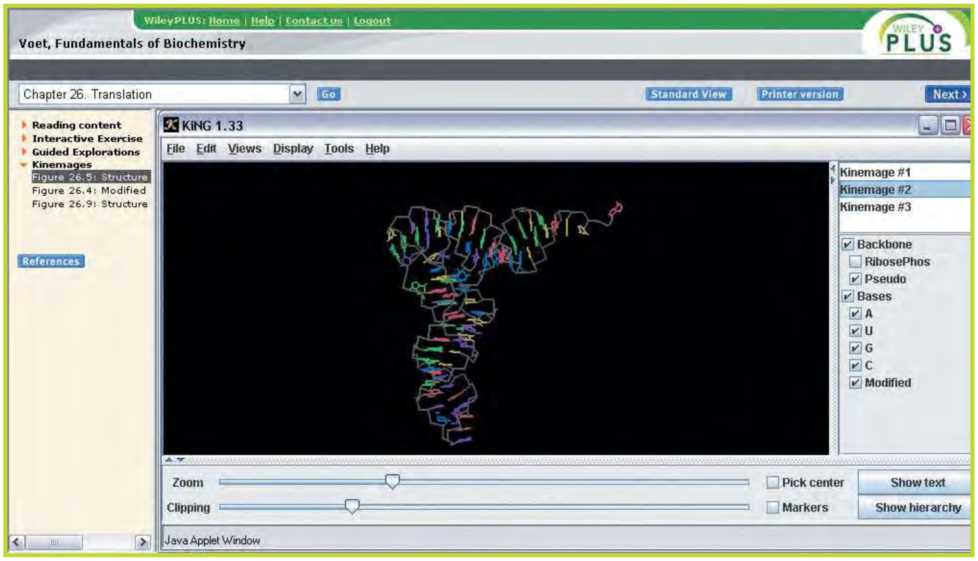
WileyPLUS: Home | Help | Contact us | Logout
Voet, Fundamentals of Biochemistry
WILEY PLUS
Chapter 26. Translation
Go
Standard View
Printer version
Next ›
Reading content
Interactive Exercise
Guided Explorations
Kinemages
Figure 26.5: Structure
Figure 26.4: Modified
Figure 26.9: Structure
References
KiNG 1.33
File
Edit
Views
Display
Tools
Help
Kinemage #1
Kinemage #2
Kinemage #3
☑ Backbone
☐ RibosePhos
☑ Pseudo
☑ Bases
☑ A
☑ U
☑ G
☑ C
☑ Modified
Zoom
Clipping
☐ Pick center
☐ Markers
Show text
Show hierarchy
Java Applet Window

KINEMAGES

A set of 22 exercises comprising 55 individual 3-dimensional images of selected proteins and nucleic acids can be manipulated by users as suggested by an accompanying script.

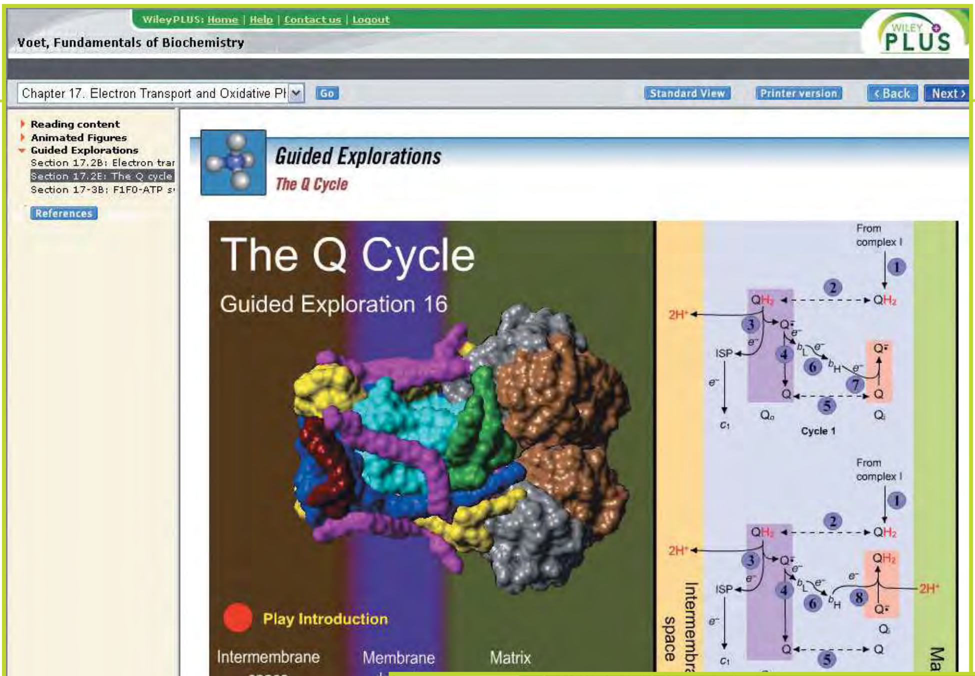
WileyPLUS: Home | Help | Contact us | Logout
Voet, Fundamentals of Biochemistry
WILEY PLUS
Chapter 17. Electron Transport and Oxidative Ph
Go
Standard View
Printer version
‹ Back
Next ›
Reading content
Animated Figures
Guided Explorations
Section 17.2B: Electron tran
Section 17.2E: The Q cycle
Section 17-3B: F1F0-ATP s
References
Guided Explorations
The Q Cycle
The Q Cycle
Guided Exploration 16
Play Introduction
Intermembrane space
Membrane
Matrix
From complex I
2H⁺
QH₂
Q⁻
ISP
e⁻
c₁
Qₒ
Qᵢ
b_L
b_H
Cycle 1
Intermembrane space
Ma

GUIDED EXPLORATIONS

These 30 self-contained presentations enhance key topics from the text with extensive animated computer graphics, which in many cases are narrated.

INTERACTIVE EXERCISES

59 molecular structures from the text have been chosen for presentation in a browser-independent format that allows students to manipulate the structures and answer questions based on that experience.

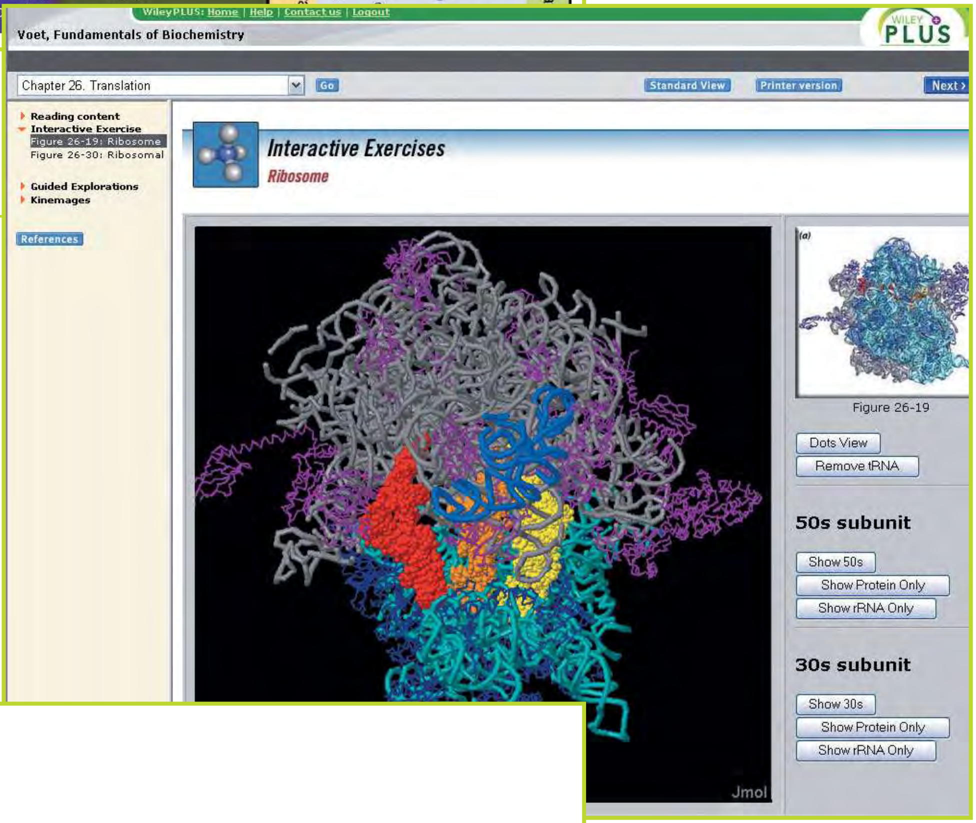
WileyPLUS: Home | Help | Contact us | Logout
Voet, Fundamentals of Biochemistry
WILEY PLUS
Chapter 26. Translation
Go
Standard View
Printer version
Next ›
Reading content
Interactive Exercise
Figure 26-19: Ribosome
Figure 26-30: Ribosomal
Guided Explorations
Kinemages
References
Interactive Exercises
Ribosome
Jmol
(a)
Figure 26-19
Dots View
Remove tRNA
50s subunit
Show 50s
Show Protein Only
Show rRNA Only
30s subunit
Show 30s
Show Protein Only
Show rRNA Only

ANIMATED FIGURES

67 figures from the text, illustrating various concepts, techniques, and processes, are presented as brief animations.

Glossary

Numbers and Greek letters are alphabetized as if they were spelled out.

***A*.** See Absorbance.

A site. See aminoacyl site.

aa–tRNA. See aminoacyl–tRNA.

aaRS. See aminoacyl–tRNA synthetase.

ABC transporter. A member of a large family of transmembrane proteins that use the free energy of ATP to mediate the transport of polar or nonpolar substances across a membrane.

ABO blood group antigens. The oligosaccharide components of glycolipids on the surfaces of erythrocytes and other cells.

Absolute configuration. The spatial arrangement of chemical groups around a chiral center.

Absorbance (*A*). A function of the amount of light transmitted through a solution (I) relative to the incident light (I_0) at a given wavelength: $A = \log(I_0/I)$. Also called optical density.

Absorptivity (ε). A constant that relates the absorbance of a solution to the concentration of the solute at a given wavelength. Also called the extinction coefficient.

Acceptor stem. The base-paired region of a tRNA molecule that contains the 5′ end and the 3′ end, to which an amino acid is attached.

Accessory pigment. A molecule in the photosynthetic system that absorbs light at wavelengths other than those absorbed by chlorophyll.

Acid. A substance that can donate a proton.

Acid–base catalysis. A catalytic mechanism in which partial proton transfer from an acid or partial proton abstraction by a base lowers the free energy of a reaction's transition state. See also general acid catalysis and general base catalysis.

Acidic solution. A solution whose pH is less than 7.0 ($[H^+] > 10^{-7}$ M).

Acidosis. A pathological condition in which the pH of the blood drops below its normal value of 7.4.

Action potential. The wave of transient depolarization and repolarization that constitutes the electrical signal generated by a nerve cell.

Active site. The region of an enzyme in which catalysis takes place.

Active transport. The transmembrane movement of a substance from low to high concentrations by a protein that couples this endergonic transport to an exergonic process such as ATP hydrolysis.

Activity. A solute's concentration, corrected for its nonideal behavior at concentrations greater than infinite dilution.

Acyl-carrier protein. A phosphopantetheine-containing protein that binds the intermediates of fatty acid synthesis as thioesters.

Acyl–enzyme intermediate. An intermediate of peptide bond hydrolysis in which the carbonyl carbon of the scissile bond is covalently bound to the enzyme nucleophile that attacked it.

Acyl group. A portion of a molecule with the formula —COR, where R is an alkyl group.

Adenylate cyclase system. A signal transduction pathway in which hormone binding to a cell-surface receptor activates a G protein that in turn stimulates adenylate cyclase to synthesize the second messenger 3′,5′-cyclic AMP (cAMP) from ATP.

Adenylylation. Addition of an adenylyl (AMP) group.

Adipocyte. Fat cell, which is specialized for the synthesis and storage of triacylglycerols from free fatty acids.

Adipose tissue. Fat cells; distributed throughout an animal's body.

ADP–ATP translocator. A membrane transport protein with an adenine nucleotide–binding site that alternately allows ADP to enter and ATP to exit the mitochondrial matrix.

Adrenoreceptor. A cell surface receptor that binds and responds to adrenal hormones such as epinephrine and norepinephrine. Also called an adrenergic receptor.

Aerobe. An organism that uses O_2 as an oxidizing agent for nutrient breakdown.

Affinity chromatography. A procedure in which a molecule is separated from a mixture of other molecules by its ability to bind specifically to an immobilized ligand. See also metal chelate affinity chromatography.

Affinity labeling. A technique in which a labeled substrate analog reacts irreversibly with, and can thereby be used to identify, a group in an enzyme's active site.

Agarose. Linear carbohydrate polymers, made by red algae, that form a loose mesh.

Agonist. A substance that binds to a receptor so as to evoke a cellular response.

Alcoholic fermentation. A metabolic pathway that synthesizes ethanol from pyruvate through decarboxylation and reduction.

Alditol. A sugar produced by reduction of an aldose or ketose to a polyhydroxy alcohol.

Aldol cleavage. A carbon–carbon cleavage reaction of an aldol (an aldehyde or ketone with a β hydroxyl group) that yields smaller carbonyl compounds.

Aldonic acid. A sugar produced by oxidation of an aldose aldehyde group to a carboxylic acid group.

Aldose. A sugar whose carbonyl group is an aldehyde.

Alkalosis. A pathological condition in which the pH of the blood rises above its normal value of 7.4.

Allele. An alternate form of a gene; diploid organisms contain two alleles for each gene, which may or may not be identical.

Allosteric effector. A small molecule whose binding to a protein affects the function of another site on the protein.

Allosteric interaction. The binding of ligand at one site in a macromolecule that affects the binding of other ligands at other sites in the molecule. See also cooperative binding.

αα motif. A protein motif consisting of two α helices packed against each other with their axes inclined.

α-amino acid. See amino acid.

α anomer. See anomers.

α/β barrel. A β barrel in which successive parallel β strands are connected by α helices such that a barrel of α helices surrounds the β barrel.

α carbon. The carbon atom of an amino acid to which the amino and carboxylic acid groups are attached.

α cell. A pancreatic islet cell that secretes the hormone glucagon in response to low blood glucose levels.

α-glycoside. See glycoside.

α helix. A regular secondary structure of polypeptides, with 3.6 residues per right-handed turn, a pitch of 5.4 Å, and hydrogen bonds between each backbone N—H group and the backbone C═O group that is four residues earlier.

Alternative splicing. The tissue-specific patterns of splicing of a given pre-mRNA that result in variations in the excision and retention of exons and introns.

Alzheimer's disease. A neurodegenerative disease characterized by the precipitation of β amyloid protein in the brain.

Ames test. A method for assessing the mutagenicity of a compound from its ability to cause genetically defective strains of bacteria to revert to normal growth.

Amido group. A portion of a molecule with the formula —CONH—.

Amino acid. A compound consisting of a carbon atom to which are attached a primary amino group, a carboxylic acid group, a side chain (R group), and an H atom. Also called an α-amino acid.

Amino group. A portion of a molecule with the formula $—NH_2$, —NHR, or $—NR_2$, where R is an alkyl group. Amino groups are usually protonated at physiological pH.

Amino sugar. A sugar in which one or more OH groups are replaced by an amino group, which is often acetylated.

Amino terminus. The end of a polypeptide that has a free amino group. Also called the N-terminus.

Aminoacyl site (A site). The ribosomal site where a tRNA with an attached aminoacyl group binds during protein synthesis.

Aminoacyl–tRNA (aa–tRNA). The covalent ester complex between an "activated" amino acid and a tRNA molecule.

Aminoacyl–tRNA synthetase (aaRS). An enzyme that catalyzes the ATP-dependent esterification of an amino acid to a tRNA with high specificity for the amino acid and the tRNA molecule.

Amphibolic. A term to describe a metabolic process that can be either catabolic or anabolic.

Amphipathic substance. See amphiphilic substance.

Amphiphilic substance. A substance that contains both polar and nonpolar regions and is therefore both hydrophilic and hydrophobic. Also called an amphipathic substance.

Amyloid. Insoluble extracellular aggregates of fibrous protein that characterize such diseases as Alzheimer's disease and the transmissible spongiform encephalopathies.

Anabolism. The reactions by which biomolecules are synthesized from simpler components.

Anaerobe. An organism that does not use O_2 as an oxidizing agent for nutrient breakdown. An obligate anaerobe cannot grow in the presence of O_2, whereas a facultative anaerobe can grow in the presence or absence of O_2.

Anaplerotic reaction. A reaction that replenishes the intermediates of a metabolic pathway.

Androgen. A steroid that functions primarily as a male sex hormone.

Anemia. A condition caused by insufficient red blood cells.

Angina. Chest pain due to insufficient blood supply to the heart.

Anion exchanger. A cationic matrix used to bind anionic molecules in ion exchange chromatography.

Anneal. To maintain conditions that allow loose base pairing between complementary single polynucleotide strands so that properly paired double-stranded segments form.

Anomeric carbon. The carbonyl carbon of a monosaccharide, which becomes a chiral center when the sugar cyclizes to a hemiacetal or hemiketal.

Anomers. Sugars that differ only in the configuration around the anomeric carbon. In the α anomer, the OH substituent of the anomeric carbon is on the opposite side of the ring from the CH_2OH group at the chiral center that designates the D or L configuration. In the β anomer, the OH substituent is on the same side.

Antagonist. A substance that binds to a receptor but does not elicit a cellular response.

Antenna chlorophyll. A chlorophyll group that absorbs light energy and passes it on to a photosynthetic reaction center by exciton transfer.

Anti conformation. A purine or pyrimidine nucleotide conformation in which the ribose and the base point away from each other. See also syn conformation.

Antibody. A protein produced by an animal's immune system in response to the introduction of a foreign substance (an antigen); it contains at least one pair each of identical heavy and light chains. Also called an immunoglobulin (Ig).

Anticodon. The sequence of three nucleotides in tRNA that recognizes an mRNA codon through complementary base pairing.

Anticodon arm. The conserved stem–loop structure in a tRNA molecule that includes the anticodon.

Antigen. A substance that elicits an immune response (production of antibodies) when introduced into an animal; it is specifically recognized by an antibody.

Antioxidant. A substance that destroys an oxidative free radical such as $O_2^-\cdot$ or $OH\cdot$.

Antiparallel. Running in opposite directions.

Antiport. A transmembrane channel that simultaneously moves two molecules or ions in opposite directions. See also symport and uniport.

Antisense RNA. A single-stranded RNA molecule that forms a double-stranded structure with a complementary mRNA so as to block its translation into protein.

Antisense strand. The DNA strand that serves as a template for transcription; it is complementary to the RNA. Also called the noncoding strand.

AP site. An apurinic or apyrimidinic site; the deoxyribose residue remaining after the removal of a base from a DNA strand.

Apoenzyme. An enzyme that is inactive due to the absence of a cofactor.

Apolipoprotein. The protein component of a lipoprotein. Also called an apoprotein.

Apoprotein. A protein without the prosthetic group or metal ion that renders it fully functional. See also apoenzyme and apolipoprotein.

Apoptosis. Cell death by a regulated process in which the cell shrinks and fragments into membrane-bounded portions for phagocytosis by other cells. See also necrosis.

Aptamer. A nucleic acid whose conformation allows it to bind a particular ligand with high specificity and high affinity.

Aquaporin. A tetrameric membrane protein that mediates the rapid diffusion of water molecules but not protons or other ions across a membrane.

Archaea. One of the two major groups of prokaryotes (the other is eubacteria). Also known as archaebacteria.

Archaebacteria. See archaea.

Assay. A laboratory technique for detecting, and in many cases quantifying, a macromolecule or its activity.

Asymmetric center. See chiral center.

Atherosclerosis. A disease characterized by the formation of cholesterol-containing fibrous plaques in the walls of blood vessels, leading to loss of elasticity and blockage of blood flow.

ATP mass action ratio. The ratio $[\mathrm{ATP}]/[\mathrm{ADP}][\mathrm{P}_i]$, which influences the rate of electron transport and oxidative phosphorylation.

ATP synthase. See F_1F_0-ATPase.

ATPase. An enzyme that catalyzes the hydrolysis of ATP to $\mathrm{ADP} + \mathrm{P}_i$.

Attenuation. A mechanism in prokaryotes for regulating gene expression in which the availability of an amino acid determines whether an operon (consisting of genes for the enzymes that synthesize the amino acid) is transcribed.

Attenuator. A prokaryotic control element that governs transcription of an operon according to the availability of an amino acid synthesized by the proteins encoded by the operon.

Autocatalytic reaction. A reaction in which a product molecule can act as a catalyst for the same reaction; the reactant molecule therefore appears to catalyze its own reaction.

Autoimmune disease. A disease in which the immune system has lost some of its self-tolerance and produces antibodies against certain self-antigens.

Autolysis. An autocatalytic process in which a molecule catalyzes its own degradation.

Autophosphorylation. The kinase-catalyzed phosphorylation of itself or an identical molecule.

Autoradiography. A process in which X-ray film records the positions of radioactive entities, such as proteins or nucleic acids, that have been immobilized in a matrix such as a nitrocellulose membrane or an electrophoretic gel.

Autotroph. An organism that can synthesize all its cellular components from simple molecules using the energy obtained from sunlight (photoautotroph) or from the oxidation of inorganic compounds (chemolithotroph).

Axial substituent. A group that extends perpendicularly from the plane of the ring to which it is bonded. See also equatorial substituent.

BAC. See bacterial artificial chromosome.

Backbone. The atoms that form the repeating linkages between successive residues of a polymeric molecule, exclusive of the side chains. Also called the main chain.

Bacteria. The organisms comprising the two major groups of prokaryotes, the archaea and the eubacteria.

Bacterial artificial chromosome (BAC). A plasmid-derived DNA molecule that can replicate in a bacterial cell. BACs are commonly used as cloning vectors.

Bacteriophage. A virus specific for bacteria. Also known as a phage.

Barr body. The condensed and darkly staining inactive X chromosome in the nucleus of a female mammalian cell.

Base. (1) A substance that can accept a proton. (2) A purine or pyrimidine component of a nucleoside, nucleotide, or nucleic acid.

Base excision repair (BER). The removal and replacement of a damaged nucleotide in DNA that is initiated by the removal of the base.

Base pair. The specific hydrogen-bonded association between nucleic acid bases. The Watson–Crick base pairs are $A \cdot T$ and $G \cdot C$.

Basic helix–loop–helix (bHLH) motif. A eukaryotic protein motif that includes a basic DNA-binding region followed by two amphipathic helices connected by a loop. The second helix, which mediates protein dimerization, is often continuous with a leucine zipper motif.

Basic solution. A solution whose pH is greater than 7.0 ($[\mathrm{H}^+] < 10^{-7}$ M).

Beer–Lambert law. The equation that describes the relationship between a solute's absorbance (A) and its concentration (c): $A = \varepsilon c l$ where ε is the solute's molar absorptivity and l is the length of the light path.

BER. See base excision repair.

Beriberi. A disease caused by a deficiency of thiamine (vitamin B_1), which is a precursor of the cofactor thiamine pyrophosphate.

βαβ motif. A protein motif consisting of an α helix connecting two parallel strands of a β sheet.

β anomer. See anomers.

β barrel. A protein motif consisting of a β sheet rolled into a cylinder.

β bend. See reverse turn.

β bulge. An irregularity in a β sheet resulting from an extra residue that is not hydrogen bonded to a neighboring chain.

β cell. A pancreatic islet cell that secretes the hormone insulin in response to high blood glucose levels.

β-glycoside. See glycoside.

β hairpin. A protein motif in which two antiparallel β stands are connected by a reverse turn.

β oxidation. A series of enzyme-catalyzed reactions in which fatty acids are progressively degraded by the removal of two-carbon units as acetyl-CoA.

β sheet. A regular secondary structure in which extended polypeptide chains form interstrand hydrogen bonds. In parallel β sheets, the polypeptide chains all run in the same direction; in antiparallel β sheets, neighboring chains run in opposite directions.

bHLH motif. See basic helix–loop–helix motif.

Bilayer. An ordered, double layer of amphiphilic molecules in which polar segments point toward the two solvent-exposed surfaces and the nonpolar segments associate in the center.

Bile acid (bile salt). An amphiphilic cholesterol derivative that acts as a detergent to solubilize lipids for digestion and absorption.

Binding change mechanism. The mechanism whereby the subunits of the F_1F_0-ATP synthase adopt three successive conformations to convert ADP + P_i to ATP as driven by the dissipation of the transmembrane proton gradient.

Bioavailability. A measure of the fraction of a drug that reaches its target tissue, which depends on the drug's dosage and pharmacokinetics.

Biochemical standard state. A set of conditions including unit activity of the species of interest, a temperature of 25°C, a pressure of 1 atm, and a pH of 7.0.

Biofilm. A surface-associated aggregate of bacterial cells and extracellular polysaccharides that protect the cells from environmental assault.

Bioinformatics. The study of biological information in the form of molecular sequences and structures; e.g., structural bioinformatics.

Biopterin. A pterin derivative that functions as a cofactor in the hydroxylation of phenylalanine to produce tyrosine.

Blastoderm. The single layer of cells surrounding a yolk-like core that forms during the early development of an insect larva.

Blunt ends. The fully base-paired ends of a DNA fragment that has been cleaved by a restriction endonuclease that cuts the DNA strands at opposing sites.

Bohr effect. The decrease in O_2 binding affinity of hemoglobin in response to a decrease in pH.

bp. Base pair, the unit of length used for DNA molecules. Thousands of base pairs (kilobase pairs) are abbreviated kb.

Bradford assay. A spectroscopic technique for determining protein concentration in solution from the absorbance of a dye bound to the protein.

Branch migration. The movement of a crossover point in a Holliday junction during DNA recombination.

Breathing. The small conformational fluctuations of a protein molecule.

Bromodomain. A protein module that binds acetylated Lys residues in histones.

Buffer. A solution of a weak acid and its conjugate base in approximately equal quantities. Such a solution resists changes in pH on the addition of acid or base.

Buffering capacity. The ability of a buffer solution to resist pH changes on addition of acid or base. Buffers are most useful when the pH is within one unit of its component acid's p*K*.

C-terminus. See carboxyl terminus.

C value. A measure of the quantity of an organism's unique genetic material.

C-value paradox. The occurrence of exceptions to the rule that an organism's DNA content (C value) is correlated to the complexity of its morphology and metabolism.

Cahn–Ingold–Prelog system (*RS* system). A system for unambiguously describing the configurations of molecules with one or more asymmetric centers by assigning a priority ranking to the substituent groups of each asymmetric center.

Calvin cycle. The sequence of photosynthetic dark reactions in which ribulose-5-phosphate is carboxylated, converted to three-carbon carbohydrate precursors, and regenerated. Also called the reductive pentose phosphate cycle.

Calmodulin (CaM). A small Ca^{2+}-binding protein that binds to other proteins in the presence of Ca^{2+} and thereby regulates their activities.

CaM. See calmodulin.

CAM. See crassulacean acid metabolism.

cAMP. 3′,5′-Cyclic AMP, an intracellular second messenger.

Cap. A 7-methylguanosine residue that is posttranscriptionally appended to the 5′ end of a eukaryotic mRNA.

Capillary electrophoresis (CE). Electrophoretic procedures carried out in small diameter capillary tubes.

Carbamate. The product of a reaction between CO_2 and an amino group: —NH—COO^-.

Carbohydrate. A compound with the formula $(C \cdot H_2O)_n$ where $n \geq 3$. Also called a saccharide.

Carbonyl group. A portion of a molecule with the formula $\rangle\text{C═O}$.

Carboxyl group. A portion of a molecule with the formula —COOH. Carboxyl groups are usually ionized at physiological pH.

Carboxyl terminus. The end of a polypeptide that has a free carboxylate group. Also called the C-terminus.

Carcinogen. An agent that damages DNA so as to induce a mutation that leads to uncontrolled cell proliferation (cancer).

Caspase. A heterotetrameric cysteine protease that hydrolyzes cellular proteins, including caspase zymogens, as part of the process of apoptosis.

Catabolism. The degradative metabolic reactions in which nutrients and cell constituents are broken down for energy and raw materials.

Catabolite repression. A phenomenon in which the presence of glucose prevents the expression of genes involved in the metabolism of other fuels.

Catalyst. A substance that promotes a chemical reaction without itself undergoing permanent change. A catalyst increases the rate at which a reaction approaches equilibrium but does not affect the free energy change of the reaction.

Catalytic perfection. The ability of an enzyme to catalyze a reaction as fast as diffusion allows it to bind its substrates.

Catalytic triad. The hydrogen-bonded Ser, His, and Asp residues that participate in catalysis in serine proteases.

Cataplerotic reaction. A reaction that drains the intermediates of a metabolic pathway.

Catecholamine. A hydroxylated tyrosine derivative, such as dopamine, norepinephrine, or epinephrine.

Catenate. To interlink circular DNA molecules like the links of a chain.

Cation exchanger. An anionic matrix used to bind cationic molecules in ion exchange chromatography.

CCAAT box. A eukaryotic promoter element with the consensus sequence CCAAT that is located 70 to 90 nucleotides upstream from the transcription start site.

cDNA. See complementary DNA.

CE. See capillary electrophoresis.

Cell cycle. The sequence of events between eukaryotic cell divisions; it includes mitosis and cell division (M phase), a gap stage (G_1 phase), a period of DNA synthesis (S phase), and a second gap stage (G_2 phase) before the next M phase.

Cellular immunity. Immunity mediated by T lymphocytes (T cells).

Central dogma of molecular biology. The paradigm that DNA directs its own replication as well as its transcription to RNA, which is then translated into a polypeptide. The flow of information is from DNA to RNA to protein.

Centromere. The eukaryotic chromosomal region that attaches to the mitotic spindle during cell division; it contains high concentrations of repetitive DNA.

Ceramide. A sphingosine derivative with an acyl group attached to its amino group.

Cerebroside. A ceramide with a sugar residue as a head group.

C_4 plant. A plant in which photosynthesis relies on CO_2 that has been concentrated by incorporating it into oxaloacetate (a C_4 compound).

Chain-terminator procedure. A technique for determining the nucleotide sequence of a DNA using dideoxy nucleotides so as to yield a collection of daughter strands of all different lengths. Also called the dideoxy method.

Channeling. The transfer of an intermediate product from one enzyme active site to another in such a way that the intermediate remains protected by the protein.

Chaotropic agent. A substance that increases the solubility of nonpolar substances in water and thereby tends to denature proteins.

Chaperone. See molecular chaperone.

Chargaff's rules. The observation, first made by Erwin Chargaff, that DNA has equal numbers of adenine and thymine residues and equal numbers of guanine and cytosine residues.

Chemical potential. The partial molar free energy of a substance.

Chemiosmotic theory. The postulate that the free energy of electron transport is conserved by the formation of a transmembrane proton gradient. The electrochemical potential of this gradient is used to drive ATP synthesis.

Chemolithotroph. An autotrophic organism that obtains energy from the oxidation of inorganic compounds.

Chimera. See recombinant.

Chiral center. An atom whose substituents are arranged such that it is not superimposable on its mirror image. Also called an asymmetric center.

Chirality. The property of being asymmetric. A chiral molecule cannot be superimposed on its mirror image.

Chloroplasts. The plant organelles in which photosynthesis takes place.

Chromatin. The complex of DNA and protein that comprises the eukaryotic chromosomes.

Chromatin-remodeling complex. An ATP-dependent multisubunit protein in eukaryotes that transiently disrupts DNA–histone interactions so as to alter the accessibility of DNA in nucleosomes.

Chromatography. A technique for separating the components of a mixture of molecules based on their partition between a mobile solvent phase and a porous matrix (stationary phase).

Chromodomain. A protein module that binds methylated Lys residues in histones.

Chromophore. A light-absorbing group or molecule.

Chromosome. The complex of protein and a single DNA molecule that comprises some or all of an organism's genome.

Chylomicrons. Lipoprotein particles that transport dietary triacylglycerols and cholesterol from the intestines to the tissues.

Cis conformation. An arrangement of the peptide group in which successive C_α atoms are on the same side of the peptide bond.

Cis peptide. A conformation in which successive C_α atoms are on the same side of the peptide bond.

Cistron. An archaic term for a gene.

Citric acid cycle. A set of eight enzymatic reactions, arranged in a cycle, in which free energy in the form of ATP, NADH, and $FADH_2$ is recovered from the oxidation of the acetyl group of acetyl-CoA to CO_2. Also called the Krebs cycle and the tricarboxylic acid (TCA) cycle.

Clathrin. A three-legged protein that polymerizes to form a polyhedral structure defining the shape of membranous vesicles that travel between the plasma membrane and intracellular organelles such as the Golgi apparatus.

Clinical trials. A three-phase series of tests of a drug's safety, effectiveness, and side effects in human subjects.

Clone. A collection of identical cells derived from a single ancestor.

Cloning. The production of exact copies of a DNA segment or the organism that harbors it.

Cloning vector. A DNA molecule such as a plasmid, virus, or artificial chromosome that can accommodate a segment of foreign DNA for cloning.

Closed system. A thermodynamic system that can exchange energy but not matter with its surroundings.

Coated vesicle. A membranous intracellular transport vesicle that is encased by clathrin or another coat protein.

Coding strand. See sense strand.

Codon. The sequence of three nucleotides in DNA or RNA that specifies a single amino acid.

Coenzyme. A small organic molecule that is required for the catalytic activity of an enzyme. A coenzyme may be either a cosubstrate or a prosthetic group.

Coenzyme Q. An isoprenoid that functions in electron-transport pathways as a lipid-soluble electron carrier. Also called ubiquinone.

Cofactor. A small organic molecule (coenzyme) or metal ion that is required for the catalytic activity of an enzyme.

Coiled coil. An arrangement of polypeptide chains in which two α helices wind around each other, as in α keratin.

Cointegrate. The product of the fusion of two plasmids, which occurs as an intermediate in transposition.

Colligative property. A physical property, such as freezing point depression or osmotic pressure, that depends on the concentration of a dissolved substance rather than on its chemical nature.

Colony hybridization. A procedure in which DNA from multiple cell colonies is transferred to a membrane or filter and incubated with a DNA or RNA probe to test for the presence of a desired DNA fragment in the cell colonies. Also called *in situ* hybridization.

Combinatorial chemistry. A method for rapidly and inexpensively synthesizing large numbers of related compounds by systematically varying a portion of their structure.

Compartmentation. The division of a cell into smaller functionally discrete systems.

Competitive inhibition. A form of enzyme inhibition in which a substance competes with the substrate for binding to the enzyme active site and thereby appears to increase K_M.

Complementary DNA (cDNA). A DNA molecule, usually synthesized by the action of reverse transcriptase, that is complementary to an mRNA molecule.

Composite transposon. A genetic sequence that may include a variety of genes and is flanked by IS-like elements; such transposons apparently arose by the association of two independent IS elements.

Condensation reaction. The formation of a covalent bond between two molecules, during which the elements of water are lost; the reverse of hydrolysis.

Conjugate acid. The compound that forms when a base accepts a proton.

Conjugate base. The compound that forms when an acid donates a proton.

Conjugate redox pair. An electron donor and acceptor that form a half-reaction. Also called a redox couple.

Conservative replication. A hypothetical mode of DNA duplication in which the parental molecule remains intact and both strands of the daughter duplex are newly synthesized.

Conservative substitution. A change of an amino acid residue in a protein to one with similar properties, e.g., Leu to Ile or Asp to Glu.

Constant region. The C-terminal portion of an antibody (immunoglobulin) subunit, which does not exhibit the high sequence variability of the antigen-recognizing (variable) region of the antibody.

Constitutive enzyme. An enzyme that is synthesized at a more or less steady rate and that is required for basic cell function. Also called a housekeeping enzyme. See also inducible enzyme.

Contact inhibition. The inhibition of proliferation in cultured animal cells when the cells touch each other.

Contour length. The end-to-end length of a stretched-out polymer molecule.

Contour map. A map containing lines (contours) that trace positions of equal value of some property of the map (e.g., height above sea level, electron density).

Convergent evolution. The independent development of similar characteristics in unrelated species or proteins.

Cooperative binding. A situation in which the binding of a ligand at one site on a macromolecule affects the affinity of other sites for the same ligand. Both negative and positive cooperativity occur. See also allosteric interaction.

Corepressor. A substance that acts together with a protein repressor to block gene transcription.

Cori cycle. An interorgan metabolic pathway in which lactate produced by glycolysis in the muscles is transported via the bloodstream to the liver, where it is used for gluconeogenesis. The resulting glucose returns to the muscles.

Cosubstrate. A coenzyme that is only transiently associated with an enzyme so that it functions as a substrate.

Coupled enzymatic reaction. A technique in which the activity of an enzyme is measured by the ability of a second enzyme to use the product of the first enzymatic reaction to produce a detectable product.

Covalent catalysis. A catalytic mechanism in which the transient formation of a covalent bond between the catalyst and a reactant lowers the free energy of a reaction's transition state.

CpG island. A cluster of CG dinucleotides located just upstream of many vertebrate genes; such sequences occur elsewhere in the genome at only one-fifth their randomly expected frequency.

Crassulacean acid metabolism (CAM). A variation of the C_4 photosynthetic cycle in which CO_2 is temporarily stored as malate.

Cristae. The invaginations of the inner mitochondrial membrane.

Cross talk. The interactions of different signal transduction pathways through activation of the same signaling components, generation of a common second messenger, or similar patterns of target protein phosphorylation.

Cryoelectron microscopy (cryo-EM). A technique in electron microscopy in which a sample is rapidly frozen to very low temperatures so that it retains its native shape to a greater extent than in conventional electron microscopy.

C3′-*endo*. A ribose conformation in which C3′ is displaced toward the same side of the ring as C5′.

C_3 plant. A plant in which photosynthesis proceeds by the incorporation of CO_2 into three-carbon compounds.

C2′-*endo*. A ribose conformation in which C2′ is displaced toward the same side of the ring as C5′.

Curved arrow convention. A notation for indicating the movement of an electron pair in a chemical reaction by drawing a curved arrow emanating from the electrons and pointing to the electron-deficient center that attracts the electron pair.

Cyanosis. A bluish skin color indicating the presence of deoxyhemoglobin in the arterial blood.

Cyclic symmetry. A type of symmetry in which the asymmetric units of a symmetric object are related by a single axis of rotation.

Cyclin. A member of a family of proteins that participate in regulating the stages of the cell cycle and whose concentrations change dramatically over the course of the cell cycle.

Cytochrome. A redox-active protein that carries electrons via a prosthetic Fe-containing heme group.

Cytochrome P450. Heme-containing monooxygenases that catalyze the addition of OH groups to drugs and toxins in order to detoxify them and facilitate their excretion.

Cytoplasm. The entire contents of a cell excluding the nucleus.

Cytoskeleton. The network of intracellular fibers that gives a cell its shape and structural rigidity.

Cytosol. The contents of a cell excluding its nucleus and other membrane-bounded organelles.

D. Dalton, a unit of molecular mass; 1/12th the mass of a ^{12}C atom.

D arm. A conserved stem–loop structure in a tRNA molecule that usually contains the modified base dihydrouridine.

Dark reactions. The portion of photosynthesis in which NADPH and ATP produced by the light reactions are used to incorporate CO_2 into carbohydrates.

ddNTP. An abbreviation for any dideoxynucleoside triphosphate.

Deamination. The hydrolytic removal of an amino group.

Debranching. The enzymatic removal of side chains from a branched polymer such as glycogen.

Degenerate code. A code in which more than one "word" encodes the same entity.

$\Delta\mathscr{E}$. Electromotive force. Change in reduction potential.

$\Delta G^{\ddagger}$. See free energy of activation.

$\Delta\Psi$. See membrane potential.

Denature. To disrupt the native conformation of a polymer.

Deoxy sugar. A saccharide produced by replacement of an OH group by H.

Deoxynucleotide. See deoxyribonucleotide.

Deoxyribonucleic acid. See DNA.

Deoxyribonucleotide. A nucleotide in which the pentose is 2′-deoxyribose. Also known as a deoxynucleotide.

Depolarization. The loss of membrane potential that occurs during electrical signaling in cells such as neurons.

Desaturase. An enzyme that introduces double bonds into a fatty acid.

Desensitization. A cell's or organism's adaptation to a long-term stimulus through a reduced response to the stimulus.

Dextrorotatory. Rotating the plane of plane-polarized light clockwise from the point of view of the observer; the opposite of levorotatory.

Diabetes mellitus. A disease in which the pancreas does not secrete sufficient insulin (also called type I, insulin-dependent, or juvenile-onset diabetes) or in which the body has insufficient response to circulating insulin (type II, non-insulin-dependent, or maturity-onset diabetes). Diabetes is characterized by elevated levels of glucose in the blood.

Dialysis. A procedure in which solvent molecules and solutes smaller than the pores in a semipermeable membrane freely exchange with the bulk medium, while larger solutes are retained, thereby changing the solution in which the larger molecules are dissolved.

Diazotroph. A bacterium that can fix nitrogen.

Dideoxy method. See chain-terminator procedure.

Diet-induced thermogenesis. See thermogenesis.

Diffraction pattern. The record of the destructive and constructive interferences of radiation scattered from an object. In X-ray crystallography, this takes the form of a series of discrete spots resulting from a collimated beam of X-rays scattering from a single crystal.

Diffusion. The transport of molecules through their random movement.

Diffusion-controlled limit. The theoretical maximum rate of an enzymatic reaction in solution, about 10^8 to $10^9\ M^{-1} \cdot s^{-1}$.

Dihedral angle. See torsion angle.

Dihedral symmetry. A type of symmetry in which the asymmetric units are related by a twofold rotational axis that intersects another rotation axis at a right angle.

Dimer. An assembly consisting of two monomeric units (protomers).

Dinucleotide binding fold. A protein structural motif consisting of two βαβαβ units, which binds a dinucleotide such as NAD^+. Also called a Rossmann fold.

Dipeptide. A polypeptide consisting of two amino acids.

Diphosphoryl (pyrophosphoryl) group. Two phosphoryl groups linked by a phosphoanhydride bond $(—O_3P—O—PO_3—)^{2-}$.

Diploid. Having two equivalent sets of chromosomes.

Dipolar ion. A compound bearing oppositely charged groups. Also called a zwitterion.

Disaccharide. A carbohydrate consisting of two monosaccharides linked by a glycosidic bond.

Dissociation constant (*K*). The ratio of the products of the concentrations of the dissociated species to those of their parent compounds at equilibrium.

Disulfide bond. A covalent —S—S— linkage.

DNA. Deoxyribonucleic acid. A polymer of deoxynucleotides whose sequence of bases encodes genetic information in all living cells.

DNA chip. See DNA microarray.

DNA fingerprinting. A technique for distinguishing individuals on the basis of DNA polymorphisms, such as the number of short tandem repeats (STR).

DNA glycosylase. An enzyme that initiates base excision repair of DNA by cleaving the glycosidic bond that links a nucleotide base to ribose.

DNA library. A set of cloned DNA fragments representing some or all of an organism's genome.

DNA microarray. A set of DNA segments of known sequence that are immobilized on a solid support for the purpose of hybridizing with nucleic acids in test samples. Also called a DNA chip.

dNTP. A deoxyribonucleoside triphosphate.

Dolichol. An isoprenoid that serves as a lipid-soluble carrier of an *N*-linked oligosaccharide during its synthesis in the endoplasmic reticulum.

Domain. A group of one or a few polypeptide segments of about 40–200 residues that folds into a globular unit.

Double-displacement reaction. A reaction in which a substrate binds and a product is released in the first stage, and another substrate binds and another product is released in the second stage.

Double-reciprocal plot. See Lineweaver–Burk plot.

Drug–drug interactions. Increases or decreases in the bioavailability of a drug caused by the metabolic effects of another drug.

$\mathcal{E}$. See reduction potential.

$\mathcal{E}°'$. Reduction potential under biochemical standard conditions.

E site. See exit site.

EC classification. The Enzyme Commission's system for classifying and numbering enzymes according to the type of reaction catalyzed.

Edman degradation. A procedure for the stepwise removal and identification of the N-terminal residues of a polypeptide.

EF hand. A widespread helix–loop–helix structural motif that forms a Ca^{2+}-binding site.

Eicosanoids. C_{20} compounds derived from the C_{20} fatty acid arachidonic acid and which act as local mediators. Prostaglandins, prostacyclins, thromboxanes, leukotrienes, and lipoxins are eicosanoids.

Electrochemical cell. A device in which two half-reactions occur in separate compartments linked by a wire for transporting electrons and a salt bridge for maintaining electrical neutrality; the simultaneous activity of the half-reactions forms a complete oxidation–reduction reaction.

Electrochemical potential. The partial molar free energy of a substance (chemical potential) in the presence of an electrical potential.

Electrogenic transport. The transmembrane movement of a charged substance in a way that generates a charge difference across the membrane.

Electromotive force (emf). $\Delta\mathcal{E}$. Change in reduction potential.

Electron crystallography. A technique for determining molecular structure, in which the electron beam of an electron microscope is used to elicit diffraction from a two-dimensional crystal of the molecules of interest.

Electron density. The arrangement of electrons that gives rise to a diffraction pattern in X-ray crystallography.

Electron-transport chain. A series of membrane-associated electron carriers that pass electrons from reduced coenzymes (NADH and $FADH_2$) to molecular oxygen so as to recover free energy for the synthesis of ATP.

Electrophile. A group that contains an unfilled valence electron shell, or contains an electron-deficient atom. An electrophile (electron-lover) reacts readily with a nucleophile (nucleus-lover).

Electrophoresis. See gel electrophoresis.

Electrospray ionization (ESI). A method for vaporizing macromolecules for their mass spectrometry in which a macromolecular solution is sprayed from a narrow capillary at high voltage to produce fine, highly charged droplets that rapidly evaporate leaving the now charged macromolecule in the gas phase.

Electrostatic catalysis. A catalytic mechanism in which the distribution of charges about the catalytic site lowers the free energy of a reaction's transition state.

Elementary reaction. A simple one-step chemical process, several of which may occur in sequence in a chemical reaction.

ELISA. See enzyme-linked immunosorbent assay.

Elongase. An enzyme that adds acetyl units to a fatty acid previously synthesized by fatty acid synthase.

Elongation factor. A protein that interacts with tRNA and/or the ribosome during polypeptide synthesis.

Eluant. The solution used to wash material through a chromatographic column.

Elution. The process of dislodging a molecule that has bound to a chromatographic matrix.

Emergent property. A property of a complex system that is not attributable to any of its individual components but becomes apparent when all components are present.

emf. Electromotive force. Change in reduction potential.

Enantiomers. Molecules that are nonsuperimposable mirror images of one another. Enantiomers are a type of stereoisomer.

Endergonic process. A process that has an overall positive free energy change (a nonspontaneous process).

Endocrine gland. A tissue in higher animals that synthesizes and releases hormones into the bloodstream.

Endocytosis. The internalization of extracellular material through the formation of a vesicle that buds off from the plasma membrane; the opposite of exocytosis. See also receptor-mediated endocytosis.

Endoglycosidase. An enzyme that catalyzes the hydrolysis of the glycosidic bonds between two monosaccharide units within a polysaccharide.

Endonuclease. An enzyme that catalyzes the hydrolysis of the phosphodiester bonds between two nucleotide residues within a polynucleotide strand.

Endopeptidase. An enzyme that catalyzes the hydrolysis of a peptide bond within a polypeptide chain.

Endoplasmic reticulum (ER). A labyrinthine membranous organelle in eukaryotic cells in which membrane lipids are synthesized and some proteins undergo posttranslational modification.

Endosome. A membrane-bounded vesicle that receives materials that the cell ingests via receptor-mediated endocytosis and passes them to lysosomes for degradation.

Enediol intermediate. A reaction intermediate containing a carbon–carbon double bond and a hydroxyl group attached to each carbon.

Energy coupling. The conservation of the free energy of electron transport in a form that can be used to synthesize ATP from ADP + P_i.

"Energy-rich" compound. See "High-energy" compound.

Enhanceosome. A complex containing several transcription factors that regulates gene expression in eukaryotes.

Enhancer. A eukaryotic DNA sequence located some distance from the transcription start site, where an activator of transcription may bind.

Enthalpy (*H*). A thermodynamic quantity, $H = U + PV$, that is equivalent to the heat absorbed at constant pressure (q_P).

Entropy (*S*). A measure of the degree of randomness or disorder of a system. It is defined as $S = k_B \ln W$, where k_B is the Boltzmann constant and W is the number of equivalent ways the system can be arranged in its particular state.

Enzyme. A biological catalyst. Most enzymes are proteins; a few are RNA.

Enzyme-linked immunosorbent assay (ELISA). A technique in which a molecule is detected, and in many cases quantified, by its ability to bind an antibody to which an enzyme with an easily detected reaction product is attached.

Enzyme saturation. A state in which the substrate concentration is so high that essentially all the enzyme molecules are in the ES form.

Epigenetics. The inheritance of patterns of gene expression that are maintained from generation to generation independent of DNA's base sequence. This occurs, for example, through the methylation of DNA.

Epimers. Sugars that differ only by the configuration at one C atom (excluding the anomeric carbon).

Equatorial substituent. A group that extends largely in the plane of the ring to which it is bonded. See also axial substituent.

Equilibrium. The point in a process at which the forward and reverse reaction rates are exactly balanced so that it undergoes no net change.

Equilibrium constant (K_{eq}). The ratio, at equilibrium, of the product of the concentrations of reaction products to that of its reactants. K_{eq} is related to ΔG° for the reaction: $\Delta G^\circ = -RT \ln K_{eq}$. Usually abbreviated K.

ER. See endoplasmic reticulum.

Erythrocyte. A red blood cell, which functions to transport O_2 to the tissues. It is essentially a membranous sack of hemoglobin.

Erythrocyte ghost. Membranous particles derived from erythrocytes, which retain their original shape but are devoid of cytoplasm.

ES complex. The enzyme–substrate complex, whose formation is a key component of the Michaelis–Menten model of enzyme action. Also called the Michaelis complex.

ESI. See electrospray ionization.

Essential amino acid. An amino acid that an animal cannot synthesize and must therefore obtain in its diet.

Essential fatty acid. A fatty acid that an animal cannot synthesize and must therefore obtain in its diet.

EST. See expressed sequence tag.

Ester group. A portion of a molecule with the formula —COOR, where R is an alkyl group.

Estrogen. A steroid that functions primarily as a female sex hormone.

Ether. A molecule with the formula ROR′, where R and R′ are alkyl groups.

Eubacteria. One of the two major groups of prokaryotes (the other is archaea).

Euchromatin. The transcriptionally active, relatively uncondensed chromatin in a eukaryotic cell.

Eukarya. See eukaryote.

Eukaryote. An organism consisting of a cell (or cells) whose genetic material is contained in a membrane-bounded nucleus.

Evolution. The gradual alteration of an organism or one of its components as a result of genetic changes that are passed from parent to offspring.

Exciton transfer. A mode of decay of an energetically excited molecule, in which electronic energy is transferred to a nearby unexcited molecule. Also known as resonance energy transfer.

Exergonic process. A process that has an overall negative free energy change (a spontaneous process).

Exit site (E site). The ribosomal binding site that accommodates a tRNA molecule that has previously transferred its peptidyl group to an incoming aminoacyl–tRNA and is ready to dissociate from the ribosome.

Exocytosis. The release outside the cell of a vesicle's contents through the fusion of the vesicle membrane with the plasma membrane; the opposite of endocytosis.

Exoglycosidase. An enzyme that catalyzes the hydrolytic excision of a monosaccharide unit from the end of a polysaccharide.

Exon. A portion of a gene that appears in both the primary and mature mRNA transcripts. Also called an expressed sequence.

Exonuclease. An enzyme that catalyzes the hydrolytic excision of a nucleotide residue from one end of a polynucleotide strand.

Exopeptidase. An enzyme that catalyzes the hydrolytic excision of an amino acid residue from one end of a polypeptide chain.

Expressed sequence. See exon.

Expressed sequence tag (EST). A cDNA segment corresponding to a cellular mRNA, that can be used to identify genes that are transcribed.

Expression vector. A plasmid containing the transcription and translation control sequences required for the production of a foreign DNA gene product (RNA or protein) in a host cell.

Extinction coefficient. See absorptivity.

Extrinsic protein. See peripheral protein.

$\mathcal{F}$. Faraday, the electrical charge of one mole of electrons.

F_1F_0-ATPase. A multisubunit protein consisting of a proton-translocating membrane-embedded component (F_0) linked to a soluble catalytic component (F_1) that catalyzes ATP synthesis in the presence of a protonmotive force. Also called ATP synthase.

Fab fragment. A proteolytic fragment of an antibody molecule that contains the antigen-binding site. See also Fc fragment.

Facilitated diffusion. See passive-mediated transport.

Familial hypercholesterolemia. See hypercholesterolemia.

Fat. A mixture of triacylglycerols that is solid at room temperature.

Fatty acid. A carboxylic acid with a long-chain hydrocarbon side group.

Fc fragment. A proteolytic fragment of an antibody molecule that contains the two C-terminal domains of its two heavy chains. See also Fab fragment.

Fe–S cluster. See iron–sulfur cluster.

Feedback inhibition. The inhibition of an early step in a reaction sequence by the product of a later step.

Feedforward activation. The activation of a later step in a reaction sequence by the product of an earlier step.

Fermentation. An anaerobic catabolic process.

Fibrous protein. A protein characterized by a stiff, elongated conformation, that tends to form fibers.

First-order reaction. A reaction whose rate is proportional to the concentration of a single reactant.

Fischer convention. A system for describing the absolute configurations of chiral molecules by relating their structures to that of D- or L-glyceraldehyde.

Fischer projection. A graphical convention for specifying molecular configuration in which horizontal lines represent bonds that extend above the plane of the paper and vertical lines represent bonds that extend below the plane of the paper.

5′ end. The terminus of a polynucleotide whose C5′ is not esterified to another nucleotide residue.

Flip-flop. See transverse diffusion.

Flipase. An enzyme that catalyzes the translocation of a membrane lipid across a lipid bilayer (a flip-flop).

Fluid mosaic model. A model of biological membranes in which integral membrane proteins float and diffuse laterally in a fluid lipid bilayer.

Fluorescence. A mode of decay of an excited molecule, in which electronic energy is emitted in the form of a photon.

Fluorescence recovery after photobleaching (FRAP). A technique for assessing the diffusion of membrane components from the rate at which the fluorescently labeled component moves into an area previously bleached by a pulse of laser light.

Fluorophore. A fluorescent group or molecule.

Flux. (1) The rate of flow of metabolites through a metabolic pathway. (2) The rate of transport per unit area.

fMet. The formylated methionine that initiates ribosomal polypeptide synthesis in prokaryotes.

Footprinting. A procedure in which the DNA sequence to which a protein binds is identified by determining which bases are protected by the protein from chemical or enzymatic modification.

Fractional saturation (Y). The fraction of a protein's ligand-binding sites that are occupied by ligand. For example, Y_{O_2} is the fractional saturation of a protein's oxygen-binding sites.

Fractionation procedure. A laboratory technique for separating the components of a mixture of molecules through differences in their chemical and physical properties.

Frameshift mutation. An insertion or deletion of nucleotides in DNA that alters the sequential reading (the frame) of sets of three nucleotides (codons) during translation.

FRAP. See fluorescence recovery after photobleaching.

Free energy (G). A thermodynamic quantity, $G = H - TS$, whose change at constant pressure is indicative of the spontaneity of a process. For spontaneous processes, $\Delta G < 0$, whereas for a process at equilibrium, $\Delta G = 0$. Also called Gibbs free energy.

Free energy of activation ($\Delta G^{\ddagger}$). The free energy of the transition state minus the free energies of the reactants in a chemical reaction.

Free radical. A molecule with an unpaired electron.

Functional group. A portion of a molecule that participates in interactions with other substances. Common functional groups in biochemistry are acyl, amido, amino, carbonyl, carboxyl, diphosphoryl (pyrophosphoryl), ester, ether, hydroxyl, imino, phosphoryl, and sulfhydryl groups.

Furanose. A sugar with a five-membered ring.

Futile cycle. See substrate cycle.

G. See free energy.

$G^{\ddagger}$. The free energy of the transition state. See also free energy of activation.

G protein. A guanine nucleotide–binding protein, most of which are involved in signal transduction, that is inactive when it binds GDP and active when it binds GTP. The GTPase activity of the G protein limits its own activity. Heterotrimeric G proteins consist of three subunits, which dissociate to form G_α (to which GTP binds) and $G_{\beta\gamma}$ components on activation.

G-quartet. A cyclic tetramer of hydrogen-bonded guanine groups. Stacks of G-quartets result from the antiparallel association of G-rich telomeric DNA hairpin structures.

Ganglioside. A ceramide whose head group is an oligosaccharide containing at least one sialic acid residue.

Gap genes. See segmentation genes.

Gap junction. An intercellular channel for ions and small molecules that is formed by protein complexes in the membranes of apposed cells.

Gastrulation. The stage of embryonic development in which cells migrate to form a triple-layered structure.

Gates and fences model. A model for membrane structure that includes cytoskeletal proteins that prevent or limit the free diffusion of other membrane proteins.

Gating. The opening and closing of a transmembrane channel in response to a signal such as mechanical stimulation, ligand binding, presence of a signaling molecule, or a change in membrane voltage.

Gel electrophoresis. A procedure in which macromolecules are separated on the basis of charge or size by their differential migration through a gel-like matrix under the influence of an applied electric field. In polyacrylamide gel electrophoresis (PAGE), the matrix is cross-linked polyacrylamide. Agarose gels are used to separate molecules of very large masses, such as DNAs. See also SDS-PAGE and pulsed-field gel electrophoresis.

Gel filtration chromatography. A procedure in which macromolecules are separated on the basis of their size and shape. Also called size exclusion or molecular sieve chromatography.

Gene. A unique sequence of nucleotides that encodes a polypeptide or RNA; it may include nontranscribed and nontranslated sequences, some of which have regulatory functions.

Gene cluster. A region of DNA containing multiple copies of genes, usually tRNA or rRNA genes, whose products are required in large amounts.

Gene duplication. An event, such as aberrant crossover, that gives rise to two copies of a gene on the same chromosome, each of which can then evolve independently.

Gene expression. The decoding, via transcription and translation, of the information contained in a gene to yield a functional RNA or protein product.

Gene knockout. A genetic engineering process that deletes or inactivates a specific gene in an animal.

Gene product. The RNA or protein that is encoded by a gene and that is the end point of the gene's expression through transcription and translation.

Gene therapy. The transfer of genetic material to the cells of an individual in order to produce a therapeutic effect.

General acid catalysis. A catalytic mechanism in which partial proton transfer from an acid lowers the free energy of a reaction's transition state.

General base catalysis. A catalytic mechanism in which partial proton abstraction by a base lowers the free energy of a reaction's transition state.

General transcription factor (GTF). One of a set of eukaryotic proteins that are required for the synthesis of all mRNAs.

Genetic anticipation. A pattern of inheritance of a genetic disease, in which the age of onset of symptoms decreases with each generation.

Genetic code. The correspondence between the sequence of nucleotides in a nucleic acid and the sequence of amino acids in a polypeptide; a series of three nucleotides (a codon) specifies an amino acid.

Genetic engineering. See recombinant DNA technology.

Genome. The complete set of genetic instructions in an organism.

Genomic library. A set of cloned DNA fragments representing an organism's entire genome.

Genomics. The study of the size, organization, and gene content of organisms' genomes.

Genotype. An organism's genetic characteristics.

Gibbs free energy. See free energy.

Globin. The polypeptide components of myoglobin and hemoglobin.

Globoside. A ceramide whose head group is a neutral oligosaccharide.

Globular protein. A water-soluble protein characterized by a compact, highly folded structure.

Glucocorticoid. A steroid hormone that affects a range of metabolic pathways and the inflammatory response.

Glucogenic amino acid. An amino acid whose degradation yields a gluconeogenic precursor. See also ketogenic amino acid.

Gluconeogenesis. The synthesis of glucose from noncarbohydrate precursors.

Glucose–alanine cycle. An interorgan metabolic pathway that transports nitrogen to the liver in which pyruvate produced by glycolysis in the muscles is converted to alanine and transported to the liver. There the alanine is converted back to pyruvate and its amino group is used to synthesize urea for excretion. The pyruvate is converted, via gluconeogenesis, to glucose, which is returned to the muscles.

Glucose–fatty acid cycle. The downregulation of glycolysis by fatty acid oxidation, caused by the acetyl-CoA–induced inhibition of phosphofructokinase by citrate. Also called the Randle cycle.

Glycan. See polysaccharide.

Glycerophosphate shuttle. A metabolic pathway that uses the interconversion of dihydroxyacetone phosphate and 3-phosphoglycerol to transport cytosolic reducing equivalents into the mitochondria.

Glycerophospholipid. An amphiphilic lipid in which two fatty acyl groups are attached to a glycerol-3-phosphate whose phosphate group is linked to a polar group. Also called a phosphoglyceride.

Glycoconjugate. A molecule, such as a glycolipid or glycoprotein, that contains covalently linked carbohydrate.

Glycoforms. Glycoproteins that differ in the sequence, location, and number of covalently attached carbohydrates.

Glycogen. An $\alpha(1 \rightarrow 6)$ branched polymer of $\alpha(1 \rightarrow 4)$-linked glucose residues that serves as a glucose storage molecule in animals.

Glycogen storage disease. An inherited disorder of glycogen metabolism affecting the size and structure of glycogen molecules or their mobilization in the muscle and/or liver.

Glycogenolysis. The enzymatic degradation of glycogen to glucose-6-phosphate.

Glycolipid. A lipid to which carbohydrate is covalently attached.

Glycolysis. The 10-reaction pathway by which glucose is broken down to 2 pyruvate with the concomitant production of 2 ATP and the reduction of 2 NAD^+ to 2 NADH.

Glycomics. The study of the structures and functions of all of a cell's carbohydrates, including large glycans and the small oligosaccharides of glycoproteins.

Glycoprotein. A protein to which carbohydrate is covalently attached.

Glycosaminoglycan. An unbranched polysaccharide consisting of alternating residues of uronic acid and hexosamine.

Glycoside. A molecule containing a saccharide and another molecule linked by a glycosidic bond to the anomeric carbon in the α configuration (α-glycoside) or β configuration (β-glycoside).

Glycosidic bond. The covalent linkage (acetal or ketal) between the anomeric carbon of a saccharide and an alcohol (*O*-glycosidic bond) or an amine (*N*-glycosidic bond). Glycosidic bonds link the monosaccharide residues of a polysaccharide.

Glycosylation. The attachment of carbohydrate chains to a protein through *N*- or *O*-glycosidic linkages.

Glyoxylate pathway. A variation of the citric acid cycle in plants that allows acetyl-CoA to be converted quantitatively to gluconeogenic precursors.

Glyoxysome. A membrane-bounded plant organelle in which the reactions of the glyoxylate cycle take place. It is a specialized type of peroxisome.

Golgi apparatus. A eukaryotic organelle consisting of a set of flattened membranous sacs in which newly synthesized proteins and lipids are modified.

Gout. A disease characterized by elevated levels of uric acid, usually the result of impaired uric acid excretion. Its most common manifestation is painful arthritic joint inflammation caused by the deposition of sodium urate.

GPCR. G protein–coupled receptor, a cell-surface protein with seven transmembrane helices that interacts with an associated G protein on ligand binding.

GPI-linked protein. A protein that is anchored in a membrane via a covalently linked glycosylphosphatidylinositol (GPI) group.

Gram-negative bacterium. A bacterium that does not take up Gram stain, indicating that its cell wall is surrounded by a complex outer membrane that excludes Gram stain.

Gram-positive bacterium. A bacterium that takes up Gram stain, indicating that its outermost layer is a cell wall.

Grana (*sing.* granum). The stacked disks of the thylakoid in a chloroplast.

gRNA. See guide RNA.

Group I intron. An intron in an rRNA molecule whose self-splicing reaction requires a guanine nucleotide and generates a cyclized intron product.

Group II intron. An intron in a eukaryotic rRNA molecule whose self-splicing reaction does not require a free nucleotide and generates a lariat intron product.

Growth factor. A protein hormone that stimulates the proliferation and differentiation of its target cells.

GTF. See general transcription factor.

GTPase. An enzyme that catalyzes the hydrolysis of GTP to GDP + P_i.

Guide RNA (gRNA). Small RNA molecules that pair with an immature mRNA to direct its posttranscriptional editing.

***H*.** See enthalpy.

Half-life. See half-time.

Half-reaction. The single oxidation or reduction process, involving an electron donor and its conjugate electron acceptor, that occurs in electrical cells but requires direct contact with another such reaction to form a complete oxidation–reduction reaction.

Half-time ($t_{1/2}$). The time required for half the reactant initially present to undergo reaction. Also called half-life.

Halobacteria. Bacteria that thrive in (and may require) high salinity.

Haploid. Having one set of chromosomes.

HAT. See histone acetyltransferase.

Haworth projection. A representation of a sugar ring in which ring bonds that project in front of the plane of the paper are represented by heavy lines and ring bonds that project behind the plane of the paper are drawn as light lines.

HDL. High density lipoprotein; see lipoprotein.

Heat shock protein (Hsp). See molecular chaperone.

Helicase. An enzyme that unwinds a double-stranded nucleic acid.

Helix cap. A protein structural element in which the side chain of a residue preceding or succeeding a helix folds back to form a hydrogen bond with the backbone of one of the helix's four terminal residues.

Helix–turn–helix (HTH) motif. An ~20-residue protein motif that forms two α helices that cross at an angle of ~120°. This motif, which occurs in numerous prokaryotic DNA-binding proteins, binds in DNA's major groove to specific base sequences.

Heme. A porphyrin derivative whose central Fe(II) atom is the site of reversible oxygen binding (in myoglobin and hemoglobin) or oxidation–reduction (in cytochromes).

Hemiacetal. The product of the reaction between an alcohol and the carbonyl group of an aldehyde.

Hemiketal. The product of the reaction between an alcohol and the carbonyl group of a ketone.

Hemolytic anemia. Loss of red blood cells through their lysis (destruction) in the bloodstream.

Henderson–Hasselbalch equation. The mathematical expression of the relationship between the pH of a solution of a weak acid and its p*K*: $\text{pH} = \text{p}K + \log([\text{A}^-]/[\text{HA}])$.

Heptad repeat. A sequence of seven residues that is repeated in the same polymer.

Heterochromatin. Highly condensed, nonexpressed eukaryotic DNA.

Heterogeneous nuclear RNA (hnRNA). Eukaryotic mRNA primary transcripts whose introns have not yet been excised.

Heterologous DNA. A segment of DNA consisting of imperfectly complementary strands.

Heterolytic cleavage. Cleavage of a bond in which one of two chemically bonded atoms acquires both of the electrons that formed the bond.

Heteropolysaccharide. A polysaccharide consisting of more than one type of monosaccharide.

Heterotrimeric G protein. See G protein.

Heterotroph. An organism that obtains free energy from the oxidation of organic compounds produced by other organisms.

Heterozygous. Having one each of two gene variants.

Hexose monophosphate shunt. See pentose phosphate pathway.

"High-energy" intermediate. A substance whose degradation is highly exergonic (yields at least as much free energy as is required to synthesize ATP from ADP + P_i; $\geq 30.5\ \text{kJ} \cdot \text{mol}^{-1}$ under standard biochemical conditions). Also called an "energy-rich" compound.

High-performance liquid chromatography (HPLC). An automated chromatographic procedure for fractionating molecules using precisely fabricated matrix materials and pressurized flows of precisely mixed solvents.

Highly repetitive DNA. Clusters of nearly identical sequences of up to 10 bp that are repeated thousands of times; these sequences are present at $>10^6$ copies per haploid genome. Also known as short tandem repeats (STRs).

Hill coefficient. The exponent in the Hill equation. It provides a measure of the degree of cooperative binding of a ligand to a molecule.

Hill equation. A mathematical expression for the degree of saturation of ligand binding to a molecule with multiple binding sites as a function of the ligand concentration.

Histone acetyltransferase (HAT). An enzyme that catalyzes the sequence-specific acetylation of histones so as to regulate gene transcription.

Histone code. The correlation between the pattern of histone modification and the transcriptional activity of the associated DNA.

Histones. Highly conserved basic proteins that constitute the protein core to which DNA is bound to form a nucleosome.

HIV. Human immunodeficiency virus, the causative agent of acquired immunodeficiency syndrome (AIDS).

HMG protein. A member of the high mobility group (HMG) of nonhistone chromosomal proteins whose abundant charged groups give them high electrophoretic mobility.

hnRNA. See heterogeneous nuclear RNA.

Holliday junction. The four-stranded structure that forms as an intermediate in DNA recombination.

Holoenzyme. A catalytically active enzyme–cofactor complex.

Homeobox. See homeodomain.

Homeodomain. An ~60-amino acid DNA-binding motif common to many genes that specify the identities and fates of embryonic cells; such genes encode transcription factors. Also called a homeobox.

Homeostasis. The maintenance of a steady state in an organism.

Homeotic selector genes. Insect genes that specify the identities of body segments.

Homolactic fermentation. The reduction of pyruvate to lactate with the concomitant oxidation of NADH to NAD^+.

Homologous end-joining. A pathway in which DNA with double-strand breaks is repaired nonmutagenically through recombination with an intact homologous chromosome.

Homologous proteins. Proteins that resemble each other due to their evolution from a common ancestor.

Homologous recombination. See recombination.

Homolytic cleavage. Cleavage of a bond in which each participating atom acquires one of the electrons that formed the bond.

Homopolysaccharide. A polysaccharide consisting of one type of monosaccharide unit.

Homozygous. Having two identical copies of a particular gene.

Hoogsteen base pair. A form of base pairing in which thymine or uracil atom N3 hydrogen bonds to adenine atom N7 and adenine N6 hydrogen bonds to thymine or uracil O4. See also Watson–Crick base pair.

Hormone. A substance (e.g., a peptide or a steroid) that is secreted by one tissue into the bloodstream and which induces a physiological response (e.g., growth and metabolism) in other tissues.

Hormone response element (HRE). A DNA sequence to which a hormone–receptor complex binds so as to enhance or repress the transcription of an associated gene.

Hormone-sensitive lipase. An adipose tissue enzyme that releases fatty acids from triacylglycerols in response to a hormonally generated increase in cAMP. Also known as hormone-sensitive triacylglycerol lipase.

Housekeeping enzyme. See constitutive enzyme.

***Hox* gene.** A gene encoding a transcription factor that includes a homeodomain.

HPLC. See high-performance liquid chromatography.

HRE. See hormone response element.

Hsp. Heat shock protein. See molecular chaperone.

HTH motif. See helix–turn–helix motif.

Humoral immunity. Immunity mediated by antibodies (immunoglobulins) produced by B lymphocytes (B cells).

Hybridization. The formation of double-stranded segments of complementary DNA and/or RNA sequences.

Hybridoma. The cell clones produced by the fusion of an antibody-producing lymphocyte and an immortal myeloma cell. These are the cells that produce monoclonal antibodies.

Hydration. The molecular state of being surrounded by and interacting with several layers of solvent water molecules, that is, solvated by water.

Hydrogen bond. A largely electrostatic interaction between a weakly acidic donor group such as O—H or N—H and a weakly basic acceptor atom such as O or N.

Hydrolase. An enzyme that catalyzes a hydrolytic reaction.

Hydrolysis. The cleavage of a covalent bond accomplished by adding the elements of water; the reverse of a condensation.

Hydronium ion. A proton associated with a water molecule, H_3O^+.

Hydropathy. A measure of the combined hydrophobicity and hydrophilicity of an amino acid residue; it is indicative of the likelihood of finding that residue in a protein interior.

Hydrophilic substance. A substance whose high polarity allows it to readily interact with water molecules and thereby dissolve in water.

Hydrophobic collapse. A driving force in protein folding, resulting from the tendency of hydrophobic residues to avoid contact with water and hence form the protein core.

Hydrophobic effect. The tendency of water to minimize its contacts with nonpolar substances, thereby inducing the substances to aggregate.

Hydrophobic interaction chromatography. A procedure in which molecules are selectively retained on a nonpolar matrix by virtue of their hydrophobicity.

Hydrophobic substance. A substance whose nonpolar nature reduces its ability to be solvated by water molecules. Hydrophobic substances tend to be soluble in nonpolar solvents but not in water.

Hydroxide ion. OH^-, a product of the ionization of a water molecule.

Hydroxyl group. A portion of a molecule with the formula —OH.

Hyperammonemia. Elevated levels of ammonia in the blood, a toxic situation.

Hyperbolic curve. The graphical representation of the mathematical equation that describes the noncooperative binding of a ligand to a molecule or the rate of a reaction catalyzed by a Michealis–Menten enzyme.

Hypercholesterolemia. High levels of cholesterol in the blood, a risk factor for heart disease. Familial hypercholesterolemia usually results from an inherited defect in the LDL receptor.

Hyperchromic effect. The increase in DNA's ultraviolet absorbance resulting from the loss of stacking interactions as the DNA denatures.

Hyperglycemia. Elevated levels of glucose in the blood.

Hypervariable residue. An amino acid residue occupying a position in a protein that is occupied by many different residues among evolutionarily related proteins. The opposite of a hypervariable residue is an invariant residue.

Hypoxia. A condition in which the oxygen level in the blood is lower than normal.

I-cell disease. A hereditary deficiency in a lysosomal hydrolase that leads to the accumulation of glycosaminoglycan and glycolipid inclusions in the lysosomes.

IDL. Intermediate density lipoprotein; see lipoprotein.

IEF. See isoelectric focusing.

Ig. Immunoglobulin. See antibody.

Imaginal disk. A patch of apparently undifferentiated but developmentally committed cells in an insect larva that ultimately gives rise to a specific external structure in the adult.

Imino group. A portion of a molecule with the formula $>\text{C}{=}\text{NH}$.

Immune system. The cells and organs that respond to microbial infection by producing antibodies and by killing pathogens and infected host cells.

Immunoaffinity chromatography. A procedure in which a molecule is separated from a mixture of other molecules by its ability to bind specifically to an immobilized antibody.

Immunoassay. A procedure for detecting, and in some cases quantifying the activity of, a macromolecule by using an antibody or mixture of antibodies that reacts specifically with that substance.

Immunoblot. A technique in which a molecule immobilized on a membrane filter can be detected through its ability to bind to an antibody directed against it. A Western blot is an immunoblot to detect an immobilized protein after electrophoresis.

Immunofluorescence microscopy. A technique in microscopy in which a fluorescence-tagged antibody is used to reveal the presence of the antigen to which it binds.

Immunoglobulin (Ig). See antibody.

Immunoglobulin fold. A disulfide-linked domain consisting of a sandwich of a three-stranded and a four-stranded antiparallel β sheet that occurs in antibody molecules.

Imprinting. The differential expression of maternal and paternal genes according to their patterns of DNA methylation.

in silico. In a computer simulation (electronic circuits are mainly silicon-based).

in situ. In place.

***in situ* hybridization.** See colony hybridization.

in vitro. In the laboratory (literally, in glass).

in vivo. In a living organism.

Inactivator. An inhibitor that reacts irreversibly with an enzyme so as to inactivate it.

Indirect readout. The ability of a DNA-binding protein to detect its target base sequence though the sequence-dependent conformation and/or flexibility of its DNA backbone rather than through direct interaction with its bases.

Induced fit. An interaction between a protein and its ligand, which induces a conformational change in the protein that increases the protein's affinity for the ligand.

Inducer. A substance that facilitates gene expression.

Inducible enzyme. An enzyme that is synthesized only when required by the cell. See also constitutive enzyme.

Inhibition constant (K_I). The dissociation constant for an enzyme–inhibitor complex.

Inhibitor. A substance that reduces an enzyme's activity by affecting its substrate binding or turnover number.

Initiation factor. A protein that interacts with mRNA and/or the ribosome and which is required to initiate translation.

Inorganic compound. A compound that lacks the element carbon.

Insertion sequence. A simple transposon that is flanked by short inverted repeats. Also called an IS element.

Insertion/deletion mutation. A genetic change resulting from the addition or loss of nucleotides; also called an indel.

Insulator. A segment of DNA that delimits the effective range of a transcription-regulating element.

Insulin resistance. The decreased ability of cells to respond to insulin by increasing their glucose uptake.

Integral protein. A membrane protein that is embedded in the lipid bilayer and can be separated from it only by treatment with agents that disrupt membranes. Also called an intrinsic protein.

Intercalation agent. A substance, usually a planar aromatic cation, that slips in between the stacked bases of a double-stranded polynucleotide.

Interconvertible enzyme. An enzyme that undergoes covalent modification/demodification, usually phosphorylation/dephosphorylation, so as to modulate its activity.

Interfacial activation. The increase in activity when a lipid-specific enzyme contacts the lipid–water interface.

Intermembrane space. The compartment between the inner and outer mitochondrial membranes. Because of the porosity of the outer membrane, the intermembrane space is equivalent to the cytosol in its small-molecule composition.

Internal conversion. A mode of decay of an excited molecule, in which electronic energy is converted to heat (the kinetic energy of molecular motion).

Intervening sequence. See intron.

Intrinsic protein. See integral protein.

Intron. A portion of a gene that is transcribed but excised prior to translation. Also called an intervening sequence.

Invariant residue. A residue in a protein that is the same in all evolutionarily related proteins. The opposite of an invariant residue is a hypervariable residue.

Ion exchange chromatography. A fractionation procedure in which ions are selectively retained by a matrix bearing oppositely charged groups.

Ion pair. An electrostatic interaction between two ionic groups of opposite charge. In proteins, it is also called a salt bridge.

Ionophore. An organic molecule, often an antibiotic, that increases the permeability of a membrane to a particular ion. A carrier ionophore diffuses with its ion through the membrane, whereas a channel-forming ionophore forms a transmembrane pore.

Iron–sulfur protein. A protein that contains a prosthetic group consisting most commonly of equal numbers of iron and sulfur ions (i.e., [2Fe–2S] and [4Fe–4S]) and that usually participates in oxidation–reduction reactions.

IS element. See insertion sequence.

Isoaccepting tRNA. A tRNA that carries the same amino acid as another tRNA.

Isoelectric focusing (IEF). Electrophoresis through a stable pH gradient such that a charged molecule migrates to a position corresponding to its isoelectric point.

Isoelectric point (p*I*). The pH at which a molecule has no net charge and hence does not migrate in an electric field.

Isoforms. See isozymes.

Isolated system. A thermodynamic system that cannot exchange matter or energy with its surroundings.

Isomerase. An enzyme that catalyzes an isomerization reaction.

Isopeptide bond. An amide linkage between an α-carboxylate group of an amino acid and the ε-amino group of Lys, or between the α-amino group of an amino acid and the β- or γ-carboxylate group of Asp or Glu.

Isoprenoid. A lipid containing five-carbon units with the same carbon skeleton as isoprene.

Isoschizomers. Restriction endonucleases that cleave at the same nucleotide sequence.

Isozymes. Enzymes that catalyze the same reaction but are encoded by different genes. Also called isoforms.

Jaundice. A yellowing of the skin and whites of the eyes as a result of the deposition of the heme degradation product bilirubin in those tissues. It is a symptom of liver dysfunction, bile-duct obstruction, or a high rate of red cell destruction.

Junk DNA. See selfish DNA.

K. See dissociation constant and equilibrium constant.

k. See rate constant.

k_B. Boltzmann constant ($1.3807 \times 10^{-23}\ \text{J} \cdot \text{K}^{-1}$); it is equivalent to R/N, where R is the gas constant and N is Avogadro's number.

kb. Kilobase pair; 1 kb = 1000 base pairs (bp).

k_{cat}. The catalytic constant for an enzymatic reaction, equivalent to the ratio of the maximal velocity (V_{max}) and the enzyme concentration ($[\text{E}]_T$). Also called the turnover number.

k_{cat}/K_M. The apparent second-order rate constant for an enzyme-catalyzed reaction; it is a measure of an enzyme's catalytic efficiency.

kD. Kilodaltons; 1000 daltons (D).

K_{eq}. See equilibrium constant.

Ketogenesis. The synthesis of ketone bodies from acetyl-CoA.

Ketogenic amino acid. An amino acid whose degradation in animals yields compounds that can be converted to fatty acids or ketone bodies. See also glucogenic amino acid.

Ketone bodies. Acetoacetate, D-β-hydroxybutyrate, and acetone; these compounds are produced from acetyl-CoA by the liver for use as metabolic fuels in peripheral tissues.

Ketose. A sugar whose carbonyl group is a ketone.

Ketosis. A potentially pathological condition in which ketone bodies are produced in excess of their utilization.

K_I. See inhibition constant.

Kinase. An enzyme that transfers a phosphoryl group between ATP and another molecule.

Kinase cascade. A set of reactions in which kinase-catalyzed phosphorylation activates the next kinase in a series, thereby amplifying the effect of the initial kinase.

K_M. See Michaelis constant.

K_M^{app}. The apparent (observed) Michaelis constant for an enzyme-catalyzed reaction, which may differ from the true value due to the presence of an enzyme inhibitor.

k_{-1}. The rate constant for a reverse reaction, e.g., the breakdown of the ES complex to E + S.

Krebs cycle. See citric acid cycle.

k_2. The rate constant for the second step of a simple enzyme-catalyzed reaction that follows Michaelis–Menten kinetics, that is, the conversion of the ES complex to E + P.

K_w. The ionization constant of water; equal to 10^{-14}.

L. See linking number.

Lactose intolerance. The inability to digest the disaccharide lactose due to a deficiency of the enzyme β-galactosidase (lactase).

Lagging strand. A newly synthesized DNA strand that extends 3′ → 5′ in the direction of travel of the replication fork. This strand is synthesized as a series of discontinuous fragments that are later joined.

Lateral diffusion. The movement of a lipid within one leaflet of a bilayer.

LBHB. See low-barrier hydrogen bond.

LDL. Low density lipoprotein; see lipoprotein.

Lead compound. A drug molecule that serves as the starting point for the development of more effective drug molecules.

Leader peptide. See signal peptide.

Leader sequence. (1) A nucleotide sequence that precedes the coding region of an mRNA. (2) A signal sequence.

Leading strand. A newly synthesized DNA strand that extends $5' \rightarrow 3'$ in the direction of travel of the replication fork. This strand is synthesized continuously.

Lectin. A protein that binds to a specific saccharide.

Lesch–Nyhan syndrome. A genetic disease caused by the deficiency of hypoxanthine–guanine phosphoribosyltransferase (HGPRT), an enzyme required for purine salvage reactions. Affected individuals produce excessive uric acid and exhibit neurological abnormalities.

Leucine zipper. A protein structural motif in which two α helices, each with a hydrophobic strip along one side, associate as a coiled coil. This motif, which has a Leu at nearly every seventh residue, mediates the association of many types of DNA-binding proteins.

Leukocyte. White blood cell.

Levorotatory. Rotating the plane of polarized light counterclockwise from the point of view of the observer; the opposite of dextrorotatory.

LHC. See light-harvesting complex.

Ligand. (1) A small molecule that binds to a larger molecule. (2) A molecule or ion bound to a metal ion.

Ligand-gated channel. A channel whose opening and closing (gating) is controlled by the binding of a specific molecule (ligand).

Ligase. An enzyme that catalyzes bond formation coupled with the hydrolysis of ATP.

Ligation. The joining together of two molecules such as two DNA segments.

Light-harvesting complex (LHC). A pigment-containing membrane protein that collects light energy and transfers it to a photosynthetic reaction center.

Light reactions. The portion of photosynthesis in which specialized pigment molecules capture light energy and are thereby oxidized. Electrons are transferred to generate NADPH and a transmembrane proton gradient that drives ATP synthesis.

Limited proteolysis. A technique in which a polypeptide is incompletely digested by proteases.

Lineweaver–Burk plot. A graph of a rearrangement of the Michaelis–Menten equation to a linear form that permits the determination of K_M and $V_{\max}$. Also called a double-reciprocal plot.

Linker DNA. The ~55-bp segment of DNA that links nucleosome core particles in chromatin.

Linking number (*L*). The number of times that one strand of a covalently closed circular double-stranded DNA winds around the other; it cannot be changed without breaking covalent bonds.

Lipid. Any member of a broad class of biological molecules that are largely or wholly hydrophobic and therefore tend to be insoluble in water but soluble in organic solvents such as hexane.

Lipid bilayer. See bilayer.

Lipid-linked protein. A protein that is anchored to a biological membrane via a covalently attached lipid such as a farnesyl, geranylgeranyl, myristoyl, palmitoyl, or glycosylphosphatidylinositol group.

Lipid raft. A semicrystalline region of a cell membrane containing tightly packed glycosphingolipids and cholesterol.

Lipid storage disease. A defect in a lipid-degrading enzyme that causes the substrate for the enzyme to accumulate in lysosomes.

Lipoprotein. A globular particle consisting of a nonpolar lipid core surrounded by an amphiphilic coat of protein, phospholipid, and cholesterol. Lipoproteins, which transport lipids between tissues via the bloodstream, are classified by their density as high, low, intermediate, and very low density lipoproteins (HDL, LDL, IDL, and VLDL).

Liposome. A synthetic vesicle bounded by a single lipid bilayer.

Lipoyllysyl arm. An extended structure, consisting of lipoic acid linked to a lysine side chain, that delivers intermediates between active sites in multienzyme complexes such as the pyruvate dehydrogenase complex.

London dispersion forces. The weak attractive forces between electrically neutral molecules in close proximity, which arise from electrostatic interactions among their fluctuating dipoles.

Low-barrier hydrogen bond (LBHB). An unusually short and strong hydrogen bond that forms when the donor and acceptor groups have nearly equal p*K* values so that the hydrogen atom is equally shared between them.

Lung surfactant. The amphipathic protein and lipid mixture that prevents collapse of the lung alveoli (microscopic air spaces) on the expiration of air.

Lyase. An enzyme that catalyzes the elimination of a group to form a double bond.

Lymphocyte. Types of white blood cells that mediate the immune response. Mammalian B lymphocytes develop in the bone marrow, and T lymphocytes in the thymus.

Lysis. The disintegration of cells by rupturing their cell walls.

Lysophospholipid. A glycerophospholipid derivative lacking a fatty acyl group at position C2 that acts as a detergent to disrupt cell membranes.

Lysosome. A membrane-bounded organelle in a eukaryotic cell that contains a battery of hydrolytic enzymes and which functions to digest ingested material and to recycle cell components.

Macronutrient. A nutrient that is required in relatively large amounts, such as proteins, carbohydrates, and fats. See also micronutrient.

Main chain. See backbone.

Major groove. The groove on a DNA double helix onto which the glycosidic bonds of a base pair form an angle of $>180°$. In B-DNA, this groove is wider than the minor groove.

Malaria. A mosquito-borne disease caused by protozoa of the genus Plasmodia, most notably *Plasmodium falciparum,* which reside in red blood cells during much of their life cycle.

Malate–aspartate shuttle. A metabolic circuit that uses the malate and aspartate transporters and the interconversion of malate, oxaloacetate, and aspartate to ferry reducing equivalents into the mitochondrion.

Malignant tumor. A mass of cells that proliferate uncontrollably; a cancer.

Mass spectrometry. A technique for identifying molecules by measuring the mass-to-charge ratios of molecular ions in the gas phase.

Maternal-effect genes. Insect genes whose mRNA or protein products are deposited by the mother in the ovum and which define the polarity of the embryonic body.

Matrix. The gel-like solution of enzymes, substrates, cofactors, and ions in the interior of the mitochondrion.

Mechanism-based inhibitor. A molecule that chemically inactivates an enzyme only after undergoing part or all of its normal catalytic reaction. Also called a suicide substrate.

Mechanosensitive channel. A channel whose opening and closing (gating) is controlled by stimuli such as touch, sound, and changes in osmotic pressure.

Mediated transport. The transmembrane movement of a substance through the action of a specific carrier protein; the opposite of nonmediated transport.

Melting temperature (T_m). The midpoint temperature of the melting curve for the thermal denaturation of a macromolecule.

Membrane-enveloped virus. A virus produced by budding from the surface of a host cell such that the viral particle is surrounded by a membrane derived from the host cell.

Membrane potential ($\Delta\Psi$). The electrical potential difference across a membrane.

Memory B cell. A B cell that can recognize its corresponding antigen and rapidly proliferate to produce specific antibodies weeks to years after the antigen was first encountered.

Mercaptan. A compound containing an —SH group.

Messenger RNA (mRNA). A ribonucleic acid whose sequence is complementary to that of a protein-coding gene in DNA. In the ribosome, mRNA directs the polymerization of amino acids to form a polypeptide with the corresponding sequence.

Metabolic fuel. A molecule that can be oxidized to provide free energy for an organism.

Metabolic syndrome. An obesity-related disorder that includes insulin resistance, hypertension, and atherosclerosis.

Metabolism. The total of all degradative and biosynthetic cellular reactions.

Metabolite. A reactant, intermediate, or product of a metabolic reaction.

Metabolomics. The study of all the metabolites produced by a cell under a given set of conditions, including their concentrations and functions.

Metal chelate affinity chromatography. A procedure in which a molecule bearing metal-chelating groups is separated from a mixture of other molecules by its ability to bind to metal ions attached to a chromatographic matrix.

Metal ion catalysis. A catalytic mechanism that requires the presence of a metal ion to lower the free energy of a reaction's transition state.

Metalloenzyme. An enzyme that contains a tightly bound metal ion cofactor, typically a transition metal ion such as Fe^{2+}, Zn^{2+}, or Mn^{2+}.

Methanogen. An organism that produces CH_4.

Micelle. A globular aggregate of amphiphilic molecules in aqueous solution that are oriented such that polar segments form the surface of the aggregate and the nonpolar segments form a core that is out of contact with the solvent.

Michaelis complex. See ES complex.

Michaelis constant (K_M). For an enzyme that follows the Michaelis–Menten model, $K_M = (k_{-1} + k_2)/k_1$; K_M is equal to the substrate concentration at which the reaction velocity is half-maximal.

Michaelis–Menten equation. A mathematical expression that describes the activity of an enzyme in terms of the substrate concentration ([S]), the enzyme's maximal velocity ($V_{\max}$), and its Michaelis constant (K_M): $v_0 = V_{\max}[S]/(K_M + [S])$.

Micro RNA (miRNA). See short interfering RNA.

Microarray. See DNA microarray.

Microfilament. A 70-Å-diameter cytoskeletal element composed of actin.

Microheterogeneity. The variability in carbohydrate composition in glycoproteins.

Micronutrient. A nutrient that is required in relatively small amounts, including vitamins and minerals. See also macronutrient.

Mineral. An inorganic substance required for metabolic activity, including sodium, potassium, chloride, and calcium. Minerals such as iron, copper, and zinc, which are required in small amounts, are known as trace elements.

Mineralocorticoid. A steroid hormone that regulates the excretion of salt and water by the kidneys.

Minor groove. The groove on a DNA double helix onto which the glycosidic bonds of a base pair form an angle of $<180°$. In B-DNA, this groove is narrower than the major groove.

(–) end. The end of a polymeric filament where growth is slower. See also (+) end.

miRNA. Micro RNA. See short interfering RNA.

Mismatch repair (MMR). A postreplication process, in which mispaired nucleotides are excised and replaced, that distinguishes between the parental (correct) and daughter (incorrect) strands of DNA.

Mitochondria (*sing.* mitochondrion). The double-membrane-enveloped eukaryotic organelles in which aerobic metabolic reactions occur, including those of the citric acid cycle, fatty acid oxidation, and oxidative phosphorylation.

Mitochondrial matrix. See matrix.

Mixed inhibition. A form of enzyme inhibition in which an inhibitor binds to both the enzyme and the enzyme–substrate complex and thereby differently affects K_M and $V_{\max}$. Also called noncompetitive inhibition.

MMR. See mismatch repair.

Moderately repetitive DNA. Segments of hundreds to thousands of base pairs that are present at $<10^6$ copies per haploid genome.

Modification methylase. A bacterial enzyme that methylates a specific sequence of DNA as part of a restriction–modification system.

Molecular chaperone. A protein that binds to unfolded or misfolded proteins so as to promote normal folding and the formation of native quaternary structure. Also known as a heat shock protein (Hsp).

Molecular cloning. See recombinant DNA technology.

Molecular sieve chromatography. See gel filtration chromatography.

Molecular weight. See M_r.

Molecularity. The number of molecules that participate in an elementary chemical reaction.

Molten globule. A collapsed but conformationally mobile intermediate in protein folding that has much of the native protein's secondary structure but little of its tertiary structure.

Monocistronic mRNA. The RNA transcript of a single gene.

Monoclonal antibody. A single type of antibody molecule produced by a clone of hybridoma cells, which are derived by the fusion of a myeloma cell with a lymphocyte producing that antibody.

Monomer. (1) A structural unit from which a polymer is built up. (2) A single subunit or protomer of a multisubunit protein.

Monoprotic acid. An acid that can donate only one proton.

Monosaccharide. A carbohydrate consisting of a single saccharide (sugar).

Morphogen. A substance whose distribution in an embryo directs, in part, the embryo's developmental pattern.

Motif. See supersecondary structure.

Motor protein. An intracellular protein that couples the free energy of ATP hydrolysis to molecular movement relative to another protein that often acts as a track for the linear movement of the motor protein.

M_r. Relative molecular mass. A dimensionless quantity that is defined as the ratio of the mass of a particle to 1/12th the mass of a ^{12}C atom. Also known as molecular weight. It is numerically equal to the grams/mole of a compound.

mRNA. See messenger RNA.

Multienzyme complex. A group of noncovalently associated enzymes that catalyze two or more sequential steps in a metabolic pathway.

Multiple myeloma. A disease in which a cancerous B cell proliferates and produces massive quantities of a single antibody known as a myeloma protein.

Multisubunit protein. A protein consisting of more than one polypeptide chain (subunit).

Mutagen. An agent that induces a mutation in an organism.

Mutase. An enzyme that catalyzes the transfer of a functional group from one position to another on a molecule.

Mutation. A heritable alteration in an organism's genetic material.

Myocardial infarction. The death of heart tissue caused by the loss of blood supply (a heart attack).

Myofibril. The bundle of fibers that are arranged in register in striated muscle cells.

Myristoylation. The attachment of a myristoyl group to a protein to form a lipid-linked protein.

N-end rule. The correlation between the identity of a polypeptide's N-terminal residue and its half-life in the cell.

***N*-glycosidic bond.** See glycosidic bond.

***N*-linked oligosaccharide.** An oligosaccharide linked via a glycosidic bond to the amide group of a protein Asn residue in the sequence Asn-X-Ser/Thr.

N-terminus. See amino terminus.

Native structure. The fully folded conformation of a macromolecule.

Natural selection. The evolutionary process by which the continued existence of a replicating entity depends on its ability to survive and reproduce under the existing conditions.

ncRNA. See noncoding RNA.

NDP. A ribonucleoside diphosphate.

Near-equilibrium reaction. A reaction whose ΔG value is close to zero, so that it can operate in either direction depending on the substrate and product concentrations.

Necrosis. Trauma-induced cell death that results in the unregulated disintegration of the cell and the release of proinflammatory substances. See also apoptosis.

Negative cooperativity. See cooperative binding.

NER. See nucleotide excision repair.

Nernst equation. An expression of the relationship between reduction potential difference ($\Delta\mathscr{E}$) and the concentrations of the electron donors and acceptors (A, B): $\Delta\mathscr{E} = \Delta\mathscr{E}^\circ - RT/n\mathscr{F} \ln ([A_{red}][B_{ox}]/[A_{ox}][B_{red}])$.

Neurotransmitter. A substance released by a nerve cell that alters the activity of another nerve cell.

Neutral drift. Evolutionary changes that become fixed at random rather than through natural selection.

Neutral solution. A solution whose pH is equal to 7.0 ($[H^+] = 10^{-7}$ M).

NHEJ. See nonhomologous end-joining.

Nick translation. The progressive movement of a single-strand break (nick) in duplex DNA through the coordinated actions of a $5' \rightarrow 3'$ exonuclease function that removes residues from the 5′ side of the break and a polymerase function that adds residues to the 3′ side.

Nitrogen assimilation. The incorporation of fixed nitrogen (e.g., ammonia) into a biological molecule such as an amino acid.

Nitrogen cycle. The series of reactions in which N_2 and ammonia are interconverted, often via nitrate and nitrite, by various organisms.

Nitrogen fixation. The process by which atmospheric N_2 is converted to a biologically useful form such as NH_3.

NMD. See nonsense-mediated decay.

NMR. See nuclear magnetic resonance.

Noncoding RNA (ncRNA). An RNA molecule, such as rRNA, tRNA, or another small RNA, that is not translated.

Noncoding strand. See antisense strand.

Noncompetitive inhibition. (1) A synonym for mixed inhibition. (2) A special case of mixed inhibition in which the inhibitor binds the enzyme and enzyme–substrate complex with equal affinities ($K_I = K_I'$), thereby reducing the apparent value of V_{max} but leaving K_M unchanged.

Noncooperative binding. A situation in which binding of a ligand to a macromolecule does not affect the affinities of other binding sites on the same molecule.

Nonessential amino acid. An amino acid that animals can synthesize from common intermediates.

Nonhomologous end-joining (NHEJ). An error-prone pathway for repairing DNA with double-strand breaks.

Nonmediated transport. The transmembrane movement of a substance through simple diffusion; the opposite of mediated transport.

Nonpolar molecule. A molecule that lacks a group with a permanent dipole.

Nonreceptor tyrosine kinase. An intracellular tyrosine kinase that is indirectly activated by ligand binding to a receptor.

Nonrepetitive structure. A segment of a polymer in which the backbone has an ordered arrangement that is not characterized by a repeating conformation.

Nonsense codon. See Stop codon.

Nonsense-mediated decay (NMD). The degradation of an mRNA that contains a premature Stop codon.

Nonsense mutation. A mutation that converts a codon that specifies an amino acid to a Stop codon, thereby causing the premature termination of translation.

Nonsense suppressor tRNA. A mutated tRNA that recognizes a Stop codon so that its attached aminoacyl group is appended to the polypeptide chain; it mitigates the effect of a nonsense mutation in a structural gene.

Northern blotting. A procedure for identifying an RNA containing a particular base sequence through its ability to hybridize with a complementary single-stranded segment of DNA or RNA. See also Southern blotting.

nt. Nucleotide.

NTP. A ribonucleoside triphosphate.

Nuclear magnetic resonance (NMR). A spectroscopic method for characterizing atomic and molecular properties based on the signals emitted by radiofrequency-excited atomic nuclei in a magnetic field. It can be used to determine the three-dimensional molecular structure of a protein or nucleic acid.

Nuclease. An enzyme that hydrolytically degrades nucleic acids.

Nucleic acid. A polymer of nucleotide residues. The major nucleic acids are deoxyribonucleic acid (DNA) and ribonucleic acid (RNA). Also known as a polynucleotide.

Nucleolus (*pl.* nucleoli). The dark-staining region of the eukaryotic nucleus, where ribosomes are assembled.

Nucleophile. A group that contains unshared electron pairs that readily reacts with an electron-deficient group (electrophile). A nucleophile (nucleus-lover) reacts with an electrophile (electron-lover).

Nucleoside. A compound consisting of a nitrogenous base and a five-carbon sugar (ribose or deoxyribose) in *N*-glycosidic linkage.

Nucleosome. The complex of a histone octamer and ~200 bp of DNA that forms the lowest level of DNA organization in the eukaryotic chromosome.

Nucleosome core particle. The complex of histones and ~146 bp of DNA that forms a compact disk-shaped particle in which the DNA is wound in ~2 helical turns around the outside of the histone octamer.

Nucleotide. A compound consisting of a nucleoside esterified to one or more phosphate groups. Nucleotides are the monomeric units of nucleic acids.

Nucleotide excision repair (NER). A multistep process in which a portion of DNA containing a lesion is excised and replaced by normal DNA.

Nucleotide sugar. A saccharide linked to a nucleotide by a phosphate ester bond, the cleavage of which drives the formation of a glycosidic bond.

Nucleus. The membrane-enveloped organelle in which the eukaryotic cell's genetic material is located.

Nutrition. The intake and utilization of food as a source of raw materials and free energy.

***O*-glycosidic bond.** See glycosidic bond.

***O*-linked oligosaccharide.** An oligosaccharide linked via a glycosidic bond to the hydroxyl group of a protein Ser or Thr side chain.

Oil. A mixture of triacylglycerols that is liquid at room temperature.

Okazaki fragments. The short segments of DNA formed in the discontinuous lagging-strand synthesis of DNA.

Oligomer. (1) A short polymer consisting of a few linked monomer units. (2) A protein consisting of a few protomers (subunits).

Oligopeptide. A polypeptide containing a few amino acid residues.

Oligosaccharide. A polymeric carbohydrate containing a few monosaccharide residues.

Oligosaccharide processing. The cellular pathway in which a newly glycosylated protein undergoes the enzymatic removal and addition of monosaccharide residues.

Oncogene. A mutant version of a normal gene (a proto-oncogene), which may be acquired through viral infection; it interferes with the mechanisms that normally control cell growth and differentiation and thereby contributes to uncontrolled proliferation (cancer).

Open complex. The separated DNA strands at the transcription start site.

Open reading frame (ORF). A portion of the genome that potentially codes for a protein. This sequence of nucleotides begins with a Start codon, ends with a Stop codon, contains no internal Stop codons, is flanked by the proper control sequences, and exhibits the same codon-usage preference as other genes in the organism.

Open system. A thermodynamic system that can exchange matter and energy with its surroundings.

Operator. A DNA sequence at or near the transcription start site of a gene, to which a repressor binds so as to control transcription of the gene.

Operon. A prokaryotic genetic unit that consists of several genes with related functions that are transcribed as a single mRNA molecule.

Optical activity. The ability of a molecule to rotate the plane of polarized light.

Optical density. See absorbance.

Ordered mechanism. A sequential reaction with a compulsory order of substrate addition to the enzyme.

ORF. See open reading frame.

Organelle. A differentiated structure within a eukaryotic cell, such as a mitochondrion, ribosome, or lysosome, that performs specific functions.

Organic compound. A compound that contains the element carbon.

Orphan gene. A gene, usually identified through genome sequencing, with no known function.

Orthologous genes. Related genes in different species that have the same function.

Orthophosphate cleavage. The hydrolysis of ATP that yields ADP + P_i.

Osmosis. The movement of solvent across a semipermeable membrane from a region of low solute concentration to a region of high solute concentration.

Osmotic pressure. The pressure that must be applied to a solution containing a high concentration of solute to prevent the net flow of solvent across a semipermeable membrane separating it from a solution with a lower concentration of solute. The osmotic pressure of a 1 M solution of any solute separated from solvent by a semipermeable membrane is ideally 22.4 atm.

Overproducer. A genetically engineered organism that produces massive quantities of a foreign DNA gene product.

Oxidation. The loss of electrons. Oxidation of a substance is accompanied by the reduction of another substance.

Oxidative phosphorylation. The process by which the free energy obtained from the oxidation of metabolic fuels is used to generate ATP from ADP + P_i.

Oxidizing agent. A substance that can accept electrons from other substances, thereby oxidizing them and becoming reduced.

Oxidoreductase. An enzyme that catalyzes an oxidation–reduction reaction.

Oxonium ion. A resonance-stabilized carbocation such as occurs during the lysozyme-catalyzed hydrolysis of a glycoside.

Oxyanion hole. A structure in an enzyme active site that preferentially binds and thereby stabilizes the oxyanionic tetrahedral transition state of the reaction.

Oxygen debt. The postexertion continued elevation in O_2 consumption that is required to replenish the ATP consumed by the liver during operation of the Cori cycle.

Oxygenation. The binding of molecular oxygen, e.g., to a heme group.

P site. See peptidyl site.

P/O ratio. The ratio of the number of molecules of ATP synthesized from ADP + P_i to the number of atoms of oxygen reduced.

PAGE. Polyacrylamide gel electrophoresis. See gel electrophoresis.

Pair-rule genes. See segmentation genes.

Palindrome. A word or phrase or a nucleotide sequence that reads the same forward or backward.

Palmitoylation. The attachment of a palmitoyl group to a protein to form a lipid-linked protein.

Paralogous genes. Related genes in the same organism derived from a gene duplication event.

Partial oxygen pressure (pO_2). The concentration of gaseous O_2 in units of pressure (e.g., torr).

Passive-mediated transport. The thermodynamically spontaneous carrier-mediated transmembrane movement of a substance from high to low concentration. Also called facilitated diffusion.

Pasteur effect. The greatly increased sugar consumption of yeast grown under anaerobic conditions compared to that of yeast grown under aerobic conditions.

Pathogen. A disease-causing microorganism.

PCR. See polymerase chain reaction.

Pellagra. The human disease resulting from a deficiency of the vitamin niacin (nicotinic acid), a precursor of the nicotinamide-containing cofactors NAD^+ and $NADP^+$.

Pentose phosphate pathway. A pathway for glucose degradation that yields ribose-5-phosphate and NADPH. Also called the hexose monophosphate shunt.

Peptidase. An enzyme that hydrolyzes peptide bonds. Also called a protease.

Peptide. A polypeptide of less than about 40 residues.

Peptide bond. An amide linkage between the α-amino group of one amino acid and the α-carboxylate group of another. Peptide bonds link the amino acid residues in a polypeptide.

Peptide group. The planar —CO—NH— group that encompasses the peptide bond between amino acid residues in a polypeptide.

Peptidoglycans. The cross-linked bag-shaped macromolecules consisting of polysaccharide and polypeptide chains that form bacterial cell walls.

Peptidyl site (P site). The ribosomal site that accommodates a tRNA with an attached peptidyl group during protein synthesis.

Peptidyl transferase. The catalytic activity of the ribosome, which carries out peptide bond synthesis by promoting the nucleophilic attack of an incoming aminoacyl group on the growing peptidyl group.

Peptidyl–tRNA. The covalent complex between a tRNA molecule and a growing polypeptide chain during protein synthesis.

Peripheral protein. A protein that is weakly associated with the surface of a biological membrane. Also called an extrinsic protein.

Periplasmic compartment. The space between the cell wall and the outer membrane of gram-negative bacteria.

Peroxisome. A eukaryotic organelle with specialized oxidative functions.

Perutz mechanism. A model for the cooperative binding of oxygen to hemoglobin, in which O_2 binding causes the protein to shift conformation from the deoxy (T state) to the oxy (R state).

PFGE. See pulsed-field gel electrophoresis.

p_{50}. For a gaseous ligand, the ligand concentration, in units of pressure (e.g., torr), at which a binding protein such as hemoglobin is half-saturated with ligand.

pH. A quantity used to express the acidity of a solution, equivalent to $-\log [H^+]$.

Phage. See bacteriophage.

Pharmacogenomics. The study of how an individual's genetic makeup influences a drug's effectiveness.

Pharmacokinetics. The behavior of a drug in the body over time, including its tissue distribution and rate of elimination or degradation.

Phenotype. An organism's physical characteristics.

ϕ (phi). The torsion angle that describes the rotation around the C_α—N bond in a peptide group; the dihedral angle made by the bonds connecting the C—N—C_α—C atoms in a peptide chain.

Phosphagen. A phosphoguanidine whose phosphoryl group-transfer potential is greater than that of ATP; these compounds can therefore phosphorylate ADP to generate ATP.

Phosphatase. An enzyme that hydrolyzes phosphoryl ester groups. See also protein phosphatase.

Phosphatidic acid. The simplest glycerophospholipid, consisting of two fatty acyl groups attached to glycerol-3-phosphate.

Phosphodiester bond. The linkage in which a phosphate group is esterified to two alcohol groups, e.g., the phosphate groups that join the adjacent nucleoside residues in a polynucleotide.

Phosphoglyceride. See glycerophospholipid.

Phosphoinositide pathway. A signal transduction pathway in which hormone binding to a cell-surface receptor induces phospholipase C to catalyze the hydrolysis of phosphatidylinositol-4,5-bisphosphate (PIP_2), which yields inositol-1,4,5-trisphosphate (IP_3) and 1,2-diacylglycerol (DAG), both of which are second messengers.

Phospholipase. An enzyme that hydrolyzes one or more bonds of a glycerophospholipid.

Phosphoprotein phosphatase. See protein phosphatase.

Phosphorolysis. The cleavage of a chemical bond by the substitution of a phosphate group rather than water.

Phosphoryl group. A portion of a molecule with the formula $—PO_3H_2$.

Phosphoryl group-transfer potential. A measure of the tendency of a phosphorylated compound to transfer its phosphoryl group to water; the opposite of its free energy of hydrolysis.

Photoautotroph. An autotrophic organism that obtains energy from sunlight.

Photon. A packet of light energy. See also Planck's law.

Photooxidation. A mode of decay of an excited molecule, in which oxidation occurs through the transfer of an electron to an acceptor molecule.

Photophosphorylation. The synthesis of ATP from ADP + P_i coupled to the dissipation of a proton gradient that has been generated through light-driven electron transport.

Photoreactivation. The conversion of pyrimidine dimers, a form of DNA damage, to monomers using light energy.

Photorespiration. The consumption of O_2 and evolution of CO_2 by plants (a dissipation of the products of photosynthesis), resulting from the competition between O_2 and CO_2 for binding to ribulose bisphosphate carboxylase.

Photosynthesis. The reduction of CO_2 to $(CH_2O)_n$ in plants and bacteria as driven by light energy.

Photosynthetic reaction center. The pigment-containing protein complex that undergoes photooxidation during the light reactions of photosynthesis.

Phylogenetic tree. A reconstruction of the probable paths of evolution of a set of related organisms, usually based on sequence variations in homologous proteins and nucleic acids; a sort of family tree.

Phylogeny. The study of the evolutionary relationships among organisms.

p*I*. See isoelectric point.

PIC. See preinitiation complex.

Ping Pong reaction. A group-transfer reaction in which one or more products are released before all substrates have bound to the enzyme.

Pitch. The distance a helix rises along its axis per turn; 5.4 Å for an α helix, 34 Å for B-DNA.

p*K*. A quantity used to express the tendency for an acid to donate a proton (dissociate); equal to $-\log K$, where K is the acid's dissociation constant. Also known as pK_a.

Planck's law. An expression for the energy (E) of a photon: $E = hc/\lambda = h\nu$, where c is the speed of light, λ is its wavelength, ν is its frequency, and h is Planck's constant (6.626×10^{-34} J · s).

Plaque. (1) A region of lysed cells on a "lawn" of cultured bacteria, which indicates the presence of infectious bacteriophage. (2) A deposit of insoluble material in an animal's tissues.

Plasmalogen. A glycerophospholipid in which the C1 substituent is attached via an ether rather than an ester linkage.

Plasmid. A small circular DNA molecule that autonomously replicates in a bacterial or yeast cell. Plasmids are often modified for use as cloning vectors.

PLP. Pyridoxal-5′-phosphate, a cofactor used mainly in transamination reactions.

(+) end. The end of a polymeric filament where growth is faster. See also (−) end.

pmf. See protonmotive force.

Point mutation. The substitution of one base for another in DNA. Point mutations may arise from mispairing during DNA replication or from chemical alterations of existing bases.

Polar molecule. A molecule with one or more groups that have permanent dipoles.

Polarimeter. A device that measures the optical rotation of a solution. It can be used to determine the optical activity of a substance.

Poly(A) tail. The sequence of adenylate residues that is posttranscriptionally appended to the 3′ end of eukaryotic mRNAs.

Polyacrylamide gel electrophoresis (PAGE). See gel electrophoresis.

Polycistronic mRNA. The RNA transcript of a bacterial operon. It encodes several polypeptides.

Polycythemia. A condition characterized by an increased number of erythrocytes.

Polyelectrolyte. A macromolecule that bears multiple charged groups.

Polymer. A molecule consisting of numerous smaller units that are linked together in an organized manner. Polymers may be linear or branched and may contain one or more kinds of structural units (monomers).

Polymerase. An enzyme that catalyzes the addition of nucleotide residues to a polynucleotide through nucleophilic attack of the chain's 3′-OH group on the α-phosphoryl group of the incoming nucleoside triphosphate. DNA- and RNA-directed polymerases require a template molecule with which the incoming nucleotide must base pair.

Polymerase chain reaction (PCR). A procedure for amplifying a segment of DNA by repeated rounds of replication centered between primers that hybridize with the two ends of the DNA segment of interest.

Polymorphism. A variation in DNA or amino acid sequences between individuals.

Polynucleotide. See nucleic acid.

Polypeptide. A polymer consisting of amino acid residues linked in linear fashion by peptide bonds.

Polyprotic acid. A substance with more than one proton that can be donated. Polyprotic acids have multiple ionization states.

Polyribosome. An mRNA transcript bearing multiple ribosomes in the process of carrying out translation. Also called a polysome.

Polysaccharide. A polymeric carbohydrate containing multiple monosaccharide residues. Also called a glycan.

Polysome. See polyribosome.

Polyunsaturated fatty acid. A fatty acid that contains more than one double bond in its hydrocarbon chain.

Porphyrias. Genetic defects in heme biosynthesis that result in the accumulation of porphyrins.

Positive cooperativity. See cooperative binding.

Posttranscriptional modification. The removal or addition of nucleotide residues or their modification following the synthesis of RNA.

Posttranslational processing. The removal or derivatization of amino acid residues following their incorporation into a polypeptide, or the cleavage of a polypeptide.

$p\mathrm{O}_2$. See partial oxygen pressure.

pre-mRNA. See heterogeneous nuclear RNA.

pre-rRNA. An immature rRNA transcript.

pre-tRNA. An immature tRNA transcript.

Prebiotic era. The period of time between the formation of the earth ~4.6 billion years ago and the appearance of living organisms at least 3.5 billion years ago.

Precursor. The entity that gives rise, through a process such as evolution or chemical reaction, to another entity.

Preinitiation complex (PIC). The assembly of eukaryotic transcription factors bound to DNA that renders the DNA available for transcription by RNA polymerase.

Prenylation. The attachment of an isoprenoid group to a protein to form a lipid-linked protein.

Preproprotein. A protein bearing both a signal peptide (preprotein) and a propeptide (proprotein).

Preprotein. A protein bearing a signal peptide that is cleaved off following the translocation of the protein through the endoplasmic reticulum membrane.

Pribnow box. The prokaryotic promoter element with the consensus sequence TATAAT that is centered at around the −10 position relative to the transcription start site.

Primary active transport. Transmembrane transport that is driven by the exergonic hydrolysis of ATP.

Primary structure. The sequence of residues in a polymer.

Primary transcript. The immediate product of transcription, which may be modified before becoming fully functional.

Primase. The RNA polymerase responsible for synthesizing the RNA segment that primes DNA synthesis.

Primer. An oligonucleotide that serves as a starting point for additional polymerization reactions catalyzed by DNA polymerase to form a polynucleotide. A primer base-pairs with a segment of a template polynucleotide strand so as to form a short double-stranded segment that can then be extended through template-directed polymerization.

Primosome. The protein complex that synthesizes the RNA primers in DNA synthesis.

Prion. A protein whose misfolding causes it to aggregate and produce the neurodegenerative symptoms of transmissible spongiform encephalopathies and related diseases. Misfolded prions induce properly folded prions to misfold and thereby act as infectious agents.

Probe. A labeled single-stranded DNA or RNA segment that can hybridize with a DNA or RNA of interest in a screening procedure.

Processive enzyme. An enzyme that catalyzes many rounds of a polymerization reaction without dissociating from the growing polymer.

Prochirality. A property of some nonchiral molecules such that they contain a group whose substitution by another group yields a chiral molecule.

Product inhibition. A case of enzyme inhibition in which product that accumulates during the course of the reaction competes with substrate for binding to the active site.

Proenzyme. An inactive precursor of an enzyme.

Prokaryote. A unicellular organism that lacks a membrane-bounded nucleus. All bacteria are prokaryotes.

Promoter. The DNA sequence at which RNA polymerase binds to initiate transcription.

Proofreading. An additional catalytic activity of an enzyme, which acts to correct errors made by the primary enzymatic activity.

Propeptide. A polypeptide segment of an immature protein that must be proteolytically excised to activate the protein.

Proprotein. The inactive precursor of a protein that, to become fully active, must undergo limited proteolysis to excise its propeptide.

Prostaglandin. See eicosanoids.

Prosthetic group. A cofactor that is permanently (often covalently) associated with an enzyme.

Protease. See peptidase.

Proteasome. A multiprotein complex with a hollow cylindrical core in which cellular proteins are degraded to peptides (recycled) in an ATP-dependent process.

Protein. A macromolecule that consists of one or more polypeptide chains.

Protein kinase. An enzyme that catalyzes the transfer of a phosphoryl group from ATP to the OH group of a protein Ser, Thr, or Tyr residue.

Protein phosphatase. An enzyme that catalyzes the hydrolytic excision of phosphoryl groups from proteins.

Proteoglycan. An extracellular aggregate of protein and glycosaminoglycan.

Proteomics. The study of all of a cell's proteins, including their quantitation, localization, modifications, interactions, and activities.

Proto-oncogene. The normal cellular analog of an oncogene; the mutation of a proto-oncogene may yield an oncogene that contributes to uncontrolled cell proliferation (cancer).

Protomer. One of two or more identical units of an oligomeric protein. A protomer may consist of one or more polypeptide chains.

Proton jumping. The sequential transfer of protons between hydrogen-bonded water molecules. Proton jumping is largely responsible for the rapid rate at which hydronium and hydroxyl ions appear to move through an aqueous solution.

Proton wire. A group of hydrogen-bonded protein groups and water molecules that serves as a conduit for protons to traverse a membrane via proton jumping.

Protonmotive force (pmf). The free energy of the electrochemical proton gradient that forms during electron transport.

Proximity effect. A catalytic mechanism in which a reaction's free energy of activation is reduced by the prior bringing together of its reacting groups.

PRPP. 5-Phosphoribosyl-α-pyrophosphate, an "activated" form of ribose that serves as a precursor in the synthesis of histidine, tyrosine, and purine and pyrimidine nucleotides.

Pseudo-first-order reaction. A bimolecular reaction whose rate appears to be proportional to the concentration of only a single reactant because the second reactant is present in large excess.

Pseudogene. An unexpressed sequence of DNA that is apparently the defective remnant of a duplicated gene.

ψ (psi). The torsion angle that describes the rotational position around the C_α—C bond in a peptide group; the dihedral angle made by the bonds connecting the N—C_α—C—N atoms in a peptide chain.

PSI. Photosystem I, the protein complex that reduces $NADP^+$ during the light reactions of photosynthesis.

PSII. Photosystem II, the protein complex that oxidizes H_2O to O_2 during the light reactions of photosynthesis.

Pulse-labeling. A technique for tracing metabolic fates, in which cells or a reacting system are exposed briefly to high levels of a labeled compound.

Pulsed-field gel electrophoresis (PFGE). An electrophoretic procedure in which electrodes arrayed around the periphery of an agarose slab gel are sequentially pulsed so that DNA molecules must continually reorient, thereby allowing very large molecules to be separated by size.

Purine nucleotide cycle. The conversion of aspartate to fumarate, which replenishes citric acid cycle intermediates, through the deamination of AMP to IMP.

Purines. Derivatives of the compound purine, a planar aromatic, heterocyclic compound. Adenine and guanine, two of the nitrogenous bases of nucleotides, are purines.

Pyranose. A sugar with a six-membered ring.

Pyrimidine dimer. The cyclobutane-containing structure resulting from UV irradiation of adjacent thymine or cytosine residues in DNA.

Pyrimidines. Derivatives of the compound pyrimidine, a planar aromatic, heterocyclic compound. Cytosine, uracil, and thymine, three of the nitrogenous bases of nucleotides, are pyrimidines.

Pyrophosphate cleavage. The hydrolysis of ATP that yields $AMP + PP_i$.

Pyrophosphoryl group. See diphosphoryl group.

q. The thermodynamic term for heat absorbed.

Q cycle. The cyclic flow of electrons accompanied by the transport of protons, involving a stable semiquinone intermediate of CoQ in Complex III of mitochondrial electron transport and in photosynthetic electron transport.

q_P. The thermodynamic term for heat absorbed at constant pressure.

Quantum (*pl.* quanta). A packet of energy. See also photon.

Quantum yield. The ratio of molecules reacted to photons absorbed in a light-induced reaction.

Quaternary structure. The spatial arrangement of a macromolecule's individual subunits.

R group. A symbol for a variable portion of an organic molecule, such as the side chain of an amino acid.

R state. One of two conformations of an allosteric protein; the other is the T state. The R state is usually the catalytically more active state.

Racemic mixture. A sample of a compound in which both enantiomers are present in equal amounts.

Radioimmunoassay (RIA). A technique for measuring the concentration of a molecule based on its ability to block the binding of a small amount of the radioactively labeled molecule to its corresponding antibody.

Radionuclide. A radioactive isotope.

Ramachandran diagram. A plot of ϕ versus ψ that indicates the sterically allowed conformations of a polypeptide.

Randle cycle. See glucose–fatty acid cycle.

Random coil. A totally disordered and rapidly fluctuating polymer conformation.

Random mechanism. A sequential reaction without a compulsory order of substrate addition to the enzyme.

Rate constant (k). The proportionality constant between the velocity of a chemical reaction and the concentration(s) of the reactant(s).

Rate-determining step. The step with the highest transition state free energy in a multistep reaction; the slowest step.

Rate enhancement. The ratio of the rates of a catalyzed to an uncatalyzed chemical reaction.

Rate equation. A mathematical expression for the time-dependent progress of a reaction as a function of reactant concentration.

Rational drug design. See structure-based drug design.

Reaction coordinate. The path of minimum free energy for the progress of a reaction.

Reaction order. The sum of the exponents of the concentration terms that appear in a reaction's rate equation.

Reading frame. The grouping of nucleotides in sets of three whose sequence corresponds to a polypeptide sequence.

Receptor. A binding protein that is specific for its ligand and elicits a discrete biochemical effect when its ligand is bound.

Receptor-mediated endocytosis. A process in which an extracellular ligand binds to a specific cell-surface receptor and the resulting receptor–ligand complex is engulfed by the cell.

Receptor tyrosine kinase. A hormone receptor whose intracellular domain is activated, as a result of hormone binding, to phosphorylate tyrosine residues on other proteins and/or on other subunits of the same receptor.

Recombinant. A DNA molecule constructed by combining DNA from different sources. Also called a chimera.

Recombinant DNA technology. The isolation, amplification, and modification of specific DNA sequences. Also called molecular cloning or genetic engineering.

Recombination. The exchange of polynucleotide strands between separate DNA segments. Homologous recombination occurs between DNA segments with extensive homology, whereas site-specific recombination occurs between two short, specific DNA sequences.

Recombination repair. A mechanism for repairing damaged DNA, in which recombination exchanges a portion of a damaged strand for a homologous segment that can then serve as a template for the replacement of the damaged bases.

Redox center. A group that can undergo an oxidation–reduction reaction.

Redox couple. See conjugate redox pair.

Reducing agent. A substance that can donate electrons, thereby reducing another substance and becoming oxidized.

Reducing equivalent. A term used to describe the number of electrons that are transferred from one molecule to another during a redox reaction.

Reducing sugar. A saccharide bearing an anomeric carbon that has not formed a glycosidic bond and can therefore reduce mild oxidizing agents.

Reduction. The gain of electrons. Reduction of a substance is accompanied by the oxidation of another substance.

Reduction potential ($\mathcal{E}$). A measure of the tendency of a substance to gain electrons.

Reductive pentose phosphate cycle. See Calvin cycle.

Regular secondary structure. A segment of a polymer in which the backbone adopts a regularly repeating conformation.

Release factor. A protein that recognizes a Stop codon and thereby helps induce ribosomes to terminate polypeptide synthesis.

Renaturation. The refolding of a denatured macromolecule so as to regain its native conformation.

Repetitive DNA. Stretches of DNA of up to several thousand bases that occur in multiple copies in an organism's genome; they are often arranged in tandem.

Replica plating. The transfer of yeast colonies, bacterial colonies, or phage plaques from a culture plate to another culture plate, a membrane, or a filter in a manner that preserves the distribution of the cells on the original plate.

Replication. The process of making an identical copy of a DNA molecule. During DNA replication, the parental polynucleotide strands separate so that each can direct the synthesis of a complementary daughter strand, resulting in two complete DNA double helices.

Replication fork. The branch point in a replicating DNA molecule at which the two strands of the parental molecule are separated and serve as templates for the synthesis of the daughter strands.

Replicon. A unit of eukaryotic DNA that is replicated from one replication origin.

Replisome. The DNA polymerase–containing protein assembly that catalyzes the synthesis of both the leading and lagging strands of DNA at the replication fork.

Repolarization. The recovery of membrane potential that occurs during electrical signaling in cells such as neurons.

Repressor. A protein that binds at or near a gene so as to prevent its transcription.

RER. See rough endoplasmic reticulum.

Residue. A term for a monomeric unit of a polymer.

Resonance energy transfer. See exciton transfer.

Respiratory distress syndrome. Difficulty in breathing in prematurely born infants, caused by alveolar collapse resulting from insufficient synthesis of lung surfactant.

Restriction endonuclease. A bacterial enzyme that recognizes a specific DNA sequence and cleaves the DNA as part of a restriction–modification system.

Restriction–modification system. A matched pair of bacterial enzymes that recognize a specific DNA sequence: a modification methylase that methylates bases in that sequence, and a restriction endonuclease that cleaves the DNA if it has not been methylated in that sequence. It is a defensive system that eliminates foreign (e.g., viral) DNA.

Reticulocyte. An immature red blood cell, which actively synthesizes hemoglobin.

Retrotransposon. A transposon whose sequence and mechanism of transposition suggest that it arose from a retrovirus.

Retrovirus. A virus whose genetic material is RNA that must be reverse-transcribed to double-stranded DNA during host cell infection.

Reverse transcriptase. A DNA polymerase that uses RNA as its template.

Reverse turn. A polypeptide conformation in which the chain makes an abrupt reversal in direction; usually consisting of four successive residues. Also called a β bend.

Rho factor. A prokaryotic helicase that separates DNA and RNA to promote transcription termination.

RIA. See radioimmunoassay.

Ribonucleic acid. See RNA.

Ribonucleoprotein. A complex of protein and RNA.

Ribonucleotide. A nucleotide in which the pentose is ribose.

Ribosomal RNA (rRNA). The RNA molecules that constitute the bulk of the ribosome, the site of polypeptide synthesis. rRNA provides structural scaffolding for the ribosome and catalyzes peptide bond formation.

Ribosome. The organelle that synthesizes polypeptides under the direction of mRNA. It consists of around two-thirds RNA and one-third protein.

Riboswitch. An mRNA structure that regulates gene expression through alterations in its structure triggered by the presence of the metabolite that is synthesized by the encoded protein.

Ribozyme. An RNA molecule that has catalytic activity.

Rickets. The vitamin D-deficiency disease in children that is characterized by stunted growth and deformed bones.

Rigor mortis. The stiffening of muscles after death.

RNA. Ribonucleic acid. A polymer of ribonucleotides. The major forms of RNA include messenger RNA (mRNA), transfer RNA (tRNA), and ribosomal RNA (rRNA).

RNA editing. The posttranscriptional insertion, deletion, or alteration of bases in mRNA.

RNA interference (RNAi). A form of posttranscriptional gene regulation in which a short double-stranded RNA segment triggers the degradation of the homologous mRNA molecule.

RNAi. See RNA interference.

RNAP. RNA polymerase, the enzyme that synthesizes RNA using a DNA template.

Rossmann fold. See dinucleotide binding fold.

Rotational symmetry. A type of symmetry in which the asymmetric units of a symmetric object can be brought into coincidence through rotation.

Rough endoplasmic reticulum (RER). That portion of the endoplasmic reticulum associated with ribosomes; it is the site of synthesis of membrane proteins and proteins destined for secretion or residence in certain organelles.

rRNA. See ribosomal RNA.

***RS* system.** See Cahn–Ingold–Prelog system.

***S*.** See entropy.

S. Svedberg, a unit for the sedimentation coefficient, equivalent to 10^{-13} s.

Saccharide. See carbohydrate.

Salt bridge. See ion pair.

Salting in. The increase in solubility of a protein (or other molecule) with increasing (low) salt concentration.

Salting out. The decrease in solubility of a protein (or other molecule) with increasing (high) salt concentration.

Salvage pathway. A metabolic pathway for converting free purines and pyrimidines to their nucleotide forms.

SAM. *S*-Adenosylmethionine, a nucleotide cofactor that functions mostly as a methyl group donor. Also called AdoMet.

Sarcomere. The repeating unit of a myofibril, consisting of thin and thick filaments that slide past each other during muscle contraction.

Saturated fatty acid. A fatty acid that does not contain any double bonds in its hydrocarbon chain.

Saturation. The state in which all of a macromolecule's ligand-binding sites are occupied by ligand. See also enzyme saturation and saturated fatty acid.

Schiff base. An imine that forms between an amine and an aldehyde or ketone.

SCID. See severe combined immunodeficiency disease.

Scrapie. See transmissible spongiform encephalopathy.

Screening. A technique for identifying clones that contain a desired gene.

Scurvy. A disease caused by vitamin C (ascorbic acid) deficiency, which results in inadequate formation of 4-hydroxyprolyl residues in collagen, thereby reducing the collagen's stability.

SDS-PAGE. Polyacrylamide gel electrophoresis (PAGE) in the presence of the detergent sodium dodecyl sulfate (SDS), which denatures and imparts a uniform charge density to polypeptides and thereby permits them to be fractionated on the basis of size rather than inherent charge.

Second messenger. An intracellular ion or molecule that acts as a signal for an extracellular event such as ligand binding to a cell-surface receptor.

Second-order reaction. A reaction whose rate is proportional to the square of the concentration of one reactant or to the product of the concentrations of two reactants.

Secondary active transport. Transmembrane transport that is driven by the energy stored in an electrochemical gradient, which itself is generated utilizing the free energy of ATP hydrolysis or electron transport.

Secondary structure. The local spatial arrangement of a polymer's backbone atoms without regard to the conformations of its substituent side chains. α helices and β sheets are common secondary structural elements of proteins.

Secretory pathway. The series of steps in which an integral membrane or secretory protein is recognized by the signal recognition particle as it emerges from the ribosome, is translocated across the endoplasmic reticulum membrane via a translocon, and is cleaved by a signal peptidase.

Sedimentation coefficient. A measure of a particle's rate of sedimentation in an ultracentrifuge, usually expressed in Svedberg units (S).

Segment polarity genes. See segmentation genes.

Segmentation genes. Insect genes that specify the correct number and polarity of body segments. Gap genes, pair-rule genes, and segment polarity genes are all segmentation genes.

Selectable marker. A gene whose product has an activity, such as antibiotic resistance, such that, under the appropriate conditions, cells harboring the gene can be distinguished from those that lack the gene.

Selfish DNA. Genomic DNA that has no apparent function. Also called junk DNA.

Semiconservative replication. The natural mode of DNA duplication in which each new duplex molecule contains one strand from the parent molecule and one newly synthesized strand.

Semidiscontinuous replication. The mode of DNA replication in which one strand is replicated as a continuous polynucleotide strand (the leading strand) while the other is replicated as a series of discontinuous fragments (Okazaki fragments) that are later joined (the lagging strand).

Sense strand. The DNA strand complementary to the strand that is transcribed; it has the same base sequence (except for the replacement of U with T) as the synthesized RNA. Also called the coding strand.

Sequential model of allosterism. A model for allosteric behavior in which the subunits of an oligomeric protein change conformation in a stepwise manner as the number of bound ligands increases.

Sequential reaction. A reaction in which all substrates must combine with the enzyme before a reaction can occur; it can proceed by an Ordered or Random mechanism.

Serine protease. A peptide-hydrolyzing enzyme characterized by a reactive Ser residue in its active site.

Severe combined immunodeficiency disease (SCID). An inherited disease that greatly impairs the immune system. One such defect is a deficiency of the enzyme adenosine deaminase.

Shear degradation. The fragmentation of DNA by the mechanical force of shaking or stirring.

Shine–Dalgarno sequence. A purine-rich sequence ~10 nucleotides upstream from the start codon of many prokaryotic mRNAs that is partially complementary to the 3′ end of the 16S rRNA. This sequence helps position the ribosome to initiate translation.

Short interfering RNA (siRNA). A naturally occurring RNA of 18 to 25 nucleotides that inhibits gene expression through RNA interference. Also known as micro RNA (miRNA).

Short tandem repeat (STR). See highly repetitive DNA.

Shotgun cloning. The cloning of an organism's genome in the form of a set of random fragments.

Sickle-cell anemia. An inherited disease in which erythrocytes are deformed and damaged by the presence of a mutant hemoglobin (Glu 6β → Val) that in its deoxy form polymerizes into fibers.

σ factor. A component of the bacterial RNA polymerase holoenzyme that recognizes a gene's promoter and is released once chain initiation has occurred.

Sigmoidal curve. The S-shaped graphical representation of the cooperative binding of a ligand to a molecule.

Signal-gated channel. A channel whose opening and closing (gating) is controlled by the binding of an intracellular signaling molecule.

Signal peptide. A short (13–36 residues) N-terminal peptide sequence that targets a nascent secretory or transmembrane protein to the endoplasmic reticulum (in eukaryotes) or plasma membrane (in prokaryotes). This leader peptide is subsequently cleaved away by signal peptidase.

Signal recognition particle (SRP). A protein–RNA complex that binds to the signal peptide of a nascent transmembrane or secretory protein and escorts it to the endoplasmic reticulum (in eukaryotes) or plasma membrane (in prokaryotes) for translocation through the membrane.

Signal transduction. The transmittal of an extracellular signal to the cell interior by the binding of a ligand to a cell-surface receptor so as to elicit a cellular response through the activation of a sequence of intracellular events that often include the generation of second messengers.

Silencer. A DNA sequence some distance from the transcription start site, where a repressor of transcription may bind.

Single-displacement reaction. A reaction in which a group is transferred from one molecule to another in a concerted fashion (with no intermediates).

Single nucleotide polymorphism (SNP). A single base difference in the genomes of two individuals; such differences occur every 1250 bp on average in the human genome.

Single-strand binding protein (SSB). A tetrameric protein, many molecules of which coat single-stranded DNA during replication so as to prevent formation of double-stranded DNA.

siRNA. See short interfering RNA.

Site-directed mutagenesis. A technique in which a cloned gene is mutated in a specific manner.

Site-specific recombination. See recombination.

Size exclusion chromatography. See gel filtration chromatography.

Sliding filament model. A mechanism for muscle contraction in which interdigitated thin and thick filaments move past each other so as to shorten the overall length of a sarcomere.

Small nuclear ribonucleoprotein (snRNP). A complex of protein and small nuclear RNA that participates in mRNA splicing.

Small nuclear RNA (snRNA). Highly conserved 60- to 300-nt RNAs that participate in mRNA splicing.

Small nucleolar RNA (snoRNA). Eukaryotic RNA molecules of 70 to 100 nt that pair with immature rRNAs to direct their sequence-specific methylation.

SNARE. A membrane-associated protein that participates in vesicle fusion; SNAREs from the two fusing membranes form a bundle of four helices that holds the membranes in close proximity.

snoRNA. See small nucleolar RNA.

SNP. See single nucleotide polymorphism.

snRNA. See small nuclear RNA.

snRNP. See small nuclear ribonucleoprotein.

Soap. A salt of a long-chain fatty acid, which contains a polar head group and a long hydrophobic tail.

Solvation. The state of being surrounded by several layers of ordered solvent molecules. Hydration is solvation by water.

Somatic hypermutation. The greatly increased rate of mutation that occurs in the immunoglobulin genes of proliferating B lymphocytes and leads, over several cell generations, to antibodies with higher antigen affinity.

Somatic recombination. Genetic rearrangement that occurs in cells other than germline cells.

Sonication. Irradiation with high frequency sound waves. Such treatment is used to disrupt cells and subcellular membranous structures.

SOS response. A bacterial system that recognizes damaged DNA, halts its replication, and repairs the damage, although in an error-prone fashion.

Southern blotting. A procedure for identifying a DNA base sequence after electrophoresis, through its ability to hybridize with a complementary single-stranded segment of labeled DNA or RNA. See also Northern blotting.

Special pair. The set of two closely spaced chlorophyll groups in a photosynthetic system that undergo photooxidation.

Spherocytosis. A hereditary abnormality in the erythrocyte cytoskeleton that renders the cells rigid and spheroidal and which causes hemolytic anemia.

Sphingolipid. A derivative of the C_{18} amino alcohol sphingosine. Sphingolipids include the ceramides, cerebrosides, and gangliosides. Sphingolipids with phosphate head groups are called sphingophospholipids.

Sphingomyelin. The most common sphingolipid, consisting of a ceramide bearing a phosphocholine or phosphoethanolamine head group.

Spliceosome. A 60S particle containing proteins, snRNPs, and pre-mRNA; it carries out the splicing reactions whereby a pre-mRNA is converted to a mature mRNA.

Splicing. The usually ribonucleoprotein-catalyzed process by which introns are removed and exons are joined to produce a mature transcript. Some RNAs are self-splicing.

Spontaneous process. A thermodynamic process that occurs without the input of free energy from outside the system. Spontaneity is independent of the rate of a process.

Squelching. The inhibition of the activity of a transcription factor by another transcription factor that competes with it for binding to DNA.

SR. See SRP receptor.

SRP. See signal recognition particle.

SRP receptor (SR). The endoplasmic reticulum protein that serves as a docking point for the signal recognition particle (SRP) during the synthesis of a transmembrane or secretory protein.

SSB. See single-strand binding protein.

Stacking interactions. The stabilizing van der Waals interactions between successive (stacked) bases and base pairs in a polynucleotide.

Standard state. A set of conditions including unit activity of the species of interest, a temperature of 25°C, a pressure of 1 atm, and a pH of 0.0. See also biochemical standard state.

Starch. A mixture of linear and branched glucose polymers that serve as the principal energy reserves of plants.

STAT. A member of a family of proteins that function as signal transducers and activators of transcription (STAT) by binding to DNA in response to tyrosine phosphorylation.

State function. Quantities such as energy, enthalpy, entropy, and free energy, whose values depend only on the current state of the system, not on how they reached that state.

Steady state. A set of conditions in an open system under which the formation and degradation of individual components are balanced such that the system does not change over time.

Steady state assumption. A condition for the application of the Michaelis–Menten model to an enzymatic reaction, in which the concentration of the ES complex remains unchanged over the course of the reaction.

Stem–loop. A secondary structural element in a single-stranded nucleic acid, in which two complementary segments form a base-paired stem whose strands are connected by a loop of unpaired bases.

Stereoisomers. Chiral molecules with different configurations about at least one of their asymmetric centers but which are otherwise identical.

Steroid. Any of numerous naturally occurring lipids composed of four fused rings; many are hormones that are derived from cholesterol.

Sterol. An alcohol derivative of a steroid.

Sticky end. The single-stranded extension of a DNA fragment that has been cleaved at a specific sequence (often by a restriction endonuclease) in a staggered cut such that this single-stranded extension is complementary to those of similarly cleaved DNAs.

Stop codon. A sequence of three nucleotides that does not specify an amino acid but instead causes the termination of translation. Also called a nonsense codon.

STR. Short tandem repeat. See highly repetitive DNA.

Striated muscle. The voluntary or skeletal muscles, which have a striped microscopic appearance.

Stroma. The concentrated solution of enzymes, small molecules, and ions in the interior of a chloroplast; the site of carbohydrate synthesis.

Stromal lamellae. The membranous assemblies that connect grana in a chloroplast.

Strong acid. An acid that is essentially completely ionized in aqueous solution. A strong acid has a dissociation constant much greater than unity ($pK < 0$).

Structural bioinformatics. See bioinformatics.

Structural gene. A gene that encodes a protein.

Structure-based drug design. The synthesis of more effective drug molecules as guided by knowledge of the target molecule's structure and interactions with other drug molecules. Also called rational drug design.

Substrate. A reactant in an enzymatic reaction.

Substrate cycle. Two opposing metabolic reactions that function together to hydrolyze ATP, but provide a control point for regulating metabolic flux. Also called a futile cycle.

Substrate-level phosphorylation. The direct transfer of a phosphoryl group to ADP to generate ATP.

Subunit. One of several polymer chains that make up a macromolecule.

Sugar. A simple mono- or disaccharide.

Suicide substrate. See mechanism-based inhibitor.

Sulfhydryl group. A portion of a molecule with the formula —SH.

Supercoiling. The topological state of covalently closed circular double-helical DNA in which the double helix is twisted around itself. It arises through the over- or underwinding of the double helix. Also called superhelicity.

Superhelicity. See supercoiling.

Superoxide radical. $O_2^{-}\cdot$, a partially reduced oxygen species that can damage biomolecules through free radical reactions.

Supersecondary structure. A common grouping of secondary structural elements. Also called a motif.

Suppressor mutation. A mutation that cancels the effect of another mutation.

Surface labeling. A technique in which a lipid-insoluble protein-labeling reagent is used to identify the portion of a membrane protein that is exposed to solvent.

Surroundings. In thermodynamics, the universe other than the particular system that is of interest.

Symbiosis. A mutually dependent relationship between two organisms.

Symmetry model of allosterism. A model for allosteric behavior in which all the subunits of an oligomeric protein are constrained to change conformation in a concerted manner so as to maintain the symmetry of the oligomer.

Symport. A transmembrane channel that simultaneously transports two different molecules or ions in the same direction. See also antiport and uniport.

Syn conformation. A purine nucleotide conformation in which the ribose and the base are eclipsed. See also anti conformation.

Syncytium. A single cell containing multiple nuclei that results from repeated nuclear division without the formation of new plasma membranes.

Synonymous codons. Codons that specify the same amino acid.

System. In thermodynamics, the part of the universe that is of interest; the rest of the universe is the surroundings. See also closed system, isolated system, and open system.

Systems biology. The computer-based collection and analysis of data sets for the purpose of discerning relationships between dynamic or multifactorial biological entities.

***T*.** See twist.

$t_{1/2}$. See half-time.

T state. One of two conformations of an allosteric protein; the other is the R state. The T state is usually the catalytically less active state.

T → R transition. A shift in conformation of an allosteric protein induced by ligand binding.

TAFs. TBP-associated factors, which, along with TBP, constitute the general transcription factor TFIID required for the transcription of eukaryotic structural genes.

TATA box. A eukaryotic promoter element with the consensus sequence TATAAAA located 10 to 27 nucleotides upstream from the transcription start site.

Tautomers. Isomers that differ only in the positions of their hydrogen atoms and double bonds.

Taxonomy. The study of biological classification.

Tay-Sachs disease. A fatal sphingolipid storage disease caused by a deficiency of hexosaminidase A, the lysosomal enzyme that breaks down ganglioside G_{M2}.

TBP. TATA-binding protein, a DNA-binding protein that is required for transcription of all eukaryotic genes.

TCA cycle. Tricarboxylic acid cycle. See citric acid cycle.

Telomerase. An RNA-containing DNA polymerase that, using the RNA as a template, catalyzes the repeated addition of a specific G-rich sequence to the 3′ end of a eukaryotic DNA molecule to form a telomere.

Telomere. The end of a linear eukaryotic chromosome, which consists of tandem repeats of a short G-rich sequence on the 3′-ending strand and its complementary sequence on the 5′-ending strand.

Tertiary structure. The entire three-dimensional structure of a single-chain polymer, including that of its side chains.

Tetrahedral intermediate. An intermediate of peptide bond hydrolysis in which the carbonyl carbon of the scissile bond has undergone nucleophilic attack so that it has four substituents.

Tetramer. An assembly consisting of four monomeric units.

Therapeutic index. The ratio of the dose of a drug that produces toxicity to the dose that produces the desired effect.

Thermodynamics. The study of the relationships among various forms of energy.

Thermogenesis. The generation of heat by muscle contraction (shivering) or by fuel oxidation without ATP synthesis (also called diet-induced thermogenesis).

Thermophile. An organism that thrives at high temperatures.

θ structure. The appearance of a circular DNA molecule undergoing replication by the progressive separation of its two strands.

THF. Tetrahydrofolate, a cofactor for reactions that transfer one-carbon units in various oxidation states.

Thick filament. The sarcomere element that is composed primarily of several hundred myosin molecules.

Thin filament. The sarcomere element that is composed primarily of actin, along with tropomyosin and troponin.

30-nm fiber. A condensed chromatin structure in which nucleosomes fold in a zigzag manner to form a fiber with a diameter of ~30 nm.

3′ end. The terminus of a polynucleotide whose C3′ is not esterified to another nucleotide residue.

Thylakoid. The innermost compartment in chloroplasts, which is formed by invaginations of the chloroplast's inner membrane. The thylakoid membrane is the site of the light reactions of photosynthesis.

Titration curve. The graphic presentation of the relationship between the pH of an acid- or base-containing solution and the degree of proton dissociation (roughly equal to the number of equivalents of strong base or strong acid that have been added to the solution).

T_m. See melting temperature.

TM protein. See transmembrane protein.

Topoisomerase. An enzyme that alters DNA supercoiling by catalyzing breaks in one or both strands, passing DNA through the break, and resealing the break.

Topology. The study of the geometric properties of an object that are not altered by deformations such as bending and stretching

Torsion angle. The dihedral angle described by the bonds between four successive atoms. The torsion angles ϕ and ψ indicate the backbone conformation of a peptide group in a polypeptide.

TPP. Thiamine pyrophosphate, a cofactor for reactions in which α-keto acids undergo decarboxylation.

TψC arm. A conserved stem–loop structure in a tRNA molecule that usually contains the sequence TψC, where ψ is pseudouridine.

Trace element. See mineral.

Trans conformation. An arrangement of the peptide group in which successive C_α atoms are on opposite sides of the peptide bond.

Trans peptide. A conformation in which successive C_α atoms are on opposite sides of the peptide bond.

Transamination. The transfer of an amino group from an amino acid to an α-keto acid to yield a new α-keto acid and a new amino acid.

Transcription. The process by which RNA is synthesized using a DNA template, thereby transferring genetic information from the DNA to the RNA. Transcription is catalyzed by RNA polymerase as facilitated by numerous other proteins.

Transcription factor. A protein that promotes the transcription of a gene by binding to DNA sequences at or near the gene or by interacting with other proteins that do so.

Transcriptomics. The study of all the mRNA molecules that a cell transcribes.

Transfer RNA (tRNA). The small L-shaped RNAs that deliver specific amino acids, which have been esterified to the tRNA's 3′ ends, to ribosomes according to the sequence of a bound mRNA. The proper tRNA is selected through the complementary base pairing of its three-nucleotide anticodon with the mRNA's codon, and the growing polypeptide is transferred to its aminoacyl group.

Transferase. An enzyme that catalyzes the transfer of a functional group from one molecule to another.

Transformation. (1) The permanent alteration of a bacterial cell's genetic message through the introduction of foreign DNA. (2) The genetic changes that convert a normal cell to a cancerous cell.

Transgene. A foreign gene that is stably expressed in a host organism.

Transgenic organism. An organism that stably expresses a foreign gene (transgene).

Transition. A mutation in which one purine (or pyrimidine) replaces another.

Transition state. A molecular assembly at the point of maximal free energy in the reaction coordinate diagram of a chemical reaction.

Transition state analog. A stable substance that geometrically and electronically resembles the transition state of a reaction.

Transition temperature. The temperature at which a lipid bilayer shifts from a gel-like solid to a more fluid liquid crystal form.

Translation. The process of transforming the information contained in the nucleotide sequence of an RNA to the corresponding amino acid sequence of a polypeptide as specified by the genetic code. Translation is catalyzed by ribosomes and requires the additional participation of messenger RNA, transfer RNA, and a variety of protein factors.

Translocation. (1) The movement of a polypeptide through a membrane during the synthesis of a secreted protein. (2) The movement, by one codon, of the ribosome relative to the mRNA after peptide bond synthesis.

Translocon. A multisubunit protein that forms an aqueous pore across the endoplasmic reticulum membrane for the purpose of translocating a protein as part of the secretory pathway.

Transmembrane (TM) protein. An integral protein that completely spans the membrane.

Transmissible spongiform encephalopathy (TSE). An invariably fatal neurodegenerative disease resulting from prion infection, such as scrapie in sheep.

Transpeptidation. The ribosomal process in which a tRNA-bound nascent polypeptide is transferred to a tRNA-bound aminoacyl group so as to form a new peptide bond, thereby lengthening the polypeptide by one residue at its C-terminus.

Transposable element. See transposon.

Transposition. The movement (copying) of genetic material from one part of the genome to another or, in some cases, from one organism to another.

Transposon. A genetic unit that can move (be copied) from one position to another in a genome; some transposons carry genes. Also called a transposable element.

Transverse diffusion. The movement of a lipid from one leaflet of a bilayer to the other. Also called flip-flop.

Transversion. A mutation in which a purine is replaced by a pyrimidine or vice versa.

Treadmilling. The addition of monomeric units to one end of a linear aggregate, such as an actin filament, and their removal from the opposite end such that the length of the aggregate remains unchanged.

Triacylglycerol. A lipid in which three fatty acids are esterified to a glycerol backbone. Also called a triglyceride.

Tricarboxylic acid (TCA) cycle. See citric acid cycle.

Triglyceride. See triacylglycerol.

Trimer. An assembly consisting of three monomeric units.

Tripeptide. A polypeptide containing three amino acids.

tRNA. See transfer RNA.

TSE. See transmissible spongiform encephalopathy.

Tumor suppressor. A protein whose loss or inactivation may lead to cancer.

Turnover number. See k_{cat}.

Twist (*T*). The number of complete revolutions that one strand of a covalently closed circular double-helical DNA makes around the duplex axis. It is positive for right-handed superhelical coils and negative for left-handed superhelical coils.

Two-dimensional (2D) gel electrophoresis. A technique in which proteins are first subjected to isoelectric focusing, which separates them by net charge, and then to SDS-PAGE in a perpendicular direction, which separates them by size.

Tyrosine kinase. An enzyme that catalyzes the ATP-dependent phosphorylation of a Tyr side chain.

***U*.** The thermodynamic symbol for energy.

Ubiquinone. See coenzyme Q.

Ubiquitin. A small, highly conserved protein that is covalently attached to a eukaryotic intracellular protein so as to mark it for degradation by a proteasome.

Ultracentrifugation. A procedure that subjects macromolecules to a strong centrifugal force (in an ultracentrifuge), thereby separating them by size and/or density and providing a method for determining their mass and subunit structure.

Uncompetitive inhibition. A form of enzyme inhibition in which an inhibitor binds to the enzyme–substrate complex and thereby decreases its apparent K_M and its apparent $V_{\max}$ by the same factor.

Uncoupler. A substance that allows the proton gradient across a membrane to dissipate without ATP synthesis so that electron transport proceeds without oxidative phosphorylation.

Uniport. A transmembrane channel that transports a single molecule or ion. See also antiport and symport.

Unsaturated fatty acid. A fatty acid that contains at least one double bond in its hydrocarbon chain.

Urea cycle. A catalytic cycle in which amino groups donated by ammonia and aspartate combine with a carbon atom from HCO_3^- to form urea for excretion and which provides the route for the elimination of nitrogen from protein degradation.

Uridylylation. Addition of a uridylyl (UMP) group.

Uronic acid. A sugar produced by oxidation of an aldose primary alcohol group to a carboxylic acid group.

***v*.** Reaction velocity, typically measured as the rate of appearance of product or disappearance of reactant.

Vacuole. An intracellular vesicle for storing water or other molecules.

van der Waals distance. The distance of closest approach between two nonbonded atoms.

van der Waals forces. The noncovalent associations between molecules that arise from the electrostatic interactions among permanent and/or induced dipoles.

van't Hoff plot. A graph of K_{eq} versus $1/T$ that is used to determine $\Delta H°$ and $\Delta S°$ and therefore $\Delta G°$ for a chemical reaction.

Variable arm. A nonconserved region of a tRNA molecule that contains 3 to 21 nucleotides and that may include a base-paired stem.

Variable region. The N-terminal portions of an antibody molecule, where antigen binding occurs and which are characterized by high sequence variability.

Variant. A naturally occurring mutant form.

Vector. See cloning vector.

Vesicle. A fluid-filled sac enclosed by a membrane.

Virulence. The disease-evoking power of a microorganism.

Virus. A nonliving entity that co-opts the metabolism of a host cell to reproduce.

Vitamin. A metabolically required substance that cannot be synthesized by an animal and must therefore be obtained from the diet.

VLDL. Very low density lipoprotein; see lipoprotein.

$V_{\max}$. Maximal velocity of an enzymatic reaction.

$V_{\max}^{app}$. The observed maximal velocity of an enzymatic reaction, which may differ from the true value due to the presence of an inhibitor.

v_o. Initial velocity of an enzymatic reaction.

Voltage-gated channel. A channel whose opening and closing (gating) is controlled by a change in membrane potential.

***W*.** (1) See writhing number. (2) The number of energetically equivalent ways of arranging the components of a system.

***w*.** The thermodynamic term for the work done by a system on its surroundings.

Water of hydration. The shell of relatively immobile water molecules that surrounds and interacts with (solvates) a dissolved molecule.

Watson–Crick base pair. A stable pairing of nucleotide bases, either adenine with thymine or guanine with cytosine, that occurs in DNA and, to a lesser extent, in RNA. See also Hoogsteen base pair.

Weak acid. An acid that is only partially ionized in aqueous solution. A weak acid has a dissociation constant less than unity ($pK > 0$).

Western blot. See immunoblot.

Wild type. The naturally occurring version of an organism or gene.

Wobble hypothesis. An explanation for the permissive tRNA–mRNA pairing at the third anticodon position that includes non-Watson–Crick base pairs. This allows many tRNAs to recognize two or three different (degenerate) codons.

Writing number (W). The number of turns that the duplex axis of a covalently closed circular double-helical DNA makes around the superhelix axis. It is a measure of the DNA's superhelicity.

X-Ray crystallography. A method for determining three-dimensional molecular structures from the diffraction pattern produced by exposing a crystal of a molecule to a beam of X-rays.

Xenobiotic. A molecule that is not normally present in an organism.

***Y*.** See fractional saturation.

YAC. See yeast artificial chromosome.

Yeast artificial chromosome (YAC). A linear DNA molecule that contains the chromosomal structures required for normal replication and segregation in a yeast cell. YACs are commonly used as cloning vectors.

Ylid. A molecule with opposite charges on adjacent atoms.

Y_{O_2}. See fractional saturation.

Z-scheme. A Z-shaped diagram indicating the sequence of events and their reduction potentials in the two-center photosynthetic electron-transport system of plants and cyanobacteria.

Zero-order reaction. A reaction whose rate does not vary with the concentration of any of its reactants.

Zinc finger. A protein structural motif, often involved in DNA binding, that consists of 25 to 60 residues that include His and/or Cys residues to which one or two Zn^{2+} ions are tetrahedrally coordinated.

Zwitterion. See dipolar ion.

Zymogen. The inactive precursor (proenzyme) of a proteolytic enzyme.

This page intentionally left blank

Index

Page numbers in **bold face** refer to a major discussion of the entry. F after a page number refers to a figure. T after a page number refers to a table. Positional and configurational designations in chemical names (e.g., 3-, α, *N-*, *p-*, *trans,* D-) are ignored in alphabetizing. Numbers and Greek letters are otherwise alphabetized as if they were spelled out.

A
A, *see* Adenine; Aminoacyl site
Aβ (amyloid-β protein), 169
A antigens, 242F
aaRSs, *see* Aminoacyl-tRNA synthetases
aa-tRNA, *see* Aminoacyl-tRNA
A bands, 198
Abasic sites, 921
ABCA1 (ATP-cassette binding protein A1), 729
ABC transporters, 311, **314–316,** 315F
Abdominal cavity, adipose tissue in, 796
Ab initio protein design, 163
ABO blood group antigens, 242
Abortive initiation, 948
Absolute configuration, 83
Absorbance, 95–96
Absorbance spectroscopy, 95
Absorption spectrum, 96
Absorptivity, 95
Abx (anteriobithorax) mutant, 1092
AC, *see* Adenylate cyclase
ACAT (acyl-CoA:cholesterol acyltransferase), 684F, 725
ACC (acetyl-CoA carboxylase), 805
Acceptor stem (tRNA), 991F
Accessory BChl, 648
Accessory pigments, 644–645
Acesulfame, 228
Acetal:
  cyclic, 225
  nonenzymatic acid-catalyzed hydrolysis, 344F
Acetaldehyde, 327
  from alcoholic fermentation, 505
  geometric specificity, 326
Acetamide, 319
Acetaminophen, 399, 719
Acetate, cholesterol biosynthesis from, **722–725**
Acetic acid, titration curve, 34F
Acetimidoquinone, 400
Acetoacetate:
  in amino acid degradation, 747F
  decarboxylation, 334F
  in ketogenesis, 698–699F
  in ketone body conversion to acetyl-CoA, 700F
  from phenylalanine/tyrosine breakdown, 760–761F
  from tryptophan breakdown, 758, 760F
Acetoacetyl-ACP, in fatty acid synthesis, 705F
Acetoacetyl-CoA:
  in ketogenesis, 699, 699F
  in ketone body conversion to acetyl-CoA, 700F
Aceto-α-hydroxybutyrate, 772
Acetolactate, 772
Acetone, geometric specificity, 326
Acetyl-ACP, in fatty acid synthesis, 705F
Acetylcholine, hydrolysis, 349
Acetylcholinesterase, 349, 371T
Acetyl-CoA (acetyl-coenzyme A), 451–452, 468–469, 801, 1060. *See also* Ketone bodies
  in amino acid degradation, 747F
  in citric acid cycle, 568F, **570–573,** 584F, 585–587
  in fatty acid synthesis, 705F
  in glyoxylate cycle, 591F
  in ketogenesis, 699, 699F
  in ketone body conversion to acetyl-CoA, 700F
  mammalian metabolism, 792F, 793, 797
Acetyl-CoA-ACP transacylase, in fatty acid synthesis, 705F
Acetyl-CoA carboxylase (ACC), 805
Acetyl-coenzyme A, *see* Acetyl-CoA
N-Acetylglucosamine (NAG, GlcNAc), 232, 340, 343, 346, 347
N-Acetyl-D-glucosamine, 232F, 237F
N-Acetylglutamate, 747
N-Acetylglutamate synthase, 747
Acetyl-Lys binding sites, 1062F
ε-*N*-Acetyllysine, 86F
N-Acetylmuramic acid (NAM, MurNAc), 237F, 340, 343, 346
N-Acetylneuraminic acid (NANA), 225F
Acetyl phosphate, 461T, 465, 497
Acids, 32–34
  as buffering agents, 36
  conjugate bases, 32
  polyprotic, 35, 35F
  strength, 32–34
Acid-base catalysis (enzymes), **331–333**
Acid-base chemistry, **32–34**
  and proton jumping, 30–31
  standard state conventions, 17
Acidic solutions, 31
Acidosis, 36
Aconitase:
  in citric acid cycle, 568F, **578–579,** 587
  in glyoxylate cycle, 591F
  stereospecificity of, 325
Aconitate, 567
ACP (acyl-carrier protein), 703–704
Acquired immunodeficiency syndrome (AIDS), 377, 384–385
Acridine orange, as intercalating agent, 873F, 919
Acromegaly, 411
Actin, **207–209,** 628
  myosin-actin interaction, 203F
  structure, 202F, 203F
α-Actinin, 204
β-Actinin, 205
Actinomycin D, 954
Action potentials, 302–303
Action potential time course, 302F
Activation domains, 1068
Activation energy, **328–330**
Activators (regulatory proteins), 1067
Active membrane transport, 276, 297, **297–310**
  ATP-driven, **311–314**
  endergonic process, 311
  ion-gradient-driven, **316–318**
  sodium and potassium, 312F
Active site (enzymes), 323
Active transporters, 299, 311–318
Active transport systems, 316
Activity, 17
Activity site, 833
Acute intermittent porphyria, 778
Acute lymphoblastic leukemia, 751
Acute pancreatitis, 357
Acyclovir, 844
Acyl-carnitine, 687
Acyl-carrier protein (ACP), 703–704
Acyl-CoA:cholesterol acyltransferase (ACAT), 684F, 725
Acyl-CoA dehydrogenase, 688–689F
Acyl-CoA oxidase, 698
Acyl-CoA synthetases, 686, 687F

Acyl-dihydroxyacetone phosphate, in triacylglycerol biosynthesis, 710F
Acyl-dihydroxyacetone phosphate reductase, in triacylglycerol biosynthesis, 710F
Acyl-enzyme, tetrahedral intermediate, 357F
Acyl-enzyme intermediate, chymotrypsin, 354
1-Acylglycerol-3-phosphate acyltransferase, in triacylglycerol biosynthesis, 710F, 711
2-Acylglycerols, 678–679
Acyl phosphates, 465
N-Acylsphingosine, 714, 718F
Acyl thioester, 498
Adaptor, 418
ADAR2, 976
Addison's disease, 215T, 255
Adenine (A), 40, 41T
  base pairing, 46F, 49F, 851F, 866–868
  Chargaff's rules and, 44
  as common nucleotide, 42
  modified forms in tRNA, 992F
  oxidative deamination, 917F
  stacking interactions, 867F
Adenine nucleotide translocase, 599–600
Adenine phosphoribosyltransferase (APRT), 823
Adenine ribonucleotide synthesis, 821–822
Adenosine, 41T, 460, 840F
Adenosine-3′,5′-cyclic monophosphate, *see* cAMP
Adenosine-5′(β,γ-imido)triphosphate (AMPPNP, ADPNP), 202F, 415, 422F
Adenosine deaminase, 378, 841F
Adenosine diphosphate, *see* ADP
Adenosine monophosphate, *see* AMP
Adenosine triphosphate, *see* ATP
Adenosylcobalamin, 697
S-Adenosylhomocysteine, 754, 1063
S-Adenosylmethionine (SAM, AdoMet), 753–754, 966, 1055, 1063, 1064
Adenylate cyclase (AC), 428–429, 432–434, 432F, 434F, 546, 797, 801
Adenylate kinase, 467F, 513–514
Adenylic acid, *see* AMP
Adenylosuccinate, in IMP conversion to AMP/GMP, 822
Adenylosuccinate lyase:
  in IMP conversion to AMP/GMP, 821F
  in IMP synthesis, 819F
Adenylosuccinate synthetase, in IMP conversion to AMP/GMP, 821F
Adenylylation, 766
Adenylyltransferase, 766
ADH (alcohol dehydrogenase reaction), 327
Adipocytes, 248F, 796, 805
Adiponectin, 806, 806F
Adiponectin receptors, 806
Adipose tissue, 248, 454
  brown, 632
  mammalian metabolism in, 793, 794F, **795–796,** 797
A-DNA, 852T
  conformation, 856F–857
AdoMet, *see S*-Adenosylmethionine
ADP (adenosine diphosphate), 42
  citric acid cycle regulator, 585
  in glycolysis, 487F, 488
ADP-ATP translocator, 599–600
ADP-glucose, 42, 42F, 561
ADP-glucose pyrophosphorylase, 669
ADPNP, *see* Adenosine-5′(β,γ-imido) triphosphate
Adrenal cortex, 255
Adrenal glands, 255, 406F, 409–410, 799
Adrenaline, *see* Epinephrine
Adrenergic receptors (adrenoreceptors), 409, 551–552
α-Adrenergic receptors, 409, 552
β-Adrenergic receptors, 409, 551
Adrenocortical steroids, 410
Adult respiratory distress syndrome, 250
Adverse reactions, 397
Aequorea victoria, 87
Aerobes, 449
Aerobic metabolism, 7, 505, 567F. *See also* Citric acid cycle; Electron transport
  antioxidant mechanisms, **636–637**
  coordinated control, **633–634**
  electron transport in, 597
  in heart, 795
  physiological implications, **634–637**
Affinity chromatography, 97, 101F
Affinity chromatography nucleic acids, 872
Affinity labeling, 348
African sleeping sickness, 504
Agarose gel, 367
  for nucleic acid electrophoresis, 52, 872–873
  for protein chromatography, 98
Aging:
  and free radicals, 636
  and telomerase, 915
Agonists, 409
Agre, P., 306
AICAR (5-Aminoimidazole-4-carboxamide ribonucleotide), 774, 775F, 819F, 820
AICAR transformylase, in IMP synthesis, 819F
AIDS, *see* Acquired immunodeficiency syndrome
AIR carboxylase, in IMP synthesis, 819F, 820
AIR synthetase, in IMP synthesis, 819F
Akt protein, 443F
Ala, *see* Alanine
ALA (δ-aminolevulinic acid), in heme biosynthesis, 776F, 777
Alanine (Ala):
  α helix/β sheet propensities, 140T
  biosynthesis, 764–765F
  breakdown, 747F, 748–751
  as common amino acid, 93
  glucose–alanine cycle, **799,** 799F
  ionizable groups, 76T, 79F
  nonpolar side chain, 79, 79F
  side chain hydropathy, 156T
  transamination, 559
  from tryptophan breakdown, 758, 760F
Alanine transaminase (ALT), 742
Alanine tRNA (tRNA^{Ala}), 991
β-Alanine, in pyrimidine catabolism, 845F
Alber, T., 881
Alberts, B., 949
Albumin, 685
Alcaptonuria, 477, 762
Alcohol, functional group and linkages, 4T
Alcohol dehydrogenase, 324
  as bisubstrate reaction, 375
  in fructose metabolism, 517F
Alcohol dehydrogenase reaction (ADH), 327
Alcoholic fermentation, 322, **506–509**
Aldehyde, 4T, 330
Alditols, 224
Aldohexoses, 220F
Aldolase:
  in Calvin cycle, 665F
  enzymatic mechanism of, 493
  in glycolysis, 487F, **492–494,** 492F
Aldol cleavage, 492
Aldonic acids, 224
Aldopentoses, 220F
Aldoses, 220F
D-Aldoses, 220F
Aldosterone, 255F, 410
Aldotetroses, 220F
Aldotrioses, 220F
Alkalosis, 36
Alkylacylglycerophospholipids, 716–717
Alkylating agents, mutagenic effects, 918
O^6-Alkylguanine-DNA alkyltransferase, 921
Alkyltransferases, 921
Allantoic acid, 842F–843
Allantoin, 842F–843
Allantoinase, in uric acid degradation, 842F
Allele, 66
Allis, D., 1060
1,6-Allolactase, 1047
Allopurinol, 843
D-Allose, 220F
Allosteric control:
  enzymes, 324, 386–390, 458
  glycogen phosphorylase, 543, 545
  glycogen synthase, 542–543, 545
  metabolic flux, 457
  phosphofructokinase, 512–513F
Allosteric effectors, 386, 559–560

Allosteric modifiers:
  structural change, 390
Allosteric proteins, **192–194**
Allosterism:
  interactions, allosteric, 192
  sequential model of, 193F
  symmetry model of, 193F
Alloxanthine, 843
Allysine, 139F
Almassy, R., 820
α (Soret) band, 610
αβ barrel (TIM barrel), 148, 149, 495–496
α helix, **129–132,** 129F, 132F, 265–267
α keratins, 134, 136
α proteins, 148
ALT (alanine transaminase), 742
Alternative name, 324
Alternative splicing, 973–975
Altman, S., 980
D-Altrose, 220F
Alu elements, 1043F
Alu family, 1045
Alzheimer's disease, 169–170, 636, 1087
Amanita phalloides, 955
α-Amanitin, 955
Amatoxins, 955
Amber codon, 990
Amber suppressor, 1028
Ames, B., 919
Ames test, 919F, 920
Amethopterin, 838
Amides, functional group and linkages, 4T
Amidophosphoribosyl transferase, in IMP synthesis, 818, 819F
Amines, 330
  functional group and linkages, 4T
  reaction with carboxylic acids, 3F
Amino acids:
  abbreviations, 76–77T, 81–82
  abundance, 93
  acid–base properties, **81**
  biologically active, **86–89,** 88F
  charged polar side chains, 77T, 78, 80–81
  as chemical messengers, 88
  classification and characteristics, **78–81**
  derivatives in proteins, **86–89,** 86F
  energy recovery by citric acid cycle, 567
  essential, 764T
  general properties, **74–78**
  genetic code specification, 989T
  glucogenic, 747
  hydrophobic effect, 80
  intracellular protein degradation, **733–735**
  ketogenic, 747–748
  nomenclature, 81–82, 82F
  nonessential, 764T
  nonpolar side chains, 76T, 79, 79F
  nutritive importance, 74
  occurrence, 76–77T
  peptide bonds, **78**
  p*K* values of ionizable groups, 76–77T
  specification by codon, 986
  stereochemistry, **82–86**
  structures, **74–82,** 76T
  transport between tissues, 798–799
  uncharged polar side chains, 77T, 79–80, 79F
α-Amino acids, 74F, 84F
D-Amino acids, **84,** 84–85
L-Amino acids, **84**
L-α-Amino acids, 84
Amino acid biosynthesis:
  citric acid cycle intermediates, 589
  essential amino acids, **769–774**
  mammalian metabolism, 792F–793
  nonessential amino acids, **764–769**
Amino acid breakdown, **747–763,** 747F
  branched-chain amino acids, 757–758
  common intermediates, 747F
  mammalian metabolism, 792F–793, 797–798
Amino acid catabolism, 739F
Amino acid deamination, **738–742**
  oxidative, **742**
  transamination, **738–742**
Amino acid derivatives, **86–89**
Amino acid metabolism, 86–89
  heme biosynthesis, **775–778**
  heme degradation, **778–780**
Amino acid residues, 78
  α helix/β sheet propensities, 140T
  conservative substitution, 116
  hydropathics, 156T
  hypervariable, 116
  invariant, 116
  pH effects, 332
  polypeptide chain interior, 81
Amino acid sequencing, *see* Protein sequencing
Amino acid stem (tRNA), 991F
Aminoacrylate, 749
Aminoacyl-adenylate, 994
Aminoacyl (A) site, 1006
Aminoacyl–tRNA (aa-tRNA), 994F–995, 1009F, 1021
Aminoacyl–tRNA synthetases (aaRSs), **994–998**
  class I vs. class II, 994–995
  organisms lacking, 998
  proofreading (editing) step, 997–998
  and unique structural features of tRNA, 995–997
p-Aminobenzoic acid, 754
γ-Aminobutyric acid (GABA), 88, 780
Aminoglycosides, 1024
5-Aminoimidazole-4-carboxamide ribotide, *see* AICAR
5-Aminoimidazole-4-(*N*-succinylocarboxamide) ribotide (SACAIR), in IMP synthesis, 819F, 820
5-Aminoimidazole ribotide (AIR), in IMP synthesis, 819F, 820
β-Aminoisobutyrate, in pyrimidine catabolism, 845F
α-Amino-β-ketobutyrate, 749
α-Amino-β-ketobutyrate lyase, 748F–749
δ-Aminolevulinic acid (ALA), 776F, 777
δ-Aminolevulinic acid synthase, in heme biosynthesis, 776F
Aminopterin, 838
Amino sugars, 225
Amino terminus, *see N*-terminus
Aminotransferase, 739, 845F
Ammonia, 743
Ammonification, 788
Ammonium ion, titration curve, 34F
Ammonium sulfate, for protein salting out, 97F
AMP (adenosine monophosphate), 41T
  animal catabolism pathway, 840F
  from IMP, 821F
  synthesis, 819F, **821–822**
AMP deaminase, 840
AMP-dependent protein kinase (AMPK), 703, 804–805F
Amphibolic pathways, 588
Amphipathic molecules, 28–29
Amphiphilic molecules, 28–29
AMPK, *see* AMP-dependent protein kinase
AMP nucleosidase, catalytic power, 323T
AMPPNP, *see* Adenosine-5′-(β,γ-imido) triphosphate
Amp$^{\text{R}}$ gene, 62
Amylase, 231
Amylo-1,6-glucosidase deficiency (Cori's disease), 538, 539
Amyloid, 168–169
Amyloid-β protein (Aβ), 169
Amyloidoses, 168
Amylopectin, 230, 544
α-Amylose, 230F, 231F, 544
Amylo-(1,4→1,6)-transglycosylase (branching enzyme), 538, **543–544**
Amylo-1,4→1,6-transglycosylase deficiency (Andersen's disease), 538
Amytal, 603
Anabolic steroids, 411
Anabolism, 448, 457
Anaerobes, 449
Anaerobic gylcolysis, 506
Anaerobic metabolism, 7, 505, 634–635, 795. *See also* Fermentation
Anaerobiosis, 488
Analbuminemia, 685
Anaplerotic reactions, 589
Andersen's disease, 538, 539
Androgens, 255F, 410
Anencephaly, 755
Anfinsen, C., 159
Angelman syndrome (AS), 1067

Angina pectoris, 781
Animal cells, 8F
Anion channels, 305
Anion exchangers, in chromatography, 98
Anion-selective pore, 305
Ankyrin, 273F, 274
Ankyrin repeats, 274F
Annealing:
  of DNA, 866
  in DNA manipulation, 61
α Anomers, 222F–223F
Anomeric forms, 222–223
Antagonists, 409
ANT-C (antennapedia complex), 1094
Antenna chlorophyll, 643F
Antennapedia complex (ANT-C), 1094
Antennapedia mutant *(antp),* 1092
Anteriobithorax mutant *(abx),* 1092
Anterograde transport, 283
Anthranilate, 773
Antibiotics:
  arsenicals as, 576
  effects on protein synthesis, 1024–1025
  peptidoglycan-specific, 238
  transcription inhibitors, 953–955
  as transition state analogs, 339
  type II topoisomerase inhibitors, 865
Antibiotic-resistant transposons, 938
Antibodies, **209–215**
  binding of, to antigens, **212–214**
  defined, 209
  diversity of, **214,** 1081
  for immunoassays, 95
  interaction of, with antigen, 214F
  monoclonal, 212, 213
  structure, **209–212**
Anticodons, 987
  codon–anticodon interactions, **998–999**
  recognition by aminoacyl-tRNA synthetases, 995
Anticodon arm (tRNA), 991F
Anti conformation, 856F
Antifolates, 838
Antigen–antibody binding, **212–214**
Antigens, 95, 209, 214F
Antimycin A, 603
Antioxidants, 636
Antiparallel β sheet, 132–134
Antiparallel strands, DNA, 45
Antiport, 310
Antisense RNA, 1034, 1075
Antisense (noncoding) strand, 944, 945F
Antp (antennapedia) mutant, 1092
Ap$_5$A, 467
Apaf-1 (apoptosis protease-activating factor-1), 1090
AP endonuclease, 921
Apical domain, 277
ApoA-I (apolipoprotein A-I), 682
ApoB (apolipoprotein B), 975
ApoB-48 (apolipoprotein B-48), 975
ApoB-100 (apolipoprotein B-100), 682, 975
Apoenzymes, 327
Apolipoproteins, 682
Apolipoprotein A-I (apoA-I), 682
Apolipoprotein B (apoB), 975
Apolipoprotein B-48 (apoB-48), 975
Apolipoprotein B-100 (apoB-100), 682, 975
Apoproteins, 682
Apoptosis, 420F, 924, 1086
  cellular death, 1082
  essential process, 1086–1087
  extrinsic and intrinsic pathways, 1088–1089
  programmed cell death, 1086–1087
Apoptosis extrinsic pathway, 1089F
Apoptosis protease-activating factor-1 (Apaf-1), 1090
Apoptosome, 1090, 1090F
Apoptotic bodies, 1087
Aβ precursor protein (βPP), 169
APRT (Adenine phosphoribosyltransferase), 823
APS/Cbl complex, 442
AP sites, 921
Aptamers, 1055
Apurinic (AP) sites, 921
Apyrimidinic (AP) sites, 921
AQP1, 306, 307F
Aquaporins, **306–307**
  kidneys, 306
  lacrimal glands, 306
  salivary glands, 306
  water molecules, 306
Aquaporin AQP1, 306F
Arabidopsis thaliana, 593, 961F
D-Arabinose, 220F
Arachidic acid, 247T
Arachidonic acid, 247T, 259F
Archaea, 9F
Archaeal rhodopsin family, 266
Archaebacteria, 9
Architectural proteins, 1058
Arg, *see* Arginine
Arginase, in urea cycle, 744, 746
Arginine (Arg):
  α helix/β sheet propensities, 140T
  biosynthesis, 768–769
  breakdown, 747F, 751–752F
  charged polar side chain, 80
  genetic code specification, 988, 989T
  ionizable groups, 77T
  as NO precursor, 781
  side chain hydropathy, 156T
  in urea cycle, 744F
Argininosuccinase, in urea cycle, 746
Argininosuccinate, in urea cycle, 744F, 746
Argininosuccinate synthetase, in urea cycle, 744, 746
Arg residues, 306, 318
Aromatic amino acid decarboxylase, in neurotransmitter synthesis, 781F
Arrhenius, S., 32
ARS (autonomously replicating sequences), 912
Arsenate, 528
Arsenicals, 576
Arsenic poisoning, 576
Arsenite, 576
Arthritis, rheumatoid, 215T, 733
Artificial sweeteners, 228
AS (Angelman syndrome), 1067
Ascorbic acid, 137. *See also* Vitamin C
Asn, *see* Asparagine
Asn residues, 307
AsnRS, 998
Asp, *see* Aspartic acid
L-Asparaginase, 751
Asparagine (Asn):
  acid-base catalysis by, 332
  α helix/β sheet propensities, 140T
  biosynthesis, 764–765F
  breakdown, 747F, 751
  covalent catalysis by, 335
  genetic code specification, 989T
  ionizable groups, 77T
  side chain hydropathy, 156T
  uncharged polar side chain, 79
Asparagine synthetase, 765
Aspartame, 228, 762
Aspartate, 80. *See also* Aspartic acid
  from amino acid degradation, 738, 747F
  biosynthesis, 764–765F
  breakdown, 751
  reaction with carbamoyl phosphate, 386
  in urea cycle, 743, 744F
Aspartate aminotransferase, 556
Aspartate/ATCase reaction, 387F
Aspartate transaminase (AST), 742
Aspartate transcarbamoylase (ATCase), 386–390
  conformational changes, 389F
  in UMP synthesis, 825F
Aspartic acid (Asp):
  α helix/β sheet propensities, 140T
  charged polar side chain, 80, 80F
  genetic code specification, 989T
  ionizable groups, 77T
  side chain hydropathy, 156T
Aspartic protease, 384
Aspartokinase, 770
Aspartyl phosphate residue, 312
Aspartyl-β-phosphate, 770
Aspartyl-tRNA synthetase (AspRS), 996–997
Aspirin, 719
AspRS (aspartyl-tRNA synthetase), 996–997
Assays, proteins, 95–97

Assimilation, 782, 786–788
AST (aspartate transaminase), 742
Asthma, 410, 435
Asturias, F., 1056, 1070
Asx, 82. *See also* Asparagine; Aspartic acid
Asymmetric centers, 83
Ataxia telangiectasia (ATM), 1084
ATCase, *see* Aspartate transcarbamoylase
Atherosclerosis, 727–728. *See also* Myocardial infarction
ATM (ataxia telangiectasia), 1084
ATP (adenosine triphosphate), 42. *See also* Electron transport; Oxidative phosphorylation
  AMP-to-ATP ratio, 804
  ATCase inhibition, 387
  biological importance, 460–461
  in Calvin cycle, 664, 665F
  chemical potential energy, 42
  coupled reactions involving, 463, 463T
  dissipation in dark reactions, 641, 664, 672–673F
  DNA ligase activation, 907F
  free energy of phosphate hydrolysis, 461T
  in fructose metabolism, 517F
  in galactose metabolism, 519F
  in gluconeogenesis, 553F, 554F, 557–558
  in glycolysis, 486–492, 487F, 490–491, 499, 503–504
  group transfer, **460–462**
  hydrolysis by type II topoisomerases, 863–864
  in mannose metabolism, 520F
  metabolic role overview, 451F
  and muscle contraction, 510, 795
  production control, **631–634**
  production in light reactions, 641, 647, 650–651F, 661–663
  regeneration, 464–465, 631
  and standard free energy, 462
ATPase(s), 165
  A-type, 311
  Ca^{2+}–, 313–314F
  F-type, 311
  P-type, 311
  $(Na^+–K^+)$–, 311F–313, 316
  V-type, 311
ATP-cassette binding protein A1 (ABCA1), 729
ATP-citrate lyase, in fatty acid synthesis, 702
ATP-driven active transport, **311–314**
ATP driven complexes, 1056
ATP hydrolysis, 311, 313
ATP mass action ratio, 631
ATP synthase (F_1F_0-ATPase), 618, **622–629**
  binding change mechanism, 624–629
  chloroplasts, 661
  F_0 component, 623–624
  F_1 component, 622–623
ATR protein kinase, 1086
Attenuators, **1051–1054**
A-type ATPases, 311
Autocatalytic trypsinogen activation, 357
Autoimmune diseases, **214–215,** 811
Autoinhibitor segments, 433
Autolysis, 357
Automated DNA sequencing, **55–56**
Autonomously replicating sequences (ARS), 912
Autophosphorylation, 413
Autoradiography, 367
  colony hybridization application, 64
  protein purification application, 102
  sequencing gel, 55F
Autotrophs, 449
Avery, O., 48
Avidin, 481
Avogadro's number, 13
Azathioprine, 844
3′-Azido-3′-deoxy thymidine (AZT, zidovudine), 384
Azotobacter vinelandii, 783
AZT (3′-Azido-3′-deoxythymidine, zidovudine), 384

B
BACs, *see* Bacterial artificial chromosomes
Bacillus anthracis, 444–445
Bacillus stearothermophilus, 512
Bacitracin, 563
Backbone, proteins, 127–129
Bacteria. *See also specific headings, e.g.:* Photosynthetic bacteria
  cell walls, **235–238,** 236F, 237F
  evolutionary studies, **9–11**
  fatty acids, 247
  gene insertion sequences, 1043–1044
  lipid bilayer fluidity modification, 262–263
  lysozyme action, 339–340
  microfossil, 2F
  tetracycline-resistant, 1025
  transformed pneumococci, 48F
Bacterial artificial chromosomes (BACs), 61
Bacterial biofilms, 234
Bacterial oxalate transporter, 310
Bacteriochlorophyll *a* (BChl *a*), 642F
Bacteriochlorophyll *b* (BChl *b*), 642F
Bacteriophages, 51
Bacteriophage 434, repressor, 876–877F
Bacteriophage , 60, 63F
Bacteriophage SP01, 947
Bacteriophage T4:
  genetic code, 986
  wild-type reversion rate, 909
Bacteriopheophytin (BPheo), 647
Bacteriorhodopsin, 265F
  proton pumping in, 608–609
  structure, 265F–266
Baker's yeast *(Saccharomyces cerevisiae):*
  codon usage bias, 999
  DNA chips, 479F
  80S rRNA, 1008F
  proteins from, 94
Baltimore, D., 912
*Bam*HI–DNA complex, 876
B antigens, 242F
Banting, F., 475, 811, 812
Barcroft, J., 191
Barnett, J., 307
Barr bodies, 1057F
Bases, 32–34
  conjugate acids, 32
  nucleotide, *see* Nucleotide bases
  strength, 33–34
Base excision repair (BER), **921–923**
Base-flipping, 921
Base pairs (bp), 46, 47, 851F
Basic helix–loop–helix (bHLH), 726, 882–883
Basic solutions, 31
Basolateral domain, 277
Bassham, J., 663
Bcd (bicoid) gene, 1092
B cells (B lymphocytes), 209
BChl *a* (bacteriochlorophyll *a*), 642F
BChl *b* (bacteriochlorophyll *b*), 642F
Bcl-2 family, 1089
B-DNA, 849, 851, 852T
  conformation, 850, 856F–857
  dimer stacking energies, 868T
Beadle, G., 49
Becker muscular dystrophy (BMD), 205
Beer–Lambert law, 95
Behenic acid, 247T
Benson, A., 663
Benzoic acid, 686
BER (base excision repair), **921–923**
Berg, P., 997
Beriberi, 509
Berman, H., 138
Bernal, J. D., 125, 182, 697
Berson, S. A., 408
Best, C., 475, 811, 812
βαβ Motif, 146
β anomers, 223F
β (Soret) band, 610
β barrels, 148
  transmembrane protein, 267
β bends, 134
β bulge, 139
β cells, pancreatic, *see* Pancreatic β cells
β-clamp, 630, 906
β hairpin motif, 146
β keratins, 134–136
β oxidation, 686, **688–690,** 698

βPP, *see* Aβ precursor protein
β propeller, 431
β proteins, 148
β sheet, **132–134,** 132F, 133F
β subunit, 906
b_H (cytochrome b_{562}), 148, 612
BHA, 290–291, 290F, 291F
bHLH (basic helix–loop–helix), 726, 882–883
Bibliome, 478
Bicarbonate:
  as buffer, 36
  role in carbon dioxide transport, 189
Bicoid (bcd) gene, 1092
Bicoid protein, 1092
Bidirectional replication, 894
Bilayers, *see* Lipid bilayers
Bile acids, 678, 678F
  cholesterol conversion to, 725
  and lipid absorption, 630
Bile salts, 678, 678F
Bilirubin, in heme degradation, 778, 779F
Biliverdin, in heme degradation, 778, 779F
Bimolecular nucleophilic substitution reactions, 336–337
Bimolecular reactions, 336–337, 365
Binding change mechanism, 624–629
Bioavailability, and toxicity, 396
Biochemical constants, 13
Biochemical signaling:
  and heterotrimeric G proteins, **428–436**
  and metabolic regulation, 803–804
  and phosphoinositide pathway, **436–445**
  and receptor tyrosine kinases, **412–428**
Biochemistry, 1, 13
Biocytin, 318T, 554
Biofilms, 234
Bioinformatics, **151–154**
Biological membranes, *see* Membranes
Biomolecule bond energies, 25T
Biopterin, 760
Biosphere, energy flow in, 18F
Biosynthetic pathways, 452
Biotin, 480–481
Biotin group, 554, 555F
Biotinyllysine, 554, 555F
1,3-Bisphosphoglycerate (1,3-BPG), 465
  in Calvin cycle, 665F, 666
  free energy of phosphate hydrolysis, 461T
  in gluconeogenesis, 553F
  in glycolysis, 487F, 497–499
2,3-Bisphosphoglycerate (2,3-BPG):
  binding of, to fetal hemoglobin, 191
  and blood oxygen carrying capacity, 502
D-2,3-Bisphosphoglycerate (BPG), 191
Bisphosphoglycerate mutase, 502
2,3-Bisphosphoglycerate phosphatase, 502
Bisubstrate reactions (enzyme kinetics), **375–376,** 375F
Bithorax complex (BX-C), 1094
Bithorax mutant *(bx),* 1092
b_L (cytochrome b_{566}), 612
Black, J., 844
Blackburn, E., 914
Blastocyst, 1066
Blastoderm, 1090
Blobel, G., 280, 1008
Bloch, K., 701, 721
Blood-brain barrier, 396
Blood buffering, 35–36
Blood coagulation:
  cascade, 358–359
  multidomain protein, 120F
Blood glucose:
  allowable levels, 794
  glucagon secretion and, 797
  and gluconeogenesis, 559F
  and liver glucose conversion to G6P, 796–797
  normal vs. non-insulin-dependent diabetics, 813F
Blood oxygen carrying capacity, 502
Bloodstream, 793
  fatty acid release into, 796
  triacylglycerol release into, 797
Blood types, 242
Blow, D., 351
Blue-green algae, *see* Cyanobacteria
Blunt ends, 52
Blunt end ligation, 908
B lymphocytes (B cells), 209
BMD (Becker muscular dystrophy), 205
Bohr, C., 189
Bohr effect, 189–190
Boltzmann constant (k_B), 13, 372
Bonaparte, N., 576
Bond energies, 25T
BoNT/A (botulinum neurotoxin A), 288
BoNT/G (botulinum neurotoxin G), 288
Bordetella pertussis, 435
Botulism, 288
Bovine carboxypeptidase A, 134F
Bovine chymotrypsinogen, hydropathic index plot, 157F
Bovine Complex I, 605F
Bovine cytochrome *c,* 612
Bovine cytochrome *c* oxidase, 616F
Bovine F_1-ATPase, 623F
Bovine insulin, 92F, 104
Bovine pancreatic RNase A, 333F
Bovine pancreatic trypsin inhibitor (BPTI), 356F
Bovine protein kinase A, 433F
Bovine rhodopsin, 429F
Bovine spongiform encephalopathy (BSE, mad cow disease), 169, 171
Boyer, H., 61
Boyer, P., 625
bp, *see* Base pairs
1,3-BPG, *see* 1,3-Bisphosphoglycerate
2,3-BPG, *see* 2,3-Bisphosphoglycerate
BPheo (bacteriopheophytin), 647
B protein, 971
BPTI (bovine pancreatic trypsin inhibitor), 356F
Bradford assay, 96
Brain:
  blood–brain barrier, 396
  mammalian metabolism in, **793–794,** 794F
Branched-chain amino acid degradation, 757–758
Branched-chain α-keto acid dehydrogenase, 580, 757
Branching enzyme (amylo-(1,4→1,6)-transglycosylase), 538, **543–544**
Branch migration, 927F, 928
Branden, C.-I., 667
Braunstein, A., 740
BRCA1, 934
BRCA2, 934
BRE, 959F
Breaker, R., 1055
Breathing, 158
Brenner, S., 986
Briggs, G. E., 369
Brittle bone disease, 137
Broad beans, 526
Broad-spectrum antibiotics, 1025
Brodsky, B., 138
Bromodomains, 1061–1063
5-Bromouracil (5BU), 940
Brønsted, J., 32
Brown, A., 366
Brown adipose tissue, 632
Brown fat, 632
BSE (bovine spongiform encephalopathy), 169
b-type cytochromes, 611–612
Bubonic plague, 426
Buchanan, J., 818
Buchner, E., 322
Buffers, **34–36**
Buffering capacity, 36
Bundle-sheath cells, 674
Bunick, G., 885
Burk, D., 373
Burley, S., 961, 962
αβ-trans-Butenoyl-ACP, 705F
N-Butyldeoxynojirimycin, 721
Butyramide, 319
Butyryl-ACP, in fatty acid synthesis, 705F
BX-C (bithorax complex), 1094
Bx (bithorax) mutant, 1092

C

C, *see* Cytosine
C2′-*endo* conformation, 856F
C3′-*endo* conformation, 856F

C3G, 443F
C_3 plants, 674
C_4 cycle, 673–674
C_4 plants, 674
Ca, *See under* Calcium
CA1P (2-carboxyarabinitol-1-phosphate), 671
Ca^{2+} ion:
  and calmodulin, 439–440
  citric acid cycle control, 587
  and glycogen breakdown control, 546–547
  with metal-activated enzymes, 335
  with proteins, 93
  and tropomyosin, 207F
  vitamin D control of, 256–257
Ca^{2+}–ATPase (Ca^{2+} pump), 313–314F
Cadmium (Cd^{2+}) ion, Zn^{2+} ion replacement, 326
Caenorhabditis elegans, 418, 1075, 1076
Caffeine, 435
Cahn, R., 85
Cahn–Ingold–Prelog (*RS*) system, 85
CAIR (Carboxyaminoimidazole ribotide), in IMP synthesis, 819F, 820
Cairns, J., 894, 919
CAK (cdk-activating kinase), 1082
Calcineurin (PP2B), 428
Calcium, and muscle contraction, 207. *See also under* Ca
Calf thymus histones, 884T
Calmodulin (CaM), 438–440, 547
Calnexin, 1033
Calreticulin, 1033
Calvin, M., 663
Calvin cycle (reductive pentose phosphate cycle), **663–669F,** 664F, 665F
  control, **670–671**
  free energy changes for reactions, 670T
CaM (calmodulin), 438–440, 547
CAM (crassulacean acid metabolism), 675
Cambillau, C., 679
Camels, fat storage in hump of, 677
cAMP (adenosine-3′,5′-cyclic monophosphate), 428, 546, 712
cAMP-dependent protein kinase (cAPK), 432, 546
CAM plants, 674–675
cAMP-phosphodiesterases (cAMP-PDEs), 436
cAMP receptor protein, 1050–1051, 1051F
Cancer, 488
  abnormal DNA methylation patterns, 1067
  L-asparaginase as anticancer agent, 751
  gangliosides and, 253
  and oncogenes, 421
  and telomerase, 915
  thymidylate synthesis inhibition, 838
  type II topoisomerases as anticancer agent, 865
Candida albicans, 594
Cantor, C., 873
CAP (Cbl-associated protein), 443F
CAP (catabolite activator protein, cAMP receptor protein), 1050–1051, 1051F
Cap-binding protein, 1014
Capillaries, oxygen transport in, 189–190
Capillary electrophoresis (CE), 103
cAPK (cAMP-dependent protein kinase), 432, 546
Capping, 915
Capping enzyme, 966
Cap structure, eukaryotic mRNA, 966F
CapZ, 205
Carbamate, 190, 745
N-Carbamoylaspartate, 386
Carbamoyl aspartate, in UMP synthesis, 825F
Carbamoyl phosphate, 460
  reaction with aspartate, 386
  in UMP synthesis, 825F
  in urea cycle, 743, 744F, 745
Carbamoyl phosphate, in urea cycle, 695
Carbamoyl phosphate synthetase (CPS) I, in urea cycle, 743, 745
Carbamoyl phosphate synthetase (CPS) II, in UMP synthesis, 824–825F
Carbinolamine intermediate, 330
Carbohydrates, **219–242**. *See also* Glycoprotein(s); Monosaccharides; Oligosaccharides; Polysaccharides
  catabolism overview, 452F
  defined, 219
  energy recovery by citric acid cycle, 567
  Fischer convention: D and L sugars, 221
  in gangliosides, 253F
  metabolism in liver, 796
  from photosynthesis, 640–641, 663–675
  and recognition events, 219, 241–242
Carbohydrate recognition markers, 286
Carbon, oxidation states of, 453
α Carbon, amino acids, 74–75, 83
Carbon—carbon bonds, 453
Carbon dioxide:
  from C_4 cycle, 673–674
  permeability to intermembrane space, 599
  from photorespiration, 671–675
  in photosynthesis, 640–641, 663–664
Carbon fixation, by photosynthesis, 640
Carbonic anhydrase, 189
  catalytic power, 323T
  Michaelis–Menten parameters, 371T
  Zn^{2+} role in, 336F
Carbon monoxide dehydrogenase, 693
Carboxymethylcysteine, 497
Carboxyaminoimidazole ribotide (CAIR), in IMP synthesis, 819F, 820
2-Carboxyarabinitol-1-phosphate (CA1P), 671
γ-Carboxyglutamate, 86F
Carboxyl group, 26F
Carboxylic acids:
  functional group and linkages, 4T
  reaction with amines, 3F
Carboxyl terminus, *see* C-terminus
Carboxymethylcysteine, 497
Carboxymethyl (CM) groups, in cation exchangers, 98
Carboxypeptidase A:
  β sheet, bovine, 134F
  catalytic power, 323T
2-Carboxypropyl-CoA, 694, 694F
Carcinogens, **919–920**
Cardiac glycosides, 313
Cardiolipin, 716
Carnitine, 687
Carnitine palmitoyl transferase I, 687, 805
Carnitine palmitoyl transferase II, 687
β-Carotene, 69, 257, 645
Carotenoids, 643F, 645
Carriers, 297
Carrier ionophores, 297
Cartilage, 235
Caspases, apoptosis participation, 1087–1088
Caspases (cysteinyl aspartate-specific proteases), 1087
Caspase-3, 1088
Caspase-7, 1088, 1088F
Caspase-8, 1088
Caspase-9, 1090
Caspase-10, 1088
Caspase-activated DNase, 1088
Cassette exons, 974
CAT (chloramphenicol acetyltransferase), 1068
Catabolism, 448
  overview, 452F
  purine ribonucleotides, **839–842**
  thermodynamics, 457
Catabolite gene activator protein (CAP), 1050–1051, 1051F
Catabolite repression, **1050–1051**
Catalase, 324, 371T, 636
Catalysis:
  electrostatic, 337
  lysozyme mechanism, 344
  proximity/orientation effects, 336–338
Catalysts, 6, 19. *See also* Enzymes
Catalytic constant, 371
Catalytic mechanism:
  chymotrypsin, 352–357
  lysozyme, 343–347
Catalytic perfection, 496
Catalytic triad, 350F–351
Cataracts:
  and diabetes, 811F
  and galactitol, 519
Catechol, 409, 780

Catecholamines, 409, 780–781F, 801
Catenation, 860F
CATH (database), 153
Cathepsins, 733
Cathepsin D, 286
Cation channels, 305–306
Cation exchanger, in chromatography, 98
Caveolae, 278
Caveolins, 278
CCAAT box, 959
CCVs (clathrin-coated vesicles), 284–285, 285F, 685
Cd^{2+} ion, Zn^{2+} ion replacement, 326
Cdks (cyclin-dependent protein kinases), 1082
Cdk2 (cyclin-dependent protein kinase 2), 1082
Cdk4/6-cyclin D complexes, 1086
Cdk7 (cyclin-dependent protein kinase 7), 1082
Cdk-activating kinase (CAK), 1082
cDNA (complementary DNA), 912
CDP–Diacylglycerol, 716
CDP–glucose, 561
CE (capillary electrophoresis), 103
CE (computer program), 153
Cech, T., 977–978
Celecoxib (Celebrex), 398, 719
Cells. *See also* Cancer; Eukaryotes; Prokaryotes
  components, 6–7F
  evolution, **5–7**
  lysing in protein purification, 94
  metabolic pathways in, 453–455
  microfilaments in nonmuscle, 207–209
Cell–cell recognition:
  cell-surface carbohydrates, 241–242
  gangliosides and, 253
Cell cycle, 883, 1081–1084
Cell cycle arrest, 1086
Cell membranes, 5–6, 8F. *See also* Membranes
Cell nucleus, 8F
Cell signaling, *see* Signal transduction
Cellular immunity, 209
Cellulase, 230
Cellulose, 228, **228–230,** 229F
Cell wall(s):
  bacterial, **235–238,** 236F, 237F
  Chaetomorpha, 229F
Central dogma of molecular biology, 49, 849, 942, 985
Centrioles, 8F
Centromeres, 1043
Ceramides, 252
  biosynthesis, 718F
  in sphingoglycolipid degradation, 720F
Cerebrosides, 252, 717, 718
CF_1CF_0 complex, 661
CFTR (cystic fibrosis transmembrane conductance regulator), 315–316
cGMP, 436
cGMP–PDEs, 436
CGN (cis Golgi network), 282
C_H (constant region), 212
C_H1, 212
C_H2, 212
C_H3, 212
Chain elongation:
  polypeptide synthesis, **1008–1010**
  RNA polymerase, **947–950**
Chain initiation:
  polypeptide synthesis, **1010–1014,** 1013F
Chain initiation codons, 990–991
Chain termination:
  polypeptide synthesis, **1026–1028,** 1026F
  RNA polymerase, **950–952**
Chain-terminator method, nucleic acid sequencing, **53–56,** 54F
Chair conformation, 342F
Chamberlin, M., 950
Changeux, J.-P., 193
Channels, 297
Channel-forming ionophores, 297
Channel-forming proteins, 267
Channeling, 745–746, 774
Chaotropic agents, 159, 263–264
Chaperones, molecular, 165–168
Chaperonins, 165–166
Chargaff, E., 44, 48
Chargaff's rules, 44, 47, 48
Charifson, P., 1088
Checkpoints, cell cycle, 1082
Chemical energy, transformation of light energy to, **645–647**
Chemical equilibria, *see* Equilibrium
Chemical evolution, **3–5**
Chemical kinetics, **364–366**. *See also* Enzyme kinetics
Chemical mutagenesis, **916–919**
Chemical potential, 16, 296
Chemical potential difference, membranes, 296
Chemical protons, 618
Chemiosmotic theory, **618–622**
Chemolithotrophs, 449
Cheng, Xiaodong, 1065
Chicken, muscle troponin, 204F
Chimera, 61
Chipman, D., 346
Chiral centers, 83
Chirality, 83
Chiral organic synthesis, 86
Chi sequence, 930
Chitin, 230
Chk2 (activated protein kinase), 1084
Chl *a* (chlorophyll *a*), 642F
Chl *b* (chlorophyll *b*), 642F
Chloramphenicol, 1025
Chloramphenicol acetyltransferase (CAT), 1068
Chloride ions, and transmembrane movement, 305
Chlorocruorins, 181
Chlorophylls, 642F, 643–645
  absorption spectra, 643F
  antenna, 643F
  electronic states, 646F
Chlorophyll *a* (Chl *a*), 642F
Chlorophyll *b* (Chl *b*), 642F
Chloroplasts, 8, **641–645,** 641F
  evolution, 10
  light-absorbing pigments, **643–645**
  oxygen generation, 655F
  oxygen yield per flash, 655F
  thylakoid membrane, **641–642**
Chloroquine, 394
Chocolate, 435
Cholecalciferol (Vitamin D_3), 256
Cholera toxin, 253, 435
Cholesterol, 254
  biosynthesis, **721–725**
  isotopic tracer studies, 476
  as membrane fluidity modulator, 262–263
  synthesis regulation, **725–727**
  transport, 683F, **727,** 729, 729F
  uses, 725
Cholesteryl esters, 254, 725
Cholesteryl stearate, 254
Choline, 349, 715, 249T
Chondroitin-4-sulfate, 232F
Chondroitin-6-sulfate, 232F
Chorea, 1045
Chorismate, 773
Chorismate mutase, catalytic power, 323T
Chou, P., 140, 163
Chromatin, 8F
  ATP-driven complexes, 1056
  electron micrograph, 887F
  higher level organization, **887–890**
  histones, **884,** 884T
  nucleosomes, **884–887,** 885F
  structure, 889F, **1055–1067**
Chromatin decondensation, 1060
Chromatin filaments, 887F–888
Chromatin-remodeling complexes, 1056–1058
Chromatography:
  affinity, 97, 101
  gel filtration, 97, **100–101**
  high-performance liquid (HPLC), 98
  hydrophobic interaction, 97
  hydroxyapatite, 872
  immunoaffinity, 101
  ion exchange, **97,** 99F
  metal chelate affinity, 101
  molecular sieve, **100–101**
  nucleic acids, **872**

  proteins, **101**
  size exclusion, **100–101**
Chromodomains, 1064
Chromophore, 96
Chromosomes, 47, 883F
  eukaryotic, **883–890**
  histone-depleted metaphase, 888F
  histones, **884,** 884T
  recombination, 938F
  replication of linear, 914F
Chromosome inactivation, 1057
Chronic myelogenous leukemia (CML), 424–425
Chylomicrons, 681, 809
Chylomicron remnants, 683
Chymotrypsin, 1068
  activation effects on active site, 358
  active site, 348, 352F
  catalytic mechanism, **352–357**
  function, 348
  geometric specificity, 326
  polypeptide degradation, 738
  specificity, 107T, 351
  tosyl-L-phenylalanine chloromethylketone binding, 348
  X-ray structure, 348–352
Chymotrypsinogen, 351
  activation effects on active site, 358
  hydropathic index plot, bovine, 157F
Cigarette smoking, protease inhibitor effects, 356
Ciliated protozoa, alternative genetic code in, 991
Cinchona tree, 394
Ciprofloxacin, 444, 865
Circular duplex DNA, 857F
Cis cisternae, 282
Cis conformation, 127
Cis Golgi network (CGN), 282
Cisternae, 282
Cisternal progression, 283
Cistron, 945
Citrate, 325, 567
  in amino acid degradation, 747F
  in citric acid cycle, 568F, 578–579, 584F
  in glyoxylate cycle, 591F
Citrate synthase:
  citric acid cycle, **577–578**
  in citric acid cycle, 568F
  in glyoxylate cycle, 591F
Citric acid cycle (Krebs cycle, tricarboxylic acid cycle, TCA cycle), 452
  acetyl-CoA synthesis, **570–574**
  aconitase, **578–579,** 587
  amino acid degradation, 747F
  amphibolic functions, 588F
  citrate synthase, **577–578,** 586
  coordinated control, 634F
  electron transport sites, 597F
  energy-producing capacity, 584
  evolution, 592–593
  fumarase, **583**
  and gluconeogenesis, 556
  glyoxylate cycle, **590–594,** 591F
  α-ketoglutarate dehydrogenase in, **585–587,** 586T
  malate dehydrogenase in, 568F, **583**
  NAD$^+$-dependent isocitrate dehydrogenase in, **579–580,** 579F, 586–587
  pathways using citric acid cycle intermediates, **588–589**
  products of, 584F
  purine nucleotide, 841
  pyruvate dehydrogenase in, 568F, 570–573
  related reactions, **588–591**
  replenishment of citric acid cycle intermediates, **589–590**
  succinate dehydrogenase in, 568F, **582,** 582F
  succinyl-CoA synthetase in, 568F, **580–582,** 581F
Citrulline, in urea cycle, 744F, 746
Citryl-CoA, 578
CJD (Cruetzfeldt–Jakob disease), 169–170
CKIs (cyclin-dependent kinase inhibitors), 1083
Cl$^-$ (chloride), 299
C$_L$ (constant region), 212
Clamp loader, 906–907
Class I aminoacyl-tRNA synthetases, 994–995
Class II aminoacyl-tRNA synthetases, 994–995
Class II genes, 1067
Class II gene promoters, 1069
Classification number (enzymes), 324–325
Clathrin, 284
Clathrin-coated pits, 685
Clathrin-coated vesicles (CCVs), 284–285, 285F, 685
Clathrin flexible cage, 285–286
Clathrin light chain (LCa), 275
Clathrin light chain (LCb), 275
Clay, and chemical evolution, 3
ClC Cl$^-$ channels, 305–306, 305F
Cl$^-$ channels, 305–306
Cleavage and polyadenylation specificity factor (CPSF), 966
Cleland, W. W., 375
Clinical trials, 396–398
Clones, 60
Cloned DNA, and selection, 61–62
Cloning, 51
  inclusion bodies, 94F
  shotgun, 63
  techniques, 60–62
Cloning vectors, 60–61
Closed systems, 18
Clostridium botulinim, 917
Clotting, *see* Blood coagulation
Clp, 737
ClpA, 737
ClpP, 737
ClpX, 737
CM (carboxymethyl) groups, in cation exchangers, 98
CML (chronic myelogenous leukemia), 424–425
CMP (cytidine monophosphate), 41T, 845F
Cn3D (computer program), 154
Co^{2+}, as cofactor, 335
CoA, *see* Coenzyme A
Coactivators, 1061
Coagulation, *see* Blood coagulation
Coagulation cascade, 358–359
CoA moiety, 1061
CoASH, *see* Coenzyme A
Coated vesicles, 283
  clathrin, 284–285
  protein transportation, 283–285
Coatomer, 285
Cobalamin, 692
Cobalamin coenzymes, 693
Cobra venom enzyme, 251F
Cochaperones, 165
Cockayne syndrome (CS), 924
Coding (sense) strand, 945F
Codons, 986, 989T
  chain initiation, 990–991
  evolution, 990
  frequently used, 999
  phenotypically silent, 990
  Stop, 974, 990, 1026
  synonyms, 989–990
Codon–anticodon interactions, **998–999**
Coenzymes, **327–328**
Coenzyme A (CoA, CoASH), 451–452, 468–469, 569. *See also* Acetyl-CoA
Coenzyme Q (ubiquinone), 257, 606F
Coenzyme Q$_6$, 606
Coenzyme Q$_8$, 606
Coenzyme Q$_{10}$, 606
Coenzyme Q–cytochrome *c* oxidoreductase, *see* Complex III
Coenzyme QH·, 606F
Coenzyme QH$_2$, 606F, 621
Cofactors, **326–328**
  metal ions as, 335–336
  prosthetic groups, 327
Cohen, P., 743
Cohen, S., 61
Coils, polypeptides, 139
Coiled coil structure, 134–135, 135F
Cointegrate, 937F
Colipase, 679
Collagen, 98T, 136–139F, 232
Collagen diseases, 137
Colligative properties, 29

Collins, F., 56, 57
Collip, J., 812
Colony hybridization, 64F–65
Colony-stimulating factors, genetically engineered, 67T
Combinatorial chemistry, 395
Compartmentation, cells, 5, 6F
Competition, 309
Competitive enzyme inhibition, **377–381,** 379F–380F
Competitive inhibitors, 377, 379
Complementarity, 5, 5F
  electronic, 325
  geometric, 325
Complementary base pairing, DNA, 46F
Complementary DNA (cDNA), 912
Complex I (NADH–coenzyme Q oxidoreductase), 602–603, **604–609**
  coenzymes of, 605–606
  electrons in, 606–607
  hydrophilic domain of, 607F
  reduction potentials, 604F
Complex II (succinate–coenzyme Q oxidoreductase), 602–603, 604F, **609–611**
Complex III (coenzyme Q–cytochrome *c* oxidoreductase; cytochrome bc_1), 602–603, 604F, **611–615,** 649–650
Complex IV (cytochrome *c* oxidase), 602–603, **615–618**
  control, 631
  reduction potentials, 604F
Complex V (ATP synthase; proton-pumping ATP synthase; F_1F_0-ATPase), 618, **622–629**
Composite transposons, 936F
Concerted acid–base catalyzed reactions, 331
Condensation reactions, 3, 78, 78F
Congenital erythropoietic porphyria, 778
Conjugate acids, 32
Conjugate bases, 32
Conjugate redox pair, 471
Connexins, 307, 308
Connexons, 308
Conservative replication, 893
Conservative substitution, amino acid residues, 116
Constant region (C_H), 212
Constant region (C_L), 212
Constitutive enzymes, 950
Contour length, 883
Contour maps, 141–142
Controlled rotation mechanism, 860, 862–863
Convergent evolution, 352
Coomassie brilliant blue, 96
Cooperative oxygen binding, 186–194
Cooperativity:
  hemoglobin oxygen binding, **186–194**
  protein denaturation, 158
  synergy, 1069
Cooperman, B., 833
COPI, 284–285
COPII, 285
Coproporphyrinogen III, in heme biosynthesis, 776F
Coproporphyrinogen oxidase, in heme biosynthesis, 776F
CoQ, *see* Coenzyme Q
Cordycepin, 983
Core, two-domain, 1049
Core enzyme, 943, 947
Core histones, posttranslational modifications, 1059
Corepressors, 1051
Core promoter element, 958
Core proteins, 234–235F
Corey, R., 127, 130, 132
Cori, C., 533, 798
Cori, G., 533, 798
Cori cycle, **798,** 798F
Cori's disease, 538, 539
Corn:
  chloroplast, 641F
  evolution, 59F
  transposition in, 934–935
Corrin ring, 693
Cortex, 409
Cortisol, 255F, 410
Cosubstrates, 327
  nicotinamide adenine dinucleotide (NAD^+), 327
  nicotinamide adenine dinucleotide phosphate ($NADP^+$), 327
Coulomb (unit), 13
Coupled enzymatic reactions, 95
Coupled reactions, high-energy compounds in, **462–464**
Covalent bond energies, 25T
Covalent catalysis, **333–335**
Covalent modification:
  enzymes, 324
  glycogen phosphorylase, 534, **546**
  glycogen synthase, **545, 550**
  for metabolic flux control, 458
  protein phosphorylation, 390–393
  proteins, 93
  pyruvate dehydrogenase, 585
COX, 718
COX-1, 719
COX-2, 719
COX-3, 719
Coxibs, 719
CP43 (PsbC), 653
CP47 (PsbB), 653
CpG islands, 918, 958, 1040
  chromosome inactivation, 1057
  palindromes, 1065
CPSF (cleavage and polyadenylation specificity factor), 966
CPS I, 743–745
CPS II, 745
Cramer, W., 656
Crassulacean acid metabolism (CAM), 675
Creatine kinase, 466, 513
Creatine phosphate, 460
Crick, F., 44, 49, 126, 200, 849–850F, 850, 893, 942, 986, 990
Cristae, 598
CrkII, 443F
Crohn's disease, 215T
Crossing-over, 927F
Cross talk, 421
Cruciforms, 891
Cruetzfeldt–Jakob disease (CJD), 169–170
Cryoelectron microscopy (cryo-EM), 1002
Cryptic splice sites, 974
CS (Cockayne syndrome), 924
CTCF, 1070
CTD (C-terminal domain), 391F, 955–956
C-terminal α helix, 1049
C-terminal cytoplasmic domain, 303
C-terminal domain (CTD), 391F, 955–956
C-terminus (carboxyl terminus), 78
  dynamics, 158
  as working end of polypeptide synthesis, 1008–1009
CTP (cytidine triphosphate):
  ATCase inhibition, 387
  synthesis, **826**
CTP synthetase, 826–827F
c-type cytochromes, 150
CuA center, cytochrome *c* oxidase, 616
CuB, cytochrome *c* oxidase, 617
Cubic symmetry, 155F
Cu ion:
  as cofactor, 326, 335
  Cu_A center, 616
  Cu_B, cytochrome *c* oxidase, 617
Curie, E., 408
Curved arrow notation, 330
Cushing's syndrome, 256
Cutaneous anthrax, 444
C-value paradox, 1038
Cyanide (CN^-), 603
Cyanobacteria, 640, 643F, 645. *See also* Photosynthetic bacteria
Cyanogen bromide, 108F
Cyanosis, 194
Cyclic symmetry, 155
Cyclins, 1082–1084
Cyclin A, 1082
Cyclin-dependent kinase inhibitors (CKIs), 1083
Cyclin-dependent protein kinases (Cdks), 1082
Cyclin H, 1082
Cyclooxygenase, 718
Cyclopentanoperhydrophenanthrene, 254
Cyclosporin A, 428

Cys, *see* Cysteine
Cys$_2$–His$_2$ zinc finger, 158F
Cys$_2$–His$_2$ zinc finger, 879F–881
Cys$_6$ zinc finger, 879F–881
CysRS, 998
Cystathionine, 754
Cysteine (Cys):
  acid–base catalysis by, 332
  α helix/β sheet propensities, 140T
  biosynthesis, 769
  breakdown, 747F, 748–751
  covalent catalysis by, 335
  disulfide bonds, 80F
  genetic code specification, 989T
  as rare amino acid, 93
  side chain hydropathy, 156T
Cysteine proteases, 1087
Cysteinyl aspartate-specific proteases (caspases), 1087
Cystic fibrosis, 56
Cystic fibrosis transmembrane conductance regulator (CFTR), 315–316
Cyt, *see* Cytosine
Cytidine, 41T, 845F
Cytidine deaminase, 845F, 976
Cytidine monophosphate (CMP), 41T, 845F
Cytidine triphosphate, *see* CTP
Cytochromes:
  function, 610–611
  heme prosthetic group, 327
Cytochrome *a,* 616
Cytochrome a_3, 616
Cytochrome *b,* 611–612
Cytochrome b_6, 656
Cytochrome b_6f complex, 650–651F, 656–657, 656F
Cytochrome b_{559}, 653
Cytochrome b_{560}, 610
Cytochrome b_{562} (b_H), 148, 612
Cytochrome b_{566} (b_L), 612
Cytochrome bc_1, *see* Complex III
Cytochrome *c,* 150, 151F, 602–603, 649F–650, 1089–1090
  in apoptosis, 1089–1090
  electron transport, 602–605
  evolution, **114–117,** 119F
  isoelectric point, 98T
  occurrence, 150
  as peripheral membrane protein, 269
  phylogenetic tree, 116–117F
  side chain location, horse heart, 147F
  as soluble electron carrier, 615
  species, 114–115T
Cytochrome c_1, 611–612
Cytochrome *c* oxidase, *see* Complex IV
Cytochrome *c* reductase, *see* Complex III
Cytochrome *d,* 621
Cytochrome *f,* 656–657
Cytochrome P450, **398,** 398–400
Cytokines, 422, 1070
Cytokine receptors, 1071
Cytoplasm, 8
Cytoplasmic domains, 314
Cytoplasmic loops, 305
Cytosine (Cyt), 40, 41T, 1065
  base pairing, 46F, 851F, 866–868
  Chargaff's rules and, 44
  as common nucleotide, 42
  modified forms in tRNA, 992F
  oxidative deamination, 917F
  reaction with hydroxylamine, 940
Cytoskeleton, 8, 274
Cytosol, 8. *See also* Fatty acid biosynthesis; Gluconeogenesis; Glycolysis; Pentose phosphate pathway; Urea cycle
  acetyl-CoA transport from mitochondria, for fatty acid biosynthesis, **701–702**
  heme biosynthesis in, 776F
  metabolic functions, 455T
  metabolite transport between mitochondria and, in gluconeogenesis, 556–557, 557F
Cytosolic (outer) faces, 283
Cytosolic palmitoyl-CoA, 805
Cytosolic reducing equivalents, 599

D
D (dalton), 13
D (Fischer convention), 83–84
D1 (PsbA), 652
D$_1$ proteins, 971
D2 (PsbD), 652
D$_2$ proteins, 971
D$_3$ proteins, 971
DAG, *see* 1,2-Diacylglycerol
Dalgarno, L., 1011
Dali (computer program), 153
Dalton (D), 13
Dam methyltransferase, 918
Danio rerio, 57T
Dansyl chloride, 105–106, 106F
Dark reactions, photosynthesis, 641, **663–675**
D Arm (tRNA), 991F
Darnell, J., 1071
Darst, S., 943
Darwin, C., 11, 59, 576
Darwinian evolution. *See* Evolution
Davies, D., 773
Davis, R., 61
Dawkins, R., 11
Dayhoff, M., 117
D-channel, 618
Dcm methyltransferase, 918
DCMU [3-(3,4-dichlorophenyl)-1,1-dimethylurea], 650
ddC (2′,3′-dideoxycytidine, Zalcitabine), 384
ddI (2′,3′-dideoxyinosine, Didanosine), 384
ddNTP, 54
Deadenylases, 1074
DEAE (diethylaminoethyl) groups, in anion exchangers, 98
Deamination, 732
Death ligand, 1088
Death receptor, 1088
5-Deazatetrahydrofolate (5dTHF), 820
Debranching enzyme, 231, 533, **536–537**
Decapping enzyme, 1074
Decoding, 1014
deDuve, C., 534
Deep View (computer program), 153
Degeneracy, codon, 999
Degenerate code, 986, 999T
Degradative pathways, 451–452
7-Dehydrocholesterol, 256
Dehydrogenases, sequential reaction mechanism, 375–376
Deletion mutations, 916–919
Δ^4-fatty acyl desaturase, 708
Δ^5-fatty acyl desaturase, 708
Δ^6-fatty acyl desaturase, 708
Δ^9-fatty acyl desaturase, 708
Demethylases, 1065
Denaturation:
  DNA, **864, 866,** 866F
  proteins, 94, **158–160**
Denatured (fully unfolded) proteins, 139
Denaturing conditions, 263–264
Denitrification, 788
5′-Deoxyadenosylcobalamin, 692, 693F
Deoxyhemoglobin, 183F
  bisphosphoglycerate (BPG) binding to, 191
  ion pairs and hydrogen bonds, 187F
Deoxyhemoglobin S, 196F
Deoxyribonucleic acid, *see* DNA
Deoxyribonucleotides, 40, 41F, **828–838**
β-D-2′-Deoxyribose, 40, 224, **828–834**
Deoxy sugars, 224
Deoxythymidine, 41T, 845F
Deoxythymidine monophosphate (deoxythymidylic acid, dTMP), 41T
Depolarization, 302
Depsipeptides, 955
Dermatan sulfate, 232F
Desaturases, 707–708
Desensitization, 430
Desert-dwelling succulent plants, 675
Detergents:
  membrane disruption, 263–264
  protein denaturation, 158–160
Development, molecular basis of, **1090–1097**
Dextrorotatory molecules, 84
DHAP, *see* Dihydroxyacetone phosphate
DHF (dihydrofolate), 835
DHFR (dihydrofolate reductase), 754, 836–837F

Diabetes mellitus, 215T, 475, **811–814.** *See also* Insulin
1,2-Diacylglycerol (DAG), 251, 437–438, 679
  activation of protein kinase C by, 440–442
  in fatty acid synthesis, 714
  in triacylglycerol biosynthesis, 710F
Diacylglycerol acyltransferase, in triacylglycerol biosynthesis, 710F, 711
Diacylglycerophospholipids, synthesis, 714–716
Dialysis, 30F
Diazotrophs, 782–783
Dicer, 1075
3-(3,4-Dichlorophenyl)-1,1-dimethylurea (DCMU), 650
Dickerson, R., 45, 351
Didanosine (2′,3′-Dideoxyinosine, ddI), 384
2′,3′-Dideoxycytidine (ddC, Zalcitabine), 384
2′,3′-Dideoxyinosine (ddI, Didanosine), 384
2′,3′-Dideoxynucleoside triphosphate, 54
3,5–2,4-Dienoyl-CoA isomerase, 692
2,4-Dienoyl-CoA reductase, 690
Diethylaminoethyl (DEAE) groups, in anion exchangers, 98
Diet-induced thermogenesis, 808
Differential gene splicing, 58
Diffraction patterns, 141F
Diffusion, **29–30**
  facilitated, 276, 297
  lipid bilayers, 261F
  thermodynamics, 296–297
Diffusion-controlled limit, 371
Digestion, 74
Digitalin, 313
Digitalis, 313, 394
Digitoxin, 313
Dihedral angles, polypeptides, 128
Dihedral symmetry, 155
7,8-Dihydrobiopterin, 762
Dihydroceramide, 718F
Dihydroceramide reductase, 718F
Dihydrofolate (DHF), 835
Dihydrofolate reductase (DHFR), 754, 837F
Dihydrolipoamide, in citric acid cycle, 573
Dihydrolipoyl dehydrogenase (E_3), 571, 574F, 580
Dihydrolipoyl transacetylase (E_2), 571, 575–576
Dihydrolipoyl transsuccinylase, 580
Dihydroorotase, in UMP synthesis, 825–826, 825F
Dihydroorotate, in UMP synthesis, 825–826, 825F
Dihydroorotate dehydrogenase, in UMP synthesis, 825–826, 825F
Dihydropteridine reductase, 762–763F
Dihydrouracil, in pyrimidine catabolism, 845F
Dihydrouracil dehydrogenase, in pyrimidine catabolism, 845F
Dihydrouridine, 992, 992F
Dihydroxyacetone, 221
Dihydroxyacetone phosphate (DHAP):
  in Calvin cycle, 665F, 666
  in fructose metabolism, 517F
  in glycolysis, 487F, 492–494
  in triacylglycerol biosynthesis, 710F
Dihydroxyacetone phosphate acyltransferase, in triacylglycerol biosynthesis, 710F, 711
1α,25-Dihydroxycholecalciferol, 256
Dihydroxyphenylalanine (L-DOPA), synthesis from tyrosine, 780–781F
Dihydroxythymine, in pyrimidine catabolism, 845F
Diimine, 786
Diisopropylphosphofluoridate (DIPF), 348
  neurotoxicity, 349
  as serine protease inhibitor, 355
Dimers, 44
N^6,N^6-Dimethyladenine, 977
Dimethylallyl pyrophosphate, 722–723F
5-Dimethylamino-1-naphthalenesulfonyl chloride, 105–106, 106F
5,6-Dimethylbenzimidazole, 693
N^2,N^2-Dimethylguanosine, 992F
Dimethyl sulfate, mutagenic effects, 917
2,4-Dinitrophenol (DNP), 630–631
Dintzis, H., 1008
Dinucleotide-binding (Rossmann) fold, proteins, 150
Dipalmitoyl phosphatidylcholine (DPPC), 250, 261F
Dipeptides, 78
DIPF, *see* Diisopropylphosphofluoridate
Diphosphate ester, functional group and linkages, 4T
Diphosphatidylglycerol, 249T
Diploid organisms, 47
Dipolar ions, 75F
Dipole–dipole interactions, 25F, 25T
Direct repeats, 935F
Disaccharides, **227**
Dissociation constant *(K)*:
  selected acids, 33T
  water, 31
Disulfide, functional group and linkages, 4T
Disulfide bonds:
  cleavage in protein sequencing, 106–107
  cysteine, 80F
  keratin, 136
  position determination, 112F
  and protein folding, 157–158
Diversity, 1079, 1081
DMD (Duchenne muscular dystrophy), 205
DNA (deoxyribonucleic acid), 39–40. *See also* B-DNA; Genes; Mutations; Nucleic acids; Nucleotides; RNA
  A-DNA, 852T
  base composition, **44**
  base pairing, 46F, 851F, **866–868**
  base stacking interactions, 867–868, 867F
  complementary strands, 46F
  contour length, 883
  denaturation, **864,** 864F, **866**
  double helix, **44–47,** 45F, **849–864**
  dynamic nature of, and evolution, 58–59
  evolution, 871
  flexibility, **855–857**
  forensic testing, 66
  as genetic information carrier, **47–48**
  geometry, **849–864**
  Hoogsteen base pairs, 866F
  hybridization, 866
  ionic interactions, **868**
  lack of uracil in, 921
  melting curve, 866, 866F
  methylation, 918
  nontranscribed, **1043–1046,** 1056
  nucleotides, 42
  palindrome sequences, 51–52F
  renaturation, **866,** 866F
  repetitive sequences, 1043
  selfish (junk), 1046
  shear degradation, 883
  supercoiled, *see* Supercoiled DNA
  unexpressed, 1038
  Watson-Crick base pairs, 46, 851F
  Z-DNA, 852–853F, 852T, 854, 857
DnaA protein, 903
DnaB protein, 903
DNA catalog, 49–50
DNA chips, 479F–480
DNA damage, *see* Mutation
DNA-directed DNA polymerases, 894, 895F
DNA fingerprinting, 66
DNA glycosylases, 921
DnaG protein, 904
DNA gyrase, 863
DnaJ, 1028–1029
DnaK, 1028–1029
DNA libraries, **62–65**
DNA ligase, 61, 896, 907F
DNA manipulation:
  applications, 67–70
  genomic libraries, **62–65**
  polymerase chain reaction, 65–67, 65F
DNA methylation (eukaryotes), 1066–1067
DNA methylation levels (epigenetic reprogramming), 1066
DNA methylation sites, 1042
DNA methyltransferases (DNA MTases), 1065

DNA microarrays, 479–480
DNA MTases (DNA methyltransferases), 1065
DNA photolyases, 920F
DNA polymerases, 894, 895F, 949
DNA polymerase I, *see* Pol I
DNA polymerase II (Pol II), 902
DNA polymerase III (Pol III), 902
DNA polymerase IV, 926
DNA polymerase V, 926
DNA polymerase β (pol β), 910
DNA polymerase γ (pol γ), 911
DNA polymerase η (pol η), 925
DNA-protein interactions, **874–883**
  eukaryotic transcription factors, **879–883**
  prokaryotic transcriptional control motifs, **876–879**
  restriction endonucleases, **875–876,** 875F, 876F
DNA recombination, *see* Recombination
DNA repair, **920–926**. *See also* Recombination
  base excision repair (BER), **921–923**
  direct damage reversal, **920–921**
  introduction of errors, **925–926**
  mismatch repair, **924–925**
  nucleotide excision repair (NER), **923–924**
  and Pol I, 899–900
  by recombination, **932–934**
  SOS response, **926**
DNA replication, 48, 48F, 58, 849. *See also* Eukaryotic DNA replication; Gene expression; Prokaryotic DNA replication
  complementarity and, 5
  overview, **894–896**
  postreplication repair, 932–933F
  replication forks, 894
  RNA primers, 896, 899F
  semiconservative, 893
  semidiscontinuous, 896
DNase, caspase-activated, 1088
DNase I, 899
DNMT1 protein, 1066
DNMT3a (DNA MTase), 1066
DNMT3b (DNA MTase), 1066
DNP (2,4-dinitrophenol), 630–631
dNTPs, 53
  and replication fidelity, 909
  synthesis, 833–834
  use in PCR, 64, 65F
Docking protein, 279
Dolichol-PP-oligosaccharide synthesis pathway, 562F
Dolichol pyrophosphate, 561F–562
Domains:
  apical, 277
  basolateral, 277
  protein duplication, 120
  protein evolution, 118
  proteins, **149–150,** 150F
Donohue, J., 44, 850
L-DOPA (dihydroxyphenylalanine), synthesis from tyrosine, 780–781F
Dopamine, 88, 780–781F
Dopamine β-hydroxylase, in neurotransmitter synthesis, 781F
Dosage compensation, 1057
Double blind tests, 397
Double-displacement reactions, 376
Double helix, **44–47,** 45F, **849–864**
Double-reciprocal plot, *see* Lineweaver-Burk plot
Double-stranded breaks (DSBs), 925–926
Double-stranded DNA (dsDNA), 899
Double-stranded RNA, 1075, 1076
Doudna, J., 1030
Down's syndrome, 169
Doxorubicin, 865
DPE, 959F
DPPC (dipalmitoyl phosphatidylcholine), 250, 261F
Drew, H., 45
Drosophila sp., 1070
  development, 1090–1091
  histone genes reiteration, 1042
Drosophila melanogaster:
  calmodulin, 439F
  development, 1090–1097
  genome sequencing, 57T
  26S proteasome, 735F
Drug design, **394–400**
  bioavailability and toxicity, 396
  clinical trials, 396–398
Drug–drug interactions, 398–400
Druker, B., 425
DSBs (double-stranded breaks), 925–926
DSCAM protein, 974
dsDNA (double-stranded DNA), 899
D segment, 1079
dTMP (deoxythymidine monophosphate), 41T
Dual-specificity tyrosine phosphatases, 426
Duchenne muscular dystrophy (DMD), 205
dUTP diphosphohydrolase (dUTPase), 834F
Dwarfism, 411
Dystrophin, 205, 968

E
$\mathscr{E}$, *see* Reduction potential
E (exit) site, 1006
E. coli, see Escherichia coli
E_1, *see* Pyruvate dehydrogenase
E_1 (conformational state), 312
E-1 (low-affinity lactose binding site), 317
E1 (ubiquitin-activating enzyme), 734
E_2 (conformational state), 312
E_2 (dihydrolipoyl transacetylase), 571, 575–576
E-2 (high-affinity lactose binding site), 317
E2s (ubiquitin-conjugating enzymes), 734
E2F family (of transcription factors), 1086
E3, *see* Ubiquitin-protein ligase
E_3 (dihydrolipoyl dehydrogenase), 571, 574F, 580
E3a, 735
E_3 binding protein, 572
E4P, *see* Erythrose-4-phosphate
Early genes, 947
EC classification number, 324–325
*Eco*RI endonuclease, 52T, 875F–876
*Eco*RV endonuclease, 52T, 876, 876F
Edema, 256
Edema factor (EF), 444–445
Edidin, M., 270
Editing, RNA, 975
Edman, P., 109
Edman degradation, 106, **109–110,** 109F, 111
Edman's reagent, 109
eEF1A, 1025
eEF1B, 1025
eEF2, 1025–1026
EF (edema factor), 444–445
Effector (executioner) caspase, 1088
EF-G, 1022
EF hands, 438, 439F
EF-Ts, 1015
EF-Tu, 1015–1016, 1018
EGF (epidermal growth factor) receptor, 421
Ehlers–Danlos syndromes, 137
Eicosanoids, **258–259,** 259F
eIF2, 1013
eIF2B (initiation factor), 1077
eIF2 phosphatase, 1077
eIF4A, 1014
eIF4E, 1014
eIF4F, 1014
eIF4G, 1014
eIF5B, 1014
18S rRNA, 977, 1007
80S ribosome, 1008F
Eisenberg, D., 667
EJC (exon-junction protein complex), 1074
Eklund, H., 829
Elastase:
  function, 348
  polypeptide degradation, 738
  proelastase activation to, 358
  specificity, 107T
  substrate specificity, 351
  X-ray structure, 348–352
Elastin, 351
ELC (Essential light chains), 201
Electrical potential difference, 471
Electroblotting, 874

Electrochemical cells, 471F–472
Electrochemical gradients, 312, 316
Electrochemical potential, 296
Electrogenic antiport, 600
Electromagnetic radiation, 645
Electromotive force (emf), 472
Electron acceptors, 470–471
Electron beam, 266
Electron crystallography, 265, 266
Electron crystal structures, 308, 310F
Electron density, 142
Electron density maps, 141
Electron donors, 470–471
Electronic complementarity (enzymes), 325
Electron micrographs, 283F
Electron-transfer flavoprotein (ETF), 688
Electron-transfer reactions, 469, 474
Electron transport, 504
  bacteria, 621
  Complex I, 605
  Complex II, 609
  Complex III: Q cycle, 612–614
  Complex IV, 618
  Complex V (ATP synthase), **618–622**
  photosynthetic bacteria, **647–650**
  sequence of, 602–604, 647–662
  thermodynamics, 601
  two-center, photosynthesis, **650–663**
Electron-transport chain, **597–618**
  inhibitors, 603–604
  reduction potentials, 604F
Electrophoresis:
  agarose gel, 872–873
  capillary (CE), 103
  nucleic acids, **872–873,** 873F
  nucleic acid sequencing, **52–53,** 52F, 54F, 55F
  polyacrylamide gel (PAGE), **101–103**
  protein purification, 101–103
  proteins, **101–103**
  pulsed-field gel (PFGE), **873**
  SDS-PAGE, 102–103
Electrospray ionization (ESI), 111F
Electrospray ionization mass spectrometry (ESI-MS), 347
Electrostatic catalysis, **337**
Electrostatic interactions, proteins, 156–157
Elementary reactions, 364
Eliminations, 453
Elion, G., 838, 844
ELISA (enzyme-linked immunosorbent assay), 95F, 102
Elk-1, 420F
Elongases, 707–708
Elongation factors, 1012T, 1015
Elongator, 965
Eluant, 99
Elution, 99
Embden, G., 486
Embden–Meyerhoff–Parnas pathway, 486
Embryonic mouse paw cell death, 1087F
Emergent properties, 444
Emf (electromotive force), 472
Enantiomers, 83–86
Endergonic processes, 14, 448–449
End groups, 104–105
End group analysis, 104–106
endo conformation, 856–857
Endocrine glands, 406
Endocrine hormones, 406–407
Endocrine system, 406F, 799
Endocytosis, 278
  clathrin-coated vesicles, 286
  receptor-mediated, **684–685**
Endoglycosidases, 226–227
Endonucleases, 51, 858–859
Endopeptidases, 107, 107T
Endopeptidase V8, specificity, 107T
Endoplasmic reticulum (ER), 8, 8F, 438. *See also* Rough endoplasmic reticulum (RER)
  glycosylated protein synthesis in, 239
  lipid biosynthesis, 275
  smooth, 8F, 455T
Endosome, 290
Endosomes, 685
Endosymbiosis, 10
Endothelium-derived relaxing factor, 781
Endotoxic shock, 782
Enediol (enediolate) intermediate, 494
Energy, 12
  activation, **328–330**
  conservation of, 12
  flow in biosphere, 18F
  as state function, 15
  transformation of light energy to chemical energy, 645–647
Energy coupling, 618
Energy reserves, fats vs. glycogen, 248–249
Energy-rich compounds, *see* High-energy compounds
Engrailed (en) gene, 1091
Enhanceosome, 1068
Enhancers, 959–960, 1067
Enolase, in glycolysis, 487F, **500**
Enolate, in glycolysis, 492F
Enolpyruvate, 502
Enoyl-ACP reductase, in fatty acid synthesis, 705F
Enoyl-CoA hydratase, 688
Enoyl-CoA isomerase, 690
3,2-Enoyl-CoA isomerase, 690
Enteropeptidase, 357
Enthalpy, 12, 14–15
Entropy:
  and hydrophobic effect, 26–27
  and life, 17–19
  and second law of thermodynamics, 13–14
  as state function, 15
Enzymatic interconversion, *see* Covalent modification
Enzymes, 19. *See also* Protein(s); *specific enzymes and classes of enzymes*
  activation energy, **328–330**
  catalysis of reactions of metabolic pathways, 452–453
  catalytic efficiency, 329–330
  catalytic perfection, 496
  catalytic power of selected, 323T
  channeling, 774
  classification by reaction type, 324T
  coenzymes, **327–328**
  cofactors, **326–327**
  constitutive, 950
  coupled enzymatic reactions, 95
  electrophilic groups, 335F
  general properties, **323–328**
  geometric specificity, 326
  inducible, 950
  isozymes, 455
  metabolic thermodynamics, 455–457
  metal-activated, 335–336
  nomenclature, **324–325**
  nucleophilic groups, 335F
  processive, 896–897
  reaction coordinate, **328–330**
  stereospecificity, 325–326
  substrate specificity, 324, **325–326**
  synthesis by genes, 49–50
  X-ray crystallography, 340, 342
Enzyme action, 369
Enzyme activity regulation, **386–393**
  allosteric control, 386–390
  covalent modification, 390–393
  mechanism of, 324
Enzyme inactivator, 385
Enzyme inhibition, **377–385**
  competitive, **377–381,** 379F, 380F, 381T
  mixed, 381T, **382–383,** 383F
  noncompetitive, 382–383
  transition state analogs, 339
  uncompetitive, **381–382,** 381T, 382F
Enzyme inhibitors, 377
Enzyme kinetics, 364, **366–376**
  bisubstrate reactions, **375–376,** 375F
  data analysis, 364, **372–375**
  Michaelis–Menten equation, 368–372
  steady state kinetic measurements, 374–375
  transition state theory and, 372
Enzyme-linked immunosorbent assay (ELISA), 95F
Enzyme mechanisms:
  acid–base catalysis, **331–333**
  covalent catalysis, **333–335**
  electrostatic catalysis, **337**
  metal ion catalysis, **335–336**
  orientation effects, **336–338,** 336F

  - pH effects, 332
  - preferential transition state binding, **338–339,** 338F
  - proximity effects, **336–338**
- Enzyme saturation, 370
- Enzyme–substrate complex, 325F, 338–339, 367
- Enzyme system, as enzymatically interconvertible, 545–546F
- Enzyme–transition state complex, 338–339
- Enzymology, 322, 363–364, 475
- EPA (fatty acid), 247T
- Epidermal growth factor (EGF), 120F
- Epidermal growth factor receptor, 421
- Epigenetic genome changes, 1066
- Epigenetic programming, aberrations, 1067
- Epigenetic reprogramming, DNA methylation levels, 1066
- Epimers, 221
- Epimerization, 224
- Epinephrine (adrenaline), 407, 409
  - and fatty acid metabolism, 712
  - fight or flight reaction, 551
  - and fuel metabolism, 799, 801–803
  - glycogen metabolism effects, 552
  - insulin as antagonist, 552
  - synthesis from tyrosine, 780, 781F
- E proteins, 971
- Equal®, 228
- Equilibrium, **15–17**
  - near-equilibrium reactions, 456, 631
  - temperature and, 16–17
- Equilibrium constant (K_{eq}), 16
- ER, *see* Endoplasmic reticulum
- eRF1, 1026
- Ergocalciferol (Vitamin D_2), 256
- Ergosterol, 256
- ERKs (extracellular-signal-regulated kinases), 419
- ER-resident proteins, 286–287
- Erythrocytes, 181
  - antigenic determinants, 242F
  - 2,3-BPG synthesis, 502
  - carbon dioxide transport, 189–190
  - glycocalyx, 241F
  - glycophorin A, 264F
  - heme biosynthesis in, 777–778
  - lysis, 194
  - membranes, **272–274,** 273F
- Erythrocyte ghosts, 272
- Erythrocyte glucose transporter (GLUT1), 307
- Erythropoietic protoporphyria, 778
- Erythropoietin, genetically engineered, 67T
- D-Erythrose, 220F
- Erythrose-4-phosphate (E4P):
  - in Calvin cycle, 665F, 666
  - in pentose phosphate pathway, 521F, 524
- D-Erythrulose, 221F
- *Escherichia coli (E. coli),* 8, 316, 386
  - alternative splice site selection, 975F
  - biosynthesis thiamine pyrophosphate, 1054
  - catabolite repression, 1050–1051
  - cellular contents, 988
  - chromosome, 895F
  - cloning vectors from, 60–62
  - codon usage bias, 999
  - cross section, 6F
  - DNA polymerases, 896–902
  - and DNA polymerases, 53
  - fatty acid biosynthesis, 703
  - gene number, 1039
  - genome sequencing, 57T
  - *his* operon, 1053
  - hot spots, 941
  - *ilv* operon, 1053
  - *lac* operon, **1048–1050**
  - *lac* repressor, 1048–1050
  - lactose metabolism, 1046
  - leading and lagging strand synthesis, **904–905,** 905F
  - *met* repressor, 878F
  - molecular cloning techniques, 1049
  - nontranscribed DNA, 1043
  - nucleotide excision repair, 923F
  - polypeptide synthesis in, 1011
  - primosome, 904
  - proteins from, 94
  - pyrimidine synthesis regulation, 827F
  - recombination in, 928–930, 929F–930F
  - replication fidelity, 909
  - replication termination, 908–909
  - replisome, 904–905F
  - ribosome, components of, 1001T
  - RNA polymerase, 943F–945
  - RNA primers, 896, 899F
  - rRNA posttranscriptional processing, 976F
  - SOS response, 926
  - transcription, 943–952
  - tRNA posttranscriptional processing, 976F
  - *trp* operon, genetic map, 1051F–1054
  - *trp* repressor, 877F–878
  - type III topoisomerase, 860–861F
  - wild-type reversion rate, 909
- *Escherichia coli* complex II, 609–611
- *Escherichia coli* maltoporin, 298–299
- *Escherichia coli* OmpF porin, 267F, 298
- ES complex, 325F, 338–339, 367
- ESEs (exonic splicing enhancers), 975
- ESI (electrospray ionization), 111F
- ESI-MS (electrospray ionization mass spectrometry), 347
- Essential amino acids, 764T, **769–774**
- Essential fatty acids, 293
- Essential light chains (ELC), 201
- ESSs (exonic splicing silencers), 975
- Esters, functional group and linkages, 4T
- Ester group, 4T
- β-Estradiol, 255F, 410
- Estrogens, 255, 410
- ESTs (expressed sequence tags), 1040
- ETF (electron-transfer flavoprotein), 688
- ETF:ubiquinone oxidoreductase, 688
- Ethanol, 326, 327, 379
- Ethanolamine, 715, 249T
- Ether, functional group and linkages, 4T
- Ethidium ion, as intercalating agent, 873F
- Ethylene gylcol, 379
- O^6-Ethylguanine, 921
- Ethylnitrosurea, mutagenic effects, 917
- Etoposide, 865
- Ets-1, 420F
- Eubacteria, 9
- Euchromatin, 1056
- Eukarya, 9F
- Eukaryotes, **7–9**
  - cell cycle, 883, 1081F
  - chromosome structure, **883–890**
  - citric acid cycle in, 570
  - classification, 9
  - evolution, 9–10
  - gene clusters, 1042
  - gene number, selected organisms, 1039T
  - lipid biosynthesis, 275F
  - membranes, 263
  - metabolic functions, 455T
  - new membrane generation, 277
  - nucleus, 1056F
  - photosynthesis in, 641
  - polypeptide synthesis in, 1025–1026
  - protein degradation in, 734–735
  - pyruvate dehydrogenase complex, 571–572
  - repetitive DNA, 1044–1046
  - transposons, 935, 938–939
- Eukaryotic DNA replication, **910–915**
  - multiple origins, **911–914**
  - telomerase, **914–916**
  - telomeres, **914–916**
- Eukaryotic gene expression, **1055–1097**
  - chromatin structure, **1055–1067**
  - molecular basis of development, **1090–1097,** 1091F
  - posttranscriptional control mechanisms, **1073–1077**
  - selective, by differentiated cells, 960
  - somatic recombination, **214**
  - transcription control, **1067–1073**
  - transcription factors, **879–883**
  - translational control, **1076–1077**
- Eukaryotic motifs, structure of, 879–881
- Eukaryotic mRNAs, 965–976
- Eukaryotic pre-tRNAs, 981–982
- Eukaryotic ribosomes, **1007–1008**
- Eukaryotic rRNAs, 977–978

Eukaryotic transcription, **952–965**
  RNA polymerase promoters, **958–965**
  RNA polymerases, **953–958**
  transcription factors, **960–965**
Eukaryotic tRNAs, 980–982
Evans, P., 512, 694
Even-chain fatty acid oxidation, 686
Even-skipped gene *(eve),* 1093F
Evolution. *See also* Mutation
  352, 345
  amino acids, 74
  chemical, **3–5**
  citric acid cycle, 592–593
  DNA, 871
  genetic code, 990
  histones, 884
  natural selection, 114
  nucleic acid sequence and, 58–59
  nucleotides, 40l
  organismal domains of, **9–10**
  principles of, 11
  proteins, 92, **114–117**
  serine proteases, 352F
Evolutionarily conservative proteins, 116
Exciton transfer, 646–647
Executioner (effector) caspase, 1088
Exergonic processes, 14, 448–449
Exit channel, 618
Exit (E) site, 1006
exo conformation, 857
Exocrine glands, 407
Exocytosis, 287
Exoglycosidases, 226–227
Exons (expressed sequences), 967
  splicing, 969F–971
Exonic splicing enhancers (ESEs), 975
Exonic splicing silencers (ESSs), 975
Exon-junction protein complex (EJC), 1074
Exon skipping, 970–971
Exonucleases, 51
Exopeptidases, 107
Exosomes, 1074
Expressed sequences, *see* Exons
Expressed sequence tags (ESTs), 1040
Expression, *see* Gene expression
Expression vector, 67
Extinction coefficient, 95–96
Extracellular apoptosis, 1088–1090
Extracellular factors, gene expression, 1070
Extracellular fluids, buffering, 35–36
Extracellular-signal-regulated kinases (ERKs), 419
Extremophiles, 475
Extrinsic membrane proteins, **269**
Extrinsic pathway, apoptosis, 1088
Extrinsic pathway, blood coagulation cascade, 358
Eyring, H., 328

F
$\mathscr{F}$ (Faraday), 471
F_1F_0-ATPase, *see* ATP synthase
F1P, *see* Fructose-1-phosphate
F2,6P (fructose-2,6-bisphosphate), 512, 558–559
F6P, *see* Fructose-6-phosphate
Fab fragments, 210F, 211
Fabry's disease, 720
Facilitated diffusion, 276, 297
F-actin, 202, 204F
Factor V, 358
Factor Va, 359
Factor VII, 358
Factor VIIa, 359
Factor VIII, 358
Factor VIIIa, 359
Factor IX, 67T, 358
Factor IXa, 359
Factor X, 67T, 358
Factor Xa, 359
Factor XI, 358
Factor XIII, 358
Facultative anaerobes, 449
FAD (flavin adenine dinucleotide), **469–470.** *See also* $FADH_2$
  in citric acid cycle, 568F, 569, 570, 572T, 582
  in glyoxylate cycle, 591F
  reduction to $FADH_2$, 470F
FADD (fas-associating death domain-containing protein), 1088
$FADH_2$ (flavin adenine dinucleotide, reduced form). *See also* FAD
  in citric acid cycle, 567, 569, 570
  FAD reduction to, 470F
  P/O ratio in oxidative phosphorylation, 629–630
$FADH_2$ (flavin adenine dinucleotide, reduced form), 452
FAICAR (5-formaminoimidazole-4-carboxamide ribotide), in IMP synthesis, 819F, 820
Familial hypercholesterolemia (FH), 728
Faraday ($\mathscr{F}$), 13, 471
Farber's lipogranulomatosis, 720
Farnesyl pyrophosphate, 723, 723F
Farnesyl residue, 268
Fas (transmembrane protein), 1088
Fas-associating death domain-containing protein (FADD), 1088
FasL (fas ligand), 1088
Fas ligand (FasL), 1088
Fasman, G., 140, 163
Fasting:
  amino acid metabolism during, 797–798
  brain effects, 794
  gluconeogenesis during, 530, 552
  and glucose–alanine cycle, 799
  lysosomal protein degradation, 733
Fast-twitch muscle fibers, 511, 798
Fats, 248
Fat cells, *see* Adipocytes
Fat-soluble vitamins, 257, 450
Fatty acids, **246–249,** 247T
  amphiphilic nature of anions, 28F
  energy recovery by citric acid cycle, 567
  essential, 293
  membrane proteins, 267–269
Fatty acid binding protein, 680F
Fatty acid biosynthesis, **701–711,** 701F
  acetyl-CoA carboxylase, **702–703**
  cellular location, 453–454
  citric acid cycle intermediates, 589
  desaturases, 707–708
  elongases, 707–708
  fatty acid synthase, **703–707**
  mitochondrial acetyl-CoA transport to cytosol, **701–702**
  triacylglycerols, **711**
  triclosan, 708
Fatty acid metabolism:
  mammalian, 792F, 793, 797
  regulation, **711–714**
Fatty acid oxidation, **685–698**
  activation, **686**
  AMPK and promotion of, 805
  β oxidation, 686, **688–690,** 701F
  β oxidation, peroxisomal, **698**
  electron transfer in, 597
  even-chain fatty acids, 686
  mammalian metabolism, 792F, 793
  odd-chain fatty acids, 686, **692–697**
  thermodynamics, 690
  transport across mitochondria, **686–687**
  unsaturated fatty acids, **690–692**
Fatty acid synthase, **703–707,** 801
Fatty acid synthesis, mammalian metabolism, 792F, 793, 797
Fava beans, 526
Favism, 526
FBP, *see* Fructose-1,6-bisphosphate
FBPase, *see* Fructose-1,6-bisphosphatase
FBPase-2 (fructose bisphosphatase-2), 558
Fc fragment, 211–212
Fd (ferredoxin), 660
FdUMP (5-fluorodeoxyuridylate), 838
Fe^{2+}:
  as cofactor, 335
  in heme group, 178F–179
Fe^{3+}:
  as cofactor, 326, 335
  in ribonucleotide reductase, 829F
Feedback inhibitors, 387
Feedforward activation, 823
Feigon, J., 1058
Female sex hormones, 410, 411
FeMo-cofactor, in nitrogenase, 784
Fen (fenfluramine), 397
FEN1 (flap endonuclease-1), 911

Fenfluramine (fen), 397
Fe-protein, in nitrogenase, 783
Fermentation, 322, 485, **504–510**
  alcoholic, **506–509**
  energetics of, 509–510
  homolactic, **505–506**
  thermodynamics, **509–510**
Ferredoxin (Fd), 660, 785
Ferredoxin-$NADP^+$ reductase (FNR), 652
Ferredoxin–thioredoxin reductase, 671
Ferritin, 69
Ferrochelatase, in heme biosynthesis, 776F
Ferryl oxidation state, 617
Fe–S clusters, *see* Iron–sulfur clusters
Fetal hemoglobin, 118, 191, 1043
Ffh, 1030
FGAM (formylglycinamidine ribotide), in IMP synthesis, 819F, 820
FGAM synthetase, in IMP synthesis, 819F
FGAR (formylglycinamide ribotide), in IMP synthesis, 819F, 820
FH (familial hypercholesterolemia), 728
Fibrin, 168, 358
Fibrinogen, 119, 168, 358
  isoelectric point, 98T
Fibrinopeptides, evolution rate, 119F
Fibronectin, 120F
Fibrous proteins, **134–139**
50S subunit, 1001–1006
"Fight or flight" reaction, 551
Fire, A., 1075
FirstGlance (program), 153
First law of thermodynamics, **12**
First-order reactions, 364–365, 365F
Fischer, E., 83, 325, 369
Fischer convention, 84F, 221
Fischer projections, 84
Fish, lipid bilayer fluidity modification, 262
5.8S rRNA, 977, 1007
5′ End, nucleic acids, 43–44
5S RNA, 868–869, 976
5dTHF (5-deazatetrahydrofolate), 820
Flap endonuclease-1 (FEN1), 911
Flavin adenine dinucleotide, *see* FAD
Flavin coenzymes:
  Ping Pong reaction mechanism, 376
Flavin mononucleotide (FMN), 606, 606F
Flavoprotein dehydrogenase, 599
Fleming, A., 238
Fletterick, R., 391
Flexibility, of DNA, **855–857**
Flipases, 276
Flip-flop, 261
Fluid mosaic model, membranes, **270–272**
Fluorescence, 646
Fluorescence photobleaching recovery measurements, 270–271F
Fluorochlorobromomethane, enantiomers, 83F
5-Fluorocytosine, 1065
5-Fluorodeoxyuridylate (FdUMP), 838
Fluorophore, 270
Flux, 309, **456–459**
fMet (*N*-formylmethionine), 1011
$\text{fMet-tRNA}_{\text{f}}^{\text{Met}}$, 1012–1013
FMN (flavin mononucleotide), 606, 606F
FMNH· (flavin mononucleotide, reduced form radical), 606F
$FMNH_2$ (flavin mononucleotide, reduced form), 606F
FMRP, 1044
FNR (ferredoxin–$NADP^+$ reductase), 652
Folate, reduction to THF, 754–756F
Folding funnel, 162
Folic acid, 754
Following substrates, 376
Fomaldehyde, geometric specificity, 326
Footprinting, 946
Forensic DNA testing, 66
5-Formaminoimidazole-4-carboxamide ribotide (FAICAR), in IMP synthesis, 819F, 820
Formate, 310
N-Formiminoglutamate, 752
N^5-Formimino-tetrahydrofolate (N^5-Formimino-THF), 752F
Formylglycinamide ribotide (FGAR), in IMP synthesis, 819F, 820
Formylglycinamidine ribotide (FGAM), in IMP synthesis, 819F, 820
N-Formylmethionine (fMet), 1011
48S initiation complex, 1014
Fos, 419, 1070
Fossil record, 9, 59
[4Fe–4S], *see* Iron–sulfur clusters
45S rRNA, 977
434 Repressor, 876–877F
Fowler's solution, 576
Foxglove plant, 394
F proteins, 971
Fractional saturation, of oxygen in myoglobin, 179–180
Fractionation:
  nucleic acids, **872–874**
  proteins, 97F
Fragile X syndrome, 1044, 1044T
Frameshift mutations, 986
Frank, J., 1002, 1008, 1019
Franklin, R., 44, 850
Free energy (*G*), **14–15**
  ATP and, 462
  chemical reactions, 14–17
  standard state, 17
  as state function, 15
Free energy of activation, 18–19, 328–330, 338–339, 372
Free radicals, 606
Fridovich, I, 636
Friedrich's ataxia, 1044T
Frozen-accident theory of codon evolution, 990
α-D-Fructofuranose, 222F
β-Fructofuranosidase, 366
Fructokinase, in fructose metabolism, 516, 517F
Fructose, 221, 228
  intolerance, 518
  metabolism, **516–518,** 517F
D-Fructose, 221F, 222F
Fructose-1,6-bisphosphatase (FBPase), 514–515F, 801
  in Calvin cycle, 665F, 666, 670–671
  in gluconeogenesis, 557
Fructose-1,6-bisphosphate (FBP):
  in Calvin cycle, 664, 665F
  in gluconeogenesis, 553F, 558
  in glycolysis, 487F, 491
Fructose-1-phosphate (F1P), 516, 517F, 797
Fructose-1-phosphate aldolase, in fructose metabolism, 516, 517F
Fructose-2,6-bisphosphate (F2,6P), 512, 558–559, 804
Fructose-6-phosphate (F6P):
  in Calvin cycle, 665F, 669
  free energy of phosphate hydrolysis, 461T
  in fructose metabolism, 517F
  glucokinase inhibition, 796–797
  in gluconeogenesis, 553F, 557
  in glycolysis, 487F, 490–491
  in mannose metabolism, 520F
  in pentose phosphate pathway, 521F, 524
Fructose bisphosphatase-2 (FBPase-2), 558
Fructose intolerance, 518
Fruit fly, *see Drosophila*
FSSP (database), 153
F-type ATPases, 311
Ftz (fushi tarazu) gene, 1093F
L-Fucose, 224
Fuel metabolism, hormonal control of, **799–804**
  and catecholamines, 801
  disturbances, 809–815
  and glucagon, 801–803
  and glucose, 800
  and homeostasis, 799. *See also* Metabolic homeostasis
  insulin, 800–803
  and liver gluconeogenesis/glycogenolysis, 801
  receptors, 803
  signaling pathways, 803
  and storage of fuel, 800–801
Fumarase, 332
  in citric acid cycle, 568F, **583**
  pH effects, 332
  in urea cycle, 744F

Fumarate, 567
  in amino acid degradation, 747F
  in citric acid cycle, 377, 568F, 582, 584F
  in urea cycle, 743, 744F
Functional groups, 3, 26F. *See also specific functional groups*
Furan, 222
Furanoses, 222
Furylfuramide, 920
Fushi tarazu (ftz) gene, 1093F
Fusion, vesicle, **287–291**
Fusion peptide, 290
Futile cycle, 514
Fyn, 422

G
G, *see* Guanine
G, see Free energy
$\overline{G}_A$ (partial molar free energy), 296
G_0 phase (in cell cycle), 1082
G1,6P (glucose-1,6-bisphosphate), 537
G1P, *see* Glucose-1-phosphate
G_1 phase, 1082
G_2 phase, 1082
G6P, *see* Glucose-6-phosphate
G6Pase (Glucose-6-phosphatase), 538, 801
G6PD, *see* Glucose-6-phosphate dehydrogenase
G6P translocase, 539
Gab-1 (Grb2-associated binder-1), 442
GABA (γ-Aminobutyric acid), 88, 780
G-actin, 202
Gaia hypothesis, 10
GAL4, 880F–881
Galactitol, 519
Galactocerebrosides, 252, 720F
D-Galactosamine, 225
D-Galactose, 220F, 221, **518–520,** 519F
Galactose-1-phosphate, in galactose metabolism, 518, 519F
Galactose-1-phosphate uridylyl transferase, 518
Galactosemia, 519
β-Galactosidase, 227, 1047
β-Galactosidase activity, 1097
Galactoside permease, *see* Lactose permease
Galactosyltransferase, 560
Gallus gallus (chicken), 57T
GalNAc transferase, 561
Gamblin, S., 1064
γ (Soret) band, 610
γc cytokine receptor, 70
γ complex, Pol III holoenzyme, 906
γ-globulin, isoelectric point, 98T
Gangliosides, 253F, 717, 720F
Ganglioside G_{M1}, 253F, 720F
Ganglioside G_{M2}, 253F, 720F
Ganglioside G_{M3}, 253F, 720F
GAP, *see* Glyceraldehyde-3-phosphate; GTPase-activating protein
GAP334-Ras-GDP-AlF_3 complex, 419F
GAPDH, *see* Glyceraldehyde-3-phosphate dehydrogenase
Gap junctions, 307
GAR (glycinamide ribotide), in IMP synthesis, 819F, 820
Garrod, A., 477, 762
GAR synthetase, in IMP synthesis, 819F
GAR transformylase, in IMP synthesis, 819F, 820
Gas constant *(R),* 13
Gastrula, 1066
Gastrulation, 1090
Gated ion channels, 302
Gates and fences model, membranes, 274
Gating, ion channel, 302
Gating machinery, 303
Gaucher's disease, 720
GCN4, 881F–882
GDP (guanosine diphosphate), 278, 568F, 569, 570, 581
GDPNP (guanosine-5′-(β,γ-imido) triphosphate; GMPPNP), 1016
GEF (guanine nucleotide exchange factor), 418
Gehring, W., 1094
Geiger counter, 367
Gel electrophoresis, *see* Electrophoresis
Gel filtration chromatography, **97, 100F**
  molecular sieve, 99–100
  size exclusion, 99–100
GenBank, 56, 113T
Genes, 48
  early, 947
  exons and introns, 967–973
  expression, 50
  function identification, 1040–1046
  gap, 1091
  late, 947
  manipulations, and metabolic pathways, 477
  maternal-effect, 1091
  middle, 947
  orthologous, 118
  paralogous, 118
  protein synthesis direction, **49–50**
  pseudogenes, 119
  recombination, **926–939**
  segmentation, 1091
  segment polarity, 1091
  structural, 944
  transgenes, 68–69
  transposition, 58
Gene activation, prokaryotes, **1050–1051**
Gene clusters, **1042–1043,** 1042F
Gene duplication, **117–120,** 118
Gene expression, 50, 944, **1038–1097.** *See also* Eukaryotic gene expression; Prokaryotic gene expression; Transcription factors
  enhancers, 959–960
  gene clusters, **1042–1043,** 1042F
  gene number, **1038–1042**
  genome organization, **1038–1046**
  molecular basis of development, **1090–1097,** 1091F
  nontranscribed DNA, **1043–1046**
  overview, 849
  and σ factors, 947
  tissue specificity, 1055
  transcriptomics, 50
  Z-DNA and, 854
Gene identification, exons/introns, 1040
Gene knockouts, 69, 477
Gene number, **1038–1042,** 1039T
Gene products, 945
General acid catalysis, 331
General base catalysis, 331
General (homologous) recombination, **926–932**
General transcription factor (GTF), 960, 961T
Gene silencing, 1062
Gene splicing, differential, 58
Gene therapy, 69–70
Genetically engineered hybrid protein, 1069
Genetically modified foods, 69
Genetic anticipation, 1044
Genetic code, **986–991**
  deciphering, **987–988**
  evolution, 990
  nature of, **988–991**
  nonuniversality of, 991
  standard, 989T
  triplet codons, **986–988**
  triplets, **986–987**
Genetic control, of metabolic flux, 459
Genetic engineering. *See also* Recombinant DNA technology
Genetic markers, 1042
Genetic mutations, *see* Mutation
Genome, 47, 478
  organization, **1038–1046**
  sequencing projects, 57T
Genome sequencing, **57–58**
Genomics, 50, 478, 1038
Genomic imprinting, 918, 1067
Geometric complementarity, 325
Geometric permissiveness, 1069
Geometric specificity, 326
George III, King of England, 778
Geranylgeranyl residue, 268
Geranyl pyrophosphate, 723, 723F
Gerhart, J., 387
GH, *see* Growth hormone
Ghost erythrocytes, 272
Ghrelin, 807
$G_{i\alpha}$ protein, 431
Giant gene, 1092
Gibbs, J. W, 14

- Gibbs free energy *(G),* 14. *See also* Free energy
- Gigantism, 411
- Gilbert, W., 1049
- Gilman, A., 430
- Gilroy, J., 843F
- G_L (glycogen-binding subunit), 548–549
- Glc, *see* Glucose
- GlcNAc (*N*-Acetylglucosamine), 232, 340, 343, 346, 347
- Gleevec (imatinib), 424–425F
- Gln, *see* Glutamine
- GlnRS (Glutaminyl–tRNA synthetase), 995–996, 996F
- Globin family, 176–178
  - chain synthesis and fetal development, 1043F
  - DNA methylation, 918
  - genealogy, 118–119F
  - gene organization, 1043F
- α-Globin gene cluster, 1043F
- β-Globin gene cluster, 1043F
- Globosides, 720F
- Globular proteins, 134–136, 145–146
- γ-Globulin, isoelectric point, 98T
- Glu, *see* Glutamic acid
- Glucagon, 550, 797
  - countering of insulin effects by, 801–803
  - and fatty acid metabolism, 712
  - and fuel metabolism, 407
  - glycogen metabolism effects, 550
- Glucocerebrosides, 252, 720F
- Glucocorticoids, 255F, 410
- Glucocorticoid receptor (GR), 1073, 1073F
- Glucocorticoid response element (GRE), 1073
- Glucogenic amino acids, 747
- Glucokinase, 489, 516, 796, 796F, 800, 801
- Glucokinase regulatory protein, 796
- Gluconeogenesis, 454, 486, 530, **552–560**
  - AMPK and inhibitation of, 805
  - and citric acid cycle, 556, 588–589
  - and fuel metabolism, 407
  - glycolysis compared, 553F
  - hydrolytic reactions, **557–558**
  - insulin blocking of, 801
  - mammalian metabolism, 792, 792F
  - oxaloacetate from glyoxylate cycle, 590–591
  - pyruvate to phosphoenolpyruvate, **552–560**
  - regulation, **558–560**
  - during starvation, 810
- Gluconic acid, 225
- 1,5-Gluconolactone, 542
- α-D-Glucopyranose, 222, 222F
- β-D-Glucopyranose, 223F
- D-Glucosamine, 225
- D-Glucose (Glc), 220F
- Glucose (Glc), 228, 809. *See also* Blood glucose
  - aerobic and anaerobic metabolism contrasted, 634–635
  - in amino acid degradation, 747F
  - AMPK and uptake of, 805
  - complete oxidation, 596–597
  - in gluconeogenesis, 553F
  - in glycolysis, 487F, 489–490
  - and insulin release, 800
  - levels of, during starvation, 809–810
  - mammalian metabolism, 794
  - metabolic energy, 485
- Glucose-1,6-bisphosphate (G1,6P), 537
- Glucose-1-phosphate (G1P):
  - covalent modification, 391
  - free energy of phosphate hydrolysis, 461T
  - in galactose metabolism, 518
  - in glycogen breakdown, 533
  - in glycogen synthesis, 540F
- Glucose-6-phosphatase (G6Pase), 538, 801
- Glucose-6-phosphatase deficiency (von Gierke's disease), 538, 539
- Glucose-6-phosphate (G6P), 463, 489, 800
  - covalent modification, 392–393
  - fats in liver, 797F
  - free energy of phosphate hydrolysis, 461T
  - in gluconeogenesis, 553F
  - in glycogen breakdown, 534
  - in glycolysis, 487F, 489
  - high muscle exertion conditions, 795
  - hydrolysis free energy, 466
  - in pentose phosphate pathway, 521F
  - possible fates, 531F
- Glucose-6-phosphate dehydrogenase (G6PD):
  - deficiency, 526
  - in pentose phosphate pathway, 521F
- Glucose–alanine cycle, 798–799, 799F
- Glucose binding sites, 307
- Glucose concentration, 311
- Glucose–fatty acid cycle (Randle cycle), 634
- Glucose hydroxyl groups, 299
- Glucose metabolism:
  - overview, 531F
  - substrate cycles, 558F
- Glucose transporters, **798–799**
- Glucose transport intestinal epithelium, 317F
- Glucose transport model, 307F
- [1-^{13}C]Glucose, 476F
- β-D-Glucose, 223F
- D-Glucose, 221, 222F
- α-Glucosidase, 231
- α-1,4-Glucosidase deficiency (Pompe's disease), 538, 539
- Glucosyl residue, 299
- D-Glucuronic acid, 224
- Glu residue, 318
- GLUT1, 307, 309, 311, 805
- GLUT2, 539, 802F
- GLUT4, 442, 552, 800, 800F, 802F, 805
- Glutamate (Glu), 80. *See also* Glutamic acid
  - from amino acid breakdown, 738, 742, 747F
  - biosynthesis, 764–765F
  - breakdown, 751–752F
  - proline synthesis from, 768–769
  - in urea cycle, 744F
- Glutamate-5-phosphate, 768F
- Glutamate-5-semialdehyde, 752, 768
- Glutamate dehydrogenase, 589, 742
- Glutamate synthase, 787
- Glutamic acid (Glu):
  - α helix/β sheet propensities, 140T
  - charged polar side chain, 80
  - as common amino acid, 93
  - genetic code specification, 989T
  - ionizable groups, 77T
  - side chain hydropathy, 156T
- Glutaminase, 695, 751–752F
- Glutamine (Gln):
  - acid–base catalysis by, 332
  - α helix/β sheet propensities, 140T
  - biosynthesis, 764–765F
  - breakdown, 747F, 751–752F
  - genetic code specification, 989T
  - ionizable groups, 77T
  - side chain hydropathy, 156T
  - uncharged polar side chain, 79–80, 79F
- Glutamine synthetase, 764–767
- Glutaminyl–tRNA synthetase (GlnRS), 995–996, 996F
- γ-Glutamyl kinase, 768
- γ-Glutamylphosphate, 765
- Glutathione (GSH), 88, 400F, 526, 637
- Glutathione peroxidase, 526, 637
- Glutathione reductase, 526
- Gluthathione disulfide (GSSG), 88
- Glu–tRNA$^{\text{Gln}}$ amidotransferase, 998
- Glx, 81–82. *See also* Glutamic acid; Glutamine
- Gly, *see* Glycine
- Glycans, *see* Polysaccharides
- Glyceraldehyde, 220F, 516
- *(S)*-Glyceraldehyde, 85
- D-Glyceraldehyde, 84F, 220F
- L-Glyceraldehyde, 84F, 85
- Glyceraldehyde-3-phosphate (GAP):
  - in Calvin cycle, 664–666, 665F, 668
  - in fructose metabolism, 517F
  - in glycolysis, 486, 487F, 492–494
  - in pentose phosphate pathway, 521F, 524
- Glyceraldehyde-3-phosphate dehydrogenase (GAPDH):
  - in Calvin cycle, 665F
  - domains, 150F
  - in glycolysis, 487F, **497–499**

- Glyceraldehyde kinase, in fructose metabolism, 516
- Glycerate, from photorespiration, 672
- Glycerol, 224, 248, 249T, 517F
- Glycerol-3-phosphate, 249F
  - in adipose tissue, 796
  - free energy of phosphate hydrolysis, 461T
  - in fructose metabolism, 517F
  - hydrolysis free energy, 466
  - in triacylglycerol biosynthesis, 710F
- Glycerol-3-phosphate acyltransferase, in triacylglycerol biosynthesis, 710F, 711
- Glycerol-3-phosphate dehydrogenase, in triacylglycerol biosynthesis, 710F
- Glycerol kinase, in fructose metabolism, 517F
- Glycerol phosphate dehydrogenase, in fructose metabolism, 517F
- Glyceroneogenesis, 711
- Glycerophospholipids, **249–252,** 249F
  - common classes, 249T
  - hydrolysis, 250–252
  - synthesis, **714–717**
- Glycinamide ribotide (GAR), in IMP synthesis, 819F, 820
- Glycine (Gly):
  - α helix/β sheet propensities, 140T
  - biosynthesis, 769
  - breakdown, 747F, 748–751
  - as chemical messenger, 88
  - as common amino acid, 93
  - genetic code specification, 989T
  - in heme biosynthesis, 776F
  - ionizable groups, 76T
  - nonpolar side chain, 79
  - side chain hydropathy, 156T
- Glycine cleavage system, 749
- Glycocalyx, 241F
- Glycoconjugates, 241
- Glycoforms, 240
- Glycogen, 231
  - as glucose stockpile, 530
  - heart, 795
  - starch contrasted as fuel reserve, 544
  - structure, 532F
  - structure optimization, 544
- Glycogen branching enzyme, 540, **543–544**
- Glycogen breakdown, *see* Glycogenolysis
- Glycogen debranching enzyme, 231, 533, **536–537**
- Glycogen degradation, 793
- Glycogen granules, 532
- Glycogenin, 543
- Glycogen metabolism:
  - allosteric control, **545**
  - covalent modification control, **545–550**
  - hormonal control, **550–552**
  - opposing pathways, 540F
- Glycogenolysis (glycogen breakdown), 314, 531F, **532–539**
  - glycogen debranching enzyme, 533, **536–537**
  - glycogen phosphorylase, 533, **534–536**
  - insulin blocking of, 801
  - mammalian metabolism, 792F, 797
  - muscle contraction link, 547
  - overview, 532–534
  - phosphoglucomutase, 533, **537–539**
- Glycogen phosphorylase, 231, 391F, 533, **534–536**
  - allosteric control, **545**
  - conformational changes, 392F
  - covalent modification, 391, **546**
  - and fructose, 518
  - interconvertible enzyme system, 545–546F
  - McArdle's disease and, 538
  - reaction mechanism of, 535
- Glycogen storage diseases, 538–539
- Glycogen synthase, 540, **541–543,** 805
  - allosteric control, 542, **545**
  - covalent modification, **545, 550**
- Glycogen synthase kinase 3β (GSK3β), 552
- Glycogen synthesis, 492, 530–531, 531F, **540–544**
  - aldolase, 492–494
  - glycogen branching enzyme, 540, **543–544**
  - glycogen synthase, **541–543**
  - mammalian metabolism, 792F, 793
  - UDP-glucose pyrophosphorylase, **540–541**
- Glycolate, from photorespiration, 672
- Glycolate oxidase, 672
- Glycolate phosphatase, 672
- Glycolipids, 225, 274, 286
- Glycolysis. *See also* Fermentation
  - aldolase, **492–494,** 492F
  - AMPK activation of, 804–805
  - anaerobic, 506
  - cellular location, 453–454
  - control of, **510–515**
  - coordinated control, 634F
  - coupling to citric acid cycle, 567F
  - electron transport sites, 597F
  - Embden–Meyerhoff–Parnas pathway, 486
  - energy-generating capacity, aerobic vs. anaerobic, 584
  - enolase, **500**
  - first stage summary, 486, 496F
  - free energy changes in, 511F
  - gluconeogenesis compared, 553F
  - glyceraldeyde-3-phosphate dehydrogenase (GAPDH), **497–499**
  - hexokinase (HK), **489–490,** 490F
  - mammalian metabolism, 792F–793, 795, 797
  - metabolic key, 487F
  - net reaction, 489
  - overview, **486–488,** 487F
  - and pentose phosphate pathway, 525F
  - phosphofructokinase (PFK), **491–492, 511–514**
  - phosphoglucose isomerase (PGI), **490–491**
  - phosphoglycerate kinase, **499**
  - phosphoglycerate mutase (PGM), **499–500,** 501F
  - pyruvate kinase (PK), **501**
  - stage 2 summary, 488, 503–504
  - substrate cycles, **514–515**
  - substrate cycling, **514–515**
  - triose phosphate isomerase (TIM), **494–496,** 495F
- Glycophorin A, 264F, 265F
- Glycoprotein(s), **234–242**
  - bacterial cell walls, **235–238**
  - glycosylated proteins, **238–240**
  - membrane, 274
  - oligosaccharide functions, **240–242**
  - P-, 314–315
  - proteoglycans, **234–235**
  - sialic acids in, 225
- Glycosaminoglycans, **232–234,** 286
  - disaccharide units of selected, 232F
  - in proteoglycans, 235F
- Glycosides, 225F
- α-Glycosides, 225–226, 225F
- β-Glycosides, 225–226, 225F
- Glycosidic bonds, 225–226, 560–561
- Glycosphingolipids, 252
- Glycosylated proteins, **238–240**
- Glycosylation, 238
- Glycosylphosphatidylinositol-linked protein (GPI-linked protein), 268
- Glycosyltransferases, 239
- Glyoxylate cycle, 590–594, 591F
- Glyoxylic acid, in uric acid degradation, 842F
- Glyoxysomes, 590–591F, 698
- G_{M1}, *see* Ganglioside G_{M1}
- G_{M2}, *see* Ganglioside G_{M2}
- G_{M3}, *see* Ganglioside G_{M3}
- G_{Ml}, gangliosidosis, 720F
- GMP (guanosine monophosphate), 41T
  - animal catabolism pathway, 840F
  - from IMP, 821F
  - synthesis, **821–822,** 821F
- GMP synthase, in IMP conversion to AMP/GMP, 821F
- G_M subunit, 548
- Gobind Khorana, H., 988
- Goldberg, J., 925
- Golgi apparatus, 8, 8F, 282, 286. *See also* Plasma membrane; Posttranslational modification
  - glycosylated protein synthesis in, 239
  - metabolic functions, 455T

Gonads, 410
Gout, 843–844
GPCRs (G protein-coupled receptors), 428, 429
GPI-linked protein (Glycosylphosphatidylinositol-linked protein), 268
G proteins, 416, 546, 971. *See also* Heterotrimeric G proteins
G protein-coupled receptors (GPCRs), 428, 429
G-quartet, 914, 915F
GR (glucocorticoid receptor), 1073, 1073F
Gram, C., 236
Gram-negative bacteria, 236, 316
Gram-positive bacteria, 236
Granum, 641F, 642
Graves' disease, 215T
Grb2, 418F
GRE (glucocorticoid response element), 1073
Greek key motif, 146
Greenberg, G. R., 818
Green fluorescent protein, 87
Green sulfur bacteria, 658
gRNAs (guide RNAs), 975
GroEL, X-ray structure, 165–166, 166F
GroEL–GroES–(ADP)$_7$ complex, 166F
  chaperones, barrel structure of, 165–166
  conformational changes in, 166–168
GroES, X-ray structure, 166F
Group I introns, 978, 979F
Group II introns, 978
Group-transfer reactions, 453
  cofactors for, 326
  phosphoryl group-transfer potentials, 461, 461T
  Ping Pong reactions, 376
Growth factor receptors, 233
Growth hormone, 67T
Growth hormone (GH), 411–412
G$_{s\alpha}$, 431
GSH (glutathione), 88, 400F, 526, 637
GSK3β (glycogen synthase kinase 3β), 443F, 552
GSSG (gluthathione disulfide), 88
GTF (general transcription factor), 960, 961T
GTP (guanosine triphosphate), 278, 553F, 554F
GTPase-activating protein (GAP), 418–419
GTP-binding factors, 1027
Guanidinium ion, as chaotropic agent, 159
Guanidino group, 466
Guanine (G), 40l, 41T
  base pairing, 46F, 851F, 866–868
  Chargaff's rules and, 44
  as common nucleotide, 42
  modified forms in tRNA, 992F
  in purine catabolism, 840F
  tautomeric forms, 44F
Guanine deaminase, in purine catabolism, 840F
Guanine-7-methyltransferase, 966
Guanine nucleotide exchange factor (GEF), 418
Guanine ribonucleotide synthesis, 821–822
Guanosine, 41T, 840F
Guanosine diphosphate, *see* GDP
Guanosine monophosphate, *see* GMP
Guanosinc triphosphate, *see* GTP
Guanosine-5′-(β,γ-imido)triphosphate (GMPPNP, GDPNP), 1016
Guanylate cyclase, 436
Guanylic acid, *see* GMP
Guide RNAs (gRNAs), 975
D-Gulose, 220F

H
H (heavy chains), 201, 210, 285
H1 histones, 884, 884T, 887F
H2A histones, 854T, 884–886F, 887, 888
H2B histones, 884, 884T, 885F, 886F, 887, 888
H3 histones, 884, 884T, 885F, 886F, 888
H4 histones, 119, 884, 884T, 885F, 886F, 887–888
HA (hemagglutinin), 289–291
HA1, 290F
HA2, 290F
H (enthalpy), 12
Haber-Bosch process, 786
Haemophilus haemolyticus, 1065
Haemophilus influenzae, 57T
Hairy gene, 1092
Haldane, J. B. S., 2, 369
Half-cell, 471F–472
Half-chair conformation, 342F
Half-life, 365–366
Half-reactions, 470–471
  biological significance, 473–474
  selected reaction reduction potentials, 473T
Half-time, 365–366
Haloarcula marismortui, 869F, 1002
Halobacter halobium, 266
Halobacteria, 9
Halobacterium salinarium, 266, 608–609
Hamm, H., 430
Hammerhead ribozyme, 870F
Hanson, J., 200
H antigens, 242F
Haploid DNA, 47
Haploid genome DNA contents, 1039F
Harden, A., 485
Harrison, S., 863, 876
HATs (histone acetyltransferases), 1060–1061
Hatch, M., 674
Haworth projections, 222
Hb, *see* Hemoglobin
HCC (hepatocellular carcinoma), 480F
HD, *see* Huntington's disease
HDACs (histone deacetylases), 1062
  gene silencing, 1062
  transcriptional repression, 1062
HDL (high density lipoproteins), 685, 728–729
Heart, 795
  AMPK-activated glycolysis in, 804–805
  citric acid cycle in, 586
  muscle ATP production energetics, 511T
Heart attack, *see* Myocardial infarction
Heart-specific enzymes, as indicators of myocardial infarction, 635
Heat *(q),* 12
Heat-labile enterotoxin, 435
HEAT sequence, 426
Heat shock proteins (Hsp), 165
Heavy chains (H), 201, 210, 285
HECT domain, 734
Helicase, 903
Helicase II (UvrD), 924
Helices, left- vs. right-handed, 45F
Helicobacter pylori, 1038F
Helix capping, 140
Helix–turn–helix (HTH) motif, 876, 877F
Hemagglutinin (HA), 289–291
Heme *a,* 611F
Heme *b,* 611F
Heme *c,* 611F
Heme c_i, 657
Heme-controlled protein synthesis, 1077F
Heme *f,* 657
Heme groups:
  biosynthesis, **775–778**
  degradation, **778–780**
  hemoglobin, 186F
  iron porphyrins, 488
  isotopic tracer studies, 476
  myoglobin, 177, 178F, 342
  oxygenation, 178
Heme-regulated inhibitor (HRI), 1077
Hemerythrin, 181
Heme *x,* 657
Hemiacetals, 211–222F, 344F
Hemiketals, 211–222F
Hemin, 777
Hemocyanin, 181
Hemoglobin (Hb), 94, 177, **181–197,** 309, 390
  abnormal, 195T
  allosteric proteins, **192–194,** 193F
  BPG (2,3-D-bisphosphoglycerate) binding, 191
  and carbon dioxide transport, 189–190
  deoxy, 182–183F
  erythrocyte shape and, 272

Hemoglobin (Hb) (*cont.*)
  evolution rate, 119F
  fetal, 118, 191, 1043
  function, 181–184, 191
  and globin family, 118–119
  high-altitude adaptation, 192
  Hill plot, 185F
  isoelectric point, 98T
  mutations, **194–197**
  and other oxygen-transport proteins, 181
  oxy, 182–183F
  oxygen binding, **184–186**
  oxygen binding cooperativity, **186–194**
  oxygen binding curve, 184F
  R and T conformational states (Perutz mechanism), 186F–189
  structure, 126F, **181, 182–184**
Hemoglobin S (sickle-cell hemoglobin), 194–197
Hemolymph, 181
Hemolytic anemia, 194
Hemophilia a, 359
Hemophilia b, 359
Henderson, R., 266
Henderson–Hasselbalch equation, 34
Hen egg white (HEW) lysozyme. *See also* Lysozyme
Henri, V., 368
Henseleit, K., 569, 743
Heparan, 232F–233F, 233
Heparan sulfate (HS), 233
Hepatitis B surface antigen, 67T
Hepatocellular carcinoma (HCC), 480F
Hepatomegaly, 538
Heptad repeats, 881–882
Heptoses, 221
HER2 receptor, 213, 425
Herceptin (trastuzumab), 213, 425
Hereditary nonpolyposis colorectal cancer syndrome, 924
Hereditary spherocytosis, 273
Hers' disease, 538, 539
Hershko, A., 734
Heterochromatin, 1056
Heterochromatin protein 1 (HP1), 1064
Heterogeneous nuclear mRNAs (hnRNAs), 967
Heterokaryon, 271F
Heterologous DNA, 926
Heterolytic cleavage, 695
Heteropolysaccharides, 226
Heterotrimeric G proteins, **428–436,** 430F, 1070
  and adenylate cyclase, 432–434
  components of, 428
  dissociation of, 430–432
  and phosphodiesterases, 435–436
  transmembrane helices in, 429–430
Heterotrophs, 449
Heterozygotes, 195
Hexokinase (HK), 463
  activity relative glucokinase, 796F
  in glycolysis, 487F, **489–490,** 490F, 511
  in mannose metabolism, 520F
Hexose, 221
  chair and half-chair conformations, 342F
  metabolism of non-glucose, **516–520**
Hexose-monophosphate shunt, 521
Hexosiminidase A deficiency, and Tay-Sachs disease, 720–721
Hg^{2+} ion, zinc ion replacement, 326
hGH (human GH), 411–412F
hGHbp, 412
HGPRT (hypoxanthine–guanine phosphorihosyl transferase), 824
High-altitude adaptation, 192
High density lipoproteins (HDL), **681,** 685, 728–729
High-energy bonds, 461
High-energy compounds, 459–469. *See also specific compounds, especially* ATP
  ATP and phosphoryl group transfer, **460–462**
  coupled reactions, **462–464**
  thioesters, **468–469**
"High-energy" intermediates, 459
Highly repetitive DNA sequences, 1044
High mobility group (HMG), 1058
High-performance liquid chromatography (HPLC), 98
High-throughput screening, 395
HI/HA (hyperammonemia), 742, 747
Hill, A., 184
Hill coefficient, 185
Hill equation, 184–186
Hill plot, 185F
Hinkle, P., 630
Hippuric acid, 686
His, *see* Histidine
his operon, *E. coli,* 1053
His residues, 306, 318
His tag, 628
Histamine, 88, 780
Histidine (His):
  acid–base catalysis by, 332
  α helix/β sheet propensities, 140T
  biosynthesis, 774, 775F
  breakdown, 747F, 751–752F
  charged polar side chain, 80
  covalent catalysis by, 335
  genetic code specification, 989T
  ionizable groups, 77T
  as rare amino acid, 93
  side chain hydropathy, 156T
  structure, 77T
Histones:
  calf thymus, 884T
  chromatin fiber interaction, 887F–890
  covalently modified, 1059–1060
  DNA binding, 875
  and DNA replication, 914
  gene clusters, selected organisms, 1042F
  H1, 884, 884T, 887F
  H2A, 884, 884T, 885F, 886F, 887, 888
  H2B, 884, 884T, 885F, 886F, 887, 888
  H3, 884, 884T, 885F, 886F, 888
  H4, 119, 884, 884T, 885F, 886F, 887–888
  isoelectric point, 98T
  linking nucleosomes, 886–887
Histone acetylation, 1060
Histone Acetyl-Lys, 1060
Histone acetyltransferases (HATs), 1060
Histone code, 1060
Histone deacetylases (HDACs), 1062
Histone-depleted metaphase chromosomes, 888F
Histone–DNA interactions, 1059–1060
Histone Lys, 1060, 1063
Histone methylation, 1063
Histone methyl-Lys residues, 1064F
Histone methyltransferases (HMTs), 1063
Histone modifications, nucleosome core particle, 1059T
Histone tail modifications, histone code, 1060
Hitchings, G., 838, 844
HIV (human immunodeficiency virus), 912–913
HIV-1 reverse transcriptase, 912–913
HIV-1 reverse transcriptase inhibitors, 384–385
HIV protease inhibitors, 381, 384–385
HK, *see* Hexokinase
HMG (high mobility group), 1058
HMG1, 1080
HMG2, 1080
HMG box, 1058
HMG-CoA (β-Hydroxy-β-methylglutaryl-CoA):
  in cholesterol biosynthesis, 722–723F
  in ketogenesis, 699, 699F, 805
HMG-CoA lyase, in ketogenesis, 699, 699F
HMG-CoA reductase, 684F, 805
  in cholesterol synthesis, 722–723F
  statins, inhibition by, 726–727
HMG-CoA synthase, in ketogenesis, 699, 699F
HMG proteins, 1058
  gene expression, 1058–1059
  regulatory proteins, 1058
HMTs (histone methyltransferases), 1063
hnRNAs (heterogeneous nuclear mRNAs), 967
Hodgkin, D. C., 125, 182, 692, 697
Holden, H., 206, 695
Holley, R., 50, 991

Holliday, R., 926
Holliday junction, 926, 927F–928F, 934
Holoenzyme:
  PP2A, 427
  RNA polymerase, 943F, 946
Homeobox, 1095
Homeodomain, 1095
Homeostasis, 407, 799. *See also* Metabolic homeostasis
Homeotic mutation, 1097
Homeotic selector genes, 1092
Homocitrate, 784
Homocysteine, 754
Homocysteine methyltransferase, 770
Homocysteinuria, 755
Homodimers, 305
Homogentisate, in phenylalanine breakdown, 477F
Homogentisate dioxygenase, 762
Homogentisic acid, 477, 762
Homolactic fermentation, **505–506**
Homologous end-joining, 934
Homologous proteins, 116–117F
Homologous (general) recombination, **926–932**
Homology, 1040
Homology modeling, 163
Homolytic cleavage, 695
Homopolysaccharides, 226
Homo sapiens, 57T
Homotetramers, 304
Homozygotes, 195
Hoogsteen base pairs, 866
Hormones, **405–412.** *See also* Glucagon; Insulin
  adrenal glands, 409–410
  endocrine, 406–407
  fuel metabolism regulation, 407–408, **799–804**
  glycogen metabolism control, 550–552
  growth, 411–412
  mammalian metabolism role, 791
  pancreatic, 407–408
  steroid, 410–411
Hormone activated nuclear receptors, 1072–1073
Hormone response elements (HREs), 1072–1073
Hormone-sensitive lipase, 685
Hormone-sensitive triacylglycerol lipase, 633, 712
Horseshoe crab, 181
Horwich, A., 166
Hot spots, 941
Hox genes, 1095–1097
HP1 (heterochromatin protein 1), 1064
HPLC (high-performance liquid chromatography), 98
HPRT (hypoxanthine phosphoribosyl transferase), 213
HREs (hormone response elements), 1072–1073
HRI (heme-regulated inhibitor), 1077
HS (heparin sulfate), 233
HS4 insulator, 1070
Hsp40, 165
Hsp70, 165
Hsp90, 165
HTH (helix–turn–helix) motif, 876, 877F
Huber, R., 355–356, 736
Humans. *See also specific organs, cell types, diseases, etc.*
  arachidonic acid, as most important eicosanoid precursor, 259
  daily metabolic energy needs, 631
  fuel reserves, normal 70-kg man, 778T, 810T
  gene number, 1039
  genome sequencing, 56
  hemoglobin variants, 195T
  human-mouse cell fusion, 271F
Human cyclin-dependent kinase-2, 1083F
Human genome:
  genes associated with disease, 1041–1042
  sequence variations, 1041
human GH (hGH), 411–412F
Human growth hormone, genetically engineered, 67T
Human histone methyltransferase, 1064F
Human immunodeficiency virus (HIV), 912–913
Human p53 DNA-binding domain, 1085F
Human TAF1 double bromodomain, 1062F
Humoral immunity, 209
Hunchback (hb) genes, 1091
Hunchback protein, 1092
Huntingtin, 1044
Huntington's disease (HD), 636, 1044, 1044T, 1087
Hurwitz, J., 943
Huxley, A., 200
Huxley, H., 200
Hyaluronate, 232F
Hyaluronic acid, 232, 235F
Hybridization (RNA–DNA), 866
Hybridoma cells, 213
Hyde, C., 773
Hydration, 26
Hydrocortisone, 255F, 410
Hydrogen bond (defined), 23
Hydrogen bonds, 24F
  bond energy, 25T
  functional groups, 26F
  nucleic acids, 867
  proteins, 156–158
Hydrolases, reaction type catalyzed, 324T
Hydrolysis, 3, 312, 313
Hydronium ion, 30
Hydropathy, 156
Hydropathy scale, 156T
Hydrophilic substances, 26
Hydrophobic collapse, 161
Hydrophobic effect, **26–29**
  amino acids, 80
  membrane proteins, 266–267
  nucleic acids, 867–868
  proteins, 156
Hydrophobic forces, 28–29
Hydrophobic interaction chromatography, **97**
Hydrophobicity, 1060
Hydrophobic substances, 26–27
Hydropyrimidine hydratase, in pyrimidine catabolism, 845F
β-Hydroxyacyl–ACP dehydrase, in fatty acid synthesis, 705F
L-Hydroxyacyl-CoA, 688
L-Hydroxyacyl-CoA dehydrogenase, 688
Hydroxyapatite, and nucleic acid chromatography, 872
β-Hydroxy-β-methylglutaryl-CoA (HMG-CoA), *see* HMG-CoA
D-β-Hydroxybutyrate, in ketone body conversion to acetyl-CoA, 698, 700F
β-Hydroxybutyrate dehydrogenase, in ketone body conversion to acetylCoA, 700F
D-β-Hydroxybutyryl-ACP, in fatty acid synthesis, 705F
Hydroxyethylthiamine pyrophosphate, 508
Hydroxylamine, 940
Hydroxyl group, 26F
Hydroxyl radical, 636
5-Hydroxylysyl (Hyl), 137
Hydroxymethylbilane, 777
Hydroxymethylglutaryl-CoA reductase (HMG-CoA reductase), 805
p-Hydroxyphenylpyruvate, in phenylalanine breakdown, 477F
4-Hydroxyproline, 86F
3-Hydroxyprolyl, 137
4-Hydroxyprolyl (Hyp), 137
Hydroxypyruvate, from photorespiration, 672
5-Hydroxytryptamine, 780
Hydroxyurea, 196
5-Hydroxyurea, 847
Hyl (5-Hydroxylysyl), 137
Hyp (4-Hydroxyprolyl), 137
Hyperammonemia (HI/HA), 742, 747
Hyperbolic binding curve, 179–180
Hypercholesterolemia, 726
Hyperchromic effect, 864
Hyperglycemia, 256, 811
Hyperhomocysteinemia, 755
Hyperlysinemia, 758
Hyperlysinuria, 758
Hypermutation, somatic, 214, 1081
Hyperphenylalaninemia, 762
Hyperproliferative signals, 1086

Hyperthermophiles, 159
Hypervariable residues, 116
Hypervariable sequences, 212
Hyperventilation, and alkalosis, 36
Hypoglycemia, 518, 538
Hypothalamus, 406F, 807
Hypotonic environments, bacterial cell walls and, 235–236
Hypoxanthine, 72, 818, 840F
Hypoxanthine–guanine phosphoribosyl transferase (HGPRT), 824
Hypoxanthine phosphoribosyl transferase (HPRT), 213
Hypoxia, 192
H zone, 198, 199F

I
I band, 198, 199F
Ibuprofen, 85F, 719
ICAT (isotope-coded affinity tags), 480–481F
Ice, 24F
I-cell disease, 286
ICLs (intracellular loops), 315F
Icosahedral symmetry, 155, 155F
IDL (intermediate density lipoproteins), 681, 683
D-Idose, 220F
Iduronate, 233
IEF (isoelectric focusing), 103
IFs (initiation factors), 1012–1014, 1012T
IF$_1$, 633
IF-1, 1012
IF-2, 1012
IF-3, 1012
I-FABP (intestinal fatty-acid binding protein), 680F
Ig, *See* Immunoglobulin
IgA (immunoglobulin A), 210
IgD (immunoglobulin D), 211
IgE (immunoglobulin E), 211
IgG (immunoglobulin G), 211F
IgM (immunoglobulin M), 210
Ile, *see* Isoleucine
IleRS, 997
ilv operon, *E. coli,* 1053
Imaginal disks, 1091
Imatinib, 424–425F
Imidazole, reaction with *p*-nitrophenylacetate, 336
Imine (Schiff Base), 330
Imine, functional group and linkages, 4T
Immune system, **209**. *See also* Antibodies
  and adenosine deaminase, 840
  induced apoptosis, 1087
Immunoaffinity chromatography, 101
Immunoassays, 95
Immunoblotting, 102, 874
Immunofluorescence microscopy, 207
Immunoglobulin (Ig), **209–212**. *See also* Antibodies
Immunoglobulin A (IgA), 210
Immunoglobulin D (IgD), 211
Immunoglobulin E (IgE), 211
Immunoglobulin fold, 148, 212F
Immunoglobulin G (IgG), 211F
Immunoglobulin M (IgM), 210
IMP (inosine monophosphate):
  as AMP/GMP precursor, 818
  animal catabolism pathway, 840F
  conversion to AMP or GMP, 821F
  pathway regulation, 822–823
  synthesis, **818–821,** 819F
IMP cyclohydrolase, in IMP synthesis, 819F
IMP dehydrogenase, in IMP conversion to AMP/GMP, 821F
Inactivation, 309
Inactivation ball, 304
Inactivators, 377
Inclusion bodies, 94F
Indirect readout, 878
Indole, 773–774
Indole-3-glycerol phosphate, 773
Induced fit, 325
Inducers, 1047
Inducible enzymes, 950
-ine (suffix), 82
Influenza virus, 289
Ingold, C., 85
Ingram, V., 195
Inheritance, 48. *See also* DNA
Inhibition, enzyme, *see* Enzyme inhibition
Inhibition constant, (K_I), 368, 378–381
Inhibitors, 377
Inhibitor-1 (phosphoprotein phosphatase inhibitor 1), 548
Initial velocity of reaction (v_o), 370
Initiation factors (IFs), 1012–1014, 1012T
Initiator caspases, 1088
Inorganic pyrophosphatase, 464, 465F
Inosine, 840F, 992F
Inosine monophosphate, *see* IMP
myo-Inositol, 224
Inositol polyphosphate 5-phosphatase, 441
Inositol-1,4,5-triphosphate (IP$_3$), 437
Inr (initiator) element, 959
Insertion mutations, 916, 919
Insertion sequence (IS), 935F
In silico models, 482
In situ hybridization, 64F–65
Insulators:
  heterochromatin spreading, 1070
  limit enhancers, 1070
Insulin, 92, **800–803**
  and catecholamines, 801
  diabetes mellitus, 811–813
  discovery, 812
  epinephrine as antagonist, 552
  and fatty acid metabolism, 712
  and fuel storage, 800–801
  genetically engineered, 67T
  and glucagon, 801–803
  glucose and triggering of, 800
  isoelectric point, 98T
  and liver gluconeogenesis/glycogenolysis, 801
  primary structure of bovine, 92F, 104
  pyruvate dehydrogenase phosphatase activation, 585
  receptor, 413F
Insulin-dependent diabetes mellitus, 215T, 811–812
Insulin receptor (IR), 433F
Insulin receptor substrate 1 (IRS-1), 416
Insulin receptor substrate 2 (IRS-2), 416
Insulin resistance, 813
Insulin signaling system, 442, 443F
Insulin-stimulated protein kinase, 436, 548
Integral membrane proteins, **263–264,** 263F
Integral proteins, 263–264
Integrases, 939
Intercalating agents, 873, 919
Intercalation, **873**
Intercellular channels, 308
Interconvertible enzyme system, 545–546F
Interfacial activation, 679F
Interferons, 422, 972
Intermediates, 364
Intermediate density lipoproteins (IDL), 681, 683
Intermembrane space, 599
Internal conversion, 646
Internal hydrophilic cavity, 318
Internal resolution site, 936
Interorgan metabolic pathways, **798–799**
  Cori cycle, **798,** 798F
  glucose–alanine cycle, **798–799,** 799F
  glucose transporters, **798–799**
Intervening sequences, *see* Introns
Intestinal epithelium, 317F
Intestinal fatty acid-binding protein (I-FABP), 630
Intestinal mucosa, 630
Intestine, fuel availability after meals, 793
Intracellular apoptosis, 1088–1090
Intracellular fluids, buffering, 35–36
Intracellular loops (ICLs), 315F
Intracellular signaling, *see* Signal transduction
Intrasteric mechanisms, 440
Intrinsic factor, 696
Intrinsic membrane proteins, *see* Integral membrane proteins
Intrinsic pathway, apoptosis, 1088
Intrinsic pathway, blood coagulation cascade, 358–359
Introns, 67
Introns (intervening sequences), 967
  discovery, 968
  eukaryotic pre-tRNAs, 981–982

  group I, 978, 979F
  group II, 978
  lariat structure, 970
Invariant residues, 116
Inverted repeats, 935F
In vitro assessment, 394
Iodoacetate, 107
Ion, solvation, 25–26, 26F
Ion-binding sites, 311
Ion channels, **299–302**
Ion exchange chromatography, **97,** 99F
Ion-gradient-driven active transport, **316–318**
Ionic interactions, 24–25, 25T
Ionizable groups, p*K* values of, **81**
Ionization, water, **30–32**
Ionophores, **297–298**
Ion pair, 157
Ion specificity, 302
IP_3 (inositol-1,4,5-trisphosphate), 437
IPTG (isopropylthiogalactoside), as inducer, 1047
IR (insulin receptor), 433F
Iron (element), *See under* Fe
Iron porphyrins, 488
Iron–sulfur clusters:
  [2Fe–2S], 605
  [4Fe–4S], 579, 605
Iron–sulfur protein (ISP), 605, 612
Irreversible inhibitor, 385
IRS-1 (insulin receptor substrate 1), 416
IRS-2 (insulin receptor substrate 2), 416
IS (insertion sequence), 935F
IS1, 935
IS2, 935
Islets of Langerhans, 407
Isoaccepting tRNAs, 995, 998
Isocitrate, 325
  in amino acid degradation, 747F
  in citric acid cycle, 568F, 578–580, 584F
  in glyoxylate cycle, 591F
  lsocitrate dehydrogenase, in citric acid cycle, 568F, 579–580, 586–587
Isocitrate lyase, in glyoxylate cycle, 591, 591F
Isoelectric focusing (IEF), 103
Isoelectric point, amino acids, 81
Isoforms, 391, 398
Isolated systems, 18
Isoleucine (Ile):
  α helix/β sheet propensities, 140T
  biosynthesis, 771–773
  breakdown, 747F, 757–758
  genetic code specification, 989T
  ionizable groups, 76T
  nonpolar side chain, 79, 79F
  side chain hydropathy, 156T
  structure, 76T, 79F
Isomerases, 324T, 453
Isomerizations, 453
Isopentyl pyrophosphate, 722–723F
Isopeptide bond, 88, 734
Isoprene, 257, 721
Isoprene units, 268, 721
Isoprenoid group, 268
Isoprenoids, 257
Isopropylthiogalactoside (IPTG), as inducer, 1047
Isoproterenol, 409
Isoschizomers, 72
Isotope-coded affinity tags (ICAT), 480–481F
Isotopic labeling, 367
Isotopic tracers, 475–476
Isozymes, 391, 398, 455
ISP (iron–sulfur protein), 605, 612
Iwata, S., 318

J
Jaenisch, R., 1067
JAK (Janus kinase), 1071
JAK-STAT pathway, 1071–1072, 1071F
Janus kinase (JAK), 1071
Jap, B., 306
Jaundice, 780
Jelly roll, 149
J_λ, 1079
Jmol, 153
Johnson, L., 391
Joliet, P., 655
Jones, M. E., 826
Jorgensen, R., 1075
J subunit, 210
Jun, 419, 1070
Junk DNA, 972, 1046
Juvenile-onset diabetes mellitus, 811

K
K, see Dissociation constant
*k (*rate constant), 364
k_1, 368
k_{-1}, 368
k_2, 368
Kaback, R., 318
Kabat, E., 212
Kandler, O., 9
κ chain gene family, 1078F–1079
Karplus, M., 158
k_B (Botzmann constant), 13–14, 372
kb (kilobase pairs), 47
k_{cat}, 371
k_{cat}/K_M, 371–372, 371T
K^+ channels, 299–302, 618
KcsA K^+ channel, 299–303, 300F, 301F
kD (kilodaltons), 13
KDEL receptors, 286
KDPG (2-keto-3-deoxy-6-phosphogluconate), 529
Keilin, D., 610, 619
Kendrew, J., 126, 177, 182, 200, 968
Kennedy, E., 686
K_{eq} (equilibrium constant), 16
Keratan sulfate, 232F, 233, 235F
Keratins, 134–136
α Keratins, 134, 136
β Keratins, 134–136
Kerr, J., 1086
Ketals, cyclic, 225
2-Keto-3-deoxy-6-phosphogluconate (KDPG), 529
2-Keto-3-deoxy-D-arabinoheptulosonate-7-phosphate, 773
α-Keto acid, from amino acid transamination, 738–741F
2-Keto acid dehydrogenases, 580
β-Ketoacyl–ACP reductase, in fatty acid synthesis, 705F
β-Ketoacyl–ACP synthase, in fatty acid synthesis, 705F
Ketoacyl-CoA thiolase, 688, 689–690
3-Ketoacyl-CoA transferase, in ketone body conversion to acetyl-CoA, 700F
α-Ketobutyrate, 754, 772
Keto–enol tautomerization, 331F
Ketogenesis, 698, 699F
Ketogenic amino acids, 747–748
α-Ketoglutarate, 567, 595
  amino acid biosynthesis from, 764–769
  from amino acid degradation, 738, 742, 747F, 751–752F
  in citric acid cycle, 568F, 579–580, 584F
  in urea cycle, 744F
α-Ketoglutarate dehydrogenase, 580, 586–587
  in citric acid cycle, 568F, 580
  malate dehydrogenase, 583
  NAD^+-dependent isocitrate dehydrogenase, 579–580, 579F, 586–587
  net reaction, 569–570
  overview, 567–570, 568F
  pathways using citric acid cycle intermediates, 588–589
  pyruvate dehydrogenase complex, 570–573
  pyruvate dehydrogenase complex regulation, 584–585
  rate-controlling reactions, 585–587, 586T
  reactions replenishing citric acid cycle intermediates, 589–590
  regulation, 583–587, 587F
  related reactions, 535–539
  succinate dehydrogenase, 582, 582F
  succinyl-CoA synthetase, 580–582, 581F
Keto group, hydrogen bonding, 26F
Ketone, 4T, 330
Ketone bodies, **698–700**
  conversion to acetyl-CoA, 700F
  in diabetes, 811
  as energy source during starvation, 810–811
  mammalian metabolism, 794, 797

Ketose, 220
D-Ketose, 221F
Ketosis, 700, 811
3-Ketosphinganine, 718F
3-Ketosphinganine reductase, 718F
3-Ketosphinganine synthase, 718F
KFERQ proteins, 733
K_I (inhibition constant), 368, 378–381
Kidney, 406F, **798**
Kidney stones, 843
Kilobase pairs (kb), 47
Kilodaltons (kD), 13
Kim, J.-J., 688
Kim, P., 881
Kim, S.-H., 869, 1083F
Kinases, 376, 406, 465. *See also* *specific kinases*
Kinase cascades, **416–422**
  completion of signaling pathway by, 419–420
  and GAPs, 418–419
  in mammalian cells, 420F
  and scaffold proteins, 420, 422
  and SH3 domains, 417–418
Kinemages, 153
Kinetics, **364–376**. *See also* Enzyme kinetics
Kinetically stable, 461
KiNG (program), 153
K^+ ion, 299, 335
Klenow fragment, 900F
Klentaq1, 900–902, 901F
Klinefelter's syndrome, 411
Klug, A., 869, 870, 879, 886
K_M (Michaelis–Menten constant), 369–371, 371T
  Lineweaver–Burk plot for, 373
  sample calculation, 373
knirps gene, 1092
Knirps protein, 1092
Knoop, F., 475, 569, 686
Knowles, J., 496
Köhler, G., 213
Kok, B., 655
Kornberg, A., 533, 896, 898
Kornberg, R., 884, 953, 961, 1056, 1069, 1070
Kornberg, T., 1094, 1096
Kornfeld, S., 239
Koshland, D., 193
Kraut, J., 354
Krebs, E. G., 533
Krebs, H., 567, 569, 743
Krebs cycle, *see* Citric acid cycle
krüppel gene, 1092
Krüppel protein, 1092
K_S, 371
Ku70 subunit, 925
Ku80 subunit, 925
Kühne, W., 200
Ku protein, 925
Kuru, 169
K_v channels, 303F–304F
Kv1.2 channels, 303–304F
K_W, ionization constant of water, 31
Kwashiorkor, 789
Kynureninase, 758

L

L (Fischer convention), 84
L (linking number), 827
L23 protein, 1028
lac operator, 1048F
lac operon, 945F, 1048
lac repressor, **1046–1050**
α-Lactalbumin, 560
β-Lactamase, 238, 936
Lactase, 227
Lactate:
  from homolactic fermentation, **505–506**
  isozyme action, 455
  muscle fatigue and, 795
Lactate dehydrogenase (LDH), 148, 455, 505
Lactic acid, 190
Lactose, 227
  E. coli metabolism, 1046
  synthesis, 560
Lactose analog, 318
Lactose binding site, 318
Lactose intolerance, 227
Lactose permease (galactoside permease), 316, 1047
  in *E. coli,* 317F–318F
  proton gradient, 316–318
Lactose synthase, 560
Lactosyl ceramide, 720F
lacZ coding sequence, 1097
LADH (liver alcohol dehydrogenase), 509
Lagging strand, 896, **904–905,** 905F
λ chain, 1079
Lander, E., 57
Lands, W., 716
Lanosterol, 724
Large (50S) ribosomal subunit, 1001–1006, 1001T
Lariat structure, 970
Late genes, 947
Lateral diffusion, in lipid bilayers, 261
Lathyrism, 137
Lauric acid, 247T
LBHBs (low-barrier hydrogen bonds), 355
LCa (clathrin light chain), 285
LCAT (lecithin–cholesterol acyltransferase), 685
lck, 422
LDH (lactate dehydrogenase), 148, 455, 505
LDL, *see* Low density lipoproteins
Lead compound, 394–395
Leader sequence, 1051F–1052
Leading strand, 896, **904–905,** 905F
Leading substrates, 376
Lecithin, 249T, 715F
Lecithin–cholesterol acyltransferase (LCAT), 685
Lectins, 241
Leeuwenhoek, A. van, 200
Leghemoglobins, 181
Lehninger, A., 686
Leischmaniasis, 504
Leloir, L., 533
Lenski, R., 11
Leptin, 806F–807
Lesch–Nyhan syndrome, 70, 824, 844
Leslie, A., 623F
Lethal factor (LF), 444–445
Leucine (Leu):
  α helix/β sheet propensities, 140T
  biosynthesis, 771–773
  breakdown, 747F, 757–758
  as common amino acid, 93
  genetic code specification, 988, 989T
  nonpolar side chain, 79
  side chain hydropathy, 156T
  structure, 76T
Leucine zippers, 881F–882
Leukocytes, 241–242
Leukocyte elastase, inhibition, 356
Leukotrienes, 258, 259F
Leupeptin, 350F
Levinthal, C., 161
Levorotatory molecules, 84
Lewis, E. B., 1095
Lewis, M., 1049
LexA, 926
LF (lethal factor), 444–445
LH-2, 644F
LHC (light-harvesting complex), 644, 662
Lienhard, G., 338
Life. *See also* Cells; Evolution
  cellular architecture, **5–7**
  chiral molecules and, 84–86
  organismal evolution, **9–10**
  origin, **2–5**
  thermodynamics and, **17–19**
  water and, 22
Li–Fraumeni syndrome, 1084
Ligands, 101, 180
Ligand binding, 437–438
Ligand-gated channels, 302
Ligases, 453
Ligases, reaction type catalyzed, 324T
Ligation, 61
Light-absorbing pigments, photosynthetic, **643–645**
Light chains (L), 201, 210
Light chain (in clathrin), 285
Light energy, transformation of, to chemical energy, **645–647**

Light-harvesting complex (LHC), 644, 662
Light reactions, photosynthesis, 641, **645–663**
Lignin, 229–230
Lignoceric acid, 247T
Limited proteolysis, 108
Limulus polyphemus, 181
LINEs (long interspersed nuclear elements), 939, 1045
Lineweaver, H., 373
Lineweaver–Burk plot (double-reciprocal plot), 373–374
  competitive inhibition, 380F, 381T
  mixed inhibition, 381T, 383F
  uncompetitive inhibition, 381T, 382F
Linkages, 3
Linker, hinge binding DNA, 1049
Linker DNA, 884
Linker histones, 886–887
Linking number, supercoiled DNA, 858
Link proteins, 234
Linoleic acid, 246, 246F, 247T, 690, 709
α-Linolenic acid, 246F, 247, 247T
γ-Linolenic acid, 247T
Lipases, 678–679F, 685, 796
Lipids. *See also* Glycerophospholipids; Membranes
  asymmetrical distribution in membranes, **274–278**
  biological functions, 245–246
  catabolism overview, 452F
  classification, **246–259**
  digestion and absorption, **678–680**
  fatty acids, **246–249,** 247T
  glycerophospholipids, **249–252**
  hydrophobicity, 245, 245F
  miscellaneous lipids, **257–259**
  sphingolipids, **252–253,** 253F
  steroids, **254–257**
  transport, **680–685**
  triacylglycerols, **248–249**
Lipid bilayers, 28F, 245, **260–263.** *See also* Membranes
  fluidity, 262–263
  formation, **260–263,** 260F
  lipid mobility in, **261–262**
  phase transition, 262–263
  phospholipid diffusion in, 261F
Lipid biosynthesis:
  endoplasmic reticulum, 275F
  and pentose phosphate pathway, 520–527
Lipid-linked membrane proteins, **267–269**
Lipid metabolism, 677, 711F
Lipidomics, 482
Lipid raft, 277
Lipid storage diseases, 718, 720–721
Lipmann, F., 460, 619
Lipoamide, in citric acid cycle, 572–573, 573F
Lipogenesis, AMPK and inhibition of, 805
Lipoic acid, 572–573, 572T
Lipolysis, AMPK and inhibition of, 805
Lipoproteins, **680–681,** 796
Lipoprotein lipase, 682
Liposomes, 260–261
Lipoyllysyl arm, dihydrolipoyl dehydrogenase, 575F
Lipscomb, W., 388
Liquid crystals, lipid bilayers as, 262
Liquid scintillation counting, 367
Liver:
  alanine transport to from muscles, 798–799
  AMPK-inhibited lipogenesis/gluconeogenesis in, 805
  epinephrine response, 552
  glucagon secretion, 797
  glucose generation in, 537–539
  glycogen in, 231F
  glycogen storage capacity, 530
  insulin and blocking of gluconeogenesis/glycogenolysis in, 801, 802F
  lactate transport to from muscles, 798
  mammalian metabolism in, 793–794F, **796–797**
  metabolic function, 454
  phosphoprotein phosphatase-1 activity control, 548
Liver alcohol dehydrogenase (LADH), 509
Liver glycogen synthase deficiency, 539
Liver phosphorylase deficiency (Hers' disease), 538, 539
L_λ, 1079
Loewenstein, W., 308
Lon, 737
London dispersion forces, 25
  bond energy, 25T
  defined, 25
Longevity, and caloric intake, 811
Long interspersed nuclear elements (LINEs), 939, 1045
Long terminal repeats (LTRs), 1046
Long-term regulation, 713
Long-term regulation, gluconeogenesis, 559
Lovelock, J., 10
Low-barrier hydrogen bonds (LBHBs), 355
Low density lipoproteins (LDL), **681,** 684
  atherosclerosis, 727–729
  receptor-mediated endocytosis, **684F–685**
Lowenstein, J., 841
Lowry, T., 32
LTB4, 259F
LTRs (long terminal repeats), 1046
Lu, P., 1049
Lührmann, R., 972
Lung surfactant, 250
Lyases, 453
Lyases, reaction type catalyzed, 324T
Lydon, N., 425
Lysidine, 992F
Lysine (Lys):
  acid–base catalysis by, 332
  α helix/β sheet propensities, 140T
  biosynthesis, 770–771
  breakdown, 747F, 758
  charged polar side chain, 80F
  covalent catalysis by, 335
  genetic code specification, 989T
  ionizable groups, 77T
  side chain hydropathy, 156T
Lysis, 194
Lysophosphatidic acid, 251, 710F, 711
Lysophospholipid, 251F
Lysosome, 8F
Lysosomes, 8, 278
  metabolic functions, 455T
  protein degradation in, **733**
Lysozyme, 168, 238, **339–343**
  catalytic mechanism, **343–347,** 361
  cleavage site, 340F
  isoelectric point, 98T
  model building studies, 340–343
  strain effects, 346
  structure, **339–343,** 341F
  substrate interactions, 343F
  transition state analog inhibition, 346
Lysozyme catalysis, 347F
Lysozyme catalytic mechanism, 344
Lysozyme mechanism, experimental support, 346
Lysozyme reaction, covalent intermediate, 343–347
Lysozyme reaction mechanism, 345, 345F
Lysyl oxidase, 139F
D-Lyxose, 220F

M
m^{4}C (N^4-methylcytosine), 918
m^{5}C (5-methylcytosine), 918, 1065
m^{6}A (N^6-methyladenine), 918
m^{7}G (7-methylguanosine), 966
m^{7}GDP, 1014
McArdle's disease, 531, 538–540
McCarty, M., 48
McClintock, B., 934–935
MacKinnon, R., 300, 303, 305
McKnight, S., 881
MacLeod, C., 48
MacLeod, J. J. R., 812
Macronutrients, 449–450
Mad cow disease (bovine spongiform encephalopathy; BSE), 169
Magnesium ion, *See* Mg^{2+} ion
Main chain, proteins, 127–129
Maintenance methylation, 1066, 1066F

Maize, *see* Corn
Major grooves, DNA, 46, 852–853F
Malaria, and sickle-cell anemia, 197, 527
Malate, 556, 567
  in citric acid cycle, 568F, 584F
  in glyoxylate cycle, 591F
  in urea cycle, 744F
Malate–aspartate shuttle, 599
Malate dehydrogenase, 556
  in citric acid cycle, 568F, **583**
  in urea cycle, 744F
Malate synthase, in glyoxylate cycle, 591, 591F
Malathion, 349
Male sex hormones, 410–411
Malic enzyme, 696
Malignant transformations, 421
Malignant tumors, 421. *See also* Cancer
Malonate, succinate dehydrogenase inhibition, 377–378
Malonic semialdehyde, in pyrimidine catabolism, 845F
Malonyl–ACP, in fatty acid synthesis, 705F
Malonyl–CoA, 805
  in fatty acid synthesis, 701, 705F
  from pyrimidine catabolism, 845F
Malonyl-CoA–ACP transacylase, in fatty acid synthesis, 705F
Maltodextrins, 298
Maltoporin, 298
Maltoporin subunit, 299F
Maltose, 228
Mammals:
  foreign DNA, 1076
  placental, 1057
Mandelkow, E., 1096
Manipulating DNA, 59–70
D-Mannose (Man), 220F, 520
Mannose-6-phosphate:
  in mannose metabolism, 520F
  recognition marker, 286
MAPs, *see* Microtubule-associated protein
MAPKAP kinase, 420F
MAP kinase kinase kinases (MKKKs), 420
MAP kinase kinases (MKKs), 419, 420
MAPKs (mitogen-activated protein kinases), 419
Maple syrup urine disease, 758
Margoliash, E., 115
Margulis, L., 10
Marmur, J., 866
Marsupials, X chromosome in, 1057
Martius, C., 569
Martz, E., 153
Mass spectrometry, 110–111
Maternal-effect genes, 1091
Mating type switching, 1056
Matrix, mitochondria, 598
Matthaei, H., 988
Maturation, 283
Maturity-onset diabetes mellitus, 811
Max, 420F
Maximal reaction velocity, *see* V_{max}
Max protein, 882F
Mb, *see* Myoglobin
MCM, 911
M disk, 198, 199F
mdm2 gene, 1084
Mdm2 protein, 1084
MDR (multidrug resistance) transporter, 314
Mechanism-based inhibitors, 838
Mechanosensitive channels, 302
Mediated membrane transport, **296–297**
Mediated transport, 309
Mediators:
  adaptors, 1069
  coactivator, 1069
  complex, 1069
  head domain, 1070
  middle domain, 1070
  tail domain, 1070
Medium-chain acyl-CoA dehydrogenase, 638
Medulla, 409
MEK, 419
Melanin, 762
Mello, C., 1075
Melting curve, DNA, 866, 866F
Melting temperature (T_m), DNA, 866F
Membranes. *See also* Lipids; Lipid bilayers
  assembly, **278–282**
  erythrocytes, **272–274,** 273F
  fluid mosaic model, **270–272**
  gates and fences model, 274
  glycerophospholipids in, 249–250
  lipid asymmetry, **274–278**
  lipid synthesis, **714–719**
  protein asymmetry, 265
  proton gradient dissipation, 630–631, 632F
  secretory pathway, **278–282**
  skeleton, 271–274
  sphingolipids in, 252–253
  structure, **269–278,** 270F
Membrane anchor, 280
Membrane-enveloped virus, 289
Membrane potential, 296
Membrane proteins, **263–269,** 263F, 266
  integral, **263–264,** 263F
  lipid-linked, **267–269**
  lipoproteins, **680–681**
  peripheral, **269**
  protein-lipid ratios, 263–264
  secretory pathway, **278–282**
  signal hypothesis, 278F–280
  transmembrane, **265**
Membrane subdomains, 277–278
Membrane transport, **295–318**
  active transport, **297–310**
  ATP-driven active, **311–314**
  ion-gradient-driven active, **316–318**
  mediated, **296–297**
  nonmediated, 296–297
  passive-mediated transport, **297–310**
  thermodynamics, **296–297**
Memory B cells, 210
Menaquinone, 258, 647
Mendel, G., 10, 47–48
Mendelian laws, 1066
Menten, M., 368
Mercaptans, for disulfide bond cleavage, 106–107
2-Mercaptoethanol, 103, 106
6-Mercaptopurine, 844
Mercury (Hg^{2+}) ion, zinc ion replacement, 326
Mertz, J., 61
Meselson, M., 893, 894
Mesophiles, 159
Mesophyll cells, 674
Messenger RNA, *see* mRNA
Metabolic disturbances, **809–815**. *See also* Fasting
  diabetes mellitus, 475, **811–814**
  obesity, 515, **814–815**
  starvation, **809–811**
Metabolic fate tracing, **475–477**
Metabolic flux, 456–459
Metabolic homeostasis, **804–808**
  and adaptive thermogenesis, 808
  and adiponectin, 806
  and AMP-dependent protein kinase, 804–805
  and ghrelin, 807
  and leptin, 806–807
  and $PYY_{3\text{-}36}$, 808
Metabolic inhibitors, 384, 477
Metabolic maps, 454
Metabolic pathways, **451–455.** *See also specific pathways and cycles, e.g.:* Interorgan metabolic pathways
  committed step, 456–457
  common intermediates, 451–452
  enzyme catalysis, 452–453
  evolution, 7
  experimental approaches to study of, **475–482**
  mammalian fuel metabolism, 792F
  near-equilibrium nature of, 456, 631
  organizing, 454
  short- and long-term regulation, 713
Metabolic studies, 488
Metabolic syndrome, 815
Metabolism. *See also* Aerobic metabolism; Anaerobic metabolism
  changing external conditions, 791

  - experimental approaches to study of, **475–482**
  - fructose, **516–518,** 517F
  - galactose, **518–520,** 519F
  - glucose, *see* Glucose metabolism; Glycolysis
  - hexoses other than glucose, **516–520**
  - hormonal control of fuel metabolism, **799–804**
  - interrelationships among brain, adipose tissue, muscle, and liver, 794F
  - mannose, **520,** 520F
  - metabolic fate tracing, **475–477**
  - metabolic flux control, **457–459**
  - nucleotide, 839F
  - nutrition, **449–450**
  - overview, **449–459**
  - system perturbation, **477**
  - systems biology and study of, **477–482**
  - thermodynamics, **455–457**
- Metabolites, 451
- Metabolome, 478
- Metabolomics, 482
- Metal-activated enzymes, 335–336
- Metal chelate affinity chromotography, 101
- Metal ions. *See also* Metalloenzymes; *specific metal ions*
  - as catalysts, 6, **335–336**
  - as cofactors, 326
  - nucleic acid stabilization by, 868
  - protein cross-linking, 157–158
- Metal ion catalysis, 6, **335–336**
- Metalloenzymes, 335
- *Methanococcus jannaschii,* 280–281F
- Methanogens, 9
- Methemoglobin, 179
- N^5,N^{10}-Methenyltetrahydrofolate, 920
- Methionine (Met):
  - α helix/β sheet propensities, 140T
  - biosynthesis, 770–771
  - breakdown, 747F, 753–754
  - genetic code specification, 988–989, 989T
  - ionizable groups, 76T
  - nonpolar side chain, 79
  - as rare amino acid, 93
  - side chain hydropathy, 156T
  - structure, 76T
- Methionine synthase, 770
- Methotrexate, 838
- 9-Methyladenine, 867F
- N^6-Methyladenine (m^{6}A), 918
- 1-Methyladenosine, 992F
- Methylamine methyltransferase, 1000
- Methylated histones, 1063–1064
- Methylation, DNA, 918
- Methylcobalamin, 770
- 3-Methylcytidine, 992F
- 5-Methylcytosine (m^{5}C), 918, 1065
- N^4-Methylcytosine (m^{4}C), 918
- N^5,N^{10}-Methylene-tetrahydrofolate, 749, 835–837F
- N^5,N^{10}-Methylene-tetrahydrofolate reductase (MTHFR), 755
- Methylglyoxal, 495
- Methyl groups, 1060
- 2-Methylguanine, 977
- O^6-Methylguanine, 917, 921
- 7-Methylguanosine (m^{7}G), 965–966
- N^7-Methylguanosine, 992F
- 3-Methylhistidine, 86F
- Methylmalonic semialdehyde, in pyrimidine catabolism, 845F
- Methylmalonyl-CoA, from pyrimidine catabolism, 845F
- Methylmalonyl-CoA mutase, 692, 695–696
- Methylmalonyl-CoA racemase, 692
- *N*′-Methyl-*N*′-nitro-*N*-nitrosoguanidine (MNNG), 917
- $O^{2'}$-Methylribose, 977
- N^5-Methyltetrahydrofolate, 754
- 2′-*O*-Methyltransferase, 966
- Methyltransferases, 918
- Methyltransferase flip target bases, 1065–1066
- Metmyoglobin, 179
- *met* repressor, *E. coli,* 878F
- Metzler, D., 740
- Mevalonate, in cholesterol synthesis, 722–723F
- Mevalonate-5-phosphotransferase, in cholesterol synthesis, 722–723F
- Meyerhof, O., 486
- Mg^{2+} ion:
  - in chlorophyll, 643, 647
  - as cofactor, 335
  - free nucleotides with, 42
  - with metal-activated enzymes, 335
  - nucleic acid stabilization by, 868
- M.HhaI, 1065F
- Micelles, 28F
  - defined, 28
  - lipid bilayers, 260
- Michaelis, L., 368
- Michaelis complex, 368
- Michaelis constant, *see* K_M
- Michaelis–Menten kinetics, 796
- Michaelis–Menten equation, 368–372, 376, 379F, 381T
- Micrococcal nuclease, 884, 886
- Microdomains, 277
- Microfilaments, 207–209
- Microheterogeneity, 234
- Micronutrients, 450
- Microradiography, 367
- Micro RNAs (miRNAs), 1075
- Microscopy, immunoflourescence, 207
- Middle genes, 947
- Miescher, F., 48
- Miles, E., 773
- Miller, S., 2
- Milligan, R., 206
- Milstein, C., 213
- Miltefosine, 320
- Minerals, 3, 450. *See also* Metal ions; *specific metal ions*
- Mineral acids, 34
- Mineralocorticoids, 255F, 410
- Minor grooves, DNA, 46, 852–853F
- Minot, G., 696
- (–) end, 203, 208F
- miRNAs (micro RNAs), 1075
- Mismatch repair (MMR), 918, **924–925**
- Mitchell, E., 618
- Mitchell, P., 618–619
- Mitochondria, 8, **597–600**. *See also* Amino acid breakdown; Citric acid cycle; Fatty acid oxidation; Oxidative phosphorylation; Urea cycle
  - acetyl-CoA transport to cytosol, in fatty acid biosynthesis, **701–702**
  - ADP–ATP translocator, 599–600
  - citric acid cycle in, 570
  - electron-chain component reduction potentials, 604F
  - evolution, 10
  - fatty acid elongation, 709F
  - fatty acid transport, **686–687**
  - free-radical damage, 636
  - genetic code variants, 991
  - glyoxylate cycle in, 590–591F
  - heme biosynthesis in, 776F
  - membranes, 263
  - metabolic functions, 455T
  - metabolite transport between cytosol and, in gluconeogenesis, 556–557, 557F
  - transport systems, **599–600**
- Mitochondrial electron-transport chain, 474, 597, 604F. *See also* Electron-transport chain
- Mitochondrial matrix, 598
- Mitochondrial membranes, 599F
- Mitochondrion, 8F
- Mitogen-activated protein kinases (MAPKs), 419
- Mixed enzyme inhibition, 381T, **382–383,** 383F
- MKKs, *see* MAP kinase kinases
- MKKKs (MAP kinase kinase kinases), 420
- MLCK (myosin light chain kinase), 439–440
- *MM3* gene, 1096
- MMDB (Molecular Modeling Database), 154
- MMR (mismatch repair), 918, **924–925**
- MNNG (*N*′-Methyl-*N*′-nitro-*N*-nitrosoguanidine), 917
- Mobile phase, 98
- Moderately repetitive DNA sequences, 1046
- Modification methylase, 51

MoFe-protein, in nitrogenase, 783
Molecular chaperones, **165–168**
Molecular cloning experiments, 1068. *See also* Cloning
Molecularity, 365
Molecular Modeling Database (MMDB), 154
Molecular sieve chromatography, 99–100, 1004F
Molecular weight, 13
Molten globule, 161
2-Monoacylglycerol, in triacylglycerol biosynthesis, 710F
2-Monoacylglycerol acyltransferase, in triacylglycerol biosynthesis, 710F
Monocistronic mRNA, 945
Monoclonal antibodies, 212, 213
Monod, J., 193
Monomers, 44, 305
Monooxygenases, 398
Monosaccharides, **219–224.** *See also specific monosaccharides*
  anomeric forms, 222–223
  classification, **219–224**
  configuration and conformation, **221–224**
  derivatives, **224–226**
Monosodium glutamate (MSG), 74, 764
Monoubiquitination, 735
Moore, P., 869, 1002
Moras, D., 996
Morphogens, 1092
Mosaics, protein, 120
Motifs, proteins, 146
Motor proteins, 205–206
Mouse:
  Hox-3.1 gene expression, 1097
  mouse-human cell fusion, 271F
  normal vs. obese, 807F
  protein kinase A, 433F
M phase, 1081
M-protein, 205
mRNA (messenger RNA), 49, 49F, 942
  affinity chromatography, 872
  base pairing with rRNA, 1011–1012
  degradation, 1074
  editing, 975
  monocistronic, 945
  polycistronic, 945
  posttranscriptional processing, **965–976**
MSG (monosodium glutamate), 74, 764
MTE, 959F
MTHFR (N^5,N^{10}-Methylene-tetrahydrofolate reductase), 755
mTOR, 443F
Mucolipidosis II, 286
Mucosa, 630
Mulder, G. J., 74
Müller, C., 1072
Muller-Hill, B., 1049
Mullis, K., 65
Multidrug resistance (MDR) transporter, 314
Multienzyme complexes, 570
Multiple myeloma, 212
Multiple sclerosis, 215T
Multisubunit complexes, 1069
Multisubunit proteins, 92
Murine, 210F
MurNAc, *see N*-Acetylmuramic acid
Murphy, W., 696
Muscle:
  alanine transport to liver, 798–799
  Bohr effect and, 190
  dicarboxylate recovery by citric acid cycle, 567
  epinephrine response, 550
  force generation mechanism of, 206F
  glycogen synthase, 542
  glycolytic ATP production, 510
  lactate dehydrogenase in, 505
  lactate transport to liver, 798
  mammalian metabolism in, **794–795,** 794F
  myoglobin function in, 179–180
  phosphocreatine energy source, 466
  phosphofructokinase in, **511–514**
  striated structure, **198–205**
  thick filament structure, **198,** 199F
  thin filament structure, 199F, **204**
Muscle contraction, **198–209,** 313–314
  and Cori cycle, 798
  and glycogen breakdown, 547, 549F
  high exertion, anaerobic, 795
  and myosin heads, 205–207
  striated muscle structure, **198–205**
  unconventional myosin V, 1088–1090
Muscle fatigue, 506, 795
Muscle fibers, slow- vs. fast-twitch, 510
Muscle phosphofructokinase deficiency (Tarui's disease), 538–539
Muscle phosphorylase deficiency (McArdle's disease), 531, 538–540
Mushroom poisoning, 955
Mus musculus, 57T
Mutagens, 477, 916
Mutagenesis, 68F, **916–919**
Mutases, 453, 500
Mutations, 11, **916–920**. *See also* Evolution
  Ames test, 919F
  built-in protection against, within genetic code, 990
  carcinogens, **919–920**
  chemical mutagenesis, **916–919**
  deletion, 916–919
  and evolution, 58–59
  frameshift, 986
  and free radicals, 636
  insertion, 916, 919
  neutral drift, 116
  nonsense, 1027–1028
  point, 58, 636, 916–919
  and protein synthesis, 49
  random nature of, 919
  suppressor, 986
  transitions, 916
  transversions, 916
Mutational hotspot, 1085
MutH, 925
MutL, 924–925
MutS, 924–925
Myasthenia gravis, 215T
Myc, 419, 1070, 1085
Mycobacterium tuberculosis, 594
Mycophenolic acid, 822
Mycoplasma genitalium, 57T
Myelinated membranes, 263
Myelin sheath, 253F
Myeloma, multiple, 212
Myoadenylate deaminase deficiency, 841
Myocardial infarction (heart attack), 455, 635, 728
Myofibrils, 198, 199F
Myoglobin (Mb), **177–180,** 309, 342
  function, **179–180,** 189F
  and globin family, 118
  heme group, 178, 178F, 342
  Hill plot, 185F
  ion pairs in, 157F
  isoelectric point, 98T
  molecular dynamics, 158F
  oxygen binding curve, 180F
  oxygen binding saturation function, 370
  oxygen binding site, 178F
  structure, **177–179,** 177F
  X-ray diffraction photo, sperm whale, 141F
  X-ray studies, 126
Myo-Inositol, 249T
Myomensin, 205
Myosin, 201F, 203F, **205–207**
Myosin-binding protein C, 205
Myosin head, 201, 204F
Myosin light chain kinase (MLCK), 439–440
Myotonic dystrophy, 1044, 1044T
Myristic acid, 247T, 268
Myristoylation, 268

N
NAD$^+$ (nicotinamide adenine dinucleotide), 327F, **469–470**
  and cell signaling, 435
  in citric acid cycle, 568F, 569, 570, 572T, 583
  cosubstrate, 327
  DNA ligase activation, 907F
  in fatty acid oxidation, 688
  in fructose metabolism, 517F
  in glycolysis, 487F

  in glyoxylate cycle, 591F
  in ketone body conversion to acetyl-CoA, 700F
  reduction to NADH, 469F
  in urea cycle, 744F
NAD^+-dependent isocitrate dehydrogenase, in citric acid cycle, **579–580,** 579F, 586–587
Na^+-dependent symport, 316
NADH (nicotinamide adenine dinucleotide, reduced form), 327F, 452
  in citric acid cycle, 567, 569, 570, 585
  electron-transfer coenzyme, 474
  in fructose metabolism, 517F
  function of, 474
  in gluconeogenesis, 553F
  in glycolysis, 504
  impermeability to inner membrane space, 599
  NAD^+ reduction to, 469F
  P/O ratio in oxidative phosphorylation, 629–630
  redox center, 597
  reducing equivalents, 556, 599
  thermodynamics of oxidation, 601
  in triacylglycerol synthesis, 710F
NADH–coenzyme Q oxidoreductase, *see* Complex I
$NADP^+$ (nicotinamide adenine dinucleotide phosphate), 327F
  cosubstrate, 327
  metabolic role overview, 451F
  in pentose phosphate pathway, 520–523
  reduction in photosynthesis, 641, 650–652
NADPH (nicotinamide adenine dinucleotide phosphate, reduced form), 327F
  in Calvin cycle, 664–665F
  dissipation in dark reactions, 641, 664, 672–673F
  in fatty acid synthesis, 705F
  in heme degradation, 779F
  production in light reactions, 641, 650–652
  in triacylglycerol synthesis, 710F
NADPH oxidase, 638
NAG (*N*-Acetylglucosamine), 232, 340, 343, 346, 347
NAG2FGlcF (NAGβ(1→4)-2-deoxy-2-fluoro-β-D-glucopyransosyl fluoride), 347
Na^+ ion, 299
  and DNA melting temperature, 868
  with metal-activated enzymes, 335
(Na^+–K^+)–ATPase, 794
NAM, *see* *N*-Acetylmuramic acid
NANA (*N*-Acetylneuraminic acid), 225F
Nanos gene, 1092
Nanos protein, 1092
Native (folded) proteins, 139
Natural selection, 114, 116. *See also* Evolution
  and chemical evolution, 5
  nucleic acid sequence and, 58
NBDs (nucleotide-binding domains), 315F
ncRNAs (noncoding RNAs), 1041
NDB (Nucleic Acid Database), 152
NDP (nucleoside diphosphates), 467
Near-equilibrium reactions, 456, 631
Nebulin, 205
Necrosis, 1087
Negative feedback regulation, of metabolic flux, 458
Negatively cooperative oxygen binding, 185
Negative regulators, 1050
N-end rule, 735
NER (nucleotide excision repair), **923–924,** 923F
Nernst, W., 471
Nernst equation, **470–472**
Nerve cells, phosphocreatine energy source, 466
Nerve impulses, 302–303
Nerve poisons, 349
Nervonic acid, 247T
Neural tube defects, 755
Neuroglobin, 179
Neuropeptide Y, 807
Neurotoxins, 349
Neurotransmitters, 287, 313–314, 349
  amino acids as, 88
  synthesis from tyrosine, 780–781F
Neutral drift, 116
Neutral solutions, 31
Nevirapine, 384
Newsholme, E., 515
New variant CJD (nvCJD), 171
NFAT4, 420F
NHEJ (nonhomologous end-joining), 925
NHP6A, 1058
Ni^{2+}-nitriloacetic acid, 628
Niacin (nicotinic acid), 450. *See also* Nicotinamide
Nick translation, 899, 905
Nicolson, G., 270
Nicotinamide, 435, 450, 450F, 488, 847
Nicotinamide adenine dinucleotide, *see* NAD^+
Nicotinamide adenine dinucleotide, reduced form, *see* NADH
Nicotinamide adenine dinucleotide phosphate, *see* $NADP^+$
Nicotinamide adenine dinucleotide phosphate, reduced form, *see* NADPH
Nicotinamide coenzymes, 327F
Nicotinamide mononucleotide (NMN^+), 907
Nicotinic acid (niacin), 450
Niedergerke, R., 200
Niemann–Pick disease, 720
19S caps, 735, 737
Nirenberg, M., 988
Nitrate reductase, 788
Nitric oxide (NO), **781–782**
Nitric oxide synthase, 781–782
Nitrification, 788
Nitrogenase, **783–788**
Nitrogen cycle, 788
Nitrogen excretion, 841–842F
Nitrogen fixation, 733, **782–788**
Nitrogen mustard, mutagenic effects, 917
Nitroglycerin, 781
p-Nitrophenolate ion, 336
p-Nitrophenylacetate, reaction with imidazole, 336
N-linked oligosaccharides, 234–235, 238–240
  formation, 561–562
  synthesis, 239F
NMD (nonsense-mediated decay), 1074
NMN^+ (nicotinamide mononucleotide), 907
NMR, *see* Nuclear magnetic resonance
No-go decay, 1074
Noller, H., 1001
Nomenclature:
  amino acids, **81–82,** 82F
  enzymes, **324–325**
Noncoding RNAs (ncRNAs), 1041
Noncoding (antisense) strand, 944, 945F
Noncompetitive enzyme inhibition, *see* Mixed enzyme inhibition
Noncooperative oxygen binding, 185
Nonessential amino acids, **764–769,** 764T
Nonheme iron proteins, 605
Nonhomologous end-joining (NHEJ), 925
Non-insulin-dependent diabetes mellitus, 811, 813–814
Nonketotic hyperglycinemia, 749
Nonmediated membrane transport, 296–297
Nonmediated transport, 309
Nonpolar molecules, 26–28
Nonreceptor tyrosine kinases (NRTKs), 422, 1071
Nonreducing sugars, 226
Nonsense codons, 990
Nonsense-mediated decay (NMD), 1074
Nonsense mutation, 1027–1028
Nonshivering thermogenesis, 515, 632
Nonsteroidal anti-inflammatory drugs (NSAIDs), 719
Non-stop decay, 1074
Nontranscribed DNA, **1043–1046,** 1056
Nonviral retrotransposons, 939
Non-Watson–Crick base pairs, 866–867F
Noradrenaline, *see* Norepinephrine
Norepinephrine (noradrenaline), 407, 409
  and fatty acid metabolism, 712
  fight or flight reaction, 551

- Norepinephrine (noradrenaline) (*cont.*)
  - and fuel metabolism, 799, 801
  - glycogen metabolism effects, 550
  - synthesis from tyrosine, 780–781F
  - and thermogenesis, 632–633, 808
- Northern blot, 874
- *Notophthalmus viridescens,* gene clusters, 1042F
- Novobiocin, 865
- NRTKs (nonreceptor tyrosine kinases), 422, 1071
- NSAIDs (nonsteroidal anti-inflammatory drugs), 719
- N-terminal cytoplasmic domain, 303
- N-terminal domain, 391F
- N-terminal “headpiece,” 1049
- N-terminal tails, 1060
- N-terminus (amino terminus), 78
  - dynamics, 158
  - end-group analysis, 104–105
  - as starting end of polypeptide synthesis, 1008
- NTP (nucleoside triphosphates), 467–468
- Nuclear magnetic resonance (NMR):
  - metabolic pathway studies, 476F–477
  - proteins, 143–144
  - 2D nuclear magnetic resonance spectroscopy, 144
  - yeast structure, 1059F
- Nuclear membrane, 8F
- Nuclear receptor superfamily, 1072
- Nucleases, 95
  - EDTA inhibition, 872
  - participation in RNAi, 1075–1076
- Nucleic acids, 39, 41T. *See also* DNA and RNA
  - chromatography, **872**
  - dietary, 839
  - electrophoresis, **872–873,** 873F
  - fractionation, **872–874**
  - function, **47–49**
  - ionic interactions, **868**
  - single-stranded, **47**
  - as source of biological information, 849
  - stabilizing forces, **864–871**
  - stacking interactions, **867–868,** 867F
  - structure, **43–47,** 43F
- Nucleic Acid Database (NDB), 152
- Nucleic acid sequencing, **50–59**
  - automated, **55–56**
  - chain-terminator method, **53–56,** 54F
  - databases, 112–114, 1038
  - and ethics, 70
  - gel electrophoresis, **52–53,** 52F, 54F, 55F
  - mutations and evolution, **58–59**
  - projects ongoing, 57T
  - restriction endonucleases, **51–52**
- Nucleolus, 8F, 953, 977
- Nucleophilic catalysis, 333–335
- Nucleosidases, 840F
- Nucleosides, 41, 41T
- Nucleoside diphosphates (NDP), 467
- Nucleoside diphosphate kinases, 467, 822
- Nucleoside monophosphate kinases, 822
- Nucleoside phosphorylases, 840F
- Nucleoside triphosphates (NTPs), 467–468
- Nucleosomes, **884–887,** 885F
  - core particle, 884, 885F
  - DNA in eukaryotes, 1056
- Nucleosome remodeling, 1058F
- Nucleotidase:
  - in purine catabolism, 840F
  - in pyrimidine catabolism, 845F
- Nucleotides, 39, 41–42, 41T
  - degradation, **839–846**
  - metabolism, 839F
  - phosphate groups, 42
  - structure and function, **40–42**
  - and sugar–phosphate backbone, 856F
  - torsion angles and conformation, 855F
- Nucleotide bases, 41T
  - DNA base composition, **44**
  - tautomeric forms, 44, 44F
- Nucleotide-binding domains (NBDs), 315F
- Nucleotide derivatives, 42
- Nucleotide excision repair (NER), **923–924,** 923F
- Nucleotide residues, 43–44
- Nucleotide sugar, 561
- Nucleus, 7, 455T, 1007, 1056F. *See also* DNA replication; Posttranslational modification; Transcription
- Nusslein-Volhard, C., 1092
- Nutrasweet®, 228, 762
- Nutrition, **449–450**
- nvCJD (new variant CJD), 171

O

- *O*-Linked oligosaccharides, 561
- Obesity, **814–815**
  - and appetite regulators, 807–808
  - fat reserve and survival, 810–811
  - and leptin, 806–807
  - and thermogenesis, 515
  - and type II diabetes, 813
- Obligate aerobes, 449
- Obligate anaerobes, 449, 469
- Ochoa, S., 533
- Ochre codon, 990
- Octanoyl-CoA, 688
- Odd-chain fatty acid oxidation, 686, **692–697**
- OEC (oxygen-evolving center), 653, 654–656
- Official (systematic) name, 324
- Ogston, A., 579
- Oils, 248
- Okazaki, R., 896
- Okazaki fragments, 896, 897F, 899, 904, 907
- Oleate, amphiphilic nature of, 28F
- Oleic acid, 246, 246F, 247T, 690
- Oligomers, 44, 154
- Oligopeptides, 78
- Oligosaccharides:
  - as antigenic determinants, 242F
  - functions, **240–242**
  - *N*-linked, 234–235, 238–240
  - *O*-linked, 234, 240
  - processing, 238–240
  - in proteoglycans, 235F
  - recognition events, mediation of, 241–242
  - structural effects, 240–242
- *O*-Linked oligosaccharides, 234, 240
- OMP (orotidine-5′-monophosphate), in UMP synthesis, 825F, 826
- OMP decarboxylase, in UMP synthesis, 825F, 826, 828
- OmpF porin, 256F, 288
- Oncogenes, 420, 421
- Opal codon, 990
- Oparin, A., 2
- Open complex, 947
- Open reading frame (ORF), 58, 482, 1040
- Open systems, 18
- Operators, 876, 1048F
- Operons, 945, 1042
- Opsin, 429
- Optical density, 95
- Optically active molecules, 82
- Ordered mechanism, sequential reactions, 375
- ORF (open reading frame), 58, 482, 1040
- Organelles, 8
- Organic arsenicals, 576
- Organic compounds, 2
- Organismal evolution, domains of, **9–10**
- Organogenesis, 1090
- Organ specialization, **792–799**
  - adipose tissue, **795–796**
  - brain, **793–794**
  - kidney, **798**
  - liver, **796–797**
  - metabolic function, 454–455
  - muscle, **794–795**
- *oriC* locus, 903
- Orientation effects (enzymes), **336–338,** 336F
- Origin-independent replication restart, 933
- Ornithine:
  - biosynthesis, 768–769
  - in urea cycle, 744F, 746
- Ornithine-δ-aminotransferase, 769
- Ornithine transcarbamoylase, in urea cycle, 744, 746
- Orotate, in UMP synthesis, 825F, 826
- Orotate phosphoribosyl transferase, in UMP synthesis, 825F, 826

Orotic aciduria, 828
Orotidine-5′-monophosphate (OMP), in UMP synthesis, 825F, 826
Orphan genes, 1040
Orthologous genes, 118
Orthophosphate cleavage, 464
Oryza sativa, 57T
Osmosis, **29–30**
Osmotic balance, 299
Osmotic pressure, 29, 30F
Osmotic water content, 312
Osteogenesis imperfecta (brittle bone disease), 137
Ouabain, 313
Ova, 410
Ovalbumin:
  chicken mRNA, 967F
  isoelectric point, 98T
Ovaries, 255, 406F, 410
Overproducers, 67
Oxalate, 310
Oxalate transporter, 309–310
Oxaloacetate, 567
  amino acid biosynthesis from, 589–590, 764–769
  in amino acid degradation, 738, 747F, 751
  in citric acid cycle, 568F, 584F
  in gluconeogenesis, 553, 556
  in glyoxylate cycle, 591F
  from mammalian metabolism, 793
  in urea cycle, 744F
Oxalosuccinate, in citric acid cycle, 528, 579, 579F
Oxidation, 453
Oxidation–reduction reactions, 449, **469–474**
  cofactors for, 326
  FAD, **469–470**
  metal ion catalysis, 335–336
  NAD^+, **469–470**
  Nernst equation, **470–472**
  redox centers, 597
  reduction potential measurements, **472–474**
Oxidative deamination, **742,** 917F
Oxidative metabolism, 314. *See also* Aerobic metabolism
Oxidative phosphorylation, 452, 465, **618–631,** 792F–793, 797
  ATP mass action ratio, 631
  ATP synthase, 618, **622–629**
  chemiosmotic theory, **618–622**
  control, **631–633,** 633–634
  P/O ratio, **629–630**
  thermodynamic efficiency, 601
  uncoupling, **630–631**
Oxidized (term), 452
Oxidizing agents, 470–471
Oxidoreductases, 324T, 453
2,3-Oxidosqualene, 724
OxlT, 309–310
8-Oxoguanine (oxoG), 917
Oxonium ion, 344
6-Oxo-PGF1a, 259F
Oxyanion hole, 354, 356–357
Oxygen. *See also* Respiration
  adaptation of life to, 7
  binding by hemoglobin, **184–190**
  binding by myoglobin, **177–180**
  Bohr effect, 189–190
  permeability to intermembrane space, 599
  from photosynthesis, 640, 641, 654–656
  physiological implications of oxidation, **634–637**
  reactive species, 635–636
Oxygenation:
  hemoglobin, 178–179
  myoglobin, 178–179
Oxygen binding curve:
  hemoglobin, 184
  myoglobin, 180F
Oxygen debt, 798
Oxygen-evolving center (OEC), 654–656
Oxygen tension, 180
Oxygen-transport proteins, 181
Oxyhemoglobin, *see* Hemoglobin

P
P (peptidyl) site, 1006
$p14^{ARF}$, gene encoding, 1085
$p21^{Cip1}$, 1084
p51, 913
p53, 420F, 1084
p53 gene, 1085–1086
p66, 912
$p90^{rsk}$, 420F
p680, 654
p700, 658
p870, 648
PA (protective antigen), 444–445
PAB II (Poly(A) binding protein II), 966
Pabo, C., 879, 1096
PABP (Poly(A) binding protein), 966–967
PAF65α, 1060
PAF65β, 1060
PAGE, *see* Polyacrylamide gel electrophoresis
pAgK84, restriction digests, 53F
Pair-rule genes, 1091, 1093F
  even-skipped (eve), 1092
  fushi tarazu (ftz), 1094
  hairy, 1092
  primary, 1092–1093
  runt, 1092
  secondary, 1093F
PALA (*N*-(phosphonacetyl)-L-aspartate), 388
Palindrome DNA sequences, 51–52F, 875–876
Palmitate:
  amphiphilic nature of, 28F
  in fatty acid synthesis, 705F
Palmitic acid, 246, 247T, 268
1-Palmitoleoyl-2-linoleoyl-3-stearoylglycerol, 248
1-Palmitoyl-2,3-dioleoyl-glycerol, 678
Palmitoyl-ACP, in fatty acid synthesis, 705F
Palmitoylation, 268
Palmitoyl thioesterase, 268, 705F
Pancreas, 406F, 799–800
  glucagon secretion, 712
  insulin secretion, 712, 811–812
Pancreatic β cells, 811–812
Pancreatic DNase I, 858–859
Pantothenic acid (vitamin B_3), 468–469
PAP (Poly(A) polymerase), 966
Papain, 211
Paper chromatography, 98
Parallel β sheet, 132, 133–134
Paralogous genes, 118
Paraoxonase, 349
Parathion, 349
Parkinson's disease, 636, 780, 1087
Parnas, J., 486
Paromomycin, 1035
Partial molar free energy ($\overline{G}_A$), 16
Partial oxygen pressure ($p\text{O}_2$):
  hemoglobin, 184–186
  myoglobin, 180
Passive-mediated glucose uniport, 316
Passive-mediated transport, **297–310**
  aquaporins, **306–307**
  ion channels, **299–302**
  ionophores, **297–298**
  porins, **298–299**
  transport proteins, **307–310**
Pasteur, L., 322, 485
Pasteur effect, 510
Patel, D., 1055
Pathogens, 209
Pauling, L., 127, 130–132, 195, 200, 338, 369, 850
P body (processing body), 1074
pbx (postbithorax) mutant, 1092
PC, *see* Plastocyanin
PCAF complex, 1060
PCC (protein-conducting channel), 1032
P-cluster, in nitrogenase, 784
PCNA (proliferating cell nuclear antigen), 910–911
PCR (polymerase chain reaction), 65–67, 65F
PDB (Protein Data Bank), 151–154
PDI (protein disulfide isomerase), 163–165, 164F
PDK1 (phosphoinositide-dependent protein kinase-1), 442

PE (phosphatidylethanolamine), 249T, 275, 275F, 715F
Pearse, B., 285
Pectins, 233
Pellagra, 450
Penicillin, 238
Penicillinase, 238
Pentose, 221
Pentose phosphate pathway, 486, **520–527,** 521F
  carbon skeleton rearrangements, 525F
  control, **524–527**
  and glycolysis, 525F
  mammalian metabolism, 797
PEP, *see* Phosphoenolpyruvate
PEP carboxykinase, 556–557
PEPCK (PEP carboxykinase), in gluconeogenesis, 554, 556
PEPCK (PEP carboxykinase) mechanism, 556F
Pepsin, 384
  isoelectric point, 98T
  polypeptide degradation, 738
  specificity, 107T
  X-ray studies, 125
Peptidases, 85
Peptides, 92, **127–129,** 278
Peptide bonds, **78**
Peptide-N^4-(*N*-acetyl-β-D-glucosaminyl)-asparagine amidase F, 149
Peptidoglycans, 236–237F
  238, 225
  lysozyme action in, 237F
Peptidomimetic drugs, 384
Peptidyl homoserine lactone, 108F
Peptidyl (P) site, 1006
Peptidyl transferase, 1008, 1009F, 1019
Peptidyl–tRNA, 1006, 1009F, 1021
Peptidyl–tRNA hydrolase, 1035
Peripheral membrane proteins, **269**
Permeases, 297
Pernicious anemia, 696
Peroxidase, 718
Peroxisomal β oxidation, **698**
Peroxisomes, 8, 455T, 672. *See also* Amino acid breakdown
Pertussis, 435
Pertussis toxin, 435
Perutz, M., 181, 182, 186, 200, 850
Perutz mechanism, hemoglobin, 186F–189
PEST proteins, 735
PFGE (pulsed-field gel electrophoresis), **873**
PFK, *see* Phosphofructokinase
PFK-2 (phosphofructokinase-2), 558–559
PFK-2/FBPase-2, 804
2PG, *see* 2-Phosphoglycerate
3PG, *see* 3-Phosphoglycerate
PGF$_{2\alpha}$, 259F
PGH$_2$, 259F
PGI, *see* Phosphoglucose isomerase
PGK, *see* Phosphoglycerate kinase
P-glycoprotein, 314–315
PGM, *see* Phosphoglycerate mutase
pH, 31
  biochemical standard state, 17
  common substances, 32T
  enzyme effects, 332
  Henderson–Hasselbalch equation for, 34
  protein effects, 332
  protein effects, renaturing, 159
Phage λ, 61, 63F
Pharmacogenomics, 400
Pharmacokinetics, 396
PHD finger, 1064
Phe, *see* Phenylalanine
Phen (phentermine), 397
Phenotypes, 59
Phenotypically silent codons, 990
Phentermine (phen), 397
Phentolamine, 409
Phenylacetic acid, 686
Phenylaceturic acid, 686
Phenylalanine (Phe):
  α helix/β sheet propensities, 140T
  biosynthesis, 773
  breakdown, 477F, 747F, 760–763F
  genetic code specification, 989T
  ionizable groups, 76T, 79F
  nonpolar side chain, 79, 79F
  side chain hydropathy, 156T
Phenylalanine hydroxylase, 760–761F, 763F
Phenylethanolamine *N*-methyltransferase, in neurotransmitter synthesis, 781F
Phenylisothiocyanate (PITC), in Edman degradation, 109, 109F
Phenylketonuria (PKU), 228, 762
Phenylpyruvate, 762
Phenylthiocarbamyl (PTC), in Edman degradation, 109, 109F
Phenylthiohydantoin (PTH), in Edman degradation, 109, 109F
Pheophytin *a* (Pheo *a*), 653
ϕ Angle, 128, 128F
Philadelphia chromosome, 424
Phillips, D., 340, 341, 347
Phillips, S., 878
Phorbol-13-acetate, 441, 441F
Phosophoimagers, 361
Phosphagens, 466
Phosphatases, 406
Phosphate carrier, 600
Phosphate diester, functional group and linkages, 4T
Phosphate ester, functional group and linkages, 4T
Phosphate ion. *See also* ATP
  titration curve, 34F
  titration curve, polyprotic ion, 35F
Phosphatidic acids, 249, 249T, 710F
Phosphatidic acid phosphatase, in triacylglycerol biosynthesis, 710F
Phosphatidylcholine (lecithin), 249T, 715F
Phosphatidylethanolamine (PE), 249T, 275, 275F, 715F
Phosphatidylethanolamine transferase, 715
Phosphatidylglycerol, 249T, 715, 717F
Phosphatidylglycerol phosphate, 716
Phosphatidylinositol, 249T, 259, 715, 717F
Phosphatidylinositol-4,5-bisphosphate (PIP$_2$), 437, 438F
Phosphatidylserine, 249T
Phosphatidylserine, synthesis, 715
Phosphoanhydrides:
  hydrolysis, 463F, 464
  resonance/electrostatic stabilization, 461F
Phosphoanhydride bond, 460F
Phosphoarginine, 466
Phosphocreatine, 461T, 466
Phosphodiesterases, 435–436
Phosphodiester bond, 43
Phosphoenolpyruvate (PEP):
  free energy of phosphate hydrolysis, 461T, 463
  in gluconeogenesis, 554F
  in glycolysis, 487F, 500–501F
  hydrolysis of, 503F
  metabolite transport, 556–557
Phosphoenolpyruvate carboxykinase, 801
Phosphoester bond, 460F
Phosphofructokinase (PFK):
  citrate inhibition, 634
  deactivation by thioredoxin, 671
  in glycolysis, 487F, **491–492, 511–514**
Phosphofructokinase-2 (PFK-2), 558–559
Phosphoglucomutase, 519F, 533, **537–539**
6-Phosphogluconate, in pentose phosphate pathway, 521F, 522
6-Phosphogluconate dehydrogenase, in pentose phosphate pathway, 521F, 523
6-Phosphoglucono-δ-lactone, in pentose phosphate pathway, 521F–522
6-Phosphogluconolactonase, in pentose phosphate pathway, 521F, 522
Phosphoglucose isomerase (PGI), 487F, **490–491,** 491F, 796
2-Phosphoglycerate (2PG), 20
  in gluconeogenesis, 553F
  in glycolysis, 487F, 499–500
3-Phosphoglycerate (3PG), 20
  amino acid biosynthesis from, 769
  in Calvin cycle, 663, 665F
  in gluconeogenesis, 553F
  in glycolysis, 487F, 499–500
Phosphoglycerate kinase (PGK):
  in Calvin cycle, 665F
  in glycolysis, 487F, **499**
Phosphoglycerate mutase (PGM), in glycolysis, 487F, **499–500,** 501F

Phosphoglycerides, *see* Glycerophospholipids
Phosphoglycohydroxamate, 494
2-Phosphoglycolate, 494, 672
Phosphoguanidines, 466
Phosphoinositide-dependent protein kinase-1 (PDK1), 442
Phosphoinositide 3-kinases (PI3Ks), 442
Phosphoinositide pathway, **436–445,** 437F
  and calmodulin, 438–440
  and diacylglycerol, 440–442
  and ligand binding, 437–438
Phospholipase, 251, 275
Phospholipase A_2, 251, 251F
  lipid digestion, 630
Phospholipase C (PLC), 251, 437–438
Phospholipids. *See also* Glycerophospholipids; Sphingomyelins
  transport across membranes, 276–277
  in triacylglycerol biosynthesis, 710F
Phospholipid translocases, 276
Phosphomannose isomerase, in mannose metabolism, 520F
Phosphomevalonate kinase, in cholesterol synthesis, 722
N-(Phosphonacetyl)-L-aspartate (PALA), 388
Phosphopentose epimerase, in Calvin cycle, 665F, 666
Phosphoprotein phosphatase, 393
Phosphoprotein phosphatase-1 (PP1), 426, 546–550
Phosphoprotein phosphatase inhibitor 1 (inhibitor 1), 548
β-5-Phosphoribosylamine, in IMP synthesis, 818, 819F
5-Phosphoribosyl-α-pyrophosphate (PRPP), 774, 818, 819F, 822
Phosphoribulokinase, 665F, 666
Phosphorlyase kinase deficiency, 539
Phosphorolysis, 391
Phosphorylase, *see* Glycogen phosphorylase
Phosphorylase *a,* 391, 546
Phosphorylase *b,* 391, 546
Phosphorylase kinase, 393, 546–547, 801
Phosphorylated compounds, 459, 460
Phosphorylation:
  protein, 390–393
  substrate-level, 465. *See also* Photophosphorylation
Phosphoryl group transfer, **460–462**
Phosphoryl group-transfer potentials, 461, 461T
O-Phosphoserine, 86F
Photoautotrophs, 449
Photon absorption, 643, 646, 648–649
Photooxidation, 647
Photophosphorylation, 465, 650, **661–663**
Photoreactivation, 920
Photorespiration, **671–675,** 673F
Photosynthesis, 6–7, 18, 488, **640–675**
  Calvin cycle, **663–669F,** 665F
  Calvin cycle control, **670–671**
  chloroplasts, **641–645,** 641F
  dark reactions, 641, **663–675**
  electron transport, **647–662**
  light reactions, 641, **645–663**
  net reaction, 640
  photoautotrophs, 449
  photophosphorylation, 650, **661–663**
  photorespiration, 640–641, **645–663**
  transformation of chemical energy to light energy, **645–647**
  two-center electron transport, **650–663**
  Z-scheme, 652, 652F
Photosynthetic bacteria:
  electron transport in, **647–650**
  light-absorbing pigments in, 643–645, 643F
  plasma membrane, 641–642
  purple, 647F–649
Photosynthetic reaction center:
  excitation energy trapping, 647F
  photosynthesis in, 643–644, 647F–649
  from *Rhodobacter sphaeroides,* 648F
  from *Rhodopseudomonas viridis,* 648
  as transmembrane protein, 647–648
Photosystem I, *see* PSI
Photosystem II (PSII), 650–651F, 652–654, 662
Phycocyanin, 643F
Phycocyanobilin, 645
Phycoerythrin, 643F
Phycoerythrobilin, 645
Phylloquinone, 658
Phylogenetic trees, homologous proteins, 116–117F
Phylogeny, **9**
  inferring from amino acid sequences of homologous proteins, 116–117F
  inferring from nucleic acid sequence, 58–59
p*I,* 81
PI3Ks (phosphoinositide 3-kinases), 442
PIC (preinitiation complex), 960, 962F
Pickart, C., 737
Picot, D., 656
P_{II} (regulatory protein), 766
Ping-Pong reactions, 376
PIP_2 (phosphatidylinositol-4,5-bisphosphate), 437, 438F
PITC (phenylisothiocyanate), in Edman degradation, 109, 109F
Pitch, α helix, 131
Pituitary, 406F
PK, *see* Pyruvate kinase
p*K:*
  acid proton donation, 32
  amino acid ionizable groups, 75, 76–77T, 78, **81**
  selected acids, 33T
PKA, *see* Protein kinase A
PKB (protein kinase B), 443F
PKC, *see* Protein kinase C
PKU (phenylketonuria), 228, 762
Placebo, 397
Planck's constant, 13, 266, 372, 645
Planck's law, 645
Plants, 581F, 640, 641. *See also* Photosynthesis
  C3, 674
  C4, 674
  CAM, 674–675
  light-absorbing pigments in, 643F
Plant cells, 8
Plaque(s), 62
  Alzheimer's disease, 169
  atherosclerosis, 728
Plasmalogens, 251–252, 716
Plasma membrane, 270F
  as lipid biosynthesis site, 275
  photosynthetic bacteria, 641–642
Plasmids, 60, 935
  antibiotic-resistant transposons, 938
  expression vectors, 67
  insulin gene, 1068
Plasmodium falciparum, 57T, 197, 394, 527
Plastocyanin (PC), 652, 652F, 657, 662
Plastoquinol, 651
Plastoquinone, 651, 662
PLC (phospholipase C), 437–438
Pleated β sheet, 133, 133F
PLP, *see* Pyridoxal-5′-phosphate
(+) end, 203, 208F
Pmf (protonmotive force), 620
PMP (pyridoxamine-5′-phosphate), 739F
PNP (purine nucleoside phosphorylase), in purine catabolism, 840
Point mutations, 58, 636, 916–919
Pol I (DNA polymerase I), 53, 896–897
  discovery, 898
  exonuclease function, 897F, 899F
  Klenow fragment, 900F
  and replication fidelity, 909
  use in PCR, 65F
  use in site-directed mutagenesis, 68
Pol II (DNA polymerase II), 902
Pol III (DNA polymerase III), 902
Pol III holoenzyme, 909
  β subunit, 906
  leading and lagging strand synthesis, 879–880F, 904–905F

Pol α (DNA polymerase α), 910
Polarimeter, 83F
Polar molecules, 23–24
Pol β, 910
Pol ε, 911
Pol η (DNA polymerase η), 925
Pol γ (DNA polymerase γ), 911
Pole cells, 1090
Polpot, J.-L., 656
Poly(A), 988
Poly(C), 988
Poly(Lys), 988
Poly(Pro), 988
Poly-*N*-acetylglucosamine, 234
Polyacrylamide gel electrophoresis (PAGE), 367
  nucleic acids, 52, 872
  proteins, 102F
  SDS (SDS-PAGE), 102–103
Poly(A) binding protein (PABP), 966–967
Poly(A) binding protein II (PAB II), 966
Poly(A) polymerase (PAP), 966
Poly(A) tails, 966, 967
Polycistronic mRNA, 945
Polycythemia, 194
Polyelectrolytes, 98
Poly-D-glucuronate, 234
Polymers, 3
Polymerase α, 910
Polymerase β, 910
Polymerase ε, 911
Polymerase chain reaction (PCR), **65–67,** 65F
Polymorphic cytochromes P450, 400
Polymorphic gene, 1044
Polymorphisms, 66
Polynucleotide phosphorylase, 987
Polynucleotides, 43. *See also* Nucleic acids
Polypeptides, 78. *See also* Proteins
  chain conformations, **127–129**
  cleavage in protein sequencing, **107–108**
  diversity, **92–93**
  hydrolysis, 107
  Ramachandran diagram, 129F
  reverse turns, 135F
  theoretical number of, 92
Polypeptide synthesis, **1008–1028**
  chain elongation, 1008–1010, **1014–1026**
  chain initiation, **1010–1014,** 1013F
  chain termination, **1026–1028,** 1026F
Polyproteins, 384
Polyprotic acids, 35, 35F
Polyribosomes (polysomes), 1010F
Polysaccharides, 219, **226–234, 228–230.** *See also* Oligosaccharides; *specific polysaccharides*
  glycosaminoglycans, **232–234**
  storage, **230–231**
  structural, **228–230**
Polysomes (polyribosomes), 1010F
Polytopic transmembrane proteins, 281
Polyubiquitin, 734
Polyunsaturated fatty acids, 247
Pompe's disease, 538, 539
P/O ratios, **629–630**
Porcine pancreatic elastase, 356
Porins, 267, 267F, **298–299,** 599
Porphobilinogen, in heme biosynthesis, 776F, 777
Porphobilinogen deaminase, in heme biosynthesis, 776F, 777
Porphobilinogen synthase, in heme biosynthesis, 776F, 777
Porphyrias, 778
Porphyrin, 178
Positively cooperative oxygen binding, 185
Positive regulators, 1050
postbithorax mutant *(pbx),* 1092
Postreplication repair, 932–933F
Postsynaptic membrane, 287
Posttranscriptional control mechanisms, **1073–1077**
Posttranscriptional modification, 965
Posttranscriptional processing, **965–982**
  mRNA, **965–976**
  rRNA, **976–980**
  tRNA, **980–982**
Posttranslational modification, 280
  histones, 884
  proteins, 280
Posttranslational protein processing, **1028–1031**
Posttranslocational state, 1022
PP1 (Phosphoprotein phosphatase-1), 426, 546, 547–550
PP2A, 426–428, 427F
PP2B (calcineurin), 428
PP$_i$ (pyrophosphate), 461
PPM family, 426
PPP family, 426
Prader–Willi syndrome (PWS), 1067
pRb, tumor suppressor, 1086
Prebiotic era, **2–3**
Precursors, 6
Preferential transition state binding, **338–339,** 338F
Preinitiation complex (PIC), 960, 962F
Prelog, V., 85
Pre-mRNAs, 967
Prenylation, 268
Prenyl transferase, 722
Prephenate, 773
Preproproteins, 1030
Preproteins, 280, 1030
Pre-rRNAs, 976
Presequences, 280
Presynaptic membrane, 287
Pretranslocational state, 1022
Pre-tRNAs, 981–982
Pribnow, D., 946
Pribnow box, 946F
Priestley, J., 640
Primaquine, 526, 527
Primary active transport, 311
Primary pair-rule genes, 1093
Primary structure (proteins), **91–120**
Primary transcripts, 965
Primase, 896
Primer, for chain-terminator method, 54
Primosome, 904
Prion, 170
Prion diseases, 169–171
Prion protein (PrP), 170–171
Pristanic acid, 731
Pro, *see* Proline
Probe, for colony hybridization, 64
Procarboxypeptidase A, 358
Procarboxypeptidase B, 358
Procaspases (single-chained zymogens), 1087
Procaspase-7, 1088
Procaspase-8, 1088
Procaspase-9, 1090
Procaspase-10, 1088
Processing body (P body), 1074
Processivity:
  DNA polymerase, 896–897
  RNA polymerase, 949
Prochiral molecules, 325
ProCysRS, 998
Product inhibition, 378
Proelastase, 358
Proenzymes, 357
Proflavin, as intercalating agent, 873F, 919
Progeria, 915
Progestins, 411
Programmed cell death, apoptosis, 1086
Proinsulin, 1030
Prokaryotes, **7–9,** 7F
  classification, 9
  DNA economy of, 1043
  gene clusters, 1042
  gene number, selected organisms, 1039T
  lipid biosynthesis, 275
  protein degradation in, 735
  transposons, 935
Prokaryotic DNA replication, **896–909**
  DNA polymerases, **896–902,** 899F
  fidelity, **909**
  initiation, **903–904**
  leading and lagging strand synthesis, **904–905**
  termination, **908–909**
Prokaryotic gene expression, **1046–1055**
  attenuation, **1051–1054**
  catabolic repression, **1050–1051**
  gene activation, **1050–1051**
  lac repressor, **1046–1050**

- riboswitches, **1054–1055**
- transcriptional control motifs, **876–879**

Prokaryotic ribosomes, **1001–1007**
Prokaryotic transcription, 943–952
Proliferating cell nuclear antigen (PCNA), 910–911
Proline (Pro):
- α helix/β sheet propensities, 140T
- biosynthesis, 768–769
- breakdown, 747F, 751–752F
- genetic code specification, 989T
- nonpolar side chain, 79
- side chain hydropathy, 156T
- structure, 76T

Proline racemase, inhibition, 339
Prolyl hydroxylase, 137
Promoters, 945–946
- core promoter element, 958
- upstream promoter element, 958

Proofreading, 897, 997–998
Prophospholipase A_2, 358
Propionibacterium shermanii, 694, 694F
Propionyl-CoA, 753F
Propionyl-CoA carboxylase, 692
Propranolol, 409
Proproteins, 1029
Propyl group, 307
Prostacyclins, 258, 259F
Prostaglandin H_2 synthase, 718
Prostaglandins, 259F, 709, 718–719
Prosthetic groups, 326, 327
Protease inhibitors, 355–356
Proteases, 95, 107
Proteasome, **735–738,** 736F
Protective antigen (PA), 444–445
Protein(s), 74. *See also* Amino acids; Enzymes; specific proteins and classes of proteins
- allosteric, **192–194**
- αα motif, 146
- α helix, **129–132,** 131F
- amino acid derivatives in, **86–89,** 86F
- assaying, 95–97
- βαβ motif, 146
- β barrel, 148
- β bulge, 139
- β hairpin motif, 146
- β sheet, **132–134,** 132F, 133F
- as buffering agents, 36
- catabolism overview, 452F
- coated vesicles, transport, 283–285
- composition of selected, 93T
- core, 234
- dinucleotide-binding fold, 150
- domains, **149–150,** 150F
- domain shuffling, 120
- evolutionarily conservative, 116
- fibrous, **134–139**
- functions, 91–92
- as fuel reserves, 798
- globular, *see* Globular proteins
- glycosylated, **238–240**
- homologous, 116
- integral, 263–264, 267
- isoelectric point of selected, 98T
- isotopic labeling, 367
- link, 234–235F
- in membranes, *see* Membrane proteins
- motifs, **146**
- motor, 205–206
- nuclear magnetic resonance, 143
- peptide group, 92, **127–129**
- pH effects, 332
- polypeptide diversity, **92–93**
- posttranslational processing, 282F
- preproteins, 280
- primary structure, **91–120**
- quaternary structure, 126F, **154–155**
- receptor, 395, 405
- Rossmann fold, 150
- secondary structure, 126F, **127–140**
- side chain location, 145–146
- solubility, **97–98**
- stabilizing, 94–95
- steroid hormone binding, 255
- tertiary structure, 126F, **140–154**
- transport, **307–310**
- visualizing, 145
- water-soluble, 267
- X-ray crystallography, 141–142

α_1-Proteinase inhibitor, 356
Protein-carbohydrate interactions, 240–242
Protein-conducting channel (PCC), 1032
Protein crystals, 141F
Protein Data Bank (PDB), 151–154
Protein degradation:
- intracellular, **733–735**
- lysosomal, **733**
- proteasome, **735–738,** 736F
- ubiquitin, **734–735**

Protein denaturation, 94, 139, **158–160**
Protein design, 163
Protein disulfide isomerase (PDI), 163–165, 164F
Protein domains, 120
Protein evolution, 92, **114–117**
- evolutionarily conservative proteins, 116
- gene duplication, **117–120,** 119F
- rates of, selected proteins, 119F
- sequence evolution, **114–117**

Protein Explorer (computer program), 152
Protein families, **118–120,** 150–151
Protein folding, **161–172**
- denaturation, 94, 139
- diseases, from misfolding, **168–172**
- energy–entropy diagram, 162F
- molecular chaperones, **165–168**
- pathways, **161–162,** 161F
- PDI, catalysis by, **163–165**
- renaturation, 161F

Protein function, **176–215**
Protein kinases, 251, 391
Protein kinase A (PKA), 432, 433F. *See also* cAMP-dependent protein kinase (cAPK)
Protein kinase B (PKB), 443F
Protein kinase C (PKC), 440–442
Protein-modifying reagents, 344
Protein modules, 1061
Protein mosaics, **120**
Protein phosphatases, 253, 391, 425–428
Protein phosphorylation, 390–393
Protein purification, **94–103**
- affinity chromatography, 101, 101F
- capillary electrophoresis (CE), 103
- chromatography, **98–101**
- electrophoresis, **101–103**
- gel filtration chromatography, 100–101, 1004F
- general approach to, **94–97**
- hydrophobic interaction chromatography, 99–100
- immunoaffinity chromatography, 101
- ion exchange chromatography, 98–99, 99F
- polyacrylamide gel electrophoresis (PAGE), 102F
- protein solubility, **97–98**
- SDS-PAGE, 102–103, 102F

Protein renaturation, **158–160,** 161F
Protein sequence identity, 120
Protein sequencing, **104–114,** 163
- databases, 112–114
- disulfide bond cleavage, 106–107
- Edman degradation, 106, **109–110,** 109F
- end group analysis, 104–105
- polypeptide cleavage, **107–108**
- preliminary steps, **104–107**
- sequence reconstruction, **112–114**

Protein Ser/Thr phosphatases, 426
Protein stability, 156–160
- denaturation, **158–160**
- renaturation, **158–160**

Protein structure(s):
- bioinformatics, structural, **151–154**
- irregular structures, **139–140**
- nonrepetitive structure, **139–140**
- primary structure, 92. *See also* Polypeptides; Protein evolution; Protein purification; Protein sequencing
- quaternary structure, 126, 154–155
- secondary structure, 126, 127–140
- stabilizing forces, 156–158
- structural genomics, 163
- symmetry, **155,** 155F
- tertiary structure, 126, **140–154**

Protein synthesis, 985. *See also* Ribosomes; Translation
- chain elongation, **1008–1010**

Protein synthesis (*cont.*)
  chain initiation, **1010–1014,** 1013F
  chain termination, **1026–1028,** 1026F
  heme-controlled, 1077F
  by recombinant DNA techniques, **49–50,** 60, 67, 67T
  ribosome role in, 49, 942, 1000–1001, 1010
  translational accuracy, 1026F
protein tyrosine kinases (PTKs), 413
Protein tyrosine phosphatases (PTPs), 425–426
Proteoglycans, 235F
Proteome, 50, 478, 480
Proteomics, 50, 480–482
Prothrombin, 358
Protomers, 154
Proton gradient, 316–318
  mitochondrial membranes, 597
  oxidative phosphorylation, 621
Proton jumping, 30–31, 31F
Protonmotive force (pmf), 620
Proton pump, 266, 608
Proton-pumping ATP synthase, *see* ATP-synthase
Proton translocation, 318
Proton wire, 608
Protoporphyrin IX, 610, 776F, 777
Protoporphyrinogen IX, in heme biosynthesis, 776F
Protoporphyrinogen oxidase, in heme biosynthesis, 776F, 777
Protosterol, 724
Proximity effects (enzymes), **336–338**
PrP (prion protein), 170–171
PRPP, *see* 5-Phosphoribosyl-α-pyrophosphate
Prusiner, S., 170
PsaA, 658
PsaB, 658
PsaC–E, 658
PsaF, 658
PsaI–M, 658
PsaX, 658
PsbA (D1), 652
PsbB (CP47), 653
PsbC (CP43), 653
PsbD (D2), 652
Pseudo-first-order reaction, 366
Pseudogenes, 119
Pseudouridine, 977, 992F
PSI (photosystem I), 650–651F
  electron pathways, 658–661
  segregation, 662
  X-ray structure, 659F
ϕ angles, 128, 128F
D-Psicose, 221F
PSII (photosystem II), 650–651F, 652–654, 662
Psoriasis, 215T
PTC (phenylthiocarbamyl), in Edman degradation, 109, 109F
Pteridine, 760–761F
Pterins, 760–761F
PTH (phenylthiohydantion), in Edman degradation, 109, 109F
PTKs (protein tyrosine kinases), 413
PTPs (protein tyrosine phosphatases), 425–426
P-type ATPases, 311
PUC18, 60F, 62
Pulmonary emphysema, 356
Pulsed-field gel electrophoresis (PFGE), **873**
Pulse-labeling, 895F
Pumped protons, 618
PurE, 820
Pure noncompetitive inhibition, 383
Purine, 40, 856F
Purine nucleoside phosphorylase (PNP), in purine catabolism, 840
Purine nucleotide cycle, 841F
Purine ribonucleotides, **40–42,** 41F. *See also* Adenine; Guanine
  AMP synthesis, 819F, **822–823F**
  catabolism, **839–842**
  GMP synthesis, 819F, **822–823F**
  IMP synthesis, **818–824,** 819F
  salvage, **823–824**
  synthesis, **818–824,** 819F
  synthesis regulation, **822–823**
PurK, 820
Puromycin, 1024
Purple photosynthetic bacteria, 647F–649
PWS (Prader–Willi syndrome), 1067
Pyl, *see* Pyrrolysine
Pyran, 222
Pyranoses, 222
Pyridine nucleotides, 327F
Pyridoxal-5′-phosphate (PLP), 739F–741F
  as covalent catalyst, 335
  as glycogen phosphorylase cofactor, 534
Pyridoxamine-5′-phosphate (PMP), 739F
Pyridoxine, 739F
Pyrimidine, 40
  dimers, 916
  sterically allowed orientations, 856F
Pyrimidine biosynthesis pathway, 387F
  regulation of, 827F
Pyrimidine ribonucleotides, **40–42,** 41F. *See also* Cytosine; Thymine; Uracil
  CTP synthesis, **826**
  degradation of, **845–846**
  synthesis, **824–828**
  synthesis regulation, **827–828**
  UMP synthesis, **824–828**
  UTP synthesis, **826**
Pyrobaculum aerophilum, 971
Pyrolobus fumarii, 159
Pyrophosphate (PP_i), 461
Pyrophosphate cleavage, 464, 465F
Pyrophosphomevalonate decarboxylase, 722
Pyrrole-2-carboxylate, proline racemase inhibition, 339
Δ-1-Pyrroline-2-carboxylate, proline racemase inhibition, 339
Δ^1-Pyrroline-5-carboxylate, 768
Pyrroline-5-carboxylate reductase, 768
Pyrrolysine (Pyl), 1000
Pyruvate:
  amino acid biosynthesis from, 764–768
  in amino acid degradation, 747F, 748F–749
  in citric acid cycle, 568F, 570–573
  in gluconeogenesis, **552–560,** 589–590
  in glycolysis, 487F, 501–504
  isozyme action, 455
  mammalian metabolism, 793, 795
  metabolic fate, 505F
Pyruvate carboxylase:
  in gluconeogenesis, **552–560,** 559
  two-phase reaction mechanism of, 555F
Pyruvate decarboxylase, 506
Pyruvate dehydrogenase (E_1), 797
  in citric acid cycle, 568F, **570–573**
  coenzymes and prosthetic groups, 572T
  regulation, **584–585**
Pyruvate:ferredoxin oxidoreductase, 593
Pyruvate–H^+ symport, 570
Pyruvate kinase (PK), 463
  deficiency, 502
  in glycolysis, 487F, **501–504,** 511
Pyruvate–phosphate dikinase, 674
Pyuvate ketoglutarate dehydrogenase, 797
$PYY_{3\text{-}36}$, 808

Q
Q, *see* Coenzyme Q
q (heat), 12
Q Cycle, 612–614, 651F
q_P (heat at constant pressure), 12
Q-SNAREs, 287, 288, 289F
Quanta, 645
Quantum yield, 649
Quaternary structure (proteins), 126F, **154–155**
Quinine, 394, 394F
Quinol oxidase, 621

R
R (gas constant), 13
R5P, *see* Ribose-5-phosphate
Rabbit:
  glycogen phosphorylase, 391F
  muscle actin, 202F
  muscle phosphorylase kinase, 547F
Racemic mixtures, 84

Racker, E., 622
Rad51, 934
Radioimmunoassay (RIA), 95, 408
Radionuclides, 367
Raff, M., 1087
Raf kinase, 419
RAG1, 1080
RAG2, 1080
Ramachandran, G. N., 129
Ramachandran diagram, 129F
Ramakrishnan, V., 1002
Randle cycle (glucose-fatty acid cycle), 634
Random coils, proteins, 139
Random mechanism, sequential reactions, 375
Rapamycin, 443F
Ras, 417, 419F
RasGAP, 418–419
Ras signaling cascade, 417F, 803, 1070, 1085
Rat:
  intestinal fatty-acid binding protein (I-FABP), 680F
  liver cytoplasmic 40S subunit, 1007T
  liver enzymes half-lives, 733F
  testis calmodulin, 438F
Rate constant *(k),* 364
Rate-determining step, 329
Rate enhancement, 329, 338
Rate equations, 365–366
Rational drug design, 395
Ratner, S., 743
Rayment, I., 206, 745
Reaction coordinate, **328–330**
Reaction coordinate diagram, 328F
Reaction kinetics, **364–376.** *See also* Enzyme kinetics
Reaction order, 365
Reactive oxygen species, 611
Reading frame, 986
Rearrangements, 453
RecA-mediated pairing, 929F
RecA-mediated strand exchange, 930F
RecA protein, 926, 929F–930F
RecBCD protein, 930
Receptors, 550, 801
Receptor-mediated endocytosis, 290, **684F–685**
Receptor protein, 395, 405
Receptor tyrosine kinases (RTKs), **412–428,** 1070
  and kinase cascades, 416–422
  and nonreceptor tyrosine kinases, 422–425
  and protein phosphatases, 425–428
  signal transmission by, 413–416
Recombinant, 61F
Recombinant DNA technology, **59–60,** 61F, 70. *See also* Cloning
Recombination, 58, **926–939**
  general or homologous, **926–932**
  repair by, **932–934**
  transposition, 58, **934–939**
Recombination repair, 925, **932–934**
Recombination signal sequences (RSS), 1080
Redox centers, 597
Redox cofactors, 609–611
Redox couples, 471
Redox reactions, *see* Oxidation–reduction reactions
Red tide, 676
Reduced (term), 397–398
Reducing agents, 470–471
Reducing end, 231
Reducing equivalents, 556
Reducing sugars, 226
Reduction, 453
Reduction potential, 472
  measurement, **472–474**
  selected half-reactions, 473T
Reductive pentose phosphate pathway, *see* Calvin cycle
Reef, 22F
Rees, D., 783
Regeneration:
  ATP, 464–465, 631
  coenzymes, 327–328
Regular secondary structures (proteins), 129
Regulatory light chains (RLC), 201
Regulatory proteins:
  activators, 1067
  repressors, 1067
Reichard, P., 829
Relaxed circles, 857F, 859
Release factor (RF), 1012T, 1026F–1027
Remington, J., 578
Renaturation:
  DNA, **866,** 866F
  proteins, **158–160F**
Repair, DNA, *see* DNA repair
Repetitive DNA sequences, 1043–1046
Replica plating, 64
Replication, 48
  of DNA, *see* DNA replication
  of linear chromosome, 914F
  of molecules, 5F
Replication forks, 894
Replicons, 913
Replisome, 904–905F
Repolarization, 302
Repressors, 876
  corepressors, 1051
  regulatory proteins, 1067
RER, *see* Rough endoplasmic reticulum
Resolvase, 938
Resonance energy transfer, 646–647
Respiration, 488
  ATP resupply by, 795
  brain tissue, 793
  hemoglobin/myoglobin function, 189F
  and inner mitochondrial membrane surface area, 599
  physiological implications, **634–637**
Respiratory distress syndrome, 250
Restart primosome, 933
Restriction endonucleases:
  cloning application, 61
  DNA–protein interactions, **875–876,** 875F
  for nucleic acid sequencing, **51–52**
  recognition and cleavage sites of selected, 52T
Restriction–modification system, 51–52
Reticulocyte heme-controlled protein synthesis, 1077
Reticulocytes, 778, 1077, 1077F
Retinal, 257
Retinal residue, 263
Retinoblastoma, 1086
Retinol binding protein, 149
Retro aldol condensation, 492
Retrograde transport, 283
Retrotransposons, 939, 1046
Retroviruses, 912, 938–939
Reverse transcriptase (RT), 384, 912–913
Reverse turns, 134
RF (release factor), 1012T, 1026F–1027
RF-1, 1026
RF-2, 1026
RF-3, 1027
R groups, amino acids, 75
Rhamnose, 233
Rheumatoid arthritis, 215T, 733
Rhizobium, 782F
Rhodopsin, 429
Rho factor, 951
RIA (radioimmunoassay), 95, 408
Ribitol, 224
Riboflavin (vitamin B_2), 470
Ribonuclease, *see* RNase
Ribonucleic acid, *see* RNA
Ribonucleoproteins, 914
Ribonucleotides, 40, 41F
Ribonucleotide reductase, 617, 828–834, 830F
Ribose, 220F, 221
  conformations in DNA, 856F
  in ribonucleotides, 40
D-Ribose, 220F
α-D-Ribose-5-phosphate, in IMP synthesis, 819F
Ribose-5-phosphate (R5P):
  in Calvin cycle, 665F, 666
  in pentose phosphate pathway, 521F–522
Ribose phosphate isomerase, in Calvin cycle, 665F, 666
Ribose phosphate moiety, 826
Ribose phosphate pyrophosphokinase, in IMP synthesis, 818, 819F
Ribosomal RNA, *see* rRNA
Ribosomal synthesis, 279F

Ribosomes, 8F, **1001–1008.** *See also* Protein synthesis
  eukaryotic, **1007–1008**
  membrane protein synthesis in, 278–282
  prokaryotic, **1001–1007**
  subunit self-assembly, 1007
  and transpeptidation, 1019–1021
Ribosome recycling factor (RRF), 1027
Riboswitches, **1054–1055**
Ribozymes, 323, 870
Ribulose, 221F
D-Ribulose, 221F
Ribulose-1,5-bisphosphate (RuBP), in Calvin cycle, 664, 665F, 666
Ribulose-5-phosphate epimerase, in pentose phosphate pathway, 521F–523
Ribulose-5-phosphate isomerase, in pentose phosphate pathway, 521F
Ribulose-5-phosphate (Ru5P):
  in Calvin cycle, 663F–664
  in pentose phosphate pathway, 521F–522, 521F–523
Rich, A., 854, 869
Richardson, D., 153
Richmond, T., 885
Rickets, 256–257
Rickettsia prowazekii, 57T
Rieske center, 611
Rifampicin, 954
Rifamycin B, 954
Rigor mortis, 217
RING finger, 734, 735
RISC (RNA-induced silencing complex), 1075–1076
Ritonavir, 384, 385
Rittenberg, D., 476, 775
RLC (regulatory light chains), 201
RNA (ribonucleic acid), 39–41. *See also* DNA replication; mRNA; Nucleic acids; rRNA; Transcription; Translation; tRNA
  A-DNA type helix formation, 854–855
  base-catalyzed hydrolysis, 871
  catalytic properties, 323
  as enzyme, 978
  hybridization, 866
  nucleotides, 42
  single-stranded nucleic acids in, 47
  structure, **868–871**
  synthesis by recombinant DNA techniques, 60
RNA-dependent RNA polymerase, 1076
RNA–DNA hybrids, 866
RNA editing, 975
RNAi (RNA interference), 1075–1076
RNA-induced silencing complex (RISC), 1075–1076
RNA interference (RNAi), 1075–1076
RNA interference mechanism, 1075F
RNAP, *see* RNA polymerase
RNAP II-Mediator complex, 1069–1070
RNA polymerase (RNAP), 904, 942, 946
  binding of, to promoters, **945–946**
  chain growth, **947–950**
  collisions with DNA polymerase, 949
  eukaryotes, *see* Eukaryotic transcription
  heavy metal substitution for Zn^{2+}, 326
  processivity, 949
  structure, **943–944,** 944F
  transcription termination at specific sites, **950–952**
RNA polymerase core enzyme, 943
RNA polymerase holoenzyme, 943F, 946
RNA polymerase I (RNAP I), 953, 958–964
RNA polymerase II (RNAP II), 953, 957–958, 959F
RNA polymerase III (RNAP III), 953, 960
RNA primers, 896, 899F, 905F
RNA-recognition motifs (RRM), 975
RNase III, 976
RNase A (ribonuclease A):
  bovine pancreatic, 332–333
  isoelectric point, 98T
  renaturation, 159–160F
RNase B, 241F
RNase D, 977
RNase E, 976
RNase F, 976
RNase H, 912
RNase H1, 911
RNase M5, 977
RNase M16, 977
RNase M23, 977
RNase P, 976, 980–981
RNA triphosphatase, 966
RNA world, 47, 871
Roberts, R., 967, 1065
Roberts, R. J., 968
Rodnina, M., 1021
Rofecoxib (Vioxx), 719
Rose, L., 491
Rose, W. C., 75
Rosenberg, J., 875
Rossmann (Dinucleotide-binding) fold, 150
Rotational symmetry (proteins), 155
Rotenone, 603
Rothman, J., 275, 287
Rough endoplasmic reticulum (RER), 8F
  membrane protein synthesis in, 278
  metabolic functions, 455T
Rous sarcoma virus (RSV), 421
RPA, 911
Rpb1 subunit, 955–956
Rpb2 subunit, 956
RRF (ribosome recycling factor), 1027
RRM (RNA-recognition motifs), 975
rRNA (ribosomal RNA), 49, 942. *See also* Ribosomes
  double-stranded segments, 868–869
  gene clusters, 1042
  posttranscriptional processing, **976–980**
  ribosomal RNA processing, 976–980
  self-splicing, 977–978F
RSC complex, 1056
R-SNAREs, 287, 288, 289F
RSS (recombination signal sequences), 1080
RS (Cahn-Ingold-Prelog) system, 85
R state, 186–189, 192–194, 393F
R subunit (of protein kinase A), 433
RSV (rous sarcoma virus), 421
RT (reverse transcriptase), 384, 912–913
RTKs, *see* Receptor tyrosine kinases
Rubisco, 672
RuBP (ribulose-1,5-bisphosphate), in Calvin cycle, 664, 666
RuBP carboxylase, 665F, 666–668, 670–671
RuBP carboxylase activase, 668
RuBP carboxylase–oxygenase (Rubisco), 672F. *See also* Ribulose-1,5-bisphosphate
Runt gene, 1092
Ru5P, *see* Ribulose-5-phosphate
Rutter, W., 1068
RuvA protein, 931F
RuvB protein, 931–932
RuvC protein, 932

S
S (entropy), 13
S1P, *see* Site-1 protease
S2P, *see* Site-2 protease
S4 helix, 303
S6′, 737
S6 kinase, 420F
S7P, *see* Sedoheptulose-7-phosphate
SACAIR (5-Aminoimidazole-4-(*N*-succinylocarboxamide) ribotide), in IMP synthesis, 819F, 820
SACAIR synthetase, in IMP synthesis, 819F
Saccharides, 219. *See also* Carbohydrates; Monosaccharides; Polysaccharides
Saccharine, 228
Saccharomyces cerevisiae, see Baker's yeast
Saccharomyces uvarum, pyruvate decarboxylase, 507F
Saccharopine, 758
Sacchettini, J., 630
SAGA, 1060
Sali, A., 1008
Salmine, isoelectric point, 98T
Salmonella typhimurium, 305
  glutamine synthetase, 766F
  SDS-PAGE purification, 102F
  tryptophan synthase, 773F–774
Salts, solvation in water, 26
Salt bridge, 157
Salting in, 97

Salting out, 97
Salvage pathways, 823
SAM, *see S*-Adenosylmethionine
Sandhoff's disease, 720
Sanger, F., 53, 104–105, 697, 968
Santi, D., 835
Saquinavir, 384, 385
Sarcomas, 421, 1084
Sarcomere, 198, 199F
Sarcoplasmic reticulum, 207, 313
Sarin, 349
Sarko, A., 229
Saturated enzyme, 370
Saturated fatty acids, 247, 247T
Saturation, 309
  enzymes, 370
  oxygen in myoglobin, 180
Sav1866 (ABC transporter), 315
Sayle, R., 153
SBP (sedoheptulose-1,7-bisphosphate), in Calvin cycle, 665F, 666, 670–671
SBPase (sedoheptulose-1,7-bisphosphatase), in Calvin cycle, 665F, 666, 670–671
Scaffold proteins, 420, 422
Scalar protons, 618
SCAP (SREBP cleavage-activating protein), 725
Scatchard plot, 414
Schachman, H., 387
Schiff base, 330
  formation (transimination), 740–741F
  imine, 330
Schirmer, T., 299
Schulz, G., 467
SCID (severe combined immunodeficiency disease), 70, 840–841
SCID-X1, 70
Scintillation counters, 367
SCOP (database), 154
Scott, M., 1095
Scott, W., 870
Screening, of genomic libraries, 64–65
Scr protein, 416
Scrunching, 948
Scurvy, 137
SdhA, 610
SdhB, 610
SdhC, 610
SdhD, 610
SDS (sodium dodecyl sulfate), 102–103
SDS-PAGE (sodium dodecyl sulfate-polyacrylamide gel electrophoresis), 102–103, 102F. *See also* Polyacrylamide gel electrophoresis
Sec, *see* Selenocysteine
Sec61, 280
Secondary active transport, 311, 316
Secondary lysosome, 684F
Secondary pair-rule genes, 1093F
Secondary structure (proteins), 126F, **127–140**
  defined, 126
  fibrous proteins, 134–139
  nonrepetitive structure, 139–140
  peptide group, 127–129
  regular secondary structure, 128–134
  supersecondary structure, 146
Second law of thermodynamics, **13–14**
Second messengers, 405–406, 429, 550
Second-order reactions, 365, 366
β-Secretases, 169
γ-Secretases, 169
Secretory pathway, **278–282**
Secretory vescicles, 282F
SecY, 280
SecYEG, 1032
Sedimentation coefficients, 735
Sedoheptulose-1,7-bisphosphate (SBP), in Calvin cycle, 665F, 666, 670–671
Sedoheptulose-7-phosphate (S7P):
  in Calvin cycle, 665F
  in pentose phosphate pathway, 521F, 524
Sedoheptulose bisphosphatase (SBPase), in Calvin cycle, 665F, 666, 670–671
Segmentation genes, 1091
Segment polarity genes, 1091
SELB, 1000
Selectable markers, 62
Selectins, 241–242
Selectivity filter, 301
Selenocysteine (Sec), 1000
Self-comparmentalized proteases, 737
Selfish DNA, 1046
Sem-5 protein, 418
Semiconservative replication, 893, 894F
Semidiscontinuous replication, 896
Semi-invariant positions (tRNA), 992
Sendai virus, 271F
Senescence, 915
Sense RNA, 1075
Sense (coding) strand, 944, 945F
Septic shock, 445
Sequence analysis, 309
Sequencing, *see* Nucleic acid sequencing; Protein sequencing
Sequential model of allosterism, 193, 193F
Sequential reactions, 375–376
Serine (Ser), 249T
  α helix/β sheet propensities, 140T
  biosynthesis, 769
  breakdown, 747F, 748–751
  as common amino acid, 93
  covalent catalysis by, 335
  genetic code specification, 988, 989T
  ionizable groups, 77T
  side chain hydropathy, 156T
  structure, 77T
  uncharged polar side chain, 79, 79F
Serine carboxypeptidase II, 352F
Serine dehydratase, 748–749F
Serine hydroxymethyltransferase, 749–751, 837F
Serine proteases, **347–357.** *See also* Chymotrypsin; Elastase; Trypsin
  active site, **348,** 352F
  catalytic mechanism, **352–357,** 353F
  catalytic triad, 350F
  preferential transition state binding, 354F
  X-ray structure, **348–352**
Serotonin, 780
Serum albumin, 98T
Serum glutamate–oxaloacetate transaminase (SGOT), 742
Serum glutamate-pyruvate transaminase (SGPT), 742
SET7/9, 1063–1064F
SET domain, 1063
70S ribosome, 1001T
Severe combined immunodeficiency disease (SCID), 70, 840–841
Sex hormones, 410–411
SGOT (serum glutamate-oxaloacetate transaminase), 742
SGPT (serum glutamate-pyruvate transaminase), 742
SH2 (Src homology 2) domains, 416F, 422–424, 423F, 1061
SH3 domains, 417–418F, 423F–424
Sharon, N., 346
Sharp, E., 967
Sharp, P. A., 968
Shc protein, 442
Shear degradation, 883
Shearing, of DNA, 63
Shemin, D., 476, 775
Shine, J., 1011
Shine–Dalgarno sequence, 1011–1012, 1055
Short interfering RNAs (siRNAs), 1075
Short interspersed nuclear elements (SINEs), 1045
Short tandem repeats (STRs), 66, 1044
Short-term regulation, 713
Shotgun cloning, 63
Shotton, D., 351
SHP-2, 426, 443F
Shulman, G., 813
Sialic acid, 225
Sickle-cell anemia, 70, 194F–197, 527
Sickle-cell hemoglobin (hemoglobin S), 194–197
Side chains, 1059–1060
Side chain distribution, 145–146
Sigler, P., 166, 430, 877, 962
σ^{70}, 947
σ Factor, 943
σ^{gp28}, 947
$\sigma^{gp33/34}$, 947

Sigmoidal binding curve, 184F
Signal-anchor sequences, 281
Signal-gated channels, 302
Signal hypothesis, membrane protein transport, 278F–280
Signaling, biochemical, *see* Biochemical signaling
Signal peptidase, 280
Signal peptides, 278
Signal recognition particle (SRP), 278, 428
Signal recognition particle receptor, 278–280
Signal strength, 302
Signal transduction, 299
Signal-transduction pathways, 1070
Signature sequence (TVGYG), 301
Signer, R., 850
Sildenafil, 436
Silencers, 1067
Simian virus 40 (SV40), 959
Simple sugars, *see* Monosaccharides
SINEs (short interspersed nuclear elements), 1045
Singer, S., 270
Single blind tests, 397
Single-chained zymogens (procaspases), 1087
Single-displacement reactions, 375–376
Single nucleotide polymorphisms, (SNPs), 1041
Single-strand binding protein (SSB), 904, 904F–905F
Single-stranded nucleic acids, 47
siRNAs (short interfering RNAs), 1075
Site-1 protease (S1P), 726
Site-2 protease (S2P), 726
Site-directed mutagenesis, 68F, 344
Site-specific recombination, 926
SI units, 13
16S rRNA, 976
Size exclusion chromatography, 100–101
Skehel, J., 290
Skeletal muscles. *See also* Striated muscle
  adipose tissue in, 796
  oxygen usage, 795
Ski7p protein, 1074
Skin, 796
Skou, J., 311
Slack, R., 674
SLI, 964
Sliding clamp, 905–906
Sliding filament model, 201
Slow-twitch muscle fibers, 510, 798
Small intestine, 809
Small nuclear ribonucleoproteins (snRNPs), 971
Small nuclear RNAs (snRNAs), 971
Small nucleolar RNAs (snoRNAs), 977
Small (30S) ribosomal subunit, 1001–1006, 1001T
Small ubiquitin-related modifier (SUMO), 1029
Smith, C., 873
Smith, E., 115
Smith, J., 656
Smith, M., 68
Smoking, protease inhibitor effects, 356
Smooth endoplasmic reticulum, 8F, 455T
Sm proteins, 971
Sm RNA motif, 971
S_N2 reaction, 337F
Snake venoms, *see* Venoms
SNAP-25, 287F
SNAREs, 287F, 288, 289F, 800
Snell, E., 740
snoRNAs (small nucleolar RNAs), 977
SNPs (single nucleotide polymorphisms), 1041
snRNAs (small nuclear RNAs), 971
snRNP core protein, 971
snRNPs (small nuclear ribonucleoproteins), 971
SOD (superoxide dismutase), 636
Sodium dodecyl sulfate (SDS), 102–103
Sodium ion, *See* Na^+ ion
$(Na^+–K^+)$–ATPase, 311F–313, 316
$(Na^+–K^+)$ pump, 311
Solvation, 25–26, 26F
Solvent, water as, **25–26**
Somatic hypermutation, 214, 1081
Somatic recombination, **214**
Somatostatin, 407
Sonication, 638
D-Sorbose, 221F
Sørenson, S., 31
Soret bands, 610
Sos protein, 418
SOS response, **926**
Southern, E., 874
Southern blotting, 874F
Sowadski, J., 433
Specialization, cells, 8
Special pair, 648–650
Specificity site, 833
Spectrin, 272F
Speed and specificity, 309
Sperm, 410
S phase, 1082
Sphinganine, 718F
Sphingoglycolipids, 717
Sphingolipids, **252–253,** 253F
  degradation, 720–721
  synthesis, **717–718**
Sphingolipid storage diseases, 253, 720–721
Sphingomyelins, 252F, 253, 720F
Sphingophospholipids, 252
Sphingosine, 252
Spina bifida, 755
Spinobulbar muscular atrophy, 1044T
Splenda®, 228
Spliceosome, 971
Splicing, introns and exons, 967, 969–972
Spontaneous processes, 12, 13
Sprang, S., 430
Squalene, 722–725
Squalene epoxidase, 724
Squalene oxidocyclase, 724
Squalene synthase, 724
Squelching, 1069
SR-BI, 685
Src activation, 423F
Src–AMPPNP, 422F
Src family, 422
Src homology 2 (SH2) domains, 416F, 422–424, 423F, 1061
SRE (sterol regulatory element), 725
SREBP (sterol regulatory element binding protein), 725
SREBP cleavage-activating protein (SCAP), 725
SRP (signal recognition particle), 278, 428
SRP9, 1031F
SRP14, 1031F
SRP54, 1032
SRP receptor, 279
SR proteins, 975
SSB (single-strand binding protein), 904, 904F–905F
Stacking interactions, **867–868**
Stadtman, E., 766
Stahl, E., 893, 894
Standard reduction potential, 472, 473T
Standard state, 15–17
Staphylococcal nuclease catalytic power, 323T
Staphylococcus aureus, cell wall, 236
Starch, **230–231**
  as glucose stockpile, 530
  glycogen contrasted as fuel reserve, 544
Starch synthase, 669, 669F
Stark, H., 972
Starvation, **809–811.** *See also* Fasting
  and blood glucose levels, 809–810
  gluconeogenesis during, 810
  and immediate allocation of absorbed fuels, 809
  ketone bodies as energy source during, 810–811
  and longevity, 811
Stat3β, 1072
State functions, 15
Statins, 726–727
Stationary phase, 98
Stats, 1071
Ste5p, 422
Steady state, 18–19, 368, 374–375
Steady state assumption, 368, 369
Stearic acid, 246, 246F, 247T
1-Stearoyl-2-oleoyl-3-phosphatidylcholine, 250F

Steitz, J., 971, 1002
Steitz, T., 869, 900, 996
Stem–loop structures, 47F
Stercobilin, in heme degradation, 779F, 780
Stereochemistry, amino acids, **82–86**
Stereoelectronic control, 495
Stereoisomers, 83–84
Stereospecificity, 325–326
Steroids, **254–257,** 255F, 410–411
Steroid hormones, 254–257, 1070
Steroid receptors, 165, 410, 1073
Sterols, 254
Sterol regulatory element (SRE), 725
Sterol regulatory element binding protein (SREBP), 725
Sterol-sensing domain, 726
Stevia, 228
Sticky ends, 52, 61
Stigmatellin, 614
Stop codons, 974, 990, 1026
  gene identification, 1040
  and nonsense mutation, 1027–1028
Storage diseases, 720–721
Storage polysaccharides, **230–231**
STRs (short tandem repeats), 66, 1044
Strand-passage mechanism, 860
Streptavidin, 628
Streptomyces lividans, 300
Streptomycin, 1024–1025
Striated muscle structure, **198–205.** *See also* Skeletal muscles
  thick filaments, 198, 199F
  thin filaments, 198, 199F
Stroke, 635, 728
Stroma, 641F, 642
Stromal lamellae, 641F, 642
Strominger, J., 236
Strong acids, 33
Stroud, R., 351
Structural bioinformatics, **151–154**
Structural genes, 944
Structural polysaccharides, **228–230**
Structure-based drug design, 395
Stubbe, J., 830
*su*3 (amber suppressor), 1028
Submitochondrial particles, 638
Substitutional editing, 975
Substrates, 324
  leading vs. following, 376
  Michaelis–Menten parameters of selected, 371T
  suicide substrates, 838
Substrate cycles, 458–459
  glucose metabolism, 558F
  glycolysis, **514–515**
Substrate-level phosphorylation, 465. *See also* Oxidative phosphorylation; Photophosphorylation
Subtilisin, 352F
Subunits, 92, 154–155
Subunit IV, 656
Succinate, 567, 595
  in citric acid cycle, 377, 568F, 582, 584F
  in glyoxylate cycle, 591F
  in ketone body conversion to acetyl-CoA, 700F
Succinate–Coenzyme Q oxidoreductase, *see* Complex II
Succinate dehydrogenase:
  in citric acid cycle, 568F, **582**
  malonate inhibition, 377–378
Succinate semialdehyde, 595
Succinate thiokinase, in citric acid cycle, 568F, **580–582,** 581F
Succinyl-CoA, 469
  in amino acid degradation, 747F, 753–758
  in citric acid cycle, 568F, 580, 584F
  in heme biosynthesis, 776F
  in ketone body conversion to acetyl-CoA, 700F
Succinyl-CoA synthetase, in citric acid cycle, 568F, **580–582,** 581F
Succinyl-phosphate, in citric acid cycle, 581
Sucralose, 228
Sucrose, 227, 228, 366
Sucrose-phosphate phosphatase, 669
Sucrose-phosphate synthase, 669
Sugars, 220–221, 226. *See also* Disaccharides; Monosaccharides
Suicide substrates, 838
Sulbactam, 225
Sulfa drugs, 756
Sulfanilamide, 756
Sulfatide, in sphingoglycolipid degradation, 720F
Sulfonamides, 756, 820
Sulston, J., 57
Sumner, J., 322–323
SUMO (small ubiquitin-related modifier), 1029
Supercoiled DNA, **857–859,** 857F, 858F
  progressive unwinding, 859F
  and topoisomerase, 859
  during transcription, 948F
Supercoiling, 857, 857F
Superhelicity, 857
Superoxide dismutase (SOD), 636
Superoxide radical, 635
Supersecondary structures, 146
Supply–demand process, 459
Suppressor mutations, 986
Surface labeling, 264
Surroundings, 12
Sutherland, E., 428, 533, 550
Suv39h, 1064
SV40 (simian virus 40), 959
Svedberg (unit), 735
Sweet N Low®, 228
SWI/SNF, 1056
Swiss-Pdb Viewer, 153
Swiss roll, 149
Switch regions, 431
SXL protein, 974
Symbiosis, 10
Symmetry model of allosterism, 193F
Symport, 310
Synapses, 287, 349
Synaptic cleft, 287
Synaptic vesicles, 287
Synaptobrevin, 287F
Synchrotron, 141
Syn conformation, 856F
Syncytium, 1090, 1091F
Synechocystis sp., 57T
Synergy, 1069
Synonym codons, 989–990
Syntaxin, 287
Synthase, 707F
Syphilis, arsenicals for, 576
Systematic (official) name, 324
Systemic lupus erythematosus, 215T
Systems, 12, 18
Systems biology, **477–482**
Szent-Györgyi, A., 200, 569

T
T, *see* Thymine
T (supercoiled DNA twist), 858F
T. elongatus, 659F
$t_{1/2}$ (half-life), 365–366
TAFs (TBP-associated factors), 963
TAF1, 1060
TAF5, 1060
TAF6, 1060
TAF9, 1060
TAF10, 1060
TAF12, 1060
D-Tagatose, 221F
Tainer, J., 834
D-Talose, 220F
Tangier disease, 729
Taq polymerase, 65
Target DNA sites:
  enhancers, 1067
  silencers, 1067
T Arm (tRNA), 991F
Tarui's disease, 538–539
TATA-binding protein (TBP), 961, 961F
TATA box, 959
Tatum, E., 49
Taurine, 678
Tautomers, 44, 44F
Taxonomy, **9**
Taylor, E., 206
Taylor, S., 433
Tay–Sachs disease, 253, 720–721
TBHA2, 291
TBP (TATA-binding protein), 961, 961F
TBP-associated factors (TAFs), 963
TC10 protein, 442

TCA cycle, *see* Citric acid cycle
T cells (T lymphocytes), 209
T cell receptors, 422
Telomerase, **914–916**
Telomeres, **914–916,** 1043
Temin, H., 912
Teosinte, 59F
TerA site, *E. coli* chromosome, 908F
TerB site, *E. coli* chromosome, 908F
TerC site, *E. coli* chromosome, 908F
TerD site, *E. coli* chromosome, 908F
TerE site, *E. coli* chromosome, 908F
TerF site, *E. coli* chromosome, 908F
TerG site, *E. coli* chromosome, 908F
Terminal deoxynucleotidyl transferase, 1080
Terminal desaturases, 708
Termolecular reactions, 365
Terpenoids, 257
Tertiary structure (proteins), 126F, **140–154**
  determination of, 141–145
  families, protein, 150–151
  polarity, side chain location and, 145–146
  supersecondary structures, 146–148
Testes, 255, 406F, 410
Testicular feminization, 411
Testosterone, 255F, 410
Tetanus, 288
Tetracycline, 1025
Tetracycline-resistant bacteria, 1025
Tetrahedral intermediate, chymotrypsin, 352, 356–357
Tetrahedral symmetry, 155, 155F
5,6,7,8-Tetrahydrobiopterin, 762
Tetrahydrofolate (THF), 754–756F, 755T
Tetrahymena:
  GCN5 X-ray structure, 1061F
  self-splicing, 978F
  telomerase, 914F
Tetrahymena thermophila, 979F, 1061
Tetraloop, 979
Tetramers, 44
Tetramethyl-*p*-phenylenediamine, 629
Tetroses, 221
TeTx (tetanus neurotoxin), 288
TFIIA, 963F
TFIIB, 962, 963F
TFIIB$_C$, 962
TFIIB$_N$, 962
TFIID, 961
TFIIE, 962, 964
TFIIF, 962, 964
TFIIH, 962, 964
TFIIIA, 879
TFIIIB, 964
TGN (trans Golgi network), 282
Thalidomide, 85–86
ThDP, *see* Thiamine pyrophosphate
Theobromine, 435
Theophylline, 435
Therapeutic index, 398
Thermodynamics, **11–19**
  catabolic vs. anabolic pathways, 457
  chemical equilibria, **15–17**
  diffusion, 296–297
  electron transport, 601
  fatty acid oxidation, 690
  fermentation, **509–510**
  first law, **12**
  free energy, **14–15**
  membrane transport, **296–297**
  metabolism, **455–457**
  near-equilibrium reactions, 456
  oxidative phosphorylation, 601
  second law, **13–14**
  standard state conventions, 17–18
Thermogenesis, 515, 632, 808
Thermogenin, 632, 808
Thermolysin, specificity, 107T
Thermophiles, 9
Thermus thermophilus, 606F, 607F, 1022F
θ replication, 895F
θ structures, 894
THF, *see* Tetrahydrofolate
Thiamine (vitamin B$_1$), **499,** 509
Thiamine pyrophosphate (TPP, ThDP), 572–573, 572T
  as cofactor for pyruvate decarboxylate, 507–508
  as covalent catalyst, 335
Thiazolinone, 109F
Thiazolium ring, 508
Thi box, 1055
Thick filaments, **198,** 199F, 202F
Thin filaments, **198,** 199F
Thioesters, 4T, **468–469**
Thiogalactoside transacetylase, 1047
Thiohemiacetal, 498
Thiokinases, 686, 687F
Thiol, functional group and linkages, 4T
Thiolase, 688, 689–690
  in ketogenesis, 699F
  in ketone body conversion to acetyl-CoA, 700F
Thioredoxin, 671
Thioredoxin reductase, 832F
30-nm fiber, 887
30S subunit, 1001–1006, 1001T
Thompson, L., 812
Thr, *see* Threonine
Threading, 163
3′ end, nucleic acids, 44
Threonine (Thr):
  α helix/β sheet propensities, 140T
  biosynthesis, 770–771
  breakdown, 747F, 748–751
  discovery, 75
  genetic code specification, 989T
  ionizable groups, 77T
  side chain hydropathy, 156T
  structure, 77T
  uncharged polar side chain, 79
Threonine dehydrogenase, 749
D-Threose, 220F
Thrombin, 358
Thromboxanes, 258, 259F
ThrRS, 998
Thylakoid membrane, **641–642,** 641F, 651F, 661F
Thymidine, isotopic labeling, 367
Thymidylate synthase, 835–838
Thymidylate synthesis, 835–837
Thymine (T), 40, 41T
  base pairing, 46F, 851F, 866–868
  Chargaff's rules and, 44
  as deoxynucleotide, 42
  origin, **834–838**
  in pyrimidine catabolism, 845F
  tautomeric forms, 44F
Thymine dimer, 916F
Thyroid, 406F
Thyroid hormones, 1072
Thyroxine, 88, 1072
TIM barrel, 148, 149, 495–496
Tissues, metabolic function, 455
Tissue factor, 358
Tissue-type plasminogen activator, genetically engineered, 67T
Titin, 92, 204–205, 967, 968
Titration curves, 34F–35
Tjian, R., 1062F
T loops, 1082
T lymphocytes (T cells), 209
T_m, DNA, 866F
T_m, melting temperature, DNA, 866
TMDs (transmembrane domains), 303, 315F
Tn3 transposon, 936F
TNBS (trinitrobenzenesulfonic acid), 275, 275F
TnC, 204
TnI, 204
tnpA gene, 936
TnpA transposon, 936
tnpR gene, 936
TnpR transposon, 936
TnT, 204
Tofu, 361
Topoisomerases:
  inhibitors as antibiotics and anticancer agents (Type II), 865
  supercoiling, 859–864
  Type IA, **859–860F**
  Type IB, **860, 862–863**
  Type II, 859, **863–864**
Topoisomerase I, 859–864
Topoisomerase III, 860–861F
Topology(-ies):
  of α, β, and αβ proteins, 148
  of strands in β sheet, 134

Torsion angles, polypeptides, 128
Tosyl-L-lysine chloromethylketone, trypsin binding, 348
Tosyl-L-phenylalanine chloromethylketone (TPCK), chymotrypsin binding, 348
Toxicity, and bioavailability, 396
Toxoplasma gondii, 826F
Toxoplasmosis, 826
Toyoshima, C., 314
TPCK (tosyl-L-phenylalanine chloromethylketone), 348–349F
TPP, *see* Thiamine pyrophosphate
TPP-sensing mRNA element, 1055
TPP-sensing riboswitch, 1054F
TψC Arm (tRNA), 991F
Transaldolase, in pentose phosphate pathway, 521F, 523–524
Transaminases:
  Ping Pong reaction mechanism, 376
  in urea cycle, 744F
Transamination, 559, **738–742**
Trans cisternae, 282
Transcobalamins, 696
Trans conformation, 127
Transcortin, 410
Transcription, 49F, 849. *See also* RNA polymerase
  chain elongation, **947–950**
  control in eukaryotes, **1067–1073**
  control in prokaryotes, **876–879**
  eukaryotic promoters, **958–965**
  eukaryotic RNA polymerases, **953–958**
  eukaryotic transcription factors, **960–965**
  inhibitors, 953–955
  initiation of, at promoter, **944–947**
  posttranscriptional control, **1073–1077**
  posttranscriptional processing, **965–982**
  primary transcripts, 965
  prokaryotic, 943–952
  rate of, 949–950
  termination at specific sites, **950–952**
Transcriptional activators mediator interface, 1069–1070
Transcriptional activities:
  acetylation, 1062
  carcinoma, 480F
Transcriptional coactivators, protein modules, 1061
Transcriptional control motifs, **876–879,** 876F, 877F
Transcriptional control systems, 1068
Transcriptional initiation complex model, 1063F
Transcriptional machinery, 1070
Transcriptional regulation, 1073
Transcriptional repression, 1057, 1062
Transcription factors, 419, 1068
  DNA-protein interactions, 875F, 876F, **879–883**
  eukaryotic, **960–965**
  leucine zippers, 881F–882
  transcription patterns, 1069
Transcriptome, 50, 478–479
Transcriptomics, 50, 478–479
Transferases, 324T, 375
Transfer RNA, *see* tRNA
Transformation:
  of cloning vectors, 61–62
  of organisms by DNA, 48
Transgenes, 68–69
Transgenic organisms, 68–69
Transgenic plants, 70
α(1→4) Transglycosylase, 536–537
Trans Golgi network (TGN), 282
Transimination (Schiff base formation), 740–741F
Transition metal ions, as cofactors, 335–336
Transition mutations, 916
Transition state analogs, 339, 378
Transition state diagram, 328F–329F
Transition state theory, **328–330,** 339
  enzyme kinetics, 372
  enzyme preferential transition state binding, **338–339,** 338F, 354F
Transition temperature, lipid bilayers, 262
Transketolase:
  in Calvin cycle, 665F, 666
  in pentose phosphate pathway, 521F, 523–524
Translation, 49F, 849. *See also* Posttranslational modification
  accuracy, 1026F
  chain elongation, **1008–1010**
  chain initiation, **1010–1014,** 1013F
  chain termination, **1026–1028,** 1026F
  and control, **1076–1077**
  posttranslational protein processing, **1028–1031**
  ribosome read, direction of, 1010
Translational control, **1076–1077**
Translocation, 1015
Translocation process, 299
Translocation systems, 310F
Translocon, 279
  multifunctional transmembrane pore, 280–281
  transmembrane helix insertion, 281–282
Transmembrane domains (TMDs), 303, 315F
Transmembrane helices, 265, 305, 429–430
Transmembrane helix insertion, 281–282
Transmembrane proteins, **265**
  β barrels, 267
  polytopic, 281
Transmissible spongiform encephalopathies (TSEs), 170
Transmission coefficient, 372
Transpeptidation, 1015, 1019–1021
Transport cycle, 307–308
Transporters, 297
Transport proteins, 295, **307–310,** 454
Transport protein, vesicle, **282–288**
Transport speed, 302
Transposable elements, **935–936**
Transposase, 935
Transposition, 58, **934–939**
Transposons, 926, **935–936**
Transverse diffusion, in lipid bilayers, 261
Transversion mutations, 916
TRA protein, 974
Trastuzumab (Herceptin), 425
Treadmilling, 208–209
Triacylglycerols, **248–249,** 678, 809
  in adipose tissue, 796
  biosynthesis, **710F–711**
  digestion and absorption, **678–680**
  in liver, 797
  transport, 683F
Triacylglycerol lipase, 633, 678–679F, 712
Tricarboxylate transport system, 702
Tricarboxylic acid cycle, *see* Citric acid cycle
TRiC chaperonin, 168
Triclosan, 708
Trifluoroacetic acid, 109
Trigger factor, 165, 1028–1029
Triglycerides, *see* Triacylglycerols
Trimers, 44
Trimethoprim, 838
Trinitrobenzenesulfonic acid (TNBS), 275, 275F
Trinucleotide repeats, 1044
Trinucleotide repeat diseases, 1044–1045, 1044T
Trioses, 220
Triose phosphate isomerase (TIM):
  β barrels, 149F
  in Calvin cycle, 665F
  catalytic power, 323T
  in fructose metabolism, 517F
  in glycolysis, **494–496**
Tripeptides, 78
Triskelions, 285F
Tris(2,3-dibromopropyl)phosphate, 920
tRNA (transfer RNA), 49, 49F, 942
  aminoacyl-tRNA synthetase, **994**
  cloverleaf secondary structure, 987F, 991F
  gene clusters, 1042
  isoaccepting, 995, 998
  modified bases, 992, 992F
  posttranscriptional processing, **980–982**
  proofreading, 997–998
  recognition of more than one codon by, **998–999**
  stacking interaction stabilization, 869F
  structure, **991–993,** 991F
  tertiary structure, 993F
tRNA^{Ala} (alanine tRNA), 991
tRNA^{Asp}, 996

tRNA$_{\text{f}}^{\text{Met}}$, 1010–1011
tRNA$^{\text{Gln}}$, 996
tRNA$_{\text{i}}^{\text{Met}}$, 1013
tRNA$_{\text{m}}^{\text{Met}}$, 1010–1011
tRNA nucleotidyltransferase, 982
tRNA$^{\text{Phe}}$:
  transfer RNA, covalent complex Phe, 869
  yeast, 993F, 998
tRNA$^{\text{Pyl}}$, 1000
tRNA$^{\text{Sec}}$, 1000
tRNA$^{\text{Tyr}}$, 982
Tropomodulin, 205
Tropomyosin, 204F, 207F
  isoelectric point, 98T
α-Tropomyosin, 973
Troponin, 204F, 438
Trp, *see* Tryptophan
trpL mRNA, 1052F
trp operon, 945, 1051F–1054
trp operon attenuation, 1053F
trp repressor, 877F–878
Trypanosomiasis, arsenicals for, 576
Trypsin, 107
  activation effects on active site, 357
  function, 348
  inhibitors, 358
  Ping Pong reaction mechanism, 376
  for polypeptide cleavage, 107
  polypeptide degradation, 738
  specificity, 107T
  substrate specificity, 351
  tosyl-L-lysine chloromethylketone binding, 348
  trypsinogen activation to, 357, 357F
  X-ray structure, 348–352
Trypsinogen:
  activation effects on active site, 357
  activation to trypsin, 357, 357F
Tryptophan (Trp):
  α helix/β sheet propensities, 140T
  biosynthesis, 773
  breakdown, 747F, 758, 760F
  as corepressor to *trp* operon (*E. coli*), 1051–1052
  genetic code specification, 988–989, 989T
  ionizable groups, 76T
  nonpolar side chain, 79
  as rare amino acid, 93
  side chain hydropathy, 156T
Tryptophan synthase, 773
TSEs (transmissible spongiform encephalopathies), 170
T state, 186–189, 192–194, 393F
Tswett, M., 98
Tubular particles, 308
Tumor necrosis factor-α, 806
Tumor suppressors, 1084
Turner's syndrome, 411
Turnover number, 371
Tus gene, 908
Tus protein, 908
TVGYG (signature sequence), 301
20S proteasome, 735–737
23S rRNA, 976, 1001
26S proteasome, 735, 735F, 737
28S rRNA, 977, 1007
Twist, supercoiled DNA, 858F
[2Fe–2S] clusters, *see* Iron–sulfur clusters
Two-center electron transport, photosynthesis, **650–663**
Two-dimensional (2D) gel electrophoresis, 480
Two-dimensional (2D) nuclear magnetic resonance spectroscopy, 144
TxB2, 259F
Type IA topoisomerases, **859–860F**
Type IB topoisomerases, **860, 862–863**
Type I diabetes mellitus, 811–812
Type I glycogen storage disease, 538–539
Type II diabetes mellitus, 813–814
Type II topoisomerases, **863–864,** 863F
Tyrosine (Tyr):
  acid-base catalysis by, 332
  α helix/β sheet propensities, 140T
  biosynthesis, 773
  breakdown, 747F, 760–763F
  genetic code specification, 989T
  ionizable groups, 77T
  in neurotransmitter synthesis, 781F
  in phenylalanine breakdown, 477F
  side chain hydropathy, 156T
  structure, 77T
  uncharged polar side chain, 79
Tyrosine hydroxylase, in neurotransmitter synthesis, 781F
Tyrosine kinase-associated receptors, 422
TyrRS, 998

U
U, *see* Uracil
U (energy), 12
U1-70K, 972
U1-A, 972
U1-C, 972
U1-snRNA, 971
U2-snRNP, 971
U2-snRNP auxiliary factor (U2AF), 974
U4-snRNP, 971
U5-snRNP, 971
U6-snRNP, 971
Ubiquinol (QH$_2$), 606F
Ubiquinone (coenzyme Q), 257, 606F
Ubiquitin, **734–735**
Ubiquitin-activating enzyme (E1), 734
Ubiquitin-conjugating enzymes (E2s), 734
Ubiquitin isopeptidases, 734
Ubiquitin-protein ligase (E3), 734
UCP1, 808
UCP2, 808
UCP3, 808
UDG (uracil-DNA glycosylase), 921, 922F
UDP (uridine diphosphate), 518
UDP-galactose, in galactose metabolism, 518, 519F
UDP-galactose-4-epimerase, 518–519F
UDP-glucose, 519F, 540
UDP-glucose pyrophosphorylase, **540–541,** 540F
Ultraviolet radiation, *see* UV radiation
Umami, 764
UMP (uridine monophosphate), 41T
  catabolism, 845F
  synthesis, **824–826**
Unbound transription factors, 1069
Uncompetitive enzyme inhibition, **381–382,** 382F
Uncouplers, 630–631
Uncoupling protein, 632
Unidirectional replication, 894
Unimolecular reactions, 365F, 367
Uniport, 310
UniProt data base, 113
Units, 13
Unsaturated fatty acids, 247, 247T, **690–692**
Unwin, N., 265, 266
Upstream enhancer, 1070
Upstream promoter element, 958
Upstream transcription factors, 1068–1069
Uracil (U), 40, 41T
  excision, 921
  lack of, in DNA, 921
  modified forms in tRNA, 992F
  in pyrimidine catabolism, 845F
  as ribonucleotide, 42
Uracil-DNA glycosylase (UDG), 921, 922F
Urate oxidase, in uric acid degradation, 842F
Urea, 319
  as chaotropic agent, 159
  in urea cycle, 743, 744F
  from uric acid breakdown, 842F
Urea cycle, **743–747,** 744F
Urease, 322–323, 371T
Ureido group, 554
β-Ureidoisobutyrate, in pyrimidine catabolism, 845F
β-Ureidopropionase, in pyrimidine catabolism, 845F
β-Ureidopropionate, in pyrimidine catabolism, 845F
Urey, H., 2
Uric acid, 743, 818, **842–844**
Uridine, 41T, 845F
Uridine diphosphate (UDP), 518
Uridine monophosphate, *see* UMP
Uridine phosphorylase, in pyrimidine catabolism, 845F
Uridine triphosphate (UTP), 540F, 826–828
Uridylic acid, *see* UMP
Uridylylation, 766–767

Uridylyl-removing enzyme, 766–767
Uridylyltransferase, 766
Urobilin, in heme degradation, 778, 779F
Urobilinogen, in heme degradation, 779F
Uronic acids, 224
Uroporphyrinogen decarboxylase, in heme biosynthesis, 776F, 777
Uroporphyrinogen III, in heme biosynthesis, 776F, 777
Uroporphyrinogen III cosynthase, in heme biosynthesis, 776F, 777
Uroporphyrinogen synthase, in heme biosynthesis, 777
UTP (uridine triphosphate), 540F, 826–828
UTR (untranslated region), 1044
U4-U6-snRNP, 971
UvrABC endonuclease, 923
UV (ultraviolet) radiation:
  and Cockayne syndrome (CS), 924
  DNA repair, 920
  polypeptides, absorption by, 96
  and xeroderma pigmentosum (XP), 924
UvrA gene, 923
UvrA protein, 923
UvrB gene, 923
UvrB protein, 923
UvrC gene, 923
UvrC protein, 923
UvrD (helicase II), 924

V
v (velocity of reaction), 364
v_o (initial velocity of reaction), 370
Vacuoles, 8, 8F
Valine (Val):
  α helix/β sheet propensities, 140T
  biosynthesis, 771–773
  breakdown, 747F, 757–758
  as common amino acid, 93
  genetic code specification, 989T
  ionizable groups, 76T
  nonpolar side chain, 79
  side chain hydropathy, 156T
Valinomycin, 297–298F
ValRS, 997–998
Vancomycin, 225
van der Waals contact, 356
van der Waals diameter, 306
van der Waals distance, water, 23
van der Waals forces, 25, 25T
Vane, J., 719
Van Schaftingen, E., 796
Van't Hoff plot, 16
Variable arm (tRNA), 991F
Variable region (V_H), 212
Variable region (V_L), 212
Variants (hemoglobin), 194, 195T
Varshavsky, A., 735
VAST (computer program), 154
v-*ebrB* oncogene, 421
Vectorial protons, 618
Vectors, 60
Velocity, of reaction (v), 364
Venoms:
  cobra venom enzyme, 251F
  phospholipases in, 251
Venter, C., 57
Very low density lipoproteins (VLDL):
  degradation, 681, **683**
  liver secretion, 797
Vesicles:
  as first cells, 5
  fusion, **287–291**
  secretory, 282F
  transporting, **282–288**
v-*fos* viral gene, 421
V_H (variable region), 212
Viagra (sildenafil), 436
Vibrio cholerae, 435, 478
Vinyl ether group, 252
Vioxx, 398, 719
Viral fusion protein, 289
Virulence, bacterial cell walls and, 236
Viruses, 7
  double-stranded RNA, 1076
  Ebola, 277
  HIV, 277
  influenza, 277
  measles, 277
  RNA in, 854, 871
Virus-induced human cancer, 488
Vitamins, 256–257, 450
Vitamin A, 69
Vitamin B_1 (thiamine), **499,** 509
Vitamin B_2 (riboflavin), 470
Vitamin B_3 (pantothenic acid), 468–469
Vitamin B_6 (pyridoxine), 534, 739
Vitamin B_{12} (cobalamin), 692, 696, 697
Vitamin C, 130, 137
Vitamin D, 256–257
Vitamin D_2 (ergocalciferol), 256
Vitamin D_3 (cholecalciferol), 256
Vitamin E, 258F
Vitamin K, 258F
V(D)J joining, 1080
V(D)J recombinase, 1080
v-*jun* viral gene, 421
V_L (variable region), 212
V_λ, 1079
VLDL, *see* Very low density lipoproteins
V_{max} (maximal reaction velocity), 370
  Lineweaver–Burk plot for, 373–374
  sample calculation, 373
Voltage-gated channels, 302
Voltage-gated ion channels, 302
Voltage gating in K_v, 303–304
Voltage sensor, 303
von Euler, U., 258
von Gierke's disease, 538, 539
von Liebig, J., 322
v-*ras* oncogene, 421
v-Ras protein, 421
v-*src* gene, 421
V-type ATPases, 311

W
W (number of equivalent configurations), 13
w (work), 12
Waksman, G., 900
Walker, J., 622
Wallin, I., 10
Wang, A., 854
Wang, J., 863
Warburg, O., 460, 488, 569
Water, **22–36,** 249T. *See also* Acid-base chemistry
  activity, 17
  buffers, **34–36**
  chemical properties, **30–36**
  diffusion, **29–30**
  in fatty acid synthesis, 705F
  in gluconeogenesis, 553F
  in glyoxylate cycle, 591F
  hydrocarbon transfer to nonpolar solvent thermodynamics, 27T
  hydrogen bonds in, 24F
  hydrophobic effect, **26–29**
  ionization, **30–32**
  molecular structure, 23F
  nitrogen excretion to conserve, 843
  osmosis, **29–30**
  in pentose phosphate pathway, 521F
  photosynthesis role, 18F, 640, 641, 650–652, 655
  physical properties, **23–30**
  as solvent, **25–26**
  structure, **23–26**
Water of hydration, 30–31, 306
Water-soluble vitamins, 450–451
Water-splitting enzyme, 654–655
Watson, H., 351
Watson, J., 44, 126, 200, 849–850F, 850, 893, 1001
Watson–Crick base pairs, 851F, 866–867
Watson–Crick structure, of DNA, 44–47
WD repeat, 726
Weak acids, 33
Weintraub, H., 1056
Weiss, S., 943
Western blot, 874
Western blotting, 102
Wheelis, M. L., 9
Wild type, 68
Wiley, D., 290
Wilkins, M., 850
Wilson, K., 1088
Withers, S., 346, 347
Wobble hypothesis, 999, 999T

Wobble pairs, 999F
Woese, C. R., 9
Wolfenden, R., 338, 361, 1021
Work *(w),* 12
Writhing number, supercoiled DNA, 858
Wüthrich, K., 144, 170
Wyman, J., 193

X

Xanthine, 822, 840F
Xanthine oxidase, 840F, 841–842
Xanthomas, 728
Xanthosine, in purine catabolism, 840F
Xanthosine monophosphate (XMP), 821F–822
X Chromosome Inactivation, 1057
Xenobiotics, 396
Xeroderma pigmentosum (XP), 924
Xfin protein zinc finger, 879F
X-gal, 62
Xist gene, 1057
X-linked phosphorylase kinase deficiency, 539
XMP (xanthosine monophosphate), 821F–822, 840F
XP (xeroderma pigmentosum), 924
X-ray crystallography, 342
  enzymes, 340, 342
  hemoglobin, 182
  protein tertiary structure, 141–142
Xu5P, *see* Xylulose-5-phosphate
Xylitol, 224
D-Xylose, 220F, 221
D-Xylulose, 221
Xylulose-5-phosphate (Xu5P) in Calvin cycle, 521F, 522, 665F, 666

Y

Y_{O_2} (fractional saturation for O$_2$):
  hemoglobin, 184–186
  myoglobin, 179–180
YACs, *see* Yeast artificial chromosomes
YADH (yeast alcohol dehydrogenase), 509
Yalow, A., 408
Yalow, R., 407, 408
Yanofsky, C., 1053
Yeast, 485. *See also* Baker's yeast
  electron microscopy, 1056–1057F
  fermentation, 485, 505, 507F
Yeast alcohol dehydrogenase (YADH), 509
Yeast artificial chromosomes (YACs), 61, 63–64
Yeast hexokinase, 490F
Yeast RNA polymerase II holoenzyme, 1070F
Yersinia pestis, 426
-yl (suffix), 82
Ylid, 508
Yonath, A., 1002
YopH, 426
Yoshikawa, S., 616
Young, W., 485

Z

Zalcitabine (2′,3′-dideoxycytidine, ddC), 384
Zα, 854
Zamecnik, P., 1000
Z disk, 198, 199F
Z-DNA, 852–853F, 852T, 854, 857
Zero order reactions, 366
Zidovudine (3′-Azido-3′-deoxythymidine, AZT), 384
Zif268, zinc finger motif, 158F, 879F
Zinc fingers:
  Cys$_2$-His$_2$, 158F, 879F–881
  Cys$_6$, 880F–881
  DNA binding motifs, 879F–881
Zn^{2+} coordination center, 1073
Zn^{2+} ion:
  as cofactor, 326, 335, 336
  with proteins, 93
  with yeast alcohol dehydrogenase, 509
Zovir (acyclovir), 844
Z-scheme, 652, 652F
Zymogens, 357, 1087